F 1103

R

REVUE ROUMAINE DE CHIMIE

04

REFERÁLVA

TOME 15
N° 1
Janvier 1970

ÉDITIONS DE L'ACADÉMIE DE LA RÉPUBLIQUE SOCIALISTE DE ROUMANIE

Rev. Roumaine Chim. 15, 1–138 (1970), Bucarest

COMITÉ DE RÉDACTION

Rédacteur en chef :

C. D. NENIŢESCU, membre de l'Académie de la République Socialiste de Roumanie.

Rédacteurs en chef adjoints :

A. T. BALABAN et V. E. SAHINI, membres correspondants de l'Académie de la République Socialiste de Roumanie.

Collège de rédaction :

C. DRĂGULESCU, RALUCA RIPAN, CR. SIMIONESCU, membres de l'Académie de la République Socialiste de Roumanie; EM. BRATU, membre correspondant de l'Académie de la République Socialiste de Roumanie, Pr G. OSTROGOVICH, MARG. AVRAM, F. BADEA, I. D. MARCHIDAN, D. NEGOIU et D. SĂNDULESCU.

Les manuscrits, les livres et les revues proposés en échange, ainsi que toute correspondance seront envoyés à la rédaction :

REVUE ROUMAINE DE CHIMIE

23, str. Dumbrava Roşie, Bucarest, Roumanie.

F 1103

REVUE ROUMAINE DE CHIMIE

Tome 15, N° 1 Janvier 1970

Page

I. G. MURGULESCU and I. MIHALCEA, Radiolysis of the hexamminocobaltic nitrate in aqueous solutions . . . . 3– 10 ✓

V. E. SAHINI and C. I. GHIRVU, Pariser-Parr treatment of substituted benzenes. II. Charge-transfer configurations of the benzenesulphonic acid . 11– 14

O. BENALI BAITICH, M. MEKLATI et M. ACHOUR, Interprétation des spectres électroniques d'ions complexes cyanes de fer (II) et de fer (III) dans l'approximation de la théorie du champ cristallin 15– 25

G. COSTEANU, ORTANSA LANDAUER et CORNELIA MATEESCU, L'influence du solvant sur la vitesse de réaction. L'hydrolyse alcaline de l'acétate de *n*-butyle dans le solvant mixte eau-dioxane 27– 32

MARTHA PAUČÍROVÁ, K. MATIAŠOVSKÝ and M. MALINOVSKÝ, Volume properties of the melts of the systems LiF-AlF_3 and NaF–AlF_3 . . . . 33– 41 ✓

RODICA VÎLCU and FLORICA IRINEI, Excess functions for mixed electrolyte solutions 43– 51

ILEANA PETRUȘ, Reactions in solid media. II. Kinetics of the formation of the double oxide of powder mixtures in nitrogen atmosphere . . . . . 53– 57 ✓

H. NEBELL, Thermodynamic properties of liquid magnesium-lead, magnesium-indium and magnesium-gallium alloys 59– 65

T. CHIRULESCU and E. SEGAL, Gas chemisorption on ferromagnetic powder. IV. Hydrogen, oxygen ferrites system at liquid nitrogen temperature . . 67– 69

AL. FRUMA, D. L. CRĂCIUNESCU et C. GHIRVU, L'influence de la structure électronique sur l'effet catalytique des complexes cuivre-aniline substituée 71– 76

MARIA FITI, La cinétique de compétition dans l'étude des intermédiaires instables. I. Les ions Co^+, Mn^+, Zn^+, Cd^+ et Ni^+ 77– 85

V. M. BHATNAGAR, The cell parameters of synthetic fluorapatite, $Ca_{10}(PO_4)_6F_2$ 87– 89

S. SOLACOLU, P. BALTĂ and GEORGETA JITIANU, The kinetics of changes of the vitreous structures in some lithium-silicate glasses 91–101

J. DICK und ANNA MAURER, Neue Komplexverbindungen der Pyrazolonreihe. VI . . . . 103–114 ✓

E. POPPER, LUCIA CHIOREAN and IULIA PITEA, Photocolorimetric study of Pd(II) and the α-ethyl-isonicotinic acid thioamide 115–118

Rev. Roumaine Chim. 15, 1–138 (1970), Bucarest

Page

A. ŞUTEU und CARMEN MANIU, Kolorimetrische Bestimmung des Hydrazins mit Phosphomolybdowolframsäure 119–121

L. BALABÁN and L. PREISLER, The evolution of gaseous products during the photo-oxidative degradation of polypropylene 123–128

LEONIA STOICESCU-CRIVETZ, ELENA MĂNTĂLUŢĂ et I. ZUGRĂVESCU, Polyhydantoïnes-Triazines 129–134

I. OPREAN, C. BODEA and V. FĂRCĂŞAN, On the synthesis of 3-nitro-10-methyl-phenothiazine 135–138

Revue Roumaine de Chimie, **15**, 3–10 (1970)

RADIOLYSIS OF THE HEXAMMINOCOBALTIC NITRATE IN AQUEOUS SOLUTIONS

I. G. MURGULESCU and I. MIHALCEA
Laboratory of Physical Chemistry, Bucharest University,
B-dul Republicii 13

Received February 25, 1969

The kinetics and the mechanism of the hexamminocobaltic nitrate decomposition in aqueous solutions under the action of γ-radiations are studied. The decomposition of the $[Co(NH_3)_6]\,(NO_3)_3$ takes place according to a reduction mechanism of Co(III) to Co(II) by hydrogen atoms. The radiolysis process is studied for various concentrations of the hydrogen ions and the rate constant of the complex with the hydrogen atoms is determined. The influence of the dose rate and of the temperature on the yield of the complex decomposition is studied. The activation energy of the process is determined.

Although a few studies [1–4] were recently made on the radiolysis of the aqueous solutions of complex ammines, the problem of the reactivity of the water radiolysis products in the presence of these complexes, as well as the mechanism of these reactions are not yet elucidated. For instance, some authors [2–4] consider that the decomposition of the complexes in the irradiated solutions is a reaction of the reduction of Co(III) to Co(II), while others [5,6] assume that it is a hydrolytic mechanism. The results of the different authors referring to the kinetics of the complex ammine radiolysis in aqueous solutions are not similar. Therefore this problem necessarily requires a thorough kinetic study.

In this paper, we intend to investigate the kinetics of the radiolysis of hexamminocobaltic nitrate in aqueous solutions, as well as the influence of various factors on this process.

[1] A. V. Egunov and P. T. Dolin, *Doklady Akad. Nauk. S.S.S.R.*, **142**, 1 (1962).

[2] D. Katakis and A. O. Allen, *J. Phys. Chem.*, **68**, 1359 (1964).

[3] J. Halpern and J. Rabani, *J. Amer. Chem. Soc.*, **88**, 699 (1966).

[4] I. G. Murgulescu and I. Mihalcea, *Rev. Roumaine Chim.*, **12**, 763 (1967).

[5] L. N. Neocladnova and G. A. Saghisultanova, *Doklady Akad. Nauk. S.S.S.R.*, **149**, 5 (1963).

[6] L. N. Neocladnova and G. A. Saghisultanova, *Radiokhimiya*, **3**, 305 (1963).

EXPERIMENTAL

The Co(III) hexammine was obtained and purified by techniques described in literature.[7] The other substances made use of in this work were "chemically pure". The solutions were always recently prepared, before each irradiation, with triply distilled water. The irradiations were carried out with a $Co^{60} - \gamma$ source having the activity of 50 gr. equiv. Ra. The irradiation technique and the form of the cells in which the solutions were irradiated have been described in a previous paper. [8] The doses were determined by means of Fricke's dosimeter assuming that $G(Fe^{+3}) = 15.6$.

The variation of the complex concentration with the irradiation time was measured spectrophotometrically at 470 mμ.

RESULTS

Since, when irradiating solutions of complexes in a neutral medium, a $Co(OH)_2$ precipitate is formed [1] which makes the spectrophotometric determination of the complex concentration impossible, we had to add to the initial solutions nitric acid in known concentrations from 0.005 M/l–0.045 M/l. The radiochemical yield G of decomposition of $[Co(NH_3)_6](NO_3)_3$ as a function of the acid concentration is given in table 1.

Table

Variation of the rate constant and of yield G with

0.005 M/l				0.0066 M/l				00.1	
t min	$k_1' \times 10^4$ min^{-1}	$k_0 \times 10^{-14}$ $\frac{molec}{sec}$	G	t min	$k_1' \times 10^4$ min^{-1}	$k_0 \times 10^{-14}$ $\frac{molec}{sec}$	G	t min	$k_1' \times 10^4$ min^{-1}
50	20.50	0.383	1.570	29	16.7	0.330	1.350	62	14.3
80	21.60	0.396	1.610	87	17.7	0.330	1.350	127	15.6
124	23.69	0.414	1.680	127	18.5	0.331	1.350	200	16.9
213	25.99	0.398	1.620	155	18.9	0.332	1.355	280	17.2
250	27.37	0.395	1.610	180	19.2	0.329	1.340	323	18.5
—	—	—	—	—	—	—	—	338	19.1
—	—	—	—	—	—	—	—	—	—
—	—	—	—	—	—	—	—	—	—

---

[7] N. G. KLIUCHNICOV, "Rukovodstvo po neorganicheskomu sintezu" Izd. Khimia, Moscow, 1965 p. 356.

[8] I. G. MURGULESCU, T. ONCESCU, J. PĂUN and I. MIHALCEA, *Rev. Roumaine Chim.*, **12**, 573 (1967).

The order of the reactions is changing from zero to one with the acid concentration increase.

The influence of the complex concentration on yield G is given in table 2. The acid concentration remained constantly, equal to 0.02 M/l.

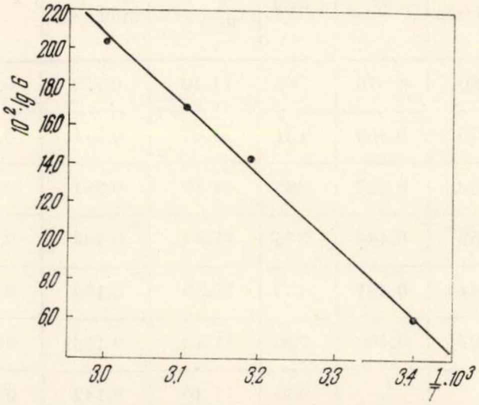

Fig. 1. – Dependence of log G on the $1/T$.
[Complex] = 0.002 M/l; [HNO_3] = 0.005 M/l.
Dose rate= 1.78×10^{15} eV/ml. sec.

1

the acid conc. Complex conc.=0.002 M/l

M/l		0.02 M/l				0.045 M/l			
$k_0 \times 10^{-14}$ $\frac{\text{molec}}{\text{sec}}$	G	t min	$k_1' \times 10^4$ min^{-1}	$k_0 \times 10^{-14}$ $\frac{\text{molec}}{\text{sec}}$	G	t min	$k_1' \times 10^4$ min^{-1}	$k_0 \times 10^{-14}$ $\frac{\text{molec}}{\text{sec}}$	G
0.286	1.125	88	11.60	0.224	0.715	95	6.20	0.121	0.384
0.295	1.160	131	11.20	0.211	0.675	122	6.19	0.119	0.377
0.292	1.145	285	11.80	0.201	0.638	160	6.04	0.116	0.370
0.285	1.120	375	11.40	0.186	0.591	615	5.94	0.100	0.317
0.290	1.140	435	11.30	0.179	0.569	790	6.21	0.099	0.314
0.292	1.145	720	11.40	0.156	0.495	1 180	6.00	0.087	0.275
–	–	900	11.30	0.142	0.451	1 225	6.13	0.087	0.276
–	–	1 285	10.80	0.117	0.372	1 585	6.08	0.078	0.249

At this concentration G increases with the complex concentration increase, the reaction being of the first order.

Table

Influence of the complex conc. on the rate const.

0.00125 M/l				0.002 M/l				0.004	
t min	$k_1' \times 10^4$ min^{-1}	$k_0 \times 10^{-14}$ molec/sec	G	t min	$k_1' \times 10^4$ min^{-1}	$k_0 \times 10^{-14}$ molec/sec	G	t min	$k_1' \times 10^4$ min^{-1}
82	15.20	0.180	0.576	88	11.40	0.224	0.715	132	10.40
150	15.55	0.175	0.559	131	11.00	0.211	0.675	210	10.20
190	15.40	0.168	0.537	285	11.80	0.201	0.638	343	10.40
306	15.02	0.152	0.486	375	11.40	0.186	0.591	485	10.30
396	15.15	0.144	0.461	435	11.30	0.179	0.569	788	10.10
565	15.05	0.127	0.406	720	11.40	0.156	0.495	952	10.30
—	—	—	—	900	11.30	0.142	0.451	1 070	10.00
—	—	—	—	1 285	10.80	0.117	0.372	1 175	10.10

Table

Influence of the dose rate on the yield G.

0.565×10^{15} eV/ml.s			1.2×10^{15} eV/ml.s			1.78×10^{15} eV/ml.s		
t min	$k_0 \cdot 10^{-14}$ $\frac{\text{molec}}{\text{sec}}$	G	t min	$k_0 \cdot 10^{-14}$ $\frac{\text{molec}}{\text{sec}}$	G	t min	$k_0 \cdot 10^{-14}$ $\frac{\text{molec}}{\text{sec}}$	G
290	0.0610	1.080	200	0.1310	1.090	132	0.1970	1.110
550	0.0614	1.185	390	0.1370	1.140	160	0.2070	1.160
775	0.0651	1.153	455	0.1345	1.120	361	0.2070	1.160
1 280	0.0632	1.120	600	0.1390	1.160	440	0.2050	1.150
1 605	0.0636	1.125	855	0.1345	1.120	—	—	—
—	—	—	—	—	—	—	—	—

We also studied the dose rate influence on yield G. The results obtained are recorded in table 3.

In order to determine the activation energy of the radiolytic process of the hexamminocobaltic nitrate in aqueous solution, we studied the decomposition of this complex at various temperatures and determined the G variation with temperature. The results thus obtained are represented in figure 1 which shows that G varies with T according to a simple equation of Arrhenius type. The activation energy thus determined is 1.65 kcal/mol.

2

and on the yield G. Acid conc. = 0.02 M/l

M/l		0.005 M/l				0.01M /l			
$k_0 \times 10^{-14}$ molec/sec	G	t min	$k_1' \times 10^4$ min^{-1}	$k_0 \times 10^{-14}$ molec/sec	G	t min	$k_1' \times 10^4$ min^{-1}	$k_0 \times 10^{-14}$ molec/sec	G
0.394	1.250	215	9.48	0.428	1.367	220	6.48	0.612	2.01
0.366	1.160	285	9.48	0.416	1.329	420	6.27	0.555	1.91
0.356	1.130	327	9.60	0.416	1.329	780	6.25	0.482	1.65
0.338	1.070	840	9.40	0.324	1.033	825	6.20	0.487	1.67
0.290	0.922	1 065	9.40	0.298	0.952	940	6.35	0.482	1.65
0.264	0.839	1 285	9.55	0.276	0.892	1 040	6.50	0.487	1.67
0.248	0.787	1 435	9.47	0.269	0.859	—	—	—	—
0.237	0.753	—	—	—	—	—	—		—

3

[Complex] = 0.002 M/l in HNO_3 0.01 M/l

2.24×10^{15} eV/ml.s			2.45×10^{15} eV/ml.s		
t min	$k_0 \cdot 10^{-14}$ $\frac{\text{molec}}{\text{sec}}$	G	t min	$k_0 \cdot 10^{-14}$ $\frac{\text{molec}}{\text{sec}}$	G
90	0.267	1.190	62	0.286	1.170
140	0.272	1.210	127	0.295	1.200
183	0.263	1.170	200	0.292	1.190
368	0.248	1.100	280	0.285	1.160
405	0.250	1.110	323	0.290	1.180
500	0.253	1.125	338	0.292	1.190

DISCUSSIONS OF RESULTS

When the aqueous solutions of $[Co(NH_3)_6](NO_3)_3$ are irradiated with ionizing radiations, the reduction of Co(III) to Co(II) takes place through the water radiolysis products.

The absorption of γ-radiation by the water yields, according to the theory of the free radicals, the following radical species : e_{aq}^-, H and OH. In acid solutions, e_{aq}^- is converted into H according to reaction (1)

$$e_{aq}^- + H^+ \rightarrow H \tag{1}$$

where the rate constant is equal to 2×10^{10}l. $M^{-1} sec^{-1}$ [9] so that the only species to be taken into consideration are H and OH. The acetone presence in the solutions to be irradiated did not affect yield G, which indicates that all hydrated electrons were converted into hydrogen atoms.

From table 1, we see that the reduction process of Co(III) into Co(II) obeys a zero or first order kinetics as a function of the concentration of hydrogen ions. Thus, when $[H^+]$ is equal to or less than 10^{-2} M/l, the reaction order is equal to zero, while at higher concentrations we have a reaction of first order. The same table shows that G decreases when the hydrogen ion concentration increases. This suggests the idea that the hydrogen ion enters the competition reaction for the hydrogen atom.

Concomitantly with the increase of the complex concentration, the yield G increases, at expected, thus demonstrating the existence of competitive reactions in the system under study (table 2).

From table 3, one can see that G does not vary with the dose rate which indicates that, at small dose rate the principal reactions of the radicals in the solution volume are those with dissolved substances and there are no recombination reactions or these are so small as to be negligible under these conditions.

According to data in tables 1, 2 and 3, it may be assumed that the principal reactions taking place, in the given system, by irradiation with γ-rays, are the following :

$$[Co(NH_3)_6]^{+3} + H \xrightarrow{k_1} Co^{+2} + H^+ + 6\,NH_3 \tag{2}$$

$$H^+ + H \xrightarrow{k_2} H_2^+ \tag{3}$$

$$NO_3^- + 2H \xrightarrow{k_3} NO_2^- + H_2O \tag{4}$$

The rate of the complex decomposition reaction is

$$-\frac{d\,(a-x)}{dt} = k_1\,(a-x)\cdot[H] \tag{5}$$

where a is the initial concentration of the complex in solution, x — the concentration decrease and [H] — the concentration of the hydrogen atoms.

Since on the one hand, the hydrogen atoms are formed by the water radiolysis with an yield of $G_{(H)} = G_H + G_{e_{aq}^-}$ and on the other hand these atoms disappear in reactions (2) — (4), their concentration at any given moment will be constant, so that we can apply the steady state principle as follows :

$$\frac{G_{(H)}\,I}{100\ N} = k_1\,(a-x)\,[H] + k_2\,[H]\,[H^+] + k_3\,[NO_3^-]\,[H]^2 \tag{6}$$

where I is the dose rate.

---

[9] J. P. Keene, *Radiation Res.*, **22**, 1 (1964).

Assuming that the term in $[H]^2$ is small enough, we obtain

$$[H] = \frac{G_{(H)}\,I}{100\,N} \cdot \frac{1}{k_1\,(a - x) + k_2\,[H^+]} \tag{7}$$

and then, substituting [H] in (5),

$$\frac{dx}{dt} = k_1\,(a - x) \cdot \frac{G_{(H)}\,I}{100\ N} \cdot \frac{1}{k_1\,(a - x) + k_2\,[H^+]} \tag{8}$$

After separating the variables and integrating, we shall have :

$$k_1 = \frac{100\,N\,k_2\,[H^+]}{G_{(H)}\,I\,t} \cdot \frac{2.303}{t} \log \frac{a}{a - x} + \frac{k_1\,x\,100\ N}{G_{(H)}\,I\,t} \tag{9}$$

1) When $[H^+] \rightarrow 0$, i.e. in the case of weak acid or neutral solutions,

$$x = \frac{G_{(H)}\,I}{100\ N}\,t \tag{10}$$

which means that the complex decomposition follows a zero order kinetic law.

Table 1 shows that this equation is verified well enough, the reaction being of the zero order at low concentrations of hydrogen ions.

2) In an acid medium it is the term in $[H^+]$ that predominates, i. e.

$$k_1 = \frac{2.303\,k_2\,100\ N[H^+]}{G_{(H)}It} \log \frac{a}{a - x} \tag{11}$$

or

$$k_1' = \frac{k_1 G_{(H)} I}{k_2\,100\ N[H^+]} = \frac{2.303}{t} \log \frac{\varepsilon.}{\varepsilon} \tag{12}$$

As shown in table 1, equation (12) is experimentally verified, the complex decomposition following a kinetics of first order. This equation helps to determine the relative rate constant k_1/k_2.

The calculations we made for the radiolysis of the complex solution of 0.002 M/l concentration in an acid of 0.045 M/l gave $k_1/k_2 = 3.9$. If one of these constants is known, the other can be easily deduced. The literature [10] gives the value $k_2 = 2.6 \times 10^3$ l. mole^{-1} sec^{-1}, from which we deduce $k_1 = 1.0 \times 10^4$l. mole^{-1} sec^{-1}. This result agrees with that found by Halpern [3] which showed the $k_1 < 10^5$l. mole^{-1} sec^{-1}.

The rate constant of reaction (2) was also determined by us by the method of the competitive reactions.

Indeed, if we consider that the principal reactions are (2) and (3), their kinetic equation will be :

$$G = \frac{G_{(H)}}{1 + \dfrac{k_2\,[H^+]}{k_1\,[\text{complex}]}} \tag{13}$$

---

[10] F. Dainton and S. A. Silles, *Proc. Chem. Soc.*, **1962**, 223.

or

$$\frac{1}{G} = \frac{1}{G_{(H)}} + \frac{k_2}{k_1 G_{(H)}} \cdot \frac{[H^+]}{[\text{complex}]} \tag{14}$$

Thus, if yield G is determined as a function of ratio $[H^+]/[\text{complex}]$, we shall be able to determine the relative rate constant k_1/k_2. In our experiments, we maintained constant the concentration of one of the dissolved substances and varied the other one and then vice versa.

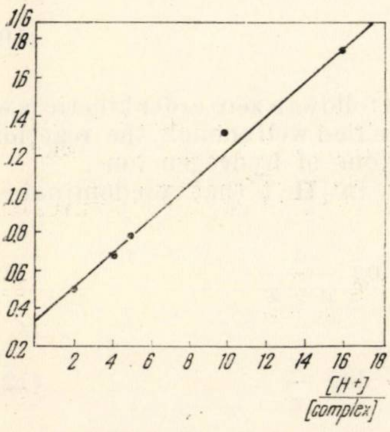

Fig. 2. — Dependence of $1/G$ on the ratio $[H^+]/[\text{Complex}]$.
[Complex] is varied. Dose rate = 2.45×10^{15} eV/ml. sec.

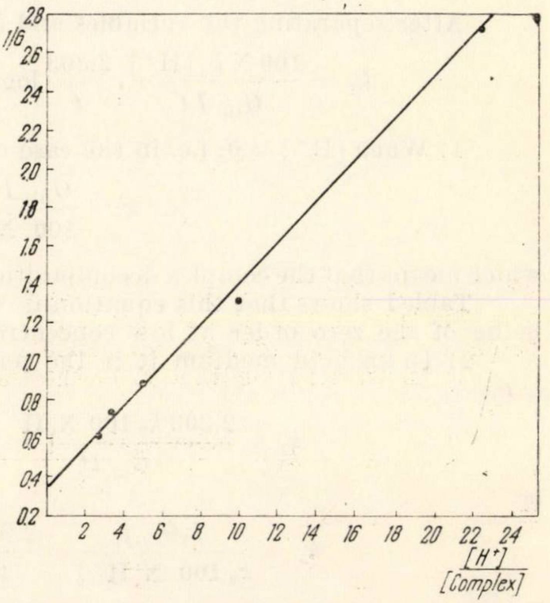

Fig. 3. — Dependence of $1/G$ on the ratio $[H^+]/[\text{Complex}]$.
$[H^+]$ is varied. Dose rate = 2.45×10^{15} eV/ml. sec.

Figure 2 represents the dependence of $1/G$ on the ratio $[H^+]/[\text{complex}]$ on the assumption that $[H^+] =$ const. and complex is varied, while figure 3, represents the same on the assumption that $[H^+]$ is varied and [complex] is constant.

The slopes of these straight lines allowed us to calculate the value of ratio k_1/k_2 which was found to be equal to 3.5. From this and the k_2 value, we deduced $k_1 = 0.8 \times 10^4$ l. mole^{-1} sec^{-1}.

Revue Roumaine de Chimie, **15**, 11–14 (1970)

PARISER-PARR TREATMENT OF SUBSTITUTED BENZENES. II *

CHARGE-TRANSFER CONFIGURATIONS OF THE BENZENESULPHONIC ACID

V. E. SAHINI and C. I. GHIRVU **

Institute of Physical Chemistry of the Academy, Str. Dumbrava Roşie 23, Bucharest

Received July 22, 1969

The π-electron energy levels of the benzenesulphonic acid has been calculated using a method due to Longuet-Higgins and Murrell, the imaginary orbitals of benzene and a vacant orbital for the substituent being considered.

INTRODUCTION

In their study of the electronic spectra of the monosubstituted benzenes, Longuet-Higgins and Murrell have proposed a simplified method, [1,2] further developed by Nagakura and his coworkers,[3,4] a variant of the ASMO—CI method, [5,6] in which the locally excited configurations of benzene (and even of the substituents) and intramolecular charge-transfer configurations are used as starting configurations.

For the electron releasing substituents the method has first been applied by Longuet-Higgins and Murrell [1,2] and further by Kimura and Nagakura, [3] while for the electron withdrawing substituents this method has been dealt with by Nagakura, Kojima and Moruyama. [4]

In the present paper we used Nagakura, Kojima and Moruyama's scheme with two simplifying approximations. First, we used for benzene the imaginary orbitals and secondly, a vacant orbital for the substituent was considered.

So, the diagonal matrix elements corresponding to locally excited configurations are those indicated by Pariser and Parr[6] for benzene. The diagonal matrix elements corresponding to intramolecular charge-transfer configurations have been calculated as indicated by Longuet-Higgins and

---

* Previous part V. E. Sahini and C. I. Ghirvu, *Rev. Roumaine Chim.*, **13**, 851 (1968).

** Permanent address : The "Al. I. Cuza" University, Physical Chemistry Laboratory, Calea 23 August 11, Jassy, Romania

[1] H. C. Longuet-Higgins and J. N. Murrell, *Proc. Phys. Soc.*, A **68**, 601 (1955).

[2] J. N. Murrell, *Proc. Phys. Soc.*, A **68**, 969 (1955).

[3] K. Kimura and S. Nagakura, *Mol. Phys.*, **9**, 117 (1965).

[4] S. Nagakura, M. Kojima and Y. Moruyama, *J. Mol. Spectroscopy*, **13**, 174 (1964).

[5] M. Goeppert-Mayer and A. L. Sklar, *J. Chem. Phys.*, **6**, 645 (1938).

[6] R. Pariser and R. G. Parr, *J. Chem. Phys.*, **21**, 466, 767 (1953).

Murrell.[1] This slightly modified scheme has been applied to calculate the transition energies of benzenesulphonic acid. All necessary integrals were estimated as indicated by Pariser and Parr.[6]

CALCULATION METHOD

We consider the marking of the atoms given in figure 1 and denote by $\Phi_0, \Phi_1, \Phi_{-1}, \Phi_2, \Phi_{-2}, \Phi_3$ the molecular orbitals of benzene of which are given by[7]

$$\Phi_k = \frac{1}{\sqrt{6}} \sum_{j=0}^{5} \omega^{kj} \varphi_j \tag{1}$$

where $\omega = \exp(2 \pi i / 6)$, $k = 0, \pm 1, \pm 2, 3$ and φ_j are the atomic orbitals according to figure 1.

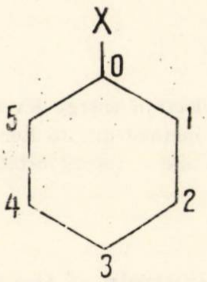

Fig. 1. — Marking of the atoms for monosubstituted benzenes.

At the same time we denote by $\Phi_X = \varphi_X$, the vacant orbital of the substituent.

The starting configurations to be taken into consideration will be as follows

$$\left.\begin{aligned}
\Psi_N &= |\Phi_0 \overline{\Phi}_0 \Phi_1 \overline{\Phi}_1 \Phi_{-1} \overline{\Phi}_{-1}| \\
\Psi_{-12} &= \frac{1}{\sqrt{2}} \{ | \Phi_0 \overline{\Phi}_0 \Phi_1 \overline{\Phi}_1 \Phi_{-1} \overline{\Phi}_2 | + | \Phi_0 \overline{\Phi}_0 \Phi_1 \overline{\Phi}_1 \Phi_2 \overline{\Phi}_{-1} | \} \\
\Psi_{-1-2} &= \frac{1}{\sqrt{2}} \{ | \Phi_0 \overline{\Phi}_0 \Phi_1 \overline{\Phi}_1 \Phi_{-1} \overline{\Phi}_{-2} | + | \Phi_0 \overline{\Phi}_0 \Phi_1 \overline{\Phi}_1 \Phi_{-2} \overline{\Phi}_{-1} | \} \\
\Psi_{12} &= \frac{1}{\sqrt{2}} \{ | \Phi_0 \overline{\Phi}_0 \Phi_1 \overline{\Phi}_2 \Phi_{-1} \overline{\Phi}_{-1} | + | \Phi_0 \overline{\Phi}_0 \Phi_2 \overline{\Phi}_1 \Phi_{-1} \overline{\Phi}_{-1} | \} \\
\Psi_{1-2} &= \frac{1}{\sqrt{2}} \{ | \Phi_0 \overline{\Phi}_0 \Phi_1 \overline{\Phi}_{-2} \Phi_{-1} \overline{\Phi}_{-1} | + | \Phi_0 \overline{\Phi}_0 \Phi_{-2} \overline{\Phi}_1 \Phi_{-1} \overline{\Phi}_{-1} | \} \\
\Psi_{1X} &= \frac{1}{\sqrt{2}} \{ | \Phi_0 \overline{\Phi}_0 \Phi_1 \overline{\Phi}_X \Phi_{-1} \overline{\Phi}_{-1} | + | \Phi_0 \overline{\Phi}_0 \Phi_X \overline{\Phi}_1 \Phi_{-1} \overline{\Phi}_{-1} | \} \\
\Psi_{-1X} &= \frac{1}{\sqrt{2}} \{ | \Phi_0 \overline{\Phi}_0 \Phi_1 \overline{\Phi}_1 \Phi_{-1} \overline{\Phi}_X | + | \Phi_0 \overline{\Phi}_0 \Phi_1 \overline{\Phi}_1 \Phi_X \overline{\Phi}_{-1} | \}
\end{aligned}\right\} \tag{2}$$

---

[7] R. G. Parr, "The Quantum Theory of Molecular Electronic Structure", W. A. Benjamin Inc., New York, 1964, p. 62.

Since the configurations Ψ_{-12} and Ψ_{1-2}, Ψ_{12} and Ψ_{-1-2} and Ψ_{1x} and Ψ_{-1x} are degenerated pairs we shall take the plus and minus configurations[8]

$$\left.\begin{aligned}
\Psi_{12}^{+} &= \frac{1}{\sqrt{2}}(\Psi_{12} + \Psi_{-1-2})\,; & \Psi_{-12}^{-} &= \frac{i}{\sqrt{2}}(\Psi_{-12} - \Psi_{1-2}) \\
\Psi_{12}^{-} &= \frac{i}{\sqrt{2}}(\Psi_{12} - \Psi_{-1-2})\,; & \Psi_{1x}^{+} &= \frac{1}{\sqrt{2}}(\Psi_{1x} + \Psi_{-1x}) \\
\Psi_{-12}^{+} &= \frac{1}{\sqrt{2}}(\Psi_{-12} + \Psi_{1-2})\,; & \Psi_{1x}^{-} &= \frac{i}{\sqrt{2}}(\Psi_{1x} - \Psi_{-1x})
\end{aligned}\right\} \quad (3)$$

Now, it is necessary to calculate the matrix elements of the Hamiltonian $\hat{H}$, given as Pariser and Parr indicated,[6] namely the differences $E(\Psi_{ij}) - E(\Psi_N)$. For the locally excited states of benzene these are those from Pariser-Parr's theory.[7] Since there is a slight interaction between Ψ_{1x} and Ψ_{-1x} we shall have

$$\left.\begin{aligned}
E(\Psi_{1x}^{+}) - E(\Psi_N) &= E(\Psi_{1x}) - E(\Psi_N) + \langle\Psi_{1x}|\hat{H}|\Psi_{-1x}\rangle \\
E(\Psi_{1x}^{-}) - E(\Psi_N) &= E(\Psi_{-1x}) - E(\Psi_N) - \langle\Psi_{1x}|\hat{H}|\Psi_{-1x}\rangle
\end{aligned}\right\} \quad (4)$$

where

$$E(\Psi_{1x}) - E(\Psi_N) = E(\Psi_{-1x}) - E(\Psi_N) = I_B - A_X - J_{1x} \quad (5)$$

I_B being the ionisation potential of benzene, A_X the electron affinity of the substituent and $J_{1x} = J_{-1x}$ the corresponding coulomb integral. For the nonzero off-diagonal matrix we get:

$$\left.\begin{aligned}
\langle\Psi_N|\hat{H}|\Psi_{1x}^{+}\rangle &= \frac{2}{\sqrt{6}}\beta_{0x}\,; & \langle\Psi_{-12}^{+}|\hat{H}|\Psi_{1x}^{+}\rangle &= \frac{1}{\sqrt{6}}\beta_{0x} \\
\langle\Psi_{12}^{+}|\hat{H}|\Psi_{1x}^{+}\rangle &= \frac{1}{\sqrt{6}}\beta_{0x}\,; & \langle\Psi_{-12}^{-}|\hat{H}|\Psi_{1x}^{-}\rangle &= -\frac{1}{\sqrt{6}}\beta_{0x} \\
\langle\Psi_{12}^{-}|\hat{H}|\Psi_{1x}^{-}\rangle &= \frac{1}{\sqrt{6}}\beta_{0x}\,; & &
\end{aligned}\right\} \quad (6)$$

where β_{0x} is the resonance integral between 0 and X (figure 1). This integral has been evaluated as $\beta_{0x} = k\,\beta_0$, β_0 being the standard resonance integral between two adjacent carbon atoms in benzene.

Finally, we must only calculate J_{1x} of Eq. (5) and $\langle\Psi_{1x}|\hat{H}|\Psi_{-1x}\rangle$ of Eq. (4). We make these calculations by reducing the integrals over molecular orbitals to those over atomic orbitals, which we calculate by Pariser-Parr's approximation.

---

[8] R. G. Parr, *J. Chem. Phys.*, **33**, 1184 (1960).

RESULTS AND DISCUSSIONS

For benzenesulphonic acid, studied earlier by us,[9,*] the following parameters have been used: $\beta_{0x} = 0.6\,\beta_0(\beta_0 = 2.371$ eV[8]), $I - A = 10.01$ eV (Hinze and Jaffé [10]), and for the electron affinity of the sulphonic group we chose the value 0.16 eV. The C—C and C—S bond lengths of benzenesulphonic acid were those of reference, [11] ($d_{C-S} = 1.90$ Å, $d_{C-C} = 1.40$ Å). The wave functions and the energy levels are given in table 1, and calculated and experimental transition energies are given in table 2.

Table 1

Energy levels and wave functions for benzenesulphonic acid

Energies (eV)	Ψ_i / Ψ_{ij}	Ψ_N	Ψ^+_{-12}	Ψ^-_{-12}	Ψ^+_{12}	Ψ^-_{12}	Ψ^+_{1X}	Ψ^-_{1X}
$E_0 = 0.2839$	Ψ_0	0.9701	0.0221	0.0000	0.0196	0.0000	0.2373	0.0000
$E_1 = 4.2042$	Ψ_1	0.0000	0.0000	0.7393	0.0000	−0.1492	0.0000	−0.6566
$E_2 = 4.4919$	Ψ_2	−0.2278	0.3484	0.0000	0.2255	0.0000	0.8808	0.0000
$E_3 = 5.3190$	Ψ_3	0.0000	0.0000	0.6686	0.0000	0.2779	0.0000	0.6897
$E_4 = 6.1383$	Ψ_4	0.0535	0.9206	0.0000	−0.2641	0.0000	−0.2827	0.0000
$E_5 = 6.9436$	Ψ_5	0.0496	0.1750	0.0000	0.9376	0.0000	−0.2946	0.0000
$E_6 = 6.9468$	Ψ_6	0.0000	0.0000	−0.0796	0.0000	−0.9489	0.0000	−0.3052

Table 2

Experimental and theoretical transition energies for benzenesulphonic acid

Transition	Transition energies (eV)	
	Calculated	Experimental [a)]
$E_0 \rightarrow E_1$ $E_0 \rightarrow E_2$	$\left.\begin{matrix}4.49\\4.77\end{matrix}\right\}$	4.59–4.91
$E_0 \rightarrow E_3$	5.60	5.71
$E_0 \rightarrow E_4$	6.42	—
$E_0 \rightarrow E_5$	7.23	—
$E_0 \rightarrow E_6$	7.23	—

a) Reference *.

The calculations of this paper as well as theoretical considerations reveal the fact that the electronic spectra of the monosubstituted benzenes with electron withdrawing substituents will be of some charge-transfer character in the near ultraviolet part.

---

[9] V. E. Sahini, C. I. Ghirvu and V. P. Macovei, *Rev. Roumaine Chim.*, **12**, 237 (1967).

[10] J. Hinze and H. H. Jaffé, *J. Amer. Chem. Soc.*, **84**, 540 (1962).

[11] Tables of Interatomic Distances and Configurations in Molecules and Ions. Special Publication No. 11, London, The Chemical Society, Burllington House, 1958.

Revue Roumaine de Chimie, **15**, 15–25 (1970)

INTERPRÉTATION DES SPECTRES ÉLECTRONIQUES D'IONS COMPLEXES CYANES DE FER (II) ET DE FER (III) DANS L'APPROXIMATION DE LA THÉORIE DU CHAMP CRISTALLIN

O. BENALI BAITICH, M. MEKLATI et M. ACHOUR

Département de Chimie, Faculté des Sciences d'Alger, 2, Rue Didouche Mourad

Reçu le 5 mai 1969

La détermination des spectres électroniques de quelques ions monosubstitués du ferrocyanure et du ferricyanure est reprise en vue de l'indexation des différentes bandes. L'utilisation de la méthode du champ cristallin sous sa forme semi-empirique nous permet de proposer une indexation cohérente des bandes *d-d* et de déterminer les paramètres introduits par cette méthode pour les deux séries d'ions complexes.

I. INTRODUCTION

L'objet de ce travail consiste en l'interprétation des spectres électroniques d'absorption de deux séries d'ions complexes cyanés de Fer (II) et de Fer (III) à l'aide de la méthode du champ cristallin. Les ions complexes cyanés étudiés ici dérivent du ferrocyanure et du ferricyanure par substitution à un cyanure des coordinats suivants : H_2O, NH_3 et NO_2^-.

Aucune interprétation des spectres électroniques de ces ions n'a été proposée jusqu'à présent, alors qu'il existe plusieurs études sur les ions ferrocyanure, [1,2] ferricyanure, [3,4] nitroprussiate. [5,6] Même les données spectroscopiques sont rares, puisque les seuls renseignements concernant les ions complexes de Fer (II) sont ceux de Shinra et Masuda [7] qui ne précisent pas la position des bandes, et pour les ions complexes de Fer (III) ceux de Matsuoka et Shimura [8] qui indiquent la position des bandes et leur nature. C'est pourquoi, il nous a semblé nécessaire de reprendre la détermination des spectres d'absorption, avant d'entreprendre l'indexation des différentes bandes. A cet effet, les niveaux de plus basses énergies pour les ions

---

[1] H. B. Gray et N. A. Beach, *J. Amer. Chem. Soc.*, **85**, 2922 (1963).

[2] J. J. Alexander et H. B. Gray, *Coord. Chem. Rev.*, **2**, 29 (1967).

[3] C. S. Naiman, *J. Chem. Phys.*, **35**, 323 (1961).

[4] G. Basu et R. L. Belford, *J. Chem. Phys.*, **37**, 1933 (1962).

[5] H. B. Gray et C. J. Ballhausen, *J. Chem. Phys.*, **36**, 1151 (1962).

[6] P. T. Manoharan et H. B. Gray, *J. Amer. Chem. Soc.*, **87**, 3340 (1965).

[7] K. Shinra et I. Masuda, *J. Chem. Soc. Japan*, **75**, 1211 (1954).

[8] N. Matsuoka et Y. Shimura, *Nippon Kagaku Zasshi*, **84**, 496 (1963).

complexes de configuration d^6 et d^5 de symétrie C_{4v} sont déterminés en fonction des paramètres du champ cristallin et des paramètres de répulsions électroniques, dans l'approximation du champ fort et en se limitant aux termes diagonaux.

II. SPECTRES ÉLECTRONIQUES D'ABSORPTION

Les spectres dans le visible et le proche ultra-violet de ces ions complexes ainsi que ceux du ferrocyanure et du ferricyanure, ont été obtenus en solution à l'aide d'un spectrophotomètre Karl Zeiss PMQ II à monofaisceau. Tous les sels de ces ions complexes sont solubles dans l'eau, à l'exception de celui de l'amminopentacyanoferrate (III) qui peut toutefois être dissous dans une solution diluée d'ammoniaque (3 %). Nous avons admis que, ni la symétrie, ni la composition de l'ion complexe ne sont altérées lors de la mise en solution. Les résultats obtenus, pour les spectres des ions ferrocyanure et ferricyanure sont en acord avec ceux de la littérature.[1,9] Les ions complexes de Fer (II) présentent deux bandes dans le visible conformément à l'étude de Shinra et Masuda, [7] mais nous avons pu mettre en évidence une bande située aux courtes longueurs d'onde, domaine non prospecté par ces derniers (vers 225 mμ). Les longueurs d'onde des maxima des différentes bandes, les nombres d'onde calculés et les logarithmes des coefficients d'extinction correspondants sont résumés dans le tableau 1. Ainsi les spectres des ions aquo- et amminopentacyanoferrate (II) sont très voisins du point de vue de la position des bandes, comme de celui de leurs intensités. Compte tenu de celles-ci, les deux premières bandes sont vraisemblablement dues à des transitions *d-d*, alors que la dernière est sans doute imputable à un transfert de charge du fait de sa grande intensité (log ε voisin de 4) et de son énergie très voisine de la première bande de transfert de charge de l'ion ferrocyanure.

Les trois ions complexes de Fer (III) étudiés ici présentent des spectres très semblables comportant quatre bandes chacun dont les caractéristiques sont reproduites dans le tableau 1. Nos résultats sont conformes à ceux de la référence 8, pour les ions aquo - et nitropentacyanoferrate (III) ; par contre, pour l'amminopentacyanoferrate (III) nous trouvons, pour la première bande située à 556 mμ un coefficient d'extinction dont le logarithme est 2,22 au lieu de 0,54 pour la référence citée. Ceci rétablit une similitude totale entre le spectre de ces trois ions, analogue à celle constatée pour les ions complexes de Fer (II).

La très grande intensité de ces bandes ne permet pas de préciser leur nature avec certitude. Cependant, une attribution de ces bandes, par comparaison avec le spectre de l'ion ferricyanure interprété par Naiman [3] est proposée. Nous admettrons en accord avec Matsuoka et Shimura [8] que la deuxième bande dont la position se retrouve à 395 mμ est une bande de transfert de charge correspondant à la première bande de transfert de charge du spectre de l'ion ferricyanure (416 mμ). Par suite de sa très forte

---

[9] A. V. Kiss, J. Abraham et I. Hegedus, *Z. anorg. Chem.*, **244**, 98 (1940).

Tableau 1

Spectres électroniques des ions complexes cyanes de Fer (II) et de Fer (III)

$[Fe(CN)_5H_2O]^{3-}$			$[Fe(CN)_5NH_3]^{3-}$			$[Fe(CN)_6]^{4-}$			Nature des transitions
λ	$\bar{\nu}$	log ε	λ	$\bar{\nu}$	log ε	λ	$\bar{\nu}$	log ε	
560	17 860	1,49	520	19 230	1,48	425	23 530	0,4	*d-d* [a]
420	23 810	2,41	405	24 690	2,57	322	31 050	2,54	,,
230	43 480	2,80	225	44 440	4,04	270	37 040	3,25	,,
—	—	—	—	—	—	218	45 870	4,35	*TC* [b]
—	—	—	—	—	—	200	50 000	4,05	,,

$[Fe(CN)_5H_2O]^{2-}$			$[Fe(CN)_5NH_3]^{2-}$			$[Fe(CN)_5NO_2]^{3-}$			$[Fe(CN)_6]^{3-}$			
λ	$\bar{\nu}$	log ε	λ	$\bar{\nu}$	log ε	λ	$\bar{\nu}$	log ε	λ	$\bar{\nu}$	log ε	
540	18 520	2,51	556	17 990	2,22	545	18 340	2,40	550	18 180	0,05	*d-d*
395	25 310	2,90	396	25 260	2,76	395	25 310	2,81	416	24 040	3,01	*TC*
355	28 170	2,91	364	27 480	2,93	345	28 980	2,92	320	31 250	3,05	*d-d*
288	34 720	3,12	285	35 090	3,20	250	40 000	3,80	303	33 000	3,22	*TC*
	—			—			—		280	35 710	3,04	*d-d*
	—			—			—		261	38 310	3,08	*TC*
	—			—			—		226	44 250	3,44	,,

λ en mμ et $\bar{\nu}$ en cm^{-1};

[a] *d–d* = transition de champ cristallin

[b] *TC* = transition de transfert de charge

intensité la quatrième bande doit être de même nature. Quant à la seconde, elle est sans doute imputable à une transition *d-d*. Cependant, pour ce qui est de la première bande, nous pensons, contrairement à ces auteurs, qu'elle est due à une transition *d-d* et non à un transfert de charge et cela, en raison de son énergie relativement élevée très voisine par ailleurs de l'énergie de la première bande *d-d* du spectre de l'ion ferricyanure.

III. CALCUL DES NIVEAUX DE PLUS BASSES ÉNERGIES POUR LA CONFIGURATION d^6

La théorie du champ cristallin est appliquée suivant l'approximation du champ fort, en négligeant le couplage spin-orbite. L'approximation du champ fort se justifie ici par les propriétés magnétiques de ces ions. [10] C'est ainsi que, pour un complexe octaédrique, l'ordre des perturbations est le suivant : $V_0 > \sum_{i \neq j} e^2/r_{ij}$. Les cinq orbitales d, initialement dégénérées, vont se trouver décomposées par l'action de V_0 en t_{2g} trois fois dégénérées et e_g deux fois dégénérées, d'énergies respectives $\varepsilon_0 - 4D_q$ et $\varepsilon_0 + 6D_q$, [11,12] ε_0 étant une constante et D_q le paramètre correspondant à la perturbation octaédrique. Les six électrons se placent d'abord sur l'orbitale t_{2g} puis, sur l'orbitale e_g, donnant lieu ainsi à plusieurs configurations ; chaque configuration à son tour va se décomposer en plusieurs termes sous l'influence des répulsions électroniques, et les énergies de ces termes devraient être obtenues par résolution des déterminants séculaires de perturbation correspondants qui impliquent la connaissance de tous les paramètres. Suivant l'approximation de champ fort et dans le but de simplifier les calculs, nous avons été conduits à négliger les éléments non diagonaux des matrices de perturbation, c'est-à-dire l'interaction des termes de même symétrie et de même multiplicité provenant des différentes configurations. Dans ces conditions, l'énergie d'un terme se trouve égale à l'élément matriciel diagonal, et s'exprimera analytiquement en fonction des paramètres du champ cristallin et des paramètres de répulsions électroniques. Ces paramètres peuvent alors être considérés comme des paramètres empiriques que l'on détermine grâce aux données spectroscopiques.

Pour le groupe O_h, les matrices complètes de perturbation pour les configurations d^1 à d^9 ont été établies par Tanabe et Sugano. [13] Nous avons directement utilisé leurs résultats, compte tenu de l'approximation formulée précédemment pour déterminer les transitions de plus basses énergies $t_{2g}^6 \rightarrow t_{2g}^5\, e_g$ intervenant dans le spectre de l'ion ferrocyanure.

Le champ cristallin dans les ions pentacyanés dont la symétrie la plus probable est C_{4v} est traité à nouveau comme une faible perturbation quadratique du champ octaédrique.[11,12] Le problème de la détermination des niveaux d'énergie se ramène alors à l'application des trois perturbations qui se présentent ici dans l'ordre : $V_0 > V_q > \sum_{i \neq j} e^2/r_{ij}$. En effet les spectres des ions pentacyanés n'étant pas constitués par une décomposition des bandes du spectre de l'ion hexacyané, l'hypothèse de classement des perturbations indiquée ci-dessus se trouve justifiée. L'effet du champ quadratique se manifestera par la décomposition de l'orbitale t_{2g} en e et b_2 et l'orbitale e_g en a_1 et b_1 comme le représente la figure 1.

---

[10] G. Foex, C. J. Gorter et C. J. Smits, «Constantes sélectionnées-Diamagnétisme et Paramagnétisme — Relaxation paramagnétique», Masson, Paris, 1957.

[11] W. Moffitt et C. J. Ballhausen, *Ann. Rev. Phys. Chem.*, **7**, 107 (1956).

[12] C. J. Ballhausen, « Introduction to Ligand Field Theory », McGraw-Hill Book Company Inc., 1962.

[13] Y. Tanabe et S. Sugano, *J. Phys. Soc. Japan*, **9**, 753 (1954).

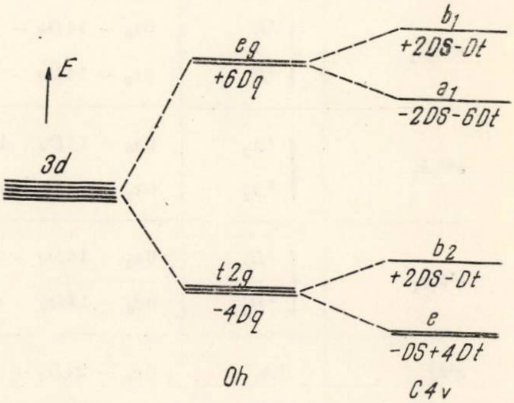

Fig. 1. — Décomposition des orbitales d dans un champ octaédrique et dans un champ de symétrie C_{4v}.

Deux nouveaux paramètres Ds et Dt sont introduits. Le classement des orbitales e, b_2, a_1, b_1 dépend des grandeurs et signes de ces paramètres. Pour une élongation axiale Ds et Dt sont positifs, tandis que pour une compression, ils sont négatifs. Cependant, pour une faible perturbation quadratique, nous pourrons prévoir que les orbitales e et b_2 seront plus stables que a_1 et b_1. Dans ces conditions, les configurations de plus basses énergies pour six électrons sont alors : $e^4 b_2^2$, $e^4 b_2 a_1$, $e^3 b_2^2 a_1$, $e^4 b_2\ b_1$, $e^3 b_2^2 b_1$... Nous avons déterminé pour chacune de ces configurations l'énergie des termes résultants des intéractions électroniques. A cette fin, nous avons d'abord formé les fonctions d'onde correspondant à chaque terme en utilisant les propriétés de symétrie, puis, évalué les énergies de répulsion. Le tableau 2 regroupe le résultat de ces calculs.

IV. INTERPRÉTATION DES SPECTRES DES IONS COMPLEXES DE FER (II)

1° *Bandes d-d*

Le spectre de l'ion ferrocyanure nous ayant servi de base pour l'étude des ions de plus basse symétrie, son indexation [1] est reprise ici pour le calcul des paramètres $10D_q$, B et C par l'utilisation des termes diagonaux des matrices de perturbation de la référence 13

Tableau 2

Configurations	Termes	Energies
$e^3b_2^2b_1$	^1E	$6\varepsilon_0 - 14Dq + 3Ds + 9Dt + 15A - 18B + 14C$
	^3E	$6\varepsilon_0 - 14Dq + 3Ds + 9Dt + 15A - 24B + 12C$
$e^3b_2^2a_1$	^1E	$6\varepsilon_0 - 14Dq - Ds + 4Dt + 15A - 26B + 14C$
	^3E	$6\varepsilon_0 - 14Dq - Ds + 4Dt + 15A - 28B + 12C$
$e^4b_2b_1$	$^1A_2$	$6\varepsilon_0 - 14Dq + 14Dt + 15A - 30B + 14C$
	$^3A_2$	$6\varepsilon_0 - 14Dq + 14Dt + 15A - 30B + 12C$
$e^4b_2a_1$	$^1B_2$	$6\varepsilon_0 - 14Dq - 4Ds + 9Dt + 15A - 14B + 14C$
	$^3B_2$	$6\varepsilon_0 - 14Dq - 4Ds + 9Dt + 15A - 22B + 12C$
$e^4b_2^2$	$^1A_1$	$6\varepsilon_0 - 24Dq + 14Dt + 15A - 30B + 15C$

$$
\begin{array}{lllll}
^1A_1 & (t_{2g}^6) & \rightarrow {}^3T_1\,(t_{2g}^5\,e_g) & 23530\ \mathrm{cm}^{-1} & : 10D_q - 3C \\
,, & ,, & \rightarrow {}^1T_1 \quad ,, & 31050\ \ ,, & : 10D_q - C \\
,, & ,, & \rightarrow {}^1T_2 \quad ,, & 37040\ \ ,, & : 10D_q + 16\,B - C
\end{array}
$$

Nous déduisons alors la valeur des paramètres

$$10\,D_q = 34810\ \mathrm{cm}^{-1}\ B = 375\ \mathrm{cm}^{-1}\ C = 3760\ \mathrm{cm}^{-1}.$$

La considération uniquement des deux bandes permises de spin n'aurait permis de déterminer que B (375 cm^{-1}). Il faudrait fixer à priori la valeur de C pour atteindre $10D_q$. C'est ainsi que Gray et Beach, [1] en prenant $C = 2800\ \mathrm{cm}^{-1}$, proposent $10D_q = 33800\ \mathrm{cm}^{-1}$. En général, le choix de la valeur de C est dicté par celle du rapport C/B. Il est admis en effet dans les diagrammes de Tanabe et Sugano [14] que la valeur de ce rapport pour le complexe reste égale à celle pour l'ion libre (4,4). Dans ces conditions Jørgensen [15] propose $10D_q = 31400\ \mathrm{cm}^{-1}$ et $B = 400\ \mathrm{cm}^{-1}$. Nos résultats s'écartent davantage de ces derniers surtout en ce qui concerne la valeur de C. Cet écart est dû, d'une part, à la considération de toutes les bandes observées pour la détermination des paramètres, et d'autre part, à l'approximation utilisée pour l'évaluation de l'énergie des transitions.

Par la suite, pour les ions pentacyanés dérivés du ferrocyanure, nous n'observerons pas expérimentalement un nombre suffisant de transitions pour pouvoir calculer les différents paramètres ($10D_q$, Ds, Dt, B, C) On est donc obligé de faire des hypothèses supplémentaires : nous admettons que les valeurs de $10D_q$, B et C de l'ion hexacyané se conservent lors de la descente de symétrie. Ces hypothèses nous permettront alors de calculer les valeurs de Ds et Dt en n'utilisant que les deux bandes *d-d* observées. Les ions aquo- et amminopentacyanoferrate (II) ayant des spectres semblables, l'indexation de leurs bandes sera faite de la même manière.

---

[14] Y. Tanabe et S. Sugano, *J. Phys. Soc. Japan.*, **9**, 766 (1954).

[15] C. K. Jørgensen, «Absorption Spectra and Chemical Bonding in Complexes», Pergamon Press, Addison Wesley Publishing Compagny Inc, 1962.

L'état fondamental étant ${}^1A_1$, seules les transitions ${}^1A_1 \rightarrow {}^1E$ et ${}^1A_1 \rightarrow {}^1A_1$ seront permises de spin et d'orbitale dans le groupe C_{4v}. Les deux bandes *d-d* sont d'intensité notablement différentes ; il est donc logique de faire correspondre à la plus intense (deuxième bande) une transition permise d'orbitale, et à la moins intense (première bande) une transition de type ${}^1A_1 \rightarrow {}^1A_2$ ou ${}^1A_1 \rightarrow {}^1B_2$. D'après le tableau 2, nous constatons que la transition ${}^1A_1\,(e^4 b_2^2) \rightarrow {}^1A_2\,(e^4 b_2 b_1)$ indépendante de Ds et Dt ($10D_q - C$) est équivalente en énergie à la transition ${}^1A_1 \rightarrow {}^1T_1$ du ferrocyanure (31050 cm^{-1}). Elle ne peut donc indexer la première bande de ces complexes. Par contre la transition ${}^1A_1\,(e^4 b_2^2) \rightarrow {}^1B_2\,(e^4 b_2 a_1)$ d'énergie $10D_q - 4Ds - 5Dt + 16B - C$ pourrait convenir à l'indexation de cette bande. Il en résulte que l'orbitale a_1 serait plus stable que b_1. Aussi à la deuxième bande *d-d* ne pourra-t-on faire correspondre que la transition :

$$ {}^1A_1\,(e^4 b_2^2) \rightarrow {}^1E\,(e^3 b_2^2 a_1) : 10\,D_q - Ds - 10Dt + 4B - C. $$

En prenant comme valeurs de $10D_q$, B et C celles déterminées précédemment pour le ferrocyanure, nous obtenons : pour l'ion $[\mathrm{Fe(CN)_5H_2O}]^{3-}$: $Dt = 450\ \mathrm{cm}^{-1}$ $Ds = 4231\ \mathrm{cm}^{-1}$ et pour l'ion $[\mathrm{Fe(CN)_5NH_3}]^{3-}$: $Dt = 389\ \mathrm{cm}^{-1}$ $Ds = 3967\ \mathrm{cm}^{-1}$.

Vu que ces paramètres sont relatifs au substituant, nous pouvons les classer de la manière suivante :

substituant	H_2O	NH_3	CN^-
Dt (cm^{-1})	450	339	0
Ds (cm^{-1})	4231	3969	0

Ainsi Dt et Ds sont positifs et décroissent de H_2O à CN^-, ce qui est conforme, compte tenu du choix qui a prévalu à leur définition, [12] à la position des coordinats dans la série spectrochimique. En effet, le paramètre Dt pour un complexe MX_5Y peut être relié, dans le modèle du champ cristallin simple, à la différence $Dq_X - Dq_Y$. [16] Comme $Dq_{H_2O} < Dq_{NH_3} < Dq_{CN^-}$, il s'ensuit que l'on a bien pour Dt le classement trouvé. D'après les valeurs obtenues, ces deux complexes devraient présenter une élongation axiale par rapport à la symétrie octaédrique, l'importance de l'élongation axiale étant de même sens que le paramètre Dt. Cette prédiction reste à vérifier par radiocristallographie.

2° *Bandes de transfert de charge*

Les deux bandes de transfert de charge du ferrocyanure sont dues à des transitions Métal →Coordinat,[1] et plus précisément, d'après le calcul par la méthode des orbitales moléculaires de Alexander et Gray,[2] à : $2t_{2g} \rightarrow 4t_{1u}$ et $2t_{2g} \rightarrow 2t_{2u}$, les orbitales $4t_{1u}$ et $2t_{2u}$ étant localisées sur l'orbitale antiliante π^* du cyanure. Pour les ions pentacyanés, une seule bande de transfert de charge est observée. L'énergie de cette bande est d'ailleurs voisine de la première bande homologue du ferrocyanure. Elle est très probablement due à la transition : $b_2 \rightarrow \pi^*$ (CN). La faible différence (de l'ordre de 1000 cm^{-1}) des bandes de transfert de charge pour les deux complexes aquo- et amminopentacyanoferrate (II) argumente cette indexation.

---

[16] R. A. Wentworth et T. S. Piper, *Inorg. Chem.*, 4, 709 (1965).

V. INTERPRÉTATION DES SPECTRES DES IONS COMPLEXES DE FER (III)

1° *Bandes d-d*

En reprenant l'indexation des bandes du spectre de l'ion ferricyanure[3], nous déterminons comme précédemment la valeur des paramètres $10Dq$, B et C par l'utilisation des trois bandes *d-d* observées

$$\begin{array}{llllll}
{}^2T_2\,(t_{2g}^5) & \rightarrow {}^4T_1 & (t_{2g}^4\,e) & 18180 & \text{cm}^{-1}: & 10Dq - 5B - 4C \\
,, \quad ,, & \rightarrow {}^2A_2\,,\,{}^2T_1 & ,, & 31250 & ,, \quad : & 10Dq - 2B - C \\
,, \quad ,, & \rightarrow {}^2E & ,, & 35710 & ,, \quad : & 10Dq + 7B - C
\end{array}$$

$10Dq = 36100 \text{ cm}^{-1} B = 496 \text{ cm}^{-1} C = 3860 \text{ cm}^{-1}$

Naiman[3] propose les valeurs suivantes :

$$10Dq = 34950 \text{ cm}^{-1} \quad B = 720 \text{ cm}^{-1} \quad C = 3286 \text{ cm}^{-1}$$

Cette dernière valeur de B nous semble un peu élevée, comparée à celle du ferrocyanure compte tenu de la série néphélauxétique.[15]

Les niveaux de plus basses énergies correspondant à d^5 dans un champ de symétrie C_{4v} sont obtenus comme précédemment en considérant les configurations suivantes : $e^4 b_2$, $e^3 b_2^2$, $e^4 a_1$, $e^3 b_2 a_1$, $e^4 b_1$, $e^3 b_2 b_1$... Nous avons calculé pour toutes ces configurations les énergies correspondantes et celles des termes résultants des interactions électroniques (voir tableau 3).

Les ions complexes cyanés de Fer (III) étant de bas spin, l'état fondamental sera un doublet. Leur spectre comporte deux bandes *d-d* : le log ε de la première est voisin de 2,4, celui de la deuxième étant de 2,9. Ces deux bandes correspondent à des transitions permises de spin. Si l'état fondamental est ${}^2B_2$, les seules transitions permises sont ${}^2B_2 \rightarrow {}^2B_2$ et ${}^2B_2 \rightarrow {}^2E$. Mais dans ce cas, puisqu'il n'y a pas d'autre terme ${}^2B_2$ en dehors de l'état fondamental, et compte tenu des énergies de répulsions électroniques, seules les transitions suivantes sont à considérer : ${}^2B_2\,(e^4 b_2) \rightarrow \rightarrow {}^2E\,(e^3 b_2^2)$, ${}^2B_2 \rightarrow {}^2E\,(1)\,(e^3 b_2 a_1)$ et ${}^2B_2 \rightarrow {}^2E(1)\,(e^3 b_2 b_1)$. La première de ces transitions dont l'énergie $3Ds - 5Dt$ correspond à l'écart entre l'orbitale b_2 et e ne peut être de l'ordre de 18000 cm^{-1} en vertu de l'hypothèse de travail ($V_0 > V_q$). Il convient donc d'attribuer les deux bandes *d-d* aux deux autres transitions :

$$\begin{array}{ll}
{}^2B_2\,(e^4 b_2) \rightarrow {}^2E\,(1)\,(e^3 b_2 a_1) : & 10Dq - Ds - 10Dt + 7B - C \\
,, \qquad ,, \quad \rightarrow {}^2E\,(1)\,(e^3 b_2 b_1) : & 10Dq + 3Ds - 5Dt - C
\end{array}$$

Tableau 3

Configurations	Termes	Energies
$e^3 b_2 b_1$	^4E	$5\varepsilon_0 - 10Dq + Ds + 10Dt + 10A - 23B + 6C$
	$^2E(2)$	$5\varepsilon_0 - 10Dq + Ds + 10Dt + 10A - 14B + 9C$
	$^2E(1)$	$5\varepsilon_0 - 10Dq + Ds + 10Dt + 10A - 20B + 9C$
$e^4 b_1$	$^2B_1$	$5\varepsilon_0 - 10Dq - 2Ds + 15Dt + 10A - 20B + 10C$
$e^3 b_2 a_1$	^4E	$5\varepsilon_0 - 10Dq - 3Ds + 5Dt + 10A - 19B + 6C$
	$^2E(2)$	$5\varepsilon_0 - 10Dq - 3Ds + 5Dt + 10A - 9B + 9C$
	$^2E(1)$	$5\varepsilon_0 - 10Dq - 3Ds + 5Dt + 10A - 13B + 9C$
$e^4 a_1$	$^2A_1$	$5\varepsilon_0 - 10Dq - 6Ds + 10Dt + 10A + 10C$
$e^3 b_2^2$	^2E	$5\varepsilon_0 - 20Dq + Ds + 10Dt + 10A - 20B + 10C$
$e^4 b_2$	$^2B_2$	$5\varepsilon_0 - 20Dq - 2Ds + 15Dt + 10A - 20B + 10C$

La détermination des paramètres Ds et Dt d'après cette indexation nous conduit à un résultat incompatible avec le choix de l'état fondamental. En effet, on trouve que $3Ds-5Dt$ est négatif, ce qui signifie que l'orbitale b_2 est plus stable que l'orbitale e. Dans ces conditions, nous sommes amenés à choisir comme état fondamental $^2E(b_2^2\, e^3)$, et par conséquent à considérer deux nouvelles configurations : $b_2^2\, e^2\, a_1$ et $b_2^2\, e^2\, b_1$. La décomposition de ces deux configurations conduit aux termes suivants :
$b_2^2\, e^2\, a_1 : {}^4A_2 + {}^2A_1 + {}^2A_2 + {}^2B_2 + {}^2B_1$ et $b_2^2\, e^2\, b_1 : {}^4B_2 + {}^2A_1 + {}^2A_2 + {}^2B_2 + {}^2B_1$
Compte tenu des règles de sélection, seules les transitions $^2E \rightarrow {}^2A_1$ et $^2E \rightarrow {}^2E$ seront à considérer. C'est pourquoi le calcul de l'énergie pour ces deux configurations n'est effectué que pour le terme $^2A_1$. Nous obtenons :

$$^2A_1\,(b_2^2\, e^2\, a_1) = 5\varepsilon_0 - 10Dq + 10A - 12B + 11C$$

$$^2A_1\,(b_2^2\, e^2\, b_1) = 5\varepsilon_0 - 10Dq + 4Ds + 5Dt + 10\,A - 8B + 9C$$

Nous proposons alors l'indexation suivante :

$^2E\ (b_2^2\, e^3) \rightarrow {}^2A_1(b_2^2\, e^2\, a_1)$ 1re bande : $10Dq - Ds - 10Dt + 8B + C$
„ $\rightarrow {}^2A_1(b_2^2\, e^2\, b_1)$ 2e bande : $10Dq + 3Ds - 5Dt + 12B - C$

De cette indexation nous déduisons pour les trois ions complexes la valeur des paramètres Ds et Dt qui se classent de la manière suivante :

substituant	NH_3	H_2O	NO_2^-	CN^-
Dt (cm^{-1})	2529	2464	2456	0
Ds (cm^{-1})	645	766	1023	0

Ces résultats sont compatibles avec le choix de l'état fondamental. Cependant, contrairement à la série homologue du Fer (II), nous n'observons pas ici une décroissance simultanée des deux paramètres. Par ailleurs, l'ordre de classement des coordinats suivant *Dt* s'intervertit pour H_2O et NH_3. Ceci provient de la position même des deux bandes *d-d* dont les énergies ne sont pas dans l'ordre de la série spectrochimique. L'expérience démontre donc que, dans ces conditions, il n'est pas possible de comparer les paramètres de perturbation quadratique des deux séries de complexes.

2° *Bandes de transfert de charge*

Dans l'ion ferricyanure, les transitions Coordinat → Métal peuvent apparaître dans le visible car l'orbitale t_{2g} n'est pas saturée. D'après Naiman, [3] les deux premières bandes de transfert de charge seraient dues à des transitions aboutissant à l'orbitale du métal t_{2g}, tandis que les deux dernières à l'orbitale e_g.

La bande commune aux trois ions pentacyanés située à 395 mμ pourrait être attribuée à une transition d'une orbitale moléculaire, localisée sur une orbitale du cyanure, à l'orbitale la plus basse incomplètement remplie du métal. Dans ce cas, il s'agirait de la transition : $C_1(CN) \rightarrow$ $\rightarrow e\,(b_2^2 e^4)$.

La deuxième bande de transfert de charge pourrait correspondre soit à la transition C_1 (CN) $\rightarrow a_1(b_2^2\, e^3\, a_1)$, soit à une transition d'une autre orbitale moléculaire plus basse, localisée sur le cyanure à la même orbitale e : $C_2(CN) \rightarrow e\,(b_2^2 e^4)$.

L'écart entre les deux bandes de transfert de charge étant de l'ordre de 10000 cm^{-1} pour l'aquo- et l'amminopentacyanoferrate (III), et de l'ordre de 14 500 cm^{-1} pour le nitropentacyanoferrate (III), nous suggérons la transition : $C_1(CN) \rightarrow a_1\,(b_2^2\, e^3\, a_1)$.

En effet, si l'on ne tient pas compte des répulsions électroniques, cet écart est égal à la différence d'énergie $a_1 - e$ $(10Dq - Ds - 10Dt)$. D'après la valeur des paramètres calculés précédemment, cette différence est de l'ordre de 10 500 cm^{-1}, résultat très voisin de l'écart observé pour les complexes aquo- et ammino mais trop faible pour le complexe nitro.

VI. CONCLUSION

L'étude spectrophotométrique préliminaire de quelques ions complexes cyanés monosubstitués de Fer (II) et de Fer (III), nous a amené à constater une similitude entre les spectres des ions de chaque série.

L'application de la théorie du champ cristallin sous sa forme semi-empirique nous a permis de proposer une indexation cohérente des bandes *d-d*. Les paramètres 10*Dq*, *Ds*, *Dt*, *B* et *C* sont déterminés pour les deux séries d'ions complexes. Les valeurs de *Ds* et *Dt* se classent conformément à la série spectrochimique des coordinats pour la série du Fer (II), et entraînent l'ordre suivant pour les orbitales du métal : $e < b_2 < a_1 < b_1$.

Lors de l'interprétation des spectres des ions de Fer (III), l'ambiguïté sur le choix de l'état fondamental est apparue ; mais les résultats les plus cohérents semblent nous suggérer $^2E\,(b_2^2 e^3)$ comme état fondamental, c'est-à-dire l'ordre suivant pour les orbitales du métal : $b_2 < e < a_1 < b_1$.

Enfin, l'utilisation des paramètres du champ cristallin pour cette série, nous a permis de situer la deuxième bande de transfert de charge.

REMERCIEMENTS

Nous adressons nos remerciements à M. E. Wendling, maître de conférences à la Faculté des Sciences d'Alger pour les conseils fructueux qu'il nous a prodigués et pour la correction du manuscrit.

Revue Roumaine de Chimie, **15**, 15–25 (1970)

Revue Roumaine de Chimie, 15, 27–32 (1970)

L'INFLUENCE DU SOLVANT SUR LA VITESSE DE RÉACTION

L'HYDROLYSE ALCALINE DE L'ACÉTATE DE *n*-BUTYLE DANS LE SOLVANT MIXTE EAU-DIOXANE

G. COSTEANU, ORTANSA LANDAUER et CORNELIA MATEESCU

Laboratoire de Chimie Physique, Institut Polytechnique, Bucarest, 132, str. Griviţei

Reçu le 28 octobre 1968

On étudie l'hydrolyse alcaline de l'acétate de *n*-butyle dans différents mélanges eau-dioxane à 20°, 30°, 40° et 50°. Les résultats obtenus sont mis en corrélation avec la constante diélectrique du solvant mixte. La variation de la constante de vitesse de l'hydrolyse alcaline en fonction de la teneur en dioxane du solvant mixte est attribuée à la solvatation du complexe activé et des molécules réagissantes.

Nous avons étudié la vitesse d'hydrolyse alcaline de l'acétate de *n*-butyle dans différents mélanges eau-dioxane, à 20°, 30°, 40° et 50°. Dans ces conditions la réaction d'hydrolyse s'écrit [1,2]

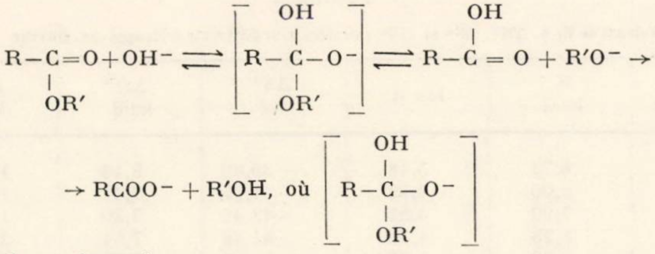

$$R-\underset{OR'}{C}=O+OH^- \rightleftharpoons \left[R-\overset{OH}{\underset{OR'}{C}}-O^-\right] \rightleftharpoons R-\overset{OH}{C}=O+R'O^- \rightarrow$$

$$\rightarrow RCOO^- + R'OH, \text{ où } \left[R-\overset{OH}{\underset{OR'}{C}}-O^-\right]$$

est le complexe formé.

PARTIE EXPÉRIMENTALE

Les substances utilisées dans nos recherches étaient à l'état très pur [3] notamment le dioxane a été purifié et séché d'après la méthode de Hess et Frahm. [4]

---

[1] C. K. Ingold "Structure and Mechanisme in Organic Chemistry", Cornell Univ. Press Ithoco, New York, 1953, p. 754.

[2] J. Hine "Physical Organic Chemistry" 2e éd., McGrawHill Book Company Inc., New York, 1962, p. 277.

[3] G. Costeanu, O. Landauer et C. Mateescu, *Rev. Roumaine Chim.*, **13**, 155 (1968).

[4] "Technique of Organic Chemistry", vol. 7, IIe éd., "Organic Solvents", New York, *Interscience Publishers Inc. London,* 1955, p. 731.

La concentration initiale de l'ester, déterminée par hydrolyse totale, était approximativement de 0,01 mole/l, et celle de l'hydroxyde de sodium, constante à toutes les déterminations, était de 0,015 mole/l.

RÉSULTATS EXPÉRIMENTAUX

Les constantes de vitesse, calculées au moyen de l'équation cinétique des réactions du seconde ordre figurent dans le tableau 1.

Tableau 1

Valeurs des constantes de vitesse en l mole^{-1} s^{-1}, à 20°, 30°, 40° et 50°

% g dioxane	$10^2 k_{20}°$	$10^2 k_{50}°$	$10^2 k_{40}°$	$10^2 k_{50}°$
16,24	4,81	7,64	11,89	18,40
26,79	4,69	7,08	10,90	15,90
37,11	4,15	6,52	9,02	14,33
47,27	3,16	5,79	6,96	12,88
57,10	2,46	4,08	5,90	10,80
66,64	1,96	3,37	5,56	9,56
76,35	1,79	3,16	5,51	9,31

Les résultats expérimentaux nous ont permis de calculer l'énergie d'activation (E), le facteur préexponentiel (A), l'enthalpie d'activation (ΔH^*), l'entropie d'activation (ΔS^*) et l'enthalpie libre d'activation (ΔG^*), au moyen des relations déjà connues [3] (tabl. 2).

Tableau 2

Valeurs de E, A, ΔH^*, ΔS^* et ΔG^* calculées pour différents mélanges eau-dioxane

% g dioxane	E kcal	log A	ΔS^* u.é	ΔH^* kcal	ΔG^* kcal
16,24	8,74	5,18	−39,40	8,14	19,88
26,79	8,00	4,62	−41,96	7,41	19,92
37,11	7,90	4,51	−42,47	7,30	19,95
47,27	8,23	4,73	−41,46	7,64	20,00
57,10	9,38	5,38	−38,48	8,78	20,25
66,64	10,52	6,10	−35,19	9,93	20,42
76,35	10,75	6,24	−34,55	10,16	20,45

La constante de vitesse d'hydrolyse alcaline de l'acétate de *n*-butyle décroît avec la teneur en dioxane du solvant mixte (fig. 1).

On voit (tableau 1) que par la variation de la concentration du dioxane de 16,24% à 76,35%, la constante de vitesse décroît respectivement de 2,68 ; 2,42 ; 2,15 et 1,98 fois la valeur de cette constante à la concentration de 16,24 % dioxane, aux températures déjà mentionnées.

Dans d'autres réactions du même genre[5], telle que l'hydrolyse alcaline de l'acétate de méthyle, ou de l'acétate d'éthyle en solution dans des solvants mixtes, eau-alcool méthylique, ou eau-alcool éthylique, la constante de vitesse décroît 8 fois, pour la première réaction, et 10 fois pour la seconde réaction, quand la teneur en alcool varie de 10 à 50%.

---

[5] S. Villermaux, J. Villermaux et R. Gibert, *J. Chem. Phys.*, **63**, 10 (1966).

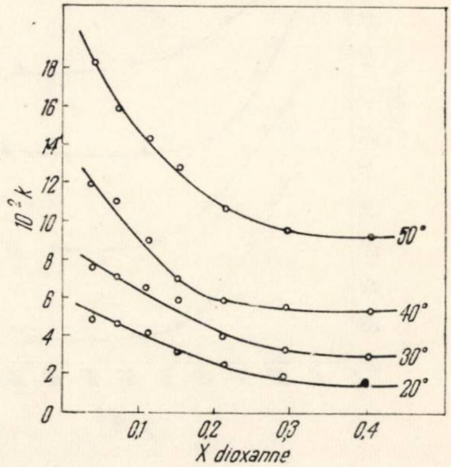

Fig. 1. — Variation de la constante de vitesse en fonction de la teneur en dioxane du solvant mixte.

La variation de la constante de vitesse en fonction de la concentration en alcool du solvant mixte est attribuée à deux effets :

1°. la variation du degré de solvatation du complexe activé et des molécules réagissant avec la teneur en alcool.

2°. le déplacement de l'équilibre de la réaction, représentée plus haut, à cause de l'existence de l'équilibre

$$OH^- + EtOH \rightleftharpoons H_2O + EtO^-.\ [6]$$

Nous admettons que, dans notre cas, la variation de la constante de vitesse avec la teneur en dioxane est due uniquement au premier effet.

En comparant la constante de vitesse d'hydrolyse alcaline de l'acétate de *n*-butyle, calculée pour une solution à 70 % dioxane à 20°, avec celles trouvées dans les mêmes conditions, par d'autres chercheurs [7], en étudiant l'hydrolyse alcaline de l'acétate de méthyle et de l'acétate d'éthyle, on constate que leurs valeurs se situent dans l'ordre : acétate de méthyle > acétate d'éthyle > acétate de *n*-butyle (tableau 3).

Tableau 3

Constantes de vitesse d'hydrolyse alcaline de quelques acétates

Substances	10^2 k l·mole^{-1} s^{-1} 70 % dioxane ; *t* : 20°
Acétate de méthyle	5,4
" d'éthyle	3,5
" de *n*-butyle	1,9

---

[6] E. Tommila, *Suomen Kem.*, **B 23**, 73 (1966).

[7] E. Tommila et S. Maltamo, *Acta Chem. Scand.*, **8**, 1152 (1954).

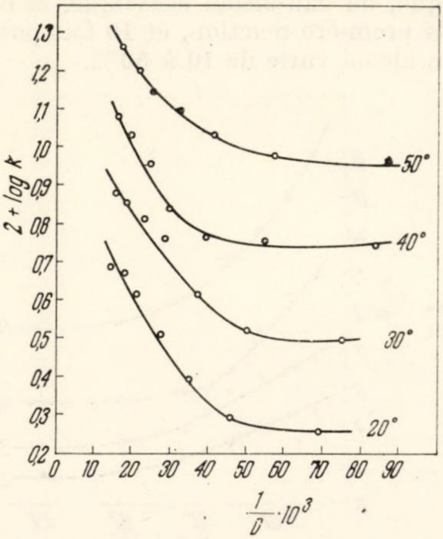

Fig. 2. — Variation de log k en fonction de $\frac{1}{D}$.

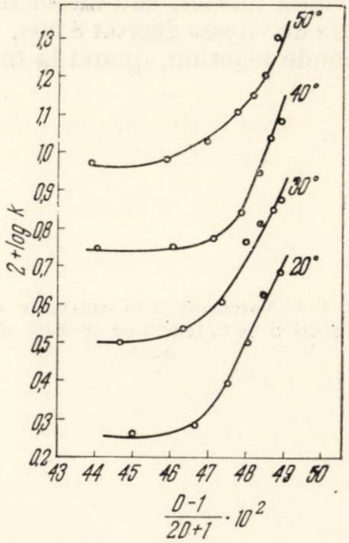

Fig. 3. — Variation de log k en fonction de $\frac{D-1}{2D+1}$.

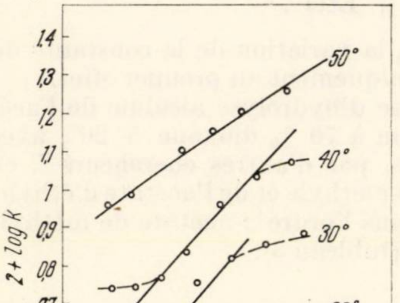

Fig. 4. — Variation de log k en fonction de D.

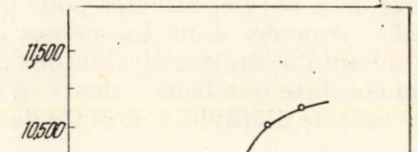

Fig. 5. — Variation de l'énergie d'activation en fonction de la teneur en dioxane du solvant mixte.

On a trouvé de même, que la constante de vitesse d'hydrolyse alcaline de l'acétate de *n*-butyle, déterminée dans une solution à 70 % dioxane, à 30°, est 40 fois plus grande que celle obtenue dans les mêmes conditions, pour l'hydrolyse alcaline de l'acétate du tertiaire butyle.[8]

Ceci vérifie l'ordre dans lequel se situent les vitesses d'hydrolyse des esters des différents alcools

$$^{k}(\text{alcool primaire}) > {}^{k}(\text{alcool secondaire}) > {}^{k}(\text{alcool tertiaire}).$$

Nous avons essayé de montrer l'influence du facteur électrostatique sur la constante de vitesse en faisant appel aux théories d'Amis [9] ou de Kirkwood. [10] Ces théories sont vérifiées dans toutes les solutions contenant de 16,24 à 57,10 % dioxane.

On remarque sur les figures 2 et 3 que le log k varie linéairement avec $\frac{1}{D}$ ou $\frac{D-1}{2D+1}$, dans ce domaine de concentration. La pente de la droite est négative, dans le premier cas, et positive, dans le second cas.

On trouve une variation beaucoup plus linéaire en représentant le log k en fonction de D [11] (fig. 4).

Sur la figure 4 on voit que la partie linéaire des courbes s'étend sur un domaine d'autant plus grand que la température de la réaction est plus élevée.

On admet l'existence dans ce domaine des interactions non électrostatiques dont l'intensité décroît au moment où la température s'élève.

L'énergie d'activation varie avec la concentration du dioxane et passe par un minimum à 37 % de dioxane (fig. 5).

L'existence de ce minimum a été remarqué aussi par d'autres chercheurs en étudiant l'hydrolyse alcaline des esters dont le radical acide de la molécule a un groupement alkyl ou aryl. Le groupement CH_3— du radical acide, et le groupement n-C_4H_9—de l'alcool manifestent une attraction pour le composant organique du solvant mixte (dioxane), alors que les groupements chargés électriquement sont hydrophiles.

On suppose qu'à une concentration du dioxane de 37,11 % la solvatation du complexe activée est minimale ; ceci correspondrait aux valeurs minimales de E et A à cette concentration. On admet, d'autre part, qu'une solvatation plus grande des molécules réagissantes, par rapport à la solvatation du complexe activé, se traduit par une augmentation de l'énergie d'activation, alors qu'une solvatation plus grande du complexe activé est accompagnée d'une diminution de l'énergie d'activation [12].

---

[8] Sh. Shalom, Lin Tsai, et S. Melvin, *J. Amer. Chem. Soc.*, **78**, 5420 (1956).

[9] E. S. Amis, *J. Chem. Educ.*, **30**, 351 (1953).

[10] J. K. Kirkwood, *J. Chem. Phys.*, **2**, 351 (1934).

[11] E. Tommila, A. Koivisto, S. P. Lyyra, V. Anatoll et S. Heimo, *Ann. Acad. Sci. Fenniae*, **A**, **II.**, **47**, (1952).

[12] A. Vöipio, *Ann. Acad. Sci. Fenniae*, **A**, **II**, **92** (1959).

En représentant le log $A-E$ (fig. 6) on obtient deux droites partant du minimum de l'énergie d'activation dont les pentes sont égales à 0,77 pour les solutions à 16,24 —37,11% dioxane, et à 0,60 pour les solutions à 37,17 — 76,35% dioxane, c'est-à-dire une valeur moyenne de 0,68 (fig. 6).

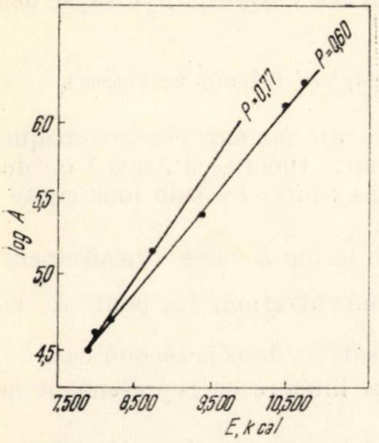

Fig. 6. — Variation de log A en fonction de E.

Revue Roumaine de Chimie, **15**, 33–41 (1970)

VOLUME PROPERTIES OF THE MELTS OF THE SYSTEMS $LiF-AlF_3$ AND $NaF-AlF_3$

MARTHA PAUČÍROVÁ, K. MATIAŠOVSKÝ and M. MALINOVSKÝ

Institute of Inorganic Chemistry of the Slovak Academy of Sciences, Dubrovska Cesta,
Bratislava, Czechoslovakia

Received March 27, 1969

The density of the melts of the binary systems $LiF-AlF_3$ and $NaF-AlF_3$ was measured using a hydrostatic method. On the basis of the measured values the excess volume and the partial molar volumes of the components of molten binary mixtures were determined.

INTRODUCTION

The study of the density of molten fluorides is of interest both from the technical and theoretical points of view. The technical importance of this study is evident considering the utilization of fluoride melts as electrolytes in electrometallurgy, especially in the electrolytic production of aluminium. From the theoretical point of view, the study of the volume properties may furnish important information on the structure of fluoride melts.

The density of the melts of the system $NaF-AlF_3$ has been measured by Lundina,[1] Abramov and Kozunov, [2] Vajna [3] and by Edwards et al.[4] All published density isotherms are of the same general character with a maximum in the concentration range 20–25 mole % AlF_3. However, the corresponding values of the density of pure molten NaF and of the binary $NaF-AlF_3$ mixtures, presented by different authors, are substantially different. On the other hand, the density of the molten $LiF-AlF_3$ mixtures has not yet been systematically studied. The only published data are those of Kostyukov [5] who measured the density of the melts containing 10, 22.5, 25, 30 and 35 mole % AlF_3 the measured data being used in the study of the viscosity of the melts of the system $LiF-AlF_3$.

---

[1] Z. F. Lundina, *Trudy VAMI*, **13**, 5 (1936).

[2] G. A. Abramov and P. A. Kozunov, *Trudy Leningrad, politekhn. inst., Razdel metallurgia*, **1**, 60 (1939).

[3] A. Vajna, *Alluminio*, **19**, 541 (1950).

[4] J. D. Edwards, C. S. Taylor and A. S. Russel, *J. Electrochem. Soc.*, **100**, 508 (1953).

[5] M. M. Kostyukov and G. I. Sipria, *Zhur. priklad. Khim.*, **36**, 1905 (1963).

EXPERIMENTAL

For the preparation of the LiF-AlF_3 and NaF$-AlF_3$ mixtures LiF and NaF of a purity "for monocrystals" were used. Pure aluminium fluoride, containing 99.5 wt. % AlF_3 was prepared by sublimation of the technical product in a Pt apparatus according to.[6] The density was determined using a hydrostatic method [7] with an accuracy of $\pm 0.2\%$. From the measured data if follows that in the chosen temperature range the polytherms of density of individual mixtures are a linear function of temperature (Table 1 and 2). The dependence of the density of the melts on the composition of the LiF$-AlF_3$ mixtures at different temperatures is presented in figure 1. In figure 2 the corresponding dependence for the melts of the system NaF$-AlF_3$ is presented.

Table 1

Values of constants in the equation $\rho_t = a - b.t$ for LiF$-AlF_3$ mixtures in the temperature range 850–1050°

Composition (Mole %)		a	$b \times 10^{-3}$
AlF_3	LiF		
0	100	2.2004	0.47
5	95	2.2970	0.48
10	90	2.4940	0.61
15	85	2.6112	0.67
20	80	2.6810	0.71
25	75	2,8180	0.84
30	70	2.8940	0.94
35	65	2.9240	1.03
40	60	2.8360	1.02
45	55	2.6660	0.94

Table 2

Values of constants in the equation $\rho_t = a - b.t$ for NaF$-AlF_3$ mixtures in the temperature range 1000–1100°

Composition (Mole %)		a	$b \times 10^{-3}$
AlF_3	NaF		
0	100	2.5812	0.636
10	90	2.6910	0.648
15	85	2.8445	0.765
20	80	2.9962	0.898
23	77	3.0120	0.912
25	75	3.0220	0.920
30	70	2.9745	0.920
35	65	2.9125	0.935
40	60	2.7490	0.890
45	55	2.5062	0.782
50	50	2.3065	0.690

On the basis of the measured density values the molar volumes, V, of the melts of both binary systems were calculated. Using the least square method the equations $V = f(x_2)$ were calculated, the accuracy being sufficient if for x_2 a polynom of the 3rd degree was used :

$$V = a + bx_1 + cx_1^2 + dx_1^3 = V_1^0 + bx_2 + cx_2^2 + dx_2^3 \qquad (1)$$

---

[6] K. Matiašovský, M. Malinovský, E. Plkšo and C. Kubík, *Chem. Zvesti*, **14**, 487 (1960).

[7] M. Malinovský, M. Paučírová and K. Matiašovský, *Chem. Zvesti*, **23**, 27 (1969).

where x_i – molar ratio

V_1^0 – molar volume of the pure component 1.

According to,[8] the partial molar volumes of the components of a binary system, $\overline{V}_1$ and $\overline{V}_2$, can be calculated using the equation:

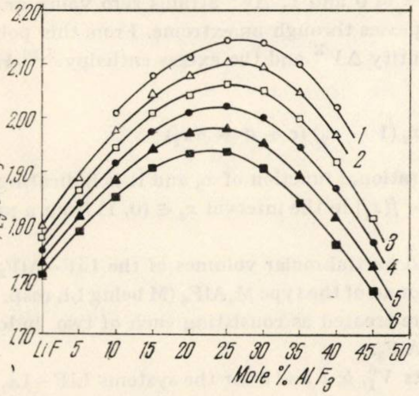

Fig. 1. – Densities of LiF – AlF$_3$ mixtures
1, 800°; 2, –850°; 3, –900°; 4, –950°, 5, –1000°; 6, –1050°.

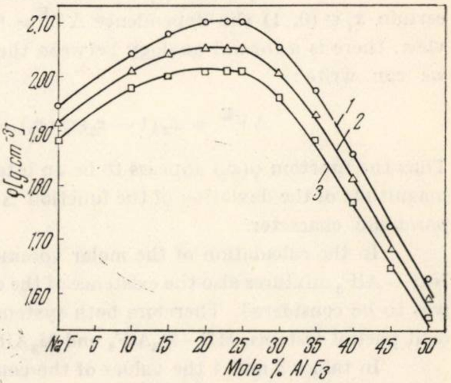

Fig. 2. – Densities of NaF – AlF$_3$ mixtures
1, 1000°; 2, –1050°; 3, –1100°.

$$\overline{V}_1 = V - x_2\left(\frac{\partial V}{\partial x_2}\right)T,\ P \tag{2}$$

After introducing for V the expression from the equation (1) and carrying out the indicated operations the equation is obtained:

$$\overline{V}_1 = V_1^0 - cx_2^2 - 2dx_2^3 \tag{3}$$

Analogously, for $\overline{V}_2$ the following equation is valid:

$$\overline{V}_2 = V + x_1\left(\frac{\partial V}{\partial x_2}\right)T,\ P \tag{4}$$

After introducing for V the expression from the equation (1) and rearranging:

$$\overline{V}_2 = V_1^0 + b + c + d - (c + 3d)\,x_1^2 + 2dx_1^3 \tag{5}$$

For $x_2 = 1$, according to the equation (1)

$$(V)_{x_2=1} = V_2^0 = V_1^0 + b + c + d \tag{6}$$

From the equations (5) and (6) it follows that

$$\overline{V}_2 = V_2^0 - (c + 3d)\,x_1^2 + 2\,dx_1^3 \tag{7}$$

An important quantity appears to be the value of the deviation, ΔV^E, of the real molar volume from the ideal molar volume, V_{id}. This excess volume is given by the equation:

$$\Delta V^E = V - V_{id} = x_1\overline{V}_1 + x_2\overline{V}_2 - (x_1V_1^0 + x_2\,V_2^0) \tag{8}$$

---

[8] E. Hála and A. Reiser, "Fysikální chémie I.," Publishing house ČSAV, Prague, 1960, p. 206.

After introducing for V_1^0 and $\overline{V}_2$ the expressions from the equations (3) and (7) into the equation (8) and rearranging, the follwing expression for ΔV^E is obtained:

$$\Delta V^E = -(c+d)\,x_2 + cx_2^2 + dx_2^3 \tag{9}$$

From the equation (9) it follows that for $x_i = 0$ and 1, ΔV^E attains zero value and for certain $x_i \in (0, 1)$ the dependence $\Delta V^E = f(x_i)$ passes through an extreme. From this point of view, there is a formal analogy between the quantity ΔV^E and the excess enthalpy.[9,10] Hence we can write:

$$\Delta V^E = x_2(1-x_2)\,\varphi(x_2) = -\,x_2(1-x_2)(c+d+dx_2) \tag{10}$$

Thus the function $\varphi(x_2)$ appears to be an integral rational function of x_2 and it is indicating the magnitude of the deviation of the function $\Delta V^E = f(x_i)$ in the interval $x_2 \in (0, 1)$ from a purely parabolic character.

In the calculation of the molar volumes and partial molar volumes of the $LiF-AlF_3$ and $NaF-AlF_3$ mixtures also the existence of the compound of the type M_3AlF_6 (M being Li, resp. Na) was to be considered. Therefore both systems were treated as consisting each of two independent partial systems, $MF-M_3AlF_6$ and $M_3AlF_6-AlF_3$.

In tables 3 and 4 the values of the constants V_1^0, b, c and d for the systems $LiF-Li_3AlF_6$ and $NaF-Na_3AlF_6$ are presented including the average error at different temperatures. The partial molar volumes calculated using equations (3) and (7) and the molar volume V at 1000° are presented in figures 3 and 4. In figures 5 and 6 the dependence of the excess volume ΔV^E and of the expression $\Delta V^E / x_2(1-x_2)$ on the composition at 1000° is presented.

Table 3

Values of constants in the equation $V = V_1^0 + bx_2 + cx_2^2 + dx_2^3$ for $LiF-Li_3AlF_6$ mixtures at different temperatures

Temperature (°C)	V_1^0	b	c	d	Mean error
950	14.794	61.201	6.829	−2.734	±0.037
1000	14.975	62.527	6.701	−2.413	±0.029
1050	15.107	64.063	6.079	−1.742	±0.037

Table 4

Values of constants in the equation $V = V_1^0 + bx_2 + cx_2^2 + dx_2^3$ for $Li_3AlF_6-AlF_3$ mixtures at different temperatures

Temperature (°C)	V_1^0	b	c	d	Mean error
950	80.088	−36.767	−0.297	33.790	±0.047
1000	81.788	−37.326	4.268	28.068	±0.048
1050	83.568	−38.192	11.286	18.922	±0.058

In the system $NaF-AlF_3$, beside cryolite, Na_3AlF_6, the incongruently melting chiolite, $Na_5Al_3F_{14}$, exists. However, the existence of this compound was not considered in the study of volume properties of $NaF-AlF_3$ mixtures since it is decomposed completely by a peritectic

---

[9] O. J. Kleppa and L. S. Hersh, *Discuss. Faraday Soc.* **32**, 99 (1961).

[10] O. J. Kleppa and J. M. Toguri, "Selected Topics in High Temperature Chemistry", T. Förland, K. Grjotheim, K. Motzfeldt and S. Urnes, eds. Universitetsforlaget, Oslo, 1960, p. 25.

reaction at 739°.[11] In the system LiF-AlF_3 no compound of this type has been determined. On the other hand, in both systems the existence of the compound of the type $MAlF_4$ was determined[12-15] and the existence of the complex AlF_4^- anion was confirmed by Malinovský and Matiašov-

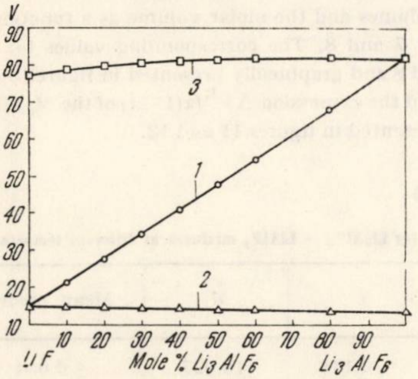

Fig. 3. — Dependence of the molar volume and the partial molar volumes on concentration for LiF—Li_3AlF_6 mixtures at 1000°.

1, molar volume; *2*, $\overline{V}_{LiF}$; *3*, $\overline{V}_{Li_3AlF_6}$.

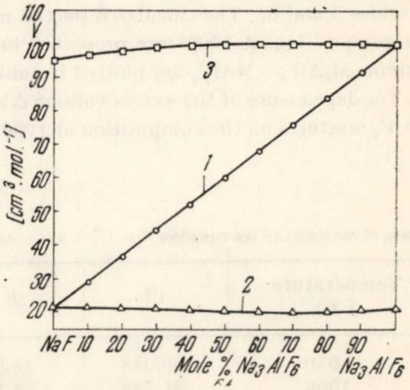

Fig. 4. — Dependence of the molar volume and the partial molar volumes on concentration for NaF-Na_3AlF_6 mixtures at 1000°.

1, molar volume; *2*, $\overline{V}_{NaF}$; *3*, $\overline{V}_{Na_3AlF_6}$.

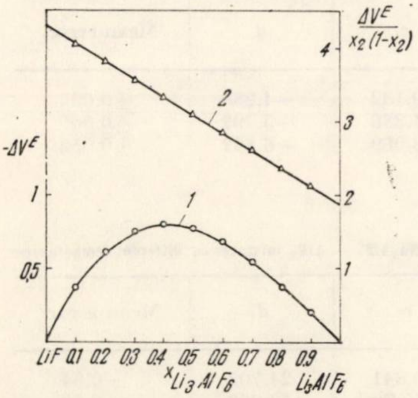

Fig. 5.— Dependence of ΔV^E and $\Delta V^E/x_2$ $(1-x_2)$ on concentration for LiF—Li_3AlF_6 mixtures at 1000°.

1, $\Delta V^E = f(x_2)$; *2*, $\Delta V^E/x_2(1-x_2) = \varphi(x_2)$.

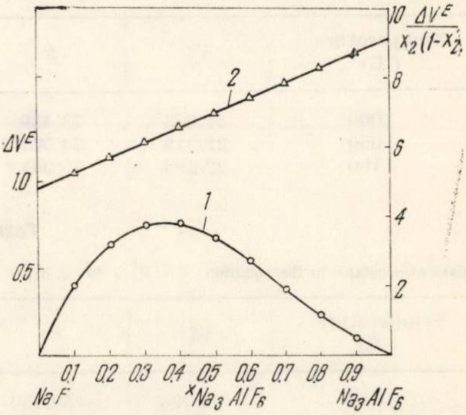

Fig. 6. — Dependence of ΔV^E and $\Delta V^E/x_2$ $(1-x_2)$ on concentration for NaF — Na_3AlF_6 mixtures at 1000°.

1, $\Delta V^E = f(x_2)$; *2*, $\Delta V^E/x_2(1-x_2) = \varphi(x_2)$.

[11] K. Grjotheim, J. L. Holm, C. Krohn and J. Thonstad, "Selected Topics in High Temperature Chemistry", T. Förland, K. Grjotheim, K. Motzfeldt, S. Urnes, eds. Universitetsforlaget, Oslo 1960, p. 151.

[12] R. F. Porter and E. A. Zeller, *J. Chem. Phys.*, **33**, 858 (1960).

[13] D. L. Hildebrand and L. P. Theard, *U. S. Dept. Com. Offico Techn. Serv.*, AD **258**, 410 (1961).

[14] L. D. Mc Cory, R. C. Paulo and J. L. Margrave, *J. Phys. Chem.*, **67**, 1086 (1963).

[15] G. Garton and B. M. Vanklyn, *J. Inorg. Nuclear Chem.*, **27**, 2461 (1965).

ský[16] by means of the cryoscopic measurements in the system Li_3AlF_6-KCl. Therefore, in the calculation of the molar volumes and partial molar volumes the possibility of the existence of this compound was also considered.

The calculated values of the constants V_1^0, b, c, d for the M_3AlF_6-AlF_3 mixtures are listed in tables 5 and 6. The calculated partial molar volumes and the molar volume as a function of the composition at 1000° are presented in figures 7 and 8. The corresponding values for the systems $M_3AlF_6-MAlF_4$ are plotted in tables 7 and 8 and graphically presented in figures 9 and 10. The dependence of the excess volume ΔV^E and of the expression $\Delta V^E/x(1-x)$ of the $M_3AlF_6-MAlF_4$ mixtures on the composition at 1000° are presented in figures 11 and 12.

Table 5

Values of constants in the equation $V = V_1^0 + bx_2 + cx_2^2 + dx_2^3$ for Li_3AlF_6 – $LiAlF_4$ mixtures at different temperatures

Temperature (°C)	V_1^0	b	c	d	Mean error
950	80.088	−24.508	−0.148	10.027	±0.054
1000	81.788	−24.881	1.881	8.331	±0.043
1050	83.567	−25.408	4.824	5.754	±0.067

Table 6

Values of constants in the equation $V = V_1^0 + bx_2 + cx_2^2 + dx_2^3$ for $NaF-Na_3AlF_6$ mixtures at different temperature

Temperature (°C)	V_1^0	b	c	d	Mean error
1000	21.603	73.439	9.132	−4.288	±0.034
1050	21.949	74.567	11.386	−5.792	±0.005
1100	22.293	75.941	13.069	−6.862	±0.052

Table 7

Values of constants in the equation $V = V_1^0 + bx_2 + cx_2^2 + dx_2^3$ for Na_3AlF_6 – AlF_3 mixtures at different temperatures

Temperature (°C)	V_1^0	b	c	d	Mean error
1000	99.926	−58.154	20.841	24.703	±0.54
1050	102.158	−59.677	25.570	19.068	±0.56
1100	104.486	−60.268	22.704	24.329	±0.41

Table 8

Values of constants in the equation $V = V_1^0 + bx_2 + cx_2^2 + dx_2^3$ for $Na_3AlF_6-NaAlF_4$ mixtures at different temperatures

Temperature (°C)	V_1^0	b	c	d	Mean error
1000	99.930	−38.771	9.261	7.324	±0.55
1050	102.158	−39.787	11.364	5.653	±0.56
1100	104.487	−40.181	10.089	7.213	±0.42

---

[16] M. Malinovský and K. Matiašovský, *Chem. Zvesti*, (in press).

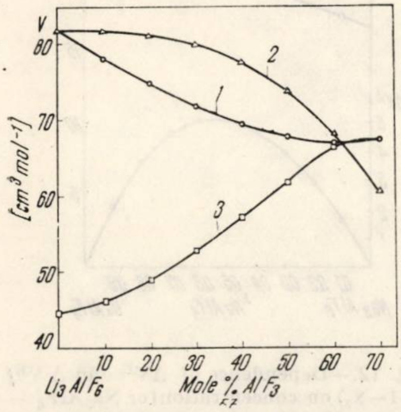

Fig. 7. — Dependence of the molar volume and the partial molar volumes on concentration for Li_3AlF_6 — AlF_3 mixtures at 1000°

1, molar volume; *2*, $\overline{V}_{Li_3AlF_6}$; *3*, $\overline{V}_{AlF_3}$.

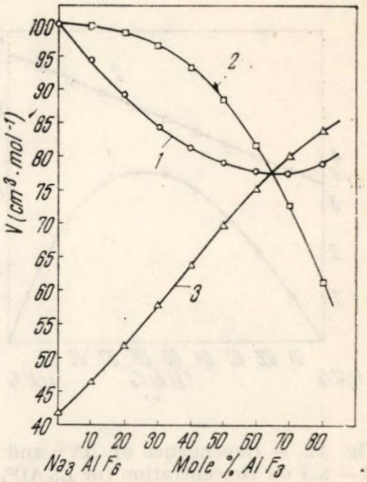

Fig. 8. — Dependence of the molar volume and the partial molar volumes on concentration for Na_3AlF_6—AlF_3 mixtures at 1000°

1, molar volume; *2*, $\overline{V}_{Na_3AlF_6}$; *3*, $\overline{V}_{AlF_3}$.

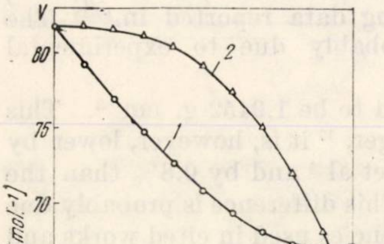

Fig. 9. — Dependence of the molar volume and the partial molar volumes on concentration for Li_3AlF_6—$LiAlF_4$ mixtures at 1000°.

1, molar volume; *2*, $\overline{V}_{Li_3AlF_6}$; *3*, $\overline{V}_{LiAlF_4}$.

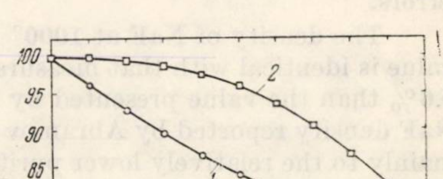

Fig. 10. — Dependence of the molar volume and the partial molar volumes on concentration for Na_3AlF_6—$NaAlF_4$ mixtures at 1000°.

1, molar volume; *2*, $\overline{V}_{Na_3AlF_6}$; *3*, $\overline{V}_{NaAlF_4}$.

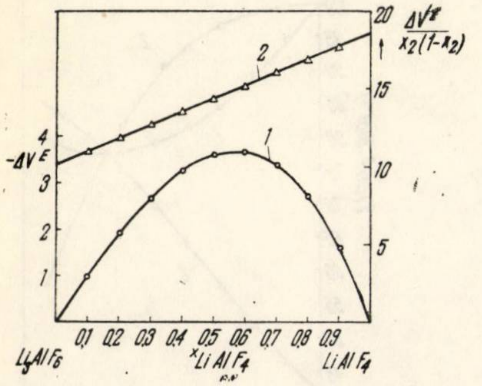

Fig. 11. — Dependence of ΔV^E and $\Delta V^E / x_2 (1 - x_2)$ on concentration for $Li_3AlF_6 - LiAlF_4$ mixtures at 1000°.

1, $-\Delta V^E = f(x_2)$; *2*, $-\Delta V^E / x_2 (1 - x_2) = \varphi(x_2)$.

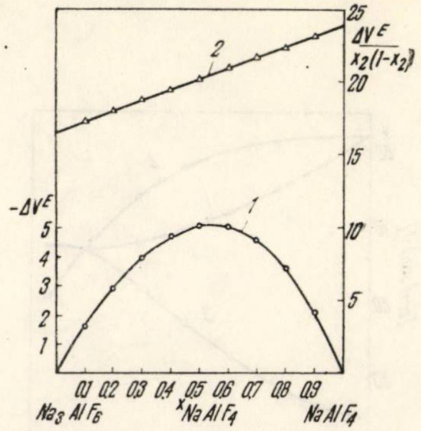

Fig. 12. — Dependence of ΔV^E and $\Delta V^E / x_2(1 - x_2)$ on concentration for $Na_3AlF_6 - NaAlF_4$ mixtures at 1000°.

1, $\Delta V^E = f/x_2/$; *2*, $\Delta V^E / x_2 (1 - x_2) = \varphi(x_2)$.

DISCUSSION OF RESULTS

The measured value of the density of LiF at 1000°, 1.7330 g/cm^{-3}, is in a good agreement with the corresponding data reported in.[17,18] The somewhat lower value reported by[6] is probably due to experimental errors.

The density of NaF at 1000° was found to be 1.9452 g. cm^{-3}. This value is identical with that measured by Jaeger, [17] it is, however, lower by 0.6% than the value presented by Edwards et al [4] and by 0.8% than the NaF density reported by Abramov et al. [19] This difference is probably due mainly to the relatively lower purity of reagencies used in cited works and it does not greatly exceeds the experimental error reported in. [4,19]

In figure 13, the measured polytherm of the density of Li_3AlF_6 is compared with the data reported by Kostyukov,[5] Mashovets[20] and Maltsev.[21]

In this case, the discrepancies among the reported data may be due, beside the purity of the Li_3AlF_6 used, also to the experimental complications caused by the corrosion of the suspended Pt wire of the melt with the gaseous phase.

---

[17] F. M. Jaeger, *Z. anorg. Chem.*, **101**, 180 (1917).

[18] H. W. Vornhusen, "Physikalische Stoffwerte von Fluoridsalzschmelzen, spezielle Anwendung auf das Mosel-Reaktorkonzept", 1965, 11 s. — Ord. Nr. Jül — 268 — RG.

[19] G. A. Abramov, M. M. Vetyukov, I. P. Gupalo, A. A. Kostyukov and L. N. Lozhkin, "Teoreticheskiye osnovy elektrometallurgii alyuminiya", Metallurgizdat, Moscow, 1953.

[20] V. P. Mashovets and V. I. Petrov, *Zhur. priklad. Khim.*, **32**, 1526 (1959).

[21] V. T. Maltsev and G. A. Buchalova, *Zhur. priklad. Khim.*, **40**, 532 (1967).

The measured values of the density of Na$_3$ AlF$_6$ (Fig. 14) agree with the data reported by Mashovets and Petrov [20] and by Abramov et al. [19] within the experimental error.

The measured isotherms of the density of NaF – AlF$_3$ mixtures (Fig. 2) are in a good agreement with the published data, [1–4] the maxima being slightly shifted from the coordinate corresponding to the cryolite composition towards NaF. The density isotherms of the LiF-AlF$_3$ mixtures (Fig. 1) have a similar general character. However, in this case at lower temperatures the maxima are shifted towards LiF whilst with the increasing temperature it is displaced towards AlF$_3$. This shift of the maximum with increasing temperature is probably due to the increasing temperature of the AlF$_6^{3-}$ions.

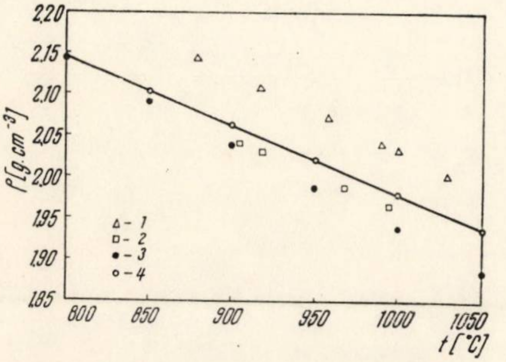

Fig. 13. — Densities of molten Li$_3$AlF$_6$.
1 – according to Mashovets,[19], 2 – according to Kostyukov,[5] 3– according to Maltsev,[21] 4 – this work.

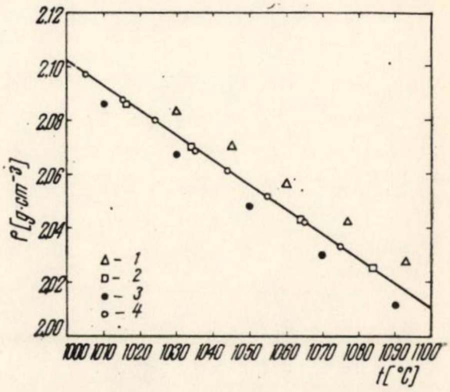

Fig. 14. — Densities of molten Na$_3$AlF$_6$
1 – according to Abramov, [20] 2 – according to Mashovets,[19] 3 – according to Edwards,[4] 4– this work.

Considering the dependence of the molar volume and of the partial molar volumes on the composition (Fig. 3, 4), the systems LiF–Li$_3$AlF$_6$ and NaF–Na$_3$AlF$_6$ differ but slightly from an ideal behaviour with a minimum $\bar{V}_i (i = 1, 2)$ for $x_i \rightarrow 0$, this being most probably due to a predominating influence of the large complex AlF$_6^{3-}$ on the volume properties of these melts.

From figures 5, 6, 9 and 10 presenting the dependence of the molar volume and of the partial molar volumes on the composition in the systems of the type M$_3$AlF$_6$ –AlF$_3$ and M$_3$AlF$_6$-MAlF$_4$ respectively, it is evident that in both cases there are strongly expressed deviations of the real volume from an additive value (Fig. 11, 12). The possible reasons of these deviations will be discussed in the subsequent paper.

Revue Roumaine de Chimie, 15, 43–51 (1970)

EXCESS FUNCTIONS FOR MIXED ELECTROLYTE SOLUTIONS

RODICA VÎLCU and FLORICA IRINEI
Laboratory of Physical Chemistry, University of Bucharest, Bd. Republicii nr. 13

Received January 9, 1969

The excess enthalpies of the KBr-NaBr-H_2O ternary system were determined by a method of adiabatic calorimetry for 1 m and 2 m total molalities of the dissolved salts at 288. 15, 298.15 and 308.15°K. The experimental values of heats of mixing were confirmed by data calculated with the help of Harned's laws. A computing method is shown for the excess functions and the activity coefficients in the case when electrolytes are in the presence of other electrolytes in solution, by means of a measurable deviation coefficient. This computing method was equally applied to the KCl−NaCl−H_2O system.

INTRODUCTION

Interactions between ions of electrolytes in aqueous solutions determine macroscopic effects revealed by various experimental operations.

In this paper, the behaviour of some electrolytes in ternary mixtures was characterized by calorimetry, as well as by data based on colligative properties of solutions. Although quite different as experimental processes, these methods were associated with a view to establishing the interaction rate between ions of electrolytes in aqueous solutions. The non-ideality of such systems, exteriorized by the values of excess functions or of other quantities of ideality deviation, were pointed out in previous papers.[1,2] The relation between the mixing enthalpies of their derived excess quantities — calorimetrically determined — and the thermodynamic activity coefficients — as deduced from cryometric data — was expressed by equations

$$H^M = -RT^2\left(x_{012}\frac{\partial \ln \gamma_{012}}{\partial T} + x_{12}\frac{\partial \ln \gamma_{12}}{\partial T}\right) \quad (1)$$

$$G^E = RT\,(x_{012}\ln \gamma_{012} + x_{12}\ln \gamma_{12}) \quad (2)$$

---

[1] R. Vîlcu and F. Stanciu, *Rev. Roumaine Chim.*, **13**, 7 (1968).
[2] R. Vîlcu and F. Stanciu, *Rev. Roumaine Chim.*, **13**, 253 (1968).

where:

x_{012} denotes the solvent molar fraction in the ternary system (electrolyte)$_1$ — (electrolyte)$_2$ — water
x_{12} „ the molar fraction of the solute electrolytes in the ternary system
γ_{012} „ the solvent activity coefficient in the ternary system
γ_{12} „ the activity coefficient of the solute substances in the ternary system.

Such correlations throw into relief the solute electrolyte deviations from the ideal behaviour.

COMPUTATIONS

The present paper gives explicitly the relation between the thermodynamic excess functions and a deviation (quantity) δ expressing the effect of the ionic interactions upon the macroscopic quantities of the systems. With the help of the same quantity, the activity coefficients can be indirectly computed for some electrolytes in a mixture with another electrolyte in a ternary system. Quantity δ that gives quantitative information on the modifications of the interionic actions within the thernary solutions of electrolytes in regard to the actual interactions between the respective binary systems, can be defined as a function of the supposed deviation from the addivity of the Gibbs thermodynamic potential of the electrolytes dissolved into the ternary mixture [3]:

$$RT \ln \delta = \frac{m_1 G_1 + m_2 G_2}{m_1 + m_2} - G_{12} \tag{3}$$

where Gibbs molar potentials in binary systems are denoted by G_1 and G_2, while G_{12} denotes the free molar energy of the ternary system. Electrolytes molalities in the ternary system are denoted by m_1 and m_2.

The thermodynamic treatment of this equation (3) allows to express quantity δ as a function of activity coefficients γ_1, γ_2 and γ_{12} of electrolytes 1 and 2 dissolved in binary systems and respectively of the two electrolytes in the ternary solution formed by mixing the binaries:

$$\log \delta = m_1 \log \gamma_1 + m_2 \log \gamma_2 - m \log \gamma_{12} \tag{4}$$

The activity coefficients in this equation are determined from cryometric and ebulliometric data [4] so that deviation quantity δ could be deduced, for various temperatures, as a function of the molalities of the given solutions.

The form of activity coefficent γ_{12} can be deduced, from equation (4), as the geometric average of the activity coefficients characterizing electrolytes 1 and 2 in the ternary mixture.

$$\gamma_{12}^{m} = (\gamma_1)_{12}^{m_1} (\gamma_2)_{12}^{m_2} \tag{5}$$

---

[3] I. G. Murgulescu and O. Landauer *Analele Universității "C. I. Parhon", București, Seria St. Naturii*, **18**, 23 (1958).

[4] R. Vîlcu *Analele Universității București, Seria St. Naturii*, 35, 27 (1962).

By applying the logarithms, one obtains :

$$m \log \gamma_{12} = m_1 \log (\gamma_1)_{12} + m_2 \log (\gamma_2)_{12} \tag{5'}$$

Quantities $(\gamma_1)_{12}$ and $(\gamma_2)_{12}$, as quantities characterizing an electrolyte in the presence of another one, include interaction corrections. Harned's laws [5] throw that into relief :

$$\log (\gamma_1)_{12} = \log \gamma_1 - \alpha_{12} m_2 - \beta_{12} m_2^2 + \cdots \tag{6 a}$$

$$\log (\gamma_2)_{12} = \log \gamma_2 - \alpha_{21} m_1 - \beta_{21} m_1^2 \tag{6 b}$$

where α, β are corrective coefficients.

In most cases, the terms in β having negligible values are neglected and one obtains

$$\log (\gamma_1)_{12} = \log \gamma_1 - \alpha_{12} m_2 \tag{7 a}$$

$$\log (\gamma_2)_{12} = \log \gamma_2 - \alpha_{21} m_1 \tag{7 b}$$

By combining relations (6 a) and (6 b) with Gibbs-Duhem's equation, their treatment leads to the following differential equation :

$$2(\alpha_{12} + \alpha_{21})\, y\, \mathrm{d}y - 2\, \alpha_{12}\, \mathrm{d}y = \frac{2\mathrm{d}\, \Phi}{2.303\, m} \tag{8}$$

Quantity y characterizes the proportions of the two electrolytes in the mixture, so that

$$m_1 = my \text{ and } m_2 = m(1 - y)$$

For equimolal concentrations ($y = 0.5$), the integration of equation (8), between the limits of infinite dilution and given concentration, leads to relation

$$\frac{\alpha_{12} + \alpha_{21}}{4} = \alpha_{21} + \frac{2}{2.303\, m} (\Phi_y - \Phi_0) \tag{9}$$

where

Φy denotes the osmotic coefficient of the considered ternary solution,

Φ_0 " the osmotic coefficient of the binary solution.

Harned's coefficients and deviation quantity are correlated by taking into account equations (4), (5), (7a) and (7 b):

$$\log \delta = m_1\, m_2\, (\alpha_{12} + \alpha_{21}) \tag{10}$$

In the case of very exact computations, the second members of equation (10) are supplemented with corrective factors β_{12}, β_{21}, etc. which are equal to deviation δ logarithm.

---

[5] H. S. HARNED and B. B. OWEN, "The Physical Chemistry of Electrolytic Solutions", Reinhold Publ. Corp., New York, 1963, p. 603.

From the combination of the last two equations, one will obtain the expression of Harned's coefficient α_{21}:

$$\alpha_{21} = \frac{\log \delta}{m_1 m_2} - \frac{2}{2.303\ m} (\Phi_y - \Phi_0) \qquad (11)$$

Therefore, coefficients α_{21} and implicitly α_{12} can be calculated, for a total concentration m of the ternary, directly from the experimental data. Consequently, Harned's equations allow to compute the activity coefficients $(\gamma_1)_{12}$ and $(\gamma_2)_{12}$ of electrolytes 1 and 2 when other electrolytes are present in the solution. Such quantities are inaccessible to direct measurements.

The excess thermodynamic functions of electrolyte solutions can also be expressed with regard to deviation δ.

For solutions consisting of two uni-univalent electrolytes, respecting Harned's laws, the following equations of the excess thermodynamic functions were established [6, 7]:

$$G^E = -2.303\ RT x_1 x_2\, m \left[(\alpha_{12} + \alpha_{21}) + \frac{2m}{3}(2\beta_{12} + \beta_{21}) - \right.$$

$$\left. - \frac{2mx_2}{3}(\beta_{12} - \beta_{21}) \right] \qquad (12)$$

where

x_1 denotes the molar fraction of electrolyte 1 in the ternary system

x_2 " the molar fraction of electrolyte 2 in the ternary system.

From relation (12), combined with Gibbs-Helmholtz' equation, one obtains the molar mixing enthalpy:

$$H^M = 2.303\ RT^2 x_1 x_2\, m \frac{\partial}{\partial T} \left[(\alpha_{12} + \alpha_{21}) + \frac{2m}{3}(2\beta_{12} + \beta_{21}) - \right.$$

$$\left. - \frac{2m\, x_2}{3}(\beta_{12} - \beta_{21}) \right] \qquad (13)$$

For equal molar fractions of the solutes, $x_1 = x_2 = 0.5$, the equations reduce themselves to:

$$G^E = -\frac{2.303\ RT\, m}{4} [(\alpha_{12} + \alpha_{21}) + m\,(\beta_{12} + \beta_{21})] \qquad (14\text{ a})$$

and

$$H^M = \frac{2.303\ RT^2}{4} \frac{m\partial}{\partial T} [(\alpha_{12} + \alpha_{21}) + m\,(\beta_{12} + \beta_{21})] \qquad (14\text{ b})$$

---

[6] K. S. Pitzer and L. Brewer, "Thermodynamics", McGraw-Hill Book Comp., New York, 1961, p. 572.

[7] J. H. Stern and C. W. Anderson, *J. Phys. Chem.*, 68, 2528 (1964).

It should be remarked the advantage offered by the substitution of the corrective terms appearing in these equations of the single δ correction, experimentally accessible [2,4] (see eq. 4). According to equation (10), established in this paper, the excess functions in the last two equations take the forms:

$$G^E = -\frac{2.303\ RT\,m}{4}\ \frac{\log \delta}{m_1\,m_2} \tag{15}$$

and

$$H^M = \frac{2.303\ RT^2\,m}{4\ m_1\,m_2}\ \frac{\partial \log \delta}{\partial T} \tag{16}$$

and are expressed in regard to a quantity capable to show the modifications corresponding to the purely ionic interactions when mixing binary aqueous solutions of electrolytes.

WORKING TECHNIQUE

The mixing enthalpies were first determined with an adiabatic calorimeter described in a previous paper. [8] For system $NaBr-KBr-H_2O$ and its associated binaries, deviations δ were borrowed from the results of a differential cryometry work, while their variation with the temperature, for a given composition, were estimated by means of a combination between the cryometric measurements and the results of a differential ebulliometry[4] work, in binary and ternary systems of electrolytes. The $NaCl.KCl-H_2O$ ternary was characterized by means of the cryometric and thermochemical data.

EXPERIMENTAL RESULTS AND DISCUSSION

a. *System* $NaBr-KBr-H_2O$. The thermal effects were determined in the case of mixing aqueous solutions of KBr and NaBr, in concentrations such that the total molality of ternary $KBr-NaBr-H_2O$ be equal to 1 and 2. By holding constant the total molality of this ternary, variable molar fractions of the binaries were chosen, between 0.2 and 0.8, in regard to KBr. The measurements were repeated at three temperatures : 288.15 ; 298.15 and 308. 15° K. [9]

If the total molality of the mixture is equal to 1 m, the experimental values of the excess enthalpies (of mixing) are correlated, in composition and temperature by the following empirical equation

$$H^M = 2.303\ RT^2 m\ x_1 x_2(-9.55 \times 10^{-5} + 0.48 \times 10^{-5}\ x_2)$$

where x_1 denotes the NaBr molar fraction
x_2 " the KBr molar fraction.

---

[8] R. Vîlcu and F. Stanciu, *Rev. Roumaine Chim.*, **10**, 6 (1965).

[9] R. Vîlcu and F. Irinei, *J. Chem. Thermodynamics* (in press).

Similarly formulated, but with other constants, the equation still holds its validity to a total concentration of 2 m:

$$H^M = 2.303\ RT^2\ m\ x_1x_2\ (-\ 8.56 \times 10^{-5} + 0.05\ \times 10^{-5}x_2).$$

Beside these empirical equations for estimating the heats of mixing, the excess enthalpies were computed for molar fractions equal to those of the KBr and NaBr solutions according to equation (14). In view of this computation, the thermal coefficient of deviation δ between 269.4 and 329°K was estimated with the help of cryometric and ebulliometric data resulting from the slope dependence of log δ in regard to T, for a total concentration of $m = 1.4$. This slope is hardly influenced by the concentration, so that practically it maintains its value (0.0047×10^{-3}) within a concentration range from 1 to 2 m. The standard mixing enthalpy computed for a total concentration of 1 m has the value of -9.70 cal/mol which differs from the experimental one by 2.6 %, i.e. by less than 0.3 cal. Such a difference is not to be taken into consideration, since however sharp the experimental measurements, this difference will be within the measurement errors. The same good agreement between computation and experiment is found for the total concentration of 2 m. The comparative values are recorded in table 1.

Table 1

Comparative data for the heats of mixing and the thermodynamic excess functions of the NBr – KBr–H_2O – system, at 298 15° K: $x_1 = x_2 = 0.5$

Total molality (m)	H^M(cal/mol)			G^E(cal/mol)	TS^E (cal/mol)
	Present work		Exptl.[10]	(Present work)	(Present work)
	Exptl.	Calc.			
1	−9.42	−9.70	−9.43	−4.83	−4.59
2	−17.27	−19.40		−9.66	−7.61

This table gives also the standard excess free energies, as well as the products TS^E. The standard G^E was computed by means of equation

$$\frac{G^E_{298}}{298} = \frac{G^E_2}{T_2} - \int_{T_2}^{298} \frac{H^M}{T^2}\mathrm{d}T \tag{15}$$

Index 2 marks the quantities corresponding to the freezing point of the solution.

The free energy at the freezing point was calculated, for a solution whose total molality was 1 or 2, by means of equation (13), where log $\delta = 5.60\ \times 10^{-3}$ (at $T = 269.4$°K).

The above equation can be valued, within the limits available for δ, for any concentration and temperature.

From the values of the mixing enthalpy and of the excess free energies, the excess entropy can be deduced:

$$TS^E = H^M - G^E \tag{16}$$

---

[10] R. W. Wood and R. W. Smith, *J. Phys. Chem*, **69**, 2974 (1965).

In the case of system KBr-NaBr$-H_2O$, comparative data for G^E and S^E are not available. Analogies with related systems, such as KCl$-$NaCl$-H_2O$, show a considerable similarity between the values of these excess functions, which leads to the conclusion that the substitution of anion Br^- to Cl^- does not change the level of ionic interactions in the systems with moderate concentrations.

b. *System NaCl$-$KCl$-H_2O$* was thermodynamically characterized by the activity coefficients of electrolytes NaCl and KCl as computed in the ternary mixture and by the excess free enthalpies. The activity coefficients of the mixture electrolytes were estimated by means of equations (7a) and (7b).

Harned's coefficients α_{12} and α_{21} in equations (7a) and (7b) were determined for both NaCl and KCl electrolytes from the NaCl$-$KCl$-H_2O$, system, by making use of equation (11).

By taking into account that α_{12} and α_{21} hardly vary with the concentration, their values, established for m $= 1.6$ within the molal 1 and 2 interval were considered valid.

Coefficients α_{12} and α_{21} were calculated with m $= 1.6$ molal, a concentration framed by a higher number of experimental data.

Table 2

Harned's coefficients of the KCl$-$NaCl$-H_2O$ system

m	α_{12}		α_{21}	
	Present work	Lit.[11]	Present work	Lit.[11]
1		-0.0084		0.0235
1.6	-0.0059		0.0235	
2		-0.0095		0.0230

In table 2 are recorded the values of Harned's coefficients, we obtained for system NaCl$-$KCl$-H_2O$ at 1.6 molal, as well as the values we deduced from isopiestic measurements [11] of vapour tensions.

The activity coefficients, computed for the freezing point of the solutions, were transposed for standard conditions by equation :

$$\log \gamma_{298.1} = \log \gamma_T - \frac{y}{\nu} \bar{L}_{2(298.1)} + \frac{z}{\nu} \bar{J}_{2(298.1)}$$

where

$$y = \frac{298.1 - T}{2.303\, R\, 298.1\, T} \quad \text{and} \quad z = 298.1\, y - \frac{1}{R} \log \frac{298.1}{T}$$

---

[11] R. A. Robinson, *J. Phys. Chem.*, **65**, 662 (1963).

The thermochemical quantity $\overline{L}_2$ represents the partially molar relative thermal content of the solute component, while $\overline{J}_2$ denotes the partially molar relative thermical capacity of the solution.

The activity coefficient of the NaCl in the binary solution was computed for 298.1°K in another paper [8].

In order to compute the activity coefficient of KCl at the standard temperature, we had to use values of $\overline{J}_2$ and $\overline{L}_2$ from the literature [6].

The comparison between the values so obtained for $(\gamma_{NaCl})_{mixture}$ and $(\gamma_{KCl})_{mixture}$ and the results given by Stahanova, Vasilev and Epihin[12] lead to satisfactory agreements. For $(\gamma_{KCl})_{mixture}$, the difference, appearing between the two series of values, can be largely attributed to the thermochemical data used in computing the standard values of the activity coefficients. Table 3 records the values of the activity coefficients at 298.15°K for each of the considered electrolytes in the ternary system, as well as in their respective binaries.

Table 3

Standard activity coefficients of KCl and NaCl in binary and ternary solutions

m	$(\gamma_1)_{12}$		$(\gamma_2)_{12}$		γ_1	γ_2
	Present work	Lit.[12]	Present work	Lit.[12]	Lit.[8]	Lit.[5]
2	0.562	0.585	0.634	0.634		0.670

Table 4 contains the Gibbs' free energies of excess, obtained from calorimetric measurements, given comparatively with the values computed by equation (15), for a total concentration of 2 molal, taking into account deviations δ as estimated from cryometric data. [8]

Table 4

Standard excess free enthalpies of the KCl – NaCl – H_2O system

m	G^E cal/mol		
	Present work		Lit.[7]
	Calorimetry	Cryoscopy	
2	−9.27	−14.30	−9.30

The experimental Gibbs' free energy of excess was estimated from the heat of mixing values at 283.15 ; 298.15 and 313.15°K. The difference between the calorimetrically and cryometrically obtained values, though of only 5 cal/mol is proportionally large if the small values of the free energy of excess are taken into account. The value of deviation δ which appears in the determination of the free energy of excess, can be affected by a small uncertainty : the correct valuation of this quantity implies extremely exact determinations of the freezing temperatures for the binary systems

---

[12] M. S. STAHANOVA, V. A. VASILIEV and A. EPIHIN, *Zhur. fiz. Khim.*, **37**, 354 (1963).

$NaCl-H_2O$ and $KCl-H_2O$ as well as for the ternary $NaCl-KCl-H_2O$. Besides, the method of estimating the activity coefficient from cryometric data is affected by the errors of the graphic solving of the integrals in the activity coefficient expression.

From the excellent agreement between the calculated and the experimental values of the excess functions, there results that the calculation errors are reduced to a minimum by applying the new formulations of the equations defining the excess thermodynamic quantities. Even in the case of large enough concentrations, the incertainties introduced by corrective terms α_{12}, α_{21}, . . . are removed by replacing them by a single correction δ, accessible to measurements. Quantity δ contains implicitly, the whole set of terms that should be contained in Harned's laws if we want to have a rigorous representation of the behaviour of the non-ideal systems.

We thus step forward in order to establish a relation between the microscopic representation and the macroscopic parameter values (the excess functions) of the system.

Contrary to the theory of Brønsted-Guggenheim[13] which does not anticipate changes in the specific interactions between ions in the case of two electrolytes with common ions and therefore recommends to equalize the excess thermodynamical functions to zero, both the computing method chosen for the excess quantities and the experimental results for the ternary systems lead to excess values different from zero. This result can be considered as a measure of the deviations from Brønsted-Guggenheim's theory and consequently attributed to interaction differencies between equally charged ions. The result is also confirmed by the system $NaBr-KBr-H_2O$ and by the system $KCL-NaCl-H_2O$ which have a similar behaviour, and are studied in this paper, as well as by other alkali halides in mixtures.[7, 9-15]

---

[13] E. A. Guggenheim, *Phyl. Mag.*, **19**, 588 (1935).

[14] T. F. Young and M. B. Smith, *J. Phys. Chem.*, **58**, 716 (1954).

[15] T. F. Young, Y. C. Wu and A. A. Krawetz, *Discuss. Faraday Soc.*, **24**, 27, 77, 80 1957).

Revue Roumaine de Chimie, 15, 53–57 (1970)

REACTIONS IN SOLID MEDIA. II[1]

KINETICS OF THE FORMATION OF THE DOUBLE OXIDE OF POWDER MIXTURES IN NITROGEN ATMOSPHERE

ILEANA PETRUŞ

Institute of Physical Chemistry of the Academy
Bucharest, str. Dumbrava Roşie 23

Received January 30, 1969

The kinetics of the reaction $CoO + Al_2O_3$ in a molar ratio 1: 2 and nitrogen atmosphere was studied and the kinetic law was deduced.

The first part of this work[1] published in 1968 showed the results ensuing after the investigation of the reaction $CoO + Al_2O_3$ in a 1:1 mol mixture, in tablets, in nitrogen atmosphere, and in the temperature range 900 to 1050°.

As previously shown this reaction was studied by several authors; but their works do not contain data on the kinetics of the reaction. Since the mechanism of the reaction is unknown, we might consider it somewhat similar to that proposed by Schmalzried [2–4] in the study carried out by him on the reaction with platinum wire marking and natural marking, poly and mono-crystalline phases, for the mixture of the two oxides CoO polycrystalline and Al_2O_3 monocrystalline.

If this mechanism were applicable to powders, the kinetics of the reaction would not depend on the ratio of the two constituents, as one of these, CoO, reacting in gasform would have a higher evaporation rate than the reaction rate of $CoO + Al_2O_3$.

However the diagram given by Schmalzried is applied to temperatures around 1400 °. This diagram could possibly not be applicable at lower temperatures, when the gasification rate of the CoO would become negligible.

A kinetic study of the reaction could give us nevertheless certain hints as to the possibility of applying the suggested mechanism to a reaction among monocrystals or polycrystals and monocrystals.

[1] Part I: D. Cismaru and S. Zervudis, *Rev. Roumaine Chim.*, **13**, 275 (1968).
[2] H. Schmalzried, *Z. phys. Chem.* (*Frankfurt*), **32**, 76 (1962).
[3] W. Rogola and H. Schmalzried, *Naturwiss.*, **50**, 593 (1967).
[4] H. Schmalzried, *Ber. deutsch. Keram. Soc.*, **1**, 11 (1965).

In the present paper we aimed at studying the reaction $CoO + Al_2O_3$ in a 2 :1 mol ratio also in nitrogen atmosphere.

EXPERIMENTAL

The alumina used for the mixture was obtained from active chromatographic Merck Al_2O_3, by heating in a platinum crucible at 1200° for approximately 6 hours, till constant weight was reached.

The cobalt oxide was obtained from CO_3O_4 (Merck) through calcination at 1000° in nitrogen atmosphere for 1 hour, cooling also in nitrogen atmosphere and heating again at 1000° for another hour in nitrogen atmosphere.

For both oxides the size passing through the 13,000 mesh/sq. cm sieve was used.

The aluminium oxide, as well as the cobalt II oxide, after being mixed in a 2 :1 mol proportion, were homogenized by stirring for 48 hours. The mixture was stamped into 1 g and 12 mm diameter tablets at a pressure of 3100 kg per cm^2. The homogeneity of the tablets was determined by analysis.

The samples were heated in the platinum crucible introduced into the quartz tube, and this into an electric furnace at fixed time-intervals and temperatures, maintaining the reaction temperature constant with a maximum deviation of $\pm$ 2.5°.

The temperature was measured with a thermocouple Pt-PtRh placed near the sample.

A purified nitrogen flow passed through the quartz tube. Purification is achieved through a reduction column with CuO heated at 400° and then dried by passing it through drying flasks with H_2SO_4 conc., NaOH rotulis, $CaCl_2$, silicagel $Mg(ClO_4)_2$ H_2SO_4 conc.

At the end of the reaction the quartz tube was taken out of the electric furnace and cooled without interrupting the nitrogen flow. One has then proceeded to the grinding of the tablets and the separation of the unreacted CoO of the spinel and the unreacted alumine by treating the ground product with 1 :1 HCl and then filtering it.

After filtering the Co^{2+} of the solution was dosed with αα'-dipyridyl, and the quantity of CoO transformed into spinel was calculated.

RESULTS AND DISCUSSION

The obtained results were used to determine the rate constant, by making use of the following two equations :

1. $1 - (1 - z)^{2/3} - 2/3\, z = k_G . t$ (the Ghinstling-Brounstein-Cismaru's equation [5,6])

2. $z = 1 - \frac{6}{n^2} \sum_{n=1}^{n=\infty} \frac{1}{n^2} \exp\,(-\, n^2\, k_s \cdot t)$ (the Serin-Ellikson's equation [7])

In both equations, z is the transformed substance fraction, k is the rate coefficient including also the diffusion coefficient of a constituent

---

[5] A. M. Ghinstling and B. I. Brounstein, *Zhur. priklad. Khim.*, **23**, 1249 (1950).

[6] D. Cismaru, *Studii și Cercetări Fiz., Acad. R. P. Română*, **3**, 435 (1955).

[7] B. Serin and R. T. Ellikson, *J. Chem. Phys.*, **9**, 742 (1941).

into the reaction product, t is the reaction time, and in equation (2), n is a whole number taking values from 1 to ∞.

In figure 1, one gives the variation of z *versus* t (in minutes).

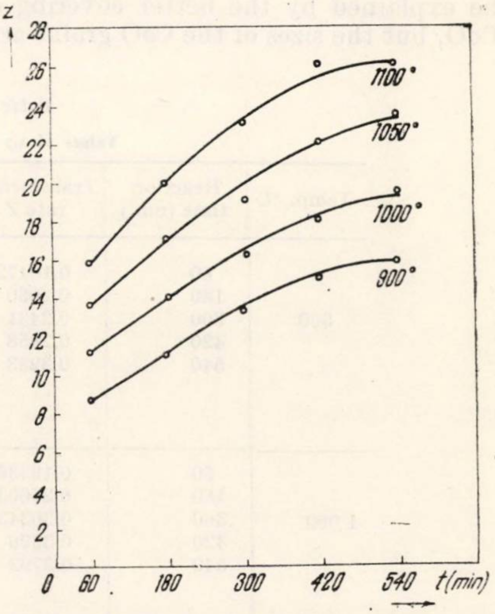

Fig. 1. – Variation of z *versus* time t (in minutes).

The following tables give the results obtained for a value of the rate constant k, computed by means of equation (1) and (2).

$k_G = k$ inferred from equation (1)

$k_S = k$ inferred from equation (2)

by applying Arrhenius'equation

$$k = Ae^{-E/RT}$$

one has determined the activation energy E, using for k the values of the rate constants k_G and k_S

One has thus obtained for the activation energy the values $E = 20{,}000$ cal/mol when using the rate constants (eq. 1) and $E = 30{,}000$ cal/mol when using (eq. 2).

The pre-exponential coefficients in both cases have been computed. Their values are : $A_G = 1.202 \times 10^{-4}$ and $A_S = 6.761 \times 10^{-4}$.

By comparing the values in the case of the same reaction with a 1 :1 mol mixture, one notices that the reaction is much quicker in the case of a 2 :1 mol mixture.

Table 3 holds the values of the rate constants and activation energies using only one of the equations, namely Serin-Ellikson's equation.

The fact that there exist some differences between the rate characteristics obtained in the mixture of 1 :1 mol and 2 :1 mol CoO :Al_2O_3, could be explained by the better covering of the Al_2O_3 grain's surface by the CoO, but the sizes of the CoO grains are much smaller than those of Al_2O_3.

Table 1

Values of k_G and k_S

Temp. °C	Reaction time (min)	Transformed rate Z	k_G *	k_S **
900	60	0.16472	5.04	1.00
	180	0.2080	2.3	3.00
	300	0.2431	2.24	2.60
	420	0.2858	2.42	2.40
	540	0.3233	2.60	2.40
			M : 2.40	M : 2.60
1 000	60	0.19336	7.55	—
	180	0.26603	5.00	5.00
	300	0.30343	3.40	3.30
	420	0.3396	3.60	3.00
	540	0.3792	3.57	3.00
			M : 4.05	M : 3.575
1 050	60	—	—	—
	180	0.3216	5.81	6.60
	300	0.3453	5.27	4.40
	420	0.4122	5.49	4.00
	540	0.4411	5.07	3.50
			M : 5.41	M : 4.55
1 100	60	—	—	—
	180	0.3767	10.67	0.00
	300	0.4327	8.73	5.80
	420	0.4821	8.00	5.00
	540	0.4815	6.20	4.00
			M : 8.40	M : 5.7

* $k_G = k$ deduced from Ghinstling-Brounstein-Cismaru's eq.
** $k_S = k$ deduced from Serin-Ellikson's eq.

The CoO grains have sizes harmonizing with those of the colloidal particles, as they are forming colloidal suspensions passing through filter paper, while those of Al_2O_3 have larger sizes and their suspension is not colloidal and does not pass through filter paper.

It we admit that Schmelzreid's mechanism may be also applied to powders, by comparing the result we could draw the conclusion that in the case of the ratio CoO : Al_2O_3 at 2 : 1, the CoO quantity would be sufficient to give the quantity of vapours necessary to cover the Al_2O_3 grains and the formed spinel, at the working temperature.

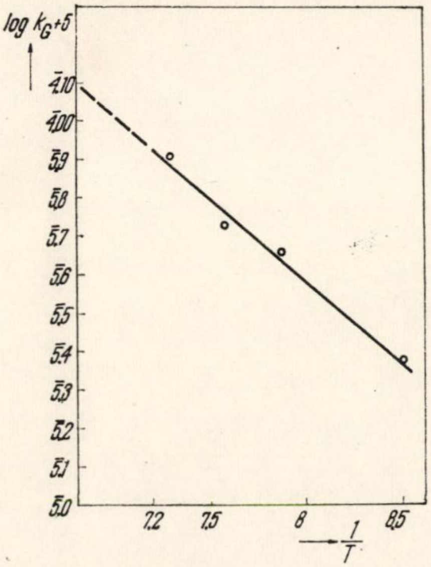

Fig. 2. — Dependency of rate constant k_G on temperature.

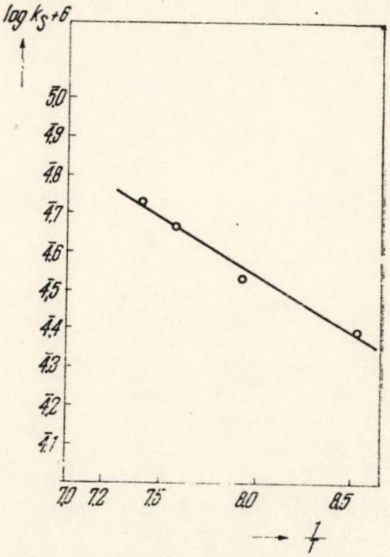

Fig. 3. — Dependency of rate constant k_S on temperature.

Table 2

Values of k_G and k_S

Temp. °C	$1/T$	log. k_G+5	E cal/mol	$A.\ 10^4$	$\log k_S+6$	E cal/mol	$A.\ 10^4$
900	0.085	0.38	20,000	1.202	0.415	30,000	6.761
1 000	0.0875	0.67			0.530		
1 050	0.0757	0.73			0.658		
1 100	0.073	0.92			0.74		

Table 3

Rate constants and activation energies for the reactions $CoO + Al_2O_3$ in molar ratio 1 : 1 and 2 :1

Temp. °C	$CoO+Al_2O_3$ 1 : 1			$CoO + Al_2O_3$ 2 : 1		
	$k_S.\ 10^5$	E cal/mol	$A.\ 10^6$	$k_S.\ 10^4$	E cal/mol	$A.\ 10^5$
900	0.28	57,000	9,833	0.60	30,000	7,079
1 000	2.66			3.40		
1 050	6.20			4.55		
1 100	—			5.50		

Nevertheless, the better coverage of the Al_2O_3 grains by those of CoO could supposedly play an important role too.

Revue Roumaine de Chimie, 15, 59–65 (1970)

THERMODYNAMIC PROPERTIES OF LIQUID MAGNESIUM-LEAD, MAGNESIUM-INDIUM AND MAGNESIUM-GALLIUM ALLOYS

H. NEBELL *)

Center of Chemical Physics, Bucharest, Str. Galaţi 31

Received March 20, 1969

The thermodynamic properties of liquid Mg-Pb, Mg-In and Mg-Ga alloys have been determined between 450° and 650° by measuring the EMF of the galvanic cells,

$$Mg_{(s)}|MgF_2-LiCl-KCl|\ (Mg-Me)_1$$

where Me is Pb, In and Ga. Special attention has been given to the construction of the cell and to the composition of the electrolyte. The functioning of the cell was checked by measuring the time dependence of the EMF of the cell.

Several studies have been made of the thermodynamic properties of liquid Mg-Pb alloys. Wagner and Engelhardt, [1] Lantratov, [2] Knappwost, [3] Stryvalin et al [4] and Wilson [5] used the electromotive-force method. Scheil and Wolf [6] and Schmal and Sieber [7] applied the transpiration technique, and Eldrige, Miller and Komarek [8] utilized the phase diagram to determine the activity of magnesium in liquid Mg-Pb alloys. The results of these studies were not in very good agreement. Therefore Eldrige, Miller and Komarek [9] also studied the Mg-Pb system by an isopiestic technique. The reinvestigation of the liquid Mg-Pb alloy described in this paper was mainly undertaken in order to control the functioning of the galvanic cell.

Very little information is available on the thermodynamic properties of liquid Mg-In and Mg-Ga alloys. Recently Danilian and Yazenko[10]

---

*) Present address : Resalandvegenll I. Øvre Årdal, Norway.

[1] C. Wagner and G. Engelhardt, *Z. phys. Chem.*, **159**, 241 (1932).

[2] M. F. Lantratov, *Zhur. neorg. Khim.*, **4**, 1415 (1959).

[3] A. Knappwost, *Z. phys. Chem.*, **21**, 358 (1959).

[4] I. T. Stryvalin, O. A. Esin and B. M. L. Lepinskikh, *Zhur. fiz. Khim.*, **38**, 637 (1964).

[5] J. R. Wilson, Queens University, Kingston, Ontario, Canada, March 1966 (private communication).

[6] E. Scheil and F. Wolf, *Z. Metallk.*, **50**, 229 (1959).

[7] N. G. Schmal and P. Sieber, Paper 2K. pl. -16, HMSO, London, 1959.

[8] J. M. Eldridge, E. Miller and K. L. Komarek, *Trans. Met. Soc. AIME*, **233**, 1303 (1965).

[9] J. M. Eldridge, E. Miller and K. L. Komarek, *Trans. Met. Soc. AIME*, **239**, 570 (1967).

[10] B. H. Danilian and S. P. Yazenko, *Zhur. fiz. Khim.*, **42**, 734 (1968).

published values for the integral heat of mixing of liquid magnesium and liquid gallium. Their experimental values agree fairly well with the results obtained in this investigation.

EXPERIMENTAL

It is well known[11] that magnesium is to some extent dissoluble in its own molten halides. Therefore, the EMF of the galvanic cell,

$$Mg_{(s)} \,|\, MgCl_2 \,|\, (Mg - Me)_{(l)}$$

will always decrease with time because of metallic diffusion. In this investigation the metallic diffusion is reduced by choosing a favourable electrolyte (a eutectic mixture of LiCl and KCl with a 5 weight % MgF_2 addition), by working at relatively low temperatures (below the melting temperature of magnesium, 650°) and by separating the electrodes by means of an alumina tube with a small hole at the bottom. The effect of the still remaining diffusion is lowered by using a great amount of magnesium in the liquid alloy compared to the minute amount of magnesium which dissolves from the solid electrode. In this way, the decrease in the EMF becomes much smaller so that it is negligible during the experimental period of six to seven hours.

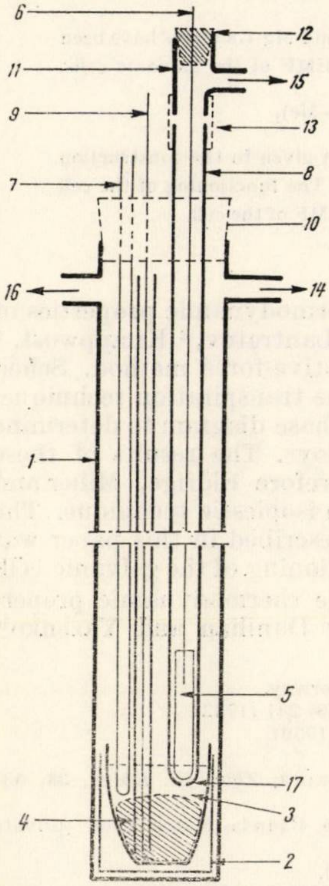

Fig. 1. — The cell

1, quartz tube; *2*, iron crucible; *3*, electrolyte; *4*, alloy; *5*, magnesium reference electrode *6*, wolfram wire to reference electrode; *7*, thermoelement; *8*, alumina tube; *9*, wolfram wire for alloy contact; *10*, rubber stopper; *11*, glass connection; *12*, rubber stopper; *13*, rubber fitting; *14*, to argon container; *15* — to argon container; *16* — vacuum; *17* — hole for contact.

Apparatus. The arrangement of the cell is shown in figure 1. A porcelain crucible, protected by an outer crucible of iron and a vacuum tight quartz-tube, contains the electrolyte and the liquid alloy. Wolfram wires protected by alumina tubes carry the current from the electrodes to the top of the cell assembly. The solid reference electrode is placed in an alumina tube with a small hole at the bottom. The vapour pressure in this tube always equals the outer pressure. A classical vertical furnace was employed for this investigation. Temperature and EMF were recorded simultaneously with a high precision potentiometer. The Pt/Pt10Rh thermoelement was standardized against the melting point of pure aluminium metal.

Procedure. The alloys were prepared by melting the appropriate amounts of magnesium, the other metal component and the previously dried and previously molten electrolyte in an inert atmosphere of purified argon. The original atmosphere was previously removed by evacuating the quartz tube.

---

[11] J. D. Corbett, in B. R. Sudheim, "Fused Salts", McGraw-Hill, New York 1964.

Because of its good wetting properties and its low specific weight, the electrolyte facilitates the production of an homogeneous alloy at the bottom of the porcelain crucible. Approximately 4—10 g of the alloy, depending upon the magnesium content, and 3 g of the electrolyte were placed in the crucible. While preparing the alloy, the solid reference electrode and the wolfram wire contact to the alloy were kept in an upper position. Then they were lowered into position and a constant temperature of about 640° was maintained for about 50 minutes until the EMF of the cell was stabilized, which indicated the attainment of the thermodynamic equilibrium. Then the temperature was lowered continuously at a rate of 0,5° /min and the measurements started.

Chemicals. The salts, KCl, LiCl and MgF_2, of *p. a.* quality, were dehydrated by bubbling pure hydrogen chloride through the molten mixture for several hours. All the metals were spectrochemically pure. The argon gas was purified by passing through a tube with metallic copper at 500° and two water absorption towers.

EXPERIMENTAL RESULTS

The experimental EMF values, given by tables 1a, 1b and 1c vary linearly with the temperature. Hence, in this temperature range, the change in enthalpy, ΔH^{s}_{Mg} and entropy, $\Delta \bar{S}^{s}_{Mg}$, for the cell reaction;

$$Mg_{(s)} \rightarrow Mg \text{ (in liquid alloy)}$$

are both independent of temperature within the experimental limits of error.

Tables 2a, 2b and 2c give $\Delta \bar{G}^{s}_{Mg}$, $\Delta \bar{S}^{s}_{Mg}$, and $\Delta \bar{H}^{s}_{Mg}$ at 650°, the melting point of pure magnesium *versus* the molfraction of added metals. The partial thermodynamic functions are calculated according to the well known formulas :

$$\Delta \bar{G}^{s}_{Mg} = -nFE$$

$$\Delta \bar{S}^{s}_{Mg} = nFT\,(\mathrm{d}E/\mathrm{d}T)$$

$$\Delta \bar{H}^{s}_{Mg} = -nFE + nFT\,(\mathrm{d}E/\mathrm{d}T),$$

Table 1a

EMF of the cell: $Mg_{(s)}$ Mg F_2 — LiCl—KCl (Mg — Pb)$_{(l)}$ for different weighed-in amounts of X_{Pb} *versus* temperature, °C

$X_{Pb} = 0.190$		$X_{Pb} = 0.314$		$X_{Pb} = 0.435$		$X_{Pb} = 0.478$		$X_{Pb} = 0.627$		$X_{Pb} = 0.822$	
temp. °C	E, mV	temp. °C	E, mV	temp. °C	E, mV	temp. °C	E, mV	temp. °C	E, mV	temp. °C	E, mV
562	10.0	572	35.1	562	72.4	563	80.9	567	111.6	563	152.5
578	10.9	585	36.0	573	73.0	572	81.2	579	112.7	581	154.0
594	11.7	596	36.7	584	73.7	587	82.6	587	113.2	596	155.9
608	13.0	608	37.5	599	75.0	599	82.7	601	114.6	611	157.5
626	14.1	614	37.8	609	75.5	612	84.1	615	116.0	628	159.0
641	15.1	621	38.2	628	77.0	628	84.9	627	116.8	638	160.1
—	—	643	39.1	639	77.8	642	86.2	641	118.0	647	161.2

Table

EMF of the cell: $Mg_{(s)}$ Mg F_2 – LiCl – KCl (Mg – In $_{(l)}$ for different weighed-

$X_{In} = 0.205$		$X_{In} = 0.283$		$X_{In} = 0.403$		$X_{In} = 0.497$		$X_{In} = 0.542$	
temp. °C	E, mV	temp. °C	E, mV	temp. °C	E, mV	temp. °C	E, mV	temp. °C	E, mV
537	5.6	466	11.8	466	35.2	466	51.1	471	62.3
551	6.4	523	15.6	522	38.9	511	54.4	503	64.9
576	8.0	601	20.9	582	42.9	552	57.8	553	69.0
603	9.5	643	23.5	625	45.7	601	61.5	611	74.1
618	10.8	—	—	—	—	631	63.6	639	76.3
642	12.1	—	—	—	—	—	—	—	—

Table

EMF of the cell; $Mg_{(S)}$|MgF_2 – LiCl – KCl|$(Mg – Ga)_{(l)}$ for

$X_{Ga} = 0.193$		$X_{Ga} = 0.290$		$X_{Ga} = 0.408$		$X_{Ga} = 0.438$		$X_{Ga} = 0.504$	
temp. °C	E, mV	temp. °C	E, mV	temp. °C	E, mV	temp. °C	E, mV	temp. °C	E, mV
516	2.2	465	7.4	469	29.4	465	35.3	466	65.5
559	4.4	507	9.4	501	30.4	507	36.8	513	68.3
625	7.6	585	13.5	546	31.9	593	40.0	568	71.1
645	8.4	633	16.4	596	33.4	639	41.8	621	73.7
—	—	—	—	640	34.8	—	—	639	74.6

where E is the measured electromotive force at 650° n is here two, and F is the Faraday constant : 23, 066 kcal/volt. For practical reasons[9] liquid magnesium is usually chosen as standard state. Tables 2a, 2b, and 2c give therefore also $\Delta\bar{H}^1_{Mg}$ and $\Delta\bar{S}^1_{Mg}$ for the cell reaction,

$$Mg_{(1)} \rightarrow Mg_{(\text{in alloy})} \ (\text{at } 650°)$$

These latter values are obtained by subtracting the heat of fusion and entropy of fusion of pure magnesium, –2.1 kcal and 2.27 e.u. [12] from the former. Obviously, at 650°, the melting point of pure magnesium, $\Delta\bar{G}^s_{Mg} = \Delta\bar{G}^1_{Mg}$. Figures 2a, 2b and 2c give the experimental partial thermodynamic function of magnesium in liquid magnesium-lead alloys at 650°. The partial free energy curve and the partial enthalpy curve are compared. with the best values found in literature, those given by Eldrige, Miller and Komarek. [9] Their values are based upon own investigations and previous studies.[1–8]

In figures 3a, 3b and 3c the integral free energies, entropies and enthalpies of mixing of the three systems are compared with the ideal values. The integral values are calculated by Margules formula which is a modification of the Gibbs-Duhems formula.

---

[12] O. KUBASCHEWSKI, E. EVANS and C. B. ALCOCK, "Metallurgical Termochemistry", 4th Pergamon Press, London, 1967, p. 303.

1b

in amounts of X_{In} *versus* temperature, °C

$X_{In} = 0.584$		$X_{In} = 0.642$		$X_{In} = 0.646$		$X_{In} = 0.792$	
temp. °C	E, mV	temp. °C	E, mV	temp. °C	E, mV	temp. °C	E, mV
464	71.4	462	85.5	481	90.1	461	118.1
497	74.1	476	87.6	535	95.5	501	122.2
546	78.0	517	91.5	576	99.2	532	126.6
605	83.8	564	96.1	606	103.2	574	131.1
642	87.0	618	102.3	631	105.0	599	134.5
—	—	647	104.9	—	—	635	139.1

1c

different weighed-in amounts of X_{Ga} *versus* temperature °C

$X_{Ga} = 0.522$		$X_{Ga} = 0.572$		$X_{Ga} = 0.652$		$X_{Ga} = 0.686$		$X_{Ga} = 0.798$	
temp. °C	E, mV	temp. °C	E, mV	temp. °C	E, mV	temp. °C	E, mV	temp. °C	E, mV
468	78.4	464	83.7	468	109.2	469	117.1	470	153.3
501	80.3	499	85.8	493	111.0	497	119.8	505	157.1
547	82.7	547	88.3	554	115.6	540	124.3	545	161.6
614	86.3	625	92.5	630	121.8	618	130.0	627	168.4
636	87.2	640	93.2	648	123.5	646	131.9	646	170.4

Table 2a

EMF $\Delta\overline{G}^s$, $\Delta\overline{S}^s$ and $\Delta\overline{H}^s$ for the cell-reaction, $Mg_{(s} \rightarrow Mg_{(in\ alloy)}$ and $\Delta\overline{S}^l$ and $\Delta\overline{H}^l$ for the cell-reaction, $Mg_{(l)} \rightarrow Mg_{(in\ alloy)}$ at 650° *versus* X_{Pb}

X_{Pb}	0.190	0.314	0.435	0.478	0.627	0.822
E (mV)	15.4	39.5	79.0	86.9	118.9	161.6
$-\Delta\overline{G}^s$(kcal)	0.71	1.82	3.64	4.01	5.53	7.45
$\Delta\overline{S}^s$ (e.u.)	2.5	2.7	3.2	3.3	4.0	4.6
$\Delta\overline{H}^s$ (kcal)	1.6	0.7	−0.7	−1.0	−1.8	−3.2
$\Delta\overline{S}^l$ (e.u)	0.2	0.4	0.9	1.0	1.7	2.3
$-\Delta\overline{H}^l$ (kcal)	0.5	1.4	2.8	3.1	3.9	5.3

Table 2b

EMF, $\Delta\overline{G}^s$, $\Delta\overline{S}^s$ and $\Delta\overline{H}^s$ for the cell-reaction, $Mg_{(s)} \rightarrow Mg_{(in\ alloy)}$ and $\Delta\overline{S}^l$ and $\Delta\overline{H}^l$ for the cell-reaction, $Mg_{(l)} \rightarrow Mg_{(in\ alloy)}$ at 650°C *versus* X_{In}

X_{In}	0.205	0.283	0.403	0.497	0.542	0.584	0.642	0.646	0.792
E (mV)	12.5	23.9	47.5	65.2	77.3	87.2	105.0	107.1	140.2
$-\Delta\overline{G}^s$ (kcal)	0.529	1.10	2.19	3.01	3.56	4.02	4.83	4.93	6.44
$\Delta\overline{S}^s$ (e. eu.)	2.54	2.72	2.97	3.52	3.81	3.94	4.47	4.53	5.33
$\Delta\overline{H}^s$ (kcal)	1.83	1.41	0.55	0.24	−0.04	−0.30	−0.72	−0.75	−1.53
$\Delta\overline{S}^l$ (e.u.)	0.27	0.45	0.70	1.25	1.54	1.67	2.20	2.26	3.06
$-\Delta\overline{H}^l$ (kcal)	0.27	0.69	1.65	1.86	2.14	2.40	2.82	2.85	3.63

The three liquid alloys are all characterized by relatively strong heats of mixing. The minimum integral enthalpies are -1.5 kcal for Mg-In, -2.5 kcal for Mg-Pb and -2.6 kcal for Mg-Ga at the compositions

Table 2c

EMF, $\Delta\bar{G}^s$, $\Delta\bar{S}^s$ and $\Delta\bar{H}^s$ for the cell-reaction, $Mg_{(s)} \rightarrow Mg_{(in\ alloy)}$ and $\Delta\bar{S}^l$ and $\Delta\bar{H}^l$ for the cell-reaction, $Mg_{(l)} \rightarrow Mg_{(in\ alloy)}$ at 650 °C *versus* X_{Ga}.

X_{Ga}	0.193	0.209	0.408	0.434	0.504	0.522	0.572	0.653	0.686	0.798
E(mV)	8.9	17.2	34.9	42.1	75.1	88.5	94.2	123.6	132.1	170.6
$-\Delta\bar{G}^s$ (kcal)	0.410	0.793	1.61	1.94	3.46	4.07	4.34	5.69	6.10	7.85
$\Delta\bar{S}^s$ (e.u.)	2.2	1.9	1.3	1.6	2.5	2.5	2.4	3.5	3.8	4.4
$\Delta\bar{H}^s$ (kcal)	1.6	1.0	−0.4	−0.5	−1.2	−1.8	−2.1	−2.5	−2.6	−3.8
$\Delta\bar{S}^l$ (e.u.)	−0.1	−0.4	−1.0	−0.7	0.2	0.2	0.1	0.2	0.4	1.3
$-\Delta\bar{H}^l$ (kcal)	0.5	1.1	2.5	2.6	3.2	3.8	4.2	4.5	4.7	5.9

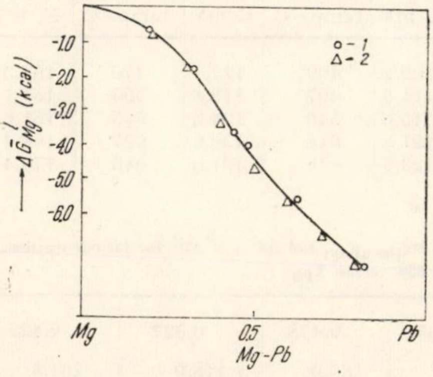

Fig. 2a. — $\Delta\bar{G}^l_{Mg}$ for the cell reaction; Mg(1) → Mg(in Mg-Pb) *versus* X_{Pb} at 650°; 1) this investigation; 2) Eldridge, Miller and Komarek (9)

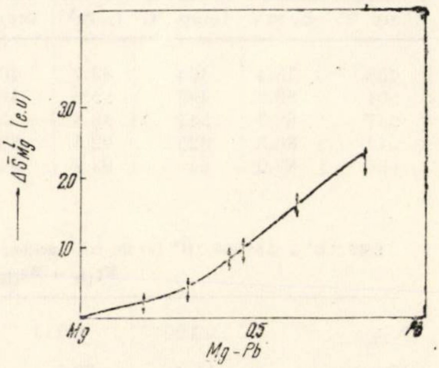

Fig. 2b. — $\Delta\bar{S}^l_{Mg}$ for the cell reaction; Mg(1) → Mg(in Mg-Pb) *versus* X_{Pb} at 650°

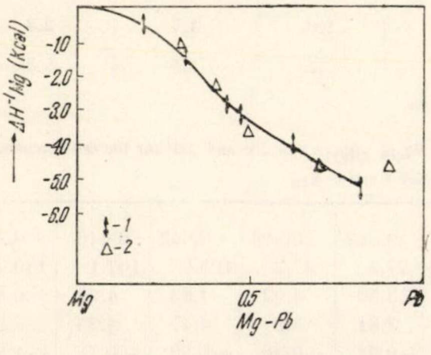

Fig. 2c. — $\Delta\bar{H}^l_{Mg}$ for the cell reaction; Mg (1)→Mg(in Mg−Pb) *versus* X_{Pb} at 650°; 1) exp. values; 2) Eldridge, Miller and Komarek (9)

55.60 and 50 mol% magnesium, respectively. These minimum values may be compared with data given in literature, -2.3 kcal at 60 mol% magnesium for the system Mg-Pb[9] and -2.5 kcal at 60 mol% magnesium for the system Mg-Ga.[10]

Especially the Mg-Ga, but also to some extent the Mg-Pb system, show strong ordering tendencies. These tendencies are indicated by their phase diagrams with compounds like Mg_2Pb, Mg_5, Ga_2, Mg_2Ga, MgGa and $MgGa_2$. However, since the integral entropy of the system Mg-Ga is negative at some composition, a considerable effect of vibrational and electronic terms has to be assumed for liquid Mg-Ga alloys.

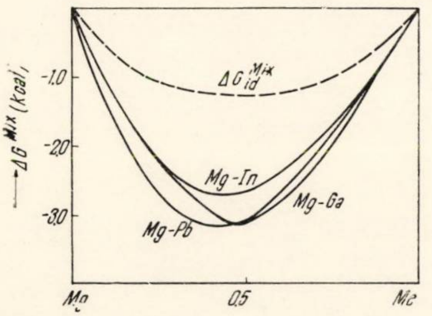

Fig. 3a. — ΔG^{Mix} for the reaction ; Mg(1) + Me(1) → (Mg — Me)$_1$ *versus* X_{Me} at 650°

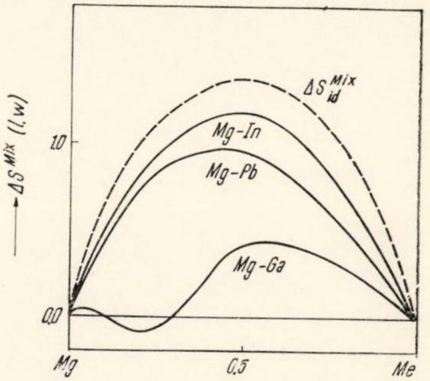

Fig. 3b. — ΔS^{Mix} for the reaction ; Mg(1) + Me(1) → (Mg + Me)$_1$ *versus* X_{Me} at 650°

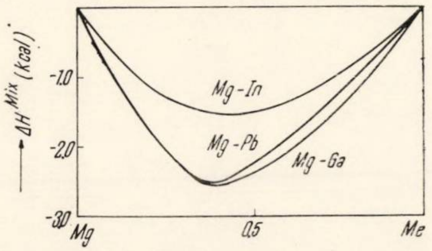

Fig. 3c. — ΔH^{Mix} for the reaction ; Mg(1) + Me(1) → (Mg + Me)$_1$ *versus* X_{Me} at 650°

Acknowledgements. I wish to express my deep gratitude to the Academy of the Socialist Republic of Romania which offered a fellowship and also to Professor I. G. Murgulescu, Research Director of the Institute of Physical-Chemistry, for the facilities he arranged to encourage my experiments and for the great interest he constantly showed in my work.

Revue Roumaine de Chimie, **15**, 67–69 (1970)

GAS CHEMISORPTION ON FERROMAGNETIC POWDER. IV* HYDROGEN, OXYGEN FERRITES SYSTEM AT LIQUID NITROGEN TEMPERATURE

T. CHIRULESCU and E. SEGAL

Institute of Physical Chemistry of the Academy, Bucharest, str. Dumbrava Roşie 23

Received January 25, 1969

The variations in the magnetization of some perminvar ferrites induced by the hydrogen and oxygen chemisorption at liquid nitrogen temperature, are studied. A possible interpretation of the results according to Néel's ferrimagnetic theory is also given.

In carrying on our research on gas chemisorption on perminvar ferrites, we present in this paper the study of the magnetization modifications of these ferrites under the influence of hydrogen and oxygen chemisorption at 77° K. In previous papers we stressed their collective paramagnetism[1,2] and discussed the magnetization changes induced by the hydrogen and oxygen chemisorption at room temperature.[3]

EXPERIMENTAL

The experimental set up has been previously described[4]; the method for obtaining and purifying the gases has also been presented in an earlier work. [3]

By using a polystyrene cylindrical flask filled with liquid nitrogen, the measurements were performed at liquid nitrogen temperature.

For each measurement a quantity of about 3 g of ferrite has been used. The measuretments were performed on five perminvar ferrites finely divided. These are zinc-nickel ferrites with a very small cobalt addition. The ZnO/NiO ratio increases from the PA to PH ferrite.

---

* Previous part : T. Chirulescu and E. Segal, *Rev. Roumaine Chim.*, **13**, 1577 (1968)

[1] C. P. Bean and I. S. Jacobs, "Magnetism", (G. T. Rado and H. Suhl, eds.), vol. 3, Academic Press, New York and London, 1963, p. 271.

[2] T. Chirulescu, *Studii şi Cerc. Şti. Chim. Acad. R. S. România*, **16**, 789 (1968).

[3] T. Chirulescu and E. Segal, *Rev. Roumaine Chim.*, **12**, 1285 (1967).

[4] T. Chirulescu and E. Segal, *Rev. Roumaine Chim.*, **11**, 1367 (1966).

The thermogravimetric and thermodifferential analyses of the studied ferrites have shown that during heating in air, at temperatures higher than the evacuation temperature, our samples did not show any mass decrease.

RESULTS AND DISCUSSION

In a previous paper we have shown that the ferrites we studied at liquid nitrogen temperature do not show any hysteresis loop. This remark induces us to state that at this temperature (77°K) our samples show collective paramagnetism.[1]

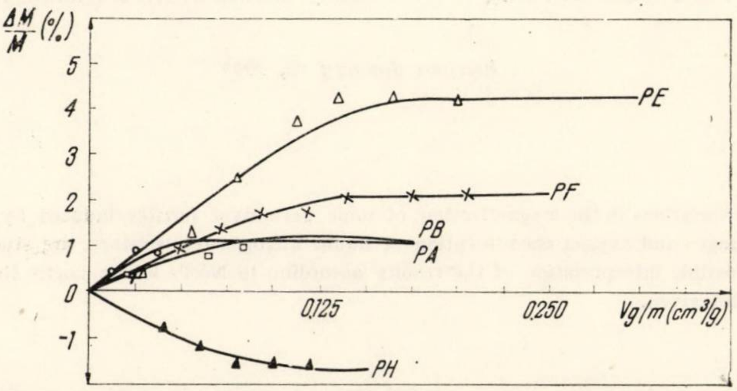

Fig. 1. — Hydrogen magnetization-volume isotherms.

Figure 1 shows the hydrogen volume-magnetization isotherms for PA, PB, PE, PF and PH ferrites at 77°K. One sees that the initial slopes of the PA, PB, PE and PF isotherms are positive, showing a magnetization increase after hydrogen chemisorption. It should be noticed that hydrogen chemisorption on the PA, PB, PE and PF ferrites leads to a magnetization increase, both at 296 and 77°K.

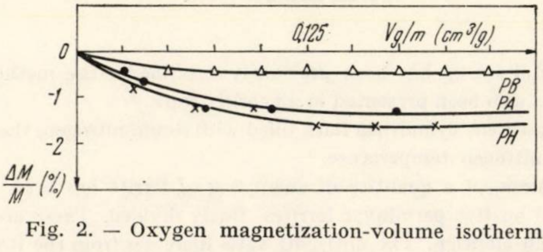

Fig. 2. — Oxygen magnetization-volume isotherms.

The effect of oxygen chemisorption on the considered ferrites is emphasized by the volume-magnetization isotherms plotted in figure 2. In this figure the PE and PF isotherms were not plotted on account of the small variation of the magnetization produced by the oxygen chemisorption on these ferrites. It may be observed that the isotherms have negative slopes, showing a magnetization decrease after the oxygen chemisorption. This behaviour is similar to that corresponding to the oxygen chemisorption at room temperature.[3]

For the interpretation of the results at 77°K, we shall assume that, at least, in a superficial layer, involved into the interaction with the gases, the ferrites tend to pass into the normal structure, i.e. the trivalent iron ions pass into the octahedral interstices (sublattice B) and the divalent zinc and nickel ions pass into the tetrahedral interstices (sublattice A). We shall also assume that the cobalt ions in very small concentrations, have no influence on the chemisorptive properties of the perminvar ferrites. According to Néel's ferrimagnetic theory,[5] the total magnetic moment M of a ferrite is

$$M = |M_B - M_A| (\mu_B)$$

where M_A and M_B are the magnetic moments of the two sublattices.

After the hydrogen chemisorption, the donor interaction with sublattice A leads to a decrease in the number of the uncoupled electrons and thus to a decrease in the magnetic moment of this sublattice. Thus the total magnetization of the ferrite increases. When the zinc ion concentration increases, the interaction passes to the sublattice B, and leads to a decrease in the magnetization of the ferrite. In this way, the smaller magnetization decrease in the case of the PF ferrite (as PB ferrite) and the relative decrease of the PH ferrite magnetization may be explained.

The oxygen chemisorption leads to a magnetization increase of the sublattice, where the oxygen interacts. In the case of the PA and PB ferrites, the interaction with the sublattice A leads to a decrease in the magnetization of these ferrites. When the zinc ion concentration increases, the interaction between the sublattices A and B weakens and $A-B$ interaction becomes more important. This latter interaction produces an antiparallel orientation of the magnetic moments.[6] The oxygen interaction with the divalent nickel ions of the sublattice A, corresponding to a certain value of the zinc ion concentration, higher than the critical value, leads probably to a relative magnetization decrease in the PH ferrite, more marked than in the case of the other studied ferrites.

---

[5] L. Néel, *Ann. Physique*, **3**, 137 (1948).

[6] S. Cedighian, "Ferite", Editura Tehnică, Bucharest, 1966, p. 39.

Revue Roumaine de Chimie, 15, 71–76 (1970)

L'INFLUENCE DE LA STRUCTURE ÉLECTRONIQUE SUR L'EFFET CATALYTIQUE DES COMPLEXES CUIVRE-ANILINE SUBSTITUÉE

AL. FRUMA, D. L. CRĂCIUNESCU et C. GHIRVU
Institut de Chimie Physique, 23, Str. Dumbrava Roşie, Bucarest

Reçu le 21 janvier 1969

On étudie l'influence de la structure électronique des complexes de type $(CuCl_n)H_{n-2}2An$ sur l'effet catalytique dans la décomposition de l'eau oxygénée et la cinétique de décomposition des solutions de H_2O_2 entre 25°–70°. Les résultats obtenus sont mis en corrélation avec les résultats du calcul de la charge électronique de l'azote aminique effectué par une méthode OM simple, en utilisant la variante perturbationnelle de Nagakura et Tanaka. On observe une activité plus accusée aux complexes azotés qu'à ceux halogénés, les complexes clorurés étant plus actifs que ceux bromurés. L'étude en IR des complexes n'a pas conduit à des écarts caractéristiques en fonction des substituants. L'équation d'Arrhenius se vérifie entre 25°–70°, et l'énergie d'activation est comprise entre 14,8 et 19,5 kcal/mole.

Ces derniers temps les travaux qui cherchent à élucider la structure moléculaire des complexes selon leurs propriétés catalytiques sont de plus en plus nombreux.

Aussi, une série de chercheurs [1,2] ont-ils utilisé la réaction de décomposition catalytique de l'eau oxygénée pour confirmer les résultats obtenus par RES sur la structure moléculaire. On sait que de nombreuses amines, telles que l'aniline et la diphénylamine sont inhibitrices [3] pour la réaction de décomposition de l'H_2O_2 catalysée par Fe^{+3} et dans laquelle l'ion Cu^{+2} joue le rôle de promoteur.[4–7] D'ici l'intérêt particulier des complexes cuivre-aniline, complexes qui possèdent une partie promotrice et une partie inhibitrice. Les différents substituants de l'amine ont une influence remarquable sur la liaison Cu-amine et, donc, sur l'activité catalytique. Dans un travail antérieur [8] nous avons établi que les constan-

[1] H. Siegel et U. Mueller, *Helv. Chim. Acta*, **49**, 671 (1966).
[2] H. Erlenmeyer, U. Mueller et H. Siegel, *Helv. Chim. Acta*, **49**, 681 (1966).
[3] V. Anderson et J. Taylor, *J. Amer. Chem. Soc.*, **45**, 605 (1921).
[4] A. Bohnson et V. Robertson, *J. Amer. Chem. Soc.*, **45**, 2512 (1923).
[5] A. Bohnson et V. Robertson, *J. Amer. Chem. Soc.*, **47**, 1299 (1925).
[6] V. S. Barb et S. P. Baxendale, *Trans. Faraday Soc.*, **47**, 462 (1951).
[7] J. H. Walton et J. Filson, *J. Amer. Chem. Soc.*, **54**, 3226 (1932).
[8] D. Crăciunescu et Al. Fruma, *Rev. Roumaine Chim.*, **14**, 653 (1969).

tes de vitesse de réaction de décomposition catalytique de l'H_2O_2 en présence de la Cu-diphénylamine diminuent par l'augmentation du degré de saturation des positions de coordination du cuivre. Dans le présent travail nous nous sommes proposé d'étudier l'influence des substituants sur la stabilité des complexes Cu-aniline substitués, par la corrélation des résultats expérimentaux cinétiques avec les résultats théoriques du calcul OM, en utilisant une variante perturbationnelle.

TECHNIQUE EXPÉRIMENTALE

Pour la détermination du volume de l'oxygène résulté de la décomposition des solutions de H_2O_2, on a utilisé l'installation en verre, thermostatée, décrite dans un travail antérieur.[8] On a étudié l'action des complexes[9] $(CuCl_4)H_2\cdot 2An$[*] Cl (*ortho* et *méta*) $(CuCl_4)H_2\cdot 2AnBr$ (*o* et *m*) ; $(CuCl_4)H_2\cdot 2AnNO_2$ (*o*) et $(CuCl_4)H_2\cdot 2Bz$[**] sur la décomposition des solutions de H_2O_2 2%, 6% et 10%, catalysées par le Fe^{3+}.

Pour obtenir des données comparables, on a choisi les proportions suivantes : complexe-solution dans l'eau 0,05 moles, 1 ml ; $FeCl_3$ solution dans l'eau 0,05 moles, 1 ml ; H_2O_2 2%—4 ml ou 6%— 1,33 ml ou 10% —0,81 ml. Le calcul des constantes de vitesse de réaction a été réalisé en considérant que la réaction est du premier ordre. [10,11] Dans ce cas

$k = 2{,}303/t\cdot \log V_f/V_f - V_v$ ou V_f = le volume d'oxygène dégagé dans la décomposition totale de l'H_2O_2 ; V_v = le volume d'oxygène dégagé jusqu'au moment t.

Les déterminations en IR ont été effectuées à l'aide d'un appareil UR 10 Karl Zeiss Jéna.

RÉSULTATS ET DISCUSSIONS

Dans le tableau 1 nous avons porté les constantes de vitesse de la réaction de décomposition catalytique de l'H_2O_2 en présence de certains complexes, dans le cas de concentrations différentes de l'H_2O_2. Nous avons comparé ces résultats aux constantes de vitesse de la même réaction, effectuée en l'absence du complexe.

On observe que tous les complexes produisent une diminution de la constante de vitesse, ce qui indique que l'effet global du complexe Cu-aniline substitué est inhibiteur et que l'influence promotrice de l'ion Cu^{2+} est écranée par l'influence fortement inhibitrice du groupe aminique. Cette observation a un caractère qualitatif, du fait qu'une comparaison quantitative de l'effet inhibiteur est irréalisable dans nos conditions à cause de la quantité de cuivre mise en liberté par les différents complexes qui diffère chaque fois. Nos considérations ci-dessus ne seront pas affectées par cette observation, parce que nous avons comparé les complexes entre eux, la quantité du cuivre mise en liberté étant toujours proportionnelle avec l'activité des complexes. Les complexes les plus stables sont, évidemment, les plus inhibiteurs, étant donné le nombre réduit d'ions Cu^{2+} mis en liberté et, également, l'impossibilité probable du métal de venir en contact avec la solution, à cause du très grand volume de l'amine par rapport au volume réduit de l'ion métallique. Il est intéressant de remarquer que les substituants halogénés conduisent à une grande stabilité du complexe, la liaison Cu-azote étant considérablement forte. C'est ainsi que viennent d'apparaître les valeurs inférieures de la constante de vitesse. Dans le cas de l'aniline bromurée, les constantes de vitesse sont d'environ 20 % inférieures à celles obtenues dans le cas de l'aniline chlorurée à cause de la stabilité plus grande présentée par l'aniline bromurée, en comparaison de l'aniline chlorurée.

---

[9] M. BREZEANU, C. GHEORGHIU et F. ZĂLARU, *Analele Univ. Bucureşti Sec. St. Nat.*, **15**, 81 (1966).

[*] An = aniline.

[**] Bz = benzidine

[10] H. ZELLE et H. SIEGEL, *Helv. Chim. Acta*, **49** 870 (1966).

[11] A. KONOPLENA et L. A. NICOLAEV, *Zhur. fiz. Khim.*, **40**, 442 (1966).

Tableau 1

Constantes de vitesse de la réaction de décomposition catalytique des solutions de H_2O_2 à 25° (min^{-1})

Concentrations	2 %	6 %	10 %
$FeCl_3$	0,162	0,215	0,245
$(CuCl_4)H_22An$	0,045	0,052	0,065
$(CuCl_4)H_22AnCl(o)$	0,039	0,034	0,071
$(CuCl_4)H_22AnCl(m)$	0,041	0,060	0,073
$(CuCl_4)H_22AnBr(o)$	0,031	0,042	0,052
$(CuCl_4)H_22AnBr(m)$	0,031	0,041	0,050
$(CuCl_4)H_22AnNO_2$	0,105	0,152	0,181
$(CuCl_4)H_22Bz$	0,057	0,048	0,062

On observe également, une légère augmentation de la stabilité du composant *ortho* par rapport aux complexes *méta* substitués (complexes chlorurés). Ces différences sont très petites en marge de la sensibilité de la méthode expérimentale, ainsi que nous n'en insisterons plus. Dans le cas des substituants azotés, les constantes de vitesse sont beaucoup plus grandes par rapport aux constantes de vitesse d'autres composants. La stabilité du complexe possédant les substituants azotés est, donc, très réduite. Pour une comparaison plus poussée on a étudié le complexe $(CuCl_4)H_2Bz$, possédant une structure similaire aux autres complexes cités, mais ayant une plus complète saturation des positions de coordination du cuivre. Ce phénomène se manifeste par des valeurs plus basses pour la constante de vitesse, ce qui confirme une série d'observations antérieures[8] suggérant que le complexe $CuCl_26NH\,Ph_2$*** présente une activité inférieure de 30 % à l'activité du complexe $CuCl_2$ NH Ph_2.

La variation de la constante de vitesse en fonction de l'augmentation de la concentration de l'H_2O_2, en conservant, pourtant, une quantité égale d'oxygène dégageable est conforme aux hypothèses de travail : parallèlement à l'augmentation de la concentration, la réaction est accélérée, donc la constante de vitesse est augmentée, respectivement.

*** Cu Cl_2 6 NH Ph_2 ; $CuCl_2$ NHPh_2 = complexes cuivre-diphénylamine.

Pour le calcul de l'énergie d'activation nous avons effectué des expériences à des températures différentes de 25°. Ainsi, nous avons étudié deux complexes $(CuCl_4)H_2.2An\cdot Br(m)$ et $(CuCl_4)H_2.2AnNO_2$ (*o*) dans l'intervalle de 25° à 70°. Le premier complexe présente la plus grande stabilité, alors que le second, possède la plus petite stabilité des complexes.

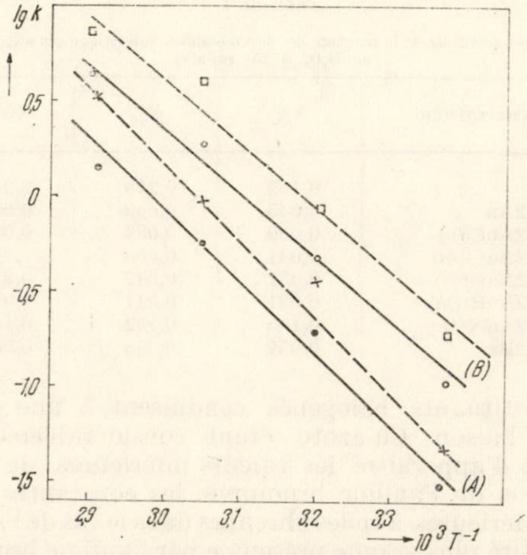

Fig. 1. — Variation de la constante de vitesse avec la température pour le complexe $(CuCl_4)H_2 2AnBr(m)$ (courbes A) et pour le complexe $(CuCl_4)H_2 2AnNO_2$ (courbes B) aux concentrations de l'H_2O_2 de 2 % (courbes continues) et 10 % (courbes pointillées)

Dans la figure 1 on a représenté la variation de la constante de vitesse en fonction de la température. On met en évidence que, parallèlement à l'augmentation de la température la constante de vitesse varie selon l'équation d'Arrhenius. Le fait que les différents points sont parfaitement placés sur des droites plaide pour l'idée que par l'augmentation de la température, le mécanisme de réaction ne se modifie pas. L'énergie d'activation ainsi calculée est comprise entre 14,8—19,5 kcal/mole, valeurs comparables aux résultats obtenus par d'autres chercheurs dans des études sur d'autres complexes. [12]

Par un calcul OH Hückel simple on peut facilement déduire qualitativement [13] que la vitesse de réaction dans la décomposition catalytique de H_2O_2 en présence des complexes du cuivre avec des amines varie en fonction de la densité électronique du groupe aminique. Certaines expériences effectuées avec le complexe $(CuCl_4)H_2\cdot en$ (en=éthylènediamine) nous ont permis d'observer que les substances appartenant à cette classe ont un effet plus inhibiteur que les complexes qui possèdent des amines aromatiques ($k = 0{,}011$ à 25 ° et H_2O_2 2 %). Ce phénomène peut être expliqué théoriquement par le fait que dans le cas des amines aromatiques les deux électrons libres de l'azote aminique entrent en conjugaison avec les électrons π du reste aminique (le groupe $-NH_2$ étant connu comme un chromophore puissant). Il s'ensuit l'augmentation de la vitesse de réaction, due à l'affaiblissement de la liaison N-Cu. D'autre part, si dans le reste aminique on introduit de nouveaux substituants qui provoquent l'augmentation ou l'affaiblissement de la conjugaison des électrons libres de l'azote, avec les électrons π du reste, la vitesse de réaction sera dépendante de la nature électronique du substituant (donneur ou accepteur d'électrons) et de la position des substituants par rapport au groupe aminique. Il résulte donc, très clairement (tabl. 1) que la vitesse de réaction est beaucoup augmentée dans le cas où l'on introduit dans la molécule d'aniline le groupe NO_2, qui possède de fortes propriétés d'attraction pour les électrons.

---

[12] T. V. Vorobieva, V. V. Voevodski et A. P. Purmal, *Zhur. fiz. Khim.*, **36**, 532 (1962).

[13] E. Hückel, *Z. Physik*, **70**, 204 (1931).

Nous avons calculé par la méthode OM simple en utilisant la variante perturbationnelle de Nagakura et Tanaka [14], la charge électronique de l'azote aminique. Cette charge est de 1,845 [15] dans l'aniline (en utilisant pour le paramètre α_{NH_2} la valeur $\alpha + 1{,}2\,\beta$ et $K_{C-NH_2} = 1$). En considérant l'orbitale vacante de l'aniline, possédant l'énergie $\alpha - 1{,}431\beta$ qui a la forme

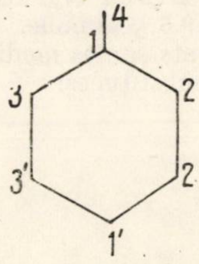

$\psi = 0{,}2001\,(\varphi_2 + \varphi_3) + 0{,}3297\,(\varphi_{2'} + \varphi_{3'}) - 0{,}5585\,\varphi_1 + 0{,}2384\,\varphi_4 -$
$-0.5771\,\varphi_1$ on a trouvé pour la charge électronique de l'azote aminique les valeurs suivantes :

q_{NH_2} (orthochloraniline) $= 1{,}845 + (0{,}0060)^2$
q_{NH_2} (métachloraniline) $= 1{,}845 + (0{,}01)^2$
q_{NH_2} (*o*-bromaniline) $= 1{,}845 + (0{,}0081)^2$
q_{NH_2} (*m*-bromaniline) $= 1{,}845 + 0{,}0148)^2$
Les paramètres utilisés : $\alpha Cl = \alpha + 2\beta$ [16]
$\alpha Br = \alpha + 1{,}5\ \beta$[16]
$\beta C - Cl = 0{,}4\ \beta$[16]
$\beta C - Br = 0{,}5\ \beta$ (fixé)

---

[14] S. Nagakura et J. Tanaka, *J. Chem. Phys.*, **22**, 236 (1954).

[15] N. Mataga, *Bull. Chem. Soc. Japan.*, **36**, 1607 (1963).

[16] A. Stuitwieser, jr. «Molecular Orbital Theory for Organic Chemists», John Weleyand Sons, Inc., New York, Londres, 1962, p. 131.

On voit clairement que dans le cas des complexes avec brome, la vitesse est, théoriquement, plus basse ; les résultats théoriques sont en concordance avec les résultats expérimentaux du tableau 1.

Par l'étude en IR, nous n'avons par réussi de mettre en évidence les modifications (augmentation ou affaiblissement dans la liaison cuivre-azote du complexe, en fonction de la nature des substituants de la molécule d'aniline. Les déplacements qui ont lieu dans les spectres après la complexation ne sont pas concluants et il nous faut souligner encore une fois que le critère de l'activité catalytique est plus efficace que le critère spectroscopique dans le cas des complexes mentionnés.

CONCLUSIONS

On remarque une nette concordance entre les résultats du calcul de la densité électronique par atome d'azote aminique (avec des implications dans la modification de la liaison coordinative (Cu-N) et l'effet catalytique des complexes cités. Les amines azotées présentent un effet plus prononcé que les amines halogénées et les complexes avec chlore dans la molécule sont plus actifs que ceux qui possèdent du brome. L'équation d'Arrhenius est vérifiée de 25° à 70°. L'énergie d'activation a été évaluée dans le cas du plus actif complexe à environ 14,8 kcal/mole ; dans le cas du plus inactif complexe on a trouvé 19,5 kcal/mole. L'étude en IR ne nous a pas conduit à des résultats concluants sur les modifications de la liaison Cu—N pour les différentes anilines substituées.

Revue Roumaine de Chimie, **15**, 77–85 (1970)

LA CINÉTIQUE DE COMPÉTITION DANS L'ÉTUDE DES INTERMÉDIAIRES INSTABLES. I

LES IONS Co^+, Mn^+, Zn^+, Cd^+ ET Ni^+

MARIA FITI

Institut de Physique Atomique, Bucarest, P. O. B. 35

Reçu le 31 janvier 1969

On étudie les possibilités de la méthode cinétique de compétition dans l'étude des réactions des ions Me^+, produites dans la radiolyse des solutions aqueuses de certains sulfates $Me^{2+}SO_4(Me^{2+} = Co^{2+}, Mn^{2+}, Zn^{2+}, Cd^{2+}, Ni^{2+})$, avec divers solutés réductibles. Les constantes de vitesse des réactions des ions Zn^+, Cd^+ et Ni^+ sont comparées à d'autres résultats obtenus par la technique de la radiolyse-éclair.

INTRODUCTION

La nature des réactions des intermédiaires instables, produites dans les processus radiolytiques, constitue en cinétique chimique un problème d'actualité qui a été résolu récemment dans de nombreux cas par la technique de la radiolyse-éclair.

Dans le présent travail, en utilisant la méthode cinétique de compétition, on a étudié indirectement quelques réactions des ions Co^+, Mn^+, Zn^+, Cd^+, Ni^+ produits dans les solutions de $Me^{2+}SO_4$ sous l'action des rayons γ du radio-cobalt. Des intermédiaires Me^+ formés par capture d'un électron hydraté ont déjà été observés,

$$Me^{2+} + e^-_{aq} \rightarrow Me^+ \tag{1}$$

grâce aux spectres optiques obtenus dans la radiolyse-éclair[1] de même qu'aux spectres RPE de solutions irradiées à −196°. [2] En l'absence de capteurs, les ions Me^+ réagissent entre eux

$$2Me^+ = Me^{2+} + Me^\circ \tag{2}$$

Les réactions de certains ions Me^+ avec les acides halogéno-aliphatiques, [3] ainsi que des réductions par les ions Zn^+, Cd^+, Ni^+ ont été récemment signalées. [4]

---

[1] J. H. Baxendale, F. M. Fielden et J. P. Keene, *Proc. Chem. Soc.*, **1963**, 242.

[2] P. N. Moorthy et J. J. Weiss, *Nature*, **211**, 1317 (1964).

[3] M. Anbar et P. Neta, *J. Chem. Soc. (A)*, **1967**, 841.

[4] D. Meyerstein et W. A. Mulac, *J. Phys. Chem.*, **72**, 784 (1968).

Dans ce qui suit, on utilisera la transformation de e_{aq}^- en Me^+ par l'intermédiaire de la réaction (1), en vue d'étudier les réactions de ces espèces avec divers solutés réductibles.

Dans le cas général de la radiolyse d'une solution aqueuse d'ions Me^{2+} qui captent efficacement e_{aq}^- en présence d'un soluté S, bon capteur à la fois de e_{aq}^- et de Me^+, les processus suivants ont lieu

$$Me^{2+} + e_{aq}^- \rightarrow Me^+ \tag{1}$$

$$2\,Me^+ \Rightarrow Me^{2+} + Me^\circ \tag{2}$$

$$Me^+ + S = Me^{2+} + S^- \tag{3}$$

$$e_{aq}^- + S \rightarrow S^- \tag{4}$$

Les réactions des radicaux H et OH avec Me^{2+} ou Me^+ sont éliminées par un capteur spécifique, par exemple, à l'aide d'un alcool inférieur.

Pour étudier la réaction (3) qui nous intéresse il est nécessaire de supprimer (2) et (4), ce que l'on peut faire par le choix approprié des concentrations S et Me^{2+} ; de plus, la condition

$$k_1 \cdot [Me^{2+}] \gg k_4 \cdot [S] \tag{A}$$

doit être réalisée, afin d'obtenir $G_{Me^+} = G_{e_{aq}^-}$.

On peut alors étudier la compétition entre deux capteurs S et S_1 pour l'ion Me^+

$$Me^+ + S = Me^{2+} + S^- \tag{3}$$

$$Me^+ + S_1 = Me^{2+} + S_1^- \tag{5}$$

et déterminer soit l'une des constantes k_3 ou k_5, si l'autre est connue, soit leur rapport.

Le fait que S_1 peut réagir avec l'électron hydraté

$$S_1 + e_{aq}^- \rightarrow S_1^- \tag{6}$$

implique encore la condition

$$k_1 \cdot [Me^{2+}] \gg k_6 \cdot [S_1] \tag{B}$$

Pratiquement, si $[S]$ est constant et $[S_1]$ varie dans les limites des conditions *(A) et (B)*, on peut obtenir la variation du rendement radiolytique des produits de réduction, S^- ou S_1^- en fonction du rapport $[S_1]\,/[S]$.

Dans tous les cas que nous avons examinés, on a vérifié que les conditions *(A) et (B)* soient réalisées. Les valeurs k_1 et k_6 étant connues, on a choisi les concentrations Me^{2+} et S appropriées.

Si l'on considère la compétition entre les réactions (3) et (5), on peut écrire l'équation suivante

$$\frac{G_{(S^-)}}{G(Me^+)^-} = \frac{k_3 \cdot [S]}{k_3 \cdot [S] + k_5 \cdot [S_1]} \tag{C}$$

soit

$$\frac{1}{G(S_1^-)} = \frac{1}{G(\mathrm{Me}^+)}\left(1 + \frac{k_5\,[S_1]}{k_3\,[S]}\right) \tag{D}$$

En traçant $1/G(S^-)$ en fonction du rapport $[S_1]/[S]$, la droite qu'on obtient correspond précisément à la compétition entre (3) et (5), sans réaction secondaire, et par conséquent, la pente de cette droite donne le rapport k_5/k_3 et son ordonnée à l'origine la valeur de $G(\mathrm{Me}^+)$.

TECHNIQUES EXPÉRIMENTALES

Les solutions ont été préparées en utilisant de l'eau tétradistillée et des produits de qualité *pro analysis* Merck.

On a utilisé $MeSO_4$ (Me= Co^{2+}, Mn^{2+}, Zn^{2+}, Cd^{2+}, Ni^{2+} et des solutés réductibles comme $NaNO_3$, $NaIO_3$, $CuSO_4$ et H_3O^+ dont la concentration a été choisie selon leur réactivité avec e_{aq}^- et Me^+.

On a ajouté à chaque solution de l'alcool éthylique 10^{-2} M, afin de capter les radicaux H et OH.

Sauf indication contraire, le pH des solutions était compris entre 5 et 8.

Les solutions ont été soigneusement désaérées et irradiées dans des ampoules de 10 ml environ.

Les irradiations ont été effectuées avec une source γ du radio-cobalt de 500 Ci, le débit de la dose ayant été de $3{,}2.10^{18}$ eV/ml.h (en prenant $G_{Fe^{3+}} = 15{,}6$).

La durée d'irradiation a été choisie de manière que les réactions secondaires des produits finals de la radiolyse soient évitées.

Il importe de noter que l'H_2O_2 issue de la radiolyse ne peut réagir avec les ions Me^+, même si elle est très réactive envers ceux-ci parce que $[H_2O_2] \ll [S]$ et $[S_1]$; il revient donc aux réactions (5) et (3) seulement à réagir avec les ions Me^+.

On a dosé le nitrite, formé par réduction radiolytique du nitrate à l'aide de la formation d'un colorant azoïque ; la solution irradiée a été traitée avec de l'acide sulfanilique en milieu chlorhydrique, puis avec du chlorhydrate de naphtal-éthylène-diamine. [5] On a mesuré l'intensité de la coloration à 535 mμ au spectrophotomètre CF4-Optica-Milano (le coefficient d'extinction est de 48 000 M^{-1} cm^{-1}).

L'hydrogène a été extrait de la solution irradiée, selon une technique bien connue, [6] et dosé par chromatographie en phase gazeuse sur une colonne de tamis moléculaire 5 A, à la température ambiante, en utilisant l'argon comme gaz porteur.

RÉSULTATS ET DISCUSSIONS

Le caractère réducteur des intermédiaires Me^+ a été mis en évidence en calculant le potentiel rédox du couple Me^{2+}—Me^+. [7] Il nous a donc paru intéressant d'examiner le comportement chimique de ces ions envers divers solutés réductibles.

[5] G. Charlot, «Méthodes de Chimie Analytique», éd. Masson, Paris, 1961, p. 411.

[6] M. Chouraqui et J. Sutton, *Trans. Faraday Soc.*, **62**, 211 (1966).

[7] J. H. Baxendale, R. S. Dixon, *Z. Physik. Chem.*, **43**, 161 (1964).

La réaction avec NO_3^- a été étudiée relativement à la réduction radiolytique de NO_3^- dont le mécanisme est bien connu.

En présence d'un alcool inférieur la réduction de NO_3^- par e_{aq}^- a lieu avec un rendement égal au rendement des électrons

$$G(NO_2^-) = G_{e_{aq}^-}$$

L'alcool capte les radicaux H et OH pour former le radical CH_2CHOH :

$$CH_3CH_2OH + OH = CH_3CHOH + H_2O \tag{7}$$

$$CH_3CH_2OH + H = CH_3CHOH + H_2 \tag{8}$$

En l'absence de l'alcool, NO_3^- réagit avec e_{aq}^- d'après les réactions

$$NO_3^- + e_{aq}^- + H_2O = NO_2 + 2OH^- \tag{9}$$

$$2NO_2 + H_2O = NO_3^- + NO_2^- + 2H^+ \tag{10}$$

En présence de l'alcool, la réaction de dismutation (10) est éliminée par suite de la réaction

$$NO_2 + CH_3CHOH = NO_2^- + CH_3CHO + H \tag{11}$$

Un mécanisme analogue de réduction par un composé intermédiaire a lieu dans le cas de réduction de NO_3^- en présence de formiate[8] et de phosphite.[9] Il importe de noter que le radical CH_2CHOH ne réagit ni avec Me^+.[4, 10]

Si l'ion Me^{2+}, capteur efficace pour e_{aq}^-, est présent dans la solution, a lieu aussi la réaction (1) qui conduit à la formation de Me^+ avec un rendement des électrons hydratés.

Dans ce cas, la réduction de NO_3^- est produite par l'intermédiaire de Me^+

$$NO_3^- + Me^+ + H_2O = NO_2^- + 2OH^- + Me^{2+} \tag{12}$$

réaction suivie par (11).

Il résulte de ce schéma que

$$G(NO_2^-) = G(Me^+) = G_{e_{aq}^-}$$

On sait [9,11] que les valeurs récentes pour $G_{e_{aq}^-}$ en solution neutre varient entre 2,5 et 2,7.

Les *courbes de dilution* représentées sur la figure 1 montrent que $G(NO_2^-)$ déterminé pour $[NO_3^-]=2\cdot10^{-3}$ M, s'approche de la valeur moyenne $G = 2{,}6$ dans le cas de Zn^+ et Cd^+ et Co^+, il est plus petit pour Mn^+ et devient négligeable pour Ni^+, variation conforme à la réactivité avec NO_3^-.

---

[8] E. Hayon, *Trans. Faraday Soc.*, **61**, 734 (1965).

[9] M. Haissinsky, *J. Chim. phys.*, **10**, 1141 (1965).

[10] S. Gordon, E. J. Hart, M. S. Matheson, J. Rabani et J. K. Thomas, *Discuss. Faraday Soc.*, **36**, 193 (1963).

[11] B. H. J. Bielski et A. O. Allen, *J. Phys. Chem.*, **71**, 4544 (1967).

Nous avons arrêté les expériences correspondant aux courbes de dilution à la concentration $NO_3^- = 2.10^{-3}$, avant le palier, afin de rester toujours dans les limites de la condition (*A*). D'autre part, comme on le verra plus tard sur les figures 2 et 3, nous obtenons les $G(NO_2^-)$ au palier, qui vont nous intéresser, en extrapolant les droites de compétition (les ordonnées à l'origine). Les valeurs $G(Me^+)$ que l'on déduit varient entre 2,3 et 2,8, ce qui vérifie les hypothèses qui sont à la base de la méthode utilisée ; c'est-à-dire

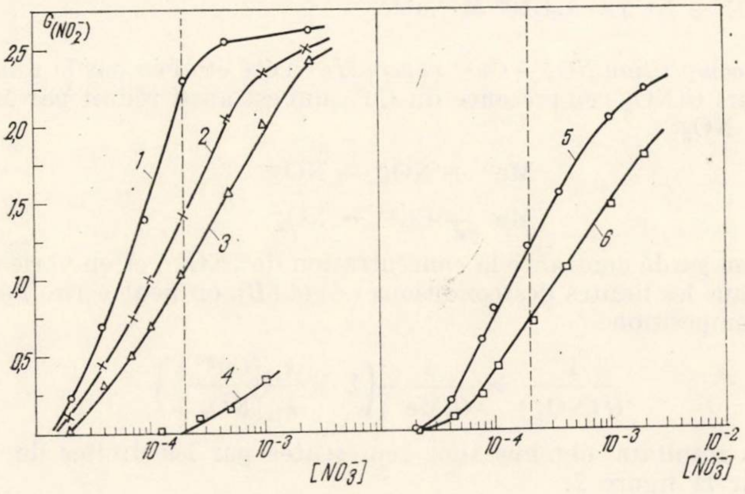

Fig. 1. — Courbes de dilution concernant la réduction radiolytique du NO_3^-.

1, C_2H_5OH $10^{-2}M$, *2*, C_2H_5OH $10^{-2}M$, $ZnSO_4$ 0,1M, *3*, C_2H_5OH $10^{-2}M$, $CdSO_4$ $10^{-2}M$, *4*, C_2H_5OH $10^{-2}M$, $NiSO_4$ $10^{-2}M$, *5*, C_2H_5OH $10^{-2}M$, $CoSO_4$ $10^{-2}M$, *6*, C_2H_5OH $10^{-2}M$, $MnSO_4$ 0,5M.

$$G(NO_2^-) = G(Me^+) = G_{e^-_{aq}}$$

Les courbes de dilution représentées sur la figure 1 correspondent à la réduction du NO_3^- par des radicaux différents : e^-_{aq}, Co^+, Mn^+, Zn^+, Cd^+ et Ni^+ dont les rendements sont cependant égaux, pour former le même produit NO_2^-. Il est donc évident que pour la même concentration du NO_3^-, dans le domaine linéaire de ces courbes, $G(NO_2^-)$ sera déterminé par la réactivité de chacun vis-à-vis de NO_3^-.

En première approximation on voit que l'ordre de réactivité est le suivant : $Zn^+ > Co^+ > Cd^+ > Mn^+ > Ni^+$ ce qui correspond pour les ions $Zn^+ > Cd^+ > Ni^+$ à l'ordre de réactivité trouvé par Meyerstein et Mulac.[4]

Ci-après, en partant de la réaction déjà connue du NO_3^- avec Me^+, on peut utiliser la méthode de compétition décrite, pour étudier d'autres réactions de ces ions.

La réduction de NO_3^- est convenable, comme réaction de référence, grâce à la grande sensibilité et à la reproductibilité de l'analyse du nitrite, ainsi qu'à la grande réactivité du NO_3^- envers les ions Me^+. De plus, du travail on connaît les valeurs des constantes de vitesse suivantes :

$$k(NO_3^- + Zn^+) = 2{,}1.10^9\ M^{-1}.s^{-1},\quad k(NO_3^- + Cd^+) = 3{,}5.10^8\ M^{-1}.s^{-1}$$

et $k(NO_3^- + Ni^+) = 1{,}4.10^6\ M^{-1}.s^{-1}$.

La compétition $NO_3^- - Cu^{2+}$ envers Me^+ a été étudiée par la diminution des valeurs $G(NO_2^-)$ en présence du Cu^{2+} qui est aussi réduit par Me^+ sans produire NO_2^-

$$Me^+ + NO_3^- \rightarrow NO_2^- \tag{12}$$

$$Me^+ + Cu^{2+} \nrightarrow NO_2^- \tag{13}$$

Si on garde constante la concentration de $[NO_3^-]$ et on varie celle de $[Cu^{2+}]$ dans les limites des conditions (A) et (B), on peut écrire l'équation de la compétition

$$\frac{1}{G(NO_2^-)} = \frac{1}{G(Me^+)}\left(1 + \frac{k_{13}[Cu^{2+}]}{k_{12}[NO_3^-]}\right) \tag{E}$$

Les résultats obtenus sont représentés par les droites de compétition sur la figure 2.

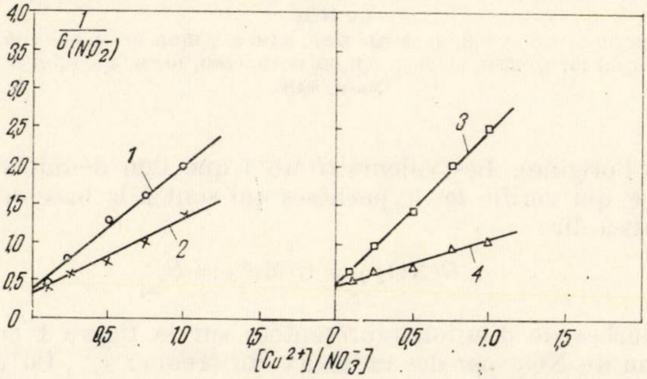

Fig. 2. — La compétition $NO_3^- - Cu^{2+}$; la solution aqueuse de $NO_3^- \cdot 10^{-3}M$, C_2H_5OH 10^{-2} M, Cu^{2+} variable et *1*, $ZnSO_4$ 0,1M; *2*, $CdSO_4$ $10^{-2}M$; *3*, $CoSO_4$ $10^{-2}M$; *4*, $MnSO_4$ 0,5M.

On tire de ces droites la pente qui représente $\frac{1}{G(Me^+)} \cdot \frac{k_{13}}{k_{12}}$ et l'ordonnée à l'origine qui correspond à $1/G(Me^+)$.[4]

De ces valeurs et des valeurs connues pour k_{12} on calcule k_{13}. Les valeurs obtenues sont présentées sur le tableau 1.

L'unité qui exprime les constantes de vitesse est $M^{-1}S^{-1}$. Toutes les valeurs marquées par astérisque sont déterminées par radiolyse-éclair. [4]

Tableau 1

Valeurs de $G(Me^+)$ et constantes relatives des réactions $Me^+ + Cu^{2+}$ par rapport aux $Me^+ + NO_3^-$

Me^+	Zn^+	Cd^+	Co^+	Mn^+
$G(Me^+)$	2,7 ± 0,1	2,6 ± 0,1	2,8 ± 0,1	2,3 ± 0,1
k_{13}/k_{12}	4,5 ± 0,2	3,1 ± 0,2	5,2 ± 0,2	1,6 ± 0,2
k_{13}	(9,4 ± 0,2).10⁹	(1,1 ± 0,2)10⁹	—	—
	2,5.10⁸ *	1,2.10⁸ *	—	—

La compétition $NO_3^- - IO_3^-$ envers Me^+ a été poursuivie d'une manière analogue

$$Me^+ + NO_3^- \rightarrow NO_2^- \qquad (12)$$

$$Me^+ + IO_3^- \nrightarrow NO_2^- \qquad (14)$$

Il en résulte l'équation de compétition suivante

$$\frac{1}{G(NO_2)} = \frac{1}{G(Me^+)}\left(1 + \frac{k_{14}[IO_3^-]}{k_{12}[NO_3^-]}\right) \qquad (F)$$

Les résultats sont représentés sur la figure 3 et les valeurs qu'on en tire dans le tableau 2.

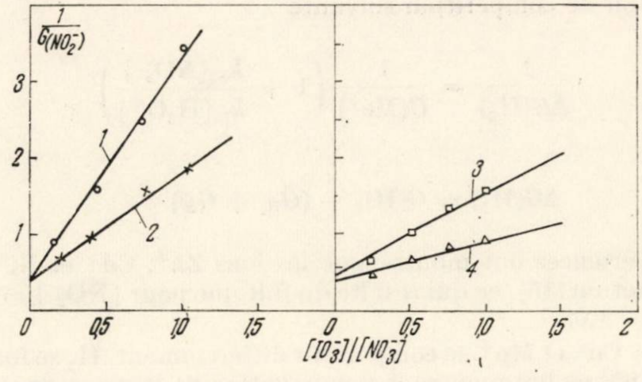

Fig. 3. — La compétition $NO_3^- - IO_3^-$; la solution aqueuse de NO_3^- — 10^{-3}M C_2H_5OH 10^{-2} M, IO_3^- variable et *1*, $ZnSO_4$ 0,1M; *2*, $CdSO_4$ 10^{-2}M; *3*, $CoSO_4$ 10^{-2}M; *4*, $MnSO_4$ 0,5 M.

La compétition $NO_3^- - H_3O^+$ envers Me^+ a été étudiée en provoquant les réactions

$$Me^+ + NO_3^+ \nrightarrow H \qquad (12)$$

$$Me^+ + H_3O^+ \rightarrow H \qquad (15)$$

Tableau 2

Valeurs des $G(Me^+)$ et constantes relatives des réactions $Me^+ + IO_3^-$ par rapport aux $Me^+ + NO_3^-$

Me^+	Zn^+	Cd^+	Co^+	Mn^+
$G(Me^+)$	2,8 ± 0,1	2,8 ± 0,1	2,6 ± 0,1	2,4 ± 0,1
k_{14}/k_{12}	8,2 ± 0,2	5,4 ± 0,2	2,7 ± 0,2	1,4 ± 0,1
k_{14}	$(1,6 \pm 0,1).10^{10}$	$(2,1 \pm 0,2).10^{9}$	—	—
	$3,6.10^{9}$ *	$2,3.10^{9}$ *	—	—

Cette compétition a été indirectement poursuivie en transformant en H_2, par l'intermédiaire de la réaction (8), tout l'hydrogène atomique produit dans la solution irradiée, $k(H_3O^+ + k_{aq}) = 2,3.10^{10}\ M^{-1}s^{-1}$.[12]

Dans notre cas H_2 va provenir de la radiolyse de l'eau ($G_{H_2} = 0,45$ et $G_H = 0,60$) et de la réaction (15) qui selon nos hypothèses doit correspondre à $G(Me^+)$ et implicitement à $G_{e_{aq}^-}$.

Pratiquement on a utilisé une concentration constante du H_3O^+($p_H = 2$ par addition de H_2SO_4) et on a varié NO_3^- tel que les conditions (A) et (B) soient réalisées.

Au fur et à mesure que NO_3^- croît, H_2 va diminuer grâce à la réaction (12) d'une quantité qui doit correspondre à $G(Me^+)$. C'est ainsi qu'on peut écrire l'équation de compétition suivante

$$\frac{1}{\Delta G(H_2)} = \frac{1}{G(Me^+)}\left(1 + \frac{k_{12}[NO_3^-]}{k_{15}[H_3O^+]}\right) \qquad (G)$$

où

$$\Delta G(H_2) = G(H)_2 - (G_{H_2} + G_H)$$

Nos expériences ont montré que les ions Zn^+, Cd^+ et Ni^+ ne subissent pas la réaction (15), ce qui résulte du fait que pour $[NO_3^-] = 0$, $G(H_2) = G_{H_2} + G_H = 1,05$.

Les ions Co^+ et Mn^+ se comportent différemment, H_2 se forme d'un G supérieur à 1,05, ce qui montre la participation de la réaction (15).

Les résultats que l'on obtient de la compétition des réactions (12) et (15) dans le cas des ions Co^+ sont représentés sur la figure 4 et les valeurs qu'on en tire sont

$$G(Me^+) = 2,85 \pm 0,1\ ; \quad k_{12}/k_{15} = 112$$

---

[12] M. Anbar et P. Neta « A compilation of specific bimolecular rate constants for the reactions of hydrated electrons, H-atoms and OH-radicals with inorganic and organic compounds in aqueous solution», IA– 1079, Israel Atomic Energy Commission, 1966.

L'ion Mn^+ forme H_2, $G(H_2)=2{,}6$ dans nos conditions, mais il le forme de même dans les solutions neutres, ce qui a été expliqué [13] par la réaction avec les molécules de l'H_2O

$$Mn^+(H_2O)_n + H_2O = Mn^{2+}(OH)(H_2O)_{n-1} + H_2 + OH^- \qquad (16)$$

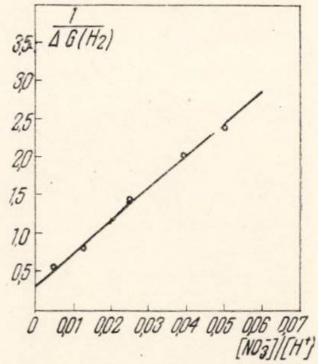

Fig. 4. — La compétition $NO_3^- - H_3O^+$; la solution aqueuse au $pH = 2$, C_2H_5OH 10^{-2} M, NO_3^- variable et $CoSO_4$ 10^{-2}M.

Le rendement en milieu neutre $G(H_2) = 1{,}6$ est donc inférieur à la valeur correspondant au $p_H = 2$ mais il est difficile à séparer l'effet des deux réactions (15) et (16).

On pourrait dire en première approximation que la réactivité de Mn^+ envers les ions H_3O^+ n'est pas négligeable.

En analysant l'ensemble de nos résultats on observe que les ions Me^+ à l'exception du Ni^+ sont de bons réducteurs. Leur grande réactivité a été expliquée [2,14] par le fait que l'électron additionnel est localisé dans l'orbitale S, pendant que dans le cas de Ni^+ il est localisé dans une orbitale inférieure.

On observe que les ions Co^+ et Mn^+ réagissent aussi avec les ions H_3O^+ ce qui les approche du comportement chimique de e^-_{aq}, tandis que Zn^+, Cd^+, Ni^+ ressemblent plutôt à l'atome H.

Les valeurs des constantes de vitesse obtenues par notre méthode sont plus élevées que celles obtenues par radiolyse-éclair, [4] à l'exception de la réaction $Cd^+ + IO_3$ pour laquelle la valeur est la même que celle de [4] aussi bien que l'ordre de la réactivité $Zn^+ > Cd^+ > Ni^+$.

En ce qui concerne les valeurs de $G(Me^+)$ qu'on peut prendre comme des valeurs pour Ge^-_{aq} on voit qu'à l'exception du $G(Mn^+)$ elles sont en accord avec les valeurs récemment publiées. [9,11]

On peut donc conclure que malgré ses limites la cinétique de compétition représente une méthode satisfaisante dans l'étude des intermédiaires instables et peut se conjuguer aux méthodes récentes de la chimie moderne: radiolyse et photolyse-éclair et résonance paramagnétique électronique.

---

[13] M. Anbar, Advances in Chemistry, Series, 50, « Solvated Electron », 1965, p. 73.
[14] T. Feldmann, A. Treinin et V. Volterra, *J. Chem. Phys.*, **42**, 3366 (1965).

Revue Roumaine de Chimie, **15**, 77–85 (1970)

Revue Roumaine de Chimie, **15**, 87–89 (1970)

THE CELL PARAMETERS OF SYNTHETIC FLUORAPATITE, $Ca_{10}(PO_4)_6F_2$

V. M. BHATNAGAR *)

Fisk University, Nashville, Tennessee, U.S.A.

Received June 21, 1969

Calcium fluorophosphate, generally known as fluorapatite, $Ca_{10}(PO_4)_6F_2$, is one of the most studied mineral structures. It has a structure practically identical with the hydroxyapatite, $Ca_{10}(PO_4)_6(OH)_2$, which is the chief component of bones and teeth. The X-ray single crystal structure determinations on mineral fluorapatite were carried out as early as 1923 by Hentschel [1] and in 1930 by Mehmel[2] and Náray-Szabó[3] who showed that the space group is C_{6h}^2 ($C6_3/m$) and the unit cell contained 42 atoms or one molecule of $Ca_{10}(PO_4)_6F_2$.

A more accurate and interesting determination of the fluorapatite structure was made by Beevers and McIntyre[4] (1946) who showed that the unit cell of the structure has two equal edges inclined at 120° to one another. These two edges are of length $a = 9.37$ Å while the third edge is at right angle to these and has a length of 6.88 Å. The linkage of the Ca—O columns by the PO_4 groups produces a hexagonal network like a honeycomb with channels extending right through the structure in the *c*-direction. The walls of these channels are lined with oxygen atoms, the arrangement being such that in the wall of each channel there are six caves or holes per unit length. Into these caves calcium atoms are just fit, one calcium going about half-way into each. Thus about half the area of each calcium is left exposed the inside the channels and the fluorine atoms just fit between the group of the three calcium at one level. Young and Elliott [5] (1966) have recently shown that the fluorine tends to contract the calcium triangle as the Ca—F distance is about 2.288 Å in fluorapatite as compared to 2.355 Å for the corresponding distance in hydroxyapatite. This contraction of the Ca—F distance has been suggested to cause a change in the *a*- axis of fluorapatite.

---

*) Present adress : Department of Chemistry, University of New Brunswick, Fredericton, Canada.

[1] H. Hentschel, *Cent. Min.*, **20**, 609 (1923).
[2] M. Mehmel, *Zeit. Krist.*, **75**, 323 (1930).
[3] S. Náray-Szabó, *Zeit. Krist.*, **75**, 387 (1930).
[4] C. A. Beevers and D. B. McIntyre, *Min. Mag.*, **27**, 254 (1946).
[5] R. A. Young and J. C. Elliott, *Arch. Oral. Biol.*, **11**, 699 (1966).

Table 1

The cell parameters of synthetic fluorapatite, $Ca_{10}(PO_4)_6F_2$, Radiation = Cuλ = 1.54178 Å;
I/I_1 = diffractometer; system = hexagonal;
a = 9.3680 Å; c = 6.8868 Å; c/a = 0.735, volume = 523.4 $Å^3$.

h	*k*	*l*	I/I_1	dÅ (observed)	dÅ (calculated)
0	1	0	11	8.08	8.11
0	1	1	2	5.25	5.25
1	1	0	2	4.676	4.684
0	2	0	8	4.053	4.056
1	1	1	7	3.873	3.873
0	2	1	2	3.493	3.495
0	0	2	19	3.440	3.443
0	1	2	7	3.167	3.170
1	2	0	24	3.063	3.066
1	2	1	100	2.801	2.801
1	1	2	27	2.772	2.774
0	3	0	67	2.702	2.704
0	2	2	18	2.624	2.625
0	3	1	6	2.516	2.517
1	3	0	30	2.250	2.250
2	2	1	2	2.217	2.217
1	3	1	6	2.139	2.139
1	1	3	4	2.060	2.061
0	4	0	4	2.029	2.028
2	2	2	22	1.935	1.937
1	3	2	12	1.881	1.884
2	3	0	5	1.861	1.861
1	2	3	24	1.835	1.838
2	3	1	17	1.796	1.797
0	4	2	12	1.747	1.748
0	0	4	7	1.720	1.722
2	2	3	8	1.639	1.639
2	3	2	5	1.634	1.637
1	3	3	2	1.607	1.607
2	4	0	5	1.534	1.533
0	4	3	4	1.520	1.520
1	2	4	2	1.501	1.501
2	4	1	2	1.497	1.497
0	5	2	7	1.469	1.468
0	3	4	4	1.453	1.452
2	3	3	4	1.446	1.446
1	5	1	7	1.426	1.426
3	4	0	1	1.335	1.334
3	4	1	7	1.311	1.309
2	5	0	4	1.300	1.299
2	5	1	4	1.276	1.277
3	4	2	2	1.247	1.244
1	6	0	2	1.238	1.237
1	4	4	6	1.235	1.234
1	5	3	5	1.231	1.230
1	6	1	7	1.217	1.218
4	4	0	2	1.172	1.171
4	4	1	5	1.154	1.154
2	4	4	4	1.146	1.145
1	1	6	2	1.115	1.115
3	5	2	6	1.100	1.098
1	7	3	4	0.974	0.973

The high-precision, computer-refined values of the cell parameters of synthetic fluorapatite were determined with an X-ray diffractometer, internally standardized by means of sodium chloride. Two computer programmes CELFIT (Bracher[6], 1967) and GENRAT (Pistorius [7], 1968), were used for calculating the cell parameters of apatite and for indexing the diffraction lines. The programmes were written into Fortran IV in order to be compatible with the IBM digital computer model 360/40. The CELFIT programme when supplied with sets of Miller indices, corresponding values of the Bragg angle, and a set of approximate unit cell dimensions, refines any or all of the latter by the method of the least squares until the shifts in these parameters fall below specified limits. The GENRAT programme, when supplied with sets of unit cell dimensions, generates all possible $h\ k\ l$ reflections between two specified values of the Bragg angle. A Phillips wide range goniometer model PW-1050 was used for all determinations. The results obtained are shown in table 1. The cell parameters quoted are based on the best fit obtained by the least squares programme. Both calculated and observed interplanar spacings have been included for the sake of completeness. The angular positions of all peaks were taken at points in the centre of the peaks, one-third of the distance between the actual top of the peaks and their base lines. The intensities listed for the various $h\ k\ l$ reflections have been given in terms of their heights above background, taken relative to the strongest peak as intensity 100.

Acknowledgements. The apatite investigation was supported by research grant DE-02105 of the Unites States Department of Health, Education and Welfare. The author wishes to thank Dr. W. R. Liebenberg, Dr. S. A. Hiemstra and Dr. H. V. R. von Rahden of the National Institute for Metallurgy — South Africa for their interest and valuable help and Professor Nelson Fuson and Professor James R. Lawson of the Fisk University for fruitful discussions.

[6] B. H. Bracher, *U. K. A. E. R. E.*, (1967), R-5412.
[7] C. W. F. T. *Pistorius*, C. S. I. R. Pretoria, 1968.

Revue Roumaine de Chimie, **15**, 91–101 (1970)

THE KINETICS OF CHANGES OF THE VITREOUS STRUCTURES IN SOME LITHIUM-SILICATE GLASSES*

S. SOLACOLU, P. BALTĂ and GEORGETA JITIANU

Institute of Physical Chemistry of the Academy
23 Dumbrava Roşie, Bucharest, Romania

Received June 21, 1969

The study of structural changes taking place in glasses of the Li_2O-SiO_2 system, containing 50–100 % $Li_2O.2SiO_2$ was undertaken using as basic method the classical differential thermal analysis (DTA), some variants based on the same principle as well as electronic microscopy and roentgen-structural analysis. New data concerning the influence of composition on the temperatures of glassy microphases separation and crystallization are provided by the thermograms ; most of the thermal effects as indicated by these thermograms are due to lithium disilicate. On the basis of electron-microscope photographs, the kinetics and mechanism of glassy phases separation are discussed in correlation with data available in literature. The isothermal differential analysis gives the kinetic curves which allow the estimation of nucleation process duration as well as the rate of crystal growth. It follows that the methods based upon DTA and electron microscopy give multilateral information about structural changes taking place in glasses.

As known, from the structural standpoint, the glassy state is characterized by a lower degree of order than the crystalline solid. The glass, considered as under–cooled liquid is metastable and permanently tends to the lower energy state corresponding to the crystal, the level of thermal energy having a decisive influence. Consequently the glassy structure is determined, besides the composition, by the so-called "thermal history"[1,2] which makes possible the obtaining of other properties without any composition change. This possibility is outstandingly important for practice ; from the theoretical point of view it requires the knowledge of the nature of structural transformations produced by temperature and the way they influence the properties. During the last years theoretical arguments [1] and experimental data [3-7] attested the possibility of structural changes in glass melts at high temperatures. It is also known that in a given temperature range all glasses tend to crystallize. The nucleation and crystallization processes were the subject matter of many works which led to interesting results. [8-12] X-ray diffraction with small angles [13] and electron microscopy [14-18] showed that in some glasses a microliquation phenomenon (glassy phases separation) might take place.

---

* Communicated at the 1st National Conference of Pure and Applied Physical Chemistry, Bucharest, September 1968.

[1] W. A. Weyl and C. Marboe, "The Constitution of Glasses a Dynamic Interpretation", Interscience Publishers, New York, 1964, chap. I.

[2] P. Baltă, *Studii şi Cercetări Chim. Acad. R.S.R.*, **15**, 433 (1967).

The laws of these phenomena, their interdependence and sequence as well as their influence upon properties are not yet wholly elucidated. That is why in the present paper we aimed at contributing to a better knowledge of structural changes occurring in glasses and their kinetics by using as basic method the DTA the possibilities of which have already been outlined [2-4] as well as the electron microscopy. For this study, glasses from the Li_2O-SiO_2 system were chosen in order to take advantage of the results accumulated so far. Special attention was given to phenomena occurring at relatively low temperatures belonging to the interval between the beginning of endothermal effects and the end of exothermal ones. As known, it is just within this temperature range that the glassy phases separation and crystallization of glasses occur.

The separation of glassy phases in the Li_2O-SiO_2 system

Within certain composition limits the separation of the glassy phase takes place easily in the glasses of the Li_2O-SiO_2 system.

This phenomenon is related to the specific properties of the lithium ion. Its strong electrostatic field determines the formation of some vitreous structures [19] with distinct properties (surface tension, viscosity) and as a result, its separation tendence as independent glassy phase.

---

[3] S. Solacolu and P. Baltă, *Ind. chim. belge*, Compte rendu XXXVI-e Congrès Internat. de Chimie Ind., **2**, 513 (1966).

[4] S. Solacolu and P. Baltă, *Rev. Roumaine Chim.*, **4**, 208 (1967).

[5] E. Zarjiţki, "Travaux du IVe Congrès Internat. du Verre", Paris, 1956, p. 323–330.

[6] E. Plumat, G. Periaux, R. Marit, J. Dela Ruye and J. Mairesse, *Silic. ind.* **19**, 517 (1964).

[7] V. A. Florinscaia "Steklobrazovoe sostaianiye", vol. II, Izd. A. N. S. S. S. R., Moscow-Leningrad, 1960, p. 177–194.

[8] V. Dunning, "Khimia tverdova sostaianiye", Izd. inostr. lit., Moscow, 1961, p. 213, 224.

[9] W. B. Hilling, "Kinetics of High-Temperature Processes", John Wiley Chappman Hall, New York, 1959, p. 127–135.

[10] L. A. C. Staveley, "The Vitreous State", Sheffield, Great Britain, 1955, p. 85–90.

[11] I. Gutzov, S. Toshev, M. Marinov and E. Popov, "Proceeding of the 9-th Conference on the Silicate Industry", Budapest, Siliconf., 1967, 256–259.

[12] I. Gutzov, S. Toshev, M. Marinov and E. Popov, *Kristall und Technik*, **3**, 37 (1968).

[13] E. A. Porai-Koşiţ, "Steklobraznoe sostoianje", vol. II, Izd. A. N. S.S.S.R., Moscow, Leningrad, 1960, p. 14–25.

[14] W. Vogel, "Struktur und Kristallisation der Gläser", VEB-Deutscher Verlag für Grunstoffindustrie, Leipzig, 1965.

[15] V. I. Averianov and E. A. Porai-Koşiţ, "Structurnyie prevraschenia v steklakh pri povyshenih temperaturah", Izd. A. N. S. S. S. R. Moscow, Leningrad, 1965, p. 76–100.

[16] J. W. Chan, and R. J. Charles, *Physics Chem. Glasses*, **6**, 181 (1965).

[17] R. J. Charles, *J. Am. Ceram. Soc.*, **2**, 55, (1966).

[18] M. R. Marinov and M. S. Radenkova-Janeva, "Proceeding of the 9-th Conference on the Silicate Industry", Budapest, Siliconf., 1967, p. 248–250.

[19] S. Urnes, *Trans. Br. Ceram. Soc.*, **60**, 85 (1961).

Unlike the oxide systems which present domains of stability of two immiscible liquids (regions which in the case of glasses extend under the liquidus and solidus curves), in the Li_2O-SiO_2 system part of the liquidus curve, between $Li_2O.2SiO_2$ and SiO_2, has an S shape (figure 1); this is considered an indication for the existence of an immiscibility region under the liquidus curve.[20] A good deal of researches carried out on the glasses of this system [14–18,20] allowed the delimitation, on the phase equilibrium diagram (figure 1), of composition and temperature limits where, for the studied glasses, distinct glassy micro-phases appear and develop, in terms of thermal history. The diagram records the limits of this domain established in papers.[17,18] The precision of the delimitation is rather low, the data in the two works presenting important discrepancies.

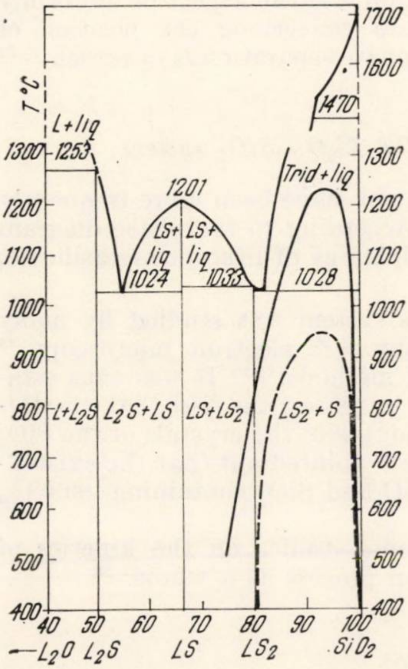

Fig. 1. — Domain of the phases separation in the Li_2O-SiO_2 system, solid line after Charles,[17] dashed line after Marinov and al. [18]

As regards the mechanism of phase separation, the most interesting seems to be Chan and Charles [16] conception. They advance the idea that a phase is stable against the infinitesimal fluctuation of its composition and density, if the chemical potential of each component increases with the increasing density of the component. In some system for a given composition, there are temperatures for which this stability condition is not satisfied. In the domain thus delimited a spinodal curve separates the regions with various phase separation mechanism. In the space delimited by this spinodal, the glass is unstable and spontaneously separates into two glassy phases (spinodal decomposition), the composition of which varies with temperature and time until the equilibrium is reached. The separated particles have a micelle aspect.

---

[20] J. Robredo, *Silic. ind.*, **30**, 647 (1965).

Between the spinodal and the phases separation limit there is a metastability region in which two phases may separate only by nucleation and the growth of one of them. In this case the separated glassy phase has a well defined and invariable composition and the aspect of uniformly distributed spheres. The experimental data concerning the position of spinodals are still very poor. The study of phase separation is of present[21,22] interest.

The crystallization of glasses of the Li_2O-SiO_2 system

In glassy state the masses in this system have been more frequently studied in the range $Li_2O.SiO_2$ and SiO_2. According to the phase diagram (fig. 1) this region includes the stability domains of lithium metasilicate, lithium disilicate and silicon dioxide.

The crystallization of glasses in this system was studied by many researchers using DTA[23,24] roentgenography [25,26] electron microscopy,[15] high temperature microscopy, [27] and other methods.[28,29] It was thus established that as the temperature of glasses increases, the first that crystallize are the lithium silicates and only at about 900° the crystals of the SiO_2 polymorphic modifications appear. Glasser [30] pointed out that the existence of some solid solution, between $Li_2O.2SiO_2$ and SiO_2 containing 80.08% –84.00% SiO_2, is possible.

These data are supplemented by some studies on the kinetics of crystal growth [27] and of the crystallization process as a whole. [26]

EXPERIMENTAL

As raw materials quartz sand (98% SiO_2) and p. a. Li_2CO_3 were used ; the chosen compositions were fused in a silicon carbide rods electric furnace at 200–300° over the corresponding liquidus temperature, to ensure in this way, a good loosening and homogenizing. All compositions are located in the domain of the glassy phase separation.

The melting was carried out in alumina crucibles and, taking into account the corrosive action of alkali oxides, some compositions were melted in platinum crucibles. The melt was rapidly cooled by pouring on a metal plate in air.

---

[21] W. Haller, *J. chem. Phys.*, **42**, 686 (1965).

[22] Y. Moriya, D. H. Warington and R. W. Douglas, *Physics Chem. Glasses*, **8**, 19 (1967).

[23] V. Velea, Doctoral Thesis, Moscow, 1959.

[24] T. Thiagarajan, *Centr. Glass. Ceram. Res. Inst. Bull.*, **132**, 33 (1966).

[25] A. M. Kalinina, V. N. Filipovici, V. A. Koleseva and I. A. Bondari, "Steklobraznoe sostoianiye katalizirovanaia krist. stekla", Izd. A. N. S. S. S. R., Moscow, Leningrad, 1963, p. 53–66.

[26] E. Rindone, *J. Am. Ceram. Soc.*, **45**, 7 (1962).

[27] J. G. Morley, *Glass. Technol.*, **6**, 69 (1965).

[28] Jro Matsuda Eiji, *Kogyo Kogaku Zasshi*, **67**, 884 (1964).

[29] T. Moriya Sakaina, *Chem. Soc. Japan. Industr. Chem. Sec.*, **63**, 1129 (1960).

[30] F. P. Glasser, *Physics Chem. Glasses*, **8**, 224 (1967).

The sample so obtained underwent the following measurements: DTA (10°/min. speed of heating), isothermal differential analysis, according to a method inspired by Jen Chiu's paper [31] who used it for glassy polymers, and adapted by us to inorganic glasses, X-ray analysis by Debye-Scherer method and electron microscopy with platinum and carbon replica.[15]

Structural changes evidenced by DTA

The thermograms obtained for 4 rapidly cooled glass samples containing between 50 and 100% $Li_2O.2SiO_2$ (calculated according to the composition are represented on figure 2.

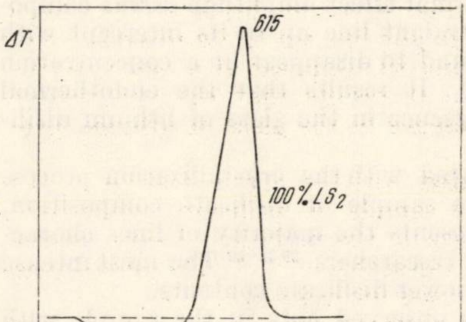

Fig. 2. — Thermograms of studied glasses.

Fig. 3. — Variation of the amplitude of endothermal effects (solid line) and of the temperature T_g (dashed line) *versus* concentration of lithium disilicate.

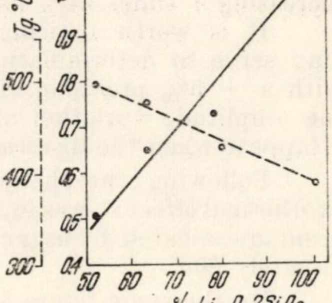

All curves present an endothermal effect which corresponds to the domain of structural changes. Recently communicated works [32] as well as our determinations showed that the temperature of the 1st inflexion (the endothermal effect) corresponds satisfactorily to T_g, the temperature of the beginning of structural changes determined on the basis of viscosity.

---

[31] Jen Chiu, *Analyt. Chem.*, **36**, 2058 (1964).

[32] Akira Yamamoto, "Detection of Characteristic Points of Commercial Glasses by Differential Thermal Analysis", First Intern. Thermal Analysis Conference, Aberdeen, 1965, p. 125.

The nature of structural changes is still debatable; contributions to its elucidation are given here and elsewhere. [33]

The variation of T_g and the amplitude of the endothermal effect *versus* the concentration of lithium disilicate in glasses is plotted in figure 3. The structural transformations begin at a temperature which is as lower as the disilicate concentration is higher. This phenomenon evidences the stabilizing role of rigid SiO_2 matrix the presence of which hinders the structural changes, that is the displacement of bulky polysilicic anions and alkali cations. The change of endothermal effect amplitude *versus* composition is also linear. Extending the straight line up to its intercept with abscissa, the endothermal effect is found to disappear at a concentration of lithium disilicate lower than 10%. It results that the endothermal effect is related exclusively to the presence in the glass of lithium disilicate.

The exothermal effects are correlated with the crystallization process of glasses. The roentgenogram of the sample of disilicate composition, crystallized during DTA (figure 4) presents the majority of lines characteristic of disilicate as found by other researchers. [25,34–37] The most intense lines are also found in samples having lower disilicate contents.

The second exothermal effect is observed only in the sample with 50% disilicate. The first exothermal effect also presents variation with the disilicate concentration (figure 5).

The temperature of the maximum of exothermal effect decreases linearly with the increase in the disilicate content so that the glass with 100% $Li_2O.2SiO_2$ crystallizes at about 150° lower than the glass with 50% $Li_2O.2SiO_2$. The amplitude of exothermal effect has a reverse variation increasing 7 times at a doubling of disilicate concentration.

It is worth noticing that the two magnitudes mentioned above may serve to determinations of disilicate concentration in such glasses with a $\pm$ 5% precision. The slope of the straight line which represents the amplitude variation of the exothermal effect shows that this must disappear when the disilicate concentration decrease at 40%.

Following the change in the temperature of the maximum of the exothermal effect it was found out that at the same concentration the maximum investigated by us is confused with the new one which occurs at approximately 900°.

On the same figure 5 it is shown that the variation of the surface between the exothermal effect and the base line *versus* disilicate concentration can be satisfactorily approximated by a straight line. The heat evolved is then proportional to the quantity of vitreous phase which crystallizes.

---

[33] S. Solacolu, P. Baltă and G. Jitianu "Change Correlation of the Vitreous Structures with the Temperature and Electric Conductivity", Communicated at the 1st National Conference of Pure and Applied Physical Chemistry, Bucharest, Sept. 1968.

[34] A. E. Austin, *J.. Am. Ceram. Soc.*, **71**, 218 (1948).

[35] R. Roy and F. Osborn, *J. Am. Ceram. Soc.*, **71**, 2086 (1949).

[36] K. P. Müller, M. Kolterman and K. Gruner, *Ber. dtsch. keram. Ges.*, **43**, 283 (1966).

[37] L. I. Mirkin, "Spravochinic po rengenostructurnomu analizu polikristalov", Gos. Izd. fiz. mat. lit., Moscow, 1961, p. 489.

The correlation of these data with the thermal equilibria in the system (figure 1) was attempted and important discrepancies due to the state of undercooled melt characteristic of glasses were found. The order of the compounds crystallization is the reversed of that for a slowly cooled melt and the domain of disilicate primary crystallization is much

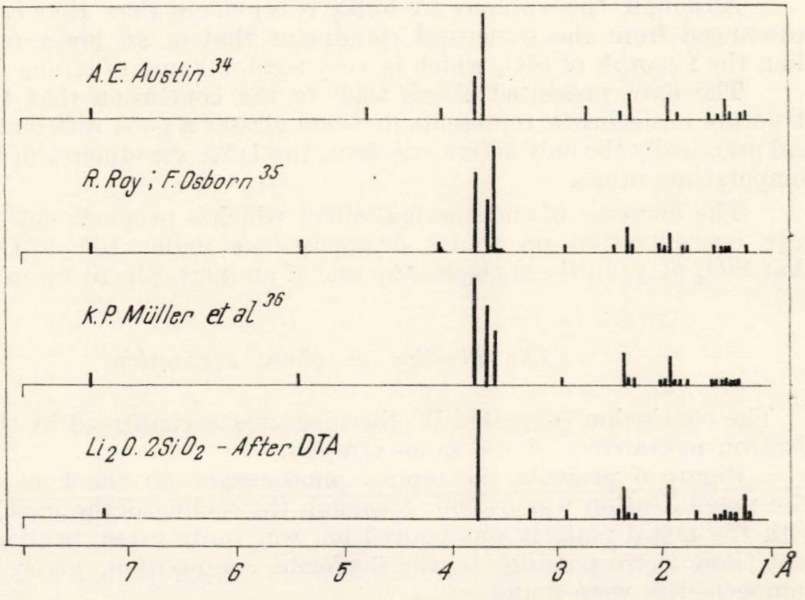

Fig. 4. — Identified lines on the sample disilicate composition roentgenogram, after the DTA, compared with those found by other researchers.

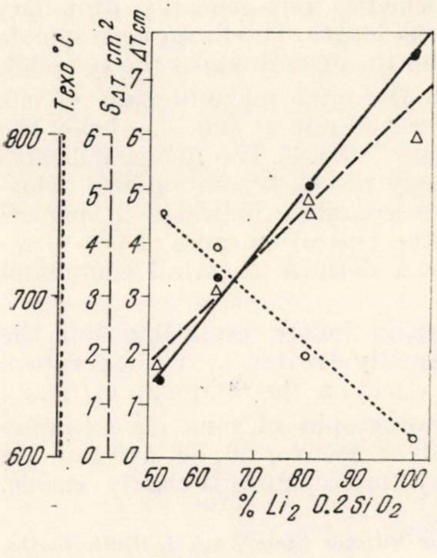

Fig. 5. — Variation of the amplitude of exothermal effects (solid line), of temperature of maximum of exothermal effects (dotted line) and of the surface between the exothermal effect and the base line *versus* disilicate concentration of lithium disilicate (dashed line).

extended to the detriment of the primary crystallization of SiO_2. The crystallization takes place much under the liquidus temperature. At such undercooling the crystallization process is controlled by the mass transfer so that it should be triggered at the moment the viscosity is small enough to allow the displacement of structural elements. According to Mackenzie [38] for alkali oxides contents up to 20%, the basic structural elements are the random network of SiO_2 and anions of the form $(Si_6O_{15})^{6-}$ up to $(Si_{24}O_{51})^{6-}$ with dimensions of 6-28Å.

Although these anions are bulky it is evident that they can be easier rearranged from the structural standpoint that is at lower temperatures, than the network of SiO_2 which is very rigid because of strong Si-O bonds.

The data presented above lead to the conclusion that the vitreous structure of disilicate represents in these glasses a good differentiated phase and practically the only active one from the DTA standpoint, in the studied temperature range.

The decrease of endothermal effect which is proportional to the disilicate concentration up to its disappearance under 10% $Li_2O.SiO_2$ shows that SiO_2 plays in these glasses the role of an inert diluent up to about 900°.

The kinetics of phase separation

The conclusion suggested by thermograms as confirmed by the results of electron microscopy of the same samples.

Figure 6 presents the replica photographs for the 4 glass samples. The magnification was 54,000. Although the cooling of the melt, in contact with the metal plate it was poured on, was quite rapid, in all samples, except these corresponding to the disilicate composition, glassy micro-nonhomogeneities were found.

It is noticed that the micro-nonhomogeneities were generally drop-like, very frequently linked as chains of various length. This image corresponds to that indicated by Chan and Charles[16] for the domain under the spinodal.

Figure 7 shows the photograph with the same magnification of one sample of disilicate composition, treated for 30 min at 500 ° i.e. below the limit of phase separation indicated elsewhere [17] (fig. 1). The image indicates that the transition in the domain of glassy phases separation was achieved. It results that the limit of phase separation indicated in paper[17] is nearer to reality. The establishing of the separation cause of two vitreous phases from a glass corresponding to a definite chemical compound appears very difficult.

To study the glassy phases separation before crystallization the samples of non-annealed glass were thermally treated at a temperature corresponding to the end of endothermal effect on the thermogram (fig. 2). On figure 8 the electron-microscope photographs of some glass samples with 62.7% $Li_2O.2SiO_2$, thermally treated at 645° for 30, 60, 120 min are given. The dimensions increase of glassy microphases is clearly visible.

---

[38] J. D. MACKENZIE, "Modern Aspects of the Vitreous State", vol. I, Butterworths, 1960, p. 188–219.

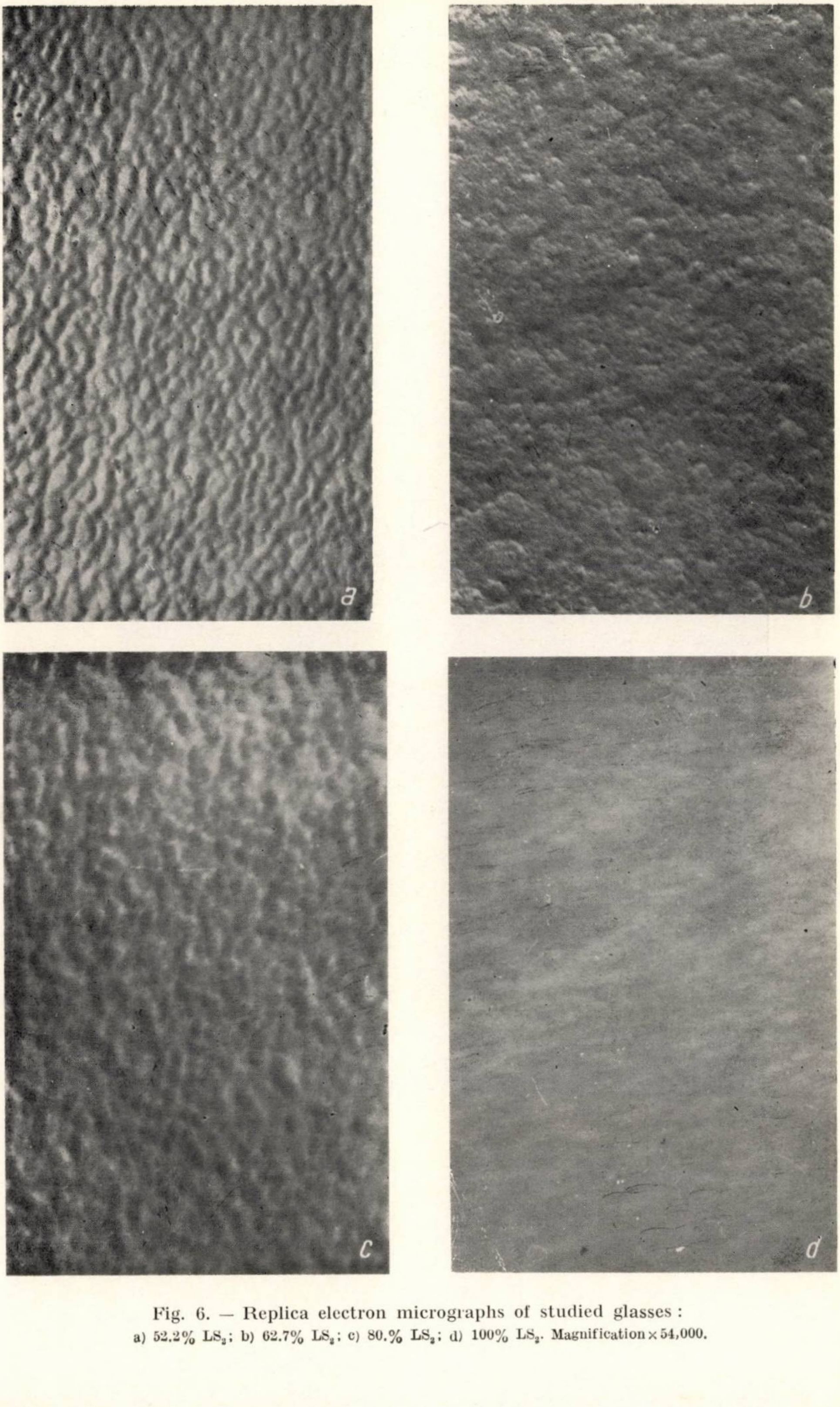

Fig. 6. — Replica electron micrographs of studied glasses :
a) 52.2% LS$_2$; b) 62.7% LS$_2$; c) 80.% LS$_2$; d) 100% LS$_2$. Magnification × 54,000.

Fig. 7. — Replica electron micrograph of sample of disilicate composition after 30 min treatment at 500°.

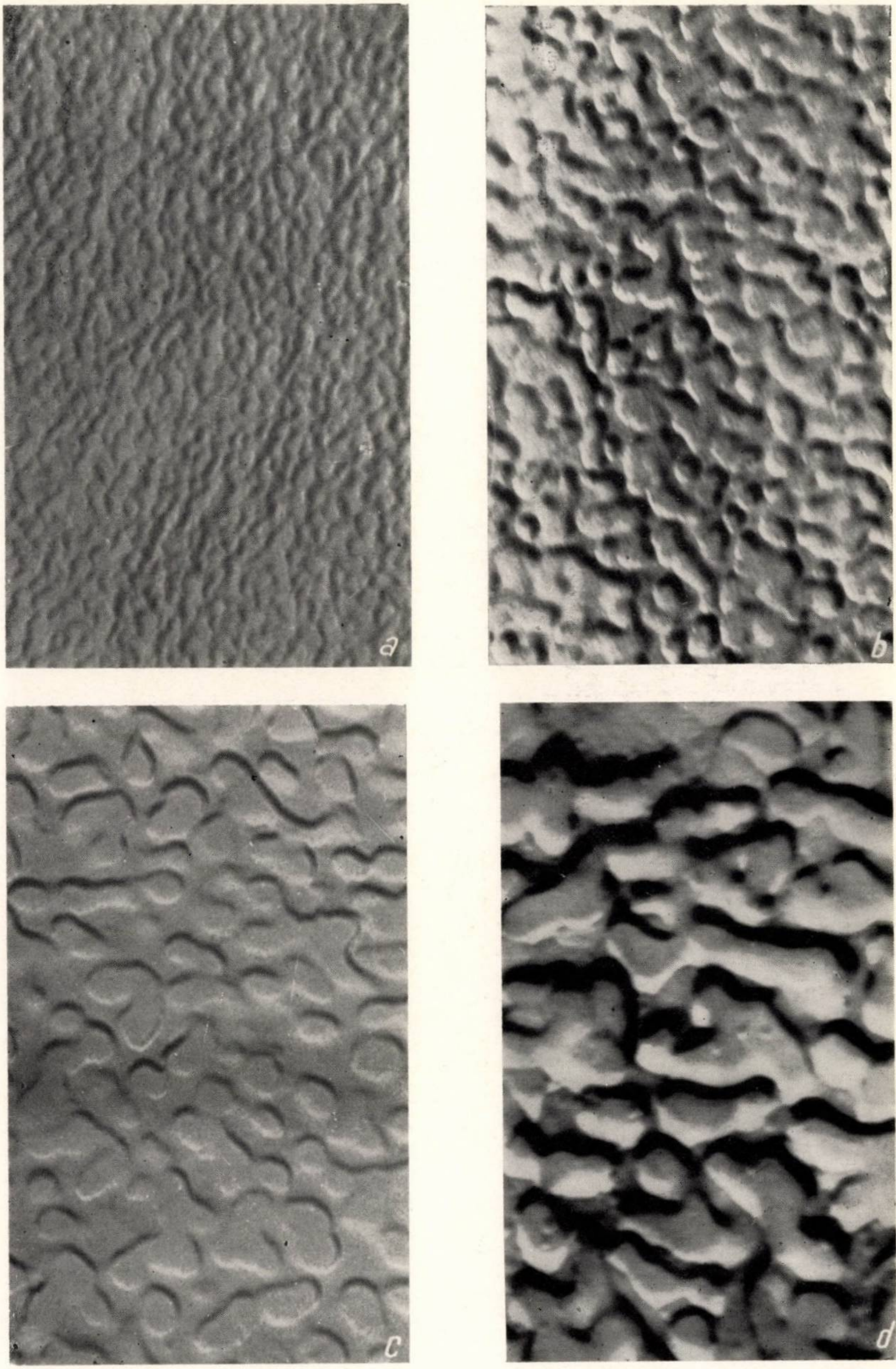

Fig. 8. — Electron micrographs of the glass samples with 62.7 % LS_2:
a) rapidly cooled from the melt, b) after 30 min at 645°, c) after 60 min at 645°, d) after 120 min at 645°.

Considering that the chains with micelle aspect are formed by the joining of some spheres, an average radius of these elementary microphases could be determined.

Figure 9 shows that the average radius is proportional with the time

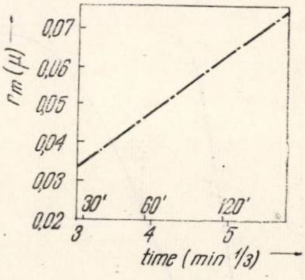

Fig. 9. – Time dependence of the mean radius (r_m) of the microphases at 645°.

raised at the third power, thus confirming Haller's [21] idea. He considers that to such relation, between the dimensions of glassy microphases and time, corresponds a mechanism where their rate of increase is determined by the diffusion process over large distances. This idea was supported by the results of other authors [22] too.

The photographs in figure 8 suggest another interesting remark; the length of chains formed by the joining of several spherical drops remains practically constant for a long time and only after a two-hour treatment a sensible increase is found, probably caused by the joining of individual drops which were numerous enough before.

The study of phase separation, started with the determinations reported above is being continued, both the specification of its mechanism and its kinetics being under consideration.

The kinetics of crystallization process

To obtain additional data on the crystallisation process as a whole, a method which allows the recording of crystallisation thermal effect at constant temperature was used. The method called isothermal differential analysis, was already used with interesting results in the study of crystallization kinetics in some semiconductor glasses, with V_2O_5.[39, 40] In principle it consist in heating the sample up to the temperature of the process and maintaining this temperature constant all throughout the determination; the thermal process is recorded versus time and the area between the exothermal curve and the base line is proportional to the quantity of crystal formed in a given time. By representing the percentage area *versus* time one obtains a curve which rigorously reflects the evolution of crystallization in time. In figure 10 curves obtained at two temperatures, in the domain of exothermal effect for glass samples with 62.7% $Li_2O.2SiO_2$ are presented.

---

[39] P. Baltă and E. Baltă, *Rev. Roumaine Chim.*, **12**, 1435 (1967).

[40] P. Baltă and M. Biale, "The Influence of the Impurities on the V_2O_5 Glasses", Proceeding of the 9th Conference on the Silicate Industry, Budapest, Siliconf., 1967, p. 33–39.

One should remark the interesting shape of these curves with an inflexion point indicating that at the beginning the crystallization process is accelerated and at the end is slowed down.

According to this shape the crystallization process of glasses in the $Li_2O.2SiO_2$ system looks like a chain reaction.[41] The analogy can be further carried out if we take into account that the chain reaction begins due to some active particles, (atoms or free radicals) which determine the transformation of a great quantity of substance and which, in our case, could be considered as crystallization nuclei.

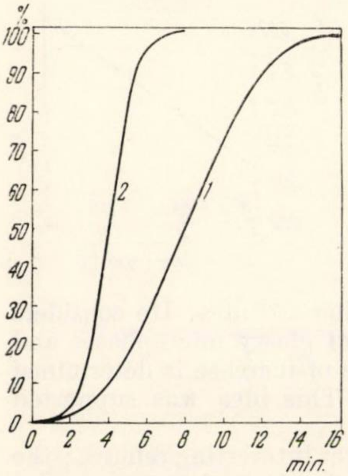

Fig. 10. — Kinetic curves obtained through differential isothermic analysis of sample with 62.7 % LS_2 at two temperatures in the exothermic effect domain : 1) at 678°, 2) at 740°.

Similar curves have been obtained by Rindone[26] when determining crystal concentration by X-ray; in glasses of other composition similar results have been obtained by the same method.[39, 40] It results that the first part of the curve, the induction period, must be related to the nucleation process. Such an interpretation is based on the results of Gutzov et all.[11] which determined directly the concentration of platinum nuclei formed in an alkali phosphate glass.

The intermediary part of the curve, which is practically linear represents the crystal growth rate. This was recently proved by Morley[27] with the high temperature microscope by measuring the crystal growth directly. The final part of the kinetic curve indicates the tendency to hinder the process due to the gradual exhaustion of the glassy phase which crystallizes.

It is obvious that the isothermal differential analysis reflects all crystallization processes, the curve we obtained giving information on the nucleation as well as on the growth phenomena which, in the case of studied glasses, could not be separated in time. The improvement of equipement will allow the extension of the isothermal differential analysis up to temperatures close to the liquidus curve so that on the basis of the kinetic curves the variation of the nucleation and crystal growth rates will be established in the whole temperature range which is of interest.

---

[41] * * * "Noţiuni de cinetică chimică", Translation from Russian, Ed. Teh., Bucharest, 1963, p. 169, 199.

CONCLUSIONS

The structural changes taking place in glasses of the Li_2O-SiO_2 system, in the composition range 50–100% $Li_2O.2SiO_2$ were multilaterally studied by methods based on thermal differential analysis, X-ray analysis and electron microscopy.

The thermograms showed that in the composition range under consideration the vitreous structure of the lithium disilicate behaves in glasses as a well differentiated phase, the only which undergoes structural changes up to 900°, while up to this temperature SiO_2 appears like an inert diluant.

The study of glassy phases separation provides arguments for the spinodal separation theory and allows the obtaining of some data on the process kinetics.

By isothermal differential analysis kinetic curves, offering information on the nucleation as well as on the crystal growth rate, were obtained.

It was proved that the DTA and electron microscopy supply very useful, multilateral information on the structural transformations occurring in glasses while the possibilities of this method are not yet being exhausted.

ACKNOWLEDGEMENTS

The authors wish to thank Mr. N. Butucescu (I.C.M.P.C. Bucharest) for his valuable help in recording the electron micrographs of the glass samples used in this study.

Revue Roumaine de Chimie, **15**, 103–114 (1970)

NEUE KOMPLEXVERBINDUNGEN DER PYRAZOLONREIHE. VI[1–5]

J. DICK und ANNA MAURER

Aus der Abteilung für Anorganische Chemie der Akademie, Forschungsstelle Timişoara,
B-dul Mihai Viteazul 24

Eingegangen am 26. Dezember 1968

Es werden die komplexbildenden Eigenschaften des Platins (II) u. (IV) und Palladiums (II) mit Liganden der Pyrazolonreihe und verschiedenen Anionen untersucht. Dabei wurden sowohl Salze der komplexen Anionen $[Me^{II}X_4]^{-2}$ und $[Me^{IV}X_6]^{-2}$ als auch Chelatverbindungen des Typs $[Me^{II}Lig_nX_2]$ erhalten. Platin (II) u. (IV) bildet keine Chelatverbindungen. Die Verbindungen werden durch UV-,IR-Spektren und thermischen Abbau charakterisiert. Auf Grund experimenteller Ergebnisse wird die wahrscheinliche Struktur dieser Verbindungen besprochen.

In unseren Arbeiten I — V haben wir Pyrazolonkomplexverbindungen des Co(II), Ni(II), Cd(II), Zn(II), Be(II), Hg(II), Bi(III), Tl(III), In(III) und Ge(IV) beschrieben. [1–5] Die Struktur dieser Verbindungen wurde durch IR-Spektren erläutert.[6]

Auf dem Gebiete der Pyrazolonkomplexverbindungen des Antipyrins und der 4-Amino-antipyrinderivate mit Platin und Palladium liegen keine systematischen Arbeiten vor und die Reaktionen zwischen $[PtCl_6]^{-2}$ und $[PdCl_4]^{-2}$ und einigen der genannten Liganden wurden bloß gelegentlich analytischer Auswertungen beschrieben. [7–9]

In vorliegender Arbeit werden die komplexbildenden Eigenschaften des Platins (II) und (IV) und des Palladiums (II) mit den 4-Amino-antipyrinderivaten untersucht.

---

[1] J. Dick und C. Drugărin, *Studii şi Cercetări Şti. Chim., Baza Cercetări Şti., Timişoara*, **8**, 205 (1961).

[2] J. Dick und A. Maurer, *Studii şi Cercetări Şti. Chim., Baza Cercetări Şti., Timişoara*, **9**, 257 (1962).

[3] J. Dick und A. Maurer, *Studii şi Cercetări Şti. Chim., Baza Cercetări Şti., Timişoara*, **10**, 61 (1963).

[4] J. Dick und A. Maurer, *Rev. Roumaine Chim.*, **10**, 633 (1965).

[5] J. Dick und A. Maurer *Rev. Roumaine Chim.*, **14**, 1603 (1969).

[6] J. Dick, R. Bacaloglu und A. Maurer, *Rev. Roumaine Chim.*, **12**, 607, 617, 629 (1967).

[7] L. Knorr, *Liebigs Ann. Chem.*, **238**, 204 (1887).

[8] R. Weehuizen, *Pharm. Weekblad*, **43**, 1105 (1906).

[9] E. Sudo, *Sci. Repts. Tohoku Univ. Ser. A.* **8**, 367 (1956).

Mit $[PtX_6]^{-2}$ wo X= Cl, Br, SCN und $[PtCl_4]^{-2}$ werden in sauren Lösungen die Verbindungen $[PtX_6](HPyr)_2$ und $[PtCl_4](HPyr)_2$ wo Pyr= 4-Dimethylamino-1-phenyl-2,3-dimethylpyrazolon, und zwar:

I $[PtCl_6](HPyr)_2$
II $[PtBr_6](HPyr)_2$
III $[Pt(SCN)_6](HPyr)_2$
IV $[PtCl_4](HPyr)_2$

erhalten.

Selbst in konzentrierten Lösungen von $H_2[PtCl_6]$ und Pyramidon in wasserfreiem Alkohol, wird I erhalten. Komplexe Anionen des Platins müssen beständiger als seine Komplexverbindungen sein, da mit Pyramidon in absolutem Alkohol, statt $[PtLig_2X_2]X_2$ die Salze

V $[PtBr_4](HPyr)_2$
VI $[PtJ_4](HPyr)_2$

erhalten wurden. In diesem Falle hat einerseits eine Redox-Reaktion zwischen Pt(IV) und Pyramidon stattgefunden, anderseits können vorhandene Spuren von $H_2[PtX_6]$ in PtX_4 die Salzbildung katalysieren.

Die Verbindung IV wurde, nur nach vorheriger Reduktion des $[PtCl_6]^{-2}$ zu $[PtCl_4]^{-2}$ erhalten.

Palladium (II) bildet in sauren wäßrigen Lösungen die Verbindungen:

VII $[PdCl_4](HPyr)_2$
VIII $[PdBr_4](HPyr)_2$
IX $[Pd(SCN)_4(HPyr)_2$

und in neutralen wäßrigen Lösungen die Chelate:

X $[PdPyrCl_2]$
XI $[PdPyrBr_2]$

Palladiumkomplexe mit der Koordinationszahl 4 weisen im allgemeinen eine planquadratische Struktur auf. [10] Da das Pyramidon ein zweizähliger Ligand ist, müssen die erhaltenen Verbindungen in der *cis*-Form vorliegen.

Die Verbindungen wurden auf ihre UV- und IR-Spektren, sowie thermischen Abbau untersucht.

EXPERIMENTELLES

I. $[PtCl_6](HPyr)_2$ wird auf zwei Wegen erhalten:

A. — Aus einer salzsauren konzentrierten Lsg von 0,5 g $H_2[PtCl_6]$. $6H_2O$ in 2 ml 2n HCl und 1 g Pyramidon in 5 ml 2n HCl. Nach 2 Std. wird der organgefarbige kristalline Niederschlag filtriert, mit kleinen Mengen Wasser, Alkohol und Äther gewaschen und über $CaCl_2$ getrocknet.

---

[10] K. A. Jensen, *Z. anorg. Chem.*, **241**, 215 (1939).

B.— Die eisgekühlte Lösung von 0,5 g$[H_2PtCl_6]\cdot 6H_2O$ in 5 ml wasserfreiem Alkohol wird mit 1 g Pyramidon in 5 ml wasserfreiem Alkohol versetzt. Es bildet sich ein gelber Niederschlag der Zusammensetzung I. Sogar beim Kochen der Verbindung in der Mutterlösung (mit absolutem Alkohol verdünnt) und nachherigem Abkühlen auf Eis wurde I erhalten. Es ist schwer löslich in Wasser und organischen Lösungsmitteln, löslich in Acetonitryl.

II. $[PtBr_6]\,(HPyr)_2\cdot 4H_2O$. 1 g Pyramidon in 15 ml Wasser wird mit HBr auf pH 1 gebracht und mit 0,4 g $H_2[PtBr_6]\cdot 9H_2O$ (aus $H_2[PtCl_6]\cdot 6H_2O$ durch wiederholtes Abrauchen mit HBr nach [11] hergestellt) in 3 ml 2n HBr versetzt. Der orangefarbene Niederschlag nimmt binnen 3 Std. unter Eiskühlung und zeitweisem Umrühren kristalline Form an und färbt sich rot. Nach 6 Std. wird filtriert, mit wenig eisgekühltem Wasser, Alkohol und Äther gewaschen und wie bei I getrocknet. Löslichkeit wie bei I.

III. $[Pt(SCN)_6]\,(HPyr)_2$. Man fügt zu einer eisgekühlten Lsg von 0,5 g $H_2[Pt(SCN)_6]$ (aus $H_2[PtCl_6]\cdot 6H_2O$ nach [12] hergestellt) in 15 ml Wasser von pH 1 (H_2SO_4), unter ständigem Umrühren eine eisgekühlte, schwefelsaure Lsg (pH 1) von 0,5 g Pyramidon in 15 ml Wasser. Eventuelle Verharzungen werden entfernt. Es bildet sich ein gelber Niederschlag, welcher weiter wie II behandelt wird. F = 134—135°. Schwer löslich in Wasser, Alkohol und Äther, leicht löslich in organischen Lösungsmitteln.

IV. $[PtCl_4]\,(HPyr)_2$. Zu 2 ml einer salzsauren Lsg von 0,3 g $H_2[PtCl_4]$ (durch Reduktion von $H_2\,[PtCl_6]$ mit Hydrazynsulfat erhalten [13]), fügt man 1 g Pyramidon in 6 ml 2n HCl. Es fällt langsam ein kristalliner orangerosa gefärbter Niederschlag aus, der nach 24 Std. filtriert, und wie I weiterbehandelt wird. Schwer löslich in Wasser und organischen Lösungsmitteln. Schmp. 229—230° (zers.).

V. $[PtBr_4]\,(HPyr)_2$. Unter ständigem Rühren wird die eisgekühlte Lsg von 0,8 g $PtBr_4$ (durch Glühen des $H_2[PtBr_6]$. 9 H_2O bei 170—180° erhalten) in 10 ml absolutem Alkohol mit 0,8 g Pyramidon in 10 ml wasserfreiem Alkohol versetzt. Der entstandene flockige, dunkle Niederschlag geht beim Stehen unter Eiskühlung in eine feinkörnige und ockergelb gefärbte Form über. Nach 5 Std. wird filtriert, gut abgesaugt, mit Äther gewaschen und über $CaCl_2$ getrocknet. Schwer löslich in Wasser, Alkohol, Äther, leicht löslich in Aceton und Acetonitryl.

VI. $[Pt\,J_4]\,(HPyr)_2$ wird wie V erhalten. Dazu wird das nach [14] hergestellte PtJ_4 verwendet. Der anfangs sehr feine, braune Niederschlag wird nach 3—5stündigem Stehen kristallin, wird durch Wasser zersetzt und ist etwas löslicher in organischen Lösungsmitteln als V.

VII. $[PdCl_4]\,(HPyr)_2$. 7 ml einer 2n HCl-Lsg von 0,2 g $PdCl_2$ wird mit 1 g Pyramidon in 5 ml 2n HCl umgesetzt. Langsam kristallisiert ein braungelber Niederschlag aus. Man filtriert, wäscht mit kleinen Mengen Wasser und trocknet über $CaCl_2$ im Vakuum. Fast unlöslich in Wasser, wenig löslich in organischen Lösungsmitteln, löslich in Acetonitryl.

VIII. $[PdBr_4]\,(HPyr]_2$. Wird wie VII aus 2n HBr-Lsg von $H_2[PdBr_4]$ (aus $PdCl_2$ nach [15] hergestellt) und Pyramidon bei Eiskühlung erhalten. Zunächst bildet sich ein rotbrauner, amorpher Niederschlag, welcher allmählich in eine mikrokristalline Form übergeht. Nach ungefähr 3 Std. wird filtriert und wie bei VII behandelt. Löslichkeitsverhältnisse wie bei VII.

IX. $[Pd(SCN)_4]\,(HPyr)_2\cdot 6H_2O$. Man versetzt 0,5 g (nach [16] erhaltenes) $K_2[Pd(SCN)_4]$ in 10 ml Wasser mit H_2SO_4 auf pH 1 gebracht, mit einer schwefelsauren Lsg von 1 g Pyramidon in 40 ml Wasser.

[11] A. Gutbier und F. Bauriedel, *Ber. dtsch. chem. Ges.*, **42**, 4246 (1909).

[12] W. N. Iwanov, *Chem. Ztg.*, **47**, 209 (1923).

[13] G. Brauer "Handbook of Preparativ Inorganic Chemistry" 2. Bd. 2. Aufl. Acad. Press, New York, London, 1965, S. 1570.

[14] H. Topse, *Overs Danske Selsk. Forh.*, **1869**, 77.

[15] A. Gutbier und C. Fellner *Z. anorg. Chem.*, **95**, 136 (1960).

[16] O. Grube und D. Beischer, *Z. Elektrochem.*, **39**, 134 (1933).

Es bildet sich ein rosaroter Niederschlag, welcher beim Stehen kristallin wird. Weiterverarbeitung wie bei VIII. Leichter löslich in organischen Lösungsmitteln als VII und VIII.

X. [*PdpyrCl$_2$*]. Man versetzt unter ständigem Umrühren 0,5 g $PdCl_2$ und 3 g KCl in 60 ml Wasser mit 1,5 g Pyramidon in 50 ml Wasser. Es bildet sich allmählich ein sehr feiner ockergelber Niederschlag der in kristalline Form übergeht. Nach 20 Std. wird filtriert, mit kleinen Mengen eisgekühltem Wasser, Alkohol und Äther gewaschen und bei 50° getrocknet. Unlöslich in Wasser und organischen Lösungsmitteln.

XI. [*PdPyrBr$_2$*] wird aus 1 g [$PdPyrCl_2$] durch Verreiben mit 2 g KBr, bis die Farbe in orangengelb übergeht, erhalten. Nachher wird mit Wasser behandelt, filtriert und wie X gewaschen und getrocknet. Löslichkeitsverhältnisse wie bei X.

ANALYSE

Platin wurde als Metall, Palladium als Metall oder mit Dimethylglyoxim, Halogen und Pseudohalogen potentiometrisch oder gewichtsanalytisch und Stickstoff nach Pregl bestimmt.

Die analytischen Ergebnisse sind in Tabelle 1 zusammengefaßt.

Tabelle 1

Analysenergebnisse der Verbindungen

	Komplexverbindung	Molargewicht, *ber.*:	*Ber.*: %			*Gef.* %.		
			Metall	Halogen	N	Metall	Halogen	N
I	$[PtCl_6](HPyr)_2$	872,27	22,38	24,39	9,65	22,36	24,08	9,55
II	$[PtBr_6](HPyr)_2.4H_2O$	1211,00	16,12	39,59	6,94	16,12	39,27	6,86
III	$[Pt(SCN)_6](HPyr)_2$	995,85	19,59	33,74	16,86	19,79	33,62	16,58
IV	$[PtCl_4](HPyr)_2$	801,35	24,36	17,70	10,49	24,07	17,65	10,60
V	$[PtBr_4](HPyr)_2$	979,19	19,94	32,64	8,58	20,32	33,06	8,38
VI	$[PtJ_4](HPyr)_2$	1167,25	16,73	43,49	7,20	17,00	43,79	7,05
VII	$[PdCl_4](HPyr)_2$	712,52	14,93	19,90	11,80	15,05	19,80	11,58
VIII	$[PdBr_4](HPyr)_2$	890,36	11,95	35,90	9,44	12,08	35,72	9,80
IX	$[Pd(SCN)_4](HPyr)_2.6H_2O$	892,92	11,92	23,99	15,69	11,82	24,02	15,55
X	$[PdPyrCl_2]$	408,46	26,05	17,36	10,29	26,15	17,14	10,08
XI	$[PdPyrBr_2]$	497,38	21,39	32,13	8,45	20,95	31,95	8,75

Der thermische Abbau wurde bei gleichmäßigem Erhitzen der Verbindung von 5°/Min. zwischen 30—600° durchgeführt. Das Verhalten der Platin- und Palladiumkomplexverbindungen ist aus Abbildung 1 und 2 ersichtlich.

Die UV-Spektren wurden mit dem Spektrophotometer UNICAM SP 800 im Bereiche 200—350 nm im Vergleich mit reinen Lösungsmitteln aufgenommen. Dazu werden 1.10^{-4} molare Lösungen der Komplexverbindungen in Wasser und Methanol verwendet. Die Verbindungen mit Brom sind lichtempfindlich; ihre Absorptionsspektren wurden 3 Min nach der Herstellung ihrer Lösungen aufgezeichnet. Die Absorptionsspektren sind aus Abb. 3 und 4 ersichtlich,

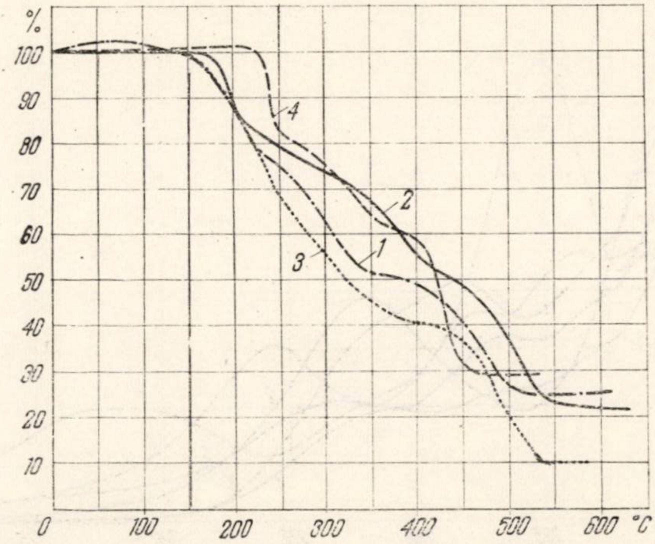

Abb. 1. — Thermogravimetrische Kurven der Pt-Komplexverbindungen.
1. $[PtCl_6](HPyr)_2$; 2. $[PtBr_6](HPyr)_2$; 3. $[Pt(SCN)_6](HPyr)_2$; 4. $[PtCl_4](HPyr)_2$.

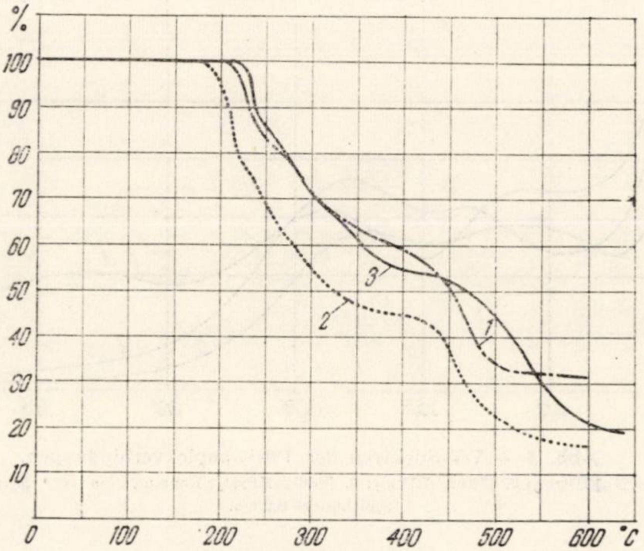

Abb. 2. — Thermogravimetrische Kurven der Pd-Komplexverbindungen.
1. $[PdPyrCl_2]$; 2. $[PdCl_4](HPyr)_2$; 3. $[PdBr_4](HPyr)_2$.

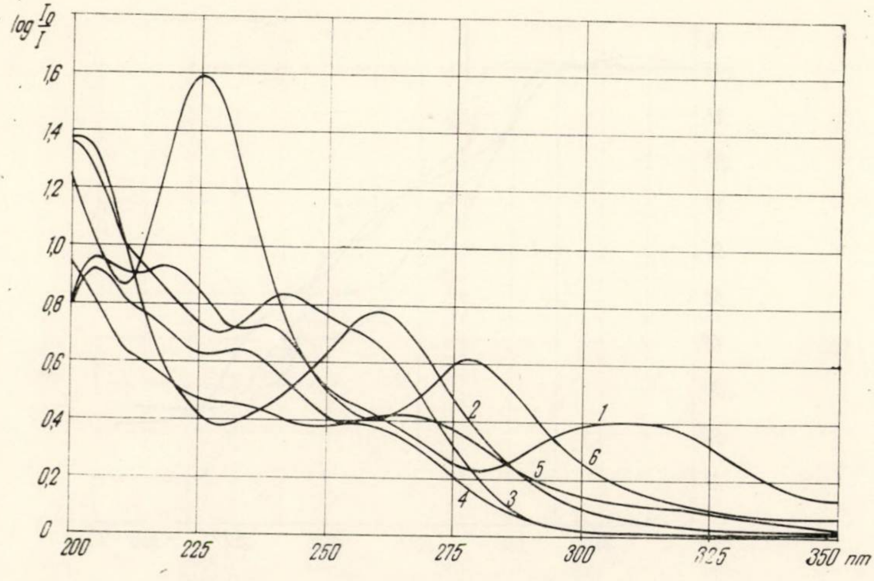

Abb. 3. — UV-Spektren der Pt-Komplexverbindungen.

1, $[PtBr_6](HPyr)_2$; 2, $[PtCl_6](HPyr)_2$; 3, $[Pt(SCN_6)](HPyr)_2$; 4, $[PtCl_4](HPyr)_2$ 5, $[PtJ_4](HPyr)_2$; 6, $[PtBr_4](HPyr)_2$; Konzentration 10^{-4} M in Wasser, Schichtdicke 0,2 cm.

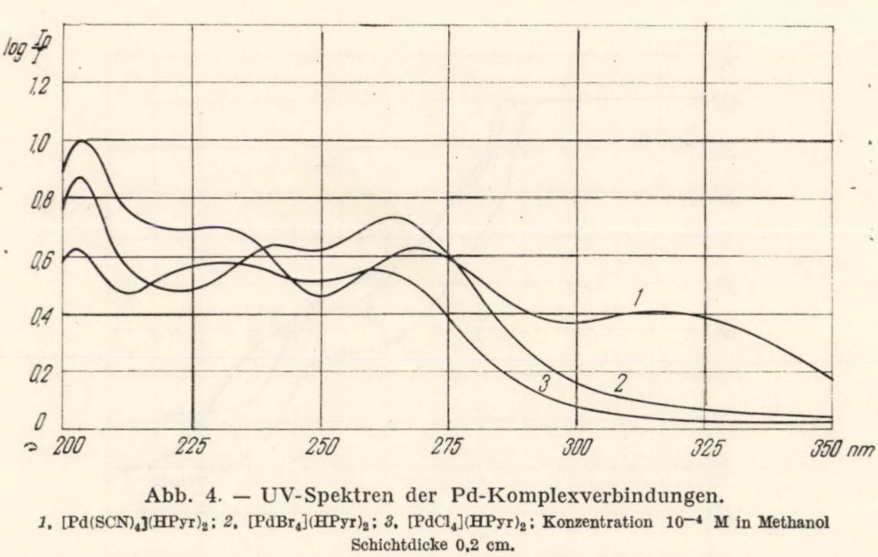

Abb. 4. — UV-Spektren der Pd-Komplexverbindungen.

1, $[Pd(SCN)_4](HPyr)_2$; 2, $[PdBr_4](HPyr)_2$; 3, $[PdCl_4](HPyr)_2$; Konzentration 10^{-4} M in Methanol Schichtdicke 0,2 cm.

während die Absorptionsmaxima (λ_{max}) und die entsprechenden molaren Extinktionskoeffizienten ($\log \varepsilon_{max}$) in Tabelle 2 verzeichnet sind.

Gleichzeitig wurden unter denselben Bedingungen (wäßrige Lsg, Konzentration 1.10^{-4} M, bzw. 2.10^{-4} M) die Absorptionsspektren von $H_2[PtCl_6]$. $6H_2O$ und Pyramidon aufgenommen, Abb. 5.

Tabelle 2

Absorptionsmaxima und die entsprechenden molaren Extinktionskoeffizienten aus den UV-Spektren der Verbindungen

Verbindung	λ_{max} nm	log ε_{max}	λ_{max} nm	log ε_{max}	λ_{max} nm	log ε_{max}	λ_{max} nm	log ε_{max}
$[PtCl_6](HPyr)_2$	—		260	4,54			202	4,84
$[PtBr_6](HPyr)_2$	313	4,30	226	4,90			<200	
$[Pt(SCN)_6](HPyr)_2$			242	4,62			197	4,83
$[PtCl_4](HPyr)_2$			255*	4,31	230*	4,36	<200	
$[PtBr_4](HPyr)_2$			265	4,32	233	4,51	205	4,66
$[PtJ_4](HPyr)_2$	278	4,48	238	4,56	218	4,67	205	4,68
$[PdCl_4](HPyr)_2$			261	4,45	230	4,46	203	4,49
$[PdBr_4](HPyr)_2$			265	4,55	241	4,49	203	4,65
$[Pd(SCN)_4(HPyr)_2$	317	4,31	269	4,48	231*	4,54	204	4,70
$[PtCl_6]H_2.6H_2O$			262	4,34			202	4,57
Pyramidon			265	3,95	225	3,97	<200	

* Schulter

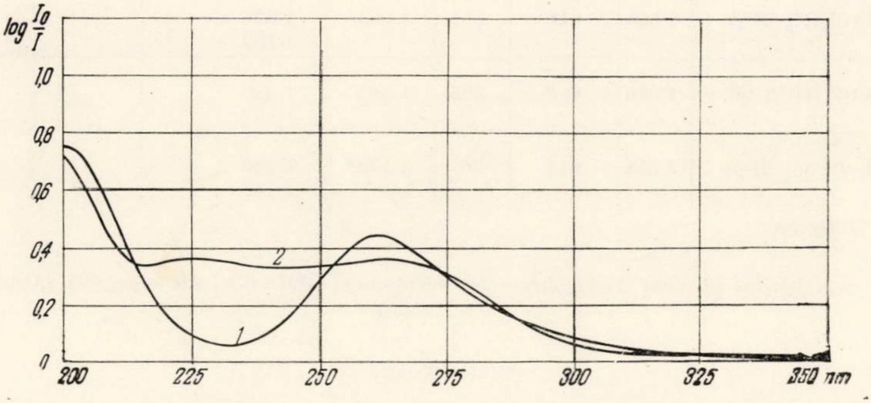

Abb. 5. — UV-Spektren des Pyramidons.
1, $[PtCl_6]\ H_2.6H_2O$; *2*, Pyramidon Konzentrationen 10^{-4} bzw. 2.10^{-4} M in Wasser, Schichtdicke 0,2 cm.

Die IR-Spektren wurden mit dem Doppelstrahlgerät UR-10, VEB Carl Zeiss Jena und Prismen aus KBr (400—700 cm^{-1}), NaCl (700—1800 cm^{-1})und LiF (1800—4000 cm^{-1}) vermessen. Dazu wurden KBr-Preßlinge der Verbindungen I, III, IV, VI, VII, IX und X verwendet. In

Tabelle 3 ist die Lage der charakteristischen Banden der an der Chelat- oder Salzbildung beteiligten Gruppen, im Vergleich zu den Schwingungen des freien Liganden, sowie die der SCN-Gruppe verzeichnet.

Tabelle

Charakteristische Banden aus den

	Verbindung	Ligand					Chelatver		
		$>C=O$			$>C=C<$	$>C-NR_2$	Chelatring		
		$\nu_{C=O}$	$\delta_{O=C-N}$	$\gamma_{C=O}$	$\nu_{C=C}$	ν_{C-N}	ν_{C-O}	ν_{Me-O} oder ν_{Me-N}	ν_{C-N}
	Dimethylamino-antipyrin	1 665	603	560	1 556	1 315 1 130			
X	$[PdPyrCl_2]$						1 010	495	1 325 1 145
III	$[Pr(SCN)_6](HPyr)_2$								
IX	$[Pd(SCN)_4(HPyr)_2$								
VI	$[PtJ_4](HPyr)_2$								
I	$[PtCl_6]H_2 \cdot 2Pyr$	1 660	618	565	1 563	1 320 1 132			
IV	$[PtCl_4]H_2 \cdot 2Pyr$	1 660	618	565	1 565	1 320 1 132			
VII	$[PdCl_4]H_2 \cdot 2Pyr$	1 655	618	565	1 570*	1 320 1 132			

* Schulter

Als Beispiel wird das IR-Spektrum der Verbindung $[PdPyrCl_2]$ wiedergegeben (Abb. 6).

DISKUSSION

Platin neigt besonders zur Salzbildung u. zw. Salze der komplexen Anionen $[PtX_4]^{-2}$ und $[PtX_6]^{-2}$, die kristallin und sowohl in festem Zustand als auch in Lösung beständig sind. Die Bromverbindungen sind in Lösung lichtempfindlich. Die Verbindungen I—IX sind schwer löslich in Wasser und organischen Lösungsmitteln, außer jenen mit SCN, welche in organischen Lösungsmitteln gut löslich sind. Im allgemeinen ist die Löslichkeit der Salze des $[PtX_4]^{-2}$ etwas größer als jene des $[PtX_6]^{-2}$. Löslichkeitsverhältnisse und Beständigkeiten der Palladiumkomplexe sind ähnlich.

Da die Reaktion zur Bildung des [$PdPyrCl_2$] quantitativ verläuft und die Verbindung fast unlöslich ist, kann sie als Grundlage einer quantitativen Bestimmungsmethode des Palladiums dienen.

3

IR-Spektren der Verbindungen

bindungen		Salze								
Pyrazolonring		C–OH				C–NR_2	Me–S=C=N			
$\nu_{C=N}$	$\nu_{C=C}$	ν_{C-O}	δ_{OH}	γ_{OH}	ν_{OH}	ν_{C-N}	ν_1 $\nu_{as SCN}$	ν_3 $\nu_{s SCN}$	ν_2 δ_{SCN}	$2 \cdot \nu_2$
1 600	1 565									
1 630	?	1 025	1 380	630 645	2 650	1 330 1 135	2 120	710	465	935 840
1 620	1 570*	1 025	1 390	630 645	2 600 2 710	1 330 1 135	2 105 2 115	690*	475	930 855 870
1 620	1 570*	1 025	1 380	635 640	2 700	1 330 1 135				

Das Verhalten der Verbindungen bei höheren Temperaturen ist aus den Thermogrammen ersichtlich.

Die Pyramidonsalze komplexer Anionen gliedern sich nach der Temperaturbeständigkeit folgendermaßen: Pt(II) > Pd(II) > Pt(IV). Im Falle der Chlorverbindungen beginnt die Zersetzung des [$PtCl_4$] $(HPyr)_2$ bei 228 – 230°, des [$PdCl_4$]$(HPyr)_2$ bei 186° und des [$PtCl_6$]$(HPyr)_2$ bei 131°. Die Salze komplexer Anionen mit Br weisen eine höhere Temperaturbeständigkeit als jene mit Cl auf. Beginn der Zersetzung [$PtBr_6$]$(HPyr)_2$ – 180°, [$PdBr_4$]$(HPyr)_2$ – 224°. (Schmelzpunkte beider Verbindungen fallen mit dem Beginn der Zersetzung zusammen). Die Verbindungen [Pt $(SCN)_6$]$(HPyr)_2$ zersetzt sich bereits bei 142°.

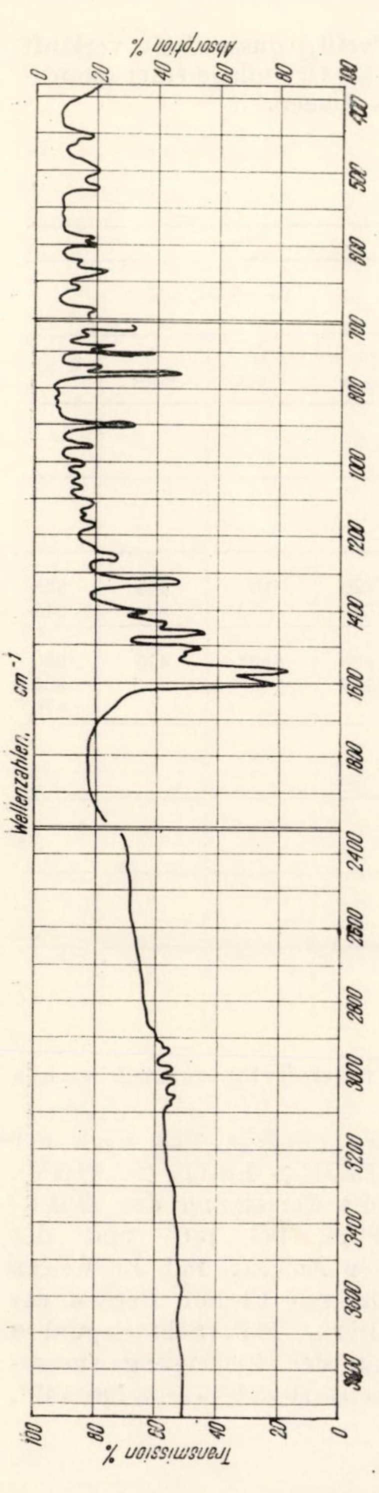

Abb. 6. — IR-Spektrum des [$PdPyrCl_2$].

Die Chelate des Palladiums sind temperaturbeständiger als seine Salze; so ist [$PdPyrCl_2$] (Beginn der Zersetzung bei 202°) beständiger als [$PdCl_4$] ($HPyr)_2$.

Da die Thermolyse nur bis 600° geführt werden konnte, hinterließen die Platinkomplexe ein Gemisch von Oxiden an Stelle von metallischem Platin. Die Verbindung [$Pt(SCN)_6$] ($HPyr)_2$ hinterläßt einen Rückstand von nur 10,5% an Stelle von 19,59 % Pt bzw. ca. 22,80% PtO_2. Es ist möglich, daß das während der Zersetzung der SCN-Gruppe entstandene Kohlenoxid mit Pt flüchtige Carbonylverbindungen bildet, wodurch Verluste hervorgerufen werden.

Die Verbindungen werden auch durch die UV-Spektren charakterisiert. Im Falle des [$PtCl_6$]($HPyr)_2$ sind die Absorptionsmaxima im Vergleich zu jenen der freien Säure kaum verschoben. Hingegen ist ein Anstieg der molaren Extinktionskoeffizienten bei [$PtCl_6$] ($HPyr)_2$ zu verzeichnen, da das Dimethylamino-antipyrin in demselben Bereiche absorbiert.

Größeren Beitrag zur Struktur der Verbindungen leisteten die IR-Spektren. Ihre Auswertung erfolgt, da bereits Pyrazolonkomplexe (Chelate, Salze mit komplexen Anionen und einfache Komplexe) mit anderen Metallen von uns weitläufig erläutert wurden,[6] nur im Bereich von Banden der an der Chelatbildung beteiligten Gruppen; C=O (5), $-NH_2$(4) und SCN.

Wie aus Tabelle 3 ersichtlich, werden im Spektrum der Verbindung [$PdPyrCl_2$] an Stelle der der Carbonylgruppe zugeschriebenen Bande von 1670—1645 cm^{-1} zwei andere Banden im Bereiche 1020—960 cm^{-1} 1620—1600 cm^{-1} vorgefunden, welche der einfachen Bindung C—O und der Doppelbindung C=N entsprechen. Die leichte Verlagerung der Schwingungen der C=N Gruppe (N der Aminogruppe) läßt auf die Koordination des Metallions durch das N-Atom schließen. Die Valenzschwingungen Me—O und Me—N der verwendeten Metalle sind schwer zu erkennen, da sie mit anderen Schwingungen gekoppelt sind.

Aus diesen Feststellungen ergibt sich, daß [$PdPyrCl_2$] ein Chelat des Typs ON ist, und wie folgt formuliert werden kann :

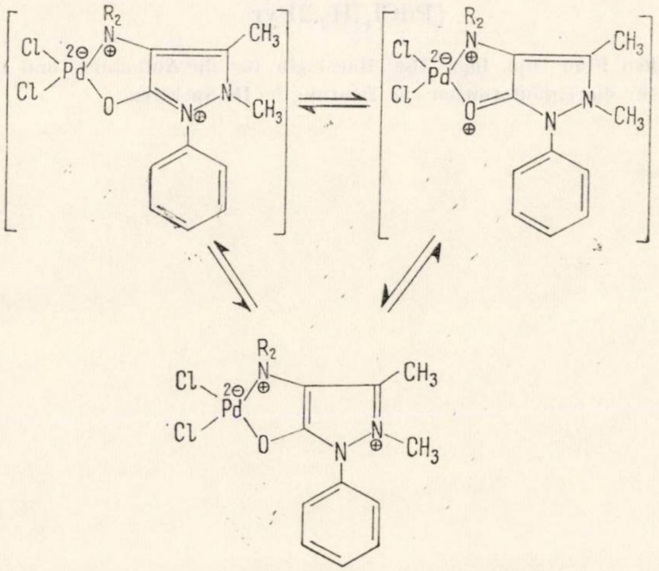

Zieht man die Absorptionsspektren der Verbindungen III, VI und IX in Betracht, so können diese als Salze komplexer Anionen mit Pyramidonium, in welchem das Proton an das Carbonylsauerstoffatom gebunden ist und mit dem Aminstickstoff eine Chelatprotonbindung bildet,[6] betrachtet werden. Die SCN-Gruppen werden in den Verbindungen III und IX durch das S-Atom vom Zentralatom Pt und Pd (Übergangselemente der dritten und zweiten Reihe) koordiniert. Dieses wird hauptsächlich durch die Schwingungen ν_2 (ν_{CS} oder $\nu_{s\,SCN}$) im Werte von ungefähr 700 cm^{-1} nach[17–19] und ν_1($\nu_{C=N}$ oder $\nu_{as\,SCN}$) im Werte von ungefähr 2100 cm^{-1} (wenn man den hypsochromen Effekt der Komplexbildung in Betracht zieht) veranschaulicht.

Untersucht man die Spektren der Verbindungen I, IV und VII d.h. die Salze der komplexen Anionen mit Cl, so wird festgestellt, daß sich diese kaum von jenen des Liganden als solchem unterscheiden; es werden die der Carbonyl- und Aminogruppe entsprechenden Banden bei fast densel-

---

[17] K. Nakamoto, "Infrared Spectra of Inorganic and Coordination Compounds", J. Willey, New York, London, 1963, S. 173.

[18] L. Lewis, R. S. Nyholm und P. W. Smith *J. Chem. Soc.*, **1961**, 4590.

[19] L. H. Jones *J. Chem. Phys.*, **25**, 1069 (1956).

ben Wellenzahlen wie im Ligand wiedergefunden. Demnach können diese Verbindungen zunächst wie folgt formuliert werden:

$$[PtCl_6]H_2.2Pyr$$

$$[PtCl_4]H_2.2Pyr$$

$$[PdCl_4]H_2.2Pyr$$

Wir danken Frau Dipl.-Ing. Ilse Bacaloglu für die Aufnahme und Herrn Dr.-Ing. R. Bacaloglu für die Erläuterungen zur Deutung der IR-Spektren.

Revue Roumaine de Chimie, 15, 115–118 (1970)

PHOTOCOLORIMETRIC STUDY OF Pd (II) AND THE α-ETHYL-ISONICOTINIC ACID THIOAMIDE

E. POPPER, LUCIA CHIOREAN and IULIA PITEA
Laboratory of Analytical Chemistry, Faculty of Pharmacy
Cluj, Str. Pasteur Nr. 6

Received November 25, 1968

A new method is described for photometric dosing of Pd (II) with α-ethyl-isonicotinic acid thioamide. The brownish-yellow complex is stable at pH 4–4.5 with a maximal absorption at $\lambda = 400$ nm. The combining ratio between the two reagents has been determined by applying the method of continuous variations and of molar ratio. By both methods the 1 Pd : 1 R ratio has been obtained. We determined the instability constant obtaining a K mean value of 1.22×10^{-3} and a value of the stability constant K_s of 8.17×10^2.

We have shown, in a previous paper,[1] that α-ethyl-isonicotinic acid thioamide is a colour reagent for osmium, giving a brownish-yellow complex at pH 5–7. The hydrosoluble complex formed allowed the photometric determination of this element, the maximum absorption being at $\lambda = 470$ nm.

A permanent concern of our group is to extend the use of this substance as a colour reagent for other metals too.

Thus, Pd (II) gives in ethanolic medium at pH 4–4.5 with α-ethyl isonicotinic acid thioamide a brownish-yellow stable complex with the maximum absorption at $\lambda = 400$ nm. This complex allowed the photometric determination of Pd (II) in concentrations in the range 0.23 to 2.99 μg/ml.

EXPERIMENTAL

Apparatus. The determinations have been made by means of a FEK–56 photometer at room temperature by using the 3 cm tube and the filter no 3 ($\lambda = 400$ nm).

Reagents. An acid (hydrochloric acid) palladium chloride solution has been used with pH 3.5 and a 5.932 μg/ml content of Pd.

As reagent 0.01 g % solution of α-ethyl-isonicotinic acid thioamide in ethanol has been used.

Method. In 25 ml graduated flasks volumes from the palladium solution have been measured with a burette, the concentration in Pd/ml being in the range 0.23 to 2.99 μg. To the metal solution 5 ml reagent were added stirred for one minute and then ethanol to 25 ml of volume was poured, pH 4—4.5. The colour formed was read 30 minutes following addition of the reagent, as against control samples prepared from the same quantity of reagent, ethanol and distilled water at the same pH as the samples.

---

[1] E. Popper, I. Grecu, I. Pitea, L. Chiorean and I. Gocan, *Studii și Cercetări de Chim. Acad. R. P. Română*, **12**, 387 (1964).

RESULTS AND DISCUSSIONS

The pH effect. It has been established that the optimum working pH is in the series 4 to 4.5, in which interval the complex is stable. This pH is achieved by simply mixing the palladium and reagent solutions. At lower pH values the colour given by the complex interferes with the yellow colour given by the reagent with hydrochloric acid and which deepens at pH lowering. At pH values higher than 4.5 a slight opalescence and even precipitation is observed.

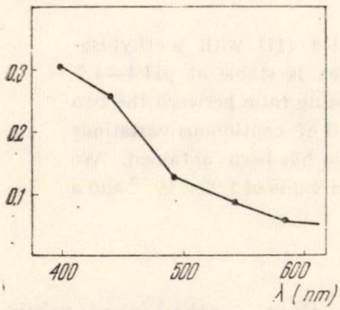

Graph 1. — The absorbance variation depending on the wavelength.

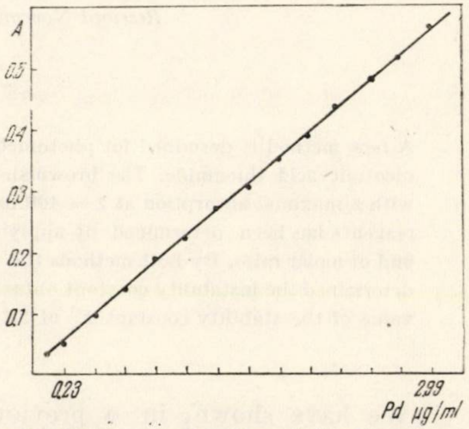

Graph 2. — Verification of Lambert-Beer's law.

Time stability. The coloured complex formed is stable, 30 minutes following reagent addition, for 4 hours at room temperature.

Wavelength effect. In graph 1 the absorbance variation depending on the wavelength is given. A maximum absorbance results for λ = 400 nm and a decrease of the extinction for other wavelength values.

Establishing of the standard curve. From graph 2 one can see that the Lambert-Beer law is observed within the concentration limits 0.23 and 2.99 μg Pd/ml.

THE DETERMINATION OF THE REACTION RATIO BETWEEN Pd (II) AND α-ETHYL-ISONICOTINIC ACID THIOAMIDE

In order to determine the reaction ratio between Pd (II) and α-ethyl-isonicotinic acid thioamide Jobb's [2] method of continuous variations and Yoe and Jones' [3] method of molar ratio have been used.

---

[2] P. Jobb, *Liebigs Ann. Chem.*, **10**, 113 (1928).

[3] J. H. Yoe and A. L. Jones, *Ind. Eng. Chem. Anal. Ed.*, **16**, 111 (1944).

To apply Jobb's method of continuous variations equimolecular palladium and reagent solutions were prepared for three concentrations: *1*, 0.557×10^{-5} m; *2*, 1.115×10^{-5} m; *3*, 1.672×10^{-5} m. This has been done in 25 ml graduated flasks in which 1...3...9 ml palladium solution were measured by means of a burette. To this solution volumes of reagent solution were added up to 10 ml total reagent solution. The volume is completed to 25 ml with ethanol and the extinctions are read 5 minutes following preparation.

For each concentration a combining ratio of 1 Pd: 1 R has been obtained, the results being given in graph 3.

The molar ratio method has been applied by using palladium and reagent equimolecular solutions, with a concentration of 2.230×10^{-5} m.

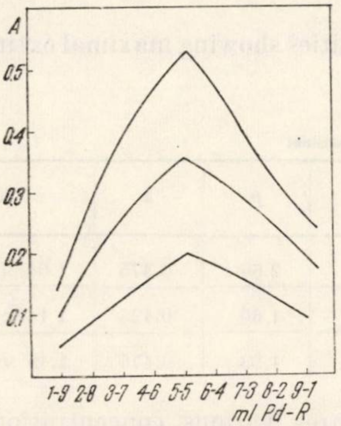

Graph 3. — Determination of the combining ratio by Jobb's method of continuous variations. *1*, 0.557×10^{-5} m; *2*, 1.115×10^{-5}m; *3*, 1.672×10^{-5} m.

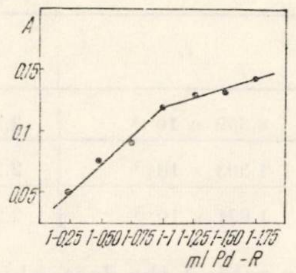

Graph 4. — Determination of the combining ratio by the molar ratio method of Yoe and Jones.

The palladium quantity was kept constant and the reagent quantity varied. 25 ml balloon flasks were used with 1 ml of palladium solution to which 0.25; 0.50; 0.75; 1; 1.25; 1.50; 1.75 ml of reagent solution were added. The volume supplemented up to 25 ml with ethanol, and reading occurred 5 minutes after preparation.

The results are given in graph 4, again obtaining a 1 Pd : 1 R combining ratio thus confirming the result obtained by the continuous variation method.

DETERMINATION OF THE COMPLEX STABILITY

In order to determine the instability constant of the complex we used the continuous variation method, working with nonequimolecular palladium and reagent solutions. The determinations were made in the same conditions as those of the combining ratio.

The computing of the instability constant was performed by applying the formula:

$$K = \frac{C_1^{m+n-1}\ p^{n-1}[(pm+n)\,x - n]^{m+n}}{m^{n-1}\cdot n^{m-1}\,(p-1)^{m+n-1}\ [n-(m+n)\,x]}$$

where m and n are the coefficients of the two components from the coefficients of the complex $[m = n = 1]$

c_1 is the molar concentration of the solution palladium.

c_2 is the molar concentration of the reagent solution.

$$p = \frac{c_2}{c_1}$$

x is the ratio of Pd and reagent quantities showing maximal extinction.

Table 1

Complex instability constant

No	c_1	c_2	p	x	K
1	8.359×10^{-5}	2.235×10^{-4}	2.66	0.375	1.04×10^{-3}
2	1.393×10^{-4}	2.235×10^{-4}	1.60	0.425	1.14×10^{-3}
3	1.671×10^{-4}	2.235×10^{-4}	1.33	0.475	1.49×10^{-3}

In table 1 the data obtained for three various concentrations are given. The mean value of the instability constant is: $K = 1.223 \times 10^{-3}$, the stability constant $K_s = 8.17 \times 10^2$.

Revue Roumaine de Chimie, 15, 119–121 (1970)

KOLORIMETRISCHE BESTIMMUNG DES HYDRAZINS MIT PHOSPHOMOLYBDOWOLFRAMSÄURE

A. ŞUTEU und CARMEN MANIU

von der Chemischen Fakultät der „Babeş-Bolyai"-Universität
Cluj, str. Arany Janos 11

Eingegangen am 3. Februar 1969

In vorliegender Arbeit wird gezeigt, daß Hydrazin in Mengen von 0,015–0,2 mg durch kolorimetrische Bestimmung der durch Reduktion der Phosphomolybdowolframsäure entstehenden blauen Farbe (Absorptionsmaximum bei λ = 75nm) bestimmt werden kann. Der Molextinktionskoeffizient für λ= 680 nm beträgt $\varepsilon = 2700$. Die blaue Verbindung wird aus 0,75–1,25 N H_2SO_4 Lösung mit n-Buthylalkohol extrahiert und kolorimetriert.

Zur kolorimetrischen Bestimmung des Hydrazins wurden verschiedene organischen Reagenzien benützt. Watt und Chrisp[1] bestimmen Hydrazin mit alkoholischer Dimethylazobenzaldehidlösung, wobei das intensiv rote *p*-Dimethylaminobenzaldazin entsteht, welches bei $\lambda = 458$ nm kolorimetriert wird. Durch dieselbe Reaktion bestimmen Freier und Resch [2] Hydrazinspuren in Wasser. Dombrauskos und Herbert [3] wenden zur Hydrazinbestimmung aus verschiedenen Materialien eine gegen die Wattsche etwas abgeänderte Methode an.

Riley [4] bestimmt Hydrazin mit 2, 4, 8-Trinitrochlorbenzol in $HCCl_3$, wobei das bei λ=494 nm kolorimetrierbare violette Hexanitrohydrazobenzol entsteht.

In vorliegender Arbeit wird die durch Reduzierung der Phosphomolybdowolframsäure entstandene blaue Verbindung kolorimetriert, und das Hydrazin bestimmt. Die Phosphomolybdowolframsäure wurde von Kokorin[5] synthetisiert und wir haben sie schon zur kolorimetrischen Fe^{2+} —Bestimmung benützt. [6]

---

[1] C. W. Watt und D. Chrisp, *Analyt. Chem.*, **24**, 2006 (1952).

[2] R. Freier und G. Resch, *Z. Analyt. Chem.*, **149**, 177 (1956).

[3] T. Dombrauskos und H. Herbert, *Ann. Ind. Hyg. Assoc. J.*, **23**, 151 (1962).

[4] J. P. Riley, *Analyst*, **79**, 76 (1954).

[5] H. A. Kokorin *Zhur. obshchei Khim.*, **26**, 1 (1956).

[6] A. Şuteu und C. Maniu *Rev. Roumaine Chim.*, **13**, 1201 (1968).

Es wurde festgestellt, daß die durch Reduktion der Phosphomolybdowolframsäure entstehende blaue Farbe stark pH-abhängig ist; daher war es nötig dessen Einfluß auf den Ablauf der Reaktion zu untersuchen.

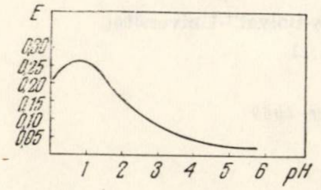

Abb. 1. — pH-Abhängigkeit der Extinktion der durch Reduktion der Phosphomolybdowolframsäure entstandenen blauen Verbindung.
Hydrazinkonzentration 0,5 g/l; Phosphomolybdowolframsäurekonzentration 0,8 g/l.

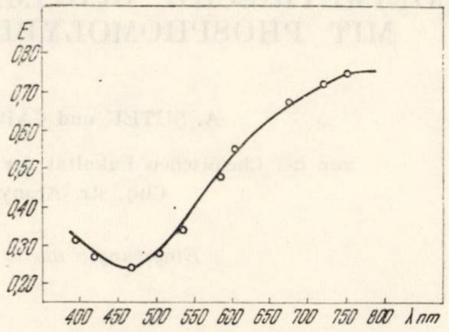

Abb. 2. — Absorptionskurve in n-Buthylalkohol.
Hydrazinkonzentration 0,09 mg; 25 ml n-Buthylalkohol; 4 ml 2% ige Phosphomolybdowolframsäure.

Abb. 1 zeigt die pH-Abhängigkeit der Extinktion von 0,5 g/l Hydrazin und 0,8 g/l Phosphomolybdowolframsäure enthaltenden Lösungen.

Der pH-Wert der Lösungen wurde mit 2N H_2SO_4 von 0 bis 6 eingestellt.

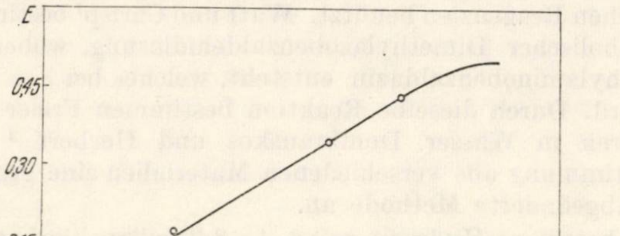

Abb. 3. — Anwendungsbereich des Lambert-Beerschen Gesetzes.

Aus Abb. 1 ist ersichtlich, daß maximale Extinktion bei pH = 1 erhalten wird. Weiter wurde die Zeitabhängigkeit der Reduktion der Phosphomolybdowolframsäure mit Hydrazin untersucht und festgestellt, daß sie bei Zimmertemperatur langsam abläuft. Erhitzt man aber auf siedendem Wasserbad, erhält man nach 8 Min. eine gleichbleibende Farbe, welche zur Stabilisation mit n-Buthylalkohol extrahiert wird. Dabei muß der Säuregehalt zwischen 0,75—1,25 N H_2SO_4 liegen. Für diese in n-Buthylalkohol extrahierte Farbe wurde die Absorptionskurve (siehe Abb. 2) aufgestellt, wobei der Hydrazingehalt 0,09 mg war und 4 ml 2%-ige Phosphomolybdowolframsäure benützt wurden.

Die blaue Verbindung wurde aus der 1 NH_2SO_4-Lösung mit 25 ml n-Buthylalkohol extrahiert. Wie ersichtlich, liegt das Absorptionsmaximum bei λ=750 nm. Die Absorptionsbestimmungen wurden mit einem Pulfrichphotometer durchgeführt.

Die Konzentrationsgrenzen, innerhalb welcher das Lambert-Beersche Gesetz gültig ist, mußten ebenfalls bestimmt werden. Die Daten sind in Abb. 3 dargestellt.

Aus Abb.3 ist ersichtlich, daß die in 25 ml n-Buthylalkohol befindliche Hydrazinmenge zwischen 0,015—0,2 mg liegen muß. Der Molextinktionskoeffizient wurde errechnet und beträgt $\varepsilon = 2700$ ($\lambda = 680$ nm).

ARBEITSWEISE

Die 0,015—0,2 mg Hydrazin enthaltende Lösung wird mit destilliertem Wasser auf 10 ml gebracht und mit H_2SO_4 auf pH = 1 eingestellt. Man gibt 4 ml 2% ige Phosphomolybdowolframsäure zu und erwärmt 8 Min. lang auf siedendem Wasserbad. Zur erkalteten Lösung werden 3 ml H_2SO_4 1 : 1 hinzugegeben und danach 2 malmit je 10 ml n-Buthylalkohol extrahiert. Wasserspuren werden aus dem Extrakt mit wasserfreiem Na_2SO_4 entfernt und durch Watte filtriert. Die so erhaltene Lösung wird auf 25 ml aufgefüllt, wonach in einer 0,5 cm Kuvette bei λ = 750 nm kolorimetriert wird.

Andere Reduktionsmittel wie Fe^{2+}, Sn^{2+}, Sb^{3+}, Hydroxylamin, Harnstoff, Askorbinsäure usw. stören die Hydrazinbestimmung mit Phosphomolybdowolframsäure.

SCHLUSSFOLGERUNGEN

In vorliegender Arbeit, wird gezeigt, daß das Hydrazin auf Grund seiner reduzierenden Einwirkung auf die Phosphomolybdowolframsäure auch kolorimetrisch bestimmt werden kann. Die Phosphomolybdowolframsäure wird reduziert und es entsteht eine Verbindung von blauer Farbe, welche mit n-Buthylalkohol extrahiert wird. So können 0,015—0,2 mg Hydrazin quantitativ bestimmt werden.

Revue Roumaine de Chimie, 15, 123–128 (1970)

THE EVOLUTION OF GASEOUS PRODUCTS DURING THE PHOTO-OXIDATIVE DEGRADATION OF POLYPROPYLENE

L. BALABÁN and L. PREISLER

Research Institute of Macromolecular Chemistry, Tkalcovská 2, Brno, Czechoslovakia

Received November 11, 1968

During the photo-oxidative degradation of polypropylene the evolution of gaseous products has been studied. The presence of acetaldehyde (Ac), acetone (An), propionic aldehyde (Pr), carbon monoxide (CMO), carbon dioxide (CDO) and methane has been determined by the chromatographic method. All the measurements have been carried out in the temperature range 75–90°. The following energies of activation have been found: $E_{\mathrm{Ac}} = 24.5$ kcal/mol, $E_{\mathrm{An}} = 34.3$ kcal/mol, $E_{\mathrm{Pr}} = 39.5$ kcal/mol, $E_{\mathrm{CMO}} = 31.8$ kcal/mol, $E_{\mathrm{CDO}} = 33.4$ kcal/mol.

INTRODUCTION

The oxidative degradation of polymers can be initiated by the heat, by an ultraviolet radiation, by a high energy radiation, by metal catalysts, or by mechanical scission of polymeric chains. One of the most important initiating reactions of the degradation of polypropylene is the photolytic generation of free radicals near the irregularities of the polymeric chain[1] which starts the autocatalytic oxidative degradation of the polymer. In recent works dealing with the photo-oxidative degradation of polypropylene the changes of the polymer solid phase were studied. The concentrations of carbonyl and hydroxyl bonds during the photo-oxidative degradation were determined by infrared spectroscopy. [2] In other papers the hydroperoxide concentration in the early stage of photo-oxidation [3] of the polymer and also the changes in infrared spectra of near infrared region were measured. [4] Other authors studied the oxygen absorption, [5,6] the influence of metals [7] and followed the inhibited photo-oxidative degradation in the presence of UV absorbers. [5,8–10]

[1] L. Balabán, Thesis, ČSAV, Prague, 1966.

[2] L. Balabán and J. Majer, *J. Polymer Sci.*, Papers presented at the Symposium on Macromolecular Chemistry, Brussels, 1967.

[3] K. Veselý, D. Ryšavý and L. Balabán, *Oesterr. Chem. Ztg.*, **67**, 154 (1966).

[4] A. A. Hitz and D. L. Beck, *Textile Res. J.*, **35**, 716 (1965).

[5] L. Balabán, *Chem. průmysl*, **13**, 45 (1963).

[6] M. B. Neiman, V. Ja. Efremov and B. V. Rozynov, *Plast. Massy*, **9**, *4* (1062).

[7] T. Takahashi and K. Suzuki, *Kobunshi Kagaku*, **21**, 494 (1964).

[8] A. F. Strobel and S. C. Catino, *Ind. Eng. Chem.*, **1**, 264 (1962).

[9] R. C. Hirt, N. Z. Searle and R. G. Schmitt, *Soc. Plast. Eng. Trans.*, **1**, 1 (1961).

[10] A. P. Pivovarov, Ju. A. Ershov and A. F. Lukovnikov, *Plast. Massy*, **10**, *7* (1966).

Our work deals with the problem of photo-oxidative degradation of polypropylene studied by the gaseous products analysis. The experimental results enabled us to propose the mechanism of the formation of these low molecular products.

EXPERIMENTAL

The atactic polypropylene used in our experiments has been isolated by propane extraction of a mixture of isotactic and atactic polymer prepared by the stereospecific polymerization. The atactic part of the polymer has been dissolved in hexane and stored under nitrogen at 0°. This polymer was defined by the following parameters: the average number molecular weight ($Mn = 5.6 \times 10^4$); the concentration of Ti ($Ti < 0.005$ %); the concentration of Al ($Al < 0.005$ %).

The foils needed for our measurement have been prepared by evaporating the solvent from the hexane polymer solution on glass plates, first on air and then under vacuum at room temperature. The thickness of the foils has been 10^{-2} mm when the homogeneous absorption of the sample can be assumed. The absence of the solvent in the foils has been controlled by the chromatographic method. The foils of atactic polypropylene have been irradiated in quartz tubes filled with pure oxygen at atmospheric pressure in the temperature range 75—90°. (The scheme of the apparatus used for the degradation processes has been described in a recent paper. [5]) The gaseous phase consisting of oxygen and of low molecular compounds as the products of the photo-oxidative degradation has been analysed by gas chromatography. Each volume of the gaseous mixture taken for analysis has been replaced by pure oxygen to keep the constant pressure. The analysis has been carried out using a special chromatograph developed in our institute equipped with a flame ionisation detector. For the separation of the components a column 1 m in length and 4.5 mm in diameter packed with Sterchamol (particle size 0.3—0.4 mm) containing 20% tris-[β-cyanoethoxy] propane was used. The flow rates of the carrier gas (nitrogen) were 50 cm^3/min. The products of the oxidative degradation were identified by comparing the retention times with published values[11,12] and also by checking the retention times with those obtained for model compounds, on three different columns containing Apiezon L, or didecylphthalate and/or tris-[β-cyanoethoxy]-propane. Carbon oxides and methane were separated, on the column packed with activated carbon. The detection of these components occurred as follows: after separating CO, CH_4 and CO_2, the components passed through an oven, where CO and CO_2 were hydrogenated on a nickel catalyst at 300° to methane,[13,14] which was detected by means of the flame ionization detector. Three peaks were observed which represented the concentration of CO, methane and CO_2. The quantitative calculation of the concentration of all components was made by measuring the peak area.

RESULTS

The analysis of the gas phase has shown the presence of acetaldehyde, propionaldehyde, acetone, methane, carbon monoxide and carbon dioxide. The increase of the concentration of all components with time in the tem-

---

[11] R. Kaiser, "Chromatographie in der Gasphase", Bibliographisches Institut, Mannheim, 1962.

[12] E. Bayer, "Chromatografija Gazov", Izdatelstvo Inostrannoj Literatury, Moscow, 1961.

[13] U. Schwenk, Hachenberg and M. Förederrenter, *Brennstoff-Chem.*, **42**, 295 (1961).

[14] K. Porter and D. H. Volman, *Analyt. Chem.*, **34**, 748 (1962).

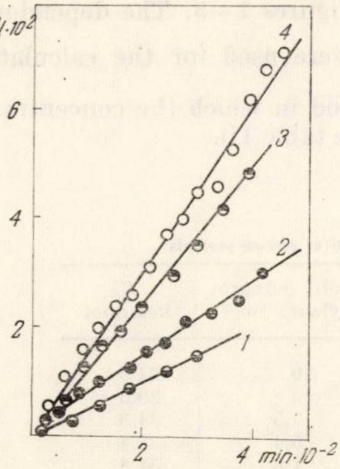

Fig. 1. — Evolution of acetaldehyde.
1, 75°; *2*, 80.4°; *3*, 85°; *4*, 90°.

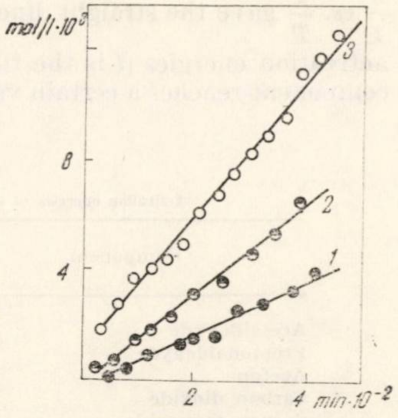

Fig. 2. — Evolution of propionaldehyde.
1, 80.4°; *2*, 85°; *3*, 90°.

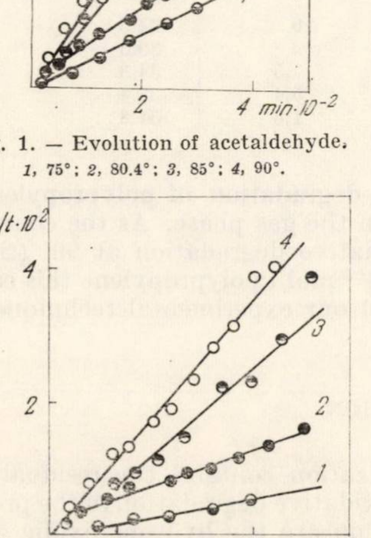

Fig. 3. — Evolution of acetone.
1, 75°; *2*, 80.4°; *3*, 85°; *4*, 90°.

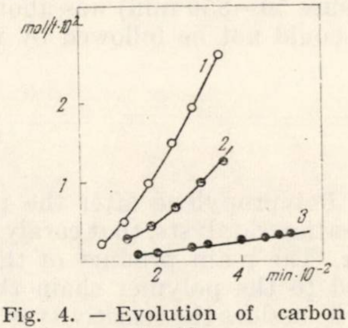

Fig. 4. — Evolution of carbon dioxide.
1, 90°; *2*, 85°; *3*, 75°.

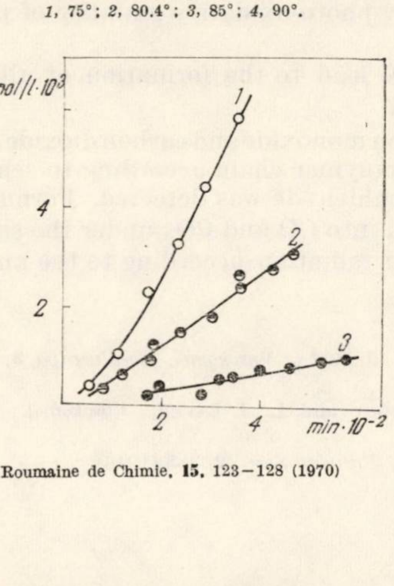

Fig. 5. — Evolution of carbon monoxide.
1, 90°; *2*, 85°; *3*, 75°.

perature range of 75— 90° is shown in figures 1—5. The dependences of $\log \frac{1}{t}$ *vs.* $\frac{1}{T}$ gave the straight lines and were used for the calculation of the activation energies (t is the time period in which the concentration of the component reaches a certain value (see table 1)).

Table 1

Activation energies of the formation of gaseous products

Component	mol/l polypropylene. 10^{-3}	E_a kcal/mol
Acetaldehyde	10	24.5
Propionaldehyde	3	39.5
Acetone	7,5	34.3
Carbon dioxide	5,4	33.4
Carbon monoxide	1,6	31.8

Contrary to the thermo-oxidative degradation of polypropylene [15,16] only traces of formaldehyde appeared in the gas phase. As the concentration of methane during the photo-oxidative degradation at 90° (time of exposure 50—350 min) was about 5×10^{-5} mol/l polypropylene this component could not be followed by means of our experimental technique.

DISCUSSION

Polypropylene after the polymerization contains the residual polymerization catalysts, that catalyze the oxidative degradation in the presence of air. The main product of this reaction are the hydroperoxidic groups bound to the polymer chain that are photolytically very easily splitted what is, besides the sensitivity of the polymer to the chain transfer reactions, one of the most important causes of low photo-oxidative stability of polypropylene.

The reaction paths denoted by X lead to the formation of alkoxy radicals that invoke the chain reaction.

Formaldehyde, acetaldehyde, carbon monoxide and carbon dioxide may form as a result of the splitting of the polymer chain according to scheme B. Only a small concentration of formaldehyde was detected. Formaldehyde is probably immediately converted into CO and CO_2 under the simultaneous action of oxygen and ultraviolet radiation according to the known radical mechanism. [17]

---

[15] D. Ryšavý, L. Balabán, V. Slavík and J. Růža, *Vysokomol. Soedineniya*, **3**, 1110 (1961).

[16] V. B. Miller, M. B. Neiman, V. S. Pudov and L. J. Lafer, *Vysokomol. Soedineniya*, **1**, 1696 (1959).

[17] D. W. G. Style and D. Summers, *Trans. Faraday Soc.*, **42**, 388 (1946).

The Reaction Scheme

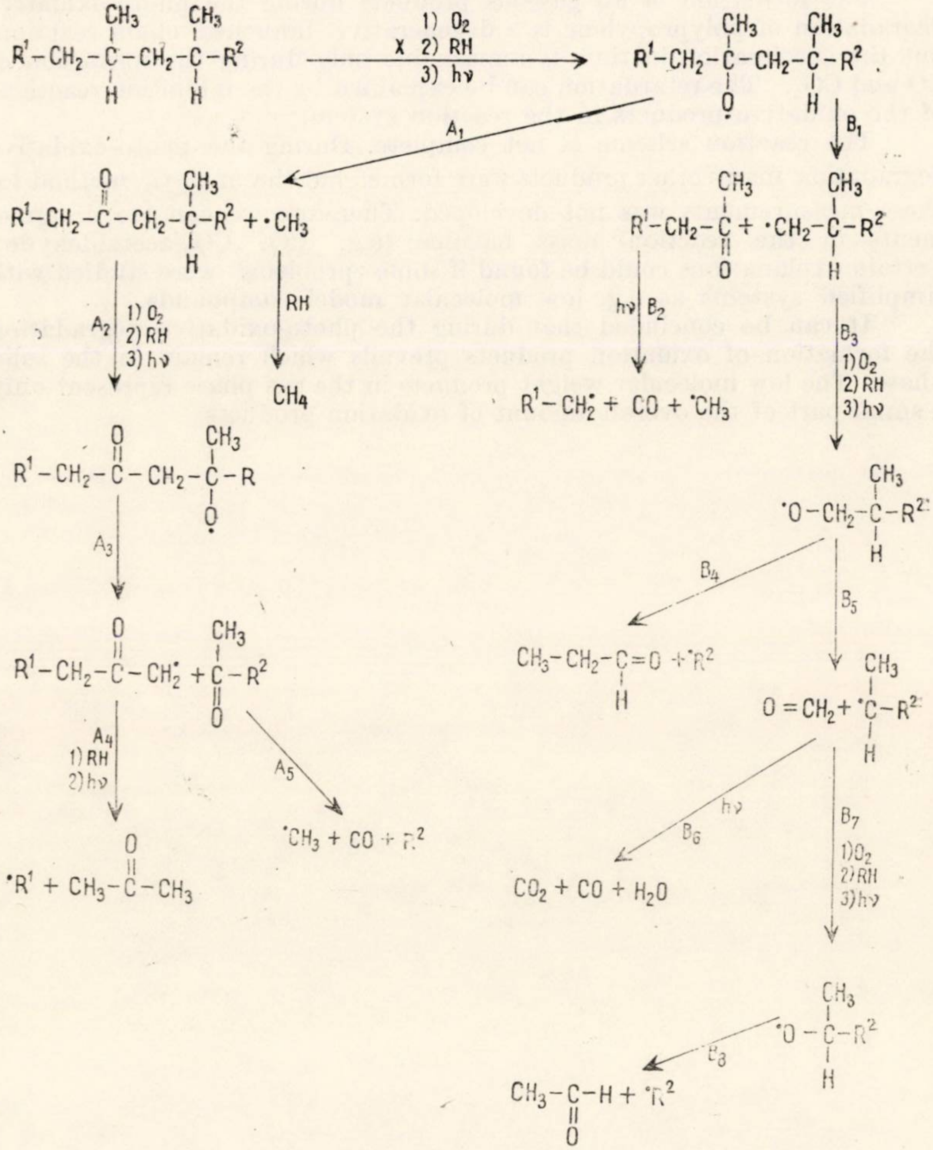
1) O2
2) RH
3) hν
X
A1
B1
RH
hν B2
A2
B3
A3
A4
1) RH
2) hν
A5
B4
B5
hν
B6
B7
B8

The reaction mechanism expressed by the reaction path A leads to the formation of methane, acetone or to the photolytic products according to the reaction A_5.

The formation of all gaseous products during the photo-oxidative degradation of polypropylene is a degenerative branched chain reaction, but the acceleration in time is remarkable only during the formation of CO and CO_2. The retardation can be explained by the inhibition reactions of the oxidative products in the reaction system.

The reaction scheme is not complete. During the photo-oxidative degradation many other products were formed but the analytic method for these measurements was not developed. Therefore we can see disagreements in the reaction mass balance (e.g. CO, CO_2/acetaldehyde). Certain explanations could be found if some problems were studied with simplified systems as e.g. low molecular model compounds.

It can be concluded that during the photo-oxidative degradation the formation of oxidation products prevails which remain in the solid phase. The low molecular weight products in the gas phase represent only a small part of the overall amount of oxidation products.

Revue Roumaine de Chimie, **15**, 129–134 (1970)

POLYHYDANTOÏNES-TRIAZINES

LEONIA STOICESCU-CRIVETZ, ELENA MĂNTĂLUŢĂ et I. ZUGRĂVESCU

Institut de Chimie Macromoléculaire «P. Poni» de l'Académie,
filiale de Jassy, 41A, Aleea Gr. Ghica Vodă

Reçu le 11 juin 1969

On a étudié la réaction des esters glyciniques de la *s*-triazine sur les isocyanates aromatiques et les conditions de cyclisation des uréido-esters formés, en hydantoïnes. Les poly-hydantoïnes-triazines obtenues, ont été caractérisées par les spectres en infrarouge, les analyses élémentaires et thermogravimétriques. Les polymères présentent un seuil de décomposition vers 300° à l'air. On peut tourner des films à partir d'une solution dans la N-méthylpyrrolidone.

Les possibilités offertes par les réactifs chlorotriaziniques pour préparer des polymères thermostables n'ont fait jusqu'à présent l'objet que d'un nombre limité de publications.[1–3]

Le chlorure de cyanuryle réagit par ses trois atomes de chlore avec les composés dont la structure présente un hydrogène mobile, comme les amines, les alcools. Nous avons mis à profit cette réactivité pour préparer de nouveaux dérivés de s.triazine qui pourraient nous conduire à des polymères thermostables. On a choisi le cycle triazinique à cause de sa haute stabilité thermique, due à sa symétrie moléculaire et à son aromaticité.[4] En effet la 2,4-dichloro-6-phényl-s.triazine réagit avec le glycinate de méthyle pour donner soit la 2,4-diglycinates-6-phényl-s.triazine (B) soit la 2-chloro-4-glycinate-6-phényl-s.triazine (A), suivant les conditions de réaction.

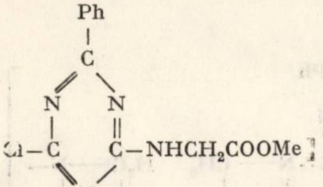

(A)

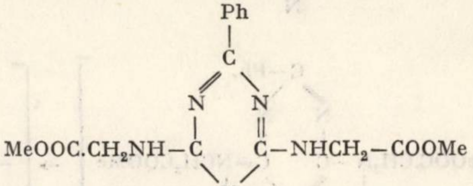

(B)

[1] H. K. Reimschuessel, A. M. Lovelace et E. M. Hagermann, *J. Polymer Sci.*, **40**, 270 (1959).

[2] R. Audebert et J. Néel, *J. Polymer Sci.*, *C*, **16**, 3245 (1968).

[3] G. F. Ehlers et J. D. Ray, *J. Polymer Sci.*, *A-1*, **4**, 1645 (1966), *J. Polymer Sci.*, *A-1*, **2**, 4989 (1964).

[4] D. R. Anderson et J. M. Holovka, *J. Polymer Sci.*, *A-1*, **4**, 1689 (1966).

Par l'addition de l'isocyanate de phényle sur le composé (B) il se forme tout d'abord un uréido-ester, réaction apparentée à celle de Wheeler et Hoffman [5] qui se transforme en hydantoïne par une conversion thermique ou par une conversion chimique, en utilisant un acide minéral comme catalyseur

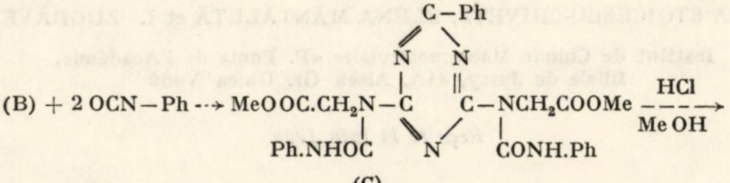
(B) + 2 OCN−Ph
MeOOC.CH₂N−C
C−Ph
N
N
C−NCH₂COOMe
Ph.NHOC
N
CONH.Ph
HCl
Me OH

(C)

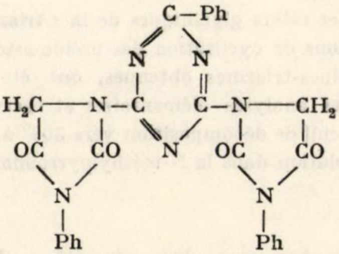
C−Ph
N
N
H₂C
N−C
C−N
CH₂
OC
CO
N
OC
CO
N
N
Ph
Ph

(D)

Nous avons essayé l'extension de cette réaction à la polycondensation de 2,4-diglycinester-6-phényl-s.triazine (B) avec les diisocyanates de dibenzyl (DIBB), diisocyanate de 2,4-tolyle(DIT) et diisocyanate de ditolyméthane (DITM). Nous avons obtenu des poly(hydantoïnes-triazines) d'après le schéma

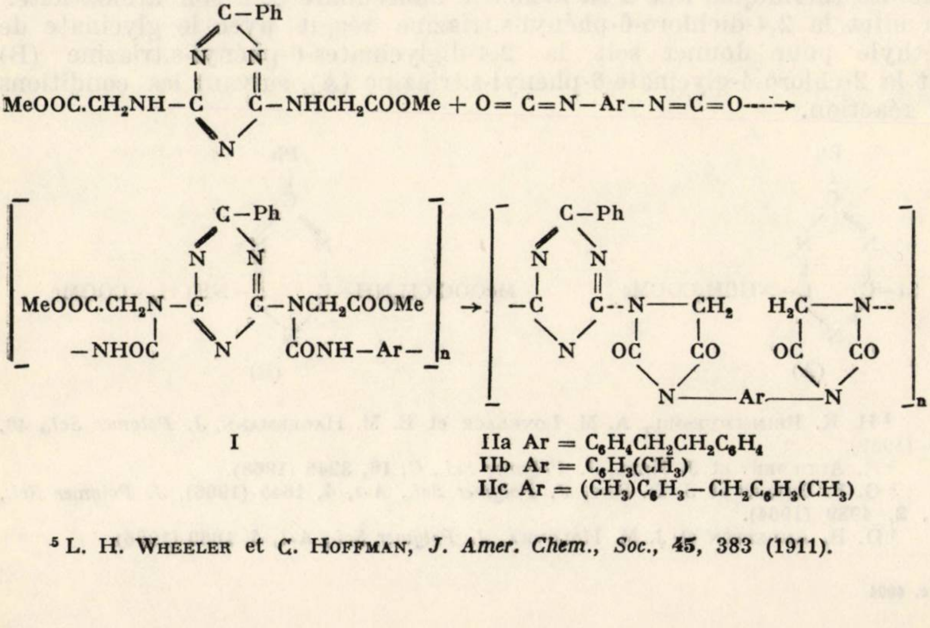
C−Ph
N
N
MeOOC.CH₂NH−C
C−NHCH₂COOMe + O=C=N−Ar−N=C=O
N
MeOOC.CH₂N−C
C−NCH₂COOMe
−NHOC
CONH−Ar−
n
−C
C−N
CH₂
H₂C
N
OC
CO
OC
CO
N
Ar
N
n

I

IIa Ar = $C_6H_4CH_2CH_2C_6H_4$

IIb Ar = $C_6H_3(CH_3)$

IIc Ar = $(CH_3)C_6H_3-CH_2C_6H_3(CH_3)$

---

[5] L. H. Wheeler et C. Hoffman, *J. Amer. Chem., Soc.*, **45**, 383 (1911).

RÉSULTATS ET DISCUSSIONS

Cette réaction de polyaddition-cyclocondensation a été récemment étudiée pour la préparation des polyhydantoïnes aromatiques, par fusion des réactifs, en l'absence de solvant [6] et en solution de *méta*-crésol.[7] Dans le cas des composés de s.triazine, il nous a été impossible d'atteindre des degrés de condensation plus élevés en utilisant comme solvant le *m*-crésol. En chauffant des quantités équimoléculaires de (B) et de diisocyanates dans une solution de N-méthylpyrrolidone (NMP), à 50°, sous atmosphère inerte, on obtient en première étape un prépolymère de type uréido-ester triazinique (I), ayant une viscosité inhérente de 0,29 et une stabilité thermique plus faible par rapport aux polyamides aromatiques. Cette stabilité devrait se trouver augmentée par la transformation du polyurée-ester en un système dont les atomes azote ne soient plus liés à des hydrogènes. Dans ce sens, le chauffage ultérieur de la solution de polyuréido-ester en NMP, en présence de l'acide chlorhydrique comme catalyseur, produit la hétérocyclisation, conduisant à une polyhydantoïne-triazine (II). On peut diriger la réaction sans la séparation du prépolymère. La conversion de polyuréido-ester en polyhydantoïne a été suivie spectrophotométriquement, par la disparition des bandes d'absorption (NH) à 3330 cm^{-1} et -(C-O-C) à 1190 et 1018 cm^{-1} qui sont caractéristiques pour les uréido-esters et l'apparition dans les spectres en IR des bandes 4-oxo et 2-oxo dans les régions 1780 cm^{-1}, respectivement 1698—1720 cm^{-1} ,attribuées au cycle hydantoïnique.[8] L'examen des spectres en IR montre qu'après les opérations subies, la cyclisation en hydantoïne n'est pas achevée, et que l'on est en présence d'un mélange de polyurée-esters et polyhydantoïnes. Par un traitement thermique supplémentaire de 3—4 h à 200°, sous vide, la réaction d'hétérocyclisation en polyhydantoïnes est terminée. Ce fait est confirmé par les analyses élémentaires et l'examen des spectres en IR des polymères préparés, qui sont comparables au spectre de la hydantoïne (D) préparée comme modèle.

PROPRIÉTÉS DES POLYMÈRES

Les polyhydantoïnes II, obtenues dans ce travail, sont des solides blancs ou très légèrement teintés en jaune, insolubles dans les solvants polaires tels que : diméthylformamide, diméthylacétamide, diméthylsulfoxyde. Ils sont solubles dans l'acide sulfurique et dans le N-méthylpyrrolidone (NMP), contenant 3% LiCl. De cette solution on peut obtenir par évaporation des films transparents.

Des indications relatives au poids moléculaire des polymères ont été obtenues en mesurant à 20° les viscosités inhérentes ($\eta_{\text{inh}}^{20°}$) des divers

[6] R. H. Sallé, B. Sillion et G. de Gaudemaris, *J. Polymer Sci.*, *A-1*, **4**, 2903 (1966) ; *Bull. Soc. chim. France*, **1968**, 3378.

[7] Y. Imai, *J. Polymer Sci.*, *A-1*, **5**, 2289 (1967).

[8] J. Derkosch, *Monatsh.*, **92**, 361 (1961).

échantillons en NMP avec 3 % LiCl. Comme on peut le voir sur le tableau 1, le polymère IIb présente la viscosité inhérente la plus petite. La difficulté d'obtenir un poids moléculaire plus grand s'explique par la grande différence de réactivité des deux fonctions isocyanates du diisocyanate de 2,4-toluène, cette différence étant due à l'effet stérique du méthyle.[9] La vitesse de réaction de cette fonction sur le groupement N-aminoacétate de la s.triazine est très faible, la réaction de polycondensation procède lentement, nécessitant un chauffage prolongé.

Tableau 1

Caractéristiques des poly-(hydantoïnes-triazines) II

N°	Ar	P. Fus. 0°	η inh. Conc 0,5 %	Analyses						A.T.G. perte en poids %	
				C %		H %		N %			
				Calculé	Trouvé	Calculé	Trouvé	Calculé	Trouvé	300°	400°
Ia	$C_6H_4CH_2CH_2C_6H_4$	315 décomp.	0,29					16,46	15,99		
IIa	$C_6H_4CH_2CH_2C_6H_4$	360	0,42	65,52	64,30	4,98	5,05	18,44	16,54	17,9	35,8
IIb	$-C_6H_3(CH_3)-$	310	0,15	59,86	60,30	3,42	3,73	22,21	18,34	17,6	43,4
IIc	$-(CH_3)C_6H_3CH_2C_6H_3(CH_3)$	340	0,29	66,04	67,95	4,25	4,48	17,97	15,95	11,8	29,0

La stabilité thermique des produits II a été étudiée par thermogravimétrie, en opérant sur des prises d'essais préalablement pulvérisés

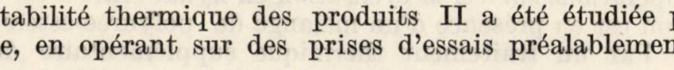

Fig. 1. — Stabilité thermique des polymères. II.

——— Polyhydantoïne IIa; – – – Polyhydantoïne IIb; —·—·— Polyhydantoïne IIc.

---

[9] L. L. Ferstandig et R. A. Scherrer *J. Amer. Chem. Soc.*, **81**, 4838 (1959).

et en réglant la vitesse d'élévation de la température à 6° par minute. Les échantillons commencent généralement à se décomposer vers 300° à l'air. Les courbes de stabilité des polymères sont portées sur la figure 1. On constate que les polyhydantoïnes présentent une stabilité thermique inférieure aux autres polyhétérocycles. Probablement le cycle hydantoïnique subit lui-même une décomposition, à cause de son aromaticité plus faible.

PARTIE EXPÉRIMENTALE

Monomères et produits intermédiaires

La 2,4-dichloro-6-phényl-s.triazine a été préparée selon le procédé de Fairfull [10] et contrôlée par son analyse et son point de fusion à 121°.

2-chloro-4-(méthoxycarbonylméthyl)N-amino-6-phényl-s.triazine. (*A*) A une suspension de 2,4-dichloro-6-phényl-s.triazine 3g dans 10 ml dioxanne et 10 ml eau, refroidie à 0°, on ajoute le chlorhydrate de glycinate de méthyle (1,65 g) dissous dans 10 ml eau. On ajoute ensuite sous agitation une solution d'hydroxyde de sodium (1,15 g dans 15 ml eau) en maintenant la température au-dessous de 5°. On chauffe à 50° pendant 4 h. Après refoidissement le produit séparé est filtré, lavé à l'eau, séché.

P. Fus. 153° (éthanol).

$C_{12}H_{11}ClN_4O_2$ (278,69)

Calculé : C 51,71 ; H 3,97 ; N 20,10 %

Trouvé : C 51,65 ; H 4,07 ; N 20,58 %

2,4-bis (méthoxycarbonylméthyl)N,N-diamino-6-phényl-s.triazine (*B*). A une suspension de 2,4-dichloro-6-phényl-s.triazine (2g) dans 10 ml dioxanne et 15 ml eau à 0° on ajoute le chlorhydrate de glycinate de méthyle (2,22 g) dissous dans 10 ml eau. On agite pendant 30 minutes, on ajoute 10 ml pyridine, en maintenant l'agitation à la température ambiante pendant 4 h. On chauffe à 90° − 95° pendant 6 h. Après refroidissement on filtre le produit cristallin séparé. P. Fus. =270° (acide acétique). Rendement 67 %.

$C_{15}H_{17}N_5O_4$ (331,32)

Calculé : C 54,36 ; H 5,17 ; N 21,13 %

Trouvé : C 54,27 ; H 5,05 ; N 21,04 %

Absorption IR 1740 (C = O), 1026 (C − O − C) 3247 (NH)

2,4-bis (phényl-3'-imidazolidinedione-2,4)yl-1,1,6-phényl-s.triazine (*D*). Dans un ballon maintenu sous atmosphère inerte et muni d'un agitateur, d'une arrivée de gaz et d'un réfrigérant ascendant on mélange 1g de (B) avec l'isocyanate de phényle (0,71 g) dans 10 ml métacrésol. Ce mélange est agité et chauffé 5 h à 50°, sous courant d'azote. On ajoute 1 ml acide chlorhydrique dans 10ml *m*-crésol et on continue l'agitation pendant 7h à 50°. On verse le contenu dans un excès d'éthanol. Le produit solide séparé est filtré, lavé à l'éthanol et séché sous vide à 100°. On obtient 0,95 g.P. Fus.= 290°.

$C_{27}H_{19}N_7O_4$ (505,47)

Calculé : C 64,15 ; H 3,80 ; N 19,39 %

Trouvé : C 64,44 ; H 3,83 ; N 19,22 %

Absorption IR : 1798 cm^{-1} et 1727 cm^{-1} (C = O) hydantoïne

---

[10] A. E. Fairfull et D. A. Peak, *J. Chem. Soc.*, **1955**, 803.

Polymérisation

Nous avons utilisé comme monomère triazinique pour la réaction de polyaddition-cyclocondensation le produit (B) et les diisocyanates de dibenzyl, de 2,4-tolyle et de ditolyméthane, qui ont été purifiés par distillation sous pression réduite.

La réaction de polyaddition en solution a été effectuée en chauffant des quantités équimoléculaires de réactifs à 50° dans la N-méthyl-pyrrolidone, sous atmosphère inerte, pendant plusieurs heures. L'hétérocyclisation des polyuréido-esters obtenus dans la première étape a été effectuée par chauffage de la solution des esters dans NMP en présence de l'acide chlorhydrique. Les polymères sont isolés par précipitation dans l'éthanol, filtrés, lavés à l'éthanol puis portés à poids constants par chauffage sous vide.

Les principales caractéristiques des produits obtenus sont indiquées dans le tableau 1. Nous donnons à titre d'exemple la préparation du polymère IIa.

Polyhydantoïne-triazine IIa

Un ballon à trois tubulures est muni d'un agitateur et d'une arrivée de gaz. Il est purgé de son air et sera maintenu sous atmosphère inerte pendant toute la durée de la réaction par un fort courant d'azote sec. On mélange dans le ballon 1 g (B) et 0,79 g (DIDB) en 10 ml (NMP) à 50°. On agite pendant 7 h à cette température. Le mélange devient visqueux. On le verse dans l'éthanol, on filtre le produit séparé, on lave plusieurs fois à l'éthanol, on sèche sous vide. Le prépolymère est une poudre blanche, soluble dans les DMF, DMA, DMSO. Il se décompose vers 300°.

$C_{31}H_{29}N_7O_6$ (595,59)
Calculé : N 16,46 %
Trouvé : N 15,99 %
Absorption IR : 3330 cm^{-1} (NH), 1745 cm^{-1} (C = O), 1195 et 1018 cm^{-1} (—C—O—C—)

Pour la cyclisation en polyhydantoïne on met dans le ballon le prépolymère avec 10 ml NMP, on ajoute 1 ml acide chlorhydrique et on agite à 50° pendant 6 h ; la solution est transparente. On verse dans 100 ml éthanol et le produit séparé est filtré, lavé à l'éthanol, séché sous vide.

Par un traitement thermique ultérieur de 4 h à 200° sous vide, on achève la cyclisation.

$C_{29}H_{21}N_7O_4$(531,51)
Calculé : C 65,52 ; H 4,98 ; N 18,44 %
Trouvé : C 64,30 ; H 5,05 ; N 16,54 %
Absorption IR : 1770 cm^{-1} et 1710 cm^{-1} (C= O hydantoïne)

Pour les polymères IIb, IIc on n'a pas séparé la phase intermédiaire.

Les spectres en IR ont été enregistrés à l'aide d'un spectrophotomètre Unicam 100, les échantillons étant dispersés dans le bromure de potassium.

Les viscosités inhérentes ont été mesurées à 20° pour des concentrations de 0,5 % dans le NMP et 3 % LiCl.

Les courbes de stabilité thermique ont été enregistrées à l'aide d'un dérivatographe F. Paulik, pour une montée en température de 6° par minute.

Revue Roumaine de Chimie, **15**, 135–138 (1970)

ON THE SYNTHESIS OF 3-NITRO-10-METHYL-PHENOTHIAZINE

I. OPREAN, C. BODEA and V. FĂRCĂŞAN
Institute of Chemistry of the Academy, Str. Donath 59–65, Cluj

Received April 21, 1969

The nitration of 10-methyl-phenothiazine, (I), with HNO_3 (d = 1.42) is accompanied by oxidation at the level of the sulfur atom. The only reaction product is 3-nitro-10-methyl-phenothiazine-5-oxide, (III), which forms by recrystallization from benzene a molecular combination containing 1/2 mole benzene. 3-Nitro-10-methyl-phenothiazine, (II), was prepared by condensation of *o*-methyl-aminothiophenol, (VI), with 2,4-dinitro-chlorobenzene, (VII).

★

The synthesis of 3-nitro-10-methyl-phenothiazine, (II) is of particular interest for the preparation of stable amino-phenothiazines, with the amino group located in *para* position to the nitrogen atom, amines used as intermediary products in the preparation of other phenothiazine derivatives. There is a confusion in the literature about the preparation and the properties of this nitro-derivative.

The nitration of 10-methyl-phenothiazine, (I) was first carried out by Schmalz and Burger [1] who stated that by the action of HNO_3(d = =1.42), 3-nitro-10-methyl-phenothiazine (II) is formed. After recrystallization from benzene the product is described as yellow crystals, m.p. 119–120°. Repeating these experiments Skorodumov et al.[2] reported that under the above mentioned conditions a mixture of two yellow substances is obtained, one of them showing the m.p. indicated by Schmalz and Burger, and considered as II, and another with m.p. 176–177° which is 3-nitro-10-methyl-phenothiazine-5-oxide (III).

A great amount of nitration reactions of phenothiazine derivatives carried out in our laboratory using HNO_3 of various concentrations under different conditions [3] led us to the conclusion that the nitration with HNO_3 is always accompanied by oxidation at the level of the sulfur bridge, leading to 5-oxides or even to 5,5-dioxides .[4] It has been also observed that the mono- and dinitro-derivatives which are not oxidated at the level of the sulfur atom, compounds obtained by methods other than nitration with HNO_3, are dark-brown. The yellow colour is, in exchange, a common feature of all the nitro-5-oxides of phenothiazine.

---

[1] A. C. Schmalz and A. Burger, *J. Amer. Chem. Soc.*, **76**, 5458 (1954).

[2] V. A. Skorodumov, E. N. Ilitschenko and S. V. Juravlev, *Zhur. obshchei Khim.*, **30**, 1680 (1960).

[3] C. Bodea, V. Fărcăşan, I. Oprean, *Studii şi Cercetări Chim.* Acad. R.P.R. – Fil. Cluj, **14**, 173 (1963) ; *Chem. Abstr.*, **61**, 16067h (1964).

[4] G. P. Brown, J. W. Cole and T. I. Crowell, *J. Org. Chem.*, **20**, 1772 (1955).

These reasons determined us to reinvestigate the nitration of 10-methyl-phenothiazine under the conditions described by Skorodumov et al.[2]

Observing by means of a Boetius microscope the behaviour on melting of the product with m.p. 119–120°, obtained by recrystallization from benzene, we noted that at 96° the crystals begin to change shape and at 120° a homogeneous mass is formed. Gradual growing of new crystals takes then place and these crystals show finally a sharp m.p.179–180°.

If the product with m.p. 119–120° is recrystallized from aqueous acetic acid the substance with m.p. 176–177° (capillary) is obtained. When the melting of this substance is observed by means of Boetius microscope, melting occurs at 179–180°, without any foregoing transformation. On recrystallizing from benzene, this product is transformed into the compound with m.p. 119–120°.

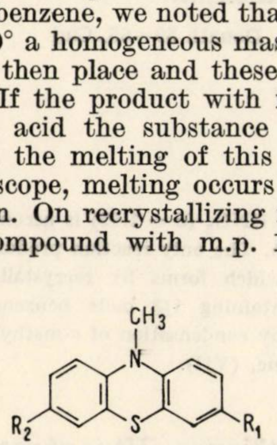

$I : R_1 = R_2 = H$
$II : R_1 = NO_2 ; R_2 = H$
$IV : R_1 = NO_2 ; R_2 = Cl$

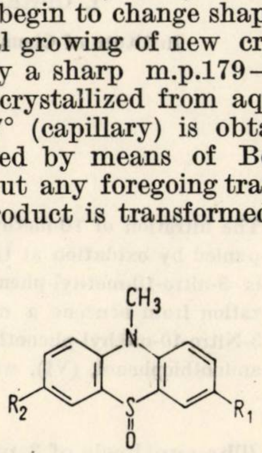

$III : R_1 = NO_2 ; R_2 = H$
$V : R_1 = R_2 = H$

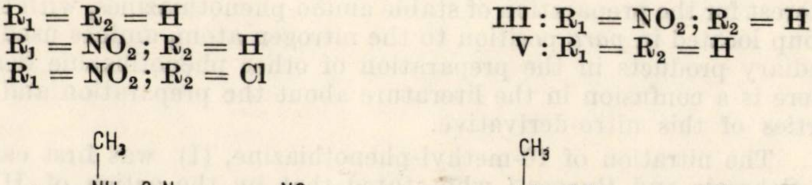

Both substances show, by thin-layer chromatography, the same R_f, they present identical UV spectra, in their IR spectra the band assigned to ν_{SO} appears at 1040 cm^{-1} and under the action of concentrated HCl they are converted into 3-nitro-7-chloro-10-methyl-phenothiazine (IV).[3]

This behaviour suggests that we have to do with two forms of the same substance as in the case of 10-methyl-phenothiazine-5-oxide (V). Polymorphism of V has already been reported.[4]

The thermogravimetrical analysis of the product with m.p. 119–120° proved that this substance is the 3-nitro-10-methyl-phenothiazine-5-oxide, (III), crystallized with 1/2 mole benzene (see fig. 1).

It is worth mentioning that the proportion of carbon and hydrogen of the 5-oxide, (III), crystallized with 1/2 mole benzene (C % 61.33, H% 4.19) is close to that of 3-nitro-10-methyl-phenothiazine (II), (C % 60.45, H % 3.91) a fact which may account for the confounding of the two substances.

To remove any doubt about the products under consideration, we carried out an independent synthesis of 3-nitro-10-methyl-phenothiazine, (II), using *o*-methylamino-thiophenol (VI) and 2,4-dinitro-chlorobenzene (VII) as starting materials. The 2,4-dinitro-diphenylsulfide, (VIII), thus obtained, was cyclized *via* the Smiles rearrangement [5] to II. The product of this reaction, melting at 145—146° has, as expected, not the yellow colour characteristic of phenothiazine-5-oxides, but a red one. The characteristic differences between phenothiazines and the corresponding 5-oxides,[6] can be observed by comparing the spectra of II and III in the region 250—700 mμ. Finally, II was converted by oxidation into III, which was found identical in all respects with the product obtained by nitration with HNO_3.

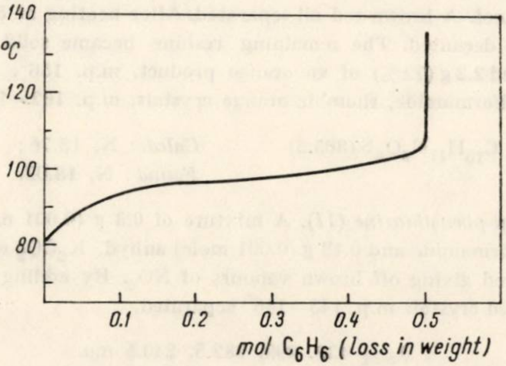

Fig. 1. — Thermogram of compound with m. p. 119—120°.

In experiments aiming at obtaining II by nitration of 10-methyl-phenothiazine using $Cu(NO_3)_2$ in acetic anhydride, a method successfully applied to prepare nitrothiophenes,[7] the oxidation at the level of the sulfur atom could not be avoided, the reaction product being the 5-oxide III.

Further studies shall supply more information about the tendency of nitroderivatives of phenothiazines to form molecular combinations with aromatic hydrocarbons.

EXPERIMENTAL

Nitration of 10-methyl-phenothiazine (I) was performed according to Skorodumov et al.[3]

Thin-layer chromatography of the two forms of III was carried out on Silicagel G, using as solvent for the substance toluene, and the system toluene-ethanol 3 :1, as eluent ; identical R_f (0.61) was obtained for both forms.

[5] Kiichi Fujii, *J. Pharm. Soc. Japan*, **77**, 3 (1957) ; *Chem. Abstr.*, 51, 8756 (1957).

[6] R. J. Warren, I. B. Eisdorfer, W. E. Thompson and J. E. Zarembo, *J. Pharm. Sci.*, **55**, 144 (1966).

[7] S. Gronowitz and N. Gjos, *Acta Chem. Scand.*, **21**, 2855 (1967).

IR spectra of the two forms of III recorded on a double beam spectrophotometer, Carl Zeiss Jena, type UR-10, in KBr pellets show: ν_{SO} 1035 cm^{-1}, ν_{NO_2} 1335 and 1510 cm^{-1}.

Electronic spectra of the two forms of III, recorded in chloroform on a DK-2A Beckmann spectrophotometer show bands at λ_{max} 362, 286.7, 254 (shoulder), and 228.5 mμ.

2.4-Dinitro-2'-methylamino-diphenylsulphide (VIII). 1.4 g (0.4 mole) *o*-Methylaminothiophenol, (VI) and 0.23 g Na (0.01 mole) were mixed in 3 ml absolute ethanol. The resulted Na salt of VI was added to a solution of 2.02 g (0.01 mole) 2.4-dinitrochloro-benzene (VII) in 14 ml absolute ethanol. A brown-red oil separated. After heating at 50—60° for 1 hour the ethanolic solution was decanted. The remaining residue became solid on standing. Maceration with ethanol yielded 2.2 g (72%) of an orange product, m.p. 156°. After recrystallization from aqueous dimethylformamide, rhombic orange crystals, m.p. 162—163°.

$C_{13}H_{11}N_3O_4S$ (305.3) *Calcd.*: N, 13.76;
Found: N, 13.02.

3-Nitro-10-methyl-phenothiazine (II). A mixture of 0.3 g (0.001 mole) diphenylsulphide, (VIII), 2 ml dimethylformamide and 0.13 g (0.001 mole) anhyd. K_2CO_3 were boiled for 20 min. The solution became red giving off brown vapours of NO_2. By adding 2—3 drops of water, 0.22 g (yield 88%) of red crystals m.p. 145—146° separated.

λ_{max} 422, 299, 282.5, 240.5 mμ
IR spectrum ν_{SO} absent
ν_{NO_2} 1325 and 1508 cm^{-1}

$C_{13}H_{10}N_2O_2S$ (258.3) *Calcd.*: N, 10.85;
Found: N, 11.05.

Oxidation of 3-nitro-10-methyl-phenothiazine (II). To 0.1 g II a cooled mixture of HNO_3 (d = 1.4) and acetic acid 1 : 1 was added in drops till the red colour of the solution became yellow. Then the mixture was poured immediately into water. By salting out the mixture with sodium acetate and keeping it overnight 0.07 g yellow crystals separated. Mixed m. p. with 3-nitro-10-methyl-phenothiazine-5-oxide (III) obtained by nitration of 10-methyl-phenothiazine (I) showed no depression.

By boiling III in concentrated HCl orange-red crystals, identical with 3-chloro-7-nitro-10-methyl-phenothiazine[3] (m. p. 188—189°) were obtained.

Nitration of 10-methyl-phenothiazine (I) with $Cu(NO_3)_2$ in acetic anhydride. 1.2 g powdered $Cu(NO_3)_2 \cdot 3H_2O$ (0.005 mole) were suspended in 7 ml acetic anhydride by stirring and cooling with ice.

A solution of 2.13 g (0.01 mole) 10-methyl-phenothiazine (I) in 40 ml acetic anhydride were added, under continuous stirring and cooling. The mixture was allowed to stand for 2 hours at room temperature, then filtered and the filtrate poured into water. After removal of the supernatant the brown resinous product became solid. Recrystallization from benzene-glacial acetic acid yielded 1 g (36%) 3-nitro-10-methyl-phenothiazine-5-oxide, (III), m.p. 174—176°. The mixed m.p. with the product obtained by nitration with nitric acid in acetic acid showed no depression.

La REVUE ROUMAINE DE CHIMIE paraît 12 fois par an. Le prix d'un abonnement annuel est de: £ 5.0.0; $ 12,—; FF 60,—; DM 48,—. Toute commande de l'étranger (fascicules ou abonnements) sera adressée à CARTIMEX, Boîte postale 134—135, Bucarest, Roumanie, ou à ses représentants à l'étranger.

R.P. d'ALBANIE, Ndermarja Shtetnore e Botimeve Tirana; R.D. ALLEMANDE, Deutscher Buch Export und Import Leipzig, 701, Leninstrasse 16; R.P. de BULGARIE, Hemus, Place Slaweikov, 11, Sofia; R. P. de CHINE, Waiwen Shudian P. O. B. 88, Peking; R.P.D. CORÉENNE, Chulphanmul, Phenian; RÉPUBLIQUE CUBA, Cubartimpex Simon Bolivar 1, Palacio Aldamo, Habana; R.P. HONGROISE, Kultúra, P.O.B. 149, Budapest 62; R.P. MONGOLE, Mongolgosknigotorg, Ulan Bator; R. P. de POLOGNE, Ruch Ul. Wronia 23, Warszawa; R.S. TCHÉCOSLOVAQUE, Artia, Ve Smeckach 30-Praha II; U.R.S.S., Mejdunarodnaia Kniga, Moskva G-200; R. D. du VIETNAM, So Xuat Nhap Khau Sach Bao, 32 Hai Ba Trung, Hanoi; R.S.F. de YOUGOSLAVIE, Jugoslovenska Knjiga Terazije 27, Belgrad; Prosveta 16/1, Terazije, Belgrad; Forum Voïvode Misica, Novi Sad; ARGENTINE, Editorial Sudaminter S.A., Alsina 500, Buenos Aires; AUSTRALIE, Current Books Ltd. Distributors 168—174, Day Street Sydney; AUTRICHE, Globus Zeitungs Drucks und Verlagsanstalt GmbH. 1200, Wien, Höchstädplatz 3; BELGIQUE, Du Monde Entier 5, Place St. Jean-Bruxelles, Agence Messageries de la Presse 14—22, Rue du Persil, Bruxelles; CANADA, Progress Books 44 Stafford St. Toronto, Ontario, W.M. Dawson Subscriptions Service Ltd., Six Thorneliffe Park Drive, Toronto 17, Ontario; COLOMBIE, Liberia Buchholz Galeria, av. Jiménez de Quesada 8—40 Bogotá; DANEMARK, Ejnar Munksgaard, Noregade 6, Kopenhavn; ESPAGNE, Libreria Herder, Calle de Balmés 26, Barcelona 7; ÉTATS-UNIS, Fam Book Service 69, Fifth Avenue, Suite 8 F., New York, 10003 N. Y.; Continental Publications, 111, South Mermanec Ave., St. Louis Missouri 63105; Turner Subscription Agency 235, Park Avenue South, New York 3 N. Y.; FINLANDE, Akateeminen Kirjakauppa P.O.B. 10128, Helsingfors, 10; FRANCE, Nouvelles Messageries de la Presse Parisienne, 111, Rue Rémur, Paris II, Europériodiques S.A. 72. Boul, Senard, 22 Saint Cloud; GRANDE-BRETAGNE, Collet's Holdings Ltd. Dennington Estate, Weillingborough, Northants Central Books Ltd. 37, Inn Road London W.c. 1; ISRAËL, Lepac Ltd., P.O.B., 1136 Tel-Aviv; Haiflepac Ltd. P.O.B. 1794, Haifa; ITALIE, So. Co. Lib. Ri. Piazza Margana 33 — Roma; Messagerie Italiane Sp. A. Milano, Via Priv. Renzo e Lucia 7. JAPON, Nauka Ltd. 30—19 Minami — Ikebukuro 2 chome Toshima Ku, Tokyo; PAYS—BAS, N. V. Martinus Nijhoff, P.O.B. 269, Den Haag; Swetz & Zeitlinger, Keizersgracht 471—487, Amsterdam C.; NORVÉGE, Tryggve Juul Moller—Boekhandel Øvre Slottsgate 15 Oslo 1; R.F. d' ALLEMAGNE, Kubon & Sagner, P.O.B. 68, München 34; Presse Vertriebsgesellschaft GmbH 6, Frankfurt/Main Börsenstrasse 13—15; Kunst und Wissen, Erich Biber P.O.B. 46, 7000 Stuttgart 1; SUISSE, Pinkus & Cie Froschaugasse 7 Zürich, Fachbücherei Berne, P.O.B. 397, 3001 Berne.

En Roumanie vous pourrez vous abonner par les bureaux de poste, chez votre facteur ou directement par les services de presse des entreprises et institutions.

La REVUE ROUMAINE DE CHIMIE paraît 12 fois par an. Le prix d'un abonnement annuel est de: £ 5.0.0; $ 12.–; Fr 60.–; DM 48.–. Toute commande de l'étranger (fascicules ou abonnements) sera adressée à CARTIMEX, Boîte postale 134–135, Bucarest, Roumanie, ou à ses représentants à l'étranger.

R.P. d'ALBANIE, Ndermarja Shtetnore e Botimeve Tirana; R.D. ALLEMANDE, Deutscher Buch-Export und Import, Leipzig 701, Leninstrasse 16; R.P. de BULGARIE, Hemus, Place Slaveikov, 11, Sofia; R.P. de CHINE, Waiwen Shudian P.O.B. 88, Peking; R.P.D. CORÉENNE, Chulphanmul, Phenian; RÉPUBLIQUE CUBA, Cubartimpex Simon Bolivar 1, Palacio Aldama, Habana; R.P. HONGROISE, Kultura, P.O.B. 149, Budapest 62; R.P. MONGOLE, Mongolgosknigotorg, Ulan Bator; R.P. de POLOGNE, Ruch Ul. Wronia 23, Warszawa; R.S. TCHÉCOSLOVAQUE, Artia, Ve Smeckach 30, Praha 2; U.R.S.S., Mejdunarodnaia Kniga, Moskva G-200; R.D. du VIETNAM, So Xuat Nhap Khau Sach Bao, 32 Hai Ba Trung, Hanoi; R.S.F. de YOUGOSLAVIE, Jugoslovenska Knjiga Terazije 27, Beograd; Prosveta 16, Terazije, Beograd; Forum Vojvode Misica, Novi Sad; ARGENTINE, Editorial Sudamericana S.A., Alsina 500, Buenos Aires; AUSTRALIE, Current Books Pty. Distributors 185–174, Day Street Sydney; AUTRICHE, Globus Zeitungs Druck und Verlagsanstalt GmbH., 1200, Wien, Höchstädtplatz 3; BELGIQUE, Du Monde Entier 5, Place St. Jean Bruxelles, Agence Messageries de la Presse 14–22, Rue du Persil, Bruxelles; CANADA, Progress Books 44 Stafford St. Toronto, Ontario, W.M. Dawson Subscriptions Service Ltd. Six Thorncliffe Park Drive, Toronto 17, Ontario; COLOMBIE, Libreria Buchholz Galeria, av. Jiménez de Quesada 8–40 Bogotá; DANEMARK, Ejnar Munksgaard, Nörregade 6, Kopenhavn; ESPAGNE, Libreria Herder, Calle de Balmes 26, Barcelona 7; ETATS-UNIS, Fam Book Service 69, Fifth Avenue, Suite 8 F., New York, 10003 N.Y.; Continental Publications, 111, South Meramec Ave., St. Louis Missouri 63105; Turner Subscription Agency 235, Park Avenue South, New York 3 N.Y.; FINLANDE, Akateeminen Kirjakauppa P.O.B. 10128, Helsinki 10; FRANCE, Nouvelles Messageries de la Presse Parisienne, 111, Rue Réaumur, Paris 2, Europériodiques S.A. 72 Boul. Sénard, 92 Saint Cloud; GRANDE-BRETAGNE, Collet's Holdings Ltd. Dennington Estate, Wellingborough, Northants; Central Books Ltd. 37, Grays Inn Road London W.C. 1; ISRAEL, Heskel Ltd. P.O.B. 1436, Tel-Aviv; Haifepac Ltd. P.O.B. 1794, Haifa; ITALIE, Sa. Co. Lib. Ri. Piazza Margana 33 – Roma; Messaggerie Italiane Sp. A. Milano, Via Paolo Ranzo e Lucia 2; JAPON, Nauka Ltd. 30–19 Minami – Ikebukuro 2chome Toshima Ku, Tokyo; PAYS-BAS, N.V. Martinus Nijhoff P.O.B. 269, Den Haag; Swets & Zeitlinger, Keizersgracht 471–487, Amsterdam C.; NORVÈGE, Tryggve Juul Møller—Bokhandel Øvre Slottsgate 15 Oslo 1; R.F. d'ALLEMAGNE, Kubon & Sagner, P.O.B. 68, München 34; Presse Vertriebsgesellschaft GmbH 6, Frankfurt/M Savignystrasse 13–15; Kunst und Wissen, Erich Bieber P.O.B. 46, 7000 Stuttgart 1; SUISSE, Pinkus & Co. Froschaugasse 7 Zürich, Fachbücherei Berne, P.O.B. 397, 3001 Berne.

En Roumanie vous pourrez vous abonner par les bureaux de poste, chez votre facteur ou directement par les services de presse des entreprises et institutions.

NOTE POUR LES AUTEURS

La *Revue Roumaine de Chimie* publie des articles en anglais, français, russe, allemand ou espagnol. Les auteurs sont priés d'envoyer des articles, notes, communications et comptes rendus inédits.

Les manuscrits seront dactylographiés à deux intervalles. Les tableaux seront dactylographiés sur feuilles séparées, de même que la légende des figures. Les diagrammes seront tracés à l'encre de Chine sur papier calque. Les tableaux et les figures seront numérotés par des chiffres arabes, en nombre strictement nécessaire. Prière de ne pas inscrire les mêmes données dans les tableaux et les figures. Les formules chimiques seront incluses dans le texte ; en outre, elles seront transcrites sur des feuilles séparées. Les auteurs sont priés d'indiquer les caractères italiques (en soulignant les lettres au crayon), ainsi que tout autre caractère spécial. L'ordre des références bibliographiques sera celui de leur mention dans le texte ; le nom de l'auteur sera précédé de l'initiale du prénom ; les publications périodiques seront présentées suivant les prescriptions internationales. Les références seront ajoutées à la fin de l'article ; elles paraîtront comme des notes, au bas de la page. Le texte sera précédé d'un résumé, comprenant 15 lignes au maximum.

L'entière responsabilité du contenu des articles appartient aux auteurs. On publie des articles dus aux collaborateurs roumains ou étrangers. Les auteurs recevront 50 tirés à part.

PRINTED IN ROMANIA

1970 MAR 2 3

TRAVAUX PARUS AUX ÉDITIONS DE L'ACADÉMIE DE LA RÉPUBLIQUE SOCIALISTE DE ROUMANIE

CORNEL BODEA et collab., **Tratat de biochimie vegetală**, partea I, **Fitochimie** (Traité de biochimie végétale, Ire partie, Phytochimie), Ier vol., 1964, 747 p. + 4 annexes + 2 pl., 41 lei; IIe vol., 1265, 1962, p., 1 pl., 56 lei; III vol., 1967, 773 p., 35 lei.

V. GHEŢIE et V. MICUŞAN, **Analiza imunochimică. Teorie şi practică** (Analyse immunochimique. Théorie et pratique), 1966, 369 p., 28 lei.

SILVIA IONESCU, **Reacţii chimice induse de radiaţiile ionizante** (Réactions chimiques produites par les radiations ionisantes), 1963, 271 p., 15 lei.

MARIETA NICOLAE, **Fizico-chimia proceselor fotografice** (Physico-chimie des processus photographiques), 1964, 426 p. + 4 pl., 35 lei.

R. PORTOCALĂ et L. POPA, **Acizii ribonucleici celulari şi virali** (Les acides ribonucléiques cellulaire et viraux), 1966, 375 p., + 8 pl., 26 lei.

D. PURDELA et R. VÎLCEANU, **Chimia compuşilor organici ai fosforului şi ai acizilor lui** (La chimie des composés organiques du phosphore et de ses acides), 1965, 540 p., 37 lei.

CRISTOFOR SIMIONESCU, MARGARETA GRIGORAŞ et AGATA CERNĂTESCU-ASANDEI, **Chimia lemnului din R.P.R.** (La chimie du bois en Roumanie), 1964, 239 p. + 6 pl., 27 lei.

CRISTOFOR SIMIONESCU et CLEOPATRA VASILIU-OPREA, **Mecanochimia compuşilor macromoleculari** (La mécanochimie des composés macromoléculaires), 1967, 344 p., 23,50 lei.

I. V. MAXIM, **Materiale nucleare** (Matériaux nucléaires), 1969, 444 p., 4 pl., 30 lei.

I.P.I. — c. 4004

43 436

Lei 25.—

F 1103

RESTRÁLVA

04

REVUE ROUMAINE DE CHIMIE

R

TOME 15
N° 2
Février 1970

ÉDITIONS DE L'ACADÉMIE DE LA RÉPUBLIQUE SOCIALISTE DE ROUMANIE

Rev. Roumaine Chim.

15, 139–296 (1970), Bucarest

COMITÉ DE RÉDACTION

Rédacteur en chef :

C. D. NENIŢESCU, membre de l'Académie de la République Socialiste de Roumanie

Rédacteurs en chef adjoints :

A. T. BALABAN et V. E. SAHINI, membres correspondants de l'Académie de la République Socialiste de Roumanie

Collège de rédaction :

C. DRĂGULESCU, RALUCA RIPAN, CR. SIMIONESCU, membres de l'Académie de la République Socialiste de Roumanie ; EM. BRATU, membre correspondant de l'Académie de la République Socialiste de Roumanie ; Pr G. OSTROGOVICH, MARG. AVRAM, F. BADEA, I. D. MARCHIDAN, D. NEGOIU et D. SĂNDULESCU.

Les manuscrits, les livres et les revues proposés en échange, ainsi que toute correspondance seront envoyés à la rédaction :

REVUE ROUMAINE DE CHIMIE

23, str. Dumbrava Roşie, Bucarest, 9, Roumanie

F 1103

REVUE ROUMAINE DE CHIMIE

Tome 15, No 2 Février 1970

Page

I. G. MURGULESCU and IOANA DEMETRESCU, Kinetics of the reactions between benzyl bromide and normal alcohols . . . . 141–147 ✓

MIHAELA HILLEBRAND, O. MAIOR and V. EM. SAHINI, Charge transfer complexes of the aromatic heterocycles. I. CT-Complexes of some phenoxathiin derivatives 149–152

K. A. LEVISON and P. G. PERKINS, The electronic structure and geometry of aluminium borohydride 153–159

D. CISMARU, E. SEGAL et SANDA FĂTU, Étude de la chimisorption de l'oxygène sur des couches minces d'argent par des mesures de force thermo-électromotrice 161–165

O. RADOVICI and M. E. MACOVSCHI, Hydrogen overvoltage on thin evaporated metal films. II. Application of Tafel equation to thin metal films. . 167–173 ✓

RODICA VÎLCU and AL. BÎRHALĂ, Differential vapour-pressure measurements and the thermodynamic properties of benzil-CCl_4, benzil-$CHCl_3$, biphenyl-CCl_4 and biphenyl-$CHCl_3$ solutions 175–187

N. PETRESCU and MARIA PETRESCU, Self-diffusion of liquid bismuth from its melting point to 700° 189–199

MARTHA PAUČÍROVÁ, K. MATIAŠOVSKÝ and M. MALINOVSKÝ, Contribution to the study of the structure of molten $LiF-AlF_3$ and $NaF-AlF_3$ mixtures 201–208

TATIANA ONCESCU, On the intermediate in the reaction mechanism of Me(III) oxalato complexes decomposition 209–212

I. GANOVICI and LUCIA GANOVICI, Self-diffusion of liquid cadmium from its melting point to 500° 213–219

CAMELIA BELDIE, Activity coefficients in ternary systems phenol-water-electrolyte 221–228

I. TEOREANU and TRAN van HUINH, The mineralizing influence of apatite on the formation of portland cement clinker 229–238

C. ANDREI, D. MIHĂIŢĂ, I. HOGEA and D. MUNTEANU, Grafting of maleic anhydride on ethylene vinyl acetate copolymer in homogeneous medium in presence of peroxide initiators . . . . 239–245 ✓

A. ARSENE, MARIA PARASCHIV and A. T. BALABAN, Reaction of ethyl *o*-phenylene arsenite with tropolone 247–252

MALVINA FĂRCAŞIU and RODICA ISTRĂŢOIU, The donor-acceptor complexes of N-substituted maleimides with amines, and their role in nucleophilic addition reaction. 253–258

Rev. Roumaine Chim. 15, 139–296 (1970), Bucarest

Page

S. ROŞCA and C. D. NENITZESCU, The resolution of enantiomeric amino-derivatives of arene-tricarbonyl-chromium (O) 259–263

MARIA IONESCU und KLARA MAKKAY, Das Verhalten einiger Oxazolidone-(4). VIII. Über den Reaktionsmechanismus bei der Bildung der 2,5-disubstituierten Oxazolidone-(4) 265–272

N. I. IONESCU, About the mechanism of electrical resistance variations in thin copper and silver films during oxygen chemisorption 273–281

J. MÁTHÉ, Evidence of neighbour cation influence and correlation effect from ligand field calculations 283–290

D. CISMARU and D. MANOLESCU, Crystal structure studies of solid solutions in the system $Al_2O_3-Cr_2O_3-Li_2O$ 291–295

Revue Roumaine de Chimie, **15**, 141–147 (1970)

MŰSZAKI KÖNYVTÁR

KINETICS OF THE REACTIONS BETWEEN BENZYL BROMIDE AND NORMAL ALCOHOLS

I. G. MURGULESCU and IOANA DEMETRESCU

Physical Chemistry Department, Bucharest University, Bd. Republicii 13

Received April 28, 1969

The system

$$C_6H_5CH_2Br + ROH \rightarrow C_6H_5CH_2OR + HBr,$$

in which $R = CH_3$, C_2H_5, C_3H_7, and C_4H_9, was studied in a temperature range from 50° to 85°. Evolution of the reactions was investigated by determining the resulting HBr through a direct conductometric method. Independence of the rate constants with regard to the initial concentration of benzyl bromide was found. For every reaction both the apparent energy of activation and the pre-exponential factor were determined. Experimental data are discussed according to the theory of dipole-dipole reactions, comprising the kinetics of the studied reactions.

INTRODUCTION

The action of normal alcohols on benzyl bromide was little investigated. One may mention von Halban and Gast's work [1] restricted however only to ethyl alcohol, they being concerned mainly with kinetics of reactions between organic halides and mixtures of alcohol, water, and acetone.

The present work was carried out in view of a more complete characterization of nucleophylic substitutions.

EXPERIMENTAL

Schuchardt benzyl bromide and Austranal *p.a.* alcohols have been used. In order to anhidrize the methyl and ethyl alcohols 4 Å molecular sieves have been employed. The remaining water has been dosed by means of Karl Fischer's reagent.

The concentrations have been determined by a direct conductometric method, utilizing calibration curves given in a previous work.[2] We have used a conductivity cell with two compartments, closed by flame-melting at every determination in order to avoid a possible loss of resulting HBr, owing to the relative high working temperature. The cell, provided with platinized platinum electrodes, has been introduced directly into the thermostat. The resistance measurements have been made by means of a Wheatstone bridge, utilizing a cathode-ray oscilloscope as null indicator.

---

[1] H. von Halban und W. Gast, *Z. phys. Chem.*, **91**, 591 (1916).

[2] I. Demetrescu. *Rev. Roumaine Chim.*, to be published.

RESULTS

The reaction

$$C_6H_5CH_2Br + ROH \rightarrow C_6H_5CH_2OR + HBr \tag{I}$$

is a bimolecular one and its rate is given by the well known equation:

$$\frac{\mathrm{d}x}{\mathrm{d}t} = k\,(a - x)\,(b - x), \tag{1}$$

where x is the diminution of concentration, while a and b are the initial concentrations of the reactants.

Since x is negligible with respect to b (the alcohol concentration), the rate equation takes the form:

$$\frac{\mathrm{d}x}{\mathrm{d}t} = kb\,(a - x),$$

which on being integrated leads to:

$$k = \frac{2.303}{bt} \log \frac{a}{a - x}. \tag{2}$$

In order to prove the validity of equation (2) we give in table 1 the evolution of the measurements we have performed in order to find a kinetic constant.

Table 1

$C_6H_5\ CH_2\ Br + C_4H_9OH$; $T = 65°$; $a = 0.000165$ molcm^{-3}; $b = 0.0104$ molcm^{-3}

t min	$X \cdot 10^3$ Ω^{-1}cm^{-1}	x molcm^{-3}	a-x molcm^{-3}	k cm^{3}mol^{-1}min^{-1}
0		0	0.000165	—
100	0.234	0.0000210	144	1.25 10^{-1}
120	260	225	142	1.19
160	320	275	138	1.10
170	341	290	136	1.09
250	450	440	121	1.17
400	580	640	101	1.07
500	640	720	093	1.10
600	750	850	080	1.13
660	780	900	075	1.14
920	900	1080	057	1.10
				$k_m = 1.14 \times 10^{-1}$

The rate constant kept its value when various initial concentrations were taken.

In table 2 the rate constants of alcoholysis reactions of benzyl bromide at various temperatures are listed, together with the apparent energies of activation, $E_{\exp}$, determined by the least square method.

Table 2

Rate constants and energies of activation for the sytem $C_6H_5CH_2Br$ + ROH

ROH	k, $cm^3mol^{-1}sec^{-1}$							E cal-mol^{-1}
	50°	60°	65°	70°	75°	80°	85°	
CH_3OH	—	2.28×10^{-3}	4.30×10^{-3}	6.10×10^{-3}	1.06×10^{-2}	1.52×10^{-2}	—	22 416
C_2H_5OH	—	—	2.93×10^{-3}	4.92×10^{-3}	7.38×10^{-3}	—	1.66×10^{-2}	21 501
C_3H_7OH	5.11×10^{-4}	—	2.51×10^{-3}	4.01×10^{-3}	5.51×10^{-3}	—	—	21 134
C_4H_9OH	—	1.14×10^{-3}	1.90×10^{-3}	2.76×10^{-3}	3.90×10^{-3}	—	—	20 140

It may be seen that the obtained values show a slight decrease as the chain of alcohol grows longer. In figure 1 the straight lines plotted according to Arrhenius's equation run almost parallelly with each other.

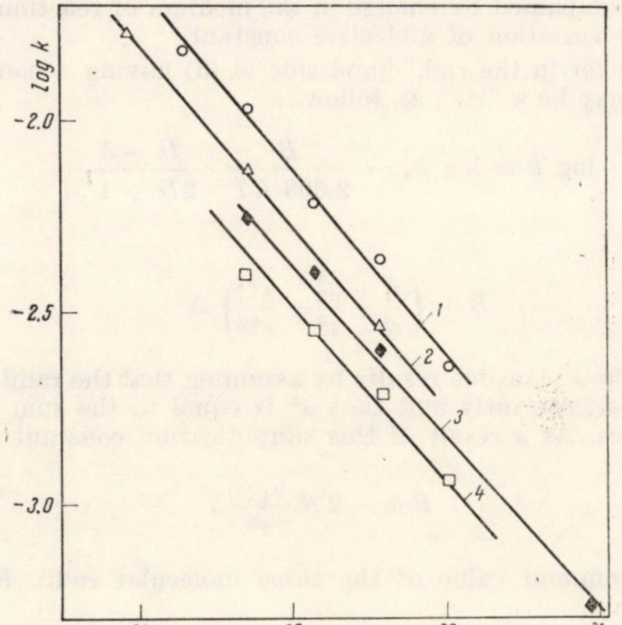

Fig. 1. — Alcoholysis reactions of benzyl bromide
1, CH_3OH; 2, C_2H_5OH; 3, C_3H_7OH; 4, C_4H_9OH.

The reaction (I) between benzyl bromide and the alcohols is a dipole-dipole reaction in which the solvent is at the same time reactant. In many cases the kinetics of dipole-dipole reactions suits a well known equation,[3] derived by means of the activated complex theory and using the result, obtained by Kirkwood, concerning the energy of transferring a dipole from a medium the dielectric constant of which equals the unity into a medium with a dielectric constant as great as D. Neglecting the interactions of the van der Waals's type, this equation may be written as follows

$$\log k = \log k_0 - \frac{N}{2.303\,RT} \cdot \frac{D-1}{2D+1}\left(\frac{\mu_1^2}{r_1^3} + \frac{\mu_2^2}{r_2^3} - \frac{\mu^{*2}}{r^{*3}}\right) \tag{3}$$

in which μ_1 and μ_2 are the moments of the two dipoles, r_1 and r_2 the radii of the molecules (presumed spherically) in which they are contained, and μ^* and r^* the moment and the radius of the activated complex. The constant k_0 corresponds, as it may be easily seen, to a medium with a dielectric constant $D = 1$. The other quantities involved have the usual meanings.

It is to be noted that in reaction (I) one of the reactants, the alcohol is at the same time medium of reaction. Thus, replacing of an alcohol by another is accompanied by change in the medium of reaction and by the corresponding variation of dielectric constant.

The bracket in the right-hand side of (3) having a constant value, equation (3) may be written as follows :

$$\log\ k = \log\ k_0 - \frac{B}{2.303\,RT} \cdot \frac{D-1}{2D+1}, \tag{4}$$

where

$$B = \left(\frac{\mu_1^2}{r_1^3} + \frac{\mu_2^2}{r_2^3} - \frac{\mu^{*2}}{r^{*3}}\right) N .$$

One reaches plausible results by assuming that the radii r_1, r_2, and r^* do not differ significantly and that μ^* is equal to the sum $(\mu_1 + \mu_2)$ of the two dipoles. As a result of this simplification constant B becomes :

$$B = -2\,N\,\frac{\mu_1\,\mu_2}{r^3}, \tag{5}$$

r being the common value of the three molecular radii. Equation (3) takes the form :

$$\log\ k = \log\ k_0 + \frac{2\,N\mu_1\mu_2}{2.303\,RTr^3} \cdot \frac{D-1}{2\,D+1} \tag{6}$$

As seen in figure 2, at each temperature of the experiments log k depends linearly on the ratio $(D-1)\,/\,(2D+1)$ and thus it suits equation (6). The dielectric constants were taken from a previous work.[4]

---

[3] S. Glasstone, K. J. Laidler, H. Eyring, "The Theory of Rate Processes", New York, London, 1941, p. 419.

[4] I. G. Murgulescu, D. Oancea and G. Mincu, *Rev. Roumaine Chim.*, **14**, 3 (1969).

From the slope of the straight lines in figure 2 the value of the constant B is obtained, from which we derive the radius r. In this way we obtain $|B| = 6.95 \times 10^{11}$ CGS units. With the value 1.66D for the dipole moments of the alcohols and 1.88 D for the moment of benzyl bromide, from equation (5)

$$r = 1.76\ \text{Å}$$

results.

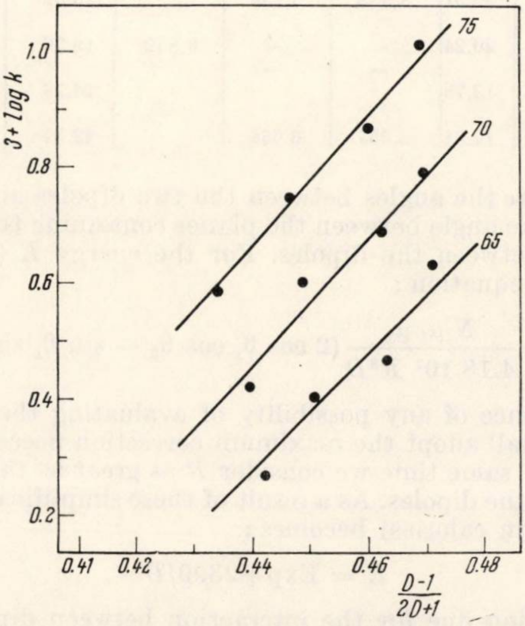

Fig. 2. – Dependence of the rate constants of the alcoholysis reactions of benzyl bromide on the dielectric constants of alcohols.

Keeping in mind the simplifying assumptions we made, this result is a plausible one and proves the usefulness of equation (6).

Table 3 allows a comparison between the values of the experimentally found rate constants and those calculated by means of (6). The agreement between the two series of values is satisfactory. It is to be noted that k_0 depends only on the temperature; it does not depend on the nature of the alcohol.

In order to estimate now the real activation energy, E, we have to correct the apparent activation energy, E_{exp}, experimentally found, by taking into account the interaction between dipoles. The dipole-dipole interaction potential Φ is given by:

$$\Phi = -\frac{\mu_1 \mu_2}{DR^3} (2 \cos \theta_1 \cos \theta_2 - \sin \theta_1 \sin \theta_2 \cos \varphi) \qquad (7)$$

Table

Comparison between the experimentally found kinetic

Alcohols	60°				65°			
	10gk_0	D	log k		log k_0	D	log$k$	
			exper.	calc.			exper.	calc.
CH_3OH		26.31	$\bar{3}.358$	$\bar{3}.358$		25.52	$\bar{3}.633$	$\bar{3}.590$
C_2H_5OH	$\bar{8}.329$	20.24	—	—	$\bar{8}.852$	19.70	$\bar{3}.466$	$\bar{3}.507$
C_3H_7OH		13.78	—	—		14.79	$\bar{3}.400$	$\bar{3}.387$
C_4H_9OH		12.84	$\bar{3}.057$	$\bar{3}.058$		12.37	$\bar{3}.278$	$\bar{3}.294$

where θ_1 and θ_2 are the angles between the two dipoles and the axis joining them, φ is the angle between the planes containing the dipoles and R is the distance between the dipoles. For the energy E (in cal per mol) we find then the equation :

$$E = E_{\text{exp}} + \frac{N\,\mu_1\,\mu_2}{4.18.10^7\,R^3 D}(2\cos\theta_1\cos\theta_2 - \sin\theta_1\sin\theta_2\cos\varphi) \qquad (8)$$

In the absence of any possibility of evaluating the angles and the distance R, we shall adopt the maximum correction necessary when $\theta_1 = \theta_2 = 0$. At the same time we consider R as great as the minimum distance $2r$ between the dipoles. As a result of these simplifications the energy of activation E (in calories) becomes :

$$E = \text{Exp} + 2390/D$$

The correction due for the interaction between dipoles is a relatively small one.

In table 4 are listed, for each of the studied reactions, the energy E and the corresponding pre-exponential factor of the Arrhenius's equation. In the last column we give also the experimental factors calculated in the classical approach of chemical reactions by intermolecular collisions :

$$A = N\sigma_{12}^2\left[8\pi RT\left(\frac{1}{M_1}+\frac{1}{M_2}\right)\right]^{1/2}\ \text{cm}^3\ \text{mol}^{-1}\ \text{sec}^{-1} \qquad (9)$$

where all symbols have the known meanings. In the absence of the required data σ was calculated by assuming that the volume of molecules is as great as that actually occupied by them :

$$\sigma = 1.184\times10^{-8}\ V_m^{1/3} = 1.184\times10^{-8}\left(\frac{M}{d}\right)^{1/3} \qquad (10)$$

M being the molecular mass and d the density of the liquid. The densities were taken from a previous work.[5]

The constants A as calculated by means of (9) are greater than those computed by using Arrhenius's equation and activation energies. We

---

[5] I. G. Murgugesccu and Fl. Bărbulescu, *Rev. Roumaine Chim.*, **2**, 153 (1963).

3

constants and those computed using equation (6).

70°				75°			
log k_0	D	log$k$		log k_0	D	log k	
		exper.	calc.			exper.	calc.
$\bar{8}.684$	24.74	$\bar{3}.785$	$\bar{3}.782$	$\bar{8}.906$	24.03	$\bar{2}.025$	$\bar{3}.981$
	19.20	$\bar{3}.691$	$\bar{3}.691$		18.62	$\bar{3}.868$	$\bar{3}.887$
	14.28	$\bar{3}.603$	$\bar{3}.554$		13.78	$\bar{3}.741$	$\bar{3}.744$
	11.91	$\bar{3}.440$	$\bar{3}.449$		11.48	$\bar{3}.591$	$\bar{3}.635$

do not find results in better agreement with the experimental ones even by using other equations, as for example[6] :

$$A = 3\ \pi\sigma\eta/2\ m \tag{11}$$

in which η is the viscosity of the solvent and m and σ are the mass and the diameter of the molecules of the solved substance.

Table 4

Comparison between the constants A, derived from experimental data and from equation (9)

Alcohols	E calmol^{-1}	Å	log A	
			Exper.	Calc.[9]
CH_3OH	22 509	4.94	12.138	14.412
C_2H_5OH	21 624	5.20	11.480	14.359
C_3H_7OH	21 298	5.41	11.184	14.349
C_4H_9OH	20 337	5.58	10.408	14.344

CONCLUSIONS

Reactions of nucleophylic substitution of the form of (I) are of the dipole-dipole type.

The introduction of dielectric constants into the expression of the rate constants (equation (3)) alows the unitary treatment of the kinetics of the alcoholysis processes of benzyl bromide. The kinetic constants for various alcohols depend linearly on the ratio $(D - 1)\ /\ (2D + 1)$. The alcohols having the same dipole moments, the kinetic constants depend, at constant temperature, only on this ratio.

By taking into account the dipole-dipole interactions it is possible to derive the actual activation energies and the pre-exponential constants A of Arrhenius's equation. These constants are smaller than those calculated by means of the classical approach of intermolecular collisions.

---

[6] E. A. MOELWYN HUGHES, "The Kinetics of Reactions in Solution", Oxford, 2nd edition, 1947, p. 200.

Revue Roumaine de Chimie, 15, 149–152 (1970)

CHARGE TRANSFER COMPLEXES OF THE AROMATIC HETEROCYCLES. I

CT-COMPLEXES OF SOME PHENOXATHIIN DERIVATIVES

MIHAELA HILLEBRAND, O. MAIOR and V. EM. SAHINI
Department of Physical Chemistry University of Bucharest, Bdul Republicii 13

Received July 23, 1969

Optical spectra of the CT-complexes of some phenoxathiin derivatives with tetracyanoethylene and dichlorodicyanobenzoquinone are presented and discussed ; the ionisation potentials estimated from the CT-band energy are correlated with the energy of the last occupied molecular orbital.

The donor character of phenoxathiin was already discussed in relation to the formation of the positive radical ion and of the charge transfer complexes. Charge transfer complexes of phenoxathiin with iodine and chloranil were studied by Kuboyama [1] and those of some phenoxathiin derivatives with tetrachloro phthalic anhydride (TPA) were reported previously by us. [2]

In the present paper, optical spectra of phenoxathiin CT-complexes obtained in solution with the stronger acceptors tetracyanoethylene (TCNE) and dichlorodicyanobenzoquinone (DDQ) are presented and discussed.

EXPERIMENTAL

The synthesis and properties of the donors: 2F–,2Cl–,2CH_2Cl–,2CH_3–,3CH_3–,2,3$(CH)_2^{\cdot}$, 2, 3, 8$(CH_3)_3$-phenoxathiin were reported elsewhere. [2] As acceptors we used TCNE and DDQ. The complexes were obtained by mixing the methylene chloride or nitromethane solutions of both components, optimal concentrations being 10^{-2} M for TCNE and 3.5×10^{-3} M. for DDQ. The donor concentrations were modified in the range $1-6 \times 10^{-2}$ M. for the complexes with TCNE, respectively in the range $5 \times 10^{-3}-1.5 \times 10^{-2}$ M. for DDQ. The spectra were recorded with a Beckmann DK–2 spectrophotometer using cells with 0.5–1 cm. pathlength, in the range of 350—900 mμ. The broad aspect of the CT-bands and the spectral region where they are placed introduce some uncertainty in the location of the charge transfer maximum. The precision was therefore estimated as ± 5 mμ.

---

[1] A. Kuboyama, *J. Amer. Chem. Soc.*, **86**, 164 (1964).

[2] M. Hillebrand, O. Maior, V. Sahini and E. Volanschi, *J. Chem. Soc. Phys. Org.* B, **6**, 755 (1969).

RESULTS AND DISCUSSION

The absorption spectra of the CT-complexes studied consist of two bands in the case of TCNE, located in the range 390—460 mμ, and, respectively, 600—750 mμ, and of a single band in the range 700—850 mμ, when DDQ is used as acceptor. Absorption bands of the acceptors or donors could not be detected in either of these regions. The bands present a broad aspect and the first CT-band of the complexes with TCNE is apparent in some cases as a shoulder only. This band cannot be observed in polar solvents, like nitromethane. The maxima of the absorption bands are listed in table 1.

Table 1

Visible bands (mμ) of the charge transfer complexes

Donors / Acceptor	TCNE		DDQ	
	CH_2Cl_2	CH_3NO_2	CH_2Cl_2	CH_3NO_2
2F-phenoxathiin	415 645	590	735	710
2Cl-phenoxathiin	400—425 650	590	745	710—715
$2CH_2Cl$-phenixathiin	405—440 660—665	610	765	725
Phenoxathiin	435 675	620	765—770	735—740
$2CH_3$-phenoxathiin	450 695	655	790	770
$3CH_3$-phenoxathiin	425—450 700	650	795—800	770
2, 3 $(CH_3)_2$-phenoxathiin	440—460 725	680	830	800
2, 3, 8 $(CH_3)_3$-phenoxathiin	460—470 750	700	855	830

It may be observed that the shift of the charge transfer bands for different donors agrees with the electronegativity and inductive effects of the substituents. In all the complexes there is a bathocromic shift in the order F—, Cl—, CH_2Cl—, $2CH_3$—, $3CH_3$—, $2,3(CH_3)_2$—, $2,3,8(CH_3)_3$—phenoxathiin, pointing out that the greater the electronegativity of the substituents is, the more energy is required for the formation of the CT-complexes; especially the presence of several methyl groups enhances the donor capacity of the molecule. In nitromethane, all bands are shifted towards blue, comparatively to their position in methylene chloride. Thus the polarity of the solvent acts in the same direction as the electronegative substituents.

The presence of two absorption bands in the spectra of the CT-complexes of TCNE has been mentioned by Kuroda et al.[3] and Lepley[4]. As the longest wavelength band of a CT-complex is usually assigned to a transition from the last occupied molecular orbital of the donor to the lowest empty molecular orbital of the acceptor, the second band was explained as being due to a transition from the last but one occupied molecular orbital of the donor to the same unfilled orbital of the acceptor. An argument for this assignment is the agreement of the difference between the energies of the two charge transfer bands with the energy differences of the two last occupied molecular orbitals, estimated from the UV spectrum of the molecule, supposing a correct assignment of the electronic transitions. This is verified in the case of phenoxathiin, where the difference of the energies of the two CT-bands is 1 eV, a value nearly equal with 0.94 eV, the difference between the energies of the two last occupied molecular orbitals[2].

For the complexes with TCNE two linear dependencies between the energy of the CT-band and the ionisation potential of the donor were given.[5,3]

$$(h\,\nu)_{\mathrm{CT}} = 0.487\,I_p - 1.30\ \mathrm{eV}$$

$$(h\,\nu)_{\mathrm{CT}} = 0.87\ \ I_p + 4.86\ \mathrm{eV}$$

The first equation was established for the complexes of methyl substituted benzenes, the second one for a larger class of compounds including polycyclic aromatic hydrocarbons. Therefore, we used the second dependence to interpolate the ionisation potential of the donors, in order to compare them with the previously obtained values from a similar study of phenoxathiin-T.P.A. complexes. The results are collected in table 2; all these new values are smaller than those previously reported, but they are with in the range accepted in literature (7.6 eV [1] — 7.98 eV [6])

Table 2

Ionisation potentials of the donors obtained from the charge transfer complexes study

Donor	$(h\nu)_{\mathrm{CT}}$	I_p	h_{X} *)
2F-phenoxathiin	1.92	7.79	1.5
2Cl-phenoxathiin	1.91	7.78	1.2
$2CH_2Cl$-phenoxathiin	1.87	7.73	—
Phenoxathiin	1.84	7.70	0
$2CH_3$-phenoxathiin	1.79	7.64	−0.5
$3CH_3$-phenoxathiin	1.77	7.62	−0.5
2, 3 $(CH_3)_2$-phenoxathiin	1.71	7.55	—
2, 3, 8 $(CH_3)_3$-phenoxathiin	1.65	7.48	—

***) h_{X} = inductive parameter for the substituent x.**

---

[3] H. Kuroda, M. Kobayashi, M. Kinoshita and S. Takomotu, *J. Chem. Phys.*, **36**, 457 (1962).

[4] A. R. Lepley, *Tetrahedron Letters*, **39—40**, 2823 (1964).

[5] P. E. Merrifield and D. Phillips, *J. Amer. Chem. Soc.*, **80**, 2778 (1958).

[6] P. Nounou, *J. Chim. Phys.*, **63**, 997 (1966).

The difference between the ionisation potentials obtained in the two charge transfer studies are possibly due to the different values of the ionisation potentials of the donors used in establishihg the dependence $(h\nu)_{CT} - I_p$. Thus, Basu and Chowdhury [7] in their study on T.P.A. charge transfer complexes considered mass-spectrometric values for the ionisation potentials of the donors, while Kuroda et al. used the values obtained by Briegleb and Czekalla from CT-complexes study; these latter values are smaller than the former ones.

It is interesting to remark that even these ionisation potentials are somewhat different from those obtained previously, they also can be correlated with the energy of the last occupied molecular orbital calculated by an inductive model for the monosubstituted derivatives (Fig. 1).

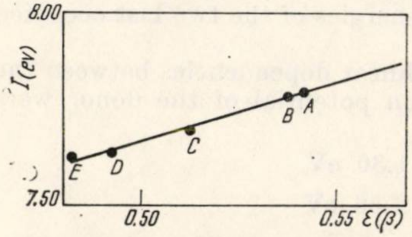

Fig. 1. — Correlation curve between the ionisation potentials and the highly occupied molecular orbital for :

A, 2F – phenoxathiin; *B*, 2Cl-phenoxathiin; *C*, phenoxathiin; *D*, $2CH_3$ – phenoxathiin; *E*, 3 CH_3 – phenoxathiin.

This implies that the parameters established previously [2] for the substituents, (Table 2) account well for their inductive effects.

Comparing the energies of the CT-bands in the complexes with *TCNE* and DDQ, it may be concluded that DDQ appears as a stronger acceptor than TCNE, and that both are stronger than T.P.A.

---

[7] M. Chowdhury and S. Basu, *Trans. Faraday Soc.*, **56**, 335 (1960).

Revue Roumaine de Chimie, **15**, 153–159 (1970)

THE ELECTRONIC STRUCTURE AND GEOMETRY OF ALUMINIUM BOROHYDRIDE

K.A. LEVISON and P. G. PERKINS

Department of Chemistry, University of Strathclyde, Glasgow, C. 1

Received September 16, 1969

The electronic structures of two models of aluminium borohydride are calculated by the self-consistent molecular orbital method. Basis sets of 3*s*, 3*p*, and contracted and diffuse 3*d* orbitals plus all valence electrons were employed for the aluminium atom. Two geometries were considered; the first was one in which the six bridging hydrogen atoms form a trigonal prism (overall symmetry D_{3h}) and the second in which they form an octahedron around the central aluminium atom (symmetry D_{3d}). The results of the calculations show that the first model has, overall, the lower energy of the two independently of how the 3*d* orbitals are included. The 3*d* orbitals contribute surprisingly little to the bonding, although this does increase when they are contracted. The dominant interactions stem from the 3*s*, and 3*p* orbitals and these stay approximately constant on inclusion of *d* orbitals.

INTRODUCTION

Aluminium borohydride, $Al(BH_4)_3$ was synthesized in 1940 [1] and, in the same year, it was demonstrated by electron diffraction [2] that the aluminium atom is bonded to all three borons with B-Al-B angles close to 120°. The similarity of the infra-red spectrum to that of diborane led Price [3] to conclude that the molecular structure is essentially trigonal prismatic (Figure 1).

Each boron atom appears to be bonded to the aluminium *via* two hydrogen bridge bonds. If the line joining the bridge hydrogen atoms (H^b) is perpendicular to the AlB_3 plane, then the molecular symmetry is D_{3h} and the six H^b atoms form a trigonal prism around the aluminium. If, however, the tetrahedral BH_4 units are rotated by approximately 50° about the Al-B bonds (the exact value depends upon the bond lengths) a trigonal antiprism is obtained. The symmetry of the AlH_6^b group is then D_{3d}: however the presence of the terminal hydrogen (H^t) further lowers the molecular symmetry to D_3. The symmetry of all intermediate models is also D_3 (The prismatic and antiprismatic models were first suggested by Longuet-Higgins [4]).

---

[1] H. I. Schlesinger, R. T. Sanderson, and A. B. Burg, *J. Amer. Chem. Soc.*, **62**, 3421 (1940).

[2] J. Y. Beach, and S. H. Bauer, *J. Amer. Chem. Soc.*, **62**, 3440, (1940).

[3] W. C. Price, *J. Chem. Phys.*, **17**, 1044 (1949).

Price [3] considered both models and decided that the prismatic model was the most likely. The same conclusion was reached from studies of the Raman spectrum [5] and the nuclear magnetic resonance spectrum [6] of the molecule. Furthermore, recent work by Almennigen, Gundersen and Haaland,[4] using the electron scattering pattern from gaseous $Al(BH_4)_3$, seems to rule out the antiprismatic model. These workers concluded that the molecular symmetry is either D_{3h} or perhaps slightly deformed into D_3. The $Al(BH_4)_3$ molecule is therefore an interesting one for theoretical study because it is important to determine whether the stability is due to the change of nuclear repulsion energy alone with different geometry or whether the inclusion of the $3d$ orbitals is the factor which militates against a particular geometry.

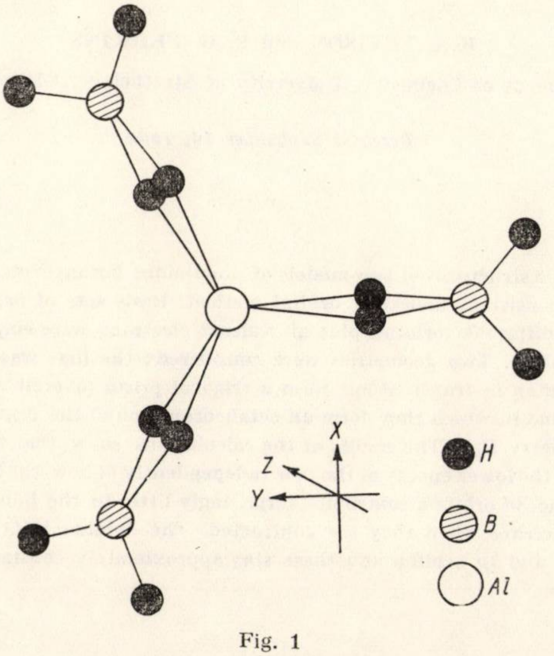

Fig. 1

Two models were considered: the first was the *trigonal prismatic* model, (as in Figure 1) in which the Al, B, and H^t atoms all lie in the same plane with the H^b atoms in a plane perpendicular to it; in the second each of the BH_4 groups was rotated by 54°44′ (half the tetrahedral angle) about the Al-B bond so that the bridging hydrogen atoms formed an *octahedral* arrangement around the aluminium atom. The experimental bond distance and angles[7] for both structures are shown in Table 1 with molecular axes defined in Figure 1.

---

[4] H. C. Longuet-Higgins, *J. Chem. Soc.*, **1946**, 139.

[5] A. R. Emery, and R. C. Taylor, *Spectrochim. Acta.* **16**, 1455 (1960).

[6] R. A. Ogg, and J. D. Ray, *Discuss. Faraday Soc.*, **1946**, 139.

Table 1

Geometrical Parameters for $Al(BH_4)_3$

	Bond Distance Å
$Al-B$	2.143
$Al-H_b$	1.801
$B-H_b$	1.283
$B-H_t$	1.196
$<H^b-Al-H^b$	73.4°
$<H^b-B-H^b$	114.0°
$<H^t-B-H^t$	116.2°

METHOD OF CALCULATION

This was based essentially on the S.C.M.O. method originated by Pople, Segal and Santry[8] which assumes that molecular orbitals for both σ and π electrons may be written as linear combinations of basis orbitals sited on dfferent atoms. This leads to a Fock interaction matrix with diagonal elements

$$F_{\mu\mu} = H_{\mu\mu} - \frac{1}{2} P_{\mu\mu}\gamma_{\mu\mu} + \sum_{\sigma(\neq\mu)} P_{\sigma\sigma}\gamma_{\mu\sigma}$$

and off-diagonals,

$$F_{\mu\nu} = H_{\mu\nu} - \frac{1}{2} P_{\mu\nu}\gamma_{\mu\nu}$$

In these equations the quantities $H_{\mu\mu}$, $H_{\mu\nu}$, $P_{\mu\mu}$, $P_{\mu\nu}$, $\gamma_{\mu\mu}$, and $\gamma_{\mu\nu}$ are the diagonal and off-diagonal elements of the core Hamiltonian matrix, the density matrix, and the electron repulsion matrix respectively, Basis sets chosen included the 3*d* orbitals of aluminium in diffuse or contracted form and in order to assess the contribution of these excited states to the energy, control calculations which neglected them completely were also performed. Our mode of choosing the input data for the core matrix and the electron repulsion matrix differed from that suggested by Pople *et al* and a full account of our derived Coulomb, repulsion and overlap integrals has been given elsewhere.[9]

The calculations were performed on the Newcastle University KDF9, the Strathclyde University ICT1905, and the S.R.C. Chilton Atlas Computers.

RESULTS AND DISCUSSION

In the following Tables the calculations denoted by (*a*) and (*b*) refer to the use of diffuse and contracted 3*d* functions respectively. The results are discussed under two heads.

---

[7] A. Almenningen, G. Gundersen, and A. Haaland, Private Communication.

[8] J. A. Pople, D. P. Santry, and G. A. Segal, *J. Chem. Phys.*, **43**, S129 (1965). D. P. Santry and G. A. Segal, *J. Chem. Phys.*, **48**, 335 (1968).

[9] K. A. Levison and P. G. Perkins, *Theor. Chim. Acta*, in the press; K. A. Levison and P. G. Perkins, *Discuss. Faraday Soc.*, Cambridge, 1969.

(i) *Molecular Energies*

Table 2 shows the energies computed for the trigonal prismatic and octahedral models based on the diffuse and contracted aluminium orbitals. It is reasonable to compare the two energies directly since both models involve the same atoms, the structures merely differing by minor changes in the positions of the hydrogen atoms.

Table 2

Molecular Energies of $Al(BH_4)_3$

Energies (eV)	Trigonal Prismatic Model		Octahedral Model	
	A1 *3d* orbitals omitted	A1 *3d* orbitals included	A1 *3d* orbitals omitted	A1 *3d* orbitals included
Electronic Energy (*a*)	−1917.820	−1917.966	−1947.066	−1947.232
(*b*)	—	−1918.339	—	−1947.665
Nuclear Energy	1524.696	1524.696	1563.145	1563.145
Total Energy (*a*)	− 393.124	− 393.271	−383.921	− 384.087
(*b*)	—	−393.644	—	− 384.520
Lowering of Total (*a*)	—	0.147	—	0.166
Energy by *d*-orbital-mixing (*b*)	—	0.520	—	0.599

We find that, independently of the mode of including the *3d* orbitals, the molecule of Al $(BH_4)_3$ is theoretically more stable in the trigonal prismatic form : this result is in satisfying agreement with the experimental conclusions. It is striking that the *electronic* energy of the octahedral is greater than that of the trigonal prismatic form but it is the *nuclear* repulsion energy which finally determines the favoured geometry. The energy difference between the two models is 9.184 eV (calcn. (a)) and (calcn. (b)). Since the CNDOSCMO method generally over-estimates absolute molecular electronic energies the discrepancy in energy between the two structures is probably even greater than these figures imply. This argues that we should not expect a labile equilibrium between the two forms.

The inclusion of the *3d* orbitals does indeed have the effect of slightly stabilising each structure but, for a diffuse function, the energy lowering (Table 2) is very small. The effect of *3d* contraction is to markedly increase this stabilising energy (by ∼ 4 times) and it seems clear that the *3d* orbitals do play an important rôle in the bonding of this compound. It is interesting that the participation of these orbitals is apparently greater in the 'octahedral' (D_3) model but it is consistent with the behaviour of transition metal hexa-coordinate compounds. In the case of Al $(BH_4)_3$ the *d* orbitals may be subjected to a linear transformation which redefines them as in a transition metal compound. However, as aforestated, it is the nuclear repulsion energy which dictates the geometry of the molecule.

(ii) *Charge Distribution*

Tables 3, 4, 5, and 6 detail the electronic charge distribution both in terms of atomic charges and bond orders between atoms. The following discussion will be mainly confined to the trigonal prismatic structure in

Table 3

Charge Densities in Al $(BH_4)_3$

	Trigonal Prismatic Model		
	Al 3*d* orbitals omitted		Al 3*d* orbitals included
Electron Density on Aluminium			
Al 3*s*	1.612	(*a*)	1.612
		(*b*)	1.610
Total Al 3*p*	0.342	(*a*)	0.343
		(*b*)	0.343
Total Al 3*d*	—	(*a*)	0.008
		(*b*)	0.038
Total Charge on Aluminium	1.954	(*a*)	1.963
		(*b*)	1.991
Electron Density on Boron			
B 2*s*	1.445	(*a*)	1.449
		(*b*)	1.456
Total B 2*p*	1.685	(*a*)	1.674
		(*b*)	1.651
Total Charge on Boron	3.130	(*a*)	3.123
		(*b*)	3.107
Electron Density on Bridging Hydrogen			
H 1*s*	1.149	(*a*)	1.149
		(*b*)	1.154
Electron Density on Terminal Hydrogen			
H 1*s*	0.961	(*a*)	0.962
		(*b*)	0.960

Table 4

Bond Orders contributing to the $B-H^b$ bond in Al $(BH_4)_3$

	H^b 1*s*		
	Trigonal Prismatic Model		
	Al 3*d* orbitals omitted		Al 3*d* orbitals included
2*s*	0.374	(*a*)	0.375
		(*b*)	0.373
$2p_x$	—	(*a*)	—
		(*b*)	—
$2p_y$	0.286	(*a*)	0.286
		(*b*)	0.288
$2p_z$	0.628	(*a*)	0.626
		(*b*)	0.620

Table 5

Bond Orders contributing to the Al$-$H^b bond in Al (BH$_4$)$_3$

	H^b 1s Trigonal Prismatic Model		
A1	Al 3d orbitals omitted		Al 3d orbitals included
3s	0.284	(a)	0.283
		(b)	0.283
$3p_x$	—	(a)	—
		(b)	—
$3p_y$	0.099	(a)	0.098
		(b)	0.096
$3p_z$	0.213	(a)	0.213
		(b)	0.214
$3d_{xz}$	—	(a)	—
		(b)	—
$3d_{yz}$	—	(a)	0.025
		(b)	0.068
$3d_{xy}$	—	(a)	—
		(b)	—
$3d_{z^2}$	—	(a)	0.004
		(b)	0.010
$3d_{x^2-y^2}$	—	(a)	0.008
		(b)	0.003

Table 6

Bond Orders contributing to the Al$-$B bond in Al (BH$_4$)$_3$

Trigonal Prismatic Model

		B			
Al		2s	$2p_x$	2py	$2p_z$
		*0.161	—	*0.146	—
3s	(a)	0.162	—	0.146	—
	(b)	0.162	—	0.147	—
		—	*0.034	—	—
$3p_x$	(a)	—	0.036	—	—
	(b)	—	0.037	—	—
		*0.109	—	*0.133	—
$3p_y$	(a)	0.110	—	0.133	—
	(b)	0.113	—	0.133	—
		—	—	—	*0.184
$3p_z$	(a)	—	—	—	0.184
	(b)	—	—	—	0.184
$3d_{xz}$	(a)	—	—	—	—
	(b)	—	—	—	—
$3d_{yz}$	(a)	—	—	—	0.024
	(b)	—	—	—	0.064
$3d_{xy}$	(a)	—	0.035	—	—
	(b)	—	0.042	—	—
$3d_z{}^2$	(a)	0.015	—	—	—
	(b)	0.039	—	0.001	—
$3d_x{}^2-{}_y{}^2$	(a)	0.022	—	0.001	—
	(b)	0.051	—	0.013	—

* Al 3d orbitals not included.

which the contracted 3*d* function was employed in the calculation. Perhaps the most striking feature of the charge distribution is the extremely small electron population on the central aluminium atom (Table 3). In particular the $3p$ orbitals are very little occupied. It seems that the six bridging hydrogens are responsible for removing considerable charge from aluminium and the latter is left positively charged to the extent of ~ 1 unit. The bridge hydrogens carry a negative charge of 0.15 electrons and this may be somewhat exaggerated since Burnelle and Kaufman,[10] from an *ab initio* calculation, found that the bridge hydrogens of diborane were only slightly negatively charged.

Perhaps the most interesting point is that in a compound, aluminium can be both strongly positively charged (present work) or negatively charged (as in the methyl aluminium compounds[9]). This means that spectroscopic techniques which yield a measure of charge density on an atom (such as, in this case, the ^{27}Al n.m.r. spectrum) should be extremely useful in investigation of these compounds.

Bond Orders

The most interesting interactions occur in the Al-H-B bridging unit. The three bonds comprising this entity are taken in turn.

B-H^b bond (Table 4). Overall, the bond orders here are almost completely unaffected by inclusion of d orbitals on aluminium either in diffuse or contracted form. It is interesting that despite the lower energy of the boron $2s$ orbital, and hence its "energy compatibility" with the hydrogen $1s$, the largest bond order is between the favourably orientated $2p_z$ orbital and the hydrogen. This reflects the relative importance of these two factors in B-H bridge bond formation.

Al-H^{bridge} bond. It may be seen (Table 5) that the inclusion of d orbitals again has almost no effect on bond orders involving Al $3s$ and $3p$ orbitals. When d interactions are considered these increase with the contraction of the d function but the only bond of any significance is that between d_{yz} and $1s$ i.e. where the d orbital is orientated appropriately. This situation parallels that in the methyl aluminium hydrides[9] where also the Al-H^b bond does not have any significant d character.

Al-B bond. Here again the role played by the $3s$ and $3p$ orbitals remains almost unaffected by inclusion of the d orbitals. In fact, contrary to the situation in Me_2AlBH_4[10] the latter do not play a particularly important part in the Al-B bonds. At first this seems somewhat surprising but it must be borne in mind that there are three boron atoms around the central aluminium and so the separate bonding effects are necessarily somewhat "diluted" by this situation.

We thank the S.R.C. for financial support.

---

[10] K. A. Levison and P. G. Perkins, *Theor. Chim. Acta*, in the Press.

Revue Roumaine de Chimie, 15, 161–165 (1970)

ÉTUDE DE LA CHIMISORPTION DE L'OXYGÈNE SUR DES COUCHES MINCES D'ARGENT PAR DES MESURES DE FORCE THERMOÉLECTROMOTRICE

D. CISMARU, E. SEGAL et SANDA FĂTU

Institut de Chimie Physique de l'Académie, Bucarest, 23, rue Dumbrava Roşie

Reçu le 23 janvier 1968

On met en évidence la modification de la force thermoélectromotrice absolue des couches minces d'argent comme suite de l'adsorption de l'oxygène. Cette modification peut être interprétée en tenant compte du fait que, pour l'argent, la surface Fermi se trouve en contact avec les faces (111) de la zone Brillouin.

INTRODUCTION

Les propriétés électriques, magnétoélectriques et thermoélectriques des couches minces métalliques sont profondément influencées par le phénomène de chimisorption, comme suite de l'interaction du métal et des molécules de gaz adjacentes. L'étude de ces propriétés, ainsi que de leurs modifications dues à l'interaction de la couche mince et des molécules de sa surface, offre la possibilité d'obtenir les informations pour caractériser et déceler le mécanisme de la chimisorption.

Pour étudier le phénomène de la chimisorption sur métaux, on utilise couramment les méthodes suivantes : la méthode de la modification de la conductivité électrique,[1,2] la méthode de la modification du travail d'extraction,[3] la méthode de la modification de la tension Hall,[4] ainsi que la méthode de la modification de la force thermoélectromotrice,[5] moins appliquée dans ce genre de recherches, mais avec des perspectives au moins égales.

Dans cette note on présente les résultats préliminaires concernant la chimisorption de l'oxygène sur des couches minces d'argent, résultats obtenus pendant l'étape de vérification du dispositif expérimental.

[1] R. SUHRMANN et K. SCHULTZ, *Z. phys. Chem.* (*Frankfurt*), **1**, 69 (1954).
[2] I. G. MURGULESCU et N. I. IONESCU, *Rev. Roumaine Chim.*, **11**, 1267 (1966).
[3] I. G. MURGULESCU et M. VASS, *Rev. Roumaine Chim.*, **11**, 299 (1966).
[4] I. G. MURGULESCU et G. COMŞA, *Rev. Roumaine Chim.*, **11**, 1253 (1966).
[5] H. WENZEL, thèse, Hanovre (1968).

PARTIE EXPÉRIMENTALE

Pour obtenir un vide avancé, on a utilisé une installation (fig. 1) composée d'une pompe à vide préliminaire PVP, une pompe de diffusion type IFA, PD, des pièges à azote liquide T et un getter à titane G.

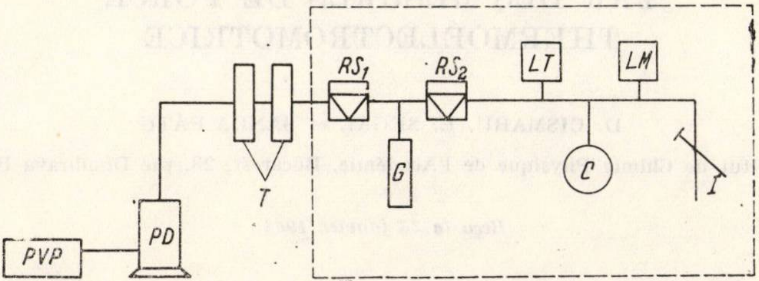

Fig. 1. — Schéma de l'installation :
PVP, pompe à vide préliminaire ; *PD*, pompe de diffusion ; *T*, pièges à azote liquide ; *RS_1*, *RS_2*, robinets à rodage sphérique ; *C*, cellule : *LT*, *LM*, lampes manométriques

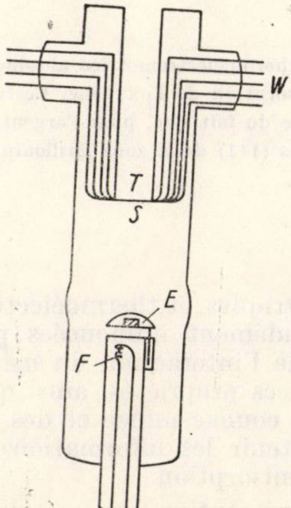

Fig. 2. — Cellule de mesure :
S, support : *T*, tube ; *E*, écran ; *F*, filament ; *W*, électrodes

On a raccordé à cette installation une cellule C, pour obtenir les couches minces et pour étudier les propriétés thermoélectriques. L'oxygène nécessaire pour la chimisorption se trouve dans l'introducteur de gaz I, construit d'après Murgulescu et Vass.[3]

La cellule[6], représentée dans la figure 2, comprend un cylindre en verre razotherme, muni d'un filament de wolfram *F*, dont l'échauffement produit des vapeurs métalliques, et d'un écran *E* qui permet de masquer le support *S* sur lequel, après avoir dégasé, on dépose la couche mince métallique à la température de l'azote liquide.

Pendant l'évaporation de la couche mince, on introduit dans le tube *T* de l'azote liquide, pour refroidir le support. Sur le support *S* (figure 3), on a installé aux extrémités deux petits fours *C*, grâce auxquels on obtient le gradient de température mesuré avec un thermocouple différentiel *TD*. La température moyenne du support est mesurée avec le thermocouple *T* Tous les deux thermocouples sont confectionnés en cuivre et constantan. La tension électromotrice résultée à la suite de l'application d'un gradient de température sur la couche mince a été mesurée avec des électrodes d'argent *E*, fixées sur le support de quartz avec de l'argent coloïdal, électrodes servant aussi à la mesure de la résistance de la couche mince, pendant le dépôt. La ligne pointillée représente l'extrémité d'un écran de verre qui protège les soudures du thermocouple pendant le dépôt de la couche mince. Les petits fours sont alimentés de courant électrique par l'intermédiaire des fils *F*.

---

[6] R. Grigorovici, N. Croitoru et A. Dévény, *Rev. Roumaine Phys.*, **11**, 869 (1966).

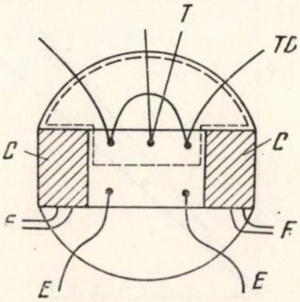

Fig. 3. — *S*, Support ; *T*, thermocouple ; *TD*, thermocouple différentiel ; *C*, petits fours ; *F*, résistance de chauffage ; *E*, électrodes.

On a mesuré la pression de l'installation avec des lampes manométriques LT et LM (fig. 1). L'installation de vide proprement dite, comprenant une pompe de vide préliminaire, une pompe de diffusion, des pièges et un getter, est séparée de la partie de mesure à l'aide d'un robinet à rodage sphérique RS_2.

On a mesuré la tension apparue dans les thermocouples avec un compensateur de type YTWK—1, et la force thermoélectromotrice de la couche mince d'argent soumise à un gradient de température, à l'aide d'un montage de compensation de type Lindeck-Rothe [7]. La résistance de la couche mince pendant le dépôt a été contrôlée avec un ohmmètre électronique type URV—2. En connaissant la valeur de la résistance de la couche mince, on a pu déduire, grâce à la formule Fuchs-Sondheimer [8], la valeur approximative de l'épaisseur de la couche.

Après avoir obtenu un vide à peu près égal à 5.10^{-5} torr, l'installation (cellules, introducteur de gaz, lampes manométriques, robinets à rodage sphériques et getter à titane) a été chauffée dans un four à 430—450° pendant quelques heures (le four est représenté en pointillé dans la figure 1).

Au moment où le vide atteint environ 5.10^{-8} torr, la couche métallique se dépose par évaporation, en contrôlant la résistance et en maintenant le support à la température de l'azote liquide. Après le dépôt, la couche a été stabilisée par échauffement à 100° à l'aide d'un petit four électrique.

Les petits fours *C* (fig. 3) ont permis de créer aux extrémités de la couche un gradient de température et on a interrompu ensuite l'alimentation pour éviter l'apparition de courants parasites. La force thermoélectromotrice de la couche mince et le gradient de température ont été mesurés par la méthode de la compensation.

Dans la seconde étape, après avoir isolé la cellule de l'ensemble de pompage grâce au robinet à rodage sphérique RS_2 (fig. 1), on a introduit de l'oxygène dans l'installation.

En assurant le même gradient de température, on a mesuré la force thermoélectromotrice de la couche mince sur la surface de laquelle se trouve maintenant de l'oxygène chimisorbé.

---

[7] P. Manolescu, « Măsurarea mărimilor electrice », Ed. tehnică, Bucarest, 1966, p. 164·

[8] K. Fuchs, *Proc. Camb. Phil. Soc.*, **34**, 100 (1938).

RÉSULTATS ET DISCUSSIONS

Dans la figure 4 on a représenté la variation de la tension électromotrice apparue aux extrémités de la couche mince en fonction du gradient de température, pour le couple composé de Ag massif/Ag couche mince pur, ainsi que pour le couple correspondant à une couche mince d'argent avec de l'oxygène chimisorbé.

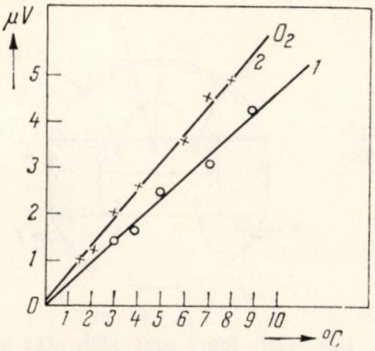

Fig. 4. — Variation de la tension électromotrice avec le gradient de température ;

1, pour le couple Ag massif/Ag couche mince pure ; *2*, pour le couple Ag massif/Ag couche mince avec de l'oxygène chimisorbé.

Les pentes des droites obtenues permettent de calculer les valeurs des forces thermoélectromotrices différentielles.

Pour une couche mince ayant l'épaisseur d'environ 80 Å à la température moyenne de 320°K, on obtient une force thermoélectromotrice du couple $|\alpha|$ de valeur absolue égale à 4,39 μV/degré. La valeur résultée pour la couche mince sur laquelle on a chimisorbé de l'oxygène est de $|\alpha| = 6$ μV/degré.

En tenant compte du signe négatif de la force thermoélectromotrice différentielle du couple formé par les électrodes d'argent massif et la couche mince d'argent,[9] on peut calculer les valeurs φ suivantes pour la force thermoélectromotrice absolue de la couche dans le vide et en présence de l'oxygène chimisorbé

$$\varphi_{\text{Ag couche}} = -2{,}87\ \mu\text{V/degré}$$

$$\varphi_{\text{Ag couche + oxygène chimisorbé}} = -4{,}48\ \mu\text{V/degré}.$$

On peut donner une interprétation probable de la décroissance de la force thermoélectromotrice de la couche mince d'argent à la suite de la chimisorption de l'oxygène, en considérant l'expression théorique suivante de la force thermoélectromotrice absolue [5*]

$$\varphi = -\frac{\pi^2 k^2 T}{3|\mathrm{e}|E_F}\left\{\frac{\mathrm{d}\ln \mathrm{l}_0}{\mathrm{d}\ln E}\left(1-\frac{\mathrm{d}\ln\psi}{\mathrm{d}\ln X}\right)+\frac{\mathrm{d}\ln A}{\mathrm{d}\ln E}\right\} \qquad (1)$$

---

[9] F. Savornin, *Compt. rend.*, **254**, 3348 (1962).

[*] Dans le raisonnement ci-dessus, on n'a pas tenu compte de la variation de l'épaisseur des couches minces d'argent à la suite de la chimisorption. D'après Murgulescu et Ionescu [2], cette variation est d'une couche atomique. Pour l'épaisseur de la couche mince utilisée, nous considérons que la modification du rapport X introduite par la variation mentionnée ne peut affecter sensiblement le résultat.

où ψ représente la fonction Fuchs-Sondheimer, X est le rapport entre l'épaisseur de la couche et le libre parcours moyen l_0 du matériel massif, A représente l'aire de la surface Fermi, E l'énergie des électrons du métal et E_F l'énergie Fermi.

Conformément à la formule (1), la différence entre les forces thermoélectromotrices absolues pour la couche mince recouverte et la couche pure peut s'exprimer sous la forme

$$\varphi-\varphi_{\text{pur}}=\frac{\pi^2k^2T}{3|e|E_F}\left(1-\frac{d\ln\psi}{d\ln X}\right)\left[\left(\frac{d\ln l_0}{d\ln E}\right)_{E=E_F}-\left(\frac{d\ln l_0}{d\ln E}\right)_{E=E_F}\text{pur}\right]-$$
$$-\frac{\pi^2k^2T}{3|e|E_F}\left[\left(\frac{d\ln A}{d\ln E}\right)_{E=E_F}-\left(\frac{d\ln A}{d\ln E}\right)_{E=E_F}\text{pur}\right] \qquad (2)$$

En général, le libre parcours moyen augmente avec l'énergie des électrons, ce qui fait que le quotient différentiel $\frac{d\ln l_0}{d\ln E}$ soit positif. Vu que, à la suite de la chimisorption de l'oxygène, gaz typiquement accepteur, d'une part le libre parcours moyen se réduit par l'introduction de nouveaux défauts superficiels, et d'autre part, l'énergie Fermi se réduit aussi, les valeurs du quotient différentiel $\frac{d\ln l_0}{d\ln E}$ pour la couche mince pure et recouverte sont proches, donc le premier terme de l'équation (2) est négligeable.

Etant donné que pour l'argent la surface Fermi se trouve en contact avec les faces (1 1 1) de la zone Brillouin,[10] il en résulte qu'à la suite de l'absorption, l'aire de la surface Fermi s'accroît. En tenant compte du fait qu'après l'adsorption de l'oxygène la valeur de l'énergie Fermi se réduit, il en résulte que la différence

$$\left(\frac{d\ln A}{d\ln E}\right)_{E=E_F}-\left(\frac{d\ln A}{d\ln E}\right)_{E=E_F}\text{pur}$$

est positive, le second terme de l'équation (2) est négatif, donc la différence $\varphi-\varphi_{\text{pur}}$ sera négative, ce qui concorde avec les données expérimentales.

CONCLUSIONS

1. On a mis en évidence la modification de la force thermoélectromotrice absolue des couches minces d'argent, comme suite de l'adsorption de l'oxygène.

2. La décroissance de la force thermoélectromotrice observée expérimentalement peut être interprétée en tenant compte du fait que, pour l'argent, la surface Fermi se trouve en contact avec les faces de la zone Brillouin.

---

[10] R. J. WEISS, « Fizica Tverdogo Tela », Atomizdat, Moscou, 1968, p. 300.

Revue Roumaine de Chimie, 15, 161–165 (1970)

Revue Roumaine de Chimie, 15, 167–173 (1970)

HYDROGEN OVERVOLTAGE ON THIN EVAPORATED METAL FILMS. II[1]

APPLICATION OF TAFEL EQUATION TO THIN METAL FILMS

O. RADOVICI and M. E. MACOVSCHI

Institute of Physical Chemistry of the Academy Bucharest, str. Galați 31

Received February 20, 1969

The applicability of Tafel equation to thin metal films is discussed; the deviation from linearity of the plotting E *vs.* $\lg(I/S)$ of films deposited on insulating supports is explained related to the film's own high resistance.

INTRODUCTION

It is well known that the hydrogen overvoltage phenomenon on metals is described by the Tafel equation:

$$\eta = a + b \ln (I/S) \tag{1}$$

in which $b = RT/\alpha F$ and "a" represents the η value for the current density I/S equal to the unit. The validity of relation (1) was proved by many authors for a very wide range of current densities,[2] between 10^{-9} and 10^{2} A.cm^{-1}. The working surface of solid metal electrodes is equipotential and for this reason the $E-I$ dependence in any of its points is identical with the $E-I$ dependence of the whole electrode.

The same $E-I$ dependence – relation (1) – was observed in the case of the thin metal films deposed on a conductor support [3] (made of metal or of coal). These films are equipotential too, but they present the disadvantage, caused by the presence of a film/support bimetal couple in the solution, consisting of the fact that the nature of the support may greatly influence the electrochemical behaviour of the film (see ref. 3).

Thin metal films deposited on insulating supports (by vacuum evaporation) allow the film/contact-wire couple to remain outside the solution. But these films comply with relation (1) only for small or very small current densities; when the current density increases, E is getting larger and larger values compared to those required by relation (1) [1] – figure 1. This phenomenon may be explained by taking into account the important value, of hundreds or even thousands of ohms, reached by the film's own resistance at very small thickness. In this case, the film is not equipotential any more and the dependence *E vs.*lg (I/S) is deflected from a straight line, though Tafel equation is valid for every point of the film.

---

[1] O. Radovici and M. E. Macovschi – *Rev. Roumaine Chim.*, 14, 159 (1969).

[2] K. J. Vetter, "Elektrochemische Kinetik", Springer Verlag, Berlin, Göttingen, Heidelberg, 1961, p. 430.

[3] R. Piontelli, B. Rivolta and L. Giuliani, *Electrochim. Metal.*, 3, 1 (1968).

The influence of the electrode's own resistance on the hydrogen overvoltage phenomenon was observed for solid metal too, the calculus made for very long wire electrodes being already experimentally verified.[4]

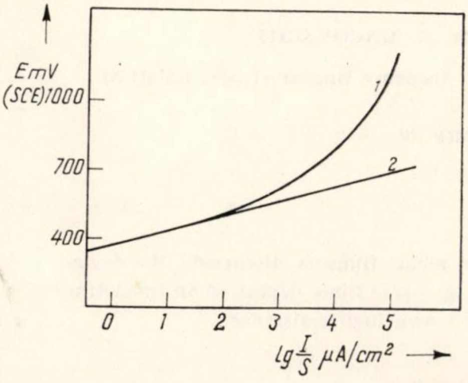

Fig. 1. — Dependence E vs. lg (I/S).
1, gold film on glass, symetrically supplied; ≠ 525 Å; R about 20 ohm. *2*, the normal Tafel dependence.

THE CALCULUS OF E–I RELATION FOR THIN METAL FILMS

The potential in any point of the electrode, fulfils the Tafel equation in differential form:

$$\eta = a + b \ln (\mathrm{d}i/\mathrm{d}s) \qquad (2)$$

where $\mathrm{d}i/\mathrm{d}s$ is the current density leaving the film in the point for which η is measured. In the same time η varies on the electrode surface due to the ohmic fall of voltage inside the film:

$$\mathrm{d}U = i\,\mathrm{d}R \qquad (3)$$

The precise form of relation (3) depends on the geometry of a given film.

It must be underlined that the position of Luggin capillary on the film surface (when the solution resistance is negligible) has no influence upon the stationary state, established for a given external voltage E because the real value of potential in any point of the film is the difference between the voltage E measured outside the solution and the ohmic voltage fall inside the film.

A. Rectangular electrode supplied at both ends

On a rectangular electrode of length L, width l and resistance R, supplied at both ends — figure 2 — the potential varies as shown in figure 3 A. At a distance "x" from the electrode middle, the potential is:

$$E_x = \eta_x = E - Ir - U_x \qquad (4)$$

---

[4] J. Wojtowicz, L. Laliberte and B. E. Conway, *Electrochim. Acta*, **13**, 361 (1968).

where r is the resistance of contact wires and of the film between the solution surface and the external measuring point of potential — figure 2 B. E_x is correlated with the current density $\mathrm{d}i/\mathrm{d}s = \mathrm{d}i/l\,\mathrm{d}x$ passing from the film into the solution at the level "x" by the relation :

$$E_x = E - Ir - U_x = a + b \ln (\mathrm{d}i/l\,\mathrm{d}x) \tag{5}$$

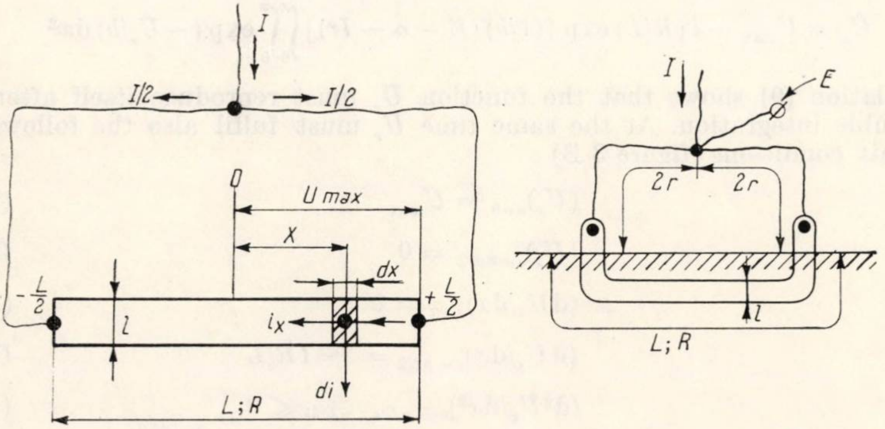

Fig. 2. — Notations used in the calculus and the practical achievement of the electrode.

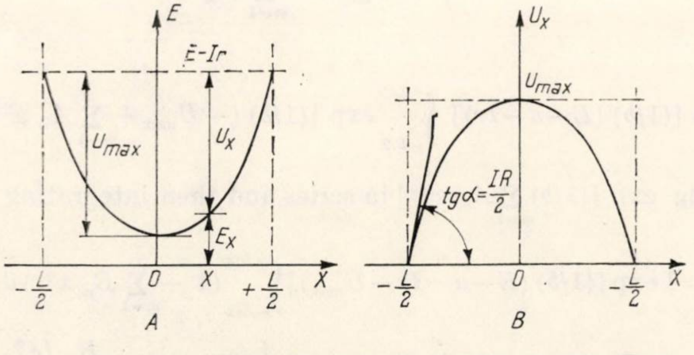

Fig. 3. — Potential variation (A) and voltage fall in the film (B) on an electrode similar to that shown in figure 2.

where

$$\mathrm{d}i = l \exp\,[(1/b)\,(E - a - Ir - U_x)] \tag{6}$$

and

$$I = l \exp\,[(1/b)\,(E - a - Ir)] \int_{-L/2}^{+L/2} \exp\,(-U_x/b)\,\mathrm{d}x \tag{7}$$

In order to explicite relation (7) that gives the $E-I$ dependence it is necessary to know the function U_x. We have (figure 3 B):

$$U_x = U_{\max} - \int_0^x \mathrm{d}U = U_{\max} - \int_0^x i_x \,\mathrm{d}R = U_{\max} - R/L \int_0^x i_x \,\mathrm{d}x \tag{8}$$

and taking into account (6):

$$U_x = U_{\max} - l\,(R/L) \exp\,[(1/b)\,(E - a - Ir)] \int_0^x\!\!\int_0^x \exp\,(-U_x/b)\,\mathrm{d}x^2 \tag{9}$$

Relation (9) shows that the function U_x must reproduce itself after a double integration. At the same time U_x must fulfil also the following limit conditions (figure 3 B):

$$(U_x)_{x=0} = U_{\max} \tag{10}$$

$$(U_x)_{x=\pm L/2} = 0 \tag{11}$$

$$(\mathrm{d}U_x/\mathrm{d}x)_{x=0} = 0 \tag{12}$$

$$(\mathrm{d}U_x/\mathrm{d}x)_{x=\pm L/2} = \mp IR/L \tag{13}$$

$$(\mathrm{d}^2 U_x/\mathrm{d}x^2)_{x\in[-L/2;\,+L/2]} \leqslant 0 \tag{14}$$

All these conditions are fulfilled by the function:

$$U_x = U_{\max} - \sum_{m=1} A_m\, x^{2m} \tag{15}$$

Thus:

$$I = l \exp\,[(1/b)\,(E-a-Ir)] \int_{-L/2}^{+L/2} \exp\,[(1/b)\,(-U_{\max} + \sum_{m=1} A_m\, x^{2m})]\,\mathrm{d}x \tag{16}$$

Developing $\exp\,[(1/b) \sum_{m=1} A_m\, x^{2m}]$ in series and then integrating it results:

$$\begin{aligned} I &= l \exp\,[(1/b)\,(E-a-Ir-U_{\max})] \int_{-L/2}^{+L/2} (1 + \sum_{m=1} B_m\, x^{2m})\,\mathrm{d}x = \\ &= L\, l \exp\,[(1/b)\,(E-a-Ir-U_{\max})] \left[1 + \sum_{m=1} \frac{B_m\, L^{2m}}{(2m+1)\cdot 2^{2m}}\right] \end{aligned} \tag{17}$$

where

$$\sum_{m=1} B_m\, x^{2m} = \sum_{n=1} [(1/n!\, b^n)\,(\sum_{m=1} A_m\, x^{2m})^n] \tag{18}$$

Writing $E = E_{(I)}$ and taking into account (11) and (15) it results:

$$\begin{aligned} E &= a + b \ln\,(I/lL) + Ir + \\ &+ b \left\{ \sum_{m=1} (A_m\, L^{2m}/b\, 2^{2m}) - \ln\left[1 + \sum_{m=1} \frac{B_m\, L^{2m}}{(2m+1)\, 2^{2m}}\right]\right\} \end{aligned} \tag{19}$$

Relation (19) shows that actually E values are getting higher as compared to those required by relation (1) (when m → ∞ the first sum increases more quickly than the logarithm of the second).

$U_{\max}$ and A_m coefficients can be calculated for different degrees of accuracy by identifying the coefficients in the following identity :

$$\sum_{m=1} A_m x^{2m} \equiv l \exp\{(1/b)[E-a-Ir-\sum_{m=1} A_m (L/2)^{2m}]\} \int_0^x\!\!\int_0^x \Bigg[1 + \sum_{n=1} \frac{(\sum_{m=1} A_m x^{2m})^n}{b^n \cdot n\,!}\Bigg] \mathrm{d}x^2 \tag{20}$$

and with the help of the additional relations (derived from the limit conditions) :

$$\sum_{m=1} 2m\, A_m\, (L/2)^{2m-1} = IR/L \tag{21}$$

$$U_{\max} = \sum_{m=1} A_m\, (L/2)^{2m} \tag{22}$$

It is obvious that A_m coefficients, as well as $U_{\max}$, depend on the film parameters and the given stationary state.

As a rough approximation :

$$U_x = U_{\max} - A_1\, x^2 \tag{23}$$

Under such conditions, only 2 coefficients must be determined and therefore relation (20) is no longer necessary, the limit conditions (21) and (22) being sufficient. We have :

$$U_x = IR/4 - (IR/L^2)\, x^2 \tag{24}$$

and

$$E = a + b \ln (I/lL) + Ir + b \ln \frac{1 + \sum_{n=1} (IR/4b)^n\, (1/n\,!)}{1 + \sum_{n=1} \{(IR/4b)^n\, (1/n\,!)\, [1/(2m+1)]\}} \tag{25}$$

B. Rectangular electrode supplied at one end

The notations used in the calculus (similar to the previous ones) are presented in figure 4. The potential at the distance "x" from the-solution surface is :

$$E - Ir - U_x = a + b \ln (\mathrm{d}i/l\, \mathrm{d}x) \tag{26}$$

Writing (26) as a function of i and integrating it results :

$$I = l \exp\, [(1/b)\, (E - a - Ir)] \int_0^L \exp\, (-U_x/b)\, \mathrm{d}x \tag{27}$$

To explicate the $E-I$ dependence (relation (27) similar with relation (7) it is necessary to know function U_x. We have:

$$U_x=\int_0^x \mathrm{d}U=\int_0^x i_x\,\mathrm{d}R=(R/L)\int_0^x\left(I-\int_0^x \mathrm{d}i\right)\mathrm{d}x=IRx/L-\int_0^x\left(\int_0^x \mathrm{d}i\right)\mathrm{d}x \tag{28}$$

Combining relations (28) and (26) it results:

$$U_x=(IR/L)\,x-(R/L)\,l\exp\,[(1/b)\,(E-a-Ir)]\int_0^x\int_0^x \exp\,(-U_x/b)\,\mathrm{d}x^2 \tag{29}$$

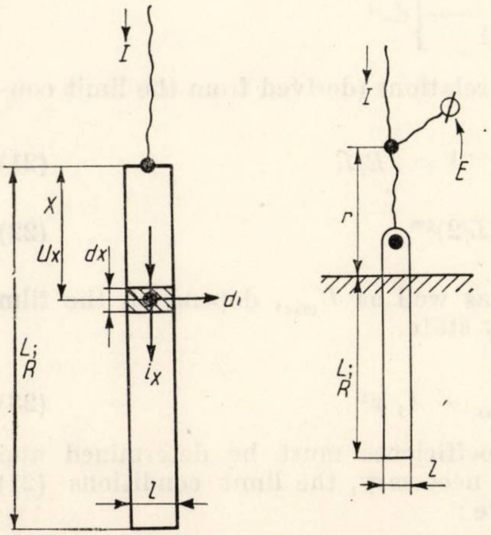

Fig. 4 — Notations used in the calculus and the practical achievement of the electrode.

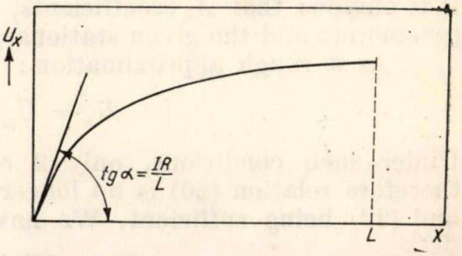

Fig. 5. — Variation of the ohmic fall inside the film.

The function U_x, whose shape is presented in figure 5, must reproduce itself again after a double integration. It must also, at the limit, fulfill the conditions:

$$(U_x)_{x=0}=0 \tag{30}$$

$$(\mathrm{d}U_x/\mathrm{d}x)_{x=0}=IR/L \tag{31}$$

$$(\mathrm{d}^2U_x/\mathrm{d}x^2)_{x\in[0;L]}\leqslant 0 \tag{32}$$

These conditions are fulfilled by the function:

$$U_x=\sum_{m=1}A_m\,x^m \tag{33}$$

Then:

$$I=l\exp\,[(1/b)\,(E-a-Ir)]\int_0^L \exp\,[-(1/b)\sum_{m=1}A_m\,x^m]\,\mathrm{d}x \tag{34}$$

Developing $\exp\,[-(1/b)\sum\limits_{m=1}A_m\,x^m]$ in series and integrating it results:

$$\begin{aligned}I&=l\exp\,[(1/b)\,(E-a-Ir)]\int_0^L(1+\sum_{m=1}B_m\,x^m)\,\mathrm{d}x=\\&=lL\exp\,[(1/b)\,(E-a-Ir)]\left(1+\sum_{m=1}\frac{B_m\,L^m}{m+1}\right),\end{aligned} \tag{35}$$

where

$$\sum_{m=1} B_m x^m = \sum_{n=1} \{[(1-)^n/(n\,!b^n)]\,(\sum_{m=1} A_m x^m)^n\} \tag{36}$$

Pointing out relation $E = E_{(I)}$ we have:

$$E = a + b \ln (I/lL) + Ir + b \ln \{1/[1 + \sum_{m=1} B_m L^m/(m + 1)]\} \tag{37}$$

In relation (37) (in contrast with relation (19)) the positive sign of the correction term (the last term) is not evident, because the coefficients B_m appear from summation or different terms positive as well as negative — relation (36).

A_m coefficients are calculated by identifying the coefficients in the identity:

$$\begin{gathered}\sum_{m=1} A_m x^m \equiv IRx/L - \\ -(Rl/L) \exp [(1/b)(E-a-Ir)] \int_0^x\!\!\int_0^x \{1 + \sum_{n=1} [(-1)^n/n\,!b^n)]\,(\sum_{m=1} A_m x^m)^n\} \mathrm{d}x^2\end{gathered} \tag{38}$$

In the case of the simplest approximation we have:

$$U_x = IRx/L \tag{39}$$

and

$$E = a + b \ln (I/lL) + Ir + b \ln \{IR/b\,[1 - \exp(-IR/b)]\} \tag{40}$$

In relation (40) the positive sign of the correction term is evident.

CONCLUSIONS

From the above the following conclusions may be drawn:

— the electrochemical measurements on thin metal films are strongly influenced by the conductibility as well as by the nature of the support on which they are deposited;

— it is preferably to deposite films on insulating supports and to place the film/contact-wire bimetal couples outside the solution;

— the measurements must be performed only at those current intensities for which the film can be considered equipotential, otherwise it becomes difficult to explain the results;

— the rather high resistance, of the thin metal films causes deviation of the dependence E — lg (I/S) from the Tafel line in direction of a limitation of the total current I at increasing overvoltages;

— at a given external voltage E the position of Luggin capillary on the film surface has no influence on the stationary state if solution resistance is neglected.

Experimental verification of this theory is going to be the subject of a future paper.

Revue Roumaine de Chimie, 15, 167–173 (1970)

whence

$$[illegible] \qquad (36)$$

Taking out solution $Z = [illegible]$, we have:

$$Z = [illegible] \qquad (37)$$

In relation (37) in contrast with relation (36) the positive sign of the corresponding term (the last term) [illegible] coefficients [illegible] from [illegible] of different sign [illegible] as well as negative [illegible] relation (36).

a_n coefficients are calculated by identifying the coefficients of the identity:

$$[illegible] \qquad (38)$$

In the case of the adopted approximation we have:

$$[illegible] \qquad (39)$$

and

$$Z = [illegible] \qquad (40)$$

In relation (40) the negative sign of the [illegible] term is [illegible].

CONCLUSIONS

From the above the following conclusions may be drawn:

— the electrochemical measurements on thin metal films are strongly influenced by the conductibility as well as by the nature of the support on which they are deposited;

— it is preferable to deposit films on insulating supports and to place the film contact connections outside the solution;

— the measurements must be performed only at those current intensities for which the film can be considered equipotential, otherwise it becomes difficult to explain the results;

— the rather high resistance of the thin metal films causes deviation of the dependence $E = \lg(i/i_0)$ from the Tafel line in direction of a limitation of the total current I at increasing overvoltages;

— at a given external voltage E the position of Luggin capillary on the film surface has no influence on the stationary state if solution resistance is neglected.

Experimental verification of this theory is going to be the subject of a future paper.

Revue Roumaine de Chimie, 15, 175–187 (1970)

DIFFERENTIAL VAPOUR-PRESSURE MEASUREMENTS AND THE THERMODYNAMIC PROPERTIES OF BENZIL-CCl_4, BENZIL-$CHCl_3$, BIPHENYL-CCl_4 AND BIPHENYL-$CHCl_3$ SOLUTIONS

RODICA VÎLCU and AL. BÎRHALĂ
Institute of Physical Chemistry of the Academy, Bucharest, str. Galați 31

Received February 10, 1969

Gibbs free energies and enthalpies of dilution were measured by a differential vapour-pressure micromethod in the binary mixtures Benzil-CCl_4, Benzil-$CHCl_3$, Biphenyl-CCl_4-Biphenyl-$CHCl_3$. A vapourometer of our own manufacture was used. The measurements were carried out at temperatures of 298.57, 308.67 and 318.51°K within the concentration range 0.01 – 0.1 molar. The experimental data were checked by calculating the molecular weights of the solutes.

The pressure of saturated vapours produced at a certain temperature by a solvent in solution might give useful information about the nature of the solute and the thermodynamic behaviour of the solution.

One of the static methods, of the differential type for vapour pressure measurement was initiated by Hill.[1] This micromethod called thermoelectric (vapourometric) * allows the measurement of the difference between vapour pressure of the solution and that of the pure solvent; only small quantities of solution (drops) are needed.

In solvent vapour-saturated atmosphere at a determined temperature two drops, one of solvent, the other of solution, are placed upon the active region of two temperature detectors (transducers). As the vapour pressure of the solvent in the solution drop is smaller than in the pure solvent drop, the solvent vapours condense at a higher rate on the solution drop than on the pure solvent one. The produced condensing heat increases the solution drop temperature, while the solvent drop stays at the initial temperature.

After a certain time the system reaches a steady regime, that is for a given concentration of the solution (at constant temperature) a

---

* The method is known as: Vapour Pressure Osmometry, Vapour Membrane Osmometry, Vapour Phase Osmometry.

[1] A. V. Hill, *Proc. Roy. Soc.*, **A 127**, 9 (1930).

ΔT, temperature difference between solution and solvent drops is obtained; ΔT is proportional to the vapour pressure difference between solvent and solution.

The earliest works based on vapourometric technique used thermoelements [2-6] as temperature detectors, but the measurements of the very small voltages generated by them is rendered difficult because of parasite voltage noises.

The replacement of thermoelements by thermistors [7] eliminated these difficulties and small temperature difference measurement were much facilitated.

The vapourometric method was applied in determinations of molecular weights,[2-22] molecular associations [23,24] and only scarcely applied to the thermodynamic characterization of solutions.[25-28]

Theoretical treatment of the method and possibilities to apply it can be found in papers.[29-33]

The present paper presents the design of a vapourometer and the thermodynamic study of benzil ($C_6H_5 \cdot CO \cdot CO \cdot C_6H_5$) and biphenyl solutions, in carbon tetrachloride and chloroform, in the concentration range 0.01–0.1 mol/l, at temperatures of 298.57°K, 308.67°K and 318.51°K.

---

[2] E. J. Baldes, *J. Sci. Instr.*, **11**, 223 (1934).

[3] B. B. Westfall and E. M. Landis, *J. Biol. Chem.*, **116**, 727 (1936).

[4] N. Lifson and V. Lorber, *J. Biol. Chem.*, **158**, 209 (1945).

[5] M. N. Fineman and J. W. Mc Bain, *J. Phys. Colloid. Chem.*, **52**, 881 (1948).

[6] G. B. Taylor and M. B. Hall, *Analyt. Chem.*, **23**, 947 (1951).

[7] A. P. Brady, H. Huff and J. W. Mc Bain, *J. Phys. Colloid Chem.*, **55**, 304 (1951).

[8] R. H. Müller and H. J. Stolten, *Analyt. Chem.*, **25**, 1103 (1953).

[9] B. R. Y. Iyengar, *Rec. Trav. chim.*, **73**, 789 (1954).

[10] B. R. Y. Iyengar, *J. Sci. Ind. Res. India*, **13 B**, 73 (1954).

[11] W. I. Higuchi, M. A. Schwartz, E. G. Rippie and T. Higuchi, *J. Phys. Chem.*, **63**, 996 (1959).

[12] J. J. Neumayer, *Analyt. Chim. Acta*, **20**, 519 (1959).

[13] C. Tomlinson, *Mikrochim. Acta.*, **1961**, 457.

[14] W. R. Moore and B. M. Tidswell, *Chem. Ind.*, **1967**, 61.

[15] F. M. Goyan and R. D. Johnson, *J. Pharm. Sci.*, **52**, 390 (1963).

[16] F. M. Goyan and R. D. Johnson, *J. Pharm. Sci.*, **53**, 328 (1964).

[17] V. J. Filipic, J. A. Connelly and C. L. Ogg, Proceedings, 1961, "International Symposium on Microchemical Techniques" (N. Cheronis, ed.) vol. 2, Wiley (Interscience) New York, 1962.

[18] D. Wegmann, C. Tomlinson and W. Simon, "Proceedings", 1961 International Symposium on Microchemical Techniques.

[19] Ch. Chylewski, Promotionsarbeit, ETH, Zürich, 1964.

[20] W. Simon, J. T. Clerc and R. F. Dohner, *Microchem. J.*, **10**, 495 (1966).

[21] R. F. Dohner, A. H. Wachter and W. Simon, *Helv. Chim. Acta.*, **50**, 2193 (1967).

[22] J. Biroš, *Chem. listy*, **61**, 1513 (1967).

[23] F. E. Schrier, *J. Chem. Educ.*, **45**, 176 (1968).

[24] D. Voisin, Annie Hout and B. Gastambride, *Ann. Chim. (France)*, **3**, 497 (1968).

[25] C. G. Mc Gee and B. R. Iyengar, *Indian J. Phys.*, **26**, 61 (1952).

[26] D. E. Burge, *J. Phys. Chem.*, **67**, 2590 (1963).

[27] R. D. Johnson and F. M. Goyan, *J. Pharm. Sci.*, **56**, 757 (1967).

[28] W. Brown, *J. Appl. Polymer Sci.*, **11**, 2381 (1967).

[29] C. Tomlinson, Ch. Chylewski and W. Simon, *Tetrahedron*, **19**, 949 (1963).

[30] Ch. Chylewski and W. Simon, *Helv. Chim. Acta*, **47**, 515 (1964).

[31] A. C. Meeks and I. J. Goldfarb, *Analyt. Chem.*, **39**, 908 (1967).

[32] E. Yu. Bekhli, D. D. Novikov and S. G. Entelis, *Vysokomol. Soedineniya*, A **9** 2754 (1967).

[33] J. van Dam, *Rec. Trav. chim.*, **83**, 129 (1964).

EXPERIMENTAL

The equipment consists of a differential vapourometer with thermistors (figure 1), Wheatstone bridge for the measurement of resistance difference between the two thermistors (figure 2) the thermosetting device, and a system for the measurement of the working temperature.

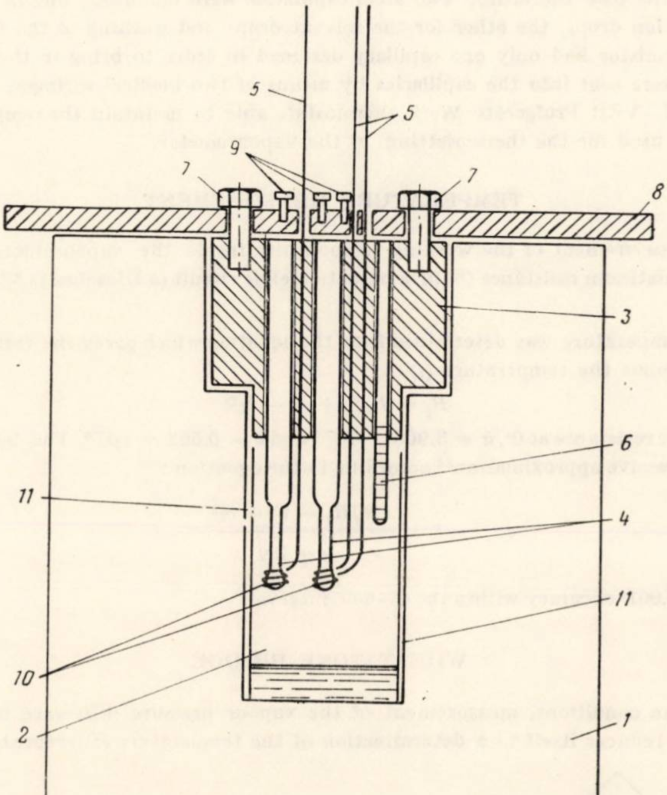

Fig. 1. — Vapourometer.

1, aluminium block; *2*, measuring cell; *3*, teflon stopper; *4*, thermistors; *5*, stainless steel capillaries; *6*, platinum-resistance thermometer; *7*, screws; *8*, PMMA plate; *9*, terminals of the thermistors; *10*, platinum wire turns; *11*, filter paper.

The vapourometer (figure 1) manufactured by ourselves according to existing similar equipment consists of an aluminium block (1) in which the measuring cell (2) is tightened by a teflon stopper (3); this stopper constitutes the support of the two thermistors (4), the stainless steel capillaries ($\O_i = 0.6$ mm) (5), and the platinum-resistance thermometer (6) which measures the temperature in the cell. The thermistors are of G A 51 P 68 Fenwal Electronics type; their resistance is $10^5\ \Omega$ at 25° with a thermal coefficient of $-4.6\,\%/°$. The platinum resistance thermometer is of a DIN 43760-Degussa type with $10^2\ \Omega$ at 0°.

The teflon stopper is fixed with screws (7) to a PMMA plate (8) and on this plate are mounted the terminals (9) of the two thermistors.

To maintain the drops on the ends of the thermistors two platinum wire turns (10) were used ; 2—3 cm^3 of solvent were poured at the bottom of the cell to create the saturated vapour atmosphere ; for the same purpose the vertical walls were covered with filter paper (11).

The right side thermistor is the test, while the other one is the standard. In the neighbourhood of the test thermistor two steel capillaries were mounted : one in order to bring into the solution drops, the other for the solvent drops and washing of the thermistor. The standard thermistor had only one capillary designed in order to bring in the solvent drops. The liquids were sent into the capillaries by means of two medical syringes.

A NBE—VEB Prüfgeräte Werk thermostat, able to maintain the temperature within ± 0.02°, was used for the thermosetting of the vapourometer.

TEMPERATURE MEASUREMENT

The measurement of the working temperature inside the vapourometer was carried out with the platinum resistance (6) in a potentiometric circuit (a Dieselhorts VEB Meßtechnik-Mellenbach).

The temperature was determined from the equation which gives the variation of resistance (R_t) versus the temperature (t)

$$R_t = R_0(1 + at + bt^2)$$

where R_0 is the resistance at 0°, $a = 3.908 \times 10^{-3}$ and $b = 0.562 \times 10^{-6}$. The temperature was found by successive approximation[34] according to the equation :

$$t = \frac{(R_t/R_0 - 1) + bt^2}{a + 2bt}$$

This gives a 0.001° accuracy within the 0—600° interval.

WHEATSTONE BRIDGE

In these conditions, measurement of the vapour pressure difference between solvent and solution, reduces itself to a determination of the temperature difference between the two drops on the thermistors. This is proportional to the resistance change when pure solvent and solution drops are on the standard thermistor and on the test one. This resistance change is proportional to the concentration of the solution (figures 3 and 4), and was measured with

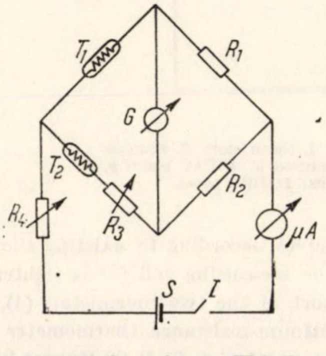

Fig. 2. — Wheatstone bridge.

T_1, T_2, thermistors; R_1, R_2, standard resistors; R_3, decade resistor; R_4 potentiometer; G galvanometer; S, battery; I, switch.

---

[34] M. M. Popov, "Termometria i Calorimetria", Izdat. Moscow Univ., 1954, p. 192·

a symmetrical Wheatstone bridge (figure 2) having on two arms the T_1 and T_2 thermistors, and on the other two, the standard resistors R_1 and R_2. The R_3 decade resistor was used to balance the bridge supplied by a 6 V battery. A light-beam galvanometer was used as null detector.

The R_4 potentiometer adjusts the current in the bridge; the maximum admitted value was 0.1 mA, but in order to prevent self-heating by Joule effect, it was maintained between 0.30–0.45μA.

WORKING TECHNIQUE

As soon as the temperature in the cell reached equilibrium, a solvent drop was placed on each of the two thermistors; the bridge was balanced and the resistance was recorded. A solution drop was then placed on the test thermistor (only after complete removal of the solvent), and when thermal equilibrium was reached again, the bridge was balanced and the new value of resistance was recorded; the difference of the two resistance values yields the ΔR. The time allowed for establishing of thermal equilibrium was 5 minutes for benzil and biphenyl in CCl_4 and 4 minutes for solutions with $CHCl_3$.

SOLVENTS AND SOLUTES

The solvents used were: CCl_4 (M = 153.82, d = 1.59 g/ml) and $CHCl_3$ (M = 119.38, d = 1.47 g/ml) spectroscopically pure.

The solutes were: *p.a.* benzil and biphenyl. The benzil was purified 3 times through recrystallization from absolute ethanol.

RESULTS AND DISCUSSION

The thermistor resistance dependence on temperature is approximately reproduced by the equation:

$$R = R_0 \exp \ B\left(\frac{1}{T} - \frac{1}{T_0}\right)$$

which holds on a range of some hundreds of degrees. R and R_0 are the thermistor resistances at T and T_0 respectively, and B a constant which depends on the nature of the semiconductor, and is related to the thermal coefficient of thermistor resistance, $a = \frac{1}{R}\frac{\mathrm{d}R}{\mathrm{d}T}$, by the equation:

$$a = -\frac{B}{T^2}$$

It ensues that the temperature variation of resistance is:

$$\frac{\mathrm{d}R}{\mathrm{d}T} = -R\frac{B}{T^2}$$

which emphasizes the higher sensitivity of the thermistor at lower temperatures.

Using high resistance thermistors to measure small temperature variations, the resistance variations become proportional to the temperature variations, even if resistance-temperature curves of the thermistors, are not linear. Taking into account this proportionality, the following equation is obtained :

$$\Delta R = K_1 \, \Delta T \tag{1}$$

where ΔR is the resistance change of test thermistor corresponding to a ΔT temperature difference.

If K_1 is known, the heat of vaporization, Δh_1, of the solvent in ideal diluted solutions can be determined by means of Clapeyron equation :

$$\Delta h_1 = \frac{RT^2}{\Delta T} x_2 \tag{2}$$

x_2 being the molar fraction of the solute, and R the gas constant.

CALCULATION OF ACTIVITIES AND THERMODYNAMIC PARAMETERS

A proportionality between ΔT and $\Delta\mu_1$, the difference of the chemical potential of pure solvent and solvent in solutions, was assumed by Burge [26] and Brown [28]; a relationship was established between thermodynamic magnitudes and vapourometric data :

$$\Delta T = K_2 \, \Delta\mu_1 \tag{3}$$

or

$$\Delta R = K_1 K_2 \, \Delta\mu_1 = K_3 \, \Delta\mu_1 \tag{3a}$$

$\Delta \mu$ allows the thermodynamic characterization of the solution by means of the activity of the solvent a_1, and its osmotic rational coefficient g, with which it is related by the well known equations discussed by Robinson and Stokes [35] :

$$\Delta\mu_1 = -RT \ln a_1 = g \, RT \, x_2 \tag{4}$$

A combination of equations (3a) and (4) at a given temperature leads to the relation :

$$\Delta R = - K_4 \ln a_1 \tag{5}$$

where :

$$K_4 = K_3 \, RT$$

or :

$$\Delta R = K_4 \, g \, x_2 \tag{5a}$$

For $x_2 \to 0$, $g \to 1$ and

$$\lim_{x_2 \to 0} \frac{\Delta R}{x_2} = K_4 \tag{6}$$

---

[35] R. A. Robinson and R. H. Stokes, "Electrolyte Solutions", Butterworths Scientific Publications, London 1959, 2nd ed., chapter 2.

K_4 is consequently determined as ordinate at the origin of the $\Delta R/x_2$ *versus* x_2 dependence, and allows the calculation of a_1 activity (equation 5).

The constant K_4 is a calibration constant (table 1) for a given solvent and temperature, and may be obtained by measuring ΔR at a series of concentrations for a solute of known molecular weight.

For molecular weight determinations by vapourometric method the molal constant k is usually used ; it is given by the ordinate intercept on a plot $\Delta R/m_2$ *versus* m_2, where m_2 is the molal concentration of the solute. In terms of this constant we get :

$$\Delta R\ M_1/(k_1 \cdot 1000) = -\ln a_1 \tag{7}$$

M_1 is the molecular weight of the solvent.

Once in possession of thermodynamic activity of the solvent in solution, we may find the molar change of the dilution Gibbs free energy :

$$\Delta G_1 = RT \ln a_1 \tag{8}$$

If experimental data at several temperatures are available, the thermal coefficient of the Gibbs free energy and implicitely the dilution heat may be determined by :

$$\Delta H_1 = \frac{\partial(\Delta G_1/T)}{\partial\left(\frac{1}{T}\right)} \tag{9}$$

ΔH_1 is graphically estimated from the slope of $\Delta G_1/T$ *versus* the reciprocal of absolute temperature plot. If now on a rectangular plot ΔG_1 is represented on the ordinate and the absolute temperature on the abscissa, the slope of the straight line (on the given temperature interval) represents the dilution entropy :

$$\Delta S_1 = -\frac{\partial(\Delta G_1)}{\partial T} \tag{10}$$

In order to standardize the apparatus, substances were used which form ideal solutions and keep the proportionality

$$\Delta R = K c$$

where K is the constant of the apparatus and c the concentration of solute.

In this work benzil ($C_6H_5.CO.CO.C_6H_5$) was used for standardization (figures 3 and 4).

The constant of the apparatus was computed by Tomlinson,[29] Chylewski [19] and Adicoff and Murbach [36] from data referring to the geometry of the measuring cell, factors of thermal balance such as solvent evaporation from the cell, thermal conduction, the diffusion of solute through the drop, diffusion of solvent through the cell atmosphere.

---

[36] A. Adicoff and W. J. Murbach , *Analyt. Chem.*, **39**, 302 (1967).

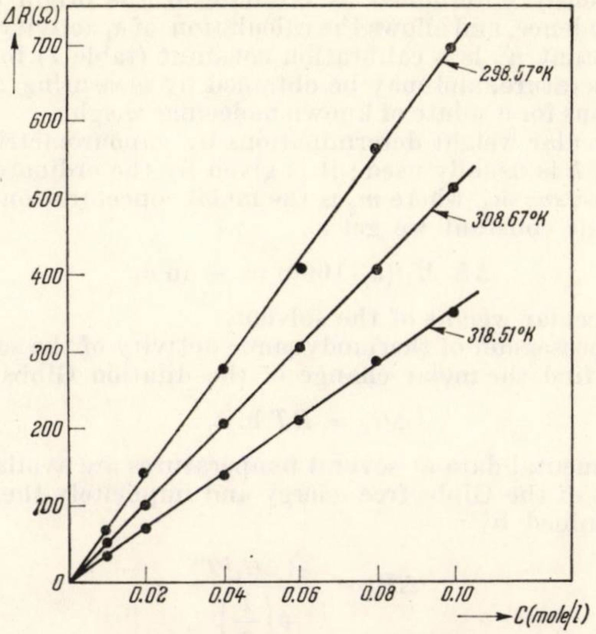

Fig. 3. — **Signal measured for benzil in CCl_4, as a function of the molarity of the solution.**

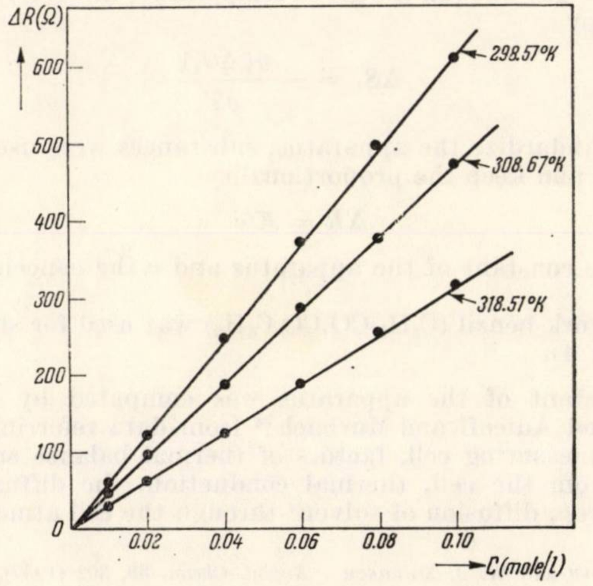

Fig. 4. — **Signal measured for benzil in $CHCl_3$, as a function of the molarity of the solution.**

Graphically, the intrument constants (table 1) have been determined for each solvent as ordinate intersection on a plot
$\Delta R/x_2$ *versus* x_2 — the molar fraction of the solute or of
$\Delta R/m_2$ *versus* m_2 — the solute molality.

Table 1

Calibration constants

Solvent	298.57°K		308.67°K		318.51°K	
	k molal	K_4 mole fraction	k molal	K_4 mole fraction	k molal	K_4 mole fraction
$CHCl_3$	10,340 ±38*)	86,500 ± 295	7,520 ±25	62,850 ±167	5,120 ±14	42,800 ±135
CCl_4	9,843 ±18	64,125 ±104	7,590 ±17	49,350 ±113	4,920 ±12	32,037 ±67

*) Standard deviation.

The lines were drawn by the least square method.

Table 1 shows that these constants are different for different solvents and decrease as temperature increases.

Once the calibration constant determined, the first checking of the vapourometer was achieved by calculating the molecular weights of benzil and biphenyl within the concentration range of 0.01—0.1 mol/l. The molecular weights were computed by the relation :

$$M = \frac{(K_4 - \Delta R) g_{\text{solute}}\, M_{\text{solvent}}}{\Delta R \cdot g_{\text{solvent}}}$$

Table 2

Benzil and biphenyl molecular weights in CCl_4 at 298.57°K

Concentration mol/l	$\Delta R(\Omega)$		M (molecular weight)	
	Benzil	Biphenyl	Benzil $M = 210.24$	Biphenyl $M = 154.21$
0.01	62	63	209	151
0.02	125	127	210	150
0.04	249	252	208	151
0.06	374	370	207	155
0.08	496	490	208	154
0.10	610	609	211	155
		average :	208.8±1.7*)	152.7±1.1

* Standard deviation

As may be seen in table 2 and 3, values very close to the theoretic ones were obtained, the differences being small.

Table 3

Benzil and biphenyl molecular weights in $CHCl_3$ at 298.57°K

Concentration mol/l	$\Delta R(\Omega)$		M (molecular weight)	
	Benzil	Biphenyl	Benzil $M = 210\cdot24$	Biphenyl $M = 154\cdot21$
0.01	70	70	210	154
0.02	143	142	208	152
0.04	278	283	211	152
0.06	415	420	212	155
0.08	564	558	208	154
0.10	694	690	211	155
		average :	210.0±1.4*)	153.7±1.7

*) Standard deviation.

Table

Thermodynamic magnitudes of benzil$-CCl_4$ system

Concentration mol/l	$\Delta R(\Omega)$			$\Delta R\cdot1{,}000/K_4 = -\ln a_1$		
	298.57°K	308.67°K	318.51°K	298.57°K	308.67°K	318.51°K
1		2			3	
0.01	62	48	31	0.96	0.97	0.96
0.02	125	96	63	1.95	1.94	1.96
0.04	249	189	124	3.89	3.83	3.87
0.06	374	286	189	5.84	5.79	5.90
0.08	496	378	251	7.73	7.66	7.83
0.10	610	473	314	9.51	9.58	9.80

*) Average value, computed with $-\ln a_1$ values from (3) and (4) columns

**) Standard deviation

Table

Thermodynamic magnitudes of biphenyl$-CCl_4$ system

Concentration mol/l	$\Delta R(\Omega)$			$\Delta R\cdot1{,}000/K_4 = -\ln a_1$		
	298.57°K	308.67°K	318.51°K	298.57°K	308.67°K	318.51°K
1		2			3	
0.01	63	47	31	0.98	0.95	0.96
0.02	127	96	61	1.98	1.94	1.92
0.04	252	193	125	3.93	3.92	3.90
0.06	370	289	189	5.77	5.86	5.90
0.08	490	377	252	7.64	7.64	7.87
0.10	609	464	311	9.50	9.40	9.71

*) Average value, computed with $-\ln a_1$ values from (3) and (4) columns.

**) Standard deviation.

By means of equations (5) and (7) the logarithm of CCl_4 and $CHCl_3$ activity in benzil and biphenyl solutions was determined and with these values the range of dilution Gibbs free energies ΔG_1 calculated. These values are listed in tables 4–7, together with the dilution heats ΔH_1, found from $\Delta G_1/T$ versus $1/T$ plots.

These last tables are stressing the change of thermodynamic magnitudes with temperature and concentration. The sign of these changes is the same for the four studied systems : the dilution Gibbs free energy as well as dilution heat increases (in absolute value) with increasing concentration.

Both molecular weights values and those of thermodynamic magnitudes, were characterized by standard deviations.

In the absence of comparison values for the dilution thermodynamic magnitudes, the confirmation of their validity was achieved by means of molecular weights computed as seen above. The reproducibility and

4

at different concentrations and temperatures

$\Delta R \cdot M_1/k = -\ln a_1$			$-\Delta G_1$*) $= RT \ln a_1$(cal/mol)			$-\Delta H_1$ cal/mol
298.57°K	308.67°K	318.51°K	298.57°K	308.67°K	318.57°K	
4			5			6
0.96	0.97	0.96	574±11**)	596±18	612±13	3.3±0.05
1.95	1.94	1.97	1,157±15	1,192±15	1,245±22	161±8.
3.90	3.83	3.88	2,310±22	2,349±18	2,451±12	—
5.85	5.79	5.91	3,468±25	3,554±14	3,737±28	581±12
7.75	7.66	7.85	4,593±12	4,697±15	4,962±14	726±15
9.53	9.58	9.82	5,649±7	5,878±15	6,207±7	2727±67

5

at different concentrations and temperatures

$\Delta R \cdot M_1/k = -\ln a_1$			$-\Delta G_1$*) $= RT \ln a_1$ (cal/mol)			$-\Delta H_1$ (cal/mol)
298.57°K	308.67°K	318.51°K	298.57°K	308.67°K	318.51°K	
4			5			6
0.98	0.95	0.96	583±15**)	584±14	612±13	—
1.98	1.94	1.92	1,176±9	1,192±15	1,215±10	−578±11
3.94	3.92	3.91	2,333±8	2,404±20	2,471±29	−276±9
5.78	5.86	5.90	3,426±13	3,591±19	3,733±25	1165±14
7.66	7.64	7.88	4,537±14	4,685±7	4,982±29	2144±12
9.40	9.40	9.72	5,640±11	5,766±30	6,148±25	2027±19

Table

Thermodynamic magnitudes of benzil-CHCL$_3$ system

Concentration mol/l	$\Delta R(\Omega)$			$\Delta R\cdot 1{,}000/K_4 = -\ln a_1$		
	298.57°K	308.67°K	318.51°K	298.57°K	308.67°K	318.51°K
1	2			3		
0.01	70	51	35	0.80	0.81	0.81
0.02	143	103	70	1.65	1.64	1.63
0.04	278	207	140	3.21	3.29	3.27
0.06	415	306	210	4.80	4.87	4.91
0.08	564	410	284	6.52	6.52	6.63
0.10	694	513	352	8.02	8.16	8.22

*) Average value, computed with $-\ln a_1$ values from (3) and (4) columns.
**) Standard deviation.

Table

Thermodynamic magnitudes of biphenyl–CHCl$_3$ system

Concentration mol/l	$\Delta R(\Omega)$			$\Delta R\cdot 1{,}000/K_4 = -\ln a_1$		
	298.57°K	308.67°K	318.51°K	298.57°K	308.67°K	318.57°K
1	2			3		
0.01	70	52	35	0.80	0.82	0.81
0.02	142	104	69	1.64	1.65	1.61
0.04	283	209	141	3.27	3.32	3.29
0.06	420	310	214	4.85	4.93	5.00
0.08	558	415	282	6.45	6.60	6.59
0.10	690	520	353	7.98	8.27	8.25

*) Average value, computed with $-\ln a_1$ values from (3) and (4) columns.
**) Standard deviation.

the agreement with theoretic molecular weights support the validity of our data. The dilution magnitudes are directly related to vapourometric measurements by equations rigorously founded thermodynamically.

The differential method for vapour pressure measurements of solutions compared with pure solvents, may be applied to the characterization of the thermodynamic behaviour of solutions of non-volatile solutes in volatile solvents.

The reduction of the sample to drops enables the method fit to be used for substances available in very small quantities. To this may be added the advantage of rapid measurements and full liberty in choosing solvents and working temperatures.

6

at different concentrations and temperatures

$\Delta R \cdot M_1/k = -\ln a_1$			$-\Delta G_1$*) $= RT \ln a_1$ (cal/mol)			
298.57°K	308.67°K	318.51°K	298.57°K	308.67°K	318.51°K	$-\Delta H_1$ (cal/mol)
4			5			6
0.80	0.80	0.81	479±5**)	497±9	516±15	77± 5
1.65	1.63	1.63	980±10	1,004±9	1,033±14	−169± 9
3.21	3.29	3.26	1,905±17	2,017±10	2,067±20	513±14
4.79	4.86	4.90	2,844±12	2,982±15	3,101±9	1008±15
6.51	6.51	6.62	3,865±8	3,996±9	4,195±13	1087±16
8.01	8.14	8.21	4,756±15	5,000±13	5,199±7	1859±23

7

at different concentrations and temperatures

$\Delta R M_1/k = -\ln a_1$			$-\Delta G_1$*) $= RT \ln a_1$ (cal/mol)			
298.57°K	308.67°K	318.51°K	298.57°K	308.67°K	318.51°K	$-\Delta H_1$ (cal/mol)
4			5			6
0.80	0.82	0.81	479±5**)	506±5	516±15	—
1.64	1.65	1.61	973±8	1,013±18	1,019±7	—
3.27	3.32	3.29	1,939±12	2,037±10	2,082±16	187±17
4.85	4.92	4.99	2,878±8	3,021±25	3,161±22	1350±18
6.44	6.59	6.57	3,824±7	4,045±24	4,165±18	1255±21
7.97	8.26	8.23	4,729±10	5,068±19	5,214±17	2484±23

Revue Roumaine de Chimie, **15**, 189–199 (1970)

SELF-DIFFUSION OF LIQUID BISMUTH FROM ITS MELTING POINT TO 700°

N. PETRESCU and MARIA PETRESCU

Physical Chemistry Research Center, Bucharest, Str. Galaţi 31

Received: February 18, 1969

The self-diffusion coefficient in liquid bismuth was determined through the capillary—reservoir method with the radioactive tracer Bi^{210} incorporated in the alloy of the reservoir. From the analysis of the experimental results, the following expression was derived for the temperature dependence of the diffusion coefficient: $D = (38.3 \pm 1.1) \times 10^{-5} \exp\left(-\frac{2\,507 \pm 124}{RT}\right)$ cm²/s. The values of the activation energy and of the pre-exponential factor of the equation are compared with the values predicted by empirical relations or by the expressions derived from the quasicrystalline model of the liquid. The self-diffusion coefficients are corroborated with the data on the viscosity of the metal. The values of the self-diffusion coefficients obtained experimentally are then interpreted in terms of the polynomial type temperature dependences implying diffusion mechanism based on cooperative motion modes of atoms in the liquid.

In the last few years, liquid metals and alloys have got an increasing number of applications in important technical fields as nuclear power generators, magnetohydrodynamics, fuel cells and so on. At the same time, precise information about the kinetic and equilibrium characteristics of metallic melts are required, to an ever growing extend, in order to elucidate the mechanism of processes applied in the practice of metal extraction and refining; they are also necessary in the theoretical approach and the practical managing of solidification processes.

In the present paper there are presented the results on the diffusivity in liquid bismuth. In the fifth group of the periodic table bismuth has the most pronounced metallic character and it serves as an alloying element for a large variety of non-ferrous alloys.

A recent review [1] on self-diffusion in liquid metals shows that self-diffusion coefficients have been determined up to the present in 11 pure liquid metals, distributed as follows in the periodic table:

---

[1] N. H. Nachtrieb, *Adv. Phys.*, **16**, 309 (1967).

— group Ia : sodium[2] and potassium[3]
— group Ib : copper[4] and silver[5,6]
— group IIb : zinc[7,8], mercury[9–12] and cadmium[13]
— group IIIa : gallium[14] and indium[15,16]
— group IV : tin[16,17] and lead.[18]

The study on self-diffusion in liquid bismuth, presented in this paper, adds another metal to the above list including in it also the fifth group of the periodic classification.

The self-diffusion coefficients experimentally determined in liquid pure metals served as a starting point as well as a validity criterion for a series of recent theories[1,19,20] on the diffusion mechanism in metallic melts. It may be mentioned that some of this new points of view are of interest not only for the diffusion process in the particular class of liquids under consideration, but they also represent a contribution to a better understanding of the liquid state.

Besides self-diffusion determinations in liquid pure metals, diffusivities have been studied in a series of liquid alloys, either on account of the technological interest of the respective alloys, or in order to treat more complexely the diffusion phenomenon in metallic melts by taking into account new variables as the valency effect, the relative atomic size, the solute-solvent interactions and so on. Among these investigations there are a number of studies undertaken on bismuth alloy systems.[21–26] In theoretical approaches to diffusion in liquid alloys a series of correlating expressions have been proposed ; to check them, information about diffusivities in pure components in the liquid state are needed in many cases.

In the present paper, self-diffusion in pure bismuth was studied in a large temperature range starting from 275° up to 700°.

---

[2] R. E. Mayer and N. H. Nachtrieb, *J. Chem. Phys.*, **23**, 1851 (1955).

[3] J. Rohlin and A. Lodding, *Z. Naturforsch. A*, **17**, 1081 (1962).

[4] J. Henderson and L. Yang, *Trans. Met. Soc. AIME*, **221**, 72 (1961).

[5] L. Yang, G. Derge and M. Kado, *Trans. Met. Soc. AIME*, **212**, 628 (1958).

[6] V. G. Leak and R. A. Swalin, *Trans. Met. Soc. AIME*, **230**, 426 (1964).

[7] W. Lange, W. Pippel and F. Bendel, *Z. phys. Chem.* (Lepzig), **212**, 238 (1959).

[8] N. H. Nachtrieb, E. Fraga and C. Wahl, *J. Phys. Chem.*, **67**, 2353 (1963).

[9] R. E. Hoffman, *J. Chem. Phys.*, **20**, 1567 (1952).

[10] N. H. Nachtrieb and J. Petit, *J. Chem. Phys.*, **24**, 746 (1956).

[11] R. E. Mayer, *J. Phys. Chem.*, **65**, 567 (1961).

[12] D. S. Brown and D. G. Tuck, *Trans. Faraday Soc.*, **60**, 1230 (1964).

[13] M. Mirshamsi, A. Cosgarea and W. R. Upthegrove, *Trans. Met. Soc. AIME*, **236**, 122 (1966).

[14] J. Petit and N. H. Nachtrieb, *J. Chem. Phys.*, **24**, 1056 (1956).

[15] A. Lodding, *Z. Naturforsch. A*, **11**, 200 (1956).

[16] G. Careri, A. Paoletti and M. Vicentini, *Nuovo Cim.*, **10**, 1088 (1958).

[17] C. H. Ma and R. A. Swalin, *J. Chem. Phys.*, **36**, 3014 (1962).

[18] S. J. Rothman and L. D. Hall, *Trans. Met. Soc. AIME*, **206**, 199 (1956).

[19] M. H. Cohen and D. Turnbull, *J. Chem. Phys.*, **31**, 1164 (1959) ; **34**, 120 (1961).

[20] R. A. Swalin, *Acta Met.*, **7**, 736 (1959).

[21] S. J. Rothman and L. D. Hall, *Trans. Met. Soc. AIME*, **206**, 199, 1580 (1956).

[22] K. Niwa, M. Shimoji, K. Kado, Y. Watanabe and T. Yokokawa, *Trans. Met. Soc. AIME*, **209**, 839 (1957).

[23] R. Grace and G. Derge, *Trans. Met. Soc. AIME*, **203**, 389 (1955).

[24] T. V. Vasilenko and E. I. Harkov, *Ukrain. fiz. Zhur.*, **7**, 1345 (1962).

[25] R. D. Stover and F. O. Shuck, *Trans. Met. Soc. AIME*, **242**, 768 (1968).

[26] N. Petrescu, to be published.

EXPERIMENTAL

Determinations were made through the capillary-reservoir method, with the radioactive tracer included in the reservoir. The tracer used was Bi^{210}, obtained through an (n, γ) reaction in a nuclear reactor. Bi^{210} is a β and α emitter with a rather short half-life ($T_{1/2} = 4.989$ days). Thus the necessity arose to carefully verify if the measured radioactivity belonged entirely to the tracer, Bi^{210}. The radiochemical purity of the irradiated bismuth was checked through experimental determination of the decay curve. The experimental points placed themselves on a straight line corresponding to the decay time of Bi^{210}.

Bismuth of similar chemical purity was used for filling the capillaries. The capillary bore (1 mm in diameter and length l about 20 mm) was drilled in a spectrally pure graphite electrode of 5 mm in diameter. As a distinctive feature the apparatus[27] used for the diffusion experiments offered the possibility of changing the samples without solidification of the liquid radioactive metal in the reservoir. This was particularly useful when working with bismuth which expands upon freezing and could have broken the reservoir.

When filling the capillary with metallic bismuth, the volumetric anomaly of this material upon melting (3.32% shrinkage) was taken into account. For this reason, the immersion filling was preferred; it was carried out in an apparatus similar to that used for the diffusion annealings. After solidification an outgrowth formed at the open end of the capillary. Upon remelting the sample in order to perform the diffusion, this excess volume was reabsorbed within the capillary. As the diffusion runs were carried out always at a temperature greater than that of the capillaries filling the liquid expansion resulted in a small excess drop at the open end of the capillary. The presence of this droplet was considered necessary in order to perform a good diffusion run. This drop could, to a certain extent, counterbalance the immersion error [28] (loss of material from the capillary mouth through mechanical sweaping during immersion). On the other hand, if a thin film of oxide had been present, it would have been carried with the droplet into the bath, so that a perfectly clean capillarly-bath interface became available for diffusion.

The diffusion annealings were carried out in an atmosphere of pure hydrogen. Hydrogen is inactive against bismuth, it dissolves neither in solid bismuth nor in liquid bismuth, but it acts as a good reducing agent of bismuth oxides. The temperature was maintained constant during the diffusion run with an accuracy of ± 1°.

The diffusion coefficients have been computed from the integrated equation of Fick's second law. For the boundary and initial conditions used ($c = 0$ for $0 < x < l$ at $t = 0$ and $c = c_0$ for $x < 0$ at $t \geqslant 0$; $x = 0$ at the bath capillary interface), the integrated equation has the form:

$$\frac{\bar{c}}{c_0} = 1 - \frac{8}{\pi^2} \sum_{\nu=0}^{\nu=\infty} \frac{1}{(2\nu + 1)^2} \exp\left[- (2\nu + 1)^2 \frac{\pi^2}{4} \frac{Dt}{l^2} \right] \tag{1}$$

where:

D = self-diffusion coefficient, (cm^2/s)
t = diffusion time, (s)
l = length of the liquid capillary column in which diffusion takes place, (cm)
$\bar{c}$ = average specific radioactivity of the capillary sample after diffusion, (counts/min, g)
c_0 = specific radioactivity of the bath in the reservoir, (counts/min, g)

---

[27] N. Petrescu, St. Zămîrcă, L. Ganovici and I. Ganovici, *Rev. Roumaine Chim.*, **13**, 865 (1968).

[28] C. A. Angell and J. W. Tomlinson, *Discussions Faraday Soc.*, **32**, 237 (1961).

The reference samples for measuring c_0 were taken from the radioactive bath in a manner similar to that described for filling the diffusion capillaries. Their radioactivity was counted in the same conditions as those of the diffusion samples, after taking them out from the graphite sheath.

To compute the diffusion coefficient D from the measurements data by means of eq. (1), a numerical tabulation of the function $\overline{c}/c_0 = f(\theta)$ was used (where $\theta = Dt/l^2$). A computer was used to this purpose and enough terms in the right-hand side of eq. (1) were taken to ensure the convergence of the series.

RESULTS AND DISCUSSION

The results of the experimental determinations are given in table 1 and the temperature dependence of diffusion coefficients is plotted in fig. 1

Table 1

Experimental determinations of the self-diffusion in liquid bismuth

Temperature °C	t Time of diffusion s.	l Length of capillary cm	$\overline{c}$ Average specific radioactivity of capillary after diffusion counts/min. g	c_0 Specific radioactivity of bath counts/min.g	θ	$D \cdot 10^5$ cm²/s	$\overline{D} \cdot 10^5$ cm²/s	ε standard deviation %
275	3 600	2.016	51 923	255800	0.032362	3.65	3.94±0.30	7.6
		1.890	59 658		0.042721	4.24		
285	3 300	1.872	53 129	251500	0.035049	3.72	3.82±0.10	2.6
		1.913	53 390		0.035396	3.93		
300	4 200	2.180	52 440	260200	0.031900	3.61	4.06±0.55	13.5
		2.198	58 146		0.039222	4.51		
350	3 600	2.148	61 493	253500	0.046216	5.92	5.50±0.42	7.6
		2.158	56 680		0.039265	5.08		
400	3 000	2.181	62 664	262100	0.044651	7.08	6.17±0.90	14.6
		2.181	53 899		0.033215	5.27		
500	2 100	2.120	53 902	264500	0.032619	6.98	6.98	—
600	1 620	2.151	53 943	258000	0.034335	8.82	8.71±0.61	7.0
		2.050	50 837		0.030500	7.91		
	1 800	2.143	53 497	247000	0.036841	9.40		
700	1 500	2.065	56 291	249200	0.040075	11.39	11.39	—

One can see that the experimental points place themselves on a straight line representing an Arrhenius type equation in logarithmic form. The statistical analysis of the data resulted in the following Arrhenius equation :

$$D = (38.3 \pm 1.1) \times 10^{-5} \exp\left(-\frac{2507 \pm 124}{RT}\right) \text{cm}^2/\text{s} \qquad (2)$$

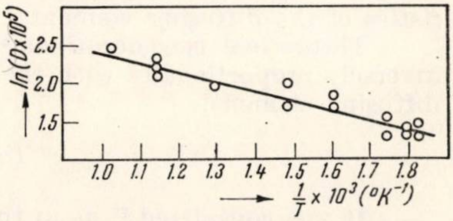

Fig. 1. – Experimental values of the self-diffusion coefficient in liquid bismuth ; least square line calculated according to an Arrhenius type temperature dependence.

Though the physical significance of the parameters in the Arrhenius equation used for liquid diffusion and even the correctness of using it to express the temperature dependence of diffusivities in metallic melts was criticized in the last time,[1] it may still be used to allow comparison among different metals. As concerns the parameters in the Arrhenius equation, the pre-exponential factor D_0 and the activation energy Q, whatever their significance, it may be noted that their experimental values agree with some simple calculating relations.

Saxton and Sherby,[29] in an analysis of the experimental information available up to that time on viscosity and diffusion in pure liquid metals, propose an expression for calculating the activation energy Q, of the same type as that derived theoretically by Bockris.[30]

$$Q = KRT_m \qquad (3)$$

where T_m is the melting point in °K, R is the gas constant in cal/°K, mol, and K is a constant. A correlation between Q and T_m was proposed empirically also by Grosse.[31] When analyzing the experimental data, Saxton and Sherby discriminate the role of the structure prior to melting and propose $K = 3$ for typical metals and $K = 2.75$ for semimetals. The rhombohedric structure of bismuth ranges it among the semimetals. Using $K = 2.75$ we obtained for liquid bismuth $Q_{\text{calc.}} = 2974$ cal/mol, while the value obtained directly from the experimental data was $Q_{\text{exp.}} = 2507$ cal/mol.

The idea concerning the influence of the structure prior to melting on the parameters of the Arrhenius equation for diffusion in metallic melts seems to offer good possibilities for the rationalisation of experimental data.

The listed values for K were obtained from the average slope of plots of the diffusion data computed from viscosities. As soon as more new experimental data on diffusion in metallic melts are going to be available, it will be possible to use them directly for a better choice of constant K. For the time being we mention that from the few existing data on diffusion in liquid semimetals there results for K a value less than 2.75, e.g. for bismuth (present paper) $K = 2.32$, for mercury [9-12] $K = 2.37 \div 2.50$ and for tin [32] $K = 2.56 \div 2.77$.

---

[29] H. J. Saxton and O. D. Sherby, *Trans. Am. Soc. Metals,* **55** ; 826 (1962).

[30] J.O'M. Bockris and G. W. Hooper, *Discussions Faraday Soc.*, **32**, 218 (1962).

[31] A. V. Grosse, *Rev. Hautes Tempér. et Réfract.*, **4**, 171 (1967).

The second parameter in the Arrhenius equation, the pre-exponential factor D_0, can be also evaluated in several ways [33-36] from the characteristics of the diffusing element.

Theoretical considerations [33,36] allow to appreciate that D_0 varies inversely proportionally with the square root of the atomic mass of the diffusing element.

$$D_0 = C/\sqrt{M} \tag{4}$$

It was considered,[29] as in the case of activation energy Q, that the structure in solid state influences the value of D_0 by means of the constant C. This constant has the value $C = 7 \times 10^{-3}$ for metals with a body-centered cubic structure in solid state, and $C = 3.5 \times 10^{-3}$ for prior close-packed metals (having a face-centered cubic structure or a close-packed hexagonal structure). For semimetals C has a variable value which depends on the number of covalent bonds in the structure of the solid material. The authors quoted above [29] have determined this dependence by using values of the diffusivities calculated from viscosity data. As the present paper has increased the number of diffusion determinations in liquid semimetals we could plot the curve from figure 2 by using directly the experimental values of D_0. From figure 2 it may be seen that the effect of the coordination number is manifest in these melts, but its influence

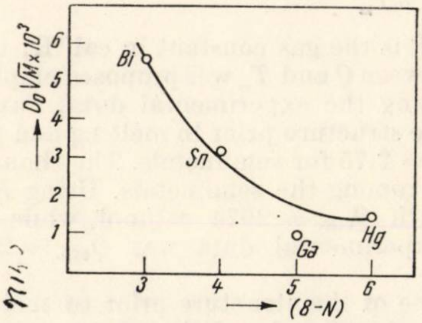

Fig. 2. — Possible dependence of the mass corrected pre-exponential factor D_0 of liquid semimetals, on the coordination number in solid state.

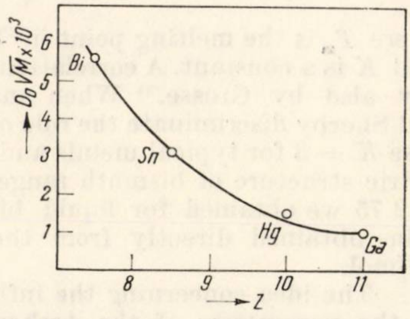

Fig. 3. — Suggested dependence of the mass corrected pre-exponential factor D_0 of liquid semimetals, on the coordination number in liquid state.

---

[32] Y. P. Gupta, *Acta Met.*, **14**, 1007 (1966).

[33] S. Glasstone, K. J. Lardler and H. Eyring, "The Theory of Rate Processes" McGraw-Hill, New York, 1941, p. 525.

[34] J. Frenkel, "Kinetic Theory of Liquids", Dover Publications, New York, 1955, p. 31.

[35] J. A. Cahill and A. V. Grosse, *J. Phys. Chem.*, **69**, 518 (1965).

[36] C. Zener, *J. Appl. Phys.*, **22**, 372 (1951).

is somewhat less pronounced than in the curve plotted when diffusivities computed from viscosities were used.[29] In figure 3 we plotted the value $D_0\sqrt{M}$ for semimetals function of the coordination numbers in liquid state, determined through X-ray diffraction studies.[37] It is to be mentioned that the results place themselves in a more satisfactory manner on the curve.

However, in order to establish a quantitative correlation among liquid state diffusivity, mass of diffusing particle and coordination number, there are required still more experimental data on self-diffusion in liquid state.

From Frenkel's kinetic theory of liquids, Grosse [31,35] points out the following expression for the pre-exponential factor D_0 :

$$D_0 = \frac{k}{6h\,(N_{Av})^{2/3}}\,\theta_D\cdot(V_{at})^{2/3} \tag{5}$$

where V_{at} is the atomic volume of the liquid metal at the melting point θ_D is the Debye temperature of the metal, and k, h and N_{Av} are the usual universal constants. By applying relation (5) we obtained for the factor D_0 of the self-diffusion in liquid bismuth the following values; 44.32×10^{-5}; 43.20×10^{-5} and 33.87×10^{-5}, corresponding to different values given in literature for the Deby temperature of bismuth. The value $D_0 = 38.3 \times 10^{-5}$ we obtained experimentally is situated between these values.

To calculate the self-diffusion coefficients from viscosities, Saxton and Sherby used equation (6)

$$D_{\mathrm{calc}} = S\,\frac{T}{\eta d_i}\,. \tag{6}$$

For the constant S, the authors proposed the value 2×10^{-17} ergs per °K, which results from the predominant slope when plotting the viscosity and diffusion data for 8 metals, for which there were available determinations of self-diffusion in liquid state. As the scatter of the data was at a minimum when Pauling's univalent ionic diameter was used for d_i, this was taken by the quoted authors as the best indicator of relative atomic size in pure liquid metals.

Equation (6), as it can be observed, represents the generalized form of the various theoretical expressions correlating viscosity and diffusivity. The chief theoretical relations of this type are presented in table 2. By calculating the conversion constant S for each relation in table 2, one may note that in Sutherland's equation this constant takes a value which is very close to the value 2×10^{-17} found from experimental data. Thus Sutherland's equation seems the most suitable for predicting diffusivities of liquid metals from viscosity data. For liquid bismuth too, Sutherland's relation correlates the experimental data in the best way. Indeed, by calculating the radius of the diffusing particle in liquid bismuth by means of the relations given in table 2, it appears that Sutherland's equation leads to a value very close to Pauling's univalent ionic radius, while the other expressions result in either overestimated or underestimated values as compared to the possible atomic size parameters. The computation of the radius of the diffusing particle was made at 750°K, situated in the middle of the temperature range for which we studied the self-diffusion in liquid bismuth. The value of the viscosity of bismuth was taken from the data of Ofte and Wittenberg.[38]

---

[37] R. M. Waghorne, V. G. Rivlin and G. I. Williams, *Adv. Phys.*, **16**, 215 (1967).

Table 2

Radius of diffusing particle in liquid bismuth, calculated from self-diffusion data

Theory	Relation	Conversion constant S in eq. (5) ergs/°K	Computed value of the radius of the diffusing particle
Eyring	$D=\frac{k}{2}\frac{T}{\eta r}$	13.800×10^{-17}	6.10
Stokes-Einstein	$D=\frac{k}{6}\frac{T}{\eta r}$	1.465×10^{-7}	0.65
Sutherland	$D=\frac{k}{4}\frac{T}{\eta r}$	2.197×10^{-17}	0.97
Walls-Upthegrove	$D=\frac{k}{2\,(2b+1)}\frac{T}{\eta r}$	2.391×10^{-17}	1.06

metallic radius (Goldschmidt) 1.55÷1.74 A°
tetrahedric covalent radius =1.46 A°
Pauling univalent ionic radius=0.98 A°
$r_{\mathrm{Bi}}^{3+}=0.96$ A°;] $r_{\mathrm{Bi}}^{5+}=0.74$ A° ;

The agreement with ionic radius given by Sutherland's expression, checked also in the present paper, has led to the idea that in liquid metals the diffusion process can be visualized as the migration of ions in the continuum formed by free electrons. Though attractive, this image has to be considered with caution since it does not take into account the interactions between the diffusing ions and the oppositely charged continuum of electrons. On the other hand, the values of the radii of the diffusing particle computed from the relations in table 2 are not constant but are slightly temperature dependent.

The hole theory, which predicts for liquid state diffusion an Arrhenius type temperature dependence, implies a diffusion mechanism similar to the vacancy diffusion in solids. As Nachtrieb [1] points out, when structural particularities of the liquids are taken into account, it appears that this "jump mechanism" is neither the unique possible mechanism nor the most probable. In liquids there may be found a whole spectrum of elementary diffusive motions, the "jump distance" being not necessarily of molecular size. From Egelstaff's determinations of inelastic scattering of neutrons in liquids [39] it may be concluded that this "free diffusion" may be more important than the "jump diffusion".

---

[38] D. Ofte and L. J. Wittenberg, *Trans. Met. Soc. AIME*, **227**, 706 (1963).

Such point of view is taken in the small fluctuation theory of Swalin.[20] It is considered that diffusion in metallic melts occurs through displacement of atoms on small distances of variable size, based on the local density fluctuations. The energy required for the atomic diffusive movement is the energy necessary to produce the density fluctuation. By expressing the variation of the interatomic potential through a Morse function and by treating the size distribution of the fluctuations according to Fürth, Swalin gets an expression for the diffusion coefficient which contains no activation energy, e.g :

$$D = 3.59 \times 10^{-7} \frac{Z}{K} T^2 \tag{7}$$

where : Z = mean coordination number in liquid
K = force constant of the interatomic bond, dyne/cm.

In a revaluation of the theory, Swalin,[6] uses a Boltzmann type statistical treatment instead of Fürth distribution, and reduces the numerical constant in eq. (7) to two thirds of its initial value :

$$D = 2.39 \times 10^{-7} \frac{Z}{K} T^2 \tag{7'}$$

By plotting in fig. 4 the experimental data on the self-diffusion in liquid bismuth function of the square of the absolute temperature, the experimental points placed themselves on a straight line according to eq. (7).

The least square analysis of the experimental data reaches the following expression for this temperature dependence

$$D = 1.194 \times 10^{-10} T^2 \tag{8}$$

By identifying eq. (8) and eq. (7) the value of the force constant K of the interatomic bond in bismuth was derived, using for the coordination number in liquid bismuth the value $Z = 7.5$ obtained by Hendus from X-ray diffraction determinations.[40] The value of the force constant obtained in this manner was $K = 22.6 \times 10^3$ dyne/cm when using the numerical coefficient from eq(7), or $K = 14.9 \times 10^3$ dyne/cm when the numerical coefficient from eq. (7') was used. Since we had not at our disposal the value of the force constant in bismuth derived from compressibility measurements or from spectroscopic data, we could not check the above values. At any rate they are of the correct order of magnitude as can be seen when comparing them with the force constant data given by Waser and Pauling, [41] for other elements.

[39] P. A. Egelstaff, *Adv. Phys.*, **11**, 203 (1962).

[40] H. Hendus, *Z. Naturforsch. A*, **2**, 505 (1947).

[41] J. Waser and L. Pauling, *J. Phys. Chem.*, **18**, 787 (1950).

In figure 5 we plotted experimental data in coordinates D, T according to a first power temperature dependence proposed by Reynik [42]. In the quoted paper, the author considers that a correct application of the transition state theory to the small fluctuations diffusion mechanism results in this kind of temperature dependence of the diffusion coefficients in liquid metals.

From figure 5 it appears that a good correlation of the data is obtained when the straight line is not obliged to pass through the origin of the coordination axes (the corresponding equation is $D = -5.27 \times 10^{-5} + 0.01658 \times 10^{-5}\,\mathrm{T}$). The correlation is less satisfactory when the straight line passes through the origin of the coordination axes (the corresponding equation being in this case $D = 0.009367 \times 10^{-5}\mathrm{T}$).

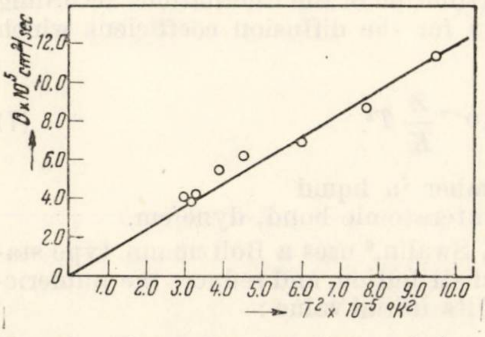

Fig. 4. — Temperature dependence of the self-diffusion coefficients in liquid bismuth on the square of the absolute temperature (Swalin's theory).

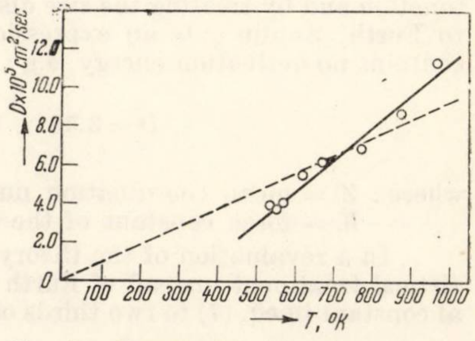

Fig. 5. — Temperature dependence of the self-diffusion coefficients in liquid bismuth on the first power of the absolute temperature (Reynik's and Nachtrieb's relation).

A recent theoretical model for the mechanism of diffusion in liquid metals is that proposed by Nachtrieb.[1] He analyzed how adequately was described the temperature dependence of the self-diffusion coefficient in a number of liquid metals (for which reliable experimental diffusion data were available) by different mathematical functions, e.g. $D = f\left(e^{-\frac{1}{T}}\right)$, $D = f(T^2)$, $D = f(T)$, $D = f(T^{1/2})$. On account of this analysis Nachtrieb suggested the idea that it may be possible that more than one mode of motion, at different time scales, may contribute to the liquid diffusion; moreover, the relative importance of each contribution may be different at different temperatures. Nachtrieb considers that such a contribution to the diffusion process in liquid state can be ascribed to the cooperative motion of the atoms resulting from the irreversible displacement of the "center" of the oscillatory motion executed by each atom. The expression of the diffusion coefficient derived from these considerations is:

$$D = \frac{k^2\,\theta_D}{h\,K}\,T \tag{9}$$

---

[42] R. J. Reynik, *Appl. Phys. Letters*, **9**, 239 (1966).

where : D = self-diffusion coefficient, cm^2/s
T = absolute temperature (°K)
k = Boltzman constant, (erg/°K)
h = Planck constant (erg.sec)
θ_D = Debye characteristic temperature, (°K)
K = force constant of the interatomic bond, dyne/cm.

For a series of metals having cubic structures in solid state (K, Na, Cu, Ag), the self-diffusion coefficient in liquid state at the melting point computed from eq. (9) is close enough to the experimental value. This agreement is considered by Nachtrieb as indicating that the proposed mechanism is responsible of the entire diffusion process. Keeping this fact in mind, the large discrepancies obtained for Zn, In and Sn, with structures in solid state pronouncedly anisotropic, are considered to indicate a persistance of a short range anisotropic order in liquid state too. In this case, the use of the force constant corresponding to nearest neighbours for computation purposes would result in calculated values of the diffusion coefficient smaller than the experimental ones.

By applying relation (9) for liquid bismuth at the melting point, we obtained for the force constant the value $K = 4.97 \times 10^3$ dyne/cm. For computation we used our experimental data on self-diffusion in liquid bismuth. As can readily be seen, the value of the force constant calculated by means of eq. (9) is but 1/3 or 1/4 of its value calculated from eq. (7) or eq. (7′). Taking into account the anisotropic rhombohedral structure of solid bismuth, this result can be interpreted according to Nachtrieb's consideration on Zn, In and Sn, as indicating a short range anisotropic order in liquid bismuth. Yet we consider that this theory should be previously checked with more numerous data on diffusion in liquid metals, before quantitative evaluation of short-range order formations in liquid state would be available on this basis.

Acknowledgement. The authors gratefully acknowledge the most valuable help from and stimulating discussions with Professor I. G. Murgulescu from the University of Bucharest.

Revue Roumaine de Chimie, **15**, 201–208 (1970)

CONTRIBUTION TO THE STUDY OF THE STRUCTURE OF MOLTEN LiF–AlF$_3$ AND NaF–AlF$_3$ MIXTURES

MARTHA PAUČÍROVÁ, K. MATIAŠOVSKÝ and M. MALINOVSKÝ

Institute of Inorganic Chemistry of the Slovak Academy of Sciences, Dubrovska cesta, Bratislava, Czechoslovakia

Received March 27, 1969

An attempt was made to determine the structure of the melts of the system LiF–AlF$_3$ based upon the study of the volume properties of these melts. The results of this study indicate that in the concentration range 0–20 mole % AlF$_3$ the melts in both systems dissociated most probably under the formation of the complex AlF$_6^{3-}$ anions which partially dissociated into AlF$_4^-$ and F$^-$ anions. At the higher AlF$_3$ concentrations the presence of other complex anions, probably of Al$_3$F$_{14}^{5-}$, is to be considered.

INTRODUCTION

From the phase diagrams of the systems LiF – AlF$_3$[1–5] and NaF–AlF$_3$[6–10] it is evident that in both systems a congruently melting compound of the type M$_3$AlF$_6$ (M being Li, resp. Na) is formed. In both cases, the flattening of the maximum indicates a pronounced dissociation of this compound in the melt.

The dissociation of sodium cryolite, Na$_3$AlF$_6$, was studied by several authors. Grjotheim[10,11] assumes that molten cryolite entirely dissociates into Na$^+$ cations and complex AlF$_6^{3-}$ anions, the last being further

---

[1] N. Puschin, A. Baskoff, *Z. anorg. Chem.*, **81**, 347 (1913).

[2] P. P. Fedotieff, L. Timofeeff, *Z. anorg. Chem.*, **206**, 263 (1932).

[3] P. Drossbach, *Z. Elektrochem.*, **42**, 65 (1936).

[4] E. P. Dergunov, Doklady Akad. Nauk S.S.S.R., **60**, 1185 (1948).

[5] M. Malinovský, I. Čakajdová, K. Matiašovský, *Chem. zvesti* **21**, 794 (1967).

[6] P. P. Fedotyev, V. I. Ilyinskij, *Izv. SPB Politekhn. Inst.*, **18**, I., 147 (1912).

[7] N. A. Puschin, A. B. Baskov, *Izv. SPB Elektrotekhnicheskovo Inst.*, **7**, 395 (1912).

[8] N. W. F. Phillips, R. H. Singleton, E. A. Hollingshead, *J. Electrochem. Soc.*, **102**, 690 (1955).

[9] K. Grjotheim, J. L. Holm, C. Krohn, J. Thonstad, in "Selected Topics in High Temperature Chemistry", T. Förland, K. Grjotheim, K. Motzfeldt, S. Urnes, eds. Universitetsforlaget, Oslo 1960, p. 151–178.

[10] K. Grjotheim, "Contribution to the Theory of Aluminium Electrolysis", Det Kgl. Norske Videnskabers Selskabs Skrifter Nr. 5. Bruns Bokhandel, Trondheim, 1956.

[11] K. Grjotheim, C. Krohn, *Chem. zvesti*, **21**, 762 (1967).

partially dissociated.Concerning the dissociation of the complex AlF_6^{3-} anions, Grjotheim considered the following possibilities :

$$2AlF_6^{3-} \rightleftarrows Al_2F_{11}^{5-} + F^- \tag{1}$$

$$2AlF_6^{3-} \rightleftarrows Al_2F_{10}^{4-} + 2F^- \tag{2}$$

$$2AlF_6^{3-} \rightleftarrows Al_2F_9^{3-} + 3F^- \tag{3}$$

$$AlF_6^{3-} \rightleftarrows AlF_5^{2-} + F^- \tag{4}$$

$$AlF_6^{3-} \rightleftarrows AlF_4^- + 2F^- \tag{5}$$

$$AlF_6^{3-} \rightleftarrows Al^{3+} + 6F^- \tag{6}$$

The theoretical liquidus curve for the scheme (5) appears to be in good agreement with the experimentally determined liquidus curve, the equilibrium constant being $K = 0.03 - 0.04$ and the degree of dissociation $\alpha = 0.23 - 0.25$. However, Grjotheim does not exclude the possibility of a simultaneous dissociation according to schemes (5) and (6).

Frank and Foster[12] have studied the dissociation of Na_3AlF_6 on the basis of the density data of molten NaF-AlF_3 mixtures. They have considered the following schemes of dissociation :

$$Na_3AlF_6 \rightleftarrows 3NaF + AlF_3 \tag{7}$$

$$3Na_3AlF_6 \rightleftarrows 4NaF + Na_5Al_3F_{14} \tag{8}$$

$$Na_3AlF_6 \rightleftarrows 2NaF + NaAlF_4 \tag{9}$$

the schemes (7) resp. (9) being equal to the schemes (6) resp. (5) proposed by Grjotheim, since the difference lies only in the different form of presentation (ionic resp. molecular) due to the different methods used in the above mentioned works. With the scheme (9) Frank and Foster obtained a very good agreement between the calculated and experimentally determined values of the density for the equilibrium constant $K = 0.09$.

Vetyukov [13] determined the dissociation degree of Na_3AlF_6 on the basis of the isotherm of the molar volumes of NaF$-NaAlF_4$ mixtures. The determined value was $\alpha = 0.25$. The same method was used already by Pearson and Waddington[14] for the system NaF$-AlF_3$.

The values of the equilibrium constant of dissociation, calculated by [10-12] are in relatively good agreement for the concentration range 0$-$25 mole % AlF_3. However, at higher concentrations of AlF_3 there are large discrepancies among the published data. According to Cochran,[15] this is due to the presence of another complex ion, namely of $Al_3F_{14}^{5-}$, beside AlF_6^{3-} and AlF_4^- . The corresponding compound, $Na_5Al_3F_{14}$ (chiolite) forms in the system NaF$-AlF_3$ as an incongruently melting compound.

---

[12] W. B. FRANK, L. M. FOSTER, *J. Phys. Chem.*, **64**, 95 (1960).

[13] M. M. VETYUKOV, "Fizicheskaya khimia rasplavlennykh solei i shlakov", Trudy vsesoyuznovo soveshchaniya po fizicheskoi khimii solei i shlakov, Metallurgizdat, Moscow, 1962, p. 77.

[14] T. G. PEARSON, J. WADDINGTON, *Discuss. Faraday Soc.* **1**, 307 (1947).

[15] C. N. COCHRAN, *Trans. Met. Soc. AIME*, **239**, 1056 (1967).

Cochran assumes the following dissociation schemes:

$$Na_3AlF_6 \rightleftarrows NaAlF_4 + 2NaF \tag{10}$$

$$Na_5Al_3F_{14} \rightleftarrows Na_3AlF_6 + 2NaAlF_4 \tag{11}$$

Using the method of comparison of the calculated and experimental liquidus curves, he determined the corresponding equilibrium constants $K_{10} = 0.0194$ and $K_{11} = 0.0877$.

METHOD OF CALCULATION

The dissociation degree of the complex anion AlF_6^{3-} in molten Li_3AlF_6, resp. Na_3AlF_6 was determined on the basis of the experimental values of the density of molten LiF$-$AlF$_3$ and NaF$-$AlF$_3$ mixtures[16] using the method suggested by Frank and Foster[12] and by Vetyukov.[13]

The molar volumina of the melts of the system $(LiF)_6-(LiAlF_4)_{3/2}$ and $(NaF)_6-(NaAlF_4)_{\frac{3}{2}}$ calculated on the basis of the experimentally determined values of the density of these melts using the method proposed in[13] are presented in figure 1 and 2.

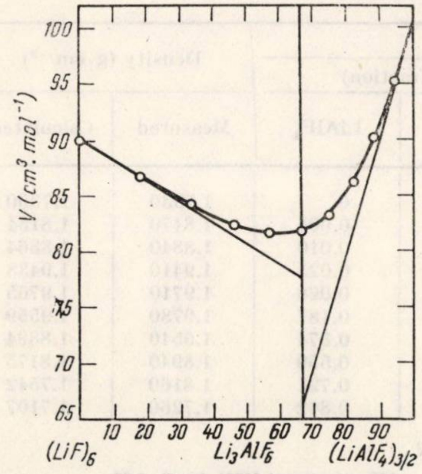

Fig. 1. — Molar volume of $(LiF)_6$ — $(LiAlF_4)_{3/2}$ mixtures at 1000°.

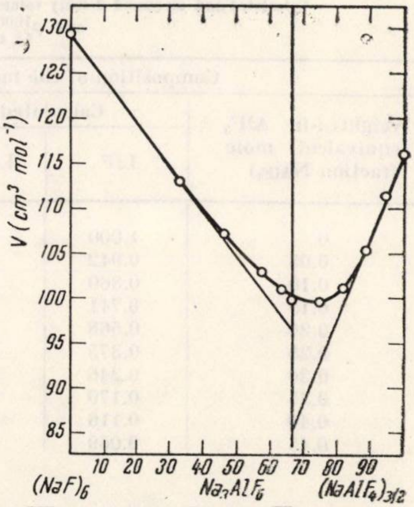

Fig. 2. — Molar volume of $(NaF)_6$ — $(NaAlF_4)_{3/2}$ mixtures at 1000°.

The equilibrium constant K for the systems MF$-$AlF$_3$ was calculated by a method used by Frank and Foster.[12] For this purpose, in both cases the dissociation scheme (9) has been accepted:

$$M_3AlF_6 \rightleftarrows 2MF + MAlF_4$$

The equilibrium constant of this reaction is given by the equation:

$$K = \frac{[MF]^2 \cdot [MAlF_4]}{[M_3AlF_6]} \tag{12}$$

For various selected values of the equilibrium constant K the corresponding composition of the melt (the hypothetical equilibrium concentrations of MF, MAlF$_4$ and M$_3$AlF$_4$) was calculated.

---

[16] M. Paučírová, K. Matiašovský, M. Malinovský, *Rev. Roumaine Chim.*, (in print).

For each value of K the density of the corresponding MF—AlF_3 mixture was calculated using the equation

$$\rho_{mix} = \frac{100}{\dfrac{\text{wt. \% MF}}{\rho_{MF}} + \dfrac{\text{wt. \% } M_3AlF_6}{\rho_{M_3AlF_6(nd)}} + \dfrac{\text{wt. \% } MAlF_4}{\rho_{MAlF_4}}} \qquad (13)$$

For the hypothetical density of non-dissociated (nd) M_3AlF_6 at 1000° the following values have been accepted : $\rho^{1000°}_{Li_3AlF_6(nd)} = 2.10$ g.cm^{-3}, $\rho^{1000°}_{Na_3AlF_6(nd)} = 2.22$ g.cm^{-3}. The density of $NaAlF_4$ was found to be $\rho^{1000°}_{NaAlF_4} = 1.63$ g.cm^{-3}.

In the system LiF—AlF_3 the density measurement was carried out in the concentration range 0—45 mole % AlF_3. The density of $LiAlF_4$ could not be determined experimentally owing to the high vapour pressure of this compound. The density value determined by extrapolation was $\rho^{1000°}_{NaAlF_4} = 1.646$ g.cm^{-3}.

The calculated values of the density of the LiF—AlF_3 and NaF—AlF_3 mixtures at 1000° are presented in figures 3 and 4, and the corresponding data are reported in tables 1 and 2.

Table 1

Calculated and measured density values of LiF — AlF_3 mixtures at 1000° (for K = 0.06 and $\rho^{1000°}_{Li_3AlF_6}$ /nd/ = 2.10 g. cm^{-3}

Composition of the melt				Density (g.cm^{-3})	
Weighted-in AlF_3 (equivalent mole fraction N_{AlF_3})	Calculated (mole fraction)				
	LiF	Li_3AlF_6	$LiAlF_4$	Measured	Calculated
0	1.000	0	0	1.7330	1.7330
0.05	0.942	0.055	0.004	1.8170	1.8154
0.10	0.860	0.129	0.010	1.8840	1.8864
0.15	0.741	0.233	0.025	1.9410	1.9438
0.20	0.568	0.364	0.068	1.9710	1.9765
0.25	0.375	0.438	0.187	1.9780	1.9559
0.30	0.246	0.379	0.374	1.9540	1.8894
0.35	0.170	0.270	0.559	1.8940	1.8175
0.40	0.116	0.163	0.721	1.8160	1.7542
0.45	0.069	0.069	0.862	1.7260	1.7107

Table 2

Calculated and measured density values of NaF — AlF_3 mixtures at 1000° (for K=0,06 and $\rho^{1000°}_{Na_3AlF_6}$ /nd/ = 2.22 g.cm^{-3})

Composition of the melt				Density (g.cm^{-3})	
Weighted-in AlF_3 (equivalent mole fraction N_{AlF_3})	Calculated (mole fraction)				
	NaF	Na_3AlF_6	$NaAlF_4$	Measured	Calculated
0	1.000	0	0	1.9452	1.9452
0.05	0.942	0.055	0.004	—	1.9967
0.10	0.860	0.129	0.010	2.0430	2.0431
0.15	0.741	0.233	0.025	2.0795	2 0805
0.20	0.568	0.364	0.068	2 0982	2.0942
0.25	0.375	0.438	0.187	2.1020	2.0488
0.30	0.246	0.379	0.374	2.0545	1.9514
0.35	0.170	0.270	0.559	1.9775	1.8500
0.40	0.116	0.163	0.721	1.8590	1.7609
0.45	0.069	0.069	0.862	1.7242	1.6862

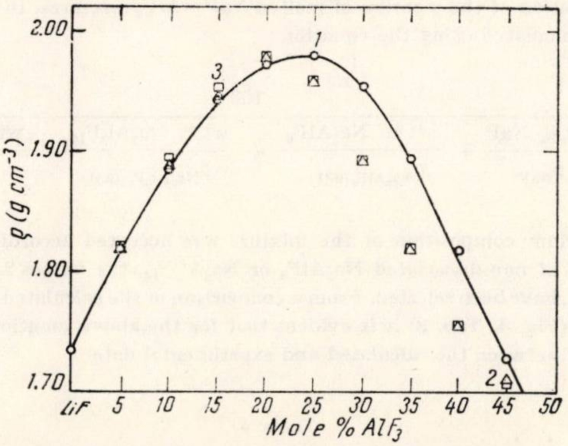

Fig. 3. — Density of LiF–AlF$_3$ mixtures at 1000°.
1, experimental values, *2*, calculated values for K = 0.06, *3*, calculated values for K = 0.10.

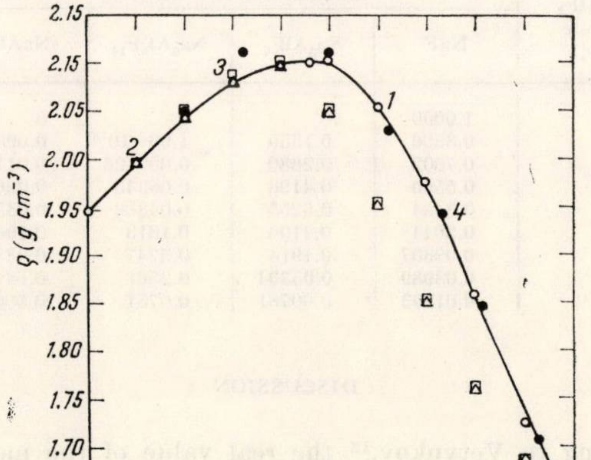

Fig. 4. — Density of NaF–AlF$_3$ mixtures at 1000°
1, experimental values, *2*, calculated values for K = 0.06, *3*, calculated values for K = 0.08, *4*, values calculated according to the equation (14).

According to Cochran,[15] in the melts of the system $NaF—AlF_3$, beside the anions AlF_6^{3-} and AlF_4^-, the complex anions $Al_3F_{14}^{5-}$ are also present. This assumption was also considered in the calculation of the density of molten $NaF-AlF_3$ mixtures. In this case the density of a mixture was calculated using the equation :

$$\rho_{\mathrm{mix}} = \frac{100}{\dfrac{\mathrm{wt\,\%\ NaF}}{\rho_{\mathrm{NaF}}} + \dfrac{\mathrm{wt\,\%\ Na_3AlF_6}}{\rho_{\mathrm{Na_3AlF_6(nd)}}} + \dfrac{\mathrm{wt\,\%\ Na_5Al_3F_{14}}}{\rho_{\mathrm{Na_5Al_3F_{14}(nd)}}} + \dfrac{\mathrm{wt\,\%\ NaAlF_4}}{\rho_{\mathrm{NaAlF_4}}}} \tag{14}$$

The equilibrium composition of the mixture was accepted according to[15] and for the hypothetic density of non-dissociated Na_3AlF_6 or $Na_5Al_3F_{14}$, the values 2.22 $g.cm^{-3}$ and 2.00 $g.cm^{-3}$ respectively, have been selected. From a comparison of the calculated and experimentally determined values (Fig. 4, Tab. 3) it is evident that for the above mentioned values there is the best agreement between the calculated and experimental data.

Table 3

Calculated and measured density values of NaF – AlF_3 mixtures at 1000°
(for $\rho^{1000°}_{Na_3AlF_6}$ /nd/ = 2.22 $g.cm^{-3}$, $\rho^{1000°}_{Na_5Al_3F_{14}}$ /nd/ = 2.00 $g.cm^{-3}$)

Composition of the melt					Calculated density ($g.cm^{-3}$)
Weighted-in AlF_3 (equivalent mole fraction N_{AlF_3})	Calculated (mole fraction)				
	NaF	Na_3AlF_6	$Na_5Al_3F_{14}$	$NaAlF_4$	
0	1.0000	0	0	0	1.9452
0.0988	0.8606	0.1359	1.96×10^{-5}	0.00356	2.0540
0.1601	0.7002	0.2880	0.000426	0.01139	2.1100
0.1978	0.5500	0.4196	0.00346	0.02689	2.1340
0.2500	0.3454	0.5255	0.04366	0.08538	2.1100
0.3111	0.2044	0.4196	0.1813	0.1947	2.0290
0.3665	0.09807	0.1914	0.3247	0.3858	1.9426
0.4085	0.03989	0.05334	0.2568	0.6499	1.8480
0.4642	0.01293	0.00781	0.0731	0.9062	1.7070

DISCUSSION

According to Vetyukov,[13] the real value of the molar volume of non-dissociated Na_3AlF_6 in the molten $NaF-NaAlF_4$ mixtures can be determined graphically as the common point of intersection of the tangents to the molar volumes isotherm in the points corresponding to the molar volumes of NaF and $NaAlF_4$ with the co-ordinate corresponding to the cryolite composition. However, this hypothesis was not confirmed in the present work, since there is no common point of intersection of the tangents to the molar volumes isotherm with the co-ordinate corresponding to Li_3AlF_6, resp. Na_3AlF_6 (Fig. 1, 2). The erroneous conclusion made by Vetyukov is probably due to the fact that in[13] the density of the $(NaF)_6-(NaAlF_4)_{3/2}$ mixtures was experimentally measured only to the concentration of approximately 85 mole % $(NaAlF_4)_{3/2}$ and the molar volume of $NaAlF_4$ was determined by the graphical extrapolation. Furthemore, the assumption concerning the additivity of the molar volumes, which is a fundamental condition, is fulfilled only in the partial systems $MF-M_3AlF_6$, whilst it is not valid in the partial systems $M_3AlF_6-MAlF_4$.[16]

The density values of the $MF-AlF_3$ mixtures calculated according to scheme (9) proposed by Frank and Foster [12] are in good agreement with the experimental data up to the concentration of 20 mole % AlF_3 (Fig. 3, 4). In this concentration range the equilibrium constant for both systems has the same value, $K = 0.06$, this corresponding to the dissociation degree $\alpha = 0.3$. These values of K and α are in good agreement with those determined by Grjotheim [11] in the system $NaF-AlF_3$ on the basis of the liquidus curves method. At higher AlF_3 concentrations there are relatively large discrepancies between the experimental and calculated data. Hence, it may be assumed that scheme (9) does not describe entirely the process of dissociation. The very good agreement between the measured and calculated values reported by Frank and Foster [12] is due most probably to the irrationally high value of the density of $NaAlF_4$ (1.873 g. cm^{-3}) which was accepted in.[12] The density of $NaAlF_4$, experimentally determined in the present work, at 1000° was found to be $\rho^{1000°}_{NaAlF_4} = 1.63$ g.cm^{-3}, this being in a good agreement with the values obtained by the extrapolation based on the density data measured by.[17–20] The extrapolated values, range in the interval 1.60 – 1.72 g.cm^{-3}. Thus it is evident that the extremely high density value accepted by Frank and Foster is not physically justified.

The calculation of the molar volumes in [12] is based on the following assumption :

$$V_{\text{mix.}(A+B)} = x_A V_A + (1 - x_A)\, V_B$$

However, from our previous work [16] it follows that this assumption may be considered to be satisfactorily fulfilled only in the partial systems $MF-M_3AlF_6$, whilst in the systems $M_3AlF_6-AlF_3$, resp. $M_3AlF_6-MAlF_4$ there are large deviations from the above mentioned expression. A relatively good agreement between the calculated and the experimental data in the systems $MF-M_3AlF_6$ up to the concentration 20 mole % AlF_3 (in the concentration co-ordinates $MF-AlF_3$) is due to the fact that in this concentration range there practically exist simultaneously only two anionic species, AlF_6^{3-} and F^-, anions AlF_4^- being present only in a minor concentration (Tab. 3, 4). On the other hand, in the systems $M_3AlF_6-MAlF_4$ actually in the whole concentration range at least 3, more probably 4 anions are present, namely AlF_6^{3-}, AlF_4^-, F^- [12] and most probably also $Al_3F_{14}^{5-}$.[15]

[17] Z. F. Lundina, *Trudy VAMI*, **13**, 5 (1936).

[18] G. A. Abramov, P. A. Kozunov, *Trudy Leningrad. politekhn. inst., Razdel metallurgia*, **1**, 60 (1939).

[19] A. Vajna, *Alluminio*, **19**, 541 (1950).

[20] J. D. Edwards, C. S. Taylor, A. S. Russel, *J. Electrochem. Soc.*, **100**, 508 (1953).

Therefore, the density of the NaF—AlF_3 mixtures was calculated assuming that the co-existence of Na_3AlF_6, $NaAlF_4$ and $Na_5Al_3F_{14}$. The calculated density values are in a very good agreement with the experimental data (Fig. 4), thus supporting the assumption of the existence of the $Al_3F_{14}^{5-}$ anions in the melt.

An analogous calculation for the system LiF—AlF_3 could not be carried out since in the study of the phase equilibria in this system no compound of the type $M_5Al_3F_{14}$ or any other complex compound was determined.[1-5]

Revue Roumaine de Chimie, 15, 209–212 (1970)

ON THE INTERMEDIATE IN THE REACTION MECHANISM OF Me(III) OXALATO COMPLEXES DECOMPOSITION

TATIANA ONCESCU

Department of Physical Chemistry, University of Bucharest, Bd. Republicii 13

Received February 6, 1969

The present paper brings some physico-chemical arguments to establish the nature of the radical-ion appeared on decomposition of Me (III) oxalato complexes in solution.

* * *

There is an extensive literature on the thermal[1–4] and photochemical[3–8] decomposition of oxalato complexes of some trivalent transitional metals like iron, cobalt and manganese.

Irrespective of the adopted mechanism concerning the first step of the reaction — spontaneous decomposition or solvent participation — the presence of a radical ion resulted from an oxalate group by an internal electron transfer process, was unanimously admitted.

In our papers [9,10] concerning the thermal decomposition of Co(III) and Mn (III) oxalato complexes, we admitted the existence of $C_2O_4^{\cdot -}$ radical ion in solution, which appears according to the following scheme:

$$[\mathrm{Me}(C_2O_4)_3]^{-3} + H_2O \rightleftharpoons [\mathrm{Me}(C_2O_4)_2\,OC_2O_3H_2O]^{-3} \qquad \text{(I)}$$

$$[\mathrm{Me}(C_2O_4)_2OC_2O_3H_2O]^{-3} \rightleftharpoons [\mathrm{Me}(C_2O_4)_2]^{-2} + H_2O + C_2O_4^{\cdot -} \qquad \text{(II)}$$

$$[\mathrm{Me}(C_2O_4)_3]^{-3} + C_2O_4^{\cdot -} \rightarrow [\mathrm{Me}(C_2O_4)_2]^{-2} + 2CO_2 + C_2O_4^{-2} \qquad \text{(III)}$$

Taube [1] and others assume that in solution the fast reaction:

$$C_2O_4^{\cdot -} \rightarrow CO_2^{\cdot -} + CO_2$$

[1] H. Taube, *J. Amer. Chem. Soc.*, **70**, 1216 (1948).

[2] A. W. Adamson, H. Ogata, J. Grossman and R. Newbury, *J. Ionorg. Nucl. Chem.*, **6**, 319 (1958).

[3] T. B. Copstake and N. Uri, *Proc. Roy. Soc.*, A 228, 252 (1955).

[4] F. D. Graziano and G. M. Harris, *J. Phys. Chem.*, **63**, 330 (1959).

[5] I. G. Murgulescu, *Bull. Soc. Sc. Cluj*, **8**, 1933 (1935).

[6] C. Furlani and A. Ciana, *Ann. Chim.* (Ital), **47**, 1081 (1957).

[7] A. W. Adamson and A. H. Sporer, *J. Amer. Chem. Soc.*, **80**, 3865 (1958).

[8] C. A. Parker and C. G. Hatchard, *J. Phys. Chem.*, **63**, 22 (1959).

[9] I. G. Murgulescu and T. Oncescu, *Z. Phys. Chem.* (*Leipzig*), **214**, 238 (1960).

[10] I. G. Murgulescu and T. Oncescu, *Rev. Roumaine Chim.*, **10**, 3 (1965).

is also possible and therefore the $CO_2^{\cdot -}$ is the radical ion that takes part in reaction III. Stranks, Dainton et al.[11] consider that $CO_2^{\cdot -}$ appears even from the descomposition of the monoaquaeted complex (reaction II), as follows:

$$[Co(C_2O_4)_2OC_2O_3H_2O]^{-3} \rightleftharpoons [Co(C_2O_4)_2]^{-2} + H_2O + CO_2^{\cdot -} + CO_2 \qquad (II')$$

Their conclusion is grounded as follows in solution a fast exchange must establish itself:

$$C_2O_4^{\cdot -} \rightleftharpoons \overset{*}{C}_2O_4^{-2}$$

and if exchange is rapid, thermal decomposition should yield radioactive $\overset{*}{C}O_2$ (using C^{14}). Experiments with the tris-oxalatocobalt (III) in the presence of radiocobalt as Co(II) in oxalate solution, showed the absence of any significant radioactivity in the evolved carbon dioxide. Dainton concluded that most probably $CO_2^{\cdot -}$ takes part in reaction III. He explained the reduced activity in the evolved CO_2 as due to a very slow electron transfer reaction between Co (II) oxalato/Co (III) oxalato complexes, followed by the decomposition of the active trisoxalato-complexes:

$$[Co(C_2O_4)_3]^{-3} + \left[\overset{*}{Co}(C_2O_4)_n\right]^{2-2n} \rightleftharpoons \left[\overset{*}{Co}(C_2O_4)_3\right]^{-3} + [Co(C_2O_4)_n]^{2-2n}$$

Shagisultanova[12] tries to evidence by ESR spectra on UV iradiation of $[Co(C_2O_4)_3]K$, the presence of $C_2O_4^{\cdot -}$ radical ion, but concluded that it is not possible to notice the respective signal because of a "cage effect".

Because of the controversy concerning this intermediate, we thought it worthwhile investigating this problem, to obtain further proofs on its nature.

RESULTS

In our experiments we have used the manganese bisoxalato complex $[Mn(C_2O_4)_2\ (H_2O)_2]K$, which decomposes in the same way as the trisoxalato complex, producing the same radical ion but more quickly.

The essential properties of this intermediate, the precipitation of calomel in the presence of $HgCl_2$, or the polymerization of some monomers like vinyl acetate, metamethylacrylate, acrylonitrile, were already showed by various researchers.[13, 3, 10, 14]

We have assumed that if this radical ion can initiate the polymerization, it also can close the chain[15] and infrared spectrum will show this fact.

---

[11] F. S. Dainton, G. S. Laurence, W. Schneider, D. R. Stranks and M. S. Vaidya, "Radioisotopes in Scientific Research", Pergamon-Press, London, 1958 pp. 305–325.

[12] A. L. Pozniak and G. A. Shagisultanova, *Doklady. Akad. Nauk. S.S.S.R.*, **173**, 612 (1967).

[13] J. M. Eder, *Chem. Ber.*, **XIII** 502 (1880).

[14] R. Inoue, T. Yamauchi and T. Ozechi, *Chem. High Polymers (Japan)*, **11**, 489 (1955).

[15] I. G. Murgulescu, T. Oncescu and I. Vlagiu, Communicated at the 1st National Conference on Physical Chemistry Bucharest, Sept 1968.

To this purpose we have prepared polyacrylonitrile in the presence of a small amount of $[Mn(C_2O_4)_2(H_2O)_2]K$ (below 1 cg) in a water-alcohol mixture (2 : 1) slowly acidified with nitric acid, by bubbling argon. The obtained polymer has a great colouring ability, due to the presence of the free carboxylic groups, at the ends of the chain, unlike the polymers prepared on the irradiation of acrylonitrile with γ rays emitted by Co^{60}, also by bubbling argon. From the comparative analysis of the infrared spectra (using the potassium bromide disk method) of the two kind of polymers, results the presence of the characteristic $C=O$ stretching frequency of about 1740 cm^{-1}, in the case of the polymer prepared under the complex action (Fig. 1).

The $>C=O$ bonding can be

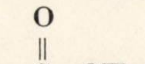

$$-\overset{\displaystyle O}{\overset{\|}{C}}-OH$$

either from the $-\overset{O}{\overset{\|}{C}}-OH$ group, or from the $-O-\underset{\displaystyle O}{\underset{\|}{C}}-\underset{\displaystyle O}{\underset{\|}{C}}-OH$ one, re-

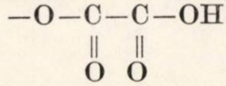

$$-O-\underset{\displaystyle O}{\underset{\|}{C}}-\underset{\displaystyle O}{\underset{\|}{C}}-OH$$

sulted from $CO_2^{\cdot -}$ or $C_2O_4^{\cdot -}$ radical ion.

To verify its nature we have treated the polymer with dilute NaOH at 30° for a few minutes, filtered it and the obtained solution treated according to the indication of Paget and Berger[16] with phenylhidrazine chloride. A pink colour of high sensitivity (1 γ) only to oxalic acid, appeared. The test with chromotropic acid,[17] specific only to formic acid, was negative.

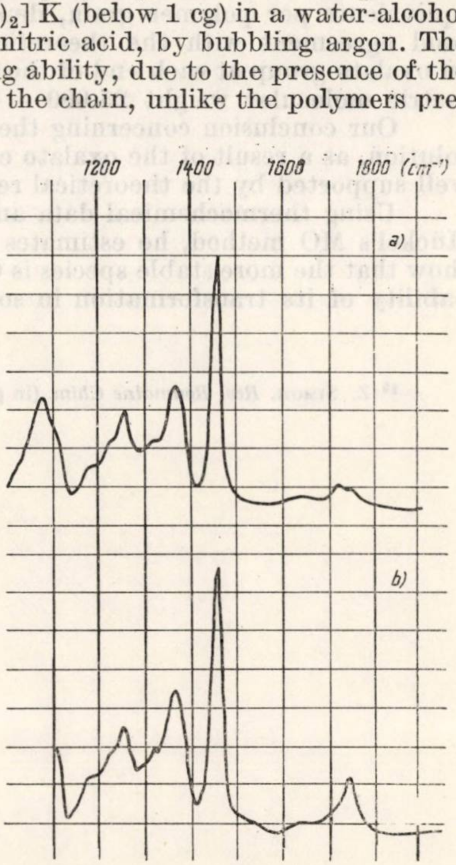

Fig. 1. — IR spectra of the polyacrylonitrile prepared ;
a, on the γ rays irradiation, *b*, under the Me (III) oxalato complex action.

In addition we have titrated with KOH the dissolved polymer in dimethylformamide, in the presence of NaCl and phenol red according to Urbanovicz.[18]

By using the formula : $\dfrac{N f 10^{-3} V}{n g}$ in which,

N = ml KOH n/20 used at the titration
f = the factor of KOH n/20 solution
V = the volume in which the polymer dissolved
g = the amount (in grams) of dissolved polymer
n = ml, the volume of the titrated sample

---

[16] M. Paget and R. Berger, *Bull. biol. pharm.*, **70**, 2(1938).
[17] E. Eegriwe, *Z. anal. Chem.*, **110**, 22, (1937).
[18] S. Urbanovicz, *Chem. Analit.*, **4**, 575 (1961).

we have found results, in the range $0.67 \times 10^{-4} - 1.03 \times 10^{-4}$ COOH equivalents per polymer gram, depending on the prepared polymer, in good agreement with the theoretical ones : $(0.5-0.8)10^{-4}$ (considering an oxalato group at each end of the chain, for the polymers with a viscosimetric molecular weight 25.000 — 40.000).

Our conclusion concerning the presence of the $C_2O_4^{\cdot-}$ radical ion in solution, as a result of the oxalato complexes decomposition, is also quite well supported by the theoretical results of Simon.[19]

Using thermochemical data and conjugation energies calculated by Hückel's MO method, he estimates the $C_2O_4^{\cdot-}$ stability. His calculations show that the more stable species is $C_2O_4^{\cdot-}$ and not $CO_2^{\cdot-}$, hence the improbability of its transformation in solutions into $CO_2^{\cdot-}$.

[19] Z. Simon, *Rev. Roumaine Chim.* (in print).

Revue Roumaine de Chimie, **15**, 213–219 (1970)

SELF-DIFFUSION OF LIQUID CADMIUM FROM ITS MELTING POINT TO 500°

I. GANOVICI and LUCIA GANOVICI

Physical Chemistry Research Center, Bucharest, str. Galaţi 31

Received January 31, 1969

Self-diffusion coefficients of liquid cadmium have been measured by the capillary-reservoir method using the radioactive isotope Cd^{115}. The temperature dependence of diffusivity from its melting point to 500° was investigated. The results can ber epresented by the equation $D = 7.54 \times 10^{-4} \exp(-4419/RT)$. The self-diffusion data D_0 and E_D are compared with the values of cadmium neighbours in the periodical system both vertically and horizontally.

There is little information on the diffusivity of pure liquid metals because of the considerable difficulties of the experimental technique particularly at high temperatures. At present there have been determined self-diffusion coefficients on only nine metals.

In several synthetical works, concerning the transport properties in liquid metals [1–3] cadmium is not listed among the metals whose self-diffusion coefficients were measured. Yet, we found only one paper published by Mirshamsi [4] which presents the self-diffusivity values of Cd and Pb in the binary-liquid Cd–Pb system; in this work are presented also experimental values of self-diffusion coefficients of liquid cadmium.

It is the purpose of the present investigation to complete available experimental data necessary for understanding the diffusion mechanism in liquid metals. It also tries to complete the subgroup IIb of the periodical system since both the viscosity and self-diffusion of Zn and Hg have been measured.

---

[1] H. J. Saxton and O. D. Sherby, *Trans. A.S.M.*, **55**, 826 (1962).

[2] J. R. Wilson, *Metallurgical Rev.*, **10**, 445 (1965).

[3] A. V. Grosse, *Rev. Inst. Hautes Tempér. et Refract.*, **4**, 171 (1967).

[4] M. Mirshamsi, *Trans. A.I.M.E.*, **236**, 125 (1966).

EXPERIMENTAL

The self-diffusion coefficients of liquid cadmium have been determined by the capillary-reservoir method using the radioactive tracer Cd^{115}. The presentation of this method including a discussion of the experimental techniques required for precise measurements, has been published in a previous paper. [5]

In our experiments, an amount of 70 g cadmium 99.999 pct purity was made radioactive by adding about 1 mCi of Cd^{115}. A quartz crucible containing this material served as a reservoir.

The diffusion experiments were carried out in purified hydrogen atmosphere after the installation was successively pumped out and then filled with hydrogen several times. The choice of hydrogen as a protective atmosphere was determined by the absence of the solubility of hydrogen in liquid cadmium. On the other hand since the cadmium oxides are reduced from about 250°–300° in hydrogen atmosphere, we had the possibility to purify the surface of the liquid metal by keeping the reservoir for five minutes at 450° before each diffusion run.

The investigated temperature range had a top limit of 500° because of the volatility of liquid Cd (the vapour pressure of Cd at 500° is 13 mm Hg while at 600° it is 83 mm Hg). The temperature both of the reservoir and samples was maintained constant within ± 1° precision during about 1–2 hours for homogenization at operating temperature.

Two samples at a time were employed for each diffusion experiment. They were made of spectrally pure graphite about 20 mm in length and 1 mm inside diameter (to avoid convection currents) and were filled by means of a previously described technique. [5] Before filling the length of the capillaries has been measured with a 0.01 mm precision. The samples were sharpened at the open end in order to avoid drawing out of metal from the reservoir. After the capillaries were slowly raised out of the melt, they were solidified before being taken out of the furnace, otherwise the solidification front can favour at some samples a sedimentation of oxide impurities owing to a higher density (8.2 g/cm³) than liquid cadmium (8.01 g/cm³ at 330° and 7.82 g/cm³ at 500°). This effect has been observed at some of our samples in determining the radioactivity penentration curve.

The self-diffusion coefficients have been computed both from the integral radioactivity of the samples ($\overline{C}/C_0$) after diffusion and from radioactivity penetration curve using relations (1) and (2) respectively:

$$\frac{\overline{C}}{C_0} = 1 - \frac{8}{\pi^2} \sum_{n=0}^{\infty} \frac{1}{(2n+1)^2} \exp\left[-\frac{(2n+1)^2\pi^2}{4} \cdot \frac{Dt}{l^2}\right] \tag{1}$$

$$\frac{C}{C_0} = 1 - \frac{4}{\pi} \sum_{n=0}^{\infty} \frac{1}{(2n+1)} \sin\frac{(2n+1)\pi}{2}\frac{x}{l} \exp\left[-\frac{(2n+1)^2 \cdot \pi^2}{4}\frac{Dt}{l^2}\right] \tag{2}$$

where C_0 is the specific radioactivity of molten metal in the reservoir; t, is the diffusion time (s); l, is the capillary length (cm); x, is the distance from the open end of capillary (cm) and D, the self-diffusion coefficient (cm²/s).

The relations (1) and (2) have been obtained by integrating Fick's second law; the initial and boundary conditions in our experiments being: $C = 0$ for $t = 0$ and $0 < x < l$; $C = C_0$ for $x = 0$ and $\frac{\partial c}{\partial x} = 0$ for $x = l$ when $t > 0$.

After the diffusion run the metal rods were separated, weighed and measured in the same geometrical conditions. All good rods were then cut into about 1.5 mm pieces which were weighed and whose radioactivity was measured. From the counting results the $C/C_0 = f(x_k/l)$ penetration curves were constructed. We have considered in our calculations $x_k/l = \sum_{i=1}^{k} g_i/G$ where $\sum_{i=1}^{k} g_i$ is the weight of all pieces from the open end of the capillary and G, is the total weight of the samples. In this way, no correction for contraction of the sample was necessary.

---

[5] N. Petrescu, St. Zămîrcă, Lucia Ganovici and I. Ganovici, *Rev. Roumaine Chim.*, **13**, 865 (1968).

To compute the self-diffusion coefficients, both (1) and (2) relations were tabled by a CET–500 computer after two parameters $\theta = Dt/l^2$ and $\delta = x_k/l$.

RESULTS. DISCUSSION

We have determined the self-diffusion coefficients of liquid Cd in the temperature range from 330° to 500° for six different temperatures. The results for the good runs are shown in table 1 where the values in column 5 are an average of the diffusion coefficients calculated by the two methods.

Table 1

Experimental diffusivity data for liquid Cd

Run	Diffusion temperature, °C	Diffusion time, s	Length of capillary, cm	$D.10^5$, cm²/s	
				Experim.	Average
I 12 S	330	13500	2.034	2.09	1.99±0.14
II 1 S	330	9000	2.068	1.89	
I 11 S	350	12600	1.944	2.40	2.20±0.14
II 5 S	350	9000	2.041	2.08	
II 7 S	350	7200	1.972	2.17	
II 7 D	350	7200	1.907	2.14	
I 4 D	390	7200	1.875	2.48	2.38±0.13
I 4 S	390	7200	1.991	2.52	
I 10 D	390	10800	1.950	2.21	
I 10 S	390	7200	2.043	2.47	
II 6 D	390	7200	1.913	2.35	
II 8 S	390	6480	1.686	2.25	
I 3 D	430	6420	2.070	2.91	2.96±0.42
I 3 S	430	6420	1.983	3.10	
I 9 D	430	9000	2.064	2.55	
I 9 S	430	9000	2.005	2.47	
II 11 S	430	6315	2.094	2.78	
II 10 S	430	4470	1.801	3.26	
II 10 D	430	4470	1.633	3.67	
I 8 D	470	7200	2.028	4.45	3.87±0.78
I 8 S	470	7200	2.012	4.18	
II 12 D	470	5400	2.032	2.98	
I 1 D	500	4500	2.070	4.60	4.52±0.33
I 1 S	500	4500	1.983	4.49	
I 7 D	500	6300	2.034	4.70	
II 3 S	500	4500	2.006	3.97	
II 3 D	500	4500	2.048	4.84	

Revue Roumaine de Chimie, **15**, 213–219 (1970)

We have considered that a run was good if the experimental points of the radioactivity penetration curve superposed over theoretical curve (2).

Nearly 40 pct of the runs were disqualified in this way, some of these exhibiting a perturbation of radioactivity distribution along the sample (fig. 1).

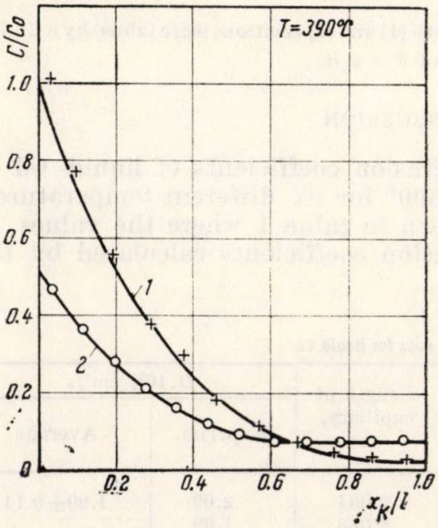

Fig. 1. — Radioactivity distribution obtained by sectioning of sample.
1, sample solidified in the furnace; *2*, sample solidified after being taken out of the furnace.

Fig. 2. — Self-diffusion coefficients calculated from the curves shown in fig. 1, using eq. (2); *1*, sample solidified in the furnace; *2*, sample solidified after being taken out of the furnace.

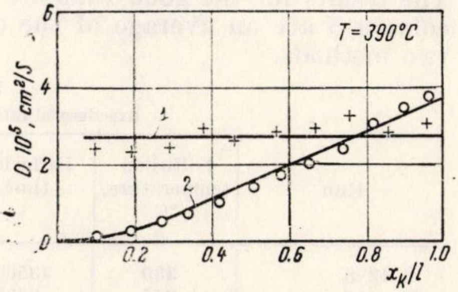

The decrease of radioactive concentration at the open end of the sample, together with an increase at the closed end leads to an increase of self-diffusion coefficients along the sample (fig. 2). This effect was more obvious at higher temperatures. In accordance with our previous considerations it is due to the sedimentation of oxide impurities, a phenomenon which increases with the temperature. In order to diminish this effect we have cooled the samples in the furnace and thus, the number of disqualified samples became smaller.

Both an average self-diffusion coefficient and its corresponding mean square error were calculated for every operating temperature, so that the average of relative error was 10 pct.

The best representation of our experimental values on a $\log D = f(1/T)$ plot by the least squares analysis is a straight line in terms of an equation of the Arrhenius type:

$$D = 7.54 \times 10^{-4} \exp(-4419/RT) \tag{3}$$

Data on liquid Cd being now available, it is appropriate to compare them with those belonging to its neighbours in the subgroup IIb of the periodical system, namely, zinc[6] and mercury[7] as shown in table 2.

In line with decreasing melting points in the sequence Zn→Cd→Hg the activation energy of diffusivity E_D, decreases, the same behaviour being also noticed for the pre-exponential factor D_0. Since Zn and Cd have the same crystal structure (typical metals) it is to be

[6] N. H. Nachtrieb, E. Fraga and C. Wahl, *J. Phys. Chem.*, **67**, 2353 (1963).

[7] D. Z. Brower and D. G. Tuck, *Trans. Faraday Soc.*, **60**, 1230 (1964).

Table 2

Experimental and calculated diffusivity data for Zn, Cd, Hg

Element	$T_{\text{m.p.}}$ °K	Crystal structure	D_0, cm²/s. 10^4		e^{γ}	E_D, cal/g.atom		E_D, cal/g. at from η exp.
			Exp.	Calc. eq. (5)		Exp.	Calc. eq. (4)	
Zinc	692.7	H.c.p.	8.2	4.64	1.77	5090	4600	4800
Cadmium	594	H.c.p.	7.54* 3.621**	3.80	1.98	4419* 3305**	3971	3520
Mercury	234.3	Rhomb.	1.26	2.44	0.52	1160	1330	1330

* Present work
** Mirshamsi's values

expected that their D_0 and E_D values should be very close. Our experimental values for Cd confirm this supposition. Mercury having an open structure (semimetal) has a smaller activation energy.

In order to illustrate these considerations the use of a homologous reciprocal temperature is appropriate in comparing diffusivity behaviour of Zn, Cd, and Hg (fig. 3).

It is possible to evaluate both the values E_D and D_0. Thus, E_D can be calculated by one of the empirical relations of Bockris,[8] Saxton and Sherby[1] or Grosse.[3] We have calculated E_D using Grosse's relation :

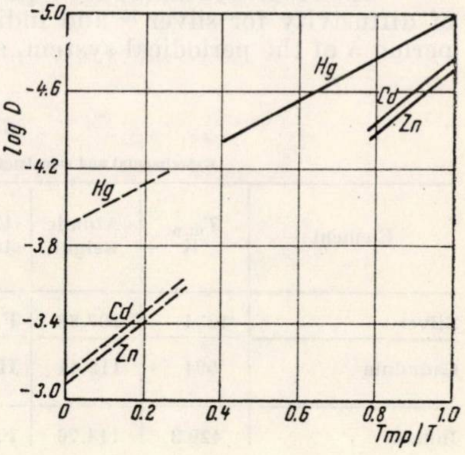

Fig. 3. — Plot of diffusivity data as $\log D = f(T_{\text{m.p.}}/T)$ for liquid Zn, Cd, and Hg. Solid lines indicate experimental temperature range investigated ; dashed lines are extrapolations of data to $T_{\text{m.p.}}/T = 0$.

$$E_D = 3.53\,T_{\text{m.p.}}^{1.10}\ ;\quad (T_{\text{m.p.}}\ \text{in °K}) \tag{4}$$

which is more reliable since it is based on a large number of experimental data for liquid metals. The agreement between calculated and experimental values for Cd is very satisfactory.

---

[8] L. O'M Bockris and G. W. Hooper, *Discuss. Faraday Soc.*, **32**, 218 (1962).

The D_0 value can be calculated also on the basis of Frenkel's[9] theory from the expression:

$$D_0^{\text{theor}} = \frac{k\Theta}{6h}\left(\frac{V_{\text{at}}}{N_{\text{Av}}}\right)^{2/3} \tag{5}$$

where k and h are the Boltzman and Planck's constants; Θ, is the Debye temperature; V_{at}, the liquid atomic volume at the melting point.

Experimental values of D_0 cannot be compared directly with D_0^{theor} since there appears an entropy factor of the system as it results from Frenkel's theory. This factor, $e^{\gamma} = D_0^{\text{exp}}/D_0^{\text{theor}}$ can also be evaluated from viscosity data, its average value for all metals being in a first approximation 1. Our experimental value 1.98 is in good agreement, as much as can be expected considering the scattering of experimental data, both for viscosity and for diffusivity.

The E_D value obtained in our experiments (4419 cal/g.at.) and that of Mirshamsi (3305 cal/g. at.) are also in good agreement with the value $E_D = 3971$ cal/g.at. calculated by Grosse's relation (4); thus, our E_D is by 10 pct higher and Mirshamsi's E_D by 17 pct smaller. It is possible that the higher values of D_0 and E_D obtained in the present work, might be caused by the sedimentation of oxide impurities, a phenomenon leading to a small increase of self-diffusion coefficients at higher temperatures.

The results obtained for liquid Cd also fit in the experimental values of diffusivity for silver[10] and indium,[11] the nearest neighbours of Cd in period 5 of the periodical system, as may be seen in table 3.

Table 3

Experimental and calculated diffusivity data for Ag, Cd, and In.

Element	$T_{\text{m.p.}}$ °K	Atomic weight,	Crystal structure	D_0, cm²/s . 10^4 Exp.	Calc. eq. (5)	e^{γ}	E_D, cal/g. atom Exp.
Silver	1234	107.88	F.c.c.	7.2	4.64	1.55	7660
Cadmium	594	112.41	H.c.p.	7.54* 3.621**	3.80	1.98	4419* 3305**
Indium	429.3	114.76	F.c.t.	4.25	3.32	1.28	2200

* Present work
** Mirshamsi's values

From theoretical considerations one should expect that the D_0 values of the metals with similar crystal structures and very close atomic masses, would but little differ. This expectation is experimentally confirmed for Ag, Cd and In which have a close-packed structure.

---

[9] J. Frenkel, "Kinetic Theory of Liquids", Dover Publications, New York, 1955, p. 31.

[10] V. G. Leak and R. A. Swalin, *Trans. A.I.M.E.*, **230**, 426 (1964).

[11] A. Lodding, *Z. Naturforsch.*, **1956** 200.

Using our experimental values of D at 400° and η values reported in [12] we had the possibility to calculate the radius of diffusing particle either from Sutherland's equation:

$$D = \frac{kT}{4\pi r\eta} \tag{6}$$

or from Walls and Upthegrove's equation [13]:

$$D = \frac{kT}{2\pi r(2b+1)\eta} \tag{7}$$

where b, is the ratio between the radius of the diffusing particle and interatomic distance in the liquid.

Comparing the value $r = 0.54$ Å and $r = 0.74$Å calculated by eq. (6) and (7) respectively, with Pauling's ionic univalent radius $r = 1.14$Å one may observe that Walls and Upthegrove's equation which contains also a geometrical paramater b, leads to a good approximation for the radius of the diffusing particle.

For the sake of comparison we have adopted Pauling's ionic univalent radius since it is a better indicator of relative ionic size in pure metals than multivalent values, all multivalent values being strongly dependent upon the amount of bonding deformation.

---

[12] * * * "Liquid Metals Handbook", Washington, 1952, p. 40.

[13] H. A. WALLS and W. R. UPTHEGROVE, *Acta Metall.*, **12**, 461 (1964).

Revue Roumaine de Chimie, **15**, 213 – 219 (1970)

– c. 4126

Revue Roumaine de Chimie, **15**, 221–228 (1970)

ACTIVITY COEFFICIENTS IN TERNARY SYSTEMS PHENOL-WATER-ELECTROLYTE

CAMELIA BELDIE

Department of Physical Chemistry of Jassy University
Calea 23 August, 11

Received February 11, 1969

The nonelectrolyte activity coefficients in salt solution were calculated both for the phenol-water- and for the water-phenol-electrolyte systems. The first component is solvent and the second, the solute nonelectrolyte. Following electrolytes were used : alkaline chlorides, bromides, iodides, sulphates and nitrates, sodium citrate and oxalate, oxalic acid, malonic acid, succinic acid, picric acid, resorcine, hydroquinone, citric acid, camphoric acid, and benzylic acid. The results are compared with those obtained for the furfural-water system. The k_s interaction parameter was also calculated and was found strongly influenced at the same time by the nature of the solvent. We believe that the k_i self-interaction nonelectrolyte parameter is influenced by the solvent.

In earlier papers [1–5] we investigated the influence of different electrolytes on the phenol solubility in water, respectively on the water solubility in phenol and it has been ascertained that electrolytes can be divided, from this viewpoint, into two categories: electrolytes producing a salting out by decreasing the nonelectrolyte solubility in salt solution and electrolytes giving a salting in by raising the nonelectrolyte solubility.

The activity coefficient of a nonelectrolyte in salt solution may be considered as a measure of the salt effect on the nonelectrolyte solubility. One of the most usual ways to determine the effect of salts on the activity coefficient of a nonelectrolyte is the comparison of nonelectrolyte solubility in salt solution to that in pure solvent, respectively in pure water, when an aqueous solution is used.

The experimental data usually obey the Setschenow's equation. [6],

$$\log S_i^0/S_i = K_s c_s = \log f_i \qquad (1)$$

---

[1] E. Papafil, M. Papafil and C. Beldie, *Anal. Sti. Univ. "Al. I. Cuza" Iaşi Sect. I* **4**, (fasc. 1), 153 (1958).

[2] E. Papafil and C. Beldie, *Ibid.*, **7**, (fasc. 1), 147 (1961).

[3] E. Papafil and C. Beldie, *Ibid.*, **10**, (fasc. 2), 105 (1964).

[4] E. Papafil and C. Beldie, *Ibid.*, **11**, (fasc. 2), 117 (1965).

[5] C. Beldie and E. Papafil, *Ibid.*, **12**, (fasc. 2), 97 (1966).

[6] J. Setschenow, *Ann. chim. phys.*, **6**, 226 (1891).

where S_i^0 is the nonelectrolyte solubility in pure solvent, S_i — the nonelectrolyte solubility in salt solution, K_s — the Setschenow's constant, c_s — the electrolyte concentration in moles/l and f_i — the nonelectrolyte activity coefficient in salt solution.

Equation (1) represents a first approximation of the theoretical equation, suggested by Long and McDevit [7] based on thermodynamical reasons;

$$\log f_i = k_s\, c_s + k_i\, c_i \tag{2}$$

where k_s is the ion-nonelectrolyte interaction parameter, k_i — the self-interaction parameter of the nonelectrolyte and c_i—the nonelectrolyte concentration in salt solution.

Combining this equation with the usual equilibrium expression in saturated solutions, one obtains [7]

$$\log f_i/f_i^0 = \log S_i/S_i^0 = k_s\, c_s + k_i\,(S_i - S_i^0) \tag{3}$$

When the nonelectrolyte solubility is very low, one may admit that f_i^0 is equal to one and then the $k_i\,(S_i - S_i^0)$ term becomes negligible, since in this case k_i will have an extremely low value.

When k_i cannot be neglected, it has to be determined by another method, so that k_s may be evaluated.

The ion-nonelectrolyte interaction parameter represents the salting parameter, which characterizes the salt influence on the nonelectrolyte solubility. Therefore it must take characteristic values for every electrolyte.

Usually the equation correlating the nonelectrolyte solubility to its activity coefficient, is applied in form (1). The limit concentration up to which expression (1) is admissible depends on the nonelectrolyte concentration (about 4m).

RESULTS AND DISCUSSION

In this paper are presented the data for the nonelectrolyte activity coefficients calculated for phenol-water-[1, 3, 4] and water-phenol-electrolyte[2, 5] systems (in which the first component is solvent and the second, the nonelectrolyte solute), the interaction parameter k_s, discussions and their correlated expressions.

We used the equation deduced by Long and McDevit, in the form (3), for the water-phenol system (in which the water is solvent and the phenol is nonelectrolyte solute) and for which the k_i value is known.

In the case of the phenol-water and the furfural-water systems, where k_i is not known, the Setschenow's approximate equation was used

$$\log S_i^0/S_i = k_s\, c_s = \log f_i$$

In this expression, beside neglecting the value of the k_i $(S_i - S_i^0)$ term one uses also the approximation $f_i^0 = 1$ (the nonelectrolyte activity coefficient in pure solvent), so that the calculated activity coefficients of a nonelectrolyte in salt solution are, in fact, only relative activity coefficients, considering the activity coefficient in pure solvent equal to unit.

---

[7] F. A. Long and W. F. McDevit, *Chem. Rev.*, **51**, 119 (1952).

In the present paper we shall also consider the k_s parameter values calculated from expression (1) for the phenol-water mixture and with the help of equation (3) for the water-phenol mixture.

Average values for the same salt effects are listed in tables 1 and 2.

Table 1

k_s Values (phenol-water)

Electrolyte	18°	25°	32°	Electrolyte	18°	25°	32°
NaCl	4.09	3.602	2.997	$(NH_4)_2SO_4$	4.115	—	—
KCl	2.865	2.485	2.127	$NaNO_3$	2.39	—	—
NH_4Cl	2.256	2.116	1.814	KNO_3	1.554	—	—
RbCl	2.021	1.821	1.756	NH_4NO_3	1.287	—	—
CsCl	—	0.995	0.814	Natrium citrate	—	19.262	—
NaBr	3.82	3.436	2.712	Natrium oxalate	—	14.149	—
KBr	2.587	2.404	2.096	Ammonium oxalate	—	5.956	—
NH_4Br	2.083	1.966	1.702	Oxalic acid	—	0.431	—
RbBr	1.903	1.703	1.590	Succinic acid	—	−0.426	—
NaI	3.30	2.548	2.204	Picric acid	—	−0.311	—
KI	2.136	1.864	1.767	Resorcinol	—	−0.303	—
NH_4I	1.623	1.478	1.388	Malonic acid	—	−0.265	—
RbI	1.460	1.303	1.360	Citric acid	—	−0.210	—
Na_2SO_4	9.717	—	—	Hydroquinone	—	−0.203	—
K_2SO_4	5.708	—	—	Camphoric acid	—	−0.108	—
				Benzylic acid	—	−0.051	—

Table 2

k_s Values (water-phenol)

Electrolyte	18°	25°	32°	Electrolyte	18°	25°	32°
NaCl	0.193	0.173	0.217	$(NH_4)_2SO_4$	0.137	—	—
KCl	0.160	0.136	0.160	$NaNO_3$	0.120	—	—
RbCl	0.115	0.092	0.146	KNO_3	0.063	—	—
NH_4Cl	0.096	0.085	0.118	NH_4NO_3	0.030	—	—
NaBr	0.146	0.135	0.183	Camphoric acid	—	0.530	—
KBr	0.114	0.097	0.141	Natrium citrate	—	0.463	—
RbBr	—	—	0.116	Natrium oxalate	—	0.377	—
NH_4Br	0.069	0.061	0.088	Ammonium oxalate	—	0.360	—
NaI	0.083	0.079	0.116	Oxalic acid	—	0.346	—
KI	0.040	0.044	0.061	Citric acid	—	0.181	—
RbI	—	—	0.032	Benzylic acid	—	0.156	—
NH_4I	—	—	0.034	Ammonium succinate	—	0.127	—
Na_2SO_4	0.173	—	—	Succinic acid	—	0.049	—
K_2SO_4	0.160	—	—	—	—	—	—

In order to compare these three systems we shall also consider the results obtained with the furfural-water mixtures [8] (table 3). In this table are listed the k_s parameter values calculated with the help of the same equation (1).

Table 3

k_s Values (furfural-water) 25°

Electrolyte	k_s	Electrolyte	k_s	Electrolyte	k_s
HCl	5.34	NH_4Br	3.37	Oxalic acid	−0.742
NaCl	28.58	RbBr	3.50	Malonic acid	−0.654
KCl	13.37	NH_4NO_3	0.901	Benzylic acid	−0.553
NH_4Cl	13.31	Citric acid	−1.11	Resorcinol	−0.532
RbCl	9.85	Adipic acid	−0.901	Hydroquinone	−0.469
NaBr	8.04	Succinic acid	−0.812	Pyrocatechol	−0.347
KBr	3.52	—	—	—	—

From tables 1—3 we ascertain that for all inorganic electrolytes used, the interaction electrolyte-nonelectrolyte parameter has positive values which decrease with the raising of the cation ionic volume, respectively anion-ionic volume. This was to be expected since the solvation numbers of the respective ions calculated by Azzam [9] (table 4), decrease in the same order.

Table 4

Solvation numbers calculated by Azzam[9]

Ions	Li^+	Na^+	K^+	Rb^+	Cs^+	H_3O^+	F^-	Cl^-	Br^-	I^-
Ion radius	0.7	1.0	1.33	1.52	1.7	1.38	1.33	1.80	1.96	2.2
Solvation number	6	4.5	2.9	2.3	0	2.9	4.7	2.9	2.4	0

For the organic ions the positive values obtained are much increased in case they give a salting out; and when a salting in is produced, the obtained values are negative. The absolute values are comparable with those obtained for inorganic electrolytes.

If one considers the three mixtures in which the solvent is successively water, phenol and furfural, one notes that the value of the k_s parameter increases in the same order as the respective molecular dipole moments (water = 0.184D ; phenol = 1.56D ; furfural = 3.57D), whence we concluded that the k_s parameter which represents the interaction ion-nonelectrolyte depends also upon the solvent. This fact is proved by the data listed in tables 1—3. The values of the k_3 parameter for the same nonelectrolyte and the same salt but in different solvents (phenol, furfural) are different.

We also found a variation with the temperature of the k_s parameter. This variation decreases from chlorine to iodine, and from sodium to rubidium respectively, so that for rubidium iodide, the variation amounts actually to zero.

---

[8] C. Beldie and Fl. Bărbulescu, *Rev. Roumaine Chim.* (in print).

[9] A. M. Azzam, *Z. Elektrochem.*, **50**, 889 (1954).

Therefore the temperature influence may also be correlated to the same considerations concerning the ion dimensions in solution.

The values of the k_s interaction parameter we calculated are comparable with the corresponding literature data, in those cases in which they exist (table 5).

Table 5

Comparison of our k_S values with those in the literature[7] (water-phenol) 30°

Salt	Conc. (molality)	k_s (our data)	k_s (from the literature)
NaCl	0.94	—	0.229
	0.54	0.217	—
KCl	0.93	—	0.191
	0.5	0.180	—
$NaNO_3$	0.3	0.120	—
	0.93	—	0.148
KNO_3	0.91	—	0.107
	0.664	0.063	—

As we have already mentioned, we arrived at the conclusion that the k_s parameter as well as the k_i parameter greatly depend on the solvent.

If the k_s parameter depended only upon the ion-nonelectrolyte parameter then k_s should have the same value in various solvents, a fact we could not confirm experimentally.

According to the literature k_i represents the nonelectrolyte self-interaction parameter but we think the k_i value depends upon the solvent too. If this were not so, then the interaction parameter of the same nonelectrolyte in different solvents would be the same, but this fact does not actually happen. In the case of the water-phenol mixture $k_i = -0.14$[7].

We are not able to discuss the problem of the k_i parameter, since we did not investigate this matter; neither are the necessary data to be found in the literature. Research in this field deals with the behaviour of different nonelectrolytes in salt solution and not with the influence exerted by the solvent. It is a task of the future to check up the above assumption.

The activity coefficients of nonelectrolytes were calculated by using equations (1) and (3). The values are greater than one for all these substances that produce salting out and less than one for those that yield salting in.

Therefore, when one adds an electrolyte to a nonelectrolyte solution in a solvent which decreases the nonelectrolyte solubility, the activity coefficient of the latter increases with respect to its value in pure solvent, in the other case it decreases.

Plotting log f_i against m (salt molality), in most cases one obtains straight lines and from their slope one can determine the k_s parameter. Results obtained agree with average calculated values for k_s.

Examples are given in figures 1—5.

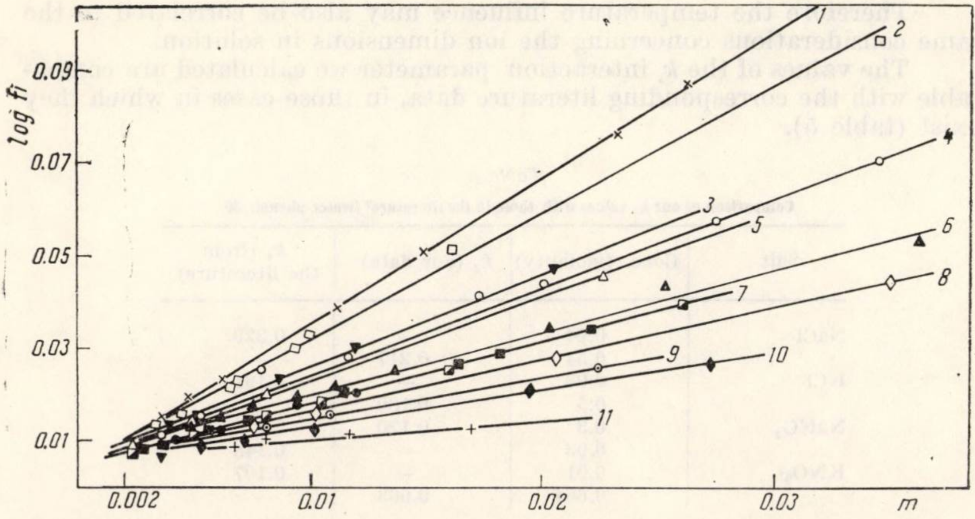

Fig. 1. — Phenol-Water 25°.

1, NaCl; **2**, NaBr; **3**, NaI; **4**, KCl; **5**, KBr; **6**, NH_4Cl; **7**, RbCl;, KI, NH_4 Br; **8**, RbBr; **9**, NH_4I; **10**, RbI; **11**, CsCl.

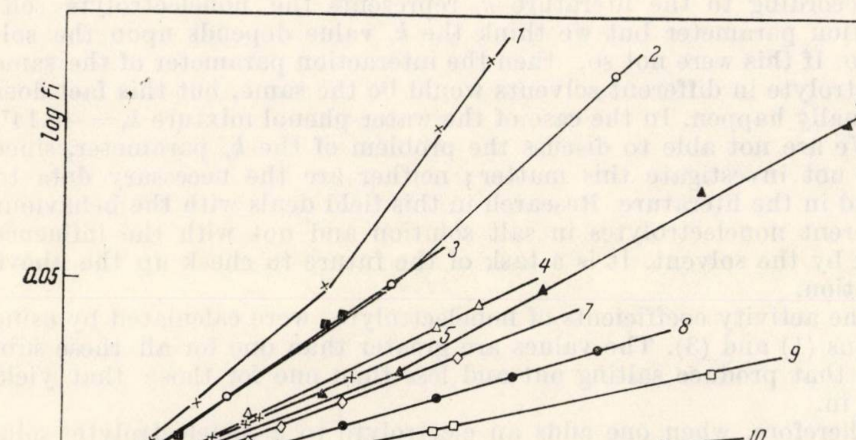

Fig. 2. — Water-Phenol 25°.

1, NaCl; **2**, KCl; **3**, NaBr; **4**, KBr; **5**, RbCl; **6**, NH_4Cl; **7**, NaI; **8**, NH_4Br; **9**, KI; **10**, NH_4 I.

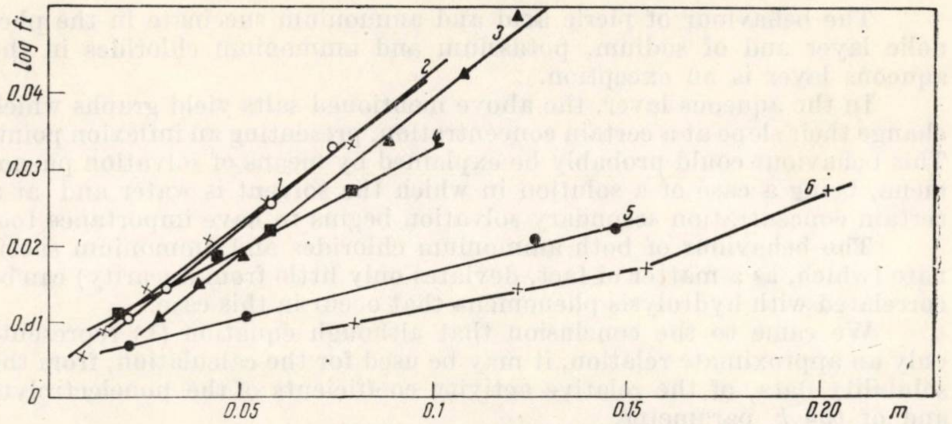

Fig. 3. — Water-phenol 25°.
1, camphoric acid; 2, natrium citrate; 3, natrium oxalate; 4, ammonium oxalate; 5, citric acid; 6, ammonium succinate.

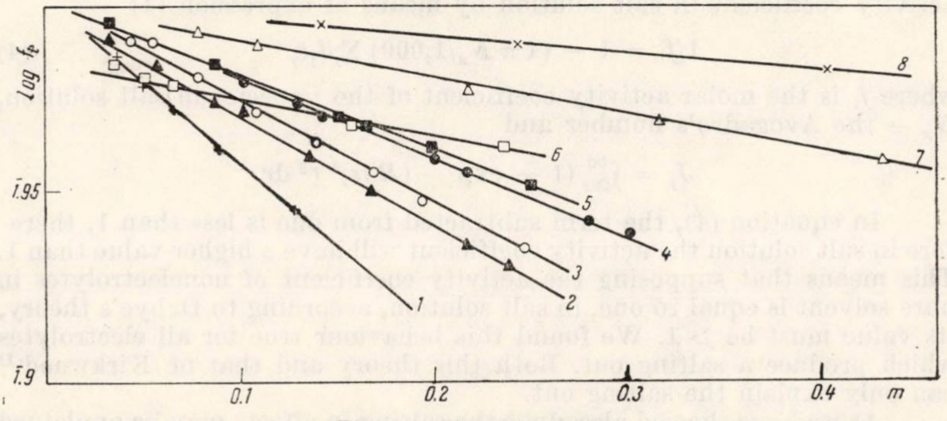

Fig. 4. — Phenol-Water 25°.
1, succinic acid; 2, resorcinol; 3, malonic acid; 4. citric acid; 5, hydroquinone; 6, picric acid; 7, camphoric acid; 8, benzylic acid.

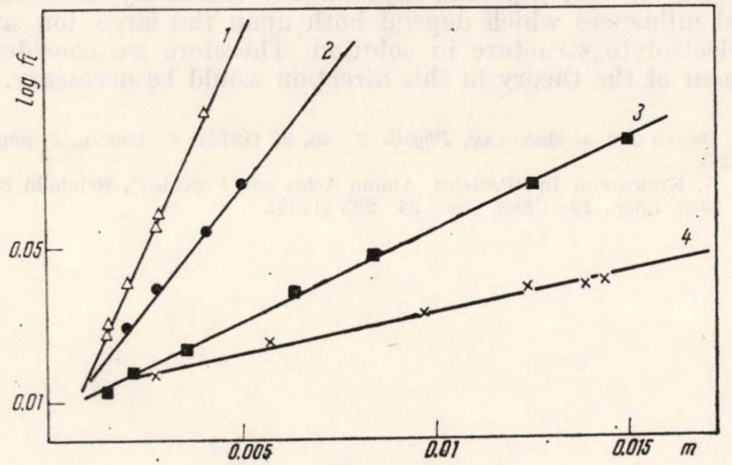

Fig. 5. — Phenol-Water 25°.
1, sodium citrate; 2, sodium oxalate; 3, ammonium oxalate; 4, oxalic acid.

The behaviour of picric acid and ammonium succinate in the phenolic layer and of sodium, potassium and ammonium chlorides in the aqueous layer is an exception.

In the aqueous layer, the above mentioned salts yield graphs which change their slope at a certain concentration, presenting an inflexion point. This behaviour could probably be explained by means of solvation phenomena, being a case of a solution in which the solvent is water and at a certain concentration secondary solvation begins to have importance too.

The behaviour of both ammonium chlorides and ammonium succinate (which, as a matter of fact, deviates only little from linearity) can be correlated with hydrolysis phenomena that occur in this case.

We came to the conclusion that although equation (1) represents only an approximate relation, it may be used for the calculation, from the solubility data, of the relative activity coefficients of the nonelectrolyte and of the k_s parameter.

Concerning salting out our results are in agreement with the theory[7]; the Debye-McAulay's electrostatic theory [10] explains the nonelectrolyte activity coefficient in salt solution by means of expression (4)

$$1/f_i = 1 - (4\,\pi\, N_A/1{,}000)\, \Sigma_j J_j c_j \tag{4}$$

where f_i is the molar activity coefficient of the i species in salt solution, N_A — the Avogadro's number and

$$J_j = \int_{\Omega j}^{\infty} (1 - \exp - (R_j/r)^4\, r^2\, \mathrm{d}r$$

In equation (4), the term subtracted from one is less than 1, therefore in salt solution the activity coefficient will have a higher value than 1. This means that supposing the activity coefficient of nonelectrolytes in pure solvent is equal to one, in salt solution, according to Debye's theory, its value must be > 1. We found this behaviour true for all electrolytes which produce a salting out. Both this theory and that of Kirkwood [11] can only explain the salting out.

As we have showed already, [8] the salting in effects may be explained by the internal pressure theory developed by Long and McDevit. But this theory gives only a partial explanation. Certainly there must exist additional influences which depend both upon the large ion and upon the nonelectrolyte structure in solution. Therefore we consider that a development of the theory in this direction would be necessary.

---

[10] P. DEBYE and J. MCAULAY, *Physik. Z.*, **26**, 22 (1925); P. DEBYE, *Z. physik. Chem.*, *130*, 55 (1927).

[11] J. G. KIRKWOOD, In "Proteins, Amino Acids and Peptides", Reinhold Publ. Corp., New York, 1943, Chap. 12; *Chem. Rev.*, **24**, 233 (1939).

Revue Roumaine de Chimie, **15**, 229–238 (1970)

THE MINERALIZING INFLUENCE OF APATITE ON THE FORMATION OF PORTLAND CEMENT CLINKER

I. TEOREANU and TRAN VAN HUINH

Polytechnic Institute, Bucharest, str. Polizu 1

Received August 6, 1969

The additions of apatite affects the process of clinker formation in all its stages. For certain proportions of apatite and certain burning temperatures, both the processes in the solid state and the processes taking place after the appearance of the liquid state are accelerated. This has positive consequences on the mineralogic composition and structure of the clinkers. The mechanic strength achieved is in this manner improved.

1. The use of apatite as a mineralizing agent represents a simple and efficient way to speed up the formation process of portland cement clinkers.

In spite of the studies carried out so far [1–4] the mechanism of the mineralizing effect of apatite is not yet completely understood. In the present study an effort is made to elucidate this problem using roentgenographic, microscopic and chemical techniques as well as differential thermal analysis. The experiments were carried out with clinker having the following characteristics: lime saturation factor $S_k = 0.96$; silica ratio $M_{Si} = 2.2$; alumina ratio $M_{Al} = 2.0$. Apatite of vietnamese origin was added in the raw mixture in proportion of 0.5%, 1%, 3% and 6%. The chemical constitution of the raw materials used for the synthesis of the clinkers is given in table 1.

2. The experiments show that apatite has a complex influence in all the stages of the process of clinker formation.

---

[1] B. V. Volkonski, P. F. Konovalov and S. D. Makashev, "Mineralizatory v tsementnoi promyshlenosti", Izd. Lit. po Stroit., Moscow, 1964, ch. 3.

[2] W. Eitel, "Silicate Science", vol. V, Acad. Press, New York-London, 1966, section C.

[3] M. M. Sychev and V. I. Korneev, *Tsement*, **31**, 6 (1965).

[4] Bui Van Thien, Iu. M. Butt and M. A. Vorobieva, *Silikaty Trudy Tekhn. Inst.*, Moscow, **59**, 247 (1969).

Table 1

Chemical constitution of the raw materials used for the synthesis of the clinkers

Components of the raw mixture	CaO	SiO_2	Al_2O_3	Fe_2O_3	MgO	SO_3	P_2O_5	F	Calcination loss %	Alkalies %
Calcium carbonate	55.8	0.01	0.05	0.01	—	—	—	—	43.86	0.20
Sand	0.25	98.15	1.18	0.10	—	—	—	—	0.13	0.30
Alumina	—	—	100	—	—	—	—	—	—	—
Ferric oxide	—	—	—	100	—	—	—	—	—	—
Vietnamese apatite	49.09	7.00	1.57	1.22	0.30	0.29	37.60	1.80	1.01	0.20

2.1. In order to elucidate the processes occurring in the solid phase of the system and the way in which the additions influence them, parallel differential thermal analyses were performed on samples with and without the mineralizing agent. The DTA curve of the samples without apatite, in the 20—1150° range of temperature shows, the existence of three endothermal and one exothermal effects (curve a, fig. 1). The most prominent endothermal effect is indicated by a peak corresponding to a temperature of 920° which is generated by calcium carbonate decomposition. The second endothermal peak appears at 575° which represents the conversion point of α-quartz into β-quartz. The third peak at 1130° corresponds to the thermal decomposition of gehlenite. The exothermal effect, with the peak at 1100° is due to the formation of gehlenite, as well as of dicalcium silicate and of

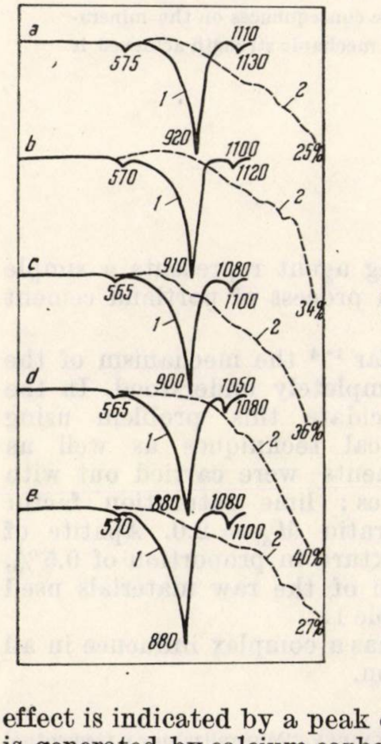

Fig. 1. — Thermograms (1) and volume variations (2) curves of samples with and without mineralizing agent addition;

a, without addition; *b*, with 0.5% apatite; *c*, with 1% apatite; *d*, with 3% apatite; *e*, with 6% apatite.

some calcium aluminates and calcium ferrites (the formation of the latter compounds occurs also at lower temperatures, however, at smaller rates and yields, so that their corresponding exothermal effects is masked by the endothermal effects of $CaCO_3$ decomposition). These effects may also be seen on the DTA curves of the samples containing 0.5—6% apatite but at lower temperatures (curve b,c,d and e, fig. 1). This fact emphasizes the accelerating influence of apatite on the solid phase reactions.

In order to find out the components appearing at different temperatures, the samples with and without mineralizing agent were burnt at the chosen temperatures and then the roentgenographic analyses were performed. In this way, it was possible to better point out, on a comparative basis, the influence of apatite on the solid phase reactions and on the nature of the phases generated in the system.

The diffractogram of the samples free of apatite did not show in the range of 500—700° any lines indicative of new components (curve a and b, fig. 2). These appeared only in the samples burnt at higher temperatures beginning with 800° (curve c, fig. 2). On the other hand, the analysis of the samples containing apatite indicates the presence of lines of dicalcium silicate, monocalcium aluminate and dicalcium ferrite at lower burning temperature. Thus, the roentgenogram of the sample with 1% apatite shows the existence of the above mentioned components, accompanied by $CaCO_3$, $Ca_3(PO_4)$, SiO_2, Fe_2O_3, at a burning temperature as low as 700° (curve a, fig. 3). In the case of samples burnt at 1020°, the roentgenogram (curve b, fig. 3) contains the specific lines of gehlenite, $2CaO.SiO_2$, $CaO.Al_2O_3$, $4CaO.\ Al_2O_3.Fe_2O_3$ and CaO, the calcium carbonate decomposition being practically completed at this temperature (in the samples free of apatite the specific lines of gehlenite and $4CaO.\ Al_2O_3 \cdot Fe_2O_3$ appear only for burning temperatures larger than 1100° (curve e, fig. 2)).

The accelerating effect of apatite on the solid phase reactions is due mainly to its P_2O_5 content. Of course, the presence of fluorine in the apatite should not be ignored, but it is necessary to take into account the fact that the amounts of fluorine involved are much smaller than those of P_2O_5 *).

---

*) The influence of the fluorine compounds on the solid phase processes has been intensively studied.[1,2,5-14] It was observed that fluorine acts more vigorously in the presence of P_2O_5.

[5] H. F. W. Taylor, "The Chemistry of Cements" vol. I, Acad. Press, London and New York, 1964, ch. 3.

[6] N. A. Toropov and I. A. Bondur, *Izvest. Akad. Nauk S.S.S.R, Otdel. khim. Nauk,* **1959**, 1520.

[7] A. M. Palei, *Tsement*, **24**, 23 (1958).

[8] E. Bereczki, *Epitöanyag*, **16**, 357 (1964).

[9] I. G. Konovalov, *Tsement*, **18**, 14 (1952).

[10] J. Mukerji, *J. Amer. Ceram. Soc.*, **48**, 210 (1965).

[11] M. I. Gherman and N. V. Sahmagon, *Tsement*, **25**, 17 (1959).

[12] I. Covaliu, S. Tîrziu and I. Sîrbu, *Revista Construcţii şi Materiale de Construcţii,* **14**, 309 (1962).

[13] R. B. Sosman, *Trans. Brit. Ceram. Soc.*, **54**, 655 (1955).

[14] A. Nagy, *Rev. Mat. Constr.*, **1968**, 428.

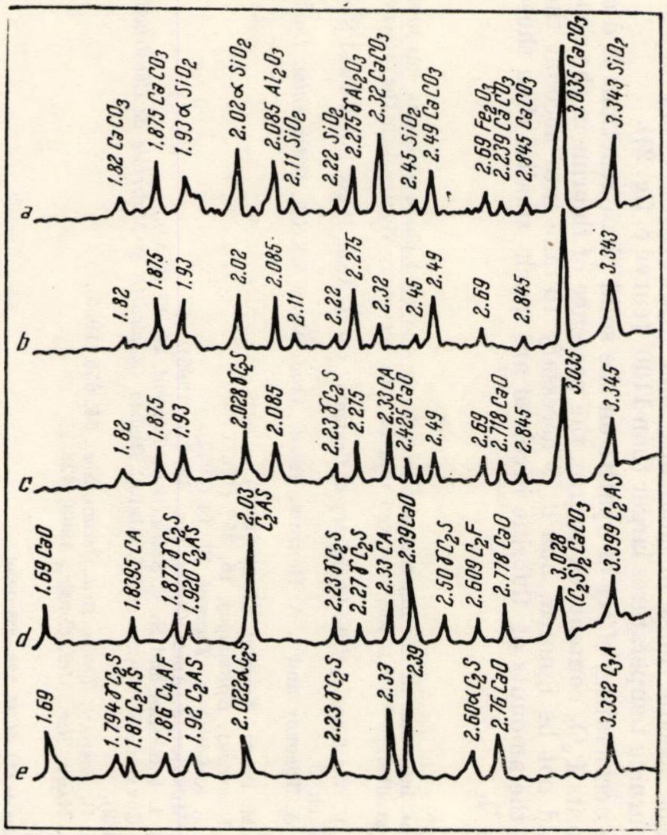

Fig. 2. — Roentgenograms of samples without apatite addition burnt;
a, at 600°; *b*, at 700°; *c*, at 800°; *d*, at 1020°; *e*, at 1110°.

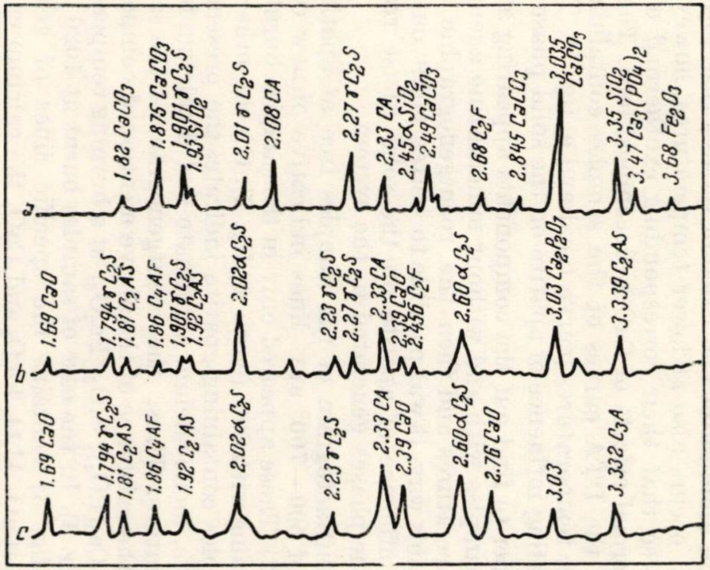

Fig. 3. — Roentgenograms of samples with 1% apatite burnt
a, at 700°; *b*, at 1020°; *c*, at 1150°.

The mineralizing agents exert a labilization effect on the silica crystalline network and this fact has a great influence upon the whole ensemble of reactions taking place in solid phase. In this manner the silica activity is increased and consequently its reaction capacity with calcium oxide is increased too, calcium silicates being formed. As a result, the calcium carbonate decomposition is accelerated and simultaneously the formation rates of other components, such as aluminates, ferrites, are increased too. As the values of the ionic radius of silicium and phosphorus are close to each other, the latter is able to displace silicium from the silica network. Being pentavalent (and not tetravalent as silicium) distorted tetrahedrons $(PO_4)^{3-}$ are formed; this fact brings about an unbalancing of charge in the silica network; consequently the lability of the network increases. This could account for the increased rate of the polymorphous conversions of silica with consequences upon the rate of formation in the solid phase of some silicates, aluminates and ferrites.

2.2. Using the high temperature microscope one found that the apatite additions speed up the appearance of the liquid phase in the system. Namely, the melting point of the samples with apatite droped down by approx. 50° as compared with that of the samples free of apatite. This earlier appearance of the liquid phase leads to an acceleration of the diffusion processes and as a consequence to an increase in the binding rate of calcium oxide. The mineralogical composition of the clinkers is accordingly modified. Logically, the apatite addition should accelerate the binding of calcium oxide and promote the tricalcium silicate formation. The fraction of calcium oxide which is assimilated at different temperatures and also the corresponding mineralogical composition of the clinkers showed, however, that the mechanism by which the apatite acts is much more intricate in this stage of clinker formation, since it is linked not only to the speeding up of the appearance of the liquid phase but also to other factors.

In order to determine the fraction of calcium oxide, which is assimilated, samples with and without apatite burnt at 1350, 1400 and 1450° were analysed. The content in free lime is given in table 2.

Table 2

Content in free lime

Sample number	Added apatite %	Free lime (%) at		
		1350°	1400°	1450°
1	0	2.76	1.69	0.91
2	0.5	10.02	5.77	0.46
3	1.0	6.17	0.32	0.19
4	3.0	7.50	0.39	0.23
5	6.0	11.65	5.98	0.78

From table 2 it can be inferred that at 1350° the apatite addition is far from accelerating the binding of calcium oxide, and in fact hinders it. The fraction of CaO assimilated is increased only at 1400–1450° especially for additions of 1–3% apatite. These results agree fairly well with the mineralogical composition data obtained from microscopic and roentgenographic determinations (table 3 and fig. 4—6). They show the existence at some burning temperatures of an optimum apatite addition too ; for this optimum one obtains a considerable increase of the tricalcium silicate content, especially due to the calcium saturation of dicalcium silicate.

On the basis of all these data it can be concluded that, in this stage of clinker formation, the influence of apatite is the result of its effect on the diffusion processes (therefore on the binding capacity of calcium oxide) and of its effect on the stability of the hydraulic components of the clinker (particularly of $3CaO.SiO_2$).

Table 3

Mineralogical composition of the clinkers

Burning temperature	Added apatite %	Mineralogical components, % wt				
		$3CaO.SiO_2$	$2CaO.SiO_2$	$3CaO.Al_2O_3$	$4CaO.Al_2O_3.Fe_2O_3$	$5CaO.3Al_2O_3$
1350°	0	43.2	28.9	10.4	10.5	3.7
	0.5	20.4	38.0	10.7	9.4	3.8
	1.0	39.5	28.8	11.7	9.6	3.4
	3.0	32.8	33.7	11.3	9.5	3.6
	6.0	20.1	37.9	10.5	9.2	3.8
1400°	0	53.0	19.4	11.4	10.5	3.7
	0.5	32.3	35.9	11.4	9.5	3.6
	1.0	60.0	14.6	10.0	10.4	3.8
	3.0	58.0	15.5	11.6	9.8	3.8
	6.0	41.5	28.0	11.3	9.4	4.6
1450°	0	61.0	14.0	11.2	10.2	2.0
	0.5	62.0	14.0	10.2	9.9	2.1
	1.0	64.1	12.0	9.3	10.1	3.0
	3.0	61.2	14.3	11.0	10.0	2.5
	6.0	56.8	18.0	11.2	10.1	2.7

Various authors [8,15–17] report that fluorine and P_2O_5 bring about, in specific conditions, the instability of tricalcium silicate. In the synthesis of tricalcium silicate, fluorine (in the form of fluorides and fluosilicates) induces not only an increase in the formation rate of $3CaO.SiO_2$ but also an increase in its decomposition rate during the cooling stage. For alite, containing both Al_2O_3 and MgO, the stability of the resulting product is however fair. [8] This is somewhat the case of the syntheses performed in the present study*). By using apatite as a mineralizing agent, the predominant influence on the stability of the alite formed in the clinker is due undoubtedly to phosphorus, in a degree depending

---

[15] N. A. Toropov and A. I. Borisenko, *Tsement*, **20**, 10 (1954).

[16] J. H. Welch and W. Gutt, "Chemistry of Cement, Proceedings of the Fourth International Symposium", Washington, 1960, p. 59.

[17] R. E. Simanovskaia and S. Ia. Spunt, *Doklady Akad. Nauk S.S.S.R.*, **101**, 917 (1955).

*) It is to be mentioned that the fluorine introduced into the system by the addition of apatite represents maximum 0.108%.

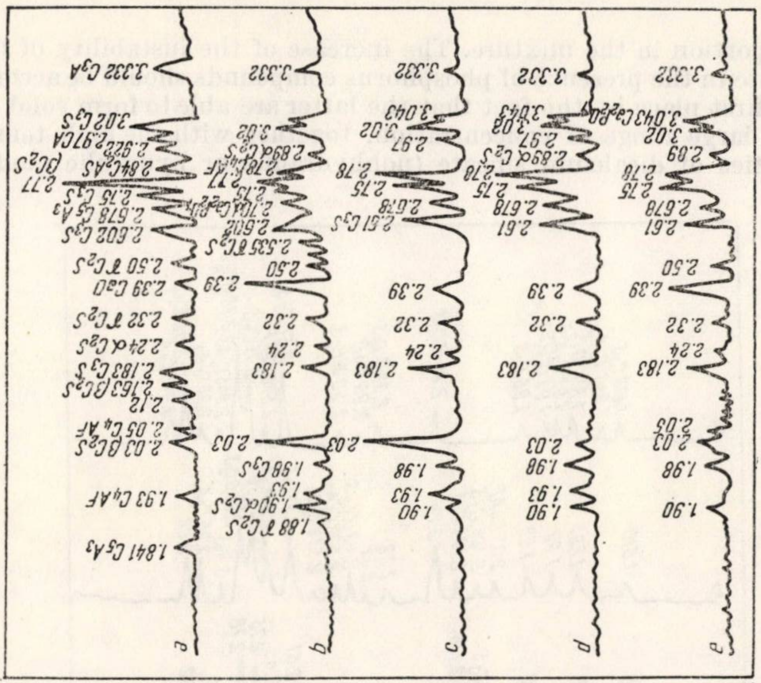

Fig. 5. – Roentgenograms of samples burnt at 1400°;

a, without apatite addition; *b*, with 0.5% apatite; *c*, with 1% apatite; *d*, with 3% apatite; *e*, with 6% apatite.

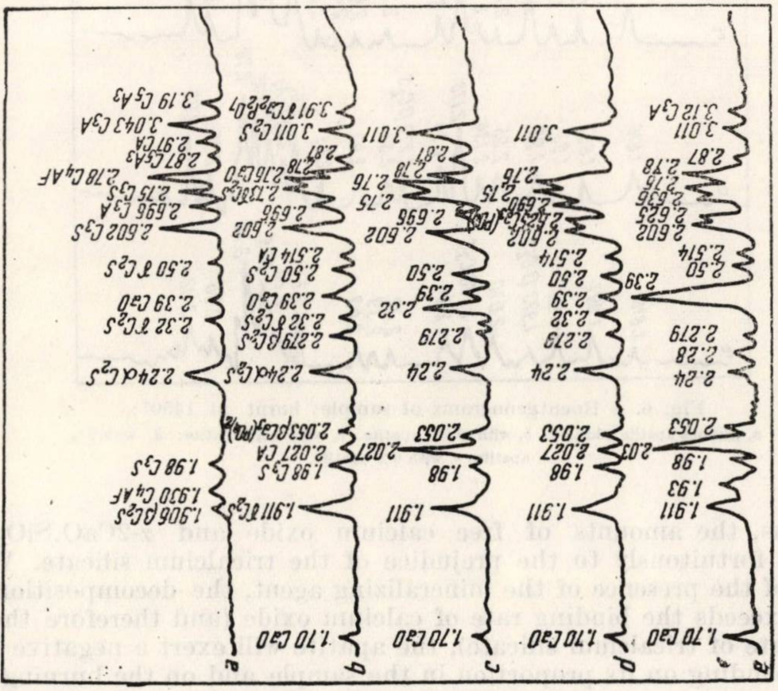

Fig. 4. – Roentgenograms of samples burnt at 1350°;

a, without apatite addition; *b*, with 0.5% apatite; *c*, with 1% apatite; *d*, with 3% apatite; *e*, with 6% apatite.

on its proportion in the mixture. The increase of the instability of tricalcium silicate in the presence of phosphorus compounds should be accounted for in the first place by the fact that the latter are able to form solid solutions in a large range of concentration, together with the high temperature varieties of dicalcium silicate (nonhydraulic or hydraulic modifications).

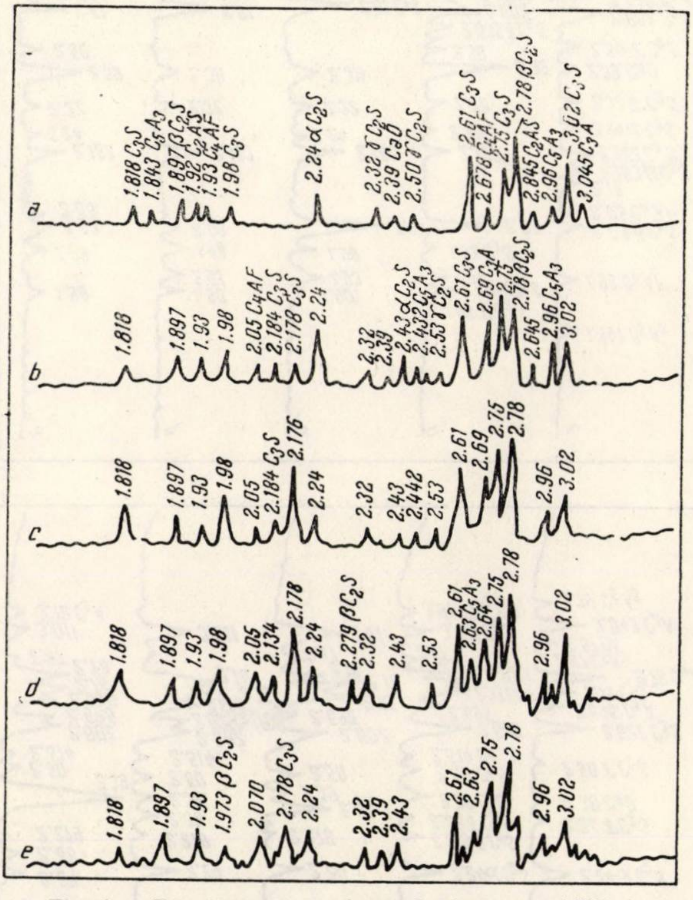

Fig. 6. – Roentgenograms of samples burnt at 1450°; *a*, without apatite addition; *b*, with 0.5% apatite; *c*, with 1% apatite; *d*, with 3% apatite; *e*, with 6% apatite.

Thus, the amounts of free calcium oxide and α-$2CaO.SiO_2$ are increased fortuitously to the prejudice of the tricalcium silicate. When, because of the presence of the mineralizing agent, the decomposition rate of alite exceeds the binding rate of calcium oxide (and therefore the formation rate of tricalcium silicate), the apatite will exert a negative influence, depending on its proportion in the sample and on the burning temperature.

As concerns the aluminate formation in the clinker containing an apatite addition and burnt at 1400–1500° one may notice a certain insta-

Fig. 7. — Microphotograph of the clinker burnt at 1450° without apatite addition (× 400).

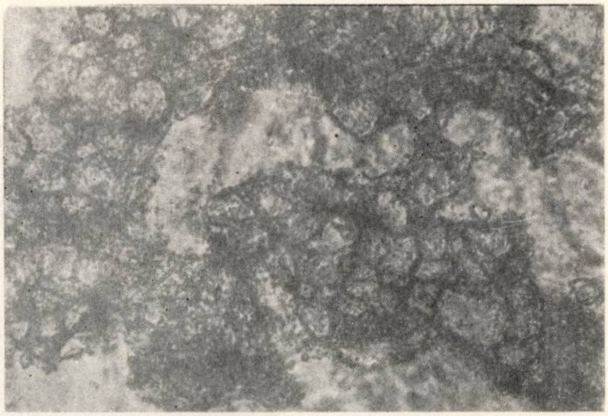

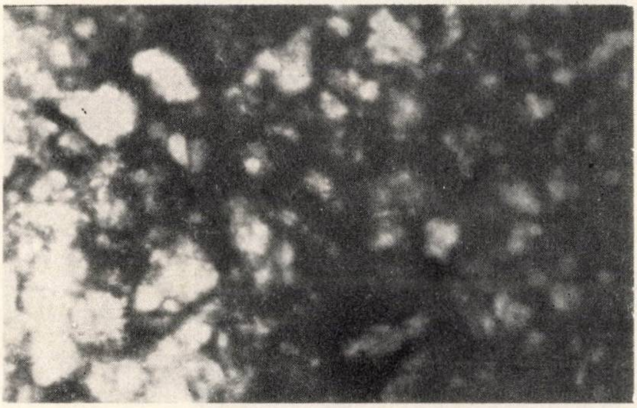

Fig. 8. — Microphotograph of the clinker burnt at 1450° with 0.5% apatite (× 4000).

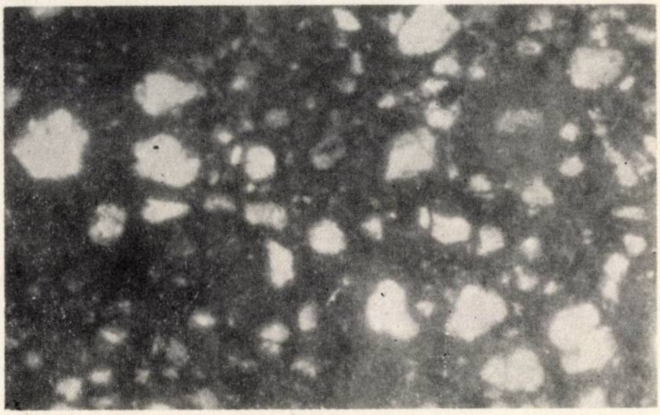

Fig. 9. — Microphotograph of the clinker burnt at 1450° with 1% apatite (× 400).

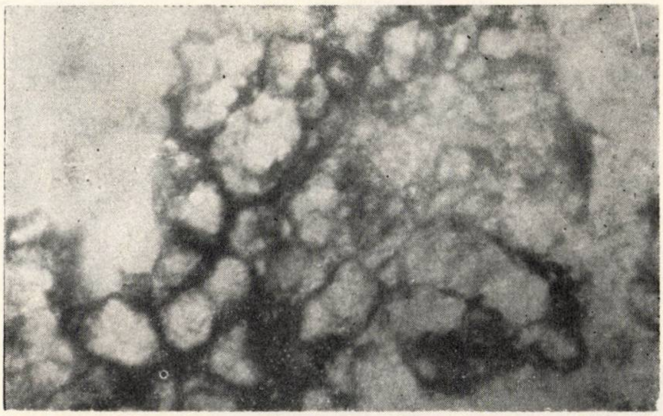

Fig. 10. — Microphotograph of the clinker burnt at 1450° with 3% apatite (× 400).

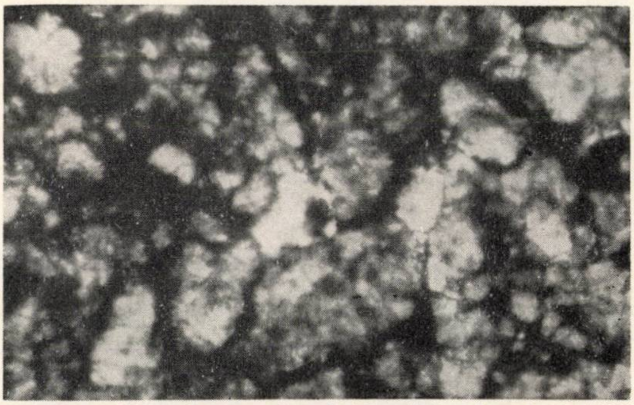

Fig. 11. — Microphotograph of teh clinker burnt at 1450° with 6% apatite (× 400).

bility of the tricalcium aluminate whose content decreases to the benefit of aluminates less rich in calcium oxide ($5CaO.3Al_2O_3$) ; no increase in the content of free calcium oxide takes however place. The process proceeds probably according to the following reactions :

$$\frac{\begin{array}{c}3(3CaO.Al_2O_3) \rightarrow 5CaO.3Al_2O_3 + 4CaO \\ 4(2CaO.SiO_2) + 4CaO \rightarrow 4(3CaO.SiO_2)\end{array}}{3(3CaO.Al_2O_3) + 4(2CaO.SiO_2) \rightarrow 5CaO.3Al_2O_3 + 4(3CaO.SiO_2)}$$

2.3. Petrographic observations indicate an important influence o apatite additions on the crystallization processes occurring during the formation of clinkers. In the samples burnt at 1450° without apatite addition, the alite and belite crystals are poorly outlined, of irregular form and contain numerous inclusions (the size of alite and belite crystals is in the range of $5-35$ μ and $5-30$ μ respectively (fig. 7)).

The structure of the clinker improves with increasing amounts of added apatite (fig. 8—10). The best results in this respect are obtained with additions of $1-3\%$ and especially for the samples with 1% apatite. In this case, the mineralogic components of clinkers are able to form distinctive and regular crystals (the size of alite and belite crystals is in the range of $10-60$ μ and $3-40$ μ respectively). The alite crystals are predominant in clinkers, whilst the calcium oxide crystals are not visible. By increasing the amount of added apatite up to 6%, the clinker structure deteriorates. The alite crystals especially, become poorly distinctive grains, having belite and calcium oxide inclusions, generated as a result of alite decomposition under the influence of apatite, as shown before (fig. 11).

It seems natural that apatite by influencing favourably within a certain range of concentration the mineralogic composition and the structure of clinker, will also improve its mechanical strength. As a checking of this assumption, tests of mechanical strength were carried out on microsamples after 3, 7 and 28 days of hardening. The results of these tests (table 4) agree with the roentgenographic and petrographic analyses. Indeed, it was shown that clinkers burnt at 1400—1450° and containing 1% added apatite had a much better mechanical strength than the clinkers free of apatite, especially regarding the compression strength. Though clinkers containing 3% apatite have an improved structure and a somewhat higher content of tricalcium silicate, they have however no better mechanical strength, since, as revealed by roentgenograms, a large part of dicalcium silicate is present in the α modification.

3. On the basis of experiments carried out it may be concluded that :

— Added apatite influences the formation process of portland cement clinker in all its stages.

— Apatite addition exerts at suitable temperatures an advantageous effect at concentrations around 1%, the main influencing factor being the P_2O_5 content of the apatite. The solid phase processes (calcium carbonate decomposition, polymorphous transformations of silica, formation of silicates and aluminates) are accelerated. The appearance of the liquid phase is speeded up and as a result, the rate of the diffusion processes

Table 4

Mechanical strength of the clinkers

Burning temperature	Added apatite %	Compression strength (kg/cm²) of microsamples after a setting of:			Bending strength (kg/cm²) of microsamples after a setting of:		
		3 days	7 days	28 days	3 days	7 days	28 days
1350°	0	216	233	300	16.4	19.2	20.8
	0.5	48	52	56	3.6	5.6	6.8
	1.0	84	112	140	8.6	10.4	16.0
	3.0	52	56	84	3.4	5.8	8.1
	6.0	42	50	58	3.2	5.0	5.8
1400°	0	232	252	389	17.4	19.6	23.0
	0.5	160	180	246	11.4	17.0	21.0
	1.0	256	318	430	19.0	29.0	34.0
	3.0	236	254	392	17.0	20.0	30.0
	6.0	202	232	360	9.2	11.8	16.8
1450°	0	272	334	458	20.4	27.2	31.2
	0.5	278	338	464	22.0	27.4	30.4
	1.0	304	368	536	24.0	29.2	31.6
	3.0	268	304	428	20.6	27.2	29.5
	6.0	234	254	326	17.6	20.4	24.0

is increased. This, in turn, leads to an increased rate of assimilation and to the promotion of alite formation. Also, the clinker structure is improved.

— At optimum amounts of added apatite, clinkers of higher mechanical strength are obtained.

— Owing to the porous structure of the clinkers mineralized with the aid of apatite, the grinding process is easier to be performed.

Revue Roumaine de Chimie, 15, 239–245 (1970)

GRAFTING OF MALEIC ANHYDRIDE ON ETHYLENE VINYL ACETATE COPOLYMER IN HOMOGENEOUS MEDIUM IN PRESENCE OF PEROXIDE INITIATORS *)

122

C. ANDREI, D. MIHĂIŢĂ, I. HOGEA and D. MUNTEANU **)

Research Laboratory, Petrochemical Works Ploieşti, Brazi, jud. Prahova

Received February 11, 1969

This paper studies the grafting of maleic anhydride on binary ethylene vinyl acetate copolymer (E-VA) in homogeneous medium in presence of peroxide initiators. The influence of the nature and concentration of initiators, of the concentration of copolymer, temperature and reaction time on grafting is investigated. The infra-red spectrum of the grafted copolymer gives indications on its structure. According to the reaction kinetics and the copolymer structure, a reaction mechanism is proposed.

INTRODUCTION

For some time the idea was accepted that maleic anhydride does not homopolymerize and that it participates merely in copolymerization reactions. The main reason for this phenomenon was attributed to the steric hindrance existing in this 1,2 ethylene disubstituted compound.

Both Lang and co-workers [1,2] as well as Joshi [3,4] refuted this hypothesis in their works and indicated conditions for homopolymerization of maleic anhydride

Joshi showed that the homopolymerization process characterizes itself by a very high chain transfer constant between the monomer and the initiator, which he attributed to the mobile hydrogen atoms present in the maleic anhydride cycle and which he considered as being responsible for the great difficulties in homopolymerization of maleic anhydride.

With regard to the use of maleic anhydride as modification agent of some polymers, most information on this subject is found in patent literature; on the other hand, as pointed out by Gabara and Porejko in their works,[5-7] only very few suggestions exist, on the mechanism of grafting of various polymers.

---

*) Paper presented at the First National Conference of Macromolecular Chemistry held on September 18–24, 1968, Jassy, Romania

**) Present address: Petrochemical Works, Piteşti

[1] J. L. Lang, W. A. Pavelich and H. D. Clarey, *J. Polymer Sci.*, **55**, S31 (1961).

[2] J. L. Lang, W. A. Pavelich and H. D. Clarey, *J. Polymer Sci.*, *A*, **1**, 1123 (1963).

[3] R. M. Joshi, *Makromol. Chem.* **53**, 33 (1962).

[4] R. M. Joshi, *Makromol. Chem.*, **55**, 35 (1962).

Some types of binary copolymers are known which were obtained by grafting of maleic anhydride on macromolecular catenary. Thus, maleic anhydride was grafted on polyethylene,[5,6] on atactic polypropylene[8], natural rubber[9], both by radical and ionic systems.

The purpose of the present paper is to study and to give information on the mechanism of grafting maleic anhydride (MA) on binary ethylene vinyl acetate copolymer (E-VA) in homogeneous medium in presence of peroxide initiators.

EXPERIMENTAL

Materials

The grafting of maleic anhydride was carried out on an ethylene vinyl acetate copolymer, having 7% vinyl acetate ($\overline{M} = 27.000$) manufactured by I.C.I. by mass process at high pressure.

This was purified by solving in *p*-xylene, precipitating with acetone, filtering and drying at 50° in vacuum to constant weight.

Maleic anhydride (U.S.S.R.), benzoyl peroxide (BP) (Carlo-Erba), *p*-xylene (Reactivul, Bucharest, Romania), were chemically pure.

α', α'-Azoisobutironitrile (AIBN) was recrystallized from diethylether.

WORKING TECHNIQUE

The process of grafting maleic anhydride on ethylene vinyl acetate copolymer was carried out in a three-necked flask with stirrer, refrigerant and thermometer. The temperature in the flask was maintained by thermostatic oil bath at the required fixed value to an accuracy of ± 1°.

A quantity of ethylene vinyl acetate copolymer, determined by weighing (about 1 g) and 112 ml *p*-xylene (96.4 g) were introduced into the flask.

When the polymer had dissolved completely and the solution had reached a constant temperature, maleic anhydride (15% concentration) and the respective initiator (BP or AIBN) were introduced, their concentrations being expressed in mole of peroxide per 100 grams of 15% maleic anhydride solution.

From that moment the time of reaction was recorded.

After the reaction, the cooled solution was poured into acetone (200 ml), attaining thus an acetone : solution ratio of 2 : 1.

The precipitated polymer, separated by filtering on a filter crucible (G. 4, G.5), continued to be washed with acetone until the maleic anhydride and poly (maleic anhydride) (PMA) disappeared from the acetone used for washing and then it was dried in vacuum at 50° to constant weight.

---

[5] W. GABARA and S. POREJKO, *J. Polymer Sci.*, *A—1*, **5**, 1547 (1967).

[6] S. POREJKO, W. GABARA and J. KULESZA, *J. Polymer Sci.*, *A—1*,**5**, 1563 (1967).

[7] W. GABARA and S. POREJKO, *J. Polymer Sci.*, *A—1*, **5**, 1539 (1967).

[8] A. ROMANOV, *Plaste und Kautschuk*, **12**, 521 (1965).

[9] J. LE BRAS, *Kautschuk und Gummi*, **10**, 521 (1965).

Quantitative purification by washing was checked by comparing the results of elementary analysis of the product after first and repeated purification, the results being similar, and by infra-red analysis of grafted copolymer and acetone used for extraction, which analysis also showed absence of maleic anhydride.

The degree of grafting was determined as percentage of increase in weight of initial copolymer.

The losses during these operations, determined on the pure ethylene vinyl acetate copolymer with the aid of blank tests, were between 1–3%.

Grafting in nitrogen medium was carried out in the same manner and it has to be mentioned that from beginning nitrogen was continuously bubbled into the reaction medium by a bubbler, and was dried beforehand by passing it through a vessel with H_2SO_4 and then through another recipient with $CaCl_2$.

RESULTS AND DISCUSSIONS

Properties and structure of grafted copolymer

The grafted copolymer obtained is much more rigid than the ethylene vinyl acetate copolymer and has a brown colour resembling that of poly (maleic anhydride), the colour intensifying with the increase in percentage of grafted maleic anhydride.

It does not solve in solvents characteristic of poly (maleic anhydride), (alcohol, acetone, water); it solves in *p*-xylene and tetraline at temperatures close to their boiling points.

Their solubility decreases with the increase of grafting percentage, the copolymers with contents of less than 6% grafted maleic anhydride solving even in benzene.

The degree of crystallinity was determined by comparing it by the DTA method on a Linssei instrument, both on ungrafted ethylene vinyl acetate copolymer and on copolymer having 20% grafted maleic anhydride, and a decrease in crystallinity was noticed from the initial value of 37% (E-VA) to 17% (grafted copolymer).

The infra-red spectrum confirmed the initially established hypothesis which assumed that there are grafted chains of poly (maleic anhydride) on the main catenary of ethylene vinyl acetate copolymer.

The absorption bands at 5.41 μ and 5.59 μ characteristic of valence vibrations of C=O groups which belong to a maleic anhydride cycle in the grafted copolymer spectrum are found again but shifted to 5.44 μ and 5.65 μ.

The shifting of these bands towards longer wavelengths demonstrates the disappearance of carbonyl group conjugation in the maleic anhydride cycle and shows clearly that chains of poly (maleic anhydride) were grafted on ethylene vinyl acetate copolymer and not simple cycles of maleic anhydride.

This conclusion is further confirmed by the absence in the spectrum of grafted copolymer of the absorption band from 14.38 μ characteristic of —CH=CH— group.

Influence of nature and concentration of initiators.

In figure 1 interdependence is shown between the grafting percentage and initiator concentration, this being the most important indication for the explanation of the mechanism and the elucidation of the grafting reaction. The aspects of the three curves are characteristic of grafting which occurs through chain transfer.

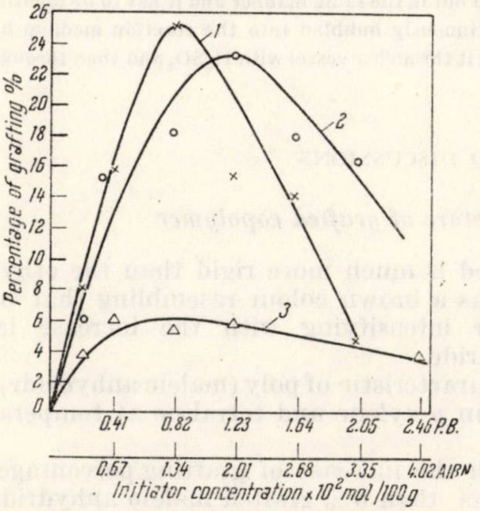

Fig. 1. — Dependence of grafting percentage on the nature and concentration of initiators.

1, Benzoyl peroxide in air

2, Benzoyl peroxide in nitrogen

3, Azoisobutironitrile in air

Solvent – *p*-xylene; working temperature 110°; time 3,5 hours.

Copolymer/maleic anhydride ratio: 0.06 g/g.

The initially increasing aspect of the curve is explained by the increase in concentration of radicals formed by decomposition of initiators and which are thus responsible for the acceleration of the chain transfer reaction.

The presence of a maximum is the result of the decrease in the length of poly (maleic anhydride) segments which continue to be grafted on the main catenary, as a consequence of diminution in the maleic anhydride concentration due to the great monomer consumption in the simultaneous homopolymerization process.

Both the more accelerated increase and the presence of the slightly higher maximum of the percentage to be grafted in air as against that to be grafted in nitrogen are probably explained by the additional existence of ethylene vinyl acetate macroradicals formed by oxidation and which also take part in grafting, the oxidation effect cumulating to that of chain transfer.

The subsequent development of the curve with concentrations over 1.23×10^{-2} mol peroxide/100 g solution when the percentage to be grafted in nitrogen exceeds clearly the percentage to be grafted in air, confirms the original hypothesis on chain transfer.

The same conclusions can be arrived at by comparing the results obtained by grafting in similar conditions in presence of BP and AIBN. The difference between the maximum value of grafting with BP (25%) and

AIBN (6%) can be explained only by accepting the hypothesis of grafting by transfer of catenary, since it is well-known that the reactivity of AIBN radicals in the chain transfer is very small.

Influence of copolymer concentration

In order to be able to show the influence of the ethylene vinyl acetate copolymer concentration on the percentage of grafting, the reaction was carried out with different quantities of copolymer, whereas the quantity of solution (p-xylene + maleic anhydride) and the concentration of maleic anhydride were maintained constant.

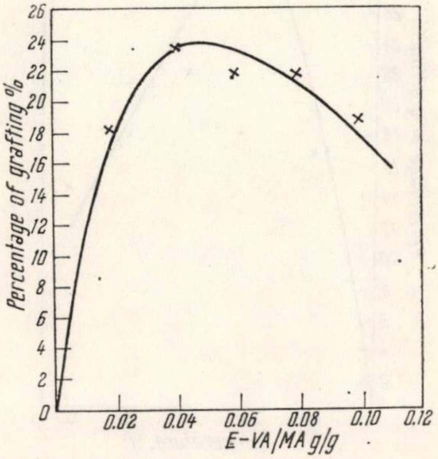

Fig. 2. – Dependence of grafting percentage on copolymer/maleic anhydride ratio.
Initiator: benzoyl peroxide 0.82×10^{-2} mol/100 g solution.
Temperature: 110°; reaction time: 3,5 hours.

The results are shown in figure 2.

In this case too the aspect of the curve is typical for grafting by chain transfer.

With the increase of copolymer concentration (increase of copolymer-monomer ratio), the reaction probability increases between the radicals and copolymer and at the same time the viscosity of the reaction mixture, which is in opposition to the development of the transfer reaction.

The two opposite tendencies explain the existence of the maximum, showing also the relationship between the phenomena.

Influence of temperature and time

Figure 3 shows the influence of temperature on the percentage of grafting. This develops concomitantly with the increase of temperature until a maximum is reached at 100°, after which it decreases again.

The effects of temperature increase are:

— increase in number of chain transfer reactions
— increase in number of homopolymerization reactions
— decrease of molecular weight of grafted segments.

The opposition between the first factor and the following two determines the curve aspect.

Figure 4 represents the interdependence between the grafting percentage and time.

In the initial portion the curve shows a sharp slope (up to one hour), whereas subsequently increase in time is insignificant.

This much sharper slope in case of grafting of maleic anhydride on E-VA copolymer, in comparison with the grafting of maleic anhydride on polyethylene,[6] can be attributed to the more reactive hydrogen adjacent to the tertiary carbon in the E-VA copolymer catenary and probably also in the esteric group to the methyl group activated by C=0, which could enter transfer reaction of the catenary.

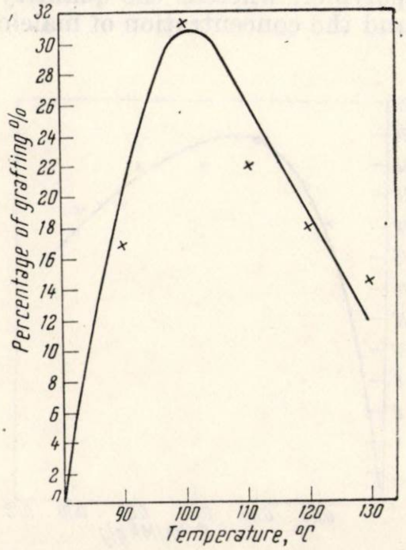

Fig. 3. — Dependence of grafting percentage on temperature.

Initiator : benzoyl peroxide 0.82×10^{-2} mol/100 g solution.

Time : 3,5 hours E-VA/MAr atio 0.06.

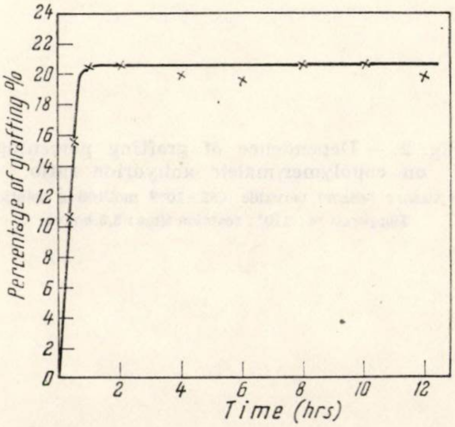

Fig. 4. — Percentage of grafting vs. time of reaction.

Temperature 110° ; benzoyl peroxide concentration 0.82×10^{-2} mol/100 g solution ; maleic anhydride concentration 15% ; copolymer monomer, 0.04 g/g.

MECHANISM OF REACTION

As a result of the study of copolymer structure and reaction kinetics, we can state that maleic anhydride grafting on ethylene vinyl acetate copolymer takes place by means of ethylene vinyl acetate macroradicals formed by the chain transfer reaction of the copolymer with the initiator (1)

AAAAA· +nB → grafted (1), where AAAA—E-VA

B—M.A.

Although the polymerization reaction of maleic anhydride has a smaller activating energy than the chain transfer reaction, no E-VA macroradicals are formed during the reaction (2),

$$BBB\cdot + AAAA \rightarrow AAAA\cdot + BBB \quad (2), \text{ where } BBB - \text{P.M.A.}$$

due to the insolubility of poly (maleic anhydride) in the solvents used. The probability of forming grafted copolymer by the reaction between the macroradicals of poly (maleic anhydride) and copolymer is very slight due both to the insolubility of poly (maleic anhydride) and to the reduced possibility of collision of the two macroradicals.

CONCLUSIONS

1. Grafting of maleic anhydride on ethylene vinyl acetate copolymer in homogeneous phase in the solvents and with the initiators mentioned takes place by means of ethylene vinyl acetate macroradicals formed by chain transfer reaction of the copolymer and the initiator.
2. The mechanism of grafting is confirmed both by the structure of the copolymer studied by infra-red absorption [chains of poly (maleic anhydride)] grafted on the main catenary of ethylene vinyl acetate copolymer and by the reaction kinetics.
3. The grafted copolymer has a high transformation ability during total or partial hydrolysis, aminolysis, alcoholysis reactions and a wide range of copolymers with different properties is obtained, which could be advantageously used for industrial application.

The authors take this opportunity to express their thanks to the Management of the Petrochemical Works Ploieşti for kind support of this work.

Although, the polymerization reaction of maleic anhydride has smaller activation energy than the chain transfer reaction, no EVA macroradicals are formed during the reaction (2):

[illegible] P.M.A.

Due to the insolubility of poly (maleic anhydride) in the solvents used, the probability of forming grafted copolymer by the reaction between the macroradicals of poly (maleic anhydride) and copolymer is very slight due both to the insolubility of poly (maleic anhydride) and to the reduced possibility of collision of the two macroradicals.

CONCLUSIONS

1. Grafting of maleic anhydride on ethylene vinyl acetate copolymer in homogeneous phase in the solvents and with the initiators mentioned takes place by means of ethylene vinyl acetate macroradicals formed by chain transfer reaction of the copolymer and the initiator.

2. The mechanism of grafting is confirmed both by the structure of the copolymer studied by infrared absorption (chains of poly (maleic anhydride) grafted on the main [illegible] of ethylene vinyl acetate copolymer) and by the reaction kinetics.

3. The grafted copolymer has a high transformation ability during total or partial hydrolysis, aminolysis, alcoholysis reactions and a wide range of copolymers with different properties is obtained, which could be advantageously used for industrial application.

The authors take this opportunity to express their thanks to the [illegible] for kind [illegible] of this work.

[illegible]

Revue Roumaine de Chimie, **15**, 247–252 (1970)

REACTION OF ETHYL *o*-PHENYLENE ARSENITE WITH TROPOLONE

A. ARSENE, MARIA PARASCHIV and A. T. BALABAN

Institute of Atomic Physics, P. O. Box 35, Bucharest, Romania

Received September 3, 1969

The structure of the crystalline product obtained from ethyl *o*-phenylene arsenite and tropolone was investigated by UV, IR and NMR spectroscopy. From the two possible formulas, the coordinated one, II, is considered less likely than the non-coordinated formula IV.

The reaction of 2-alkoxy-1,3,2-benzodioxaboroles with tropolones was shown [1-3] to afford yellow crystalline compounds (I). The presence of a coordinative bond which makes such compounds highly polar is evidenced by the dipole moment,[4] by infrared and electronic absorption spectra. In agreement with their high polarity, these compounds exhibit a marked negative solvatochromy.[5] Analogous compounds are obtained from diarylborinic esters and tropolones.[6,7] Other bidentate ligands, such as enolizable 1,3-diketones react similarly with benzodioxaboroles[8,9] or diarylborinic acids[6,10] yielding chelated compounds.

---

[1] A. T. Balaban, G. Mihai, R. Antonescu and P. T. Frangopol, *Tetrahedron*, **13**, 258 (1961).

[2] A. T. Balaban, *Rev. Roumaine Chim.*, **10**, 879 (1965).

[3] I. Bally and A. T. Balaban, *Studii și Cercetări Chim. Acad. Romînia*, **17**, 431 (1969).

[4] A. T. Balaban, I. Bally, R. J. Bishop, C. N. Renţea and L. E. Sutton, *J. Chem. Soc.*, **1964**, 2382.

[5] A. Arsene, A. T. Balaban, I. Bally, A. Barabas, M. Paraschiv and C. N. Renţea, *Spectrochim. Acta*, **23A**, 1373 (1967).

[6] I. Bally, E. Ciornei and A. T. Balaban, *Rev. Roumaine Chim.*, **13**, 1507 (1968).

[7] I. Bally, A. Arsene, M. Roman, M. Paraschiv, E. Romaş and A. T. Balaban, *Rev. Roumaine Chim*, **13**, 1225 (1968).

[8] A. T. Balaban, C. N. Renţea and M. Mocanu, *Tetrahedron Letters*, **1964**, 2049.

[9] A. T. Balaban, C. N. Renţea, M. Mocanu-Paraschiv and E. Romaş, *Rev. Roumaine Chim*, **10**, 849 (1965).

[10] I. Bally, A. Arsene, M. Băcescu-Roman and A. T. Balaban, *Tetrahedron Letters*, **1965**, 3929.

In order to test whether elements from other groups of the periodic systems may replace boron as the acceptor atom, the synthesis of an arsenic compound (II) analogous to I was attempted.

In principle, the arsenic atom in tri-coordinated structures such as III could act as electron acceptor expanding its valence shell. Such "hypervalent chelates" would require, [11] however, the presence of two co-ordinating sites giving rise to a five-coordinated trigonal-bipyramidal configuration in which the arsenic would have five valencies. The presence of only one co-ordinating site could from the outset be predicted to act unfavourably. This would give rise, however, to interesting differences between the boron and arsenic analogues.

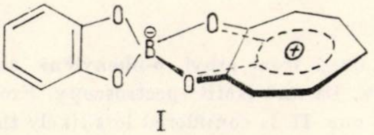

I

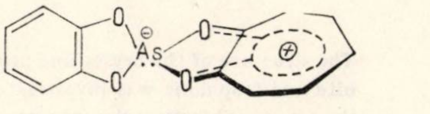

II

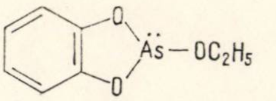

III

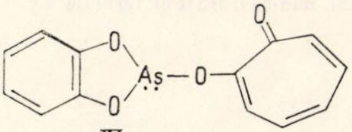

IV

By treating ethyl *o*-phenylene arsenite (III) with tropolone in benzene, a yellow product with an elementary analysis consistent with formulas II or IV was obtained. Its infrared spectrum (KBr pellet) presents bands at 1608s, 1590s, 1528s, 1490vs, 1458 vs, 1432s, 1396s, 1339m, 1299s, 1280s, 1250vs, 1210s, 1105m, 1081m, 1024m, 975m, 967m, 925, 888m, 870m, 851w, 810vs, 772s, 753s, 742s, 730s, 672s, 624s, 540s, 440m. In solution several modifications of the number and position of bands can be noted : the band from 1608 cm^{-1} appears at 1615 cm^{-1} in CCl_4 ; two bands at 1220 and 1235 (CCl_4) or 1216 and 1231 (CS_2) appear instead of the band at 1210 cm^{-1} ; only two bands instead of three appear at 745 vs and 729 s cm^{-1} (CS_2). Other differences can be observed for the 925 and 1450 cm^{-1} bands.

The ultraviolet absorption spectrum of the arsenic compound is very similar to that of I, excepting that the longest-wavelength absorption band does not present fine structure. In benzene two maxima appear at 374 ($\in$ 3800) and 326 nm ($\in$ 10400) ; in 1,2-dichloroethane the maxima are at 372 (4300), 323 (11300), 283 (6100) and 237 nm (33000). The bands at ca. 370 and 325 nm are due to the tropolonic moiety, the band at ca. 280 nm to the pyrocatecholic chromophore. However, the negative solvatochromy is much less pronounced than in the case of I, as shown

[11] J. I. Musher, *Angew. Chem.* **81**, 68 (1969).

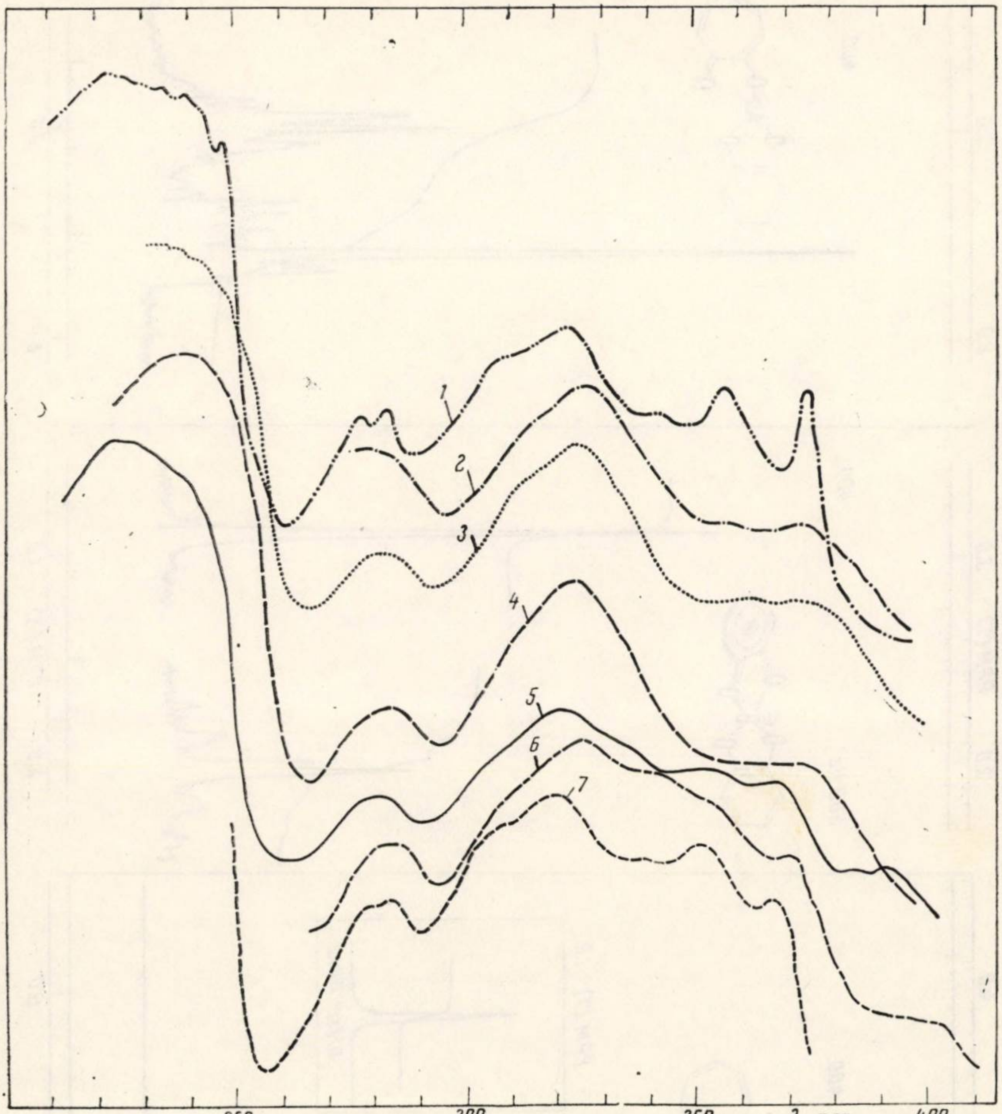

Fig. 1. — Ultraviolet absorption spectra of IV.

Solvents: *1*, cyclohexane; *2*, benzene; *3*, di-n-butyl ether; *4*, 1, 2-dichloroethane; *5*, ethanol; *6*, dimethylformamide; *7*, acetonitrile

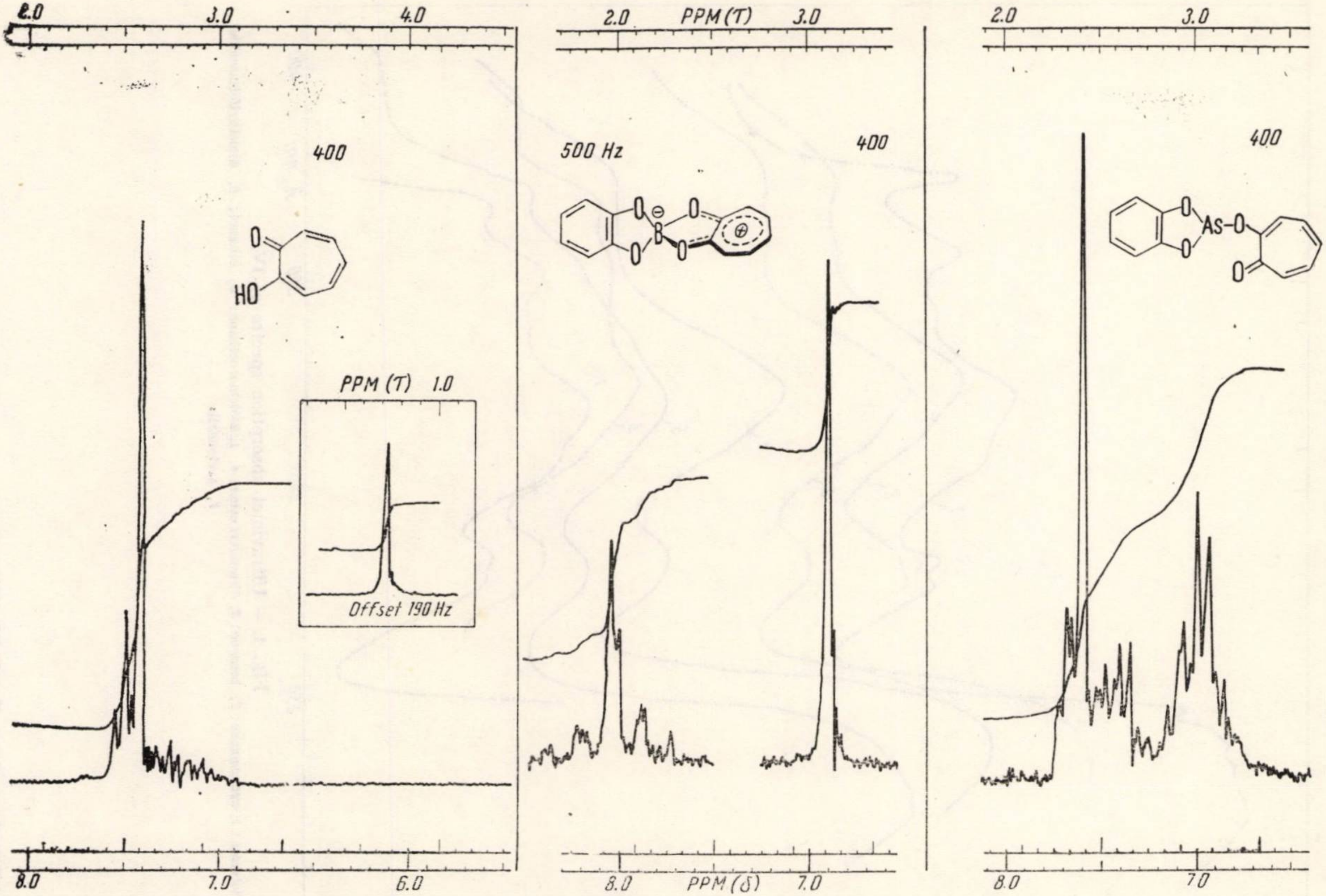

Fig. 2. – Nuclear magnetic resonance spectra in deuterochloroform (with TMS at 38°) of tropolone, I and IV.

by table 1 and fig. 1. This would be in better agreement with a nonchelated, less polar, structure IV. It is also apparent that solvents such as acetonitrile, formamide or dimethylformamide considerably affect the spectrum of the arsenic compound, unlike the boron analogue.[2,5]

Table 1

Solvatochromy of the boron and arsenic compounds

Solvent	Absorption maximum (nm)	
	I	IV
Cyclohexane	374	375
Benzene	368	374
1, 2-Dichloroethane	364	372
Acetonitrile	358	368
Formamide	355	—
Dimethylformamide	—	370
Ethanol	—	368
Di-n-butyl ether		370

A comparison of the nuclear magnetic resonance spectra of tropolone, the boron and arsenic compounds (Fig. 2) reveals interesting differences between the two last products. In the boron compound (I) the tropolonic protons form a multiplet centered at τ 2.0 which is shifted downfield from the position (τ 2.6) where they appear in tropolone. In the arsenic compound, however, these protons appear at τ 2.3 – 2. 7 as in tropolone. The four protons of the pyrocatechol moiety also appear differently in the boron and arsenic compounds : a peak at τ 3.1 in the former (cf. ref. 9 for the NMR spectrum of a related compound) and a multiplet at τ 2.8. – 3.2 in the latter compound.

In conclusion, a non-chelated structure IV is in better agreement with the spectral data than a coordinated formula II analogous to the boron compound. This difference between the boron and arsenic compounds is due both to the fact that the arsenic atom in IV has a complete electronic octet, whereas in II it would have expanded the valence shell to 10 electrons, and to the unfavourable four-coordinated structure II for arsenic which is more stable in five- or six-coordinated compounds.

In confirmation of this idea, compound III failed to react with 1,3-diketones (whereas 2-alkoxy-1,3,2-benzodioxaborole, the boron analogue of III, readily affords [7,9] chelate compounds with 1,3-diketones).

EXPERIMENTAL

Ethyl *o*-phenylene arsenite (III), m.p. 150°, b.p. 114°/10 mm was prepared according to literature data [12] from arsenic trichloride and pyrocatechol, followed by reaction of the resulted chloroderivative with ethanol in benzene in the presence of pyridine.

Equimolar amounts of III (230 mg) and tropolone (120 mg) were heated in 10 ml benzene under reflux for 10 minutes until III dissolved completely. On cooling, yellow crystals m.p. 194–195° (capillary), 181–183° (micro hot stage) separated. The m.p. does not increase on

---

[12] G. Kamai and Z. L. Khisamova, *Zhur. obshchei Khim,* **24,** 816 (1954).

Revue Roumaine de Chimie, **15**, 247–252 (1970)

recrystallization from benzene. Found : C, 51.19 ; H, 3.15 ; As, 24.58. $C_{13}H_9AsO_4$ requires : C, 51.23 ; H, 2.98 ; As, 24.63 %. The analysis for arsenic was performed according to ref. [13].

Ultraviolet and visibile absorption spectra were recorded with an Optica (Milan) CF—4 instrument, infrared spectra with a Zeiss Jena UR—10 apparatus, and nuclear magnetic resonance spectra with a Varian A60-A spectrometer.

Acknowledgements. Thanks are expressed tov. Mrs. Maria Roman for elementary C, H analyses, to Mrs. Elena Romas for the infrared spectra and to Dr. W. Silhan for the NMR spectra.

---

[13] O. WINTERSTEINER, *Mikrochem.*, **4**, 155 (1926); cf. HOUBEN-WEYL'S "Methoden der Organischen Chemie" (E. MÜLLER, ed.), vol. 2, G. Thieme Verlag, Stuttgart, 1953, p. 204.

Revue Roumaine de Chimie, 15, 253–258 (1970)

THE DONOR-ACCEPTOR COMPLEXES OF N-SUBSTITUTED MALEIMIDES WITH AMINES, AND THEIR ROLE IN NUCLEOPHILIC ADDITION REACTION

MALVINA FĂRCAŞIU and RODICA ISTRĂŢOIU

Institute of Normal and Pathologic Physiology "D. Danielopolu" Bucharest, Bd. 1 Mai. 11
and
Institute of Inframicrobiology "St. Nicolau" Bucharest, Şos. Mihai Bravu 285

Received February 25, 1969

Charge transfer bands were evidenced in the electronic spectra of the solutions of N-substituted maleimides (I) and amines, belonging to electron donor-acceptor complexes. For a tertiary amine, the equilibrium constant of the formation of the complex was determined; its small value indicated that the complexes are "contact complexes". For primary amines the C.T. bands disappeared in time, the product of the nucleophilic addition of the amine to the double bond of I being isolated. The donor-acceptor complexes are considered as intermediates in the nucleophilic addition. The N-benzyl maleimide adds two molecules of cyclohexyl amine. The donor-acceptor complexe of N-cyclohexyl maleimide and cyclohexyl amine was stable; no addition product was obtained. 2,3-Dichloro-N-cyclohexyl maleimide was found to give stronger donor-acceptor complexes with amines and 2, 3 substituted products.

Maleimide and its N-substituted derivatives possess an electron deficient double bond, manifested for instance by their philodienic reactivity. One could expect that these compounds manifest electron-acceptor properties, particularly because the related maleic anhydride was found to give donor-acceptor complexes with several donors.[1]

In the present work, the acceptor properties of N-substituted maleimides (I) relatively to aromatic and aliphatic amines (n-donors [2]) were studied.

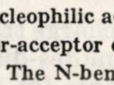

I

a. $R = C_6H_5$
b. $R = CH_2-C_6H_5$
c. $R = C_6H_{11}$ (cycloheyxl)

---

[1] *a*, D. Bryce-Smith and J. E. Lodge, *J. Chem. Soc.*, **1962**, 2675; *b*, Z. Racisjewski, "Amer. Chem. Soc. Meeting", Los Angeles, Calif., April 1–5, 1963, p. 21; *c*, S. Iwatsuki and Y. Yamashita, *Makromole. Chem.*, **89**, 205 (1965).

[2] R. S. Mulliken, *J. Chim. phys.*, **61**, 20 (1964).

The reaction between N-phenyl maleimide (I_a) and aniline, giving an addition product formulated as II_a, was described in the literature.[3]

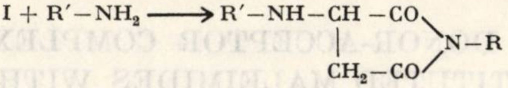

$$I + R'{-}NH_2 \longrightarrow R'{-}NH{-}CH{-}CO{\diagdown}N{-}R \quad (CH_2{-}CO{\diagup})$$

II

a. $R=R'=C_6H_5$
b. $R=C_6H_5$; $R'=C_6H_{11}$
c. $R=CH_2-C_6H_5$; $R'=C_6H_5$
d. $R=C_6H_{11}$; $R'=C_6H_5$

By reexamining this reaction, we observed that when dissolving I_a in aniline, a broad absorption band, having a maximum at 370 m μ appeared. Neither aniline nor I_a presented such "extra" band when dissolving in non-complexing solvents. All substituted maleimideamine pairs behaved similarly; the positions of the maxima of the observed absorption bands are given in the table (third column). When an addition reaction took place, this "extra" band appeared at the very moment of dissolving and disappeared gradually as the reaction progressed, and the product (which is colourless), precipitated.

It appeared of interest to study the behaviour of a tertiary amine, which cannot add to the double bond. When dimethylaniline was mixed with I_a and I_c broad absorption bands were obtained, with maxima within the range 360–380 mμ.

The width of these "extra" bands is typical for charge transfer bands.[4] The time stability of C T maximum for the maleimides-dimethylaniline systems allowed to determine the equilibrium constants for the formation of the donor-acceptor complexes in these cases. The results are given in the table. The small values thus obtained indicate that the complexes of N-substituted maleimides (I) with amines belong to the category of "contact complexes" [5] (i.e. the charge transfer band is mainly due to the electrons transfers taking place only at the random collision between donor and acceptor molecules, in solution).

For the cyclohexylamine-N-cyclohexyl maleimide (I_c) system, the charge transfer band was time-stable and appeared at longer wawelengths than for the above discussed systems. The band presents the characteristic property of charge transfer bands, to vanish on heating and to reappear on cooling.

As concerns the addition reaction of the primary amines to the double bond of I, it gave the N,N'-disubstituted amino succinimides II_{a-d}. The reaction was fast (completed in few minutes) for II_b, and slower (24 hrs,) for $II_{a,c,d}$. The last three compounds once formed, are stable in the reaction medium, while the first (II_b), if not filtered immediately after precipitation, gave a waxy untraceable material. It is noteworthy that the aniline adds to N-cyclohexyl maleimide (I_c) only when a large excess of aniline is present.

---

[3] *a*, C. Hell and R. Poliakoff, *Chem. Ber.*, **1892**, 640. *b*, S. C. Harvey, *J. Amer. Chem. Soc.*, **71**, 1121 (1949).

[4] D. Booth, *Sci. Progress*, **58**, 435 (1960).

[5] L. E. Orgel and R. .S Mulliken, *J. Amer. Chem. Soc.*, **79**, 48 39 (1957).

When the molar proportion of the reactants was 1 : 1, the donor-acceptor complex (evidenced by charge transfer band) was stable indefinitely, and the reactants could be isolated unchanged (see the Table).

Table 1

Donor-aceeptor complexes and reaction products from N-substituted maleimides and amines

Maleimide	Amine	Donor-acceptor complex		Addition product	Remark
		Ch. tr. band mμ	Equil. const. l/mol		
I_a	$C_6H_5NH_2$	370	—	II_a	see exp.
	$C_6H_{11}NH_2$	360	—	II_b	’’
	$C_6H_5N(CH_3)_2$	360–380	0.26	—	for the eq. const. see exp.
I_b	$C_6H_5NH_2$	—	—	II_c	see exp.
	$C_6H_{11}NH_2$	—	—	$III_{(a+b)}$	probable isomers mixt.
I_c	$C_6H_5NH_2$	340–350	—	does not react	component molar ratio 1/1
	$C_6H_5NH_2$	340–350	—	II_d	amine in excess
	$C_6H_{11}NH_2$	490–500	—	doesnot react	see exp.
	$C_6H_5N(CH_3)_2$	360–380	0.36	—	

The reaction of N-benzyl maleimide (I_b) with cyclohexyl amine followed a different way : a double addition involving the ring opening takes place :

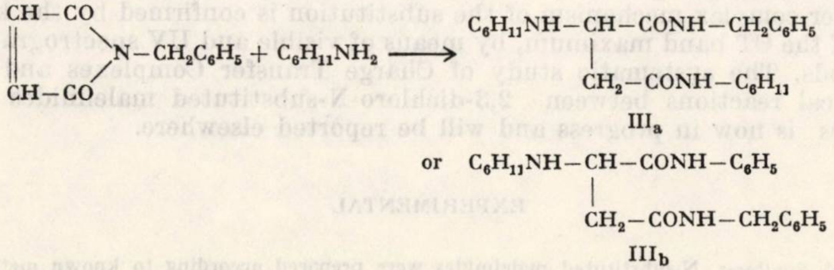

III_a

or

III_b

Quite surprisingly, cyclohexylamine did not add to N-cyclohexyl maleimide (I_c). No reaction took place even when an important excess of amine was employed at ordinary or at reflux temperature.

The rapid development of charge transfer bands when N-substituted maleimides (I) were dissolved in amines, and the disappearance of those bands as the partners reacted (in the cases when a nucleophilic addition of the amine to the double bond of the maleimide took place) seem to indicate the intervention of the donor-acceptor complexes as intermediates in these reactions. As in other cases, [1] the transfer of the electron pair, which establishes the new C—N bond can be considered to proceed stepwise, the first step being the partial transfer of one electron giving a donor-acceptor complex (IV), as represented in the scheme :

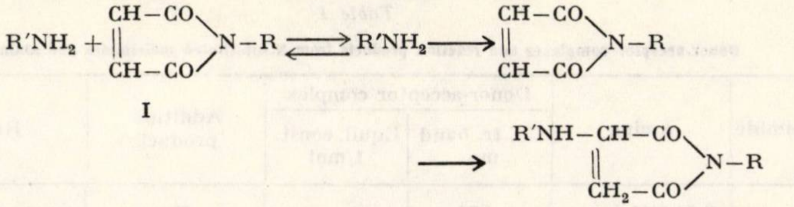
I IV II

The electron-acceptor ability of N-substituted maleimides can be increased by introducing high electronegatives substituents to the double bond, capable to reduce its electron density. It was to be supposed that 2,3 dichloro-N-substituted maleimides, would be stronger acceptors that the correspondings simply N-substituted maleimides.

Thus, by mixing 2,3 dichloro-N-cyclohexyl maleimide and pyridine a charge transfer complex was obtained, with a maximum at 550 mμ ; this maximum vanished in about 30 h, as a result of the double substitution of pyridine to the methylenic CH, giving the corresponding pyridinium salt

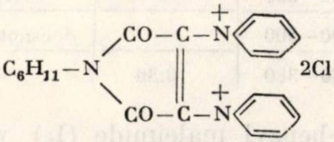
V

An analogue product of V has been recently reported. [6] The charge transfer complex mechanism of the substitution is confirmed by the kinetics of the CT band maximum, by means of visible and UV spectrographic methods. The systematic study of Charge Transfer Complexes and the chemical reactions between 2,3-dichloro-N-substituted maleimides and amines is now in progress and will be reported elsewhere.

EXPERIMENTAL

a) *Syntheses.* N-substituted maleimides were prepared according to known methods, consisting in the reaction of maleic anhydride with primary amines with subsequent cyclization of maleamic acids in presence of acetic anhydride and anhydrous sodium acetate. [7]

The reactions between N-substituted maleimides and amines, were performed in the following manner :

---

[6] M. J. Karten U. S., 3,335,147, Aug. 8, 1967. Chem. Abstr., **68**, 12867 e (1968).

[7] *a*, A. Piutti and E. Giustiniani, *Gazz. chim. Ital.*, **26**, 436 (1896) ; *b*, E. Bellack and J. B. Dewitt, *J. Agric. Food Chem.*, **2**, 1176 (1954) ; *c*, Kwan-Chung Tsou, R. J. Barrnett and A. M. Seligman, *J. Amer. Chem ; Soc.*, **77**, 4613 (1955) ; *d*, R. Istrăţoiu, M. Fărcaşiu and C. Nicolau, *Rev. Roumaine Chim.*, **12**, 1429 (1967).

1) *N-phenyl-maleimide and aniline*

a) 2g N-phenyl-maleimide were mixed at room temperature with 25 ml freshly distilled aniline. The orange solution obtained began to precipitate after 24 h. The white precipitate was filtered, washed with EtOH and three times recrystallized from i-PrOh. The product had m.p. 218°, and corresponds to $C_{16}H_{14}N_2O_2$ (Calcd : C, 72.16 ; H, 5.30 ; Found : C, 72.04 ; H, 5.49). The structure IIa given in the Table was confirmed by NMR.
b) By heating the same reactants at 60–70°, 2 h, the same product was obtained, but it was difficult to be separated from the waxy brown mass, also formed.

2) *N-phenyl-maleimide and cyclohexylamine*

a) 2 g N-phenyl-maleimide and 25 ml freshly distilled cyclohexylamine were mixed at room temperature ; a red solution was obtained and, after a few minutes, a white product precipitated. After filtration and three times recrystallization from EtOH, the product corresponds to II_b $C_{16}H_{20}N_2O_2$ (Calcd : C, 70.56 ; H, 7.40 : Found : C, 70.73 ; H, 7.25) M.p. 152–154°. The structure in the table was confirmed by NMR. If the precipitate is not immediately filtered, after 24 h red waxy unidentifiable products are obtained.
b) The same red waxy products were obtained if the cyclohexyl amine and N-phenyl maleimide solution were heated at 60–70°.

3) *N-benzyl-maleimide and aniline*

a) 0.5 g N-benzyl-maleimide dissolved in CH_2Cl_2 were mixed at room temperature with 0.5 ml freshly distilled aniline. The solvent was removed *in vacuo* and the white precipitate was three times recrystallized from EtOH. The product, m.p. 131°, corresponds to $C_{17}H_{16}N_2O_2$. (II_c in the table).

(Calcd. : C, 72.83 ; H, 5.75 ; Found : C, 72.50 ; H, 5.45).

b) 0.5 g N-benzyl-maleimide refluxed with 30 ml aniline, gave a waxy product, that could not be characterized.

4) *N-benzyl-maleimide and cyclohexylamine*

2 g N-benzyl-maleimide and 25 ml cyclohexylamine mixed at room temperature gave a red solution : by evaporating *in vacuo* the excess of amine, the white product III obtained was three times recrystallized from EtOH and water. M.p. 116°. It corresponds to $C_{23}H_{35}N_3O_2$ (see the table). (Calcd. : C, 71.80 ; H, 9.08 ; Found : C, 72.07 ; H 9.11).

5) *N-cyclohexyl-maleimide and aniline*

a) 2g N-cyclohexyl-maleimide in CH_2Cl_2 mixed with 30 ml freshly distilled aniline at room temperature gave a yellow solution. By evaporating the solution, the starting material N-cyclohexyl-maleimide I_c was recovered. Purified by sublimation it had m.p. 89° (Calcd. : C, 67.02 : ; H, 7.31 ; Found : C, 66.89 ; H. 7.60).

b) 2 g N-cyclohexylmaleimide and 30 ml aniline, refluxed 1 h, gave, after the removal *in vacuo* of the excess of aniline, a white product ; recrystallized three times from EtOH it corresponds to $C_{16}H_{20}N_2O_2$ (II_d) (Calcd. : C 70.50 ; H 7.40 ; N 10.29 ; Found : C, 70.28 ; H, 7.20 ; N, 10.58) M.p. 170°.

6) *N-cyclohexyl-maleimide and ciclohexylamine*

By mixing 2g of N-cyclohexyl-maleimide with 25 ml cyclohexylamine, either at room temperature or at reflux, a red solution was obtained ; no precipitate appeared even after 48 hours. Removing the excess of amine and recrystallizing three times from EtOH, the starting material N-cyclohexyl-maleimide I_c was obtained (Calcd. : C, 67.02 : H, 7.31 N 7.82 ; Found : C, 67.15 ; H, 7.60 ; N, 7.66).

b) *The equilibrium constants.* The equilibrium constants were derived with a method based on spectrophotometric measurements. By the spectroscopical determination the sample cell contained a maleimide-dimethylaniline solution in chloroform (Merck spectroscopic grade), the dimethylaniline being in great excess. The compensation cell was filled with the corresponding maleimide (also dissolved in chloroform) in a concentration identical with that existing initially in the sample cell.

The equilibrium constants (K) were calculated using the formula[8] ;

$$\frac{C_a \cdot 1}{D_{\text{cor}}} = \frac{1}{(\varepsilon_c - \varepsilon_a)\, C_d\, K} + \frac{1}{\varepsilon_c - \varepsilon_a}$$

where :

C_a initial concentration of acceptor (mol/l)

$D_{\text{cor}} = D_{\text{measured}} - \varepsilon_d . C_d$

ε = extinction molar coefficient

K = equilibrium constant

C_d = initial concentration of the donor (mol/l)

a, b, c — are the indices for acceptor, donor resp. complex

1 — the thickness of the cell

C_a/D_{cor} function of $1/C_d$ is graphically represented ; ε_c is deduced from the intersection with the ordinate and K from the slope.

In order to define the position of the charge transfer bands and to deduce the equilibrium constant, the spectrophotometric measurements were performed on a Carry 4 spectrophotometer.

For the equilibrium constants, the measurements were performed at 19 ± 0.5°.

---

[8] M. FĂRCAŞIU (to be published).

Revue Roumaine de Chimie, 15, 259–263 (1970)

THE RESOLUTION OF ENANTIOMERIC AMINO-DERIVATIVES OF ARENE-TRICARBONYL-CHROMIUM(O)

S. ROŞCA and C. D. NENITZESCU
Polytechnic Institute Bucharest, str. Polizu, 1

Received October 13, 1969

The resolution of racemic *o*- and *m*-toluidine-tricarbonyl-chromium(0) is reported. Optically active complexes were obtained *via* their diastereoisomeric salts with (+)- camphor-10-sulphonic acid. By acetylation of the optically active complexes of free amines, the corresponding acetylated compounds retaining optical activity were obtained. The resolution into enantiomers of the racemic 2-(3.4-dihydro)-naphthyl—piperidine-tricarbonyl-chromium(0) is also reported.

Molecular asymmetry of some metallocene derivatives has been first demonstrated by the resolution into enantiomers of ferrocenes[1–4] and cyclopentadienyl-tricarbonyl-manganese(I) derivatives.[5]

In the class of benzenoid-metal complexes two unlike substituents in *ortho* or *meta* can also give rise to optical activity. This was shown by the resolution of *m*-methoxybenzoic acid-tricarbonyl-chromium(0).[6] However, there are few other examples of resolution into enantiomers in this class.[7–9]

In the present paper we report the resolution of racemic *o*-toluidine-tricarbonyl-chromium(0) (I) and *m*-toluidinetricarbonly-chromium(0) (0) (II):

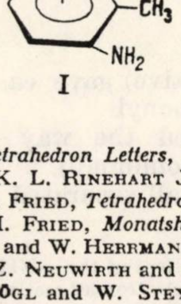

I

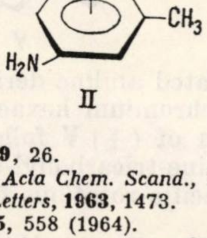

II

[1] J. B. Thomson, *Tetrahedron Letters*, **1959**, 26.

[2] L. Westman and K. L. Rinehart Jr., *Acta Chem. Scand.*, **16**, 1199 (1962).

[3] K. Schlögl and M. Fried, *Tetrahedron Letters*, **1963**, 1473.

[4] K. Schlögl and M. Fried, *Monatsh.* **95**, 558 (1964).

[5] R. Riemschneider and W. Herrmann, *Liebigs Ann. Chem.* **642**, 68 (1961).

[6] A. Mandelbaum, Z. Neuwirth and M. Cais, *Inorg. Chem.* **2**, 902 (1963).

[7] H. Falk, K. Schlögl and W. Steyer, *Monatsh.* **97**, 1029 (1966).

[8] G. Price, D. Phil. Thesis Oxford 1962 (cited by K. Schlögl, *Fortschritte der Chemischen Forschung*, **6** (3), 479 (1966).

[9] M. J. Besançon and J. Tirouflet, *Bull. Soc. chim. France*, **1967**, 751.

The resolution of **I** and **II** was achieved *via* their diastereoisomeric salts with (+)-camphor-10-sulphonic acid, which could partly be separated by recrystallization from ethylacetate, or ethylacetate and acetone mixtures.

The stability toward oxidation of the arene-tricarbonyl-chromium (0) complexes is very much reduced by the change of the functional group from amino to ammonium cation, during the formation of the diastereoisomers *). As diastereoisomers (**I***a*) and (**II***a*) were extremely sensitive to air oxidation, both in solution and in solid state, they were carefully handled under inert gas.

Optically active complexes of free amines (obtained from the diastereoisomeric salts by treatment with NaOH solution) were acetylated with acetic anhydride in pyridine, using a procedure described for acetanilide-tricarbonyl-chromium(0).[10] Acetylated compounds retained optical activity.

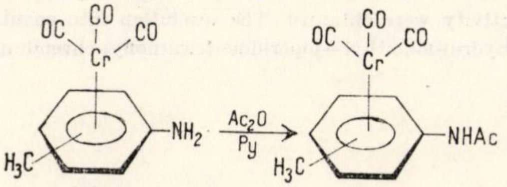

(+)-I
(+)-II
(−)-II

(+)-III
(+)-IV
(−)-IV

We report also the resolution into enantiomers of the racemic 2-(3.4-dihydro)-naphthylpiperidine-tricarbonyl-chromium(0) (**V**). This compound was obtained from 2-(3.4-dihydro)-naphthylpiperidine (**VI**) and chromium hexacarbonyl following esentially Nicholls and Whiting's method.[10] As expected, the enamine **VI** (which can be considered as a vinylogue of an N-alkylated aniline derivative) gave easily and in high yield the complex with chromium hexacarbonyl.

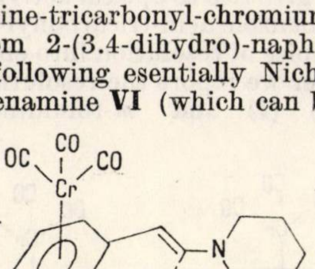

V

The resolution of (±)-**V** followed the way previously described for *o*-and *m*-toluidine-tricarbonyl-chromium(0).

In table 1 specific rotations for all separated optically active compounds are given.

---

*) This is probably due to the strong -I effect of the $-\overset{+}{N}H_3$ group and is in agreement with earlier observations according to which electron-attracting groups destabilize such complexes.

[10] B. Nicholls and M. C. Whiting, *J. Chem. Soc.*, **1959**, 551.

Table 1

Specific rotations of optically active Ar-Cr(CO)$_3$

Ar	Specific rotation $[\alpha]_D^o$ (temp.)	c (in AcOEt)
o-Toluidine	(+)−I +15.2±0.6 (22°)	1.0
o-Toluidine	(−)−I −13.6±0.8 (22°)	0.7
m-Toluidine	(+)−II + 5.2±0.7 (23°)	0.7
m-Toluidine	(−)−II − 5.5±0.4 (23°)	1.2
N-acetyl-*o*-toluidine	(+)−III +22.3±1.0 (23°)	0.5
N-acetyl-*m*-toluidine	(+)−IV + 7.3±0.9 (25°)	0.6
N-acetyl-*m*-toluidine	(−)−IV − 8.4±0.9 (25°)	0.6
2-(3.4-dihydro-naphthylpiperidine	(+)−V + 6.5±0.3 (23°)	1.7
2-(3.4-dihydro)naphthylpiperidine	(−)−V − 5.9±0.3 (23°)	1.7

EXPERIMENTAL

Melting and boiling points are uncorrected. Specific rotations were measured using an "Opton" polarimetre with a 1.91 dm cell, in ethylacetate as solvent.

Ethylacetate and acetone used for the recrystallization of the diastereoisomers were purified by the usual methods and saturated with argon before use.

Commercial (+)-camphor−10−sulphonic acid was used after recrystallization from EtOH. M. p. 193°; $[\alpha]_D^{20}$ = 24° (H_2O ; c = 5).

The chromium hexacarbonyl [11] and 2-tetralone [12] were prepared by the methods described in literature.

***o-Toluidine-tricarbonyl-chromium (0) (I) and m-toluidine-tricarbonyl-chromium(0)* (II). Title compounds were prepared according to Nicholls and Whiting. [10] From 2 g (9 mmoles) Cr(CO)$_6$ and 3 g (28 mmoles) *o*-toluidine, 1.9. g (86 %) (I) were obtained ; m.p. 129−130° from chloroform-*n*-heptane (lit. [10] 130−132). With *m*-toluidine 1.95 g (88 %) (II) were obtained ; m.p. 136° (lit. [10] 137−139°).**

***Resolution of (±)-o-toluidine-tricarbonylchromium(O).* A solution of 730 mg (3 mmoles) (±)−I in 15 ml AcOEt was placed in a Schlenk-tube previously filled with argon. A hot solution of 720 mg (3.2 mmoles) (+)-camphor-10-sulphonic acid in 20 ml AcOEt was added, and the mixture was stirred by argon bubbling for 5 min ; a yellow precipitate was formed. The Schlenk tube was then connected with two other similar tubes on of them empty (flushed with argon) and the other containing 80 ml AcOEt. After the sedimentation of the precipitate the liquid was removed by decantation into the empty tube. The following operation was then repeated four times : 20 ml of AcOEt were poured over the precipitate and the suspension heated (80° on a steam bath) with gentle stirring. After the sedimentation of the crystals formed on cooling at 0°, the liquid is poured over the previous decantate.**

Finally from the tube containing the insoluble material (fraction A) and that containing the liquid (fraction B) the solvent was evaporated to dryness in an argon stream.

---

[11] **E. O. Fischer, W. Hafner and K. Ofele, *Chem. Ber.*, 92, 3050 (1959).**

[12] **J. W. Cornforth, R. H. Cornforth and R. Robinson, *J. Chem. Soc.*, 1942, 689.**

To the solid resulting from fraction A, 15 ml of 5% NaOH solution was added and the mixture was extracted with ether. The ethereal solution was thoroughly washed with water, dried over $CaCl_2$ and the ether evaporated to afford 380 mg complex (+) -**I**; m.p. 128°; IR spectrum identical with that of the original **I**; $\alpha_D^{22} = +0.29 \pm 0.01°$ (130 mg dissolved in 13 ml AcOEt).

The solid resulting from fraction B was worked up as above to yield 125 mg complex (−)−**I**; $\alpha_D^{22} = -0\,.17 \pm 0.01^0$ (85 mg in 13 ml AcOEt).

Resolution of (±)-m-*toluidinetricarbonyl-chromium*(0). The procedure is essentially the same as described above, but instead of AcOEt as solvent, a mixture of 1 : 1 AcOEt−Me_2CO was used.

From 800 mg (3.3 mmoles) **II** and 810 mg (3.5 mmoles) (+)-camphor-10-sulphonic acid were obtained ; a) 315 mg complex from the fraction containing the insoluble material ;; m. p. 135°; IR spectrum identical with that of the original **II**; $\alpha_D^{23} = -0.13 \pm 0.01°$ (161 mg in 13 ml AcOEt) ; b) 195 mg complex from the decantated liquid, m.p. 134°; IR spectrum identical with that of the original **II**; $\alpha_D^{23} = +0.07 \pm 0.01°$ (92 mg in 13 ml AcOEt).

Acetylation of (+) *-o-toluidine-tricarbonyl-chromium(O).* A solution of 200 mg (0.8 mmoles) (+)-**I** and 130 mg (1.2 mmoles) acetic anhydride in 3 ml pyridine was kept over night at room temperature in the dark. The solution was then poured into a mixture of 10−15 g ice and 5 ml conc. HCl and extracted with ether. The extract was washed with diluted HCl and with water, dried over $CaCl_2$ and evaporated. The residue was further purified by passing through an acidic Al_2O_3 column (benzene-ether 3 :1). The solvent was removed to afford 95 mg (40%) yellow crystals of (+)−**III**; m.p. 124° (slight decp. at 118°); $\alpha_D^{23} = +0.23 \pm 0.01°$ (70 mg in 13 ml AcOEt). Found : C, 49.93 ; H, 3.95. $C_{12}H_{11}O_4NCr$ requires : C, 50.53 ; H, 3. 89.

Acetylation of (−)− *and* (+)-m-*toluidine-tricarbonyl-chromium*(*O*). The above procedure was used. 140 mg (0.6 mmoles) (−)−**II** and 130 mg (1.2 mmoles) acetic anhydride in 3 ml pyridine gave 130 mg acetylated product. Recrystallization from chloroform-light petroleum gave 110 mg (67% of (−)-**IV**; decn 138°; $\alpha_D^{25} = -0{,}09 \pm 0.01°$ (73 mg in 13 ml AcOEt). Found : C, 50.51 ; H, 4.10 ; N, 5.05 ; Cr, 18.52. $C_{12}H_{11}O_4NCr$ requires : C, 50.53 ; H, 3.89 ; N, 4.91 ; Cr, 18.24.

From 100 mg (0.4 mmoles) (+)-**II** and 130 mg (1.2 mmoles) acetic anhydride, 96 mg (82%) of (+)-**IV** were obtained; m.p. 138° (decn.); IR spectra of (+)-**IV** and of (−) -**IV** are identical; $\alpha_D^{25} = +0.08 \pm 0.01°$ (75 mg in 13 ml AcOEt).

2-(3.4-Dihydro)-naphthylpiperidine (**VI**). Title compound was obtained following an usual procedure for the preparation of enamines.[13]

A solution of 6.3 g (43 mmoles) 2-tetralone, 3.8 g (44 mmoles) piperidine and 30 mg p-toluenesulphonic acid in 60 ml benzene, placed in a 100 ml flask equipped with a downward condenser, was refluxed for 8 hours ; about 0.5 ml of water separated. The benzene was removed at normal pressure and the residue distilled at reduced pressure to give 7.2 g (79%) **IV**; b. p. 183°/1.5 mm. The product is sensitive to air and moisture. Found : C, 84.15 ; H, 9.2 ; N, 6.61. $C_{15}H_{19}N$ requires : C, 84.46 ; H, 8.98 ; N, 6.56.

2-(3,4-Dihydro)-naphthylpiperidine-tricarbonyl-chromium(0) (**V**). A mixture of 2.6 g (12 mmoles) **IV** and 3.1 g (14 mmoles) Cr $(CO)_6$ in 30 ml decaline (distilled over sodium and then saturated with argon) was heated under argon for 4 hours at 205−210°. On cooling crystallized complex precipitated. From the condenser 1.2 g Cr $(CO)_6$ were recovered. The complex was filtered and washed with light petroleum. Two recrystallizations from ether-light petroleum gave 2.2 g (77%)

[13] J. A. West, *J. Chem. Educt.*, **40**, 195 (1963).

yellow crystals of **V** ; m.p. 138 – 139° Found : C, 61.65 ; H, 5,56 ; N, 4.15 ; Cr, 15.00. $C_{18}H_{19}O_3NCr$ requires : C, 61.89 ; H, 5.48 ; N, 4,01 ; Cr, 14.89.

Resolution of (±)-*2-(3.4-dihydro)-naphthylpiperidine-tricarbonyl-chromium(O)*. The procedure is identical with that described for the resolution of (±)-**I**.

Using 700 mg (2 mmoles) (±)-**V** and 510 mg (2.2 mmoles) (+)-camphor-10-sulphonic acid, were obtained : a) 280 mg (–)-V from the decantate ; m.p. 135° ; $\alpha_D^{23} = -0.19 \pm \pm 0.01$ (220 mg in 13 ml AcOEt) and b) 250 mg (+)-**V** from the precipitate ;m.p. 136° ; ; $\alpha_D^{23} = +0.21 \pm 0.01$ (220 mg in 13 ml AcOEt).

Revue Roumaine de Chimie, 15, 265 272 (1970)

DAS VERHALTEN EINIGER OXAZOLIDONE-(4). VIII [1]

ÜBER DEN REAKTIONSMECHANISMUS BEI DER BILDUNG DER 2,5-DISUBSTITUIERTEN OXAZOLIDONE-(4)

MARIA IONESCU und KLARA MAKKAY

Von der chemischen Fakultät der Babeş-Bolyai-Universität Cluj, str. Arany Janos, 11

Eingegangen am 14. Februar 1969

Es wird der Bildungsmechanismus der 2,5-disubstituierten Oxazolidone-(4) und Spirooxazolidone-(4) neben Oxazolen, beziehungsweise 2,6-disubstituierten Cyclohexanonderivaten durch Kondensation in verschiedenen Bedingungen besprochen. Es wurde festgestellt, daß das Benzaldehyd- und Cyclohexanoncyanhydrin in freiem Zustand reagieren. In Abhängigkeit vom Reaktionsmedium und von der Elektronenaffinität der Substituenten, die in den Carbonylmolekülen enthalten sind, reagieren die Carbonylkomponenten entweder in der Chlorhydrin- oder in der Hydratform; die Kondensationsform bestimmt, ob sich diese Oxazolidone-(4) neben sekundären Reaktionsprodukten, oder ohne diese bilden.

Bei früheren Untersuchungen [2,3] wendeten wir bei der Kondensation von Benzaldehyd, *o*-, *m*-, *p*-Nitrobenzaldehyden und Cyclohexanon mit Benzaldehydcyanhydrin, oder Cyclohexanoncyanhydrin die Fischer Methode [4] an, wobei sich die entsprechenden 2,5-disubstituierten Oxazolidone-(4) und Spirooxazolidone-(4) mit ihren Nebenprodukten bildeten. Wird der trockene Chlorwasserstoffstrom durch eine verdünnte Salzsäurelösung ersetzt,[5] so bilden sich die entsprechenden Oxazolidone-(4) und Spirooxazolidone-(4) ohne Nebenprodukte.

Zur Erklärung der Bildung von Oxazolen und Oxazolidonen nach der Methode von Fischer,[4] formulierte Ingham folgenden Reaktionsmechanismus[6]:

---

[1] VII. Teil: M. Ionescu und K. Makkay, *Stud. Univ. Babeş Bolyai, Chem.*, **1**, 23 (1969).

[2] M. Ionescu und K. Makkay, *Stud. Univ. Babeş Bolyai, Chem.*, **1**, 283 (1963).

[3] M. Ionescu und K. Makkay, *Stud. Univ. Babeş Bolyai Chem.*, **1**, 115 (1966).

[4] E. Fischer, *Ber. dtsch. chem. Ges.*, **29**, 205 (1896).

[5] M. Ionescu und K. Makkay, *Stud. Univ. Babeş Bolyai Chem.*, **2**, 115 (1966).

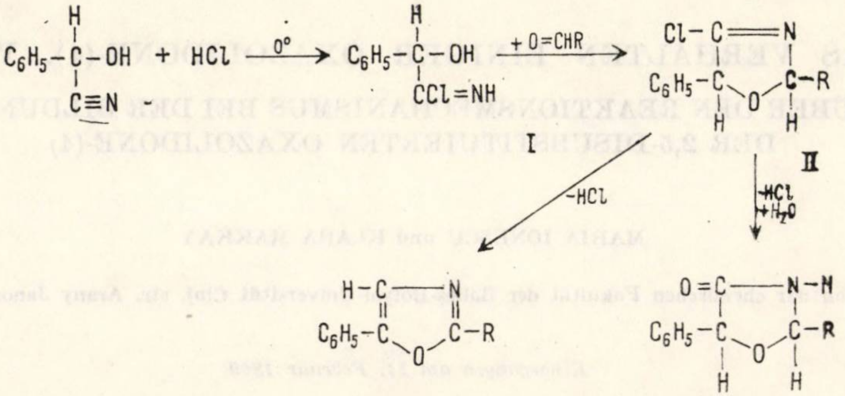

Das Verhältnis zwischen Oxazolen und Oxazolidonen-(4) wird von der Menge des im Reaktionsmedium befindlichen Wassers bestimmt.[6] In absolut wasserfreiem Medium[7] entstehen ausschließlich die Oxazole; in Gegenwart großer Wassermengen[5] erhält man die Oxazolidone-(4) ohne Nebenprodukte.

Im Gegensatz zur Mechanismustheorie von Ingham, stellten wir fest, daß das Zwischenprodukt kein Chlorimid (I) ist. Ferner konnten wir nachweisen, daß bei dieser Synthese der Oxazole und Oxazolidone das Zwischenprodukt (II) nicht auftritt[8].

Um die Mechanismustheorie von Ingham[6] zu prüfen, haben wir die Chlorimide (I) und (III) durch Einwirkung eines trockenen Chlorwasserstoffstromes auf die ätherische Lösung der Benzaldehyd-, beziehungsweise Cyclohexanoncyanhydrine, bei 0°, gesondert dargestellt

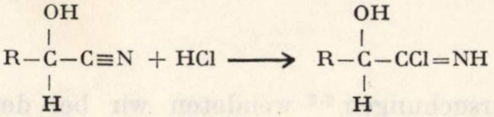

$$R-\overset{\displaystyle OH}{\underset{\displaystyle H}{C}}-C\equiv N + HCl \longrightarrow R-\overset{\displaystyle OH}{\underset{\displaystyle H}{C}}-CCl=NH$$

R: I $=C_6H_5$
R und H: III$=(CH_2)_5$

Wir haben beobachtet, daß diese relativ stabilen Chlorimide mit den obigen Aldehyden nicht mehr reagieren, und keine Oxazole und Oxazolidone-(4) ergeben. Diese Tatsache beweist, daß die Cyanhydrine in freiem Zustande reagieren.

Um die Wirkung der Carbonylkomponenten zu untersuchen, haben wir die klassische Methode abgeändert, und zwar wurde die ätherische Lösung dieser Verbindungen mit Chlorwasserstoffgas behandelt und nachträglich das Cyanhydrin hinzugegeben, wobei sich die Oxazole und Oxazolidone-(4) bildeten.

Wird in Abwesenheit von Lösungsmitteln – die Chlorwasserstoff an das Cyanhydrin übermitteln könnten – gearbeitet, so scheidet sich bei 0° unter der Wirkung trockenen gasförmigen Chlorwasserstoffes kristallines Benzaldehydchlorhydrin ab, aus welchem durch Behandlung mit Cyanhydrin, Oxazolidon-(IV) entsteht.

---

[6] B. H. Ingham, *J. Chem. Soc.*, **1927**, 697.
[7] A. Balaban und P. Frangopol, *Studii şi Cercetări Chim. Acad.*, **6**, 427 (1958).
[8] B. Ternai, *Privatmitteilung.*

Die Ergebnisse der Untersuchungen bestätigen, daß die Bildung der Oxazole und Oxazolidone-(4) sowie das Verhältnis derselben, durch die Eigenschaften der Carbonylkomponenten bestimmt werden. Wir nehmen an, daß die Carbonylverbindungen nicht frei, sondern entweder als Chlorhydrin, oder als Hydrat, an der Reaktion teilnehmen. Dieses hängt vom Reaktionsmedium bzw. der Elektronenaffinität der Substituenten in dem Molekül des Carbonylderivates ab.

A. Bei der Kondensation von Benzaldehydcyanhydrin mit aromatischen Aldehyden, bei 0°, in absolut wasserfreiem Medium, in Gegenwart von Chlorwasserstoffgas,[7] nehmen wir folgenden Reaktionsmechanismus an :

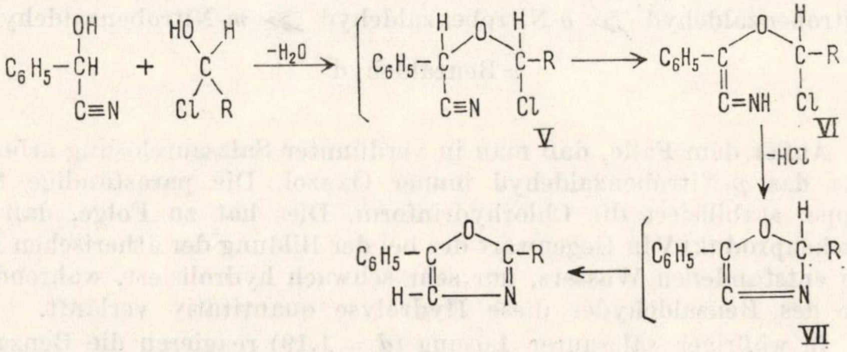

Am Anfang der Reaktion und unabhängig vom Reaktionsmedium entsteht unter Wasserabspaltung eine ätherische Bindung. Das Wasser wird aus dem System mit Hilfe eines Stromes Chlorwasserstoff entfernt, wobei Oxazol entsteht.

Wird das bei der Bildung der ätherischen Bindung entstandene Wasser aus dem Reaktionsgemisch nicht entfernt, oder wird in Anwesenheit von Wasser gearbeitet, so geht die Hydrolyse des Zwischenproduktes V zu Gunsten der Oxazolidonbildung vor sich :

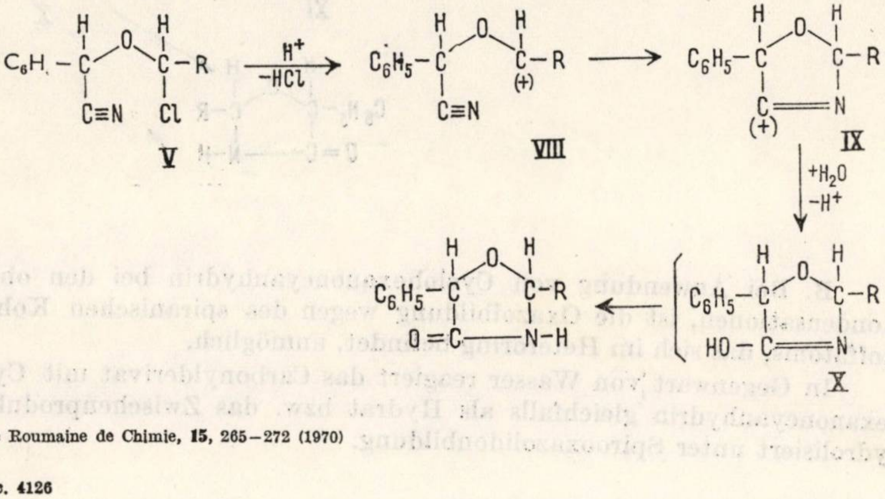

Die Oxazolidonbildung kann neben, oder ohne Bildung von Oxazol stattfinden. Dieses hängt von der Menge des hydrolysierenden Wassers und von der Stabilität des Zwischenproduktes V, bzw. von der Stabilität der Chlorhydrinform des Carbonylbestandteiles ab.

Die Gegenwart von trockenem HCl-Gas und Thyonylchlorid verhindert diese Hydrolyse,[7] wobei keine Oxazolidone-(4) entstehen. Wird dem Reaktionsgemisch nachträglich Wasser beigemengt, werden Oxazolidone-(4) neben Oxazolen erhalten.

Wir konnten folgende Reihenfolge in der Abhängigkeit der Oxazolidonbildung von der Stabilität des Zwischenproduktes V, bzw. des Chlorhydrins der Carbonylkomponente, feststellen:

p-Nitrobenzaldehyd $\gg$ *o*-Nitrobenzaldehyd $\gg$ *m*-Nitrobenzaldehyd =
=Benzaldehyd

Außer dem Falle, daß man in verdünnter Salzsäurelösung arbeitet, bildet das *p*-Nitrobenzaldehyd immer Oxazol. Die parastandige NO_2-Gruppe stabilisiert die Chlorhydrinform. Dies hat zu Folge, daß das Zwischenprodukt V in Gegenwart des bei der Bildung der ätherischen Bindung entstandenen Wassers, nur sehr schwach hydrolisiert, während im Falle des Benzaldehydes diese Hydrolyse quantitativ verläuft.

In wäßriger salzsaurer Lösung ($d = 1,19$) reagieren die Benzaldehyde als Hydrate, und es entstehen ausschließlich Oxazolidone-(4)

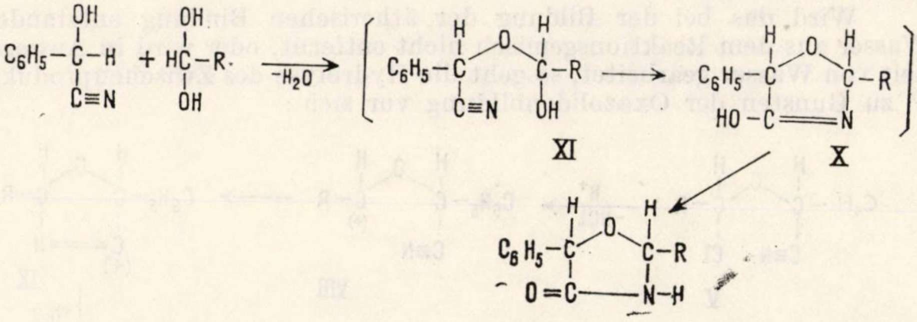

B. Bei Anwendung von Cyclohexanoncyanhydrin bei den obigen Kondensationen, ist die Oxazolbildung wegen des spiranischen Kohlenstoffatoms, das sich im Heteroring befindet, unmöglich.

In Gegenwart von Wasser reagiert das Carbonylderivat mit Cyclohexanoncyanhydrin gleichfalls als Hydrat bzw. das Zwischenprodukt V hydrolisiert unter Spirooxazolidonbildung.

Die Hydratform der Carbonylkomponente reagiert aldolisch mit Cyclohexanoncyanhydrin :

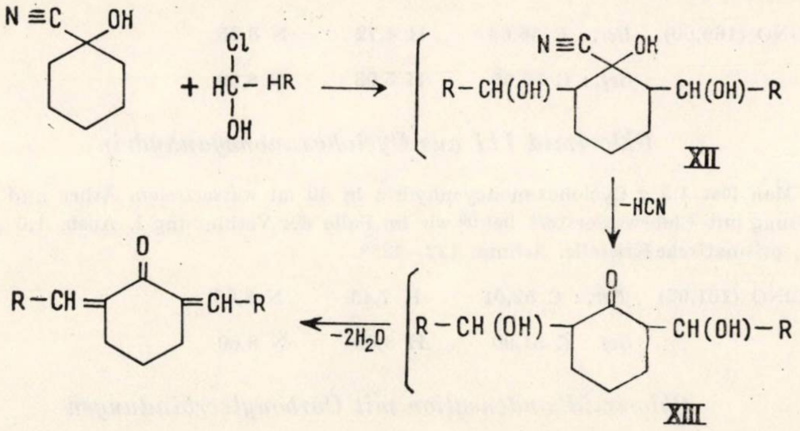

Da das Chloratom des Chlorhydrins aktiver ist als die OH-Gruppe, reagiert es mit den 2- und 6ständigen Wasserstoffatomen des Cyanhydrins durch Induktiveffekt der aktivierten C≡N Gruppe. Neben Abspaltung von 2 Molekülen Chlorwasserstoff entsteht das Zwischenprodukt XII als ein aldolisches Kondensationsprodukt. Dank des sterischen Effektes der voluminösen 2-und 6ständigen Gruppen, spaltet sich aus letzteren ein Molekül HCN ab. Das Zwischenprodukt XII geht in Folge einer Krotonisierung durch Abspaltung von 2 Wassermolekülen in XIII über.

Die relativ große Beständigkeit der Cyanhydrine in saurem Medium bestätigt unsere Annahme, daß die aldolische Kondensation und die Cyanwasserstoffabspaltung in der Cyanhydrinform und nicht in der Carbonylform des Cyclohexanons stattfindet.

In Gegenwart von einer kleinen Wassermenge vermuten wir, daß sich zwischen den zwei Additionsprodukten der Carbonylkomponente ein Gleichgewicht einstellt, was zu gleichzeitiger Bildung von Spirooxazolidon und dem entsprechenden 2,6-disubstituierten Cyclohexanon führt. Auch in diesem Falle wurde die höchste Beständigkeit des *p*-Nitrobenzaldehyd-chlorhydrins erwiesen, welches sich nur sehr wenig hydrolisiert und auch in wäßrigem salzsaurem Medium das Cyclohexanonderivat (XVII) neben Spirooxazolidon (XVIII) bildet.

BESCHREIBUNG DER VERSUCHE

Chlorimid I aus Benzaldehydcyanhydrin

Man löst 1,5 g Benzaldehydcyanhydrin in 25 ml wasserfreiem Äther, kühlt bis 0° und führt 1 Std. bei 0° trockenen Chlorwasserstoffstrom ein. Nach ungefähr 30 Min. beginnt die Abscheidung der schwachrosa Kristalle. Diese Abscheidung ist nach 24stündigem Stehenlassen bei Raumtemperatur vollendet. Man filtriert und wäscht mit wasserfreiem Äther aus, bis für Cl^- negative Reaktion eintritt, trocknet an der Luft. Ausb. 1,5 g schwachrosa Kristalle. Schmp. 98°

C_8H_8ClNO (169,60) *Ber.* : C 56,63 H 4,72 N 8,25

Gef. : C 56,95 H 5,08 N 8,30

Chlorimid III aus Cyclohexanoncyanhydrin

Man löst 1,5 g Cyclohexanoncyanhydrin in 40 ml wasserfreiem Äther und behandelt die Lösung mit Chlorwasserstoff bei 0° wie im Falle der Verbindung I. Ausb. 1,6 g (84,3%). Weiße, prismatische Kristalle. Schmp. 122–123°.

$C_7H_{12}ClNO$ (161,62) *Ber.* : C 52,01 H 7,43 N 8,66

Gef. : C 51,90 H 8,09 N 8,60

Chlorimidkondensation mit Carbonylverbindungen

a) 0,2 g I werden mit 0,3 ml Benzaldehyd in 5 ml wasserfreiem Äther behandelt. Man läßt die Mischung über Nacht bei 20° in geschlossenem Gefäß stehen. Man gießt die ätherische Lösung ab. Die unreagierten Komponenten werden quantitativ zurückgewonnen.

b) Man behandelt 0,2 g Chlorimid III mit 0,3 ml Benzaldehyd in 5 ml wasserfreiem Äther wie im Falle *a*. Die unreagierten Ausgangsstoffe können fast quantitativ zurückgewonnen werden.

c) Man schüttelt 5 Std. lang I bzw. III mit 0,4 g *p*-Nitrobenzaldehyd in 25 ml Äther gelöst. Nach 24 Std. Stehen bei 20° werden die Ausgangsstoffe fast quantitativ zurückgewonnen.

d) 0,5 g I bzw. III werden in 25 ml wasserfreiem Äther mit *p*-Nitrobenzaldehyd 30 Min. lang gekocht. Durch Abkühlen scheiden aus der ätherischen Lösung fast quantitativ die unreagierten Komponenten aus.

e) Man löst 1 g Cyclohexanoncyanhydrin in 32 ml wasserfreiem Äther, behandelt 1 Std. lang bei 0° mit Chlorwasserstoffstrom. Die ätherische Lsg aus der sich eine große Menge weißen Niederschlages abscheidet, wird mit 1 ml Benzaldehyd behandelt. Nach 24 stündigem Stehen bei 0° bleibt ungefähr 0,90 g unreagiertes Chlorimid (III) zurück. Nach Vertreiben des Äthers, bleibt eine klebrige Masse zurück, an welcher, durch Einwirkung von kaltem Äthanol, 0,10 g 2-Phenyl-5-spirocyclohexyliden-oxazolidon-(4) (XIV) erhalten wird. Schmp. 134°.

f) Man behandelt 1 g Cyclohexanoncyanhydrin mit Chlorwasserstoff, wie im Falle *e*) Nach hinzufügen von 1 g p-Nitrobenzaldehyd und nach 24 stündigem Stehen bei 20° in einem geschlossenen Gefäß, werden 0,95 g unreagiertes III, 0,90 g *p*-Nitrobenzaldehyd und 0,15 g (7%) 2,6-Bis-*p*-nitrobenzyliden-cyclohexanon (XVII) erhalten. Schmp. 206°.

g) Man löst 3 g Cyclohexanoncyanhydrin in 60 ml Äther, behandelt 25 Min. lang bei 0° mit trockenem Chlorwasserstoff. Man teilt diese Lösung in drei Portionen :

– die erste Portion versetzt man mit 1 g Benzaldehyd und läßt es bei 20° in einem geschlossenen Gefäß 48 Std. lang stehen. Ausbeute : 0,25 g (13,5%) Oxazolidon (XIV). Schmp. 135°; 1,80 g (84,7%) 2,6-Bis-Benzyliden-cyclohexanon (XVI). Schmp. 118°.

– die zweite Portion behandelt man mit 1 g *p*-Nitrobenzaldehyd in 20 ml wasserfreiem Äther gelöst, und verfährt wie im vorhergehenden Falle. Man erhält 2,0 g (70,9%) 2,6-Bis-*p*-nitrobenzyliden-cyclohexanon (XVII). Schmp. 206° (aus Äthanol).

– der dritten Portion gibt man 1 g *m*-Nitrobenzaldehyd zu und nach 40stündigem Stehen bei 20° in einem geschlossenen Gefäß, erhält man nach Vertreiben des Äthers 1,75 g

(81, 8%) 2-(*m*-Nitrophenyl)-5-spirocyclohexyliden-oxazolidon-(4) (XIX) mit Schmp. 158⁰ (aus Alkohol).

Man verdünnt die nach dem Umkristallisieren zurückgebliebene äthanolische Lsg mit einer doppelten Menge Wasser. Man erhält auf diese Weise 0,2 g (7%) hellgelbe Nadeln von 2,6-Bis-*m*-nitrobenzyliden-cyclohexanon (XX). Schmp. 186⁰.

$C_{20}H_{16}N_2O_5$ (364,34) *Ber.* :	C 65,93	H 4,42	N 7,69
Gef. :	C 66,03	H 4,63	N 7,96

Durch 2stündiges Kochen dieses Cyclohexanonderivates in 20%iger Lösung entsteht *m*-Nitrobenzoesäure.

Bildung der Oxazolidone-(4) durch Behandlung der Carbonylkomponenten mit Chlorwasserstoff

A. Kondensation von Benzaldehydcyanhydrin

a) Man löst 15 ml Benzaldehyd in 40 ml wasserfreiem Äther und behandelt ungef. 1 Std. lang mit auf $CaCl_2$ und H_2SO_4 getrocknetem Chlorwasserstoff. Man teilt diese Lösung in drei Portionen :

— die erste Portion wird mit 5 g Benzaldehydcyanhydrin vermischt, und bei 20⁰ in einem geschlossenen Gefäß 24 Std. stehen gelassen. Man filtriert 8,5 g (Ausb. 95,7%) 2,5-Diphenyl-oxazolidon-(4) (IV) mit Schmp. 190⁰. Durch Vertreiben des Äthers erhält man noch 1 g IV. Schmp. 189—90⁰.

— die zweite Portion läßt man bei 20⁰ in einem geschlossenen Gefäß 1 Std. stehen, dann versetzt man sie mit 5 g Benzaldehydcyanhydrin. Nach 24 Std. filtriert man 8,5 g Oxazolidon-(4) (IV). Schmp. 191⁰ (Ausb. 95,7%).

Nach vertreiben des Äthers wird die dritte Portion bei 20⁰ mit 5 g Benzaldehydcyanhydrin versetzt. Nach Stehenlassen bei 20⁰ über Nacht, in geschlossenem Gefäß, erhält man 8,7 g IV. Schmp. 193⁰ (Ausb. 98%).

b) Man behandelt 15 g Benzaldehyd bei 0⁰ 1 Std. lang mit auf $CaCl_2$ und H_2SO_4 getrocknetem Chlorwasserstoff. Die abgeschiedenen Kristalle werden in drei Portionen geteilt und sofort verarbeitet :

— die erste Portion löst man in 10 ml wasserfreiem Äther und behandelt sie mit 5 g Benzaldehydcyanhydrin. Nach 24stündigem Stehen bei 20⁰ erhält man 7,2 g IV. Schmp. 193⁰. Nach Vertreiben des Äthers erhält man noch weitere 1,5 g IV. Schmp. 189—90⁰ (Ausb. 98,2%).

— die zweite Portion versetzt man ohne Lösungsmittel mit 5 g Benzaldehydcyanhydrin. Nach 24stündigem Stehen bei 20⁰ in geschlossenem Gefäß erhält man 8,7 g bei 190⁰ schmelzendes Oxazolidon-(4) (IV) (Ausb. 98%).

— die dritte Portion läßt man drei Tage lang in einem geschlossenen Gefäß bei 20⁰ stehen. Die Flüssigkeit wird mit 5 g Benzaldehydcyanhydrin behandelt. Nach 24stündigem Stehen bei 20⁰ erhält man 8,72 g IV, welches nach Waschen mit Äther bei 193⁰ schmilzt. (Ausb. 98,2%).

c) Man behandelt 1 Std. lang bei 0⁰ 10 g Cyclohexanon gelöst in 30 ml wasserfreiem Äther, mit einem trocknen Strom HCl. Die rosa Lösung wird in drei Portionen geteilt.

— die erste Portion vermischt man mit 3,5 g Benzaldehydcyanhydrin, und läßt bei 20⁰ in einem geschlossenen Gefäß über Nacht stehen. Man erhält 5 g 2-Spirocyclohexyliden-5-phenyl-oxazolidon-(4) (XV). Schmp. 160⁰ (aus Äthanol).

— die zweite Portion läßt man an der Luft bis zur vollständigen Entweichung des Äthers. Den Rückstand vermischt man mit 3,5 g Benzaldehydcyanhydrin in 20 ml Äther gelöst. Nach 24stündigem Stehen bei 20⁰ im geschlossenen Gefäß gewinnt man 4,5 g Oxazolidon (XV). Schmp. 159⁰.

— aus der dritten Portion vertreibt man den Äther bei 20⁰ und läßt den Rückstand in geschlossenem Gefäß über Nacht bei 20⁰ stehen, dann behandelt man mit 3,5 g Benzaldehydcyanhydrin gelöst in 20 ml wasserfreiem Äther. Nach 24stündigem Stehen bei 20⁰ im geschlossenen Gefäß erhält man 3,5 g Oxazolidon (XV). Schmp. 160⁰. Durch Vertreiben des Äthers erhält man noch weitere 1,5 g bei 158⁰ schmelzendes XV.

d) Man löst durch Erwärmen 0,5 g *p*-Nitrobenzaldehyd in 25 ml wasserfreiem Äther, kühlt auf 0⁰ ab, und behandelt die Lösung 1 Std. lang bei 0⁰ mit einem auf $CaCl_2$ und H_2SO_4 getrockneten Chlorwasserstoffstrom. Man vermischt mit 0,5 g Benzaldehydcyanhydrin, läßt in geschlossenem Gefäß bei 20⁰ 24 Std. lang stehen, wobei 0,4 g hellgelbe Kristalle von 2-(*p*-Nitrophenyl)-5-phenyloxazol (XXI) mit Schmp. 206⁰ abscheiden (Ausb. 45,4%).

Durch Vertreiben der Äthers erhält man weiße Kristalle von 2-(*p*-Nitrophenyl)-5-phenyloxazolidon-(4) (XXII). Schmp. 160⁰ (aus Äthanol) (Ausb. 0,1 g, ungef. 10%).

B. Kondensation mit Cyclohexanoncyanhydrin

a) Man behandelt 2,5 g Benzaldehyd bei 0⁰, 30 Min. lang mit auf $CaCl_2$ und H_2SO_4 getrocknetem Chlorwasserstoff. Die ausgeschiedenen weißen Kristalle werden mit einer Lösung von 2,5 g Cyclohexanoncyanhydrin in 20 ml wasserfreiem Äther, behandelt. Man läßt bei 20⁰ in geschlossenem Gefäß über Nacht stehen. Auf diese Weise erhält man 3 g Spirooxazolidon-(4) (XIV). Schmp. 135⁰. Durch Vertreiben des Äthers erhält man noch 1,5 g 2,6-Bis-benzylidencyclohexanon (XVI). Schmp. 118⁰.

b) Man löst 0,5 g *m*-Nitrobenzaldehyd in 25 ml wasserfreiem Äther, und behandelt bei 0⁰ 1 Std. lang mit einem auf $CaCl_2$ und H_2SO_4 getrockneten HCl-Strom, darauf versetzt man mit 0,5 g Cyclohexanoncyanhydrin und läßt bei 20⁰ in einem geschlossenen Gefäß über Nacht stehen. Durch fraktionierte Umkristallisation aus Äthanol werden 0,8 g Oxazolidon XIX (Schmp. 158⁰) und 0,1 g Cyclohexanonderivat XX (Schmp. 186⁰) erhalten.

c) Man behandelt bei 0⁰ 1 Std. lang 0,5 g *p*-Nitrobenzaldehyd gelöst in 25 ml wasserfreiem Äther mit auf $CaCl_2$ und H_2SO_4 getrocknetem Chlorwasserstoff. Man versetzt mit 0,5 g Cyclohexanoncyanhydrin und läßt bei 20⁰ über Nacht stehen, wobei 0,45 g (74%) XVII (Schmp. 206⁰), und ungef. 0,05 g Oxazolidon-(4) XVIII (Schmp. 142⁰) (Ausb. ungef. 5,5%) erhalten werden.

Revue Roumaine de Chimie, 15, 273–281 (1970)

ABOUT THE MECHANISM OF ELECTRICAL RESISTANCE VARIATIONS IN THIN COPPER AND SILVER FILMS DURING OXYGEN CHEMISORPTION

N. I. IONESCU

Institute of Physical Chemistry of the Academy
Bucharest, str. Dumbrava Roşie 23

Received April 2, 1969

The comparison of the results obtained, by two methods, concerning the electrical increase in the thin copper and silver films resistance depending on temperature in the chemisorption process of oxygen has shown that, owing to the complexity of the phenomenon, it is difficult to affirm the existence of a single mechanism determining the resistance of the metal. It seems more probable that at least two mechanisms should appear simultaneously.

In some previous papers we have followed the influence of the oxygen chemisorption on electrical properties i.e. the electrical resistance and its temperature coefficient in thin silver [1,2] and copper [3–5] films.

The experimental data obtained both in silver [2,6,7] and in copper [4,5,8] have allowed to draw some conclusions on the mechanism producing resistance variations.

These conclusions were based on determinations obtained through two different techniques concerning the dependence on temperature of the resistance increase during oxygen chemisorption. According to it, in the present paper we aim at comparing the previously obtained results,[2,4,5] in order to complete the picture of the interaction between oxygen and the two metals studied (silver and copper).

RESULTS AND DISCUSSION

If a gas touches the surface of a thin metallic film, a positive variation in the electrical resistance of adsorbant is always recorded.

---

[1] I. G. Murgulescu and N. I. Ionescu, *Rev. Roumaine Chim.*, **11**, 1035 (1966).
[2] I. G. Murgulescu and N. I. Ionescu, *Rev. Roumaine Chim.*, **11**, 1267 (1966).
[3] I. G. Murgulescu and N. I. Ionescu, *Rev. Roumaine Chim.*, **13**, 1533 (1968).
[4] I. G. Murgulescu and N. I. Ionescu, *Rev. Roumaine Chim.*, **14**, 681 (1969).
[5] I. G. Murgulescu and N. I. Ionescu, *Rev. Roumaine Chim.*, **14**, 1073 (1969).
[6] N. I. Ionescu, *Rev. Roumaine Chim.*, **13**, 683 (1968).
[7] I. G. Murgulescu, G. Comşa and N. I. Ionescu, *J. Catalysis*, **12**, 102 (1968).
[8] I. G. Murgulescu, N. I. Ionescu and G. Comşa, *J. Catalysis*, **13**, 328 (1969).

Up to the present there are three main hypotheses trying to explain this fact.

I. The decrease in the number of conduction electrons in the metal yielded to the chemisorbed gas in order to form a chemisorption bond.[9]

II. The decrease in thickness of the thin film by 1—2 atom layers due to the formation of a surface complex between the metallic atoms and the gas adsorbed (loss of the metallic character of the boundary layer).[10]

III. Reductions in the mobility of electrons as a result of the change in the mean free path or in their reflexion conditions at the surface of the film.[11-13]

These hypotheses have also been used together to the same purpose : I with II,[2] I with III,[14] II with III[15] and I, II and III.[3,6]

In order to go deeper into the causes producing the variation of the electrical resistance in the thin copper and silver films during oxygen chemisorption, we have profited by the previously published data.[2,4,5] Thus, as shown before in those papers, two working ways were followed in order to obtain these results.

A. The adsorption of the gas took place first at 273°K[16] and after the process had come to an end, the nonadsorbed gaseous stage was pumped out. Then, the temperature was suddenly lowered to 77°K.

B. The adsorption of oxygen took place first at 77°K[17] and after the process had come to an end, the temperature was suddenly increased to 273°K.

In both cases the equilibrium resistances were read at the two temperatures mentioned above.

The value of the temperature coefficient of electrical resistance of the thin films α has been calculated by the relationship :

$$\alpha = \frac{1}{R_{77}} \cdot \frac{R_{273} - R_{77}}{196} \qquad (1)$$

in which R_{273} and R_{77} are the resistances of the film at 273°K and 77°K temperatures.

---

[9] R. Suhrmann and K. Schulz, *Z. phys. Chem. (Frankfurt)*, **1**, 69 (1954).

[10] W. M. H. Sachtler and G. J. H. Dorgelo, *Z. phys. Chem. (Frankfurt)*, **25**, 69 (1960).

[11] T. Toya, *J. Res. Inst. Cat.*, **10**, 236 (1962).

[12] O. A. Pancenko and Iu. G. Ptuşinski, *Izvest. Akad. Nauk S.S.S.R., seria fizicheskaia*, **28**, 1466 (1964).

[13] H. Kölbel, E. Schöttle and H. Hammer, *Z. phys. Chem. (Frankfurt)*, **46**, 88 (1965).

[14] H. Wenzel, Dissertation, Hannover, 1968.

[15] H. Kölbel, E. Schöttle and H. Hammer, *Z. phys. Chem. (Frankfurt)*, **47**, 183 (1965).

[16] R. Suhrmann, H. J. Busse and G. Wedler, *Z. phys. Chem. (Frankfurt)*, **47**, 1 (1965).

[17] R. Suhrmann, J. M. Heras, L. V. de Heras and G. Wedler, *Z. Elektrochem.*, **68**, 990 (1964).

As we have also previously shown,[2,5] information can be obtained by means of electrical resistance depending on temperature of thin metallic films when we consider the conditions :

$$\frac{\Delta R_{273}}{\Delta R_{77}} = 1 \tag{2}$$

$$\frac{\left(\frac{\Delta R}{R}\right)_{273}}{\left(\frac{\Delta R}{R}\right)_{77}} = 1 \tag{3}$$

in which ΔR_{273} and ΔR_{77} stand for the increases of the resistance due to the oxygen chemisorption at 273°K and 77°K.

Tables 1, 2 and 3 show the determinations of the resistance increases depending on temperature in thin copper films when the pressure of the gas introduced first at 273°K, is high (table 1), low (table 2) and medium (table 3).[5] Table 4 shows the same thing in silver,[2] at high pressures of the oxygen. The temperature coefficient has been calculated by means of the relationship (1).

Table 1

Temperature coefficient of the thin copper films after oxygen chemisorption at high pressures

1	2	3	4	5	6	7
Pressure of the introduced gas in torr	R_{077} Ω	R_{0273} Ω	$R_{77}(O_2)$ Ω	$R_{273}(O_2)$ Ω	$\alpha_0 \cdot 10^3$ degree^{-1}	$\alpha_1 \cdot 10^3$ degree^{-1}
1×10^{-3}	28.471	34.849	34.074	40.515	1.132	0.964
3×10^{-4}	25.825	31.686	29.234	35.277	1.158	1.055
4×10^{-4}	26.488	30.187	30.974	34.593	0.712	0.596
1×10^{-3}	27.307	33.083	32.104	37.872	1.079	0.917
6×10^{-4}	31.962	37.031	36.454	41.307	0.809	0.679
5×10^{-4}	29.447	36.642	31.708	38.759	1.247	1.134

The data presented in table 1 show that, after the oxygen chemisorption takes place in copper, the value of the coefficient α diminishes. The results in table 2 show that the coefficient α generally remains unchanged at a low pressure of the gas. Table 3 shows that α increases and diminishes in rather the same proportion, it means that in the whole it can be considered constant. It must be emphasized that relation (3) is more accurately verified when coefficient α increases. If coefficient α diminishes the relation (2) is more accurately verified.[5] The data in table 4 indicate that by oxygen chemisorption in silver the increase of the coefficient α is very low and can be considered as practically constant.

Table 2

Temperature coefficient of the thin copper films after oxygen chemisorption at low pressures

1	2	3	4	5	6	7
Pressure of the introduced gas in torr	R_{077} Ω	R_{0273} Ω	$R_{77}(O_2)$ Ω	$R_{273}(O_2)$ Ω	$\alpha_0 \cdot 10^3$ degree^{-1}	$\alpha_1 \cdot 10^3$ degree^{-1}
5×10^{-5}	37.662	46.943	42.529	52.638	1.257	1.212
5×10^{-5}	33.012	40.144	36.029	43.638	1.102	1.077
5×10^{-5}	36.366	40.467	40.933	45.535	0.575	0.574
4×10^{-5}	32.108	38.633	33.335	40.176	1.037	1.047
3×10^{-5}	31.150	37.261	33.984	40.972	1.001	1.049
4×10^{-5}	28.481	30.763	32.002	34.706	0.409	0.431

Table 3

Temperature coefficient of the thin copper films after oxygen chemisorption at medium pressures

1	2	3	4	5	6	7
Pressure of the introduced gas, in torr	R_{077} Ω	R_{0273} Ω	$R_{77}(O_2)$ Ω	$R_{273}(O_2)$ Ω	$\alpha_0 \cdot 10^3$ degree^{-1}	$\alpha_1 \cdot 10^3$ degree^{-1}
1×10^{-4}	27.186	30.405	28.692	31.704	0.604	0.536
1×10^{-4}	27.293	29.501	30.173	31.368	0.413	0.202
1×10^{-4}	31.432	35.834	35.741	40.305	0.714	0.651
1×10^{-4}	31.783	35.620	35.354	38.641	0.616	0.474
1×10^{-4}	28.976	34.805	29.780	36.031	1.026	1.071
1×5.10^{-4}	30.623	37.078	33.928	42.247	1.075	1.251
1×5.10^{-4}	30.725	35.446	33.433	39.142	0.784	0.871

Let us consider now the values of the temperature coefficient of the resistance in silver [2] and copper [4] when the adsorption takes place first at 273°K.

If the ratios determined by the formulas (2) and (3) are computed by means of this data, one obtains the results in tables 5 (for copper) and 6 (for silver). The inverse ratio, i.e. $\frac{\Delta R_{77}}{\Delta R_{273}}$ has been calculated for the fourth experiment in table 6, column 6.

It seems that relation (2) is generally more accurately verified than relation (3) as shown in tables 5 and 6.

Table 4

The temperature coefficient of the thin silver films after oxygen chemisorption at high pressures

1	2	3	4	5	6	7
Pressure of the introduced gas, in torr	R_{077} Ω	R_{0273} Ω	$R_{77}(O_2)$ Ω	$R_{273}(O_2)$ Ω	$\alpha_0 . 10^3$ degree^{-1}	$\alpha_1 . 10^3$ degree^{-1}
9×10^{-4}	13.853	15.553	14.652	16.573	0.626	0.669
3×10^{-4}	12.292	14.752	12.981	15.632	1.021	1.042
2×10^{-4}	12.525	14.808	13.208	15.666	0.930	0.949
1×10^{-4}	13.277	17.056	13.902	17.932	1.452	1.479
3×10^{-3}	12.314	16.808	13.263	18.166	1.862	1.886

Table 5

Resistance increases depending on temperature in thin copper films after oxygen chemisorption at high pressures

1	2	3	4	5	6	7
T°K	Pressure of the introduced gas, in torr	R_0 Ω	ΔR Ω	R Ω	$\frac{\Delta R_{273}}{\Delta R_{77}}$	$\frac{\left(\frac{\Delta R}{R}\right)_{77}}{\left(\frac{\Delta R}{R}\right)_{273}}$
273	3×10^{-5}	32.416	5.867	38.283	1.014	1.052
77		30.102	5.786	35.888		
273	2×10^{-5}	35.062	4.141	39.203	1.008	1.121
77		30.584	4.107	34.691		
273	6×10^{-5}	37.301	7.707	45.008	1.014	1.064
77		34.302	7.603	41.905		
273	3×10^{-5}	34.459	5.771	40.230	1.003	1.147
77		29.221	5.752	34.973		
273	2×10^{-5}	32.656	6.416	39.072	1.106	1.029
77		28.524	5.799	34.323		
273	2×10^{-5}	37.153	6.893	44.046	1.071	1.067
77		33.091	6.436	39.527		

Table 6

Resistance increases depending on temperature in thin silver films after oxygen chemisorption at high pressures.

1	2	3	4	5	6	7
T°K	Pressure of the introduced gas, in torr	R_0 Ω	ΔR Ω	R Ω	$\frac{\Delta R_{273}}{\Delta R_{77}}$	$\frac{\left(\frac{\Delta R}{R}\right)_{77}}{\left(\frac{\Delta R}{R}\right)_{273}}$
273	1×10^{-4}	19.445	1.807	21.252	1.044	1.340
77		15.202	1.731	16.933		
273	5×10^{-4}	22.382	2.344	24.726	1.149	1.278
77		16.827	2.040	18.867		
273	5×10^{-4}	21.462	2.023	23.485	1.040	1.353
77		16.694	1.945	18.639		
273	4×10^{-5}	25.111	0.942	26.053	1.004	1.481
77		17.651	0.946	18.597		
273	6×10^{-4}	14.211	1.241	15.452	1.066	1.314
77		11.034	1.164	12.198		
273	2×10^{-4}	20.841	1.693	22.534	1.253	1.102
77		16.322	1.351	17.673		

The decrease in the temperature coefficient of electrical resistance α has been interpreted as a result of its decrease in thickness [2,4] presuming that the structure of the metallic film does not change. In fact, if we admit that the structure of the film, not involved in chemisorption does not change during the process, then on considering the relation :

$$\alpha = \frac{\alpha_\infty}{\ln \frac{\beta_l}{d}} \tag{4}$$

where α_∞ is the temperature coefficient and l the mean free path of electrons in the bulk which has the same structure as the thin film, d the thickness of the film and β a constant, it results that a decrease in the coefficient α can be assigned only to a decrease in the thickness d.

On the other hand, as we have previously shown, the validity of relation (2) supposes a change in the mean free path l and in the scattering coefficient of the electrons p, either l or p, i.e. a mechanism III, whereas the verification of formula (3) shows a variation in the number of free electrons N and in the thickness d, either N or d that means the mechanisms I and II (I or II).

A decrease in the temperature coefficient of resistance α has been obtained,[2,4] by means of the values of resistance written in tables 5 and 6, i.e. mechanism II producing the resistance variation by decrease in thickness and now, by applying relations (2) and (3) a mechanism III, through a change in the mean free path of the electrons and (or) in their reflexion conditions.

As both ways of making the experiments and of computing the results are equally efficient, the most probable explanation implies the coexistence of two or more mechanisms producing this variation in the resistance of the above mentioned.

To explain the results shown, for instance in tables 5 and 6, the mechanisms II and III could exist simultaneously, which makes us presume that some superficial oxygenated compounds of copper and silver might be formed and adsorbed on the surface and also increase concomitantly the residual resistance.

In the same way the results in table 1 have proved before [5] to be a verification of the relation (2) and now, they prove a decrease in the temperature coefficient of the resistance. As in the previous case, one can speak here of a complex mechanism (II and III) influencing the electrical resistance of the metal.

In silver, at high pressures, (table 4), α can be considered as being constant. The previous results had indicated a verification of relation (3).[2,5] As the constancy of the coefficient α can be justified by the fact that the thickness of the film does not change, it follows that in this case too, the mechanisms I and II (I or II) may be valid. The constancy of the value α pleads especially for mechanism I.

In copper, at low pressures (table 2) on the one hand α is constant, on the other hand relation (3) is verified. This explanation is similar to the explanation given in the previous case, as mechanisms I and II (I or II) probably exist there.

Relation (2) is better verified at intermediate pressures (table 3) when coefficient α decreases.[5] That is why a mechanism II and III can be taken into consideration. When coefficient α increases, relation (3) is better verified.[5] This shows the occurrence possibility of mechanisms I and II (I or II). The results obtained do not allow to specify the mechanism prevailing in this case.

In this way, by the two techniques reminded before, we cross experiments of simultaneous determination, of the temperature coefficient of resistance and of the ratios value defined by relations (2) and (3). These experiments as well as the concomitent measurement of several electrical properties on one and the same film (a difficult thing from the experimental point of view [5]) can supply information on the causes producing the variations of the resistance observed in the gas adsorption in thin metallic films.

These results show, at the same time, the difficulty to draw definite conclusions on the nature of the mechanism governing the increases of the electrical resistance, experimentally recorded in the given cases.

The results obtained so far are synthesized in table 7. Instead of considering the pressure, it was the coverage degree θ that was taken into account, as the pressure and the volume of the gas introduced were known. The interval 0—1 was divided into three parts :

— the first corresponds to a low coverage degree, up to 0.3,

— the second corresponds to a medium coverage degree, from 0.3 to 0.6,

— the third corresponds to a high coverage degree, over 0.6.

The mechanisms determining the variations of the electrical resistance in thin copper and silver films during oxygen chemisorption do not appear individually but grouped according to the data shown in table 7. This conclusion leads to the application of the method of grouping together the mechanisms, formerly employed.

Table 7

Mechanisms determining the variation in the electrical resistance in thin copper and silver films during oxygen chemisorption

Metal	θ	Working ways	Variation in the temperature coefficient of the electrical resistance	$\frac{\Delta R_{273}}{\Delta R_{77}}$	$\frac{\left(\frac{\Delta R}{R}\right)_{273}}{\left(\frac{\Delta R}{R}\right)_{77}}$	Mechanisms explaying the observed variations in the electrical resistance
silver	high	B	diminishes	$=1$	$\neq 1$	II and III
silver	high	A	constant	$\neq 1$	$=1$	I and II (I or II)
copper	high	B	diminishes	$=1$	$\neq 1$	II and III
copper	high	A	diminishes	$=1$	$\neq 1$	II and III
copper	low	A	constant	$\neq 1$	$=1$	I and II (I or II)
copper	medium	A	constant	$\neq 1$	$\neq 1$	One cannot specify the mechanism prevailing

As in similar conditions the mechanisms I and II (I or II) appear once and the mechanisms II and III appear another time, the results obtained in silver create the premises to justify the simultaneous existence of the three causes.[4,6]

The data presented can also justify the calculus of the variation of the coefficient p due to the adsorption of oxygen taken into account in other papers.[3,6]

It must be mentioned that mechanism II always occurs in the interpretation of the obtained results, a fact that pleads for its generality.

As a matter of fact we have been able to show both qualitatively and quantitatively [2,4,7,8] that, if the mechanisms I and II were considered together,[2] this assumption would affect neither the magnitude nor the specific character of the decrease in thickness.[8] In other words, even by admitting simultaneously the mechanisms I and II for the interpretation of the resistance variation in thin copper and silver films during oxygen chemisorption, the hypothesis II, of Sachtler and Dorgelo remains valid.

The formation of a superficial combination assumes an electronic participation of the two constituents, which can bring an argument in favour of the existence of a variation in the number of free electrons besides the decrease in thickness.

Therefore interaction between silver and oxygen, in accordance with the above data, will probably look as follows : an oxygenated combination on the surface tends to form with the contribution of a number of free electrons. This combination remains adsorbed on the surface and simultaneously increases the residual resistance.

At the beginning of the process in copper, an oxygenated combination on the surface occurs, with the help of some free electrons of the metal, which remains adsorbed on the surface. With the increase in the coverage degree the oxygenated combination concomitantly increases the residual resistance in the same way as in silver.

The results presented in this paper are in agreement with those obtained by other researchers.[18] They showed that in copper, the temperature coefficient of resistance α remains constant within a long interval of coverage and decreases when the surface tends to be saturated. The authors consider that the fact is likely to be explained admitting of a variation in the thickness of the film.

Based on experiments concerning the chemisorption of oxygen in thin copper and silver films we can conclude that because of the complexity of the of adsorption phenomenon it would be difficult to affirm the existence of a single mechanism determining the variation in the electrical resistance of the metal. It seems more probable that at least two mechanisms should appear simultaneously.

---

[18] D. Lazarov and G. Bliznakov, *Doklady Bolgarskoi Akademii Nauk*, **20**, 209 (1967).

Revue Roumaine de Chimie, **15**, 283–290 (1970)

EVIDENCE OF NEIGHBOUR CATION INFLUENCE AND CORRELATION EFFECT FROM LIGAND FIELD CALCULATIONS

F. MÁTHÉ

Department of Physical Chemistry, Babeş-Bolyai University, Cluj, str. Arany János 11

Received February 24, 1969

Within the framework of the electrostatic theory, a study is made on transition metal fluorine compounds which manifest a strong Jahn-Teller distorsion (Cr(II), Mn(III), Cu(II)). It is pointed out that the ligand field parameters $z_{ef}<r^4>$ depend upon the type of the central ion orbitals (empty, half-filled, filled d orbitals) which interacts with the ligands and upon the effective ligand charge. The $z_{ef}<r^4>$ product is different for the fluorine ions which form a bridge between the metal ions as compared to the non-bridging anions. The poor agreement between the experimental transitions and the values calculated with the Hartree-Fock SCF radial functions is due to expansion of electron clouds by partial covalent bond formation and to the correlation effect, which is greater for the ions with more than half-filled *d* shell.

The optical spectra of transition metal compounds can be explained on the basis of ligand field theory. The optical transitions in the visible region take place between the levels arising from different d^n configurations which are split by the interaction with the field of surrounding ligand atoms. The effect of the neighbour cations is completely neglected in this theory. This is justifiable in the first approximation, because the cation-cation interaction energy is about 10^2-10^3 orders of magnitude less than the ligand field strength. In some cases as a consequence of this interaction the splitting of the $d-d$ transition bands and appearance of new satellite lines have been reported.[1–6] In other cases polarization of the

---

[1] S. Sugano and Y. Tanabe, "Magnetism", vol. 3, editors G, T. Rado and H. Suhl, Academic Press, New York, 1963, p. 243.

[2] D. S. Mc Clure, *J. Chem. Phys.*, **39**, 2850 (1963).

[3] J. Fergusson and H. J. Guggenheim, *J. Chem. Phys.*, **44**, 1095 (1966).

[4] C. E. Schäffer, *J. Inorg. Nuclear Chem.*, **8**, 149 (1958).

[5] I. Owen, *J. Appl. Phys. Suppl.*, **32/33**, 3555 (1962).

[6] R. L. Greene, D. D. Sell, W. M. Yen, A. L. Schawlow and R. M. White, *Phys. Rev. Letters*, **15**, 656 (1965).

ligand orbital by the neighbour cations is responsible for the modification of crystal field splitting parameter[7] and electron repulsion parameters.[8]

In a recent paper[9] we discussed the splitting of Russell-Saunders D term in noncubic symmetries, expressing the ligand field energies in terms of parameters, characterizing the ligand ions situated on the x, y and z axes.

The term energies are:

D_{4h} symmetry group:

$$\begin{aligned} \varepsilon(B_{1g}) &= -6\,Dq - 2\,Ds - 5\,Dt \\ \varepsilon(A_{1g}) &= -6\,Dq + 2\,Ds \\ \varepsilon(B_{2g}) &= +4\,Dq - 2\,Ds + 5\,Dt \\ \varepsilon(E_{g}) &= +4\,Dq + Ds \end{aligned} \tag{1}$$

D_{2h} symmetry group:

$$\begin{aligned} \varepsilon(A^{\bullet}_{1g}) &= -6\,Dq - 2\,Ds - 5\,Dt \\ \varepsilon(A_{1g}) &= -6\,Dq + 2\,Ds \\ \varepsilon(B_{1g}) &= +4\,Dq - 2\,Ds + 5\,Dt \\ \varepsilon(B_{2g}) &= +4\,Dq + Ds - Dr \\ \varepsilon(B_{3g}) &= +4\,Dq + Ds + Dr \end{aligned} \tag{2}$$

where

$$\begin{aligned} Dq &= \frac{8}{14}\,Dq\,(z) + \frac{3}{14}\,Dq\,(x) + \frac{3}{14}\,Dq\,(y) \\ Ds &= Ds(x) + Ds(y) - 2Ds\,(z) \\ Dt &= \frac{2}{7}\,Dq(x) + \frac{2}{7}\,Dq(y) - \frac{4}{7}\,Dq\,(z) \\ Dr &= 3[Ds\,(x) - Ds(y)] + \frac{10}{7}\,[Dq(x) - Dq(y)]. \end{aligned} \tag{3}$$

In these equations the individual ligand parameters are

$$Dq(i) = \frac{z_i\,e^2\,\langle r^4\rangle}{6R_i^5} \qquad Ds(i) = \frac{z_i\,e^2\,\langle r^2\rangle}{7\,R^{\prime 3}} \tag{4}$$

R_i is the ligand-central ion distance, $<r^k>$ stands for the radial integrals $\int R^2(r)\,r^k\,d\tau$. The radial integrals for the first-row transition metal ions computed from analytical selfconsistent wave functions have been tabula-

---

[7] J. Fergusson, K. Knox and D, L. Wood, *J. Chem. Phys.*, **35**, 2237 (1961).

[8] D. S. Mc Clure, *J. Phys. Chem. Solids*, **3**, 311 (1957).

[9] J. Máthé, *Rev. Roumaine Chim.*, **14**, 1003 (1969).

Table 1

Experimental ligand field transitions and the calculated values by means of radial functions corresponding to the central ion charges 0, +1, and +2

$\Delta_1 = \varepsilon(A_{1g}) - \varepsilon(B_{1g}),\ \Delta = \varepsilon(B_{2g}) - \varepsilon(B_{1g}),\ \Delta_2 = \varepsilon(E_g) - \varepsilon(B_{2g})$

Compound	Transition	Experimental cm^{-1}	M(0)	M(+1)	M(+2)
$KCrF_3$	Δ_1	9,150	10,145	5,235	3,595
	Δ	11,100	21,550	6,600	3,500
	Δ_2	2,900	1,630	2,095	2,060
$(NH_4)_2MnF_5$	Δ_1	12,750	9,965	4,285	3,675
	Δ	18,200	20,345	7,850	3,790
	Δ_2	2,800	2,330	1,970	1,790
CuF_2	Δ_1	7,500		2,930	2,290
	Δ	8,800		2,570	1,490
	Δ_2	2,550		1,460	1,290

ted recently.[10,11] We have calculated the ligand field $d-d$ transitions for some transition metal fluorides (Cr(II), Mn(III), Cu(II)) which manifest strong Jahn-Teller distorsions, using these radial integrals and the relations (1)—(4). As seen from table 1 the calculated $d-d$ transitions depend very much upon the central ion charge. We can obtain an acceptable agreement between the experimental and calculated values using central ion radial integrals corresponding to a metal charge close to zero. Wendling [12] obtained similar results for TiF_6^{-3}, concluding that this indicates the validity of Pauling neutrality principle.

Measuring the ligand-field $d-d$ transitions we can evaluate the effective ligand charge-radial integral products : $z_i \langle r^4\rangle_i\ (i = x, y, z)$. Table 2 summarizes the spectral and crystallografic data for some Cr(II), Mn(III), Cu(II) fluorides and the ligand field parameters $z_{sh}\langle r^4\rangle_{sh}$, $z_l\langle r^4\rangle_l$, characterizing the fluorine anions situated at a short and at a long distance from the central ion. If there are three different distances (short, medium and long) we have considered that $z_{sh}\langle r^4\rangle_{sh} = z_m\langle r^4\rangle_m$. As Table 2 indicates the products $z_{ef}\langle r^4\rangle$ are greater than the $\langle r^4\rangle$ integral for monovalent cations. This does not mean that the central ion charge is really close to zero. By delocalization of d electrons in covalent bond the radial extension of the electron cloud increases. This is in agreement with the neutron diffraction measurements which show that the magnetic electrons are extended beyond the neighbourhood of their parent atoms. Naturally the central ion charge is smaller than the formal charge because of the electron charge transfer from each ligand to the central ion.

The second factor which determines the $z_{ef} < r^4 >$ product is the effective ligand charge which acts on the central ion. The effective ligand

---

[10] F. M. O. Michel-Calendini and M. R. Kibler, *Theor. Chim. Acta*, **10**, 367 (1968).

[11] A. J. Freeman and R. E. Watson, "Magnetism", vol. 2 A, editors G. T. Rado and H. Suhl, Academic Press, New York, 1965, p. 290.

[12] E. Wendling, *Bull. Soc. chim. France*, **1967**, 2738.

Table 2

Summarized spectral, crystallografic data and ligand field parameters $z_{ef}<r^4>$ of some Mn (III), Cr (II) and Cu(II) fluorides

Compound	d-d trans. cm^{-1}	Ref.	R_{M-F} Å	$z_{ef}<r^4>$ a.u.	d orbital	Structure Ref.
MnF_3	12,000 19,000 23,000 (b)	13 14	2F 1.79 (B) 2F 1.91 (B) 2F 2.09 (B)	26.90 23.90	E HF	Perovskit 15
K_3MnF_6	9,000 17,500 21,000 (b)	14	4F 1.86 (NB) 2F 2.06 (NB)	25.95 26.77	E HF	16
NH_4MnF_5	12,750 18,200 21,000	17	2F 1.84 (NB) 2F 1.85 (NB) 2F 2.12 (B)	25.56 13.33	E HF	18
$KCrF_3$	9,150 11,100 14,000	16	2F 1.95 (B) 2F 2.00 (B) 2F 2.32 (B)	22.22 14.27	E HF	16 Perovskit
Na_2CrF_4	9,600 11,850 15,200	16	4F 1.96 (B) 2F 2.45 (NB)	20.61 24.36	E HF	19 20
CuF_2	7,500 8,800 11,350	20	4F 1.93 (B) 2F 2.27 (B)	15.73 11.20	HF F	21 Rutil
$KCuF_3$	7,200 8,900 11,550	20	2F 1.89 (B) 2F 1.96 (B) 2F 2.25 (B)	15.55 13.01	HF F	22 Perovskit
K_2CuF_4	7,800 9,200 11,900	20	2F 1.95 (NB) 4F 2.08 (B)	19.63 10.61	HF F	23 K_2NiF_4

b—band estimated
B—bridging fluorine, NB non-bridging fluorine
E, HF, F—the fluorine ion interacts with empty, half-filled and filled d orbital.
The $<r^4>$ integrals for monovalent cations are[10]: Cr^+ 13.211; Mn^+ 11.025; Cu^+ 4.595.

charge decreases on account of two sorts of charge transfer : charge transfer from the ligand to the central ion and charge transfer from the ligand to the nearest-neighbour transition metal ion if the ligand forms a bridge between the cations. It follows that the effective charge of bridging anions

---

[13] R. J. H. Clark, *J. Chem. Soc.*, **1964**, 417.

[14] T. S. Davis, J. P. Fackler and M. J. Weeks, *Inorg. Chem.*, **7**, 1994 (1968).

[15] M. A. Hepworth and K. H. Jack, *Acta Cryst.*, **10**, 345 (1957).

[16] D. Oelkrug, *Ber. Bunsenges. physik. Chem.*, **70**, 736 (1966).

[17] R. Dingle, *Inorg. Chem.*, **4**, 1287 (1965).

[18] "Tables of Interatomic Distances and Configurations in Molecules and Ion s", Supplement, The Chemical Society, London, 1965.

[19] D. Babel, *Z. anorg. Chem.*, **336**, 200 (1965).

[20] D. Oelkrug, *Z. physik. Chem. (Frankfurt)*, **56**, 325 (1967).

[21] C. Billy and H. M. Haendler, *J. Amer. Chem. Soc.*, **79**, 1049 (1957).

[22] A. Okazaki and Y. Suemune, *J. Phys. Soc. Japan*, **16**, 176 (1961).

[23] K. Knox, *J. Chem. Phys.*, **30**, 991 (1959).

is less than the effective charge of ligand ions which are bounded only to one transition metal ion, consequently the $z_{ef}<r^4>$ product is smaller for the bridging anion as compared to the non-bridging anions. Table 2 data confirm this conclusion.

In the compounds investigated there are two main kind of fluorine ions : free or non-bridging anions, which are bounded only to one transition metal ion, fluorine ions which form a bridge between the central ions. The bridge structure can be linear, while the central ion octahedra share a common corner (e.g. perovskite structures). There are bent bridges too with different M—L—M angles. In the case of bent 90° bridge, the neighbouring cations share a common octahedral edge. In rutil-type structures the anions connect three cations situated at three different distances.

In the K_3MnF_6 compound the manganese octahedra are isolated, the fluorine ions being bound to a single central ion. The effective charges of the two fluorine anions situated at different distances are approximately equal, the two products $z_{sh}\langle r^4\rangle_{sh}$ and $z_l\ \langle r^4\rangle_l$ have the same values.

The $(NH_4)_2MnF_5$ has a chain structure, the manganese octahedra have a common corner. Four fluorine ions are non-bridging, two anions situated at 2.12 Å from the manganese ion form a bent bridge. The $z_{ef}<r^4>$ for the bridging fluorine ions are approximately the half of the non-bridged anion parameter.

Another group of transition ion fluorides crystallizes in prevoskite-type structure : the metal ions lie on the corner of the cube and the fluorine ions are near the center of the cube edges, forming nearly a linear M—F—M bridge. The perovskite-type metal fluorides may exhibit two types of magnetic structures. In the G-type structure the magnetic ions are coupled antiferromagnetically to all six nearest neighbours. In the A-type structure four nearest neighbours are coupled ferromagnetically and two antiferromagnetically.[24]

In the A-type ordered MnF_3 and $KCrF_3$ the fluorine ion interacts on one side with the empty $d_{x^2-y^2}$ orbital (short distance), on the other side with the half-filled d_{z^2} orbital (long distance). The empty-half-filled orbital interaction produces the ferromagnetic coupling of the metal ions. The fluorine ions situated at a medium distance interact with two empty orbitals realizing an antiferromagnetic coupling between the ferromagnetic planes. As it results from table 2 the $z_{ef}\ \langle r^4\rangle$ data for fluorine ions which interact with the empty *d* orbitals are greater than the $z_{ef}\ \langle r^4\rangle$ value for half-filled orbitals.

In the $KCuF_3$ the fluorine anions can interact with the filled d_{z^2} orbital (long distance) and half-filled $d_{x^2-y^2}$ orbital (short distance). The two $z_{ef}\ \langle r^4\rangle$ values are different for the half-filled and filled orbitals : $(z_{ef}\ \langle r^4\rangle)_F < (z_{ef}\ \langle r^4\rangle)_{HF}$.

The K_2CuF_4 has a compressed octahedral structure, the ground term being $^2A_{1g}$. In this compound four fluorine ions form linear bridges.

---

[24] M. K. Wilkinson, "Advanced Course on Magnetic Exchange Interactions in Transition Metal Compounds", The Netherlands'-Norvegian reactor school, September, Kjeller, Norway, 1964, p. 185.

The $z_{ef}\,\langle r^4\rangle$ value for the bridging fluorine interacting with the half-filled $d_{x^2-y^2}$ orbital is approximately half as compared to the non-bridging ions.

In Na_2CrF_4 the chromium octahedra share common edges, forming 90°-bent bonds between the chromium ions. In this compound as in the above discussed cases the $z_{ef}\,\langle r^4\rangle$ product is smaller for bridging anions as compared to the non-bridging anions.

Another class of fluorine compounds has rutil-type structure, in which the anions connect three cations situated at different distances. The bonding parameters of CuF_2 have different values for different fluorine ions situated at short distance (interacting with half-filled d orbitals) and long distances from the central ion (interacting with filled d orbital).

We conclude from these results that the central ion contribution to the $z_{ef}\langle r^4\rangle$ values shows the following order: empty d orbital $\rangle$ half-filled orbital; half-filled orbital $\rangle$ filled orbital. The specific contribution of the bridging fluorine ions as compared to the non-bridging ones indicates that we cannot treat the metal oxides and halides as isolated "clusters".

Increasing of the radial integral $\langle r^4\rangle$ as compared to the corresponding integral calculated with the free ion wave function is an expression of electron cloud expansion effect (nephelauxetic effect)[25]. This effect contributes to the reduction of electron-electron repulsion parameters and spin-orbit coupling constants [26] (these being proportional with the $\langle r^{-1}\rangle$ and $\langle r^{-3}\rangle$ radial integrals) and to the increasing of $\langle r^4\rangle$ and $\langle r^2\rangle$ integral values. In analogous manner to the nephelauxetic "reduction" ratio [25,27] $\beta = B/B_0$ we can introduce new nephelauxetic "expansion" ratios defined in the following manner:

$$\gamma = \frac{\langle r^4\rangle}{\langle r^4\rangle_0} \qquad \lambda = \frac{\langle r^2\rangle}{\langle r^2\rangle_0}$$

where $\langle r^4\rangle_0$ and $\langle r^2\rangle_0$ are the radial integral values corresponding to the formal charge of central ion. The value of nephelauxetic expansion ratio change with the bond type, being different for σ and π bonds. Using the LCAO antibonding wave functions

$$\begin{aligned} \psi_\sigma &= a_\sigma\,|d_\sigma\rangle - b_\sigma \sum_x |\sigma_x\rangle \\ \psi_\pi &= a_\pi\,|d_\pi\rangle - b_\pi \sum_x |\pi_x\rangle \end{aligned} \tag{5}$$

and the nephelauxetic expansion ratios, we can evaluate the term energies in octahedral field (d^4, d^9 configurations)

---

[25] C. K. Jörgensen, "Progress in Inorganic Chemistry", vol. 4, editor A. F. Cotton, Interscience Publ., New York, 1962, p. 73.

[26] W. Marshall and R. Stuart, *Phys. Rev.*, **123**, 2048 (1961).

[27] C. K. Jörgensen, *Helv. Chim. Acta, Fasc. extr. A. Werner*, **1967**, 131.

$$\varepsilon(E_g) = -\,6\,a_\sigma^2\,\gamma_\sigma^0\,(1-\omega)\,z_L\,\frac{e^2\langle r^4\rangle_0}{6\,R^5} = -\,6\gamma_\sigma\,(1-\omega)\,Dq_0$$

$$\varepsilon(T_{2g}) = +\,4a_\pi^2\,\gamma_\pi^0\,(1-\omega)\,z_L\,\frac{e^2\langle r^4\rangle_0}{6\,R^5} = 4\,\gamma_\pi\,(1-\omega)\,Dq_0 \tag{6}$$

$$\Delta = 10\,Dq = 10\,(0.6\gamma_\sigma + 0.4\,\gamma_\pi)\,(1-\omega)\,Dq_0 = 10\,\bar{\gamma}(1-\omega)\,Dq_0$$

where z_L represents the ligand formal charge, ω is the fraction of charge transferred from the ligand to the metal ion, $\bar{\gamma}$ stands for the "mean" nephelauxetic expansion ratio expressing the σ and π bond contribution. Dq_0 is the pure electrostatic splitting parameter : $z_L\,\frac{e^2\langle r^4\rangle^0}{6\,R^5}$.

In the nephelauxetic expansion ratio $\gamma = a^2\gamma^0$ the first factor a^2 corresponds to the d-electron delocalization. This effect can be called according to Jörgensen's terminology "symmetry-restricted covalency". The second factor γ^0 expresses the radial expansion and deformation of d wave function. To the γ^0 values contribute also the "central-field" covalency effect, the reduction of central ion charge by ligand → central ion charge transfer.

Using the antibonding wave functions for the D_{4h} symmetry group we can obtain analogously the orbital energies. Because of the preponderent ionic character of the metal-ligand bond we used instead of molecular orbitals the "d" metal orbitals multiplied by the mixing coefficients.

$$|b_{1g}> = a_\sigma\,|\,d_{x^2-y^2}> -\frac{1}{2}\,b_\sigma(|\sigma_1> - |\sigma_2> + |\,\sigma_3> - |\sigma_4>)$$

$$|a_{1g}> = \alpha_\sigma\,|\,d_{z^2}> -\frac{1}{\sqrt{2}}\,b'_\sigma(|\sigma_5> + |\,\sigma_6>) +$$

$$+\frac{1}{2}\,b''_\sigma(|\,\sigma_1> + |\sigma_2> + |\sigma_3> + |\sigma_4>) \tag{7}$$

$$|b_{2g}> = a_\pi\,|\,d_{xy}> -\frac{1}{2}\,b_\pi(|\,\pi_1> + |\,\pi_2> + |\pi_3> + |\,\pi_4>$$

$$|e_g>_1 = \alpha_\pi\,|\,d_{xz}> -\frac{1}{\sqrt{2}}\,b'_\pi(|\,\pi'_1> + |\pi'_3>)$$

The term energies are :

$$\varepsilon(B_{1g}) = -6\gamma_\sigma(x^2-y^2)\mathrm{Dq} - 2\lambda_\sigma(x^2-y^2)\mathrm{Ds} - 5\gamma_\sigma(x^2-y^2)\,Dt$$

$$\varepsilon(A_{1g}) = -6\gamma_\sigma(z^2)\,Dq + 2\,\lambda_\sigma(z^2)\,Ds$$

$$\varepsilon(B_{2g}) = 4\gamma_\pi(\mathrm{x}y)\,Dq - 2\,\lambda_\pi(xy)\,Ds + 5\gamma_\pi(xy)Dt \tag{8}$$

$$\varepsilon(E_g) = 4\gamma_\pi(xz)\,Dq + \lambda_\pi(xz)\,Ds$$

The three ligand field transitions are

$$\Delta_1 = \varepsilon(A_{1g}) - \varepsilon(B_{1g}) = 6[\gamma_\sigma(x^2-y^2) - \gamma_\sigma(z^2)]Dq_0 + 2[\lambda_\sigma(x^2-y^2) + \lambda_\sigma(z^2)]Ds_0 + 5\gamma_\sigma(x^2-y^2)Dt_0 \tag{9}$$

$$\Delta = \varepsilon(B_{2g}) - \varepsilon(B_{1g}) = [6\gamma_\sigma(x^2-y^2) + 4\gamma_\pi(xy)]\,Dq_0 + 5\gamma_\sigma(x^2-y^2)\,Dt_0$$

$$\Delta_2 = \varepsilon(E_g) - \varepsilon(B_{2g}) = 4[\gamma_\pi(xz) - \gamma_\pi(xy)]Dq_0 + [\lambda_\pi(xz) + 2\lambda(xy)]Ds_0 - 5\gamma_\pi(xy)\,Dt_0$$

Table 3

Experimental ligand field parameters for some transition metal difluorides, and the calculated *Dq* values by means of radial integrals of bivalent ions

Compound	Exp. cm^{-1}	Calc. M(+2)
CrF_2	1100	338
MnF_2	830	188
FeF_2	880	158
NiF_2	730	152
CuF_2	880	149

The difference between the second and third band Δ_2 depends upon the π bond formation only. We expect in the case of Cu compounds that the calculated Δ_2 should be equal with the observed difference (the filled d orbitals do not form acceptor π bonds). The poor agreement between the experimental and calculated values (Table 1), can be explained with the Watson correlation effect, the Hartree-Fock radial wave function differs from the true function.

In table 3 there are given the experimental and calculated *Dq* values for some difluorides. The discrepancies are due mainly to the nephelauxetic expansion effect, i.e. partial covalent bond formation between the central ion and ligand. The Watson [28] correlation effect can contribute significantly to these discrepancies. This is illustrated by the sudden break of calculated *Dq* value for more than half-filled *d* shell. An analogous break was observed by Watson for the correlation energy of gaseous transition metal ions. In addition to ionic correlation the molecular extra correlation effect likewise can cause the experimental *Dq* value to be significantly different from the value predicted using the Hartree-Fock radial functions.

---

[28] R. E. Watson, *Phys. Rev.*, **118**, 1036 (1960).

Revue Roumaine de Chimie, **15**, 291–295 (1970)

CRYSTAL STRUCTURE STUDIES OF SOLID SOLUTIONS IN THE SYSTEM $Al_2O_3-Cr_2O_3-Li_2O$

D. CISMARU and D. MANOLESCU

Institute of Physical Chemistry of the Academy, Bucharest, str. Dumbrava Roşie 23

Received February 3, 1969

A α-$Al_2O_3-\alpha$-$Cr_2O_3-Li_2O$ system has been studied from the point of view of the phase composition and of the crystal structure; in all samples the Cr_2O_3 to Li_2O ratio by weight was constant and equal to 4 : 1, while the Al_2O_3 to $(Cr_2O_3-Li_2O)$ ratio was changed. All the samples were heated at 1200°.

Crystal structure, phase composition and colour of a binary system α-Al_2O_3 — α-Cr_2O_3 have made the object of studies of many workers.[1–5]

It has now been established that this binary system forms a continuous series of solid solutions; the lattice parameters of which are linearly related to the atomic percentage of one of the components (Vegard's law) and that the colour change from ruby-red to chromic oxide green is due to a gradual shift of the absorption band structure with the chromium content, brought about by changes in the crystal field where the chromium ions are placed.

The $Al_2O_3-Cr_2O_3-Me^{I,II}O$ (Me : metal) systems are known as important catalysts for dehydrocyclization (aromatization) and dehydrogenation of paraffins. However, they have not been well characterized as to their phase composition and crystal structure, the information available in the literature[6–8] till now being scarce. In this work we are concerned with this problem.

---

[1] E. Thilo and J. Iander, *Z. anorg. Chem.*, **279**, 2 (1955).

[2] L. E. Orgel, *Nature*, **179**, 1348 (1957).

[3] L. Singn, *Nature*, **181**, 1264 (1958).

[4] R. M. Springgs and S. L. Bender, *J. Amer. Ceram. Soc.*, **45**, 506 (1962).

[5] J. Graham, *J. Phys. Chem. Solid*, **17**, 18 (1960).

[6] R. G. Davis, R. H. Griffith and J. D. Marsh, *Adv. Catalysis*, **9**, 154 (1957).

[7] A. H. Rubinstein, N. A. Pribitkova, V. A. Afanasiev and A. A. Slinkin, *Kinetika i Kataliz*, **1**, 129 (1960).

[8] V. Klyucharov and S. A. Suvorov, *Izvest. Akad. Nauk S.S.S.R., Neorgn. Materialy*, **1**, 1403 (1965).

EXPERIMENTAL

Sample preparation. Merck's alumina powder and Riedel de Haën chromic oxide powder were used in this investigation; the purity of the alumina was 99.8%, most impurity being alkalis. The chromic oxide 99.6% pure, containing about 0.1 % Fe_2O_3 and 0.2% Al_2O_3 with 0.2% water. Merck lithium carbonate was about 99% pure containing about 1% water and impurity $< 0.1\%$. Alumina powder was previously calcined for 4 hours at 1250° to obtain α-Al_2O_3 100%. The chromic oxide is also of a α-Cr_2O_3 form. For both oxides the size passing through the 12500 mesh/cm^2 sieve was used. The accurately weighed powders were homogenized in absolute alcohol in the desired proportions and then dried for 12 hours at 110°. After drying, the powders were pressed in pellets of about 0.5 g and 8 mm in diameter each at a pressure of 2750 kg/cm^2. These were heated in a sinterized corundum crucible in an electric furnace at 1200° for 8 hours, the atmosphere used being air. No transformation has been observed during more than 8 hours at the same temperature. The temperature was measured with a Pt—PtRh thermocouple welded near the samples. The temperature was kept constant to ± 5°. In all prepared samples the Cr_2O_3 to Li_2O ratio by weight was constant and equal to 4 : 1 the Al_2O_3-to-(Cr_2O_3—Li_2O) ratio being continuously changed. The samples composition and the calcination losses are given in table 1.

Table 1

Composition and calcination losses

	Content, wt (%)			Calcination losses %
	Al_2O_3	Cr_2O_3	Li_2O	
1	95	4	1	0.9
2	90	8	2	0.9
3	85	12	3	0.9
4	80	16	4	0.9
5	75	20	5	0.9
6	70	24	6	0.9
7	65	28	7	0.9

Chemical analysis. To determine the composition of the components soluble in water, which may be the alkaline aluminate, chromite and chromate as shown by Rubinstein and his coworkers,[7] the water extracts produced from exact samples (from 1.5 to 2 g) were analysed by repeated extractions (10 min boiling in 50 ml H_2O each time). The extract obtained was diluted in graduated beaker to a definite volume and the individual samples were accounted iodometrically for Cr^{6+} and acidimetrically for alkalis by titrating the 0.1 N H_2SO_4 in the presence of phenolphthaleine as an indicator. The qualitative determination of Al^{3+} in the extract was also carried out first by a reaction with Alisarin-Rot alcoholic solution and then by the action of the NH_4Cl to hydrolyse the aluminate so as to form a residue. The quantitative determination of the aluminate is not possible because the concentration of Al^{3+} is smaller than 0.1%. The water extract was of a bright yellow colour. No green extracts corresponding to the Cr^{3+} have been obtained in either case. The Cr^{6+} content in extracts is practically unchanged and it does not change with the chromium content (about 0.5% for the samples 1—5 and about 1% for 6—7). The reaction of all samples was neutral.

Composition and structure. The sintered samples were broken in an agate mortar. X-ray powder patterns were obtained in a Debye camera 114.6 mm in diameter, using CuKα radiation filtered with Ni. A TUR M 60 apparatus was used throughout. Measurements were made by the Straumanis' method on five or six back reflexion lines, to reduce the random errors which appear when reliance is placed on only three reflexions. With sharp patterns this procedure results in a precision of about, ± 0.001 Å in a_0 and ± 0.002 Å in c_0, for α-$Al_2O_3-\alpha Cr_2O_3$ solid solutions, if hexagonal indices for the rhombohedral lattice are used. All measurements were made at room temperature ($20 \pm 5°$); since the thermal expansion of alumina at 20° is $6 \times 10^{-6}/°$ the errors due to temperature fluctuations are smaller than 0.0001 Å in a_0 or 0.0004 Å in c_0.

The same procedure results in a precision of about ± 0.001 Å in a_0 for $Li_2O-Al_2O_3-Li_2O.Cr_2O_3$ solid solutions.

The lithium structure aluminate was determined by the data given in the literature.[9] The compound has a spinel-type structure. The space group is : $O_h^7 - Fd\,3\,m$ (possible reflexions being : hkl : $h+k$, $k+1$, $(1+h) = 2\,n$; hhl : $1+h = 2n$; okl : $k, 1 = 2n$, $k+1 = 4n$). The lattice constant determined has a value of $a_0 = 7.890$ Å. The lithium chromite structure is unfortunately unknown. All we know is that the chromites prepared by drying are of the $Me^{II}\,Cr_2O_4$ type. They have a spinel structure i.e. of a double oxide, where voluminous ions of O_2^{2-} form a cubic closed-packed structure. In this structure the metal ions are arranged in regular tetrahedron while the chromium ions in regular octahedron being surrounded by four and six oxygens.

The powder diffraction patterns study shows the formation of two series of solid solutions: a solid solution between Al_2O_3 and Cr_2O_3 and another between $Li_2O.Al_2O_3$ and $Li_2O.Cr_2O_3$. Samples up to 4% Li_2O show the formation of a α-Al_2O_3—α-Cr_2O_3 solid solution containing about 4% Cr_2O_3 in Al_2O_3 if we consider the Cr_2O_3 lattice dilatation to be linear. Over 4% the α-Al_2O_3—α-Cr_2O_3 solid solution becomes very amorphous, which makes impossible the determination of crystallographic constants.

On the other hand the solid solution of aluminate-chromite appears from the start well constituted. As expected it has a spinel-type lattice like that of the aluminate. The results representing the lattice parameters are listed in table 2, along with the percentual composition of the two solid solutions approximately determined from the line intensities.

Table 2

Values of lattice parameters and composition

Cr_2O_3	$Al_2O_3-Cr_2O_3$		$Li_2Al_2O_4-Li_2Cr_2O_4$	$Al_2O_3-Cr_2O_3$	$Li_2Al_2O_4-Li_2Cr_2O_4$
	a	c	a	%	%
4	4.764	13.009	7.925	94	5
8	4.766	13.015	7.930	89	10
12	4.768	13.020	7.937	83	15
16			7.960	77	21
20			7.964	72	27
24			7.968	65	33
28			7.971	59	38

---

[9] A. J. Mirkin, "Spravochnic po roentgenostructurnomu analizu policristalov", Gosud. izdatel. fizico-mat. literatury, Moscow, 1961, p. 490.

The table shows the slight increase in the lattice constant with the Cr_2O_3 content for the spinel phase. This suggests that the chromite phase in the solid solution increases with the chromium content. On the other hand the values of lattice parameters for the α-Al_2O_3—α-Cr_2O_3 solid solution remain actually constant over the range studied. Over 15% Cr_2O_3 the solid solution of α-Cr_2O_3—αAl_2O_3 forms very small crystals which preclude the measurement of crystallographic constants. The samples obtained in the same conditions (heated for 8 hours at 1200°) but without lithium oxide show that up to 15% Cr_2O_3 they form only a solid solution, but above 15% Cr_2O_3 a very strong corundum phase, the Cr_2O_3 and their solid solutions appear. The colour changes gradually from ruby-red to chromic oxide green with the increase in the chromium content. In the samples which contain lithium oxide the colour remains practically unchanged with the increase in the chromium content. This confirms on the one hand that the solid solution composition remains practically unchanged within the range studied and on the other hand that the spinel phase takes place before the other solid solutions. No corundum phase was revealed. Moreover, experiments carried out at 1000—1200° show the formation of solid solutions of the same kind but worse crystallized. The formation of only continuous series of solid solutions up to 15% Cr_2O_3 is due to the temperature. Spriggs and Bender [4] showed that the formation of a continuous series of solid solutions from 100 mol % α-Al_2O_3 up to 100 mol % α-Cr_2O_3 takes place by heating to melt the samples with an oxyacetylene-flame until melting, and subsequent quenching with cold water. The results show a continuous change in the lattice parameters from 100 mol% α-Al_2O_3 to 100 mol % α-Cr_2O_3 which confirms Vegard's law. The lithium chromate could not be identified.

CONCLUSIONS

The study of the Al_2O_3—Cr_2O_3—Li_2O system shows the formation of two series of continuous solid solutions ; a solution of α-Al_2O_3 — α-Cr_2O_3 with a practically constant composition within the range studied (4—28% Cr_2O_3) and a solution of $Li_2O.Al_2O_3$ — $Li_2O.Cr_2O_3$. The formation of the latter is confirmed by the variation of the spinel-phase lattice constant from 7.890 Å to 7.971 Å. From the data here presented and assuming that only the above mentioned phases take place, the probable lattice constant of the $Li_2O \cdot Cr_2O_3$ phase was determined, its value being $a_0 = 8.13$ Å. In fact this assumption is backed up by the formation of the α-Al_2O_3—α-Cr_2O_3 solid solution with an approximately constant content of about 4 ± 1% Cr_2O_3 over the whole range in spite of the high increase in the Cr_2O_3 percentage.

Rubinstein and coworkers [7] preparing the samples at 1000—1100°, but with potassium oxide, observed the formation of only one solid solution of spinel type, which they assume to be γAl_2O_3—Cr_2O_3. This interpretation is not quite true because the potassium aluminate forms a solid solution with the potassium chromite. The potassium aluminate has a lattice parameter of $a_0 = 7.680$ Å and the results confirm even the formation of this latter solution. Furthermore taking into account the conditions in which the experiments were conducted (calcination at 1000–1100° up to a constant weight) the appearance of the corundum phase in samples containing over 20% Cr_2O_3 together with the solid solution α-Al_2O_3 – α-Cr_2O_3 is due to the conversion of γ-alumina into the α-alumina.

However, further studies, at higher temperatures, are needed for the full knowledge and explanation of these processes.

ORSZÁGOS MŰSZAKI KÖNYVTÁR ÉS DOKUMENTÁCIÓS KÖZPONT 1883

Revue Roumaine de Chimie, **15**, 291–295 (1970)

NOTE POUR LES AUTEURS

La *Revue Roumaine de Chimie* publie des articles en anglais, français, russe, allemand ou espagnol. Les auteurs sont priés d'envoyer des articles, notes, communications et comptes rendus inédits.

Les manuscrits seront dactylographiés à deux intervalles. Les tableaux seront dactylographiés sur feuilles séparées, de même que la légende des figures. Les diagrammes seront tracés à l'encre de Chine sur papier calque. Les tableaux et les figures seront numérotés par des chiffres arabes, en nombre strictement nécessaire. Prière de ne pas inscrire les mêmes données dans les tableaux et les figures. Les formules chimiques seront incluses dans le texte ; en outre, elles seront transcrites sur des feuilles séparées. Les auteurs sont priés d'indiquer les caractères italiques (en soulignant les lettres au crayon), ainsi que tout autre caractère spécial. L'ordre des références bibliographiques sera celui de leur mention dans le texte ; le nom de l'auteur sera précédé de l'initiale du prénom ; les publications périodiques seront présentées suivant les prescriptions internationales. Les références seront ajoutées à la fin de l'article ; elles paraîtront comme des notes, au bas de la page. Le texte sera précédé d'un résumé, comprenant 15 lignes au maximum.

L'entière responsabilité du contenu des articles appartient aux auteurs. On publie des articles dus aux collaborateurs roumains ou étrangers. Les auteurs recevront 50 tirés à part.

PRINTED IN ROMANIA

ORSZÁGOS MŰSZAKI KÖNYVTÁR ÉS DOKUMENTÁCIÓS KÖZPONT 1983

1970 APR 16

TRAVAUX PARUS AUX ÉDITIONS DE L'ACADÉMIE DE LA RÉPUBLIQUE SOCIALISTE DE ROUMANIE

CORNEL BODEA et collab., **Tratat de biochimie vegetală, partea I, Fitochimie** (Traité de biochimie végétale, Ire partie, Phytochimie), Ier vol., 1964, 747 p. + 4 annexes + 2 pl., 41 lei ; IIe vol., 1965, 1262 p., 1 pl., 56 lei ; IIIe vol., 1967, 773 p., 35 lei.

V. GHEȚIE et V. MICUȘAN, **Analiza imunochimică. Teorie și practică** (Analyse immunochimique. Théorie et pratique), 1966, 369 p., 28 lei.

SILVIA IONESCU, **Reacții chimice induse de radiațiile ionizante** (Réactions chimiques produites par les radiations ionisantes), 1963, 271 p., 15 lei

MARIETA NICOLAE, **Fizico-chimia proceselor fotografice** (Physico-chimie des processus photographiques), 1964, 426 p. + 4 pl., 35 lei.

R. PORTOCALĂ et L. POPA, **Acizii ribonucleici celulari și virali** (Les acides ribonucléiques cellulaires et viraux), 1966, 375 p. + 8 pl., 26 lei.

D. PURDELA et R. VÎLCEANU, **Chimia compușilor organici ai fosforului și ai acizilor lui** (La chimie des composés organiques du phosphore et de ses acides), 1965, 540 p., 37 lei.

CRISTOFOR SIMIONESCU et CLEOPATRA VASILIU-OPREA **Mecanochimia compușilor macromoleculari** (La mécanochimie des composés macromoléculaires), 1967, 344 p., 23,50 lei.

I. P. „Informația" — c. 4126

43426

Lei 25

F 1103 04

R

[illegible]ERÁLVA

REVUE ROUMAINE DE CHIMIE

TOME 15

N° 3

Mars 1970

ÉDITIONS DE L'ACADÉMIE DE LA RÉPUBLIQUE SOCIALISTE DE ROUMANIE

Rev. Roumaine Chim.

15, 297 — 486 (1970), Bucarest

COMITÉ DE RÉDACTION

Rédacteur en chef :

C. D. NENIŢESCU, membre de l'Académie de la République Socialiste de Roumanie

Rédacteurs en chef adjoints :

A. T. BALABAN et V. E. SAHINI, membres correspondants de l'Académie de la République Socialiste de Roumanie

Collège de rédaction :

C. DRĂGULESCU, RALUCA RIPAN, CR. SIMIONESCU, membres de l'Académie de la République Socialiste de Roumanie; EM. BRATU, membre correspondant de l'Académie de la République Socialiste de Roumanie, Pr G. OSTROGOVICH, MARGARETA AVRAM, F. BADEA, I. D. MARCHIDAN, D. NEGOIU et D. SĂNDULESCU.

Les manuscrits, les livres et les revues proposés en échange, ainsi que toute correspondance seront envoyés à la rédaction :

REVUE ROUMAINE DE CHIMIE

23, str. Dumbrava Roşie, Bucarest, Roumanie.

F 1103

ORSZÁGOS MŰSZAKI KÖNYVTÁR ÉS DOKUMENTÁCIÓS KÖZPONT

REVUE ROUMAINE DE CHIMIE

Tome 15, N° 3 Mars 1970

Page

I. G. MURGULESCU and D. OANCEA, Nucleophilic substitutions. II Reactions between benzyl bromide and alkali alcoxides 299–307

A. GIOABĂ, V. EM. SAHINI and ELENA VOLANSCHI, Charge transfer complexes of the aromatic heterocycles. II. CT-Complexes of Phenoxatellurine and Some of its Derivatives with TCNE 309–311

ZLATA PAVLOVIĆ and R. POPOVIĆ, Thermodynamics of the behaviour of Pb(II)-ions in acid and alkaline solution . . . . * 313–323

O. RADOVICI and VERONICA TUCSEK, The potential distribution and the surface charge at the silicon-hydrofluoric acid interface 325–332

ELENA CONSTANTINESCU and T. MARIAN, The anodic behaviour of pure aluminum in acidic solutions of potassium halides 333–341

S. STERNBERG and CONSTANŢA HERDLICKA, Interdiffusion coefficient of silver ion in molten alkali nitrates by the chronopotentiometric method 343–355

ŞTEFANIA ZUCA and M. OLTEANU. The electrical conductivity of binary molten alkali chloride systems as a function of anion polarization . . . 357–369

MIHAELA TEODORESCU and E. SEGAL, The effect of pretreatment on the electrical resistance variation of zinc oxide thin films, under irradiation and carbon monoxide chemisorption 371–376

E. J. TOMUŞ, Heat of dilution of aqueous solutions of potassium, silver and lead nitrates 377–384

CAMELIA BELDIE and FLORICA BĂRBULESCU, Salt effects in ternary systems furfural-water-electrolyte. I. Ternary Systems Furfural-Water-Uni-Univalent Electrolyte 385–393

F. M. ALBERT and AURELIA MEGHEA, Electron spin resonance (ESR) study of the oxidation of some aromatic amines with sodium chlorite 395–400

S. SOLACOLU, R. DINESCU and MARIA ZAHARESCU, Die thermischen Phasengleichgewichte des Systems BaO-TiO_2—V_2O_5 401–408

I. GRECU et ELENA CUREA, Combinaisons complexes de la dihydrazinophtalazine (DHF). Les sélénocyanates dihydrazinophtalazino-métalliques . 409–416

D. LUPU, Magnetic exchange in a heterogeneous trinuclear system 417–422

M. MARCU and M. DIMA, Coordination polymers. III. Polycoordination of 4,4'-diphenylsulphonedicarboxaldehyde bis(thiosemicarbazone) with cadmium and mercury 423–429

GEORGETA POPESCU, L'étude de la viscosité de structure des solutions de stéarate d'aluminium dans les hydrocarbures. L'influence de quelques composés polaires 431–440

Rev. Roumaine Chim. 15, 297–486 (1970), Bucarest

Page

IG. POINESCU, STELIANA MAXIM and A. CARPOV, Synthesis of the sulphuric ester of poly(vinyl alcohol) 441–450

ANTOANETA SPINZI et I.V. NICOLESCU, Propriétés physico-structurales des catalyseurs utilisés à l'oxydation des hydrocarbures. III. Propriétés électriques des systèmes oxydiques à base de V_2O_5 — MoO_3 — P_2O_5 par rapport au milieu de réaction 451–456

MARIA GRUIA, O. KÖRNER and ALA NICOLESCU, The variation of physico-structural properties of some aluminium hydroxides as against their formation conditions 457–462

A.T. BALABAN, Chemical Graphs. VIII. Valence Isomerism and General Cubic Graphs 463–484

Revue Roumaine de Chimie, **15**, 299–307 (1970)

NUCLEOPHILIC SUBSTITUTIONS. II

REACTIONS BETWEEN BENZYL BROMIDE AND ALKALI ALCOXIDES

I. G. MURGULESCU and D. OANCEA

Faculty of Chemistry of the Bucharest University, Physical Chemistry
Department, Bd. Republicii 13

Received April 30, 1969

The reactions between benzyl bromide and sodium alcoxides in alcoholic solutions have been studied using methyl, ethyl, n-propyl, n-butyl, n-amyl and n-hexyl alcohols. The rate constants of these reactions have been reported at different temperatures between 30° and 70°. The dependence of the rate constants upon dielectric constants of the solvents has been studied, regarding, these reactions as ion-dipole reactions.

The study of the displacement reactions on saturated carbon proved the existence of some obscure mechanistic problems which remained unsolved up to now. Some compounds deviate from the general mechanisms and these deviations are subject to contradictory discussions. Such a peculiar behaviour appears in the case of nucleophilic substitution of α halogenated toluene. Solvolysis of these compounds seems to occur through an intermediate rather than a SN 1 or SN 2 mechanism. [1]

Benzyl bromide has been scarcerly studied from the mechanistic point of view regarding nucleophilic substitution. However, there are some papers dealing with solvolysis of benzyl bromide in polar solvents as water or heavy water [2] acetone-water mixtutres, [3,4] anhydrous ethanol [5] or ethanol-water mixtures [5,6]

A systematic and recent paper [7] deals with alcoholysis of benzyl bromide in four normal alcohols (methanol-n buthanol). In alcoholic solutions of alkali alcoxides the substitution reaction rates increase considerably. The first studies about the reactions between benzyl bromide and alkali alcoxides have been made by Tronov and Gerschewitsch[8] and Plisov[9]. More recent papers[10,11] refer to the action of methoxide ion on benzyl bromide. All these papers report data only about the reactions between benzyl bromide and alkali methoxides or ethoxides at certain temperatures. In the present paper one has studied the reactions of benzyl bromide with sodium alcoxides. The obtained data have been correlated with dielectric constants of the medium as done in a previous paper regarding similar reactions of benzyl chloride[12]. Normal alcohols (from methyl to n-hexyl) were used as solvents and the substitution reaction rates were watched at different temperatures and concentrations.

---

[1] O. A. Reutov ,,Probleme teoretice ale chimiei organice'' Ed. Acad., Bucharest, 1964. Translation from Russian, Cha p. II

[2] P. M. Laughton and E. R. Robertson, *Canad J. Chem.*, **34**, 1714 (1956) ; **37**, 1491 (1959).

[3] J. Hine and D. E. Lee, *J. Amer. Chem. Soc.*, **73**, 22 (1951).

[4] G. R. Cowie, H. J. M. Fitches and G. Kohnstam, *J. Chem. Soc.*, **1963**, 1585.

[5] H. von Halban and W. Gast, *Z. Phys. Chem.*, **1916**, 593.

[6] J. W. Baker, *J. Chem. Soc.*, **1934**, 987.

[7] I. G. Murgulescu and I. Demetrescu, *Rev. Roumaine Chim.* (to be published).

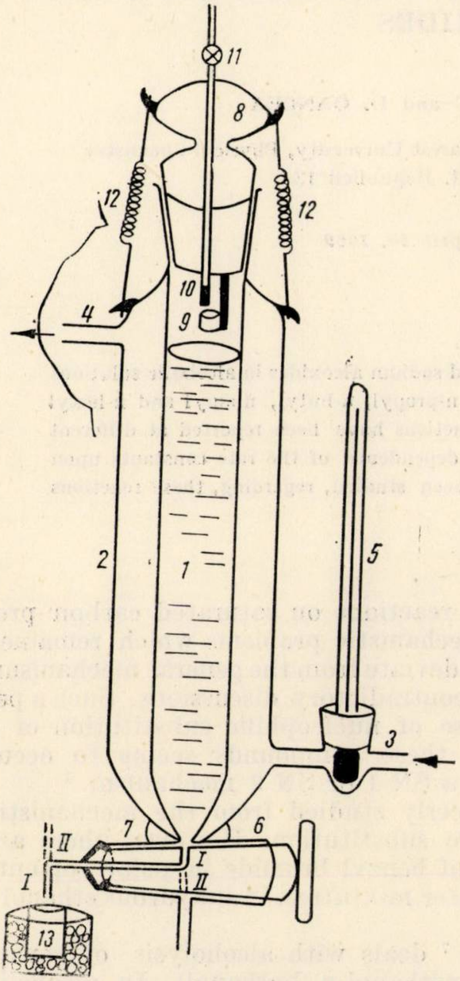

Fig. 1. – Reaction flask used for kinetic measurements

1, compartment for alcoxide solution; 2, thermostating jacket; 3, 4, sleeves for thermostating circuit; 5, thermometer; 6, 11, taps; 7, thermal insulationt with asbestos wire; 8, ground glass stopper; 9, compartment for benzyl bromide; 10, valve; 12, springs; 13, cooled vessel.

EXPERIMENTAL

Schuchardt benzyl bromide without further purificatons was used. All the alcohols used as solvents were dried before their use, since the water traces alter the dielectric constants and at the same time, give simultaneous reactions which interfere with those under investigation. For this purpose, a previously reported method was used.[12] The residual water content was determined by Karl Fischer method and was always found to be less than 0.01 %. Alkali alcoxides were prepared by dissolving pure metallic sodium in the appropriate alcohols in an inert gas (N_2) atmosphere. Precautions were taken to remove the oxygen and water traces. Alkali alcoxide solutions were standardized against 0.1 N salicylic acid in propyl alcohol in the presence of phenolphthalein.

The reactions were watched at different temperatures between 30° and 70° by using a Höppler thermostat (±0.02°) up to a conversion of about 80 %. Since at higher tempe ratures the reaction rates increase considerably (the half-life decreases to 100 sec) all the kinetic runs were performed by using an apropriate reaction flask which can be thermostated. The flask is made in such a way, that aliquots can be withdrawn at exactly known times, and the reaction can be suddenly "frozen" (fig. 1). The reagents are placed in two compartments 1 and 9, and are left for about 10 minutes so that the reagents take the temperature of the thermostat which can be read on the thermometer 5. Then, the reaction flask is suddenly overturned and thorougly shaken while the time is measured. After a determined interval of time, the tap 6 is turned in the position I (full line). The vapor pressure will push a reacting mixture amount through the tap 6 directly into the cooled vessel 13. A measured aliquot of this cooled amount is now titrated with 0.1 N salicylic acid. When a suitable amount of the reacting mixture was pushed out, the tap 6 is returned to position II (dotted line). Then it is washed with clean alcohol and dried by passing warm air. If the vapor pressure is too low and cannot push out the sample (e.g. at low temperatures or for superior alcohols) before the sample flows out, the tap 11 is turned on and an amount of dried air is introduced into the reaction flask to create some over pressure. The tap 11 is turned off and the reaction flask is ready for measurement.

---

[8] B. Tronov and A. Gerschewitsch, *Chem. Zentr.*, **1927 II**, 1145.

[9] A. K. Plisov, *Ukrain. Khim. Zhur.*, **4** Sci **Pt.**, 241 (1929).

[10] G. Klopman and R. F. Hudson, *Helv. Chim. Acta*, **44**, 1914 (1961).

[11] J. B. Stothers and A. N. Bourns, *Canad. J. Chem.*, **40**, 2007 (1962).

[12] I. G. Murgulescu, D. Oancea and G. Mincu, *Rev. Roumaine Chim.*, **14**, 3 (1969).

The reagents were kept in Pellet burettes protected from atmospheric moisture by tubes filled with anhydrous $CaCl_2$.

RESULTS

Simultaneous reactions occur between benzyl bromide and sodium alcoxides in the respective alcohols, according to the following scheme:

$$PhCH_2Br + RONa \rightarrow PhCH_2OR + NaBr \tag{a}$$

$$PhCH_2Br + ROH \rightarrow PhCH_2OR + HBr \tag{b}$$

$$HBr + RONa \rightarrow ROH + NaBr \tag{c}$$

where $R = CH_3$, C_2H_5, nC_3H_7, nC_4H_9, nC_5H_{11}, nC_6H_{13}
Reaction (b) has a much smaller rate as compared to reaction (a) and consequently can be neglected. This is reasonably because the rate constants of the reaction (b) are about 2×10^4 times smaller than the rate constants of the reaction (a), as shown in table 1.

Table 1

Rate constants for reactions between benzyl bromide and sodium alcoxides (k_2) comparatively with the corresponding values for reactions between benzybromide and respective alcoholos (k_2')* at70°

Alcohol	k_2 (cc mol^{-1} sec^{-1})	$10^3\times k_2'$ (cc mol^{-1} sec^{-1})	$\rho=k_2/k_2'$
CH_3OH	80.00	6.10	1.31×10^4
C_2H_5OH	105.7	4.92	2.14×10^4
n-C_3H_7OH	83.20	4.01	2.07×10^4
n-C_4H_9 OH	57.01	2.76	2.06×10^4

* ref. 7)

In this table are given the rate constants, k_2, for the reactions between benzyl bromide and different alcoxides (second column) and k'_2, for the reactions between benzyl bromide and respective alcohols [7] (third column). The ratio $\rho = k_2 : k_2'$ which is about 2×10^4 is given in the last column. All values are reported for 70°. These results show that reactions II and III are negligibly slow, and consequently reaction kinetics can be rightly described by equation :

$$PhCH_2Br + RONa \rightarrow PhCH_2OR + NaBr$$

Kinetic mesurements showed that up to a 80% conversion, the process is bimolecular and verifies the equation :

$$k_2 = \frac{2.303}{t\,(a-b)} \log \frac{(a-x)b}{(b-x)a} \tag{1}$$

where a and b are initial concentrations of reagents and x is the decrease in concentration according to time t.

When $a = b$, one can use the equation :

$$k_2 = \frac{1}{t}\left(\frac{1}{a-x} - \frac{1}{a}\right) \tag{2}$$

Two kinetic runs and respective rate constants are given, for exemplification, in table 2 and 3.

It can be seen that the rate constants obey the proposed equation, deviations being within the limits of experimental errors.

Table 2

A kinetic run for reaction between benzyl bromide and sodium methoxide

T = 50° $a = b = 0.1$ mol l^{-1}

t(sec)	$(a-x)\times 10^4$(mol cc^{-1})	k(cc mol^{-1} sec^{-1})
300	0.660	17.16
780	0.440	16.31
1260	0.325	16.48
1680	0.260	16.94
2160	0.230	15.49
2400	0.200	16.66
3000	0.165	16.86
		$k = 16.55 \pm 0.21$

Table 3

A kinetic run for reaction between benzyl bromide and sodium hexoxide

$T = 50°$ $a = b = 0.1$ mol l^{-1}

t (sec)	$(a-x)\times 10^4$ (mol cc^{-1})	k(cc mol^{-1} sec^{-1})
300	0.815	7.62
600	0.680	7.84
900	0.590	7.71
1200	0.514	7.90
1600	0.448	7.70
1800	0.412	7.98
2400	0.348	7.78
		$k = 7.79 \pm 0.07$

At the same temperature the studied rate constants depend neither upon the initial concentrations of the reagent nor on the ratio between the initial concentrations of the reagents, as shown in table 4.

Table 4

Rate constants of the reaction $PhCH_2Br + RO^- \rightarrow PhCH_2OR + Br^-$ for different initial concentrations

$T = 50°$ a = alcoxide concentration (mol. l^{-1})
b = benzyl bromide concentration (mol. l^{-1})

System PhCH Br +	b	a	$a:b$	k
CH_3O^-	0.1	0.1	1 :1	16.62
	0.1	0.2	2 :1	16.71
	0.1	0.05	1 :2	16.54
	0.2	0.1	1 :2	16.60
$C_2H_5O^-$	0.1	0.1	1 :1	21.07
	0.1	0.2	2 :1	20.91
	0.1	0.05	1 :2	20.97
	0.2	0.1	1 :2	21.08
$nC_3H_7O^-$	0.1	0.1	1 :1	18.60
	0.1	0.2	2 :1	18.92
	0.1	0.05	1 :2	18.71
	0.2	0.1	1 :2	18.57
$nC_4H_9O^-$	0.1	0.1	1 :1	13.98
	0.1	0.2	2 :1	13.98
	0.1	0.05	1 :2	13.80
	0.2	0.1	1 :2	14.03
$nC_5H_{11}O^-$	0.1	0.1	1 :1	8.95
	0.1	0.2	2 :1	9.05
	0.1	0.05	1 :2	9.12
	0.2	0.1	1 :2	8.93
$nC_6H_{13}O^-$	0.1	0.1	1 :1	7.79
	0.1	0.2	2 :1	7.81
	0.1	0.05	1 :2	7.84
	0.2	0.1	1 :2	7.75

Table 5 gives the rate constants for the studied reactions at different working temperatures.

Table 5

Rate constants of the reactions between benzyl bromide and sodium alcoxides at different temperatures ($cm^3mol^{-1} sec^{-1}$)

System $PhCH_2Br +$ / Temperature	30°	40°	50°	60°	70°
CH_3ONa	2.723	5.561	16.62	36.98	80.00
C_2H_5ONa	3.815	9.292	21.07	48.16	105.7
$n-C_3H_7ONa$	3.391	7.956	18.20	41.20	83.20
$n-C_4H_3ONa$	2.368	6.004	13.98	29.12	57.01
$n-C_5H_{11}ONa$	1.724	4.247	8.951	19.82	40.07
$n-C_6H_{13}ONa$	1.503	3.390	7.791	15.85	33.10

Since alkali alcoxides are dissociated in the respective alcohols and benzyl bromide is a dipolar substance, it is necessary to take into account the electrostatic interactions between reactant particles immersed in the medium having a definite dielectric constant.

For this purpose a relationship taking into account the electrostatic energy between ions and dipolar molecules was used. Since the rate constants under investigation do not depend significantly upon the ionic strength of the medium, the relationship refers to the ion-dipole interactions in a medium of given dielectric constant and zero ionic strength :

$$k_{D,o} = k_0 \exp\left(-\frac{NZ_B \varepsilon \mu_A \cos\theta}{Dr_0^2 RT}\right) =$$

$$= A \exp(-E/RT) \exp\left(-\frac{NZ_B \varepsilon \mu_A \cos\theta}{Dr_0^2 RT}\right) \tag{3}$$

Where, $k_{D,o}$ is the experimental rate constant and k_0 is a theoretical value of this rate constant when $D \to \infty$, that is to say without electrostatic interactions. The constant k_0 was expressed by the Arrhenius equation. In the logarithmic form equation (3) becomes :

$$\log k_{D,o} = \log A - \frac{E}{2.303\,RT} - \frac{N \varepsilon \mu \cos\theta}{2{,}303\,Dr_0^2 RT} \tag{4}$$

where $Z_B = 1$, μ is the dipole moment of benzyl bromide, D is the dielectric constant of the solvent, r_0 is the distance between the ion and the dipole, θ is the angle of inclination of the polar axis to the line joining its centre to that of the ion, the other symbols having their usual meanings.

The dielectric constants and their dependence upon the temperature were taken from a previous paper. [12]

Plotting $\log k_2$ against $1/D$ there must result a straight line, as eq. (4) suggests. According to the theoretical prediction of the Amis equation, [13] if the reaction proceeds through the nucleophilic attack of the alcoxide ion on saturated carbon, the slope of this line must be negative. Figure 2 confirms these expectations.

Only the points regarding reactions which occur in methyl alcohol are not on this line.

At the same temperature, the lines plotted in figure 2 can be described by using the following equation :

$$\log k_2 = \log k_0 - B/D \tag{5}$$

By comparing with equation (4), one can now obtain the meaning of both curve slopes and intercepts on the log k axis :

$$\log k_0 = \log A - E/2.303\ RT \tag{6}$$

$$B = \frac{N \varepsilon \mu \cos\theta}{2.303\, r_0^2 RT} \tag{7}$$

---

[13] E. A. Amis, "Solvent Effects on Reaction Rates and Mechanisms", Academic Press, New York and London 1966, p. 42.

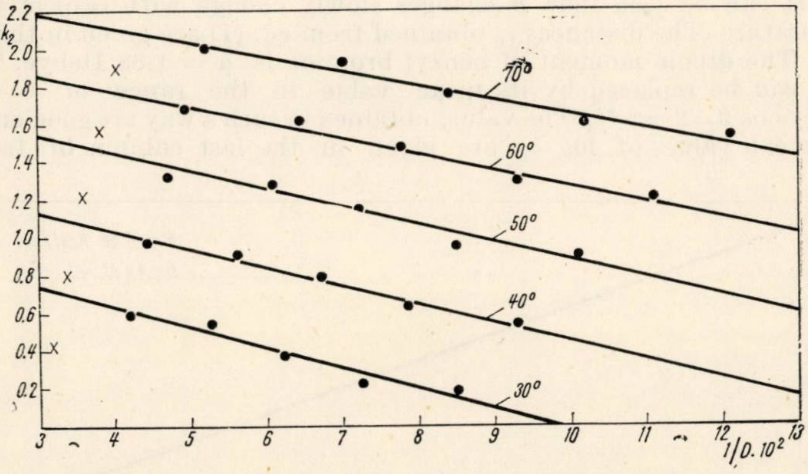

Fig. 2. — Influence of dielectric constants on the reaction rates.

The values log k_0 calculated by using equation (5) are given in table 6.

Table 6

The values of log k_0 ($cm^3\ mol^{-1}\ sec^{-1}$) calculated by using equation (5), at differen temperatures

System PhCH$_2$Br + / Temperature	30°	40°	50°	60°	70°
CH_3ONa	(0.753)*	(1.139)	(1.543)	(1.890)	(2.222)
C_2H_5ONa	1.022	1.395	1.749	2.102	2.434
nC_3H_7ONa	1.079	1.441	1.821	2.161	2.473
nC_4H_9ONa	1.028	1.424	1.798	2.122	2.418
$nC_5H_{11}ONa$	0.993	1.383	1.721	2.083	2.407
$nC_6H_{13}ONa$	1.066	1.424	1.806	2.140	2.475

* The values given in brackets, regarding sodium methoxide, were not included in the mean value of log k_0.

Here, log k_2 are experimental rate constants for bimolecular reactions under investigation (log $k_2 = \log k_{D,o}$) and B was determined at the different temperatures from the slopes of the plots given in figure 2. The values of B constant are given in table 7.

Table 7

Values of B, r_0 and (log $k_0)_{\text{mean}}$ at different temperatures

T^0	B	r_0(Å)	(log k_0) m
30	10.47	2.44	1.04
40	9.61	2.50	1.41
50	9.04	2.54	1.78
60	8.46	2.58	2.12
70	7.88	2.64	2.44

It can be seen that B changes slowly enough with respect to the temperature. The distances r_0 obtained from eq. (7) are given in the same table. The dipole moment of benzyl bromide is $\mu = 1.88$ Debye, [14] and $\cos\,\theta$ can be replaced by its mean value in the range of $0 - \pi/2$, namely $\cos\,\theta = 2/\pi \simeq {}^2/_3$. The values obtained in such a way are good enough. The mean values of $\log\,k_0$ are given in the last column of table 7.

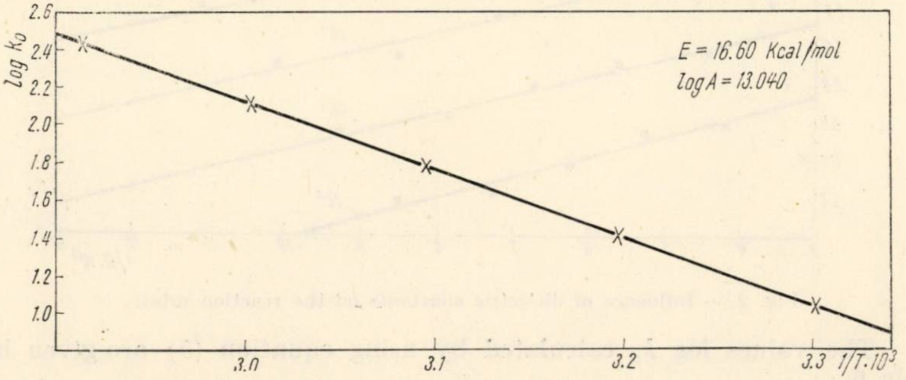

Fig. 3. — Influence of temperature on the reaction rates.

Each mean value was calculated by mediating $\log\,k_0$ for all systems, except methyl alcohol, at the same temperature. These mean values of $\log\,k_0$ can be used for estimation of the Arrhenius energy of activation E and A constant, applying the usual graphical method (fig. 3).

All the reactions under investigation occur with the same activation energy namely 16.600 kcal mol^{-1}. The reactions with sodium methoxide have a special behaviour, making an exception from these regularities. The A factor of Arrhenius equation is smaller than the calculated values obtained by using the simple collision theory. Thus, we have found $\log A_{\text{exp}} = 13.040$ compared to the calculated value $\log A_{\text{calc}} = 14.339$. The latter figure is a mean value for all studied systems, calculated at the mean working temperature (50°) as done in a previous paper [12].

DISCUSSION

Experimental data show that the studied reactions are ion-dipole reactions. The theoretical equation used for taking into account the solvent influence on the electrostatic interactions, harmonizes well with experimental data. Taking into account these interactions, one can conclude that all reactions occur with the same activation energy, namely 16.000 kcal mol^{-1}. This figure is by 4.300 kcal mol^{-1} smaller than the corresponding value for benzyl chloride-sodium alcoxides systems [12]. This decrase in activation energy takes place to the same effect as the decrease of bond energy from 66.5 kcal mol^{-1} for C—Cl bond, to,

---

[14] H. Mohler, *Helv. Chim. Acta*, **21**, 67 (1938).

54.0 kcal mol^{-1} for C-Br bond.[15] One must expect such a change since the breaking bond energy is closely connected with the activation energy.[16] The quantitative explanation of the activation energy in such systems meets with difficulties since solvation and desolvation energies of reagents, products and transition state play a prominent part when chemical changes take place in the solution, and their accurate values are generally unknown. The deviations from the regularities recorded for these systems, in the case of the reactions taking place in methyl alcohol, are probably due to such solvation effects.

The greater dielectric constant of methyl alcohol implies a greater solvation efficiency. Thus, while all products are soluble in methyl alcohol (in the studied concentration ranges), in the other alcohols, sodium bromide as a product resulting from the reaction is insoluble (hardly soluble) and separates from the system as a precipitate (in the same concentration range). The insoluble product occurring in the course of reaction favours perhaps the evolution of the transition state towards final products, increasing the reaction rate. The preponderance of this effect in comparison with the dielectric constant changing effect might explain the reaction rate increase when passing from methyl to ethyl alcohol. When reactions occur in all the other alcohols, except methyl alcohol, the changes in rate constants depending on the reacton medium can be properly explained on the basis of the dielectric constant variation.

The decrease of the experimental pre-exponential factor A in comparison with the calculated value by using the collision theory ($\log A_{\text{exp}} = 13.040$ as compared to $\log A_{\text{calc}} = 14.339$) is perhaps due to a "cage" effect. Because of this effect the "encounter" number between reactant particles is diminished. This effect is more pronounced for benzyl bromide than for benzyl chloride,[12] since the greater halogen volume makes the escape from the "cage" more difficult.

The studied reactions occur through nucleophilic attack of the alcoxide ion on saturated carbon, according to a mechanims previously proposed.[12] However, the transition-state structure is more complicated because of the solvent molecule assistance and the reaction mechanism cannot be reduced to the simple image of backside attack.

---

[15] O. A. Reutov, *loc. cit.*, Annex, Table 4.

[16] E. F. Caldin, *J. Chem. Soc.*, **1959**, 3345.

Revue Roumaine de Chimie, **15**, 309–311 (1970)

CHARGE TRANSFER COMPLEXES OF THE AROMATIC HETEROCYCLES. II*

CT-COMPLEXES OF PHENOXATELLURINE AND SOME OF ITS DERIVATIVES WITH TCNE

A. GIOABĂ, V. EM. SAHINI and ELENA VOLANSCHI

Department of Physical Chemistry
University of Bucharest, Bdul Republicii 13

Received July 23, 1969

Optical spectra of the CT- complexes of phenoxatellurine and some substituted derivatives with tetracyanoethylene are given and discussed. Ionisation potentials of the donors are determined and correlated with Hückel MO calculations.

Charge transfer complexes with phenoxatellurine as donor were not mentioned in literature till 1969, when the complexes with s-trinitrobenzene and picric acid were reported. [1] In the present paper, the spectral behaviour of the charge transfer (CT) complexes obtained with tetracyanoethylene (TCNE) as acceptor, and phenoxatellurine and its 2, 8 — substituted derivatives as donors, were studied. The results are correlated with ionisation potentials and MO calculations, in the frame work of the Hückel method.

EXPERIMENTAL

Phenoxatellurine, 2,8-difluoro, 2,8-dichloro-and 2,8-dimethyl-phenoxatellurine were synthetised and purified as described in previous works.[2,3]

Tetracyanoethylene was used as electron acceptor and anhydrous carbon tetrachloride, methylene chloride and nitromethane as solvents. The range of concentrations was 5×10^{-3}—5×10^{-2} M for both donor and acceptor. The spectra were recorded at a Beckmann DK-2 spectrophotometer in the range 350—900 mμ, using a path length of 1 cm.

---

* Note I — M. Hillebrand, O. Maior and V. Sahini, *Rev. Roumaine Chim.* (in press).

[1] B. Hetnarski and W. Hofman, *Bull. Acad. Polonaise Sci.*, **17**, 1 (1969).

[2] A. Gioabă, V. Em. Sahini and El. Volanschi, *Rev. Roum. Chim.* (to be published).

[3] G. Vasiliu and A. Gioabă, Rev. Chim. (Bucureşti), **20**, 357 (1969).

RESULTS AND DISCUSSION

The formation of a CT-complex between TCNE and the studied donors is characterized by the appearance of a band on the range 600—750 mμ, which does not exist in the spectra of the individual components. The broad shape of these CT-bands prevents very accurate measurement of peak maxima. Therefore the absorption maxima are located in a range of ±5 mμ. The experimental data are listed in table 1.

Table 1

Optical spectra ($\lambda_{m\mu}$) of the charge transfer complexes

Solvent Donor	CCl_4	CH_2Cl_2	NO_2CH_3
Phenoxatellurine	700±3	707±3	665±5
2,8-dimethyl-phenoxatellurine	717±3	730±5	700±5
2,8-dichloro-phenoxatellurine	655±5	660±3	610±5
2,8-difluoro-phenoxatellurine	620±5 infl.	640±3	610±3

A general remark made throughout this work was the lack of stability of these complexes at room temperature. Therefore the spectra were taken at a slightly lower temperature (about 10—12°).

It may be seen from table 1 that polar solvents like nitromethane shift the CT-band towards shorter wavelengths. This might be due to the solvatation of the tellurium atom which renders more difficult the formation of the charge transfer complex.

It was also stated that methyl substitution in the rings of the donor molecule facilitates the CT-transition, that is, shifts it towards longer wavelengths in all the solvents used. On the contrary, the fluoro-or chloro-substitution diminishes the donor properties of phenoxatellurine.

H. Kuroda et al.[4] give a correlation curve of the frequency of the CT-band to the ionisation potentials of the donors; the curve was obtained in the study of the CT-complexes of TCNE with several donors in methylene chloride. Using their equation:

$$0.87\, I_p = h\nu_{CT} + 4.86 \text{ eV},$$

with our $h\nu\ CT$ data, the ionisation potentials of the donors were obtained. They are given in table 2 and they are ordered as expected from the inductive effect of the substituents.

The ionisation potential may be correlated with the highest occupied MO by a linear relation. Hückel calculations on phenoxatellurine

---

[4] H. Kuroda, M. Kobayashi, M. Kinoshita and S. Takomotu, *J. Chem. Phys.*, **36**, 457 (1962).

Table 2

Ionisation potentials and the energy of the highest occupied molecular orbital

Donors	I_p (eV)	OM (β units)
Phenoxatellurine	7.60	0.4808
2,8-dimethyl- -phenoxatellurine	7.54	0.4651
2,8-dichloro- -phenoxatellurine	7.74	0.5239
2,8-difluoro- -phenoxatellurine	7.81	0.5361

2,8-dimethyl- and 2,8-dichloro-phenoxatellurine were performed in a previous work and were discussed related to the UV spectra of these compounds.[2]

For 2,8-difluoro-phenoxatellurine, an inductive model was used with :

$$\alpha_F = \alpha_C + 1.5\ \beta$$

$$\beta_{CF} = \beta_{CC}$$

The parameters of the tellurium and oxygen atoms were the same as those used for the other phenoxatellurines, i.e. $h_{Te} = 1.00$, $k_{CTe} = 0.57$, $h_0 = 2.00$, $k_{CO} = 0.71$.[2]

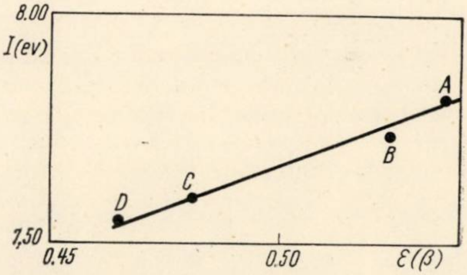

Fig. 1.—Dependence of the I_p of the donors on the highest occupied MO energy.

A, 2,8-difluorophenoxatellurine. *B*, 2,8-dichlorophenoxatellurine: *C*, phenoxatellurine *D*,2,8-dimethylphenoxatellurine.

The plot of the ionisation potentials obtained above *vs.* the energy of the highest occupied MO in β units indicates a good linear dependence, as it may be observed in figure 1.

Revue Roumaine de Chimie, **15**, 313–323 (1970)

THERMODYNAMICS OF THE BEHAVIOUR OF Pb(II)-IONS IN ACID AND ALKALINE SOLUTION

ZLATA PAVLOVIĆ and R. POPOVIĆ

Department of Analytical Chemistry, Faculty of Technology, Tuzla, Yugoslavia

Received November 12, 1968

Taking into account the dependence of ΔG°-values on the hydrolysis products of lead ions and the number of the linking OH^--groups it can be concluded that for mononuclear hydrolysis products this dependence expressed as a linear function differs from the same dependence when this concerns polynuclear products. The ΔG°-values for the ions existing in strong alkaline solution were considered in a similar way. The values assumed for the free energy of formation are:

$$\Delta G^\circ_{PbO_2^{2-}} = -63 \text{ kcal/mol}$$

$$\Delta G^\circ_{Pb(OH)_2} = -97 \text{ kcal/mol}$$

$$\Delta G^\circ_{Pb(OH)_3^-} = -138 \text{ kcal/mol}$$

$$\Delta G^\circ_{Pb(OH)_4^{2-}} = -177 \text{ kcal/mol}$$

All these ΔG°-values were checked by considering the homogeneous and the heterogeneous equilibria in the considered system and they may be taken as most probable.

INTRODUCTION

The present thermodynamical consideration has its inception in an effort to obtain data on the free energy of formation of ΔG° (kcal/mol) of PbO_2^{2-}-ions and the dissolved Pb-hydroxide, which could not be found in literature. In other words, the hydrolysis process of Pb(II)-ions was treated from the standpoint of electrochemical thermodynamics and the amphoteric behaviour of the Pb(II)-hydroxide as well.

The ΔG°-values for some polynuclear species are calculated from hydrolysis constants given by Carrel and Olin [1] and Pajdowsky and Olin [2] who discovered some unknown polynuclear hydrolysis products of Pb(II)-ions.

Our earlier considerations pointed out that the dependence between the ΔG°-values of hydrolysis products and the number of the consisting OH^--groups can be considered as close to linear.[3,4] This fact was observed considering these relations for various bivalent metal ions, and rather good agreements with the experimental results from several authors were reached, as for instance for zinc with the data of Charlot,[5] for mercury with the data of Ahlberg,[6] or for cadmium according to Biederman.[7]

---

[1] B. Carrel and Å. Olin, *Acta Chem. Scand.*, **16**, 2350 (1962).

[2] L. Pajdowsky and Å. Olin, *Acta Chem. Scand.*, **16**, 983 (1962).

In a similar way the amphoteric behaviour of the various Me(II)-hydroxides has been observed, i.e. the dependence between the $\Delta G°$-values of the products of acid ionisation of Me(II)-hydroxides and the number of the liberated hydrogen ions, starting from the $\Delta G°$-values of the dissolved Me(II)-hydroxide.[8] The considerations of the above mentioned relations have made possible the prediction of the unknown $\Delta G°$-values of some types of Me(II)-ions existing in aqueous solutions within the pH-range 0—14. The graphical representations of homogeneous and heterogeneous equilibria for such a system were made with the aim to check the probability of the predicted $\Delta G°$-values of the dissolved $Pb(OH)_2$, PbO_2^{2-}-ions and $Pb(OH)_3^-$- and $Pb(OH)_4^{2-}$-ions as well.

The known thermodynamical interpretation of the system Pb-aqueous solution by Pourbaix[9] can be made more complete due to these thermodynamical considerations.

THE STANDARD FREE ENERGY OF FORMATION $\Delta G°$ (kcal/mol) OF Pb(II)-HYDROLYSIS PRODUCTS

First, all the known $\Delta G°$-values of the existing Pb(II)-ions in acid and alkaline solutions were collected and also $\Delta G°$ of the solid Pb(II)-hydroxide according to Latimer[10] and Pourbaix,[9] and those calculated according to the data of Charlot.[5] The $\Delta G°$-values of the polynuclear hydrolysis products were calculated from the equilibrium constants of Pb-hydrolysis process[1]. and represented in table 1.

The relationship between the $\Delta G°$-values for the Pb(II)-hydrolysis products and the number of the linking OH^--groups is represented graphically in figure 1.

In the given diagram $\Delta G°$-n.OH^- (Fig.1), the $\Delta G°$-value of Pb(II)-ions is taken as the starting point (at n.OH^- =0). For the final product of hydrolysis of Pb(II)-ions, i.e. for the solid Pb(II)-hydroxide the known $\Delta G°$-value is inserted at n.OH^- =2[10]. At the same time the calculated

---

[3] T. Marković and Z. Pavlović, *Werkstoffe u. Korrosion*, **6**, 472 (1965).

[4] T. Marković, Z. Pavlović and E. Nad, *Werkstoffe u. Korrosion*, **17**, 957 (1966).

[5] G. Charlot, "Les méthodes de la Chimie analytique", Paris, 1963, Masson et Cie, p. 44.

[6] I. Ahlberg, *Acta Chem. Scand.*, **16**, 887 (1962).

[7] G. Biedermann and L. Chiavatta, *Acta Chem. Scand.*, **15**, 1347 (1961); **16**, 2221 (1962).

[8] Z. Pavlović, D. Dodig and J. Grganović, *Thermodynamics of Formation of* $Cu(OH)_2$, $Cu(OH)_3^-$ *- and* $Cu(OH)_4^{2-}$ *- Ions and the Experimental Verification of the Processes*, 2nd J.U.P.A.C. -Congress, Beograd, 1966.

[9] M. Pourbaix, "Atlas d'équilibres électrochimiques", Paris, Gauthier-Villars et Cie, 1963, p. 485.

[10] M. W. Latimer, "Oxidation Potentials", New York, Prentice-Hall, p. 150.

$\Delta G°$-values of $Pb(OH)_2\downarrow$ after Charlot's data are inserted into the same diagram. Consequently, the $\Delta G°$-value of the mononuclear Pb(II)-hydrolysis product is inserted at $n.OH^- = 1$.

Table 1

Standard free energy of formation $\Delta G°$ (kcal/mol) on lead

Formula	$\Delta G°$ kcal/mol
Pb^{2+}	$-\ 5.81$[10]
$Pb(OH)_2\downarrow$	-100.6[10]
	(-101.48) (-102.84)[1,5]
$PbOH^+$	$-\ 51.73$[1]
Pb_2OH^{3+}	$-\ 59.70$[1]
$Pb_3(OH)_4^{2+}$	-213.22[1]
$Pb_4(OH)_4^{4+}$	-223.75[1]
$Pb_6(OH)_8^{4+}$	-430.99[1]
$HPbO_2^-$	$-\ 81.00$[9,12]
H_2O	$-\ 56.69$[10]
OH^-	$-\ 37.595$[10]

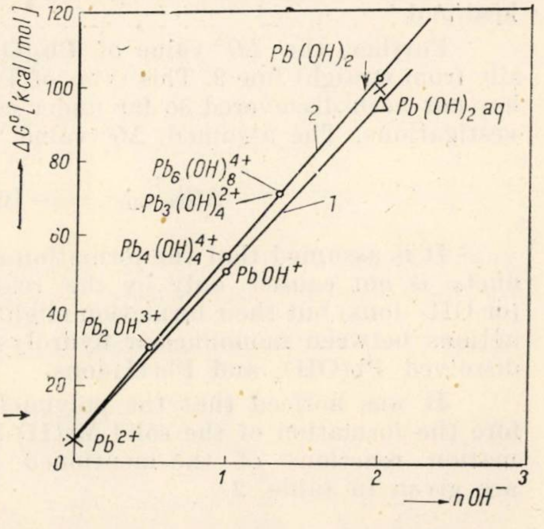

Fig. 1. — Dependence of $\Delta G°$-values of → Pb-hydrolysis products and the number of the linking OH^--groups.

1, Latimer's data; *2*, calculated values from the known equilibria constants; *3*, graphically predicted values.

As for polynuclear hydrolysis products Pb_2OH^{3+}, $Pb_3(OH)_4^{2+}$ and others[1] the respective $\Delta G°$-values are inserted into the same diagram at the number of OH^--groups relating to one lead atom.

From earlier analogous considerations on hydrolysis products of some Me(II)-ions the following conclusion has been obtained: the respective $\Delta G°$-values of polynuclear hydrolysis products of Me(II)-ions lie either very close to the straight line, obtained by connecting the point for Me(II)-ions and that for the solid Me(II)-hydroxide,[11] or just upon it. In the diagram (Fig. 1) it is represented by straight line 2.
After connecting the starting point with the points for the mentioned polynuclear hydrolysis products and taking the latter to be strictly correct, the straight line 2 is obtained. In this way the graphically predicted $\Delta G°$-value of the solid Pb(II)-hydroxide would be:

$$\Delta G° Pb(OH)_2\downarrow\ = -103 \text{ kcal/mol.}$$

This value is slightly different from the known and from the calculated values, as can be seen from table 1. Comparing the $\Delta G°$-values, of the dissolved Pb(II)-hydroxide it is apparent that the transformation of the dissolved form into the solid state is spontaneous. In other words, the formation of the dissolved Pb(II)-hydroxide precedes the formation of the solid phase which can be given by the reaction

$Pb(OH)_2 \rightarrow Pb(OH)_2\downarrow$ developing with the $\Delta G°$-change as $\Delta G^°_R = -3.6$ kcal/mol taking into account Latimer's data. According to Charlot's data, this value would be within the range of -4.48 and -5.84 kcal/mol. Finally, using the graphically obtained ΔG°-value for the solid Pb(II)-hydroxide, the change of ΔG°-values of the mentioned transformation would be -6 kcal/mol.

---

[11] J. Brenet, Z. Pavlović and Dodig, *J. Chem. phys.*, **66**, 78 (1969).

[12] A. B. Garret, S. Vellenga and C. M. Fontana, *J. Amer. Chem. Soc.*, **61**, 367 (1939).

Further, the ΔG°-value of $Pb_2(OH)_3^+$-ions was predicted graphically from straight line 2. This type of Pb-polynuclear hydrolysis product has not been discovered so far under conditions of the experimental investigations. The assumed ΔG°-value would be

$$\Delta G^\circ_{Pb_2(OH)_3^+} = -160 \text{ kcal/mol.}$$

It is assumed that the formation of the polynuclear hydrolysis products is not caused only by the reaction between Pb-ions and water (or OH^--ions) but their formation might also be a consequence of interactions between mononuclear hydrolysis products $PbOH^+$-ions and the dissolved $Pb(OH)_2$ and Pb(II)-ions.

It was noticed that the polynuclear species were formed just before the formation of the solid Me(II)-hydroxide. All the supposed formation reactions of the mentioned polynuclear hydrolysis products are given in table 2.

Table 2

ΔG°-values of the reactions of the formation of the polynuclear hydrolysis products

	Chemical reaction	ΔG_R° kcal/mol
1.	$Pb^{2+} + OH^- \rightleftharpoons PbOH^+$	-8.33
2.	$2Pb^{2+} + OH^- \rightleftharpoons Pb_2OH^{3+}$	-10.50
	$PbOH^+ + Pb^{2+} \rightleftharpoons Pb_2OH^{3+}$	-2.16
3.	$3Pb^{2+} + 4OH^- \rightleftharpoons Pb_3(OH)_4^{2+}$	-45.41
	$Pb^{2+} + 2Pb(OH)_2 \rightleftharpoons Pb_3(OH)_4^{2+}$	-13.41
	$2PbOH^+ + Pb(OH)_2 \rightleftharpoons Pb_3(OH)_4^{2+}$	-12.76
	$Pb^{2+} + PbOH^+ + Pb(OH)_2 \rightleftharpoons Pb_3(OH)_4^{2+}$	-58.68
4.	$4Pb^{2+} + 4OH^- \rightleftharpoons Pb_4(OH)_4^{4+}$	-60.13
	$Pb^{2+} + 2PbOH^+ + Pb(OH)_2 \rightleftharpoons Pb_4(OH)_4^{4+}$	-17.48
	$4PbOH^+ \rightleftharpoons Pb_4(OH)_4^{4+}$	-16.83
	$2Pb(OH)_2 + 2Pb^{2+} \rightleftharpoons Pb_4(OH)_4^{4+}$	-18.13
5.	$2Pb^{2+} + 3OH^- \rightleftharpoons Pb_2(OH)_3^+$	-35.59
	$PbOH^+ + Pb(OH)_2 \rightleftharpoons Pb_2(OH)_3^+$	-11.27
6.	$6Pb^{2+} + 8OH^- \rightleftharpoons Pb_6(OH)_8^{4+}$	-95.64
	$Pb^{2+} + 3Pb(OH)_2 + 2PbOH \rightleftharpoons Pb_6(OH)_8^{4+}$	-30.72
	$Pb_2OH^{3+} + PbOH^+ + 3Pb(OH)_2 \rightleftharpoons Pb_6(OH)_8^{4+}$	-28.56
	$Pb_4(OH)_4^{4+} + 2Pb(OH)_2 \rightleftharpoons Pb_6(OH)_8^{4+}$	-13.24

The ΔG°-values of the quoted reactions imply that the supposed mechanism of the hydrolysis process be thermodynamically possible. It is quite evident that this mechanism would be very difficult to prove experimentally.

In a similar way the mechanism of the formation of the solid Pb(II)-hydroxide was considered, i.e. through the calculation of the ΔG°-

values of the formation reactions of the solid Pb(II)-hydroxide, where all the mentioned components of the hydrolysis products are taken into account.

Table 3

ΔG°-values of reactions of formations of the solid Pb-hydroxide

Chemical reaction	ΔG°_R kcal/mol $Pb(OH)_2\downarrow$
1. $Pb^{2+} + 2OH^- \rightleftharpoons Pb(OH)_2\downarrow$	-20.60
2. $Pb_2OH^{3+} + 3OH^- \rightleftharpoons 2Pb(OH)_2\downarrow$	-14.56
3. $PbOH^+ + OH^- \rightleftharpoons Pb(OH)_2\downarrow$	-11.27
4. $Pb_3(OH)_4^{2+} + 2OH^- \rightleftharpoons Pb(OH)_2\downarrow$	$-\ 4.46$
5. $Pb_4(OH)_4 + 4OH^- \rightleftharpoons 4Pb(OH)_2\downarrow$	$-\ 7.07$
6. $Pb_2(OH)_3 + OH^- \rightleftharpoons 2Pb(OH)_2\downarrow$	$+\ 1.79$
7. $Pb_6(OH)_8 + 4OH^- \rightleftharpoons 6Pb(OH)_2\downarrow$	$-\ 3.70$
8. $Pb(OH)_2 \rightleftharpoons Pb(OH)_2\downarrow$	$-\ 3.60$

Comparing the obtained ΔG°-values of the quoted reactions, it can be concluded that the spontaneousness of these reactions decreases as higher polynuclear hydrolysis products take part in the observed reactions. However all the mentioned reactions can be taken as thermodynamically possible.

AMPHOTERIC BEHAVIOUR OF THE Pb(II)-HYDROXIDE

The dissolution process of the solid Pb(II)-hydroxide in sufficiently alkaline solutions is considered from the standpoint of the electrochemical thermodynamics too. After the classical conception of amphoteric behaviour of Pb(II)-hydroxide in alkaline solution, the following reactions can be written:

$$Pb(OH)_2 \rightarrow HPbO_2^- + H^+$$

$$Pb(OH)_2 \rightarrow PbO_2^{2-} + 2H^+$$

The ΔG°-value of PbO_2^{2-}-ions could not be found in literature. In similar considerations for zinc[4] and copper,[8] the ΔG°-values of similar kind of ions were known, or could have been calculated from the respective equilibrium constants. The ΔG°-values of the dissolved metal hydroxides could be calculated as well. In the above cases a very close linear relationship existed between the ΔG°-values of mentioned ions and the number of the released H^+-ions.

Applying this conclusion to the considered system it is possible to predict graphically the unknown ΔG°-value for the PbO_2^{2-}-ions.

In figure 2 the ΔG°-n.OH^- (n.H^+)-diagram is represented. As can be seen from straight line 3, the ΔG°-value of the dissolved Pb(II)-hydroxide is taken as the starting point (at n.$H^+ = 0$). The known ΔG° of $HPbO_2^-$-ions is plotted against the number of released H^+-ions (n.H^+=1).

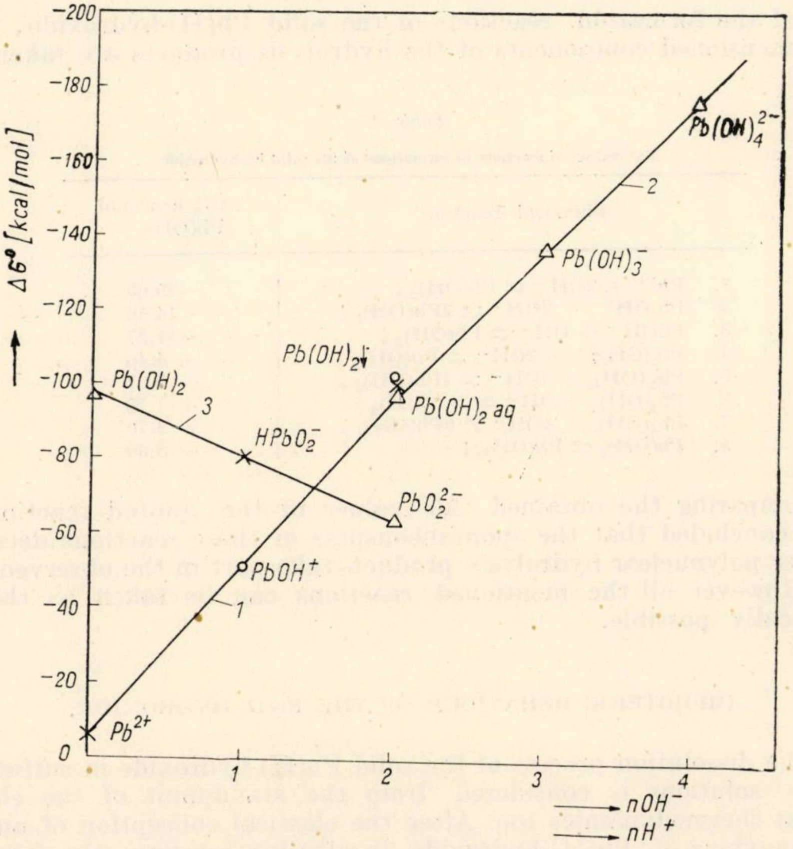

Fig. 2. $-\Delta G^\circ$ (kcal/mol)-n.OH^-(n.H^+)-diagram for the mononuclear species of Pb(II)-ions.

Thus, the predicted ΔG°-value of the PbO_2^{2-}-ions (at $nH^+ = 2$) would be :

$$\Delta G_{PbO_2^{2-}} = -63 \text{ kcal/mol}$$

However, according to a more recent theory of complex ions the formation of the previously considered ions is observed over the formation of tri- and tetra-hydroxocomplexes, as shown by the following reactions :

$$Pb(OH)_2 + OH^- \rightleftharpoons Pb(OH)_3^-$$

$$Pb(OH)_2 + 2OH^- \rightleftharpoons Pb(OH)_4^{2-}$$

In a sufficient concentration of OH^--ions the dissolved Pb(II)-hydroxide reacts with OH^--ions producing $Pb(OH)_3^-$ and $Pb(OH)_4^{2-}$, respectively. These complexes can be transformed into the above mentioned ions by the dehydration process :

$$Pb(OH)_3^- \rightleftharpoons HPbO_2^- + H_2O$$

$$Pb(OH)_4^{2-} \rightleftharpoons PbO_2^{2-} + 2H_2O$$

In all the similar systems so far observed, the ΔG°-change of the dehydration reaction was so low that it could be neglected.

Taking into account the known ΔG°-value of $HPbO_2^-$-ions and the predicted ΔG°-value of $HPbO_2^-$ -ions, as a probable one, and using the hydration reaction the ΔG°-values of hydrocomplexes could be calculated:

$$\Delta G^\circ_{Pb(OH)_3^-} = -138 \text{ kcal/mol}$$

$$\Delta G^\circ_{Pb(OH)_4^{2-}} = -177 \text{ kcal/mol}$$

In figure 2 ΔG°-values of the mononuclear hydroxocomplexes depending on the number of the consisting $OH^=$-groups are represented by straight lines 1 and 2. That means: the straight line 1 refers to the mononuclear $PbOH^+$-ions up to the formation of the dissolved $Pb(OH)_2$ and further, straight line 2 represents the relationship of the terms if the number of the linking OH^--groups is greater than those in the dissolved Pb-hydroxide. The slopes of these two straight lines are different, which can be considered as reasonable, since the ways of the linking of OH^--ions are different too.

Using the above mentioned ions and hydroxides as a basis, the following scheme may be given for the behaviour of the solid $Pb(OH)_2$ in alkaline solution:

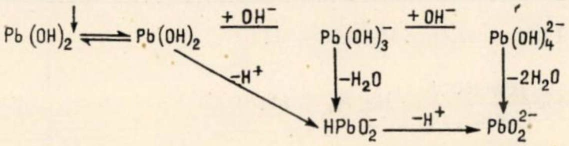

In the above scheme the formation of $HPbO_2^-$- and PbO_2^{2-}-ions is represented according to the theory of complex ions. Tri- and tetra-$Pb(OH)_3^-$ and $Pb(OH)_4^{2-}$ undergo dehydration thus being transformed into $HPbO_2^-$- and PbO_2^{2-}-ions. The equilibrium between two phases of Pb-hydroxide (solid and dissolved) is shifted permanently during the formation of the mentioned hydroxocomplexes. The classical explanation of the behaviour of amphoteric hydroxides in alkaline solution, is also included. The dissolved Pb(II)-hydroxide may ionize as in acid forming $HPbO_2^-$ -ions as the first product and PbO_2^{2-} -ions as the second product of the ionisation respectively.

DISTRIBUTION OF MONONUCLEAR Pb-HYDROXOCOMPLEXES AS A FUNCTION OF pH-VALUE OF SOLUTION

Both the predicted and the calculated ΔG°-values of the mentioned species of Pb-ions are checked by considering pH-region of the stability of the mentioned Pb-ions. In other words, the homogeneous equilibria are observed.

Using the already known and the predicted ΔG°-values of all the components, the ΔG°-values of various reactions, which are possible within the considered system, were calculated. According to the well known expression

$$\Delta G^\circ_R = -RT \ln K$$

and for 25°

$$\Delta G^\circ_R = -1.3463 \log K$$

the equilibrium constants are calculated. The ΔG°_R represents the difference between the sum of the ΔG°-values of products $(\Sigma \Delta G^\circ_p)$ and the sum of the ΔG°-values of reactants $(\Sigma \Delta G^\circ_r)$ for each of the given reactions.

$$\Delta G^\circ_R = \sum \Delta G^\circ_p - \sum \Delta G^\circ_r$$

In table 4 all the considered reactions are represented and also the most convenient expressions for the graphical representations.

Table 4

Chemical reactions and respective expressions to construct the diagram of homogeneous equilibria

Chemical reaction and respective expression	pK
1. $Pb^{2+} + H_2O \rightleftharpoons PbOH^+ + H^+$	
$\log \frac{[PbOH^+]}{[Pb^{2+}]} = \log K_1 + pH$	7.9
2. $PbOH^+ + H_2O \rightleftharpoons HPbO_2^- + 2H^+$	
$\log \frac{[HPbO_2^-]}{[PbOH^+]} = \log K_2 + 2pH$	20.1
3. $HPbO_2^- \rightleftharpoons PbO_2^{2-} + H^+$	
$\log \frac{[PbO_2^-]}{[HPbO_2^-]} = \log K_3 + pH$	13.2
4. $Pb^{2+} + 2H_2O \rightleftharpoons Pb(OH)_2 + 2H^+$	
$\log \frac{[Pb(OH)_2]}{[Pb^{2+}]} = \log K_4 + 2pH$	16.2
5. $Pb(OH)_2 + H_2O \rightleftharpoons Pb(OH)_3^- + H^+$	
$\log \frac{[Pb(OH)_3^-]}{[Pb(OH)_2]} = \log K_5 + pH$	11.5
6. $Pb(OH)_3^- + H_2O \rightleftharpoons Pb(OH)_4^{2-} + H^+$	
$\log \frac{[Pb(OH)_4^{2-}]}{[Pb(OH)_3^-]} = \log K_6 + pH$	13.1

The reactants in the given reactions are marked *A* and the products *B* respectively in the following graphical representations. Reactions 1, 2 and 3 are represented in figure 3. It can be seen from the diagram that the formation of the simple hydrolysis product $PbOH^+$ can occur if the pH is above 7. This sort of ions can be transformed into $HPbO_2^-$-ions if the pH-value of solution is within 9–11. Further, the formation of the final product of an acid ionisation of Pb-hydroxide, i.e. the formation of PbO_2^{2-}-ions, is possible in a strong alkaline solution (pH >13).

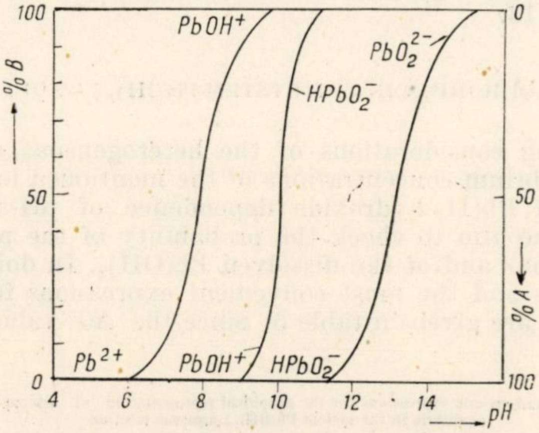

Fig. 3. — Dependence of the distribution of Pb^{2+}-, $PbOH^+$-, $HPbO_2^-$- and PbO_2^{2-}-ions in solution, on pH-values.

In the same manner, the stability of Pb^{2+}-ions, relating to the formation of the dissolved $Pb(OH)_2$, and further the pH-region of the stability of tri- and tetra-hydrocomplexes are represented in figure 4.

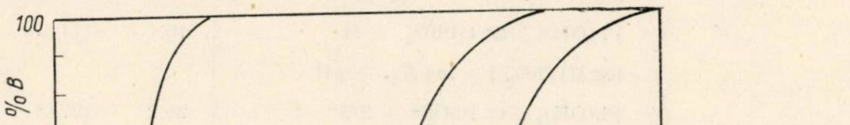

Fig. 4. — Graph of homogeneous equilibriums between Pb(II) -ions, $Pb(OH)_2$ (diss), and $Pb(OH)_3^-$ and $Pb(OH)_4^{2-}$-ions.

It is obvious that the pH-region of Pb(II)-ions-stability against the dissolved $Pb(OH)_2$ is possible if the pH-value is below 7. The dissolved Pb-hydroxide can be formed within pH-range 7 — 10. The increase of pH-value causes the transformation of the dissolved $Pb(OH)_2$ into $Pb(OH)_3^-$-ions. The stability of $Pb(OH)_4^{2-}$-ions is expressed if the pH-value is above 13.

HETEROGENEOUS EQUILIBRIA IN THE SYSTEM $Pb(OH)_2\downarrow$ —AQUEOUS SOLUTION

The following considerations of the heterogeneous equilibria, i.e. the possible equilibrium concentrations of the mentioned ions in the presence of the solid Pb(II)-hydroxide dependence of pH-solution, were also made with the aim to check the probability of the predicted $\Delta G°$-values of PbO_2^{2-}-ions and of the dissolved $Pb(OH)_2$. In doing so, certain chemical reactions and the most convenient expressions for the graphical representation are given in table 5. Since the $\Delta G°$-values of the solid Pb(II)-hydroxide are different, all calculations were made using the two extreme $\Delta G°$-values for the solid $Pb(OH)_2$. The results, i.e. the calculated equilibrium constants obtained by the use of $\Delta G°$-value of $Pb(OH)_2\downarrow$ after Latimer, are given in parenthesis in table 5, and in the graphical representations by dashed lines. Taking into account the expressions in table 5, the diagram log a_i-pH for the system $Pb(OH)_2\downarrow$ —aqueous solution can be represented.

Table 5

Chemical equations and expressions for the graphical representation of heterogeneous equilibria in the system $Pb(OH)_2\downarrow$-aqueous-solution

	Chemical reaction and respective expression	pK	
1′	$Pb^{2+} + 2H_2O \rightleftarrows Pb(OH)_2 + 2H^+$	11.9	(13.8)
	$\log [Pb^{2+}] = -\log K_{1'} - 2\,pH$		
2′	$PbOH^+ + H_2O \rightleftarrows Pb(OH)_2 + H^+$	3.9	(5.7)
	$\log [PbOH^+] = -\log K_{2'} - pH$		
3′	$Pb(OH)_2 \rightleftarrows Pb(OH)_2$	4.4	(2.6)
	$\log [Pb(OH)_2] = -\log K_{3'}$		
4′	$Pb(OH)_2\downarrow \rightleftarrows HPbO_2^- + H^+$	16.1	(14.35)
	$\log [HPbO_2^-] = \log K_{4'} + pH$		
5′	$Pb(OH)_2\downarrow \rightleftarrows PbO_2^{2-} + 2H^+$	29.2	(27.5)
	$\log [PbO_2^{2-}] = \log K_{5'} + 2pH$		

Obviously, the different $\Delta G°$-values of the solid $Pb(OH)_2\downarrow$ taken in calculations have no influence on the pH-values of intersections of the given straight lines referring to the equilibrium concentrations for the considered Pb-ions. However, the values of the ions concentrations at the given pH-values differ remarkably. Considering the characteristic pH-region for the given sorts of Pb-ions, it may be seen that Pb^2-ions predominate in the system if the pH-value is below 8. Within the pH-range 8—10 the concentration of $PbOH^+$-ions is higher than that of unhydrolysed Pb(II)-ions. The lowest solubility of the Pb(II)-hydroxide is at pH = 10, where the concentrations of $HPbO_2^-$ - and $PbOH^+$-ions

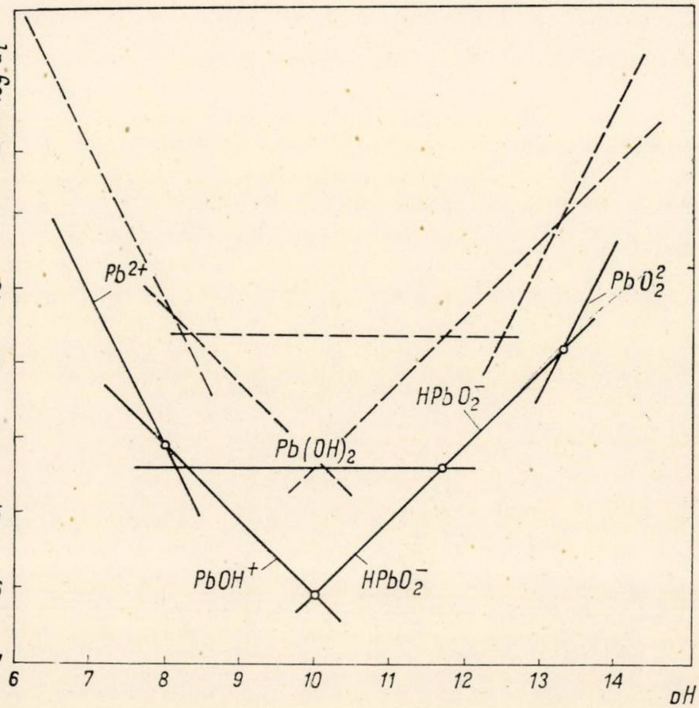

Fig. 5.—Log a_i-pH diagram of the system $Pb(OH)_2$-aqueous solution.

are equal. The intersection between the straight lines referring to $HPbO_2^-$- and PbO_2^{2-} -ions is at pH = 13.3. This implies that PbO_2^{2-}-ions predominate in the strong alkaline solution (pH >14).

If the dashed straight lines are considered in a similar way, it is obvious that within each of the above mentioned pH-regions remarkably higher equilibrium concentrations of Pb-ions may exist.

Of course, only with the results of experimental investigations of the system $Pb(OH)_2 \downarrow$ -aqueous solution it would be possible to prove which of all the mentioned ΔG°-values of $Pb(OH)_2 \downarrow$ might be taken as quite correct. But this is not the subject of the present thermodynamical considerations.

In any case, these thermodynamical considerations make the already well-known E(volt)-pH-diagram by Pourbaix more complete.

Revue Roumaine de Chimie, 15, 325–332 (1970)

THE POTENTIAL DISTRIBUTION AND THE SURFACE CHARGE AT THE SILICON-HYDROFLUORIC ACID INTERFACE

O. RADOVICI and VERONICA TUCSEK

Institute of Physical Chemistry of the Academy, Bucharest, str. Galaţi 31

Received March 6, 1969

The potential and charge distributions at the silicon-hydrofluoric acid interface have been measured by differential capacity measurements. The changes of these distributions due to the addition of copper ions to the solutions have been studied.

INTRODUCTION

An important characteristic of the semiconductor-electrolyte interface is the distribution of the potential difference over the double layer, the semiconductor surface film and the semiconductor space-charge region. A convenient way to study this characteristic is the comparison of the differential capacity of the interface *versus* potential, with the theoretical values computed for the semiconductor space charge. This problem, extensively studied for the germanium-electrolyte systems,[1-4] has been investigated by Memming[5] for the Si-HF case. He has observed that in the case of n-type Si, and 10 M HF, and with measurements carried out in the potential range +200 . . . −400 mV *vs.* saturated calomel electrode at 140 Kc, the experimental curves coincide with the theoretical ones. He has concluded that in this case the interface potential is completely confined to the semiconductor space-charge region.

In a preceding note [6] it has been shown that at 8000 c, in the potential range −300 . . . −500 mV the differential capacity values for n-type Si in 2.5 N HF are in agreement with the theoretical predictions for the semiconductor space-charge region, in the vicinity of the flat band potential. (A 1.3 rugosity factor has been assumed).

[1] K. Bohnenkamp and H. J. Engell, *Z. Elektrochem.*, **61**, 1184 (1957).
[2] M. Hofman-Pérez and H. Gerischer, *Z. Elektrochem.*, **65**, 771 (1961).
[3] W. H. Brattain and P. J. Boddy, *J. Electrochem. Soc.*, **109**, 574 (1962).
[4] P. J. Boddy and W.H. Brattain, *J. Electrochem. Soc.*, **109**, 812 (1962).
[5] R. Memming and G. Schwandt, *Surface Science*, **5**, 97 (1966).
[6] O. Radovici and Veronica Tucsek, *Rev. Roumaine Chim.*, **13**, 1549 (1968).

In the present paper the differential capacity measurements of Si-HF system for n-type silicon, 2.5 M HF are presented at the frequencies 800 and 8000 c, and the $+200 \ldots -700$ mV potential range. They allow us to study the potential and charge distributions at the interface.

EXPERIMENTS

(1, 1, 1) oriented, n-type, 100 Ω cm resistivity silicone single crystal electrodes[6] were used. The 2.5 M solution has been prepared by using HF e.g.; dilute solution of cupric sulfate was introduced into the HF solution at 10^{-6} M and 10^{-4} M concentrations.

The impedance of the interface, expressed by a capacity parallel connected with a conductance, was measured by using a Wayne Kerr a.c. bridge type 641 B, with both an external generator and an external null instrument. The electrode has been polarized by using a potentiostate. The a.c. measuring voltage superposed on the electrode potential was less than 10 mV. The measurements have been carried out, starting from the cathodic region to the anodic one, balancing the bridge for each value of the potential, for both requencies. The measuring time for each potential was about five minutes.

RESULTS

The current-voltage characteristic and the differential capacity curves for the Si-HF system were simultaneously determined on the polarization curve. It should by noticed (fig. 1.1) that the potential range $+200 \cdots -700$ mV, measured *vs.* saturated calomel electrode, corresponds to the blocked region of the semiconductor. This allows [6] the use of the reduced equivalent circuit (fig. 2 *a*). The significance of the elements Rs and Cs has to be determined.

The differential capacity curves, plotted in the same potential range (fig. 3) at 800 and 8000 c, have a rough logarithmic dependence of potential. At about 200 mV a shoulder (more pronounced at the lower frequency) may be observed.

The polarization and differential capacity curves for the Si-HF system with an addition of divalent copper ions in 2.5 M HF solution in a 10^{-6} M concentration, have been plotted (fig. 1.2, fig. 4). The presence of the copper ions changes both the polarization current (an increase of one order of magnitude has been observed) and the differential capacity. The variation of the capacity in the presence of copper ions is observed especially in the anodic range and at the lower frequency.

At higher Cu^{++} concentrations the polarization current is higher and the differential capacity changes qualitatively (fig. 5). In the cathode region the differential capacity is approximately independent of the potential, closely connected to the value of Cu-HF system. Compared with the preceding concentration (fig. 4) it increases with one order of magnitude. In the anodic region, in the $-200 \ldots -300$ mV range, it decreases with two orders of magnitudes intersecting the low concentration curve at -100 mV.

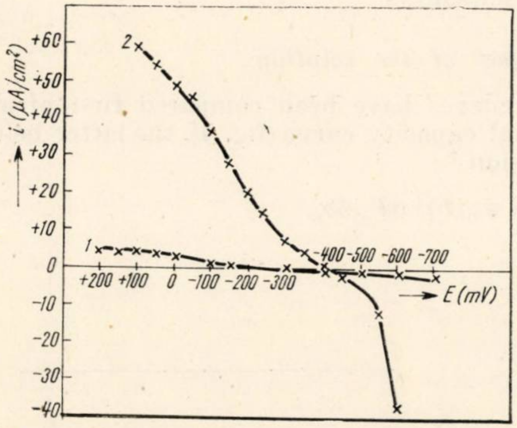

Fig. 1. — *1*, Current-voltage characteristic of Si-HF interface ; *2*, Current-voltage characteristic of Si-HF interface with 10^{-6} M Cu^{++} addition.

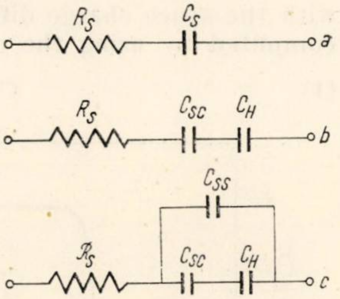

Fig. 2. — Equivalent circuit of Si-HF interface.

a) the reduced equivalent circuit; *b*) contribution of double layer; *c*) contribution of Cu^{++}.

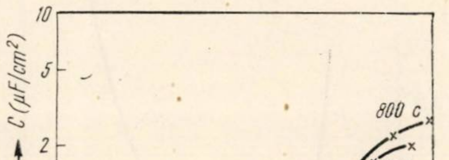

Fig. 3. — Differential capacity curves of Si-HF interface.

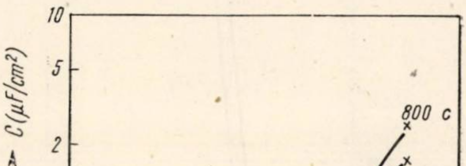

Fig. 4. — Differential capacity curves of Si-HF interface with 10^{-6}M Cu^{++} addition.

DISCUSSIONS

a) *The effect of the solution*

The differential capacity curves have been compared first of all, with the space charge differential capacity curve (fig. 6), the latter being computed by using the expression[7]:

$$C_{\mathrm{sc}} = (K \epsilon_0 / L) \, | \mathrm{d}F_{\mathrm{s}} / \mathrm{d}v_{\mathrm{sc}} | \tag{1}$$

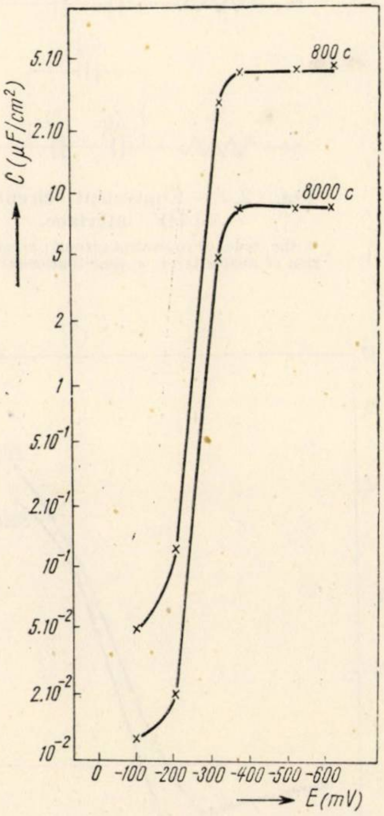

Fig. 5. — Differential capacity curves of Si-HF interface with 10^{-4}M Cu^{++} addition.

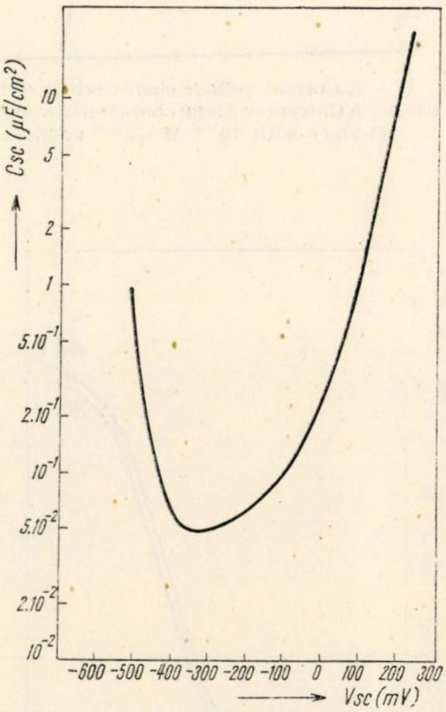

Fig. 6. — Calculated differential capacity of silicon space-charge.

where $L \equiv (K \epsilon_0 kT / q^2 N_{\mathrm{D}})^{1/2}$ represents the effective Debye length; K is the dielectric constant of silicon; ϵ_0 is the permittivity of the free space; q is the electronic charge; k is the Boltzmann's constant;

---

[7] A. MANY, Y. GOLDSTEIN and N. B. GROVER, "Semiconductor Surfaces", North-Holland Publ. Comp., Amsterdam, 1965, p. 222.

T is the absolute temperature; N_D is the concentration of the donor impurities, and

$$dF_s/dv_{sc} = (1/\sqrt{2})\,[\exp v_{sc} - \exp(-2u - v_{sc}) - 1]\,[\exp v_{sc} - \\ - \exp(-2u - v_{sc}) - v_{sc} - 1]^{-1/2}$$

where $u = \Phi q/kT$; and $v_{sc} = V_{sc}q/kT$; Φ represents the position of Fermi level reported to the middle of the energy gap, and V_{sc} is the barrier height at the silicon surface, related to the bulk potential; a 1.3 rugosity factor was considered.

One observes a good agreement between the measured capacity for the Si-HF system (fig. 3) and the computed one (fig.6), by comparing the two curves in the $-300\ldots-500$ mV range. For more negative potentials, the experimental curves have a saturation tendency whereas for more positive potentials the experimental curves are smaller than the theoretical ones with one order of magnitude.

The analysis of the experimental data suggests that the capacity Cs is composed of two capacities series connected: C_{sc}, the silicon space charge capacity and another capacity C_H, due to the double layer (fig. 2 b). In this case the double layer takes over a part V_H of the potential difference V_s.

In order to compute the values of C_H and V_H, one considers the equations which can be derived from the equivalent circuit (fig. 2b) observing the condition that the measured potential E will be referred to the same null potential as the potential V_{sc}. This correspondence has been realized by superposing the experimental curves $C_s(V_E)$ on the computed one $C_{sc}(V_{sc})$ in their range of coincidence. We notice that $E = -300$ mV corresponds to $V_{sc} = 0$ mV. The measured potential E expressed in this scale has been denoted by V_s.

The equations are:

$$V_s = V_{sc} + V_H \tag{2}$$

$$\frac{1}{C_s} = \frac{1}{C_{sc}} + \frac{1}{C_H} \tag{3}$$

$$Q = C_H V_H = C_s V_s \tag{4}$$

$$C_{sc} = f(V_{sc}) \tag{5}$$

The capacities C_s and C_{sc} have been calculated by integrating the differential capacity curves of fig. 6; Q represents the electrical charge of the interface; the function f has been expressed analytically by equation (1).

From equations (2–5) one obtains the expression:

$$C_s(1 - C_s/C_H)^{-1} = f\,[V_s(1 - C_s/C_H)] \tag{6}$$

which can be written again as follows:

$$\ln C_s = \ln(1 - C_s/C_H) + \ln f(\ln\exp[\ln V_s + \ln\{1 - C_s/C_H\}]). \tag{7}$$

Equation (7) may be solved graphically by representing in a double logarithmic plot the values $C_s = C_s(V_s)$ and $C_{sc} = f(C_{sc})$. According to eq. (7) there exists a correspondence among the points of the two curves, i.e. two corresponding points are connected by a straight line sloping at 45° in the double logarithmic plane. The projection of the segment on the two coordinate axes represents the corresponding value of $1-C_s/C_H$.

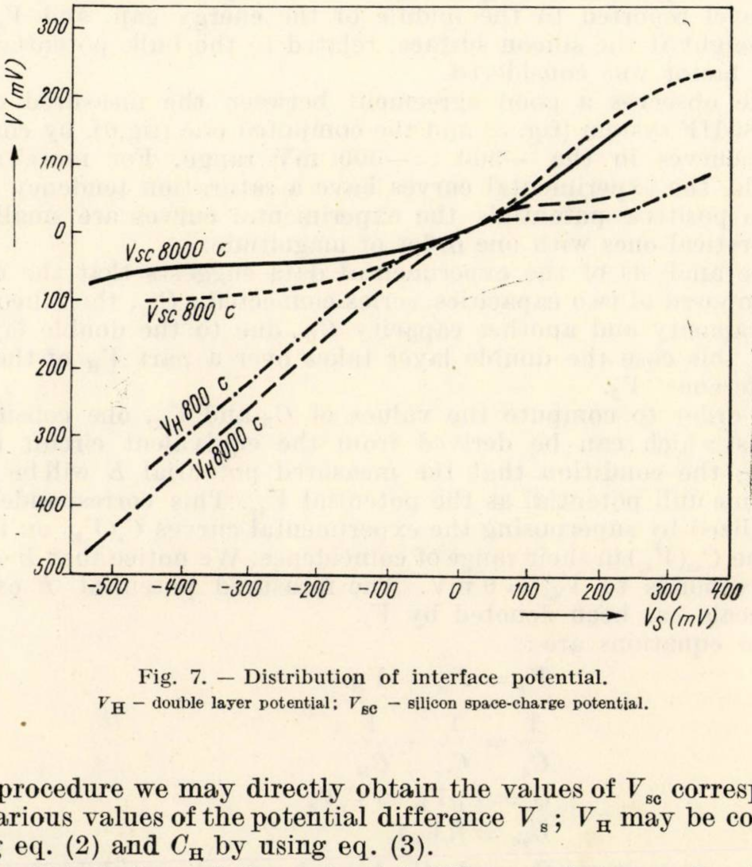

Fig. 7. — Distribution of interface potential.
V_H – double layer potential; V_{sc} – silicon space-charge potential.

By this procedure we may directly obtain the values of V_{sc} corresponding to the various values of the potential difference V_s; V_H may be computed by using eq. (2) and C_H by using eq. (3).

The distribution of the potential difference between the two elements V_{sc} and V_H has been represented in figure 7. From figure 7 we see that in the anodic range the potential difference is taken over mostly by V_H and only a small part drops on the silicon. In the cathodic region the potential difference is taken over mainly by the silicon, the contribution of the solution being small. This result is reflected in the polarization curve too (fig. 1a), which shows that in the considered potential range the semiconductor surface is more blocked in the cathodic region than is the anodic one, i.e. the cathodic V_{sc} is greater than the anodic V_{sc}.

The distribution of the interface charge, computed from eq. (4) has been represented in figure 8, considering $Q = 0$ for $V_s = 0$.

The accuracy of this method depends on the accuracy with which the correspondence of the curves C_s and C_{sc} has been realized.

In our case the superposition method is not reliable enough and the choice of the null potential at $V_s = -300$ mV introduces an error $\pm V_s$, which is reflected in the value of the potential V_{H} by an error $\mp V_{\mathrm{H}}$ and in the value of the capacity by

$$C_{\mathrm{H}} = C_{\mathrm{H}}(V_{\mathrm{H}} \mp \Delta V_s) - C_{\mathrm{H}}(V_{\mathrm{H}}) \simeq \mp \Delta V_s \left(\frac{\partial C_{\mathrm{H}}}{\partial V}\right)_{V_{\mathrm{H}}}.$$

b) *The effect of the copper ions*

The increase of the differential capacity in the anodic region in the presence of copper ions is dependent on the measuring frequency. This suggests the introduction of a capacity in parallel to the capacity measured in the absence of Cu^{++} which expresses the ionisation of the silicon surface states by the Cu^{++} present in the solution. The phenomenon takes place as if the presence of the double layer were hindering the approach of Cu^{++} to the electrode surface. The resulting equivalent circuit is shown in figure 2 c, where C_{ss} actually represents the effect of the silicon surface layer which has been mentioned in the introduction. The increase of the polarization current in the presence of Cu^{++} ions (fig. 1.2) suggests the possibility of a Faraday component contribution to the values of C_{ss}.

On taking the difference of the differential capacity curves (measured at 800 c) from figure 4 and figure 3 one may compute the surface layer contribution to the differential capacity. The capacity C_{ss} may be obtained by integration from figure 2c. The interface charge Q_{ss} due to Cu^{++} is represented in figure 8.

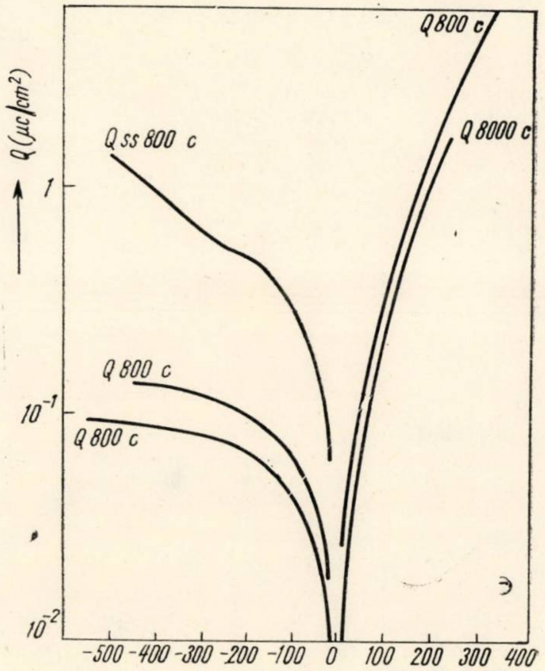

Fig. 8. — Distribution of interface charge.
Q — the charge of Si-HF interface; Q_{SC} — the charge due to Cu^{++}.

On analysing the curves in figure 7, corresponding to high Cu^{++} concentrations, it may be seen that in the cathodic region the electrode behaves as a copper electrode. This suggests the presence of a compact atomic copper layer deposited on the silicon surface. In the anodic region the differential capacity curves intersect the curves which are characteristic for silicon. We have thus a cathode copper electrodeposition on the silicon stand, followed by anodic dissolution.

CONCLUSIONS

The results of the differential capacity measurements carried out with an impedance bridge, at 800 and 8000 c frequencies show that the potential difference of the interface is distributed between the silicon space charge layer and the double layer. In the anodic range the potential is taken over mostly by the double layer, whereas in the cathodic range the potential is taken over by the silicon.

The interface charge in the presence of the copper ions has been increasing. The increase is due to the ionization of the silicon surface states.

Revue Roumaine de Chimie, **15**, 333 – 341 (1970)

THE ANODIC BEHAVIOUR OF PURE ALUMINUM IN ACIDIC SOLUTIONS OF POTASSIUM HALIDES

ELENA CONSTANTINESCU and T. MARIAN

Laboratory of Physical Chemistry, University of Bucharest, Bd. Republicii 13

Received April 18, 1969

Anodic polarization curves, under controlled potential, have been recorded for pure aluminum in 1 N, 0.1 N and 0.01 N potassium halide solutions in 0.5 N H_2SO_4. The current-potential curves and micrographs of the aluminum electrodes are analysed. In order to explain the results obtained, a plausible mechanism is suggested for the local destruction by the halogen ions, of the oxide layer which passivates aluminum.

INTRODUCTION

Aluminum is a strongly electronegative metal, whose standard potential is – 1.67 V. However, because of passivation, aluminum presents quite a high resistance to water, as well as to many neutral and acidic solutions, a fact which is of great importance for its practical use.

Not only oxygen or oxidizing agents, but even water itself is a passivator for aluminum, which is therefore in a passive state in most aqueous solutions, both neutral and slightly acidic. For this reason, the electrode potential of aluminum becomes more positive, than its normal equilibrium potential, by about 1 V.

Aluminum passivity is produced by the presence on the metal surface of a protective film made up of successive Al_2O_3 layers, with different degrees of hydration.

It has been established that aluminum is particularly sensitive to the halogen ions which partially destroy the passivating film. In the present work, we have intended to study comparatively the anodic behaviour of pure aluminum in potassium halide H_2SO_4 solutions. The interest for such a study was aroused by Tomashov and Modestova's earlier paper ,[1] which has a rather similar topic.

The analysis of both the controlled-potential polarization curves and the aluminum anodes micrographs has pointed out several regularities concerning the nature and the strength of the corrosive attack, under the mentioned conditions. We succeeded in explaining these facts on the basis of a plausible mechanism for the local destruction of the metal-covering oxide film, by the halogen ions.

---

[1] N. D. Tomashov and V. N. Modestova, *Trudy Inst. Fiz. Khim. Akad. Nauk S.S.S.R* No 5, Issledovania po Korozii Metalov, 4, 75 (1955).

EXPERIMENTAL

Cell and electrodes. A glass cell with two compartments, as shown in figure 1, was used.

The working electrode consisting of an aluminum disk with an area of 1 cm^2 was glued at the end of a glass tube having the same external diameter. The electric contact was achieved by means of mercury. As counter and reference electrodes, a platinum plate of about 10 cm^2 and the saturated calomel electrode were respectively used. The working and the reference electrodes were connected by a Haber-Luggin capillary.

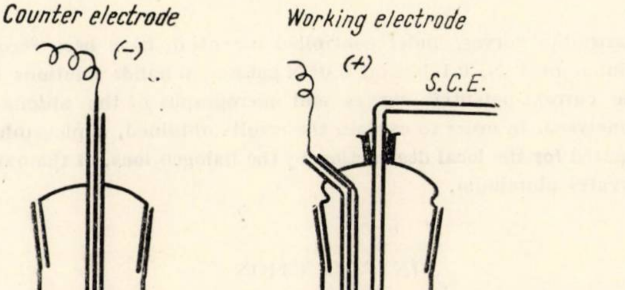

Fig. 1. — Electrolytic cell.

Instrumentation. The aluminum electrode potential was controlled, varied and measured by means of a Tacussel potentiostatic equipment made up of a PRT 20—2 potentiostat, a 9/A Servovit automatic pilot and a S6/G4R millivoltmeter. The current-potential curves were obtained by means of a Graphispot recording galvanometer.

Chemicals. 1N, 0.1 N and 0.01 N KX (X = F, Cl, Br, I) solutions in 0.5 N H_2SO_4 were used. The solutions have been prepared from *p.a.* chemicals and doubly distilled water. The studied electrodes were made of 99.95% aluminum.

Procedures. The aluminum samples were previously polished electrochemically in a cooled mixture of 95% glacial acetic acid and 5% perchloric acid.

All the measurements were performed in the presence of air, at 25.0 ± 0.1°. The solutions in the anodic compartment were stirred magnetically. The rate increase of the working electrode potential was 300 mV/min.

The corroded aluminum plates were photographed by means of a MIM-7 metallographic microscope. The micrographs obtained represent only portions of the plate surfaces, 200 times greater.

RESULTS

The recorded polarization curves are shown in figure 2. They are reproducible. We mention that the final parts of the polarization curves are spread on a surface of approximately ± 0.010 V in 1 N, ± 0.020 V in 0.1 N and ± 0.100 V in 0.01 N KX solutions. One notices that in the initial part of all curves, the reproducibility is far better.

The initial potential of all anodic curves is −0.537 V. This potential, at which the current through the electrolytic cell is zero, must be considered the equilibrium potential of passive state aluminum.

We thought that the current-potential curves are well characterized by the average E/i and the actual dE/di anodic polarization values in the points corresponding to the current densities $i=0.3, 1.5, 7.5$ mA/cm². These average and actual polarizations are listed in tables 1 and 2.

Table 1

Average anodic polarizations E/i (V cm²/mA)

Conc.	i mA/cm²	KF	KCl	KBr	KI
1 N	0.3	−0.040	−1.767	−1.290	−0.707
	1.5	0.242	−0.324	−0.224	−0.108
	7.5	0.142	−0.057	−0.035	−0.014
0.1 N	0.3	−0.123	−1.000	−0.706	0.543
	1.5	0.342	−0.091	−0.017	0.233
	7.5	0.221	0.014	0.042	0.085
0.01 N	0.3	1.627	0.833	1.293	2.377
	1.5	0.917	0.550	0.742	1.039
	7.5	0.361	0.222	0.281	0.344
H_2SO_4	0.3	1.543			
	1.5	1.092			
	7.5	0.424			

The polarization curves show distinct resemblances in the case of the Cl^-, Br^-, I^- ions and they point to a special position in the F^- ions case.

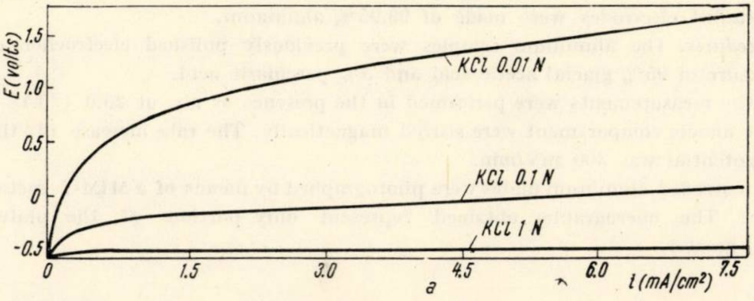

Fig. 2 a. – Current-potential curves for aluminum in KCl solutions in 0.5 N H_2SO_4.

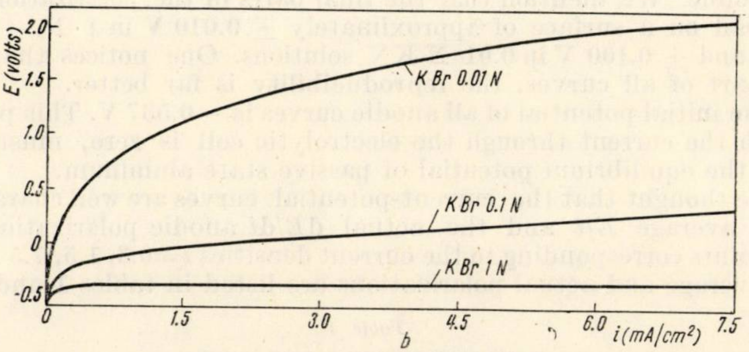

Fig. 2 b. – Current-potential curves for aluminum in KBr solutions in 0.5 N H_2SO_4.

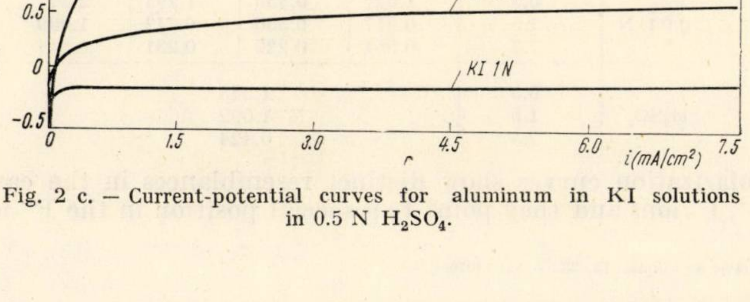

Fig. 2 c. – Current-potential curves for aluminum in KI solutions in 0.5 N H_2SO_4.

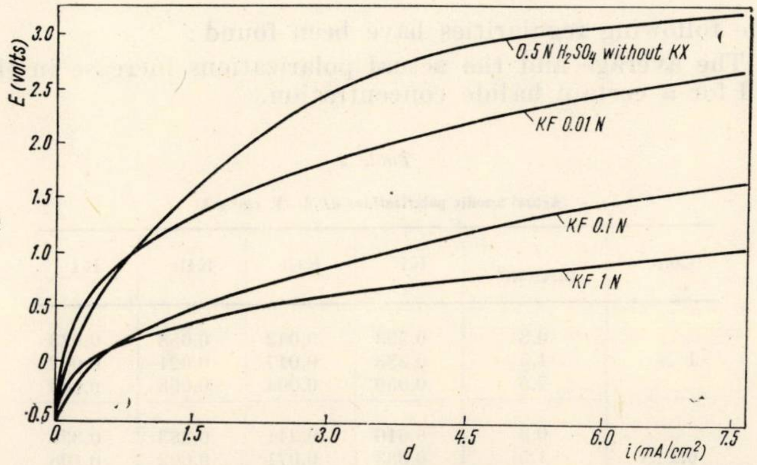

Fig. 2 d. — Current-potential curves for aluminum in KF solutions in 0.5 N H_2SO_4 and in 0.5 N H_2SO_4 without potassium halides.

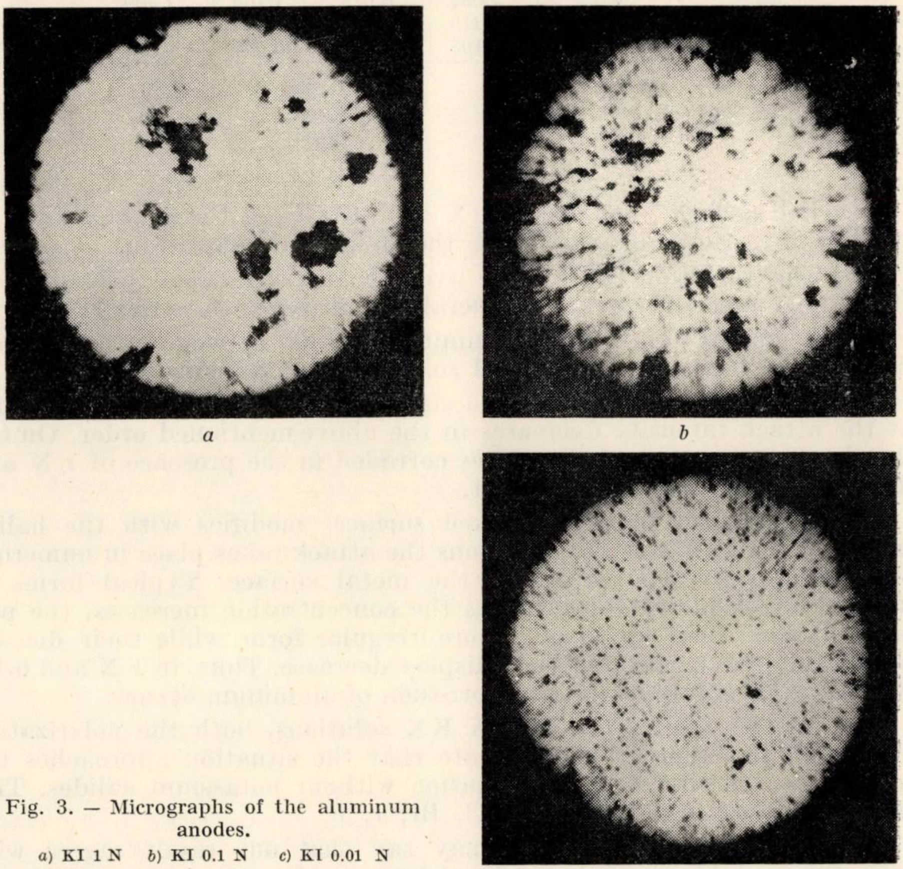

Fig. 3. — Micrographs of the aluminum anodes.
a) KI 1 N *b*) KI 0.1 N *c*) KI 0.01 N

The following regularities have been found :

1. The average and the actual polarizations increase in the order Cl, Br, I for a certain halide concentration.

Table 2

Actual anodic polarizations dE/di (V. cm^2/mA)

Conc.	i mA/cm^2	KF	KCl	KBr	KI
1 N	0.3 1.5 7.5	0.533 0.233 0.050	0.042 0.017 0.004	0.058 0.021 0.006	0.083 0.017 0.008
0.1 N	0.3 1.5 7.5	0.616 0.383 0.092	0.241 0.071 0.025	0.283 0.092 0.033	0.333 0.108 0.033
0.01 N	0.3 1.5 7.5	2.082 0.416 0.108	0.916 0.267 0.067	1.100 0.333 0.075	1.499 0.416 0.092
H_2SO_4	0.3 1.5 7.5	1.499 0.666 0.100			

2. For each X^- ion species ($X = F, Cl, Br, I$) the average and the actual polarizations decrease with the halide concentration.

3. The variation rate of the average and the actual polarizations with the X^- ions concentration generally increases in the series F, Cl, Br, I.

The general aspect of the aluminum anodes as well as their micrographs given here only for the KI solutions (fig. 3) show that :

4. Aluminum is attacked in a similar way by the Cl^-, Br^-, I^- ions but the attack intensity decreases in the above mentioned order. On the other hand, the aspect of the plates corroded in the presence of 1 N and 0.1 N KF solutions is different.

5. The aspect of the attacked surfaces modifies with the halide concentration. In 0.01 N KX solutions the attack takes place in numerous points, uniformly overspread on the metal surface. Typical forms of pinpoint corrosion are obtained. As the concentration increases, the pits become larger, deeper and of a more irregular form, while their density and the uniform character of their display decrease. Thus, in 1 N and 0.1N KCl, KBr, KI solutions, pitting corrosion of aluminum occurs.

6. In the case of the 0.01 N KX solutions, both the polarization curves and the micrographs indicate that the situation approaches the limit case of the 0.5 N H_2SO_4 solution without potassium halides. This tendency increases in the order Cl, Br, I, F.

As a general remark, we may say that our results agree with those obtained by Tomashov, by galvanostatic measurements, in the absence of air.[1]

DISCUSSION

Aluminum resistance to corrosion is chiefly determined by the behaviour of the superficial layer which causes the metal's passivity. This layer is an electron-conducting film of partially hydrated aluminum oxide. [2] Its thickness varies, being however of the order of 100 Å.

The oxide layer prevents the electrochemical dissolution of aluminum in 0.5 N H_2SO_4. On the other hand this reaction is facilitated by the presence of the halogen ions and by the potential increase.

The above results show that the F^- ions attack of the oxide film has certain specific features which require a separate discussion. Nevertheless, it is obvious that the way of attacking of the X^- ions ($X = Cl$, Br, I) is the same, but there are differences concerning the attack intensity.

It is therefore but natural that for the latter case we should admit the following :

1. The anodic process has two important stages,

(A) The local destruction of the oxide film, determined by the X^- ions.

(B) The metallic aluminum dissolution, there where the protecting layer was removed.

2. Stage (A), which involves a different contribution of the X^- ions, is the rate-controlling stage.

Let us examine the situation closer. Once in the force field of the anode surface, the X^- ions are adsorbed preferentially in the neighbourhood of the Al^{3+} ions at the external limit of the oxide film. The X^- anions action, combined with the applied positive potential, loosens the bond between the neighbouring Al^{3+} ions and the whole oxide lattice. In favourable cases, one Al^{3+} ion is taken out of the lattice, it hydrates and desorbs itself, entering the solution with its disturbing X^- ions :

$$Al^{3+}_{lattice} + nX^-_{ads} \xrightarrow{H_2O} Al^{3+}_{ads} \cdot mH_2O \cdot nX^- \xrightarrow{H_2O} [Al(H_2O)_6]^{3+} + nX^-$$

where $m < 6$, $n < 4$.

As a consequence, the supplementary O^{2-} ion undergoes one of the processes :

$$\text{(I)} \quad O^{2-} + H_2O \rightarrow 2\,OH^- \rightarrow 2OH_{ads} + 2\,e^-$$

$$2\,OH_{ads} \rightarrow H_2O + O_{ads}$$

$$\text{(II)} \quad O^{2-} \rightarrow O^- + e^-$$

$$O^- \rightarrow O_{ads} + e^-$$

Path (I) seems more probable due to the presence of the water molecules at the metal surface. The released electrons pass through the oxide film and are caught by the anode. The oxygen adatoms join in molecules which desorb and leave the electrode.

---

[2] M. Pourbaix, "Atlas d'équilibres électrochimiques à 25°C", Gauthier-Villars, Paris 1963, p. 175.

We notice that the small number of attack positions on the aluminum surface shows that out of the X^- adions, only a few succeed in removing Al^{3+} ions. The small probability of this act implies that the corresponding energy barrier be high. Very rough considerations have pointed to an order of magnitude of 10 eV. The positive potential applied to the electrode cannot supply this energy so that the perturbation caused by the X^- adions is essential.

Vacancies and steps at the film surface being created, the attack of the halogen ions is successful especially in their neighbourhood. Thus, areas of the X^- ions action efficiency are formed, in which the oxide film is progressively destroyed in its depth. It is easy to understand that the greater the halogen ions concentration, the larger the gaps.

There, where the aluminum surface is cleared of the protecting film, the anodic dissolution (B) of the metallic lattice takes place :

$$Al + 6H_2O \rightarrow [Al(H_2O)_6]^{3+} + 3\ e^-$$

The aluminum electrodissolution occurs in stages, inversely than the electrocrystallisation.[3]

The X^- ions also interfere in stage (B), resisting the formation of a new oxide layer on the active surface of aluminum. A dynamic equilibrium between the incipient oxide layer formation and destruction processes is achieved.

In the slow stage (A), the halogen ions have different contributions, on account of the differences between their sizes. As the ionic radius decreases, the aggressivity of the X^- ions increases owing to the possibility of a more favourable geometrical ion disposition, on the one hand, and of a more energetic interaction between the X^- adions and the marginal Al^{3+} ions, on the other hand. Accordingly, it is to be expected that the anodic process rate and the pits sizes should increase in the order I, Br, Cl, for equal halide concentrations and that it should also increase with the concentration of each kind of ions.

The criterion of the ionic radius size explains rather well the regularities underlined, if we take into account that the more hindered the anodic process, i.e. the smaller its rate, the higher the polarization.

We discuss now the case of the KF solutions. The anodic process occurs also in stages (A) and (B). We shall present only the peculiar features of the F^- ions action, without insisting on the facts completely similar to those discussed in the previously analysed case.

In stage (A), the F^- ions are able to attack the oxide layer very strongly. There are two competitive reactions for the removal of the Al^{3+} ions out of the oxide lattice :

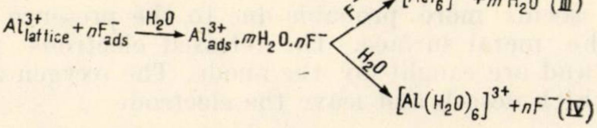

$$\begin{tikzcd} & {[AlF_6]^{3-} + m\,H_2O\ (III)} \\ Al^{3+}_{lattice} + nF^-_{ads} \arrow[r, "H_2O"] & Al^{3+}_{ads}.mH_2O.nF^- \arrow[u, "F^-"] \arrow[d, "H_2O"'] \\ & {[Al(H_2O)_6]^{3+} + nF^-\ (IV)} \end{tikzcd}$$

where m, $n < 6$.

---

[3] J. O'M. BOCKRIS and A. DAMJANOVIC, "The Mechanism of the Electrodeposition of Metals" in J. O'M. BOCKRIS and B. E. CONWAY, "Modern Aspects of Electrochemistry", vol. 3, Butterworths, London, 1964, p. 224.

The weight of the former reaction increases with the fluoride concentration.

The oxygen release and the anodic dissolution (B) of the aluminum lattice take place as in the previous case.

In 1 N KF solution, reaction (III) is prevailing. As a result, the $[AlF_6]^{3-}$ ions combine in fluoroaluminates $K[AlF_4]$ and $K_2[AlF_5]$, whose anions have a polymeric structure with octahedron units AlF_6, linked by common edges.[4] The presence of the insoluble fluoroaluminates on the aluminum anode surface, as a layer less compact than the partially substituted oxide layer hinders both processes (A) and (B). It seems likely that in this case, (B) would be the slow stage, responsible for the high electrode polarization.

In 0.1 N and 0.01 N KF solutions the weight of reaction (III) is much smaller than that of reaction (IV), so that the polymeric fluoroaluminates formation is no longer possible. The rate-controlling process (A) is hindered to a greater extent than in the case of the other halides, because the F^- ions effective concentration is smaller, part of them being consumed in the formation of the very stable complex $[AlF_6]^{3-}$ ions. Consequently, the anodic polarization is higher and pinpoint corrosion occurs.

We mention that in all the cases, the oxide film destruction by the halogen ions takes place simultaneously with the destructive action of the sulphate ions and with the reaction between the H_3O^+ ions and the amphoteric oxide $Al_2O_3 . xH_2O$. But the last two reactions are much less efficient.

Only in diluted (0.01 N) KX solutions, they become competitive with the X^- ions action, owing to the much higher H_2SO_4 concentration. This fact explains why, in this case, the experimental situation tends to approach, in the order $Cl < Br < I < F$, that existing in the case of the 0.5 N H_2SO_4 solution, without potassium halides.

In conclusion, we consider that the advanced outline for the aluminum electrodissolution process accounts satisfactorily for the above experimental results.

---

[4] G. V. Akimov and N. E. Paleolog, *Trudy Inst. Fiz. Khim. Akad. Nauk S.S.S.R.* No 2, Issledovania po Korozii Metalov, **1**, 5 (1951).

Revue Roumaine de Chimie, **15**, 343–355 (1970)

INTERDIFFUSION COEFFICIENT OF SILVER ION IN MOLTEN ALKALI NITRATES BY THE CHRONOPOTENTIOMETRIC METHOD

S. STERNBERG and CONSTANȚA HERDLICKA

Institute of Physical Chemistry of the Academy, Bucharest, str. Galați, 31

Received April 7, 1969

The interdiffusion coefficients of silver ion in molten $NaNO_3$, $RbNO_3$ and $CsNO_3$ have been measured by the chronopotentiometric method. The interdiffusion coefficients change with temperature according to the following Arrhenius type equations :

$NaNO_3$ $\log D = 1.07 \times 10^{-3} \exp(-4645/RT)$, $(318-397°)$
$RbNO_3$ $\log D = 1.66 \times 10^{-3} \exp(-5600/RT)$, $(336-417°)$
$CsNO_3$ $\log D = 1.84 \times 10^{-3} \exp(-5800/RT)$, $(426-480°)$

The interdiffusion coefficients for Ag^+ in all the series of molten alkali nitrates have been correlated with other transport phenomena as cation and anion selfdiffusion and solvent viscosity. The following three factors influence the interdiffusion phenomenon : the radius of interdiffusing cation, the ratio of diffusing cation radius to solvent cation radius and viscosity of the solvent. It was shown that Stokes-Einstein equation is obeyed at solvent melting point both for Ag^+ interdiffusion coefficient and for the selfdiffusion coefficients of solvent cation and anion.

The interdiffusion coefficients in molten salts systems have been studied in only a few cases due to experimental difficulties involved.

Three methods have been used to measure the interdiffusion coefficients in molten salts.

Laity and Miller [1] used a constant mass diffusion cell to investigate concentrated mixtures of $AgNO_3$-$NaNO_3$, at 310 °.

Sjöblom[2] initiated a gravimetric technique with porous frit for diffusion measurements in molten salts and checked it on $AgNO_3$ diffusion in $NaNO_3$ and KNO_3 also for concentrated mixtures. Very recently Sjöblom[3] extended the method to interdiffusion studies in diluted solutions of $AgNO_3$ in molten alkali nitrates.

---

[1] R. W. LAITY and M. P. MILLER, *J. Phys. Chem.*, **68**, 2145 (1964).

[2] C. A. SJÖBLOM, *Z. Naturforsch.*, **20a**, 1572 (1965).

[3] C. A. SJÖBLOM and A. BEHN, *Z. Naturforsch.*, **23a**, 1774 (1968).

Different authors applied the chronopotentiometric method to the determination of interdiffusion coefficients of $AgNO_3$ in $NaNO_3^{4,5}$, KNO_3^5, $CsNO_3^4$ and $KNO_3 + NaNO_3^{5,6}$ of equimolecular composition.

In a previous work we determined the interdiffusion coefficient and activation energy for $AgNO_3$ in $LiNO_3$ and KNO_3 by the chronopotentiometric method .[7] In this paper we present the interdiffusion data for Ag^+ in $NaNO_3$, $RbNO_3$ and $CsNO_3$ also obtained by the chronopotentiometric method. The results we obtained for the silver ion diffusion in all the series of alkali nitrates are discussed in connection with the nature of the solvent and correlated with other transport magnitudes.

EXPERIMENTAL

The experimental device and details concerning its operation are given elsewhere .[7] We used a chronopotentiometric circuit consisting of three electrodes. The working electrode was a platinum plate of 0.32 cm^2 surface area. The counterelectrode was also a platinum plate of greater area than the working electrode ($\sim$4 cm^2). The reference electrode was a silver wire immersed in a diluted solution of $AgNO_3$ in the respective solvent and having a concentration approximately equal to the working solution. The contact with the melt in the cell was achieved through a hole in the wall of the test tube containing the silver wire and nitrates mixture; this hole was filled with asbestos string.

The thermosetting was ensured by a photoresistance thermoregulator within $\pm$ 0.5° and measured with a Pt-PtRh thermocouple.

The potential-time curves were recorded by a magneto-optic oscillograph. The transition time was taken as the average of three or more recordings made for the same current density. The transition time was measured for different densities between 5 − 10 mA/cm^2 and $AgNO_3$ concentrations of $1.45 - 2.40 \times 10^{-2}$ mol/l. In these conditions the transition time was between 0.3 and 2 seconds.

We use analytical grade reagents which were purified by reiterated recrystallization then dried and melted.

RESULTS AND DISCUSSION

The interdiffusion coefficient of Ag^+ in $NaNO_3$ in a temperature range of 318 − 397 °, in $RbNO_3$ (336 − 417°) and in $CsNO_3$ (426 − 480°) were calculated. The chronopotentiometric method for the calculation of diffusion coefficient requires $i\,\tau^{1/2}$ (i is the current density and τ the transition time) to be constant at different current densities and $i\,\tau^{1/2}/C$, where C is the concentration of electroactive ion (Ag^+), to be constant at any concentration: these conditions were accomplished in all studied systems. This results from figure 1 where the relation $i\,\tau^{1/2}$ *versus* i for the three systems is given. On figure 2, the variation of $i\,\tau^{1/2}$ *versus* the concentration of $AgNO_3$ in $NaNO_3$ for some temperatures is plotted.

---

[4] C. E. THALMAYER, S. BRUCKENSTEIN and D. M. GRUEN, *J. Inorg. Nuclear Chem.*, **26**, 347 (1964).

[5] K. KAWAMURA, *Electrochim. Acta*, **12**, 1233 (1967).

[6] D. INMAN and J. O'M. BOCKRIS, *J. Electroanalyt. Chem.*, **3**, 126 (1962).

[7] S. STERNBERG and C. HERDLICKA, *Rev. Roumaine Chim.*, **14**, 991 (1969).

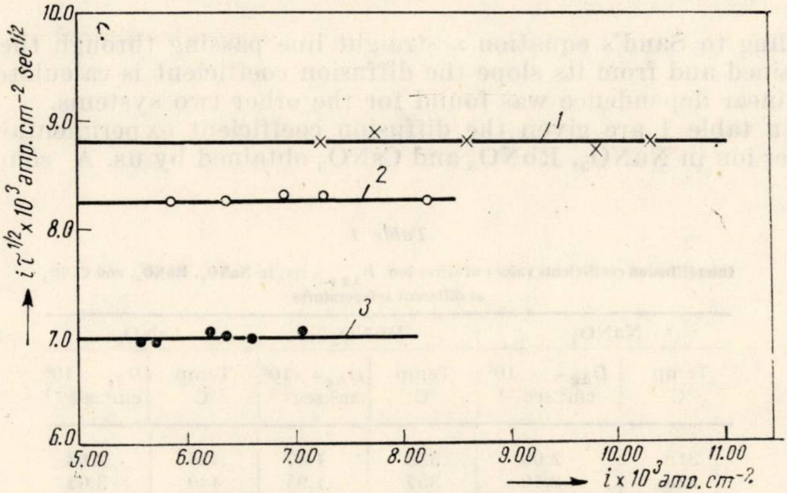

Fig. 1. — Variation of $i\ \tau^{1/2}$ with current density

1, $AgNO_3-CsNO_3$, $C_{Ag^+} = 1.86 \times 10^{-5}$ mol/cc, 440°;
2, $AgNO_3-RbNO_3$, $C_{Ag^+} = 2.18. \times 10^{-5}$ mol/cc, 357°;
3, $AgNO_3-NaNO_3$, $C_{Ag^+} = 1.59 \times 10^{-5}$ mol/cc, 365°.

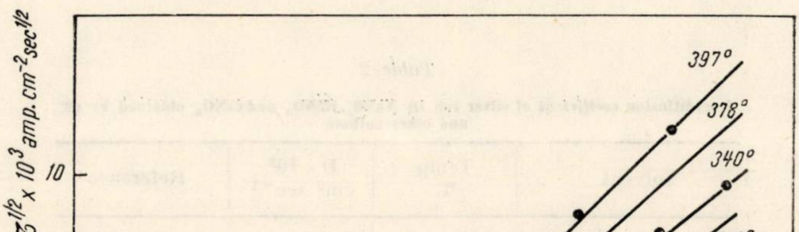

Fig. 2. — Variation of $i\ \tau^{1/2}$ with $AgNO_3$ concentration in $NaNO_3$.

According to Sand's equation a straight line passing through the origin is obtained and from its slope the diffusion coefficient is calculated. The same linear dependence was found for the other two systems.

In table 1 are given the diffusion coefficient experimental values of silver ion in $NaNO_3$, $RbNO_3$ and $CsNO_3$ obtained by us. A comparison between our data and values available in literature obtained by the same method or other methods, is made in table 2. It is remarkable that a very good agreement exists between our results and data published by other authors obtained mainly by the chronopotentiometric method. The values given by the porous frit method are only slightly higher than ours and this is probably due to the concentration difference of $AgNO_3$ in the two methods (0.5 mol/l in porous frit method against maximum 0.025 mol/l in the chronopotentiometric one).

Table 1

Interdiffusion coefficients values of silver ion, $D_{Ag^+} \times 10^5$, in $NaNO_3$, $RbNO_3$, and $CsNO_3$ at different temperatures

$NaNO_3$		$RbNO_3$		$CsNO_3$	
Temp °C	$D_{Ag^+} \times 10^5$ $cm^2.sec^{-1}$	Temp °C	$D_{Ag^+} \times 10^5$ $cm^2.sec^{-1}$	Temp °C	$D_{Ag^+} \times 10^5$ $cm^2.sec^{-1}$
318	2.09	336	1.57	426	2.83
328	2.19	357	1.95	440	3.02
340	2.36	378	2.18	460	3.45
350	2.50	396	2.41	480	3.82
365	2.62	417	2.77		
378	2.88				
383	3.11				
397	3.28				

Table 2

Interdiffusion coefficient of silver ion in $NaNO_3$, $RbNO_3$ and $CsNO_3$ obtained by us and other authors

Solvent	Temp °C	$D \times 10^5$ $cm^2\ sec^{-1}$	Reference
$NaNO_3$	310	1.94	our result
	310	1.93	Thalmayer [4]
	315	2.01	Kawamura [5]
	310	2.05	Sjöblom[3]
	310	1.96	Laity [1]
$RbNO_3$	360°	1.94	our result
	360°	1.98	Sjöblom[3]
$CsNO_3$	428	2.86	our result
	428	2.89	Thalmayer[1]
	428	2.88	Sjöblom[3]

The interdiffusion coefficients of Ag^+ in the three solvents varies with temperature according to an equation of Arrhenius type : $D=D_0 \exp(-E/RT)$, where D_0 is the pre-exponential factor and E the activation energy of diffusion. These are temperature-independent constants.

Fig. 3. — Arrhenius plots of the silver ion interdiffusion coefficient in : *1*, $CsNO_3$; *2*, $RbNO_3$; *3*, $NaNO_3$.

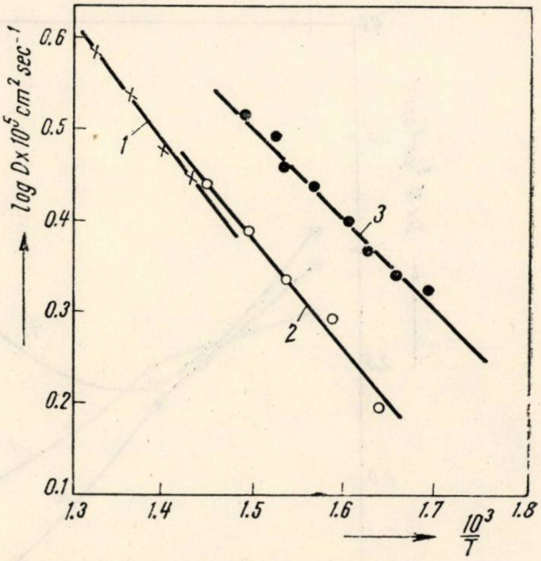

In figure 3 it is represented the linear charge of log *D versus* the reciprocal absolute temperature which corresponds to the following equation :

$$AgNO_3-NaNO_3;\ \log D=1.07\times10^{-3}\exp\left(-\frac{4645}{RT}\right),\ (318-397°)\quad (1)$$

$$AgNO_3-RbNO_3;\ \log D=1.66\times10^{-3}\exp\left(-\frac{5600}{RT}\right),\ (336-417°)\quad (2)$$

$$AgNO_3-CsNO_3;\ \log D=1.84\times10^{-3}\exp\left(-\frac{5800}{RT}\right),\ (426-480°)\quad (3)$$

The numerical values of D_0 and E have been obtained from the experimental data by the method of the least squares. The mean values of activation energies obtained by us for Ag^+ diffusion in $NaNO_3$ and $RbNO_3$ are very close to the mean values of E obtained by Sjöblom[3] which are 4800 and 5400 cal respectively. A good agreement between the activation energies we have obtained for the diffusion of Ag^+ in $NaNO_3$ and $CsNO_3$ and Thalmayer's[4] data, 4500 and 5100 cal respectively, is obtained too.

Figures 4 and 5 represent the interdiffusion coefficients of silver ion, D_{Ag^+} (inter) in the alkali nitrates series at 350° and the temperature of solvent melting. Their values were calculated according to equations

1, 2, 3 for $NaNO_3$ and $CsNO_3$ obtained in the present work and $D = 16.1 \times 10^{-3} \exp(-7900/RT)$ and $D = 1.86 \times 10^{-3} \exp(-4340/RT)$ obtained in a previous work[7] for $LiNO_3$ and KNO_3 respectively. The same figures reproduce the selfdiffusion coefficients of alkali cations,[8] D_{Me^+} (self), and the anion,[8] $D_{NO_3^-}$ (self), as well as the viscosities,[9] η, of alkali nitrates. The selfdiffusion coefficient of Rb^+ in $RbNO_3$ was approximately calculated with only one value of D_{Rb^+} (self) available, found by Ketelaar [10] and assuming an activation energy of 5500 cal. For $D_{NO_3^-}$ (self) in $RbNO_3$ there is no reference in literature and the dotted portion in figure 5 was imaginarily drawn by us.

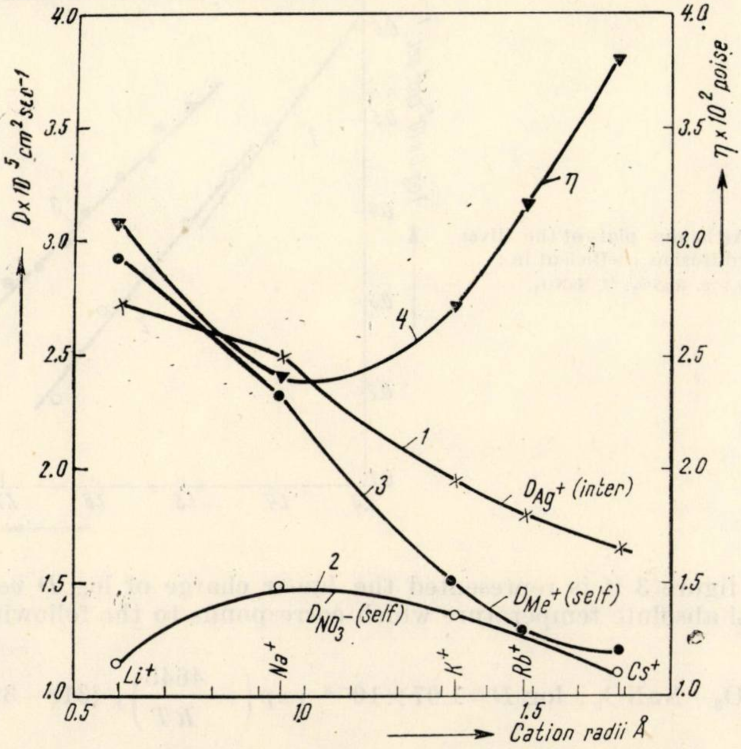

Fig. 4. — *1*, Interdiffusion coefficient of silver ion, D_{Ag^+} (inter); *2*, selfdiffusion coefficient of anion, $D_{NO_3^-}$ (self); *3*, selfdiffusion coefficient of alkali cation, D_{Me^+} (self); *4*, solvent viscosity, η as a function of the alkali cation radii at 350°.

The melting points for $LiNO_3$, $NaNO_3$, KNO_3, $RbNO_3$ and $CsNO_3$ are 254, 310, 337, 316 and 417° respectively.

---

[8] A. S. Dworkin, R. B. Escue and E. R. Van Arstdalen, *J. Phys. Chem.*, **64**, 872 (1960).

[9] S. Zuca and R. Borcan, *Rev. Roumaine Chim.*, (to be published).

[10] J. A. A. Ketelaar and J. C. Th. Kwak, *J. Phys. Chem.*, **71**, 1149 (1967).

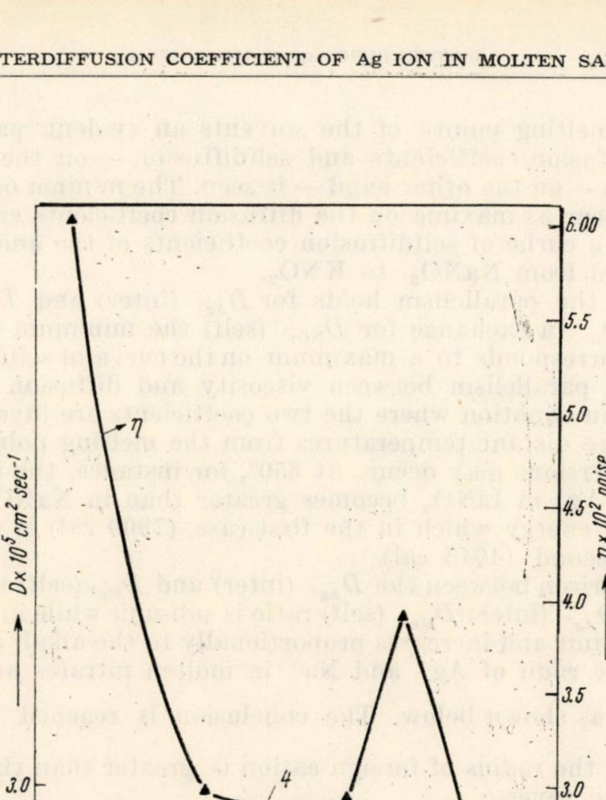

Fig. 5. — *1*, Interdiffusion coefficient of silver ion, D_{Ag^+} (inter) ; *2*, selfdiffusion coefficient of anion, $D_{NO_3^-}$ (self) ; *3*, selfdiffusion coefficient of alkali cation, D_{Me^+} (self): *4*, solvent viscosity, η as a function of the alkali cation radii at the temperature of solvent melting.

At the melting points of the solvents an evident parallelism between interdiffusion coefficients and selfdiffusion — on the one hand — and viscosities — on the other hand — is seen. The minima on the viscosities curve appear as maxima on the diffusion coefficients curves and the reverse. On the curbe of selfdiffusion coefficients of the anion, the maximum is shifted from $NaNO_3$ to KNO_3.

At 350° the parallelism holds for D_{Ag^+} (inter) and D_{Me^+} (self) except for $LiNO_3$. In exchange for $D_{NO_3^-}$ (self) the minimum on the viscosities curve corresponds to a maximum on the curve of selfdiffusion coefficients. This parallelism between viscosity and diffusion results from Stokes-Einstein equation where the two coefficients are inversely proportional. At more distant temperatures from the melting point of the solvent some inversions may occur. At 350°, for instance, the interdiffusion coefficient of Ag^+ in $LiNO_3$ becomes greater than in $NaNO_3$ because of the activation energy which in the first case (7900 cal) is much greater than in the second (4645 cal).

A comparison between the D_{Ag^+} (inter) and D_{Me^+} (self) indicates that in $LiNO_3$ the D_{Ag^+} (inter)/D_{Me^+} (self) ratio is sub-unit while in the other nitrates is over-unit and increases proportionally to the alkali cation radius.

The ionic radii of Ag^+ and Na^+ in molten nitrates are very close to each other as shown below. The conclusion is reached that $\frac{D_{inter}}{D_{self}}$ is sub-unit when the radius of foreign cation is greater than that of solvent cation and the reverse.

A similar behaviour of the ratio between the interdiffusion coefficient of the foreign cation, D_{inter}, and the selfdiffusion coefficient of solvent cation is found from other data available in the literature.

Ketelaar[11] studied the diffusion of four tracer alkali cations in $NaNO_3$, KNO_3, $RbNO_3$ and $CsNO_3$. He found out that for each fused nitrate there is a maximum value of the diffusion coefficient which corresponds in all cases to the diffusion of the tracer in its own salt.

If Ketelaar's observation is re-formulated in terms of "interdiffusion" and "selfdiffusion" the same conclusion concerning the value of the ratio D_{inter}/D_{self} with ours is reached. For the interdiffusion of K^+ ion in alkali nitrates this behaviour is illustrated in figure 6 drawn according to Ketelaar data.[12]

A satisfactory explanation for the correlation of transport phenomena in alkali nitrates could be obtained by Stokes-Einstein equation

$$D = \frac{KT}{a \pi r \eta} \tag{4}$$

where "a" is a constant, r is the radius of the diffusing ion and the other magnitudes have well known significances. In the classical formulation the value of a is 6 for the diffusion of a big particle. Li and Chang[13] have obtained a modified S-E equation in which the constant a has the value 4 corresponding to a small diffusing particle.

---

[11] J. A. A. KETELAAR and E. P. HONIG, *J. Phys. Chem.*, **68**, 1598 (1964).

[12] E. P. HONIG and J. A. A. KETELAAR, *Trans. Faraday Soc.*, **62**, 190 (1966).

[13] J. C. U. LI and P. CHANG, *J. Chem. Phys.*, **23**, 518 (1955).

The chronopotentiometric method determines in fact the limit interdiffusion coefficients (corresponding to the infinite dilution state) which by definition are equal to the diffusion coefficient of tracer ion.[14]

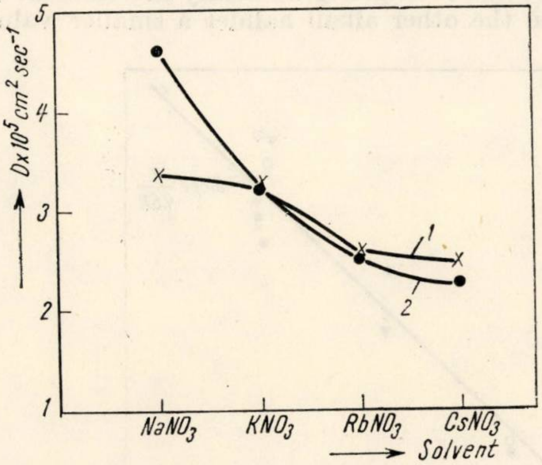

Fig. 6. — *1*, Diffusion coefficient of potassium ion in $NaNO_3$, KNO_3, $RbNO_3$ and $CsNO_3$; *2*, Cation selfdiffusion in alkali nitrates.

In these conditions the viscosity (η) in Stokes-Einstein equation is that of alkali nitrate and we get

$$\frac{D_+\,(\text{inter})}{D_+\,(\text{self})} = \frac{r_+}{r_+^*} \tag{5}$$

where r_+^* is the foreign cation radius and r_+ the radius of solvent cation. It is equally obtained

$$\frac{D_+\,(\text{self})}{D_-\,(\text{self})} = \frac{r_-}{r_+} \tag{6}$$

where r_- and D_- refer to NO_3^- anion.

Table 3

Relationships between the diffusion coefficients and ionic radii at the melting point of the solvents

Solvent	D_{Ag^+} (inter)/D_{Me^+} (self)	r_{Me^+}/r_{Ag^+}	$D_{NO_3^-}$ (self)/D_{Me^+} (self)	r_{Me^+} (self)/$r_{NO_3^-}$(self)
$LiNO_3$	0.65	0.60	0.35	0.34
$NaNO_3$	1.10	0.95	0.64	0.54
KNO_3	1.32	1.33	0.89	0.76
$RbNO_3$	1.44	1.48	—	0.84
$CsNO_3$	1.41	1.69	0.96	0.96
$AgNO_3$			0.59	0.56

---

[14] R. W. Laity and J. D. E. McIntyre, *J. Amer. Chem. Soc.*, **87**, 3806 (1965).

In order to use further S-E equation some considerations concerning the radius of silver ion are needed. The radius of silver ion found in literature is $r_{Ag^+} = 1.13$ Å and comes from the difference $d_{AgF^-} r_{F^-}$ where d refers to the interionic separation roentgenographically determined. If the same reasoning is applied to the other alkali halides a smaller value for r_{Ag^+} is found. By applying the relation $r_{Ag^+} = d_{AgX^-} r_{X^-}$ in the four halides AgX and by averaging the results $r_{Ag^+} = 0.96$ Å is obtained. Similar conclusions are reached if the study of thermodynamic properties of AgX + Alk. X systems is considered.[15] It could be assumed that in alkali nitrates the radius of silver ion is somewhat smaller than 1.13 and very close to that of natrium ion. From equation (5) one can calculate an average kinetic radius of silver ion in molten nitrates. A $r_{Ag^+} = 1.00$ Å value is obtained and which will be used in all further considerations.

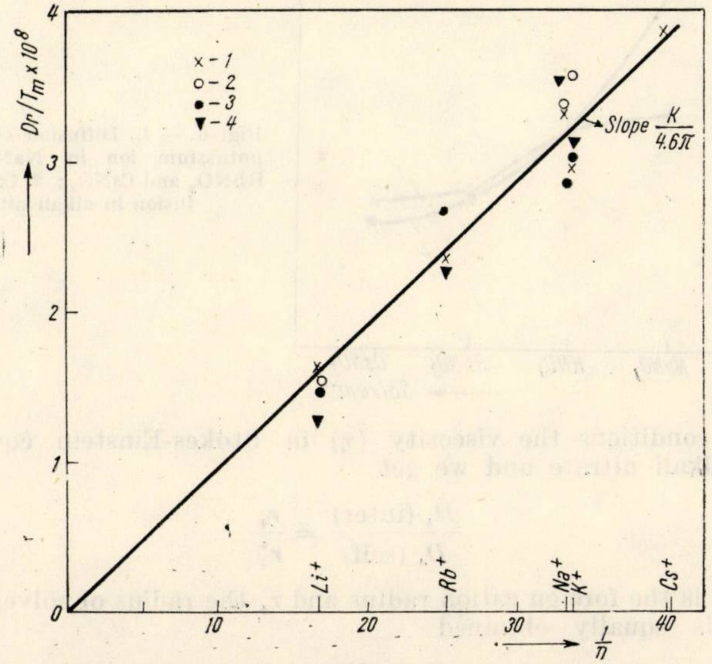

Fig. 7. — Variation of Dr/T_m versus $1/\eta$ at the temperature of solvent melting. *1*, Ag^+ interdiffusion, our results; *2*, NO_3^- selfdiffusion; *3*, cation selfdiffusion; *4*, Sjöblom results.[3]

As seen in table 3 equations (5) and (6) are satisfactorily checked and this accounts for the regularity observed in D_{inter} / D_{auto} ratio. For r_{Ag^+} the value 1.00 Å was taken and for $r_{NO_3^-}$ 1.77 (a value calculated from the $\frac{r_{Me^+}}{r_{NO_3^-}}$ ratio given by Pauling[16]).

---

[15] I. G. Murgulescu and S. Sternberg, *Z. phys. Chem.* (*Leipzig*), **219**, 114 (1962).

[16] L. Pauling, "The Nature of Chemical Bond", Cornell University Press, New York 1960, p. 547.

Figure 7 represents the verification of S—E equation for D_{Ag^+} (inter), D_{Me^+} (self) and $D_{NO_3^-}$ (self) at melting points of alkali nitrates. The values of r_{Ag^+} and $r_{NO_3^-}$ are taken as specified above. The S—E equation applies satisfactorily for a mean value of "a" constant of 4.6. This value was found by Forcheri[17] too for the selfdiffusion coefficient of Tl in $TlNO_3$ and other diffusion coefficients in alkali nitrates.

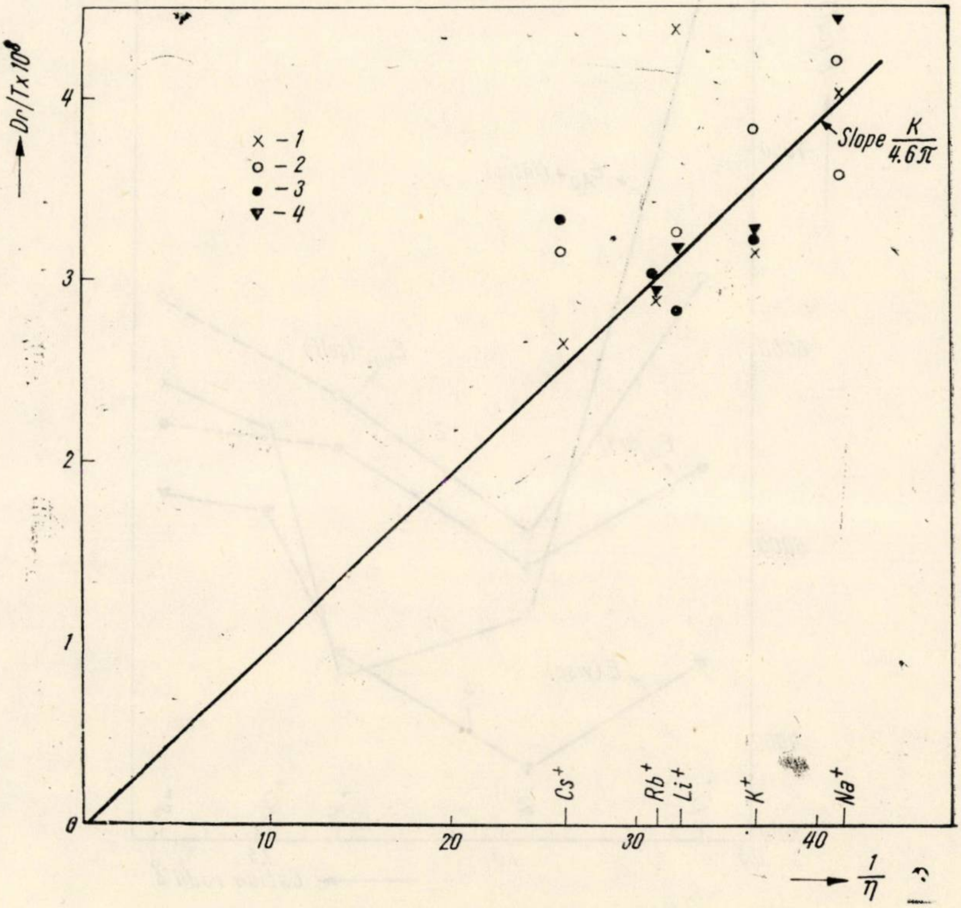

Fig. 8. — Variation of Dr/T versus $1/\eta$ at 350°.

1, Ag+ interdiffusion, our results; *2*, NO_3^- selfdiffusion; *3*, cation selfdiffusion, *4*, Sjöblom results.[3]

It is worth mentioning that at temperatures different from the melting ones the deviations from S-E equation become much higher (figure 8).

In figure 9 are plotted the activation energies for interdiffusion, selfdiffusion and viscosity. For the interdiffusion of silver ion, the very high values for $LiNO_3$ and the existence of a minimum for KNO_3 are remarkable. This could be explained as follows : the Ag^+ interdiffusion in alkali nitrates is of course influenced by the number and volume of cation holes. In lithium nitrate at the melting point the "average hole volume'

---

[17] S. Forcheri and V. Wagner, *Z. Naturforsch*, **22a**, 1171 (1967).

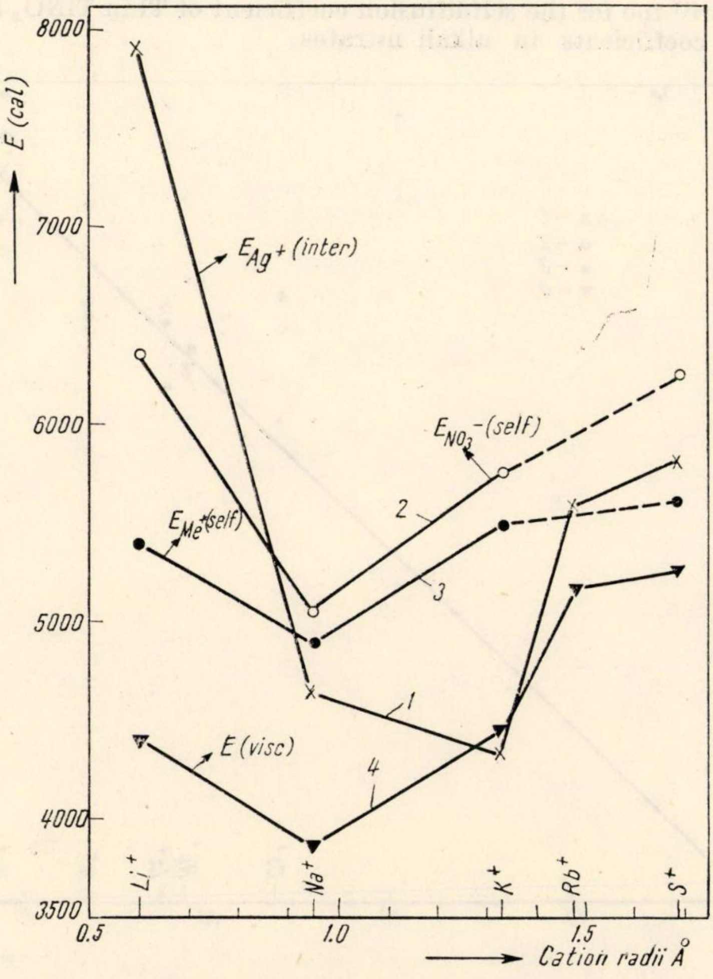

Fig. 9. — Activation energies as function of cationic radii for :
1, Ag^+ interdiffusion ; *2*, NO_3^- selfdiffusion ; *3*, cation selfdiffusion ; *4*, viscosity.

is probably smaller than the volume of silver ion and this hinders the interdiffusion. As the temperature increases the number of holes with a greater volume increases ; this explains the more pronounced increase of D_{Ag^+} (inter) *versus* temperature and the higher activation energy. In the other solvents with greater cations than silver the mean volume of holes is greater than the diffusing ion. The activation energies are much lower than in $LiNO_3$ and they steadily increase from K to Cs in the same way as the viscosity increase.

This standpoint is supported by the comparison of activation energies of cation inter- and self-diffusion. Thus, when the radius of the foreign cation is greater than the radius solvent cation $E_{\text{inter}} \gg E_{\text{self}}$. In the other cases when the radius of foreign cation is smaller than the solvent cation radius $E_{\text{inter}} < E_{\text{self}}$ except for $CsNO_3$ where E_{Cs^+} (self) is by 200 cal smaller than E_{Ag^+} (inter). The experimental data of selfdiffusion activation energies for $RbNO_3$ are not available.

Figure 9 shows that the change in the activation energy *versus* alkali cation radius has the same evolution for all the four cases discussed, but for interdiffusion the minimum is for KNO_3 while for cation and anion selfdiffusion and viscosity the minimum corresponds to sodium nitrate.

From the above analysis it ensues that the interdiffusion phenomenon is determined by three factors; the solvent viscosity, the radius of diffusing foreign cation and its ratio to the radius of solvent cation.

This standpoint is supported by the comparison of activation energies of cation inter- and self-diffusion. Thus, when the radius of the foreign cation is greater than the radius of solvent cation $E_{inter} \gg E_{self}$. In the other cases when the radius of foreign cation is smaller than the solvent cation radius $E_{inter} < E_{self}$ except for CsNO$_3$ where E_{a} (self) is by 200 cal smaller than E_{a} (inter). The experimental data of self-diffusion activation energies for RbNO$_3$ are not available.

Figure 8 shows that the change in the activation energy versus alkali cation radius has the same evolution for all the four cases discussed, but for interdiffusion the minimum is for KNO$_3$ while for cation and anion self-diffusion and viscosity the minimum corresponds to sodium nitrate.

From the above analysis it emerges that the interdiffusion phenomenon is determined by three factors: the solvent viscosity, the radius of diffusing foreign cation and its ratio to the radius of solvent cation.

Revue Roumaine de Chimie, **15**, 357–369 (1970)

THE ELECTRICAL CONDUCTIVITY OF BINARY MOLTEN ALKALI CHLORIDE SYSTEMS AS A FUNCTION OF ANION POLARIZATION

STEFANIA ZUCA and M. OLTEANU

Institute of Physical Chemistry of the Academy, Bucharest, Str. Galaţi, 31

Received March 14, 1969

The electrical conductivity and density of (Na–Rb)Cl, (Na–Cs)Cl, (K–Rb)Cl, (K–Cs)Cl and (Rb–Cs)Cl sytems are reported. These results and the available data for (Na–K)Cl and (K–Li)Cl mixtures are discussed in terms of the polarization model of Lumsden. The electrical conductivity deviations from additivity are found to obey the equation :

$$\Delta\lambda = -a\,\alpha\left[\frac{1}{(r_{\mathrm{Me_I Cl}} - d)^2} - \frac{1}{(r_{\mathrm{Me_{II} Cl}} + d)^2}\right]^2,$$

this indicating that the polarization of common anion owing to the different cation sizes, is the main hindrance to electrical transport in mixtures.

In the fused alkali halides mixtures there is no evidence of the complex ions formation; they are considered the simplest systems of molten salts completely dissociated in constituent ions. As a rule in such mixtures the systematic negative deviations from additivity of the conductivity isotherms must be assigned to the simple ionic interactions.[1]

Concerning the interaction potential significance in the fused salts two views have been expressed : Førland[2–4] assumed this interaction potential to come from the Coulomb interactions between the next-nearest neighbours. According to Lumsden[5–6] the most important contribution is due to the polarization effect of the common ion by the two uncommon ions from the mixture. Starting from this point of view Lumsden[5–6] successfully related the equilibrium properties of the binary mixtures with common anion to the polarization effect. [5-6] Referring to the transport properties, the recent results on conductivity and ionic mobility[7-10] as well as on the viscosity[11-12] of some binary mixtures could be satisfactorily explained by the anion polarization model.

---

[1] I. G. Murgulescu and Şt. Zuca, *Rev. Chim. Acad. R.P.R.*, **7**, 227 (1959).

[2] T. Førland, *J. Phys. Chem.*, **59**, 152 (1955).

[3] T. Førland, *Norg. Tekn. Vitenskapakad.*, **2**, 4 (1957).

[4] M. Blander, "Molten Salt Chemistry", Interscience Publishers, New York, 1964, p.149.

[5] J. Lumsden, *Discuss. Faraday Soc.*, **32**, 138 (1961).

[6] J. Lumsden, "Thermodynamics of Molten Salt Mixtures", Academic Press, London, 1966, p. 70.

Recently we performed[13-14] a comprehensive investigation on the electrical conductivity of binary alkali halides mixtures with common cation in which polarization of common ion is considered[6] to be very low. To explain the observed regularities of the electrical conductivity behaviour of these systems, it was necessary to take into account beside Coulomb interactions the polarization effect too.

The present communication refers to the molten binary alkali chloride mixtures with common anion. We report here the results concerning the density and the electrical conductivity of the following mixtures: (Na—Rb)Cl, (Na—Cs)Cl, (K—Rb)Cl, (K—Cs)Cl, (Rb—Cs)Cl for which no data are available. From this category of mixtures only the (Na—K)Cl and (K—Li)Cl[15-17] systems have been investigated; in the following discussion where these two mixtures are involved, reference will be made to Yaffe and Van Artsdalen's[15] experimental data.

EXPERIMENTAL AND RESULTS

The experimental set up for the density and for the conductivity measurements is similar to that previously employed. [1,13] All chemicals used in experiments were Merck p.a. reagents recrystallized and molten by a special technique pseviously described. [13] During the melting of the mixtures a thoroughly dried argon gas was bubbled for a long time through the melt, in order to eliminate any HCl trace. All salts were tested for neutrality with phenolphthalein, both before and after experiment.

The density and the specific conductivity were measured as a function of temperature at three molar fractions ($x_1 = 0.25$; 0.50; 0.75) for each system.

Table 1 gives the experimentally determined specific conductivity at different temperatures, for each investigated mixture. The corresponding data for simple salts (NaCl, KCl, RbCl and CsCl), as well as the agreement with recent literature conductivity data, were discussed elsewhere. [13,14]

The density (d), as a function of the temperature (t°C) is accurately represented by the equation

$$d = a - bt \qquad (1)$$

Numerical values of the a and b constants as determined by the least squares method, are listed in table 2—6 along with the applicable temperature range. Simultaneously, the A

---

[7] C. T. Moynihan and R. W. Laity, *J. Phys. Chem.*, **68**, 3312 (1964).

[8] V. Wagner and S. Forcheri, *Z. Naturforsch.*, **22a**, 891 (1967).

[9] V. Wagner, and S. Forcheri, *ibid.*, **23a**, 925 (1968).

[10] V. Wagner, E. Berra and S. Forcheri, *ibid.*, (in press).

[11] I. G. Murgulescu and S. Zuca, *Electrochim. Acta*, **11**, 1383 (1966).

[12] I. G. Murgulescu and S. Zuca, *ibid.*, (in press).

[13] St. Zuca, and L. Ionescu-Vasu, *Rev. Roumaine Chim.*, **12**, 1285 (1967).

[14] St. Zuca and M. Olteanu, *ibid.*, **13**, 1567 (1968).

[15] E. R. van Artsdalen and I. S. Yaffe, *J. Phys. Chem.*, **59**, 118 (1955).

[16] F. R. Duke and C. L. Bissell, *J. Electrochem. Soc.*, **3**, 717 (1964).

[17] Y. Matsumura, M. Mizeno and K. Nishihara, *Memoir of the Faculty of Engineering, Kyoto University*, **vol. XXIX**, Part 4, October 1967.

and E_λ values are reported; they represent the pre-exponential factor and respectively the activation energy in the Arrhenius equation :

$$\lambda = A\, e^{-E_\lambda/RT} \tag{2}$$

which expresses the dependence of the equivalent conductivity upon temperature (T°K).

According to the reported density data, the molar volume of investigated mixtures does not exceed additivity by more than 0.5%, the only exception is the sodium – caesium chloride system where the differences reach 1%.

Figure 1 illustrates the isotherms of molar volume at 850°. Contrary to the approximate linear behaviour of the molar volumes, the isothorms of equivalent conductivity (fig. 2) show important negative deviations from additivity. (We notice that, the x_1 molar fraction always refers to the first component concentration in the mixture).

DISCUSSIONS

The experimental values, λ, of the equivalent conductivity, the λ_e values calculated by the relation of additivity :

$$\lambda_e = x_1\,\lambda_1 + x_2\,\lambda_2 \tag{3}$$

(where x_1 and x_2 stand for the molar fractions of the two components), and the λ_M values, calculated by Markov's[18] equation :

$$\lambda_M = x_1{}^2\lambda_1 + x_2^2\lambda_2 + 2\ x_1 x_2 \lambda_1 \tag{4}$$

for the present studied mixtures and for (K–Na) Cl and (K–Li)Cl mixtures[15] are listed in table 7. The two last columns of this table indicate percent deviations of the observed electrical conductivity from both additivity and Markov's equations. When comparing these values, it is evident that generally eq. (4) predicts the experimental data better than eq. (3) does. However the agreement is satisfactory ($\sim$ 0.5%) only for (Rb–Cs)Cl system. At the same time a clear distinction exists between these systems regarding their departure from eq. (4). It is possible to group together on the one hand the (K–Rb)Cl, (K–Cs)Cl, (Rb–Cs)Cl and (Na–K)Cl mixtures for which the experimental data do not deviate by more than 2% and on the other hand the (Na–Rb)Cl, (Na–Cs) Cl and (K–Li)Cl mixtures where the deviations are approximately ten times higher.

Markov[18] pointed out that the more complicated the phase diagram of the binary system is, the larger are the departures from eq. (4), namely the percentage deviations increase in the sequence : solid solution $<$ solid solution with solubility gap $<$ eutectic system $<$ incongruently melting compounds $<$ congruently melting compounds.

Checking this correlation for the seven above mentioned alkali chloride mixtures it has been ascertained that the phase diagrams of

---

[18] I. K. Delimarski and B. F. Markov, "Electrokhimia rasplavlenykh solei" Metallurgizdat, Moscow, 1960, chap. I.

Table 1

Specific conductivity for investigated alcali chlorides

System NaCl–CsCl						System NaCl–RbCl					
$x_{NaCl} = 0.75$		$x_{NaCl} = 0.5$		$x_{NaCl} = 0.25$		$x_{NaCl} = 0.75$		$x_{NaCl} = 0.5$		$x_{NaCl} = 0.25$	
t°C	χ(ohm^{-1}cm^{-1})	t°C	χ(ohm^{-1}cm^{-1})	t°C	χ(ohm^{-1}cm^{-1})	t°C	χ(ohm^{-1}cm^{-1})	t°C	χ(ohm^{-1}cm^{-1})	t°C	χ(ohm^{-1}cm^{-1})
767.7	2.171	775.0	1.772	773.7	1.529	773.4	2.491	780.5	2.049	776.0	1.784
776.0	2.192	786.5	1.800	779.5	1.542	780.7	2.511	795.0	2.075	785.5	1.807
785.0	2.215	794.2	1.815	789.5	1.560	789.8	2.537	806.5	2.098	792.7	1.821
800.0	2.251	803.2	1.835	798.0	1.577	796.6	2.550	816.2	2.129	804.3	1.845
810.0	2.276	811.0	1.853	804.8	1.591	798.5	2.561	823.7	2.138	817.0	1.875
821.0	2.301	818.5	1.868	812.3	1.605	817.0	2.592	834.6	2.169	830.0	1.903
828.7	2.319	822.3	1.873	819.2	1.618	831.0	2.625	840.8	2.172	839.0	1.919
833.3	2.325	828.2	1.889	825.7	1.632	835.0	2.649	850.7	2.198	847.5	1.936
843.0	2.347	835.0	1.901	833.0	1.644	847.0	2.660	856.3	2.213	854.2	1.944
851.4	2.360	853.3	1.939	846.8	1.670	854.5	2.680	866.6	2.228	863.0	1.965
855.5	2.371	860.4	1.953	851.8	1.680	865.0	2.702	875.1	2.252	871.0	1.980
862,5	2.380	868.4	1.967	864.0	1.702	867.0	2.712	882.0	2.267	882.0	2.001
866.5	2.397	873.7	1.978	875.5	1.720	876.0	2.734			887.0	2.013
873.7	2.404	879.0	1.989	880.0	1.734	882.6	2.751				

Table 1 (continued)

System KCl – CsCl						System KCl RbCl					
$x_{KCl}=0.75$		$x_{KCl}=0.5$		$x_{KCl}=0.25$		$x_{KCl}=0.75$		$x_{KCl}=0.5$		$x_{KCl}=0.25$	
t°C	χ(ohm^{-1}cm^{-1})	t°C	χ(ohm^{-1}cm^{-1})	t°C	χ(ohm^{-1}cm^{-1})	t°C	χ(ohm^{-1}cm^{-1})	t°C	χ(ohm^{-1}cm^{-1})	t°C	χ(ohm^{-1}cm^{-1})
778.4	1.873	751.0	1.611	794.0	1.560	790.7	2.025	793.5	1.889	783.6	1.749
789.4	1.901	765.6	1.638	798.0	1.570	803.6	2.058	800.0	1.909	791.7	1.766
798.6	1.925	771.4	1.651	806.5	1.588	815.5	2.088	805.8	1.926	796.6	1.776
808.5	1.948	779.0	1.670	814.5	1.604	822.8	2.106	810.6	1.936	806.2	1.798
823.4	1.981	783.5	1.683	823.0	1.620	828.4	2.120	813.3	1.944	815.5	1.816
836.5	2.010	792.2	1.700	828.0	1.629	838.0	2.140	820.0	1.956	822.6	1.828

846.0	2.031	800.2	1.714	837.4	1.644	844.8	2.156	828.8	1.977	830.0	1.845
852.7	2.045	808.7	1.738	846.4	1.662	850.0	2.170	833.3	1.984	840.0	1.865
862.5	2.064	815.5	1.752	855.6	1.680	856.5	2.180	840.0	2.003	848.6	1.884
875.5	2.089	821.5	1.760	862.8	1.695	862.5	2.193	851.8	2.027	853.3	1.893
887.8	2.120	830.6	1.780	866.6	1.701	875.0	2.218	855.4	2.033	862.3	1.915
894.5	2.130	835.8	1.791	873.5	1.715	881.4	2.232	862.5	2.047	872.2	1.938
		843.3	1.807	880.5	1.725	889.0	2.249	876.6	2.075		
		853.7	1.828			901.4	2.275	885.6	2.091		
		863.7	1.848			908.0	2.291	902.5	2.126		
		870.6	1.865			915.5	2.308	916.8	2.157		
		879.5	1.885								

Table 1 (continued)

System RbCl – CsCl					
$x_{RbCl} = 0.75$		$x_{RbCl} = 0.5$		$x_{RbCl} = 0.25$	
t°C	$\chi(\text{ohm}^{-1}\text{cm}^{-1})$	t°C	$\chi(\text{ohm}^{-1}\text{cm}^{-1})$	t°C	$\chi(\text{ohm}^{-1}\text{cm}^{-1})$
775.3	1.551	753.8	1.447	780.6	1,445
781.8	1.565	768.0	1.469	786.5	1.459
789.7	1.581	778.6	1.490	796.0	1.475
799.0	1.603	786.2	1.504	801.0	1.488
805.2	1.615	793.0	1.518	806.2	1.495
810.3	1.624	800.2	1.531	815.0	1.512
817.8	1.639	807.4	1.547	825.0	1.527
825.0	1.653	815.3	1.566	827.8	1.534
830.4	1.661	821.2	1.574	836.5	1.548
836.0	1.673	823.7	1.582	843.7	1.562
842.6	1.685	832.6	1.595	851.4	1.574
846.4	1.692	841.0	1.610	858.0	1.585
855.6	1.711	850.2	1.625	864.6	1.595
862.0	1.723	858.3	1.639	868.8	1.603
868.7	1.734	866.3	1.654	879.8	1.625
879.8	1.755	871.5	1.663		
888.8	1.772	879.8	1.679		
		885.0	1.689		
		891.5	1.702		

Table 2

System NaCl–RbCl

x_{NaCl}	a	$b \times 10^3$	Standard deviations	Temperature range °C	$A \times 10^{-2}$	E_λ kcal/mol	Standard deviations for E_λ	Temperature range °C
1	1.9903	0.5444	0.0002	809–905	4.41	2.53	0.015	810–950
0.75	2.3852	0.7988	0.0005	730–900	4.85	3.19	0.015	750–890
0.50	2.4957	0.7303	0.0007	730–880	5.04	3.50	0.018	770–890
0.25	2.6905	0.8016	0.0007	720–880	5.21_5	3.65	0.013	750–895
0	2.8537	0.8514	0.0009	740–960	5.46	3.75	0.028	740–920

Table 3

System NaCl–CsCl

x_{NaCl}	a	$b \times 10^3$	Standard deviations	Temperature range °C	$A \times 10^{-2}$	E_λ kcal/mol	Standard deviations for E_λ	Temperature range °C
1	1.9903	0.5444	0.0002	809–905	4.41	2.53	0.015	810–950
0.75	2.5445	0.7616	0.0009	750–870	4.57_5	3.24	0.010	750–870
0.50	2.9623	0.9410	0.0010	730–870	5.21	3.65	0.004	750–880
0.25	3.2261	0.9853	0.0009	720–870	5.36	3.77	0.007	750–880
0	3.5023	1.0849	0.0008	660–820	6.06	4.00	0.010	670–860

Table 4

System KCl – RbCl

x_{KCl}	a	$b \times 10^3$	Standard deviations	Temperature range °C	$A \times 10^{-2}$	E_λ kcal/mol	Standard deviations for E_λ	Temperature range °C
1	1.9564	0.5583	0.0002	780–940	5.53	3.44	0.012	780–920
0.75	2.2265	0.6694	0.0005	780–920	5.76	3.64_5	0.008	780–920
0.50	2.4348	0.7264	0.0010	780–900	5.82	3.74	0.016	760–920
0.25	2.6808	0.8249	0.0006	750–880	5.53	3.71	0.037	780–920
0	2.8537	0.8514	0.0009	740–960	5.46	3.75	0.028	740–920

Table 5

System KCl – CsCl

x_{KCl}	a	$b \times 10^3$	Standard deviations	Temperature range °C	$A \times 10^{-2}$	E_λ kcal/mol	Standard deviations for E_λ	Temperature range °C
1	1.9564	0.5583	0.0002	780–940	5.53	3.44	0.012	780–920
0.75	2.4491	0.7654	0.0006	750–875	5.79	3.69	0.029	750–900
0.50	2.8429	0.8840	0.0006	720–870	6.08_5	3.90	0.011	750–890
0.25	3.1863	0.9898	0.0007	690–870	5.92	3.91	0.011	760–890
0	3.5023	1.0849	0.0008	660–820	6.06	4.00	0.010	670–860

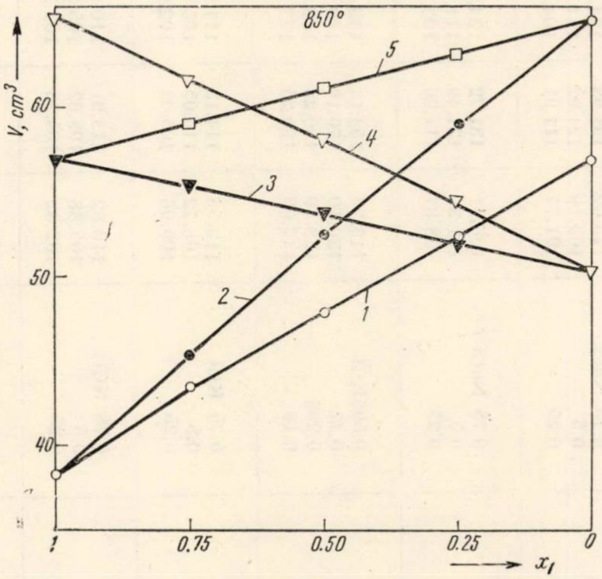

Fig. 1. — The isotherms of molar volume of alkali chloride mixtures at 850°

1, (Na–Rb)Cl; *2*, (Na–Cs)Cl; *3*, (K–Rb)Cl; *4*, (K–Cs)Cl; *5*, (Rb–Cs)Cl.

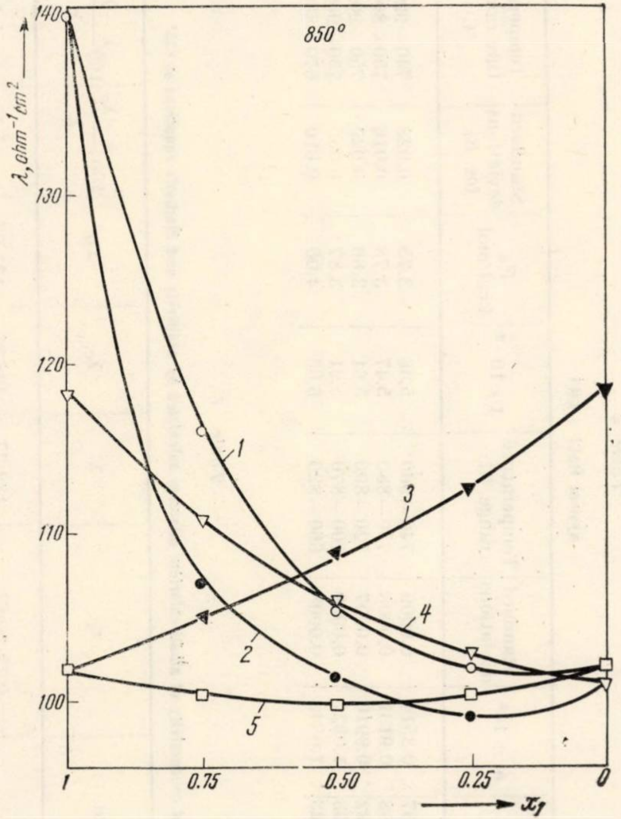

Fig. 2. — The isotherms of equivalent conductivity of alkali chloride mixtures at 850°:

1, (Na–Rb)Cl; *2*, (Na–Cs)Cl; *3*, (K–Rb)Cl; *4*, (K–Cs)Cl; *5*, (Rb–Cs)Cl.

Table 6

System RbCl – CsCl

x_{RbCl}	a	$b \times 10^3$	Standard deviations	Temperature range °C	$A \times 10^{-2}$	$E\lambda$ kcal/mol	Standard deviations for $E\lambda$	Temperature range °C
1	2.8537	0.8514	0.0009	740–960	5.46	3.75	0.028	740–920
0.75	3.0238	0.9131	0.0008	750–880	5.47	3.78	0.016	750–890
0.50	3.2022	0.9910	0.0007	720–890	5.61	3.86	0.029	750–900
0.25	3.3493	1.0327	0.0009	700–870	5.61	3.87	0.055	750–900
0	3.5023	1.0849	0.0008	660–820	6.06	4.00	0.010	670–860

Table 7

Equivalent conductivity of alkali chlorides mixtures calculated by additivity and Markov's equations at 850°

System	x_1	λ	λ_C	λ_M	$100\,\dfrac{\lambda-\lambda_C}{\lambda}$	$100\,\dfrac{\lambda-\lambda_M}{\lambda}$
(Na–K)Cl	0.73 NaCl	129.77	136.36	131.63	– 5.1	– 1.4
	0.51	122.88	131.13	125.06	– 6.7	– 1.8
	0.20	118.01	123.71	119.75	– 4.8	– 1.5
(Na–Rb)Cl	0.75 NaCl	115.92	131.93	124.42	–13.81	– 7.33
	0.5	105.19	121.92	111.91	–15.90	– 6.39
	0.25	101.77	111.91	104.40	– 9.96	– 2.58
(Na–Cs) Cl	0.75 NaCl	106.91	131.72	124.04	–23.21	–16.02
	0.5	101.30	121.49	111.26	–19.93	– 9.83
	0.25	98.87	111.26	103.59	–12.53	– 4.77
(Li–K)Cl	0.595KCl	115.74	154.14	133.09	–33.18	–14.99
(K–Li)Cl	0.41	126.10	170.18	149.01	–34.96	–18.17
	0.296	129.89	180.28	162.05	–38.86	–24.82
	0.18	147.99	190.25	177.22	–28.56	–19.75
(K–Rb)Cl	0.75 KCl	112.56	114.13	111.07	– 1.13	+ 1.32
	0.5	108.72	110.05	105.98	– 1.22	+ 2.52
	0.25	105.06	105.98	102.92	– 0.88	+ 2.04
(K–Cs)Cl	0.75 KCl	110.82	113.91	110.69	– 2.79	+ 0.12
	0.5	105.88	109.62	105.33	– 3.53	+ 0.52
	0.25	102.82	105.33	102.11	– 2.43	+ 0.69
(Rb–Cs)Cl	0.75 RbCl	100.60	101.69	101.52	– 1.08	– 0.91
	0.5	99.45	101.48	101.26	– 2.04	– 1.82
	0.25	99.05	101.26	101.09	– 2.23	– 2.06

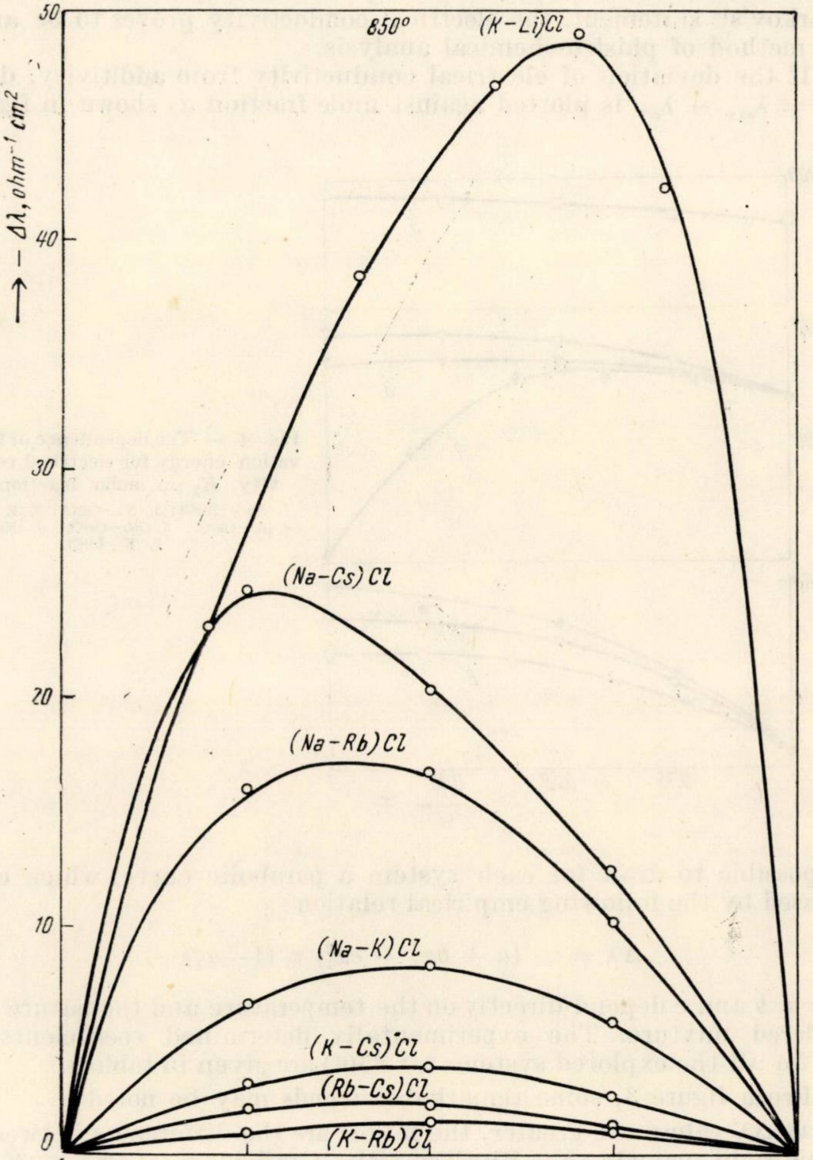

Fig. 3. — The dependence of the deviations from additivity $\Delta\lambda$ on the molar fraction x_1.

all four systems from the first group indicate[19,20] the formation of solid solution while the last three mixtures give eutectic systems.[21,22] According to Markov's[18] statement, the electrical conductivity proves to be an efficient method of phisico-chemical analysis.

If the deviation of electrical conductivity from additivity, defined as $\Delta\lambda = \lambda_{\text{exp}} - \lambda_c$, is plotted against mole fraction as shown in figure 3,

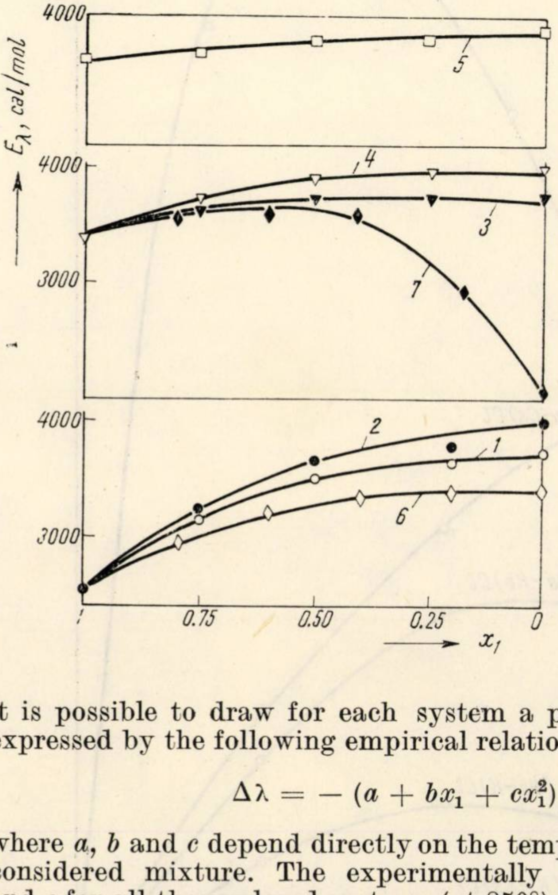

Fig. 4. — The dependence of the activation energy for electrical conductivity, E_λ on molar fraction x_1: *1*, (Na – Rb)Cl; *2*, (Na – Cs)Cl; *3*, (K – Rb)Cl; *4*, (K – Cs)Cl; *5*, (Rb – Cs)Cl; *6*, (Na – K)Cl; *7*, (K – Li)Cl.

it is possible to draw for each system a parabolic curve, which can be expressed by the following empirical relation:

$$\Delta\lambda = -(a + bx_1 + cx_1^2)\, x_1\, (1 - x_1) \tag{5}$$

where a, b and c depend directly on the temperature and the nature of the considered mixture. The experimentally determined coefficients a, b and c for all the explored systems (at 850°) are given in table 8.

From figure 3, some remarkable trends may be noted:

a) $\Delta\lambda$ values are greater, the larger are the differences between the cationic radii, namely (K – Rb)Cl < (Rb – Cs)Cl < (K – Cs)Cl < (K – Na) Cl < (Na – Rb)Cl < (Na – Cs)Cl < (Li – K)Cl.

---

[19] S. Zemczuzny and F. Rambach, *Z. anorg. Chem.*, **65**, 403 (1910).

[20] E. K. Akopov and A. G. Bergman, *Zhur. obschchei Khim.*, **24**, 1524 (1954).

[21] E. Aukrust, B. Björge, H. Flood and T. Førland, *Ann. New York Acad. Sci.*, **79**, 830 (1960).

[22] I. G. Murgulescu and S. Sternberg, *Z. phys. Chem. (Leipzig)*, **219**, 114 (1962).

b) the asymmetry of $\Delta\lambda$ *vs.* x_1 curves becomes more pronounced in the series following the same order. These two behaviours may be qualitatively explained in terms of the polarization model of Lumsden. [5,6] According to this model, in a binary mixture with a common anion, let us say $(\mathrm{Me_I}-\mathrm{Me_{II}})\mathrm{Cl}$ where $r_{\mathrm{Me}_\mathrm{I}^+} < r_{\mathrm{Me}_\mathrm{II}^+}$, r denoting the alkali cation radius, the common anion becomes polarized by the unsymmetrical electric field due to the different sizes of the two cations. As a result of induced anion polarization, sort of associated cation-anion groups, as $\mathrm{Me_I}-\mathrm{Cl}-\mathrm{Me_{II}}$, appear in the melt; the common anion being displaced towards the smaller cation. Consequently, the latter moves against the nearest Cl^- ion, with more difficulty in the mixture than in the simple salt. Hence the mobility and implicitly the electrical conductivity will be smaller in mixtures compared to the simple salts. The effect being more marked as the difference between the two cations is greater, we expect $\Delta\lambda$ values to increase in the same way, as may be clearly seen in figure 3.

Table 8

The values of constants a, b, c, of eq. (5) at 850°

System	*a*	*b*	*c*
(Na–K)Cl	27.3674	13.0799	−3.5942
(Na–Rb)Cl	46.9521	17.5527	44.9680
(Na–Cs)Cl	88.3738	−162.3000	294.5687
(K–Li)Cl	304.9500	−415.3200	234.2600
(K–Rb)Cl	7.1438	−14.1789	21.0863
(K–Cs)Cl	6.8115	23.1438	−13.6581
(Rb–Cs)Cl	17.8179	−28.9137	19.0096

A strengthening of the attractive force between the smaller cation and the common anion, $(\mathrm{Me_I}-\mathrm{Cl})$, when the second component $(\mathrm{Me_{II}Cl})$ is added in the melt, leads to an initial drop of electrical conductivity which is more rapid as $r_{\mathrm{Me}_\mathrm{I}^+} \ll r_{\mathrm{Me}_\mathrm{II}^+}$. Therefore the maximum of $\Delta\lambda vs. x_1$ curves will shift towards the $\mathrm{Me_ICl}$ rich region, more definitely as $r_{\mathrm{Me}_\mathrm{I}^+} \ll r_{\mathrm{Me}_\mathrm{II}^+}$. If changes in relative mobility are to be attributed to changes in the cation-anion bond energy, it is reasonable to expect a corresponding change in the activation energy for the electrical conductivity of the mixture. A plot of E_λ versus x_1, as in figure 4, shows the activation energy of mixtures to be always higher than that calculated additively. The increases in the excess energy, ΔE_λ, follow the development observed in figure 3 for $\Delta\lambda$. (The E_λ values for (Na–K)Cl and (K–Li)Cl systems were calculated from data in papers[15,17]).

If the above discussed model is correct, we consider that $\Delta\lambda$ has to be quantitatively correlated to the anion polarization. The polarization energy of a bond $\mathrm{Me_I}-\mathrm{Cl}-\mathrm{Me_{II}}$ is given by Debye's equation:

$$E_p = -\frac{\alpha}{2} F^2 \tag{6}$$

where α is the anion polarization and F the electric field. According to Lumsden[5,6] this last term is given by the relation :

$$F = e\left[\frac{1}{r^2_{\mathrm{Me_IC l}}} - \frac{1}{r^2_{\mathrm{Me_{II}Cl}}}\right] \tag{7}$$

and finally the expression for polarization energy becomes :

$$E_p = -\frac{e^2}{2}\alpha\left[\frac{1}{r^2_{\mathrm{Me_ICl}}} - \frac{1}{r^2_{\mathrm{Me_{II}Cl}}}\right]^2 \tag{8}$$

where $r_{\mathrm{Me_ICl}}$ and $r_{\mathrm{Me_{II}Cl}}$ refer to the interionic separation in single salts. Multiplying eq. (8) by N one obtains the polarization energy due to a gram mole of ion each polarized by two unlike ions.

Recently, Sternberg and Herdlicka,[23] extending the theory of strict regular solutions to ionic liquids, obtained for polarization energy, the following relation :

$$E_p = -\frac{e^2}{2}\alpha\left[\frac{1}{(r_{\mathrm{Me_ICl}} - d)^2} - \frac{1}{(r_{\mathrm{Me_{II}Cl}} + d)^2}\right]^2 \tag{9}$$

where

$$d = 0.1274\,\frac{r_{\mathrm{Me_ICl}} - r_{\mathrm{Me_{II}Cl}}}{r_{\mathrm{Cl^-}}} \tag{10}$$

In figure 5 the observed $\Delta\lambda$ values for equimolecular mixtures are plotted against $\alpha\left[\frac{1}{(r_{\mathrm{Me_ICl}} - d)^2} - \frac{1}{(r_{\mathrm{Me_{II}Cl}} + d)^2}\right]^2$ parameter. It can be seen that there is a proportionality and a straight line can be drawn through the obtained points and the origin of the coordinate system. The most notable exception is the already mentioned (Na$-$Cs)Cl system. In fig. 5 the value of Kordes[24] for the anion polarizability was used, the interionic separations were taken from Wychoff[25] and "d" values from the previously quoted paper.[23]

The results in figure 5 prove that $\Delta\lambda$ can be expressed as :

$$\Delta\lambda = -a\alpha\left[\frac{1}{(r_{\mathrm{Me_ICl}} - d)^2} - \frac{1}{(r_{\mathrm{Me_{II}Cl}} + d)^2}\right]^2 \tag{11}$$

where "a" is a factor changing very little with the temperature and molar fraction of the mixture, (lines with only very little different slope can be drawn for different temperatures and concentrations). For 850° and $x_1 = x_2 = 0.5$, "a" is equal to 7.501×10^3. It means that the line drawn on figure 5 has a slope $\sim$ 10 times less than calculated by eq. (9). The result is open to serious discussions. As a matter of fact it is difficult at the present time to make a realistic estimate of the numerical multiplying factor of eqs. (8) and (9).[5,6]

---

[23] S. Sternberg and C. Herdlicka, *Rev. Roumaine Chim.*, **13**, 13 (1968).

[24] E. Kordes, *Z. Electrochem.*, **59**, 551 (1955).

[25] R. W. G. Wyckoff, "Crystal Structure", Interscience, New York, 1948.

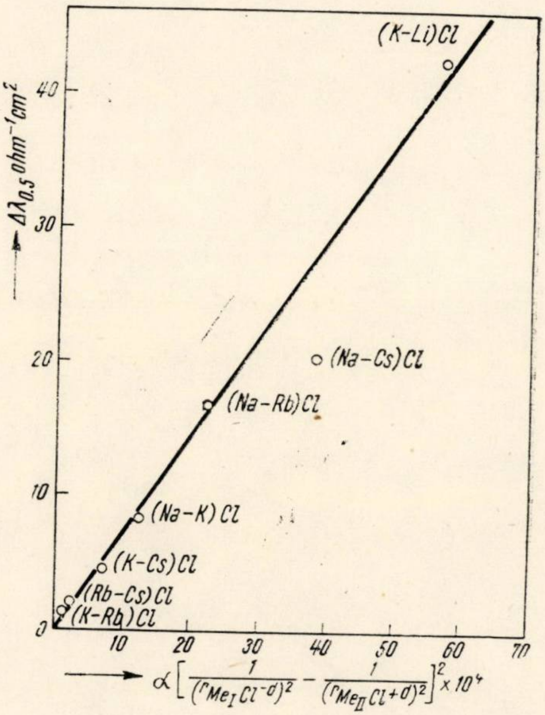

Fig. 5. — The dependence of $\Delta\lambda_{0,5}$ on the $\alpha\left[\frac{1}{(r_{\mathrm{Me_I Cl}}-d)^2}-\frac{1}{(r_{\mathrm{Me_{II}Cl}}+d)^2}\right]^2$ parameter.

In conclusion, it is apparent that the alkali chlorides mixtures behave in a manner which is generally consistent with the polarization model. In a first approximation, the deviations of the electrical conductivity isotherms from additivity are related, in these mixtures, to a function of anion polarization and interionic distances.

Revue Roumaine de Chimie, **15**, 371–376 (1970)

THE EFFECT OF PRETREATMENT ON THE ELECTRICAL RESISTANCE VARIATION OF ZINC OXIDE THIN FILMS, UNDER IRRADIATION AND CARBON MONOXIDE CHEMISORPTION

MIHAELA TEODORESCU and E. SEGAL

Institute of Physical Chemistry of the Academy, Bucharest, str. Dumbrava Roşie 23

Received February 6, 1969

Results are given which refer to the chemisorptive and photosorptive properties of thin zinc oxide films pretreated as follows: thermally, by irradiation and by previous oxygen chemisorption. Evidence is brought of the influence of carbon monoxide chemisorption, in the dark and under irradiation, on the future behaviour of zinc oxide films.

Zinc oxide is a catalyst used in many and various chemical processes. Its catalytic action in oxidizing carbon monoxide both under irradiation and in the dark is well known.[1]

This paper presents the influence of pretreatment on the chemisorptive and photosorptive properties of zinc oxide films.

EXPERIMENTS AND RESULTS

The experimental device and the method used for obtaining the films were already described in a previous paper.[2] The zinc oxide films thickness was 2000 Å. The changes of the film properties due to pretreatment, irradiation and chemisorption, were studied by the variation of the electrical resistance. The working temperature was 77°K.

In a first set of experiments, the carbon monoxide chemisorption on zinc oxide films was studied in the following conditions:

1. — The zinc oxide film was outgassed for 5 hours at 450° and then stabilized at 77°K. It was maintained in the dark during carbon monoxide chemisorption.

2. — The zinc oxide film with carbon monoxide or oxygen previously chemisorbed on, was outgassed again. The value of the electrical resistance after outgassing and reaching of the temperature of 77°K, was greater than that corresponding to a clean film.

3. — The zinc oxide film was successively irradiated and maintained in the dark in vacuum, for nearly 10 minutes, until the electrical resistance in the dark or under irradia-

---

[1] W. Doerffler and K. Hauffe, *J. Catalysis*, **3**, 170 (1964).

[2] E. Segal and M. Teodorescu, *Rev. Roumaine Chim.*, **11**, 1449 (1968).

tion become constant. Carbon monoxide was introduced both in the dark and under irradiation.

4. — The outgassed zinc oxide film was maintained in the dark, and oxygen pretreated. The oxygen chemisorption causes also the increase of the electrical resistance.[3]

In all four cases presented, the carbon monoxide chemisorption leads to an increase of the electrical resistance of the film (that is, a positive variation).

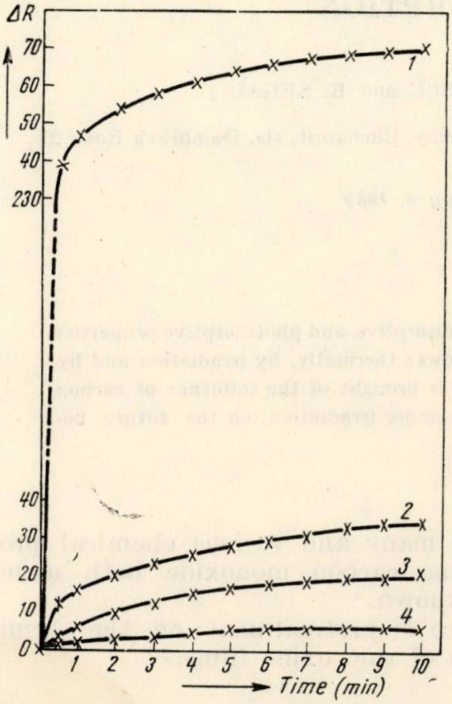

Fig. 1. — Plot $\Delta R = f(t)$ for the carbon monoxide chemisorption on untreated zinc oxide film ;
1, 2, 3, 4, successive gas introduction.

In figure 1, it is possible to see the curve of the film resistance variation (ΔR) as a function of time for the experiment described at point 1.

In another set of experiments, the zinc oxide film was pretreated in vacuum, undergoing periods of irradiation followed by periods when it was maintained in the dark. The values of the resistance variation obtained in this case for two films of nearly the same thickness are shown in figures 2 and 4.

The great variation produced by the first irradiation can be remarked. After the third irradiation, the absolute value of the electrical resistance variation in the dark becomes nearly equal to that obtained under irradiation. The variation in the dark is the same after every irradiation.

The electrical resistance variation after saturation, when carbon monoxide was introduced and chemisorbed on the film in the dark, is shown in figure 3.

One may notice that irradiation produces a negative variation whose value is greater than the corresponding value in vacuum. The maximum variation of the electrical resistance corresponding to the period in the dark is also greater than in vacuum. It has been observed

---

[3] E. Segal and M. Teodorescu, *Rev. Roumaine Chim.*, **12**, 75 (1967).

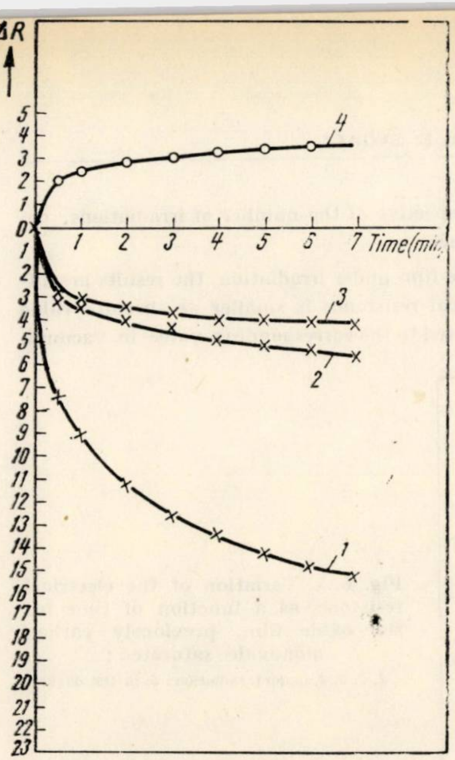

Fig. 2. — Variation of the electrical resistance as a function of time, for zinc oxide film in vacuum ;

1, 2, 3, under irradiation ; *4,* in the dark.

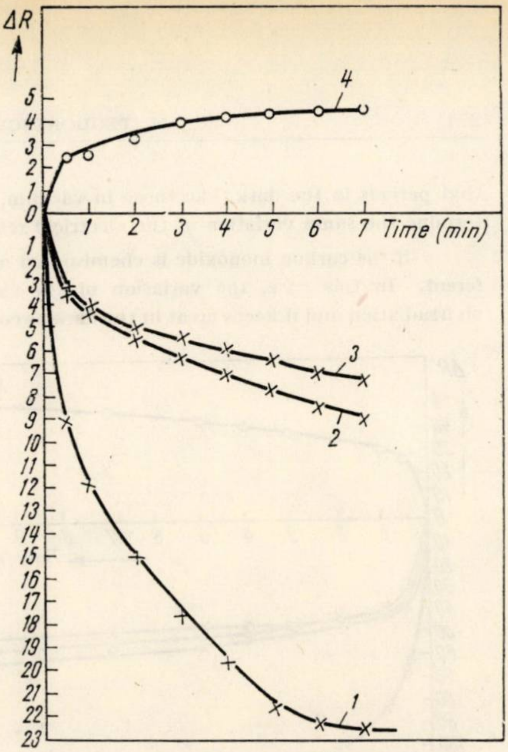

Fig. 3. — Variation of the electrical resistance as a function of time using the zinc oxide film shown in figure 2, after previous carbon monoxide chemisorption in the dark ;

1, 2, 3, under irradiation ; *4,* in the dark.

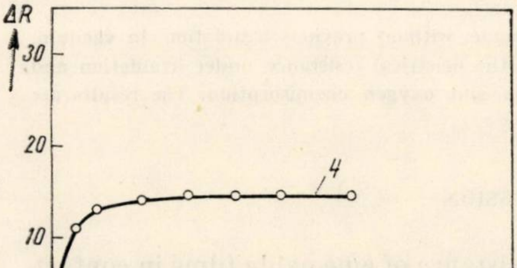

Fig. 4. — Variation of the electrical resistance as a function of time for zinc oxide film in vacuum ;

1, 2, 3, under irradiation ; *4,* in the dark.

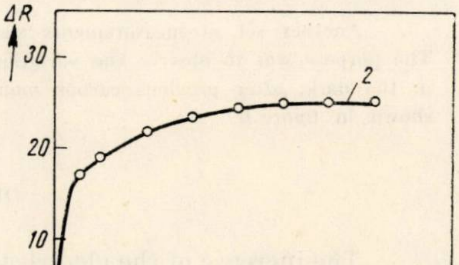

Fig. 5. — Variation of the electrtical resistance as a function of time using the zinc oxide film shown in figure 4, after previous carbon monoxide chemisorption on irradiated film ;

1, under irradiation ; *2,* in the dark.

that periods in the dark, like those in vacuum, irrespective of the number of irradiations, determine the same variation of the electrical resistance.

If the carbon monoxide is chemisorbed on the film under irradiation, the results are different. In this case, the variation of the electrical resistance is smaller as absolute value on irradiation and it keeps great in the dark as compared to the corresponding value in vacuum.

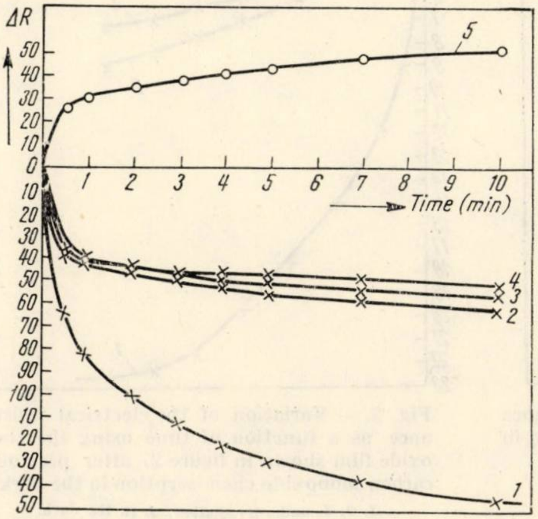

Fig. 6. — Variation of the electrical resistance as a function of time for zinc oxide film, previously carbon monoxide saturated;
1, 2, 3, 4, under irradiation; *5,* in the dark.

Another set of measurements were made without previous irradiation in vacuum. The purpose was to observe the variation of the electrical resistance under irradiation and in the dark, after previous carbon monoxide and oxygen chemisorption. The results are shown in figure 6.

DISCUSSION

The increase of the electrical resistance of zinc oxide films in contact with carbon monoxide at 77°K points to the chemical character of this interaction even at low temperature. The explanation of this phenomenon is similar to that made in a previous paper[2] for the interaction of carbon monoxide with zinc oxide films at room temperature.

On pretreatment with oxygen of the zinc oxide films the situation does not change qualitatively, the interaction of carbon monoxide being achieved by partial reactions with different kinds of negatively charged chemisorbed oxygen. Their presence on the surface is due both to previous oxygen chemisorption and to the method of preparing the zinc oxide films by oxidizing the metal zinc. The forms O_2^{--}, O_2^{-}, O^{-} were brought out.[4,5] Some of these forms are retained on the surface even after long outgassing, the fact being confirmed by the greater value of the electrical resistance after outgassing (experiment 2).

[4] Kozo Hirota and Masazumi Chono, *Sci. Papers Inst. Phys. Chem. Res.*, **58**, 115 (1964).

[5] I. P. Solonitzin, *Kinetika i Kataliz*, **3**, 433 (1965).

The carbon monoxide pretreatment does not seem to have any influence on oxygen chemisorption, this being adsorbed while realizing new electrically charged forms on the surface.

The behaviour of zinc oxide films in vacuum, in the dark and under irradiation, can also be explained by the different kinds of ionic oxygen chemisorbed on the surface. The negative resistance variations when irradiating present a partial reversibility, which can be assigned to the fact that the interaction between irradiation and the film leads both to the discharge of some of the chemisorbed oxygen forms, and to desorption. The oxygen desorbed under irradiation is adsorbed again when stopping irradiation, in the same quantity after every irradiation, the fact being proved by the same positive resistance variation obtained in the dark (fig. 2 and 4).

The photodesorption phenomenon can be interpreted by the electronic theory of chemisorption and catalysis on the sign of the photoeffect.[6-9]

The positive resistance variation in the dark, in a carbon monoxide atmosphere, is greater than in vacuum (fig. 3 and 5). This allows to presume that both oxygen and carbon monoxide desorbed during irradiation are readsorbed. Previous irradiation produces a greater number of O_2^- ions, due both to the irreversible discharge of O_2^{--} under irradiation, and to the reversible oxygen adsorption in the form of O_2^-.

Because O_2^- ions work like chemisorptive centers for carbon monoxide, it is evident that this one will be stronger and correspondingly, the resulting electrical resistance variation will be higher.

This effect is even more marked (fig. 5 — positive variation) if the contact between carbon monoxide and the film is achieved under irradiation, the surface concentration of O_2^- adsorption centers being respectively greater.

The absolute value of the electrical resistance variation, greater under irradiation in a carbon monoxide atmosphere and after saturation of the film with carbon monoxide in the dark, than the corresponding value in vacuum, can be explained taking into account the fact that due to previous irradiation in vacuum, the quantity of carbon monoxide adsorbed in the dark is greater. Then correspondingly, the quantity which can be photodesorbed due to the irradiation is greater, and thus a greater absolute value of the resistance variation is obtained.

Under irradiation the quantity of carbon monoxide which can be chemisorbed on a pretreated film is smaller (saturation is more quickly realized). For following irradiations, the quantity desorbed is smaller, and consequently the resistance variations will be smaller (fig. 5).

The phenomenon can be treated like a special case of memory effect. Solonitzin[10] studies the memory effect on pretreated zinc oxide

---

[6] F. F. Volkenstein, "The Electronic Theory of Catalysis on Semiconductors", Pergamon Press, Oxford, London-New York, Paris, 1963, chap. 10.

[7] F. F. Volkenstein and S. M. Kogan, *Zhur. fiz. Khim.*, **55**, 483 (1958).

[8] F. F. Volkenstein and I. V. Karpenko, *Kinetika i Kataliz*, **1**, 72 (1962).

[9] F. F. Volkenstein, *Kinetika i Kataliz*, **2**, 481 (1961).

[10] I. P. Solonitzin, Thesis, Leningrad, 1965.

and stresses the fact that chemisorption is stronger on a pretreated film, while photosorption is weaker. In another paper[11] evidence is brought of the "postaction" effect, which consists in keeping the continuity character of the photosorption phenomenon, even when irradiation stops. The same theoretical explanation was given[12] for the two effect types.

The memory observed by us, refers to the films behaviour after preirradiation and after chemisorption until saturation. Zinc oxide "remembers" the way in which the carbon monoxide chemisorption was made, (in the dark or under irradiation) and behaves differently.

CONCLUSIONS

The interaction of carbon monoxide at 77°K with zinc oxide films which were pretreated thermally, by irradiation and oxygen chemisorption, leads to an effect which can be interpreted by means of the electronic theory of chemisorption and photosorption on semiconductors.

A memory effect, manifest after pretreatment by irradiation and carbon monoxide chemisorption until saturation, is apparent.

[11] R. Coekelbergs, A. Crucq, J. Decot, L. Degols, M. Randoux and L. Timerman, *J. Phys. Chem. Solids*, **26**, 1983 (1965).

[12] F. F. Volkenstein and V. G. Baru, *Zhur. fiz. Khim.*, **1317**, 6 (1968).

Revue Roumaine de Chimie, **15**, 377–384 (1970)

HEAT OF DILUTION OF AQUEOUS SOLUTIONS OF POTASSIUM, SILVER AND LEAD NITRATES

E. J. TOMUŞ

Laboratory of Physical Chemistry, University of Bucharest, Bd. Republicii 13

Received March 19, 1969

The heats of dilution of aqueous solutions of KNO_3, $AgNO_3$ and $Pb(NO_3)_2$ have been measured, at 25°, calorimetrically. The measurements in the range of dilute solutions have been carried out using a resistance thermometer sensitive to temperature changes of 10^{-5}°, while in the range of concentrated solutions a mercury thermometer giving 0.01° has been used. A relationship for the heat of dilution as function of concentration, valid at all concentrations, has been developed.

INTRODUCTION

Heats of dilution data are of a general interest, the process of dilution being always involved in processes occurring in solutions. A special interest has been shown in measurements of heats of dilution of dilute solutions in order to provide a proof of Debye-Hückel limiting law for electrolytic solutions. This explains, presumably, why data on the heats of dilution in the range of dilute solutions are available[1] now for the most of aqueous electrolytic solutions while, for many of these, such data are lacking in the range of concentrated solutions. For example, the heat of dilution of dilute aqueous potassium nitrate solutions have been measured by Lange and Monheim[2] but there are no measurements of heats of dilution of concentrated aqueous potassium nitrate solutions.

In this paper the heats of dilution, at 25°, of aqueous solutions of three nitrates, potassium, silver and lead nitrates, are reported, the measurements being carried out for dilute as well as for concentrated solutions.

EXPERIMENTAL

Substances. The potassium nitrate and lead nitrate used for measurements were pure chemical reagent grade, of 99.98% purity, produced by "Reactivul-Bucureşti". Before use they were recrystallized from water and dried at 110°. The silver nitrate was pure grade. It was dried in vacuum before use.

---

[1] E. Lange and A. L. Robinson, *Chem. Rev.*, **9**, 89 (1931) ; F. D. Rossini, "Selected Values of Chemical Thermodynamic Properties", National Bureau of Standards, Circular 500 (1961).

[2] E. Lange and J. Monheim, *Z. phys. Chem.*, **150A** 349 (1930).

Apparatus. In the case of measurements of heats of dilution of concentrated solutions the calorimeter [3] has been provided with a mercury thermometer giving 0.01 degrees. A resistance thermometer sensitive to temperature changes of 10^{-5} degrees, described in a previous paper, [3] has been used in measurements of heats of dilution of dilute solutions.

Procedure. In order to determine the heat of dilution (to infinite dilution) of a solution of a given concentration, a series of experiments of dilution with finite amounts of pure solvent are necessary, and then the extrapolation of these results is to be carried out. The range of concentrations was divided into one of molalities $m < 0.1$ and another of $m > 0.1$. In a first group of experiments samples of solutions of various concentrations ranging from 0.1 to 0.001 molal were diluted with the quantity of water necessary to form a 0.001 molal solution. The total quantity of water in the resulting solutions was 400 g. Each of the different samples of initial solution contained 4×10^{-4} moles of solute. The measured quantity in these experiments was the intermediate heat of dilution from the molality m to 0.001, i.e. $\Delta H_{\text{dil}}^{m \to 0.001}$. In the second group of experiments samples of solutions of concentrations higher than 0.1 molal were diluted by an amount of water so that a 0.1 molal solution be formed. Each sample of initial solution of this group contained 0.04 moles of solute. The intermediate heat of dilution, $\Delta H_{\text{dil}}^{m \to 0.1}$, measured in these experiments, combined with data obtained for dilute solutions ($m < 0.1$), was used to find values for the heat of dilution to infinite dilution, $\Delta H_{\text{dil}}^{m \to 0}$, as function of concentration.

RESULTS

The molar heats measured by dilution to 0.001 molality of solutions of concentrations $m < 0.1$, are given in table 1 for aqueous solutions of KNO_3, $AgNO_3$ and $Pb(NO_3)_2$. These data were plotted against $\sqrt{m}$ and the extrapolation to infinite dilution was carried out. The intercept of the extrapolated curves with the ordinate gives, with opposite sign, the heat of dilution of the 0.001 molal solution, $\Delta H_{\text{dil}}^{0.001 \to 0}$. This value is found to be -18 cal/mole for KNO_3, -17 cal/mole for $AgNO_3$ and -61 cal/mole for $Pb(NO_3)_2$ aqueous solutions. If this value is added to measured intermediate heats of dilution, $\Delta H_{\text{dil}}^{m \to 0.001}$, the heats of dilution to infinite dilution at those concentrations are found :

$$\Delta H_{\text{dil}}^{m \to 0} = \Delta H_{\text{dil}}^{m \to 0.001} + \Delta H_{\text{dil}}^{0.001 \to 0}. \quad (1)$$

The values obtained for $\Delta H_{\text{dil}}^{m \to 0}$ are also given in table 1. The value referring to 0.1 molal solution, $\Delta H_{\text{dil}}^{0.1 \to 0}$, is of a particular interest, because this value is to be added to the measured values of intermediate heats of dilution, $\Delta H_{\text{dil}}^{m \to 0.1}$, of solutions of concentrations higher than 0.1 molal, in order to obtain the heats of dilution to infinite dilution, $\Delta H_{\text{dil}}^{m \to 0}$, of those solutions, according to the equation

$$\Delta H_{\text{dil}}^{m \to 0} = \Delta H_{\text{dil}}^{m \to 0.1} + \Delta H_{\text{dil}}^{0.1 \to 0}. \quad (1a)$$

The molar heats measured by dilution to $m = 0.1$ of solutions of concentrations higher than 0.1 molal, $\Delta H_{\text{dil}}^{m \to 0.1}$, are given in table 2 for KNO_3,

---

[3] I. G. MURGULESCU and E. TOMUŞ, *Anal. Univ. Bucureşti, Ser. Ştiinţele Naturii*, **41**, 97 (1963).

Table 1

Heats of dilution of the dilute aqueous solutions of KNO_3, $AgNO_3$ and $Pb(NO_3)_2$, at 25°, in cal/mole

m, $\frac{\text{moles}}{1000\ \text{gH}_2\text{O}}$	KNO_3		$AgNO_3$		$Pb(NO_3)_2$	
	$\Delta H_{\text{dil}}^{m\to 0.001}$	$\Delta H_{\text{dil}}^{m\to 0}$	$\Delta H_{\text{dil}}^{m\to 0.001}$	$\Delta H_{\text{dil}}^{m\to 0}$	$\Delta H_{\text{dil}}^{m\to 0.001}$	$\Delta H_{\text{dil}}^{m\to 0}$
0.10	+63	+45	−56	−73	+88	+ 27
0.090	+53	+35	−58	−75	+61	0
0.0625	+25	+ 7	−60	−77	− 9	− 70
0.0400	+ 3	−15	−57	−74	−61	−122
0.0225	−12	−30	−48	−65	−87	−148
0.0100	−17	−35	−32	−49	−80	−141
0.0064	−16	−34	−24	−41	−66	−127
0.0036	−11	−29	−15	−32	−44	−105
	−		−		−	
0.0010	0	(−18)	0	(−17)	0	(−61)
	+		+		+	
	extrapolated values					
0.00	(+18)	0	(+17)	0	(+61)	0

Table 2

Heat of dilution of concentrated aqueous KNO_3 solutions, at 25°

m, $\frac{\text{moles}}{1000\ \text{gH}_2\text{O}}$	$\Delta H_{\text{dil}}^{m\to 0.1}$ cal/mole	$\Delta H_{\text{dil}}^{m\to 0}$ cal/mole	m, $\frac{\text{moles}}{1000\ \text{gH}_2\text{O}}$	$\Delta H_{\text{dil}}^{m\to 0.1}$ cal/mole	$\Delta H_{\text{dil}}^{m\to 0}$ cal/mole
0.10	0	+45	2.00	1242	1287
0.20	+98	143	2.50	1468	1513
0.30	187	232	3.00	1676	1721
0.50	349	394	3.50	1872	1917
0.75	529	574	3.77	(1995)	(1995)
1.00	691	736	(satd)		(extrapolated)
1.50	983	1028			

Table 3

Heat of dilution of concentrated aqueous $AgNO_3$ solutions, at 25°

m, $\frac{\text{moles}}{1000\ \text{gH}_2\text{O}}$	$\Delta H_{\text{dil}}^{m\to 0.1}$ cal/mole	$\Delta H_{\text{dil}}^{m\to 0}$ cal/mole	m, $\frac{\text{moles}}{1000\ \text{gH}_2\text{O}}$	$\Delta H_{\text{dil}}^{m\to 0.1}$ cal/mole	$\Delta H_{\text{dil}}^{m\to 0}$ cal/mole
0.10	0	−73	5.00	1380	1307
0.20	+29	−44	6.00	1546	1473
0.30	68	− 5	7.0	1690	1617
0.50	142	+69	8.0	1807	1734
0.75	237	164	9.0	1891	1818
1.00	327	254	10.0	1958	1885
2.00	654	581	11.0	2001	1928
3.00	933	860	12.0	2033	1960
4.00	1183	1110	13.0	2044	1971
			14.2		(1970)
			(satd.)		(extrapolated)

in table 3 for $AgNO_3$ and in table 4 for $Pb(NO_3)_2$ aqueous solutions, at concentrations indicated in the first column. In the third column of these tables the heats of dilution to infinite dilution, $\Delta H_{dil}^{m \to 0}$, obtained by eq. (1a), are also given. The first values in these columns, $\Delta H_{dil}^{0.1 \to 0}$, are taken from table 1.

Table 4

Heat of dilution of concentrated aqueous $Pb(NO_3)_2$ solutions, at 25°

m, moles / 1000 gH_2O	$\Delta H_{dil}^{m \to 0.1}$ cal/mole	$\Delta H_{dil}^{m \to 0}$ cal/mole	m, moles / 1000 gH_2O	$\Delta H_{dil}^{m \to 0.1}$ cal/mole	$\Delta H_{dil}^{m \to 0}$ cal/mole
0.10	0	+27	0.80	1616	1643
0.20	264	291	1.00	2003	2030
0.30	517	544	1.10	2188	2215
0.50	983	1010	1.20	2371	2398
0.60	1204	1231	1.40	2718	2745
			1.707 (satd)		(3260) (extrapolated)

The concentration dependence of the heat of dilution, for the three investigated solutions, is shown graphically in figure 1.

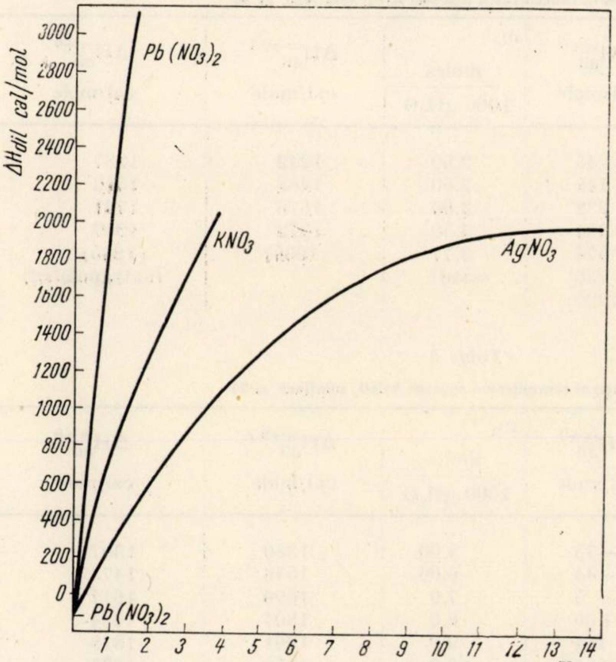

Fig. 1. — Heats of dilution of KNO_3, $AgNO_3$ and $Pb(NO_3)_2$ aqueous solutions at 25° plotted against molality.

DISCUSSION

The above data of heats of dilution in the domain of dilute solutions seem to support the requirements of the limiting law

$$\Delta H_{dil} = - S^\circ \sqrt{m} \tag{2}$$

written as a consequence of the Debye-Hückel's ionic interaction theory of electrolytic solutions.[4a]

An equation to give the concentration dependence of the heat of dilution is developed here on the basis of the following analogy between the heat of dilution and lattice energy of ionic crystals. The heat of dilution, ΔH_{dil}, accompanies the process of increasing the distances between the ions from a solution of a given concentration to infinity (by addition of an infinite amount of water), while the lattice energy, ΔH_r, accompanies the process of increasing the distances between the ions of a crystal from a given value to infinity, in vacuum. There are, of course, a number of dissimilitudes in this analogy, which are to be taken in account in order to obtain a formula for the heat of dilution starting from the known formula for the lattice energy:

$$\Delta H_r = \alpha \frac{Ne^2}{r_0}. \tag{3}$$

First of all, the dielectric constant, D, of the medium separating the ions in solution is to be taken into account. At higher concentrations this is expected to differ from the value D_0 of the dielectric constant of the pure solvent, because the thickness r_h of the solvation layer is not to be neglected compared with the distance r between two neighbour ions. If we consider that the dielectric constant has, inside the solvation layer, a value D_h different of that of the pure solvent, than the average value D of the dielectric constant of the medium separating the ions in a solution may be written as

$$D = \frac{D_0 (r - 2r_h) + 2D_h r_h}{r} = D_0 \left[1 + 2\frac{r_h}{r}\left(\frac{D_h}{D_0} - 1\right)\right]. \tag{4}$$

As the distance r is a function of the concentration and r_h and D_h cannot be accurately known, the last formula may be rewritten as

$$D = D_0 (1 + Bc^n) \tag{4a}$$

where B is a constant involving r_h and D_h/D_0, and c is the concentration. The thickness of the solvation layer, r_h, may be also dependent on the distance r between the ions, owing to the interactions between solvent dipoles of this layer and the neighbouring ions. Therefore, we assume that $r_h \sim 1/r^3$.

Another change in formula (3) refers to the parameters r_0 of the elementary cell of the crystal. For a crystal, r_0 has a definite value, specific for a given substance, while for a solution the distance r between neighbour ions depends on concentration. If we divide the solution into small cubes each containing one ion in their center, then, if the solution contains,

---

[4] H. S. HARNED and B. B. OWEN, "The Physical Chemistry of Electrolytic Solutions", Reinhold Publ. Corp., 1958 a) p. 334; b) p. 707–708

per 1000 cm^3, c moles of solute dissociating in ν ions, the distance r is given by the following formula:

$$1/r = \frac{(\nu N)^{1/3}}{10} c^{1/3}. \tag{5}$$

Thus, the exponent n in eq. (4a) may be assumed to be $n = 4/3$.

The quantity α of eq. (3) is finally to be adapted. For a given crystal it has a well definite value (Madelung's constant). In the development of eq. (3) the constant α represents a convergent series arising from the summation of contributions of alternating opposite charged ions. In solution, in order to evaluate α, we divide the space surrounding an ion in elementary spherical shells. In such a shell only the excedent of ions of opposite charge with the central ion contribute to the total electrostatic interaction energy with this central ion, owing to reciprocal cancellation of the contributions of each pair of opposite charged ions. This excedent of ions of opposite charge to the central ion may be considered as proportional to the volume $4\pi R^2 dR$ of the elementary spherical shell of radius R and thickness dR, and inversely proportional to the volume of the whole sphere of radius R. Beyond a certain distance R_0, this excess of opposite charged ions may be considered to vanish. The integration of the contributions of all these elementary shells gives

$$\alpha = \int_r^{R_0} \frac{4\pi R^2 dR}{\frac{4\pi}{3} R^3} = 3 \ln \frac{R_0}{r} . \tag{6}$$

When r is replaced by c according to eq. (5), parameter R_0 must also be replaced by an analogous expression, in which instead of c we put c_0. We obtain

$$\alpha = \ln \frac{c}{c_0} . \tag{7}$$

Now, taking into account all these remarks, formula (3) may be rewritten as follows, to give the heat of dilution as function of concentration:

$$\Delta H_{dil} = \frac{N^{4/3} \nu^{1/3}}{10} \frac{e^2}{D_0} \frac{c^{1/3}}{1 + Bc^{4/3}} \ln \frac{c}{c_0} . \tag{8}$$

If we want to use the molality m (moles/1000 g solvent) instead of molarity c, according to the relation

$$c = md/\ (1 + mM/1000) \tag{9}$$

where d is the density of the solution (in g/cm^3) and M the molecular weight of the solute, we may approximate that the quantity $d/(1 + mM/1000)$ depends linearly on the square root of molality *m*. With this assumption we have $c^{1/3} \sim m^{1/2}$ and $c^{4/3} \sim m^2$. Thus, in terms of m, we have

$$\Delta H_{dil} = A \frac{m^{1/2}}{1 + Bm^2} \ln \frac{m}{m_0} \tag{10}$$

where A involves the constants N, e, D_0 and ν (a constant for a given electrolyte), explicitly appearing in eq. (8).

Equation (10) is in good agreement with experimental data at high concentrations but gives a deeper minimum in the range of low concentrations. The agreement is obtained even in the range of low concentrations if the quantity $m_0/9$ is added to both numerator and denominator of the logarithm argument. So, the following formula has been found to give results in very good agreement with experimental data at all concentrations :

$$\Delta H_{dil} = 2.303\ A \frac{m^{1/2}}{1 + Bm^2} \log \frac{m + m_0/9}{10\ m_0/9} \cdot \qquad (11)$$

As a limiting law, when m → 0, this formula gives

$$\Delta H_{dil} = -2.303\ A\, m^{1/2}. \qquad (11a)$$

Equation (11a) confers to the quantity 2.303 A the significance of a limiting slope.

The values of the three parameters, 2.303 A, B and m_0, of eq. (11) are given, for investigated solutions, in table 5. These values have been determined using three experimental points ; m_0 is the value (non-zero) of the molality at which the heat of dilution passes from negative to positive values. The values of A and B have been determined from other two experimental points at higher concentrations.

Table 5

Parameters of eq. (11) for the heat of dilution as function of concentration, at 25°

Solute	2.303 A, cal/mole$^{3/2}$	B	m_0 moles/1000gH_2O	$m_0/9$	$-\log(10m_0/9)$
KNO_3	610	0.0038	0.0555	0.00617	1.2095
$AgNO_3$	550	0.0034	0.320	0.0356	0.4490
$Pb(NO_3)_2$	2020	0.000	0.090	0.010	1.000
NaCl	390	0.0162	0.856	0.0951	0.0220
NaBr	408	0.0085	0.781	0.0868	0.0615
KCl	328	0.0034	0.820	0.0911	0.0400
KBr	413	0.0050	0.541	0.0601	0.2210
$NaNO_3$	485	0.0060	0.153	0.0170	0.7695

In addition to the systems experimentally investigated in this paper, the values of parameters A, B and m_0 have been determined and included in table 5 for a few other systems for which the necessary experimental data are available[4b]. For example, in figure 2 experimental heats of dilution of NaCl aqueous solutions, at 25°, are compared with the values calculated by the following equation :

$$\Delta H_{dil} = 390 \frac{m^{1/2}}{1+0.0162\ m^2} [0.0220 + \log(m + 0.0951)] \qquad (12)$$

obtained by substitution of the three parameters of eq. (11) by their nummerical values taken from table 5 for NaCl.

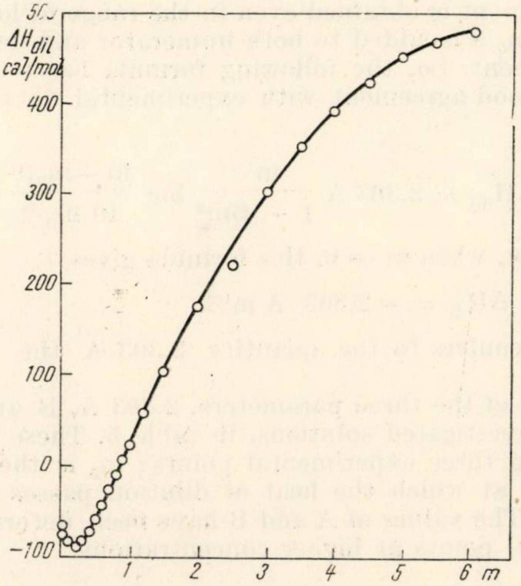

Fig. 2. — Comparison between calculated (by eq. (11)) and experimental values of the heat of dilution of NaCl aqueous solutions;

1, (o) experimental values; *2*, (———) calculated values.

Equation (11) has been used also in carrying out extrapolations to infinite dilution of the heats of dilution of the investigated systems, together with graphical extrapolations.

Revue Roumaine de Chimie, **15**, 385–393 (1970)

SALT EFFECTS IN TERNARY SYSTEMS

FURFURAL-WATER-ELECTROLYTE. I

TERNARY SYSTEMS FURFURAL-WATER-UNI-UNIVALENT ELECTROLYTE

CAMELIA BELDIE and FLORICA BĂRBULESCU

Department of Physical Chemistry
University of Jassy

Received February 11, 1969

The salt out effects in furfural-water inorganic electrolyte systems were measured. It was used a furfural-water solution saturated at 25°. The inorganic electrolytes were the following: HCl, NaCl, KCl, RbCl, NH_4,Cl, NaBr, KBr, NH_4Br, and NH_4NO_3. The activity coefficients of the nonelectrolyte (water) in salt solution were computed. We have calculated, too, the interaction parameter k_s from the equation log $S_0/S = k_sc_s$ and by using the plots log f_i *vs.* . The obtained results verify the salt effect theory and, at the same time, our data for the phenol-water system.

Continuing a study begun some years ago upon the phenol-water system, we have investigated the influence exerted by some inorganic electrolytes on the binary system furfural-water at the equilibrium temperature, 25°.

The furfural-water system as the phenol-water one is partly miscible, but the furfural has a different chemical structure and the water solubility in furfural is much lower than in phenol.

Therefore the two systems can be compared from the viewpoint of the influence that different electrolytes exert on the water solubility in the two organic solvents, implicitly on the activity coefficients.

Commonly, in order to determine the salt effects upon the non-electrolyte activity coefficient, one compares the solubility in salt solution with that in pure solvent. In this case the furfural is solvent and the water is the nonelectrolyte solute.

Usually the data are correlated by Setschenow's equation

$$\log S_0/S = k_s c_s$$

where S_0 and S are the nonelectrolyte solubilities in moles/liter, in pure solvent and in salt solution respectively, c_s is the concentration of salt in moles/liter and k_s — the Setschenow's constant, the salt effect parameter, that represents the ion-nonelectrolyte interaction in first approximation.

In fact there are several kinds of interactions, such as the self-interaction of the nonelectrolyte and the solvent-nonelectrolyte one. These interactions, in a more accurate expression are characterized by another parameter.

In order to compare the experimental salt effects with the theory or the salt effects of two nonelectrolytes with a various solubility, it will be necessary to distinguish between these two parameters.

As a rule, most theories of the salt effects[1] correlate only the ion-nonelectrolyte interaction parameter.

The activity coefficient of a solute species, referred to infinite dilute solution, can be correlated by equation[1] (1)

$$\log f_i = k_s c_s + k_i c_i \tag{1}$$

where s and i indices refer to salt and nonelectrolyte, respectively, k_s and k_i are the ion-nonelectrolyte interaction parameter and the self-interaction parameter of the nonelectrolyte.

Since the well known equilibrium equation in the saturate solution is[2]

$$f_i S = f_i^0 S_0$$

while

$$\log f_i^0 = k_i S_0$$

we may write

$$\log f_i/f_i^0 = \log S_0/S = k_s c_s + k_i (S - S_0) \tag{2}$$

When the nonelectrolyte solubility is decreased, f_i^0 is equal to uni and the term $k_i(S - S_0)$ is negligible.

In this case k_s parameter can be obtained from the plots log S_0/S *versus* c_s.

When the solubility is increased, the latter term of the equation (2) is not negligible, and in this case k_s could be determined only if we know the value of k_i parameter.

EXPERIMENTAL

The technical equipment has been described previously. [3,4]

A turbidimetric method, tested with a photoelectric one was used. We used a photocolorimeter, thermostated to maintain the temperature constant within ± 0.05°, and a ultrathermostat U_{10}.

---

[1] F. A. Long and W. F. McDevit, *Chem. Rev.*, **51**, 119 (1952).

[2] W. F. McDevit and F. A. Long, *J. Amer. Chem. Soc.*, **74**, 1090 (1952).

[3] E. Papafil, M. Papafil and C. Beldie, *Anal. Şti. Univ. "Al. I. Cuza" Iaşi, Sect. I*, **4**, 153 (1958).

[4] E. Papafil and C. Beldie, *Ibid.*, **7**, 147 (1961).

The substances were purified and analysed before the investigations; the water purity was tested by measuring the electric conductivity with a conductometer OK-102. Furfural was purified by distillation under low pressure and the refraction index varied between 1.526—1.535. This change of the refractive index has no influence on the solubility.

The following electrolytes were used : hydrogen chloride, sodium, potassium, ammonium, rubidium chlorides and bromides, as well as ammonium nitrate. The other substances used in the phenol-water system, do not influence the water solubility in furfural, but they salt out from solution. This phenomenon occurred with alkaline sulphates and nitrates and some organic salts. In the case of alkaline iodides an oxidation-reduction reaction takes place.

Therefore we have confined ourselves to the electrolytes that behave as in phenol-water mixture, in order to compare the two systems.

The electrolytes used were *p.a.* grade reagent Merck, AnalAR or BDH. Where necessary the substances were purified.

In order to calculate the interaction k_s parameter and the activity coefficients of the nonelectrolyte (water) in salt solution the water solubility in furfural in a 10—50° temperature range was measured. These data are summarized in table 1.

Table 1

The water solubility in furfural

m	t°C	m	t°C
2.3843	13.95	3.2773	34.5
2.4135	14.45	3.2826	34.55
2.4646	15.95	3.2986	35.1
2.5424	17.9	3.4484	38.1
2.6079	20.0	3.5404	39.95
2.6915	21.75	3.6384	41.15
2.7403	22.85	3.7417	43.15
2.8460	24.95	3.7708	43.95
3.0376	29.4	3.9013	45.95
3.0690	29.85	4.0151	47.85

During the investigations the composition of the furfural-water mixture was maintained constant (saturated solution at 25°); we have varied the electrolyte concentration and we have measured Δt, the displacement of the equilibrium temperature.

All electrolytes used produce a salting out, lowering the water solubility in furfural.

The experimental data are listed in table 2.

In the first column the electrolyte concentrations in molalities, in the second, experimental Δt, in the third, calculated Δt, in the fourth, k_s parameter and in the fifth, the activity coefficients are summarized.

RESULTS AND DISCUSSION

To test the accuracy of the experimental data, we have used the empirical equation[3,4]

$$\Delta t = am^b \tag{3}$$

Table 2

Salting data on the furfural-water system

m	Δt	$\Delta t_{\text{calc.}}$	k_s	f_i
$a = 254.3$ HCl $b = 0.71$				
0.02173	16°75	16°77	4.980	1.2829
0.01754	14°2	14°41	5.237	1.2355
0.01332	11°85	—	5.811	1.1951
0.007232	7°2	7°68	6.685	1.1178
0.005598	6°5	6°40	8.240	1.1090
0.005222	6°05	6°09	7.807	1.0984
0.004978	5°9	—	7.911	1.0949
$a = 5843$ NaCl $b = 1.05$				
0.004287	19°8	19°07	29.986	1.3445
0.003248	14°25	—	28.279	1.2355
0.002398	10°15	10°36	27.690	1.1652
0.002236	9°65	9°63	28.524	1.1582
0.001907	8°15	8°146	28.553	1.1336
0.001881	8°1	8°03	28.591	1.1318
0.001526	6°3	6°45	28.080	1.1037
0.001304	5°55	5°47	29.126	1.0914
0.001213	5°05	—	28.417	1.0826
$a = 6769$ KCl $b = 1.23$				
0.01081	23°15	25°83	14.080	1.4200
0.009230	21°55	21°27	15.261	1.3831
0.007564	16°65	—	14.148	1.2794
0.004747	9°6	9°39	13.297	1.1564
0.004725	9°5	9°33	13.219	1.1547
0.003485	6°45	6°42	12.495	1.1054
0.003315	6°25	6°036	12.718	1.1019
0.002631	4°55	—	11.756	1.0738
0.001448	2°15	2°18	—	1.0352
$a = 2640$ NH_4Cl $b = 1.05$				
0.009284	20°3	19°40	14.20	1.3550
0.008134	17°1	16°88	13.522	1.2882
0.007867	16°3	—	13.376	1.2742
0.005074	10°45	10°28	13.473	1.1704
0.004837	9°7	9°78	13.186	1.1582
0.003179	6°25	6°29	13.262	1.1019
0.002751	5°35	—	13.297	1.0878
0.001175	2°05	2°21	12.144	1.0334
0.001099	1°95	1°89	12.311	1.0316
0.000787	1°55	1°45	14.350	1.0263

Table 2 (continuation)

m	Δt	$\Delta t_{calc.}$	k_s	f_i
$a = 6702$ RbCl $b = 1.25$				
0.009685	16°15	15°82	10.741	1.2708
0.008722	14°2	13°88	10.459	1.2337
0.007409	11°55	11°32	10.123	1.1885
0.006002	8°7	—	9.63	1.1423
0.005433	7°7	7°68	9.525	1.1265
0.005277	7°45	7°41	9.420	1.1213
0.004797	6°45	6°57	9.076	1.1054
$a = 1890.7$ NaBr $b = 1.09$				
0.01404	17°35	18°07	7.961	1.2935
0.01341	17°2	—	8.291	1.2917
0.01070	13°8	13°76	8.352	1.2285
0.008864	10°9	10°95	8.005	1.1775
0.007494	9°2	9°12	8.157	1.1513
0.005510	6°45	6°52	7.902	1.1054
0.004105	4°7	—	7.881	1.0773
0.004070	4°65	4°69	7.773	1.0756
$a = 1249$ KBr $b = 1.21$				
0.03213	19°15	—	3.859	1.3304
0.02300	13°05	13°01	3.668	1.2144
0.02279	12°75	12°87	3.619	1.2091
0.01767	9°55	9°46	3.572	1.1564
0.01588	8°35	8°31	3.513	1.1371
0.01413	7°4	7°23	3.518	1.1213
0.01230	6°1	—	3.314	1.0984
0.01213	6°05	6°00	3.361	1.0984
0.007239	3°6	3°21	3.383	1.0580
$a = 1443$ RbBr $b = 1.25$				
0.02604	14°5	15°10	3.586	1.2399
0.02406	13°6	13°68	3.662	1.2249
0.01970	10°65	10°65	3.503	1.1724
0.01841	9°9	9°79	3.535	1.1617
0.01752	9°2	—	3.489	1.1511
0.01716	9°15	8°96	3.523	1.1494
0.01633	8°2	8°36	3.371	1.1343
0.01539	7°85	7°82	3.407	1.1283
0.01507	7°7	7°62	3.424	1.1265

Table 2 (continuation)

m	Δt	$\Delta t_{\text{calc.}}$	k_s	f_i
$a = 803.2$ NH_4Br $b = 1.11$				
0.02581	13°8	13°86	3.463	1.2285
0.02249	11°9	—	3.441	1.1951
0.01905	9°8	9°90	3.382	1.1592
0.01710	8°65	8°78	3.380	1.1423
0.01511	7°8	7°65	3.470	1.1283
0.01450	7°3	7°31	3.381	1.1195
0.005996	2°8	—	3.237	1.0455
$a = 281.8$ NH_4NO_3 $b = 1.25$				
0.07531	11°25	11°12	0.976	1.1845
0.06310	8°9	8°91	0.937	1.1459
0.04811	6°35	—	0.890	1.1037
0.04759	6°3	6°28	0.898	1.1037
0.03713	4°6	4°59	0.852	1.0756
0.02187	2°65	2°37	0.854	1.0439

where Δt is the raising of the equilibrium temperature, m — the salt molality, a and b, two constants : a, specific to the electrolyte and b another constant specific to the liquid mixture. Their values are summarized in table 2.

The b constant varies between 1.05 and 1.25 except for hydrogen chloride which for b is equal to 0.71 ; a has a certain value for an electrolyte.

For two salts that bring about the same salting, respectively the same raising of the equilibrium temperature, the molality ratio has constant value and it gives us the solubility order for the respective salts in furfural-water solvent mixture.

The m_1/m_2 values are listed in table 3.

As table 3 shows the solubility order is :

$$NaCl < KCl < NH_4Cl < RbCl$$

and

$$NaBr < KBr < NH_4Br \simeq RbBr \text{ except}$$

KCl and NH_4Cl at 40°.

The values of k_s parameter from the equation $\log S_0/S = k_s\, c_s$ are much greater than the same values in the phenol-water mixture and the same order (as in phenol-water mixture) was maintained for chlorides[3] only.

Table 3

Values of the m_1/m_2 ratio (furfural-water 25°)

Electrolyte	m_1/m_2		
	$\Delta t = 5°$	10°	15°
$\dfrac{\mathrm{NaCl}}{\mathrm{KCl}}$	0.470	0.461	0.445
$\dfrac{\mathrm{KCl}}{\mathrm{NH_4Cl}}$	0.927	0.990	1.036
$\dfrac{\mathrm{NH_4Cl}}{\mathrm{Rb\ Cl}}$	0.645	0.752	0.770
$\dfrac{\mathrm{NaBr}}{\mathrm{KBr}}$	0.413	0.442	0.454
$\dfrac{\mathrm{KBr}}{\mathrm{NH_4Br}}$	0.995	0.943	—
$\dfrac{\mathrm{KBr}}{\mathrm{RbBr}}$	0.944	0.983	0.996

In table 4 are listed the k_s values.

Table 4

Values of k_s parameter in the furfural-water system (25°)

Electrolyte	NaCl	KCl	NH_4Cl	RbCl	NaBr	KBr	RbBr	NH_4Br	NH_4NO_3	HCl
k_s	28.58	13.37	13.31	9.85	8.04	3.52	3.50	3.37	0.901	5.34

k_s Values for potassium, rubidium and ammonium bromides are very close to each other, as can be seen on the plots $\log f_i$ *versus* m, from which the values of k_s parameter are obtained (Fig. 1).

To calculate the activity coefficient of the water in furfural-electrolyte mixture, the following equation[1] was used :

$$\log f_i = k_s\, c_s = \log S_0/S$$

in which we have made two approximations ; the activity coefficient of the nonelectrolyte in pure solvent is equal to 1 and the $k_i\,(S - S_0)$ term from the equation (2) is negligible.

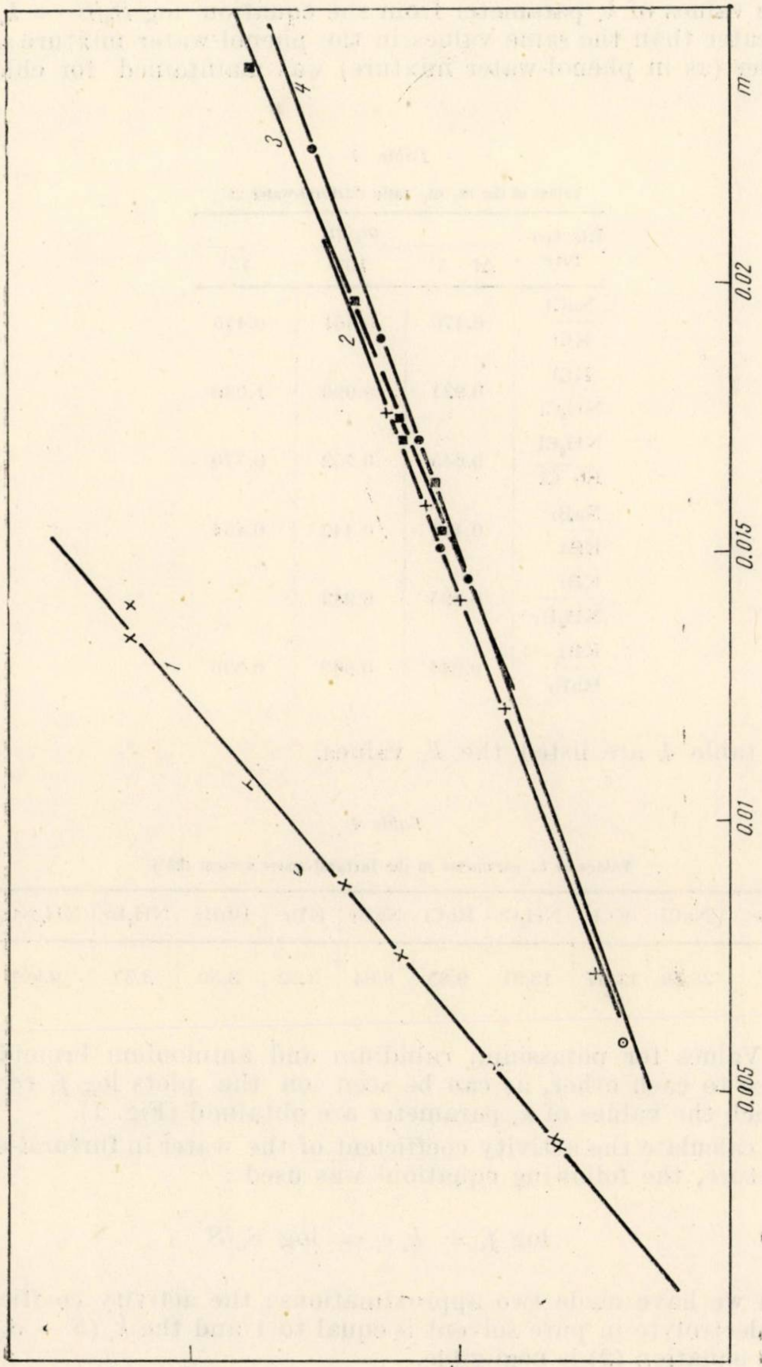

Fig. 1. Furfural-water 25°-
1, NaBr; 2, KBr; 3, RbBr; 4, NH_4 Br.

The activity coefficients calculated in this way are listed in table 2, fifth column. From the results obtained it can be seen that the activity coefficients have values much greater than 1 and this fact proves both the salting theory[1,5] and, at the same time, the results in phenol as solvent.[3]

From the experimental results given here, we can conclude that the interaction parameter k_s, which in first approximation represents the ion-nonelectrolyte interaction, is strongly influenced by the kind of solvent. Such a conclusion results from the fact that the interaction parameter k_s, for the same couple ion-nonelectrolyte has various values in different solvents. A comparison of the k_s values, when either furfural or phenol are used as solvent, will be discussed in a forthcoming paper.

---

[5] P. Debye, *Z. Physik. Chem.*, **130**, 55 (1927).

Revue Roumaine de Chimie, **15**, 385–393 (1970)

The activity coefficients calculated in this way are listed in table 3, [illegible] column. From the results obtained it can be seen that the activity coefficients have values much greater than 1 and this fact proves both the solvation theory [illegible] and, at the same time, the results in [illegible] as sol-vent.

From the experimental results given here, we can conclude that the interaction parameter k_s, which in first approximation represents the ion-nonelectrolyte interaction, is strongly influenced by the kind of solvent. Such a conclusion results from the fact that the interaction parameter k_s for the same couple ion-nonelectrolyte has various values in different solvents. A comparison of the k_s values, when ether furfural or phenol are used as solvents, will be discussed in a forthcoming paper.

[illegible] Z. physik. Chem., 138, [illegible]

[illegible]

Revue Roumaine de Chimie, **15**, 395–400 (1970)

ELECTRON SPIN RESONANCE (ESR) STUDY OF THE OXIDATION OF SOME AROMATIC AMINES WITH SODIUM CHLORITE

F. M. ALBERT and AURELIA MEGHEA

Polytechnic Institute Bucharest,
Department of General Chemistry, Calea Griviţei 132

Received March 12, 1969

The ESR method was used to study the oxidation mechanism with sodium chlorite. The existence of an equilibrium in solution between the chlorite ion and the free chlorine dioxide was confirmed in this way and also the possibility of the latter to be an intermediate in the oxidation reaction with sodium chlorite. The sodium chlorite belongs to the class of oxidizing agents which by reaction with aromatic amines leads to polymeric products with paramagnetic properties. The paramagnetic product was obtained from aniline and five of its substitute derivatives (N-methyl- and N-ethyl-aniline, *o*- and *m*-toluidine, diphenylamine).

The oxidation of aromatic amines with sodium chlorite has been formerly investigated[1] for analytical purposes in connection with their spectrophotometric identification and quantitative determination. There was also presented an indirect volumetric method for the determination of aromatic amines which consisted in their oxidation with sodium chlorite, followed by the iodometric titration of the excess reagent.[2,3]

In this paper the ESR method was used to study the paramagnetic compounds which appear in the oxidation reaction of aromatic amines with sodium chlorite.

EXPERIMENTAL

The nature of the oxidation products of aromatic amines with sodium chlorite depends on the concentration of reagents, on the pH and the reaction time.

---

[1] Gr. Popa, F. M. Albert and E. Rădulescu-Grigore, *Z. analyt. Chem.*, **193**, 324 (1963); *Anal. Univ. Bucureşti* (Ser. St. Nat.-Chimie), **42**, 73 (1963); *Z. analyt. Chem.*, **207**, 346 (1965); *Rev. Roumaine Chim.*, **11**, 1449 (1966).

[2] Gr. Popa, F. M. Albert and E. Grigore, *Z. analyt. Chem.*, **199**, 210 (1964).

[3] F. M. Albert, V. Cimpu, M. Văleanu and E. Rădulescu-Jercan, *Rev. Roumaine Chim.*, **11**, 1443 (1966).

The development of the reaction is marked by the appearance of a number of coloured compounds leading finally to a green precipitate.

The minimal concentration at which the beginning of the reaction could be observed depended on the involved amine. In each case, the higher the concentration of reagents and acidity of the solution the more advanced is the oxidation.

For aniline, the first pink coloured stage could be observed for concentrations of amine higher than 10^{-2} M and only after addition of a minimal amount of 10% HCl (0.03 ml).

The reaction of N-methyl-aniline, N-ethyl-aniline, *o*- and *m*-toluidine was less complicated than for aniline, being characterized by a sequence of three stages in bright colours: red, blue and finally a green amorphous precipitate.

In solution of N,N-dimethyl- and diethyl-aniline or *p*-toluidine, the reaction stopped at the first red-violet stage.

The reaction of diphenylamine developed through all stages leading to the green amorphous precipitate. Dried and stored some days, without previous refinement, the green powder changed into bright blue crystals.

For all amines, aqueous solutions 10^{-4} M to 1 M of amine hydrochloride were prepared and mixed in equal volumes (1 :1) with 10% aqueous solutions of 50% purity sodium chlorite.

Diphenylamine is insoluble in water, therefore a 0.2 M benzenic solution was used to which sodium chlorite in suspension was added and then dry gaseous HCl was bubbled through.

Samples of the reacting mixture have been examined by ESR during the reaction to observe the appearance of paramagnetic compounds.

All measurements were performed with a JEOL X-band spectrometer using 100 Kc/sec field modulation.

For aniline samples of concentrations lower than 10^{-2} M a spectrum of four equally intense overlapping lines was observed (fig. 1 a), having the following parameters : the hyperfine spliting (hfs) constant was of 16,7 gauss, the overall width was of 50 gaus The widh fine splitting (hfs) constant was of 16.7 gauss, the overall width was of 50 gauss. The width of a hfs component as measured between the points of maximum slope was of 8 gauss. At higher concentration (5×10^{-2} M) and slight heating (40°) a single-line spectrum superposed on the four lines (fig. 1 b) is obtained. At 7×10^{-2} M concentration the quartet could not be observed any more and only the singlet spectrum remained increasing in time and with the added amount of hydrochloric acid (fig. 2).

Similar results have been obtained for N-methyl-aniline, N-ethyl-aniline, *o*- and *m*-toluidine, but at higher concentrations.

THE ASSIGNMENT OF ESR SPECTRA

The four-line spectrum, characteristic of low-concentration solutions, which do not exhibit the coloured stages formerly discussed, was assigned to a paramagnetic intermediate appearing in the mechanism of the oxidation with sodium chlorite.

In fact, solutions of sodium chlorite acidulated with hydrochloric acid have the same quartet ESR spectrum with the same dependence on time and pH. The same is true for solutions of gaseous chlorine dioxide in water, benzene, carbon tetrachloride, acetic acid. The best resolved quartet spectrum was obtained in acetic acid. The parameters measured on this spectrum are in agreement with those formerly presented by

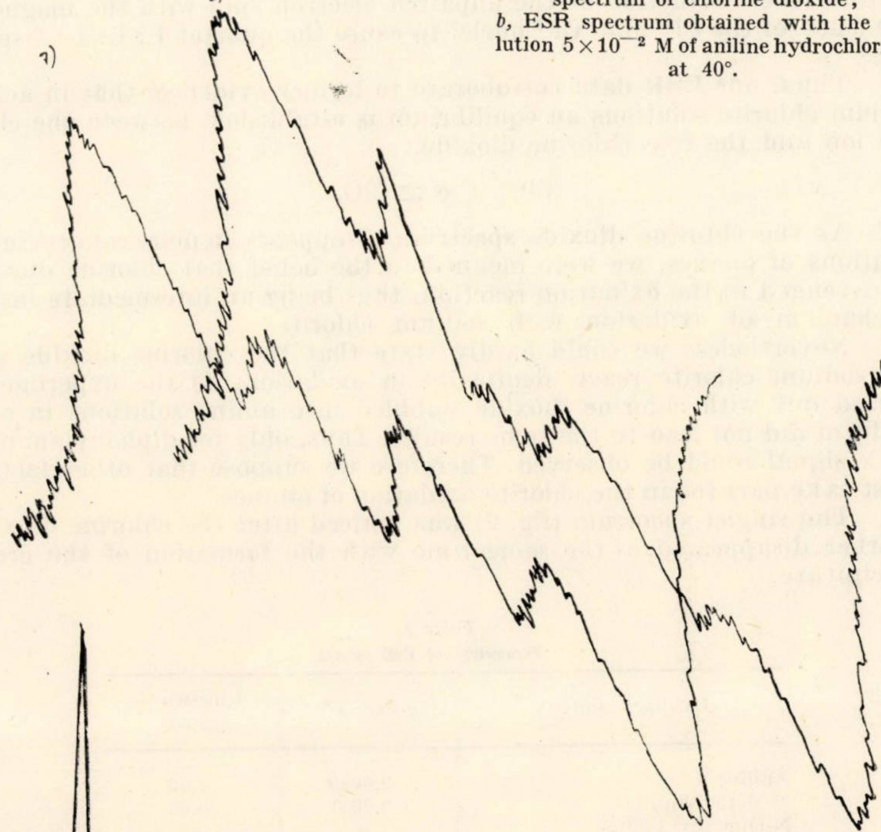

Fig. 1. — *a*, First derivative of the ESR spectrum of chlorine dioxide; *b*, ESR spectrum obtained with the solution 5×10^{-2} M of aniline hydrochloride at 40°.

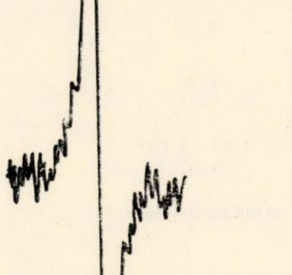

Fig. 2. — ESR spectrum of the paramagnetic compound.

Bennett and Ingram[4,5] for solutions of chlorine dioxide. These authors consider the interaction of the unpaired electron spin with the magnetic moments of the Cl^{35} and Cl^{37} nuclei to cause the quartet 1 : 1 : 1 : 1 splitting.

Thus, our ESR data corroborate to former evidence[6] that in acidic sodium chlorite solutions an equilibrium is established between the chlorite ion and the free chlorine dioxide.

$$ClO_2 + e \rightleftarrows ClO_2^-$$

As the chlorine dioxide spectrum disappears in more concentrated solutions of amines, we were inclined to the belief that chlorine dioxide is scavenged in the oxidation reaction, thus being an intermediate in the mechanism of oxidation with sodium chlorite.

Nevertheless we could hardly state that the chlorine dioxide and the sodium chlorite react identically in oxidation, as the experiments carried out with chlorine dioxide bubbled into amine solutions in acid medium did not lead to the same results. Thus, only for diphenylamine a weak signal could be observed. Therefore we suppose that other factors must take part too in the chlorite oxidation of amines.

The singlet spectrum (fig. 2) was noticed after the chlorine dioxide quartet disappeared, at the same time with the formation of the green precipitate.

Table 1

Parameters of ESR spectra

Oxidized amine	*g*-Factor*	Line-width (gauss)
Aniline	2.0029	1.00
N-Methyl-aniline	2.0031	0.85
N-Dimethyl-aniline	—	—
N-Ethyl-aniline	2.0029	1.12
N-Diethyl-aniline	—	—
o-Toluidine	2.0026	0.85
m-Toluidine	2.0029	0.85
p-Toluidine	—	—
Diphenylamine (pp. green)	2.0029	1.90—2.10
Diphenylamine (pp. blue)	2.0029	8.46

* The *g*-factor of spectroscopical splitting was calculated *vs.* the peroxylamine-disulfonate marker for which the $g = 2.0055$

The data in table 1 point, for all studied amines, to a *g*-factor of 2.0029, a value which is very close to that corresponding to the free electron. The line width is about the same for methyl-aniline, *o*- and *m*-toluidine and slightly greater for ethyl-aniline and aniline. The diphenylamine leads to a compound with twice as wide a line (but still no wider than 2 gauss). Stored for about 3 months it changes into a crystalline blue powder with a signal of about 8 gauss.

---

[4] J. E. Bennett and D. J. E. Ingram, *Phil. Mag.*, [8] **1**, 109 (1956).

[5] J. E. Bennett, D. J. E. Ingram and D. Schonland, *Proc. Phys. Soc.*, **69 A**, 556 (1956).

[6] N. V. Trotskaia and I. E. Flis, *Zhur. fiz. Khim.*, **33**, 1614 (1959).

The amine oxidation is known as a complex reaction, leading to a variety of compounds whose nature is determined by the oxidizing agent and the oxidation conditions.

From this point of view the oxidizing agents can be divided into two classes.[7]

The first class gives oxygen to the amine molecule, while the second class takes hydrogen from the amino group with formation of quinone-imine groups.

With oxidizing agents of the first class (e.g. H_2O_2, H_2SO_5) the products are monomolecular compounds (as phenylhydroxalymine-, nitrozo-, nitro- and *p*-benzoquinone derivatives) and dimolecular ones (azo- or azoxy-, N-phenyl *p*-quinonedi-imine-derivatives).

Two types of paramagnetic intermediates are described in the literature for these cases :

— the aminium cation-radical[8,9] 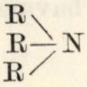 $R_3N^{\cdot +}$ and

— the nitroxide radical 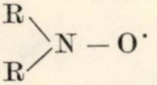 $R_2N-O^{\cdot}$

both of them having a wider ESR spectrum, which consists of many hyperfine components.

The second class of oxidants (e.g. CrO_3, PbO_2, hot H_2SO_4, $NaClO_3$) leads to di- and polymolecular compounds. When *ortho* hydrogen atoms are involved phenazine derivatives appear, while with amino-hydrogens linear polymers are obtained.

A series of works in the literature[10-13] are concerned with the paramagnetism of these polymeric compounds. In all cases singlet spectra with a g-factor of 2.00 and a width of 2 to 8 gauss were formed.

It is obvious that our oxidizing agent has to be classified into the second class not only by chemical analogy to sodium chlorate but also by the nature of the product, whose ESR spectra resemble closely those previously described for polymeric species. The only difference observed regards the line width, which is smaller for most of our compounds.

---

[7] N. V. Sidgwich, "The Organic Chemistry of Nitrogen", 3rd ed., Oxford Univ. Press, 1966, p. 150.

[8] R. I. Walter, *J. Amer. Chem. Soc.*, **77**, 599 (1955); K. Kurwata and D. H. Geske, *ibid.*, **86**, 2101 (1964).

[9] H. van Willigen, *J. Amer. Chem. Soc.*, **89** (9), 2229 (1967); R. F. Nelson, R. N. Adams, *Amer. Chem. Soc., Div. Fuels Chem., Preprints*, **11** (1), 74–6 (1967); L. Hagopian and collab. *J. Chem. Phys.*, **71** (7), 2229–6 (1967).

[10] V. P. Parini, Z. S. Cazacova and A. A. Berlin, *Vysokomol. Soedineniya*, **3**, 1870 (1961).

[11] T. Laederich and Ph. Traynard, *Compt. rend.*, **257** (1), 84 (1963).

[12] A. A. Berlin, L. A. Bliumenfeld, M. I. Cercașin, A. E. Calmansov and O. G. Selscaia, *Vysokomol. Soedineniya*, **1**, 1361 (1959); A. A. Berlin and N. G. Matveeva, *ibid.*, **1**, 1643 (1959); L. A. Bliumenfeld, A. A. Berlin, N. G. Matveeva and A. E. Calmansov, *ibid.*, **1**, 1647 (1959); V. P. Parini, Z. S. Kazacova, M. H. Ocorocova and A. A. Berlin, *ibid.*, **3**, 402 (1961).

[13] V. I. Maltsev, V. B. Lebedev, V. A. Tincovici and A. A. Petrov, *Vysokomol. Soedineniya*, **4**, 848 (1962); V. I. Maltsev and V. A. Tincovici, *ibid.*, **5**, 1367 (1963).

The origin of the paramagnetism of polymers with conjugated double bond system in the main chain is a still unsolved question.

Some authors[12] consider the paramagnetism of such systems to be a property of the fundamental state, appearing as a result of the total delocalization of the π-electrons in the polymeric chain. The corresponding ESR signal presenting no longer hfs, the line narrowing appears as a measure of the delocalization degree. The mobility of the electrons in the molecule is confirmed by the g-value of the polymeric species, very close to the free electron g-factor.

According to another opinion[13] the paramagnetism of polymers with high conjugated double bond systems is due to donor-acceptor interactions not only between the quinone and imine groups, but also between different polymer fractions having different electron affinities.

Revue Roumaine de Chimie, **15**, 401–408 (1970)

DIE THERMISCHEN PHASENGLEICHGEWICHTE DES SYSTEMS $BaO-TiO_2-V_2O_5$*)

S. SOLACOLU, R. DINESCU und MARIA ZAHARESCU

aus dem Institut für Physikalische Chemie der Akademie Bukarest, str. Dumbrava Roşie 23

Eingegangen am 9. September 1969

Es wurden die thermischen Phasengleichgewichte des Systems $BaO-TiO_2-V_2O_5$ bestimmt. Für die Begrenzung der primären Kristallisationsfelder der einzelnen Phasen wurde die Methode der Hochtemperaturmikroskopie benützt. Die sich im thermischen Gleichgewichtszustand befindenden festen Phasen wurden röntgenographisch, mikroskopisch und mit der elektronischen Mikrosonde bestimmt. Es wurde das Phasendiagramm aufgestellt, welches die Eutektika und Peritektika und die Grenzlinien der primären Kristallisationsfelder sowohl der unären und binären Verbindungen enthält, als auch der ternären Verbindung der Zusammensetzung $3BaO.3TiO_2.2V_2O_5$, welche röntgenographisch und mikroskopisch charakterisiert wurde.

1. EINLEITUNG

Die Bariumtitanate und -vanadate weisen dielektrische Eigenschaften und elektrische Leitfähigkeit auf, welche für die Elektrotechnik von Interesse sind. Aus diesem Grunde wurde die Prüfung der thermischen Phasengleichgewichte des Systems $BaO-TiO_2-V_2O_5$ in Angriff genommen. Vorher wurden die zugehörigen binären Systeme untersucht. Rase und Roy[1] berichten über das Vorkommen von 5 Verbindungen im System $BaO-TiO_2$ und zwar: $2BaO.TiO_2$ und $BaO.TiO_2$ welche bei 1860° bzw. 1618° kongruent schmelzen, $BaO.2TiO_2$, beständig im Temperaturbereich 1210 –1322°, $BaO.3TiO_2$ welches unkongruent bei 1367° schmilzt und $BaO.4TiO_2$, mit dem unkongruenten Schmelzpunkt bei 1428°. In letzter Zeit hat Tillmanns[2] mit der elektronischen Mikrosonde neben $BaO.4TiO_2$ auch kleine Mengen Kristalle $BaO.5TiO_2$ gefunden. Jonker und Kwestroo[3] berichten über das Vorhandensein von nichtbeständigen $2BaO.5TiO_2$- und $2BaO.9TiO_2$-Kristallen, welche aber in Gegenwart von kleinen Mengen SnO_2 oder ZrO_2 beständig werden.

---

*) Vorgetragen auf der Landeskonferenz für Allgemeine und Angewandte Physikalische Chemie, Bukarest 2.–5. September 1968.

[1] D. E. Rase und R. Roy, *J. Amer. Ceram. Soc.*, **38**, 102 (1955).

[2] E. Tillmanns, *Naturwiss*, **55**, 81 (1968).

[3] G. H. Jonker und W. Kwestroo, *J. Amer. Ceram. Soc.*, **41**, 390 (1958).

Das System $BaO-V_2O_5$ wurde von Kohlmuller und Perraud[4] untersucht. Durch Reaktionen in Lösungen gelang das Aufbereiten von drei Bariumvanadaten : $BaO.V_2O_5$, $2BaO.V_2O_5$ und $3BaO.V_2O_5$. Für $2BaO.V_2O_5$ werden zwei polymorphe Formen angegeben und zwar ein metastabiles $2BaO.V_2O_5$ (I) und ein stabiles $2BaO.V_2O_5$ (II) mit der Umwandlungstemperatur bei 700°. Das Studium der thermischen Phasengleichgewichte des Systems hat das Vorhandensein von nur zwei Verbindungen bestätigt und zwar $BaO.V_2O_5$, dessen Röntgenogramm mit demjenigen der gleichen aber in Lösung erhaltenen Verbindung, übereinstimmt, und $2BaO.V_2O_5$ mit der Struktur der stabilen Phase (II). Das Vorhandensein der Verbindung $3BaO.V_2O_5$ konnte mangels einer klaren thermischen Umwandlung bei 1140° nicht mit Sicherheit bestätigt werden.

Beljaev und Nestorova[5] stellen eine minimale Löslichkeit der Endglieder im System $TiO_2-V_2O_5$ fest.

Die thermischen Phasengleichgewichte des ternären Systems $BaO-TiO_2-V_2O_5$ sind noch nicht untersucht worden; es wird an verschiedenen Stellen[6,7] lediglich auf eine Beeinflussung der dielektrischen Eigenschaften des $BaO.TiO_2$ durch kleine Mengen V_2O_5 hingewiesen.

Die vorliegende Arbeit verfolgt die Feststellung der thermischen Phasengleichgewichte sowohl in den binären Systemen $BaO-V_2O_5$ und $TiO_2-V_2O_5$, als auch im ternären System $BaO-TiO_2-V_2O_5$.

2. ARBEITSMETHODEN

Die verwendeten Reagenzien waren analysenrein : TiO_2 (Anatas) – 99,80 %; V_2O_5 – 99,60 % und $BaCO_3$ – 99,80 %.

Bei der Aufbereitung der untersuchten Massen wurden die jeweiligen Oxide als Pulver der Feinheit 60 μm 10 Std. lang im Form von Wasserschlamm geschüttelt.

2.1. *Orientative Bestimmung der Liquidustemperaturen*

Die orientative Bestimmung der Liquidustemperaturen wurde mit einem Hochtemperaturmikroskop MHO 2, mit horizontalem Ofen der Firma Zeiss, ausgeführt. Bei der Eichung des Thermoelementes wurden analysenreine Reagenzien verwendet, und zwar : das Eutektikum $KCl + Na_2SO_4$ (517°), KCl (774°), NaCl (801°), Na_2SO_4 (884°) und K_2SO_4 (1069°).

Die Probekörper aus der jeweiligen mit Kanadabalsam gekneteten Masse, welche in den Ofen des Mikroskopes eingeführt wurden, hatten die Form von kleinen Kegeln mit dem Basisdurchmesser von 0,5 mm und wurden senkrecht in kleinen Platinringen aufgehängt. Die Aufheizungsgeschwindigkeit bis in die Nähe des Schmelzintervalles war von 10–12°/min und in diesem Intervalle von ungefähr 3°/min. Als Liquidustemperatur wurde diejenige Temperatur angenommen, bei welcher der Kegel in einen runden Tropfen übergegangen ist.

Die vom Prospekt des Apparates angegebene Fehlergrenze für Temperaturmessungen liegt bei ±15°. Durch aufmerksame Eichungen konnte diese Fehlergrenze auf ± 5° eingeschränkt werden.

---

[4] R. Kohlmuller und J. Perraud, *Bull. Soc. chim. France*, **1964**, 642.

[5] I. N. Beljaev und A. K. Nestorova, *Zhur. obshchei Khim.*, **22**, 402 (1952).

[6] E. G. Fesenko, O. I. Prokopalo, V. D. Komarov und I. A. Shpolyanskii, *Izvest. Leningr. Elektrotekhn. Inst.*, **61**, 252 (1963).

[7] G. Lapluye, G. Morinet und P. Palla, *Compt. rend.*, **250**, 79 (1960).

2.2. *Phasenanalyse*

Die Phasenanalyse wurde röntgenographisch lichtmikroskopisch, sowie mit der elektronischen Mikrosonde ausgeführt.

2.2.1. *Die Röntgenogramme* wurden nach Debye-Scherrer mit $Cu_{K\alpha}$-Strahlen ausgeführt.

2.2.2. *Die mikroskopischen Bestimmungen* wurden mit einem Polarisationsmikroskop MIN-5 durchgeführt. Die Probekörper wurden verschiedenen Temperaturen ausgesetzt, zu dünnen Schliffen verarbeitet und im polarisierten Licht analysiert.

2.2.3. *Die Phasenanalyse mit Hilfe der elektronischen Mikrosonde* wurde an einem Apparat Jeol vom Typ JXA 3A ausgeführt. Die Messungen wurden bei einer Elektronenbeschleunigungsspannung von 16 kV vorgenommen. Die quantitativen Auswertungen wurden nach dem Verfahren von Philibert[8] vorgenommen, das von Duncumb und Shields[9] geändert und von Kusman[10] für oxidische Verbindungen geeicht wurde.

3. VERSUCHSERGEBNISSE

3.1. *Chemische Verbindungen im System*

Die Phasenanalyse der binären Systeme hat die Bestimmung als kristalline Phasen im thermischen Gleichgewicht für folgende Verbindungen ermöglicht: TiO_2 (Rutil), V_2O_5, BaO, $BaO.V_2O_5$, $2BaO.V_2O_5$, $3BaO.V_2O_5$, $2BaO.TiO_2$, $BaO.TiO_2$, $BaO.3TiO_2$ und $BaO.4TiO_2$.

Außer diesen unären und binären Verbindungen wurde das Vorhandensein eines ternären, in der Fachliteratur bisher unbekannten Bariumtitanatvanadats, und zwar $3BaO.3TiO_2.2V_2O_5$, festgestellt.

3.1.1. *Das System $BaO-TiO_2$.* Die synthetisierten Bariumtitanate haben die in der Literatur[1] angegebene Diffraktionslinien aufgewiesen.

3.1.2. *Das System $BaO-V_2O_5$.* In diesem System wurde das Vorhandensein der drei von Kohlmuller und Perraud[4] angeführten chemischen Verbindungen bestätigt.

Die Diffraktionslinien des $3BaO.V_2O_5$, welches sowohl durch Schmelzen einer Masse aus BaO und V_2O_5 im Verhältnis 3 : 1, als auch durch Reaktion im festen Zustand bei 900° erhalten wurde, bestätigen die von Kohlmuller theoretisch errechnete Form.[4] Der Verlauf der Schmelzkurven einiger ternären Schnittebenen, welche in die Zone der primären Kristallisation des $3BaO.V_2O_5$ fallen, weisen auf den kongruenten Charakter dieser Verbindung im Rahmen des ternären Systems hin.

---

[8] J. Philibert, Publications de l'Irsid, ser **B**, **1965**, 1.

[9] P. Duncumb und P. K. Shields, "The Electron Microprobe", Wiley, New York, 1966, S. 350.

[10] L. Kusman, *Silicat. Ind.*, **34**, 13 (1969).

Die Diffraktionslinien des $2BaO.V_2O_5$, welches ebenfalls durch Reaktionen im festen Zustand bei 705° erhalten wurde, sind annährend gleich mit den von Kohlmuller für die beständige Form (II) des Pyrobariumvanadates angegebenen Linien.

Obwohl die Schmelzpunkte in beiden Fällen die gleichen waren 705°, unterscheidet sich die Struktur des Metabariumvanadates von der die Kohlmuller vorgeschlagen hatte.[4] Das in der vorliegenden Arbeit gefundene Debyegramm ist aus Tabelle 1 ersichtlich.

Tabelle 1

Gitterkonstanten der Verbindungen des System $BaO-TiO_2-V_2O_5$

$BaO.V_2O_5$		$3BaO.3TiO_2.2V_2O_5$	
d(h k l)	I	d(h k l)	I
4,532	s. s. sch.[a]		
3,511	s. s. sch.	3,561	m. st.
		3,404	m. st.
3,341	st.[b]		
3,185	s. sch.[c]	3,183	m. st.
		3,074	m. st.
2,988	s. s.sch.		
2,853	m. st.[d]		
		2,759	st.
2,690	s. s. sch.		
		2,482	s. sch.
2,397	s. sch.		
2,218	sch.[e]		
2,124	sch.	2,174	sch.
		2,123	s. sch.
1,984	s. sch.	1,946	s. sch.
		1,908	s. sch.

[a] s.s. schw. = sehr sehr schwach
[b] st. = stark
[c] s.sch. = sehr.schwach
[d] m. st. = mittelstark
[e] sch. = schwach

Abbildung 1 (*a*, *b*, *c*) zeigt die mikroskopischen Aufnahmen der chemischen Verbindungen des binären Systems $BaO-V_2O_5$, deren optische Eigenschaften in Tabelle 2 angegeben sind.

3.1.3. *Das System $TiO_2-V_2O_5$*. Durch die Röntgenogramme des Systems $TiO_2-V_2O_5$ konnten keine binären chemischen Verbindungen nachgewiesen werden. Mit Hilfe der Röntgendiffraktion und der Lichtmikroskopie wurde beobachtet, daß Rutil und V_2O_5 gleichzeitig in allen Mischungen dieses Systems vorkommen, in denen die Konzentration des TiO_2 größer ist als 4%.

Es wird darauf hingewiesen, daß, obwohl TiO_2, das als Ausgangsstoff diente, als Anatas kristallisiert war, nach seiner Erwärmung in Gegenwart von V_2O_5, selbst wenn diese bei Temperaturen unterhalb der Umwandlungstemperatur Anatas $\xrightarrow{800^\circ}$ Rutil stattfand, in allen Massen nur als Rutil vorzufinden war. Hieraus geht die mineralisierende Wirkung des V_2O_5 auf die Umwandlung Anatas → Rutil klar hervor.

Tabelle 2

Optische Eigenschaften der Verbindungen des Systems $BaO-TiO_2-V_2O_5$

Nr.	Verbindung	Form der Kristalle	Farbe	Brechungsindex	Extinktionswinkel
1	$BaO.V_2O_5$	prismatisch folienartig	gelblich grau	>2,10	~45°
2	$2BaO.V_2O_5$	prismatisch gestreckt	gelblich grau	>2,10	~26°
3	$3BaO.V_2O_5$	prismatisch	weißlich grau	>2,10	0°
4	$3BaO.3TiO_2.$ $.2V_2O_5$	körnig	gelblich	>2,10	—

Das gleichzeitige Vorhandensein des V_2O_5 und des Rutils wurde auch in den Röntgenogrammen der ternären Mischungen gefunden, die in der sauren Zone des Systems liegen. Auf diese Weise wurde das primäre Kristallisationsfeld dieser beiden Verbindungen bestätigt.

3.1.4. *Das System $BaO-TiO_2-V_2O_5$*. Im ternären System wurde das Vorhandensein einer einzigen chemischen Verbindung gefunden, für welche die Formel $3BaO.3TiO_2.2V_2O_5$ vorgeschlagen wird. Das Debyegramm dieser Verbindung ist in Tabelle 1 wiedergegeben.

Abb. 1 *c* zeigt die mikroskopische Aufnahme der Verbindung, während ihre optischen Eigenschaften in Tabelle 2 wiedergegeben sind. Aus dem Verlauf der Schmelzkurven wurde bestimmt, daß $3BaO.3TiO_2.2V_2O_5$ kongruent bei 1248° schmilzt.

Nachdem die klassischen chemischen Methoden der Phasenanalyse bei der Bestimmung der genauen oxidischen Zusammensetzung der identifizierten Verbindung zu keinem aufschlußreichen Ergebnis führten, wurde die elektronische Mikrosonde in Anspruch genommen.

Die qualitative Verteilung des V_2O_5, TiO_2 und BaO in der Mischung von obiger Zusammensetzung, welche in festem Zustand reagierte, ist in Abb. 2 (*a*, *b*, *c*, *d*) wiedergegeben. Eine erste Näherung zeigt, daß die Verteilung der drei Komponenten, sowohl im untersuchten A-Kristall (Abb. 2 *a*) als auch im Rest der Masse, einheitlich ist. Bei den Kristallen B (Abb. 2 *a*) ist eine gewisse Zunahme der TiO_2 Konzentration zu beobachten, die entweder einer nicht vollständigen Reaktion, oder einer ungenügenden Homogenisierung zugeschrieben werden kann.

Die quantitativen Berechnungen die anhand der oben genannten Methoden durchgeführt werden, haben die für die identifizierte ternäre Verbindung vorgeschlagene Formel bestätigt.

Die Röntgenogramme und der Verlauf der Schmelzkurven in einer Nachbarzone des primären Kristallisationsfeldes des $3BaO.3TiO_2.2V_2O_5$ mit einem kleineren Gehalt an V_2O_5, schienen die Bildung einer zweiten chemischen ternären Verbindung zum Ausdruck zu bringen. Mit Hilfe der Mikrosonde konnte mit Bestimmtheit festgestellt werden, daß keine ternäre Verbindung, sondern ein Gemisch von zwei Kristallarten vorliegt. Die Verteilung des TiO_2, V_2O_5 und BaO (Abb. 3 *a*, *b*, *c*, *d*) in der untersuchten Masse zeigt ein Zusammenhäufen des TiO_2 in den B-Kristallen und sein vollkommenes Fehlen in dem Rest der Masse. Daraus konnte man schließen, daß die beiden Kristallarten einerseits Rutil (B) und andererseits Kristalle sind die nur aus V_2O_5 und BaO bestehen. Die quantitativen Rechnungen haben für diese letzten Kristalle die Zusammensetzung $3BaO.V_2O_5$ bestätigt.

3.2. *Die thermischen Phasengleichgewichte des Systems $BaO-TiO_2-V_2O_5$*

Die für die ternären Mischungen gefundenen Schmelzpunkte und ihre Phasenanalysen haben die Bestimmung der Grenzlinien ermöglicht, welche die primären Kristallisationsfelder der einzelnen Phasen abgrenzen, sowie die Bestimmung der invarianten Punkte.

Tabelle 3

Die Teilsysteme des ternären Systems $BaO-TiO_2-V_2O_5$

Nr.	Das Teilsystem	Inv. punkt	Zusammensetzung %			Schmelzpunkt °C
			BaO	TiO_2	V_2O_5	
I	$TiO_2-V_2O_5-BaO.V_2O_5$	E_1	17	15	68	520
II	$TiO_2-BaO.V_2O_5-3BaO.3TiO_2.2V_2O_5$	G_2	22,5	25	52,5	680
III	$BaO.V_2O_5-2BaO.V_2O_5-3BaO.$ $.3TiO_2.2V_2O_5$	G_3	40,5	7	52,5	630
IV	$2BaO.V_2O_5-3BaO.V_2O_5-3BaO..$ $.3TiO_2.2V_2O_5$	G_4	47	6	47	645
V	$TiO_2-3BaO.V_2O_5-3BaO.3TiO_2.$ $2V_2C_5$	E_5	43	37	26	1200
VI	$TiO_2-3BaO.V_2O_5-BaO.4TiO_2$	E_6	41,5	49,5	9	—
VII	$BaO.4TiO_2-BaO.3TiO_2-3BaO.V_2O_5$	G_7	42,5	7	9,5	—
VIII	$BaO.3TiO_2-BaO.2TiO_2-3BaO.V_2O_5$	G_8	47	44,5	8,8	—
IX	$BaO.2TiO_2-BaO.TiO_2-3BaO.V_2O_5$	G_9	48	44	8	1210
X	$BaO.TiO_2-2BaO.TiO_2-3BaO.V_2O_5$	G_{10}	64,5	26,5	9	1250
XI	$BaO-3BaO.V_2O_5-2BaO.TiO_2$	G_{11}	69,5	15,5	14	1350

Das thermische Phasengleichgewichtsdiagramm des Systems $BaO-TiO_2-V_2O_5$ ist in Abb. 4 wiedergegeben. Das System wird in 11 Teilsysteme zergliedert, die in Tabelle 3 wiedergegeben sind.

Man bemerkt, daß die primären Kristallisationsfelder der binären und ternären Verbindungen, sowie auch die ternären Eutektika und Peritektika, in dem basischen Teil des Systems liegen.

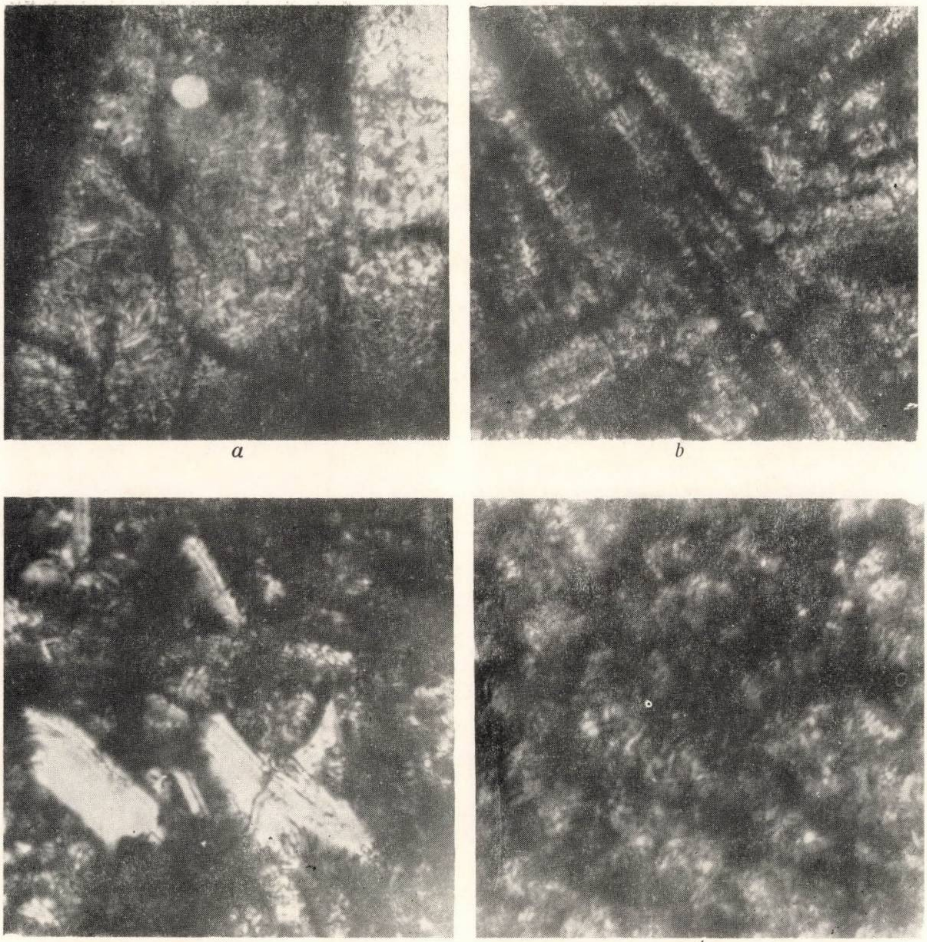

a b c d

Abb. 1. — Mikroskopische Aufnahmen der chemischen Verbindungen des Systems $BaO - TiO_2 - V_2O_5$ (× 450).

a, $BaO.V_2O_5$; *b*, $2BaO.V_2O_5$; *c*, $3BaO.V_2O_5$; *d*, $3BaO.3TiO_2.2V_2O_5$.

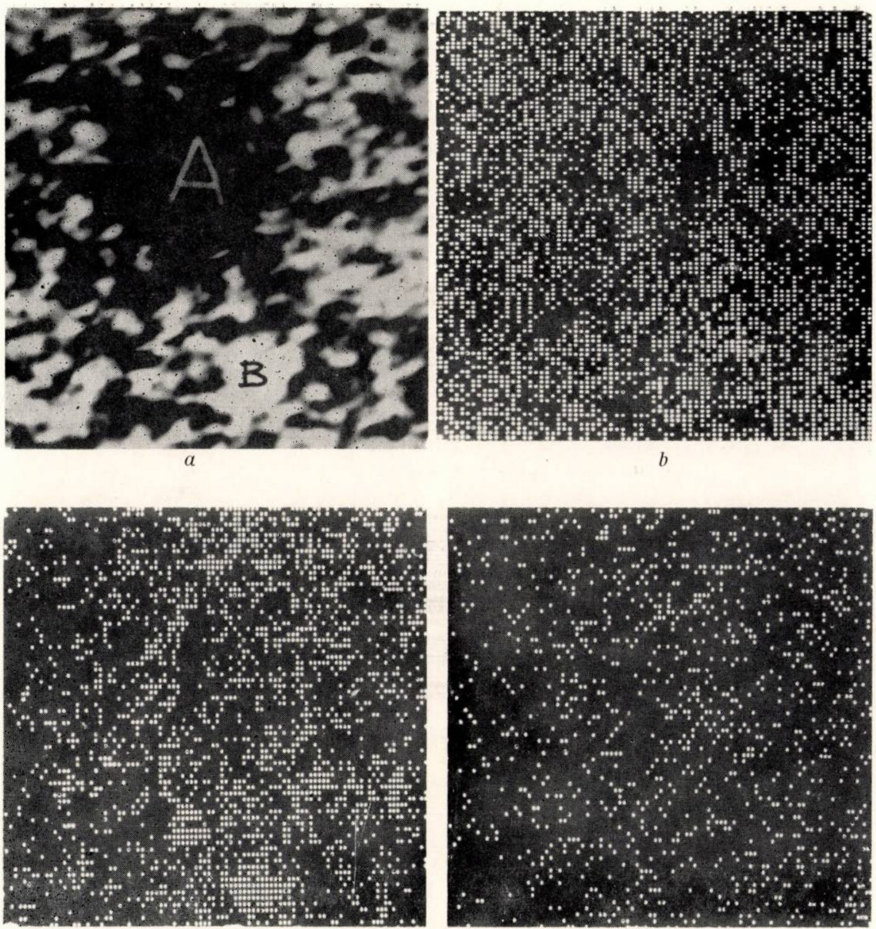

a *b* *c* *d*

Abb. 2. — Verteilung der einzelnen Oxide in der Masse der Zusammensetzung $3BaO.\ 3TiO_2.2V_2O_5$ (× 1400)

a, Elektronenmikroskopische Aufnahme; *b*, Verteilung des $V_2\ O_5$; *c*, Verteilung des TiO_2; *d*, Verteilung des BaO.

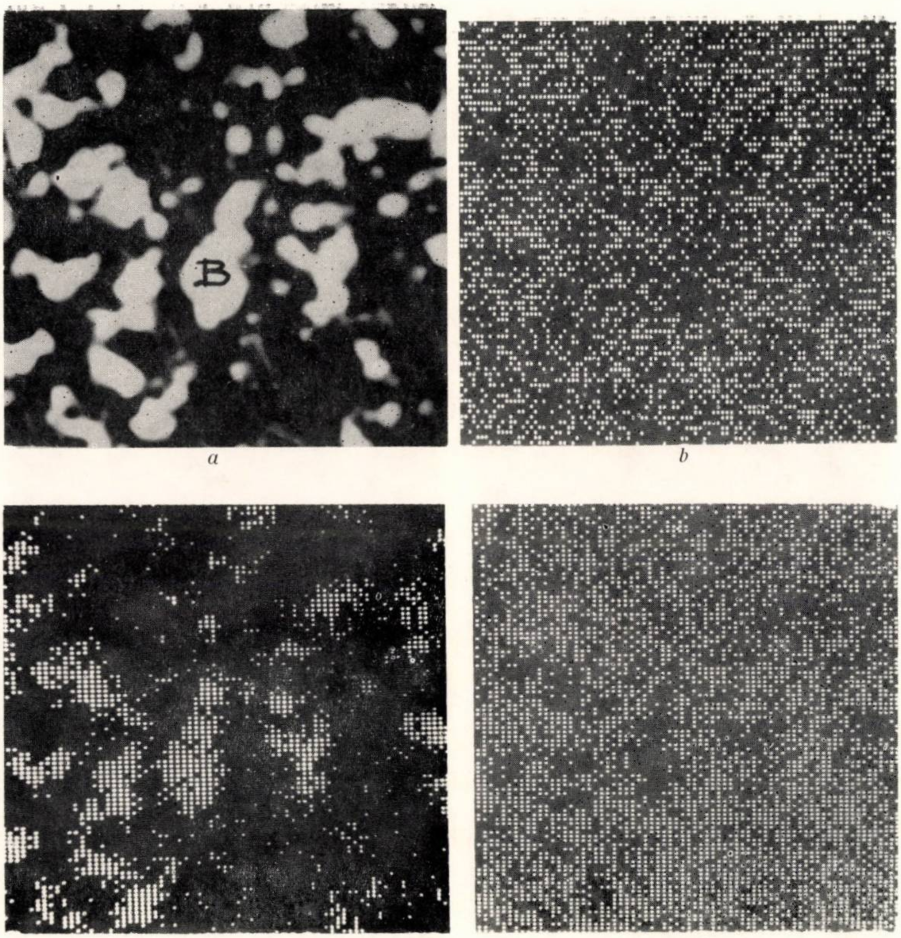

a *b*

c *d*

Abb. 3. — Verteilung der einzelnen Oxide in der Masse der Zusammensetzung $2BaO.\ 3TiO_2.V_2O_5$ (×3750)

a, Elektronenmikroskopische Aufname; *b*, Verteilung des V_2O_5; *c*, Verteilung des TiO_2; *d*, Verteilung des BaO

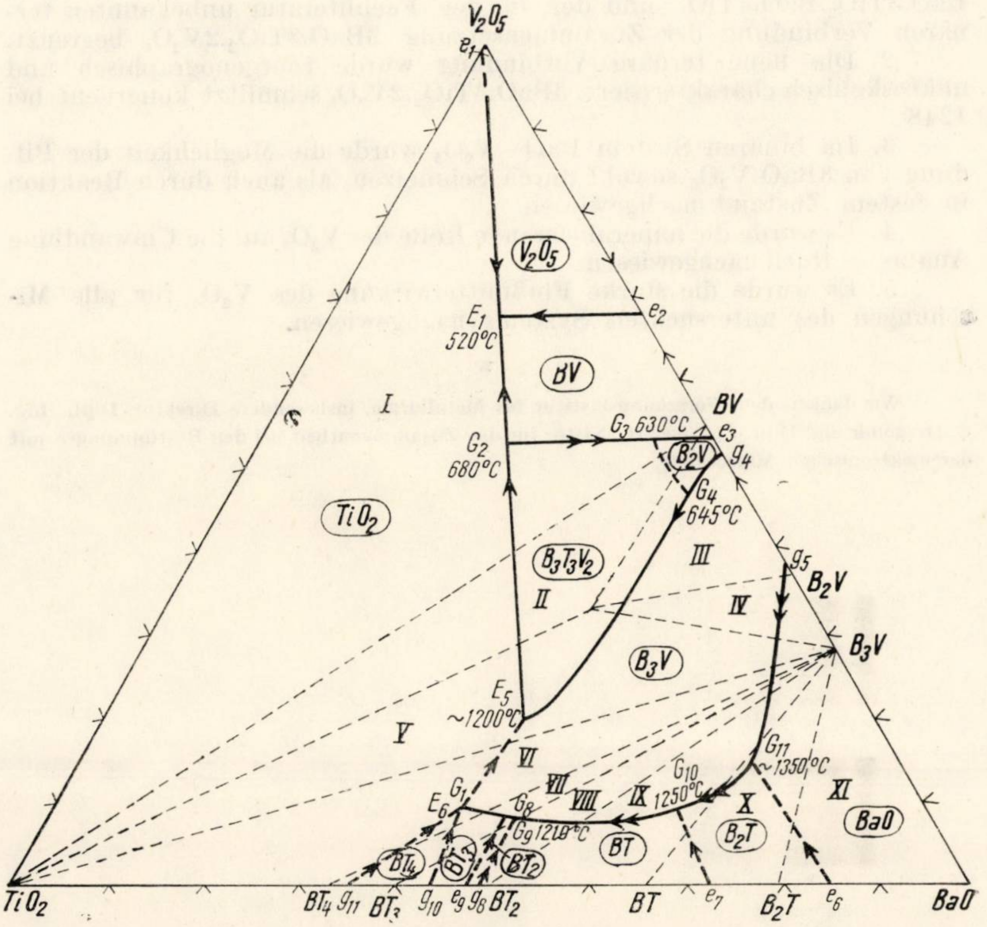
V2O5
e1
V2O5
E1
520°C
e2
BV
BV
I
G3 630°C
e3
G2
680°C
B2V
g4
G4
645°C
TiO2
B3T3V2
III
g5
B2V
II
IV
B3V
B3V
E5
~1200°C
V
VI
G11
~1350°C
G10
1250°C
XI
G1
VII
VIII
IX
X
E6
G8
G9 1210°C
BT
B2T
BaO
BT4
BT3
BT2
TiO2
BT4
g11
BT3
g10
e9
g8
BT2
BT
e7
B2T
e6
BaO

Abb. 4. — Thermisches Phasengleichgewichtsdiagramm des Systems $BaO-TiO_2-V_2O_5$.

Die sauere Zone wird von dem primären Kristallisationsfeld des TiO_2 fast gänzlich bedeckt.

Es wird der starke Flußmitteleffekt des V_2O_5 für die Massen dieses Systems hervorgehoben: in Gegenwart von nur 2,5% V_2O_5 sinkt der Schmelzpunkt des $BaO.TiO_2$ um ungefähr 275°.

4. SCHLUSSFOLGERUNGEN

1. Es wurde das thermische Phasengleichgewichtsdiagramm des Systems $BaO-TiO_2-V_2O_5$ aufgestellt und die primären Kristallisationsfelder der unären und binären Verbindungen: V_2O_5, BaO, TiO_2 (Rutil), $BaO.V_2O_5$, $2BaO.V_2O_5$, $3BaO.V_2O_5$, $2BaO.TiO_2$, $BaO.TiO_2$, $BaO.2TiO_2$,

$BaO.3TiO_2.BaO.4TiO_2$ und der, in der Fachliteratur unbekannten ternären Verbindung der Zusammensetzung $3BaO.3TiO_2.2V_2O_5$ begrenzt.

2. Die neue ternäre Verbindung wurde röntgenographisch und mikroskopisch charakterisiert. $3BaO.3TiO_2.2V_2O_5$ schmiltzt kongruent bei 1248°.

3. Im binären System $BaO-V_2O_5$ wurde die Möglichkeit der Bildung von $3BaO.V_2O_5$ sowohl durch Schmelzen, als auch durch Reaktion in festem Zustand nachgewiesen.

4. Es wurde die mineralisierende Rolle des V_2O_5 auf die Umwandlung Anatas → Rutil nachgewiesen.

5. Es wurde die starke Flußmittelwirkung des V_2O_5 für alle Mischungen des untersuchten Systems nachgewiesen.

*

Wir danken dem Forschungsinstitut für Metallurgie, insbesondere Direktor Dipl. -Ing. C. Dragomir und Dipl.-Physiker R. Nistor für die Zusammenarbeit bei den Bestimmungen mit der elektronischen Mikrosonde.

Revue Roumaine de Chimie, **15**, 409 – 416 (1970)

COMBINAISONS COMPLEXES DE LA DIHYDRAZINOPHTALAZINE (DHF)

LES SÉLÉNOCYANATES DIHYDRAZINOPHTALAZINO-MÉTALLIQUES

I. GRECU et ELENA CURÉA

Faculté de Pharmacie, Chaire de chimie minérale, Cluj, 4 b, str. Pasteur

Reçu le 29 mars 1969

On décrit les sélénocyanates métalliques de la dihydrazinophtalazine (DHF), nouvelles combinaisons complexes du type :

$[Me_m(DHF)(SeCN)_n]$. xH_2O où Me(II) = Cu, Zn, Cd, Mn, Co, Ni.

On expose les méthodes de préparation, les résultats analytiques et quelques propriétés physico-chimiques, ainsi que la solubilité et leur comportement au chauffage. La structure la plus probable de ces combinaisons est discutée en tenant compte des données chimiques, spectrales en IR et magnétiques obtenues.

En étudiant la possibilité de l'emploi de la dihydrazinophtatalazine comme ligand dans la chimie coordinative nous avons décrit dans nos travaux antérieurs les thiocyanates,[1] les sulfates[2] et les benzoates métalliques de la DHF.[3]

Dans le présent travail nous donnons les résultats, concernant les sélénocyanates dihydrazinophtalazino-métalliques, complexes inconnus jusqu'à présent dans la littérature, dont la formule générale est

$$[Me_m(DHF)(SeCN)_n]\cdot xH_2O \text{ où}$$

$$Me(II) = Cu, Zn, Cd, Mn, Co, Ni \quad m, n = 1, 2$$

Leur préparation a été faite par l'action des quantités stœchiométriques de nitrates (acétates) des métaux de transition dissous dans l'eau sur une solution de DHF (base) en présence de KSeCN.

Les complexes obtenus sont microcristallins de couleur jaune-orange, jusqu'au brun-violet.

---

[1] I. Grecu et E. Curea, *Farmacia*, **14**, 719 (1966).

[2] I. Grecu et E. Curea, *Rev. Roumaine Chim.*, **13**, 781 (1968).

[3] I. Grecu et E. Curea, *Il Farmaco ed. pr.*, **23**, 603 (1968)

Ils sont difficilement solubles dans l'eau, l'éther, le chloroforme, l'acétone et l'alcool éthylique, solubles dans la formamide ; leur solubilité dans l'eau augmente qualitativement de gauche à droite dans la série : Co, Ni, Cu, Cd, Zn, Mn.

PARTIE EXPÉRIMENTALE

Synthèse et analyse

1. $[Cu_2DHF(SeCN)_2].4H_2O$

Préparation. On dissout 1,20 g de $Cu(NO_3)_2.3H_2O$ dans 10 ml d'eau distillée et on le traite à 1,4 g de DHF (base) dissoute dans 100 ml d'eau à chaud, 50 ml d'alcool à 96° et 1,0 de KSeCN dissous dans 50 ml d'eau. De cette solution on sépare, après décantation, un précipité brun microcristallin que l'on filtre sur Büchner ; on le lave à plusieurs reprises à l'eau distillée, avec 2—3 ml d'alcool éthylique, à 96°, et 2—3 ml d'éther éthylique et on le sèche à l'air sur une plaque poreuse.

2. $[Zn\ DHF\ (SeCN)_2].\ 2H_2O$

Préparation. On dissout 0,92 g $Zn(CH_3.COO)_2$ dans 30 ml d'eau distillée et on le traite à 1 g de DHF dissoute dans 100 ml d'eau distillée à chaud et 1 g de KSeCN, dissous dans 50 ml d'eau. On ajoute 50 ml d'alcool à 96°. Le précipité formé est traité selon les mêmes procédés que ci-dessus.

3. $[Cd\ DHF\ (NCSe)_2]$

Préparation. On dissout 1,33 g de $Cd(CH_3\text{-}COO)_2.2H_2O$, dans 10 ml d'eau distillée et contenant 1,4 g de DHF, 50 ml d'alcool à 96° et 1 g de KSeCN. Le précipité est traité de la même manière qu'au premier point.

4. $[Mn\ DHF(NCSe)_2]$

Préparation. On dissout 2 g de $Mn(CH_3-COO)_2$ dans 30 ml d'eau et on le traite à 1,0 g de DHF dissoute dans 100 ml d'eau et 1,0 g de KSeCN dissous dans 10 ml d'eau. Le précipité formé est traité de la manière décrite ci-dessus.

5. $[Co\ DHF(SeCN)_2].2H_2O$

Préparation. On dissout 1,45 g $Co(NO_3)_2.\ 6H_2O$ dans 20 ml d'eau distillée et on le traite à 150 ml de solution contenant 1,0 g de DHF et 1,5 g de KSeCN. On ajoute 100 ml d'eau chaude et 50 ml d'alcool à 96°. Le mélange est chauffé au bain-marie lorsqu'il se forme un précipité brun-violet qui este traité de la même manière que le complexe n° 1.

6. $[Ni\ DHF\ (SeCN)_2].2H_2O$

Préparation. On dissout 1,45 g $Ni(NO_3)_2.6H_2O$ dans 20 ml d'eau distillée et on le traite de la même manière qu'au point 5.

Dans le tableau 1 sont indiquées les données concernant la composition, la couleur et les résultats de l'analyse quantitative des complexes décrits.

ÉTUDE THERMOGRAVIMÉTRIQUE

Les déterminations thermogravimétriques ont été faites entre 30—800° à l'aide d'une thermobalance à régime de chauffage de 5°/m.

Les données expérimentales obtenues, ainsi que les résultats de la détermination thermogravimétrique des éléments respectifs sous forme d'oxyde sont mentionnés dans le tableau 2.

Tableau 1

Données de l'analyse chimique des complexes synthétisés

N° crt.	Composé	Couleur	Analyse					
			Calculé			Trouvé		
			Me	N	Se	Me	N	Se
1	$[Cu_2(DHF)(SeCN)_2].4H_2O$	brun	21,21	18,77	26,35	20,70	19,00	26,43
2	$[Zn(DHF)(SeCN)_2].2H_2O$	jaune-orange	13,03	22,33	30,81	12,87	22,22	31,04
3	$[Cd(DHF)(NCSe)_2]$	jaune-orange	21,94	21,95	30,81	21,72	22,07	29,75
4	$[Mn(DHF)(NCSe)_2]$	jaune-verdâtre	12,07	24,67	34,63	12,05	24,97	34,32
5	$[Co(DHF)(SeCN)_2].2H_2O$	brun-violet	11,90	22,73	31,90	12,04	22,81	31,72
6	$[Ni(DHF)(SeCN)_2].2H_2O$	brun verdâtre	11,86	22,74	31,91	12,32	23,20	31,65

Les thermogrammes (fig. 1—3) indiquent une décomposition thermique brusque avec la participation du ligand chez les complexes de Cu(I) (140°) de Cd(II) et de Ni(II) (190°), de Co(II) (160°) et une décomposition relativement lente chez les complexes de Zn(II) et de Mn(II).

Les paliers observés dans l'intervalle de 100 à 190° chez les complexes de Co(II), Ni(II), Cu(I) et Zn(II) correspondent à la perte des molécules d'eau ; les paliers rencontrés dans l'intervalle de 150 à 380°, dans les thermogrammes de Co(II), de Ni(II) et de Cu(I), correspondent aux sélénocyanures respectifs.

Dans la série : Cu—Zn—Co—Mn—Ni—Cd la stabilité thermique des complexes augmente à partir du cuivre au cadmium.

ÉTUDE SPECTROPHOTOMÉTRIQUE (IR)

Nous avons effectué aussi les spectres en IR des complexes synthétisés à l'état solide (pastilles de KBr) dans l'intervalle spectral de 400 à 3600 cm^{-1} à l'aide d'un UR 10 Zeiss-Jéna.

La comparaison du spectre fourni par les complexes avec celui du ligand (tableau 3) donne ce qui suit :

— Déplacement par coordination de la bande νs NH_2 et ν as NH_2 d'environ 100—150 cm^{-1} vers les nombres d'onde moins petits.

— Les vibrations de déformation de la liaison du δ a N—H et du δs a N—H du groupement NH_2 sont peu affectées.

L'ion $SeCN^-$ a un comportement analogue à celui de l'ion SCN^- [4–14] et peut être lié au cation par l'azote ou par le soufre. La différenciation

---

[4] W. A. Baker et G. J. Jones, *Chem. Commun.*, **15**, 369 (1965) ; *Inorg. Chem.* ; **3**, 1184 (1964).

[5] F. Basolo et J. L. Burmeister, *J. Amer. Chem. Soc.*, **85**, 1700 (1963).

[6] J. Burmeister et L. Williams, *Inorg. Chem.*, **5**, 1113 (1966).

[7] J. J. Lewis, R. S. Nyholm et P. W. Smith, *J. Chem. Soc.*, **1961**, 4590.

[8] M. Mark, J. Chaberlain et C. Bailov, *J. Amer. Chem. Soc.*, **81**, 64 (1959).

[9] H. W. Morgan, *J. Inorg. Nuclear Chem.*, **16**, 367 (1961).

[10] P. C. Mitchell et R. J. Williams, *J. Chem. Soc.*, **1960**, 1912.

[11] O. Pecile, *Inorg. Chem.*, **5**, 210 (1966) ; **5**, 11 (1966).

[12] A. Sabatini, et J. Bertini, *Inorg. Chem.*, **4**, 1663 (1965) ; **4**, 959 (1965).

[13] A. Turco et C. Pecile. *Nature*, **191**, 66 (1961).

[14] A. Turco, C. Pecile et M. Nicolini, *J. Chem. Soc.*, **1962**, 3008.

Tableau 2

Données de l'analyse thermogravimétrique des complexes synthétisés

Composé	Décomposition thermique				Analyse thermogravimétrique					
	a	b	c	d	Quantité pesée mg	Oxyde correspondant (mg)		Métal correspondant (mg)		Erreur %
						théoriquement	pratiquement	théoriquement	pratiquement	
Cu_2 (DHF) $(SeCN)_2.4H_2O$	60	150–530	140–150	>530	96,0	23,00	23,30	21,21	21,45	+1,30
Zn(DHF) $(SeCN)_2.2H_2O$	60	175–600	–	>600	90,20	14,30	14,90	13,03	13,27	+1,85
Cd(DHF)$(NCSe)_2$	160	200–720	190–200	>720	128,80	32,27	32,00	21,94	21,75	–0,84
Mn(DHF)$(NCSe)_2$	70	140–650	–	>650	96,70	15,90	15,39	12,05	13.33	+3,30
Co(DHF)$(SeCN)_2.2H_2O$	70	380–630	160–170	>630	55,18	8,35	8,29	11,90	11,81	–0,75
Ni(DHF)$(SeCN)_2.2H_2O$	70	400–670	190–200	>670	154,40	23,31	24,10	11,86	12,26	+3,40

a, Température initiale de décomposition; *b*, Décomposition lente; *c*, Décomposition accentuée; *d*, Température où le résidu est constant.

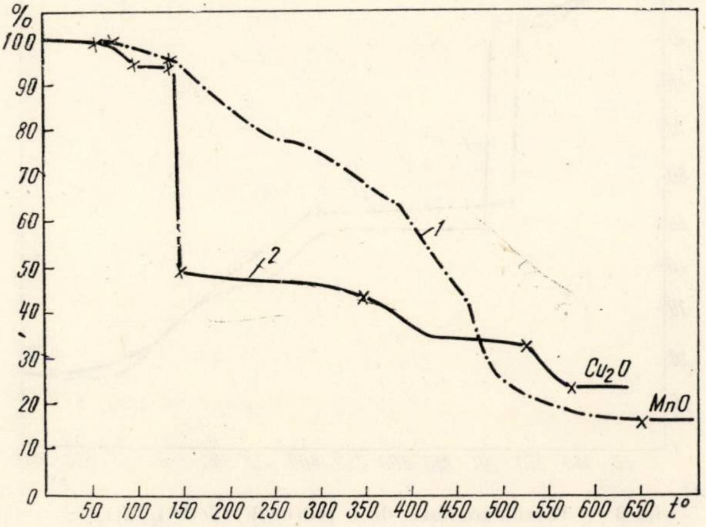

Fig. 1. — Thermogrammes de *1* [Mn (DHF) $(NCSe)_2$] ;
2 [Cu_2(DHF) $(SeCN)_2$].$4H_2O$.

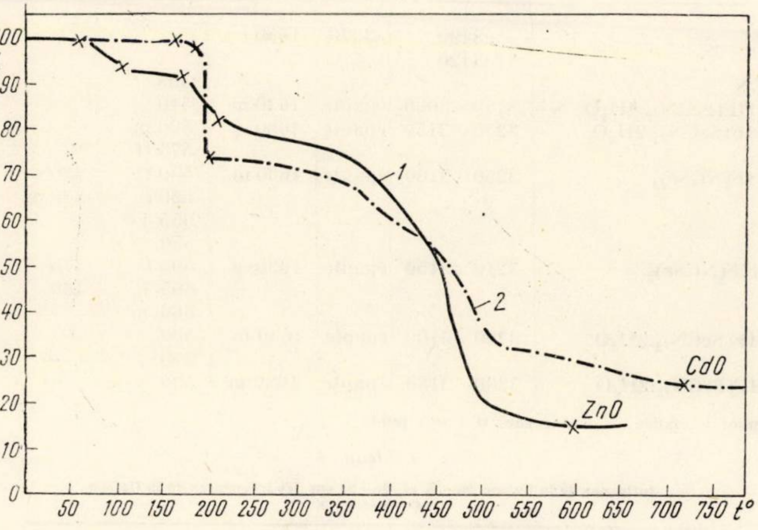

Fig. 2. — Thermogrammes de *1* [Cd(DHF) $(NCSe)_2$] ;
2 [Zn(DHF) $(SeCN)_2$].$2H_2O$.

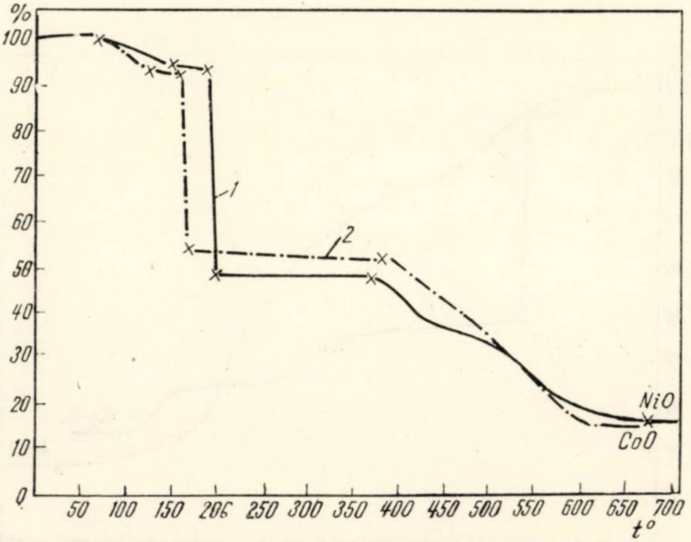

Fig. 3. — Thermogrammes de *1* $[Ni(DHF)(SeCN)_2].2H_2O$;
2 $[Co(DHF)(SeCN)_2].2H_2O$.

Tableau 3

Données de l'analyse spectrale en IR des complexes synthétisés

Nº crt.	Composé	—NH—NH₂			—SeCN		
		νa NH₂	νsNH₂	δNH₂	νC—Se	δC—Se	νC—N
1	DHF	3490 3420	3320	1630 i			
2	KSeCN	—	—	—	558		2068 i
3	$Cu_2DHF(SeCN)_2.4H_2O$	3150—3060	épaule	1630 m	510 s	—	2110 i
4	$ZnDHF(SeCN)_2.2H_2O$	3250—3150	épaule	1630 m	500 m 575 tf	——	2060 2120 i
5	$CdDHF(NCSe)_2$	3250—3100	épaule	1630 m	530 f 650 i 655 i 550	430 s 480 m	2070 i
6	$MnDHF(NCSe)_2$	3210—3150	épaule	1630 m	505 f 665 i 660 m	475 480	2070 i
7	$CoDHF(SeCN)_2.2H_2O$	3260—3190	épaule	1630 m	500 570	—	2110 i
8	$NiDHF(SeCN)_2.2H_2O$	3280—3180	épaule	1630 m	505	—	2120 i

i = intense; f = faible; m = moyenne; tf = très faible.

Tableau 4

Influence de la liaison Me—N et Me—Se sur les fréquences de la liaison C≡N et C—S

	Me — NCSe	Me — SeCN
ν(C≡N)	<2062	>2100
ν(C—Se)	> 558	< 558
δ(C—Se)	> 400	< 400

de ceux-ci peut être faite surtout par la position des bandes de liaisons de valence ν (C ≡ N), ν (C—Se) et δ (C—Se) (tableau 4).

En tenant compte des données spectrales en IR nous supposons que la liaison Me-anion se fait par l'intermédiaire de l'atome de sélénium chez les complexes de Cu(I), Zn(II), Co(II) et Ni(II) et de l'atome d'azote chez les complexes de Cd(II) et Mn(II).

Le scindement de la bande ν (C ≡ N) du complexe de Zn(II) (2060 et 2120 cm^{-1}) peut être attribué à une faible tendance de formation des ponts Zn—SCN—Zn, soit à l'influence de l'état cristallin sur les oscillations des composants du complexe.[15]

Tableau 5

Données magnétiques des complexes synthétisés

N° crt.	Composé	$\mu_{eff.}$	χ_g	T_k	B.M. $\mu_{eff.}$ expér.
1	$[Cu_2DHF(SeCN)_2].4H_2O$	—	—	—	0
2	$[MnDHF(NCSe)_2]$	4,90	$27{,}95.10^{-6}$	· 297	5,53
3	$[Co\ DHF(SeCN)_2].2H_2O$	3,88	$11{,}00.10^{-6}$	,,	3,69
4	$[Ni\ DHF(SeCN)_2].2H_2O$	2,83	$7{,}36.10^{-6}$	,,	3,01

DÉTERMINATIONS MAGNÉTIQUES

On a déterminé les moments magnétiques pour les complexes de Cu(I) Mn(II), Co(II) et Ni(II) ; on utilise la méthode de Faraday, [16] à la température de 297°K, en employant comme étalon le Hg $[Co(SCN)_4]$.

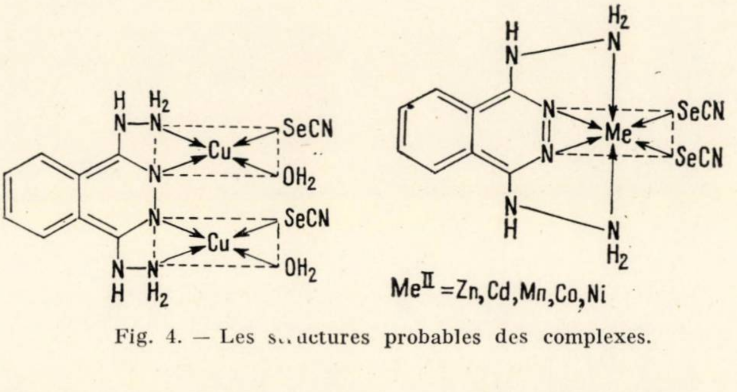

Fig. 4. — Les structures probables des complexes.

---

[15] I. Haritonov et G. V. Tindadze, *Zhur. neorg. Khim.*, **10**, 35 (1965).

[16] B. N. Figgis et R. S. Nyholm, *J. Chem. Soc.*, **1958**, 4190 ; *J. Chem. Soc.*, **1959**, 338.

Le moment magnétique effectif a été calculé d'après la relation[17]

$$\mu_{eff} = 2{,}839[\chi_M \cdot T]^{1/2} \quad \chi_M = \chi_g \cdot M$$

après l'utilisation de la correction pour le diamagnétisme des ions.

Les résultats sont rendus dans le tableau 5.

En tenant compte des données spectrales et magnétiques et des résultats analytiques concernant le rapport des constituants on peut attribuer aux complexes les structures probables indiquées dans la figure 4.

---

[17] B. N. Figgis et R. L. Martin, *J. Chem. Soc.*, **1956**, 3837.

Revue Roumaine de Chimie, **15**, 417–422 (1970)

MAGNETIC EXCHANGE IN A HETEROGENEOUS TRINUCLEAR SYSTEM

D. LUPU

Institute of Chemistry of the Academy,
Department of Inorganic Chemistry, Cluj, str. Donath 59–65

Received April 25, 1969

Molecular weight and electric conductivity measurements proved the existence of the $[Fe^{II}Fe_2^{III}(CH_3COO)_6O \cdot 3H_2O] \cdot 2H_2O$ trimer, similar to the well-known trinuclear acetates of Fe(III) and Cr(III). From the magnetic susceptibility data on powder samples, in the range 90°–300° K, the magnitude of the magnetic exchange interactions between Fe(III)-Fe (III) and Fe (II)-Fe (III) in this compound are obtained.

INTRODUCTION

Chrétien and Lous[1] prepared a compound formulated as $Fe^{II} Fe_2^{III} (CH_3COO)_6(OH)_2.4H_2O$ on the basis of elemental analysis. Since no other suitable solvent was found at that time, cryoscopic measurements were conducted in aqueous solution. A too low value was thus obtained for the molecular weight and the authors concluded that hydrolysis reactions took place in this system.

The compound is very similar to the trinuclear basic acetates[2] of Fe(III) and Cr(III), containing, according to the above mentioned authors, six acetate groups and two hydroxy groups for three metal ions. It may be now considered[3–4] that the structure of the trinuclear basic acetates contains the $[M_3(CH_3COO)_6O.3H_2O]^+$ skeleton, with M = Fe(III) or Cr (III) octahedrally co-ordinated ; the three octahedra, each containing one trivalent metal ion, have a common vertex, which is occupied by an oxygen atom.

Since little was known about the compound, cryoscopic, conductometric and magnetic susceptibility studies were performed in order to obtain some experimental data about its structure.

---

[1] A. Chrétien and E. Lous, *Bull. Soc. Chim. France*, **11**, 446 (1944).
[2] R. F. Weinland and E. Gussmann, *Ber.*, **42**, 3881 (1909).
[3] L. E. Orgel, *Nature*, **187**, 504 (1960).
[4] B. N. Figgis and G. B. Robertson, *Nature*, **205**, 694 (1965).

EXPERIMENTAL

Cryoscopic measurements were carried out in pyridine, using a platinum resistance thermometer, as described by Beckman and Waentig.[5] Nickel (II)-diethyldithiophosphate, a compound soluble in pyridine without decomposition[6] was used as a standard; the precision was ± 2%.

Electric conductivity was measured with a LP Conductoscope, at 25° and 5000 Hz.

The magnetic susceptibility of the compound in the solid state was measured by means of the Faraday method (with ± 1% error), using $Co(SCN)_4Hg$ as a calibrant[7] ($\chi_g = 16.44 \times 10^{-6}$ c.g.s. units at 20°). The temperature was maintained constant within ± 0.5°. The susceptibility of the solution was measured by the Gouy method, with benzene as a calibrant[8] ($\chi_g = -0.702 \times 10^{-6}$ at 25°).

RESULTS AND DISCUSSION

The molecular weight obtained for concentrations of 0.5–0.8% W/W in pyridine, is 624 as compared to 627.7, corresponding to the formula $Fe^{II}\ Fe_2^{III}\ (CH_3COO)_6(OH)_2.4H_2O$ deduced by Chrétien and Lous.

The equivalent electric conductivity in pyridine, immediately after dissolution, is zero, a fact suggesting that the complex is a nonelectrolyte.

The molar magnetic susceptibility of the compound dissolved in pyridine, calculated for M = 627.7 and corrected for diamagnetism (see ref. 8, p. 78), is $\chi_M = 12{,}770 \times 10^{-6}$ at 23°, very close to that found for the solid sample at the same temperature, $\chi_M = 13{,}240 \times 10^{-6}$ as it is the case with the trinuclear basic acetates in aqueous solutions.[9] This is another evidence that the structure of the compound is not affected by dissolution. These values correspond to the effective magnetic moments $\mu_{eff} = 3.19$ BM per iron atom, in solution, and $\mu_{eff} = 3.24$ BM in the solid state. They are well below the spin-only value for high-spin Fe(III) and even for Fe(II). The small value of the effective magnetic moment per iron atom makes possible to formulate the hypothesis that in this compound too, magnetic exchange interactions take place, as it is the case with the other trinuclear acetates mentioned above.

All these data show that the compound is of the same type as the trinuclear Fe(III) and Cr(III) basic acetates and may be formulated as $[Fe^{II}\ Fe_2^{III}\ (CH_3COO)_6O.3H_2O].2H_2O$, one Fe(III) ion being substitued with Fe(II).

The values of the molar magnetic susceptibility obtained on powder samples, are given in table 1.

The increase of the effective magnetic moment per iron atom with temperature, is in agreement with the hypothesis of the antiferromagnetic interactions in the system.

The temperature dependence of the magnetic susceptibilities of some trinuclear Fe(III) and Cr(III) acetates (Welo's compounds) was

---

[5] E. Beckman and P. Waentig, *Z. anorg. Chem.*, **67**, 17 (1910).

[6] C. K. Jörgensen, *J. Inorg. Nuclear Chem.*, **24**, 1571 (1962).

[7] B. N. Figgis and R. S. Nyholm, *J. Chem. Soc.*, **1958**, 4190.

[8] P. W. Selwood, "Magnetochemistry", Interscience Publ., New York 1956, p. 25.

[9] J. Lewis, *Pure Appl. Chem.*, **10**, 11 (1965).

Table 1

Temperature dependence of the molar magnetic susceptibility, corrected for diamagnetism, χ_M, for $Fe^{II}Fe_2^{III}(CH_3COO)_6(OH)_2 \cdot 4H_2O$. The effective magnetic moment per iron atom was calculated from the formula $\mu_{eff} = 2.839\sqrt{(\chi_M/3).T}$

T (°K)	$\chi_M \cdot 10^6$	μ_{eff}/Fe atom
296	13,240	3.24
294	13,370	3.24
262	14,050	3.14
228	15,370	3.07
209	16,060	3.00
200	16,550	2.98
186	17,240	2.93
160	18,700	2.83
151	19,870	2.84
128	22,110	2.76
106	25,350	2.69
97	27,010	2.65
94	27,670	2.64

successfully explained by Kambe,[10] using the Heisenberg-Dirac-Van Vleck (HDVV) spin-coupling Hamiltonian for three interacting magnetic ions. Recently, Adams and co-workers[11] used the same model to obtain the value of the exchange interactions in trinuclear Fe(III) alcoxides and Ginsberg, [12] for the linear bis (acetylacetonato) nickel(II) trimer.

In a trinuclear system of the same type as Welo's compounds, containing one high-spin Fe(II) ion (S=2) and two high-spin Fe(III) ions (S=5/2), the HDVV spin-coupling Hamiltonian is

$$H_{ex} = -2J[(S_1.S_2) + (S_2.S_3)] - 2\mathcal{J}\ (S_3.S_1) \tag{1}$$

considering the two Fe (III) ions equivalents with respect to Fe(II) ion. S_1 and S_3 are the spin operators for Fe(III) and S_2 for Fe(II); J and $\mathcal{J}$ are the exchange integrals between Fe(II)-Fe (III) and Fe(III) Fe(III) ions respectively.

Following the same procedure as Ginsberg and co-workers,[12] we obtained the spin levels given in table 2.

The magnetic susceptibility, χ_M, of the system is the average of the individual spin levels susceptibilities, each weighted by its degeneracy and the corresponding Boltzman factor:

$$\chi_M = \frac{Ng^2\beta^2}{kT} \cdot [2\exp(-y/2) + 2\exp(-2x + 3y/2) + 2\exp(-6x + 11y/2) +$$
$$2\exp(-12x + 23y/2) + 10\exp(-6y) + 10\exp(-2x - 4y) +$$
$$10\exp(-6x) + 10\exp(-12x + 6y) + 10\exp(-20x + 14y) +$$
$$28\exp(-2x - 10y) + 28\exp(-6x - 6y) + 28\exp(-12x) +$$
$$28\exp(-20x + 8y) + 28\exp(-30x + 18y) + 60\exp(-6x - 14y) +$$

---

[10] K. Kambe, *J. Phys. Soc. Japan*, **5**, 48 (1950).

[11] R. W. Adams, C. G. Baraclough and R. L. Martin, *Inorg. Chem.*, **5**, 346 (1966).

[12] A. P. Ginsberg, R. L. Martin and R. C. Sherwood, *Inorg. Chem.*, **7**, 932 (1968).

Table 2

Spin levels for a triangular system containing an atom with four unpaired electrons and two atoms, each with five unpaired electrons (S-the total spin of the trimer, S′-the total spin of the two atoms with five unpaired electrons). E(S, S′) are the energies of the spin levels, taking the state with S = 0 and S′ = 0 as ground state

S	S′	H_{ex}	E (S, S′)
7	5	$-69J/4-25\mathcal{J}/2$	$-26J\ -30\mathcal{J}$
6	5	$-33J/4-25\mathcal{J}/2$	$-17J\ -30\mathcal{J}$
	4	$-53J/4-5\mathcal{J}/2$	$-22J\ -20\mathcal{J}$
5	5	$+35J/4-25\mathcal{J}/2$	$-30\mathcal{J}$
	4	$-5J/4-5\mathcal{J}/2$	$-10J\ -20\mathcal{J}$
	3	$-37J/4+11\mathcal{J}/2$	$-18J\ -12\mathcal{J}$
4	5	$+75J/4-25\mathcal{J}/2$	$+10J\ -30\mathcal{J}$
	4	$+35J/4-5\mathcal{J}/2$	$-20\mathcal{J}$
	3	$+3J/4+11\mathcal{J}/2$	$-8J\ -12\mathcal{J}$
	2	$-21J/4+23\mathcal{J}/2$	$-14J\ -6\mathcal{J}$
3	5	$+107J/4-25\mathcal{J}/2$	$+18J\ -30\mathcal{J}$
	4	$+67J/4-5\mathcal{J}/2$	$+8J\ -20\mathcal{J}$
	3	$+35J/4+11\mathcal{J}/2$	$-12\mathcal{J}$
	2	$+11J/4+23\mathcal{J}/2$	$-6J\ -6\mathcal{J}$
	1	$-5J/4+31\mathcal{J}/2$	$-10J\ -2\mathcal{J}$
2	4	$+91J/4-5\mathcal{J}/2$	$+14J\ -20\mathcal{J}$
	3	$+59J/4+11\mathcal{J}/2$	$+6J\ -12\mathcal{J}$
	2	$+35J/4+23\mathcal{J}/2$	$-6\mathcal{J}$
	1	$+19J/4+31\mathcal{J}/2$	$-4J\ -2\mathcal{J}$
	0	$+11J/4+35\mathcal{J}/2$	$-6J$
1	3	$+81J/4+11\mathcal{J}/2$	$+23J/2-12\mathcal{J}$
	2	$+57J/4+23\mathcal{J}/2$	$+11J/2-6\mathcal{J}$
	1	$+41J/4+31\mathcal{J}/2$	$+3J/2-2\mathcal{J}$
	0	$+33J/4+35\mathcal{J}/2$	$-J/2$
0	2	$+59J/4+23\mathcal{J}/2$	$+6J\ -6\mathcal{J}$
	1	$+43J/4+31\mathcal{J}/2$	$+2J\ -2\mathcal{J}$
	0	$+35J/4+35\mathcal{J}/2$	0

$$
\begin{gathered}
60\exp(-12x-8y)+60\exp(-20x)+60\exp(-30x+10y)+\\
110\exp(-12x-18y)+110\exp(-20x-10y)+110\exp(-30x)+\\
182\exp(-20x-22y)+182\exp(-30x-17y)+280\exp(-30x-26y)]/\\
[1+\exp(-2x+2y)+\exp(-6x+6y)+3\exp(-y/2)+\\
3\exp(-2x+3y/2)+3\exp(-6x+11y/2)+3\exp(-12x+23y/2)+\\
5\exp(-6y)+5\exp(-2x-4y)+5\exp(-6x)+\\
5\exp(-12x+6y)+5\exp(-20x+14y)+7\exp(-2x-10y)+\\
7\exp(-6x-6y)+7\exp(-12x)+7\exp(-20x+8y)+\\
7\exp(-30x+18y)+9\exp(-6x-14y)+9\exp(-12x-8y)+\\
9\exp(-20x)+9\exp(-30x+10y)+11\exp(-12x-18y)+\\
11\exp(-20x-10y)+11\exp(-30x)+13\exp(-20x-22y)+\\
13\exp(-30x-17y)+15\exp(-30x-26y]
\end{gathered}
\tag{2}
$$

where $x = -\mathcal{J}/kT$ and $y = -J/kT$

By a trial and error procedure, the best fitting between experimental data and eq. (2) is obtained for $g=2$, $\mathcal{J}=-36\ \mathrm{cm}^{-1}$ and the values of J given in figure 1. at three different temperatures.

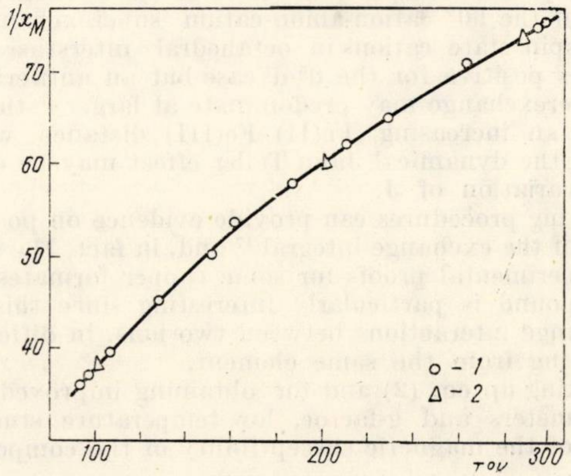

Fig. 1. — Temperature dependence of the reciprocal molar magnetic susceptibility of $Fe^{II}Fe_2{}^{III}(CH_3COO)_6(OH)_2 \cdot 4H_2O$.

1, experimental points; *2*, theoretical points obtained from the eq. (2) for $g = 2$, $\mathcal{J} = -36\ \mathrm{cm}^{-1}$ and $J = 2.8\ \mathrm{cm}^{-1}$ (at 100.7 °K). $J = -6.7\ \mathrm{cm}^{-1}$ (at 201 4°K), $J = -10\ \mathrm{cm}^{-1}$ (at 288° K).

It is rather surprising that the g-factor has the spin-only value since with Fe(II) high-spin ion in O_h symmetry, an orbital contribution to the effective magnetic moment is to be expected. The hexa-coordinated Fe(II) complex with protoporphyrin[13] has $\mu_{eff} = 4.83-5.02$ but this compound was studied at room temperature only. However, the t_{2g} electron delocalization may bring the magnetic moment closer to the spin-only value.

In a recent paper,[14] Ham demonstrated that the dynamical Jahn-Teller effect for Fe(II) in octahedral symmetry, simulates the effect of covalent bonding in reducing the magnitude of certain parameters of the system (spin-orbit coupling constant, g-factor). Koswig and co-workers[15] give experimental evidence concerning the Jahn-Teller effect on Fe(II) included in AgCl and AgBr lattices (O_h symmetry): the splitting ΔE of the E_g excited state increases approximately linearly with temperature in the range 80° – 300° K.

---

[13] W. P. Hambright, A. N. Thorpe and C. C. Alexander, *J. Inorg. Nuclear. Chem.*, **30**, 3139 (1968).

[14] F. S. Ham, *Phys. Rev.*, **138**, A 1727 (1965).

[15] H. D. Koswig, U. Retter and W. Ulrici, *Phys. stat. sol.*, **24**, 605 (1967).

The magnitude of the exchange integral between Fe(III) ions, $\mathcal{J} = -36\ \mathrm{cm}^{-1}$, is close to that found for trinuclear Fe(III) basic acetates by Kambe and remains constant in the temperature range considered here. On the other hand, the exchange integral J, between Fe(II)-Fe(III), is temperature dependent (see fig. 1). Goodenough[16] showed that the sign of the 90° cation-anion-cation superexchange interactions between high-spin state cations in octahedral interstices that share a common face is positive for the d^6-d^5 case but an antiferromagnetic 90° correlation superexchange may predominate at larger cation-cation separations. Thus, an increasing Fe(II)-Fe(III) distance with increasing temperature or the dynamical Jahn-Teller effect may be correlated with the observed variation of J.

Curve-fitting procedures can provide evidence on possible temperature variation of the exchange integral[17] and, in fact, Martin and Waterman[18] give experimental proofs for some copper formates, dimers.

The compound is particularly interesting since this is a case of magnetic exchange interactions between two ions, in different oxidation states, originating from the same element.

For checking-up eq. (2) and for obtaining improved values of the exchange parameters and g-factor, low-temperature studies, down to liquid helium, of the magnetic susceptibility of the compound would be quite desirable.

Acknowledgments. The author wishes to thank dr. Iuliu Pop of the Department of Physics, "Babeş-Bolyai" University, Cluj, for useful discussions in the field and also, to all those who helped him by stimulating comments.

---

[16] J. B. Goodenough, "Magnetism and The Chemical Bond", Interscience Publ., John Wiley ed., New York, 1963, p. 190.

[17] J. S. Smart, "Magnetism", (G. T. Rado and H. Suhl eds.) Vol. 3, Academic Press, New York, 1963, p. 74.

[18] R. L. Martin and H. Waterman, *J. Chem. Soc.*, **1959**, 2960.

Revue Roumaine de Chimie, **15**, 423–429 (1970)

COORDINATION POLYMERS. III

POLYCOORDINATION OF 4,4′-DIPHENYLSULPHONEDICARBOXALDEHYDE BIS(THIOSEMICARBAZONE) WITH CADMIUM AND MERCURY

M. MARCU and M. DIMA

Institute of macromolecular chemistry "P. Poni",
Jassy, Aleea Grigore Ghica Vodă, 41 A

Received March 3, 1969

The 4,4′-diphenylsulphonedicarboxaldehyde bis(thiosemicarbazone) ligand is sinthetized in ethanol-water-glacial acetic acid medium. By the reaction between the ligand in DMF and cadmium or mercury acetates in ethanol, one obtains coordination polymers as yellow powders. Elementary analysis and IR spectra confirm the structure of the compounds. The coordination polymers obtained are semiconductors. The thermic stability in air was also studied.

The synthesis of the coordination polymers obtained by polycoordination of terephthalic and isophthalic bis(thiosemicarbazones) with cadmium and mercury acetate, was given in two former papers.[1, 2]

Chakravarty and Drinkard,[3] obtained coordination polymers with a good thermic stability by the synthesis of naphthazarine bis(thiosemicarbazone) and the reaction of this ligand with zinc and nickel.

In the present paper we deal with the synthesis of the 4,4′-diphenylsulphonedicarboxaldehyde bis(thiosemicarbazone) (I) obtained by the reaction between thiosemicarbazide and 4,4′-diphenylsulphonedicarboxaldehyde, in ethanol-water-glacial acetic acid medium.

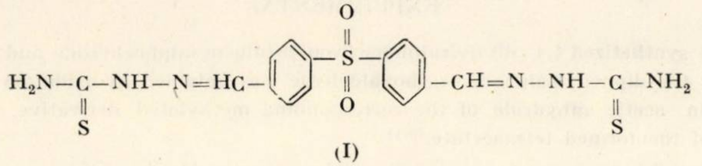

(I)

By the reaction between the stoichiometric quantities of ligand dissolved in DMF and the cadmium or mercury acetates in ethanol, one obtains coordination polymers as yellow powders. The coordination polymers are separated from the mixture of solvents.

---

[1] Part II: M. Marcu and M. Dima, *Rev. Roumaine Chim.*, **13**, 359 (1968).
[2] M. Marcu and M. Dima, *Rev. Roumaine Chim.*, **11**, 1353 (1967).
[3] D. N. Chakravarty and W. C. Drinkard, *J. Indian Chem. Soc.*, **37**, 517 (1960).

One has also tried the synthesis of coordination polymers with Cu^{2+}. To this end the reaction has been carried out of the ligand, the solute in DMF and copper acetate, acetylacetonate, sulphate, nitrate or chloride in ethanol or DMF. The yield was every time yellow-green precipitates, which on elementary analysis and magneto-chemical measurements have been found to be a mixture of compounds with Cu^{2+} and Cu^{1+}. The fact that thiosemicarbazones reduce part of the Cu^{2+} to Cu^{1+}, which then reacts with the unoxidized thiosemicarbazone this type of reaction being common to the organic compounds containing oxidizable sulphur, [4-8]

$$2R - S^- + 2Cu^{2+} \longrightarrow R - S - S - R + 2Cu^{1+}$$

results in the obtention of products that are not unitary in their chemical composition.

The synthesis of the coordination polymers with zinc and nickel has been also attempted. Therefore stoichiometric quantities of ligand and zinc or nickel acetate in DMF were stirred for three hours, at room temperature, the compounds obtained being precipitated from water. The same reaction was tried at 100° and on solvent refluxing. Elementary analysis and IR spectra show that for the first two experiments (by cooling) the reaction does not occur, while for the last two (by heating), a partial destruction of the ligand takes place, accompanied by the separation of metal sulphur.

After identifying the cadmium and mercury coordination polymers by elementary analysis and IR spectra, we assign the following structure to the macromolecular chain unit (II)

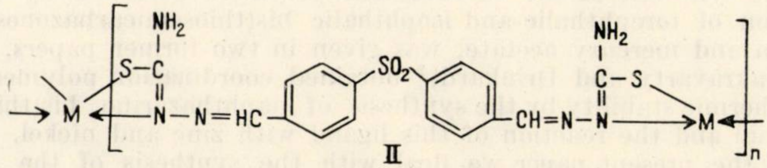

II

in which M is cadmium or mercury.

EXPERIMENTAL

One has synthetized 4,4′-ditolylsulphone from *p*-toluenesulphochloride and toluene with $AlCl_3$.[9] The 4,4′-diphenylsulphonedicarboxaldehyde was obtained by oxidation with chromic anhydride in acetic anhydride of the corresponding methylated derivative, and by the hydrolysis of the formed tetraacetate.[10,11]

---

[4] R. Weiss and H. Venner, *Z. physiol. Chem.*, **317**, 82 (1952).

[5] K. A. Jensen and E. Rancke-Madsen, *Z. anorg. Chem.*, **219**, 243 (1934).

[6] R. Kuhn and F. Zillikon, U. S. Patent 2.695.911, 1954.

[7] E. Cattelain, *Bull. Soc. chim. France*, **1945**, 49.

[8] V. N. Pochainova, E. I. Krilov and D. I. Riabcicov, *Zhur. neorg. Khim.*, **1**, 406 (1956).

[9] C. Holt and B. Pagdin, *J. Chem. Soc.*, **1960**, 2508.

[10] H. Burton and P. F. Hu, *J. Chem. Soc.*, **1948**, 601.

[11] J. Bernstein, H. L. Yale, K. Losse, M. Holsing, J. Martins and W. A. Lott, *J. Amer. Chem. Soc.*, **73**, 911 (1951).

Bernstein and co-workers,[11] obtain 4,4′-diphenylsulphonedicarboxaldehyde bis(thiosemicarbazone) by boiling, under stirring, for two hours a glacial acetic acid and thiosemicarbazide mixture with a solution of ethanol-glacial acetic acid of 4,4′-diphenylsulphonedicarboxaldehyde.

The 4,4′-diphenylsulphonedicarboxaldehyde bis(thiosemicarbazone) synthetized by us was obtained according to Sah and Daniels[12] method.

1. *4,4′-diphenylsulphonedicarboxaldehyde bis(thiosemicarbazone)*

In a three-neck flask of 1 liter, fitted out with reflux refrigerent, stirrer and dropping funnel 5 gr of 4,4′-diphenylsulphonedicarboxaldehyde dissolved in 200 ml of ethanol are introduced.

The solution is brought to refluxing and by dropping under constant stirring, a solution of 3.33 g thiosemicarbazide in 150 ml water and 15 ml glacial acetic is added. A yellow compound separates. The reaction mixture is continuously stirred on refluxing for one hour, filtered hot, washed with hot water and then with alcohol. It recrystallizes from a DMF-water mixture. Yield: 65%. M.p. 264° with decomposition.

$C_{16}H_{16}N_6O_2S_3$	C %	H %	N %	S %
Calcd.:	45.72	3.81	20.00	22.85
Found:	45.45	3.76	20.05	22.90

2. *Synthesis of coordination polymers*

a) Cadmium polymer

To 0.002 mol (0.84 gr) ligand dissolved in 75 ml of DMF, a solution of 0.002 mol (0.533 g) dihydrated cadmium acetate in 75 ml ethanol is added, by dropping and magnetic stirring. Towards the end of the addition, a yellow suspension forms: stirring continues for one hour then the suspension is separated on G_3 washed with ethanol, water and again with ethanol. The product is dried at 110° and then in vacuum.

$(C_{16}H_{14}N_6O_2S_3Cd)_n$	C %	H %	N %	S %	Cd %
Calcd.:	36.19	2.66	15.82	18.12	21.18
Found:	35.75	2.80	15.76	18.09	20.65
Calcd.:	N/Cd=6.00		S/Cd=3.00		
Found:	N/Cd=6.16		S/Cd=3.08		

b) Mercury polymer

For the synthesis of the mercury polymer, one starts from the same quantities (in mol) of ligand solved in DMF and mercury acetate in ethanol, to which 1 ml of glacial acetic acid is added.

$(C_{16}H_{14}N_6O_2S_3Hg)_n$	C %	H %	N %	S %	Hg %
Calcd.:	31.03	2.28	13.57	15.53	32.41
Found:	31.18	2.35	13.43	15.42	32.67
Calcd.:	N/Hg = 6.00			S/Hg=3.00	
Found:	N/Hg = 5.89			S/Hg=2.89	

---

[12] P. T. SAH and T. C. DANIELS, *Rec. Trav. chim.*, **69**, 1545 (1950).

RESULTS AND DISCUSSIONS

IR spectra

The IR spectra of the 4,4'-diphenylsulphonedicarboxaldehyde bis(thiosemicarbazone) ligand and of the cadmium and mercury coordination polymers, were registered as KBr tablets with a UNICAM SP_{200} spectrophotometer.

The IR spectrum of the ligand has three ν_{NH} vibrations at 3200, 3300 and 3460 cm^{-1}, in the range of the valence vibration NH (3050 – 3500 cm^{-1}). In the 1600 cm^{-1} range there is a strong band obtained by superposition of $\nu_{C=C}$ and $\nu_{C=N}$ at 1610 cm^{-1}. The SO_2 group presents two intense bands, corresponding to ν_s at 1110 and 1160 cm^{-1}, as well as ν_a at 1300 and 1330 cm^{-1}. At 950 cm^{-1} there exists a medium frequency band which we assign to the $\nu_{C=S}$ vibration.

Looking at the IR spectrum of the ligand as compared to the IR spectra of the coordination polymers with cadmium and mercury, in the above mentioned ranges, one notices that, in the range of the NH (3050–3500 cm^{-1}) vibration of the cadmium and mercury coordination polymers, there are only two ν_{NH} vibrations, at 3350 and 3500 cm^{-1}, respectively at 3350 and 3460 cm^{-1}. In the 1600 cm^{-1} range, in the case of the two coordination polymers, besides the strong band noticed for the ligand, there appears another band due to the re-arrangement of the double bonds in conjugated system in the ligand's molecule, namely $\nu_{C=N} = 1630$ cm^{-1} for the cadmium polymer and $\nu_{C=N} = 1628$ cm^{-1} for the mercury polymer.

The SO_2 group remains also in the case of the coordination polymers as follows : for the cadmium polymer $\nu_s = 1110$ and 1160 cm^{-1} and $\nu_a = 1300$ and 1330 cm^{-1} ; for the mercury polymer ν_s 1110 and 1160 cm^{-1} and $\nu_a = 1300$ cm and 1330 cm^{-1}.

We find the diminished vibration band $\nu_{C=S} = 950$ cm^{-1} of the ligand very much attenuated in the case of the cadmium and mercury polymer.

This proves that the synthetized coordination polymers have at the ends $C{\Leftarrow}S$ groups from the ligand.

One may draw the conclusion that the alteration of the IR spectra of the coordination polymers, as compared to the IR spectrum of the ligand, exactly confirms the structure of the macromolecular chain unit suggested above (II).

Variation of the electric conductivity with temperature

The electric conductivity σ of the synthetized coordination polymers has been determined with a TESLA-283 Megaohmmeter, on polymer tablets obtained by pressing at $10 t/cm^2$, in a temperature range of 25 to 125°, using aluminium electrodes. Measurements were made in air. To eliminate the influence of adsorbed gas and moisture, the tablets were initially heated to 150°, after which the variation of the electric conductivity with the temperature was measured during cooling off.

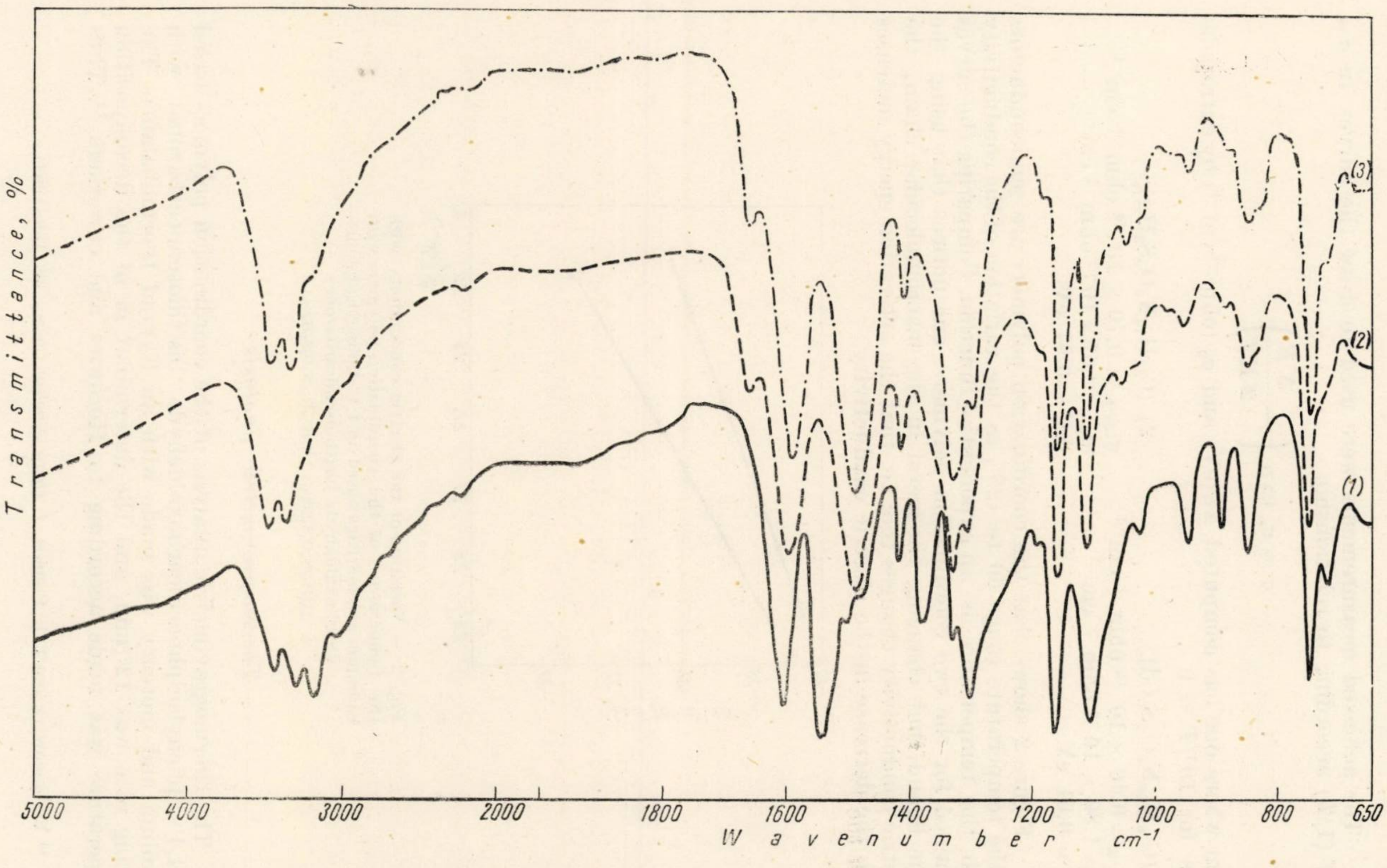

Fig. 1. — IR spectra of 4,4′-diphenylsulphonedicarboxaldehyde bis(thiosemicarbazone) and its coordination polymers with cadmium and mercury.

1, $C_{16}H_{16}N_6O_2S_3$; *2*, $(C_{16}H_{14}N_6O_2S_3Cd)_n$; *3*, $(C_{16}H_{14}N_6O_2S_3Hg)_n$.

The achieved measurements were used to draw the curves $\ln \sigma = f(1/T)$ according to relationship

$$\sigma = \sigma_0 \exp \left(-\frac{\Delta E}{2\,KT} \right)$$

from where one has computed ΔE(eV) and σ_0 ($\text{ohm}^{-1}\,\text{cm}^{-1}$) by extrapolation for $10^3/T = 0$

1) $(C_{16}H_{14}N_6O_2S_3Cd)_n$	2) $(C_{16}H_{14}N_6O_2S_3Hg)_n$
$\sigma_{298°K} = 0.40 \times 10^{-13}\ \text{ohm}^{-1}\,\text{cm}^{-1}$	$\sigma_{298°K} = 0.70 \times 10^{-14}\ \text{ohm}^{-1}\,\text{cm}^{-1}$
$\sigma_0 = 1.80 \times 10^{-9}\ \text{ohm}^{-1}\,\text{cm}^{-1}$	$\sigma_0 = 2.07 \times 10^{-7}\ \text{ohm}^{-1}\,\text{cm}^{-1}$
$\Delta E = 0.61$ eV	$\Delta E = 0.97$ eV

Figure 2 shows that the coordination polymers are semiconductors in the temperature range 50 to 125°, as the variation of the conductivity with the temperature is an exponential function. Comparing the curves obtained for the two coordination polymers, one notices that using the same ligand, but changing the metal in the macromolecular chain, the electric conductivity changes too; i.e. that the activation energy increases with the decrease in the electric conductivity.

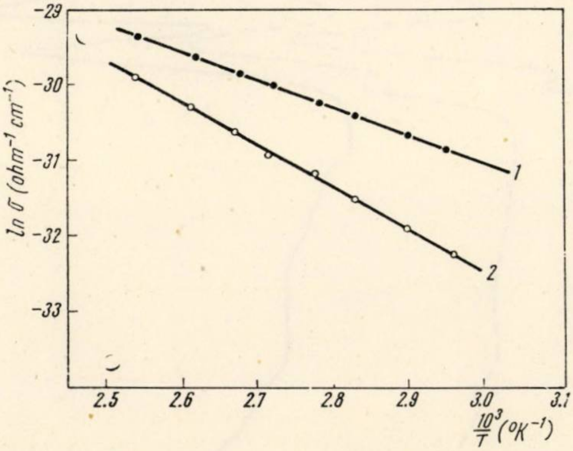

Fig. 2. — Variation of the electric conductivity with the temperature of the coordination polymers with cadmium and mercury based on 4,4′-diphenylsulphonedicarboxaldehyde bis(thiosemicarbazone). *1*, $(C_{16}H_{14}N_6O_2S_3Cd)_n$; *2*, $(C_{16}H_{14}N_6O_2S_3Hg)_n$.

Thermogravimetric analysis

The thermogravimetric analysis of the coordination polymers based on 4,4′-diphenylsulphonedicarboxaldehyde bis(thiosemicarbazone) with cadmium and mercury was made with an Eyraud thermobalance. The heating rate was 12°/min, and the determination of the decomposition temperature was made according to Horowitz and coworkers.[13] Thus the decomposition temperature of the cadmium polymer is 305° and that of the mercury polymer 265°, decomposition temperatures higher than those corresponding to the coordination polymers with cadmium and mercury based on terephthalic bis(thiosemicarbazone)[1] and isophthalic bis(thiosemicarbazone).[2] Up to the decomposition temperature, the cadmium polymer loses about 5% of its weight, while no loss is noticed for the mercury polymer. After these temperatures, the loss in weight for the cadmium polymer is greater than that of the mercury polymer by approximately 5%, and at 415° the loss is the same for both polymers, namely 26%. Over this temperature the loss in weight is greater for the mercury polymer, reaching 78% at 700°, against 72% at same temperature for the cadmium polymer. After this temperature, one does not observe any additional loss in weight for the cadmium polymer, since CdO, which is stable up to 900°, is already forming, while for the mercury polymer, starting from 500°, the loss is progressive, and is explained by the fact that the forming HgO, decomposes over this temperature.

---

[13] E. Horowitz and T. P. Perros, *J. Inorg. Nuclear Chem.*, **26**, 139 (1964).

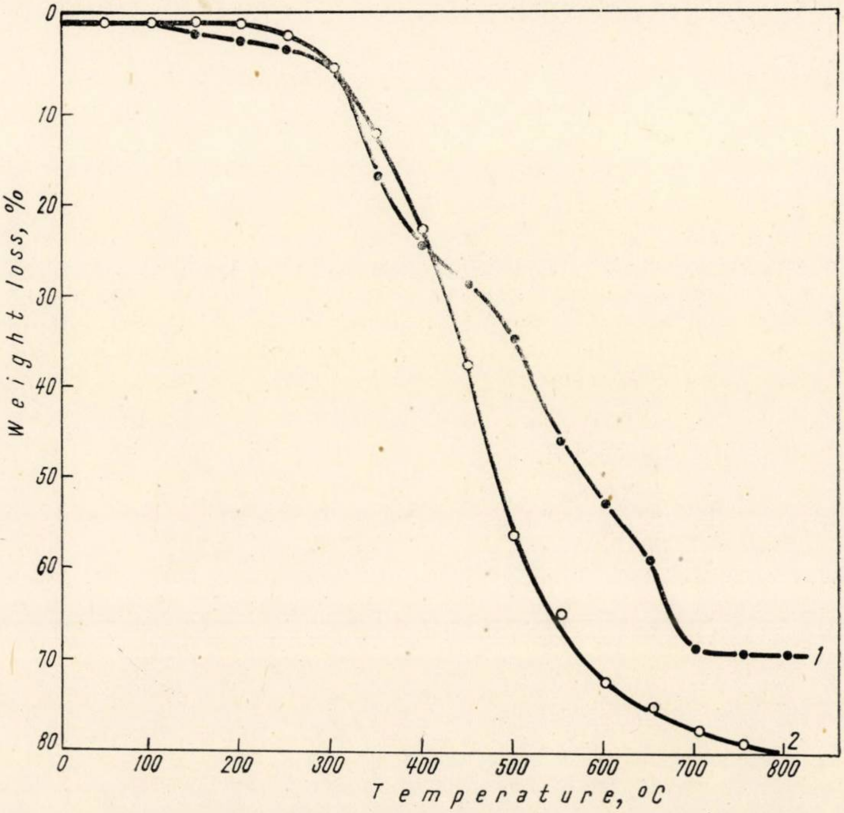

Fig. 3. — Thermogram of the coordination polymers with cadmium and mercury based on 4,4′-diphenylsulphonedicarboxaldehyde bis(thiosemicarbazone) *1*, $(C_{16}H_{14}N_6O_2S_3Cd)_n$; *2*, $(C_{16}H_{14}N_6O_2S_3Hg)_n$.

Revue Roumaine de Chimie, 15, 431–440 (1970)

L'ÉTUDE DE LA VISCOSITÉ DE STRUCTURE DES SOLUTIONS DE STÉARATE D'ALUMINIUM DANS LES HYDROCARBURES

L'INFLUENCE DE QUELQUES COMPOSÉS POLAIRES

GEORGETA POPESCU

Institut de Chimie Macromoléculaire «P. Poni» de l'Académie, Secteur des Colloïdes, Bucarest, 89 Spl. Independenței

Reçu le 28 mars 1969

On étudie la viscosité de structure des solutions de stéarate d'aluminium dans différents hydrocarbures (aromatiques, cycliques. aliphatiques), en déterminant l'influence exercée par quelques alcools et crésols. On met en évidence la structure de réseau du polymère de savon et les changements dans la structure des particules colloïdales.

Parmi les propriétés mécaniques concernant la structure des colloïdes, la viscosité de structure présente un grand intérêt parce qu'elle dépend de la forme des particules[1] et par conséquent elle peut indiquer les changements qui interviennent sous l'influence de différents facteurs.

Dans des recherches antérieures nous avons étudié la viscosité de structure des solutions visqueuses d'oléate de sodium et nous avons montré que la résistance structurale et les effets thixotropiques augmentent lorsqu'on ajoute au système du crésol.[2] Pour les solutions qui contiennent de grandes quantités de crésol, correspondant au minimum de viscosité, l'allure de la courbe d'écoulement peut être interprétée en admettant le changement de la forme anisodiamétrique des micelles dans une forme isodiamétrique.[3] La viscosité de structure constitue donc une méthode adéquate d'étude des systèmes dispersés.

Les solutions de stéarate d'aluminium et particulièrement de mono- et distéarate ont été étudiées du point de vue du comportement viscosimétrique dans différents solvants, surtout dans des hydrocarbures aromatiques.[4-7] Néanmoins des études systématiques concernant l'influence exercée par la nature du solvant d'une part et par l'adjonction de différents composés d'autre part, sur les propriétés rhéologiques du stéarate neutre d'aluminium font complètement défaut. C'est pourquoi nous nous sommes proposé d'étudier dans ce travail la viscosité de structure des solutions de stéarate neutre d'aluminium dans des hydrocarbures à différentes structures (aliphatiques, cycliques, aromatiques), ainsi que l'influence exercée par quelques composés polaires (alcools, crésols).

---

[1] W. Philippoff, *Koloid-Z.*, **71**, 1 (1935).

[2] E. P. Schipanova, G. Popescu et A. A. Trapeznicov, *Rev. Roumaine Chim.*, **9**, 465 (1964).

[3] E. Angelescu et G. Popescu, *Rev. Roumaine Chim.*, **11**, 503 (1966).

PARTIE EXPÉRIMENTALE

Nous avons préparé les solutions de stéarate d'aluminium (produit Merck) dans le benzène, le toluène, l'*o*- et le *p*-xylène, le cyclohexane, la décaline et le *n*-décane. La concentration du savon a été exprimée en moles par 1 kg de solution. Les hydrocarbures ont été purifiés par distillation, séchés sur sodium et caractérisés par l'indice de réfraction et par chromatographie. Nous avons purifié et caractérisé de façon analogue les alcools et le crésol employés.

En vue d'étudier les propriétés mécaniques des solutions, nous avons utilisé un viscosimètre aux cylindres coaxiaux Rotovisko Haake K.G., et déterminé les courbes d'écoulement, c'est-à-dire le gradient moyen de la vitesse D en fonction de la tension de cisaillement τ, des solutions hydrocarbonées de stéarate d'aluminium de différentes concentrations, en l'absence et en présence des alcools ou crésols. Nous avons utilisé le corps de rotation NV, de 40,2 mm de diamètre qui permet la détermination des viscosités dans l'intervalle 4—10 000 cP avec une précision de $\pm$ 1,5%, en maintenant constante la température (20 $\pm$ 0,1°) et en introduisant la même quantité de solution dans l'appareil (20 ml). Nous avons calculé la tension de cisaillement τ, le gradient moyen de la vitesse D et la viscosité η, d'après les relations

$$\tau = A.S. \text{ (dyne cm}^{-2}\text{)}; \qquad D = \frac{B}{\text{UM}} \text{ (s}^{-1}\text{)}; \qquad \eta = \text{UM}.S.K \text{ (cP)}$$

où A et B sont les facteurs de cisaillement correspondant au corps de rotation employé, K sa constante d'étalonnage ; le produit UM, indiqué par C_t (nombre de tours), représente le facteur de vitesse et S les gradations de l'aiguille indicatrice.

RÉSULTATS ET DISCUSSIONS

Dans la figure 1 on a représenté les courbes d'écoulement pour les solutions de stéarate d'aluminium dans le toluène, d'une concentration de 0,1 (8,8%), 0,2 (17,5%), 0,25 (21,9%) et 0,3 M (26,3%), déterminées à 20°.

On a constaté que les solutions de stéarate d'aluminium dans le toluène présentent une viscosité de structure d'autant plus marquée

---

[4] W. Ostwald et E. K. Riedel, *Kolloid-Z.*, **70**, 67 (1935).

[5] H. Sheffer, *Canad. J. Research*, **26B**, 481 (1948).

[6] T. Inone et Yasuji Iida, *J. Chem. Soc. Japan*, **73**, 71 (1952) ; *Chem. Abstr.*, **46**, 5401 (1952).

[7] M. Nakagaki et M. Nishino, *Yakagaku Zasshi*, **82**, 821 (1962) ; **83**, 185, 1137 (1963) ; *Chem. Abstr.*, **57**, 15264 (1962).

que la concentration du savon augmente. On n'a pu obtenir que la branche de structure de la courbe générale, parce que la précision de l'appareil ne permet pas la détermination des gradients de la vitesse pour des tensions de cisaillement trop petites. Les courbes d'écoulement obtenues sont semblables à celles des corps pseudoplastes. [8]

Pour mettre en évidence l'influence du solvant sur la structure du savon d'aluminium, nous avons déterminé, les courbes d'écoulement

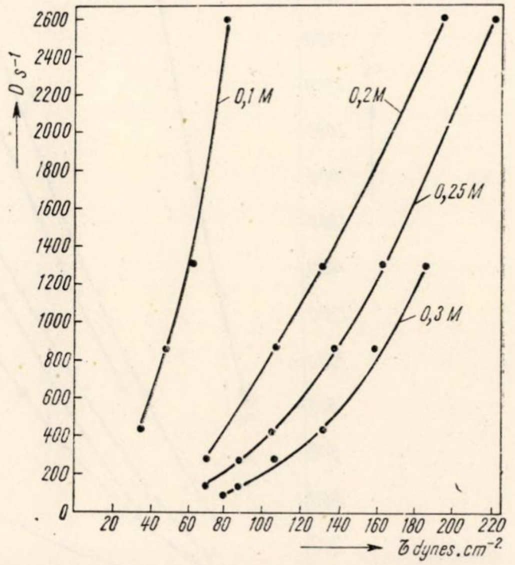

Fig. 1. — Courbes d'écoulement des solutions de stéarate d'aluminium dans le toluène, ayant les concentrations : 0,1, 0,2, 0,25 et 0,3 M, à 20°.

des solutions de stéarate d'aluminium d'une concentration de 0,2 M, dans les solvants de différentes structures : hydrocarbures aliphatiques (*n*-décane), cycliques (cyclohexane, décaline) et aromatiques (benzène, toluène, *o*- et *p*-xylène). Comme on peut voir dans la figure 2, les courbes sont déplacées vers les tensions de cisaillement plus élevées dans l'ordre : *n*-décane < *p*-xylène < cyclohexane < benzène < toluène < *o*-xylène <décaline.

A l'exception de la solution de stéarate d'aluminium dans le *n*-décane qui présente un comportement newtonien, toutes les autres solutions présentent une viscosité de structure d'autant plus marquée que le volume moléculaire du solvant augmente.

Il est à remarquer la différence de comportement entre les solutions du savon dans les deux isomères du xylène qui ont des structures différentes : dans le cas de l'*o*-xylène (courbe *5*) la courbe d'écoulement est déplacée vers des tensions de cisaillement plus grandes en comparaison de celle du *p*-xylène (courbe *6*). On peut attribuer cette différence de comportement au moment dipolaire de l'*o*-xylène. Les solutions dans l'*o*-xylène et spécialement dans la décaline présentent la viscosités la plus marquée.

---

[8] K. Steiger-Trippi et A. Ory, *Pharm. Acta Helv.*, **36**, 205 (1961).

Ces résultats sont en concordance avec les données obtenues par certains auteurs[9,10] qui, en étudiant les propriétés des sols et gels des savons d'aluminium dans des hydrocarbures, ont établi que les molécules forment par association de longues micelles fibrillaires. On a même considéré ces savons comme de hauts polymères formés par des liaisons d'hydrogène, [5-7,11] en présentant une puissante viscosité de structure. [4, 10]

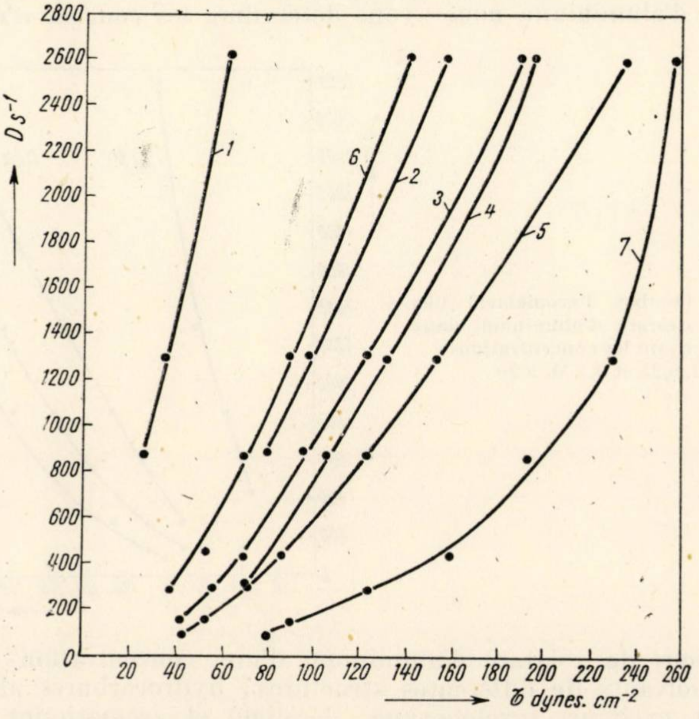

Fig. 2. — Courbes d'écoulement des solutions de stéarate d'aluminium dans différents solvants

n-décane (c. *1*); cyclohexane (c.*2*); benzène (c.*3*); toluène (c.*4*); *o*-xylène (c.*5*); *p*-xylène (c.*6*); décaline (c.*7*); température = 20°.

La viscosité de structure a été attribuée à une structure de réseau ayant des liaisons faibles entre les points de contact ou aux terminaisons des micelles. [11,12] D'après Ludke[13] les micelles peuvent avoir la structure des unités de polymère orientées dans la direction de l'axe de l'atome d'oxygène coordonné à l'octaèdre d'aluminium.

---

[9] V. R. Gray, *Trans. Faraday Soc.*, **42B**, 196 (1964); V. R. Gray et A. E. Alexander, *J. Phys. Coll. Chem.*, **9**, 53 (1949).

[10] J. W. McBain et E. B. Working, *J. Phys. Coll. Chem.*, **51**, 947 (1947).

[11] W. H. Bauer, N. Weber et S. E. Wiberley, *J. Phys. Chem.*, **62**, 106 (1958).

[12] C. G. McGee, *J. Amer. Chem. Soc.*, **71**, 278 (1949).

[13] W. O. Ludke, S. E. Wiberley, J. Goldenson et W. H. Bauer, *J. Phys. Chem.*, **59**, 222 (1955).

Dans la figure 3 nous avons représenté la variation de la viscosité des solutions de stéarate d'aluminium de concentration 0,2 M dans les solvants indiqués ci-dessus, en fonction de la tension de cisaillement appliquée.

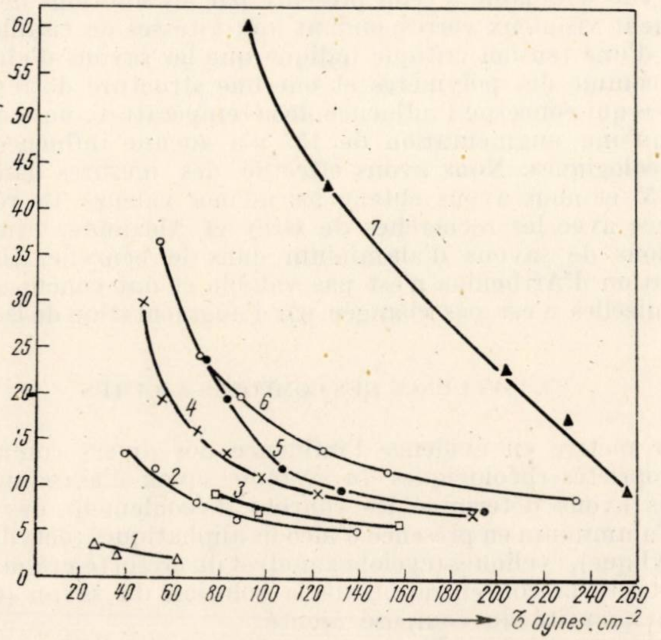

Fig. 3. — Variation de la viscosité de la solution de stéarate d'aluminium 0,2 M dans différents solvants, en fonction de la tension de cisaillement.

n-décane (c.*1*); *p*-xylène (c.*2*); cyclohexane (c.*3*); benzène (c.*4*); toluène (c.*5*); *o*-xylène (c.*6*); décaline (c.*7*); température = 20°.

Dans le cas des solutions dans les hydrocarbures aromatiques : benzène (courbe *4*), toluène (courbe *5*), *o*-xylène (courbe *6*) et *p*-xylène (courbe *2*), la viscosité baisse fortement au début jusqu'à atteindre un domaine critique de tension de cisaillement (compris à peu près entre 100—160 dynes cm^{-2}) et ensuite elle diminue lentement. Dans le cas des hydrocarbures cycliques saturés, l'allure des courbes change : on remarque une nette différence entre les courbes *3* et *7*, respectivement entre la solution dans l'hydrocarbure à un seul cycle (cyclohexane) ou à deux cycles (décaline). La solution dans la décaline est plus visqueuse et dans le domaine des tensions de cisaillement exploré, sa viscosité baisse fortement et continuellement au fur et à mesure que la tension croît, tandis que la courbe de viscosité de la solution dans le cyclohexane présente une très faible décroissance. La solution dans le *n*-décane présente la plus basse viscosité, d'ailleurs on a vu qu'elle a un comportement tout à fait différent.

Cette différence de comportement des solutions de stéarate d'aluminium dans différents solvants peut être attribuée à une résistance différente de la structure du réseau.

D'après ce que l'on a montré, le comportement à l'écoulement des solutions de savons d'aluminium dans les hydrocarbures est à plusieurs points de vue semblable à celui présenté par les solutions de polymères. [14] L'écoulement visqueux correspondant aux vitesses de cisaillement situées au-dessus d'une tension critique indique que les savons d'aluminium sont dispersés comme des polymères et ont une structure de réseau.

En ce qui concerne l'influence de la température, nos expériences ont montré qu'une augmentation de 15° n'a aucune influence sur les propriétés rhéologiques. Nous avons effectué des mesures dans le domaine de 20 à 35° et nous avons obtenu les mêmes valeurs. Ce résultat est en concordance avec les recherches de Grey et Alexander [9] sur la viscosité des solutions de savons d'aluminium dans le benzène. Ils ont trouvé que l'équation d'Arrhenius n'est pas valable et ont conclu que la dimension des micelles n'est pas changée par l'augmentation de la température.

L'INFLUENCE DES COMPOSÉS AJOUTÉS

Pour mettre en évidence l'influence des divers composés polaires sur les propriétés rhéologiques du système savon d'aluminium-hydrocarbure, nous avons déterminé les courbes d'écoulement des solutions de stéarate d'aluminium en présence d'alcools aliphatiques (octylique, iso-octylique, nonylique), cycliques (cyclohexanol) et du crésol (*o*-crésol.) On a maintenu constante la concentration de la solution du savon (0,2 M) et on a varié la quantité du composé ajouté.

De même que dans le cas du système savon-hydrocarbure, les solutions de stéarate d'aluminium en présence des composés polaires présentent une puissante viscosité de structure, les courbes d'écoulement étant semblables à celles des corps pseudoplastes. Dans la figure 4 nous avons représenté les courbes d'écoulement des solutions de stéarate d'aluminium 0,2 M dans le toluène, en présence d'une quantité de 1 % de composé ajouté et dans la figure 5 les courbes d'écoulement de la même solution de savon mais dans le benzène, en contenant des quantités croissantes d'*o*-crésol.

On constate que les courbes sont déplacées vers des tensions de cisaillement plus élevées (fig. 4) dans l'ordre : cyclohexanol $<$ alcool octylique $<$ nonylique $<$ iso-octylique $<$ *o*-crésol, et au fur et à mesure que la quantité du composé ajouté croît, elles sont situées vers des tensions plus petites (fig. 5). On voit bien l'influence exercée par la longueur de la chaîne hydrocarbonée de l'alcool (fig. 4, courbes *2* et *3*), ainsi que sa ramification (courbes *2* et *4*), surtout aux gradients élevés de vitesse.

Pour mieux mettre en évidence l'influence des composés polaires sur les solutions de savon d'aluminium dans l'hydrocarbure, nous avons représenté dans les figures 6 et 7 la variation de la viscosité des solutions

---

[14] W. Philippoff et K. Hess, *Z. phys. Chem.*, **B 31**, 237 (1936).

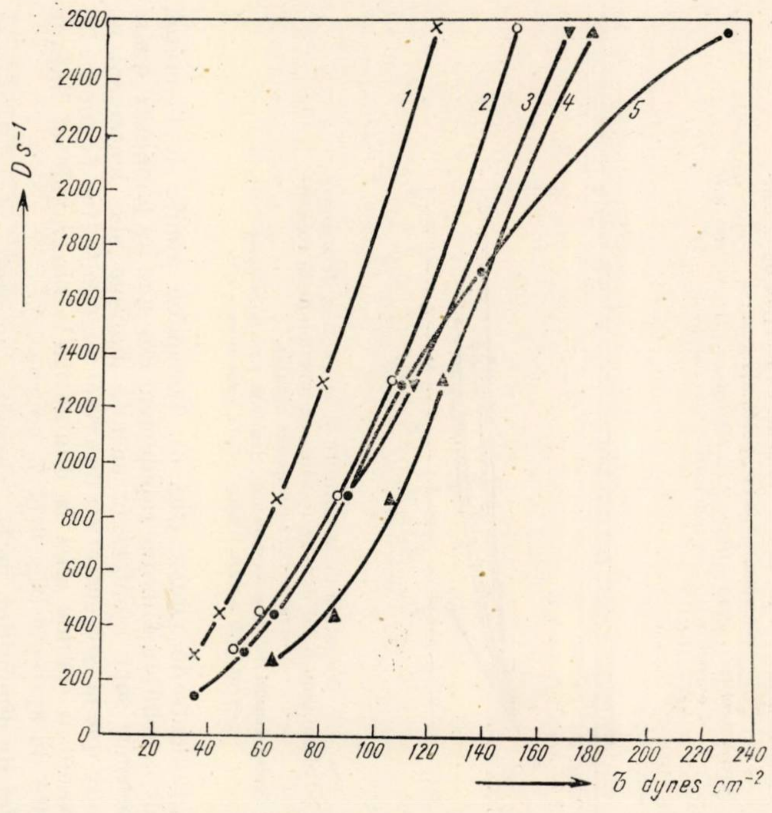

Fig. 4. — Courbes d'écoulement de la solution de stéarate d'aluminium 0,2 M dans le toluène + 1 % composé ajouté.

cyclohexanol (c.*1*) ; alcool octylique (c.*2*) ; nonylique (c.*3*) ; iso-octylique (c.*4*) ; *o*-crésol (c.*5*) ; température = 20°.

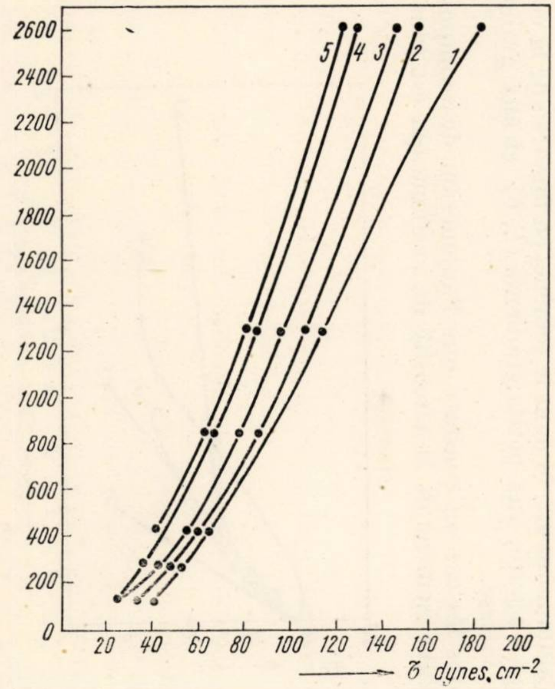

Fig. 5. — Courbes d'écoulement de la solution de stéarate d'aluminium 0,2 M dans le benzène + quantités croissantes de l'*o*-crésol.

1% (c.*1*) ; 2% (c.*2*) : 4,5% (c.*3*) ; 6,5% (c.*4*) et 9% (c.*5*) ; température = 20°.

de stéarate d'aluminium 0,2 M dans le toluène, en fonction de la concentration du composé ajouté, aux petits gradients (C_t 6) et aux gradients élevés (C_t 1) de vitesse.

Dans tous les cas on constate que l'adjonction des composés polaires mène à l'abaissement de la viscosité du système qui est plus marqué aux petits gradients de vitesse (fig. 6). Lorsqu'on ajoute de l'*o*-crésol, la viscosité de la solution diminue rapidement dès que les premières quantités de substance sont ajoutées et ensuite diminue plus lentement au fur et à mesure que la concentration du crésol augmente (fig. 6, courbe 5). Le cyclohexanol a comme effet la diminution la plus rapide et linéaire de la viscosité du système (fig. 6 et 7, courbe 1.).

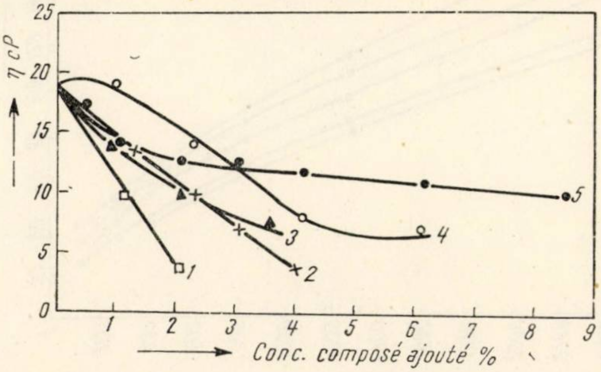

Fig. 6. — Variation de la viscosité de la solution de stéarate d'aluminium 0,2 M, dans le toluène, en fonction de la concentration des composés ajoutés.
cyclohexanol (c.*1*); alcool octylique (c.*2*); nonylique (c.*3*); iso-octylique (c.*4*) et *o*-crésol (c.*5*); nombre de tours = C_t 6; température = 20°.

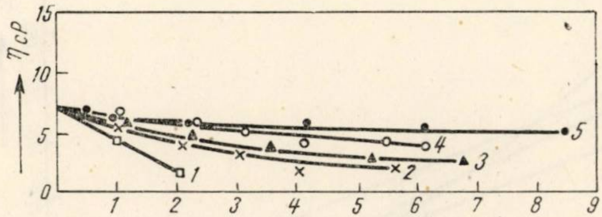

Fig. 7. — Variation de la viscosité de la solution de stéarate d'aluminium 0,2M dans le toluène, en fonction de la concentration des composés ajoutés.
Cyclohexanol (c.*1*); alcool octylique (c.*2*); nonylique (c.*3*); iso-octylique (c.*4*); *o*-crésol (c.*5*) nombre de tours = C_t 1; température = 20°.

Cet effet de diminution de la viscosité apparaît plus clairement lorsqu'on examine les courbes inscrites dans la figure 8. Il est d'autant plus accentué que le gradient de vitesse est plus petit, respectivement le nombre de tours est plus grand (C_t 9) (courbes continues).

Pour la solution dans le *n*-décane, l'allure des courbes change : la viscosité augmente légèrement en passant par un maximum bien aplati (courbes interrompues).

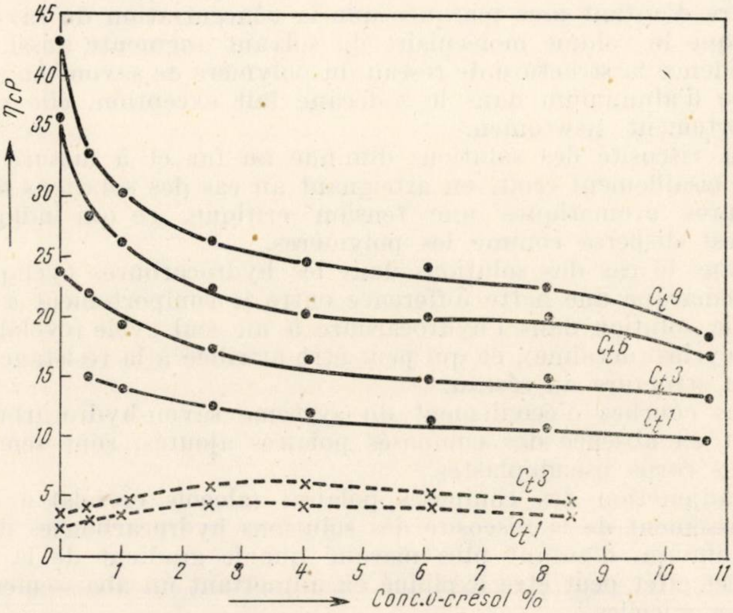

Fig. 8. — Variation de la viscosité des solutions de stéarate d'aluminium 0,2 M dans la décaline (courbes continues) et dans le *n*-décane (courbes interrompues), à différents gradients de vitesse, en fonction de la concentration de l'*o*-crésol ajouté ; température = 20°.

Ces résultats peuvent être interprétés en tenant compte que par l'adjonction des composés polaires comme les alcools ou les crésols, dans un système de savon d'aluminium-hydrocarbure, il y a lieu une interaction des molécules du composé ajouté et du polymère de savon. Ceci détermine un abaissement de la longueur des micelles [11] et un affaiblissement des forces d'attraction des terminaisons du polymère.

Dans le cas des solutions de stéarate d'aluminium dans le *n*-décane nous avons constaté qu'elles ont un comportement tout à fait différent. L'apparition d'un maximum de viscosité produit par l'adjonction du crésol peut être attribuée à une croissance des nombres de liaisons d'hydrogène formées entre les molécules du crésol, ce qui correspond à une augmentation de la viscosité de la solution. Lorsqu'on ajoute des quantités plus grandes de crésol, il intervient le phénomène d'abaissement des micelles et par conséquent la viscosité diminue.

CONCLUSIONS

L'étude de la viscosité de structure des solutions de stéarate d'aluminium dans différents hydrocarbures nous conduit aux conclusions suivantes :

— Les solutions de stéarate d'aluminium présentent une viscosité de structure d'autant plus marquée que la concentration du savon augmente et que le volume moléculaire du solvant augmente aussi, ce qui met en évidence la structure de réseau du polymère de savon. La solution de stéarate d'aluminium dans le *n*-décane fait exception, elle présente un comportement newtonien.

— La viscosité des solutions diminue au fur et à mesure que la tension de cisaillement croît, en atteignant au cas des solutions dans les hydrocarbures aromatiques une tension critique, ce qui indique que le savon est dispersé comme les polymères.

— Dans le cas des solutions dans les hydrocarbures cycliques saturés on remarque une nette différence entre le comportement à l'écoulement de la solution dans l'hydrocarbure à un seul cycle (cyclohexane) et à deux cycles (décaline), ce qui peut être attribué à la résistance différente de la structure du réseau.

— Les courbes d'écoulement du système savon-hydrocarbure, en présence et en absence des composés polaires ajoutés, sont semblables à celles des corps pseudoplastes.

— L'adjonction des composés polaires (alcools, crésols) a comme effet l'abaissement de la viscosité des solutions hydrocarbonées de stéarate d'aluminium, d'autant plus marqué que le gradient de la vitesse diminue ; cet effet peut être expliqué en admettant un abaissement de la longueur des micelles.

— Dans le domaine des gradients élevés de vitesse on remarque l'influence de la longueur de la chaîne hydrocarbonée d'alcool, ainsi que de son branchement.

Nous tenons à exprimer nos plus vifs remerciements à M. le Dr Max Solomon de l'Institut de Métrologie, Laboratoire de Mesures Analytiques, pour tout l'appui accordé au cours des travaux effectués.

Revue Roumaine de Chimie, **15**, 441–450 (1970)

SYNTHESIS OF THE SULPHURIC ESTER OF POLY(VINYL ALCOHOL)

IG. POINESCU, STELIANA MAXIM and A. CARPOV

Institute of Macromolecular Chemistry "P. Poni", Jassy, Aleea Gr. Ghica Vodă, 41 A

Received February 27, 1969

In the present paper one presents the synthesis of the sulphuric ester of poly(vinyl alcohol). The latter was obtained by sulphatation of poly(vinyl alcohol) with the trioxide sulphur nitromethane system. The reaction conditions were determined. Products with a maximum transformation degree of 0.42 were obtained.

The speciality literature shows the sulphatation of poly(vinyl alcohol) and its derivatives in order to obtain certain polymers with specific features (emulsifiers, stabilizing agents of emulsions, ion exchanger membranes or fibres, etc.)

Different sulphatation agents are recommended.

Takahashi[1] uses sulphuric acid (85%) and obtains poly(acid vinyl sulphate) with a maximum transformation degree of 0.40, the polymer suffering a slight decrease in molecular weight.

Fingauz[2] and co-workers note that the alcoholysis of the poly(vinyl acetate) in ethyl alcohol solution with sulphuric acid (as cataylst) is accompanied by a secondary reaction, leading to the formation of a certain quantity of poly(acid vinyl sulphate).

Starting from this study, the authors have intended to investigate the possibilities of sulphating the polymer during the alcoholysis in ethanol. They have used sulphuric acid (100%), SO_3, or chlorosulphonic acid, obtaining a polymer with 10.0 to 15.0% sulphur.

Ushakov[3] and coworkers produce poly(acid vinyl sulphate) by processing the poly(vinyl alcohol) with chlorosulphonic acid, obtaining thus products with a maximum transformation degree of 0.42.

Karrer[4] and Takahashi,[1] afford the sulphuric ester of poly(vinyl alcohol) by processing the polymer with an adduct of sulphur trioxide with pyridine. One reaches a maximum esterification degree of 0.7, without any degradation of the polymer.

---

[1] A. Takahashi, M. Nagasawa and I. Kagawa, *Kogyo Kagaku Zasshi*, **61**, 1614 (1958); *Chem. Abstr.*, **56**, 7496 (1962).

[2] I. M. Fingauz, A. F. Vorobeva, G. A. Shirikova and M. P. Dokuceaeva, *J. Polymer Sci.*, **56**, 245 (1962).

[3] S. N. Ushakov and I. R. Gruz, *Zhur. priklad. Khim.*, **39**, 1534 (1966).

[4] P. Karrer and F. Schulz, *Helv. Chim. Acta*, **27**, 1427 (1944).

Jones[5] and Korneva,[6] show the esterification of poly(vinyl alcohol) with the adduct SO_3-pyridine (dimethylamine) in the presence of the salts of chlorosulphonic acid with alkaline metals. One obtains partially esterified products, used in the industry of photographic materials.

Sakurada[7] and coworkers have prepared alkyl substituted poly-(sodium vinyl sulphate), from dodecyl(hexadodecyl) substituted poly-(vinyl alcohol) and sulphamic acid, in presence of urea at 130°.

Besides the sulphuric ester of the poly(vinyl alcohol) with a linear structure, the literature also describes polymers with a tridimensional (cross-linked) structure by which the $-SO_3H$ group is bound to the carbon atom either by means of the oxygen, or directly. These macromolecular products are used as cation exchangers.[8-12]

We know from literature that sulphur trioxide, as adducts or solved in different solvents, presents the advantage of a great reactivity variation and a decrease of the secondary destructive effects given by the classical sulphonating agents (H_2SO_4, HSO_3Cl, etc.)

Hesselbjerg-Christensen,[13] has shown the use of a sulphur trioxide and nitromethane mixture for the sulphonation of iodobenzene.

We have used, for the first time, this system at the sulphonation of the copolymer styrene-divinylbenzene.[14, 15]

One presents below the results concerning the esterification of poly(vinyl alcohol) with sulphur trioxide solved in nitromethane, a system never used up to now to this purpose.

EXPERIMENTAL

To obtain poly(acid vinyl sulphate) one has used poly(vinyl alchool) of the "Mowiol N_{70-98}" type[16] with the following characteristics : $K_w = 70$ and an acetyl group content of 2%. Other products, manufactured in Romania, were submitted to esterification, for instance polyvinyl alcohol), poly(vinyl acetate) and the copolymer of vinyl chloride with vinyl acetate (80 :20).

---

[5] R. V. Jones, (to Phillips Petroleum Co.), U. S. 2 623 037, 25 Aug., 1949; *Chem. Zentr.*, **1955**, 11466.

[6] E. D. Korneva, O. K. Smirnov and V. M. Uvarova, *Zhur. priklad. Khim.*, **39**, 1876 (1966).

[7] I. Sakurada, H. Noma, E. Koniski and T. Ishitaba, (to Daüchi Kogyo Seiyaku Co.), Jap., 11245 ('61), Fev. 10; *Chem. Abstr.*, **56**, 2586 (1962).

[8] Chemische Fabrik Budenheim Akt.-Ges., Oe. P. 180.908, Aug. 25, 1955; *Chem. Zentr.*, **1956**, 1693.

[9] Prospectus "Gelvatol" — Tèchnical Bulletin No. 6082, Monsanto Company, U.S.A., p. 14.

[10] M. W. Fogle (to Eltra Corp.,) U.S. 3 275 575, Sept. 27, 1966; *Chem. Abastr.*, **66**, 3429 (1967).

[11] A. L. Volf, I. A. Meos and A. S. Inkina, *Zhur. priklad. Khim.*, **35**, 2047 (1962).

[12] L. M. Sergeeva, A. D. Virnik and Z. A. Rogovin, *Khim. Volokna*, **1967**, 25.

[13] H. Hesselbjerg-Christensen, *Acta Chem. Scand.*, **15**, 1507 (1961).

[14] Ig. Poinescu, A. Carpov and M. Dima, *Rev. Roumaine Chim.*, **11**, 573 (1966).

[15] M. Dima, Ig. Poinescu and A. Carpov, Patent No 49760, April 24, 1967, O.S.I.R.S., Romania.

[16] Prospectus "Mowiol", Farbwerke Hoechst A. G., vormals Meister Lucius & Brüning, Frankfurt (M)-Hoechst.

Sulphur trioxide was obtained by distillating oleum (65 % SO_3).

The solution of sulphur trioxide in nitromethane was achieved according to the formerly described method.[13, 14]

The esterification reaction was carried out in a three-neck flask, fitted out with a stirrer, a thermometer and a condenser closed with a tube containing anhydrous calcium chloride. Poly(vinyl alcohol) and 25 % of the total nitromethane quantity are introduced. The concentration of the poly(vinyl alcohol) in nitromethane is about 4 %. After complete esterification, the reaction mixture is precipitated in methanol, obtaining an amorphous product, whose colour changes from dark brown to black according to the reaction conditions. The precipitate is filtered off and washed on the filter until the sulphate ions are totally removed, then dried in vacuum at 40°, for 10 hours. The poly(acid vinyl sulphate) thus obtained is insoluble in water. The poly(sodium vinyl sulphate) was obtained from the free acid through neutralization with sodium hydroxide.

The free "soluble" acid of the sodium salt was obtained according to Ushakov's[3] indications, by passing the aqueous poly(sodium vinyl sulphate) solution over a column with a strongly acid cation exchanger (Amberlite IR-120).

The sulphur content of the poly(acid vinyl sulphate) was determined by Haslam[17] and Wilson's[18] methods.

RESULTS AND DISCUSSIONS

To find the optimum esterification conditions of poly(vinyl alcohol) with sulphur trioxide solved in nitromethane, we decided to observe the influence of different factors (the molar ratio poly(vinyl alcohol) SO_3, temperature, the esterification reaction time etc.) on the transformation degree α.[19, 20]

It is known that at room temperature the sulphur trioxide solution in nitromethane decomposes gradually, losing its activity,[13, 14, 21] according to the reactions :

$$CH_3.NO_2 \xrightarrow{SO_3} CO + NH_2OH$$

$$NH_2OH + SO_3 \longrightarrow NH_2\,OSO_3H$$

$$NH_2OH + SO_2 \longrightarrow NH_2SO_3H$$

One also observes the formation of sulphur dioxide during the reaction.

Taking these indications as a starting point we decided to watch the degradation, respectively the activity decrease in time of the sulphur trioxide solution in nitromethane. This degradation was observed at 40°. Below 40°, the degradation is slow and requires long periods of time ;

---

[17] J. Haslam, D. Sc., F.R.I.C., and H. A. Willis, B. Sc., "Identification and Analysis of Plastics", London, Iliffe Books Ltd., 1965, p. 3.

[18] N. H. Wilson, M. R. Pearson and M. D. Fitzgerald, *J. Appl. Chem.*, **4**, 488 (1954).

[19] I. Scondac and M. Dima, *Studii şi Cercetări Şti. Chim. Fil. Iaşi*, **13**, 205 (1962).

[20] I. Scondac and M. Dima, *Studii şi Cercetări Şti. Chim. Fil. Iaşi*, **13**, 217 (1962).

[21] H. A. Lehmann, G. Kempe and M. Ruppert, *Z. anorg. Chem.*, **297**, 311 (1958).

at temperatures over 40°, the degradation is very rapid, and cannot be studied. One has used the same molar ratio, sulphur trioxide/nitromethane, as in the case of the esterification reaction of the poly(vinyl alcohol) described below. The degradation products were determined by titration with a potassium bromate-bromide solution.[22] The obtained data being represented graphically, one has marked down on the ordinate the consumption of the 0.02n potassium bromate-bromide solution, corresponding to the total reducing activity, owing to the decomposition products, and on the abscissa, the time (fig.1).

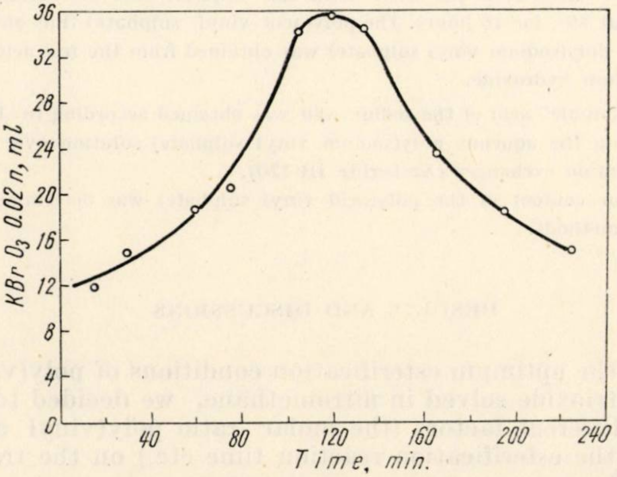

Fig. 1 — Degradation curve in time of a sulphur trioxide solution in nitromethane at 40° (molar ratio SO_3/CH_3NO_2 ; 1/3).

The first part of the curve shows a very high degradation the first two hours, in good agreement with the literature.

In the second part of the curve, the consumption of bromate-bromide solution decreases. This behaviour makes us think that the reaction products undergo chemical re-combinations (secondary reactions take place) leading to a marked loss of the reducible activity.

The esterification reaction takes place in the heterogeneous phase, and is very energetic in the first 15 to 30 minutes. As the reaction advances in time, the mixture colours. The colouration gets intense with the increase of the poly(vinyl alcohol)/SO_3 ratio.

The esterification of poly(vinyl alcohol) with different quantities of sulphur trioxide shows a great increase of the transformation degree α only up to the molar ratio polymer/SO_3 of 1 :7 ($\alpha = 0.41$) (fig. 2).

The attempts to a higher transformation degree than 0.41, by increasing the quantities of SO_3, have not had the desired results. For the molar ratio polymer/SO_3 of 1 :10 one obtains only a transformation degree of $\alpha = 42.40\%$.

---

[22] I. M. Kolthoff "Treatise on Analytical Chemistry", vol. 5, Part II, New York Interscience Publishers, 1961, p. 289.

By variating the concentration of poly(vinyl alcohol) *versus* nitromethane and keeping the ratio polymer/SO_3 constant, one obtains products with a maximum transformation degree of 0.41 (table 1).

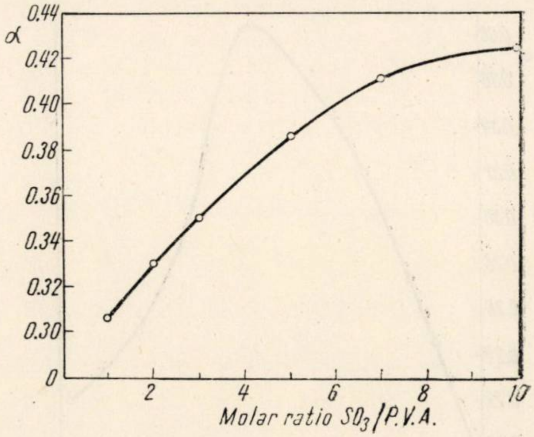

Fig. 2 — Influence of the molar ratio SO_3/P.V.A. on the transformation degree α (50° and 5 hrs).

Table 1

Dependence of the transformation degree α on the concentration of PVA in nitromethane

No	P.V.A./SO_3 mol	Conc. P.V.A. in nitromethane %	Sulphur %	Transf. degree α
1	1 : 5	1.0	14.50	0.30
2	1 : 5	2.0	14.70	0.32
3	1 : 5	3.0	15.00	0.33
4	1 : 5	5.0	16.20	0.37
5	1 : 5	7.0	17.00	0.41

Neither does one obtain a higher degree of transformation than 0.40 (fig. 3) by increasing the duration of the esterification reaction over 5 hours.

The impossibility of complete esterification of the poly(vinyl alcohol) in the above reaction conditions may be explained through steric factors hindering the interaction of the sulphatation agent with each elementary link of the poly(vinyl alcohol) as the distance between the two carbon atoms containing —OH groups and located at the same level, is of only 2.52 Å. [2, 23]

Another reason is the activity decrease in time of the SO_3 solution in nitromethane, as shown above.

The esterification reaction of poly(vinyl alcohol) is especially influenced by temperature. If one represents graphically the transformation

---

[23] S. N. Ushakov, "Polivinilovyi Spirt i evo Proivodnyie", vol. 1, Moscow, Izd.Akad. Nauk SSSR, 1960, p. 263.

degree α, as a function of temperature, the curve presents a maximum ($\alpha = 0.38$) for the temperature of 50° (fig. 4).

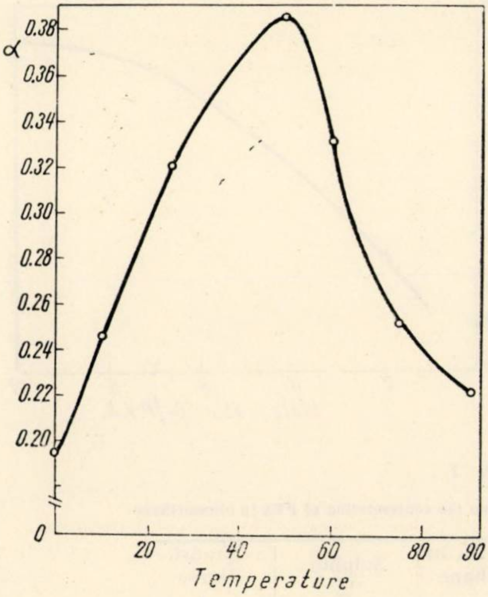

Fig. 3 — Influence of temperature on the transformation degree α (molar ratio P.V.A./SO_3; 1/5 and 5 hrs).

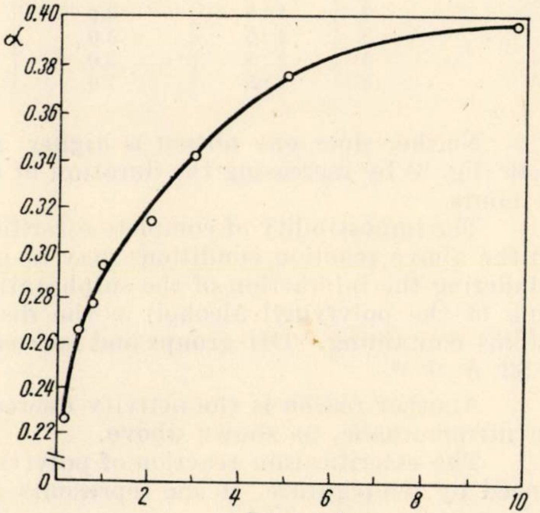

Fig. 4 — Influence of the esterification duration (in hours) on the transformation degree α (50° and molar ratio P.V.A./SO_3; 1/5).

This decrease of the transformation degree over a certain temperature may be explained by the fact that sulphatation is a reversible reaction, the reaction of opposite direction being the acid hydrolysis of the $-SO_3H$ groups. The rate of this reaction increases with the temperature and the decrease of the sulphatating agent's concentration.[2] In our case the decrease of the esterification agent's concentration is due to the SO_3 consumption in the sulphation reaction on the one hand, and to the degradation in time and at high temperature of the mixture SO_3/CH_3NO_2, on the other hand.

The esterification degree of the poly(vinyl alchol) depends on the value of Fikentscher's constant, and is at its maximum for $K_w = 70$ (fig. 5).

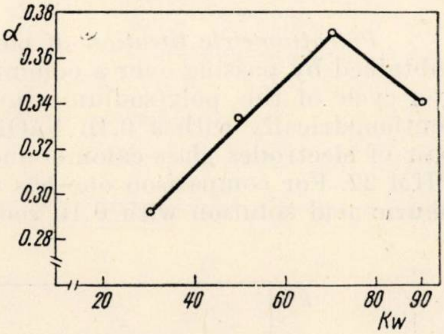

Fig. 5 — Dependence of the transformation degree α on the value of K_w (Fikentscher's constant) (molar ratio P.V.A./SO_3 1/5, 50° and 5 hrs).

This behaviour of macromolecular compounds was also observed for the chlormethylation or sulphonation of polystyrene.

In a series of experiments one has watched the influence of the acetyl group content of the poly(vinyl alcohol) on its esterification degree. The values of the transformation degree obtained in this case do not exceed those of former experiments (table 2).

Table 2

Dependence of the transformation degree α on the acetyl groups content in PVA

No	Macromolecular compound	Acetyl Group %	K_w	Transformation degree α
1	Poly(vinyl alcohol) "Mowiol"	2.0	30.0	0.29
2	Poly(vinyl alcohol) "Mowiol"	12.0	30.0	0.35
3	Poly(vinyl acetate)	50.0	31.0	0.36

It is likely that in the case of copolymers with a high content also in acetyl groups, one cannot obtain completely sulphatated products, because of steric hindering.

Beside Mowiol type poly(vinyl alcohol) one has also submitted to the sulphatation reaction poly(vinyl alcohol), poly(vinyl acetate) and the vinyl chloride-vinyl acetate copolymer manufactured in Romania. The results obtained are given in table 3.

Table 3

Dependence of sulphur content on macromolecular compound nature

No	Macromolecular Compound	Acetyl Groups %	Sulphur %
1	Poly(vinyl alcohol)	5.0	16.68
2	Poly(vinyl acetate)	50.0	14.37
3	Vinyl chloride– vinyl acetate copolymer (80:20)	20.0	10.76

Potentiometric titration of poly(acid vinyl sulphate). The free acid (obtained by passing over a column with Amberlite IR-120 in the hydrogen cycle of the poly(sodium vinyl sulphate) solution) was titrated potentiometrically with a 0.1n NaOH solution (fig. 6). One has used the pair of electrodes glass-calomel and the Radiometer potentiometer/type PHM 22. For comparison one has titrated potentiometrically a 0.1n sulphuric acid solution with 0.1n sodium hydroxide (fig. 6).

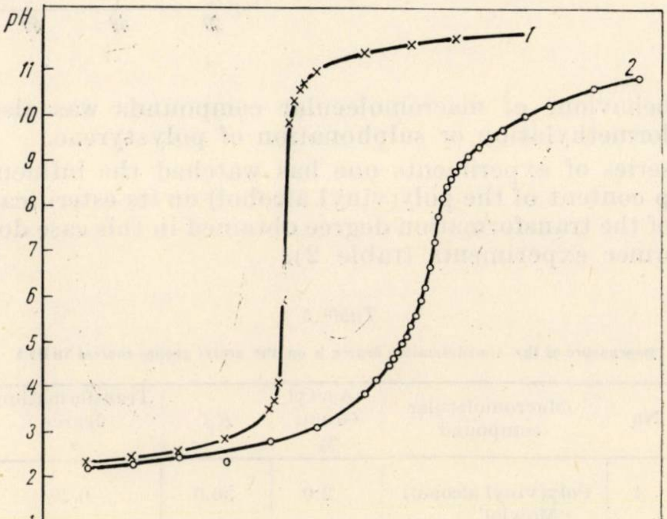

Fig. 6 — Potentiometric titration of poly(acid vinyl sulphate).
1, sulphuric acid; *2*, poly(acid vinyl sulphate).

By comparing the titration curves one notices that the poly(acid vinyl sulphate) behaves like a strong acid.

From the results of the potentiometric titration one has computed the sulphur content, respectively the transformation degree, the obtained data being then compared to those determined by the sulphur analysis (table 4).

Table 4

Concordance of transformation degree α, calculated from the potentiometric titration curves and determinated from sulphur content

No	Transformation degree α, computed through	
	Sulphur content	Potentiometric titration
1	0.21	0.22
2	0.28	0.27
3	0.34	0.34
4	0.40	0.39

Viscosimetric measurements. Viscosity measurements were carried out with aqueous solutions of poly(vinyl alcohol) and poly(sodium vinyl sulphate) (fig. 7) at 25°, with an Ubbelhode viscosimeter.

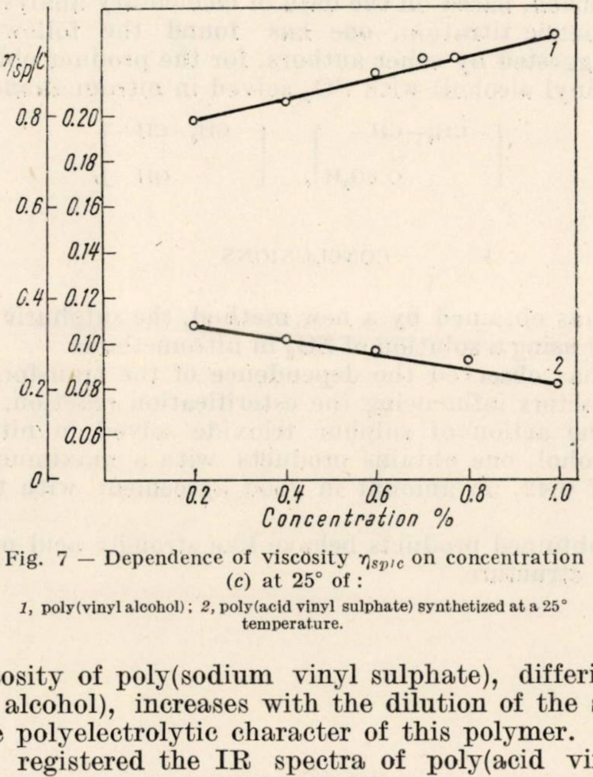

Fig. 7 — Dependence of viscosity $\eta_{sp/c}$ on concentration (*c*) at 25° of :

1, poly(vinyl alcohol); *2*, poly(acid vinyl sulphate) synthetized at a 25° temperature.

The viscosity of poly(sodium vinyl sulphate), differing from that of poly(vinyl alcohol), increases with the dilution of the solution, thus explaining the polyelectrolytic character of this polymer.

One has registered the IR spectra of poly(acid vinyl sulphate) and of poly(vinyl alcohol). A UNICAM SP 200 apparatus was used. The specimen tabletted with potassium bromide.

By comparing the IR spectra of these two polymers one notices the appearance of absorption bands characteristic of the $-SO_3H$ group (1200 and 1030 cm^{-1}) and the absorption change of the characteristic band of the $-OH$ group (2090 cm^{-1}).

Based on the results of the elementary analysis one has computed the number of structural units reacting a $-SO_3H$, (X) and unreacting (Y), referred to 100 units [19, 20] (Table 5).

Table 5

Elementary analysis of sulphuric ester of poly(vinyl alcohol)

No	Found C %	Found H %	Computed O (difference)	Found S %	Structural units %	
					X	Y
1	41.30	6.88	42.12	9.70	17.57	82.43
2	37.19	6.20	44.41	12.21	24.11	75.89
3	34.19	5.70	45.18	14.92	32.66	67.34

In conclusion, based on the data of elementary analysis, IR analysis and potentiometric titration, one has found the following structural formula, as suggested by other authors, for the product obtained by processing poly(vinyl alcohol) with SO_3 solved in nitromethane.

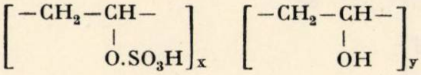

$$\left[-CH_2-\underset{O.SO_3H}{\underset{|}{CH}}-\right]_x \left[-CH_2-\underset{OH}{\underset{|}{CH}}-\right]_y$$

CONCLUSIONS

1. One has obtained by a new method, the sulphuric ester of poly(vinyl alcohol) using a solution of SO_3 in nitromethane.

2. One has observed the dependence of the transformation degree on different factors influencing the esterification reaction.

3. By the action of sulphur trioxide solved in nitromethane on poly(vinyl alcohol) one obtains products with a maximum transformation degree of 0.42, an amount in good agreement with the data in literature.

4. The obtained products behave like strongly acid polyelectrolytes with a linear structure.

Revue Roumaine de Chimie, **15**, 451–456 (1970)

PROPRIÉTÉS PHYSICO-STRUCTURALES DES CATALYSEURS UTILISÉS À L'OXYDATION DES HYDROCARBURES. III *

PROPRIÉTÉS ÉLECTRIQUES DES SYSTÈMES OXYDIQUES À BASE DE $V_2O_5-MoO_3-P_2O_5$ PAR RAPPORT AU MILIEU DE RÉACTION

ANTOANETA SPINZI et I. V. NICOLESCU

Centre de Recherches de Chimie Physique de l'Académie, Bucarest, 89, Spl. Independenţei

Reçu le 4 mars 1969

On examine par la méthode de la conductivité électrique l'influence de l'additif P_2O_5 sur le V_2O_5 et le système catalytique V_2O_5 - MoO_3 (1 : 0,33 mole). On étudie le système binaire $V_2O_5-P_2O_5$ (1 : 0,1 mole) et ternaire $V_2O_5-MoO_3-P_2O_5$ (3 : 1 : 0,33 mole) dans un milieu d'air, d'hydrogène et de mélange butènes (2 % vol)- air dans un intervalle de température de 200 à 440°. Les résultats présentés comparativement aux résultats obtenus pour les oxydes primaires, V_2O_5 et MoO_3 permettent d'attribuer au P_2O_5, adjoint au système catalytique $V_2O_5-MoO_3$, un rôle de promoteur textural.

Les travaux et les brevets [1-8] attestent des résultats positifs obtenus dans la réaction d'oxydation des alkènes ou bien des hydrocarbures aromatiques et alcoyl aromatiques, par l'utilisation des catalyseurs à base de $V_2O_5-MoO_3$ promus par P_2O_5, comparativement au même catalyseur non promu. On considère que l'adjonction de quelques pour-cents de P_2O_5 ($<8\%$) dans le système catalytique de base produit la baisse de la température de réaction et par conséquent l'amélioration de la sélectivité du catalyseur.

---

[*] IIe Partie — A. Spinzi et I. V. Nicolescu, *Rev. Roumaine Chim.* (sous presse).

[1] Soc. Chempatents, Brev. Fr. 1 170 866, 20 janv. 1959.

[2] Fr. Weis et J. Modiano, Brev. Fr. 1 260 597, 29 janv. 1960.

[3] M. Robert et B. Egbert, Brev. Fr. 1 262 809, 24 avr. 1961.

[4] Badische Anilin und Soda Fabrik, Brev. Fr., 1 261 073, 4 avril 1961.

[5] Brev. Belg. 614 363, 1961 ; *Chem. Abstr.*, **58**, 452h (1963).

[6] W. A. Skimer et D. Tieszen, *Ind. Eng. Chem.* **53**, 557 (1961).

[7] B. L. Moldavski et Iyu. D. Kernos, *Vestnik. tehn. econ. inform.*, **9**, 15 (1962).

[8] Iu. D. Kernos, B. Moldavski et E. A. Klionskaia, *Kinetika i Kataliz*, **2**, 272 (1962)

Des études REP et IR [9-12] ont démontré la formation des solutions solides par l'interaction du P_2O_5 et du V_2O_5 ou bien des $V_2O_5-MoO_3$. Il nous a paru intéressant d'étudier la variation de la conductivité électrique de tels systèmes pour préciser si l'adjonction du P_2O_5 influe sur les propriétés du catalyseur, comme promoteur structural ou bien textural. Cela, surtout, étant donné, le fait que dans quelques travaux antérieurs[13] nous avons étudié la conductivité électrique des systèmes $V_2O_5-K_2O$ et $V_2O_5-MoO_3$.

En dehors des oxydes primaires, V_2O_5 et MoO_3, pris en guise de référence, on a examiné les combinaisons $V_2O_5-P_2O_5$ (1:0,1 mole) et $V_2O_5-MoO_3-P_2O_5$ (3 : 1 : 0,33 mole). Dans tous les deux cas, la teneur en P_2O_5 a été de 7%, alors que le rapport V_2O_5 : P_2O_5 a été constant et égal à 1 : 0,1 mole. Le rapport $V_2O_5-MoO_3$ (1 : 0,33 mole) correspond au catalyseur d'activité optimale d'après les auteurs cités. [11, 14]

PARTIE EXPÉRIMENTALE

Nos expériences ont porté sur des oxydes purs, V_2O_5 et MoO_3, préparés par la décomposition thermique, à 350°, 2h et à 500°, 4h, du métavanadate d'ammonium et du paramolybdate d'ammonium *p.a.*

Les oxydes mixtes, binaires $V_2O_5-P_2O_5$ et ternaires $V_2O_5-MoO_3-P_2O_5$ ont été obtenus par imprégnation du V_2O_5, préparé comme ci-dessus, d'une solution de phosphate où bien de phosphomolybdate d'ammonium, suivie d'essorage à 110°, décomposition à 350°, 2h, et calcination à 500°, 6h. Les poudres obtenues après broyage ont été pastillées sous pression constante.

L'étude de la conductivité électrique a été effectuée à l'aide de l'appareil et selon la méthode présentés dans un travail antérieur. [13] On a choisi comme réaction test l'oxydation des *n*-butènes. Les mesurages ont été réalisés en présence de l'air et dans un mélange de butène (2%vol)-air, en fonction de la température où bien du temps, à 400°, par le traitement consécutif du catalyseur pastillé avec : hydrogène → azote → air et butène (2% vol)-air → azote → air. De cette manière, on a pu poursuivre les relations entre la variation de la conductivité électrique et l'état actif du catalyseur pendant la réaction.

RÉSULTATS ET DISCUSSIONS

Dans la figure 1*a*, *b* on présente comparativement la variation du $\log \sigma = f(1/T)$ dans un milieu d'air, respectivement butène (2% vol)-air, tant pour les systèmes simples V_2O_5 et MoO_3 que pour les systèmes mixtes

---

[9] I. I. Ioffe et L. Iya. Margolis, The III-th International Congress on Catalysis, Amsterdam, 1964.

[10] B. E. Zaițzev, Z. I. Ezhkova et I.I. Ioffe, *Kinetika i Kataliz*, **4**, 755 (1966).

[11] V. B. Kazanski, Z. I. Ezhkova, A. G. Liubarski, I. V. Voevodski et I. I. Ioffe, *Kinetika i Kataliz*, **6**, 862 (1961).

[12] Z.I. Ezhkova, I. I. Ioffe, V. B. Kazanski, A.V. Krylova, A. G. Liubarski et L. Iya. Margolis, *Kinetika i Kataliz*, **5**, 861 (1964).

[13] I. V. Nicolescu et A. Suceveanu, *Rev. Roumaine Chim.*, **11**, 123 (1966).

[14] M. Blanchard et J. C. Delgrange, *Compt. rend.*, **262**, 1231 (1966).

$V_2O_5-P_2O_5$ (1 : 0,1 mole) et $V_2O_5-MoO_3-P_2O_5$ (3 : 1 : 0,33 mole). D'après le diagramme il résulte :

1) Un domaine de valeurs basses pour la conductivité électrique du MoO_3, avec un haut coefficient de température tant en présence de l'air, que dans le milieu de réaction, butène-air.

2) La conductivité électrique des oxydes mixtes des systèmes binaire $V_2O_5-P_2O_5$ et ternaire $V_2O_5-MoO_3-P_2O_5$ est située dans le domaine des valeurs supérieures de la conductivité électrique dans l'ordre : $V_2O_5 < V_2O_5-P_2O_5 < V_2O_5-MoO_3-P_2O_5$.

3) Par le traitement des catalyseurs avec le mélange de réaction, butène-air, les valeurs de la conductivité électrique sont légèrement élevées, en gardant la même alternance qu'en présence de l'air.

Les résultats ci-dessus permettent d'apprécier que l'influence électronique du P_2O_5 sur le réseau du V_2O_5 n'est pas essentielle ce qui confirme d'ailleurs les données de certains mesurages pour le travail d'extraction.[9] En échange, la conductivité électrique élevée du système $V_2O_5-MoO_3-P_2O_5$ est évidente, surtout dans le mélange de réaction butène-eau.

Conformément à une étude antérieure effectuée sur le système $V_2O_5-MoO_3$ [4] un tel effet est maximal pour le rapport des composants $V_2O_5-MoO_3$ égal à 1 : 0,33 mole, ce qui correspond à la limite de solubilité du MoO_3 dans le réseau du V_2O_5. On y retrouve le même rapport dans l'oxyde ternaire $V_2O_5-MoO_3-P_2O_5$.

Dans la figure 2 on a représenté les isothermes de la conductivité électrique des systèmes mentionnés, effectuées à 400°, en coordonnées $\log \sigma = f$ (temps). A cette occasion, on a étudié l'influence du traitement des catalyseurs à l'hydrogène et successivement à l'air, après un lavage préalable à l'azote pur. De cette façon, on obtient des informations sur les transformations électroniques des composants actifs, ainsi que des oxydes mixtes, $V_2O_5 - P_2O_5$ et $V_2O_5-MoO_3-P_2O_5$, dans un milieu donneur (hydrogène) et accepteur (air).

Les résultats obtenus permettent les observations suivantes :

1) Les variations de la conductivité électrique sont excessivement intenses par rapport au temps, dans un milieu donneur (H_2), en dépassant quatre ordres de grandeur dans le cas du MoO_3 et 1—2 ordres de grandeur en d'autres cas.

2) On remarque, également, un comportement différent du V_2O_5 dans un milieu réducteur, en comparaison des systèmes mixtes à base de V_2O_5. Pour le V_2O_5 l'équilibre électronique se réalise par étapes, pendant 200 mn, tandis que l'adjonction de P_2O_5 facilite une stabilisation rapide du système catalytique, jusqu'à un certain état de valence du vanadium.

3) Dans le cas du système ternaire $V_2O_5-MoO_3-P_2O_5$ on observe une tendance plus nette de stabilisation dans un milieu d'hydrogène, le transfert électronique est légèrement diminué et le processus oxydo-réducteur est pratiquement irréversible. C'est ici le cas de mettre en discussion l'influence du MoO_3 et du P_2O_5 tant sur l'abaissement du niveau oxydo-réducteur, que sur sa stabilisation.

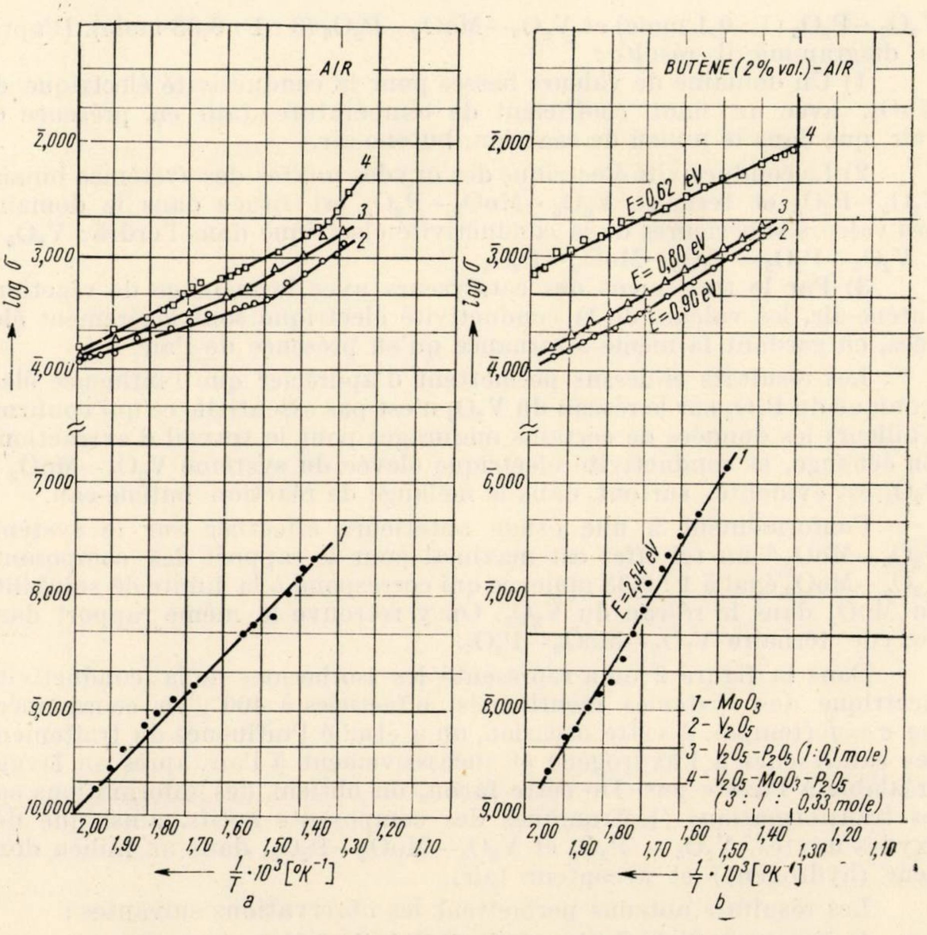

Fig. 1. — Variation de la conductivité électrique en fonction de la température des oxydes primaires V_2O_5, MoO_3, binaires $V_2O_5-P_2O_5$ et ternaires $V_2O_5-MoO_3-P_2O_5$. *a*, Air; *b*, butène (2% vol)-air

Par suite, on a représenté les isothermes de la conductivité électrique des mêmes systèmes pour la température de 400°, dans les conditions de réaction, mélange butène (2% vol)-air, et ensuite d'oxydation avec air, après insufflation d'azote pur.

L'allure générale des courbes, ainsi que le déplacement des valeurs de la conductivité électrique révèlent un comportement différent des oxydes étudiés, dans un milieu d'hydrocarbure, par rapport à l'hydrogène pur. Pour le V_2O_5, $V_2O_5-P_2O_5$ et le $V_2O_5-MoO_3-P_2O_5$ l'allure des courbes est presque parallèle, en indiquant une stabilisation dès les 30 premières mn. Le transfert électronique milieu de réaction — catalyseur est beaucoup diminué, comme suite du caractère donneur-accepteur du mélange gazeux. On ne remarque plus le rôle de stabilisateur du MoO_3 et du P_2O_5. L'alternance des courbes est modifiée dans l'ordre : $V_2O_5 < V_2O_5-P_2O_5 < V_2O_5-MoO_3-P_2O_5$.

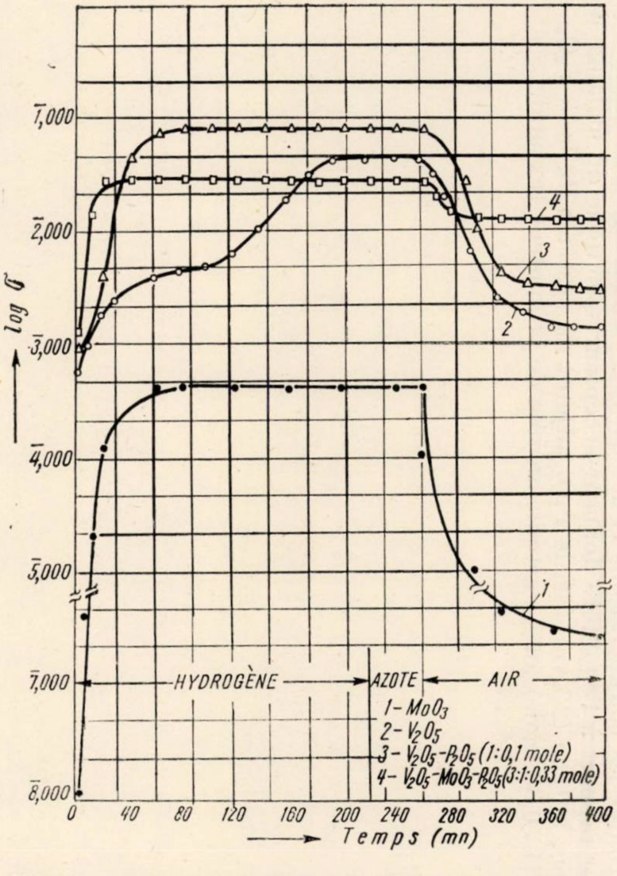

Fig. 2. – Isothermes de la conductivité électrique à 400°, en fonction du temps au traitement successif à l'hydrogène, à l'azote et à l'air

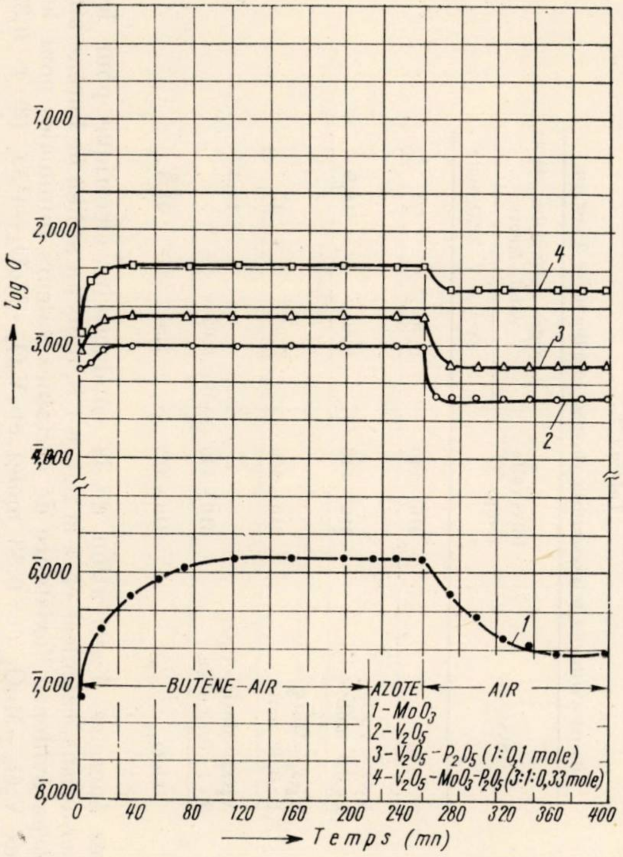

Fig. 3. – Isothermes de la conductivité électrique à 400°, en fonction du temps au traitement successif à mélange de butène (2 % vol)-air, d'azote et d'air.

Tableau 1

Energie d'activation de la conductivité électrique en milieu butène (2%vol)-air

Système	Intervalle temp. °C	Énergie activation de la cond. électr.	
		ev	kcal/mole
V_2O_5	316–440	0,90	21
$V_2O_5-P_2O_5$ 1 : 0,1 mole	316–440	0,80	18,5
$V_2O_5-MoO_3$ 1 : 0,33 mole	316–440	0,67	15
$V_2O_5-MoO_3-P_2O_5$ 3 : 1 : 0,33 mole	316–440	0,62	14,3
MoO_3	316–385	2,54	58,5

Les énergies d'activation de la conductivité électrique pour les oxydes ci-dessus, calculées cf. à la figure 1 b, dans un milieu de butène-air, mettent en évidence l'existence de certaines valeurs minimales pour les systèmes $V_2O_5-MoO_3$ (1 : 0,33 mole) et $V_2O_5-MoO_3-P_2O_5$ (3 : 1 : 0,33 mole) (voir tabl. 1). L'abaissement du seuil énergétique à des valeurs similaires (0,62–0,67 ev) tant pour le système binaire $V_2O_5-P_2O_5$, que pour le système ternaire $V_2O_5-MoO_3-P_2O_5$ paraît être dû, exclusivement, à la présence du MoO_3 dans le système.

Toutes les considérations ci-dessus nous conduisent à la conclusion que par rapport à l'équilibre donneur-accepteur spécifique du mélange de réaction, butène (2%vol)-air, le P_2O_5 adjoint au système de base $V_2O_5-MoO_3$ (1 : 0,33 mole) joue, surtout, un rôle de promoteur textural.

Revue Roumaine de Chimie, 15, 457–462 (1970)

THE VARIATION OF PHYSICO-STRUCTURAL PROPERTIES OF SOME ALUMINIUM HYDROXIDES AS AGAINST THEIR FORMATION CONDITIONS

MARIA GRUIA, O. KÖRNER and ALA NICOLESCU

Physical Chemistry Research Center of the Academy
Department of Catalysis, Spl. Independenţei 89

Received March 31, 1969

The preparation method of some aluminium hydroxides, in presence of admixtures which modify the surface activity of their formation medium is described. The obtained aluminium hydroxides are characterized by a series of physical methods. The essential differences between the IR spectra, especially in the field in which vibrations of the constitutional OH groups appear are insisted upon.

The studies concerning active alumina are becoming ever more the topics of papers, illustrating the continuous interest aroused by this problem. From the different structural forms, the eta and gamma-alumina[1] have shown to be the most interesting for catalysis purposes.

The obtention of a special polymorphic form of alumina, by the aluminium hydroxide transformation is conditioned, to a great extent, by the crystallographic structure of the raw hydroxide, then by the crystallites size and their homogeneity, by their packing in secondary particles and at last, by the phase transformation due to the thermal treatment. These topics are widely discussed in literature.[2,3]

In the present paper, the main target was the study of the influence of some tensio-active admixtures on the structural modifications of aluminium hydroxides obtained by the precipitation of aluminium nitrate with ammonia solution.

EXPERIMENTAL

The aluminium hydroxides preparation

The HE hydroxide. The raw materials are : aluminium nitrate solution 18% and ammonium hydroxide solution 10%.

---

[1] D. S. Mac Iver, W. Wilmot and J. M. Bridges, *J. Catalysis*, 3, 502 (1964)
[2] B. C. Lippens, Doctoral Thesis, Technische Hogeschool, Delft, The Netherlands, 1961.
[3] M.E. Winfield, in "Catalysis" (P.H. Emmett, ed.), vol. 7, Reinhold Publ. Corp., New York, 1960, p. 93–182.

Both solutions are simultaneously introduced, in drops, into a jar which contains 300 ml distilled water, previously treated with ammonia to a pH = 9.5, being steadily and thoroughly stirred. During the precipitation, the pH is maintained in the range 9.5—10. The time limit for a precipitation of a bulk of 1000 ml aluminium nitrate solution is of about 30—35 min. The working temperature is of about 22°.

After the precipitation, the obtained suspension is maintained in the mother-liquor and left to age for 24 hours, at room temperature. During the aging, the bulk of the suspension decreased by 5%. Then, the suspension was filtered by centrifugation, and washed with distilled water, to the complete removal of the NO_3^- ion (tested with nitron). About 15 litres of distilled water were used for this operation. The precipitate is then dried in drying cabinet in an air-stream, at 120°, for 6—8 hours.

The HP hydroxide. We have used the same method as for the HE hydroxide. The only difference lies in the fact that into the precipitation medium, i.e. the aluminium nitrate solution, an admixture of polyacrilamide was introduced, having a concentration of 0.3% *versus* the bulk of the nitrate solution. Aging took place in the presence of this admixture. Most of the polyacrilamide was removed by washing, during the filtration. The drying of the hydroxide was performed in the same conditions as for the HE hydroxide.

The HC hydroxide. Also for this hydroxide, the same method and the same raw materials were used, except for the admixture, which in this case was neutral carboxymethylcellulose (CMC), 0.3% *versus* the nitrate solution, in view of the modification of the surface activity of the precipitation medium. As in the previous case, most of the CMC was removed during the washing of the precipitate.

The characterization of aluminium hydroxides

We studied the physical and structural properties of the hydroxides HE, HP and HC — by IR spectroscopy and X-ray analysis — and the results are listed in table 1 and figures 1 A and 1 B.

Table 1

Physical and structural properties of aluminium hydroxides

Aluminium hydroxides	D_r g/cm^3	D_{ap} g/cm^3	V_p cm^3/g	Ignit. losses g to 100 g hydroxide	Physic. adsorb. water g/100 g hydroxide	X-ray structure
HE	2.69	1.92	0.15	32.5	9.3	Bayerite + some pseudo-bohemite
HP	2.55	1.77	0.17	34.5	8.4	Bayerite + Nordstrandite
HC	2.60	1.87	0.15	23.1	7.0	Pseudo-bohemite + traces of bayerite

D_r = real density; D_{ap} = apparent density; V_p = pore volume.

From the data of table 1, it has been stated that the tensio-active admixture used in the precipitation medium has a particular importance, at first in the evolution of the crystallographic species. The comparison hydroxide, HE, obtained in the absence of the admixture, evolves by aging into bayerite, the pseudo-bohemite amount representing a minor part of the product (about 5%). In the non-aged sample, only pseudo-bohemite is obtained. In the hydroxide sample obtained in the presence of polyacrilamide, HP, the evolution into more organised crystallographic species is even more marked, obtaining in this case a mixture of bayerite and nordstrandite.

As for the HC sample, the carboxymethylcellulose admixture stops the evolution of the pseudo-bohemite into trihydroxides; only a very minute amount of pseudo-bohemite passes into bayerite.

In this manner, the significant role of the tensio-active admixtures, in the hydroxide formation medium, is seen.

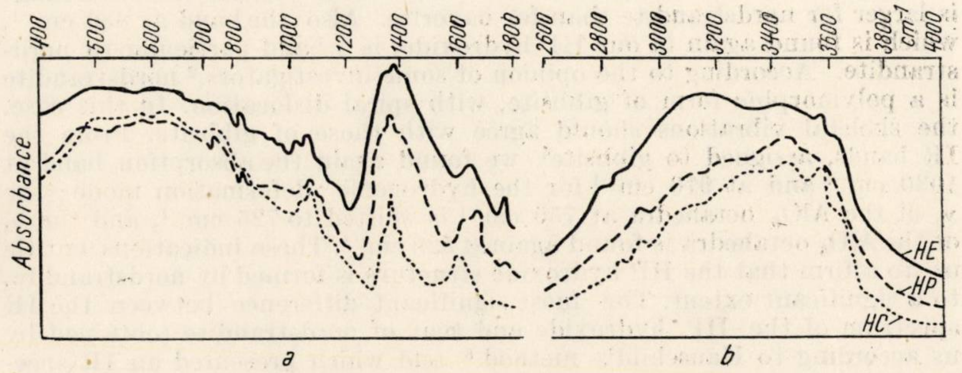

Fig. 1. — IR spectra of aluminium hydroxides.
a, 400–1800 cm^{-1} range; *b*, 2600–3800 cm^{-1} range.

The water loss, on hydroxide ignition, also confirms that the HP hydroxide is made up of aluminium trihydroxide, while the others possess variable amounts of pseudo-bohemite. The porosities of the hydroxide samples are close to one another. The hydroxide has a specific surface of 248 sq.m/g, which shows that the pore size is very small, and the *t* method enables to ascertain that the pores are filled with a multilayer, i.e. they are penlike.

The IR spectra presented in figure 1 confirm the hydroxide structure, determined by X-ray diagrams. In figure 1 A, we represented the absorption bands of the skeletal vibrations placed in the 400–1200 cm^{-1} range[4] which include the fundamental vibration modes of the octahedral and tetrahedral coordinated aluminium, and the deformation modes of the constitutional hydroxides.

The prevailing bayerite structure of the HE hydroxide (curve 1) is characterized by the doublet at 1000 cm^{-1}, as well as by the ν_3 value of the AlO_6 octahedra, at 750 cm^{-1}.

The HC aluminium hydroxide, which – as already seen – has a pseudo-bohemite structure, shows the hydrogenic deformation modus, in the IR spectra (curve 3) at 1070 cm^{-1}; at 755 cm^{-1} it shows the hydrogenic torsion mode; at 620 cm^{-1} it shows the ν_3 vibration of the AlO_6 octahedra and it absorbs in the 520 cm^{-1} range, which is characteristic of the ν_4 vibration of the AlO_6 octahedra . These absorption bands, according to,[4] attest the presence of the bohemite structure.

---

[4] A. J. Léonard, F. Van Cauwelaert and J. J. Fripiat, *J. Phys. Chem.*, **71**, 695 (1967).

In the case of HP hydroxide (curve 2), the IR spectrum is more complex, as we have a mixture of trihydroxides. The bayerite doublet at 1000 cm^{-1} is very much broadened, extending from 1030 cm^{-1} to 870 cm^{-1} and involving the somewhat shifted band at 1060 cm^{-1}, assigned by Hauschild[5] to nordstrandite.

However, according to this author, the OH valence vibration range is larger for nordstrandite than for bayerite. Also the band at 830 cm^{-1}, which is found again in our HP hydroxide, is a band particular to nordstrandite. According to the opinion of some investigators,[2] nordstrandite is a polymorphic form of gibbsite, with spiral dislocation. In this case, the skeletal vibrations should agree with those of gibbsite. From the IR bands, assigned to gibbsite[4] we found again the absorption band at 1030 cm^{-1} and at 970 cm^{-1} for the hydrogenic deformation mode; the ν_3 of the AlO_6 octahedra at 750 cm^{-1} is shifted to 725 cm^{-1}, and the ν_4 of the AlO_6 octahedra is found again at 525 cm^{-1}. These indications entitle us to affirm that the HP hydroxide structure is formed by nordstrandite, to a significant extent. The most significant difference between the IR spectrum of the HP hydroxide and that of nordstrandite (obtained by us according to Hauschild's method [5] and which presented an IR spectrum identical to that described by the author) is situated in the range 850—1100 cm^{-1}, where we have the interference of the hydrogenic deformation mode of bayerite and nordstrandite.

The IR spectrum range within 1200—1400 cm^{-1} is referring to the deformation vibrations of the OH,[6] bound to the lattice. In the case of our hydroxides, the absorption maximum is placed for the HE hydroxide at 1380 cm^{-1}, for the HP hydroxide at 1385 cm^{-1} and for that of HC at 1375 cm^{-1}. In this range the shape of the spectrum should be also noticed, namely we have a broad spectrum of strong absorption for the HE hydroxide, which points to great amounts of OH groups and are bound by hydrogen bridges. For the HP hydroxide, the situation is similar, the amount of hydroxides would be somewhat lower, while for the HC hydroxide a sharp peak is observed, indicating the loss of interactions between the hydroxilic groups. A low absorption is also noticed, which means a diminished amount of constitutional OH on the surface. These facts might be related to the crystallographic structure of the hydroxide and to the preferentially exposed face. It is well known that bayerite crystallizes in a hexagonal pattern, containing 2 hydroxide molecules in the elementary cell and having as maximum density face, that of the basic pinacoid. That means, that for every elementary cell, we have 6 neighbour OH groups, which can interact by hydrogen bridges; this can justify the intense and broad spectrum in this field. For the HE hydroxide, the electron-microscope photograph confirms that it is formed by hexagonal thin platelets.

---

[5] U. Hauschild, *Z. anorg. Chem.*, **324**, 15 (1963).

[6] M. Avram and G. D. Mateescu, "Spectroscopia în infraroşu. Aplicaţii în chimia organică", Editura Tehnică, Bucharest, 1966, p. 100.

As known, bohemite crystallizes in the orthorhombic pattern, containing 2 molecules of hydroxide in the elementary cell. If the face of greatest density is exposed, the OH groups are much scarcer. The interactions between the groups are much less frequent and consequently, the spectrum has a sharp form, and the intensity is much slighter.

The vibration bands of the molecular water physically adsorbed in the lattice are sited in the field of $1500-1800$ cm^{-1}. From figure 1A significant differences among the hydroxides are noticed. These differences were noticed also when we determined the amount of water retained by the hydroxides, up to the temperature at which the conversion of hydroxide into oxide begins. These results are listed in table 1. In the IR spectrum, the HE hydroxide shows two absorption maxima, for the physically adsorbed water; one at 1630 cm^{-1} and another, smaller, at 1760 cm^{-1}. The HP hydroxide has a pronounced maximum at 1660 cm^{-1} and a small one at 1770 cm^{-1}; the HC hydroxide has a single maximum at 1615 cm^{-1}. The explanation of these differences is likely to be found in the crystallite packing in the secondary particle.

In figure 1B, the IR spectrum of our hydroxides is shown in the $2600-4000$ cm^{-1} field. This region is characteristic of surface hydroxiles vibrations, both singular (vibration band at 1680 cm^{-1}) and bound by hydrogen bridges. This range can be interpreted as that at $1200-1400$ cm^{-1}, since it presents the same interaction phenomena by hydrogen bridges of the OH groups, and agrees also as intensity, with every hydroxide under consideration.

The studied hydroxides yielded by thermal transformation the corresponding aluminium oxides. The physico-structural properties, as well as their catalytic activity related to the cyclohexene isomerization and to the n-butyl-alcohol dehydration-isomerization reactions, are the subject-matter of a previous paper.[7] The obtained results point to the fact that although the oxides structure corresponds to the eta polymorphic form, their catalytic properties vary considerably. In the quoted paper, a satisfactory correlation was established between the catalytic activity and the amount of electron-acceptor centers, determined by E P R.

The present study, too, proves that the structures of the initial hydroxide grants to the basic properties of the final product — alumina — but a direct correlation was not yet established.

The IR studies of the adsorbed species, (see Fink's paper[8]) proved that the 1100 to 1500 cm^{-1} field of the IR spectrum is very sensitive as to the adsorbed species. Therefore, starting from alumina, with no IR absorption bands in this field, it has been found that by adsorption — for example — of NH_3 or C_2H_5OH — a series of characteristic bands are obtained, whose intensity varies function of the adsorbate concentration. That is, there is a modification of the spectrum just in the range with essential modifications when passing from hydroxide to oxide. For example, in the presence of alcohol, 1400 cm^{-1} bands also appear again, that is, in the region where the constitutional OH groups disappeared. This suggests the idea that it would be interesting to follow up the modification of IR spectra of the adsorbed species on alumina, as against the spectrum of the raw hydroxide.

---

[7] I. V. Nicolescu, A. Nicolescu, M. Gruia, A. Terlecki-Baricevič, M. Dardan, Em. Angelescu and A. Ionescu, Preprint no. 78; Fourth International Congress on Catalysis, Moscow, 1968.

[8] H. Dunken and P. Fink, *Acta Chim. Acad. Sci. Hung.*, **53**, 179 (1967).

Revue Roumaine de Chimie, 15, 463–486 (1970)

CHEMICAL GRAPHS. VIII.[1,2]

VALENCE ISOMERISM AND GENERAL CUBIC GRAPHS

A. T. BALABAN

Institute of Atomic Physics, P.O.B. 35, Bucharest, Romania

Received October 31, 1969

A complete chart of general cubic graphs (regular graphs of degree 3 which can have loops and multiple bonds) of orders up to 10 is presented. On this basis, one is able to rationalize the numbers of valence isomers of cyclopolyenes $C_{2n}H_{2n}$ and all other unsaturated systems such as hydrocarbons $C_{2n+1}H_{2n+2}$, heterocycles $C_{2n}H_{2n}X$, $C_{2n}H_{2n}X_2$, $C_{2n+1}H_{2n+2}X$, etc. Specific examples are discussed.

I. DEFINITIONS

Following the terminology of graph theory,[3-9] a *graph* is a figure consisting of points (vertices) and lines (edges or bonds) connecting some of these points. The lines of the graph thus determine unordered pairs of points. By definition, such *simple graphs* do not have lines joining a point with itself (loops), or two distinct lines joining the same pair of points (double bonds). If the definition is generalized to permit multiple bonds between a pair of points, the result is called a *multigraph*. If the graph is allowed to have loops, it is called a *loop-graph*. A *general graph* can have both loops and multiple edges; an alternative name is *pseudograph*.[9]

---

[1] Preceding part, A. T. Balaban, *Tetrahedron*, 25, 2949 (1969).

[2] Presented at the Iupac Symposium on Valence Isomerization, Karlsruhe, 9–12 September 1968.

[3] D. König, "Theorie der endlichen und unendlichen Graphen", Akad. Verlag, Leipzig, 1936; reprinted, Chelsea Publ. Comp., New York, 1950.

[4] C. Berge, "Théorie des graphes et ses applications", Duond, Paris, 1958; English translation, Methuen, London, 1962.

[5] O. Ore, "Theory of Graphs", Amer. Math. Soc. Coll. Publ. Nr. 38, Providence, Rhode Island, 1962; ,,Graphs and Their Uses", Random House, New York, 1963.

[6] R. G. Busacker and T. L. Saaty, "Finite Graphs and Networks. An Introduction with Applications", McGraw-Hill Book Comp., New York, 1965.

[7] G. Avondo-Bodino, ,,Economic Applications of the Theory of Graphs", Gordon and Breach, New York, 1962.

[8] F. Harary, in "Graph Theory and Theoretical Physics" (F. Harary, editor), Academic Press, London, 1967.

[9] F. Harary, "Graph Theory", Addison-Wesley Publ. Comp., Reading, Massachusetts, 1969.

A pair of points joined by a line, or a pair of lines meeting in a point are called *adjacent*. A point is *incident* to a line which joins it. The number of lines to which a point is incident is called the *degree* (valence or local degree) of that point. A loop is equivalent to two edges in this count. A *regular graph* has equal degrees for all its points : a regular graph of degree 3 is called a *cubic graph*. It is easily demonstrated that the number of points p (called the *order*) of a cubic graph must be an even number and that its number of edges is $q = 3p/2$.

Connected graphs are those in which every vertex is connected by some route along the edges of the graph with every other vertex ; only connected graphs are included in the present discussion. A *planar graph* is one that can be drawn in the plane so that its edges interesect only in vertices of the graph.

Two graphs are *isomorphic* if there is a one-to-one correspondence between their sets of points which preserves adjacency.

As yet there is no general consensus on the definitions of *valence isomer* and *valence isomerization*. Structural (valence isomers being defined according to structural criteria), mechanistic (valence isomerization being defined as a concerted or pericyclic process), and technical definitions (valence isomerization being defined by the reaction techniques employed, such as photochemical and thermal isomerizations) were proposed. Since the technical criteria are often misleading, and since mechanistic definitions could only be applied to reactions whose mechanism is already known, we favour the structural definition of valence-isomers and isomerism ; valence isomerization is the interconversion between two valence isomers.

By valence isomeric structures (or formulas) we denote those non-isomorphic connected graphs which conserve the degree of every point of the graph (univalent atoms, or points, and bonds incident to them, being excluded). This definition can be illustrated by examples from the C_4H_4 and C_6H_6 isomeric series. From the nine formulas I—IX, III is not a connected graph and must be excluded ; it does not represent even an isomer of C_4H_4. All the rest are isomers ; I and II are valence isomers according to the above definition ; so are also V, VI , and VII on one hand, and IV, VIII and IX on the other hand. Of course, owing to steric strain, compounds VI, VII and VIII would not be stable. In the C_6H_6 series the number of isomers (connected graphs) is about one hundred; half of these are not prohibitingly strained. Only 19 graphs are displayed, which form five groups of valence isomers according to above definition : X to XV, XVI to XIX, XX to XXII, XXIII to XXV, and XXVI to XXVIII.

These formulas were drawn so as to emphasize structural and graph-theoretical similarities, not the molecular geometry. Though lines cross in several graphs, only one (XV) is non-planar.

Most intramolecular concerted processes, including 1,5-hydrogen transfers,[10] are valence isomerizations according to the above definition. The identity of the points whose degrees are conserved, should be preserved, as far as possible. As already pointed out,[11] the above definition also includes as valence isomerism some cases of allylic isomerism, such as 1,4- and 1,3-cyclohexadienes.

---

[10] A. T. Balaban, *Rev. Roumaine Chim.*, **12**, 875 (1967).

[11] A. T. Balaban, *Rev. Roumaine Chim.*, **11**, 1097 (1966); Erratum, *ibid.*, **12**, Nr. 1, last page (not numbered) (1967).

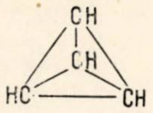
I

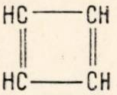
II

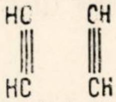
III

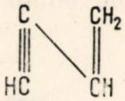
IV

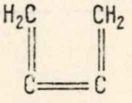
V

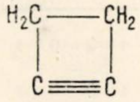
VI

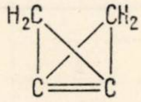
VII

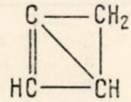
VIII

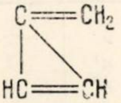
IX

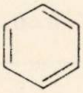
X

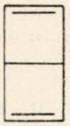
XI

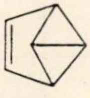
XII

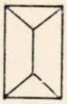
XIII

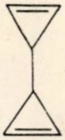
XIV

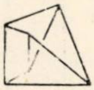
XV

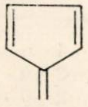
XVI

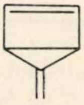
XVII

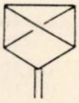
XVIII

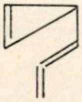
XIX

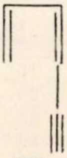
XX

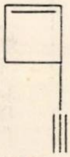
XXI

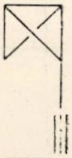
XXII

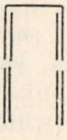
XXIII

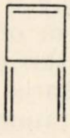
XXIV

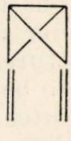
XXV

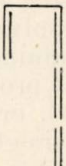
XXVI

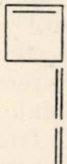
XXVII

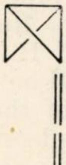
XXVIII

II. INTRODUCTION

In a previous paper,[11] the known valence isomers of cyclopolyenes $(CH)_p$ with $p = 4, 6, 8$, and 10 were discussed on the basis of the exhaustive list of cubic multigraphs (regular multigraphs of degree 3). It was thus found that the numbers of cubic multigraphs of orders $p = 4, 6, 8,$

and 10 with 0, 1, . . ., p/2 double bonds are those indicated in Tables 1 and 2 (adapting tables 1 and 4 of the previous paper[11]). The multigraphs are classified into classes $\varkappa^{\circ}, \ldots, \varkappa^{p/2}$ according to[12] the number β of double bonds they possess (p/2, . . .,0).

Table 1

Numbers of valence isomers of (CH_p) hydrocarbons, or of cubic multigraphs of order p.

p	Class	Bonds		Valence isomers (multigraphs)		
		Double	Single	Nr.	Total nr.	Notation
	$\varkappa^{\circ}$	2	2	1		4−2−0−1
4	$\varkappa^1$	1	4	0	2	—
	$\varkappa^2$	0	6	1		4−0−0−1
	$\varkappa^{\circ}$	3	3	1		6−3−0−1
6	$\varkappa^1$	2	5	2	6	6−2−0−1 and 6−2−0−2
	$\varkappa^2$	1	7	1		6−1−0−1
	$\varkappa^3$	0	9	2		6−0−0−1 and 6−0−0−2
	$\varkappa^{\circ}$	4	4	1		8−4−0−1
	$\varkappa^1$	3	6	4		8−3−0−1 to 8−3−0−4
8	$\varkappa^2$	2	8	5	20	8−2−0−1 to 8−2−0−5
	$\varkappa^3$	1	10	5		8−1−0−1 to 8−1−0−5
	$\varkappa^4$	0	12	5		8−0−0−1 to 8−0−0−5
	$\varkappa^{\circ}$	5	5	1		10−5−0−1
	$\varkappa^1$	4	7	7		10−4−0−1 to 10−4−0−7
10	$\varkappa^2$	3	9	16	91	10−3−0−1 to 10−3−0−16
	$\varkappa^3$	2	11	25		10−2−0−1 to 10−2−0−25
	$\varkappa^4$	1	13	23		10−1−0−1 to 10−1−0−23
	$\varkappa^5$	0	15	19		10−0−0−1 to 10−0−0−19

A procedure for counting cubic graphs of a given order has been found by Robinson,[13] thus solving an older problem of the theory of graphs.[14] However, for obtaining the pictures of the graphs, recourse must still be had to recurrent procedures (to be presented in a subsequent section of the present paper), or to computer programmes[15] (which are not completely safe from oversights[11,15]). Pictures of simple cubic graphs of higher orders may be found in references[15−18].

---

[12] E. E. van Tamelen, *Angew. Chem.*, **77**, 759 (1965).

[13] R. W. Robinson, unpublished (private communication and ref. 9).

[14] F. Harary, *Publ. Math. Inst. Hung. Acad. Sci.*, **5A**, 63 (1960).

[15] J. Lederberg, *Proc. Natl. Acad. Sci. U.S.A.*, **53**, 134 (1965); ,,Topology of Molecules in the Mathematical Siences'', MIT Press, Cambridge, Massachusetts, 1970;

J. Lederberg, G. L. Sutherland, B. G. Buchanan, E. A. Feigenbaum, A. V. Robertson, A. M. Duffield and C. Djerassi, J. *Amer. Chem. Soc.*, **91**, 2973 (1969).

[16] A. T. Balaban, R. O. Davies, F. Harary, A. Hill and R. Westwick, *J. Austral. Math. Soc.*, in press.

[17] D. W. Grace, Stanford Computation Center Technical Report CS 15 (1956).

[18] M. Brückner, "Vielecke und Vielfläche", Teubner, Leipzig, 1900.

p \ β	0	1	2	3	4	5
4	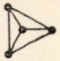 4-0-0-1	—	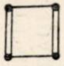 4-2-0-1	—	—	—
6	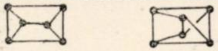 6-0-0-1 (6-0-0-2)	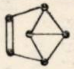 6-1-0-1	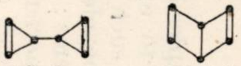 6-2-0-1 6-2-0-2	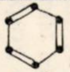 6-3-0-1	—	—
8	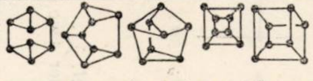 8-0-0-1 8-0-0-2 (8-0-0-3) 8-0-0-4 (8-0-0-5)	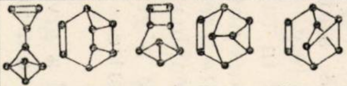 8-1-0-1 8-1-0-2 8-1-0-3 8-1-0-4 (8-1-0-5)	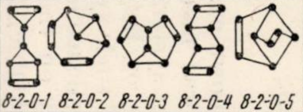 8-2-0-1 8-2-0-2 8-2-0-3 8-2-0-4 8-2-0-5	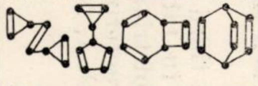 8-3-0-1 8-3-0-2 8-3-0-3 8-3-0-4	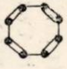 8-4-0-1	—
10	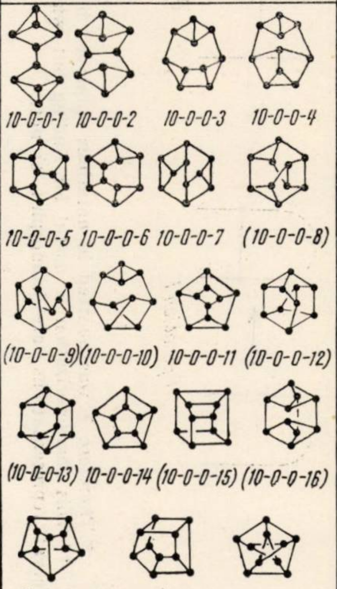 10-0-0-1 10-0-0-2 10-0-0-3 10-0-0-4 10-0-0-5 10-0-0-6 10-0-0-7 (10-0-0-8) (10-0-0-9)(10-0-0-10) 10-0-0-11 (10-0-0-12) (10-0-0-13) 10-0-0-14 (10-0-0-15) (10-0-0-16) (10-0-0-17) (10-0-0-18) (10-0-0-19)	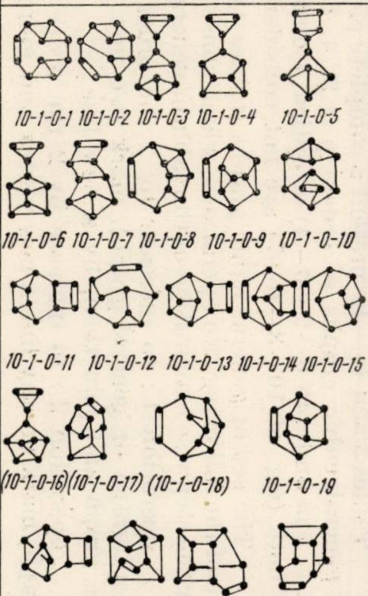 10-1-0-1 10-1-0-2 10-1-0-3 10-1-0-4 10-1-0-5 10-1-0-6 10-1-0-7 10-1-0-8 10-1-0-9 10-1-0-10 10-1-0-11 10-1-0-12 10-1-0-13 10-1-0-14 10-1-0-15 (10-1-0-16)(10-1-0-17) (10-1-0-18) 10-1-0-19 (10-1-0-20) (10-1-0-21)(10-1-0-22) (10-1-0-23)	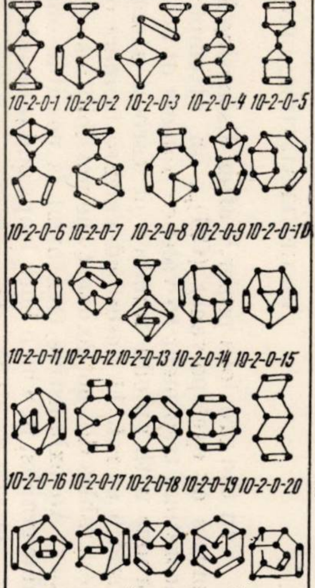 10-2-0-1 10-2-0-2 10-2-0-3 10-2-0-4 10-2-0-5 10-2-0-6 10-2-0-7 10-2-0-8 10-2-0-9 10-2-0-10 10-2-0-11 10-2-0-12 10-2-0-13 10-2-0-14 10-2-0-15 10-2-0-16 10-2-0-17 10-2-0-18 10-2-0-19 10-2-0-20 10-2-0-21 10-2-0-22 (10-2-0-23)(10-2-0-24)(10-2-0-25)	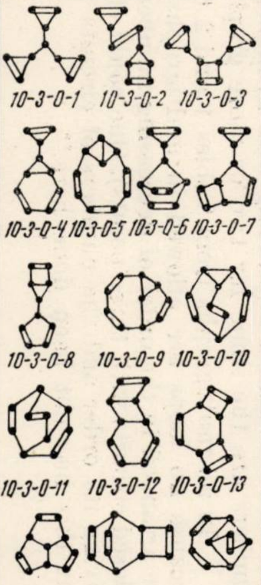 10-3-0-1 10-3-0-2 10-3-0-3 10-3-0-4 10-3-0-5 10-3-0-6 10-3-0-7 10-3-0-8 10-3-0-9 10-3-0-10 10-3-0-11 10-3-0-12 10-3-0-13 10-3-0-14 10-3-0-15 10-3-0-16	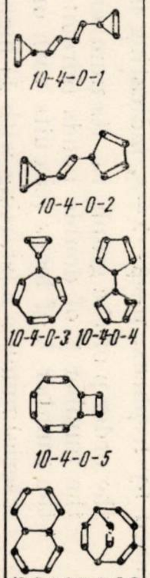 10-4-0-1 10-4-0-2 10-4-0-3 10-4-0-4 10-4-0-5 10-4-0-6 10-4-0-7	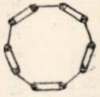 10-5-0-1

The notation of graphs in the presen t paper consists of four numbers joined by hyphens, $p-\beta-\lambda-s$, indicating in order:

the order p of the graph, i.e. its number of atoms with valence $\geqslant 2$;
the number β of double bonds (circuits with two vertices);
the number λ of loops (circuits with one vertex);

a serial number s (starting with 1) higher when the preceding three numbers are the same for two or more graphs.

In all multigraphs from Tables 1 and 2 the third number λ is zero because no loops are allowed in multigraphs.* In table 2, the graphs are arranged in the order of decreasing numbers of triangles they possess (closed circuits with three points). One could characterize a graph by specifying its order and the numbers of circuits with 1, 2, 3, 4, ... points but this has not been done here.**

III. GENERAL CUBIC GRAPHS

In the previous paper,[11] after discussing known examples of valence isomers of cyclopolyenes $(CH)_p$, an attempt was made to extend the theoretical treatment to valence isomers of other systems, such as hydrocarbons with an odd number of carbon atoms or heterocycles. Tables 5 and 6 of ref. 11 described valence isomers of such systems; however, these tables did not exhaust the possibilities of valence isomerism in these cases. An exhaustive treatment is possible only on the basis of general cubic graphs, in which both loops and multiple (double) bonds are allowed.

Tables 3 and 4a—4e present a complete picture (up to isomorphism) of general cubic graphs of orders p = 2, 4, 6, 8, and 10. Geometrical (e. g. *syn* and *anti* 8—2—0—4) or optical isomers (e.g. of 10—2—0—14) or both (e.g. of 10—3—0—7) are not considered in tables 1 through 4.

The set of general cubic graphs (tables 4) was obtained by making use of the following two operations, which constitute a recurrent procedure for the stepwise elaboration of the table of general cubic graphs:

operation 1: to increase by 2 the order of a given cubic graph (mulitgraph or general graph), mark two new vertices on any line(s) of the graph and join them by a new line;

operation 2: to increase by 2 the order of a given general cubic graph, mark on any line a new vertex and join it to a loop.

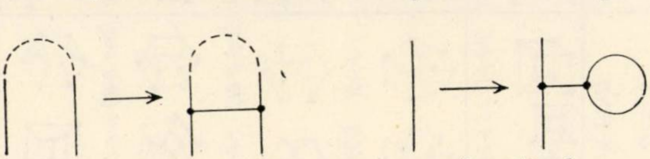

---

* Therefore λ was omitted in notations employed in ref. 11.

** This characterization is useful for finding out whether two complicated graphs, in different representations, are isomorphic or not.

Table 3

Numbers of general cubic graphs of orders 2–10

No of points p	Double bonds β / Loops λ	0	1	2	3	4	5	Total
2	0	0	1					1
	1	0	0					0
	2	1	0					1
	Total	1	1					2
4	0	1	0	1				2
	1	0	1	0				1
	2	0	1	0				1
	3	1	0	0				1
	Total	2	2	1				5
6	0	2	1	2	1			6
	1	1	1	2	0			4
	2	1	2	1	0			4
	3	1	1	0	0			2
	4	1	0	0	0			1
	Total	6	5	5	1			17
8	0	5	5	5	4	1		20
	1	4	6	6	3	0		19
	2	5	6	6	1	0		18
	3	3	4	2	0	0		9
	4	2	2	0	0	0		4
	5	1	0	0	0	0		1
	Total	20	23	19	8	1		71
10	0	19	23	25	16	7	1	91
	1	19	33	32	18	4	0	106
	2	23	34	31	13	1	0	102
	3	15	21	16	3	0	0	55
	4	9	11	5	0	0	0	25
	5	4	3	0	0	0	0	7
	6	2	0	0	0	0	0	2
	Total	91	125	109	50	12	1	388

Table 4a—4c

General cubic graphs of orders $p=2$, 4, and 6

$\lambda \backslash \beta$	0	1
0	—	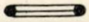 2-1-0-1
1	—	—
2	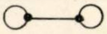 2-0-2-1	—

$p=2$

$\lambda \backslash \beta$	0	1	2
0	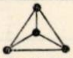 4-0-0-1	—	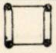 4-2-0-1
1	—	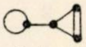 4-1-1-1	—
2	—	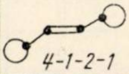 4-1-2-1	—
3	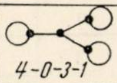 4-0-3-1	—	—

$p=4$

$\lambda \backslash \beta$	0	1	2	3
0	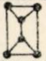 6-0-0-1 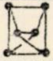 (6-0-0-2)	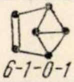 6-1-0-1	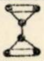 6-2-0-1 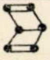 6-2-0-2	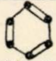 6-3-0-1
1	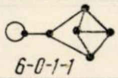 6-0-1-1	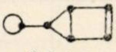 6-1-1-1	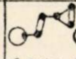 6-2-1-1 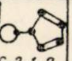 6-2-1-2	—
2	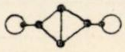 6-0-2-1	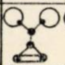 6-1-2-1 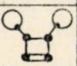 6-1-2-2	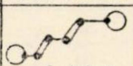 6-2-2-1	—
3	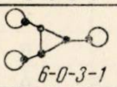 6-0-3-1	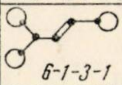 6-1-3-1	—	—
4	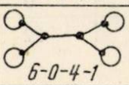 6-0-4-1	—	—	—

$p=6$

General cubic graphs of order 8

β λ	0	1	2	3	4
0	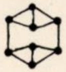 8-0-0-1 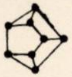 8-0-0-2 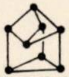 (8-0-0-3) 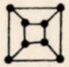 8-0-0-4 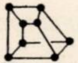 (8-0-0-5)	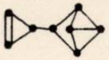 8-1-0-1 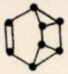 8-1-0-2 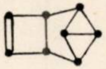 8-1-0-3 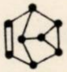 8-1-0-4 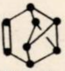 (8-1-0-5)	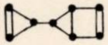 8-2-0-1 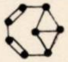 8-2-0-2 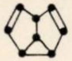 8-2-0-3 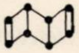 8-2-0-4 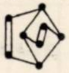 8-2-0-5	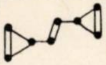 8-3-0-1 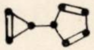 8-3-0-2 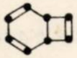 8-3-0-3 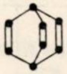 8-3-0-4	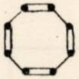 8-4-0-1
1	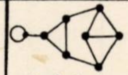 8-0-1-1 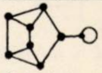 8-0-1-2 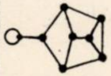 8-0-1-3 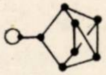 (8-0-1-4)	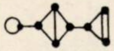 8-1-1-1 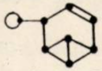 8-1-1-2 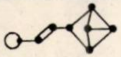 8-1-1-3 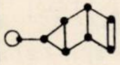 8-1-1-4 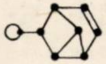 8-1-1-5 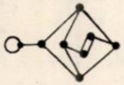 8-1-1-6	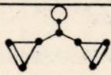 8-2-1-1 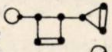 8-2-1-2 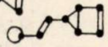 8-2-1-3 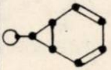 8-2-1-4 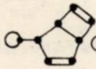 8-2-1-5 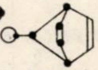 8-2-1-6	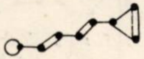 8-3-1-1 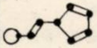 8-3-1-2 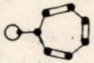 8-3-1-3	—
2	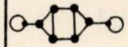 8-0-2-1 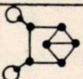 8-0-2-2 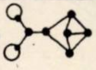 8-0-2-3 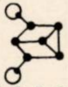 8-0-2-4 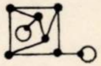 8-0-2-5	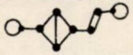 8-1-2-1 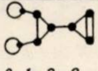 8-1-2-2 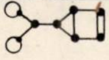 8-1-2-3 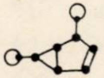 8-1-2-4 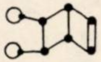 8-1-2-5 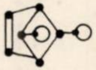 8-1-2-6	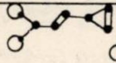 8-2-2-1 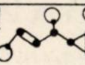 8-2-2-2 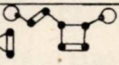 8-2-2-3 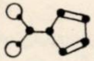 8-2-2-4 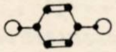 8-2-2-5 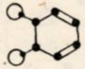 8-2-2-6	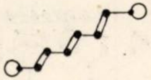 8-3-2-1	—
3	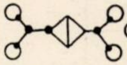 8-0-3-1 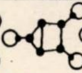 8-0-3-2 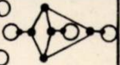 8-0-3-3	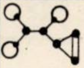 8-1-3-1 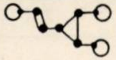 8-1-3-2 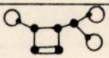 8-1-3-3 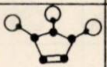 8-1-3-4	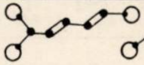 8-2-3-1 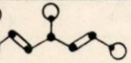 8-2-3-2	—	—
4	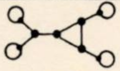 8-0-4-1 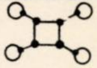 8-0-4-2	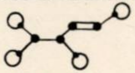 8-1-4-1 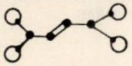 8-1-4-2	—	—	—
5	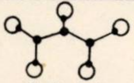 8-0-5-1	—	—	—	—

Table 4e

General cubic graphs of order 10

λ \ β	0	1	2	3	4	5
0	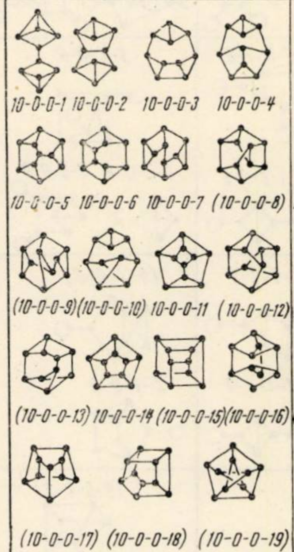 10-0-0-1 10-0-0-2 10-0-0-3 10-0-0-4 10-0-0-5 10-0-0-6 10-0-0-7 (10-0-0-8) (10-0-0-9)(10-0-0-10) 10-0-0-11 (10-0-0-12) (10-0-0-13) 10-0-0-14 (10-0-0-15)(10-0-0-16) (10-0-0-17) (10-0-0-18) (10-0-0-19)	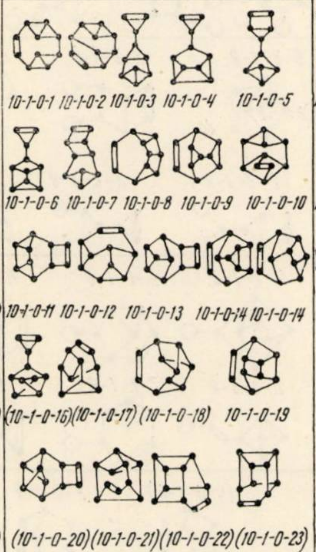 10-1-0-1 10-1-0-2 10-1-0-3 10-1-0-4 10-1-0-5 10-1-0-6 10-1-0-7 10-1-0-8 10-1-0-9 10-1-0-10 10-1-0-11 10-1-0-12 10-1-0-13 10-1-0-14 10-1-0-14 (10-1-0-16)(10-1-0-17) (10-1-0-18) 10-1-0-19 (10-1-0-20)(10-1-0-21)(10-1-0-22)(10-1-0-23)	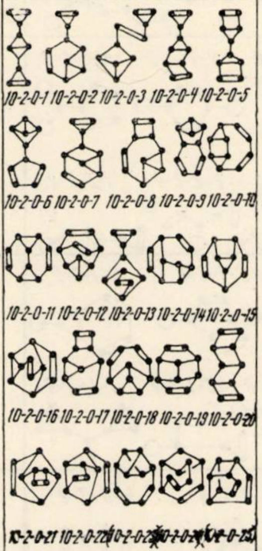 10-2-0-1 10-2-0-2 10-2-0-3 10-2-0-4 10-2-0-5 10-2-0-6 10-2-0-7 10-2-0-8 10-2-0-9 10-2-0-10 10-2-0-11 10-2-0-12 10-2-0-13 10-2-0-14 10-2-0-15 10-2-0-16 10-2-0-17 10-2-0-18 10-2-0-19 10-2-0-20 10-2-0-21 10-2-0-22 (10-2-0-23)(10-2-0-24)(10-2-0-25)	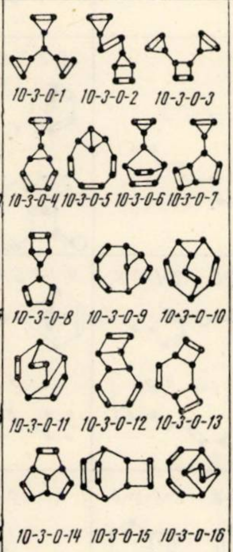 10-3-0-1 10-3-0-2 10-3-0-3 10-3-0-4 10-3-0-5 10-3-0-6 10-3-0-7 10-3-0-8 10-3-0-9 10-3-0-10 10-3-0-11 10-3-0-12 10-3-0-13 10-3-0-14 10-3-0-15 10-3-0-16	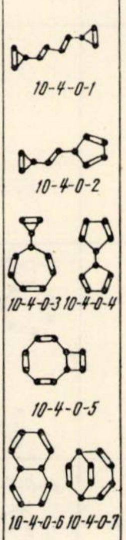 10-4-0-1 10-4-0-2 10-4-0-3 10-4-0-4 10-4-0-5 10-4-0-6 10-4-0-7	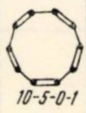 10-5-0-1

Table эp (continued)

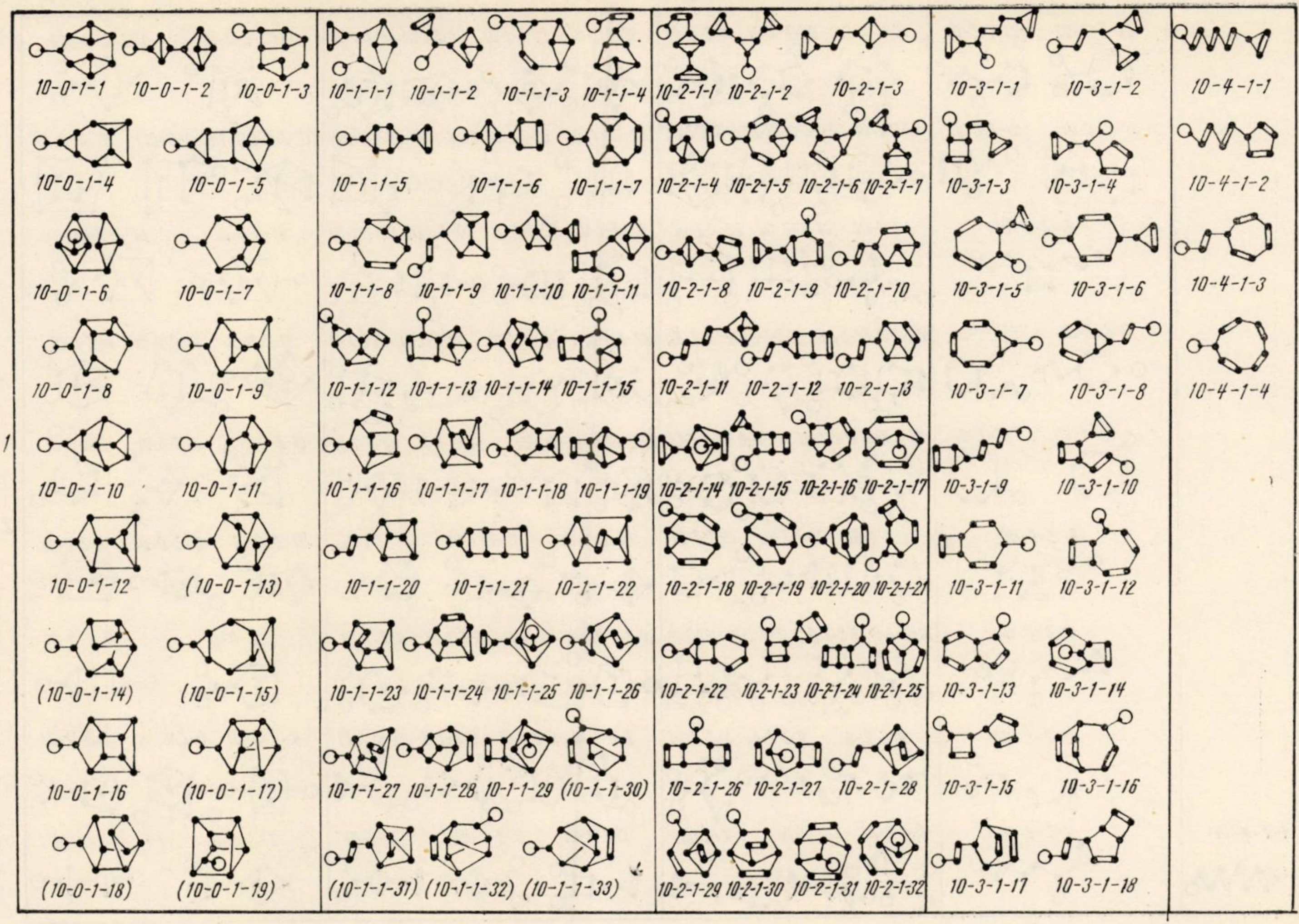
10-0-1-1
10-0-1-2
10-0-1-3
10-0-1-4
10-0-1-5
10-0-1-6
10-0-1-7
10-0-1-8
10-0-1-9
10-0-1-10
10-0-1-11
10-0-1-12
(10-0-1-13)
(10-0-1-14)
(10-0-1-15)
10-0-1-16
(10-0-1-17)
(10-0-1-18)
(10-0-1-19)
10-1-1-1
10-1-1-2
10-1-1-3
10-1-1-4
10-1-1-5
10-1-1-6
10-1-1-7
10-1-1-8
10-1-1-9
10-1-1-10
10-1-1-11
10-1-1-12
10-1-1-13
10-1-1-14
10-1-1-15
10-1-1-16
10-1-1-17
10-1-1-18
10-1-1-19
10-1-1-20
10-1-1-21
10-1-1-22
10-1-1-23
10-1-1-24
10-1-1-25
10-1-1-26
10-1-1-27
10-1-1-28
10-1-1-29
(10-1-1-30)
(10-1-1-31)
(10-1-1-32)
(10-1-1-33)
10-2-1-1
10-2-1-2
10-2-1-3
10-2-1-4
10-2-1-5
10-2-1-6
10-2-1-7
10-2-1-8
10-2-1-9
10-2-1-10
10-2-1-11
10-2-1-12
10-2-1-13
10-2-1-14
10-2-1-15
10-2-1-16
10-2-1-17
10-2-1-18
10-2-1-19
10-2-1-20
10-2-1-21
10-2-1-22
10-2-1-23
10-2-1-24
10-2-1-25
10-2-1-26
10-2-1-27
10-2-1-28
10-2-1-29
10-2-1-30
10-2-1-31
10-2-1-32
10-3-1-1
10-3-1-2
10-3-1-3
10-3-1-4
10-3-1-5
10-3-1-6
10-3-1-7
10-3-1-8
10-3-1-9
10-3-1-10
10-3-1-11
10-3-1-12
10-3-1-13
10-3-1-14
10-3-1-15
10-3-1-16
10-3-1-17
10-3-1-18
10-4-1-1
10-4-1-2
10-4-1-3
10-4-1-4

Table 4e (continued)

2

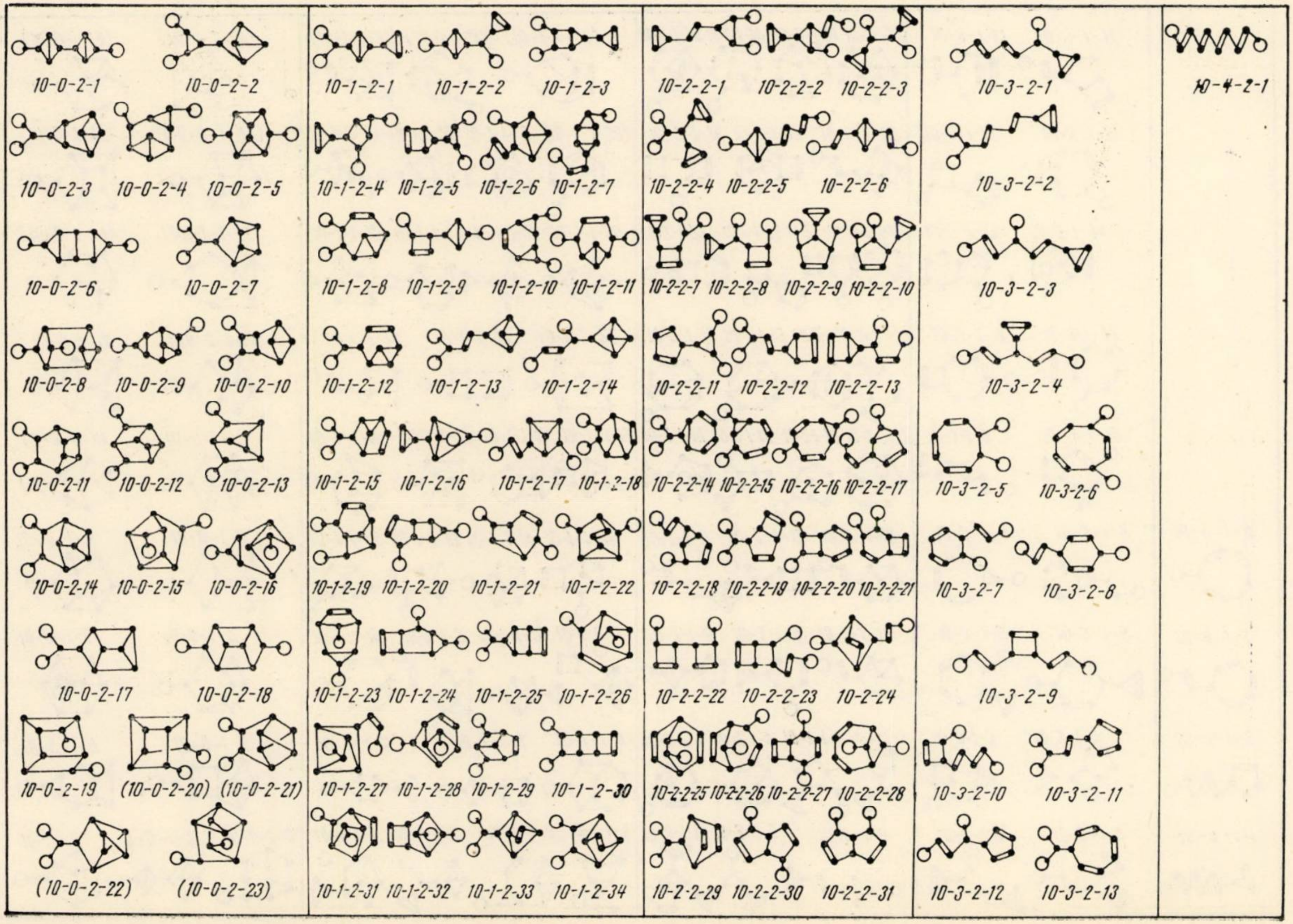
10-0-2-1
10-0-2-2
10-0-2-3
10-0-2-4
10-0-2-5
10-0-2-6
10-0-2-7
10-0-2-8
10-0-2-9
10-0-2-10
10-0-2-11
10-0-2-12
10-0-2-13
10-0-2-14
10-0-2-15
10-0-2-16
10-0-2-17
10-0-2-18
10-0-2-19
(10-0-2-20)
(10-0-2-21)
(10-0-2-22)
(10-0-2-23)
10-1-2-1
10-1-2-2
10-1-2-3
10-1-2-4
10-1-2-5
10-1-2-6
10-1-2-7
10-1-2-8
10-1-2-9
10-1-2-10
10-1-2-11
10-1-2-12
10-1-2-13
10-1-2-14
10-1-2-15
10-1-2-16
10-1-2-17
10-1-2-18
10-1-2-19
10-1-2-20
10-1-2-21
10-1-2-22
10-1-2-23
10-1-2-24
10-1-2-25
10-1-2-26
10-1-2-27
10-1-2-28
10-1-2-29
10-1-2-30
10-1-2-31
10-1-2-32
10-1-2-33
10-1-2-34
10-2-2-1
10-2-2-2
10-2-2-3
10-2-2-4
10-2-2-5
10-2-2-6
10-2-2-7
10-2-2-8
10-2-2-9
10-2-2-10
10-2-2-11
10-2-2-12
10-2-2-13
10-2-2-14
10-2-2-15
10-2-2-16
10-2-2-17
10-2-2-18
10-2-2-19
10-2-2-20
10-2-2-21
10-2-2-22
10-2-2-23
10-2-24
10-2-2-25
10-2-2-26
10-2-2-27
10-2-2-28
10-2-2-29
10-2-2-30
10-2-2-31
10-3-2-1
10-3-2-2
10-3-2-3
10-3-2-4
10-3-2-5
10-3-2-6
10-3-2-7
10-3-2-8
10-3-2-9
10-3-2-10
10-3-2-11
10-3-2-12
10-3-2-13
10-4-2-1

Tabela 4e (continued)

3	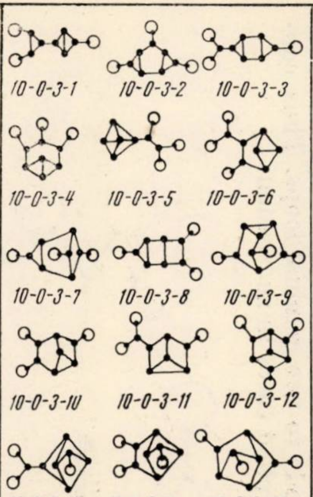 10-0-3-1 10-0-3-2 10-0-3-3 10-0-3-4 10-0-3-5 10-0-3-6 10-0-3-7 10-0-3-8 10-0-3-9 10-0-3-10 10-0-3-11 10-0-3-12 10-0-3-13 10-0-3-14 10-0-3-15	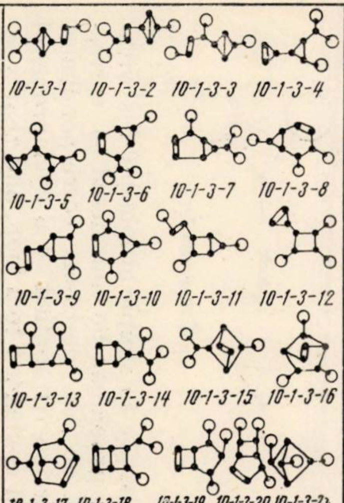 10-1-3-1 10-1-3-2 10-1-3-3 10-1-3-4 10-1-3-5 10-1-3-6 10-1-3-7 10-1-3-8 10-1-3-9 10-1-3-10 10-1-3-11 10-1-3-12 10-1-3-13 10-1-3-14 10-1-3-15 10-1-3-16 10-1-3-17 10-1-3-18 10-1-3-19 10-1-3-20 10-1-3-21	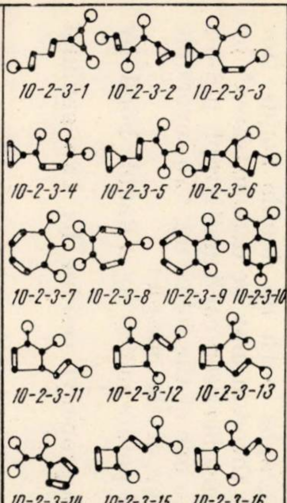 10-2-3-1 10-2-3-2 10-2-3-3 10-2-3-4 10-2-3-5 10-2-3-6 10-2-3-7 10-2-3-8 10-2-3-9 10-2-3-10 10-2-3-11 10-2-3-12 10-2-3-13 10-2-3-14 10-2-3-15 10-2-3-16	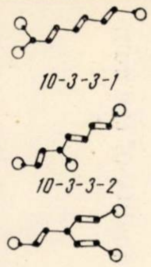 10-3-3-1 10-3-3-2 10-3-3-3	—	—
4	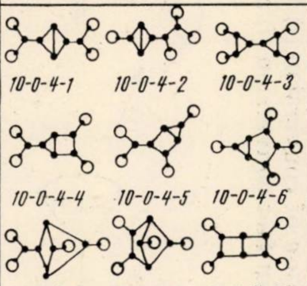 10-0-4-1 10-0-4-2 10-0-4-3 10-0-4-4 10-0-4-5 10-0-4-6 10-0-4·7 10-0-4-8 10-0-4-9	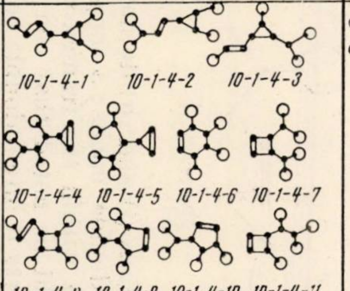 10-1-4-1 10-1-4-2 10-1-4-3 10-1-4-4 10-1-4-5 10-1-4-6 10-1-4-7 10-1-4-8 10-1-4-9 10-1-4-10 10-1-4-11	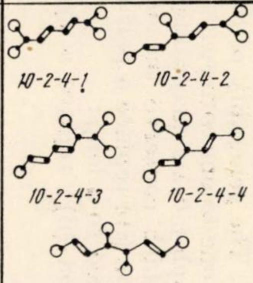 10-2-4-1 10-2-4-2 10-2-4-3 10-2-4-4 10-2-4-5	—		—
5	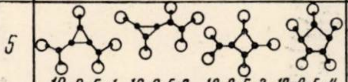 10-0-5-1 10-0-5-2 10-0-5-3 10-0-5-4	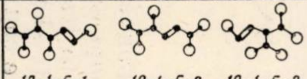 10-1-5-1 10-1-5-2 10-1-5-3	—	—	—	—
6	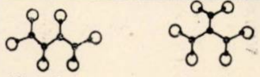 10-0-6-1 10-0-6-2	—	—	—	—	—

Theorem 1. If the number of graphs of order p with λ loops and β double bonds is denoted by G (p, β, λ), one can see from table 3 that

$$G\ (p, 1, 0) = G\ (p, 0, 2)$$

This can be demonstrated by the fact that one can establish a one-to-one correspondence between a graph with one double bond and a graph with only two loops.

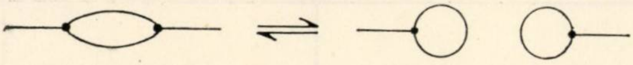

Theorem 2. A second observation from table 3 is the equality of the numbers

$$\sum_{\beta} G\ (p,\ \beta,\ 0) = \sum_{\lambda} G\ (p, 0,\ \lambda)$$

In other words, for a given order p, the number of multigraphs (for which $\lambda = 0$) equals the number of loop-graphs with no double bonds (for which $\beta = 0$). The generality of this theorem may be demonstrated* by establishing a one-to-one correspondence between each multigraph p-β-0-s and a loop-graph p-0-λ-s′ according to one of the following two reversible conversions which conserve the order of the graph :

conversion (i) : replace a pair of points joined by a double bond by a point attached to a loop ;

conversion (ii) : replace a cyclopropenyl residue by two geminal loops.

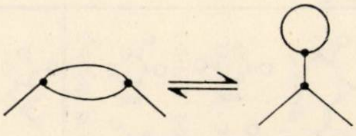

Conversion (i)

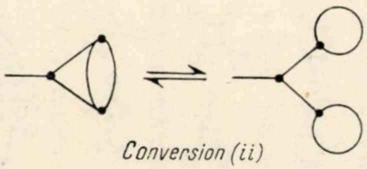

Conversion (ii)

Conversions (i) and (ii) do not apply to simple graphs p-0-0-s without loops or double bonds ; a simple graph can be considered to correspond to itself within the framework of this one-to-one correspondence.

It should be noted that conversion (i) applied to a cyclopropenyl residue converts it into a double bond connected to a loop, and that a second application of conversion (i) leads to two geminal loops. Thus conversion (ii) is in fact conversion (i) applied twice in succession.

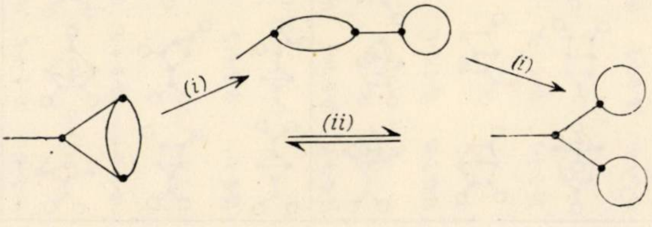

---

* Discussions with prof. Frank Harary and Dr. Paul Stockmeyer are acknowledged.

It is easily seen that these two conversions exhaust all possible cases : in a cubic multigraph the single bonds adjacent to a double bond can either meet, as in conversion (ii), or not, as in conversion (i) ; conversely, in a cubic loop-graph with more than 2 points, every point with a loop must be adjacent to a point without a loop, which in turn can either be adjacent to two points without a loop as in conversion (i), or to at least a point with a loop as in conversion (ii).

Because of the one-to-one correspondence rules (i) and (ii), the number of multigraphs G $(p, \beta, 0)$ without cyclopropenyl residues equals the number of loop-graphs G $(p, 0, \lambda)$ with $\beta = \lambda$. If c cyclopropenyl residues are present in a cubic multigraph p-β-0-*s*, this is converted by conversions (ii) into a loop-graph p-0-λ-s′ with $\lambda = \beta + c$. The one-to-one correspondences required for the demonstration can be established by applying conversions (i) and (ii) as appropriate, once or several times in succession, as exemplified in Table 5, proving theorem 2.

Since operations (1) and (2) increase the order of the cubic graph by two, whereas conversions (i) and (ii) preserve the order, one can arrive at tables 4 from table 2 either by applying operations (1) and (2), or conversions (i) and (ii) ; however, the main use of operations (1) and (2) is for expanding the table of cubic graphs to higher orders, whereas conversions (i) and (ii) serve as a check for the completeness of the expanded table.

The recurrent procedure for obtaining simple cubic graphs by making use of operation (1) has been discussed by Johnson.[19, 20] No mention of operation (2) or conversions (i) and (ii) has apparently been published.

From the standpoint of graph theory and of chemical applications, the following items are of interest in a general cubic graph :

its order p, the numbers β of double bonds and λ of loops ; whether it is planar or non-planar (no molecule whose formula is a non-planar graph has as yet been prepared)* ; the numbers of circuits with 3, 4, . . . points ; the symmetry, indicating the possibility of geometrical or optical isomerism ; the numbers of equivalent points, bonds, or loops, determining the numbers of isomers when identifying the points with atoms or groups of atoms ; the minimum number of cuts which can convert the connected graph into a non-connected one ; the steric strain of the molecule pictures by the given graph.

IV. APPLICATIONS

Hydrocarbons with an odd number of carbon atoms cannot be represented by cubic graphs ; at least one point of the graph, i. e. of the structural formula from which the hydrogen and other univalent atoms have been omitted, must have a degree different from 3. If this degree is 2,

---

* In tables 2 and 4, all planar graphs have been drawn without crossing bonds. The notation of non-planar graphs, which have crossing bonds, is enclosed in brackets.

[19] E. L. Johnson, Operations Research Center Technical Report ORC 63–28 (RR) University of California, Berkeley.

[20] O. Ore, "The Four-Colour Problem", Academic Press, New York, 1967.

Table 5

Application of conversion rules (i) and (ii) to the cubic graphs or order six

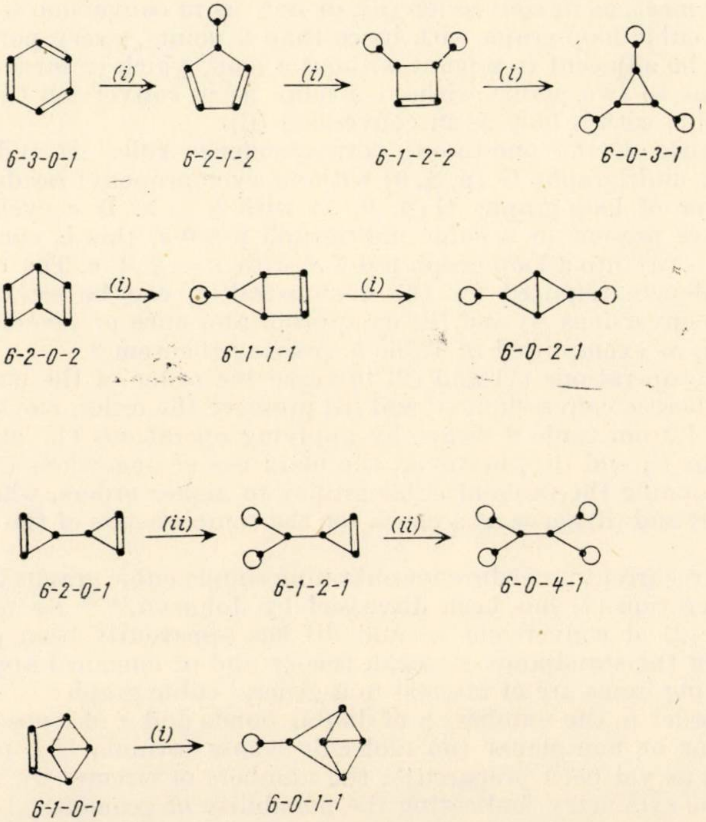

the corresponding point can be represented by the point of attachment of a loop in a general cubic graph. The same is true for a heteroatom with connectivity 2 in a heterocyclic system.

Thus general cubic graphs can, by omitting the loops, represent irregular graphs, in which some points have degree 3, and other points (to which loops had been attached) have degree 2.

Valence isomers of five-membered aromatic heterocycles $(CH)_4X$ (e.g. furan, azoles). Table 6 presents[*] the four possible valence isomers of five-

Table 6

Possible valence isomers of five-membered aromatic heterocyclic compounds

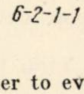

6-2-1-1

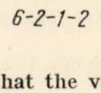

6-2-1-2

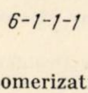

6-1-1-1

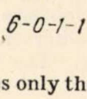

6-0-1-1

---

[*] In order to evidence that the valence isomerization involves only the reorganization of bonds, tables 6—8 contain crossing bonds even for planar graphs.

membered aromatic heterocyclic compounds $(CH)_4X$. These correspond to the four general cubic graphs of order six with one loop 6-β-1-s (table 4c). In the previously published paper (table 6 of ref. 11), graph 6—2—1—1, with the loop attached to a double bond, was missing. We shall discuss first chemical evidences for compounds derived from this graph.

Though interconversions between cyclopentenes and vinylcyclopropanes are well documented,[21–23] little is known about the valence isomerization of cyclopentadienes and 3-vinylcyclopropenes. Heteroanalogues of vinylcyclopropanes, e.g. vinylaziridines, behave analogously, forming thermally 3-pyrrolines.[24] The first observation involving a compound derived from graph 6—2—1—1 was made in 1965 by Wynberg in the study of photochemical transformations of thiophene derivatives, heteroanalogues of cyclopentadiene : 2-phenylthiophene was found to rearrange photochemically to 3-phenylthiophene.[25] Isotopic labelling[26] and further studies[27] evidenced that the intermediately formed valence isomer XXIX can recyclize in any of the two equivalent positions of the cyclopropene ring, accounting for the isomerization. An analogous isomerization was observed by Van Tamelen in the furan series.[28]

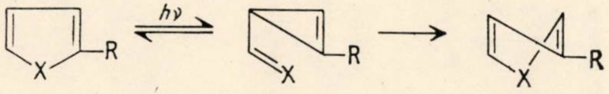

XXIX XXX

Similar observations were made by Ullman, Schmid, and others, on heterocyclics with two heteroatoms : isoxazoles are converted photochemically into oxazoles,[29] benzisoxazoles into benzoxazoles,[30] pyrazoles and their benzoderivatives yield imidazoles[31]; oxa- and thiadiazoles behave similarly.[32]

---

[21] R. N. Warrener and J. B. Bremner, *Rev. Pure Appl. Chem.*, **16**, 117, 156 (1966).

[22] S. Sarel, J. Yovell and M. Sarel-Imber, *Angew. Chem.*, **80**, 592 (1968).

[23] H. M. Frey, *Adv. Phys. Org. Chem.*, **4**, 155 (1966).

[24] R. S. Atkinson and C. W. Rees, *Chem. Commun.*, **1967**, 1232;
A. Padwa and W. Eisendardt, *ibid.*, **1968**, 380.

[25] H. Wynberr and H. van Driel, *J. Amer. Chem Soc.*, **67**, 3998 (1965).

[26] H. Wynberg and H. van Driel, *Chem. Commun.*, **1966**, 203; H. Wynberg and R. M. Kellogg, Proc. 152 nd Natl. Meeting Amer. Chem. Soc., New York, Sep. 10—16, 1966, S 35.

[27] H. Wynberg, R. M. Kellogg, H. van Driel and G. E. Beekhuis, J. *Amer. Chem. Soc.*, **89**, 3501 (1967) and previous papers in the series.

[28] E. E. van Tamelen and T. H. Whitesides, *J. Amer. Chem. Soc.*, **90**, 3895 (1968).

[29] E. F. Ullman and B. Singh, *J. Amer. Chem. Soc.*, **88**, 1844 (1966); B. Singh and E. F. Ullman, *ibid.*, **89** 6911 (1967).

[30] H. Göth and H. Schmid, *Chimia, (Aarau)* **20**, 148 (1966).

[31] T. Tiefenthaler, W. Dorschein, H. Göth and H. Schmid, *Helv. Chim. Acta*, **50**, 2244 (1967).

[32] T. S. Cantrell and W. S. Haller, *Chem. Commun.*, **1968**, 977.

Table 7

Possible valence isomers of pyran, pyrone, etc.

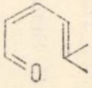
8-3-2-1

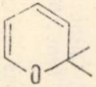
8-2-2-6

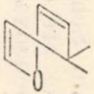
8-2-2-5

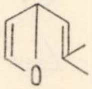
8-2-2-3 a

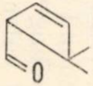
8-2-2-3 b

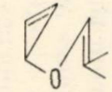
8-2-2-2 a

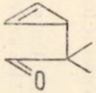
8-2-2-2 b

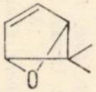
8-1-2-6

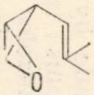
8-1-2-1 a

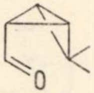
8-1-2-1 b

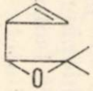
8-1-2-2

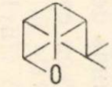
(8-0-2-5)

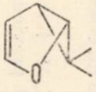
8-1-2-4 a

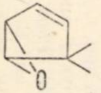
8-1-2-4 b

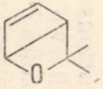
8-1-2-5

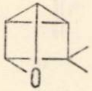
8-0-2-4

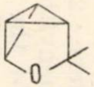
8-0-2-2

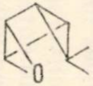
8-0-2-1

As to the other graphs mentioned in table 6, besides literature data quoted previously,[11] structures related to 6—1—1—1 were postulated and discussed;[33–35] an X-ray study of the valence tautomer derived from graph 6—0—1—1 of cyclopentadienone was reported,[36] and related derivatives were described.[37]

Valence isomers of six-membered systems with two heteroatoms $(CH)_4XY$. When X is oxygen and Y represents a CR_2 group or a carbonyl CO, pyran and pyrone are obtained, respectively. Table 7 presents the possible valence isomers for these systems. They correspond to the general cubic graphs of order 8 with two loops 8—β—2'—s (table 4d). When the loops are equivalent (i.e. symmetrical relatively to a plane perpendicular to the graph), one isomer results on replacing the two loops together with their points of attachment by X and Y; when the loops are not equivalent, two isomers result, which are indicated by the letters a and b in table 7. Of course, graphs with two geminal loops (8—0—2—3, 8—1—2—3, 8—2—2—1 and 8—2—2—4) cannot correspond to molecules in this case.

It may be noted that, as in the case of 1,3- and 1,4-cyclohexadiene mentioned in the first section (Definitions), 2-pyran appears as a valence isomer of 4-pyran (8—2—2—6 and 8—2—2—5, respectively). It is interesting in this respect that 4-pyrones can be converted into 2-pyrones.[38]

The valence tautomerism between 2-pyrans and *cis*-2,4-dien-1-onses, mentioned in ref. 11, has been studied by several research workers (8—3—2—1 and 8—2—2—6).[39,40] Benzo-2-pyrans present an analogous valence isomerism.[41] The *cis- trans* isomerization of 2,4-dienals was postulated to proceed through a 2-pyranic valence isomer.[42]

The valence tautomerism of 2-pyrone, mentioned in ref. 11, d does not only involve a bicyclic structure derived from graph 8—1—2—5,[43,45] but also a tricyclic one derived from graph 8—0—2—2, in photochemical reactions.[45] Other systems related to graph 8—2—2—6 afford photo-

---

[33] J. I. Brauman, L. E. Ellis and E. E. van Tamelen, *J. Amer. Chem. Soc.*, **88**, 846 (1966);
L. Skattebol, *Tetrahedron*, **23**, 1107 (1967).

[34] H. Prinzbach and U. Fischer, *Helv. Chim. Acta*, **50**, 1692 (1967).

[35] S. Masamune, R. T. Seidner, H. Zenda, M. Wiesel, N. Nakatsuka and G. Bigam, *J. Amer. Chem. Soc.*, **90**, 5286 (1968).

[36] J. Trotter, C. S. Gibbons, N. Nakatsuka and S. Massamune, *J. Amer. Chem. Soc.*, **89**, 2794 (1967).

[37] C. S. Gibbons and J. Trotter, *J. Chem. Soc.* (*A*), **1967**, 2027.

[38] A. Schönberg and R. von Ardenne, *Chem. Ber.*, **101**, 343, 356 (1968).

[39] A. T. Balaban, W. Schroth and G. Fischer, in "Advances in Heterocyclic Chemistry" (A. R. Katritzky and A. J. Boulton, editors), vol. 10, p. 241, Academic Press, New York, 1969.

[40] T. A. Gosinck, Ph. D. Thesis, Oregon State Univ., 1966; *Dissertation Abs.*, **27** B, 3852 (1967).

[41] R. S. Becker and J. Michl, *J. Amer. Chem. Soc.*, **88**, 5931 (1966); J. Cole and R. S. Becker, *J. Phys. Chem.*, **71**, 4045 (1967); K. R. Huffman and E. F. Ullman, *J. Amer. Chem. Soc.*, **89**, 5629 (1967).

[42] P. Schiess, H. L. Chia and C. Suter, *Tetrahedron Letters*, **1968**, 5747.

[43] E. J. Corey and J. Streith, *J. Amer. Chem. Soc.*, **86**, 950 (1964).

[44] M. Rosenblum and C. Gatsonis, *J. Amer. Chem. Soc.*, **89**, 5074 (1967).

[45] W. H. Pirkle and L. H. McKendry, *J. Amer. Chem. Soc.*, **91**, 1179 (1969); E. J. Corey and W. H. Pirkle, *Tetrahedron Letters*, **1967**, 5255.

chemically bicyclic structures 8—1—2—5 similarly to 2-pyrone, e.g. dimethyl 1,2-dihydropyridazine-1,2-dicarboxylate.[46] Ring contractions of 4-pyran derivatives can be explained by valence isomerization to structures derived from graph 8—2—2—3b.[47]

The concerted process with a cyclic 6-membered transition state converting 1,3,5-hexatrienes (XXXII) into cyclohexadienes (XXXIII) thermally [10,48-51] can take a different course leading to structure XXXI derived from graphs 8—1—2—4a or 8—1—2—4b. Though this has been observed also in the pyran series,[52,53] most examples which are described in the literature refer to cyclohexadienone derivatives, where X is CR_2 and Y is CO.[49,54,55] Analogous photochemical cyclizations occur with *o*-vinylstyrene.[56] The valence isomerism between structures 8—3—2—1 and 8—2—2—6 with both X and Y heteroatoms being sulphur has been described by Schroth and coworkers.[57]

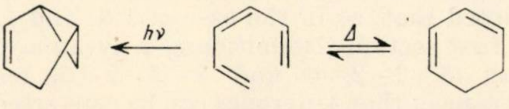

XXXI XXXII XXXIII

Valence isomers of seven-membered cyclopolyenes $(CH)_6X$. Systems with X = CR_2 (tropylidene derivatives) or X = CO (tropone) may theoretically have the valence isomers presented in Table 8. These correspond to the 19 general cubic graphs of order 8 with one loop, 8—β—1—s (table 4d). In the previously published[11] table 6, four graphs (8—3—1—2, 8—3—1—1, 8—2—1—3 and 8—1—1—3, with the loop connected to the double bond) were missing.

In addition to the literature references quoted in the previous paper [11], the following newer literature data can be indicated.

---

[46] L. J. Altman, M. Semmelhack, R. B. Hornby and J. C. Vederas, *Chem. Commun.*, **1968**, 686.

[47] J. d'Angelo and Vu Moc Thuy, *Bull. Soc. Chim. France*, **1968**, 2823.

[48] E. F. Ullman, W. A. Henderson Jr. and K. R. Huffman, *Tetrahedron Letters*, **1967**, 935.

[49] H. E. Zimmerman, D. S. Crumrine, D. Dopp and P. S. Huyffer, *J. Amer. Chem. Soc.*, **91**, 434 (1969) and previous papers in the series.

[50] W. G. Dauben and J. H. Smith, *J. Org. Chem.*, **32**, 3244 (1967).

[51] P. Courtot and O. Le Goff-Hays, *Bull. Soc. Chim. France*, **1968**, 3401.

[52] E. F. Ullman and W. A. Henderson, *J. Amer. Chem. Soc.*, **88**, 4942 (1966); **89**, 4340 (1967).

[53] M. M. Bursey and L. R. Dusold, *Tetrahedron Letters*, **1967**, 2649.

[54] D. W. Swatton and H. Hart, *J. Amer. Chem. Soc.*, **89**, 5075 (1967); D. W. Swatton, *Dissertation Abs.*, **28** B, 3659 (1968).

[55] J. Griffiths and H. Hart, *J. Amer. Chem. Soc.*, **90**, 3297 (1968).

[56] J. Meinwald and P. H. Marzochi, *J. Amer. Chem. Soc.*, **89**, 696 (1967); M. Pomerantz, *ibid.*, 694.

[57] W. Schroth, F. Billig and G. Reinhold, *Angew. Chem.*, **79**, 685 (1967).

Table 8

Possible valence isomers of tropylidene, tropone, oxepin, etc.

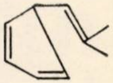
8-3-1-2

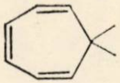
8-3-1-3

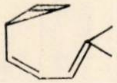
8-3-1-1

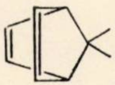
8-2-1-6

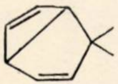
8-2-1-5

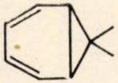
8-2-1-4

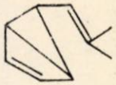
8-2-1-3

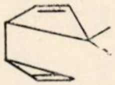
8-2-1-2

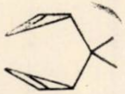
8-2-1-1

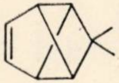
8-1-1-6

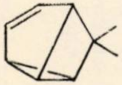
8-1-1-5

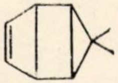
8-1-1-4

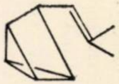
8-1-1-3

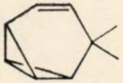
8-1-1-2

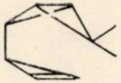
8-1-1-1

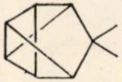
(8-0-1-4)

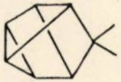
8-0-1-3

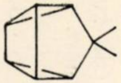
8-0-1-2

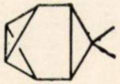
8-0-1-1

Many new data appeared on the valence isomerism between tropylidene (8—3—1—3) and norcaradiene (8—2—1—4)[58–64] Interconversions between isomeric tropylidenes occur *via* 1,5 hydrogen shifts.[10,65] The valence isomerism may initiate further rearrangements in carbonium ions occuring in the solvolysis of (7-cycloheptatrienyl)-methyl 3,5-dinitrobenzoate.[66] Benzo- and quino-tropylidenes behave similarly.[67,68] In the heterocyclic seven-membered series, the valence isomerism between oxepin and benzene-oxide is now well documented.[69] However, in the azepine[70] or 1,2-diazepine series[71–73] only one isomer is found; this is 8—3—1—3 for 1H-azepine or 4H-1,2-diazepine, but 8—2—1—4 for 5H-1,2-diazepine or 3,4-diazanorcaradiene.

Photochemical reactions convert tropylidenes (8—3—1—3) into other valence isomers than 8—2—1—4: system 8—2—1—5,[74-76] system 8—1—1—4;[77] bicycloheptadienes (8—2—1—6) are converted thermally into tropylidenes (8—3—1—2)[78,79] and photochemically into quadricyclanes (8—0—1—2)[80,81] which revert thermally into tropylidenes. Oxa-[82,83]

---

[58] G. Maier, *Angew. Chem.*, **79**, 446 (1967).

[59] J. A. Berson and M. R. Willcott III, *Record Chem. Progr.*, **27**, 139 (1966).

[60] J. A. Berson, P. W. Grubb, R. A. Clark, D. R. Hartter and M. R. Willcott III, *J. Amer. Chem. Soc.*, **89**, 4076 (1967).

[61] E. Ciganek, *J. Amer. Chem. Soc.*, **89**, 1454, 1458 (1967).

[62] M. Jones Jr., S. D. Reich, L. T. Scott and L. E. Sullivan, *Angew. Chem.*, **80**, 631 (1968).

[63] T. Mukai, H. Kubota and T. Toda, *Tetrahedron Letters*, **1967**, 3581.

[64] K. W. Egger, *J. Amer. Chem. Soc.*, **90**, 1, 6 (1968).

[65] K. W. Egger, *J. Amer. Chem. Soc.*, **89**, 3688 (1967).

[66] G. D. Sargent, N. Lowry and S. D. Reich, *J. Amer. Chem. Soc.*, **89**, 5985 (1967).

[67] M. Pomerantz and G. W. Gruber, *J. Amer. Chem. Soc.*, **89**, 6799 (1967).

[68] B. Föhlisch *et al.*, *Chem. Ber.*, **101**, 2717 (1968).

[69] E. Vogel and W. Gunther, *Angew. Chem.*, **79**, 429 (1967).

[70] L. A. Paquette and D. E. Kuhla, *Tetrahedron Letters*, **1967**, 4517; L. A. Paquette, J. H. Barrett and D. E. Kuhla, J. *Amer. Chem. Soc.*, **91**, 3616 (1969).

[71] G. Maier and T. Sayrac, *Chem. Ber.*, **101**, 1354 (1968) and previous papers.

[72] G. Maier and U. Heep, *Chem. Ber.*, **101**, 1371 (1968); M. A. Battiste and T. J. Barotn, *Tetrahedron Letters*, **1967**, 1227.

[73] O. Buchardt, C. L. Pedersen, U. Svanholm, A. M. Duffield and A. T. Balaban, *Acta Chim. Scand.*, in press.

[74] M. R. Willcott III and E. Goerland, *Tetrahedron Letters*, **1966**, 6341.

[75] L. B. Jones and V. K. Jones, *J. Amer. Chem. Soc.*, **89**, 1880 (1967).

[76] L. A. Paquette and J. H. Barrett, *J. Amer. Chem. Soc.*, **88**, 1718 (1966).

[77] H. Prinzbach and E. Druckrey, *Tetrahedron Letters*, **1968**, 4285.

[78] M. R. Willcott III and C. J. Boriack, *J. Amer. Chem. Soc.*, **90**, 3287 (1968).

[79] R. K. Lustgarten and H. G. Richey Jr., *Tetrahedron Letters*, **1966**, 4655.

[80] H. Prinzbach and J. Rivier, *Angew. Chem.*, **79**, 1101, 1102, 1103 (1967); *Tetrahedron Letters*, **1967**, 3713.

[81] H. Prinzbach, *Chimia (Aarau)*, **20**, 432 (1966); *Pure Appl. Chem.*, **16**, 17 (1968).

[82] H. Prinzbach, P. Vogel and W. Auge, *Chimia (Aarau)*, **21**, 469 (1967); H. Prinzbach, P. Würsch, P. Vogel, W. Tochterman and C. Franke, *Helv. Chim. Acta*, **51**, 911 (1968).

[83] P. Deslongchamps and J. Kallos, *Canad. J. Chem.*, **45**, 2235 (1967).

and aza- heterocyclic analogues[84] present similar reactions. Two further systems were described with oxygen heteroatoms, namely 8–1–1–4) (the epoxide of Dewar benzene, which is converted by light or heat into the valence isomeric mixture of benzene-oxide-oxepin)[85] and 8–2–1–1 (tetraphenyl derivative, undergoing isomerization into 8–2–1–6).[86]

---

[84] H. Prinzbach, R. Fuchs and R. Kitzing, *Angew. Chem.*, **80**, 78 (1968); P. Kitznig, R. Fuchs, M. Joyeux and N. Prinzbach, *Helv. Chim. Acta*, **51**, 888 (1968).

[85] E. E. van Tamelen and D. Carty, *J. Amer. Chem. Soc.*, **89**, 3922 (1967).

[86] A. W. Dow II, *Dissertation Abs.*, **28** B, 2338 (1967).

Revue Romaine de Chimie, **15**, 463–486 (1970)

ORSZÁGOS MŰSZAKI KÖNYVTÁR ÉS DOKUMENTÁCIÓS KÖZPONT 1883

La *Revue Roumaine de Chimie* paraît 12 fois par an. Le prix d'un abonnement annuel est de £5.0.0 ; $ 12, — ; FF 60,— ; D.M. 48, — . Toute commande l'étranger (fascicules ou abonnements) sera adressée à CARTIMEX, Boîte postale 134—135, Bucarest, Roumanie, ou à ses représentants à l'étranger :

ALBANIA Ndërmarja Shtetëtrore E. Tregëtimit Të Librit Tirana ; AUSTRIA Globus Buchvertrieb Salzgries 16 Wien I ; BELGIUM Du Monde Entier 5, Place St. Jean Bruxelles ; Librairie Claeys-Verheughe 8, Volderstraat Gand ; Maison des Langues Vivantes 65, Rue du Midi Bruxelles ; Office International de Librairie 30, Av. Marnix Bruxelles 5 ; Vander Editeur 10, Munstraat Louvain ; BULGARIA Hemus Pl. Slaveikov 11-Sofia ; CANADA Canadian Slavic Studies Loyola Colege Montreal 262 ; Librairie Lidec Inc. 1083 Van Home Montreal ; Panonia Books 2, Spadina Road Toronto 4 Ontario ; CHINA Waiwen Shudian P.O. Box 88 Peking ; COLOMBIA Libreria Karl-Bucholz Av. Jimenez 8—40 Bogota ; CUBA Cubartimpex P.O. Box 6540 La Habana ; CZECHOSLOVAKIA Artia Ve Smerckach 30 Praha I ; DENMARK Munksgaard 6 Norregade Copenhagen K ; N. J. Hasses-Bogimport 8, Loerstraede Copenhagen K. ; FINLAND Akateeminen Kirjakauppa Postfach 10128 Helsinki 10 ; FRANCE Agence Littéraire et Artistique Parisienne 7, Rue Debelleyme Paris 3-e ; Eyrolles Editeur 61, Boulevard Saint-Germain Paris 5-e ; Librairie de l'enseignement technique (Stand permanent des livres techniques et scientifiques roumains) 61, Boul. Saint-Germain, Paris 5-e; Librairie Hachette 25, Rue des Cévennes Paris 5-e ; Librairie Joseph Gibert 26—30, Boul. Saint-Michel Paris 6-e ; Libella 12, Rue Saint-Louis-en-l'Ile Paris 4-e ; Maison du Livre Italien 46, Rue des Ecoles Paris 5-e ; Office International de Documentation et Librairie 48, Rue Gay-Lussac Paris 5-e ; Presses Universitaires de France 17, Rue Soufflot Paris 5-e ; THE GERMAN DEMOCRATIC REPUBLIC Deutscher Buch-Export-und-Import Leninstrasse 16 Leipzig C. 1 ; THE FEDERAL REPUBLIC OF GERMANY Kubon Sagner P.O. Box 68 München 34 ; Reise und Verkehrsverlag Hönigwiesenstrasse, 25 7 Stuttgart-Veihingen ; Zumsteins Landkartenhaus Liebherrstrasse, 5 8 München 22; GREAT BRITAIN Bailey Bros & Swinfen Ltd. Warner House 48, Upper Thames Street London E.C. 4 City 6521 ; Blackwell's Foreign Department Broad Street Oxford ; Central Books Ltd. 37, Grays Inn Road London W.C.1 ; Collet's Holdings Ltd. Denington Estate London Road Wellingborough Northans N & G Goyle Ltd. 119—125 Charring Cross Road London W.C. 2 ; Parker & Son 103, Walton Street Oxford ; HOLLAND Antiquariat Junk Walderstraat 10 Lochem ; Boekhandel Pegasus Leidsestraat 25 Amsterdam ; Intertaal Van Baerlesstraat 150 Amsterdam Zuit ; Meulenhoff Beulingstraat 2 Amsterdam C ; Swets & Zeitlinger Keizersgracht 471—487 Amsterdam ; HUNGARY Kultura Fö utca 32 Budapest 1 ; ISRAEL Haiflepac Ltd. 11, Arlosorov St. Haifa ; Lepac Ltd, 15, Rambam St. Tel-Aviv ; Lotus Ltd. Achad Haam St. Tel-Aviv ; ITALY SO, CO, LIB, RI Export-Import Piazza Margana 33 Roma ; JAPAN Maruzen Ltd. 6 Tory Michome Nihombashi Tokyo ; Nauka Ltd. Imp. Departm. 30—19 Minami Ikebukuro 2, Chome, Toshima-Ku Tokyo ; DEMOCRATIC PEOPLE'S REPUBLIC OF KOREA Chulpanmul ; MEXICO Editorial Grijalbo S. A. Aparatado 28568 Mexico. 17.D.F. ; MONGOLIA Mongolgosknigotorg Ulan Bator ; NORWAY Norsk Bokimport Postboks 3267 Oslo ; POLAND Ars Polona Krakowskie Przedmiescie 7 Warszawa ; PORTUGAL Libreria Bucholz Avenida Libertade Lisboa ; SPAIN Libreria Bucholz Paseo de Recoletos Madrid ; Libreria Cientifica General Preciados no. 48 Madrid 13 ; SWEDEN Almqvist & Wiksell 26, Gamla Brogatan Stockholm K. ; C. E. Fritze Fredgatan 2 Stockholm 16 ; Gumperts AB P. O. Box 346 Göteborg I ; SWITZERLAND Fachbücherei Postfach 1420 3001-Berna ; Herbert-Lang Ecke Munzgraben 2 Berna ; Librairie Payot 1-Rue de Bourg Ch-1002 Lausanne ; Librairie Rousseau 36, Rue Jean-Jacques Rousseau Genève ; Pinkus & Co. Froschaugasse 7 Zürich I ; THE UNITED ARAB REPUBLIC Dar El Tahrir et Publishing 21 Kasr el Nil St. (Dar el Shark Bookshop) Cairo ; THE U.S.A. Angelescu Book Service 3645, Barham Street Detroit 24 Michigan ; American Chemical Society 1155, Sixteenth Street NW Washington DC 20036 ; Fam Book Service 69, Fifth Avenue Suite 8 F ; New York 10003, N.Y. Franklin Square-Subscription Agency Teaneck (New Jersey 07666) ; W. S. Heinman 400, East 72nd Street New York, 21, N. Y. ; McGraw-Hill Book Company 330, West 42nd Street New York, N.Y. 10036 ; Moore-Cottrell Subscr. Agency Worth Cohocton, New York 14868 ; Nicoară Travel Service 17432, Woodward Ave. Detroit Michigan 48203 ; Shoenhof's Foreign Books, Inc. 1280, Massachusetts Avenue Cambridge, Massachusetts 02138 ; Henry M. Snyder & Co. Inc. 440 Fourth Avenue New York, N.Y. 10016 ; Twayne Publishers, Inc. 31 Union Square West New York 3, N. Y. ; Zeitein & Ver Brugge Booksellers 815 No. La Cienaga BLVD Los Angeles 69, California ; THE U.S.S.R. Mejdunarodnaia Kniga Moscow C. 200 ; THE DEMOCRATIC REPUBLIC OF VIET-NAM Xunhasaba 32, Hai Ba Trung Hanoi ; YUGOSLAVIA Forum V. Misica, 1 Novi Sad ; Jugoslovenska Knjiga Terazije, 27 Beograd ; Libertatea Z. Zrenjanina, 7 Pancevo ; Prosveta Terazije 16 I Beograd ;

1970 MAJ 21

TRAVAUX PARUS AUX ÉDITIONS DE L'ACADÉMIE DE LA RÉPUBLIQUE SOCIALISTE DE ROUMANIE

CORNEL BODEA et collab., **Tratat de biochimie vegetală**, partea I, **Fitochimie** (Traité de biochimie végétale, Ire partie, Phytochimie), Ier vol., 1964, 747 p. + 4 annexes + 2 pl., 41 lei, IIe vol., 1965, 1262 p., 1 pl., 56 lei, IIIe vol., 1967, 773 p., 35 lei.

V. GHEŢIE et V. MICUŞAN, **Analiza imunochimică. Teorie şi practică** (Analyse immunochimique. Théorie et pratique), 1966, 369 p., 28 lei.

R. PORTOCALĂ et L. POPA, **Acizii ribonucleici celulari şi virali** (Les acides ribonucléiques cellulaires et viraux), 1966, 375 p. + 8 pl., 26 lei.

D. PURDELA et R. VÎLCEANU, **Chimia compuşilor organici ai fosforului şi ai acizilor lui** (La chimie des composés organiques du phosphore et de ses acides), 1965, 540 p., 37 lei.

CRISTOFOR SIMIONESCU, MARGARETA GRIGORAŞ et AGATA CERNĂTESCU-ASANDEI, **Chiima lemnului din R.P.R.** (La chimie du bois en Roumanie), 1964, 239 p. + 6 pl., 27 lei.

CRISTOFOR SIMIONESCU et CLEOPATRA VASILIU-OPREA, **Mecanochimia compuşilor macromoleculari** (La mécanochimie des composés macromoléculaires), 1967, 344 p., 23,50 lei.

CARMEN SABĂU. **Schimbul ionic, teoria şi aplicaţiile sale în chimia analitică** (L'échange ionique. Théorie et applications à la chimie analytique), 1967, 307 p., 12 lei.

I. MAXIM, **Materiale nucleare** (Matériaux nucléaires), 1969, 444 p., 30 lei.

CR. SIMIONESCU, C. UGLEA, **Fracţionarea compuşilor macromoleculari** (Le fractionnement des composés macromoléculaires), 1969, 292 p., 18,50 lei.

I. P. „Informaţia" c. 4207

43 426

Lei 25

F 1103

P.Z.TERALVA

R

REVUE ROUMAINE DE CHIMIE

TOME 15
N° 4
Avril 1970

ÉDITIONS DE L'ACADÉMIE DE LA RÉPUBLIQUE SOCIALISTE DE ROUMANIE

Rev. Roumaine Chim. 15, 487–666 (1970), Bucarest

COMITÉ DE RÉDACTION

Rédacteur en chef :

C. D. NENIŢESCU, membre de l'Académie de la République Socialiste de Roumanie.

Rédacteurs en chef adjoints :

A. T. BALABAN et V. E. SAHINI, membres correspondants de l'Académie de la République Socialiste de Roumanie.

Collège de rédaction :

C. DRĂGULESCU, RALUCA RIPAN, CR. SIMIONESCU, membres de l'Académie de la République Socialiste de Roumanie ; EM. BRATU, membre correspondant de l'Académie de la République Socialiste de Roumanie ; Pr G. OSTROGOVICH, MARGARETA AVRAM, F. BADEA, I. D. MARCHIDAN, D. NEGOIU et D. SĂNDULESCU.

Les manuscrits, les livres et les revues proposés en échange, ainsi que toute correspondance seront envoyés à la rédaction :

REVUE ROUMAINE DE CHIMIE

23, str. Dumbrava Roşie, Bucarest, Roumanie.

REVUE ROUMAINE DE CHIMIE

Tome 15, N° 4 Avril 1970

ORSZÁGOS MŰSZAKI KÖNYVTÁR ÉS DOKUMENTÁCIÓS KÖZPONT

Page

I. G. MURGULESCU and M. I. VASS, Surface potential variation during nitrogen adsorption on thin copper films 489–493

V. E. SAHINI, C. PODINĂ et V. CONSTANTIN, L'étude des picolines par spectrométrie de masse 495–499

A. GIOABĂ, V. E. SAHINI and ELENA VOLANSCHI, Spectral study of phenoxatellurine and some of its derivatives 501–509

A. BALINT, Z. SIMON and M. MRACEC, Molecular orbital calculations in the 2,5-diamino-1,4-benzoquinone series. III. Pariser-Parr-Pople calculations for 2,5-bisphenylamino-1,4-benzoquinone 511–513

O. RADOVICI and M. V. POPA, The kinetics of cobalt corrosion process. . 515–526 R

S. STERNBERG and MARIANA TERZI, The surface tension of binary molten mixtures of silver chloride with sodium and potassium chloride . . . . 527–537 R

V. MINCU et E. SEGAL, Propriétés magnétiques des combinaisons complexes des halogénures des métaux bivalents avec des composés pyridiniques . 539–541

S. LICĂ, L'électrolyte pâteux utilisable dans les accumulateurs électriques . 543–551

LUCIA TUDOR, Radiolysis processes in aqueous solution of KI in the presence of KH_2PO_4 and $NaNO_3$ 553–557

RALUCA RIPAN et V. CORDIŞ, Une nouvelle synthèse de l'acide phospho-12-vanadique au moyen des échangeurs d'ions 559–562

C. DRĂGULESCU, T. SIMONESCU, GIZELLA NEMES und MARIA TOTAN, Untersuchungen der Komplexe Th-Alizarin und Th-Chinalizarin durch Extraktion mit Butanol-1 . . . . 563–571 R

FR. MIHAI und R. NUŢIU, Verbindungen der Dilitursäure mit Anilin und Phenylendiaminen . . . . 573–581 R

C. LITEANU, E. CORDOŞ and LIANA MĂRGINEANU, Automatic potentiometric titration in molten media. I. A new automatic continuous procedure for potentiometric titration in molten media with solid standard . 583–587

GR. POPA and D. N. TODOR, Determination of the siderite and ankerite content by thermal analysis methods 589–595

D. COSTACHE and P. JUNIE, Kinetic measurement of cobalt traces. I. With magnezon 1 . . . . 597–603 R

M. E. MACOVSCHI and VIORICA NIŢU, Photometric determination of copper traces without extraction 605–606

A. SZURKOS and P. NAGY, A polarographic study on styrilcyanines. I. Substituent effects in the polarographic reduction of the styrilcyanines according to Brown-Okamoto equation 607–614

T. HODIŞAN, A. ŞUTEU und V. GOREA, Eine neue kolorimetrische Bestimmungsmethode des Urans(VI) 615–617

MARIA CAPROŞU, MAGDA PETROVANU et I. ZUGRĂVESCU, L'addition des philodiènes sur la 1-méthyl-phtalazine et sur la β-phényl-vinyl-phtalazine 619–626

A. BALINT, The synthesis of some new 3,6-dichloro-2,5-bisphenylamino-1,4-benzoquinone derivatives with electron-donor and electron-acceptor groups 627–634

A. T. BALABAN, A. ARSENE, IOANA BALLY, A. BARABÁS, MARIA PARASCHIV, MARIA ROMAN and ELENA ROMAŞ, Heterocyclic organoboron compounds. XII. 2,4,6-Trisubstituted-1,3,2-dioxaborinium salts . . 635–653

V. TĂMAŞ and C. BODEA, $TiCl_4$-carotenoid complexes. VII. Action of $TiCl_4$ on 5,8-epoxy-carotenoids (5,8-epoxy-β-carotene, 5,8-epoxy-cryptoxanthin and 5,8-epoxy-zeaxanthin) 655–659

E. CORDOŞ, An automatic ratemeter for consecutive slope measurements . . 661–666

Revue Roumaine de Chimie, **15**, 489–493 (1970)

ORSZÁGOS MŰSZAKI KÖNYVTÁR ÉS DOKUMENTÁCIÓS KÖZPONT

SURFACE POTENTIAL VARIATION DURING NITROGEN ADSORPTION ON THIN COPPER FILMS

I. G. MURGULESCU and M. I. VASS
Institute of Physical Chemistry of the Academy, Bucharest, str. Dumbrava Roşie, 23

Received March 20, 1969

Retarding field diode has been used to measure the surface potential variation during nitrogen adsorption on thin copper films at 77°K. A value of +0.20 V was obtained and the possible forms of nitrogen bonding at 77°K are discussed.

It is well known that nitrogen forms at room as well as at high temperatures, atomic chemisorbed layers on the surface of the transitional metals: W[1–4], Mo,[5,6] Ta,[7] Fe,[8,9] Ni[10,11] whose structures have been proved to be complex, involving different adsorbed species with different bonding energies.[12] The structures of the adsorbed nitrogen layers at low temperatures is until now unsufficiently known; the appearance of a molecular chemisorption with the partial breaking of the triple $N \equiv N$ bond is supposed [13] to occur. It is interesting that both iron, which is very active in chemisorption at high temperatures and nickel which is slightly active towards nitrogen in the same conditions, produce at low temperatures, small values of the surface potential: +0.20 V for iron [14] and +0.22 V for nickel.[15] This finding leads us to the supposition that on the two metals at 77°K the bond has an identic nature. The exact nature of the bond: either molecular chemisorption or physical adsorption without breaking of the triple bond is still a disputable problem. The marked lack of distinction between the behaviour of the two metals guided us to the conclusion that surface potential variation may also take place at low temperatures on other metals, as for example on so-called sp metals, whose activity at room temperature against nitrogen is negligible.

That is why we decided to study the nitrogen adsorption on thin copper films at 77°K.

---

[1] J. A. Becker and. C. D. Hartman, *J. Phys. Chem.*, **57**, 153 (1953).

[2] G. Ehrlich, *J. Chem. Phys.*, **24**, 482 (1956).

[3] P. Kisliuk, *Phys. Rev.*, **122**, 405 (1961).

[4] P. A. Redhead, Proc. Symp. on Electron and Vacuum Phys., Hungary, 1962, p. 89.

[5] A. A. Parry and J. A. Pride, *Brit. J. Appl. Phys.*,**18** 329 (1967).

[6] R. S. McKee and M. V. Roberts, *Chem. Comm.*, **1965** , p. 59.

[7] R. Griffith and J. A. Pride, *Trans. Faraday Soc.*, **63**, 2522 (1967).

[8] V. Ponec and Z. Knorr, *J. Catalysis*, **10**, 74 (1968).

[9] O. Beeck, W. A. Cole and A. Wheeler, *Discuss. Faraday Soc.*, **8**, 314 (1950).

[10] H. H. Madden and H. E. Farnsworth, *J. Chem. Phys.*, **34** 1186 (1961).

[11] L. H. Germer, *J. Chem. Phys.*, **36**, 1555 (1962).

[12] G. Ehrlich, *J. Chem. Phys.*, **35**, 1421 (1961).

[13] B. M. W. Trapnell, *Trans. Faraday. Soc.*, **52**, 865 (1956).

[14] P. M. Gundry, J. Haber and F. C. Tompkins, *J. Catalysis*, ,**1** 363 (1962).

[15] J. C. Mignolet, *Discuss. Faraday Soc.*, **8**, 105 (1950).

EXPERIMENTAL

Retarding field diode method has been used for the following of surface potential variations during adsorption. The thin copper films were prepared inside the cell by evaporation of 4 mg spec. pure Johnson-Matthey copper. The nitrogen was obtained in a device adapted to the previous described system [16] for the filling of gas phials, by thermal decomposition of sodium azide. First experiments were carried out with chemically purified nitrogen by passing cylinder nitrogen through: silicagel, magnesium perchlorate, reduced copper deposited on Kisselgur, H_2SO_4 conc., silicagel, phosphor pentoxide and a column packed with active charcoal and cooled with liquid nitrogen. In spite of all possible care taken during purification, the values of surface potential differences obtained by using this nitrogen were not reproducible enough and we have given up this method.

Copper deposition was effected at 77°K and was followed by thermal sinterisation at 353°K for 5—10 min. to stabilize the crystalline lattice. The film thickness deduced from geometrical area, was about 600 Å. The pressure during deposition was $2-5\times10^{-9}$ torr, having a 20 s pulse of 1×10^{-8} torr at the maximum sintering temperature.

The experimental details, measuring circuits, working method, gas handling, as well as the advantages of using the retarding field diode in adsorption studies, were previously described. [16,17]

On figure 1 the shifts of the logarithm of anodic current *versus* retarding applied potential curves at the step dose interaction with nitrogen are plotted. The deviation from parallelism deduced from the plots is lower than 0.01 V, filling the criterion of the working method.

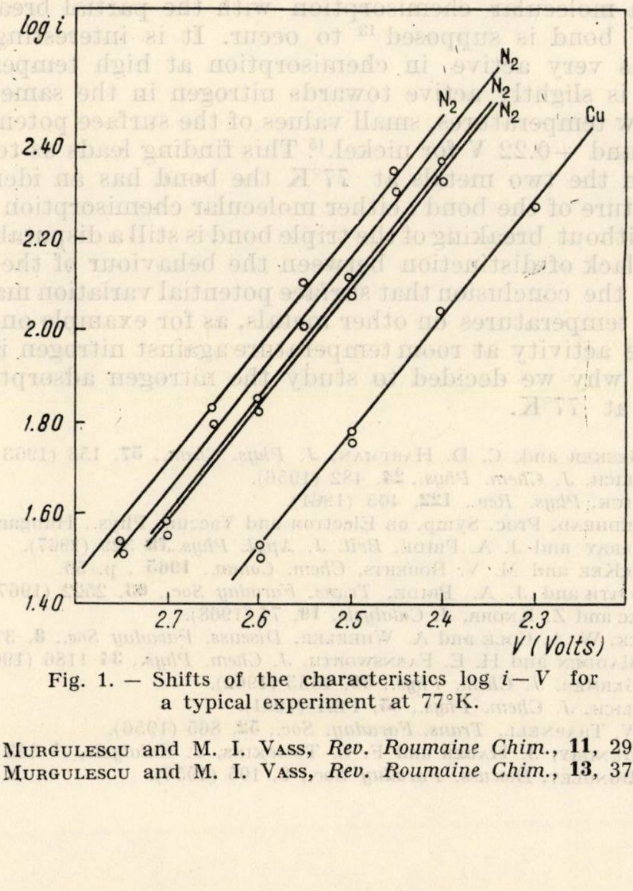

Fig. 1. — Shifts of the characteristics log $i-V$ for a typical experiment at 77°K.

---

[16] I. G. Murgulescu and M. I. Vass, *Rev. Roumaine Chim.*, **11**, 299 (1966).

[17] I. G. Murgulescu and M. I. Vass, *Rev. Roumaine Chim.*, **13**, 373 (1968).

RESULTS AND DISCUSSIONS

The experiments were performed only at 77°K; the surface potential variation (ΔV) with the number of adsorbed molecules on cm² (n_a), the time variation as well as ΔV occurring at sudden temperature changes have been measured.

Figure 2 shows the ΔV *versus* number of adsorbed molecules. It must be emphasized at first the appearance of positive maximum value $+ 0.20$ V at the medium coverage of $2.6-2.8 \times 10^{14}$ molecules/cm². The small ΔV value is in agreement with the observed values [18, 19] for the nitrogen adsorption on other metals at the same temperature.

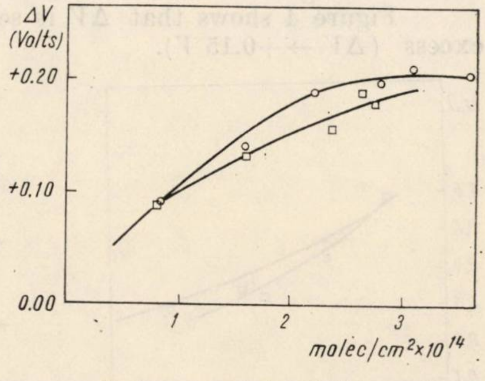

Fig. 2. — Surface potential variations with the number of adsorbed molecules at 77°K.

The nitrogen molecule covers [20], in a monomolecular layer physically adsorbed on an inert surface, an area of 16.1 Å.² If we assume the same adsorption condition in the N_2-Cu system, at saturation, the number of adsorbed molecules found by us, covers only 43 per cent from geometrical area. However, taking into account that ΔV_{max} has a sensible value close to that for covalent adsorption, we can suppose that the area occupied by a molecule is increased. It is likely that nitrogen molecule will "cover" four adsorption sites, forming an adsorbed complex of $\underset{/\backslash/\backslash}{[N = N]^+}$ type, so that it disposes of a double area to justify ΔV saturation at the observed $n_{a\,max}$. The increasing of the occupied area of the molecule can be understood as the formation of the charge transfer bonds towards the metal, being known the existence of labile $w\pi$ orbitals in the nitrogen molecule. The possibility of the gas phase formation of charge species N_2^+ cannot also be completely avoided. Indeed, the utilisation of a retarding field diode with electron gun as emitter, has proved the forming,[21] by the nitrogen interaction with electronic beam of N_2^+, N^+, N_2^{++} ions, evidently at great negative potentials (15—64 V).

As to the system N_2-Ni, there are[22] spectroscopic evidences on the adsorbed $Ni- [N \equiv N]^+$ type complexes. The molecule polarization in the surface field cannot be avoided as a possible explanation [23] either.

---

[18] P. L. Jones and B. A. Pethica, *Proc. Roy. Soc.*, *A* **256**, 454 (1960).

[19] H. W. H. Sachtler and G. J. H. Dorgelo, *J. Chim. phys.*, **54**, 27 (1957).

[20] D. M. Young and A. D. Crowell, "Physical Adsorption of Gases", Butterworth, London, 1962, p. 226.

[21] R. N. Lee and H. E. Farnsworth, *Surface Sci.*, **3**, 461 (1965).

[22] R. F. Eischens and J. Jacknow, Proc. III Int. Congress Catal., North Holland Publishing Co., Amsterdam, 1965, p. 627.

[23] P. M. Gundry and F. C. Tompkins, *Trans. Faraday Soc.*, **56**, 846 (1950).

The above hypotheses account for the variations sense of ΔV, namely explain the formation of an adsorbed layer which reduces the work function of copper.

The variation of the dipole moment value with n_a (evidently, admitting the applicability of the Helmholtz equation at the low coverages) seems to support the hypothesis of charged adsorbed species forming. On figure 3 it can be observed that $\mu_{\theta\to 0} = \frac{1}{2}\mu_{\theta\to 0}$ which is a proof of sufficient strong interaction between adsorbed dipoles.

Figure 4 shows that ΔV is sensitive to the removing of the gas excess $(\Delta V \to +0.15\ V)$.

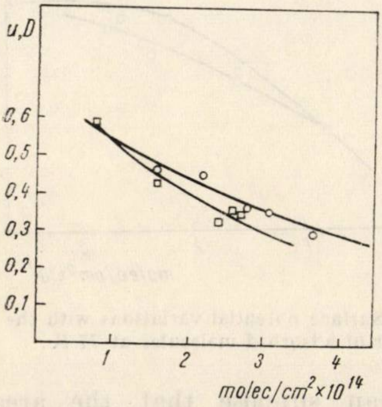

Fig. 3. — Variation of the dipole moment of the bond with the number of adsorbed molecules at 77°K.

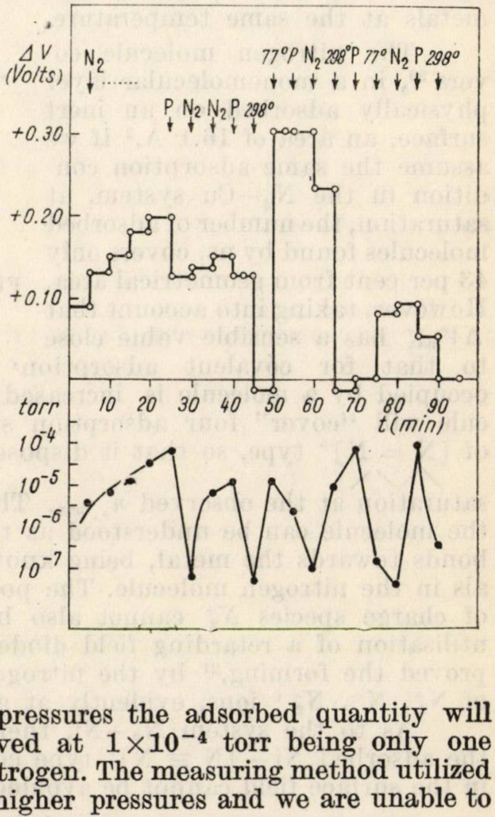

Fig. 4. — Surface potential variations in time for dose introduction of nitrogen (N_2) at 77°K for sudden temperature change (298°K) and gas excess pumping (P) for a typical experiment; in the lower part the simultaneous pressure variation in the system is plotted.

We conclude that at higher pressures the adsorbed quantity will be increased, the species we observed at 1×10^{-4} torr being only one of the possible forms of adsorbed nitrogen. The measuring method utilized in this work cannot be applied to higher pressures and we are unable to say something about other adsorbed forms.

Newly introduced doses, after evacuating the gas excess, lead to the increase in n_a to 4.5×10^{14} molec/cm² but the ΔV value is only partially returning. This observation supports the previous statement about the n_a increase with the pressure.

If after pumping, the system is heated 298°K, ΔV decreases to zero and n_a to$\leqslant 0.5\times10^{14}$ molec/cm², which is in agreement with other authors' observations [13] that nitrogen does not form adsorbed layers on copper at room temperature. It is clear that the previously described bond at 77°K is a weak one, the molecule being unable to pass into chemisorbed state.

Cooling the system in the presence of the desorbed quantity ΔV becomes $+0.30$ V but n_a does not return to the initial value. Pumping the desorbed gas and cooling again the system, an increase in 0.05 V is obtained. This is perhaps a variation due to the metallic lattice structure modifications after the cooling-heating cycle. Neglecting the contamination as unlikely, we suppose that among the readsorbed molecules there are N_2^{++} or N^+ species issued from the interaction of nitrogen with the hot filament or with the electronic beam. The hypothesis of a new molecular layer polarized by the first one cannot be applied as long as the first adsorbed layer is not completed.

Revue Roumaine de Chimie, **15**, 489 – 493 (1970)

Revue Roumaine de Chimie, **15**, 495 – 499 (1970)

L'ÉTUDE DES PICOLINES PAR SPECTROMÉTRIE DE MASSE

V. E. SAHINI, C. PODINĂ et V. CONSTANTIN

Laboratoire de Chimie Physique, Université de Bucarest, 13, Bd. Republicii

Reçu le 7 juin 1969

On étudie les mécanismes d'obtention des principaux ions qui paraissent dans les spectres de masse des isomères de la picoline, ainsi que l'influence de la position du groupement méthyle sur les processus de dissociation des ions moléculaires. On donne aussi les spectres de masse de la 2,4-diméthylpyridine et de la 2,4,6-triméthylpyridine.

L'établissement des mécanismes de fragmentation des molécules de différents composés au bombardement électronique a une importance particulière pour la corrélation des spectres de masse avec la structure des molécules respectives.

Les composés organiques qui contiennent dans leurs molécules un atome d'azote peuvent être souvent reconnus dans les spectres de masse par leurs ions moléculaires de masses impaires. La présence d'un électron non couplé dans de tels ions aboutit à la formation des ions doublement chargés, qui peuvent être facilement détectés, grâce à leur masse spécifique demi-entière. L'existence de ces ions doublement chargés dans les spectres de masse facilite l'établissement de la structure de certains ions fragmentaires et permet la précision de certaines réactions de fragmentation.

Les spectres de masse de divers composés aromatiques qui contiennent de l'azote [1, 2] montrent que la dissociation des ions moléculaires est en grande mesure influencée par la présence de cet atome d'azote qui détermine le principal processus de fragmentation : l'élimination d'une molécule neutre de HCN ou du radical H_2CN, processus qui dans la majorité des cas est confirmé par la présence du pic métastable respectif.

Dans ce travail on étudie les mécanismes de dissociation au bombardement électronique des isomères de la picoline.

---

[1] H. Budzikiewicz, C. Djerassi et D. H. Williams, «Interpretatsia mass-spectrov organicheskikh soedinenii», Izd. «Mir», Moscou, 1966, p. 286–311.

[2] V. E. Sahini, V. Constantin et C. Podină, *Rev. Roumaine Chim.*, **12**, 1405 (1967).

Les déterminations ont été effectuées à l'aide d'un spectromètre de masse du type MI-1305. Pour tous les composés étudiés on a employé les paramètres suivants : courant d'ionisation 1,5 mA, tension d'ionisation 52 V, tension d'accélération 4 kV. On a effectué les calculs des diagrammes moléculaires en approximation Hückel, sur un modèle inductif, avec les paramètres suivants : $\alpha_N = \alpha_C + h\beta$; $\beta_{CN} = \beta_{CC}$ et $\alpha_C^{CH_3} = \alpha - 0{,}5\beta$, où $\alpha_C^{CH_3}$ représente l'intégrale coulombienne du carbone adjacent du méthyle, et h a été varié entre 0,2 et 2. Pour le calcul des diagrammes moléculaires on a utilisé un calculateur électronique du type CET-501.

Les résultats expérimentaux sont présentés dans le tableau 1. Chaque pic du spectre de masse représente le pourcentage de l'ion respectif par rapport à la somme des intensités de tous les ions obtenus dans le spectre du composé. Dans le tableau on a donné seulement les pics dont l'intensité dépasse 1% de l'abondance ionique totale.

On a mis en évidence les transitions métastables qui aboutissent aux masses apparentes : 48,2 ; 46,8 ; 45,9 ; 33,3 ; 24,3 et 23,4, ainsi que les ions doublement chargés correspondant à m/e = 46,5 ; 45,5 ; 44,5 ; 33,5 ; 32,5 et 31,5.

DISCUSSION DES RÉSULTATS

L'analyse des spectres de masse des composés étudiés montre la grande stabilité des molécules de ceux-ci au bombardement électronique. Les ions moléculaires paraissent avec des intensités assez considérables, 30% environ de l'abondance ionique totale constituant, dans tous le cas, les pics de base des spectres.

Généralement si les molécules contiennent des atomes qui possèdent des électrons non liants, les ions moléculaires se forment par l'éloignement de l'un de ces électrons. Il existe aussi des cas où l'ionisation peut avoir lieu par l'élimination d'un électron du système conjugué.[3, 4] La détermination des potentiels d'ionisation et le calcul de l'énergie des liaisons π pour la pyridine et ses dérivés alcoylés, montrent que l'ionisation a lieu par l'éloignement d'un électron non-liant et par la localisation de la charge positive de l'ion moléculaire sur l'atome d'azote.[5-7]

Les intensités dont les ions moléculaires paraissent dans les spectres des trois isomères de la picoline (tableau 1) sont en concordance avec les valeurs des potentiels d'ionisation de ceux-ci [6] déterminées par impact électronique : 9,66 ; 9,71 et 9,56 pour 2 ; 3 et respectivement 4-picoline.

---

[3] A. Streitwieser jr., «Sovremennye problemy fizicheskoi organicheskoi Khimii», Izd. «Mir», Moscou, 1967, p. 28.

[4] P. B. Terentiev, P. A. Hmelnitski, A. A. Poliakova, A. N. Kost et L. V. Mochentseva, *Zhur. org. Khim.*, **4**, 938 (1968).

[5] H. Baba, I. Omura et K. Higashi, *Bull. Chem. Soc. Japan*, **29**, 521 (1956).

[6] K. Higashi, I. Omura et H. Baba, *J. Chem. Phys.*, **24**, 623 (1956).

[7] I. Omura, H. Baba et K. Higashi, *Bull. Chem. Soc. Japan*, **30**, 633 (1957).

Tableau 1

Spectres de masse des isomères de la picoline, 2,4-diméthylpyridine et 2,4,6-triméthylpyridine

m/e	2-picoline	3-picoline	4-picoline	2,4-diméthylpyridine	2,4,6-triméthylpyridine
121					28,1
120					8,1
107				29,5	2,8
106				9,5	5,6
93	29,2	28,1	30,2		1,3
92	6,0	8,5	6,8	4,6	
80				2,0	1,4
79				7,0	8,3
78	5,1	1,1	1,2	1,2	
77				2,4	4,1
67	2,8	3,4	2,7		
66	11,7	11,0	10,7	1,6	
65	4,8	7,8	6,4	3,6	1,4
64	1,3	1,5	1,3		
63	2,0	2,8	2,2	1,3	
53	1,4	0,8	1,9	1,2	2,2
52	2,6	1,0	1,7	1,7	1,9
51	4,8	2,1	3,1	2,4	
50	2,6	1,2	1,7	1,2	
42				1,1	1,9
41	1,3	1,1	1,3	1,4	1,3
40	2,5	4,4	3,7	1,4	
39	7,0	11,0	8,6	6,5	4,9
38	2,1	3,0	2,3	1,2	

Le plus important processus de dissociation de l'ion moléculaire est l'élimination de l'azote sous forme de HCN (1, fig. 1), processus confirmé par le pic métastable $m^* = 46{,}8$. L'ion *d*, m/e 66, représente approximativement 11% de l'abondance ionique totale, étant le plus intense ion fragmentaire des spectres des picolines. Le fait que la grandeur de ce pic ne dépend pas de la position du méthyle, nous montre que l'atome d'hydrogène de HCN qui s'élimine provient du noyau pyridinique. (Ce qui est confirmé par le spectre de masse de la 2,4,6-triméthylpyridine (tableau 1) à laquelle l'élimination de HCN n'a pas lieu, le processus découle d'une manière analogue, mais avec élimination d'acétonitrile.)

La perte d'un atome d'hydrogène de l'ion moléculaire *a*, m/e 93 (2, fig. 1) conduit à l'ion *f*, m/e 92, qui paraît dans les spectres de masse avec un poids notable. Il est à supposer que l'élimination de l'atome d'hydrogène a lieu du groupement méthyle. Cette réaction peut être assimilée à une rupture β de la chaîne latérale, qui est généralement caractéristique des composés aromatiques alcoyles.[1] Le fait que l'intensité de l'ion *f*, m/e 92 est sensiblement plus grande pour la 3-picoline que pour les autres isomères s'explique par la densité d'électrons relativement plus grande au carbone lié au méthyle en 3-picoline (Q_3) par rapport aux densités électroniques des carbones des positions correspondantes en 2 et 4-picoline (Q_2) et respectivement (Q_4). Le calcul des diagrammes moléculaires à paramètres divers pour l'intégrale coulombienne de l'atome d'azote mène à la même répartition relative de charge au carbone lié au méthyle : $Q_3 > Q_4 > Q_2$. Par exemple, les valeurs obtenues pour $h = 1$ sont

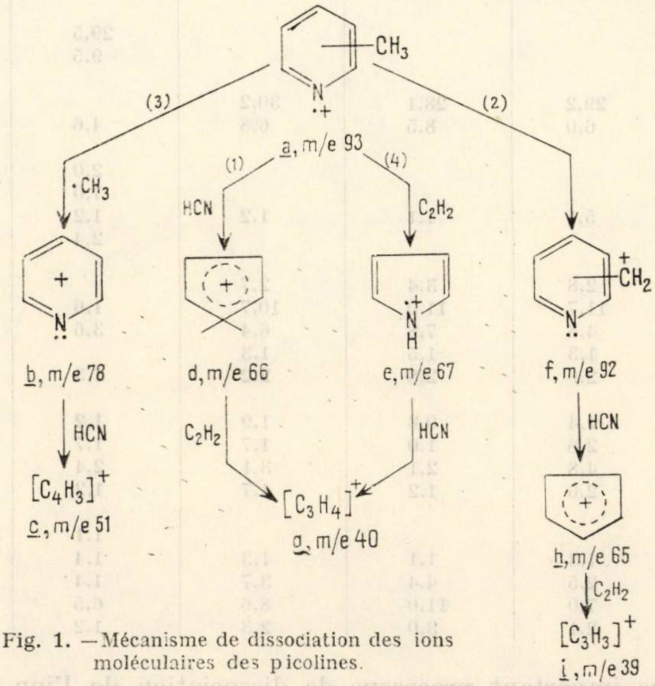

Fig. 1. — Mécanisme de dissociation des ions moléculaires des picolines.

$$Q_2 : Q_3 : Q_4 = 0{,}6666 : 0{,}8130 : 0{,}7148.$$

L'ion *f*, m/e 92 se dissocie plus loin par élimination de HCN et ensuite de C_2H_2 (2, fig. 1). Cette succession de réactions est imposée par la présence des pics métastables $m^* = 45{,}9$ et respectivement 23,4 dans les spectres des trois isomères. En même temps, on constate que les intensités des ions *h*, m/e 65 et *i*, m/e 39 respectent avec approximation la proportion des ions *f*, m/e 92 dont ils proviennent.

La dissociation de l'ion moléculaire avec la formation de l'ion ***b***, m/e 78 par une rupture α de la chaîne latérale (3, fig. 1) a un poids notable seulement au cas de la 2-picoline, ce qui est en quelque sorte similaire au phénomène d'« orthoeffet » rencontré à certains composés aromatiques substitués,[8, 9] mais dans ce cas il est plus difficile à expliquer. L'existence du pic métastable m* = 33,3 indique la continuation de la réaction 3 par l'élimination de l'azote de l'ion *b*, m/e 78 sous la forme de HCN. Du tableau 1 on voit que les intensités des ions *b*, m/e 78 et *c*, m/e 51, dans les spectres des trois isomères, respectent la même proportion.

Le quatrième processus primaire de dissociation des ions moléculaires consiste dans l'élimination d'une molécule neutre de C_2H_2 (4, fig. 1). Dans ce processus se forme, par réarrangement, l'ion de pyrrole *e*, m/e 67. Une telle réaction est en quelque sorte inaccoutumée pour un processus primaire, parce que dans les processus primaires s'éliminent d'habitude des fragments stables qui contiennent l'hétéroatome (HCN ou H_2CN, CO ou HCO, H_2O, etc.). L'abondance relativement grande de l'ion *e*, m/e 67 pourrait être expliquée en ce cas particulier par le fait que tant la molécule neutre qui s'élimine (C_2H_2), que l'ion pseudomoléculaire qu'on obtient sont des fragments stables, ce qui favorise thermodynamiquement la réaction. La dissociation de l'ion moléculaire avec la formation d'un ion de masse 67 est confirmée par le pic métastable m* = 48,2 mis en évidence dans tous les trois spectres de masse analysés. L'existence du groupement d'ions doublement chargés aux masses 33,5 ; 32,5 et 31,5 indique la présence de l'atome d'azote dans l'ion *e*, m/e 67, ce qui exclut la forme hydrocarbonée de cet ion et donc d'autres possibilités d'obtention.

L'ion *g*, m/e 40 s'obtient à la suite de certains processus secondaires tant de l'ion *d*, m/e 66 par la perte d'une molécule neutre de C_2H_2 (m* = 24,3), que par la décomposition de l'ion *e*, m/e 67 avec élimination de HCN.

---

[8] G. Spiteller, *Monatsh.*, **92**, 1147 (1961).

[9] T. Aczel et H. E. Lumpkin, *Analyt. Chem.*, **33**, 386 (1961).

aromatiques substitués[7,8] mais dans ce cas il est plus difficile à expliquer. L'existence du pic métastable $m^* = 53,8$ indique la confirmation de la réaction 3 par l'élimination de l'azote de l'ion A, m/e 78 sous la forme de HCN. Du tableau 1 on voit que les intensités des ions b, m/e 78 et c, m/e 51, dans les spectres des trois isomères, respectent la même proportion.

Le quatrième processus primaire de dissociation des ions moléculaires consiste dans l'élimination d'une molécule neutre de C_2H_2 (c, fig. 1). Dans ce processus se forme, par réarrangement, l'ion de pyrrole e, m/e 67. Une telle réaction est en quelque sorte inaccoutumée pour un processus primaire, parce que dans les processus primaires s'éliminent d'habitude des fragments stables qui contiennent l'hétéroatome, HCN ou H_2CN, CO ou HCO, H_2O, etc. L'abondance relativement grande de l'ion e, m/e 67 pourrait être expliquée en ce cas particulier par le fait que tant la molécule neutre qui s'élimine (C_2H_2), que l'ion pseudo-moléculaire qu'on obtient sont des fragments stables, ce qui favorise thermodynamiquement la réaction. La dissociation de l'ion moléculaire avec la formation d'un ion de masse 67 est confirmée par le pic métastable $m^* = 48,2$ mis en évidence dans tous les trois spectres de masse analysés. L'existence du groupement d'ions doublement chargés aux masses 33,5; 33,0 et 31,5 indique la présence de l'atome d'azote dans l'ion e, m/e 67, ce qui exclut la forme hydrocarbonée de cet ion et donc d'autres possibilités d'obtention.

L'ion g, m/e 40 s'obtient à la suite de certains processus secondaires tant de l'ion d, m/e 66 par la perte d'une molécule neutre de C_2H_2 ($m^* = 24,3$), que par la décomposition de l'ion e, m/e 67 avec élimination de HCN.

[7] G. Spiteller, Monatsh., 92, 1147 (1961).
[8] T. Aczel et H. E. Lumpkin, Analyt. Chem., 33, 386 (1961).

Revue Roumaine de Chimie, **15**, 501 – 509 (1970)

SPECTRAL STUDY OF PHENOXATELLURINE AND SOME OF ITS DERIVATIVES

A. GIOABĂ, V. E. SAHINI and ELENA VOLANSCHI

Physical Chemistry Department, University of Bucharest, Bdul. Republicii 13

Received November 12, 1969

Optical spectra of phenoxatellurine and some of its tellurium—and ring—subtituted derivatives are presented in different solvents. Effects of substitution are discussed in the frame of Hückel L.C.A.O. — MO calculations.

INTRODUCTION

Phenoxatellurine and its analogy with phenoxathiine was reported in literature in 1926,[1] coloured complexes with strong acids being mentioned. Crystallographic measurements for phenoxathiine, phenoxaselenine and phenoxatellurine were made in 1941 [2] and it was stated that all the compounds are folded around an axis uniting the heteroatoms.

As for its methyl- and halogen-substituted derivatives at tellurium or in the 2,8 ring-positions, only syntheses are reported.[1,3,4]

Optical spectra of these compounds and their correlation with the electronic structure form the object of the present paper. HMO calculations are performed and they account satisfactorily for substitution and solvent effects.

EXPERIMENTAL

The following substances were synthesized and purified :

- — phenoxatellurine, m.p. 78–79°[1]
- — phenoxatellurine-10,10-dichloride, m.p. 265°[1].
- — phenoxatellurine-10,10-dibromide, m.p. 290° (decomp.)[1]
- — phenoxatellurine-10,10-diiodide, m.p. 270° (decomp.)[1]
- — 2,8-dimethyl-phenoxatellurine, m.p. 48–49°[3]
- — 2,8-dimethyl-phenoxatellurine-10,10-dichloride, m.p. 285–286°[3]
- — 2,8-dichloro-phenoxatellurine, m.p. 111–112°[4]

---

[1] H. D. K. Drew, *J. Chem. Soc.*, **1926**, 223, 3054.

[2] R. G. Wood, C. H. McCale and G. Williams, *Phil. Mag.*, **31**, 71 (1941).

[3] A. Gioabă and G. Vasiliu, *Anal. Univ. Buc. – Seria Chimie* **15**, 89 (1966).

[4] G. Vasiliu and A. Gioabă, *Rev. Chim. București*, **19**, 253 (1968).

— 2,8-dichloro-phenoxatellurine-10,10-dichloride, m.p. 308—309°[4].

— 2,8-dichloro-phenoxatellurine-10,10-dibromide, m.p. 327—329° (decomp.)[4]

— 2,8-dichloro-phenoxatellurine-10,10-diiodide, m.p. 267—271° (decomp.)[4]

— 2,8-dimethyl-phenoxatellurine-10,10-dibromide :

1.486 g Br_2 solved in 10 cc. carbon tetrachloride were added at 0°, in dark, in small portions, to a solution of 3 g 2,8-dimethyl-phenoxatellurine in 50 cc. anhydrous carbon tetrachloride. About 10 minutes later, a yellow amorphous precipitate of 2,8-dimethyl-phenoxatellurine-10,10-dibromide is separated from the reaction mixture. The precipitate was filtered in dark, washed with anhydrous carbon tetrachloride and dried; its melting point is 292—294° with decomposition. After three recrystallizations from acetone, its m.p. is 295—296° (decomp.). Yield : 72.77%. The elementary analysis for $C_{14}H_{12}Br_2O$ Te gives :

Te % calculated : 26.38, found : 26.12

—2,8-dimethyl-phenoxatellurine-10,10-diiodide :

A solution of 2 g. 2,8-dimethyl-phenoxatellurine in 20 cc. chloroform was added at room temperature in small portions, stirring continuously, to a solution of 1.57 g. iodine solved in 80 cc. anhydrous chloroform. A red-yellow precipitate is immediately observed; it was filtered 3—4 hours later, washed with anhydrous chloroform and dried. After three recrystallizations from anhydrous acetone, the product has a melting point of 290—292° (decomp.). The yield was 92.69%. The elementary analysis for $C_{14}H_{12}I_2O$ Te gives :

Te % calculated : 22.08, found : 22.31.

Optical spectra in the range 225—500 mμ were obtained with Unicam SP—500 and Beckmann DK-2 spectrophotometers. The solvents were chosen of different dielectric constants : heptane, cyclohexane, methylene chloride and methyl-alcohol. The p.a. reagents were distilled and anhydrized. The concentrations of the solutions were in the range $1 \times 10^{-4} - 2 \times 10^{-3}$ M. The vapour spectrum of phenoxatellurine was taken at a PGS-2 spectrograph, with a dispersion of 7.4 Å/mm., in a quartz absorption tube of 40 cm. in length, provided with electrical heating and outgassed. The temperature of the sample was varied from 40 to about 100°.

MO calculations were performed at CET—501 and IBM-360 electronic computers

MO CALCULATIONS

The transition energies, charge diagrams and transition moments of phenoxatellurine, simple and substituted, were carried out in the frame of the Hückel method. The lack of information in literature about the parameters of the tellurium atom led us to calibrate one set of parameters to give the best agreement with the experimental spectrum of phenoxatellurine. The same set was used throughout the calculations performed on ring-substituted derivatives.

It was considered that :

$$\alpha_O = \alpha_C + h_O \beta_{CC} \qquad \beta_{CO} = k_{CO}\beta_{CC}$$

$$\alpha_{Te} = \alpha_C + h_{Te}\beta_{CC} \qquad \beta_{CTe} = k_{CTe}\beta_{CC}$$

where α and β have the usual significance in the Hückel theory.

The parameters of the oxygen atom were considered constant for all these compounds : $h_O = 2.00$ and $k_{CO} = 0.71$; the same values were used with satisfactory results in the discussion of the optical and ESR spectra of phenoxathiine. [5]

The parameters of the tellurium atom h_{Te} and k_{CTe} were varied within the limits 0.80–1.25 and, respectively, 0.3–0.9 and chosen to account the best for the spectral transitions of phenoxatellurine, with the same assignment of the bands as in the case of phenoxathiine. The values of the tellurium atom parameters listed in table 1 are reasonable, in comparison with those used by other authors for sulphur in phenoxathiine [5] and for selenium in benzoselenazoles.[6]

The ring-substituents were described in two different ways :

a) using an inductive model, with h_X varying between 0.8 and 1.5 for chlorine and between −0.8 and −0.1 for the methyl group.[7] The resonance integral between the substituted carbon atom and its ring neighbours was considered constant.

b) using a "heteroatom model", with h_X between 2.0 and 3.3 and k_{CX} between 0.5 and 0.8.

The effect of the polar solvents on the optical spectrum of phenoxatellurine was taken into account using a higher coulombian parameter for the tellurium atom, according to.[8]

The parameters used in the calculations are listed in table 1.

Table 1

Parameters used in the calculations

Substance	h_{Te}		k_{CTe}	h_o	k_{CO}	$h_5 = h_{11}$	$h_{15} = h_{16}$	$k_{5-15} = k_{11-16}$
Phenoxatellurine (PhXTe)	Heptane	1.00	0.57	2.00	0.71	—	—	—
	CH_3OH	1.15	0.57	2.00	0.71	—	—	—
2,8-dichloro PhXTe	I.M.¹)	1.00	0.57	2.00	0.71	1.00	—	—
	H.M.²)	1.00	0.57	2.00	0.71	—	1.8	0.5
2,8-dimethyl-PhXTe	I.M.	1.00	0.57	2.00	0.71	−0.8	—	—
	H.M.	1.00	0.57	2.00	0.71	—	2.00	0.5
10, 10-dichloroPhXTe		1.05	0.65	2.00	0.71	—	—	—

1) Inductive Model
2) Heteroatom Model

---

[5] B. Lamotte and G. Berthier, *J. Chim. phys.*, **63**, 369 (1966).

[6] N. M. Atherton, J. N. Okwell, *J. Chem. Soc.*, A, **1967**, 771.

[7] A. Streitwieser, "Molecular Orbital Calculations", John Wiley & Sons, New York, London, 1963.

[8] M. Broze, Z. Luz and B. L. Silver, *J. Chem. Phys.*, **46**, 4891 (1967).

Table 2

Spectral data

	Phenoxatellurine λmμ (PhxTe)		10,10-dichloro-PhxTe λmμ		10,10-dibromo-PhxTe λmμ		10,10-diiodo-PhxTe λmμ	
	CH_3OH	heptane	CH_3OH	DCM	CH_3OH	DCM	CH_3OH	DCM
Unsubstituted	232 infl	233 infl	—	—	—	—	—	—
	249–53 sh	257.5 m	—	—	—	—	—	250 sh
			279 m	—	280 m	—		
	294 sh	295 sh	299 m	300 sh	298 m	300 infl	298 m	292 m
	344 infl	359 m	—	—	—	—	338 m 370 sh	340 sh 370 sh
2,8-dichloro PhxTe		244 sh	—	—	—	—	—	—
	258 sh	262 m	—	—	—	—	254 sh	—
	297 m. small	302 m	295 infl	311 m	295 sh	303 infl	—	293 m
	—	357 m	307 m	—	308 m	—	352 m	380 sh
2,8-dimethyl-PhxTe	240 infl	240	—	—	—	—	—	236 small
	257 infl	260 m	—	—	—	—	249 infl. vague	—
	294 m. small	298	290 m	315 m	289 m	300 infl	—	292 m
	344 infl	358 m	308 m	—	309 m	—	370 infl	370 sh

m – maximum
sh – shoulder
infl. – inflexion

RESULTS AND DISCUSSIONS

The spectral data of the compounds studied in heptane, methyl alchool and methylene chloride DCM are collected in table 2. It may be seen that the spectra of the 10,10-dichloro- and dibromo-derivatives are quite similar; the presence of iodine in the 10,10-diiodo-derivatives determines the appearance of two new absorption peaks in the visible range of the spectrum (the compounds are intensively coloured). Taking into account the peculiar character of the iodine atom and the analogy of the chloro- and bromo-derivatives, MO calculations were performed only on phenoxatellurine, 10,10-dichloro-, 2,8-dichloro-and 2,8-dimethylphenoxatellurine. In order to facilitate the discussion, the experimental data for these compounds are listed in table 3, together with the calculated transition energies and the assignments made for them.

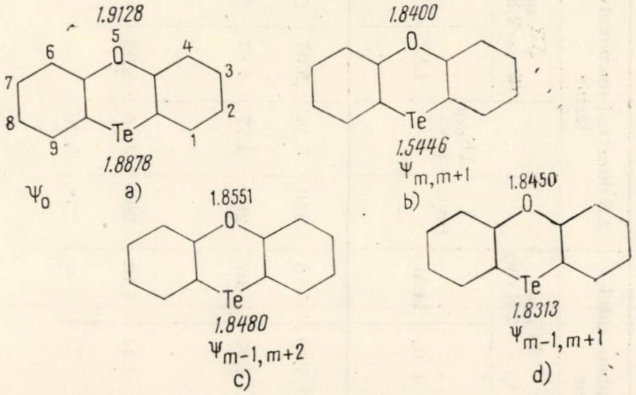

Fig. 1. — Charge diagrams of phenoxatellurine in the fundamental (*a*) and excited states (*b*, *c*, *d*).

As the band at 295 mμ appears in all the studied compounds, ring- or tellurium-substituted, it seems to be related to the conjugation in the median ring. The comparison of the charge diagrams of the fundamental ψ_0 and excited $\psi_{m,\,m+1}$ $\psi_{m-1,\,m+1}$ and $\psi_{m-1,\,m+2}$ states (Fig. 1) reveals the $\psi_0 \rightarrow \psi_{m,\,m+1}$ transition to be the most dependent on the tellurium atom, and therefore the band at 295 mμ was assigned to this transition. The participation of the oxygen atom in the aromatic conjugation seems to be reduced, as it appears from the small shift of the considered band (0.2 eV) for a relatively large variance of the h_0 parameter (from 2.2 to 1.42). The same dependence of the band at 295 mμ on the heteroatom in the median ring was observed in the case of phenoxathiine,[9] when the ionisation or the sulphur-substitution determined a bathocromic shift and the splitting into two peaks. As the chloro-substitution at

---

[9] M. Hillebrand, O. Maior, V. Em. Sahini and E. Volanschi, *J. Chem. Soc.*, (in press).

Table 3

Experimental data and calculated transitions energies

Phenoxatellurine						2,8-dichloro-phenoxatellurine				2,8-dimethyl-phenoxatellurine				10,10-dichloro-phenoxatellurine			Transition
Heptane			Methyl alcohol					$\Delta E_{calc.}$ ($\beta = -2.8$ eV)				$\Delta E_{calc.}$ ($\beta = -2.8$ eV)					
$\lambda_{m\mu}$	ΔF_{ex} (eV)	$\Delta E_{calc.}$ ($\beta = -2.8$ eV)	$\lambda_{m\mu}$	ΔE_{ex} (eV)	$\Delta E_{calc.}$ ($\beta = -2.8$ eV)	λ (mμ)	ΔF_{exp} (eV)	I.M.	H.M.	λ (mμ)	ΔE_{exp} (eV)	I.M.	H.M.	λ (mμ)	ΔF_{exp} (eV)	$\Delta E_{calc.}$ ($\beta = -2.8$)	
233	5.32	5.36	232	5.34	5.38	244	5.08	5.10	5.16	240	5.17	5.07	5.17	—	—	—	$\psi_0 - \psi_{m-1,m+2}$
257.5	4.81	5.19	249	4.94	5.21	262	4.73	4.77	5.07	260	4.77	4.87	5.09	—	—	—	$\psi_0 - \psi_{m-1,m+1}$
														279	4.44	4.49	$\psi_0 - \psi_{m,m+3}$
295	4.20	4.15	294	4.22	4.27	302	4.10	3.44	4.10	298	4.16	3.93	4.10	299	4.15	4.04	$\psi_0 - \psi_{m,m+1}$
359.5	3.44	—	344	3.60	—	357	3.47	—	—	358	3.46	—	—	—	—	—	n$-\pi^*$

*) ψ_m – highly occupied MO

I.M. – Inductive model

H.M. – Heteroatom model

the tellurium atom is accompanied by its partial positivation, the same splitting of the band at 295 mμ into two maxima at 279 and 299 mμ is visible in the spectrum of 10,10-dichlorophenoxatellurine in methyl alcohol (fig. 2).

The new peak at 279 mμ could be assigned by analogy with the phenoxathiine-radical ion to the $\psi_0 \rightarrow \psi_{m, m+3}$; a good enough agreement with the experimental spectrum was obtained by modifying the participation of the tellurium atom in the aromatic conjugation, according to the parameters listed in table 1. A comparison of the transition moments (Q^2) reveals that the $\psi_0 \rightarrow \psi_{m, m+3}$ transition (0.0377), which does not appear in the experimental spectrum of phenoxatellurine, is the second as intensity in the spectrum of phenoxatellurine-10,10-dichloride (0.0987). The most intensive (0.8635) is $\psi_0 \rightarrow \psi_{m, m+1}$, a fact which is also in agreement with the experimental spectrum.

We remark that this splitting effect was not observed in a less polar solvent as methylene chloride (heptane could not be used because of the lack of solubility of the derivatives), a fact which justifies the hypothesis [8] that polar solvents act in a similar way with the electronegative substituents.

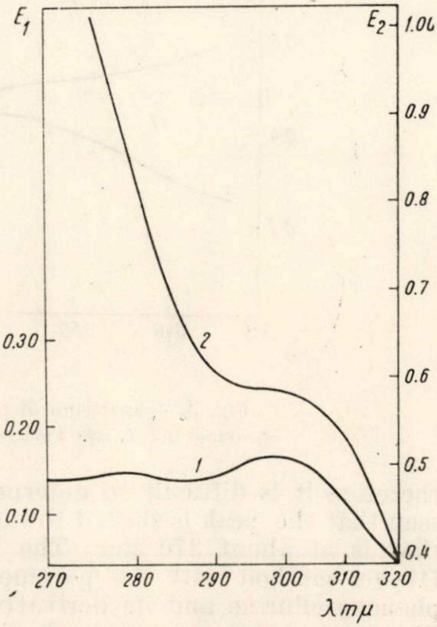

Fig. 2. — Spectrum of 10,10-dichlorophenoxatellurine.
1, in methyl alcohol; *2*, in methylene chloride.

The band at 257.5 mμ and the inflexion at 232 mμ were assigned respectively to the transitions $\psi_0 \rightarrow \psi_{m-1, m+1}$ and $\psi_0 \rightarrow \psi_{m-1, m+2}$; they both exist in the spectrum of phenoxathiine but become distinct only in the ion or fluoro-substituted derivatives.[9] Our assignment seems reasonable, taking into account the smaller electronegativity of tellurium comparatively to sulphur.

The band at 359 mμ in the spectrum of phenoxatellurine in heptane was associated to a $n \rightarrow \pi^*$ transition, determined by the unshared electrons of the tellurium atom. It is indeed shifted towards small wavelengths in polar solvents; in methyl alcohol it appears like a vague inflexion at 344 mμ. If HCl is bubbled through the solution of phenoxatellurine in an inert solvent in which the band is clearly visible, the peak at 359 mμ disappears (fig. 3). It is noted that in these conditions no chloroderivative at the tellurium atom is to be obtained, since it would precipitate.

The fact that ring-substituents determine only small shifts of that band while substitution with chlorine or bromine at the tellurium atom brings about its disappearance is another argument that it involves the unshared electrons. In the vapour spectrum this band is very flat and therefore it is difficult to determine its maximum. However, it may be seen that the peak is shifted towards longer wavelengths than in solvents, that is at about 370 mμ. The MO calculations, in the frame of the Hückel method with the parameters used for the $\pi \rightarrow \pi^*$ transitions in phenoxatellurine and its derivatives, do not account for this transition. The same statement was made in the study of the azines-$n \rightarrow \pi^*$ transitions.[10]

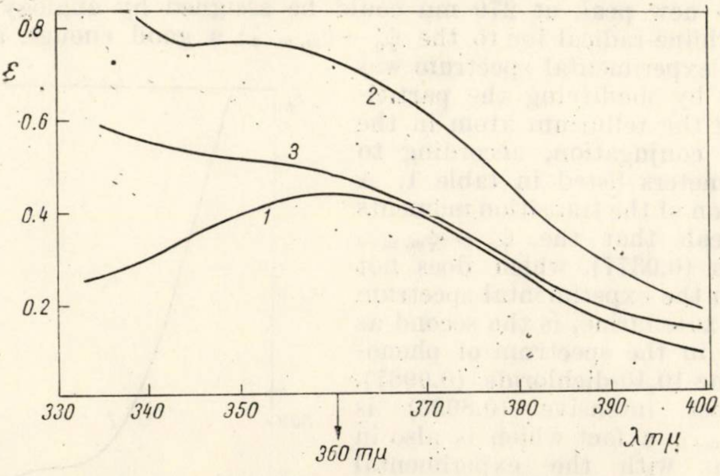

Fig. 3. — Spectrum of phenoxatellurine in cyclohexane.
1, without HCl; 2, after 3 min bubbling HCl; 3 after 6 min bubbling HCl.

As far as the influence of the substituents on the spectrum is concerned, it was stated that ring-substitution (Cl, CH_3) shifts all the transitions, but does not change the general aspect of the spectrum.

The spectral data for 2,8-dichloro- and 2,8-dimethyl-phenoxatellurine are presented in table 3, with the transitions calculated in the frame of the inductive and conjugative models; it may be seen that a better agreement with the experimental transitions as a whole is obtained for both compounds using the "heteroatom" model with the parameters listed in table 1. This statement agrees with the remark already made in the study of other substituted heterocycles,[11] that conjugative substituents bring generally about bathocromic shifts of the $\pi \rightarrow \pi^*$ and hypsochromic shifts of the $n - \pi^*$ transitions. One sees from table 2 that the transitions $\psi_0 \rightarrow \psi_{m,m+1}$, $\psi_0 \rightarrow \psi_{m-1,m+1}$, $\psi_0 \rightarrow \psi_{m-1,m+2}$ for phenoxatellurine and $\psi_0 \rightarrow \psi_{m,m+3}$ for the 10,10-dichloro-or dibromo-derivatives (all $\pi \rightarrow \pi^*$) are shifted towards longer wavelengths by both ring-substituents, while the 359 mμ ($n \rightarrow \pi^*$) presents a small shift towards the blue region of the spectrum.

---

[10] L. Goodman, *J. Mol. Spectroscopy*, **6**, 109 (1961).

[11] L. Goodman and R. W. Harrell, *J. Chem. Phys.*, **30**, 1131 (1959).

Apart from the $n \rightarrow \pi^*$ transition, the polar solvents as compared to the inert ones determine only small shifts of all the transitions towards smaller wavelengths. A MO calculation starting from the hypothesis that the effective electronegativity of the tellurium atom is enhanced as a result of solvent interaction[8] leads to a set of calculated transitions shifted towards greater energies. As the experimental effects of the solvents are small, the results of the Hückel calculations must be treated with reserve; however, the shift of the set of calculated transitions in the same direction with the experimental ones seems to support the idea that solvent effect may be taken into account by modifying the coulombian parameter of the heteroatom.

In conclusion, it is noted that, in spite of the simplifying hypotheses involved by Hückel calculations, the results agree satisfactorily with the experimental ones for all the compounds studied concerning the $\pi \rightarrow \pi^*$ transition energies.

Apart from the $n \to \pi^*$ transition, the polar solvents as compared to the non-polar ones determine only small shifts of all the transitions towards shorter wavelengths. By calculation starting from the hypothesis that the effective electronegativity of the hydroxyl oxygen atom is increased as a result of solvent interaction leads to a set of calculated transitions shifted towards greater energies. As the experimental effects of the solvents are small, the results of the Hückel calculations must be regarded with reserve; however, the shift of the set of calculated transitions in the same direction with the experimental ones seems to support the idea that solvent effects may be taken into account by modifying the coulombic parameter of the heteroatom.

In conclusion, it is found that in spite of the simplifying hypotheses involved in the calculations, the results agree satisfactorily with the experimental values for all the compounds concerning the $\pi \to \pi^*$ transition energies.

Revue Roumaine de Chimie, 15, 511 – 513 (1970)

MOLECULAR ORBITAL CALCULATIONS IN THE 2,5-DIAMINO-1,4-BENZOQUINONE SERIES. III[1]

PARISER-PARR-POPLE CALCULATIONS FOR 2,5-BISPHENYLAMINO-1,4- BENZOQUINONE

A. BALINT, Z. SIMON and M. MRACEC

Chemical Research Center of the Academy, Timişoara, Bd. Mihai Viteazul, 24

Received March 4, 1969

P–P–P-calculations for 2,5-bisphenylamino-1,4-benzoquinone are performed and the first two $\pi-\pi^*$ transitions are explained on this basis.

In two previous papers[1,2] we have tried to explain the spectra of some 3,6-dichloro-2,5-bisphenylamino-1,4-benzoquinone-derivatives with electron-donor and electron-acceptor groups. The transitions calculated using a HMO method with parameters based on Klessinger's P–P–P-calculations for 2,5-diamino-1, 4-benzoquinone, were in a good agreement with the experimental data.

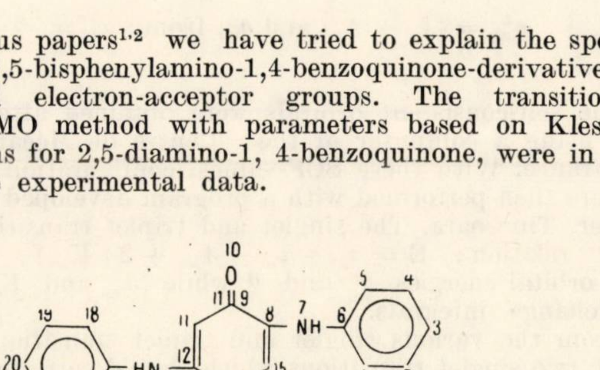

In the present paper P–P–P-calculations for 2,5-bisphenylamino-1,4-benzoquinone are performed. The geometrical data and the energetic parameters are the same as Klessingers has used for 2,5-diamino 1,4-benzoquinone and aniline,[3,4] e.g. :

$$r_{C-C}\,(\text{benzoquinone}) = 1.46\ \text{Å} \qquad \beta_{C-C} = -1.899\ \text{eV}$$

$$r_{C=C}\,(\text{benzoquinone}) = 1.36\ \text{Å} \qquad \beta_{C=C} = -2.907\ \text{eV}$$

---

[1] A. Balint and Z. Simon, *Rev. Roumaine Chim.*, **13**, 1635 (1968).

[2] A. Balint and Z. Simon, *Rev. Roumaine Chim.*, **13**, 1427 (1968).

[3] M. Klessinger, *Theor. Chim. Acta*, **5**, 236 (1966).

[4] M. Klessinger, *Theor. Chim. Acta*, **5**, 251, 259 (1966).

$r_{C-N} = 1.43$ Å $\qquad \beta_{C-N} = -2.30$ eV

$r_{C=O} = 1.22$ Å $\qquad \beta_{C=O} = -2.67$ eV

$r_{C\underline{..}C}$ (benzene) $= 1.40$ Å $\qquad \beta_{C-C} = -2.3194$ eV

For the "H" matrix ($\alpha_{\mu}^{\text{core}}$ and $\beta_{\mu\nu}^{\text{core}}$) the starting values were those above mentioned and (for $\alpha_{\mu}^{\text{core}} = I_{\mu}$, the ionization potentials) the following:

$$I_C = -11.22 \text{ eV}, \; I_N = -22.69 \text{ eV and } I_o = -17.92 \text{ eV}.$$

For the "G" matrix ($\gamma_{\mu\mu}$ and $\gamma_{\mu\nu}$) the starting values were calculated on the basis of Mataga and Nishimoto's [5] formulae:

$$\gamma_{\mu\mu} = \frac{14.3994}{a_{\mu\mu}} \qquad \gamma_{\mu\nu} = \frac{14.3994}{a_{\mu\nu} + r_{\mu\nu}}$$

where $r_{\mu\nu}$ = the distance between the atoms μ and ν in Å and a = the average covalent radii. $a_{\mu\mu}$ were calculated using the relation:

$$\underline{e}^2_{\mu\mu} = |I_\mu + A_\mu| \text{ and } a_{\mu\nu} \text{ from: } a_{\mu\nu} = \frac{a_\mu + a_\nu}{2}.$$

The self-consistent orbitals were obtained after 14 P—P—P-iterations using a computer of the "Centre de Mécanique Ondulatoire", Paris, France. With these SCF-values, configuration interaction calculations were then performed with a program developed for the MECIPT-2-computer, Timişoara. The singlet and triplet transitions were calculated by the relation: $E = \varepsilon_n - \varepsilon_m - J_{mn} + 2(K_{mn})$, where ε_m and ε_n are the orbital energies $\underline{m}$ and $\underline{n}$ while J_{mn} and K_{mn} are the Coulomb and exchange integrals.

From the various singlet and triplet transitions we have selected the first two singlet transitions which should correspond to the first and second $\pi-\pi^*$ bands.

The first two $\pi-\pi^*$ singlet transitions ($^1A_g-^1A_g$ and $^1A_g-^1B_u$) correspond to 2.646 eV and 3.109 eV respectively while the first two $\pi-\pi^*$ triplet transitions ($^1A_g-^3A_g$ and $^1A_g-^3B_u$) to 1.986 eV and 1.988 eV respectively. Thus, for the first band we should have $\lambda_{\max} = 469$ mμ and a relatively low intensity (as the $^1A_g-^1A_g$ transition is simmetry forbidden), for the second $\lambda_{\max} = 399$ mμ and a high intensity. As a matter of fact, the spectrum of 2,5-bisphenylamino-1,4-benzoquinone shows the first two maxima at about 520 mμ ($\varepsilon_{\max} = 885$) and 390 mμ ($\varepsilon_{\max} = 15400$).[6] The slight discrepancy in the case of the first $\pi-\pi^*$ transition appears also in the case of 2,5-diamino-1,4-benzoquinone and could be explained on the same basis.[4]

The SCF atomic charges and bond orders are given in table 1.

---

[5] N. MATAGA and K. NISHIMOTO, *Z. physik. Chem.*, NF **12**, 335; **13**, 140, (1957).

[6] E. A. BRAUDE, *J. Chem. Soc.*, **1945**, 490.

Table 1

Charge densities and bond orders of 2,5-bisphenylamino-1,4-benzoquinone

Atoms	Charge density	Bonds	Bond order
1,18	1.04199	1–2,18–19	0.67273
2,19	0.98810	2–3,19–20	0.66309
3,20	1.01852	3–4,20–21	0.66084
4,21	0.99187	4–5,21–22	0.67543
5,22	1.04557	5–6,22–17	0.62490
6,17	1.00856	6–7,17–16	0.33745
7,16	1.72993	7–8,16–12	0.39939
8,12	0.96798	8–9,12–13	0.23837
9,13	0.67878	9–10,13–14	0.82200
10,14	1.44761	9–11,13–15	0.33349
11,15	1.08110	11–12,8–15	0.84261

Acknowledgements. We are indebted to Professor H. Normant, member of the Academy of Science, and Mr. O. Chalvet from the "Centre de Mécanique Ondulatoire", Paris, France, by the courtesy of which we had the opportunity to obtain our SCF orbitals with an appropriate computer.

Revue Roumaine de Chimie, **15**, 515 – 526 (1970)

THE KINETICS OF COBALT CORROSION PROCESS

O. RADOVICI and M. V. POPA

Institute of Physical Chemistry of the Academy, Bucharest, str. Galaţi, 31

Received April 9, 1969

The kinetics of cobalt dissolution in phosphoric, oxalic, chromic acids and in natrium hydroxide was studied at different temperatures using the potentiostatic technique. The results show that the kinetics parameters of cobalt dissolution have been influenced by the temperature, by the potential applied to the electrode and by the nature of the ions in solution.

INTRODUCTION

Few works have been carried out on the corrosion of pure cobalt in different media, such as : 0.2N NaOH, sulphuric and chromic acid to 25°[1] acetic acid, ammonium hydroxide, phosphoric concentrated acid, citric acid, hydrofluoric acid,[2] sulphuric acid in the presence of KI and tetrabutylammonium sulfate,[3] perchloric acid.[4]

Iofa and Bei Bao-Min,[5] Rotinian and Simonova[6] have also studied the pH medium influence on the corrosion rate as well as cobalt anodic dissolution.

In spite of the intensive investigation, the mechanism of cobalt active dissolution has not been known completely so far.

Ebersbach and collab.[7] show that cobalt dissolution is related to the following reactions :

$$Co + H_2O \rightleftarrows CoOH + H^+ + e^- \qquad (1)$$

or :

$$Co + H_2O \rightleftarrows CoOH^+ + H^+ + 2e^- \qquad (2)$$

---

[1] M. H. Tikkanen, T. Tuominen and A. Laurila, Proceedings Second International Congress on Metallic Corrosion, 1963, p. 563.

[2] J. S. Pettibone, "Corrosion Resistance of Metals and Alloys", 2nd ed. Reinhold Publishing Corporation, New York, 1963, p. 626.

[3] S. Rashkov, K. L. Hampartzumian and N. A. Pangarov, *Electrochim.* Acta, **9**, 841 (1964).

[4] Z. A. Iofa, V. V. Batrakov and Cho-Ngok-Ba, *Electrochim. Acta*, **9**, 1645 (1964).

[5] Z. A. Iofa and Bei Bao-Min. *Zhur. fiz. Khim.*, **36**, 2558 (1962).

[6] A. L. Rotinian and M. V. Simonova, *Elektrokhimia*, **1**, 1407 (1965).

[7] U. Ebersbach, K. Schwabe and K. Ritter, *Electrochim. Acta*, **12**, 927 (1967).

The reaction:

$$CoOH^{+} + H^{+} \rightleftarrows Co^{2+} + H_2O \qquad (3)$$

is considered as an intermediary stage.

Unlike Rotinian, Simonova and Ebersbach, Heusler[8] supposes the forming of an intermediary stage on the electrode surface having catalytic characteristics and existing under two forms corresponding to cathodic and anodic reactions. The forming of this compound has been linked neither to the sign of the electrode surface charge, nor to the acidity of the medium.

The principal object of the work, based on the potentiostatic method, consists of the kinetic study of metallic cobalt behaviour in phosphoric, oxalic, chromic acids and in natrium hydroxide at different temperature, as well as under the influence of Cl^- ion adsorbed on the metallic surface in these media.

EXPERIMENTAL

The tests have been carried out on a pure metallic cobalt disc electrode, having 1 cm^2 surface. The rotating electrode has a rotation of ~1270 rot/min.

A glass cell provided with separated anodic and cathodic compartments was used (fig. 1).

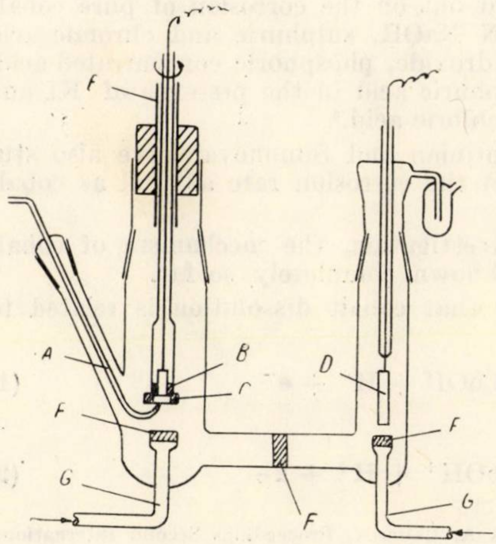

Fig. 1. — The working cell.

***A*, Haber-Luggin capillary; *B*, teflon plug; *C*, cobalt electrode; *D*, platinum electrode; *E*, stirrer guide; *F*, gas frite; *G*, gas inlet.**

The working electrode has been polished mechanically, degreased in benzene and cleaned in acetone. Before the experiments the solution was deaerated by bubbling pure argon, previously purified of water and oxygen rests by four-hour passing over silica gel, active copper

---

[8] K. E. Heusler, *Z. Elektrochem.*, **62,** 582 (1958).

and metallic copper. The temperature in the cell was kept at 25°, 50°, 75° approximately ± 0.5°.

Before the experiments a 30-minute cathodic polarisation at a current density of 1.5 mA/cm^2 has also been performed, in order to reduce the oxide film formed in the air on the electrode surface.

A Wenking electronic potentiostat was used for determining the cathodic and anodic polarisation curves. Every 10 min a 20 – 50 mV step potential was applied to the electrode by means of a precision potentiometer. The determinations were made beginning with negative current values (cathodic polarisation), then passing continuously to the anodic polarisation.

All the potential values in this study are referred to the saturated calomel electrode. Platinum was used as a counter electrode.

RESULTS AND DISCUSSION

The results obtained on studying the cobalt behaviour in phosphoric acid are reproduced in figures 2 and 3, respectively in the absence and the presence of halogen ions, at different temperatures.

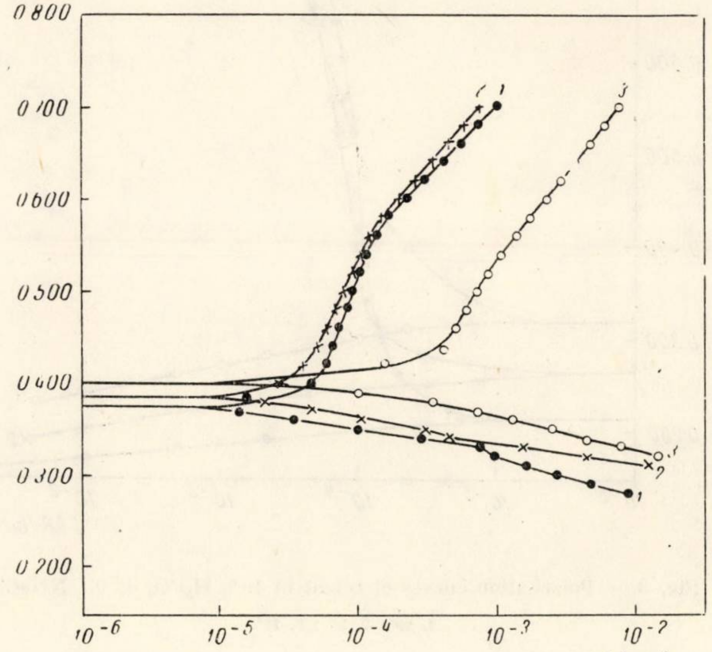

Fig. 2. — The polarisation curves of cobalt in 10%H_3PO_4.
1, 25°; *2*, 50°; *3*, 75°.

The curves show that the anodic dissolution of cobalt in this medium is fast. Hence, the fact that the corrosion process rate is controlled only by the cathodic reaction (the hydrogen evolution) is evident.

The cobalt corrosion rate in phosphoric acid increases with the temperature and decreases with the addition of halogen ions. Thus, the specific adsorption of halogen ions leads to the reduction of the corrosion rate. It is also noticed that the addition of halogen ions brings about an important variation in the electrode potential — an argument favouring the existence of some anion OH^- and possiblly PO_4^{3-} anion cobalt complexes, ligands being replaced by ligand Cl^-.

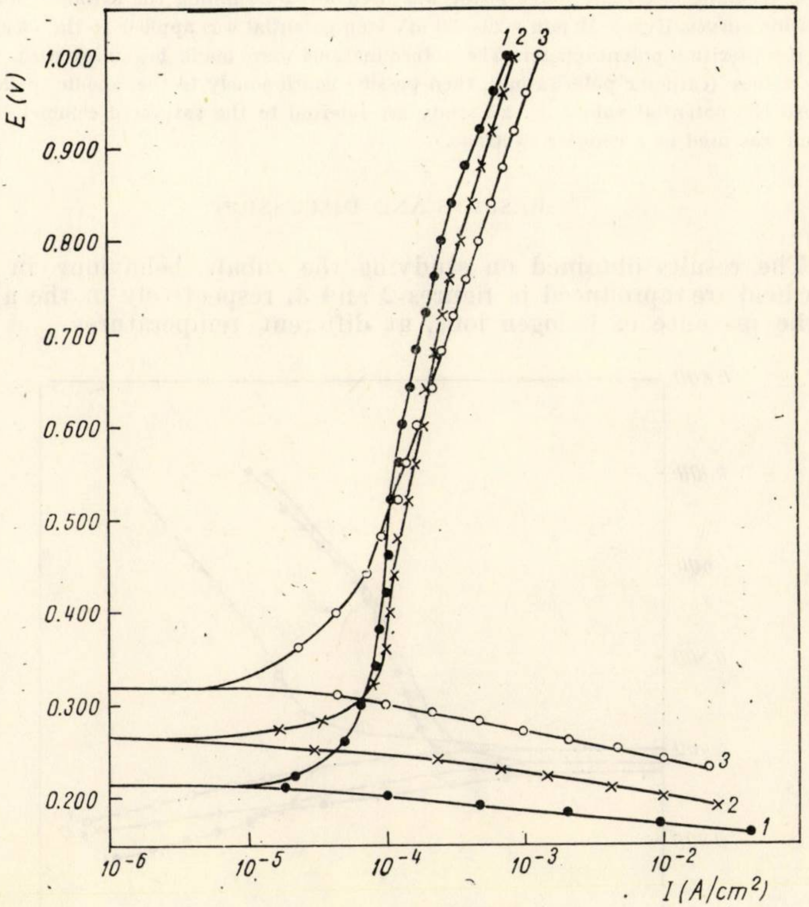

Fig. 3. — Polarisation curves of cobalt in 10% H_3PO_4 + 0.1 NNaCl.

1, 25°; *2*, 50°; *3*, 75°.

The corrosion currents, I_1, I_2 and the steady state potential, E_s, for cobalt in phosphoric acid, are reproduced in table 1.

Table 1

Steady state potential (E_S) and corrosion currents values (i) of cobalt in 10% H_3PO_4 and 10% H_3PO_4 + 0. 1N NaCl, at 25°, 50° and 75°

Solution	10% H_3PO_4			10% H_3PO_4 + 0.1N NaCl		
Temperature	25°	50°	75°	25°	50°	75°
$-E_s$ (V)	0.375	0.385	0.400	0.215	0.265	0.320
i_1(A/cm^2)	0.45×10^{-4}	0.35×10^{-4}	3.0×10^{-4}	0.35×10^{-4}	0.69×10^{-4}	0.38×10^{-4}
i_2(A/cm^2)	0.75×10^{-5}	$1.2\ \times10^{-5}$	1.9×10^{-4}	0.65×10^{-5}	$3.1\ \times10^{-5}$	0.40×10^{-4}

Chromic acid

The cathodic and anodic behaviour of cobalt in chromic acid, respectively in the absence and the presence of halogen ions, is reproduced on figures 4 and 5.

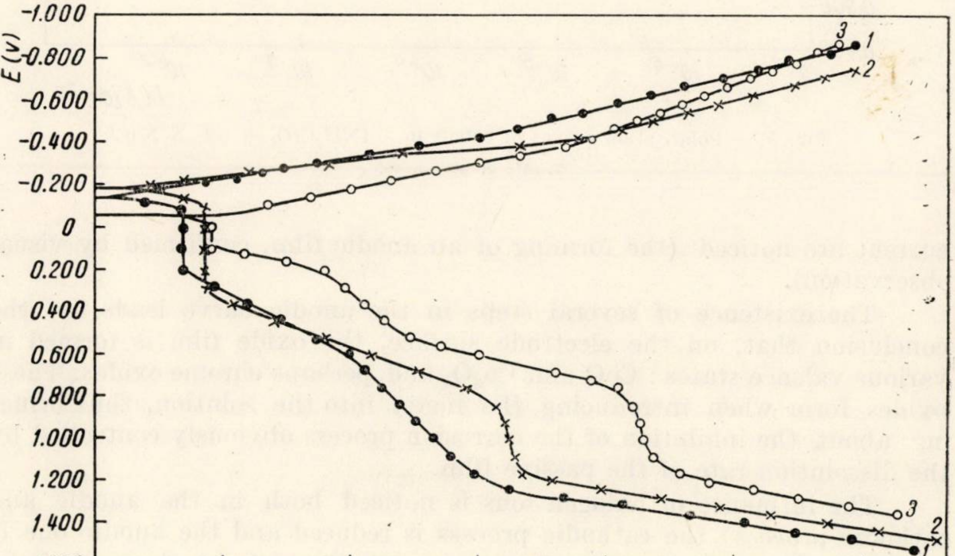

Fig. 4. — Polarisation curves of cobalt in 0.1N H_2CrO_4.

1, 25°; *2*, 50°; *3*, 75°.

The cathodic curves show a rapid evolution of the hydrogen to the electrode. Nevertheless, the anodic curves present some characteristics differing from those in phosphoric acid. Thus, the limiting values of the

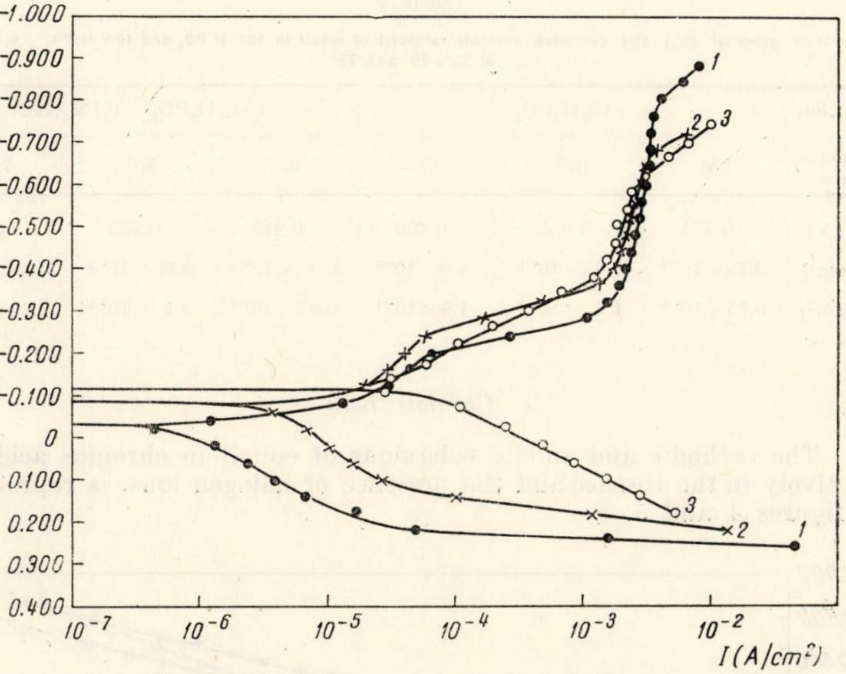

Fig. 5. — Polarisation curves of cobalt in 0.1NH$_2$CrO$_4$ + 0.1 N NaCl.
1, 25°; *2*, 50°; *3*, 75°.

current are noticed (the forming of an anodic film, confirmed by visual observation).

The existence of several steps in the anodic curve leads to the conclusion that, on the electrode surface, the oxide film is formed in various valence states : CoO and Co_3O_4 and, perhaps chrome oxides. These oxides form when introducing the metal into the solution, thus bringing about the inhibition of the corrosion process obviously controlled by the dissolution rate of the passive film.

The influence of halogen ions is noticed both in the anodic and cathodic process : the cathodic process is reduced and the anodic one is characterized by the increase in the current, therefore by decreasing the corrosion resistance of the anodic films. The phenomenon is similar to other metals, such as : Fe, Al, Ni.

It is noticed that the dissolution rate of cobalt is extremely low in chromic acid, showing a great stability of cobalt in a wide potential range.

The values of the cathodic currents i_1, i_2 the steady state potential, E_s, and passivation currents, i_{p1}, i_{p2} at different temperatures and in the absence or the presence of halogen ions, have been given in table 2.

Table 2

Steady state potential (E_S), corrosion currents (i) and passivation currents (i_p) values of cobalt in 0.1N H_2CrO_4 and 0.1 H_2CrO_4 + 0.1N NaCl, at 25°, 50° and 75°

Solution	0.1N H_2CrO_4			0.1N $H_2CrO_4 + 0.1$ N NaCl		
Temperature	25°	50°	75°	25°	50°	75°
$-E_s$(V)	0.140	0.180	0.060	0.030	0.085	0.115
i_1 (A/cm^2)	0.12×10^{-7}	0.16×10^{-7}	1.0×10^{-7}	0.24×10^{-6}	0.95×10^{-6}	22.0×10^{-6}
i_2(A/cm^2)	0.12×10^{-6}	1.8×10^{-6}	2.0×10^{-6}	—	—	—
i_{p1}(A/cm^2)	$0.5\ \times10^{-7}$	0.75×10^{-7}	0.80×10^{-7}	$0.14-0.6\times$ $\times10^{-5}$	$0.7-1.7\times$ $\times10^{-5}$	—
i_{p2}(A/cm^2)	$0.15-0.65\times$ $\times10^{-5}$	$1.7-2.0\times$ $\times10^{-5}$	$1.7-2.0\times$ $\times10^{-4}$	—	—	—

The shape of the cathodic curves show that besides the hydrogen evolution process, a reduction process of the chromic acid on the metallic surface takes place beforehand, too.

Oxalic acid

The cathodic and anodic curves in oxalic acid have been reproduced in figures 6 and 7, the cathodic curves being similar to those in phosphoric acid. Still, the anodic curve is typical of the anodic processes characterized by active-passive-transpassive regions.

The values of the corrosion currents, i, the steady state potential, the Flade potential, E_F, and the passivation currents, i_p, values at different temperatures and in the presence or the absence of halogen ions are presented in table 3.

The great value of the passivation current is an argument that, a porous, film which does not resist to corrosion is formed in oxalic acid, due to the formation of oxalic acid cobalt complexes.

When the passivation domain is much lower and the passivation currents have high values, the influence of halogen ions is particularly important for the anodic processes.

The polarisation curves show that, in this case, the corrosion rate is controlled by the anodic process, because the cathodic current value is smaller than the anodic passivation current value.

Natrium hydroxide

The polarisation curves, figures 8 and 9, are similar to those in chromic acid. The cathodic curves show a rapid hydrogen evolution. Like chromic acid, the anodic curves show some characteristics, namely the formation of two oxidation steps : CoO and Co_3O_4.

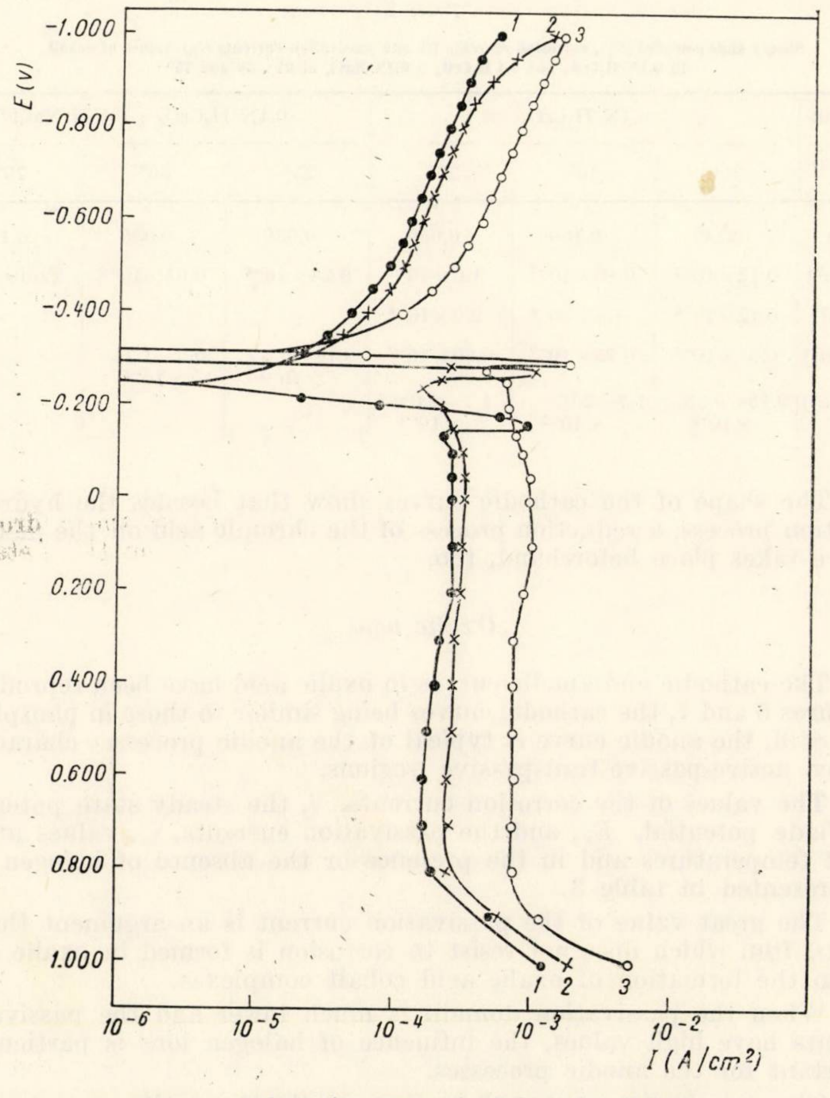

Fig. 6. — Polarisation curves of cobalt in 3% $H_2C_2O_4$.

1, 25°; *2*, 50°; *3*, 75°.

It has been noticed that the influence of halogen ions does not lead to the reduction of the passivation domain, but it increases the corrosion current values. On the other hand, the cathodic curves have not been affected to a great extent by halogen ions.

The steady state potential and corrosion currents values, i, as well as the passivation currents, I_{p1}, I_{p2} for the respective working temperatures and in the presence or absence of halogen ions have been given in table 4.

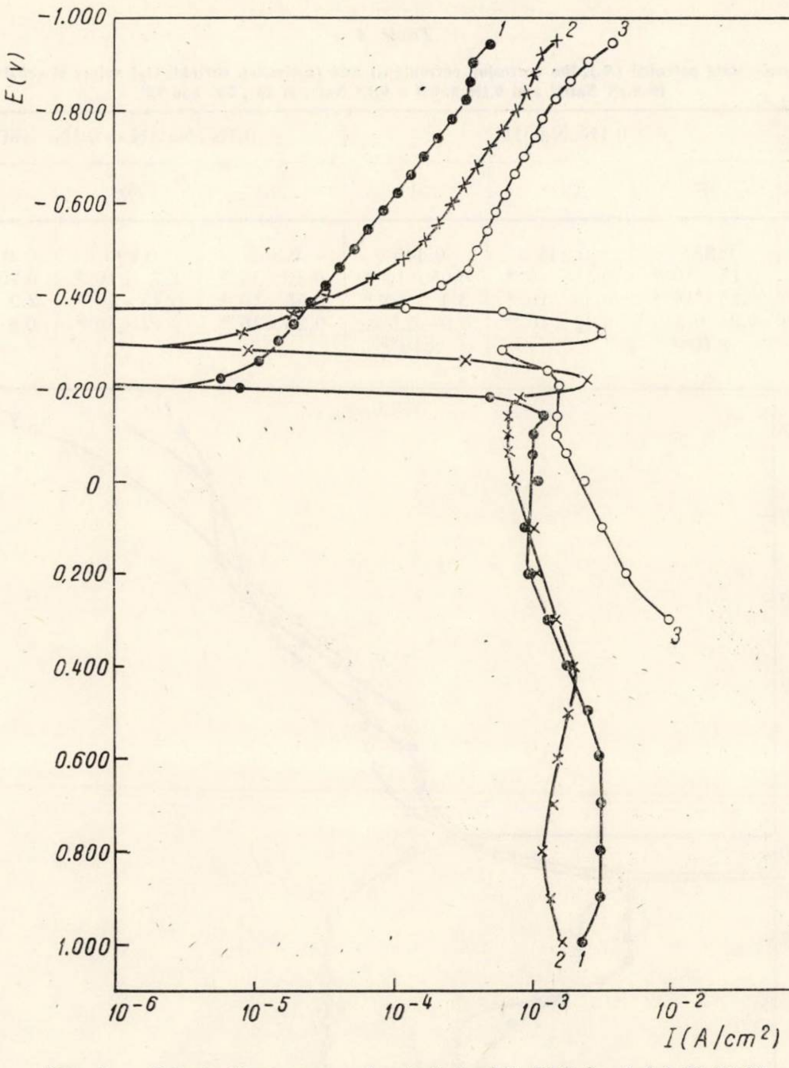

Fig. 7. — Polarisation curves of cobalt in 3% $H_2C_2O_4$ + 0.1 N NaCl.
1, 25°; *2*, 50°; *3*, 75°.

Table 3

Steady state potential (E_S), the Flade potential (E_F), the corrosion currents (i) and passivation currents (i_p) values of cobalt in 3% $H_2C_2O_4$ and 3% $H_2C_2O_4$ + 0.1N NaCl, at 25°, 50° and 75°

Solution	3% $H_2C_2O_4$			3% $H_2C_2O_4$ + 0.1N NaCl		
Temperature	25°	50°	75°	25°	50°	75°
$-E_S$(V)	0.245	0.290	0.315	0.210	0.295	0.375
$-E_F$(V)	0.100	0.200	0.260	0.100	0.140	0.200
i (A/cm²)	0.39×10^{-4}	0.55×10^{-4}	1.5×10^{-4}	0.95×10^{-4}	0.52×10^{-4}	2.6×10^{-4}
i_p (A/cm²)	$1.7-2.7 \times 10^{-4}$	$2.5-3.2 \times 10^{-4}$	$7.5-9.9 \times 10^{-4}$	$0.9-3.2 \times 10^{-3}$	$0.69-1.9 \times 10^{-3}$	1.6×10^{-3}

Table 4

Steady state potential (E_s), the corrosion currents (i) and passivation currents (i_p) values of cobalt in 0.1N NaOH and 0.1N NaOH + 0.1N NaCl, at 25°, 50° and 75°

Solution	0.1N NaOH			0.1N NaOH + 0.1N NaCl		
Temperature	25°	50°	76	25°	50°	75°
$-E_s$(V)	0.355	0.345	0.445	0.355	0.290	0.445
i(A/cm^2)	0.15×10^{-6}	0.55×10^{-6}	0.65×10^{-6}	0.40×10^{-6}	$1.7\ \times10^{-6}$	0.75×10^{-6}
i_{p1}(A/cm^2)	0.15×10^{-6}	0.35×10^{-6}	$3.4\ \times10^{-5}$	0.55×10^{-6}	0.45×10^{-6}	$2.2\ \times10^{-5}$
i_{p2}(A/cm^2)	$0.2-0.5\times$ $\times10^{-5}$	0.32×10^{-5}	$5.0-6.5\times$ $\times10^{-5}$	0.25×10^{-5}	0.12×10^{-5}	$0.8-1.6\times$ $\times10^{-4}$

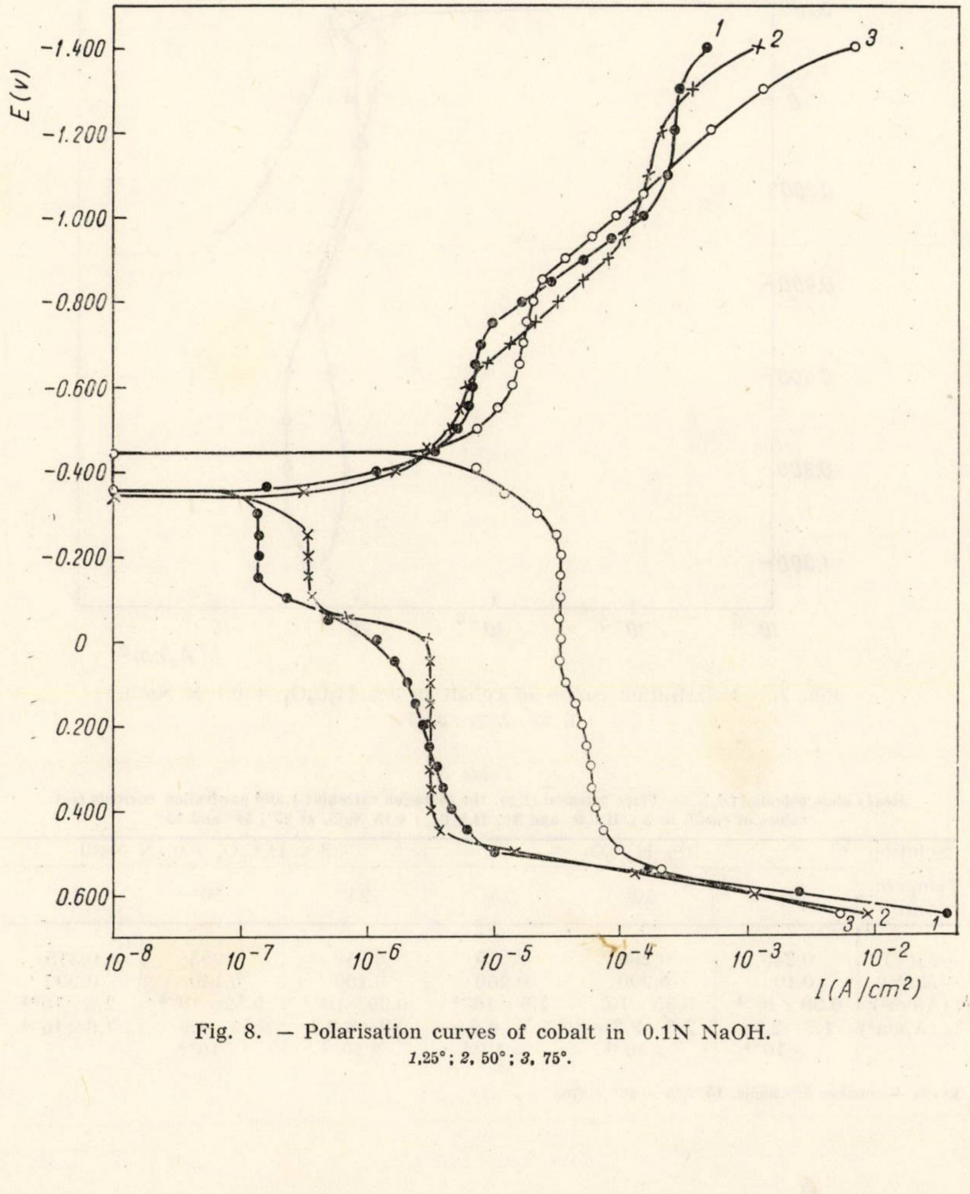

Fig. 8. — Polarisation curves of cobalt in 0.1N NaOH.
1,25°; *2*, 50°; *3*, 75°.

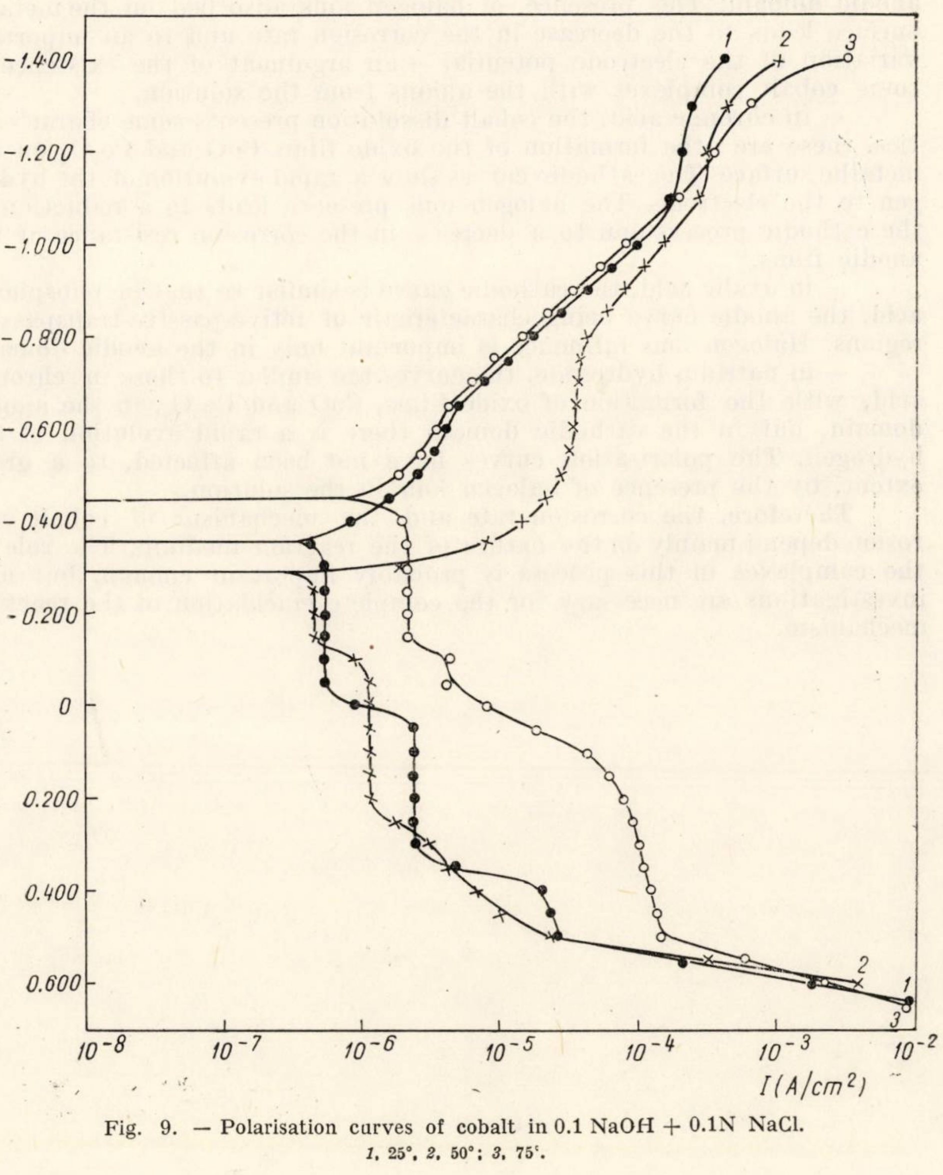

Fig. 9. — Polarisation curves of cobalt in 0.1 NaOH + 0.1N NaCl.
1, 25°, *2*, 50°; *3*, 75°.

CONCLUSIONS

The kinetic study on cobalt corrosion behaviour in different acid and alkaline media shows that:

— in phosphoric acid medium, the process is controlled only by the cathodic reaction, a rapid dissolution of cobalt taking place in the anodic domain. The presence of halogen ions adsorbed on the metallic surface leads to the decrease in the corrosion rate and to an important variation of the electrode potential — an argument of the existence of some cobalt complexes with the anions from the solution.

— in chromic acid, the cobalt dissolution presents some characteristics, these are : the formation of the oxide films CoO and Co_3O_4 on the metallic surface. The cathodic curves show a rapid evolution of the hydrogen to the electrode. The halogen ions presence leads to a reduction of the cathodic process and to a decrease in the corrosion resistance of the anodic films.

— in oxalic acid, the cathodic curve is similar to that in phosphoric acid, the anodic curve being characteristic of active-passive-transpassive regions. Halogen ions influence is important only in the anodic domain.

— in natrium hydroxide, the curves are similar to those in chromic acid, with the formation of oxide films, CoO and Co_3O_4, in the anodic domain, but in the cathodic domain there is a rapid evolution of the hydrogen. The polarisation curves have not been affected, to a great extent, by the presence of halogen ions in the solution.

Therefore, the corrosion rate and the mechanism of cobalt corrosion depend mainly on the nature of the reaction medium. The role of the complexes in this process is probably important enough, but new investigations are necessary for the complete elucidation of the reaction mechanism.

Revue Roumaine de Chimie, **15**, 527 – 537 (1970)

THE SURFACE TENSION OF BINARY MOLTEN MIXTURES OF SILVER CHLORIDE WITH SODIUM AND POTASSIUM CHLORIDE

S. STERNBERG and MARIANA TERZI

Institute of Physical Chemistry of the Academy, Bucharest, str. Galaţi, 31

Received April 7, 1969

The surface tension of pure molten KNO_3, AgCl, NaCl, KCl and molten AgCl + NaCl, AgCl + KCl mixtures was measured, and its dependence on temperature and composition was studied. The method used to determine the surface tension is based on the measurement of the force which is necessary to detach an object from the surface of the melt. The surface tension isotherms show that both systems present negative deviations from additivity as well as from the Guggenheim relationship. These deviations are explained by the existence of an enrichment of the surface layer in the component of lower surface tension. Both the enrichment factor and the surface layer molar fractions are calculated on the basis of the Eberhart equation. It is shown that the Eberhart relationship is not applied to the complex-forming systems.

The surface tension of simple salts has been the object of many studies,[1–3] but the results for the molten salts mixtures published in the literature are still insufficient. In the present paper, the results obtained from the surface tension measurements of the binary molten mixtures of silver chloride with sodium chloride and silver chloride with potassium chloride are presented.

EXPERIMENTAL

The surface tension was determined by a "detachment method"; it consists of measuring the maximum force necessary to detach a platinum cylinder from the surface of the melt. The apparatus, which allows simultaneous measurement of both the surface tension and density of the melt, is similar to that used by Janz and Lorenz.[4] The major details of

---

[1] F. M. Jaeger, *Z. anorg. Chem.*, **101**, 1 (1917).

[2] R. B. Ellis, J. E. Smith and E. B. Baker, *J. Phys. Chem.*, **62**, 766 (1958).

[3] G. J. Janz and M. R. Lorenz, *J. Electrochem. Soc.*, **108**, 1052 (1961).

[4] G. J. Janz and M. R. Lorenz, *Rev. Sci. Instr.*, **31**, 18 (1960).

the apparatus are shown in figure 1. The main part which plays the principal role in this method is a platinum cylinder welded at the bottom of a platinum body, having the geometrical shape shown in figure 1.

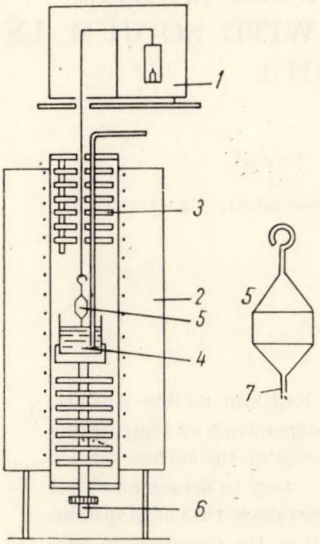

Fig. 1. — Apparatus for measuring the surface tension of molten salts.

1, Analytical balance; *2*, furnace; *3*, ceramic screens; *4*, crucible with the melt; *5*, platinum bob; *6*, lifting device for the sample; *7*, platinum cylinder.

For density measurements the bob is immersed entirely into the melt, while for surface tension measurements only the lower end of this bob is introduced into the melt.

The surface tension cylinder, of which the lower end is perfectly flat, is introduced into the melt at a depth of only 2mm. This cylinder is suspended from the arm without pan of an analytical balance placed on a marble plate above the furnace. The furnace is designed so that a uniform temperature zone exists around the position where the crucible with the melt is situated. In order to have a minimum temperature gradient a spiral winding was applied on the ceramic tube. The pitch of the spiral winding was greater in the central zone of the furnace and smaller at the ends. For this purpose too, two metallic lids seal hermetically the tube of the furnace, as well as a number of ceramic screens are positioned above and below the crucible containing the sample of the melt. During the experiment the temperature was maintained constant by help of an electronic thermoregulator with photoresistance. For surface tension measurements, the furnace was provided, at its lower end, with a device allowing a very slow and uniform motion of the crucible containing the melt.

The relation suggested by Janz [4] to evaluate the surface tension by this method, takes into account the expansion of the cylinder at high temperatures and is of the form:

$$\sigma = \left(\frac{A}{1 + \alpha \, \Delta T} \right) G \tag{1}$$

where A is a constant which depends on the cylinder radius according to the expression $A = g/2\pi r$, α is the coefficient of linear expansion of platinum and has a value of 8.868×10^{-6}, and G represents the difference between the weight of the bob when the film of liquid which adheres to the cylinder surface has a maximum stretching, and the weight of the bob after its detachment from the melt surface.

In the absence of reliable data for molten salts, distilled water and different organic liquids with exactly known surface tensions such as benzene, toluene, carbon tetrachloride, were used for the calibration of apparatus. By plotting the surface tensions of these reference substances as a function of the weight differences G measured with our cylinder at 20°, one obtains a straight line whose slope is the constant A. We obtained for A the value of 3.543×10^3.

RESULTS AND DISCUSSIONS

The surface tension of molten KNO_3 was measured in the range of temperature 373–477° to check up the method on molten salts. The results were compared with the values published in the literature and obtained by the maximum bubble pressure method by Bloom and coworkers, [5] and by the same method by Janz.[4] This comparison is illustrated in figure 2. It can be seen that our value is in a good agreement with the values of the authors quoted, the differences being of the order of ±1%. The temperature coefficient of the surface tension of KNO_3 obtained by Janz [4] has the same value as ours.

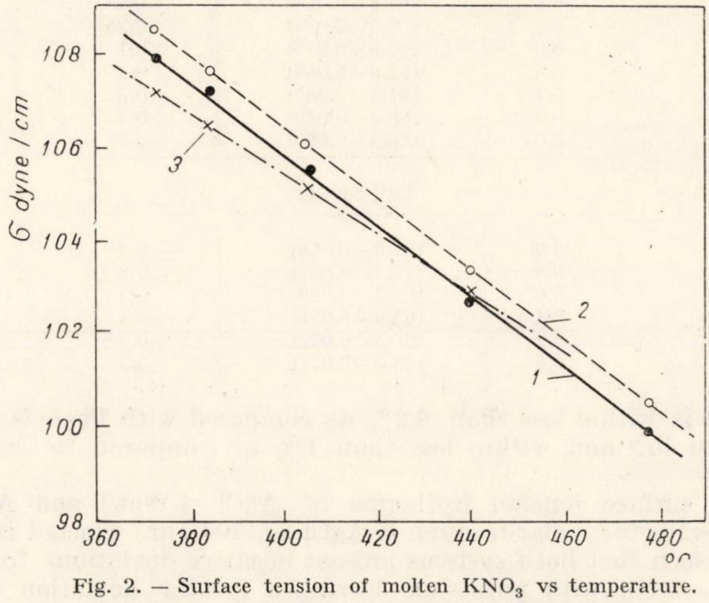

Fig. 2. — Surface tension of molten KNO_3 vs temperature.
1, our results; *2*, Janz and Lorenz [4]; *3*, Bloom, David and James. [5]

The surface tension as a function of temperature was measured both on pure molten salts AgCl, NaCl, KCl and on their mixtures. In all cases, the surface tensions both of simple salts and of mixtures can be expressed as linear functions of the temperature, of the $\sigma = a - bt$ type, t being the temperature in °C. These results are given in table 1. The precision of the method, determined by the least square method is of ± 0.3 dyne/cm.

---

[5] H. Bloom, F. G. Davies and D. W. James, *Trans. Faraday Soc.*, **56**, 1179 (1960).

By comparing the surface tensions of pure salts from table 1 with the data published in the literature a good agreement will be found. Thus the data for NaCl agrees within 1% with Jaeger's data,[1] with those cited in,[6] as well as with those obtained by Bloom. [5] In the case of KCl, the agreement is within less than 0.2% as compared with Peake's data[7] and those cited in,[6] and within less than 1% as compared to the data of Boom.[5]

Table 1

The equations of surface tension for molten simple salts and mixtures

AgCl+NaCl

AgCl molar fraction	Surface tension dyne/cm	Average error dyne/cm
1.0	209.2−0.0564t	±0.1
0.8	195.8−0.068t	±0.5
0.7	193.5−0.075t	±0.25
0.6	192.3−0.079t	±0.1
0.5	192.6−0.083t	±0.4
0.4	191.4−0.087t	±0.5
0.2	188.8−0.089t	±0.2
0.0	186.9−0.090t	±0.6
	AgCl+KCl	
0.9	187.8−0.058t	±0.4
0.8	177.3−0.060t	±0.3
0.6	168.2−0.0695t	±0.3
0.4	165.9−0.078t	±0.1
0.2	160.3−0.076t	±0.35
0.0	153.0−0.071t	±0.2

The surface tension isotherms of AgCl + NaCl and AgCl+KCl systems *versus* the molar fraction of AgCl, at 700°, are plotted in figure 3. It can be seen that both systems present negative deviations from linearity, the system with potassium having a greater deviation than that with sodium. The isotherm shape of AgCl + KCl system, as well as the magnitude of the deviation from linearity (fig. 3) are the same as those of Boardman, Palmer and Heymann[8] measured by the maximum bubble pressure method.

Assuming that the mixtures have an ideal behaviour, we can make use of the following equation given by Guggenheim,[9] to calculate the surface tension of the mixture,

$$\sigma = \frac{\sigma_A + \sigma_B}{2} - \frac{(\sigma_B - \sigma_A)^2 a}{8\,k\,T} \tag{2}$$

---

[6] I. D. Sokolova and N. K. Voskresenskaia, *Uspekhi Khim.*, **35**, 1186 (1966).

[7] J. S. Peake and M. R. Bothwell, *J. Amer. Chem. Soc.*, **76**, 2656 (1954).

[8] N. K. Boardman, A. R. Palmer and E. Heymann, *Trans. Faraday Soc.*, **51**, 277 (1955).

[9] E. A. Guggenheim, "Mixtures", Clarendon Press, Oxford, 1952, chap. 9.

where σ_A and σ_B represent the surface tensions of the pure components, and a is the average area of the surface per molecule. Relation (2) is valid only for an equimolecular ideal mixture. The average area is

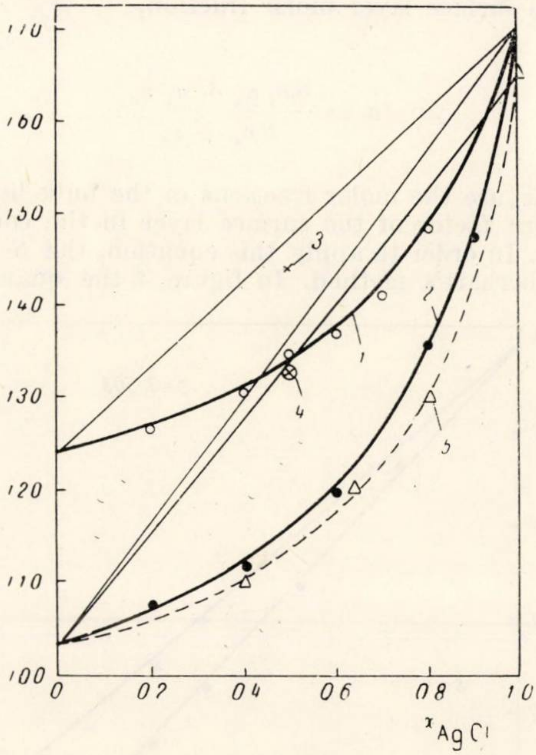

Fig. 3. — Surface tension isotherms of molten mixtures AgCl+NaCl and AgCl + KCl at 700°.

Our experimental data: *1*, AgCl + NaCl; *2*, AgCl + KCl. Values calculated after Guggenheim: *3*, AgCl + NaCl, *4*, AgCl + KCl; *5*, Boardman's data for the AgCl + KCl system; *1*, *2* Curves calculated after Eberhart's relation.

evaluated from molar volume measurements, after Boardman,[8] thus:

$$a = \frac{1}{2}\left(\frac{M_A}{Nd_A}\right)^{2/3} + \frac{1}{2}\left(\frac{M_B}{Nd_B}\right)^{2/3} \tag{3}$$

where M_A and M_B are the molecular weights of the components, d_A and d_B the densities, and N is Avogadro's number.

By computing the surface tension values after Guggenheim, for the systems studied (fig. 3), one can observe that there is a great discrepancy between the calculated and experimental values. This behaviour can be qualitatively explained by the fact that the surface layer of the liquid is enriched in the component of lower surface tension (NaCl), thereby minimizing the surface tension of the mixture.

Recently, Eberhart[10] has been suggested an equation for the surface tension of binary liquid mixtures, by assuming that it is a linear function of the surface layer molar fraction,

$$\sigma = \frac{Sx_A\,\sigma_A + x_B\,\sigma_B}{Sx_A + x_B} \tag{4}$$

where x_A and x_B are the molar fractions in the bulk liquid phase, and S is an enrichment factor of the surface layer in the component of lower surface tension. In order to apply this equation, the S factor was determined after Eberhart's method. In figure 4 the quantity ξ is plotted

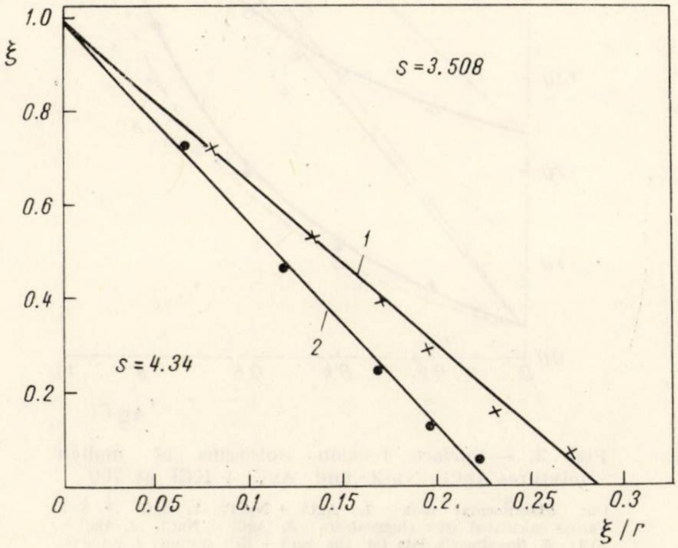

Fig. 4. — Diagram for the determination of the enrichment factor S for the AgCl+NaCl and AgCl +KCl systems.

1, AgCl + NaCl; *2*, AgCl + KCl.

versus the ratio ξ/r, ξ and r being defined by the relationships:

$$\xi = \frac{\sigma - \sigma_A}{\sigma_B - \sigma_A} \quad \text{and} \quad r = \frac{x_B}{x_A} \tag{5}$$

For both systems a straight line was obtained whose slope is S, according to equation:

$$\xi = -S(\xi/r) + 1 \tag{6}$$

---

[10] J. G. Eberhart, *J. Phys. Chem.*, **70**, 1183 (1966).

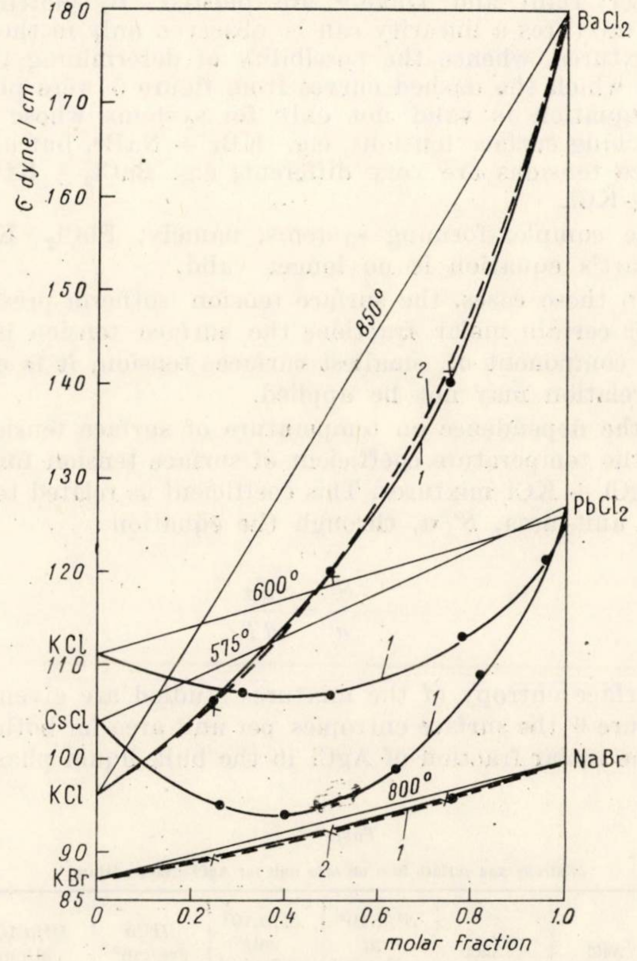

Fig. 5. — Surface tension isotherms of some binary systems of molten salts.

1, experimental curves; *2*, theoretical curves after Eberhart.

The values of S namely 3.508 for AgCl + NaCl and 4.34 for AgCl+KCl were used in relation (4) to calculate the curves plotted in figure 3. As may be seen, there is a good agreement between the theoretical curve calculated after Eberhart's relation and the experimental points.

We have tried to apply the Eberhart's equation to other binary systems of molten salts studied by other authors. In figure 5 the surface tension isotherms for four systems, namely KBr + NaBr at 800°

after Bertozzi,[11] $BaCl_2+KCl$ at 850° after Bertozzi and Soldani,[12] $PbCl_2 + KCl$ at 600° after Boardman and coworkers,[8] and $PbCl_2 + CsCl$ at 575° after Dahl and Duke,[13] are plotted. By plotting ξ *vs* ξ/r for all these mixtures a linearity can be observed only in the case of the first two mixtures, whence the possibility of determining the S factor by means of which the dashed curves from figure 5 were plotted. Thus, Eberhart's equation is valid not only for systems whose components have approaching surface tensions, e.g. KBr + NaBr, but also for those whose surface tensions are very different, e.g. $BaCl_2$ + KCl, AgCl + NaCl, AgCl+KCl.

For the complex-forming systems, namely, $PbCl_2+KCl$, $PbCl_2+CsCl$, Eberhart's equation is no longer valid.

Since in these cases, the surface tension isotherm presents a minimum and for certain molar fractions the surface tension is lower than that of the component of smallest surface tension, it is evident that Eberhart's relation may not be applied.

From the dependence on temperature of surface tension, we have determined the temperature coefficient of surface tension for the AgCl+NaCl and AgCl + KCl mixtures. This coefficient is related to the surface entropy per unit area, S^s/a, through the equation:

$$-\frac{S^s}{a}=\frac{d\sigma}{dT} \tag{7}$$

The surface entropy of the mixtures studied are given in tables 2 and 3. In figure 6 the surface entropies per unit area for both systems are plotted *vs* the molar fraction of AgCl in the bulk liquid phase. It can be

Table 2

Entropy and surface heat on area unit for AgCl+NaCl mixture

x_{AgCl}	x^σ_{AgCl}	$S^s/a.10^2$ erg/cm² grad	$S^s/a.10^9$ cal/cm² grad	H^s/a erg/cm²	$H^s/a.10^6$ cal/cm²
1.0	1.00	5.64	1.35	224.7	5.37
0.8	0.53	6.8	1.63	214.4	5.12
0.7	0.40	7.5	1.79	214	5.11
0.6	0.30	7.9	1.89	213.9	5.11
0.5	0.22	8.3	1.98	215.3	5.14
0.4	0.16	8.7	2.08	215.1	5.13
0.2	0.07	8.9	2.13	213.1	5.09
0.0	0.00	9.0	2.15	211.5 (216.2)	5.06

The value in parenthesis obtained by Bloom and collab. [5] is given for comparison

---

[11] G. Bertozzi, *J. Phys. Chem.*, **69**, 2606 (1965).

[12] G. Bertozzi and G. Soldani, *J. Phys. Chem.*, **70**, 1838 (1966).

[13] J. Dahl and F. R. Duke, *J. Phys. Chem.*, **62**, 1142 (1958).

Table 3

Entropy and surface heat on area unit for AgCl + KCl mixture

x_{AgCl}	x^{σ}_{AgCl}	$S^s/a.10^2$ erg/ cm² grad	$S^s/a.10^9$ cal/ cm² grad	H^s/a erg/cm²	$H^s/a.10^6$ cal/cm²
1.0	1.00	5.64	1.35	224.7	5.37
0.9	0.68	5.8	1.38	203.6	4.86
0.8	0.48	6.0	1.43	193.7	4.63
0.6	0.26	6.95	1.66	187.1	4.47
0.4	0.13	7.8	1.86	187.2	4.47
0.2	0.06	7.6	1.81	181.0	4.35
0.0	0.00	7.1	1.70	172.4(175.1)	4.12

The value in paranthesis is obtained by Bloom and collab. [5]

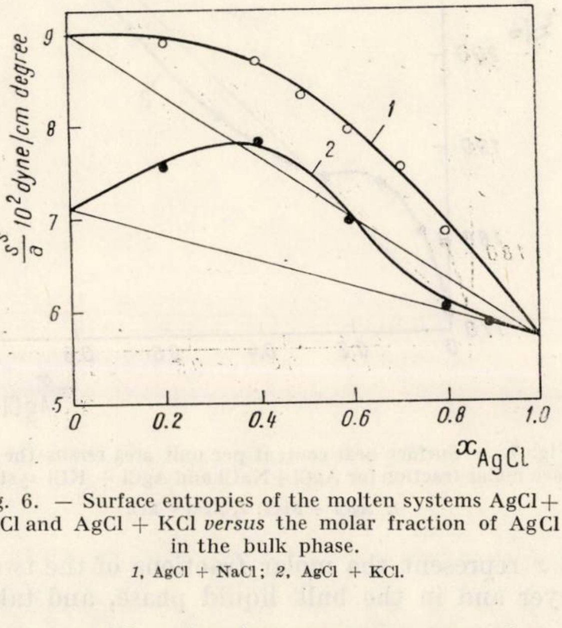

Fig. 6. — Surface entropies of the molten systems AgCl + NaCl and AgCl + KCl *versus* the molar fraction of AgCl in the bulk phase.
1, AgCl + NaCl; *2*, AgCl + KCl.

seen that the system with potassium presents somewhat greater deviations from additivity than the system with sodium.

By the help of the equation:

$$H^s/a = \sigma - (T d\sigma/dT) \tag{8}$$

the surface heat content per unit area was computed both for their mixtures (fig. 7). The results are listed in tables 2 and 3. The surface heat content per unit area is a constant for each salt and is independent of temperature.

Knowing the values of the enrichment factor S of the surface layer in the component of lower surface tension defined by Eberhart[10] as follows:

$$S = \frac{x_A^\sigma / x_B^\sigma}{x_A / x_B} \tag{9}$$

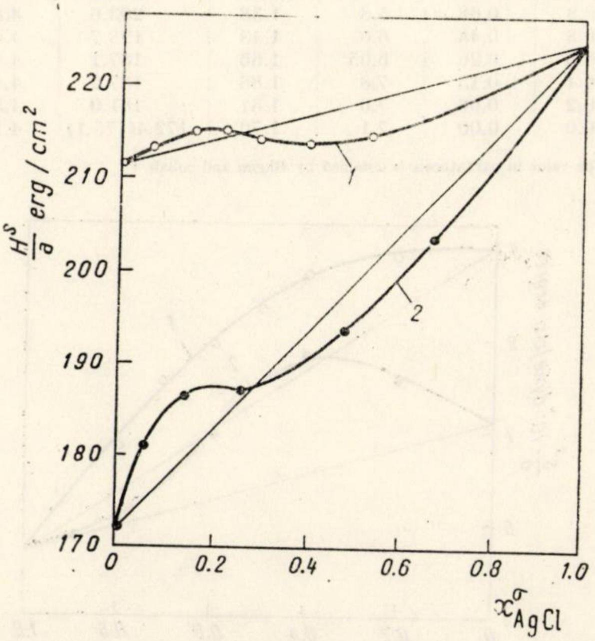

Fig. 7. — Surface heat content per unit area *versus* the surface molar fraction for AgCl+NaCl and AgCl + KCl systems.

1, AgCl + NaCl; *2*, AgCl + KCl.

where x^σ and x represent the molar fractions of the two components in the surface layer and in the bulk liquid phase, and taking into account the relation:

$$x_A^\sigma + x_B^\sigma = 1 \tag{10}$$

we have calculated the molar fractions of the components in the surface layer of the liquid; they are listed in tables 2 and 3. In figure 8 the measured values of the surface tensions of the two systems are plotted against the molar fraction of AgCl in the surface layer, at 700°. It can be seen that the experimental points are situated on a line, that is $\sigma = x_A^\sigma \sigma_A + x_B^\sigma \sigma_B$, which is an alternative way to check up Eberhart's equation.

On the basis of the above results, the following conclusions could be drawn:

The concept of "active surface substance" can be applied also in the case of molten salts. As has been shown, the salts of lower surface tension play the role of active surface substances; they lower the surface tension of the mixture considerably more than additively. At the same time, it has been shown that Eberhart's relation is no longer valid in the case of complex combinations and that it may be used eventually as a criterion to prove their existence.

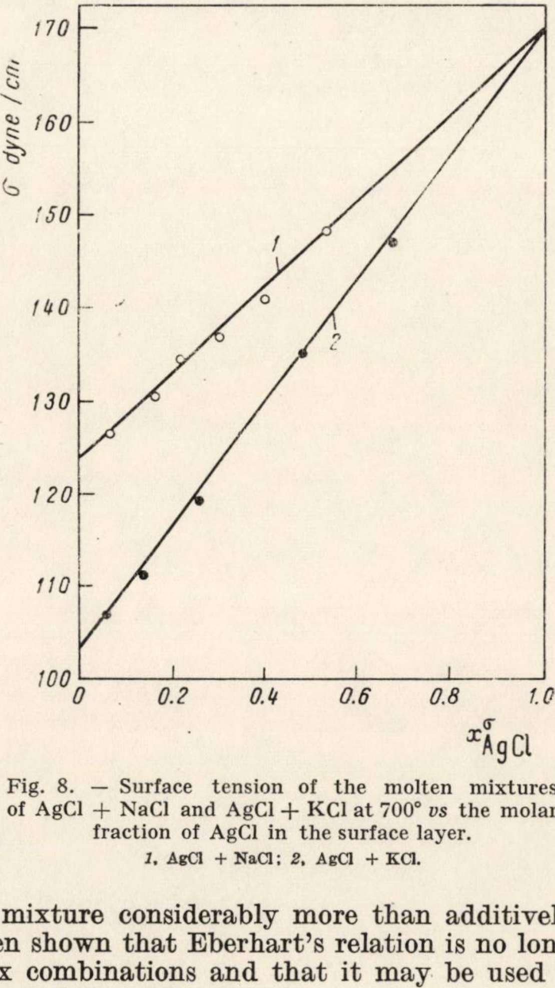

Fig. 8. — Surface tension of the molten mixtures of AgCl + NaCl and AgCl + KCl at 700° *vs* the molar fraction of AgCl in the surface layer.
1, AgCl + NaCl; *2*, AgCl + KCl.

Revue Roumaine de Chimie, **15**, 539 – 541 (1970)

PROPRIÉTÉS MAGNÉTIQUES DES COMBINAISONS COMPLEXES DES HALOGÉNURES DES MÉTAUX BIVALENTS AVEC DES COMPOSÉS PYRIDINIQUES

V. MINCU et E. SEGAL

Chaire de Chimie Physique, Université de Bucarest, 13, Bd. Republicii

Reçu le 15 juillet 1969

On présente une étude du comportement magnétique de quelques combinaisons complexes pyridiniques des chlorures de cobalt et de nickel.

En étudiant les combinaisons complexes pyridiniques des chlorures de Co(II) et de Ni(II), on a démontré que leur décomposition jusqu'au chlorure anhydre s'effectue en passant par certains composés avec un contenu intermédiaire de pyridine, conformément à la séquence [1-3]

$$MePy_4Cl_2(s) \rightarrow MePy_2Cl_2(s) \rightarrow MePyCl_2(s) \rightarrow MePy_{2/3}Cl_2(s)$$

Pour obtenir des renseignements concernant la structure de tous les termes de cette séquence, les auteurs se sont proposé d'étudier leurs propriétés magnétiques. On présente plus loin les résultats obtenus en étudiant la susceptibilité magnétique des composés susmentionnés.

PARTIE EXPÉRIMENTALE

On a utilisé :

— le complexe tétrapyridinique du chlorure de cobalt $CoPy_4Cl_2$;

— le complexe tétrapyridinique du chlorure de nickel, $NiPy_4Cl_2$, synthétisés et analysés conformément aux méthodes décrites dans la littérature.[4]

Les combinaisons complexes avec un contenu intermédiaire de pyridine ont été obtenues en décomposant ces deux substances dans le dérivatographe et en arrêtant l'échauffe-

---

[1] L. R. Ocone, J. R. Soulen et B. P. Block, *J. Inorg. Nuclear Chem.*, **15**, 76 (1960).

[2] J. R. Allan, D. H. Brown, R. M. Nuttal et D. W. A. Sharp, *J. Inorg. Nuclear Chem.*, **26**, 1895 (1964).

[3] I. G. Murgulescu, E. Segal et D. Fătu, *J. Inorg. Nuclear Chem.*, **27**, 2677 (1965).

[4] F. Reitzenstein, *Z. anorg. Chem.*, **11**, 254 (1896).

[5] P. N. Selwood, «Magnetochemistry», Interscience Publishers Inc., New York-Londres, 1956, p. 21.

ment à la température correspondant à la stabilité thermique du composé désiré. Dans ce but, on a utilisé un dérivatographe MOM Budapest, type Paulik, Paulik Erdey.

Les mesurages magnétiques ont été effectués à la température ambiante, par la méthode Faraday,[5] en utilisant un électroaimant Weiss et une balance de déflection nulle, de sensibilité 0,02 mg. Comme étalon on a utilisé du $Hg[Co(SCN)_4]$.

RÉSULTATS ET DISCUSSIONS

Dans le tableau 1 on a mentionné les combinaisons complexes (col. 1), les valeurs des susceptibilités magnétiques à 298°K (col. 2), les valeurs du moment magnétique effectif μ_{ef} (col. 3) et, pour comparaison, les valeurs du moment magnétique correspondant à l'absence d'une composante orbitale (col. 4).

Le moment magnétique effectif a été calculé à l'aide de la formule

$$\mu_{ef} = 2{,}828\sqrt{\chi_{Me(II)}T}$$

où $\chi_{Me(II)}$ représente la susceptibilité magnétique du métal de la combinaison complexe, résultée des valeurs expérimentales.

En examinant les valeurs présentées dans le tableau 1, on constate dans tous les cas l'existence d'une importante composante orbitale. Si l'on observe la variation du moment magnétique en fonction de la teneur

Tableau 1

Les propriétés magnétiques des composés étudiés

Composé	$10^6\chi_{Me(II)}$	μ_{ef} (MB)[a]	μ_{ef}^s (MB)
$CoPy_4Cl_2$	10 720	5,03	3,87
$CoPy_2Cl_2$	9 650	4,77	3,87
	(8280)[b]	(4,42)[b]	
	(11230)[b]	(5,15)[b]	
$CoPyCl_2$	12,230	5,37	3,87
$CoPy_{2/3}Cl_2$	12,230	5,37	3,87
$CoCl_2$		4,97...5,3[c]	3,87
$NiPy_4Cl_2$	4 260	3,17	2,83
$NiPy_2Cl_2$	4 930	3,41	2,83
		(3,37)[d]	
$NiPyCl_2$	5 100	3,47	2,83
$NiPy_{2/3}Cl_2$	5 310	3,54	2,83
$NiCl_2$		3,04...3,46[c]	2,83

a Pour toutes les valeurs déterminées, on a admis une erreur de ± 0,05 MB.

b La valeur de 4,42 MB. correspond à la forme bleue et celle de 5,15 MB à la forme violette, d'après Gill, Nyholm et collab.[6]

c Les valeurs sont égales à celles indiquées dans les tableaux de la référence.[7]

d Valeurs déterminées par Gill, Nyholm et collab.[6]

---

[6] N. S. Gill et R. S. Nyholm et (partiellement) G. A. Barclay, T. I. Christine et P. J. Pauling, *J. Inorg. Nuclear Chem.*, **18**, 88 (1961).

[7] Tables de Constantes et Données Numériques 7. Constantes Sélectionnées ; G. Foex, «Diamagnétisme et Paramagnétisme» ; G. J. Gorter et L. J. Smits, «Relaxation Paramagnétique», Masson et Cie Ed., Paris, 1957, p. 238, 257.

en pyridine, on remarquera que pour les sels du nickel, celui-ci augmente conformément à la série $NiPy_4Cl_2(s) \rightarrow NiPy_2Cl_2(s) \rightarrow NiPyCl_2(s) \rightarrow NiPy_{2/3}Cl_2(s)$, tandis que pour les composés du cobalt, cette série est interrompue au composé $CoPy_2Cl_2$. La valeur que nous avons déterminée pour la susceptibilité Co(II) dans la combinaison complexe (9650.10^{-6}) correspond à la moyenne des valeurs fournies par Gill, Nyholm et collab.[6] (9760.10^{-6}) pour la forme bleue (coordination tétraédrique) et pour la forme violette (coordination octaédrique). Contrairement aux opinions antérieures conformément auxquelles la forme bleue, instable, se transforme intégralement en forme violette dans un intervalle de quelques heures, nous considérons qu'à un moment donné on obtient un équilibre entre les deux formes. En mesurant à des intervalles de temps espacés la susceptibilité magnétique du même échantillon de $CoPy_2Cl_2$, obtenue au dérivatographe, on n'a remarqué aucune variation de cette grandeur.

CONCLUSIONS

On a déterminé les susceptibilités magnétiques et les moments magnétiques des $CoPy_4Cl_2$, $CoPy_2Cl_2$, $CoPyCl_2$, $CoPy_2/_3Cl_2$, $NiPy_4Cl_2$, $NiPy_2Cl_2$, $NiPyCl_2$ et $NiPy_{2/3}Cl_2$. Les valeurs obtenues indiquent l'existence d'une importante composante orbitale.

Revue Roumaine de Chimie, **15**, 543 – 551 (1970)

L'ÉLECTROLYTE PÂTEUX UTILISABLE DANS LES ACCUMULATEURS ÉLECTRIQUES

S. LICĂ

Académie Militaire, Bucarest, 81–83, Bd. Coşbuc

Reçu le 12 juillet 1969

On présente des données sur la réalisation d'un électrolyte pâteux qui peut être utilisé dans les accumulateurs de type Zn/KOH/AgO. Des expériences effectuées sur la conductibilité spécifique des solutions de KOH de différentes concentrations avec et sans addition d'alcool polyvinylique et de chlorure polyvinylique, il résulte que les solutions ayant les concentrations de 35 à 40% KOH ont la conductibilité la plus indiquée pour être utilisées dans les accumulateurs. Les déterminations voltamétriques sur les potentiels de déchargement de l'hydrogène et de l'oxygène de ces solutions ont révélé que l'addition des ingrédients cités n'influe pas sur ces phénomènes. Les expérimentations des accumulateurs avec ces électrolytes pâteux ont donné des résultats comparables aux résultats obtenus au cas des accumulateurs sans ces additions.

★

Dans un ouvrage antérieur [1] on a montré l'influence de l'addition des ions étrangers dans l'électrolyte des accumulateurs de la classe Zn(KOH)AgO.

L'ouvrage présent est une continuation de ces recherches et se réfère à l'introduction dans l'électrolyte des accumulateurs électriques de différents ingrédients qui immobilisent la solution, ce qui permet de réaliser un accumulateur demi-sec.

Cela constitue un avantage important dans l'exploitation des accumulateurs électriques du fait que l'électrolyte ne coule pas.

On a effectué peu de recherches[2,3] en ce qui concerne l'électrolyte des accumulateurs de la classe Zn(KOH)AgO, ces accumulateurs n'étant employés en pratique qu'en 1941. C'est à André [4] que l'on attribue la première tentative d'utiliser dans le système électrochimique Zn/KOH/AgO la cellophane comme séparateur.

Dirkse [5] a étudié la composition et les propriétés des solutions de KOH saturées de ZnO. Ces solutions ont été préparées d'une solution de KOH saturée de ZnO et conservée pendant quelques semaines.

De cette solution de KOH saturée de ZnO on a obtenu d'autres solutions par l'addition de l'eau. Les solutions ont été conservées en vases de verre pirex quelques mois et puis on a analysé le zinc et le potassium.

---

[1] I. Burlacu et S. Lică, *Rev. Roumaine Chim.*, **12**, 1099 (1967).

[2] T. P. Dirkse, *J. Electrochem. Soc.*, **102**, 497 (1955).

[3] T. Baker et I. Trachtenberg, *J. Electrochem. Soc.*, **114**, 1045 (1967).

[4] H. André, *Bull. Soc. chim. France*, **1**, 132 (1941).

[5] T. P. Dirkse, *J. Electrochem. Soc.*, **106**, 154 (1959).

L'ouvrage a eu comme but l'étude de la stabilisation des solutions de zincate en fonction du temps afin de trouver les conditions les plus favorables pour leur utilisation dans les accumulateurs Zn/KOH/AgO.

On est arrivé à la conclusion que les solutions de KOH saturées de ZnO qui contiennent 15% K et 1,83% Zn de densité 1,2258 g/ml ont la viscosité relative 1,865 poise et la conductibilité spécifique 0,521 ohm^{-1} cm^{-1}.

C'est la raisòn que les solutions ayant cette concentration sont utilisées dans les accumulateurs.

Baker et Trachtenberg[3] ont repris ces recherches et ont déterminé la conductibilité des solutions de KOH et KOH saturées de ZnO entre +36° jusqu'à −66°. Des courbes présentées il résulte que la conductibilité spécifique du KOH aussi bien que celle du KOH + ZnO diminuent avec la baisse de la température.

Les auteurs mentionnés[3] ont fait des recherches sur la variation de la conductibilité spécifique en fonction de la concentration. Pour les deux électrolytes, des déterminations ont été effectuées à des concentrations de 25, 30, 34 et 39%.

On constate que dans l'intervalle de température de +36° à −26°, la conductibilité spécifique du KOH a des valeurs proches indifférement des concentrations et elle se situe entre les limites : 0,631−0,620 ohm $^{-1}$ cm $^{-1}$.

Cela est aussi valable pour l'électrolyte formé de KOH saturé de ZnO, bien que, dans ce cas, la différence entre les conductibilités des solutions de diverses concentrations soit plus grande, demeurant cependant dans des limites assez rapprochées (0,252−0,399 ohm $^{-1}$ cm $^{-1}$).

Dans les deux cas, si la température baisse de −20° à −60° les différences deviennent plus grandes.

De ces déterminations il résulte que la solution de concentration 35−40%, tant celle de KOH que celle de KOH saturé de ZnO, a la plus grande conductibilité spécifique.

Les solutions de cette concentration présentent un grand intérêt puisqu'elles sont utilisées en pratique à l'accumulateur Zn/KOH/AgO. A cette concentration de l'électrolyte, la solubilité des Ag_2O et AgO est minime, phénomène observé également par d'autres chercheurs.[6,7]

Une communication récente[8] a porté sur l'influence des additions plastifiantes (mélanges d'oxydes métalliques et alcool polyvinylique ou de chlorure polyvinylique) au KOH.

Cet ouvrage présente des données sur l'utilisation des électrolytes pâteux dans les accumulateurs électriques.

Il en résulte que les électrolytes utilisés dans les accumulateurs aussi bien acides que basiques ne perdent pas leurs qualités si l'on ajoute du polychlorure ou de l'alcool polyvinylique. Ce phénomène a l'avantage de permettre la réalisation d'un accumulateur demi-sec.

---

[6] R. Amlie et P. Rüetschi, *J. Electrochem. Soc.*, **108**, 813 (1961).

[7] T. P. Dirkse, *J. Electrochem. Soc.*, **111**, 629 (1964).

[8] I. Burlacu et S. Lică, Conf. rep. de Chimie fizică generală şi aplicată (Communication), 2−5 sept. 1968.

PARTIE EXPÉRIMENTALE

Pour l'étude des électrolytes pâteux pouvant être utilisés dans les accumulateurs électriques on a effectué trois sortes de déterminations:

— déterminations de la conductibilité spécifique, exécutées sur les solutions de KOH ou KOH saturées de ZnO.

A ces solutions on a ajouté graduellement de l'alcool et différents oxydes métalliques. Les mêmes expériences ont été effectuées avec addition de PVC.

— déterminations voltamétriques des solutions de KOH avec ou sans addition d'alcool PV ou de PVC sur les potentiels de décharge de l'hydrogène et de l'oxygène ;

— déterminations sur des paramètres caractéristiques des accumulateurs, exécutées avec des électrolytes pâteux semblables et la comparaison de ces caractéristiques avec celles des accumulateurs exécutés sans additions.

La première série de déterminations qui se réfère à la conductibilité spécifique a eu comme but la vérification des résultats obtenus dans les accumulateurs expérimentés, publiés antérieurement. [1]

On a déterminé la conductibilité spécifique dans une cellule de conductibilité habituelle avec les électrodes de platine platiné à l'aide d'un pont Kohlrausch.

On a déterminé la variation de la conductibilité spécifique à 24°±0,5° pour les solutions de KOH, KOH saturées de ZnO, KCl, KBr et KI en fonction de la concentration.

Les résultats de ces déterminations sont présentés dans le tableau 1.

On a également déterminé la conductibilité spécifique du mélange de KOH et KCl, KOH et KBr et KOH et KI de différentes propoattions tel qu'il résulte du tableau 2.

Dans le tableau 3 sont présentées des données sur la variation de la conductibilité spécifique de la solution de KOH à laquelle on a ajouté du PVC en différentes proportions et puis divers oxydes métalliques.

De ces tableaux il résulte que, en général, à une température constante, la conductibilité spécifique des solutions de KOH et KOH saturées de ZnO diminue avec la baisse de la concentration, dans toutes les déterminations effectuées.

De même, pour le mélange de KOH 1N avec les halogénures de potassium, la conductivité spécifique suit la règle connue de l'additivité.

Les solutions d'halogénures à ces concentrations ont des conductivités sensiblement égales à celles du KOH.

En ce qui concerne la conductibilité de la solution de KOH 40% à laquelle on ajoute de l'alcool PV ou PVC avec différents oxydes métalliques, la conductivité présente de petites variations.

Ce phénomène présente une grande importance pour l'industrie des accumulateurs de type Zn/KOH/AgO parce qu'il offre la possibilité de réaliser des accumulateurs à électrolyte pâteux.

Vu que les déterminations de la conductibilité spécifique sur l'électrolyte utilisé dans les accumulateurs citées plus haut ont été satisfaisantes, on a passé à une deuxième série d'expériences afin de voir si ces additions influent ou non sur le déchargement de l'hydrogène et de l'oxygène de ces solutions, phénomène qui dans le fonctionnement des accumulateurs revêt une importance majeure.

Dans ce sens on a utilisé la voltamétrie à l'aide d'un polarographe enregistreur LP 60 avec une cellule qui est représentée sur la figure 1.

La cellule comporte un vase de verre d'une capacité de 10 ml et ∅ = 1,5 cm, munie d'une part et d'autre de deux ramifications avec ∅ = 0,8 cm.

Tableau 1

Variation de la conductibilité spécifique en fonction de la concentration. λ (ohm^{-1} cm^{-1})

N°	SOLUTION	CONCENTRATION								
		8N	4N	1N	2.10^{-1}N	10^{-1}N	10^{-2}N	10^{-3}N	10^{-4}N	10^{-5}N
1	Cond. KOH	0,369	0,368	0,081	0,022	0,0109	0,00124	13.10^{-5}	$12{,}2.10^{-6}$	41.10^{-7}(=24 ± 0,5)
2	Cond. KOH saturé de ZnO	0,359	0,361	0,082	0,021	0,0110	0,0016	18.10^{-5}	16.10^{-6}	56.10^{-7} ,,
3	,, KCl	—	—	0,101	—	0,0121	0,0013	13.10^{-5}	15.10^{-6}	32.10^{-7} ,,
4	,, KBr	—	—	0,076	—	0,0108	0,0013	$13{,}5.10^{-5}$	$15{,}2.10^{-6}$	42.10^{-7} ,,
5	,, KJ	—	—	0,074	—	0,0106	0,0012	$13{,}2.10^{-5}$	2.10^{-6}	35.10^{-7} ,,

Tableau 2

Conductibilité spécifique du mélange de KOH avec halogénures (λ = ohm^{-1} cm^{-1})

N°	MÉLANGE	PROPORTION ml KOH/ml hlg.				
		4 : 0	3 : 1	2 : 2	1 : 3	0 : 4
1	N KOH + N KCl	0,102	0,101	0,104	0,103	0,101
2	N KOH + N KBr	0,106	0,102	0,106	0,101	0,088
3	N KOH + N KJ	0,100	0,101	0,103	0,096	0,072

Tableau 3

Conductibilité spécifique des solutions de KOH 40% avec différentes additions

Nº	ÉLECTROLYTE	Cond. spéc. $ohm^{-1}cm^{-1}$	Nº	ÉLECTROLYTE	Cond. spéc. $ohm^{-1}cm^{-1}$
1	100 ml KOH 40%	0,368	9	100 ml KOH 40% 30 g PVC 10 g ZnO	0,338
2	100 ml KOH 40% 10 g PVC	0,368	10	100 ml KOH 40% 30 g PVC 20 g ZnO	0,334
3	100 ml KOH 40% 20 g PVC	0,367	11	100 ml KOH 40% 30 g PVC 30 g ZnO	0,329
4	100 ml KOH 40% 30 g PVC	0,347	12	100 ml KOH 40% 30 g PVC 40 g ZnO	0,320
5	100 ml KOH 40% 40 g PVC	0,337	13	100 ml KOH 40% 30 g PVC 10 g MgO	0,337
6	100 ml KOH 40% 10 g PVC 10 g Al_2O_3	0,352	14	100 ml KOH 40% 30 g PVC 20 g MgO	0,334
7	100 ml KOH 40% 10 g PVC 20 g Al_2O_3	0,332	15	100 ml KOH 40% 30 g PVC 30 g MgO	0,333
8	100 ml KOH 40% 10 g PVC 30 g Al_2O_3	0,316	16	100 ml KOH 40% 30 g PVC 40 g MgO	0,324

Dans ces ramifications, d'un côté on a soudé un fil de Pt avec ∅ = 0,3 mm, qui, au bout entrant dans la cellule, a été fondu sous forme de sphère à ∅ = 1,5 mm.

Dans l'autre ramification, le bout du fil de Pt qui entre dans la cellule a été soudé à une lame de Pt avec la surface de 1 cm². Dans les ramifications latérales on a ajouté de l'Hg qui a servi de contact avec le conducteur conduisant au polarographe. A l'exécution de la cellule les recherches antérieures [9,10] ont été d'un réel profit.

Les voltamogrammes ont été enregistrés autant aux tensions qui augmentent qu'à une tension qui diminue ; on a travaillé avec une sensibilité petite $\frac{1}{1000}$ pour avoir la possibilité de contrôler la pente des courbes enregistrées.

Dans la figure 2 sont présentés les voltamogrammes en solutions de KOH 40% avec et sans addition de PVC. On a utilisé seulement le PVC vu que dans les déterminations de conductibilité spécifique aussi bien que dans les expérimentations des accumulateurs, l'addition des oxydes métalliques à côté du PVC ne détermine pas une grande amélioration des caractéristiques électriques des accumulateurs.

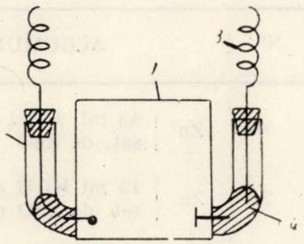

Fig. 1. — La cellule voltamétrique.

1, Corp de la cellule ; *2*, ramification latérale ; *3*, fil conducteur ; *4*. hydrargirum.

---

[9] S. LICĂ et G. TUDORACHE, *Bul. Inst. Politehn. București*, XXVIII, 25 (1966).

[10] J. GINER, *J. Electrochem. Soc.*, **111**, 376 (1964).

Dans le tableau 4 sont présentées les caractéristiques électriques plus importantes des modèles de microaccumulateurs expérimentaux de type Zn/KOH/AgO dont l'électrolyte a été modifié par l'introduction de différentes additions au cycle 4 de chargement-déchargement.

Le mode d'exécution des accumulateurs a été le même que celui de notre ouvrage antérieur. [1]

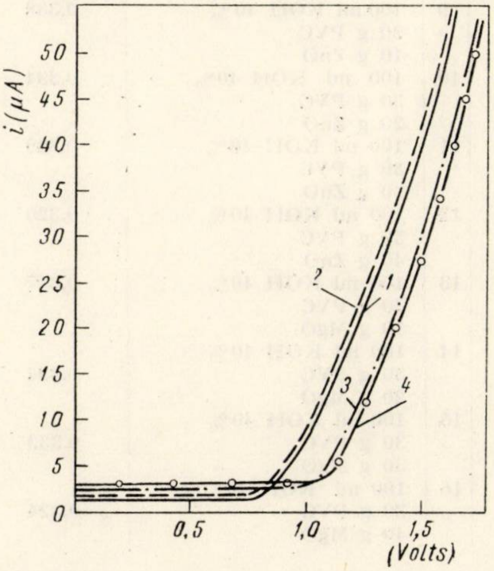

Fig. 2. — Voltamogrammes de déchargement de H_2 et O_2.

1, **Déchargement d'oxygène (potentiel croissant 400 mV/mn) ;** *2*, **Déchargement d'oxygène (potentiel décroissant 400 mV/mn) ;** *3*, **Déchargement d'hydrogène (potentiel croissant 400 mV/mn) ;** *4*, **Déchargement d'hydrogène (potentiel décroissant 400 mV/mn).**

Tableau 4

Paramètres des accumulateurs expérimentés

N°	ACCUMULATEUR			$E°$ (V)	I_{cc} (A)	γ (V)	i_{sc} (A)
1	Zn	15 ml KOH 40% sat. de ZnO	AgO	1,860	0,43	1,73	1,25
2	Zn	15 ml KOH 40% sat. de ZnO et 2 g PVC	AgO	1,863	0,35	1,50	1,05
3	Zn	15 ml KOH 40% sat. de ZnO et 3 g PVC	AgO	1,861	0,37	1,48	1,03
4	Zn	15 ml KOH 40% sat. de ZnO et 5 g PVC	AgO	1,860	0,35	1,47	1,00
5	Zn	15 ml KOH 40% sat. de ZnO et 3 g PVC et 3 g MgO	AgO	1,866	0,33	1,49	1,00

Les paramètres du tableau ont été obtenus de la manière suivante : la tension de la cellule en circuit ouvert ($E°$) a été mesurée directement à l'aide d'un potentiomètre enregistreur à grande impédance d'entrée avec la précision de ±0,5 mV, le courant de court-circuit (i_{sc}) a été mesuré directement à l'aide d'un ampermètre, la constante de tension de la cellule (γ) a résulté de la pente de la courbe ($i-E$) représentée semi-logarithmiquement pour la croissance du courant sollicité de l'accumulateur pour une unité logarithmique et la constante du courant (I_{cc}) a résulté du prolongement de la pente de la courbe de la cellule à la tension $E°$, comme il résulte de la figure 3. Ces paramètres ont été théoriquement déduits par d'autres chercheurs.

Du tableau 4 et de la figure 3 il résulte que les paramètres des accumulateurs qui ont du PVC dans l'électrolyte sont proches de ceux des accumulateurs sans additions.

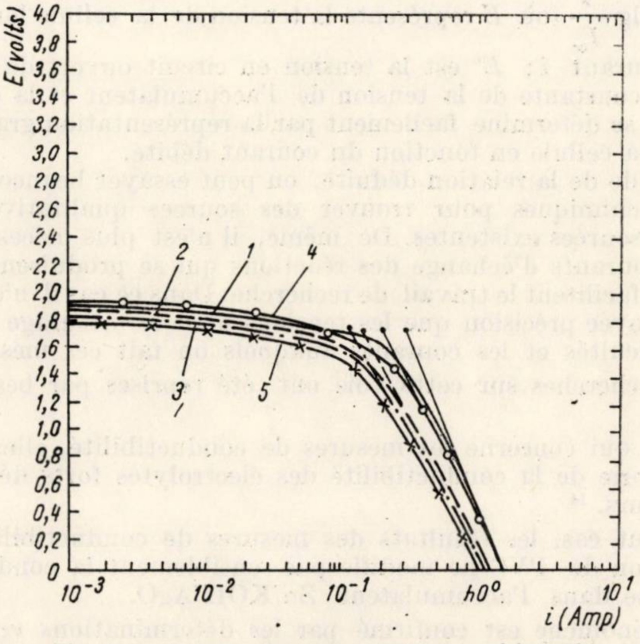

Fig. 3. — Courbes des accumulateurs expérimentés.

1, acc. Zn | KOH 40% 15 ml | AgO;

2, acc. Zn | KOH 40% 15 ml +1 g PVC | AgO;

3, acc. Zn | KOH 40% 15 ml + 3 g PVC | AgO;

4, acc. Zn | KOH 40% 15 ml +5 g PVC | AgO;

5, acc. Zn | KOH 40% 15 ml +3 g PVC + +3 g MgO | AgO.

DISCUSSION

Le grand nombre de recherches effectuées à présent sur la réalisation de nouvelles sources d'énergie ont abouti à des méthodes adéquates de l'interprétation rapide des résultats expérimentaux.

Il y a une décennie, dans le domaine des systèmes électrochimiques générateurs d'énergie chimique on appliquait seulement les principes thermodynamiques.

Parallèlement au développement de la cinétique électrochimique, les recherches se sont également orientées vers l'application des principes de la cinétique à l'étude des générateurs de l'énergie. Des recherches amples sur l'application de ces principes ont été exécutées par Green,[11] Stern et Geary,[12] qui ont abouti à une équation similaire à la relation de Tafel, entre le potentiel d'une électrode et le courant qui passe par l'interface électrode-électrolyte.

Dans le cas de sources chimiques de courant, la relation a la forme $E = E^\circ - \gamma \lg \frac{i}{I_{cc}}$, où E représente la tension de la cellule lorsque celle-ci débite le courant i; E° est la tension en circuit ouvert de la cellule et γ et I_{cc} la constante de la tension de l'accumulateur et la constante du courant qui se détermine facilement par la représentation graphique de la tension de la cellule en fonction du courant débité.

A l'aide de la relation déduite, on peut essayer beaucoup de systèmes électrochimiques pour trouver des sources qualitativement supérieures aux sources existentes. De même, il n'est plus nécessaire de connaître les courants d'échange des réactions qui se produisent sur chaque électrode et facilitent le travail de recherche. Dans ce cas il n'est nécessaire de mesurer avec précision que les tensions dont le mesurage ne comporte pas de difficultés et les courants auxquels on fait ces mesurages.

Les recherches sur cette voie ont été reprises par beaucoup d'auteurs.[13,15]

En ce qui concerne les mesures de conductibilité, elles s'accordent avec la théorie de la conductibilité des électrolytes forts développés par divers auteurs. [14]

En tout cas, les résultats des mesures de conductibilité montrent que l'addition de PVC ne modifie pas sensiblement la conductibilité du KOH, utilisé dans l'accumulateur Zn/KOH/AgO.

Ce phénomène est confirmé par les déterminations voltamétriques — d'où il résulte que les potentiels de déchargement de H_2 et O_2 ne présentent pas de modification par l'addition de PVC en différentes proportions — ainsi que par les courbes des accumulateurs ($E - i$) présentées sur la figure 3, les paramètres E°, γ, I_{cc} étant très proches.

Cependant il faut mentionner qu'au stockage prolongé l'électrolyte des accumulateurs Zn/KOH/Ag devient marron.

On ne constate pas ce phénomène au stockage d'un mélange de H_2SO_4 et PVC.

Le polychlorure de vinyle a un comportement semblable à celui au cas de l'exposition à des radiations mentionné dans,[16] où on montre que par irradiation, le PVC donne des réticulations intermoléculaires à petits rendements et interfère avec l'oxygène.

---

[11] B. Green et N. D. Green, Sci. Reports, AF 19, 604, 8377 (1962).

[12] M. J. Stern et A. L. Geary, *J. Electrochem. Soc.*, **104**, 56 (1957) .

[13] S. Lică, *Rev. Chim.* (*Bucureşti*), **19**, 316 (1968).

[14] G. Niac, «Chimie fizică , Ed. didactică şi pedagogică, Bucarest, 1966, p. 405.

[15] D. R. Cogley et N. J. Butler, *J. Electrochem. Soc.*, **113**, 1074 (1966).

[16] S. Ionescu, «Reacţii chimice induse de radiaţiile ionizante», Ed. Academiei, Bucarest, 1963, p. 216.

Dans l'accumulateur Zn/KOH/AgO, l'O_2 nécessaire au processus provient de la réaction de décomposition de AgO avec libération de O_2 d'après la réaction

$$2AgO \rightarrow Ag_2O + 1/2\ O_2$$

L'apparition de la couleur peut être attribuée à la formation des doubles liaisons conjuguées, apparition qui peut avoir lieu avec la libération du HCl de la molécule, qui est immédiatement consommée par KOH d'après le schéma

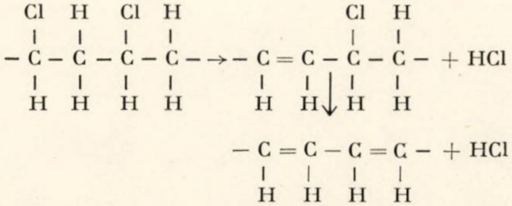

$$-\underset{\mathrm{H}}{\overset{\mathrm{Cl}}{\mathrm{C}}}-\underset{\mathrm{H}}{\overset{\mathrm{H}}{\mathrm{C}}}-\underset{\mathrm{H}}{\overset{\mathrm{Cl}}{\mathrm{C}}}-\underset{\mathrm{H}}{\overset{\mathrm{H}}{\mathrm{C}}}-\rightarrow-\underset{\mathrm{H}}{\mathrm{C}}=\underset{\mathrm{H}}{\mathrm{C}}-\underset{\mathrm{H}}{\overset{\mathrm{Cl}}{\mathrm{C}}}-\underset{\mathrm{H}}{\overset{\mathrm{H}}{\mathrm{C}}}-+\mathrm{HCl}$$

$$\downarrow$$

$$-\underset{\mathrm{H}}{\mathrm{C}}=\underset{\mathrm{H}}{\mathrm{C}}-\underset{\mathrm{H}}{\mathrm{C}}=\underset{\mathrm{H}}{\mathrm{C}}-+\mathrm{HCl}$$

L'élucidation de ce phénomène exige une recherche plus détaillée.

On peut conclure que l'utilisation du PVC dans l'électrolyte des accumulateurs alcalins n'influe pas sensiblement sur les caractéristiques électriques de ces accumulateurs.

Néanmoins, par l'addition du PVC à l'électrolyte, l'électrolyte est mobilisé dans le temps d'exploitation.

Revue Roumaine de Chimie, **15**, 543 – 551 (1970)

Revue Roumaine de Chimie, **15**, 553 – 557 (1970)

RADIOLYSIS PROCESSES IN AQUEOUS SOLUTION OF KI IN THE PRESENCE OF KH_2PO_4 AND $NaNO_3$

LUCIA TUDOR

Institute of Atomic Physics, Bucharest, P. O. Box 35

Received December 19, 1968

The paper studies the variation of the yields of the main radiolysis outcomes, $G_{(I_2)}$ and $G_{(N\bar{O}_3)}$, in the $KI-KH_2PO_4-NaNO_3-H_2O$ system function of the absorbed integral dose and on the concentration of KI, KH_2PO_4 and $NaNO_3$. The irradiations have been made from a radiocobalt source and at an integral dose in the range of 4.6×10^{18} and 3.6×10^{19} eV/ml. Based on experimental results some hypotheses regarding the mechanism of reactions that may take place in this system have been advanced.

INTRODUCTION

The radiolysis of the KI aqueous solutions is the topic of some earlier works,[1–3] as well as of more recent studies.[4–6] The oxidation reaction of the I^- ion on account of the OH radicals resulting from the water radiolysis is unanimously accepted.

The evidences of the reversibility of the oxidations reaction have been brought by studying the effect of the KH_2PO_4 addition [5] (buffer and scavenger for the hydrated electron):

$$I^- + OH \rightleftarrows I + OH^- \qquad (1)$$

The shift of the balance towards the right side is due to the following reactions of the acid anion $H_2PO_4^-$:

$$H_2PO_4^- + OH^- \rightarrow HPO_4^{2-} + H_2O \qquad (2)$$

$$H_2PO_4^- + \bar{e}_{aq} \rightarrow HPO_4^{2-} + H_2O + H \qquad (3)$$

---

[1] R. Johnson, *J. Phys. Chem.*, **21**, 1417 (1953).

[2] H. A. Schwarz, I. P. Losee and O. Allen, *J. Amer, Chem. Soc.*, **76**, 4693 (1954).

[3] J. C. B. Senvar and E. J. Hart, Proc. Second. Intern. Conf. Peaceful Uses of Atomic Energy, Genève, vol. 29, 1958 p. 19.

[4] J. Iove and J. Pucheault, *J. Chim. phys.*, **61**, 711 (1964).

[5] I. A. Atanasiu and M. Fiti, *Rev. Roumaine Chim.*, **12**, 297 (1967).

[6] G. V. Buxton and F. S. Dainton, *Proc. Roy. Soc. A.*, **287**, 427 (1965).

The effect has been subsequently studied, as regards the possibilities of its use in chemical dosimetry.[7]

As a sequel to these results, the action of NO_3^- (powerful trapper of e_{aq}^-) on the radiolytic oxidation of the I^- ion, has been studied by the present paper.

EXPERIMENTAL

The solutions, prepared from analytically pure reactives, Merck products, in tetradistilled water, have been irradiated from a radio-cobalt source of ~ 500 Ci. The work has been carried out in usual conditions in the presence of air, in the dose range of $4.6 \times 10^{18} - 3.68 \times 10^{19}$ eV/ml.

The KI concentration varied between 10^{-4} and 1 M, and the KH_2PO_4 and $NaNO_3$ concentration between 10^{-3} and 1 M.

The characteristic pH of the solutions changed between 4 and 8, having minimal values at the maximum of KH_2PO_4 concentrations. The molecular iodine and nitrite anion, as products of radiolysis have been analysed.

The proportioning of iodine has been made by classical methods and the nitrite has been measured colorimetrically[8] with a photocolorimeter ∅ 3 K–M.

RESULTS

The first series of experiments has traced the variation of the $G_{(I_2)}$ yields depending on the concentration of the system components and on the integral absorbed dose.

Figure 1 shows the variation of the $G_{(I_2)}$ yields depending on the concentration in potassium iodide, for various $NaNO_3$ and KH_2PO_4 concentrations, when $D = 1.84 \times 10^{19}$ eV/ml.

One notices that the oxidation of I^- ion is favoured by the increase in the concentration of all components of the system, $G_{(I_2)}$ having a maximum value for 1 M concentrations of the components.

Figure 2 shows the dependence of the $G_{(I_2)}$ yield upon the absorbed integral dose, for various concentration of KI.

In all cases, KH_2PO_4 and $NaNO_3$ have a concentration of 1 M. For doses higher than 2×10^{19} eV/ml one can notice a constant value of the $G_{(I_2)}$ factor equal to (3.2 ± 0.5) molecules /100 eV for a concentration of 10^{-2} M in KI solutions.

Parallel to the determination of the molecular iodine, the quantity of nitrite resulted from the radiolytic reduction of nitrate has been dosed.

Thus, figure 3 shows the variation of the nitrite yields $G_{(NO_2^-)}$ — depending on the KI concentration for two concentrations of KH_2PO_4 and $NaNO_3$ and for two different values of the dose.

For KI concentrations higher than 10^{-2} M, when the concentrations of KH_2PO_4 and $NaNO_3$ are 10^{-2} M, the yield $G_{(NO_2^-)}$ amounts to (3.5 ± 0.25).

It is noteworthy that for KI concentrations of 10^{-3} M, the yield $G_{(NO_2^-)}$ amounts to (0.59 ± 0.01) irrespective of the dose and the concentration

---

[7] M. Fiti and L. Tudor, *Rev. Roumaine Phys.*, **12**, 583 (1967).

[8] N. L. Allport, "Colorimetric Analysis", Ed. Chapman and Hall, 3rd ed., London, 1951, p. 152.

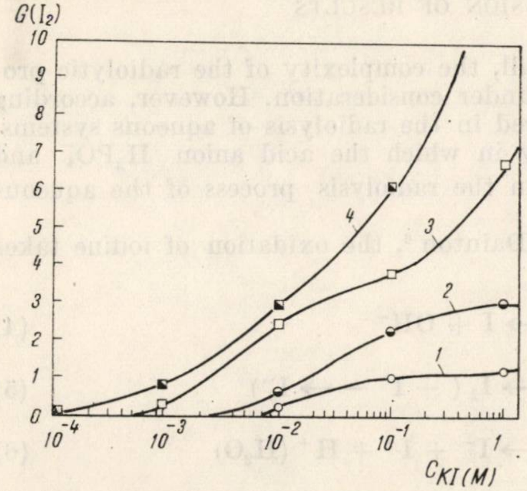

Fig. 1. — Variation of the iodine ($G_{(I_2)}$) *versus* the KI concentrations for different concentrations in KH_2PO_4 and $NaNO_3$ for the integrally absorbed dose. $D = 1.84 \times 10^{19}$ eV/ml.

1, KH_2PO_4 10^{-3} M, $NaNO_3$ 10^{-3} M; *2*, – KH_2PO_4 10^{-2} M, $NaNO_3$ 10^{-2} M; *3*, KH_2PO_4 10^{-1} M, $NaNO_3$ 10^{-1} M; *4*. – KH_2PO_4 1 M, $NaNO_3$ 1 M.

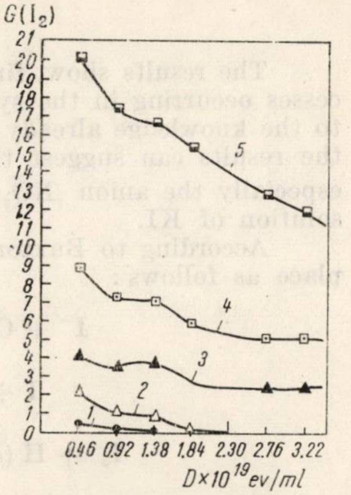

Fig. 2. — Variation of the iodine yield *versus* the integrally absorbed dose for KH_2PO_4 1 M, $NaNO_3$ 1 M

1, KI 10^{-4} M; *2*, KI 10^{-3} M; *3*, KI 10^{-2} M; *4*, KI 10^{-1} M; *5*, KI 1M.

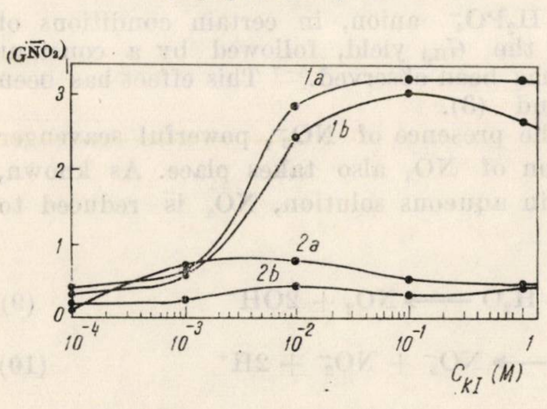

Fig. 3. — Variation of the $G_{(N\bar{O}_2)}$ yield *versus* the concentration KI.

1, $KH_2PO_4 \times 10^{-2}$ M, $NaNO_3$ 10^{-2} M; a) $D = 0.46 \times 10^{19}$ eV/ml; *2*, $KH_2PO_4 10^{-3}$M, $NaNO_3$ 10^{-3} M; b) $D = 0.92 \times 10^{19}$ eV/ml

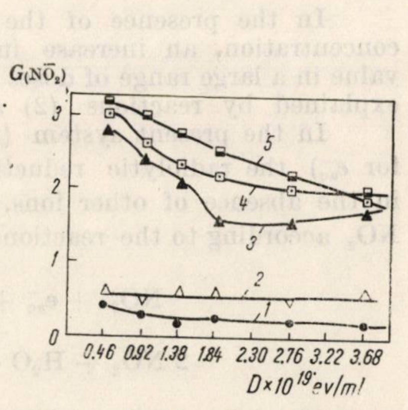

Fig. 4. — Variation of the $G_{(N\bar{O}_2)}$ yield *versus* the integrally absorbed dose for $KH_2PO_4 \cdot 10^{-2}$ M; $NaNO_3 \cdot 10^{-2}$ M.

1. KI.10^{-4} M; *2*, KI 10^{-3} M; *3*, KI.10^{-2} M; *4*, KI.10^{-1} M; *5*, KI 1 M.

of the other components. This effect is better outlined in figure 4, which shows the variation of $G_{(N\bar{O}_2)}$ function of the integral dose absorbed by the system for different concentrations of KI and for KH_2PO_4 10^{-2}M and $NaNO_3 10^{-2}$ M.

DISCUSSION OF RESULTS

The results show, first of all, the complexity of the radiolytic processes occurring in the system under consideration. However, according to the knowledge already acquired in the radiolysis of aqueous systems, the results can suggest the way in which the acid anion $H_2PO_4^-$ and especially the anion $\overline{NO}_3$ step in the radiolysis process of the aqueous solution of KI.

According to Buxton and Dainton [6], the oxidation of iodine takes place as follows:

$$I^- + OH \longrightarrow I + OH^- \tag{4}$$

$$I + I \longrightarrow I_2\ (+ I^- \longrightarrow I_3^-) \tag{5}$$

$$I_3^- + H\ (e_{aq}^-) \longrightarrow I_2^- + I^- + H^+\ (H_2O) \tag{6}$$

$$I_3^- + H_2O_2 \longrightarrow 3\ I^- + 2H^+ + O_2 \tag{7}$$

In the presence of oxygen, the hydrogen atom reacts by means of the HO_2 radical:

$$I^- + HO_2 + H^+ \longrightarrow I + H_2O_2 \tag{8}$$

In the presence of the $H_2PO_4^-$ anion, in certain conditions of concentration, an increase in the $G_{(I_2)}$ yield, followed by a constant value in a large range of doses has been observed.[5-7] This effect has been explained by reactions (2) and (3).

In the present system (the presence of NO_3^-, powerful scavenger for e_{aq}^-) the radiolytic reduction of $\overline{NO}_3$ also takes place. As known, in the absence of other ions, in aqueous solution, $\overline{NO}_3$ is reduced to $\overline{NO}_2$ according to the reactions:

$$NO_3^- + e_{aq}^- + H_2O \longrightarrow NO_2 + 2OH^- \tag{9}$$

$$2\ NO_2 + H_2O \longrightarrow NO_3^- + NO_2^- + 2H^+ \tag{10}$$

The increase in the yields of $G_{(I_2)}$ and $G_{(NO_2^-)}$ simultaneously to the increase in the I^- and NO_3^- concentration over 10^{-3} M, suggest the occurrence of the following reaction

$$NO_2 + I^- \longrightarrow NO_2^- + I \tag{11}$$

At KI concentrations lower than 10^{-2} M (figure 3) the value $G_{(NO_2^-)} = (0.59 \pm 0.01)$ remains much below (3.05 ± 0.25) which corresponds to the concentration 10^{-2} M in KI and 10^{-2} M in $NaNO_3$.

This great difference could be explained by the fact that in the region of small concentrations, reaction (11) cannot take place (having probably a small rate constant), the oxidation processes of the ion I^- and reduction processes of $N\overline{O}_3$ yielding independently.

The low value of the $G_{(N\overline{O}_2)}$ yield can also suggest the idea that, in this system, the reduction of $N\overline{O}_3$ competes with the oxidation reaction of NO_2^- formed through the radiolysis.

The higher is the dose absorbed by the system, the stronger is the intervention of these reactions, this resulting from the decrease in the $G_{(N\overline{O}_2)}$ yield with the increase in the absorbed integral dose (Figure 4).

The values of $G_{(I_2)}$ develop similarly with the dose, a fact accounted for by the reduction in the molecular iodine accumulated in the system.

The sharp increase in the $G_{(I_2)}$ yield, in solutions (of a higher concentration than 0.1 M) may be explained by the "direct action" effect of the radiations upon I^- and $N\overline{O}_3$. Hyder[9] has recently studied this effect and the influence of the presence of the I^- ion on the $G_{(N\overline{O}_2)}$ yield in the radiolysis of the concentrated $NaNO_3$ solutions.

In conclusion the results allow the qualitative interpretation of the radiolytic processes taking place within the system and which can be used as premises for further studies.

---

[9] M. L. Hyder. *J. Phys. Chem.*, **69**, 1858 (1965).

Revue Roumaine de Chimie, **15**, 553 – 557 (1970)

Revue Roumaine de Chimie, **15**, 559 – 562 (1970)

UNE NOUVELLE SYNTHÈSE DE L'ACIDE PHOSPHO-12-VANADIQUE AU MOYEN DES ÉCHANGEURS D'IONS

RALUCA RIPAN et V. CORDIȘ

Institut de Chimie de l'Académie, Filiale de Cluj, 59–65, Str. Donath

Reçu le 31 octobre 1969

Dans ce travail on présente la méthode de préparation de l'acide phospho-12-vanadique de ses composants NaH_2PO_4 et $NaVO_3$ au moyen des échangeurs d'ions.

A la différence des acides phosphomolybdique, phosphotungstique, silicomolybdique et silicotungstique (que l'on a pu isoler) à l'état libre par la méthode éthérée et de la cristallisation,[1] l'acide phosphovanadique n'a pu être obtenu de cette manière. Nos essais pour la préparation de cet acide par l'extraction avec l'éther, ainsi qu'avec d'autres solvants organiques (acétone, alcool isobutylique, 1-butanol, alcool amylique, alcool isopropylique, etc.) de la solution de son sel de sodium acidulée par un acide minéral, n'ont pas donné de résultats positifs. C'est pourquoi la seule possibilité c'est de l'en obtenir en solution, par les échangeurs d'ions.

L'isolement de cet acide à l'état solide n'a pu être réalisé, car, par l'évaporation de la solution d'acide, soit sur le bain d'eau, soit par son exposition à l'air, on obtient un résidu solide brun-roux peu soluble dans l'eau chaude, qui, à la suite de l'analyse, ainsi que basé sur les spectres d'absorption dans le visible s'est avéré un produit de décomposition.

La préparation de l'acide phospho-12-vanadique peut être réalisée, soit par passage sur un échangeur cationique d'une solution de phosphovanadate de sodium,[2] soit par le passage d'un mélange approximativement stœchiométrique de solutions aqueuses de phosphate monosodique et métavanadate de sodium ou d'ammonium, sur un échangeur d'ions mixte. Cette dernière variante fera l'objet de cet ouvrage.

La méthode est fondée sur le comportement différent des résines échangeuses d'ions envers les ions à petit poids moléculaire et ceux à grand poids moléculaires, tels que les hétéropolyanions de la série 12.[3]

---

[1] E. A. Nikitina, *Zhur. priklad. Khim.*, **7**, 1194 (1937); *Zhur. obshchei Khim.*, **7**, 2609 (1937); *Zhur. obshchei Khim.*, **8**, 751 (1938); P. M. Zavelewich, *Zhur. obshchei Khim.*, **18**, 1762 (1948).

[2] R. Ripan, A. Duca et V. Cordiș, *Rev. Roumaine Chim.*, **12**, 375 (1967).

[3] Charreton et G. Bertho, *Compt. rend.*, **261**, 2903 (1965).

Si l'on passe un mélange formé d'hétéropolyanions et d'ions plus simples sur un échangeur anionique et un échangeur cationique, tous les ions simples seront retenus et, éventuellement, une petite partie des hétéropolyanions. De cette façon on peut obtenir un hétéropolyacide pur, en tenant compte du domaine de pH dans lequel l'hétéropolyacide est stable.

À l'aide de cette méthode ont été préparés les anions phosphotungstiques des séries 12 et 11 $[PO_4(WO_3)_{12}]^{3-}$et $[PO_6(WO_3)_{11}]^{7-}$, ainsi que les hétéropolyacides mixtes de phosphore, vanadium et molybdène.[3]

1. PRÉPARATION DE L'ACIDE PHOSPHO-12-VANADIQUE

Les substances initiales et les échangeurs d'ions utilisés ont été : NH_4VO_3 pss. (Reanal), $NaVO_3.1,5H_2O$ préparé du NH_4VO_3[4] et du NaH_2PO_4 *p.a.* La résine mixte : Amberlite, monobed résine MB-1 mixture 1 : 2 IR-120 et IRA 400 (Serva) ; Amberlite IR-120 (H), Schuchardt (München). La régénération de l'échangeur cationique IR-120 (H) et de la résine mixte a été effectuée avec HCl 2,5 N, et l'excès d'acide a été éliminé par lavage avec beaucoup d'eau. Echangeur anionique Dowex de type 3, forme R.OH (Serva). La régénération a été réalisée par une solution de NaOH 2,5 N, et l'excès a été éliminé par lavage avec beaucoup d'eau.

Pour la préparation de l'acide phospho-12-vanadique on a utilisé des solutions aqueuses de $NaVO_3$ ou NH_4VO_3 et NaH_2PO_4 prises approximativement en quantités stœchiométriques. Si à une solution de phosphate on ajoute approximativement la quantité stœchiométrique d'une solution de métavanadate de sodium ou d'ammonium et si l'on passe sur une colonne remplie d'un mélange formé d'un échangeur cationique (H^+) et d'un échangeur anionique (OH^-) , tous les cations seront échangés contre des ions H^+, et les anions plus petits contre des ions OH^- . L'effluent consiste en acide phospho-12-vanadique.

On a utilisé une colonne échangeuse en verre, 25 cm de long, à un diamètre intérieur de 2,8 cm et remplie de résine, à une hauteur de 5 cm.

Pour 32 ml NaH_2PO_4 0,05 M on a ajouté 50 ml $NaVO_3$ 0,25 M (le rapport 1P : 12 V) et on a passé par la colonne échangeuse remplie de résine mixte Amberlite MB-1, forme RH et RCl. La vitesse de passage de la solution par la colonne a été assez grande, approximativement de 70—80 gouttes/mn, car par un passage lent de la solution peut avoir lieu la réduction de l'hétéropolyacide.[5]

Ensuite, l'effluent rouge a été passé sur l'échangeur anionique Dowex de type 3, forme R—OH, pour la rétention des traces éventuelles d'anions Cl^-, anions qui proviennent de la résine mixte. Enfin, on a passé aussi l'effluent sur l'Amberlite IR-120 (H) pour l'élimination totale du sodium. (La vérification a été effectuée flammephotométriquement et on a trouvé, après le premier passage du mélange sur la résine mixte, des traces de sodium dans l'effluent.)

Nos essais de remplacer le NaH_2PO_4 par H_3PO_4 n'ont pas donné de résultats positifs. Par l'analyse de l'effluent on a trouvé le rapport 1 P : 12 V.

---

[4] I. V. Kariakin et I. I. Angelov, «Chistye khimicheskie reaktivy», Goskhimizdat, Moscou, 1955, p. 369.

[5] L. C. W. Baker, B. Loew et Thomas P. Mc.Cutcheon, *J. Amer. Chem. Soc.*, **72**, 2374 (1950).

2. TITRAGE CONDUCTOMÉTRIQUE ET POTENTIOMÉTRIQUE DE L'ACIDE PHOSPHO-12-VANADIQUE

Pour identifier l'acide phospho-12-vanadique obtenu, on a d'abord effectué l'analyse chimique, en déterminant le vanadium et le phosphore, dont le rapport a été trouvé égal à 12. Le phosphore a été déterminé colorimétriquement, [6] et le vanadium par titrage à sel de Mohr.

Par des titrages conductométriques et potentiométriques on a obtenu des informations sur la basicité de l'acide.

Les titrages conductométriques ont été effectués avec NaOH $1,5.10^{-1}$ N et $TlCH_3COO$ ($T_{Tl}=0,02$). On a pris 15 ml de solution d'hétéropolyacide à $T_V = 0,0008922$, qu'on a titré par une solution de NaOH $1,5.10^{-1}$ N. La courbe de titrage conductométrique est représentée dans la figure 1.

On obtient le point d'inflexion de la courbe pour une consommation de 0,5 ml NaOH ce qui correspond au rapport de 12 V : 3 NaOH. Au point d'équivalence a lieu la formation du sel de sodium selon la réaction suivante :

$$H_7PV_{12}O_{36} + 3\,NaOH = Na_3H_4PV_{12}O_{36} + 3\,H_2O$$

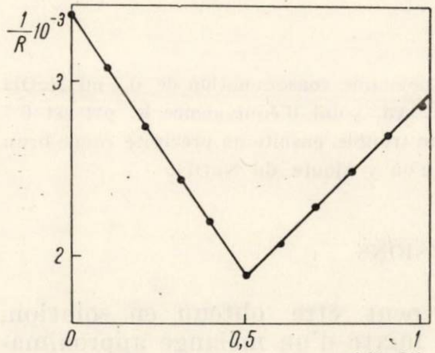

Fig. 1. — Courbe de titrage conductométrique de l'acide phospho-12-vanadique avec NaOH $1,5.10^{-1}$ N.

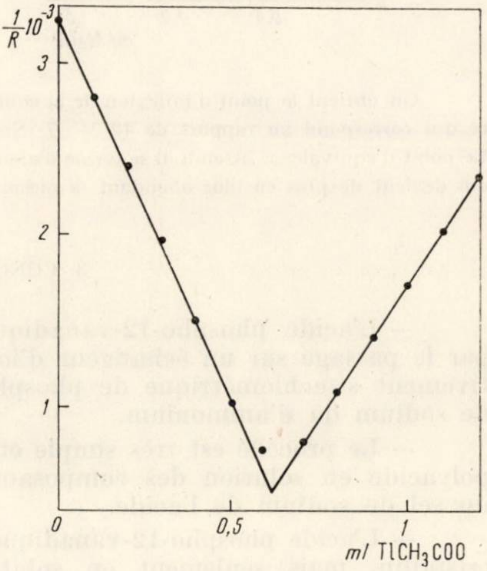

Fig. 2. — Courbe de titrage conductométrique de l'acide phospho-12-vanadique avec $TlCH_3COO$.

Pour le titrage conductométrique avec $TlCH_3COO$ on a pris 7 ml d'hétéropolyacide ($T_V = 0,0008922$) ; on obtient le point d'inflexion pour une consommation de 0,62 ml

---

[6] Iu. N. Knipowich et Iu. V. Morachewski, «Analis mineralnowo syria », Goskhimizdat Leningrad, 1956, p. 329.

$TlCH_3COO$, ce qui correspond au rapport de 12 V : 7 Tl (fig. 2). Pendant le titrage se forme un précipité brun.

Pour le titrage potentiométrique on a pris 5 ml d'hétéropolyacide avec $T_V = 0{,}00182$, qui ont été dilués avec 5 ml d'eau et puis on a titré avec NaOH $1{,}5.10^{-1}$ N (fig. 3).

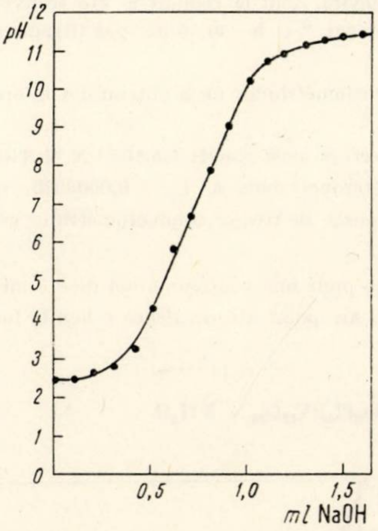

Fig. 3. — Courbe de titrage potentiométrique de l'acide phospho-12-vanadique avec NaOH $1{,}5.10^{-1}$ N.

On obtient le point d'inflexion de la courbe pour une consommation de 0,7 ml NaOH, ce qui correspond au rapport de 12 V : 7 NaOH. Au point d'équivalence le pH est 6,7. Le point d'équivalence atteint, il se forme d'abord un trouble, ensuite un précipité rouge-brun, qui devient de plus en plus abondant à mesure qu'on y ajoute du NaOH.

3. CONCLUSIONS

— L'acide phospho-12-vanadique peut être obtenu en solution, par le passage sur un échangeur d'ions mixte d'un mélange approximativement stœchiométrique de phosphate monosodique et métavanadate de sodium ou d'ammonium.

— Le procédé est très simple et il permet l'obtention de ce hétéropolyacide en solution des composants, sans la synthèse, au préalable, du sel de sodium de l'acide.

— L'acide phospho-12-vanadique ne peut pas être obtenu à l'état cristallin, mais seulement en solution.

Revue Roumaine de Chimie, **15**, 563 – 571 (1970)

UNTERSUCHUNGEN DER KOMPLEXE Th-ALIZARIN UND Th-CHINALIZARIN DURCH EXTRAKTION MIT BUTANOL-1

C. DRĂGULESCU, T. SIMONESCU, GIZELLA NEMES und MARIA TOTAN

von der Forschungsstelle der Akademie, Zweigstelle Timişoara, Bd. Mihai Viteazul 24

Eingegangen am 17. November 1969

Es wurden die optimalen Bedingungen für die Thoriumextraktion mit butanolischen Alizarin- und Chinalizarinlösungen in Gegenwart von Trichloressigsäure (TCE) festgesetzt. Die beiden Komplexe wurden in butanolischem Medium untersucht, und ihre Zusammensetzung bestimmt. Gleichzeitig wurden auch die Stabilitätskonstanten für [Th – A] : $K = 5{,}8.10^4$ und für [Th–ChA] : $K = 2{,}68.10^5$, berechnet. Auch der Einfluß mehrerer fremder Ionen wurde untersucht.

In der Fachliteratur kennt man mehrere Arbeiten, die sich auf die Thoriumbestimmung mit Alizarin S in wäßrigem Medium [1,2] beziehen, der Komplex Th – Alizarin S wurde mit quaternären langkettigen Alkylammoniumsalzen extrahiert.[3]

Der Komplex Th-Chinalizarin wurde in wäßrigem-azetonischem Medium [4] und Buthylcellosolv [5] untersucht.

Der Zweck unserer Arbeit war die Festsetzung der Extraktionsbedingungen des Thoriums in Gegenwart von TCE – Säure, mit Alizarin bzw. Chinalizarinlösungen in Butanol, sowie die Untersuchungen der im butanolischen Medium gebildeten Komplexe, zwecks Ausarbeitung extraktiv-spektrophotometrischen Bestimmungsmethoden für Thorium.

EXPERIMENTELLES

Apparatur:

Die Absorptionsspektren wurden mit einem Spektrophotometer „Unicam SP 800" Cambridge-England bestimmt, während die andern spektrophotometrischen Messungen mit

---

[1] D. V. N. SARMA und BH. SV. RADHOVA RAO, *Analyt. Chim. Acta*, **13**, 142 (1955).

[2] SARENDRA NATH SINHA und ARUN K DEY, *Z. analyt. Chem.*, **195**, 416 (1963).

[3] TAICHI SATO und M. L. GOOD, *J. Inorg. Nuclear Chem.*, **28**, 2733 (1966).

[4] A. PURUSHOTTAM, *Z. analyt. Chem.*, **145**, 245 (1955).

[5] F. TH. BARRA und S. B. SEEGER, *Rev. Real. Acad. Cienc. Exacta*, **61**, 827 (1967); *Chem. Abstr.*, **69**, 24277 w (1968).

einem Spektrophotometer „Spekol" – Carl Zeiss Jena DDR durchgeführt wurden. Die pH-Werte wurden mit einem pH-Meter MV 11 Claman & Grahnert Dresden DDR gemessen.

Reagenzien:

– Die 10^{-2} M Thoriumnitratlösung wurde durch Auflösen von ungefähr 5,52 g $Th(NO_3)_4 \cdot \times H_2O$ Merck (mit einem Gehalt an ThO_2 von min. 46%) in 1 l doppelt destiliertem Wasser hergestellt. Der Titer der Lsg wurde gravimetrisch für die ThO_2-Form bestimmt.

– Die 10^{-3} und 2.10^{-4} M Thoriumnitratlösungen wurden durch Verdünnen der obenangeführten Lsg erhalten.

– Die 10^{-3} M butanolische Alizarinlösung wurde durch Auflösen von 0,2401 g Alizarin Riedel de Häen *p.a.*, beim Erwärmen, in 1 l Butanol-1, präpariert.

– Die 2.10^{-4} M butanolische Chinalizarinlösung wurde durch Auflösen, beim Erwärmen, von 0,2722 g Chinalizarin Merck *p.a.* (gereinigt durch Sublimation) in 1 l Butanol-1 erhalten.

– Die ungefähr 2 M TCE-Säurelösung wurde durch Auflösen der entsprechenen TCE-Menge in doppelt destilliertem Wasser erhalten.

– Das verwendete Butanol war die Fraktion, die bei 117–118,5° während der Destillation des durch Gährung erhaltenen Butanols, übergeht.

Arbeitsweise. Um Thorium mit einer butanolischen Alizarinlösung zu extrahieren, wurden 20 ml einer wäßrigen Thoriumnitratlösung, die 0,4 ml ungefähr 2 M TCE-Säure enthielt (pH = 2,8), mit 10 ml butanolischer Alizarinlösung versetzt und 2 minutenlang geschüttelt. Nach der Phasenabtrennung wurde die Extraktion noch einmal mit 10 ml Butanol-1 wiederholt, nachdem vorher aber 0,2 ml ungefähr 2 M TCE-Lsg zugesetzt wurde und der pH-Wert von neuem auf 2,8 eingestellt worden war.

Nach dem Vereinigen der butanolischen Phasen in einem 25 ml Meßkolben und nach dem Auffüllen zur Marke mit Butanol-1, wurden die spektrophotometrischen Bestimmungen durchgeführt.

Bei der Thoriumextraktion mit butanolischer Chinalizarinlösung wurde genau wie oben vorgegangen, mit dem Unterschied, daß in diesem Fall bei einem pH-Wert von 3,5 gearbeitet wurde.

Alle Messungen wurden bei Zimmertemperatur durchgeführt.

ERGEBNISSE UND DISKUSSIONEN

Während der Thoriumextraktion aus wäßrigen Lösungen bei pH = 2,8, mit einer butanolischen Alizarinlösung und bei pH = 3,5, mit einer butanolischen Chinalizarinlösung, bilden sich zwei Farbkomplexe. Aus den in Abb. 1 dargestellten Absorptionskurven folgt, daß der Komplex [Th–A] bei 550 mμ und der Komplex [Th-ChA] bei 600 mμ ein Absorptionsmaximum aufweist.

Da, für jeden einzelnen Fall, der Addend praktisch keine Absorption aufweist, wurden die spektrophotometrischen Messungen bei den erwähnten Wellenlängen durchgeführt.

Aus dem parallelen Studium der Thoriumextraktion mit butanolischen Alizarin- und Chinalizarinlösungen folgt, daß eine Umrührzeit von 2 Minuten genügt, um das Verteilungsgleichgewicht zu erreichen. Die spektrophotometrischen Bestimmungen für das Butanolextrakt können gleich nach der Extraktion durchgeführt werden. Die gebildeten Komplexe sind wenigstens zwei Tage lang beständig.

Um die optimalen Bedingungen, unter denen sich die Thoriumkomplexe mit Alizarin und Chinalizarin bilden und extrahiert werden können zu bestimmen, wurde der Einfluß des pH-Wertes und der TCE-Säurekonzentration untersucht. Die Kurven *1* und *2* aus Abb. 2 zeigen, daß in beiden Fällen der günstigste pH-Wert in relativ enge Bereiche fällt. Demnach wurde die Extraktion mit butanolischer Alizarinlösung bei dem pH-Wert = 2,8 und die mit butanolischer Chinalizarinlösung bei dem pH-Wert = 3,5 durchgeführt.

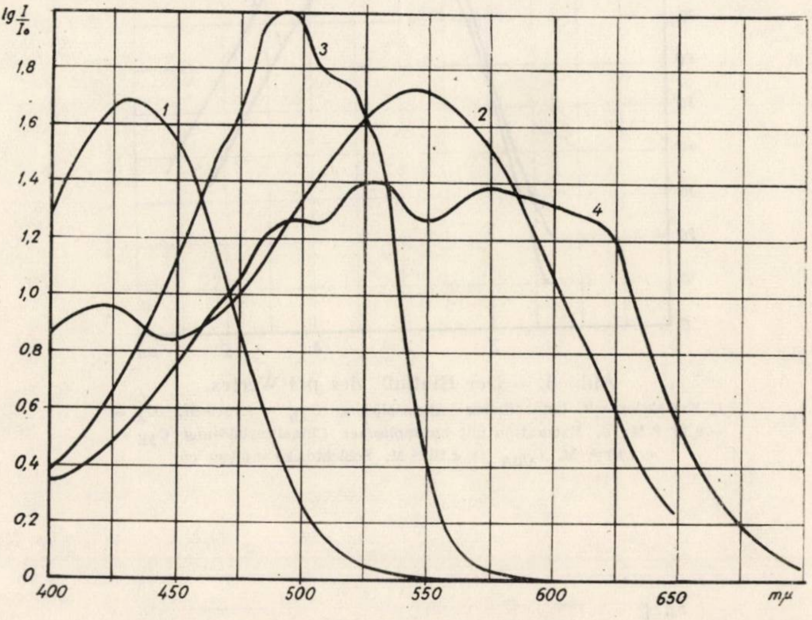

Abb. 1. — Absorptionskurven.

1, butanolische Alizarinlösung, $C_A = 8.10^{-5}$ M; *2*, der Komplex [Th–A], $C_{Th} = 8.10^{-5}$ M, $C_A = 8.10^{-5}$ M; *3*, butanolische Chinalizarinlösung, $C_{ChA} = 4.10^{-5}$ M; *4*, der Komplex [Th–ChA], $C_{Th} = 4.10^{-5}$ M, $C_{ChA} = 4.10^{-5}$ M, Schichtdicke = 4 cm. Auf der Ordinate lg $\frac{I_0}{I}$.

Aus Abb. 3 folgt, daß die TCE-Säure die Thoriumextraktion mit butanolischer Alizarin- bzw. Chinalizarinlösung stark beeinflußt. Ohne TEC-Säure beträgt die prozentuelle Extraktion nur 25,6% bzw. 12,6%; die Extraktion wächst parallel mit der TCE-Säurekonzentration bis zu einer gegebenen Grenze, um dann abzunehmen.

Bei der Thoriumextraktion mit einer butanolischen Alizarinlösung, genügt eine Menge von 0,1–0,2 ml ungefähr 2 M TCE-Lösung, um eine praktisch totale Extraktion zu bewirken. Weil aber unter diesen Bedingungen die Phasenabtrennung sehr langsam vor sich geht und von dem Auftreten eines Films an der Trennungsoberfläche begleitet ist, wurden 0,4 ml TCE-Lösung benützt. In diesem Fall erreicht

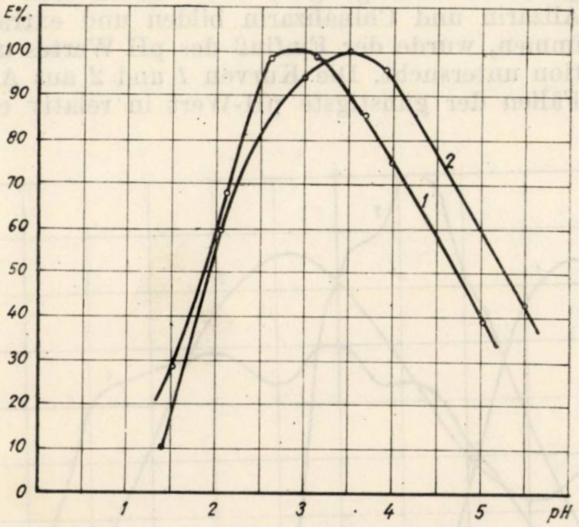

Abb. 2. — Der Einfluß des pH-Wertes.

1, Extraktion mit butanolischer Alizarinlösung $C_{Th} = 8.10^{-5}$ M, $C_A = 8.10^{-5}$ M; 2, Extraktion mit butanolischer Chinalizarinlösung $C_{Th} = 4.10^{-5}$ M, $C_{ChA} = 4.10^{-5}$ M. Schichtdicke = 0,999 cm.

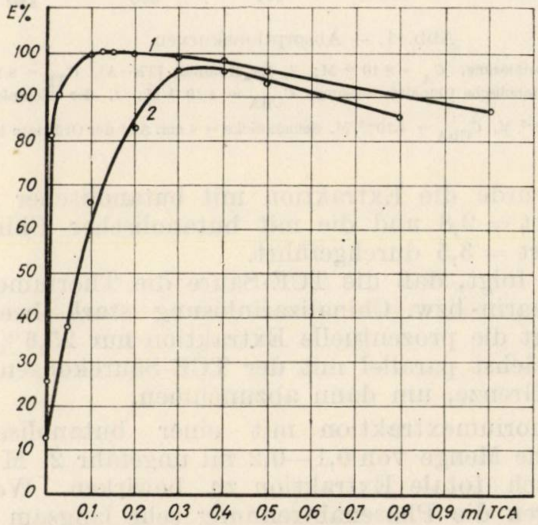

Abb. 3. — Der Einfluß der TCE-Säurekonzentration.

1. Extraktion mit butanolischer Alizarinlösung $C_{Th} = 8.10^{-5}$ M, $C_A = 1{,}6.10^{-4}$ M; 2,Extraktion mit butanolischer Chinalizarinlösung $C_{Th} = 4.10^{-5}$, $C_{ChA} = 4.10^{-5}$ M. Schichtdicke — 0.999 cm.

die prozentuelle Extraktion 98%, die Phasen trennen sich gut ab und sind auch genügend klar. Bei der selben TCE-Säurekonzentration und mit einer butanolischen Chinalizarinlösung wurde eine prozentuelle Extraktion von 96,5% erreicht.

Das Lambert-Beersche Gesetz und die spektrophotometrische Bestimmung des Thoriums

Die Gültigkeit des Lambert-Beerschen Gesetzes wurde für das ganze Konzentrationsbereich, in dem gearbeitet wurde, geprüft. Im Falle des Komplexes [Th—A] gilt dieses Gesetz bis zu wenigstens 60 µg/ml, während es im Falle des Komplexes [Th—ChA] bis zu 10 µg/ml gültig ist.

Die spektrophotometrische Thoriumbestimmung kann mit Hilfe einer Eichkurve durchgeführt werden. Der Bestimmungsfehler beträgt 3—5%.

Der Einfluß fremder Ionen

Das Verhalten der verschiedenen Ionen bei der Thoriumbestimmung durch Extraktion mit butanolischer Alizarinlösung zeigt, daß: Ni^{2+}, Co^{2+}, Cd^{2+}, Ba^{2+}, Pb^{2+}, Ti^{4+} und PO_4^{3-}-Ionen nicht störend wirken bis zu 100fachen Mengen; während La^{3+} und Ce^{3+}-Ionen bis zu einem 10fachen Überschuß nicht stören. Die Ionen Al^{3+}, Fe^{3+}, UO_2^{2+}, Zr^{4+} und WO_4^{2-} stören jedoch.

Der Einfluß des Kupfers wurde durch Maskierung mit Thioharnstoff beseitigt.

Im Falle der Thoriumbestimmung durch Extraktion mit einer butanolischen Chinalizarinlösung stören die Ionen Ti^{4+} und PO_4^{3-}; die andern Ionen verhalten sich genau so wie im Falle der Thoriumbestimmung mit Alizarin.

Die Zusammensetzung und die Stabilität der Komplexe [Th—A] und [Th—ChA].

Die Komplexe [Th-A] und [Th—ChA] wurden im butanolischen Medium spektrophotometrisch untersucht. Ihre Absorptionskurven bei verschiedenen Molverhältnissen, dargestellt in Abb. 4 und 5 haben die gleiche Form und die Maxima bei denselben Wellenlängen. Diese Tatsache beweist die Bildung eines einzigen Komplexes in beiden Fällen.

Für die Feststellung der Komplexzusammensetzung wurde die Methode der kontinuierlichen Veränderungen [6] mit äquimolaren Lösungen bei verschiedenen Wellenlängen und Konzentrationen angewendet. Die Kurven „Job" aus der Abb. 6 und 7 zeigen für beide Komplexe ein Kombinationsverhältnis [Me : Addend] = 1 : 1 an.

---

[6] P. Job, *Ann. Chim.* (*France*), **9**, 113 (1928).

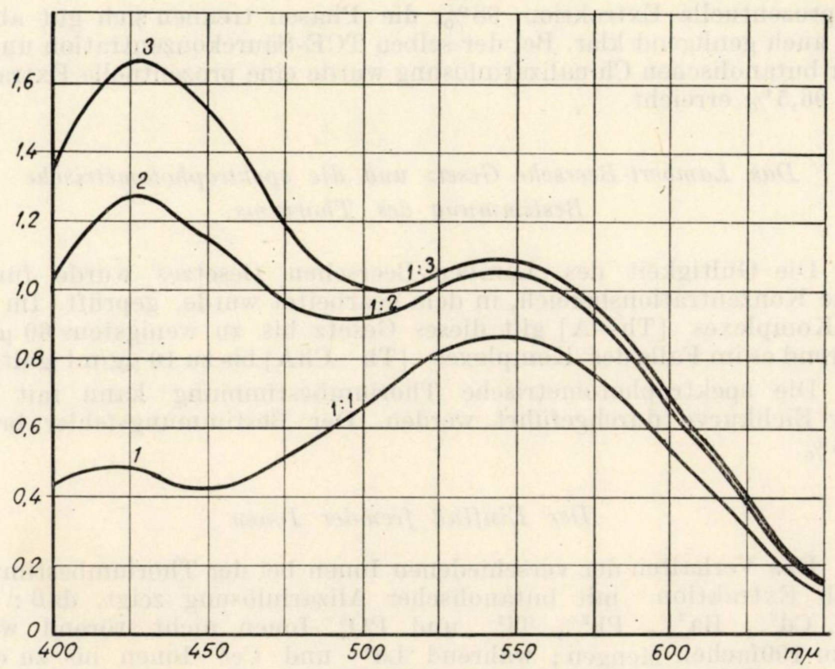

Abb. 4. — Absorptionskurven der Gemische von Thorium- und Alizarinlösungen: $C_{\mathrm{Th}} = 8.10^{-5}$ M.

1, $C_{\mathrm{A}} = 8.10^{-5}$ M, *2*, $C_{\mathrm{A}} = 1{,}6.10^{-4}$ M, *3*, $C_{\mathrm{A}} = 2{,}4.10^{-4}$ M. Schichtdicke = 0,999 cm. Auf der Ordinate lg $\frac{I_0}{I}$

Die Methode des Neigungsverhältnisses[7] (Abb. 8, 9) und die Methode der Molverhältnisse[8] (Abb. 10) bestätigen die erhaltenen Ergebnisse. Die Kurven aus Abb. 10 beweisen für beide Komplexe die Existenz eines Dissoziationsprozesses.

Die Bildungskonstante der beiden Komplexe wurde mit Hilfe einer von Majumdar und Chakrabartty[9] ausgearbeiteten Methode bestimmt. Die Kurven aus den Abb. 6 und 7 ermöglichten die Berechnung dieser Bildungskonstante, die für den Komplex [Th—A] $K = 5{,}8\ 10^4$ und für den Komplex [Th—ChA] $K = 2{,}68.10^5$ war.

SCHLUSSFOLGERUNGEN

— Es wurden die optimalen Extraktions- und Bildungsbedingungen der Alizarin- und Chinalizarinkomplexe bestimmt.

— Die Gegenwart der TCE-Säure ermöglicht die Thoriumextraktion bei pH = 2,8 mit einer butanolischen Alizarinlösung und bei pH = 3,5 mit einer butanolischen Chinalizarinlösung.

---

[7] A. E. HARVEY und D. L. MANNING, *J. Amer. Chem. Soc.*, **72**, 4488 (1950).

[8] J. H. YOE und A. L. JONES, *Ind. Eng. Chem. Anal. Ed.*, **16**, 111 (1944).

[9] A. K. MAJUMDAR und M. M. CHAKRABARTTY, *Analyt. Chim. Acta*, **19**, 372 (1958).

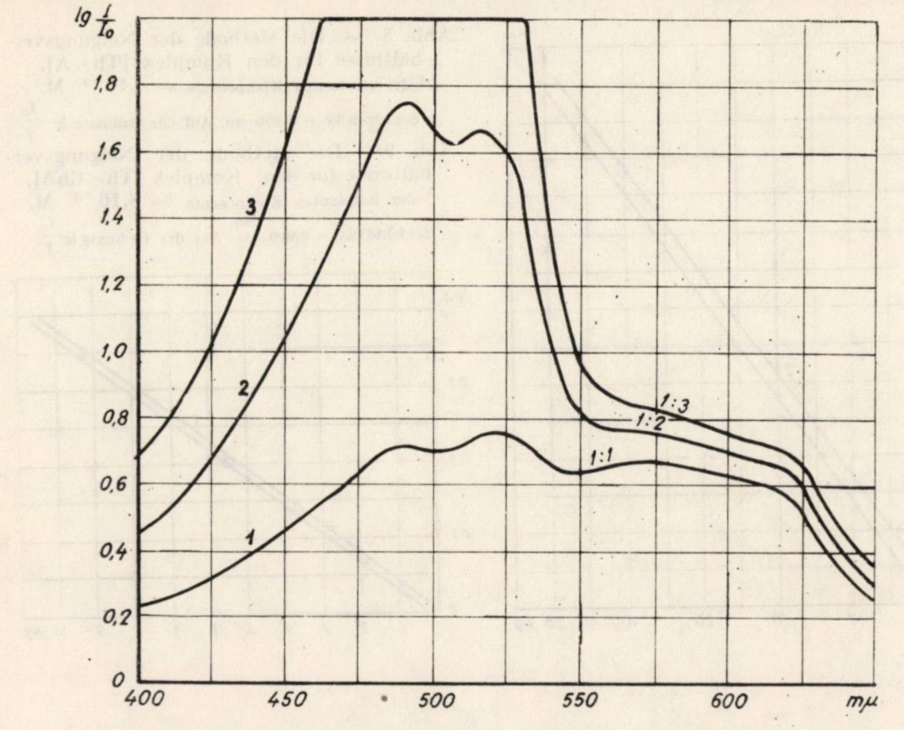

Abb. 5. — Absorptionskurven der Gemische von Thorium- und Chinalizarinlösungen : $C_{\mathrm{Th}} = 4.10^{-5}$ M. Auf der Ordinate lg $\frac{I_0}{I}$

1, $C_{\mathrm{ChA}} = 4.10^{-5}$ M. *2*, $C_{\mathrm{ChA}} = 8.10^{-5}$ M. *3*, $C_{\mathrm{ChA}} = 1{,}2.10^{-4}$ M. Schichtdicke = 0,999 cm.

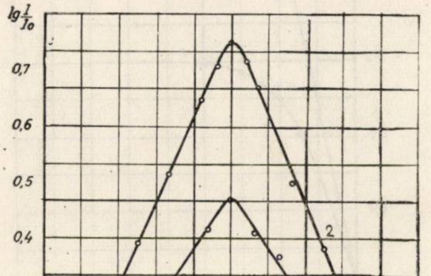

Abb. 6. — Absorptionskurve der kontinuierlichen Veränderung für den Komplex [Th-A]. Auf der Ordinate lg $\frac{I_0}{I}$

1, $C = 1{,}2.10^{-4}$ M. *2*, $C = 2{,}4.10^{-4}$ M. Schichtdicke = 0,999 cm.

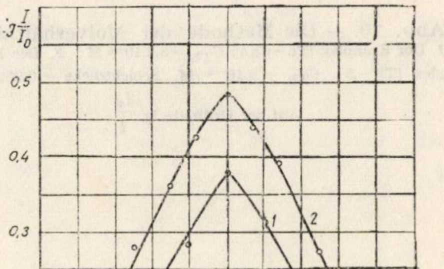

Abb. 7. — Absorptionskurve der kontinuierlichen Veränderung für den Komplex [Th—ChA]. Auf der Ordinate lg $\frac{I_0}{I}$

1, $C = 8.10^{-5}$ M; *2*, $C = 1{,}12.10^{-4}$ M. Schichtdicke = 0,999 cm.

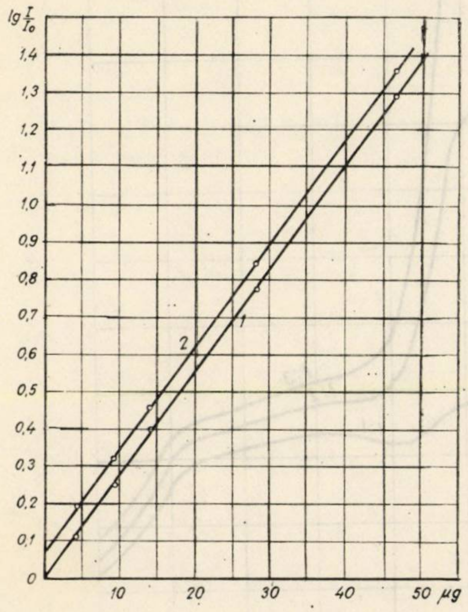

Abb. 8. – Die Methode der Neigungsverhältnisse für den Komplex [Th–A], $C_{\text{der konstanten Komponente}} = 4.10^{-4}$ M. Schichtdicke = 0,999 cm. Auf der Ordinate lg $\frac{I_0}{I}$

Abb. 9. – Die Methode der Neigungsverhältnisse für den Komplex [Th–ChA], $C_{\text{der konstanten Komponente}} = 8.10^{-5}$ M. Schichtdicke = 0,999 cm. Auf der Ordinate lg $\frac{I_0}{I}$

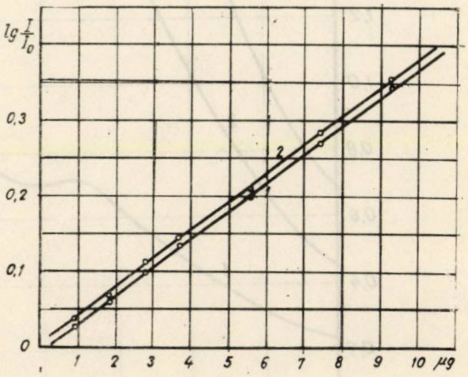

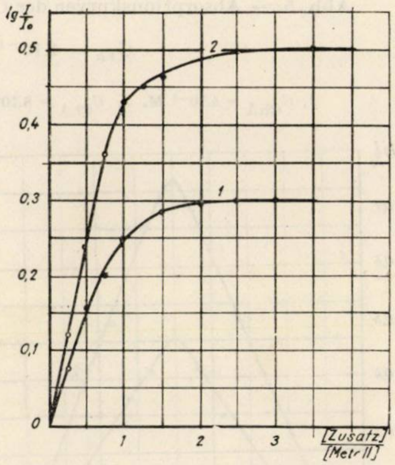

Abb. 10. – Die Methode der Molverhältnisse. 1. Der Komplex [Th–ChA] $C_{Th} = 3{,}2.10^{-5}$ M; 2. Der Komplex [Th–A]. $C_{Th} = 8.10^{-5}$ M. Schichtdicke = 0,999 cm. Auf der Ordinate lg $\frac{I_0}{I}$

– Die prozentuelle Extraktion mit butanolischen Alizarin- und Chinalizarinlösungen beträgt 98 % bzw. 96,2 %.

– Das Lambert-Beersche Gesetz gilt für den [Th–A]-Komplexen bis zu wenigstens 60 µg/ml und für den [Th–ChA]-Komplexen bis zu wenigstens 10 µg/ml, eine Tatsache, die die Ausarbeitung extraktiv – spektrophotometrischer Bestimmungsmethoden für Thorium mit butanolischen Alizarin- und Chinalizarinlösungen, ermöglichte.

— Außer den Ti^{4+} und PO_4^{3-}-Ionen, die bei der Thoriumextraktion mit butanolischer Chinalizarinlösung störend wirken, haben alle andern studierten Ionen denselben Einfluß. Die Ionen Ce^{3+} und La^{3+}, bis zu einem Verhältnis 1:10 und die Ionen der zweiwertigen Elemente stören nicht, bis zu einem Verhältnis von 1 : 100, außer Kupfer. Die Ionen der dreiwertigen Metalle und verschiedene Anionen wirken störend.

— Die äquimolare Zusammensetzung der beiden Komplexe wurde durch die Methoden der kontinuierlichen Veränderungen, der Molverhältnisse und der Neigungsverhältnisse, bestätigt.

— Die Bildungskonstante des Komplexes [Th—A] ist $K = 5{,}8.10^4$ und die des Komplexes [Th—ChA] $K = 2{,}68.10^5$.

Revue Roumaine de Chimie, **15**, 573 – 581 (1970)

VERBINDUNGEN DER DILITURSÄURE MIT ANILIN UND PHENYLENDIAMINEN

FR. MIHAI und R. NUŢIU
vom Lehrstuhl für Chemie der Fakultät für Physik, Universität Timişoara,
Bd. V. Pårvan 4

Eingegangen am 28. Juni 1968

In Fortsetzung unserer Forschungen über die Dilitursäure wurden eine Reihe von Verbindungen mit folgenden organischen Basen präpariert : Anilin, *o*, *m*- und *p*-Phenylendiamin. Die Phenylendiamine reagieren mit der Dilitursäure in beiden Wertigkeitsstufen, wobei sowohl mono- als auch di-Diliturate erhalten werden. Es wurden thermogravimetrische Untersuchungen der erhaltenen Verbindungen vorgenommen und die Aktivierungsenergien der Dehydratierungsprozesse der hydratierten Verbindungen bestimmt. Desgleichen wurde die Wasserlöslichkeit der neuen Diliturate bei 10° und 25° bestimmt, und es wurde eine neue gravimetrische Methode zur Bestimmung von *p*-Phenylendiamin als di-Diliturat ausgearbeitet.

Die Eigenschaft der Dilitursäure (5-Nitrobarbitursäure), schwer lösliche Salze zu bilden, wurde zur Ausarbeitung einiger vorteilhafter Bestimmungsmethoden von Metallkationen verwendet.[1] Redemann und Nieman[2] machten schon im Jahre 1940 auf die Tatsache aufmerksam, daß einige organische Basen mit Dilitursäure als schwerlösliche Verbindungen gefällt werden. Dennoch wurden keine Bestimmungsmethoden der organischen Basen mit diesem Reagens ausgearbeitet, mit Ausnahme von Äthylendiamin und Chinin.[3] Im Fachschrifttum sind keine Angaben über die Natur dieser Verbindungen vorhanden.

In der vorliegenden Arbeit wurde in Fortsetzung früherer Untersuchungen 1,4 über Salze der Dilitursäure, die Herstellung und Charakterisierung der Diliturate des Anilins und der Phenylendiamine verfolgt. Da die Phenylendiamine eine sehr geringe Basizität aufweisen und folglich ihre Bestimmung durch Neutralisierung sehr schwierig ist, wurde gleichzeitig die Möglichkeit ihrer Bestimmung auf gravimetrischem Wege verfolgt. Es wurden folgende Verbindungen präpariert :

---

[1] Fr. Mihai, B. Roch und A. Moraru, *Bul. Şti. Tehn. Inst. Polit. Timişoara*, **26**, 441 (1967).

[2] C. E. Redemann und C. Nieman, *J. Amer. Chem. Soc.*, **62**, 590 (1940).

[3] A. Berlin und J. Robinson, *Analyt. Chim. Acta*, **24**, 319 (1961).

[4] Fr. Mihai, *Rev. Roumaine Chim.*, **11**, 657 (1966).

(I) Anilindiliturat ($C_4H_3O_5N_3.C_6H_7N$)
(II) Trihydratiertes *o*-Phenylendiamin-di-Diliturat
($C_4H_3O_5N_3)_2$ *o*-$C_6H_8N_2.3H_2O$
(III) Trihydratiertes *m*-Phenylendiamin-di-Diliturat
$(C_4H_3O_5N_3)_2.m-C_6H_8N_2.3H_2O$
(IV) *p*-Phenylendiamin-di-Diliturat $(C_4H_3O_5N_3)_2 \, . \, p-C_6H_8N_2$
(V) *o*-Phenylendiamin-mono-Diliturat $C_4H_3O_5N_3.o\text{-}C_6H_8N_2$
(VI) *p*-Phenylendiamin-mono-Diliturat $C_4H_3O_5N_3.p-C_6H_8N_2$

Sämtliche Verbindungen sind kristallin, von weißer oder schwachgelber Farbe. Zum Unterschied von den di-Dilituraten, welche ziemlich beständig sind, dunkeln die mono-Diliturate unter Lichteinwirkung nach.

Sie wurden durch vollständige chemische Analyse, sowie durch thermogravimetrische Analyse charakterisiert, und im Falle der Hydrate wurde der Dehydratierungsvorgang auch kinetisch untersucht.

EXPERIMENTELLER TEIL

Darstellung der Verbindungen

Zwecks Darstellung dieser Verbindungen wurden zusätzlich gereinigte Phenylendiamine (Firma „CHINOIN" und „REANAL") verwendet, sowie Dilitursäure, die durch Nitrierung aus Barbitursäure (Firma MERCK") synthetisiert worden war. [5]

Die 1%igen wäßrigen Lsgen der Amine werden mit einem 2,5-3fachen Überschuß einer 50%igen alkoholischen Dilitursäurelösung m/10 versetzt, so daß das Molverhältnis größer als 1 : 2 ist. Der Inhalt des Kolbens wird gut durchgeschüttelt (er muß gut verschlossen sein, damit der Luftzutritt verhindert wird). Alle Operationen müssen im Dunkeln vorgenommen werden. Die Reaktionsprodukte kristallisieren nach einigen Sekunden. Nach Abkühlung mit Eis werden die kristallinen Produkte abfiltriert, mit einer 50% igen alkoholischen Lsg von Dilitursäure m/10, gekühltem Alkohol und Äther gewaschen.

Im Falle der Reaktionsprodukte (III) wurde die Fällung in der Wärme vorgenommen, um einen leichter filtrierbaren Niederschlag zu erhalten. Zur Fällung der Verbindungen (V) und (VI) wurde ein Molverhältnis zwischen Phenylendiamin und Dilitursäure von 1 : 1 benutzt.

In Tabelle 1 sind die Analysenergebnisse für C, H und N angeführt.

Die Richtigkeit der molekularen Formeln wurde durch die Bestimmung des Dilituratanions als Zinksalz überprüft. [6]

Thermogravimetrische Untersuchungen

Die thermische Zersetzung der organischen Verbindungen der Dilitursäure unterscheidet sich grundsätzlich von der der metallischen Diliturate, die sich zum größten Teil bis zum Metalloxid zersetzen. Die untersuchten Diliturate der organischen Basen zersetzen sich ohne Rückstand. Ihre Untersuchung erlaubt die thermische Stabilität sowohl der Hydrate als auch der wasserfreien Verbindungen zu verfolgen. Aus den in den Abbildungen 1 und 2 dargestellten thermolytischen Kurven (die mit einer Erwärmungsgeschwindigkeit von 5°/Min. unter den in einigen früheren Arbeiten angeführten Bedingungen erhalten wurden [1-4]) ist ersichtlich, daß die Trihydrate (II) und (III) sich unter 75° dehydratieren, während die wasserfreien Produkte bis zu 150—195° stabil sind. Die mono-Diliturate (I), (V) und (VI) haben eine gerin-

---

[5] W. W. HARTMANN und O. E. SHEPARD, "Organic Syntheses", 2 Coll. vol., 1943, S. 440.

[6] FR. MIHAI und B. ROCH, *Studii și Cercetări Ști. Chim.. Baza Cercetări Ști., Timișoara.* 5, 113 (1958).

Tabelle 1

Ergebnisse der Elementaranalyse, %

Substanz	C		H		N	
	ber.	*gef.*	*ber.*	*gef.*	*ber.*	*gef.*
$C_4H_3O_5N_3.C_6H_7N$(I)	45,10	44,89 44,64	3,78	3,97 3,88	21,03	20,50 20,74
$(C_4H_3O_5N_3)_2$.*o*-$C_6H_8N_2.3H_2O$(II)	33,07	33,10 32,82	3,98	3,94 4,06	22,02	21,83 21,60
$(C_4H_3O_5N_3)_2$.*m*-$C_6H_8N_2.3H_2O$(III)	33,07	32,60 32,20	3,98	4,11 4,27	22,02	21,74 21,52
$(C_4H_3O_5N_3)_2$.*p*-$C_6H_8N_2$ (IV)	37,00	36,40 36,70	3,10	3,05 2,90	24,66	23,56 23,80
$C_4H_3O_5N_3$.*o*-$C_6H_8N_2$ (V)	42,69	42,20 42,42	3,90	4,02 3,81	24,53	24,62 24,65
$C_4H_3O_5N_3$.*p*-$C_6H_8N_2$ (VI)	42,69	41,82 42,02	3,90	3,92 4,34	24,53	24,28 23,89

gere thermische Stabilität (bis zu 90—120°). Dadurch unterscheiden sie sich von den Dilituraten der aliphatischen Diamine,[3] bei welchen eine größere thermische Stabilität festgestellt wurde (bis zu 240°).

Kinetik der Dehydratierung

Zur Untersuchung der Kinetik der Dehydratierung wurde die Methode der isothermen Erhitzung gewählt, die bei den metallischen Dilituraten angewendet wurde, [7] weil der Wert der Geschwindigkeitskonstanten aus den Versuchsergebnissen bestimmt werden kann. Aus der Veränderung derselben mit der Temperatur kann die Aktivierungsenergie und der Vorexponentialfaktor berechnet werden, um die Arrheniussche Gleichung auszudrücken.

Während des thermischen Zersetzungsvorgangs dieser Diliturate stellt die Entziehung des Wassers einen gesonderten Zersetzungsvorgang der wasserfreien Verbindungen dar, wie im Falle der metallischen Diliturate.[7] Der Dehydratierungsvorgang findet bei viel niedrigeren Temperaturen als die Zersetzung der wasserfreien Verbindung statt, welche von einer leichten Explosion begleitet wird.

Die Dehydratierung der Phenylendiamindiliturate gliedert sich in den thermischen Zersetzungsprozeß fest — gasförmig :

$$(R)_2\cdot FAM\cdot 3H_2O \longrightarrow (R)_2\cdot FAM + 3H_2O$$

---

[7] Fr. Mihai, *Studii și Cercetări Chim. Acad. România*, **13**, 825 (1964).

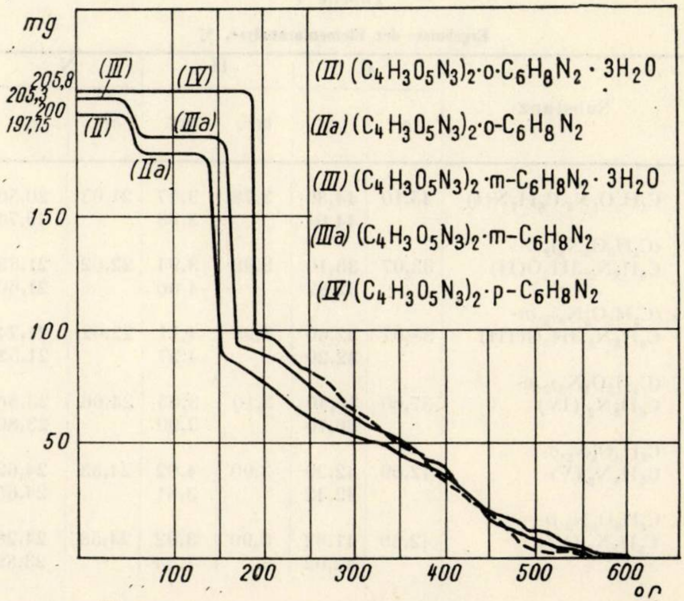

Abb. 1. — Thermogramme der Dilitursäureverbindungen mit den Phenylendiaminen (II—IV).

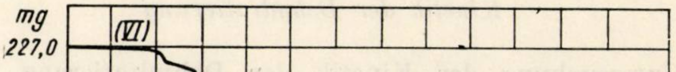

Abb. 2. — Thermogramme der Dilitursäureverbindungen mit Anilin und den Phenylendiaminen (I, V und VI).

Die Art und Weise der Wasserentziehung wird aus der thermolytischen Kurve abgeleitet, auf welcher stöchiometrische horizontale Stufen erscheinen.[8] Um vergleichbare Daten zu erhalten, wurden die Bestimmungen mit gleichen Substanzmengen durchgeführt, die auf der gleichen Oberfläche verteilt wurden.

Die Deutung der Versuchsergebnisse wurde mit Hilfe der kinetischen Gleichung erster Ordnung vorgenommen, wodurch die Linearität des Vorgangs ausgedrückt wird.[9]

Von beiden Verbindungen wurde eine Menge von $s = 400$ mg untersucht, denen eine Menge von $a = 42{,}4$ mg entzogenes Wasser entspricht.

In Abbildung 3 wurden die Isothermen des Dehydratierungsvorganges der Verbindung (II) dargestellt, und in Tabelle 2 wurden die Versuchwerte für k und $1/T$ angegeben. Aus diesen Werten wurde mit Hilfe der Methode der kleinsten Quadrate[10] der Vorexponentialfaktor A und die Neigung p der Geraden berechnet.

Tabelle 2

Die k- und T- Werte für o- und m-Phenylendiamin-di-Diliturat

T°K / Substanz		333	343	353	363	373
II	k	—	0,078	0,158	0,203	0,441
III	k	0,026	0,061	0,120	0,220	0,392

Aus diesen Daten geht hervor: $\log A = 7{,}764$; $A = 5{,}815.10^7$; $p = -3{,}041.10\ ^3$; $E = 13{,}9$ kcal/Mol und die Arrheniusche Gleichung:

$$\log k = 7{,}764 - \frac{13{,}9}{4{,}573 \cdot T \cdot 10^3}.$$

In Abbildung 4, Gerade *1*, wurde $\log k = f\ (1/T)$ dargestellt. Die Gerade wurde durch die aus der Arrheniuschen Gleichung berechneten Punkte geführt:

$$1/T \cdot 10^3 = 2{,}66 \qquad \log k = \bar{1}{,}67$$

$$1/T \cdot 10^3 = 2{,}90 \qquad \log k = \bar{2}{,}94$$

In Abbildung 5 wurden die Isothermen des Dehydratierungsvorganges der Verbindung (III) dargestellt, und in Tabelle 2 wurden die

---

[8] A. C. ZETLENMAYER, C. H. SCHEIDER, H. V. ANDERSON and R. I. FUCHS, *J. Phys.-Chem.*, **61**, 991 (1957).

[9] I. G. MURGULESCU und E. I. SEGAL, *Anal. Univ. Buc.*, *Şti. Nat.*, **22**, 75 (1959).

[10] L. M. BATUNER und M. E. POZIN, ,,Metode matematice în tehnica chimică'' (Übers. a. d. Russ.), Ed. tehnică, Bukarest, 1956, S. 482.

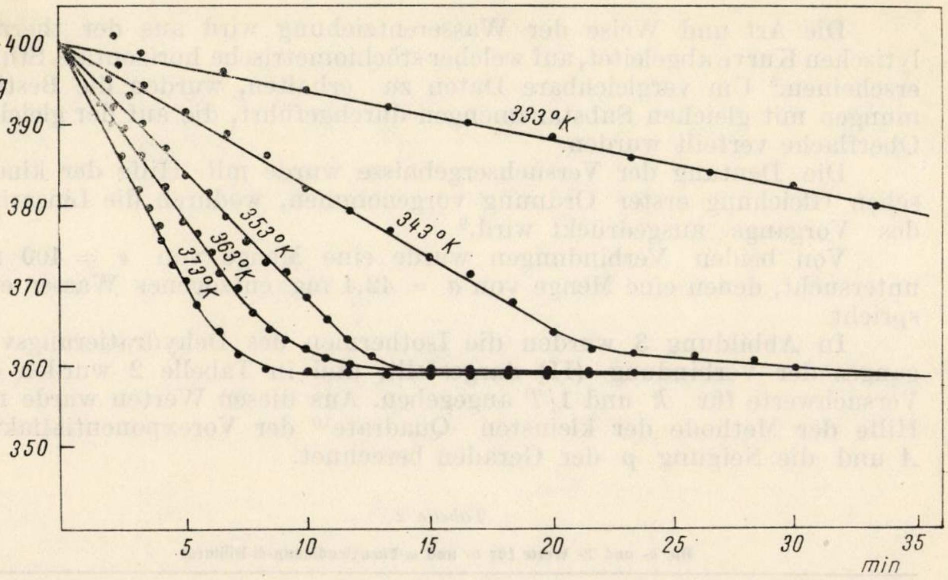

Abb. 3. — Isothermen des Dehydratierungsvorgangs von *o*-Phenylendiamin-di-Diliturat.

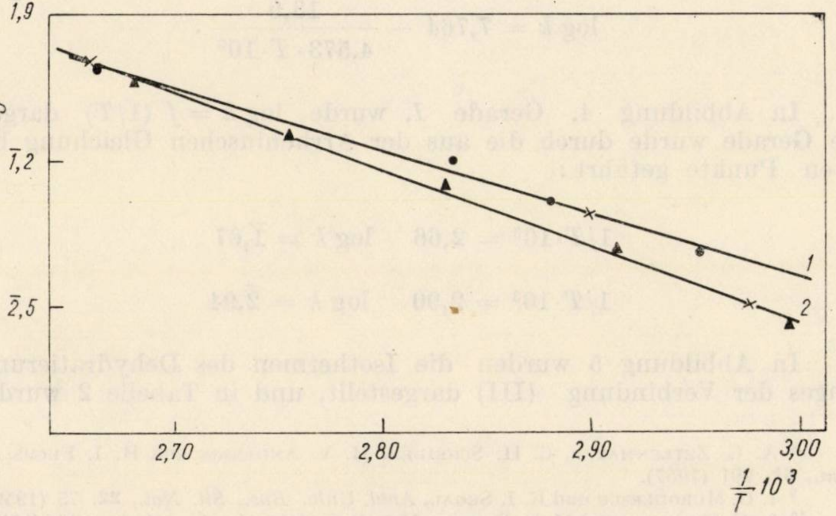

Abb. 4. Änderung von log *k* gegen 1/*T*.

1 *o*-Phenylendiamin-di-Diliturat; *2*. *m*-Phenylendiamin-di-Diliturat.

Versuchswerte für k und T angeführt; die Geschwindigkeitskonstante wurde wie im ersten Falle berechnet.

Aus diesen Daten geht hervor: $\log A = 9{,}378$; $A = 2{,}39.10^9$; $p = -3{,}642.10^3$; $E = 16{,}7$ kcal/Mol und die Arrheniussche Gleichung:

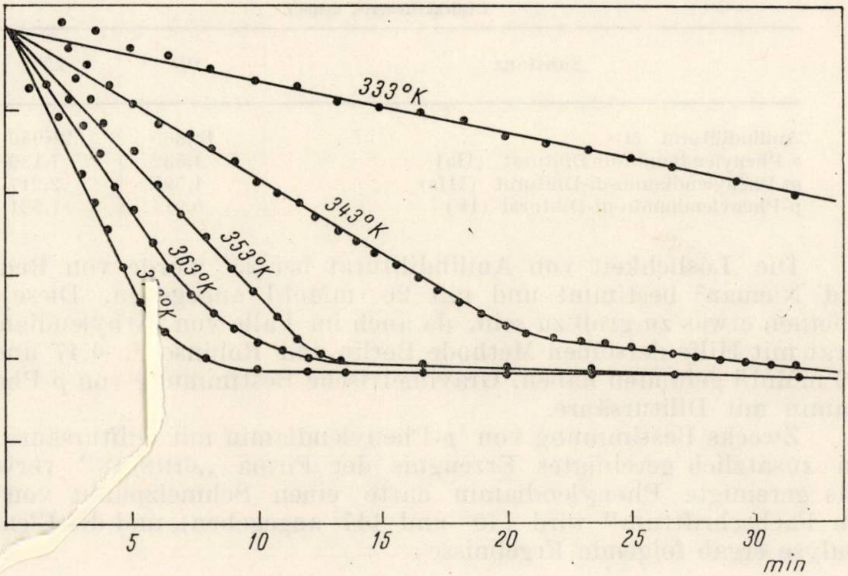

Abb. 5. — Isotherme des Dehydratierungsvorgangs von *m*-Phenylendiamin-di Diliturat.

$$\log k = 9{,}378 - \frac{16{,}7}{4{,}573 \cdot T \cdot 10^3}$$

In Abbildung 4, Gerade *2*, wurde $\log k = f\,(1/T)$ dargestellt. Die Gerade wurde durch die aus der Arrheniusschen Gleichung berechneten Punkte geführt:

$$1/T \cdot 10^3 = 2{,}66 \qquad \log k = \bar{1}{,}69$$

$$1/T \cdot 10^3 = 2{,}98 \qquad \log k = \bar{2}{,}52$$

Die Versuchswerte für $\log k$ nähern sich in beiden Fällen zufriedenstellend der Geraden.

Bestimmung der Löslichkeit

Zwecks Festsetzung einiger gravimetrischer Bestimmungsmethoden der Phenylendiamine mit Dilitursäure wurde die Löslichkeit der Diliturate des Anilins und der di-Diliturate der *o*-, *m*- und *p*-Phenylendiamine bei 10° und 25° mit der von Berlin und Robinson gegebenen Methode bestimmt. [3]

Die erhaltenen Versuchsergebnisse sind in Tabelle 3 angeführt.

Tabelle 3

Löslichkeitswerte, mMol/l

Substanz	10°	25°
Anilindiliturat (I)	13,865	21,950
o-Phenylendiamin-di-Diliturat (IIa)	4,532	7,130
m-Phenylendiamin-di-Diliturat (IIIa)	1,599	2,917
p-Phenylendiamin-di-Diliturat (IV)	0,914	1,531

Die Löslichkeit von Anilindiliturat bei 25° wurde von Redemann und Nieman[2] bestimmt und mit 26 mMol/l angegeben. Diese Daten scheinen etwas zu groß zu sein, da auch im Falle von Äthylendiamindiliturat mit Hilfe derselben Methode Berlin und Robinson[3], 0,47 und nicht 0,6 mMol/l gefunden haben. Gravimetrische Bestimmung von *p*-Phenylendiamin mit Dilitursäure.

Zwecks Bestimmung von *p*-Phenylendiamin mit Dilitursäure wurde ein zusätzlich gereinigtes Erzeugnis der Firma „CHINOIN" verwendet. Das gereinigte Phenylendiamin hatte einen Schmelzpunkt von 139,5° (im Fachschrifttum[11] wird 140° und 147° angegeben), und die Elementaranalyse ergab folgende Ergebnisse :

ber. : N 25,91 ; *gef* : N 25,81 %
25,74

Zu Fällung wurde eine 50 %ige alkoholische Lösung von Dilitursäure m/20, die in der Kälte präpariert und filtriert worden war und eine wäßrige Lösung von *p*-Phenylendiamin m/20 verwendet. Die zur Fällung gebrauchten Substanzmengen entsprechen dem Molverhältnis 2,5 : 1. Es bildete sich sofort ein Niederschlag, und nach 10—15 Minuten Abset-

Tabelle 4

Ergebnisse der Bestimmung von *p*-Phenylendiamin, mg

Zur Untersuchung genommene Menge	*gef.*	*ber.*	Δ
10,80	44,60	45,44	−0,84
13,51	55,80	56,80	−0,80
16,20	67,45	68,16	−0,71
27,03	112,90	113,60	−0,70
40,53	169,00	170,40	−1,40
54,06	228,10	227,21	+0,89
81,11	339,80	340,81	−1,01
108,14	454,00	454,42	−0,42

---

[11] I. HEILBRON, "Dictionary of Organic Compounds — The Constitution of Physical and Chemical Properties...", 3. Bd., Izdatelsvo inostranoi literatury, Moskau 1949, s. 403.

zen bei Raumtemperatur wurde mit Eis gekühlt und durch einen G4 Tiegel filtriert. Der Niederschlag wird mit einer eisgekühlten 50%igen alkoholischen Dilitursäurelösung m/20 auf den Tiegel gebracht. Sodann wird der im Tiegel befindliche Niederschlag 3—4mal mit je 2—3 ml gekühltem 96%igem Äthylalkohol und danach mit Äthyläther gewaschen. Nach dem Trocknen mit der Wasserstrahlpumpe wurde dieses Produkt bei 110° im Trockenschrank auf konstantes Gewicht gebracht. Die Analysenergebnisse sind in Tabelle 4 angeführt.

SCHLUSSFOLGERUNGEN

Die Dilitursäure bildet kristalline Niederschläge mit einigen schwachen organischen Basen wie Anilin und die Phenylendiamine. Mit *o*- und *p*-Phenylendiamin werden sowohl mono- als auch di-Diliturate erhalten, während man mit *m*-Phenylendiamin nur di-Diliturate erhält.

Die geringe Löslichkeit dieser di-Diliturate erlaubt eine quantitative Bestimmung der Phenylendiamine auf gravimetrischem Wege. Im Falle von *p*-Phenylendiamin befinden sich die Fehler der von uns ausgearbeiteten Methode innerhalb der erlaubten Grenzen.

Der niedrige Wert der Aktivierungsenergie läßt die Schlußfolgerung zu, daß das Kristallwasser dieser Verbindungen in das Gitter eingebaut ist.

Die Untersuchung der Struktur dieser Verbindungen wird Gegenstand künftiger Arbeiten sein.

Revue Roumaine de Chimie, **15**, 573 – 581 (1970)

Revue Roumaine de Chimie, **15**, 583 – 587 (1970)

AUTOMATIC POTENTIOMETRIC TITRATION IN MOLTEN MEDIA. I

A NEW AUTOMATIC CONTINUOUS PROCEDURE FOR POTENTIOMETRIC TITRATION IN MOLTEN MEDIA WITH SOLID STANDARD

C. LITEANU, E. CORDOŞ and LIANA MĂRGINEANU

Division of Analytical Chemistry, University "Babeş-Bolyai"
Cluj, str. Arany János, 11

Received July 15, 1969

Acido-basic titrations in molten media are laborious since they are made point-by-point and a weighing is required after each reagent adding. The present paper describes a new procedure that offers the possibility of making continuous potentiometric titrations in molten media. The standard is prepared in the form of a stick and continually introduced by a mechanical device into the melt which contains the sought for species. Recording the e.m.f. of the indicator electrode, the titration curve is directly obtained in a much shorter time than by the point-by-point procedure. The titration curves and the results of their processing are presented.

The reactions in molten media are the subject-matter of an even greater number of papers, specially after 1950; one can say that by now every branch of chemistry is involved in one way or another, in their[1] study. This is easy to understand since the molten media open a wide field for research and they are often very important from the practical point of view.[2,3]

The analytical chemistry is interested in molten media reactions because they bring new ways for solving some problems of analysis and permit the extension of the analytical theories over other media than aqueous or organic nonaqueous ones. For example, after the acido-basic concepts, developed for molten media by Lux,[4] Flood and Forland,[5] a base is an oxygen donor substance and an acid is an acceptor one:

$$\text{Acid} + O^{2-} \rightleftharpoons \text{Conjugated Base}$$

$$\text{Base} \rightleftharpoons O^{2-} + \text{Conjugated Acid}$$

---

[1] G. J. Janz, *J. Chem. Educ.*, **44**, 581 (1967).
[2] C. Liteanu and E. Cordoş, *Rev. Roumaine Chim.*, **12**, 985 (1967).
[3] B. R. Sundheim, *Analyt. Chem.*, **30**, 1892 (1958).
[4] H. Lux, *Z. Elektrochem.*, **45**, 303 (1939).
[5] H. Flood and T. Forland, *Acta Chem. Scand.*, **1**, 592 (1947).

According to these definitions $Cr_2O_7^{2-}$, PO_3^-, $P_2O_7^{4-}$, CrO_3 are acids and CO_3^{2-}, HCO_3^-, Na_2O_2, PO_4^{3-} are bases. [6, 7] As a matter of fact a reaction like that between bichromate and carbonate is a neutralization reaction[8]:

$$Cr_2O_7^{2-} + CO_3^{2-} = 2CrO_4^{2-} + CO_2$$

There is, principially, a chance of turning to account for analytical purposes some acido-basic reactions in molten media, using the titration. The main question is that of final point detection which, at least now, cannot be made chemically, that is with indicators. The only way is that of the instrumentalization of the final point detection the potential jump being particularly useful for this purpose. [9]

In principle, such a titration is accomplished by adding weighed portions of the solid standard to the melt with the sought-for species, followed by the determination of indicator electrode e.m.f. after each reagent addition. As one can see, the titration is laborious, requiring a great many weighings in order to plot a curve. This might be the reason why acido-basic titrimetry in molten media is not enough developed. If the time for melting the solvent were included, a point-by-point titration would last over three hours. The long time required for titration, beside being a disadvantage in itself, allows the developing of secondary reactions which in some cases distort the result.

This paper is concerned with continuous procedure for the titration in molten media, in order to avoid the numerous weighings, to reduce the time required by titration and record directly the titration curve. In fact all these tasks could be fulfilled by finding a proper method of continuously introducing the standard into the melt. There are, theoretically, the following possibilities for solving this problem :

First, the melting of the standard and its adding to the melt. This technique could be worked out but it is difficult.[10]

Another possibility would be the adding of the standard as a powder, uniformly, by a mechanical device. It has been rejected because this kind of devices are very delicate, specially if one takes into account the small quantity of standard. Neither in this instance can the uniformity of standard adding be assured, since the powders could dehomogenize prior to pouring, because of trepidations, if they are not absolutely uniformly granulated. If the powder is very fine, and it must be, then the convectional streams above the melt recipient become a serious source of trouble.

Finally, we figured out a third possibility, used in the present work, that is to prepare the solid standard as a stick and to introduce it uniformly into the melt that contains the sought-for species. In this case the stick must have a uniform cross-section all over its length and the stick substance must melt just when it contacts the molten solvent and not before or after.

---

[6] J. M. Schlegel, *J. Chem. Educ.*, **43**, 362 (1967).

[7] N. Coumert, M. Porthault and J. C. Merlin, *Bull. Soc. chim. France*, **1965**, 910.

[8] A. M. Shams El Din and A. A. Gerges, *J. Electroanalyt. Chem.*, **4**, 309 (1962).

[9] A. M. Shams El Din, *Electrochim. Acta*, **7**, 285 (1962).

[10] J. Jordan, J. Meier, E. J. Billingham and J. Pendergrast Jr., *Analyt. Chem.*, **31**, 1439 (1959); **32**, 651 (1960).

The stick could be made of pure standard or a solidified solution of the standard in a certain solvent. To this purpose, the same solvent in which the sought-for species is dissolved, could be preferably used.

EXPERIMENTAL

The instrumentation for acido-basic titration in molten media is shown in figure 1. The sought-for species is dissolved in the melt (1) from the crucible (2) placed in a furnace. The indicator electrode (3), reference electrode (4) and a thermocouple (5) for temperature control are introduced into the melt.

An oxygen electrode has been used as indicator electrode.[11] It has been made of a platinized platinum foil introduced into a glass tube through which oxygen gas, electrolytically obtained, has been bubbled. The melt volume being smaller than 25—30 ml and the electrode immersed until the bottom, the oxygen, delivered with a frequency of 5—6 bubbles per second, served for homogenizing the melt.

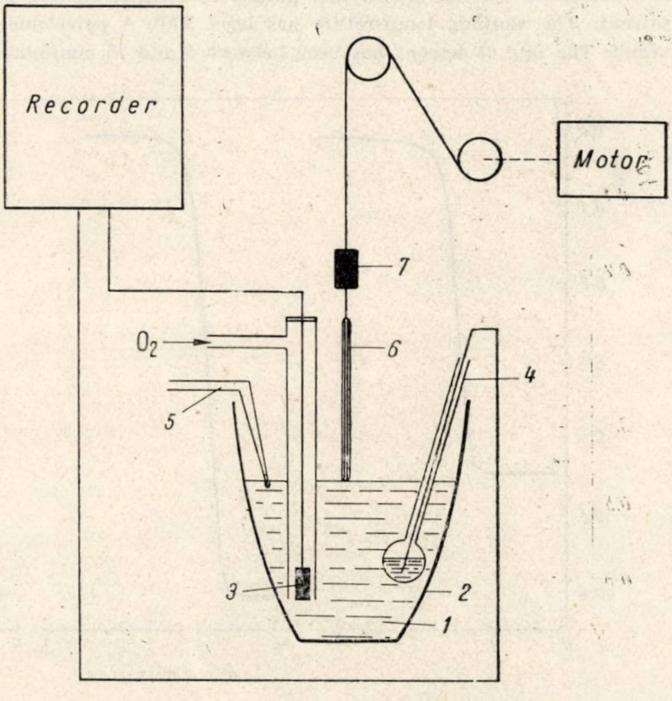

Fig. 1. — Instrumentation scheme for automatic continuous potentiometric titration in molten media. *1*, melt; *2*, crucible; *3*, indicating electrode, *4*, reference electrode; *5*, thermocouple; *6*, stick of solid standard; *7*, counterweight.

The reference electrode has been a silver electrode made of silver wire, 1 mm in diameter, introduced into a thin-wall glass tube containing potassium nitrate with 2.04% silver nitrate.[12]

---

[11] A. M. Shams El Din, *J. Electroanalyt. Chem.*, **6**, 131 (1963).

[12] D. G. Ives and G. J. Janz, "Reference Electrodes", J. Wiley, New York, 1961, p. 524.

The potential difference between the electrodes has been recorded by a Zeiss Jena recorder, type GlBl with 10 M input impedance.

The standard stick, hanged by a thread having a counterpoise, is introduced into the melt by a system of sheaves and a motor that assures a uniform descent with desired speed.

The technique of manufacturing the sticks, is the following:

The standard is melted together with the solvent, in a known ratio. After the homogenizing of the melt, this is sucked up in capillary tubes with very fine walls (made from vial glass) and let to solidify. The glass is then carefully broken and the sticks taken out. The uniformity of the stick is tested by means of a micrometer, with a 0.02 mm tolerance and the inadequate portions are removed. Sticks of potassium bichromate in sodium nitrate (1 : 5) have been manufactured.

By the above procedure a series of titrations have been accomplished, using potassium bichromate as acid and sodium carbonate, sodium hydroxide and sodium peroxide as bases. A eutectic of sodium nitrate and potassium nitrate, melting point 220°, has been used as solvent. The working temperature has been 300°. A porcelaine crucible served as titration vessel. The rate of descent has been between 5 and 15 mm/minute.

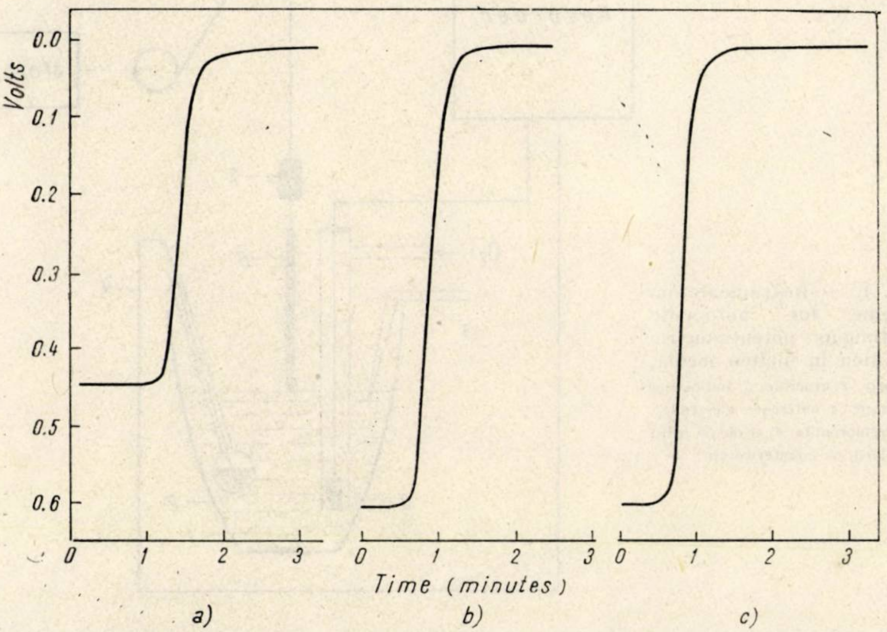

Fig. 2. — Titration curves of sodium carbonate (a), potassium hydroxide (b) and sodium peroxide (c) by potassium bichromate at 300°.

The moment when the stick touches the surface of the melt and the moment the titration is completed and the motor stops, are marked on the chart recorder. From the content in standard substance of the stick by unit of length, from the used length of the stick or from its weight one can calculate the amount of standard reacted every moment of titration.

The titration itself lasts about 5 to 10 minutes. All preliminaries considered, (melting the solvent, introducing the electrodes, etc.) each determination takes up to 40 minutes.

A series of titration curves, with classical feature, similar to those from the point-by-point titration, are obtained. They could be linearized so that the equivalent point has been calculated both by the linearization method[13] and by the Hahn-Weiller method.[14] Figure 2 shows the titration curves of sodium carbonate (a), sodium peroxide (b) and potassium hydroxide (c) by potassium bichromate. For all the determinations the amounts of taken substance have been found with satisfactory accuracy as seen in table 1.

Table 1

Results of continuous titration of sodium carbonate, potassium hydroxide and sodium peroxide by potassium bichromate at 300°

Titrated substance	Taken mg	Found mg	Relative error %
Na_2CO_3	3.60	3.57	−0.9
	4.60	4.57	−0.7
	20.40	20.52	+0.6
	45.70	45.38	−0.7
KOH	2.30	2.25	−2.2
	2.40	2.43	+1.2
	3.60	3.55	−1.4
Na_2O_2	5.60	5.40	−3.5
	2.50	2.45	−2.1
	1.40	1.46	+4.3
	6.20	6.16	−0.6
	4.60	4.65	+1.1

It can be concluded that the use of standard as sticks and its immersion into the melt that contains the sought-for species, enables a continuous titration and allows to record directly, in a short time, the titration curve. The equivalent points could be calculated by the usual methods and the amounts of substances are determined with satisfactory accuracy.

---

[13] C. Liteanu and M. Mioşcu, *Rev. Roumaine Chim.*, **13**, 1185 (1968).
[14] F. L. Hahn and G. Weiller, *Z. analyt. Chem.*, **69**, 417 (1926).

Revue Roumaine de Chimie, **15**, 589 – 595 (1970)

DETERMINATION OF THE SIDERITE AND ANKERITE CONTENT BY THERMAL ANALYSIS METHODS

GR. POPA and D. N. TODOR
University of Bucharest, Spl. Independenţei, 89
and
Geological Prospection Enterprise, Bucharest, Str. Caransebeş, 1

Received July 14, 1969

The determination of the siderite and ankerite content by methods of thermal analysis is based on their decomposition under the action of thermal energy. The mass variation, graphically registered by the curves GT and GTD, as a result of the eduction of CO_2, allows to determine successfully the siderite and ankerite content in different mixtures with other minerals. The specific temperature ranges of these decompositions are 450–600° for siderite, and 700–900° for ankerite. One notices that very often the presence of iron in the analysed samples is not bound to carbonates; this is evidenced only by the curve DTA, through an exothermal effect, between 400 and 460°. In the case of a mixture of several carbonates: siderite, ankerite, calcite, dolomite, etc., the thermal effects registered by the curve following the decomposition, influence one another but do not superpose.

Thermal analysis methods, giving good results have been used for the determination of the siderite and ankerite content, mineral carbonates frequently met in iron ore deposits.

The transformations of these minerals are minutely rendered in the speciality literature, [1–7] but they are based only on the curves of differential thermal analysis. The study of these curves enables no quantitative determination and only qualitative specifications are possible.

The combining of thermal methods, under the name of "combined thermal method", or "thermal derivatography", has permitted successful determinations of carbonate minerals. The subject studied by us aims at achieving the quantitative determination of ankerite and siderite by means of DTA, TG and DTG curves.

[1] F. L. Cuthbert and R. A. Rowland, *Amer. Min.*, **32**, 111 (1947).
[2] P. F. Kerr and J. L. Kulp, *Amer. Min.*, **32**, 678 (1947).
[3] A. F. Frederickson, *Amer. Min.*, **33**, 372 (1948).
[4] A. F. Rowland and E. C. Joans, *Amer. Min.*, **34**, 550 (1949).
[5] V. J. Kaurkvskii, *Zhur. priklad. Khim.*, **27**, 136 (1954).
[6] V. J. Kaurkvskii and A. P. Polikin, *Trudy Voronezh. Gosudarst. Univ.*, **49**, 121 (1958).
[7] V. Schwab, in "Handbook of Differential Thermal Analysis", Chemical Publishing Co., New York, 1966.

EXPERIMENTAL

The data given in this paper were obtained with a derivatograph, using the following experimental parameters :

- maximum heating temperature — 1000°
- temperature increase rate in the furnace — 10° per minute
- quantity of sample processed — 0.5—0.6 g.
- the inert standard substance — aluminium oxide
- the atmosphere in the furnace — air at room pressure.

EXPERIMENTAL DATA

1. Transformations of siderite : the first transformation undergone by siderite under the action of thermal energy is brought about by the decomposition of iron carbonate ($FeCO_3 \rightarrow FeO + CO_2$). This takes place with heat absorption and is recorded by the thermal curves through an endothermal effect and a loss in weight, corresponding to the quantity of CO_2 released. The temperature range of decomposition is 450—600°, with maximum effect at 580°. This interval naturally changes with the heating rate, the quantity of the sample and its purity. Further, with the temperature increase, and immediately after the completion of carbonate decomposition, the oxidation of the ferrous acid occurs as a result of this decomposition.

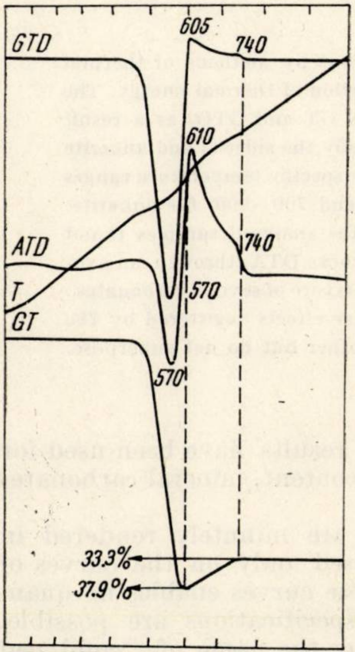

Fig. 1. — Sample No 1 — monomineral siderite, Teliuc.

$$(3\ FeO + 1/2\ O_2 \rightarrow Fe_3O_4).$$

This oxidation is marked on the thermal curves, through a large exothermal effect, and an increase in weight (fig. 1). The oxidation temperature is variable : data found in literature are very contradictory, as the oxidation is influenced in the first place by the atmosphere in the furnace. In an inert atmosphere, the oxidation does not take place, or it occurs only partially. Secondly, the oxidation is related to the volume of the sample, the crucible shape as well as to the covering or uncovering of the sample. This last experimental factor is very important, and as seen from figures 2 and 3, the characteristic temperatures, as well as the reactions, are strongly influenced. The covering of the sample has a considerable influence on the appearance of the reactions, especially when there is a change in weight. The reactions accompanied by a loss in weight may take place through the covering of the sample, but they result in a temperature gap of the thermal effect's peak.

Oxidations, reactions accompanied by an increase in weight, may be entirely inhibited or not well defined. Therefore, in such cases, experiments should be carried out with uncovered sample, and the literature data, if they do not render the experimental conditions, should be considered only for the sake of orientation.

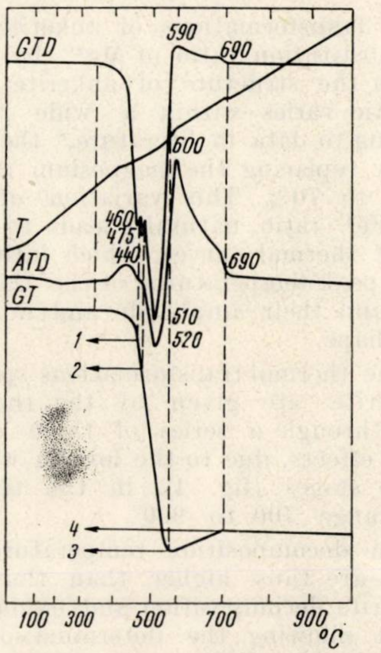

Fig. 2. — Sample No 2 — siderite with hydrated iron oxides, Teliuc (analysis carried out with uncovered sample).

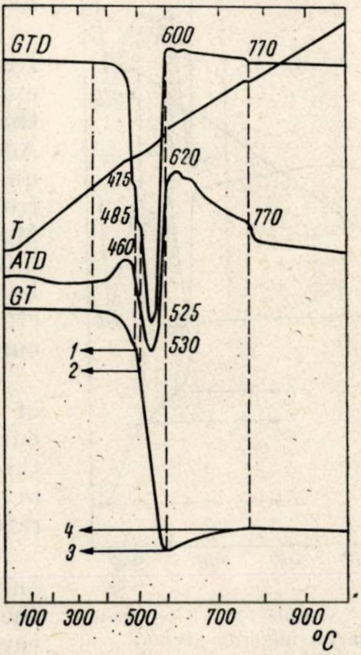

Fig. 3. — Sample No 2 — siderite with hydrated iron oxides, Teliuc (analysis carried out with covered samples).

Another question that has given rise to much controversy in the literature is the beginning of oxidation and up to the form it reaches. Some authors [7] consider that the only possible reaction, in the case of oxidation is : $3\ FeO + CO_2 \rightarrow Fe_3O_4 + CO$, and others [4] demonstrate that the oxidation takes place due to the oxygen found in the furnace and not to carbon dioxide. They have therefore carried out experiments in a CO_2 atmosphere and have proved that the oxidation did not take place. Ker and Kulp[2] have raised some doubts about the possibility of immediate oxidation of ferrous acid, which after decomposition of the carbonate shows as a very fine powder protected from the CO_2 resulted from decomposition.

In conclusion, based on the thermal phenomena registered by the curves TG and DTG, we believe, contrarily to the above mentioned authors, who have taken into consideration only the thermal effects on DTA curve, that the oxidation process takes place immediately after the decomposition of the carbonate, when working with an uncovered sample, and that oxidation yields Fe_3O_4 at room atmosphere. The very marked exothermal effect registered by the DTA curve, is due to the summation of two factors, one being the oxidation, and the other a structure change, representing the passing of the oxide from the triagonal to the cubic structure of magnetite.

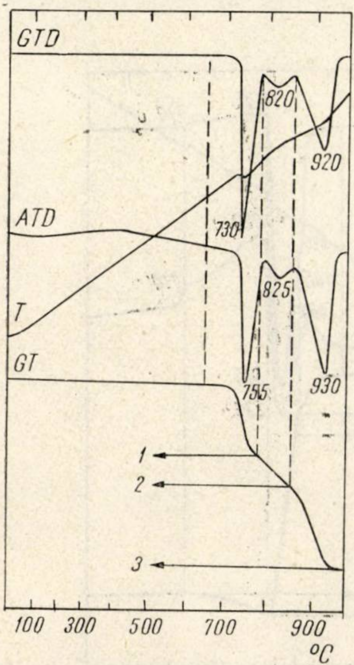

Fig. 4. — Sample No 3 — mono-mineral ankerite, Teliuc.

2. Transformations of ankerite. No fixed substitution ratio of Mg^{2+} by Fe^{2+} exists in the structure of ankerite since this ratio varies within a wide range. According to data in literature,[8] the iron quantity replacing the magnesium ranges from 5 to 70%. This variation of the $Mg^{2+}—Fe^{2+}$ ratio, naturally leads to very different thermal curves, which influence but the peak temperatures of the thermal effects and their amplitude and not the curve shape.

The thermal transformations specific of ankerite, are given by the thermal curves through a series of three endothermal effects, due to the loss in weight in three stages (fig. 4), in the temperature range 700 to 900°.

The decomposition temperatures of ankerite are thus higher than those of the siderite decomposition and oxidation, this fact allowing the determination of ankerite beside siderite.

The three reactions which bring about the appearance of the three endothermal effects are :

1. $Ca(Mg, Fe)\,(CO_3)_2 \rightarrow MgO + CO_2 + (Fe, Ca)\,(CO_3)_2$
2. $(Fe, Ca)\,(CO_3)_2 \rightarrow FeO + CO_2 + CaCO_3$
3. $CaCO_3 \rightarrow CaO + CO_2$

The thermal decomposition of ankerite has been mentioned in literature,[9-11] from a qualitative point of view, by the method of differential thermal analysis. From our own findings, also mentioned in literature,[12] it results that the bigger the iron quantity in the ankerite lattice, the lower the decomposition temperature of the first effect, naturally followed by the two others. At first sight one would believe an exothermal effect might also exist on the thermal curves, after the second endothermal effect, brought about by the oxidation of the FeO released from the ankerite's lattice; but this can not exist since, as shown in the case of siderite, the oxidation does not occur in CO_2 atmosphere.

---

[8] J. L. Kulp, P. Kent and P. F. Kerr, *Amer. Min.*, **36**, 92 (1951).

[9] C. W. Beck, *Amer. Min.*, **35**, 985 (1950).

[10] S. Guigue, *Publs. serv. carte géol. Algérie Bull.*, **5**, 43 (1955).

[11] V. Tolnay and V. Koblennez, *Magy. Allami Foldt. Ins. Evi. Jelentese*, **1967**, 369.

[12] R. C. Mackenzie, "The Differential Thermal Investigation of Clays", Mineralogical Society, London, 1957.

DETERMINATION OF MINERALS ON THERMAL CURVES

The mineralogical composition of carbonate samples from the iron ore deposits can be very different. The prevailing minerals found in iron ore deposits in different proportions are: siderite, ankerite, calcite, dolomite, hydrated or anhydrous iron oxides, and sulphides. Among these, the carbonate minerals are very well suited for quantitative determinations through thermal methods.[13] The present oxides and sulphides can be interpreted only qualitatively.

The calculation of the carbonate content, according to the size and shape of the curves, is carried out in the following way: from every upper point of inflexion of each thermal effect registered by the curve DTG, one draws perpendicular lines to curve TG, which divide it into segments proportional to every thermal effect separately, respectively to every change in weight.

The ratio of the total height in mm of the total loss in weight, to the height in mm of each segment on the TG curve, gives the content of the change in weight, specific of each thermal effect.

CONCLUSIONS

Research undertaken on six samples of various ores, listed in table 1, results in a very good characterization of the thermal effects specific

Table 1

Stages of weight changes of analysed samples

Weight changes			Origin of weight changes
Interval on figure	phenomenon	%	
Sample No 1, Teliuc, monomineral siderite, fig. 1			
0–1	$-CO_2$	–37.9	decomposition of $FeCO_3$
1–2	$+O_2$	+ 4.6	FeO oxidation of Fe_3O_4
Sample No 2, Teliuc, siderite with hydrated iron oxide, fig. 2			
0–1	$-H_2O$	– 4.1	dehydration of oxide
1–2	$-H_2O$	– 3.9	dehydration of oxide
2–3	$-CO_2$	–25.2	decomposition of $FeCO_3$
3–4	$+O_2$	+ 3.0	FeO oxidation of Fe_3O_4

---

[13] D. N. Todor, Proceedings of the National Conference on Soil Science, Publ. SNRS, No 5, 1967.

Table 1 (continued)

Interval on figure	Weight changes		Origin of weight changes
	phenomenon	%	
Sample No 3, Teliuc, monomineral ankerite, fig. 4			
0–1	$-CO_2$	−16.8	decomposition of $MgCO_3$ from ankerite
1–2	$-CO_2$	− 7.2	decomposition of $FeCO_3$ from ankerite
2–3	$-CO_2$	−17.7	decomposition of $CaCO_3$ from ankerite
0–3		−41.7	
Sample No 4, Delniţa, dolomite with oxide and sulphides, fig. 5			
0–1	$-CO_2$	−14.5	decomposition $MgCO_3$ from dolomite
1–2	$-CO_2$	−14.9	decomposition $CaCO_3$ from dolomite
0–2		−29.4	
Sample No 5, Işalniţa, magnesite with ankerite, etc. fig. 6			
0–1	$-CO_2$	−22.1	decomposition $MgCO_3$ from magnesite
1–2	$-CO_2$	− 3.3	decomposition $MgCO_3$ from ankerite
2–3	$-CO_2$	− 1.1	decomposition $FeCO_3$ from ankerite
3–4	$-CO_2$	− 5.5	decomposition $CaCO_3$ from ankerite
0–4		−31.7	
Sample No 6, Ghelar, siderite, ankerite, calcite, etc., fig. 7			
0–1	$-H_2O$	− 2.1	dehydration of oxide
1–2	$-CO_2$	−16.5	decomposition $FeCO_3$ from siderite
2–3	$+O_2$	+ 2.1	FeO oxidation of Fe_3O_4
3–4	$-CO_2$	− 6.4	decomposition $MgCO_3$ from ankerite
4–5	$-CO_2$	− 2.3	decomposition $FeCO_3$ from ankerite
5–6	$-CO_2$	− 9.6	decomposition $CaCO_3$ from ankerite
6–7	$-CO_2$	− 1.8	decomposition $CaCO_3$ from calcite
0–7		−36.6	

of the present components. By applying the above calculation, one could establish the mineralogical composition, which is conclusive with the chemical analysis and the macro- and micromineralogical descriptions. The analytical data of the ores, comparable to those obtained through thermal methods, are shown in table 2.

Table 2

Content in components of minerals analysed by thermal method, compared to data of chemical analysis

No of sample and origin	Thermal methods						Chemical analysis					
	CO_2 total	Fe of siderite	Fe of ankerite	Mg of ankerite	Mg of magnezite	Ca of ankerite	Ca of calcite	Carbonate total	CO_2	Fe	Mg	Ca
1 Teliuc	37.9	48.0	—	—	—	—	—	99.7	37.5	48.4	—	—
2 Teliuc	25.2	32.0	—	—	—	—	—	66.3	26.4	42.3	—	—
3 Teliuc	41.7	—	9.1	9.3	—	16.1	—	91.1	40.8	9.6	9.0	16.4
4 Delniţa	29.4	—	—	—	8.0	—	13.6	61.7	30.0	24.4	8.3	13.2
5 Işalniţa	31.1	—	1.4	1.8	12.2	4.7	—	63.3	31.1	23.9	14.6	4.8
6 Ghelar	36.6	20.6	2.9	3.5	—	8.7	1.7	87.8	37.4	36.2	3.2	10.7

Nevertheless, on the thermal curves shown in figures 5, 6, 7, one notices small shifts of peak temperatures of the thermal effects as against those of the monominerals in figures 1, 2 and 4, shifts which may be explained by the reciprocal influence of physico-chemical changes brought about by the temperature.

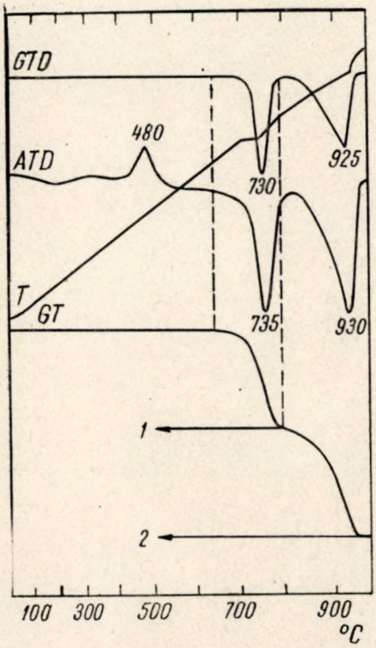

Fig. 5. — Sample No 4 — dolomite with iron oxides and sulphides, Delniţa.

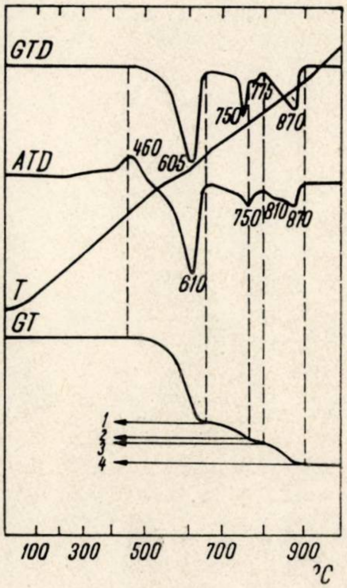

Fig. 6. — Sample No 5 — mixture of ankerite magnesite, iron oxide and sulphides, Işalniţa.

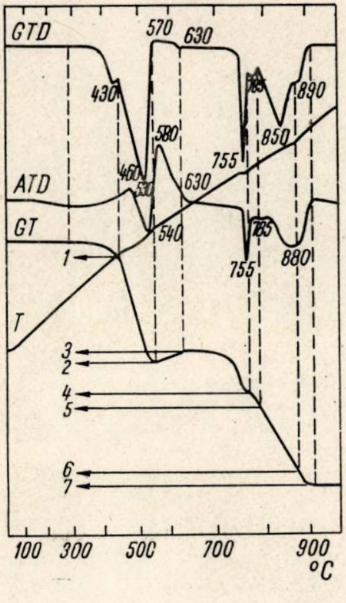

Fig. 7. — Sample No 6 — mixture of siderite, ankerite, calcite, iron oxides and sulphides, Ghelar — Hunedoara.

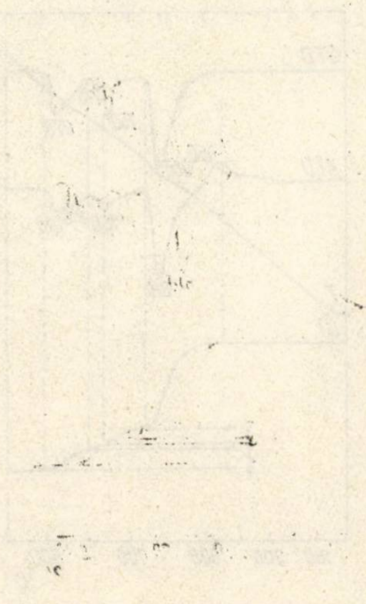

Fig. 6. — Sample No. 5. — [illegible]

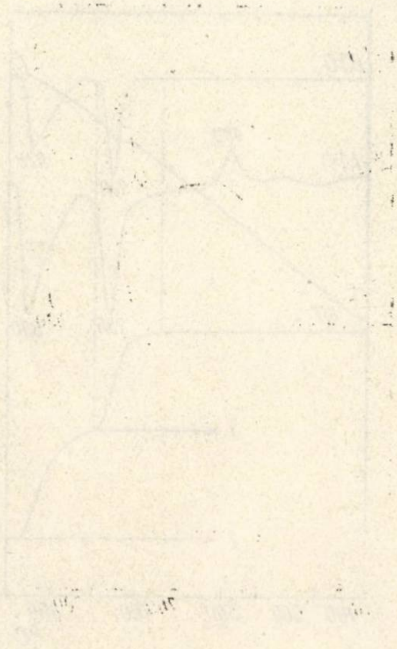

Fig. 5. — Sample No. 4. — [illegible]

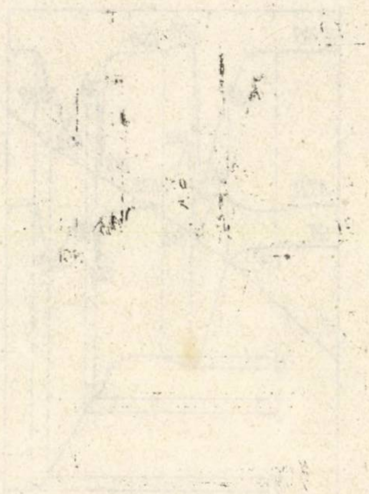

Fig. 7. — Sample No. 7. — [illegible]

Revue Roumaine de Chimie, **15**, 597 – 603 (1970)

KINETIC MEASUREMENT OF COBALT TRACES. I WITH MAGNEZON 1

D. COSTACHE and P. JUNIE

Department of Analytical Chemistry, University of Bucharest
Splaiul Independenţei, 89

Received July 29, 1969

One determines the cobalt by the kinetic method using the oxidation reaction of magnezon with peroxide in alkaline medium. The reaction rate is measured spectrophotometrically at $\lambda = 533$ nm. Optimum conditions, gauging curve, interference and reproductivity are given. The rate constants and influence of temperature are calculated. The method suggested allows the measurement of cobalt in the concentration range 3.25×10^{-9} to 24.36×10^{-9} g Co/ml.

The concentration of a substance is determined either directly, or through a special feature which is measured and finds itself in a certain dependency on its concentration.

In the kinetic methods of analysis, the recorded feature is the reaction rate, which changes according to the concentration of the substance to be determined, substance having a catalytic role. The literature mentions cobalt determinations by the kinetic method. [1-20]

---

[1] J. Bognar, *Magyar Kém. Folyóirat*, **59**, 25 (1953).

[2] J. Bognar and O. Jellinek, *Acta Chim. Acad. Sci. Hung.*, **29**, 131 (1961); **29**, 139 (1961); **29**, 319 (1961).

[3] J. Laszlovski, *Mikrochim. Acta*, **1961**, 289.

[4] E. Schulek and J. Laszlovski, *Mikrochim. Acta*, **1960**, 41.

[5] J. Bognar, *Mikrochim. Acta*, **1963**, 801.

[6] N. B. Parhomenko, G. A. Prik and K. B. Iatsimirski, *Žhur. analit. Khim.*, **16**, 599 (1961).

[7] J. Bognar and L. Sipoş, *Mikrochim. Acta*, **1963**, 442.

[8] J. Bognar and O. Jellinek, *Acta Chim. Acad. Sci. Hung.*, **29**, 21 (1961).

[9] A. K. Babko and N. M. Lukovskaia, *Ukrain. Khim. Zhur.*, **28**, 968 (1962).

[10] J. Bognar, *Mikrochim. Acta*, **1961**, 901.

[11] V. M. Peskova, J. F. Dolmanova and N. M. Cemenova, *Zhur. analit. Khim.*, **18**, 1228 (1963).

[12] E. A. Bozhevolnov and S. U. Kreingold, *Tr. Vses. Nauk* in Ref. *Zhur. Khim.*, **26**, 204 (1966).

[13] S. G. Oradovski, *Khim. Protsesy Moyakh Okeanakh Akad. Nauk*, **1966**, 78.

[14] S. U. Kreingold and E. A. Bozhevolnov, *Metody Anal. Khim. Reaktiv i Preparatov*, **11**, 49 (1965).

[15] J. Laszlovski, *Magyar Khém. Folyóirat*, **71**, 260 (1965); **71**, 99 (1965).

[16] A. K. Babko and N. M. Lukovskaia, *Ukrain. khim. Zhur.*, **30**, 508 (1964).

All these works use as reaction indicator the oxidation of some organic substances containing two hydroxyls in *ortho* position, with peroxide, in alkaline medium.

In the present paper, as in papers [21,22] one makes use of the oxidizing reaction of a substance presenting a hydroxyl group in *ortho* against an azo group:

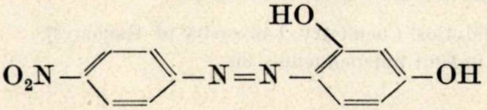

Magnezon 1

which widens considerably the domain in which the kinetic methods for the determination of cobalt may be applied.

EXPERIMENTAL

The reacting solution was obtained by dissolving magnezon 1 in ethylic alcohol: the concentration obtained was 0.016 g %.

Peroxide obtained by diluting perhydrol had a 3.69 M concentration.

The potassium hydroxide solution ensuring the reaction medium had a 1 M concentration.

The cobalt solution was obtained by solving spectrally pure metallic cobalt in diluted sulphuric acid, of which, through successive dilutions, one has obtained a working solution having a 4.06×10^{-8} g Co/ml concentration.

To obtain all the solutions, as well as to bring to the mark in the calibrated flasks one has used thrice distilled water. Horizontal Pulfrich Zeiss Jena and V.S.U.1 spectrophotometers were used and the method was worked out at $\lambda = 533$ nm wavelength.

Working method

The solutions were mixed in 25 ml flasks, in the following order and quantities: 1 ml reactive, 5 ml potassium hydroxide, 1 ml peroxide, from 1 to 15 ml cobalt solution.

After bringing to the mark with tridistilled water, and starting the chronometer, the content of the flask is thoroughly stirred for about one minute, and then passed into the vat of the spectrophotometer in order to have its optical density read every minute, for 20 minutes.

Water is added in the blank test vat since the solution, initially coloured, turns colourless in time.

The optimum reaction conditions were chosen after studying the influence of the pH and of the peroxide concentration, the results of which are given in figures 1 and 2.

---

[17] Gr. Popa and D. Costache, *Analele Universității București*, **16**, 107 (1967).
[18] Gr. Popa and D. Costache, *Rev. Roumaine Chim.*, **12**, 963 (1967).
[19] Gr. Popa and D. Costache, *Analele Universității București*, **17**, 21 (1968).
[20] D. Costache and Gr. Popa, *Analele Universității București*, **17**, 55 (1968).
[21] Gr. Popa and D. Costache, *Rev. Roumaine Chim.*, **13**, 573 (1968).
[22] D. Costache, (forthcoming)

It results that the reaction rate increases with the increase in the peroxide's concentration up to a 1.50×10^{-3} g/ml concentration of the latter, and then stabilizes.

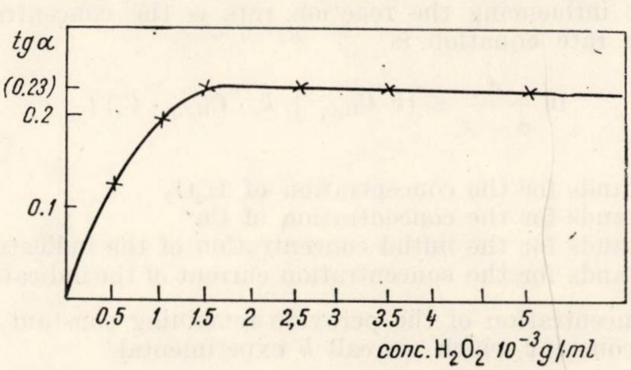

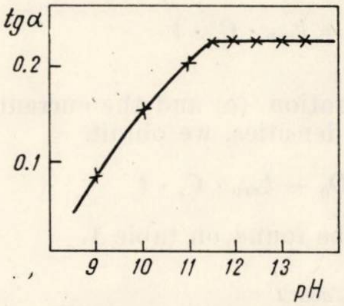

Fig. 1. — Variation of tg α *versus* peroxide concentration.

Fig. 2. — Variation of tg α *versus* the pH of the medium.

The maximum reaction rate is attained in the pH range between 11.5 and 13.5.

The concentrations of the substances in the vat are the following:

Magnezon 1 — 6.40×10^{-6} g/ml
H_2O_2 — 3.01×10^{-3} g/ml
KOH — 0.2 N
Cobalt — $3.25 \times 10^{-9} - 24.36 \times 10^{-9}$ g Co/ml

RESULTS AND DISCUSSIONS

The indicator reaction is the oxidizing reaction of the magnezon 1 with peroxide in alkaline medium. The indicator substance, the concentration variation of which is watched in time, is magnezon 1.

From the concentration ratio of peroxide and magnezon it results that the peroxide occurs in too great a quantity as against the magnezon, a fact allowing us to consider its concentration constant from the practical point of view, and the reaction as pseudomonomolecular.

In the expression of reaction rate the rate constant is a function of the peroxide's concentration, of the temperature and of the cobalt's concentration.

$$k = f([H_2O_2],\ t^\circ,\ [Co]) \tag{1}$$

Working in standard conditions (same peroxide concentration, same ionic strength, and in a thermostating regime of the samples), the only element influencing the reaction rate is the concentration of the catalyst. The rate equation is

$$\ln \frac{a}{a-x} = (k \cdot C_{\mathrm{H_2O_2}} + k_c \cdot C_{\mathrm{H_2O_2}} \cdot C_c)\, t \qquad (2)$$

in which

$C_{\mathrm{H_2O_2}}$ stands for the concentration of H_2O_2
C_c stands for the concentration of Co
a stands for the initial concentration of the indicator substance
$a-x$ stands for the concentration current of the indicator substance

The concentration of the peroxide remaining constant, we write it in the rate constant which we call k experimental

$$\ln \frac{a}{a-x} = k_{\mathrm{exp}} \cdot C_c \cdot t \qquad (3)$$

Replacing the initial concentration (a) and the current one ($a-x$) of the magnezon with the optical densities, we obtain

$$\ln D = \ln D_0 - k_{\mathrm{exp}} \cdot C_c \cdot t \qquad (4)$$

The experimental data may be found on table 1.

Table 1

Variation in time of optical densities of solutions with variable catalyst content

Uncatalytical reaction	min	2	3	4	5	6	7	8
	D	1.20	1.20	1.20	1.19	1.18	1.17	1.16
	min	9	10	11	12	13	14	15
	D	1.16	1.16	1.15	1.15	1.15	1.14	1.14
	min	16	17	18	19	20		
	20	1.14	1.13	1.12	1.11	1.11		
Co conc 3.25×10^{-9} g/ml	min	2	3	4	5	6	7	8
	D	1.12	1.09	1.07	1.05	1.04	1.03	1.01
	min	9	10	11	12	13	14	15
	D	1.00	0.99	0.98	0.96	0.94	0.93	0.92
	min	16	17	18	19	20		
	D	0.91	0.89	0.88	0.86	0.85		
Co conc 6.50×10^{-9} g/ml	min	2	3	4	5	6	7	8
	D	1.10	1.07	1.05	1.02	0.99	0.97	0.95
	min	9	10	11	12	13	14	15
	D	0.93	0.90	0.88	0.86	0.84	0.82	0.80
	min	16	17	18	19	20		
	D	0.79	0.77	0.76	0.74	0.72		

Table 1 (continued)

Co conc 9.74×10^{-9} g/ml	min	2	3	4	5	6	7	8
	D	1.06	1.03	0.99	0.95	0.92	0.89	0.87
	min	9	10	11	12	13	14	15
	D	0.84	0.81	0.79	0.77	0.75	0.73	0.70
	min	16	17	18	19	20		
	D	0.67	0.65	0.62	0.60	0.58		
Co conc 12.99×10^{-9} g/ml	min	2	3	4	5	6	7	8
	D	1.03	0.98	0.95	0.91	0.87	0.85	0.82
	min	9	10	11	12	13	14	15
	D	0.80	0.78	0.75	0.72	0.68	0.67	0.63
	min	16	17	18	19	20		
	D	0.62	0.58	0.57	0.54	0.52		
Co conc 16.24×10^{-9} g/ml	min	2	3	4	5	6	7	8
	D	0.98	0.94	0.89	0.86	0.82	0.78	0.75
	min	9	10	11	12	13	14	15
	D	0.70	0.68	0.65	0.62	0.58	0.56	0.54
	min	16	17	18	19	20		
	D	0.52	0.48	0.46	0.44	0.43		
Co conc 24.36×10^{-9} g/ml	min	2	3	4	5	6	7	8
	D	0.94	0.87	0.81	0.76	0.71	0.66	0.62
	min	9	10	11	12	13	14	15
	D	0.58	0.54	0.50	0.47	0.44	0.40	0.38
	min	16	17	18	19	20		
	D	0.35	0.33	0.30	0.28	0.26		

For the present paper one has chosen the "tangent method", and obtained figures 3 and 4, the latter being the gauging graph.

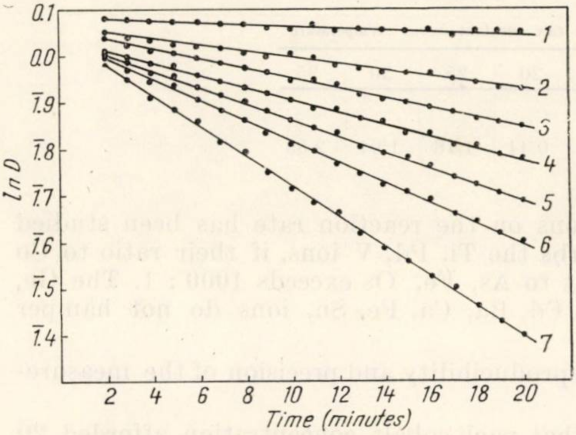

Fig. 3. — Variation of ln D *versus* time ; *1*, – g Co/ml ; *2*, 3.25×10^{-9} g Co/ml ; *3*, 6.50×10^{-9} g Co/ml ; *4*, 9.74×10^{-9} g Co/ml ; *5*, 12.99×10^{-9} g Co/ml ; *6*, 16.24×10^{-9} g Co/ml ; *7*, 24.36×10^{-9} g Co/ml.

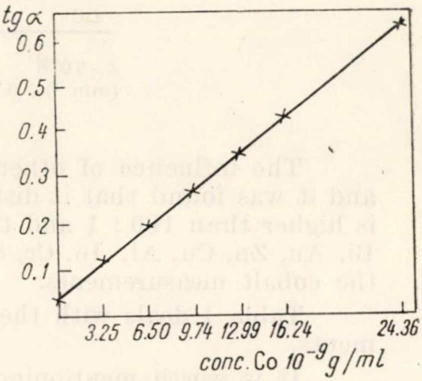

Fig. 4. — Variation of tg α *versus* cobalt concentration.

One has then computed the rate constant $k_{\text{exp.}}$ according to relationship

$$k = \frac{\ln D_1 - \ln D_2}{t_2 - t_1} \times 2.303 \tag{5}$$

in which D_1 and D_2 represent optical densities at the moments t_1 and t_2

The values of these constants in the case of samples with different catalyst concentration are given in table 2.

Table 2

Values of the rate constant *k*, for different concentrations of catalyst

Co conc. (g/ml)	k (min^{-1})
—	0.44×10^{-2}
3.25×10^{-9}	1.52×10^{-2}
6.50×10^{-9}	2.29×10^{-2}
9.74×10^{-9}	3.34×10^{-2}
12.99×10^{-9}	3.80×10^{-2}
16.24×10^{-9}	4.81×10^{-2}
24.36×10^{-9}	6.76×10^{-2}

One has also noted the influence of temperature on the reaction rate, having a cobalt concentration of 8.12×10^{-9} g Co/ml in the samples. These are shown in table 3. Working temperature, 20°.

Table 3

Variation of the rate constant *versus* temperature

t°C	15	20	25	30	35
$k \times 10^{-2}$ (min^{-1})	0.27	0.44	1.16	1.94	2.85

The influence of other ions on the reaction rate has been studied and it was found that it disturbs the Ti, Pd, V ions, if their ratio to Co is higher than 100 : 1 and that to As, Fe, Os exceeds 1000 : 1. The Ge, Bi, Au, Zn, Cu, Al, In, Cr, Sr, Cd, Ba, Ca, Fe, Sn, ions do not hamper the cobalt measurements.

Table 4 deals with the reproducibility and precision of the measurements.

It is worth mentioning that each cobalt concentration afforded 20 measurements, of which only 5 were included in the table. The average square selection error was computed for the 20 measurements. The method enables cobalt determination in a 3.25×10^{-9} to 24.36×10^{-9} g Co/ml concentration range. A measurement requires approximately 15 to 20 minutes, irrespective of the calibration graph.

Table 4

Reproducibility and precision of measurements

No of measurements	Co analysed g/ml	∡ α°	Co found in analysis g/ml × 10^{-9}	Difference g/ml × 10^{-9}	Standard square selection error s^2
	3.25×10^{-9}	7°			
1		8°	4.15	0.90	
2		7°	3.35	0.10	
3		7°	3.35	0.10	
4		7°	3.35	0.10	1.618×10^{-4}
5		6°	2.75	0.50	
	6.50×10^{-9}	11°			
1		11°	6.50	—	
2		11°	6.50	—	
3		10°	5.80	0.70	1.336×10^{-4}
4		12°	7.20	0.70	
5		11°	6.50	—	
	9.74×10^{-9}	15°			
1		15°	9.74	—	
2		14°	8.94	0.80	
3		15°	9.74	—	
4		16°	10.34	0.60	1.775×10^{-4}
5		16°	10.34	0.60	
	12.99×10^{-9}	19°			
1		19°	12.99	—	—
2		20°	13.49	0.50	
3		19°	12.99	—	
4		20°	13.49	0.50	0.869×10^{-4}
5		20°	13.49	0.50	
	16.24×10^{-9}	23°			
1		24°	17.04	0.80	
2		24°	17.04	0.80	
3		23°	16.24	—	
4		24°	17.04	0.80	1.057×10^{-4}
5		23°	16.24	—	
	24.36×10^{-9}	32°			
1		31°	23.66	0.70	
2		31°	23.66	0.70	
3		32°	24.46	0.10	
4		32°	24.46	0.10	1.456×10^{-4}
5		32°	24.46	0.10	

Revue Roumaine de Chimie, 1, 597 – 603 (1970)

Revue Roumaine de Chimie, 15, 605 – 606 (1970)

PHOTOMETRIC DETERMINATION OF COPPER TRACES WITHOUT EXTRACTION

M. E. MACOVSCHI and VIORICA NIŢU

Institute of Physical Chemistry of the Academy, Bucharest, str. Galaţi 31

Received July 17, 1969

A photometric method for the determination of copper traces with dithizone, eliminating the extraction, is presented. The method is rapid and simple and has a sensitivity of 0.5 μg Cu/ml; it may be also used as a microtitration method for copper dosage.

Usually the copper traces determination is made colorimetrically using as reagent dithizone[1] solved in CCl_4 or $CHCl_3$. The method is sensitive but supposes the extraction of copper-dithizone complex. By eliminating this extraction, the method proposed by us becomes very rapid and simple. It was elaborated to determine the width of the thin copper films deposited on glass by vacuum evaporation. Such films are especially used in solid-gas kinetic studies.

REAGENTS

Dithizone: 0.05 % solution in acetone (0.01 % for microtitration).

Standard copper solution: 3 μg Cu/ml (obtained by solving pure metallic copper in nitric acid and dilution with distilled water).

In a 25 ml measuring flask one introduces one after another the slightly acid copper solution (maximum 5 ml), distilled water up to 5 ml, 15 ml acetone and the dithizone solution, drop by drop, until the colour changes from reddish-violet to greyish-violet. Then acetone is added to the mark and the extinction is measured at $\lambda = 560$ nm, as against a diluted dithizone solution (one drop in 25 ml acetone).

The absorption spectra of dithizone and of the copper-dithizone complex are shown in figure 1. The determinations are not affected by the fact that dithizone has no absorption minimum at $\lambda=560$ nm, because dithizone is added only up to the colour change and the small excess of dithizone is balanced by using a diluted dithizone solution as blank.

---

[1] E. B. Sendel, "Colorimetric Determination of Traces of Metals", 3rd Ed. Interscience Publ. Inc. New York, 1959, p. 819.

The stability of the copper dithizone complex is satisfactory in time; however it is recommended to determine the extinction immediately after the filling of the measuring flask.

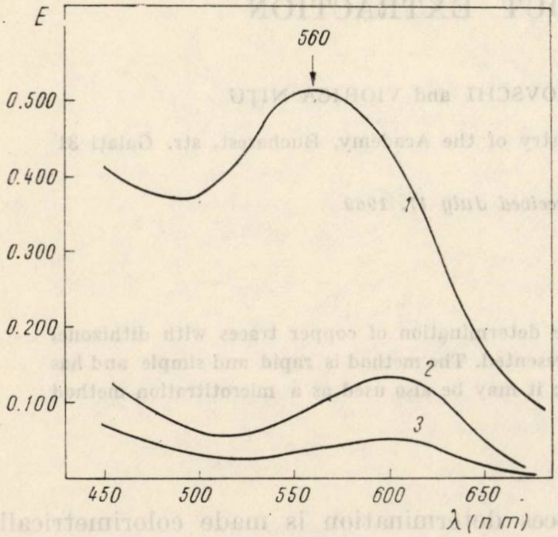

Fig. 1. — Absorption spectra of dithizone and copper-dithizone complex :

1, Copper-dithizone complex (10 µg Cu); *2*, 0.4 ml dithizone 0.05 % in 25 ml acetone; *3*, 0.2 ml dithizone in 25 ml acetone.

The Lambert-Beer's law is obeyed for the domain 0—15 µg. Cu. The sensitivity of the method is of about 0.5 µg Cu/ml; the accuracy —±5% and, for large quantities of copper, it depends also on the possibility to observe the very moment of the colour change.

The method may also be used as a microtitration method for copper dosage.

The procedure is analogue to that described above: to the slightly acid copper solution (maximum 5 ml) 15—20 ml acetone are added. The mixture is then titrated with 0.001% dithizone solution in acetone until the colour changes from reddish-violet to greyish-violet. Because the dithizone solution is not very stable it is necessary to make control determinations with standard samples.

Revue Roumaine de Chimie, **15**, 607 – 614 (1970)

A POLAROGRAPHIC STUDY ON STYRILCYANINES. I

SUBSTITUENT EFFECTS IN THE POLAROGRAPHIC REDUCTION OF THE STYRILCYANINES ACCORDING TO BROWN-OKAMOTO EQUATION

A. SZURKOS and P. NAGY

Faculty of Chemistry, Pedagogical Institute, Tg. Mureş
Str. Nicolae Iorga, 1

Received June 18, 1969

Nine compounds of 1-ethyl-2(p–X-styril)-pyridinium iodide have been prepared. The polarographic reduction of these compounds has been studied, especially with respect to pH and substituent effects. It has been observed, that the substituent effects can be described by Brown-Okamoto equation.

One of the most striking developments of physical-organic chemistry is the establishment of quantitative correlation between the structure and reactivity of organic compounds. Lately, the polarographic method in the study and elucidation of structural problems of organic molecules has been applied on a very wide scale.[1,2]

Quantitative correlations between half-wave potentials and structure of organic compounds have been described in several articles.[3–6] The most fruitful of these have proved the assumption, that there exists a dependence between the half-wave potentials and the reduction rate constants.

Hammett established the equation[7]

$$\log \frac{k}{k_0} = \rho\sigma \tag{1}$$

---

[1] P. Zuman, "Polarography 1964" Macmillan, London, 1966, p. 687.
[2] I. P. Kitaev and G. K. Budnikov, *Uspekhi Khim.*, **31**, 670 (1962).
[3] A. Maccol, *Nature*, **163**, 178 (1949).
[4] L. E. Lyons, *Nature*, **166**, 193 (1950).
[5] B. M. Covlons and W. R. Crowel, *J. Amer. Chem. Soc.*, **74**, 1294 (1952).
[6] P. Zuman, *Chem. listy*, **48**, 94 (1954).
[7] L. P. Hammett, "Physical Organic Chemistry", McGraw-Hill Book Company Inc., New York, 1940, p. 73.

where $-k$ is the rate or equlibrium constant for *meta* or *para* substituted benzene derivatives.

$-k_0$ the same for nonsubstituted derivatives.

$-\sigma$ the substituent constant, independent of the reaction type and characteristic of each substituent.

$-\rho$ the reaction constant, independent of substituent and characteristic of the reaction type.

The Hammett equation has also been used for the quantitative correlation of the half-wave potentials. Most of the electrochemical reactions of organic compounds are irreversible and $E_{1/2}$ is proportional to the logarithm of rate constant for irreversible process. [8-10]

$$E_{1/2} = \frac{RT}{\alpha nF} \cdot \ln 0.87\, k \sqrt{\frac{t}{D}} \tag{2}$$

where $-\alpha$ is the transfer coefficient

$-t$ the drop-time of the dropping mercury electrode.

$-D$ the diffusion coefficient.

$-k$ the specific rate constant of the electrode process, its value is determined by the free energy of the compound.

If $(E_{1/2})_x$ and $(E_{1/2})_0$ represent the half wave potentials of substituted, respectively unsubstituted compound for the irreversible process the following equation can be set up:

$$(E_{1/2})_x - (E_{1/2})_0 = \Delta E_{1/2} \sim \Delta \ln k = \ln \frac{k_x}{k_0} \tag{3}$$

The obtained equation is equivalent to the Hammett equation, which, presents the following form for the electrochemical process [11-13]

$$\Delta E_{1/2} = \rho_\pi \sigma \tag{4}$$

The Hammett equation has also been used for the polarographic study of heterocyclic systems.[14] It has been established, that the σ values used in the series of benzene derivatives are also valid for the substituents in the heterocyclic nucleus.[15]

Data concerning the polarographic reduction of styrilcyanines on the basis of linear free energy relationships have not been found in the current literature.

---

[8] J. Koutecky, *Coll. Czech. Chem. Comm.*, **18**, 597 (1959).
[9] R. Brdicka, *Coll. Czech. Chem. Comm.*, **19**, 41 (1954).
[10] P. Zuman, *Coll. Czech. Chem. Comm.*, **25**, 3225 (1960).
[11] O. Hanousch, *Coll. Czech. Chem. Comm.*, **25**, 2250 (1960).
[12] R. W. Brockman and D. E. Pearson, *J. Amer. Chem. Soc.*, **74**, 4128 (1952).
[13] P. Zuman, *Coll. Czech. Chem. Comm.*, **19**, 599 (1954).
[14] P. Zuman, *Coll. Czech. Chem. Comm.*, **27**, 63 (1962).
[15] Eiji Imoto, *Rev. of Polarography (Japan)*, **9**, 187 (1961).

The present paper shows a study upon the substituent effects on the polarographic reduction of the compounds of type: 1-ethyl-2(p-X-styril)-pyridinium iodide according to Brown-Okamoto equation.[16]

EXPERIMENTAL

The studied compounds have the following general formula:

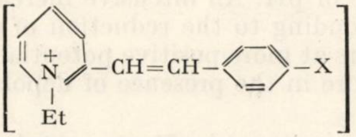

where $X = -OH, -OCH_3, -N(Et)_2, -N(Me)_2, -NH_2, -NHAc, -H, -Cl, -NO_2$.

Standard literature preparations were used for these compounds. Namely 1-ethyl-2-methyl-pyridinium iodide was condensed with *p*-substituted benzaldehides, in the presence of piperidine.[17] The purification was made by recrystallization from ethanol. Compounds IV, VI, VIII and IX are not described in literature. The purity of the compounds has been controlled by nitrogen microanalysis. The empirical formula, the melting points the molecular weights and the results of microanalysis are given in table 1.

Table 1

Compounds and their analysis data

No	X	Empirical formula	m.p. C°	MW	Analysis N %	
					calcd.	found
I.	$-OH$	$C_{15}H_{13}ONJ$	252.3	353.20	3.96	4.21
II.	$-N(Et)_2$	$C_{19}H_{26}N_2J$	200.4	408.32	6.86	7.17
III.	$-N(Me)_2$	$C_{17}H_{21}N_2J$	261.0	380.27	7.42	7.65
IV.	$-NH_2$	$C_{15}H_{17}N_2J$	231.2	352.22	7.95	8.24
V	$-OCH_3$	$C_{16}H_{18}ONJ$	227.6	367.23	3.81	4.11
VI.	$-NHAc$	$C_{17}H_{19}ON_2J$	270.6	394.25	7.10	7.46
VII.	$-H$	$C_{15}H_{16}NJ$	211.7	337.20	4.15	4.28
VIII.	$-Cl$	$C_{15}H_{15}NJCl$	229.6	371.65	3.77	4.07
IX.	$-NO_2$	$C_{15}H_{15}O_2N_2J$	240.6	382.20	7.33	7.71

The polarographic measurements have been carried out by using a polarograph, type LP-60. The polarograph was coupled to an electronic recorder with a sensitivity of 3.5×10^{-10} A/mm. The half-wave potential was determined against the SCE, using a Lingane-Laitinen cell. Solutions of 4×10^{-5} M from the studied compounds have been prepared in Britton-Robinson buffers. The precise determination of the pH value of the buffered solution was made with a pH-meter, of Radelkisz type. The measurements were performed at 22°. The capillary constants: the drop-time $t = 3.01$ s the flow rate $m = 2.37$ mg.s^{-1}.

---

[16] H. C. Brown and Y. Okamoto, *J. Amer. Chem. Soc.*, **80**, 4979 (1958).
[17] W. H. Mills and W. J. Pope, *J. Chem. Soc.*, **121**, 946 (1922).

RESULTS AND DISCUSSION

1. *The shape of polarographic curves*

The polarographic curves of the studied compounds in the range pH $= 2-11$ are given in figure 1. It can be seen, that the curves have almost the same character. In the range pH $= 2-5.7$ for the compounds V, VII, VIII and pH $= 2-8.7$ for the compounds I, II, III, IV, VI the reduction takes place in a single wave, and its limiting current is cancelled with the increasing value of pH. An intensive increase in the current can also be observed corresponding to the reduction of protons from supporting electrolyte. This occurs at more positive potentials than in the absence of the depolariser, therefore in the presence of depolariser the protons are catalytically reduced.

For the progressive values of pH the catalytic hydrogen current appears in the form of maxima (I, II, IV, V, VII, VIII) which in the basic media disappear, and the curve splits into three well distinguished waves. In the polarographic curve of compound IX, the wave appears corresponding to the reduction of the $-NO_2$ group.

According to our assumption the electrochemical reduction of the studied styrilcyanines is similar to that of N-alkyl-pyridinium ions desbribed in literature.[18] The polarographically active group is the quaternary azoatom from the pyridine nucleus. On the other hand it has been assumed, that the splitting of the curve into three waves in basic media may be due to the intricate adsorption process of the depolarizer and of the depolarization product. It has been also considered, that the second and the third wave are not resulting from another electrode process, but represent the continuation of the original reduction, at more negative potentials hindered by the adsorption phenomena.

The purpose of the present paper is not to show details of the reduction mechanism, though these are being studied.

2. *The pH effect*

It has been noted, that the half-wave potential of the first wave depends on the pH-value only for the compounds whose substituents can be protonized (i.e. $-NH_2$, $-N(Me)_2$, $-N(Et)_2$) or can dissociate (i.e. $-OH$). For the compounds V, VII, VIII the half-wave potential is independent of the pH-value (figure 2). The dependence of $E_1/_2$ on pH cannot be due to the proton participation in the reduction process. This dependence may be explained as follows : as a consequence of the protonation or dissociation, the electron distribution in the molecular conjugated system changes. For example : the unshared electron pair of the azoatom from the dimethylamino group (in compound III) takes part more or less, depending on the pH, in the conjugation of the π electron system.

---

[18] P. Topkins, *Analyt. Chem.*, **21**, 64 (1949).

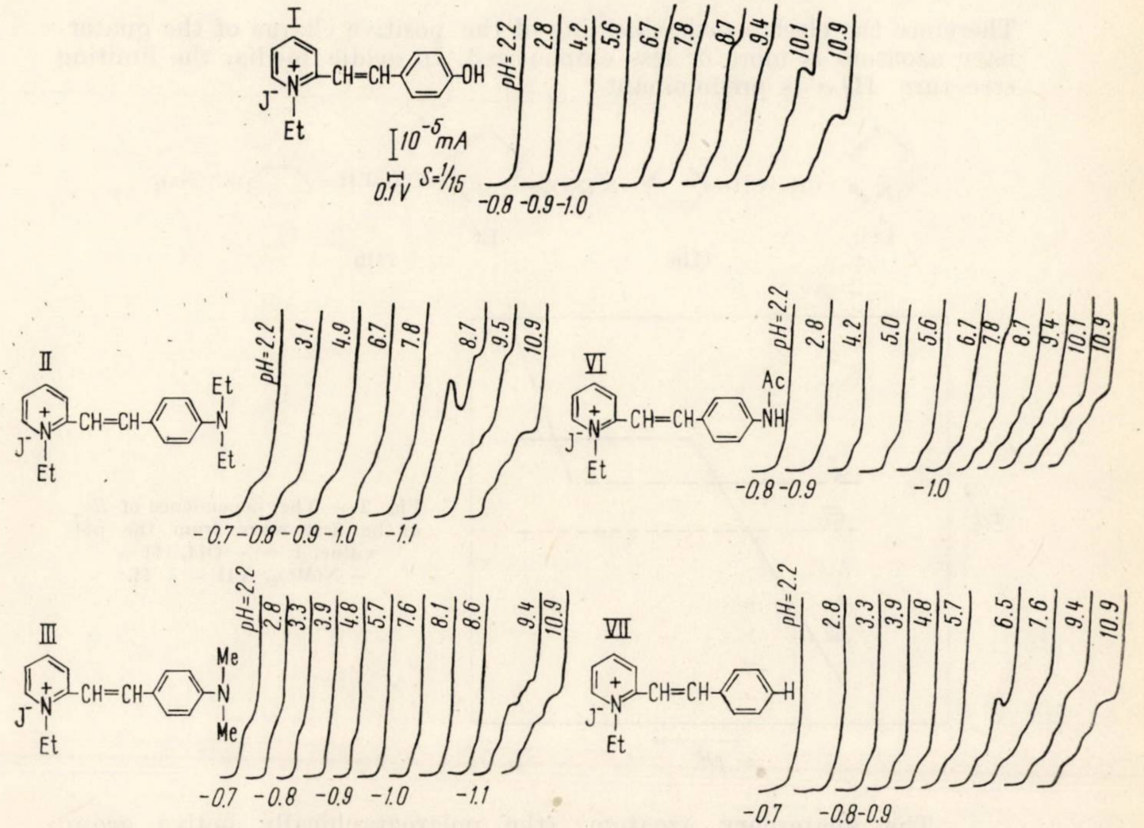

Fig. 1. — Polarographic curves of the 1-ethyl-2(*p*-X-styril)-pyridinium iodides in the pH 2 – 11 range

Therefore the electrostatic shielding of the positive charge of the quaternary azoatom is more or less emphasized. In acidic media, the limiting structure III-a is predominant:

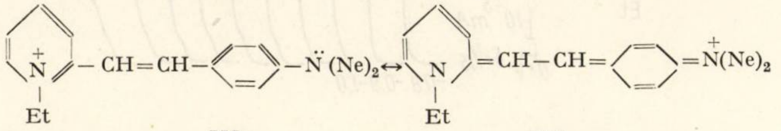

IIIa IIIb

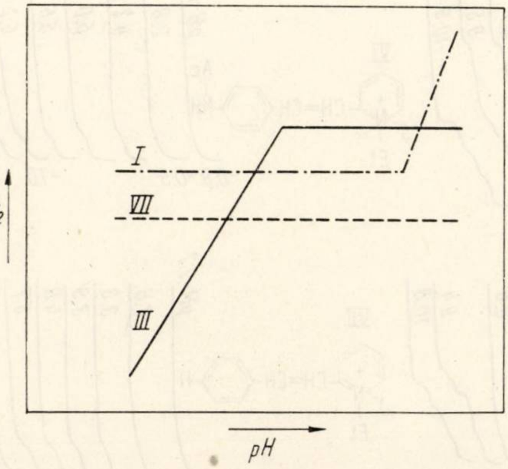

Fig. 2 — The dependence of $E_{1/2}$ of the first wave from the pH value. I = — OH, III = — N(Me)$_2$, VII = — H.

The quaternary azoatom (the polarographically active group) will have therefore, in acidic media, an entirely positive charge, which is favorable to the electrochemical process. In fact the half-wave potential in acidic media are shifted to positive values. In the basic media the limiting structure IIIb is more probable and an electrostatic shielding on the quaternary azoatom occurs. Therefore, the electrochemical reduction takes place more difficultly, and the half-wave potentials are shifted to the negative values.

The change of the half-wave potential in the basic media for the p—OH substituted compound (I) is due to the dissociation of the hydroxyl group. The electronic structure of the dissociated compound can be described with two limiting structures (Ia the amphionic and Ib the quinoidic structure). For the equilibrium stage, the limiting structure Ib (the anhydrobase) is predominant.[19,20]

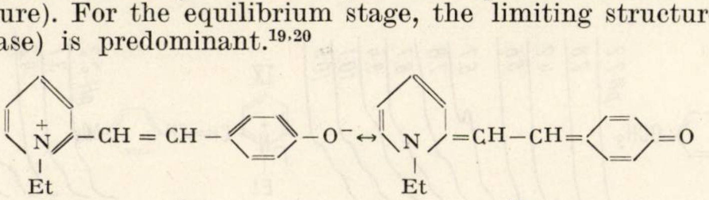

Ia Ib

---

[19] A. I. Kiprianov and F. A. Mihailenko, *Zhur. obshchei Khim.*, **10**, 600 (1940).

[20] A. I. Kiprianov and F. A. Mihailenko. *Zhur. obshchei Khim.*, **31**, 1334 (1961).

3. *The substituent effect*

We have studied the effect of *p*-substituents upon the polarographic reduction in the basic media. An influence of substituents has been observed only on the half-wave potential of the first wave. This effect for the second and the third wave is not significant (Table 2).

Table 2

$E_{1/2}$ values of the first wave in the basic media and the corresponding σ^+ constants

No.	X	$E_{1/2}$ mV	σ^+
I.	$-O^-$H	−1380	−2.23
II.	$-N(Et)_2$	−1330	−1.76
III.	$-N(Me)_2$	−1323	−1.70
IV.	$-NH_2$	−1283	−1.30
V.	$-OCH_3$	−1230	−0.78
VI.	−NHAc	−1213	−0.60
VII.	H	−1153	0.00
VIII.	Cl	−1131	$+0.227^{(\sigma)}$

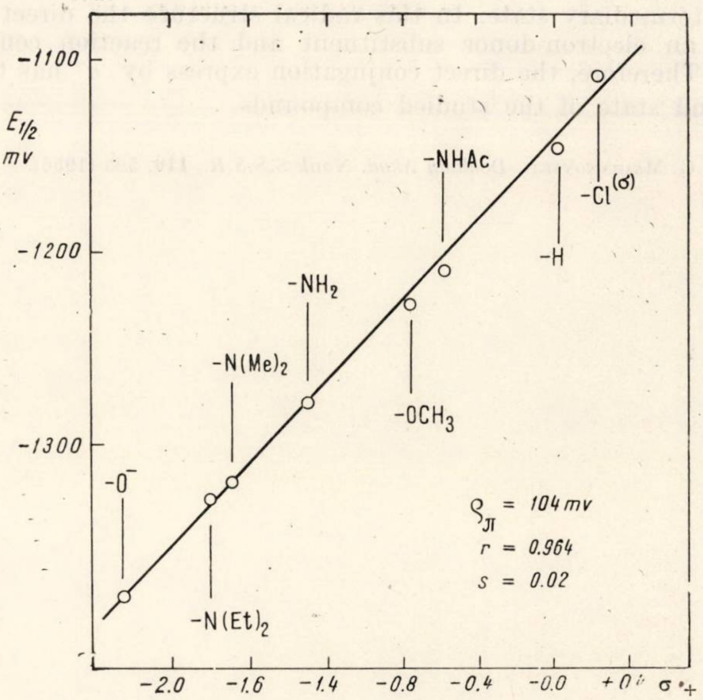

Fig. 3. — Plot of $E_{1/2}$ values against the Brown-Okamoto substituent constants.

The above data prove that the substituents possessing a positive inductive and tautomer effect make the electrochemical reduction more difficult. The half-wave potentials are shifted toward negative values, relative to the unsubstituted compound.

The half-wave potentials plotted against the σ^+ (substituent constant determined by Brown and Okamoto) give a linear correlation (Figure 3). This correlation can be described by the modified Hammett equation:

$$(E_{1/2})_x = (E_{1/2})_0 + \rho_\pi \sigma^+ \tag{5}$$

The best value of ρ_π has been calculated using the least squares method. The value of the correlation coefficient (r) shows that the precision of the correlation is good enough ($r = 0.964$).

The exclusive applicability of σ^+ for the electron donor substituents, in the studied reaction series, denotes a direct resonance between these substituents and the reaction centre. The sign of the reaction constant is positive which shows that the mechanism of the potential-determining step is nucleophilic.[10] According to the reduction mechanism described in literature for the N-alkyl-pyridinium ions,[21] the reduction takes place with the participation of a single electron, and a radical appears in the intermediary state. In this radical structure the direct resonance between an electron-donor substituent and the reaction centre is not possible. Therefore, the direct conjugation express by σ^+ has to occur in the ground state of the studied compounds.

---

[21] S. G. MAIRANOVSKII, *Doklady Akad. Nauk S.S.S.R.*, **110**, 593 (1956).

Revue Roumaine de Chimie. **15**, 615 – 617 (1970)

EINE NEUE KOLORIMETRISCHE BESTIMMUNGSMETHODE DES URANS(VI)

T. HODIŞAN, A. ŞUTEU und V. GOREA

vom Chemischen Institut der „Babeş-Bolyai"-Universität Cluj, str. Arány János 11

Eingegangen am 17. Juli 1969

Eine neue auf der Reaktion zwischen U(VI) und Pyrogallol beruhende Bestimmungsmethode des Urans. Dabei bildet sich eine gelbe Verbindung mit einem Absorptionsmaximum bei 430 nm und einem Extinktionskoeffizienten von 3420 $Mol^{-1}.cm^2$. Mit Hilfe dieser Methode können 19 bis 140 µg/ml U(VI) bestimmt werden.

In der Fachliteratur wurden eine Reihe kolorimetrischer Bestimmungsmethoden für U(VI) beschrieben. Davon erwähnen wir hier die Methoden, die folgende Substanzen verwenden: Kalium rhodanid,[1] Dibenzoylmethan,[2] Morin,[3] Arsenazo [3(-2-arsenophenylazo-)-4,5-dihydroxynaphthyldisulfonsäure],[4] PAN (1,2-Pyridyl-azo-naphthol),[5] Ferrocyanid,[6] 2-Acetoacetylpyridin,[7] Aluminon (Aurintrikarbonsäure),[8] Brompyrogallolrot,[9] Salizylaldoxim,[10] Orthohydroxybenzoesulfinsäure,[11] Tanninsäure,[12] Merkaptobernsteinsäure, [13] Chinalizarin, [14] Salizylhydroxamsäure,[15] Querzetin,[16] 2,4-Dihydroxy-5-chloracetophenon,[17] 1-Phenyl-3-

---

[1] R. R. Streden, *Analyt. Chim. Acta*, **4**, 94 (1950).

[2] R. Pribil und M. Jelinek, *Chem. listy*, **47**, 1326 (1953).

[3] Gy Almássy, Z. Nagy und J. Straub, *Acta Chim. Acad. Sci. Hung.*, **7**, 317 (1955).

[4] V. I. Kuznetsov und I. V. Nikolskaya, *Zavodskaya Lab.*, **26**, 266 (1960).

[5] L. K. Cheng, *Analyt. Chem.*, **30**, 1027 (1958).

[6] J. Cernikov und F. Guldina, *Z. analyt. Chem.*, **96**, 17 (1954).

[7] T. Hara, *Nippon Kagaku Zasshi*, **78**, 333 (1957); *Chem. Abstr.*, **52**. 7026b (1958).

[8] A. K. Mukherji und A. K. Dey, *Mikrochim. Acta*, **6**, 736 (1958).

[9] V. F. Lukyanov und E. P. Duderova, *Zhur. analit. Khim.*, **16**, 60 (1961).

[10] R. Ripan, G. Kiss und Z. Székely, *Studii și Cercetări Chim. Acad. România*, **11**, 259 (1960).

[11] I. P. Alimarin und D. I. Kuznetsov, *Doklady Akad. Nauk S.S.S.R.*, **131**, 821 (1960).

[12] M. Kibaku und Ch. Yoshimura, *Bunseki Kagaku*, **7**, 488 (1958); *Chem. Abstr.*, **54**, 16 284 e (1960).

[13] M.E. Roselli, *Anales direc. nacl. quím.*, **7**, 35 (1954).

[14] F. Pino-Pérez und J. Chabannes, *Anales edafol. y fisiol. vegetal*, **10**, 595 (1951); *Chem. Abstr.*, **47**, 443 h (1953).

[15] A. S. Bhaduri und P. Ray, *Science and Culture*, **18**, 97 (1952); *Chem. Abstr.*, **47**, 2636 c (1953).

[16] J. Komenda, *Chem. listy*, **47**, 531 (1953).

[17] S. K. Banerji und A. K. Dey, *Z. analyt. Chem.*, **159**, 293 (1958).

methyl-4-(3-karboxy-4-hydroxyphenylazo)-5-pyrazolon,[18] 2-(*o*-Arsenophenyl-azo) chromotropsäure [Neotoron][19,20] usw.

Diese Arbeit soll die Anwendungsmöglichkeiten des Pyrogallols als Reaktionsmittel zur kolometrischen Bestimmung des U(VI) studieren. In erster Reihe wurde die Absorptionskurve des aus der Reaktion zwischen U(VI) und Pyrogallol entstehenden Komplexes bestimmt. Es wurde ein Spektrophotometer Beckman-DB verwendet. Die Ergebnisse sind in Abbildung 1 wiedergegeben.

Aus Abb. 1 ist ersichtlich, daß sich während der Reaktion ein gefärbter Komplex mit einem Absorptionsmaximum von 430 nm bildet.

Da der Verlauf der Reaktion vom pH-Wert der Lösung abhängt, wurde anschließend der Einfluß der pH-Werte auf die Absorption einiger, die gleiche Menge an U(VI) und Pyrogallol enthaltender Lösungen studiert, welche auf verschiedene pH-Werte gebracht wurden.

Aus Abb. 2 geht hervor, daß sich bei einem pH-Wert $< 5{,}0$ kein gefärbter Komplex bildet. Der günstigste pH-Wert liegt bei pH $= 5{,}6$. Es wurde mit Essigsäure-Natriumacetat gepuffert. Bei pH Werten $> 6{,}5$ steigt die Absorbanz wieder an, da das Pyrogallol oxydiert wurde.

Die Versuche zeigen, daß die wässerigen Pyrogallollösungen der Oxydation zufolge unbeständig sind, weshalb alle Versuche in alkoholischen Pyrogallollösungen unternommen wurden.

Im weiteren wurde das dem Lambert-Beerschen Gesetz entsprechende Konzentrationsgebiet des U(VI) studiert. Die Daten sind in Abbildung 3 enthalten.

Aus Abb. 3 ist eine lineare Abhängigkeit zwischen Absorbanz und Urankonzentration im Bereich 19—140 μg/ml ersichtlich. Der molare Extinktionskoeffizient $\varepsilon = 3420$ Mol^{-1}.cm^{2}. Um die Dispersion der Ergebnisse in Betracht zu ziehen, wurde mit Hilfe der Statistik der geraden Linie die Gleichung der wahrscheinlichsten Geraden berechnet.

$$y = 0{,}02638 + 0{,}002927x$$

$$x = \mu\text{g U/ml}$$

$$y = \text{Extinktion}$$

Um das Verbindungsverhältnis von U(VI) mit Pyrogallol zu klären, wurde ein Studium mit Hilfe der „Methode der kontinuierlichen Änderungen unternommen.[21] Die Kurve ist in Abb. 4 dargestellt und weist ein dem Verhältnis UO_2^{2+} : Pyrogallol 1 : 3 entsprechendes Maximum auf.

ARBEITSWEISE

Die U(VI)-Lsg mit dem Konzentrationsbereich 19—140 μg UO_2^{2+}/ml wird in einen 25 cm^3 Meßkolben gebracht und auf pH 5,6 mit 10 ml Essigsäure-Natriumacetat gepuffert, 5 ml 1%ige alkoholische Pyrogallollösung hinzugefügt und die Absorbanz in einer 1 cm-Küvette gemessen. Es wurde ein blauer Filter verwendet ($\lambda = 470$ nm). Die Bestimmungen werden durch die Ionen gestört, welche mit Pyrogallol gefärbte Verbindungen bilden : Fe^{3+} (1μg/ml), Ce^{4+} (1,4μg/ml), V^{3+} (0,1 μg/ml), Au^{3+} (0,016 μg/ml), sowie durch Sb^{5+} (4,6 μg/ml), Bi^{5+} (71 μg/ml), Mo^{6+} (5μg/ml), Ta^{5+} (0,07 μg/ml) welche in sauren Lösungen schwerlösliche Verbindungen bilden.

---

[18] Gh. Baiulescu und I. C. Ciurea, *Analyt. Chim. Acta*, **24**, 152 (1961).

[19] I. Shibata und T. Matsuma, *Bull. Chem. Soc. Japan*, **31**, 377 (1958).

[20] H. Matsuyama, T. Hara und K. Kayama, *Nippon Kagaku Zasshi*, **79**, 958 (1958); *Chem. Abstr.*, **53**, 128 i (1959).

[21] P. Job, *Ann. Chim.* (*France*), **9**, 113 (1928).

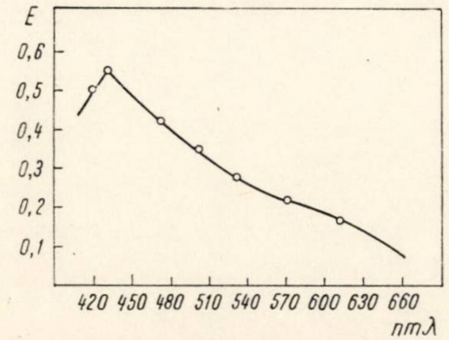

Abb. 1. — Absorptionskurve des Uran (VI)-Pyrogallolkomplexes.

Urankonzentration = 38 mg/l; Pyrogallolkonzentration M/500; pH = 5,6; 1 cm-Küvette.

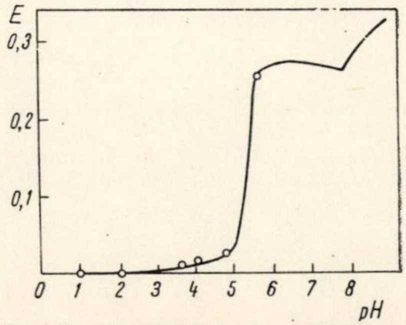

Abb. 2.— Der Einfluß des pH-Wertes auf die Farbintensität des Uran(VI)-Pyrogallolkomplexes.

Urankonzentration 38 mg/l; Pyrogallolkonzentration = M/500; λ = 430 nm; 1 cm-Küvette.

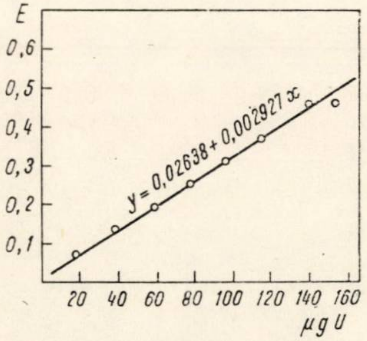

Abb. 3. — Gültigkeitsbereich des Lambert-Beerschen Gesetzes.

pH = 5,6; 1 cm-Küvette.

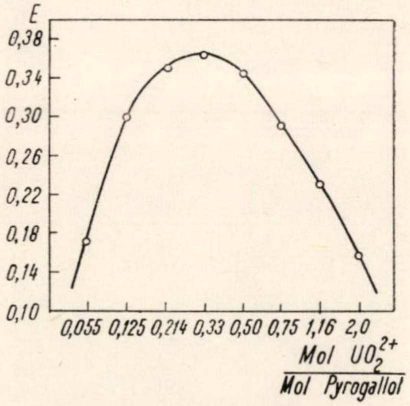

Abb. 4. — Studium des Verbindungsverhältnisses zwischen Uran und Pyrogallol mit Hilfe der Methode der kontinuierlichen Variationen.

SCHLUSSFOLGERUNGEN

Das Uranylion gibt mit Pyrogallol bei einem pH-Wert 5,6 eine gelbe, leicht lösliche Verbindung mit einem Molverhältnis UO_2-Pyrogallol 1 : 3 (Nach der Jobschen Methode). Das Absorptionsmaximum dieses Komplexes liegt bei $\lambda = 470$ mm($\varepsilon = 3420$). Die Farbintensität verändert sich linear im Konzentrationsgebiete : 19—140 μg U(VI)/ml.

Revue Roumaine de Chimie, 15, 615 – 617 (1970)

Revue Roumaine de Chimie, **15**, 619 – 626 (1970)

L'ADDITION DES PHILODIÈNES SUR LA 1-MÉTHYL-PHTALAZINE ET SUR LA β-PHÉNYL-VINYL-PHTALAZINE

MARIA CAPROŞU, MAGDA PETROVANU et I. ZUGRĂVESCU

Université « Al. I. Cuza », Laboratoire de chimie organique, Jassy 11, str. 23 August

Reçu le 12 juillet 1969

L'addition d'anhydride maléique sur la 1-méthyl-phtalazine en proportions équimoléculaires conduit à l'ylide (III) ou à la bétaïne (IV) selon les conditions expérimentales. L'addition de N-phényl-maléine-imide à la 1-méthyl-phtalazine en proportions équimoléculaires conduit à l'ylide (V). Par cyclo-addition 1,4-dipolaire de l'anhydride maléique, de l'acétylènedicarboxylate de méthyle et de l'isocyanate de phényle sur les ylides obtenus, on aboutit aux produits (VI), (VIII) et (IX). Par l'addition de l'anhydride maléique sur la β-phényl-vinyl-phtalazine on obtient l'ylide (XI) qui, par l'addition d'une nouvelle molécule d'anhydride maléique donne naissance au produit (XII).

Dans des recherches antérieures [1,2] Zugrăvescu et ses coll. ont étudié l'action de quelques philodiènes sur les N-hétérocycles appartenant à la classe des benzpyridines et benzpyridazines dans le but d'isoler des combinaisons ylidiques stables.

En faisant réagir la phtalazine et l'anhydride maléique à l'état solide en proportion équimoléculaire, Zugrăvescu et Petrovanu [1] ont isolé l'un des premiers ylides stables connu dans la littérature (I a , b).

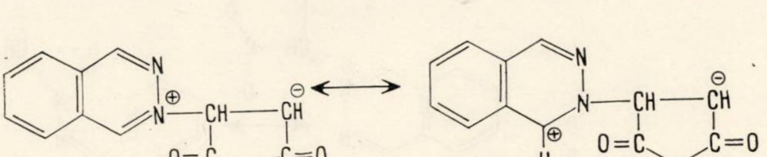

I

D'après les indications de Doering,[3] l'existence des combinaisons ylidiques C—N serait due à l'interaction électrostatique qui s'exerce entre les deux centres polaires. Mais cette seule interaction étant insuffisante à stabiliser la molécule, on rencontre beaucoup de difficultés à isoler des ylides de ce genre. Bien entendu, la possibilité d'isoler des ylides C—N dépendrait de la mesure dans laquelle les deux charges pourraient être stabilisées par divers groupements d'atomes de la molécule amphionique.

---

[1] I. Zugrăvescu, M. Petrovanu, A. Caraculacu et A. Sauciuc, *Rev. Roumaine Chim.*, **12**, 109 (1967).

[2] M. Petrovanu, A. Sauciuc, I. Gabe et I. Zugrăvescu, *Rev. Roumaine Chim.*, **13**, 513 (1968).

[3] A. W. Johnson, « Ylid Chemistry », Academic Press, vol. 7, New York et Londres, 1966, p. 251.

Tenant compte des faits susmentionnés, nous avons expliqué la stabilité du phtalazinium-ylide (I) en admettant que le reste d'anhydride maléique est un bon accepteur de charge anionique, la charge cationique étant stabilisée par le noyau benzénique accolé au cycle pyridazinique.

Poursuivant nos recherches concernant l'obtention de nouveaux phtalazinium-ylides, nous nous sommes proposé d'étudier le comportement de quelques dérivés phtalaziniques 1 substitués dans les processus de formation et stabilisation des ylides.

La réaction entre la méthyl-1-phtalazine et l'anhydride maléique, respectivement N-phényl-maléine-imide

Nous avons choisi en premier lieu la méthyl-1-phtalazine plus basique que la phtalazine grâce à l'effet exercé par le groupement méthylique.

En faisant réagir des quantités équimoléculaires de méthyl-1-phtalazine et d'anhydride maléique à l'état solide, nous avons réussi à isoler un produit amphionique auquel, basés sur les données chimiques et spectrales, nous avons attribué la structure ylidique (III a, b).

Il est à remarquer que la formation de l'ylide se produit à l'atome d'azote 3, malgré la basicité plus élevée de l'atome d'azote 2 voisin du groupement méthylique. Tenant compte de l'effet inducteur négatif exercé par le second atome d'azote du cycle[4] la force basique est répartie entre les deux hétéroatomes voisins ce qui amoindrit l'importance des effets inductifs, la direction de la réaction étant influencée surtout par l'effet stérique (du groupement méthylique).

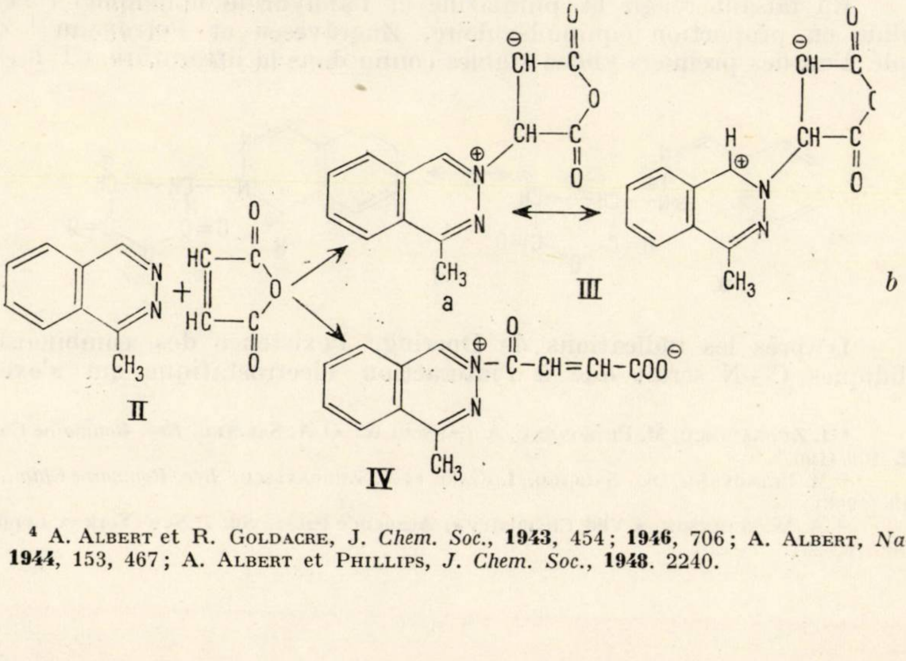

---

[4] A. Albert et R. Goldacre, J. *Chem. Soc.*, **1943**, 454 ; **1946**, 706 ; A. Albert, *Nature*, **1944**, 153, 467 ; A. Albert et Phillips, *J. Chem. Soc.*, **1948**. 2240.

La réaction entre la méthyl-l-phtalazine et l'anhydride maléique en l'absence des solvants étant fortement exothermique, on doit refroidir le mélange des réactants pour éviter la formation de résines.

On peut expliquer la formation de l'ylide par l'attaque nucléophylique énergique de l'atome d'azote 3 du noyau phtalazinique sur la double liaison éthylénique de l'anhydride maléique. En effectuant la réaction en milieu éthéré (solvant polaire aprotonique) on n'obtient plus l'ylide (III) mais la bétaïne (IV).

Il est connu que l'anhydride maléique à côté du rôle habituel de philodiène peut jouer, dans certaines réactions, le rôle d'agent d'acylation.

Dans le cas de l'obtention de la bétaine (IV), l'anhydride maléique se comporte comme agent d'acylation, la formation de la bétaïne s'expliquant par l'attaque électrophile sur l'azote 3 de la méthylphtalazine par l'anhydride maléique. Dans ce cas il faut admettre que l'effet polaire du solvant joue un rôle déterminant.

En faisant réagir la méthyl-l-phtalazine avec N-phényl-maléineimide en proportions équimoléculaires en solution benzénique nous avons réussi à isoler l'ylide stable (V a,b) selon le schéma ci-dessous

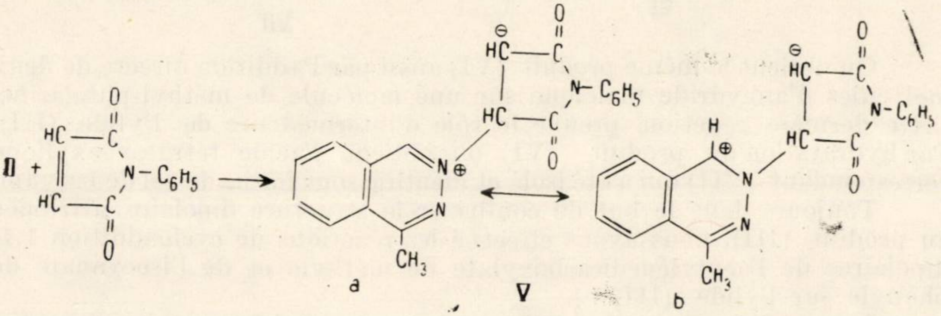

Etant donné que dans le cas de la phtalazine non substituée on n'a pas réussi à isoler un ylide du type (V), nous considérons que l'obtention d'un produit dipolaire 1 : 1 dans le cas de la méthyl-phtalazine est due à la capacité nucléophile accrue de l'azote 3 du cycle méthyl-l-phtalazinique.

Il est connu que dans les réactions de cycloaddition 1,3 et 1,4-dipolaires on admet l'apparition de produits ylidiques comme intermédiaires non isolables. Par conséquent, l'existence d'un ylide est largement prouvée s'il peut participer directement aux réactions de cycloaddition 1,3- ou 1,4-dipolaires.

Nous avons donc étudié les réactions d'addition de quelques composés philodiéniques sur l'ylide (III).

Par cycloaddition 1,4-dipolaire d'une nouvelle molécule d'anhydride maléique sur l'ylide (III, b) on obtient le produit (VI) conformément à la réaction suivante

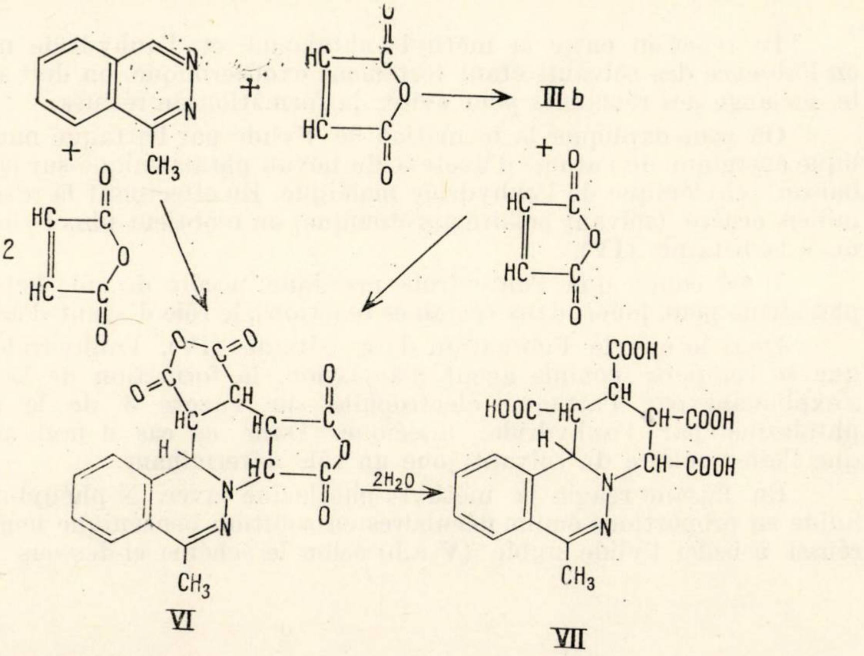

On obtient le même produit (VI) aussi par l'addition directe de deux molécules d'anhydride maléique sur une molécule de méthyl-phtalazine. Cette dernière réaction prouve le rôle d'intermédiaire de l'ylide (III). Par hydratation du produit (VI) on obtient l'acide tétracarboxylique correspondant (VII) qui a été isolé et identifié sous forme de sel de baryum.

Toujours dans le but de confirmer la structure dipolaire attribuée au produit (III), nous avons effectué les réactions de cycloaddition 1,4-dipolaires de l'acétylènedicarboxylate de méthyle et de l'isocyanate de phényle sur l'ylide (III, b).

Les produits (VIII) et (IX) obtenus selon le schéma suivant confirment aussi l'existence de la structure amphionique (III a, b).

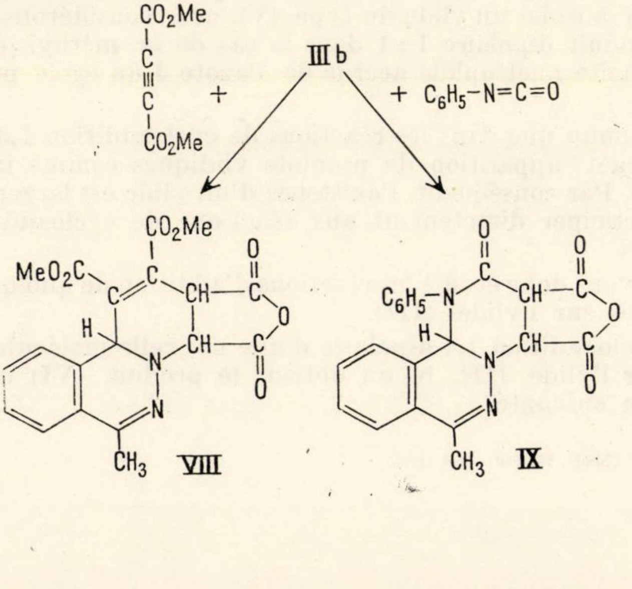

D'une manière analogue l'ylide (V) donne avec l'acétylène-dicarboylate de méthyle le produit de cycloaddition 1,4-dipolaire (X) selon la réaction ci-après.

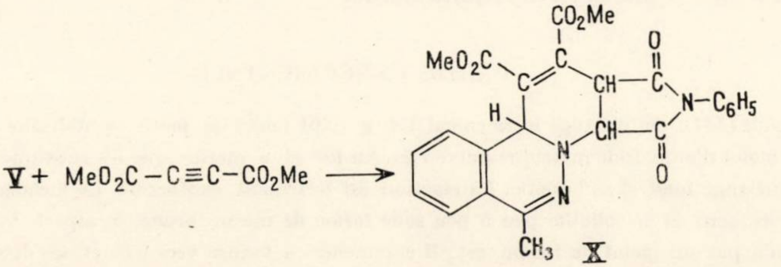

La réaction entre la β-phényl-vinyl-phtalazine et l'anhydride maléique

En faisant réagir la β-phényl-vinyl-phtalazine et l'anhydride maléique en proportions équimoléculaires, en solution benzénique, nous avons réussi à isoler l'ylide (XI a, b) conformément au schéma ci-dessous.

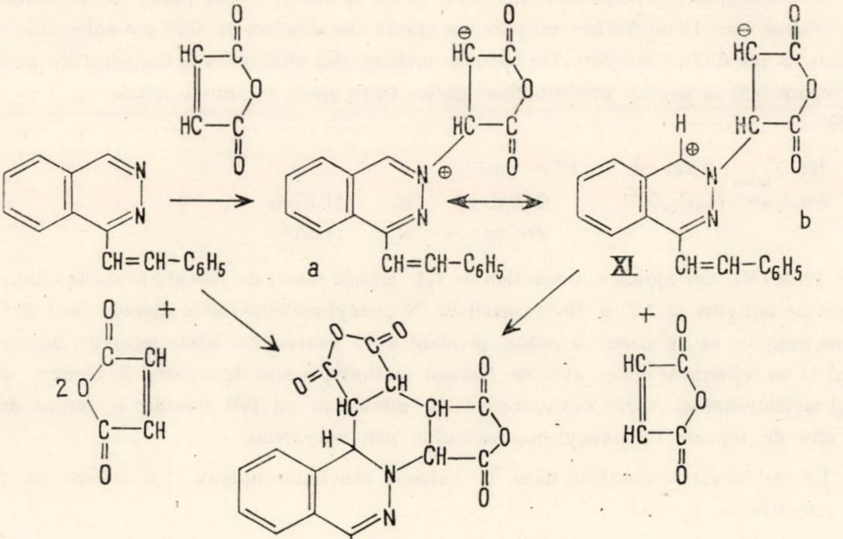

L'introduction du reste phényl-vinylique dans la molécule de la phtalazine intensifie la basicité de l'atome d'azote du cycle phtalazinique tenant compte de l'accroissement de la capacité de résonance du système.

L'existence de l'ylide (XI a, b) est prouvée dans ce cas aussi par sa capacité de participer aux cycloadditions 1,4-dipolaires.

En effet, traité par une nouvelle molécule d'anhydride maléique, l'ylide (XI) conduit au produit (XII). On obtient ce même produit (XII) par l'addition directe de deux molécules d'anhydride maléique sur une molécule de β-phényl-vinyl-phtalazine.

PARTIE EXPÉRIMENTALE

Ylide (*III*). On mélange intimement 1,4 g (0,01 mole) de méthyl-phtalazine avec 0,98 g (0,01 mole) d'anhydride maléique pulvérisé. Au fur et à mesure que les substances réagissent, le mélange fond et se liquéfie. La réaction est fortement exotherme. Le mélange liquide devient visqueux et se solidifie peu à peu sous forme de masse brune à aspect vitreux. Le produit n'a pas un point de fusion net; il commence à fondre vers 95° et se décompose à 120°.

IR λ_{max} : 1780 cm $^{-1}$, 1840 cm $^{-1}$.
Analyse : $C_{13}H_{10}O_3N_2$ *Calculé* : N 11,57%
Trouvé : N 11,37%
N 11,81%

3-N-maléyl-méthyl-phtalazinium-bétaïne (*IV*). A 1,4 g (0,01 mole) de 1-méthyl-phtalazine dissous dans 15 ml d'éther anhydre, on ajoute une solution de 0,98 g d'anhydride maléique dans 15 ml d'éther anhydre. On laisse le mélange des solutions à la température ambiante. Il se sépare peu à peu un produit blanc qu'on filtre après environ 1 heure. P_f 123°.

IR λ_{max} : 1620 cm $^{-1}$, 1750 cm $^{-1}$.
Analyse : $C_{13}H_{10}O_3N_2$ *Calculé* : N 11,57%
Trouvé : N 11,45%

Ylide (*V*). On ajoute une solution de 1,4 g (0,01 mole) de métyl-phtalazine dans 20 ml de benzène anhydre à 1,7 g (0,01 mole) de N-phényl-maléine-imide dissous dans 20 ml de benzène anhydre et on porte à reflux pendant 4–5 heures. On laisse refroidir, on chasse le solvant et on reprend le résidu avec de l'alcool méthylique afin de séparer le trimère de l'N-phényl-maléine-imide. Après l'évaporation du méthanol, on fait bouillir le résidu dans de l'eau afin de séparer l'N-phényl-maléine-imide non réactionné.

Le résidu est recristallisé dans de l'alcool éthylique aqueux. On obtient un produit blanc jaunâtre à P_f 147°.

IR λ_{max} : 1680 cm $^{-1}$, 1735 cm $^{-1}$, 2800 cm $^{-1}$, 2920 cm $^{-1}$.
Analyse : $C_{19}H_{15}O_2N_2$ *Calculé* : N 13,29%
Trouvé : N 13,09%
N 13,33%

Bis-anhydride de l'acide 11 b H-1,2,3,4-tétrahydro-pyrido-[*2,1-a*]*-7-méthyl-phtalazine-1,2,3,4-tétracarboxylique* (*VI*). On mélange intimement 1,4 g (0,01 mole) de 1-méthyl-phtalazine avec 2g d'anhydride maléique bien pulvérisé. Le mélange fond et se liquéfie; la réaction est exotherme. Au refroidissement on obtient une masse brune à aspect vitreux. Après recristallisation dans du benzène anhydre on obtient un produit blanchâtre à P_f 127°.

IR λ_{max} : 1220 cm^{-1}, 1780 cm^{-1}, 1860 cm^{-1}.
Analyse : $C_{17}H_{12}O_6N_2$ *Calculé* : N 8,23%
Trouvé : N 7,94%

On obtient le même produit en ajoutant la solution de 1,4 g de 1-méthyl-phtalazine dans 15 ml de benzène anhydre à 2 g d'anhydride maléique dissous dans 15 ml de benzène anhydre. On porte à reflux le mélange pendant 2 heures. Au refroidissement de la solution il se sépare un produit jaunâtre. Purification par dissolution dans du chloroforme et précipitation par de l'éther de pétrole.

Le produit est transformé dans l'acide tétracarboxylique respectif en le faisant bouillir avec de l'eau. On filtre et on traite avec une solution de Cl_2Ba. On obtient le sel de baryum sous forme de cristaux blancs qui n'ont pas de point de fusion.

3,4 Anhydride de l'acide 11 b H 1,2-dicarbométoxy-3,4-dihydro-pyrido-[2,1-a]-7-méthyl-phtalazine-dicarboxylique (*VIII*). On ajoute 0,7 ml d'acétylène dicarboxylate de méthyle à une solution de 1,21 g (0,05 mole) d'ylide (III) dans 30 ml de tétrahydrofuranne et on porte à reflux pendant 3—4 heures. La solution est refroidie et traitée par un excès d'éther éthylique jusqu'à la précipitation complète. On obtient un produit brun clair à P_f 114°.

Analyse : $C_{19}H_{16}O_7N_2$ *Calculé* : N 7,29%
Trouvé : N 7,89%

Anhydride de l'acide 11 b H-1-phényl-2-one-3,4-dihydro-pyrimido-[2,1-a]-7-méthyl-phtalazine-3,4-dicarboxylique (*IX*). On ajoute 1,19 ml (0,005 mole) d'isocyanate de phényle à une solution de 1,21 g d'ylide (III) (0,005 mole) dans 30 ml de tétrahydrofuranne et on porte le mélange à reflux pendant 3—4 heures. La solution est refroidie et traitée par un excès d'éther éthylique. Il se sépare un produit jaune foncé à P_f 95—100°.

IR λ_{max} ; 1(8) cm^{-1} , 1720 cm^{-1}, 1885 cm^{-1}, 2800 cm^{-1}.
Analyse : $C_{20}H_{15}O_4N_3$ *Calculé* : N 11,63%
Trouvé : N 11,19%

1,2-diméthyl-ester de l'acide 3,4-N-phényl-imide-dihydro-pyrido-[2,1-a]-7-méthyl-phtalazine-1,2,3,4-tétracarboxylique (*X*). On dissout 1,58 g d'ylide (V) et 0,71 ml d'acétylène-dicarboxylate de méthyle dans 40 ml de benzène anhydre et on porte à reflux pendant 3—4 heures. Après refroidissement de la solution et précipitation par de l'éther de pétrole on obtient un produit brun-rouge à P_f 164°.

Analyse : $C_{25}H_{21}O_6N_3$ *Calculé* : N 9,15%
Trouvé : N 8,42%
N 8,57%

Ylide (*XI*). A la solution de 2,32 g (0,01 mole) de β-phényl-vinyl-phtalazine dans 15 ml de benzène sec on ajoute 0,98 g (0,01 mole) d'anhydride maléique dissous dans 20 ml de benzène anhydre. On porte à reflux pendant 3 heures. Dans la solution refroidie il se sépare un produit brun à P_f 120—122°.

Analyse : $C_{20}H_{14}O_3N_2$ *Calculé* : N 8,48%
Trouvé : N 8,75%
N 8,25%

Bis-anhydride de l'acide 11 b H-1,2,3,4-tétrahydro-pyrido-[2,1-a]-β-phényl-vinyl-phtalazine-1,2,3,4-tétracarboxylique (XII). A 2,32 g (0,01 mole) de β-phényl-vinyl-phtalazine en solution benzénique, on ajoute 2 g d'anhydride maléique dissous dans 20 ml de benzène sec. On porte à reflux pendant 2 heures. Dans la solution refroidie il se sépare un produit beige à P_f 94–100°.

IR λ_{max} : 1770 cm^{-1}, 1845 cm^{-1}
Analyse : $C_{21}H_{16}O_6N_2$ *Calculé* : N 6,53%
Trouvé : N 6,18%

On obtient le même produit en portant à reflux pendant 3 heures un mélange du produit (XI) avec la quantité calculée d'anhydride maléique en solution benzénique.

Revue Roumaine de Chimie, **15**, 627 – 634 (1970)

THE SYNTHESIS OF SOME NEW 3,6-DICHLORO-2,5-BISPHENYLAMINO-1,4-BENZOQUINONE DERIVATIVES WITH ELECTRON-DONOR AND ELECTRON-ACCEPTOR GROUPS

A. BALINT

Center for Chemical Research of the Academy, Timişoara, Bd. Mihai Viteazu, 24

Received October 12, 1968

The synthesis, the purification and the analysis of 15 new unsymmetrical derivatives of chloranil are described. Such compounds present an appreciable interest not only for their spectra and theoretical interpretations as organic-electronic "models", but also for various possibilities in order to obtain derivatives with practical applications.

Some unsymmetrical derivatives of chloranil (2,3,5,6-tetrachloro-1,4-benzoquinone) and of 1,4-benzoquinone, were first described in a German patent.[1] In order to obtain such compounds, this patent has used the condensation of chloranil with various amines in two steps,e.g.:

I.

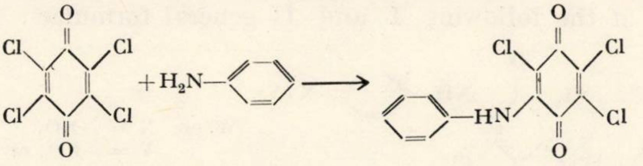

II.

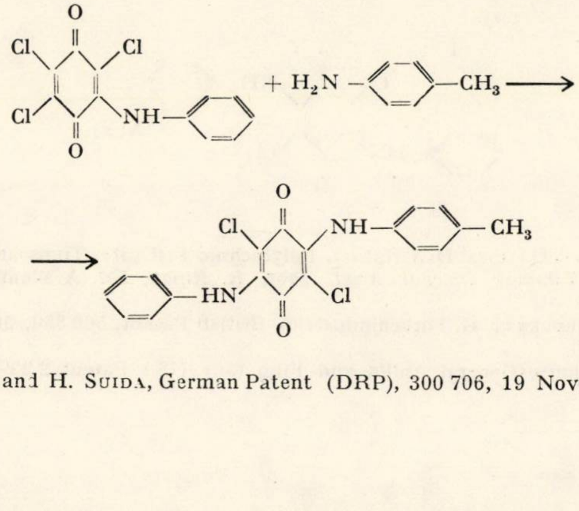

---

[1] W. Suida and H. Suida, German Patent (DRP), 300 706, 19 November 1919, *Frdl.* **13**, 353.

Such reactions can also be observed in the case of other derivatives e.g. the cyanuric chloride. We have tried to reproduce these reactions,[2] but our opinion is that for purity purposes this way is not the most indicated one. In order to obtain pure unsymmetrical substances, we have then examinated some British[3] and American[4] patents. In these patents there are described the reactions which lead to such derivatives. Starting from chloranil in methanol, the 2-methoxy-3,5,6-trichloro-1,4-benzoquinone is obtained:

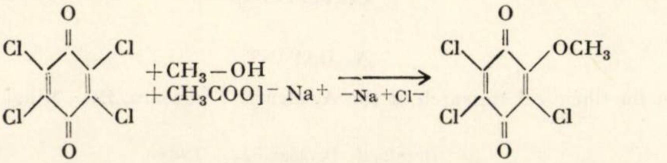

We have checked this reaction (see compound No 1 in the experimental section) and we have mentioned there some details which are not described in these patents. By condensation with aniline the 2-methoxy-5-phenylamino-3,6-dichloro-1,4-benzoquinone was then obtained:

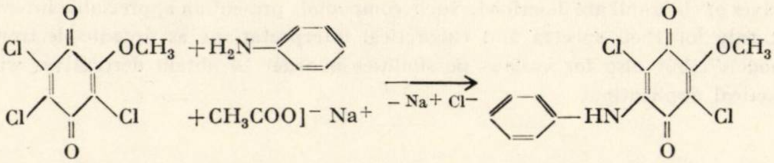

The synthesis of this compound is not described in the above mentioned patents[3,4] but its use is only mentioned in order to obtain other derivatives. We have prepared the compound (see compund No 2 in the experimental section) which was treated thereafter with various *meta* and *para*-methyl-, methoxy- or nitro-anilines. This way we have obtained substances of the following I and II general formulae:

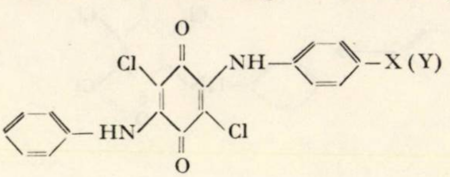

Where $X = -NO_2$
$Y = -CH_3$ or $-OCH_3$

I

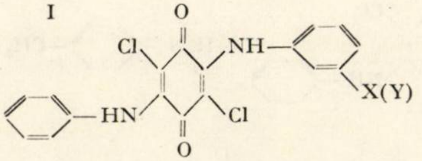

II

---

[2] A. BALINT, Doctoral Dissertation, Polytechnic Institute, Timişoara, 1964. J. Reichel and A. Balint, *Volumul omagial Acad. Prof. R. Ripan*, Ed. Academiei R. S. România, 1966, 471–479.

[3] W. W. GROVES (I. G. Farbenindustrie) British Patent, 509 890, 509 891 and 509 893, 20 July 1939.

[4] G. LANGBEIN (General Anilin and Film Co.) USA Patent 2 229 099 and 2 267 741, 31 March 1942.

In order to prepare unsymmetrical derivatives with electron-donor and electron-acceptor groups in different phenyl-rings, it was necessary to synthesize intermediate products of the following general structures (see compounds 3,4,5 and 6 in the experimental section):

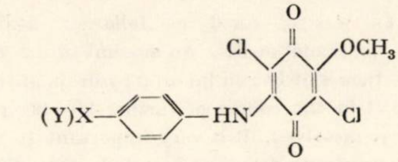

where X= $-NO_2$
Y= $-CH_3$ or $-OCH_3$

III

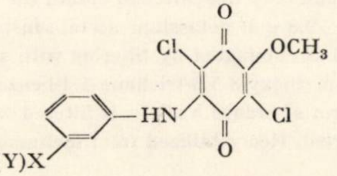

IV

From these intermediate compounds, by treating with *meta* or *para*-nitroanilines, we have obtained substances of the general formulae (see compounds 13, 14, 15 and 16 in the experimental section):

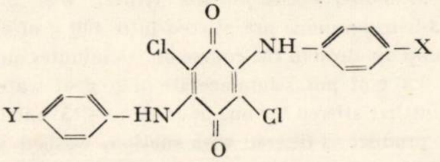

where X = $-NO_2$
Y = $-CH_3$ or $-OCH_3$

V

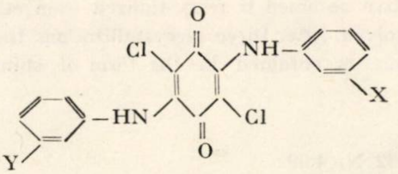

VI

CONCLUSIONS

15 New unsymmetrical derivatives of chloranil were prepared. The synthesis of such compounds presents an appreciable interest not only because they are used in order to obtain triphendioxazine dyes but also because it is possible to obtain substances with interesting properties for the most various purposes. The compounds specified in this paper present also an interest as organic-electronic "models" for the quantum chemistry calculations and for the spectral data in theses series. We have just reported the spectra, the molecular orbital calculations and the theoretical interpretations in the case of two such derivatives[5] but their synthesis

---

[5] A. Balint and Z. Simon, *Rev. Roumaine Chim.*, **13**, 1427 (1968).

and also the synthesis of other similar derivatives with electron-donor and electron-acceptor groups, are described only in the present paper.

EXPERIMENTAL*

2-Methoxy-3,5,6-trichloro-1,4-benzoquinone (No **1**), was obtained as follows: 24.6 g of chloranil are heated while stirring in 640 cmc of methanol at 60°. An amount of 8.2 g anhydrous sodium acetate in 100 cmc of methanol is then slowly run in, drop by drop, at the same temperature, in the course of 30—40 minutes and in the course of further 20—30 minutes the whole is heated to boiling until the chloranil has dissolved. It is very important to use the exactly amount of anhydrous sodium acetate or if crystallized sodium acetate is used, to weigh exactly 13.6 g of substance and only thereafter to obtain the corresponding anhydrous acetate. Therefore it is better to use 9.8 g of potassium acetate instead of anhydrous sodium acetate. The sodium chloride formed is eliminated by filtering with suction while hot, and the filtrate is allowed to cool. The 2-methoxy-3,5,6-trichloro-1,4-benzoquinone which crystallizes from the cooled filtrate in the form of orange leaflets, is filtered with suction, washed with a small amount of methanol and dried. Recrystallized from methanol it melts at 183—185° (in fused tube).

Anal. $C_7H_3Cl_3O_3$
Calcd.: C, 34.79 H, 1.25 Cl, 44.07;
Found: C, 34.64 H, 1.17 Cl, 44.19.

2-Methoxy-5-phenylamino-3,6-dichloro-1,4-benzoquinone (No **2**) was obtained as follows: 24.2 g of 2-methoxy-3,5,6-1,4-benzoquinone are stirred into 400 g of ethanol. At 40—45°, 9.3 g of aniline are introduced drop by drop in the course of 15 minutes and in the course of further 15 minutes a solution of 9.8 g of potassium acetate in 20 g of water is then slowly run in, drop by drop. The whole is further stirred for one hour at 40—45° and then for another hour while cooling with ice, the product is filtered with suction, washed with ethanol and dried. In order to eliminate the small amount of bis-phenylamino-derivative formed as a by-product, the mono-phenylamino-derivative obtained is recrystallized from ethanol, the bis-phenylamino-derivative remaining undissolved. After three recrystallizations the 2-methoxy-5-phenylamino-3,6-dichloro-1,4-benzoquinone is obtained in the form of shining dark-violet leaflets melting at 199—202°.

Anal. $C_{13}H_9Cl_2NO_3$
Calcd.: C, 52.34 H, 3.04 Cl, 23.82 N, 4.69;
Found: C, 52.30 H, 3.08 Cl, 23.64 N, 4.58.

The 2-methoxy-5-Y-phenylamino-3,6-dichloro-1,4-benzoquinone-derivatives (No **3**,**4**,**5** and **6**) were obtained exactly in the same manner by using instead of 9.3 g of aniline, 1/10 moles of amine dissolved in 100 g of ethanol. It is also possible to use 8.2 g of anhydrous sodium acetate instead of 9.8 g of potassium acetate. All the products recrystallize from ethanol in the form of dark-violet leaflets and the purity of all these compounds was checked by thin-layer chromatography with dioxane as eluent (see table 1)

The 5-phenylamino-2-Y-phenylamino-3,6-dichloro-1,4-benzoquinone-derivatives (No **7**, **8**, **9** and **10**) were obtained from 2-methoxy-5-phenylamino-3,6-dichloro-1,4-benzoquinone (1/10 moles) by treating with 1/10 moles of amine in 1000 g of ethanol in the presence of 10 g of anhydrous sodium acetate and heating to boiling for 5 hours.

The 5-phenylamino-2-X-phenylamino-3,6-dichloro-1,4-benzoquinone-derivatives (No **11** and **12**) were obtained exactly in the same manner, using 1000 g of n-butanol instead of 1000 g of ethanol (see table 2).

---

* All m. ps. are uncorrected

Y = CH_3, $-OCH_3$

Table 1

2-methoxy-5-Y-phenylamino-3,6-dichloro-1,4-benzoquinone derivatives

No	COMPOUND	m.p.	Anal.	C		H		Cl		N	
				Calcd.	Found	Calcd.	Found	Calcd.	Found	Calcd.	Found
3	2-methoxy-5-(4′-methylphenylamino)-3,6-dichloro-1,4-benzoquinone	164–166°	$C_{14}H_{11}Cl_2NO_3$	53.84	53.71	3.55	3.50	22.75	22.81	4.49	4.53
4	2-methoxy-5-(3′-methylphenylamino)-3,6 dichloro-1,4-benzoquinone	172–174°	$C_{14}H_{11}Cl_2NO_3$	–	–	–	–	22.75	22.61	4.49	4.38
5	2-methoxy-5-(4′-methoxyphenylamino)-3,6-dichloro-1,4-benzoquinone	190–192°	$C_{14}H_{11}Cl_2NO_4$	51.21	51.30	3.38	3.30	21.64	21.51	4.27	4.15
6	2-methoxy-5-(3′-methoxyphenylamino)-3,6-dichloro-1,4-benzoquinone	185–187°	$C_{14}H_{11}Cl_2NO_4$	–	–	–	–	21.64	21.73	4.27	4.32

$X = -NO_2$
$Y = -CH_3, -OCH_3$

Table 2

5-(phenylamino)-2-Y-phenylamino-3,6-dichloro-1,4-benzoquinone and 5-(phenylamino)-2-X-phenylamino-3,6-dichloro-1,4-benzoquinone-derivatives

No	COMPOUND	m.p.	Anal.	C		H		Cl		N	
				Calcd.	Found	Calcd.	Found	Calcd.	Found	Calcd.	Found
7	5-(phenylamino)-2-(4′-methylphenylamino)-3,6-dichloro-1,4-benzoquinone	291–293°	$C_{19}H_{14}Cl_2N_2O_2$	61.12	61.01	3.78	3.71	19.03	18.88	7.50	7.38
8	5-(phenylamino)-2-(3′-methylphenylamino)-3,6-dichloro-1,4-benzoquinone	301–302°	$C_{19}H_{11}Cl_2N_2O_2$	–	–	–	–	19.03	18.91	7.50	7.40
9	5-(phenylamino)-2-(4′-methoxyphenylamino)-3,6-dichloro-1,4-benzoquinone	280–282°	$C_{19}H_{14}Cl_2N_2O_2$	–	–	–	–	18.25	18.11	7.20	7.13
10	5-(phenylamino)-2-(3′-methoxylphenylamino)-3,6-dichloro-1,4-benzoquinone	254–256°	$C_{19}H_{14}Cl_2N_2O_3$	–	–	–	–	18.25	18.10	7.20	7.09
11	5-(phenylamino)-2-(4′-nitrophenylamino)-3,6-dichloro-1,4-benzoquinone	313–315°	$C_{18}H_{11}Cl_2N_3O_4$	–	–	–	–	17.57	17.40	10.40	10.31
12	5-(phenylamino)-2-(3′-nitrophenylamino)-3,6-dichloro-1,4-benzoquinone	299–301°	$C_{18}H_{11}Cl_2N_3O_4$	–	–	–	–	17.57	17.42	10.40	10.29

$X = -NO_2$
$Y = -CH_3, -OCH_3$

Table 3

5-Y-phenylamino-2-X-phenylamino-3,6-dichloro-1,4-benzoquinone-derivatives

No	COMPOUND	m.p.	Anal.	C		H		Cl		N	
				Calcd.	Found	Calcd.	Found	Calcd.	Found	Calcd.	Found
13	5-(4′-methylphenylamino)-2-(4″-nitrophenylamino)-3,6-dichloro-1,4-benzoquinone	304–307°	$C_{19}H_{13}Cl_2N_3O_4$	54.54	54.41	3.13	3.07	16.98	17.03	10.04	10.10
14	5-(3′methylphenylamino)-2-(3″-nitrophenylamino)-3,6-dichloro-1,4-benzoquinone	297–300°	$C_{19}H_{13}Cl_2N_3O_4$	–	–	–	–	16.98	16.85	10.04	9.92
15	5-(4′-methoxyphenylamino)-2-(4″-nitrophenylamino)-3,6-dichloro-1,4-benzoquinone	303–306°	$C_{19}H_{13}Cl_2N_3O_5$	52.53	52.37	3.01	2.96	16.36	16.41	9.68	9.74
16	5-(3′-methoxyphenylamino)-2-(3″-nitrophenylamino)-3,6-dichloro-1,4-benzoquinone	246–249°	$C_{19}H_{13}Cl_2N_3O_5$	–	–	–	–	16.36	16.28	9.68	9.53

The 5-Y-phenylamino-2-X-phenylamino-3,6-dichloro-1,4-benzoquinone-derivatives (No **13**, **14**, **15** and **16**), were obtained from the intermediate products presented in table 1 (1/10 moles) by treating with 1/10 moles of methyl or methoxy-anilines in ethanol or with 1/10 moles of nitro-anilines in n-buthanol, always in the presence of anhydrous sodium acetate and heating to boiling for some hours. The purification of all these compounds was accomplished by extraction with boiling ethanol, filtration with suction while hot and washing with ethanol, acetone and ether (see table 3).

All the substances specified in the present paper dissolve in conc. sulphuric acid from a red-violet or violet to blue, greenish-blue or green solution.

Revue Roumaine de Chimie, **15**, 635 – 653 (1970)

HETEROCYCLIC ORGANOBORON COMPOUNDS. XII[1, 2]

2,4,6-TRISUBSTITUTED-1,3,2-DIOXABORINIUM SALTS

A. T. BALABAN, A. ARSENE, IOANA BALLY, A. BARABÁS, MARIA
PARASCHIV, MARIA ROMAN and ELENA ROMAŞ

Institute of Atomic Physics, P. O. Box 35, Bucharest

Received November 22, 1969

The reaction of 1,3-diketones with phenylboronic acid in the presence of strong acids leads to 2,4,6-trisubstituted-1,3,2-dioxaborinium salts. An equivalent name is 2,4,6-trisubstituted 2,3-boroxaropyrylium salts. They can be prepared also by protodeboronation of diphenylborinic acid chelates with 1,3-diketones. On heating or in solution these salts readily undergo conversion into *bis*-(1,3-diketonato)-boronium salts by breaking the B – C bond and evolving the boron-bonded aryl as ArH. Infrared, ultraviolet and NMR spectra are discussed.

I. INTRODUCTION

Owing to its electron deficiency a boron atom with three covalent bonds reacts readily with lone electron pairs, giving rise to coordinative bonds. This fact makes boron fluoride a widely-used electrophilic catalyst. When the unshared electron pair belongs to an atom situated in the same molecule as the boron atom, a coordinative bond develops if sterical factors are favourable and a chelate ring is formed.

Thus, enolizable 1,3-diketones (I) react with 2-alkoxy-1,3,2-benzodioxaboroles (II) affording crystalline chelate compounds (III)[3-6] with

---

[1] Part XI : A. Barabás, E. Işfan, E. Romaş and A. Trestianu, *Rev. Roumaine Chim.*, **14**, 253 (1969).

[2] Preliminary notes : a, A. T. Balaban, A. Barabás and A. Arsene, *Tetrahedron Letters*, **1964**, 2721 ; b, A. T. Balaban, A. Arsene, I. Bally, A. Barabás, M. Paraschiv and E. Romaş, *Tetrahedron Letters*, **1965**, 3917.

[3] H. Schäfer and O. Braun, *Naturwiss.*, **39**, 280 (1952).

[4] H. Funck and H. Koch, *Wiss. Z. Univ. Halle*, **8**, 1025 (1959).

[5] A. T. Balaban, C. N. Renţea and M. Mocanu, *Tetrahedron Letters*, **1964**, 2049.

[6] A. T. Balaban, C. N. Renţea, M. Mocanu-Paraschiv and E. Romaş, *Rev. Roumaine Chim.*, **10**, 849 (1965).

six-membered chelate rings. The two oxygen atoms are equivalent when $R'=R'''$, as shown by PMR spectroscopy.[6]

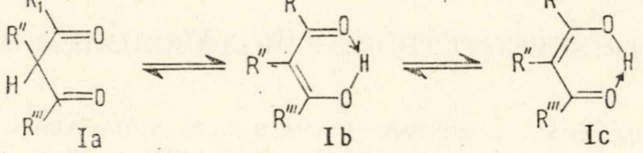

Ia Ib Ic

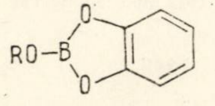

II

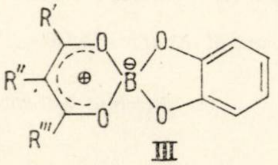

III

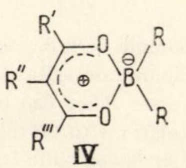

IV

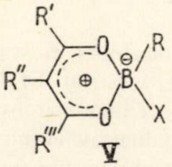

V

Similarly, 1,3-diketones react with trialkylboranes, eliminating one mole of alkane and yielding IV, $R=Alk$,[7-9] or with diarylborinic esters, eliminating one mole of alcohol and forming IV, $R=Ar$.[10] These compounds are similar to the long-known complexes IV, $R=F$, formed from 1,3-diketones and boron fluoride,[11-21] to complexes IV, $R=OAc$, formed from 1,3-diketones and pyroboracetate,[22] or to complexes IV, $R'=OAlk$,

---

[7] B. M. Mikhailov and Yu. N. Bubnov, *Izvest. Akad. Nauk S.S.S.R., Otdel. khim. Nauk*, **1960**, 1883.

[8] L. H. Toporcer, R. E. Dessy and S. I. E. Green, *Inorg. Chem.*, **4**, 1649 (1965); *J. Amer. Chem. Soc.*, **87**, 1236 (1965); L. H. Toporcer, *Diss. Abstr.*, **26**, 3640 (1966).

[9] M. F. Hawthorne and M. Reintjes, *J. Amer. Chem. Soc.*, **86**, 5016 (1964); *J. Org. Chem.*, **30**, 3851 (1965).

[10] I. Bally, A. Arsene, M. Băcescu-Roman and A. T. Balaban, *Tetrahedron Letters*, **1965**, 3929.

[11] G. T. Morgan and R. B. Tunstall, *J. Chem. Soc.*, **125**, 1963 (1924).

[12] H. Meerwein, *Ber. dtsch. Chem. Ges.*, **66**, 411 (1933); H. Meerwein and D. Vossen, *J. prakt. Chem.* (2), **141**, 149 (1934); H. Meerwein and W. Pannwitz, *ibid.*, **141**, 123 (1934); H. Meerwein, K. Bodenbrenner, P. Borner, F. Kunert and K. Wunderlich, *Liebigs Ann. Chem.*, **632**, 38 (1960).

[13] F. C. Young, F. C. Frostick, Jr., J. J. Sanderson and C. R. Hauser, *J. Amer. Chem. Soc.*, **72**, 3635 (1950); C. R. Hauser, F. C. Frostick, jr., and E. E. Man, *ibid.*, **74**, 3231 (1952); C. R. Hauser, F. M. Swamer and J. T. Adams, *Org. Reactions*, **8**, 59 (1954).

[14] H. O. House and D. J. Reif, *J. Amer. Chem. Soc.*, **77**, 6525 (1955).

[15] R. Neu, *Pharm. Ber. dtsch. pharmaz. Ges.*, **295**, 1 (1962).

[16] H. Musso and K. Figge, *Liebigs Ann. Chem.*, **668**, 1, 15 (1963).

[17] E. Leucht and W. Riedel, *ibid.*, **669**, 55 (1963).

[18] R. D. Youssefyeh, *J. Amer. Chem. Soc.*, **85**, 3901 (1963).

[19] M. Acarbay. *Liebigs Ann. Chem.*, **677**, 127 (1964).

[20] J. A. Durden and D. G. Crosby, *J. Org. Chem.*, **30**, 1684 (1965).

[21] J. D. von Mikusch-Buchberg and A. N. Sagredos, *Liebigs Ann. Chem.*, **681**, 118 (1965).

[22] W. Heimann and A. N. Sagredos, *Chem. Ber.*, **98**, 1949 (1965).

formed from dialkyl-[23] or diarylboronic esters[23,24] and 1,3-ketoesters. Diketene and benzodioxaboroles also afford such chelates.[25] More complicated organoboranes react with 1,3-diketones yielding complexes which contain chelate rings like IV.[26]

On the contrary, no unsymmetrical compound V could be isolated so far, with R=Alk or Ar, and with X=Hal, OH, OAlk or OAc. Our attempts showed that no crystalline complexes V can be isolated from 1,3-diketones and arylboronic acids (VI, X=OH) or esters (VI, X=OAlk). It may be noted that the delocalization in the chelate rings of III, IV or V cannot extend through the sp^3-hybridized boron atom; the earlier statement[23a,27] that such chelates would posess aromatic character is therefore false.

However, bearing in mind that boron may take part in aromatic rings,[28] several of which were prepared by Dewar,[29,30] we attempted to treat the mixture of I + VI with strong acids, hoping that the non-isolable compound V would split off water (or alcohol) forming a boron-containing cation VII.

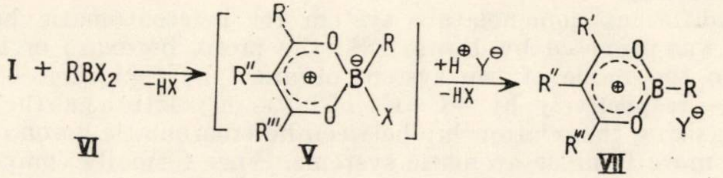

Indeed, treatment of a solution containing equimolar amounts of dibenzoylmethane and phenylboronic acid or its di-*n*-butyl ester in dichloromethane with a solution of anhydrous perchloric acid in the same solvent[31] at low temperatures afforded a crystalline perchlorate (VII, R′=R‴=Ar=Ph, R″=H) m.p. ca. 105° with decomposition and formation of a higher melting solid (see below).

---

[23] a. W. Gerrard, M. F. Lappert and R. Shafferman, *J. Chem. Soc.*, **1958**, 3648; *Chem. and Ind.*, **1958**, 722; b. L. A. Duncansson, W. Gerrard, M. F. Lappert, H. Pyszora and R. Shafferman, *J. Chem. Soc.*, **1958**, 3652.

[24] R. Neu, *Arch. Pharm.*, **294**, 173 (1961); *Experientia*, **19**, 68 (1963).

[25] J. R. Horder and M. F. Lappert, *Chem. Commun.*, **1967**, 485.

[26] G. W. Rotermund and R. Köster, *Liebigs Ann. Chem.*, **686**, 153 (1965); R. Köster and G. W. Rotermund, *ibid.*, **689**, 40 (1965).

[27] W. Gerrard, "The Organic Chemistry of Boron", Academic Press, Inc., New York, 1961, p. 91.

[28] a. A. T. Balaban, *Studii și Cercetări Chim. Acad. R. P. România*, **7**, 257 (1959); b, A. T. Balaban and Z. Simon, *Tetrahedron*, **18**, 315 (1962); c, A. T. Balaban and Z. Simon, *Rev. Roumaine Chim.*, **10**, 1059 (1965).

[29] P. M. Maitlis, *Chem. Rev.*, **62**, 223 (1962).

[30] a, M. J. S. Dewar, in "Progress in Boron Chemistry", vol. 1, (H. Steinberg and A. L. McCloskey, editors), Pergamon Press, Oxford, 1964, p. 235; b, M. J. S. Dewar, in "Boron-Nitrogen Chemistry", "Adv. in Chemistry Series" No. 42, (Amer. Chem. Soc., Washington, D.C., p. 227.

[31] F. Klages and P. Hegenberg, *Angew. Chem.*, **74**, 902 (1962).

A different method for the preparation of the same product IX consists in the protodeboronation of the chelate VIII (IV, $R=R'=R'''=Ph$, $R''=H$) formed from dibenzoylmethane and diphenylborinic ester.[10]

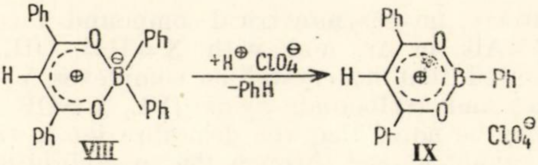

II. NOMENCLATURE

According to the Chemical Abstracts nomenclature, compounds VII should be called 1,3,2-dioxaborinium salts, the numeration starting from one of the oxygen atoms, continuing with the boron, oxygen and carbon atoms. Therefore cation IX should be named 2,4,6-triphenyl-1,3,2-dioxaborinium.

A different nomenclature system for heteroaromatic boron compounds was proposed by Dewar[30,32]: the prefix boroxaro or borazaro is added to the name of the system obtained by replacing $-B=O-$ or $-B=N-$ respectively, by $-C=C-$. This nomenclature has the advantage of emphasizing the relationship between heteroaromatic boron compounds and the more familiar aromatic systems. Since formally compounds VII can be obtained from pyrylium salts X through replacement of a $-C=C-$ grouping by a $-B=O-$ grouping, they should be named 2,3-boroxaropyrylium salts. The numerotation is identical to the previously discussed one. It is necessary to indicate the position of the boron and oxygen atoms in order to avoid confusion, e.g. with the closely related 2,4,6-triphenyl-4,3-boroxaropyrylium cation (XI), which has not yet been prepared.

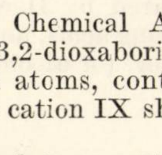

X

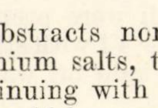

XI

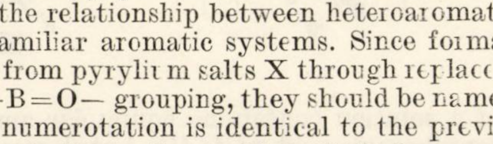

---

[32] M. J. S. Dewar and R. Dietz, *J. Chem. Soc.*, **1959**, 2728.

According to formulae IXa-IXc, the positive charge of the cation manifests itself most strongly in positions 4 and 6 (as in IXc). One of the probable reasons why salts VII with aliphatic R′ and R‴ substituents are unstable is that alkyl groups are less effective stabilizing factors for carbonium ions than aryl groups. Even better than aryl groups should be $-O^{\ominus}$ (leading to boroxaropyrones), $-OAlk$ or $-NAlk_2$ groupings in positions 2, 4 or 6.

III. SYNTHESIS

A. *From an arylboronic acid derivative and an 1,3-diketone in the presence of strong acids*

As outlined in the introduction, treatment of a dichloromethane solution of dibenzoylmethane and phenylboronic acid or its *n*-butyl ester, in equimolar amounts, with anhydrous perchloric acid in the same solvent affords at low temperatures a crystalline yellow perchlorate (IX). A hexachloroantimonate of the same cation was obtained from dibenzoylmethane, phenylboronic acid and antimony pentachloride in acetonitrile containing some hydrochloric acid (infrared spectra of the two salts were identical excepting bands due to the perchlorate anion).

The same method applied to several 1,3-diketones and boronic acids afforded the salts presented in table 1. An excess of perchloric acid over the stoichiometric amount has an adverse effect on the yield and must therefore be avoided.

When starting from dialkyl arylboronates the salt obtained (in the case of VIIa or IX) was purer than when employing the free arylboronic acid, because in the former case the reaction afforded an alcohol, which could be more easily removed from the reaction product than the water formed in the latter case.

B. *From 2,2-diaryl-1,3,2-dioxaborines by protodeboronation*

It was pointed out in the introduction the chelates IV prepared from borinic acids and 1,3-diketones split off a boron-carbon bond on treatment with strong acids, affording a cation VII and a hydrocarbon RH. Thus, treatment of chelate VIII in dichloromethane with anhydrous perchloric acid at low temperatures yielded the perchlorate IX, identical to that obtained by the previous method. The benzene which was formed during the course of this reaction was evidenced gas-chromatographically in the amount requested by this process.

IV. DECOMPOSITION

An interesting feature of 2,4,6-triphenyl-1,3,2-dioxaborinium perchlorate (IX) is its behaviour on heating. It presents a double melting point, with decomposition at 120° in capillary or 105° on a Koffler block, and resolidification to a higher melting perchlorate (XII). The decomposition process takes place easily even at lower temperatures, in solution; therefore attempts to purify the product by recrystallization (e.g. from acetonitrile) resulted in partial decomposition, causing some confusion in the preliminary note, [2a] corrected afterwards. [2b] The purification of the product is best carried out by dissolving it in the necessary amount of dichloromethane at room temperature, and adding then petroleum ether.

The structure of the decomposition product XII is that of a *bis*-(1,3-diketonato)-boronium salt,[33] as proved by comparison with authentic specimens prepared by various methods, e.g. from boron trichloride and 1,3-diketones.[34] Indeed, the higher-melting decomposition product from VIIa and VIIc can be prepared from boron trichloride and dibenzoylmethane, while the decomposition product of VIIb can be obtained from boron trichloride and di-*p*-anisoyl-methane.

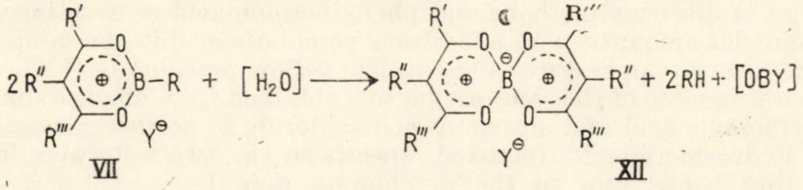

VII, a, R, R′, R‴=Ph; R″=H.
b, R, = Ph; R″=H; R′ R‴ = p-$C_6H_4OCH_3$.
c, R′, R‴ = Ph; R″ = H; R = p-$C_6H_4OCH_3$

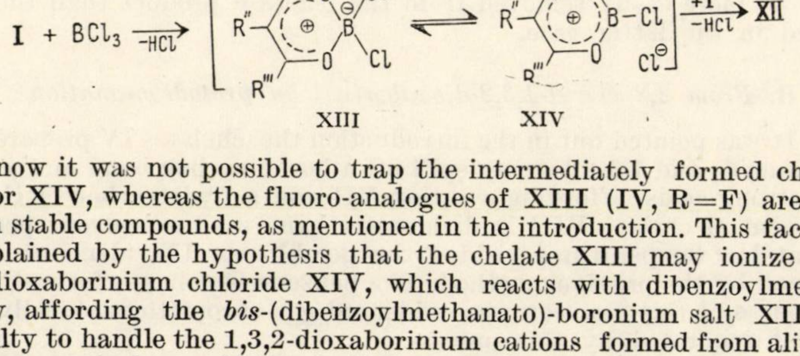

Until now it was not possible to trap the intermediately formed chelates XIII or XIV, whereas the fluoro-analogues of XIII (IV, R=F) are well-known stable compounds, as mentioned in the introduction. This fact may be explained by the hypothesis that the chelate XIII may ionize to an 1,3,2-dioxaborinium chloride XIV, which reacts with dibenzoylmethane readily, affording the *bis*-(dibenzoylmethanato)-boronium salt XII. The difficulty to handle the 1,3,2-dioxaborinium cations formed from aliphatic 1,3-diketones is due probably to their easy decomposition by the process outlined above.

The relationship between dioxaborinium salts and benzene suggested by formula IXa indicates that dioxaborinium salts should possess aromatic character. Irrespective which criterion is adopted as definition for aromaticity (literature cited in[28b]), a certain conjugation energy is expected to be associated with aromatic systems. The ready decomposition of 1,3,2-dioxaborinium salts affording *bis*-(1,3-diketonato)-boronium salts indicates that this conjugation energy is small. This agrees with the high "aromaticity constant"[28b, c] of system VII. Even pyrylium salts[35, 36] with only one oxygen heteroatom are readily converted into aliphatic compounds by reaction with nucleophiles. The driving force of the decomposition IX→XII is the increase from 3 to 4 of the coordination number of the boron atom and the spread of the positive charge over two oxa-oxonia-pentadiene units in XII instead of one as in IX.

---

[33] W. DILTHEY, *Liebigs Ann. Chem.*, **344**, 300 (1905).

[34] a, A. BARABÁS, E. IŞFAN, M. ROMAN, M. PARASCHIV, E. ROMAŞ and A. T. BALABAN, *Tetrahedron*, **24**, 1133 (1968); b, A. TRESTIANU, H. NICULESCU-MAJEWSKA, I. BALLY, A. BARABÁS and A. T. BALABAN, *ibid.*, **24**, 2499 (1968).

The second reaction product formed in the thermal decomposition of VII is ArH. When starting from phenylboronic acid in the preparation of VII (a,b), the decomposition should afford benzene, whereas the decomposition of VIIc, prepared from *p*-anisylboronic acid should afford anisole. The thermogravimetric analyses presented in table 1 and in figure 1 bear out these expectations. They evidence two processes in which the weight decreases, corresponding to the two melting points observed under the microscope or in the capillary; the first process (i) at lower temperature corresponds to the loss of the RH residue, i.e. benzene from VIIa and VIIb, and anisole from VIIc. The second process (ii) is the decomposition of the *bis*-(1,3-diketonato)-boronium salt ending (in air) in a residue consisting of boric oxide. For perchlorates both processes are exothermal as shown by the DTA curve in figure 1; slightly for (i), strongly for (ii). By carrying out the decompositions in vacuo in a closed system and freezing out the volatile product evolved in process(i), a chemical identification of benzene (from VIIa, VIIb and VIId) and of anisole (from VIIc) was effected by dinitration[37] and characterization of the dinitroderivatives by m.p., mixed m.p. and eutectic m.p. [38]

In order to get more insight into the course of this decomposition process, dibenzoylmethane was tritiated at its methine group (and at the enolic proton) by refluxation in ethanol-tritiated water. Then by reaction with phenylboronic acid and anhydrous perchloric acid in dichloromethane, 2,4,6-triphenyl-5-*t*-1,3,2-dioxaborinium perchlorate was prepared in 85% yield. Its specific activity (Ci/mole) was half of the specific activity of the labelled dibenzoylmethane started from, the enolic hydrogen being eliminated during the conversion into VII. The decomposition into *bis*-(dibenzoylmethanato)-boronium perchlorate and benzene was per-

---

[35] K. Dimroth and. K. H. Wolf, in "Newer Methods of Preparative Organic Chemistry" (W. Foerst, editor), Academic Press, Inc., New York, 1964, vol. 3, p. 357.

[36] A. T. Balaban, W. Schroth and G. Fischer, in "Advances of Heterocyclic Chemistry", vol. 10 (A. R. Katritzky and A. J. Boulton, editors), Interscience Publ., Inc., New York, 1970, p. 241.

[37] E. H. Huntress and S. P. Mulliken, "Identification of Pure Organic Compounds", Wiley, New York, 1957.

[38] L. Koffler and A. Koffler, "Thermomikromethoden", Verlag Chemie, Weinheim, 1954.

formed in vacuo at 100° for 40 min. in the usual manner and the specific activities of the two reaction products were measured after purification (details are indicated in [39]). Benzene had a specific activity about eleven times smaller than the specific activity of the parent dioxaborinium perchlorate. This finding agrees with one of the two mechanisms indicated below :

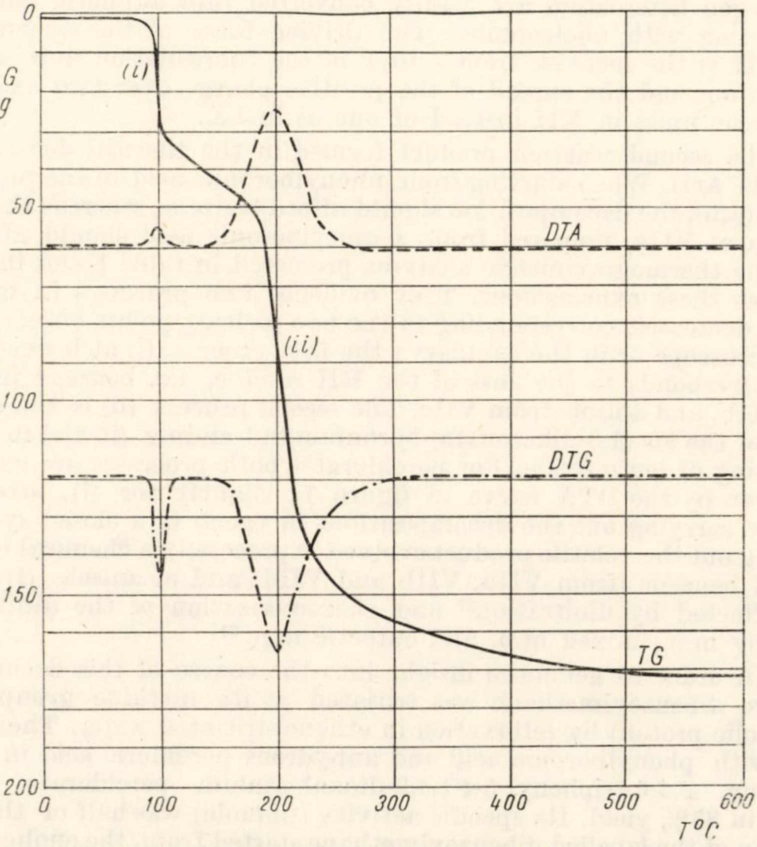

Fig. 1. — Thermogravimetric analysis of 2,4,6-triphenyl-1,3,2-dioxaborinium perchlorate (IX), (200 mg sample).

1. A homolytic breaking of the boron-phenyl bond; the reactive phenyl radical thus formed may abstract a hydrogen atom with equal probability from the methine carbon or from the ten phenyl hydrogens of the dibenzoylmethane. Examples of homolytic breaking of boron-carbon bonds have been discussed in the literature.[40, 41]

---

[39] A. Barabás, C. Măntescu, D. Duţă and A. T. Balaban, *Tetrahedron Letters*, **1965**, 3925.

[40] J. E. Leffler, E. Dolan and T. Tanigaki, *J. Amer. Chem. Soc.*, **87**, 927 (1965).

[41] S. I. Weissman and H. von Willigen, *ibid.*, **87**, 2285 (1965); M. A. Kuck and G. Urry, *ibid.*, **88**, 89 (1966); M. A. Kuck, *Diss. Abstr.*, **26**, 1339 (1965).

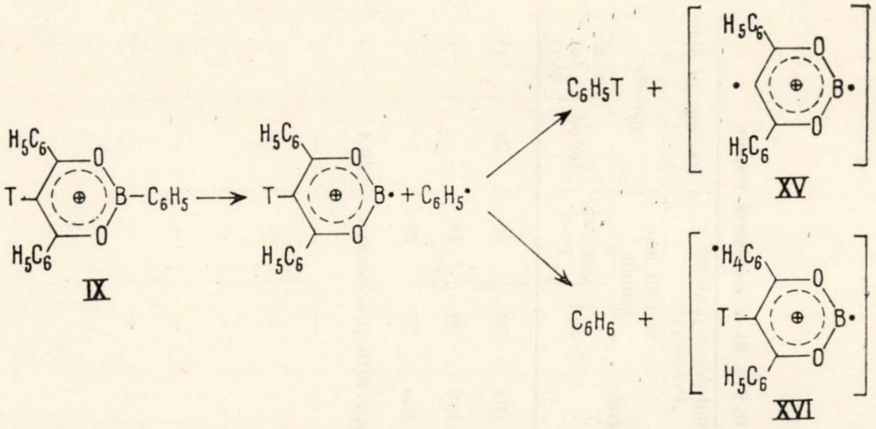
IX
XV
XVI
C_6H_5T +
C_6H_6 +
$C_6H_5^{\cdot}$

2. A homolytic breaking of a bond within the covalently-bonded anion, with formation of a reactive free radical.[42] It is uncertain whether the formation of the *bis*-(dibenzoylmethanato)-boronium salt involves free dibenzoylmethane as postulated in the latter mechanism, or whether it is a direct process as admitted in the former mechanism.

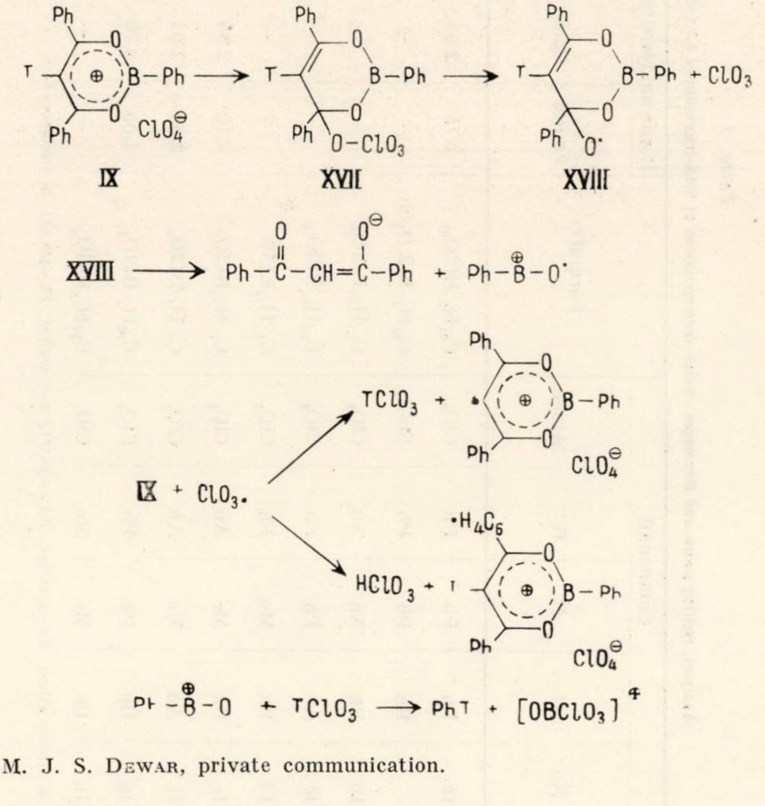
IX
XVII
XVIII
$ClO_4^{\ominus}$
$O-ClO_3$
$+ ClO_3$
XVIII → $Ph-\overset{\overset{O}{\|}}{C}-CH=\overset{\overset{O^{\ominus}}{|}}{C}-Ph + Ph-\overset{\oplus}{B}-O^{\cdot}$
IX + $ClO_3\cdot$
$TClO_3$ +
$HClO_3$ +
$Ph-\overset{\oplus}{B}-O + TClO_3 \longrightarrow PhT + [OBClO_3]^{+}$

---

[42] M. J. S. Dewar, private communication.

Table 1

Analyses, melting points and thermogravimetric decompositions of 2,4,6-trisubstituted 1,3,2-dioxaborinium salts (VII, R″ = H) at atmospheric pressure.

Compound					Formula	Boron analysis, %		Melting point °C	Thermal decomposition Process (i)			Residue at 550°	
										Weight loss g/mole		g/mole	
No	R	R′	R‴	Anion		Found	Calc.		Temp. range °C	found	calc. for RH	found	calc. for B_2O_3
VIIa	Ph	Ph	Ph	ClO_4	$C_{21}H_{1}BClO_{6}$	2.75	2.63	104[b]	95–104	80	78	29	34
	Ph	Ph	Ph	$SbCl_{6}$	$C_{21}H_{1}BCl_{}O_2Sb$	—	—	148[b]	120–140	90	78	—	—
VIIb	Ph	An	An	ClO_4	$C_{23}H_{20}BClO_{3}$	—	—	140	115–130	77	78	—	—
VIIc	An	Ph	Ph	ClO_4	$C_{22}H_{1}BClO_{7}$	—	—	194	overlaps with process(ii)			36.4	34
VIId	Ph	Me	Ph	ClO_4	$C_{1}H_{14}BClO_{6}$	—	—	100	—	—	—	—	—
VIIe	Ph	Me	An	ClO_4	$C_{17}H_{16}BClO_7$	3.12	2.85	123	—	—	—	—	—
VIIf	An	Me	An	ClO_4	$C_{1}H_{1}BClO_8$	2.86	2.64	250	—	—	—	—	—
VIIg	Bu	Ph	Ph	ClO_4	$C_{14}H_{1}BClO_{6}$	4.05	3.79	148	—	—	—	—	—
VIIh	Ph	Me	Me	ClO_4	$C_{11}H_{12}BClO_{3}$	—	—	90	—	—	—	—	—

a, Abbreviations: An = *p*-anisyl; Bu = *n*-butyl; Me = methyl; Ph = phenyl. b, Decomposition.

The fate of the second atom of boron is not known; species like ($OBClO_4$) or ($OBClO_3$) as written above are probably formed. The specific activity of the *bis*-(dibenzoylmethanato)-boronium perchlorate isolated in the above reaction was found to be a little higher than the initial specific activity of the dioxaborinium salt; no conclusion could be drawn from this figure on the nature of the reaction leading to compound XII.

V. SPECTRA

A. *Infrared absorption spectra*

Some relevant infrared spectra of boron compounds dealt with in this paper are presented in Table 2, together with some tentative assignments of the observed absorption frequencies. It may be observed that IR spectra can discriminate between these compounds. The most obvious differences are in the 3000−3100 and 700−800 cm $^{-1}$ regions, where the vibrations of the aryl hydrogens occur. Compounds with only one kind of phenyl groups present a single absorption peak in the region of aromatic CH stretching vibrations (an exception is pinacolyl benzeneboronate), whereas rather complicated patterns arise for compounds with different phenyl groups. In the spectra of *bis*-(dibenzoylmethanato)-boronium salts XIIa (e.g. triiodide, chloride, tetrachloroferrate, tetrachloroaluminate, hexachlorostannate [34a]) with one kind of phenyl groups, two strong infrared bands appear at ca. 720 and 780 cm $^{-1}$. In the spectra of the iodide, hexachloroantimonate or perchlorate of XIIa these bands may appear split, e.g. the perchlorate has partly overlapping bands at 720, 727 cm^{-1}. This splitting is probably due to the fact that owing to crystal packing the out-of-plane vibrations of phenyl hydrogens are not equivalent for the four phenyl groups. A similar observation was reported for diphenylboronic acid[43]; in accordance to this latter statement, the corresponding chelate IV (R, R′, R‴ = Ph, R″ = H) also presents a split phenyl vibration at 750, 760 cm $^{-1}$, which was attributed to the boron-bonded phenyl groups. As expected, in the spectra of compounds IV, and VIIa (or IX) with two different kind of phenyl groups four distinct bands due to out-of-plane vibrations are present. A comparison with properly chosen reference compounds as has been done in Table 2, enabled the assignment of these bands to the boron-bonded and carbon-bonded phenyl groups respectively.

---

[43] L. J. Bellamy, W. Gerrard, M. F. Lappert and R. C. Williams, *J. Chem. Soc.*, **1958**, 2412; E. W. Abel, W. Gerrard and M. F. Lappert, *ibid.*, **1957**, 3833.

Table 2

Infrared absorption spectra of boron compounds in KBr pellets. a, neat liquid film.

$PhB(OH)_2$	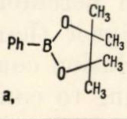 a,	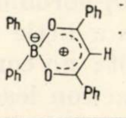	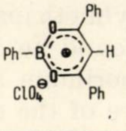	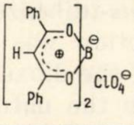	Assignments
3700ms	—	—	—	—	νOH
—	—	3130vw	3135vw	3140mw	νCH, chelate ring
3100mw	3088ms	3085vw	—	—	
—	3060s	3060mw	3070mw	3070mw	νCH, phenyl groups
—	3030ms	3040mw	—	—	
—	—	3010mw	3020mw	—	
—	—	3000mw	—	—	
—	2990vvs	—	—	—	νCH, methyl
—	2940vs	—	—	—	groups
1610s	1610vs	1600m	1600m	1602s	νC=C,phenyl groups
—	—	1540vs	1540vs	1570–	νC=O chelate
				–1520vvs	νC=C ring
1510m	1510vs	1490s	1490vs	1490vs	νC=C, phenyl
—	1470ms	—	—	—	groups
1450vs	1445vs	1430m	1440mw	—	νB-Ph, ref. [43–43]
—	—	—	—	1432s	—
1400–	1410–	1360s	1370ms	1380vs	νB-O and δCH,
–1340vvs	–1330vvs	—	1355s	1360vs	methyl groups
1320vs	1312vs	1310m	1310mw	1310vs	—
1280ms	—	1270w	1270w	—	—
—	—	1240m	1240m	1255vs	—
1195vs	1220s	1205ms	1195mw	1192m	—
—	1160vs	1180mw	—	1170m	—
—	—	1160m	—	—	—
—	—	1140m	—	—	—
1100vs	1100vs	—	1120–	1120–	νCl-O in ClO_4^-
—	—	1090m	–1090s	–1080vvs	
1080ms	1072ms	1070mw	—	—	—
1035s	1032vs	1040mw	1030m	1040vs	—
1015s	—	1005mw	1000m	1000s	—
—	970vs	980ms	985m	—	—
930m	932mw	930w	920mw	910ms	—
—	868vs	880ms	—	850mw	—
—	840m	870ms	850w	840w	—
—	—	—	830w	830w	—
810ms	820m	820w	—	815w	—
—	—	780ms	780mw	786ms	δCH, C-phenyls
770s	770s	760ms	760m	—	δCH, B-phenyl
—	—	750ms	—	—	
—	—	720ms	728m	727ms	δCH, C-phenyls
—	—	—	—	720ms	
705s	708vs	712ms	710m	—	δCH, B-phenyl
660mw	672vs	680m	680m	652s	—
638vs	657vs	660mw	640m	—	—
620w	620w	615mw	615m	623s	νCl-O in ClO_4^-
—	—	605mw	—	607s	—
582ms	580 m	560m	550mw	568m	—

[41] F. K. BUTCHER, W. GERRARD, M. HOWARTH, E. F. MOONEY and H. A. WILLIS, *Spectrochim. Acta*, **20**, 79 (1964).

[45] R. HEMMING and D. G. JOHNSTON, *J. Chem. Soc.*, **1964**, 466; *ibid.*, **1966**, **B**, 314.

[46] J. E. BURCH, W. GERRARD, M. GOLDSTEIN, E. F. MOONEY and H. A. WILLIS, *Spectrochim. Acta*, **18**, 1403 (1962).

[47] E. NYILAS and A. H. SOLOWAY, *J. Amer. Chem. Soc.*, **81**, 2681 (1959).

[48] G. SMOLINSKY, *J. Org. Chem.*, **26**, 4915 (1961).

B. *Ultraviolet absorption spectra*

The ultraviolet absorption spectra of 2,4,6-triphenyl-1,3,2-dioxaborinium perchlorate (IX) were recorded in acetonitrile and dichloromethane. As reported previously,[50] in acetonitrile the absorption maxima appear at 282 (lg ε 4.07) and 374 nm (lg ε 4.54) with a shoulder at ca. 385 nm. As shown in figure 2, the spectrum of the acetonitrile solution changes in time presenting three isosbestic points at 262, 302 and 355 nm, and becoming identical after two hours to the spectrum of a mixture of boric acid and dibenzoylmethane. [51–54] In dichloromethane,[2a] the maxima appear at 271, 277, 293 and 368 nm (major band) with shoulders at ca. 264 and 386 nm; the dichloromethane solution also changes its absorbance in time, more slowly in the presence of anhydrous perchloric acid. The absorption bands of *bis*-(dibenzoylmethanato)-boronium perchlorate (XII) appear in acetonitrile [2a,50] at 305, 378 and 396 nm, and in dichloromethane[34] at 277 (lg ε 4.25), 310 (4.45), 382 (5.05) and 400 nm (5.13).

Like 2,4,6-triarylpyrylium salts (X), 2,4,6-triaryl-1,3,2-dioxaborinium salts (IX) fluorescence in solution. A comparison between the electronic absorption spectra of 2,4,6-triphenylpyrylium salts[49,55] and 2,4,6-triphenyl-1,3,2-dioxaborinium salts (table 3) shows that the replacement of aC = C grouping by a B=O grouping causes a marked hypsochromic effect, in agreement with molecular orbital calculations. [28c]

C. *Nuclear magnetic resonance spectra*

The ^{1}H and ^{11}B NMR data summarized in table 4 are consistent with the proposed structure of an 1,3,2-dioxaborinium salt for compounds 6 and 7 from this table.

A comparison between pmr spectra of compounds 5, 6, 7 and 10 provides the location of peaks due to the different phenyl groups in compound 7; it may be seen that both C—Ph and B—Ph groups are present in the spectrum of this compound. The location of the olefinic C—H signal in compounds 7 and 10 is rather difficult, is it because covered by the phenyl multiplet.

The ^{11}B spectrum of compound 7 clearly shows its boron atom in a planar sp^2 hybridization state, its chemical shift being closest to that of a simple phenylboronic ester (compound 4). This may be surprising as compound 7 contains some additional deshielding factors, relatively to compound 4: an extended conjugated system and a positive charge. It was pointed out however,[56] that the correlation between electron den-

---

[49] A. T. Balaban, V. E. Sahini and E. Keplinger, *Tetrahedron*, **9**, 163 (1960).

[50] A. Arsene, A. T. Balaban, I. Bally, A. Barabás, M. Paraschiv and C. N. Rențea, *Spectrochim. Acta*, **23 A**, 1373 (1967) .

[51] B. Eistert, F. Weygand and E. Csendes, *Chem. Ber.*, **84**, 745 (1951).

[52] P. Karrer, J. Kerble and R. M. Thakkar, *Helv. Chim. Acta*, **33**, 174 (1950).

[53] P. Karrer, J. Kerble and V. Albers-Schonberg, *ibid.*, **34**, 1014 (1951).

[54] G. S. Hammond, W. G. Borduin and G. A. Guter, *J. Amer. Chem. Soc.*, **81**, 4682 (1959).

[55] A. T. Balaban, M. Mocanu and Z. Simon, *Tetrahedron*, **20**, 119 (1964).

[56] R. Schaeffer, "Nuclear Magnetic Resonance Spectroscopy of Boron Compounds" in "Progress in Boron Chemistry", (H. Steinberg and A. L. McCloskey, editors). Pergamon Press, Oxford, 1964, vol. 1, p. 417.

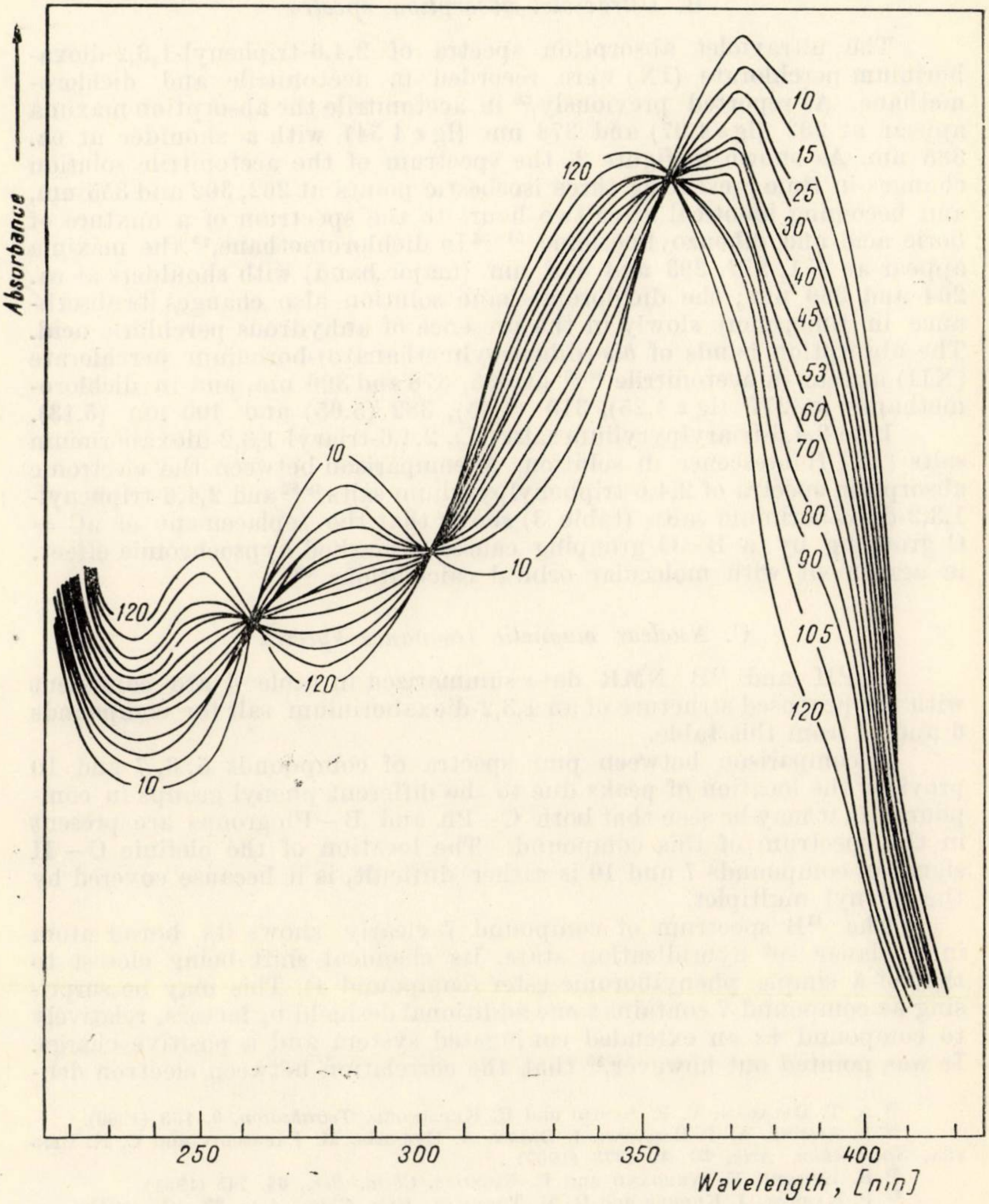

Fig. 2. — Ultraviolet absorption spectrum of 2,4,6-triphenyl-1,3,2-dioxaborinium perchlorate (IX) in acetonitrile at 10, 15, 25, 30, 40, 45, 53, 60, 70, 80, 90, 105 and 120 minutes after dissolution.

Table 3

Comparison of experimental and theoretical electronic absorption spectral data for 2,4,6-triphenyl-1,3,2,dioxaborinium (IX) and 2,4,6-triphenylpyrylium (X) cations.

Compound	Absorption frequencies (cm^{-1})		
	Experimental		Theoretical[28c]
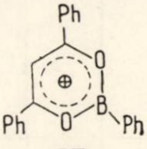 IX	25,800[a] 27,200 34,100 36,100 36,900	26,000[b] 26,800 — 35,500 —	21,100 27,100 28,600 31,400 35,000
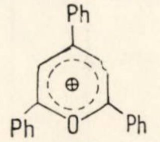 X	24,600[c] 27,700 36,000 — —	24,100[d] 30,100 35,400 — —	23,000 26,000 33,200 40,000 43,400

Solvents: a, dichloromethane; b, acetonitrile; c, acetic acid[49]; d, dichloromethane.[49]

sity and boron chemical shift was not yet clearly understood. Nevertheless it must be admitted that the considerable difference between the ^{11}B chemical shifts of compounds 7 and 1, the latter of which surely contains a boron atom involved in a benzenoid resonance, makes the aromaticity of compound 7 at least questionable. This is consistent with our above reported observations on the low stability of the 1,3,2-dioxaborinium salts.

EXPERIMENTAL

Methods and apparatus

Melting points determined in capillary are not corrected. Melting points determined on the Koffler micro hot stage are corrected. Infrared absorption spectra were determined in potassium bromide pellets or nujol mulls with a double-beam Jena UR-10 spectrophotometer. Ultraviolet absorption spectra were recorded with an Optica-Milano CF-4 spectrophotometer. Thermogravimetric measurements were effected with an Orion-Derivatograph. Gas chromatographic analyses were run with a Carlo Erba gas chromatograph.

Table 4

^{1}H and ^{11}B-nmr spectra of boron compounds

No	Compound	^{1}H chemical shifts (δ)				^{11}B chem. shifts$^{b.}$	References
		$C-C_6H_5^{a}$,	$B-C_6H_5^{a}$,	$C-H$	$-CH_3$		
1	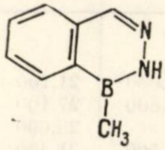	—	—	—	—	38.5	57,58
2	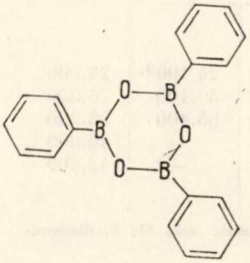	—	7.60(3H) 8.25(2H)	— —	— —	33.3	c, d,
3	$CH_3(CH_2)_3B(OH)_2$	—	—	—	—	32.4	59
4	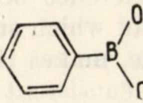	—	—	—	—	28.5	59
5	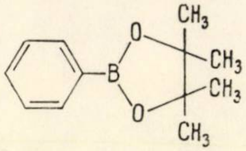	—	7.30(3H) 7.75(2H)	1.30	1.30 12(H)		c,
6	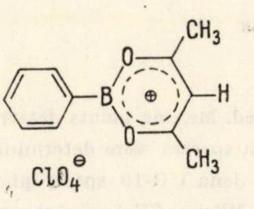	—	6.67(3H) 7.31(2H)	6.04 (1H)	2.25 (6H)	—	c,

---

[57] M. J. S. Dewar and R. Jones, *J. Amer. Chem. Soc.*, **89**, 2408 (1967).

[58] F. A. Davis and M. J. S. Dewar, *J. Org. Chem.*, **33**, 3324 (1968).

[59] W. D. Phillips, H. C. Miller and E. L. Muetterties, *J. Amer. Chem. Soc.*, **81**, 4496 (1959).

Table 4 (continued)

No	Compound	¹H chemical shifts (δ)				¹¹B chem. shifts[b]	Refe-rences
		$C-C_6H_5^a$	$B-C_6H_5^a$	$C-H$	$-CH_3$		
7	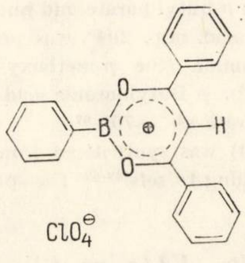	7.62 (6H) 8.10 (2H) 8.20 (2H)	6.72 (3H) 7.30 (2H)	7.30 (?)	—	29 27 26	e, f, g,
8	$B(OH)_3$		—	—	—	18.8	[60], h,
9	$B(OCH_3)_3$		—	—	—	18.1	[60]
10	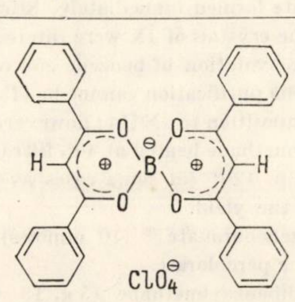	7.70 (12H) 8.25 (4H) 8.35 (4H)	—	sub-merged	—	4.6 4.5	i, j, k,

a, groups of multiplets centered on; b, ¹¹B chemical shifts downfield from $BF_3.Et_2O$ as external standard (if otherwise, recalculated); c, PMR spectrum in $CDCl_3$, this work; d, ¹¹B spectrum in Py, ref. [59]; e, ¹¹B spectrum in DMF, this work; f, ¹¹B spectrum in DMSO, this work; g, ¹¹B spectrum in MeCN, this work; h, in H_2O; i, ¹¹B spectrum of the ClO_4 salt in MeCN; j, ¹¹B spectrum of the $SbCl_6^-$ salt in MeCN; the ¹¹B spectra from this table will be discussed in detail in a forthcoming paper to be published jointly with Prof. J.A.S. Smith; k, the PMR spectra of these compounds were recorded in liquid SO_2 solutions and some discussion on them was already published in ref. [34b]

Reagents

Dichloromethane and acetonitrile were purified by drying over phosphorus pentoxide, then fractionated. Dibenzoylmethane (m. p. 78° from methanol) was prepared from dibromochalcone and sodium methoxide, or was a commercial product. *p*-Methoxyacetophenone, m.p. 37°, b.p. 120—125°/5 mm, (obtained by acetylating anisole in the presence of iodine catalyst [61]) was condensed [62] with ethyl acetate in the presence of sodium powder, affording *p*-anisoylacetone, m.p. 54° from ethanol. Di-*p*-anisoylmethane, m.p. 120° from ethanol, was prepared by condensing ethyl *p*-anisoate with *p*-methoxyacetophenone in the presence of sodium. *p*-Anisoylbenzoylmethane was prepared similarly [62] from ethyl benzoate and *p*-methoxyacetophenone. Benzoylacetone was obtained [63] from ethyl acetate and acetophenone in the presence of sodium ethoxide. *p*-Anisoylacetone was prepared from ethyl acetate and *p*-methoxy-acetophenone in the presence of sodium. [62]

---

[60] T. P. Onak, H. Landesmann, R. W. Williams and I. Shapiro, *J. Phys. Chem*,. **63**, 1553 (1959).

[61] X. A. Dominquez, B. Gomez, J. Silin, D. Giesecke and E. Ureta, *J. Amer. Chem. Soc.*, **76**, 5150 (1954).

[62] A. Horeau and J. Jacques, *Bull. Soc. chim. France*, (5), **15**, 57 (1948).

Benzeneboronic acid, m.p. 218°, was synthetised from *n*-butyl borate and phenylmagnesium bromide at −60°, see ref.[64] *p*-Methoxybenzeneboronic acid, m.p. 204°, was prepared [64,65] from *n*-butyl borate and *p*-methoxyphenylmagnesium bromide (the *p*-methoxy-bromobenzene being obtained by brominating anisole in acetic acid [66]). *n*-Butylboronic acid was synthetised from *n*-butylmagnesium bromide and trimethylborate at −70°. [67]

Pinacolyl benzeneboronate (compound 5 in Table 4) was synthetised from benzeneboronic acid (or anhydride) and pinacol hexahydrate according to refs.[68,69] The product was twice distilled at 110°/12 mm.

2,4,6-Triphenyl-1,3,2-dioxaborinium salts (VIIa or IX)

A. The perchlorate was obtained from 2.3 g (10 mmoles) dibenzoylmethane and 1.3 g (10 mmoles) benzeneboronic acid dissolved in 20 ml dichloromethane, cooled at −30° and treated gradually with stirring with a cold solution of 1 g (10 mmoles) of anhydrous perchloric acid [31] in 16 ml dichloromethane. A yellow precipitate formed immediately. Stirring was continued until the solution reached room temperature. The crystals of IX were filtered off and dried in vacuum. Yield 4 g , m.p. 102° with decomposition, evolution of benzene and resolidification to a mixture of XIIa and boric oxide perchlorate. The purification cannot be effected by recrystallization at temperatures over 45° because of decomposition to XIIa ; however, suspension of the crude perchlorate in a large amount of dichloromethane heated at 40°, filtration and treatment with petroleum ether gives a product with m.p. 120° (in some cases even 128°). An excess of perchloric acid during the synthesis lowers the yield.

B. A similar procedure employing di-*n*-butylbenzeneboronate [70] (10 mmoles) instead of benzeneboronic acid, at −40°, gave a somewhat purer perchlorate.

C. The hexachloroantimonate was obtained from dibenzoylmethane (3 g, 13 mmoles) and 1.5 g (13 mmoles) benzeneboronic acid in 20 ml acetonitrile ; into this solution cooled at −10°, a solution of 1.8 ml (4 g, 13 mmoles) antimony pentachloride and 1.5 ml (13 mmoles) conc. hydrochloric acid in 10 ml acetonitrile was added with cooling and stirring. The crystalline yellow precipitate which was formed (7 g) was filtered off, dried on a porous plate and in vacuum, m.p. 145—146°. The product decomposes on recrystallization.

D. The perchlorate was prepared also from the chelate VIII of diphenylboronic acid with dibenzoylmethane (2,2,4,6-tetraphenyl-1,3,2-dioxaborine) [10] in dichloromethane solution at 0° by treatment with an equivalent amount of anhydrous perchloric acid in dichloromethane. The precipitated perchlorate was identical (m.p. and IR spectrum) with IX. Gas chromatographic analysis of the filtrate showed that the dichloromethane contained benzene in the amount requested by the stoichiometry of the reaction.

---

[63] C. Beyer and L. Claisen, *Ber. dtsch. Chem. Ges.*, **20**, 2180 (1887).

[64] F. R. Bean and J. R. Johnson, *J. Amer. Chem. Soc.*, **54**, 4415 (1932).

[65] W. Konig and W. Scharrenbeck, *J. prakt. Chem.*, **128**, 152 (1930).

[66] K. H. Slotta and H. Heller, *Ber. dtsch. Chem. Ges.*, **63**, 3043 (1930).

[67] H. R. Snyder, J. A. Kuck and J. R. Johnson, *J. Amer. Chem. Soc.*, **60**, 107 (1938).

[68] H. G. Kuivila, H. G. Keough and E. J. E. J. Soboczenski, *J. Org. Chem.*, **19**, 780 (1954).

[69] J. M. Sugihara and C. M. Brown, *J. Amer. Chem. Soc.*, **80**, 2443 (1958).

[70] P. B. Brindley, W. Gerrard and M. F. Lappert, *J. Chem. Soc.*, **1955**, 2956.

2,4,6-Trisubstituted-1,3,2-dioxaborinium perchlorates, VIIb—h

These compounds were prepared as above under A from equimolar amounts of arylboronic acid, 1,3-diketone and anhydrous perchloric acid in dichloromethane.

Thermal decomposition of 2,4,6-triaryl-1,3,2-dioxaborinium salts VIIa—e

A. Thermoderivatograms were recorded photographically for 200 mg dry samples of 1,3,2-dioxaborinium salts in air in the temperature range 20—600° with a heating rate of 4—5°/min. The inert substrate in the differential thermal analysis was powdered quartz.

B. Preparative thermal decompositions with VIIa -d and tritiated VIIa were effected in a vacuum line at 100°, trapping the volatile products with liquid nitrogen. Benzene from VIIa, b,d, and anisole from VIIc was identified by dinitration.[37,38] The residue remaining in the heated flask was recrystallized from acetonitrile and identified by means of mixed m.p. and infrared spectra with the corresponding *bis*-(1,3-diketonato)-boronium perchlorate prepared[34] from boron trichloride and 1,3-diketones, in the case of VIIa -d.

Hydrolysis of 2,4,6-triphenyl-1,3,2-dioxaborinium perchlorate (IX)

Brief refluxation (2 min) of the perchlorate IX with distilled water affords after cooling and filtration dibenzoylmethane in 85% yield (if copper acetate is added, the yield of dibenzoylmethane as cupric chelate, is raised to 97%). The second product of hydrolysis, benzeneboronic acid, was isolated in 30% yield from the acid aqueous filtrate by neutralisation with potassium hydroxide, evaporation to dryness, acidification with acetic acid, extraction with ethanol and evaporation of the solvent.

Acknowledgements : Thanks are expressed to Drs. Cyryl Parkanyi and Rudolf Zahradnik (Praha) for theoretical MO calculations of the energy levels of 1,3,2-dioxaborinium salts. The recording of NMR spectra is acknowledged to Mrs. Alice Trestianu from our laboratory and Mr. F. Chiraleu, Institute for Organic Chemistry, Bucharest (PMR spectra) and to Prof. J.A.S. Smith, University of Warwick, Coventry, England (^{11}B-spectra).

Revue Roumaine de Chimie, **15**, 635 – 653 (1970)

Revue Roumaine de Chimie, **15**, 655 –659 (1970)

$TiCl_4$-CAROTENOID COMPLEXES. VII*

ACTION OF $TiCl_4$ ON 5,8-EPOXY-CAROTENOIDS (5,8-EPOXY-β-CAROTENE, 5,8-EPOXY-CRYPTOXANTHIN AND 5,8-EPOXY-ZEAXANTHIN)

V. TĂMAŞ and C. BODEA

Institute of Agronomy "Dr. Petru Groza", Department of Chemistry, Cluj, str. Mănăştur, 3

Received July 16, 1969

New titanochloro-carotenoid complexes were obtained by the action of $TiCl_4$ on 5,8-epoxy-carotenoids. The acetonolysis of these complexes yielded retrodehydro-carotenoids. In this way 5,8-epoxy-β-carotene was converted into retrodehydro-carotene, 5,8-epoxy-cryptoxanthin into retrodehydro-cryptoxanthin and retrobis-dehydro-carotene, and 5,8-epoxy-zeaxanthin into eschscholtzxanthin and anhydro-eschscholtzxanthin.

It is known that 5,6- and 5,8-epoxy-carotenoids can lose the epoxydic oxygen under the action of certain reagents, with regeneration of the starting carotenoid. Some 5,6-epoxy-carotenoids can be partialy de-epoxidated on treatment of their chloroformic solution with chloroform-HCl[1] with regeneration of the basic carotenoid and formation of 5,8-epoxy-carotenoid.

A general method of de-epoxidation of 5,6- and 5,8-epoxycarotenoids consisting in the reduction with $LiAlH_4$ was described by Cholnoky and al. [2] (scheme 1).

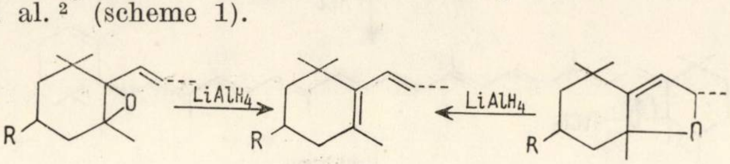

R=H or HO

In previous papers we have shown that $TiCl_4$ can be attached to the C=C double bond and to the oxygen the functional group of oxygenated carotenoids. In the case of hydroxy-carotenoids $TiCl_4$ is predominantly attached to the C=C double bond and secondarily to the hydroxyl group.[3-5] In the case of carbonyl-carotenoids the $TiCl_4$ is attached only to the carbonyl oxygen.[6]

---

* Part VI.: V. Tămaş and C. Bodea, *Rev. Roumaine Chim*, **14**, 1591 (1969).

[1] P. Karrer and E. Jucker, *Helv. Chim. Acta*, **28**, 427 (1945).

[2] L. Cholnoky, J. Szabolcs and G. Toth, *Liebigs Ann. Chem.*, **708** 218 (1967).

Continuing our studies about $TiCl_4$-carotenoid complexes we acted with $TiCl_4$ on some 5,8-epoxy-carotenoids. All the investigated 5,8-epoxy-carotenoids were de-epoxidated and transformed with high yields (60—80%) into retrodehydro-carotenoids.

By the action of $TiCl_4$ on 5,8-epoxy-β-carotene (I), in benzene solution, a titanochloro-carotenoid complex was obtained, to which structure IIa is assigned (but structure IIb or IIc are not to be excluded). This complex is transformed by acetonolysis into retrodehydro-carotene (III).

The sequences of the transformation of I into II are outlined in scheme 2.

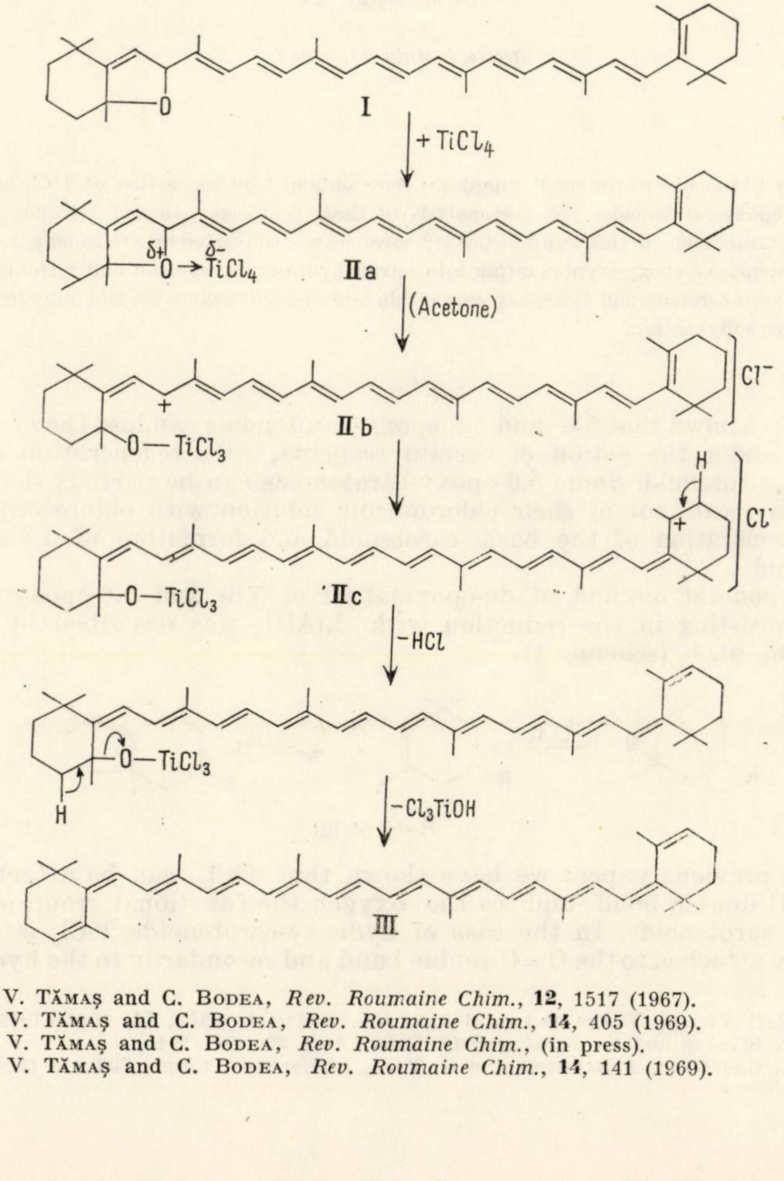

---

[3] V. Tămaş and C. Bodea, *Rev. Roumaine Chim.*, **12**, 1517 (1967).

[4] V. Tămaş and C. Bodea, *Rev. Roumaine Chim.*, **14**, 405 (1969).

[5] V. Tămaş and C. Bodea, *Rev. Roumaine Chim.*, (in press).

[6] V. Tămaş and C. Bodea, *Rev. Roumaine Chim.*, **14**, 141 (1969).

The structure of IIa was deduced from the results of the chlorine analysis (Cl = 19.00%) and the electronic spectrum ($\lambda_{max.}$ = 458 nm, in dimethylformamide).

It is interesting to notice that IIa is transformed into III very easily, even during the determination of λ_{max} in dimethylformamide, a behaviour not observed in the case of other types of titanochlorocarotenoid complexes.

The course of the transformation of II into III is shown in figure 1.

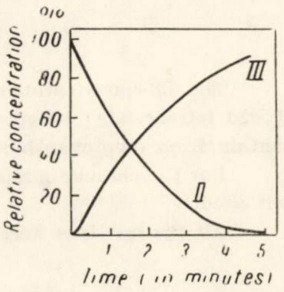

Fig. 1. — Transformation of II into III.

The acting of TiCl$_4$ upon 5,8-epoxy-cryptoxanthin (IV), in the conditions of the conversion of II into III leads to a mixture of two retrodehydro-carotenoids, namely: retrodehydro-cryptoxanthin (V) and retrobisdehydro-carotene (VI) (scheme 3).

The isolation of V indicates that the first stage in the transformation of IV into VI is a de-epoxidation followed by dehydration.

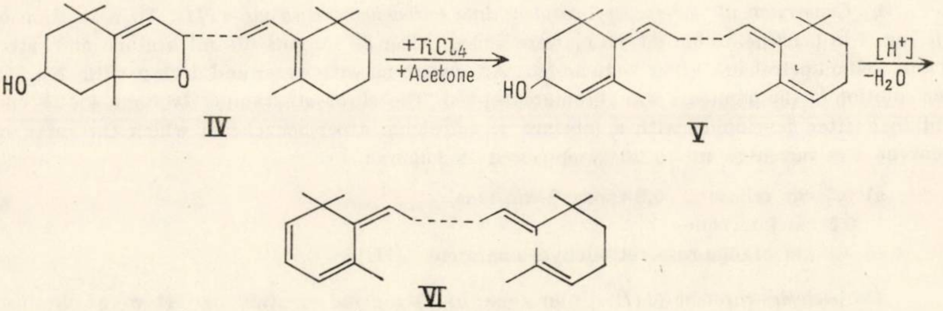

IV

V

VI

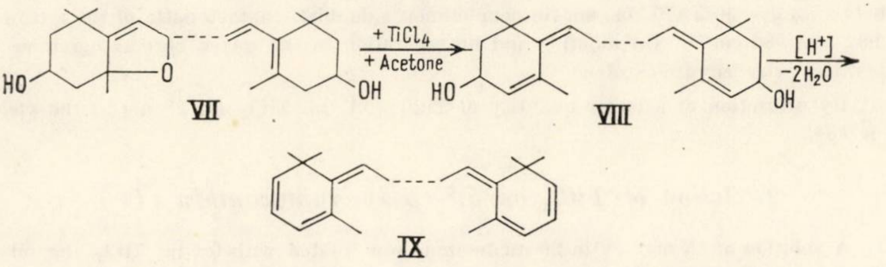

VII

VIII

IX

Under similar reaction conditions 5,8-epoxy-zeaxanthin (VII) yields a mixture of eschscholtzxanthin (VIII) and anhydroeschscholtzxanthin (IX) (scheme 4).

The de-epoxidation mechanism of IV and VII, is that shown in scheme 1.

In conclusion the reaction of 5,8-epoxy-carotenoids with $TiCl_4$ constitutes a practical method to convert carotenoids of the β-carotene type into retrodehydro-carotenoids.

EXPERIMENTAL

The 5,8-epoxy-carotenoids used were partial synthetical products prepared by the aid of lead tetraacetate; 5,8-epoxy-β-carotene was obtained from β-carotene,[7] 5,8-epoxy-cryptoxanthin from cryptoxanthin[8] and 5,8-epoxy-zeaxanthin from zeaxanthin.[9]

For the chromatographical separations a mixture of MgO-sand (ratio 2 : 1, in weight) was used.

All the reactions were carried out at room temperature (18—20°).

1. *Action of $TiCl_4$ on 5,8-epoxy-β-carotene (I)*

a) *Preparation of II.* 20 mg I were solved in 5 ml benzene, 0.05 ml $TiCl_4$ were added, and the mixture stirred several times.

After 10 min, the precipitate was filtered off and washed thrice with benzene; 15 mg dark powder (II) containing 19.00% Cl were obtained. II showed only a maximum at 458 nm (in dimethyl-formamide).

b) *Conversion of 5,8-epoxy-β-carotene into retrodehydro-carotene (III).* To a solution of 25 mg I in benzene, 0.05 ml $TiCl_4$ were added. After 30 seconds 40 ml acetone and after 5 min 100 ml petroleum ether were added. After washing with water and drying with Na_2SO_4 the solution of the pigments was chromatographed. The chromatogramme (column 4×25 cm) obtained after developing with a mixture of petroleum ether-benzene in which the ratio of benzene was increased up to 20%, appeared as follows:

a) 0.5 cm yellow 5,8-epoxy-β-carotene
0.5 cm interzone
b) 4.0 cm orange-rose retrodehydro-carotene (III)

Retrodehydro-carotene (III). From zone b) 15 mg red crystals of III were obtained (from ether). The pigment showed all the properties corresponding to retrodehydro-carotene, namely: λ_{max} = 501, 470, 445 nm (in neophaline), a doublet, characteristic of the retro form, at 962 and 980 cm^{-1} (in nujol)[10] and no separation in the mixed chromatogramme with authentical retrodehydro-carotene.

By utilization of a larger quantity of $TiCl_4$ (0.1 ml $TiCl_4$ for 25 mg I) the yield in III is 80%.

2. *Action of $TiCl_4$ on 5,8-epoxy-cryptoxanthin (IV)*

A solution of 15 mg IV in 20 ml benzene was treated with 0.1 ml $TiCl_4$, the mixture stirred 30 seconds and then 50 ml acetone were added. After 5 min the solution of the pigments was diluted with 60 ml petroleum ether and worked up as described under 1.b. After developing with petroleum ether + 3% benzene, the following chromatogramme (3×20 cm) was obtained :

---

[7] C. Bodea and M. Florescu, *Studii şi Cercetări Biochim.*, **3**, 13 (1960).

[8] C. Bodea and V. Tămaş, *Liebigs Ann. Chem.*, **671**, 57 (1964).

[9] C. Bodea and V. Tămaş, *Studii şi Cercetări Biochim.*, **5**, 359 (1962).

[10] E. Nicoară, V. Tămaş, G. Neamţu and C. Bodea, *Liebigs Ann. Chem.*, **697**, 201 (1966).

a) 0.5 cm yellow	5,8-epoxy-cryptoxanthin
b) 0.7 cm orange-red	retrodehydro-cryptoxanthin (V)
c) 0.5 cm interzone	
d) 3.0 cm rose-red	retrobisdehydro-carotene (VI)

From zone b) red crystals of V were obtained. The structure of pigment was confirmed by the following properties : $\lambda_{max}=500$, 470, 445 nm (in neophaline) ; in the IR spectrum a doublet at 962 and 982 cm^{-1} (in nujol) and a band at 1029 cm^{-1} (HO allylic) ; in the system petroleum ether — 95% methanol, 45% hypophasic partition. By treatment in chloroformic solution, with chloroform-HCl V was converted into VI.

Retrobisdehydro-carotene (*VI*). From zone b) 6 mg VI were obtained (from ether). The structure of the pigment resulted from the following properties : $\lambda_{max}=517$, 488, 460 nm (in neophaline), in the IR spectrum the characteristic doublet (960 and 980 cm^{-1}, in nujol) and no separation in mixed chromatogramme with authentical retrobisdehydrocarotene.

By utilization of a larger quantity of $TiCl_4$ (0.15 ml $TiCl_4$ for 15 mg IV) the yield in VI can be increased up to 70%.

3. *Action of $TiCl_4$ on 5,8-epoxy-zeaxanthin (VII)*

To a solution of 15 mg VII in 50 ml benzene, 0.15 ml $TiCl_4$ were added and the mixture stirred several times. After 30 seconds 50 ml acetone and after another 10 min 100 ml petroleum ether were added. After developing with a mixture of petroleum ether and 50% benzene the column (30×20 cm) appeared as follows :

a) 0.2 cm yellow	5,8-epoxy-zeaxanthin
b) 0.8 cm orange-red	eschscholtzxanthin (VIII)
1.0 cm interzone	
c) 3.0 cm red-violet	anhydroeschscholtzxanthin (IX)

Eschscholtzxanthin (*VIII*). From zone b) red crystals of VIII were obtained. The structure of VIII was confirmed as follows: $\lambda_{max}=501$, 470, 444 nm (in neophaline), in the IR-spectrum a doublet at 960 and 980 cm^{-1} and a band at 1028 cm^{-1} (for HO allylic), no separation in the mixed chromatogramme with authentical eschscholtzxanthin. On treating VIII with chloroform-HCl, IX was obtained.

Anhydroeschscholtzxanthin (*IX*). From zone a) 5 mg red powder were obtained (from ether). The electronic spectrum of IX showed λ_{max} at 532, 498, 465 nm (in neophaline) and the IR spectrum a doublet, characteristic for the retro-form. In the mixed chromatogramme with authentical anhydroeschscholtzxanthin there was no separation.

Revue Roumaine de Chimie, **15**, 655 – 659 (1970)

Revue Roumaine de Chimie, 15, 661 – 666 (1970)

AN AUTOMATIC RATEMETER FOR CONSECUTIVE SLOPE MEASUREMENTS

E. CORDOȘ

Department of Chemistry, University "Babeș-Bolyai", Cluj, str. Arany János, 11

Received June 23, 1969

The integration methods for determining the slope are the most convenient for adaptation to consecutive measurement since the results are not affected by the absolute value of the input signal. The paper presents a ratemeter which makes consecutive measurements on the same kinetic curve. The instrument has a logic part that assures a 28 second measurement cycle. In this time is included the integration period, the readout time and the period for erasure of the result and starting a new cycle. The ratemeter has been tested, with satisfactory results, both on synthetic signals and chemical systems.

The automatic measurement of reaction rate is an important step in the automation of kinetic analysis methods. Both in the analytical research and other fields one gets the problem of consecutive slope determination in different parts of the same kinetic curve. Among the known methods for automatic slope determination[1] those based on integration[2] are the most convenient for adaptation to consecutive measurements.

In this paper an integration technique is applied in order to make consecutive slope measurements and the diagram of a ratemeter built for this purpose is presented.

Principle

The slope determination by integration is based on the following principle : the transducer signal is integrated on two equal time increments, Δt, between t_1, t_2 and t_3 (fig. 1). The difference ΔA, of the areas A_1 and A_2, defined by the two time increments is the parallelogram ABCD, which is proportional to the slope according to relation :

$$\mathrm{tg}\alpha = \Delta A / (\Delta t)^2 \tag{1}$$

If the instrument that works on the above principle can be reset to make a new integration on other two time increments between t_4, t_5 and t_6 then the difference $A_4 - A_3$ is again proportional to the slope after the relation 1. In the integration method the first area obtained by integration is taken as reference for the measurement.

---

[1] H. L. Pardue, *Rec. of Chem. Progress*, **27**, 151 (1966).

[2] E. Cordoș, S. R. Crouch and H. V. Malmstadt, *Analyt. Chem.*, **40**, 1812 (1968).

As it has been shown[3] the results are also valid for a longer integration time, when the integrated portion of the curve cannot be assimilated with a straight line. In this case the difference between the two areas is proportional with the tangent to kinetic curve in the point that corresponds to the middle of integration period. In this way one can get a series of results which are useful both for analytical and/or kinetic purposes.

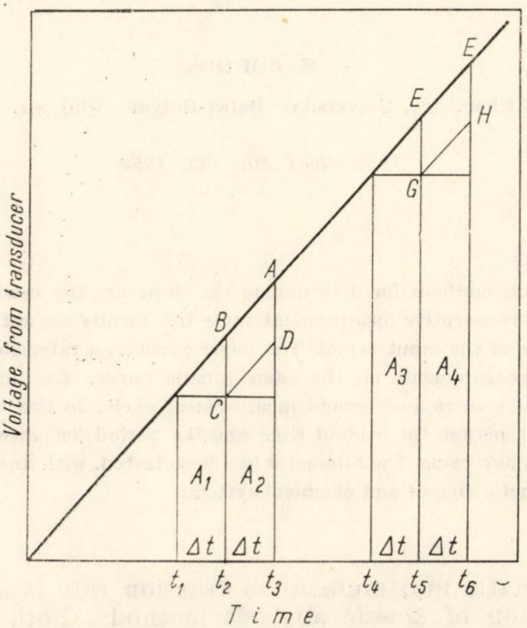

Fig. 1. — Consecutive slope measurement by integration and subtraction on two different portions of a rate curve.

INSTRUMENTATION

The diagram of the ratemeter for consecutive measurements on the same kinetic curve is shown in figure 2. The ratemeter has three basic circuits : the integration and subtraction circuit, the relay drivers block and the logic circuit. The integration and subtraction circuit is composed of two operational amplifiers set as integrators and connected to the signal source by five relays. The transducer signal is integrated by these two integrators on two equal time increments. The difference between the output voltages is proportional to the slope of the input signal. The way that this circuit is working is minutely described in a previous paper.[2]

---

[3] E. Cordoş, *Stud. Univ. Babeş-Bolyai Chem.*, 1969 (in press)

The operations in the integrating and subtraction circuit are controlled by the logic circuits which act the relay drivers (RD) and direct the signal to one integrator or to another. Beside this the logic circuit assures a period for reading the result, then erases it and begins a new measurement. This circuit is made of two pairs of J.K. flip flops (I, II and A, B) seven Nand gates (G_1 to G_7) and a Binary Counting Decoder (B.C.D.). The relays are activated according to the following sequence : 20-second measurement period (two 10-second integrating period), 7-second display of the result on digital voltmeter and 1-second erasure of result. The cycle lasts 28 seconds.

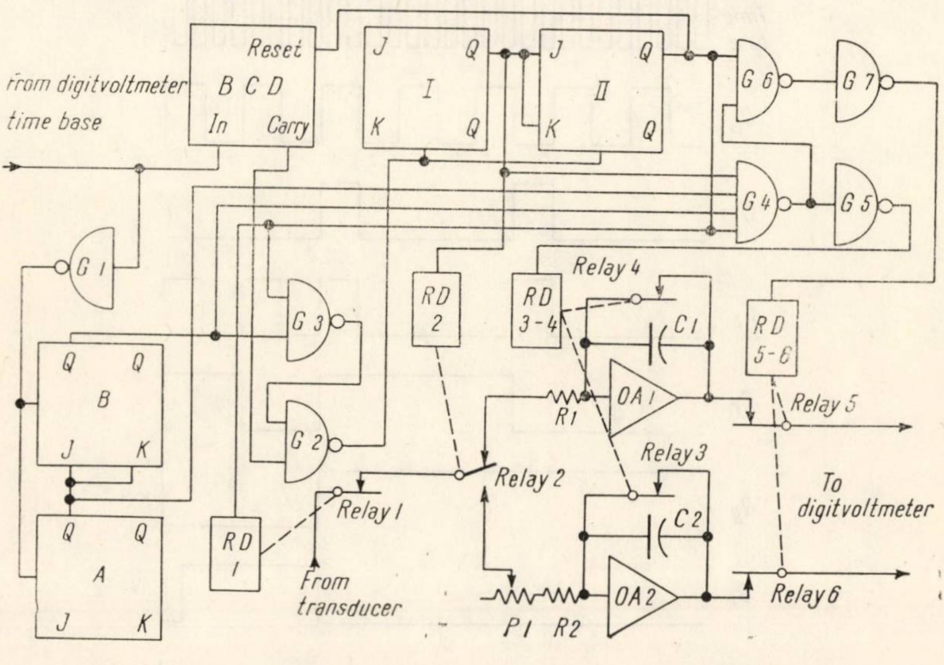

Fig. 2. — Diagram of the ratemeter showing integration and subtraction circuit and logic circuit.

I, II, A, B – J.K. flip flops; G1 to 7 – Nand gates; RD1 to 6 – Relay drivers; R1 and R2 – 450 K; C1 and C2 – 1 μf; P1 – 10 K pot; OA1 and OA2 – Operational amplifiers.

The logic part works, as it can be seen from the output waveforms (fig. 3), by modelling square-wave impulses. The J.K. flip flops I and II activate relays 2 and 1 respectively. Ten-second impulses are produced by the B.C.D. which receives very accurate one-second impulses from the time base of the digitvoltmeter. When the measurement period is over, the pair of flip flops A and B produce two impulses of 7 seconds each to provide the total time for read-out and erase the result. The combination of gates G_6 and G_7 provide the 7-second impulse which activates relays 5 and 6, thereby connecting the outputs to the digital voltmeter during the readout period. Gates G_4 and G_5 activate relays 3 and 4 for one second and after the read-out period is over shorts the 1μf capacitors to prepare the circuit for a new cycle.

The ratemeter designed to make consecutive measurements has been built on a Heath Binary Information Module EU 801-12. The components of the circuit have been wired on the cards, introduced into the module and connected according to the diagram. A Universal Digital Instrument Heath EU 801-X has been used as a readout system and 1-second impulse source.

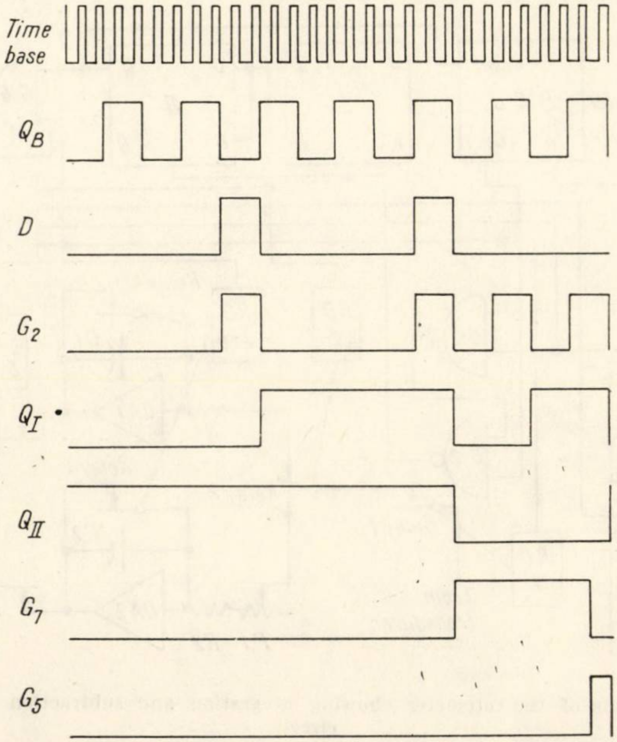

Fig. 3. — Output waveform in main points of the logic circuit.

Table 1

Automatic consecutive measurements of synthetic signal slopes

Input rate mV/sec	1.0	3.2	5.8	9.0	11.8	14.2
Digital readout mV	45.1 45.3 45.1 44.9 44.9 45.0 45.0 45.1 44.9 44.8	143.9 144.3 144.1 144.1 143.8 143.7 144.2 144.3 144.1 144.0	262.4 261.7 261.9 262.0 262.3 261.8 262.5 261.5 262.1 262.0	405.1 405.8 406.5 406.1 405.2 405.8 406.1 405.5 406.3 405.9	530.9 531.8 532.4 532.2 532.1 531.0 532.8 532.1 532.0 532.1	636.0 639.0 640.1 640.2 639.9 641.0 640.5 639.5 639.0 639.9
Average	45.01	144.05	262.02	405.83	531.94	639.91
Relative standard deviation %	0.32	0.14	0.12	0.11	0.11	0.10
Proportionality constant	45.01	45.01	45.17	45.09	45.07	45.06

RESULTS AND DISCUSSION

The ratemeter has been tested by measuring the slope of synthetic signals (Table 1). The results from this table have been obtained by measuring ten times a constant slope during 280 seconds. The output voltage of the ratemeter is constant for all the measurements, as indicated by the relative standard deviation, and it is a linear function of the input signal slope, as seen from the proportionality constant.

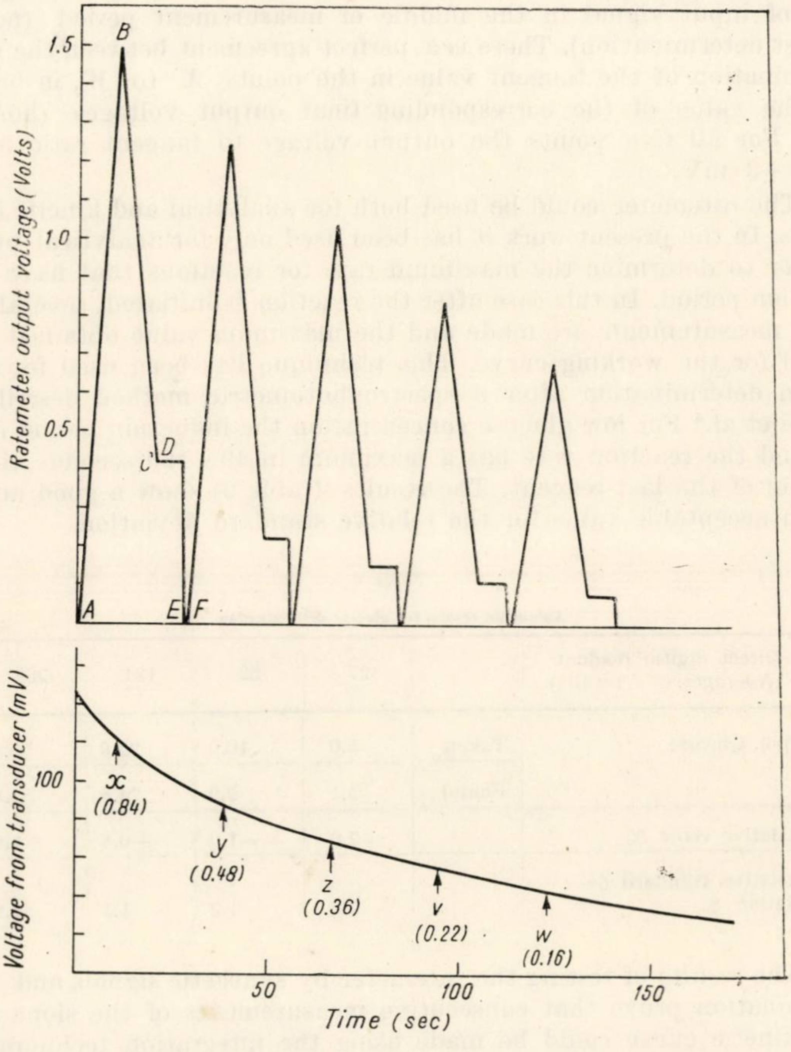

Fig. 4. — Simultaneous recording of the ratemeter output voltage (above) and the kinetic curve used as input signal (below).

Figure 4 shows the recording of the ratemeter output voltage (above) and a portion of a kinetic curve used as input signal. The increasing output voltage from *A* to *B* corresponds to the charging of first integrator and the decreasing output voltage *BC* to the charging of the second one (see fig. 2). The output voltage in *C* is proportional to the slope of input signal in the middle of measurement period (point *X* for first determination). There is a perfect agreement between the graphic determination of the tangent value in the points *X* to *W*, in brackets, and the value of the corresponding final output voltages (horizontal lines). For all five points the output voltage to tangent ratio is equal $5 \times 10^2 \pm 2$ mV.

The ratemeter could be used both for analytical and kinetic investigations. In the present work it has been used only for analytical purposes in order to determine the maximum rate for reactions that have a long induction period. In this case after the reaction is initiated, several consecutive measurements are made and the maximum value obtained is considered for the working curve. This technique has been used for kinetic glucose determination after a spectrophotometric method described by Pardue et al.[4] For low glucose concentration the induction period is quite long and the reaction rate has a maximum in 40—120 seconds after the addition of the last reagent. The results (table 2) show a good accuracy and an acceptable value for the relative standard deviation.

Table 2

Automatic results for glucose determination

Direct digital readout (Averages of 5 results)		27	52	131	269
Ppm Glucose	Taken	5.0	10.0	25.0	50.0
	Found	5.1	9.9	24.8	50.8
Relative error %		+2.0	−1.0	−0.8	+1.6
Relative standard deviation %		2.2	1.2	1.1	1.9

The results of testing the ratemeter by synthetic signals and glucose determination prove that consecutive measurements of the slope on the same kinetic curve could be made using the integration technique. The main condition for the instrument built to this purpose is to have a logic part which can assure the proper readout time and reset the instrument for starting a new measurement without external triggering.

Acknowledgment. The author is greatly indebted to Professor H. V. Malmstadt, in whose laboratory this work was carried out, for his constant interest and advice.

---

[4] H. L. Pardue, M. F. Burke and D. O. Jones, J. *Chem. Educ.*, **44**, 684 (1967).

ORSZÁGOS MŰSZAKI KÖNYVTÁR DOKUMENTÁCIÓS KÖZPONT 1883

NOTE POUR LES AUTEURS

La *Revue Roumaine de Chimie* publie des articles en anglais, français, russe, allemand ou espagnol. Les auteurs sont priés d'envoyer des articles, notes, communications et comptes rendus inédits.

Les manuscrits seront dactylographiés à deux intervalles. Les tableaux seront dactylographiés sur feuilles séparées, de même que la légende des figures. Les diagrammes seront tracés à l'encre de Chine sur papier calque. Les tableaux et les figures seront numérotés par des chiffres arabes, en nombre strictement nécessaire. Prière de ne pas inscrire les mêmes données dans les tableaux et les figures. Les formules chimiques seront incluses dans le texte ; en outre, elles seront transcrites sur des feuilles séparées. Les auteurs sont priés d'indiquer les caractères italiques (en soulignant les lettres au crayon), ainsi que tout autre caractère spécial. L'ordre des références bibliographiques sera celui de leur mention dans le texte ; le nom de l'auteur sera précédé de l'initiale du prénom ; les publications périodiques seront présentées suivant les prescriptions internationales. Les références seront ajoutées à la fin de l'article ; elles paraîtront comme des notes, au bas de la page. Le texte sera précédé d'un résumé, comprenant 15 lignes au maximum.

L'entière responsabilité du contenu des articles appartient aux auteurs. On publie des articles dus aux collaborateurs roumains ou étrangers. Les auteurs recevront 50 tirés à part.

PRINTED IN ROMANIA

TRAVAUX PARUS AUX ÉDITIONS DE L'ACADÉMIE DE LA RÉPUBLIQUE SOCIALISTE DE ROUMANIE

CORNEL BODEA et collab., **Tratat de biochimie vegetală**, partea I, **Fitochimie** (Traité de biochimie végétale, Ire partie, Phytochimie), Ier vol., 1964, 747 p. + 4 annexes + 2 pl., 41 lei ; IIe vol., 1965, 1262 p., 1 pl., 56 lei ; IIIe vol., 1967, 773 p., 35 lei.

V. GHEŢIE et V. MICUŞAN, **Analiza imunochimică. Teorie şi practică** (Analyse immunochimique. Théorie et pratique), 1966, 369 p., 28 lei.

R. PORTOCALĂ et L. POPA, **Acizii ribonucleici celulari şi virali** (Les acides ribonucléiques cellulaires et viraux), 1966, 375 p. + 8 pl., 26 lei.

D. PURDELA et R. VÎLCEANU, **Chimia compuşilor organici ai fosforului şi ai acizilor lui** (La chimie des composés organiques du phosphore et de ses acides), 1965, 540 p., 37 lei.

CRISTOFOR SIMIONESCU, MARGARETA GRIGORAŞ et AGATA CERNĂTESCU-ASANDEI, **Chimia lemnului din R.P.R.** (La chimie du bois en Roumanie), 1964, 239 p. + 6 pl., 27 lei.

CRISTOFOR SIMIONESCU et CLEOPATRA VASILIU-OPREA, **Mecano-chimia compuşilor macromoleculari** (La mécanochimie des composés macromoléculaires), 1967, 344 p., 23,50 lei.

CARMEN SABĂU, **Schimbul ionic, teoria şi aplicaţiile sale în chimia analitică** (L'échange ionique. Théorie et applications à la chimie analytique), 1967, 307 p., 12 lei.

I. V. MAXIM, **Materiale nucleare** (Matériaux nucléaires), 1969, 444 p., 30 lei.

CR. SIMIONESCU, C. UGLEA, **Fracţionarea compuşilor macromoleculari** (Le fractionnement des composés macromoléculaires,) 1969, 292 p., 18,50 lei.

I.P.I. — c. 5088

43426

Lei 25.—

F 1103

R

09 REZERVA

REVUE ROUMAINE DE CHIMIE

TOME 15
N° 5
Mai 1970

ÉDITIONS DE L'ACADÉMIE DE LA RÉPUBLIQUE SOCIALISTE DE ROUMANIE

Rev. Roumaine Chim.
15, 667 — 834 (1970), Bucarest

COMITÉ DE RÉDACTION

Rédacteur en chef :

C. D. NENIŢESCU, membre de l'Académie de la République Socialiste de Roumanie.

Rédacteurs en chef adjoints :

A. T. BALABAN et V. E. SAHINI, membres correspondants de l'Académie de la République Socialiste de Roumanie.

Collège de rédaction :

C. DRĂGULESCU, RALUCA RIPAN, CR. SIMIONESCU, membres de l'Académie de la République Socialiste de Roumanie ; EM. BRATU, membre correspondant de l'Académie de la République Socialiste de Roumanie, Pr G. OSTROGOVICH, MARG. AVRAM, F. BADEA, D. I. MARCHIDAN, D. NEGOIU et D. SĂNDULESCU.

Les manuscrits, les livres et les revues proposés en échange, ainsi que toute correspondance seront envoyés à la rédaction :

REVUE ROUMAINE DE CHIMIE

23, str. Dumbrava Roşie, Bucarest, Roumanie.

REVUE ROUMAINE
DE
CHIMIE

ORSZÁGOS MŰSZAKI KÖNYVTÁR ÉS DOKUMENTÁCIÓS KÖZPONT

Tome 15, N° 5 Mai 1970

Page

I. G. MURGULESCU, E. POPA et EUGENIA IVANA, Le spectre d'absorption des halogénures de plomb fondus 669–673

V. E. SAHINI and MARGARETA CRAIU, Depolarization ratio of the Raman lines of molecules containing carbonyl group 675–678

V. E. SAHINI and MARIANA DOBRESCU, On the carbonyl stretching frequency of halogen-substituted benzophenones 679–681

O. RADOVICI and N. TOTIR, The anodic oxidation of acetylene and methane on porous platinum and palladium electrodes 683–691

J. ZSAKÓ, Kinetic analysis of thermogravimetric data. II. Improvement of T. Ozawa's integral method 693–704

MARCELA MUSA, Absorption spectra of $CoCl_2$ and $CoBr_2$ isolated in benzene matrix 705–709

V. NEMES, I. GÖRBE and P. NAGY, Correlation between the structure and basicity constants of the *p*-dimethylamino-*p′*-*m′*-X-azobenzenes based on Hammett and Ismailow equations 711–717

RALUCA RIPAN, N. PASCU, ANA UNGUREANU et V. CORDIŞ, Contribution à l'étude de la cyanuration et du conditionnement des minerais aurifères de type Baia de Arieş 719–729

P. SPACU and ELENA ANTONESCU, Complexes of lanthanide halogenoacetates with 1,10-phenanthroline and 2–2′-dipyridyl 731–739

S. SOLACOLU, P. BALTĂ et GEORGETA JITIANU, L'analyse elcothermique — méthode d'étude des transformations structurales dans les verres 741–748

C. LITEANU et ELENA HOPÎRTEAN, Étude sur les électrodes-membranes polymère + plastifiant. I. L'obtention et le comportement électrodique de la membrane de PCV et tricrésylphosphate sensible aux ions d'hydrogène 749–756

G. CIUHANDU et M. MRACEC, Dosage photométrique du benzène et de la *m*-phénylènediamine 757–759

D. COSTACHE and GR. POPA, Kinetic determination of cobalt traces. II. With tropeoline O 761–765

Rev. Roumaine Chim. 15, 667–834 (1970), Bucarest

Page

MINODORA RADU, Electrical conductivity in relation with dispersion degree of lyophilic colloids. XI. 0.2 Sodium stearate aqueous solutions with additions of *o*-cresol and various hydrocarbons 767–773

I. MÂNDRU, Surface-active cationic substances of the type alkyl-ether-trimethyl-ammonium and alkyl-ether-pyridinium halides. II. Study on the micelle formation of the dodecylpolyoxiethylene-trimethyl-ammonium and dodecylpolyoxiethylene-pyridinium chlorides 775–782

AGLAIA CIOBANU, LUCIA ROMAN, M. BOSTAN, N. VOICULESCU et DIANA GIURGIU, Combinaisons zinc-diarylamides. II. L'échange entre le diphénylzinc et les amines aromatiques primaires 783–788

C. CHIRIAC et I. ZUGRĂVESCU, Pyrazoles. I. N-arylation des pyrazoles avec des dérivés chlorurés aromatiques activés par les groupements nitro 789–798

G. OSTROGOVICH und M. SAFTA, Studien auf dem Gebiet der symmetrischen Triazine (Neue Serie). IV. 2,4-Dioxo-6-(*p*-X-β-styryl)-tetrahydro-s-triazine; Elektronenspektroskopie der Basen und ihrer Protonierung 799–817

V. TĂMAŞ and C. BODEA, $TiCl_4$-Carotenoid complexes. VIII. Cyclization of lycopene and δ-carotene 819–822

M. RĂILEANU and EUGENIA DOBRE, Volumetric dosage with phenothiazon-(3). III. The dosage of the thiolic compounds with phenothiazone-(3) 823–827

O. L. HORER and M. BADEA, UV irradiation of UMP on paper 829–834

Revue Roumaine de Chimie, 15, 669–673 (1970)

MŰSZAKI KÖNYVTÁR

LE SPECTRE D'ABSORPTION DES HALOGÉNURES DE PLOMB FONDUS

I. G. MURGULESCU, E. POPA et EUGENIA IVANA
Centre de Chimie Physique de l'Académie,
Str. Dumbrava Roşie, 23, Bucarest 9, Roumanie

Reçu le 1er octobre 1969

On étudie le spectre d'absorption du chlorure et du bromure de plomb dans le domaine de 280 à 500 mμ, pour l'intervalle de température de 25 à 520°. Les modifications spectrales observées sont le résultat de la variation de la température et des actions interioniques.

INTRODUCTION

Les halogénures de plomb ont été l'objet de nombreuses études spectrales en solutions aqueuses,[1–3] à l'état cristallin [4–8] et à l'état fondu. A cause des propriétés particulières de l'ion de plomb de former des complexes avec des ions d'halogène (vu que, dans les solutions diluées, il y a aussi des ions de type PbX^+ [9]), la plupart des recherches ont été orientées vers la détermination des différents types des complexes et de la stabilité de ceux-ci.

Le spectre à l'état fondu des halogénures de plomb a été étudié en mélange avec des halogénures alcalins [10–11] et à l'état pur, [12–14] mais pour les halogénures purs fondus on a étudié seulement la marge de la bande d'absorption. Récemment, on a obtenu le spectre des vapeurs du fluorure de plomb fondu.[15]

Dans le présent travail nous avons étudié l'influence de la température sur le spectre d'absorption du $PbCl_2$ et du $PbBr_2$.

---

[1] L. Nilson et. G. P. Haight, Jr., *Acta Chem. Scand.*, **20**, 486 (1966).
[2] M. Lebl, J. Trnka et A. Bohun, *Czech. J. Phys.*, **B 17**, 43 (1967).
[3] J. Trnka, *Czech. J. Phys.*, **B 18**, 102 (1968).
[4] A. Bohun, J. Sak et J. Doljesi, *Phys. Solid. State*, **9**, 341 (1965).
[5] A. Bohun, V. Piskaskova et J. Trnka, *Czech. J. Phys.*, **B 16**, 898 (1966).
[6] M. Lebl, *Czech. J. Phys.*, **B 16**, 902 (1966).
[7] A. Kaldor et G. A. Somorjai, *J. Phys. Chem.*, **70**, 3538 (1966).
[8] K. J. de Vries et J. H. von Santen, *Physica*, **30**, 2051 (1964).
[9] a) M. H. Panckhurst et H. N. Parton, *Trans. Faraday Soc.*, **51**, 806 (1955).
b) A. I. Biggs, M. H. Panckhurst et H. N. Parton, *Trans. Faraday Soc.*, **51**, 802 (1955).
[10] G. P. Smith, D. W. James et C. R. Boston, *J. Chem. Phys.*, **42**, 2249 (1965).
[11] K. Balasubrahmanyan et L. Nanis, *J. Chem. Phys.*, **40**, 2657 (1964).
[12] T. Retschinsky, *Ann. Physik*, **27**, 100 (1908).
[13] B. R. Sundheim et J. Greenberg, *J. Chem. Phys.*, **28**, 439 (1958).
[14] J. Greenberg, *J. Chem. Phys.*, **40**, 3126 (1964).
[15] R. H. Hange, J. W. Hastie et J. L. Margrave, *J. Phys. Chem.*, **72**, 3510 (1968).

PARTIE EXPÉRIMENTALE

Les déterminations spectrales ont été effectuées à l'aide d'un spectrophotomètre Beckman DK-2. Dans l'espace des cuves a été introduit un fourneau qui nous a permis d'atteindre une température de 600°. La température a été déterminée à l'aide d'un thermocouple Pt-Pt-Ph. On a thermostaté le fourneau à l'aide d'un photothermorégulateur avec une variation de température de ±5°.

Pour obtenir les spectres on a besoin d'une épaisseur de la couche absorbante de l'ordre des microns. A cette fin nous avons utilisé deux lamelles en quartz très peu distancées entre elles et collées aux bords, qu'on pouvait remplir par capillarité. L'épaisseur de la couche dans ces « cuves » atteignait 11 ± 2 microns.

La fusion du sel et le remplissage des cuves ont été effectués dans un fourneau à l'aide duquel nous avons pu obtenir la température souhaitée dans un bref intervalle de temps. Toutes les opérations ont été effectuées dans une boxe à gaz inerte (argon). Le chlorure et le bromure de plomb ont été obtenus à partir de l'azotate de plomb recristallisé et de l'acide chlorhydrique, respectivement bromhydrique. Les sels ont été séchés à 120°. Les déterminations spectrales à 20° et 200° ont été effectuées à l'aide des films obtenus par le refroidissement du sel fondu.

RÉSULTATS

Le spectre électronique à l'état fondu des halogénures est caractérisé par l'existence de deux domaines :

— un domaine complètement transparent ;

— un domaine à très grande absorption, qui devient opaque aux couches d'ordre des dixièmes de millimètre.

Dans les travaux antérieurs on a étudié l'influence de la température sur la partie inférieure de la bande d'absorption. [13–14] À l'aide des cuves à des épaisseurs de couche convenables d'ordre des microns nous avons réussi à enregistrer les courbes d'absorption des deux halogénures de plomb fondus. Les courbes sont reproduites sur les figures 1 et 2 où, sur l'abscisse sont inscrites les longueurs d'onde en millimicrons et sur l'ordonnée–les extinctions. Dans le tableau 1 sont données les constantes d'absorption K du chlorure de plomb et du bromure de plomb, aux températures de 510°, 520°, respectivement 380°, 410°. Les constantes K ont été calculées selon la formule

$$\varepsilon = K \cdot c \bullet d.$$

où ε = l'extinction, d = l'épaisseur de la couche en cm et c = la concentration en mole/1000 cm^3. Les déterminations aux températures plus élevées ne sont pas reproductibles à cause de la décomposition du sel et de la variation de l'épaisseur de la couche absorbante à la suite de la vaporisation.

Le coefficient d'absorption K pour les températures de 25° et 200° n'a pu être calculé à cause des erreurs introduites par l'apparition des creux au refroidissement des films de sel fondu. Le refroidissement est accompagné aussi de la variation du volume et de la cristallisation du film en directions différentes.

Tableau 1

Les constantes d'absorption du chlorure et du bromure de plomb fondus

λ(mμ)	K . 10^{-2}			
	$PbCl_2$		$PbBr_2$	
	t = 510°C	520°C	380°C	410°C
342	1,253	1,238	1,236	1,152
344	1,253	1,238	1,236	1,152
346	1,253	1,240	1,236	1,152
348	1,257	1,240	1,236	1,152
350	1,257	1,241	1,236	1,152
354	1,259	1,241	1,236	1,152
356	1,260	1,241	1,236	1,152
358	1,261	1,240	1,236	1,152
359	1,261	1,240	1,236	1,152
360	1,259	1,240	1,236	1,152
362	1,259	—	—	—
364	1,230	1,240	1,236	1,152
366	1,190	1,236	1,236	1,152
368	1,078	1,227	1,236	—
370	1,023	1,207	1,236	1,151
372	—	1,170	1,236	1,151
374	—	1,105	1,236	1,151
378	0,462	—	1,236	1,151
380	0,392	0,807	1,236	1,151
386	0,244	—	1,236	1,147
390	0,176	0,369	1,236	1,146
400	0,068	0,156	1,236	1,142
410	—	—	1,236	1,142
425	—	—	1,210	1,142
430	—	—	1,158	1,142
435	—	—	1,050	—
445	—	—	—	0,940
450	—	—	0,440	0,586
500	—	—	0,044	0,067

Dans les figures 1 et 2 ont été tracées les courbes d'absorption à l'état solide du chlorure et du bromure de plomb à 25° et 200° et aussi à l'état fondu à 510° et 520°, respectivement à 380° et 410°.

DISCUSSIONS

Les spectres d'absorption du chlorure et du bromure de plomb sont caractérisés par une absorption presque uniforme et par une région où l'absorption décroît brusquement. Cependant, pour le chlorure de plomb on observe un maximum, assez faiblement précisé (tabl. 1).

L'influence de la température sur le spectre est caractérisée par une décroissance de l'absorption et par un déplacement de la longueur d'onde vers de petites énergies, auxquelles l'absorption commence à décroître (tabl. 2.). Le déplacement peut être le résultat de deux phénomènes qui agissent en même sens:

— l'élargissement de la bande à l'accroissement de la température ;
— la déstabilisation de l'état fondamental.

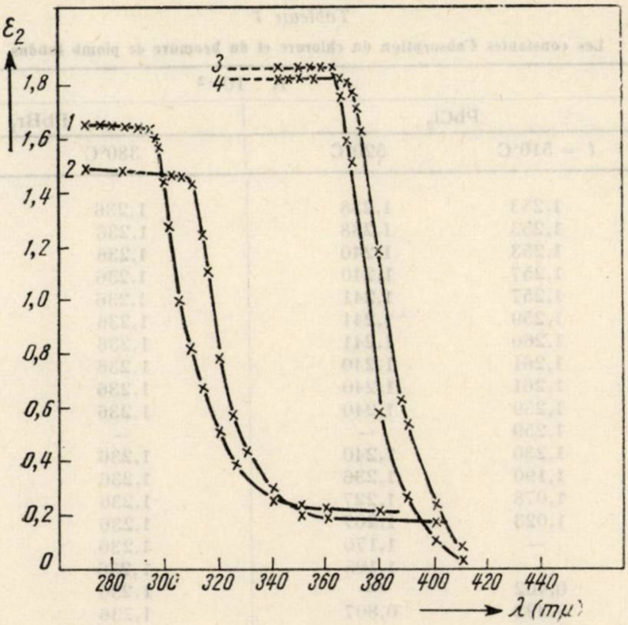

Fig. 1. — Spectre d'absorption du chlorure de plomb.
1, *t* = 25° ; *2*, *t* = 200° ; *3*, *t* = 500° ; *4*, *t* = 520°.

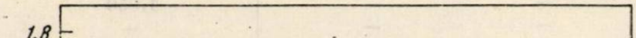

Fig. 2. — Spectre d'absorption du bromure de plomb.
1, *t* = 25° ; *2*, *t* = 200° ; *3*, *t* = 380° ; *4*, *t* = 410°.

La déstabilisation diminue la différence d'énergie entre l'état fondamental et l'état excité.

La décroissance de l'absorption à l'accroissement de la température peut être attribuée à la diminution de la densité du liquide, donc du nombre des espèces qui absorbent, ainsi qu'à la destruction des associations et des ions pairs ou à la dissociation des ions complexes, si ceux-ci existent. Les espèces ioniques possibles dans les halogénures de plomb purs fondus sont : Pb^{+2}, X^-, PbX^+, PbX_3^- ($X = Cl^-, Br^-$), parmi lesquels les moins probables sont les ions PbX_3^- qui n'ont pas été mis en évidence dans le spectre Raman[11] du sel pur fondu.

Tableau 2

Variation de la longueur d'onde λ_0 en fonction de la température

t°C	$PbCl_2$	$PbBr_2$
	λ_0 (mμ)	λ_0 (mμ)
25	295	350
200	309	366
380	—	420
410	—	430
510	362	—
520	366	—

Le chlorure de plomb à l'état solide à basses températures a trois bandes d'absorption en UV, dont les maximums sont situés approximativement à 187 mμ, 200 mμ (maximum large) et à 270 mμ. La bande[16] située vers la région des grandes longueurs d'onde est caractérisée par un maximum aigu et correspond à la transition d'un électron de la bande de valence vers l'ion pair $PbCl^+$. Etant donné les fortes interactions existantes dans les liquides ioniques et donc les grandes possibilités d'association, nous supposons que, le maximum d'absorption (de la région de 350 à 366 mμ), dont la marge d'absorption décroît brusquement dans la région des petites énergies, correspond à la transition d'un électron de l'ion Cl^- à l'ion pair $PbCl^+$.

L'effet de la température sur l'absorption étant celui de déplacement et, surtout, d'élargissement des bandes, nous pouvons admettre que les bandes correspondant aux ions Pb^{+2}, Cl^-, $PbCl^+$ se recouvrent entre elles, en résultant la bande large d'absorption observée expérimentalement.

---

[16] K. J. Best, *Z. Physik*, **163**, 309 (1961).

Revue Roumaine de Chimie, **15**, 675–678 (1970)

DEPOLARIZATION RATIO OF THE RAMAN LINES OF MOLECULES CONTAINING CARBONYL GROUP

V. E. SAHINI and MARGARETA CRAIU

Institute of Physical Chemistry of the Academy
Bucharest, str. Dumbrava Roşie, 23

Received August 2, 1969

The depolarization ratios ρ of the Raman lines corresponding to $\nu C = O$ and $\nu C = C$ (ring) for pure acetophenone and its 2M; 1M; 0,5 M and 0.25 M solutions in cyclohexane have been measured. A difference of the ρ values has been observed between the pure liquid and the solutions.

INTRODUCTION

Outstanding works in Raman spectroscopy have dealt with the determination and correction of the depolarization ratio of the Raman lines in pure liquids [1–5] and to a smaller extent in solutions.[6–8]

Shorygin [8] investigated the depolarization ratio of the Raman lines due the $C = O$ and $C = C$ (ring) vibrations for pure acetophenone and benzophenone in solution. The smaller value of $\rho (C = O)$ for benzophenone in solution than for pure acetophenone was interpreted in terms of conjugation of $C = O$ group at two systems of multiple bonds. Kroto and Yoh-Han Pao [7] qualitatively investigated the effect of solvents and of intermolecular interactions upon the depolarization ratio. Studying the Raman spectra of some solutions they observed an increase of ρ value for the benzene line at 992 cm^{-1} in benzene-acetone solution and a decrease of ρ for the same line in benzene-cyclohexane solution. This fact was assumed to an effect of intermolecular interactions between the solute and solvent molecules.

---

[1] G. Herzberg, "Infrared and Raman Spectra of Polyatomic Molecules", D. van Nostrand Company, N. Y., 1960, p. 248.

[2] J. T. Edsall and E. B. Wilson Jr., *J. Chem. Phys.*, **6**, 124 (1938).

[3] H. J. Bernstein and G. Allen, *J. Opt. Soc. Amer.*, **45**, 237 (1955).

[4] D. H. Rank and R. E. Kagarise, *J. Opt. Soc. Amer.*, **40**, 89 (1950).

[5] R. N. Jones, J. B. DiGiorgio, J. J. Elliott and G. A. Anonnenmacher, *J. Org. Chem.*, **30**, 1822 (1965).

[6] J. A. Koningstein and H. J. Bernstein, *Spectrochim. Acta*, **18**, 1249 (1962).

[7] H. W. Kroto and Yoh-Han Pao, *J. Opt. Soc. Amer.*, **58**, 479 (1968).

[8] P. P. Shorygin, *Doklady Akad. Nauk. S.S.S.R.*, **78**, 469 (1951).

After Koningstein and Bernstein [6] the effect of intermolecular interactions is to change $\alpha_i''^2$ and $\beta_i'^2$ from the relation [1]:

$$\rho_n = \frac{6\beta_i'^2}{45\,(\alpha_i'')^2 + 7\beta_i'^2} \tag{1}$$

into $\alpha_i''^2 = \alpha'^2_{i\,\mathrm{gas}}\ (1 + K_\alpha)$ and $\beta_i'^2 = \beta'^2_{i\,\mathrm{gas}}\ (1 + K_\beta)$ (for nonpolar solvents and solutes), where K_α and K_β depend both on the normal mode of vibration and on the strength of intermolecular field. The authors have shown that this effect decreases the value of ρ_{liquid} with about 10% from the value of ρ_{gas} for the completely polarized or depolarized lines. For solutions they found intermediate values between ρ_{liquid} and ρ_{gas}.

The aim of the present paper is to study the behaviour of the depolarization ratio of the Raman lines corresponding to the C = O and C = C (ring) vibrations of pure acetophenone and its solutions in cyclohexane at different concentrations. We compare also the corrected values for ρ obtained using Koningstein and Bernstein's correction [6] and Rank and Kagarise's method.[4]

EXPERIMENTAL

The Raman spectra of the pure acetophenone and of 2M, 1M, 0.5M and 0.25 M acetophenone in cyclohexane solutions were recorded using an ISP-51 spectrograph, Scientia Gevaert 68A56 plates and the polaroid cylinder technique.

The spectroscopic grade acetophenone in cyclohexane was freshly distilled and for each solution the refractive index measured.

RESULTS AND DISCUSSION

The technique of the polaroid cylinders without transverse baffles around the sample tube is frequently utilised in Raman spectroscopy. If the incident radiation strikes the sample tube obliquely the observed depolarization ratio is given by [6]:

$$\rho_{\mathrm{obsd}} = T\rho_{\mathrm{true}}\left(1 - \frac{\sin^2\bar{\theta}}{n^2}\right) + \frac{T\sin^2\bar{\theta}}{n^2} \tag{2}$$

where $\bar{\theta}$ is the averaged angle of the incidence, n — the refractive index, ρ_{true} — the depolarization ratio at perpendicular irradiation and T — the transmission factor that takes account of the polarizers optical transmission and the transmission effects within the optical system of the spectrograph. The values for transmission factor T and $\sin^2\bar{\theta}$ can be obtained for each Raman set from measurements on completely polarized and completely depolarized lines.

The true values of the depolarization ratio for a completely polarized and a completely depolarized line substituted in (2) give:

$$\rho_{obsd} = \frac{T \sin^2 \bar{\theta}}{n^2} \quad \text{for} \quad \rho_{true} = 0$$

$$\rho_{obsd} = 6/7\, T + \frac{T \sin^2 \bar{\theta}}{7n^2} \quad \text{for} \quad \rho_{true} = 6/7 \qquad (3)$$

Using ρ_{obsd} values [9] for the Raman lines of carbon tetrachloride respectively 459 cm^{-1} and 314 cm^{-1} substituted in (3) we get: $T = 1.075$ and $\sin^2\bar{\theta} = 0.118$ for $n_{CCl_4} = 1.458$. These values substituted in (2) give:

$$\rho_{obsd} = 1.075\, \rho_{true} \left(1 - \frac{0.118}{n^2}\right) + \frac{1.075 \times 0.118}{n^2} \qquad (4)$$

We make use of the above relation (4) to correct the observed values of the depolarization ratio obtained for pure and 2M, 1M, 0.5 M and 0.25 M acetophenone in cyclohexane solutions. The observed values where also corrected utilising a correction curve obtained in our previous paper.[9]

A variation of the depolarization ratio with the increase in the solvent quantity being not observed for any of the studied C = O or C = C (ring) lines, the mean values for ρ_{obsd} and ρ_{true} are given in table 1.

Table 1

Values of the depolarization ratio of ν_{CO} and ν_{CC} lines of acetophenone

Vibration		$\bar{\rho}_{obsd}$	$\bar{\rho}^*$	$\bar{\rho}^+$
C=O	pure	0.425	0.364	0.363
	solution	0.372	0.313	0.307
C=C	pure	0.750	0.672	0.682
	solution	0.624	0.547	0.546

ρ^* – corrected after Rank and Kagarise's method

ρ^+ – corrected with relation (4)

The data show a good correspondence between the corrected values on experimental curve and those corrected with relation (4).

The corrected values of the depolarization ratio of the Raman lines of pure acetophenone are similar to Shorygin's [8] data.

An analysis of the obtained experimental data shows a decrease in the value of the depolarization ratio of the solution in respect of the pure acetophenone. The decrease of the depolarization ratio of the solution can be explained according to Kroto and Yoh-Han Pao [7] as a result of the action of intermolecular forces. On the other hand Jones and co-workers [5] have observed that all C = O stretching bands appear to be strongly polarized; so the decrease of the ρ $(C = O)$ for acetophenone in cyclohexane is that of a strongly polarized line.

---

[9] V. E. Sahini, R. Beldie and M. Damaschin, *Rev. Roumaine Chim.*, **11**, 1361 (1966)

We have found the value of the depolarization ratio for $C = C$ (ring) approximately the same in acetophenone solutions as found by Shorygin[8] in benzophenone solution, but ρ $(C = O)$ are quite different between acetophenone and benzophenone, both in solution. This difference has been explained by Shorygin as being due to the difference of the conjugation of the $C = O$ group. The decrease in the value of $\bar{\rho}^{*}(C=O)$ or $\bar{\rho}^{+}(C = O)$ for acetophenone solution can be explained starting from relation (1) where ρ depends on the polarizability and anisotropy variations of the molecule. A decrease in the depolarization ratio for cyclohexane solution notes a small anisotropy of the scattering tensor and some modifications of the polarizability derivatives with regard to normal coordinates.

A decrease in the ρ value in the case of a conjugation of the $C = O$ group simultaneously at two systems of multiple bonds (benzophenone case[8]) corresponds to two significant and equal values and a third smaller value for $\frac{\partial \alpha_i}{\partial Q_n}$.

In the molecules with systems of conjugated bonds the electronic transitions are related to the excitation of valence electrons and to a displacement of these electrons along the bonds. In the case of a great effectiveness of such electronic transitions the polarizability components and their derivatives may be particularly great along the conjugated bonds. Then, the depolarization ratio of the Raman line may be modificated accordingly; hence the depolarization ratio for $C = O$ line depends on the geometrical configuration of the whole system of the conjugated multiple bonds, result in accordance with the experimental data.

Revue Roumaine de Chimie, **15**, 679–681 (1970)

ON THE CARBONYL STRETCHING FREQUENCY OF HALOGEN-SUBSTITUTED BENZOPHENONES

V. E. SAHINI and MARIANA DOBRESCU

Physical Chemistry Laboratory of the University
Bd. Republicii 13, Bucharest, Romania

Received July 7, 1969

FG-matrix method is applied for the computation of carbonyl stretching frequency of symmetric halogen-substituted benzophenones.

Infrared absorption spectra of symmetric halogen-substituted benzophenones evidence a relative constant value of the carbonyl stretching frequency, regardless of the halogen and the position of the substitution.[1] The aim of the present paper is the computation of the carbonyl stretching frequency of symmetric halogen-substituted benzophenones using the *FG*-matrix method of Wilson.[2]

In the normal coordinated treatment we used, the phenyl group substituted or not, was considered point mass, the problem being thus reduced to that of a plane four-atom molecule belonging to C_{2v} point group. The corresponding vibration representation is

$$\Gamma_{\text{vibr}} = 3A_1 + 2B_1 + B_2,$$

the vibration of B_2-class being out-of-plane. The bond lenghts and the angles (fig. 1) are the following [3] :

$$D = 1.25\ \text{Å};\ d_1 = d_2 = 1.50\ \text{Å};\ \alpha = 126°;$$
$$\beta_1 = \beta_2 = 117°,$$

and we considered all to be unaffected by the halogen substitution.

As a result, the following set of coefficients of potential energy general expression (table 1) was used for all four cases we were dealing with ; the values of the force constants (table 2) were found to comply with those considered in a similar calculation of benzophenone.[4]

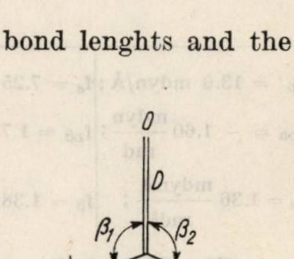

Fig. 1. — Bond lengths and angles of benzophenones

---

[1] E. J. Moriconi, W. F. O'Connor, and W. F. Forbes, *J. Amer. Chem. Soc.*, **84**, 3928 (1962).

[2] E. B. Wilson, J. C. Decius and P. C. Cross, "Molecular Vibrations. The Theory of Infrared and Raman Vibrational Spectra", McGraw-Hill, New York, 1955.

[3] S. Ramaseshan and K. Venkatesan, *Experientia* **14**, 237 (1958).

[4] P. Puranik, E. V. Rao, *Indian J. Phys.*, **37**, 121, 328 (1963).

In order to improve the computed results, a small modification of the carbonyl stretching force constant was also considered, the values used being : 12.85 ; 12.95 ; 13.00 and 13.10 for difluoro-, dichloro-, dibromo- and di-iodo benzophenone respectively.

Table 1

Coefficients of potential energy

	ΔD	Δd_1	Δd_2	$\Delta\alpha$	$\Delta\beta_1$	$\Delta\beta_2$
ΔD	f_D	f_{Dd}	f_{Dd}	$df_{D\alpha}$	$df_{D\beta}$	$df_{D\beta}$
Δd_1		f_d	f_{dd}	$df_{d\alpha}$	$df_{d\beta}$	$df'_{d\beta}$
Δd_2			f_d	$df_{d\alpha}$	$df'_{d\beta}$	$df_{d\beta}$
$\Delta\alpha$				d^2f_α	$d^2f_{\alpha\beta}$	$d^2f_{\alpha\beta}$
$\Delta\beta_1$					d^2f_β	$d^2f_{\beta\beta}$
$\Delta\beta_2$						d^2f_β

The following symmetry coordinates for A_1 and B_1-class vibrations were considered, only the first class including the carbonyl stretching vibration :

$$S_1 = \Delta D$$

$$A_1 \quad S_2 = \frac{1}{\sqrt{2}}(\Delta d_1 + \Delta d_2) \qquad B_1 \quad S_4 = \frac{1}{\sqrt{2}}(\Delta d_1 - \Delta d_2)$$

$$S_3 = \frac{1}{\sqrt{6}}(2\,\Delta\alpha - \Delta\beta_1 - \Delta\beta_2) \qquad S_5 = \frac{1}{\sqrt{2}}(\Delta\beta_1 - \Delta\beta_2)$$

Table 2

Values of the force constants

$f_D = 13.0$ mdyn/Å ;	$f_d = 7.25$ mdyn/Å ;	$f_{dd} = 2.75$ mdyn/Å ;	$f_{Dd} = 2.3$ mdyn/Å
$f_{D\alpha} = -1.60\,\frac{\text{mdyn}}{\text{rad}}$;	$f_{D\beta} = 1.75\,\frac{\text{mdyn}}{\text{rad}}$;	$f_{d\alpha} = -1.94\,\frac{\text{mdyn}}{\text{rad}}$:	$f_{d\beta} = 0.82\,\frac{\text{mdyn}}{\text{rad}}$; $f'_{d\beta} = 0.16\,\frac{\text{mdyn}}{\text{rad}}$
$f_\alpha = 1.36\,\frac{\text{mdynÅ}}{\text{rad}^2}$;	$f_\beta = 1.38\,\frac{\text{mdynÅ}}{\text{rad}^2}$;	$f_{\alpha\beta} = -0.36\,\frac{\text{mdynÅ}}{\text{rad}^2}$	$f_{\beta\beta} = -0.29\,\frac{\text{mdynÅ}}{\text{rad}^2}$

The *F* and *G* matrices were obtained using respectively Wilson's and Decius' methods. The frequency values, computed with the benzophenone set of parameters (I) as well as with the modified one (II) and those experimentally obtained,[1] are presented in table 3 and they are in a satisfactory agreement.

The fact that relatively good results can be reached using such a simple model for the computation of carbonyl stretching frequency proves that the approximation of phenyl group (substituted or not) as a point mass can be accepted as satisfactory, taking into account also that in our calculation the respective mass was modified progressively nearly up to threefold. It results that symmetric halogen substitu-

Table 3

Frequency values of benzophenones

	$\nu_{C=O}$ Obs cm^{-1}	I		II	
		f_D mdyn/Å	$\nu_{C=O}$calc. cm^{-1}	f_D mdyn/Å	$\nu_{C=O}$calc. cm^{-1}
Benzophenone	1665				
2 : 2′-Difluorobenzophenone	1667.5	13	1685.4	12.85	1674.6
3 : 3′-Difluorobenzophenone	1671.5				
4 : 4′-Difluorobenzophenone	1665.5				
2 : 2′-Dichlorobenzophenone	1667.0	13	1674.7	12.95	1672.6
3 : 3′-Dichlorobenzophenone	1671.5				
4 : 4′-Dichlorobenzophenone	1668.5				
2 : 2′-Dibromobenzophenone	1668.0	13	1673	13	1673
3 : 3′-Dibromobenzophenone	1671.5				
4 : 4′-Dibromobenzophenone	1667.5				
2 : 2′-Di-iodobenzophenone	—	13	1663.6	13.1	1667.7
3 : 3′-Di-iodobenzophenone	1670.0				
4 : 4′-Di-iodobenzophenone	1666.0				

tion of benzophenone influences to a small extent this vibration, in accordance with the infrared data obtained in the case of substituted acetophenone .[5]

---

[5] J. Norman, W. F. Forbes and W. A. Miller, *Canad. J. Chem.*, **35**, 504 (1957).

Revue Roumaine de Chimie, 15, 683–691 (1970)

THE ANODIC OXIDATION OF ACETYLENE AND METHANE ON POROUS PLATINUM AND PALLADIUM ELECTRODES

O. RADOVICI and N. TOTIR

Institute of Physical Chemistry of the Academy Bucharest, str. Galați 31

Received April 28, 1969

One has studied the anodic oxidation of acetylene and methane on porous electrodes by means of the cyclic voltammetry. The measurements were carried out in acid (H_2SO_4) as well as in alkaline (NaOH) solutions at 25 ± 0.1° on porous electrodes of platinum and palladium and on porous electrodes with PORVIC support, proving that the first step of the oxidation process is the chemisorption of the methane and acetylene.

INTRODUCTION

The study of anodic oxidation of hydrocarbons is particularly important from the practical point of view, as they can represent idea fuel for the fuel cells. The behaviour of hydrocarbons on platinum electrodes or on those of other metals with catalytic properties has been generally studied.[1-7] The study of the same process on porous electrodes, made of a single metal, or on anodes with a more complex structure [8-11] is highly actual, as the solving of this problem would make it easier to obtain hydrocarbon fuel cells and in a more convenient way from the practical point of view. The results obtained in this field have rendered evident the complexity of the phenomenon, the hydrocarbon fuel cells being much inferior to those with hydrogen.

---

[1] J. O'M Bockris, H. Wroblowa, E. Gileadi and B. J. Piersma, *Trans. Faraday Soc.*, **61**, 2531 (1965).

[2] S. Gilman, "Hydrocarbon Fuel Cell Technology", B. S. Baker, Ed., Academic Press, New York, 1965, p. 349.

[3] A. H. Taylor and S. B. Brummer, *J. Phys. Chem.*, **72**, 2856 (1968).

[4] S. B. Brummer, J. I. Ford and M. J. Turner, *J. Phys. Chem.*, **69** 3424 (1965).

[5] E. J. Cairns, A. M. Breitenstein and A. J. Scarpelling, *J. Electrochem. Soc.*, **115**, 569 (1968).

[6] E. Gileadi, G. Stoner and J. O'M. Bockris, *J. Electrochem. Soc.* **113**, 585 (1966).

[7] L. W. Niedrach and M. Tochner, *J. Electrochem. Soc.*, **114**, 17 (1967)

[8] L. W. Niedrach and M. Tochner, *J. Electrochem. Soc.*, **114**, 233 (1967).

[9] W. T. Grubb and C. J. Michalske, *J. Electrochem. Soc.*, **111**, 1015 (1964).

[10] E. J. Cairns and E. J. Mc Ineraey, *J. Electrochem. Soc.*, **114** 980 (1967).

[11] W. T. Grubb, *J. Electrochem. Soc.*, **113**, 191 (1966).

The hydrocarbon fuel cells built so far may be grouped into two categories: the first category contains the fuel cell based on direct oxidation of hydrocarbon on the anode, an oxidation which can take place at low or high temperature. The high temperature fuel cell presents the advantage of leaving out the expensive anodes and of using for fuel a larger range of materials, as well as that of using unpurified air. The second category contains the fuel cells using for the anodic oxidation products obtained by reforming the hydrocarbons in the presence of water or of steam. Each of the methods presents advantages as well as disadvantages, the principal deficiencies of the methods consisting in the lack of a cheap catalyst.

The oxidation mechanism of acetylene on platinum [12-14] and gold [15-16] electrodes has been widely studied. By studying the anodic oxidation of methane in phosphoric acid [17] and in solid electrolytes [18] one has noted its low electrochemical reactivity. Neidroch using electrodes of a special [17, 19, 20] construction also notes the low reactivity of the methane on the anodes.

The present paper deals with the anodic oxidation of methane and acetylene on porous electrodes obtained from Pt and Pd powder, as well as on porous electrodes obtained by metal deposition on a PORVIC support. The measurements have been made in acid, as well as in alkaline media.

EXPERIMENTAL

The porous electrodes used in the anodic oxidation of methane and acetylene were obtained by pressing metallic powders with 2.8 t/cm². The powders used were of *p.a.* purity. To obtain working electrodes one has weighed 400 mg of powder which was pressed into a die with a 1.5 cm. diameter, after which an electrode with a 3 mm diameter was cut and sintered at 500° for half an hour in a purified argon atmosphere. The deposit of metallic powder on a PORVIC support was obtained by reduction with formaldehyde. An electrode of platinized platinum was used as auxiliary electrode and a saturated calomel one as reference electrode. The solutions were prepared from conductivity water and *p.a.* reagents. The methane and the acetylene were introduced into the cell by bubbling. The measurements were carried out in the cell shown in figure 1.

The temperature was kept constant by recirculating a water current from a thermostat bath.

In every case the recording was made after bubbling the methane or acetylene for 5 minutes. The anodic oxidation of methane and acetylene was studied by means of the cyclic voltmmetric method, using a Tacussel type apparatus.

---

[12] J. W. Johnson, H. Wroblowa and J. O'M. Bockris, *J. Electrochem. Soc.*, **111**, 863 (1964).

[13] S. Gilman, *Trans. Faraday Soc.*, **62**, 466, 481 (1966).

[14] G. Bianchi, *Chimica e Industria*, **47**, 830 (1965).

[15] J. W. Johnson, J. L. Reed and W. J. James, *J. Electrochem. Soc.*, **114**, 572 (1967).

[16] J. L. Reed, *Diss. Abstr.*, **B 27** **(12)**, 4377 (1967).

[17] W. T. Grubb and C. J. Michalske, *Nature*, **201** (4916), 287 (1964).

[18] A. L. Lvov and E. N. Gushchina, *Elektrokhimya*, **3**, 689 (1967).

[19] L. W. Niedrach, S. Gilman and I. Weinstock, *J. Electrochem. Soc.*, **112**, 1161 (1965).

[20] L. W. Niedrach, *J. Electrochem. Soc.*, **113**, 645 (1966).

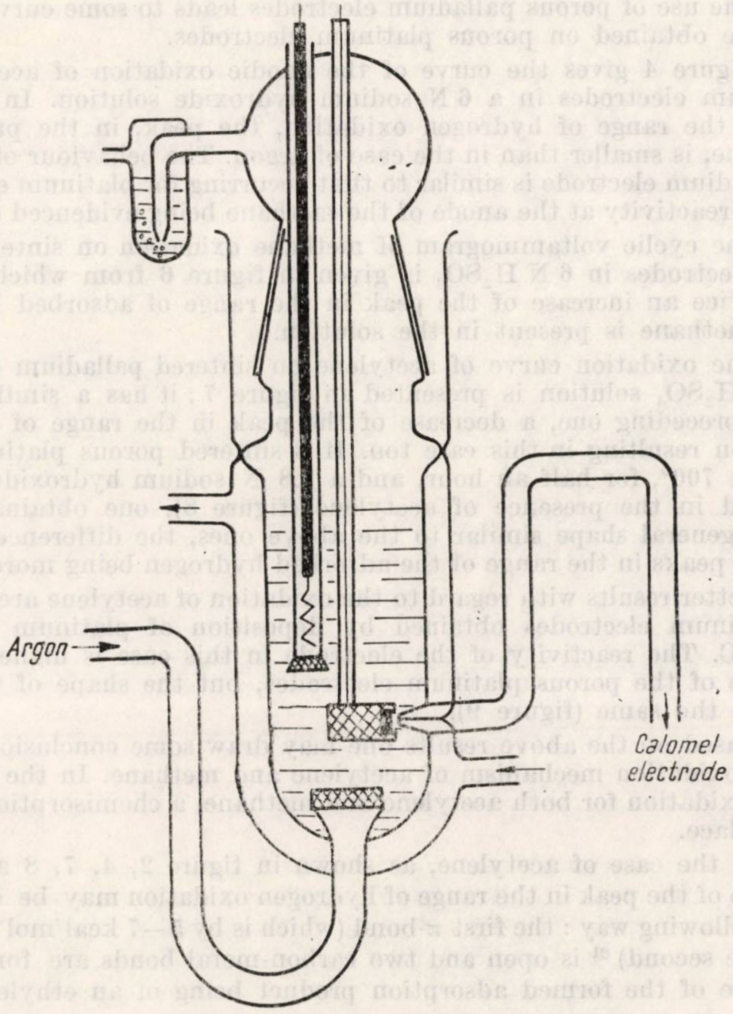

Fig. 1. – Electrolytic cell.

RESULTS AND DISCUSSION

The cyclic voltammogram of anodic oxidation of acetylene on porous platinum electrode in a $6NH_2SO_4$ solution is presented in figure 2 (curve 2).

Curve 1 is obtained with a solution in which argon was bubbled. The figure shows that in the case of anodic oxidation of acetylene, in our experimental conditions, two peaks appear in the same range with the oxidation of the absorbed hydrogen and the formation of oxide layer on the electrode's surface, the former being smaller and the latter bigger than in the case of the basic solution.

The use of porous palladium electrodes leads to some curves similar to those obtained on porous platinum electrodes.

Figure 4 gives the curve of the anodic oxidation of acetylene on palladium electrodes in a 6 N sodium hydroxide solution. In this case too, in the range of hydrogen oxidation, the peak, in the presence of acetylene, is smaller than in the case of argon. The behaviour of methane on palladium electrode is similar to that occurring for platinum electrodes, the low reactivity at the anode of the methane being evidenced (figure 5).

The cyclic voltammogram of methane oxidation on sintered palladium electrodes in 6 N H_2SO_4 is given in figure 6 from which we may also notice an increase of the peak in the range of adsorbed hydrogen, when methane is present in the solution.

The oxidation curve of acetylene on sintered palladium electrodes in 6 N H_2SO_4 solution is presented in figure 7 ; it has a similar aspect to the preceding one, a decrease of the peak in the range of hydrogen oxidation resulting in this case too. If a sintered porous platinum electrode at 700°, for half an hour, and a 1.8 N sodium hydroxide solution are used in the presence of acetylene (figure 8), one obtains a curve with a general shape similar to the above ones, the difference between the two peaks in the range of the adsorbed hydrogen being more marked.

Better results with regard to the oxidation of acetylene are obtained on platinum electrodes obtained by deposition of platinum black on PORVIC. The reactivity of the electrode in this case is higher than in the case of the porous platinum electrodes, but the shape of the curve remains the same (figure 9).

Based on the above results one may draw some conclusions on the anodic oxidation mechanism of acetylene and methane. In the first step of the oxidation for both acetylene and methane, a chemisorption process takes place.

In the case of acetylene, as shown in figure 2, 4, 7, 8 and 9 the decrease of the peak in the range of hydrogen oxidation may be explained in the following way : the first π-bond (which is by $5-7$ kcal/mol^{-1} weaker than the second) [21] is open and two carbon-metal bonds are formed, the structure of the formed adsorption product being of an ethylenic type.

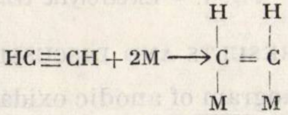

$$HC\equiv CH + 2M \longrightarrow \underset{\substack{|\\ M}}{\overset{\substack{H\\ |}}{C}} = \underset{\substack{|\\ M}}{\overset{\substack{H\\ |}}{C}}$$

The formation of the adsorbed vinyl radical takes place in the presence of the adsorbed hydrogen :

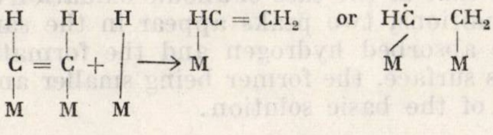

$$\underset{\substack{|\\ M}}{\overset{\substack{H\\ |}}{C}} = \underset{\substack{|\\ M}}{\overset{\substack{H\\ |}}{C}} + \underset{\substack{|\\ M}}{\overset{\substack{H\\ |}}{|}} \longrightarrow \underset{M}{\overset{\substack{HC = CH_2\\ |}}{}} \quad \text{or} \quad \dot{H\!C} - \underset{\substack{|\\ M}}{CH_2} \;\; {}_{\diagup M}$$

---

[21] G. C. Bond, "Catalysis", Ed. P. H. Emmett, 1954, p. 109.

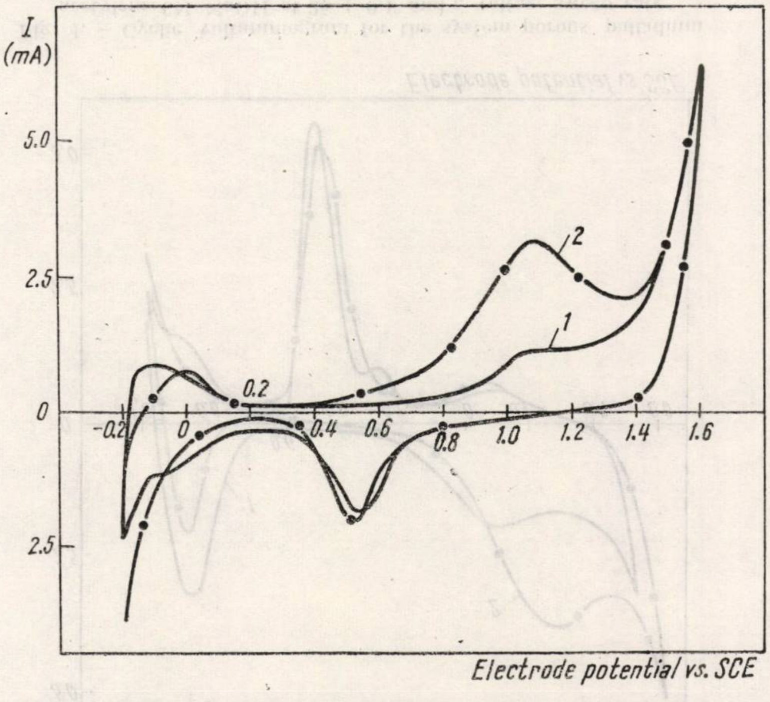

Fig. 2. — Cyclic voltammogram for the system, porous platinum-acetylene-$6NH_2SO_4$ at 25 ± 0.1° and a voltage-sweep rate of 16.6 mV/s.

1, argon; *2*, acetylene.

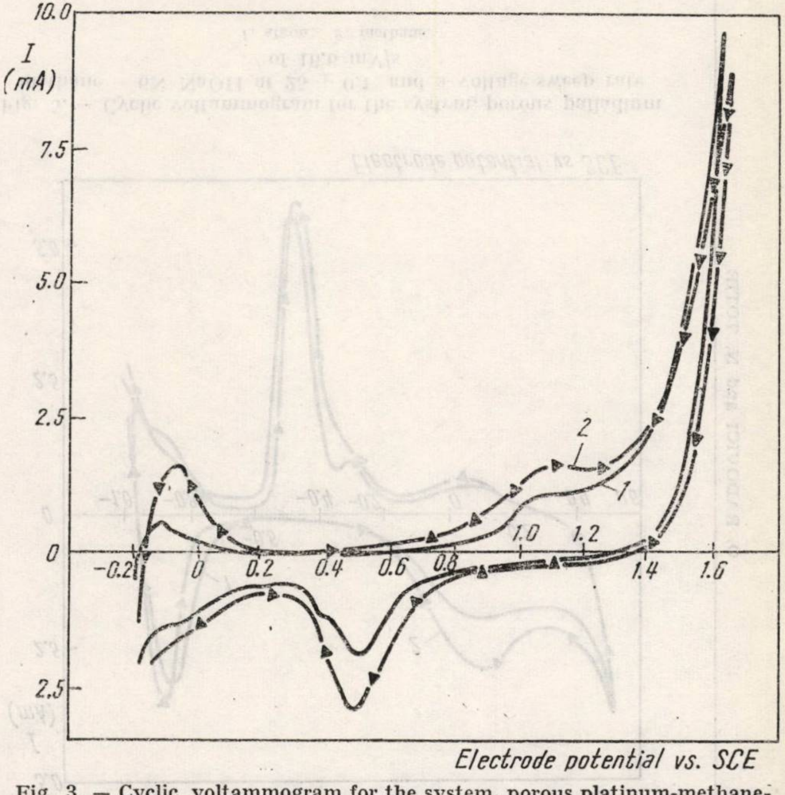

Fig. 3. — Cyclic voltammogram for the system, porous platinum-methane-$6NH_2SO_4$ at 25 ± 0.1° and a voltage-sweep rate of 16.6 mV/s.

1, argon; *2*, methane.

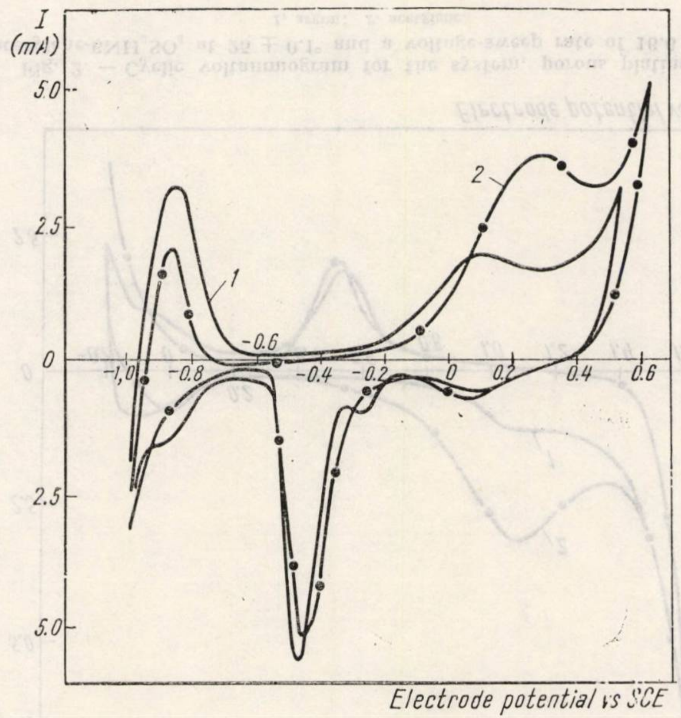

Fig. 4. — Cyclic voltammogram for the system porous palladium acetylene 6N NaOH at 25 ± 0.1° and a voltage-sweep rate of 16.6 mV/s

1, argon; *2*, acetylene.

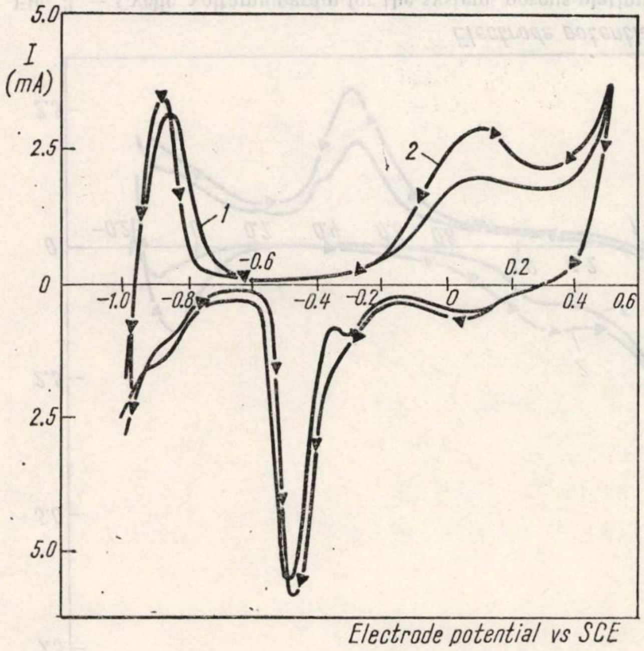

Fig. 5. — Cyclic voltammogram for the system, porous palladium methane — 6N NaOH at 25 ± 0.1° and a voltage-sweep rate of 16.6 mV/s

1, argon; *2*, methane.

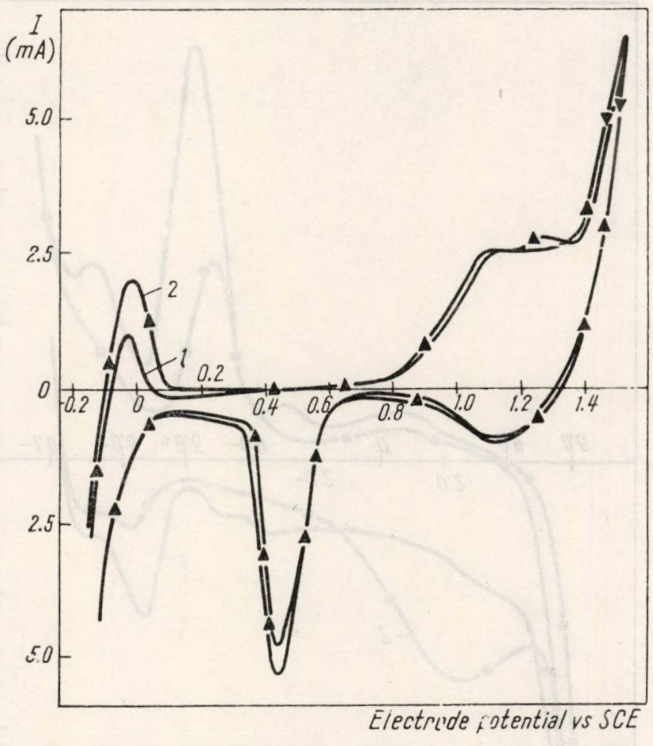

Fig. 6. — Cyclic voltammogram for the system, porous palladium methane — 6 NH_2SO_4 at 25 ± 0.1° and a voltage-sweep rate of 16.6 mV/ s.

1, argon; *2*, methane.

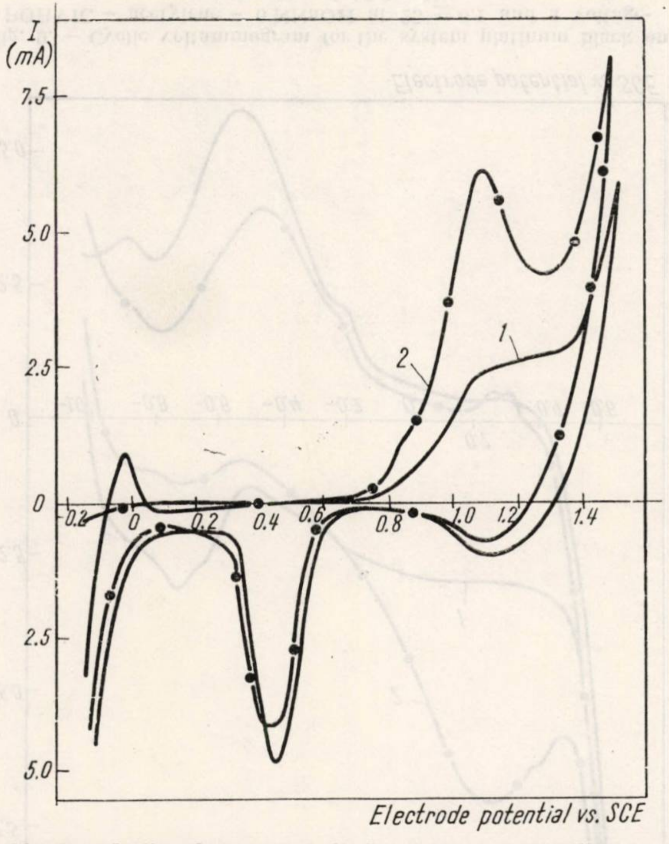

Fig. 7. — Cyclic voltammogram for the system, porous palladium-acetylene — 6 N H_2SO_4 at 25 ± 0.1° and a voltage-sweep rate of 16.6 mV/s

1, argon; *2*, acetylene.

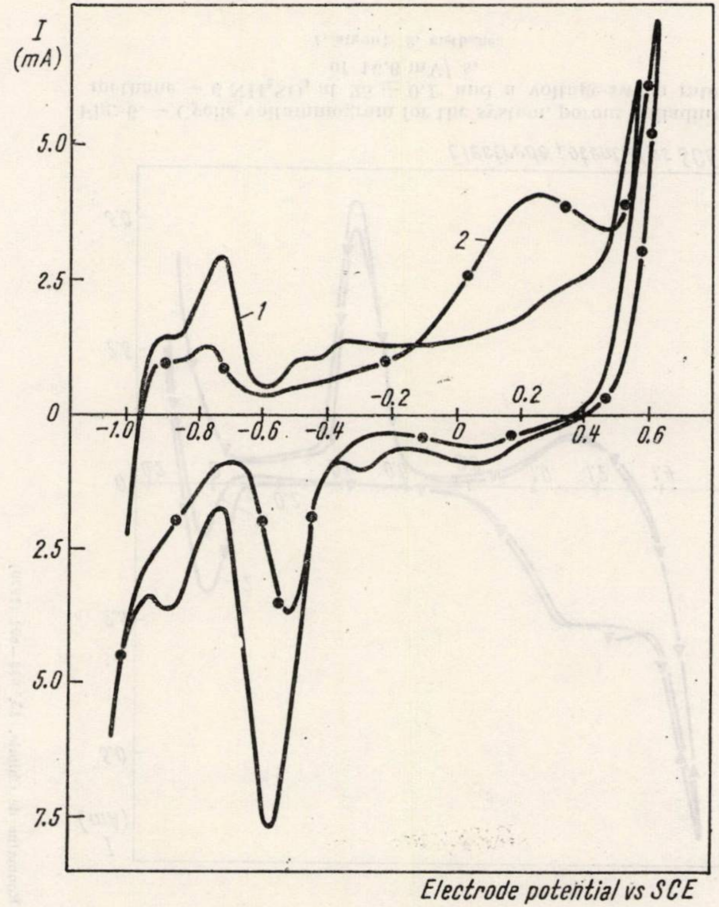

Fig. 8. — Cyclic voltammogram for the system, porous palladium-acetylene 1.8 N NaOH at 25 ± 0.1° and a voltage-sweep rate of 16.6 mV/s

1, argon; *2*, acetylene

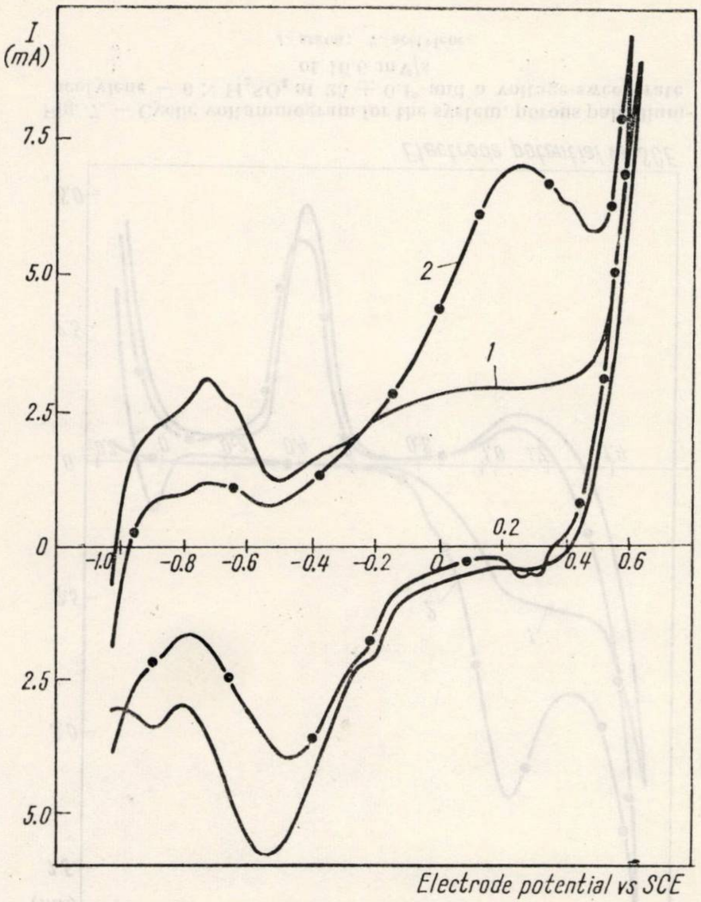

Fig. 9. — Cyclic voltammogram for the system platinum black on PORVIC — acetylene — 6 NNaOH at 25 ± 0.1 and a voltage-sweep rate of 16.6 mV/s.

1, argon; *2*, acetylene

which may exist in a normal, or in a free radical form, according as a carbon-metal bond is broken or the opening of the second π-bond of the acetylene molecule [22] occurs.

The participation of the adsorbed hydrogen in the formation reaction of the vinyl radical explains the decrease of the peak in the range of adsorbed hydrogen in the case of acetylene being present on the electrode surface. The free radical formed on the surface of the electrode may then initiate a polymerization process, a phenomenon outlined on gold electrodes by Johnson and Reed.[15]

In the first step, in the case of anodic oxidation of methane on sintered platinum or palladium electrodes, a chemisorption process takes place, that can be represented schematically in the following way :

$$CH_4 + 2M \rightarrow M - CH_3 + MH$$

and in the next phase:

$$M - H \rightarrow M + H^+ + e$$

which can explain the increase of the peak in the range of the adsorbed hydrogen oxidation.

---

[22] G. C. Bond, "Catalysis by Metals", Academic Press, 1962, p. 281.

Revue Roumaine de Chimie, **15**, 693 – 704 (1970)

KINETIC ANALYSIS OF THERMOGRAVIMETRIC DATA. II

IMPROVEMENT OF T. OZAWA'S INTEGRAL METHOD

J. ZSAKÓ*

Faculty of Chemistry, "Babeş-Bolyai" University, Cluj, str. Arany János 11

Received November 25, 1968

Ozawa's integral method has been modified, taking into account that in a logarithmic plot of the heating rate *versus* reciprocal temperature the slope of the straight line depends upon the frequency factor *Z* in Arrhenius' equation. A new method has been suggested as well on the basis of the main idea of Ozawa's method. The kinetic parameters *E* and *Z* are determined from the parameters of the straight line, obtained in a logarithmic plot of heating rate *versus* reciprocal temperature and the reaction order is derived from a new parameter, characterizing the shape of thermogravimetric curves.

Ozawa's method [1] is based on the general equation of thermogravimetric curves, suggested by Doyle [2]:

$$g(\alpha) = \frac{ZE}{Rq}\, p\,(x) \tag{1}$$

where α stands for the fraction of initial compound reacted. The function $g(\alpha)$ means

$$g(\alpha) = \int_0^\alpha \frac{\mathrm{d}\alpha}{f(\alpha)} \tag{2}$$

in which the function $f(\alpha)$ expresses the dependence of the reaction rate $\mathrm{d}\alpha/\mathrm{d}t$ from α in isothermal conditions, according to the equation

$$\frac{\mathrm{d}\alpha}{\mathrm{d}t} = kf(\alpha) \qquad (3$$

In this expression k stands for the apparent rate constant. Further, in equation (1), Z stands for the frequency factor of Arrhenius' equation,

---

* PART I: J. Zsakó, *J. phys. Chem.*, **72**, 2406 (1968).

[1] T. Ozawa, *Bull. Chem. Soc. Japan*, **38**, 1881 (1965).

[2] C. D. Doyle, *J. Appl. Polym. Sci.* **5**, 285 (1961).

E for the activation energy, R for the general gas constant, q for the heating rate and $p\,(x)$ for the integral

$$p\,(x) = -\int_{\infty}^{x} \frac{\mathrm{e}^{-x}}{x^2}\,\mathrm{d}x \tag{4}$$

The meaning of x is the following

$$x = \frac{E}{RT} \tag{5}$$

Ozawa has suggested to record the thermogravimetric curves at different heating rates q. Since $g\,(\alpha)$ does not depend upon the heating rate, for a given transformation degree the function $g\,(\alpha)$ will have the same value, irrespective of q. Thus, from equation (1) the following equation can be derived:

$$\frac{ZE}{Rq_1}\,p\left(\frac{E}{RT_1}\right) = \frac{ZE}{Rq_2}\,p\left(\frac{E}{RT_2}\right) = \ldots = \frac{ZE}{Rq_i}\,p\left(\frac{E}{RT_i}\right) = \ldots \tag{6}$$

where T_i stands for the absolute temperature at which α reaches a given value, by using the heating rate q_i. These equations (6) are used by Ozawa for the determination of the activation energy E. By taking the logarithm of equations (6) and by using for $p\,(x)$ the following expansion

$$\lg p\left(\frac{E}{RT_i}\right) \approx -2.315 - 0.4567\,\frac{E}{RT_i} \tag{7}$$

given by Doyle [3] for $x > 20$, the following equations have been derived by the above mentioned author:

$$-\lg\,q_1 - 0.4567\,\frac{E}{RT_1} = -\lg\,q_2 - 0.4567\,\frac{E}{RT_2} = \ldots \tag{8}$$

Equations (8) show the linear variation of lg q with the reciprocal absolute temperature, the slope of the straight line being

$$m = -\,0.4567\,\frac{E}{R} \tag{9}$$

That is why Ozawa suggests a plot of lg q *versus* $1/T$ and the determination of m from the equation of the obtained straight line

$$\lg\,q = m\,\frac{1}{T} + b \tag{10}$$

According to (9), the approximate value of the activation energy will be obtained by means of the relation

$$E = -4.349\ m \tag{11}$$

---

[3] C. D. Doyle, *J. Appl. Polym. Sci.* **6**, 639 (1962).

We can obtain a clear image on the accuracy of the method and especially of equation (11), by taking, instead of the expansion (7), a more accurate one, e.g. the Schlömilch expansion

$$p\,(x) \approx \frac{e^{-x}}{x\,(x+2)} \tag{12}$$

which was found by Doyle[4] to be a very good one, giving an error less than 1 p.c. even for $x = 15$. With this approximate formula we obtain instead of (7) the following expression

$$\lg p\left(\frac{E}{RT}\right) = -\,0.4343\,\frac{E}{RT} - \lg \frac{E}{RT} - \lg \frac{E+2RT}{RT} \tag{13}$$

It is clear, that the linearity can be only approximate, and even if this linearity can be assumed in first approximation, the coefficient of m in equation (11) cannot have the constant value of 4.349. It must depend upon the value of x, especially if x is small. By taking the logarithm of equation (1), we can give for $\lg p\,(x)$ the following formula:

$$\lg p\,(x) = \lg g\,(\alpha) + \lg Rq - \lg Z - \lg E \tag{14}$$

The magnitude of $\lg p\,(x)$ is determined mainly by the $\lg Z$ value. If we consider a thermal decomposition, the variation of $\lg g\,(\alpha)$ is only 1.279 in the case of a zero order reaction and even for a second order reaction it is only 2.558 if α varies from 0.05 to 0.95. The possibilities of varying the heating rate q are also very limited in the conditions of thermogravimetric analysis. The activation energies, which occur in practical cases cover also a not quite wide interval. The most frequent $\lg E$ values are situated between 4.0 and 4.6. Thus, $\lg Z$, which can be situated approximately between 2 and 30–40, is obviously the main factor in determining the numerical value of $\lg\, p\,(x)$.

In order to verify the linear variation of $\lg q$ with $1/T$, supposed by Ozawa, we have calculated the temperature corresponding to $\alpha = 0.5$ for various hypothetical thermal decompositions. To this purpose equation (14) has been used. For a given E and Z pair the value of q has been varied and the corresponding $\lg p(x)$ values have been calculated. The integrals $p\,(x)$ have been tabulated for different T and E values in our earlier paper,[5] which enabled us to obtain the needed temperature values by means of a simple interpolation. The plot of $\lg q$ *versus* $1/T$ has given indeed a good linearity, as seen in figure 1. But, by calculating the activation energy by means of equation (11), we have found $E = 30.44$ kcal/mole, instead of 30.00 kcal/mole, and $E = 13.18$ kcal/mole, instead of 12.00 kcal/mole, respectively. The former value can be considered to be acceptable, but the latter is only a very rough approximation. These results confirm our supposition concerning the coefficient of m in equation (11). Since the linearity is very good, there is a possibility to improve

---

[4] C. D. Doyle, *Nature*, **207**, 290 (1965).

[5] J. Zsakó, *J. Phys. Chem.*, **72**, 2406 (1968).

Ozawa's method, by giving the right coefficient which multiplies the slope m to give E. This coefficient cannot be the same for all practical cases and it must depend mainly upon the lg Z value.

Since the theoretical deduction of this coefficient is difficult, we accepted an empirical method. To this purpose the $\alpha = 0.5$ temperature has been calculated for about 2000 hypothetical cases carrying out a systematic variation of the different parameters q, Z and E and taking for $f(\alpha)$ different functions of the type $f(\alpha) = (1 - \alpha)^n$. In these calculations the temperature corresponding to $\alpha = 0.5$ has been taken, because it can be determined most accurately from experimental data and at the same time it is relatively little influenced by the reaction order n.[6]

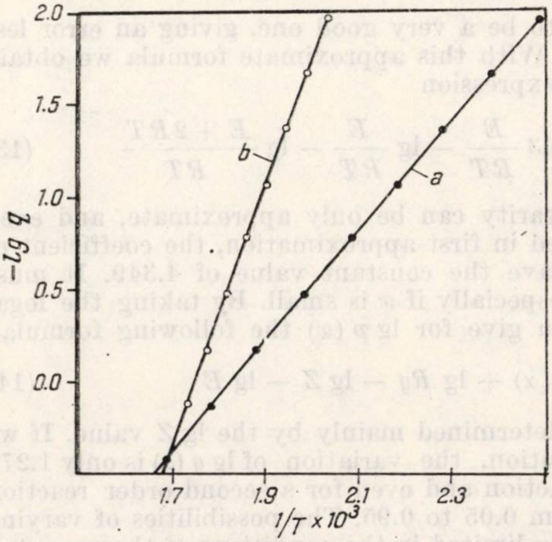

Fig. 1. — Plot of lg q *versus* $1/T_{0.5}$. a, $E = 12$ kcal/mole; $Z = 10^3$ s^{-1}; b, $E = 30$ kcal/mole, $Z = 10^{10}$ s^{-1}.

The influence of the apparent reaction order n has been first studied. This parameter influences only the value of $g(\alpha)$. Since the lg $g(\alpha)$ value shows a very moderate variation with n, it is -0.301 for $n = 0$ and 0.000 for $n = 2$, the slope of the straight line cannot be influenced sensibly by it. Our calculations with the following n values: 0, 1/3, 1/2, 2/3, 1 and 2, have shown indeed that m is independent of n. Thus, for a reaction with $E = 30$ kcal/mole and $Z = 10^{10}$ s^{-1} the calculated m values showed no systematic variation with n. They were only scattered, covering the range between 7.007×10^3 and 7.020×10^3.

Further the influence of E and Z has been studied. Our calculations have shown, that m is mainly determined by E, but it varies systematically with Z. Calculating the coefficient

$$c_m = \frac{E}{m} \tag{15}$$

---

[6] J. Zsakó, *J. Chim. phys.*, **66**, 1041 (1969).

we have found it to be a univocal function of Z. In figure 2 the full line curve gives the variation of this coefficient c_m with lg Z. The horizontal dotted line at $c_m = 4.349$ corresponds to the formula given by Ozawa. One can see, that Ozawa's method offers in many cases only a very rough approximation. Meanwhile, figure 2 enables us to obtain much more accurate values if Z is known.

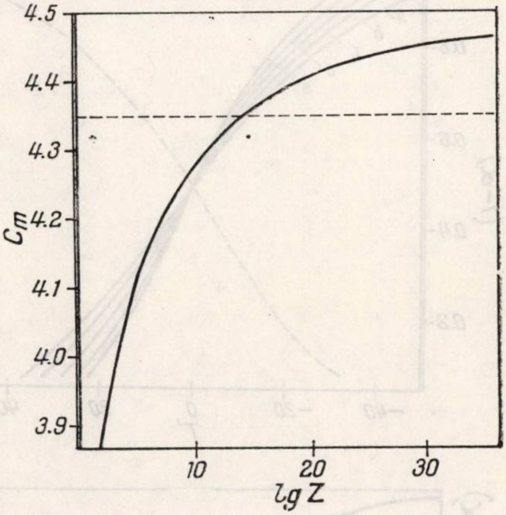

Fig. 2. – Relation between the coefficient c_m and lg Z. The dotted line corresponds to the value given by Ozawa.

In order to determine the parameter Z, Ozawa has suggested the following procedure. By plotting $1 - \alpha$ *versus* $1/T$ a thermogravimetric curve is obtained for each heating rate q. By means of a parallel shift these curves can be superposed and a master thermogravimetric curve is obtained. This master curve is considered by Ozawa to be better than the individual thermogravimetric curves, offering an elimination of experimental errors. By using this master curve and the earlier determined E value, obtained accordingly to equation (11), a plot of $1 - \alpha$ *versus* $\lg \frac{E}{Rq} p\left(\frac{E}{RT}\right)$ is carried out. By means of a parallel shift this curve can be superposed with some standard curves, obtained theoretically, by plotting $(1 - \alpha)$ *versus* $\lg \frac{ZE}{Rq} p\left(\frac{E}{RT}\right)$. These standard curves are constructed for various n values. A comparison of the shape of the experimental curve with these standard curves gives the apparent reaction order. The magnitude of the parallel shift, necessary to superpose the experimental curve with the corresponding standard curve, gives directly the value of lg Z.

We have made a thorough analysis of Ozawa's procedure. In order to clear up the problem of the master curves, theoretical thermogravimetric curves have been calculated for various heating rates. These curves, obtained by plotting $1 - \alpha$ both *versus* T and $1/T$, have been shifted in parallel direction until a superposition at $\alpha = 0.5$ has been realized. An example is given in figure 3. The full line curves correspond

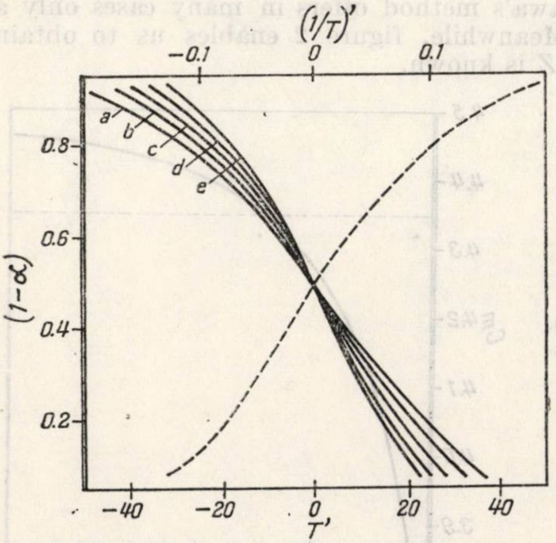

Fig. 3. — Superposition of thermogravimetric curves. $n = 1$, $E = 20$ kcal/mole, $Z = 10^7$ s^{-1}.

a, $q = 8/3$; b, $q = 2/3$; c, $q = 1/6$; d, $q = 1/24$; e, $q = 1/96$ °C s^{-1}.

The dotted line corresponds to the master curve, suggested by Ozawa.

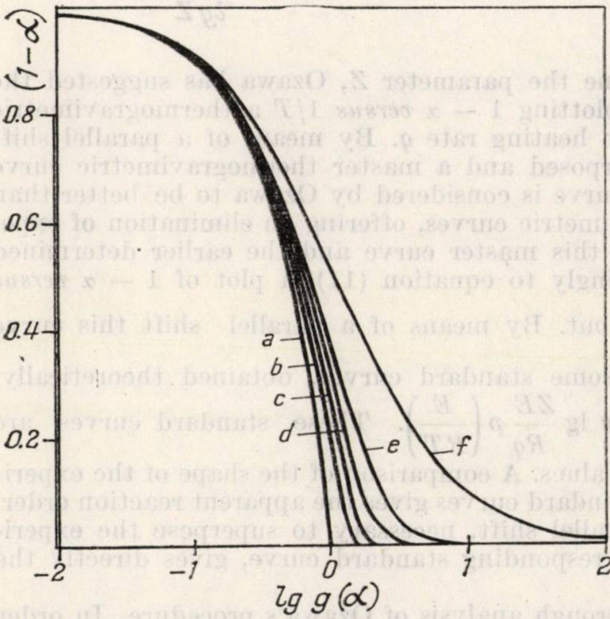

Fig. 4. — Standard thermogravimetric curves.

a, $n = 0$; b, $n = 1/3$; c, $n = 1/2$; d, $n = 2/3$; e, $n = 1$; f, $n = 2$.

to a plot *versus* $T' = T - T_{0.5}$, where $T_{0.5}$ stands for the temperature corresponding to $1 - \alpha = 0.5$. It is obvious, that in this plot a superposition is impossible. The dotted line corresponds to a plot *versus* $(1/T)' = 1/T - 1/T_{0.5}$. One can see, that in this plot a quite good superposition can be reached and the master curve is rather well defined, although a systematic variation of $1/T'$ can be observed. This variation is the largest at very little α values and at α values close to unity. This variation is, however, less than the experimental errors. Thus, in the case considered in figure 3, the magnitude of this variation can be seen from the following data obtained for $1 - \alpha = 0.9$:

q, °C s^{-1}	8/3	2/3	1/6	1/24	1/96
$(1/T)' \times 10^3$	0.17103	0.17162	0.17238	0.17313	0.17368

The reciprocal temperature range covered by this variation is too small to be indicated in figure 3. In conclusion, we can accept the construction of master curves, the principle being sound.

Concerning the standard curves, we have some objections with regard to the figure given by Ozawa.[1] In this figure the given curves correspond to the reaction orders $n = 0, 1, 2$ and 3. In the thermogravimetric analysis the most frequent reaction orders, found both theoretically and experimentally,[5] are $n = 0, 1/3, 1/2, 2/3$ and 1. Thus, it seems to be more correct to give these curves even for these reaction orders and perhaps for $n = 2$, in order to enable us to evaluate the apparent reaction order in the rare cases when n is above unity. Moreover, the figure given by Ozawa is not correct, since the curve given for $n = 1$ is situated entirely in the negative range of the $\lg \dfrac{ZE}{Rq}\, p(x)$ values. That is why we give here the correct standard curves for the above mentioned 6 reaction orders in plot *versus* $\lg g(\alpha)$, which is perfectly equivalent with Ozawa's plot, taking into account equation (1). The standard curves are given in figure 4.

On the basis of our results the following modification of Ozawa's method can be suggested. The first approximation of E is determined according to the initial method, by plotting $\lg q$ *versus* $1/T$ and by calculating E by means of equation (11). The first approximation of $\lg Z$ is determined as well by means of the method suggested by Ozawa, by using the standard curves given in figure 4. This gives the apparent reaction order too. By using the $\lg Z$ value, a more correct c_m value is obtained, by means of figure 2. With this c_m value the second approximation for E can be calculated by using the formula

$$E = c_m m \tag{16}$$

With the second approximation for E is calculated further the second approximation for $\lg Z$ in the same way as the first one. This iteration cycle is repeated until the obtained values are the same as in the former cycle. Due to the suggested modification Ozawa's method becomes much more accurate.

Ozawa's initial method, as well as the above suggested modified method, is in essence a curve fitting method. We have tried to find a possibility to simplify the method, without diminishing its accuracy. To this purpose we have studied parameter b in equation (10). This parameter must depend mainly upon the lg Z and lg E values. We have calculated the magnitude defined by the formula

$$\Delta = b - \lg Z - \lg E + 4 \tag{17}$$

and we have found it to be a univocal function of lg Z and n. Figure 5 gives a plot of Δ *versus* lg Z for $n = 0$ and $n = 1$. The curves for $n = 0$ are shifted in parallel direction in comparison with the curve for $n = 0$. The value of this shift has been found to be proportional with n, viz.

$$\Delta_n = \Delta_0 - 0.141\ n \tag{18}$$

where Δ_n and Δ_0 stand for the magnitude defined by (17), corresponding to reaction order n and 0, respectively. Thus lg Z can be calculated from b if E and n are known.

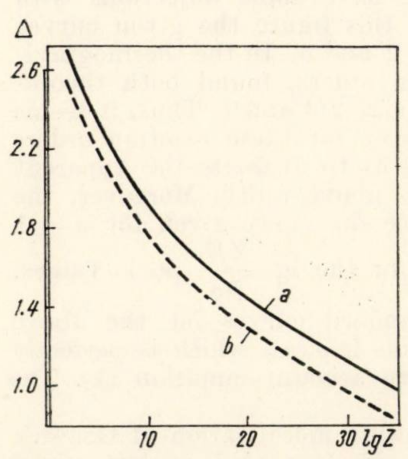

Fig. 5. — Correction term Δ as a function of lg Z.
a, $n = 0$; b, $n = 1$.

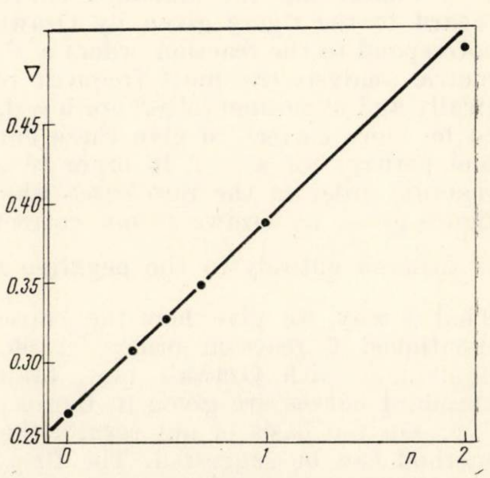

Fig. 6. — Relation between the parameter ∇ and reaction order n.

In a previous paper[6] we have studied the theoretical shape of thermogravimetric curves. We could observe that the shape of the curve is much more influenced by the reaction order if $0.5 > (1 - \alpha) > 0.1$, than in the range $0.9 > (1 - \alpha) > 0.5$. Taking into account the fact, that in a plot $1 - \alpha$ *versus* $1/T$ the thermogravimetric curves can be superposed by means of a parallel shift, we supposed that reaction order can be characterized by the magnitude

$$\nabla = \frac{1/T_{0.5} - 1/T_{0.1}}{1/T_{0.9} - 1/T_{0.1}} \quad \frac{T_{0.9}\,(T_{0.1} - T_{0.5})}{T_{0.5}\,(T_{0.1} - T_{0.9})} \tag{19}$$

where $T_{(1-\alpha)}$ stands for the absolute temperature at which the fraction of the initial compound is equal to $1 - \alpha$.

A great number of ∇ values have been calculated for 6 different reaction orders, by varying E from 10 to 60 kcal/mole and Z from 10^2 to 10^{33} s^{-1}. These calculations confirmed the validity of our supposition and showed the existence of a univocal relation between ∇ and n. Figure 6 gives the mean values of ∇ for the reaction orders under consideration. This plot is nearly linear, but in order to ensure more accuracy, the relation between ∇ and n has been approximated with a second order polynomial. By means of the method of least squares the following relation has been derived :

$$\nabla = 0.2670 + 0.125\ n - 0.0048\ n^2 \tag{20}$$

Thus, the apparent reaction order n can be obtained by determining the temperatures at which the fraction of the nondecomposed compound is equal to 0.9, 0.5 and 0.1, respectively. The magnitude ∇ is calculated accordingly to (19) and the reaction order is given by the formula

$$n = \frac{0.125 - \sqrt{0.015625 - 0.0192\,(\nabla - 0.2670)}}{0.0096} \tag{21}$$

On the basis of the above considerations we suggest the following new method, based on the main idea of Ozawa's method.

DESCRIPTION OF THE SUGGESTED METHOD

Thermogravimetric curves are recorded by several different constant heating rates q_i. By plotting $1 - \alpha$, or simply the weight of the sample *versus* temperature, the temperatures $T_{0.9}$, $T_{0.5}$ and $T_{0.1}$ are determined. By using these values the apparent reaction order is obtained by means of equations (19) and (21).

The $\lg q_i$ values are plotted *versus* $1/T_{0.5}$ and the parameters m and b are obtained for equation (10), in graphical way or by means of the least square method. From these parameters E and Z are obtained, by using a successive approximation scheme.

From equation (17) the following expression can be derived

$$\lg Z = b - \lg E + 4 - \Delta_0 + 0.141\ n \tag{22}$$

In our successive approximation scheme this equation can be written in the following form :

$$\lg Z_i = b - \lg E_i + 4 - \Delta_{0i} + 0.141\ n \tag{23}$$

where the index i indicates the i-th approximation. The i-th approximation of E and Δ_0 will be always determined by means of the $(i-1)$-th approximation of $\lg Z$ in the following way. By using $\lg Z_{i-1}$, the value of c_{mi} will be determined, by means of figure 2, but it is better to make a linear interpolation of the data given in table 1.

With this c_{mi} value the approximate activation energy is calculated, with the aid of the relation

$$E_i = c_{mi}\ m \tag{24}$$

which corresponds to equation (16).

The correction term Δ_{0i} can be obtained graphically from figure 5, but it is better to take it from table 2, by carrying out a linear interpolation.

In the first approximation cycle the zero order approximation for $\lg Z$, necessary for obtaining E_1 and Δ_{01} can be assimilated with b, i.e. $\lg Z_0 = b$.

Table 1

Coefficient c_m from the equation (16) for different lg Z values

lg Z	c_m	lg Z	c_m	lg Z	c_m
2	3.900	13	4.331	24	4.430
3	3.990	14	4.345	25	4.434
4	4.060	15	4.358	26	4.438
5	4.115	16	4.370	27	4.442
6	4.159	17	4.381	28	4.446
7	4.196	18	4.391	29	4.450
8	4.227	19	4.400	30	4.453
9	4.254	20	4.408	31	4.456
10	4.277	21	4.415	32	4.459
11	4.297	22	4.421	33	4.462
12	4.315	23	4.426	34	4.465

Table 2

Corrections Δ_0 for zero order reactions corresponding to different lg Z values

lg Z	Δ_0	lg Z	Δ_0	lg Z	Δ_0
2	2.679	13	1.737	24	1.306
3	2.544	14	1.685	25	1.274
4	2.428	15	1.637	26	1.242
5	2.324	16	1.592	27	1.210
6	2.229	17	1.550	28	1.179
7	2.141	18	1.511	29	1.148
8	2.059	19	1.474	30	1.117
9	1.983	20	1.439	31	1.086
10	1.913	21	1.405	32	1.056
11	1.853	22	1.372	33	1.026
12	1.793	23	1.339	34	0.996

These iteration cycles will be repeated until the n-th approximation will be equal to the $(n-1)$-th one.

APPLICATION

In order to illustrate the suggested method, we give below two examples.

1. For the first reaction we presumed the following kinetic parameters : $n = 1$, $E = 34$ kcal/mole, $Z = 10^{17}$ s^{-1}. By using these para-

meters, equation (14) and the table of integrals given in our previous paper,[5] the temperatures $T_{0.1}$, $T_{0.5}$ and $T_{0.9}$ have been calculated, by assuming different heating rates. The temperature values have been used for the calculation of the magnitude ∇ according to equation (19). By plotting $\lg q_i$ *versus* $1/T_{0.5}$, the parameters m and b have been determined. The obtained values are the following :

$$\nabla = 0.3843 ; \qquad m = 7759 ; \qquad b = 18.924$$

In practice these parameters are derived from experimental data, as shown above. In these examples they have been calculated and will be considered below as "experimental" data, in order to illustrate the efficiency of the suggested method.

The reaction order, given by the formula (21), is $n = 0.975$, in acceptable agreement with the presumed $n = 1$ value. Thus, equation (23) will have the following form :

$$\lg Z_i = 18.924 - \lg E_i + 4 - \Delta_{0i} + 0.137$$

By applying the above approximation scheme, this equation gives the following approximate values :

i	c_{mi}	E_i	Δ_{0i}	$\lg Z_i$
0	—	—	—	18.924
1	4.399	34132	1.474	17.054
2	4.382	34000	1.548	16.982
3	4.381	33992	1.551	16.979
4	4.381	33992	1.551	16.979

As seen, the intermediate values converge very quickly and the $E = 33.992$ kcal/mole and $Z = 0.953 \times 10^{17}\ \mathrm{s}^{-1}$ values are in very good agreement with the presumed kinetic parameters.

2. By taking the kinetic parameters $n = 1$, $E = 24$ kcal/mole and $Z = 10^{10}\ \mathrm{s}^{-1}$, the following "experimental" data can be calculated :

$$\nabla = 0.3878 ; \qquad m = 5635 ; \qquad b = 12.167$$

From this ∇ value the reaction order $n = 1.005$ can be obtained by means of equation (21). Equation (23) becomes

$$\lg Z_i = 12.167 - \lg E + 4 - \Delta_{0i} + 0.142$$

By applying the same approximation scheme, the following approximate values have been obtained :

i	c_{mi}	E_i	Δ_{0i}	lg Z_i
0	—	—	—	12.167
1	4.319	24332	1.784	10.139
2	4.280	24118	1.905	10.022
3	4.277	24101	1.912	10.015
4	4.277	24101	1.912	10.015

The $E = 24.101$ kcal/mole and $Z = 1.035 \times 10^{10}$ s^{-1} values are also in good agreement with the presumed kinetic parameters.

In conclusion, the method suggested by us is much simpler than Ozawa's curve fitting method. At the same time, it is much more accurate, since the dependence of m on Z has been taken into account. Thus, the suggested method can assure the same accuracy as the modified Ozawa method, also given in the present paper.

Revue Roumaine de Chimie, **15**, 705–709 (1970)

ABSORPTION SPECTRA OF $CoCl_2$ AND $CoBr_2$ ISOLATED IN BENZENE MATRIX

MARCELA MUSA

Institute of Physics of the Academy, Bucharest, Calea Victoriei 114

Received January 18, 1969

The absorption spectra of $CoCl_2$ and $CoBr_2$ isolated in benzene matrix were measured and the energy states of these molecules compared with those previously found on gaseous samples. The presence of tetrahedral melt complexes was avoided due to the matrix method. The experimental results were discussed pointing out the possibility that dimeric species exist both in matrix and gaseous state.

INTRODUCTION

In a previous paper [1] the gaseous $CoCl_2$ and $CoBr_2$ spectra were given; these molecules belong to the $D_{\alpha h}$ symmetry and the study of their spectra allows the verification of the crystal field theory. [2-4] Paper [1] pointed to a vibrational structure not mentioned in [2] and suggested that the broad maximum in the 12,000–17,000 cm^{-1} spectral range is due to the liquid phase condensed on the windows of the experimental tube. In the chloride melt salts[5] the Co^{2+} complex symmetry is tetrahedral, T_d, exhibiting probably more intense maxima than the $D_{\alpha h}$ complexes due to the lack of an inversion element in the T_d point group. The $^4\Gamma_2(^4F) - {}^4\Gamma_4(^4P)$ spin-allowed band of $[CoCl_4]^{2-}$ at 1,000°, is placed in nearly the same spectral range, 13,000–17,000 cm^{-1}, as the main band of the linear $CoCl_2$.[1,5] As compared to the gaseous method the matrix isolation presents the advantage of removing the liquid phase, the pure solid $CoCl_2$ or $CoBr_2$ compounds having a characteristic octahedral spectrum, even in polycrystalline state, with $^4\Gamma_4(^4F) - {}^4\Gamma_4(^4P)$ spin-allowed band situated in 16,500–18,500 cm^{-1} region.[6,7]

This paper aimed at avoiding the ambiguity arising from [1] concerning the band assignment of the gaseous sample spectra; in a sense this goal was reached.

---

[1] A. Truția and M. Musa, *Spectrochim. Acta*, **23**, 1161 (1967).

[2] J. T. Hougen, G. E. Leroi and T. C. James, *J. Chem. Phys.*, **34**, 1670 (1961).

[3] D. M. Gruen and C. W. DeKock, *J. Chem. Phys.*, **43**, 3395 (1965).

[4] C. W. DeKock and D. M. Gruen, *J. Chem. Phys.*, **44**, 4387 (1966).

[5] D. M. Gruen and R. L. McBeth, *Pure Appl. Chem.*, **6**, 23 (1963).

[6] J. Ferguson, D. L. Wood and K. Knox, *J. Chem. Phys.*, **39**, 881 (1963).

[7] A. Truția and M. Musa, *Phys. Stat. Sol.*, **8**, 663 (1965).

EXPERIMENTAL

Benzene was chosen as isolating material because it is inert against $CoCl_2$ and $CoBr_2$ and exhibits a suitable melting point, 6°, since the lowest working temperature was that of liquid nitrogen.

The cryostat was described in[8] (see also Fig. 1). This was improved by making a liquid nitrogen circulatory system around the sample support, which was a thin plate of quartz. The support temperature was that of nitrogen melting point, $-210°$, realized by a strong evaporation of the liquid in cryostat until solid nitrogen was obtained.

The temperature of the $CoCl_2$ or $CoBr_2$ furnaces was established at an appropriate value to deposit simultaneously with benzene on the support, during 5—6 minutes, a diffuse light-blue layer for $CoCl_2$ or a light-green sample for $CoBr_2$. The cryostat pressure during evaporation was of $10^{-5}-10^{-4}$ Torr.

The optical single-beam equipment consisted of a VSU-1 Carl Zeiss monochromator and an EMI 9558 QB or a M-13 gek. Zeiss photomultiplier on the exit slit, as receiver. The photocurrent was recorded by a GRVAC-Sefram galvanometer, of 10^{-9} A/mm sensitivity. The system which acted the paper of the recorder was connected to the wavelength drum of the monochromator; this way we recorded the photomultiplier current response in terms of wavelength, in cm^{-1} units.

RESULTS AND DISCUSSIONS

The lowest ^4F term of the Co^{2+} ion of d^7 electron configuration splits in the $D_{\alpha h}$ anion field into $^4\Phi_g$, $^4\Sigma_g^-$, $^4\pi_g$ and $^4\Delta_g$ and the excited ^4P term decomposes into $^4\Sigma_g^-$ and $^4\pi_g$ components.[2,4] The A_2 and $A_4-D_{\alpha h}$ crystal field parameters are positive. The computed energy states were taken from [4] where it was assumed that $A_2/A_4 = 9.0$ and that the free state energy difference decreases in the ligand field to the value $E\ (^4P)-$ $-E\ (^4F) = 12{,}520\ cm^{-1}$. Figure 2 presents the calculated energy states,[2,4] those experimentally found on gaseous $CoCl_2$ or $CoBr_2$[1,4] and those obtained in the present work.

The spectra realized on benzene matrices are not so well developed as those taken on gaseous states, the vibrational structure being not evidenced. The absorption bands are wide and shifted towards red in comparison with the maxima found on gaseous samples; the 12,000—17,000 cm^{-1} gaseous main band appears in this case too.

The broadening of the absorption bands may be explained by:

a. The existence of van der Waals type interactions between the matrix molecules and those of the isolated substance (benzene—$CoCl_2$ or $CoBr_2$).

b. The interaction among the isolated molecules: the cobalt salt concentrations in matrices are probably greater than those necessary for a perfect isolation.

c. The support temperature might not have been low enough and diffusion of the isolated molecules through the matrix bulk could have taken place.

---

[8] R. A. Jitnikov and I. V. Kolesnikov, *Pribori i Tekhnika Experimenti*, **3**, 189 (1964).

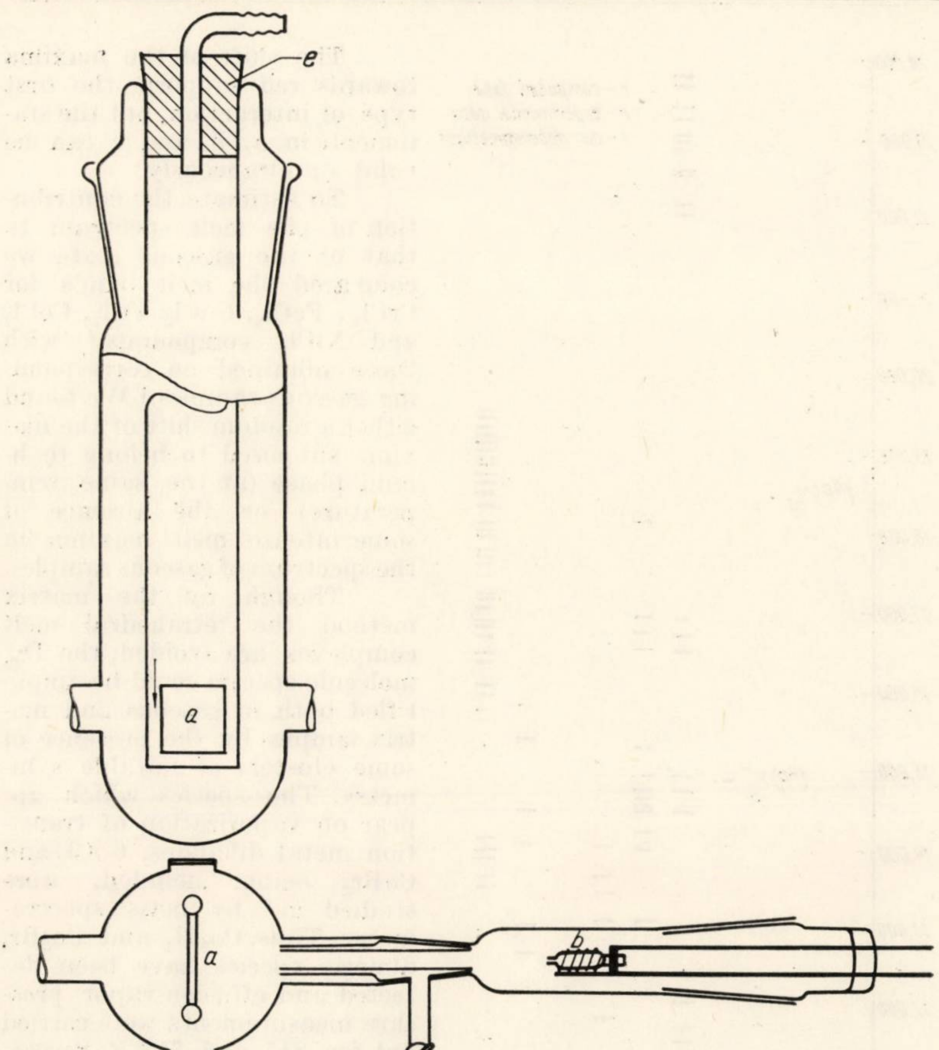

Fig. 1. — Cryostat :
a, sample support ; *b*, $CoCl_2$ or $CoBr_2$ evaporation furnace ; *c*, benzene ampoule ; *d*, piece of iron isolated in glass, magnetically acted to break the ampoule c ; *e*, rubber stopper for the forced evaporation of liquid nitrogen.

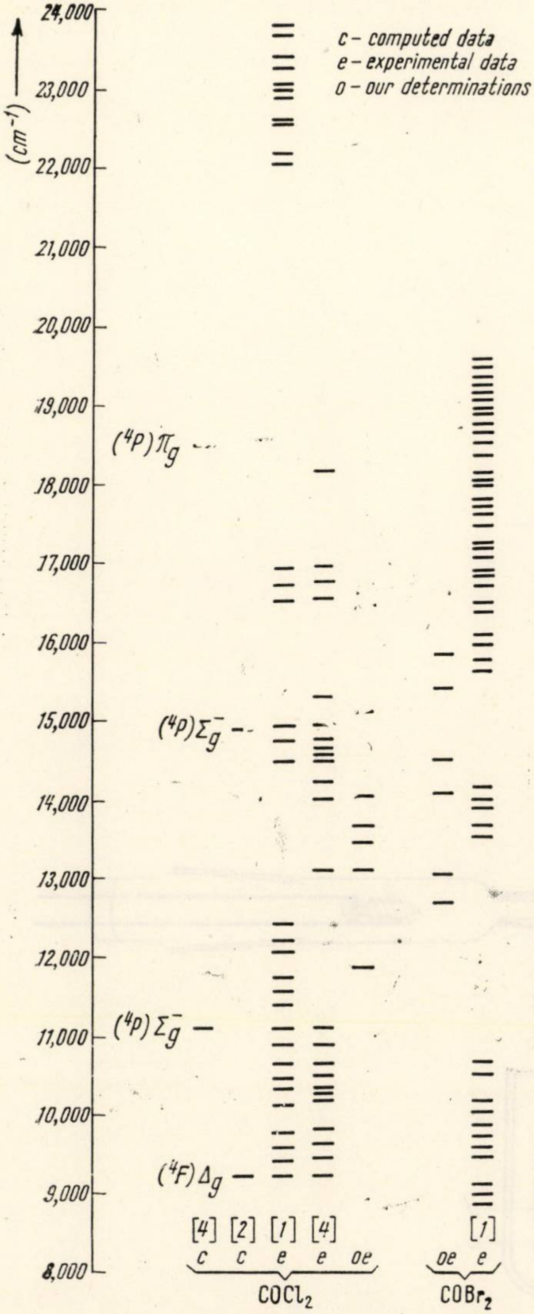

Fig. 2. — Maximum positions in the absorption spcetra of $CoCl_2$ and $CoBr_2$.

The shift of the maxima towards red supports the first type of interaction, but the statements in a, b, and c can be valid simultaneously.

To estimate the contribution of the melt spectrum to that of the gaseous state we compared the melt bands for $CrCl_2$, $FeCl_2$, $CuCl_2$ VCl_2, $CoCl_2$ and $NiCl_2$ compounds,[5] with those obtained on corresponding gaseous samples.[4] We found either a random shift of the maxima supposed to belong to liquid phase (at the same temperature) or the absence of some intense melt maxima in the spectrum of gaseous samples.

Though by the matrix method the tetrahedral melt complexes are avoided, the $D_{\alpha h}$ molecule spectra could be impurified both in gaseous and matrix samples by the presence of some clusters of suitable symmetry. The species which appear on vaporization of transition metal dihalides, $CoCl_2$ and $CoBr_2$ being included, were studied in [9] by mass spectrometry. Thus, Co_2Cl_4 and Co_2Br_4 dimeric species have been detected and effusion vapor pressure measurements were carried out for 817 and 717°K respectively. The pressure values, 2.38×10^{-7} for Co_2Cl_4 and $3.44 \times$ $\times 10^{-7}$ atm for Co_2Br_4 are to be compared with 1.61×10^{-5} and 7.40×10^{-6} atm the monomeric pressures respectively. Accordingly, in the benzene matrices the dimeric species are collected and though their quantity is small the corresponding optical transitions could be observed if the spatial positions of atoms gave at the Co^{2+} site a point group symmetry which should not contain an inversion centre. It is generally accepted that the absorption coefficient ratios for the Co^{2+} ion in tetrahedral and octahedral symmetry is $\sim 10^2$. If this value holds also for dimer to monomer ratios the high dimer band intensities can compensate for their low concentration and dimeric bands can be observed in gaseous or matrix sample spectrum.

---

[9] R. C. Schoonmaker and A. H. Friedman, *J. Chem. Phys.*, **31**, 1586 (1959).

It would be of great interest to know the spatial structure of dimers or the dimer to monomer ratios for several evaporation temperatures. In the last case one could possibly achieve matrices either without dimers or with known dimer to monomer proportions ; such samples could emphasize whether or not the monomeric spectrum is actually impurified by the dimeric one.

Acknowledgments. We would like to thank Dr. A. Truţia for useful discussions and suggestions.

group symmetry which should not confuse an [illegible]. It is generally accepted that the absorption [illegible] ratio for the Co²⁺ ion in tetrahedral and octahedral symmetry is ~ 100. If this value holds also for dimer to monomer [illegible] the high dimer band intensities can compensate for their low concentration and [illegible] bands can be observed in aqueous or [illegible] spectra.

It would be of great interest to know the [illegible] structure of [illegible] as the dimer to monomer ratios for several [illegible]. In the last case one could possibly [illegible] with KCNS in order to [illegible] samples could [illegible] whether or not the monomeric spectrum is [illegible] the dimeric one.

Acknowledgements—We would like to thank [illegible] for useful discussions and suggestions.

Revue Roumaine de Chimie, **15**, 711 – 717 (1970)

CORRELATION BETWEEN THE STRUCTURE AND BASICITY CONSTANTS OF THE *p*-DIMETHYLAMINO-*p′*-*m′*-X-AZOBENZENES BASED ON HAMMETT AND ISMAILOW EQUATIONS

V. NEMES, I. GÖRBE and P. NAGY

Faculty of Chemistry, Pedagogical Institute Tg. Mureş, Str. N. Iorga, 1

Received May 31, 1969

Nine compounds of the type *p*-dimethylamino-*p′*-*m′*-X-azobenzenes have been prepared. By a spectrophotometric method the basicity constants of these compounds in ethanol-water mixtures of 15, 30 and 45% have been determined. The applicability of Hammett and Ismailow equations for these compounds has been pointed out.

The chemical behaviour of the *p*-dimethylamino-azobenzenes was studied by several authors. Hantzsch recognized in 1908 that in acidic media these compounds appear in two different forms. In one of them the proton is linked to the azoatom of the azo-group, whereas in the second form, to the azoatom of the dimethylamino-group.[1]

According to Kehrmann's spectrophotometric studies the addition of the second, respectively of the third proton to these compounds is possible. The forming ions have characteristic spectra.[2] The above research permitted the quantitative estimation of the structural changes. Bernstein and Hinsburg have studied the pH and the substituent effect in the following tautomer equilibria :[3]

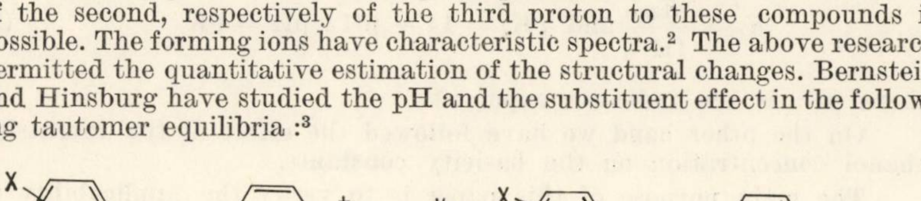

It has been established that in the presence of sulphuric acid in ethanol-water solution the value of the tautomer equilibrium constant (K_t) increased proportionally with the concentration of sulphuric acid. It has also been observed that there is a linear dependence between log K_t and the Hammett acidity function (H_0), respectively log K_t and the electronic effects of the substituents.

---

[1] A. Hantzsch, *Ber. dtsch. chem. Ges.*, **41**, 1161 (1908); *ibid.* **52**, 509 (1919).

[2] F. Kehrmann, *Ber. dtsch. chem. Ges.*, **48**, 1933 (1915).

[3] I. J. Bernstein and O. F. Hinsburg, *Doklady Akad. Nauk. SSSR.*, **180**, 98. (1968); *Zhur. org. Khim.*, 3, 2032 (1967).

Rogers and co-workers[4] determined the first and second ionization constant (pK_{a1} and pK_{a2}) of the mono- and diprotonized compounds, quoted before, by a spectrophotometric method. They have found that the effect of *p'*-substituents on the ionization constants can be expressed by the Hammett equation.[5]

The present paper carries out a study on the basicity constants of some *p*-dimethylamino-*p'*-*m'*-substituted-azobenzenes based on the following equilibrium :

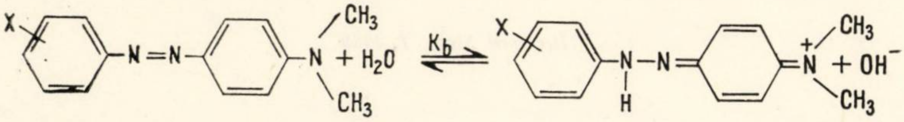

or

$$I + H_2O \overset{K_b}{\rightleftharpoons} HI^+ + OH^-$$

For the quantitative estimation of the substituent effects we have chosen the basicity constants of the compounds. Therefore

$$K_b = \frac{[IH^+].[OH^-]}{[I]} = \frac{[IH^+].K_{H_2O}}{[I].[H^+]} \qquad (1)$$

In our conditions $[HI^+] = [I]$

$$K_b = \frac{K_{H_2O}}{[H^+]} \text{ and } pK_b = 14 - pH \text{ ; } pH = pK_i \qquad (2)$$

where pK_i is the indicator exponent.

On the other hand we have followed the effect of the increasing ethanol concentration on the basicity constants.

The main purpose of this paper is to verify the applicability of Hammett and Ismailow equations, as well as of the general equation proposed by Zsakó.[6-8]

---

[4] M. T. Rogers, T. W. Campbell and M. W. Maatman, *J. Amer. Chem. Soc.*, 73 5122 (1951).

[5] L. P. Hammett, *Chem. Rev.*, **17**, 125 (1935).

[6] J. Zsakó, L. Almási, M. Giurgiu and A. Hantz, *Studii şi Cercetări Chim.*, *Fil. Cluj*, 14, 271 (1963).

[7] J. Zsakó, L. Almási, M. Giurgiu and A. Hantz, *Zhur. obshchei Khim.*, **35**, 1866 (1965).

[8] A. Benkö, J. Zsakó and P. Nagy, *Chem. Ber.* **100**, 2178 (1967).

EXPERIMENTAL

Preparation of p-dimenthylamino-p'-m'-substituted-azobenzenes

Standard literature preparations were used for these compounds.[9] Namely, the substituted diazoderivatives were coupled with N-dimethylaniline. The purification was made by recrystallization from ethanol or acetone.

Determination of pK_i *values*

The pK_i values of the studied compounds were determined by photocolorimetry, using a photocolorimeter type : FEK-56. The measurements were performed with 10^{-5} mol/l solutions (final concentration of the compounds). Since the solubility in water of these compounds, especially for the progressive values of the pH, is reduced, the solution was prepared with 15, 30 and 45% ethanol (volume percentage).

In order to fix the pH values, the solutions were buffered with glycine/HCl. The proton concentration varied in the range pH = 1.4—3.68. The pH difference of two consecutive solutions was of about 0.2 pH units. A precise determination of the pH was made by using a Radelkisz pH-meter (with a precision of 0.05 pH units).

The extinction of the prepared solutions was determined with several filters (λ_{max} = = 440, 490, 540, 580 nm (fig. 1)). The 2 cm solution was placed in two consecutive cells of 1 cm each (cell 1 and cell 2). Distilled water served as comparative solution (cell 3). The extinction values were plotted against the pH (fig. 2).

The extinction (when $[HI^+] = [I]$) "$E_{\lambda i}$" was determined by using cell 1 for the solution of the protonized form (pH = 0) and cell 2 for the solution of the nonprotonized form (pH = 10).

The indicator exponent pK_i was determined by reading the pH value corresponding to the "$E_{\lambda i}$" from the graph $E = f_{(pH)}$. Deviations from the average value were ± 0.06 in pK_i.

We used the absorption spectra of HI^+ and I, and chose filters which had maximum values of extinction. We proceeded with separated cells in order to assure the equality of concentrations of the forms HI^+ and I, and therefore the presence of the turning colour.

RESULTS AND DISCUSSION

The exponents of the basicity constants (pK_b) have been calculated from the experimentally determined pK_i values according to equation (2). The calculated values are given in table 1.

If the pK_b values are represented against the σ (substituent constant), linear correlation are obtained (fig. 3).

The substituent effects upon the protonization of the studied compounds can be described by the Hammett equation :

$$(pK_b)_x = (pK_b)_0 - \rho\sigma \tag{3}$$

where ρ is the reaction constant, expressing the sensitivity of the reaction to the electronic effects of the substituents.

A linear least squares correlation analysis has been used to determine the best values of $(pK_b)_0$ and ρ. The accuracy was estimated by the value of correlation coefficient (r).

---

[9] L. M. Jagupolski, *Zhur. obshchei Khim.*, 35, 1252 (1965).

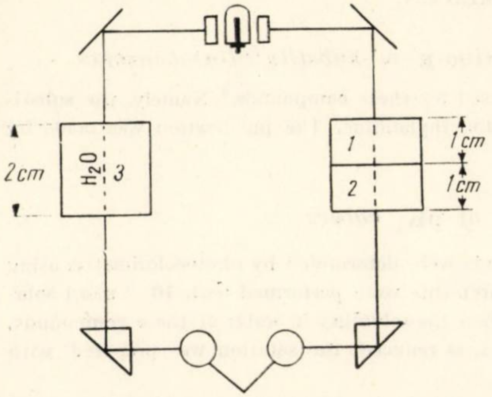

Fig. 1. — a) Determination of the extinction value of the buffered solutions. In the cell 1 and 2 the same buffered solutions were put. b) Determination of the "$E\lambda_i$" (the extinction value when $[HI^+] = [I]$). In cell 1, $pH = 0$, and in cell 2, $pH = 10$.

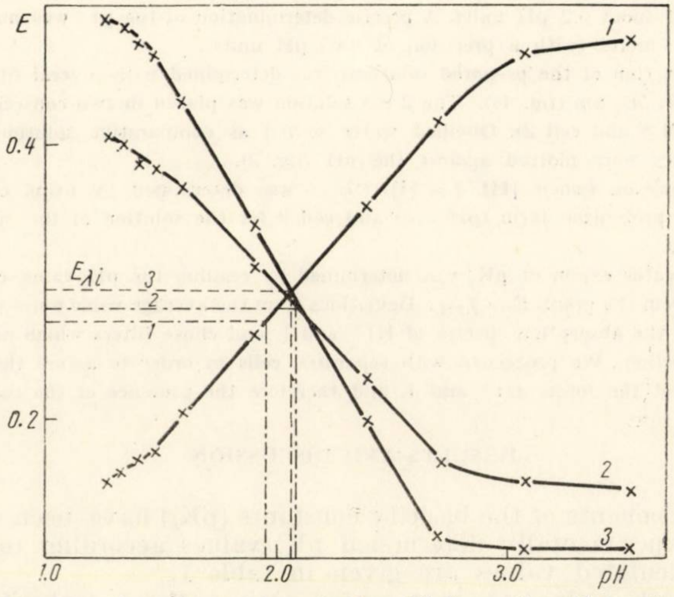

Fig. 2. — Dependence of extinction (E) from the pH for the compound "a" in the 45% ethanol-water mixture using the filters $\lambda = 440$ (1), 490 (2) and 540 nm (3). "$E\lambda_i$" when $[HI^+] = [I]$ 1. 0.273; 2. 0.282; 3. 0.296.

The calculated values of ρ and (r) are given in table 2.

The effect of solvent composition on the basicity of compounds can be described by the Ismailow equation.[10]

$$(pK_b)_M = (pK_b)_{H_2O} + \log \gamma^0_{H^+} + \log \frac{\gamma^0_I}{\gamma^0_{HI^+}} \qquad (4)$$

---

[10] N. A. Ismailow, "Elektrokhimia rastvorov," Izd. Kharkovsk. Univ. Kharkow, 1959, p. 795.

Table 1

The pK_b values in the ethanol-water mixtures

X	σ	pK_b Et–OH % 15	30	45
a. $p-CH_3$	–0.170	10.85	11.33	11.98
b. $m-CH_3$	–0.069	10.89	11.38	12.07
c. p–NH–Ac	0.000	10.97	11.46	12.16
d. –H	0.000	10.90	11.44	12.11
e. $p-SO_3^-$	+0.090	11.01	11.50	12.17
f. p–CHO	+0.216	11.14	11.65	12.25
g. p–Cl	+0.227	11.17	11.63	12.26
h. m–COOH	+0.350	11.26	11.79	12.35
i. $m-NO_2$	+0.710	11.55	11.99	12.58

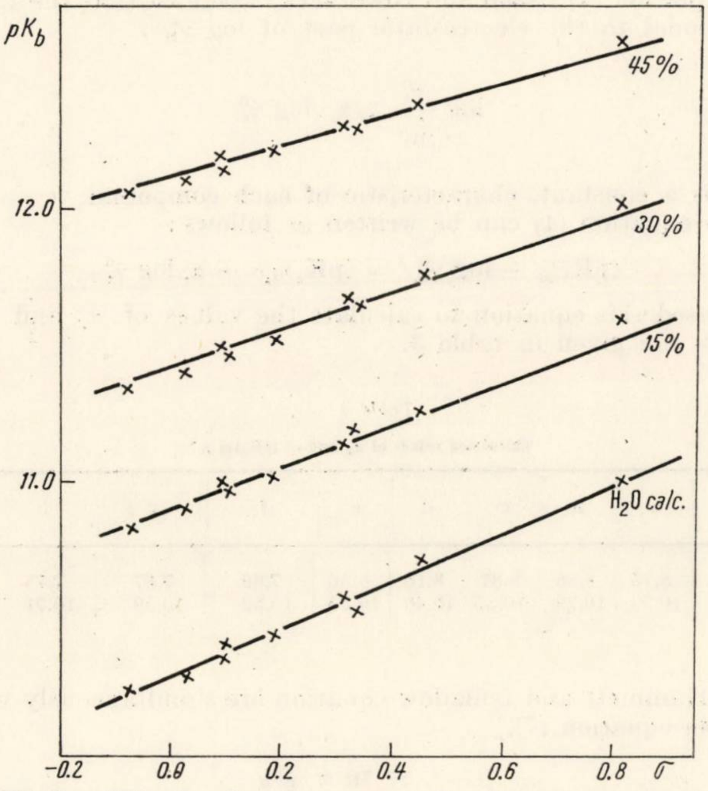

Fig. 3. — Plot of pK_b values against the Hammett substituent constant.

where $(pK_b)_M$ and $(pK_b)_{H_2O}$ represent the basicity exponents in the ethanol-water solution with composition M, respectively in water. The activ-

Table 2

Values of the reaction constant and of the correlation coefficient

Et–OH %	ρ	*r*
15	-0.773	0.915
30	-0.699	0.944
45	-0.557	0.910

ity coefficients have been determined so as to represent the change in chemical potentials by the term $RT \cdot \log \gamma^{\circ}$, when one grammion or one mol of particles passes from the infinite diluted aqueous solution into solution *M* with the same dilution.

The value of γ° in ethanol-water mixtures for protons was determined by Alexandrow and Ismailow.[11]

In equation (4) Zsakó and coworkers [6] assumed that the third term is proportional to the electrostatic part of $\log \gamma^0_{\mathrm{H}^+}$.

$$\log \frac{\gamma^0_{\mathrm{I}}}{\gamma^0_{\mathrm{HI}^+}} \cong \alpha_x \cdot \log \gamma^0_{\mathrm{el}} \tag{5}$$

where α_x is a constant, characteristic of each compound.

Thus equation (4) can be written as follows:

$$(\mathrm{pK}_b)_M - \log \gamma^0_{\mathrm{H}^+} = (\mathrm{pK}_b)_{\mathrm{H_2O}} + \alpha_x \log \gamma^0_{\mathrm{el}} \tag{6}$$

We have used this equation to calculate the values of α_x and $(\mathrm{pK}_b)_{\mathrm{H_2O}}$. The results are given in table 3.

Table 3

Calculated values of α_x and of $(\mathrm{pK}_b)_{\mathrm{H_2O}}$

X	a	b	c	d	e	f	g	h	i
α_x	8.75	8.56	8.81	8.16	8.36	7.69	7.87	7.78	6.65
$(\mathrm{pK}_b)_{\mathrm{H_2O}}$	10.23	10.29	10.35	10.40	10.43	10.52	10.59	10.71	11.10

The Hammett and Ismailow equation are simultaneously valid cnly if α_x follows equation (7).[7]

$$\alpha_x = \alpha_{\mathrm{H}} + \rho\sigma_\alpha \tag{7}$$

The validity of the above equation has been proved for the studied compounds and for $\rho_\alpha = 2.159$. In the same way the calculated values of $(\mathrm{pK}_b)_{\mathrm{H_2O}}$ plotted against σ give a linear correlation (see fig. 3) with the slope $\rho_{\mathrm{H_2O}} = -0.892$.

---

[11] W. W. ALEXANDROW and N. A. ISMAILOW, *Zhur. fiz. Khim.*, 32, 404 (1958).

From equations (3), (6), (7) Zsakó[8] deduced a general equation for the dependence of the reaction constant on the solvent composition :

$$\rho_M = \rho_{H_2O} + \rho_\alpha \log \gamma_{el}^0 \tag{8}$$

The experimental values of ρ_M and those calculated on the basis of equation (8) are given in table 4.

Table 4

Calculated and the experimental values of ρ_M in ethanol-water mixtures

	H_2O	Et–OH %		
		15	30	45
$\rho_{M_{exp}}$		−0.773	−0.699	−0.557
$\rho_{M_{calc.}}$	−0.892	−0.776	−0.672	−0.549

These data show that the sensitivity of the reaction to the substituent effects (in absolute value) decreases for increasing ethanol concentrations. The negative sign of ρ seems to indicate a nucleophile center and an electrophile mechanism of the reaction.

Acknowledgment. The authors are indebted to dr. J. Zsakó for helpful discussions.

[illegible] (Fig. 17) [illegible] a general equation [illegible]

$$[illegible]$$

The [illegible] values of [illegible] are given in Table [illegible].

[illegible]

[illegible]	[illegible]	[illegible]	[illegible]	[illegible]
[illegible]	[illegible]	[illegible]	[illegible]	[illegible]
[illegible]	[illegible]	[illegible]	[illegible]	[illegible]

[illegible] and of considerable [illegible] of the reaction.

[illegible]

[illegible]

Revue Roumaine de Chimie, **15**, 719 – 729 (1970)

CONTRIBUTION À L'ÉTUDE DE LA CYANURATION ET DU CONDITIONNEMENT DES MINERAIS AURIFÈRES DE TYPE BAIA DE ARIEŞ

RALUCA RIPAN, N. PASCU, ANA UNGUREANU et V. CORDIŞ

Institut de Chimie de l'Académie, Filiale de Cluj, 59—65, str. Donath

Reçu le 5 août 1969

On établit sur des échantillons de minerais aurifères de type Baia de Arieş les causes de l'extraction réduite de l'or et on précise également les paramètres optimums de la cyanuration permettant d'augmenter de 27 % l'extraction actuelle. On constate notamment, au moyen d'une étude minéralogique, qu'il s'agit de minerais argileux, minéralisés à leur surface par des sulfures minéraux métalliques, dont le mispickel est un porteur d'or. On démontre que dans le processus de cyanuration le grillage préalable des minerais permet d'augmenter la proportion de l'extraction de l'or de 64,22 % — valeur obtenue pour les produits non grillés — à 91,65 % pour les produits grillés.

INTRODUCTION

La cyanuration compte parmi les procédés hydrométallurgiques employés pour l'extraction de l'or à partir des minerais aurifères.[1–3]

Le mécanisme de ce procédé est donné par les réactions ci-dessous[4–8, 9–16]

---

[1] J. W. Mellor « Comprehensive Treatise on Inorganic and Teoretical Chemistry », vol. 3, Longmans, 1923, p. 499.

[2] J. S. Mac-Arthur, R. W. Forrest et W. Forrest, Brit. Pat. 14, 174, 1887, US Pat. 403,202, 1889, US Pat. 418,137 1889.

[3] J. S. Mac-Arthur, *J. Soc. Chem. Ind.*, **9**, 267 (1906); *Mining and Science Press* **112**, 851 (1916).

[4] L. Elsner, *J. prakt. Chem.*, **37**, 441 (1846).

[5] Jr. L. Janin, *Eng. Min. J.*, **46**, 548 (1888); *Mineral Industry*, **1**, 239 (1892).

[6] J. S. Maclaurin, *J. Chem. Soc.*, **63**, 724 (1893).

[7] S. B. Christy, *Amer. Inst. Min. Metall. Eng. Trans.*, **26**, 735 (1896).

[8] G. Bodländer, *Z. Angew. Chem.*, **9**, 583 (1896).

[9] G. Brasky, S. J. Swainson et N. Hedley, *Amer. Inst. Min. Metall. Eng. Trans.*, **112**, 660 (1934).

[10] B. Boonstra, *Karros. Metallschutz*, **19**, 146 (1943).

[11] P. F. Thompson, *Trans. Electrochem. Soc.*, **91**, 41 (1947).

[12] M. Kameda, *Sci. Rept. Research Inst. Tohoku Univ. Japan, Ser. A.*, **1**, 133 (1949);, **1**, 223 (1949); **1**, 435 (1949).

[13] V. Lund, *Acta Chem. Scand.*, **5**, 555 (1951).

[14] W. C. Schumb, C. N. Satterfield et R. L. Wentworth, « ACS Monograph », Reinhold, New York, 1955, p. 40.

[15] V. Kudryk et H. H. Hellogg, *J. Metals*, **6**, 541 (1954).

[16] G. A. Deitz et J. M. Halpern, *J. Metals*, **6**, 541 (1953).

$$O_2 + 2H_2O + 2e^- \longrightarrow 2OH^- + H_2O_2$$

$$Au \longrightarrow Au^+ + e^-$$

$$Au^+ + CN^- \longrightarrow AuCN$$

$$AuCN + CN^- \longrightarrow [Au(CN)_2]^-$$

La réaction générale

$$2Au + 4CN^- + O_2 + 2H_2O \longrightarrow 2[Au(CN)_2]^- + 2OH^- + H_2O_2$$

La vitesse de cyanuration [17-28] peut être calculée d'après l'équation

$$\text{Vitesse} = \frac{2AD_{CN^-}\,D_{O_2}[CN^-][O_2]}{\delta\,\{D_{CN^-}[CN^-] + 4D_{O_2}[O_2]\}}$$

où

$[CN^-]$ et $[O_2]$ = concentration (en moles/ml) du cyanure et respectivement de l'oxygène dissous ;

D_{CN^-} et D_{O_2} = coefficients de diffusion du cyanure et de l'oxygène dissous $1{,}83 \times 10^{-5}$ et respectivement $2{,}76 \times 10^{-5}$ cm^2, s^{-1} ;

A = superficie en cm^2 du métal venant en contact avec la phase aqueuse.

δ = épaisseur de la couche de séparation qui varie entre 2 et 9×10^{-3} cm, en fonction de la vitesse et de la méthode d'agitation.

La vitesse est exprimée en g. équiv., s^{-1}.

La vitesse de dissolution est maximale lorsque le rapport molaire $\frac{[CN^-]}{(^-O_2)} = 6$. Si $[CN^-] \ll 6\,[O_2]$, la vitesse de cyanuration est indépendante de la concentration de l'oxygène. Au cas où $[CN^-] \gg 6\,[O_2]$, la vitesse de cyanuration est indépendante de la concentration du cyanure.

Certains ions ont le pouvoir d'accélérer (Pb^{2+}) ou de ralentir (Pb^{2+}, Fe^{2+}, S^{2-}, Zn^{2+}, Cu^{2+}, Ni^{2+}, Mn^{2+}) la vitesse de dissolution de l'or, [29-47] par la consommation de l'oxygène et du cyanure libre de la solution dans les réactions d'oxydation, la formation des cyanures complexes, l'absorption

---

[17] J. R. LAMBERT, *Canad. Min. J.*, **74**, 57 (1953).

[18] G. THOMAS, *Canada Dept. Mines Tech. Surveyes, Mines Branch Tech. Paper*, **1954**, 9.

[19] E. ABEL, *Monatsh. Chem.*, **86**, 536 (1955).

[20] A. KAKOVSKII, *Izvest. Akad. Nauk S.S.S.R., Otdel. tekhn. Nauk*, **7**, 29 (1957).

[21] K. J. CATHRO et D. F. A. KOCH, *Australasian Inst. Min. Metall. Proc.*, **210**, 111 (1964).

[22] K. J. CATHRO et D. F. A. KOCH, *J. Electrochem. Soc.*, **111**, 1416 (1964).

[23] I. A. KAKOVSKII, Proc. 6th intern. Congr. Mineral Processing, Cannes, **1963**, 125.

[24] A. N. LEBEDEV et I. A. KAKOVSKII, *Tsvetn. Metally*, **38**, 17 (1965).

[25] F. HABASHI, *J. Chem. Educ.*, **42**, 318 (1965).

[26] F. HABASHI, *Trans. Soc. Min. Eng., AIME*, **235**, 236 (1966).

[27] H. A. WHITE, *J. Chem. Metall. Min. Soc., S. Africa*, **35**, 1 (1934).

[28] H. A. WHITE, *J. Chem. Metall. Min. Soc., S. Africa*, **20**, 1 (1919).

ayant lieu sur le matériel gangue, et par la formation des pellicules à la surface du métal. [48–53]

Pour les minerais aurifères complexes où l'or figure lié aux sulfures minéraux [54–58] et qui enrobent, en tant que composants de base, des minerais argileux, [59–60] la cyanuration n'est efficiente qu'après un traitement préalable. [61–76] Tels minerais se trouvent à Baia de Arieş où

---

[29] L. Cambi, *Atti accad. nazl. Lincei, Rend. Classe sci. fis., mat. e nat.*, **24**, 129 (1958).

[30] L. A. Kakovskii et Yu B. Kholmanskikh, *Izvest. Akad. Nauk S.S.S.R., Otdel. tekhn. Nauk, Met. i Toplivo*, **1959**, 97.

[31] W. E. Johnston, *Canad. Inst. Min. Metall. Bull.*, **254**, 224 (1933).

[32] E. S. Leaver, J. A. Woolf et N. K. Karchmer, *U.S. Bioc. Mines Rept. Invest.*, **1933**, 3064, 3436.

[33] E. S. Leaver et J. A. Woolf, *U.S. Bur. Mines Tech. Paper*, **1931**, 494.

[34] N. Hedley et H. Tabachnick, *American Cyanamid. Tech. Bull.*, **1958**, 23.

[35] R. J. Lemmon, *Chem. Eng. E. Min. Rev.*, **32**, 227 (1940).

[36] M. D. Ivanovskii, *Sbornik Nauchi Trudov Inst. Tsvetnoi Metal. i Zolota*, Moscou, **27**, 52 (1957); 283 (1958).

[37] I. N. Plaksin et M. D. Ivanovskii, *Met. i Metalloved. Akad. Nauk S.S.S.R.*, **1958**, 182.

[38] J. Berard, *Anales Real Soc. Espan Fis. Quim. Sez.*, **B 61**, 375 (1965).

[39] T. Haden, *Inst. Min. Metall. Trans.*, **47**, 381 (1938).

[40] C. G. Fink et G. L. Putnam, *Amer. Inst. Min. Metall, Eng. Trans.*, **187**, 952 (1950).

[41] I. N. Plaksin et V. V. Sulova, *Sovjet. Zolotoprom.*, **1936**, 41.

[42] I. N. Plaksin et N. A. Suvorovskii, *Annaly Inst. Obshch. i neorg. Khim., Izves. Sekt. Fiz. Khim. Anal., Akad. Nauk S.S.S.R.*, **10**, 187 (1938).

[43] A. B. Beck et H. Gartell, *Austral. Inst. Min. Metall. Proc.*, **100**, 499 (1935).

[44] E. Beyers, *J. Chem. Metall. Min. Soc., S. Africa*, **37**, 37 (1936).

[45] P. F. Thompson, *Trans. Electrochem. Soc.*, **91**, 41 (1947).

[46] M. Kameda, *Sci. Rept. Research Inst. Tohoku Univ., Japan Ser. A.*, **2**, 787 (1950).

[47] V. L. Zablotskaya, *Zhur. priklad. Khim.*, **28**, 1055 (1955).

[48] I. N. Plaksin, et M. D. Ioanovskii, *Yubileinyi Sbornik Nauk. Trudov Inst. Tsvetnykh. Metal i Zolota*, **1940**, 409.

[49] N. Gritzuk, *Canad. Min. J.*, **63**, 4941 (1942).

[50] J. J. Andereyew, *Z. Electrochem.*, **19**, 667 (1913).

[51] I. N. Plaksin et A. I. Sinel'nikova, *Zolotaya Prom.*, **3**, 33 (1939).

[52] H. H. Mc. Creedy, C. C. Clark et W. A. Gow, *Canad. Dept. Mines Tech. Surveyes, Mines Branch Rept. I.R.*, **1961**, 61.

[53] M. B. Barbin, *Izvest. V.U.Z.M.V.O. S.S.S.R., Gornyi Zhur.*, **9**, 173 (1961).

[54] J. P. Dick, *Canad. Mining Met. Bull.*, **347**, 111 (1941).

[55] J. G. Hart, *Chem. Eng. Mining Rev.*, **31**, 9 (1938).

[56] H. V. Warren, W. H. White et P. Davis, *Canad. Mining Met. Bull.*, **348**, 143 (1941).

[57] C. H. Madsen, *Canad. Mining Met. Bull.*, **349**, 203 (1941).

[58] A. A. Golovin, K. A. Karasev, L. D. Sokolova et M. B. Barbin, *Trudy Ural. Politekhn. Inst. im S. M. Kirova*, **98**, 139 (1960).

[59] I. K. Skobeev, K. D. Ignatéva et I. I. Chechulina, *Nauchi. Tr. Irkutskogo Gos. Nauchn. - Issled. Inst. Redkikh Metal.*, **12**, 315 (1965).

[60] J. T. Woodcock, *Commonwealth Sci. Ind. Res. Organ. Mining Dept. Univ. Melbourne, Ore-Dressing Invest., Rept.*, **1965**, 654.

[61] J. B. Mc. Kay et J. V. Thompson, US Pat. 2, 596, 580, 13 mai 1952.

[62] F. A. Forward et A. G. Lyle, *Bull. Inst. Mining Met.*, **47**, 16 (1945).

[63] J. A. Woolf et T. A. Jackson, *US Bur. Mines Rept. Investigation*, **3425**, 15 (1938).

[64] L. A. Abel et H. W. Garbrell, *Chem. Eng. Mining Rev.*, **31**, 51 (1938).

[65] H. M. Haward, *Canad. Mining J.*, **61**, 421 (1940).

[66] Gh. Vanici et G. Matezeanu, *Studii şi Cercetări Met.*, **2**, 137 (1957).

[67] Gh. Vanici, *Studii şi Cercetări Met.*, **6**, 341 (1961).

[68] H. W. Mc. Culloch, *Gov. Met. Lab. Repub. S. Afr.*, **1966**, 28–62.

[69] J. V. Thompson, USPat, 2, 4777, 469, 26 juillet 1949.

l'extraction de l'or ne donne pas de rendements satisfaisants par le procédé actuellement employé, à savoir : flottation suivie de la cyanuration des queues qui en résultent. Pour augmenter l'extraction, R. Ripan et ses collaborateurs ont déterminé par marquage à l'or radioactif 198 les paramètres réels de la durée des opérations de flottation [77] et de cyanuration [78] des minerais.

Bodiu, [79] en étudiant le minerai et le stérile de flottation obtenu à Baia de Arieş pour établir l'influence des différentes valeurs du pH et de la nature des agents d'alcalinité additionnés ($CaOH_2$, NaOH et NH_4OH) sur la vitesse de cyanuration, est arrivé à la conclusion que les pH inférieurs à 11 n'influent que très peu sur la vitesse de dissolution de l'or, tandis que les pH supérieurs déterminent la baisse brusque de cette vitesse.

Les résultats du présent travail, qui d'ailleurs ont fait l'objet d'un patent [80], ont démontré — dans la phase de laboratoire — que la cyanuration des queues résultées de la flottation après un traitement préalable permet d'augmenter la proportion de l'extraction de l'or.

ÉTUDE EXPÉRIMENTALE

La présente étude minéralogique du minerai aurifère a porté sur des échantillons représentatifs prélevés des silos d'alimentation des métallurgies aurifères de Baia de Arieş et a comporté les analyses suivantes : granulométrie, analyses spectrales semi-quantitatives, analyses chimiques quantitatives, analyses thermodifférentielles et thermogravimétriques.

Le produit obtenu de la flottation (stérile) a été grillé en courant d'air à 550—600°.

La cyanuration des échantillons a été faite dans des verres Berzelius non recouverts, sous agitation, à la température ambiante. On a établi que pour le produit final, grillé ou non grillé, les conditions optimales de cyanuration sont les suivantes :

1. Produit non grillé (cru)

— rapport solide-liquide : 1 : 2,33 ;

— concentration du cyanure de sodium % : 0,05 ;

— concentration de l'hydroxyde de calcium % : 0,05 ;

— pH de la turbidité de la lessive : 8,25—11 ;

— durée de la cyanuration : 8 h ;

— vitesse de l'agitation : 120 *t*/mn ;

---

[70] Dorr Co, Brit. Pat. 677, 050, 6 août 1952.

[71] Gh. Vanici, *Rev. Roumaine Métall.*, **6**, 269 (1961).

[72] M. Kheruvimova, V. Angelova et Al. Boyadzhiev, *Rudodobiev Sofia*, **19**, 24 (1964).

[73] R. Carter et C. S. Samis, *Canad. Mining Met. Bull.*, **479**, 160 (1952).

[74] G. A. Walker et G. M. Lawi, *Chem. Eng. Mining Rev.*, **31**, 451 (1939).

[75] G. A. Walker, *Chem. Eng. Mining Rev.*, **32**, 122 (1940).

[76] J. Cornelius et E. K. Penrose, *Proc. Australasian Inst. Mining Met.*, **126**, 107 (1942).

[77] R. Ripan, N. Pascu et I. Todoruţ, *Rev. Min. Bucureşti*, **14**, 546 (1953).

[78] R. Ripan, N. Pascu et I. Todoruţ, *Rev. Min. Bucureşti*, **14**, 381 (1963).

[79] A. P. Bodiu, *Studii şi Cercetări Metal.*, **10**, 205 (1965).

[80] R. Ripan, N. Pascu, A. Ungureanu et V. Cordiş, Roum. Pat. 49819, 8 novembre 1967.

2. *Produit grillé*

- rapport solide-liquide : 1 : 2,33 ;
- concentration du cyanure de sodium % : 0,05 ;
- concentration de l'hydroxyde de calcium % : 0,35 ;
- pH de la turbidité de la lessive : 8,5 – 10,0 ;
- durée de la cyanuration : 8 h ;
- vitesse de l'agitation : 120 *t*/mn.

Une fois cyanurés, les échantillons ont été filtrés sous vide, puis lavés à l'eau. Ensuite la teneur en or a été déterminée aussi bien sur des épreuves initiales de matériel de flottation, que sur des résidus de la cyanuration, selon une méthode spectrochimique. Quant à la teneur en or des lessives, elle a été calculée de la différence entre la concentration de l'or des épreuves initiales et la concentration des résidus de la cyanuration.

Le pH de la turbidité des lessives de la cyanuration a été déterminé à l'aide d'un pH-mètre soviétique type L P 5.

RÉSULTATS ET DISCUSSIONS

1. *Étude minéralogique du minerai*

L'étude minéralogique a porté sur des échantillons de minerai formés de fragments d'andésite – roches éruptives minéralisées.

Les roches éruptives avaient une structure porphyrique et comportaient des phénocristaux de feldspath, d'amphibole, de séricite, d'apatite et de quartz, tous mêlés dans une pâte microlitique, formée, elle aussi, des mêmes minerais.

Sur les sections polies des échantillons on a pu constater la prédominance des minerais suivants : pyrite, marcassite, mispickel ; la blende, la chalcopyrite, la galène, la pyrrhotine, le leucoxène et la magnétite ne se rencontrent que sporadiquement, étant d'importance secondaire.

Ci-après on donne la description des minerais qui encaissent l'or, dont le mispickel en premier lieu, et la pyrite plus rarement.

Le mispickel prédomine dans les croûtes noires, dans certaines portions, sa concentration étant directement proportionnelle au degré de silicification des croûtes, ce qui témoigne aussi du degré de minéralisation de ces dernières.

Nous avons également constaté la riche teneur en mispickel des croûtes silicifiées de la surface des blocs rocheux, minerai qui diminue graduellement vers l'intérieur des fragments d'andésite, pour disparaître complètement au centre de ces fragments. La baisse de la teneur en mispickel a été aussi constatée dans la minéralisation des remous et sur la verticale, baisse qui entraîne aussi la réduction de la teneur en or de ces dernières, ce qui constitue une preuve évidente que l'or est uniquement associé au mispickel.

Le mispickel se rencontre sous forme de cristaux idiomorphes, prismatiques ou de losanges, de petites dimensions, variant de 0,075 à 0,05 mm, réunis en agrégats granulaires ou associés à la pyrite ou à la marcassite qu'ils contournent, tels des blocs dentellés, formés de cristaux disposés autour du minerai qu'ils recouvrent. L'analyse granulocytaire révèle la prédominance des granulations menues, de l'ordre des dixièmes de micron.

La pyrite est répandue aussi bien dans les cristaux de quartz de couleur noire grisâtre, que dans la masse des fragments d'andésite, répartie de manière relativement uniforme dans la structure de la roche, ou se substituant, totalement ou en partie, aux minerais pétrogéniques. Les cristaux blancs de quartz contiennent eux aussi de la pyrite, mais en quantité plus réduite. La teneur en minerai du pyrite est de 3 à 5% environ.

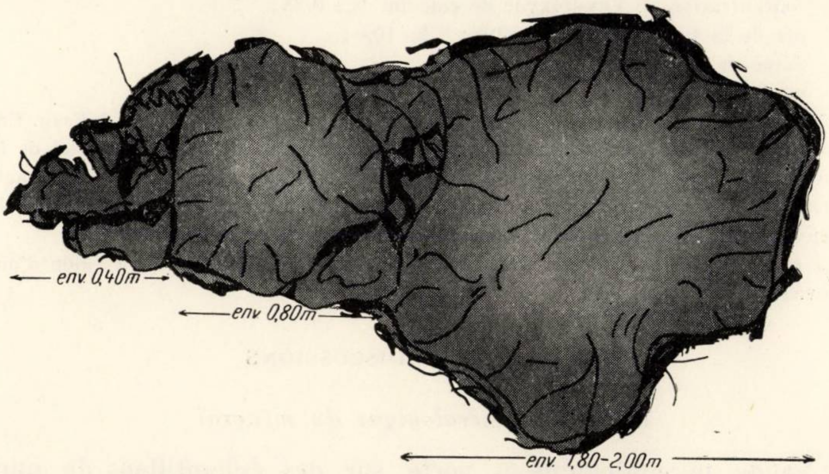

Fig. 1. — Sections dans des blocs d'andésite de différentes épaisseurs avec l'indication du degré d'imprégnation (marqué par la différence des nuances de la couleur grise). La partie centrale, à l'intérieur des blocs, colorée en blanc indique la zone stérile.

Ce sulfure se présente au cours de deux, voire même trois générations associé au mispickel, dont les cristaux le recouvrent comme une broderie, cu sous forme de cristaux idiomorphes ou hipidiomorphes recouverts de marcassite.

La classification granulométrique démontre qu'un peu plus de la moitié de la teneur en pyrite est à l'état de granulations menues (entre 0,01—0,05 mm jusqu'à 0,25 mm) et que seulement le reste des grains est de 0,25 mm.

Tableau

Analyse spectrale

N°. crt.	Élément Épreuve	Ag	Cu	Zn	Pb	V	As	Cr
1	Reversement du classeur	0,01	0,01	0,01	0,01	0,1	0,1	0,01
2	Alimentation cyanuration	0,01	0,01	t	0,01	0,1	0,1	0,01
3	Stérile final	0,01	0,01	0,01	0,01	0,1	0,1	0,01

Dans les minerais aurifères de type Baia de Arieş étudiés par nous, l'or figurait lié au mispickel, minerai qui se présente sous forme de grains très menus (la plupart de quelques dizaines de microns), en phase disperse et formant un cristallosol intimement mêlé dans le réseau cristallin minerai-hôte.

2. *Analyse granulométrique*

L'analyse granulométrique du produit improprement dénommé stérile, résultant de la flottation, a démontré que 62% du minerai broyé apparaît sous forme de grains d'une extrême finesse dont la dimension est inférieure à 0,75 mm. Conformément aux études minéralogiques cette fraction est la plus riche en or, étant donné qu'elle contient la majorité des grains menus porteurs d'or (le mispickel et, parfois, la pyrite).

Tableau 1

Analyse granulométrique du stérile de flottation

Maille de tamis/pouce	mm	Minerai g	Minerai %
30	50	—	—
60	25	4	4
100	0,15	9	9
150	0,10	5	5
200	0,075	20	20
−200	−0,075	62	62
	Total	100	100

3. *Analyse spectrale semi-quantitative*

En comparant les résultats des analyses spectrales pratiquées sur des échantillons de différente nature, à savoir : (minerai original) obtenu à partir des reversements du classeur, matériel résulté de l'opération d'alimentation-cyanuration (improprement dénommé stérile de flottation) et stérile final de la cyanuration, on a observé, excepté certains éléments, que par suite de la flottation et de la cyanuration, les concentrations de l'or ne diffèrent pas, bien que ces deux processus déterminent la séparation de quelques-uns des éléments en certaines quantités données.

2

semi-quantitative enpour-cent

Mo	Mn	Fe	Ni	Ti	Ga	Ca	Mg	Al	Si	Te
0,01	0,1	0,1	0,01	0,1	0,01	0,01	0,01	0,01	$\mathrm{fff_i}$	—
t	0,1	0,1	0,01	0,1	0,01	0,01	0,01	0,01	$\mathrm{fff_i}$	—
t	0,1	0,1	0,01	0,1	0,01	0,01	0,01	0,01	$\mathrm{fff_i}$	—

La grande majorité des éléments constituant la structure des minerais argileux qui forment la base du minerai aurifère ne peuvent être flottés et ne sont pas solubles dans les solutions de cyanure de sodium. C'est pourquoi leurs concentrations ne varient pas de manière significative par suite des opérations ci-dessus. Les autres éléments métalliques présents dans le minérai en petites concentrations à l'état de sulfures minéraux sont mis en évidence grâce à l'extrême sensibilité de la méthode d'analyse spectrale même si, partiellement, ils subissent la flottation et la cyanuration. Cette analyse vient compléter l'analyse chimique quantitative du minerai aurifère.

4. *Analyse chimique quantitative*

La teneur élevée en bioxyde de silice et en oxyde d'aluminium vient confirmer la nature argileuse des composants de base des minerais aurifères qui broyés dans une proportion de 62% en grains d'une finesse au-delà de 0,075 mm, dans un milieu alcalin de cyanure de sodium, absorbent et retiennent une partie de l'or cyanuré et du cyanure de sodium, en déterminant ainsi une baisse du niveau de l'extraction.

Tableau 3

Analyse chimique quantitative

Spécification de l'épreuve	Résultat analytique pour les éléments %											g/t	
	SiO_2	Al_2O_3	Fe_2O_3	TiO_2	CaO	MgO	As	S	Cu	Pb	Zn	Au	Ag
Minerais aurifères	60,25	15,10	3,25	0,30	0,60	0,25	0,15	2,30	0,01	0,03	0,01	7,7	2,0

Bien que les autres éléments se trouvent en concentrations réduites, quelques-uns peuvent toutefois influencer la cyanuration de l'or étant donné la consommation de l'oxygène dans la solution (Fe) et du cyanure libre, la formation de complexes cyaniques (Cu, Zn, Ni) et thiocyaniques (S), la solubilité réduite dans la lessive de cyanure du mispickel et de la pyrite, minerais porteurs d'or, et enfin la formation de pellicules à la surface du métal (FeS, $Pb(CN)_2$, CaO_2).

La cyanuration des minerais aurifères, préalablement soumis à la flottation, procédé pratiqué à Baia de Arieş, a pour résultat d'entraîner certains réactifs de flottation, tel le xantate, qui en déterminant la formation à la surface de l'or de pellicules fines empêchent l'accès du cyanure de sodium.

Tous les facteurs ci-dessus contribuent à la réduction de la proportion de l'extraction aurifère, ce qui explique pourquoi les minerais aurifères argileux, minéralisés par des minerais métalliques, sont d'habitude impropres à une extraction directe.

5. *Analyse thermodifférentielle et thermogravimétrique*

Les réactions secondaires qui accompagnent la cyanuration des minerais aurifères qui affectent tant la vitesse de dissolution que le coefficient de l'extraction de l'or peuvent être supprimées pour la plupart, excepté les phénomènes d'adsorption, par le traitement préalable du minerai. Le traitement appliqué par nous comporte le grillage du minerai ou du produit (stérile) résultant de la flottation, exposé à un courant d'air et à une température de 550 à 600°.

Par des études thermodifférentielles et thermodynamiques nous avons pu préciser la température optimale du grillage.

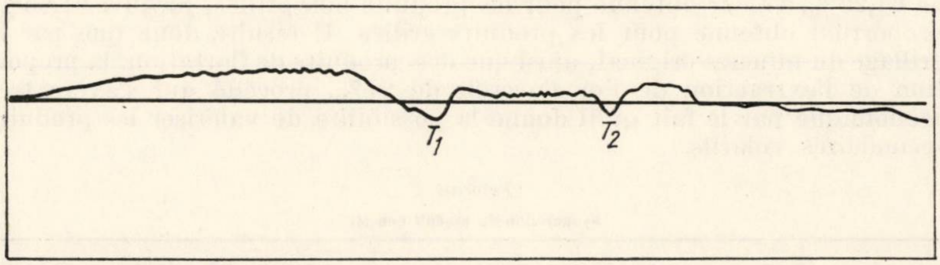

Fig. 2. — Thermogramme différentiel du minerai.
Vitesse de chauffage 2°/mn, vitesse d'enregistrement 60 mm/h ; sensibilité 0,1 mV ; T_1 = 418°, T_2 = 550°.

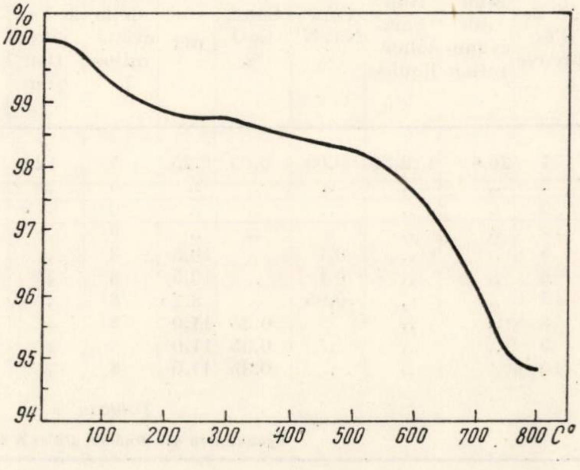

Fig. 3. — Thermogramme gravimétrique du minerai.
Vitesse de chauffage 6°/mn.

Le thermogramme différentiel met en évidence deux effets exothermiques d'intensité réduite, le premier à 418°, le deuxième à 550°. Ces deux effets marquent le début et la fin des réactions exothermiques d'oxydation des sulfures minéraux existants dans le minerai.

Le thermogramme gravimétrique permet d'observer une baisse progressive de la courbe jusqu'à 150° due à la déshydratation, après quoi les écarts de valeurs sont sans importance jusqu'à 550°, intervalle pendant lequel le soufre est graduellement éliminé sous forme de bioxyde de soufre, pour que, à 800°, la courbe décroisse brusquement de 2% à plus de 5%, par suite de la volatilisation des oxydes de zinc et d'arsenic.

Au cours du grillage des minerais aurifères étudiés par nous, les sulfures de certains éléments composants empêchent la cyanuration en phase gazeuse des produits volatils tels que le ZnO, As_2O_3, SO_2. Parallèlement, l'or sous forme colloïdale dispersé dans le réseau cristallin du mispickel, étant mis en liberté, se dissout dans la lessive de cyanure de sodium.

6. *Cyanuration des produits grillés ou non (crus) résultés de la flottation (stérile)*

La cyanuration permet d'augmenter le niveau de l'extraction de l'or de 64,22 %, valeur obtenue pour les produits non grillés, jusqu'à 91,65 %, proportion obtenue pour les produits grillés. Il résulte donc que par le grillage du minerai original, ainsi que des produits de flottation, la proportion de l'extraction de l'or s'accroît de 27 %, procédé qui s'avère très économique par le fait qu'il donne la possibilité de valoriser les produits secondaires volatils.

Tableau 4

Cyanuration du produit non grillé

N° de l'épreuve	Minerais cyanuration	Rapport solide-liquide	Conc. NaCN %	Conc. CaO %	pH	Durée de la cyanuration L	Vitesse de l'agitation t/mn	Minerai Au g/t	Résidu cyanuration Au g/t	Lessive cyanuration Au g/t	Extraction Au g/t	Extraction moyenne Au g/t
1	36,6	1 :2,33	0,05	0,05	8,25	5	120	3,8	1,4	2,4	63,1	
2	,,	,,	,,	,,	,,	5	,,	3,8	1,4	2,4	63,1	
3	,,	,,	,,	,,	,,	6	,,	3,8	1,6	2,2	58,2	
4	,,	,,	,,	,,	,,	6	,,	3,8	1,4	2,4	63,1	
5	,,	,,	0,1	,,	10,5	8	,,	3,8	1,2	2,6	68,4	64,22
6	,,	,,	0,1	,,	10,5	8	,,	3,8	1,2	2,6	68,4	
7	,,	,,	0,05	,,	8,25	8	,,	7,7	2,3	5,4	70,1	
8	,,	,,	,,	0,35	11,0	8	,,	7,7	2,7	5,0	64,9	
9	,,	,,	,,	0,35	11,0	8	,,	7,7	3.0	4,7	61,0	
10	,,	,,	,,	0,35	11,0	8	,,	6,27	2,2	4,07	64,9	

Tableau 5

Cyanuration des produits grillés à 600°

N° de l'épreuve	Minerai cyanuration	Rapport solide-liquide	Conc. NaCN %	Conc. CaO %	pH	Temps de cyanuration h	Vitesse d'agitation t/mn	Minerai Au g/t	Résidu cyanuration Au g/t	Lessive cyanuration Au g/t	Extraction Au %	Extraction moyenne Au %
1	36,6	1: 2,33	0,05	0,35	8,5	8	120	7,70	0,65	7,05	91,5	
2	,,	,,	,,	,,	,,	,,	,,	7,70	0,65	7,05	91,5	
3	,,	,,	,,	1,05	10,0	,,	,,	7,70	0,60	7,10	92,2	
4	,,	,,	,,	0,35	8,5	,,	,,	7,70	0,75	6,95	90,2	
5	,,	,,	,,	,,	,,	,,	,,	7,70	0,65	7,05	91,5	
6	,,	,,	,,	,,	10,0	,,	,,	7,70	0,25	7,45	96,7	91,65
7	,,	,,	,,	,,	8,5	,,	,,	7,70	0,50	7,20	93,5	
8	,,	,,	,,	,,	,,	,,	,,	7,70	0,80	6,90	89,6	
9	,,	,,	,,	,,	,,	,,	,,	7,70	0,75	6,95	90,2	
10	,,	,,	2	,,	,,	,,	,,	7,70	0,80	6,90	89,6	

CONCLUSIONS

1. Il a été établi que dans les minerais du type étudié par nous, l'or figure intimement mêlé au mispickel, minerai qui se présente sous forme de grains menus, en phase disperse constituant un cristallosol.

2. La plus grande partie du stérile (62 %) résulté de la flottation et qui est soumis à la cyanuration est préalablement broyé en grains d'une finesse au-delà de 0,075 mm.

3. Les analyses spectrales semi-quantitatives et les analyses chimiques quantitatives ont confirmé la nature argileuse des composants de base des minerais étudiés, qui ainsi que la majorité des éléments présents en petites concentrations déterminent un rendement réduit de l'extraction de l'or au cours de la cyanuration.

4. Par les analyses thermodifférentielles et thermogravimétriques on a établi que l'intervalle de température optimale pour le grillage des minerais aurifères s'étend de 550 à 600°.

5. L'étude de la proportion de l'extraction de l'or par cyanuration faite sur du stérile de flottation grillé et non grillé a permis d'établir que dans le premier cas, le pourcentage est en moyenne de 64 % et de 91 % dans le dernier cas. Le pourcentage de l'extraction de l'or s'accroît de 27 % et permet de valoriser les produits volatils en phase gazeuse.

Revue Roumaine de Chimie, **15**, 731–739 (1970)

COMPLEXES OF LANTHANIDE HALOGENOACETATES WITH 1,10-PHENANTHROLINE AND 2–2′-DIPYRIDYL

P. SPACU and ELENA ANTONESCU

Institute of Physical Chemistry of the Academy, Bucharest, Dumbrava Roşie, 23

Received August 19, 1969

The paper presents some new rare earth compounds with halogenoacetic acids 5,6-dimethylphenanthroline and 5-nitro-phenanthroline, as well as some new adducts of lanthanide trihalogenoacetates with piperdine. By the infrared study of [Ln (HalAc)$_3$ dipyridyl] complexes, the ultraviolet study of [Ln(HalAc)$_3$B] compounds (where B = phenanthroline, dipyridyl and phenanthroline derivatives) and a study on the fluorescence properties of Europium halogenoacetate compounds with the above cited ligands, the paper supplements also an earlier contribution.

In the previous note [1] we showed that we extended the study of rare earth compounds with aromatic amines also to some compounds with phenanthroline and dipyridyl derivatives. In the present paper in order to examine the influence of phenanthroline nucleus substituents on the formation, behaviour and stability of rare earth compounds, new compounds with 5,6-dimethyl-1,10-phenanthroline and with 5-nitro-1, 10-phenanthroline were synthetized. These ligands form with rare earth some stable compounds whose general form is [Ln(HalAc)$_3$B] where Ln = La, Pr, Sm, Eu, Er, Dy.

HalAc = CCl_3COO^- ; CCl_2HCOO^- ; $CClH_2COO^-$ and

B = 5,6-dimethyl, 1,10-phenanthroline and 5-nitro-1,10-phenanthroline.

SPECTROPHOTOMETRY

UV absorption spectra in methylic alcoholic solution were determined for complexes, for ligands with nitrogen and for mixtures of the two ligands in the ratio occurring in complexes.

From the following graphs it results that whereas absorption curve for complexes generally fits in that of nitrogenic ligands in the zone of absorption peaks, the mixture of the two ligands shows in all cases a shift of the peak situated at larger wavelengths and a vanishing of the peak situated at smaller wavelenghts. A donor-acceptor bond is doubtless

---

[1] P. Spacu and E. Antonescu, *Rev. Roumaine Chim.*, **14**, 201 (1969).

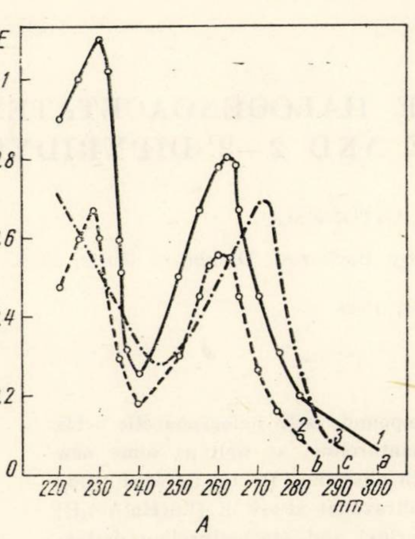

Fig. 1 A. — Absorption spectra :

1, Eu $(CCl_3COO)_3$ phen ; *2,* Phenanthroline ; *3,* $(CCl_3COO)_3$ phen.

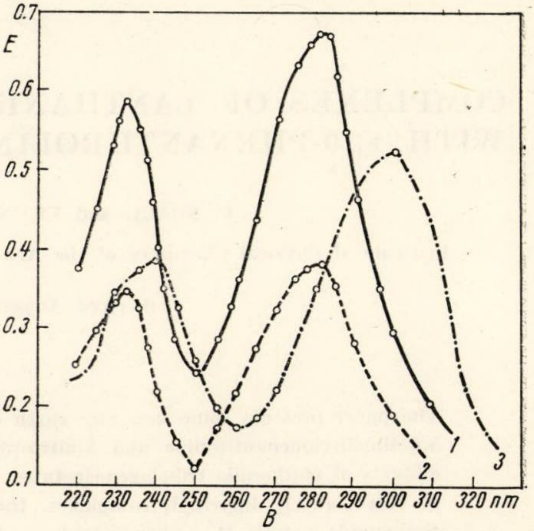

Fig. 1 B. — Absorption spectra :

1, Eu $(CCl_3COO)_3$dip $2H_2O$; *2,* Dipyridyl ; *3,* $(CCl_3COO)_3$dip.

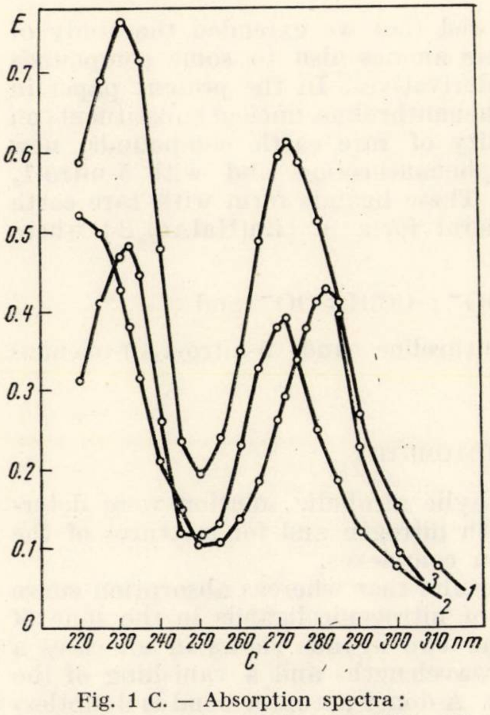

Fig. 1 C. — Absorption spectra :

1, Eu $(CCl_3COO)_3$ 5,6 $(CH_3)_2$ – 1,10 phen ; *2,* 5,6 $(CH_3)_2$ – 1,10-phenanthro line ; *3,* $(CCl_3COO)_3$ 5,6 $(CH_3)_2$ – 1,10 phen.

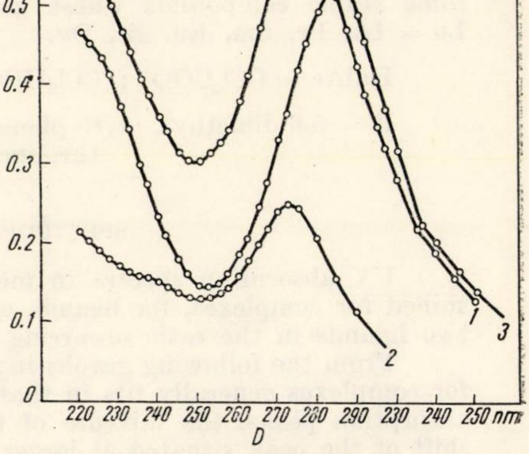

Fig. 1 D. — Absorption spectra :

1, Eu $(CCl_3COO)_3$ 4.7-diphenyl – 1,10 phen ;
2, 4,7-diphenyl – 1,10 phenanthroline ;
3, $(CCl_3COO)_3$ 4,7 diphenyl – 1,10 phen.

established between halogenoacetic acids and nitrogen-containing bases, leading to this spectral change; however the bond does not occur when lanthanide is present. This fact was considered an additional proof beside that already showed that each of the two ligands is directly bound to the lanthanide atom.

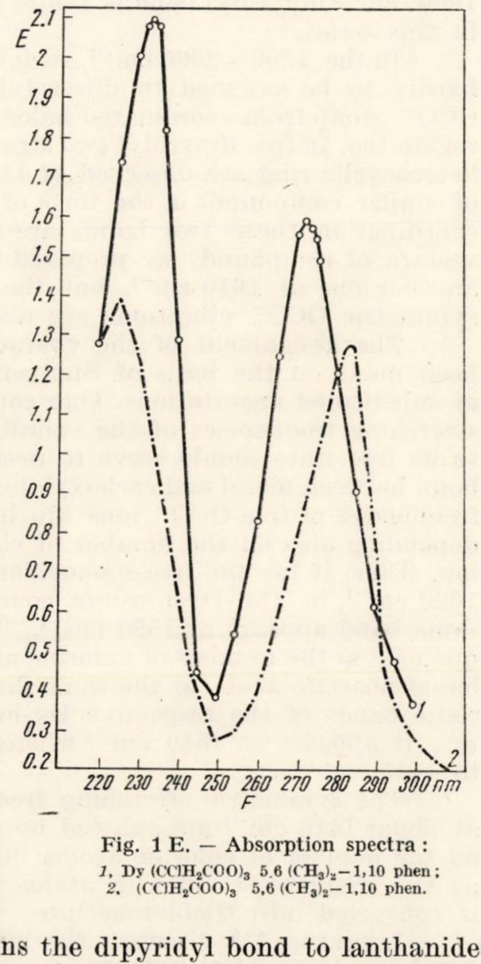

Fig. 1 E. — Absorption spectra :
1. Dy $(CClH_2COO)_3$ 5.6 $(CH_3)_2-1,10$ phen ;
2. $(CClH_2COO)_3$ 5,6 $(CH_3)_2-1,10$ phen.

Infrared spectra of $[Ln(HalAc)_3dip]$ *compounds*

The assignment of frequencies in the spectra of rare earth halogenoacetates containing dipyridyl has been made by taking into account the two kinds of ligands from the respective complex : halogenoacetic ion and dipyridyl. The sufficiently complicated shape of infrared spectra has been however explained by considering that the characteristic frequency ranges corresponding to the different vibration modes of the two ligands are generally not superposed.

The assignment of spectral bands due to coordinated dipyridyl on lanthanides has been made on the basis of Sinha [2] and Carassiti [3] works, who studied compounds of type $Lndip_2Cl_3$.

In the 700 — 900 cm^{-1} region the dipyridyl spectrum has a strong band at 755 cm^{-1} assigned to out-of-plane deformation of C — H [4]. The coordination of dipyridyl to lanthanides leads to the splitting of this band (740 — 765 cm^{-1}). A more important difference between free ligand and compound spectra which explains the dipyridyl bond to lanthanides is found in the 900 — 1200 cm^{-1} regions. Considering dipyridyl as an *ortho*-substituted pyridyne, the peak at 990 cm^{-1} in dipyridyl is assigned to the pyridine breathing mode. Due to chelation the band appears to be intensified and shifted towards higher frequencies so much the more as the ionic radius of rare earth cation has a lower value. Thus for the Sm and Eu compound a band at 1015 cm^{-1} occurs, whereas for the Dy compound the band is situated at 1020 cm^{-1}. This shift is explained by the fact that two nitrogen atmos of dipyridyl release a pair of electrons each to the central metallic atom forming a coordinate covalent bond. Owing probably to the same *ortho*-substituted pyridine vibrations the 1060 cm^{-1} dipyridyl band is found again for all compounds we prepared in this series.

---

[2] S. P. Sinha, *Spectrochim. Acta*, **20**, 879 (1964).

[3] V. Carassiti, A. Seminara and A. Seminara-Musumeci, *Ann. Chim.* (Ital.). **54**, 1025 (1964).

[4] A. A. Schilt and R. C. Taylor, *J. Inorg. Nucl. Chem.*, **9**, 211 (1959).

In the 1200—2000 cm^{-1} region the bands of the complex spectra are hardly to be assigned to dipyridyl, while bands corresponding to the OCO^- group from coordinated halogenoacetic acids are found in the same region too. In free dipyridyl two strong absorption bands generated by the heterocyclic ring are observed at 1420 cm^{-1} and 1585 cm^{-1}. The study of similar compounds in the form of Ln dip_2Cl_3 [3] shows that by dipyridyl coordination these two bands are shifted to higher frequencies. In the spectra of compounds we prepared a band appeared at 1440 cm^{-1} and another one at 1610 cm^{-1}, but the bands due to symmetric and antisymmetric OCO^- vibrations are also situated at the same frequencies.

The assignment of the characteristic OCO^- vibration bands has been made on the basis of Spinner's work [5] on the vibrational spectra of substituted acetate ions. One could expect that the perturbations of stretching frequencies of the coordinated carboxylate ion as compared to its free state should serve to measure the strength and nature of the bond between metal and carboxylate group. The antisymmetric stretching frequencies of free OCO^- ions are lowered in compounds, the shift value depending also on the number of chlorine atoms in the halogenoacetate ion. Thus, if for the free monochloroacetic acid the band is situated at 1603 cm^{-1}, in the Dysprosium compound prepared by the authors the same band appears at 1590 cm^{-1}. This band moves towards higher frequencies as the number of chlorine atoms increases in the free state of the halogenoacetic acid; to the same direction are also shifted the characteristic bands of the respective Dy-halogenoacetates : for Dy-dichloroacetate it appears at 1610 cm^{-1} whereas for the trichloroacetate it moves to 1615 cm^{-1}.

The symmetric stretching frequencis of the free OCO^- occurring at about 1416 cm^{-1} are splitted by complexation; the gap depends also on the number of chlorine atoms in the halogenoacetic ion. It decreases as the number of chlorine atoms increases, i.e. as monochloroacetate is converted into trichloroacetate.

Literature [6-8] discusses the influence of coordination on the stretching frequencies of OCO^-; four types of bonding on the carboxylate anion to the metal may be distinguished :

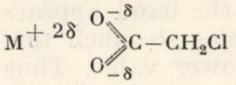

I. — Ionic bonding

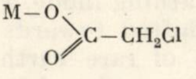

II. — Unidentate bonding

---

[5] E. SPINNER, *J. Chem. Soc.*, **1964**, 4217.

[6] K. NAKAMOTO, "Infrared Spectra of Inorganic and Coordination Compounds", J. Wiley, New York, 1963, p. 198.

[7] S. S. KRISHNAMURTHY and S. SOUNDARARAJAN, *J. Less Common Metals*, **16**, 1 (1968).

[8] S. S. KRISHNAMURTHY and S. SOUNDARARAJAN, *J. Less Common Metals*, **13**, 263 (1967).

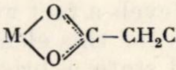

III. — Bidentate bonding

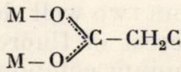

IV. — Bidentate bridge bonding

Since the unperturbed chloroacetate ion itself has a low symmetry (C_{2v}), no great differences in the infrared spectrum would be expected for the various structures. The effect due to the different metal ions would however largely depend on the structural type. In the cited works the splitting of the symmetric OCO^- stretching frequencies is explained only in terms of structure III where the chloroacetate ion is functioning as a bidentate ligand. A bridge structure as IV has been ruled out in the study on rare earth acetates by Mehrota and al.[9] and the same considerations can be expected to hold in the case of halogenoacetates too. If in a series of compounds as those studied the bonding structure were II then the antisymmetric OCO^- stretching frequencies should increase, while the symmetric OCO^- stretching frequencies should decrease as the $M-O$ bond becomes stronger. In the present study the infrared spectra of three halogenoacetates of Sm, Eu and Dy with dipyridyl were examined : the antisymmetric stretching frequency showed a small decrease in the sequence Sm >Eu >Dy, while the split symmetric stretching frequency remained almost unaltered. Undoubtedly in our compounds there is a bidentate bonding of the halogenoacetate ion to the rare-earth ion too. If the above discussed spectral perturbances of compounds compared with the free dipyridyl are also considered, it may be concluded that the dipyridyl is also directly bonded, like the halogenoacetate ion, to the rare-earth ion. Considering that the two ligands are both acting as bidentates we may state that the coordination number of $[Ln(HalAc)_3dip]$ compounds is eight.

Study of fluorescence properties

As pointed out [10–13] the ion of Europium coordinated with ligands containing oxygen or nitrogen as donors shows a very strong characteristic fluorescence when submitted to ultra-violet light. This is due to the indirect excitation of rare earth ions by intramolecular energy transfer within the chelates, from the excited electronic state of organic ligands to the 4f energy levels of coordinated rare earth ions. Crosby, Whan and Freeman[14] showed that for obtaining this energy transfer which results in fine emission, the lowest triplet state energy level of the ligands should be nearly equal to or lie above a resonance level of the considered rare earth ion. Europium presents an uncommon situation, since it shows fluorescence from two well defined resonance levels a fact which ascertains the special interest of fluorescence properties for this element.

---

[9] S. N. Misra, T. N. Misra and R. C. Mehrota, *J. Inorg. Nucl. Chem.*, **25**, 201 (1963).

[10] E. Butter and K. Kreher, *Wiss. Z.*, **4**, 881 (1965).

[11] S. P. Sinha, *J. Inorg. Nucl. Chem.*, **28**, 189 (1966).

[12] K. Kreher, E. Butter and W. Seifert, *Z. Naturforsch.*, **22b**, 3, 242 (1967).

[13] N. Filipescu, S. Bjorklund, N. McAvoy and C. R. Hurt, *Canad. J. Chem.*, **45**, 1714 (1967).

[14] G. A. Crosby, R. E. Whan and J. J. Freeman, *J. Phys. Chem.*, **66**, 2493 (1962).

Our Europium compounds show in solid state a bright red fluorescence at room temperature; this fluorescence is less intense in alcoholic solution due to the very low solubility in ethanol or methanol, and more intense in dimethylformamide where solubility is higher.

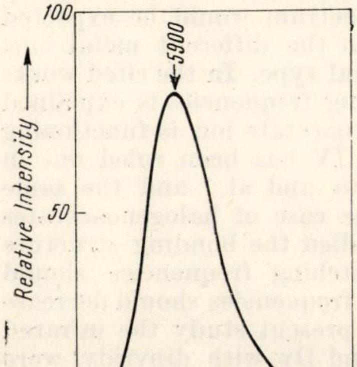

Fig. 2. — Fluorescence spectra; $Eu(CCl_3COO)_3$ dip . $2H_2O$ in solution 2×10^{-3} M (CH_3OH).

Europium chelates with phenanthroline, dipyridyl and some phenanthroline derivatives were excited in the solid state or in methanolic solution with ultra-violet light having a wavelength within the maximum absorption range of the concerned ligand; in the existing working conditions we could not obtain all the lines corresponding to $^5D_0 \rightarrow {}^7F$ transitions but only a band involving the whole range where the two $^5D_0 \rightarrow {}^7F_1$ and $^5D_0 \rightarrow {}^7F_2$ strong transitions occurred. The peak of this band was found as follows: for [$Eu(CCl_3COO)_3$phen] at 600 mμ (excitation wavelength, 265 mμ); for [$Eu(CCl_3COO)_3$ dimethyl-phen] and [$Eu(CCl_3COO)_3$dip] $2H_2O$ at 590 mμ (excitation wavelength, 296.7 mμ for dimethylphenanthroline compound and 313 mμ for dipyridyl compound); for [$Eu(CCl_3COO)_3$ diphenylphen] at 580 mμ (excitation wavelength, 296.7 mμ).

It was observed that in equally concentrated solutions, the fluorescence of phenathroline compounds increases as follows: $Eu(HalAc)_3$ phen < $Eu(HalAc)_3$ 4,7 $(C_6H_5)_2$-phen < $Eu(HalAc)_3$5,6$(CH_3)_2$ phen.

The situation was to be expected due to donor properties of CH_3-groups in *para* position, determining an increase in the electron density around the nitrogen, i.e. in the co-ordination sites of phenanthroline. Thus a better orbital overlap of ligand-metal bond is possible, and a more effective energy transfer results, with consequent increase in fluorescence.

Adducts with piperidine

As stated in an earlier work [1] the solubility of [$Ln(CCl_3COO)_3$dip] . . $2H_2O$ type compounds in piperidine is much higher than that of other similar rare-earth mono- or dichloroacetates. This fact was related to the presence of the two water molecules from trichloroacetates, which would eventually be substituted by a molecule of piperidine. Chemical analysis and ultra-violet and infrared spectra showed however that dipyridyl is substituted by three molecules of piperidine. The base substitution by piperidine does not occur in the case of mono- or dichloroacetates from the same series, as well as for the compound in the phenanthroline series. The most favourable value of Ln : CCl_3COOH : piperidine ratio as concerns stability was found to be 1 : 3 : 3, since all attempts to increase the amount of piperidine up to 1 : 3 : 4 led to easily degradable compounds. Also attempts to obtain some piperidine adducts in the same way as $[Ln(CCl_3COO)_3dip] \cdot 2H_2O$ compounds, i.e. by adding piperidine to $Ln(CCl_3COO)_3$ in alcoholic solution, always resulted in hydroxide or a gelatinous alkaline salt. The compound with piperidine was obtained indirectly from that with dipyridyl. Adducts with piperidine have been directly obtained only in the case of compounds with β-dicethones characterized by a very strong metal-ligand bond.[15,16] From rare earth chlorides some compounds with piperidine were directly obtained[17] by using anhydrous salts, but the amount of piperidine somewhat varied.

The shape of ultraviolet spectrum for the prepared piperidine compounds as compared to that of dipyridyl compounds clearly shows the substitution of dipyridyl by piperidine. Figure 3 presents the absorption spectrum of piperidine adduct. The piperidine spectrum has a slightly marked peak at 258 mμ; for the compound, the characterstic peaks of dipyridyl appearing in $[Eu(CCl_3COO)_3dip]$ spectrum are replaced by a single peak at 275 mμ.

Infrared spectra lead to the same conclusions: the bands appearing at 1440 cm^{-1} and 1610 cm^{-1} in dipyridyl compounds spectra have not been found in those of compounds with piperidine, where another band characteristic of the piperidine ring, appeared at 1340 cm^{-1}.

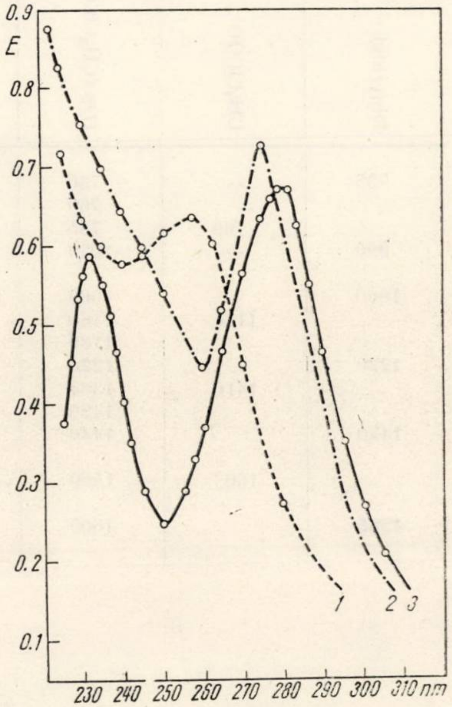

Fig. 3. — Absorption spectra:
1, Piperidine; 2, Eu $(CCl_3COO)_3$. 3 pip; 3, Eu $(CCl_3COO)_3$ dip $2H_2O$.

EXPERIMENTAL

The adducts with piperidine were prepared from $[Ln(CCl_3COO)_3dip] \cdot 2H_2O$ by adding an equivalent amount of piperidine. The resulted yellow-brown oil is dissolved in a very small amount of benzene, then the compound is extracted from the benzenic solution by adding 25 ml petroleum ether.

The complexes of the $[Ln(HalAc)_3B]$ type were prepared by adding the solid ligands (5,6-dimethyl-1,10-phenanthroline and 5-nitro-1,10 phenanthroline) in the ratio of mol/1 mol of lanthanide halogeno-acetate, dissolved in absolute ethanol at room temperature.

---

[15] R. G. Charles and R. C. Ohlman, *J. Inorg. Nucl. Chem.*, **27**, 119 (1965).

[16] E. Butter and K. Kreher, *Z. Naturforsch.*, **20 a**, 3, 408 (1965).

[17] E. M. Kirmse and U. Schilbach, *Z. Chem.*, **7**, 6, 238 (1967).

Table 1

Infrared absorption maxima (cm⁻¹)

Dipyridyl	CH_2ClCOO^-	$[Dy(CH_2ClCOO)_3dip]$	$[Dy(CHCl_2COO)_3dip]$	$[Dy(CCl_3COO)_3dip]$	Probable assignment
755	—	730	730	745	CH out-of-plane
		760	760	765	
	769	785	785	785	C−Cl
990	—	1020	1020	1020	pyridyne cycle
1060	—	1069	1069	1069	—
	1166	1160	1160	1160	
		1180	1180	1180	
1220	—	1220	1220	1220	
	1416	1385	1385	1385	OCO^- symmetric
		1420	1395	1390	
1420		1440	1442	1448	dipyridyl band
	1603	1590	1610	1615	OCO^- antisym.
1585		1605	1610	1615	dipyridyl band

Table 2

Analytical data

No	Formula of the compound	Me %		C %		H %		N %	
		calcd.	found	calcd.	found	calcd.	found	calcd.	found
1	$La(CCl_3COO)_3(CH_3)_2C_{12}H_6N_2$	16.65	16.92	28.79	28.72	1.44	1.54	3.35	3.52
2	$Pr(CCl_3COO)_3(CH_3)_2C_{12}H_6N_2$	18.85	16.71	28.72	28.67	1.44	1.75		
3	$Sm(CCl_3COO)_3(CH_3)_2C_{12}H_6N_2$	17.78	17.67	28.40	28.21	1.43	1.80		
4	$Eu\ (CCl_3COO)_3(CH_3)_2C_{12}H_6N_2$	17.93	17.92	28.34	28.38	1.42	1.75		
5	$Er(CCl_3COO)_3(CH_3)_2C_{12}H_6N_2$	19.39	19.42	27.84	27.42	1.40	1.89		
6	$Eu(CH_2ClCOO)_3(CH_3)_2C_{12}H_6N_2$	23.73	23.80	37.49	37.70	2.83	3.37	4.37	4.42
7	$Sm(CH_2ClCOO)_3(CH_3)_2C_{12}H_6N_2$	23.53	23.52	37.58	37.42	2.83	3.07	4.38	4.62
8	$Dy(CH_2ClCOO)_3(CH_3)_2C_{12}H_6N_2$	24.96	24.62	36.89	36.88	2.78	3.14	4.30	4.51
9	$Sm(CHCl_2COO)_3(CH_3)_2C_{12}H_6N_2$	20.25	20.20	32.35	32.51	2.03	2.31		
10	$Eu(CHCl_2COO)_3(CH_3)_2C_{12}H_6N_2$	20.43	20.40	32.28	32.18	2.03	2.40		
11	$Dy(CHCl_2COO)_3(CH_3)_2C_{12}H_6N_2$	21.54	21.59	31.84	31.99	2.00	2.15		
12	$Eu\ (CCl_3COO)_3NO_2 . C_{12}H_7N_2$	17.59	17.23	25.01	25.45	0.81	1.20	4.86	5.24

$(CH_3)_2C_{12}H_6N_2$ = 5,6-dimethyl-1,10-phenanthroline

$NO_2 . C_{12}H_7N_2$ = 5-nitro-1,10-phenanthroline

Spectrophotometry

The ultraviolet study was performed with a VSU-2 Zeiss-Jena spectrophotometer; the infrared study was performed with a UR-10 spectrophotometer in KBr pellets. The fluorescence spectra were recorded by a spectrofluorimeter provided with double monochromator developed at the Research Institute of Physiology, Bucharest. It was excited by a 500 W mercury lamp, reading being made with an RCA 931 A photomultiplyer fed from a stabilized 1000 ± 1 V source.

Revue Roumaine de Chimie, **15**, 731–739 (1970)

Revue Roumaine de Chimie, 15, 741–748 (1970)

L'ANALYSE ELCOTHERMIQUE – MÉTHODE D'ÉTUDE DES TRANSFORMATIONS STRUCTURALES DANS LES VERRES

S. SOLACOLU, P. BALTĂ et GEORGETA JITIANU

L'Institut de Chimie Physique de l'Académie, 23, str. Dumbrava Roşie, Bucarest,

Reçu le 13 novembre 1969

On présente une nouvelle méthode d'étude des transformations structurales des verres, aux températures supérieures à T_g : l'analyse électroconductothermique (par abréviation elcothermique), basée sur la mesure de la variation de conductivité électrique d'un échantillon de verre sous forme de disque, réchauffé à une vitesse constante dans un four électrique. Les résultats obtenus montrent qu'on peut déterminer, par cette méthode, les températures correspondant au commencement des transformations structurales (T_g), au commencement et à la fin de la cristallisation. Les études au microscope électronique font ressortir l'absence d'une relation directe entre l'aspect et les dimensions des microphases et la variation de la conductivité en fonction de la température. On présente une interprétation des inflexions qui existent dans les elcothermogrammes.

Les modifications qui ont lieu dans le verre dans le domaine dénommé « des transformations structurales » se reflètent fortement dans les propriétés de ce verre à la température normale. Ceci explique pourquoi, le long des années, de nombreuses recherches ont été consacrées à l'étude de la nature des changements qui ont lieu dans la structure du verre sous l'influence de la temperature et du temps et qui se manifestent par l'apparition d'inflexions caractéristiques sur les courbes propriété-température.

En tenant compte du fait que les propriétés électriques sont intimement liées à la structure, les auteurs ont expérimenté une série de méthodes qui permettent de suivre par l'intermédiaire de ces propriétés les transformations structurales qui ont lieu en fonction de la température.

Dans ce qui suit, on présente les résultats obtenus avec la méthode qu'on nomme par abréviation analyse elcothermique (AECT).

TRAVAUX EXPÉRIMENTAUX

Appareils et technologie

L'analyse elcothermique permet de mesurer la variation de la conductivité avec la température par l'utilisation du dispositif représenté schématiquement dans la figure 1. Ce dispositif comporte deux électrodes en platine, soutenues par deux disques en verre de silice.

Cet ensemble est posé sur un support formé d'un tube céramique. Entre les disques en platine on introduit l'échantillon de verre, sous forme d'un disque ayant le diamètre d'environ 20 mm et l'épaisseur d'approximativement 0,7 mm. Pour assurer un bon contact électrique, le système est pressé par un deuxième tube céramique, qui pèse 200 g. Le dispositif est introduit dans un four électrique ayant une résistance en Kantal et qui peut être chauffé à une vitesse réglable. Dans la présente recherche on a utilisé une vitesse de chauffage de 10°/mn. La résistance électrique du verre, dans un courant alternatif de 50 Hz, a été mesurée avec un pont électronique et après, en tenant compte des dimensions de l'échantillon, on a calculé sa résistivité.

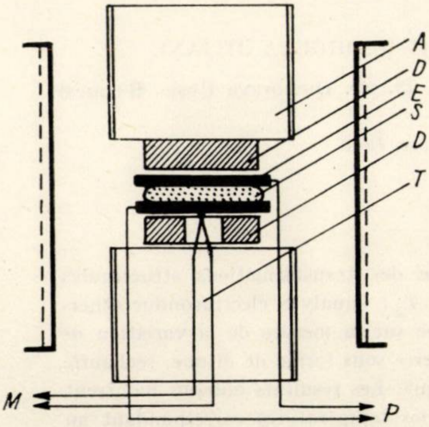

Fig. 1. — Schéma de la disposition de l'échantillon dans l'appareil pour l'analyse elcothermique.

M, millivoltmètre ; A, tube d'alumine ; D, disc du quartz ; E, électrode en platine ; S, l'échantillon ; T, thermocouple ; P, pont de mesure.

On a accordé une attention particulière aux contacts électriques. Attendu que le but de cet ouvrage était l'obtention d'informations sur les transformations structurales et pas précisément la mesure des valeurs absolues de la résistivité, on a eu soin que le métal utilisé comme contact n'influe pas sur les transformations structurales du verre aux températures élevées. C'est pourquoi on n'a pas procédé à l'argenture ou à la dorure des surface de l'échantillon, comme dans d'autres ouvrages,[1] [2] mais on a utilisé des électrodes en platine sous forme de plaques, en considérant que, de cette manière, la diffusion du métal dans le verre sera négligeable, ainsi que son influence sur la nucléation et sur la cristallisation. Le soudage des contacts directement dans l'échantillon de verre, utilisé en d'autres ouvrages [3] ne correspond pas aux buts des auteurs, parce que de cette manière on introduit un paramètre supplémentaire, qui altère la structure du verre et diminue la reproductibilité. Les échantillons de verre silico-lithique ou silico-sodique ont été obtenus en fondant dans un four électrique à silites, à approximativement 1400°, les quantités appropriées de sable quartzeux, contenant plus de 98 % de SiO_2, et de carbonates de qualité *p.a.* On a utilisé des creusets en alumine fritté et par conséquent, en analysant les verres, on a constaté la présence d'une certaine quantité de Al_2O_3, qui atteint la concentration maxima de 2,6 % dans le cas du verre de composition correspondant au disilicate de lithium (19,8 % Li_2O).

Les disques ont été obtenus en versant la fonte dans des formes en graphite. Ils ont été recuits ensuite et polis jusqu'aux dimensions mentionnées plus haut.

On a mis en corrélation la variation de la résistivité avec les résultats obtenus par l'étude des même verres aux rayons X, au spectrophotomètre d'infrarouge (UR-10), au microscope électronique (JEM-7A) et par analyse thermique différentielle.

---

[1] G. Philips et P. W. McMillan, *Glass Technol.*, **6**, 46 (1965).

[2] R. J. Charles, *J. Amer. Ceram. Soc.*, **46**, 235 (1963).

[3] B. Lengyel, *Silikatteh.*, **14**, 46 (1963).

DISCUSSION DES RÉSULTATS

Dans la figure 2 on présente les elcogrammes de quelques verres ayant des teneurs différentes en Li_2O, ainsi que des verres contenant du Na_2O. On a choisi comme coordonnées $\log \rho$ et $10^3/T$, parce que, conformément à la relation exponentielle classique (Rasch-Hinrichsen), [4] qui peut être exprimée aussi par la formule : $\log \rho = A + B/T$ on aurait dû obtenir des lignes droites, mais on obtient des courbes présentant des inflexions, déterminées évidemment par les transformations structurales qui ont lieu au-dessus de la température T_g. L'allure des courbes correspond à l'allure des courbes obtenues par différents auteurs. [1-6]

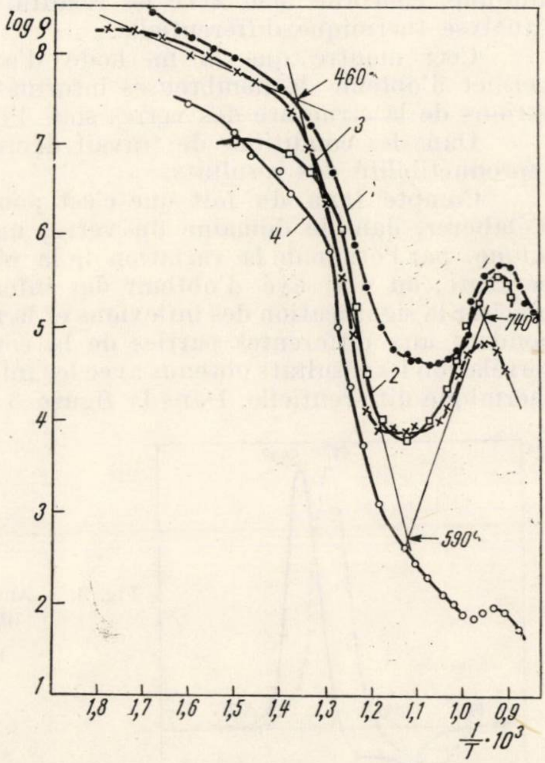

Fig. 2. — Variation du logarithme de la résistivité avec la température, pour les verres étudiés.

La première inflexion correspond à la température du commencement des transformations structurales et apparaît chez la majorité des verres.

La deuxième inflexion est attribuée au commencement de l'apparition d'une phase cristalline dans la masse vitreuse et la troisième inflexion correspond à la fin de la cristallisation. Le décalage des courbes sur la verticale met en relief le fait que, dans le cas des verres contenant du Li_2O, la valeur de la conductivité atteint un maximum à mesure que la concentration de l'oxyde alcalin augmente entre 10% et 20%.

---

[4] W. A. Weyl et E. C. Marboe, « The Constitution of Glasses », IIe vol., part. 2, Interscience Publishers, New York, 1962, p. 895.

[5] Y. Haven et B. Verkerk, *Phys. Chem. Glasses*, **6**, 38 (1965).

[6] H. Kaneko et I. O. Isard, *Phys. Chem. Glasses*, **9**, 84 (1968).

La plus grande conductivité du verre ayant la composition du disilicate de sodium doit être mise en corrélation avec la plus grande mobilité de l'ion de sodium. Le déplacement vers les températures supérieures des branches ascendantes des courbes qui présentent le déroulement du processus de cristallisation, quand la concentration en Li_2O diminue, concorde bien avec les résultats obtenus dans l'ouvrage[7] par l'analyse thermique différentielle.

Ceci montre que la méthode d'analyse elcothermique élaborée permet d'obtenir de nombreuses informations précieuses sur les modifications de la structure des verres sous l'influence de différents facteurs.

Dans les conditions de travail décrites on réalise aussi une bonne reproductibilité des résultats.

Compte tenu du fait que c'est pour la première fois qu'on essaie d'élaborer, dans le domaine du verre, une méthode d'analyse elcothermique, par l'étude de la variation de la résistivité en fonction de la température, on a essayé d'obtenir des informations supplémentaires pour préciser la signification des inflexions et la nature des processus qui correspondent aux différentes parties de la courbe. A cette fin on a mis en corrélation les résultats obtenus avec les informations fournies par l'analyse thermique différentielle. Dans la figure 3 on représente les thermogrammes du verre ayant la composition du disilicate de lithium, obtenus avec un échantillon refroidi rapidement (non recuit) et un échantillon recuit à 480°, dans les mêmes conditions que l'échantillon utilisé pour l'analyse elcothermique. La différence entre les deux courbes reflète les modifications structurales produites par le traitement thermique de recuisson. Il est évident que la courbe elcothermique doit être comparée avec le thermogramme de l'échantillon recuit.

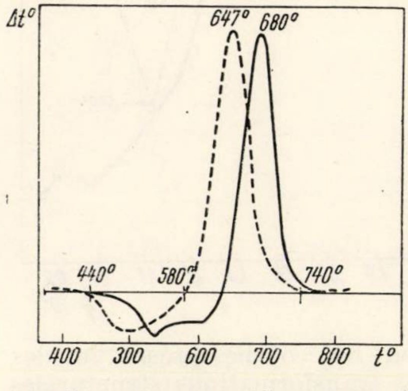

Fig. 3. — Analyse thermique différentielle de l'échantillon contenant 19,8% Li_2O.

1, non recuit; 2, recuit à 480°

En étudiant la position des points caractéristiques, c'est-à-dire : T_g (470°) le commencement de la cristallisation, respectivement le commencement de l'effet exothermique sur le thermogramme (580°) et la fin de l'effet exothermique (740°), on constate une très bonne correspon-

---

[7] S. Solacolu, P. Baltă et G. Jitianu, *Rev. Roumaine Chim.*, **15**, 91 (1970).

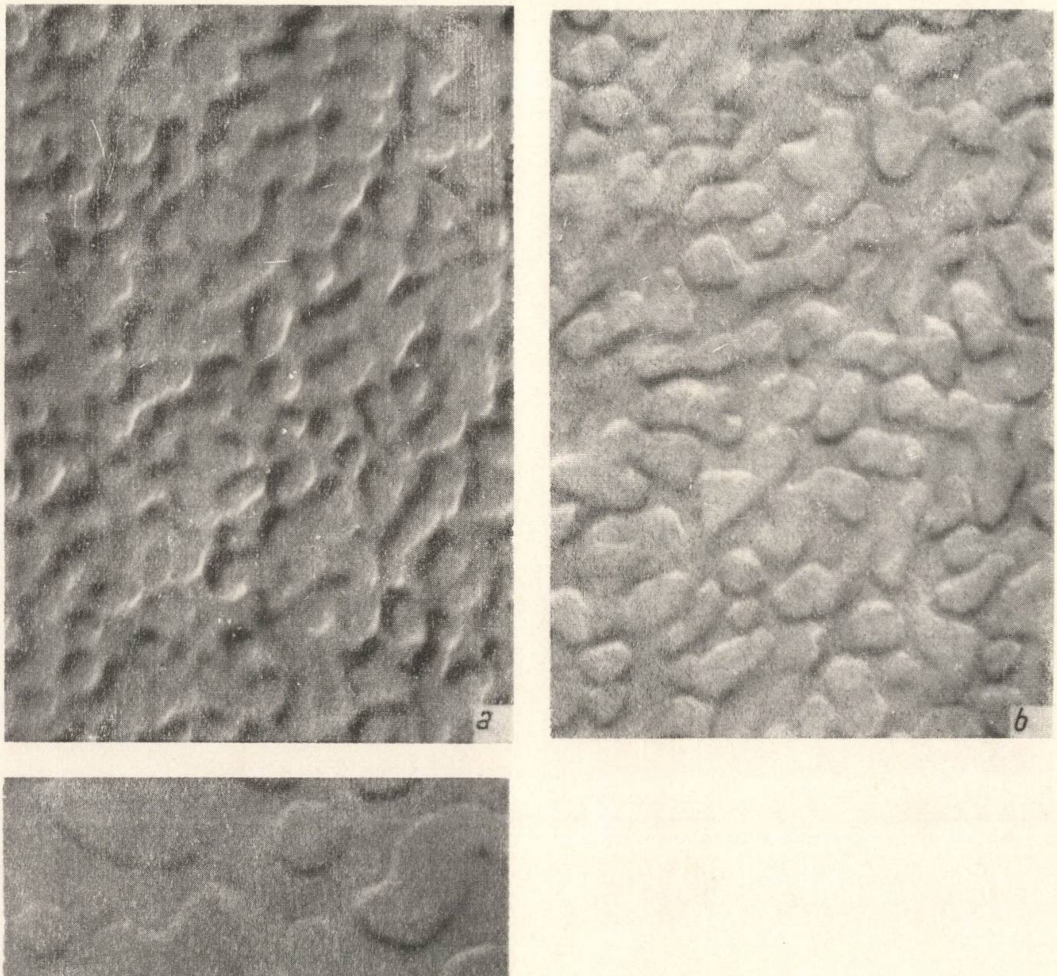

Fig. 4. — Photographies au microscope électronique des répliques des échantillons des verres contenant 10,4 % Li_2O.

a, recuit à 480° ; *b*, chauffé à une vitesse de 10°/mn jusqu'à 645° ; *c*, idem jusqu'à 805°. Grossissement × 39 000.

dance, les différences maxima entre les températures obtenues par les deux méthodes ne dépassant pas 5—10°. En tenant compte du fait que la signification des effets thermiques sur le thermogramme est bien établie [7] les résultats mentionnés plus haut représentent des arguments décisifs en ce qui concerne l'interprétation des inflexions sur l'elcothermogramme.

Les verres du domaine étudié du système Li_2O-SiO_2 présentent, comme on le sait, le phénomène intéressant de la séparation des phases. En conséquence, on a considéré utile d'étudier le mode de comportement des microphases dans les conditions de l'analyse elcothermique. A cette fin, on a chauffé des échantillons de verre contenant 10,4% de Li_2O dans le four d'analyse elcothermique, avec une vitesse constante de chauffage de 10°/mn, jusqu'aux températures choisies : la fin de la portion descendant de la courbe $\log\rho/10^3/T$, respectivement le commencement de la cristallisation (645°) et la fin de la cristallisation (805°). Après l'obtention de ces températures, on a cessé de chauffer le four et les échantillons ont été refroidis rapidement par leur évacuation du four. Les photographies au microscope électronique des répliques (platines + carbone) de ces échantillons sont présentéess dans la figure 4. Pour la comparaison on a ajouté un échantillon de verre recuit tel qu'il a été utilisé pour effectuer l'analyse elcothermique. On peut constater que les microphases grandissent sensiblement pendant les déterminations. L'augmentation des microphases est relativement petite (d'un diamètre de 512 Å à un diamètre de 680 Å), dans la période où la résistivité diminue rapidemant et assez grande dans la période correspondant à l'augmentation de la résistivité (à la cristallisation) de l'échantillon (de 680 Å à 1280 Å). Une corrélation intéressante des dimensions et de l'aspect des microphases avec les propriétés électriques (spécialement diélectriques) a été présentée par Charles. [2]

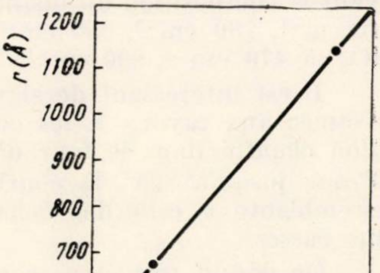

Fig. 5. — Variations du rayon moyen des microphases en fonction de $\Delta T^2.10^{-3}$ (C°).

La croissance des microphases est continuelle et elle s'accélère à mesure que la température augmente, tandis que, sur la courbe résistivité-température apparaissent les inflexions mentionnées plus haut. Ainsi qu'il résulte de la figure 5, ces résultats semblent indiquer une dépendance directement proportionnelle des rayons moyens des microphases avec le carré de la différence de température en rapport avec l'échantillon initial, la pente de la ligne droite étant inversement proportionnelle à la vitesse d'augmentation de la température. Cette corrélation peut être très utile en pratique pour estimer l'évolution des microphases existantes dans un échantillon donné, en fonction de son histoire thermique.

Il en résulte toutefois que, dans les conditions de travail des auteurs, la variation de la résistivité pendant l'analyse elcothermique ne peut être mise en corrélation simplement et directement avec la variation des dimensions et de l'aspect des microphases vitreuses, ainsi qu'on a réussi à le faire dans des conditions différentes. [2]

D'autres chercheurs [8] ont rencontré des difficultés analogues dans la corrélation des propriétés électriques avec les microphases.

Dans le cas présent, il résulte que, simultanément avec la croissance des microphases, d'autres processus structuraux ont lieu comme la diminution du degré d'ordre et aux températures plus élevées, la cristallisation, qui influe plus directement et plus fortement sur la mobilité des ions et, par conséquent, sur les propriétés électriques.

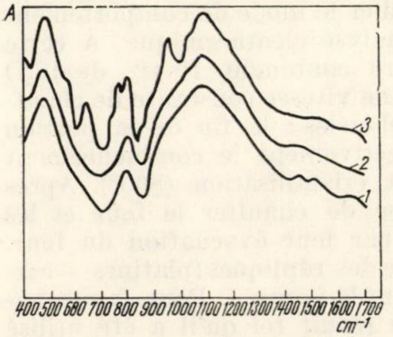

Fig. 6. — Spectres en IR du verre contenant 10,4 % Li_2O.

1, chauffé à une vitesse de 10°/mn jusqu'à 645°: 2, idem jusqu'à 895°: 3, traité thermiquement pendant 2 heures à 805°.

Pour les mêmes échantillons on a enregistré aussi les courbes d'absorption dans l'infrarouge, qui sont représentées dans la figure 6. On peut remarquer une évolution graduelle des courbes, à mesure que la température augmente vers la courbe obtenue après un traitemmet thermique de 2 heures, à 805°. Dans ce dernier échantillon, le disilicate de lithium est complètement cristallisé et à l'examen par rayons X, on décèle aussi des cristaux de spodumène, formé à cause de l'Al_2O_3 dissous du creuset dans lequel on a exécuté la fusion.

Les maxima d'absorption de cette courbe coïncident de manière satisfaisante à ceux obtenus par d'autres auteurs pour des échantillons ayant la composition du disilicate de lithium [9-11] (à 560 cm^{-1}, 640 cm^{-1}, 740 cm^{-1}, 760 cm^{-1}, 950 cm^{-1}). On observe aussi ceux correspondant à SiO_2 (à 470 cm^{-1}, 800 cm^{-1}, 1100 cm^{-1}). [10,11]

Il est intéressant de signaler que, bien qu'on puisse identifier par l'examen aux rayons X les constituants cristallisés même dans l'échantillon chauffé dans le four d'analyse elcothermique, avec la vitesse de 10°/mn, jusqu'à 805°, la courbe d'absorption dans l'infrarouge est plus ressemblante à celle des échantillons vitreux traités aux températures plus basses.

On déduit que, dans certains cas, l'analyse elcothermique (comme l'analyse thermique différentielle) est plus sensible aux transformations structurales rapides, qui ont lieu dans le verre, que la spectroscopie dans l'infrarourge.

On rencontre, encore, des difficultés dans la compréhension de la nature des transformations structurales qui déterminent l'apparition de la première inflexion (correspondant à T_g) sur la courbe $\log \rho - 10^3/T$.

---

[8] O. V. Mazurin et V. B. Borilovski, « Steklobrazovanie sostoianie », Izd. Akad. Nauk S.S.S.R., Moscou, 1963, p. 183.

[9] M. Krishna et E. M. Kriby, *J. Amer. Ceram. Soc.*, 45, 328 (1962).

[10] A. M. Kalinina, V. N. Filipovich et V. Kolesova, « Steklobrazovanie sostoianie », Izd. Akad. S.S.S.R. Moscou, 1963, p. 76.

[11] A. N. Lazarev, « Kolebetelnie spektry i stroenie silikatov », Izd. Akad. Nauk S.S.S.R., Leningrad, 1968, p. 89.

Lc conduction du courant dans les verres simples silico-alcalins est pratiquement assurée, aux températures relativement basses, par les seuls ions alcalins. Dans certains ouvrages on parle d'une dissociation électrolytique des éléments structuraux polaires $Na^+O^-SiO_{3/2}$ (Smekal, cité dans la référence [4], Müller cité dans la référence [12]), et en d'autres ouvrages, [13] on admet que quelques ions alcalins ont une plus grande mobilité que les autres. Haven et Verker, [5] en étudiant la conductivité et la diffusion des ions de sodium dans un verre binaire, arrivent à la conclusion que tous les ions de sodium participent en général en proportion égale aux deux processus. Le mécanisme de la conductivité consiste dans leur déplacement par sauts dans les lacunes et interstices du réseau. Ce mécanisme de la conductivité a été confirmé plus récemment par Kaneko et Isard. [6]

Les défauts atteignent des concentrations de jusqu'à 1% à 123° et d'approximativement 2% à 400°. La diminution plus brusque de la résistivité au-dessus de la température T_g s'explique [5] par l'augmentation plus rapide de la concentration des défauts dans cet intervalle de températures, à cause de la modification de la coordinance des ions d'oxygène non liés en pont. [14]

A la lumière des connaissances actuelles, l'inflexion qui fait l'objet de cette discussion peut être comprise ainsi que l'on indique dans les paragraphes suivants.

Conformément à la théorie de Frenkel, l'augmentation de la concentration des défauts au-dessus d'une certaine limite explique le ramollissement et la fusion du solide dans la mesure de la disproportion des liaisons chimiques. A cause de la disproportion, on peut admettre que, dans le réseau déjà désordonné du verre, apparaît un plus grand nombre d'ions alcalins plus faiblement liés. Ainsi, la dissociation électrolytique est facilitée et la concentration des ions portants de courant augmente plus rapidement qu'aux températures plus basses.

En tenant compte des estimations de Müller [15] pour les températures plus élevées, dans le domaine des transformations structurales, beaucoup moins de 1% des groupes structuraux polaires Na^+O^- doivent être dissociés électrolytiquement. Les valeurs élevées des résistivités des verres étudiées, aux températures précédant T_g, rendent possible la modification de la pente observée sur la courbe expérimentale (fig. 2), même pour une faible variation de la concentration des porteurs de courant.

Evidemment, il serait intéressant de calculer effectivement la concentration de ces porteurs de courant avant et après T_g; ceci constitue un but pour des recherches futures. On doit prendre en considération aussi la croissance parallèle de la mobilité en même temps que la croissance du volume libre.

[12] P. Tartre, *Bull. Soc. Franc. Ceram.*, **58**, 20 (1963).

[13] M. Taro, *Bull. Tokyo Inst. Technology*, **66**, 29 (1965).

[14] E. D. Lacy, *J. Amer. Ceram. Soc.*, **51**, 150 (1968).

[15] R. L. Müller, « Electricheskie sostoianie i stroenie stecla », Izd. Khimia, Moscou-Leningrad, 1964, p. 15.

Revue Roumaine de Chimie, **15**, 741–748 (1970)

La deuxième inflexion (le minimum sur la courbe) met en relief la diminution de la mobilité et de la concentration des porteurs de courant à mesure que les ions alcalins sont fixés dans les cristaux qui se forment.

La troisième inflexion (le maximum sur la courbe) est le résultat des influences en sens contraire exercées sur la mobilité des ions alcalins par le processus de cristallisation et par l'élévation du niveau de l'énergie thermique du système. A un moment donné, la diminution de la mobilité par la cristallisation est compensée et l'influence du désordre du réseau vitreux coexistant devient prédominante, sous l'influence de l'agitation thermique de plus en plus intense.

CONCLUSIONS

L'appareil et la méthode d'analyse elcothermique présentés permettent d'obtenir des informations particulièrement précieuses sur les transformations structurales qui ont lieu dans le verre aux températures supérieures à T_g.

Les résultats de l'étude des mêmes échantillons au microscope électronique indiquent le fait qu'on peut réaliser une corrélation simple, directe, entre l'aspect et les dimensions des microphases et la conductivité électrique du verre. Il paraît plus vraisemblable que cette dernière est déterminée essentiellement par d'autres facteurs structuraux plus intimes, qui influencent la mobilité des ions, comme la concentration des défauts et sa variation avec la température et le degré d'ordre de la structure.

Revue Roumaine de Chimie, **15**, 749–756 (1970)

ÉTUDE SUR LES ÉLECTRODES-MEMBRANES POLYMÈRE + PLASTIFIANT. I

L'OBTENTION ET LE COMPORTEMENT ÉLECTRODIQUE DE LA MEMBRANE DE PCV ET TRICRÉSYLPHOSPHATE SENSIBLE AUX IONS D'HYDROGÈNE

C. LITEANU et ELENA HOPÎRTEAN

Chaire de Chimie analytique, Université « Babeş-Bolyai », Cluj, 11, str. Arany János

Reçu le 14 avril 1969

Le travail présente un nouveau type d'électrode sensible aux ions d'hydrogène, consistant dans une membrane de nature organique, homogène, à base de polychlorure de vinyle et tricrésylphosphate. Le potentiel de l'électrode-membrane dépend de l'activité des ions d'hydrogène, de la nature et de la concentration des autres espèces chimiques présentes dans la solution externe, ainsi que de la température.

La première électrode-membrane employée et considérée jusqu'à présent la meilleure est l'électrode de verre (1909). [1] Cette électrode, utilisée à la mesure du pH constitue un exemple spécial d'électrode-membrane. Les électrodes de verre ont été beaucoup étudiées au début de l'année 1930 ; on a établi des rapports entre leur comportement, la structure et la composition du verre.

D'après le modèle de l'électrode de verre, de nombreux auteurs ont essayé d'obtenir d'autres électrodes spécifiques pour différents ions, de la sorte que pendant les 15 dernières années toute une série de travaux [2–8] utilisent les propriétés électrodiques des membranes échangeuses d'ions. La fonction électrodique de ces membranes permet leur emploi notamment dans les titrages potentiométriques comme électrodes indicatrices réversibles pour certains ions.

---

[1] F. Habes et Z. Klemensiewicz, *Z. phys. Chem.*, **67**, 385 (1909).

[2] J. I. Parsons, *Analyt. Chem.*, **30**, 1262 (1958).

[3] S. K. Sinha, *J. Indian Chem. Soc.*, **31**, 572 (1954) ; **32**, 25 (1955).

[4] R. Geyer et P. Nicklas, *Z. analyt. Chem.*, **177**, 166 (1960).

[5] A. S. Basu, *J. Indian Chem. Soc.*, **39**, 717 (1962).

[6] E. A. Materova et V. I. Jurchenko, *Zhur. analit. Khim.*, **16**, 388 (1961).

[7] E. Pungor, *Analyt. Chem.*, **39**, 28 A (1967).

[8] A. V. Gordievskii, E. L. Filipov, V. S. Sterman et V. V. Trizno. *Zhur. analit. Khim.*, 1164 (1965).

Le premier essai de ce genre revient à Sinha [9] qui a fait le titrage potentiométrique de l'acide chlorhydrique par l'hydroxyde de sodium, en employant comme électrode indicatrice une membrane cationique permsélective, aussi bien que par le nitrate d'argent en présence d'une électrode indicatrice consistant en une membrane anionitique.

Bien que les propriétés physiques et chimiques du verre et celles des échangeurs d'ions organiques soient essentiellement différentes, leurs propriétés électrodiques sont analogues, conditionnées par l'échange ionique phase solide-solution. La théorie de l'échange ionique sur la surface de l'électrode de verre peut être appliquée aux électrodes-membranes en résines ionitiques de sélectivité idéale. [10]

Les membranes possédant une bonne fonction électrodique, du moins entre certaines limites, peuvent servir à la détermination des activités.[2, 11–15] Des nombreux travaux parus dans la littérature il résulte que les électrodes membranes aussi bien de nature inorganique qu'organique pénètrent de plus en plus dans l'analyse chimique étant employées avec succès aussi à l'analyse des traces. [16]

Dans ce travail on présente un nouveau type d'électrode formée d'une membrane de nature organique qui peut être considérée comme homogène et dont le potentiel dépend de l'activité des ions d'hydrogène.

1. PRÉPARATION ET CERTAINES CARACTÉRISTIQUES DE LA MEMBRANE

On prépare la membrane par la plastification du polychlorure de vinyle par le tricrésylphosphate, en mélangeant dans une capsule une pâte de polychlorure de vinyle (en suspension, passée par le tamis de 4900 mailles/cm^2) et de tricrésylphosphate, en proportion de 1-PCV pour 1,8—1,9-tricrésylphosphate. La gélification de la pâte a lieu en quelques secondes, dans l'intervalle de température compris de 140 à 160°.

On a poursuivi l'obtention d'une membrane en bulle, analogue à l'électrode de verre. A cette fin la gélification a été conduite à l'extrémité d'une baguette de verre, terminée par une bulle d'environ 1 cm de diamètre.

La bulle et une portion d'environ 1 cm de longueur de la baguette, recouvertes d'une couche de pâte mince, ont été chauffées à une petite flamme de gaz, sans l'y plonger, jusqu'au moment où la pâte devient transparente. Après l'avoir maintenue 10—20 secondes à la température de gélification (140—160°), on laisse refroidir à la température ambiante et après, la membrane formée est détachée avec soin de la bulle de verre. Pour obtenir des membranes de différentes épaisseurs on peut réaliser la gélification en couches successives.

Observation. Pour les qualités physico-mécaniques de la membrane (résistance électrique, élasticité), il est très important que la fluidité de la pâte soit adéquate par le maintien du rapport optimum indiqué entre le polychlorure de vinyle et le tricrésylphosphate. A une quantité accrue de plastifiant, la membrane devient collante, difficilement détachable du support et ne présente pas une résistance mécanique satisfaisante. Au cas où la pâte est trop concentrée en polychlorure de vinyle, donc trop visqueuse, on ne peut obtenir ni de membranes minces ni de membranes d'épaisseur uniforme. Une condition importante c'est la maintien de l'intervalle de température nécessaire à une gélification rapide. A une température inférieure à 140°, la gélification n'a pas lieu dans les 10—20 secondes et à une température plus élevée il apparaît la dégradation thermique des composants de la pâte (brunissement).

---

[9] S. K. Sinha, *J. Indian Chem. Soc.*, **30**, 529 (1953).

[10] F. A. Belinskaya et E. A. Materova, *Vestnik Leningrad Univ.*, **12**, *16*, *Ser. Fiz. i Khim.*, **1957**, 3,85.

[11] A. S. Basu et S. K. Sinha, *J. Indian Chem. Soc.*, **32**, 751 (1955).

[12] A. P. Gregor et K. Sollner, *J. phys. Chem.*, **58**, 409 (1954).

[13] C. E. Marshall et H. Eyne, *J. Amer. Chem. Soc.*, **70**, 1302 (1948).

[14] B. Chaterjee et C. E. Marshall, *J. Phys. Coll. Chem.*, **54**, 671 (1950).

[15] E. A. Materova et Z. J. Alagova, *Zhur. fiz. Khim.*, **34**, 2572 (1960).

[16] G. A. Rechnitz, M. R. Kresz et Z. B. Zamochnik, *Analyt. Chem.*, **38**, 973 (1966).

Les membranes obtenues des pâtes d'une fluidité appropriée sont jaunes pâles, d'une épaisseur d'environ 0,15—0,33 mm, présentent une bonne résistance mécanique et une grande élasticité.

La conductivité spécifique des membranes $\varkappa$ a été déterminée d'après la méthode de Gregor et Sollner[17] et Manecke,[18] c'est-à-dire en courant alternatif, sans le contact des électrodes avec la membrane. Le dispositif expérimental utilisé comporte le montage de conductivité en pont d'après Kohlrausch, la cellule de conductivité étant celle utilisée dans un travail antérieur.[19] Les mesures de la résistance électrique de la membrane ont été effectuées avec la membrane à l'équilibre avec la solution de HCl 0,1 N.

Les résultats obtenus pour deux membranes, d'épaisseurs différentes, sont donnés dans le tableau 1.

Tableau 1

Influence de l'épaisseur de la membrane sur la résistance électrique

Épaisseur (mm)	Résistance électrique R_M (ohm)	Conductivité spécifique $\varkappa$ (ohm^{-1}.cm^{-1})
0,15	$1{,}74.10^5$	$1{,}97.\ 10^{-5}$
0,35	$2{,}17.10^5$	$1{,}57.\ 10^{-5}$

On peut affirmer que la membrane possède une résistance électrique plus grande, respectivement une conductivité spécifique plus faible que les membranes hétérogènes échangeuses d'ions.[20] On a observé également que la résistance électrique de la membrane introduite dans une solution de NaOH 0,1 N ne se modifie pas sensiblement.

Comportement électrodique de la membrane

L'électrode membrane a été obtenue en fixant la membrane sous forme de bulle, contenant la solution interne, à l'extrémité d'une électrode saturée de calomel (figure 1 *a*), ou à l'extrémité d'un tube en verre, le potentiel étant prélevé dans la solution interne avec un fil en platine (figure 1 *b*).

---

[17] H. P. Gregor et K. Sollner, *J. Phys. Chem.*, **50**, 53 (1946).

[18] G. Manecke, *Z. Elecktrochem.*, **55**, 672 (1951).

[19] C. Liteanu et E. Hopîrtean, *Rev. Roumaine Chim.*, **12**, 517 (1967).

[20] E. Sélegny et J. Prigent, *Bull. Soc. Chim. France*, **9**, 3615 (1968).

Le potentiel a été mesuré avec un pH-mètre MV 11 S, en utilisant la chaîne électrolytique.

(—) ESC | sol. interne | membrane | sol. externe | ESC (+)
respectivement
(—) Pt | sol. interne | membrane | sol. externe | ESC (+)

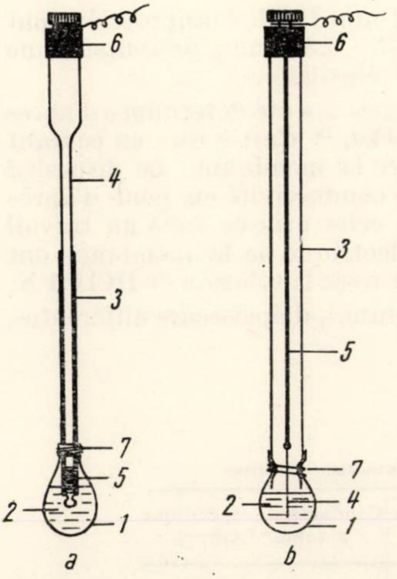

Fig. 1. — L'électrode-membrane.
1.*a* *1*, membrane; *2*, solution interne; *3*, tube en plastique; *4*, ESC; *5*, bouchon rodé; *6*, borne de contact; *7*, fil en plastique.
1.*b* *1*, membrane; *2*, solution interne; *3*, tube en verre; *4*, fil en Pt; *5*, fil en Cu; *7*, fil en plastique.

Comme solution interne on a utilisé généralement HCl 10^{-4} N et en quelques cas H_3BO_3 ou la solution tampon $CH_3COOH + CH_3COONa$ au pH = 4,57. Le potentiel de l'électrode-membrane s'établit rapidement (environ 2—4 minutes après son immersion dans la solution), étant stable dans le temps. Il faut mentionner que la membrane en forme de bulle a un potentiel d'asymétrie de 30—60 mV.

Pour l'étude de la fonction électrodique, les mesures de potentiel de l'électrode-membrane ont été effectuées parallèlement aux mesures de potentiel de l'électrode d'hydrogène, les deux électrodes étant immergées dans la même solution. Le potentiel de l'électrode-membrane a été représenté graphiquement en fonction du pH de la solution externe modifié à la suite de l'adjonction de la solution de NaOH 0,2 N. Les valeurs du pH ont été mesurées à l'aide de l'électrode d'hydrogène. Evidemment, dans la solution externe, outre l'acide étudié, il y a aussi son sel de sodium, formé à la suite de l'addition de la solution de NaOH, en vue de modifier les valeurs du pH.

Sur la figure 2 est représentée l'influence de la manière de prélèvement du potentiel dans la solution interne sur la fonction électrodique, la solution externe étant formée d'acide chlorhydrique. On remarque qu'au cas où le potentiel est prélevé dans la solution interne avec un fil en platine, la pente moyenne de la courbe ($\Delta E / \Delta \mathrm{pH} = 20{,}3$ mV) est peu différente de la pente de la courbe (22,4 mV) résultée au cas où le potentiel est prélevé à l'aide de l'électrode saturée de calomel. Le domaine de linéarité, ainsi que la pente des deux droites sont pratiquement les mêmes. Par la suite, dans tous les cas présentés le potentiel a été prélevé dans la solution interne avec l'électrode saturée de calomel.

La valeur du potentiel de l'électrode-membrane dépend, pour le même pH, de la nature des espèces chimiques présentes dans la solution externe, ce qui résulte de la figure 3 et du tableau 2 où est présentée l'influence de la nature de la solution externe sur la fonction électrodique. Pour la portion linéaire des courbes, respectivement jusqu'au pH $\simeq$ 4,7 la pente des droites ($\Delta E/\Delta \mathrm{pH}$) dépend de la nature de l'acide de la solution externe (colonne 6).

L'influence de la nature de la solution interne sur la fonction électrodique est représentée sur la figure 4 et le tableau 2.

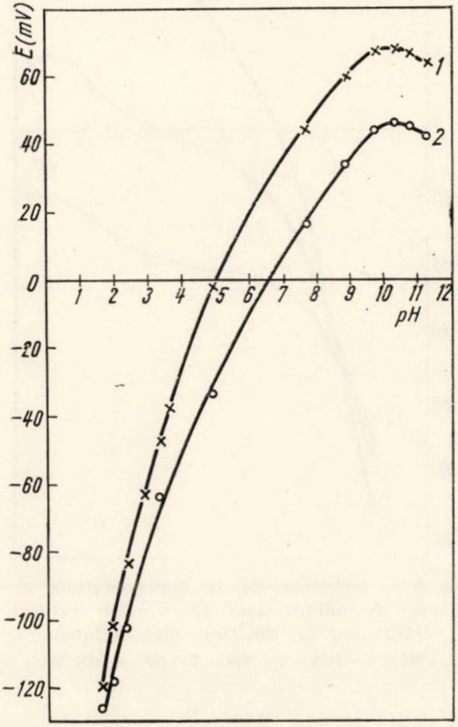

Fig. 2. — Influence de la manière de prélèvement du potentiel dans la solution interne, sur la fonction électrodique.
1 – Pt ; 2 – ESC.

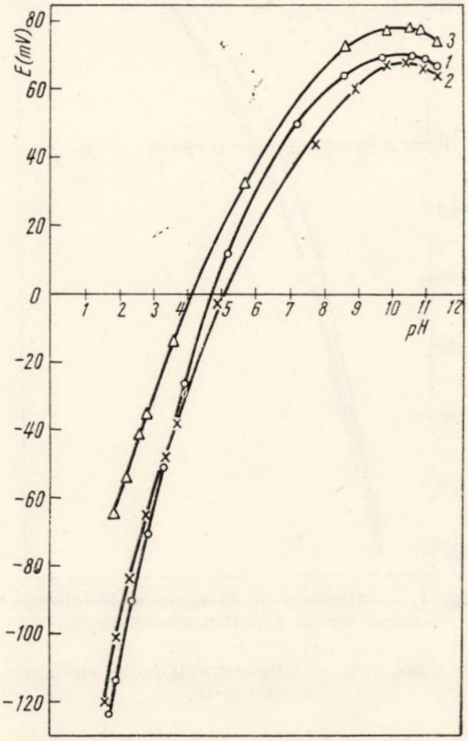

Fig. 3. — Influence de la nature de la solution externe sur la fonction électrodique.
1 – H_2SO_4 ; 2 – HCl ; 3 – $HClO_4$.

Tableau 2

Influence de la nature de la solution externe et interne sur la fonction électrodique

N° 1	Solution interne 2	Solution externe 3	Intervalle de pH 4	ΔE (mV) 5	$\Delta E/\Delta$pH(mV) 6
1	Acide borique 0,1 M	H_2SO_4	1,7–4,7	120,0	40,0
2	Acide borique 0,1 M	$HClO_4$	1,8–4,8	79,0	29,6
3	Acide borique 0,1 M	HCl	1,7–4,7	110,0	36,6
4	$CH_3COOH + CH_3COONa$ pH = 4,57	HCl	1,7–4,7	112,0	37,3
5	Acide chlorhydrique 10^{-4}N	HCl	1,7–4,7	108,0	36,0

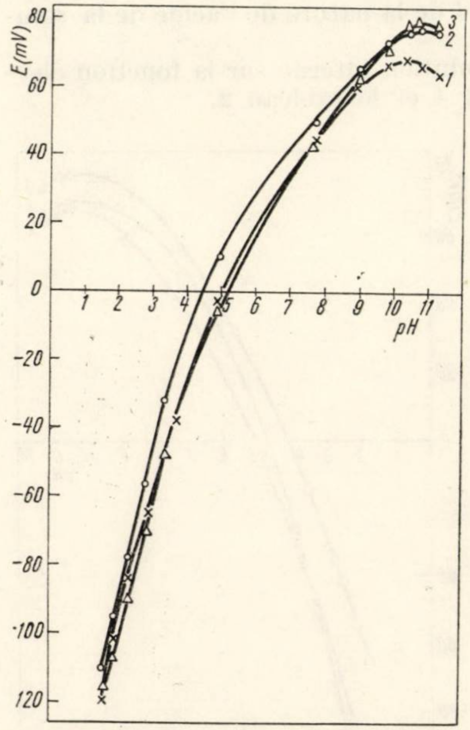

Fig. 4. — Influence de la nature de la solution interne sur la fonction électrodique.

1 – H_3BO_3 0,1 M ; 2 – $CH_3COOH+CH_3COONa$, pH = 4,57 ; 3 – HCl 10^{-4}N.

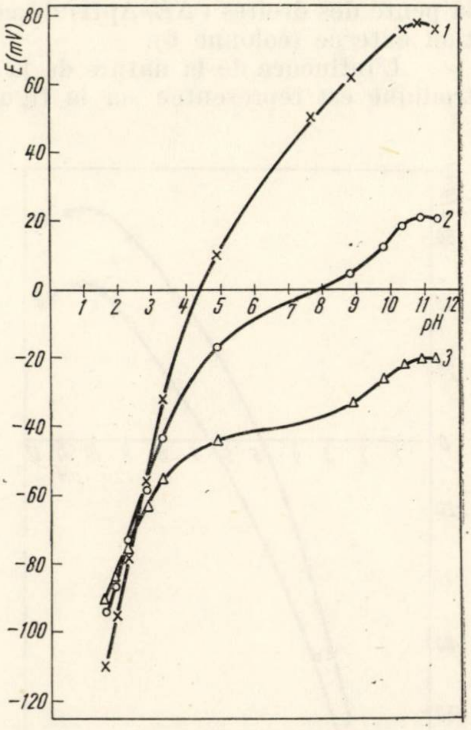

Fig. 5. — Influence de la concentration du chlorure de sodium dans la solution externe (HCl) sur la fonction électrodique.

1 – HCl ; 2 – HCl + 1% NaCl ; 3 – HCl + 10% NaCl.

On remarque que jusqu'au pH $\simeq$ 4,7 la nature de la solution interne n'a aucune influence significative sur la pente de la courbe ($\Delta E / \Delta pH$ = = 36 mV, tableau 2, colonne 6).

Une influence prononcée sur la fonction électrodique est manifestée par la concentration des électrolytes dans la solution externe (fig. 5, tabl. 3).

Tableau 3

Influence de la concentration du chlorure de sodium dans la solution externe sur la fonction électrodique

N°	Solution interne	Solution externe	Intervalle de pH	ΔE(mV)	$\Delta E/\Delta$pH(mV)
1	2	3	4	5	6
1	$CH_3COOH + CH_3COONa$ pH = 4,57	HCl	1,7–4,7	114,0	38,0
2	$CH_3COOH + CH_3COONa$ pH = 4,57	HCl + 1 % NaCl	1,7–4,0	61,0	26,5
3	$CH_3COOH + CH_3COONa$ pH = 4,57	HCl + 10 % NaCl	1.7–3,0	24,0	18,4

A mesure que la concentration du chlorure de sodium augmente dans la solution externe, le domaine du pH où il existe une dépendance linéaire entre le potentiel de l'électrode-membrane et le pH de la solution externe diminue, ainsi que la valeur du rapport $\Delta E / \Delta pH$ (tabl. 3, colonne 6). L'allure de la courbe se modifie sensiblement avec l'accroissement de la concentration du chlorure de sodium dans la solution externe. Une influence similaire sur la fonction électrodique ont aussi les oxydants ($KMnO_4$, $K_2Cr_2O_7$, Br_2) présents dans la solution externe.

On a étudié l'effet de la température sur le comportement électrodique de la membrane, en utilisant l'acide chlorhydrique aussi bien comme solution interne (10^{-4} N) qu'externe. Sur la figure 6 et le tableau 4 (colonne 7) on constate que la pente de la courbe dans la région linéaire croît avec la température. On remarque aussi que, pour les valeurs du pH supérieures à 5, le potentiel augmente avec la température.

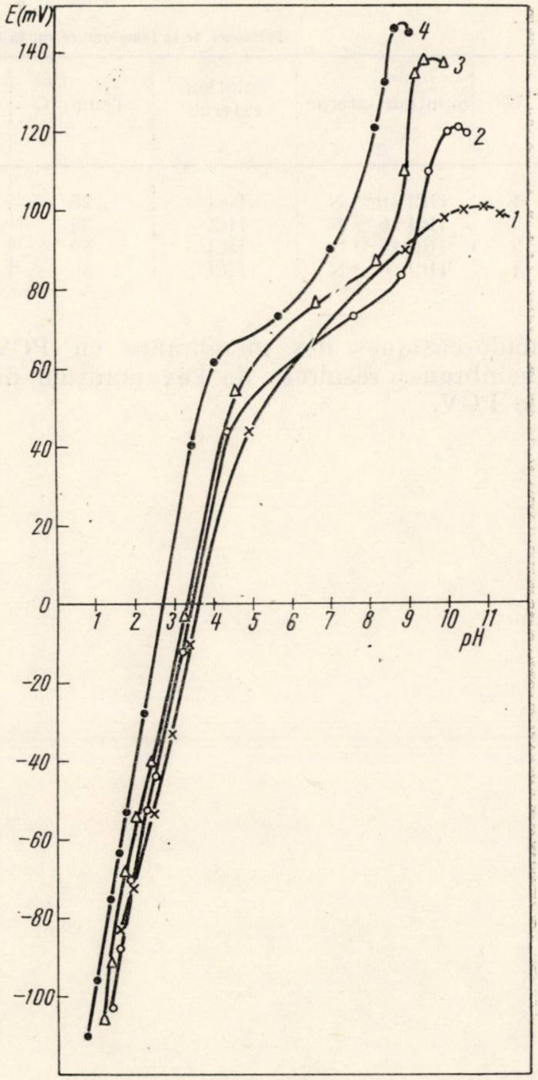

Fig. 6. — Influence de la température sur la fonction électrodique.

1–20° ; 2–30° ; 3–50° ; 4–80°.

De l'étude sur la fonction électrodique de la membrane obtenue par la plastification du polychlorure de vinyle avec du tricrésylphosphate dans les conditions mentionnées on peut conclure que pour une certaine valeur du pH le potentiel de l'électrode-membrane dépend sensiblement aussi bien de la nature et de la concentration des autres espèces chimiques présentes dans la solution externe, que de la température.

L'utilisation de cette électrode-membrane dans des titrages potentiométriques fera l'objet d'un autre travail. On étudiera également les propriétés électrodiques et l'utilisation dans les titrages potentiométriques

Tableau 4

Influence de la température sur la fonction électrodique

N° 1	Solution interne 2	Solution externe 3	Temp. °C 4	Intervalle de pH 5	ΔE (mV) 6	$\Delta E/\Delta$pH (mV) 7
1	HCl 10^{-4} N	HCl	20	1,7–4,7	120,0	40,0
2	HCl 10^{-4} N	HCl	35	1,4–4,4	148,0	49,3
3	HCl 10^{-4} N	HCl	50	1,2–4,0	146,0	52,1
4	HCl 10^{-4} N	HCl	80	0,8–3,5	152,0	56,2

acido-basiques des membranes en PCV + autres plastifiants ou des membranes résultées de l'évaporation du dissolvant dans les solutions de PCV.

Revue Roumaine de Chimie, **15**, 757–759 (1970)

DOSAGE PHOTOMÉTRIQUE DU BENZÈNE ET DE LA *m*-PHÉNYLÈNEDIAMINE

G. CIUHANDU et M. MRACEC
Laboratoire de Chimie Organique, Université de Timişoara, 4, Bd. Pârvan

Reçu le 7 août 1969

Les auteurs étudient une méthode fondée sur la conversion du benzène en *m*-phénylènediamine (*m*-PD), suivie par la copulation de celle-ci avec la bis-diazobenzidine et la photométrie du colorant à 486 nm. La sensibilité atteint 1 μg de benzène et 0,8 μg de *m*-PD. L'écart relatif : 3,4 % pour le benzène et 2,3 % pour la *m*-PD.

Au cours de leurs recherches concernant le comportement de la *m*-phénylènediamine (*m*-PD) envers certains diazoïques, Mužik et Allan ont démontré la formation des colorants dis- et tris-azoïques, même à partir de quantités équimoléculaires de diazoïque et de diamine.[1] Dans un travail antérieur, nous avons utilisé cette réaction au dosage de la *m*-PD et de quelques composés convertibles en diamine—benzène, nitro- et *m*-dinitrobenzène, *m*-nitraniline — par la copulation de la base avec la diazo-N_1, N_1-diéthylesulfanilamide, sélectionnée parmi certains dérivés de l'acide sulfanilique. La méthode [2] comporte l'extraction du tris-azoïque dans de l'alcool amylique et la photométrie à 425 nm.

Dans le présent travail, nous avons effectué la réaction avec la bis-diazobenzidine. A la suite de l'activation réciproque des deux groupements diazo, le tétrazoïque réagit aussitôt à l'une des extrémités ; mais, après copulation, l'activation par le reste aryle-azoïque faiblit sensiblement et le deuxième groupement devient beaucoup moins réactif.[3] Avec un excès suffisant de bis-diazobenzidine il résulte le trisazoïque correspondant, rouge

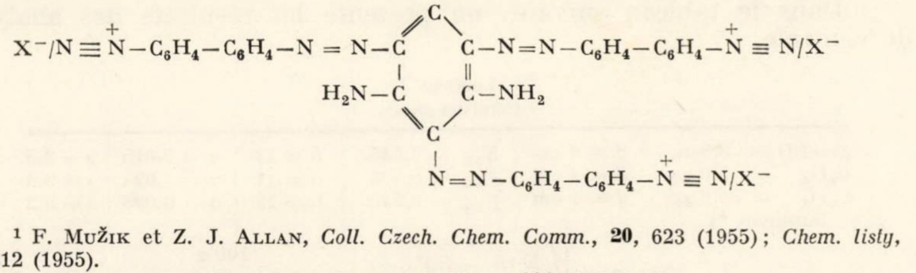
H
C
X⁻/N ≡ N⁺ – C₆H₄ – C₆H₄ – N = N – C
C – N = N – C₆H₄ – C₆H₄ – N⁺ ≡ N/X⁻
H₂N – C
C – NH₂
C
N = N – C₆H₄ – C₆H₄ – N⁺ ≡ N/X⁻

---

[1] F. Mužik et Z. J. Allan, *Coll. Czech. Chem. Comm.*, **20**, 623 (1955) ; *Chem. listy*, **49**, 212 (1955).

[2] G. Ciuhandu et M. Mracec, *Z. analyt. Chem.*, **238**, 104 (1968).

[3] H. Zollingér, « Azo and Diazo Chemistry », New York — Londres, Intersci. Publ., 1961, p. 262.

La structure d'ion de diazonium confère au colorant une solubilité en milieu aqueux, mais en même temps une certaine sensibilité envers la lumière et une relative instabilité, surtout en solution neutre ou peu acide. Pour ces raisons après la copulation rapide en milieu tamponné par de l'acétate alcalin (pH = 6—7) on rend la solution aussitôt acide (HCl, pH = 1).

La tétrazotation de la benzidine et la copulation doivent être exécutées à l'abri de la lumière, en protégeant l'éprouvette par du papier noir.

MODE OPÉRATOIRE

Le benzène est retenu dans un mélange nitrant de volumes égaux d'acide sulfurique et nitrique concentrés. Diluer 2 ml de la solution avec 5 ml d'eau, en refroidissant par de l'eau glacée, ajouter 0,5 ml de phosphate trisodique à 20%, neutraliser avec de l'hydroxyde de sodium à 20% (pH = 7,5), extraire enfin par 10, puis par 5 ml d'éther. Il faut exécuter très soigneusement la séparation de la couche aqueuse. Evaporer les extraits réunis dans une éprouvette, en portions, au bain-marie. Chauffer le résidu avec 5 ml d'eau, 1 ml d'HCl N et environ 0,2 g de Zn en poudre, pendant 15 mn au bain-marie bouillant, en agitant souvent. Refroidir, diluer à 10 ml, en filtrer 8 ml (petit filtre sec) dans une éprouvette graduée, tamponner par 1 ml d'acétate de sodium 5 M et ajouter 1 ml de *réactif tétrazo*. Agiter et, après copulation de 60 secondes, acidifier par 2 ml d'HCl 10 N, puis photométrer aussitôt.

La solution de *m*-PD (8 ml) sera traitée de la même manière.

Le *réactif tétrazo* se prépare en traitant 1 ml de benzidine à 1% en solution acétique par 1 ml d'HCl 10 N et par 1 ml de nitrite de sodium à 1% fraîchement préparé. On laisse diazoter 2 minutes (exactement) en refroidissant à l'eau courante, on ajoute quelques cristaux de sulfamate d'ammonium, on dilue à 10 ml et on utilise aussitôt.

RÉSULTATS

Le spectre (Unicam SP $_{800}$) présente un maximum à 486 nm (fig. 1).

La stabilité en milieu chlorhydrique peut être comparée à celle en milieu d'acétate-acide acétique, dans la figure 2.

La coloration est pratiquement stable pendant 60 minutes dans l'obscurité ; mais, l'altération ne peut pas être évitée à la lumière dans un intervalle plus long, tandis qu'en milieu acétique la décomposition survient vite, même dans l'obscurité.

Les courbes d'étalonnage pour le benzène et pour la *m*-PD sont tracées dans la figure 3.

Dans le tableau suivant, on présente les résultats des analyses de contrôle.

Tableau 1

Calcul des erreurs

m—PD = 3,8 µg	$d = 4$ cm	$\overline{E}_{486} = 0,645$	$n = 13$	$\sigma = 0,015$	$s = 2,3$
C_6H_6 = 8,0 µg	$d = 4$ cm	$\overline{E}_{486} = 0,705$	$n = 11$	$\sigma = 0,024$	$s = 3,4$
C_6H_6 = 30,6 µg butanone *)	$d = 1$ cm	$\overline{E}_{570} = 0,540$	$n = 12$	$\sigma = 0,028$	$s = 5,2$

$$\sigma = \sqrt{\frac{\Sigma\,(\overline{E} - E_i)^2}{n-1}} \qquad s = \frac{100\,\sigma}{\overline{E}}$$

* Photométré 5 minutes après l'addition du KOH.

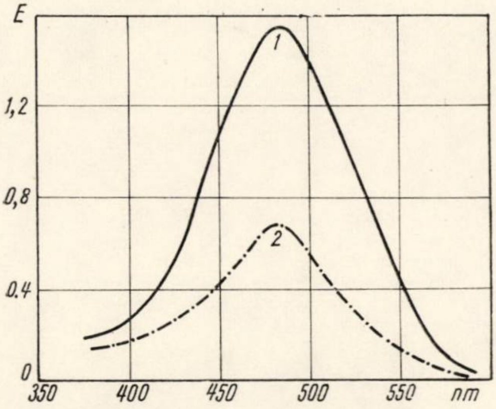

Fig. 1. — Courbes de couleur.
1, 9,8 μg *m*-PD ; *2*, 6,4 μg C_6H_6.

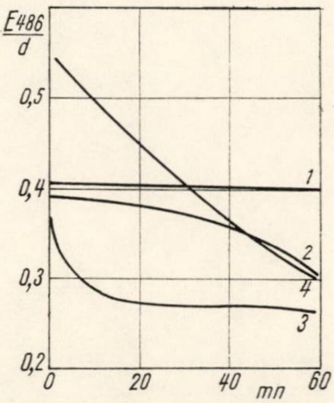

Fig. 2. — Stabilité de la coloration.
1, 9,8 μg *m*—PD en milieu chlorhydrique, dans l'obscurité ; *2*, idem, à la lumière ; *3*, 9,8 μg *m*—PD en milieu d'acétate-acide acétique dans l'obscurité ; *4*, 30,6 μg C_6H_6 dans 10 ml de butanone.

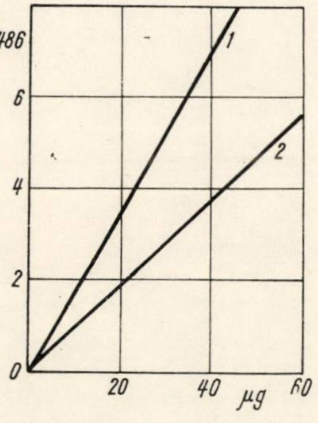

Fig. 3. — Courbes d'étalonnage.
1, *m*—PD—4 cm — 486 nm ; *2*, C_6H_6 — 4 cm — 486 nm.

Il est à remarquer que l'écart relatif de 3,4% est nettement inférieur à celui enregistré avec la butanone.

La sensibilité atteint 1 μg de benzène et 0,8 μg de *m*-PD dans une épreuve à analyser.

La méthode est avantageuse du fait qu'elle ne nécessite pas d'extraction avec des solvants organiques.

Revue Roumaine de Chimie, **15**. 761–765 (1970)

KINETIC DETERMINATION OF COBALT TRACES. II*
WITH TROPEOLINE O

D. COSTACHE and GR. POPA

Department of Analytical Chemistry, University of Bucharest,
Splaiul Independenței, 89

Received 29 July, 1969

Cobalt traces are determined according to the catalytic action of cobalt on the oxidation reaction of tropeoline O with hydrogen peroxide in an alkaline medium. The reaction rate is determined spectrophotometrically at $\lambda = 533$ mμ. The concentration range in which the method is applied is 3.25×10^{-9} – 32.50×10^{-9} g Co/cm³.

It has been previously established that cobalt traces have a catalytic effect on the oxidation rate of some organic compounds with hydrogen peroxide in alkaline medium. These compounds must have two hydroxyl groups in *ortho* position. In the speciality literature determinations of cobalt by the kinetic method and the use of dioxiderivates are well known.[1–14]

We have later found a new class of substances, namely azoderivates presenting a hydroxyl group in *ortho* position towards the azo group, the oxidizing reaction of which with hydrogen peroxide is influenced by the presence of cobalt traces. One of these methods has appeared in a former paper,[15] others are under print.

---

[*] Part I, D. Costache and P. Junie, *Rev. Roumaine Chim.*, **15**, 597 (1970).

[1] J. Bognar and O. Jellinek, *Acta Chim. Acad. Sci. Hung.*, **29**, 21 (1961).

[2] J. Bognar, *Mikrochim. Acta*, **4**, 801 (1963).

[3] E. Schulek and J. Laszlovski, *Mikrochim. Acta*, **1**, 41 (1960).

[4] N. B. Parhomenko, G. A. Prik and K. B. Iatsimirski, *Zhur. analit. Khim.*, **16**, 599 (1961).

[5] J. Laszlovski, *Mikrochim. Acta*, **2**, 269 (1961).

[6] J. Bognar, *Magyar Kem. Folyóirat*, **59**, 25 (1963).

[7] R. Kucharkowski and H. G. Döge, *Z. analyt. Chem.*, **4**, 238 (1968).

[8] V. M. Peshcova, E. K. Astakova, I. F. Dolmanova and V. M. Savostina, *Acta Chem. Acad. Sci. Hung.*, **53**, 121 (1967).

[9] A. K. Babko and N. M. Lukovskaia, *Ukrain. Khim. Zhur.*, **28**, 968 (1962).

[10] J. Bognar and O. Jellinek, *Acta Chim. Acad. Sci. Hung.*, **35**, 13 (1963).

[11] Gr. Popa and D. Costache, *Analele Universității București*, **16**, 107 (1967).

[12] Gr. Popa and D. Costache, *Rev. Roumaine Chim.*, **12**, 963 (1967).

[13] Gr. Popa and D. Costache, *Analele Universității București*, **17**, 21 (1968).

[14] D. Costache and Gr. Popa, *Analele Universității București*, **17**, 55 (1968).

[15] Gr. Popa and D. Costache, *Rev. Roumaine Chim.*, **13**, 573 (1968).

The present paper is a continuation of this study, the reactive used being of the same above mentioned class, and known under the appellation of tropeoline O.

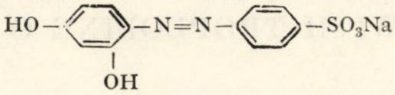

EXPERIMENTAL

Reactives: The reacting solution was obtained by solving tropeoline O in water (0.030 %).

The peroxide obtained by diluting hydrogen peroxide had a 5.018 % concentration.

The reaction medium resulted from the use of a buffer solution, obtained by solving 5 g Sorensen boric acid in 1000 cm^3 of NaOH 0.4 N.

The cobalt solution was obtained by solving spectrally pure metallic cobalt in weak sulphuric acid.

Tridistilled water was used for all solutions.

Working method: the reaction mixture was prepared in 25 cm^3 flasks in the following order and quantities: 1 cm^3 reactive, 5 cm^3 buffer solution, 2 cm^3 hydrogen peroxide and variable cobalt quantities. One brings to mark with tridistilled water. The chronometer is started, the content of the flask is well stirred and then poured into the spectrophotometer's vat, the optic density being read every minute. As a result of the oxidizing reaction, the tropeoline O, initially coloured, loses its colour so that water is transferred into the reference sample vat.

With a view to establishing optimum reaction conditions, one has undertaken some preliminary determinations: the influence of the pH, of the hydrogen peroxide's concentration, and so on.

The influence of the pH on the reaction rate is given in graph 1.

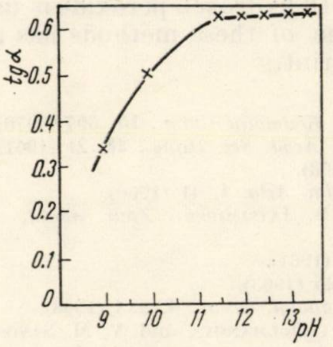

Fig. 1. — Influence of pH on reaction rate.

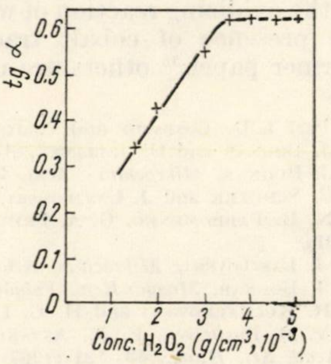

Fig. 2. — Influence of H_2O_2 concentration on reaction rate

The influence of hydrogen peroxide on the reaction rate is shown in graph 2.

It results from these graphs that the reaction rate is at its highest in the pH range 11.5—13.4 and the concentration field of H_2O_2 3.50×10^{-3} to 4.80×10^{-3} g H_2O_2/cm^3.

DISCUSSION

An essential problem of the kinetic analysis methods is the fixing of the order of reaction in view of applying correctly the kinetic relationships. The reaction order was established by the fractioning time method and the graphic method. The results have led to the conclusion that it is a matter of reactions well described by order one relationships.

Though the coloured organic reactive exists in the reaction medium, hydrogen peroxide and cobalt solution, this latter does not enter the kinetic order of the reaction, and the hydrogen peroxide concentration, compared to that of tropeoline, is such that practically it is considered constant. It results that only tropeoline O changes concentration during the reaction, and we can therefore say that we are in a case of pseudo-monomolecular reactions.

The corresponding kinetic relationship is:

$$\ln \frac{a}{a-x} = (k \cdot C_{H_2O_2} + k_C \cdot C_{H_2O_2} \cdot C_{Co})\, t \tag{1}$$

Relationship (1) shows that even in the absence of cobalt, the reaction has a certain very low rate, thus also describing the uncatalytic phenomenon. Figuring all constant terms by one constant that we shall call *k experimental*, and relating the concentration of the organic reactive to the optic density, we obtain relationship:

$$\ln \frac{D_o}{D} = k_{exp.}\, t \tag{2}$$

or

$$\ln D = \ln D_o - k_{exp.}\, t \tag{3}$$

For the determination of the cobalt we have chosen the tangent method, consisting in the graphic representation of the value ln D *versus* time (thus obtaining, according to relationship (3) straight lines); the angles made by these lines with the abcissa are determined and the value of the tangentae to these angles are represented *versus* the cobalt concentration.

Results are shown in graphs 3 and 4.

Graph 4 serves as a gauging graph. In the case of an unknown sample, the determining of the reaction rate takes place in the same way, and the unknown cobalt concentration is found out by means of the gauging graph.

We have found out the value of the rate constants *versus* the concentration of the cobalt ions by means of the relationship

$$k = \frac{\lg D_1 - \lg D_2}{t_2 - t_1} \cdot 2.303 \tag{4}$$

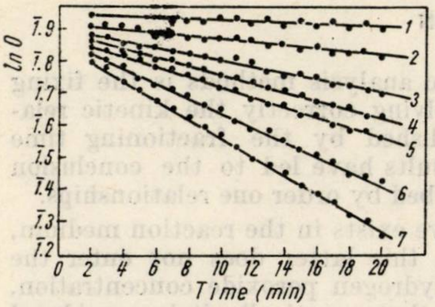

Fig. 3. — Variation in time of ln D value :

1, – g Co/cm^3; *2*, 3.25 × 10^{-9} g Co/cm^3, 8.12 × 10^{-9} g Co/cm^3; *4*, 13.00 × 10^{-9} g Co/cm^3; *5*. 16.24 × 10^{-9} g Co/cm^3; *6*, 24.36 × 10^{-9} g Co/cm^3; *7*, 32.50 × 10^{-9} g Co/cm^3.

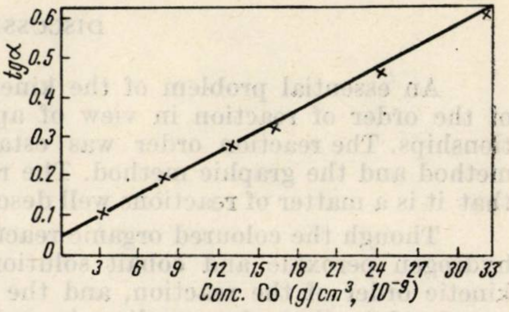

Fig. 4. — Variation of tg α value *versus* cobalt concentration.

Results are shown in table 1.

Table 1

Values of the rate constants k for different concentration of catalyst

Co. conc. g/cm^3	k (min^{-1})
—	0.53×10^{-2}
3.25×10^{-9}	1.20×10^{-2}
8.12×10^{-9}	2.25×10^{-2}
13.00×10^{-9}	3.07×10^{-2}
16.24×10^{-9}	3.77×10^{-2}
24.36×10^{-9}	5.26×10^{-2}
32.50×10^{-9}	6.87×10^{-2}

We have further studied the influence of temperature on the rate constants. Results are shown in table 2.

Table 2

Variation of the rate constant k *versus* temperature

t°C	15	20	25	30	35
$k \times 10^{-2}$ (min^{-1})	0.19	0.53	1.02	1.57	3.01

Table 2 shows that the reaction rate is greatly affected by temperature and that to avoid one of the sources of error, and obtain a good reproducibility it is necessary to keep strict thermostatic conditions during the determinations. For the present paper determinations were carried out at 20°.

We have found out that between the rate constant k, and the cobalt concentration there exists a proportionality relationship of type :

$$k = f\,(\text{conc. Co}) \tag{5}$$

By representing graphically the data of table 1, one obtains a new type of standard graph which can be used for the determination of the cobalt.

Compared to the tangent method (where tg α dependent magnitude is obtained geometrically) it presents the advantage of rapidity (k is obtained analytically).

Cobalt determinations through this method are affected by the presence of following alien ions: Ti^{4+}, Hg^{2+}, Fe^{2+}, Fe^{3+} if their ratio to cobalt exceeds 1.000 : 1.

The method's reproducibility is shown in table 3.

Table 3

Reproducibility of the method

No of determinations	Co analysed (g/cm³)	$\sphericalangle \alpha^\circ$	tg α	Co found in analysis (g/cm³ . 10^{-9}	Difference (g/cm³. 10^{-9})
	3.25×10^{-9}	6	0.105	—	—
1		6	0.105	3.25	—
2		5	0.087	2.27	0.98
3		7	0.122	4.22	0.97
4		6	0.105	3.25	—
5		6	0.105	3.25	—
	8.12×10^{-9}	11	0.194	—	—
1		11	0.194	8.44	0.32
2		12	0.212	9.74	1.62
3		11	0.194	8.44	0.32
4		10	0.176	7.47	0.65
5		11	0.194	8.44	0.32
	13.00×10^{-9}	15	0.267	—	—
1		16	0.286	13.97	0.97
2		15	0.267	13.32	0.32
3		14	0.249	12.03	0.97
4		15	0.267	13.32	0.32
5		15	0.267	13.32	0.32
	16.24×10^{-9}	18	0.324	—	—
1		19	0.344	17.54	1.30
2		18	0.324	16.24	—
3		18	0.324	16.24	—
4		19	0.344	17.54	1.30
5		17	0.305	15.27	0.97
	24.36×10^{-9}	25	0.466	—	—
1		24	0.445	23.71	0.65
2		26	0.487	25.26	1.30
3		25	0.466	24.36	—
4		25	0.466	24.36	—
5		24	0.445	25.71	0.65
	32.50×10^{-9}	31	0.600	—	—
1		30	0.577	30.87	1.63
2		32	0.624	34.12	1.62
3		31	0.600	32.50	—
4		31	0.600	32.50	—
5		29	0.554	29.90	2.60

To conclude, this method enables us to determine cobalt in the concentration range $3.12 \times 10^{-9} - 32.50 \times 10^{-9}$ g Co/cm³.

Revue Roumaine de Chimie, **15**, 767–773 (1970)

ELECTRICAL CONDUCTIVITY IN RELATION WITH DISPERSION DEGREE OF LYOPHILIC COLLOIDS. XI*

0.2 SODIUM STEARATE AQUEOUS SOLUTIONS WITH ADDITIONS OF *o*-CRESOL AND VARIOUS HYDROCARBONS

MINODORA RADU

Institute of Macromolecules of the Academy
Division of Macromolecular Physical Chemistry and Colloids
Bucharest, Splaiul Independenţei 89

Received 10 April, 1969

The influence of hydrocarbons on several physico-chemical properties of electrolytical association colloids with addition of *o*-cresol has been investigated. To this purpose the electrical conductivity and the viscosity of 0.2 M sodium stearate aqueous solutions with additions of *o*-cresol and hydrocarbons (n-decane, n-dodecane, n-hexadecane and cyclohexane) have been measured at 50 and 60°. It has been noticed that with the increase in hydrocabon concentration, the electrical conductivity decreases and the viscosity increases. The effects of *o*-cresol addition upon the electrolytical association colloids are not modified by the presence of hydrocarbons except in low concentration range of *o*-cresol (maximum viscosity range). The solubilization of the hydrocarbons increases by the addition of large *o*-cresol amounts. The presence of hydrocarbons does not change the dispersion degree of the colloidal system.

The investigations on the solubilization phenomena of various organic substances in aqueous solutions of electrolytical association colloids, have established two different sorts of solubilization.

One of them refers to non-polar constituents (hydrocarbons) added to micellar solutions; these are solubilized by penetration into the internal hydrocabon (liquid) part of the micelle.[1−11]

---

* Part X. E. Angelescu and M. Radu, *Rev. Roumaine Chim.*, **14**, 441 (1969).

[1] K. Hess, H. Kiessig and W. Philippoff, *Fette und Seifen*, **48**, 377 (1941).

[2] W. D. Harkins and H. Oppenheimer, *J. Chem. Phys.*, **16**, 1000 (1948).

[3] G. S. Hartley, *Nature*, **163**, 767 (1949).

[4] W. D. Harkins and R. Mittelmann, *J. Colloid Sci.*, **4**, 367 (1949).

[5] W. Philippoff, *J. Colloid Sci.*, **5**, 169 (1950).

[6] J. W. Smith, *Science Progress*, **39**, 292 (1951).

[7] H. B. Klevens, *J. Amer. Chem. Soc.*, **72**, 3581, 3780 (1950); **74**, 4624 (1952).

[8] B. A. Winsor, *Chem. and Ind.*, 632 (1960).

[9] I. Nakagava and K. Tori, *Kolloid-Z.*, **194**, 143 (1964).

[10] N. N. Ticurina, Z. N. Markina and P. A. Chirova, *Kolloid. Zhur.*, **30**, 443 (1968).

[11] N. Müller and R. H. Birkhahn, *J. Phys. Chem.*, **71**, 957 (1967).

The other mode of solubilization refers to polar molecules (alcohols, amines, fatty acids, etc.) that penetrate into the micelle and are orientated parallel to the micelle molecules and polar groups towards water, forming mixed micelles. [2,6–8,12,13]

At the same time, the studies carried out by means of X-ray diffraction, nuclear magnetic resonance, or other methods, have revealed the increase in the particle volume (swelling of micelles) on hydrocarbons solubilization.[1–8,11,13,14]

Therefore the change in physico-chemical properties of the electrolytical association colloids, when adding various organic substances, will be determined by the structure of molecules of solubilized substances, the added amount, their influence both on the micelles and on the dispersion medium. In this way, without changing the chemical structure of electrolytical colloids, the hydrophile-lipophile balance of the system may vary either toward hydrophile properties, or toward lipophile ones, thus changing the dispersion degree of the system.

Starting from these premises and our earlier results,[15,16] concerning the influence of added cresol on the sodium salts of higher fatty acids in the presence or absence of other substances, the present paper deals with the effects of simultaneous addition of hydrocarbons and cresol on several physico-chemical properties of 0.2 M sodium stearate solution.

With this object, 0.2 M sodium stearate solution have been investigated in the presence of *o*-cresol, added in various concentrations ranging from 0.50% to 10.66% as well as of hydrocarbons (n-decane, n-dodecane, n-hexadecane and cyclohexane) added in various amounts (the highest concentration 3.88%).

In our conditions, the concentration ratio of additions was limited by the solubilizing capacity of surfactant. To every solution with a determined concentration of cresol, various amounts of hydrocarbon were added up to the maximum possible concentration, so that the solutions should remain clear.

Taking into account that both dispersion degree and solubilization variations, are revealed by certain physical chemical properties, the electrical conductivity and viscosity have been measured at 50° and 60°.

These temperatures have been selected because only in this range, all solutions remained homogeneous and showed constant and reproducible values of electrical conductivity and viscosity.

EXPERIMENTAL RESULTS

Sodium stearate BDH and *o*-cresol p.a. FLUKA which was distilled before every series of determinations, have been used. The hydrocarbons have been purified by distillation, dried with Na wire and characterized through chromatography and refractive index.

---

[12] K. Passinen and Per Ekwall, *Acta Chem. Scand.*, **10**, 1215 (1956).

[13] J. François, B. Grilg, P. A. Spegt and A. E. Skoulios, *J. Colloid and Interf. Sci.*, **21**, 293 (1966).

[14] R. W. Mattoon, R. S. Stearns and W. D. Harkins, *J. Chem. Phys.*, **15**, 209 (1947).

[15] E. Angelescu and M. Radu, *Studii și cercetări Chim. Acad. R.P.R.* **9**, 603 (1961).

[16] E. Angelescu and M. Radu, *Rev. Roumaine Chim.*, **11**, 113 (1966).

The concentration of sodium stearate has been expressed in moles per 1 kg solution and that of additions in g addition % g solution.

The installations used for electrical conductivity, for viscosity and density have been described in previous paper.* [17]

The electrical conductivity and relative viscosity of solution *versus* hydrocarbon concentration at 60° are plotted in figures 1–4. Since the variation curves of both electrical conductivity and of relative viscosity maintain the same shape while lowering the temperature (50°), differing only as values, at 50° the values of only one solution have been plotted in the case of electrical conductivity variation (fig. 2) and of viscosity variation (fig. 4).

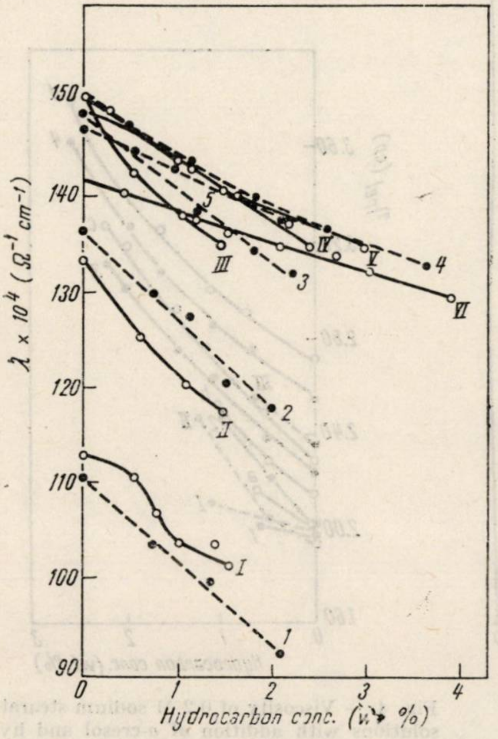

Fig. 1. — Electrical conductivity of 0.2 M sodium stearate solutions with addition of *o*-cresol and hydrocarbon : (— —) dodecane and (——) decane, *versus* hydrocarbon concentrations (60°). *o*-Cresol concentrations :

I, 1.91% ; *II*, 3.24% ; *III*, 5.48% ; *IV*, 6.94% ; *V*, 8.32% ; *VI*, 10.66% ; *1*, 1.60% ; *2*, 3.48% ; *3*, 5.40% ; *4*, 7.29% ; *5*, 8.88%.

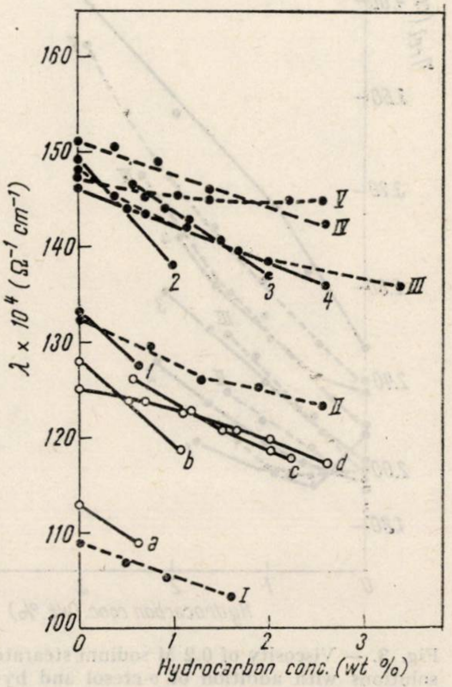

Fig. 2.—Electrical conductivity of 0.2 M sodium stearate solutions with additions of *o*-cresol and hydrocarbons: (— —) cyclohexane and (——) hexadecane ((●) at 60° and (o) at 50°) *versus* hydrocarbon concentrations. *o*-Cresol concentrations :

1 and *a*, 3.38% ; *2* and *b*, 5.21% ; *3* and *c*, 7.21% ; *4* and *d*, 9.23% ; *I*, 1.64% ; *II*, 3.08 ; *III*, 5.07% ; *IV*, 7.11%, *V* 9.53%.

Notwithstanding the amount of *o*-cresol added to the sodium stearate solution, the addition of hydrocarbon lowers the electrical conductivity and generally increases the viscosity of the system.

---

[17] E. Angelescu and M. Radu, *Rev. Roumaine Chim.*, **11**, 131 (1966).

Since the effects of *o*-cresol addition on the lyophilic character and the dispersion degree of electrolytical association colloid are already known and in order to find out the modifications induced by the addition of hydrocarbons with various number of carbon atoms in their molecule or with different molecular structure, the variation on the electrical conductivity and viscosity of solutions with 1% and 0.5% hydrocarbon addition (extrapolated values) *versus* the *o*-cresol concentration has been plotted.

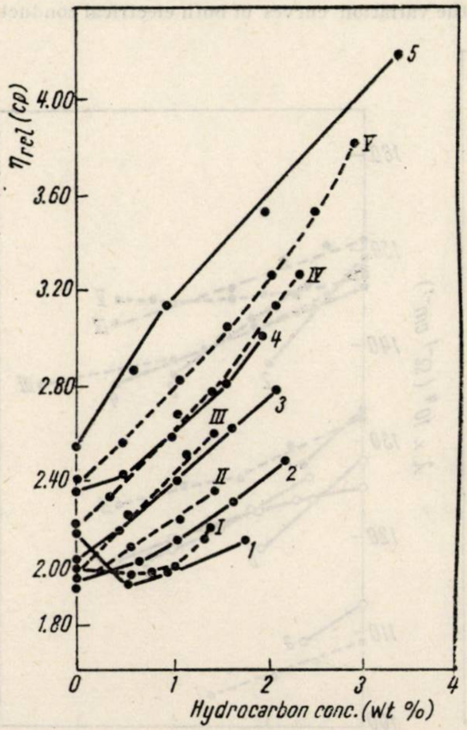

Fig. 3. — Viscosity of 0.2 M sodium stearate solutions with addition of *o*-cresol and hydrocarbons : (— — —) dodecane and (——) decane *versus* hydrocarbon concentrations (60°). *o*-Cresol concentrations :

I, 1.91% ; *II*, 3.24% ; *III*, 5.48% ; *IV*, 6.94% ; *V*, 8.32% ; *1*, 1.74% ; *2*, 3.24% ; *3*, 5.50% ; *4*, 7.23 % ; *5*, 9.13%.

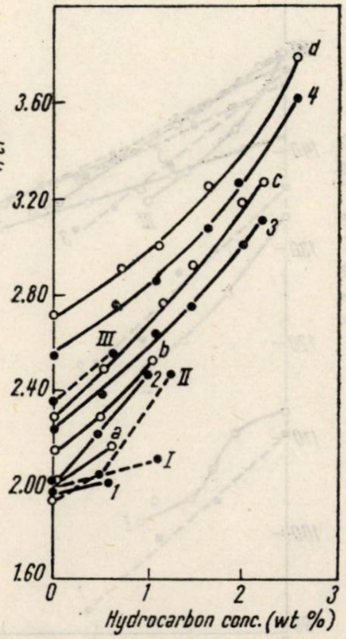

Fig. 4. — Viscosity of 0.2 M sodium stearate solutions with addition of *o*-cresol and hydrocarbons : (— — —) cyclohexane and (——) hexadecane ((●) at 60° and (○) at 50°) *versus* hydrocarbon concentrations. *o*-Cresol concentrations :

(I) 3.00% ; (II) 4.97% ; (III) 7.15% ; (1 and a) 3.38% ; (2 and b) 5.21% ; (3 and c) 7.21% ; (4 and d) 9.23%.

It has been established that irrespective of the concentration or nature of the hydrocarbon and of the temperature, the curves had the same shape. That is why, this paper shows only the graphs of the solutions with 1% or 0.5% added hydrocarbon at 60° (figures 5 and 6).

One may notice that the variation in the electrical conductivity of sodium stearate solution with *o*-cresol and hydrocarbon additions *versus* cresol concentration is similar to that of solutions without hydrocarbon addition.

The viscosity of investigated solution increases with the increase in the cresol concentrations.

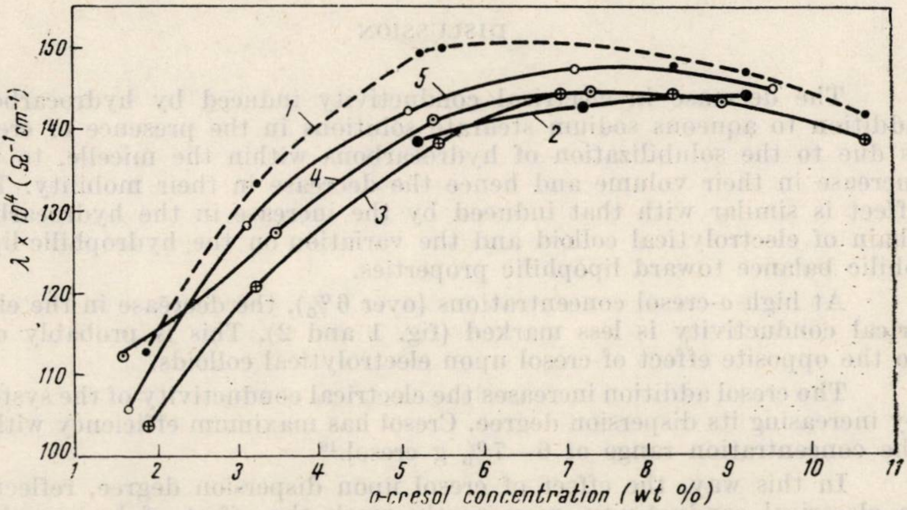

Fig. 5. — Electrical conductivity of 0.2 M sodium stearate solutions.

1, (– – –) without addition and (——) with addition; 2, hexadecane; 3, dodecane; 4, decane and 5, cyclohexane versus *o*-cresol concentration (60°).

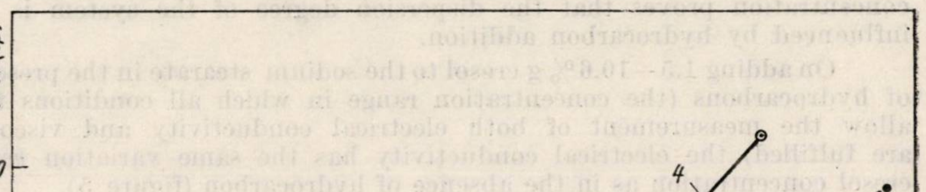

Fig. 6. Viscosity of 0.2 M sodium stearate solutions.

1, (– – –) without addition and (——) with addition; 2, hexadecane; 3, dodecane; 4, decane and 5, cyclohexane versus *o*-cresol concentration (60°).

DISCUSSION

The decrease in electrical conductivity induced by hydrocarbons addition to aqueous sodium stearate solutions in the presence of cresol is due to the solubilization of hydrocarbons within the micelle, to the increase in their volume and hence the decrease in their mobility. The effect is similar with that induced by the increase in the hydrocarbon chain of electrolytical colloid and the variation on the hydrophilic-lipophilic balance toward lipophilic properties.

At high *o*-cresol concentrations (over 6 %), the decrease in the electrical conductivity is less marked (fig. 1 and 2). This is probably due to the opposite effect of cresol upon electrolytical colloids.

The cresol addition increases the electrical conductivity of the system by increasing its dispersion degree. Cresol has maximum efficiency within the concentration range of 6 – 7 % g cresol.[16]

In this way, the effect of cresol upon dispersion degree, reflected in electrical conductivity, may partly mask the effect of hydrocarbon addition.

The linear decrease in the electrical conductivity *versus* hydrocarbon concentration proves that the dispersion degree of the system is not influenced by hydrocarbon addition.

On adding 1.5 – 10.6 % g cresol to the sodium stearate in the presence of hydrocarbons (the concentration range in which all conditions that allow the measurement of both electrical conductivity and viscosity are fulfilled) the electrical conductivity has the same variation *versus* cresol concentration as in the absence of hydrocarbon (figure 5).

Therefore, regardless of the added hydrocarbon, cresol is solubilized in micelle soap by penetration into the palissade layer of the micelle and solvates the particles, the colloidal system undergoing every consequence. [15]

However the effect upon the lowering of the electrical conductivity is the greater, the larger is the carbon number in the hydrocarbon molecule (fig. 5) : cyclohexane $<$ decane $<$ dodecane $<$ hexadecane.

Previous investigations [7,18] have pointed out that the alcohol or phenol additions increase the solubilizing ability for hydrocarbons. The investigation of 0.2 M sodium stearate with added *o*-cresol and non-polar substances confirms these results. The solubilization of hydrocarbons increases when adding several larger amounts of 7 % cresol (the solubilized hydrocarbon amount with 7 – 10 % *o*-cresol is larger than that with 1.5 % g cresol).

The increase in the hydrocarbon solubilization at high cresol concentrations may be due to the increase in the number of mixed spherical micelles (soap-cresol), an effect brought forth by the presence of cresol,[15] as well as by the easening of hydrocarbon penetration into micelle created by the presence of solvatation layer with cresol around the particles.

---

[18] P. A. Demcenco and E. P. Scorobogatco, *Ukrain. Khim. Zhur.*, **28**, 203 (1962)

In our conditions, the viscosity of solutions increases when adding hydrocarbons (fact established also in other cases,[19,20] except for the solutions with cresol concentrations smaller than 2%. *

The increase in micellar volume by hydrocarbon solubilization leads to the increase in the relative viscosity of the colloidal system. The viscosity decrease of solutions with lower cresol concentration, when adding small hydrocarbon amounts (fig. 3) is due, probably, to the change in the micelle shape, from asymmetrical micelles (the shape assumed in previous investigations about soap-water-cresol system [20]) to spherical micelles,by varying the micelle bend when solubilizing hydrocarbons. Subsequently to the addition of larger hydrocarbon amounts, the viscosity increases as is the case with all solutions with higher cresol concentrations (fig. 3 and 4).

These conclusions are supported by the relative viscosity variation *versus* cresol concentration (figure 6).

Viscosity of all solutions with added *o*-cresol and hydrocarbons is higher than that of solutions only with cresol addition (curve 1).

It is worth mentioning that even within the range of viscosity maximum ("Angelescu effect"), the hydrocarbon additions cancel the effects of cresol upon the micelles.

In the higher concentration range of added *o*-cresol, the viscosity variation (as well as the electrical conductivity variation) proves that in presence of hydrocarbons, the *o*-cresol acts undisturbedly upon the colloidal system (solubilization, increase in the dispersion degree simultaneously with external solvatation of micelles) in addition with the swelling of micelles by the concomitant solubilization of hydrocarbons.

In conclusion, the addition of hydrocarbons to the solutions of electrolytical association colloids in the presence of *o*-cresol, does not modify the dispersion degree of the system, bringing about but some changes in the shape of micelles within the range of lower cresol concentrations.

---

* Solutions with added hexadecane and cyclohexane could not be prepared otherwise than with cresol concentrations higher than 3%.

[19] A. B. Chinnikova, Z. N. Markina and N. Z. Kostova, *Kolloid. Zhur.*, **30**, 613 (1968).

[20] E. Angelescu and G. Popescu, *Kolloid-Z.*, **1**[illegible]**1**, 130 (1963).

Revue Roumaine de Chimie, 15, 775–782 (1970)

SURFACE-ACTIVE CATIONIC SUBSTANCES OF THE TYPE ALKYL-ETHER-TRIMETHYL-AMMONIUM AND ALKYL-ETHER-PYRIDINIUM HALIDES. II*)

STUDY ON THE MICELLE FORMATION OF THE DODECYL-POLYOXIETHYLENE-TRIMETHYL-AMMONIUM AND DODECYL-POLYOXIETHYLENE-PYRIDINIUM CHLORIDES

I. MÂNDRU

Bucharest University, Faculty of Chemistry, Bd. Republicii 13

Received August 6, 1969

The micelle formation of the dodecyl-polyoxyethylene-trimethyl-ammonium chlorides and of the dodecyl-polyoxyethilene-pyridinium chlorides has been studied. The presence of one or several — OCH_2CH_2 — groups between the alkyl chain and the ionic head group brings about the decrease in CMC as against the compounds lacking these groups. Due to this decrease a certain hydrophobic value has been assigned to each oxyethylene group, and that has been expressed by the number of carbon atoms determining the same CMC lowering as the oxiethylene groups. Considering these groups as part of the hydrophobic group of the amphiphile molecule, one has suggested the supplementing of Klevens relation about the variation of CMC by the number of carbon atoms with the corresponding hydrophobic values for the compounds of the type alkyl-polyoxyethylene-trimethyl-ammonium respectively pyridinium halides.

The amphiphile molecules made up of a nonpolar, hydrocarbon part and a polar part, in a solution of a certain concentration called the critical micellar concentration (CMC) are able to form supramolecular aggregates called association micelles.

The association ability of these molecules is determined by the nature and size of the nonpolar part (alkyl chain) as well as by the nature of the polar part.

For a given polar part CMC is function either of the length of the alkyl chain or of the number of carbon atoms.

Several works [1-4] showed that the decrease in the CMC occurs concomitantly with the increase in the number of carbon atoms. Kle-

---

*) First part : I. Mândru, *Rev. Chim.* (Bucharest), in press.

[1] A. Lottermoser and F. Püschel, *Kolloid-Z.*, **63**, 175 (1933).

[2] J. Stauff, *Z. phys. Chem.* (*Leipzig*), **A183**, 55 (1938).

[3] H. B. Klevens, *J. Phys. and Colloid Chem.*, **52**, 130 (1948).

[4] H. V. Tartar and A. L. Lelong, *J. Phys. Chem.*, **59**, 1185 (1955).

vens[5] has found out of experimental data the following relation between CMC and the number of carbon atoms for the ionic salts with normal paraffinic radical

$$\lg \mathrm{CMC} = A - Bm \tag{1}$$

where A and B are the constants for a homologue series and a given temperature and m is the number of carbon atoms in the normal paraffinic chain.

Subsequently relation (1) has been also theoretically inferred [6,7] as follows

$$\ln \mathrm{CCM} = -\frac{mw}{kT} - K_g \ln C_i + K_1 \tag{2}$$

where m — number of carbon atoms in the alkyl chain;
w — change in the free cohesion energy of a methylene group while passing from solution into micelle;
C_i — total concentration of counterions equal to CMC + C_s, C_s being the concentration of the added salt, in mol/1;
K_g — a constant.

Equation (1) has been checked up both for nonionic surfactants [8–10] up to C_{12}, with hydrophilous group of the same length, and for the amphoteric surfactants of the type alkyl-betaines,[11] alkyl-dimethyl-amino-propane-sulfonates [12] and also in the case of alkyl-dimethyl-amino-oxides.[13]

Shinoda [7] has noticed that relation (1) of the CMC variation with the number of carbon atoms is no longer applied in the case of hexadecyl-ether-sodium sulfates considered by Weil and collab.[14]

Within the present paper there was determined the critical micellar concentration of the n-dodecyl-polyoxiethylene-trimethyl-ammonium chlorides (abridged $C_{12}EO_nTMACl$) and of the n-dodecyl-polyoxiethylene-pyridinium chlorides (abridged $C_{12}EO_nPyCl$) of the type

$$\text{n - } C_{12}H_{25}(OCH_2CH_2)_n\overset{+}{N}(CH_3)_3Cl^- \text{ and n - } C_{12}H_{25}(OCH_2CH_2)_n\overset{+}{N}C_5H_5Cl^-$$

where n = 0,1 and 2.

By introducing the polar groups — OCH_2CH_2 — between the hydrophobic chain and the ionic head group the solubility of the compounds in water markedly increases as against those with $n = 0$, a fact that might bring about also an increase in the CMC.

---

[5] H. B. Klevens, *J. Amer. Oil Chemists'Soc.*, **30**, 74 (1953).

[6] K. Shinoda, *Bull. Chem. Soc. Japan*, **26**, 101 (1953).

[7] K. Shinoda T. Nakagawa, B. Tamamushi and T. Isemura "Colloidal Surfactantes", Academic Press, New York—London, 1963, p. 58.

[8] M. J. Schick, *J. Colloid Sci.*, **17**, 801 (1962).

[9] J. E. Carless, R. A. Challis and B. A. Mulley, *J. Colloid Sci.*, **19**, 201 (1964).

[10] K. Shinoda, Tokio Yomaguchi and R. Hori, *Bul. Soc. Chem. Japan*, **34**, 237 (1960).

[11] K. Tori, K. Kuriama and T. Nakagawa, *Kolloid-Z.*, **191**, 48 (1963).

[12] K. W. Hermann, *J. Colloid and Interface Sci.*, **22**, 352 (1966).

[13] K. W. Hermann, *J. Phys. Chem.*, **66**, 295 (1962).

[14] J. K. Weil, R. G. Bistline Jr. and A. I. Stirton, *J. Phys. Chem.*, **62**, 1083 (1958).

It has been experimentally established that as the number of $-OCH_2CH_2-$ groups increases, the CMC considerably decreases as against the compound with $n = 0$.

One can raise the question whether a small number of oxiethylene groups should be considered as pertaining either to the hydrophilous or the hydrophobic group. It is well known that compounds of the type $C_{12}H_{25}(OCH_2CH_2)_nOH$ with n below four are insoluble in water, and therefore bear a predominantly hydrophobic character.

Neither under the modified form advanced by Klevens [5]:

$$\lg CMC = A' - B'L \qquad (1')$$

where L = the length of the alkyl chain from the last hydrogen to the atom carrying the electrical charge, can relation (1) be applied to the compounds we have studied.

We think that for these compounds one would no longer consider either the length of the alkyl chain or the number of carbon atoms in the usual meaning, since the chain is broken by the polar ethereal groups.

The presence of ethereal groups, able to hydrate strongly, between the alkyl chain and the ionic head, brings about changes in the structure of the micelle surface and consequently in the factors which determine their formation and stability.

The critical micellar concentration of the above compounds has been determined using two pathways : the variation in the surface tension and the variation in the electrical conductance with the concentration.

PREPARATION OF MATERIALS

Dodecyl-monoether-glycols have been unitary products prepared by Williamson synthesis of dodecyl-chloride and the monosodium salt of the ethylene-, diethylene- and triethylene-glycol according to methods presented in literature[15-18]. Dodecyl-monoether-glycols have been converted into the corresponding chlorides by chlorination with thionyl chloride in the presence of pyridine.

The quaternary trimethyl-ammonium and pyridinium chlorides have been obtained by heating the corresponding chlorides with an excess of 30% either trimethyl-amine or pyridine in a sealed glass tube, for 20—24 h, at 130°.

Purification of quaternary salts occurred by extraction with petrol ether and recrystallization from anhydrous acetone up to the complete vanishing of the minimum on the curve of surface tension concentration around CMC.

Lauryl alcohol with chromatographically checked purity has been used for the preparation of dodecyl chloride.

The physical characteristics and the detailed description of the substances and of the synthesis and purification methods are given in first part.

---

[15] R. Fordyce, E. D. Lovell and Hibbert, *J. Amer. Chem. Soc.*, **61**, 1905 (1939).

[16] B. A. Gingras and G. H. Bayley, *Canad. J. Chem.*, 35, 599 (1957).

[17] N. Chakovskoy, R. A. Martin and R. Van Neckel, *Bull. Soc. chim. belges*, **65**, 453 (1956).

[18] J. M. Corkill, J. F. Goodman and R. H. Ottewil, *Trans. Faraday Soc.*, **57**, 1627 (1961).

Determination of the surface tension

The surface tension has been determined according to Du Nöuy and making use of Harkins' and Jordan's[19] corrections. Organic solvents have been used as standard liquids. The primary solution has been prepared by weighing of the substance directly in a graduated flask and after the vanishing of the foam it has been brought to the mark. The following solutions have been prepared by volumetric dilution in the determination vessel.

The surface tension has been determined 30 minutes after dilution in order to achieve the surface equilibrium. Over CMC the dynamic surface tension is very small and the equilibrium is reached within 2–3 minutes, but it becomes appreciable below CMC.

The water used has been thrice distilled from $KMnO_4$ and NaOH and keeps its surface tension unchanged in time.

Determination of electrical conductance

The electrical conductance has been determined by means of a conductance bridge with a frequency of 1000 cycles/s. The cell had platinum coated electrodes and the constant 0.460 cm^{-1} which has been determined with standard potassium chloride solutions. The water used has been thrice distilled, with specific conductance $2-4 \times 10^{-6}\Omega^{-1}.\ cm^{-1}$. Dilution occurred directly, volumetrically, in the conductance cell. The conductance has been determined 30 minutes after the preparation of the solution.

The determinations have been carried out at 25 ± 0.1°.

RESULTS

Figure 1 shows the variation curves of equivalent conductance function of the square root of the concentration for the series $C_{12}H_{25}(OCH_2CH_2)_nNC_5H_5Cl$.

It has been noticed that the equivalent conductance at CMC is increasing from $n = 0$ to $n = 2$. A change in the variation slope of the equivalent conductance with the concentration below CMC also occurs. The order of the increase ranges from $C_{12}PyCl$ to $C_{12}EO_2PyCl$.

Figure 2 represents the curves of the surface tension function of lg C for the pyridinium series $C_{12}EO_nPyCl$.

It has been noticed that for $n = 0,1$ and 2 the surface tension over CMC is actually constant; the increase does not pass beyond 0.3 dynes . cm^{-1} and for all three substances is actually the same. Below CMC the first part is linear.

The slope of the straight lines is the same for every substance, which proves that the surface area of the molecules in the adsorption layer is the same in accordance with Gibbs equation.

The CMC values determined by the two methods are listed in table 1.

For the trimethyl-ammonium series, $C_{12}EO_nTMACl$, figure 3 represents the equivalent conductances function of the square root in the concentration.

---

[19] W. D. Harkins and H. Jordan, *J. Amer. Chem. Soc.*, **52**, 1751 (1930).

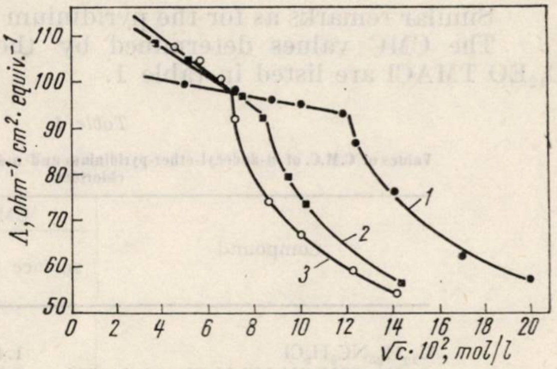

Fig. 1. — Equivalent conductance of n — $C_{12}H_{25}(OCH_2CH_2)_nNC_5H_5Cl$ solutions *vs.* concentration at 25°:

1, *n* = 0; *2*, *n* = 1; *3*, *n* = 2.

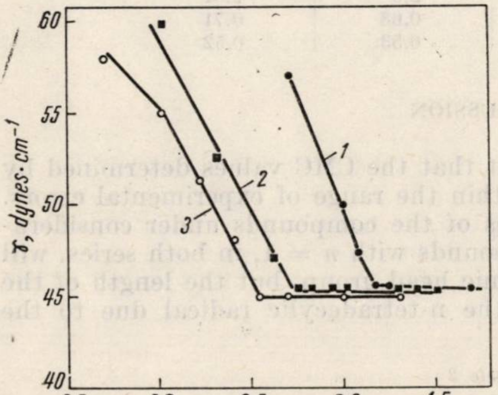

Fig. 2. — Surface tension of n — $C_{12}H_{25}(OCH_2CH_2)_nNC_5H_5Cl$ solutions *vs.* lgC, at 25°:

1, *n* = 0; *2*, *n* = 1 and *3*, *n* = 2.

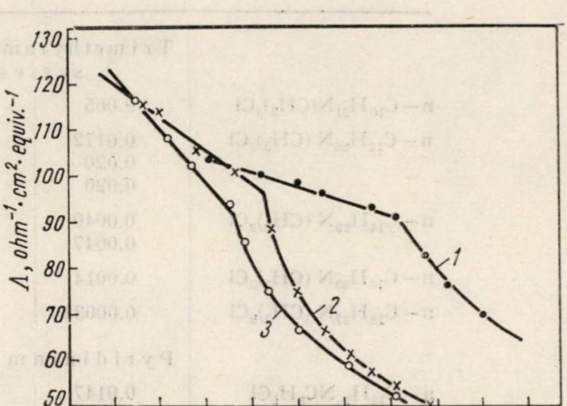

Fig. 3. — Equivalent conductance of n — $C_{12}H_{25}(OCH_2CH_2)_nN(CH_3)_3Cl$ solutions *vs.* concentrations at 25°:

1, *n* = 0; *2*, *n* = 1 and *3*, *n* = 2

Similar remarks as for the pyridinium series are to be made.

The CMC values determined by the two methods for the series $C_{12}EO$ TMACl are listed in table 1.

Table 1

Values of C.M.C. of n-dodecyl-ether-pyridinium and n-dodecyl-ether-trimethylammonium chlorides

Compound	CMC 10^2, mol/l, from	
	surface tension	electrical conductance
$C_{12}H_{25}NC_5H_5Cl$	1.48	1.56
$C_{12}H_{25}OCH_2CH_2NC_5H_5Cl$	0.58	0.69
$C_{12}H_{25}(OCH_2CH_2)_2NC_5H_5Cl$	0.40	0.49
$C_{12}H_{25}N(CH_3)_3Cl$	2.0	2.01
$C_{12}H_{25}OCH_2CH_2N(CH_3)_3Cl$	0.68	0.71
$C_{12}H_{25}(OCH_2CH_2)_2N(CH_3)_3Cl$	0.53	0.52

DISCUSSION

From table 1 one can see first that the CMC values determined by the two methods are very close within the range of experimental errors.

If we analyze the CMC values of the compounds under consideration by using relation (1), the compounds with $n = 1$, in both series, will have 14 carbon atoms up to the ionic head group, but the length of the whole chain is greater than for the n-tetradecylic radical due to the presence of the oxygen atom.

Table 2

Value of CMC of alkyl-trimethylammonium and alkyl-pyridinium chlorides

Compound	C.M.C. mol/l	Temperature °C	References
	Trimethylammonium series		
$n-C_{10}H_{21}N(CH_3)_3Cl$	0.065	25	[5]
$n-C_{12}H_{25}N(CH_3)_3Cl$	0.0172	25	[20]
	0.020	25	This work
	0.020	30	[21]
$n-C_{14}H_{29}N(CH_3)_3Cl$	0.0040	30	[5]
	0.0047	30	[20]
$n-C_{16}H_{33}N(CH_3)_3Cl$	0.0014	30	[22]
$n-C_{18}H_{37}N(CH_3)_8Cl$	0.00034	25	[23]
	Pyridinium series		
$n-C_{12}H_{25}NC_5H_5Cl$	0.0147	25	[24]
	0.0148	25	This work
	0.0156		
$n-C_{16}H_{33}NC_5H_5Cl$	0.0009	30	[25]
$n-C_{18}H_{37}NC_5H_5Cl$	0.00024	25	[23]

According to relation (1), CMC of the compounds with $n = 1$, should be similar to CMC of the tetradecyl-trimethyl-ammonium respectively pyridinium chloride, and in accordance with relation (1′) CMC should be smaller, since in this case the chain length, by virtue of Klevens' definition,[5] is greater.

The compound with $n = 2$ has 16 carbon atoms up to the ionic head group.

By the agency of literature data, listed in table 2, for the CMC of the alkyl-trimethyl-ammonium chloride and of the alkyl-pyridinium chlorides, in figure 4 there has been represented lg CMC in terms of the number of carbon atoms (solid curves). From these straight lines the following values of the constants A and B have been calculated by relation (1) at 25° : for the series of alkyl-trimethyl-ammonium chlorides $A = 1.80$ and $B = 0.298$, and for the series of alkyl-pyridinium chlorides $A = 1.67$ and $B = 0.298$.

The dotted curves in figure 4 represent lg CMC for the alkyl-ether-trimethyl-ammonium chlorides and the alkyl-ether-pyridinium chlorides function of the total amount of carbon atom up to the ionic head group. It has been first established that the lg CMC dependence function of the total amount of carbon atoms up to the ionic head group is no longer linear. The CMC values, when the alkyl chain is broken by the oxygen atoms, are greater than in the case of continuous chains with the same number of carbon atoms.

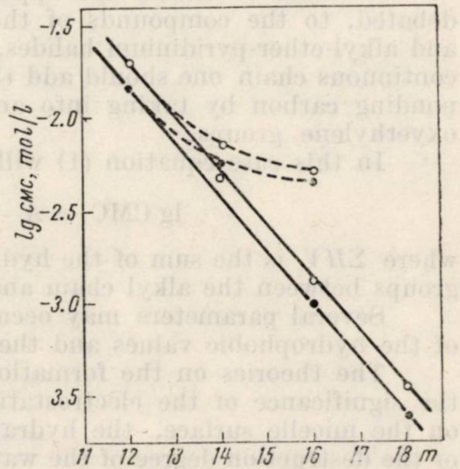

Fig. 4. — Plot of critical micellar concentration *vs.* all carbon atoms up to ionic head group :

● - pyridinium series ; ○ - trimethylammonium series. Dashed line for n-dodecyl-ether-pyridinium and dodecyl-ether-trimethylammonium chlorides.

Since by the insertion of the $- OCH_2CH_2 -$ groups between the hydrophobic part and the ionic head group, there occurs a CMC decrease as related to compounds with n = 0, a certain hydrophobic value expressed by the number of carbon atoms, might be assigned to those groups. We shall call the hydrophobic value *HV* the number of carbon atoms which bring about the same decrease in the CMC as the $- OCH_2CH_2 -$ groups inserted between the hydrophobic part and the ionic head group.

---

[20] H. W. Hoyer and Anne Marmo, *J. Phys. Chem.*, **65**, 1807 (1961).

[21] A. W. Ralston, D. N. Eggenberger and P. L. Du Brow, *J. Amer. Chem. Soc.*, **70**, 977 (1948).

[22] A. W. Ralston, D. N. Eggenberger, H. J. Harwood and P. L. Du Brow, *J. Amer. Chem. Soc.*, **69**, 2095 (1947) ; **71**, 672 (1949).

[23] P. F. Grieger and C. A. Kraus, *J. Amer. Chem. Soc.*, **70**, 3803 (1948).

[24] W. P. J. Ford, R. H. Ottewil and H. C. Parreira, *J. Colloid Sci.* **21**, 522 (1966).

[25] G. S. Hartley, *J. Chem. Soc.*, **1938**, 1968.

Figure 4 clearly shows that the hydrophobic value of the first group $- OCH_2CH_2 -$ is much greater than that of the second group. For both series the hydrophobic value of the first group $- OCH_2CH_2 -$ is about 1.5 carbon atoms while for the second group 0.35 carbon atoms.

The hydrophobic value may be assigned to the oxiethylene groups if the bonding degree of counterions on the micellar surface or the apparent dissociation degree remains the same, irrespective of the number of $- OCH_2CH_2 -$ groups. The theories of the formation of micelles and the experimental data clearly ascertain the strong influence of the bonding degree of counterions over the CMC value and micellar size.

In order to enable the application of the relation (1), previously debated, to the compounds of the type alkyl-ether-ammonium halides and alkyl-ether-pyridinium halides, to the total amount of carbon in the continuous chain one should add the total amount of equivalent, corresponding carbon by taking into account the hydrophobic values of the oxyethylene groups.

In this case equation (1) will be

$$\lg \mathrm{CMC} = A - B\,(m + \sum HV) \tag{3}$$

where ΣHV is the sum of the hydrophobic values of the $- OCH_2CH_2 -$ groups between the alkyl chain and the ionic head group.

Several parameters may occur while accounting for the magnitude of the hydrophobic values and their significance.

The theories on the formation and stability of micelles [26-29] state the significance of the electrostatic repulsion among ionic head groups on the micelle surface, the hydration degree of the ionic head groups or the destruction degree of the water structure by the ionic head groups, the part of the hydrocarbon surface implied in hydrophobic bonds with water according to Poland and Scheraga.[29]

We think that one of the most important factors is the change in the electrostatic repulsion among terminal ionic head groups. The electrostatic repulsion undergoes modifications due to the changes in the distances among ionic head groups as well as to the change in the dielectric constant owing to the strong solvation of the ether groups. To the above causes the changes in the bonding degree of counterions to micelle may be added, and also the alteration of the cohesion energy of the oxiethylene groups while passing from solution into micelle.

In order to find out the contribution of each of these factors to the CMC change they should be separately analysed in forthcoming papers.

---

[26] P. Debye, *J. Phys. Chem.*, **53**, 1 (1949).

[27] P. Debye, *Ann. New York Acad. Sci.*, **51**, 575 (1949), from [28].

[28] Reich Irving, *J. Phys. Chem.*, **60**, 254 (1956).

[29] C. D. Poland and A. H. Scheraga, *J. Colloid and Interface Sci.*, **21**, 273 (1966).

Revue Roumaine de Chimie, **15**, 783–788 (1970)

COMBINAISONS ZINC-DIARYLAMIDES. II *

L'ÉCHANGE ENTRE LE DIPHÉNYLZINC ET LES AMINES AROMATIQUES PRIMAIRES

AGLAIA CIOBANU, LUCIA ROMAN, M. BOSTAN, N. VOICULESCU et DIANA GIURGIU

Institut de Chimie Macromoléculaire « Petru Poni » de l'Académie, Filiale de Jassy, 41A, Aleea Grigore Ghica Vodă

Reçu le 1er novembre 1968

Par l'échange entre le diphénylzinc et les arylamines primaires, respectivement aryldiamines comme : α- et β-naphtylamine, N,N-diéthyl-*p*-phénylènediamine, benzidine, 3,3'-diméthylbenzidine, 3,3'-diméthoxybenzidine, on a synthétisé une série de combinaisons zinc-arylamides ou zinc-aryldiamides. Les composés ont été caractérisés par l'analyse chimique, par les spectres X, par la thermolyse. On a proposé un mécanisme de réaction.

Les réactions d'acidolyse entre les amines et les composés zinc-organiques ont été peu étudiées. On connaît quelques méthodes de préparation des produits de la réaction d'acidolyse avec des amines.

Abraham et Hill [1, 2] ont étudié la cinétique de l'acidolyse du dialkylzinc avec *p*-toluidine, cyclohexylamine, qui est de premier ordre en ce qui concerne le dialkylzinc et l'amine. Les auteurs ont trouvé que les vitesses d'acidolyse du di-*n*-propylzinc avec une série d'amines dans l'éther di-iso-propylique comme solvant sont dans l'ordre *p*-toluidine > cyclohexylamine > diphénylamine > acétanylide. Les produits de la réaction n'ont pas été isolés.

Noltes [3] a préparé une série de composés organozinc-amides $RZnNR'_2$ par l'acidolyse du diorganozinc avec des amines secondaires à 80–100°

$$R_2Zn + R'_2NH \longrightarrow RZnNR'_2 + RH$$

Coates et Ridley [4] ont montré que la diphénylamine donne le dimère $(RZnNPh_2)_2$ avec le diméthylzinc et le diéthylzinc, avec la structure

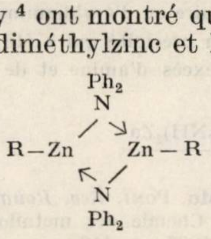

où $R = C_2H_5$ et CH_3

---

[*] S. Fișel, L. Roman, I. Popescu et Mg. Poni, *Rev. Roumaine Chim.*, **12**, 511 (1967).

[1] M. H. Abraham et J. A. Hill, *Proc. Chem. Soc.*, **1964**, 175.

[2] M. H. Abraham et J. A. Hill, *J. Organometal. Chem.*, **7**, 23 (1967).

[3] J. G. Noltes, *Rec. Trav. chim.*, **84**, 126 (1965).

[4] G. E. Coates et D. Ridley, *J. Chem. Soc.*, **1965**, 1870.

et le diméthylzinc avec la diméthylamine forme le bis-diméthylaminozinc $[(Me_2N)_2Zn]_n$ insoluble, certainement polymère.

En continuant nos études sur les zinc-arylamides,[5] dans cet ouvrage, nous présentons les produits obtenus par la réaction d'acidolyse entre le diphénylzinc et des amines aromatiques primaires et diamines aromatiques.

On a employé les amines : α-et β-naphtylamine, N,N-diéthyl-*p*-phénylènediamine, benzidine, 3,3'-diméthylbenzidine et 3,3'-diméthoxybenzidine.

PARTIE EXPÉRIMENTALE

Le diphénylzinc a été préparé d'après les indications données par Krause et Grosse.[6]

Les amines ont été purifiées soit par distillation, soit par recristallisation et séchage sous vide.

La tolidine a été obtenue dans le laboratoire par la méthode donnée dans la littérature.[7]

Les solvants — l'éther éthylique, l'éther de pétrole, l'hexane, le cyclohexane — ont été séchés, refluxés sur sodium métallique en présence du benzophénone comme indicateur d'anhydrisation et distillés juste avant l'utilisation.[8]

Pour enlever les traces d'air retenues par le solvant, on a procédé d'après les indications données par Eisch et King.[9]

L'obtention des combinaisons diphénylzinc, zinc-arylamides et zinc-diarylamides, ainsi que leur manipulation ont été effectuées dans des vases Schlenk sous courant d'azote ou d'argon purifié, selon la technique donnée par Thomas.[8]

On a déterminé la teneur en zinc et en azote des produits obtenus.

Les courbes thermogravimétriques ont été tracées avec une thermobalance Ugine-Eyraud avec la vitesse de chauffage de 15°/mn en atmosphère inerte.

Les debyegrammes ont été enregistrés avec l'appareil TUR-M-60, la radiation CuKα et le filtre de nickel. Toutes les épreuves ont été exposées durant 3—4 heures à 12 mA et 40 KV.

Le mode d'obtention des composés de la réaction du diphénylzinc avec des amines aromatiques primaires et des diamines aromatiques a été le même.

Le diphénylzinc préparé, sous courant d'azote ou d'argon séché et exempt d'oxygène, dans un vase Schlenk, par le chauffage du mélange de diphénylmercure (5g) et des copeaux du zinc (4 g), a été extrait avec de l'éther éthylique anhydre. La solution éthérée du diphénylzinc a été filtrée par une fritte poreuse G_4 dans un vase Schlenk, l'opération ayant lieu en atmosphère inerte. A la solution éthérée du diphénylzinc on a ajouté, à la température ambiante, une solution éthérée d'amine aromatique primaire ou d'aryldiamine par un entonnoir Schlenk. La réaction est exothermique ; il se sépare un précipité qui a été lavé plusieurs fois avec de l'éther éthylique séché pour éloigner tout excès d'amine et de diphénylzinc. Le composé résulté a été séché sous vide.

$\underline{(C_{10}H_7NH)_2Zn}$ (I)

---

[5] S. Fişel, L. Roman, I. Popescu et Mg. Poni, *Rev. Roumaine Chim.*, **12**, 511 (1967).

[6] E. Krause et A. V. Grosse, «Die Chemie der metallorganischen Verbindungen », Verlag von Gebrüder Borntraeger, Berlin, 1937, p. 118.

[7] B. Rassow et K. Rülke, *J. prakt. Chem.*, **65**, 117 (1902) ; P. S. Yazma, *Chem. Zentr.*, **1930**, 2239.

[8] G. Thomas, *Chem. Ztg. Chemische Apparatur*, **85**, 563 (1961).

[9] J. Eisch et R. B. King, «Organometallic Syntheses », Ier vol., Transition-Metal-Compounds, Academic Press, New York, Londres, 1965, p. 21.

De 3,3 g diphénylzinc et 3 g α-naphtylamine, les deux en solution éthérée, on a obtenu 4,7 g poudre blanche, qui devient verdâtre sous l'influence de la lumière et de l'humidité de l'air. Rendement 90 %.

Analyse : *Trouvé* : N 8,00 ; Zn 18,95 %
Calculé : N 8,01 ; Zn 18,70 %

$(C_{10}H_7NH)_2Zn$ (II)

Le composé avec la β-naphtylamine a été obtenu dans les mêmes conditions que ceux du composé précédent. C'est une poudre blanche sensible à la lumière et à l'humidité atmosphérique. Rendement 4,5 g, 86,5 %.

Analyse : *Trouvé* : N 7,82 ; Zn 18,43 %
Calculé : N 8,01 ; Zn 18,70 %

$[(C_2H_5)_2NC_6H_4NH]_2Zn$ (III)

La N,N-diéthyl-*p*-phénylènediamine (4,5 g) fraîchement distillée sous courant d'azote a été ajoutée à une solution éthérée de diphénylzinc (3,3 g). Le produit formé est une poudre blanche, très sensible à la lumière, à l'oxygène et à l'eau. Rendement 2,88 g, 49,65 %

Analyse : *Trouvé* : N 14,28 ; Zn 16,98 %
Calculé : N 14,29 ; Zn 16,69 %

$C_6H_5ZnNHC_6H_4C_6H_4NH_2$ (IV)

A la solution de 3,3 g de diphénylzinc dans de l'éther éthylique on a graduellement ajouté une solution éthérée de benzidine (1,4 g). Il précipite un produit qui a une couleur rose faible, sensible à la lumière et à l'humidité atmosphérique. rendement 2 g, 46 %.

Analyse : *Trouvé* : N 8,65 ; Zn 20,67 %
Calculé : N 8,60 ; Zn 20,06 %

$C_6H_5ZnNH(CH_3)C_6H_3C_6H_3(CH_3)NH_2$ (V)

De 3,3 g diphénylzinc et 1,4 g 3,3′-diméthylbenzidine, introduits dans de l'éther éthylique, manipulés dans les conditions mentionnées plus haut, on a obtenu 2,4 g poudre grise violacée. Rendement 45 %.

Analyse : *Trouvé* : N 7,96 ; Zn 18,85 %
Calculé : N 7,92 ; Zn 18,49 %

$C_6H_5ZnNH(OCH_3)C_6H_3C_6H_3(OCH_3)\ NHZnC_6H_5\ .\ O(C_2H_5)_2$ (VI)

Le produit obtenu du diphénylzinc (3,3 g) et 3,3′-diméthoxybenzidine (3,3 g) dans l'éther éthylique anhydre est une poudre faiblement jaunâtre. rendement 1,85 g, 41 %.

Analyse : *Trouvé* : N 4,50 ; Zn 21,78 %
Calculé : N 4,66 ; Zn 21,76 %

ATG la perte en poids % = 25,76, calculé pour la perte d'une mole d'éther et d'une mole de benzène = 25,27.

Les composés obtenus sont photosensibles avec changement de couleur, leur conservation et manipulation nécessitant une protection contre la lumière. Ils sont sensibles à l'oxygène de l'air et à l'humidité, insolubles en solvants organiques tels que: éther de pétrole, benzène, toluène, hexane, cyclohexane. A cause de leur insolubilité il a été impossible d'effectuer des déterminations du poids moléculaire.

Les combinaisons zinc-arylamides et zinc-aryldiamides se décomposent par chauffage, sans fusion.

RÉSULTATS ET DISCUSSIONS

On connaît la capacité des composés zinc-organiques de former des complexes coordinatifs avec divers ligands qui contiennent de l'oxygène,[10-12] de l'azote,[12-16] du phosphore,[12] de l'arsenic.[12] L'énergie des orbitaux *d* du zinc, ainsi que leur interaction avec les orbitaux π-moléculaires du ligand, dépendent des groupes alkyl ou aryle liés à l'atome de zinc.[13, 15, 16] En comparaison des groupements alkyliques, les groupements phényliques plus électronégatifs accroissent la polarité de la liaison Zn—C et ainsi on favorise la formation de complexes diphénylzinc du type $(C_6H_5)_2Zn : \text{donneur}$.

Le caractère donneur du solvant — l'éther éthylique — favorise la formation des complexes du type donneur-accepteur, $R_2Zn : O\,(C_2H_5)_2$, dans lesquels les forces coordinatives sont faibles.

La présence de ces complexes coordinatifs est confirmée par Thiele,[10] qui a réussi à séparer un produit d'addition avec la formule $(CH_3)_2Zn : : O\,(CH_3)_2$ peu stable, en montrant que les dérivés d'alkylzinc forment des complexes coordinatifs stables seulement avec les éthers cycliques.[11]

Aussi les éthérats des diarylzinc[12, 17-19] sont-ils plus stables si l'on utilise les diéthers et les groupes aryliques liés au zinc contiennent des substituants accepteurs d'électrons.

En présence de l'amine, le complexe $(C_6H_5)_2Zn : O\,(C_2H_5)_2$ conduit, par la substitution du donneur, au complexe avec amine $(C_6H_5)_2Zn : NH_2Ar$, qui évolue, par l'élimination du benzène, en un composé avec liaison covalente Zn—N.

Le mécanisme de l'acidolyse du diphénylzinc avec des amines aromatiques primaires peut être représenté par la chaîne des réactions

$$(C_6H_5)_2Zn : O(C_2H_5)_2 + NH_2Ar \longrightarrow (C_6H_5)_2Zn : NH_2Ar + O\,(C_2H_5)_2 \longrightarrow$$
$$\longrightarrow C_6H_5Zn{-}NHAr + C_6H_6$$

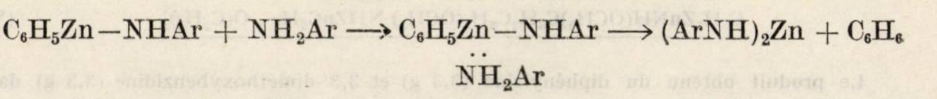

$$C_6H_5Zn{-}NHAr + NH_2Ar \longrightarrow C_6H_5\underset{NH_2Ar}{\underset{\cdot\cdot}{Zn}}{-}NHAr \longrightarrow (ArNH)_2Zn + C_6H_6$$

---

[10] K. H. Thiele, *Z. anorg. Chem.*, **319**, 183 (1962).

[11] K. H. Thiele, *Z. anorg. Chem.*, **322**, 71 (1963).

[12] J. G. Noltes et J. W. G. Van Den Hurk, *J. Organometal. Chem.*, **1**, 377 (1964).

[13] J. G. Noltes et J. W. G. Van Den Hurk, *J. Organometal. Chem.*, **3**, 222 (1965).

[14] J. G. Noltes et J. Boersma, *J. Organometal. Chem.*, **9**, 1 (1967).

[15] K. H. Thiele, *Z. anorg. Chem.*, **325**, 156 (1963).

[16] K. H. Thiele et J. Köhler, *Z. anorg. Chem.*, **387**, 260 (1965).

[17] N. I. Sheverdina, L. V. Abramova et K. A. Kocheshkov, *Doklady Akad. Nauk S.S.S.R.*, **128**, 320 (1959).

[18] N. I. Sheverdina et L. V. Abramova, *Doklady Akad. Nauk S.S.S.R.*, **134**, 853 (1960).

[19] N. I. Sheverdina, L. V. Abramova et K. A. Kocheshkov, *Doklady Akad. Nauk S.S.S.R.*, **124**, 602 (1959).

ou dans le cas des diamines aromatiques

$$(C_6H_5)_2Zn : O(C_2H_5)_2 + NH_2{-}R{-}R{-}NH_2 \longrightarrow (C_6H_5)_2Zn : NH_2{-}R{-}$$
$$-R{-}NH_2 + O(C_2H_5)_2 \longrightarrow C_6H_5Zn{-}NH{-}R{-}R{-}NH_2 + C_6H_6.$$

Dans le composé avec *o*-dianisidine (VI), la base a les deux groupes $-NH_2$ engagés en liaisons covalentes avec le zinc.

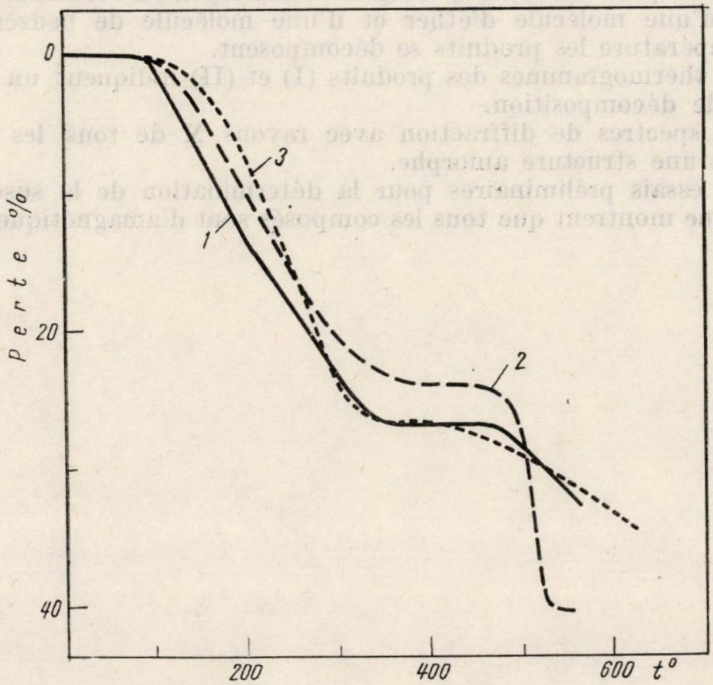

Fig. 1. — Thermogrammes.

1, Thermogramme du composé (IV) ; *2*, Thermogramme du composé (V) ; *3*, Thermogramme du composé (VI).

Un mécanisme pareil a été proposé par Abraham et Hill [2] pour l'acidolyse du dialkylzinc avec des amines primaires.

La réaction d'acidolyse des amines primaires aromatiques est suffisamment forte, les échanges ayant lieu à la température ambiante, fait observé aussi par Frankland [20] dans le cas de l'action des amines primaires avec le diéthylzinc. Dans les mêmes conditions de la réaction, ou même au chauffage, avec une amine aromatique secondaire (N, N'-diphénylbenzidine), on n'a pu séparer un produit unitaire, mais un mélange des produits non isolables.

Les courbes thermogravimétriques montrent des transformations dans les intervalles de température de 80–374°, 109–404°, 98–326° pour les composés (IV), (V), (VI) (fig. 1).

---

[20] E. Frankland, *Proc. Roy. Soc.*, **8**, 502 (1856–7), cité d'après [2].

Les pertes de 27% (IV) et de 24,11% (V) sont attribuées à la possibilité de l'élimination d'une molécule du benzène, avec la réorganisation interne de la molécule du composé.

La courbe thermogravimétrique de la combinaison (VI) montre une stabilité jusqu'à la température de 98°, au-delà de laquelle le produit commence à perdre en poids jusqu'à la température 326°, quand on établit un palier. La perte de 25,76% enregistrée correspond à l'élimination concomitante d'une molécule d'éther et d'une molécule de benzène. Après cette température les produits se décomposent.

Les thermogrammes des produits (I) et (II) indiquent un processus continu de décomposition.

Les spectres de diffraction avec rayons X de tous les composés indiquent une structure amorphe.

Les essais préliminaires pour la détermination de la susceptibilité magnétique montrent que tous les composés sont diamagnétiques.

Revue Roumaine de Chimie, **15**, 789–798 (1970)

PYRAZOLES. I.

N-ARYLATION DES PYRAZOLES AVEC DES DÉRIVÉS CHLORURÉS AROMATIQUES ACTIVÉS PAR LES GROUPEMENTS NITRO

C. CHIRIAC et I. ZUGRĂVESCU

Institut de Chimie macromoléculaire « P. Poni » de l'Académie, Filiale de Jassy, 41 A, Aleea Grigore Ghica-Vodă

Reçu le 11 octobre 1969

On étudie les réactions de N-arylation des pyrazoles avec des dérivés chlorurés aromatiques tels que : le 4-nitrochlorobenzène, 2,4-dinitrochlorobenzène et le chlorure de picryle. La N-arylation des pyrazoles avec le 2,4-dinitrochlorobenzène et le chlorure de picryle a lieu à l'état fondu par le chauffage des produits à une température de 170 à 220°. La réaction de N-arylation avec le 4-nitrochlorobenzène a été effectuée avec des dérivés pyrazoliques N-sodés dans le diméthylsulfoxyde à 100°. Ces réactions nous ont permis de synthétiser des N-arylpyrazoles, plus difficilement obtenus par les méthodes connues. L'étude des spectres en UV des dérivés 1-picrylpyrazoles montre que le 1-picryl-3,5-diphénylpyrazole présente un fort effet hypsochrome, expliqué par l'existence d'un phénomène d'empêchement stérique de la résonance, dû à la torsion du cycle benzénique par rapport au plan de la molécule.

INTRODUCTION

Dans une note antérieure,[1] nous avons étudié la réaction de N-arylation du cycle pyrazolique N-sodé avec des dérivés aromatiques : C_6H_5X ($X = Cl, Br, I$) dans des solvants aprotiques dipolaires.

La N-arylation des pyrazoles avec des dérivés halogénés aromatiques activés avec des groupements nitro a été peu étudiée.

Elguero et Jacquier [2-4] ont obtenu des dérivés pyrazoliques N-arylés par le chauffage des pyrazoles dans une solution alcoolique avec le 2,4-dinitrofluorobenzène, le chlorure de picryle ou le 4-nitrofluorobenzène, dans un tube scellé à haute température.

---

[1] C. Chiriac, L. Stoicescu-Crivetz et I. Zugrăvescu, *Rev. Roumaine Chim.*, **14**, 1263 (1969).

[2] R. Jacquier et J. Elguero, *Bull. Soc. chim. France*, **1959**, 474.

[3] R. Jacquier et J. Elguero, *Bull. Soc. chim. France*, **1959**, 1445.

[4] R. Jacquier et J. Elguero, *Bull. Soc. chim. France*, **1962**, 233.

Reimlinger et Oth [5] ont préparé le 1-(2,4-dinitrophényl)-pyrazole et le 1-picryl-pyrazole par l'action du 2,4-dinitrofluorobenzène et du chlorure de picryle sur le pyrazole dans l'éther. A l'exception du chlorure de picryle (très réactif), les autres dérivés halogénés aromatiques activés avec des groupements nitro utilisés jusqu'à présent contiennent comme halogène le fluor, qui est l'élément le plus réactif dans la série de Bunnett,[6] concernant la substitution aromatique nucléophile.

Dans nos investigations sur les pyrazoles, nous avons étudié les réactions de N-arylation avec des dérivés chlorurés comme : 4-nitrochlorobenzène (NCB), 2,4-dinitrochlorobenzène (DNCB) et trinitrochlorobenzène (TNCB).

RÉSULTATS ET DISCUSSIONS

Dans la substitution aromatique nucléophile, à côté de la réactivité du halogène aromatique, un rôle décisif joue la réactivité du composé azoté, auquel on a effectué la substitution. Cette réactivité dépend de la densité électronique au niveau de l'atome d'azote, qui est approximativement proportionnelle à la basicité.[7] Par exemple, la pipéridine qui a une basicité bien plus grande que les pyrazoles réagit avec le NCB, à une $t = 100°$, avec un grand rendement,[8] tandis que la réaction avec les pyrazoles, d'après nos investigations, ne peut pas être effectuée, même à 240–250°.

Elguero et Jacquier [7] ont essayé sans succès à N-aryler les dérivés pyrazoliques avec le DNCB. Nous avons réalisé cette réaction en travaillant à l'état fondu à haute température et avons constaté que la réaction n'a pas lieu dans les solvants suivants : toluène, xylène, DMSO, *m*-crésol, bien que quelques-uns des solvants utilisés aient des points d'ébullition plus grands que la température à laquelle a lieu la réaction. La DMF ne peut être utilisée du fait qu'elle réagit avec le DNCB.[9]

La réaction de N-arylation avec le TNCB, en solution, est connue pour les dérivés pyrazoliques avec des substituants alcoylés, ayant une basicité plus forte.[7] Nous avons réussi l'extension de la réaction avec le TNCB aux dérivés pyrazoliques ayant des substituants tels que : Cl, Br, NO_2 et C_6H_5, qui diminuent la basicité du cycle pyrazolique, et qui ne réagissent pas d'après les méthodes connues.

Dans les mêmes conditions, le DNCB réagit aussi avec les dérivés pyrazoliques ayant dans le cycle des substituants tels que : Cl, Br, NO_2

---

[5] H. Reimlinger et J. F. Oth, *Chem. Ber.*, **97**, 331 (1964).
[6] J. F. Bunnett, *Chem. Rev.*, **22**, 134 (1951).
[7] J. Elguero et R. Jacquier, *Bull. Soc. chim. France*, **1966**, 2837.
[8] E. Lellman et W. Geller, *Ber. dtsch. chem. Ges.*, **21**, 2281 (1888).
[9] W. M. Lord et A. T. Peters, *J. Chem. Soc.*, **1968** (sér. C), 783.

et C_6H_5. La N-arylation des pyrazoles avec le DNCB et le TNCB a lieu d'après le schéma 1

Schéma 1

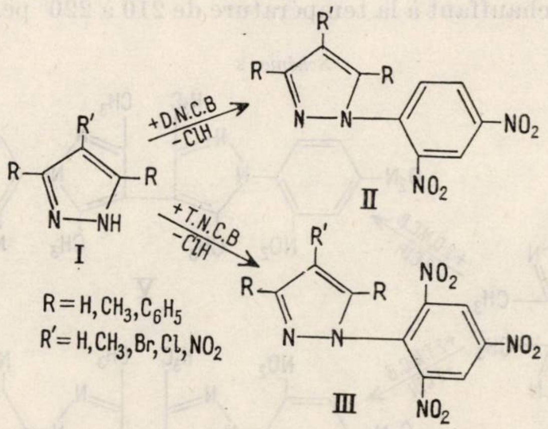

Les résultats de l'étude de ces réactions sont présentés dans le tableau 1.

Dans les réactions illustrées dans le tableau 1, le rapport molaire des produits de réaction dépasse légèrement 1 : 1 en faveur du dérivé halogéné (l'excès du dérivé halogéné ne conduit pas à un rendement meilleur). On observe aussi (tableau 1) que la réaction du TNCB et, en spécial, la réaction du DNCB avec le 3,5-diphénylpyrazole nécessite des

Tableau 1

Réactions de N-arylation des pyrazoles avec le 2,4 dinitrochloro-benzène et le chlorure de picryle

N°	Dérivé halogéné	Pyrazole I R, R'	Temps de réaction h	t° C	Pyrazole II, III P_f °C	Rend. %
1	DNCB	H, H	8	150–160	104–106[7]*	59
2	,,	CH_3, H	,,	,,	120[7]	62
3	,,	CH_3,CH_3	,,	,,	154–155[7]	63,6
4	,,	CH_3, Br	10	,,	176–177[7]	37
5	,,	CH_3, NO_2	,,	,,	185–187 (alcool)	35,5
6	,,	CH_3, Cl	,,	,,	168–170 (alcool)	37
7	,,	C_6H_5, H	8	210–220	149[7]	42
8	,,	C_6H_5, Br	10	,,	182[7]	38,6
9	,,	C_6H_5, Cl	,,	,,	146–148 (alcool)	38
10	TNCB	H, H	6	120–130	163[7]	79
11	,,	CH_3, H	,,	,,	221[7]	80,5
12	,,	CH_3, CH_3	,,	,,	191–192[7]	82
13	,,	CH_3, Br	10	160–170	185[7]	56
14	,,	CH_3, Cl	,,	,,	182–183 (alcool)	48,5
15	,,	C_6H_5, H	,,	210–220	236–238 (acide acétique)	47
16	,,	C_6H_5, Br	,,	,,	206–208 (alcool)	45,5
17	,,	C_6H_5, Cl	,,	,,	224–225 (acide acétique)	46

* Indications bibliographiques.

conditions plus énergiques qu'au cas du pyrazole non substitué, fait connu pour des réactions du même genre.[7,10]

On a synthétisé des dérivés dipyrazoliques N-arylés, par la même réaction, en partant de 3,5′, 5,5′-tétraméthyl-4,4′-dipyrazolyl et de DNCB ou de TNCB, en chauffant à la température de 210 à 220° pendant 10 heures (schéma 2)

Schéma 2

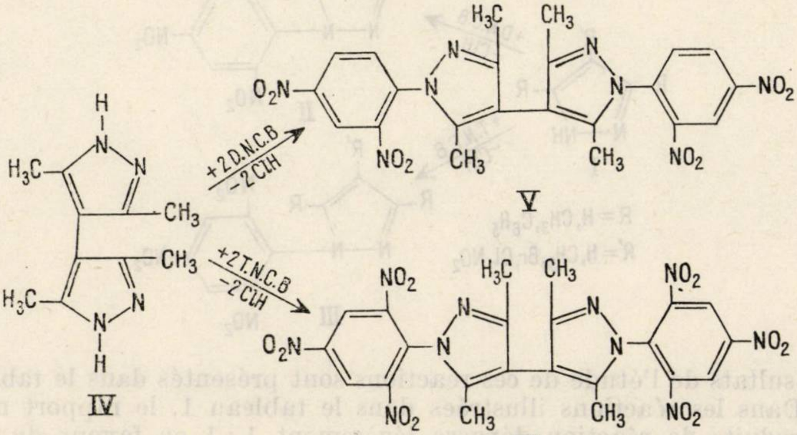

IV

V

VI

Nous avons déjà montré dans ce travail que le NCB ne réagit pas avec les pyrazoles, même à la température de 240—250°. Nous avons essayé l'arylation avec les pyrazoles N-sodés. La réaction a lieu dans des conditions bien établies (voir la partie expérimentale). Dans une solution alcoolique, la substitution n'a pas lieu, car l'éthoxyde de sodium (utilisé pour l'obtention du pyrazole N-sodé), en équilibre avec le pyrazole N-sodé, peut réagir avec le NCB, comme dans d'autres cas connus.[11]

Les solvants aprotiques dipolaires dans des réactions du même genre sont de plus en plus utilisés ce dernier temps. Parmi ces solvants, la DMF ne peut être utilisée parce qu'elle réagit avec le NCB, en donnant la *p*-nitrodiméthylaniline. Nous avons obtenu de bons résultats en utilisant le DMSO. La N-arylation des pyrazoles N-sodés avec le NCB a lieu d'après le schéma 3.

Schéma 3

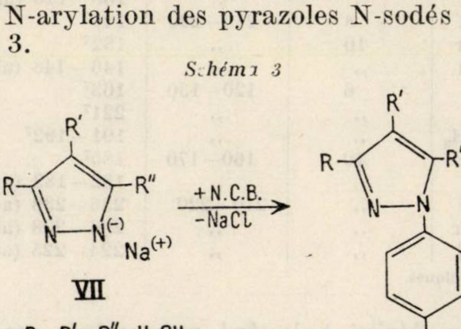

VII

VIII

R=R′=R″=H,CH₃

R, R′, R″ peuvent être: H, CH_3.

---

[10] J. F. K. Wilshire, *Austral. J. Chem.*, **19**, 1936 (1966).

[11] J. Bourdais et C. Mahieu, *Compt. rend.*, **263** (sér. C), 84 (1966).

Les résultats de l'étude de ces réactions sont présentés dans le tableau 2.

Les meilleurs résultats sont obtenus si l'on ajoute, graduellement, sous agitation, à 100°, une solution de pyrazole N-sodé (1 mole) en DMSO à une solution de NCB (1 mole) en DMSO. Pendant toute la durée de la réaction on doit avoir un excès de NCB. L'ajoutage inverse ne mène pas à de bons résultats, du fait qu'on obtient des produits secondaires.

Tableau 2

Réactions de N-arylation des pyrazoles avec le 4-nitrochlorobenzène

N°	Dérivé halogéné	Pyrazole VII R, R′, R″	Temps de réaction h	t°C	Pyrazole VIII P$_f$°C	Rend. %
1	NCB	H, H, H	6	100	169–170[7] *	68
2	,,	CH_3, H, CH_3	,,	,,	100–102[7]	74
3	,,	CH_3, CH_3, CH_3	,,	,,	115–117[7]	76
4	,,	CH_3, H, H	,,	,,	166–167[7]	72

*Indications bibliographiques.

Du tableau 2, on peut constater que la N-arylation avec le NCB n'a pas lieu aux dérivés pyrazolitiques avec des substituants : Cl, Br, NO_2, C_6H_5.

Le mécanisme des réactions de N-arylation des pyrazoles avec le TNCB, le DNCB et le NCB est probablement celui du schéma 4.

La généralisation d'un tel mécanisme, par des intermédiaires ayant une structure quinolique (XII) et (XIII) est basée sur le fait que dans les substitutions nucléophiles aromatiques connues jusqu'à présent, aux composés ayant des groupements nitro, des complexes intermédiaires colorés apparaissent, qui sont stables seulement à la température ordinaire.[12-14]

Dans les réactions des pyrazoles N-sodés avec le NCB dans le DMSO, à la température ordinaire, on observe l'apparition d'une coloration rouge, qui constitue une preuve en faveur du mécanisme proposé par nous, avec la formation d'un complexe intermédiaire (XIII). Durant le chauffage des pyrazoles non sodés avec le TNCB ou le DNCB, on n'observe aucune variation de couleur. Le complexe (XII) formé a probablement une existence très courte à cause de la grande température de réaction, de l'absence d'un solvant aprotique dipolaire et de la basicité diminuée des pyrazoles. Ces types de complexes sont stables seulement à la température ordinaire et dans les solutions des solvants aprotiques dipolaires.[12]

L'étude des spectres en UV aux dérivés 1-(2,4-dinitrophényl)-pyrazoliques témoigne de l'existence d'un phénomène d'empêchement stérique,[15] ce qui nous a déterminé à étudier ce phénomène aux 1-picrylpyrazoles et en spécial au 1-picryl-3,5-diphénylpyrazole, qui presente

---

[12] J. Sauer et R. Huisgen, *Angew. Chem.*, **72**, 296 (1960).

[13] C. C. Gitis et A. V. Ivanov, *Zhur. org. Khimii*, **1**, 901 (1965).

[14] W. Borsche, *Ber. dtsch. chem. Ges.*, **54**, 1287 (1921).

Schéma 4

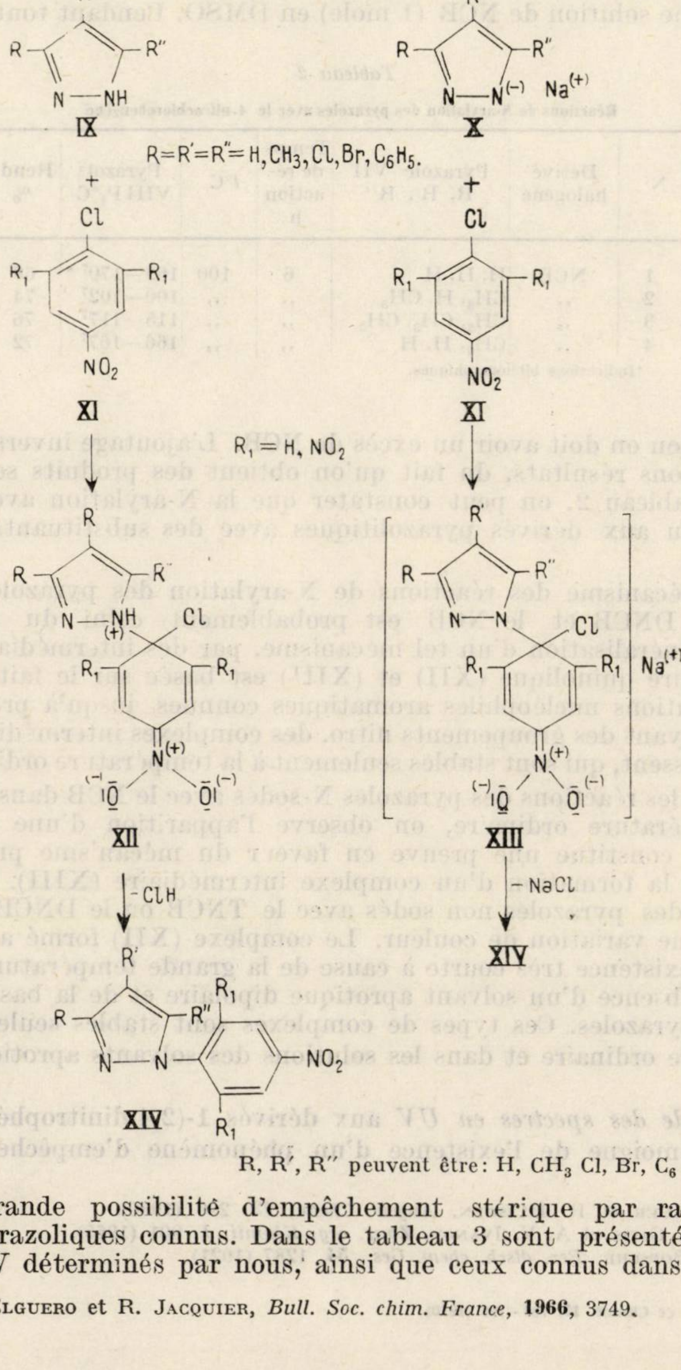
IX
X
R=R′=R″= H, CH3, Cl, Br, C6H5.
Na(+)
XI
XI
R1 = H, NO2
XII
XIII
Na(+)
− ClH
− NaCl
XIV
XIV

R, R′, R″ peuvent être: H, CH_3 Cl, Br, C_6H_5.

la plus grande possibilité d'empêchement stérique par rapport aux dérivés pyrazoliques connus. Dans le tableau 3 sont présentés les spectres en UV déterminés par nous, ainsi que ceux connus dans la littérature de spécialité, pour l'étude comparative sur l'empêchement stérique de la résonance de 1-picryl-3,5-diphénylpyrazole.

---

[15] J. Elguero et R. Jacquier, *Bull. Soc. chim. France*, **1966**, 3749.

En examinant le tableau 3, on constate que le 1-picryl-3,5-diphénylpyrazole présente un effet hypsochrome plus marqué que le 1-(2,4-dinitrophényl)-3,5-diphénylpyrazole, pour lequel on a démontré l'existence de l'empêchement stérique.[15]

Tableau 3

Spectres en UV des pyrazoles N-arylées

N°	Pyrazole	λ max	log ε	Indications bibliographiques
1	3,5-diphényl-P	209,256	4,76 ; 4,85	— *
2	1-(4-nitrophényl)-3,5-diphényl-P	248,333	4,62 ; 4,30	—
3	1-(2,4-dinitrophényl)-3,5-diphényl-P	*246,329*	4,59 ; 3,94	15
4	1-picryl-P	305	3,81	15
5	1-picryl-3,5-diméthyl-P	327—332	3,62	15
6	1-picryl-3, 4, 5-triméthyl-P	344	3,56	—
7	1-picryl-3,5-diphényl-P	*210,243*	4,54 ; 4,56	—

* Le signe (—) indique qu'aux produits respectifs les spectres en UV ne sont pas connus.

Cet effet hypsochrome, constaté par nous, ainsi que par d'autres auteurs, [15-17] aux dérivés 1-phénylpyrazoliques avec des substituants dans les positions 2′ et 6′, est dû à un phénomène d'empêchement stérique de la résonance, à cause de la torsion du cycle benzénique, phénomène rencontré au biphényle. Burness [17] considère que ce phénomène est plus prononce dans la série des 1-phénylpyrazoles que dans la série du biphényle, à cause de la liaison exocyclique C—N qui est plus courte que la liaison exocyclique C—C du biphényle. L'auteur [17] apprécie qu'à l'empêchement stérique peuvent participer aussi des électrons non participants de l'atome d'azote de la position 2 (formule 1).

Formule 1

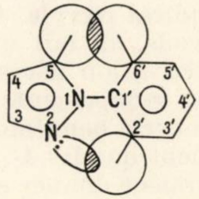

Le fort effet hypsochrome constaté au 1-picryl-3,5-diphénylpyrazole ne peut pas être attribué au déplacement en dehors du plan seulement des groupements nitro des positions 2′ et 6′ sans la torsion du cycle benzénique, comme dans d'autres cas similaires.[18,19] Si ce phénomène

[16] D. Dal Monte, A. Mangini et R. Passerini, *Gazz. chim. Ital.*, **86**, 797 (1956).
[17] D. M. Burness, *J. Org. Chem.*, **21**, 97 (1956).
[18] M. J. Kamlet et J. C. Hoffsomer, *J. Amer. Chem. Soc.*, **84**, 3925 (1962).
[19] H. G. Adolf et M. J. Kamlet, *J. Org. Chem.*, **30**, 2864 (1965).

avait lieu, le 1-picryl-3,5-diphénylpyrazole devrait présenter une absorption à une longueur d'onde approximativement égale à celle de 1-(*p*-nitrophényl)-3,5-diphénylpyrazole, parce que dans les deux cas le groupement nitro de la position 4′ reste dans le plan du cycle benzénique, en produisant un effet batochrome (conformément à la formule 2).

Formule 2

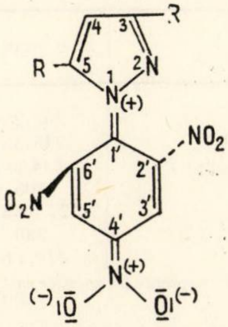

En réalité le 1-picryl-3,5-diphénylpyrazole présente une absorption à une longueur d'onde plus petite que le 1-(*p*-nitrophényl)-3,5-diphénylpyrazole (tableau 3). Donc, dans le cas du 1-picryl-3,5-diphénylpyrazole, ni le groupment nitro de la position 4′ ne participe pas à la conjugation, donc le cycle benzénique avec ses trois substituants nitro-coplanaires a subi une torsion par rapport au plan de la molécule (contrairement à la formule 2).

La coplanéité des deux groupements nitro des positions 2′ et 6′ avec le groupement nitro de la position 4′ (contrairement à la formule 2) peut être démontrée aussi par voie chimique.

Ainsi, dans une autre note,[20] nous avons montré que les 1-(2,4-dinitrophényl)-pyrazoles réagissent avec les amines, par la scission du radical 2,4-dinitrophényle et les 1-picrylpyrazoles réagissent avec l'ammoniaque par la scission du radical picryle. Ces réactions n'ont pas lieu avec les 1-(4-nitrophényl)-pyrazole, du fait qu'un seul groupement nitro ne suffit pas pour produire l'activation nécessaire de la réaction respective. Si nous supposions que les groupements nitro des positions 2′ et 6′ ne sont pas coplanaires avec le cycle benzénique (conformément à la formule 2), il résulterait logiquement que les 1-(2,4-dinitrophényl)-pyrazoles et les 1-picrylpyrazoles ne pourraient donner ces réactions, l'action inductive des groupements nitro 2′ et 6′ étant réduite. En réalité, ces réactions ont été réalisées. En plus, l'existence du cycle benzénique qui a subi une torsion (conformément à la formule 3) détermine une liaison exocyclique C—N tordue, capable de présenter les réactions indiquées plus haut.

En conclusion, l'existence d'une phénomène d'empêchement stérique chez des dérivés pyrazoliques avec des substituants moins volumineux [15–17] que le 1-picryl-3,5-diphénylpyrazole préparé par nous, ainsi que l'effet hypsochrome plus marqué de ce composé en comparaison des composés connus (le tableau 3) sont des arguments suffisants pour confirmer l'existence de ce phénomène dans notre cas. Nous pouvons donc affirmer que le radical picryle de 1-picryl-3,5-diphénylpyrazole subit une torsion par rapport au plan de la molécule, et que les groupements nitro des positions *ortho* et *para* restent dans le plan du cycle benzénique (formule 3).

---

[20] C. Chiriac et I. Zugrăvescu, *Rev. Roumaine Chim.* (sous presse).

Formule 3

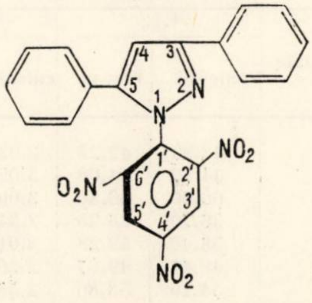

PARTIE EXPÉRIMENTALE

On prépare les dérivés pyrazoliques N-arylés présentés dans le tableau 1, par le chauffage des pyrazoles respectifs avec le DNCB ou le TNCB (avec un petit excès de dérivé halogéné), dans les conditions indiquées dans ce tableau. Dans le cas particulier de 1–(2,4 dinitrophényl)-3,5-diméthylpyrazole (II_2), on procède ainsi :

Dans un ballon on chauffe à 150–160°, pendant 8 h, 2,4 g (0,025 mole) de 3,5-diméthylpyrazole et 5,2 g (0,0257 mole) de 2,4-dinitrochlorobenzène. On obtient par recristallisation de l'alcool 4 g de 1–(2,4-dinitrophényl)-3,5-diméthylpyrazole, rendement 62%. P_f 121°.[7]

Pour les dérivés pyrazoliques N-arylés inconnus, les analyses élémentaires sont présentées dans le tableau 4.

1,1'-Di-(2,4-dinitrophényl)-3,3', 5,5'-tétraméthyl-4,4'-dipyrazolyl (V). On le prépare de 3,3', 5,5'-tétraméthyl-4,4'-dipyrazolyl[21] (1 mole) et du DNCB (2 moles), en chauffant à 210–220° pendant 10 h. P_f 210–212° (alcool).

$C_{22}H_{18}N_8O_8$	*Calculé* :	C 50,57 ; H 3,44 ; N 21,45%
	Trouvé :	C 50,70 ; H 3,38 ; N 21,40%

1,1'-Dipicryl-3,3', 5,5'-tétraméthyl-4,4'-dipyrazolyl (VI). On le prépare semblablement au dérivé (V), en partant de 3,3', 5,5'-tétraméthyl-4,4'-dipyrazolyl et de TNCB. P_f 289–291 (acide acétique).

$C_{22}H_{16}N_{10}O_{12}$	*Calculé* :	C 43,12 ; H 2,61 ; N 22,87%
	Trouvé :	C 42,89 ; H 2,22 ; N 22,29%

1-(4-Nitrophényl)-3,5-diméthylpyrazole (VIII_2). On ajoute 2,4 g (0,025 mole) de 3,5-diméthylpyrazole à une solution d'alcoolate de sodium préparée de 0,575 g (0,025 atome-gramme) de Na et 50 ml de méthanol. On évapore le méthanol, on ajoute 50–60 ml de DMSO anhydre et on chauffe jusqu'à la dissolution complète du 3,5-diméthylpyrazole N-sodé. La solution, après refroidissement à la température ambiante, est ajoutée graduellement pendant

---

[21] W. L. Mosby, *J. Chem. Soc.*, 1957, 4001.

2—3 h, sous agitation, à une solution de 4 g (0,025 mole) de 4-nitrochlorobenzène dans 40 ml de DMSO anhydre. L'opération a lieu sur un bain d'eau porté à l'ébullition. Après l'ajoutement on continue le chauffage sous agitation encore 3—4 h. On évapore le DMSO sous vide. On extrait le résidu avec 70—90 ml de ClH 18—20% et on le filtre. Au liquide filtré on ajoute une solution de NaOH 10% et de l'eau sous agitation et refroidissement. Finalement le pH doit avoir la valeur de 2—3. Le volume du liquide doit arriver à 200—250 ml. Le précipité obtenu doit être filtré, séché et recristallisé de la ligroïne ayant le point d'ébullition de 80 à 100°. Il résulte 4,1 g de 1-(4-nitrophényl)-3,5-diméthylpyrazole avec un rendement de 75%. P_f 93=95°.[7]

Tableau 4

Analyses élémentaires des pyrazoles N-arylées

N°	Pyrazole II, III	Formule minimale	C%		H%		N%	
			calculé	trouvé	calculé	trouvé	calculé	trouvé
1	II_5	$C_{11}H_9N_5O_6$	42,99	42,26	2,93	3,13	22,80	22,63
2	II_6	$C_{11}H_9ClN_4O_4$	44,59	44,08	3,09	3,13	18,24	18,66
3	II_9	$C_{21}H_{13}ClN_4O_4$	60,00	60,50	3,09	3,41	13,33	13,13
4	III_{14}	$C_{11}H_8ClN_5O_6$	38,70	38,25	2,34	2,61	20,52	20,11
5	III_{15}	$C_{21}H_{13}N_5O_6$	58,46	59,28	3,01	3,30	16,24	16,50
6	III_{16}	$C_{21}H_{12}BrN_5O_6$	49,41	49,87	2,35	2,72	13,72	13,91
7	III_{17}	$C_{21}H_{12}ClN_5O_6$	54,19	53,86	2,58	2,81	15,05	15,77

La préparation des dérivés pyrazoliques (VIII_1), (VIII_3) et (VIII_4) a lieu de la même façon.

L'étude des dérivés pyrazoliques à l'aide des spectres en UV pour démontrer l'existence du phénomène d'empêchement stérique ou 1-picryl-3,5-diphénylpyrazole préparé par nous a été effectuée dans une solution alcoolique, à l'aide d'un appareil type Unicam Sp. 800 B.

Revue Roumaine de Chimie, **15**, 799–817 (1970)

STUDIEN AUF DEM GEBIET DER SYMMETRISCHEN TRIAZINE (NEUE SERIE). IV[1]

2,4-DIOXO-6-(*p*-X-β-STYRYL)-TETRAHYDRO-s-TRIAZINE; ELEKTRONENSPEKTROSKOPIE DER BASEN UND IHRER PROTONIERUNG

G. OSTROGOVICH und M. SAFTA

aus dem Laboratorium für Organische Chemie der Technischen Hochschule,
Timişoara, str. Bocşa 6

Eingegangen am 10. Oktober 1968

Der wesentliche Gegenstand der Arbeit ist die *p*-Dimethyl-amino-β-styryl-Verbindung **2**, die (als s-Triazin-hemicyaninbase betrachtet) einen noch wenig bekannten und als solcher unerforschten Typus darstellt. Es werden präparative Beiträge und die Ergebnisse eines Studiums der elektronischen Spektren in wäßrig-äthanolischer Lösung der Base **2** und ihrer (mono- und di-)protonierten Derivate angeführt. Gleichzeitig mit der Struktur der Spektren wurden durch 8 isosbestische Punkte die verschiedenen sich in Lösungen von 2.10^{-2} Mol/l Base **2** und $0 \div 6$ Mol/l H_2SO_4 einstellenden Gleichgewichte, einschließlich das zu jedem gehörige Aziditätsintervall, erörtert. Zu diesem Zwecke wurden auch andere entsprechende β-Styryl-Derivate (**5**÷**9**, sämtlich neue Verbindungen) synthetisiert und untersucht. Die erste Protonierung der Base **2** (deren scheinbare pK_a auf ~2,8 geschätzt werden konnte), führt auch zu einem tautomeren Gleichgewicht zwischen einer roten chinoiden Form (**3***A*) und einer farblosen benzoiden Form (**3***B*), was auf diesem Gebiet scheinbar zum ersten Male festgestellt wird. Beide Formen ergeben dieselbe diprotonierte, farblose Verbindung **4**. Auf Grund der Spektren konnte auch die *trans*-Konfiguration aller in Frage kommender Verbindungen bestimmt werden.

Im Rahmen einer chemisch-analytischen, papierchromatographisch durchgeführten Untersuchung, welche den Gegenstand einer anderen Mitteilung bildet, wurde es nötig, um die Flecken des 2,4-Dioxo-6-methyl-tetrahydro-s-triazins (DMT) (Acetoguanamid, Formel **1***a*) sichtbar zu machen, eine geeignete Farbreaktion anzuwenden.

Zu diesem Zweck haben wir die säurekatalysierte (H_2SO_4) Kondensation des aktiven Methyls dieser Base mit *p*-Dimethylamino-benzaldehyd (*p*-DAB) gewählt.[2]

---

[1] G. Ostrogovich, Mitteilung III, *Bul. Şt. şi Tehn. I.P.T.*, (*Seria Chimie*), **15** (29) (1970).

[2] K. Fink, R. Cline und R. M. Fink, *Analyt. Chem.*, **35**, 389 (1963).

Wie im Jahre 1959 Hromov-Borisov und Kisareva[3] durch Kondensation in wäßriger HCl-Lösung und neuerdings auch Hickmott[4] (desgleichen in Eisessig) gezeigt haben, erhält man auf diese Weise die entsprechende *p-Dimethylamino-β-styryl-Verbindung* und zwar, im ersten

1

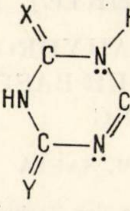
X
H
C
N
HN
C
CH3
C
N
Y

a) $(X = Y) = O$

b) $X = O;\ Y = NH$

c) $(X = Y) = NH$

Fall als Monohydrochlorid, im zweiten aber direkt als freie, durch die Formel **2** dargestellte Base. Diese ist als solche eine *orangegelbe*, bis 340° nicht schmelzende und praktisch in Wasser unlösliche Substanz (während im Gegenteil DMT leicht löslich ist).

Um vor allem einen Aspekt von präparativem Interesse hervorzuheben, sei zuerst eine unserer bei dieser Gelegenheit gemachter Fest-

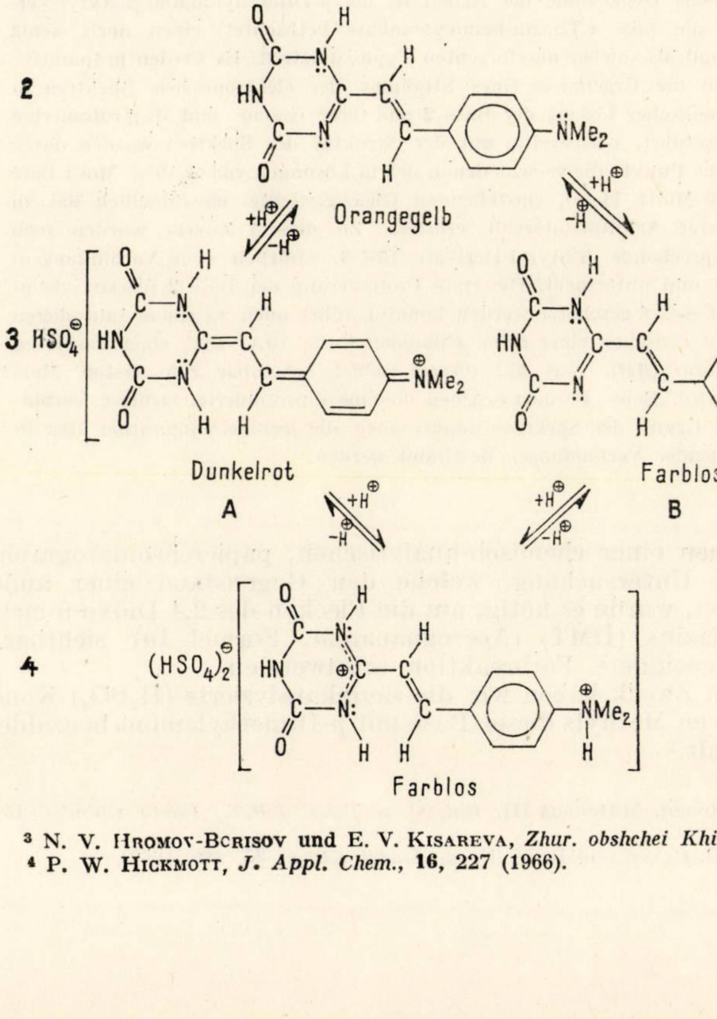
2
NMe2
Orangegelb
+H⊕
-H⊕
3
HSO4⊖
NMe2
Dunkelrot
A
Farblos
B
4
(HSO4)2⊖
NMe2
Farblos

---

[3] N. V. Hromov-Borisov und E. V. Kisareva, *Zhur. obshchei Khim.*, **29**, 3010 (1959).

[4] P. W. Hickmott, *J. Appl. Chem.*, **16**, 227 (1966).

stellungen erwähnt. Es handelt sich um die Tatsache, daß falls man die Reaktion in 96% igem Äthanol statt in Wasser verlaufen läßt und die katalytische Wirkung der Schwefelsäure heranzieht (indem man diese auf eine in bezug auf jeden der beiden Partner molare Lösung, bei einem Molverhältnis konz. H_2SO_4/Substrat = 1,2 : 1 zur Einwirkung bringt), das Kondensationsprodukt **2** mit einer Ausbeute von 96% (bei den erwähnten Verfassern 36%, beziehungsweise 50%) als Bisulfat $C_{13}H_{14}O_2N_4 \cdot H^{\oplus} SO_4H^{\ominus}$ (**3**) zugänglich wird, also in der gleichen monoprotonierten Form der Base **2** wie die von Hromov-Borisov als Monohydrochlorid synthetisierte.* Ähnlich wie dieses Hydrochlorid ist das Bisulfat **3** eine etwas leichter als die Base **2** lösliche Verbindung von dunkelroter Farbe (**3***A*), welche unter den genannten Bedingungen mit einer Ausbeute von 80% kristallin aus der Lösung ausscheidet. Aus den, durch Verdünnung mit Wasser und zusätzlicher Ansäuerung mit H_2SO_4 erhaltenen wäßrig-äthanolischen Lösungen dieses Bisulfats, fällt die Base **2** quantitativ durch Freisetzung mit wäßrigem NH_3 aus. Dadurch wird sie präparativ, wie erwähnt, mit einer 96%igen Ausbeute erhältlich.

Außerdem haben wir die geeigneten Bedingungen festgelegt, um ein zweites, farbloses, von den genannten Forschern gar nicht beobachtetes Salz darzustellen, dessen Bildung im Beisein eines Überschusses von beträchtlich höher konzentrierter wäßriger Schwefelsäure zu erwarten war. Tatsächlich geht das rotfarbige Bisulfat **3***A* auf diese Weise in eine fast farblose Lösung über, aus der das erwähnte farblose Salz beim Abkühlen im kristallinen Zustand ausscheidet. Seine Zusammensetzung entspricht der Formel eines diprotonierten Derivats der Base **2** und zwar der des Tetrasulfats $C_{13}H_{14}O_2N_4 \cdot H_2^{2\oplus}(HSO_4)_2^{2\ominus}$ (**4**).

Betreffs dieses Verhaltens der Verbindung **2**, welche augenscheinlich die Struktur eines Hemicyanins besitzt[6a] und zwar speziell zur Unterklasse der (*p*- oder *o*-)Dialkylamino-β-styryl-hemicyaninfarbstoffbasen gehört,[6b] **) halten wir es für angezeigt einen bisher im allgemeinen nicht bemerkten Aspekt sofort hervorzuheben.

Daß für Azomethin-Basen jeder Art eine ausgesprochene Halochromie bei der ersten Protonierung charakteristisch ist, bildet eine schon längst genau bekannte und klargestellte Tatsache, welche quantentheoretisch im Sinne der Formel **3***A* (und nur in diesem Sinne) selbstverständlich geworden ist. Einen entscheidenden experimentellen Beweis dafür, an den hier zu erinnern nicht ganz überflüssig erscheint, wurde eben auf diesem besonderen Gebiet der Hemicyanine erstmalig, und zwar im Falle des 2-(*p*-Dimethylamino-β-styryl)-chinolins, von Brooker[8] dadurch erbracht, daß das monoprotonierte Derivat dieser zitronengelben Base tiefrot ist, genau wie der entsprechende, echte, aus N-Methyl-chinaldiniumjodid durch Kondensation mit *p*-DAB erhaltene Hemicyaninfarbstoff, während das mit dem letzten isomere und zwar am anderen Ende quaternierte Kondensationsprodukt des Chinaldins mit Trimethyl-(*p*-formylphenyl)-ammoniumjodid im Gegensatz dazu eine farblose Verbindung bildet. Ohne weiteres voraussichtbar wurde damit auch die stark hypsochrome Auswirkung der zusätzlichen (an sich nur später und jedenfalls viel seltener erfaßten!) zweiten Protonierung,[9] welche die Absorption gleichartig bis ins Ultraviolette hinausschieben kann, wie es unser Salz **4** beweist.

---

* Es sei bemerkt, daß wie Ostrogovich[5] zeigte, auch DMT (**1** *a*) wenigstens in wäßrigem Medium nur ein Bisulfat bildet. Sicherlich ist sein neutrales Sulfat viel leichter löslich, so daß unter jedwelchen Bedingungen das aus der wäßrig-schwefelsauren Lösung der Base kristallisierbare Produkt DMT . $H^{\oplus}HSO_4^{\ominus}$ist.

**) Da das *p*-DAB als Ehrlichs Reagens für die Farbreaktion de rEiweißstoffe bekannt ist, kann beiläufig bemerkt werden, daß die Entstehung in saurem Medium der tieffarbigen konjugierten Säuren solcher Hemicyaninbasen, eine gewisse Analogie mit jener von ebenfalls azomethinartigen, violetten *p*-Dimethylamino-*benzyliden*-pyrrolenin- und -indoleninderivaten aufweist, auf denen die typische Ehrlich-Reaktion beruht.[7] Die Analogie besteht aber unbestreitbar nur in diesem sehr allgemeinen Sinne, denn jene Farbstoffe (und zwar nicht nur solche von α—, sondern auch etwaige von β-pyrroleninartiger Struktur) sind, unserer Meinung nach, nicht als echt hemicyaninisch zu betrachten.

[5] A. Ostrogovich, *Gazz. chim. Ital.*, **44**, 562 (1914).

[6] F. M. Hamer : "The Cyanine and Related Compounds", John Wiley and Sons, New York, London, 1964 : a) S. 447 ; b) Kap. XIII und Kap. XVI.

[7] H. Fischer und C. D. Nenitzescu, *Hoppe-Seyler's Z. physiol. Chem.*, **145**, 295 (1925).

Erstaunlicherweise wurde aber — soweit uns bekannt — in diesem Zusammenhang gänzlich übersehen, daß die starke energetische Bevorzugung der halochromen ersten Protonierung bei jenem Stickstoffendatom des Azomethinsystems, das zum heteroarenischen Kern gehört — also die verhältnismäßig sehr große Basizität dieses Protonenakzeptor-Zentrums — nicht unbedingt, bzw. nicht in jedem Fall den Ausschluß einer hypsochromen monoprotonierten Form vom Typus **3***B* (welche ein der farblosen Brookerschen quartären Verbindung entsprechendes Tautomer des farbigen Kations **3***A* wäre) mit sich bringt. Theoretisch ist dagegen zu erwarten, daß dieses farblose Tautomer in den Lösungen in Gleichgewicht mit dem farbigen besteht und daß bei Steigerung der Azidität das Gleichgewicht sich zu seinem Gunsten verschiebt. Auf diese Weise wird die Konzentration eines farblosen Tautomers vom Typus **3***B* gegenüber der des farbigen vom Typus **3***A* nicht unbedingt verschwindend klein bleiben (welches immer die Hemicyaninbase und die Lösungsazidität auch wäre), sondern muß bei genügend starker Azidität erfaßbar werden, so oft die Struktur des heteroarenischen Systems keinen zu großen Unterschied in der Basizität der beiden Protonenakzeptor-Zentren verursacht.

Dies ist eigentlich ebenso vorauszusehen und dementsprechend ebenso wenig befremdend als die halochrome erste Protonierung zum Salze **3***A*, denn schließlich handelt es sich offenbar um nichts anderes als um einen besonderen Fall der sonst viel erforschten und unter sehr verschiedenartigen Formen bekannten Chinoid-Benzoid Tautomerie, die hier bei einer konjugierten Säure auftritt (wie z.B. im klassischen, schon von Hantzsch erfaßten Falle der gelben, azoiden und der blauen, chinoiden Salze des *p*-Amino-azobenzols).

In unserem Falle ist hervorzuheben, daß die Base **2**, wie die entsprechenden Verbindungen der Triazine **1***b* und **1***c* (welche auch von denselben sowjetischen Verfassern bei einer vergleichenden Untersuchung der Aktivität ihrer CH_3-Gruppe synthetisiert wurden),[3] die *ersten Beispiele von Dimethylamino-β-styryl-Hemicyaninsystemen mit s-Triazinkern bilden.*

---

[8] L. G. S. Brooker und R. H. Sprague, *J. Amer. Chem. Soc.*, **63**, 3203 (1941).

[9] A. R. Katritzky und P. Simmons, *J. Chem. Soc.*, **1960**, 1511

Deswegen schien (über das anfängliche analytische Ziel hinaus, das zur Darstellung der Base **2** und zur orientierenden Prüfung ihres Verhaltens bei der Salzbildung mit Säuren Anlaß gab) eine gründliche Untersuchung dieses Verhaltens recht interessant, um so mehr als die s-Triazine (wie jede Art von 1,3-Diaza-arenen) einen besonderen Charakterzug gegenüber allen anderen Heteroarenen aufweisen, der in der Anwesenheit einer Amidingruppe im heterocyclischen Kern besteht.

Dank dieser Gruppe besitzt das Kation **3***A* eine höhere Symmetrie, so daß es der Satz der typischen isovalenten Konjugation wird, die bei den von anderen heteroarenischen Systemen stammenden β-styrylischen Hemicyanin-Farbstoffen (mit den obigen Ausnahmen) nicht möglich ist. Andererseits ist vorauszusehen, daß die Anwesenheit der Sauerstoffatome, beziehungsweise der Charakter eines N, N′-diacylierten Amidins, dieser Konstellation einen genügend starken antiauxochromen Charakter und folglich dem ganzen System noch einen etwas speziellen Zug verleihen wird. Auch solche Systeme sind bisher nur in geringer Zahl verwirklicht worden. Das Beispiel des 2-(*p*-Dimethylamino-β-styryl)-4-chinazolons [10] ist wahrscheinlich das erste teilweise Analogon von Base **2**, unter den wenigen, in der Literatur vorhandenen Fällen.

Es schien angezeigt, das Studium der besonderen Aspekte dieses Einzelfalls in zwei Richtungen einigermaßen zu erweitern und zwar: einerseits durch die Synthese anderer entsprechenden, zu Vergleichszwekken verwertbaren β-Styrylverbindungen, andererseits durch ein spektrophotometrisches Studium, welches uns eine möglichst genaue Erkenntnis der protolytischen Gleichgewichte (in erster und zweiter Stufe) und eventuell die Erfassung des im Prinzip vorauszusehenden Chinoid-Benzoid-Tautomerengleichgewichts **3***A* $\rightleftharpoons$ **3***B* gestatten sollte.

Zum Vergleich haben wir zunächst die quaternäre Ammoniumverbindung **5** synthetisiert, welche wir Trimethyl-{*p*-[β-(2,4-dioxo-tetrahydro-s-triazino-6)-vinyl]-phenyl}-ammonium-methylester-sulfat nennen. Diese ist eine neue Substanz, die durch Kondensation des Trimethyl-(*p*-formyl-phenyl)-ammonium-methylester-sulfats mit DMT (**1***a*) erhalten wurde. Die Kondensation findet mit großer Ausbeute statt, wenn die geschmolzene äquimolekulare Mischung der beiden Komponenten etwa 15 Min. bei 160° gehalten wird. Die in reinem Zustand, durch Umkristallisieren der Masse nach Abkühlung der Schmelze, mit einer 50%igen Ausbeute isolierte Verbindung **5**, welche eine dem vermeintlichen Tautomer **3***B* entsprechende Struktur besitzt, ist erwartungsgemäß farblos.

5

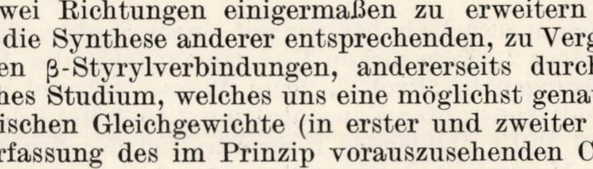

---

[10] M. T. Bogert und H. Clarck, *J. Amer. Chem. Soc.*, **46**, 1294 (1924).

Außerdem wurden (durch dasselbe Verfahren) die Verbindung **6** mit einer antiauxochromen NO_2-Gruppe in *para*-Stellung, und (durch das anfangs beschriebene Verfahren zur Herstellung der Base **2**) die Verbindungen **7**, **8**, **9** erhalten, davon die zwei letzten analog mit **2** sind, da sie auch in der *para*-Stellung auxochrome Gruppen besitzen.

6. $X = NO_2$ farblos
7. $X = H$ „
8. $X = OH$ gelblich
9. $X = OCH_3$ „

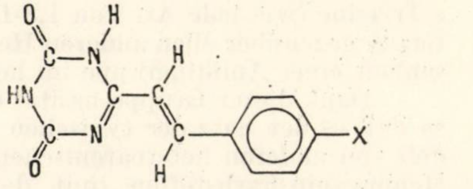

Ebenfalls zum Vergleich (und zwar besonders zur Bestimmung der IR-Spektren, welche den Gegenstand einer anderen Mitteilung bilden) haben wir durch Salzbildung mit H_2SO_4 auch die Bisulfate der Basen **6**, **7** und **9** hergestellt.

DAS SPEKTROPHOTOMETRISCHE STUDIUM IM SICHTBAREN UND ULTRAVIOLETTEN BEREICH

Zu diesem Zwecke haben wir mit einem Spektrophotometer Unicam SP 800 in einer 2,00 cm dicken Küvette zunächst die Absorptionskurven von 12 Lösungen in 50vol.-% igem Wasser-Äthanol registriert, welche eine Serie mit konstanter Konzentration 2.10^{-5} Mol/l der Base **2** und mit von 0 bis 6 Mol/l steigender Konzentration der Schwefelsäure bildeten (so daß das Molverhältnis Säure/Base zwischen die Grenzwerte 0÷300000 eingestuft wurde).

Diese Familie von 12 Kurven ist in Abbildung 1 wiedergegeben. Kurve *1* gehört der freien Base **2**, die anderen den Systemen, welche auch H_2SO_4 in stufenweise steigenden Konzentrationen enthalten.

Es ist offensichtlich, daß das *Spektrum der Base* **2** 4 Banden aufweist, von welchen eine stark ausgeprägte, für die gelbe Farbe der Substanz verantwortliche, bei 438 nm, andere zwei schwächere bei 258 und ~ 202 nm und eine sehr schwache bei 325 nm liegen. Die letzte davon konnte mit Bestimmtheit nur bei einer doppelten Konzentration (4.10^{-5} Mol/l) und in einer doppelten Schichtdicke (4 cm : Abb. 4, Kurve *13*) erfaßt werden.

Abb. 1 zeigt in klarer Weise die sukzessive Einstellung der Gleichgewichte, welche den zwei Protonierungsstufen entsprechen, das heißt die mit den Erhöhung der Säurekonzentration gleichzeitige Verschiebung dieser, welche die erste Stufe kennzeichnen, zugunsten jener die der zweiten Stufe angehören.

Wie ersichtlich, finden diese Erscheinungen ihren Ausdruck in einer Serie von 8 isosbestischen Punkten, welche bei 486 (Pi_1), 342 (Pi_2), 308 (Pi_3), 266 (Pi_4), 247 (Pi_5), ~ 235 (Pi_6), 231 (Pi_7), und ~ 199 nm (Pi_8) gelegen sind. Gleichzeitig mit der allmählichen Abschwächung bis zum Verschwinden der zur Base **2** gehörigen Banden, erscheinen und verstärken sich stufenweise neue Banden mit dem Maximum bei 516 (Kurven *4÷6*), 305 (Kurven *4÷8*), ~ 230 und ~ 223 nm (Kurven *4÷9*).

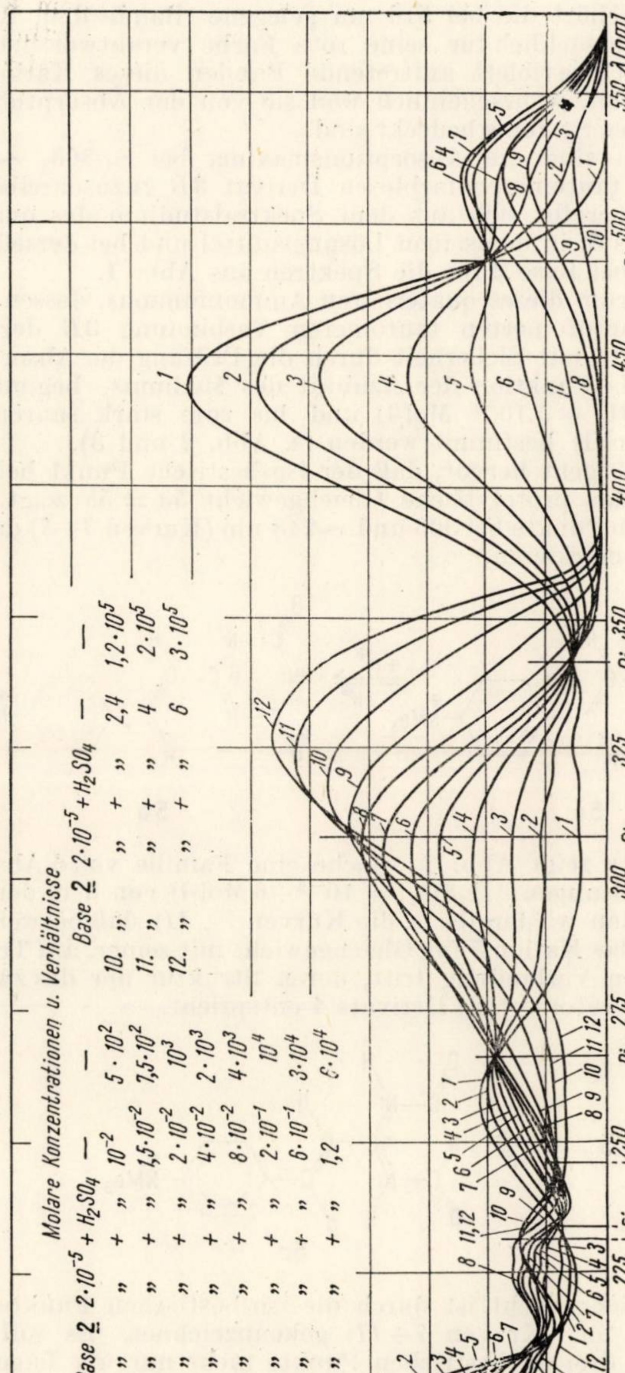

Abb. 1. — Extinktionskurven der Base **2**, ihrer monoprotonierten, tautomeren Derivate (**3** A und **3** B) und ihres diprotonierten Derivats **4**, in 50 vol.-%iger wäßrig-äthanolischer Lösung.

Offenbar gehört die bei 516 nm gelegene Bande dem Kation **3***A* an und ist hauptsächlich für seine rote Farbe verantwortlich. Andere eventuelle, im Ultraviolett auftretende Banden dieses Kations lassen sich nicht erfassen, wahrscheinlich weil sie von der Absorption anderer Komponenten des Systems bedeckt sind.

Tatsächlich sind die Absorptionsmaxima bei ~ 305, ~230 und ~223 nm dem tautomeren farblosen Derivat **3***B* zuzuschreiben. Diese Schlußfolgerung ergibt sich aus dem Spektralstudium des quaternären Ammoniumsalzes **5**, in demselben Lösungsmittel und bei derselben Konzentration, wie bei Base **2** für die Spektren aus Abb. 1.

Das Spektrum dieses quaternären Ammoniumions, dessen Struktur jener der monoprotonierten tautomeren Verbindung **3***B* der Base **2** entspricht, konnte mit Sicherheit durch die Prüfung der Absorptionsänderung von **5** als Funktion der Azidität des Mediums, beginnend vom alkalischen $[KOH] = 5.10^{-1}$ Mol/l) und bis zum stark sauren Bereich ($[H_2SO_4] = 6$ Mol/l) bestimmt werden (s. Abb. 2 und 3).

Aus Abb. 2 geht hervor, daß der isosbestische Punkt bei 273 nm (Kurven *1÷3*) das protolytische Gleichgewicht **5***a* $\rightleftharpoons$ **5***b* zeigt, während die isosbestischen Punkte bei 303 und ~248 nm (Kurven *3÷5*) das Gleichgewicht **5***b* $\rightleftharpoons$ **5** markieren.

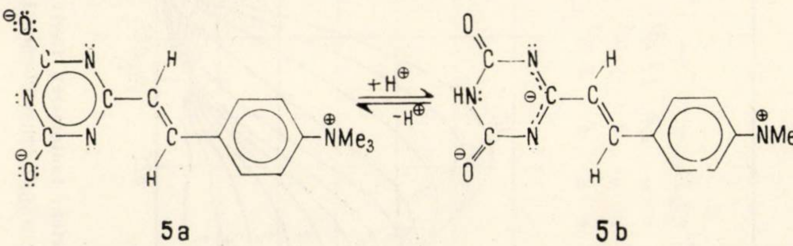

5a 5b

Andererseits zeigt Abb. 3, welche eine Familie von 6 Absorptionskurven saurer Lösungen ($[H_2SO_4] = 10^{-3}÷6$ Mol/l) von **5** in der genannten Konzentration wiedergibt (s. die Kurven *7÷11*), daß bei weiterer Aziditätserhöhung das Kation **5** ins Gleichgewicht mit seiner, am Triazinkern monoprotonierten Verbindung tritt, deren Struktur der des zweiwertig-kationischen (diprotonierten) Derivats **4** entspricht.

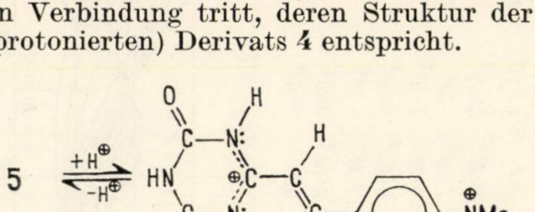

5c

Dieses Gleichgewicht ist durch die isosbestischen Punkte bei 308, 231 und ~ 197 nm (Kurven *7÷11*) gekennzeichnet. Es soll bemerkt werden, daß die drei isosbestischen Punkte nicht nur als Lage sondern auch als Intensität mit Pi_3, Pi_7 und ungefähr mit Pi_8 aus Abb. 1 übereinstimmen.

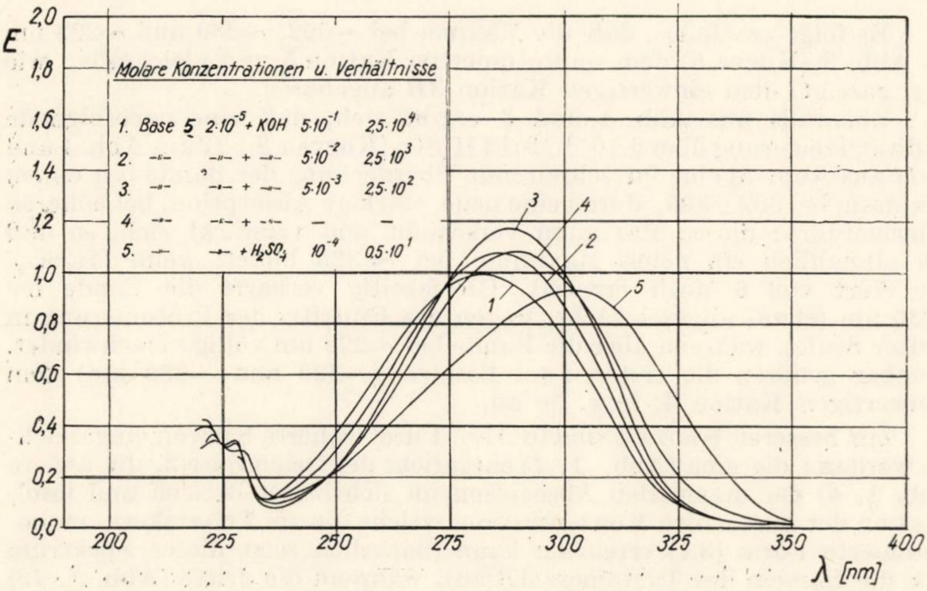

Abb. 2. — Extinktionskurven des quaternären Ammoniumions **5** und der entsprechenden (Amphi) Anionen (**5** *a* und **5** *b*) in 50 vol.-%iger wäßrig-äthanolischer Lösung.

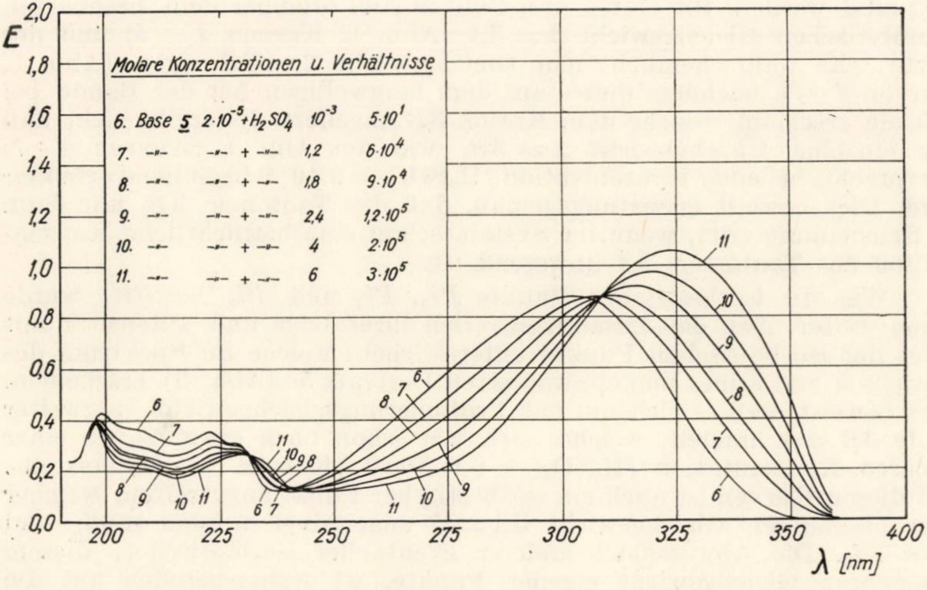

Abb. 3. — Extinktionskurven des quaternären Ammoniumions **5** und seines monoprotonierten Derivats **5** *c* in 50 vol.-%iger wäßrig-äthanolischer Lösung.

Es folgt zweifellos, daß die Maxima bei ~302, ~230 und ~223 nm aus Abb. 3 (Kurve *6*) dem unprotonierten Kation **5** und gleichfalls, wie oben gezeigt, dem einwertigen Kation **3***B* angehören.

Ebenfalls aus Abb. 1 und 3 ergibt sich, daß eine nachfolgende Aziditätssteigerung über 6.10^{-1} Mol/l H_2SO_4 (Kurven *9÷12* aus Abb. 1 und *7÷11* aus Abb. 3) eine fortschreitende Überdeckung der Bande mit einem Maximum bei 302÷305, durch eine neue, stärkere Absorption, bei höheren λ herbeiführt; dieses Maximum verschiebt und verstärkt sich, so daß sich allmählich ein neues Maximum bei ~ 325 bildet, wenn $[H_2SO_4]$ den Wert von 6 Mol/l erreicht. Gleichzeitig verharrt die Bande bei ~230 nm (etwas abgeschwächt, wegen des Eintritts der Protonierung in zweiter Stufe), während aber die Bande bei ~223 nm völlig verschwindet. Offenbar gehören die ersten zwei Banden (~325 und ~230 nm) dem zweiwertigen Kation **4**, bzw. **5***c* an.

Zur besseren Klarheit sind in Abb. 4 drei isolierte Kurven eingezeichnet worden: die eine (Abb. 1, *1*) entspricht der freien Base **2**, die andere (Abb. 1, *6*) der maximalen Absorption im sichtbaren Bereich und infolgedessen der maximalen Konzentration, welche die am Triazinkern monoprotonierte Form (**3***A*) erreichen kann (natürlich zeigt dieses Spektrum auch die Banden des Tautomers **3***B* an), während die dritte (Abb. 1, *12*) der diprotonierten Verbindung **4** (bei der von ihr maximal erreichten Konzentration) entspricht.

Mit den obigen Aspekten zusammen wird es offenbar, daß die isosbestischen Punkte Pi_1, Pi_2, Pi_4 und Pi_6 (Abb. 1) von der Einstellung der beiden Protonierungsgleichgewichte in der ersten Stufe $\mathbf{2} \rightleftharpoons \mathbf{3}A + \mathbf{3}B$ bestimmt werden. Die ersten drei Punkte sind offenbar dem besonderen protolytischen Gleichgewicht $\mathbf{2} \rightleftharpoons \mathbf{3}A$ (Abb. 1, Kurven *1 ÷ 5*) und der letzte sehr wahrscheinlich dem Gleichgewicht $\mathbf{2} \rightleftharpoons \mathbf{3}B$ eigen (Abb. 1, Kurven *4÷7*), nachdem dieses auf dem langwelligen Ast der Bande bei 230 nm erscheint, welche dem Kation **3***B* angehört. Es ergibt sich, daß das einzelne Gleichgewicht $\mathbf{2} \rightleftharpoons \mathbf{3}B$, wie aus Abb. 1 (Kurven *4÷7*) hervorgeht, bei einer Konzentration $[H_2SO_4] = 2.10^{-2}$ beginnend erfaßbar wird. Dies beweist erwartungsgemäß, daß das Tautomer **3***B*, nur dann in Erscheinung tritt, wenn im System schon eine beträchtliche Konzentration des Tautomers **3***A* anwesend ist.

Was die isosbestischen Punkte Pi_3, Pi_7 und Pi_8 betrifft, wurde schon weiter oben das Zusammentreffen ihrer Lage und Intensität mit jener der isosbestischen Punkte unterstrichen, welche im Spektrum des Kations **5** und seines monoprotonierten Derivats **5***c* (Abb. 3) erscheinen. Dies beweist, daß es sich um das Protonierungsgleichgewicht in zweiter Stufe $\mathbf{3}B \rightleftharpoons \mathbf{4}$ handelt, welches sich wie schon oben erwähnt, ab einer molaren Konzentration $[H_2SO_4] > 0{,}6$ Mol/l (Kurven *9÷12*) einstellt. Auf diesen Kurven ist auch ein isosbestischer Punkt anzutreffen, welcher dem besonderen Gleichgewicht $\mathbf{3}A \rightleftharpoons \mathbf{4}$ zugeordnet werden muß, und zwar Pi_5. Die Abwesenheit anderer eventueller isosbestischer, diesem besonderen Gleichgewicht eigener Punkte, ist wahrscheinlich auf die Überdeckung der Banden des farbigen Kations **3***A* durch die der anderen Komponenten (**3***B* und **4**) zurückzuführen. Es ist gleichfalls festzustellen daß das Gleichgewicht $\mathbf{3}A \rightleftharpoons \mathbf{4}$ erwartungsgemäß bei einer niedrigeren molaren Konzentration von H_2SO_4 erfaßbar wird, als jene dem Gleich-

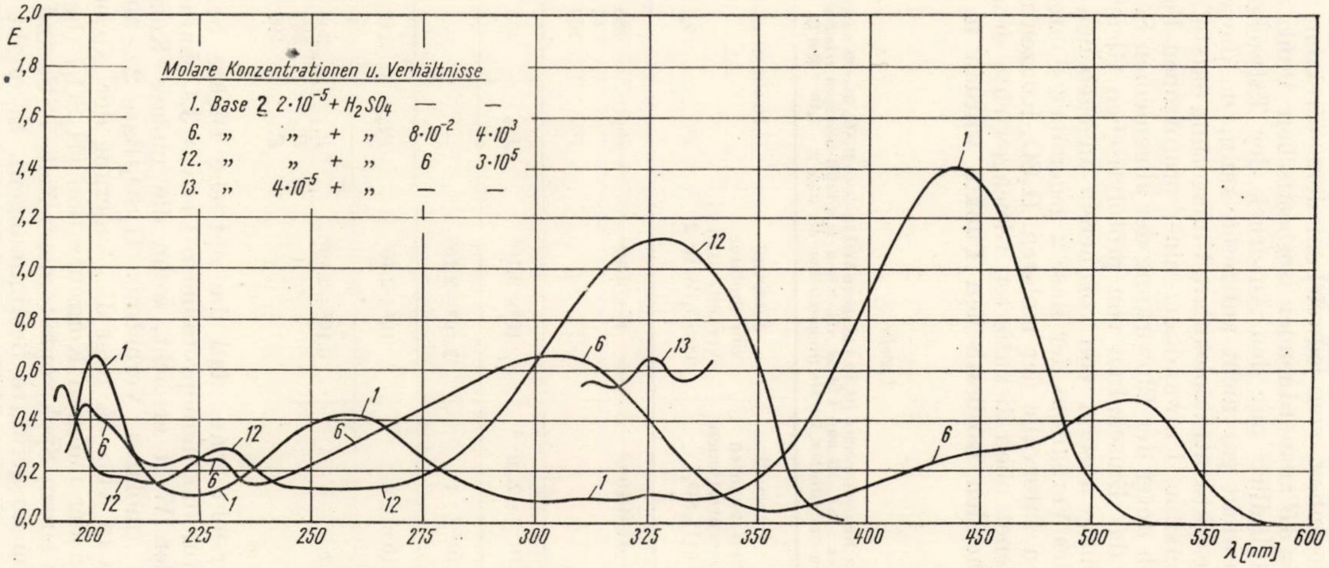

Abb. 4. – Extinktionskurve der Base **2** im Vergleich mit jenen ihrer mono- und diprotonierten Derivate **3** *A* und **4**, bei der höchsterreichten Konzentration der letzteren, in 50vol.-%iger wäßrig-äthanolischer Lösung.

gewicht $3B \rightleftharpoons 4$ entsprechende, und zwar ab $[H_2SO_4] > 0{,}2$ Mol/l (Abb. 1, Kurven *7÷11* und Abb. 5a).

Was die Abwesenheit von jedwelchem dem direkten tautomeren Gleichgewicht $3A \rightleftharpoons 3B$ zuzuordnenden isosbestischen Punk tanbelangt, stellt sie selbstverständlich nur den Ausdruck der Tatsache dar, daß ein solches Gleichgewicht gar nicht auftreten kann, da die Prototropie im allgemeinen keine echte intramolekulare Umlagerung darstellt. Tatsächlich findet die reversible Umwandlung einer prototropen Form in die andere ausschließlich unter der Einwirkung der allgemeinen Säure-Basen-Katalyse statt, die das Einschalten von protolytischen Gleichgewichten bedingt, eben im Sinne unserer von vornherein angegebenen schematischen Darstellung des Verhaltens der Base **2** gegenüber Säuren.

Die ungefähren Intervalle der molaren H_2SO_4-Konzentrationen in denen die verschiedenen oben diskutierten Gleichgewichte erfaßbar sind, sowie die entsprechenden isosbestischen Punkte wurden in Tabelle 1 wiedergegeben.

Tabelle 1

Ungefähre Intervalle von molaren Konzentrationen $[H_2SO_4]$ (molaren Verhältnissen H_2SO_4/Base 2) worin die verschiedenen Gleichgewichte zwischen den Arten 2, 3A, 3B und 4 in 50 vol.-%igen H_2O/EtOH-Lösungen erfaßbar sind, sowie die entsprechenden isosbestischen Punkte (Konzentration der Base 2 = 2.10^{-5} Mol/l)

Protolytisches Gleichgewicht	Intervall von molaren Konzentrationen $[H_2SO_4]$	Intervall von molaren Verhältnissen H_2SO_4/Base **2**	Isosbestische Punkte		
			Pi	λ_i	ε_i
$2 \rightleftharpoons 3A$	$0 \div 4.10^{-2}$	$0 \div 2.10^3$	P_{i1} Pi_2 Pi_4	486 342 266	10 100 2 620 9 500
$2 \rightleftharpoons 3B$	$2.10^{-2} \div 2.10^{-1}$	$10^3 \div 3.10^4$	Pi_6	235	3 750
$3A$ u. $3B$	$2.10^{-2} \div 4$	$2.10^3 \div 2.10^5$	—	—	—
$3A \rightleftharpoons 4$	$2.10^{-1} \div 4$	$10^4 \div 2.10^5$	Pi_5	247	4 750
$3B \rightleftharpoons 4$	$1{,}2 \div 4$	$6.10^4 \div 2.10^5$	P_{i3} P_{i7} P_{i8}	308 231 199	21 500 7 500 10 500

Aus Abb. 1 ersieht man, daß die optische Dichte bei 516 nm ($E = 0{,}49$), welche für das monoprotonierte Derivat $3A$ charakteristisch ist, seinen maximalen Wert erreicht, wenn die molare Konzentration $[H_2SO_4] \simeq 0{,}8.10^{-1}$ (molares Verhältnis H_2SO_4/Base $2 \simeq 4000$) wird.

Das Diagramm in Abb. 5a zeigt die Änderung der Absorption bei 516 nm als Funktion der molaren Konzentration $[H_2SO_4]$ (bei größerer Empfindlichkeit mit einem Spektrophotometer Zeiß VSU_1 und mit einer Küvette von 2,99 cm ausgeführte Bestimmungen). Es ergibt sich, daß in diesem wäßrig-äthanolischen Medium und bei dieser niedrigen Konzentration der Base **2** (10^{-5} Mol/l), die maximale Konzentration des mono-

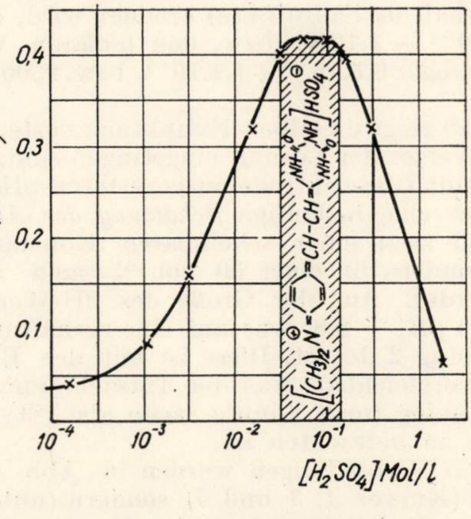

Abb. 5 a. — Änderung der Extinktion bei 516 nm als Funktion der molaren Konzentration $[H_2SO_4]$ der 50 vol.-%igen wäßrig-äthanolischen Lösungen (Anfangskonzentration der Base **2** = 10^{-5} Mol/l).

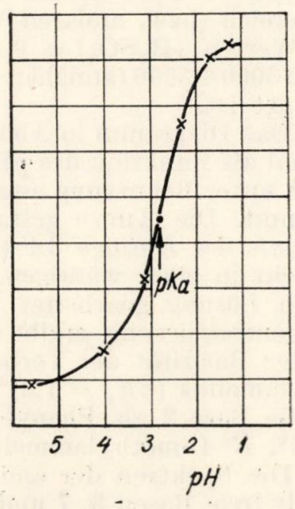

Abb. 5 b. — Änderung der Extinktion bei 516 nm als Funktion des pH-Wertes der 50 vol.-%igen wäßrig-äthanolischen Lösungen (Anfangskonzentration der Base **2** = 10^{-5} Mol/l).

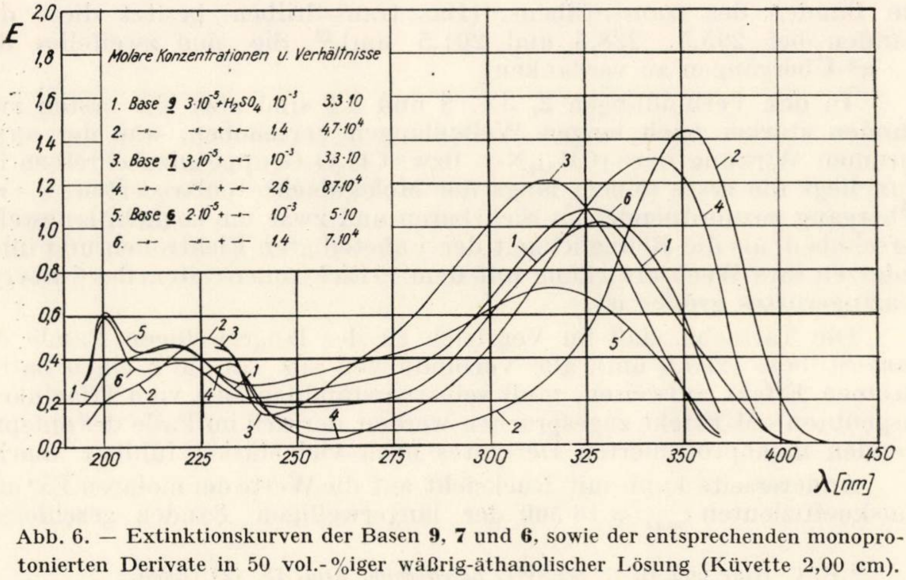

Abb. 6. — Extinktionskurven der Basen **9**, **7** und **6**, sowie der entsprechenden monoprotonierten Derivate in 50 vol.-%iger wäßrig-äthanolischer Lösung (Küvette 2,00 cm).

protonierten Derivats **3*A*** nur in einem verhältnismäßig engen Aziditätsbereich (bzw. molaren Verhältnis Säure/Base) erreicht wird, der von den Werten $[H_2SO_4] = 0{,}6\,10^{-1} \div 1.10^{-1}$, bzw. den molaren Verhältnissen $3000 \div 5000$ (annäherend sogar $0{,}5.10^{-1} \div 1{,}1.10^{-1}$, bzw. $2500 \div 5500$) begrenzt ist.

Das Diagramm in Abb. 5b zeigt dieselben Extinktionswerte, welche diesmal als Funktion des pH-Wertes der Lösung eingetragen sind. Dieser wurde unter Benutzung eines mit Glaselektrode ausgerüsteten pH-Meters bestimmt. Die Kurve gestattet eine beiläufige *Schätzung der Aziditätskonstante des Kations* **3*A*** (und zwar einer scheinbaren Konstante K'_a da nicht in einer wäßrigen, sondern in einer 50 vol.-% igen äthanolischen Lösung gearbeitet wurde). Aus der Größe des pH-Wertes bei Halbneutralisierung ergibt sich $pK'_a = 2{,}8$, was auf eine verhältnismäßig niedrige Basizität der Verbindung **2** deutet. Diese ist mit der Basizität des Ammelids ($pK_a = 1{,}8$)[11] vergleichbar, was der Tatsache entspricht, daß die Base **2** als Phenyl-Vinylog (man könnte sagen als ,,Styrylog") des N^6, N^6-Dimethylammelids zu betrachten ist.

Die Spektren der anderen Verbindungen wurden in Abb. 6 nicht nur als freie Basen **9**, **7** und **6** (Kurven *1*, *3* und *5*) sondern (unter den in der Abbildung angezeigten Bedingungen) auch als entsprechende konjugierte Säuren **9*A***, **7*A*** und **6*A*** (Kurven *2*, *4* und *6*), wiedergegeben. Die Tabelle 2 enthält die aus den Spektren in Abb. 1, 3 und 6 übernommenen Wellenlängen und Intensitäten der den Basen und entsprechenden konjugierten Säuren zugehörigen Banden.

Wie aus den Angaben der Tabelle 2 und aus Abb. 6 ersichtlich ist, zeigen die Spektren der Verbindungen **3*B***, **4**, **7**, **7*A***, **6**, **6*A***, **5**, **5*A*** eine große Ähnlichkeit mit dem Spektrum des *trans*-Stilbens, indem sie ebenfalls drei Banden aufweisen, die bei ähnlichen Wellenlängen liegen wie die Banden des *trans*-Stilbens. (Das trans-Stilben besitzt diese drei Banden bei 295,5, 228,5 und 201,5 nm).[12] Sie sind zweifellos den $\pi-\pi^*$-Übergängen zu verdanken.

In den Verbindungen **2**, **3*A***, **9** und **9*A*** sind aber die ersten zwei Banden stärker nach langen Wellenlängen verschoben, was der auxochromen Wirkung der $(CH_3)_2N$-, bzw. CH_3O-Gruppe zuzuschreiben ist. Nun liegt die erste (einem längs der Molekülachse polarisierten $\pi-\pi^*$-Übergang zuzuordnende) im Sichtbaren und zwar um so mehr langwellig verschoben, als die Beweglichkeit der unbeteiligten Elektronen und infolgedessen ihre Wechselwirkung mit dem π-Elektronensystem des β-Styryltriazingerüstes größer ist.

Die Tatsache, daß im Vergleich zu der längerwelligen Bande des *trans*-Stilbens (295,5 nm), alle Verbindungen aus Tabelle 2 einen bathochromen Effekt aufweisen, muß selbstverständlich dem vom Triazinkern ausgeübten—M-Effekt zugesprochen werden, der sich im Falle des entsprechenden monoprotonierten Derivates noch viel stärker fühlbar macht.

Andererseits kann mit Rücksicht auf die Werte der molaren Extinktionskoeffizienten $\varepsilon_{max} \gg 16\,500$ der längerwelligen Banden geschlossen

---

[11] R. C. Hirt und R. G. Schmitt, *Spectrochim. Acta*, **12**, 127 (1958).

[12] H. H. Jaffé und M. Orchin, "Theory and Applications of Ultraviolett Spectroscopy" John Wiley and Sons, New York, London, 1962, S. 276.

Tabelle 2

ε_{max}- und λ_{max}-Werte der Verbindungen

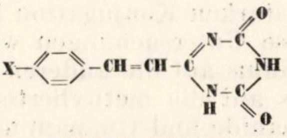

nach abnehmend auxochromem, bzw. ansteigend antiauxochromem Effekt des Substituenten X geordnet

X	Art	Bezeichnung	λ_{max}	ε_{max}	*X*	Art	Bezeichnung	λ_{max}	ε_{max}
$(CH_3)_2N$—	B	**2**	438	36 500	H	B	**7**	317	20 300
			325	2 500				232	7 500
			258	10 000				205	—
			202	17 500		$BH^{\oplus}$	**7** *A*	342	21 800
	$BH^{\oplus}$	**3A**	516	12 400				233	7 000
		3 *B*	305	16 500				200	—
			230	6 500	O_2N —	B	**6**	317	16 500
			223	7 380				218	11 500
			199	—				201	15 500
	$BH_2^{2\oplus}$	**4**	325	26 200		$BH^{\otimes}$	**6 A**	327	26 000
			232	5 250				220	9 500
			196	—				200	15 000
CH_3O —	B	**9**	350	17 500	$(CH_3)_3\overset{\oplus}{N}$ —	B	**5**	305	22 000
			238	9 300				230	7 650
			200	—				223	8 750
								200	10 750
	$BH^{\oplus}$	**9** *A*	404	24 000		$BH^{\oplus}$	**5** *A*	325	26 500
			252	8 330				230	6 500
			200	—				196	9 500

werden, daß alle Verbindungen mit stilbenähnlicher Struktur (und zwar, mit Ausnahme der Verbindung **3***A*, alle in der Tabelle 2 eingetragenen) die stabilere *trans-Konfiguration besitzen*, da festgestellt wurde, daß bei den eigentlichen Stilben-Derivaten die *cis*-Formen durch ε_{max} -Werte der längerwelligen Banden < 15 000 charakterisiert werden.[13-17] Wir bemerken bereits, daß dieser Schluß auch durch das Studium der IR-Spektren bestätigt wird, welcher den Gegenstand einer anderen Mitteilung bilden wird.

Übrigens ist auch im Falle des farbigen Kations **3***A* zu vermuten, daß es wenigstens im Kristallgitter eine streng *trans*-(und in diesem Falle gänzlich ebene) oder eine zu dieser sehr nahestehende Konformation, im Sinne der von uns angenommenen Formel **3***A*, einnimmt. Tatsächlich wäre die ebene *cis*-Konformation sterisch sehr behindert und infolgedessen

---

[13] M. Calvin und H. W. Alter, *J. Chem. Phys.*, **19**, 765 (1951).

[14] H. Suzuki, *Bull. Chem. Soc. Japan*, **33**, 379 (1960).

[15] R. Riezebos und E. Havinga, *Rec. Trav. chim.*, **80**, 446 (1961).

[16] D. Schulte-Frohlinde, H. Blume und H. Güsten, *J. Phys. Chem.*, **66**, 2486 (1962).

[17] O. H. Wheeler und H. N. Batle de Pabon, *J. Org. Chem.*, **30**, 1473 (1965).

unvereinbar mit der ausgeprägten Halochromie, welche das sichere Zeichen der sehr starken Konjugation bildet.

Diese Untersuchungen werden fortgesetzt, indem die Erweiterung des Studiums auf die anderen zwei Methyltriazin-Basen **1***b* und **1***c* und besonders auf die methylierten Derivate aller dieser Triazine (Guanamide, Guanide und Guanamine) verfolgt wird.

EXPERIMENTELLES

Nachfolgend werden die präparativen und analytischen Daten bezüglich der untersuchten Verbindungen angeführt, welche mit Ausnahme der Base **2**, alle neu sind.

Es wurde versäumt festzustellen ob die schwefelsauren Salze wasserhaltig oder -frei kristallisieren. Alle wurden nur nach einigem Verweilen im Exsikkator, also wasserfrei analysiert.

Die N %-Bestimmungen sind nach der Halbmikromethode von Kjeldahl-Parnas -Wagner, die $SO_4^{2\ominus}$ %-Bestimmungen aber gravimetrisch als SO_4Ba durchgeführt worden.

2,4-Dioxo-6-(p-dimethylamino-β-styryl)-tetrahydro-s-triazin-bisulfat (**3***A*) : $C_{13}H_{14}O_2N_4 \cdot \cdot H^{\oplus}HSO_4^{\ominus}$

a) In 10 ml Lösung von 0,66ml konz. H_2SO_4 in 96 %igem Äthanol, werden 10^{-2} Mol (= 1,27 g) **1** *a* und 10^{-2} Mol (= 1,49 g) *p*-DAB durch Erwärmen gelöst. Wie ersichtlich, wird ein Überschuß von 20 % Schwefelsäure gegenüber dem molaren Verhältnis H_2SO_4 /Base **2** = 1 : 1 verwendet.

Die Operation wird in einem Rundkolben mit Rückflußkühler auf siedendem Wasserbad ausgeführt. Anfangs färbt sich die Lösung tiefrot, dann setzen sch am Boden rotfarbige Kristalle des Bisulfats ab. Nach 4 Std. ist die Reaktion praktischi beendet. Man läß tabkühlen, filtriert und trocknet im Exsikkator. Ausbeute an **3***A* : 2,85 g, d.h. 80 % d.Th.

$C_{13}H_{16}O_6N_4S$ M = 366,36

Ber. :	N 15,72	$SO_4^{2\ominus}$	26,96 %
Gef. :	N 15,5	$SO_4^{2\ominus}$	26,6 %
	N 15,7	$SO_4^{2\ominus}$	27,0 %

b) In sehr reinem Zustand wird das Bisulfat folgendermaßen erhalten :

In ∼ 15 ml 5,5-molarer H_2SO_4 werden 2 g Base **2** aufgelöst und allmählich 65 ml heißes Wasser hinzugegeben; man erhält auf diese Weise eine ungefähr 1molare H_2SO_4-Lösung. Durch Abkühlung dieser Lösung scheiden sich bei Raumtemperatur ∼0,5 g **3** *A* (dunkelrote, nadelförmige Kristalle) aus.

Die oben angegebenen Konzentrationen der Base **2** und der Schwefelsäure wurden nach mehreren Versuchen als die günstigen befunden. Bei höherer H_2SO_4-Konzentration enthält das Produkt mehr $SO_4^{2\ominus}$ als theoretisch, bei niedrigerer werden weniger gut ausgebildete Kristalle erhalten.

2,4-Dioxo-(p-dimethylamino-β-styryl)-tetrahydro-s-triazin (**2**) : $C_{13}H_{14}O_2N_4$

a) *Die Synthese bei Säure-Katalyse* (H_2SO_4). Zu der bei der Bisulfatsynthese erhaltenen Masse gibt man 200 ml heiße, 1molare H_2SO_4-Lösung hinzu und neutralisiert nach völliger Lösung in der Wärme mit konzentrierten und weiterhin mit verdünntem Ammoniak bis zu pH ≃ 4, wobei die orangefarbige Base ausfällt. Es empfiehlt sich diesen pH-Wert nicht zu überschreiten, da sich die Base **2** bei höherem Wert wieder löst, indem sie als Säure funktioniert und ein $NH_4^{\oplus}$-Salz bildet.

Es wird filtriert, 2÷3mal mit warmem Wasser (je 5 ml), dann mit je 2÷3 ml Äthanol gewaschen und im Exsikkator getrocknet. Ausbeute = 2,48 g, d.h. 96 % d. Th.

Ein schnelleres Verfahren: die Masse des kristallisierten Bisulfats **3** *A* wird dekantiert und in 20 ml ungefähr 5molarer H_2SO_4-Lösung aufgelöst. Es wird mit wenig (30 ml) Wasser verdünnt und zum Abkühlen stehen gelassen. Zu dieser Lösung gibt man die dekantierte Mutterlösung hinzu und neutralisiert wie oben.

Das Präparat ist für gebräuchliche Zwecke genügend rein. Eine weitere Reinigung kann durch Umkristallisieren aus Formamid (~ 0,3 g aus 100 ml) erreicht werden wobei man rhombische, orangegelbe Blättchen erhält, welche bis 340° nicht, bei höherer Temperatur jedoch mit Zersetzung schmelzen. Unlöslich in Wasser, sehr wenig löslich in Äthanol, Cellosolve und Dioxan, etwas löslicher in Formamid und Eisessig.

Ber.:	M = 258,27	N 21,7 %
Gef.:		N 21,6 %
		N 21,5 %

b) *Die Synthese bei Basen(Piperidin)-Katalyse.* In 10 ml Formamid, welche 0,1 ml Piperidin enthalten, werden 5.10^{-3} Mol (= 0,63 g) **1** *a* und 5.10^{-3} Mol (= 0,745 g) *p*-DAB unter Erwärmen gelöst. Die Lösung wird auf einem Glyzerinbad bis 120° erwärmt. Nach 5 ÷ 10 Min. beginnt die Abscheidung von Kristallen der Base **2**. Die Temperatur wird 2 Std. beibehalten und dann die Lösung bei gewöhnlicher Temperatur stehen gelassen, wobei sich 0,8 g Base **2** kristallin abscheiden (Ausbeute 62 % d.Th.).

2,4-Dioxo-6- (p-*dimethylamino* - β - *styryl)-tetrahydro-s-triazin-tetrasulfat* (**4**) : $C_{13}H_{14}O_2N_4 \cdot \cdot 2H^{2\oplus}(HSO_4)_2^{2\ominus}$

In 6 ml 1 molarem H_2SO_4 werden 5.10^{-3} Mol (= 1,29 g) Base **2** aufgelöst. Nach gutem Vermischen des erhaltenen Breis (ohne Erwärmen) wird der Inhalt in einem Becher warm aufgelöst. Man erhält eine fast farblose Lösung. Durch Abkühlung kristallisieren farblose (wasserhaltige?) Nadeln des Tetrasulfats.

Durch Filtrieren entfernt man so gut wie möglich den H_2SO_4-Überschuß. Dann bringt man die Kristalle auf die trockene Platte einer Glasfilternutsche und beseitigt die an ihnen haftende Mutterlösung durch drei- bis viermal wiederholtes Auswaschen mit je 5 ml wasserfreiem Aceton.

Es wird über H_2SO_4 im Vakuum getrocknet. Das erhaltene Salz ist hygroskopisch und leicht hydrolisierbar; an der Luft geht es in das Bisulfat **3***A* über. Ausbeute = 1,36 g, d.h 60 % d.Th.

$C_{13}H_{18}O_{10}N_4S_2$

Ber.:	M = 454,43	N 12,32	$SO_4^{2\ominus}$	42,28 %
Gef.:		N 12,0	$SO_4^{2\ominus}$	41,8 %
		N 12,3	$SO_4^{2\ominus}$	42,0 %

Trimethyl-{p- [β-(*2,4-dioxo-tetrahydro-s-triazino-* 6)-*vinyl*]-*phenyl*}-*ammoniumsulfat-methylester* (**5**) : $C_{14}H_{17}O_2N_4^{\oplus}[O-SO_2-OCH_3]^{\ominus}$

In einer Ampulle werden 10^{-2} Mol (= 1,27 g) **1***a* und 10^{-2} Mol (= 2,75 g) nach Rupe und Mitarbeiter [18] hergestelltes Trimethyl(*p*-formyl-phenyl)-ammoniumsulfat-methylester erwärmt. Das geschmolzene äquimolekulare Gemisch wird 15 Min. lang bei 160° im Ölbad gehalten.

Die Reinigung erfolgt durch Umkristallisierung der abgekühlten Schmelze aus 30 ml 50 vol.-%igem wäßrigem Ätanol, der eine neue Umkristallisierung aus 15 ml einer Mischung von gleichem Volumen Äthylcellosolve und Formamid folgt. Als Endprodukt werden farblose nadelförmige Kristalle erhalten. Endausbeute: 1,92 g (50% d.Th.); Schmp. ≃ 180° unter Rotfärbung (!)

---

[18] H. RUPE, H. HAGENBACH und A. COLLIN, *Helv. Chim. Acta*, **18**, 1395 (1935).

$C_{15}H_{20}O_6N_4S$

Ber.: M = 384,41 N 14,57%

Gef.: N 14,4%

N 14,6%

2,4-Dioxo-6-(p-nitro-β-styryl)-tetrahydro-s-triazin (**6**): $C_{11}H_8O_4N_4$

Ein Gemisch von 5.10^{-3} Mol (= 0,635 g) **1***a* und 5.10^{-3} Mol (= 0,75 g) *p*-Nitrobenzaldehyd wird in eine Glasampulle gebracht, diese in der Flamme ausgezogen und verschlossen, der Inhalt geschmolzen und 30 Min. lang bei 180° im Ölbad gehalten. Die durch Abkühlung eingedickte, braunfarbige Schmelze wird mit ∼5 ml Dimethylformamid abgekocht und die heiße Suspension warm filtriert. Die Verunreinigungen und nicht reagierte Substanzen lösen sich auf. Der unlösliche Rückstand wird aus ∼10 ml Dimethylformamid umkristallisiert; die Base **6** wird so als farblose Prismen erhalten. Endausbeute 0,65 g d.h. 50%. Auch diese Verbindung schmilzt nur über 330° unter Zersetzung.

Ber.: M = 260,2 N 21,53%

Gef.: N 21,8%

N 21,7%

2,4-Dioxo-6-(p-nitro-β-styryl)-tetrahydro-s-trazinbisulfat (**6** *A*): $C_{11}H_8O_4N_4H^{\oplus} . HSO_4^{\ominus}$

In ∼ 5 ml heißer 8molarer Schwefelsäure werden 0,5 g **6** aufgelöst. Das Bisulfat kristallisiert bei Abkühlung in schwach gefärbten gelblichbraunen (wasserhaltigen?) Prismen, die nach Aufbewahren im Exsikkator der Formel **6***A* entsprechen:

$C_{11}H_{10}O_8N_4S$

Ber.: M = 358,29 N 15,64 $SO_4^{2\ominus}$ 26,81%

Gef.: N 15,5 $SO_4^{2\ominus}$ 26,9%

2,4-Dioxo-6-(β-styryl)-tetrahydro-s-triazin (**7**): $C_{11}H_9O_2N_3$

In 5 ml 96%igem Äthanol, welche $1{,}5.10^{-2}$ Mol (= 0,83 ml) konz. H_2SO_4 und $1{,}5.10^{-5}$ Mol (= 1,5ml) Benzaldehyd enthalten, werden 10^{-2} Mol (= 1,27 g) **1***a* aufgeschwämmt. Nach 30 Min. Erwärmung auf dem Wasserbad löst sich **1** *a* vollkommen auf. Es wird unter Rückfluß noch 1,5 Std. erwärmt und mit Ammoniak auf pH = 4 ÷ 5 gebracht, wobei das farblose Kondensationsprodukt als freie Base ausfällt. Man filtriert, wäscht mit wenig (∼5 ml) warmem Wasser, mit Aceton und Äther (∼ 2–3 ml) und trocknet im Exsikkator. Ausbeute: 1,7 g (∼ 80% d.Th.).

Die Reinigung erfolgt durch Umkristallisieren aus ∼60 ml Formamid; es werden farblose, nadelförmige Kristalle erhalten, deren Schmp. bei 299–300° liegt. Die Base **7** ist in Wasser, Äthanol und Äther wenig löslich.

Ber.: M = 215,21 N 19,52%

Gef.: N 19,3 %

N 19,45%

2,4-Dioxo-6-(β-styryl)-tetrahydro-s-triazinbisulfat (**7** *A*): $C_{11}H_9O_2N_3\,H^{\oplus} . HSO_4^{\ominus}$

In ∼25 ml heißer 5,5 ÷ 6 molarer Schwefelsäure werden 0,5 g **7** aufgelöst. Nach Abkühlung kristallisiert das Bisulfat in gelben Prismen. Das im Exsikkator einige Zeit aufbewahrte Salz entspricht der Formel **7** A.

$C_{11}H_{11}O_6N_3S$

Ber.: M = 313,29 N 13,41 $SO_4^{2\ominus}$ 30,66%

Gef.: N 13,2 $SO_4^{2\ominus}$ 31,2%

2,4-Dioxo-6-(p-*hydroxy-β-styryl)-tetrahydro-s-triazin* (**8**) : $C_{11}H_9O_3N$.

In 10 ml Lösung von 0,55 ml konz. H_2SO_4 ($\sim 10^{-2}$ Mol) in 96 %igem Äthanol werden 5.10^{-3} Mol (= 0,63 g) **1** und 5.10^{-3} Mol (= 0,61 g) *p*-Hydroxy-Benzaldehyd aufgelöst. Nach 3 Std. langer Erwärmung auf dem Wasserbad unter Rückfluß wird das Ganze mit Ammoniak bei pH $= 4 \div 5$ neutralisiert, das ausgefällte Produkt abfiltriert, mit wenig Wasser und Äthanol ($1 \div 2$ ml) gewaschen und im Exsikkator getrocknet. Ausbeute : 1,1 g d.h. 96 % d.Th.

Durch Umkristallisieren aus ∼ 10ml Dimethylformamid gereinigt, wird das Produkt in Form von schwach gelben Nadeln erhalten, welche nur über 330° unter Zersetzung schmelzbar sind.

Ber. :	M = 231,21	N 18,18 %
Gef. :		N 17,95 %
		N 18,0 %

2,4-Dioxo-6-(p-*methoxy-β-styryl)-tetrahydro-s-triazin* (**9**) : $C_{12}H_{11}O_3N_3$

In 10 ml Lösung von H_2SO_4 in 96 %igem Äthanol, $1,5.10^{-2}$ Mol H_2SO_4 (=0,83 ml konz. Säure) enthaltend, werden 10^{-2} Mol (= 1,27 g) **1***a* und $1,2.10^{-2}$ Mol (= 1,4 ml) *p*-Methoxy-Benzaldehyd unter Erwärmung gelöst. Nach 2stündigem Erwärmen auf dem Wasserbad wird mit Ammoniak bei pH = 4 neutralisiert, dann abgekühlt, filtriert und getrocknet. Ausbeute : 2,3 g (∼94 % d.Th.)

Durch Umkristallisieren aus 40 ml Formamid bekommt man das Produkt in Form von zitronengelben Prismen, deren Schmp. bei 305—306° liegt.

Ber. :	M = 245,23	N 17,13 %
Gef. :		N 16,8 %
		N 17,05 %

2,4-Dioxo-6-(p-*methoxy-β-styryl)-tetrahydro-s-triazinbisulfat* (**9** *A*) : $C_{12}H_{11}O_3N_3H^{\oplus} \cdot HSO_4^{\ominus}$

In 30 ml heißer 4molarer Schwefelsäure werden 0,5 g **9** aufgelöst. Beim Abkühlen kristallisiert das Salz in dunkelgelben Prismen aus, die nach Aufbewahren im Exsikkator der Formel **9***A* entsprechen :

$C_{12}H_{13}O_7N_3S$

Ber. :	M = 343,31	N 12,24	$SO_4^{2\ominus}$	27,98 %
Gef. :		N 12,1	$SO_4^{2\ominus}$	28,0 %

Revue Roumaine de Chimie, 15, 819–822 (1970)

$TiCl_4$-CAROTENOID COMPLEXES. VIII[1]
CYCLIZATION OF LYCOPENE AND δ-CAROTENE

V. TĂMAŞ and C. BODEA

Institute of Agronomy, Department of Chemistry, Cluj, Str. Mănăştur 3

Received July 8, 1969

The action of $TiCl_4$ on acyclic and half-cyclic C_{40}-carotenoids yield complexes, which are converted by acetonolysis into cyclic carotenoids with α-ionone rings and into dehydro-carotenoids. Starting with lycopene, δ-carotene, ε-carotene and 3,4-dehydro-lycopene are obtained. δ-Carotene is converted by this means into ε-carotene.

Continuing our studies about the action of $TiCl_4$ upon carotenoids[1] we have now investigated its action on acyclic and half-cyclic C_{40}-carotenoids, like lycopene (I) and δ-carotene (V). $TiCl_4$ reacts with I in benzene to give lycopene-titanochloro-complexes, as a result of the addition of $TiCl_4$ to the isolated double bond $C_1{=}C_2$, respectively $C_{1'}{=}C_{2'}$, or to the conjugated $C_5{=}C_6$ double bond. The dark reaction product contains 23.81% Cl, corresponding to a molar ratio lycopene : $TiCl_4$ = = 1 : 1.25. This ratio indicates the formation of a mixture of complexes (II, III and IV), shown in scheme 1.

SCHEME 1

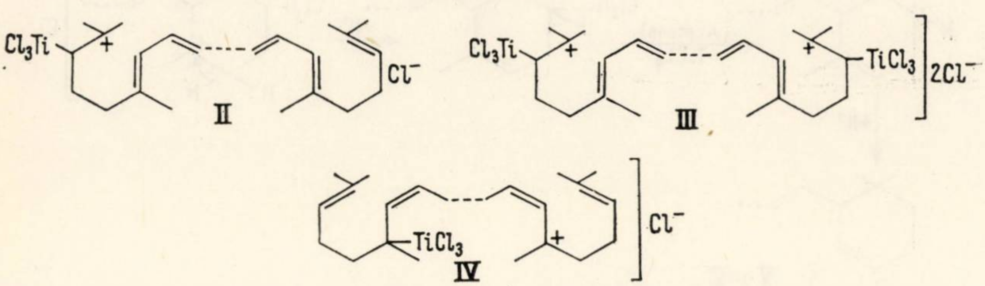

The three complexes could not be separated from the mixture.

The acetonolysis of this reaction product yields a mixture of hydrocarbon-carotenoids, easily separable by chromatography, consisting of two cyclic carotenoids with α-ionone rings, δ-carotene (V) and ε-carotene (VI) and of an acyclic dehydro-carotene, 3,4-dehydro-lycopene (VII.

---

[1] Part VII: V. TĂMAŞ and C. BODEA, *Rev. Roumaine Chim.*, 15, 655 (1970).

The transformation of lycopene under the action of $TiCl_4$ is shown in scheme 2.

SCHEME 2

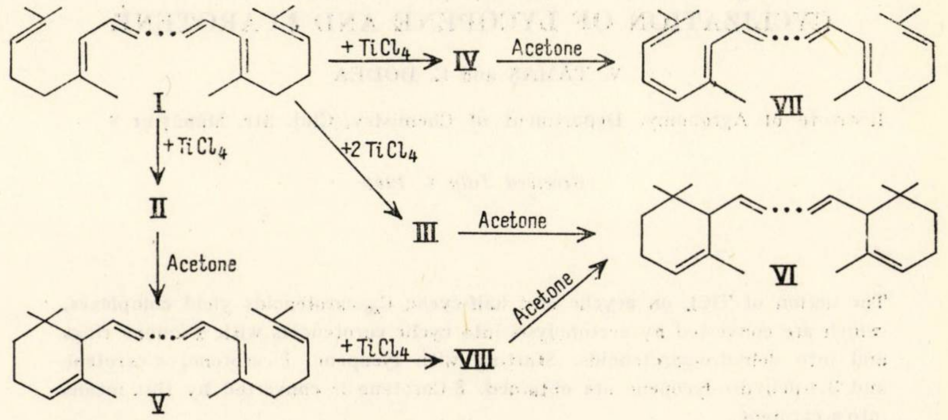
I
+ TiCl4
IV
Acetone
VII
+TiCl4
+2 TiCl4
II
III
Acetone
VI
Acetone
Acetone
+ TiCl4
VIII
V

The suggested mechanism for the cyclisation of lycopene is indicated in scheme 3.

SCHEME 3

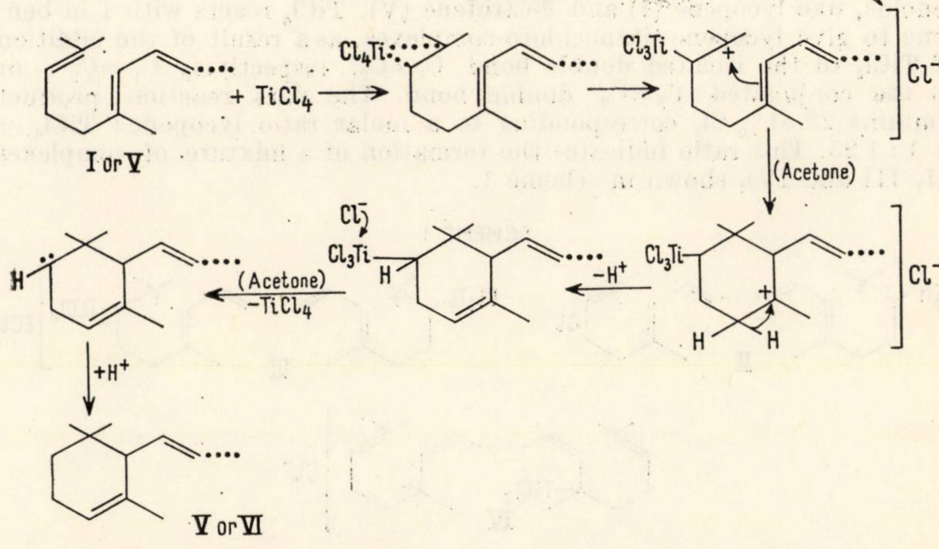
Cl4Ti:
Cl3Ti
Cl⁻
I or V
+ TiCl4
(Acetone)
Cl⁻
Cl3Ti
H
(Acetone)
-TiCl4
-H⁺
Cl3Ti
Cl⁻
H
H
+H⁺
V or VI

This mechanism is to some extent analogous to that of the cyclization of pseudoionone to give α-ionone and β-ionone under the action of D_2SO_4 and D_3PO_4, postulated by van't Hof et al.[2] and by Mursakulov et al.,[3] as well as to that of the biosynthetic cyclisation of acyclic carotenoids proposed by Goodwin.[4] It was reported that pseudoionone is cyclized by $TiCl_4$ to give β-ionone [5] and bi- and tri-cyclic ionones.[6]

---

[2] H. A. van't Hof, J. U. Veenland and Th. J. de Boer, *Tetrahedron*, **23**, 3757 (1967).

[3] I. G. Mursakulov, A. V. Semenovski, W. A. Smit and V. F. Kucherov, *Tetrahedron*, **23**, 1621 (1967).

The complexes IV are formed by the addition of $TiCl_4$ to the $C_5=C_6$ double bond, following the same steps from scheme 2. The acetonolysis of IV leads to retrodehydro-lycopene (IX), which cannot be isolated since it undergoes intramolecular stabilization through prototropic transposition resulting 3,4-dehydrolycopene (VII), as shown in scheme 4.

SCHEME 4

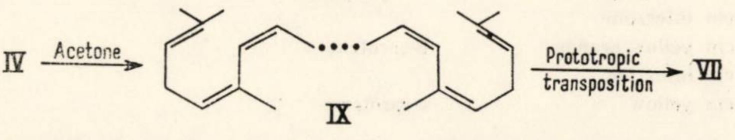

Starting with δ-carotene (V) the reaction with $TiCl_4$ leads to ε-carotene (VI) involving the complex VIII (see scheme 5).

SCHEME 5

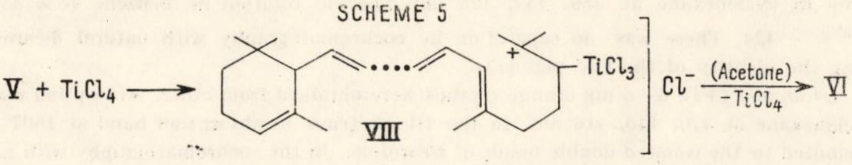

The formation of δ-carotene and ε-carotene has been proved by visible and infrared spectroscopy, specific rotation and mixed chromatography, as shown in the experimental part.

These results prove that acyclic carotenoids can be converted *in vitro* into cyclic carotenoids. We regard this as a support in favour of the proposed biosynthetical formation of cyclic carotenoids.[4]

EXPERIMENTAL

Lycopene was isolated from tomatoes [7] and purified by chromatography.

1. *Action of* $TiCl_4$ *upon lycopene (I)*

1.1. *Complex lycopene.* 1.25 $TiCl_4$. A solution of 50 mg I in 70 ml benzene, cooled to +8°, was treated with 0.1 ml $TiCl_4$. The dark blue solution was stirred several times and after 10 minutes the precipitate was filtered off and washed with benzene; 65 mg dark powder, containing 23.18 % Cl, were obtained. The electronic spectrum in dimethylformamide shows no maxima but absorption from 460 to 490 nm.

---

[4] T. W. Goodwin, *Biochem. J.*, **96**, 2 P (1965).

[5] H. R. Vogt, Thesis, Zürich, 1954.

[6] G. Büchi, E. Koller and W. Perry, *J. Amer. Chem. Soc.*, **86**, 5646 (1964).

[7] R. Willstätter and H. H. Escher, *Z. physiol. Chem.*, **64**, 47 (1910).

1.2. *Carotenoids V, VI, and VII.* A solution of 100 mg I in 100 ml benzene or 15 ml chloroform was treated with 0.15 ml $TiCl_4$ and the mixture kept 1 minute at room temperature. Then 150 ml acetone were added and after 15 minutes diluted with 400 ml petroleum ether. After washing with water and drying with Na_2SO_4, the pigments were separated by column chromatography, using as adsorbent a mixture of MgO and sand. After developing with a mixture of petroleum ether-benzene in which the ratio of benzene was increased up to 35%, the column (4 × 20) appeared as follows:

3 cm	red-violet	3,4-dehydro-lycopene
0.5 cm	interzone	
2 cm	orange-red	lycopene
1 cm	interzone	
3 cm	yellow-orange	δ-carotene
2 cm	interzone	
1.5 cm	yellow	ε-carotene

The elution of the pigments was performed with a mixture of ether-acetone-ethanol (9 : 2 : 1).

δ-Carotene (*V*). 25–27 mg dark orange crystals were obtained from ether. Absorption maxima in cyclohexane at 489, 457, 428 nm. Specific rotation in benzene (c = 33 mg), $[\alpha]_D^{25.5^\circ} = +424$. There was no separation in cochromatography with natural δ-carotene,[8] proving the identity of the two pigments.

ε-Carotene (*VI*). 6–8 mg orange crystals were obtained from ether. Absorption maxima in cyclohexane at 470, 440, 416 nm. In the IR-spectrum an absorption band at 1607 cm^{-1} is attributed to the isolated double bonds of ε-carotene. In the cochromatography with α-carotene there is a separation as ε-carotene migrates faster.

3,4-Dehydro-lycopene (*VII*). 25 mg red powder were obtained from ether, showing in cyclohexane absorption maxima at 525, 493, 462 nm. The same maxima are shown by natural VII.[9] In the IR-spectrum the doublet at 960, 980 cm^{-1}, characteristic of the *retro* form, is absent, proving the normal form of the pigment.

2. *Action of* $TiCl_4$ *upon δ-carotene (V)*

2.1. *Complex δ-carotene.* $TiCl_4$. A solution of 40 mg V in 15 ml benzene, cooled to +8°, was treated with 0.05 ml $TiCl_4$ and was stirred several times. After 15 min the precipitate was filtered off and washed with benzene; 42 mg dark powder, containing 18.82% Cl. The electronic spectrum in dimethylformamide shows a maximum at 480 nm.

2.2. *ε-Carotene* (*VI*). A solution of 33 mg δ-carotene, prepared as above, in 10 ml benzene was treated with 0.015 ml $TiCl_4$. After 1 min, 30 ml acetone and then 40 ml petroleum ether were added. The chromatogram (column 2 × 16 cm) obtained after developing with a mixture of petroleum ether-benzene in which the ratio of benzene increased up to 30% appeared as follows:

0.2 cm	orange-red	unknown
2 cm	yellow-orange	δ-carotene
0.5 cm	interzone	
5 cm	yellow	ε-carotene

Under the above mentioned conditions 10 mg ε-carotene were obtained.

---

[8] T. E. Kargl, F. W. Quackenbush and M. L. Tomes, *Proc. Amer. Soc. Horticult. Sci.*, **75**, 574 (1960), Lafayette, Ind., Purdue Univ., In : *Chem. Zentr.*, **23**, 8304 (1962).

[9] S. L. Jensen, *Phytochemistry*, **4**, 925 (1965).

Revue Roumaine de Chimie, **15**, 823–827 (1970)

VOLUMETRIC DOSAGE WITH PHENOTHIAZONE-(3). III* THE DOSAGE OF THE THIOLIC COMPOUNDS WITH PHENOTHIAZONE-(3)

M. RĂILEANU and EUGENIA DOBRE

University of Craiova, Organic Chemistry Department str. A. I. Cuza, 31

Received September 3, 1969

A method determining the thiolic compounds with phenothiazone-(3) n/100 in acetic acid was elaborated. By this method the thioglycolic acid, the cysteine, the thiourea and the thiosemicarbazide were determined. Due to thion-thiolic tautomery, the thiourea and the thiosesemicarbazide react with phenothiazone-(3) so as the thiols do. Under these conditions the phenothiazone-(3) oxidates the thiols up to the corresponding disulphides. The new determining method of the thiolic compounds is practical and very accurate.

Our previous paper [1] showed that the phenothiazone-(3) is a titrimetric substance with a redox character.

Continuing to extend the application field of this heterocycle in the analytical practice, we suggest in the present paper the dosage of thiolic compounds. With that end in view we determined with phenothiazone-(3) the thioglycolic acid, the cysteine, the thiourea and the thiosemicarbazide.

In the redox reactions due to a thion-thiolic tautomery, thiourea, [2-5] and thiosemicarbazide [6] behave like thiols.

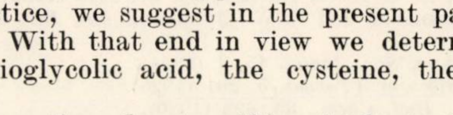

$$S = C\begin{matrix}\diagup NH_2 \\ \diagdown NH_2\end{matrix} \rightleftarrows HS-C\begin{matrix}\diagup NH_2 \\ \diagdown\!\diagdown NH\end{matrix}$$

The literature records that the thioglycolic acid is determined iodometrically,[7] iodatometrically,[8] coppermetrically [9] and mercurymetrically[10] ;

---

[*] Part II. M. Răileanu and E. Dobre, *Rev. Roumaine Chim.*, **14**, 1053 (1969).

[1] M. Răileanu and E. Dobre, *Rev. Roumaine Chim.*, **14**, 887 (1969).

[2] J. V. Dubsky, A. Okac and B. Okac, *Z. anorg. Chem.*, **216**, 486 (1934).

[3] W. Oliff, *J. Chem. Soc.*, **1965**, 2036.

[4] R. Bauer and J. Wehling, *Z. analyt. Chem.*, **199**, 171 (1964).

[5] K. Swaminathan and N. H. Irving, *J. Inorg. Nuclear Chem.*, **28**, 171 (1966).

[6] K. Jensen, *Z. anorg. Chem.*, **221** (6), 11 (1934).

[7] E. M. Hashall, *J. Assoc. Offic. Agr. Chemists*, **23**, 727 (1940).

[8] K. J. Steel, *J. Pharm. Pharmacol.*, **10**, 574 (1958).

[9] S. B. Sant and B. R. Sant, *Analyt. Chem.*, **31**, 1879 (1959).

[10] M. Wronski, *Analyt. Chem.*, **32**, 133 (1960).

also that the cysteine can be determined iodometrically,[11-15] iodatometrically,[8] bromatometrically,[16, 17] and with ferricyanide.[18]

Besides, many other determining methods of the mercaptans are known, which explain partly the difficulties met with when traying to determine with good results the compounds of this class.

Numerous determining methods of the thiourea are mentioned in the literature, too. Thus, thiourea can be determined iodometrically,[19-22] iodatometrically,[23] bromatometrically,[24] coppermetrically,[25] mercurimetrically,[26] with permanganate,[27] periodate,[28] ferricyanide,[29] iodine monochloride [30] a.s.o.

Recently the trend to use thiourea in the analytical determination of molybdenum,[31] potassium iodate [32] and cerium (IV) [33] became even more apparent.

Thiosemicarbazide is determined by iodine,[34] periodate,[35] nitrite,[36] hipobromite [37] and by other methods.

With a view to determining with phenothiazone-(3) of the thioglycolic acid, of the cysteine, of the thiourea and of the thiosemicarbazide, solutions n/100 were made under the following conditions : phenothiazone-(3) in acetic acid 95%, thioglycolic acid and cysteine in acetic acid 80%, thiourea in oxalic acid with pH=2.5 (the dissolving of the thiourea in oxalic acid is compulsory in order to obtain correct results) and thiosemicarbazide in acetic acid 95%.

The titre control of the thioglycolic acid solutions n/100 and of the cysteine n/100 was effectuated with iodine solution n/100. The thiourea

---

[11] W. A. Perlzweig and G. Debrue, *Biochem. J.*, **21**, 1416 (1927).

[12] N. Gavrilescu, *Biochem. J.*, **25**, 1190 (1931).

[13] E. J. King and C. C. Lucas, *Biochem. Z.*, **235**, 66 (1931).

[14] C. C. Lucas and E. J. King, *Biochem. J.*, **26**, 2076 (1932).

[15] R. Kuhn, L. Birkhofer and F. W. Quackenbusch, *Ber. dtsch. chem. Ges.*, **72**, 407 (1939).

[16] Y Okuda, *J. Chem. Soc. Japan*, **45**, 1 (1924).

[17] Y. Okuda, *J. Biochem.* (*Tokyo*), **5**, 201 (1925).

[18] H. L. Mason, *J. Biol. Chem.*, **86**, 623 (1930).

[19] A. Iiberti and E. Cervone, *Ann. Chim.* (*Rome*), **42**, 491 (1952).

[20] W. Scheele and C. Gensch, *Kautschuk u. Gummi*, **6**, WT 147 (1953).

[21] P. C. Gupta, *J. Indian Chem. Soc.*, **37**, 213 (1960).

[22] P. C. Gupta, *J. Indian Chem. Soc.*, **37**, 629 (1960).

[23] G. Milch, *Acta Pharm. Hung.*, **31**, 148 (1961).

[24] C. Mohr, *Z. analyt. Chem.*, **117**, 91 (1939).

[25] Z. Brada, *Analyt. Chim. Acta*, **3**, 53 (1949).

[26] H. E. Williams, *J. Soc. Chem. Ind.*, **58**, 77 (1939).

[27] K.B.S.R.P.S.P. Appa Rao and K. Neelakantam, *Indian J. Pharm.*, **14**. 50 (1952).

[28] A. Berka and J. Zýka, *Ceskoslov. farm.*, **4**, 222 (1955).

[29] M. G. Bapat and B. Sharma, *J. Sci. Research Benares Hindu Univ.*, **7**, 262 (1956–7); In : M.R.F. Ashworth, "Titrimetric Organic Analysis" (from Russian), Ed. Khimia Moscow, 1968, p. 226.

[30] B. N. Mitra and M. Srinavasan, *J. Indian Chem. Soc.*, **21**, 397 (1944).

[31] A. S. R. Murty, *Indian J. Chem.*, **3**, 517 (1965).

[32] S. K. Ghosh, *Ann. Chim.* (*France*), **48**, 141 (1966).

[33] R. P. Agarwal and S. K. Ghosh, *Ann. Chim.* (*France*), **47**, 407 (1965).

[34] K. S. Panwar, S. P. Rao and J. N. Gaur, *Anal. Chim. Acta* (*Amsterdam*), **25**, 218 (1961).

[35] A. Berka and J. Zýka, *Chem. listy*, **50**, 314 (1956).

[36] A. Miss and S. Iancu, *Rev. Chim.* (*București*), **5**, 399 (1954).

[37] J. Pijck, A. Campe and A. Claeys, *Bull, Soc. Chim. belges*, **73**, 898 (1964).

solutions n/100 and the thiosemicarbazide solution n/100 were obtained by weighing of the corresponding compounds (of analytical purity), by introduction into the graduated flask and by completing with solvent up to the mark.

In the course of analytical determinations it was found that the titre of thiourea n/100 and thiosemicarbazide n/100 solutions remains invariable only within at most two days.

The dosage with phenothiazone-(3) of the thioglycolic acid, of the cysteine, of the thiourea and of the thiosemicarbazide occurred by the indirect method, at usual temperature and without stirring in order to avoid the parallel oxidation on the mercaptans with molecular oxygen; the phenothiazone-(3) excess undemanded in the reaction was determined with sodium thiosulphate n/100.

The indirect dosage with phenothiazone-(3) of the thioglycolic acid and of the cysteine is carried out as follows: into 5 ml of thioglycolic acid n/100, or 5 ml cysteine n/100 in acetic acid 80%, 10 ml of phenothiazone-(3) n/100 in acetic acid are poured without shaking.

Then the bottle is heated to 90—100° and the phenothiazone-(3) excess immediately titrated with sodium thiosulphate n/100 till the colour changes from red to green (heating is necessary for the acceleration of the reaction).

The indirect determination of the thiourea and of the thiosemicarbazide is carried out in the same manner with the only difference that having added 10 ml of phenothiazone-(3) the closed flask is heated to 90—100° after being allowed to stay an hour, in darkness, at room temperature.

This is necessary, since the phenothiazone-(3) reacts with thiourea and thiosemicarbazide gradually, in the course of time, as the tautomeric equilibrium shifts from the thionic form to the thiolic one. Indeed, the experience shows that heating of the samples with a view of dosing the phenothiazone-(3) excess after less than 1 hour, at usual temperature, leads to inaccurate results, because unreacted thiourea decomposes while heated.

Table 1

Indirect dosage of thioglycolic acid with phenothiazone-(3) n/100

No	ml of thioglycolic acid n/100 taken during titration	ml of phenothiazone-(3) n/100 taken forthe titration of thioglycolic acid	ml of $Na_2S_2O_3$ n/100 required during retitration of phenothiazone-(3) excess n/100
1	5	10	5.01
2	5	10	5.00
3	6	10	3.99
4	6	10	4.00
5	7	10	3.01
6	7	10	2.99
7	8	10	2.00
8	8	10	2.01
9	9	10	0.99
10	9	10	1.00

The determination results with phenotihiazone-(3) of the thioglycolic acid, of the cysteine, of the thiourea and of the thiosemicarbazide are shown in tables 1, 2, 3 and 4.

Table 2

Indirect dosage of the cysteine with phenothiazone-(3) n/100

No	ml of cysteine n/100 taken during titration	ml of phenothiazone-(3) n/100 taken for the titration of cystenie	ml of $Na_2S_2O_3$ n/100 during retitration of phenothiazone (3) excess n/100
1	5	10	5.00
2	5	10	4.99
3	6	10	3.99
4	6	10	4.00
5	7	10	3.00
6	7	10	3.01
7	8	10	2.01
8	8	10	1.99
9	9	10	1.00
10	9	10	1.00

Table 3

Indirect dosage of the thiourea with phenothiazone-(3) n/100

No	ml of thiourea n/100 taken during titration	ml of phenothiazone-(3) n/100 taken for the titration of thiourea	ml of $Na_2S_2O_3$ n/100 required during retitration of phenothiazone-(3) excess n/100
1	5	10	5.00
2	5	10	4.99
3	6	10	4.01
4	6	10	4.01
5	7	10	3.00
6	7	10	2.99
7	8	10	2.00
8	8	10	2.01
9	9	10	1.00
10	9	10	1.01

Examining the experimental data registered in these tables we found an equivalent of phenothiazone-(3) consumption for an equivalent of mercaptan, whence it results that the phenothiazone-(3) oxidated the mercaptans up to the corresponding disulphides according to equation (1):

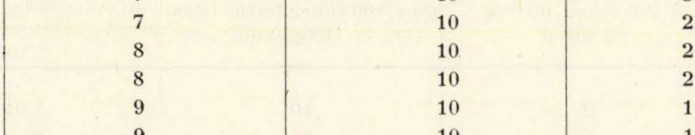

(1)

Table 4

Indirect dosage of the thiosemicarbazide with phenothiazone-(3) n/100

No	ml of thiosemicarbazide n/100 taken during titration	ml of phenothiazone – (3) n/100 taken for the titration of thiosemicarbazide	ml of $Na_2S_2O_3$ n/100 required during retitration of phenothiazone – (3) excess n/100
1	5	10	5.00
2	5	10	4.99
3	6	10	4.00
4	6	10	4.00
5	7	10	3.01
6	7	10	3.00
7	8	10	1.99
8	8	10	2.01
9	9	10	1.00
10	9	10	1.00

The reaction following the addition of the mercaptans to the quinoneiminic nucleus of the phenothiazone-(3), similar to the addition of mercaptans to p-benzoquinone [38, 39] or naphthoquinone [40] is out of question, because in this case two equivalents of phenothiazone-(3) for an equivalent of mercaptan would be consumed. From tables 1, 2, 3 and 4 it also results that the new method of indirect dosage of the thiols with phenothiazone-(3) is very accurate.

---

[38] O. Dimroth, L. Kraft and K. Aichinger, *Liebigs Ann. Chem.*, **545**, 125 (1940).

[39] M. Schubert, J. *Amer. Chem. Soc.*, **69**, 712 (1947).

[40] J. E. Little, T. J. Sproston and M. W. Foote, *J. Amer. Chem. Soc.*, **71**, 1124 (1949)

Revue Roumaine de Chimie, **15**, 829–834 (1970)

UV IRRADIATION OF UMP ON PAPER

O. L. HÖRER

"Stefan S. Nicolau" Institute for Inframicrobiology
Bucharest, Şos. Mihai Bravu 285

M. BADEA

Polytechnic Institute, Department of Physics
Bucharest, str. Polizu 1

Received July 31, 1969

The comparative appraisal of UMP photolysis in solution and on paper disks, in terms of extinction changes, is discussed, taking into account several factors such as multiple light scattering, water content and state, and a relative actinometric method is suggested.

INTRODUCTION

The interaction between light and matter in biological systems usually takes place in more or less turbid media, and multiple light scattering frequently occurs. Irradiation of nucleic acids and their constituents on paper can give useful information as a model for such biological systems, and the spectrophotometry of small paper disks impregnated with these substances permits the comparative study of a great number of UV irradiated samples, each containing less than 1 μg material.[1]

The present paper is concerned with the spectrophotometrical aspects of UMP samples irradiated on filter paper disks. The reason for choosing UMP as a test material is twofold : first — it is one of the most important photosensitive constituents of RNA, and secondly — its spectral and photochemical characteristics in solution[2] and on paper[3] are well established and it has been used for actinometric purposes.[4]

MATERIAL AND METHODS

The UMP (NBCo) solutions were prepared in distilled water or in citrate buffer (0.015 M Na Citrate) at pH 7, and in different concentrations ranging from 10^{-4} to 2×10^{-3} M.

---

[1] O. L. Hörer and M. Popescu, *Analyt. Chim. Acta*, **35**, 6 (1966).

[2] R. L. Sinsheimer, *Radiation Res.*, **1**, 505 (1954).

[3] H. Ishihara, *J. Chromatog.*, **4**, 376 (1960).

[4] D. Shugar, in "The Nucleic Acids", Vol. 3, E. Chargaff and J. N. Davidson eds., Academic Press, New York, 1960, p. 49.

The extinctions were determined by means of a VSU-1 (C. Zeiss-Jena) spectrophotometer, both in silica cells with layer depths of 0.1, 0.2 or 1.0 cm, and on previously water-cleaned and dried Schleicher-Schüll 2043 a paper disks, diameter ∅ = 0.6 cm, each disk being imbibed with 5 μl of UMP solution and then let to dry in air.[1] An improved spectrophotometric device was designed, which permits the use of several sample-holders for 24 paper disks. The corrections implied by the lack of homogeneity of the paper, as well as those due to the Na citrate on the extinction measurements have likewise been taken into account using the values at 262 and 350 nm[1].

The photochemical conversion of UMP in solutions and on paper disks, after exposure to the light of a Hanau PL 386 bactericidal lamp (with the main emission at 253.7 nm) was expressed in terms of $k = \log (E_0/E_t)$, where E_0 and E_t represent the extinctions at 262 nm of nonirradiated samples, after t seconds of exposure respectively. For the sake of uniformity all data referring to the measurements in cell will be marked with subscript c and those on paper disks with d.

The approximative UV doses D received by the samples were calculated according to the following relation :

$$D = 10^{-3} \cdot t \cdot \frac{dk/dt}{\varphi \cdot \varepsilon} \text{ einstein/cm}^2 \tag{1}$$

where t represents the exposure time, $\varphi = 2.16 \times 10^{-2}$ mol/einstein is the quantum yield,[2] and $\varepsilon = 8550$ the experimentally determined molar absorption coefficient at 253.7 nm respectively, corresponding to buffered 10^{-4} M UMP solutions.

All data are averages corresponding to 5–11 paper disks.

RESULTS AND DISCUSSION

For spectrophotometric comparison of the action of UV irradiation upon UMP in clear solutions and on paper disks as a turbid medium several factors were checked.

a) Measurements of the effective extinction coefficients of solutions ranging between 10^{-4} and 2×10^{-3} M UMP in sillica cells (E_c) and on impregnated dry paper disks (E_d) gave the following mean ratios corresponding to unbuffered (2) and buffered (2′) solutions :

$$E_d/E_c = 1.65 \pm 0.06 \tag{2}$$

$$E_d/E_c = 2.34 \pm 0.04 \tag{2'}$$

The latter value likewise agrees with that calculated for the RNA hydrolysate [5] $E_d/E_c = 2.31 \pm 0.06$, corresponding to the same ionic strength (0.09).

It results that the interaction probability between the photons and the absorbing UMP molecules is significantly increased in terms of the multiple light scattering in the paper.[6-8]

b) The data listed in table 1 exhibit similar dk/dt values for the buffered solutions irradiated simultaneously and spectrophotometrized in cells and on dried paper disks; therefore drying on paper of the irradiated solutions does not lead to a significant restoration of the damaged UMP molecules.

---

[5] O. L. Hörer, *Kolloid-Z.u.Z. Polymere*, **209**, 180 (1966).

[6] T. D. Price, P. B. Hudson and D. F. Ashman, *Nature*, **175**, 45 (1955).

[7] W. L. Butler and R. H. Norris, *Arch. Biochem. Biophys.*, **87**, 31(1960).

[8] W. L. Butler, *J. Opt. Soc. Amer.*, **52**, 292 (1962).

Table 1

Logarithmic extinction decrement rates dk_c/dt of buffered solutions, corresponding to several UMP concentrations, irradiated at various distances L from a bactericidal lamp, and spectrophotometrized in silica cells and after drying on paper disks.

L cm	Silica cells		Paper disks	
	UMP conc. 10^{-4} M	$10^4\ dk_c/dt$ sec^{-1}	UMP conc. 10^{-4} M	$10^4\ dk_c/dt$ sec^{-1}
20	1.0	1.48±0.03	5.0	1.50±0.06
21	5.0	1.30±0.02	16.0	1.31±0.01
27	7.8	0.78±0.06	7.8	0.79±0.10

c) The close k_a/k_c values obtained for the imbibed with UMP in distilled water paper disks irradiated in water saturated atmosphere and those irradiated in the "dry" state (in equilibrium with the air humidity), as seen in table 2 are probably due to the relative high water content of the latter.[9] As the physical state of the water in the paper is partly

Table 2

Logarithmic extinction decrement $k = \log(E_0/E_t)$ at 262 nm of the "wet" and "dry" paper disks containing UMP (k_d), simultaneously exposed with the reference UMP solutions in silica cells (k_c), in terms of the duration of irradiation t; the resulting dk/dt values, radiation intensities I calculated and the ratios k_d/k_c: the corrected k' values were calculated in terms of the curves corresponding to the continuous irradiation (fig. 1)

t seconds	"Wet" disks		"Dry" disks		
	k_c	k_d	k_c	k_d	k'_d
300	0.044	0.062	0.039	0.084	0.051
600	0.087	0.210	0.089	0.174	0.121
900	0.136	0.275	0.135	0.259	0.178
1200	0.184	0.429	0.177	0.335	0.248
1500	0.231	0.481	0.222	0.410	0.310
$10^4.\ dk/dt$ sec^{-1}	1.52±0.02	3.18±0.13	1.47±0.01	2.92±0.03	2.02±0.03
$I.\ 10^{10}$ *einstein* cm^2. sec	8.25±0.09	—	7.95±0.05		
k_a/k_c		2.09±0.16		1.99±0.09	1.39±0.03

---

[9] K. Macek, *Chem. listy*, **48**, 1181 (1954).

highly condensed, with an ice-like ordered structure,[10] the question arises of whether the UMP molecules should be considered as being irradiated only in "liquid" or in "frozen" solutions, implying important changes of the quantum yield.[11]

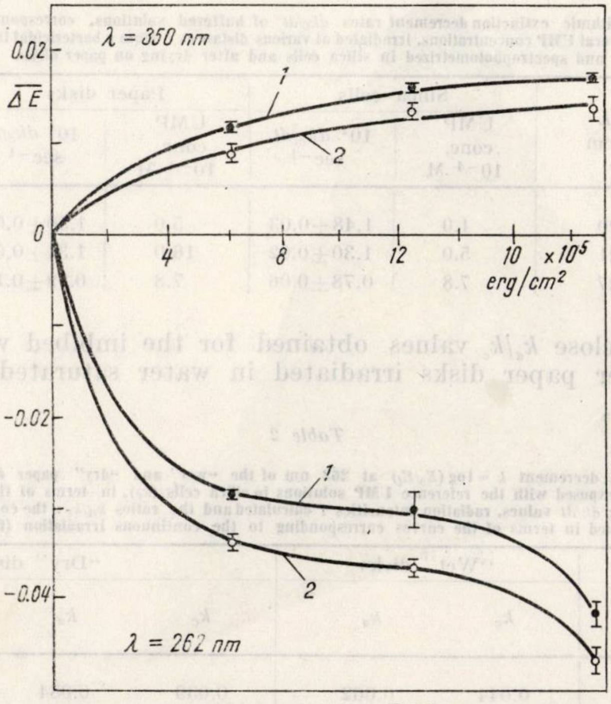

Fig. 1. — Mean extinction changes $\overline{\Delta E}$, corresponding to the wavelengths of 350 and 262 nm, of the UV irradiated substance-free paper disks in terms of received doses :

1, continuously exposed ; *2*, discontinuously exposed.

d) The extinction changes of the irradiated substance-free paper disks, determined at 262 and 350 nm (fig. 1), irrespective of whether or not they were continuously exposed, implies an adequate correction, made in terms of the data in figure 1 or directly, relative to a substance-free control disk irradiated simultaneously with the sample disks. The difference between the two methods are not significant (fig. 2, table 3 — experiment III).

The accuracy of the mean ratio $k'_d/k_c = 1.39 \pm 0.03$ (table 2) thus calculated, corresponding to $k'_d/k_d = 0.70 \pm 0.03$, suggests that paper disks containing UMP, for instance, can also be used for relative actinometric purposes, the linearity of the dose-effect curve being satisfactory (fig. 2) up

---

[10] V. K. Gorchakovskii, A. V. Finkel'shtein and D. S. Dobrovol'skii, "Materialy Konf. po itogam nauchn. issled. rabot za god, Sibirsk. Tekhnol. Inst.", Krasnoyarsk, USSR, 1965, 36 ; *Chem. Abstr.*, **65**, 9154_g (1967).

[11] K. C. Smith, *Photochem. Photobiol.*, **2**, 503 (1963).

Table 3

Logarithmic extinction decrement $k_d = \log(E_0/E_t)_d$ at 262 nm of the dry paper disks containing UMP in terms of duration of irradiation t, the corresponding corrected k_d' values obtained taking into account the extinction changes ΔE of the analogously exposed substance free paper disks, and the individual and mean k_d'/k_d values resulted: the data in brackets are calculated from direct extinction measurements with respect to simultaneously irradiated substance-free controls: I – continuous irradiation, II and III – discontinuous irradiation

Exp. code	t min	$10^3 \cdot k_d$	$10^3 \cdot k_d'$	k_d'/k_d	$\overline{k_d'/k_d}$
I	10	182± 3	130± 2	0.72±0.02	0.74±0.02
	20	352± 6	260± 6	0.74±0.03	
	30	475± 6	357± 7	0.75±0.02	
II	10	183± 6	132± 4	0.72±0.05	0.71±0.01
	20	356±10	245± 6	0.69±0.04	
	30	468± 6	336± 4	0.72±0.02	
	10	182± 4	135± 9	0.74±0.06	
			(142± 2)	(0.78±0.03)	**0.77**±0.02
III	20	371±13	293± 9	0.79±0.05	
	30	529±13	(307±10)	(0.83+0.06)	(0.79± 0.02)
			419± 8	0.79±0.03	
			(410± 7)	(0.77±0.03)	

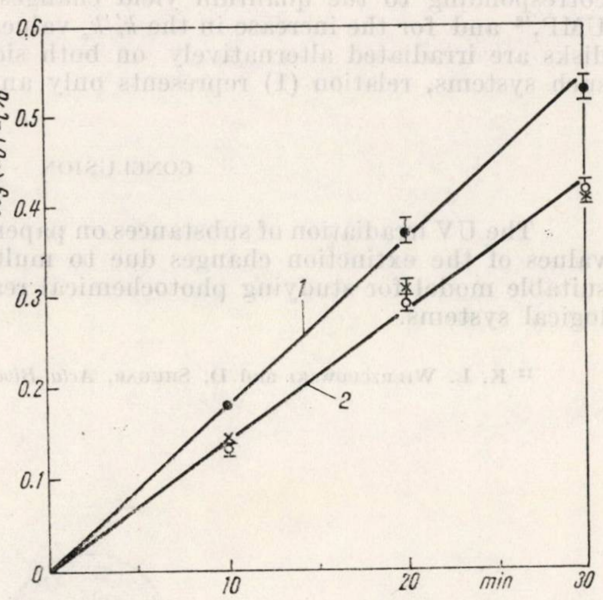

Fig. 2. — Logarithmic extinction decrement at 262 nm, log $(E_0/E_t)_d$, *versus* exposure time: as determined with respect to a non-irradiated control without correction for extinction changes due to paper irradiation, with the corresponding calculated correction, and as determined with respect to simultaneouslyirradiated substancefree controls (×).

to doses around 10^{-6} einstein/cm^2. Then, relation (1) can be applied, taking into account the k_d'/k_c ratio found.

e) Like concentrated frozen solutions, the paper disks do not conserve the homogeneous distribution of the UMP molecules during UV irradiation, the light intensity varying also significantly within the turbid medium in terms of depth and exposure time. This accounts for the more rapid flattening of all the curves in figure 2 at lower doses, than those corresponding to the quantum yield changes during UV irradiation of UMP,[12] and for the increase in the k_d'/k_c values by about 20% when the disks are irradiated alternatively on both sides (fig. 3). Therefore, for such systems, relation (1) represents only an approximate rule.

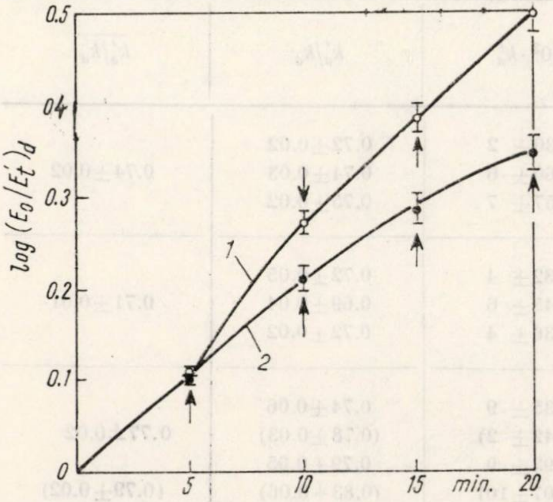

Fig. 3. — Logarithmic extinction decrement at 262 nm, $\log (E_0/E_t')_d$, of UMP irradiated on dry paper disks versus exposure time as determined with respect to simultaneously irradiated substance-free control;

1, disks exposed on one side, *2*, disks exposed on both sides successively. The arrows indicate alternation of the irradiated side.

CONCLUSION

The UV irradiation of substances on paper disks exhibiting increased values of the extinction changes due to multiple light scattering, is a suitable model for studying photochemical reactions in high turbid biological systems.

---

[12] K. L. Wierzchowski and D. Shugar, *Acta Biochim. Polon.*, **6**, 313 (1959).

ORSZÁGOS MŰSZAKI KÖNYVTÁR ÉS DOKUMENTÁCIÓS KÖZPONT 1883

CORRIGENDUM

In "Differential Vapour-Pressure Measurement and the Thermopynamic Properties of Benzil-CCl_4, Benzil-$CHCl_3$, Biphenyl-CCl_4 and Biphenyl-$CHCI_3$ solutions" by Rodica Vîlcu and Al. Bîrhală (*Revue Roumaine de Chimie*, **15**, 175 (1970)), heads of the tables 4—7 columns 3—6 should be multiplied by 10^3.

La *Revue Roumaine de Chimie* paraît 12 fois par an. Le prix d'un abonnement annuel est de £ 5.0.0 ; $ 12, — ; FF 60, — ; D.M. 48, — . Toute commande de l'étranger (fascicules ou abonnements) sera adressée à Centrala Cărţii, Oficiul de comerţ exterior Boîte postale 134—135, Bucarest, Roumanie, ou à ses représentants à l'étranger :

ALBANIA Ndërmarja Shtetëtrore E. Tregëtimit Të Librit Tirana ; AUSTRIA Globus Buchvertrieb Salzgries 16 Wien I ; BELGIUM Du Monde Entier 5, Place St. Jean Bruxelles ; Librairie Claeys-Verheughe 8, Volderstraat Gand ; Maison des Langues Vivantes 65, Rue du Midi Bruxelles ; Office International de Librairie 30, Av. Marnix Bruxelles 5 ; Vander Editeur 10, Munstraat Louvain ; BULGARIA Hemus Pl. Slaveikov 11-Sofia ; CANADA Canadian Slavic Studies Loyola Colege Montreal 262 ; Librairie Lidec Inc. 1083 Van Home Montreal ; Panonia Books 2, Spadina Road Toronto 4 Ontario ; CHINA Waiwen Shudian P.O. Box 88 Peking ; COLOMBIA Libreria Karl-Bucholz Av. Jimenez 8—40 Bogota ; CUBA Cubartimpex P.O. Box 6540 La Habana ; CZECHOSLOVAKIA Artia Ve Smerckach 30 Praha I ; DENMARK Munksgaard 6 Norregade Copenhagen K ; N. J. Hasses-Bogimport 8, Loerstraede Copenhagen K. ; FINLAND Akateeminen Kirjakauppa Postfach 10128 Helsinki 10 ; FRANCE Agence Littéraire et Artistique Parisienne 7, Rue Debelleyme Paris 3-e ; Eyrolles Editeur 61, Boulevard Saint-Germain Paris 5-e ; Librairie de l'enseignement technique (Stand permanent des livres techniques et scientifiques roumains) 61, Boul. Saint-Germain, Paris 5-e ; Librairie Hachette 25, Rue des Cévennes Paris 5-e ; Librairie Joseph Gibert 26—30, Boul. Saint-Michel Paris 6-e ; Libella 12, Rue Saint-Louis-en-l'Ile Paris 4-e ; Maison du Livre Italien 46, sRue des Ecoles Paris 5-e ; Office International de Documentation et Librairie 48, Rue Gay Lussac Paris 5-e ; Presses Universitaires de France 17, Rue Soufflot Paris 5-e ; THE GERMAN DEMOCRATIC REPUBLIC Deutscher Buch-Export-und-Import Leninstrasse 16 Leipzig C. 1 ; THE FEDERAL REPUBLIC OF GERMANY Kubon Sagner P.O. Box 68 München 34 ; Reise und Verkehrsverlag Hönigwiesenstrasse, 25 7 Stuttgart-Veihingen ; Zumsteins Landkartenhaus Liebherrstrasse, 5 8 München 22 ; GREAT BRITAIN Bailey Bros & Swinfen Ltd. Warner House 48, Upper Thames Street London E.C. 4 City 6521 ; Blackwell's Foreign Department Broad Street Oxford ; Central Books Ltd. 37, Grays Inn Road London W.C.1 ; Collet's Holdings Ltd. Denington Estate London Road Wellingborough Northans N & G Goyle Ltd. 119—125 Charring Cross Road London W.C. 2 ; Parker & Son 103, Walton Street Oxford ; HOLLAND Antiquariat Junk Walderstraat 10 Lochem ; Boekhandel Pegasus Leidsestraat 25 Amsterdam ; Intertaal Van Baerlesstraat 150 Amsterdam Zuit ; Meulenhoff Beulingstraat 2 Amsterdam C ; Swets & Zeitlinger Keizersgracht 471—487 Amsterdam ; HUNGARY Kultura Fö utca 32 Budapest 1 ; ISRAEL Haiflepac Ltd. 11, Arlosorov St. Haifa ; Lepac Ltd, 15, Rambam St. Tel-Aviv ; Lotus Ltd. Achad Haam St. Tel-Aviv ; ITALY SO, CO, LIB, RI Export-mport Piazza Margana 33 Roma ; JAPAN Maruzen Ltd. 6 Tory Michome Nihombashi Tokyo ; Nauka Ltd. Imp. Departm. 30—19 Minami Ikebukuro 2, Chome, Toshima-Ku Tokyo ; DEMOCRATIC PEOPLE'S REPUBLIC OF KOREA Chulpanmul ; MEXICO Editorial Grijalbo S. A. Aparatado 28568 Mexico. 17.D.F. ; MONGOLIA Mongolgosknigotorg Ulan Bator ; NORWAY Norsk Bokimport Postboks 3267 Oslo ; POLAND Ars Polona Krakowskie Przedmiescie 7 Warszawa ; PORTUGAL Libreria Bucholz Avenida Libertade Lisboa ; SPAIN Libreria Bucholz Paseo de Recoletos Madrid ; Libreria Cientifica General Preciados no. 48 Madrid 13 ; SWEDEN Almqvist Wiksell 26, Gamla Brogatan Stockholm 8. ; C. E. Fritze Fredgatan 2 Stockholm 16 ; Gumperts AB P. O. Box 346 Göteborg I ; SWITZERLAND Fachbücherei Postfach 1420 3001-Berna ; Herbert-Lang Ecke Munzgraben 2 Berna ; Librairie Payot 1-Rue de Bourg Ch-1002 Lausanne ; Librairie Rousseau 36, Rue Jean-Jacques Rousseau Genève ; Pinkus & Co. Froschaugasse 7 Zürich I ; THE UNITED ARAB REPUBLIC Dar El Tahrir et Publishing 21 Kasr el Nil St. (Dar el Shark Bookshop) Cairo ; THE U.S.A. Angelescu Book Service 3645, Barham Street Detroit 24 Michigan ; American Chemical Society 1155, Sixteenth Street NW Washington DC 20036 ; Fam Book Service 69, Fifth Avenue Suite 8 F ; New York 10003, N.Y. Franklin Square-Subscription Agency Teaneck (New Jersey 07666) ; W. S. Heinman 400, East 72nd Street New York, 21, N. Y. ; McGraw-Hill Book Company 330, West 42nd Street New York, N.Y. 10036 ; Moore-Cottrell Subscr. Agency Worth Cohocton, New York 14868 ; Nicoară Travel Service 17432, Woodward Ave. Detroit Michigan 48203 ; Shoenhof's Foreign Books, Inc. 1280, Massachusetts Avenue Cambridge, Massachusetts 02138 ; Henry M. Snyder & Co. Inc. 440 Fourth Avenue New York, N.Y. 10016 ; Twayne Publishers, Inc. 31 Union Square West New York 3, N. Y. ; Zeitein & Ver Brugge Booksellers 815 No. La Cienaga BLVD Los Angeles 69, California ; THE U.S.S.R. Mejdunarodnaia Kniga Moscow C. 200 ; THE DEMOCRATIC REPUBLIC OF VIET-NAM Xunhasaba 32, Hai Ba Trung Hanoi ; YUGOSLAVIA Forum V. Misica, 1 Novi Sad ; Jugoslovenska Knjiga Terazije, 27 Beograd ; Libertatea Z. Zrenjanina, 7 Pancevo ; Prosveta Terazije 16 I Beograd ;

ORSZÁGOS MŰSZAKI KÖNYVTÁR ÉS DOKUMENTÁCIÓS KÖZPONT 1983

La Revue Roumaine de Chimie paraît 12 fois par an. Le prix d'un abonnement annuel est de $ 5.00; £ 4.12; — Fr 60; — [illegible] La toute commande de l'étranger (fascicules ou abonnements) sera adressée à Cartimex, Calea Grivitei 64–66, Boîte postale 134–135, Bucarest, Roumanie, ou à ses correspondants à l'étranger.

ALBANIA: Ndermarja Shtetnore e Tregtimit, Tirana; AUSTRIA: Globus Buchvertrieb [illegible] Wien I; BELGIUM: Du Monde Entier, 5, Place St. Jean, Bruxelles; Librairie Encyclopédique [illegible] Vandenstraat [illegible] Maison des Langues Vivantes, 65, Rue du Midi, Bruxelles; Office International de Librairie 30, Av. Marnix, Bruxelles 5; Vander Editeur 10, [illegible] Louvain; BULGARIA: Hemus, Pl. Slaveikov 11, Sofia; CANADA: Canadian Slavic Studies Loyola College, Montreal 28; Librairie Québec, 1055, Van Horne, Montreal; Progress Books, 2, Spadina Road, Toronto 4, Ontario; CHINA: Guozi Shudian, P.O. Box 88 Peking; COLOMBIA: Libreria Karl Buchholz Av. Jimenez 8–40 Bogotá; CUBA: Cubartimpex, P.O. Box 6540 La Habana; CZECHOSLOVAKIA: Artia, Ve Smečkách 30 Praha 2; DENMARK: Munksgaard, 6 Nörregade Copenhagen K; [illegible] Pladsen [illegible] Copenhagen K; FINLAND: Akateeminen Kirjakauppa, Helsinki [illegible] 10 [illegible]; FRANCE: Agence Littéraire et Artistique Parisienne, 7, Rue Debelleyme, Paris 3-e; Eyrolles Editeur, 61, Boulevard Saint-Germain Paris 5-e; Librairie de l'enseignement technique (Stand permanent des livres techniques et scientifiques roumains) 61, Boul. Saint-Germain, Paris 5-e; Librairie Hachette 79, Rue des Écoles Paris 5-e; Librairie Joseph Gibert 26–30, Boul. Saint-Michel Paris 6-e; [illegible] 12, Rue Saint-Guillaume Paris 6-e; Maison du Livre Etranger 48, Rue des Écoles Paris 5-e; Office International de Documentation et Librairie 48, Rue Gay-Lussac Paris 5-e; Presses Universitaires de France 49, Rue Souflot Paris 5-e; THE GERMAN DEMOCRATIC REPUBLIC: Deutscher Buch-Export und -Import Leninstrasse 16 Leipzig C 1; THE FEDERAL REPUBLIC OF GERMANY: [illegible] P.O. Box 26 München 34; Reise und Verkehrsverlag [illegible] 27 Stuttgart-Vaihingen; Zeitungsvertrieb Lenbachstrasse 5–8 München 23; GREAT BRITAIN: Baker, Bart & Swinton Ltd. Warner House 48 Upper Thames Street London E.C. 4 City 6526; Blackwell's Foreign Department Broad Street Oxford; Central Books Ltd. 37, Grays Inn Road London W.C. 1; Collet's Holdings Ltd. Dennington Estate London Road Wellingborough Northants; H.K. Lewis Ltd. 119–125 Charing Cross Road London W.C. 2; Parker & Son 27 Broad Street, Oxford; HOLLAND: Antiquariaat Junk Wallerstraat 10 Lochem; Boekhandel Pegasus Leidsestraat 25 Amsterdam; Internationaal Van Stockumstraat 150 Amsterdam Zuid; Meulenhoff Beulingstraat 2 Amsterdam C; Swets & Zeitlinger Keizersgracht 471–487 Amsterdam; HUNGARY: Kultura Fő utca 32 Budapest 1; ISRAEL: Haifa Ltd. 11, Arlosoroff St. Haifa; Lepac Ltd. 15, Hamelach St. Tel-Aviv; Lepac Ltd. Achad Haam St. Tel-Aviv; ITALY: S.O.C.O. Lib. Esportazione [illegible] Roma; JAPAN: Maruzen Ltd. 6 Tori-Nichome Nihonbashi Tokyo; Nauka Ltd. Ippei Building 30–19 Minami Ikebukuro 2 Chome, Toshima-Ku Tokyo; DEMOCRATIC PEOPLE'S REPUBLIC OF KOREA: Chulpanmul; MEXICO: Editorial Cartago S.A. Apartado 25566 México 17 D.F.; MONGOLIA: Mongol Bookhandel Ulan Bator; NORWAY: Norsk Bokimport Postboks 2267 Oslo; POLAND: Ars Polona Krakowskie Przedmieście 7 Warszawa; PORTUGAL: Livraria Bertrand Avenida [illegible] Lisboa; SPAIN: Libreria Rubiños Paseo de Recoletos Madrid; Libreria General Francisco Carbajo, 48 Madrid 13; SWEDEN: A.B. Nordiska Wasagatan 26, Gamla Brogatan, Stockholm 16; C.E. Fritzes Fredsgatan 2 Stockholm 16; Gumperts A.B. P.O. Box 346 Göteborg 1; SWITZERLAND: Librairie Postfach 1820 3001 Bern; Herbert Lang Ecke Münzgraben 2 Bern; Librairie Payot 1 Rue de Bourg CH-1002 Lausanne; Librairie Rousseau 36, Rue Jean-Jacques Rousseau Genève; Pinkus & Co. Froschaugasse 7 Zürich 1; THE UNITED ARAB REPUBLIC: Dar El Tahrir, 24 Sh. Zakaria Ahmed [illegible] Cairo; THE U.S.A.: Angeles Book Service 7018 Barlum Street Detroit 24 Michigan; American Chemical Society 1155, Sixteenth Street N.W. Washington D.C. 20036; Bern Book Service 40 Fifth Avenue Suite 8 F New York 10011 N.Y.; Franklin Square Subscription Agency Fulton (New Jersey) 07666; N.Y. 3; Hafner 440 East 23rd Street New York 10 N.Y.; McGraw Hill Book Company 330 West 42nd Street New York 36, N.Y. 10036; Moore-Cottrell Subscription Agencies North Cohocton New York 14868; Pergamon Press 122 East 55th Street New York N.Y.; Stechert-Hafner 31 East 10th Street New York 3, N.Y.; Wayne State University Press 4841 Cass Avenue Detroit Michigan 48202; Universal Distributors 52–54 West 13th Street New York N.Y.; Cambridge Massachusetts 02138; Henry M. Snyder & Co. Inc. 440 Park Avenue South New York 10016; Twayne Publishers Inc. 31 Union Square West New York N.Y.; Victor Kamkin Bookstore 2906 14th Street N.W. Washington D.C. 20009; Four Continent Book Corporation 156 Fifth Avenue New York 10 N.Y.; Zeitlin 815 No. La Cienega Blvd. Los Angeles 46, California; THE U.S.S.R.: Mezhdunarodnaya Kniga Moskva G-200; THE DEMOCRATIC REPUBLIC OF VIETNAM: Xunhasaba 32, Hai Ba Trung Hanoi; YUGOSLAVIA: Forum 2, Novi Sad; Jugoslovenska Knjiga Terazije 27 Beograd; Nolit Terazije 27 Beograd; Prosveta Terazije 16/I Beograd.

NOTE POUR LES AUTEURS

La *Revue Roumaine de Chimie* publie des articles en anglais, français, russe, allemand ou espagnol. Les auteurs sont priés d'envoyer des articles, notes, communications et comptes rendus inédits.

Les manuscrits seront dactylographiés à deux intervalles. Les tableaux seront dactylographiés sur feuilles séparées, de même que la légende des figures. Les diagrammes seront tracés à l'encre de Chine sur papier calque. Les tableaux et les figures seront numérotés par des chiffres arabes, en nombre strictement nécessaire. Prière de ne pas inscrire les mêmes données dans les tableaux et les figures. Les formules chimiques seront incluses dans le texte ; en outre, elles seront transcrites sur des feuilles séparées. Les auteurs sont priés d'indiquer les caractères italiques (en soulignant les lettres au crayon), ainsi que tout autre caractère spécial. L'ordre des références bibliographiques sera celui de leur mention dans le texte ; le nom de l'auteur sera précédé de l'initiale du prénom ; les publications périodiques seront présentées suivant les prescriptions internationales. Les références seront ajoutées à la fin de l'article ; elles paraîtront comme des notes, au bas de la page. Le texte sera précédé d'un résumé, comprenant 15 lignes au maximum.

L'entière responsabilité du contenu des articles appartient aux auteurs. On publie des articles dus aux collaborateurs roumains ou étrangers. Les auteurs recevront 50 tirés à part.

PRINTED IN ROMANIA

TRAVAUX PARUS AUX ÉDITIONS DE L'ACADÉMIE DE LA RÉPUBLIQUE SOCIALISTE DE ROUMANIE

CORNEL BODEA et collab., **Tratat de biochimie vegetală**, partea I, **Fitochimie** (Traité de biochimie végétale, Ire partie, Phytochimie), Ier vol., 1964, 747 p. + 4 annexes + 2 pl., 41 lei, IIe vol., 1965, 1962 p., 1 pl., 56 lei, IIIe vol., 1967, 773 p., 35 lei.

V. GHEŢIE et V. MICUŞAN, **Analiza imunochimică. Teorie şi practică** (Analyse immunochimique. Théorie et pratique), 1966, 369 p., 28 lei.

SILVIA IONESCU, **Reacţii chimice induse de radiaţiile ionizante** (Réactions chimiques produites par les radiations ionisantes), 1963, 271 p,, 15 lei.

MARIETA NICOLAE, **Fizico-chimia proceselor fotografice** (Physico-chimie des processus photographiques), 1964, 426 p. + 4 pl., 35 lei.

R. PORTOCALĂ et L. POPA, **Acizii ribonucleici celulari şi virali** (Les acides ribonucléiques cellulaires et viraux), 1966, 375 p. + 8 pl., 26 lei.

D. PURDELA et R. VÎLCEANU, **Chimia compuşilor organici ai fosforului şi ai acizilor lui** (La chimie des composés organiques du phosphore et de ses acides), 1965, 540 p., 37 lei.

CRISTOFOR SIMIONESCU, MARGARETA GRIGORAŞ et AGATA CERNĂTESCU-ASANDEI, **Chimia lemnului din R.P.R.** (La chimie du bois en Roumanie), 1964, 239 p. + 6 pl., 27 lei.

CRISTOFOR SIMIONESCU et CLEOPATRA VASILIU-OPREA, **Mecanochimia compuşilor macromoleculari** (La mécanochimie des composés macromoléculaires), 1967, 344 p., 23,50 lei.

I. V. MAXIM, **Materiale nucleare** (Matériaux nucléaires), 1969, 444 p., 4 pl., 30 lei.

I. P. „Informaţia" c. 5171

43 426

Lei 25

F 1103

R 04

REFERÁLVA

REVUE ROUMAINE DE CHIMIE

TOME 15
N° 6
Juin 1970

ÉDITIONS DE L'ACADÉMIE DE LA RÉPUBLIQUE SOCIALISTE DE ROUMANIE

Rev. Roumaine Chim.

15, 835–984 (**1970**), Bucarest

COMITÉ DE RÉDACTION

Rédacteur en chef :

C. D. NENIŢESCU, membre de l'Académie de la République Socialiste de Roumanie

Rédacteurs en chef adjoints :

A. T. BALABAN et V. E. SAHINI, membres correspondants de l'Académie de la République Socialiste de Roumanie

Collège de rédaction :

C. DRĂGULESCU, RALUCA RIPAN, CR. SIMIONESCU, membres de l'Académie de la République Socialiste de Roumanie ; EM. BRATU, membre correspondant de l'Académie de la République Socialiste de Roumanie, Pr P. OSTROGOVICH, MARGARETA AVRAM, F. BADEA, I. D. MARCHIDAN, D. NEGOIU et D. SĂNDULESCU.

Les manuscrits, les livres et les revues proposés en échange, ainsi que toute correspondance seront envoyés à la rédaction :

REVUE ROUMAINE DE CHIMIE

23, str. Dumbrava Roşie, Bucarest, 9, Roumanie.

F1103

ORSZÁGOS MŰSZAKI KÖNYVTÁR DOKUMENTÁCIÓS 1883

REVUE ROUMAINE DE CHIMIE

Tome 15, N° 6 Juin 1970

Page

I. G. MURGULESCU and LAURA VASU, Correlations between electrical conductivity and diffusion in molten salts 837–841

I. G. MURGULESCU et D. TOPOR, Électromigration dans les nitrates monovalents fondus. Les ions de strontium et de baryum 843–846

CAMELIA BELDIE and FLORICA BĂRBULESCU, Salt effects in ternary systems furfural-water-electrolyte. II. Ternary systems furfural-water-organic electrolyte 847–854

D. FĂTU, SANDA FĂTU, ANCA TEODORESCU et E. SEGAL, Cinétique de la décomposition thermique de quelques combinaisons complexes des halogénures de cadmium avec des picolines 855–864

J. ZSAKÓ, E. KÉKEDY and CS. VÁRHELYI, Kinetics and mechanism of substitution reactions of complexes. XIX. Influence of heating rate on the thermal decomposition of $[Co(DH)_2\ (amine)_2]\ I$ type complexes in the conditions of thermogravimetric analysis 865–872

I. I. BĂDILESCU, Hydrogen bonds. III. HMO treatment of some chelated compounds related to 2-hydroxyacetophenone 873–879

P. NAGY, I. GÖRBE and A. SZURKOS, The substituent effects on the halfwave potential of the *p*-dimethylamino-*o*′, -*m*′, -*p*′-substituted azobenzenes 881–886

Z. GROPŞIANU, D. KOHN und A. IOVI, Wärmeübergangszahlen beim Verdampfen von Kaliumnitratlösungen 887–894

CONST. GH. MACAROVICI, F. MÁNOK und CS. VÁRHELYI, Polarographische Untersuchung der Reaktion zwischen Pentachloro-aquo-platin(IV)-Säure und 1,2-Cyclohexandiondioxim 895–899

I. PARALESCU, The molar absorptivity and stability of some complex compounds of the BA_n form 901–916

J. DICK, ANNA MAURER und Z. SZABADAI, Neue Komplexverbindungen der Pyrazolonreihe. VII. Sichtbare und UV-Spektren 917–934

ILEANA LUKÁCS, CONSTANŢA STRUSIEVICI et C. LITEANU, Sur les vanadates. XVIII. Composés mixtes $V^{5+}-V^{4+}$ obtenus en solutions aqueuses 935–944

D. COSTACHE, Kinetic measurement of cobalt traces. III. With ponceau red . 945–949

V. M. BHATNAGAR, The cell parameters of strontium hydroxyapatite, $Sr_{10}(PO_4)_6(OH)_2$ 951–953

V. M. BHATNAGAR, New observations on lead apatites 955–956

Rev. Roumaine Chim. 15, 835–984 (1970), Bucarest

S. SOLACOLU, P. BALTĂ and GEORGETA JITIANU, The influence of phosphorous pentoxide on the crystallization process of some lithium silicate glasses 957–964

ELENA NICOARĂ, DOINA OŞIANU and C. BODEA, Inchain epoxides of carotenoids. I. 9,10- and 13,14-epoxy-canthaxanthin 965–971

C. LITEANU and I. C. POPESCU, The use of membranes to indicate the equivalence point. V. The parchment-paper membrane impregnated with $BaSO_4$, indicating electrode in the Cl^-, Br^-, I^- titration 973–984

Revue Roumaine de Chimie, **15**, 837–841 (1970)

ORSZÁGOS MŰSZAKI KÖNYVTÁR ÉS DOKUMENTÁCIÓS

CORRELATIONS BETWEEN ELECTRICAL CONDUCTIVITY AND DIFFUSION IN MOLTEN SALTS

I. G. MURGULESCU and LAURA VASU
Center of Physical Chemistry of the Academy, Bucharest, str. Galați, 31

Received October 25, 1969

In this paper the difference between experimental electrical conductivity of molten alkali halides and that computed from ionic diffusion coefficients is explained by assuming the existence of a correlation factor between ionic jumps. Also, following Mullen's method, a theory of the activation energy for electrical conductivity is given in terms of compressibility coefficients of the liquid state.

Usually, by analogy with the structure of hard electrolytes, the molten alkali halides are thought of as completely dissociated systems, composed of ions that move independently. Such picture would imply a Nernst-Einstein relation between electrical mobility and diffusion coefficient for both cations and anions. However, experiments revealed differences in behaviour between electrical conductivity and coefficients of diffusion as function of temperature. Generally, the first has a slower variation with the temperature and one obtains too great values for electrical conductivity if it is calculated by a Nernst-Einstein equation.

Supposing a vacancy model for the molten salts structure, this behaviour was explained[1,2] as a result of the correlation between ionic jumps during the transport and of the ionic association.

Einstein's equation was established for perfect solids. It is known that Einstein's equation for imperfect solids differs from that for perfect solids, the difference being expressed by a constant factor[3,4]. Thus, in an electric field the ionic jumps are produced in a well defined direction, no matter if the crystal is perfect or not.

If ν is the jump frequency, we can write for the electrical conductivity $\lambda_{\text{solid}} = \alpha\nu$, where α is a function of temperature, but independent of the kind of lattice (perfect or not).

---

[1] F. Lantelme, Thèse, Université de Paris, 1965.

[2] O. P. Mehta, Thèse, Université de Paris, 1967.

[3] J. Bardeen and C. Herring, "Imperfections in Nearly Perfect Crystals", Ed. W. Shackley, N. Y., 1952, chap. 4.

[4] A. B. Lidiard, "Ionic Conductivity" in "Hanbuch der Physik", vol. 20, 1957, p. 324.

On the contrary, the diffusion, also dependent on ν, is dependent on the kind of lattice (perfect or not).

We have [5,6]

$$D = f\,G\,\nu\,d^2$$

where d is the anion-cation distance, G a numerical factor, and $f = 1$ if the lattice is perfect, but $f \neq 1$ if it is not.

The factor f has a simple meaning: suppose in a lattice an ion has just jumped from a lattice site into a neighbouring hole. Its former position is now a vacant one. If there are n neighbouring ions around a vacancy, the ion which has just jumped leaving the vacancy may return into it with a probability of $\frac{1}{n}$.

Such kind of jumps are ineffective for diffusion. To account for them in a vacancy mechanism for diffusion we must take a correlation factor $f < 1$.

Different mechanisms for different lattices were investigated [5,6]. For an interstitial mechanism it is possible that $f > 1$.[6]

Now, we may write

$$\lambda = \alpha'\,D\,f^{-1}$$

where α' is independent of the kind (perfect or not) of the lattice. This argument must remain valid also for liquids.

Instead of $\lambda_i = \frac{F^2}{RT} D_i$, we must write:

$$\lambda_i = \frac{F^2}{RT} D \cdot \frac{1}{f}$$

It may be supposed that the difference between the calculated values for electrical conductivity by a Nernst-Einstein equation (λ_1) and the experimental ones is partly due to the correlation between jumps. The ratio $\lambda_1/\lambda_{\text{exp}}$ is approximately a constant, so that jumps might be correlated in order to give a factor $f \neq 1$ (Table 1).

On the other hand, the correlation may play only an additional role in the transport process.

The great number of vacancies in the liquid state implies the presence of many groups with two or more vacancies. The possibility of associated displacements of ions must be taken into account. In simple molten salts, of NaCl type, the more mobile groups are, with the greatest probability, the pairs — the contribution to diffusion of the others groups being small.

If we take into account only the displacements of single ions and of pairs, the experimental diffusion coefficient for the i ions will be the sum for ions and pairs, i.e.

$$\left.\begin{aligned} D^+_{\text{exp}} &= x\,D^+ + (1-x)\,D_p \\ D^-_{\text{exp}} &= x\,D^- + (1-x)\,D_p \end{aligned}\right\} \text{ wherefrom } x = \frac{D^+_{\text{exp}} - D^-_{\text{exp}}}{D^+ - D^-}$$

---

[5] K. Campaan and Y. Haven, *Trans. Faraday Soc.*, **52**, 786 (1956).

[6] K. Campaan and Y. Haven, *Trans. Faraday Soc.*, **54**, 1498 (1958).

where D^+ = diffusion coefficient for cations, moving unassociated,
D_p = diffusion coefficient for pairs,
and x = fraction of single ions.

Table 1

Electrical conductivity calculated from diffusion coefficients

Salt	t°C	$D^{\pm}_{exp} \times 10^4$ cm² sec +	−	$\lambda_{1\,calc}$ ohm⁻¹cm²	$\lambda_{1\,calc}/\lambda_{exp}$ (f_1)	$\lambda_{2\,calc}$ ohm⁻¹cm²	λ_{exp}	λ^{*}_{2calc} ohm⁻¹cm²	$\lambda_{2\,calc}/\lambda_{exp}$ (f_2)
NaCl	838	0.96	0.67	164	1.17	95.9	140	(140*)	0.685
	850	0.97	0.70	162	1.18	93.6	142	(142*)	0.66
	900	1.14	0.82	189	1.27	100.6	149	147 152	0.675
	950	1.31	0.96	207.5	1.33	105.3	155.5	154 159	0.68
NaI	670	0.735	0.405	135	1.03	99.8	133.5	(133,5*)	0.75
	700	0.78	0.43	139	1.02	103.3	137	137	0.75
	750	0.865	0.49	148	1.02	106.1	144	141	0.736
	800	0.95	0.54	155	1.02	110	152	145	0.72
KCl	800	0.71	0.64	141	1.28	48	110	(110*)	0.44
	900	0.91	0.85	168	1.33	56	126	126	0.44
RbCl	750	0.481	0.428	99.6	1.16	56	86		0.65
	800	0.579	0.508	113	1.16	70.3	97		0.725
	850	0.685	0.594	128	1.20	86.4	107		0.81
LiBr	650	1.01	0.375	168	0.91	163	184	(184*)	0.89
	750	1.23	0.50	189	0.91	169.3	207	190	0.82
		$D_{exp} \times 10^5$ cm²/sec +	−						
$LiNO_3$	300	1.96	0.73	52.6	1.28	51	41	(41*)	1.24
	350	2.89	1.17	73.0	1.40	65	53	53	1.23
$NaNO_3$	315	1.81	1.16	56.6	1.26	38.4	45	(45*)	0.85
	350	2.35	1.48	68.8	1.31	47	52.5	55.9	0.895
	400	3.03	2.02	84	1.31	52	64	61.2	0.81
KNO_3	350	1.49	1.33	50.6	1.37	16.5	37	(37*)	0.45
	400	2.08	1.87	65.7	1.45	20	45.3	44.4	0.44
	450	2.77	2.54	82.2	1.51	21	54.5	48	0.39
$AgNO_3$	227	1.13	0.64	39.6	1.18	54.5	33.7		1.72
	277	1.60	0.91	51.1	1.23	69.4	41.6		1.67
	327	2.12	1.25	62.9	1.22	81	51.4		1.56

The experimental values are taken from 1, 2, 7, 8, 9, 10, 11.

---

[7] St. Zuca and L. Ionescu-Vasu, *Rev. Roumaine Chim.*, **12**, 1285 (1967).
[8] St. Zuca and M. Olteanu, *Rev. Roumaine Chim.*, (in press).
[9] J. O'M Bockris and G. W. Hooper, *Discuss. Faraday Soc.*, **32**, 218 (1961).
[10] G. Y. Janz, *Z. Naturforsch*, **A21**, 276 (1966).
[11] J. O'M Bockris, S. R. Richards and L. Nanis, *J. Phys. Chem*, **69**, 1627, (1965).

If the relation $\lambda_i = \frac{F^2}{RT} D_i x$ is valid for the single ions transport, then the equivalent conductivity of a MX salt will be :

$$\lambda_{MX} = \lambda_+ + \lambda_- = \frac{F^2}{RT}(D^+ + D^-).\ \frac{D^+_{\text{exp}} - D^-_{\text{exp}}}{D^+ - D^-}$$

Assuming a Stokes-Einstein law for diffusion of single ions, i.e a law $D_i = \frac{kT}{A\pi\eta r_i}$ or $D_i \sim \frac{1}{r_i}$ the above equation becomes :

$$\lambda_{MX} = \frac{F^2}{RT}\left(\frac{1}{r_+} + \frac{1}{r_-}\right)\frac{D^+_{\text{exp}} - D^-_{\text{exp}}}{\frac{1}{r_+} - \frac{1}{r_-}} = \frac{F^2}{RT}(D^+_{\text{exp}} - D^-_{\text{exp}})\frac{r_+ + r_-}{r_+ - r_-}$$

We applied this relation to 1 : 1 molten salts, using the experimental data for diffusion coefficients. The errors are greater as the difference $r_+ - r_-$ is smaller (see the values obtained for RbCl). The values computed in this way show the same variation with temperature as the experimental ones, i.e., for a certain salt, the ratio $\lambda_2/\lambda_{\text{exp}}$ is independent of temperature and has values ranging from 0.4 to 1.7 for different salts.

The correct formula for electrical conductivity would be :

$$\lambda_2' = \lambda_1 \cdot x f^{-1}$$

Using the f value obtained by the comparison of λ calculated with the experimental values, at a certain temperature (denoted by *), to compute the electrical conductivity of the salt at others temperatures, a very good agreement is obtained. The factors f present, for some salts, a very slight tendency to decrease as the temperature is increased, what was to be expected : as the number of vacancies increases, the probability for a vacancy to return to the same position increases and, this way, f decreases.

The $\lambda_2/\lambda_{\text{exp}}$ ratios are practically constant. That supports a physical meaning for the factor f.

At the same time, it is interesting to study the relation between diffusion and mobility through the activation energies of the processes.

In solids, where the number of mobile charge carriers (vacancies or interstitials) is small the activation energy for conductivity is the sum of the formation energy of carriers and of the energy of motion.

In fused salts, the number of holes is considerable and is not given by an exponential equation[12]. Consequently, it may be supposed that activation energy for electrical conductivity in fused salts is given only by the energy of motion.

In alkali halides melts it is very probable that the main carrier is the cation. A sufficient approximate evaluation may be made by using a comparison with the crystals.

For crystals of NaCl structure, Mullen[13] computed the energy of motion of positive – and negative – vacancies for self-diffusion and monovalent-impurity diffusion by a semiempirical procedure. The basis for the theory is the Einstein model of an ionic solid. Mullen pictures the motion process to result from the breaking of one of the Einstein springs holding an ion which is next to a vacancy. The energy of motion is postulated as the work required to move the ions which surround the jumping ion to the saddlepoint configuration. The straight-line path connecting the ion with adjoining vacancy was taken as path of the diffusing ion. The energy of motion is represented by :

---

[12] I. G. Murgulescu and G. Vasu, *Rev. Roumaine Chim.*, **11**, 681 (1966).

[13] J. G. Mullen, *Phys. Rev.*, **143**, 143, (1966).

$$E_m^s = (1 - 1/\sqrt{2})\ k_s\, r_0^2$$

$$k_s \ = \text{spring constant} = 2\ C_{11} r_0$$

$$C_{11} = \text{elastic constant}$$

The author finds values in good agreement with the experience.

Now, we attempt to make some approximation for ionic melts.

If the elasticity constants are considered inversely proportional to the compressibilities, we may write the relation :

$$\frac{E_m^s}{E_m^l} \approx \frac{\beta_l}{\beta_s} \quad \begin{array}{l} E_m^s = \text{energy of motion for ion in solid,} \\ E_m^l = \text{energy of motion for ion in melt.} \end{array}$$

The formula for estimating E_m^l is the result of an oversimplified picture. The results are shown in table 2 in comparison with experimental activation energies for electrical conductivity of some alkali halides, at the melting point. The values E_m^s calculated by Mullen are used. For the compressibilities we have used the values taken from Bockris' work.[14]

Table 2

Energy of motion for cations and activation energy for conductivity

Cation	E_m^l kcal calculated	E, kcal (experimental)
Na in NaCl	2.7	2.5
Na in NaBr	2.8	2.4
K in KCl	3.3	3.4
K in KBr	3.5	3.7
K in KI	3.6	3.5
Rb in RbCl	4.5	4.0 ; 4.4

The agreement is unexpectedly good. It is true that the E_m values decrease as the temperature increases, owing to the variation of compressibilities. (for instance, for NaCl : $E_m^l = 2.7$ kcal at 800° and 1.9 kcal at 1000°), but we have taken for the structure constant the value from the crystal $(1 - 1/\sqrt{2})$. After fusion, this constant modifies and takes values so far from the value in crystal as the temperature is raising. In addition, no mention is made about the formation energy, which may interfere to a certain extent.

---

[14] J. O'M Bockris and N. E. Richards, *Proc. Roy. Soc. (London)*, **A 241**, 44 (1957).

Revue Roumaine de Chimie, **15**, 837–841 (1970)

Revue Roumaine de Chimie, **15**, 843–846 (1970)

ÉLECTROMIGRATION DANS LES NITRATES MONOVALENTS FONDUS
LES IONS DE STRONTIUM ET DE BARYUM

I. G. MURGULESCU et D. TOPOR

Centre de Chimie Physique de l'Académie, 31, str. Galaţi, Bucarest

Reçu le 24 décembre 1969

Les études sur les mobilités électriques des ions dans les nitrates de sodium, potassium et césium fondus sont étendues aux ions de strontium et baryum. Les résultats expérimentaux renforcent les considérations déjà faites sur la migration électrique des ions alcalins, mettant en évidence la prédominance des interactions des ions simples des systèmes fondus.

Les études sur la migration électrique des ions alcalino-terreux dans les nitrates alcalins fondus sont peu nombreuses. On connaît une étude d'Arnikar [1] de 1957 sur les mobilités de ces ions dans le nitrate de sodium fondu à 350°, une autre d'Alberti, Grassini et Truco [2] de 1962 sur les mêmes mobilités dans l'eutectique $(K-Li)NO_3$ à 160°, et enfin, celle de Berlin, Ménès, Forcheri et Monfrini [3] de 1963 qui ont fait des mesures dans l'eutectique $(Na-K)NO_3$ à 270°. Du tableau 1, qui réunit les résultats publiés, on peut observer que la mobilité des ions alcalino-terreux augmente du calcium au baryum.

Tableau 1

Mobilités des ions alcalino-terreux (Résultats publiés)

Sel fondu	Température °C	Mobilités des ions alcalino-terreux u.cm^2.s^{-1} × 10^4		
		Ca^{2+}	Sr^{2+}	Ba^{2+}
$NaNO_3$	350°	1,88	1,25	2,22
$(K-Li)NO_3$	160°	—		1,3
$(Na-K)NO_3$	270°	0,45	0,55	0,79

---

[1] H. Arnikar, *Ann. Phys.*, **16**, 1291 (1959) ; *Compt. Rend.*, **244**, 2241 (1957).

[2] G. A. Alberti, G. Grassini et R. Truco, *J. Electroanalyt. Chem.*, **3**, 283 (1962).

[3] A. Berlin, F. Ménès, S. Forcheri et C. Monfrini, *J. Phys. Chem.*, **67**, 2505 (1963).

L'augmentation de la mobilité de l'ion Ca^{2+} avec la concentration en calcium, dans le système fondu $LiNO_3 - Ca(NO_3)_2$, a été observée par Kwak[4]. Ces résultats sont interprétés seulement par la diminution du volume molaire et par les interactions spécifiques dans ce système, sans appeler à la formation des associations ioniques. En effet, Kwak obtient un graphique d'Arrhenius linéaire pour la variation de la mobilité de l'ion Ca^{2+} avec la température.

PARTIE EXPÉRIMENTALE

Nous avons employé la méthode et l'installation décrites dans les travaux antérieurs ,[5] à la différence que la cellule comporte dans la paroi du tube horizontal un orifice de diamètre de 2—3 mm, afin de permettre l'introduction d'une quantité de nitrate alcalino-terreux dans la zone même de la migration.

Une fois la cellule chargée de nitrate alcalin et portée à la température de l'expérience, on a commencé le passage du courant électrique constant de 15 V environ. Les températures n'ont pas dépassé 450°, car à des valeurs supérieures les nitrates alcalino-terreux se décomposent. [6] Dans les conditions de fonctionnement rigoureusement constantes de la cellule on a ajouté une quantité de nitrate alcalino-terreux et on a noté le moment respectif comme début de l'électromigration.

La durée τ d'une détermination a été de 2 à 3 heures. Après le refroidissement de la cellule, le tube horizontal a été sectionné juste au milieu de l'orifice. Comme la position de l'orifice sur le tube horizontal est connue avec précision, elle est prise pour origine du déplacement, par migration électrique, des ions alcalino-terreux au long du tube.

Le déplacement correspondant à la durée est fixé par le maximum de la courbe de distribution de l'élément alcalino-terreux au long du tube. Cette distribution est déterminée par photométrie de flamme des fragments d'environ 3 mm d'épaisseur, sectionnés dans le tube horizontal. Un exemple typique de distribution est présenté dans la figure 1, où le déplacement de l'ion Ba^{2+} dans le nitrate de sodium à 435° est de 3,70 cm, ce qui donne une mobilité de 3.58×10^{-4} cm²/s.

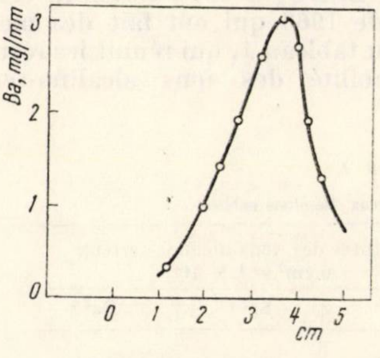

Fig. 1. — Migration du Ba^{2+} dans le nitrate de sodium à 435°.

---

[4] I. C. Th. Kwak, Thèse, Université d Amsterdam, 1967.

[5] I. G. Murgulescu et D. Topor, *Rev. Roumaine Chim.*, **9**, 815 (1964) ; **13**, 979 (1968).

[6] F. Lazarini et B. S. Brcic, *Monatsh. Chem.*, **97**, 1318 (1966).

RÉSULTATS ET DISCUSSIONS

Dans le tableau 2 sont présentés les résultats expérimentaux sur la migration électrique des ions de Ba^{2+} et de Sr^{2+} dans les nitrates fondus de sodium, potassium et césium.

Tableau 2

Mobilités des ions de strontium et baryum dans les nitrates alcalins fondus

Ion Me^{2+}	T,°C	Nitrate alcalin fondu	Mobilité du Me^{2+} u,cm². s$^{-1}\times 10^4$
Sr^{2+}	360	Na NO_3	2,18
	360	K NO_3	2,70
	450	Cs NO_3	1,06
Ba^{2+}	360	Na NO_3	2,26
	360	K NO_3	2,66
	450	Cs NO_3	1,20

La mobilité électrique du Ba^{2+} est un peu plus grande que celle du Sr^{2+}, dans le nitrate de sodium fondu à 360°, en accord avec d'autres auteurs.[1-3]

Dans le nitrate de césium fondu, à 450° les valeurs des mobilités de Sr^{2+} et Ba^{2+} sont serrées autour de celle de l'ion propre (Cs^+), de même que les mobilités des ions alcalins.[5]

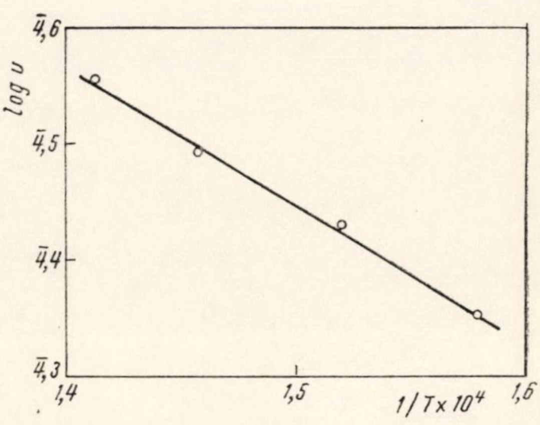

Fig. 2. — Graphique d'Arrhenius pour la migration du Ba^{2+} dans le nitrate de sodium fondu.

Un comportement similaire des mobilités de Sr^{2+} et Ba^{2+} doit se produire dans le nitrate de sodium aussi à 450°, car pour Ba^{2+} nous avons mesuré à 435° une mobilité de $3,58 \times 10^{-4}$ cm²/s. Cette valeur est correctement placée dans le groupement serré spécifique des mobilités électriques dans ce nitrate.

Les valeurs plus grandes dans le nitrate de potassium fondu sont dues à une migration plus facile des ions dont les dimensions sont très rapprochées, car d'après Pauling,[7] les rayons ioniques de K^+, Sr^{2+} et Ba^{2+} sont 1,35 Å, 1,13 Å et respectivement 1,35 Å.

Nous avons retrouvé ainsi la confirmation d'un groupement plus serré, dans les nitrates de sodium et césium, des valeurs de la mobilité électrique autour de la valeur de celle de l'ion propre.[8] Dans le nitrate de potassium les mêmes valeurs ne sont pas groupées, et cela prouve, une fois de plus, un comportement similaire à celui des ions alcalins.

Les dimensions et les charges électriques des ions, le volume libre et les interactions ioniques particulières dans ces nitrates fondus sont les grandeurs qui déterminent la mobilité électrique dans chaque paire de nitrates, sans l'introduction des associations ioniques. L'absence d'association ionique est prouvée aussi par un graphique linéaire du log u en fonction de $\frac{1}{T}$. Nous avons, par exemple, mis en évidence pour la paire $Ba(NO_3)-NaNO_3$ un graphique d'Arrhenius linéaire, qui confirme que la mobilité du baryum est propre à l'ion simple, deux fois ionisé (fig. 2).

---

[7] L. Pauling, «The Nature of Chemical Bond», Cornell Univ. Press., Ithaca, 1960.

[8] I. G. Murgulescu et D. Topor, *Rev. Roumaine Chim.*, **12**, 1279 (1967).

Revue Roumaine de Chimie, **15**, 847–854 (1970)

SALT EFFECTS IN TERNARY SYSTEMS FURFURAL-WATER-ELECTROLYTE. II*

TERNARY SYSTEMS FURFURAL-WATER-ORGANIC ELECTROLYTE

CAMELIA BELDIE and FLORICA BĂRBULESCU

Department of Physical Chemistry
University of Jassy
Calea 23 August, 11

Received February 11, 1969

The salt effects in furfural-water-organic electrolyte were measured by a turbidimetric method. The first component is solvent, the second, solute nonelectrolyte and the third, solute electrolyte. The following organic electrolytes were used : oxalic acid, malonic acid, succinic acid, adipic acid, pyrocatechin, resorcine, hydroquinone, citric acid and benzylic acid. All organic substances bring about a salting-in. We have evaluated the nonelectrolyte activity coefficients in salt solution and the k_s parameter both by using the Setschenow's equation and by a graphical method. The results both by the internal pressure theory and by the tightening of the solvent molecules around the large organic ion are explained.

In the first part of this study we have brought forward the results obtained for the furfural-water-inorganic electrolyte system.

In this paper we have investigated the organic electrolyte influence on the water solubility in furfural, respectively upon the activity coefficient, in order to compare results obtained in this case with those in the phenol-water system, and to follow the correlation between the salt effects and the ionic dimensions.

The literature mentions cases where organic electrolytes, such as tetraalkylammonium salts[1] and other organic electrolytes,[2,3] give a salting-in increasing the nonelectrolyte solubility in salt solution, when introduced into nonelectrolyte solution in pure solvent.

---

* Part I : C. Beldie and F. Bărbulescu : *Rev. Roumaine Chim.*, (in print).

[1] F. A. Long and W. F. McDevit, *Chem. Rev.*, **51**, 119 (1952).

[2] E. Papafil and C. Beldie, *Anal. Sti. Univ. "Al. I. Cuza" Iași, Sect. I*, **11 fasc. 2**, 117 (1965).

[3] C. Beldie and E. Papafil, *Ibid.*, **12 fasc. 2**, 97 (1966).

In this case, the k_s parameter of the equation

$$\log S_0/S = k_s c_s \tag{1}$$

has negative values and the nonelectrolyte activity coefficient is smaller than unit.

The salt-in effects are interesting from the viewpoint of the solubilities, since at the same temperature the nonelectrolyte solubility is higher in salt solution than in pure solvent. These salt effects are also difficult to interpret theoretically; the above facts will lead both to a development of the salting theory and to an adequate explanation of the experimental results.

One the other hand, the experimental data can be used, as we shall further see, to find the molecular weight of the organic electrolytes with large ions and likely that of the polyelectrolytes.

EXPERIMENTAL RESULTS

In order to follow the salt effect on the activity coefficient of water in salt solution, we have investigated first the water solubility in furfural in a 10—50° temperature range. The data are listed in the first part of this study, table 1.

We used a turbidimetric method tested with a photoelectric one.

The substances were purified and analysed before the determinations.

We have used the following organic electrolytes : oxalic acid, malonic acid, succinic acid, adipic acid, pyrocatechin, resorcine, hydroquinone, citric and benzylic acids. The other substances used in phenol-water system, do not influence the water solubility in furfural but they salt out from solution by cooling.

Similar phenomena were produced by some organic salts such as : alkaline oxalates, succinates and citrates.

In all investigations the furfural-water composition was maintained constant (saturated solution at 25°), various electrolyte concentrations were used and Δt — the displacement of the equilibrium temperature — was measured.

All organic electrolytes gave a salting-in by increasing the water solubility in salt solution in comparison with its solubility in pure solvent.

The experimental data obtained are illustrated in figure 1 in which we have plotted, Δt versus m (electrolyte molality).

RESULTS AND DISCUSSION

The empirical equation $\Delta t = am^b$ applies also in this case, where Δt and m have the same known significances, while a and b are two constants (see first part of the study).

In this case, too, the values of a are characteristic of the electrolyte, being different for each one. Although until now it was thought that the constant b is specific to the solvent mixture, we have found that the constant b is equal to 1 for all electrolytes producing a salting-in both in the phenol-water [2] and in the furfural-water system.

We have concluded that for electrolytes giving a salting-in in any solvent mixture, the following equation would be valid

$$\Delta t = am \qquad (2)$$

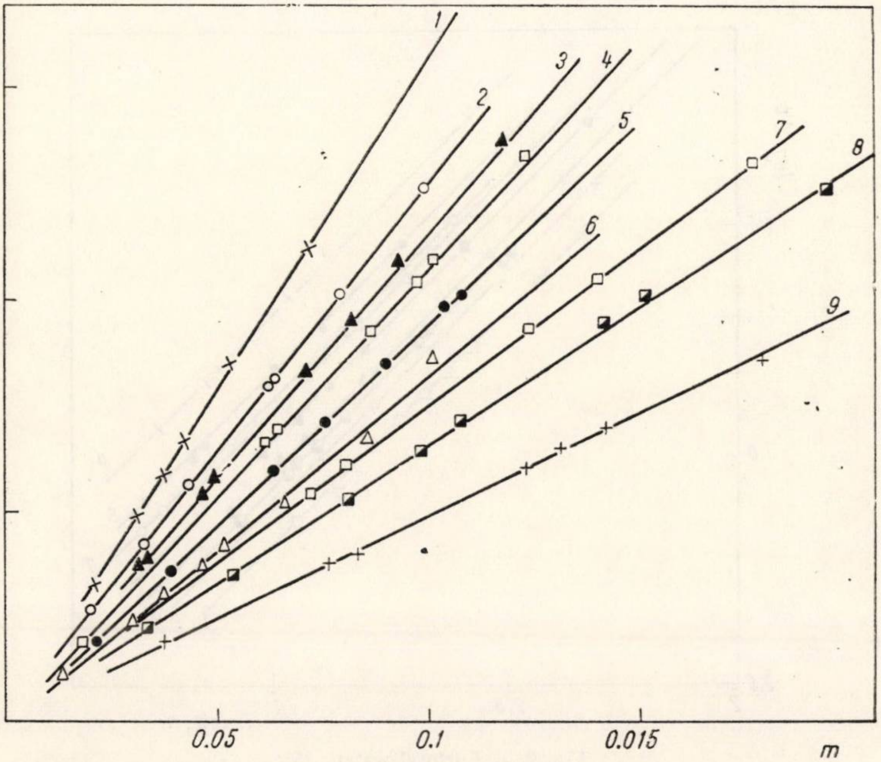

Fig. 1. — Furfural-water 25°:
1, citric acid; *2*, adipic acid; *3*, succinic acid *4*, oxalic acid; *5*, malonic acid; *6*, benzylic acid; *7*, resorcine; *8*, hydroquinone; 9, pyrocatechin.

If we plot log *t* *versus* log *m* we obtain straight lines, the slope of which is equal to 1 (Fig. 2).

For two different electrolytes when an equation (2) applies, we can write

$$\Delta t_1 = a_1 m_1$$

and

$$\Delta t_2 = a_2 m_2$$

For the same Δt

$$a_1 m_1 = a_2 m_2$$

or

$$m_1/m_2 = a_2/a_1 = \text{constant}$$

The equality of these ratios can be seen in table 1.

The solubility order is different from that found in the phenol-water mixture. Table 1 shows that this order is: citric acid < adipic acid < succinic acid < oxalic acid < malonic acid < benzylic acid < resorcine < hydroquinone < pyrocatechin.

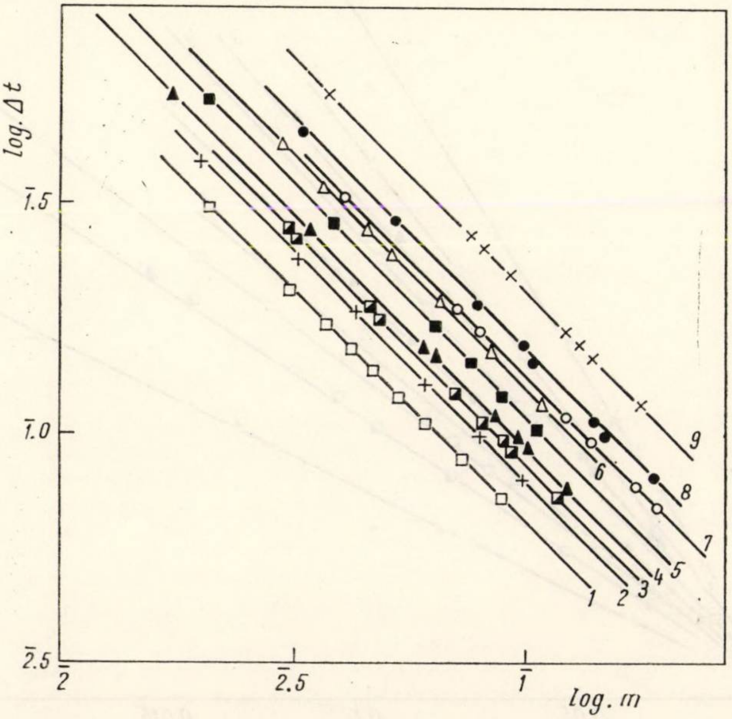

Fig. 2. — Furfural-water 25°:

1, citric acid; *2*, adipic acid; *3*, succinic acid; *4*, oxalic acid; *5*, malonic acid; *6*, benzylic acid; *7*, resorcine; *8*, hydroquinone; *9*, pyrocatechin.

The k_s parameter from equation (1) has negative values for all electrolytes producing a salting-in.

These values are summarized in table 2.

For all organic electrolytes we obtain negative values comparable, in absolute value, with our data for the inorganic electrolytes in phenol-water mixture [3].

The water activity coefficient was calculated by using equation (1). In all cases one obtains values smaller than unit, and the plots log f_i *versus* m (salt molality), results in straight lines from the slope of which we have obtained the k_s parameter (Fig. 3, 4), which agrees with the average of the calculated values k_s.

The experimental data stress that although equation (1) represents an approximate relation it can be used for the calculation both of the relative activity coefficients of the nonelectrolyte and of the interaction parameter k_s, from solubility data. Although k_s represents the ion-nonelectrolyte interaction parameter considering a thermodynamical treatment,[1] the solvent strongly influences the k_s values too.

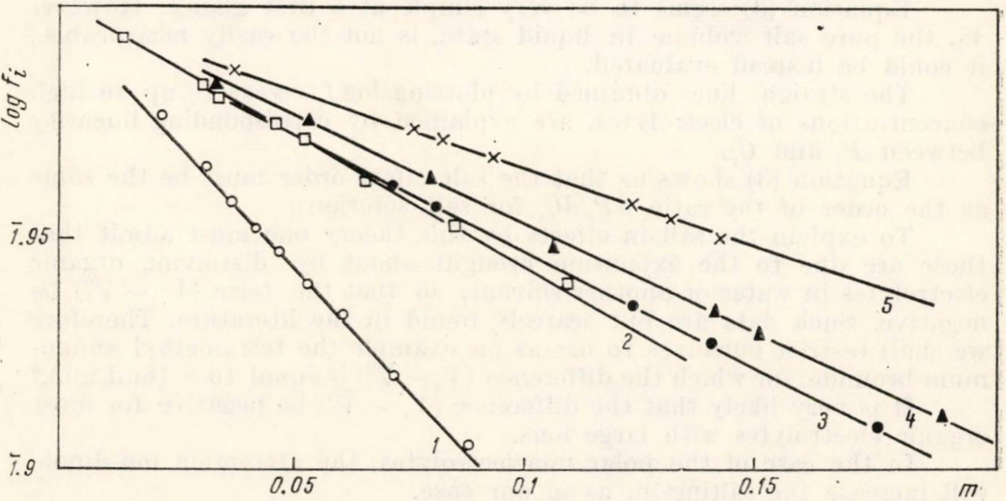

Fig. 3. — Furfural-water 25° :
1, citric acid ; *2*, benzylic acid ; *3*, resorcine ; *4*, hydroquinone ; *5*, pirocatechin.

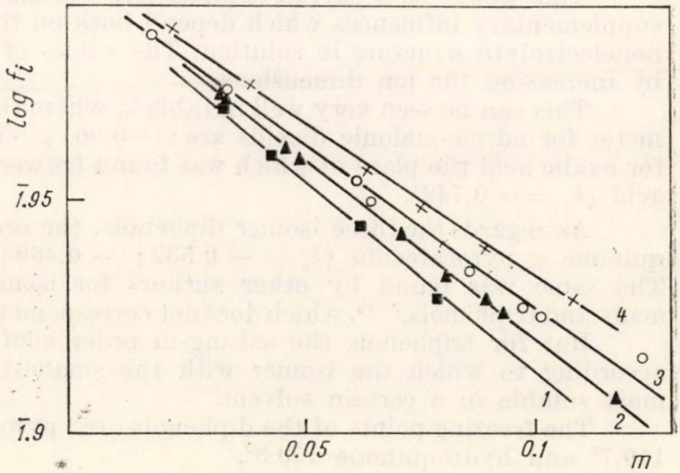

Fig. 4. — Furfural-water 25° :
1, adipic acid ; *2*, succinic acid ; *3*, oxalic acid ; *4*, malonic acid.

A partial explanation of these salt-in effects can be given by using the internal pressure theory[4] expressed by Long and McDevit equation[5]

$$k_s = \bar{V}_i^0(V_s - \bar{V}_s^0)/2.3RT\beta_0$$
$$= \lim_{C_s \to 0}(\bar{V}_i^0/2.3RT)dP_e/dC_s \qquad (3)$$

---

[4] G. Tamman, *Z. anorg. Chem.*, **158**, 17 (1926).

[5] W. F. McDevit and F. A. Long, *J. Amer. Chem. Soc.*, **74**, 1773 (1952).

where $\overline{V}_i^0$ is the partial molar volume of the nonelectrolytes at infinite dilution (l/mol); V_s — the molar volume of the pure liquid electrolyte; $\overline{V}_s^0$ — the partial molar volume of the electrolyte at infinite dilution (l/mol); β_0 — the compressibility coefficient of the pure solvent; P_e — the effective pressure exerted by salts in solution.

Equation (3) seems to be very simple at a first glance. However V_s, the pure salt volume in liquid state, is not too easily measurable; it could be instead evaluated.

The straight lines obtained by plotting $\log f_i$ *versus* C_s up to high concentrations of electrolytes, are explained by corresponding linearity between P_e and C_s.

Equation (3) shows us that the salt effect order must be the same as the order of the ratio dP_e/dC_s for salt solutions.

To explain the salt-in effects by this theory one must admit that these are due to the expansion brought about by dissolving organic electrolytes in water or another solvent, so that the term $(V_s - \overline{V}_s^0)$ be negative. Such data are but scarcely found in the literature. Therefore we shall restrict ourselves to use as an example the tetramethyl ammonium bromide, for which the difference $(V_e - \overline{V}_s^0)$ is equal to —16ml/mol.[6]

It is very likely that the difference $(V_s - \overline{V}_s^0)$ be negative for most organic electrolytes with large ions.

In the case of the polar nonelectrolytes, the attraction ion-dipole will increase the salting-in, as in our case.

This would be a partial explanation. Certainly there must be other supplementary influences which depend both on the large ion and on the nonelectrolyte structure in solution. The values of the salting-in decrease by increasing the ion dimensions.

This can be seen very well in table 2, where the values of the k_s parameter for adipic-malonic diacids are: —0.901; —0.812; —0.654 except for oxalic acid the place of which was found between malonic and succinic acid ($k_s = -0.742$).

As regards the three isomer diphenols, the order resorcine < hydroquinone < pyrocatechin ($k_s = -0.532$; -0.469; -0.347) was found. The same was found by other authors for isomerous hydroxybenzoic acids and triphenols,[7-10], which does not correspond to dipole moment order.

But for triphenols the salting-in order confirms Carnelley's rule[7] according to which the isomer with the smallest freezing point is the most soluble in a certain solvent.

The freezing points of the diphenols are: pyrocatechin 104° resorcine 110.7° and hydroquinone 170.3°.

In our case Carnelley's rule does not apply and it is not necessary to be applied, since it refers to the binary solutions and not to the ternary systems. The possibilities of the three isomers to form inter- and intramolecular hydrogen bonds are much more important, too.

---

[6] B. Lunden, *Z. phys. Chem.*, **192**, 345 (1943).

[7] A. Strătulă-Angelescu, Presentation of the doctoral thesis. Bucharest, 1964, p. 16.

[8] E. Angelescu and A. Strătulă-Angelescu, *Anal. Univ. "C. I. Parhon", Seria St. Naturii*, **30 X**, 79 (1961).

[9] E. Angelescu and A. Strătulă-Angelescu, *Ibid.*, **19 VII**, (1958).

[10] E. Angelescu and A. Strătulă-Angelescu, *Ibid.*, **26 IX**, 133 (1960).

Another explanation could be the following; for the furfural-water mixture, where the furfural is solvent and the water is solute nonelectrolyte, by adding large organic ions, the latter can gather the water molecules in a single layer around the hydrophobic ion, without directing them.

The resulting disturbance [11] of the water should show up better, since it is not compensated by an attractive ion-water dipole interaction. That is, the hydrophobic molecule does not interact attractively with, or orient the surrounding water molecules as strongly as the next shell of water molecules does. Thus, the nearest water molecules are oriented and hydrogen-bonded more strongly by the water molecules beyond them, than it would be the case if there were a counter-attraction from

Table 1

Values of the ratio m_1/m_2

Electrolyte	m_1/m_2		a_2/a_1
	Δt= 5°	10°	
Citric acid Adipic acid	0.802	0.805	0.801
Adipic acid Succinic acid	0.918	0.918	0.915
Succinic acid Oxalic acid	0.919	0.921	0.927
Oxalic acid Malonic acid	0.877	0.875	0.869
Malonic acid Benzylic acid	0.841	0.836	0.842
Benzylic acid Resorcine	0.954	0.955	0.954
Resorcine Hydroquinone	0.874	0.880	0.881
Hydroquinone Pyrocatechin	0.733	0.729	0.739

Table 2

Parameter k_s (Sechenow's constant)

Electrolyte	k_s	Electrolyte	k_s
Citric acid	−1.11	acid Malonic	−0,65
Adipic acid	−0.901	acid Benzylic	−0,553
Succinic acid	−0.812	Resorcine	−0,532
Oxalic acid	−0.742	Hydroquinone	−0,469
		Pyrocatechin	−0,347

the other side. This corresponds to a tightening of the water structure around the molecule; that is, on the internal surface of the cavity surrounding the solute. The larger and more hydrophobic the structure of the molecule, the greater is the effect.[11]

The occurrence of this tightening of the water structure, by adding an organic ion the state is such that it should decrease the number of particles in solution.

This fact will lead to a greater solubility of water in furfural. This supposition explains, too, the less than unit values for the activity coefficients we have obtained.

In fact, phenomena are much more complicated since both the solute and the solvent are dipoles. Otherwise the assumption does not explain the behaviour of the organic ions resulted from the respective salts, since by cooling they salt out from solution.

---

[11] R. M. Diamond, *J. Phys. Chem.*, **67**, 2513 (1963).

Revue Roumaine de Chimie, **15**, 855–864 (1970)

CINÉTIQUE DE LA DÉCOMPOSITION THERMIQUE DE QUELQUES COMBINAISONS COMPLEXES DES HALOGÉNURES DE CADMIUM AVEC DES PICOLINES

D. FĂTU, SANDA FĂTU, ANCA TEODORESCU et E. SEGAL
Chaire de Chimie Physique II,
Université de Bucarest

Reçu le 11 septembre 1969

On a évalué les paramètres cinétiques à partir des données thermogravimétriques pour les réactions de décomposition de quelques combinaisons complexes des halogénures de cadmium avec les picolines. Les valeurs obtenues à l'aide des méthodes Freeman–Carroll et Coats-Redfern concordent dans la limite des erreurs expérimentales. L'analyse des résultats obtenus prouve que – en fonction du nombre des molécules de ligand de la combinaison complexe – les réactions étudiées ont lieu dans un régime diffusionnel, cinétique ou mixte.

En continuant les études cinétiques sur les réactions endothermiques dans des systèmes solide-gaz, on présente les résultats obtenus pour les processus de décomposition thermique de certaines combinaisons complexes des halogénures de cadmium avec les picolines.

L'évaluation des paramètres cinétiques a été réalisée à l'aide des méthodes Freeman-Carroll[1] et Coats-Redfern[2]. Conformément aux résultats d'une étude de la stabilité thermique des combinaisons complexes de quelques halogénures de cadmium avec la pyridine et des pyridines substituées, effectuée par Allan et ses collaborateurs,[3] à la suite de l'échauffement du complexe bi-pyridinique du chlorure de cadmium, on retrouve la séquence des réactions qui conduit aux produits intermédiaires suivants:

$$CdL_2X_2 \rightarrow CdLX_2 \rightarrow CdL_{2/3}X_2 \rightarrow CdX_2$$

les mêmes qu'on rencontre dans le cas de certaines combinaisons complexes analogues de cobalt,[4] nickel,[5,6] manganèse[7] et cuivre.[8] La décomposition des combinaisons complexes pyridiques du bromure et de l'iodure de cadmium a lieu par des étapes où l'on n'a pas pu mettre en évidence des combinaisons complexes du type Cd $L_{2/3}X_2$.

---

[1] E. S. Freeman et B. Carroll, *J. Phys. Chem.*, **62**, 394 (1958).

[2] A. W. Coats et J. P. Redfern, *Nature*, **201**, 68 (1964).

[3] J. R. Allan, D. H. Brown et D. W. A. Sharp, Proceedings of the First International Conference on Thermal Analysis, Aberdeen, Scotland, MacMillan & Co LTD, Londres, 1965, p. 138.

[4] E Schönberger, D. Fătu et E. Segal, *Rev. Roumaine Chimie*, **12**, 1205 (1967).

[5] I. S. Murgulescu, E. Segal et D. Fătu, *J. Inorg. Nuclear Chem*, **27**, 2677 (1965).

[6] N. Hurduc, L. Odochian, I. A. Schneider et E. Segal, *Rev. Roumaine Chim.*, **11**, 1453 (1966).

[7] D. Fătu et S. Segal, *Rev. Roumaine Chim.* **14**, 709 (1969).

[8] D. Fătu, S. Fătu et E. Segal, *Rev. Roumaine Chim.* **14**, 1107 (1969).

PARTIE EXPÉRIMENTALE

On a utilisé :

— complexe tétra β-picolinique du chlorure de cadmium, $Cd\,Cl_2.4\beta$-pic ;

— complexe tétra γ-picolinique du chlorure de cadmium, $CdCl_2.3{,}55\gamma$-pic ;

— complexe α-picolinique du chlorure de cadmium, $CdCl_2.\ \alpha$-pic ;

— complexe tétra γ-picolinique du bromure de cadmium, $CdBr_2.4\gamma$-pic ;

— complexe di α-picolinique du bromure de cadmium, $CdBr_2.1{,}85\ \alpha$-pic ;

— complexe di β-picolinique du bromure de cadmium, $CdBr_2.\ 1{,}93\ \beta$-pic ;

— complexe di α-picolinique de l'iodure de cadmium, $CdI_2.2\alpha$-pic

qui ont été synthétisés conformément aux méthodes classiques décrites dans la littérature.[9,10]

Les combinaisons complexes ayant un contenu intermédiaire de ligand ont été obtenues par la décomposition thermique des substances mentionnées plus-haut.

Les substances ont été broyées et passées par le tamis en retenant les granules de diamètre de 0,100 à 0,090 mm.

Les courbes thermogravimétrique (TG), thermogravimétrique dérivée (DTG) et de température (T) ont été enregistrées simultanément à l'aide d'un dérivatographe MOM Budapest de type Paulik-Paulik-Erdey.

RÉSULTATS ET DISCUSSIONS

On présente ensuite les réactions de décomposition étudiées, ainsi que les valeurs respectives des paramètres cinétiques :

— l'ordre de réaction, n ;

— l'énergie d'activation, E ;

— le facteur préexponentiel A.

Pour chacune des réactions on indique :

— le poids de la poudre soumise à la décomposition W_p ;

— la valeur de la vitesse d'échauffement $\frac{dT}{dt}$

— la température de réaction t_r, considérée d'une manière conventionnelle comme la température qui correspond à la vitesse maximale de décomposition.

Dans le cas des réactions d'ordre zéro, on indique les valeurs expérimentales des facteurs préexponentiels A_{exp}, ainsi que celles calculées en considérant comme étape limitante la diffusion du composant volatil à travers la couche de corps décomposé, d'après la formule[11]

$$A_{calc} = \frac{1}{\beta} l^2 \nu \frac{9 W_c}{r^2} \tag{1}$$

---

[9] W. Lang, *Ber. dtsch. Chem. Ges.*, **21**, 1254 (1888).

[10] R. Varet, *Compt. rend.*, **115**, 465 (1892).

[11] I. G. Murgulescu et E. Segal, *Rev. Roumaine Chim.*, **10**, 307 (1965).

où

β = le rapport entre la quantité de composant volatil qui peut être éliminée dans la réaction et la quantité de poudre soumise à la décomposition ;

l—est approximé par la valeur moyenne de la constante du réseau ($l \approx \approx 10$ Å) ;

ν = la fréquence de vibration des molécules du composant volatil dans le réseau, habituellement considérée égale à $\nu = 6 \cdot 10^{12} s^{-1}$;

r = le rayon moyen du grain cristallin ;

W_c = la quantité du composant volatil qui peut être éliminée pendant la réaction.

$$CdCl_2.4\beta\text{-pic(s)} \rightarrow CdCl_2.2\beta\text{-pic(s)} + 2\beta\text{-pic (g)} \tag{I}$$

Méthode Freeman-Carroll	*Méthode Coats-Redfern*
$W_p = 0{,}0609$ g	$W_p = 0{,}0609$ g
$\frac{dT}{dt} = 10°K/mn$	$\frac{dT}{dt} = 10°K/mn$
$t_r = 130°$	
$n = 0$	$n = 0$
$E = 14{,}6$ kcal/mole	$E = 13{,}7$ kcal/mole
$A_{exp} = 1{,}6.10^4 g.s^{-1}$	$A_{exp} = 1{,}26.10^4 g.s^{-1}$
$A_{calc} = 1{,}78.10^3$ g.s^{-1}	

$$CdCl_2.2\beta\text{-pic(s)} \rightarrow CdCl_2.\beta\text{-pic(s)} + \beta\text{-pic (g)} \tag{II}$$

$W_p = 0{,}0403$ g	$W_p = 0{,}0403$ g
$\frac{dT}{dt} = 10°K/mn$	$\frac{dT}{dt} = 10°K/mn$
$t_r = 175°$	
$n = 0$	$n = 0$
$E = 25{,}6$ kcal/mole	$E = 24{,}7$ kcal/mole
$A = 1{,}4.10^{11} g.s^{-1}$	$A = 1{,}1.10^{10} g.s^{-1}$

$$CdCl_2.\beta\text{-pic(s)} \rightarrow CdCl_2.\frac{2}{3}\beta\text{-pic(s)} + \frac{1}{3}\beta \text{ pic(g)} \tag{III}$$

$W_p = 0{,}0303$ g	$W_p = 0{,}0303$ g
$\frac{dT}{dt} = 10°$ K/mn	$\frac{dT}{dt} = 10°K/mn$

Méthode Freeman-Carroll	*Méthode Coats-Redfern*
$t_r = 228°$	
$n = 1/3$	$n = 1/3$
$E = 29{,}7$ kcal/mole	$E = 30{,}6$ kcal/mole
$A = 2{,}5.10^{10}\ g^{2/3}s^{-1}$	$A = 1{,}35.10^{11}g^{2/3}.s^{-1}$
$CdCl_2 \cdot \frac{2}{3}\ \beta\text{-pic(s)} \rightarrow Cd\ Cl_2(s) + \frac{2}{3}\ \beta\text{-pic (g)}$	(IV)
$W_p = 0{,}0269$ g	$W_p = 0{,}0269$ g
$\frac{dT}{dt} = 10°$ K/mn	$\frac{dT}{dt} = 10°$ K/mn
$t_r = 322°$	
$n = \frac{1}{2}$	$n = \frac{1}{2}$
$E = 38$ kcal/mole	$E = 37{,}5$ kcal/mole
$A = 1{,}20.10^{11}g^{1/2}s^{-1}$	$A = 1{,}25.10^{11}g^{1/2}s^{-1}$
$CdCl_2.3{,}55\ \gamma\text{-pic(s)} \rightarrow CdCl_2.2\gamma\text{-pic(s)} + 1{,}55\ \gamma\text{-pic (g)}$	(V)
$W_p = 0{,}0610$ g	$W_p = 0{,}0610$ g
$\frac{dT}{dt} = 10°$ K/mn	$\frac{dT}{dt} = 10°$ K/mn
$t_r = 143°$	
$n = 0$	$n = 0$
$E = 16$ kcal/mole	$E = 16{,}9$ kcal/mole
$A_{exp} = 4{,}07.10^4\ g.s^{-1}$	$A_{exp} = 5{,}06 . 10^5\ g.s^{-1}$
$A_{calc} = 1{,}78.10^3\ g.s^{-1}$	
$CdCl_2.2\gamma\text{-pic(s)} \rightarrow CdCl_2.\gamma\text{-pic(s)} + \gamma\text{-pic(g)}$	(VI)
$W_p = 0{,}0442$ g	$W_p = 0{,}0442$ g
$\frac{dT}{dt} = 10°$ K/mn	$\frac{dT}{dt} = 10°$ K/min
$t_r = 188°$	
$n = \frac{1}{3}$	$n = \frac{1}{3}$
$E = 28{,}3$ kcal/mole	$E = 27{,}5$ kcal/mole
$A = 3{,}24.10^{10}\ g^{2/3}\ s^{-1}$	$A = 2{,}42.10^{9}g^{2/3}\ s^{-1}$

Méthode Freeman-Carroll	*Méthode Coats-Redfern*
$CdCl_2.\gamma\text{-pic(s)} \rightarrow CdCl_2.\frac{2}{3}\gamma\text{-pic(s)} + \frac{1}{3}\gamma\text{-pic (g)}$ (VII)	
$W_p = 0{,}0331$ g	$W_p = 0{,}0331$ g
$\frac{dT}{dt} = 10°K/mn$	$\frac{dT}{dt} = 10°$ K/mn
$t_r = 283°$	
$n = \frac{1}{3}$	$n = \frac{1}{3}$
$E = 4{,}58$ kcal/mole	$E = 4{,}58$ kcal/mole
$A = 2{,}1.10^{-1} g^{2/3}\ s^{-1}$	$A = 3.10^{-2}\ g^{2/3}\ s^{-1}$
$CdCl_2.\frac{2}{3}\gamma\text{-pic(s)} \rightarrow CdCl_2(s) + \frac{2}{3}\gamma\text{-pic (g)}$ (VIII)	
$W_p = 0{,}0294$ g	$W_p = 0{,}0294$ g
$\frac{dT}{dt} = 10°$ K/mn	$\frac{dT}{dt} = 10°$ K/mn
$t_r = 347°$	
$n = \frac{1}{3}$	$n = \frac{1}{3}$
$E = 28{,}8$ kcal/mole	$E = 28$ kcal/mole
$A = 7{,}6.10^5 g^{2/3}\ s^{-1}$	$A = 5{,}3.10^6\ g^{2/3}\ s^{-1}$
$CdCl_2.\ \alpha\text{-pic (s)} \rightarrow CdCl_2.\ \frac{2}{3}\ \alpha\text{-pic(s)} + \frac{1}{3}\alpha\text{-pic (g)}$ (IX)	
$W_p = 0{,}0608$ g	$W_p = 0{,}0608$ g
$\frac{dT}{dt} = 10°$ K/mn	$\frac{dT}{dt} = 10°K/mn$
$t_r = 227°$	
$n = 0$	$n = 0$
$E = 20{,}6$ kcal/mole	$E = 20{,}2$ kcal/mole
$A_{exp} = 4{,}8.10^4\ g\ s^{-1}$	$A_{exp} = 2{,}86.10^4 g.s^{-1}$

Méthode Freeman-Carrooll	*Méthode Coats-Redfern*

$$A_{calc} = 1{,}78\ g\ s^{-1}$$

$$CdCl_2 . \frac{2}{3}\ \alpha\text{-pic(s)} \rightarrow CdCl_2(s) + \frac{2}{3}\ \alpha\text{-pic(g)} \qquad (X)$$

$W_p = 0{,}0540\ g$	$W_p = 0{,}0540\ g$
$\frac{dT}{dt} = 10°\ K/mn$	$\frac{dT}{dt} = 10°\ K/mn$

$$t_r = 305°$$

$n = \frac{1}{2}$	$n = \frac{1}{2}$
$E = 26{,}1$ kcal/mole	$E = 26{,}1$ kcal/mole
$A = 5{,}5.10^6 g^{1/2}s^{-1}$	$A = 5{,}4.10^6 g^{1/2}s^{-1}$

$$CdBr_2 . 4\gamma\text{-pic(s)} \rightarrow CdBr_2 . 2\gamma\text{-pic(s)} + 2\gamma\text{-pic(g)} \qquad (XI)$$

$W_p = 0{,}0606\ g$	$W_p = 0{,}0606\ g$
$\frac{dT}{dt} = 10°K/mn$	$\frac{dT}{dt} = 10°K/mn$

$$t_r = 140°$$

$n = 0$	$n = 0$
$E = 15{,}3$ kcal/mole	$E = 15{,}6$ kcal/mole
$A_{exp} = 1{,}59.10^4 g.s^{-1}$	$A_{exp} = 2{,}49.10^4 g.s^{-1}$

$$A_{calc} = 1{,}78.\ 10^3\ g.s^{-1}$$

$$CdBr_2 . 2\gamma\text{-pic(s)} \rightarrow CdBr_2 . \gamma\text{-pic(s)} + \gamma\text{-pic(g)} \qquad (XII)$$

$W_p = 0{,}0430\ g$	$W_p = 0{,}0430\ g$
$\frac{dT}{dt} = 10°\ K/mn$	$\frac{dT}{dt} = 10°K/mn$

$$t_r = 204°$$

$n = \frac{1}{2}$	$n = \frac{1}{2}$
$E = 27{,}5$ kcal/mole	$E = 27{,}0$ kcal/mole
$A = 1{,}13.10^9 g^{1/2}$	$A = 3{,}29.10^9 g^{1/2}s^{-1}$

$$CdBr_2.\gamma\text{-pic(s)} \rightarrow CdBr_2.\frac{2}{3}\gamma\text{-pic(s)} + \frac{1}{3}\ \gamma\text{-pic(g)} \qquad \text{(XIII)}$$

Méthode Freeman-Carroll	*Méthode Coats-Redfern*
$W_p = 0{,}0342$ g	$W_p = 0{,}0342$ g
$\frac{dT}{dt} = 10°K/mn$	$\frac{dT}{dt} = 10°K/mn$
$t_r = 270°$	
$n = \frac{1}{2}$	$n = \frac{1}{2}$
$E = 36{,}8$ kcal/mole	$E = 38{,}9$ kcal/mole
$A = 1{,}22.10^{10} g^{1/2} s^{-1}$	$A = 3{,}60.10^{12} g^{1/2} s^{-1}$

$$CdBr_2.\frac{2}{3}\ \gamma\text{-pic(s)} \rightarrow CdBr_2(s) + \frac{2}{3}\ \gamma\text{-pic(g)} \qquad \text{(XIV)}$$

$W_p = 0{,}0313$ g	$W_p = 0{,}0313$ g
$\frac{dT}{dt} = 10°K/mn$	$\frac{dT}{dt} = 10°K/mn$
$t_r = 315°$	
$n = 1$	$n = 1$
$E = 41{,}2$ kcal/mole	$E = 41{,}2$ kcal/mole
$A = 4{,}2.10^{13} s^{-1}$	$A = 5{,}1.10^{13} s^{-1}$

$$CdBr_2.1{,}85\ \alpha\text{-pic (s)} \rightarrow CdBr_2.\alpha\text{-pic(s)} + 0{,}85\ \alpha\text{-pic(g)} \qquad \text{(XV)}$$

$W_p = 0{,}0608$ g	$W_p = 0{,}0608$ g
$\frac{dT}{dt} = 10°\ k/mn$	$\frac{dT}{dt} = 10°K/mn$
$t_r = 124°$	
$n = \frac{1}{2}$	$n = \frac{1}{2}$
$E = 18$ kcal/mole	$E = 17$ kcal/mole
$A = 1{,}3.10^{7}\ g^{1/2}\ s^{-1}$	$A = 3{,}6.10^{6} g^{1/2}\ s^{-1}$

$$CdBr_2.\alpha\text{-pic(s)} \rightarrow CdBr_2(s) + \alpha\text{-pic(g)} \qquad \text{(XVI)}$$

$W_p = 0{,}0500$ g	$W_p = 0{,}0500$ g
$\frac{dT}{dt} = 10°K/mn$	$\frac{dT}{dt} = 10°\ K/mn$

$t_r = 246°$

Méthode Freeman-Carroll	*Méthode Coats-Redfern*
$n = \frac{1}{2}$	$n = \frac{1}{2}$
$E = 23{,}8$ kcal/mole	$E = 24$ kcal/mole
$A = 1{,}07.10^7 g^{1/2} s^{-1}$	$A = 1{,}18.10^7 g^{1/2} s^{-1}$

$CdBr_2.1{,}93\ \beta\text{-pic(s)} \rightarrow CdBr_2.\beta\text{-pic(s)} + 0{,}93\ \beta\text{-pic(g)}$ (XVII)

$W_p = 0{,}0608$ g	$W_p = 0{,}0608$ g
$\frac{dT}{dt} = 10°K/mn$	$\frac{dT}{dt} = 10°K/mn$

$t_r = 190°$

$n = 0$	$n = 0$
$E = 20$ kcal/mole	$E = 19$ kcal/mole
$A_{exp} = 3{,}24.10^5 g.s^{-1}$	$A_{exp} = 1{,}03.10^5 g.s^{-1}$

$A_{calc} = 1{,}78.10^3\ g.s^{-1}$

$CdBr_2.\beta\text{-pic(s)} \rightarrow CdBr_2.\ \frac{2}{3}\beta\text{-pic(s)} + \frac{1}{3}\beta\text{-pic(g)}$ (XVIII)

$W_p = 0{,}0492$ g

$\frac{dT}{dt} = 10°\ K/mn$

$t_r = 213°$

$n = \frac{1}{3}$

$E = 7{,}78$ kcal/mole

$A = 0{,}73.10^{-2} g^{2/3} s^{-1}$

$CdBr_2.\ \frac{2}{3}\ \beta\text{-pic(s)} \rightarrow CdBr_2(s) + \frac{1}{2}\ \beta\text{-pic (g)}$ (XIX)

$W_p = 0{,}0450$ g	$W_p = 0{,}0450$ g
$\frac{dT}{dt} = 10°K/mn$	$\frac{dT}{dt} = 10°K/mn$

$t_r = 302°$

$n = \frac{1}{2}$	$n = \frac{1}{2}$
$E = 31$ kcal/mole	$E = 30$ kcal/mole
$A = 7.10^8 g^{1/2} s^{-1}$	$A = 1{,}58.10^8 g^{1/2} s^{-1}$

Méthode Freeman-Carroll	*Méthode Coats-Redfern*
$CdI_2.2\alpha\text{-pic(s)} \rightarrow Cd\ I_2.\alpha\text{-pic(s)} + \alpha\text{-pic(g)}$	(XX)
$W_p = 0{,}0605$ g	$W_p = 0{,}0605$ g
$\frac{dT}{dt} = 10°K/mn$	$\frac{dT}{dt} = 10°$ K/mn
$t_r = 150°$	
$n = 0$	$n = 0$
$E = 15{,}5$ kcal/mole	$E = 15{,}5$ kcal/mole
$A_{exp} = 3{,}1 \cdot 10^3$ g.s^{-1}	$A_{exp} = 1{,}44.10^3$ g.s^{-1}
$A_{calc} = 1{,}78.10^3$g.s^{-1}	

$Cd\ I_2 \cdot \alpha\text{-pic(s)} \rightarrow Cd\ I_2\text{(s)} + \alpha\text{-pic(g)}$	(XXI
$W_p = 0{,}0503$ g	$W_p = 0{,}0503$ g
$\frac{dT}{dt} = 10°$ K/mn	$\frac{dT}{dt} = 10°$ K/mn
$t_r = 244°$	
$n = \frac{1}{2}$	$n = \frac{1}{2}$
$E = 18{,}5$ kcal/mole	$E = 18{,}5$ kcal/mole
$A = 6{,}03.10^4 g^{1/2}s^{-1}$	$A = 6{,}34.10^4.g^{1/2}s^{-1}$

En analysant les données expérimentales, on conclut que l'élimination du composant volatil des combinaisons complexes picoliniques des halogénures de cadmium a lieu conformément au schéma général présenté par Allan et ses collaborateurs,[3] y compris dans certains cas les combinaisons complexes ayant quatre molécules de ligand, excepté les réactions de décomposition des corps $CdBr_2$. 2α-pic et CdI_2. 2α-pic, qui ont lieu sans la formation des intermédiaires du type $Cd\ L_2/_3X_2$.

L'ordre de réaction varie entre zéro et l'unité, en augmentant à mesure que les combinaisons complexes ayant un contenu de plus en plus réduit de ligand se décomposent. Cela indique que le déroulement de la réaction a lieu dans un régime mixte cinétique-diffusionnel. Les valeurs identiques de l'ordre de réaction pour les processus successifs VI, VII et VIII, XII et XIII, XV et XVI peuvent être dues à des phénomènes de frittage qui ont lieu au cours de l'augmentation de la température et qui compensent l'augmentation du degré de dispersion à la suite de la réaction.

La valeur zéro de l'ordre de réaction correspond à un régime purement diffusionnel. Dans ces conditions, les valeurs des facteurs préexponentiels, calculées d'après la formule 1, concordent d'une manière satisfaisante avec celles déterminées expérimentalement. Dans le cas de la réaction II, la valeur du facteur préexponentiel ne peut être établie par calcul, puisqu'on ne connaît pas les dimensions réelles des corpuscules obtenus à la suite de la décomposition de la combinaison complexe avec quatre molécules de ligand. Dans tous les cas, celles-ci sont inférieures à celles du complexe riche en composant volatil, $CdCl_2$ 4β-pic, et, pour les mêmes raisons, la valeur du facteur préexponentiel du processus II doit être supérieure à celle du processus I, fait confirmé par l'expérience.

Dans le cas de la réaction XIV, l'ordre de réaction égal à l'unité, ainsi que la valeur du facteur préexponentiel [12] prouvent qu'à la dispersion maximum, qui peut être réalisée par la réaction, on arrive au déroulement de celle-ci dans le domaine cinétique.

CONCLUSIONS

1) La décomposition de la plupart des combinaisons complexes picoliniques des halogénures de cadmum a lieu par la série de composés intermédiaires qu'on a rencontrés dans le cas des combinaisons complexes pyridiniques correspondantes, ainsi que dans le cas des combinaisons complexes des halogénures de cobalt, nickel, manganèse et cuivre avec la pyridine et les pyridines substituées.

2) Les valeurs des paramètres cinétiques calculées à l'aide des méthodes Freeman-Carroll et Coats-Redfern pour les réactions de décomposition des combinaisons complexes riches en composant volatil, ainsi que celles des combinaisons complexes intermédiaires, concordent dans la limite des erreurs expérimentales.

3) L'ordre de réaction augmente, à partir de la valeur zéro qui correspond au régime diffusionnel, jusqu'à une valeur égale à l'unité, correspondant au régime cinétique. Les valeurs intermédiaires, inférieures à l'unité, de l'ordre de réaction, correspondent à un régime mixte cinétique-diffusionnel.

---

[12] S. Glasstone, K. J. Laidler et H. Eyring, « The Theory of Rate Processes », McGraw-Hill, Londres, 1941, p. 296.

Revue Roumaine de Chimie, **15**, 865–872 (1970)

KINETICS AND MECHANISM OF SUBSTITUTION REACTIONS OF COMPLEXES. XIX[5]

INFLUENCE OF HEATING RATE ON THE THERMAL DECOMPOSITION OF $[Co(DH)_2\ (amine)_2]$ I TYPE COMPLEXES IN THE CONDITIONS OF THERMOGRAVIMETRIC ANALYSIS

J. ZSAKÓ, E. KÉKEDY and CS. VÁRHELYI

"Babeş-Bolyai" University, Cluj
Faculty of Chemistry, str. Arany János, 11

Received May 17, 1969

Thermal decomposition of 22 complexes has been studied in the conditions of thermogravimetric analysis, by using different heating rates. From the thermogravimetric curves apparent kinetic parameters of reaction (1) have been derived by means of the modified Doyle method. Apparent reaction order increases and apparent activation energy decreases with increasing heating rate. Thus the obtained kinetic parameters do not characterize the proper chemical reaction, but the complex heterogeneous process as a whole. The explanation of the observed effect is discussed.

In our previous paper [1] the thermal decomposition of $[Co(DH)_2(amine)_2]$ I type complexes has been studied in the conditions of the thermogravimetric analysis, by using a single heating rate. In the above formula DH_2 stands for a molecule of dimethylglyoxime. Our investigations have shown the first stage of the pyrolysis to be a substitution reaction according to the following equation :

$$[Co(DH)_2(amine)_2]^+ + I^- = [Co(DH)_2(amine)\ I] + amine \qquad (1)$$

Thus, one of the amine molecules in the internal co-ordination sphere is substituted by the external sphere anion, a relatively stable intermediate is formed and the liberated amine is volatilized.

For the kinetic study of this reaction Horowitz and Metzger's method [2] has been used. Since this method is not an accurate one, [3] in our further investigations the modified Doyle method has been used, which was worked out in our previous paper.[3] By means of this method the pyrolysis of the analogous bis-diphenylglyoximato-diamino-cobaltous (III) complexes has been studied.[4,5]

---

[1] J. Zsakó, Cs. Várhelyi and E. Kékedy, *J. Inorg. Nuclear Chem.*, **28**, 2637 (1966).

[2] H. H. Horowitz and G. Metzger, *Analyt. Chem.*, **35**, 1464 (1963).

[3] J. Zsakó, *J. Phys. Chem.*, **72**, 2406 (1968).

For deriving kinetic parameters from thermogravimetric curves another integral method has been proposed by Ozawa.[6] This method uses different heating rates and its application is possible only if one assumes that kinetic parameters, such as reaction order n, activation energy E_a and pre-exponential factor Z of the Arrhenius equation, are independent of the heating rate. The fundamental accuracy of this method, and its improvement possibilities, have been discussed in our previous paper.[7] If the kinetic parameters n, E_a and Z are the same, regardless of the heating rate q, the modification of the heating rate produces only a parallel shift of the thermogravimetric curve[8] and this shift depends upon the activation energy of the process.[7]

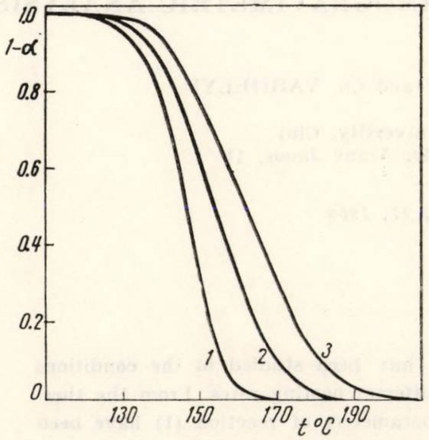

Fig. 1. – Thermogravimetric curves of $[Co(DH)_2(\beta\text{-picoline})_2]$ I at different heating rates.
1, q = 5° C/min; 2, q = 10° C/min; 3, q = 15° C/min.

In order to verify the independence of kinetic parameters of the heating rate and to apply the initial and the improved Ozawa method, thermogravimetric curves have been recorded by using different heating rates, namely 5, 10 and 15°/min respectively. Experimental results are illustrated in figure 1, which contains thermogravimetric curves of $[Co(DH)_2(\beta\text{-picoline})_2]$ I, obtained at different heating rates. As seen from this figure, the curve is shifted indeed, but its shape is modified too, namely the increase in the heating rate reduces the slope of the curve. Thus from these curves only apparent kinetic parameters can be derived whose value will depend upon the heating rate. This makes impossible the application of Ozawa's method. That is why the modified Doyle method has been used for calculating the kinetic parameters separately for each heating rate.

---

[4] Zsakó, E. Kékedy and Cs. Várhelyi, *Stud. Univ. Babeș Bolyai, Chem.* **14**, (2), 000 (1969).

[5] Part XVIII: J. Zsakó, Cs. Várhelyi and E. Kékedy, *J. Inorg. Nuclear Chem.*, (in press.)

[6] T. Ozawa, *Bull. Chem. Soc. Japan*, **38**, 1881 (1965).

[7] J. Zsakó, *Rev. Roumaine Chim.*, **15**, 000 (1970).

[8] J. Zsakó, *J. Chim. phys.*, **66**, 1041 (1969).

The basic relation used in the modified Doyle method is the following[3]:

$$B = \lg \frac{Z E_a}{R q} = \lg g(\alpha) - \lg p(x) \qquad (2)$$

where Z stands for the pre-exponential factor, E_a for the activation energy, R for the general gas constant, q for the heating rate. The functions $g(\alpha)$ and $p(x)$ have the following significance:

$$g(\alpha) = \int_0^{\alpha} \frac{\mathrm{d}\alpha}{f(\alpha)} \quad \text{and} \quad p(x) = -\int_{\infty}^{x} \frac{e^{-x}}{x^2}\,\mathrm{d}x \qquad (3)$$

where α stands for the decomposition degree of the initial compound and $f(\alpha)$ expresses the kinetic law of the decomposition in isothermal conditions, according to the equation.

$$\frac{\mathrm{d}\alpha}{\mathrm{d}t} = k\, f(\alpha) \qquad (4)$$

where k stands for the rate constant. In the integral function $p(x)$ the variable x stands for the fraction $E_a/R\,T$. Numerical values of $-\lg p(x)$ have been listed in our previous paper[3] as function of both temperature and activation energy E_a.

In eq. (2) the magnitude B depends only upon the nature of the pyrolysis process, but in the case of a given thermogravimetric curve it must have the same value for each point of the curve. The modified Doyle method is based on the constancy of B. From the thermogravimetric curves the decomposition degree can be calculated for each experimental point, according to the following relation

$$\alpha = \frac{W_0 - W}{W_0 - W_t} \qquad (5)$$

where W, W_0 and W_t stand for the actual, initial and final weight of the sample, respectively.

As concerns the shape of the function $f(\alpha)$, the most frequently functions of the following type are assumed:

$$f(\alpha) = (1 - \alpha)^n \qquad (6)$$

where n stands for the apparent reaction order. By assuming different reaction orders, the function $g(\alpha)$ can be calculated for each experimental point. The analytical shape of the function $g(\alpha)$ was given in our paper[3] for the following reaction orders: 0, 1/3, 1/2, 2/3, 1 and 2. The table with the numerical values of $-\lg p(x)$ enables us to seek for the E_a value which ensures the constancy of B during the thermal decomposition reaction. To find easily the E_a value, we gave a statistical criterion. By using the $g(\alpha)$ values, obtained for a given presumed reaction order n, and the table of integrals, B values are calculated for each experimental point, by assuming an approximate E_a value. These individual B values will be denoted by B_i. The arithmetical mean of the B_i values (denoted by $\overline{B}$), and the standard deviation of individual B_i values from the arithmetical mean are calculated.

The standard deviation, defined as

$$\delta = \sqrt{\frac{\sum(B_i - \overline{B})^2}{r}} \tag{7}$$

where r stands for the number of experimental points, gives a quantitative characterization of the constancy of B and thus, of the consistency of the assumed kinetic parameters with the experimental data. The standard deviation δ is calculated for various E_a values and its minimum indicates the best E_a value, the most consistent with the presumed reaction order. By repeating this trial-and-error procedure, for other reaction orders, too, the minimum δ values can be compared, which gives the best reaction order since the minimum δ values show a minimum for this reaction order.

The calculations have been carried out for the above mentioned six reaction orders. For each thermogravimetric curve six lg $g(\alpha)$ values have been calculated for each experimental point.

As an example we give in table 1 the fraction of the initial compound $(1 - \alpha)$, derived from the experimental thermogravimetric curves and the corresponding six lg $g(\alpha)$ values, calculated by means of the formulae given in our previous paper [3]. These data are given for the following two compounds:

$$[\mathrm{Co(DH)_2(p\text{-}ethylaniline)_2}]\,\mathrm{I} \tag{I}$$

$$[\mathrm{Co(DH)_2(o\text{-}bromaniline)_2}]\,\mathrm{I} \tag{II}$$

Table 1

lg $g(\alpha)$ values for the compounds (I) and (II) by presuming different reaction orders. (Heatings rate q = 10° C/min)

Compound	t°C	$1 - \alpha$	lg $g(\alpha)$, for reaction orders					
			$n = 0$	$n = 1/3$	$n = 1/2$	$n = 2/3$	$n = 1$	$n = 2$
(I)	180	0.9516	−1.316	−1.311	−1.310	−1.307	−1.304	−1.293
	190	0.9086	−1.040	−1.033	−1.028	−1.026	−1.019	−0.997
	200	0.8495	−0.823	−0.812	−0.806	−0.800	−0.788	−0.751
	210	0.6935	−0.513	−0.487	−0.474	−0.462	−0.436	−0.354
	220	0.4247	−0.240	−0.185	−0.157	−0.128	−0.068	+0.130
	230	0.1021	−0.047	+0.070	+0.134	+0.204	+0.358	+0.945
(II)	120	0.8982	−0.992	−0.985	−0.981	−0.977	−0.970	−0.945
	130	0.7920	−0.682	−0.665	−0.657	−0.649	−0.633	−0.581
	140	0.6327	−0.435	−0.404	−0.388	−0.373	−0.339	−0.236
	150	0.4558	−0.265	−0.214	−0.187	−0.160	−0.105	+0.072
	160	0.2035	−0.098	−0.008	+0.041	+0.092	+0.202	+0.594

Further calculations have been carried out in the following way. For each reaction order the approximate activation energy value has been estimated, by using the lg $g(\alpha)$ values and the integral table containing lg $p(x)$ values. Thus the variation of lg $g(\alpha)$ in the case of compound (*I*), assuming $n = 0$, between 180 and 230° is 1.269 (see table 1). On the other hand, the variation of lg $p(x)$ in the same temperature range is 1.239 for $E_a = 24.0$ kcal/mole and 1.333 for $E_a = 26.0$ kcal/mole, i.e. the activation energy which is the most consistent with experimental data and with the alleged reaction order $n = 0$ must be of approximately 25 kcal/mole. In order to determine more exactly the activation energy, lg $p(x)$ values have been calculated in the indicated temperature range, for intermediate E_a values, namely for 24.2, 24.4, . . . 25.6 and 25.8 kcal/mole, by means of linear interpolation, and using the integral table given in our paper.[3] With the help of these interpolated values, individual B_i values have been calculated, by using the six experimental lg $g(\alpha)$ values for $n = 0$, separately for each E_a. Arithmetical mean of these B_i values and the sums $\Sigma(B_i - \overline{B})^2$ have been calculated. The minimum of these sums indicates the best E_a value for the given reaction order. In table 2 these sums are given for several E_a values in the vicinity of the minimum. By comparing these minimum values, obtained for different reaction orders, one can choose the best reaction order, i.e. the most consistent with the experimental data. Thus, in the case of compound (I) the minimum of the sum $\Sigma(B_i - \overline{B})^2$ is the least for $n = 0$, in the case of compound (II) for $n = 1$. We can say the pyrolysis of compound (I) is apparently of zero order, with an activation energy of 25.2 kcal/

Table 2

Sums $\sum (B_i - \overline{B})^2$ calculated for the thermal decomposition of compounds (I) and (II) in the vicinity of their minimum value, by presuming different reaction orders, together with the corresponding E_a – values.

Compound	n	E_a	$\Sigma(B_i - \overline{B})^2$	n	E_a	$\Sigma(B_i - \overline{B})^2$	n	E_a	$\Sigma(B_i - \overline{B})^2$
(I)	0	25.0	0.003606	1/3	27.2	0.005691	1/2	28.2	0.008814
		25.2	0.003519		27.4	0.005679		28.4	0.008595
		25.4	0.003671		27.6	0.005760		28.6	0.008710
	2/3	29.6	0.014165	1	32.0	0.032689	2	42.4	0.212950
		29.8	0.014039		32.2	0.032653		42.6	0.212788
		30.0	0.014369		32.4	0.032969		42.8	0.213124
(II)	0	15.4	0.006543	1/3	17.0	0.004252	1/2	17.8	0.003242
		15.6	0.006438		17.2	0.004238		18.0	0.003151
		15.8	0.006487		17.4	0.004286		18.2	0.003251
	2/3	18.6	0.002404	1	20.6	0.001890	2	27.4	0.017876
		18.8	0.002301		20.8	0.001760		27.6	0.017790
		19.0	0.002344		21.0	0.001848		27.8	0.018031

/mole and that of compound (II) is of the first order, with an activation anergy of 20.8 kcal/mole.

Similar calculations have been carried out for all the studied complexes. Results are given in table 3. This table contains the best reaction order from the six we have tried, the corresponding activation energy, the standard deviation defined by relation (7), the Z value calculated on the basis of the arithmetical mean of individual B_i values, by using the obtained activation energy, according to eq. (2). The same table contains another reaction order value, too, which has been obtained using the shape of the thermogravimetric curves. In our previous paper [7] a new method was given for the determination of the apparent reaction order. This method uses the magnitude

$$\nabla = \frac{1/T_{0.5} - 1/T_{0.1}}{1/T_{0.9} - 1/T_{0.1}} \tag{8}$$

where $T_{0.1}$, $T_{0.5}$ and $T_{0.9}$ stand for the absolute temperature at which the fraction of the initial complexe $(1 - \alpha)$ reaches the indicated 0.1, 0.5 and 0.9 value, respectively. This magnitude has been found to be a univocal function of reaction order, according to the following relation:

$$\nabla = 0.2670 + 0.125\, n - 0.0048\, n^2 \tag{9}$$

In table 3 reaction orders obtained by means of relation (9) are denoted by n_∇ and those obtained with the help of the modified Doyle method are given as n_δ. By comparing the two sets of reaction orders, one can observe a quite good agreement.

Concerning the influence of heating rate on kinetic parameters, a systematic variation of these parameters can be observed with increasing heating rate. Apparent reaction order increases generally with increasing heating rate. At the same time apparent activation energy decreases nearly in all cases. A similar decrease in the activation energy with increasing heating rate has been observed by other authors,[9] too.

The explanation of this effect is, probably, the following: a linear variation of the furnace temperature is performed, but the real temperature of the sample is not the same. The lag depends upon heating rate and it is larger, when heating rate is larger. Thus, the decomposition rate is smaller, than that corresponding to the furnace temperature, a reduced thermogravimetric curve slope results, which gives a larger reaction order and a smaller activation energy. On the other hand, the volatilization of the liberated amine is not instantaneous and a lag can appear between the liberation and the volatilization of the product, which also reduces the slope of the thermogravimetric curve. This effect is larger at higher heating rates and it can explain the observed phenomenon.

The lg Z values vary parallelly with the activation energy in the same manner as in our earlier experiences.[4,5]

These results enable a single conclusion namely that the obtained kinetic parameters do not characterize the proper chemical reaction, given by eq. (1), but the complex pyrolysis process as a whole, involving, besides

---

[9] D. FURNICĂ and I. A. SCHNEIDER, *Makromol. Chem.*, **108**, 182 (1967).

Table 3

Kinetic parameters of the thermal decomposition of [Co(DH)$_2$(amine)$_2$]I type complexes at different heating rates

Amine	q = 5°C/min					q = 10°C/min					q = 15°C/min				
	n_δ	n_∇	E_a	lg Z	δ	n_δ	n_∇	E_a	lg Z	δ	n_δ	n_∇	E_a	lg Z	δ
aniline	—	—	—	—	—	1	1.36	40.8	17.9	0.131	2	2.15	36.4	16.6	0.020
o-toluidine	2/3	0.65	67.0	32.4	0.017	1	0.91	46.2	20.7	0.117	1	1.18	45.0	21.4	0.023
m-toluidine	0	0.05	54.0	25.0	0.024	1/3	0.21	43.7	19.2	0.036	1/2	0.40	37.6	13.3	0.096
p-toluidine	1/3	0.24	34.9	14.5	0.011	2/3	0.82	32.7	14.0	0.031	1	0.95	31.5	12.6	0.022
m-xylidine	2/3	0.57	39.8	18.0	0.017	2/3	0.62	31.6	13.7	0.078	2/3	0.71	28.4	12.3	0.011
o-ethylaniline	2/3	0.87	34.1	16.3	0.008	1	1.15	25.3	10.8	0.016	1	1.37	23.8	10.2	0.054
p-ethylaniline	0	0.21	27.6	10.3	0.032	1/2	0.57	25.2	8.8	0.024	1	0.93	25.9	10.4	0.025
p-propylaniline	0	0.11	41.4	17.4	0.043	0	0.19	40.8	17.0	0.043	1/3	0.46	39.2	16.6	0.024
o-anisidine	1/2	0.46	41.7	17.9	0.010	1/2	0.51	26.7	9.9	0.023	1	0.78	66.2	30.9	0.052
p-anisidine	0	0.16	64.0	25.8	0.004	1	1.05	41.6	15.5	0.124	—	—	—	—	—
o-phenetidine	1/2	0.34	38.4	16.5	0.014	2/3	0.60	33.4	14.2	0.022	1	0.93	24.0	8.8	0.038
p-phenetidine	0	0.01	20.4	6.9	0.020	0	0.09	20.4	6.9	0.015	0	0.21	20.0	7.1	0.007
o-Cl-aniline	0	0.07	30.2	14.1	0.039	1/2	0.59	29.2	13.5	0.078	1	0.97	22.1	9.7	0.027
m-Cl-aniline	1/2	0.51	61.2	31.6	0.113	2/3	0.59	30.8	13.9	0.038	2/3	0.72	29.8	13.9	0.017
p-Cl-aniline	0	−0.07	26.0	10.0	0.016	0	0.02	23.6	9.3	0.008	0	0.12	19.6	6.6	0.023
o-Br-aniline	—	—	—	—	—	1	0.79	20.8	8.7	0.015	—	—	—	—	—
p-Br-aniline	—	—	—	—	—	1/2	0.39	26.0	10.4	0.006	—	—	—	—	—
benzylamine	—	—	—	—	—	1	0.83	49.0	20.5	0.119	1	1.34	65.4	29.4	0.132
α-naphthylamine	2/3	0.73	47.0	19.4	0.023	1	1.16	45.6	18.7	0.039	1	1.52	43.4	18.1	0.016
pyridine	1	0.93	54.4	26.6	0.045	1	1.08	40.8	20.1	0.072	1	1.07	39.4	18.6	0.012
β-picoline	1	0.86	51.1	24.6	0.050	1	0.97	42.6	19.6	0.076	1	1.06	37.8	18.0	0.013
γ-picoline	0	0.03	35.8	14.4	0.022	0	0.08	31.8	12.6	0.020	0	0.19	23.4	8.0	0.052

the chemical reaction, other processes, too, as heat transfer, diffusion, formation of crystallization centres, growth of these centres, etc.

The above results can be compared with those obtained for the analogous bis-diphenylglyoximato complexes,[5] studied at a single heating rate, namely $q = 10°/\text{min}$. Nearly in all cases the apparent activation energy is larger for the bis-dimethylglyoximato — complexes than for the analogous bis-diphenylglyoximato — derivatives. This difference might be due to the differing activation energy of the chemical process.

Concerning the reproductibility of the results, it is worth mentioning, that besides the heating rate, other working conditions have a quite considerable influence. By recording the thermogravimetric curves for samples of the same weight (100 ± 0.3 mg in our experiments), and by using the same crucible, a rather good reproducibility can be reached. The activation energy values do not differ, generally, by more than 1—2 kcal/mole. This fact and the quite good agreement between the n_∇ and n_δ values plead for the possibility to characterize thermogravimetric curves by means of the kinetic parameters n, E_a and Z and to obtain these data by means of the modified Doyle method.

EXPERIMENTAL

Synthesis of the studied complexes was performed by means of the already described method[1]. Purity of the compounds has been controlled analytically, by determining the cobaltous and the halogene content. Two new compounds have been synthesized by means of the same method. Their analysis data are the following:

$[Co(DH)_2(p\text{-chloraniline})_2]I$ (Mol. wt. 671.2), red-brown needles

Co *calc.* 8.78; Co *found* 8.90;

I *calc.* 18.90; I *found* 19.10.

$[Co(DH)_2(p\text{-propylaniline})_2]I$ (Mol. wt. 686.4), brown needles

Co *calc.* 8.58; Co, *found* 8.65;

I, *calc.* 18.49; I, *found* 18.61.

Thermogravimetric curves have been recorded by means of a thermobalance, using a procedure already described.[10]

---

[10] L. Erdey and F. Paulik, *Magy. Tud. Akad. Kém. Oszt. Közl.*, **5**, 461 (1955); L. Kékedy, P. Kröbl, Á. Szurkos and E. Kékedy, *Stud. Univ. Babeş Bolyai, Chem.*, **3**, 99 (1958).

Revue Roumaine de Chimie, 15, 873–879 (1970)

HYDROGEN BONDS. III

HMO TREATMENT OF SOME CHELATED COMPOUNDS RELATED TO 2-HYDROXYACETOPHENONE *)

I. I. BĂDILESCU

Research Department, Petrochemical Works Piteşti, Piteşti, Romania

Received December 19, 1968

Ten carbonyl-containing *o*-phenols with intramolecular hydrogen bond (shown in Chart A) have been treated by the simple HMO method.

The calculated carbonyl $p_{C=O}$ bond orders *versus* $\nu_{C=O}$ frequencies of the compounds correlate satisfactorily, except for the linearly chelated 2,4-diacetylphloroglucinol; this favours the earlier suggested angular structure for the chelated 2,4-diacetylphloroglucinol. Calculated $\Delta\varepsilon = \varepsilon_{LE} - \varepsilon_{HO}$ energies correlated well with energies of the first bands in the el ectronic spectra of these compounds.

INTRODUCTION

Pauling [1] had pointed out that the differences in the strength of chelation between 2,4- and 4,6-diacetyl resorcinols could be explained on the basis of the different contribution of one Kekulé structure to the normal state of the molecules, rather than by the complete fixation of the double bonds as suggested earlier by Baker. [2,3] Accordingly, Hunsberger and his co-workers [4–8] gave a relation between the double-bond charac-

---

*) Paper presented at the National Conference of Pure and Applied Physical Chemistry. held in Bucharest, September 2–5, 1968, Part II: S. Bădilescu and I. Bădilescu, *Rev, Roumaine Chim.*., **14**, 329 (1969).

[1] L. Pauling, "The Nature of the Chemical Bond", 2nd Ed., Oxford University Press London, 1948, p. 321.

[2] W. Baker, *J. Chem. Soc.*, **1934**, 1684.

[3] W. Baker and P. Lothian, *J. Chem. Soc.*, **1935**, 628.

[4] I. M. Hunsberger, *J. Amer. Chem. Soc.*, **72**, 5626 (1950).

[5] I. M. Hunsberger, R. Ketcham and H. S. Gutowsky, *J. Amer. Chem. Soc.*, **74**, 4839 (1952).

[6] I. M. Hunsberger, D. Lednicer, H. S. Gutowsky, D. L. Bunker and P. Taussig, *J. Amer. Chem. Soc.*, **77**, 2466 (1955).

[7] I. M. Hunsberger, H. S. Gutowsky, W. Powell, L. Morin and V. Bandurco, *J. Amer. Chem. Soc.*, **80**, 3294 (1958).

[8] A. L. Porte, H. S. Gutowsky and I. M. Hunsberger, *J. Amer. Chem. Soc.*, **82**, 5057 (1960).

ter (Pauling's percentage) of the carbon-to-carbon bond holding the chelated substituents (**I**, Band *a*) and the difference $\Delta\nu_{C=O}$ of the carbonyl stretching frequencies in the chelated and unchelated (parent) compounds. Moreover, Marcinkiewicz and Green [9] correlated the C—C bond orders

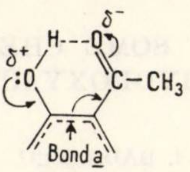

I

(p_{CC}) in benzene, naphthalene and phenanthrene, with the $\Delta\nu_{C=O}$ values reported by Hunsberger *et al.*

In two preceding paper [10,11] we showed that the relative strength of the hydrogen bonds in chelated compounds related to 2-hydroxyacetophenone (**1**) may be estimated from the shifts in the $\nu_{C=O}$ frequency of the investigated compounds with respect to that in **1**, and, on the basis of the results obtained, an angular chelated structure was assigned for 2,4-diacetyl-phloroglucinol (**9a**).

In chelated compounds of type **I** the $\nu_{C=O}$ value may be considered as dependent upon the relative importance of the canonical forms **II**a and **II**b in the chelated, conjugated molecule, and hence as dependent upon the carbonyl bond order $p_{C=O}$. Prediction concerning the

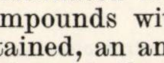

II a

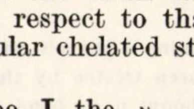

II b

strength of the hydrogen bonds of this type of compounds would be thus possible by means of the carbonyl bond orders ($p_{C=O}$), which results from molecular orbital calculations.

In this work, Hückel Molecular Orbital (HMO) calculations for the compounds related to 2-hydroxyacetophenone (shown in Chart A) are performed, in order to correlate the spectral data with the HMO calculation data and to decide on the structure of 2,4-diacetylphloroglucinol.

RESULTS AND DISCUSSIONS

In this paper the simple HMO method, without overlap, was used with parameters recommended by Streitwieser [12] or close to them. [13]

---

[9] S. Marcinkiewicz and J. Green, *J. Chem. Soc.*, **1959**, 849.

[10] S. Badilescu and I. Badilescu, *Rev. Roumaine Chim.*, **10**, 103 (1965).

[11] S. Badilescu and I. Badilescu, *Rev. Roumaine Chim.* (in press).

[12] A. Streitwieser, Jr., "Molecular Orbital Theory for Organic Chemists", John Wiley and Sons, Inc., New York — London, 1961, p. 135.

[13] B. Pullman and A. Pullman, „Quantum Biochemistry", Interscience Publishers, New York — London, 1963, chap. 3.

Chart A

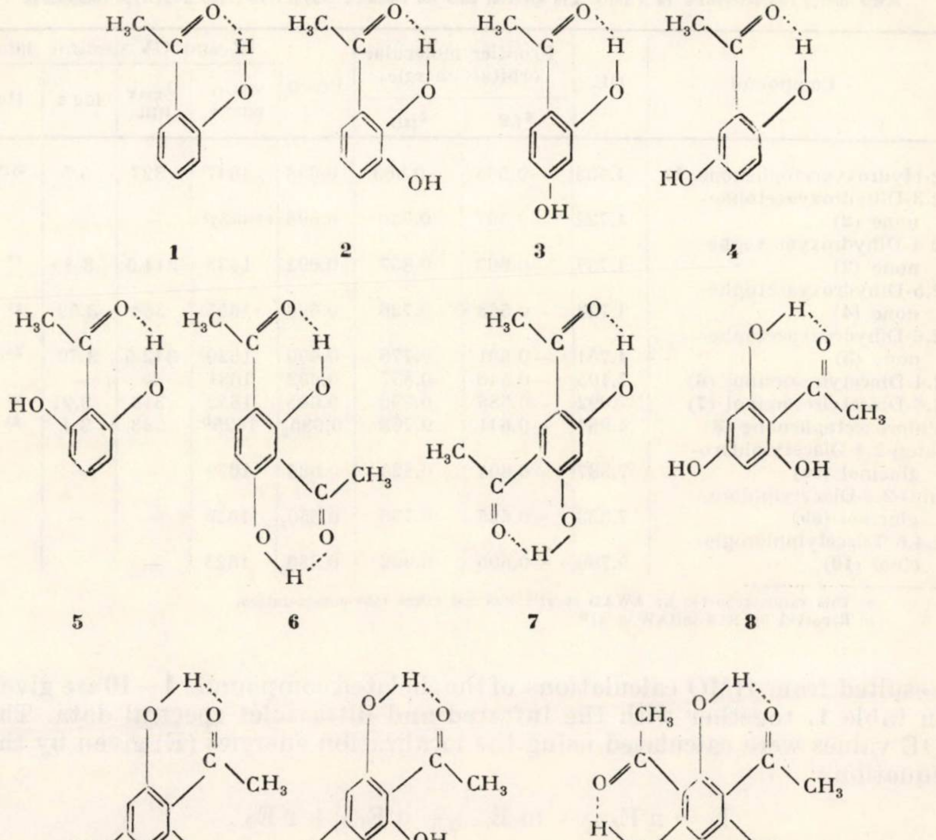

1 2 3 4 5 6 7 8 9a 9b 10

The β-exchange integrals were taken equal to β only for the C−C bonds in the phenyl ring. The coulomb integral α was taken equal to α + 2β for both oxygen atoms involved in chelation as well as for the methyl group which was considered as heteroatom. [12,13] The hydrogen bond was treated in the following manner: the same values for coulomb integrals are considered for both the OH and C = O oxygen atoms and a β-exchange integral for the hydrogen bond equal to 0.3 β is introduced. Other parameters used were: $\beta_{C-O} = 0.8\beta$, $\beta_{C=O} = \sqrt{2}\,\beta$, $\beta_{C-C_{ring}} = 0.9\,\beta$ and $\beta_{C-CH_3} = 0.6\,\beta$.

Delocalization energies (DE), the energies of the frontier molecular orbitals (ε_{HO} and ε_{LE}) and the carbonyl bond orders ($p_{C=O}$) values

Table 1

HMO energy characteristics (in β units) and spectral data for chelated 2-hydroxyacetophenone type compounds

Compound	DE	Frontier molecular orbitals energies		$p_{C=O}$	IR and UV spectral data			
		ε_{LE}	ε_{HO}		$\nu_{C=O}$ cm^{-1}	λ_{max} nm	log ε	Ref.
2-Hydroxyacetophenone (**1**)	4.535	−0.568	0.863	0.698	1647	327	3.5	14,15
2,3-Dihydroxyacetophenone (**2**)	4.722	−0.567	0.730	0.698	(1633)$^{a)}$	—	—	
2,4-Dihydroxyacetophenone (**3**)	4.737	−0.607	0.857	0.692	1638	314.5	3.89	17
2,5-Dihydroxyacetophenone (**4**)	4.724	−0.568	0.726	0.698	1655	364	3.59	18
2,6-Dihydroxyacetophenone (**5**)	4.751	−0.601	0.770	0.690	1629	342.5	3.70	19,20
2,4-Diacetylresorcinol (**6**)	7.105	−0.546	0.857	0.692	1631	—	—	
4,6-Diacetylresorcinol (**7**)	7.092	−0.586	0.896	0.695	1652	318	3.91	21
Phloroacetophenone (**8**)	4.964	−0.641	0.768	0.685_5	1625$^{b)}$	333	3.4	23
(ang)-2,4-Diacetylphloroglucinol (**9a**)	7.337	−0.604	0.820	0.686	1629	—	—	
(lin)-2,4-Diacetylphloroglucinol (**9b**)	7.333	−0.625	0.796	0.550_5	1629	—	—	
2,4,6-Triacetylphloroglucinol (**10**)	9.706	−0.605	0.942	0.686_6	1625	—	—	

a) This value, reported by AWAD et al[16] was not taken into consideration.
b) Reported by RINGSHAW et al[22]

resulted from HMO calculations of the chelated compounds **1**−**10** are given in table 1, together with the infrared and ultraviolet spectral data. The DE values were calculated using the localization energies (E) given by the equation :

$$E = n\,E_{C=C} + m\,E_{C=O} + q\,E_{CH_3} + r\,E_{\dot{O}}\ .$$

where $E_{C=C} = 2\alpha + 2\beta$, $E_{CH_3} = E_{\dot{O}} = 2\alpha + 4\beta$ and $E_{C=O} = 2\alpha + 3.732\beta$ (calculated accordingly [24]). The $\nu_{C=O}$ values were those reported [10,11] for the compounds **1**−**10** in diluted carbon tetrachloride solutions and the λ_{max} values correspond to the maxima of the first bands in the electronic spectra, in ethyl alcohol.

The $\nu_{C=O}$ frequencies were plotted against the carbonyl bond orders ($p_{C=O}$) of the investigated compounds (except **9a** and **9b**) and the

---

[14] R. A. Morton and A. L. Stubbs, *J. Chem. Soc.*, **1940**, 1347.

[15] M. B. Ledger and P. Suppan, *Spectrochim. Acta*, **23A**, 641 (1967).

[16] W. I. Awad, M. F. El-Neweihy and S. F. Selim, *J. Org. Chem.*, **25**, 1333 (1960).

[17] O. C. Musgrave, *J. Chem. Soc.*, **1957**, 1404.

[18] W. J. Horton and D. E. Robertson, *J. Org. Chem.*, **25**, 1016 (1960) .

[19] N. A. Valyashko and A. E. Lutskii, *Zhur. Obshkei Khim.*, **21**, 1091 (1951).

[20] H.—D. Dell, R. Kamp, M. Doersing and H. Jansen, *Liebigs Ann. Chem.*, **709**, 70 (1967).

[21] F. F. Cheshko and B. G. Distanov, *Zhur. Obshkei* ***Kh****im.*, **27**, 2851 (1957).

[22] D. J. Ringshaw and H. J. Smith, *Chem. and Ind.*, **1965**, 1383.

[23] P. Grammaticakis, *Compt. rend.*, **231**, 278 (1958).

[24] L. E. Orgel, T. L. Cottrell, W. Dick and L. E. Sutton, *Trans. Faraday Soc.*, **47**, 113 (1951).

correlation line thus obtained is depicted in figure 1. The equation of the correaltion line is

$$\nu_{C=O}\ (cm^{-1}) = 2210\ p_{C=O} + 109 \qquad (1)$$

Fig. 1 — The $\nu_{C=O}$ stretching frequencies *versus* the calculated carbonyl bond orders ($p_{C=O}$) of the chelated compounds **1**–**10**.

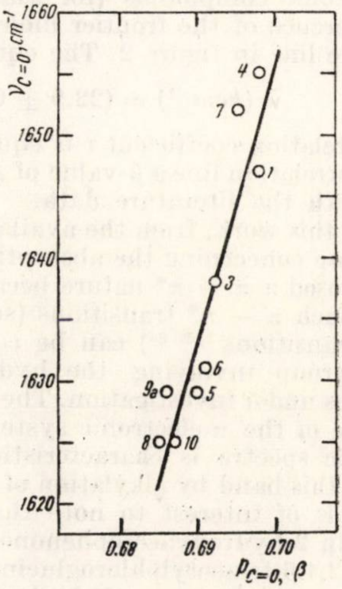

Fig. 2. — Plot of wavenumbers of the maxima of the first band in the spectra of some chelated 2-hydroxyacetophenone type compounds against calculated $\varepsilon_{LE} - \varepsilon_{HO}$ energies.

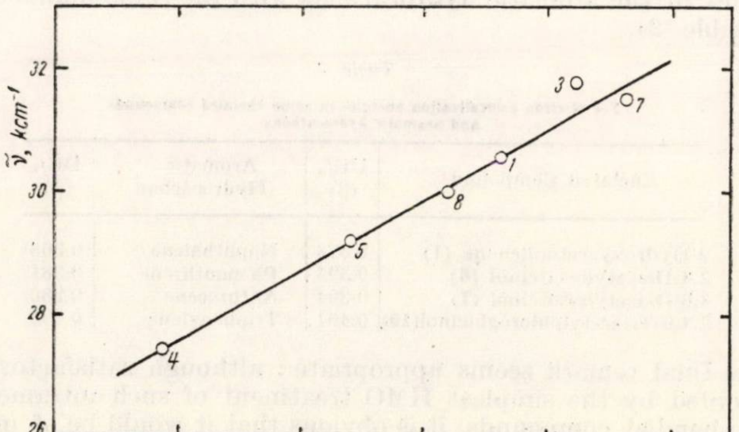

with a satisfactory value of the correlation coefficient ($r = 0.910$, $n = 8$). When the $\nu_{C=O}$ and the $p_{C=O}$ values for the angular structure of 2,4-diacetylphloroglucinol (**9a**) are taken into consideration, they give a point placed on the correlation line (with a good correlation coefficient $r = 0.975$, $n = 9$), while the point arising from the $\nu_{C=O}$ frequency and the $p_{C=O}$ value of 2,4-diacetylphloroglucinol with linear chelated structure (**9b**) does not belong to the correlation line ($r \sim 0.4$). These results give a strong evidence in favour of the angular type of chelation for 2,4-diacetylphloroglucinol which we suggested also in a previous paper.[10]

The plot of wavenumber of the first maxima in the electronic spectra of some compounds (for which spectral data are available) against the difference of the frontier molecular orbital energies ($\Delta\varepsilon = \varepsilon_{LE} - \varepsilon_{HO}$) gives the line in figure 2. The equation of this correlation line is :

$$\tilde{\nu}\ (kcm^{-1}) = (22.9 \pm 0.4)\ \ \Delta\varepsilon\ \ (\beta) - (2.2 \pm 0.6) \qquad (2)$$

The correlation coefficient r is equal to 0.988, (n = 6) and from the slope of the correlation line a β-value of about 23,000 cm^{-1} results, in good agreement with the literature data.

In this work, from the available spectral data, we took into account only those concerning the absorption bands with $\lambda_{max} > 300$ nm for which we supposed a $\pi - \pi^*$ nature because of their high intensities ($\log\varepsilon_{max} >$ 3.40). Such $\pi - \pi^*$ transitions (so-called intramolecular charge transfer (C.T.) transitions [15,25,26]) can be considered as arising from the chromophoric group involving the hydroxyphenylcarbonyl group [27,28] of the molecules under investigation. The fact that the chelation leads to a special structure of the π-electronic system, for which the first transition in the electronic spectra is characteristic, is well supported by the disappearance of this band by alkylation of the hydroxyl involved in chelation [20,29].

It is of interest to note that the per electron resonance energies (DE/n) in 2-hydroxyacetophenone (**1**), 2,4- (**6**) and 4,6-diacetylresorcinol (**7**) and 2,4,6-triacetylphloroglucinol (**10**) are very close to the corresponding values in the aromatic hydrocarbons with the same number of fused rings (table 2).

Table 2

Per electron delocalization energies in some chelated compounds and aromatic hydrocarbons

Chelated Compound	DE/$_n$ (β)	Aromatic Hydrocarbon	DE/$_n$ (β)
2-Hydroxyacetophenone (**1**)	0.378	Naphthalene	0.368
2,4-Diacetylresorcinol (**6**)	0.395	Phenanthrene	0.381
4,6-Diacetylresorcinol (**7**)	0.394	Anthracene	0.380
2,4,6-Triacetylphloroglucinol(**10**)	0.404	Triphenylene	0.403

One final remark seems appropriate : although satisfactory results were afforded by the simplest HMO treatment of such intramolecularly hydrogen-bonded compounds, it is obvious that it would be of interest to treat these compounds by more rigorous molecular orbital methods. [13,30–32]

---

[25] G. Porter and P. Suppan, *Trans. Faraday Soc.*, **61**, 1664 (1965).

[26] N. J. Turro, "Molecular Photochemistry", W. A. Benjamin, Inc., New York, 1965, p. 150.

[27] E. I. Moriconi, W. F. O'Connor and W. F. Forbes, *J. Amer. Chem. Soc.*, **82**, 5454 (1960).

[28] W. L. Dilling, *J. Org. Chem.*, **31**, 1045 (1966).

[29] D. J. Cram and F. W. Cranz, *J. Amer. Chem. Soc.*, **72**, 595 (1950).

[30] L. Paoloni, *J. Chem. Phys.*, **30**, 1045 (1959).

[31] M. Suard, *Biochim. et Biophys. Acta*, **64**, 400 (1962).

[32] I. Fischer-Hjalmars, *Act Chem. Scand,*. **12a**, 584 (1958).

CONCLUSIONS

The results obtained, although under the intrinsic limitations of the very simple model adopted and of the approximations made, afford surprisingly good agreement with the trend expected from the spectral data. Thus, the carbonyl $\nu_{C=O}$ stretching frequencies of the chelated 2-hydroxyacetophenone type compounds correlate satisfactorily with the corresponding carbonyl $p_{C=O}$ bond orders. The angular structure of chelated 2,4-diacetylphloroglucinol was demonstrated. A good correlation was also obtained by the plot of the wavenumbers of the maxima of the first band in the electronic spectra against the difference of the frontier molecular orbital energies. These results prompt us to further investigation in this field by achieving S.C.F.—L.C.A.O.—M.O. calculations of such compounds.

Acknowledgements. The author wishes to express his thanks to Prof. Dr. A. T. Balaban who suggested and facilitated this work. Thanks are due also to Dr. Z. Simon for his advice and valuable discussions and to Mr. C. Renția for the aid in performing computer calculations.

Revue Roumaine de Chimie, **15**, 881–886 (1970)

THE SUBSTITUENT EFFECTS ON THE HALFWAVE POTENTIAL OF THE *p*-DYMETHYLAMINO-*o′*, -*m′*, -*p′*-SUBSTITUTED AZOBENZENES

P. NAGY, I. GÖRBE and A. SZURKOS

Faculty of Chemistry, Pedagogical Institute, Tg. Mureş
Str. Nicolae Iorga, 1

Received July 2, 1969

The polarographic reduction of the *p*-dimetyl-amino-*o′*, -*m′*, -*p′*-substituted azobenzenes has been studied at different pH values. It has been pointed out that the substituent effects can be described by the Hammett equation. The additivity of the substituent effects has been tested. The *ortho*-effect and the polarographic *ortho*-shifst are discussed as well.

The polarographic reduction of the azo-group has been studied by several research workers. [1–7] The electrochemical reduction of the polarographically active groups in general, and of the azo-group in particular, is greatly influenced by structural changes. This dependence can be easily explained by the electron density in the electroactive group. The decrease in the electron density at the reaction center facilitates the reduction process, while the increase in this density makes it more difficult.

It has been concluded that electron-releasing substituents such as CH_3, NH_2, OH etc. move the halfwave potential, corresponding to the azo-reduction, toward negative potential values, [2–4] while the electron-withdrawing substituents act quite on the contrary.[5]

Zuman applied the Hammett equation for the halfwave potentials of substituted azobenzenes, and proved that an unambiguous correlation does exist between the electronic effects of the substituents and the halfwave potentials of these compounds. [6]

Kozeny and Velich,[7] as well as Iijima [1] found a linear correlation between the halfwave potentials of substituted *R* and *G* acids and the corresponding substituent constant. The slope of the line (the reaction constant) found by Iijima is positive. The positive slope suggests β, that the first step of the catodic reduction is the addition of an electron to each of the azo-nitrogen atoms. Therefore, Iijima proposed the following reduction mechanism:

---

[1] T. Iijima, *Review of Polarography*, **14**, 317 (1967).
[2] I. F. Vladimirchev and I. J. Postovskii, *Doklady Akad. Nauk S.S.S.R.*, **83**, 855 (1952).
[3] H. Berg, *Chem. Ing. Tech.*, **11**, 585 (1954).
[4] J. O. Carbal and H. A. Turner, *J. Soc. Dyers and Coloursits*, **72**, 158 (1956).
[5] I. Rusznyák, F. Péter and Gy. Pályi, *Acta Chim. Acad. Sci. Hung.*, **35**, 199 (1963).
[6] P. Zuman, *Coll. Czech. Chem. Comm.*, **19**, 599 (1954).
[7] M. Kozeny and V. Velich, *Coll. Czech. Chem. Comm.*, **25**, 1031 (1960).

$$R-\ddot{N}=\ddot{N}-R+2e\rightarrow R-\underset{..}{\ddot{N}}-\underset{..}{\ddot{N}}-R$$

$$R-\underset{..}{\ddot{N}}-\underset{..}{\ddot{N}}-R+2H^{+}\rightarrow R-\ddot{N}H-\ddot{N}H-R$$

On the other hand Iijima has studied the "polarographic *ortho*-shifts" for the *ortho*-substituted *R* acids.

The purpose of the present work is to verify the applicability of the Hammett equation to the polarographic reduction of *p*-dimethylamino-*m'*, -*p'*-substituted azobenzenes, as well as the additivity of the substituent effects. The effect of *ortho*-substituents on the reduction of the studied compounds has been studied as well.

EXPERIMENTAL

The compounds have the following general formula:

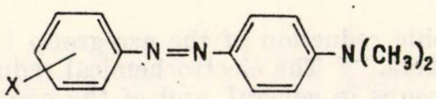

where $X = m$-Cl, m-COOH

p-CH_3, p-NHAc, p-CHO, p-COOH, p-NO_2, p-SO_3H

o-CH_3, o-Cl, o-COOH, o-NO_2

Standard literature preparations were used for these compounds.[8] The purity of studied compounds was controlled by their melting points. The polarographic measurements were performed by using solutions of 4×10^{-5} M from compounds in 80% ethanol. Acetate buffer was used to adjust the pH values of the solution (3.20; 4.76; 6.35). The current-voltage curves were obtained at 22°, by means of a recording polarograph of LP-60 type. Before every measurement methane had been bubbled through the solution for 10 minutes. The halfwave potentials were determined against the S.C.E., using a cell of Lingane-Laitinen type. (Capillary characteristics of the dropping mercury electrode: $m = 2.37$ mg/sec and $t = 3.015$ sec).

RESULTS AND DISCUSSION

1. *The applicability of the Hammett equation*

The halfwave potentials of *m'* and *p'*-substituted compounds at different pH values, as well as the corresponding substituent constants are given in table 1.

---

[8] L. M. Jagupolskii, *Zhur. obshchei Khim.*, **35**, 1252 (1965).

Table 1

$E_{1/2}$ of *m* - and *p*'-substituted compounds at different pH values

		$E_{1/2}$ mV		
X	σ	pH = 3.20	pH = 4.76	pH = 6.35
p-CH_3	−0.170	—	−425	—
m-CH_3	−0.069	−340	−424	−557
p-NHAc	0.00	—	−425	—
−H	0.00	−310	−412	−511
p-CHO	+0.216	—	−405	—
p-Cl	+0.227	—	−405	—
m-COOH	+0.350	−290	−380	−496
p-COOH	+0.406	−271	−374	−470
p-SO_3H	+0.510*	−267	−369	−476
$p-NO_2$	+0.778	−253	−343	−438

* The value of σ_{p-SO_3H} is taken from ref. 1.

If the $E_{1/2}$ values are plotted against the substituent constants (figure 1) linear correlations are obtained. These correlations cab be described by the Hammet equation :

$$(E_{1/2})_x = (E_{1/2})_0 + \rho_\pi . \sigma \qquad (1)$$

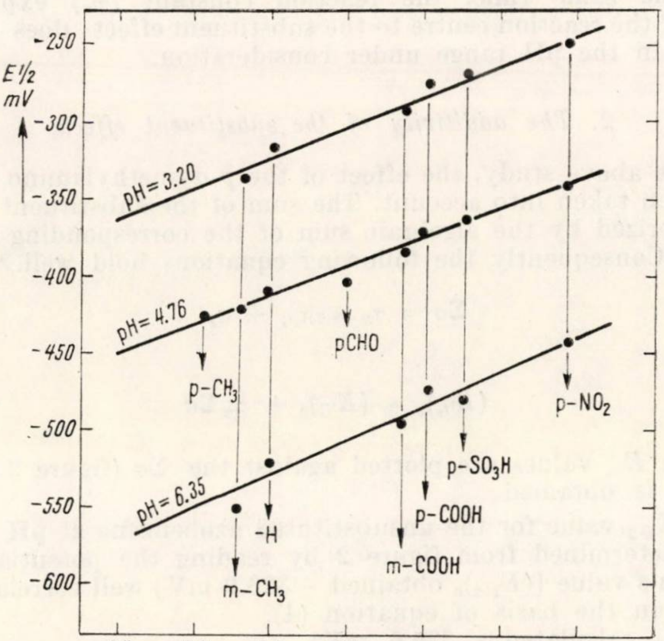

Fig. 1. — Relation between $E_{1/2}$ and σ.

It could be observed, that the electron-withdrawing substituents moved the $E_{1/2}$ values to the positive potentials, while the electron-releasing substituents acted in opposite sense. This behaviour can be obviously explained by the positive value of the reaction constant. The values of the reaction constants (ρ_π) and of the correlation coefficients (r) calculated by means of the least square method are given in table 2.

Table 2

Values of $\rho\pi$ apu r at different pH

pH	$\rho\pi$ mV	r
3.20	+ 98.0	0.970
4.76	+ 92.0	0.979
6.35	+110.0	0.930

The correlation coefficient shows that Hammett equation is applicable with good accuracy for pH 3.20 and 4.76, and only moderate accuracy for pH 6.35.

The data in table 1 and figure 1 show, that the $E_{1/2}$ values are shifted to the positive potentials for decreasing pH values. Consequently, the reduction of the azo-group is favoured by the high proton concentration. At the same time, the reaction constant (ρ_π) expressing the sensivity of the reaction centre to the substituent effects does not change essentially in the pH range under consideration.

2. *The additivity of the substituent effects*

In the above study, the effect of the *p*-dymethylamino substituent has not been taken into account. The sum of the substituent effects can be characterized by the algebraic sum of the corresponding substituent constants. Consequently the following equations hold well.[9]

$$\Sigma\sigma = \sigma_{p-\mathrm{N(CH_3)_2}} + \sigma_x \tag{2}$$

and

$$(E_{1/2})_x = (E_{1/2})_0 + \rho_\pi \Sigma\sigma \tag{3}$$

If the $E_{1/2}$ values are plotted against the $\Sigma\sigma$ (figure 2.), a linear correlation is obtained.

The $E_{1/2}$ value for the unsubstituted azobenzene at pH = 4.76 can be easily determined from figure 2 by reading the potential value for $\Sigma\sigma = 0$. This value $[(E_{1/2})_0$ obtained -336.0 mV$]$ well correlates to that calculated on the basis of equation (4).

$[(E_{1/2})_0$ calculated -335.6 mV$]$

$$E_{1/2} = -0.05 - 0.06 \text{ pH} \tag{4}$$

---

[9] P. ZUMAN, *Coll. Czech. Chem. Comm.*, **25**, 3225 (1960).

The equation (4) given by Hilson and Birnbaum[10] describes the pH dependence of the halfwave potential, corresponding to the reduction of the unsubstituted azobenzene.

Te above calculation obviously proves that substituent effects are additive for the polarographic reduction of the azo-group even if the substituents are to be found in both benzene nuclei.

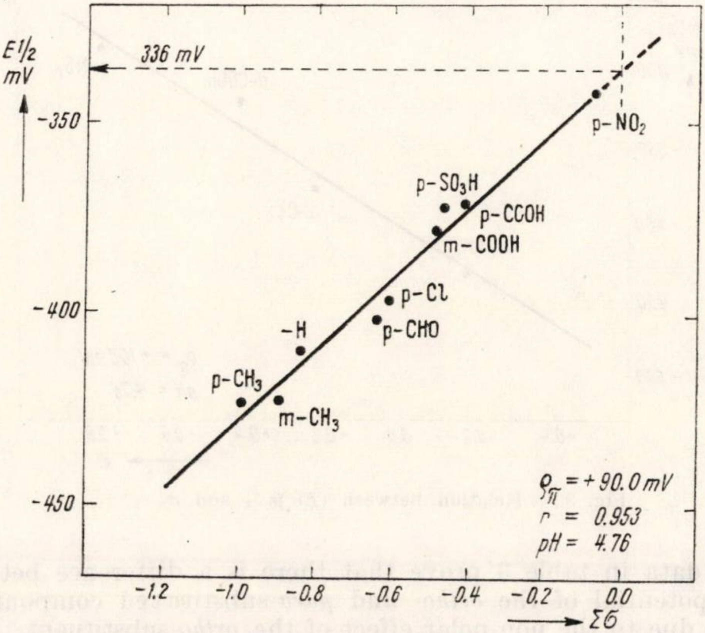

Fig. 2. – Relation between $E_{1/2}$ and $\Sigma\sigma$.
($\sigma_{p-N(CH_3)_2} = -0.83$)

3. *The ortho-effect*

The halfwave potentials of the *ortho*-substituted compounds at pH = 4.76, as well as the "polarographic *ortho*-shifts" (Δ_0)[11] are given in table 3.

Table 3

$E_{1/2}$ of the ortho substituted compounds and the Δ_0 values

X	$E_{1/2}$ mV	Δ_0
o-CH_3	−432	− 7.0
o-Cl	−374	+31.0
o-NO_2	−288	+55.0
o-COOH	−316	+58.0

---

[10] P. J. Hilson and P. B. Birnbaum, *Trans. Faraday Soc.*, **48**, 478 (1956).

[11] P. Zuman, *Coll. Czech. Chem. Comm.*, **27**, 648 (1962).

According to the theory of electronic effects, in a rough approximation, the polar effects of a substituent are the same in the *para* and *ortho* positions. Starting from this assumption, if the $(E_{1/2})_{0-x}$ values are plotted against the (σ_p), a linear correlation is obtained (figure 3).

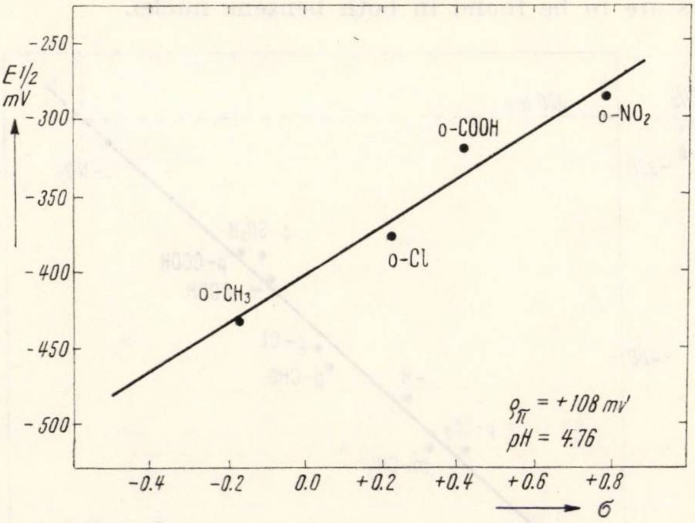

Fig. 3. — Relation between $(E_{1/2})_{0-x}$ and σ_{p-x}.

The data in table 3 prove that there is a difference between the halfwave potential of the *ortho*- and *para*-substituted compounds. This difference, due to the non-polar effect of the *ortho*-substituent, is termed by Zuman[11] the "polarographic *ortho* shift" (Δ_0) :

$$\Delta_0 = (E_{1/2})_{0-x} - (E_{1/2})_{p-x} \tag{5}$$

A negative, but insignificant $(-7.0\ \text{mV})$ *ortho*-shift has been observed for the CH_3 substituted compound. Therefore, the effect of the methyl group from the *ortho* and *para* position is nearly the same. On the other hand a positive *ortho*-shift has been observed for the NO_2, COOH and Cl substituted compounds. This means that the effect of the above substituents on the reduction process is more emphasized in the *ortho* than in the *para* position, though it should be expected that a steric hindrance of the reduction process may occur. The explanation is that a direct field effect operates between the substituent and the reaction centre in *ortho*-position.

These conclusions are not surprising in the light of Charton's recent work,[12] who concluded that the *ortho*-effect for most substituents, such as NO_2, Cl etc., is rather an electrical than a steric effect.

---

[12] M. Charton, *J. Amer. Chem. Soc.*, **91**, 615 (1969).

Revue Roumaine de Chimie, 15, 887–894 (1970)

WÄRMEÜBERGANGSZAHLEN BEIM VERDAMPFEN VON KALIUMNITRATLÖSUNGEN

Z. GROPŞIANU, D. KOHN und A. IOVI

von der Fakultät für Angewandte Chemie an der Technischen
Hochschule, Timişoara, Bd. 30 Decembrie 2

Eingegangen am 12. Juli 1969

Aufgrund experimenteller Ergebnisse wurden Gleichungen zur Berechnung der Wärmeübergangszahlen beim Sieden wäßriger Kaliumnitratlösungen verschiedener Konzentration, bei atmosphärischem Druck und bei 300 mmHg aufgestellt.

Kaliumnitrat ist sowohl für die Industrie (Glasherstellung, Lebensmittelindustrie, Pyrotechnie) als auch für die Landwirtschaft, als Düngemittel von großer Bedeutung. Es kann unmittelbar als Düngemittel verwendet werden, als Granulierungszuschlag, als Stabilisator des Ammoniumnitrates, nimmt an der Zusammensetzung der komplexen und granulierten Düngemitteln teil, usw. [1–3]

Großtechnisch kann Kaliumnitrat durch die Austauschreaktionen zwischen Natriumnitrat und Kaliumchlorid, zwischen Kaliumsulfat und Kalziumnitrat oder Salpetersäure und Kaliumchlorid [3] hergestellt werden. Im Rahmen der Prozesse, die eine Austauschreaktion verwenden, werden die Kaliumnitratlösungen durch Verdampfen konzentriert.

Zur Projektierung von Verdampfungsanlagen der Kaliumnitratlösungen ist die Kenntnis der Wärmeübergangszahl zwischen Wand und siedender Lösung nötig, jedoch sind in der Fachliteratur darüber keine Angaben zu finden.

Die Berechnung dieser Wärmeübergangszahl mit Hilfe der bekannten Gleichungen [4–5] hat den Nachteil, daß sie einerseits die Kenntnis mehrerer physikalisch-chemischer Konstanten der Lösungen voraussetzt, die ihrerseits meistens teilweise oder gänzlich fehlen und anderseits, wenn die Berechnung möglich ist, Werte liefert, die sich von den experimentell bestimmten stark unterscheiden.

---

[1] K. D. Jacob, *Comercial Fertilizer and Plant Food Industry*, **107**, 23 (1963).

[2] *Phosphorus and Potassium*, **1966**, 41.

[3] *Phosphorus and Potassium*, **1968**, 40.

[4] M. Miheev, „Fundamentals of Heat Transfer'' (Translated from the Russian) Peace Publishers, Moskau, 1956 S. 116.

[5] I. Curievici, D. Peretz und V. Macri, „Îndrumar pentru calcule de transmitere a căldurii'', Ed. didactică şi pedagogică, Bucureşti, 1962, 62.

Die gegenwärtige Arbeit hat den Zweck die Wärmeübergangszahlen beim Sieden wäßriger Kaliumnitratlösungen experimentell zu bestimmen und Beziehungen zu ihrer Berechnung, die keine physikalisch-chemische Konstanten benötigen, aufzustellen.

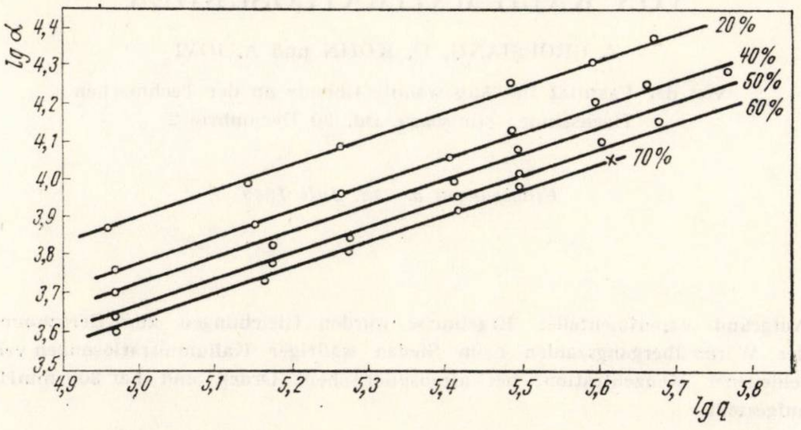

Abb. 1. — Die Veränderung von α in Abhängigkeit von q bei atmosphärischem Druck für wäßrige Kaliumnitratlösungen.

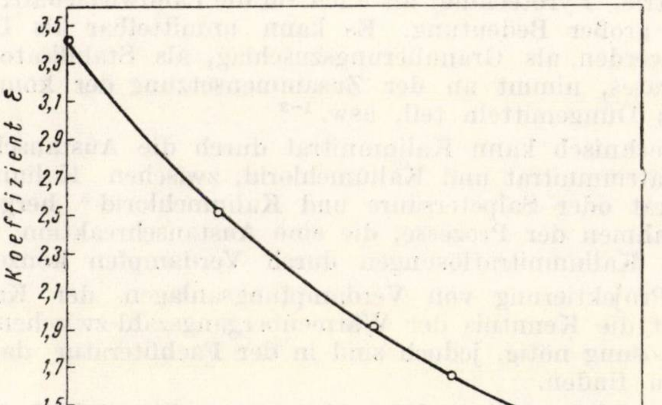

Abb. 2. — Die Abhängigkeit des Koeffizienten ε von der Konzentration der Kaliumnitratlösungen.

Die Arbeitsweise und die verwendete Laboratoriumsvorrichtung wurden in früheren Mitteilungen beschrieben.[6-7]

Die Konzentrationen der Kaliumnitratlösungen, die bei den Bestimmungen verwendet wurden, lagen zwischen 20% und 70%. Es wurde

---

[6] Z. Gropşianu, D. Kohn und A. Iovi, *Rev. Roumaine Chim.*, 14, 451 (1969).

[7] Z. Gropşianu, D. Kohn und A. Iovi, *Rev. Roumaine Chim.*, 12, 485 (1967).

eine Heizflächenbelastung zwischen $85.10^3-57.10^4 W/m^2$ verwendet und bei atmosphärischem Druck so wie auch bei 300 mmHg gearbeitet.

Die Versuchsergebnisse sind in den Abbildungen 1–8 graphisch dargestellt.

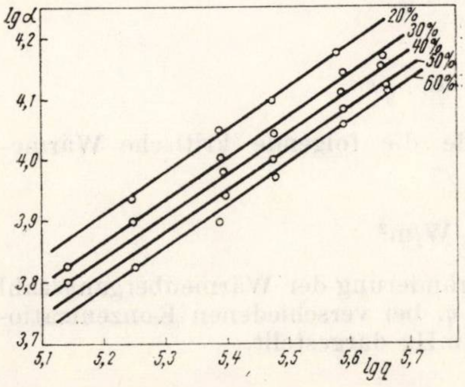

Abb. 3. – Die Veränderung von α in Abhängigkeit von q bei einem Druck von 300 mmHg für Lösungen verschiedener Konzentration.

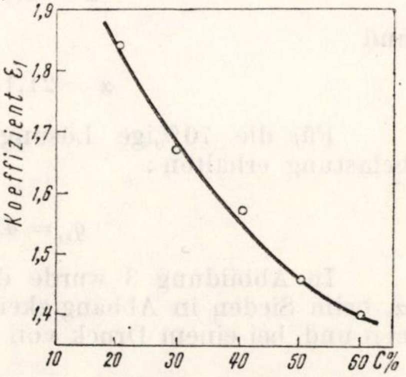

Abb. 4. – Die Abhängigkeit des Koeffizienten ε_1 von der Konzentration der Kaliumnitratlösung.

Die Veränderung der Wärmeübergangszahl α beim Sieden in Abhängigkeit von der Wärmebelastung der Heizfläche, q, für verschiedene Konzentrationen zwischen 20 % und 70 % und bei atmosphärischem Druck ist in Abbildung 1 wiedergegeben.

Aus diesem Schaubild folgt, daß α mit wachsender Wärmebelastung, q, bei allen Konzentrationen größer wird. Die Abhängigkeit, die aus diesem Schaubild abgeleitet wurde, kann durch folgende Gleichung ausgedrückt werden:

$$\alpha = \varepsilon \cdot q^{0,7}$$

wobei ε ein von der Konzentration der Lösung abhängiger Koeffizient ist (Abbildung 2).

Mit anwachsender Konzentration verkleinert sich der Wert des Koeffizienten ε, bzw. auch die Wärmeübergangszahl α, bei gleichbleibender Wärmebelastung q.

Die Beziehung zwischen ε und der Konzentration C ist folgende:

– für $C \leqslant 40\%$

$$\varepsilon = 8,95 \cdot C^{-0,386}$$

– für $40\% \leqslant C \leqslant 70\%$

$$\varepsilon = 21,15 . C^{-0,65}$$

wobei C die Konzentration der Lösung in Massenprozenten darstellt.

Folglich können folgende einfachen Beziehungen aufgestellt werden, die die Berechnung von α als Funktion der Wärmebelastung, q, bei verschiedenen Konzentrationen der wäßrigen Kaliumnitratlösungen erlauben,

$$\alpha = 8{,}95.C^{-0{,}386} \cdot q^{0{,}7}.$$

und

$$\alpha = 21{,}15 \cdot C^{-0{,}65} \cdot q^{0{,}7}$$

Für die 70%ige Lösung wurde die folgende kritische Wärmebelastung erhalten:

$$q_{kr} = 412\,000 \text{ W/m}^2$$

In Abbildung 3 wurde die Veränderung der Wärmeübergangszahl α, beim Sieden in Abhängigkeit von q, bei verschiedenen Konzentrationen und bei einem Druck von 300 mmHg dargestellt.

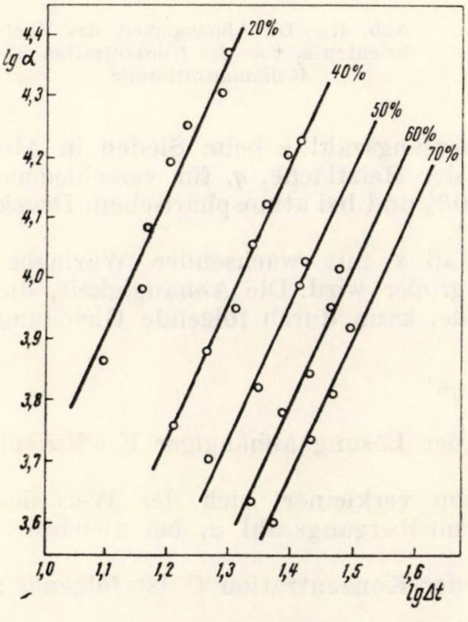

Abb. 5. — Die Veränderung von α in Abhängigkeit von Δt bei atmosphärischem Druck, für Kaliumnitratlösungen verschiedener Konzentration.

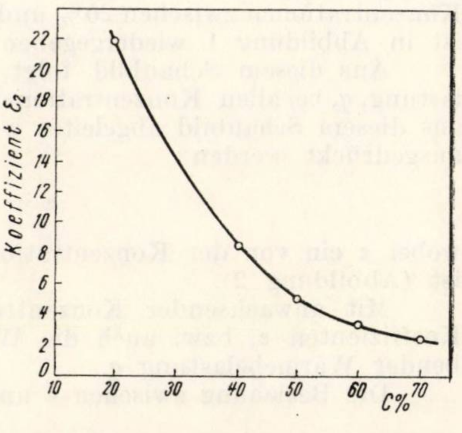

Abb. 6. — Die Abhängigkeit des Koeffizienten ε_2 von der Konzentration der Kaliumnitratlösung.

Die Wärmebelastung q übt auf α denselben Einfluß wie bei atmosphärischem Druck aus. Die Beziehung zwischen α und q ist folgende:

$$\alpha = \varepsilon_1 \cdot q^{0{,}7}$$

wobei ε_1 ein konzentrationsabhängiger Koeffizient ist (Abbildung 4).

Die Veränderung des Koeffizienten ε_1 in Abhängigkeit zur Konzentration der Lösungen wird wie folgt ausgedrückt:

— für $C \leqslant 30\%$

$$\varepsilon_1 = 3{,}42 \cdot C^{-0{,}208}$$

— für $30\% \leqslant C \leqslant 60\%$

$$\varepsilon_1 = 4{,}3 \cdot C^{-0{,}274}$$

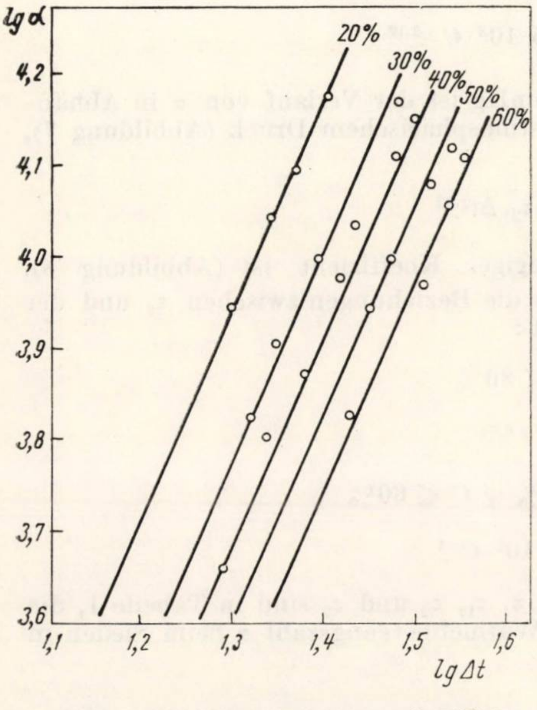

Abb — Die Veränderung von α in Abhängigkeit. von Δt bei einem Druck von 300 mmHg für Kaliumnitratlösungen verschiedener Konzentration.

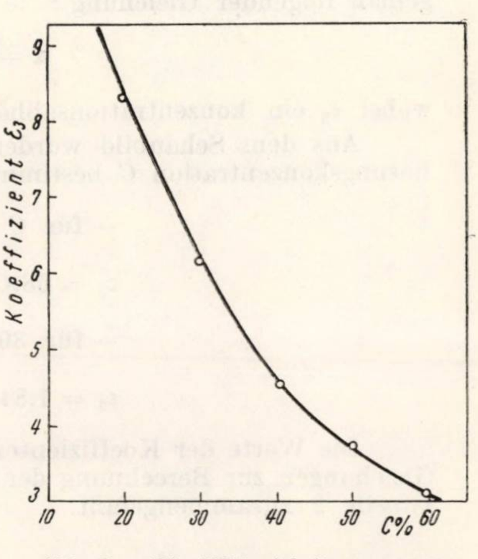

Abb. 8. — Die Abhängigkeit von ε_3 von der Konzentration der Kaliumnitratlösungen bei einem Druck von 300 mmHg.

Die in Abbildung 5 dargestellten experimentellen Ergebnisse ermöglichen die Bestimmung des Einflusses der Differenz Δt auf die Wärmeübergangszahl beim Sieden.

Unter Δt ist die Differenz zwischen den Temperaturen der Heizwand und der siedenden Lösung zu verstehen.

Mit steigender Temperaturdifferenz Δt wächst auch der Wert des Koeffizienten α, bei gleicher Konzentration, nach folgender Gleichung:

$$\alpha = \varepsilon_2 \cdot \Delta t^{2{,}33}$$

wobei ε_2 von der Konzentration der Lösung C abhängt (Abbildung 6).

Auch hier kann man eine Verringerung des Koeffizienten ε_2 und gleichzeitig eine von α, mit wachsender Konzentration feststellen. Die Beziehung zwischen ε_2 und der Konzentration ist:

– für $C \leqslant 40\%$

$$\varepsilon_2 = 1{,}27 \cdot 10^3 \cdot C^{-1.36}$$

– für $40\% \leqslant C \leqslant 70\%$

$$\varepsilon_2 = 20{,}45 \cdot 10^3 \cdot C^{-2.12}$$

Bei einem Druck von 300 mmHg ist der Verlauf von α in Abhängigkeit von Δt, ähnlich dem bei atmosphärischem Druck (Abbildung 7), gemäß folgender Gleichung:

$$\alpha = \varepsilon_3 . \Delta t^{2.33}$$

wobei ε_3 ein konzentrationsabhängiger Koeffizient ist (Abbildung 8).

Aus dem Schaubild wurden die Beziehungen zwischen ε_3 und der Lösungskonzentration C bestimmt:

– für $C \leqslant 30\%$

$$\varepsilon_3 = 68 . C^{-0.71}$$

– für $30\% \leqslant C \leqslant 60\%$

$$\varepsilon_3 = 1{,}84 \cdot 10^2 \cdot C^{-1}$$

Die Werte der Koeffizienten ε, ε_1, ε_2 und ε_3 sind in Tabelle 1, die Gleichungen zur Berechnung der Wärmeübergangszahl α beim Sieden in Tabelle 2 zusammengefaßt.

Tabelle 1

Die Werte der Koeffizienten ε, ε_1, ε_2 und ε_3

Konzentration %	ε	ε_1	ε_2	ε_3
20	2,515	1,84	22	8,3
30	—	1,69	—	6,14
40	1,92	1,57	8,57	4,52
50	1,66	1,46	5,06	3,72
60	1,482	1,4	3,45	3,06
70	1,34	—	2,58	—

Tabelle 2

Gleichungen

Konzentrationsbereich %	Gleichung	Druck, mmHg
20–40	$\alpha = 8{,}95 \cdot C^{-0{,}386} \cdot q^{0{,}7}$	760
40–70	$\alpha = 21{,}15 \cdot C^{-0{,}65} \cdot q^{0{,}7}$	
20–30	$\alpha = 3{,}42 \cdot C^{-0{,}208} \cdot q^{0{,}7}$	300
30–60	$\alpha = 4{,}3 \cdot C^{-0{,}274} \cdot q^{0{,}7}$	
20–40	$\alpha = 1{,}27 \cdot 10^3 \cdot C^{-1{,}36} \cdot \Delta t^{2{,}33}$	760
40–70	$\alpha = 20{,}45 \cdot 10^3 \cdot C^{-2{,}12} \cdot \Delta t^{2{,}33}$	
20–30	$\alpha = 68 \cdot C^{-0{,}71} \cdot \Delta t^{2{,}33}$	300
30–60	$\alpha = 1{,}84 \cdot 10^2 \cdot C^{-1} \cdot \Delta t^{2{,}33}$	

Es wurden noch die Siedetemperaturen der Kaliumnitratlösungen verschiedener Konzentration in Abhängigkeit des Druckes bestimmt, da diese zur Berechnung der Temperaturdifferenz Δt nötig sind. Die erhaltenen Ergebnisse sind in Abbildung 9 wiedergegeben.

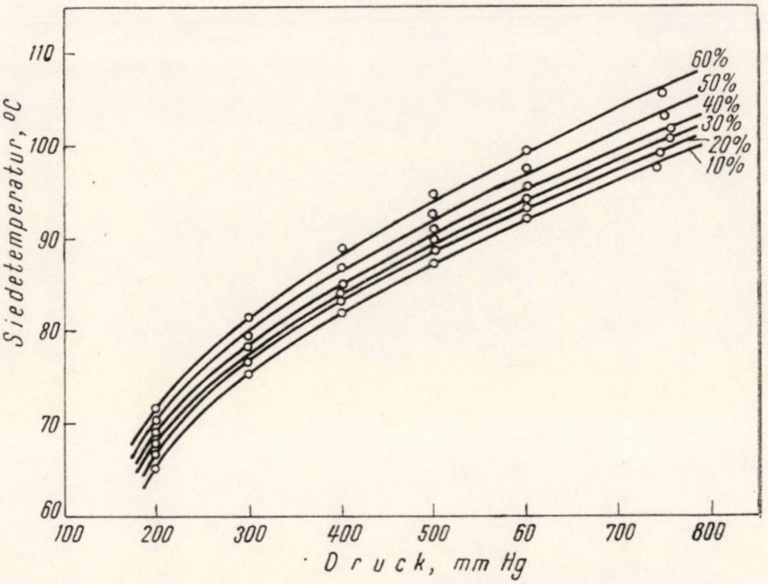

Abb. 9. — Die Siedetemperaturen der Kaliumnitratlösungen verschiedener Konzentration in Abhängigkeit des Druckes.

SCHLUSSFOLGERUNGEN

Um einfache Gleichungen zur Berechnung der Wärmeübergangszahlen α beim Sieden, von wäßrigen Kaliumnitratlösungen aufzustellen, wurden experimentelle Bestimmungen bei atmosphärischem Druck und bei einem Druck von 300 mmHg durchgeführt.

Ein Anwachsen der Wärmebelastung q, bzw. das Anwachsen der Temperaturdifferenz Δt, bestimmt eine Vergrößerung des Koeffizienten α. Die Vergrößerung der Konzentration der Lösungen hingegen bewirkt seine Verringerung.

Die Verringerung des Druckes vom atmosphärischen Druck auf 300 mmHg, bei gleicher Wärmebelastung oder gleicher Temperaturdifferenz und gleicher Lösungskonzentration, bewirkt eine Verringerung des Koeffizienten α.

Es wurden die Siedetemperaturen der Kaliumnitratlösungen verschiedener Konzentration in Abhängigkeit des Druckes bestimmt.

Revue Roumaine de Chimie, 15, 895–899 (1970)

POLAROGRAPHISCHE UNTERSUCHUNG DER REAKTION ZWISCHEN PENTACHLORO-AQUO-PLATIN(IV)-SÄURE UND 1,2-CYCLOHEXANDIONDIOXIM

CONST. GH. MACAROVICI, F. MÁNOK und CS. VÁRHELYI

Von der Chemischen Fakultät der Babeş-Bolyai-Universität-Cluj, str. Arany János Nr. 11

Eingegangen am 29. September 1969

Es wurde die Kinetik der Substitutionsreaktion zwischen $H[Pt\,Cl_5(H_2O)]$ und 1,2-Cyclohexandiondioxim (Nyoxim) unter Bildung von $[PtCl_2(NioxH)_2]$ in wässeriger Lösung untersucht. Die Änderung der Konzentration der Platinsäure wurde auf polarographischem Wege verfolgt. Die geschwindigkeitsbestimmende Reaktion ist die Dissoziation des Wassermoleküls aus $[Pt\,Cl_5(H_2O)]^-$ unter Bildung von $[PtCl_5]^-$. Dieser Vorgang ist von erster Ordnung. Aus kinetischen Daten wurden die Aktivierungsenthalpie ($\Delta H^+ = 19{,}300$ cal) als auch die Aktivierungsentropie ($\Delta S^+ = -19{,}2$ e.e.) des geschwindigkeitsbestimmenden Vorganges berechnet.

Das Hexachloroplatinat-Ion $[PtCl_6]^{2-}$ erleidet durch eine langsame Rekation einen Hydrolysenprozeß.

$$[PtCl_6]^{2-} + H_2O \rightleftarrows [PtCl_5(H_2O)]^- + Cl^- \qquad (1)$$

Dieser Vorgang ist von Sonnenlicht beschleunigt.[1,2]

Nach Davidson und Jameson[3] ist das erste Produkt der Hydrolyse : $[Pt\,Cl_5(H_2O)]^-$ eine schwache Säure mit einem pK-Wert von 3,8. Eine weitere Hydrolyse mit dem Austausch von mehreren Chlorionen in der inneren Koordinationssphäre ist praktisch vernachlässigbar, auch wenn die $H[Pt\,Cl_5(H_2O)]$-Lösung einigen Stunden lang auf 65° erwärmt wird.

Unter diesen Bedingungen ist es möglich die Substitutionsreaktionen der Pentachloro-aquo-Säuren ohne Berücksichtigung der parallelen Hydratationsvorgänge zu untersuchen. Diese Substitutionsreaktionen verlaufen im allgemeinen viel schneller als die weitgehende Hydrolyse.

In vorliegender Mitteilung wurde die Reaktion zwischen der $H[PtCl_5(H_2O)]$-Säure und 1,2-Cyclohexandiondioxim im Wasser untersucht.

---

[1] E. H. Archibald, *J. Chem. Soc.*, **117**, 1104 (1920).

[2] E. H. Archibald und W. A. Gale, *J. Chem. Soc.*, **121**, 2849 (1922).

[3] C. M. Davidson und R. F. Jameson, *Trans. Faraday Soc.*, **61**, 2463 (1965).

Zur Verfolgung der Konzentrationsänderung der Pentachloro-aquoplatin(IV)-Säure im Laufe der Substitutionsreaktion wurde die polarographische Methode angewandt.

Die gesamte Reaktion der obenerwähnten Platin-Säure mit Nyoxim ($NioxH_2$) ist folgende:

$$[Pt\,Cl_5(H_2O)]^- + 2\,NioxH_2 = [Pt\,Cl_2\,(NioxH)_2] + 2H^+ + 3\,Cl^- \quad (2).$$

In einer weiteren Reaktion reduziert sich das $[Pt\,Cl_2\,(NioxH)_2]$ unter Bildung von $[Pt\,(NioxH)_2]$.

EXPERIMENTELLER TEIL

Darstellung der $H[Pt\,Cl_5(H_2O)]$-Lösung

Es wurde 1,0 g $H_2[Pt\,Cl_6].6\,H_2O$ in 100 ml Wasser gelöst. Die Konzentration des Metalls wurde gravimetrisch nach Eindampfen eines aliquoten Teiles der Lösung und nach Glühen bei 600—700° als metallisches Platin bestimmt.

Es wurde Hexachloroplatinsäure-Lösung mit einer Konzentration von $1,844.10^{-2}$Mol bei Sonnenlicht und Zimmertemperatur zwei Wochen stehengelassen. Nach dieser Zeit wurde die Zusammensetzung der Lösung durch Titration mit 0,25 n Natronlauge bestimmt. Es wurde die Änderung des pH-Wertes der Lösung mit einem elektronischen pH-Meter (Typ L-P. 60—UdRSS) unter Verwendung von einer Glaselektrode verfolgt. Die Gesamtkonzentration der Platinkomplexe (C_{Pt}) in der untersuchten Lösung betrug $1,844.10^{-2}$. (Volumen der titrierten Lsg: 50 ml.) Die Berechnung der theoretischen pH-Werte in Beziehung zu der verwendeten 0,25 n NaOH ml Menge wurde mit Hilfe der folgenden Gleichungen ausgeführt.

$$[Na]^+ = \frac{K_{H_2O}}{[H]^+} + C_{Pt} + \frac{C_{Pt}\cdot K_a}{[H]^+ + K_a} - [H]^+ \qquad (3)$$

$$\text{wo } K_a = \frac{[H]^+\,[Pt\,Cl_5(OH)]^{2-}}{[Pt\,Cl_5\,(H_2O)]^-} = 1,59.10^{-4} \qquad (4)$$

Die Zahl der zugegebenen ml NaOH: $X = [Na]^+.200$, (5)

(Die Veränderung des Volumens im Laufe der Titration kann man vernachlässigen.)

Die völlige Überdeckung der theoretischen und experimentellen Titrationskurven bestätigt die praktisch völlige Umsetzung des Hexachloro-Komplexes in das Pentachloro-aquo-Derivat. Letzteres steht im labilen Gleichgewicht mit dem Hydroxo-pentachloro-Anion:

$$[Pt\,Cl_5(H_2O)]^- \rightleftarrows [Pt\,Cl_5(OH)]^{2-} + H^+ \qquad (6)$$

Eine andere Probe von gleichem Volumen und Konzentration mit der Vorhergehenden, wurde in einem Ultrathermostat bei 65° zwei Std. stehengelassen. Nach der Abkühlung wurde die Lösung mit 0,25 n NaOH titriert. Diese Titrationskurve ist mit der obenerwähnten Kurve völlig identisch.

Dieses Ergebnis bestätigt, daß der Hydrolysenvorgang des Monoaquo-Komplexes, der zur Substitution von mehreren Chloratomen in der inneren Koordinationssphäre führen würde, nicht stattfindet.

Polarographisches Verhalten von $H[PtCl_5\_(H_2O)]$-Säure in Anwesenheit von Nyoxim

Die polarographischen Messungen wurden mit einem Polarographen Typ OH—102 durchgeführt. Als Grundlösung wurde 0,2 M $NaNO_3$ verwendet. Vergleichselektrode: gesättigte Kalomelektrode. Die polarographische Zelle wurde bei 20° thermostatiert.

Die Reduktion der $H[Pt\,Cl_5(H_2O)]$-Säure an der Quecksilbertropfelektrode ist dem polarographischen Verhalten der Hexachloro-platin(IV)-Säure sehr ähnlich. [4,5] Die Reduktion geht am Potentialwert Null gegen gesättigte Kalomelelektrode vor sich. Nach dem Erreichen des Grenzstromwertes um $-0{,}24$ V, sinkt der Strom rasch bis zum Residualstromwert.

Diese charakteristische Erscheinung, die bei der Reduktion der anionischen Platin (IV)-Komplexe auftritt, wurde nicht völlig erklärt. Es ist wahrscheinlich, daß die Adsorption dieser Komp lexe an der Oberfläche der Quecksilbereleketrode in den obenerwähnten elektrochemischen Vorgängen eine wichtige Rolle spielt.

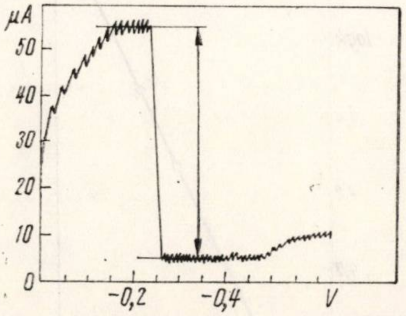

Abb. 1. — Polarogramm einer 8.10 M $H[Pt\,Cl_5(H_2O)]$-Lösung in Gegenwart von 2.10^{-3} M Nyoxim.

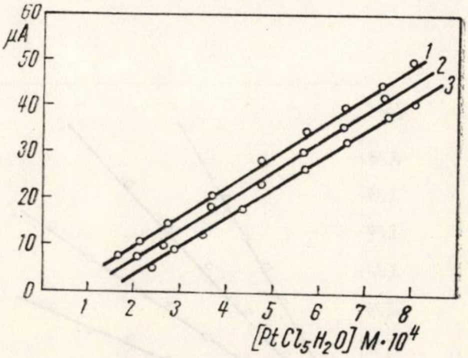

Abb. 2. — Eichkurven.

1, Nyoxim $= 2.10^{-3}$ M; *2*, Nyoxim $= 4.10^{-3}$; *3*, Nyoxim $= 6.10^{-3}$ M.

Zur Konstruktion der Eichkurven wurden die Differenzen zwischen Grenzstrom- und Residualstromwerten gegen die Konzentration der Pentachloro-aquo-platin(IV)-Säure aufgetragen (siehe Abb 1).

Wie aus Abb. 2 hervorgeht, steht die Höhe der polarographischen Stufe mit der Konzentration des Nyoxims in direktem Zusammenhang. Bei kleineren Konzentrationen des Platinkomplexes als $2{,}5.10^{-4}$, sind die Eichkurven nicht mehr linear.

Die einwandfrei reproduzierbaren polarographischen Stufen sind für die Bestimmung der Konzentration des Platin(IV)-Komplexes sehr geeignet.

Es ist bemerkenswert, daß bei Zimmertemperatur (um 20°) nach einstündigem Stehenlassen keine Verminderung der polarographischen Stufen festgestellt werden konnte. Bei diesen Arbeitsbedingung ist die Reaktion sehr langsam.

Kinetische Untersuchung der Reaktion zwischen $[Pt\,Cl_5\,(H_2O)]^-$ und Nyoxim

Die polarographische Stufe einer $H[Pt\,Cl_5(H_2O)]$-Lösung in Anwesenheit von Nyoxim nimmt ab, wenn die Mischung vorher um 60° 15 Min. lang erwärmt wurde. Nach längerem Erwärmen der Mischung der obererwähnten Verbindungen entsteht ein blaugrüner, kristalliner Niederschlag. [6]

---

[4] P. Kivalo und H. Laitinen, *J. Amer. Chem. Soc.*, **77**, 5205 (1957).

[5] A. N. Frumkin und N. V. Nikolaeva, *J. Chem. Phys.*, **26**, 1552 (1957).

[6] C. Gh. Macarovici, Cs. Várhelyi und F. Mánok, *Stud. Univ. Babeş-Bolyai, Chem.*, im Druck.

Die Bestimmung der Reaktionsordnung für den Vorgang nach Gleichung (2) wurde folgendermaßen ermittelt:

Es wurden vier Proben von $H[Pt\,Cl_5(H_2O)]$ mit gleichen Konzentrationen : $7{,}38.10\ M^{-4}$ genommen. Die Konzentration des Nyoxims in den Proben betrug $1.10^{-3}M$, $2.10^{-3}M$, $4.10^{-3}M$ und $6.10^{-3}M$. Außer diesen enthielten die Proben auch $NaNO_3$ mit der Konzentration von 0,2 M. Die Proben wurden in einem Ultrathermostat bei 60°, 30 Min. lang stehengelassen, dann

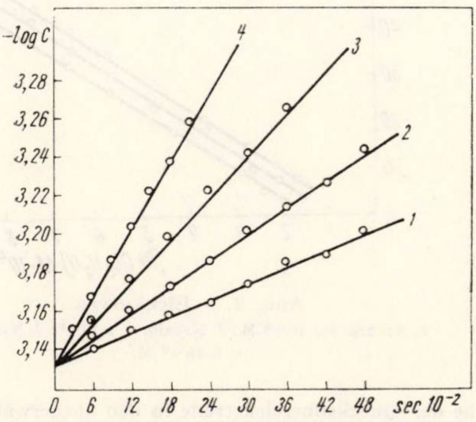

Abb. 3. — Änderung der — log C-Werte mit der Zeit.
1, 50° ; *2*, 55° ; *3*, 60° und *4*, 65°

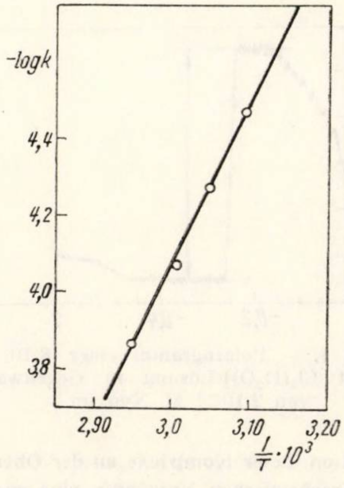

Abb. 4. — Änderung der — log K-Werte mit $1/T$. 10^3 zwischen 50—65°.

rasch abgekühlt um die Reaktion aufzuhalten. Dann wurde Wasser, bzw. Nyoxim zugegeben um die Konzentration des Nyoxims und das Volumen der Proben konstant zu halten. Die Polarogramme wurden bei 20° aufgenommen.

Es wurde beobachtet, daß die Höhen der polarographischen Stufen vollkommen identisch sind. Dieses bedeutet Reaktionsgeschwindigkeit von der Nyoximkonzentration unabhängig, und die geschwindigkeitsbestimmende Teilreaktion von erster Ordnung ist.

Die kinetischen Parameter der Reaktion wurden durch Verfolgen der Konzentrationsänderung der $H[Pt\,Cl_5(H_2O)]$-Säure in Anwesenheit von Nyoxim bei 50, 55, 60 und 65° bestimmt. Zusammensetzung der Ausgangsproben : $[Pt\,Cl_5(H_2O)]^- = 7{,}38.10^{-4}$, $[NioxH_2] = = 6.10^{-3}$, $[NaNO_3] = 0{,}2$ M. Die Konzentration des $[Pt\,Cl_5(H_2O)]^-$ -Komplexes wurde bei 20° polarographisch mit den Eichkurven bestimmt und dabei berücksichtig , daß im Laufe der Reaktion ein Teil der Nyoximmenge verschwindet.

Die graphische Darstellung von — log C(wo $C = [Pt\,Cl_5(H_2O)]^-$) gegen die Zeitdauer der Reaktion (Abb. 3.) zeigt in allen untersuchten Fällen eine gute Linearität, was bedeutet, daß die geschwindigkeitbestimmende Teilreaktion von erster Ordnung ist.

Die Geschwindigkeitskonstanten wurden mit Hilfe der Methode der kleinsten Quadrate ausgerechnet. Es wurden folgende Werte erhalten :

$$k_{50^\circ} = 3{,}55.10^{-5}, s^{-1},\ k_{55^\circ} = 5{,}37.10^{-5}\ s^{-1}$$

$$k_{60^\circ} = 8{,}30.10^{-5},\ s^{-1},\ k_{65^\circ} = 1{,}35.10^{-4}, s^{-1}$$

Die graphische Darstellung von — log k gegen $1/T.10^3$ zeigt eine gute Linearität (Abb. 5) und dies ermöglicht die Berechnung der Aktivierungsenthalpie ($\Delta H^{\overset{+}{+}}$), den Präexponentialfaktor aus der Arrheniusschen Gleichung (PZ) als auch die Aktivierungsentropie ($\Delta S^{\overset{+}{+}}$).

Die Berechnungen wurden mit Hilfe der wohlbekannten Gleichungen

$$\log k = \log PZ - \frac{\Delta H^{\overset{+}{+}}}{2{,}3\, R} \frac{1}{T} \tag{7}$$

$$\Delta S^{\overset{+}{+}} = 2{,}3 . R . \log \frac{PZ . h}{k' . T} \tag{8}$$

durchgeführt. (k' = die Boltzmannsche Konstante).

Die erhaltenen Werte sind folgende :

$$\Delta H^{\overset{+}{+}} = 19{,}3 \text{ kcal/Mol}, \quad \Delta S^{\overset{+}{+}} = -\,19{,}2 \text{ E. e.}$$

$$PZ = 3{,}9 . 10^8$$

Auf Grund der experimentellen Ergebnisse kann man folgenden wahrscheinlichen Reaktionsmechanismus aufstellen.

Es ist wahrscheinlich, daß die erste Stufe der gesamten Reaktion die geschwindigkeitsbestimmende Teilreaktion ist. Diese monomolekulare Reaktion besteht aus der Dissoziation des Wassermoleküls von der inneren Koordinationssphäre. Die Dissoziation eines zweiten Chloratoms aus dem Komplex unter Bildung des Tetrachloro-diaquo-Nichtelektrolytes : $[\mathrm{Pt\,Cl_4(H_2O)_2}]$ neben den obenerwähnten experimentellen Bedingungen findet nicht statt. Diese langsame Dissoziationsreaktion wird von zwei konsekutiven, schnellen Reaktionen unter Bildung des Nichtelektrolytes : $[\mathrm{Pt\,Cl_2(NioxH)_2}]$ gefolgt.

$$[\mathrm{Pt\,Cl_5(H_2O)}]^- \underset{}{\overset{\text{langsam}}{\rightleftarrows}} [\mathrm{PtCl_5}]^- + \mathrm{H_2O} \tag{9}$$

$$[\mathrm{PtCl_5}]^- + \mathrm{NioxH_2} \overset{\text{schnell}}{\rightleftarrows} [\mathrm{Pt\,Cl_4\,(NioxH)}]^- + \mathrm{H}^+ + \mathrm{Cl}^- \tag{10}$$

$$[\mathrm{PtCl_4(NioxH)}]^- + \mathrm{NioxH_2} \overset{\text{schnell}}{\rightleftarrows} [\mathrm{Pt\,Cl_2\,(NioxH)_2}] + 2\,\mathrm{Cl}^- + 2\mathrm{H}^+ \tag{11}$$

Die erste Stufe der gesamten Reaktion ist ein relativ langsamer Vorgang, der aus dem erheblichen Aktivierungsenthalpiewert, als auch aus der negativen Aktivierungsentropie hervorgeht.

Revue Roumaine de Chimie, **15**, 895–899 (1970)

— c. 5294

Revue Roumaine de Chimie, 15, 901–916 (1970)

THE MOLAR ABSORPTIVITY AND STABILITY OF SOME COMPLEX COMPOUNDS OF THE BA_n FORM

I. PARALESCU

Laboratory of Analytical Chemistry, Faculty of Chemistry, Bucharest
Spl. Independenţei, 89

Received October 20, 1969

The working up of the spectrophotometric data on the complex compounds of the BA_n form resulted in the possible introduction of the terms ε^n and $1/\varepsilon^n$ for the characterization of the stability or instability of the 94 complexes which are described in this paper. The identity between the obtained values and the literature data supports the validity, the utility and the extension prospects of these terms.

The basic relation of the spectrophotometry :

$$E = \varepsilon \cdot C \cdot l$$

shows that the absorbance or the extinction of a coloured system is governed by an intensive factor ε, which characterizes every absorbing species.

If the concentration C is expressed by mol-gram/1 and the thickness of the coloured layer l by centimeters, the proportionality coefficient ε is called molar extinction coefficient or molar absorptivity and is expressed by mMol^{-1}.square cm, or $1\ \text{Mol}^{-1}\ \text{cm}^{-1}$.

If $l = 1$, the molar absorptivity value is given by the relation :

$$\varepsilon = \frac{E}{C_M}$$

where C_M is the molar concentration.

The spectrophotometric study of the BA_n complex compound equilibrium is based upon a number of suitable parameters, such as : λ, pH, C_A, C_B, time, temperature, solvent, ionic strength, thickness of the coloured layer, order of the reagent adding, and so on.

For the graphic representation of the absorbance E against the concentration C, the Lambert-Beer law is defined *if* the ratio $\frac{E}{C_B}$ (which describes the slope of the straight line) has a constant value in the whole area where this law may be corroborated, according to the expression:

$$\frac{E_1}{C_{B_1}} = \frac{E_2}{C_{B_2}} = \frac{E_3}{C_{B_3}} = \ldots\ldots\ \frac{E_{i-1}}{C_{B_{i-1}}} = \frac{E_i}{C_{B_i}} = \text{constant}$$

where E_1, E_2, E_3 ... and C_{B_1}, C_{B_2}, C_{B_3} ... are the absorbances and respectively the concentrations of the dosing element, expressed in μg/ml and obtained from the Lambert-Beer calibration curve.

This constant is sub-unitary or more than 1, depending on the investigated coloured system, and may be characteristic *within the limits of the Lambert-Beer law observance only.*

If the above constant is multiplied by 1000 and by the weight of the element to be determined P_B, a new constant may be calculated (for the conditions required of the Lambert-Beer law) from the very general expression:

$$\varepsilon = \frac{E}{C_M} = \frac{E}{\dfrac{C_{BA_n}}{1000 \times P_{BA_n}}} = \frac{E}{\dfrac{C_B}{1000 \times P_B}} = \frac{E}{C_B} \times 1000 \times P_B .$$

According to Braude,[1] the molar absorptivity values — *as unique data* — of the coloured compounds, in the most favourable working conditions (i.e. if the Lambert-Beer law is observed), are tending to $\varepsilon_{\max} = 10^4 \ldots$ $\ldots 10^5$ and can be used as criteria for showing the sensitivity of the colour reactions.

We should observe that in recent treatises and papers on spectrophotometry, *the most sensitive colour reactions are described* by comparing (in reagent groups, compound types or elements) the values of the following terms:

$$\varepsilon$$

$$\varepsilon_{\text{compound}} - \varepsilon_{\text{reagent}}$$

$$\varepsilon_{\text{compound}} - \varepsilon_{\text{reagent}} - \varepsilon_{\text{metallic ion}}$$

$$\frac{P}{\varepsilon}$$

$$50\,\frac{P}{\varepsilon}$$

The term $\frac{P}{\varepsilon}$ was suggested by Sandell.[2] It may be obtained by dividing the weight (in grams) of the compound to be determined P

---

[1] E. A. BRAUDE, *J. Chem. Soc.*, **1950**, 379.

[2] E. B. SANDELL, "Colorimetric Determination of Traces of Metals", New York, Interscience Publishers, 1959, p. 84.

by the molar absorptivity value ε. The term $50\ \frac{P}{\varepsilon}$ was suggested in 1964 by Koch and Koch-Dedic.[3] Both terms are generally sub-unitarian and have similar meanings.

Tolmacev[4] proposed the term

$$\frac{\varepsilon'}{\varepsilon''}$$

for estimating the *composition* of a coloured complex, where ε' is the molar absorptivity of the compound in the presence of an excess of reagent, and ε'' the molar absorptivity in the presence of an excess of the ion to be dosed.

We should suggest in this paper the terms

$$\varepsilon^n \text{ and } \frac{1}{\varepsilon^n}$$

in order to characterize the stability or instability of the BA_n coloured complexes.

These terms were obtained by following the correlation *molar absorptivity — composition — stability (or instability) constant*, that is by a comparative processing of the spectrophotometric data of 94 BA_n coloured systems, the molar absorptivities, the combining ratios and the stability (or instability) constants of which are already demonstrated, *in identical working conditions.*

a) *Complex compounds of the BA form.* The most elementary reaction of a given ion moving into a coloured complex compound can be expressed by

$$B + A \rightleftarrows BA$$

and by

$$K_{11} = \frac{[BA]}{[B]\,[A]}$$

where B is the ion to be determined, A the reagent or the ligand, BA the coloured complex compound, K_{11} the formation or stability constant, with the combining ratio $B/A = 1/1$.

By comparing the BA coloured systems shown in table 1, a full identity may be observed between the columns of ε and K_{11}, and also that the K_{11} values of the analysed complex compounds are in most cases comprised within the limits $10^4 \ldots 10^5$ too.

Yet, many of the consulted works do mention only the instability constant K', expressed by

$$K' = \frac{1}{K}$$

---

[3] O. G. Koch and G. A. Koch-Dedic, "Handbuch der Spurenanalyse", Berlin, Springer-Verlag, 1964.

[4] V. N. Tolmacev, *Ucenye zapiski Kharkovskii Universitet*, **54**, 83 (1954).

Table 1

Verification of the terms : ε and 1/ε

No	Metallic Ion (B)	Reagent (A)	B/A $1/n$	ε	1/ε	K	K'	pK	Refe-rences
1	Mo (VI)	Quercetine	1/1	0.36×10^5	2.7×10^{-5}	—	1.1×10^{-5}	—	6
2	Mo (VI)	Tiron	1/1	2.6×10^3	3.84×10^{-4}	—	3.0×10^{-4}	—	7, 8
3	Fe (III)	2-Hydroxy-3-naphtoic acid	1/1	2,212	4.54×10^{-4}	—	4.29×10^{-4}	—	9
4	Fe (III)	Salicyladoxime	1/1	3,660	2.73×10^{-4}	—	9.30×10^{-4}	—	10
				3,620	2.76×10^{-4}	—	2.90×10^{-4}	—	
5	Fe (III)	β-Resorcylamide	1/1	1.63×10^3	6.13×10^{-4}	3.806×10^3	2.628×10^{-4}	—	11
6	Fe (III)	Oxaldihydroxamic acid	1/1	1.75×10^3	5.71×10^{-4}	$2.6-2.9 \times 10^3$	3.6×10^{-4}	—	12
7	Fe (III)	2,4-Dihydroxyacetophenone	1/1	2.10×10^3	—	0.83×10^3	—	—	13
8	Al (III)	Salicylic acid	1/1	0.43×10^4	—	$(1.65-2.86) \times 10^4$	—	—	14
9	Al (III)	Sulphosalicylic	1/1	3,883	2.58×10^{-4}	—	5.37×10^{-4}	—	15
10	Ga (III)	Salicylic acid	1/1	4,073	2.45×10^{-4}	—	$(2.02-3.54) \times 10^{-4}$	—	16
11	Ga (III)	Morine	1/1	4.8×10^4	2.08×10^{-5}	—	4.3×10^{-5}	—	17
12	Ga (III)	Acid chrome dark green C	1/1	1.65×10^4	6.0×10^{-5}	—	1.14×10^{-5}	—	18
13	Ga (III)	3′-Sulpho-2″,6″-dichloro-3,3′-dimethyl-4-hydroxyfuchsone-5,5′-dicarboxylic acid	1/1	1.00×10^4	1.0×10^{-4}	—	—	4.4—4.5	19

14	In (III)	Lumogallion	1/1	2.0×10^4	5.0×10^{-5}	—	—	5.09± 0.2	20
15	In (III)	5-(2-Pyridylazo)-2-monoethylamino-*p*-cresol	1/1	2.8×10^4	3.57×10^{-5}	—	0.65×10^{-5}	—	21
16	Tl (III)	Quercetine	1/1	15,600	6.41×10^{-5}	—	1.83×10^{-5}	—	22
17	Tl (III)	1-(2-pyridyl azo)-resorcinol	1/1	1.80×10^4	—	1.70×10^4	—	—	23
18	Tl (III)	Xylenol orange	1/1	1.98×10^4	—	7.7×10^4	—	—	23
19	Tl (III)	Phenylfluorone	1/1	31,321	3.2×10^{-5}	—	2.2×10^{-5}	—	24
20	Cu (II)	2,4-Dihydroxybenzoic acid	1/1	1,531	6.53×10^{-4}	—	2.86×10^{-4}	—	25
21	Cu (II)	Pyridine-2-azo-*p*-dimethylaniline	1/1	0.34×10^5 0.36×10^5	— —	1.3×10^5 2.1×10^5	— —	— —	26
22	Hg (II)	Pyridine-2-azo-*p*-dimethylaniline	1/1	3.93×10^4	—	8.3×10^4	—	—	26
23	Ni (II)	Pyridine-2-azo-*p*-dimethylaniline	1/1	3.28×10^4	—	1.72×10^4	—	—	26
24	Be (II)	Salicylic acid	1/1	4,468	2.23×10^{-4}	—	$(0.9-1.205) \times 10^{-4}$	—	27
25	Be (II)	Sulphosalicylic acid	1/1	3,996	2.50×10^{-4}	—	$(1.47-1.96) \times 10^{-4}$	—	27
26	Be (II)	*p*-Sulphobenzazosalicylic acid	1/1	0.182×10^5	5.49×10^{-5}	—	1.51×10^{-5}	4.82	28
27	Be (II)	Alberon	1/1	21,350	4.7×10^{-5}	—	0.6×10^{-5}	—	29
28	Zr (IV)	Kaempferol	1/1	2.65×10^4	2.17×10^{-5}	—	2.49×10^{-5}	—	30

Table 1 (continued)

No	Metallic Ion (B)	Reagent (A)	B/A (1/n)	ε	1/ε	K	K′	pK	References
29	Zr (IV)	1,5-Bis (2-hydroxy-5-sulphophenyl)-3-cyanoformazan	1/1	13,160	7.59×10^{-5}	—	1.53×10^{-5}	—	31
30	Zr (IV)	Stilbazogall I	1/1	2.7×10^{4}	3.7×10^{-5}	—	0.92×10^{-5}	—	32
31	Zr (IV)	Arsenazo	1/1	0.94×10^{4}	—	$(0.8-1.0)\times10^{4}$	—	—	33
32	W (IV)	9-(5′-Nitro-2′-hydroxyphenyl)-2,3,7-trihydroxy-6-fluorone	1/1	0.32×10^{5}	—	1.7×10^{5}	—	—	34
33	W (VI)	9-(9′-Anthracenyl)-2,3,7-trihydroxy-6-fluorone	1/1	0.352×10^{5}	—	0.6×10^{5}	—	—	34
34	Li (I)	4-[(2-Carboxy-4-nitrophenyl) azo]-3-methyl-1-phenyl-2-pyrazolin-5-one	1/1	1.65×10^{4}	6.06×10^{-5}	—	$(5.73\pm0.29)\times10^{-5}$	—	35
35	Ba (II)	Sulphonazo III	1/1	6.45×10^{4}	—	$(1.3-4.2)\times10^{4}$	—	—	36
36	Sc (III)	Methylthymol blue	1/1	1.5×10^{4}	0.7×10^{-4}	—	0.8×10^{-4}	—	37
37	Sn (IV)	Lumogallion	1/1	1.69×10^{4}	5.91×10^{-5}	—	—	4.84	38

38	Sb (III)	3,5-Dibromo-2-(2-pyridylazo)-5-diethyl-*m*-aminophenol	1/1	0.60×10^5 0.67×10^5	1.66×10^5 1.49×10^{-5}	— —	1.49×10^{-5} 1.91×10^{-5}	—	39
39	V (V)	Pyrogallol carboxylic acid	1/1	1.3×10^4	0.77×10^{-4}	—	2.4×10^{-4}	—	40
40	Ta (V)	H_2O_2	1/1	1.0×10^3	—	2.72×10^3	—	—	41
41	Bi (III)	N-Methyl-anabasin-α′-azo-diethylaminophenol	1/1	6.76×10^4	—	1.253×10^4	—	—	42
42	Gd (III)	Arsenazo III	1/1	0.535×10^5	—	2.91×10^5	—	—	43
43	Re (VII)	Methylene blue	1/1	1.1×10^5	9.0×10^{-6}	—	7.0×10^{-6}	—	44
44	U (VI)	Arsenazo III	1/1	6.0×10^4	0.16×10^{-4}	—	1.04×10^{-4}	—	45
45	Pd (II)	Palladiazo	1/1	3.7×10^4	2.7×10^{-5}	—	—	4.92	46
46	Os (IV)	Anthranilic acid	1/1	2.0×10^4	5.0×10^{-5}	—	4.6×10^{-5}	—	47
47	Pt (IV)	Anthranilic acid	1/1	2,889	3.46×10^{-4}	—	2.6×10^{-4}	—	48

In these works, the identity of the two groups of data $1/\varepsilon$ and K' is also obvious.

b) *Complex compounds of the BA_2 form.* If two coloured complexes are formed, we should distinguish :

$$\begin{array}{r} B + \ A \rightleftarrows BA \\ \underline{BA + \ A \rightleftarrows BA_2} \\ B + 2A \rightleftarrows BA_2 \end{array}$$

For these systems in equilibrium, we would write :

$$k_1 = \frac{[BA]}{[B]\,[A]}; \qquad k_2 = \frac{[BA_2]}{[BA]\,[A]}$$

$$K_{12} = \frac{[BA_2]}{[B]\,[A]^2} = k_1 . k_2 = \frac{[BA]}{[B]\,[A]} \cdot \frac{[BA_2]}{[BA]\,[A]}$$

If $k_1 \approx k_2$, both complexes are of the same order of magnitude and therefore they cannot be considered apart, by ignoring the concentration of the other. On the other hand, it is well known that for each absorbing species there is a definite characteristic molar absorptivity, which requires a correlation with the combining ratio by introducing the terms ε^2 and $1/\varepsilon^2$. The table 2 illustrates a coloured complex compound series having the combining ratio $B/A = 1/2$, the stability (or instability) constants of which have values perfectly comparable with the terms ε^2 and $1/\varepsilon^2$, respectively.

In some strictly characteristic working conditions (a certain ligand concentration, a certain H ion concentration area, a certain wavelength, a certain ionic strength, and so on) we could consider separately each of the two complexes, and nevertheless to ascertain one of the above situations, resulting in a compound with the combining ratio $B/A = 1/1$ or $1/2$, as the case may be.

c) *Complex compounds of the BA_3 form.* By the formation of coloured complex compounds of the BA_3 form we should distinguish :

$$\begin{array}{r} B + \ A \rightleftarrows BA \\ BA + \ A \rightleftarrows BA_2 \\ \underline{BA_2 + \ A \rightleftarrows BA_3} \\ B + 3A \rightleftarrows BA_3 \end{array}$$

$$k_1 = \frac{[BA]}{[B]\,[A]}; \; k_2 = \frac{[BA_2]}{[BA]\,[A]}; \; k_3 = \frac{[BA_3]}{[BA_2]\,[A]}$$

$$K_{13} = \frac{[BA_3]}{[B]\,[A]^3} = k_1 \cdot k_2 \cdot k_3 = \frac{[BA]}{[B]\,[A]} \cdot \frac{[BA_2]}{[BA][A]} \cdot \frac{[BA_3]}{[BA_2]\,[A]}$$

If the conditions for obtaining the last reaction term are achieved and the reagent is in excess, the complex compound BA_3 is formed in the system. We suggest to compare its stability (or instability) constants with the terms ε^3 and $1/\varepsilon^3$.

It is well known in the literature that if the absorption curves of the investigated coloured system are converging to some given pH values, one, two or more isosbestic points would appear. In each isosbestic point there are two coloured species simultaneously balanced.

In this respect the works of Vareille [5] are noteworthy, since he demonstrates that the percentage distribution of the three possible complexes for two distinct isosbestic points is disposed as a function of pH, following a graph where to the right or the left of each isosbestic point the highest percentage distribution characteristic of a single compound occurs.

If the practical working conditions for the formation of one of the compounds are accurately determined, it would result the most favourable conditions for yielding the compound with the combining ratio $B/A = 1/1$, or the compound with the combining ratio $B/A = 1/2$, or the compound with the combining ratio $B/A = 1/3$, as the case may be.

The data of table 3 show the full identity between the suggested terms (ε, ε^2, ε^3, $1/\varepsilon$, $1/\varepsilon^2$, $1/\varepsilon^3$) and stability (or instability) constants of some complex compounds.

.

.

.

.

n) *Complex compounds of the BA_n form.* It is possible, for all complex compounds with the combining ratio $B/A = 1/n$, which are subjected to spectrophotometric studies, to calculate the terms ε^n and $1/\varepsilon^n$, and to follow the correlation between their values and those of the stability (or instability) constants. In this respect, the data of table 4 are also instructing, since they are showing how to apply the suggested terms to the 13 germanium combinations. This table comprises also our own studies on some coloured systems.

In our opinion, the great number of the compounds which were analysed, removes any possible fortuitous identity between the two groups of data obtained by comparing the columns of the four tables, which show the ε^n and K_{1_n} values on the one hand, and the $1/\varepsilon^n$ and K'_{1_n} columns on the other hand. Moreover, this identity is fully capable to support the validity and the extension prospects of the suggested terms.

Most of the works [6–84] upon which the correlation : molar absorptivity — composition — stability (or instability) constant is based, are recent, many of them being published during the period of 1965 to 1969 and belong to a veritable school of chemistry. The greater part of the authors demonstrated the *apparent or conditional* stability (or instability) constants by Job's[85] or Harvey and Manning's[86] method, or both (that is the reason why two values are shown in the tables), and only in a small number of papers other spectrophotometric methods are mentioned for the study of the coloured system equilibrium.

---

[5] L. Vareille, *Bull. Soc. chim. France*, **1955**, 870, 872, 1493, 1496.

[6] G. Goldstein, D. L. Manning and O. Menis, *Analyt. Chem.*, **30**, 539 (1958).

[7] A. I. Busev and Czhean Fan, *Izvest. vyshih uchebnyv. zavedenie. khimia i khim. technologia*, 4, 905 (1961).

[8] A. I. Busev, "Analiticheskaia khimia elementov molibden", Moscow, Akad. Nauk. S.S.S.R. 1962, p. 42.

[9] A. K. Majumdar and C. P. Savariar, *Analyt. Chim. Acta*, **21**, 47 (1959) ; *Z. analyt. Chem.*, **174**, 153 (1960).

[10] K. R. Manolov, *Zhur. neorg. Khim.*, **12**, 2715 (1967).

[11] M. N. Desai, *Indian J. Chem.*, 4, 218 (1966).

[12] D. Monnier and C. Jegge, *Helv. Chim. Acta*, **40**, 513 (1957).

As it is not possible to discuss in detail all the 94 complex compounds shown in the table, I chose as an example the reaction of the vanadium with the N-benzoyl-N-(p-chlorophenyl)-hydroxylamine. Majumdar and

[13] M. H. Gandhi and M. N. Desai, *Analyt. Chim. Acta*, **43**, 338 (1968).

[14] B. Das and S. Aditya, *J. Indian Chem. Soc.*, **36**, 473 (1959).

[15] R. K. Nanda and S. Aditya, *J. Indian Chem. Soc.*, **40**, 660 (1963).

[16] R. C. Das, R. K. Nanda and S. Aditya, *J. Indian Chem. Soc.*, **40**, 739 (1963).

[17] E. P. Shkrobot, *Zhur. analit. Khim.*, **17**, 186 (1962).

[18] T. M. Devyatova and M. Z. Yampolsky, *Zhur. analit. Khim.*, **10**, 1468 (1968).

[19] C. D. Dwivedi, K. N. Munshi and A. K. Dey, *J. Indian Chem. Soc.*, **43**, 111 (1966).

[20] V. D. Salikhov and M. Z. Yampolsky, *Zhur. analit. Khim.*, **22**, 998 (1967).

[21] S. I. Gusev and E. M. Nikolaeva, *Zhur. analit. Khim.*, **21**, 281 (1966).

[22] R. Manczyk, J. Terpilowki and M. Kopacz, *Diss. Pharm. Pharmacol.*, **18**, 643 (1966).

[23] A. I. Busev and V. G. Tiptsova, *Zhur. analit. Khim.*, **15**, 573 (1960).

[24] M. K. Akhmedli, E. A. Bashirov and A. M. Sadykova, *Zhur. neorg. Khim.*, **12**, 476 (1967).

[25] S. L. Gupta and R. N. Soni, *J. Inst. Chem. (India)*, **40**, 31 (1968).

[26] I. M. Klotz and W.-C. L. Ming, *J. Amer. Chem. Soc.*, **75**, 4159 (1953).

[27] R. C. Das and S. Aditya, *J. Indian Chem. Soc.*, **38**, 18 (1961).

[28] L. P. Adamovich and Vu Van Nyan, *Zhur. analit. Khim.*, **23**, 994 (1968).

[29] L. P. Adamovich, O. V. Morgul-Meshkova and B. V. Yutsis, *Zhur. analit. Khim.*, **17**, 678 (1962).

[30] B. S. Garg, K. C. Trikha and R. P. Singh, *J. Indian Chem. Soc.*, **45**, 522 (1968).

[31] R. F. Khovyakhova, V. E. Blokhin, L. K. Zhuikova and I. N. Marenkova, *Tr. Ural. Plitekh. Inst.*, **163**, 28 (1967).

[32] A. I. Cherkesov and Yu. V. Pushinov, *Zhur. analit. Khim.*, **20**, 665 (1965).

[33] A. F. Kuteinikov, *Zavodskaya Lab.*, **24**, 1050 (1958).

[34] E. N. Polektova and V. A. Nazarenko, *Zhur. analit. Khim.*, **19**, 856 (1964).

[35] V. M. Dzinko, S. L. Zelichenok and I. S. Markovich, *Zhur. analit. Khim.*, **23**, 170 (1968).

[36] Z. Slovák, J. Fischer and J. Borăk, *Talanta*, **15**, 831 (1968).

[37] M. K. Akhmedli and D. G. Gambarov, *Zhur. analit. Khim.*, **22**, 1183 (1967).

[38] P. V. Marchenko and N. V. Obolonchik, *Tr. Kom. Anal. Khim., Akad. Nauk S.S.S.R., Inst. Geochim. Anal. Khim.*, **16**, 41 (1968).

[39] S. I. Gusev and L. V. Poplevina, *Zhur. analit. Khim.*, **23**, 541 (1968).

[40] S. Ya. Shaiderman and E. P. Klimenko, *Zhur. neorg. Khim.*, **12**, 2132 (1967).

[41] V. P. Vasiliev and G. A. Zaitseva, *Zhur. neorg. Khim.*, **13**, 84 (1968).

[42] E. A. Martirosov, T. Sh. Talipov, H. Ya. Dzianbaeva and Z. A. Tatarskaia, *Tr. Taskent. Universitet*, **323**, 78 (1968).

[43] T. I. Evseeva and E. P. Cherstvenkova, *Zhur. analit. Khim.*, **22**, 34 (1967).

[44] V. M. Tarayan and S. V. Vartanyan, *Doklady Akad. Nauk Armyan S.S.R.*, **45**, 121 (1967).

[45] A. A. Nemodruk and L. P. Glukhova, *Zhur. analit. Khim.*, **18**, 93 (1963).

[46] J. A. Pérez-Bustamante, C. M. Garcia and F. Burriel-Marti, *Analyt. Chim. Acta*, **44**, 95 (1969).

[47] A. K. Majumdar and J. G. Sen Gupta, *Analyt. Chim. Acta*, **20**, 532 (1959) ; *Z. analyt. Chem.*, **173**, 262 (1960) ; **174**, 157 (1960).

[48] A. K. Majumdar and J. G. Sen Gupta, *Z. analyt. Chem.*, **177**, 265 (1960).

[49] V. D. Vasilenko, M. V. Shanya and V. I. Bolbas, *Zhur. analit. Khim.*, **22**, 1818 (1967).

[50] O. Menis, D. L. Manning and G. Goldstein, *Analyt. Chem.*, **29**, 1426 (1957).

Das[56] obtained by the Job's method $K'_{12} = 3.5 \times 10^{-8}$, and by the Harvey and Manning's method $K'_{12} = 9.0 \times 10^{-8}$. Taking from the same work the combining ratio of 1/2 and $\varepsilon = 4{,}500$ we get for our own term: $\frac{1}{\varepsilon^2} = 5.0 \times 10^{-8}$ As the first two values are unquestionable, we should specify that the obtained value (5.0×10^{-8}) may be used as a criterion of this coloured system instability as well, *beside* the values characterizing it (3.5×10^{-8} and 9.0×10^{-8}). We obtained again fully comparable data by using the Job's and the Harvey and Manning's methods, and also from the term $1/\varepsilon^2$ for the coloured system: Ge (IV)-bromopyrogallol red (see table 4).

---

[51] F. S. Grimaldi and C. E. White, *Analyt. Chem.*, **25**, 1886 (1953).

[52] A. K. Majumdar and S. C. Saha, *Analyt. Chim. Acta*, **44**, 85 (1969).

[53] I. A. Tserkovnitskaya and N. A. Kustova, *Zhur. analit. Khim.*, **23**, 72 (1968).

[54] J. Halmekoski, *Soumen Kem.*, **34**, 169 (1961).

[55] E. N. Poluektova and V. A. Nazarenko, *Zhur. analit. Khim.*, **22**, 746 (1967).

[56] A. K. Majumdar and G. Das, *J. Indian Chem. Soc.*, **42**, 189 (1965).

[57] V. N. Tolmacev, *Zhur. neorg. Khim.*, **2**, 60 (1957).

[58] R. Cracuneanu and E. Florean, *Rev. Roumaine Chim.*, **31**, 105 (1968).

[59] B. Budesinsky and K. Haas, *Acta Chim. Acad. Sci. Hung.*, **39**, 7 (1963).

[60] K. Borislav, K. Donka and N. Petrana, *Talanta*, **15**, 525 (1968).

[61] L. A. Molot, I. S. Mustafin and A. P. Andronova, *Primenenie organ. reaktivov v analize. Saratov*, **1968**, 61.

[62] A. Bezdekova and B. Budesinsky, *Coll. Czech. Chem. Comm.*, **31**, 199 (1966).

[63] V. P. Antonovich and V. A. Nazarenko, *Zhur. analit. Khim.*, **23**, 1143 (1968).

[64] T. V. Malkova, N. A. Fateeva and K. B. Yatsimirski, *Zhur. neorg. Khim.*, **12**, 3342 (1967).

[65] V. M. Tarayan and A. G. Gaibakyan, *Arm. Khim. Zhur.*, **19**, 924 (1966).

[66] A. K. Majumdar and J. G. Sen Gupta, *Z. analyt. Chem.*, **178**, 401 (1961).

[67] L. V. Chaprasova, Sh. T. Talipov and R. Kh. Dzhiyanbaeva, *Nauch. Tr., Tashkent. Gos. Univ.*, **284**, 76 (1967).

[68] Gr. Popa and I. Paralescu, *Anal. Univ. "C. I. Parhon". Ser. Stiinţele Naturii. Chimie*, **9**, 104 (1960).

[69] G. Schwarzenbach and A. Willi, *Helv. Chim. Acta*, **34**, 528 (1951).

[70] L. Sommer, *Bull. Soc. chim. France*, **1959**, 862.

[71] H. K. L. Gupta and N. C. Sogani, *J. Indian Chem. Soc.*, **36**, 87 (1959).

[72] S. M. Dugar, D. N. Purohit and N. C. Sogani, *J. Indian Chem. Soc.*, **40**, 667 (1963).

[73] A. K. Majumdar and A. B. Chatterjee, *J. Indian Chem. Soc.*, **42**, 241 (1965).

[74] B. Budesinsky and K. Haas, *Z. analyt. Chem.*, **214**, 325 (1965).

[75] Sh. T. Talipov, Kh. S. Abdulaeva and G. S. Andrushko, *Uzb. Khim. Zhur.*, **11**, 17 (1967).

[76] M. Yusupov, R. Kh. Dzhiyanbaeva and Sh. T. Talipov, *Nauch. Tr., Tashkent. Gos. Univ.*, **284**, 61 (1967).

[77] I. V. Tananev and M. Spirt, "Khimia germania", Izdatelstvo Khimia, Moscow, **1967**, 202.

[78] L. I. Kononenko and N. S. Poluektov, *Zhur. analit. Khim.*, **15**, 61 (1960).

[79] Gr. Popa and I. Paralescu, *Talanta*, **15**, 272 (1968).

[80] I. Paralescu and Gr. Popa, *Rev. Chim. (Bucureşti)*, **21**, 171 (1970).

[81] V. A. Nazarenko and E. N. Poluektova, *Zhur. analit. Khim.*, **19**, 1459 (1964).

[82] T. Kanno, *Sci. Repts. Res. Inst. Tohoku Univ. Ser. A*, **10**, 250 (1958); **11**, 145 (1959).

[83] K. Pan, Z. F. Lin, S. H. Lin and P.Y. Sun, *Proc. Intern. Symp. Mol. Struct. Spectry Tokyo B*, **311**, 3 (1962).

[84] V. A. Nazarenko and L. I. Vinarova, *Zhur. analit. Khim.*, **18**, 1217 (1963).

[85] P. Job, *Ann. Chim. (France)*, **9**, 113 (1928).

[86] A. E. Harvey and D. L. Manning, *J. Amer. Chem. Soc.*, **72**, 4488 (1950).

Table 2

Verification of the terms : ε^2 and $1/\varepsilon^2$

No	Metallic Ion (B)	Reagent (A)	B/A $(1/n)$	ε	$1/\varepsilon$	ε^2	$1/\varepsilon^2$	K	K'	pK	References
48	Th (IV)	Bromopyrogallol red	1/1	2.5×10^4	4.0×10^{-5}	—	—	—	$(3.5\pm1)\times10^{-5}$	—	49
49	Th (IV)	Bromopyrogallol red	1/2	6.3×10^4	—	0.399×10^{10}	2.5×10^{-10}	—	0.63×10^{-10}	—	49
50	Th (IV)	Quercetine	1/2	33,000	—	0.11×10^{10}	9.1×10^{-10}	—	1.2×10^{-10}	—	50
—	Zr (IV)	Quercetine	1/1	—	—	—	—	—	3.3×10^{-4}	—	51
51	Zr (IV)	Quercetine	1/2	30,000	—	0.9×10^{9}	1.1×10^{-9}	—	1.3×10^{-9}	—	51
52	Ti (IV)	1-(*o*-Carboxyphenyl)-3-hydroxy-3-phenyl-triazene	1/2	12,451	—	0.155×10^{9}	6.45×10^{-9}	—	1.15×10^{-9} 2.2×10^{-9}	—	52
53	Mo (V)	Chromotropic acid	1/2	8.8×10^3	—	0.77×10^{8}	1.31×10^{-8}	—	0.35×10^{-8}	—	53
54	Mo (VI)	Acetopyrocatechol	1/2	3,190	—	1.02×10^{7}	—	0.548×10^{7}	—	—	54
55	W (VI)	Benzohydroxamic acid	1/2	6,500	—	4.23×10^{7}	—	1.3×10^{7}	—	—	55
56	V (V)	N-Benzoyl-N-(*p*-chlorophenyl)-hydroxylamine	1/2	4,500	—	0.20×10^{8}	5.0×10^{-8}	—	3.5×10^{-8} 9.0×10^{-8}	—	56
57	Zn (II)	Purpuric acid	1/2	40,000	—	0.16×10^{10}	6.2×10^{-10}	—	$(4.8\pm1.6)\times10^{-10}$	—	57

58	Co (II)	1-Benzoyl-4-phenyl-thiosemicarbazide	1/2	1.25×10^4	—	1.56×10^8	0.64×10^{-8}	—	4.86×10^{-8}	—	58
59	Ni (II)	Metallochrome violet A	1/2	11,000	—	0.12×10^9	8.33×10^{-9}	—	—	8.9	59
60	Cd (II)	Metallochrome violet A	1/2	10,300	—	1.0×10^8	1.0×10^{-8}	—	—	7.8	59
61	Fe (III)	Methylthymol blue	1/2	3.21×10^3	—	1.0×10^7	1.0×10^{-7}	—	—	6.66	60
62	Al (III)	Krumazurol S	1/2	40,700	—	0.166×10^{10}	6.02×10^{-10}	—	$(1.13 \pm 0.57) \times 10^{-10}$	—	61
63	Mg (II)	2(2′-Hydroxy-5′-sulfophenyl-azo)-chromotropic acid	1/2	15,300	—	0.234×10^9	4.27×10^{-9}	—	—	9.0	62
64	Sc (III)	Xylenol orange	1/2	7,200	—	0.52×10^8	1.92×10^{-8}	—	—	7.96	63
65	La (III)	Methylthymol blue	1/2	8.5×10^4	—	7.42×10^9	—	1.9×10^9	—	—	64
66	Nd (III)	Methylthymol blue	1/2	1.13×10^5	—	1.28×10^{10}	—	6.4×10^{10}	—	—	64
67	Ho (III)	Methylthymol blue	1/2	1.23×10^5	—	1.51×10^{10}	—	3.2×10^{10}	—	—	64
68	Re (V)	Thiosalicylic acid	1/2	6.1×10^3	—	0.37×10^8	2.70×10^{-8}	—	1.75×10^{-8}	—	65
69	Ru (III)	Anthranilic acid	1/2	4,271	—	0.18×10^8	5.55×10^{-8}	—	1.74×10^{-8}	—	66
70	Pd(II)	N-Methylanabasine-α′-azo-β-naphthol	1/2	9.417×10^3	—	8.87×10^7	—	1.38×10^7	—	—	67
71	UO_2 (II)	Chromotrop 2R	1/2	15,230	—	2.32×10^8	0.43×10^{-8}	—	0.52×10^{-8}	—	68

Table 3

Verification of the terms : ε^3 and $1/\varepsilon^3$

No	Metallic ion (B)	Reagent (A)	B/A $(1/n)$	ε	$1/\varepsilon$	ε^2	$1/\varepsilon^2$	ε^3	$1/\varepsilon^3$	K	K′	pK	References
72	Fe (III)	Tiron	1/1	0.99×10^3	—	—	—	—	—	3.4×10^3	—	—	69
—	Fe (III)	Tiron	1/2	—	—	—	—	—	—	—	9.7×10^{-6}	—	69
73	Fe (III)	Tiron	1/3	6,520	—	—	—	0.28×10^{12}	—	$(6.6-8.1) \times$ $\times 10^{12}$	—	—	69
—	Ti (IV)	Chromotropic acid	1/1	—	—	—	—	—	—	—	—	2.36	70
74	Ti (IV)	Chromotropic acid	1/2	8,346	—	7.0×10^7	$0.14 \times$ $\times 10^{-7}$	—	—	—	—	6.18	70
75	Ti (IV)	Chromotropic acid	1/3	11,500	—	—	—	0.15×10^{13}	6.66×10^{-13}	—	—	12.61	70
76	Fe (III)	3-Hydroxy-1-phenyl-3-methyl-triazine	1/3	2.8×10^3	—	—	—	0.22×10^{11}	4.54×10^{-11}	—	1.16×10^{-11}	—	71
77	Co (III)	3-Hydroxy-1-sulphonato-phenyl-3-phenyltriazine	1/3	4.833×10^3	—	—	—	0.11×10^{12}	0.9×10^{-13}	—	2.54×10^{-13}	—	72
78	Cu (II)	2-(Pyridyl-2-azo)-chromotropic acid	1/3	2.2×10^4	—	—	—	1.0×10^{13}	1.0×10^{-13}	—	2.5×10^{-13}	—	73
79	Cu (II)	Aminomethyl azo III	1/3	7.5×10^4	—	—	—	0.42×10^{15}	2.3×10^{-15}	—	—	14.8–15.4	74
80	In (III)	4-(2-N-Methyl-anabasine-azo) resorcinol	1/3	3.8×10^4	—	—	—	0.55×10^{14}	1.8×10^{-14}	—	0.35×10^{-14}	—	75
81	Tl (III)	7-[N-Methyl-anabasinyl]-8-hydroxyquinoline	1/3	1.31×10^4	—	—	—	2.25×10^{12}	—	1.895×10^{12}	—	—	76

Table 4

Verification of the terms; ε^n and $1/\varepsilon^n$

No	Metallic ion (B)	Reagent (A)	B/A $(1/n)$	ε	ε^n	$1/\varepsilon^n$	K_{in}	K'_{in}	References
82	Ge (IV)	Quinalizarine	1/1	17,000	1.7×10^4	0.58×10^{-4}	—	1.28×10^{-4}	77
83	Ge (IV)	Purpurine	1/1	8,700	0.87×10^4	1.24×10^{-4}	—	0.39×10^{-4}	77
84	Ge (IV)	6,7-Dihydroxy-2,4-dimethyl-benzopiryl chloride	1/2	5,500	3.0×10^7	—	1.9×10^7	—	78
85	Ge (IV)	7,8-Dihydroxy-2,4-dimethyl-benzopiryl chloride	1/2	2,925	0.86×10^7	—	1.3×10^7	—	78
86	Ge (IV)	6,7-Dihydroxy-2,4-diphenyl-benzopiryl chloride	1/2	25,000	6.25×10^8	—	4.8×10^8	—	78
87	Ge (IV)	7,8-Dihydroxy-2,4-diphenyl-benzopiryl chloride	1/2	15,600	2.43×10^8	—	0.8×10^8	—	78
88	Ge (IV)	Bromopyrogallol red	1/2	20,546	0.42×10^9	2.38×10^{-9}	—	2.56×10^{-9} 2.19×10^{-9}	79,80
89	Ge (IV)	Purpurogallin	1/2	34,200	0.117×10^{10}	8.54×10^{-10}	—	2.47×10^{-10}	80,81
90	Ge (IV)	Alizarine red S	1/3	8,000	1.92×10^{12}	5.2×10^{-12}	—	2.39×10^{-12}	80
91	Ge (IV)	Quercetin sulphonic acid	1/2	46,000	0.21×10^{10}	4.76×10^{-10}	—	3.28×10^{-10}	80,82
92	Ge (IV)	Quercetin sulphonic acid	1/3	51,000	0.13×10^{15}	7.69×10^{-15}	—	7.26×10^{-15}	80,82
93	Ge (IV)	Pyrocatechin violet	1/2	50,000	2.5×10^9	0.4×10^{-9}	—	6.55×10^{-9}	83,84
94	Ge (IV)	Pyrocatechin violet	1/3	55,000	1.66×10^{14}	0.60×10^{-14}	—	1.9×10^{-14}	84

The usefulness of the terms ε^n and $1/\varepsilon^n$ consists in the facility to obtain values which are *perfectly comparable* with those of the stability (or instability) constants of the coloured complexes if the two parameters, composition and molar absorptivity, ascertained *in identical working conditions*, are known.

A number of works may be also found in the literature, discussing *the formation*, *the composition* and *the stability* of the coloured complex compounds for very different working conditions. It is obvious that if the stability (or instability) constant is ascertained in some definite working conditions (a given pH, a certain wavelength, a certain solvent, a certain ionic strength, a certain temperature, and so on) and the molar absorptivity in other working conditions, and the combining ratio in quite other conditions, the correlation : molar absorptivity — composition — stability (or instability) constant is insignificant.

Also insignificant would be the results obtained by applying the suggested terms (ε^n and $1/\varepsilon^n$) to compounds with an incorrectly determined composition. In many instances various authors are reporting for the combining ratio very different values of a given compound, which was defined in identical working conditions.

Yet there are also in the literature a huge number of works in which either the molar absorptivities or the combining ratios were not determined. These works may be considered, for the time being, as an inexhaustible source of data, useful for defining the stability (or instability) of the BA_n coloured complex compounds, *beside other proceedings*, and by means of the terms :

$$\varepsilon^n \text{ and } 1/\varepsilon^n.$$

To conclude, in regard to the 94 coloured systems of BA_n, we note a close relationship between ε, $1/n$, K_{1_n} respectively K'_{1_n}, which may be represented by the general expressions :

$$K_{1_n} = y \cdot \varepsilon^n \text{ or } K'_{1_n} = \frac{1}{y \cdot \varepsilon^n}$$

where : y is a proportionality term tending *to unity*, *if* the stability, composition and area of agreement to the Lambert-Beer's law are ascertained for the best working conditions. As for the examples comprised in the 4 tables we note the small and unessential changes resulting from the proportionality term y. This should make possible to compare successfully the *two* data groups :

$$K_{1_n} \text{ and } \varepsilon^n \text{ respectively } K'_{1_n} \text{ and } \frac{1}{\varepsilon^n}.$$

Revue Roumaine de Chimie, 15, 917–934 (1970)

NEUE KOMPLEXVERBINDUNGEN DER PYRAZOLONREIHE. VII *

SICHTBARE UND UV-SPEKTREN

J. DICK, ANNA MAURER und Z. SZABADAI

aus der Abteilung für Anorganische Chemie der Akademie, Forschungsstelle Timişoara,
Bd. Mihai Viteazul 24

Eingegangen am 17. Oktober 1969

Es werden die UV- und sichtbaren Absorptionspektren einiger Koordinationsverbindungen der Pyrazolonreihe des Typs $[Me^{II}Lig(NCS)_2]$ untersucht und nachgewiesen, daß die Absorption im UV-Bereiche vom Liganden, im sichtbaren hingegen vom Zentralatom abhängt. So wurde das Elektronenspektrum der Verbindung $[Co^{II}\ Am_2(NCS)_2]$ nach der verbesserten HMO-Methode ausgewertet. Dabei wurden die Elektronenübergänge, die übrigens mit dem experimentellen Spektrum gut übereinstimmen, die Molekülbahnfunktionen (Molekülorbitalen) und ihre Symmetrie, die Ladungsverteilung auf Atome, d.h. der Charakter der Bindung Metall-Ligand annährend ermittelt und schließlich die Symmetrie und Energie der Zustände berechnet. Die untersuchte Verbindung liegt wahrscheinlich als trans-Isomer vor.

In früheren Arbeiten haben wir uns mit Koordinationsverbindungen von Übergangsmetallen mit 4-Aminoantipyrin und seinen N-methylierten Verbindungen als Ligand beschäftigt.[1–3] Die Chelatverbindungen mit der allgemeinen Formel $[Me^{II}\ Lig_2(NCS)_2]$ wurden anhand der IR-Spektren (in festem Zustand) wie folgt formuliert :

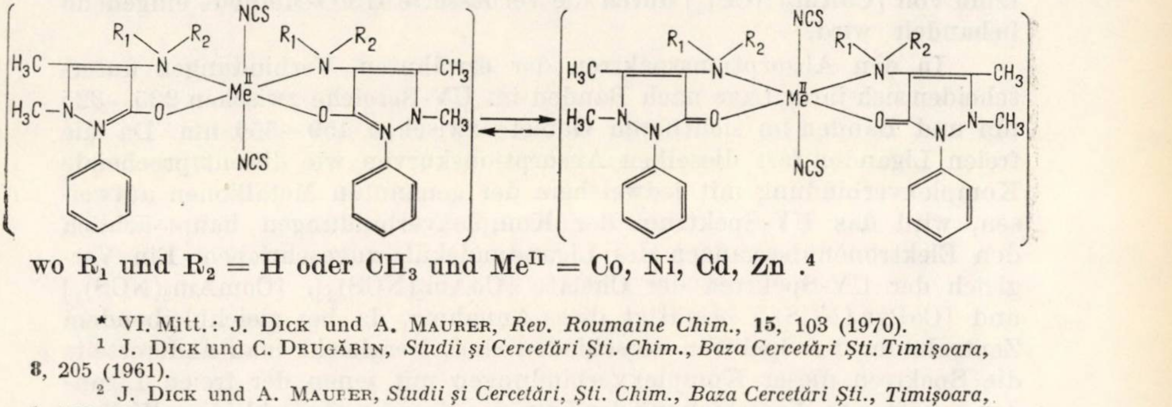

wo R_1 und R_2 = H oder CH_3 und Me^{II} = Co, Ni, Cd, Zn .[4]

---

* VI. Mitt. : J. Dick und A. Maurer, *Rev. Roumaine Chim.*, **15**, 103 (1970).

[1] J. Dick und C. Drugărin, *Studii şi Cercetări Şti. Chim., Baza Cercetări Şti. Timişoara*, **8**, 205 (1961).

[2] J. Dick und A. Maurer, *Studii şi Cercetări, Şti. Chim., Baza Cercetări Şti., Timişoara*, **9**, 257 (1962).

[3] J. Dick und A. Maurer, *Studii şi Cercetări, şti. Chim., Baza Cercetări şti., Timişoara*. **10**, 61 (1963).

[4] J. Dick, R. Bacalcglu und A. Maurer, *Rev. Roumaine Chim.*, **12**, 617 (1967).

Zur näheren Aufklärung der Struktur dieser Verbindungen in gelöstem Zustand (Methanol) wurden die UV- und sichtbaren Spektren herangezogen. Es wurden die Absorptionsspektren der Verbindungen: $[CoAm_2(NCS)_2]$; $[ComAm_2(NCS)_2]$; $[CoPyr_2(NCS)_2]$; $[NiAm_2(NCS)_2]$; $[ZnAm_2(NCS)_2]$; $[FeAm_2(NCS)_2]$; $[MnAm_2(NCS)_2]$ und $[CdAm_2(NCS)_2]$ aufgenommen, wo Am = 4-Amino-antipyrin, mAm = 4-Methylamino-antypirin und Pyr=Dimethylamino-antipyrin, wobei insbesondere das Spektrum von $[CoAm_2(NCS)_2]$ durch die verbesserte HMO-Methode eingehend behandelt wird.

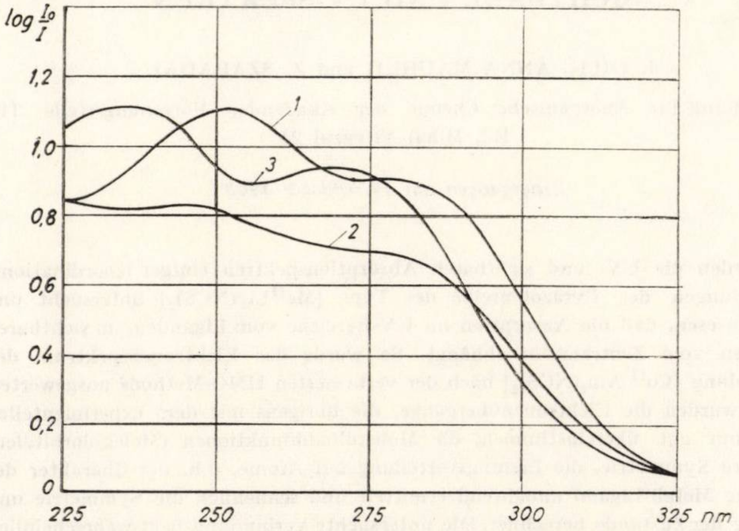

Abb. 1. — UV-Spektren der Chelatverbindungen:
1, $[CoAm_2(NCS)_2]$ — c = 0,486.10−4 M, in Methanol *p.a.*, Schichtdicke 1 cm.
2, $[ComAm_2(NCS)_2]$ — c = 0,480.10−4 M in Methhanol *p.a.*, Schichtdicke 1 cm.
3, $[CoPyr_2(NCS)_2]$ — c = 0,475.10−4 M in Methanol *p.a.*, Schichtdicke 1 cm.

In den Absorptionsspektren der erwähnten Verbindungen unterscheiden sich ihrer Lage nach Banden im UV-Bereiche zwischen 225–325 nm und Banden im sichtbaren Gebiete zwischen 450–550 nm. Da die freien Liganden fast dieselben Absorptionskurven wie die entsprechende Komplexverbindung mit jedwelchem der genannten Metallionen aufweisen, wird das UV-Spektrum der Komplexverbindungen hauptsächlich den Elektronenübergängen des Ligandmoleküls zugeschrieben. Ein Vergleich der UV-Spektren der Chelate $[CoAm_2(NCS)_2]$, $[ComAm_2(NCS)_2]$ und $[CoPyr_2(NCS)_2]$ bestätigt diese Annahme, da bei gleichbleibendem Zentralatom die Spektren verschieden sind. Vergleicht man andererseits die Spektren dieser Komplexverbindungen mit jenen der freien Liganden, so ist eine Verschiebung der Lage der Maxima gegen kleinere Wellenzahlen zu beobachten. Dieser hypsochrome Effekt verstärkt sich mit dem Anwachsen der Anzahl von Methylresten in der Amino-gruppe, also

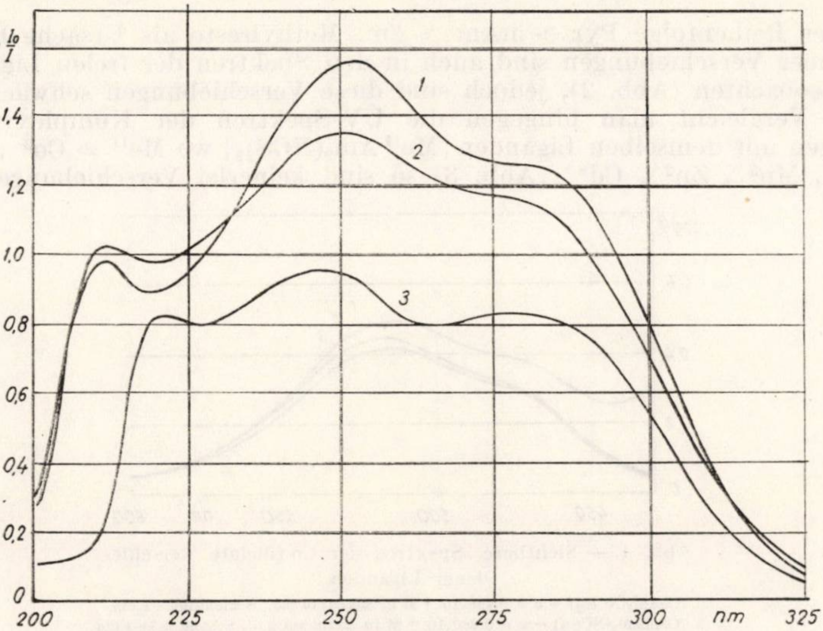

Abb. 2.—UV-Spektren der freien Liganden:

1, Amino-antipyrin – c = 1,672. 10^{-4} M in Methanol *p.a.*, Schichtdicke 1 cm.
2, Methylamino-antipyrin – c = 1,60.10^{-4} M in Methanol *p.a.*, Schichtdicke 1 cm.
3, Dimetylamino-antipyrin – c = 1,06.10^{-4} M in Methanol *p.a.*, Schichtdicke 1 cm.

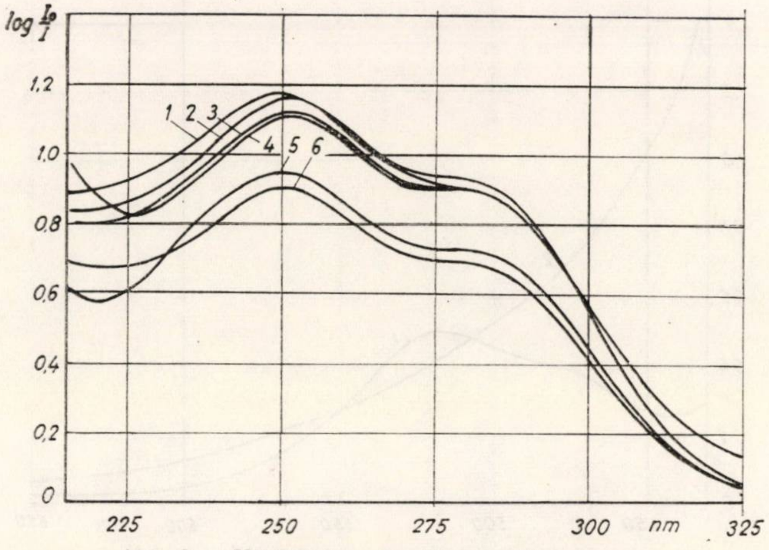

Abb. 3. – UV-Spektren der Chelatverbindungen:

1, $[FeAm_2(NCS)_2]$ – c = 0,577.10^{-4} M in Methanol *p.a.*, Schichtdicke 1 cm.
2, $[NiAm_2(NCS)_2]$ – c = 0,572.10^{-4} M in Methanol *p.a.*, Schichtdicke 1 cm.
3, $[Mn\,Am_2(NCS)^2]$ – c = 0,560.10^{-4} M in Methanol *p.a.*, Schichtdicke 1 cm.
4, $[CoAm_2(NCS)_2]$ – c = 0,520.10^{-4} M in Methanol *p.a.*, Schichtdicke 1 cm.
5, $[ZnAm_2(NCS)_2]$ – c = 0,486.10^{-4} in Methanol *p.a.* Schichtdicke 1 cm.
6, $[CdAm_2(NCS_2]$ – c = 0,472.10^{-4} M in Methanol *p.a.*, Schichtdicke 1 cm.

in der Reihenfolge Pyr > mAm > Am. Methylreste als Ursache hypsochromer Verschiebungen sind auch in den Spektren der freien Liganden zu beobachten (Abb. 2), jedoch sind diese Verschiebungen schwächer.

Vergleicht man hingegen die UV-Spektren der Komplexverbindungen mit demselben Liganden [$Me^{II}Am_2(NCS)_2$] wo $Me^{II} = Co^{2+}$, Ni^{2+}, Fe^{2+}, Mn^{2+}, Zn^{2+}, Cd^{2+} (Abb. 3) so sind keinerlei Verschiebungen der Maxima zu beobachten; dadurch wird die Voraussetzung, daß die UV-Absorptionsbanden dem Liganden zuzuschreiben sind, noch weiter verstärkt.

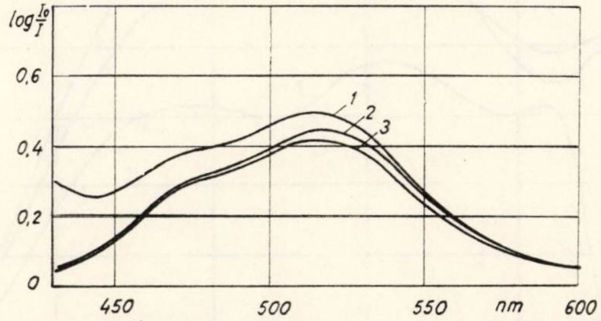

Abb. 4. — Sichtbare Spektren der Co-Chelate verschiedener Liganden:

1 [$CoAm_2(NCS)_2$] — c = $0{,}486 . 10^{-4}$ M in Methanol *p.a.*, Schichtdicke 1 cm.
2 [$ComAm_2(NCS)_2$] — c = $0{,}480 . 10^{-4}$ M in Methanol *p.a.*, Schichtdicke 1 cm.
3 [$CoPyr_2(NCS)_2$] — c = $0{,}475 . 10^{-4}$ M in Methanol *p.a.*, Schichtdicke 1 cm.

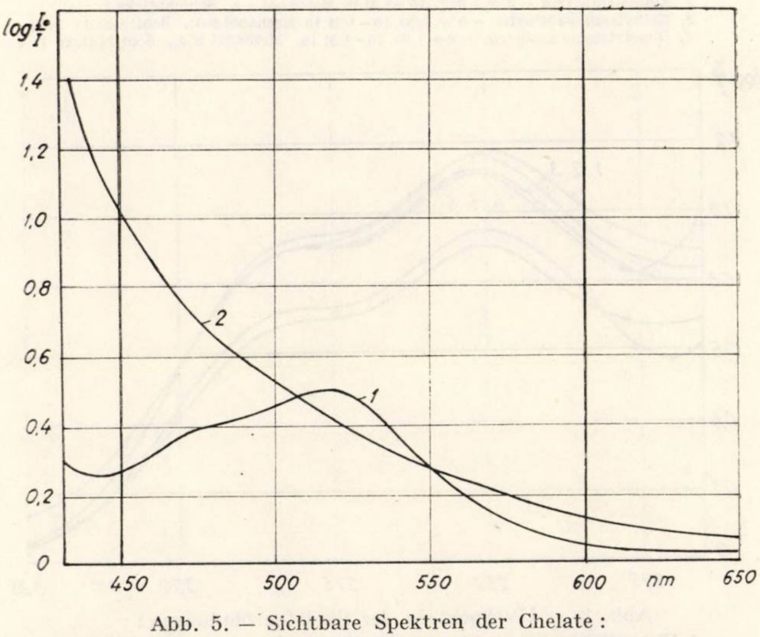

Abb. 5. — Sichtbare Spektren der Chelate:

1, [$CoAm_2(NCS)_2$] — c = $0{,}486 . 10^{-4}$ M in Methanol *p.a.*, Schichtdicke 1 cm.
2, [$FeAm_2(NCS)_2$] — c = $0{,}466 . 10^{-4}$ M in Methanol *p.a.*, Schichtdicke 1 cm.

Aus den sichtbaren Spektren der Co-Chelate mit den Liganden Pyr, mAm und Am geht hervor, daß die Lage der Maxima in den drei Verbindungen dieselbe ist, daher ist diese Absorption dem Metallion (Abb. 4) zuzuschreiben.

Zur Verstärkung dieser Voraussetzungen sei bemerkt, daß die sichtbaren Absorptionsspektren der Komplexverbindungen (verschiedener Metallionen mit demselben Liganden) wie [Co^{II} Am$_2$(NCS)$_2$] und [Fe^{II} Am$_2$ NCS)$_2$] grundverschieden sind. Während erstere ein Maximum im Bereiche 450—550 nm aufweist, fällt die Absorption letzterer im sichtbaren Bereiche ständig ab (Abb. 5).

AUSWERTUNG DES ABSORPTIONSSPEKTRUMS VON [Co^{II}Am$_2$(NCS)$_2$] NACH DER HMO-METHODE

1. *Bestimmung der Berechnungsparameter*

Die Wahl des Koordinatensystems und Bezeichnung verschiedener Atome ist aus Abb. 6 ersichtlich.

Im Molekül von [CoAm$_2$(NCS)$_2$] können 4 Bindungssysteme, davon sich jedes über mehrere Atome erstreckt, unterschieden werden.

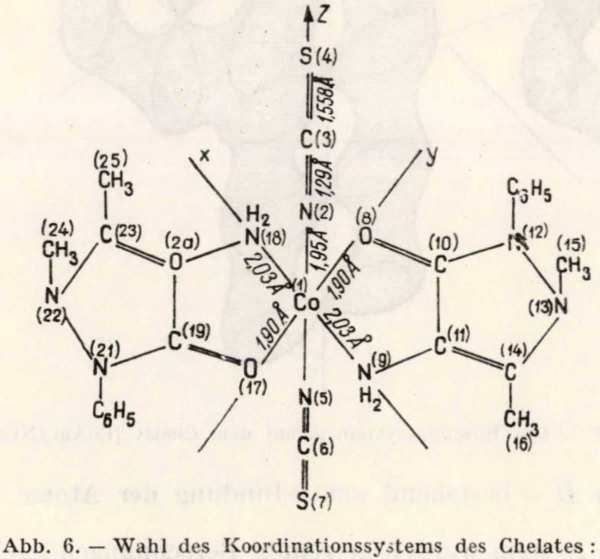

Abb. 6. — Wahl des Koordinationssystems des Chelates : [CoAm$_2$(NCS)$_2$] - und Nummerierung der Atome.

— *System A* — ein delokalisiertes π-System, welches die Atome 1, 2, 3, 4, 5, 6, 7, 8, 10, 11, 14, 17, 19, 20, 23, einschließt (Abb. 7).

— *System B* — bestehend aus π-Bindungen, über die Atome 1, 2, 3, 5, 6, delokalisiert (Abb. 8).

— *System C* — ein aus σ-Bindungen bestehendes System welches durch die Atome 1, 8, 9, 18 gebildet wird (Abb. 9)

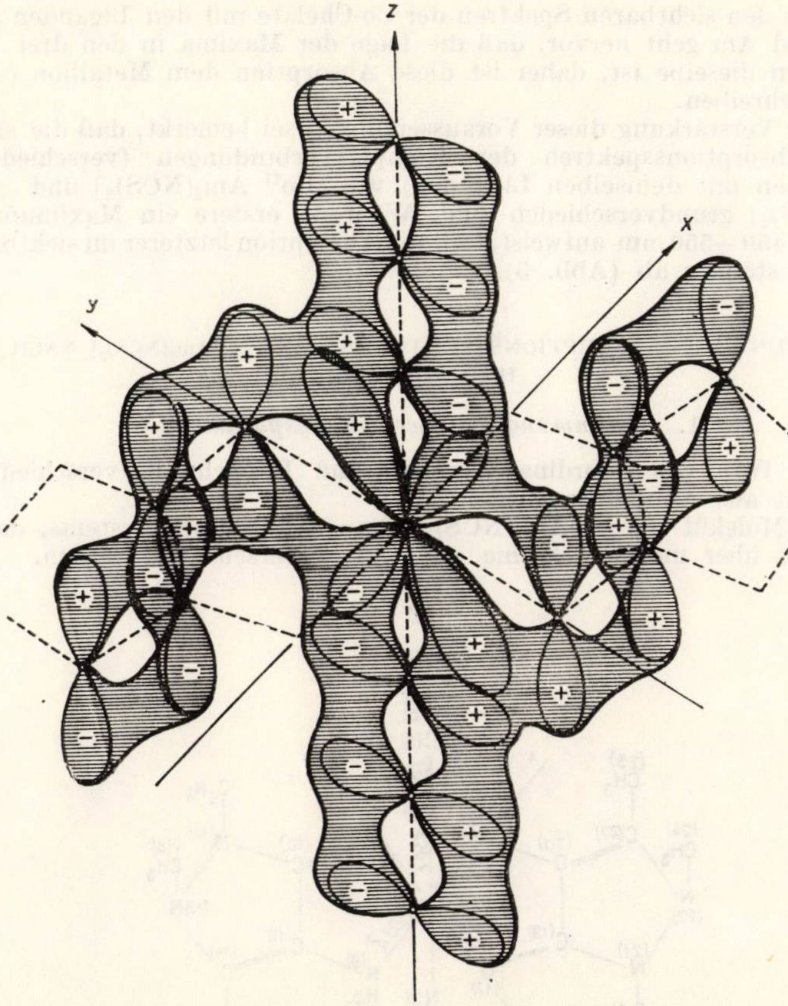

Abb. 7. – Das Bindungssystem *A* aus dem Chelat $[CoAm_2(NCS)_2]$

– *System D* – bestehend aus σ-Bindung der Atome 1, 2, 3, 4, 5, 6,7 (Abb. 10).

Für jedes System wurden getrennte Berechnungen nach der HMO-Methode ausgeführt. Die Werte der Coulomb-Integralen wurden aus den Atombahnfunktionsenergien abgeschätzt.[5] Die Austauschintegrale wurden auf Grund der von Rasch angegebenen Formel ausgewertet [6]

$$\beta_{ij} = -0{,}03996\ (I_i + I_j)\frac{S_{ij}}{1 + S_{ij}} \qquad (1)$$

---

[5] P. Herman und S. Skillmann, "Atomic Structure Calculations" Prentice-Hall, Inc., Englewood Cliffs, New-Yersey, 1963, 6, S. 25–37.

[6] G. Rasch, *Z. Chem.*, **2**, 382 (1962).

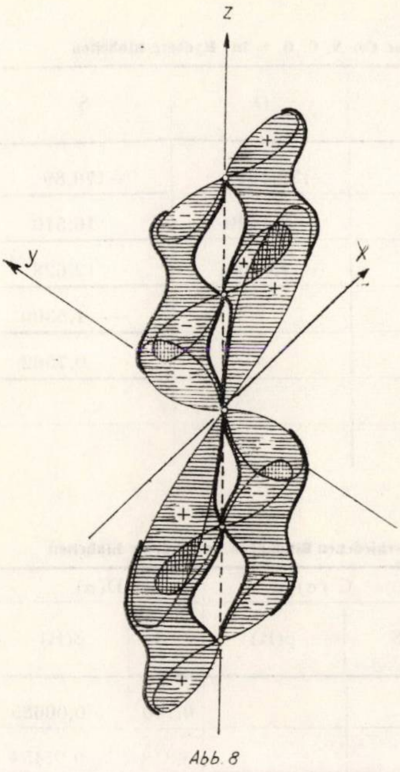

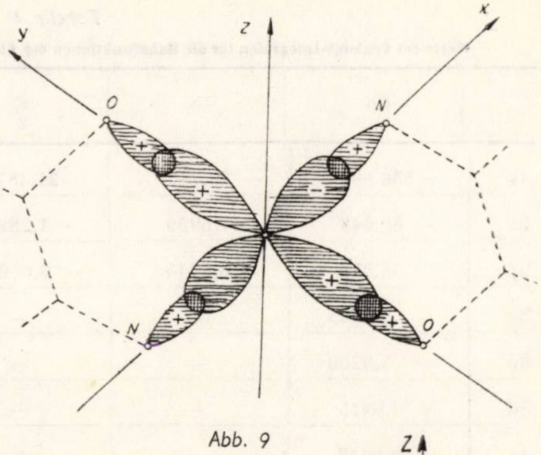
y
z
x
O
N
N
O
+
−
Abb. 9

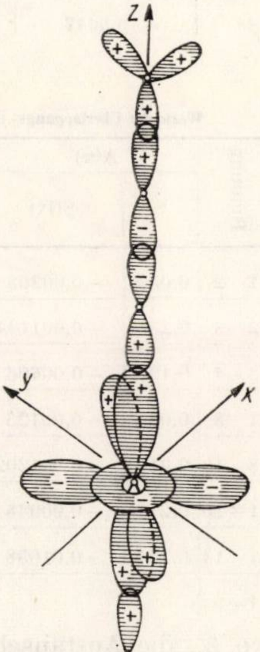

Abb. 8. – Das Bindungssystem *B* aus dem Chelat $[CoAm_2(NCS)_2]$

Abb. 9. – Das Bindungssystem *C* aus dem Chelat $[CoAm_2(NCS)_2]$

Abb. 10. – Das Bindungssystem *D* aus dem Chelat $[CoAm_2(NCS)_2]$

Tabelle 1

Werte der Coulomb-Integralen für die Bahnfunktionen der Atome Co, N, C, O, S, in Rydberg-Einheiten

	Co	N	C	O	S
1s	−558,89	− 29,737	−21,387	−39,456	−179,89
2s	− 66,648	− 1,6959	− 1,2895	− 2,1440	− 16,510
2p	− 58,358	− 0,8445	− 0,6603	− 1,0409	− 12,628
3s	− 7,8785	—	—	—	− 1,5300
3p	− 5,3200	—	—	—	− 0,7562
3d	− 1,0415	—	—	—	—
4s	− 0,5647	—	—	—	—

Tabelle 2

Werte der Überlappungs- (S) und Austauschintegralen (β) der verschiedenen Bindungen in Rydberg-Einheiten

Bindung	A(π)		B(π)		C (σ)		D(σ)	
	S	β(R)	S	β(R)	S	β(R)	S	β(R)
1−2	0,050	−0,00268	0,050	−0,00268			0,100	−0,00685
2−3	0,235	−0,001144	0,023	−0,01144			0,319	−0,01454
3−4	0,120	−0,00606					0,2244	−0,01226
1−8	0,020	−0,00125			0,0695	−0,00630		
8−10	0,215	−0,001202						
11−10	0,219	−0,00948						
11−14	0,251	−0,01058						
1−9					−0,1472	+0,0143		

wo β_{ij} die Austauschintegrale zwischen den Atomen i und j, I_i und I_j die Ionisationspotentiale in Rydberg-Einheiten der Atome i und j in entsprechenden Valenzstadien, hingegen S_{ij} die Überlappungsintegrale darstellen.

Die zur Berechnung der Integralen nötigen interatomaren Abstände wurde in Vergleich zu Komplexverbindungen mit ähnlicher Struktur, welche röntgenographisch untersucht wurden, angenommen,[7] und sind Abb. 6 zu entnehmen. Aufgrund dieser Distanzen wurde das Integral berechnet.[8]

---

[7] M. A. Porai-Koshits und E. A. Gilinskaya, „Kristallokhimia", Akad. Nauk, Moskau, 1966, 1, S. 21.

[8] S. S. Batzanov und R. A. Eviagina, „Integraly perekryvaniya i problema effektivnykh zaryadov", Bd. I, Izd. Nauka, Novo-Sibirsk, 1966, S. 306−345.

2. *Bestimmung der Energieniveaus und der möglichen Elektronenübergänge*

Durch Anwendung des Variationsprinzips für die Systeme *A*, *B*, *C* und *D* wurden die entsprechenden Sekulärdeterminanten erhalten, die zur Berechnung der Energieniveaus der Moleküle dienten, und der Koeffizienten, mit welchen sich die Atombahnfunktionen in die Molekülbahnfunktionen eingliedern. Die Energieniveaudiagramme (Abb. 11) der Systeme *A*, *B*, *C* und *D* entsprechen den vorausgesetzten Übergängen. In den Klammern sind die Wellenlängen der experimentellen Maxima in nm angegeben.

Wie ersichtlich fallen die Elektronenübergänge sämtlicher Systeme in die Bereiche, in welchen auch experimentell Absorptionsmaxima vorgefunden werden (Tabelle 3). Das Maximum bei 283 nm entspricht wahrscheinlich dem π-Phenylsystem, welches nicht in die Berechnung einbezogen wurde. Der Elektronenübergang, welcher der Wellenlänge 240 nm entspricht, wurde durch eine punktierte Linie wiedergegeben da im experimentellen Spektrum das entsprechende Maximum, fast ganz durch die gut ausgebildete Bande von 251 nm überdeckt wird (Abb. 1),

Tabelle 3

Wellenlängen entsprechend den Elektronenübergängen, welche aus den Energieniveaudiagrammen erhalten wurden, im Vergleich zu den Maxima (λ_{max}) der experimentellen Spektren (in nm)

λ_{exp} (nm)	λ theor. (nm).		
	A(π)	B (π)	D(σ)
515	532,7		
470	457,7		
	492,4	492,4	487,1
283			
251	249,5		255,1
240	239,7	238,4	236,6

3. *Die Hückelschen Molekülbahnfunktionen der Verbindung* $[Co^{II}Am_2(NCS)_2]$

In folgendem werden die Molekülorbitalen der 4 Systeme, ihre Energie in Rydberg-Einheiten und ihre Symmetrie wiedergegeben. Mit χ_i wurde die Atombahnfunktion des Atomes *i* bezeichnet

— Das System *A* :

$$\varepsilon = -\,0{,}75657\,; \qquad \Phi\,(b_g) = \frac{1}{\sqrt{2}}(0{,}99805\,\chi_4 + 0{,}06186\,\chi_3 - 0{,}00805\,\chi_2 + 0{,}00014\,\chi_1 - $$
$$-\,0{,}00805\,\chi_5 + 0{,}06186\,\chi_6 + 0{,}99805\,\chi_7)$$

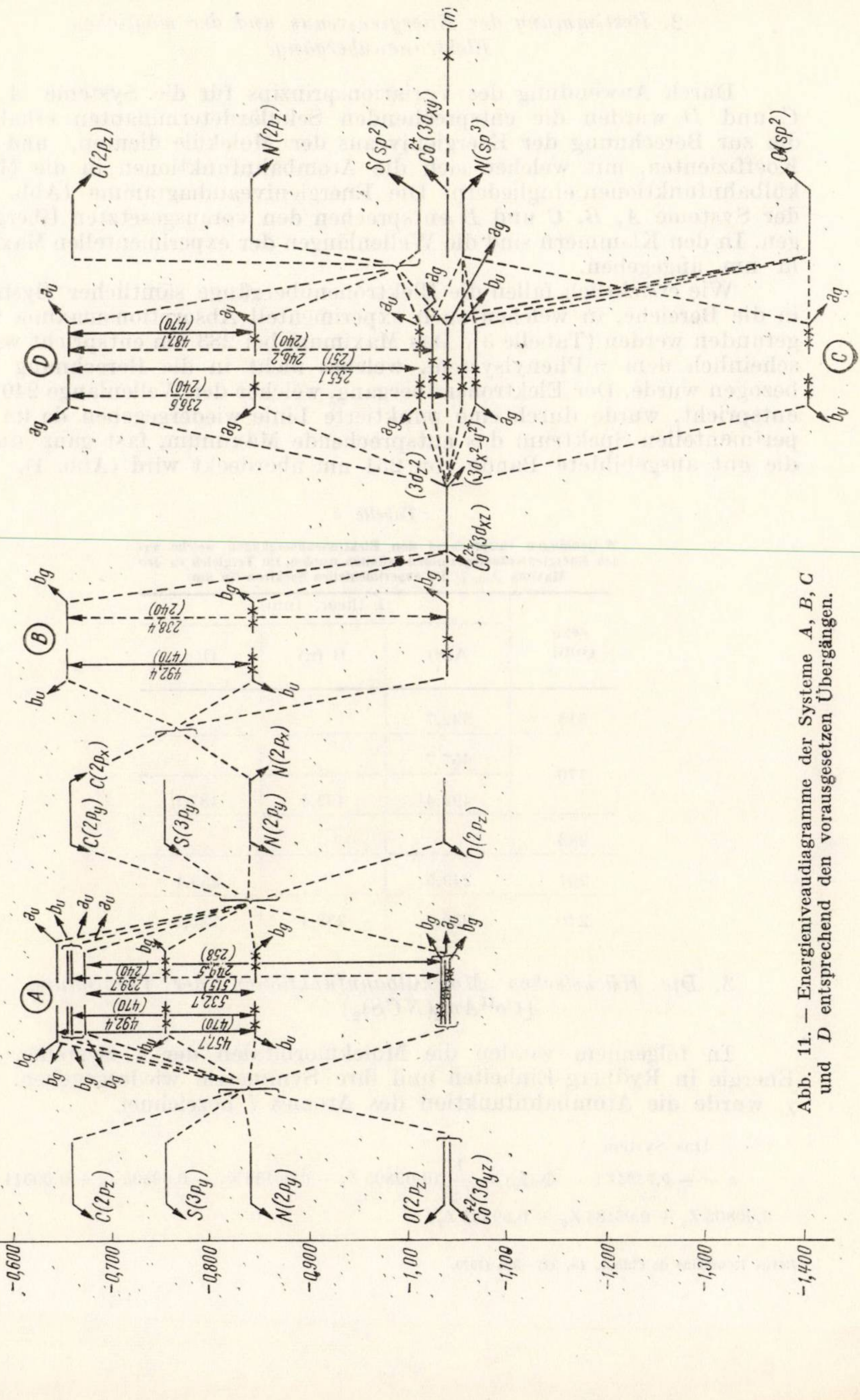
E(R)
-0,600
-0,700
-0,800
-0,900
-1,00
-1,100
-1,200
-1,300
-1,400
C(2Pz)
S(3Py)
N(2Py)
O(2Pz)
Co(3dyz)
A
457,1 (470)
492,4 (470)
532,7 (515)
249,5 (258)
239,7 (240)
C(2Py) C(2Px)
S(3Py)
N(2Py) N(2Px)
O(2Pz)
B
492,4 (470)
238,4 (240)
Co(3dxz)
D
236,6 (240)
255,1 (251)
246,2 (240)
482,4 (470)
C(2Pz)
N(2Pz)
C(Sp2)
Co(3dxy)
N(Sp3)
C(Sp2)
(3dz2)
(3dx2-y2)
(n)
C
ag
au
bg
bu

Abb. 11. — Energieniveaudiagramme der Systeme A, B, C und D entsprechend den vorausgesetzten Übergängen.

$$\varepsilon = -\,0{,}75657\,; \qquad \Phi\,(b_u) = \frac{1}{\sqrt{2}}\,(0{,}99805\,\chi_4 + 0{,}06186\,\chi_3 - 0{,}00805\,\chi_2 + 0{,}00805\,\chi_5 -$$

$$-\,0{,}06186\,\chi_6 - 0{,}99805\,\chi_7)$$

$$\varepsilon = -\,0{,}65921\,; \qquad \Phi\,(b_g) = \frac{1}{\sqrt{2}}\,(-0{,}06224\,\chi_4 + 0{,}99616\,\chi_3 - 0{,}06151\,\chi_2 + 0{,}00086\,\chi_1 -$$

$$-\,0{,}06151\,\chi_5 + 0{,}99616\,\chi_6 - 0{,}06224\,\chi_7)$$

$$\varepsilon = -\,0{,}65921\,; \qquad \Phi\,(b_u) = \frac{1}{\sqrt{2}}\,(-0{,}06224\,\chi_4 + 0{,}99616\,\chi_3 - 0{,}06151\,\chi_2 + 0{,}06151\,\chi_5 -$$

$$-\,0{,}99616\,\chi_6 + 0{,}06224\,\chi_7)$$

$$\varepsilon = -\,0{,}84521\,; \qquad \Phi\,(b_u) = 0{,}00297\,\chi_4 + 0{,}04376\,\chi_3 + 0{,}70574\,\chi_2 - 0{,}70574\,\chi_5 -$$
$$-\,0{,}04376\,\chi_6 - 0{,}00297\,\chi_7\,;$$

$$\varepsilon = -\,1{,}04128\,; \qquad \Phi\,(a_u) = 0{,}00001\,\chi_1 - 0{,}70675\,\chi_8 - 0{,}02231\,\chi_{10} - 0{,}00055\,\chi_{11} -$$
$$-\,0{,}00001\,\chi_{14} + 0{,}70675\,\chi_{17} + 0{,}02231\,\chi_{19} + 0{,}00055\,\chi_{20} + 0{,}00001\,\chi_{23}\,;$$

$$\varepsilon = -\,1{,}03965\,; \qquad \Phi\,(b_g) = 0{,}00028\,\chi_3 + 0{,}00931\,\chi_2 + 0{,}67706\,\chi_1 - 0{,}52002\,\chi_8 -$$
$$-\,0{,}01648\,\chi_{10} - 0{,}00041\,\chi_{11} - 0{,}00001\,\chi_{14} - 0{,}52003\,\chi_{17} - 0{,}01648\,\chi_{19} - 0{,}00041\,\chi_{20} -$$
$$-\,0{,}00001\,\chi_{23} + 0{,}00931\,\chi_5 + 0{,}00028\,\chi_6\,;$$

$$\varepsilon = -\,0{,}64601\,; \qquad \Phi\,(b_g) = \frac{1}{\sqrt{2}}\,(0{,}00008\,\chi_1 - 0{,}01461\,\chi_8 + 0{,}47999\,\chi_{10} - 0{,}70494\,\chi_{11} +$$

$$+\,0{,}52196\,\chi_{14} - 0{,}01461\,\chi_{17} + 0{,}47999\,\chi_{19} - 0{,}70494\,\chi_{20} + 0{,}52196\,\chi_{23})\,;$$

$$\varepsilon = -\,0{,}64601\,; \qquad \Phi\,(a_u) = \frac{1}{\sqrt{2}}\,(-0{,}01461\,\chi_8 + 0{,}47999\,\chi_{10} - 0{,}70494\,\chi_{11} + 0{,}52196\,\chi_{14} +$$

$$+\,0{,}01461\,\chi_{17} - 0{,}47999\,\chi_{19} + 0{,}70494\,\chi_{20} - 0{,}52196\,\chi_{23})\,;$$

$$\varepsilon = -\,0{,}66009\,; \qquad \Phi\,(b_g) = \frac{1}{\sqrt{2}}\,(0{,}00014\,\chi_1 - 0{,}02349\,\chi_8 + 0{,}74436\,\chi_{10} + 0{,}01326\,\chi_{11} -$$

$$-\,0{,}66723\,\chi_{14} - 0{,}02349\,\chi_{17} + 0{,}74436\,\chi_{19} + 0{,}01326\,\chi_{20} - 0{,}66723\,\chi_{23})\,;$$

$$\varepsilon = -\,0{,}66009\,; \qquad \Phi\,(a_u) = \frac{1}{\sqrt{2}}\,(-0{,}2349\,\chi_8 + 0{,}74436\,\chi_{10} + 0{,}01326\,\chi_{11} - 0{,}66723\,\chi_{14} +$$

$$+\,0{,}02349\,\chi_{17} - 0{,}74436\,\chi_{19} - 0{,}013268\,\chi_{20} + 0{,}66723\,\chi_{23})\,;$$

$$\varepsilon = -\,0{,}67442\,; \qquad \Phi\,(b_g) = \frac{1}{\sqrt{2}}\,(0{,}00010\,\chi_1 - 0{,}01519\,\chi_8 + 0{,}46318\,\chi_{10} + 0{,}70913\,\chi_{11} +$$

$$+\,0{,}53136\,\chi_{14} - 0{,}01519\,\chi_{17} + 0{,}46318\,\chi_{19} + 0{,}70913\,\chi_{20} + 0{,}53136\,\chi_{23})\,;$$

$$\varepsilon = -\,0{,}67442\,; \qquad \Phi\,(a_u) = \frac{1}{\sqrt{2}}\,(-0{,}01519\,\chi_8 + 0{,}46318\,\chi_{10} + 0{,}70913\,\chi_{11} + 0{,}53136\,\chi_{14} +$$

$$+\,0{,}01519\,\chi_{17} - 0{,}46318\,\chi_{19} - 0{,}70913\,\chi_{20} - 0{,}53136\,\chi_{23})\,;$$

$$\varepsilon = -\,1{,}04319\,; \Phi(b_g) = 0{,}00029\,\chi_3 + 0{,}00993\,\chi_2 + 0{,}73567\,\chi_1 + 0{,}47861\,\chi_8 + 0{,}01503\,\chi_{10} +$$
$$+\,0{,}00037\,\chi_{11} + 0{,}00001\,\chi_{14} + 0{,}47860\,\chi_{17} + 0{,}01503\,\chi_{19} + 0{,}00037\,\chi_{20} + 0{,}00001\,\chi_{23} +$$
$$+\,0{,}00993\,\chi_5 + 0{,}00029\,\chi_6\,;$$

$\varepsilon = -\mathit{0{,}84513}$; $\Phi(b_g) = 0{,}00298\,\chi_4 + 0{,}04376\,\chi_3 + 0{,}70561\,\chi_2 - 0{,}01926\,\chi_1 + 0{,}00012\,\chi_8 + 0{,}00012\,\chi_{17} + 0{,}70561\,\chi_5 + 0{,}04376\,\chi_6 + 0{,}00298\,\chi_7$;

— *Das System B*:

$\varepsilon = -\mathit{0{,}65959}$; $\Phi(b_g) = \frac{1}{\sqrt{2}}(0{,}99809\,\chi_3 - 0{,}06175\,\chi_2 + 0{,}00086\,\chi_1 - 0{,}06175\,\chi_5 + 0{,}99809\,\chi_6)$;

$\varepsilon = -\mathit{0{,}65959}$; $\Phi(b_u) = \frac{1}{\sqrt{2}}(0{,}99809\,\chi_3 - 0{,}06175\,\chi_2 + 0{,}06175\,\chi_5 - 0{,}99809\,\chi_6)$;

$\varepsilon = -\mathit{0{,}84520}$; $\Phi(b_u) = 0{,}04366\,\chi_3 + 0{,}70575\,\chi_2 - 0{,}70576\,\chi_5 - 0{,}04366\,\chi_6$;

$\varepsilon = -\mathit{1{,}04157}$; $\Phi(b_g) = 0{,}00040\,\chi_3 + 0{,}01362\,\chi_2 + 0{,}99981\,\chi_1 + 0{,}01362\,\chi_5 - 0{,}00040\,\chi_6$;

$\varepsilon = -\mathit{0{,}84513}$; $\Phi(b_g) = 0{,}04367\,\chi_3 + 0{,}70563\,\chi_2 - 0{,}01926\,\chi_1 + 0{,}00562\,\chi_5 + 0{,}04367\,\chi_6$;

— *Das System C*:

$\varepsilon = -\mathit{1{,}05720}$; $\Phi(b_u) = -0{,}70710\,\chi_9 + 0{,}70710\,\chi_{18}$;
$\varepsilon = -\mathit{1{,}40810}$; $\Phi(b_u) = 0{,}70710\,\chi_8 - 0{,}70710\,\chi_{17}$;
$\varepsilon = -\mathit{1{,}40831}$; $\Phi(a_g) = 0{,}02435\,\chi_1 + 0{,}70689\,\chi_8 + 0{,}70690\,\chi_{17} - 0{,}00099\,\chi_9 - 0{,}00099\,\chi_{18}$;

$\varepsilon = -\mathit{1{,}07096}$; $\Phi(a_g) = 0{,}56271\chi_1 - 0{,}01051\chi_8 - 0{,}01051\chi_{17} - 0{,}058443\chi_9 - 0{,}58443\,\chi_{18}$;

$\varepsilon = -\mathit{1{,}02751}$; $\Phi(a_g) = 0{,}82629\,\chi_1 - 0{,}01367\,\chi_8 - 0{,}01367\,\chi_{17} + 0{,}39803\,\chi_9 + 0{,}39803\,\chi_{18}$;

— *Das System D*:

$\varepsilon = -\mathit{1{,}01452}$; $\Phi(a_g) = \frac{1}{\sqrt{2}}(0{,}99939\,\chi_4 + 0{,}03471\,\chi_3 + 0{,}00291\,\chi_2 - 0{,}00147\chi_1 + 0{,}00291\,\chi_5 + 0{,}03471\,\chi_6 + 0{,}99939\,\chi_7)$;

$\varepsilon = -\mathit{1{,}01452}$; $\Phi(a_u) = \frac{1}{\sqrt{2}}(0{,}99939\,\chi_4 + 0{,}03471\,\chi_3 + 0{,}0295\,\chi_2 - 0{,}00295\,\chi_5 - 0{,}03471\,\chi_6 - 0{,}99939\,\chi_7)$;

$\varepsilon = -\mathit{0{,}65873}$; $\Phi(a_u) = -0{,}02425\,\chi_4 + 0{,}70314\,\chi_3 - 0{,}05503\,\chi_2 + 0{,}05525\,\chi_5 - 0{,}70591\,\chi_6 + 0{,}02435\,\chi_7)$;

$\varepsilon = -\mathit{0{,}84564}$; $\Phi(a_u) = 0{,}00400\,\chi_4 + 0{,}5504\,\chi_3 + 0{,}70495\,\chi_2 - 0{,}70494\,\chi_5 - 0{,}05503\,\chi_6 + 0{,}00400\,\chi_7$;

$\varepsilon = -\mathit{1{,}04197}$; $\Phi(a_g) = 0{,}00059\,\chi_4 + 0{,}00134\,\chi_3 + 0{,}03474\,\chi_2 + 0{,}99878\,\chi_1 + 0{,}03474\,\chi_5 + 0{,}00134\,\chi_6 + 0{,}00059\,\chi_7$;

$$\varepsilon = -\mathit{0{,}84516}\,;\quad \Phi(a_g) = -0{,}00399\,\chi_4 + 0{,}05511\,\chi_3 + 0{,}70408\,\chi_2 - 0{,}04912\,\chi_1 + 0{,}70408\,\chi_5 + 0{,}05511\,\chi_6 - 0{,}00399\,\chi_7\,;$$

$$\varepsilon = -\mathit{0{,}65873}\,;\quad \Phi(a_g) = -0{,}02435\,\chi_4 + 0{,}70590\,\chi_3 - 0{,}05532\,\chi_2 + 0{,}00197\,\chi_1 - 0{,}05510\,\chi_5 + 0{,}70314\,\chi_6 - 0{,}02425\,\chi_7\,;$$

4. *Berechnung der Ladungsverteilung auf die verschiedenen Atome des Moleküls im Grundzustand*

Anhand von Molekülbahnfunktionen der Komplexverbindung wurde die Ladungsverteilung auf die verschiedenen Atome des Moleküls mittels der bekannten Formel (2) berechnet

$$q_i = \sum_j c_{ij}^2 \cdot n_j \qquad (2)$$

wo mit q_i die elektrische Ladung des Atoms i (in Elektronen Einheiten), mit c_{ij} der Koeffizient der Atombahnfunktion i in der Molekülbahnfunktion j, mit n_j aber die Anzahl der Elektronen, welche der Molekülbahnfunktion j entsprechen, bezeichnet wird. In Abb. 12 sind die Ergebnisse dieser Berechnungen zu finden.

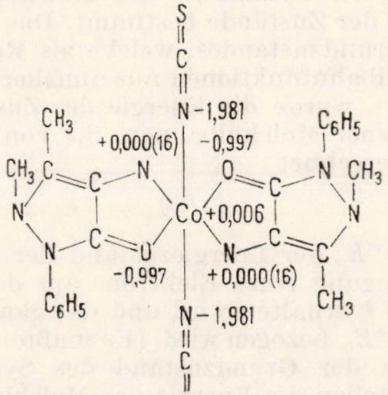

Abb. 12. — Ladungsverteilung auf die an der Bindung mit dem Metallion beteiligten Atome in Elektron-Einheiten.

Es ist zu bemerken, daß die Bindung zwischen dem Metallion Co^{2+} und dem Sauerstoff-Atom des Liganden Amino-antipyrin vorwiegend ionisch ist, ebenso die Bindung zwischen Co^{2+} und dem Stickstoffatom der NCS-Gruppe. Desgleichen geht hervor, daß die Bindung $Co^{2+} - N$ (Stickstoff der Aminogruppe des Amino-antipyrins) nur wenig polar, also entweder stark kovalent oder eine sehr labile Bindung wäre (theoretisch ungebunden). Wie aus Abb. 11 ersichtlich, sind alle Molekülbahnfunktionen des Systems C besetzt. Die kovalente Bindungsordnung zwischen $Co^{2+}-O$ und $Co^{2+}-N$ kann als gleich Null betrachtet werden; wegen dem vorwiegend polaren Charakter der Bindung im ersten Falle können wir voraussetzen, daß die Bindung $Co^{2+}-N$ (Am) sich in Methanollösung stark abschwächt (theoretisch auflöst). Auch Abb. 9 weist auf eine bestimmte Labilität dieser Bindung hin, da dieselbe durch eine negative Überlappung der Atombahnfunktion des Stickstoffs aus Amino-antipyrin mit der Bahnfunktion $d_{x^2-y^2}$ des Co-Ions entsteht.

Der ionische Charakter der Bindung zwischen dem Zentralatom und dem Liganden Amino-antipyrin erklärt auch die Tatsache, daß das Spektrum im sichtbaren Bereich der Komplexverbindung in Lösung, in größerem Maße von den Eigenschaften des Zentralmetallions, als von jenen des Liganden abhängt. Der Ligand (Am) als solcher absorbiert nicht im sichtbaren Bereiche (ist beinahe farblos); im Komplex gebunden ist er nur einer Polarisierung seitens des Metallions unterworfen, d.h. seine Struktur verändert sich nicht wesentlich. Der gebundene Ligand wird also nicht viel zum sichtbaren Spektrum der Komplexverbindung beitragen, da dieses dem entsprechenden Metallthyocyanat entspricht (dessen Lösungen im Falle des Co^{2+}, Ni^{2+} und Fe^{2+} gefärbt sind). Dadurch kann die Tatsache erklärt werden, daß die Salze $Me(NCS)_2$ in Methanollösung in vielen Fällen ähnliche Farbe wie die entsprechende Komplexverbindung $[MeAm_2(NCS)_2]$ aufweisen.

5. *Symmetrie und Energie der Zustände. Auswahlregeln*

Nach der Symmetrie der Molekülorbitale wurde die Energie und Symmetrie der Zustände bestimmt. Die Energie der Zustände wurde auf jene des Grundzustandes, welche als Referenzniveau dient, bezogen. Da die Molekülbahnfunktionen nur annähernd ermittelt sind (Repulsion vernachlässigt), wurde die Energie der Zustände nur aus der Differenz der Energien jener Molekülbahnen, die von Elektronenübergängen betroffen wurden, berechnet:

$$ {}^{m}E_{ik} - {}^{m}E_{0} = \varepsilon_{k} - \varepsilon_{i} \tag{3} $$

wo ${}^{m}E_{ik} - {}^{m}E_{0}$ der Energiezustand der Multiplizität m bedeutet, welche durch Anregung eines Elektrons aus dem Molekülzustand i zum Molekülzustand k erhalten wird und das ganze auf die Energie des Grundzustandes ${}^{m}E_{0}$ bezogen wird. (Es mußte hier die Multiplizität angegeben werden, da der Grundzustand des Systems D ein Triplett darstellt). ε_k und ε_i stellen die Energie der Molekül-Orbitalen k und i dar.

Bezeichnen wir mit Γ_k bzw. Γ_i die irreduktiblen Darstellungen, zu denen als Basisfunktionen die Molekül-Orbitale Φ_k und Φ_i gehören, dann ergibt ihr direktes Produkt $\Gamma_k . \Gamma_i$ die Symmetrie des entsprechenden Zustandes. Die Ergebnisse dieser Symmetrieuntersuchungen sind in Abb. 13, 14 und 15 wiedergegeben. Die Energien der Zustände wurden ebenfalls in Rydberg-Einheiten (R) ausgedrückt.

Zur Bestimmung der Auswahlregeln müssen die Bedingungen festgelegt werden, in welchen (4) nicht annulliert wird.

$$ < {}^{m}\Psi_{0}\, t\, {}^{m}\Psi_{ik} > \tag{4} $$

${}^{m}\Psi_{0}$ und ${}^{m}\Psi_{ik}$ stellen die Wellenfunktionen des Grundzustandes und des angeregten Zustandes welche dem Elektronenübergang $\Phi_i \rightarrow \Phi_k$ entspricht dar, hingegen bedeutet t eine der Koordinaten x, y, z (im Falle des linear polarisierten Überganges) oder eines der Produkte xy, yz, xz (im Falle des zirkular polarisierten Überganges).

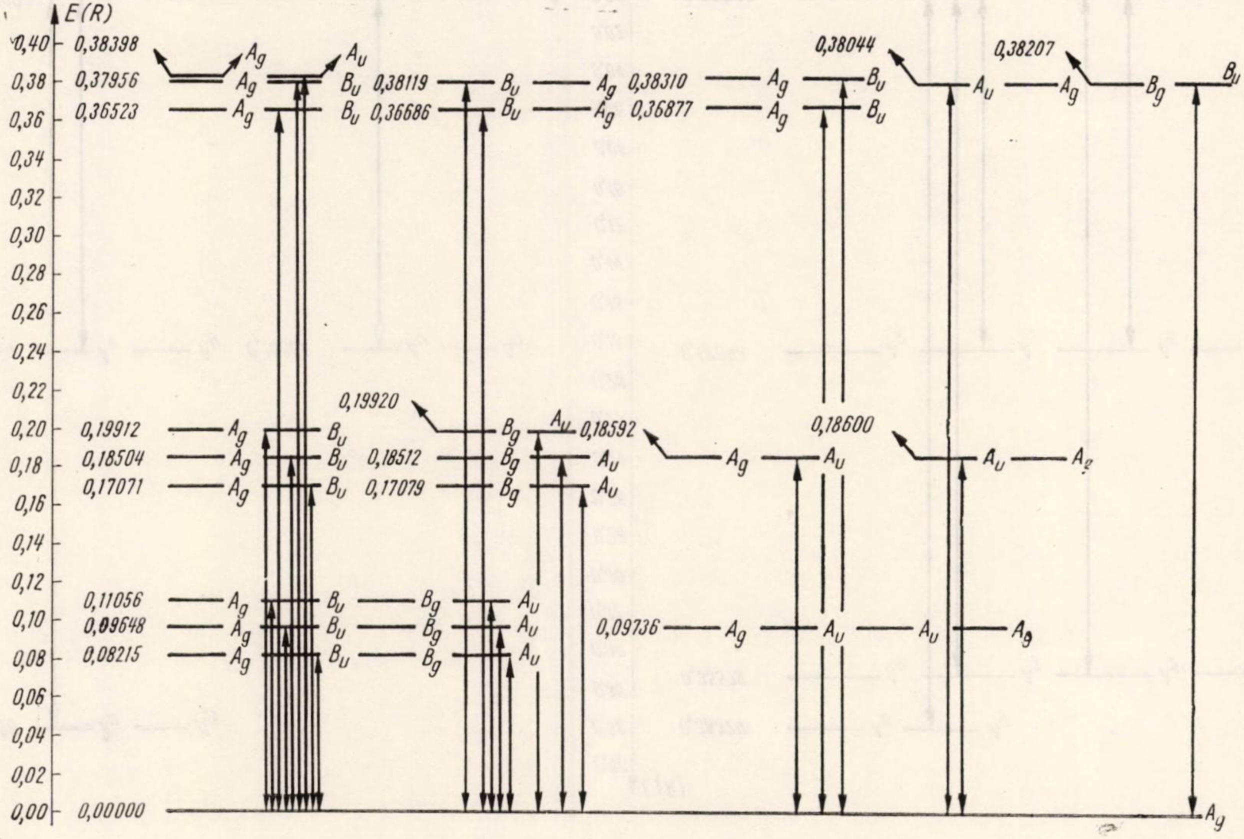
E(R)
0,40
0,38
0,36
0,34
0,32
0,30
0,28
0,26
0,24
0,22
0,20
0,18
0,16
0,14
0,12
0,10
0,08
0,06
0,04
0,02
0,00
0,38398
0,37956
0,36523
0,19912
0,18504
0,17071
0,11056
0,09648
0,08215
0,00000
0,38119
0,36686
0,19920
0,18512
0,17079
0,38310
0,36877
0,18592
0,09736
0,38044
0,18600
0,38207
Ag
Au
Bu
Bg

Abb. 13. – Energie und Symmetrie der Zustände im *A*-System.

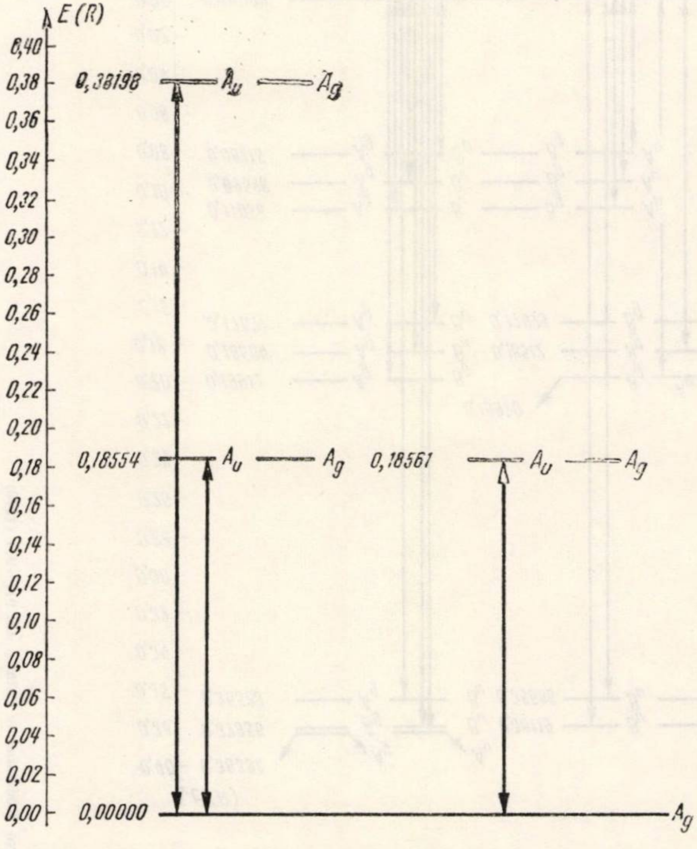
E(R)
0,40
0,38
0,36
0,34
0,32
0,30
0,28
0,26
0,24
0,22
0,20
0,18
0,16
0,14
0,12
0,10
0,08
0,06
0,04
0,02
0,00
0,38198
A_u
A_g
0,18554
A_u
A_g
0,18561
A_u
A_g
0,00000
A_g

Abb. 14. – Energie und Symmetrie der Zustände im *B*-System.

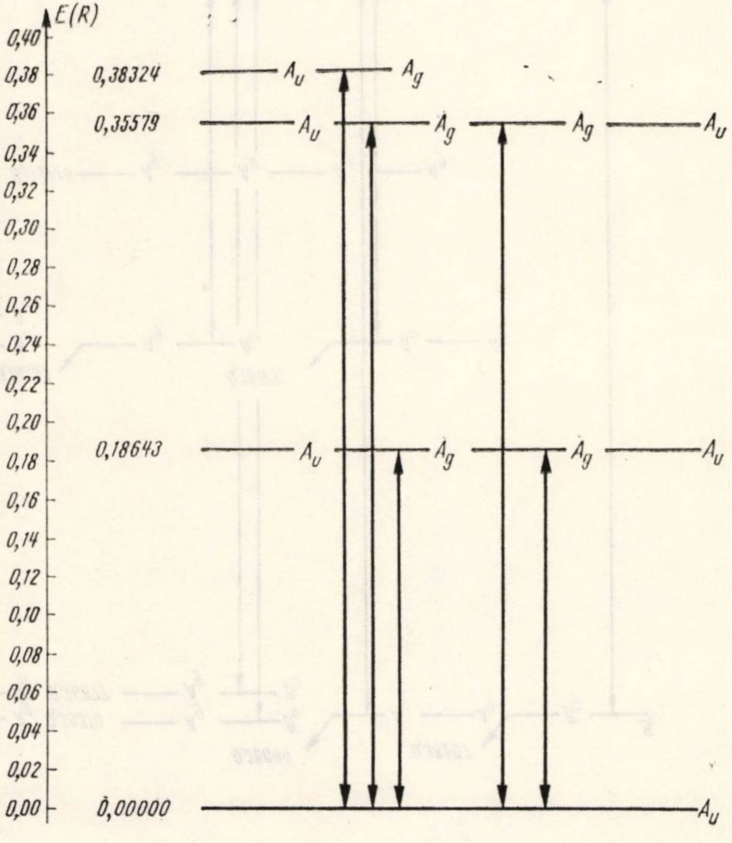
E(R)
0,40
0,38
0,36
0,34
0,32
0,30
0,28
0,26
0,24
0,22
0,20
0,18
0,16
0,14
0,12
0,10
0,08
0,06
0,04
0,02
0,00
0,38324
A_u
A_g
0,35579
A_u
A_g
A_g
A_u
0,18643
A_u
A_g
A_g
A_u
0,00000
A_u

Abb. 15. – Energie und Symmetrie der Zustände im *D*-System.

Die notwendige Bedingung, daß sich Integrale (4) nicht annulliert, ist, daß die Zerlegung in irreduktiblen Darstellungen des direkten Produktes

$$\Gamma_{m_{\psi_0}} \cdot \Gamma_{\iota} \cdot \Gamma_{m_{\Psi_{ik}}} \tag{5}$$

wenigstens einmal eine totalsymmetrische Darstellung enthalte, in unserem Falle A_g.

Es sind Übergänge mit folgender Symmetrie möglich:

Im System A:

$^1A_g \rightarrow {}^1B_u$ — zirkular polarisierter Übergang im xy-Plan des Moleküls.

$^1A_g \rightarrow {}^1A_u$ — nach z-Achse des Moleküls polarisierter Übergang.

Obwohl im A-System Übergänge aus dem Grundzustand in Zustände mit nächsthöherer Energie vom Symmetriestandpunkt aus erlaubt sind, konnten diese im untersuchten Spektralbereiche nicht beobachtet werden, da sie zu großen Wellenlängen entsprechen.

Im System B:

$^1A_g \rightarrow {}^1A_u$ — nach z-Achse polarisierter Übergang.

Im System C — sind keine Übergänge möglich, da alle Molekülbahnfunktionen besetzt sind.

Im System D — befinden sich 2 Elektronen mit gleichgerichteten Spins, folglich ist der Grundzustand ein Triplett. Der mögliche Übergang.

$^3A_u \rightarrow {}^3A_g$ — ein nach der z-Achse linear polarisierter Übergang.

Wegen den ungepaarten Elektronen aus dem D-System müßte das Molekül der untersuchten Verbindung paramagnetisch sein. Da das nichtbindende Atomorbital (n aus Abb. 11) noch ein ungepaartes Elektron aufweist, muß die Verbindung stark paramagnetisch sein. Tatsächlich konnten wir starken Paramagnetismus feststellen.

In Tabelle 3 wurden die Wellenlängen, welche den Elektronenübergängen zwischen den Energieniveaus entsprechen, wiedergegeben. Durch Symmetrieuntersuchungen der angeregten Zustände wurde bewiesen, daß die Absorptionsmaxima auch den Auswahlregeln entsprechend sind. Durch diese Regeln wurden gleichzeitig auch die Molekülorbitale festgesetzt, zwischen welchen die Übergänge stattfinden können. Dies ist besonders wichtig im Falle degenerierter Molekülbahnfunktionen.

Die theoretisch möglichen Übergänge stimmen zufriedenstellend mit den experimentellen Spektren überein.

Ähnliche Berechnungen wurden auch für *cis*-[CoAm$_2$(NCS)$_2$] aufgestellt; da die erhaltenen Resultate aber nicht mit den experimentellen übereinstimmen, ist die Wahrscheinlichkeit groß, daß die Verbindung als *trans*-Isomer vorliegt.

VERSUCHSTEIL

Die Spektren wurden mit dem Spektrophotometer UNICAM SP 800 im Bereiche 200–350 nm und 450–650 nm im Vergleich mit reinen Lösungsmitteln aufgenommen. Dazu wurden 10^{-4} molare Lösungen der Komplexverbindungen in Methanol *p.a.* verwendet.

Die Herstellung der Co-Komplexe erfolgt nach[1] des Cd nach,[2] des Zn nach,[3] während Fe- und Mn-Komplexverbindungen (ebenfalls Chelate) bisher noch nicht beschrieben wurden.

$[MnAm_2(NCS)_2]$

Wird durch Versetzen von 1,5 g $MnCl_2$ in 10 ml Wasser mit einer Lösung von 1,5 g Am, 1,5 g NH_4SCN in 25 ml Wasser erhalten. Man entfernt zuerst kleine Mengen Harz, dann bildet sich langsam ein gelblicher Niederschlag (pH der Mutterlösung = 6). Nach 2 Stunden wird filtriert, mit Wasser gewaschen und über $CaCl_2$ zwischen Filterpapier getrocknet.

$[MnAm_2(NCS)_2]$ (577,34)

Ber.:	Mn	9,52	SCN	20,12	N	19,41 %
Gef.:	Mn	9,60	SCN	20,11	N	19,19 %

$[FeAm_2(NCS)_2]$

Wird auf ähnliche Weise mit 2 g $FeSO_4$ in etwas verdünnterer Lösung erhalten (pH der Mutterlösung = 6,5). Der dunkelrote Niederschalg wird nach 1/2 — 1 Std. filtriert und wie der Mangankomplex behandelt.

$[FeAm_2(NCS)_2]$ (578,25)

Ber.:	Fe	9,66	SCN	20,09	N	19,38 %
Gef.:	Fe	9,72	SCN	20,02	N	19,25 %

Revue Roumaine de Chimie, **15**, 935–944 (1970)

SUR LES VANADATES. XVIII*

COMPOSÉS MIXTES $V^{5+}-V^{4+}$ OBTENUS EN SOLUTIONS AQUEUSES

ILEANA LUKÁCS, CONSTANȚA STRUSIEVICI et C. LITEANU

Institut de Chimie de l'Académie, Filiale de Cluj, 59–65, Str. Donath

Reçu le 13 octobre 1969

On donne les conditions de la synthèse en solutions aqueuses des composés $2K_2O.V_2O_4.2V_2O_5(K_2V^{4+}V_2^{5+}O_8)$ et $K_2O.V_2O_4.4V_2O_5.nH_2O$ (?), leurs spectres Debye-Scherrer et en IR, les valeurs de la conductivité électrique et du coefficient Seebeck.

Dans ses études [1] sur la formation des composés mixtes $V^{5+} - V^{4+}$, en solutions aqueuses, Ostrowetsky a obtenu des produits où le rapport V^{5+}/V^{4+} variait de 3/7, 2/4, 4/6, 5/5, 6/4, 7/3, 8/2, selon les conditions de préparation. Mirkin a signalé [2] la possibilité de l'existence aussi d'un composé avec le rapport V^{5+}/V^{4+} de 2/1, mais il n'a pas essayé de le séparer à l'état cristallin. Récemment on a synthétisé [3,4] les sels organiques de l'anion $[V_2^{4+}V_8^{5+}O_{28}H_4]^{4-}$, le composé $(NH_4)_2\,[V^{4+}V_2^{5+}O_8]\cdot0{,}5\,H_2O$ et les sels alcalins (Na, K) de l'anion $[V_8^{4+}V_2^{5+}O_{24}]^{6-}$.

Nous avons visé à obtenir des composés mixtes $V^{5+}-V^{4+}$ des solutions aqueuses 1M de KVO_3, respectivement de VO^{2+}, en les mélangeant à chaud, en rapport de 8/1, 6/1, 5/1, 4/1, 2/1 et 1/1.

Les résultats, quant aux rendements des réactions, compositions chimiques des précipités obtenus et pH des filtrats, sont donnés au tableau 1. Les spectres Debye-Scherrer (fig. 1 et tabl. 2) et en IR (fig. 2–4) indiquent la formation de deux types de phases : la phase A dans les produits **I–III, VI, X–XII**, stables dans les solutions au pH d'environ 5,5–6,5 et la phase B dans les produits **IV, V, VIII, IX, XIII, XIV, XVI**, stables dans les solutions au pH d'environ 2,7–4,2.

---

* XVIIe partie I. Lukács, C. Strusievici, D. Lupu, C. Mirel et C. Liteanu, *Rev. Roumaine Chim.*, **14**, 1125 (1969).

[1] S. Ostrowetsky, *Bull. Soc. chim. France*, **1964**, 1012.
[2] V. A. Mirkin et M. T. Kozlovski, *Doklady Akad. Nauk S.S.S.R.*, **150**, 317 (1963).
[3] C. Heitner-Wirguin et I. Selbin, *J. Inorg. Nuclear Chem.*, **30**, 3181 (1968).
[4] E. Hayek et U. Pallasser, *Monatsh.*, **99**, 2497 (1968).

Tableau 1

Données de l'analyse chimique des produits

Produit	KVO_3	VO^{2+}	Rendement (%) rapporté au		Composition chimique								pH du filtrat
					%				moles				
			V^{5+}	V^{4+}	K_2O	V_2O_4	V_2O_5	H_2O	K_2O	V_2O_4	V_2O_5	H_2O	
I	8	1	24	90	26,48	22,76	51,46	—	2,06	1	2,06	—	6,5
II	8	1	24	90	25,90	22,17	52,60	—	2,05	1	2,16	—	6,8
III	4	1	38	72	24,65	22,06	52,49	(0,90)	1,91	1	2,10	0,36	5,9
IV	2	1	55	25	12,79	13,69	65,62	(7,90)	1,64	1	4,30	5,30	4,2
V	1	1	100	25	8,55	14,60	67,70	(9,15)	1,03	1	4,22	5,76	3,1
VI	8	1	30	98	24,25	20,38	53,83	(1,50)	2,09	1	2,41	0,67	6,0
VII	6	1	26	47	16,16	16,35	59,96	(7,55)	1,73	1	3,34	4,25	5,2
VIII	4	1	52	62	10,42	15,95	58,83	(14,80)	1,15	1	3,36	8,55	3,8
IX	2	1	81	45	8,16	16,26	63,28	(12,30)	0,88	1	3,54	6,95	2,7
X	8	1	25	96	26,04	22,78	51,79	—	2,01	1	2,07	—	6,6
XI	8	1	24	94	25,56	23,10	51,09	—	1,95	1	2,01	—	6,6
XII	5	1	33	70	24,20	21,57	55,02	—	1,98	1	2,33	—	5,5
XIII	2	1	60	34	9,30	17,45	64,44	(8,71)	0,94	1	3,37	4,60	3,6
XIV	1	1	99	34	8,23	20,22	64,43	(7,12)	0,72	1	2,90	3,28	3,1
XV	2	1	88	85	21,35	18,27	41,85	18,53	2,06	1	2,09	9,36	6,6
XVI	3	1	79	75	9,49	15,83	64,64	(10,04)	1,05	1	3,76	5,85	3,7
XVII	4	1			5,00	7,81	33,29	(53,90)	1,12	1	3,88	63,70	3,6

Au rapport V^{5+}/V^{4+} de 8/1, le cas des produits I, II, VI, X, XI, le rendement de la réaction est d'environ 90–98 % pour V^{4+} et de 24–30 % pour V^{5+}, la composition chimique du précipité noir-mauve, identifié comme phase A, correspond à la formule $2K_2O.V_2O_4.2V_2O_5(K_2V^{4+}V_2^{5+}O_8)$, en suggérant, dans ce cas, l'équation

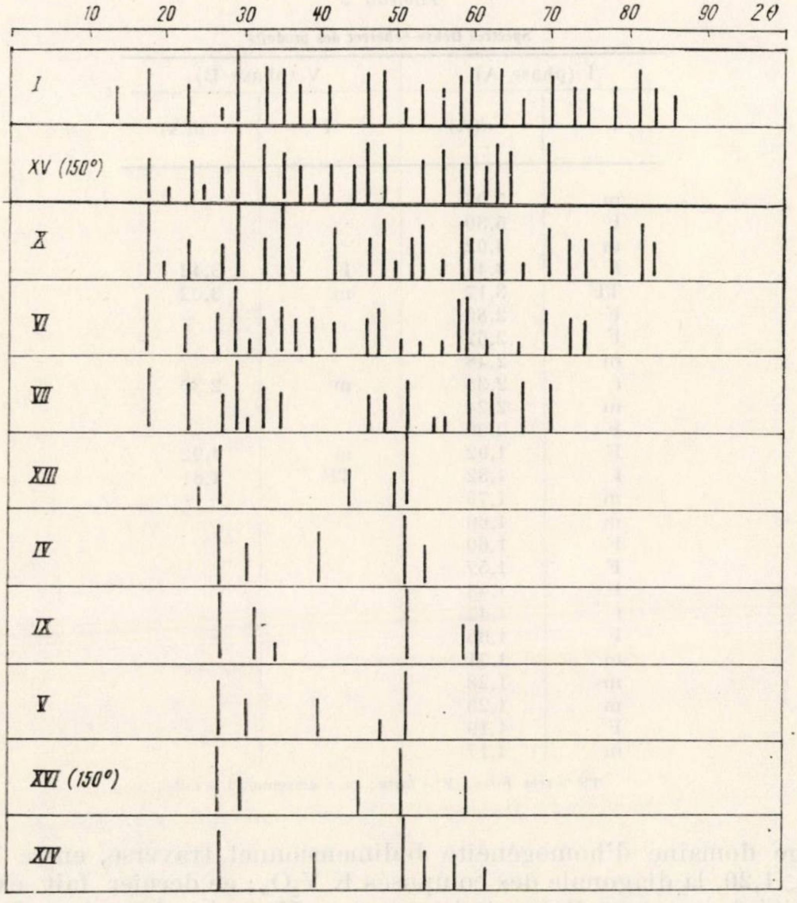

Fig. 1. — Diagrammes Debye-Scherrer des produits.

$$40K^+ + 40VO_3^- + 5VO^{2+} + 2H^+ \rightarrow$$

$$\rightarrow 5K_2V^{4+}V_2^{5+}O_8 + 30K^+ + 3V_{10}O_{28}^{6-} + H_2O \qquad (1)$$

Le composé $K_2V^{4+}V_2^{5+}O_8$ a été obtenu jusqu'à présent seulement par voie sèche et il a été identifié [5,6], comme la limite inférieure, avec $x=0$, de la phase non stœchiométrique φ, $K^+_{2-x}\ V^{4+}_{1+5x}V^{5+}_{2-3x}O^{2-}_{8+2x}$, — dont le large domaine d'homogénéité bidimensionnel traverse, entre $1{,}05 < x < 1{,}20$, la diagonale des composés $K_xV_2O_5$; ce dernier fait explique l'identité des spectres Debye-Scherrer et en IR de la phase A et de celles des produits $K_{0,9}V_2O_5$ ou $K_{1,1}V_2O_5$ (fig. 5, 6).

Tableau 2

Spectres Debye-Scherrer des produits

I (phase A)		V (phase B)	
I	d(Å)	I	d(Å)
m	7,07		
F	5,30		
m	4,02		
f	3,41	F	3,42
TF	3,17	m	3,02
F	2,80		
F	2,62		
m	2,48		
f	2,35	m	2,30
m	2,24		
F	2,00		
F	1,92	m	1,92
f	1,82	TF	1,81
m	1,75		
m	1,66		
F	1,60		
F	1,57		
F	1,48		
f	1,42		
F	1,35		
m	1,31		
m	1,28		
m	1,23		
F	1,19		
m	1,17		

TF = très forte ; F = forte ; m = moyenne ; f = faible.

Pour réaliser, même en ce qui concerne les V^{5+}, un rendement d'environ 100 %, nous avons mené la synthèse du composé $K_2V^{4+}V_2^{5+}O_8$ d'après la stœchiométrie de l'équation

$$2K^+ + 2VO_3^- + VO^{2+} + 2K^+ + 2OH^- \rightarrow$$
$$\rightarrow K_2V^{4+}V_2^{5+}O_8 + 2K^+ + H_2O \qquad (2)$$

Le produit XV (tabl. 1) obtenu de cette façon, identifié comme phase A par des spectres Debye-Scherrer et en IR (fig. 1 et 4), ayant une

---

[5] M. Pouchard, I. Galy, L. Rabardel et P. Hagenmuller, *Compt. rend.*, *Série C*, **264**, 1943 (1967).

[6] M. Pouchard, A. Casalot et S. Villeneuve, *Bull. Soc. chim. France*, **1968**, 81.

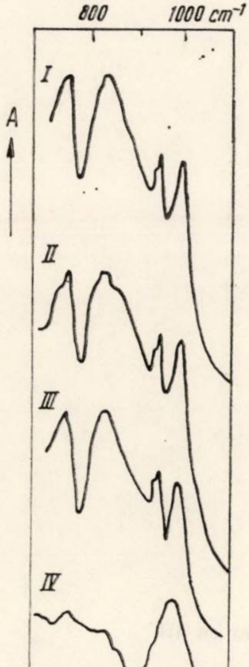

Fig. 2. — Spectres en IR des produits.

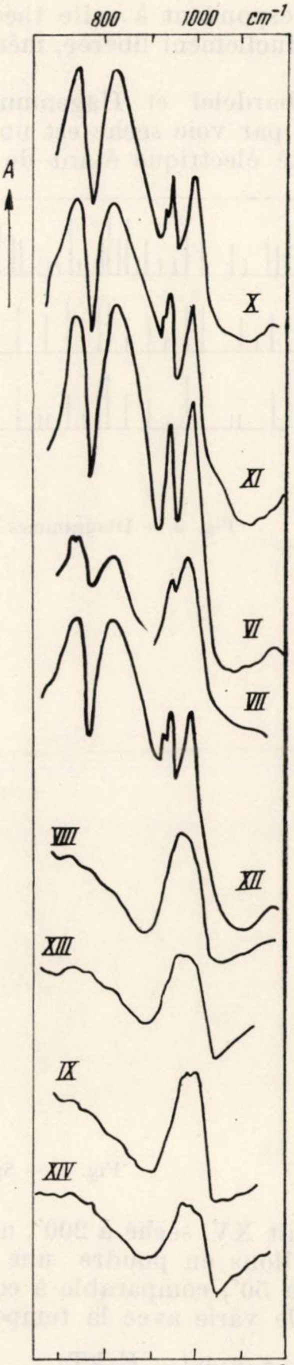

Fig. 3. — Spectres en IR des produits.

Fig. 4. — Spectres en IR des produits.

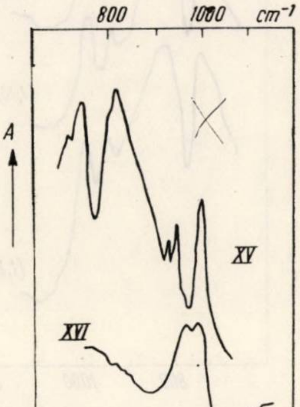

composition chimique correspondant à celle théorique, sépar avec une grande quantité d'eau, graduellement libérée, même à la température ambiante.

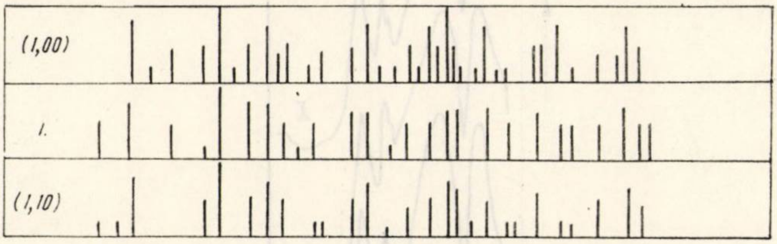

Fig. 5. — Diagrammes Debye-Scherrer.

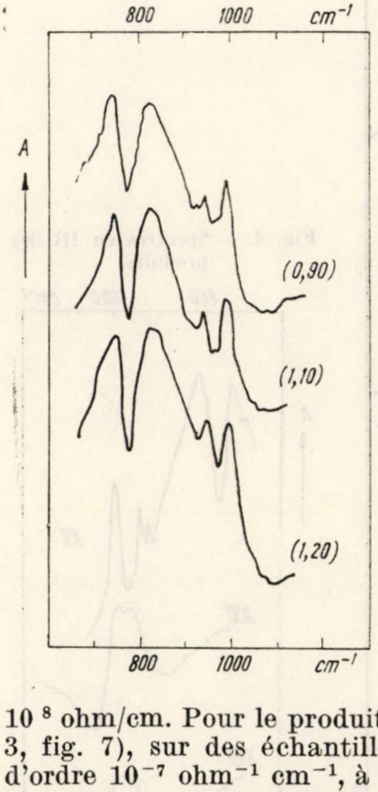

Fig. 6. — Spectres en IR.

Pouchard, Galy, Rabardelel et Hagenmuller [5] ont constaté que le composé $K_2V_3O_8$ préparé par voie sèche est un isolant, à la température ambiante sa résistivité électrique étant de beaucoup supérieure à 10^8 ohm/cm. Pour le produit XV, séché à 200°, nous avons mesuré (tabl. 3, fig. 7), sur des échantillons en poudre une conductivité électrique d'ordre 10^{-7} ohm^{-1} cm^{-1}, à 50°, comparable à celle des phases $K_xV_2O_5$ [6] avec $0,9 < x < 1,0$ laquelle varie avec la température selon la relation

$$\sigma = \sigma_0 \exp.(-E_c/kT) \tag{3}$$

Ce comportement surprenant pourrait être aussi attribué dans ce cas aux impuretés. Des études futures vont élucider ce problème.

Tableau 3

Conductivité électrique et coefficient Seebeck

Produit	Composition chimique (%)				V^{5+}/V^{4+}	$\sigma(\mathrm{ohm}^{-1}\ \mathrm{cm}^{-1})$		E_c (eV)	α (μV/°)
	K_2O	V_2O_4	V_2O_5	H_2O		50°C	200°C		
XV (séché à 200°)	25,66	22,89	51,05	(0,40)	2,03	$0{,}92.10^{-7}$	$2{,}82.10^{-6}$	0,32	+480
XVI (séché à 200°)	10,68	12,79	75,72	(0,80)	5,30	$0{,}82{,}10^{-2}$	$4{,}32.10^{-2}$	0,14	− 98

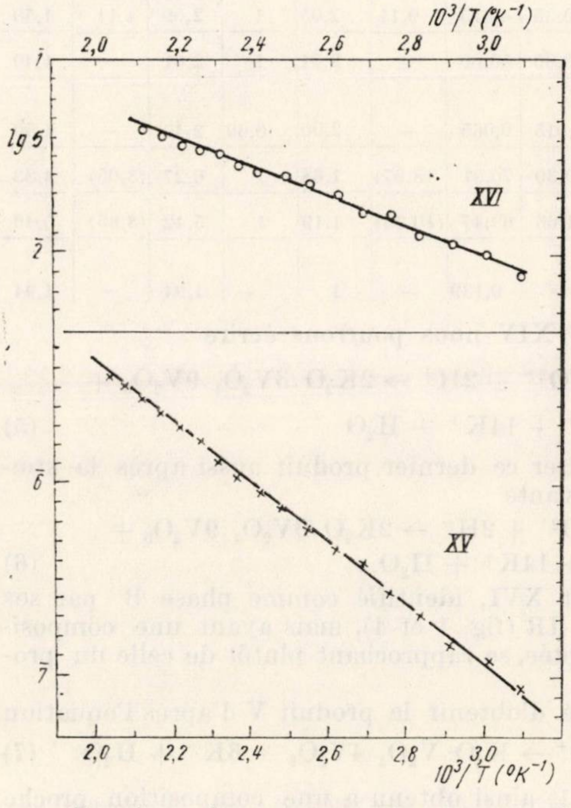

Fig. 7. — Variation de la conductivité électrique des produits en fonction de la température.

Le signe des porteurs de charge, déterminé par des mesures sur l'effet Seebeck, est positif (tabl. 3).

Le produit XV n'est pas oxydable à l'air à la température ambiante ; il résiste à l'action de l'eau bouillante (tabl. 4).

Les précipités de couleur noir verdâtre, contenant la phase B, se forment avec un rendement de 99–100% pour V^{5+} et 25–34 % pour V^{4+} au rapport V^{5+}/V^{4+} égal, 1/1 (produits V et XIV), le pH du filtrat étant d'environ 3,1. Dans le cas du produit V, l'équation probable de la réaction est la suivante

$$8K^+ + 8VO_3^- + 8VO^{2+} + 2H^+ \rightarrow K_2O.V_2O_4.4V_2O_5 + \\ + 6VO^{2+} + 6K^+ + H_2O \qquad (4)$$

Tableau 4

Action de l'eau bouillante

Produit			Composition chimique								
			%				moles				V/K
			K_2O	V_2O_4	V_2O_5	H_2O	K_2O	V_2O_4	V_2O_5	H_2O	
XV	initial		23,79	20,35	46,75	9,11	2,05	1	2,09	4,11	1,50
	traité à l'eau bouillante	résidu	26,27	23,00	50,60	–	2,01	1	2,01	–	1,49
		en solution	0,028	0,015	0,065	–	2,00	0,60	2,40	–	1,50
XVI	après 1 mois		9,82	10,30	70,91	(8,97)	1,68	1	6,27	(8,05)	4,33
	traité à l'eau bouillante	résidu	7,92	11,66	69,47	(10,95)	1,19	1	5,42	(8,65)	5,40
		en solution	0,037	–	0,139	–	1	–	1,94	–	1,94

Dans le cas du produit XIV nous pourrons écrire

$$18K^+ + 18VO_3^- + 18VO^{2+} + 2H^+ \rightarrow 2K_2O.3V_2O_4.9V_2O_5 + \\ + 12VO^{2+} + 14K^+ + H_2O \qquad (5)$$

En essayant de synthétiser ce dernier produit aussi après la stœchiométrie de l'équation suivante

$$18K^+ + 18VO_3^- + 6VO^{2+} + 2H^+ \rightarrow 2K_2O.3V_2O_4.9V_2O_5 + \\ + 14K^+ + H_2O \qquad (6)$$

nous avons obtenu le produit XVI, identifié comme phase B par ses spectres Debye-Scherrer et en IR (fig. 1 et 4), mais ayant une composition différente de celle escomptée, se rapprochant plutôt de celle du produit V (tabl. 1).

Nous avons alors essayé d'obtenir le produit V d'après l'équation

$$8K^+ + 8VO_3^- + 2VO^{2+} + 2H^+ \rightarrow K_2O.V_2O_4.4V_2O_5 + 6K^+ + H_2O \qquad (7)$$

Le produit XVII (tabl. 1) ainsi obtenu a une composition proche de celle escomptée.

Il est alors difficile à décider sur la formulation chimique de la phase B, d'autant plus que les produits contenant cette phase sont oxydables en présence de l'air, même à la température ambiante (tabl. 5), se décomposant aussi sous l'action de l'eau chaude (tabl. 4). On peut constater que la composition chimique des produits V, XVI et XVII contenant la phase B est comparable à celle des phases $K_xV_2O_5$ avec x environ 0,40 – 0,45, mais par analogie avec le composé $Na_4[V_2^{4+}V_8^{5+}O_{26}]^1$,

Tableau 5

Oxydation à l'air, à la température ambiante

Produit	Composition chimique (%)				V^{5+}/V^{4+}	Obs.
	K_2O	V_2O_4	V_2O_5	H_2O		
V	8,55	14,60	67,70	(9,15)	4,22	après 1 jour
	9,04	10,70	72,38	(7,88)	6,10	après 3 jours
	9,72	10,79	72,84	(6,65)	6,15	après 7 jours
XIV	8,23	20,22	64,43	(7,12)	2,90	après 1 jour
	8,32	11,82	72,48	(7,38)	5,60	après 1 mois
	8,17	10,97	73,12	(7,74)	6,29	après 2 mois
	8,14	10,68	74,18	(7,00)	6,30	après 3 mois
XVI	9,49	15,83	64,64	(10,04)	3,76	après 1 jour
	9,65	10,88	70,04	(9,43)	5,80	après 17 jours
	9,82	10,30	70,91	(8,97)	6,25	après 1 mois
	10,59	11,89	74,82	(2,7)	5,73	après 1 mois chauffé jusqu'à 250°
	10,55	12,12	77,20	—	5,80	— " — 350°
	10,74	17,40	72,12	—	3,75	— " — 500°

on pourra aussi formuler la composition chimique de la phase B comme $K_2H_2[V_2^{4+}V_8^{5+}O_{26}]$.

Le produit XVI (contenant la phase B) a une conductivité électrique d'ordre 10^{-2} ohm^{-1} cm^{-1}, à 50°, laquelle augmente par rapport à la température d'après la relation (3) (fig. 7). Ces données et le signe négatif de l'effet thermoélectrique, indiquant une semi-conductivité de type *n* (tabl. 3), sont comparables aux propriétés analogues des phases $K_xV_2O_5$ avec x environ 0,40–0,50 [7,8]

PARTIE EXPÉRIMENTALE

Les produits I–V ont été préparés en utilisant des solutions aqueuses 1M de KVO_3, pH ~ 7, 6, et de VOC_2O_4, pH ~ 1,2. Les solutions chauffées jusqu'à l'ébullition ont été mélangées dans les rapports donnés au tableau 1 et les précipités noirs formés ont été filtrés après 24 heures.

Pour les autres produits on a utilisé, comme source des ions VO^{2+}, des solutions aqueuses 1M de $VOSO_4$, au pH ~ 2 pour *les produits* VI–IX et au pH ~ 1,2 pour les produits X–XIV.

Le produit XV a été synthétisé en mélangeant, à froid, 50 ml de solution 1M KVO_3 avec 25 ml de solution 1M $VOSO_4$ (pH du mélange 3,7) ; en y ajoutant 2,8 g KOH, le pH augmente jusqu'à 6,8. On a fait bouillir le mélange 1 minute. Après le refroidissement, on a ajouté 25 ml de solution saturée de CH_3COOK. Le jour suivant on a filtré et lavé à l'eau le précipité noir, en le séchant sous vide 24 h.

Le produit XVI a été obtenu en mélangeant à chaud et en faisant bouillir, 1 mn, 90 ml de solution 1M KVO_3 avec 30 ml de solution 1M $VOSO_4$, acidifié avec 0,25 ml de H_2SO_4 conc. Le précipité vert-noir a été lavé à l'eau et à l'alcool et séché, sous vide, 24 heures.

---

[7] I. Lukács, C. Strusievici et C. Liteanu, *Rev. Roumaine Chim.*, **13**, 713 (1968).

[8] I. Lukács, C. Strusievici et C. Liteanu, *Rev. Roumaine Chim.*, **14**, 647 (1969).

Le produit XVII a été synthétisé en mélangeant à chaud et en faisant bouillir, 1 mn, 50 ml de solution 1M KVO_3 et 12,5 ml de solution 1M $VOSO_4$, acidifié avec 0,3 ml de H_2SO_4 conc. Le précipité de couleur vert-noir a été lavé à l'eau et séché sur P_2O_5 pendant 24 heures, puis lavé à l'alcool et séché, sous vide, pendant 24 heures.

Les spectres en IR ont été enregistrés sur des échantillons en nujol à l'aide d'un spectromètre UR-10 Zeiss, Jéna.

Les spectres Debye-Scherrer ont été obtenus avec anticathode de cuivre à l'appareillage TUR-M-60, Dresden.

Le pouvoir thermoélectrique et la conductibilité électrique ont été mesurés sur des échantillons en poudre, en présence de l'air, en utilisant une cellule aux électrodes en platine décrite dans [8].

Revue Roumaine de Chimie, **15**, 945–949 (1970)

KINETIC MEASUREMENT OF COBALT TRACES. III* WITH PONCEAU RED

D. COSTACHE

Department of Analytical Chemistry, University of Bucharest
Splaiul Independenţei, 89

Received July 29, 1969

Cobalt traces are measured by means of the kinetic method by making use of its catalytic action on the oxidation reaction between ponceau red and peroxide in an alkaline medium. The method may be used in the range 3.78×10^{-9} g Co/cm^3 – 28.35×10^{-9} gCo/cm^3.

The catalytic effect of cobalt on the oxidation reaction of some organic substances with peroxide in an alkaline medium (substances presenting two hydroxyl groups in *ortho* position) is well known in literature and different methods of measuring cobalt traces were established on this basis. [1–20]

[*] Part II: D. Costache and Gr. Popa, *Rev. Roumaine Chim.*, **15**, 761 (1970).

[1] J. Bognar, *Mikrochim. Acta*, **4**, 801 (1963).

[2] E. Schulek and J. L. Paszlovski, *Mikrochim. Acta*, **1**, 41 (1960).

[3] N. B. Parhomenko, G. A. Prik and K. B. Iatsimirski, *Zhur. analit. Khim.*, **16**, 599 (1961).

[4] J. Bognar and L. Sipoş, *Mikrochim. Acta*, **5**, 442 (1963).

[5] J. Bognar and O. Jellinek, *Acta Chim. Acad. Sci. Hung.*, **29**, 21 (1961).

[6] J. Laszlovski, *Mikrochim. Acta*, **2**, 289 (1961).

[7] J. Bognar and O. Jellinek, *Acta Chim. Acad. Sci. Hung.*, **29**, 131 (1961); **29**, 139 (1961); **29**, 319 (1961).

[8] J. Bognar, *Magyar Kém. Folyóirat*, **59**, 25 (1953).

[9] A. K. Babko and N. M. Lukovskaia, *Ukrain, khim. Zhur.*, **28**, 968 (1962).

[10] V. M. Peshkova, J. F. Dolmanova and N. M. Chemenova, *Zhur. analit. Khim.* **18**, 1228 (1963).

[11] E. A. Bozhevolnov and S. U. Kreingold, *Tr. Vses. Nauk*, from *Ref. Zhur. Khim.*, **26**, 204 (1966).

[12] J. Bognar, *Mikrochim. Acta*, **5**, 901 (1961).

[13] S. G. Oradovski, *Khim. Protsesy Moyakh Okeanakh Akad. Nauk.*, **1966**, 78.

[14] S. U. Kreingold and E. A. Bozhevolnov, *Metody Anal. Khim. Reaktiv i Preparatov*, **11**, 49 (1965).

[15] A. K. Babko and N. M. Lukovskaia, *Ukrain, Khim. Zhur.*, **30**, 508 (1964).

[16] J. Laszlovski, *Magyar Kém. Folyóirat*, **71**, 260 (1965); **71**, 99 (1965).

[17] Gr. Popa and D. Costache, *Analele Universităţii Bucureşti*, **16**, 107 (1967).

[18] Gr. Popa and D. Costache, *Rev. Roumaine Chim.*, **12**, 963 (1967).

[19] Gr. Popa and D. Costache, *Analele Universităţii Bucureşti*, **17**, 21 (1968).

[20] D. Costache and Gr. Popa, *Analele Universităţii Bucureşti*, **17**, 55 (1968).

Later on we have found out that substances of another class too, azoderivates presenting a hydroxyl group in *ortho* position as against the azo group, oxidized in the same conditions as the dioxiderivates, may be used as indicators for kinetic methods of cobalt measurements. [21]

In the present paper one makes use, as indicator reaction, of the reaction between Ponceau red, having the formula

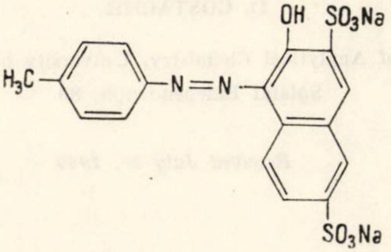

and peroxide in alkaline medium.

EXPERIMENTAL

Reactives : the reaction solution was obtained by solving Ponceau red in water (0.118 %).

The peroxide, obtained by diluting hydrogen peroxide, had a 5.14 % concentration, verified every hour by filtering with potassium permanganate.

The alkaline medium of the reaction was obtained by using a solution of potassium hydroxide 1N.

The cobalt solution was obtained by solving spectrally pure metallic cobalt in weak sulphuric acid.

For all solutions tridistilled water was used.

Apparatus : the measurements were carried out with a horizontal Pulfrich Zeiss Jena spectrophotometer at a wavelength of $\lambda = 496$ nm.

Working method : the reaction mixture is made in 25 cm^3 flasks by adding the solutions in the following order : buffer, reactive, peroxide cobalt, so that in the spectrophotometer vat the concentration of the substances be as follows :

Ponceau red	4.70×10^{-5} g/cm^3
Peroxide	4.10×10^{-3} g/cm^3
Cobalt	$3.78 \times 10^{-9} - 28.35 \times 10^{-9}$ g/cm^3

As colourless products appear after the oxidizing reaction, water is poured into the reference sample.

To establish optimum reaction conditions we have first noted the influence of the pH on the reaction rate. Results are shown on graph 1.

After examination it resulted that the reaction rate is maximum in the pH range 11.5–13.4.

The peroxide also influences the reaction rate up to a certain concentration, showing a certain stability in the range from 2.40×10^{-3} to 4.80×10^{-3} g H_2O_2/cm^3, as shown in graph 2.

---

[21] GR. POPA and D. COSTACHE, *Rev. Roumaine Chim.*, **13**, 573 (1968).

RESULTS AND DISCUSSIONS

The order of reaction is most important for the application of the corresponding kinetic relationships.

The reaction order was established by the method of fractionation time and the graphic method. Experimental results show that we are confronted with reactions well described by order one relationships.

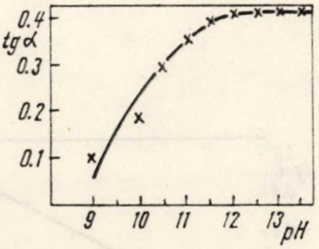

Fig. 1. — Influence of pH on reaction rate.

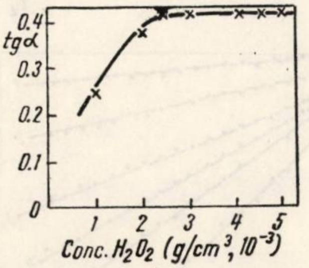

Fig. 2. — Influence of peroxide concentration on reaction rate.

This seems natural if we take into consideration the fact that cobalt is a catalyst (therefore not entering the kinetic reaction order) and the concentration of the peroxide is so high as compared to that of the reactive, that from a practical point of view it is considered constant. One can thus state that the reaction is pseudomonomolecular in regard to the concentration of the organic reactive.

The reaction rate for order one reactions is expressed by:

$$\frac{dx}{dt} = k(a - x) \tag{1}$$

After integration and binding the concentration of the reactive to the optical density of the medium by means of Lambert-Beer's relationship, we obtain

$$\ln D = \ln D_0 - kt \tag{2}$$

We have observed the variation of optical density of the reaction mixture for 20 minutes.

Representing graphically these values in semilogarithmic coordinate, we obtain graph 3.

The results will lead us, accordind to relationship (2) to straight lines, which differ from one another by their angle with the abscissa.

We have adopted the "tangent variant" which consists in the measurement of these lines' angles and the representing of the corresponding tangents *versus* the cobalt concentration, as in graph 4.

Revue Roumaine de Chimie, 15, 945–949 (1970)

This is the gauging graph, by means of which one determines the cobalt concentration in the case of an unknown sample, after having worked by the same method.

We have established the values of the rate constants for catalytic and uncatalytic reactions according to relationship :

$$k = \frac{\lg D_1 - \lg D_2}{t_2 - t_1} .2.303 \qquad (3)$$

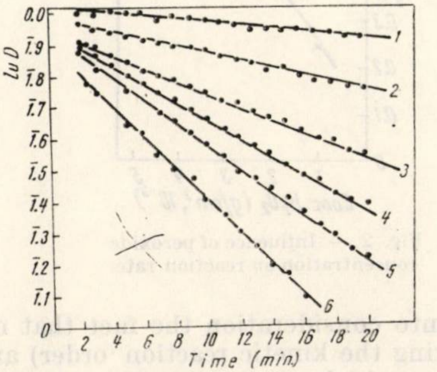

Fig. 3. — Variation of ln D value versus time ;

1, g Co/cm³; *2*, 3.78 × 10⁻⁹ g Co/cm³ ; *3*, 9.45 × 10⁻⁹ g Co/cm³ ; *4*, 15.12 × 10⁻⁹ g Co/cm³ ; *5*, 18.90 × 10⁻⁹ g Co/cm³ ; *6*, 28.35 × 10⁻⁹ g Co/cm³.

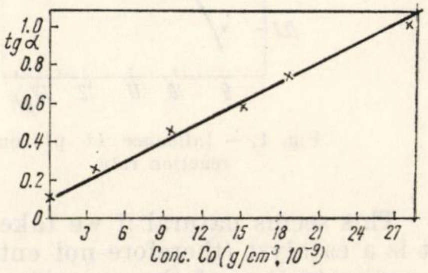

Fig. 4. — Variation of tg α value *versus* cobalt concentration.

We have represented these values *versus* the cobalt concentration, obtaining a new standard graph, that compared to graph 4 has the advantage of being quicker.

The influence of temperature on the reaction rate is shown in table 1.

Table 1

Influence of temperature on rate constant

t°C	k (min⁻¹)
15	0.46×10^{-2}
20	1.24×10^{-2}
25	2.90×10^{-2}
30	2.99×10^{-2}
35	5.54×10^{-2}

This shows that temperature strongly influences the reaction rate ; in order to preserve a good reproducibility, the measurements were made at constant temperature (20°) by adapting a metallic device which enables water, at a certain temperature, to pass around the vats.

The measurements are disturbed by the presence of the following alien ions : Ni^{2+}, Fe^{2+}, Fe^{3+}, Os^{8+} if their ratio to the cobalt is higher than 1,000 : 1.

Table 2 illustrates the reproducibility of the method.

Table 2

Reproducibility of the method

Conc. Co g/cm³	∡ α°	tg α	Conc. Co found g/cm³.10⁻⁹	Difference g/cm³.10⁻⁹
3.78×10^{-9}	13	0.230	—	—
1	13	0.230	3.78	—
2	14	0.249	4.34	0.56
3	13	0.230	3.78	—
4	12	0.212	3.21	0.56
5	13	0.230	3.78	—
9.45×10^{-9}	23	0.424	—	—
1	23	0.424	9.82	0.37
2	23	0.424	9.82	0.37
3	24	0.445	10.39	0.94
4	23	0.424	9.82	0.37
5	22	0.404	9.26	0.19
15.12×10^{-9}	30	0.577	—	—
1	30	0.577	14.55	0.56
2	29	0.554	13.98	1.13
3	28	0.531	13.23	1.89
4	31	0.600	15.30	0.19
5	30	0.577	14.55	0.56
18.90×10^{-9}	36	0.726	—	—
1	36	0.726	19.26	0.37
2	37	0.753	20.03	1.13
3	37	0.753	20.03	1.13
4	35	0.700	18.54	0.37
5	36	0.726	19.26	0.37
28.35×10^{-9}	45	1.000	—	—
1	46	1.035	29.10	0.75
2	45	1.000	28.16	0.19
3	47	1.072	30.24	1.89
4	45	1.000	28.16	0.19
5	45	1.000	28.16	0.19

It therefore results that the method allows to determine the cobalt in a range from 3.78×10^{-9} g Co/cm³ to 28.35×10^{-9} g Co/cm³ with a good reproducibility.

Revue Roumaine de Chimie, **15**, 951–953 (1970)

THE CELL PARAMETERS OF STRONTIUM HYDROXYAPATITE, $Sr_{10}(PO_4)_6\,(OH)_2$

V. M. BHATNAGAR *

Fisk University, Nashville, Tennessee 37203, USA

Received July 21, 1969

High-precision, computer-refined values of the cell parameters of strontium hydroxyapatite, $Sr_{10}(PO_4)_6(OH)_2$, have been determined with an X-ray diffractometer, internally standardized by means of sodium chloride. The results obtained are as follows : $a = 9.7667$ Å, $c = 7.2883$ Å, $c/a = 0.746$, volume = 602.1 Å^3.

The apatites form a group of structurally very closely related substances and hydroxyapatite, $Ca_{10}(PO_4)_6(OH)_2$, is well known. The ionic radii of Ca^{++}(0.99Å) and Sr^{++}(1.13 Å) are close together and strontium can replace calcium in the hydroxyapatite lattice. The X-ray structural determination on strontium hydroxyapatite was carried out as early as 1939 by Klement[1] who established the basic *ortho*phosphate configuration.

The strontium hydroxyapatite of this investigation was prepared by thoroughly mixing stoichiometric amounts of $Sr(NO_3)_2$, KOH, and KH_2PO_4 according to the following reaction :

$$10Sr(NO_3)_2 + 14\,KOH + 6\,KH_2PO_4 \rightarrow Sr_{10}\,(PO_4)_6\,(OH)_2 +$$

$$+ 20\,KNO_3 + 12\,H_2O$$

Two computer programmes were used for calculating the cell parameters and for indexing the diffraction lines. The programmes had to be re-written into Fortran IV in order to be compatible with the IBM digital computer model 360/40. The CELFIT programme,[2] when supplied with sets of Miller indices, corresponding values of the Bragg angle, and a set of approximate cell dimensions, refines any or all of the latter by the method of least-squares until the shifts in these parameters fall below specified limits. The GENRAT programme,[3] when supplied with sets of unit cell dimensions, generates all possible $h\ k\ l$ reflections between two specified values of the Bragg angle.

---

* Present address : Department of Chemistry, The University of New Brunswick, Fredericton, New Brunswick/Canada.

[1] R. Klement, *Z. anorg. Chem.*, **242**, 215 (1939).

[2] B. H. Bracher, U. K. Rep. A.E.R.E.-R5412, 1967.

[3] C. W. F. T. Pistorius, C.S.I.R., Pretoria, 1968.

Table

The Cell Parameters of Strontium Hydroxyapatite, $Sr_{10}(PO_4)_6(OH)_2$ Radiation = Cuλ 1.54178 Å ; I/I_1 = Diffractometer ; system = hexagonal ; a = 9.7667 Å, c = 7.2883 Å, c/a = 0.746, volume = 602.1 Å^3

hkl	I/I_1	dÅ (observed)	dÅ (calculated)
0 2 0	11	4.220	4.229
1 1 1	5	4.046	4.057
0 0 2	19	3.639	3.644
0 1 2	20	3.344	3.347
1 2 0	15	3.208	3.197
1 1 2	100	2.921	2.921
0 2 2	6	2.762	2.761
0 1 3	6	2.339	2.335
1 1 3	8	2.175	2.175
0 2 3	5	2.106	2.107
2 2 2	19	2.027	2.028
1 3 2	14	1.972	1.973
2 3 1	11	1.875	1.875
0 3 3	11	1.841	1.840
0 4 2	15	1.829	1.829
0 0 4	16	1.823	1.822
2 4 0	3	1.598	1.598
1 2 4	6	1.583	1.583
0 3 4	7	1.531	1.530
2 3 3	7	1.517	1.516
3 3 2	9	1.487	1.486
1 4 3	3	1.471	1.470
3 4 1	3	1.366	1.366
2 5 0	4	1.356	1.354
2 4 3	4	1.337	1.335
2 5 1	7	1.332	1.332
1 2 5	7	1.327	1.326
1 4 4	8	1.296	1.297
0 3 5	8	1.296	1.295
1 6 1	6	1.271	1.270
4 4 0	3	1.221	1.221
0 1 6	3	1.203	1.202
0 4 5	3	1.200	1.200
1 1 6	5	1.180	1.179
0 2 6	4	1.167	1.168
1 5 4	4	1.167	1.167
1 4 5	3	1.145	1.144
2 2 6	4	1.088	1.088
0 4 6	5	1.054	1.053
1 5 5	4	1.052	1.052
2 7 1	2	1.024	1.023
1 7 3	3	1.017	1.017
0 8 2	5	1.015	1.015
0 6 5	3	1.012	1.013
1 8 2	3	0.955	0.955

A Philips wide-range goniometer model PW-1050 was used with sodium chloride as an internal standard. The angular positions of all peaks were taken at points in the centre of the peaks and their baselines. The intensities listed for the various *h k l* reflections are given in terms of their heights above background, taken relative to the strongest peak as intensity *1 0 0*.

The results obtained are shown in Table. The cell parameters quoted are based on the best fit obtained by the least-squares programme. Both calculated and observed interplanar spacings have been given for the sake of completeness.

The X-ray measurements indicate that strontium hydroxyapatite crystallizes in hexagonal lattice and it may be isomorphous with calcium hydroxyapatite. The lattice constants of calcium and strontium hydroxyapatites are given below:

$Ca_{10}(PO_4)_6(OH)_2$ $a = 9.4192$ Å, $c = 6.8867$ Å, $c/a = 0.731$

$Sr_{10}(PO_4)_6(OH)_2$ $a = 9.7667$ Å, $c = 7.2883$ Å, $c/a = 0.746$

Due to the large cation, the hexagonal axes of strontium hydroxyapatite are longer than those of calcium hydroxypatite. It seems that more strontium ions are built into the lattice above each other in the direction of the *c*-axis than beside each other in the direction of the a-axis.

The apatite work was supported by research grant DE-02105 from the United States Department of Health, Education, and Welfare. I thank Dr. W. R. Liebenberg, Dr.S.A. Hiemstra, and Dr. H.V.R. von Rahden of National Institute for Metallurgy-South Africa for their interest and valuable help and Prof. Nelson Fuson and Prof. James R. Lawson of Fisk University for fruitful discussions.

Revue Roumaine de Chimie, **15**, 955–956 (1970)

NEW OBSERVATIONS ON LEAD APATITES[1]

V. M. BHATNAGAR *)

Faculté des Sciences de Toulouse, Toulouse, France

Received July 24, 1969

New methods of preparation of lead fluorapatite, $Pb_{10}(PO_4)_6F_2$, and lead hydroxyapatite, $Pb_{10}(PO_4)_6(OH)_2$, are reported. The presence of OH in hydroxyapatite sample was ascertained by infrared spectroscopy. The unit cell dimensions are as follows: $Pb_{10}(PO_4)_6F_2$, $a = 9.78$ Å, $c = 7.30$ Å, $c/a = 0.746$; $Pb_{10}(PO_4)_6(OH)_2$, $a = 9.87$ Å, $c = 7.41$ Å, $c/a = 0.750$.

Several preparations of lead fluorapatite, $Pb_{10}(PO_4)_6F_2$, were made by a new and simple procedure:

$$6(NH_4)_2HPO_4 + 9Pb(CH_3COO)_2 \rightarrow 3Pb_3(PO_4)_2 + 12CH_3COONH_4 + 6CH_3COOH$$

$$2NH_4F + Pb(CH_3COO)_2 \rightarrow PbF_2 + 2CH_3COONH_4$$

$$6(NH_4)_2HPO_4 + 2NH_4F + 10Pb(CH_3COO)_2 \rightarrow Pb_{10}(PO_4)_6F_2 + 14CH_3COONH_4 + 6CH_3COOH$$

The solutions of NH_4 were mixed and added dropwise to a continuously stirred solution of lead acetate at room temperature (23°). The lead fluorapatite which had formed was removed by filtration, washed with distilled water and dried at about 100°.

When the quantities used were,

$$(NH_4)_2HPO_4 = 3.96 \text{ g/250 ml}$$

$$NH_4F = 0.37 \text{ g/100 ml}$$

$$Pb(CH_3COO)_2 = 16.26 \text{ g/250 ml}$$

the lead fluorapatite, $Pb_{10}(PO_4)_6F_2$, with the unit cell dimensions, $a = 9.78$ Å, $c = 7.30$Å, and $c/a = 0.746$ was obtained. As the quantities

---

[1] Supported by Office National Industriel de l'Azote (France).

*) Present address: Department of Chemistry, The University of New Brunswick, Fredericton, New Brunswick/Canada.

of NH_4F were changed to halves i.e. 0.18 g/100 ml and 0.09 g/100 ml, the following results, respectively, were obtained :

$$NH_4F = 0.18\ \text{g}/100\ \text{ml}$$

$$a = 9.81\ \text{Å}$$

$$c = 7.30\ \text{Å}$$

$$c/a = 0.744$$

$$NH_4F = 0.09\ \text{gm}/100\ \text{ml}$$

$$a = 9.87\ \text{Å}$$

$$c = 7.41\ \text{Å}$$

$$c/a = 0.750$$

The experimental conditions were the same for every preparation i.e. the ammonium solutions were mixed together and added dropwise to lead acetate solution at room temperature. The lead solution was stirred continuously during ammonium addition. The precipitate was filtered, washed with distilled water and dried at 100°.

It is evident that the lowering in the quantity of NH_4F apparently affects the *a* dimension of apatite. The increase in *a* constant is as follows : $0.09 > 0.18 > 0.37$ i.e. the length of *a* axis increases as the amount of NH_4F is decreased. It seems that the fluoride ions do not take part in the reaction with 0.09 g NH_4F quantity and a product identical to lead hydroxyapatite, $Pb_{10}(PO_4)_6(OH)_2$, is formed ($a = 9.87$ Å, $c = 7.41$ Å, $c/a = 0.750$). The presence of OH in this sample was ascertained by infrared spectroscopy. Its spectrum showed clear evidence of the vibration at 3545 cm^{-1}. To see the effect of absence of NH_4F on the reaction, stoichiometric quantities of only $(NH_4)_2HPO_4$ and $Pb(CH_3COO)_2$ were used. The following lattice constants resulted from the cell based on the space group C_{6h}^2 : $a = 9.88$Å, $c = 7.41$Å, $c/a = 0.750$. Every reflection in the X-ray pattern could be indexed on the basis of the above values and the agreement between calculated and observed d-values was excellent.

The infrared spectra of lead fluorapatite, $Pb_{10}(PO_4)_6F_2$ and lead hydroxyapatite, $Pb_{10}(PO_4)_6(OH)_2$, were measured in the $4000-400\ \text{cm}^{-1}$ region with a Perkin-Elmer 337 Infrared Spectrophotometer. The KBr pellet technique was employed. Major peaks in the spectra were : for lead fluorapatite, $Pb_{10}(PO_4)_6F_2$, 535, 565 *vs* ($\nu_4PO_4^{3-}$), 935 vw ($\nu_1PO_4^{3-}$), and 950 to 1060 cm^{-1} *vs*, br($\nu_3PO_4^{3-}$). For lead hydroxyapatite, $Pb_{10}(PO_4)_6(OH)_2$, 530, 544, 565 *vs* ($\nu_4PO_4^{3-}$), 915 vw ($\nu_1PO_4^{3-}$), 950 to 1050 vs, br($\nu_3PO_4^{3-}$), and 3545 cm^{-1} (ν_sOH). Anal. *Calcd.* for $Pb_{10}(PO_4)_6F_2$: Pb, 77.30 ; PO_4, 21.27. *Found* : Pb, 77.27 ; PO_4, 21.12. *Calcd.* for $Pb_{10}(PO_4)_6(OH)_2$: Pb, 77.42 ; PO_4, 21.30. *Found* : Pb, 77.40 ; PO_4, 21.25.

The fluorapatite and hydroxyapatite melt at 1022° and 1000°, respectively. They are insoluble in several known solvents but slightly dissolve in nitric acid.

Revue Roumaine de Chimie, 15, 957–964 (1970)

THE INFLUENCE OF PHOSPHOROUS PENTOXIDE ON THE CRYSTALLIZATION PROCESS OF SOME LITHIUM SILICATE GLASSES

S. SOLACOLU, P. BALTĂ and GEORGETA JITIANU

Institute of Physical Chemistry

Bucharest, Str. Dumbrava Roşie, 23

Received December 16, 1969

Using a differential thermal analysis, electronic microscopy and roentgenography one has investigated the action of P_2O_5 on the crystallization process of some lithium-silicate glass. One has established that P_2O_5 accelerates noticeably the separation of the vitreous microphases, and determines the initiation of the crystallization process at a temperature by more than 100° lower than for any glass without P_2O_5. At higher concentrations of P_2O_5 an important increase in the rate of nucleation and the rate of crystal growth takes place.

The theoretical and practical importance of the crystallization process of glass was stimulated, especially, these later years, by the discovery of glass-ceramic masses of technical importance in different fields. The mechanism and kinetics of nucleation and crystallization of glass, as well as their influencing factors, form the subject of many a research.[1,2]

To obtain high quality glass-ceramic masses, one must control the nucleation process in order to establish optimum conditions for a uniform crystallization in the bulk of the glass and thus obtain a microcrystalline structure.

Owing to the fact that for the majority of common glass sorts the homogeneous nucleation is very low, the above mentioned conditions can be obtained only by introducing into the glass some substances with a nucleator role and thus determining a heterogeneous nucleation.

The properties of glass-ceramic masses depend on the nature and properties of the crystals appearing in the system. From this point of view, the lithium-silicate and aluminium-lithium silicate present the advantage that the formed crystalline phase, which contains lithium disilicate or lithium aluminosilicate, produces a glass ceramic mass with

---

[1] P. W. McMillan, "Glass-Ceramics", Academic Press, London and New York, 1964, p. 195.

[2] R. F. Stricland Cristable, "Kinetics and Mechanism of Crystallization", Academic Press, London, New York, 1968, p. 76.

mechanical, chemical and electrical properties of various uses. Some recent papers show that for these glass sorts, there is an advantage to use P_2O_5 rather than other nucleators both from the technological and from the crystalline mass properties point of view.[3,4].

Considering the above remarks, the authors tried to obtain further information on the nucleating action of P_2O_5 in lithium-silicate glasses and to select the proper methods to be used, both in research and industry in order to study the crystallization process.

PREPARATION OF SAMPLES

One has chosen a binary glass with 12.5% Li_2O(62.7% $Li_2O \cdot 2SiO_2$) and 1,2,3% of P_2O_5 was added to it.

The glass was melted in an electric furnace in the same conditions as in our previous work.[5] The content in P_2O_5 of the glass fell to 0.91, 1.23 and 1.73% respectively due to volatilization.

The crystallization of these samples was studied using differential thermal analysis and some variants of this method, roentgen-structural analysis, and electronic microscopy.

Determination of the nucleator's optimum content

It is known, that in the case of a reduced homogeneous nucleation the crystallization process begins at the separating interfaces of the phases, usually from the outer surface of the glass object, where the nucleation is favoured by the lack of balance of the chemical forces. One can show the influence of the surface on the crystallization process by using differential thermal analysis on pulverulent glass samples with the same composition, but with different specific surface areas (different granulometry). The thermogramme of the sample with a larger specific surface area, crystallizing easier, shows that the maximum of the exothermic effect appears at a lower temperature, than with the sample of a small specific surface area.

An interesting method to establish the optimum nucleator content consists in the comparison of its effect with the surface influence. [6] The nucleator working in the whole glass bulk will tend to blot out the influence of the difference in specific surface area. One can consider as an optimum nucleator content a concentration for which the difference between the maximum exothermal temperatures of the samples with different granulometry is null, showing therefore, that the nucleation process is uniform in the whole volume and is no longer influenced by the surface area. The temperature difference between the two maxima can be obtained by making only one differential thermal analysis, putting the sample with coarse particles instead of the reference substance. The crystallization of the sample with coarse particles appears as an endothermal effect.

---

[3] Eunio Sakka and Megumi Tashiro, *J. Ceram. Assoc. Japan*, **69**, 67 (1961).

[4] S. V. Phillips and P. W. McMillan, *Glass. Technol.*, **6**, 46 (1965).

[5] S. Solacolu, P. Baltă and G. Jitianu, *Rev. Roumaine Chim.*, (in press).

[6] T. Thiagarajan, *Central Glass Ceramic Res. Inst. Bull. India*, **13**, 33 (1966).

The thermogrammes obtained for the samples with different P_2O_5 content, using these techniques are shown in figure 1. Figure 2 represents the difference between the temperatures of the two thermal effects vs. the nucleator concentration.

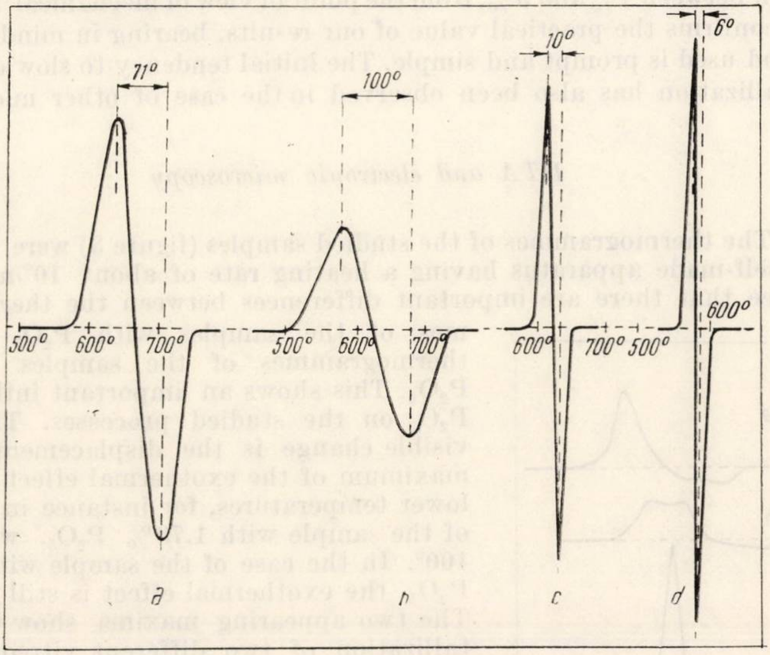

Fig. 1. — Thermogrammes of the samples containing different concentrations of P_2O_5, coarse particles serving as reference material for the fine particles : *a*, without P_2O_5 ; *b*, 0.91% P_2O_5, *c*, 1.23% P_2O_5 ; *d*, 1.73% P_2O_5.

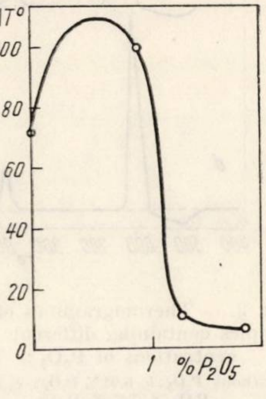

Fig. 2. — Variation of the temperature difference of the maximum exothermic effects of the samples with different granulometry at various P_2O_5 concentrations.

As can be seen, at a low P_2O_5 content (under 1%), the P_2O_5 does not help the nucleation process and even delays it.

At high concentrations, the sharp droping of the temperature difference between the two thermal effects, shows a sensible increase on the nucleator influence of P_2O_5.

From the aspect of the curve, it may be said that the optimum content of the nucleator, from the point of view of the crystallization's uniformizing process is about 2.5%.

Some works have shown as an optimum content a P_2O_5 concentration between 4% and 5%, from the point of view of mechanical strength. This confirms the practical value of our results, bearing in mind that the method used is prompt and simple. The initial tendency to slow down the crystallization has also been observed in the case of other nucleators.[3]

DTA and electronic microscopy

The thermogrammes of the studied samples (figure 3) were obtained in a self-made apparatus having a heating rate of about 10°/min. One can see that there are important differences between the thermogrammes of the samples with P_2O_5 and the thermogrammes of the samples without P_2O_5. This shows an important influence of P_2O_5 on the studied processes. The most visible change is the displacement of the maximum of the exothermal effect towards lower temperatures, for instance in the case of the sample with 1.73% P_2O_5, with over 100°. In the case of the sample with 1.91% P_2O_5, the exothermal effect is still broader. The two appearing maxima show the crystallization of two different vitreous structures and suggest that their thermal effects are interfering with one another.

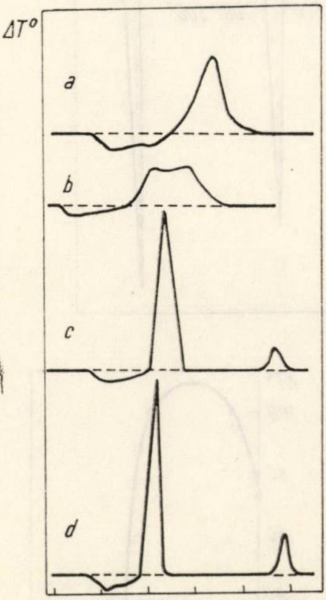

Fig. 3. — Thermogrammes of the samples containing different concentrations of P_2O_5 :
a, without P_2O_5; *b*, 0.91% P_2O_5; *c*, 1.23% P_2O_5, *d*, 1.73% P_2O_5.

From the aspect of the thermogramme one can conclude that the crystallization is slower, which corresponds entirely to the conclusions drawn from figure 2.

These particularities made us repeat the synthesis of the sample with 0.91% P_2O_5 and the determinations. The reproductibility was pretty good.

For samples with higher P_2O_5 concentrations, the exothermal effects are of higher amplitudes and narrower, showing an intensification of the crystallization process.

One notices a second smaller exothermal effect, for example at 830° for the sample with 1.23% P_2O_5 and at 880°, for the sample with 1.73% respectively.

The roentgenogrammes (figure 4) of the samples after DTA show the presence of lithium disilicate, to which, in the presence of P_2O_5, cristobalite crystals are added.

If the roentgenographic analysis is made on samples heated only up to the first exothermal effect temperature, one obtains the same patterns with visible lines of cristobalite.

This result seems to show that the second exothermal effect is not due to the crystallization of a new phase, but to an eventual transformation of one of the existing crystalline phases as was also shown in paper [7].

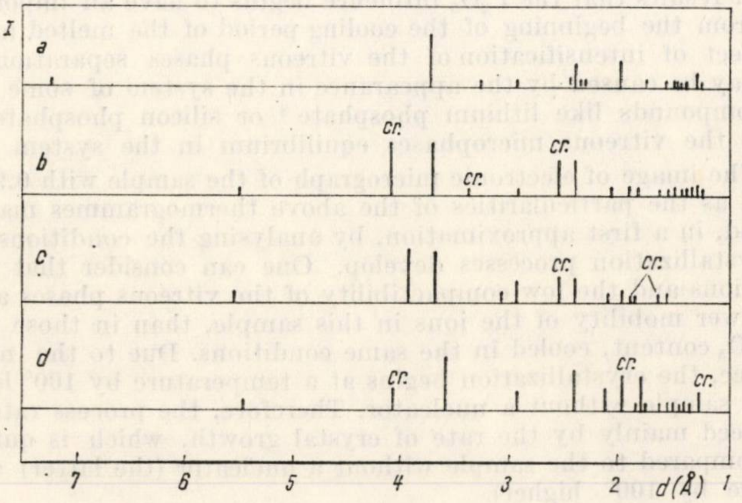

Fig. 4. — Lines which apear on the roentgenogrammes of the samples at various concentrations of P_2O_5 :
a, $Li_2O \cdot 2SiO_2$ after DTA; *b*, 0.91% P_2O_5; *c*, 1.23% P_2O_5; *d*, 1.73% P_2O_5.

The thermogrammes (figure 3) show that as the P_2O_5 concentration is growing the endothermal effect is substantially reduced both in amplitude and in temperature interval, which may be interpreted as a result of a rapid increase of the order degree by crystallization under the influence of P_2O_5 delaying or diminishing the ordinary structure transformation.

Supplementary and precious information on the action of P_2O_5 was obtained through electronic microscopy. The platinum and carbon replica micrographs of the samples with rapidly cooled different P_2O_5 contents, and of the sample crystallized by thermal treatment at a higher temperature than that of the exothermal effect, are shown in figure 5.

As can be seen, the presence of P_2O_5 brings about a very quick and massive separation of the vitreous phases, as compared with the samples without P_2O_5 (curve a).

---

[7] A. N. Lazarev, "Kolebetelnie spectry i stroenie silicatov" Izd. Nauka S.S.S.R. Leningrad, 1968, p. 89.

The sample with 0.91% P_2O_5 (curve b) contains microphases with smaller dimensions than others, and occupying the whole volume. The same thing happens, also, with other samples with P_2O_5(curves c, d).

It may be also noticed, that the microphase dimensions of the samples with a higher P_2O_5 content than 1%, are practically equal and do not grow appreciably even after the thermal treatment for crystallization (curve e).

It results that the P_2O_5 influence begins to have an important role right from the beginning of the cooling period of the melted mass, with the effect of intensification of the vitreous phases separation process. This may be caused by the appearance in the system of some phosphorous compounds like lithium phosphate [8] or silicon phosphate [9], which modify the vitreous microphases equilibrium in the system.

The image of electronic micrograph of the sample with 0.91% P_2O_5 as well as the particularities of the above thermogrammes may be understood, in a first approximation, by analysing the conditions in which the crystallization processes develop. One can consider that the small dimensions and the low compactibility of the vitreous phases are proofs of a lower mobility of the ions in this sample, than in those with over 1% P_2O_5 content, cooled in the same conditions. Due to the nucleatoric presence, the crystallization begins at a temperature by 100° lower than for the sample without a nucleator. Therefore, the process rate will be influenced mainly by the rate of crystal growth, which is quite small, even compared to the sample without a nucleator (the latter) at a temperature by 100° higher).

By admitting that the crystallization germs (P_2O_5) are concentrated especially inside the microphases, the two maxima of the exothermal effect for the sample with 0.91% P_2O_5 (fig. 3) may be considered as a reflection of the fact that the process is delayed when the crystals in their development are passing through the interface.

For the sample with a high nucleator content the germs number is higher and the mobility is also higher. As a result it is probable that the rate of crystal growth is not the dominant factor of the process, being substituted in this role, by a higher nucleation rate.

The kinetics of the crystallization process

To study the kinetics of the crystallization process, the differential thermal analysis was used. The principle of the method was described in earlier papers.[5,10,11] Figure 6 represents the curves for the samples with 1.73% P_2O_5 and without P_2O_5, at different temperatures. As has been shown, the first part of the curve allows us to obtain information regarding the nucleation process, and the central part of the curve, (a nearly straight one) regarding the rate of crystal growth.

---

[8] M. Westman, *J. Amer. Ceram. Soc.*, **49**, 310 (1966).

[9] B. Seifer, *Zhur. neorg. Khim.*, **7**, 2806 (1962).

[10] P. Baltă and E. Baltă, *Rev. Chim.*, **12**, 1435 (1967).

[11] P. Baltă and M. Biale, *Proc. of the 9-th Conf. on the Silicate Ind.*, Budapest, 1967, p. 234.

As for the two studied samples (with and without nucleator), the thermal effects take place at temperatures differing by over 100°. To compare the nucleation process, one has drawn the time corresponding

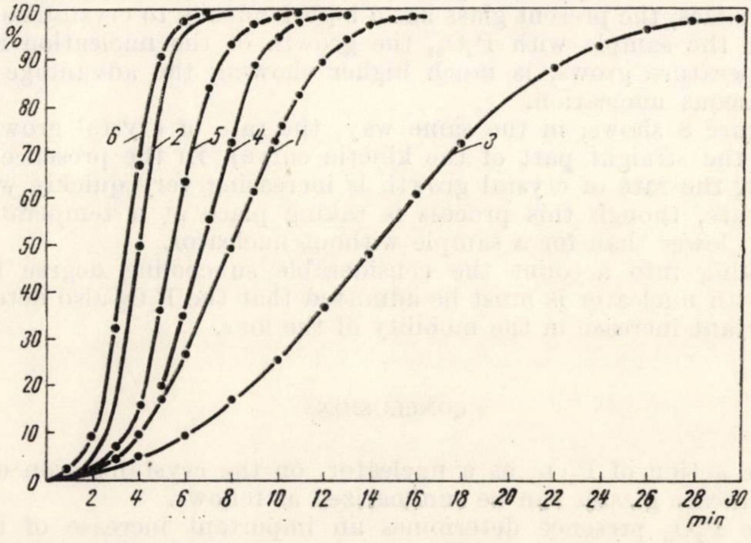

Fig. 6. — Kinetic curves obtained through differential isothermic analysis effectuated at temperatures around the maximum exothermic temperature effect ($T_{m.exo.}$):

1, without P_2O_5 at $T_{m.exo.} - 30°$; *2*, without P_2O_5 at $T_{m.exo.} + 30°$; *3*, with 1.73% P_2O_5 at $T_{m.exo.} - 15°$; *4*, with 1.73% P_2O_5 at $T_{m.exo.} + 2°$; *5*, with 1.73% P_2O_5 at $T_{m.exo.} + 5°$; *6*, with 1.73% P_2O_5 at $T_{m.exo.} + 10°$.

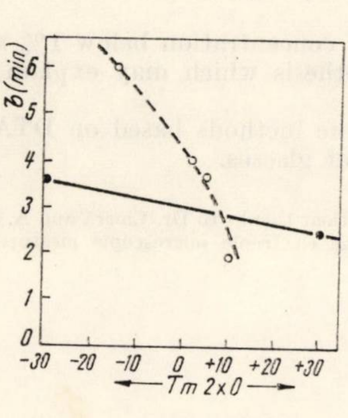

Fig. 7. — Variation of the nucleation time function of temperature, illustrated as in figure 6.

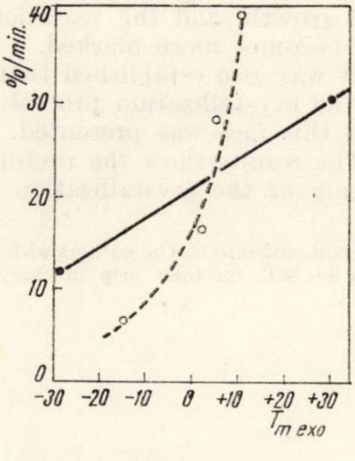

Fig. 8. — Variation of the rate crystallization function of temperature, illustrated as in figure 6.

to the first part of the curve (nucleation period) vs. the temperature, taking as reference point the temperature of the exothermal effect peak.

For glass without any P_2O_5, the period of nucleation is slowly dropping as the temperature grows, though compared to other lithium-silicate glasses, the present glass has a high tendency to crystallize.

For the sample with P_2O_5, the growth of the nucleation rate, as the temperature grows, is much higher showing the advantage of the heterogeneous nucleation.

Figure 8 shows, in the same way, the rate of crystal growth (the slope of the straight part of the kinetic curve). In the presence of the nucleator, the rate of crystal growth is increasing very quickly with the temperature, though this process is taking place at a temperature by over 100° lower than for a sample without nucleator.

Taking into account the considerable subcooling degree for the glasses with nucleator is must be admitted that the P_2O_5 also determines an important increase in the mobility of the ions.

CONCLUSIONS

The action of P_2O_5, as a nucleator, on the crystallization of some lithium-silicate glasses can be summarized as follows.

The P_2O_5 presence determines an important increase of the ion mobility in glass, which permits the initiation and development of crystallization processes at a temperature by more than 100° lower than for the glasses without P_2O_5.

The P_2O_5 presence accelerates the separation processes of vitreous phases, possibly due to the formation of the same compounds of the lithium phosphate type.

There is a big increase, both in nucleation rate and in the rate of crystal growth, and the variation of these parameters with the temperature becomes more marked.

It was also established that P_2O_5 in concentration below 1% slows down the crystallization process. A hypothesis which may explain well enough this fact was presented.

The results show the usefulness of the methods based on DTA for the study of the crystallization process of glasses.

Acknowledgements. The authors wish to express their thanks to Dr. Cioară and A. Butuceanu of I.C.M.C. for their help in carrying out the electronic microscopic measurements

Revue Roumaine de Chimie, **15**, 965–971 (1970)

INCHAIN EPOXIDES OF CAROTENOIDS. I
9,10- AND 13,14-EPOXY-CANTHAXANTHIN

ELENA NICOARĂ, DOINA OŞIANU and C. BODEA

Institute of Agronomy "Dr. Petru Groza", Department of Chemistry and Biochemistry,
Cluj, Str. Mănăştur, 3

Received December 19, 1969

Acting with perbenzoic acid upon canthaxanthin hitherto unknown inchain epoxides were obtained. The properties of 9,10- and 13,14-epoxy-canthaxanthin are described. By reduction with $NaBH_4$ the epoxides were converted into 9,10- and 13,14-epoxy-isozeaxanthin and by reduction with $LiAlH_4$ into 9-hydroxy-9,10 dihydro- and 13-hydroxy-13,14-dihydro-isozeaxanthin.

It is known that 5,6- and 5,8-epoxides of carotenoids are not only widely distributed in nature, but they undoubtedly play important roles being, as it seems, involved in electron transport, in the protection against lethal photosensitized oxidations and in conversions of carotenoids.

Semisynthetical 5,6- and 5,8-epoxides have been obtained by Karrer et al.[1] under the action of peracids upon hydrocarbon and hydroxylated carotenoids. It is to note that only the double bond 5,6 of the β-iononic rings could be epoxidized. A characteristic reaction of the 5,6-epoxides is their rearrangements into 5,8-epoxides on treatment with acids. During this reaction small quantities of the initial carotenoid are formed due to a partial loss of the epoxidic oxygen.

The purpose of this work is to explore the possibility to obtain hitherto unknown inchain epoxides of carotenoids. Taking into consideration the observation made by Bodendorf [2] that a neighbouring carbonyl group renders the epoxidation of the double bond more difficult, we have examined the action of perbenzoic acid upon canthaxanthin (4,4′-diketo-β-carotene, I).

From the chromatographic column on MgO or Al_2O_3 we could isolate two epoxides (II and III, scheme 1) which gave when treated with HCl the characteristic blue colour reaction shown by 5,6-epoxides, but the attempt to convert them into 5,8-epoxides on treatment with acids failed. Instead of that the two epoxides regenerated easily initial all-*trans* canthaxanthin along with some neo-*cis* isomers of canthaxanthin.

The relative polarity of the two epoxides, determined according to Krinsky,[3] indicated in both cases only one epoxy group.

---

[1] P. Karrer and E. Jucker, "Carotinoide", Birkhäuser, Basel, 1948, p. 76–79.

[2] K. Bodendorf, *Arch. Pharmaz.*, **268**, 491 (1930).

[3] N. I. Krinsky, *Analyt. Biochem.*, **6**, 293 (1963).

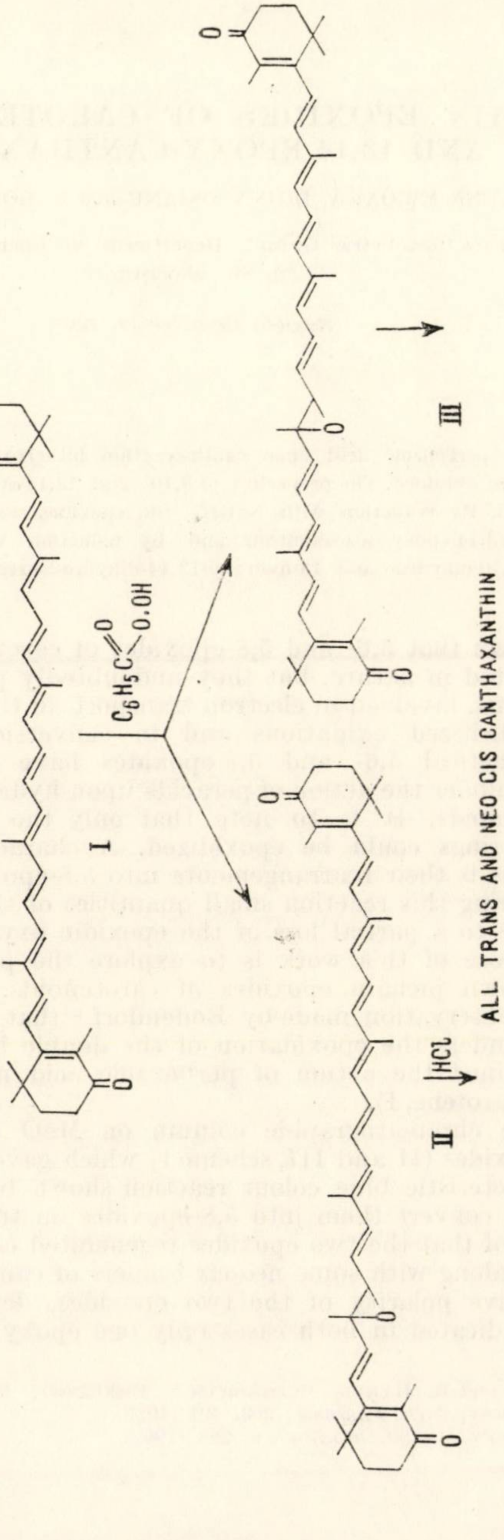
I
$C_6H_5C(=O)O.OH$
II
HCl
ALL TRANS AND NEO CIS CANTHAXANTHIN
III

Scheme 1

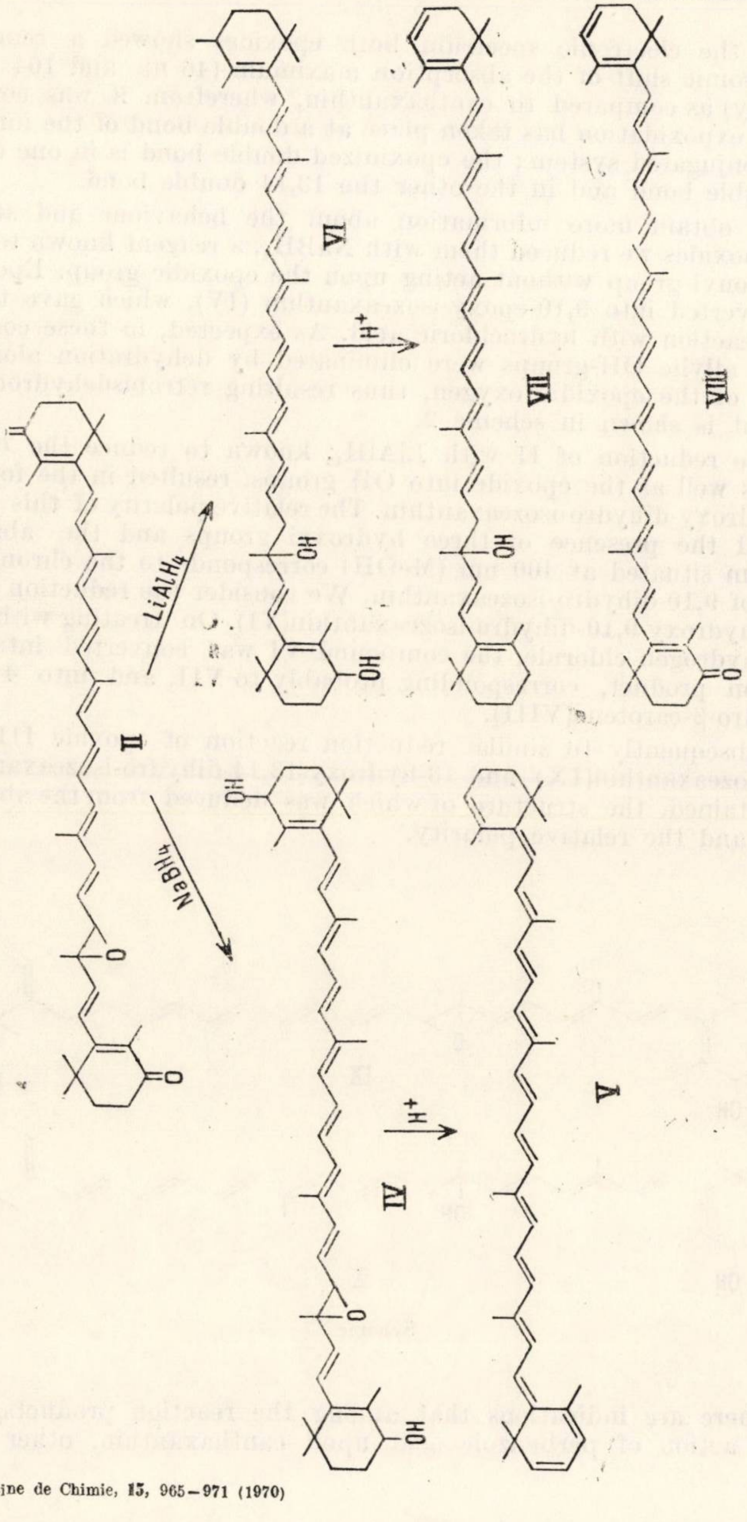
II
O
O
O
NaBH4
LiAlH4
OH
OH
OH
OH
H+
H+
IV
V
VI
VII
VIII
O

Scheme 2

In the electronic spectrum both epoxides showed a remarkable hypsochromic shift of the absorption maximum (46 nm and 104 nm respectively) as compared to canthaxanthin, wherefrom it was concluded that the expoxidation has taken place at a double bond of the inner part of the conjugated system; the epoxidized double bond is in one case the 9,10 double bond and in the other the 13,14 double bond.

To obtain more information about the behaviour and structure of the epoxides we reduced them with $NaBH_4$, a reagent known to reduce the carbonyl group without acting upon the epoxidic group. Epoxide II was converted into 9,10-epoxy-isozeaxanthin (IV), which gave the blue colour reaction with hydrochloric acid. As expected, in these conditions the two allylic OH-groups were eliminated by dehydration along with the loss of the epoxidic oxygen, thus resulting retrobisdehydrocarotene (V), as it is shown in scheme 2.

The reduction of II with $LiAlH_4$, known to reduce the carbonyl group as well as the epoxide into OH groups, resulted in the formation of a hydroxy-dihydro-isozeaxanthin. The relative polarity of this product indicated the presence of three hydroxyl groups and the absorption maximum situated at 400 nm (MeOH) corresponds to the chromophoric system of 9,10-dihydro-isozeaxanthin. We consider the reduction product to be 9-hydroxy-9,10-dihydro-isozeaxanthin(VI). On treating with chloroformic hydrogen chloride, the compound VI was converted into a dehydration product, corresponding probably to VII, and into 4-keto-3′, 4′-dehydro-β-carotene(VIII).

Subsequently to similar reduction reaction of epoxide III, 13,14-epoxy-isozeaxanthin(IX) and 13-hydroxy-13,14-dihydro-isozeaxanthin(X) were obtained, the structure of which was deduced from the absorption spectra and the relative polarity.

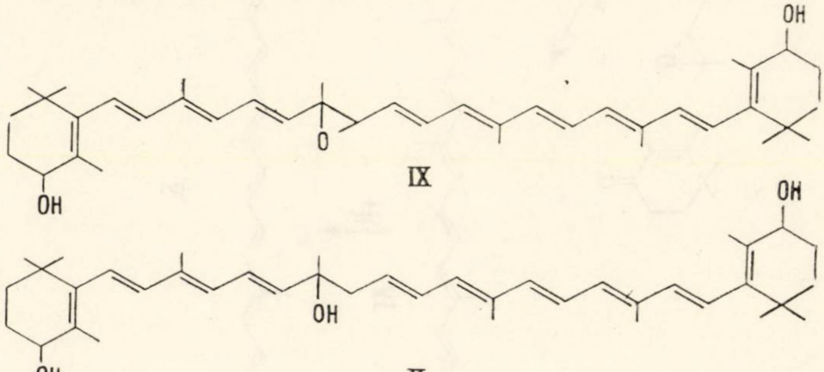

Scheme 3

There are indications that among the reaction products, formed by the action of perbenzoic acid upon canthaxanthin, other inchain epoxides might exist. These as well as the products of reaction of peracids upon other carotenoids are now under investigation.

In our opinion there are no reasons why inchain epoxides of carotenoids could not exist "in vivo" too. That they have not yet been identified in nature may be explained by their easy loss of the epoxidic oxygen. Their biological rôle might lie in the facility with which they capture and release the active oxygen.

EXPERIMENTAL

Epoxidation of canthaxanthin(I) with perbenzoic acid. Synthetic canthaxanthin (0.0018 moles) solved in chloroform (100 ml) was treated with perbenzoic acid (0.0036 moles) by addition of an ethereal solution, prepared according to Ogata and Sawaki,[4] and kept 20 h in dark at 0°. The mixture was diluted with petroleum ether (400 ml) and then washed thoroughly with aqueous sodium bisulphite and water. The solution was dried (Na_2SO_4) and chromatographed on magnesium oxide or alumina column.

a) Chromatography on magnesium oxide column. The reaction products were separated on a MgO/fine sand (1 : 2) column (8 × 40 cm) and developed with petroleum ether containing increasing concentrations of acetone (1–10 %). The chromatogram is indicated in table 1.

Table 1

Chromatogram on magnesium oxide

Length of zone (cm)	Colour	λ_{max} (nm) in benzene	Pigment
(7) 5	Ochre	—	
(6) 2	Pink-red	494	
(5) 5	Orange	452	
(4) 6	Violet	480	Unreacted canthaxanthin
(3) 2	Orange	—	
2	Colourless interzone		
(2) 3	Yellow	434	9,10-Epoxy-canthaxanthin
2	Colourless interzone		
(1) 11	Pale yellow	368	13,14-Epoxy-canthaxanthin

The pigments from the lowest zones 1 and 2 eluted in ether give, when treated with hydrochloric acid, the characteristic blue colour reaction of epoxide carotenoids.[1]

b) Chromatography on alumina column. Separation on deactivated alumina with 2 % water was carried out on column (4 × 35 cm) by the elution technique using petroleum ether containing 1 to 7 % acetone as eluant. Nine fractions were obtained. The characteristic blue colour reaction of epoxide carotenoids was more intense with the pigments from the fractions 5 and 8. Both fractions were collected after the unreacted canthaxanthin present in fraction 4.

Isolation and characterization of 9,10-epoxy-canthaxanthin(II). The pigment from zone 2 of the magnesium oxide column or from fraction 8 obtained by chromatography on alumina was rechromatographed on magnesium oxide column using petroleum ether-acetone

---

[4] Y. Ogata and Y. Sawaki, *Tetrahedron*, **23**, 3327 (1967).

(6—8%) as developing solvent. The purified epoxide II has a single λ_{max} (in benzene at 434 nm and in methanol at 424 nm) and presents a relative polarity value of 1.84 units.

The reduction of 9,10-epoxy-canthaxanthin(II) with $NaBH_4$, followed by chromatography on magnesium oxide gives the expected epoxy-isoxanthophyll IV (λ_{max} in benzene at 396 nm; blue colour reaction with hydrochlorid acid). Treatment of 9,10-epoxy-isozeaxanthin(IV) with chloroformic hydrogen chloride [5] (acidic chloroform) gives retrobisdehydrocarotene(V), identified by cochromatogram with authentic pigment prepared from isozeaxanthin by the same treatment.

Epoxide II, upon treatment with $LiAlH_4$, is converted into compound VI with λ_{max} at 400 nm in methanol and relative polarity value of 2.4 units. The compound VI gives no more colour reaction for epoxide group, but it is readily dehydrated with acidic chloroform. Chromatography on magnesium oxide column yields 4-keto-3′,4′-dehydro-β-carotene, identified by cochromatograme, and compound VIII (λ_{max} at 420 nm in methanol and partition coefficients between petroleum ether and 95% methanol 81 : 19).

Isolation and characterization of 13,14-epoxy-canthaxanthin(III). The pigment from zone 1 of the magnesium oxide column or from fraction 5 of the alumina column was purified by rechromatography on magnesium oxide, using petroleum ether with 3—5% acetone as the developing solvent. The purified pigment has a single λ_{max} at 376 nm in benzene and at 366 nm in methanol and a relative polarity value of 1.57 units, corresponding to 13,14-epoxy-canthaxanthin(III). The reduction with $NaBH_4$ of the epoxide III yields 13,14-epoxy-isozeaxanthin (IX). Upon the reduction of epoxide III with $LiAlH_4$, 13-hydroxy-13,14-dihydro-isozeaxanthin(X) is formed, with λ_{max} at 376 nm in benzene and relative polarity value of 2.6 units. On treating with acidic chloroform the pale yellow chloroformic solution of compound X turned red and the partition became epiphasic. Two red spots were observed on thin layer plates of magnesium oxide.

De-epoxidation reaction. Few drops of concentrated hydrochloric acid were added to 5 ml solution of the epoxide II or III, obtained by elution with methanol from the magnesium oxide column; the solution turned green. After 10 minutes, the mixture was shaken with an equal volume of petroleum ether and aqueous $NaHCO_3$. The upper layer was washed with water, dried (Na_2SO_4) and chromatographed on magnesium oxide column (1×15 cm). In chromatogram separates all-*trans* and neo-*cis* canthaxanthin, identified by thin-layer cochromatography with authentic pigments. The neo-*cis* isomers were obtained by melting all-*trans* canthaxanthin, according to Gansser and Zechmeister.[6]

Reduction reaction with $LiAlH_4$. The purified epoxides (II and III) were eluted from magnesium oxide column with anhydrous ether containing 1% ethanol. A slurry of $LiAlH_4$ in ether was added, until no decomposition was observed, to the epoxide solution (10 ml) cooled at 0°. The mixture was reacted in the dark at 0° for 1 h, and then neutralized by the cautious, dropwise addition of absolute ethanol containing sodium ethoxide (to solve the resulted aluminium hydroxide). Petroleum ether (25 ml) was added and after shaking with water the upper layer was chromatographed on magnesium oxide column (1×15 cm) and developed with a mixture of petroleum ether and acetone (8—10%).

Reduction reaction with $NaBH_4$. The epoxides II and III, purified by chromatography on magnesiun oxide column, were eluted with ethanol. $NaBH_4$ (15 mg) was added to the solution (10 ml) and the mixture was kept in the dark for 20—30 minutes. The reduction products were transferred in a mixture of ethylic ether and petroleum ether 2 : 1 (25 ml) by water addition. The upper layer was washed, chromatographed on magnesium oxide column (1 × 15 cm) and developed with petroleum ether containing 4—6% acetone.

---

[5] F. J. PETRACEK and L. ZECHMEISTER, *J. Amer. Chem. Soc.*, **78**, 3188 (1956).

[6] CH. GANSSER and L. ZECHMEISTER, *Helv. Chim. Acta*, **40**, 1757 (1957).

Elimination reaction of the allylic hydroxyl groups. The testing pigment, purified by column chromatography and eluted in chloroform (5 ml), was treated with acidic chloroform. The pale yellow solution of the inchain epoxy-isozeaxanthins IV and IX or of the hydroxy-dihydro-isoxanthophylls VI and X turned to deep orange and the partition, between petroleum ether : methanol 95 %, become epiphasic. The chloroformic solution was diluted with petroleum ether, washed with $NaHCO_3$ solution and then with water. The resulted dehydration products were separated by chromatography on magnesium oxide column or on chromatoplates.

Determination of relative polarity. From the M_{50} value established for the solvents system petroleum ether-aqueous methanol, the relative polarity was determined graphically on the basis of the linear relationship established by Krinsky [3].

Apparatus. The visible and ultraviolet spectra as well as the partition coefficients were performed with a Zeiss-Jena VSU-1 universal spectrophotometer.

Acknowledgement. We thank F. Hoffmann-La Roche and Co., Basle, Switzerland for gifts of canthaxanthin.

[illegible] portion of the crude [illegible] extract. The [illegible] pigment, purified by [illegible] and dried in chloroform [illegible], was treated with [illegible]. The pale yellow solution of the [illegible] IV and IX or of the hydroxy- [illegible] VI and X turned to deep orange and the partition, between petroleum ether [illegible]. The chloroform solution was diluted with petroleum ether, washed with $NaHCO_3$ solution and then with water. The purified derivatives were separated by [illegible] on [illegible] column or on [illegible] plates.

Determination of [illegible]. From the R_M value [illegible] for the solvents [illegible] the [illegible] was determined graphically on the [illegible] of the [illegible] established by [illegible].

Spectra. The visible and ultraviolet spectra as well as the [illegible] were [illegible] with a [illegible] universal spectrophotometer.

Acknowledgement. We thank [illegible] Hoffmann-La Roche and Co., Basle, Switzerland, for [illegible].

[illegible]

Revue Roumaine de Chimie, **15**, 973–984 (1970)

THE USE OF MEMBRANES TO INDICATE THE EQUIVALENCE POINT. V*

THE PARCHMENT-PAPER MEMBRANE IMPREGNATED WITH $BaSO_4$, INDICATING ELECTRODE IN THE Cl^-, Br^-, I^- TITRATION

158

C. LITEANU and I. C. POPESCU

"Babeş Bolyai" University, Cluj,
Department of Analytical Chemistry
str. Arany Janos, 11

Received August 7, 1969

The potential of the parchment-paper membrane impregnated with $BaSO_4$ is affected by the presence of foreign ions others than membranogens, in the contacting solutions. This potential-depressing effect (secondary ionic specificity) characteristic of all the membrane electrodes, was used to the determination of Br^- and I^- by zero current potentiometric titration with Ag_2SO_4. In this case the membrane acts as an indicator electrode for Br^- and I^-, respectively. The precision of the determinations is satisfactory.

The systematic study of the function of the glass electrode known and used since 1906 by Cremer [1] and Haber and Klemensiewicz [2] as well as the attempts at theoretical clearing of the occurrence of membrane [3–15] potential resulted during the first half of our century in the formation of a distinct and particularly prolific field in analytical potentiometry: the membrane electrodes as indicating electrodes.

---

* C. Liteanu, M. Mioşcu and I. Popescu, *Rev. Roumaine Chim.*, **13**, 569 (1968).

[1] M. Cremer, *Z. Biol.*, **47**, 562 (1906).

[2] F. Haber and Z. Klemensiewicz, *Z. phys. Chem.*, **67**, 385 (1909).

[3] F. G. Donnan, *Chem. Rev.*, **1**, 73 (1925).

[4] K. Horowitz, *Z. Physik*, **15**, 369 (1923).

[5] T. Teorell, *Proc. Soc., Exptl. Biol.*, **33**, 282 (1935).

[6] K. H. Meyer, and J. F. Sievers, *Helv. Chim. Acta*, **19**, 649 (1936); **19**, 665 (1936); **19**, 987 (1936).

[7] H. J. C. Tendeloo, *J. Biol. Chem.*, **113**, 333 (1936).

[8] C. E. Marshall, *J. Phys. Chem.*, **43**, 1155 (1939); **48**, 67 (1944); **52**, 1284 (1948).

[9] J. Staverman, *Trans. Faraday Soc.*, **48**, 176 (1952).

[10] G. Scatchard, *J. Amer. Chem. Soc.*, **75**, 2883 (1953).

[11] H. T. Clarke and D. Nachmansohn, "Ion Transport Across Membranes", Academic Press, Inc., New York, 1954, p. 79.

[12] R. Schlögl, "Stofftransport durch Membrane", dr. D. Steinkopf Verlag, Darmstadt, 1964, p. 115.

[13] Y. Kobatake, *J. Chem. Phys.*, **28**, 146 (1958); **28**, 146 (1958); **28**, 442 (1958).

[14] Y. Kobatake, N. Takeguchi, Y. Toyoshima and H. Fujita, *J. Phys. Chem.*, **69**, 3981 (1965); **70**, 1187 (1966).

[15] N. Lakshinarayanaiah, *J. Polymer Sci. A*, **2**, 4491 (1964).

Used in potentiometric direct determinations,[16] in potentiometric titrations at zero current,[17-19] or at non-zero constant current[20] the membrane electrodes, under certain conditions, conveniently used, offer coherent indication, to which a physical meaning about the activity of a single ion species can be ascribed.

Turning our attention to the nature of this species as regards the structure of the membrane, we can observe that almost all the works dedicated to the analytical research of the properties of the membrane electrodes are based on the behaviour of the membrane in the presence of the solution to be investigated which contains, as a species to be determined, ions identical to the counter-ions of the membrane. Thus, in the field of potentiometric titrations regardless of the reaction used (neutralizations[19-25] or precipitation[17, 18, 21b-23, 25-32]) and of the nature of the active component of the membrane (ion exchange or precipitate), the active component of the membrane (ion exchange or precipitate), the membrane is always used saturated with the counter-ion to be determined. The only exception is represented by the works of Ijsseling and van Dalen[25] who also take into consideration the possibility of the titration of ions associated to counter-ions (co-ions).

Hirsch-Ayalon[33] and afterwards Mioşcu[34] too, point out that the parchment-membrane electrode impregnated with $BaSO_4$ is also sensitive to ions (in the internal solution: Na^+, Ca^{2+}, Mg^{2+}, in the external solution F^-, Cl^-, Br^-, I^-, NO_3^-, ClO_4^-) which differ from those forming the precipitate (Ba^{2+} and SO_4^{2-}) and from the ions conferring the pH function H^+ and OH^-) on the electrode.

---

[16] L. Michaelis, *Colloid Symposium monograph.*, **5**, 135 (1937).

[17] I. M. Kolthoff and H. L. Sanders, *J. Amer. Chem. Soc.*, **59**, 416 (1937).

[18] E. M. Shobets and G. A. Kleibts, *Zhur. obshchei Khim.*, **10**, 1617 (1940).

[19] S. K. Sinha, *J. Indian Chem. Soc.*, **32**, 35 (1960).

[20] R. Geyer and P. Niklas, *Z. analyt. Chem.*, **177**, 166 (1960).

[21] a) E. A. Materova and F. A. Belinskaia, *Vestnik Leningrad Univ. Ser. Fiz. i Khim.*, No. 22, 112 (1959); No. 22, 26 (1960).

b) E. A. Materova and V. S. Yurcenko, *Zhur. analit. Khim.*, **16**, 388 (1962).

[22] M. Nakagaki, N. Koga and S. Noguchi, *Yakugaku Zasshi.*, **82**, 1124 (1962); *Chem. Abstr.*, **58**, 7387 h (1963); **83**, 885 (1963); *Chem. Abstr.*, **60**, 2313 g (1964).

[23] R. Geyer, W. Erxleben, W. Syring and K. Chojnacki, *Wiss. Z. Techn. Hochsch. Chem. Leuna-Merseburg*, **6**, 163 (1964).

[24] C. Liteanu and M. Mioşcu, *Rev. Roumaine Chim.*, **10**, 903 (1965); **11**, 864 (1966); **13**, 209 (1968); **13**, 569 (1968).

[25] F. P. Ijsseling and van Dalen, *Analyt. Chim. Acta.*, **43**, 77 (1968).

[26] J. S. Parsons, *Analyt. Chem.*, **30**, 1262 (1958).

[27] R. B. Fischer and R. F. Babcock, *Analyt. Chem.*, **30**, 1732 (1958).

[28] J. Bersier, P. Bersier, W. Trueb, and F. Hügli, *Helv. Chim. Acta*, **42**, 55 (1959); **42**, 2514 (1959).

[29] A. S. Basu, *J. Indian Chem. Soc.*, **39**, 717 (1962).

[30] E. Pungor, J. Havas and K. Toth, *Acta Chim. Acad. Sci. Hung.*, **27**, 63 (1961); **41**, 239 (1964); **48**, 17 (1966); **50**, 77 (1966); **58**, 9 (1968).

[31] R. Geyer, *Wiss. Z. Hochsch. Chem. Leuna-Merseburg*, **6**, 167 (1954); **6**, 243 (1964).

[32] G. A. Rechnitz, M. R. Kresz and S. B. Zamochnick, *Analyt. Chem.*, **38**, 973 (1966); **38**, 1786 (1966), **40**, 1054 (1968).

[33] P. Hirsch-Ayalon, *Rec. Trav. Chim.*, **80**, 365 (1961); **80**, 376 (1961).

[34] M. Mioşcu, Dissertation, Cluj, 1965.

Based on these two facts, the present paper aims at estimating analytically the so-called ionic secondary specificity of the parchment-paper membrane impregnated with $BaSO_4$: the potentiometric titration by the precipitation of Cl^-, Br^-, I^- with Ag_2So_4.

EXPERIMENTAL

The membrane electrode was prepared according to the indications of Hirsch-Ayalon [35] but in the variant studied by Liteanu and Mioşcu,[24] where the cellophane is replaced by the parchment-paper ; it is shown, as such, in figure 1.

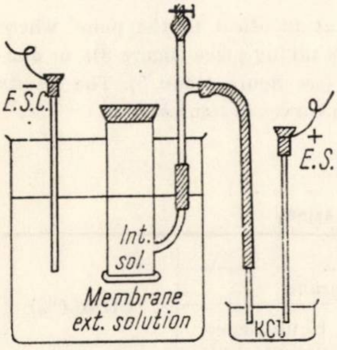

Fig. 1. — Membrane vessel placed in the take over device of the membrane potential.

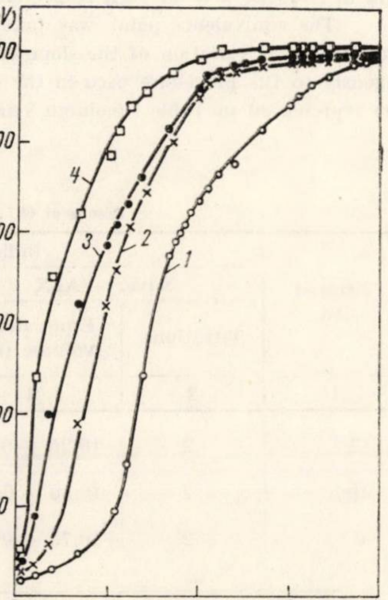

Fig. 2. — Electrodic functions E−pX : *1*, F^- ; *2*, Cl^- ; *3*. Br^- ; *4*, I^-.

The membranogens solutions $Ba(OH)_2$ and H_2SO_4 were of a 0.05 M concentration as recommended by Hirsch-Ayalon.

The measuring device. To measure the membrane potential the electrochemical chain was established :

(+) ESC/KCl sat./$Ba(OH)_2$ 0.05 M/membrane/H_2SO_4 0.05 M + NaX/KCl sat./ESC (−)
the e.m.f. of which was measured by means of a common potentiometer. During the measurements, the external solution was stirred with a magnetic stirrer.

The electrode functions $E-pX$ ($X=F^-$, Cl^-, Br^-, I^-) : resuming the experiments on the influence of F^-, Cl^-, Br^-, I^- ions on the potential of $BaSO_4$ membrane presented in,[33,34] proceeding more carefully (the 0.05 M $Ba(OH)_2$ internal solution has been changed for each series of experiments ; in the external solution, the H_2SO_4 concentration was kept constant) one has plotted the $E-pX$ curves represented in figure 2. The NaX concentration in the external solution varied between 1 M and 10^{-4} M. Within the same series of experiments

---

[35] P. Hirsch-Ayalon, *Rec. Trav. chim.*, **75**, 1064 (1956).

(that is for the same X^-) before diving the membrane electrode into more concentrated NaX solution, it was washed with distilled water and with a portion of the other solution.

Titration. Using the device from figure 1, the potentiometric titration was made by precipitation with Ag_2SO_4, 10^{-2}M (f=1), of NaX also, 10^{-2}M, where $X=Cl^-$, Br^-, I^-. The curves of titration were plotted gradually. The readings were taken when the potential of the electrode did no longer vary beyond 0.5 mV within 60 seconds.

$AgSO_4$ was used, and no other soluble salt of Ag^+ because the SO_4^{2} ion does not influence the membrane potential. To ensure the reproducibility of measurements it was also necessary to remove the precipitate from the pores of the membrane. This was achieved by the washing during one minute of the electrode in concentrated NH_4OH, for AgCl and AgBr, and in $Na_2S_2O_3$ 2N, for AgI, respectively.

The equivalence point was taken arbitrarily, either as identical to the point where the maximum variation of the slope of the titration curve is taking place (figure 3), or analogously to the procedure used in the differential titrations (see figure 4 and 5). The results are represented in Table 1 (column 5 and 6) and the titration curves in figures 3–5.

Table 1

Results of Cl^-, Br^-, I^- titrations with Ag_2SO_4

Titrated ion	Indicator electrode				Error (%)
	Silver + AgX		Membrane		
	Titrations	Equivalence volume (ml)	Titrations	Equivalence volume (ml)	
1	2	3	4	5	6
Cl^-	2	10.25 ± 0.04	4	12.46 ± 1.04	+21.56
Br^-	2	10.60 ± 0.03	3	10.61 ± 0.12	+ 0.10
I^-	2	10.75 ± 0.03	5	10.76 ± 0.07	+ 0.09

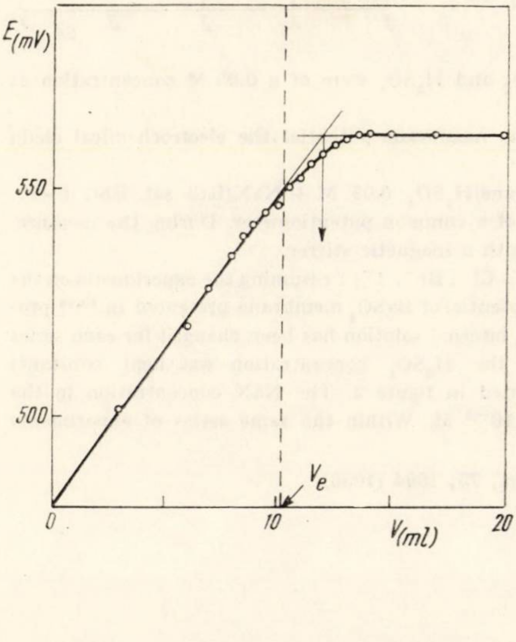

Fig. 3. — Titration curve, E—V (10 ml NaCl 10^{-2}M with Ag_2SO_4 10^{-2} M).

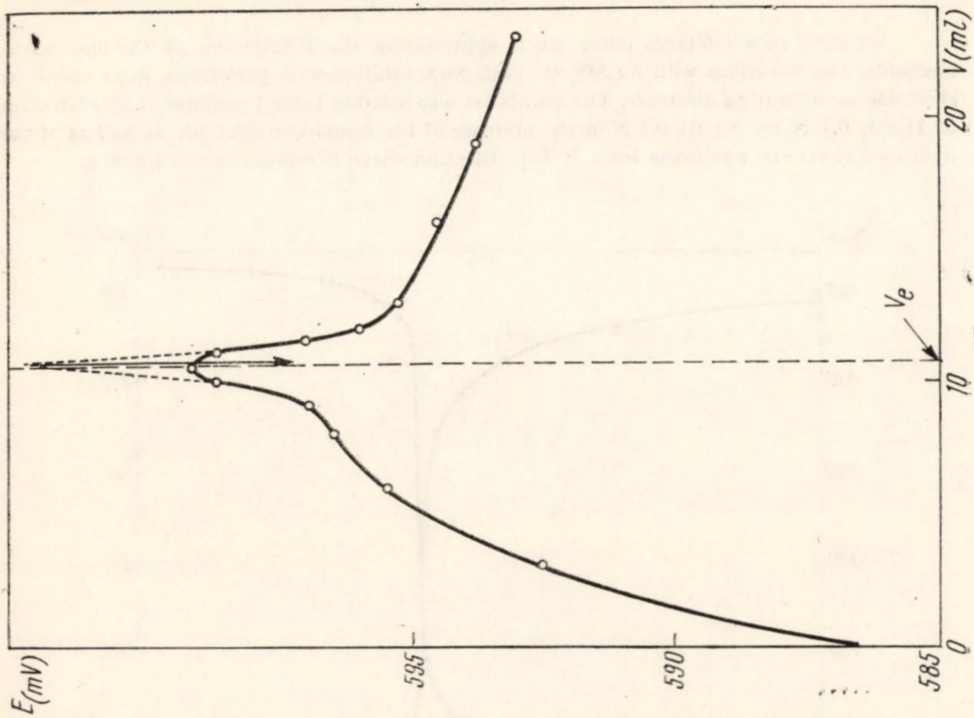

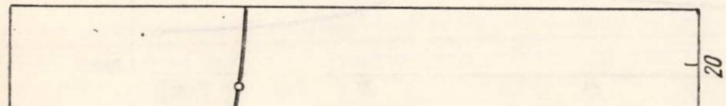

Fig. 4. — Titraion curve, E — V (10 ml NaBr 10^{-2} M with Ag_2SO_4 10^{-2} M).

Fig. 5. — Titration curve, E — V (10 ml NaI 10^{-2} M with Ag_2SO_4 10^{-2}M).

To serve as a reference point when appreciating the functioning of the membrane electrode, two titrations with Ag_2SO_4 for each NaX solution were performed, using the silver electrode as indicating electrode. The results are also listed in Table 1 (column 3). The titration of H_2SO_4 0.1 N by NaOH 0.1 N in the presence of the membrane electrode as well as of the hydrogen electrode was taken from.[34] The titration curve is represented in figure 6.

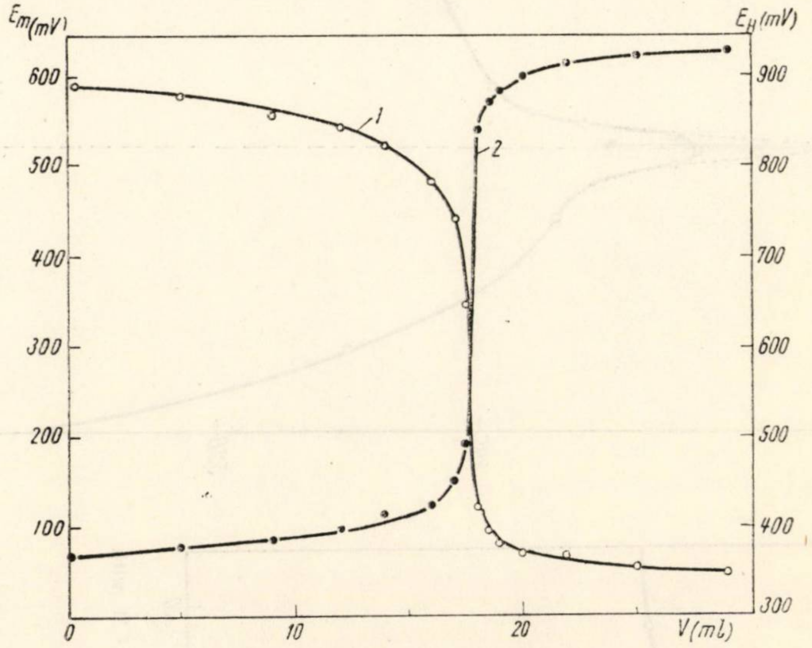

Fig. 6. — Titration curves; E—V of 20 ml H_2SO_4 0.1 N with NaOH 0.1 N; *1*, membrane electrode; *2*, hydrogen electrode.

DISCUSSION

Despite the fact that $E-pX$ measurements cover only a relatively small pX range ($0 \leqslant pX \leqslant 4$) we notice that:

a) The intensity of the potential-depressing effect decreases following the order F^-, Cl^-, I^-, in the whole investigated range.

b) The potential-depressing effect is not constant in the concentration range under consideration, that is, it reaches a minimal value towards small concentrations of NaX. Supposing that the accentuated slope of $E-pX$ curves, which occurs towards small values of pX, can be assigned to the penetration of X^- ions through the membrane, (see the results obtained by Hirsch-Ayalon) we can obtain an image of the ions capacity to penetrate the membrane. Thus was plotted the logarithm of the ions concentration at which the slope of the $E-pX$ curves (obtained by plotting the intersection of the most probable straight lines corresponding to each $E-pX$ curve for the portions neighbouring the region of the

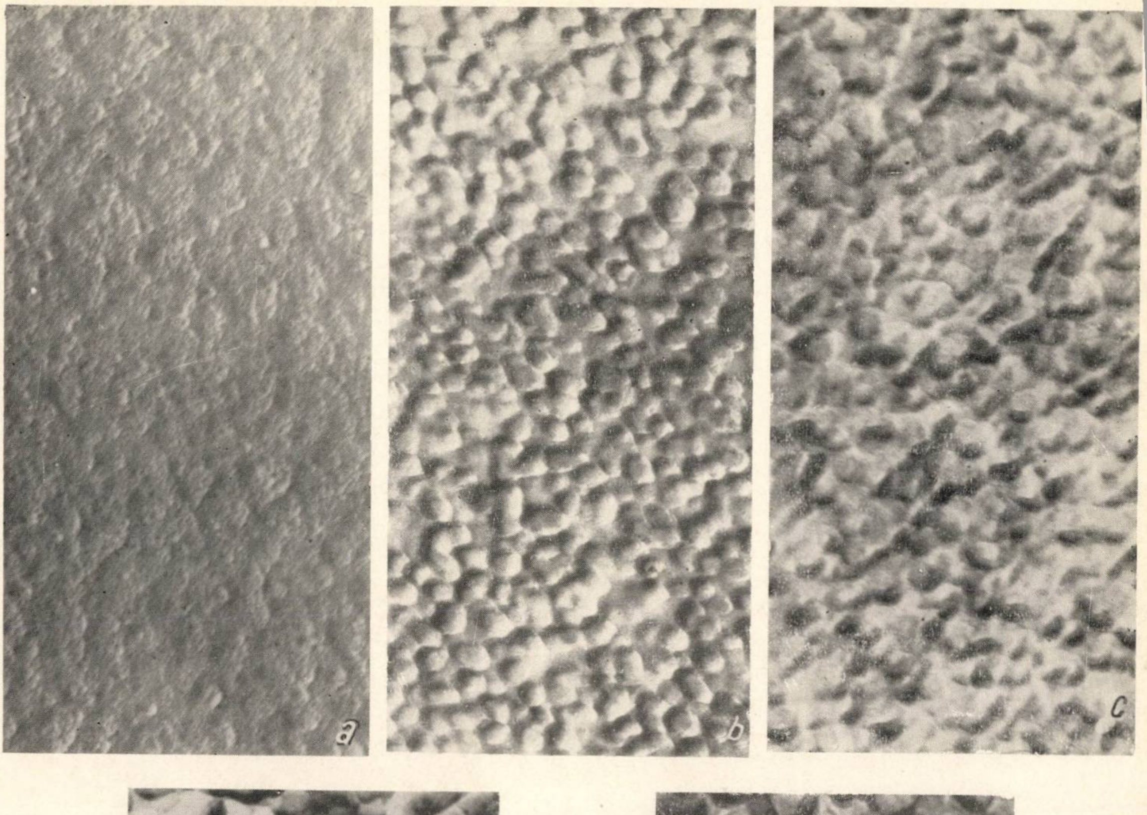

Fig. 5. —Replica electron micrographs of the samples :

a, without P_2O_5, *b*, 0,91% P_2O_5, *c*, 1,23% P_2O_5, *d*, 1.73% P_2O_5, *e*, 1.73% P_2O_5 after heating at 500° for 1 h (crystallized). Magnification × 54,000.

slope changes) changes abruptly according to the radius of the unhydrated anion [36] (figure 7).

Therefore the radius of the unhydrated ion seems to determine seriously not so much the intensity of the potential depressing effect, as the concentration threshold at which the effect occurs. When chosing the concentration of the solutions to be titrated this fact was also taken into account.

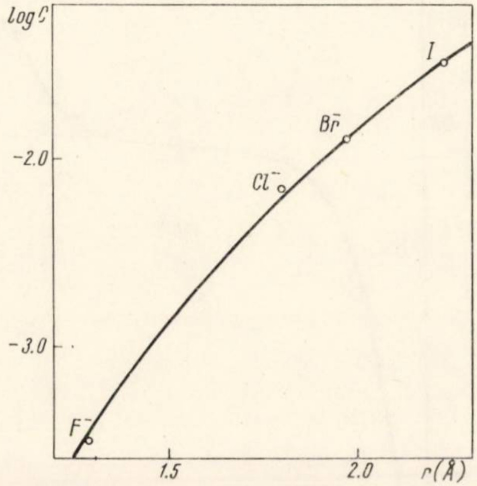

Fig. 7. — Dependence of the penetration capacity of F^-, Cl^-, I^-, anions upon the radius of the unhydrated ion.

Based on this finding it becomes obvious how the process of titration develops, when the membrane electrode is used as an indicator electrode in the titrations performed. Thus when adding the titrant the blocking of the "active ions" takes place in the precipitate. Therefore, the potential of the membrane shall increase. When the entire quantity of ions able to penetrate is exhausted to form the precipitate, the potential of the membrane is expected to remain constant. The sudden variation in the equivalence range shall be revealed by changing the slope of the $E-pX$ curve.

The titration curve of the Cl^- anion corresponds well to this interpretation, a fact which is not observed in the case of Br^- and I^- titrations.

To explain the differential behaviour of the membrane electrode, from the data $E-V$ obtained during the titration, the plots $E-pX$ ($X = Cl^-$, Br^-, I^-) were made using the corresponding data, $pX-V$ obtained by calculus (The values $S_{AgCl} = 1.7 \times 10^{-10}$, $S_{AgBr} = 3.3 \times \times 10^{-13}$, $S_{AgI} = 8.5 \times 10^{-17}$ from [37]). The curves obtained are represented in figures 8—10.

As can be seen from the figures 8—10, far clearer than in the figures 3—5, the behaviour, of the membrane electrode is clearly different in the Cl$^-$ titration to that in the I$^-$ titration, the Br$^-$ titration representing a transition between them. We add to this, the following two remarks :

---

[36] Y. Y. LURIE, "Spravochnik po analiticheskie Khimii", Izd. Khim., Moscow, 1965, p. 19.

[37] C. LITEANU, "Chimie Analitică Cantitativă, Volumetria", ed. 5, Bucharest, 1966, p. 683.

1. The ratio of the concentrations at which the potential-depressing effect of penetration occurs is the following :

$$\frac{[\mathrm{Br}^-]}{[\mathrm{Cl}^-]} = \frac{1.2 \times 10^{-2}}{6.4 \times 10^{-3}} \approx 2\ ;\ \frac{[\mathrm{I}^-]}{[\mathrm{Cl}^-]} = \frac{3.1 \times 10^{-2}}{6.4 \times 10^{-3}} \simeq 5 \qquad (1)$$

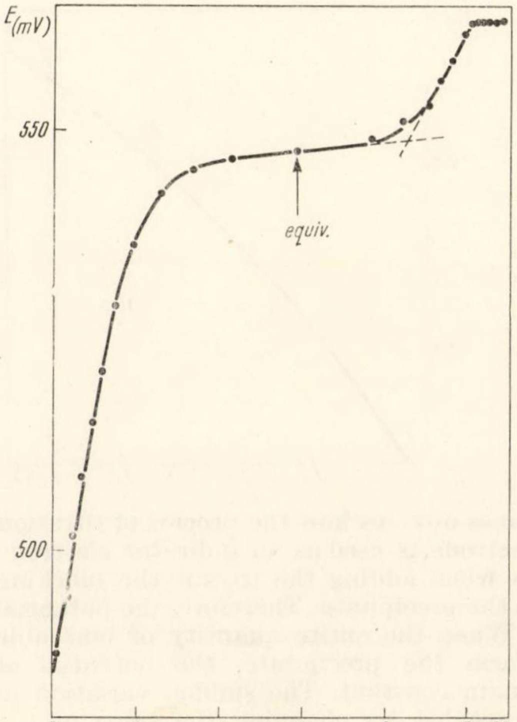

Fig. 8. — E—pCl curve from the data of the titration plotted in figure 3.

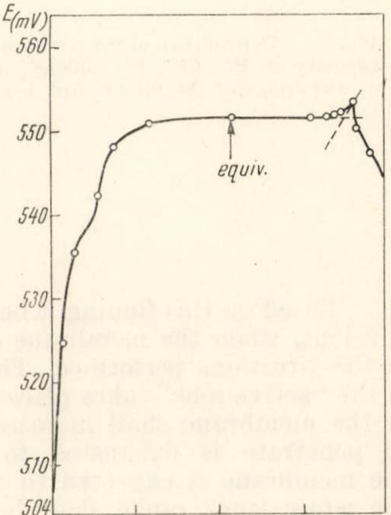

Fig. 9. — E—pBr curve from the data of the titration plotted in figure 4.

2. The ratio of AgX solubilities is :

$$\frac{[\mathrm{Cl}^-]}{[\mathrm{Br}^-]} = 22\ ;\qquad \frac{[\mathrm{Cl}^-]}{[\mathrm{I}^-]} = 1320 \qquad (2)$$

We can explain the particular functioning of the membrane electrode in the course of these titrations.

The Cl$^-$ titration. As the initial concentration of Cl$^-$ is exceeding the threshold of appearence of the potential-depressing effect, the extraction of Cl$^-$ ions of the system brings about the increase of the potential electrode. Therefore when the concentration of Cl$^-$ ions decreases beyond the value of the penetration limit through the membrane, the potential of the membrane should remain constant. As this fact is not observed experimentally it may be presumed that either an inversed penetration of the membrane is taking place, or that the Cl^- can affect the membrane potential also in another way, for instance, by adsorption on the membrane surface.

Representing in figure 11, the asymptote curve, the variation of the potential of the electrode function of the concentration of the Cl^- ions, based on the data used to draw up figure 8, in the region following the equivalence, this was found to be described by an expression similar to a Langmuir adsorption isotherm :

$$E = \frac{b.C}{1 + bC} . E_M \tag{3}$$

The linearization of the expression used in figure 11, i.e. the straight line :

$$\frac{C}{E} = \frac{1}{bE_M} + \frac{C}{E_M} \tag{4}$$

permits the calculation of the parameters E (the minimal value of the membrane potential when the phenomenon reached the maximum intensity) and b (a coefficient that indicates the strength of the forces implied in the respective phenomenon).

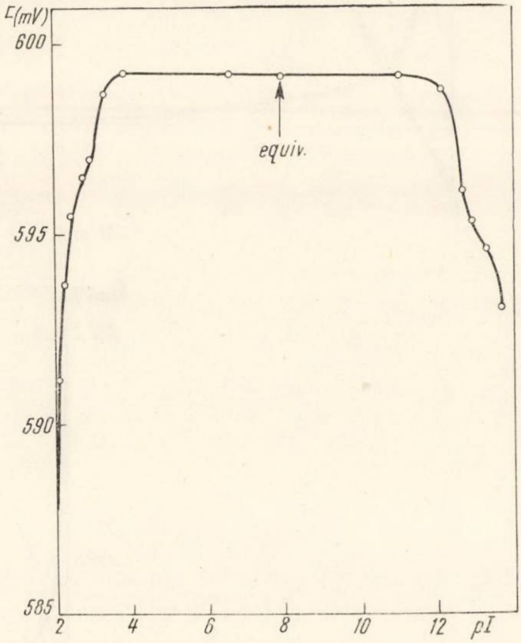

Fig. 10. — E—pI curve from the data of the titration plotted in fig. 5.

Thus for Cl^-, E_M was determined as equal to 546.3 mV and b) as equal to 2.59×10^8 mol^{-1} l.

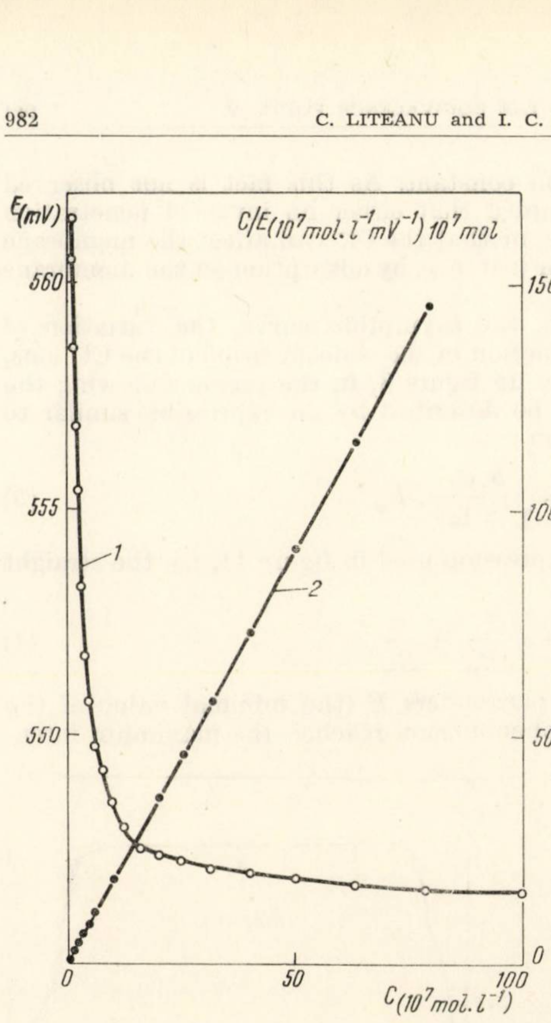

Fig. 11. — Adsorption isotherm of Cl^- on the $BaSO_4$ membrane (*1*) and its linearization (*2*).

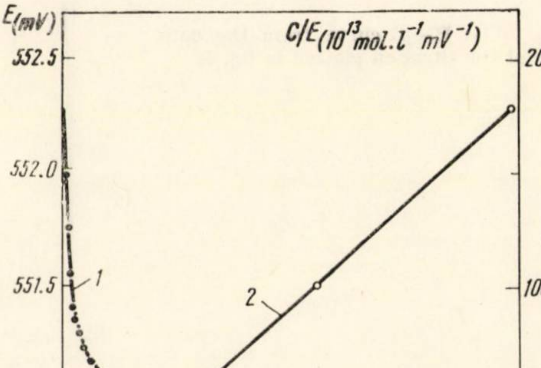

Fig. 12. — Adsorption isotherm of Br on the $BaSo_4$ membrane (*1*) and its linearization (*2*).

The small concentration at which this phenomenon occurs, as well as the fact that the time necessary to an inverse penetration able to affect the electrode potential, is much greater than the time assigned to the reading of the potential in the present experiments, lead us to assign to this phenomenon an adsorptive nature.

The Br^- titration. On the whole, the interdependence of all the phenomena presented in the previous example remains valid. Discussing in a similar way the titration curve of figure 4 by means of the relations (3) and (4) in the region following immediately the equivalence, one has obtained figure 12. The parameters $E_M = 552.2$ mV and $b = 7.45 \times 10^{10}$ mol^{-1}l indicate on the one hand the weakening of the potential-depressing effect and on the other hand the intensification of the retaining forces of Br^-.

The extraction of Br^- ions from the adsorbed state, is not complete, as shown by figure 9, a disturbing effect appearing towards the end of the titration. In this respect, we have to admit that on account of the reduced capacity of penetration through the membrane of Br^- (see the relation (1)) and the lower solubility of AgBr as compared to Cl^- (see relation (2)), the precipitation of AgBr in the pores of the membrane is possible. This leads to a greater or smaller change of the Ba SO_4 membrane electrode into one of AgBr, able to indicate the increase of the Ag concentrations in the solution. Thus knowing that in the presence of an excess of Ag ions, the precipitate has a positive charge, a decrease of the electrode potential is to be expected, a fact experimentally ascertained.

The I^- titration. Every statement made for the Br^- titration also holds in this case, but more clearly marked. Thus the extraction of I^- ions from the adsorbed state is cancelled by a still earlier precipitation of I^- in the pores of the membrane, caused by the much lesser solubility of AgI (see relation (2)). The membrane electrode being impregnated with AgI becomes sensitive to the variation of the concentration of Ag^+ ion. Thus the secondary disturbing phenomenon has a positive influence on the indication. In the case of I^- titration, direct determination of the equivalence point becomes possible from the titration curve.

In figure 13 one has shown with an illustrative character, the curve according to which the logarithm of the ions concentration is varying, when the maximum adsorption is reached (determined from figures 8—10) depending on the radii of the unhydrated ions of Cl^-, Br^-, I^-.

After these discussions the existence of two fundamental phenomena during the function of the membrane electrode: one of diffusion (penetration) and one of preliminary adsorption to the ion-exchange, becomes more probable. Although, to a certain extent their presence was established under different conditions (the first in solutions containing only $H_2SO_4-H_2O-NaX$, the second in solutions of $H_2SO_4-H_2O-NaX-$ $-AgX$) there are no reasons to doubt the above stated facts from this point of view. A proof in this respect is the nonessential difference between the experimental electrode function of pH (determined from the data represented in fig. 6), and the theoretical one calculated from the expression [33]: $E_M = \frac{RT}{zF} \ln \frac{(a_{H^+})_i}{(a_{H^+})_e}$ both represented in figure 14, in this case, too, the differences arise from the nature of the systems concerned with : the theoretical curve is set out only in the presence of $H_2SO_4-H_2O$, while the experimental one in the presence of $H_2SO_4-Na_2SO_4-H_2O$.

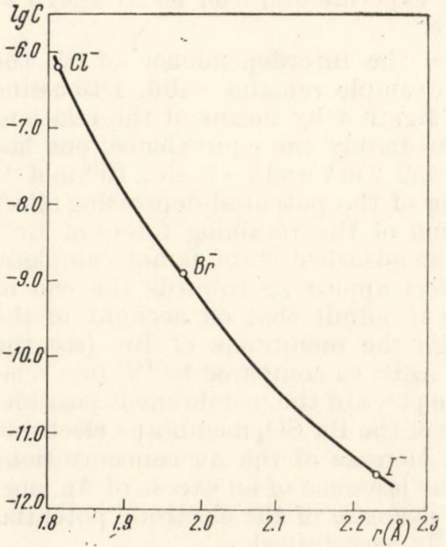

Fig. 13. — Dependence of the adsorption capacity of Cl^-, Br^-, I^- anions on the $BaSO_4$ membrane.

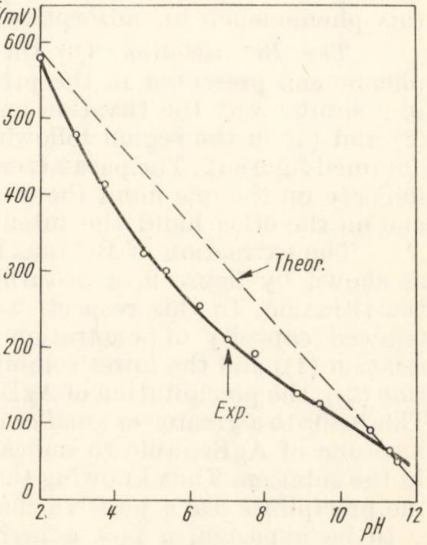

Fig. 14. — Theoretical and experimental pH electrode function of the $BaSO_4$ membrane.

CONCLUSIONS

From the potentiometric titrations made with the precipitation of Cl^-, Br^-, I^-, using the parchment-paper membrane electrode, impregnated with $BaSO_4$, as indicator electrode, the following were established :

1. The titration of Br^- and I^- develops under good conditions, the precision of the determination corresponds to the volumetric titration (1 %), the localization of the equivalence point is rather uncertain.

2. During the functioning of the membrane electrode, besides the diffusion (penetration) there also occurs an adsorption process described by a Langmuir isotherm. Both form two inseparable aspects of the potential-depressing effect.

3. The parchment-paper membrane impregnated with $BaSO_4$ is a cationic membrane with a small exchange capacity, for anions of Cl^-, Br^-, I^- (and F^-) can penetrate it. It is, therefore, immaterial if in the case of the performed experiments, the — COO^- groups in the parchment, or SO_4^{2-} groups adsorbed by the external solution, are considered responsible for its functioning. One can nevertheless contemplate the possibility, in this last case, to increase the membrane's exchange capacity.

4. Any other ions than those of Ba^{2+} and OH^- in the internal solution, respectively differing from $H^+$and SO_4^{2-} in the external solution, can be determined with more or less accuracy using the parchment-paper membrane electrode impregnated with $BaSO_4$ as indicator electrode, as a result of the potential-depressing effect.

La *Revue Roumaine de Chimie* paraît 12 fois par an. Le prix d'un abonnement annuel est de £ 5.0.0 ; $ 12,— ; FF 60,— ; D.M. 48,— . Toute commande de l'étranger (fascicules ou abonnements) sera adressée à Centrala Cărţii, Oficiul de comerţ exterior, Boîte postale 134—135, Bucarest, Roumanie, ou à ses représentants à l'étranger :

ALBANIA Ndërmarja Shtetnore E. Tregëtimit Të Librit Tirana ; AUSTRIA Globus Buchvertrieb Salzgries 16 Wien I ; BELGIUM Du Monde Entier 5, Place St. Jean Bruxelles ; Librairie Claeys-Verheughe 8, Volderstraat Gand ; Maison des Langues Vivantes 65, Rue du Midi Bruxelles ; Office International de Librairie 30, Av. Marnix Bruxelles 5 ; Vander Editeur 10, Munstraat Louvain ; BULGARIA Hemus Pl. Slaveikov 11-Sofia ; CANADA Canadian Slavic Studies Loyola Colege Montreal 262 ; Librairie Lidec Inc. 1083 Van Home Montreal ; Panonia Books 2, Spadina Road Toronto 4 Ontario ; CHINA Waiwen Shudian P.O. Box 88 Peking ; COLOMBIA Libreria Karl-Bucholz Av. Jimenez 8—40 Bogota ; CUBA Cubartimpex P.O. Box 6540 La Habana ; CZECHOSLOVAKIA Artia Ve Smerckach 30 Praha I ; DENMARK Munksgaard 6 Norregade Copenhagen K ; N. J. Hasses-Bogimport 8, Loerstraede Copenhagen K. ; FINLAND Akateeminen Kirjakauppa Postfach 10128 Helsinki 10 ; FRANCE Agence Littéraire et Artistique Parisienne 7, Rue Debelleyme Paris 3-e ; Eyrolles Editeur 61, Boulevard Saint-Germain Paris 5-e ; Librairie de l'enseignement technique (Stand permanent des livres techniques et scientifiques roumains) 61, Boul. Saint-Germain, Paris 5-e ; Librairie Hachette 25, Rue des Cévennes Paris 5-e ; Librairie Joseph Gibert 26—30, Boul. Saint-Michel Paris 6-e ; Libella 12, Rue Saint-Louis-en-l'Ile Paris 4-e ; Maison du Livre Italien 46, Rue des Ecoles Paris 5-e ; Office International de Documentation et Librairie 48, Rue Gay-Lussac Paris 5-e ; Presses Universitaires de France 17, Rue Soufflot Paris 5-e ; THE GERMAN DEMOCRATIC REPUBLIC Deutscher Buch-Export-und-Import Leninstrasse 16 Leipzig C. 1 ; THE FEDERAL REPUBLIC OF GERMANY Kubon Sagner P.O. Box 68 München 34 ; Reise und Verkehrsverlag Hönigwiesenstrasse, 25 7 Stuttgart-Veihingen ; Zumsteins Landkartenhaus Liebherrstrasse, 5 8 München 22 ; GREAT BRITAIN Bailey Bros & Swinfen Ltd. Warner House 48, Upper Thames Street London E.C. 4 City 6521 ; Blackwell's Foreign Department Broad Street Oxford ; Central Books Ltd. 37, Grays Inn Road London W.C.1 ; Collet's Holdings Ltd. Denington Estate London Road Wellingborough Northans N & G Goyle Ltd. 119—125 Charring Cross Road London W.C. 2 ; Parker & Son 103, Walton Street Oxford ; HOLLAND Antiquariat Junk Walderstraat 10 Lochem ; Boekhandel Pegasus Leidsestraat 25 Amsterdam ; Intertaal Van Baerlesstraat 150 Amsterdam Zuit ; Meulenhoff Beulingstraat 2 Amsterdam C ; Swets & Zeitlinger Keizersgracht 471—487 Amsterdam ; HUNGARY Kultura Fö utca 32 Budapest 1 ; ISRAEL Haiflepac Ltd. 11, Arlosorov St. Haifa ; Lepac Ltd, 15, Rambam St. Tel-Aviv ; Lotus Ltd. Achad Haam St. Tel-Aviv ; ITALY SO, CO, LIB, RI Export-Import Piazza Margana 33 Roma ; JAPAN Maruzen Ltd. 6 Tory Michome Nihombashi Tokyo ; Nauka Ltd. Imp. Departm. 30—19 Minami Ikebukuro 2, Chome, Toshima-Ku Tokyo ; DEMOCRATIC PEOPLE'S REPUBLIC OF KOREA Chulpanmul ; MEXICO Editorial Grijalbo S. A. Aparatado 28568 Mexico. 17.D.F. ; MONGOLIA Mongolgosknigotorg Ulan Bator ; NORWAY Norsk Bokimport Postboks 3267 Oslo ; POLAND Ars Polona Krakowskie Przedmiescie 7 Warszawa ; PORTUGAL Libreria Bucholz Avenida Libertade Lisboa ; SPAIN Libreria Bucholz Paseo de Recoletos Madrid ; Libreria Cientifica General Preciados no. 48 Madrid 13 ; SWEDEN Almqvist & Wiksell 26, Gamla Brogatan Stockholm 8. ; C. E. Fritze Fredgatan 2 Stockholm 16 ; Gumperts AB P. O. Box 346 Göteborg I ; SWITZERLAND Fachbücherei Postfach 1420 3001-Berna ; Herbert-Lang Ecke Munzgraben 2 Berna ; Librairie Payot 1-Rue de Bourg Ch-1002 Lausanne ; Librairie Rousseau 36, Rue Jean-Jacques Rousseau Genève ; Pinkus & Co. Froschaugasse 7 Zürich I ; THE UNITED ARAB REPUBLIC Dar El Tahrir et Publishing 21 Kasr el Nil St. (Dar el Shark Bookshop Cairo ; THE U.S.A. Angelescu Book Service 3645, Barham Street Detroit 24 Michigan ; American Chemical Society 1155, Sixteenth Street NW Washington DC 20036 ; Fam Book Service 69, Fifth Avenue Suite 8 F ; New York 10003, N.Y. Franklin Square-Subscription Agency Teaneck (New Jersey 07666) ; W. S. Heinman 400, East 72nd Street New York, 21, N. Y. ; McGraw-Hill Book Company 330, West 42nd Street New York, N.Y. 10036 ; Moore-Cottrell Subscr. Agency Worth Cohocton, New York 14868 ; Nicoară Travel Service 17432, Woodward Ave. Detroit Michigan 48203 ; Shoenhof's Foreign Books, Inc. 1280, Massachusetts Avenue Cambridge, Massachusetts 02138 ; Henry M. Snyder & Co. Inc. 440 Fourth Avenue New York, N.Y. 10016 ; Twayne Publishers, Inc. 31 Union Square West New York 3, N. Y. ; Zeitein & Ver Brugge Booksellers 815 No. La Cienaga BLVD Los Angeles 69, California ; THE U.S.S.R. Mejdunarodnaia Kniga Moscow C. 200 ; THE DEMOCRATIC REPUBLIC OF VIET-NAM Xunhasaba 32, Hai Ba Trung Hanoi ; YUGOSLAVIA Forum V. Misica, 1 Novi Sad ; Jugoslovenska Knjiga Terazije, 27 Beograd ; Libertatea Z. Zrenjanina, 7 Pancevo ; Prosveta Terazije 16 I Beograd.

ORSZÁGOS MŰSZ. KÖNYVTÁR ÉS DOKUMENTÁCIÓS KÖZPONT 1883

ORSZÁGOS MŰSZAKI KÖNYVTÁR ÉS DOKUMENTÁCIÓS KÖZPONT
1883

NOTE POUR LES AUTEURS

La *Revue Roumaine de Chimie* publie des articles en anglais, français, russe, allemand ou espagnol. Les auteurs sont priés d'envoyer des articles, notes, communications et comptes rendus inédits.

Les manuscrits seront dactylographiés à deux intervalles. Les tableaux seront dactylographiés sur feuilles séparées, de même que la légende des figures. Les diagrammes seront tracés à l'encre de Chine sur papier calque. Les tableaux et les figures seront numérotés par des chiffres arabes, en nombre strictement nécessaire. Prière de ne pas inscrire les mêmes données dans les tableaux et les figures. Les formules chimiques seront incluses dans le texte ; en outre, elles seront transcrites sur des feuilles séparées. Les auteurs sont priés d'indiquer les caractères italiques (en soulignant les lettres au crayon), ainsi que toute autre caractère spécial. L'ordre des références bibliographiques sera celui de leur mention dans le texte ; le nom de l'auteur sera précédé de l'initiale du prénom ; les publications périodiques seront présentées suivant les prescriptions internationales. Les références seront ajoutées à la fin de l'article ; elles paraîtront comme des notes, au bas de la page. Le texte sera précédé d'un résumé, comprenant 15 lignes au maximum.

L'entière responsabilité du contenu des articles appartient aux auteurs. On publie des articles dus aux collaborateurs roumains ou étrangers. Les auteurs recevront 50 tirés à part.

PRINTED IN ROMANIA

1970 OKT 14

TRAVAUX PARUS AUX ÉDITIONS DE L'ACADÉMIE DE LA RÉPUBLIQUE SOCIALISTE DE ROUMANIE

CORNEL BODEA et collab., **Tratat de biochimie vegetală**, partea I, **Fitochimie** (Traité de biochimie végétale, Ire partie, Phytochimie), Ier vol., 1964, 747 p. + 4 annexes + 2 pl., 41 lei, IIe vol., 1965, 1262 p., 1 pl., 56 lei, IIIe vol., 1967, 773 p., 35 lei.

V. GHEȚIE et V. MICUȘAN, **Analiza imunochimică. Teorie și practică** (Analyse immunochimique. Théorie et pratique), 1966, 369 p., 28 lei.

R. PORTOCALĂ et L. POPA, **Acizii ribonucleici celulari și virali** (Les acides ribonucléiques cellulaires et viraux), 1966, 375 p. + 8 pl., 26 lei.

D. PURDELA et R. VÎLCEANU, **Chimia compușilor organici ai fosforului și ai acizilor lui** (La chimie des composés organiques du phosphore et de ses acides), 1965, 540 p., 37 lei.

CRISTOFOR SIMIONESCU, MARGARETA GRIGORAȘ et AGATA CERNĂTESCU-ASANDEI, **Chimia lemnului din R.P.R.** (La chimie du bois en Roumanie), 1964, 239 p. + 6 pl., 27 lei.

CRISTOFOR SIMIONESCU et CLEOPATRA VASILIU-OPREA, **Mecanochimia compușilor macromoleculari** (La mécanochimie des composés macromoléculaires), 1967, 344 p., 23,50 lei.

CARMEN SABĂU, **Schimbul ionic, teoria și aplicațiile sale în chimia analitică** (L'échange ionique, Théorie et applications à la chimie analytique), 1967, 307 p., 12 lei.

I. MAXIM, **Materiale nucleare** (Matériaux nucléaires), 1969, 444 p., 30 lei.

CR. SIMIONESCU, C. UGLEA, **Fracționarea compușilor macromoleculari** (Le fractionnement des composés macromoléculaires), 1969, 292 p., 18,50 lei.

I. P. I. c. 5294 | 43 426 | **Lei 25**

F 1103

04

R

REFERALVA

REVUE ROUMAINE DE CHIMIE

TOME 15

N° 7

Juillet 1970

ÉDITIONS DE L'ACADÉMIE DE LA RÉPUBLIQUE SOCIALISTE DE ROUMANIE

Rev. Roumaine Chim.

15, 985–1140 (1970), Bucarest

COMITÉ DE RÉDACTION

Rédacteur en chef :

C. D. NENIȚESCU, membre de l'Académie de la République Socialiste de Roumanie.

Rédacteurs en chef adjoints :

A. T. BALABAN et V. E. SAHINI, membres correspondants de l'Académie de la République Socialiste de Roumanie.

Collège de rédaction :

C. DRĂGULESCU, RALUCA RIPAN, CR. SIMIONESCU, membres de l'Académie de la République Socialiste de Roumanie ; EM. BRATU, membre correspondant de l'Académie de la République Socialiste de Roumanie ; Pr G. OSTROGOVICH, MARG. AVRAM, F. BADEA, I. D. MARCHIDAN, D. NEGOIU et D. SĂNDULESCU.

Les manuscrits, les livres et les revues proposés en échange, ainsi que toute correspondance seront envoyés à la rédaction :

REVUE ROUMAINE DE CHIMIE

23, str. Dumbrava Roșie, Bucarest, Roumanie.

REVUE ROUMAINE DE CHIMIE

Tome 15, N° 7 Juillet 1970

Page

I. G. MURGULESCU und GERDA COMŞA, Adsorption von Kohlenmonoxid an dünnen Silberschichten 987–996

I. G. MURGULESCU et LETIŢIA TOPOR, L'association moléculaire des iodures alcalins en phase gazeuse 997–1004

D. I. MARCHIDAN and M. CIOPEC, Thermal properties of aluminum. High-temperature heat content. 1005–1009

G. VASU, Thermal conductivity of real dense fluids : hard sphere approximation 1011–1016

S. ŢILENSCHI und A. WOHL, Prinzipielles über die Wirksamkeit einiger Reinigungsmethoden durch Adsorption 1017–1028

C. DRĂGULESCU, R. POMOJE, I. MENESSY, M. PÎRLEA und C. MIHĂESCU, Metallkomplexe der Anthranyldiessigsäure (ANDA). VIII. Über Cr(III)-ANDA-Komplexe . . . . 1029–1038 R

RALUCA RIPAN et A. ŞUTEU, Utilisation des hétéropolycombinaisons comme échangeurs d'électrons. IV. L'utilisation du phospho-8-molybdo-2-tungsto-2-vanadate de nitron comme échangeur d'électrons 1039–1042

S. FIŞEL, GIZELLA NEMES, MARIA TOTAN und T. SIMONESCU, Der Einfluß der Trichloressigsäure (TCE) auf die Thoriumextraktion aus wäßrigen Lösungen mit Butanol-1 . . . . 1043–1047 R

T. GOINA, MARIA OLARIU and LUCIA BOCANICIU, Formation constants of the aluminium ion chelates with pyrocatechol and pyrocatechol violet 1049–1056

V. ARMEANU and L. M. BĂLOIU, Contributions to the study of the system dicyanoaurous acid-isoamyl alcohol—water 1057–1059

D. COSTACHE and GR. POPA, Kinetic dosing of the cobalt in vitamin B_{12} 1061–1063

C. CHIRIAC et I. ZUGRĂVESCU, Pyrazoles. II. Aminolyse des 1-(2,4-dinitrophényl)-pyrazoles 1065–1076

ELENA STANCIU-STOIAN, I. VLAGIU, ILEANA PETRUŞ and EMILIA NICULESCU, Radiochemical grafting of acrylonitrile on textile material in heterogeneous system . . . . 1077–1085 R

GH. FURNICĂ et V. VOICU, Rétention de certains ions radioactifs par les macromolécules inorganiques naturelles des suspensions des bassins de surface et de certaines terres actives 1087–1096

MARGARETA AVRAM, DOINA CONSTANTINESCU, I. G. DINULESCU, OANA CONSTANTINESCU-SIMON, GH. D. MATEESCU and C. D. NENITZESCU, Investigation in the cyclobutane series. XXVII. Attempted synthesis of 4.6-Dimethyl-1-*tert.*-butyl-benzo-cyclobutadiene and 4.6-Dimethyl-1-chloro-benzo-cyclobutadiene 1097–1105

J. REICHEL und R. VIDAC, Untersuchungen über Aryldiazosulfonate und Aryldiazosulfonsäuren. I. Über das photochemische Verhalten des benzoldiazosulfonsauren Natriums . . . . 1107–1119 R

C. CRISTESCU, 6-azauracil derivatives with potential cytostatic activity. IX. 6-azauracil-5-sulfonamides 1121–1125

T. RĂDULESCU und H. D. SCHELL, Quartäre Ammoniumsalze des Acetamido-benzal-fluorens 1127–1136

MARIA SZABO, Le marquage du dipholatan avec ^{35}S par synthèse 1137–1140

Revue Roumaine de Chimie, 15, 987–996 (1970)

ADSORPTION VON KOHLENMONOXID AN DÜNNEN SILBERSCHICHTEN

I. G. MURGULESCU und GERDA COMŞA
aus dem Institut für Physikalische Chemie der Akademie
Bukarest, str. Dumbrava Roşie 23

Eingegangen am 24. Dezember 1969

Es wurden Hallspannung und Widerstand 60–90 Å dicker Silberschichten während der Adsorption von Kohlenmonoxid bei 200 bzw. 77°K gemessen. Die Ergebnisse erwiesen, daß die Adsorption bei 200°K wenig wahrscheinlich ist. Tritt jedoch bei dieser Temperatur eine Adsorption auf, dann ist sie reversibel und sehr schwach. Bei 77°K hingegen verursacht Kohlenmonoxid sowohl reversible als auch irreversible Änderungen der elektrischen Parameter. Mit Hilfe der Frenkelschen Gleichung konnte aus der Desorptionskinetik der reversiblen Prozesse die Aktivierungsenergie der Desorption abgeleitet werden, und zwar 14 kcal/Mol für den bei 200°K und 5 kcal/Mol für den bei 77°K beobachteten Vorgang.

In einer Reihe früherer Arbeiten untersuchten wir den Einfluß aktiver Gase auf den Hall-Effekt und den elektrischen Widerstand sehr dünner Metallschichten. [1–4] Es handelte sich hierbei um die Systeme Cu/O_2[1,2] Cu/CO[2] und Ag/O_2.[3] Die wichtigsten qualitativen Ergebnisse können folgendermaßen zusammengefaßt werden : 1. Bei geringen Bedekkungsgraden sind die Hallspannungsänderungen positiv oder negativ, hingegen bei höheren Belegungen und bei Sättigung ausschließlich negativ[1–3]; 2. die Widerstandsänderungen sind bei allen Bedeckungsgraden positiv[1–3]; 3. unter gleichen Bedingungen (hinsichtlich Schichtstruktur und -dicke, Temperatur und Reinheit) hängen die Sättigungswerte der relativen Hallspannungs-und Widerstandsänderungen nur von der Natur des Systems Metall/Gas ab, wobei sie in der Reihenfolge Cu/O_2, Cu/CO, Ag/O_2 abnehmen. Wie von uns nachgewiesen,[3, 5, 6–9] bestätigen die Ergebnisse nicht nur qualitativ sondern auch quantitativ die Hypothese

---

[1] I. G. Murgulescu und G. Comşa, *Rev. Roumaine Chim.*, **11**, 1253 (1966).
[2] I. G. Murgulescu und G. Comşa, *Rev. Roumaine Chim.*, **12**, 1171 (1967).
[3] I. G. Murgulescu und G. Comşa, *Rev. Roumaine Chim.*, **13**, 1261 (1968).
[4] I. G. Murgulescu und G. Comşa, *Rev. Roumaine Chim.*, **14**, 825 (1969).
[5] G. Comşa, *Rev. Roumaine Chim.*, **13**, 1008 (1968).
[6] G. Comşa, *Thin Solid Films*, **4**, 1 (1969).
[7] G. Comşa, *Studii şi Cercetări Fiz.*, (im Druck).
[8] I. G. Murgulescu, G. Comşa und N. I. Ionescu, *J. Catalysis*, **12**, 102 (1968).
[9] I. G. Murgulescu, N. I. Ionescu und G. Comşa, *J. Catalysis*, **13**, 328 (1969).

von Sachtler und Dorgelo[10] bezüglich der Abnahme der effektiven Schichtdicke dünner Metallschichten bei der Adsorption von Gasen.

Als nächstes wählten wir zur Untersuchung das Ag/CO-System, wobei uns auch diesmal das Verhalten der Hallspannung und des elektrischen Widerstandes interessierte. Über die Adsorption von Kohlenmonoxid an Silber liegen nur wenige Daten vor. In Bonds Klassifikation[11] der Metalle und Nichtmetalle auf Grund ihrer adsorptiven Eigenschaften gehört Silber zu den Stoffen, an denen CO nicht adsorbiert wird. In einer von Hayward und Trapnell [12] zusammengestellten Tafel bezüglich der Adsorption von Gasen an Metallfilmen ist das Ag/CO-System mit einem Fragezeichen versehen. In ihren Arbeiten über die Änderung des Oberflächenpotentials dünner Metallschichten bei der Adsorption von Gasen befaßten sich Culver, Pritchard und Tompkins [13] auch mit dem Ag/CO-System für das sie bei 77°K den Sättigungswert + 0,32 V fanden. Dieser Wert weicht nur wenig von demjenigen ab, den dieselben Autoren am Cu/CO-System maßen. Murgulescu und Vass [14] erhielten neuerdings den Wert + 0,20 V für das Oberflächenpotential dünner Silberschichten bei Sättigung mit Kohlenmonoxid. Dégeilh, [15] der die Adsorption von Sauerstoff an Silbereinkristallen untersuchte, bemerkte u.a. an den (100)-Flächen eine stufenweise Verdrängung früher adsorbierter Gase, wie Wasserstoff, Stickstoff oder Kohlenmonoxid, durch den Sauerstoff. Wie ersichtlich, sind die erwähnten Daten einigermaßen widerspruchsvoll und beziehen sich nicht auf den Einfluß der Kohlenmonoxid-Adsorption auf die elektrischen Volumeneigenschaften des Silbers.

EXPERIMENTELLES

Versuchsanlage und Arbeitsweise sind in früheren Arbeiten beschrieben. [1-3] Die Versuche wurden an 60–90 Å dicken Silberschichten durchgeführt, die durch Aufdampfen im Vakuum unter einem Restgasdruck von 10^{-8} Torr an einer auf 77°K gekühlten Glasunterlage erzeugt und anschließend getempert wurden. Die Adsorptionsversuche fanden bei 200 bzw. 77°K statt. Es wurde der elektrische Widerstand R und die Hallspannung U_H gemessen, wobei die Änderung dieser Größen bei Einführung des Kohlenmonoxids in die Versuchszelle erfaßt wurde. Im Falle des Widerstandes wurde die relative Änderung $\Delta R/R_0$ in Abhängigkeit von der Zeit verfolgt. Dies war für die Hallspannung nicht möglich, weil das Messen dieser Größe zu langwierig ist, da jeder Meßpunkt das Mittel von ungefähr 10 Ablesungen darstellt.

ERGEBNISSE

Die Ergebnisse hinsichtlich des Ag/CO-Systems lassen folgende für beide Arbeitstemperaturen gültige Bemerkung zu: Die Resultate sind in gewissem Sinne unreproduzierbar, da bei jeder Temperatur zwei unterschiedliche Gruppen von Ergebnissen auftreten (siehe Tabelle 1). Es muß außerdem betont werden, daß zur Erzielung meßbarer Änderungen der elektrischen Parameter weit größere Mengen des zu untersuchenden Gases notwendig waren als im Falle der Systeme Cu/O_2, Cu/CO oder gar Ag/O_2.

---

[10] W. M. H. Sachtler, G. J. H. Dorgelo, *Z. phys. Chem. (Frankfurt)*, **25**, 69 (1960).

[11] G. C. Bond, „Catalysis by Metals", Academic Press, London, New York, 1962, S. 66.

[12] D. O. Hayward und B. M. W. Trapnell, „Chemisorption", II. Auflage, Butterworths, London, 1964.

[13] R. V. Culver, J. Pritchard und F. C. Tompkins, *Z. Elektrochem.*, **63**, 741 (1959).

[14] I. G. Murgulescu und M. Vass, *Rev. Roumaine Chim.*, (im Druck).

[15] R. Dégeilh, Proc. Fourth Intern. Congress on Catalysis, Moscow, 1968 (Preprint).

Tabelle 1

Die verschiedenen Gruppen von Versuchsergebnissen

Temperatur °K	Anzahl der Versuche, %	Verhalten der elektrischen Parameter (relative Änderungen)
200°	85	$\frac{\Delta U_H}{U_{H_0}} = 0$ $\frac{\Delta R}{R_0} = 0$
	15	$\frac{\Delta U_H}{U_{H_0}} = 0$ $0 < \frac{\Delta R}{R_0} < 1\,\%$ reversibel
77°	50	$\frac{\Delta U_H}{U_{H_0}} \neq 0$ $\frac{\Delta R}{R_0} \neq 0$ irreversibel
	50	$\frac{\Delta U_H}{U_{H_0}} = 0$ $0 < \frac{\Delta R}{R_0} < 1{,}5\,\%$ reversibel

1. *Adsorption bei 200°K.* : Obwohl die eingeführte Kohlenmonoxidmenge ausreichte, den Druck in der Versuchszelle schließlich bis auf ungefähr 10^{-2} Torr zu steigern, ergaben 85 % der bei 200°K durchgeführten Versuche keine Änderung der Hallspannungen oder des elektrischen Widerstandes. Um zu prüfen, ob die Oberfläche nicht vorvergiftet war, benützen wir nach jedem vergeblichen CO-Versuch als Test eine zur Sättigung ausreichende Sauerstoffmenge. Nach der Sauerstoffzufuhr stellten wir jedes Mal einen plötzlichen Anstieg des Widerstandes (Abb. 1) und einen Abfall der Hallspannung fest, wobei Vorzeichen und Größe der relativen Änderungen dieser Parameter übereinstimmten mit den früher [3] für das Ag/CO-System bei 200°K gefundenen Daten (d.h. also in Abhängigkeit von der Silberschichtdicke zwischen + 7 und + 12 % für die Widerstandsänderung und zwischen − 1 und − 4 % für die Hallspannungsänderung). Hinzufügen von Kohlenmonoxid nach der Sättigung mit Sauerstoff sowie Abpumpen des Gases aus der Versuchszelle (in den Abbildungen 1 − 4 mit dem Buchstaben *P* bezeichnet) führte im allgemeinen zu keiner bemerkenswerten Änderung der untersuchten Parameter.

Nur bei 15% der bei 200°K ausgeführten Versuche konnten wir eine Änderung des elektrischen Widerstandes feststellen. Die Änderungen sind gering (ungefähr 1%) im Vergleich zu den 10–20%-großen, an den Systemen Cu/O_2, Cu/CO und Ag/O_2 beobachteten. Charakteristisch für diese Widerstandserhöhungen ist ihre Reversibilität: durch Evakuieren stellte sich sehr rasch der Anfangswert des Widerstandes ein (Abb. 2*a*, *b*).

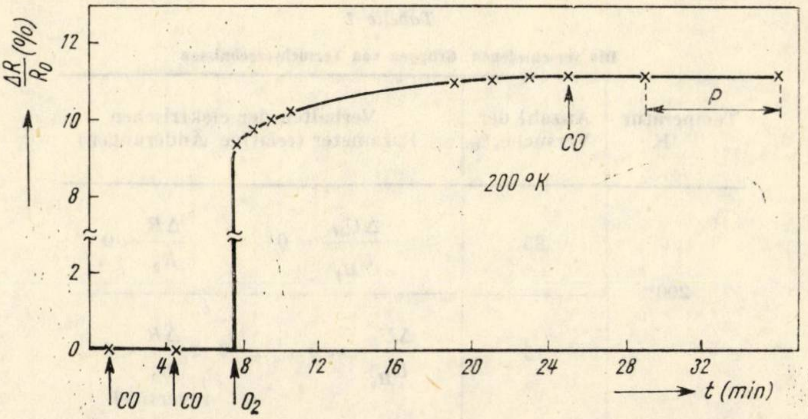

Abb. 1. – $\Delta R/R = f(t)$ – Diagramm für Versuche bei 200°K. Aufeinanderfolgende Einführung von Kohlenmonoxid und Sauerstoff.

Die Hallspannung blieb auch bei dieser Gruppe von Versuchen konstant, was plausibel scheint, wenn unsere früheren Ergebnisse in Betracht gezogen werden: Es wäre zu erwarten, daß die maximalen relativen Hallspannungsänderungen ungefähr 5-mal kleiner wären als die des Widerstandes, also kleiner als 0,2%, was weit unter der Empfindlichkeitsgrenze unserer Meßanordnung liegt. Nachträgliches Einführen von Sauerstoff bewirkt, genau wie bei der ersten Versuchsgruppe einen Anstieg des elektrischen Widerstandes und einen Abfall der Hallspannung, deren Größen mit den für das Ag/O_2-System charakteristischen Daten übereinstimmen.

2. *Adsorption bei 77°K*: Die Hälfte der bei dieser Temperatur durchgeführten Versuche ergaben völlig oder teilweise irreversible Änderungen der elektrischen Parameter, Änderungen die zwar geringer jedoch größenordnungsmäßig mit den für die Systeme Cu/O_2, Cu/CO und Ag/O_2 gefundenen vergleichbar sind. In Abbildung 3 *a*, *b*, *c* ist die Widerstandsänderung bei der Adsorption in Abhängigkeit von der Zeit für zwei derartige Versuche wiedergegeben. Die beiden Experimente unterschieden sich dadurch, daß bei dem ersten (Abb. 3*a*) die Gaszufuhr unmittelbar bei 77°K erfolgte, während bei dem zweiten (Abb. 3*b*) zuerst eine Adsorption bei 200°K versucht worden war. Bei Versuchen der ersten Art war die Änderung des Widerstandes teilweise reversibel, der maximale durch CO hervorgerufene Effekt wurde nachträglich entweder spontan oder durch Abpumpen um 24–35% abgeschwächt. Hingegen waren die Widerstandsänderungen bei Versuchen, die dem in Abb. 3*b* wiedergegebenen entsprechen, praktisch völlig irreversibel.

Die andere Hälfte der bei 77°K durchgeführten Versuche ergab nur sehr geringe und reversible Widerstandsänderungen. Die Hallspannung hingegen änderte sich nicht. In Abb. 4 sind die $\Delta R/R_0 = f(t)$ — Diagramme für 3 Versuche dieser Art aufgetragen. Wie aus diesen Diagrammen ersichtlich, bewirkt ein Evakuieren den völligen Rückgang des durch CO hervorgerufenen Effektes. Darauffolgende Einführung von Sauerstoff ruft einen plötzlichen Widerstandsanstieg hervor, der ungefähr 8mal größer ist als die reversible CO-Einwirkung. Dieser Einfluß des Sauer-

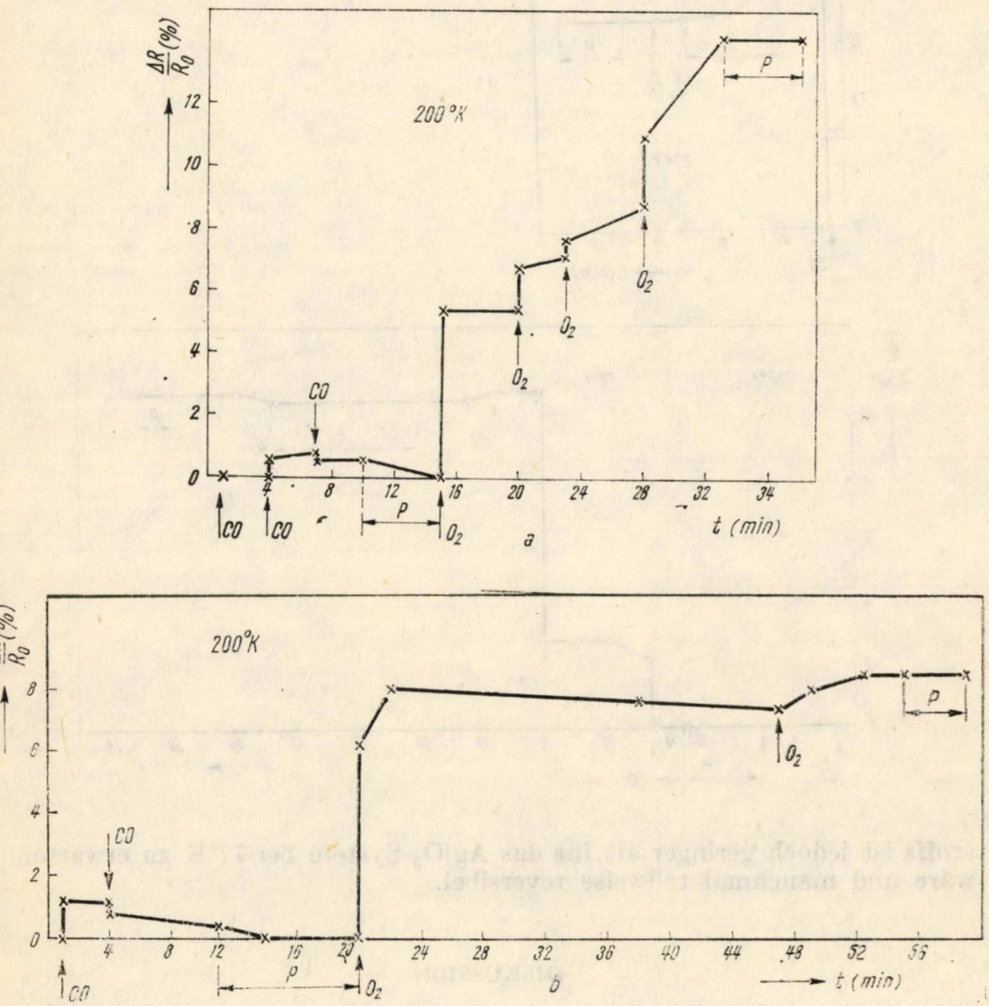

Abb. 2. — Reversible Adsorption von Kohlenmonoxid an Silber bei 200°K.

a) Evakuieren der Versuchszelle nach der CO-Adsorption bis zur völligen Desorption;

b) Fortsetzen des Evakuierens auch nach Beendigung der CO-Desorption.

Abb. 3. – Irreversible Adsorption von Kohlenmonoxid an Silber bei 77°K.

a) CO-Einführung bei 77°K ; *b*) CO-Einführung zuerst bei 200°K, anschließend Evakuieren der Zelle, Abkühlen der Probe auf 77°K und Einführung von CO.

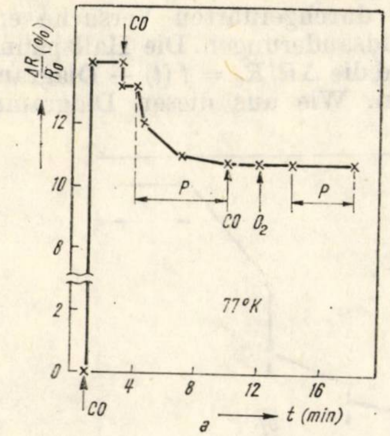

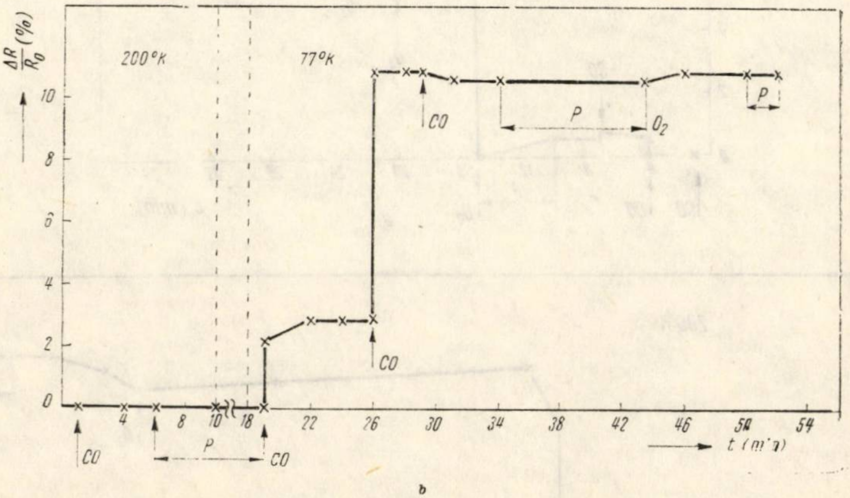

stoffs ist jedoch geringer als für das Ag/O_2-System bei 77°K zu erwarten wäre und manchmal teilweise reversibel.

DISKUSSION

Aus der in Tabelle 1 enthaltenen Statistik der Adsorptionsversuche kann gefolgert werden, daß die Wahrscheinlichkeit einer Kohlenmonoxidadsorption an Silber bei 200°K sehr gering ist. Tritt jedoch eine Adsorption auf, dann ist sie vollkommen reversibel : im Laufe weniger Minuten wurde das Kohlenmonoxid durch Abpumpen desorbiert. Bei 77°K kann Kohlenmonoxid mit gleicher Wahrscheinlichkeit sowohl reversibel als auch irreversibel adsorbiert werden. Es wäre anzunehmen, daß der, die kleinen Widerstandsänderungen bewirkende reversible Vorgang auch dann auftritt, wenn der irreversible Prozeß beobachtet wird, jedoch von den

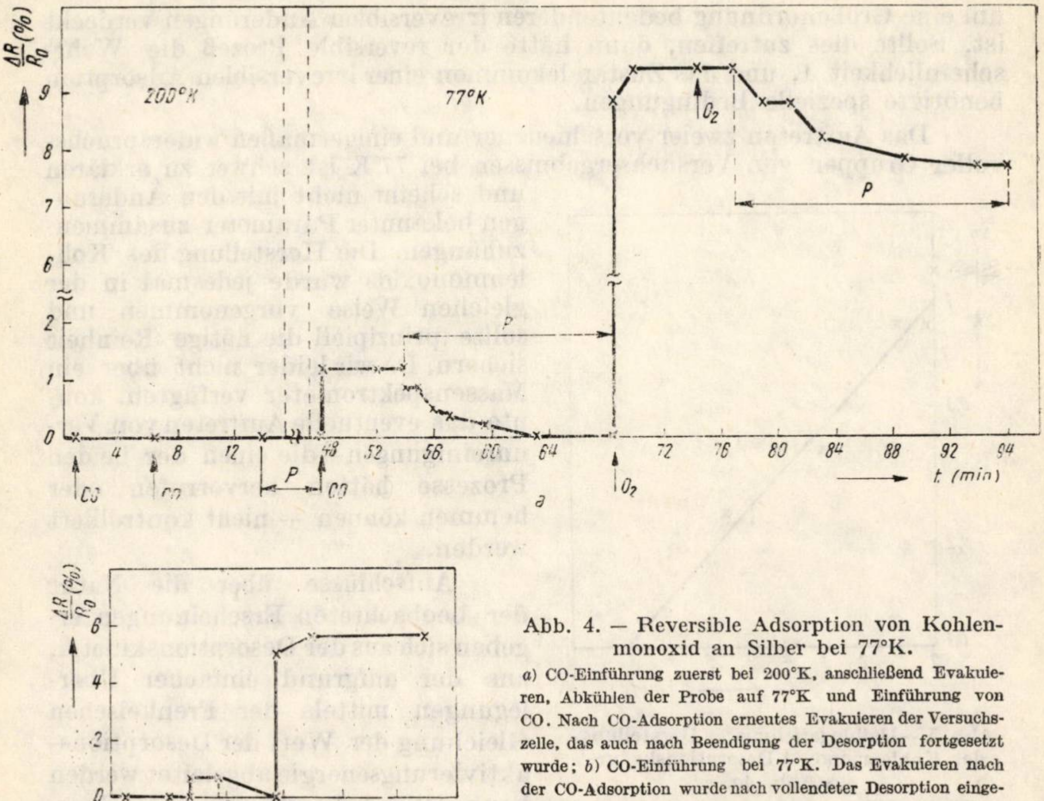

Abb. 4. — Reversible Adsorption von Kohlenmonoxid an Silber bei 77°K.

a) CO-Einführung zuerst bei 200°K, anschließend Evakuieren, Abkühlen der Probe auf 77°K und Einführung von CO. Nach CO-Adsorption erneutes Evakuieren der Versuchszelle, das auch nach Beendigung der Desorption fortgesetzt wurde; *b*) CO-Einführung bei 77°K. Das Evakuieren nach der CO-Adsorption wurde nach vollendeter Desorption eingestellt; *c*) Wie unter Punkt *a*, jedoch größere Schichtdicke.

um eine Größenordnung bedeutenderen irreversiblen Änderungen verdeckt ist. Sollte dies zutreffen, dann hätte der reversible Prozeß die Wahrscheinlichkeit 1, und das Zustandekommen einer irreversiblen Adsorption benötigte spezielle Bedingungen.

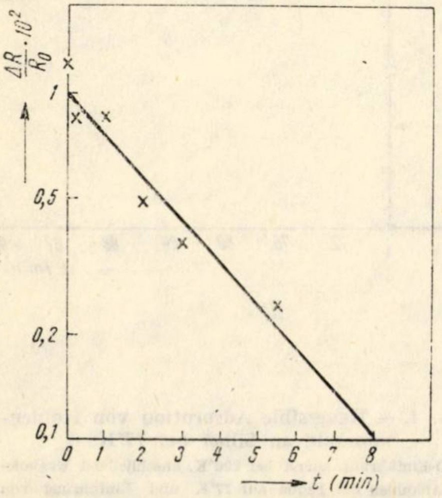

Abb. 5. — Halblogarithmische Darstellung der Kohlenmonoxid-Desorptionskurve aus Abb. 4*a*.

Das Auftreten zweier verschiedener und einigermaßen widerspruchsvoller Gruppen von Versuchsergebnissen bei 77°K ist schwer zu erklären und scheint nicht mit den Änderungen bekannter Parameter zusammenzuhängen. Die Herstellung des Kohlenmonoxids wurde jedesmal in der gleichen Weise vorgenommen und sollte prinzipiell die nötige Reinheit sichern. Da wir leider nicht über ein Massenspektrometer verfügten, konnte das eventuelle Auftreten von Verunreinigungen — die einen der beiden Prozesse hätten hervorrufen oder hemmen können — nicht kontrolliert werden.

Aufschlüsse über die Natur der beobachteten Erscheinungen ergeben sich aus der Desorptionskinetik, aus der aufgrund einfacher Überlegungen mittels der Frenkelschen Gleichung der Wert der Desorptionsaktivierungsenergie abgeleitet werden kann. (Wie bekannt, ist diese Energie im Falle einer Adsorption ohne Aktivierung gleich der Adsorptionswärme.) Zu diesem Zwecke werden wir uns einer bereits früher [3] angewendeten und dort begründeten Annahme bedienen, derzufolge die relative Widerstandsänderung $\Delta R/R_0$ beim Ag/O_2-System dem Bedekkungsgrad und demnach der Zahl der adsorbierten Moleküle proportional ist. Sollte diese Hypothese auch im Falle des Ag/CO-Systems gültig sein, dann können wir annehmen, daß die CO-Desorptionskurven in den $\Delta R/R_0 = f(t)$-Diagrammen der Abb. 2 und 4 eigentlich die Kurven $N = f(t)$, d.h. also das Abklingen — durch Desorption — der pro cm² adsorbierten Moleküle N darstellen.

Wir werden uns zunächst mit der Desorptionskurve aus Abb. 4*a* befassen, bei der wir über mehrere Punkte verfügen. Eine halblogarithmische Darstellung dieser Kurve ergibt eine Gerade (Abb. 5), woraus zu schließen ist, daß der Desorptionsvorgang ein Prozeß erster Ordnung ist:

$$N = N_0 e^{-t/\tau} \tag{1}$$

N_0 stellt die Zahl der pro cm² bei Sättigung adsorbierten Moleküle, τ die mittlere Adsorptionszeit, eine temperaturabhängige Größe, die aus der Neigung der Geraden in Abb. 5 gewonnen werden kann. Die Temperaturabhängigkeit der mittleren Adsorptionszeit ist durch die Frenkelsche Gleichung wiedergegeben:

$$\tau = \tau_0 e^{E_d/RT} \tag{2}$$

in der E_d die Desorptionsaktivierungsenergie, τ_0 die „charakteristische Zeit" [16] (d.h. der reziproke Wert des Frequenzfaktors aus der Arheniusschen Gleichung) und R die Gaskonstante ist. Für τ_0 wird üblicher Weise der Wert 10^{-13} sec eingesetzt (ein aus vereinfachenden theoretischen Überlegungen abgeleiteter Wert, der in vielen experimentellen Fällen befriedigend ist), obwohl bereits für einige Systeme dagegensprechende Versuchsergebnisse [16-18], sowie Einwürfe theoretischer Natur vorliegen [16]. Mit diesem Wert für τ_0 und dem aus Abb. 5 berechneten τ erhält man die Aktivierungsenergie des bei 77°K beobachteten Desorptionsvorganges: 5,42 kcal/Mol.

Bei den zwei $\Delta R/R_0 = f(t)$ — Diagrammen in Abb.4 sowie bei denen in Abb. 2 sind die der Kohlenmonoxiddesorption entsprechenden Kurven der fehlenden Zwischenpunkte wegen ungenau. Aus diesem Grunde sind die hieraus abgeleiteten E_d-Werte nur maximale Schätzungswerte. So ergeben sich aus den Abb. 4*b* und *c* die Werte $E_d = 5{,}4$ kcal/Mol und $E_d = 5{,}1$ kcal/Mol, hingegen aus den Abb. 2*a* und *b*, also für den bei 200°K beobachteten Adsorptionsvorgang, die Werte $E_d = 14{,}1$ kcal/Mol und $E_d = 13{,}9$ kcal/Mol.

Die Desorptionsaktivierungsenergie von ungefähr 5 kcal/Mol, die für den bei 77°K auftretenden reversiblen Vorgang gefunden wurde, fällt in den Bereich der für eine Physisorption von Kohlenmonoxid möglichen Werte. Hayward und Trapnell [12] berechneten aus der BET-Gleichung den größtmöglichen Wert der Physisorptionswärme dieses Gases, und zwar 6 kcal/Mol. Im Vergleich damit könnte also der von uns bei 77°K beobachtete reversible Adsorptionsvorgang als Physisorption gelten.

Der Wert von ungefähr 14 kcal/Mol, den wir für den bei 200°K auftretenden reversiblen Adsorptionsvorgang fanden, ist für eine Physisorption zu groß und für eine Chemisorption verhältnismäßig gering. Da keine Literaturhinweise bezüglich der Chemisorptionswärme von Kohlenmonoxid an Silber vorliegen, verglichen wir unser Ergebnis mit den von Hayward und Trapnell [12] für die Kohlenmonoxidchemisorption an dünnen Kupfer- und Goldschichten angegebenen isosterischen Adsorptionswärmen, nämlich 9 kcal/Mol. Im Vergleich damit scheint unser Ergebnis ein plausibler Wert zu sein, der darauf hinweist, daß der von uns bei 200°K beobachtete Vorgang eine Chemisorption sein könnte. Aus Gleichung (2) ist jedoch leicht zu entnehmen, daß ein Adsorptionsvorgang, dessen Desorptionsaktivierungsenergie 14 kcal/Mol beträgt und der bei 200°K reversibel ist, bei niedrigeren Temperaturen praktisch irreversibel wird. So ist z.B. bei 77°K die mittlere Adsorptionszeit von der Größenordnung 10^{26} Sekunden. Demnach könnten die irreversiblen Änderungen der elektrischen Parameter, die wir bei 77°K fanden, derselben Adsorptionserscheinung zugeschrieben werden, wie die bei 200°K beobachteten reversiblen Änderungen, nämlich einer Chemisorption mit $E_a = 14$ kcal/Mol. Diese Behauptung bedarf natürlich noch einer unmittelbaren experimentellen Bestätigung.

---

[16] L. A. PETERMANN, *Suppl. Nuovo Cimento*, V, 2, 364 (1967).

[17] D. A. DEGRAS, Thesis, CEA-R, 3123, CEN-Saclay 1966.

[18] A. CAVALERU, G. COMŞA und B. IOSIFESCU, *Vacuum*, 18, 549 (1968).

SCHLUSSBEMERKUNG

Messungen von Widerstand und Hallspannung während der Adsorption von Kohlenmonoxid an dünnen Silberschichten ergaben folgendes:

1. Die Adsorption von Kohlenmonoxid an Silber ist bei 200°K wenig wahrscheinlich, reversibel und gekennzeichnet durch eine Aktivierungsenergie der Desorption von ungefähr 14 kcal/Mol.

2. Bei 77°K konnten zwei Vorgänge beobachtet werden, eine reversible Adsorption, gekennzeichnet durch eine Desorptionsenergie von ungefähr 5 kcal/Mol, und eine in den gegebenen Versuchsbedingungen irreversible Adsorption.

Revue Roumaine de Chimie, **15**, 997–1004 (1970)

L'ASSOCIATION MOLÉCULAIRE DES IODURES ALCALINS EN PHASE GAZEUSE

I. G. MURGULESCU et LETIŢIA TOPOR

Institut de Chimie Physique de l'Académie, Bucarest, 31, str. Galaţi

Reçu le 27 décembre 1969

Les données sur l'association moléculaire des iodures de sodium, potassium, rubidium et césium ont été obtenues à partir des mesures des pressions de vapeur par la méthode du transport, en utilisant aussi les résultats fournis par la méthode Rodebush-Dixon (données déjà publiées). Nous avons calculé : les poids moléculaires moyens des vapeurs de NaI, KI, RbI et CsI ; les pressions partielles du monomère et du dimère présents dans la phase vapeur ; les chaleurs de sublimation et de vaporisation du monomère et du dimère à la température de fusion ; les chaleurs de dissociation du dimère et les valeurs de ΔH_{298}.

Les études effectuées sur la vapeur d'halogénures alcalins par diverses méthodes [1–8] ont mis en évidence la présence des polymères. Les moins étudiés ont été les iodures alcalins. La vapeur des iodures de lithium, sodium, potassium et césium en équilibre avec la phase solide à haute température a été étudiée par spectrométrie de masse[4, 9, 10]. La même méthode a été utilisée dans les études des iodures de sodium, potassium, rubidium et césium en équilibre avec la phase liquide [11]. Des mesures directes de densité de la vapeur à hautes températures ont été effectuées pour les iodures de sodium et de potassium [8].

Nous avons étudié la vapeur des iodures de sodium, de potassium, de rubidium et de césium en équilibre avec la phase liquide, en mesurant les pressions de vapeur par la méthode du transport. En combinant les données fournies par cette méthode, avec celles obtenues par la méthode

[1] R. C. Miller et P. Kusch., *J. Chem. Phys.*, **25**, 860 (1956).
[2] T. A. Milne et H. M. Klein, *J. Chem. Phys.*, **33**, 1628 (1960).
[3] J. Berkowitz, H. A. Tasman et W. A. Chupka, *J. Chem. Phys.*, **36**, 2170 (1962).
[4] J. Berkowitz et. W. A. Chupka, *J. Chem. Phys.*, **29**, 653 (1958).
[5] R. C. Schoonmaker et R. F. Porter, *J. Chem. Phys.*, **30**, 283 (1959).
[6] T. A. Milne, H. M. Klein et D. Cubicciotti, *J. Chem. Phys.*, **28**, 718 (1958).
[7] T. A. Milne, *J. Chem. Phys.*, **32**, 1275 (1960).
[8] S. Datz, W. T. Smith et E. H. Taylor, *J. Chem. Phys.*, **34**, 558 (1961).
[9] L. Friedman, *J. Chem. Phys.*, **23**, 477 (1955).
[10] P. Winchell, *Nature*, **206**, 1252 (1965).
[11] G. Platel, *J. Chim. phys.*, **10**, 1176 (1965).

Rodebush-Dixon [12,13] nous avons calculé les poids moléculaires moyens des vapeurs et les grandeurs thermodynamiques caractéristiques des processus de vaporisations et d'association.

PARTIE EXPÉRIMENTALE

La méthode de Rodebush-Dixon et celle du transport, l'appareillage et la conduite des essais ont été déjà présentés. [12,14]

On peut calculer les poids moléculaires moyens des vapeurs en utilisant les données fournies par ces méthodes et la relation

$$\overline{M} = (g/n_A)\,(P_t/p - 1) \qquad (1)$$

où g désigne le poids en mg de la substance entraînée par le gaz inerte et condensée, n est le nombre de moles du gaz inerte passé par la cellule du transport, P_t est la pression totale dans l'installation et p est la pression de vapeur déterminée par la méthode Rodebush-Dixon. Le nombre de moles de gaz inerte n a été calculé par la loi de gaz parfaits, en utilisant les valeurs lues au vase Mariotte attaché à l'installation et la relation :

$$n_A = (P_{\mathrm{atm}} - \Delta P_{\mathrm{H_2O}} - p_{\mathrm{H_2O}})\, g_{\mathrm{H_2O}}/R\,(273 + t)\, \rho_{\mathrm{H_2O}} \qquad (2)$$

où P_{atm} désigne la pression atmosphérique en mm Hg, $\Delta P_{\mathrm{H_2O}}$ la différence entre la pression du vase Mariotte et la pression atmosphérique en mm Hg, g la quantité de l'eau, en grammes, écoulée du vase Mariotte pendant une détermination, $\rho_{\mathrm{H_2O}}$ la densité de l'eau à la température t du vase Mariotte et $p_{\mathrm{H_2O}}$ la pression de vapeur de l'eau à la même température.

RÉSULTATS ET DISCUSSION

Dans les tableaux 1—4 sont inscrites les données expérimentales obtenues par la méthode du transport et les poids moléculaires moyens $\overline{M}$ des vapeurs calculés en utilisant la relation (1). P_t représente la pression totale dans l'installation et p la pression de vapeur déterminée par la méthode Rodebush-Dixon. Le nombre de moles de gaz inerte, n, a été calculé suivant la relation (2). En connaissant le poids moléculaire moyen nous avons calculé les fractions molaires x_i et les pressions partielles p_i du monomère et du dimère suivant les relations

$$x_i = (\overline{M}/M - 1) \qquad (3)$$

$$p_i = x_i\, p \qquad (4)$$

où M désigne le poids moléculaire du sel étudié et p représente la pression de vapeur obtenue par la méthode Rodebush-Dixon. Dans le tableau 5

---

[12] I. G. MURGULESCU et L. TOPOR, *Rev. Roumaine Chim.*, **11**, 1353 (1966).
[13] I. G. MURGULESCU et L. TOPOR, *Rev. Roumaine Chim.*, **12**, 1077 (1967).
[14] I. G. MURGULESCU et L. TOPOR, *Rev. Roumaine Chim.*, **13**, 1109 (1968).

Tableau 1

Données de transport et poids moléculaire moyen de la vapeur de NaI

T°C	999		1000		1050	1051	1052	1100	1101		1004
P_t	754,3							757,2			
Le vase Mariotte											
ΔP_{H_2O}	6,6										
t°C	27		26		28			26			
g_{H_2O}	101,5	102,5	100,9	101,4	51,0	51,3	57,2	51,5	52,3	52,7	52,0
n_A	3,9219	3,9606	3,9189	3,9384	1,9604	1,9719	2,1987	2,0079	2,0391	2,0547	2,0275
mg_{sel}	59,3	62,9	63,2	63,2	54,0	57,6	65,3	100,3	103,5	104,2	107,9
p	48,8	49,3			85,3	86,2	87,1	141,8	143,3		147,5
$\overline{M}$	233,7	227,1	230,6	229,4	216,0	226,4	227,5	216,7	217,4	217,3	220,0

Tableau 2

Données de transport et poids moléculaire moyen de la vapeur de KI

T°C	1000			1043		1045	1081	1082	1084
P_t	755,0			754,0					
Le vase Mariotte									
ΔP_{H_2O}	7,2								
t°C	27	28		27			28		
g_{H_2O}	104,8	109,7	100,4	62,2	61,0	63,6	51,5	50,5	50,4
n_A	4,0463	4,2135	3,8563	2,3978	2,3515	2,4517	1,9796	1,9412	1,9374
mg_{sel}	59,4	61,1	56,0	52,6	49,4	55,4	63,2	69,6	67,9
p	49,9			78,6		80,3	113,5	115,7	118,0
$\overline{M}$	207,4	204,9	205,2	188,5	180,5	190,0	180,2	197,8	188,9

Tableau 3

Données de transport et poids moléculaire moyen de la vapeur de RbI

T°C	996	998	1000		1049	1050	1051
P_t	757,4				757,9		
Le vase Mariotte							
ΔP_{H_2O}	6,6						
t°C	26						
g_{H_2O}	100,7	101,1	102,4	102,3	53,0	51,5	51,2
n_A	3,9283	3,9004	3,9946	3,9467	2,0686	2,0100	1,9983
mg_{sel}	72,6	75,8	77,3	75,8	68,2	67,8	71,3
p	53,4	54,7	55,8		94,6	95,5	96,5
$\overline{M}$	243,6	249,7	243,3	241,5	231,2	233,8	244,4

Tableau 4

Données de transport et poids moléculaire moyen de la vapeur de CsI

T°C	1003			1048	1050			1103				
P_t	751,9				752,2			755,7				
Le vase Mariotte												
ΔP_{H_2O}	7,4											
t°C	26			27		26		26				
g_{H_2O}	101,8	103,8	150,3	51,2	51,8	51,6	52,1	52,5	51,8	53,0	51,0	50,5
n_A	3,9366	4,0160	5,8151	1,9696	1,9927	1,9958	2,0152	2,0406	2,0134	2,0601	1,9823	1,9629
mg_{sel}	128,0	129,7	187,6	114,7	118,5	113,1	115,8	203,2	195,0	201,9	192,3	187,0
p	67,8			108,8	111,0			168,1				
$\overline{M}$	328,1	325,8	325,5	344,2	343,3	327,2	331,8	348,0	338,5	342,6	339,1	333,0

sont présentés les moyennes des $\overline{M}$, les poids moléculaires des iodures étudiés M, et les fractions molaires du dimère présent dans la phase vapeur.

Tableau 5

Les poids moléculaires moyens des vapeurs des iodures alcalins et les fractions molaires du dimère

La Substance	NaI	KI	RbI	CsI
$\overline{M}_{\text{moyen}}$	223,9	193,7	241,1	335,6
M	149,9	166,0	212,4	259,8
x_2	0,49	0,17	0,14	0,29

En représentant graphiquement le log p_1 ou le log p_2 en fonction de $1/T$ et en utilisant la méthode des moindres carrés, on trouve la formulation générale

$$\log p_{1(2)} = -\frac{\Delta H^0_{1(2)}}{4{,}575\,T} + \frac{\Delta C_{p_{1(2)}}}{R}\log T - I \qquad (5)$$

où $\Delta H^0_{1(2)}$ désigne la chaleur de vaporisation du monomère (dimère) et $\Delta C_{p_{1(2)}}$ la différence entre la chaleur spécifique du monomère (dimère) en phase gazeuse et en phase liquide. Les chaleurs spécifiques du monomère et du dimère ont été déduites d'après la théorie classique des chaleurs spécifique des gaz parfaits, en résultant 8,91 cal/mole.grad pour le monomère et 19,80 cal/mole. grad pour le dimère.

La chaleur spécifique de l'iodure de césium liquide est connue [15]. Pour les autres iodures liquides nous avons calculé les chaleurs spécifiques, en utilisant la différence entre les chaleurs spécifiques du gaz et du liquide, ΔC_p, et les chaleurs spécifiques des gaz, $C_{p_{\text{gaz}}}$.[16] Dans le tableau 6 sont présentées les équations qui représentent la variation des pressions de vapeur du monomère et du dimère en fonction de la température. Dans le tableau 7 sont inscrites les grandeurs thermodynamiques caractéristiques du processus de vaporisation : dans les deux premières colonnes les chaleurs de vaporisation du monomère et du dimère, dans la troisième les valeurs que nous avons obtenues sur la chaleur de dissociation du dimère, ainsi que celles publiées par d'autres auteurs [8], dans les colonnes 4—7 nos résultats sur les chaleurs de vaporisation et de sublimation du monomère et du dimère à la température de fusion et les valeurs publiées par Blander [17], dans la dernière colonne les valeurs de ΔH_{298} calculées à partir des fonctions d'énergie libre et de pression de vapeur du monomère suivant nos résultats et ceux de Brewer et Brackett[18].

---

[15] O. Kubaschewski, E. Evans et C. B. Alcock, « Metallurgical Thermochemistry », Ed. IV, Pergamon Press, Londres 1967, Tableau D.

[16] K. K. Kelley, «Contribution to the Data on Theoretical Metalurgy», Bureau of Mines Bulletin, n° 601 (1962); n° 592 (1961).

[17] M. Blander, «Molten Salt Chemistry», Interscience, New York, 1964, p. 627.

[18] L. Brewer et E. Brackett, *Chem. Rev.*, **61**, 425 (1961).

Tableau 6

Equations des pressions de vapeur du monomère et du dimère

$\log p_1$ (mm Hg)	$\log p_2$ (mm Hg)
NaI	
$-9985/T - 3{,}4224 \log T + 19{,}85$	$-11\,397/T - 5{,}8483 \log T + 28{,}50$
KI	
$-9689/T - 3{,}4626 \log T + 19{,}97$	$-11\,101/T - 5{,}9288 \log T + 28{,}05$
RbI	
$-10\,450/T - 3{,}4777 \log T + 20{,}64$	$-11\,886/T - 5{,}9500 \log T + 28{,}65$
CsI	
$-10\,103/T - 4{,}1723 \log T + 22{,}55$	$-11\,943/T - 7{,}348 \log T + 33{,}47$

La chaleur de dissociation a été calculée suivant la relation

$$\Delta H_{dis} = 2\,\Delta H_1 - \Delta H_2 \qquad (6)$$

La méthode du troisième principe [19,20] et la relation (7) ont été utilisées pour calculer ΔH_{298}

$$-R \ln p_1 = \Delta\left(\frac{\Delta F^0_T - \Delta H^0_{298}}{T}\right) + \frac{\Delta H^0_{298}}{T} \qquad (7)$$

où p_1 est la pression partielle du monomère d'après la relation (4); $\Delta\left(\frac{\Delta F^0_T - \Delta H^0_{298}}{T}\right)$ est la différence des fonctions d'énergie libre entre le gaz diatomique et la phase condensée et ces valeurs ont été calculées par Brewer et Brackett.[18]

L'analyse du tableau 7 montre une bonne concordance entre nos résultats et ceux déterminés expérimentalement [8] ou calculés [17,18] par d'autres auteurs. Pour les fractions molaires du dimère (tableau 5) nos

---

[19] J. O'M Bockris, J. L. White et J. D. Mackenzie «Physico-Chemical Measurements at High Temperatures», Butterworths, Londres, 1959, p. 353.

[20] J. L. Margrave, *J. Chem. Educ.*, **32**, 520 (1963).

Tableau 7

Chaleurs de vaporisation, de sublimation et de dissociation des iodures alcalins

ΔH_1	ΔH_2	$\Delta H_{dissoc.}$		$\Delta H_{1\,vap.}$	$\Delta H_{2\,vap.}$	$\Delta H_{1\,subl.}$	$\Delta H_{2\,subl.}$	ΔH_{298}
				à la température de fusion				
kcal/mole		T° K	kcal/mole					
			NaI					
$45{,}7-6{,}8.10^{-3}T$		1300	36,6^{a}	39,4^{a}	41,3^{a}	45,0^{a}	52,6^{a}	52,4^{a}
			42,8^{b}					
	$52{,}1-11{,}62.10^{-3}T$	1000	37,3^{a}					
			41,5^{c}	39,1^{c}	36,7^{c}	44,7^{c}	47,9^{c}	
								53,3^{d}
			KI					
$44{,}3-6{,}88.10^{-3}T$		1300	35,3^{a}	37,7^{a}	39,6^{a}	43,4^{a}	51,1^{a}	47,9^{a}
			37,3^{b}					
	$50{,}8-11{,}78.10^{-3}T$	1000	35,8^{a}					
			37,5^{c}	39,9^{c}	42,2^{c}	45,6^{c}	53,7^{c}	
								48,5^{d}
			RbI					
$47{,}8-6{,}91.10^{-3}T$	$54{,}4-11{,}84.10^{-3}T$	1000	39,3^{a}	41,4^{a}	43,5^{a}	46,7^{a}	54,0^{a}	47,7^{a}
			35,5^{c}	38,8^{c}	43,0^{c}	44,5^{c}	53,5^{c}	
								47,3^{d}
			CsI					
$46{,}2-8{,}29.10^{-3}T$	$54{,}6-14{,}6.10^{-3}T$	1000	35,8^{a}	38,7^{a}	41,5^{a}	44,3^{a}	52,8^{a}	46,1^{a}
			33,0^{c}	38,4^{c}	43,7^{c}	44,0^{c}	55,0^{c}	
								46,7^{d}

---

a = nos résultats
b = référence [8]
c = référence [16]
d = référence [17]

résultats sont en accord avec ceux de Datz [8] obtenus par des mesures directes des densités de vapeur (de 0,488 à 0,210 pour NaI entre 1212 et 1353°K et de 0,237 à 0,077 pour KI entre 1226 et 1385°K). On peut constater que la fraction molaire du dimère diminue de NaI à RbI et augmente pour CsI.

La même variation a été observée pour les chlorures et les bromures alcalins [12,14].

Un comportement particulier des halogénures de césium par rapport aux autres halogénures alcalins a été observé aussi pour autres propriétés. Par exemple, la variation du volume molaire à la fusion diminue de Li à Rb (et de F à I) mais augmente nettement pour le bromure et l'iodure de césium.[17]

En ce qui concerne la variation du rapport $\Delta H_f/RT_f\alpha^{1/3}$ (où ΔH_f représente la chaleur de fusion, T_f la température de fusion et α la polarisation) en fonction de celui des rayons du cation et de l'anion, on observe aussi une régularité pour tous les halogénures alcalins, sauf pour ceux de césium.[21]

Il est possible que la dimension de l'ion césium et les forces de polarisation aient un rôle important dans le comportement des halogénures de césium.

---

[21] H. Kanno, *Nature*, **218**, 765 (1968).

Revue Roumaine de Chimie, 15, 1005–1009 (1970)

THERMAL PROPERTIES OF ALUMINUM. HIGH-TEMPERATURE HEAT CONTENT

D. I. MARCHIDAN and M. CIOPEC

Institute of Physical Chemistry
Bucharest, Str. Galaţi 31

Received February 14, 1970

High-temperature heat contents of aluminum have been measured over the temperature range 400° to 900° K using a copper-block drop calorimeter. A tabulation of computed values is presented for heat capacity, entropy and free energy function.

The knowledge of the physico-chemical properties of metals and alloys is essential for the proper engineering of their production and processing facilities. Thermal properties are an important part of this information.

The literature on the enthalpy and heat capacity of aluminum has been well documented by McDonald [1] and Brooks. [2]

This paper presents new experimental specific heat data of aluminum from 400 to 900°K, using a copper-block drop calorimeter. [3]

EXPERIMENTAL

The experimental technique has been described in detail in a previous paper [3] and the accuracy of the measurements is considered to be within the reproducibility, which was ±0.4 per cent.

The sample was about 1.7 cm in diameter and 2.5 cm long, and weighed 11.72 g. It was machined from an ingot of high purity aluminum.

The calorimeter was calibrated using electrical calibrations. The resistance-heated furnace contained a metallic block, the temperature of which was maintained within ±0.5° by a proportional controller, using a Pt-10% Rh control thermocouple. The temperature of the sample was measured by another Pt-10% Rh thermocouple. This thermocouple was close to the sample which was suspended in the center well of the metallic block. The measuring thermocouple was checked against a Degussa (Germany) calibrated thermocouple.

---

[1] R. A. McDonald, *J. Chem. and Eng. Data*, **12**, 115 (1967).

[2] C. R. Brooks and R. E. Bingham, *J. Phys. Chem. Solids*, **29**, 1553 (1968).

[3] D. I. Marchidan and M. Ciopec, *Studii şi Cercet. Chim. Acad. R.S. România*, **17**, 737 (1969).

The sample is suspended in the metallic block by 0.1 mm diameter Cronix wires. The suspension wire is clamped between two massive kanthal electrodes which are fixed in an $x - y$ motion device that allows adjustment of the position of the heated sample from outside. The kanthal electrodes are connected by flexible copper straps to an auto-transformer. When the sample should be released the current passes through the suspension wire causing it to vaporize rapidly. Very reliable and precise release of the sample is achieved in this manner. Experiments have shown that no heat correction is required for this discharge energy.

Electrical calibration of the calorimeter was carried out over the same temperature change as the experimental drop. The energy equivalent of the calorimeter was measured by means of a small electric heater mounted inside the calorimeter. A series of 10 electrical calibrations gave an energy equivalent of 300 cal per °K with a standard deviation of ± 0.62 cal per °K.

The temperature change of the calorimeter-block is determined from the resistance of a glass-coated thermistor. The thermistor is dropped into a hole, midway between the receiver hole in the copper block and the outer wall of the block. The resistance of the thermistor is followed manually with a Wheatstone (Mellenbach) bridge. At 25° the thermistor has a resistance of 25000 ohms. A change of 0.001° causes a change of 1 ohm in the thermistor. Some difficulty is usually experienced with the stability of thermistors. In the present work the bridge (thermistor) was continuously supplied in D.C. (day and night).

RESULTS AND DISCUSSION

The experimental enthalpy measurements are presented in table 1 in order of ascending temperature.

Table 1

Enthalpy of aluminum above 350°K
(Atomic weight = 26.98)

T, °K	$H_T - H_{298.15}$ cal/mole	T, °K	$H_T - H_{298.15}$ cal/mole
370.72	449.356	673.37	2383.60
386.66	504.120	695.80	2549.649
457.66	945.000	720.99	2707.10
483.83	1122.000	774.32	3042.251
491.83	1168.22	803.260	3364.338
519.83	1374.699	852.260	3815.439
593.45	1853.60	879.260	3913.481
610.56	1996.773	—	—

Within the experimental temperature range, the following equation obtained by the method of least squares, can be used to represent the slug data:

$$H_T - H_{298.15} = -1938 + 6.01\,T + 0.633\times10^{-3}\,T^2 \qquad (1)$$

This equation is only applicable in the experimental temperature range (458° to 880°K) and should not be used for extrapolation. Enthalpies calculated from this equation at the experimental temperatures are given in table 2.

Table 2

Enthalpy of aluminum

Temperature °K	$H_T - H_{298.15}$ cal/mole		Deviation	
	Observed	Calculated Eq. (1)	cal/mole	%
457.66	945	945	0	0
483.83	1122	1118	+ 4	+0.33
491.83	1168	1171	− 3	−0.26
519.83	1374	1357	+17	+1.25
593.45	1853	1851	+ 3	+0.16
610.56	1996	1968	+28	+1.42
673.37	2383	2397	−14	−0.58
695.80	2549	2550	− 1	−0.04
720.99	2707	2724	−17	−0.62
774.32	3042	3087	−45	−1.45
803.26	3364	3398	−34	−1.00
852.26	3815	3793	+22	+0.57
879.26	3913	3935	−22	+0.55

The equation derived by the same method for the data from JANAF Thermochemical Tables,[4] is :

$$H_T - H_{298.15} = -1598 + 4.915T + 1.5\times10^{-3}T^2. \tag{2}$$

Differences in the observed enthalpy values and those calculated from the equation (2) are listed in tables 3 and 4.

The high deviations occurring at 400°K are certainly due to the form of the deduced equation which is different from JANAF equation as well as other equations given in literature for aluminum. McDonald's [1] data, for instance, follow an equation of the type :

$$H_T - H_{298.15} = -1177 + 5.04\ T + 1.425\times10^{-3}T^2 \tag{3}$$

while Wicks' [5] data verify the following equation :

$$H_T - H_{298.15} = -1605 + 4.94\ T + 1.48\times10^{-3}T^2. \tag{4}$$

---

[4] "JANAF Thermochemical Tables" (ed. D. R. Stull), Dow Chemical Company, Midland, Mich., August, 1965, No PB 168–370.

[5] C. E. Wicks and F. E. Block, "Thermodynamic Properties of 65 Elements — Their Oxides, Halides, Carbides and Nitrides", Buletin 605, Bureau of Mines, Washington, 1963, p. 91.

As these deviations are more important at lower temperatures, one can conclude that the calorimeter allows the determination of thermodynamic functions $H_T - H_{298.15}$ with a satisfactory precision ($\pm 1.5\%$) beginning with 500°K.

Table 3

Comparison of experimental values and values computed after JANAF tables

Temperature °K	$H_T - H_{298.15}$ cal/mole		Departure	
	exp.	JANAF Eq. (2)	cal/mole	%
457.66	945	965.6	−20.6	−2.13
483.83	1122	1131.0	− 9	−0.81
491.83	1168	1182.0	−14	−1.20
519.83	1374	1362.0	+12	+0.91
593.45	1853	1847.0	+ 6	+0.35
610.56	1996	1962.0	+34	+1.76
673.37	2383	2391.8	− 8.8	−0.34
695.80	2549	2548.0	+ 1.0	+0.06
720.99	2707	2725.0	−18	−0.67
774.32	3042	3007.0	+35	+1.16
803.26	3364	3317.9	+46.1	+1.40
852.26	3815	3680.0	+135	+3.67
879.26	3913	3883.0	+30	+0.78

Table 4

Departure from JANAF data

Temperature °K	$H_T - H_{298.15}$ cal/mole		Departure	
	Eq. (1)	Eq. (2)	cal/mole	%
400	567	608	−41	−6.74
500	1225	1235	−10	−0.81
600	1896	1891	+ 5	+0.26
700	2579	2578	+ 1	+0.04
800	3276	3294	−18	−0.54
900	3984	4041	−57	−1.40

The temperature dependence of heat capacity (in cal/mole. deg) for aluminum is obtained by differentiating equation (1), respectively:

$$C_p = 6.01 + 1.266 \times 10^{-3}\ \mathrm{T}. \tag{5}$$

Table 5 gives the computed values of heat capacity, enthalpy, entropy and the free energy function in the range 400° to 900°K at 50° intervals. For the free energy function, we used:

$$\frac{G_T - H_{298.15}}{T} = -S_T + \frac{H_T - H_{298.15}}{T} \tag{6}$$

in which:

$$S_T = \int_{298.15}^{T} (C_p/T)\,\mathrm{d}T + S_{298.15} \qquad (7)$$

where $S_{298.15} = 6.77$ e.u. (cal/mole. deg). If this value is introduced into equation (7) one obtains:

$$S_T = 6.01 \ln(T/298.15) + 1.266\times10^{-3}(T - 298.15) + 6.77 \qquad (8)$$

Table 5

Thermodynamic functions for aluminum

Temperature °K	C_p cal/mole. deg	$H_T - H_{298.15}$ cal/mole	S_T e.u. cal/mole. deg	$-\frac{G_T - H_{298.15}}{T}$ e.u.
400	6.51	567	8.67	7.25
450	6.58	894	9.44	7.45
500	6.64	1225	10.13	7.68
550	6.71	1558	10.77	7.94
600	6.77	1896	11.35	8.19
650	6.83	2235	11.90	8.46
700	6.90	2579	12.41	8.72
750	6.96	2925	12.89	8.99
800	7.02	3276	13.34	9.24
850	7.09	3627	13.77	9.50
900	7.15	3984	14.17	9.75

Acknowledgements. We wish to express our deep gratitude to Professor I. G. Murgulescu for the help and the interest he has shown in our work. Our thanks are also due to C. Volcovici for his help in the measurements.

Revue Roumaine de Chimie, **15**, 1011–1016 (1970)

THERMAL CONDUCTIVITY OF REAL DENSE FLUIDS: HARD SPHERE APPROXIMATION

G. VASU

Institute of Physical Chemistry of the Academy, Bucharest, str. Dumbrava Roșie 23

Received January 19, 1969

The reduction of molecular interaction to the hard sphere approximation is investigated. A new method for the computation of the hard sphere diameter is proposed, once the molecular interaction is known. The method is applied to the study of the thermal conductivity in liquid CH_4 and CF_4.

In any attempt to construct a theory of thermal conductivity of fluids, distinction must be made between the specific features, of low, mean, and high density regions. In the low density limit the thermal conductivity of a fluid composed by point-mass molecules of spherical symmetry is well described by the Chapmann-Enskog method.[1,2] This method was successfully applied to noble gas systems, and extended to describe higher density systems.[3] Extensions are also available which account for the heat transport by internal[4–7] and rotational[2] degrees of freedom in the case of polyatomic molecules. On the other hand, the heat transport in high density fluids can be treated by methods inspired from the theory of solids.[7]

In this paper we are concerned with the mean density case, and we apply the hard sphere approximation of Dymond and Alder[3] to the computation of the thermal conductivity of some real fluids. But, unlike these authors, we develop a theoretical method of computation for the effective molecular diameter, which is the fundamental parameter entering the treatment.

---

[1] J. O. Hirschfelder, C. F. Curtiss and R. B. Bird, "Molecular Theory of Gases and Liquids", John Wiley and Sons, Inc., New York and London, 1954, p. 534.

[2] S. Chapman and T. G. Cowling, "The Mathematical Theory of Non-Uniform Gases", University Press, Cambridge, 1952, Chap. 4, 7 and 16.

[3] J. H. Dymond and B. J. Alder, *J. Chem. Phys.*, **45**, 2061 (1966).

[4] A. Eucken, *Physik. Z.*, **14**, 324 (1913).

[5] J. O. Hirschfelder, *J. Chem. Phys.*, **26**, 282 (1957).

[6] E. A. Mason and L. Monchick, *J. Chem. Phys.*, **36**, 1622 (1962).

[7] J. K. Horrocks and E. McLaughlin, *Trans. Faraday Soc.*, **56**, 206 (1960); **59**, 1709 (1963).

THE EFFECTIVE DIAMETER

The efective diameter must be considered as the mean value of the shortest distance at which two molecules approach one another in a collisional process.

Let us consider a collision between two hard spheres, say 1 and 2 of velocities $\vec{C}_1$ and $\vec{C}_2$, masses m_1 and m_2, and diameters σ_1 and σ_2. In relative coordinates, the collision may be described as the reflection of molecule 2 on the surface of molecule 1, as in figure 1, so that the initial relative velocity $\vec{g} = \vec{c}_2 - \vec{c}_1$, will turn into the final relative velocity $\vec{g}' = \vec{c}_2{}' - \vec{c}'_1$ according to the law of reflection, i.e. equal angles on the two sides of the centers line at contact (in figure 1 this line is defined by the $\vec{k}$ versor) and $g = g'$.

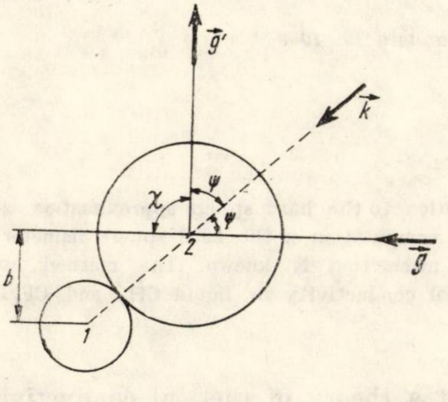

Fig. 1. – Geometry of collision. The reference system is fixed on molecule 1.

Now let us suppose the molecules are not rigorously rigid spheres, and denote by g_{11} the value of the component of $\vec{g}$ along the versor $\vec{k}$, i.e. $g_{11} = \vec{g} \cdot \vec{k} = g \cos \psi$ (obviously $g = |\vec{g}|$). Then the shortest distance at which two molecules approach one another in a collision will be directly related to the relative kinetic energy $\frac{1}{2}\,\mu g_{11}^2$, where $\mu = m_1 m_2/(m_1 + m_2)$. To find the effective diameter *, i.e. the mean shortest distance, we must find the mean value $<\mu g_{11}^2/2>$, or $<\frac{1}{2}\,\mu g^2 \cos^2 \psi>$.

The method of obtaining such mean values has been known for a long time; we do not expound it again, but give here only some results. As is well known, the following parameters may be used to describe a collision in the system of relative coordinates : the initial relative velocity $\vec{g}$, the parameter of collision b (see figure 1) and an angle ε (between 0 and 2π) determining the orientation of the plane of movement around the central line. Now, according to Eqs 3.5.1 and 4.3.4 of ref. 2, the number of collisions per volume unit and time unit with the molecular parameters $\vec{c}_1$, $\vec{c}_2$, b, ε in the ranges $d^3\vec{c}_1$, $d^3\vec{c}_2$, db, $d\varepsilon$ is given by

---

* Finally the molecules 1 and 2 are supposed identical; if they are not, we will obtain the sum of their effective radii.

$$f_1 f_2 g\, b db d\varepsilon\, d^3\vec{c}_1 d^3\vec{c}_2, \tag{1}$$

where

$$f_1 = n_1 \left(\frac{m_1}{2\pi kT}\right)^{3/2} \mathrm{e}^{-m_1 c_1^2/2kT}, \tag{2}$$

$$f_2 = n_2 \left(\frac{m_2}{2\pi kT}\right)^{3/2} \mathrm{e}^{-m_2 c_2^2/2kT}, \tag{3}$$

and where n_i $(i = 1, 2)$ denotes the density of molecules i (particles per volume):

From figure 1 we obtain

$$b = \sigma_{12} \sin \psi, \tag{4}$$

where $\sigma_{12} = (\sigma_1 + \sigma_2)/2$; we observe that $0 \leqslant b \leqslant \sigma_{12}$ and $0 \leqslant \psi \leqslant \pi/2$.

Now the variables $\vec{c}_1$, $\vec{c}_2$ are changed into variables $\vec{g}$, $\vec{G}$:

$$\vec{g} = \vec{c}_2 - \vec{c}_1, \tag{5}$$

$$\vec{G} = (m_1 + m_2)^{-1}(m_1 \vec{c}_1 + m_2 \vec{c}_2). \tag{6}$$

We obtain :

$$d^3\vec{c}_1\, d^3\vec{c}_2 = d^3\vec{g} d^3\vec{G}, \tag{7}$$

$$m_1 c_1^2 + m_2 c_2^2 = (m_1 + m_2)\, G^2 + \mu g^2. \tag{8}$$

Taking into account Eqs (1) – (4), (7), (8), the number of collisions per volume unit and time unit with the molecular parameters $\vec{g}$, $\vec{G}$, ψ, ε in he ranges $d^3\vec{g}$, $d^3\vec{G}$, $d\psi$, $d\varepsilon$ is given by

$$F(\vec{g}, \vec{G}, \psi, \varepsilon)\, d\psi\, d\varepsilon\, d^3\vec{G}\, d^3\vec{g} \tag{9}$$

where

$$F(\vec{g}, \vec{G}, \psi, \varepsilon) = n_1 n_2 \sigma_{12}^2 \left(\frac{\mu}{2\pi kT}\right)^{3/2} \left(\frac{m_1 + m_2}{2\pi kT}\right)^{3/2} \mathrm{e}^{-\frac{1}{2kT}[(m_1+m_2)G^2 + \mu g^2]} . \qquad (10)$$

From (9) and (10) it results:

$$\left\langle \frac{1}{2} \mu g^2 \cos^2 \psi \right\rangle = \frac{\mu}{2} \frac{\int \mathrm{d}^3\vec{G} \int \mathrm{d}^3\vec{g} \int_0^{2\pi} \mathrm{d}\varepsilon \int_0^{\pi/2} \mathrm{d}\psi F(\vec{g}, \vec{G}, \psi, \varepsilon) g^2 \cos^2 \psi}{\int \mathrm{d}^3\vec{G} \int \mathrm{d}^3\vec{g} \int_0^{2\pi} \mathrm{d}\varepsilon \int_0^{\pi/2} \mathrm{d}\psi F(\vec{g}, \vec{G}, \psi, \varepsilon)} = kT. \qquad (11)$$

Hence, the mean value of the kinetic energy determining the effective diameter is kT. If $\varphi(\vec{r})$, the potential energy of the molecular interaction, is known, the effective diameter will be given by the conservation of energy. In the low density limit, the effective diameter will be obtained by intersecting the $\varphi(r)$ curve with the kT level taken above zero energy, as in figure 2a. We are however interested in the high density case; in this case the molecules form an almost compact system, and the distance between neighbouring molecules nearly corresponds to the position of minimum potential energy. Therefore, in this case the effective diameter must be at the intersection of the $\varphi(r)$ curve with the kT level taken above the minimum of the potential energy, as in figure 2 b.

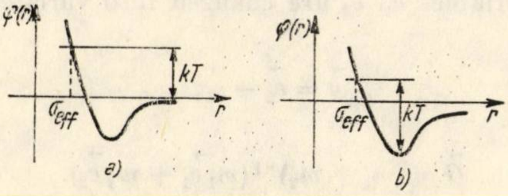

Fig. 2. — Determination of the effective diameter σ_{eff}: *a*) low density case; *b*) high density case.

Consequently, for a Lennard-Jones potential:

$$\varphi(r) = 4 \in \left[\left(\frac{\sigma_0}{r}\right)^{12} - \left(\frac{\sigma_0}{r}\right)^{6}\right], \qquad (12)$$

the effective diameter $\sigma(T)$ will be given by

$$4 \in \left[\left(\frac{\sigma_0}{\sigma(T)}\right)^{12} - \left(\frac{\sigma_0}{\sigma(T)}\right)^{6}\right] = kT - \in, \qquad (13)$$

hence

$$\sigma(T) = 2^{1/6} (1 + \sqrt{kT/\in})^{-1/6} \sigma_0, \qquad (14)$$

which is the desired result.

THE THERMAL CONDUCTIVITY OF CH_4 AND CF_4

A modified Chapman-Enskog method gives the following equation [3] for the thermal conductivity of a dense fluid :

$$\lambda = \lambda_0\left[G^{-1} + 1.2\,\frac{b}{V} + 0.755\left(\frac{b}{V}\right)^2 G\right], \tag{15}$$

where b is the van der Waals' constant, expressed by the Avogadro's number N and the effective diameter $\sigma(T)$,

$$b = \frac{2}{3}\,\pi N \sigma^3, \tag{16}$$

V is the molar volume, and λ_0 is given in terms of σ, T, and molar mass M in the form

$$\lambda_0 = \frac{2.038.10^{-4}}{\sigma^2}\sqrt{\frac{T}{M}}. \tag{17}$$

Equation (17) will give λ_0 in cal/cm s°K, if we replace σ in Ångströms. Farther, G is the value of the molecular correlation function at a distance σ. According to Reiss and co-workers, [8] G is given by

$$G(\sigma) = \frac{1}{4(1-t)} + \frac{3}{4(1-t)^2} + \frac{3t}{4(1-t)^3}, \tag{18}$$

where $t = (\pi/6)\,N\sigma^3\rho/M$, and ρ is the density. This method, with $\sigma(T)$ taken from (14), will be applied to the computation of the thermal conductivity in dense fluid state of methane and carbon tetrafluoride. The following parameters for the Lennard-Jones potential will be used [9]: for CH_4, $\epsilon/k = 148.2$°K, and $\sigma_0 = 3.817$ Å; for CF_4, $\epsilon/k = 152.5$°K, and $\sigma_0 = 4.70$ Å.

The thermal conductivities for CH_4 and CF_4 computed by (15) using the effective diameters given by (14) are listed in tables 1 and 2. At high densities the agreement with experimental values is very good. However, at lower densities the computed values are only a fraction of the entire thermal conductivity.

The meaning of our result will be clear if we observe that equation (15) accounts only for the transport of heat by translational motions of molecules. Neither the internal degrees of freedom, nor the rotational ones were taken into account. Very likely these degrees of freedom do not take part in the transport at higher densities but do take at lower ones. On the other hand, at lower densities our approximation (14) is not so good. As the density decreases, our approximation (14), which is related to figure 2b, must turn into one related to figure 2a. This means that equation (14) gives a too high value for $\sigma(T)$ at lower densities. A correction to equation (14) will correct also the values of the thermal conductivities even at lower densities.

---

[8] H. Reiss, H. L. Frisch and J. L. Lebowitz, *J. Chem. Phys.*, **31**, 369 (1959).
[9] See ref. 1, p. 1111.

Table 1

Thermal conductivities for methane *

T = 335.6°K			T = 435.3°K		
ρ g/cm³	$10^5\lambda$, cal/cm.s.°K calc.	$10^5\lambda$, cal/cm.s.°K exp.	ρ g/cm³	$10^5\lambda$, cal/cm.s.°K calc.	$10^5\lambda$, cal/cm.s.°K exp.
0.064	8.4	11.2	0.062	9.4	15.0
0.112	10.3	13.3	0.091	10.6	16.2
0.167	13.5	15.9	0.141	13.3	18.7
0.224	16.8	19.5	0.177	15.8	20.8
0.253	22.0	22.3	0.211	19.0	22.9
0.274	25.4	24.7	—	—	—

* Experimental values are taken from ref. 10

Table 2

Thermal conductivities for carbon tetrafluoride **

T = 336°K			T = 434.1°K		
ρ g/cm³	$10^5\lambda$, cal/cm.s.°K calc.	$10^5\lambda$, cal/cm.s.°K exp.	ρ g/cm³	$10^5\lambda$, cal/cm.s.°K calc.	$10^5\lambda$, cal/cm.s.°K exp.
0.529	4.1	7.4	0.616	5.5	10.7
0.732	6.3	9.1	0.785	7.7	12.7
0.957	10.4	15.6	0.907	10.0	14.6
1.082	14.3	13.8	1.000	12.3	16.3
1.158	17.2	15.3	—	—	—

** Experimental values are taken from ref. 10.

Acknowledgments. I wish to express sincere and grateful thanks to Professor I. G. Murgulescu, Member of the Academy, for the many helpful and stimulating discussions throughout this work.

---

[10] B. M. ROSENBAUM and G. THODOS, *Physica*, **37**, 442 (1962).

Revue Roumaine de Chimie, 15, 1017–1028 (1970)

PRINZIPIELLES ÜBER DIE WIRKSAMKEIT EINIGER REINIGUNGSMETHODEN DURCH ADSORPTION

ALLGEMEINE BEZIEHUNGEN

S. ŢILENSCHI
aus dem Laboratorium für Kolloidchemie—Chemische Fakultät der Universität Bukarest und

A. WOHL
vom IMNR (Projektierungs- und Forschungsinstitut für die Industrie der Nichteisen- und seltenen Metalle), Bukarest

Eingegangen am 3. Juli 1969

Durch logisch-mathematische Überlegungen wird bewiesen, daß der Endzustand des Adsorptionsgleichgewichtes, der sich in isothermen Bedingungen zwischen bestimmten Mengen vom Adsorptionsmittel und Adsorbat einstellt, von der Modalität der Kontaktierungsweise derselben bedingt ist. Man bespricht die einzelnen Zweige (aufsteigende, absteigende, positive und negative) der Isothermen der scheinbaren Adsorption. Man verbindet die Folgerungen dieser Überlegungen mit der experimentellen Tatsache, daß die Wirksamkeit der Reinigung durch Adsorption im allgemeinen auf einer Kolonne größer ist, als in statischen Bedingungen.

Die Versuche eine Flüssigkeit durch Adsorption zu reinigen haben gezeigt, daß die Entfernung der (gelösten) Verunreinigung im allgemeinen auf einer Kolonne (dynamische Adsorption) wirksamer ist, als durch Vermischung der Reaktanten (statische Adsorption). Im folgenden wird versucht, diese Tatsache theoretisch zu rechtfertigen. Es wird von Lösungen gesprochen, aber die Erwägungen haben eigentlich eine ganz allgemeine Gültigkeit, die von dem Aggregatzustand der Partner unabhängig ist.

Für die Adsorption einer Komponente (A) aus einer Lösung kann man folgende, selbst aus der Definitionsgleichung der scheinbaren Adsorption abgeleitete Beziehung schreiben :

$$c_0 - c = r . a \tag{1}$$

wobei : c_0 die Anfangskonzentration der Komponente (A) in der Lösung, [%]
c die Konzentration der Komponente (A) in der Lösung, nach der Adsorption, im Gleichgewicht, [%]

r das Verhältnis g Adsorptionsmittel/100 g Lösung,
a die scheinbare spezifische Adsorption [Gramm Komponente (A) die von 1 g Adsorptionsmittel bei der Konzentration c, festgehalten sind].

Bekanntlich ergibt die Darstellung der scheinbaren spezifischen Adsorption, a, als Funktion der Konzentration, c, Adsorptionsisothermen, die aufsteigende, oder absteigende, eventuell auch horizontale Zweige aufweisen und manchmal sogar negative Werte haben können.

Um die von uns „Kolonneneffekt" bennannte Erscheinung – d.h. die (praktisch festgestellte) größere Wirksamkeit der Reinigung durch dynamische Adsorption als durch statische Adsorption zu erklären, haben wir 3 Methoden der Kontaktierung der Lösung mit dem Adsorptionsmittel in Betracht gezogen:

– Die „einfache" (a) Methode: die Gesamtmenge der Lösung + die Gesamtmenge des Adsorptionsmittels.

– Die Methode (b) der „Adsorptionsmittelaufteilung": die Gesamtmenge der Lösung + sukzessive Fraktionen aus der Gesamtmenge des Absorptionsmittels; nach Zugabe jeder Fraktion des Adsorptionsmittels und Erreichen des Adsorptionsgleichegwichtes, wird die flüssige Phase von der festen abgetrennt.

– Die Methode (c) der „Lösungsaufteilung": sukzessive Fraktionen der Gesamtmenge der Lösung + die Gesamtmenge des Adsorptionsmittels; nach Zugabe jeder Fraktion der Lösung und Erreichen des Adsorptionsgleichgewichtes wird die flüssige Phase von der festen abgetrennt.

Jeder Fall wird einzeln untersucht. Um den Vortrag der „Aufteilungsmethoden" – (b) und (c) – zu vereinfachen, werden wir uns nur auf die Betrachtung von zwei gleichen Fraktionen begrenzen, denn die erhaltenen Ergebnisse kann man auf eine willkürliche (endliche) Zahl gleicher oder ungleicher Fraktionen erweitern.

1.a > 0

1.1. *Der aufsteigende Zweig* der Kurve a/c, also, wenn $c_i > c_j$, dann $a_i > a_j$ (a_i und a_j sind die scheinbaren spezifischen, den Gleichgewichtskonzentrationen c_i und c_j entsprechenden Adsorptionen).

Die „einfache" (a) Methode. Die Konzentration der Lösung wird nach der Adsorption

$$c_s = c_0 - r \cdot a_s. \tag{2}$$

Die Methode (b) der „Adsorptionsmittelaufteilung". Die Konzentration der Lösung wird nach ihrem Kontakt mit der ersten Fraktion des Adsorptionsmittels

$$c_1 = c_0 - \frac{r}{2} \cdot a_1 \tag{3}$$

und nach dem Kontakt mit der zweiten Fraktion:

$$c_2 = c_1 - \frac{r}{2} \cdot a_2 \tag{4}$$

a_s, a_1 und a_2 sind die scheinbaren spezifischen, den End(Gleichgewichts) konzentrationen entsprechenden Adsorptionen.

Aus (3) und (4) folgt:

$$c_2 = c_0 - \frac{r}{2}(a_1 + a_2) \tag{5}$$

$$1.11:\ a_1 > a_s$$

$$\underline{a_2 > a_s} \rightarrow c_2 > c_s \quad \text{(Voraussetzung 1.11)}$$

$$a_1 + a_2 > 2a_s \cdot \text{also:}$$

$$c_2 - \frac{r}{2}(a_1 + a_2) < c_0 - r \,.\, a_s \tag{6}$$

Aber, durch Vergleich mit (2) und (5), ergibt die Ungleichung (6): $c_2 < c_1$; das bedeutet, daß der Fall 1.11 einen Widerspruch einschließt und als solcher unmöglich ist.

$$1.12:\ a_1 > a_s$$

$$\underline{a_2 < a_s} \rightarrow c_2 < c_s \ \text{(Voraussetzung 1.12)}$$

Es gibt zwei Alternativen:

1.121 : $a_1 + a_2 > 2a_s$; daraus geht $c_2 < c_s$ hervor in Übereinstimmung mit der Voraussetzung 1.12, also foglich ist die Alternative 1.121 möglich und es folgt $c_2 < c_s$.

1.122 : $a_1 + a_2 < 2a_s$, was $c_2 > c_s$ einbezieht; das widerspricht der Voraussetzung 1.12 und macht infolgedessen die Alternative 1.122 unmöglich.

$$1.13:\ a_1 < a_s$$

$$\underline{a_2 < a_s} \rightarrow c_2 < c_s \ \text{(Voraussetzung 1.13)}$$

$a_1 + a_2 < 2a_s$, also $c_2 > c_s$ im Widerspruch mit der Voraussetzung 1.13, so daß dieser Fall unmöglich ist.

$$1.14:\ a_1 < a_s$$

$$a_2 > a_s\,.$$

Eine solche Kombination der Ungleichungen ist aber unmöglich, denn $a_1 < a_2$ wenn $c_1 > c_2$; der Vergleich der Gleichungen (3) und (5) zeigt nun offenbar, daß der Wert von c_2 höchstens gleich mit dem vom c_1 (wenn $a_2 = 0$), aber keinesfalls größer sein kann.

$$1.15:\ c_2 = c_s \rightarrow a_2 = a_s.$$

Dafür sollte $a_1 + a_2 = 2a_s$ gültig sein. Wir haben aber vorausgesetzt, daß $a_1 \neq a_2$ und a_s nicht das arithmetische Mittel zweier ungleicher Werte und gleichzeitig gleich mit einem davon sein kann.

Infolgedessen : *führt im Bereich in welchem die scheinbare spezifische Adsorption positiv ist und mit der Gleichgewichtskonzentration der Komponente (a) der Lösung zunimmt, die Methode der „Adsorptionsmittelaufteilung" notwendigerweise zu einer besseren Reinigung durch Adsorption, als die „einfache" Methode.*

Die Methode der „Lösungsaufteilung". Die Konzentration der ersten Fraktion der Lösung wird nach ihrem Kontakt mit der Gesamtmenge r des Adsorptionsmittels

$$c_1 = c_0 - 2r \, . \, a_1 \tag{7}$$

und die Konzentration der zweiten Fraktion nach dem Kontakt mit dem Adsorptionsmittel (auch vorher benützt) :

$$c_2 = c_0 - 2r \, (a_2 - a_1) \tag{8}$$

Wenn man annähme, daß c_2 kleiner ist als c_1, würde das bedeuten, daß $(a_2 - a_1) > a_1$ oder $a_2 > 2a_1$, also $a_2 > a_1$. Aber auf dem aufsteigenden Zweig der Kurve a/c können $a_2 > a_1$ und $c_2 < c_1$ nicht gleichzeitig gültig sein.

Möglich ist nur der Fall : $(a_2 - a_1) < a_1$, also $c_2 > c_1$, in Übereinstimmung mit $a_2 > a_1$, was die Bedingung $(a_2 - a_1) < a_1$ (oder $a_2 < 2a_1$) nicht ausschließt.

Die Endkonzentration c_f der zwei vereinigten Lösungsfraktionen ist das gewogene Mittel zwischen c_1 und c_2. Die Menge der ersten Fraktion (mit der Konzentration c_1) ist $50 - 2r \, (A_1 + B_1$, die der zweiten (mit der Konzentration c_2) ist $50 - 2r \, (A_2 - A_1 + B_2 - B_1)$, wo A_1, A_2 bzw. B_1, B_2 Gramm der Komponente (A) bzw. des Lösungsmittels (B) bedeuten, die von 1 g, mit den Lösungen der Konzentrationen c_1 bzw. c_2 im Gleichgewicht stehenden Adsorptionsmittel festgehalten sind. Es folgt die Gleichung :

$$c_f = \frac{[50 - 2r \, (A_1 + B_1)] \, c_1 + [50 - 2r \, (A_2 - A_1 + B_2 - B_1)] \, c_2}{100 - 2r \, (A_2 + B_2)} \tag{9}$$

Da A_1, B_1, A_2 und B_2 dasselbe (positive) Vorzeichen haben, wird die Menge der Fraktion mit der Konzentration c_2 größer als die der Fraktion von der Konzentration c_1 sein und da $c_2 > c_1$, folgt, daß c_f größer ist als das arithmetische Mittel :

$$c'_f = \frac{c_1 + c_2}{2}$$

zwischen c_1 und c_2.

Aus der Gleichung (9) ergibt sich aber, daß falls die von dem Mittel festgehaltenen Mengen (g) der Komponente (A) und des Lösungsmittels im Vergleich zu 50 (g) vernachlässigbar sind, c_f dem arithmetischen Mittel c'_f annähernd gleich sein wird. Das kann in sehr verdünnten Lösungen geschehen und wenn das Mittel kein Lösungsmittel festhält. Um das Verhältnis zwischen c'_f und c_e zu schätzen, macht man folgende Überegungen :

Aus (7) und (8) folgt:

$$c'_f = c_0 - 2r \cdot a_2 \tag{10}$$

1.16 : $c'_f > c_s$

Das bedeutet gleichzeitig (s.a. (2)) $2a_2 < a_s$ oder $a_2 < a_s$. Aber $a_2 > a_1$, so daß man auch $a_1 < a_s$ hat. Da wir uns auf dem aufsteigenden Zweig der Isotherme a/c befinden, müssen auch die Ungleichungen $c_2 < c_s$ und $c_1 < c_s$ gelten. Das schließt aber aus, daß das arithmetische Mittel (c'_f) von c_1 und c_2 größer als c_s ist.

1.17 : $c'_f < c_s$

Gegeben ist $2a_2 > a_s$, was nichts bestimmtes über das Verhältnis zwischen a_2 und a_s oder a_1 und a_s, bzw. c_2 und c_s oder c_1 und c_s sagen läßt, so daß auch die Ungleichung $c'_f < c_s$ möglich ist.

1.18 : $c'_f = c_s$

Das bedeutet $2a_2 = a_s$ oder $a_2 < a_s$ und demnach $a_1 < a_s$; daraus folgt: $c_2 < c_s$ und $c_1 < c_s$, so daß ihr arithmetisches Mittel auch nicht gleich mit c_s ist.

Infolgedessen: *führt in dem Bereich, in welchem die scheinbare spezifische Adsorption positiv ist und mit der Konzentration wächst, führt die Methode der „Lösungsaufteilung" notwendigerweise nur dann zu einer besseren Reinigung durch Adsorption als die „einfache" Methode, wenn die von dem Adsorptionsmittel festgehaltene Lösungsmenge im Vergleich mit der mit dem Adsorptionsmittel in Kontakt gesetzten Lösungsfraktion vernachlässigbar ist. Wenn die festgehaltene Lösungsmenge nennenswert ist, kann man über die Wirksamkeit der Methode der „Lösungsaufteilung" keine sichere Voraussage machen.*

1.2. *Der absteigende Zweig* der Kurve a/c, d.h. wenn $c_i > c_j$, dann $a_i < a_j$.

Die (*a*) *Methode* ergibt, wie vorher, $c_s = c_0 - r \cdot a_s$

Die (*b*) *Methode.*

1.21 : $a_1 > a_s$

$$\frac{a_2 > a_s \rightarrow c_2 < c_s \text{ (Voraussetzung 1.21)}}{a_1 + a_2 > 2a_s, \qquad \text{folglich } c_2 < c_s - \text{dieser Fall ist möglich.}}$$

1.22 : $a_1 > a_s$

$a_2 < a_s$.

Eine solche Kombination ist nicht möglich, denn $c_1 > c_2$ und demnach $a_1 < a_2$.

1.23 : $a_1 < a_s$

$$\underline{a_2 < a_s} \rightarrow c_2 > c_s \text{ (Voraussetzung 1.23)}$$

$a_1 + a_2 < 2a_s$, folglich $c_2 > c_s$ — dieser Fall ist also möglich.

1.24 : $a_1 < a_s$

$$\underline{a_2 > a_s} \rightarrow c_2 < c_s \text{ (Voraussetzung 1.24)}$$

Es gibt zwei Alternativen:

1.241 : $a_1 + a_2 < 2a_s$, woraus $c_2 > c_s$ folgt; der Widerspruch mit der Voraussetzung 1.24 macht diesen Fall unmöglich.

1.242 : $a_1 + a_2 > 2a_s$; das bedeutet $c_2 < c_s$, also ein mögliches Ergebnis.

1.25 : $c_2 = c_s$.

Die Argumentation des Absatzes 1.15 bleibt gültig, wenn bewiesen wird, daß c_2 nicht mit c_s gleich sein kann.

Infolgedessen: *kann auf dem absteigenden Zweig der Kurve a/c, die Methode der „Adsorptionsmittelaufteilung" mehr oder weniger wirksam sein als die „einfache" Methode bei der Reinigung durch Adsorption.*

Die (c) *Methode.* Die Beziehungen (7)—(10) bleiben gültig, aber $c_2 > c_1$ bedeutet diesmal $a_2 < a_1$.

1.26 : $c'_f > c_s$

Daraus folgt $a_2 < a_s$, aber nicht auch $a_1 < a_s$ und so ist es möglich, daß c'_f (das arithmetische Mittel von c_1 und c_2) größer ist als c_s.

1.27 : $c'_f < c_s$

Gegeben ist $2a_2 > a_s$ was keine Beziehung zwischen c'_f und c_{sf} aufstellt, so daß auch die obere Ungleichung möglich wird.

1.28 : $c'_f = c_s$.

Das ergibt $2a_2 = a_s$ oder $a_2 = \frac{a_s}{2}$, also $c_2 > c_s$, aber nichts Bestimmtes hinsichtlich a_1, bzw. c_1, so daß es möglich ist, daß c'_f gleich c_s ist.

Infolgedessen: *kann man auf dem absteigenden Zweig der Kurve a/c über die Wirksamkeit der Methode der „Lösungsaufteilung", bei der durch Adsorption erfolgten Reinigugn einer Lösung, im Vergleich mit der „einfachen" Methode, nicht einmal dann eine sichere Aussage machen, wenn die von dem Adsorptionsmittel festgehaltene Lösungsmenge vernachlässigbar klein ist im Vergleich mit der anfänglichen Lösungsfraktion. Es ist aber wahrscheinlicher, daß die „einfache" Methode wirksamer sein kann, denn* $c_f > c'_f$.

1.3. $a = K$ (*eine Konstante*).

In diesem Fall erhält man:

— Durch die (*a*) Methode (aus Gleichung (2)):

$$c_s = c_0 - r.K$$

— Durch die (*b*) Methode (aus Gleichung (5)):

$c_2 = c_0 - r.K$, also wie durch die ,,einfache" Methode.

— Durch die (*c*) Methode (aus Gleichung (7)):

$$c_1 = c_0 - 2r.K \text{ und aus (8) : } c_2 - c_0$$

Die Konzentration c_f der Lösung wird das gewogene Mittel von c_1 und c_2 sein, so wie es die Gleichung (9) zeigt.

Aus der Materialbilanz:

$$c_0 = \frac{c_i}{100}(100 - A_i.r - B_i.r) + A_i.r \tag{11}$$

und der Definitionsgleichung der spezifischen scheinbaren Adsorption:

$$a_i = \frac{c_0 - c_i}{r} \tag{12}$$

leitet man folgende Beziehung zwischen der spezifischen scheinbaren Adsorption (a_i) und der realen Adsorption (A_i) ab

$$a_i = A_i - \frac{c_i}{100}(A_i + B_i) \tag{13}$$

Man bemerkt, daß man folgende Gleichung haben müßte, damit a_i konstant (unabhängig von der Konzentration) ist:

$$a_i - a_j = A_i - A_j - \frac{c_i}{100}(A_i + B_i) + \frac{c_j}{100}(A_j + B_j) = 0$$

Diese Bedingung ist nur in Abwesenheit jedwelcher Adsorption rigurös erfüllt ($A_i = A_j = B_i = B_j = 0$), denn A_i, A_j, B_i und B_j sind positiv oder gleich Null. Man kann aber von einer praktisch konstanten spezifischen scheinbaren Adsorption sprechen, wenn (s. Gleichung (13)):

— die sepzifische reale Adsorption (A_i) konstant ist und

$$-\frac{c_i}{100}(A_i + B_i) \to 0 \text{ oder wenn } B_i \to 0 \text{ und } \left(1 - \frac{c_i}{100}\right) \to 0$$

Die letzte Alternative bedeutet, daß das Lösungsmittel nicht von dem Adsorptionsmittel festgehalten wird und die Lösung sehr verdünnt ist; woraus folgt, daß

$$a_i = a_j = A_i = A_j = K \text{ und } B_i = B_j = 0$$

Wenn man unter diesen Bedingungen die entsprechenden Werte von c_1 und c_2 ersetzt, erhält man für die Gleichung (9) die Form:

$$c_f = \frac{(50 - 2r.K)(c_0 - 2r.K) + 50\,c_0}{100 - 2r.K} \tag{9'}$$

Aber da $a_i \leqq c_i$ und in sehr verdünnten Lösungen $a_i \to 0$, folgt, daß $2r.K \ll 50$ (denn K ist eigentlich a_i) und $2r.K \ll 100$. Dann ergibt sich:

$$c_f \approx \frac{50\,(c_0 - 2r.K) + 50\,c_0}{100} \quad \text{oder } c_f = c_0 - r.K$$

Man kann folglich feststellen, daß man durch die Methode der „Lösungsaufteilung" eine Lösung gleicher Konzentration der Komponente (A) erhält, wie auf dem Weg der „einfachen" Methode, wenn die spezifische scheinbare Adsorption konstant (unabhängig von der Konzentration) ist, was folgende Voraussetzungen erfordert:

— sehr verdünnte Lösungen der Komponente (A);

— kein Festhalten des Lösungsmittels von dem Adsorptionsmittel;

— eine von der Konzentration unabhäbgige spezifische reale Adsorption.

Infolgendessen: *bleibt die scheinbare spezifische Adsorption positiv und von der Konzentration unabhängig, der durch Adsorption erzielte Reinigungsgrad derselbe, gleichgültig ob man die „einfache" Methode, die Methode der „Adsorptionsaufteilung", oder die der „Lösungsaufteilung" angewandt hat.*

2. a < 0 (negative Adsorption)

2.1. *Der aufsteigende Zweig* der Kurve a/c; das bedeutet in diesem Fall: wenn $c_i > c_f$, dann auch $|a_i| < |a_f|$.

Die „einfache" (a) Methode. Die Konzentration der Lösung wird nach der Adsorption

$$c_s = c_0 + r.\,|a_s|. \tag{14}$$

Die Methode (b) der Adsorptionsmittelaufteilung

$$c_1 = c_0 + \frac{r}{2}.\,|a_1| \tag{15}$$

$$c_2 = c_0 + \frac{r}{2}(|a_1| + |a_2|) \tag{16}$$

$$\begin{array}{l} 2.11:\ |a_1| > |a_s| \\ \underline{ |a_2| > |a_s|} \to c_2 < c_s \text{ (Voraussetzung 2.11)} \end{array}$$

$|a_1| + |a_2| > 2\,|a_s|$, also $c_2 > c_s$ — Widerspruch zur Voraussetzung 2.11, foglich ist dieser Fall unmöglich.

$$\begin{array}{l} 2.12:\ |a_1| > |a_s| \\ \underline{ |a_2| < |a_s|} \to c_2 > c_s \text{ (Voraussetzung 2.12).} \end{array}$$

Alternative 2.121 : $|a_1| + |a_2| > 2\,|a_s|$, woraus folgt, daß $c_2 > c_s$ in Übereinstimmung mit der Voraussetzung 2.12, so daß diese Alternative möglich ist.

Alternative 2.122 : $|a_1| + |a_2| < 2\,|a_s|$, woraus $c_2 < c_s$, im Widerspruch mit der Voraussetzung 2.12, also ist diese Alternative ausgeschlossen.

2.13 : $|a_1| < |a_s|$

$\underline{|a_2| < |a_s|} \rightarrow c_2 > c_s$ (Voraussetzung 2.13)

$|a_1| + |a_2| < 2\,|a_s| \rightarrow c_2 < c_s$ — im Widerspruch zur Voraussetzung 2.13, was diesen Fall unmöglich macht.

2.14 : $|a_1| < |a_s|$

$|a_2| > |a_s|$.

Eine solche Kombination der Ungleichungen ist nicht möglich, denn $c_1 < c_2$, folglich $|a_1| > |a_2|$.

2.15 : $c_2 = c_s$, also $|a_2| = |a_s|$ im Widerspruch zu $|a_1| \neq |a_2|$ und $|a_1| + |a_2| = 2\,|a_s|$ — demnach ausgeschlossen.

Infolgedessen : *führt auf dem aufsteigenden negativen Zweig der Kurve a/c, die Methode der „Adsorptionsmittelaufteilung" zu einer größeren Zunahme der Konzentration der Komponente (A) in der Lösung nach der Adsorption, als die „einfache" Methode.*

Die Methode (c) der. „Lösungsaufteilung".

$$c_1 = c_0 + 2r \cdot |a_1| \tag{17}$$

$$c_2 = c_0 + 2r\,(|a_2| - |a_1|). \tag{18}$$

Man beweist, wie im Falle des aufsteigenden, positiven Zweiges der Isotherme a/c, daß man $(|a_2| - |a_1|) < |a_1|$ haben muß, also $c_2 < c_1$ und folglich $|a_2| > |a_1|$.

Das gewogene Mittel (c_f) zwischen c_2 und c_1 ist wieder von der Gleichung (9) gegeben; die Menge der zweiten Fraktion ist auch diesmal größer. Dies ergibt hier aber :

$$c_f < \frac{c_1 + c_2}{2} \tag{19}$$

Aus (17) und (18) folgt :

$$c'_f = c_0 + 2r \cdot |a_2| \tag{20}$$

2.16 : $c'_f > c_s$

Das bedeutet $2\,|a_2| > |a_s|$; daraus kann man weder gewiß folgern ob $|a_2|$ und $|a_1|$ größer oder kleiner als $|a_s|$ sind, noch ob c_1 und c_2 geringer oder größer als c_s sind. Mit anderen Worten, es kann möglich sein, daß c'_f größer ist als c_s.

2.17 : $c'_f < c_s$

Daraus ergibt sich : $2\,|a_2| < |a_s|$ oder $|a_2| < |a_s|$ und umso mehr $|a_1| < |a_s|$; man hat, folglich, $c_1 > c_s$ und $c_2 > c_s$, so daß das arithmetische Mittel von c_1 und c_2 (c'_f) nicht geringer sein kann als c_s.

2.18 : $c'_f = c_s$

Daraus geht $2\,|a_2| = |a_s|$ hervor, oder $|a_2| < |a_s|$ und $|a_1| < |a_s|$, also $c_2 > c_s$ und $c_1 > c_s$, so daß $c'_f \neq c_s$.

Infolgedessen: *könnte man auf dem aufsteigenden, negativen Zweig der Kurve a/c* nur dann eine sichere Schlußfolgerung hinsichtlich der Wirksamkeit der Methode der „Lösungsaufteilung" ziehen, wenn die vom Adsorptionsmittel festgehaltene Lösungsmenge, gegen die anfangs eingeführte Lösungsfraktionsmenge vernachlässigbar wäre. Das würde jedoch eine negative spezifische scheinbare Adsorption ausschließen. Da aber $c_f < c'_f$, *kann man nicht mit Bestimmtheit voraussehen, ob die durch die Methode der „Lösungsaufteilung" durchgeführte Adsorption die Konzentration der Komponente (A) in der Lösung mehr oder weniger steigert als die „einfache" Methode.*

2.2. *Der absteigende Zweig* der Kurve a/c, also wenn $c_i > c_j$, dann $|a_i| > |a_j|$.

Die Beziehungen (14)—(19) bleiben gültig.

Die (b) Methode

2.21 : $|a_1| > |a_s|$

$\underline{|a_2| > |a_s|} \rightarrow c_2 > c_s$ (Voraussetzung 2.21)

$|a_1| + |a_2| > 2\,|a_s|$, also $c_2 > c_s$, folglich ist dieser Fall möglich.

2.22 : $|a_1| > |a_s|$

$|a_2| < |a_s|$

Diese Kombination der Ungleichungen ist nicht möglich, denn aus $c_2 > c_1$ folgt $|a_2| > |a_1|$.

2.23 : $|a_1| < |a_s|$

$\underline{|a_2| < |a_s|} \rightarrow c_2 < c_s$ (Voraussetzung 2.23)

$|a_1| + |a_2| < 2\,|a_s| \rightarrow c_2 < c_s$ — folglich ist dieser Fall möglich.

2.24 : $|a_1| < |a_s|$

$\underline{|a_2| > |a_s|} \rightarrow c_2 > c_s$ (Voraussetzung 2.24)

Alternative 2.241 : $|a_1| + |a_2| > 2\,|a_s|$, also $c_2 > c_s$ — möglich.

Alternative 2.242 : $|a_1| + |a_2| < 2\,|a_s|$, also $c_2 < c_s$ — ausgeschlossen, denn sie widerspricht die Voraussetzung 2.24.

2.25 : $c_2 = c_s$

Dieser Fall wird auf Grund der im Absatz 2.15 erörteten Beweisführung ausgeschlossen.

Infolgedessen: *kann auf dem absteigenden, negativen Zweig der Kurve a/c, die Methode der „Adsorptionsmittelaufteilung" konzentriertere oder verdünntere Lösungen der Komponente (A) liefern, als die „einfache" Methode.*

Die (c) Methode. Gegeben ist $|a_2| < |a_1|$.

2.26 : $c'_f > c_s$

Es ergibt sich : $2\,|a_2| > |a_s|$ und $2\,|a_1| > |a_s|$, aber es folgt daraus nicht, daß auch $|a_2|$ bzw. $|a_1|$ größer als $|a_s|$ sind. Demnach ist es möglich, daß c'_f größer ist als c_s.

2.27 : $c'_f < c_s$

Es ergibt sich $2\,|a_2| < |a_s|$ oder $|a_2| < |a_s|$, was aber $|a_1| < |a_s|$ nicht einschließt, so daß die Ungleichung $c'_f < c_s$ auch möglich ist.

2.28 : $c'_f = c_s$

Gegeben ist $2\,|a_2| = |a_s|$ oder $|a_2| < |a_s|$, daraus ergibt sich aber keine Schlußfolgerung hinsichtlich der Beziehung zwischen $|a_1|$ und $|a_s|$, so daß c'_f gleich mit c_s sein kann.

Infolgedessen : *kann auf dem absteigenden, negativen Zweig der Kurve a/c die Methode der „Lösungsaufteilung" Lösungen liefern, deren Konzentration verschieden oder gleich der Konzentration der durch die Anwendung der „einfachen" Methode hergestellten Lösung sein kann. Es ist aber wahrscheinlicher die in Komponente (A) verdünntere Lösungen zu erhalten, da* $c_f < c'_f$.

2.3. $a = -K$ *(eine negative Konstante)*

Die unter 1.3 wiedergegebene Beweisführung offenbart, daß die „einfache" Methode Lösungen derselben Konzentration wie auch die Methode der „Adsorptionsmittelaufteilung" gibt und zwar (s.a. Gleichungen (14) und (16) :

$$c_s = c_2 = c_0 + r \cdot |K|$$

Die Beziehung zwischen der scheinbaren und realen spezifischen Adsorption ist diesmal :

$$|a_i| = \frac{(A_i + B_i)\,c_i}{100} - A_i \qquad (21)$$

prinzipiell identisch mit (13). Die Überlegungen gemäß Absatz 1.3 bleiben also auch für den Fall der (*c*)Mezhode gültig, ebenso auch die Schlußfolgerung : *wenn die scheinbare spezifische Adsorption konstant (positiv oder negativ) bleibt, haben die Lösungen die gleiche Konzentration in Komponente (A) gleichgültig ob bei der Adsorption die „einfache" Methode, die der „Adsorptionsmittelaufteilung" oder die der „Lösungsaufteilung" angewandt wurde.*

Die Schlußfolgerungen der bisherigen Überlegungen zusammenfassend, kann man hinsichtlich der durch Adsorption gegebenen Möglichkeiten zur Entfernung einer gelösten Komponente (*A*) zur Reinigung einer Lösung) folgende Feststellungen machen :

a) Auf dem positiven, aufsteigenden Zweig der Kurve *a/c* :

— die Methode der „Adsorptionsmittelaufteilung" führt immer zu einer vollständigeren Entfernung der Komponente (*A*) durch Adsorption, als die „einfache" Methode ;

– die Methode der „Lösungsaufteilung" führt gewiß nur dann zu einer besseren Reinigung als die „einfache" Methode, wenn die von dem Adsorptionsmittel festgehaltene Menge der Lösung im Vergleich zur anfänglich eingeführten Menge der Lösungsfraktion unbedeutend gering ist; andernfalls kann die Reinigungswirksamkeit dieser Methode gleich, oder verschieden sein von der der „einfachen" Methode.

b) Auf dem positiven, absteigenden Zweig der Kurve *a/c*, können die Methoden der „Adsorptionsaufteilung" und der „Lösungsaufteilung" eine größere oder eine kleinere Wirksamkeit als die „einfache" Methode haben.

c) In dem negativen Bereich der Kurve *a/c* bringt die Adsorption eine Konzentration der Lösung in Komponente (*A*) hervor, und zwar:

Auf dem aufsteigenden Zweig:

– die Methode der „Adsorptionsaufteilung" bestimmt in einem größeren Maß als die „einfache" Methode;

– die Methode der „Lösungsaufteilung" hat den obigen Erfolg nur wenn keine signifikante Menge der Lösung von dem Adsorptionsmittel festgehalten wird.

Auf dem absteigenden Zweig kann man weder im Fall der „Adsorptionsaufteilung"- noch in dem der „Lösungsaufteilung"-Methode voraussehen ob der Effekt der Konzentration der Lösung in der Komponente (*A*) mehr oder weniger intensiv sein wird als durch die „einfache" Methode.

d) Wenn die scheinbare spezifische Adsorption unabhängig ist von der Konzentration, also konstant (positiv oder negativ), haben alle drei Methoden dasselbe Ergebnis.

Wir nehmen an, daß die obige Ausführung eine qualitative Erklärung des „Kolonneneffektes" ist, also der Tatsache, daß in manchen Fällen, durch dynamische Adsorption eine größere Reinigungswirksamkeit als durch statische Adsorption erzielbar ist. Bei der Adsorption auf einer Kolonne findet nämlich eine „Aufteilung" des Adsorptionsmittels, zugleich mit einer „Aufteilung" der Lösung dadurch statt, daß sukzessive Fraktionen der Lösung mit sukzessiven Schichten des Adsorptionsmittels von der Kolonne in Kontakt kommen.

Im zweiten Teil unserer Arbeit wird versucht werden, dieses Problem quantitativ zu behandeln.

Revue Roumaine de Chimie, **15**, 1029 – 1038 (1970)

METALLKOMPLEXE DER ANTHRANYLDIESSIGSÄURE (ANDA). VIII*

ÜBER Cr(III)-ANDA-KOMPLEXE

C. DRĂGULESCU, R. POMOJE, I. MENESSY, M. PÎRLEA und C. MIHĂESCU

von der Fakultät für Angewandte Chemie an der Technischen Hochschule,

Timişoara, str. Bocşei 6

Eingegangen am 9. Juni 1969

Es werden auf spektralphotometrischem Wege die im System Cr(III)-ANDA-H^+ stattfindenden Komplexierungsgleichgewichte untersucht. Es wurde festgestellt, daß die Anthranyldiessigsäure bei Raumtemperatur augenblicklich mit Cr(III) unter Bildung eines grüngefärbten Komplexes (I) reagiert, in welchem das Verbindungsverhältnis 1 : 1 ist. Mit der Zeit oder durch Erhitzen wird dieser in einen anderen rotvioletten, ebenfalls 1 : 1 Komplex (II) umgewandelt. Die beiden Verbindungen unterscheiden sich strukturell durch das Bestehen einer Cr (III)-N-Bindung im Komplex II, was eine größere Stabilität desselben bewirkt. In Abhängigkeit vom pH-Wert, können in der Lösung verschiedene Formen des Komplexes II existieren, [CrANDA]H und $[\mathrm{CrANDA}(H_2O)_2]$ von rotvioletter Farbe und $[\mathrm{CrANDA}(OH)_2]$ von grünlichblauer Farbe. Die Stabilität des Komplexes II, die im Vergleich mit Zn-ANDA bestimmt wurde, entspricht der Konstanten $K_{\mathrm{CrANDA}} = 4.10^{-10}$.

Die über die Reaktionen zwischen Cr(III) und Liganden vom Typ der Komplexone ÄDTA, NTA [1-3] vorgenommenen Untersuchungen haben gezeigt, daß die gebildeten Komplexe eine Reihe gemeinsamer Eigenschaften besitzen, die von der Natur des Liganden unabhängig sind. Diese Komplexe sind durch ein Verbindungsverhältnis von 1 : 1, relativ hohe Stabilität, kleine Bildungsgeschwindigkeit bei Raumtemperatur und klar ausgeprägte saure Eigenschaften des ternären Aquochelats gekennzeichnet, welche dessen Umwandlung bei ansteigenden pH-Werten in ein Hydroxokomplex von anderer Farbe bewirken.

In Fortsetzung unserer Untersuchungen über Metallkomplexe von ANDA, haben wir in der vorliegenden Arbeit die Reaktion dieses Liganden mit Cr(III) untersucht und die Natur sowie die Stabilität der in Lösung gebildeten Komplexe und die analytischen Anwendungsmöglichkeiten dieser Reaktion verfolgt.

---

* C. DRĂGULESCU, I. MENESSY und MARIA PÎRLEA, *Rev. Roumaine Chim.*, **13**, 307 (1968).

[1] G. SCHWARZENBACH und W. DIEDERMANN, *Helv. Chim. Acta*, **31**, 331 (1948).

[2] R. E. HAMM, *J. Amer. Chem. Soc.*, **75**, 5670 (1953).

[3] R. F. CELLINI und E. A. VALIENTE, *Analyt. Abstr.*, **2(8)**, Nr. 2088 (1955).

Im Verlauf der Reaktion Cr(III)-ANDA sind dieselben Etappen wie im Falle anderer Liganden vom Komplexontyp zu erkennen: beim Vermischen der Lösungen entsteht ein grüner Komplex (I), dessen Farbe mit der Zeit in rotviolett (II) übergeht. Diese Farbänderung findet um so schneller statt, je höher die Temperatur ist und geht beim Sieden augenblicklich vor sich.

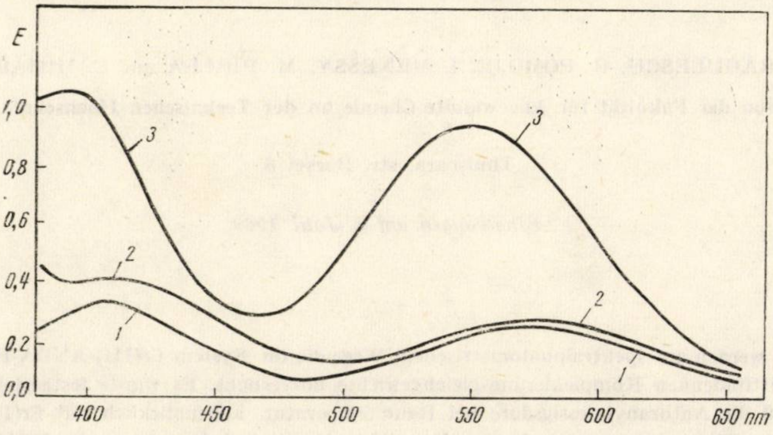

Abb. 1. — Lichtabsorption der Lösungen von Cr (III), bzw. Cr (III) und ANDA ($l = 4{,}0$ cm)

1, [Cr(III)] = 5.10^{-3}M; *2,* [Cr(III)] = [ANDA] = 5.10^{-3}M; *3,* [Cr(III)] = [ANDA] = = 5.10^{-3}M, nach dem Sieden.

Diese Veränderungen werden in Abb. 1 durch die Lichtabsorptionskurven einiger Cr(III)- bzw. Cr(III)-ANDA-Lösungen veranschaulicht, die beim Vermischen und nach dem Sieden erhalten wurden.

Um das Verbindungsverhältnis des gebildeten Komplexes (II) festzustellen, wurde die Methode der Molverhältnisse verwendet. Die erhaltenen Ergebnisse sind in Abb. 2 dargestellt, woraus hervorgeht, daß sich in diesem System eine einzige Komplexverbindung 1 : 1 von bemerkenswerter Stabilität bildet.

Die außerordentliche Stabilität dieses Komplexes wird durch das Verhalten beim Verdünnen veranschaulicht. Es wurde festgestellt, daß der molare Extinktionskoeffizient in Lösungen mit einer Konzentration von [Cr-ANDA] $= 2.10^{-3}$M-2.10^{-4}M konstant bleibt, wodurch das Fehlen jedwelcher Dissoziation des Komplexes innerhalb dieses Konzentrationsbereiches angezeigt wird. Dieselbe Sachlage ergibt sich, wenn die Verdünnung der Lösungen vor dem Sieden vorgenommen wird.

Die Veränderung des Komplexes in der Zeit wird in Abb. 3 veranschaulicht, wo die nach dem Vermischen und nach verschiedenen Zeitabschnitten erhaltenen Lichtabsorptionskurven dargestellt sind.

Demnach ergibt sich, daß sich die Absorptionsmaxima dieser Lösungen, sowohl der Position als auch der Intensität nach, denen einer Lösung welche dem Sieden unterworfen war, annähern. Die durchgeführten

Bestimmungen zeigen, daß die Bildung des Komplexes (II) in der Zeit, von einer stufenweisen Verminderung des pH-Wertes begleitet wird, und dem pH-Wert der durch Sieden erhaltenen Lösung zustrebt. Die maximale Änderung der Acidität tritt beim Freiwerden von einem Grammatom Protonen für ein Grammatom Cr(III) ein.

Abb. 2. — Veränderung der Lichtabsorption bei $\lambda = 550$ mμ, bei Lösungen mit $[Cr(III)] = 2.10^{-3}M$ und veränderlicher [ANDA] bei pH = 3,8 (l = 4,0 cm).

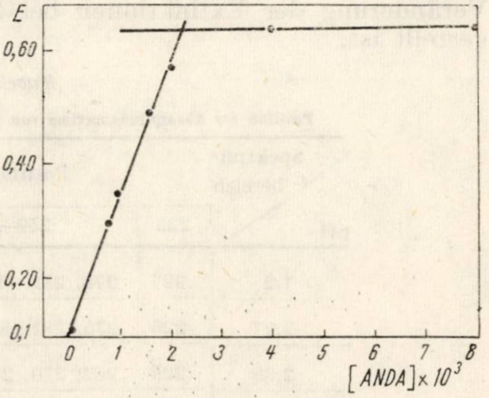

Abb. 3. — Verlauf der Lichtabsorptionskurven in Abhängigkeit von der Zeit für $[Cr(III)] = [ANDA] = 5 . 10^{-3}$ M; *1—8*, in Zeitabständen von 20 Minuten (bei 60°); *9*, nach dem Sieden.

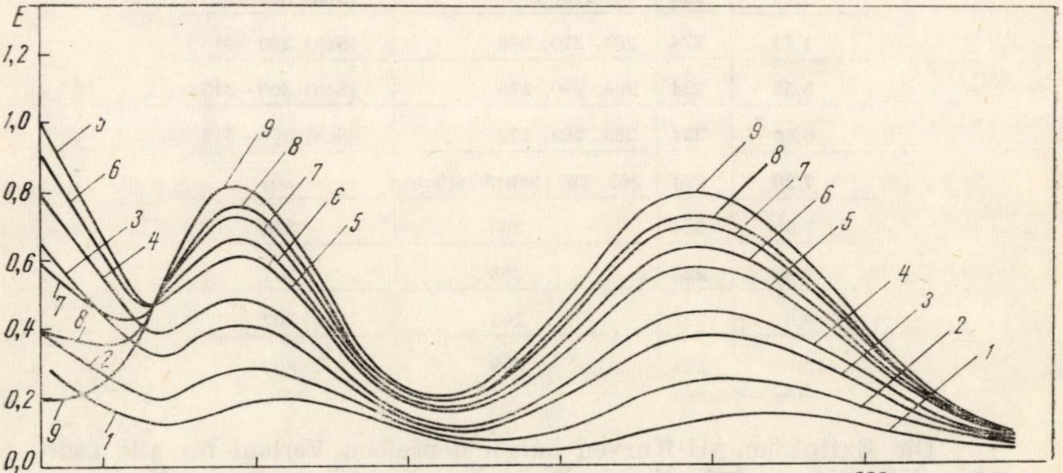

Zum Unterschied vom sichtbaren Bereich, zeigen die Lichtabsorptionskurven im UV ein anderes Verhalten, und zwar nähern sich die niedrigen Extinktionswerte denen der dem Sieden unterworfenen Lösungen, nur nachdem sie noch ein Maximum durchlaufen haben.

Um dieses Verhalten zu erklären, haben wir den Einfluß des pH-Wertes auf das Ligandenspektrum verfolgt, da die Umwandlung I→II von einer kontinuierlichen Verminderung desselben begleitet wird.

Die im Fachschrifttum vorhandenen Daten zeigen, daß das Absorptionsspektrum der Anthranylsäure und ihrer N-methyl-carboxy-Derivate [4-6] neben der Bande von 225 mμ durch das Bestehen einer Bande (des Benzens) zwischen 250—290 mμ, bzw. 300—325 mμ gekennzeichnet wird. Die Position und die Intensität der letzteren Banden wird von dem pH-Wert der Lösung stark beeinflußt.

In Tabelle 1 sind die Lichtabsorptionsbanden von ANDA in Abhängigkeit vom pH-Wert der Lösungen angeführt, während in Abb. 4 die Veränderung der Extinktionen bei $\lambda = 250$ mμ und $\lambda = 275$ mμ dargestellt ist.

Tabelle 1

Position der Absorptionsmaxima von ANDA bei verschiedenen pH-Werten

Spektralbereich / pH	Position der Maxima, mμ		
	225	250—290	300
1,2	227	275, 281, (Sch)	(Sch) 300—325
2,27	226	275, 281 (Sch)	(Sch) 300—325
2,83	225	262, 270, 276	(Sch) 300—325
3,25	224	264,270, 276	(Sch) 300—325
4,45	224	264, 270, 276	(Sch) 300—315
5,55	224	264, 270, 276	(Sch) 300—315
6,60	224	263, 269, 276	(Sch) 300—315
7,20	224	263, 267 (Sch),276(Sch)	305
7,55	224	264	308
7,95	223	263	307
9,0	223	263	307
12,0	223	259	303

(Sch = Schulter)

Die Extinktion-pH-Kurven haben denselben Verlauf für alle zwischen 250—350 mμ befindlichen Wellenlängen, und weisen ein Minimum im Bereich pH = 3—7 auf, wo die vorherrschende Form $ANDAH^{2-}$ ist.

Von diesen Banden sind für die Komplexierungsreaktion die im Bereiche 250—285 mμ befindlichen, am empfindlichsten, welche durch die batochrome Verschiebung gegen 280 mμ die Tetrakoordination des aminischen Stickstoffs kennzeichnen. [5]

Für Lösungen, welche den Komplex II enthalten, erscheint eine deutliche Bande bei 277 mμ, welche auch bei pH > 10, unter Bedin-

---

[4] P. Lumme, *Suomen Kem. B.*, **33**, 85 (1960).

[5] C. Drăgulescu, R. Pomoje, I. Menessy und C. Mihăescu, *Rev. Roumaine Chim.*, **12**, 553 (1967).

[6] C. Drăgulescu, I. Menessy, M. Pîrlea und A. Ferencz, *Bull. Soc. chim. France.* **1967**, 4740.

gungen in welchen der Ligand allein diese Bande nicht aufweist, gefunden wird; dagegen haben die Spektralkurven der Lösungen von Komplex I in diesem Bereich denselben Verlauf wie die des Liganden allein. Folglich muß der Unterschied zwischen den zwei Komplexen auf der im rotvioletten Komplex II vorhandenen Bindung Cr(III)-N beruhen. Der Strukturunterschied bewirkt die geringere Stabilität des Komplexes I gegenüber dem Komplex II. Diese Schlußfolgerung wird durch das Verhalten beim Hinzufügen von Basen bestätigt. Aus den bei Raumtemperatur erhaltenen Lösungen wird, selbst wenn sie rotviolett gefärbt sind, in schwach alkalischem Medium $Cr(OH)_3$ abgeschieden, während die gekochten Lösungen sich nicht einmal dann trüben, wenn sie stark alkalisch gemacht werden.

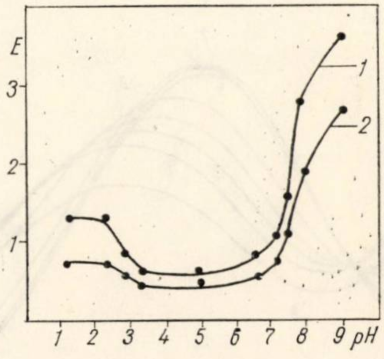

Abb. 4. – Abhängigkeit der Extinktion der ANDA-Lösungen vom pH.
[ANDA] = 2.10^{-4}M (l = 4,0 cm); *1*, λ = 250 mμ; *2*, λ = 275 mμ.

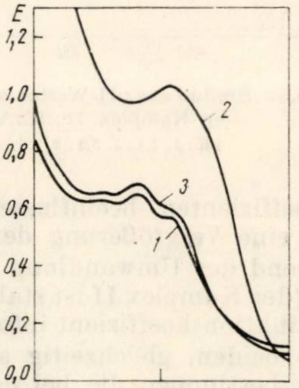

Abb. 5. – Lichtabsorption im Bereich 250–300 mμ der Lösungen:
1, [ANDA] = 4.10^{-3}m; l = 0,2 cm; pH = 3,00; *2*, [Komplex I] = 4.10^{-3}m; l = 0,2 cm; pH = 3,70; *3*, [Komplex II] = 4.10^{-3}m; l = 0,2 cm; pH = 3,15.

Beim Komplex I wurde das Verbindungsverhältnis durch die Methode des molaren Verhältnisses bestimmt, wobei als charakteristische Größe der Unterschied zwischen der Extinktion der Lösungen welche den Komplex enthalten und der Extinktion der Lösungen des Liganden bei gleicher Konzentration und $\lambda = 340$ mµ verwendet wurde. Die Ergebnisse zeigen, daß sich ein Komplex Cr(III): ANDA = 1 : 1 bildet, der aber von geringerer Stabilität ist.

Die Lichtabsorption im UV hängt sowohl von der Konzentration des Liganden, als auch vom pH ab, welche den mittleren molaren Extinktionskoeffizienten beeinflussen (die Verminderung des pH-Wertes verursacht eine Vergrößerung der Absorption — siehe Abb. 4).

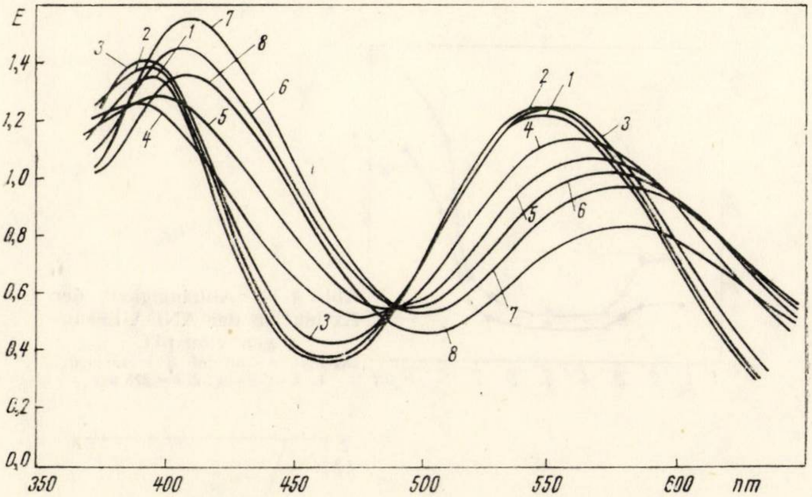

Abb. 6. — Einfluß des pH-Wertes auf die Lichtabsorptionskurven der Lösungen von Komplex II; [CrANDA] = 4.10^{-3} M; $l = 4$ cm.
pH: *1*, 1,4; *2*, 3,3; *3*, 5,8; *4*, 7,0; *5*, 8,6; *6*, 10,0; *7*, 12,2; *8*, 13,0.

Während der Umwandlung I→II nimmt die Konzentration des Liganden ab (der Komplex II ist stabiler als I), wobei gleichzeitig der mittlere molare Extinktionskoeffizient infolge Freiwerdens von Protonen abnimmt.

Diese beiden, gleichzeitig stattfindenden Einflüsse auf die Lichtabsorption, bestimmen die bei der Bildung des Komplexes II aus dem Komplex I, festgestellten Veränderungen.

Wie weiter oben gezeigt wurde, sind die Lösungen welche nur den Komplex II enthalten, stabil beim Hinzufügen von Basen. Die Veränderung des pH-Wertes beeinflußt aber merklich deren Farbe, indem die Vergrößerung der Acidität eine schwache Entfärbung verursacht, während die Vergrößerung der Basizität eine stufenweise Änderung der Farbe gegen grün, zur Folge hat.

In Abb. 6 sind die bei verschiedenen pH-Werten erhaltenen Lichtabsorptionskurven der Lösungen des Komplexes II dargestellt.

Im pH-Bereich 1—5 findet mit der Vergrößerung der pH-Werte eine schwache Intensivierung der Lichtabsorption statt, wobei die Position der Maxima ungefähr dieselbe bleibt. Über einem bestimmten pH-Wert vermindert sich die Extinktion plötzlich sehr stark, wobei gleichzeitig eine batochrome Verschiebung der beiden Banden stattfindet. Die Verschiebung ist am ausgeprägtesten im Bereich pH = 6–12, wo die Absorptionskurven einen isosbestischen Punkt bei 492 mμ aufweisen. Eine weitere Vergrößerung der pH-Werte bewirkt eine kleinere Verschiebung der Maxima und eine ausgeprägte Verminderung der Extinktion in dem gesamten untersuchten Spektralbereich, was zur Folge hat, daß bei pH = 13 die Absorptionskurve nicht mehr durch den isosbestischen Punkt geht.

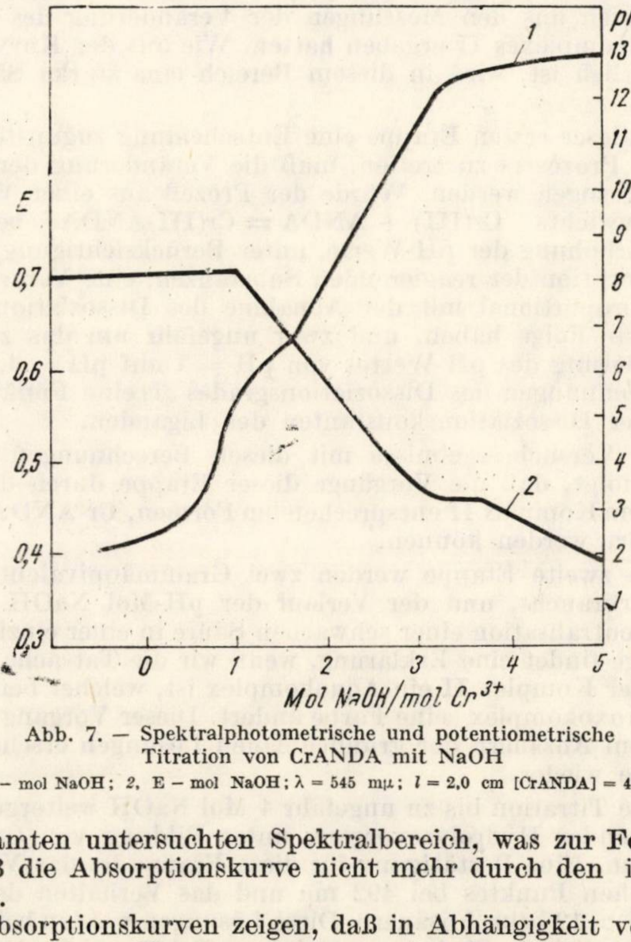

Abb. 7. – Spektralphotometrische und potentiometrische Titration von CrANDA mit NaOH

1, pH – mol NaOH; *2*, E – mol NaOH; λ = 545 mμ; *l* = 2,0 cm [CrANDA] = 4.10^{-3}M.

Die Absorptionskurven zeigen, daß in Abhängigkeit vom pH-Wert, zwischen pH = 1–5 (Kurven 1–3) entweder das Bildungsgleichgewicht des Komplexes II, oder ein Gleichgewicht zwischen zwei komplexen Formen mit annähernd gleicher Absorption besteht,

– zwischen pH = 6–12 (Kurven 4–7) ein Säure-Basen Gleichgewicht unter Beteiligung des Komplexes II vorhanden ist,

– und bei pH > 12 (Kurve 7–8) ein Zerfall des Komplexes unter Bildung von $Cr(OH)_4^-$ in der Endphase stattfindet.

Um die in diesen Lösungen stattfindenden stöchiometrischen Vorgänge zu ermitteln, wurde eine Lösung des Komplexes II mit NaOH titriert. Die Ergebnisse dieser Titration sind in Abb. 7 dargestellt worden.

Die erhaltene E-Mol NaOH (E-pH)-Kurve läßt dieselben Etappen erkennen die sich aus Abb. 6 ergeben. So stellt man bis zu pH = 5 (Kurve 2) ein leichtes Anwachsen der Extinktion fest, danach eine ausgeprägte Verminderung bis zu pH = 12, während darüber hinaus die Kurve einen Knick aufweist. In der ersten Etappe wird ein Äquivalent NaOH für 1 Mol Komplex verbraucht; dies stimmt mit den Ergebnissen überein, die sich aus den Messungen der Veränderung des pH bei der Bildung des Komplexes II ergeben hatten. Wie aus der Kurve 1, ph-Mol NaOH ersichtlich ist, wird in diesem Bereich eine starke Säure neutralisiert.

Um in dieser ersten Etappe eine Entscheidung zugunsten des einen oder anderen Prozesses zu treffen, muß die Veränderung der Extinktion in Betracht gezogen werden. Würde der Prozeß aus einer Verschiebung des Gleichgewichts $Cr(III) + ANDA \rightleftarrows Cr(III)ANDA$ bestehen, so müßte eine Erhöhung der pH-Werte, unter Berücksichtigung der äußerst geringen Absorption der reagierenden Substanzen, eine Vergrößerung der Extinktion, proportional mit der Abnahme des Dissoziationsgrades des Komplexes zur Folge haben, und zwar ungefähr um das zwanzigfache bei einer Änderung des pH-Wertes von pH = 1 auf pH = 4. Dies ergibt sich aus Berechnungen des Dissoziationsgrades als eine Funktion von α_H, auf Grund der Dissoziationskonstanten des Liganden.[6]

Da die Versuchsergebnisse mit diesen Berechnungen nicht übereinstimmen, folgt, daß die Vorgänge dieser Etappe durch das Bestehen von zwei, dem Komplex II entsprechenden Formen, Cr-ANDAH und Cr-ANDA, erklärt werden können.

Für die zweite Etappe werden zwei Grammäquivalent NaOH/Mol Cr-ANDA verbraucht, und der Verlauf der pH-Mol NaOH Kurve entspricht der Neutralisation einer schwachen Säure in einer einzigen Etappe. Diese Sachlage findet eine Erklärung, wenn wir die Tatsache in Betracht ziehen, daß der Komplex II ein Aquokomplex ist, welcher beim Übergang in einen Hydroxokomplex seine Farbe ändert. Dieser Vorgang ist umkehrbar, denn beim Ansäuern der grünlichblauen Lösungen erscheint die rotviolette Farbe wieder.

Wird die Titration bis zu ungefähr 4 Mol NaOH weitergeführt, kann ein entsprechender Hydrolysevorgang unter Bildung von $Cr(OH)_4^-$ beobachtet werden. Eine Bestätigung für diese Etappe ist das Verschwinden des isobestischen Punktes bei 492 mμ und das Verhalten der Lösungen mit einem pH > 12 beim Ansäuern. Diese Lösungen werden beim Ansäuern erst nach neuerlichem Sieden, rotviolett gefärbt, während bei vorsichtigem Ansäuern $Cr(OH)_3$ abgeschieden wird.

Die über die Komplexe II erhaltenen Versuchsergebnisse (Bestehen der Cr-N-Bindung und deren bemerkenswerte Stabilität) lassen, in Übereinstimmung mit [Cu-ANDA]H und dessen Salzen[7] folgende Strukturformeln annehmen (Abb. 8).

Zum Unterschied von den obigen Strukturen, ist im Komplex I der Stickstoff von Protonen blockiert, während Chrom durch die Carboxyl-gruppen an den Liganden gebunden wird, woraus folgt, daß der Ligand zwei- oder dreizähnig ist. Berücksichtigt man, daß die Bildung des Komplexes I nicht von einer Änderung des pH-Wertes begleitet wird, und daß bei einem entsprechenden pH-Wert der Anfangslösungen, der Ligand vor allem unter der Form $\mathrm{ANDAH^{2-}}$ existiert, kann der stattfindende Prozeß durch folgende Gleichung wiedergegeben werden:

---

[7] C. Drăgulescu, R. Pomoje und I. Menessy, „Omagiu" Acad. Prof. R. Ripan, Ed. Acad. Bukarest, 1966, S. 225.

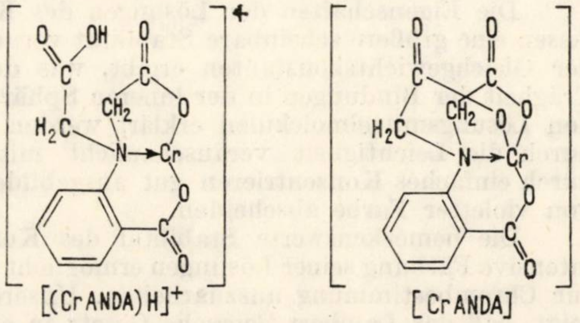

Abb. 8. — Strukturformeln von CrANDAH und CrANDA.

$$\mathrm{Cr^{3} + ANDAH^{2-} \rightleftharpoons [CrANDAH]^{+}}$$

Dieser Komplex I ist isomer mit dem Hydrogenkomplex von rotvioletter Farbe, von welchem er sich durch das Fehlen der N-Cr-Bindungen, und folglich durch eine verschiedene Zähnigkeit der Liganden unterscheidet.

Auf Grund der durchgeführten Untersuchungen kann für das System Cr (III)-ANDA-$\mathrm{H^+}$ folgendes Reaktionsschema aufgestellt werden:

$$\begin{tikzcd}
\mathrm{Cr^{3+} + ANDAH^{2-}} \arrow[r, shift left, "\mathrm{H^+}"] \arrow[d, shift right] & \mathrm{Cr(OH)_4^- + ANDA^{3-}} \arrow[l, shift left, "\mathrm{OH^-}"] \\
\begin{array}{c}[\mathrm{CrANDAH}]^+\\ \text{grün}\end{array} \arrow[u, shift right] \arrow[d, "\text{in der Zeit oder durch Erhitzen}"'] & \begin{array}{c}\mathrm{Cr(ANDA)}\\ \mathrm{(HO)_2}\\ \text{grünlichblau}\end{array} \arrow[u, "-\mathrm{H^+}"'] \arrow[d, shift right] \\
\begin{array}{c}[\mathrm{CrANDAH}]\\ \text{rotviolett}\end{array} \arrow[r, shift left, "-\mathrm{H^+}"] & \begin{array}{c}[\mathrm{CrANDA}\\ \mathrm{(H_2O)_2}]\\ \text{rotviolett}\end{array} \arrow[l, shift left] \arrow[u, shift right, "-\mathrm{H^+}"']
\end{tikzcd}$$

Um über die Stabilität des Komplexes $\mathrm{CrANDA(H_2O)_2}$ Hinweise zu erhalten, wurde die Gleichgewichtskonstante — K_e — der Reaktion bestimmt: [8]

$$\mathrm{ZnANDA + Cr \rightleftharpoons CrANDA + Zn.}$$

---

[8] C. Drăgulescu, T. Simonescu, I. Menessy und R. Anton, *Studii şi Cercetări Şti.Chim. Baza Cercetări Şti. Timişoara,* **6**, 9 (1959).

Die bei konstanten pH-Werten und für die Verhältnisse Zn/Cr = 2/1, 20/1, durchgeführten Bestimmungen ergaben für das obige Gleichgewicht den Wert $K_e = 50$.

Berücksichtigt man, daß $K_e = \frac{[\mathrm{CrANDA}]\,[\mathrm{Zn}]}{[\mathrm{ZnANDA}]\,[\mathrm{Cr}]} = \frac{K_{\mathrm{ZnANDA}}}{K_{\mathrm{CrANDA}}}$ und zieht den Wert von $K_{\mathrm{ZnANDA}} = 2\cdot10^{-8}$ in Betracht[9] so ergibt sich für $K_{\mathrm{CrANDA}} = 4\cdot10^{-10}$.

Die Eigenschaften der Lösungen des Komplexes $[\mathrm{CrANDA(H_2O)_2}]$ lassen eine größere scheinbare Stabilität vermuten, als sich aus dem Wert der Gleichgewichtskonstanten ergibt, was durch eine außergewöhnliche Trägheit der Bindungen in der inneren Sphäre des Komplexes, gegenüber den Lösungsmittelmolekülen erklärt werden kann. Diese Sachlage wird durch die Leichtigkeit veranschaulicht mit der sich aus der Lösung, durch einfaches Konzentrieren gut ausgebildete Kristalle des Komplexes, von violetter Farbe abscheiden.

Die bemerkenswerte Stabilität des Komplexes Cr-ANDA und die intensive Färbung seiner Lösungen ermöglicht es kolorimetrische Methoden zur Chrombestimmung auszuarbeiten. Unsere Bestimmungen haben gezeigt, daß das Lambert-Beersche Gesetz in einem Konzentrationsbereich von $1\cdot10^{-4} - 4\cdot10^{-3}$ M gültig ist.

Die in der vorliegenden Arbeit angeführten Bestimmungen sind mit Lösungen durchgeführt worden, die mit Hilfe von $\mathrm{Cr(NO_3)_3\cdot9\,H_2O}$ *p.a.*, und von uns synthetisierter Anthranyldiessigsäure zubereitet wurden.[8] Die Absorptionsspektren wurden mit einem Spektralphotometer UNICAM SP 800 erhalten, während die pH-Messungen mit Hilfe eines pH-Meßgerätes MV 11 mit Glaselektrode vorgenommen wurden.

---

[9] L. G. Sillen und A. E. Martell, „Stability Constants of Metal-Ion Complexes", the Chemical Society, London, 1964, S. 657.

Revue Roumaine de Chimie, **15**, 1039–1042 (1970)

UTILISATION DES HÉTÉROPOLYCOMBINAISONS COMME ÉCHANGEURS D'ÉLECTRONS. IV[1]

UTILISATION DU PHOSPHO-8-MOLYBDO-2-TUNGSTO-2-VANADATE DE NITRON COMME ÉCHANGEUR D'ÉLECTRONS

160

RALUCA RIPAN et A. ŞUTEU

Faculté de Chimie de l'Université « Babeş-Bolyai » de Cluj, Chaire de Chimie minérale,
11, str. Arany János

Reçu le 3 février

On montre que le phospho-8-molybdo-2-tungsto-2-vanadate de nitron se comporte en tant qu'échangeur d'électrons, et on détermine la capacité dynamique de réduction et d'oxydation de l'échangeur, par rapport aux ions Fe^{3+} et Fe^{2+}, ainsi que la capacité statique d'oxydation du Fe^{2+}.

Nous avons démontré dans les travaux antérieurs[1-3] que le phosphomolydbdovanadate de quinine, le phosphomolybdovanadate de nitron et le silicomolybdovanadate de nitron se comportent comme échangeurs d'électrons.

En continuant les recherches sur la possibilité d'utiliser les hétéropolycombinaisons comme échangeurs d'électrons, dans ce travail nous nous sommes proposé d'effectuer l'étude du phospho-8-molybdo-2-tungsto-2-vanadate de nitron (nitron H)$_5$ $[PMo_8W_2V_2O_{40}]$ comme nouvel échangeur d'électrons.

Nous avons préparé le phosphomolybdotungstovanadate de nitron à partir de l'acide phosphomolybdotungstovanadique, correspondant au même rapport de constituants synthétisé par la méthode de Kokorin.[4]

L'acide a été précipité par une solution aqueuse d'acétate de nitron en acide acétique et après filtration, le précipité jaune obtenu est lavé avec de l'eau chaude acidulée à H_2SO_4 ($pH \approx 1$), jusqu'à une réaction négative pour le nitron et séché à une lampe à infrarouges. Par analyse on a déterminé pour les constituants un rapport correspondant à la formule (nitron H)$_5$ $[PMo_8W_2V_2O_{40}]$.

Pour l'analyse, la substance est désagrégée par un mélange de H_2SO_4 conc. et KNO_3 et après la solubilisation on a séparé le tungstène par précipitation comme le $WO_3 \cdot H_2O$ et on l'a déterminé gravimétriquement sous forme de WO_3 ; on a déterminé après le molybdène gravimétriquement sous forme d'oxynate, le vanadium ayant été réduit au préalable jusqu'au vanadium tétravalent et puis complexé par l'EDTA, afin d'empêcher sa précipitation sous forme d'oxynate. Le vanadium a été déterminé plus tard par une autre épreuve, en calculant la différence de la somme des oxynates de molybdène et de vanadium, le phosphore colorimétriquement d'après la méthode de Charretton et ses collab.,[5] l'azote par la méthode de Dumas et l'eau par voie thermogravimétrique.

---

[1] R. Ripan et A. Şuteu, *Rev. Roumaine Chim.*, **13**, 759 (1968).
[2] R. Ripan et A. Şuteu, *Rev. Roumaine Chim.*, **12**, 1338 (1967).
[3] R. Ripan et A. Şuteu, *Rev. Roumaine Chim.*, **13**, 179 (1968).
[4] A. K. Kokorin, *Zhur. obschei. Khim.*, **26**, 1 (1956).

La capacité dynamique d'échange a été établie par la méthode des courbes d'élution.

On a déterminé au commencement la capacité dynamique d'oxydation de l'échangeur (sous forme oxydée) envers les ions Fe^{2+}.

A cette fin on passe, sur une colonne qui a contenu 2 g d'échangeur, une solution de Fe^{2+} 0,1 n acidulée avec H_2SO_4 au pH $\simeq$ 1. L'éluat est collecté par fractions de 1 ml, dans lesquelles on a titré par $KMnO_4$ 0,1 n le reste de Fe^{2+} inoxydé par l'échangeur, le Fe^{2+} oxydé par l'échangeur étant calculé par différence.

Sur la base de ces données, on a tracé un diagramme (fig. 1) dans lequel, sur l'ordonnée, on a représenté les valeurs $\frac{\text{mval}}{\text{g}}$ Fe^{2+} ox et sur l'abscisse les ml Fe^{2+} passés sur la colonne. On a planimétré la surface ABCDOA délimitée par la courbe et par l'axe des abscisses que l'on a trouvée égale à 7,025 10^3 mm².

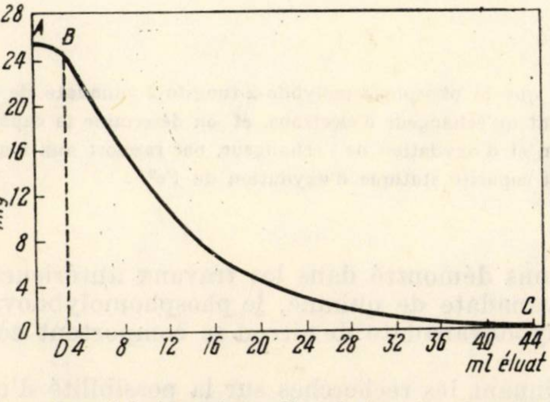

Fig. 1. — Capacité dynamique d'oxydation du phospho-8-molybdo-2-tungtso-2-vanadate de nitron, par rapport au Fe^{2+}.

Cette surface représente la capacité dynamique totale d'oxydation du Fe^{2+} par l'échangeur.

Il résulte de la construction du graphique que 1 mm² $= 8 \cdot 10^{-5}$ mval Fe^{2+} oxydés par 1 g d'échangeur. La capacité dynamique totale d'oxydation $CDT_{(OxFe^{2+})}$ rapportée à 1 g d'échangeur est donc égale à

$$CDT_{(OxFe^{2+})} = 7{,}025 \cdot 10^3 \cdot 8 \cdot 10^{-5} = 0{,}562 \text{ mval } Fe^{2+}.$$

La surface ABDOA $= 1{,}87 10^3$ mm² représente la capacité dynamique d'oxydation avant le saut rapportée à 1 g d'échangeur et est, par conséquent égale à

---

[5] B. Charreton, F. Chauveau, G. Bertho et P. Courtin, *Chim. Analyt.*, **47**, 17 (1965).

$$\mathrm{CDAS}_{(\mathrm{OxFe^{2+}})} = 1{,}87 \cdot 10^{3} \cdot 8 \cdot 10^{-5} = 0{,}150 \text{ mval } \mathrm{Fe^{2+}}.$$

Le phosphomolybdotungstovanadate de nitron en tant qu'échangeur d'électrons fonctionne réversiblement, puisque en répétant 5 fois le cycle d'oxydo-réduction, on a obtenu des résultats présentant la meilleure concordance.

Afin de déterminer la capacité statique d'oxydation du Fe^{2+} on a pesé une quantité d'échangeur que l'on a introduit dans un flacon de dosage et on a ajouté 25 ml $FeSO_4$ 0,1 n et du CO_2 ; on ferme ensuite le flacon, et 48 heures après on introduit de nouveau 25 ml $FeSO_4$ 0,1 n, puis 48 heures plus tard, le contenu est filtré en y déterminant par dosage permanganométrique le Fe^{2+} non oxydé par l'échangeur. Les résultats obtenus sont indiqués dans le tableau 1.

Tableau 1

Capacité statique d'oxydation du (nitron H)$_5$ [$PMo_8W_2V_2O_{40}$] dans la réaction d'oxydation du Fe^{2+}

N° de l'épreuve	g échangeur	$\frac{\text{mval}}{\text{g échangeur}}$	Fe^{2+}ox.	$\frac{\text{mval}}{\text{mole échangeur}}$ Fe^{2+} ox.	Nombre d'électrons accepté par une mole échangeur
1	0,5290	1,13		3,66	4
2	0,2954	1,17		3,77	
3	0,2894	1,19		3,84	

La capacité statique d'oxydation du Fe^{2+} rapportée à 1 mole phospho-8-molybdo-2-tungsto-2-vanadate de nitron a été trouvée égale à 3,69 mval Fe^{2+}, ce qui démontre que l'anion phospho-8-molybdo-2-tungsto-2-vanadate nitron se comporte comme échangeur dans la réaction d'oxydation des ions Fe^{2+} acceptant quatre électrons.

On a déterminé ensuite la capacité dynamique de réduction du phospho-8-molybdo-2-tungsto-2-vanadate de nitron (réduit par l'acide ascorbique) dans la réaction de réduction du Fe^{3+}.

A cette fin, on a passé par dessus de l'échangeur (réduit par acide ascorbique) une solution de Fe^{3+}, en titrant dans l'éluat le Fe^{2+} résulté.

La courbe d'élution est représentée dans la figure 2.

La surface ABCDOA = $9 \cdot 25 \cdot 10^{3}$ mm^2 ; le diagramme indique que 1 mm^2 = $4 \cdot 10^{-5}$ mval Fe^{3+} réd par 1 g d'échangeur, donc :

$$\mathrm{CDT}_{(\text{réd } \mathrm{Fe^{3+}})} = 9 \cdot 25 \cdot 10^{3} \cdot 4 \cdot 10^{-5} = 0{,}370 \text{ mval } \mathrm{Fe^{3+}}$$

la surface ABDOA = $1{,}82 \cdot 10^{3}$ mm^2, donc :

$$\mathrm{CDAS}_{(\text{réd } \mathrm{Fe^{3+}})} = 1{,}82 \cdot 10^{3} \cdot 4 \cdot 10^{-5} = 0{,}120 \text{ mval } \mathrm{Fe^{3+}}.$$

En examinant $\mathrm{CDT}_{(\mathrm{Ox\ Fe^{2+}})} = 0{,}562$ mval Fe^{2+} ox, en comparaison du $\mathrm{CDT}_{(\text{réd } \mathrm{Fe^{3+}})} = 0{,}370$ mval Fe^{3+} réd, on constate que la capacité dynamique de la réduction du Fe^{3+} est moindre que la capacité dynamique d'oxydation du Fe^{2+}. Cette différence s'explique par l'oxydation de la forme réduite de l'échangeur, oxydation qui se produit sous l'action de l'oxygène contenu dans l'eau de lavage effectué en vue d'éliminer l'excès d'acide ascorbique.

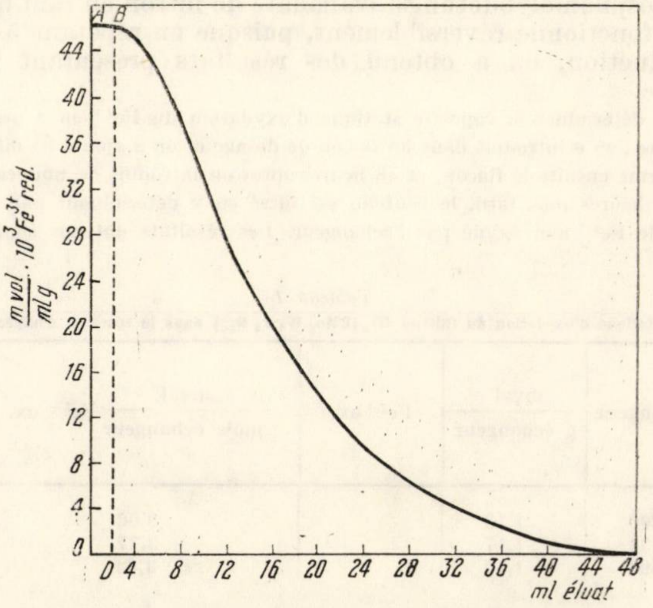

Fig. 2. — Capacité dynamique de réduction du phospho-8-molybdo-2-tungsto-2-vanadate de nitron (ramené à la forme réduite avec de l'acide ascorbique), par rapport au Fe^{3+}.

CONCLUSIONS

Les données susmentionnées permettent de tirer les conclusions suivantes :

1. Le phospho-8-molybdo-2-tungsto-2-vanadate de nitron se comporte comme un échangeur d'électrons.
2. L'échange d'électrons est réversible et l'échangeur peut être régénéré après chaque opération.
3. La capacité statique d'oxydation exercée sur le Fe^{2+} a montré que l'échangeur fonctionne en acceptant 4 électrons.
4. La forme réduite de l'échangeur est instable, au contact de l'air elle s'oxyde rapidement en passant partiellement sous forme oxydée.

Revue Roumaine de Chimie, **15**, 1043–1047 (1970)

DER EINFLUSS DER TRICHLORESSIGSÄURE (TCE) AUF DIE THORIUMEXTRAKTION AUS WÄSSRIGEN LÖSUNGEN MIT BUTANOL-1*

S. FIŞEL, GIZELLA NEMES, MARIA TOTAN und T. SIMONESCU

von der Universität „A. I. Cuza" Iaşi und Arbeitsstelle der Akademie,
Zweigstelle Timişoara, Bdul M. Viteazu 24

Eingegangen am 24. Oktober 1969

Es wurde der Einfluß der Trichloressigsäure auf die Thoriumextraktion aus wäßrigen Lösungen mit Butanol-1 aufgeklärt. Es wurde festgelegt, daß die wahrscheinlichste Formel für die extrahierte Verbindung $[Th(OH)_2A_2]_0$ ist. Die Trichloressigsäure hat auch einen Aussalzungseffekt, weil die Extraktion von der Anwesenheit großer TCE-Mengen begünstigt wird.

Im Rahmen vieler Arbeiten unseres Laboratoriums wurde die Wirksamkeit der Trichloressigsäure bei der Extraktion des Thoriums, Zirkoniums, [1] Titans, [2] sowie einiger ihrer Chelatkomplexe [3,4] aus wäßrigen Lösungen mit Butanol-1 festgestellt.

Aufgrund dieser Bemerkungen wurde ein Studium bezüglich des Einflusses der Trichloressigsäure auf die Thoriumextraktion aus wäßrigen Lösungen mit Butanol-1 unternommen, zwecks Aufklärung des Extraktionsmechanismus unter diesen Bedingungen. Zu diesem Zweck, wurde die Thoriumextraktion in Abhängigkeit von folgenden Parametern verfolgt: Metallionenkonzentration und pH-Wert der Lösungen.

EXPERIMENTELLES

Apparatur. pH-Meter MV 11 Clamann & Grahnert – Dresden DDR und Spektralkolorimeter „Spekol" – Carl Zeiss Jena, DDR.

Reagenzien

– Die 10^{-2} M Thoriumnitratlösung wurde durch Auflösen von ungefähr 5,52 g $Th(NO_3)_4 \cdot x\ H_2O$ Merck (mit einem Gehalt an ThO_2 min. 46 %) in 1 l bidestilliertem Wasser präpariert. Der Titer der Lösung wurde gravimetrisch für die ThO_2-Form bestimmt.

---

* Diese Arbeit wurde anläßlich der Landeskonferenz für analytische Chemie im September 1969 vorgetragen.

[1] C. Drăgulescu, T. Simonescu und G. Nemes, *Rev. Roumaine Chim.*, **13**, 1469 (1968).

[2] C. Drăgulescu, T. Simonescu und H. Schiff, *Rev. Roumaine Chim.*, **14**, 583 (1969).

[3] C. Drăgulescu, T. Simonescu und S. Policec, *Talanta*, **11**, 747 (1964).

[4] C. Drăgulescu, T. Simonescu, G. Nemes und M. Totan, unter Druck.

— Die 10^{-3} M Thoriumnitratlösung wurde durch Verdünnen der obenangeführten Lösung erhalten.

— Die 1 M Trichloressigsäure wurde durch Auflösen der entsprechenden Menge in bidestilliertem Wasser präpariert. Der Titer wurde alkalimetrisch bestimmt.

— 0,1 %ige Thoronlösung, in bidestilliertem Wasser.

— 0,01 M Natriumhydroxidlösung.

— Butanol-1, die Fraktion die bei 117—118,5° während der Destillierung des durch Gährung erhaltenen Butanols übergeht.

Für die Extraktion wurden Scheidetrichter von 100 ml Volumen benützt und es wurde mit gleichen Volumina der organischen Phase und der wäßrigen Phase (30 ml) gearbeitet. Um Volumenveränderungen während der Extraktion wegen der großen Azidität der wäßrigen Phase zu vermeiden, werden zuerst die Phasen untereinander vermischt. Erst nach dem Einstellen des Sättigungsgleichgewichtes können die Phasen für die Extraktion verwendet werden.

Die Verteilung des Metalles zwischen den beiden Phasen wurde durch eine Bestimmung in der wäßrigen Phase auf spektrophotometrischem Weg mit Thoron[5] verfolgt, nachdem vorher Äthanol (ca 8%ig) zugesetzt wurde, um die Klärung zu sichern.

Die Verteilung der Trichloressigsäure, wurde durch das Titrieren der wäßrigen Phase mit 0,01 M NaOH, in Gegenwart von Phenolphthalein bestimmt.

ERGEBNISSE UND DISKUSSION

Die erhaltenen Resultate, die in der Tabelle 1 wiedergegeben sind, zeigen, daß der Verteilungskoeffizient der Trichloressigsäure (D_{TCE}) mit dem Ansteigen der Säurekonzentration in der wäßrigen Phase zunimmt.

Tabelle 1

Die Änderung des Verteilungskoeffizienten von TCE

	1	2	3	4	5	6	7	8	9
$C \cdot 10^{-3}$ M	0,18	0,37	3,04	11,40	30,48	66,40	132,8	372,63	745,24
D_{TCE}	0,76	2,12	1,83	1,93	2,4	3,19	4,14	6,23	8,82

Aus dem Studium des Einflusses der Trichloressigsäurekonzentration auf die Extraktion folgt, daß die Thoriumextraktion aus wäßrigen Lösungen mit Butanol-1 nur in Gegenwart von großen Trichloressigsäuremengen stattfindet. Der Wert der Verteilungskoeffizienten D_{Th} wächst mit dem Anwachsen der TCE-Konzentration (Tabelle 2).

Tabelle 2

Die Änderung des Verteilungskoeffizienten des Thoriums

$C_{Th} = 4,8 \cdot 10^{-5}$ **M**

	1	2	3	4	5	6	7	8	9	10
$C_{TCE} \cdot 10^{-3}$ M	0	0,18	0,37	3,04	11,40	30,48	66,4	132,8	372,63	745,24
D_{Th}	0	0,11	0,17	0,20	0,24	0,28	0,76	1,68	7,4	8,68

[5] M. Pinta, „Recherche et dosage des éléments traces", Dunod, Paris, 1962, S. 161.

Das Extraktionsgleichgewicht eines Kations in Gegenwart eines Liganden (HA), kann mit Hilfe der Beziehung[6] ausgedrückt werden, wenn der pH-Wert beim Gleichgewicht in Betracht gezogen wird:

$$\log D = \log K + m \log (\mathrm{HA})_0 + n\,\mathrm{pH} \qquad (1)$$

wobei K die Extraktionsgleichgewichtskonstante darstellt. Der Index ,,o'' zeigt die Anwesenheit des Komponenten in der organischen Phase an. Durch Differenzierung der Gleichung (1) erhält man:

$$\left[\frac{\partial \log D}{\partial\, \mathrm{pH}}\right]_{(\mathrm{HA})_0} = n$$

woraus folgt, daß der Anstieg der graphischen Darstellung von log D/pH, bei konstanter Säurekonzentration in der organischen Phase, die Anzahl der Säuremoleküle angibt, welche an der Austauschreaktion teilnehmen. Auf diese Weise kann man die Ladung der Ausgangsspezie, die an der Extraktion teilnimmt, feststellen. Eine solche graphische Darstellung ist in Abb. 1 wiedergegeben, in welcher drei TCE-Konzentrationen angewendet und drei Gerade gezogen wurden.

Die pH-Veränderung wurde durch Zugabe von entsprechenden Natriumhydroxidmengen erreicht. Die verwendeten Werte der Verteilungskoeffizienten (D) befanden sich abhängig vom pH-Wert in dem Gebiet, in welches sich die Gerade einschreibt, und wurden dann statistisch mit Hilfe der Methode der kleinsten Quadrate korrigiert. So erhält man drei parallele Geraden (Abb. 1), deren Anstieg nahe dem Wert 2 ist und welcher ein Beweis dafür ist, daß an der Austauschreaktion 2 Säuremoleküle teilnehmen ($n = 2$).

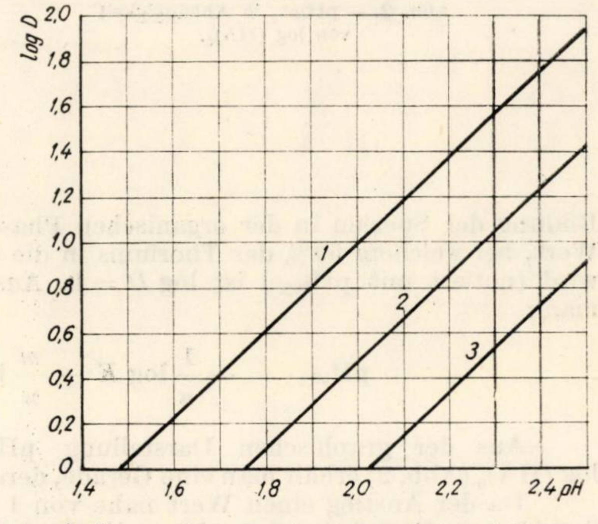

Abb. 1. — log D Abhängigkeit von dem pH-Wert der Lösung bei drei verschiedenen TCE-Säurekonzentrationen
1, – c = 2.10^{-1} m; *2*, – c = 1.10^{-1} m; *3*, – c = $0.5.10^{-1}$ m.

---

[6] R. M. Diamond und D. G. Tuck, ,,Progress in Inorganic Chemistry'', II. Bd., Interscience, New York, 1960, S. 122.

Da das Thorium in der Nitratlösung die Wertigkeit IV (Th^{4+}) hat und da die Existenz einiger Spezien mit Hydroxylgruppen im allgemeinen möglich ist, kann man bei diesem Element, sogar bei kleinen pH-Werten, annehmen, daß die Austauschreaktion nach folgendem Schema verläuft:

$$Th(OH)_2^{2+} + 2\,HA \rightleftarrows Th(OH)_2A_2 + 2H^+.$$

Die Veränderung des log D mit der Konzentration der TCE (HA) ergibt die gesamte Anzahl (m) der Säuremoleküle, welche an der Bildung der Spezien in der organischen Phase teilnehmen. Bei dem pH-Wert, bei welchem 50% des Thoriums in die organische Phase extrahiert wird (notiert mit $pH_{50\%}$) ist $\log D = 0$. Aus der Gleichung (1) erhält man:

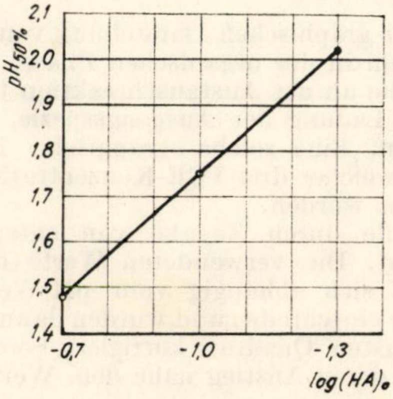

Abb. 2. – $pH_{50\%}$ in Abhängigkeit von $\log\,(HA)_0$.

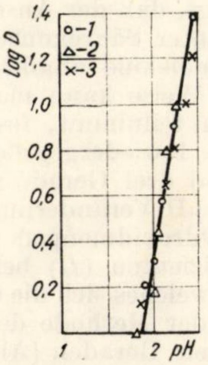

Abb. 3. – log D in Abhängigkeit von dem pH-Wert der Lösung bei drei verschiedenen Thoriumkonzentrationen.
1, 1.10^{-4}m; *2*, $2{,}44.10^{-5}$m; *3*, 5.10^{-5}m.

$$pH_{50\%} = -\frac{1}{n}\log K - \frac{m}{n}\log\,(HA)_0$$

Aus der graphischen Darstellung $pH_{50\%}$ in Abhängigkeit von $\log\,(HA)_0$ (Abb. 2) erhält man eine Gerade, deren Anstieg gleich ist mit m/n.

Da der Anstieg einen Wert nahe von 1 hat, folgt, daß m 2 ist und daß also am Extraktionsprozeß nur die Säuremoleküle teilnehmen, welche auch an dem Austauschprozeß beteiligt sind und daß die extrahierte Spezies $Th(OH)_2A_2$ ist.

Folglich kann das Gleichgewicht durch folgendes Schema dargestellt werden:

$$Th(OH)_2^{2+} + (HA)_0 \rightleftarrows [Th(OH)_2A_2]_0 + 2H^+$$

Die Veränderung des Logarithmus des Thoriumverteilungskoeffizienten in Abhängigkeit von dem pH-Wert bei konstanter TCE-Konzentration kann Aufschluß geben über die Existenz der polynuklearen Spezien im System.

Abb. 3 stellt die graphische Darstellung der Veränderung des log$D$ in Abhängigkeit vom pH-Wert bei drei verschiedenen Thoriumkonzentrationen und bei konstanter Säurekonzentration dar. Nach der Korrektur mit der Methode der kleinsten Quadrate, erhält man eine Gerade, welche anzeigt, daß sich unter den gegebenen Bedingungen sowohl in der organischen Phase als auch in der wäßrigen Phase keine polymeren Spezien bilden.

Weil die Thoriumextraktion stark von der Gegenwart großer TCE-Mengen beeinflußt ist, kann man auch den Aussalzungseffekt der Säure in Betracht ziehen, welcher die Moleküle des Kristallisationwassers des Kations beseitigt und auf diese Weise die Extraktion erleichtert.

Alle diese Betrachtungen führen zu der Schlußfolgerung, daß der wahrscheinlichste Extraktionsmechanismus durch folgendes Schema dargestellt werden kann :

$$\mathrm{Th(OH)}_2^{2+} \cdot r\,\mathrm{H_2O} + 2\,(\mathrm{HA})_0 \rightleftharpoons [\mathrm{Th(OH)_2A_2}]_0 + 2\,\mathrm{H}^+ + r\,\mathrm{H_2O}$$

Die Veränderung des Logarithmus des Thoriumverteilungskoeffizienten in Abhängigkeit von dem pH-Wert bei konstanter TCE-Konzentration kann Aufschluß geben über die Existenz der polynuklearen Species im System.

Abb. 8 stellt die graphische Darstellung der Veränderung des log D in Abhängigkeit vom pH-Wert bei drei verschiedenen Thoriumkonzentrationen und bei konstanter Säurekonzentration dar. Nach der Korrektur mit der Methode der kleinsten Quadrate, erhält man eine Gerade, welche anzeigt, daß sich unter den gegebenen Bedingungen sowohl in der organischen Phase als auch in der wäßrigen Phase keine polymeren Species bilden.

Weil die Thoriumextraktion stark von der Gegenwart großer TCE-Mengen beeinflußt ist, kann man auch den Auflösungseffekt der Säure in Betracht ziehen, welcher die Moleküle des Kristallisationswassers des Kations beseitigt und auf diese Weise die Extraktion erleichtert.

Alle diese Betrachtungen führen zu der Schlußfolgerung, daß der wahrscheinlichste Extraktionsmechanismus durch folgendes Schema dargestellt werden kann:

$$\mathrm{Th(OH)}_2^{2+} \; [illegible] + \mathrm{H_2O} + 2\,(\mathrm{HA})_2 \rightleftharpoons (\mathrm{Th(OH)_2A_2})\; [illegible] + 2\,\mathrm{H}^+ \; [illegible] + \mathrm{H_2O}$$

Revue Roumaine de Chimie, **15**, 1049 – 1056 (1970)

FORMATION CONSTANTS OF THE ALUMINIUM ION CHELATES WITH PYROCATECHOL AND PYROCATECHOL VIOLET

T. GOINA, MARIA OLARIU and LUCIA BOCANICIU

Laboratory of Inorganic Chemistry, Institute of Medicine and Pharmacy
Tîrgul Mureş Str. Gh. Marinescu 38

Received July 12, 1969

Potentiometric titration of $AlCl_3$ solution mixtures with Pyrocatechol. (H_2Py) and Pyrochatechol violet (H_4VPy) by NaOH evidences the formation of the complexes $AlPy^{+}$, $AlPy_2^{1-}$, $AlPy_3^{3-}$, respectively AlHVPy, $AlHVPy_2^{3-}$, $AlHVPy_3^{6-}$. The stability constants of these complexes were computed at constant ionic strength. The mean values of these constants are:

for $H_2Py\text{-}Al^{3+}$: $k_1 = 1.88 \times 10^{16}$; $k_2 = 3.00 \times 10^{13}$;
$k_3 = 1.00 \times 10^{9}$,
for H VPy-Al^{3+} : $k_1 = 1.32 \times 10^{25}$; $k_2 = 1.88 \times 10^{22}$;
$k_3 = 5.53 \times 10^{20}$

The interaction of the aluminium ion and pyrocatechol was the object of former studies; Dubey and Mehrotra[1] have emphasized the formation of some soluble stable complexes in the ratio pyrocatechol: Al = 1, 2,3. Results obtained by us previously[2] have shown that, in alkaline medium, aluminium forms with pyrocatechol a soluble complex with the molar ratio 1 : 2, to which we have assigned the probable formula $(HO)_2Al(OC_6H_4O)_2$.

The present paper is a continuation of our former research work, aiming at determining the stability of the complexes with pyrocatechol. At the same time we have studied the formation of aluminium ion complexes with pyrocatechol violet. Pyrocatechol violet is an indicator used in alkaline medium for Cu^{2+}, Co^{2+}, Ni^{2+}, giving complexes of the form $MeHVPy^{-}$ and $MeVPy^{0}$. It is also a specific indicator for bismuth and thorium in acid medium.[3] Spectrophotometric studies have also established the complex capacity of pyrocatechol violet with wolfram and niobium.[4]

---

[1] S. N. Dubey and R. C. Mehrotra, *J. Inorg. Nuclear Chem.*, **26**, 1543 (1964); *Chem Zentr.*, **1966**, p. 1072.

[2] T. Goina, I. Ristea and M. Olariu, *Revista Medicală*, **12**, 352 (1967).

[3] R. Pribil, "Complexonii în Chimia Analitică", Ed. Tehnică, Bucharest, 1961, p. 244.

[4] V. F. Maltsev, E. N. Pascenko, A. S. Tirovscaia and N. P. Volcova, *Zhur. neorg. Khim.*, **12**, 483 (1968).

EXPERIMENTAL

To estimate the stability of the complexes formed in the systems Al^{3+}-pyrocatechol and Al^{3+}-pyrocatechol violet, we have resorted to the calculation of the stability constants by means of the Bjerrum's potentiometric method.[5]

We have supposed that in the system Al^{3+} pyrocatechol the following reactions take place:

$$H_2Py + OH^- \rightleftarrows HPy^{1-} + H_2O \qquad \text{I}$$

$$HPy^{1-} + Al^{3+} + OH^- \rightleftarrows AlPy^{1+} + H_2O \qquad \text{II}$$

$$AlPy^{1+} + HPy^{1-} + OH^- \rightleftarrows AlPy_2^{1-} + H_2O \qquad \text{III}$$

$$AlPy_2^{1-} + HPy^{1-} + OH^- \rightleftarrows AlPy_3^{3-} + H_2Py \qquad \text{IV}$$

where H_2Py = pyrocatechol.

To compute the individual formation constants of the successive complexes, we have carried out the potentiometric titration with NaOH of H_2Py alone, on the one hand, and of the mixtures Al : H_2Py in the ratio 1 : 10 and 1 : 15 on the other hand, in the presence of KCl to maintain the ionic strength constant at 0.2.

The calculation of the value of $\bar{n}$ (indicating the mean number of ligands engaged by the metallic ion of the solution) was carried out by means of the data given in figure 1.

For every pH > 3,6 the horizontal distance between the curves 1—2, respectively 1—3, gives exactly the supplementary base consumption needed for reactions II—IV, or the total Py^{2-} anion moles number engaged in the complex. By dividing this number by the total number of Al^{3+} moles existing in the solution, one obtains $\bar{n}$.

The concentration of the Py^{2-} ions, for a given pH, was calculated from the equation expressing the balance of the ligand consumption:

$$[H_2Py]\,\text{total} = [HPy^{1-}] + [Py^{2-}] + [AlPy^{1+}] + 2\,[AlPy_2^{1-}] + 3\,[AlPy_3^{3-}]$$

Taking into account the dissociation of the phenolic protons:

$$H_2Py \rightleftarrows H^+ + HPy^{1-} \qquad \text{V}$$

$$Ka_1 = \frac{H^+ \cdot HPy^{1-}}{H_2Py} = 3.71 \times 10^{-10} \qquad (2)$$

$$HPy^{1-} \rightleftarrows H^+ + Py^{2-} \qquad \text{VI}$$

$$Ka_2 = \frac{H^+ \cdot Py^{2-}}{H\,Py^{1-}} = 1 \times 10^{-13} \qquad (3)$$

and the fact that for a certain pH:

$$[Al\,Py^{1+}] + 2\,[Al\,Py_2^{1-}] + 3\,[AlPy_3^{3-}] = \Delta\,[NaOH] \qquad (4)$$

where Δ [NaOH] represents the supplementary base consumption we have:

$$Py^{2-} = \frac{({}^{n}A - {}^{n}NaOH).1000}{\left(\dfrac{[H^+]^2}{K_1\,K_2} + \dfrac{[H^+]}{K_2} + 1\right)(V + \Delta V)}$$

---

[5] J. Bjerrum, "Metal Amine Formation in Aqueous Solution", P. Haase and Son, Copenhagen, 1941.

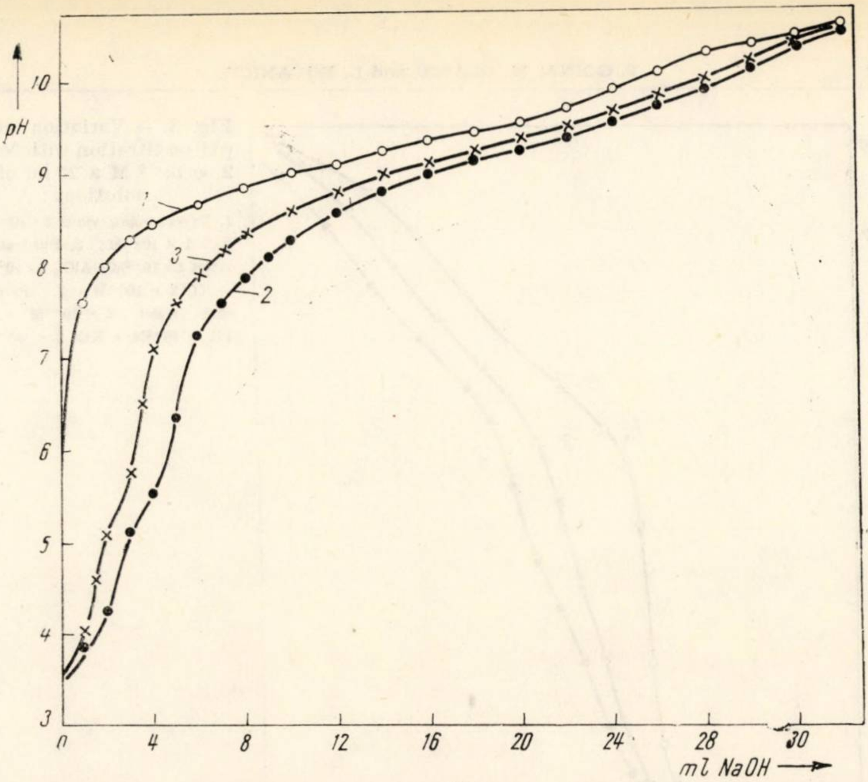

Fig. 1. — Variation of the pH on titration with NaOH 2×10^{-2} M a 25 ml of the solutions: *1*, Pyrocatechol 2×10^{-2}M + KCl 2×10^{-1}M; *2*, Pyrocatechol 2×10^{-2}M + $AlCl_3$ 2×10^{-3}M + KCl 2×10^{-1}M; *3*, Pyrocatechol 2×10^{-2}M + $AlCl_3$ 1.3×10^{-3}M + KCl 2×10^{-1}M.

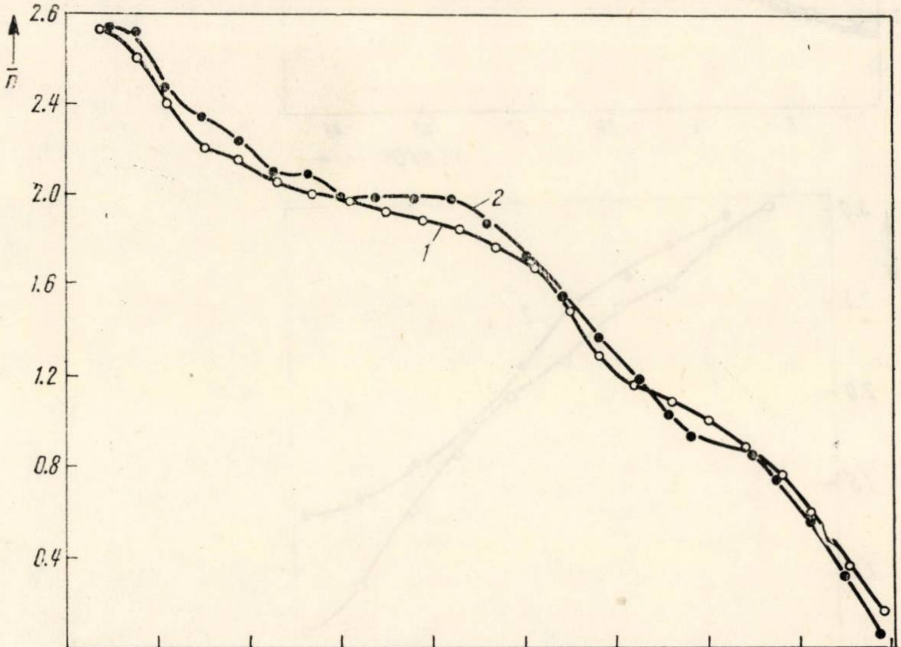

Fig. 2. — Formation curves of the system Al^{3+}-Pyrocatechol in the ratio: *1*, 1 : 10; *2*, 1 : 15.

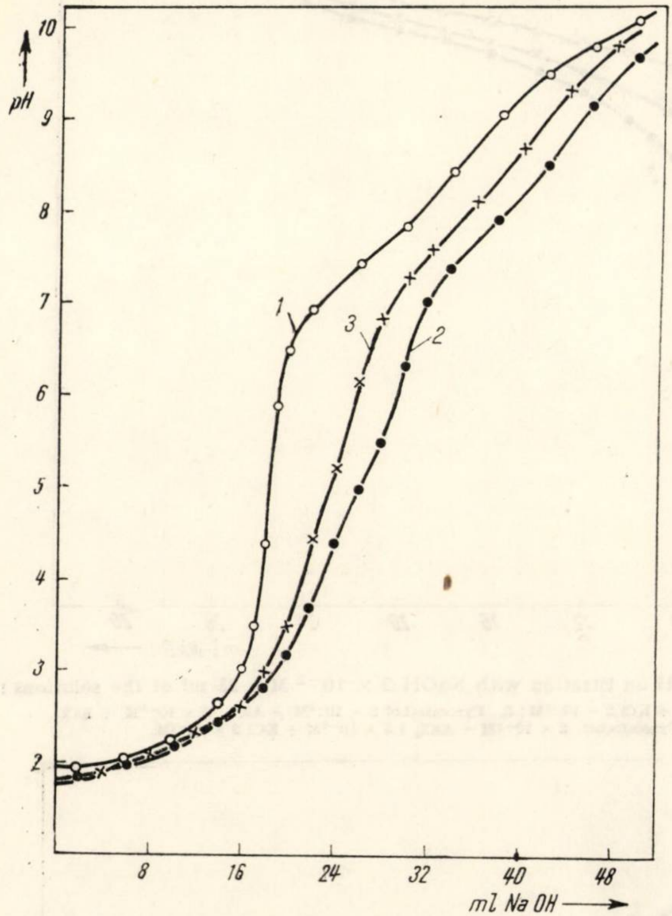

Fig. 3. — Variation of the pH on titration with NaOH 2×10^{-2} M a 25 ml of the solutions :

1, Pyrocatechol violet 2×10^{-2}M + KCl 2×10^{-1}M; *2*, Pyrocatechol violet 2×10^{-2}M + AlCl$_3$ 2×10^{-3}M + + KCl 2×10^{-1}M; *3*, Pyrocatechol violet 2×10^{-2}M + AlCl$_3$ 1.3×10^{-3}M + KCl 2×10^{-1}M.

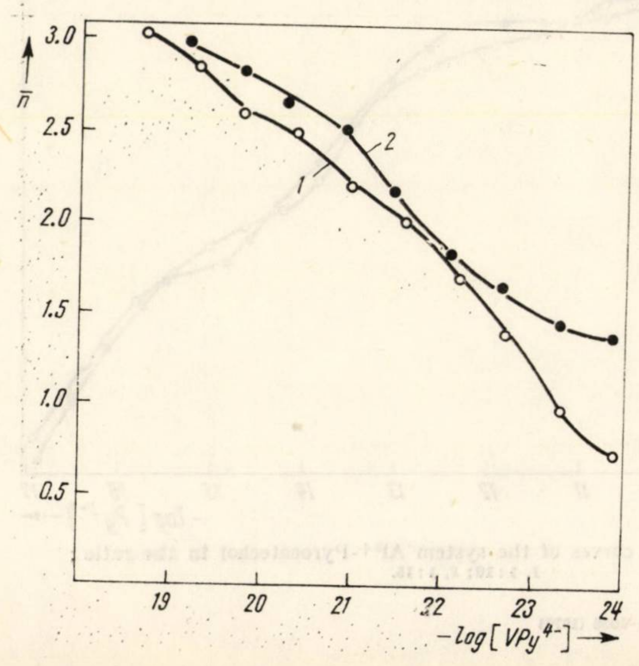

Fig. 4. — Formation curves of the system Al^{3+}-pyrocatechol in the ratio :

1, 1 : 10; *2*, 1 : 15.

Table 1

1 Al : 10 H_2Py.25 ml; μ = 0,2; $[H_2Py]$ = 2 × 10^{-2}M; $[Al^{3+}]$ = 2 × 10^{-3} M

pH	$[H^+]$	n_{Me}	n_A	mlNaOH	n_{NaOH}	$\bar{n} = \frac{n_{NaOH}}{n_{Me}}$	$[Py^{2-}]$	$P[Py^{2-}]$	log k_1	log k_2	log k_3
3.6	2.51×10^{-4}	5×10^{-5}	5×10^{-4}	0.4	0.8×10^{-5}	0.160	0.114×10^{-16}	16.943			
3.8	1.58×10^{-4}	,,	,,	0.9	1.8×10^{-5}	0.360	0.279×10^{-16}	16.554			
4.0	1.00×10^{-4}	,,	,,	1.5	3.0×10^{-5}	0.600	0.659×10^{-16}	16.101		*approximate*	
4.2	6.23×10^{-5}	,,	,,	1.9	3.8×10^{-5}	0.760	0.164×10^{-15}	15.705			
4.4	3.98×10^{-5}	,,	,,	2.2	4.4×10^{-5}	0.880	0.393×10^{-15}	15.405	16.30	13.45	8.95
4.6	2.51×10^{-5}	,,	,,	2.5	5.0×10^{-5}	1.000	0.965×10^{-15}	15.015			
4.8	1.58×10^{-5}	,,	,,	2.7	5.4×10^{-5}	1.080	0.236×10^{-14}	14.624	k_1	k_2	k_3
5.0	1.00×10^{-5}	,,	,,	2.9	5.8×10^{-5}	1.160	0.507×10^{-14}	14.231	1.99×10^{16}	2.82×10^{13}	8.91×10^{8}
5.2	6.23×10^{-6}	,,	,,	5.2	6.4×10^{-5}	1.280	0.146×10^{-13}	13.835			
5.4	3.98×10^{-6}	,,	,,	3.7	7.4×10^{-5}	1.480	0.347×10^{-13}	13.459			
5.6	2.51×10^{-6}	,,	,,	4.2	8.4×10^{-5}	1.680	0.844×10^{-13}	13.073		*corrected*	
5.8	1.58×10^{-6}	,,	,,	4.4	8.8×10^{-5}	1.760	0.207×10^{-12}	12.684	1.99×10^{16}	2.82×10^{13}	8.91×10^{8}
6.0	1.00×10^{-6}	,,	,,	4.6	9.2×10^{-5}	1.840	0.510×10^{-12}	12.292			
6.2	6.23×10^{-7}	,,	,,	4.7	9.4×10^{-5}	1.880	0.133×10^{-11}	11.876			
6.4	3.98×10^{-7}	,,	,,	4.8	9.6×10^{-5}	1.920	0.314×10^{-11}	11.503			
6.6	2.51×10^{-7}	,,	,,	4.9	9.8×10^{-5}	1.960	0.787×10^{-11}	11.104			
6.8	1.58×10^{-7}	,,	,,	5.0	10.0×10^{-5}	2.000	0.194×10^{-10}	10.712			
7.0	1.00×10^{-7}	,,	,,	5.1	10.2×10^{-5}	2.040	0.481×10^{-10}	10.317			
7.2	6.23×10^{-7}	,,	,,	5.4	10.8×10^{-5}	2.160	0.120×10^{-9}	9.920			
7.4	3.98×10^{-8}	,,	,,	5.5	11.0×10^{-5}	2.200	0.289×10^{-9}	9.539			
7.6	2.51×10^{-8}	,,	,,	6.0	12.0×10^{-5}	2.400	0.735×10^{-9}	9.133			
7.8	1.58×10^{-8}	,,	,,	6.5	13.0×10^{-5}	2.600	0.163×10^{-8}	8.787			
8.0	1.00×10^{-8}	,,	,,	6.8	13.6×10^{-5}	2.720	0.392×10^{-8}	8.406			

Table 2

1 Al: 15 H_2Py; 25 ml; = 0,2; $H_2Py = 2 \times 10^{-2}M$; $Al^{3+} = 1,3 \times 10^{-3}M$

pH	H+	n_{Me}	n_A	ml NaOH	n_{NaOH}	$\bar{n} = \frac{n_{NaOH}}{n_{Me}}$	$[Py^{2-}]$	$p\,[Py^{2-}]$	log k_1	log k_2	log k_3
3.6	2.51×10^{-4}	3.25×10^{-5}	5×10^{-4}	0.1	0.2×10^{-5}	0.061	0.134×10^{-16}	16.672			
3.8	1.58×10^{-4}	,,	,,	0.5	1.0×10^{-5}	0.307	0.285×10^{-16}	16.545			
4.0	1.00×10^{-4}	,,	,,	0.9	1.8×10^{-5}	0.554	0.717×10^{-16}	16.144		*approximate*	
4.2	6.23×10^{-5}	,,	,,	1.2	2.4×10^{-5}	0.738	0.172×10^{-15}	15.764			
4.4	3.98×10^{-5}	,,	,,	1.4	2.8×10^{-5}	0.861	0.412×10^{-15}	15.485	16.25	13.50	9.05
4.6	2.51×10^{-5}	,,	,,	1.5	3.0×10^{-5}	0.923	0.145×10^{-14}	14.838			
4.8	1.58×10^{-5}	,,	,,	1.7	3.4×10^{-5}	1.046	0.259×10^{-14}	14.586	k_1	k_2	k_3
5.0	1.00×10^{-5}	,,	,,	1.9	3.8×10^{-5}	1.169	0.501×10^{-14}	14.300	1.78×10^{16}	3.16×10^{13}	1.12×10^{9}
5.2	6.23×10^{-6}	,,	,,	2.2	4.4×10^{-5}	1.369	0.161×10^{-13}	13.793			
5.4	3.98×10^{-6}	,,	,,	2.5	5.0×10^{-5}	1.538	0.363×10^{-13}	13.416			
5.6	2.51×10^{-6}	,,	,,	2.8	5.6×10^{-5}	1.723	0.941×10^{-13}	13.026		*corrected*	
5.8	1.58×10^{-6}	,,	,,	3.0	6.0×10^{-5}	1.846	0.242×10^{-12}	12.616	1.77×10^{16}	3.17×10^{13}	1.12×10^{9}
6.0	1.00×10^{-6}	,,	,,	3.2	6.4×10^{-5}	1.969	0.572×10^{-12}	12.242			
6.2	6.23×10^{-7}	,,	,,	3.2	6.4×10^{-5}	1.959	0.147×10^{-11}	11.832			
6.4	3.98×10^{-7}	,,	,,	3.2	6.4×10^{-5}	1.969	0.357×10^{-11}	11.447			
6.6	2.51×10^{-7}	,,	,,	3.2	6.4×10^{-5}	1.969	0.898×10^{-11}	11.046			
8.8	1.58×10^{-7}	,,	,,	3.4	6.8×10^{-5}	2.092	0.222×10^{-10}	10.653			
7.0	1.00×10^{-7}	,,	,,	3.4	6.8×10^{-5}	2.092	0.555×10^{-10}	10.255			
7.2	6.23×10^{-8}	,,	,,	3.6	7.2×10^{-5}	2.215	0.132×10^{-9}	9.879			
7.4	3.98×10^{-8}	,,	,,	3.8	7.6×10^{-5}	2.336	0.334×10^{-9}	9.476			
7.6	2.51×10^{-8}	,,	,,	4.0	8.0×10^{-5}	2.461	0.870×10^{-9}	9.050			
7.8	1.58×10^{-8}	,,	,,	4.4	8.8×10^{-5}	2.708	0.189×10^{-8}	8.723			
8.0	1.00×10^{-8}	,,	,,	4.4	8.8×10^{-5}	2.708	$0{\cdot}318 \times 10^{-8}$	8.497			

Table 3

1Al : 10 H_4 V Py . 25 ml ; μ = 0.2 ; [H_4 V Py] = 2 × 10^{-2}M ; [Al^{3+}] = 2 × 10^{-3}M

pH	[H^+]	n_{Me}	n_A	ml NaOH	n_{NaOH}	$\bar{n} = \frac{n_{NaOH}}{n_{Me}}$	[$V Py^{4-}$]	$p[V Py^{4-}]$	log k_1	log k_2	log k_3
2.4	3.98×10^{-3}	5×10^{-5}	5×10^{-4}	1.4	4.00×10^{-5}	0.756	0.125×10^{-23}	23.904			
2.6	2.51×10^{-3}	,,	,,	1.8	4.86×10^{-5}	0.972	0.495×10^{-23}	23.305		*approximate*	
2.8	1.58×10^{-3}	,,	,,	2.6	7.02×10^{-5}	1.404	0.179×10^{-22}	22.747	24.95	22.52	20.20
3.0	1.00×10^{-3}	,,	,,	3.2	8.64×10^{-5}	1.728	0.666×10^{-22}	22.176			
3.2	6.23×10^{-4}	,,	,,	3.7	10.00×10^{-5}	2.000	0.262×10^{-21}	21.581	k_1	k_2	k_3
3.4	3.98×10^{-4}	,,	,,	4.2	11.34×10^{-5}	2.228	0.960×10^{-21}	21.017	8.91×10^{24}	3.35×10^{22}	1.59×10^{20}
3.6	2.51×10^{-4}	,,	,,	4.6	12.40×10^{-5}	2.480	0.375×10^{-20}	20.425			
3.8	1.58×10^{-4}	,,	,,	4.8	12.96×10^{-5}	2.592	0.148×10^{-19}	19.828			
4.0	1.00×10^{-4}	,,	,,	5.3	14.30×10^{-5}	2.860	0.535×10^{-19}	19.271		*corrected*	
4.2	6.23×10^{-5}	,,	,,	5.6	15.10×10^{-5}	3.020	0.214×10^{-18}	18.669	8.77×10^{24}	3.20×10^{22}	1.61×10^{20}

Table 4

1Al : 15 H_4V Py ; 25 ml ; μ = 0,2 ; [H_4V Py] = 2 × 10^{-2}M ; [Al^{3+}] = 1.3 × 10^{-3}M

pH	[H^+]	n_{Me}	n_A	ml NaOH	n_{NaOH}	$\overline{n} = \frac{n_{NaOH}}{n_{Me}}$	[$V Py^{4-}$]	$p[VPy^{4-}]$	log k_1	log k_2	log k_3
2.4	3.98×10^{-3}	3.25×10^{-5}	5×10^{-4}	1.4	3.78×10^{-5}	1.375	0.125×10^{-23}	23.901			
2.6	2.51×10^{-3}	,,	,,	1.8	4.86×10^{-5}	1.495	0.495×10^{-23}	23.305		*approximate*	
2.8	1.58×10^{-3}	,,	,,	2.0	5.40×10^{-5}	1.660	0.214×10^{-22}	22.669			
3.0	1.00×10^{-3}	,,	,,	2.2	5.94×10^{-5}	1.825	0.735×10^{-22}	22.133	25.25	23.10	20.9
3.2	6.23×10^{-4}	,,	,,	2.6	7.02×10^{-5}	2.160	0.292×10^{-21}	21.534			
3.4	3.90×10^{-4}	,,	,,	3.0	8.10×10^{-5}	2.490	0.108×10^{-20}	21.966	k_1	k_2	k_3
3.6	2.51×10^{-4}	,,	,,	3.2	8.64×10^{-5}	2.660	0.431×10^{-20}	20.365	1.78×10^{25}	1.26×10	8.91×10^{20}
3.8	1.58×10^{-4}	,,	,,	3.4	9.20×10^{-5}	2.830	0.165×10^{-19}	19.781		*corrected*	
4.0	1.00×10^{-4}	,,	,,	3.6	9.52×10^{-5}	2.930	0.645×10^{-19}	19.190	1.75×10^{25}	1.25×10^{23}	9.45×10^{20}

where :

^nA = number of moles of the ligand

^{n}NaOH = number of NaOH,

V = initial volume of solution

ΔV = NaOH added on titration.

A series of values of $\bar{n}$ and $[Py^{2-}]$ were obtained, corresponding to the pH range from 3,6 to 8.

In figure 2 we have shown the values of $\bar{n}$ *versus* $-\log\ [Py^{2-}]$, thus obtaining the formation curves on which we have read directly for $\bar{n} = 0{,}5$, 1,5 and 2,5 the approximate values of the formation constants, correcting them later with the recurrence formulae given by Bjerrum. Experimental data, approximate and corrected values of the formation constants are given in tables 1 and 2.

We have proceeded in the same way for the system Al^{3+} -pyrocatechol violet, supposing that the following reactions take place :

$$H_3\,VPy^- + OH^- \rightleftarrows H_2VPy^{2-} + H_2P$$
$$H_2\,VPy^{2-} + Al^{3+} + OH^- \rightleftarrows AlHVPy + H_2O$$
$$AlHVPy + H_2VPy^{2-} + OH^- \rightleftarrows AlHVPy_2^{3-} + H_2O$$
$$AlHVPy_2^{3-} + H_2VP^{2-} + OH^- \rightleftarrows AlHVPy_3^{6-} + H_2O$$

where H_4VPy is pyrocatechol violet.

The results of the titration are given by the curves in figure 3.

Knowing the values of the dissociation constants of pyrocatechol violet ($pK_1 = 7.81$; $pK_2 = 9.80$; $pK_3 = 11.73$), we have computed the necessary data for the formation curves of the respective complexes. Figure 4 permits a direct reading from the formation curves of only the values $\log k_2$ and $\log k_3$, for $\bar{n} = 1.5$ and 2.5. The value of $\log k_1$ corresponding to the complex 1 : 1 was computed by means of the formula : $\log k_1 = 3 \log k_2 - (\log k_2 + \log k_3)$

Tables 3 and 4 list the experimental data, and those computed for this system.

DISCUSSION

The important decrease in the pH in the mixtures of aluminium solutions and the ligands, attests undoubtedly the formation of chelates, involving the phenolic functions. Bjerrum's method, applied to these systems, permits the calculation of the formation constants and fairly stable soluble compounds have been pointed out.

For the compounds with pyrocatechol violet, calculations have been carried out in the range $pH = 2-4$, in which no noticeable colour changes were observed on titration with NaOH.

In the case of pyrocatechol a wider range of pH ($pH = 3.75-8$) could be used. The values of the formation constants computed by us partially agree with those computed by Dubey and Mehrotra.

Revue Roumaine de Chimie, **15**, 1057–1059 (1970)

CONTRIBUTIONS TO THE STUDY OF THE SYSTEM DICYANOAUROUS ACID-ISOAMYL ALCOHOL – WATER

V. ARMEANU and L. M. BĂLOIU

Department of Chemistry and Physics
Academy of Economic Studies, Bucharest, Piaţa Romană 6

Received August 26, 1969

The paper presents new data concerning the extraction of $H[Au(CN)_2]$ from water into isoamyl alcohol. The possibility to re-extract the complex ion in aqueous solution is discussed. On this basis, a shorter way is proposed to prepare the samples for the colorimetric determination of gold from solutions of complex cyanides.

I. INTRODUCTION

In some papers concerning the determination of gold in cyanide solutions, [1–3] the extraction with isoamyl alcohol[4] was used for the separation of the complex ion $[Au(CN)_2]^-$. We will now define more accurately the best conditions for the extraction and study if the inverse extraction, from isoamyl alcohol to water, is possible.

II. EXPERIMENTAL

We used solutions of $K[Au(CN)_2]$ with 70–240 μg Au/ml, acidulated with H_2SO_4. The potassium aurocyanide was obtained from $HAuCl_4$ and KCN, with AuCN as intermediate compound.

For extractions we used isoamyl alcohol p.a.

The saturated solution of $Ca(OH)_2$ was prepared from CaO p.a. by dissolution in water and filtration.

The gold analyses were made spectrophotometrically, with Astraviolett 3R[3] using the aqueous solutions remained after the extractions.

The pH was measured with a MV-11 Clamann & Grahnert pH-meter with glass electrode.

---

[1] R. Ripan, M. Marcu and V. Cordiş, *Rev. Chim. (Bucureşti)*, **15**, 684 (1964).
[2] V. Armeanu, M. Damian and L. M. Băloiu, *Rev. Roumaine Chim.*, **13**, 1617 (1968).
[3] V. Armeanu and L. M. Băloiu, *Analyt. Chim. Acta*, **44**, 230 (1969).
[4] D. E. Zviaghintsev and C.-I. Zaharov-Nartysov, *Zhur. priklad. Khim.*, **33**, 55 (1960).

III. DISCUSSION

Because the strong acidic solutions containing CN^- ions are difficultly handled, we envisaged the extraction of the $[Au(CN)_2]^-$ ion from a neutral or weak acid solution. Figures 1 and 2 present the results, for two different ratios alcohol : water. For a good extraction, an acidic pH is needed. The influence of the ratio alcohol : water, at two different values of pH, was also studied (Fig. 3).

We concluded that two extractions from a solution with $pH < 0.7$, with a ratio alcohol : water = 1 : 10, provide the almost complete extraction of gold (more than 99%).

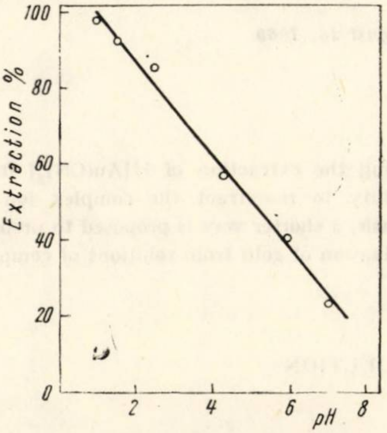

Fig. 1. — Variation of the percentage of gold extracted depending on pH, for the ratio water : alcohol = 1 : 1.

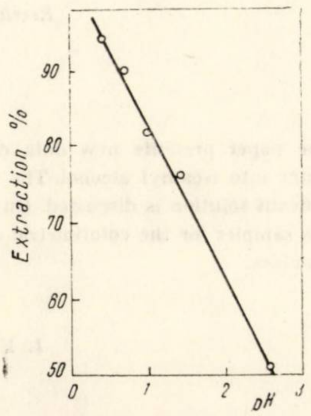

Fig. 2. — Variation of the percentage of gold extracted depending on pH, for the ratio water : alcohol = 10 : 1.

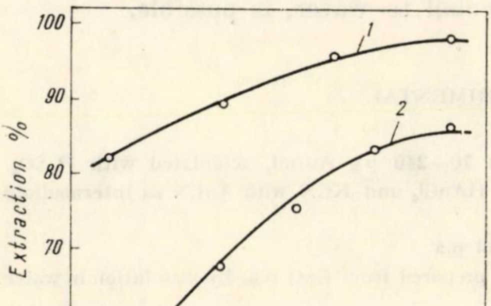

Fig. 3. — Variation of the percentage of gold extracted depending on the ratio water : alcohol. 1- pH= 1.0 ; 2- pH = 2.6.

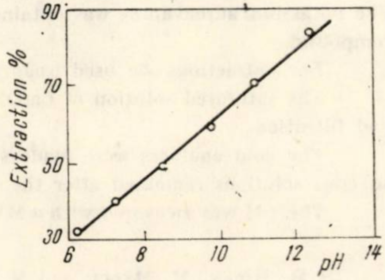

Fig. 4. — Variation of the percentage of gold extracted from alcohol in water, depending on pH.

For the colorimetric determination the $[Au(CN)_2]^-$ ion must be in aqueous solution. The complete evaporation of alcohol is long and difficult, but the re-extraction from alcohol in water may be possible. If $H[Au(CN)_2]$ is soluble in isoamyl alcohol, probably $M[Au(CN)_2]_y$, where M^{y+} is a cation which cannot form covalent bonds, will be more soluble in water.

We used for the extraction solutions of NaOH and $Ca(OH)_2$, with a ratio water : alcohol = 2 : 1, obtaining the data presented in figure 4. It must be mentioned that the values obtained with solutions of NaOH or $Ca(OH)_2$ are equal, for the same pH.

But, with the growth of pH, the separation of the phases becomes more difficult and slows down until it becomes impossible, at $pH \geqslant 13$. At this pH, only 85% of gold is extracted.

Because three extractions would be too long, we think that the best way is to make only one extraction, with an aqueous solution with a standard pH. The result of the determination is then multiplied by an empirical coefficient, calculated as to correct the incomplete extraction.

As standard solution for extraction we used a saturated solution of $Ca(OH)_2$, very easy to prepare and with a constant pH, quite close to the highest value allowed.[5] In this case, the value of the empirical parameter is $P = 1.20 \pm 0.02$ (Table 1).

Table 1

Some determinations performed in the described conditions

No.	1	2	3	4	5	6	average value
μg Au put in	34.0	34.0	34.0	27.0	27.0	27.0	
μg Au found	29.0	28.0	27.9	23.1	22.8	23.0	
P	1.17	1.21	1.22	1.19	1.21	1.20	1.20
μg Au calculated P=(1.20)	34.8	33.6	33.5	27.7	27.4	27.5	
Δ (μg Au)	+0.8	−0.4	−0.5	+0.2	−0.1	0.0	0.0
Δ (%)	+2.35	−1.18	−1.47	+0.73	−0.37	0.00	0.0

IV. CONCLUSIONS

We established that for the total extraction of $[Au(CN)_2]^-$ in isoamyl alcohol, two extractions, from an aqueous solution with $pH < 0.7$, with a volume of alcohol ten times smaller than the volume of water, is necessary. The re-extraction in the aqueous phase of about 83% of gold is possible with a saturated solution of $Ca(OH)_2$, the volume ratio being water : alcohol = 2 : 1.

Replacing the evaporation of the isoamyl alcohol by the re-extraction, the time necessary for a colorimetric determination of gold is reduced by about one hour.

---

[5] C. Luca, "PH-ul și aplicațiile sale", Edit. Tehnică, Bucharest, 1964, p. 67.

Revue Roumaine de Chimie, **15**, 1061–1063 (1970)

KINETIC DOSING OF THE COBALT IN VITAMIN B_{12}

D. COSTACHE and GR. POPA

Department of Analytical Chemistry, University of Bucharest,
Splaiul Independenţei 89

Received July 29, 1969

The kinetic method with Bordeaux S and peroxide is applied to the dosing of the cobalt in vitamin B_{12}. A gauging diagram and a table of results are given. Results obtained on the same samples by the method presently recommended by the Romanian Pharmacopoeia are also included, for the sake of comparison.

The B_{12} vitamins (several compounds are known under this name) are also called cobalamines, as they contain cobalt in their molecule.

Their chemical structure was established in 1956 by a large group of chemists, physicians, mathematicians, crystallographers and biologists, under the leadership of A. Todd. The molecule of vitamin B_{12} contains a cobalt atom coordinately bound.

Vitamin B_{12} is determined physically, chemically, biologically and microbiologically. Some of the methods employed to determine vitamin B_{12} chemically may be found in works.[1-15]

The kinetic method of analysis consists in the use of the catalytic effect of cobalt on the reaction rate of some organic compounds and peroxide, in alkaline medium.

---

[1] G. O. Rudkin and R. J. Taylor, *Z. analyt. Chem.*, **24**, 1155 (1954).
[2] J. Carneri, *Farmaco*, **10**, 31 (1953).
[3] J. Janicki, J. Pawelkiewiez and St. Stawiski, *Przemysl. Chem.*, **9**, 509 (1953).
[4] P. van Melle, *J. Amer. Pharmac. Assoc.*, **45**, 26 (1956).
[5] R. N. Boops, H. Carr and J. E. Conn, *Science*, **117**, 603 (1953).
[6] J. E. Conn, S. L. Horman and G. T. Watman, *Science*, **113**, 658 (1951).
[7] B. Jaselskie and H. Deihl, *J. Amer. Chem. Soc.*, **76**, 4345 (1954).
[8] V. Ender and H. Steeg, *Biochem. Z.*, **321**, 426 (1951).
[9] F. A. Bacher and A. E. Boley, *Analyt. Chem.*, **26**, 1146 (1954).
[10] R. R. Johnson, O. G. Bentlex and L. A. Moxon, *J. Biol. Chem.*, **218**, 379 (1950).
[11] E. L. Smith, *Radioisotope Techniques*, **1**, 281 (1953).
[12] E. L. Smith, *Analyst*, **81**, 435 (1956).
[13] K. H. Fantes and D. M. Ireland, *Biochem. J.*, **14**, 46 (1950).
[14] G. E. Boxer and J. C. Rickards, *Arch. Biochem.*, **29**, 75 (1950).
[15] G. E. Boxer and J. C. Rickards, *Arch. Biochem.*, **30**, 372 (1951); **30**, 382 (1951); **30**, 392 (1951).

Cobalt was thus measured in numerous works which appeared in literature, of which we mention.[16-23]

The present paper presents a way of applying the kinetic dosing method of cobalt which has appeared in literature.[24]

EXPERIMENTAL

We had 5 sorts of vitamin B_{12} in pure state, obtained at the antibiotic factory, Jassy, and processed for pharmaceutical use at "Biofarm" Bucharest.

The mineralization of the samples was carried out after a unanimously accepted method, described in the pharmacopoeia of numerous countries, namely by melting a certain quantity of vitamin with a 50-fold quantity of acid potassium sulphate. A clear melt is obtained, which, after cooling, is solved in water, decanted into a 1000 cm^3 calibrated flask, from which 10 cm^3 are taken, poured into a 100 cm^3 calibrated flask, and brought to mark with tridistilled water.

One obtains thus the working solution containing the cobalt ions necessary to the catalytic dosing.

Reactives : The reactive solution was obtained by solving the Bordeaux S in water (0.0271 %).

The peroxide had a 3.086 % concentration. The alkaline medium was provided by using a buffer solution obtained by solving 0.5 g Sörensen boric acid in 100 cm^3 of NaOH 0.25 N.

The reaction mixture was prepared in 25 cm^3 flasks of : 10 cm^3 Bordeaux solution in borate buffer (3/5 Bordeaux/buffer ratio), 2 cm^3 peroxide and 1 cm^3 cobalt solution, obtained by mineralizing vitamin B_{12}. One brings to mark with tridistilled water. The chronometer is started, the flask's content is well stirred and then poured into the spectrophotometer's vat, and the variation of the optical density is read every minute, having water as blank. The measurements were carried out with a horizontal Pulfrich Zeiss Jena spectrophotometer at a $\lambda = 496$ nm wavelength and a 25° temperature. A metallic thermostatic device was adapted to the spectrophotometer.

The "tangent method" consisting of the plotting of value D as function of time, obtaining straight lines, differing with one another by the angles they make with the abscissae axis, was adopted for the calculation of results.

These angles are measured, the corresponding value of their tangents is found out, and these values are plotted graphically as a function of the cobalt concentration. This graph and the same working method, record the cobalt of an unknown sample.

Graph 1 plots the calibration graph for the present case.

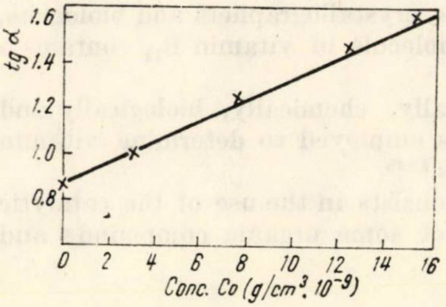

Fig. 1

---

[16] J. Bognar, *Mikrochim. Acta*, **4**, 801 (1963).

[17] E. Schulek and J. Laszlovski, *Mikrochim. Acta*, **1**, 41 (1960).

[18] N. E. Parhomenko, G. A. Prik and K. B. Iatsimirski, *Zhur. analit. Khim.*, **16**, 599 (1961).

[19] A. K. Babko and N. M. Lukovskaia, *Ukrain. khim. Zhur.*, **30**, 508 (1964).

[20] Gr. Popa and D. Costache, *Analele Universităţii Bucureşti*, **16**, 107 (1967).

[21] Gr. Popa and C. Costache, *Rev. Roumaine Chim.*, **12**, 963 (1967).

[22] Gr. Popa and D. Costache, *Analele Universităţii Bucureşti*, **17**, 21 (1968).

[23] D. Costache and Gr. Popa, *Analele Universităţii Bucureşti*, **17**, 55 (1968).

[24] Gr. Popa and D. Costache, *Rev. Roumaine Chim.*, **13**, 573 (1968).

Experimental results of cobalt dosing in vitamin B_{12} are given in table 1.

We have chosen for comparison the results obtained by the method presently recommended by the Romanian Pharmacopoeia.[25]

It hereby results that the kinetic method with Bordeaux S can be applied to the dosing of cobalt in vitamin B_{12} with good results.

Table 1

Results of determinations

Sample	Quantity under analysis g	Purity (R. Ph)	Co found on graph ($g/cm^3 . 10^{-9}$)	Total Co $g . 10^{-3}$	Vitamin B_{12} found in analysis g	Purity
I a	0.0433^7	98.30	7.41	1.830	0.0426^2	98.26
I b	0.0679^6	98.30	11.62	2.905	0.0668^1	98.31
II a	0.0311^7	97.27	5.27	1.317	0.0303^0	97.20
II b	0.0621^5	97.27	10.51	2.627	0.0604^2	97.22
III a	0.0256^0	97.74	4.34	1.085	0.0249^5	97.50
III b	0.0557^2	97.74	9.45	2.362	0.0543^4	97.52
IV a	0.0361^2	96.08	6.04	1.510	0.0347^3	96.15
IV b	0.0741^5	96.08	12.40	3.100	0.0713^0	96.16
V a	0.0515^4	96.91	8.64	2.160	0.0499^1	96.83
V b	0.0828^2	96.91	13.95	3.487	0.0802^0	96.83

---

[25] * * * "Farmacopeea Română", 8th ed., Ed. Medicală, Bucharest, 1965, p. 724.

Revue Roumaine de Chimie, **15**, 1065–1076 (1970)

PYRAZOLES. II. AMINOLYSE DES 1-(2,4-DINITROPHÉNYL)-PYRAZOLES

C. CHIRIAC et I. ZUGRĂVESCU

Institut de Chimie macromoléculaire «P. Poni» de l'Académie, Filiale de Jassy,
41 A, Aleea Gr. Ghica-Vodă

Reçu le 17 octobre 1969

On étudie les réactions des 1-(2,4-dinitrophényl)-pyrazoles avec les amines aliphatiques, l'ammoniaque et les amines aromatiques, qui ont lieu par la scission du groupement 2,4-dinitrophényle. Dans les réactions étudiées, les produits utilisés sont activés par les groupements nitro du cycle benzénique, ainsi que par le cycle pyrazolique lui-même. La réaction n'a pas lieu avec des 1-(4-nitrophényl)-pyrazoles ; un seul groupement nitro n'est pas suffisant pour produire l'activation nécessaire. Les réactions de substitution nucléophyle présentées sont influencées par des effets stériques, qui sont plus marqués chez les 1-picryl-pyrazoles. Le mécanisme de la réaction a lieu par l'intermédiaire d'un complexe de type Meisenheimer.

INTRODUCTION

Dans une note antérieure,[1] nous avons étudié la réaction N—arylation des pyrazoles avec des dérivés aromatiques chlorurés, activés par des groupements nitro comme le mono-, bi- et tri-nitrochlorobenzène. Quelques-uns des pyrazoles N-arylés obtenus présentent la propriété intéressante de réagir avec les bases fortes. Par exemple le 1-(2,4-dinitrophényl)-pyrazole forme, sous l'action de l'hydroxyde de potassium ou du méthylate de sodium, le 2,4-dinitrophénol ou le 2,4-dinitroanisole, par la scission du groupement 2,4-dinitrophényle.[2] La réaction est attribuée aux groupements nitro qui diminuent la densité électronique sur l'atome de carbone de la position 1 du cycle benzénique (le schéma 1), en facilitant l'attaque nucléophile du réactant. Cette réaction est semblable aux réactions de la 2,4-dinitroaniline ou la 2,4-dinitroaniline N-alcoylées (I) avec l'hydroxyde de potassium, où il y a aussi une substitution nucléophile avec la formation du 2,4-dinitrophénol.[3,4] De ces expériences il résulte que la liaison exocyclique C—N du 1-(2,4-dinitrophényl)-pyrazole (II) présente la même susceptibilité envers les réactants nucléophiles forts (KOH, CH_3ONa) que la liaison C—N des 2,4-dinitroanilines (I).

---

[1] C. Chiriac et I. Zugrăvescu, *Rev. Roumaine Chim.*, **15**, 789 (1970).
[2] H. R. Croker, *J. Chem. Soc.*, **1955**, 4489.
[3] C. Willgerodt, *Ber. dtsch. chem. Ges.*, **9**, 979 (1876).
[4] H. Meerwein, *Ber. dtsch. chem. Ges.*, **10**, 995 (1877).

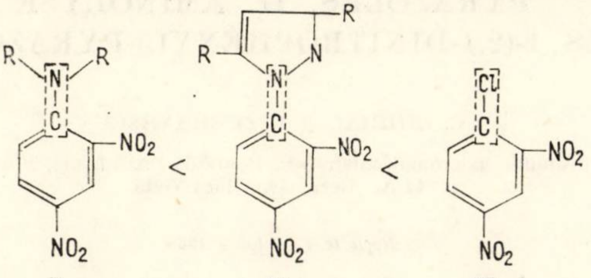

I II III

R=H, alcoyle

En continuant l'étude de ce problème, nous avons constaté que les 1-(2,4-dinitrophényl)-pyrazoles réagissent même avec des réactants nucléophiles plus faibles que le KOH ou le CH_3ONa. Ainsi avec les amines aliphatiques, l'ammoniaque et les amines aromatiques, la substitution nucléophyle des pyrazoles se produit facilement et avec un rendement presque quantitatif. La réaction présente des particularités intéressantes ; elle est influencée par des facteurs d'ordre stérique et n'est pas réalisable avec les amines (I)

RÉSULTATS ET DISCUSSIONS

La réaction de substitution nucléophile des 1-(2,4-dinitrophényl)-pyrazoles par les amines et l'ammoniaque a lieu d'après le schéma 1.

SCHÉMA 1

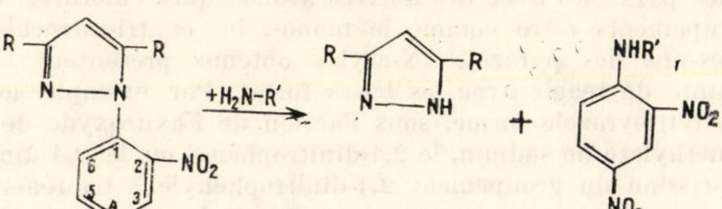

IV V VI VII

R =H,CH_3,C_6H_5

R′ =H, alcoyle, aryle

Les produits obtenus : dérivés pyrazoliques et amines substituées sont présentés dans le tableau 1.

Tableau 1

Aminolyse des 1-(2,4-dinitrophényl)-pyrazoles

Nº	Pyrazole IV R	Amine V R′	Amine VII P.f °C	Méthode utilisée *	Rend. %
1	CH_3	H	180–182 [5]	C	93
2	”	C_6H_5	156 [5]	D	98,2
3	”	CH_3	174–175 [6]	B	92
4	”	C_2H_5	112–114 [7]	B	94,2
5	”	C_3H_7	96 [8]	A, B	97
6	”	C_4H_9	89– 90[11]	A. B	97
7	”	diméthylamine	86 [9]	B	95,5
8	”	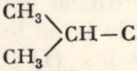 $\begin{matrix}CH_3\\CH_3\end{matrix}\!\!>CH-CH_2$	80– 81 [8]	A, B	92
9	”	pipéridine	90– 92[10]	A, B	90
10	”	pyrrolidine	104–106[13]	A, B	93,7
11	”	$p-CH_3-C_6H_4$	135–137[12]	D	95
12	H	H	179–182 [5]	C	94
13	”	C_3H_7	95– 96 [8]	A, B	96
14	”	C_4H_9	89– 90[11]	A, B	97
15	”	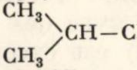 $\begin{matrix}CH_3\\CH_3\end{matrix}\!\!>CH-CH_2$	80 [8]	”	96,4
16	”	pipéridine	91– 92[10]	”	95
17	”	pyrrolidine	104–106[13]	”	94
18	C_6H_5	C_3H_7	96 [8]	”	93
19	”	C_4H_9	89– 90[11]	”	96,5
20	”	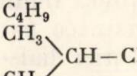 $\begin{matrix}CH_3\\CH_3\end{matrix}\!\!>CH-CH_2$	80– 81 [8]	”	90
21	”	pipéridine	90– 92[10]	”	97
22	”	H	180–182 [5]	”	91

* Les méthodes A, B, C, D sont décrites dans la partie expérimentale.

On observe dans ce tableau que la réaction est possible avec les amines aliphatiques primaires comme : méthyl-, éthyl-, propyl-, butyl- isobutyl-amine. Parmi les amines secondaires : la diméthylamine, la pyrrolidine et la pipéridine sont susceptibles de réagir, tandis que les diéthyl-, dipropyl-, dibutyl-amine, etc ne réagissent pas. Ce comportement est dû à un phénomène d'empêchement stérique qui a lieu à l'atome de carbone de la position 1 du cycle benzénique, à cause du groupement nitro de la position 2 (schéma 1).

---

[5] C. Willgerodt, *Ber. dtsch. chem. Ges.*, **9**, 978 (1876).

[6] E. Bamberger et J. Muller, *Ber. dtsch. chem. Ges.*, **33**, 111 (1900).

[7] F. Reverdin et A. de Luc, *Ber. dtsch. chem. Ges.*, **42**, 1727 (1909).

[8] P. van Romburgh et J. D. Jansen, *Rec. Trav. chim.*, **4**, 191 (1885) ; *Chem. Zentr.*, 1412 (1911), I.

[9] K. Mertens, *Ber. dtsch. chem. Ges.*, **19**, 2124 (1886).

[10] L. Spiegel et H. Kaufmann, *Ber. dtsch. chem. Ges.*, **41**, 681 (1908).

[11] Van der Kam, *Rec. Trav. chim.*, 45, 732 (1926).

[12] C. Wilgerodt, *Ber. dtsch. chem. Ges.*, **9**, 980 (1876).

[13] J. F. K. Wilshire, *Austral. J. Chem.*, **19**, 1936 (1966).

Ce phénomène d'empêchement stérique est plus marqué chez les 1-picryl-pyrazoles, qui ne réagissent qu'avec l'ammoniaque. Ces phénomènes prouvent ainsi que l'attaque nucléophile du réactant se produit sur l'atome de carbone 1 (schéma 1).

La substitution des 1-(4-nitrophényl)-pyrazoles par les amines n'est pas possible ; un seul groupement nitro n'est pas suffisant pour produire l'activation nécessaire. Ceci démontre que la présence de deux groupes nitro (*ortho* et *para*) coplanaires avec le cycle benzénique est absolument nécessaire pour la réalisation de la réaction.

On a étudié aussi comparativement la réaction des 2,4-dinitroanilines (I), avec les amines (V). Nous avons trouvé que : la 2,4-dinitro-diphénylamine, la 2,4-dinitroaniline, la 2,4-dinitrophénylpipéridine, la N-butyl-, N-isobutyl-2,4-dinitroaniline de forme générale (I) ne donnent pas de réactions de substitution nucléophile avec les amines (V), qui ont réagi avec les 1-(2,4-dinitrophényl)-pyrazoles (II ou IV). Ce genre de réactions n'est pas connu dans la littérature. Il résulte de ces expériences que la liaison exocyclique C—N des pyrazoles (II ou IV) est plus labile que la liaison C—N des 2,4-dinitroanilines (I) mentionnée plus haut. Des cas similaires d'activation exercée par les hétérocycles azoliques sont cités pour : pyrazole-, imidazole-, triazole- et tétrazole-N-acylés, chez lesquels le radical acylé réagit aisément avec des réactifs nucléophiles. La réactivité des azoles acylés (azolides) est exceptionnelle et elle est due à l'influence de l'hétérocycle.[14] L'activation produite par l'hétérocycle dans la substitution nucléophile des 1-(2,4-dinitrophényl)-pyrazoles par les amines est plus difficile à expliquer. L'une des causes pourrait être attribuée à l'isomérie atropique constatée par voie spectrale à ces composés,[15] qui détermine l'existence d'une liaison exocyclique C—N tensionnée, donc avec une capacité plus grande de réaction.

On a étudié aussi la réaction des 1-(2,4-dinitrophényl)-pyrazoles avec l'iodure de sodium dans la diméthylformamide (D.M.F.) ; nos essais n'ont pas réussi. Cette substitution a lieu dans le cas du 2,4-dinitrochlorobenzène, conduisant à 2,4-dinitroiodobenzène.[16] Ces faits montrent que la liaison exocyclique C—N des 1-(2,4-dinitrophényl)-pyrazoles (II ou IV) est moins réactive que la liaison C—Cl du 2,4-dinitrochlorobenzène (III), mais plus réactive que la liaison C—N des 2,4-dinitroanilines (I) ; donc elle occupe une position intermédiaire située entre les dérivés chlorurés et les amines tertiaires dans la série de Bunnett[17] : $F > NO_2 > \boxed{Cl} \sim Br > I > OSO_2Ar > OAr > OR > SO_2R > \boxed{NR_2} > H$.

Influence des solvants dans la réaction de 1-(2,4-dinitrophényl)-pyrazoles avec les amines et l'ammoniaque.

Les 1-(2,4-dinitrophényl)-pyrazoles réagissent avec les amines aliphatiques en solution alcoolique à reflux, mais ne réagissent pas avec l'ammoniaque gazeux dans les mêmes conditions, même après 30 h.

---

[14] H. A. Staab, *Angew. Chem.*, **74**, 418 (1962).

[15] J. Elguero et R. Jacquier, *Bull. Soc. chim. France,* **1966**, 3749.

[16] J. F. Bunnett, *J. Org. Chem.*, **23**, 305 (1958).

[17] J. F. Bunnett, *Chem. Rev.*, **51**, 273 (1951).

Si on remplace l'éthanol par le diméthylsulfoxyde (DMSO), la vitesse de réaction s'accroît. Ainsi les 1-(2,4-dinitrophényl)-pyrazoles réagissent avec les amines aliphatiques à la température ordinaire et avec l'ammoniaque à 70–100°. La réaction avec l'ammoniaque est réalisable aussi en DMF à 150–160°.

L'influence positive du DMSO constatée par nous est signalée aussi dans d'autres cas.[18]

Le mécanisme de la réaction peut être clarifié par quelques faits expérimentaux décrits pour d'autres substitutions nucléophiles connues. Dans les réactions des 1-(2,4-dinitrophényl)-pyrazoles avec des amines aliphatiques dans les solvants aprotiques bipolaires tels que : DMSO, DMF, acétonitrile, etc, on a observé l'apparition d'une couleur rouge, qui après un certain temps ou sous un faible chauffage passe en jaune. Cela dénote l'apparition d'un complexe intermédiaire instable coloré, caractéristique de la substitution nucléophyle aromatique activé par les groupements nitro.

En vertu des données obtenues jusqu'à présent on est arrivé àla conclusion que la substitution aromatique nucléophyle de l'halogène activé par des groupements nitro ne se produit pas selon un processus synchrone (VIII), mais par un intermédiaire instable coloré (IX), avec une structure quinolique,[19] dénommé le « complexe Meisenheimer ».[20]

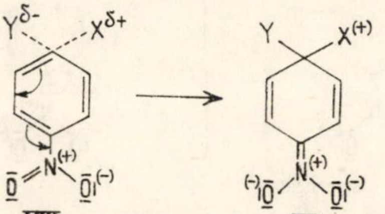

VIII IX

En tenant compte des données de la littérature, ainsi que de nos données expérimentales, le mécanisme de substitution des 1-(2,4-dinitrophényl)-pyrazoles par les amines découle d'après le schéma 2.

On peut faire sur ce mécanisme les considérations suivantes :

Dans le complexe Meisenheimer (XIII), les deux liaisons exocycliques C–N (*a* et *b* dans le schéma 2), formées à l'atome de carbone dela position 1, sont approximativement équivalentes pour une période de temps donnée. Dans le premier stade, la liaison „a" avec le pyrazole est plus forte (état de transition XII), puis suit l'étape d'égalisation dans le complexe Meisenheimer (XIII), ensuite la liaison „b" devient plus stable (état de transition XIV), et conduit finalement aux produits (XV) et (XVI).

[18] C. F. Bernasconi et M. Kaufmann, *Helv. Chim. Acta*, **49**, 2563 (1966).

[19] E. Buncel et A. R. Norris, *Quart. Rev.*, **22**, 134 (1968).

[20] J. Meisenheimer, *Liebigs Ann. Chem.*, **323**, 205 (1902).

On a isolé et étudié jusqu'à présent quelques complexes Meisenheimer plus stables,[20-22] mais dans la plupart de cas, comme dans celui étudié par nous, ce complexe n'a pas été isolé. La présence de ces intermédiaires a été mise en évidence par des études spectrophotométriques.

SCHÉMA 2

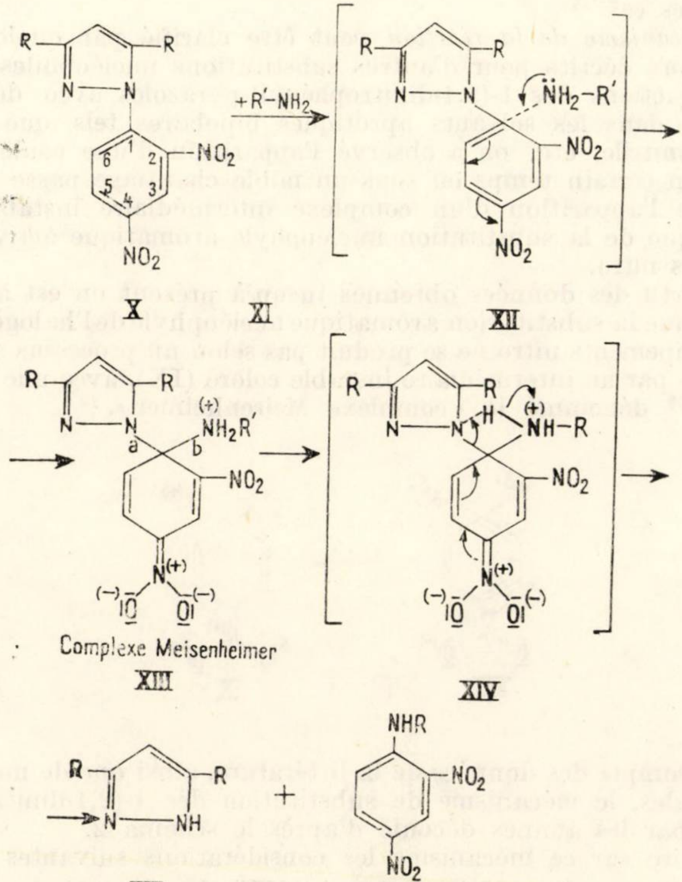
R
N
NO₂
+R'-NH₂
NH₂-R'
1
2
3
4
5
6
X
XI
XII
(+)
NH₂R'
a
b
N(+)
(−)
IO
OI
Complexe Meisenheimer
XIII
H
NH-R
XIV
NHR
NH
+
XV
XVI

L'étude du complexe coloré formé dans la réaction du 1-(2,4-dinitrophényl)-3,5-diméthylpyrazole et butylamine à l'aide des spectres dans le domaine visible

L'apparition d'une coloration rouge, transitoire dans les substitutions des 1-(2,4-dinitrophényl)-pyrazoles avec les amines aliphatiques a été étudiée spectrophotométriquement dans le cas particulier de la réaction des 1-(2,4-dinitrophényl)-3,5-diméthylpyrazoles avec la butylamine.

[21] W. E. Byrne et C. E. Griffin, *J. Org. Chem.*, **32**, 2507 (1967).
[22] J. H. Fendler et W. E. Byrne, *J. Org. Chem.*, **33**, 977 (1968).

On sait que, l'une des propriétés caractéristiques des complexes Meisenheimer est le déplacement du maximum d'absorption vers des longueurs d'ondes plus grandes, à cause de leur structure quinolique. Pour l'étude spectrale on a pris des solutions de différentes concentrations dans de différents rapports molaires pyrazole/amine (1/1 ; 1/2 ; 1/2,5 ; 1/3,5 ; 1/5 moles), qui par mélange donnent des solutions colorées. On a enregistré leurs spectres d'absorption.

L'examen de ces courbes permet d'observer deux maximums dont un se trouve à 550 mμ et est caractéristique du complexe Meisenheimer (fig. 1). Sa position dans le spectre ne change pas avec le rapport pyrazole/amine. L'autre, se trouvant à 365 mμ, est très différent du premier et correspond à l'absorption de 2,4-dinitrobutylaniline, qui se forme dans cette réaction (fig. 6). On observe que l'augmentation de la concentration molaire en butylamine produit une croissance du maximum d'absorption à 550 mμ, sans qu'un autre maximum apparaisse, ce qui confirme la présence d'un seul complexe (fig. 1, 2, 3). Ensuite le maximum décroît à cause de la transformation graduelle du complexe dans les deux composés finals jusqu'à sa disparition complète (fig. 4,5). La littérature fait mention de cas où, en présence d'un excès de réactif nucléophile, il se forme plusieurs complexes colorés avec des maximums différents, dus à la substitution dans d'autres positions en dehors de la position 1. Par exemple, les positions 3 et 5 (complexe Janovsky). [23, 24] La croissance et la décroissance du maximum d'absorption à 550 mμ sont plus rapides si la concentration molaire en butylamine est plus grande ; il a une valeur semblable aux valeurs des autres complexes Meisenheimer étudiés. [25, 26] Chaque complexe présente son maximum caractéristique, mais tous ces maximums (avec une structure semblable) sont situés dans la région 530–560 mμ, où se trouve aussi le maximum du complexe étudié par nous.

Le complexe Meisenheimer étudié est relativement stable dans les solvants aprotiques dipolaires tels que : DMSO, DMF, acétonitrile, etc. Dans les solvants polaires comme l'eau et les alcools il est instable, si l'on ajoute les solvants indiqués aux solutions colorées du complexe, la coloration disparaît. Ce comportement est analogue à celui des autres complexes Meisenheimer connus. [21, 22, 26]

En conclusion, l'existence d'un complexe de type Meisenheimer dans la substitution de 1-(2,4-dinitrophényl)-3,5-diméthylpyrazole avec la butylamine (par analogie avec d'autres amines aliphatiques) est confirmée par :

a. La couleur rouge transitoire, avec le maximum d'absorption caractéristique à 550 mμ, qui est situé parmi les autres complexes Meisenheimer connus. Nous mentionnons que le produit final, la 2,4-dinitrobutylaniline colorée en jaune présente un maximum d'absorption à 365 mμ très différent du maximum d'absorption du complexe Meisenheimer correspondant.

---

[23] R. Foster et R. K. Mackie, *J. Chem. Soc.*, **1963**, 3796.

[24] F. Cutta et J. Pisecky, *Coll. Czech. Chem. Comm.*, **23**, 628 (1958).

[25] R. Foster et R. K. Mackie, *Tetrahedron*, **18**, 161 (1962).

[26] P. Baudet, *Helv. Chim. Acta*, **49**, 545 (1966).

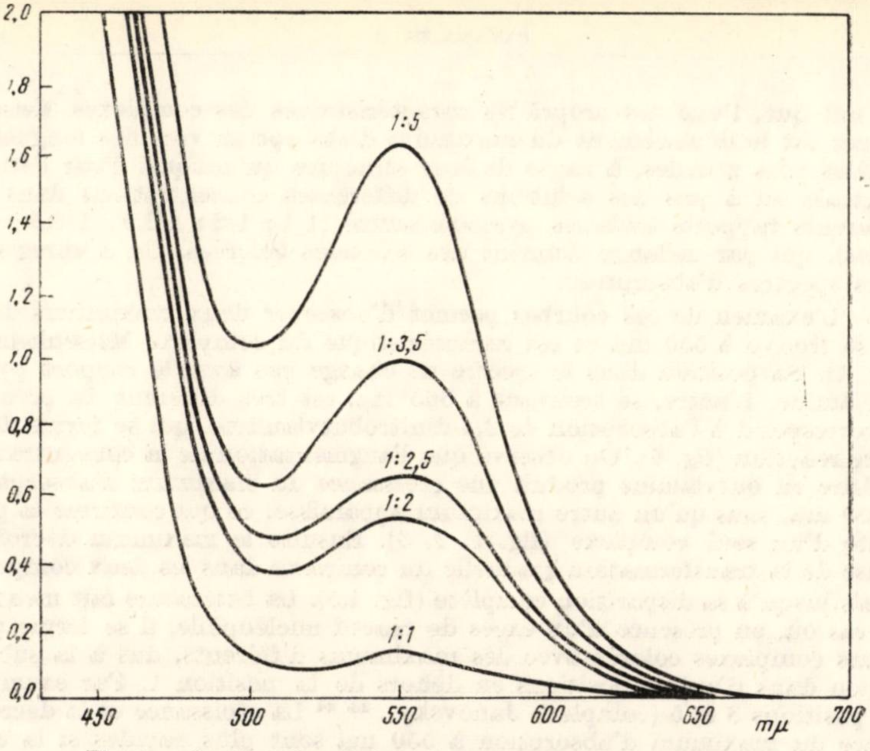

Fig. 1. — Spectres des solutions des complexes, pyrazole/amine : 1/1 ; 1/2 ; 1/2,5 ; 1/3,5 ; 1/5 mole.

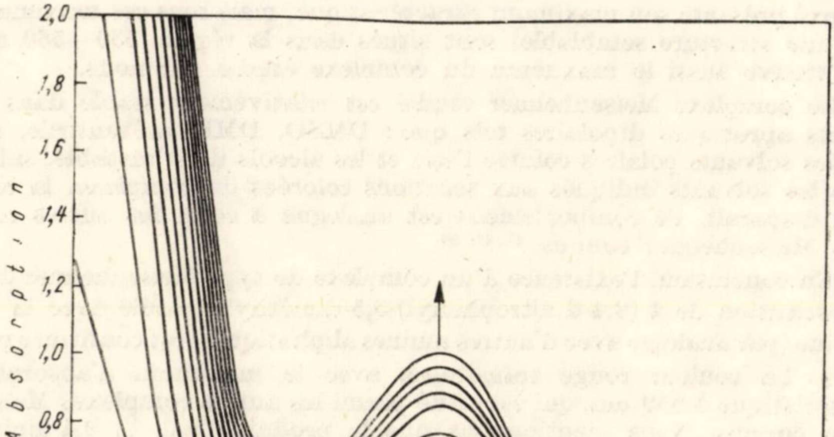

Fig. 2. — Croissance de la concentration du complexe, pyrazole/amine : 1/4,5 mole en fonction du temps. Les courbes ont été tracées de quatre en quatre minutes.

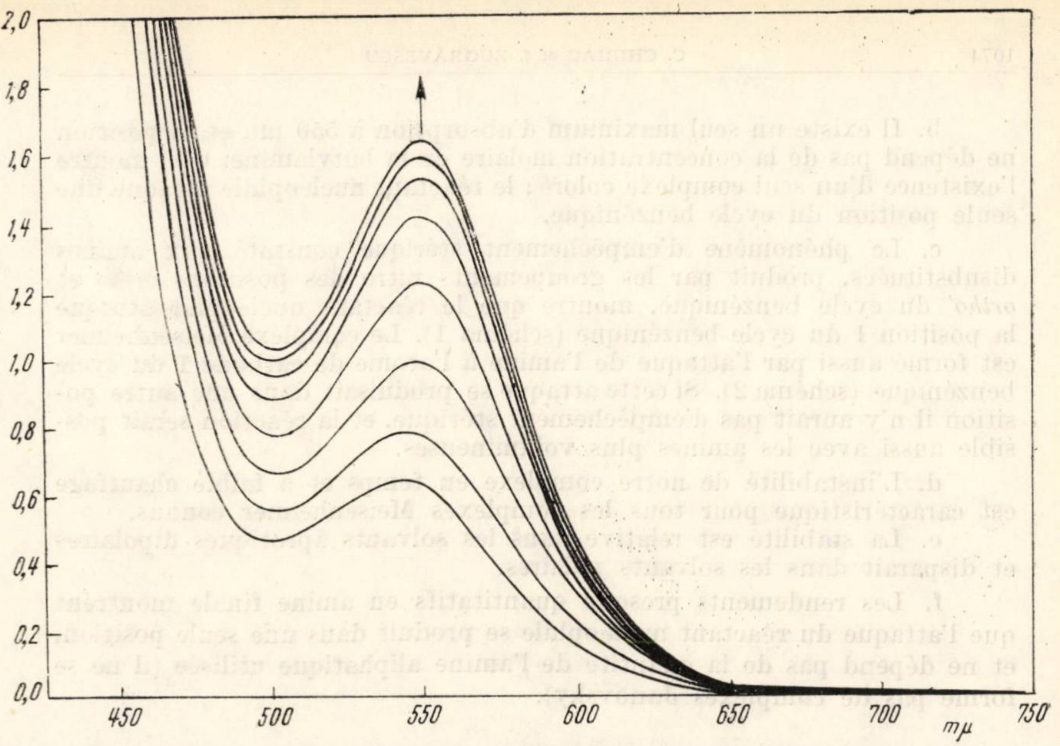

Fig. 3.— Croissance de la concentration du complexe, pyrazole/amine : 1/5 mole en fonction du temps. Les courbes ont été tracées de deux en deux minutes.

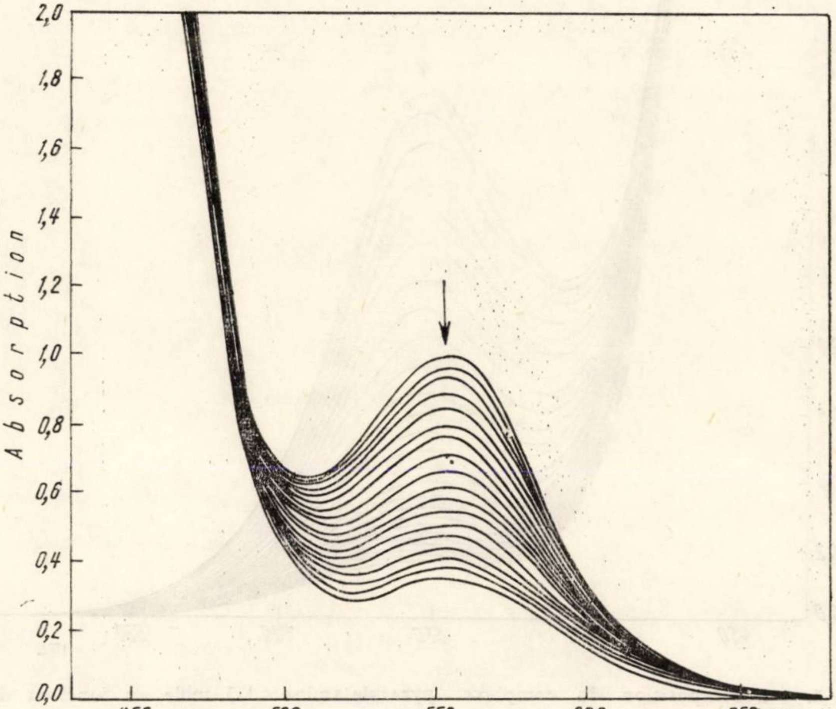

Fig. 4. — Décomposition du complexe, pyrazole/amine : 1/3,5 mole en fonction du temps. Les courbes ont été tracées de quatre en quatre minutes.

b. Il existe un seul maximum d'absorption à 550 mμ et sa position ne dépend pas de la concentration molaire de la butylamine. Ceci montre l'existence d'un seul complexe coloré ; le réactant nucléophile attaque une seule position du cycle benzénique.

c. Le phénomène d'empêchement stérique constaté aux amines disubstituées, produit par les groupements nitro des positions *ortho* et *ortho'* du cycle benzénique, montre que le réactant nucléophile attaque la position 1 du cycle benzénique (schéma 1). Le complexe Meisenheimer est formé aussi par l'attaque de l'amine à l'atome de carbone 1 du cycle benzénique (schéma 2). Si cette attaque se produisait dans une autre position il n'y aurait pas d'empêchement stérique, et la réaction serait possible aussi avec les amines plus volumineuses.

d. L'instabilité de notre complexe en temps et à faible chauffage est caractéristique pour tous les complexes Meisenheimer connus.

e. La stabilité est relative dans les solvants aprotiques dipolaires et disparaît dans les solvants polaires.

f. Les rendements presque quantitatifs en amine finale montrent que l'attaque du réactant nucléophile se produit dans une seule position, et ne dépend pas de la quantité de l'amine aliphatique utilisée (il ne se forme pas de complexes Janovsky).

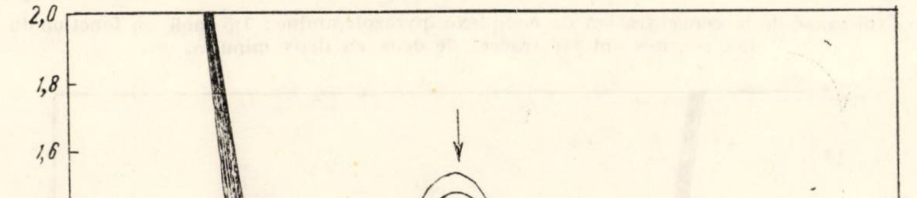

Fig. 5. — Décomposition du complexe, pyrazole/amine : 1/5 mole en fonction du temps. Les courbes ont été tracées de deux en deux minutes.

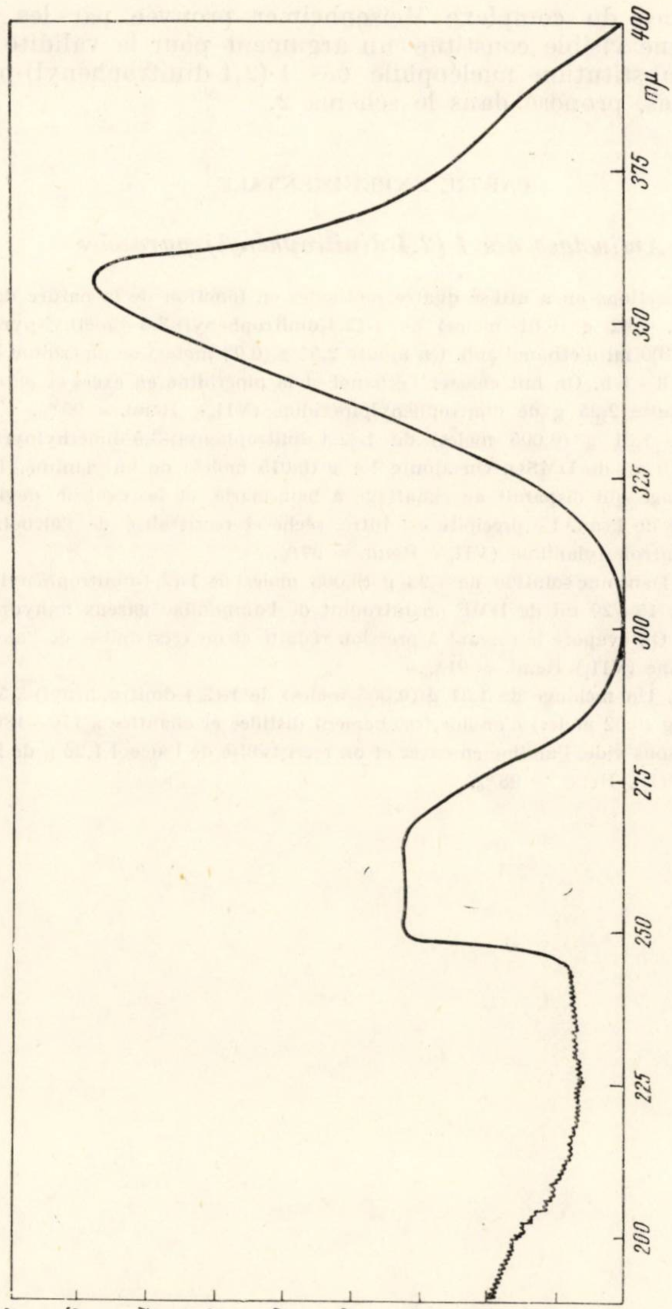

Fig. 6. — Spectre de la 2,4-dinitrobutylaniline.

L'existence du complexe Meisenheimer prouvée par les spectres dans le domaine visible constitue un argument pour la validité du mécanisme de substitution nucléophile des 1-(2,4-dinitrophényl)-pyrazoles avec les amines, proposé dans le schéma 2.

PARTIE EXPÉRIMENTALE

Aminolyse des 1-(2,4-dinitrophényl)-pyrazoles

Pour ces réactions on a utilisé quatre méthodes en fonction de la nature de l'amine :

Méthode A. 2,62 g (0,01 moles) de 1-(2,4-dinitrophényl)-3,5-diméthyl-pyrazole sont dissous dans 80—100 ml d'éthanol anh. On ajoute 2,55 g (0,03 moles) de pipéridine et on porte à reflux pendant 3—4 h. On fait chasser l'éthanol et la pipéridine en excès et on recristallise de l'alcool. Il résulte 2,25 g de dinitrophénylpipéridine (VII_9), Rend. = 90 %.

Méthode B. 1,31 g (0,005 moles) de 1-(2,4-dinitrophényl)-3,5-diméthylpyrazole sont dissous dans 8—10 ml de DMSO. On ajoute 1,1 g (0,015 moles) de butylamine. Il se forme une coloration rouge qui disparaît au chauffage à bain-marie, et la couleur devient jaune. On précipite avec de l'eau. Le précipité est filtré, séché et recristalisé de l'alcool. Il résulte 1,15 g de 2,4-dinitrobutylaniline (VII_6). Rend. = 97 %.

Méthode C. Dans une solution de 1,93 g (0,005 moles) de 1-(2,4-dinitrophényl)-3,5-diméthylpyrazole dans 15—20 ml de DMF on introduit de l'ammoniac gazeux anhydre, pendant 4 h à 150—160°. On évapore le solvant à pression réduite et on recristallise de l'alcool, 0,84 g de 2,4-dinitroaniline (VII_1). Rend. = 91 %.

Méthode D. Un mélange de 1,31 g (0,005 moles) de 1-(2,4-dinitrophényl)-3,5-diméthylpyrazole et 1,86 g (0,02 moles) d'aniline fraîchement distillée et chauffée à 170—180° pendant 4 h. On distille, sous vide, l'aniline en excès et on recristallise de l'alcool 1,26 g de 2,4-dinitrodiphénylamine (VII_2). Rend. = 98 %.

Revue Roumaine de Chimie, **15**, 1077–1085 (1970)

RADIOCHEMICAL GRAFTING OF ACRYLONITRILE ON TEXTILE MATERIAL IN HETEROGENEOUS SYSTEM

* ELENA STANCIU-STOIAN, ** I. VLAGIU, ** ILEANA PETRUŞ
and *** EMILIA NICULESCU

* Academy of Economic Studies, Bucharest, Piaţa Română 1
** Center of Physical Chemistry, Bucharest, str. Dumbrava Roşie, 23
*** U.M.B. – Pilot Station of Chemical Fibres

Received January 27, 1969

The kinetics of radiochemical grafting of acrylonitrile on a cellulose textile in the 20° to 50° temperature range and in a dose field varying from 10^5 to 10^6 r were studied. Among the reaction sensitizers used were substances of the alcohol, acid and aromatic hydrocarbon class; the percentage of grafted monomer decreases with the increase in the number of carbon atoms of the chain. The reaction was carried out in the presence and absence of air.

The action of ionizing radiations on textiles is interesting from the theoretical and particularly, from the practical point of view, this being one of the cases in which atomic energy is used for industrial purposes with a view to changing the structure of polymers and improving their physical-mechanical qualities. [1–5]

Our irradiation procedure, as well as the working systems approached according to the speciality literature, differ. [5–16]

---

[1] E. E. Magat and D. Tinner. (E. I. Du Pont de Nemours and Co). French Pat., 1,149, 305 (1957).

[2] E. E. Magat and D. Tinner. (E. I. Du Pont de Nemours and Co). Belg. Pat., 546,815 (1955).

[3] A. Charlesby, "Atomic Radiation and Polymers", Pergamon Press. London, 1960, p. 280.

[4] E. E. Magat and D. Tinner. (E. I. Du Pont de Nemours and Co). French Pat., 1,130,099 (1955).

[5] J. C. Arthur and D. J. Daigle, *Textile Res. J.*, **34**, 653 (1964).

[6] H. A. Krässing, Tappi, **1963**, 654.

[7] S. Ikuo and O. Seiji, *J. Appl. Polymer Sci.*, **7**, 2067 (1963).

[8] H. Sobue, K. Malsuzaki, H. Komogawa and A. Ishida, *J. Polymer Sci.*, Part C, **2**, 415 (1963).

[9] M. Ciubotaru, D. Feldman and Cr. Simionescu, *Cellulose Chemistry and Technology*, **2**, 131 (1968).

[10] H. A. Rutherford, *Textile Res. J.*, **30**, 546 (1960).

[11] A. A. Armstrong Jr., *Textile Res. J.*, **23**, 264 (1963).

[12] J. C. Bevington, *Nature*, **178**, 1113 (1956).

[13] V. Rusan, *Cellulose Chemistry and Technology*, **1**, 655 (1967).

[14] A. Chapiro, "Radiation Chemistry of Polymeric Systems", New York, 1962, p. 200.

[15] J. Sebban, *J. Chim. phys.*, **58**, 246 (1961).

[16] G. Odin, S. Margonie, R. Albert, K. Robert and T. Acker, *J. Polymer Sci.*, A, **1**, 639 (1963).

Among the radiochemical grafting methods more frequently employed and including the processes of free radicals we mention [14,15]:

1. Direct grafting by irradiation of the vinylic monomer in the presence of a polymer.
2. Radiochemical grafting by means of the peroxide radicals of the polymer.
3. Grafting by trapped radicals.
4. Interreticulation of two different polymers.

Chapiro [14] presents the following radiochemical grafting mechanism (also valid for our study) of a *B* monomer on an *Ap* polymer

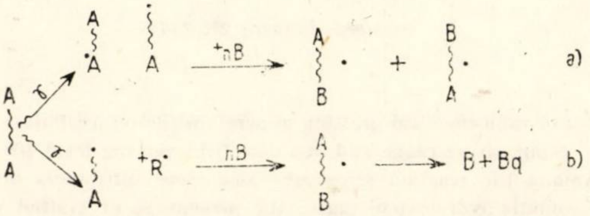

where $A \sim \cdot$ and $A \overset{\cdot}{\sim} A$ are free polymeric radicals becoming *Ap*, and $R^{\cdot}$ a radical of low molecular weight or a hydrogen atom.

Reaction (a) is expected to take place when the polymer is degradable.

By irradiation of a polymer *Ap* in the presence of oxygen a peroxidized polymer ($Ap-O_2$) is formed, leading to the formation of the grafted copolymers $Ap - Bq$:

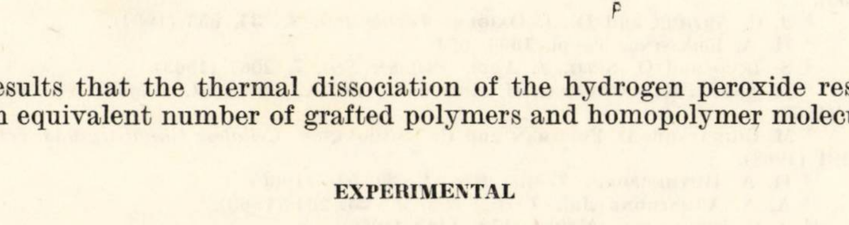

It results that the thermal dissociation of the hydrogen peroxide results in an equivalent number of grafted polymers and homopolymer molecules.

EXPERIMENTAL

The monomer (acrylonitrile) and the solvent (dimethylformamide) were purified according to the procedures known in literature. The reaction sensitizers used were p.c.

The textile (woven celofiber) was treated with warm water and washed by siphoning, then with alcohol to remove the end product, and dried in vacuum up to constant weight.

Irradiation originated in a source of Co^{60} in the dose field 10^5 to 10^6 r. The irradiation was carried out in cylindrical (a) or parallelipipedical (b) cells of glass and thermostated polystyrene (figs. 1 and 2).

The textile processed as shown was subjected to saturation by acrylonitrile (using the zag-solid system) for 180 minutes, and then irradiated.

a) (acrylonitrile-argon) – tissue + γ

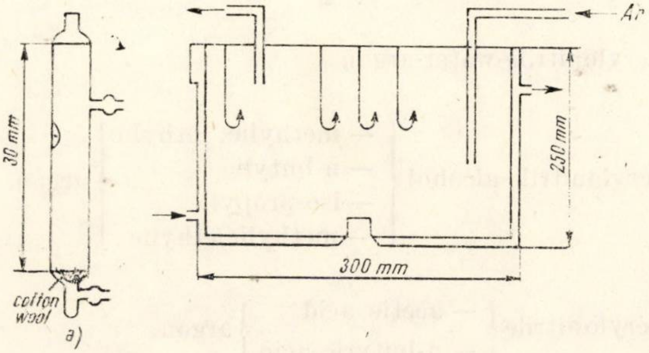

Fig. 1. – a) and b): Irradiation cells.

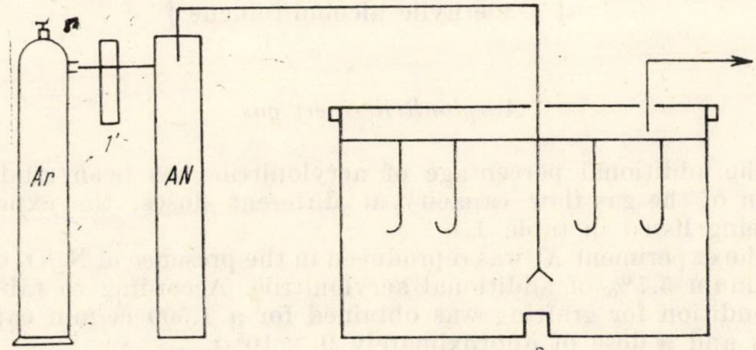

Fig. 2. – Irradiation outfit: 1 – argon bottle, 1′ – rotameter, 2 – flask, 3 – irradiation cell.

b) (acrylonitrile-argon) $\left[\begin{array}{l}\text{gas}\\ \text{gas}\end{array}\right.$ – tissue (acrylonitrile-argon) + γ gas

c) study of the grafting by after-effect

d) irradiation in the presence of N_2 with a 3 % O_2 content.

The flow capacity of the gas suitable to the grafting has varied from 480 to 2,200 cc/min, measured by rotameter.

RESULTS AND DISCUSSION

The grafting of acrylonitrile on textiles, at different doses has been studied, in the following cases :

$$1.\ \text{Acrylonitrile}\left\{\begin{array}{l}\text{argon}\\ \text{nitrogen } (O_2)\end{array}\right.$$

2. Acrylonitrile-water-argon

$$3.\ \text{Acrylonitrile-alcohol}\left\{\begin{array}{l}-\text{ methylic, ethylic}\\ -\text{ n-butylic}\\ -\text{ iso-propylic}\\ -\text{ methylic/ethylic}\end{array}\right\}\text{argon}$$

$$4.\ \text{Acrylonitrile}\left\{\begin{array}{l}-\text{ acetic acid}\\ -\text{ n-butyric acid}\end{array}\right\}\text{argon}$$

$$5.\ \text{Acrylonitrile}\left\{\begin{array}{l}-\text{ methylic alcohol/benzene}\\ -\text{ methylic alcohol/toluene}\end{array}\right\}-\text{ argon}$$

Acrylonitrile-inert gas

The additional percentage of acrylonitrile has been studied as a function of the gas flow capacity, at different doses, the experimental data being listed in table 1.

The experiment X_a was reproduced in the presence of N_2/O_2 obtaining a maximum 5.7% of additional acrylonitrile. According to table 1, the best condition for grafting was obtained for a 1,500 cc/min capacity of the gas and a dose of approximately 9×10^5 r.

The small percentage of additional acrylonitrile in the case of oxygen proves that the latter has an inhibitor role on the grafting reaction.

INFLUENCE OF THE SENSITIZERS ON GRAFTING

Among the substances, with a more or less important role as sensitizers in the grafting reaction we mention : water, methylic alcohol, [16.17] ethylic, methylic/ethylic, n-butylic, isophylic, acetic and n-butyric acid. We have also been concerned with the way in which aromatic hydrocarbons (in gaseous system) influence the grafting kinetics, the reactions being carried out in the presence of argon.

---

[17] I. Vlagiu and B. Hlevka (O.S.I.), Roum. Pat., 48,933 (1964).

In all cases, the argon was drained through the sensitizer as well as through the vessel with the monomer at the same gas flow capacity (750/750 cc/min). After a previous saturation by sensitizer (180 min) it was subjected to irradiation in the presence of the monomer (gas) at a dose of approximately 9 × 10^5 r. Experimental results are recorded in table 2.

Table 1

Influence of the dose and the gas flow capacity in percentage of additional acrylonitrile, at 17°

Sample no	Irradiation dose 10^{-5} r/h	Additional acrylonitrile %	Gas (argon) flow capacity cc/min	Remarks
X_a	0.5	2.0	1500	reaction time 4 hours
X_b	1.5	5.0	1500	
X_c	3.0	10.0	1500	
X_d	4.0	14.11	1500	
X_e	7.0	25.6	1500	
X_f	8.6	28.8	1500	
Y_f	8.6×10^5	3.5	480	
		8.6	600	
		15.0	800	
		28.8	1500	
		27.4	2200	

Table 2

Influence of the sensitizers on the percentage of additional acrylonitrile

Sensitizer	% Additional acrylonitrile	Remarks
water (softened)	17	
methylic alcohol	19.3	gas flow capacity cc/min
ethylic alcohol	17.6	
n-butylic alcohol	11.5	dose = 8.6×10^5 r
isopropylic alcohol	10.6	20°
methylic/ethylic (1 : 0.5) alcohol	18.2	reaction time = 5 hours
acetic acid	27.0	
n-butyric acid	20.4	
methylic alcohol/benzene	10.4	
methylic alcohol/toluene	9.7	
acetic acid/benzene	19.5	

As already shown, for alcohols, as the number of carbon atoms increases in the chain, the influence on the reaction output decreases. The same effect is observed in the case of acids. Compared to other studies carried out in our laboratory,[17] in the case of acrylonitrile polymerization in a heterogeneous medium the same effect has been observed, which means that the radicals developed by these substances are the more numerous as the chain is bigger or more ramified, a fact which diminishes the polymerization grafting process.

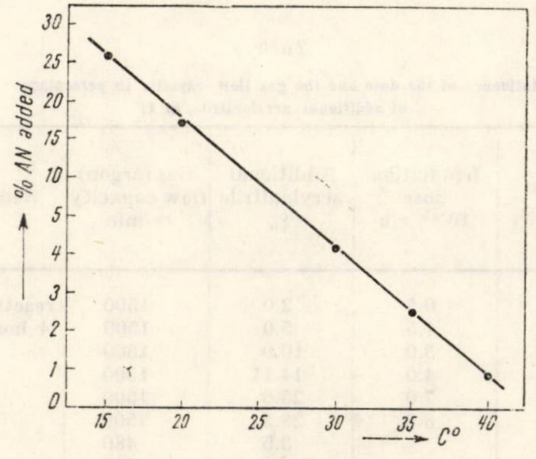

Fig. 3. — Influence of temperature on the grafting output (without sensitizer)

Table 3

Influence of temperature on grafting output

Sample	°C	*AN* % added	Remarks
methylic alcohol	20	19.3	gas flow capacity 1500 cc/min dose = 8.6×10^5r
	30	15.0	
	40	11.1	
	50	6.0	
n-butyric acid	20	20.4	
	30	16.0	
	40	10.0	
	50	4.0	

In order to lower the number of radicals, which follows the breaking of the chain caused by alcohol or acid, one has added sensitizers — respectively benzene or toluene — observing a decrease in the quantity of homopolymers, and also a decrease in the quantity of homopolymers, together with diminution in the reaction output, facts which prove the unactivating role of the aromatic hydrocarbons in the reaction system.

The influence of the reaction temperature on the grafting has also been studied in the presence of sensitizers, in the temperature range 15° to 50° (table 3, fig. 3).

As shown by the experimental data, the grafted percentage of acrylonitrile decreases with the rise in the temperature. We can assign this to two factors :

— quicker diffusion of the monomer and insufficient contact time for an eventual reaction with the P radicals ;

— more marked radiolysis of the sensitizer and inactivation of the monomer cells in excited eventual state.

DOSE EFFECT ON THE GRAFTING PROCESS
STUDY OF THE AFTER EFFECT ON THE GRAFTING

The acrylonitrile concentration in our working system (gaseous) has generally been varying between 5 and 15%, and that of the sensitizers between 2 and 12%. The polymer has been analysed for time intervals of 1, 3, 5 and 7 hours and the results shown in table 4.

Table 4

Variation of the additional acrylonitrile content in the polymer as a function of the irradiation time (after effect)

AN added %	Content in homopolymer	Irradiation time (h)	Irradiation conditions
8.0	4.0	1	dose = 1.5 × 10^5 r/h
11.0	7.0	3	20°
13.6	8.4	5	purification with argon
14.8	8.8	6	1500 cc/min

The molecular weight of the formed homopolymer is in close accordance with the quantity of radicals formed. This was determined according to the principle of Bamford's[18] method, the molecular weight (Mn) varying between 10^3 and 10^5.

By making use of Chapiro's principles on the reaction kinetics, in the simplest case of the grafting process (after effect) we may consider that this is based on the following reaction sequences :

$$\text{a)}\quad P \rightsquigarrow \gamma \xrightarrow[(G_pI)]{k_1} R^\bullet$$

$$\text{b)}\quad R^\bullet + M \xrightarrow{k_p} RM^\bullet$$

$$\text{c)}\quad R_n^\bullet + R_m^\bullet \xrightarrow{k_t} \qquad \text{inactive products}$$

$$R_n^\bullet \xrightarrow{k'_t} \qquad \text{inactive products (Q)}$$

---

[18] C. H. Bamford, A. I. Jenkins, R. Johnson and E. T. White, *Trans. Faraday Soc.*, 55, 167 (1959).

where a = the initiation, b = propagation and c = completion of the reaction stage. The reaction rate also defined by the degree of growth, can be written as:

$$-\frac{\mathrm{d}(M)}{\mathrm{d}t} = \frac{\mathrm{d}(P)}{\mathrm{d}t} = k_p (R^\bullet)(M) \tag{1}$$

but as the variation of the chain depends on the (c) stage of the process, then

$$\frac{\mathrm{d}(R^\bullet)}{\mathrm{d}t} = k_t (R^\bullet)^2 - k'_t (R^\bullet) \tag{2}$$

which can also be written

$$\frac{1}{(R^\bullet)^2}\frac{\mathrm{d}(R^\bullet)}{\mathrm{d}t} = -k_t - \frac{k'_t}{(R^\bullet)} \tag{3}$$

or

$$\frac{\mathrm{d}}{\mathrm{d}t}\left(-\frac{1}{(R^\bullet)}\right) = -k_t - \frac{k'_t}{(R^\bullet)} \tag{4}$$

Making the substitution $\frac{1}{(R^\bullet)} = y$, in equation (4) one obtains:

$$-\frac{\mathrm{d}y}{\mathrm{d}t} = -k_t - k'_t; \quad -\frac{\mathrm{d}y}{\mathrm{d}t} - k'_t y = k_t \tag{5}$$

the solution of which is

$$y = C\, \mathrm{e}^{k'_t \cdot t} - \frac{k_t}{k'_t} = \frac{1}{(R^\bullet)} \tag{6}$$

hence it results that:

$$(R^\bullet) = \frac{1}{C\, \mathrm{e}^{k'_t \cdot t} - \frac{k_t}{k'_t}} \tag{7}$$

or at the moment $t = 0$

$$(R^\bullet)_0 = \frac{1}{C - k_t/k'_t}, \tag{8}$$

After the introduction of the integration constant (c) of equations (8), (7), one finally obtains:

$$(R^{\bullet}) = \frac{k'_t\,(R^{\bullet})_0}{e^{k_t \cdot t}\,[k'_t + (R^{\bullet})_0\,k_t] - k_t\,(R^{\bullet})_0} \tag{9}$$

so that equation (1) finally becomes:

$$-\frac{d(M)}{dt} = k_p\,(R^{\bullet})\,(M) = \frac{d\,(P)/dt}{(M)} = k_p \times \frac{k'_t\,(R^{\bullet})_0}{e^{k_t \cdot t}\,[k'_t + (R^{\bullet})_0\,k_t] - k_t\,(R^{\bullet})_0}$$

or

$$\left[\frac{k'_t + k_t\,(R_0^{\bullet})}{k'_t \cdot k_t\,(R_0^{\bullet})}\right] e^{k_t \cdot t} = \frac{k_t}{k'_t \cdot k_p} + \frac{1}{k_p\,(R^{\bullet})} \tag{10}$$

Table 5

Dependence at $1/k_p$ ($R\cdot$) on irradiation time

Irradiation time in (h)	$1/k_p\,(\dot{R})$ s^{-1}	$\frac{k_t}{k'_t k_p}$	k'_t	Remarks
0.5	3.35×10^{-3}			dose 1.5×10^3 r/h
1	5.6×10^{-3}			20°
2	9.0×10^{-3}			gas flow capacity = 1500 cc/min
3	1.8×10^{-4}			
5	6.5×10^{-4}			
7	1.7×10^{-5}			
		9.76	8.14×10^{-5}	

Using equation (10) for a given value of the monomer one can study the variation of the polymerization degree as a function of the irradiation time.

Table 5 shows this variation for a 10% concentration (in grams) of the acrylonitrile.

CONCLUSIONS

a) The heterogeneous reaction medium (gas-solid) brings about better, more uniform, grafting conditions, and the quantity of homopolymers is smaller than in the solution.

b) The most favourable gas flow capacity is 1500 cc/min for a flow capacity dose of 8.6×10^5 rph.

c) The best sensitizers are water, methylic alcohols and acetic acid.

Revue Roumaine de Chimie, 15, 1087–1096 (1970)

RÉTENTION DE CERTAINS IONS RADIOACTIFS PAR LES MACROMOLÉCULES INORGANIQUES NATURELLES DES SUSPENSIONS DES BASSINS DE SURFACE ET DE CERTAINES TERRES ACTIVES

GH. FURNICĂ
Laboratoire des Rayonnements ionisants, Institut d'Hygiène,
Bucarest 15, 1, rue Leonte

V. VOICU
Institut de Physique Atomique Bucarest

Reçu le 15 mars 1969

On étudie la rétention variée des isotopes Na-22, Sr-85, Ag-110, Cs-134, Zn-65, Fe-59 et I-131 dissous dans l'eau, par la boue prélevée sur la rivière de Dîmbovitza, Bucarest, à savoir : 15 % Na, 45 % Sr, 37 % I, 97 % Zn, 95 % Fe au 98 % Cs. Par l'élution de la boue qui a fixé le Na-22, le Sr-85 au Ag-110, on observe un phénomène d'échange ionique entre les ions radioactifs et le produit naturel. Le sable retient séparément : 3,6 % Na, 22 % Ag, 72 % Zn, 8,8 % I, 99 % Cs, 93 % Sr et 94 % Fe. Le traitement du sable avec HNO_3 5 % ou le HCl 10 % modifie la capacité de rétention des ions radioactifs. Au cas de déterminations pareilles avec les bentonites de type montmorillonitique, on observe une rétention plus grande par rapport au Cs et plus petite par rapport au Na.

Par effluents radioactifs on comprend les eaux usées des laboratoires et des installations de traitement des produits radioactifs. Ces effluents contiennent, d'une manière générale, une très faible quantité d'ions radioactifs, biologiquement très nocifs, qui sont éliminés avec une forte quantité d'ions inactifs dont la nocivité biologique est faible, ou nulle. Le problème qui se pose est donc de connaître l'interaction des quantités de radioéléments de quelques 10^{-12} à 10^{-15} grammes dissous dans l'eau de la rivière et les suspensions des bassins de surface[1-2]. Si l'on introduit des radioélements dans l'eau de la rivière leur comportement ultérieur est déterminé par deux phénomènes fondamentaux. D'une part l'équilibre chimique ou physique entre les ions dans la solution et la phase solide et d'autre part le phénomènes de diffusion et de convection dans l'eau.

---

[1] J. L. Verot, J. M. Blum et R. Sarfati, « Décontamination des effluents par les zéolithes », Contract Euratom 3452/1967–1968.

[2] J. L. Verot, J. M. Blum et J. Hazera, « Étude des problèmes posés par le traitement des effluents contenant des détergents et des complexants », Contract Euratom 4192/1968.

La plupart des études existantes révèlent ce qui suit [1-15]: Selon Verot [1-2] les zéolites ont une efficience élevée de rétention pour les isotopes Co-60, Zn-65 et Ra-226. Bittel [3] soutient que la plupart des études ont ignoré l'aspect physico-chimique des isotopes radioactifs dissous dans les effluents, ce qui doit conférer un caractère a priori à toutes les études radioécologiques. L'irrigation intensive des cultures avec des eaux contaminés par effluents radioactifs est responsable du taux élevé de la contamination des plantes.[4-15] Myttenaere [4-5] montre que les facteurs de concentration entre l'eau d'irrigation et les plantes sont très élevés, ce qui souligne l'importance du contrôle du niveau d'activité des eaux, surtout pour les cultures irriguées. Collet [8] met en évidence la rétention des isotopes radioactifs Ce-141, Cs-137, I-131, P-32 et Sr-89 par la boue prélevée sur le Rhin. Hawkins [14] opine que la bentonite représente le principal composant du sol pour la rétention chimique des isotopes radioactifs.

Verot [1-2] démontre que dans l'étude de la rétention des isotopes des effluents par les zéolithes pour connaître les phénomènes physico-chimiques on doit employer au lieu des méthodes de la chimie classique, les méthodes de la micro-chimie, mais appliquées à l'étude de l'échange d'ions, entre la solution aqueuse et les corps organiques aux minéraux des suspensions.

Cette note présente succinctement les données obtenues sur la rétention des isotopes Na-22, Sr-89, Ag-110, Cs-134, Zn-65, Fe-59 et I-131 dissous dans l'eau, par la boue.

MATÉRIEL ET MÉTHODE

Comme matériel on a utilisé la boue prélevée sur la rivière de Dîmbovitza avec une turbulence maximum de 3291°, sa composition étant indiquée ci-après :

Substances humiques — 1,34 %; C-organiques — 0,78 g %; quant à la granulométrie, on a déterminé en pour-cent la répartition suivante :

[3] R. Bittel, « Radioécologie du cobalt », C.E.A. (BIB) — 130/1968, Fontenay-aux-Roses.

[4] C. Myttenaere et M. Masset, Symposion AIEA-SM-72/30. « Disposal of Radioactive Wastes into Seas, Oceans and Surface Waters ».

[5] C. Myttenaere et Ph. Bourdeau, *Giornale Fiz. Sanitaria e Protez. contro le Radiaz.*, **12**, 179 (1968).

[6] R. J. Garner et F. Morley, *Health Physics*, **13**, 465 (1967).

[7] Hwa-Shen Cheng et Hiroshi Hamaguki, *Health Physics*, **14**, 353 (1968).

[8] M. Collet et R. Maushart, „Fluss-Schlamm als Sammler für radioaktive Stoffe", Internat. Congres Internat. Radiat. Protect., Rome, 5.IX.1966.

[9] L. Argiero, G. Barzon et A. Paggi, *Giornale Fiz. Sanit. et Protezione contro le Radiaz.*, **10**, 140 (1966).

[10] Barzon, R. Nazzuoli, *Atti Soc. Tosc. Sc. Nat.*, **73**, 3 (1966).

[11] L. Baetsie, « Physico-chimie de la migration de cations dans le sol », Euratom 141/1963.

[12] Guy-Antonin Martin, *Compt. rend.* (C), **264**, 1536 (1967).

[13] R. E. Isaacks, *Agric. and Food Chemistry*, **15**, 300 (1967).

[14] R. H. Hawkins et J. H. Horton, *Health Physics*, **13**, 287 (1967).

[15] H. F. Sherry, *J. Phys. Chem.*, **70**, 1158 (1966); **71**, 1457 (1967).

	2mm	0,2– 2 mm	0,05– 0,2 mm	0,02– 0,05 mm	0,002– 0,02 mm	0,001= 0,002 mm	1.10^{-3} mm
sans gravier	–	12,45	32,70	12,20	12,00	2,35	28,30
avec gravier	21,8	9,73	25,47	9,56	9,42	1,84	22,18

La boue séchée à 105° contient $H_2O - 2{,}9\,\%$; substances humiques – 1,41 % ; C – – 0,82 % ; $CaCO_3 - 5{,}10\,\%$ et la suspension aqueuse a le $pH = 8{,}10$. Les ions échangeables en milliéquivalents/100 g sont :

$$Ca^{2+} - 18{,}04 \,;\; Mg^{2+} - 1{,}18 \,;\; K^{+} - 0{,}59 \,;\; Na^{+} - 0{,}39 \,;\; H^{+} - 0.$$

Les acides humiques extraits de substances humiques par le pyrophosphate sodique ont la composition ci-dessous :

Acides humiques – (% C-organique) – 16,68 % ;

Acides fluviques (% C-organique) – 21,8 %.

Pour la rétention des isotopes dissous dans l'eau on a employé également le sable déposé après la destruction des substances humiques, formé de 87,85 % Si total dans le gravier et 84,33 % Si dans le sable.

La boue utilisée dans notre expérience est constituée de : 30 % argiles ; 24 % poussière ; 40 % sable ; 4 % gravier et 1,5 % substances humiques. Nos expériences ont été effectuées aussi avec des alumino-silicates du type bentonite-montmorillonitique ayant la composition :

$$69-75\,\%\ SiO_2 \,;\quad 13-17\,\%\ Al_2O_3 \,;\quad 1{,}4-2{,}0\,\%\ Fe_2O_3 \,;\quad 1{,}16-1{,}61\,\%\ CaO \,;\quad 1{,}93-3{,}82\,\%\ MgO$$

et $0{,}42-1{,}86\,\%\ K_2O + Na_2O$.

Les solutions radioactives utilisées proviennent du réacteur atomique I.F.A. Bucarest, aux activités spécifiques d'ordre 0,2–2,0 nCi/ml.

L'activité a été mesurée à l'aide d'un compteur (détecteur à scintillations) à scintillateur γ à puits (produits Friescke-Hoepfner), connecté à l'échelle de comptage F.H.-49, l'étalonnage étant effectué avec des solutions étalonnées A.I.E.A. ou Amersham.

RÉSULTATS

L'efficience de la rétention des isotopes radioactifs dissous dans l'eau par la boue ou par d'autres substances a été calculée à l'aide de la relation

$$E(\%) = \frac{A_0 - A}{A_0} \cdot 100$$

A_0 = activité de la solution avant le contact avec la substance ;

A = activité de la solution après le contact avec la substance.

Les résultats obtenus sont représentés sur les figures 1–6 et au tableau 1.

Sur la figure 1 on observe que la boue retient avec un taux de 94–98% les isotopes suivants sous forme ionique : Cs^+, Zn^{2+}, Fe^{3+} et Zr^{4+}, avec une efficience de 34–36% les ions I^- et Sr^{2+} et avec une moindre efficience (15%) les ions Na^+.

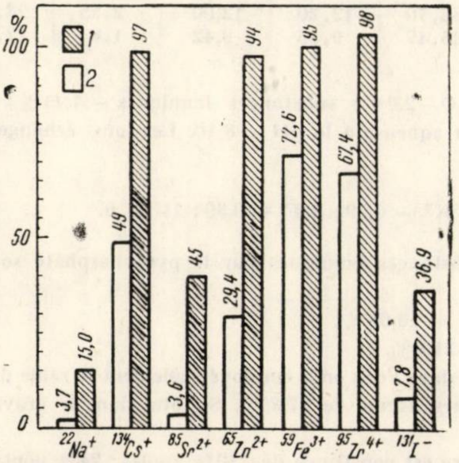

Fig. 1. — Efficience de la rétention des isotopes radioactifs dissous par la boue humide. (La concentration de la solution est 1–2 nCi/ml pour 1 g de boue et pour 50 ml de solution.)

1, eau + boue ajoutée ;
2, eau de la rivière avec une turbulence de 102°.

Fig. 2. — Efficience de la rétention des isotopes radioactifs dissous par les suspensions de l'eau de Dimbovitza.

1, eau avec une turbulence de 102° ;
2, eau avec une turbulence de 1253° ;
3, eau avec une turbulence de 3291°.

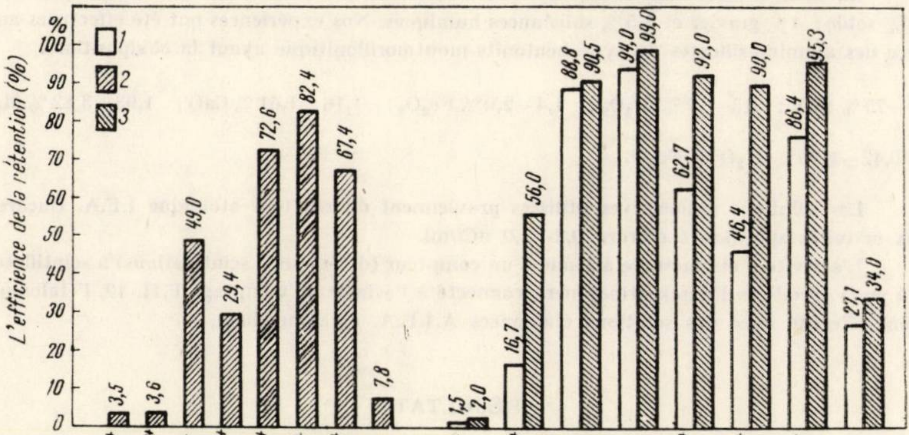

La figure 2 révèle une efficience élevée de la rétention des isotopes dissous par les suspensions de l'eau naturelle, par exemple l'eau avec une turbulence élevée (3291°).

La figure 3 représente l'influence de l'activité spécifique des solutions sur l'efficience de la rétention des isotopes par la boue. Pour l'ion Cs^+ cette influence est pratiquement négligeable pour de larges limites de concentrations (0,92–60 pCi/ml) et aussi négligeable pour l'ion Zr^{4+} entre les concentrations radioactives de 9–480 pCi/ml. La rétention des ions Na^+, Sr^{2+} et I^- est beaucoup influencée par la valeur de la concentration radioactive des solutions ; ainsi Sr^{2+} est retenu 80% à la concentration de 2pCi/ml et en petite quantité (40%) à la concentration de

61 pCi/ml. L'ion I-131 est retenu 90%, à la concentration de 1 pCi/ml, et seulement 50% à la concentration de 5 *p*Ci/ml. L'ion d'isotope Na-22 est généralement peu retenu, 15% à une concentration de 0,53 pCi/ml et 2,8% à une concentration de 60 pCi/ml.

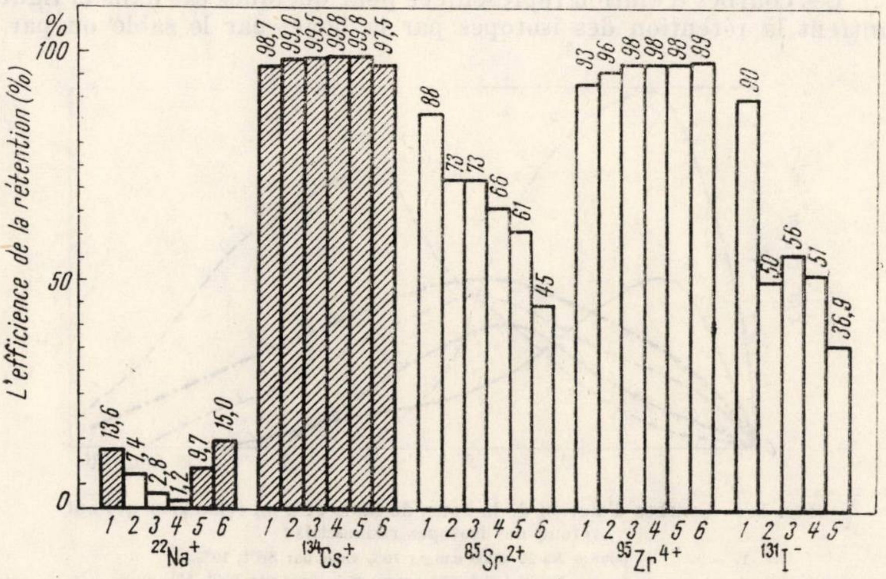

Fig. 3. — Variation de l'efficience de la rétention de la boue, en fonction de l'activité spécifique de la solution aqueuse :

Na-22 *1.* – 20 *p*Ci/ml ; *2.* – 40 *p*Ci/ml ; *3.* – 60 *p*Ci/ml ; *4.* – 0,1 *p*Ci/ml ; *5.* – 0,2 *p*Ci/ml ; *6.* – 0,53 *p* Ci/ml. Cs-132 *1.* – 18 *p*Ci/ml ; *2.* – 45 *p*Ci/ml ; *3.* – 63 *p*Ci/ml ; *4.* – 225 *p*Ci/ml ; *5.* – 0,45 *p*Ci/ml ; *6.* – 0,92 *p*Ci/ml. Sr-85 *1.* – 2 *p*Ci/ml ; *2.* – 4 *p*Ci/ml ; *3.* – 8 *p*Ci/ml ; *4.* – 9 *p*Ci/ml ; *5.* – 24 *p*Ci/ml ; *6.* – 61 *p*Ci/ml. Zr-95 *1.* – 9 *p*Ci/ml ; *2.* – 17 *p*Ci/ml ; *3.* – 28 *p*Ci/ml ; *4.* – 56 *p*Ci/ml ; *5.* – 80 *p*Ci/ml ; *6.* – 480 *p*Ci/ml. I-131 *1.* – 1 *p*Ci/ml ; *2.* – 2 *p*Ci/ml ; *3.* – 3 *p*Ci/ml ; *4.* – 5 *p*Ci/ml ; *5.* – 1,94 *p*Ci/ml.

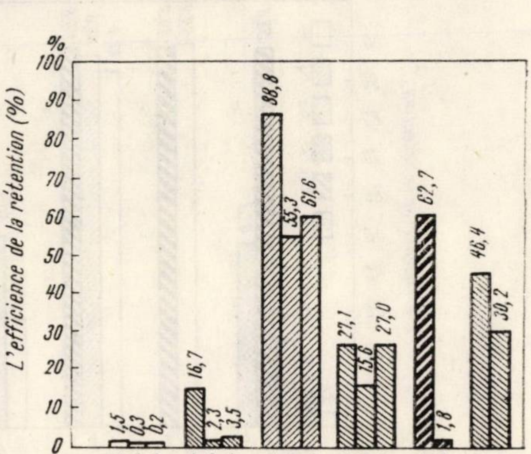

Fig. 4. — Rétention des isotopes radioactifs par les suspenisons de l'eau, ajoutées à l'échantillon avec une turbulence de 1255° :

Na-22 1. – 0,28 nCi/ml ; 2. – 0,28 nCi/ml + 40 mg $Al_2(SO_4)_3$/50 ml ; 3. – 0,28 nCi/ml + 80 mg $Al_2(SO_4)_3$/50 ml.
Sr-85 1. – 0,3 nCi/ml ; 2. – 0,3 nCi/ml + 40 mg $Al_2(SO_4)_3$/50 ml ; 3. – 0,3nCi/ml + 80 mg $Al_2(SO_4)_3$/50 ml.
Ag-110 1. – 0,3 nCi/ml ; 2. – 0,3 nCi/ml + 40 mg $Al_2(SO_4)_3$/50 ml ; 3. – 0,3 nCi/ml + 80 mg $Al_2(SO_4)_3$/50 ml.
I-131 1. – 2,7 nCi/ml ; 2. – 2,7 ml/ml + 40 mg $Al_2(SO_4)_3$/50 ml ; 3. – 2,7 nCi/ml + 80 mg $Al_2(SO_4)_3$/50 ml ; 3. – 2,7 nCi/ml + 80mg $Al_2(SO_4)_3$/50ml.
Zn – 65 1. – 1,24 nCi/ml ; 2. – 2,24 nCi/ml + 120 mg $Al_2(SO_4)_3$/50 ml.
Fe – 59 1. – 0,63 nCi/ml ; 2. – 0,63 nCi/ml + 120 ml $Al_2(SO_4)_3$/50 ml.

Sur la figure 4 on observe la rétention des isotopes dissous par les suspensions d'un échantillon d'eau avec une turbulence de 1255°. On remarque que l'adjonction dans la solution de l'$Al_2(SO_4)_3$ fait diminuer la quantité d'isotope retenue par les suspensions.

Les courbes d'élution représentées pour quelques cas dans la figure 5 montrent la rétention des isotopes par la boue, par le sable ou par un

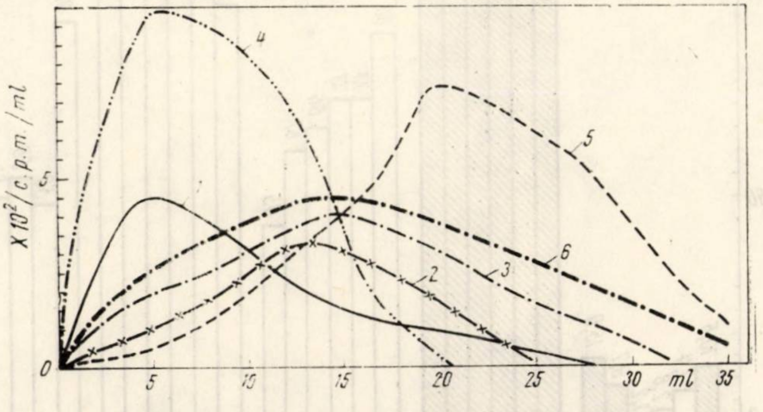

Fig. 5. — Courbes d'élution de la boue, du sable et d'un échangeur qui ont retenu des isotopes radioactifs :

1. — —— boue + Na-22 (2200 c.m.p.) 70% éluée par $SrCl_2$ 10%.
2. — × boue + Na-22 + Sr^2 (970 c.m.p.) 45% éluée par $ZnCl_2$ 5%.
3. — ·—·— boue + Sr-85 (1850 c.m.p.) 75% éluée par $ZnCl_2$ 5%.
4. — —··· — cationite + Na-22 (2300 c.m.p.) 98% éluée par $ZnCl_2$5%.
5. — — — — — cationite + Cs-134 (2400 c.m.p.) 70% éluée par $Al_2(SO_4)_3$ 2,5%.
6. — —·—·— sable + Ag-110 (1750 c.m.p.) 60% élué par HNO_3 5%.

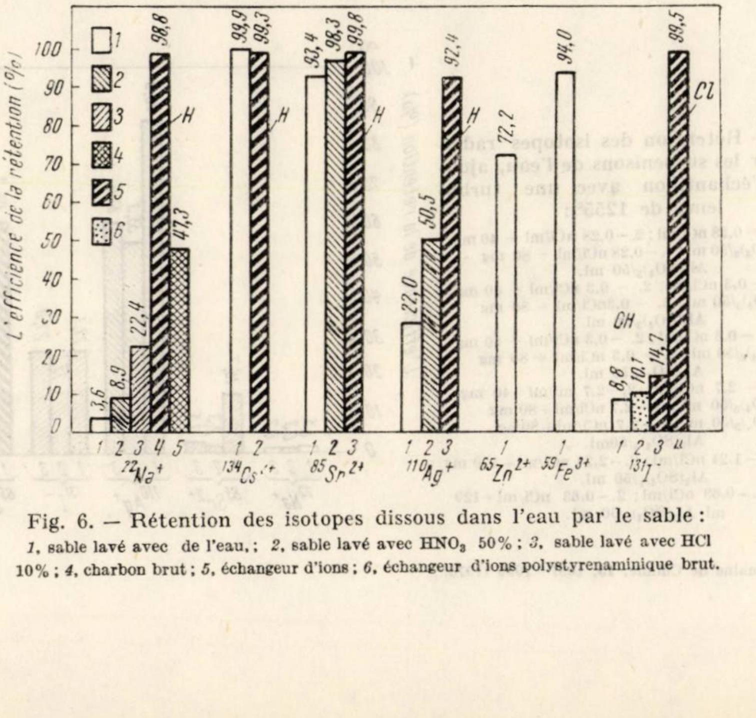

Fig. 6. — Rétention des isotopes dissous dans l'eau par le sable :
1, sable lavé avec de l'eau, ; *2*, sable lavé avec HNO_3 50% ; *3*, sable lavé avec HCl 10% ; *4*, charbon brut ; *5*, échangeur d'ions ; *6*, échangeur d'ions polystyrenaminique brut.

échangeur d'ions et on observe la possibilité de la substitution à l'aide des ions plus électropositifs ou avec plusieurs charges électriques et par les acides. Sur la figure 6 il apparaît que le sable lavé avec du HNO_3 5% ou avec du HCl 10% retient des quantités plus grandes d'isotopes radioactifs dissous dans les solutions neutres.

Tableau 1

Rétention par les bentonites montmorillonitiques des isotopes radioactifs dissous dans l'eau

L'isotope radioactif	Efficience de rétention (%) de la bentonite calcinée à		
	250°	400°	700°
Na−22	11	10	9
Cs−134	98	99	99
Sr−85	92	94	94
Co−60	97	99	98

L'analyse des résultats représentés sur le tableau 1 révèle que la bentonite retient 9−11% Na-22, 98−99% Cs-134, 92−94% Sr-85 et 97−99% Co-60 de la solution aqueuse.

DISCUSSIONS

Les résultats mentionnés relèvent le processus d'échange d'ions comme principal processus chimique qui se déroule entre les suspensions des eaux naturelles et les isotopes radioactifs dissous. On admet actuellement que la rétention des isotopes est régie par plusieurs mécanismes. Ainsi, la fonction de complexes est un phénomène possible dans les eaux naturelles, ces eaux contenant des substances comme NH_3, CN^-, SCN^-, des amines, des acides carboxyliques ou aminés, des mercaptans, etc. On admet également que les substances humiques possèdent des groupements carboxyliques, phénoliques et aminés libres.

Les phénomènes de sorption et d'échange hétérogène existent entre les eaux, d'une part, les particules en suspensions et les sédiments d'autre part et entre les sols, d'une part et les solutions des sols, d'autre part. De nombreux auteurs admettent la possibilité que les macromolécules inorganiques aient un comportement d'électrolytes amphotères[16].

---

[16] Gh. Furnică, *Rev. Roumaine de Chimie*, **13**, 225 (1968).

La dissociation des aluminosilicates en fonction du pH est possible d'après le mécanisme ci-après

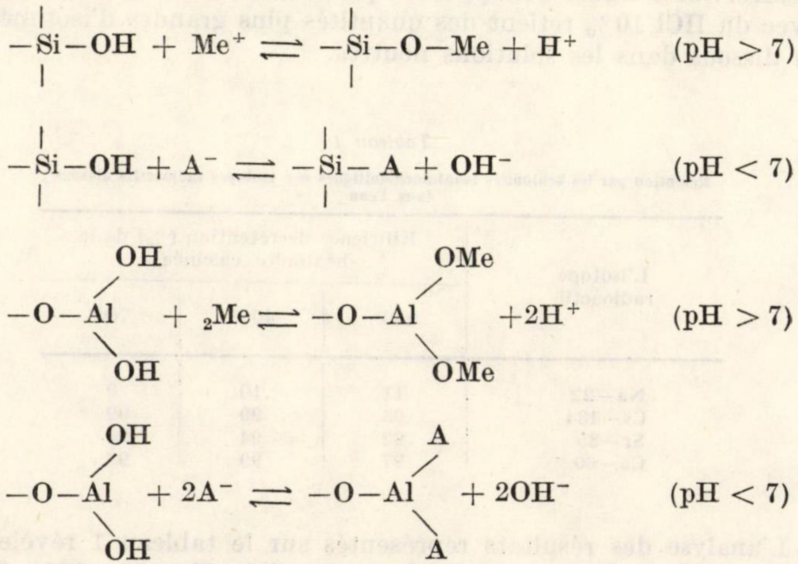

$$-\mathrm{Si}-\mathrm{OH} + \mathrm{Me}^{+} \rightleftharpoons -\mathrm{Si}-\mathrm{O}-\mathrm{Me} + \mathrm{H}^{+} \quad (\mathrm{pH} > 7)$$

$$-\mathrm{Si}-\mathrm{OH} + \mathrm{A}^{-} \rightleftharpoons -\mathrm{Si}-\mathrm{A} + \mathrm{OH}^{-} \quad (\mathrm{pH} < 7)$$

Les résultats obtenus à l'aide des bentonites (tableau 1) confirment la possibilité d'échange ionique entre les suspensions des eaux naturelles et les isotopes dissous. Sur le schéma 1 on observe la distribution spatiale de quelques macromolécules inorganiques. La distribution des groupements OH dans la structure moléculaire de montmorillonite explique les différences en ce qui concerne la rétention des ions avec des rayons ioniques inégaux. Les ions Na^+ et Cs^+ ont des propriétés chimiques très voisines, mais le rayon ionique de Na^+ est pratiquement plus grand que Cs^+, parce que l'ion Na^+ est fortement solvaté.[3,17] Hodgson [18] a étudié les réactions entre la montmorillonite et les ions radioactifs métalliques à très faible concentration, en présence d'un énorme excès d'ions non radioactifs. Dans ces conditions, l'ion radioactif semble réaliser 2 types de liaisons avec l'argile :

— une liaison relativement labile analogue à une liaison d'échange ionique ; l'ion radioactif peut alors être remplacé sur le substrat par d'autres ions ;

— une liaison où l'ion radioactif occupe probablement une position interne dans le réseau cristallin de l'argile.

Yousef [19] admet que la sorption de l'ion radioactif résulte de 2 mécanismes. Une sorption électrostatique non spécifique, qui est une adsorption au sens classique du terme en chimie des sols, phénomènes influencés par la valence de l'ion sorbé, par la densité superficielle de charges sur l'absor-

[17] W. Foerst, „Ulmans Encyklopädie der technischen Chemie", t. VIII, 1957, p. 787.

[18] J. F. Hodgson, *Soil. Sci. Soc. Am. Proc.*, **24**, 165 (1960).

[19] Y. A. Yousef et E. F. Gloyna, Rapp. U.S. atomic energy commission TID 22 878. 1966.

bant et la concentration de l'électrolyte et de la surface adsorbante en l'ion considéré et en d'autres ions (H^+, Ca^{2+}, Al^{3+}), notamment. C'est une sorption spécifique qui est surtout une interaction ions-réseau cristallin des argiles et qui dépend surtout des facteurs géométriques de l'ion et du réseau cristallin.[20] L'échange ionique est associé aussi par la formation des complexes chimiques anioniques comme forme générale[21-22] qui suit :

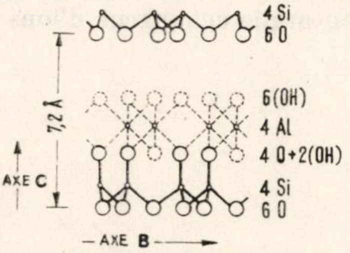
4 Si
6 O
7,2 Å
6(OH)
4 Al
4 O+2(OH)
4 Si
6 O
AXE C
— AXE B →

KAOLIN $(OH)_6Al_4Si_4O_{10}$

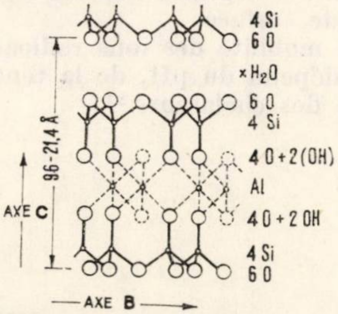
4 Si
6 O
× H₂O
6 O
4 Si
96-21,4 Å
4 O+2(OH)
Al
4 O+2 OH
4 Si
6 O
AXE C
— AXE B →

MONTMORILLONITE $(OH)_4Al_4Si_8O_{20}\times H_2O$

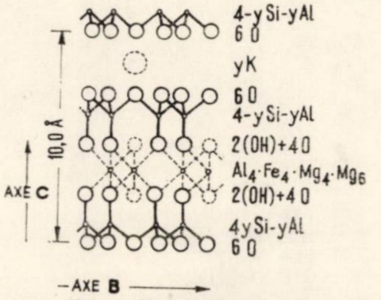
4-y Si-yAl
6 O
yK
6 O
4-y Si-yAl
10,0 Å
2(OH)+4 O
Al₄·Fe₄·Mg₄·Mg₆
2(OH)+4 O
4y Si-yAl
6 O
AXE C
— AXE B →

ILIT $(OH)_4\ K_y(Al_4\cdot Fe_4\cdot Mg_4\cdot Mg_6)(Si_{8-y}Al_y)O_{20}$

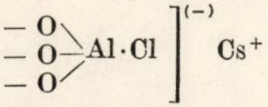

$$\left.\begin{matrix}-\mathrm{O}\\-\mathrm{O}\\-\mathrm{O}\end{matrix}\right\rangle \mathrm{Al\cdot Cl}\ \Big]^{(-)}\ \mathrm{Cs}^+$$

Cette hypothèse explique l'addition de l'eau à l'aluminium lié à l'oxygène, par des liaisons résiduelles comme celles ci-dessous :

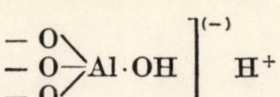

$$\left.\begin{matrix}-\mathrm{O}\\-\mathrm{O}\\-\mathrm{O}\end{matrix}\right\rangle \mathrm{Al\cdot OH}\ \Big]^{(-)}\ \mathrm{H}^+$$

---

[20] C. E. MARSHALL, "The Colloid Chemistry of the Silicates Minerals", Acad. Press, Londres, 1949.

[21] R. C. WEAST et S. M. GELBY, "Handbook of Chemistry" (47e édition), The Chemical Rubber Co., Cleveland (U.S.A.), 1966.

[22] V. LAMBRINO et GH. FURNICĂ, *Rev. Chim. București*, **19**, 464 (1968).

CONCLUSIONS

Les études radioécologiques actuelles doivent être précédées d'études physico-chimiques, les ions radioactifs dissous étant susceptibles de fournir un très grand nombre de combinaisons avec les suspensions des bassins de surface.

La mobilité des ions radioactifs dans le sol et dans les bassins de surface dépend du pH, de la teneur en argile échangeur d'ions et de la présence des chélateurs.[23]

---

[23] Roum. Pat. 53059.

Revue Roumaine de Chimie, **15**, 1097 – 1105 (1970)

INVESTIGATION IN THE CYCLOBUTANE SERIES. XXVII. [1]

ATTEMPTED SYNTHESIS OF 4.6-DIMETHYL-1-*tert.*-BUTYL-BENZOCYCLOBUTADIENE AND 4.6-DIMETHYL-1-CHLORO-BENZOCYCLOBUTADIENE

MARGARETA AVRAM, DOINA CONSTANTINESCU, I. G. DINULESCU, OANA CONSTANTINESCU-SIMON, GH. D. MATEESCU
and
C. D. NENITZESCU

Institute of Organic Chemistry of the Academy,
Bucharest, Romania

Received October 18, 1969

The synthesis of 4.6-dimethyl-1-*tert.*-butyl-benzocyclobutadiene (4) is attempted starting from 4.6-dimethyl-1-*tert.*-butyl-1-bromo-benzocyclobutene (10). The compound 4 is not stable, but its intermediate formation was proved by trapping with diphenylisobenzofuran. The synthesis of 3.4-dimethyl-1-chloro-benzocyclobutadiene (15) was also attempted. Neither is this compound stable but it can be trapped with diphenylisobenzofuran or can be obtained as a dimerisation product.

As part of our studies aiming at obtaining stable cyclobutadiene derivatives by the introduction of bulky substituents,[2,3] we reported in a previous paper the behaviour of 1-*tert.*-butyl- and 1.2-di-*tert.*-butyl-benzocyclobutadiene.[1]

In the present paper we report our attempt to synthesize 4.6-dimethyl-1-*tert.*-butyl-benzocyclobutadiene.

In order to build up the benzocyclobutene skeleton we started from trichloromethyl-mesitylene [4] which was converted to 4.6-dimethyl-1.1-dichloro-benzocyclobutene (**1**) and this in turn to 4.6-dimethyl-benzocyclobuten-1-one (**2**) according to Hart and coworkers.[5]

---

[1] Part. XXVI: M. Avram, D. Constantinescu, I. G. Dinulescu and C. D. Nenitzescu, *Tetrahedron Letters*, **1969**, 5215.

[2] M. Avram, I. G. Dinulescu, G. D. Mateescu, E. Avram and C. D. Nenitzescu, *Revue Roumaine de Chimie*, **14**, 1181 (1969).

[3] M. Avram, E. Avram, G. D. Mateescu, I. G. Dinulescu, F. Chiraleu and C. D. Nenitzescu, *Chem. Ber.*, **102**, 3996 (1969).

[4] H. Hart and R. W. Fish, *J. Amer. Chem. Soc.*, **83**, 4460 (1961).

[5] H. Hart, J. A. Hartlage, R. W. Fish and R. R. Rafos, *J. Org. Chem.*, **31**, 2244 (1966).

By condensing ketone **2** with *tert.*-butyl-magnesium chloride, 4.6-dimethyl-1-*tert.*-butyl-benzocyclobuten-1-ol (**3**) was obtained.

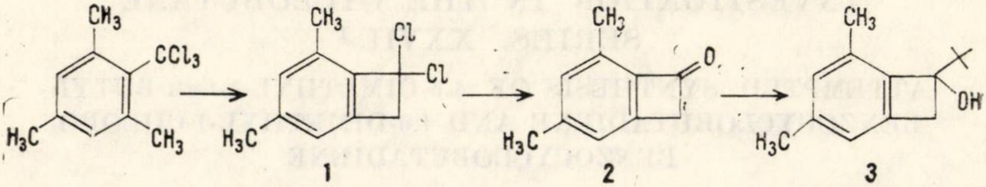

1 **2** **3**

The structure of the compound **3** is confirmed by the NMR spectrum which presents 5 signals in the ratio 2 : 6 : 9 : 1 : 2 at δ 6.60, 2.25, 1.08, 1.96 ppm, corresponding respectively to the two aromatic protons, the CH_3 groups, the *tert.*-butyl group and the proton of the hydroxy group; it has also a quartet in the region δ 2.5–3.5 ppm (J = 14.0 Hz) corresponding to the methylene group of the cyclobutene ring. In the infrared spectrum the nonassociated hydroxy group appears at 3613 cm^{-1}; the *tert.*-butyl and methyl groups present absorptions at 2871, 2925 and 2960 cm^{-1} as well as a doublet characteristic of the *tert.*-butyl group[6] at 1372–1390 cm^{-1}.

The dehydration of the tertiary alcohol **3** by heating in acetic acid, in presence of catalytic amounts of sulphuric acid yielded a liquid with b.p. 115°/2 mm, the elemental analysis of which indicated the molecular formula $C_{14}H_{18}$.

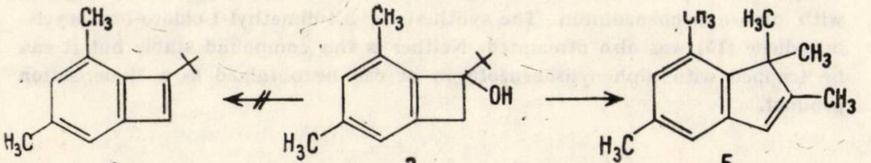

4 **3** **5**

For the latter product we took into consideration the structure of 4.6-dimethyl-1-*tert.*-butyl-benzocyclobutadiene (**4**) respectively its dimer, or the structure of products resulting by rearrangement of the cyclobutene ring.

The NMR spectrum presents the signals of the aromatic moiety at δ 6.48 and 6.65 ppm (2 H) and those of the methyl groups on the benzene ring at δ 2.20 and 2.33 ppm. It has also a signal at δ 1.16 ppm (6 H) corresponding to the saturated protons of geminal CH_3 groups, a doublet at δ 1.83 ppm (3 H) corresponding to a CH_3 group linked to the double bond of the five-membered ring, as well as a quartet with J = 1.0 Hz at δ 6.05 ppm, corresponding to the olefinic proton.

This spectrum excludes the structure of a benzocyclobutadiene **4** (or a dimer) and is in agreement with the structure of 1.1.2.5.7-pentamethyl-indene (**5**).

[6] M. Avram and G. D. Mateescu, *"Spectroscopia în infraroșu. Aplicații în chimia organică"*, Ed. Tehnică, Bucharest, 1966.

The formation of **5** from the alcohol **3** can easily be explained by a rearrangement of the neopentylic-type carbonium ion **6**. The rearrangement consists in the migration of a CH_3 group and the simultaneous enlargement of the cyclobutane ring. The carbonium ion **7** thus formed is stabilized by proton elimination leading to the indene **5**.

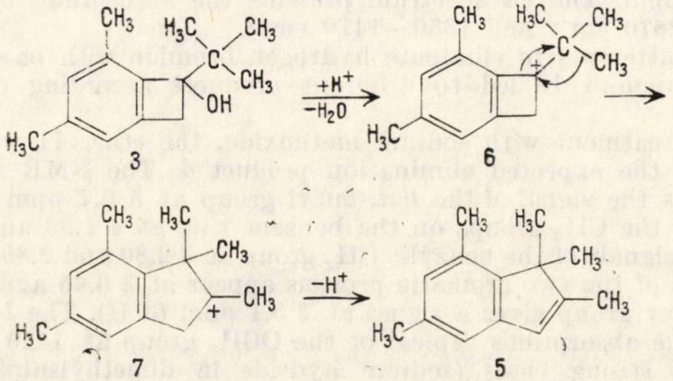

The indene structure was proved by oxidizing hydrocarbon **5** according to Lemieux.[7] A crystalline product was obtained with m.p. 175° and molecular formula $C_{14}H_{18}O_3$. The IR spectrum of the latter compound presents a broad band centered at 3335 cm^{-1}, characteristic of the associated OH group as well as a frequency corresponding to the CO group at 1683 cm^{-1}. These bands indicate the structure of the lactol **8**, a tautomer of the keto-acid **9** resulting by oxidation of a double bond from the indene ring.

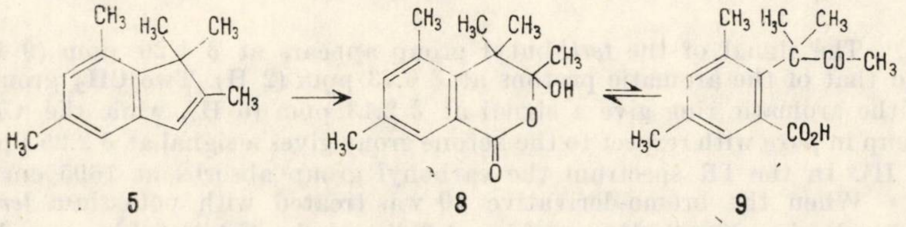

Benzocyclobutene ring opening during benzocyclobutenyl cation generation was previously observed in other cases with 1-phenyl-, methyl-[8] or *tert.*-butyl-derivatives[1].

Our observations suggested that the formation of a benzocyclobutadiene ring was unlikely in reactions involving cations of **6**-type. Therefore we converted the alcohol **3** to the bromo-compound **10** by treatment with phosphor tribromide.

---

[7] R. U. Lemieux and E. v. Rudloff, *Canad. J. Chem.*, **33**, 1701 (1955).

[8] L. Horner, P. V. Subramaniam and K. , *Liebigs Ann. Chem.*, **714**, 91 (1968).

The NMR spectrum of the bromo-derivative **10** presents a *tert.*-butyl-group signal at δ 1.1 ppm (9 H) and a quartet at δ 3.47 ppm (J = 14.5 Hz) corresponding to the benzylic methylene group of the cyclobutene ring. The CH_3 groups on the benzene ring present a signal at δ 2.23 ppm (6 H) while the aromatic protons give signals at δ 6.59 and 6.70 ppm. The IR spectrum presents the absorptions of *tert.*-butyl group at 2870 cm^{-1} and 1350–1470 cm^{-1}.

The attempts to eliminate hydrogen bromide with bases from the bromo-compound **10** led to different products according to the base utilized.

On treatment with sodium methoxide, the ether **11** was obtained instead of the expected elimination product **4**. The NMR spectrum of **11** presents the signal of the *tert.*-butyl group at δ 0.7 ppm (9 H), two signals for the CH_3 groups on the benzene ring at δ 1.96 and 2.00 ppm (6 H), the signals of the benzylic CH_2 group at δ 2.80 and 2.86 ppm, while the signals of the two aromatic protons appear at δ 6.45 and 6.50 ppm; the methoxy group gives a signal at δ 3.1 ppm (3 H). The IR-spectrum presents the absorptions typical of the OCH_3 group at 1140 cm^{-1}.

With strong bases (sodium hydride in dimethylsulphoxide) the cyclobutene ring opened and pivaloyl-mesitylene (**12**) was obtained. The structure of this ketone was proved using its NMR spectrum.

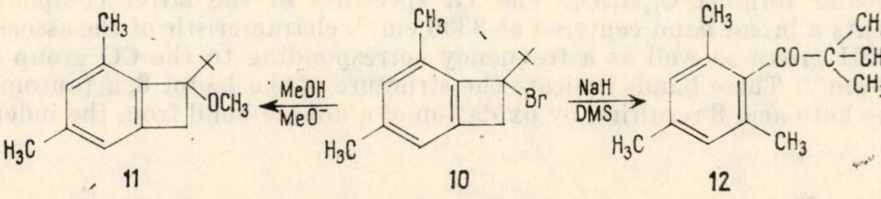

The signal of the *tert.*-butyl group appears at δ 1.20 ppm (9 H) and that of the aromatic protons at δ 6.73 ppm (2 H). Two CH_3 groups of the aromatic ring give a signal at δ 2.13 ppm (6 H), while the CH_3 group in *para* with respect to the ketone group gives a signal at δ 2.25 ppm (3 H). In the IR spectrum the carbonyl group absorbs at 1695 cm^{-1}.

When the bromo-derivative **10** was treated with potassium *tert.*-butoxide in dimethylformamide, 4.6-dimethyl-1-*tert.*-butyl-benzocyclobutadiene (**4**) was probably formed. The latter was evidenced by trapping *in situ* with 2.5-diphenylisobenzofuran.

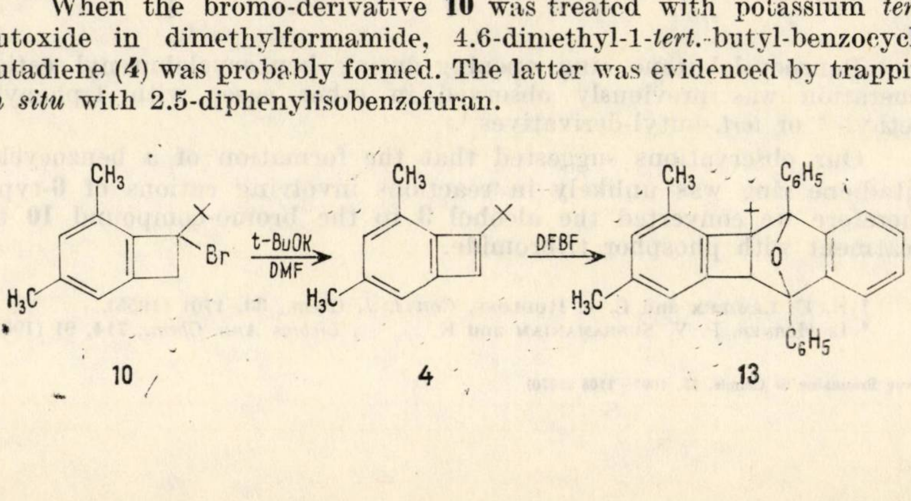

The adduct **13**, with m.p. 261–263°, presents in its NMR spectrum the signal of the *tert.*-butyl group (9 H) at δ 0.78 ppm, a multiplet in the region of the aromatic protons at δ 7.0–8.0 ppm (14 H) and two distinct signals for the two aromatic protons on the substituted benzene ring, at δ 6.11–6.59 ppm. The two methyl groups give signals at δ 1.35 and 2.13 ppm (6 H) while the bridgehead saturated proton appears at δ 3.88 ppm.

On treatment with magnesium the bromo-derivative **10** underwent a Wurtz-type reaction.

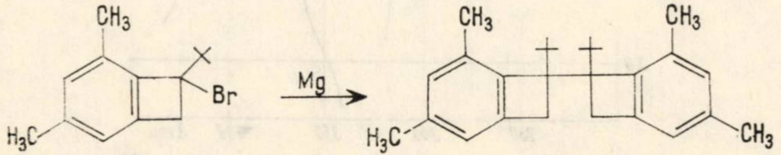

10 14

The condensation product **14** thus obtained, with m.p. 220°, has in its NMR spectrum the signal of the *tert.*-butyl group at δ 0.81 ppm (18 H), that of the CH_3 groups on the aromatic ring at δ 2.30 ppm (12 H) and those of the four aromatic protons at δ 6.60 and 6.55 ppm. A quartet between δ 2.89–3.85 ppm, due to the benzylic protons of the cyclobutene ring form an AB system, with $J_{AB} = 16$ Hz, a value typical of geminal protons of benzocyclobutene systems.

We present now some reactions of 4.6-dimethyl-1.1-dichloro-benzocyclobutene (**1**). In the attempted hydrogen chloride elimination this compound showed a behaviour similar to that of the 1.2-dibromo-benzocyclobutene prepared by Cava and coworkers.[9] By treating **1** with potassium *tert.*-butoxide in dimethylformamide a yellow crystalline compound was obtained, with m.p. 135°, the elemental analysis of which corresponds to the composition $C_{20}H_{17}Cl$.

We admit that 4.6-dimethyl-1-chloro-benzocyclobutadiene (**15**) is first formed and it then gives a Cava-type dimer **16** or **16a**. Under the action of potassium *tert.*-butoxide the latter eliminates a mole of hydrogen chloride, yielding the aromatic product **17** or **17a**.

The tetramethyl-chloro-benzo[a]biphenylene structure of **17** results also from the comparison of the UV spectrum of this compound with the UV spectrum of benzo[a]biphenylene[10].

---

[9] M. P. Cava and J. F. Stucker, *J. Amer. Chem. Soc.*, **79**, 1706 (1957).

[10] M. P. Cava and M. J. Mitchell, *"Cyclobutadiene and Related Compounds"* Academic Press, New York, 1967, p. 338; M. P. Cava and J. F. Stucker, *J. Amer. Chem. Soc.*, **77**, 6022 (1955).

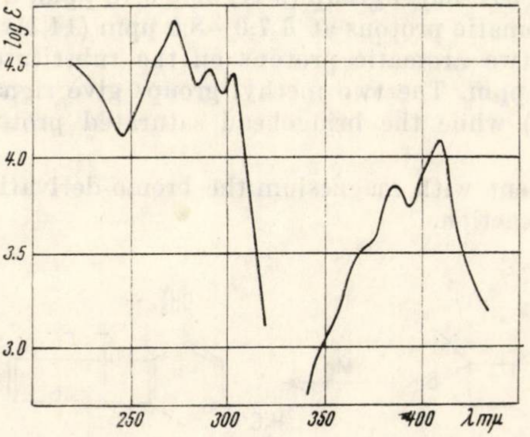

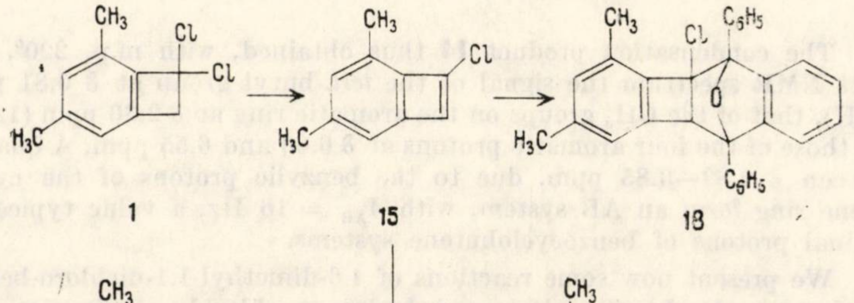
1
15
18
16
or
18 a
17
or
17 a

Fig. 1. — UV spectrum of the compound 17

When dimethyl-chloro-benzocyclobutadiene **15** was generated by treating the dichloro-derivative **1** with potassium *tert.*-butoxide in dimethylformamide, in presence of 2.5-diphenyl-3.4-benzofuran, the adduct **18**, a crystalline white product with m.p. 170°, was obtained. The NMR spectrum of the adduct **18** presents the signals of the CH_3 groups at δ 1.35 ppm (3 H) and 2.18 ppm (3 H). The signal at δ 4.0 ppm (1 H) corresponds to the bridgehead proton, a little more unshielded than in the adduct **18**, while the signals at δ 6.28 ppm (1 H) and 6.61 ppm (1 H) correspond to the aromatic protons of the benzene ring. The complex signal between δ 7.05 – 8.00 ppm (14 H) includes the other aromatic protons of the unsubstituted benzene rings.

It should be noted that when the intermediate **16** respectively **16a**, eliminates hydrogen chloride under the action of potassium *tert.*-butoxide in excess, leading to the aromatic compound **17**, the adduct **18** which results finally is stable under the reaction conditions. This stability is due to the impossibility of aromatizing the system as well as to a steric effect of the *endoxo* group.

It seems therefore that although the dimethyl-benzocyclobutadienes **4** and **15** probably formed under the conditions investigated, neither of them is stable enough to be isolated as a substance. However they can be evidenced by trapping with a reactive diene such as 2.5-diphenyl-3.4-benzofuran.

EXPERIMENTAL

The elemental analyses were performed by Miss Elvira Sliam and Mrs Violeta Daniel. IR spectra were run on a Jena UR20 spectrophotometer. NMR spectra were determined with a Varian A-60A spectrometer. UV spectra were recorded using a Jena VSU-1 spectrophotometer.

4.6-Dimethyl-1.1-dichloro-benzocyclobutene (1)

Trichloromethyl-mesitylene[4] (35.63 g, 0.15 moles) was heated for 2 hrs at 140°/80 – 100 mm; hydrogen chloride was evolved. When the evolution of hydrogen chloride subsided and the liquid became brown, the dichloro-derivative was distilled at 170°/90 mm; 27.1 g (90 %) **1** was obtained; m.p. 56°.

$C_{10}H_{10}Cl_2$ (201.1) *Calcd.*: C, 59.75; H, 5.01; Cl, 35.25;
Found: C, 59.46; H, 5.24; Cl, 35.31.

4.6-Dimethyl-benzocyclobuten-1-one (2)

The ketone **2**, m.p. 46°, was prepared according to Hart.[5] NMR spectrum (CCl_4): δ 2.26, 2.31 (6 H), 3.68 (2 H) and 6.8 and 6.96 ppm (2 H). IR spectrum (CCl_4): $\nu_{CO} = 1782$ cm.$^{-1}$

4.6-Dimethyl-1-tert.-butyl-benzocyclobuten-1-ol (3)

A solution of 13 g (0.089 moles) **2** in 100 ml anhydrous ether was added dropwise into a solution of *tert.*-butyl-magnesium chloride prepared from 7.4 g (0.31 moles) magnesium, 28.6 g (0.31 moles) *tert.*-butyl chloride and 200 ml anhydrous ether. After 1 hr at reflux, the reaction mixture was treated with water and with 50% acetic acid. The ethereal layer was washed with water and with 2% sodium hydroxide. After evaporation of solvent and distillation of the residue 14.3 g (79%) **3** were obtained : b.p. 125°/2 mm.

$C_{14}H_{20}O$ (204.2) *Calcd.* : C, 82.34 ; H, 9.87 ;
Found : C, 81.98 ; H, 9.82.

1.1.2.5.7-Pentamethyl-indene (**5**)

A solution of 1.0 g (5 mmoles) **3** in 10 ml acetic acid, to which a drop of sulphuric acid was added, was refluxed for 5 hrs. After dilution with water, the product was extracted with ether and the ethereal layer was washed with water and then with diluted sodium carbonate. Evaporation of solvent and distillation of the residue yielded 0.45 g (48%) **5**, b.p. 115°/2 mm.

$C_{14}H_{18}$ (186.2) *Calcd.* : C, 90.25 ; H, 9.76 ;
Found : C, 89.70 ; H, 9.75.

3.4.4.5.7-Pentamethyl-3-hydroxy-2-oxa-1-tetralone (**8**)

A mixture of 1.0 g (5.3 mmoles) **5**, 3.45 g (19 mmoles) sodium metaperiodate, 0.20 g (1.31 mmoles) potassium permanganate, 1.3 g (10.2 mmoles) potassium carbonate and 500 ml water was stirred at room temperature for 72 hrs. The filtered solution was concentrated, then acidified with 10% sulphuric acid and extracted with ether. After evaporation of solvent 0.6 g (43%) **8** was obtained; m.p. 175° (methanol).

$C_{14}H_{18}O_3$ (234.3) *Calcd.* : C, 71.71 ; H, 7.74 ;
Found : C, 71.63 ; H, 7.89.

IR spectrum (KBr) : $\nu_{CO} = 1683\ cm^{-1}$.

1-Bromo-4.6-dimethyl-1-tert.-butyl-benzocyclobutene (**10**)

A solution of 10.7 g (53 mmoles) **3** in 50 ml methylene chloride was added dropwise into a stirred solution of 9.5 g (35 mmoles ; 3 ml) phosphor tribromide. After 48 hrs at room temperature, the mixture was poured into water and the organic layer was washed with water and then with 5% sodium bicarbonate. Evaporation of solvent and distillation of the residue yielded 10 g (71%) **10**, b.p. 135°/2 mm.

$C_{15}H_{19}Br$ (267.2) *Calcd.* : C, 62.93 ; H, 7.16 ; Br, 29.91 ;
Found : C, 63.49 ; H, 7.19 ; Br, 29.14.

1-Methoxy-4.6-dimethyl-1-tert.-butyl-benzocyclobutene (**11**)

Into a solution of sodium methoxide (prepared from 1.0 g sodium and 25 ml methanol) 2.0 g (7.5 mmoles) **10** were added and the mixture was refluxed for 2 hrs. Water was added and the product was extracted with ether. After evaporation of solvent and distillation, 1.0 g (62%) ether **11** was obtained, b.p. 95°/4 mm.

$C_{15}H_{22}O$ (218.3) *Calcd.* : C, 82.50 ; H, 10.40 ;
Found : C, 82.10 ; H, 10.57.

Pivaloyl-mesitylene (**12**)

To 20 ml anhydrous dimethylsulphoxide 2.5 g (40%) sodium hydride were added in portions, and the mixture was left at room temperature until the hydrogen evolution subsided. Bromo-derivative **10** (2.0 g, 7.5 mmoles) was added, the mixture was shaken for 30 min. and then left for 12 hrs. The yellow mixture was then poured in water and extracted with ether. After washing with water, the ether was evaporated and the residue distilled yielding **12**, b.p. 115° /1 mm.

$C_{14}H_{20}O$ (204.3) *Calcd.* : C, 82.30 ; H, 9.87 ;
Found : C, 81.54 ; H, 9.90.

The adduct of 4.6-dimethyl-1-tert.-butyl-benzocyclobutadiene with 2.5-diphenyl-3.4-benzofuran (**13**)

Into a mixture of 1.13 g (10 mmoles) potassium *tert.*-butoxide, 1.3 g (5 mmoles) diphenyl-benzofuran and 20 ml dimethylformamide, 1.35 g (5 mmoles) **10** was added ; the mixture was then shaken until the exothermic reaction subsided. After 10 hrs it was diluted with water and extracted with ether. The ether was evaporated and the residue was treated with maleic anhydride in benzene, in order to remove unreacted diphenylbenzofuran. After working up and chromatography on alumina with ether, 0.6 g (27 %) 2′.4′-dimethyl-1.6-diphenyl-2-*tert.*-butyl-9-oxa-3.4.7.8-dibenzotricyclo [4.2.1.$0^{2.5}$] nona-3.7-diene (**13**) was obtained ; m.p. 261−263°.

$C_{34}H_{32}O$ (456.6) *Calcd.* : C, 89.43 ; H, 7.06 ;
Found : C, 88.97 ; H, 7.69.

1.1′-Bis[4.4′.6.6′-tetramethyl-1.1′-di-tert.-butyl-benzocyclobutenil] (**14**)

A solution of 2.7 g (10 mmoles) **10** in 30 ml ether was boiled with 0.12 g (5 mmoles) magnesium for 1 hr. After working up, 0.64 g (34 %) **14** was obtained ; m.p. 220° (methanol).

$C_{28}H_{38}$ (374.6) *Calcd.* : C, 89.77 ; H, 10.22 ;
Found : C, 89.18 ; H, 10.34.

2.4.7.9-Tetramethyl-5-chloro-benzo [a] biphenylene (**17**)

A solution of 2.0 g (10 mmoles) **1** in 8 ml dimethylformamide was added to a mixture of 2.3 g (20 mmoles) potassium *tert.*-butoxide in 10 ml dimethylformamide, and the resulting mixture shaken for 30 min. After 1 hr at room temperature, it was diluted with water and extracted with benzene. After solvent evaporation and recrystallization of residue from methanol 0.36 g (17 %) **17** was obtained ; m.p. 134°

$C_{20}H_{17}Cl$ (292.8) *Calcd.* : C, 82.03 ; H, 5.85 ; Cl, 12.11 ;
Found : C, 81.73 ; H, 6.02 ; Cl, 12.39.

NMR spectrum (CCl_4) : δ 2.06 (3 H), 2.22 and 2.30 (6 H), 2.85 (3 H), 6.10 (1 H), 6.15 (1 H), 6.79 (1 H). 6.84 (1 H) and 7.06 ppm (1H).

UV spectrum (cyclohexane) : λ_{max} (log ε) : 274 (4.714), 292 (4.459) 304 (4.450), 386 (3.855), 410 mμ (4.091).

The adduct of 4.6-dimethyl-1-chloro-benzocyclobutadiene with 2.5-diphenyl-3.4-benzofuran (**18**)

Into a mixture of 2.2 g (20 mmoles) potassium *tert.*-butoxide, 2.7 g (10 mmoles) diphenylbenzofuran and 40 ml dimethylformamide, a solution of 2.0 g (10 mmoles) **1** in 8 ml dimethylformamide was added, and the resulting mixture shaken until the exothermic reaction subsided. After 24 hrs the mixture was diluted with water and extracted with ether. The ether was evaporated and the excess of diphenylbenzofuran removed by treatment with maleic anhydride in benzene. After working up, an oily residue (2 g) was obtained, which was chromatographied on alumina with ether, yielding 1.8 g (62 %) 2′.4′-dimethyl-1.6-diphenyl-2-chloro-9--oxa-3.4.7.8-dibenzotricyclo [4.2.1.$0^{2.5}$] nona-3.7-diene (**18**), m.p. 170° (methanol).

$C_{30}H_{23}ClO$ (434.9) *Calcd.* : C, 82.82 ; H, 5.33 ; Cl, 8.15 ;
Found : C, 82.62 ; H, 5.50 ; Cl, 8.03.

with ether. After washing with water, the ether was evaporated and the residue distilled via [illegible] (2, b.p. 75°/1 mm.

$C_{15}H_{24}$ (204.3) Calcd.: C, 88.[illegible]; H, [illegible];
Found: C, 88.[illegible]; H, [illegible]

The adduct of 1,6-dimethyl-4-tert-butyl-benzocyclooctatriene with 2,5-diphenyl-3,4-benzofurane (13)

Into a mixture of 1.12 g (10 mmoles) potassium tert-butoxide, 1.4 g (5 mmoles) diphenylbenzofurane and 20 ml dimethylformamide 1.[illegible] g ([illegible] mmoles) [illegible] was added; the mixture was then shaken until the exothermic reaction subsided. After [illegible] hrs it was diluted with water and extracted with ether. The ether was evaporated and the residue was treated with maleic anhydride in benzene in order to remove unreacted diphenylbenzofurane. After working up and chromatography on alumina with ether, 0.8 g ([illegible]%) 2,4-dimethyl-1,6-diphenyl-[illegible]-tert-butyl-[illegible]-tricyclo[4.2.1.0^{2,5}]nona-3,7-diene (13) was obtained, m.p. 201–202°.

$C_{34}H_{32}O$ (456.6) Calcd.: C, 89.42; H, 7.06;
Found: C, 89.97; H, 7.08.

1,1'-Bis[4,6,6'-tetramethyl-1,1'-di-tert-butyl-benzocyclobutene] (14)

A solution of 2.2 g (10 mmoles) 12 in 30 ml ether was boiled with 0.12 g (5 mmoles) magnesium for 1 hr. After working up, 0.64 g (34%) 14 was obtained; m.p. 250° (methanol).

$C_{28}H_{38}$ (374.6) Calcd.: C, 89.77; H, 10.23;
Found: C, 89.18; H, 10.84.

2,4,5,9-[illegible]-5-chloro-benzo[a][illegible] (17)

A solution of 2.0 g (10 mmoles) 1 in 8 ml dimethylformamide was added to a mixture of 2.2 g (20 mmoles) potassium tert-butoxide in 40 ml dimethylformamide, and the resulting mixture shaken for 30 min. After 1 hr at room temperature, it was diluted with water and extracted with benzene. After solvent evaporation and recrystallization of residue from methanol 0.86 g ([illegible]%) 17 was obtained, m.p. 138°.

$C_{20}H_{17}Cl$ (292.8) Calcd.: C, 82.05; H, 5.86; Cl, 12.11;
Found: C, 81.75; H, 6.02; Cl, 12.36.

NMR spectrum (CCl_4): δ 2.08 (3 H), 2.22 and 2.30 ([illegible]), 2.80 ([illegible]), 6.10 (1 H), 6.15 (1 H), 6.79 (1 H), 6.84 (1 H) and 7.06 ppm (1 H).

UV spectrum (cyclohexane): λ_{max} (log ε) 234 (4.71), 262 (4.45), 304 (4.15), 338 (3.65), 412 mμ ([illegible]).

The adduct of 2,4-dimethyl-7-chloro-benzocyclooctatriene with 2,5-diphenyl-3,4-benzofurane (18)

Into a mixture of 2.2 g (20 mmoles) potassium tert-butoxide, 2.7 g (10 mmoles) diphenylbenzofurane and 40 ml dimethylformamide, a solution of 2.0 g (10 mmoles) 1 in 8 ml dimethylformamide was added, and the resulting mixture shaken until the exothermic reaction subsided. After 24 hrs the mixture was diluted with water and extracted with ether. The ether was evaporated and the excess of diphenylbenzofurane removed by treatment with maleic anhydride in benzene. After working up, an oily residue ([illegible] g) was obtained, which was chromatographed on alumina with ether, yielding 1.8 g (37%) 2,4-dimethyl-1,6-diphenyl-3-chloro-[illegible]-tetracyclo[4.2.1.0^{2,5}]nona-3,7-diene (18), m.p. 170° (methanol).

$C_{30}H_{23}ClO$ (434.9) Calcd.: C, 82.84; H, 5.33; Cl, 8.15;
Found: C, 82.62; H, 5.50; Cl, 8.08.

Revue Roumaine de Chimie, **15**, 1107–1119 (1970)

UNTERSUCHUNGEN ÜBER ARYLDIAZOSULFONATE UND ARYLDIAZOSULFONSÄUREN. I

ÜBER DAS PHOTOCHEMISCHE VERHALTEN DES BENZOLDIAZOSULFONSAUREN NATRIUMS

J. REICHEL und R. VIDAC

vom Laboratorium für Farbstoffe und Zwischenprodukte der Technischen Hochschule, Timişoara, Bd 30 Decembrie, 2 und vom Laboratorium für Angewandte Chemie der Universität, Timişoara, str. Pestalozzi 16

Eingegangen am 31. März 1969

Die spektroskopische Untersuchung im ultravioletten und sichtbaren Bereich des stabilen benzoldiazosulfonsauren Natriums in wäßriger Lösung, führte zur Schlußfolgerung, daß die feststellbare primäre Umwandlung in der Zersetzung in Diazonium- und Sulfitione besteht, begleitet von einer Photolyse der Diazoniumione zu Phenol. Nach einer länger anhaltenden Bestrahlung stellte dieses sogar das Hauptprodukt dar. Als Nebenprodukt erhält man *p*-Hydroxyazobenzol.

Die Bildung der Diazosulfonate wurde zum erstenmal von Schmidt und Lutz,[1] im Jahre 1869, beschrieben.

Wie bekannt, können die Natrium- oder Kaliumsalze der Aryldiazosulfonsäuren (ArN_2SO_3H) durch die Reaktion der Diazoniumsalze mit Natriumsulfit, in neutralem oder schwach basischem Medium, erhalten werden.[2]

Die Diazosulfonate können in zwei isomeren, einer labilen und einer stabilen Form, existieren.[3–6] Die labilen Diazosulfonate weisen noch einige der Eigenschaften der Komponenten aus denen sie präpariert wurden, also die des Diazoniumkations und die des Sulfitanions, auf: sie kuppeln mit basischen Naphthollösungen, um Azofarbstoffe zu bilden; reagieren mit Jod; durch Umsetzung mit Mineralsäuren setzen sie SO_2 frei. Dieses Verhalten wird auf die Existenz eines Gleichgewichtes zwischen den labilen Diazosulfonaten und den Diazonium- und Sulfitionen zurück-geführt. Die labilen Diazosulfonate gehen spontan in die stabile Form über, wobei die Isomerisierungsgeschwindigkeit mit dem Ansteigen der Temperatur zunimmt.[6–8] Die Resultate der kinetischen Messungen entsprechen aber keineswegs einer Kinetik erster Ordnung.

---

[1] R. Schmidt und L. Lutz, *Ber. dtsch. chem. Ges.*, **2**, 51 (1869).

[2] W. L. Hall und H. D. Gibbs, *J. Washington Acad. Sci.*, **17**, 433 (1927); *Chem. Zentr.*, **1928**, I, 34.

[3] A. Hantzsch, *Ber. dtsch. chem. Ges.*, **27**, 1702, 1715, 1726 (1894).

[4] E. Bamberger, *Ber. dtsch. chem. Ges.*, **27**, 2586, 2930 (1894).

[5] H. H. Hodgson und E. Marsden, *J. Chem. Soc.*, **1943**, 470.

[6] H. C. Freeman und R. J. W. Le Fèvre, *J. Chem. Soc.*, **1951**, 415.

Die stabilen Diazosulfonate zeigen nicht die charakteristischen Eigenschaften der Diazoniumsalze, so zum Beispiel, kuppeln sie nicht mit den Naphtholen in alkalischer Lösung und reagieren nicht mit Sulfit, eine Tatsache die beweist, daß diese nicht im Gleichgewicht mit den Diazoniumionen stehen. Die stabilen Diazosulfonate können unzersetzt jahrelang aufbewahrt werden, somit stellen sie eine Stabilisierungsform der Diazoderivate dar.

Mit Chlor[9] oder Brom[10] in saurer Lösung, oder mit Kaliumbromat in Salzsäure,[11–12] gehen sie in Diazoniumsalze über. Einige substituierte Diazosulfonate kuppeln mit Naphtholen, beim Erwärmen in alkalischer Lösung. In Gegenwart einer Kupplungskomponente dem Licht ausgesetzt, bilden sie Azofarbstoffe.[13] Diese Eigenschaften der Diazosulfonate ermöglichen ihre Anwendung in der Färberei, im Textildruck, in der Diazotypie und in der Farbphotographie.

Wegen ihrer technischen Bedeutung waren die Diazosulfonate Gegenstand vieler Untersuchungen. Für die stabilen Diazosulfonate wurde im allgemeinen eine *trans*-azo-Struktur angenommen, traditionell „anti"[3] genannt.

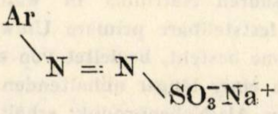

$$\overset{Ar}{\diagdown}N = N\underset{SO_3^- Na^+}{\diagdown}$$

Bezüglich der Struktur der labilen Diazosulfonate hat es viele Divergenzen gegeben. Bamberger[4] und später Hodgson und Marsden[5] verteidigten eine Diazosulfitstruktur, oder eine Diazosulfitstruktur im Gleichgewicht mit Diazoniumsulfit,

$$Ar - N = N - OSO_2^- \, Na^+ \rightleftarrows Ar - \overset{+}{N} \equiv N \, [SO_3^{2-}] \, Na^+$$

während Hantzsch,[3] und nachher Freeman und Le Fèvre[6] eine *cis*-azo-Struktur bevorzugten, „syn" genannt.

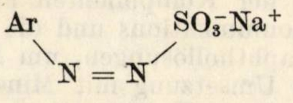

$$\overset{Ar}{\diagdown}N = N\overset{SO_3^- Na^+}{\diagup}$$

[7] A. Hantzsch und M. Schmiedel, *Ber. dtsch. chem. Ges.*, **30**, 71 (1897).

[8] E. S. Lewis und H. Suhr, *Chem. Ber.*, **92**, 3031 (1959).

[9] M. P. Schmidt, *J. prakt. Chem.*, (2), **85**, 239 (1912).

[10] E. Fischer, *Liebigs Ann. Chem.*, **199**, 304 (1897).

[11] I. C. I., DRP. 587509 (1931); *Friedländer*, **20**, 1241.

[12] M. Mendoza und A. G. Murray, I.C.I., E.P. 414681 (1933); *Chem. Zentr.*, **1935**, I, 1127.

[13] R. Pütter, „Methoden der organischen Chemie", Bd. X/3, IV. Auflage, Georg Thieme Verlag, Stuttgart, 1965, S. 577.

Gegenwärtig wiegt die Meinung vor, daß die Isomerie der Diazosulfonate höchstwahrscheinlich eine Isomerie der Konfiguration darstellt und nicht der Struktur.[14,15]

DER EINFLUSS DES LICHTES AUF DIAZOSULFONATE

Die primäre photochemische Umwandlung, welche durch Lichteinwirkung auf die stabilen Diazosulfonate eintritt, wodurch diese die Eigenschaft erringen die Kupplung mit Naphtholen und anderen Komponenten einzugehen, um Azofarbstoffe zu bilden, wird noch nicht ganz verstanden; es ist noch nicht entschieden, ob das stabile Diazosulfonat (anti) in die labile Form (syn) isomerisiert, oder ob ein unmittelbarer Übergang in Diazoniumione stattfindet.[13]

Feer [16] stellte vor etwa 80 Jahren fest, daß durch die Aussetzung der Diazosulfonate ans Licht, diese fähig werden mit Phenolen zu kuppeln. Es ist bemerkenswert, daß damals die Ansichten von Hantzsch über die Isomerie von Diazoverbindungen noch Zukunftsmusik darstellten.

Später nehmen Desai, Mehta und Thosar [17] an, daß die Aussetzung der stabilen Diazosulfonate ans Licht, deren Umwandlung in kupplungsfähige Isomere (*syn*), bestimmt. Die Forschungen dieser Autoren fußten auf jodometrischen Titrationen, auf Abwägungen des gebildeten Farbstoffes durch Kupplung mit β-Naphthol, sowie auf die periodische Feststellung des pH-Wertes. Die mit diesen Methoden erhaltenen Resultate stehen allerdings nicht im Gegensatz mit der Möglichkeit einer unmittelbaren Zersetzung der stabilen Diazosulfonate in Diazonium- und Sulfitionen. Auch Freemans und Le Fèvres [6] Resultate, welche nach der chemischen Methode erhalten wurden, sind nicht im Gegensatz zu dieser Möglichkeit.

De Jonge und Dijkstra [18] sehen es als ungerechtfertigt an, daß aus den von Freeman und Le Fèvre [6] im ultravioletten und sichtbaren Bereich unternommenen Untersuchungen, für das *anti-o*-chlorbenzoldiazosulfonsaure Natrium, Schlußfolgerungen zugunsten der Bildung anderer Produkte als für die der Diazonium- und Sulfitionen gezogen werden, weil die *o*-Chlorbenzoldiazoniumsalze, Absorptionsmaxima bei ungefähr den gleichen Wellenlängen wie das bestrahlte Produkt aufweisen. Noch viel weniger können die Schlußfolgerungen von Freeman und Le Fèvre durch Analogie auch auf andere Diazosulfonate ausgedehnt werden. Auf Grund dieser spektroskopischen Untersuchungen haben Freeman und Le Fèvre [6] folgendes Reaktionsschema vorgeschlagen:

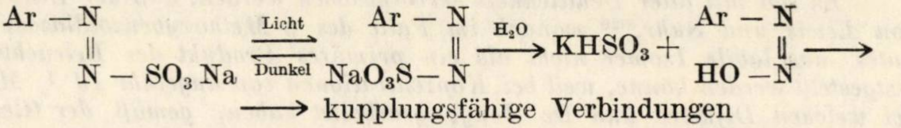

$$\begin{matrix}\mathrm{Ar-N}\\ \|\\ \mathrm{N-SO_3Na}\end{matrix} \underset{\text{Dunkel}}{\overset{\text{Licht}}{\rightleftharpoons}} \begin{matrix}\mathrm{Ar-N}\\ \|\\ \mathrm{NaO_3S-N}\end{matrix} \xrightarrow{\mathrm{H_2O}} \mathrm{KHSO_3} + \begin{matrix}\mathrm{Ar-N}\\ \|\\ \mathrm{HO-N}\end{matrix} \longrightarrow$$

$$\longrightarrow \text{kupplungsfähige Verbindungen}$$

[14] Anm. 13, S. 570.

[15] H. ZOLLINGER, ,,Azo and Diazo Chemistry Aliphatic and Aromatic Compounds'', Interscience Publishers, New York, London, 1961, S. 151.

[16] FEER, DRP 53455, 1889; *Friedländer*, **2**, 558; H. C. FREEMAN und R. J. W. LE FÈVRE, *J. Chem. Soc.*, **1951**, 415.

[17] R. L. DESAI, T. N. MEHTA und V. B. THOSAR, *J. Soc. Dyers and Colourists*, **54**, 371 (1938).

[18] J. DE JONGE und R. DIJKSTRA, *Rec. Trav. chim.*, **75**, 290 (1956).

Durch das Messen der pH-Veränderungen in den Diazosulfonatlösungen während der ultravioletten Beleuchtung und nach Unterbrechung derselben, stellten De Jonge und Dijkstra[18] eine plötzliche Steigerung des pH-Wertes bis zu einem Maximum fest, gefolgt von einem langsamen Absinken, welches sich nach der Unterbrechung der Beleuchtung beschleunigte und weiterging bis unter den anfänglichen Wert. Die plötzliche Steigerung und das langsame Absinken des pH-Wertes wurde von den Autoren folgendem Prozeß zugeschrieben:

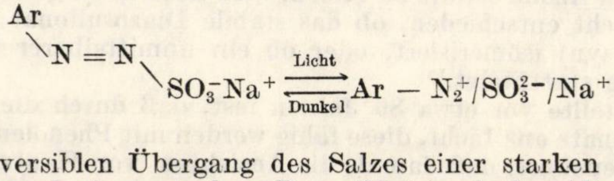

$$\mathrm{Ar{-}N{=}N{-}SO_3^-Na^+} \underset{\text{Dunkel}}{\overset{\text{Licht}}{\rightleftharpoons}} \mathrm{Ar-N_2^+/SO_3^{2-}/Na^+}$$

also dem reversiblen Übergang des Salzes einer starken Säure (Diazosulfonsäure) und einer starken Base (Natriumhydroxid), in ein Salz einer schwachen Säure (schwefelige Säure) und starken Basen (Natriumhydroxid und Diazoniumhydroxid), während das langsame Absinken des pH-Wertes unter den Anfangswert damit begründet wurde, daß während der Beleuchtung, „ein kleiner Teil" der Diazoniumionen, unter der Einwirkung des Lichtes zersetzt wird, um Phenol, Stickstoff und Wasserstoffione zu bilden:

$$\mathrm{ArN_2^+ + H_2O \xrightarrow{Licht} ArOH + N_2 + H^+}$$

Dieselben Autoren[19] stellten auf Grund kinetischer Messungen fest, daß die Aussetzung des *p*-Methoxybenzoldiazosulfonates dem ultravioletten Licht, dessen direkte Zersetzung in Diazonium- und Sulfitionen hervorruft, welche im Dunkeln das stabile Diazosulfonat zurückbilden, ohne daß inzwischen das labile Isomer auftritt. Auch bei der Herstellung des *p*-Methoxybenzoldiazosulfonates wurde das Auftreten eines instabilen Diazosulfonates oder eines anderen Zwischenproduktes oder zeitweiligen Biproduktes, ausgeschlossen, weil das Verschwinden der Kupplungseigenschaft, kolorimetrisch gemessen, streng nach einer Kinetik zweiter Ordnung in bezug auf die Diazoniumion- und Sulfitionkonzentration verlief.

Es soll mit aller Deutlichkeit hervorgehoben werden, daß der Einwand von Lewis und Suhr,[8,20] *wonach im Falle des* p-*Methoxybenzoldiazosulfonates das labile Isomer nicht als ein primäres Produkt der Beleuchtung festgestellt werden könne, weil bei Konzentrationen von ungefähr* 10^{-3} *Mol/l bei welchen Dijkstra und De Jonge gearbeitet haben, gemäß der Gleichgewichtskonstante:*

$$\mathrm{K.10^{-4}} = \frac{[syn\text{-}p\text{-}\mathrm{CH_3O\cdot C_6H_4\cdot N_2\cdot SO_3^-}]}{[p\text{-}\mathrm{CH_3O\cdot C_6H_4\cdot N_2^+}]\cdot[\mathrm{SO_3^{2-}}]} = 0{,}013$$

---

[19] R. Dijkstra und J. De Jonge, *Rec. Trav. chim.*, **77**, 538 (1958).

[20] Anm. 15, S. 62.

bestimmt von den ersten Autoren, nur 10^{-3}%, als ein syn-*Diazosulfonat im Gleichgewicht mit 99,99% Diazoniumionen, anwesend sein könnten, auf einem Rechenfehler beruht. Aus dem gleichen Gleichgewichtskonstantenwert folgt, gemäß unserer Berechnung, daß bei Konzentrationen von 10^{-3} Mol/l, bei denen Dijkstra und De Jonge arbeiteten, 10%, also um 10^4 mehr,* syn-*Diazosulfonat — angenommen, daß es sich bilden würde — im Gleichgewicht mit 99% Diazoniumionen stehen.*

Die labilen Diazosulfonate sind im allgemeinen dunkler gefärbt, als die stabilen Diazosulfonate. Freeman und Le Fèvre [6] stellten fest, daß für *o*-Chlorbenzoldiazosulfonat das Spektrum des *anti*-Isomeren ein Absorptionsmaximum im sichtbaren Bereich bei 428 mμ hat, während das des *syn*-Isomeren bei 448 mμ ein Maximum aufweist.

Van der Veen, Helfferich und Van Beek [21] — auf Grund einer Bemerkung von Freeman und Le Fèvre, nach welcher einige *cis*-Diazosulfonate, durch Bestrahlung der *trans*-Isomere erhalten, sehr stabil sind, wenn die Diazosulfonate vorher auf Filterpapier imprägniert werden — studierten spektroskopisch im sichtbaren Bereich, den Einfluß der Lichtaussetzung bei 405 und 425 mμ, auf das stabile *o*-Chlorbenzoldiazosulfonat, absorbiert auf einen durchsichtigen Film von Zellulose-Triazetat. Sie interpretierten das Ansteigen der Extinktion im Gebiete größerer Wellenlängen als die des isosbestischen Punktes bei 425 mμ, sowie ihren Rückgang im Dunkeln zum anfänglichen Niveau, als einen experimentellen Beweis für die Bildung des *syn*-Isomeren. Ein ähnliches Verhalten bewiesen auch die *p*- und *o*-Methoxybenzoldiazosulfonate, für welche dieselben Schlüsse gezogen wurden.

DIE SPEKTROSKOPISCHE UNTERSUCHUNG IM ULTRAVIOLETTEN UND SICHTBAREN BEREICH DES BENZOLDIAZOSULFONSAUREN NATRIUMS

Durch das Studium der Lichteinwirkung auf das Natriumbenzoldiazosulfonat haben wir versucht, die viel diskutierte primäre Umwandlung der Diazosulfonate aufzuklären. In der spektroskopischen Untersuchung der dem Licht ausgesetzten Lösungen zogen wir sowohl die Folgereaktionen und die eventuellen Nebenreaktionen, als auch die beträchtliche Veränderung des pH-Wertes, die im Laufe der Beleuchtung und nach der Unterbrechung derselben, im Dunkeln, zu bemerken ist, in Betracht.

Die Feststellung De Jonge's und Dijkstra's [18] bezüglich der Steigung des pH-Wertes im Laufe der Bestrahlung einiger stabiler Diazosulfonate bis zu einem maximalen Wert, welcher sich im alkalischen Bereich befindet, gefolgt von dessen langsamen Absinken, infolge der Hydrolyse „eines kleinen Teiles" der Diazoniumione, zu Phenol, Stickstoff und Wasserstoffionen, führte uns zu der Annahme, daß das gebildete Phenol eventuell mit den Benzoldiazoniumionen kuppeln könnte um *p*-Hydroxyazobenzol zu bilden. Die Anwesenheit des letzteren sogar in sehr kleinen Konzentrationen im Vergleich zu der Diazosulfonatkonzentration könnte — infolge seiner großen Extinktion bei solchen Wellenlängen, bei welchen das Diazosulfonat kleine Extinktionen aufweist — beträchtliche spektrale Veränderungen hervorrufen, kompliziert durch eine betonte Veränderung der Extinktion des Azofarbstoffes durch das langsame Absinken des pH-Wertes aus dem basischen Medium in das saure.

---

[21] J. van der Veen, J. Helfferich und L. K. H. van Beek, *Rec. Trav. chim.*, **85**, 895 (1966).

Folglich, schlugen wir folgendes Reaktionsschema vor:

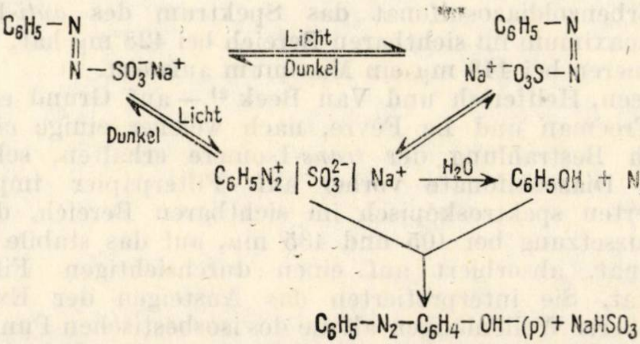

In Abb. 1, stellt die Kurve *1* das Spektrum des benzoldiazosulfonsauren Natriums dar, welches von uns bestimmt wurde, während Kurve *2* das Spektrum derselben Verbindung darstellt, welches aber von Hantzsch und Lifschitz [22] bestimmt und nur von neuem in einer der Kurve *1* entsprechenden Skala, aufgestellt wurde.

In Abb. 2 sind die Absorptionspektren jener Produkte dargestellt, die durch die Belichtung der wäßrigen Lösungen des stabilen Natriumbenzoldiazosulfonates resultieren, oder die sich durch eine nachträgliche absichtliche Alkalinisierung der beleuchteten Lösungen bilden können.

Tabelle 1

Absorptionsmaxima

Produkt	mμ (log ε)	Referenzen
Benzol-*anti*-diazosulfonat	202 (3,86) 218 (3,88), 288 (4,05),415 (2,25)	vorliegende Arbeit
	218 (3,97), 290 (4,07),410 (2,39)	8
	288 (3,77), 416 (1,88)	22
Benzol-*syn*-diazosulfonat	243 (3,76), 300 (2,32)	8

Dank seiner Instabilität, kann das Benzol-syn-diazosulfonat nicht gereinigt werden und folglich taugt es nicht für spektroskopische Bestimmungen. Lewis und Suhr [8] bestimmten das „ungefähre" Spektrum

---

[22] A. Hantzsch und J. Lifschitz, *Ber. dtsch. chem. Ges.*, 45, 3011 (1912).

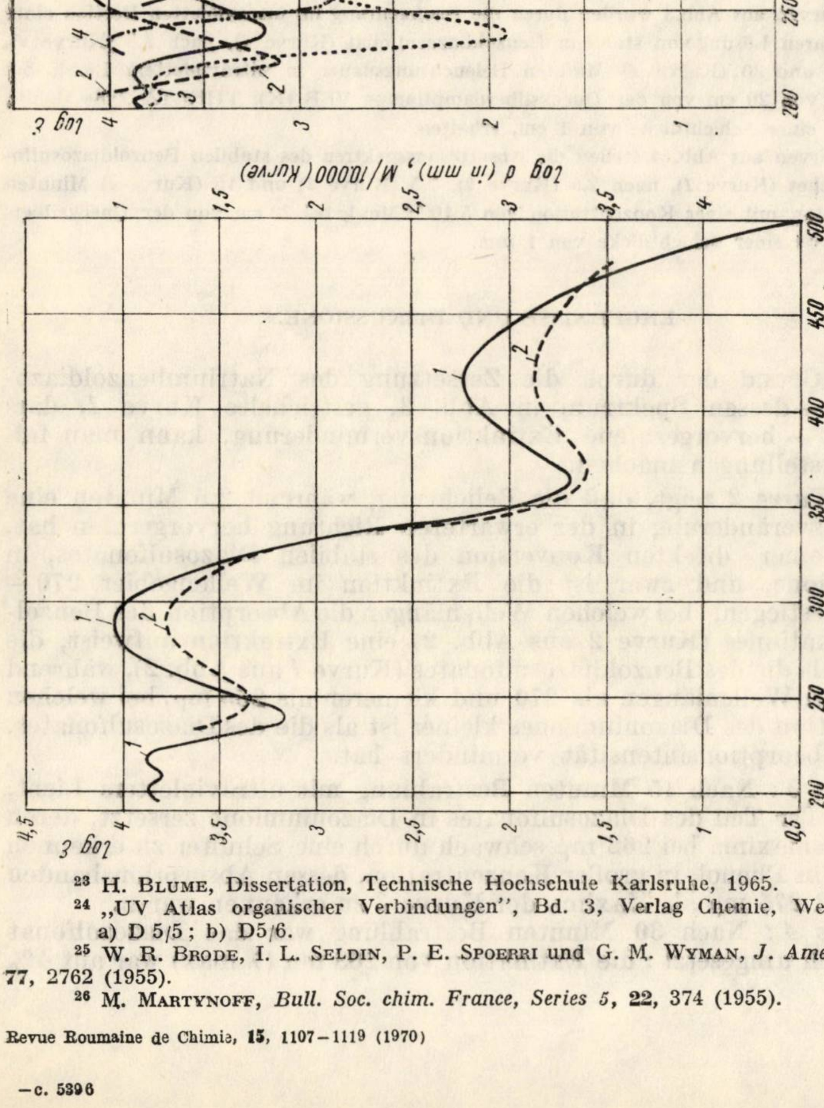

Abb. 1. – Das Absorptionsspektrum im ultravioletten und sichtbaren Bereich des stabilen Natrium-benzoldiazosulfonates (*Anti*-Isomer) von uns aufgestellt in der vorliegenden Arbeit (Kurve *1*) und von A. Hantzsch und J. Lifschitz (Kurve *2*).[22]

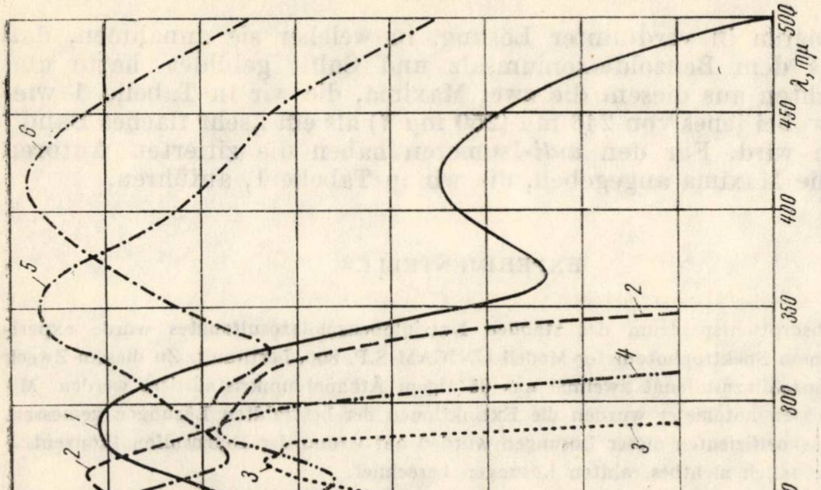

Abb. 2. – Die Absorptionsspektren im ultravioletten und sichtbaren Bereich der zum Studium des photochemischen Verhaltens des benzoldiazosulfonsauren Natriums herangezogenen Verbindungen:

1, Natrium-benzoldiazosulfonat (stabiles Isomer) in Wasser – bestimmt in der vorliegenden Arbeit; *2*, Benzoldiazoniumchlorid, in Wasser[23]; *3*, Phenol, in Wasser[24a]; *4*, Phenoxydion (Phenol in wäßrigem NaOH, pH = 12–13)[24b]; *5*, *p*-Hydroxyazobenzol in 10%igem Alkohol[25]; *6*, *p*-Hydroxyazobenzol in 0,05 N alkoholischem NaOH.[26]

---

[23] H. Blume, Dissertation, Technische Hochschule Karlsruhe, 1965.

[24] „UV Atlas organischer Verbindungen", Bd. 3, Verlag Chemie, Weinheim, 1967. a) D 5/5; b) D5/6.

[25] W. R. Brode, I. L. Seldin, P. E. Spoerri und G. M. Wyman, *J. Amer. Chem. Soc.*, **77**, 2762 (1955).

[26] M. Martynoff, *Bull. Soc. chim. France, Series 5*, **22**, 374 (1955).

Revue Roumaine de Chimie, **15**, 1107–1119 (1970)

–c. 5396

dieses Isomeren in verdünnter Lösung, in welcher sie annahmen, daß es sich aus dem Benzoldiazoniumsalz und Sulfit gebildet hatte und veröffentlichten aus diesem die zwei Maxima, die wir in Tabelle 1 wiedergeben, wobei jenes von 243 mμ (250 mμ ?) als ein „sehr flaches Band'' beschrieben wird. Für den *anti*-Isomeren haben die zitierten Autoren auch nur die Maxima angegeben, die wir in Tabelle 1, anführen.

EXPERIMENTELLES

Das Absorptionsspektrum des stabilen Natriumbenzoldiazosulfonates wurde experimentell mit einem Spektrophotometer Modell UNICAM S.P. 800, bestimmt. Zu diesem Zweck mußte das Benzoldiazosulfonat zweimal aus 95%igem Äthanol umkristallisiert werden. Mit demselben Spektrophotometer wurden die Extinktionen der bestrahlten Lösungen gemessen. Die Extinktionskoeffizienten dieser Lösungen wurden auf Grund der Diazosulfonatkonzentration der ursprünglich nichtbestrahlten Lösungen berechnet.

Die Kurven aus Abb.3 wurden durch die Beobachtung im ultravioletten Bereich einer $1{,}67.10^{-4}$ molaren Lösung von stabilem Benzoldiazosulfonat (Kurve *1*), nach 2,5 (Kurve *2*), 15 (Kurve *3*) und 30 (Kurve *4*) Minuten Beleuchtungsdauer in ultraviolettem Licht, bei einer Distanz von 20 cm von der Quecksilberdampflampe VEB (K), THELTA Zella-Mehlis, Typ Q 99, in einer Schichtdicke von 1 cm, erhalten.

Die Kurven aus Abb. 4 stellen die Absorptionsspektren des stabilen Benzoldiazosulfonates, als solches (Kurve *1*), nach 2,5 (Kurve *2*), 7,5 (Kurve *3*) und 15 (Kurve *4*) Minuten Beleuchtung dar, mit einer Konzentration von 5.10^{-3} Mol/l, bei 20 cm von der Quecksilberdampflampe und einer Schichtdicke von 1 mm.

ERGEBNISSE UND DISKUSSIONEN

Auf Grund der durch die Zersetzung des Natriumbenzoldiazosulfonates — dessen Spektrum in Abb. 3, gestrichelte Kurve *1*, dargestellt ist — hervorgerufene Extinktionsverminderung, kann man folgende Feststellungen machen.

Die Kurve 2 zeigt, daß die Belichtung, während 2,5 Minuten eine Absorptionsveränderung in der erwarteten Richtung hervorgerufen hat, im Sinne einer direkten Konversion des stabilen Diazosulfonates, in Diazoniumione, und zwar ist die Extinktion im Wellengebiet 270—235 mμ gestiegen, bei welchen Wellenlängen die Absorption des Benzoldiazoniumkationes (Kurve 2 aus Abb. 2) eine Extinktion aufweist, die größer ist als die des Benzoldiazosulfonates (Kurve *1* aus Abb. 2), während bei größeren Wellenlängen als 270 und kleineren als 235 mμ, bei welchen die Extinktion des Diazoniumiones kleiner ist als die des Diazosulfonates, sich die Absorptionsintensität vermindert hat.

Kurve 3: Nach 15 Minuten Bestrahlung mit ultraviolettem Licht, war ein großer Teil des Diazosulfonates in Diazoniumione zersetzt, deren Absorptionsmaxima bei 262 mμ schwach durch eine Schulter zu erkennen waren und in Phenol, in großer Konzentration, dessen Absorptionsbanden bei 269 und 275 mμ als Maxima der Kurve *3* zu erkennen waren.

Kurve 4: Nach 30 Minuten Bestrahlung war das Diazosulfonat fast gänzlich umgesetzt: die Extinktion von 288 mμ (λ max) war auf 4%

des anfänglichen Wertes gefallen und größtenteils auf die Absorption der anwesenden Diazoniumionen zurückzuführen, deren Maximum bei 262 mμ deutlich in Erscheinung trat. Bei 269 und 275 mμ weist die Kurve *4* das unveränderte Spektrum des Phenoles auf.

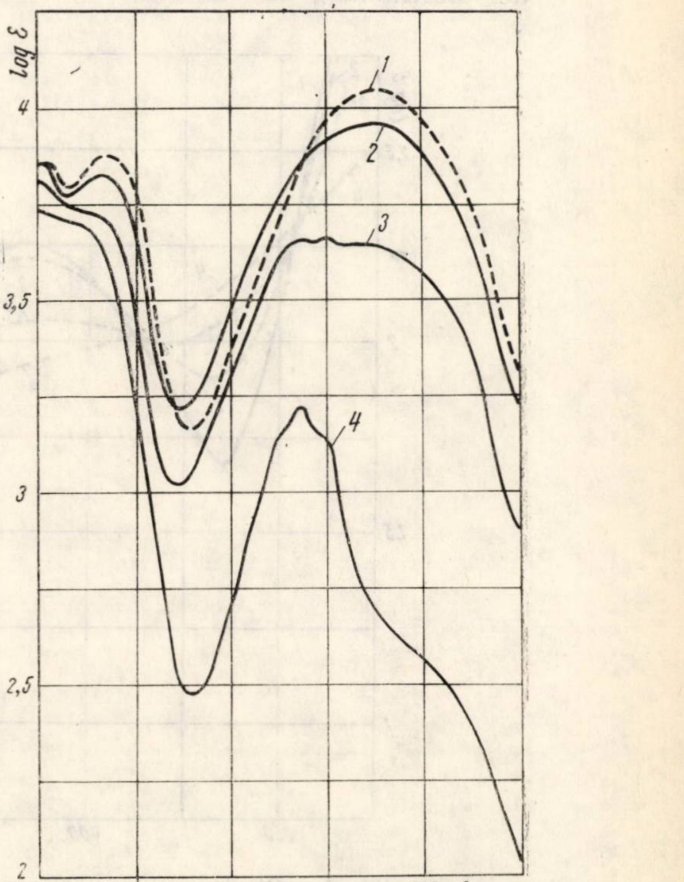

Abb. 3. — Die Absorptionsspektren im ultravioletten Bereich der wäßrigen Natrium-benzoldiazosulfonatlösungen, von einer $1{,}67 \cdot 10^{-4}$ Mol/l Konzentration, dem ultravioletten Licht ausgesetzt, bei einer Schichtdicke von 1 cm, während 2,5 (Kurve *2*), 15 (Kurve *3*) und 30 (Kurve *4*) Minuten und das Spektrum der unbestrahlten Lösung (Kurve 1).

In Abbildung 4 schreiben wir die progrediente Verminderung der Absorption bei 415 mμ, nach 2,5 (Kurve *2*), 7,5 (Kurve *3*) und 15 (Kurve *4*) Minuten Belichtungsdauer mit ultraviolettem Licht, der Verringerung der Konzentration des Benzoldiazosulfonates, infolge deren Umsetzung in Benzoldiazoniumionen und Phenol zu, dessen Absorption im sichtbaren Bereich praktisch Null ist. Diese Verringerung ist im allgemeinen von einer Steigerung der Absorption überdeckt, welche wir auf die Bildung des *p*-Hydroxyazobenzols durch Kupplung der Benzoldiazoniumione mit Phenol zurückführen. Die Bilanz dieser beiden Effekte wirkt sich aber durch ein Anwachsen der Extinktion nur bei den Wellenlängen von ungefähr 345—390 mμ und über 460 mμ aus, bei welchen das Verhältnis zwischen den molaren Extinktionskoeffizienten des *p*-Hydroxyazobenzols und des Diazosulfonates, ziemlich groß ist (siehe auch Abb. 2, Kurven *5* und *6*, im Vergleich zu *1*). Die spektralen Veränderungen werden auch noch durch das Anwachsen des pH-Wertes kompliziert, welches im Laufe der Bestrahlung zu bemerken war und welches die Absorption des *p*-Hydroxyazobenzols verändert. Auch ist eine Umsetzung eines kleinen Teiles der Diazoniumionen in Diazoanhydrid nicht auszuschließen.

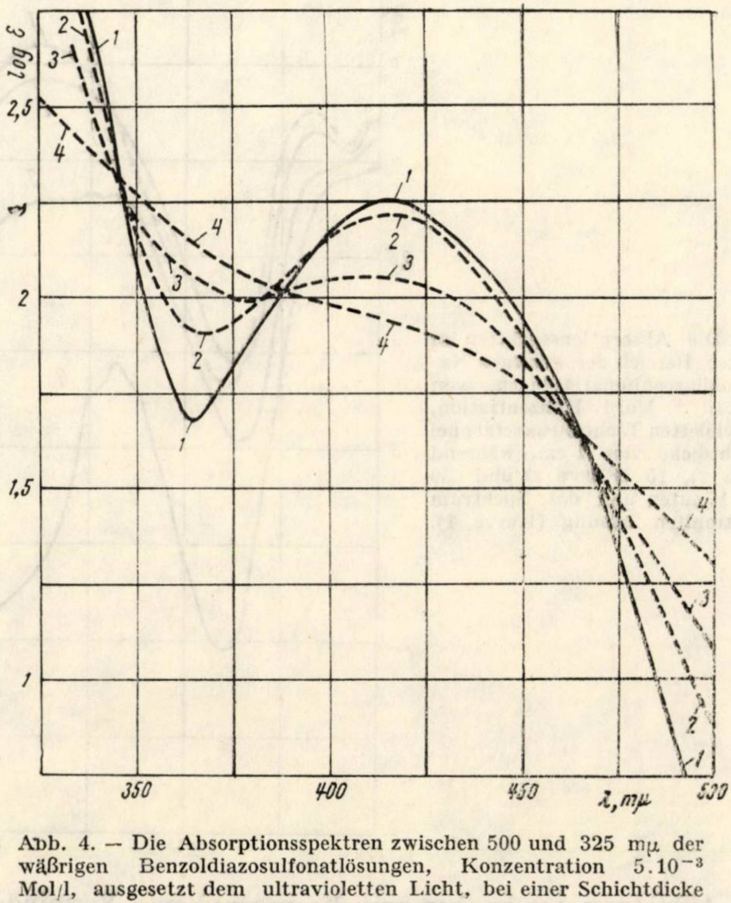

Abb. 4. — Die Absorptionsspektren zwischen 500 und 325 mμ der wäßrigen Benzoldiazosulfonatlösungen, Konzentration $5 . 10^{-3}$ Mol/l, ausgesetzt dem ultravioletten Licht, bei einer Schichtdicke von 1 mm, während 2,5 (Kurve *2*), 7,5 (Kurve *3*) und 15 (Kurve *4*) Minuten und das Spektrum der unbestrahlten Lösung (Kurve *1*).

Wenn die Bestrahlungsdauer 15 Minuten überschreitet, verändert sich die Absorption im sichtbaren Bereich nicht mehr, ein Beweis dafür, daß die Zersetzung des Diazosulfonates vollständig vor sich gegangen war und daß sich kein Azofarbstoff mehr bildet, weil das Medium angesäuert wurde, im Laufe der Photolyse der Diazoniumionen zu Phenol. Im ultravioletten Bereich fällt die Extinktion weiter bis die Umsetzung der Diazoniumionen in Phenol vollständig ist.

In Abbildung 5, stellt die Kurve *1* das Absorptionsspektrum der unbestrahlten Lösung des benzoldiazosulfonsauren Natriums dar, während die Kurven *2*—*7* für die bestrahlte Lösung nach 7,5 Minuten auf folgende Weise aufgestellt wurden :

Die Kurve 2 : für die 7,5 Minuten lang bestrahlte Lösung, gleich nach dem Entfernen der Strahlen ;

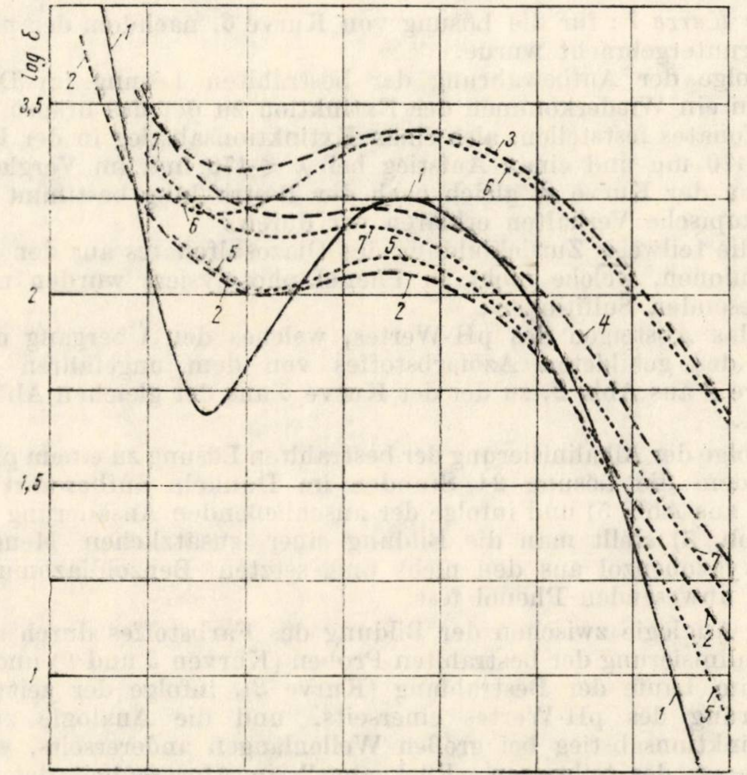

Abb. 5. — Die Absorptionsspektren der wäßrigen Natrium-benzoldiazosulfonatlösungen :

1, nicht ausgesetzt dem ultravioletten Licht ; *2*, nach 7,5 Minuten Bestrahlung ; *3*, Probe 2 von oben, bei pH = 10 ; *4*, Probe 3 von oben, bei pH = 5 ; *5*, Probe 2 von oben nach 24 Stunden Aufbewahrung im Dunklen ; *6*, Probe 5 bei pH = 10 ; *7*, Probe 6, adjustiert zu einem pH-Wert = 5.

Die Kurve 3 : für die obenangeführte Lösung nach einer Alkalinisierung zu pH=10 erhalten ;

Die Kurve 4 : ergab sich für die alkalische Lösung von Kurve 3, nach deren Ansäuerung zu pH=5.

Aus den Extinktionsveränderungen bei 470—500, 415 und 350 mμ, wird die Bildung einer zusätzlichen Menge von *p*-Oxyazobenzol, festgestellt.

Die Kurven 5—7 wurden analog mit *2—4*, mit der 7,5 Minuten lang bestrahlten Lösung, aber nach deren 24 Stunden langem Aufbewahren im Dunkeln bei 3°, erhalten.

Die Kurve 5 : für die bestrahlte Lösung, aufbewahrt im Dunkeln 24 Stunden;

Die Kurve 6 : für die Lösung von Kurve *5*, aber alkalinisiert zu pH=10;

Die Kurve 7 : für die Lösung von Kurve *6*, nachdem der pH-Wert auf 5 heruntergebracht wurde.

Infolge der Aufbewahrung der bestrahlten Lösung im Dunkeln, kann man ein Wiederkommen der Extinktion zu der des ursprünglichen Diazosulfonates feststellen, also einen Extinktionsabstieg in der Kurve *5* bei $\lambda > 470$ mμ und einen Aufstieg bei $\lambda < 470$ mμ, im Vergleich der Extinktion der Kurve *2*, gleich nach der Bestrahlung bestimmt. Dieses spektroskopische Verhalten erklären wir durch:

a) die teilweise Zurückbildung des Diazosulfonates aus den Benzoldiazoniumionen, welche nicht zu Phenol photolysiert wurden und aus den anwesenden Sulfitionen;

b) das Absteigen des pH-Wertes, welches den Übergang der Absorption des gebildeten Azofarbstoffes von dem ungefähren Verlauf der Kurve *6* aus Abb. 2, zu der der Kurve *5* aus der gleichen Abbildung, bestimmt.

Infolge der Alkalinisierung der bestrahlten Lösung zu einem pH-Wert 10, nachdem die Lösung 24 Stunden im Dunkeln aufbewahrt wurde (Kurve *6* aus Abb. 5) und infolge der anschließenden Ansäuerung (Kurve *7* aus Abb. 5) stellt man die Bildung einer zusätzlichen Menge von *p*-Hydroxyazobenzol aus den nicht umgesetzten Benzoldiazoniumionen und dem anwesenden Phenol fest.

Die Analogie zwischen der Bildung des Farbstoffes durch absichtliche Alkalinisierung der bestrahlten Proben (Kurven *3* und *6*) und dessen Bildung im Laufe der Bestrahlung (Kurve *2*), infolge der zeitweiligen Vergrößerung des pH-Wertes einerseits, und die Analogie zwischen dem Extinktionsabstieg bei großen Wellenlängen andererseits, während des Prozesses des teilweisen „Rückgangs", in Abwesenheit des Lichtes (Kurve *5*) — ein Prozeß der begleitet ist von einem Abstieg des pH-Wertes im sauren Gebiet — und dessen Verringerung, infolge der Ansäuerung der alkalinisierten Proben, also mit großem Gehalt an *p*-Hydroxyazobenzol (Kurven *4* und *7*), ist offensichtlich.

SCHLUSSFOLGERUNGEN

Die spektroskopischen Untersuchungen im ultravioletten und sichtbaren Bereich, der wäßrigen verdünnten Lösungen von benzoldiazosulfonsaurem Natrium, ausgesetzt dem ultravioletten und sichtbaren Licht, führten nicht zu der Entdeckung einiger spektralen Veränderungen, welche die Bildung des labilen Isomers (*syn*) als Primärprodukt der Bestrahlung, andeuten könnten. Das spektroskopisch bestimmbare Primärprodukt der Bestrahlung ist das Benzoldiazoniumkation welches sich seinerseits photolytisch in Phenol zersetzt — das Hauptprodukt einer langanhaltenden Bestrahlung. Als Nebenprodukt ergibt sich *p*-Hydroxyazobenzol.

Folglich können wir folgendes Umsetzungsschema vorschlagen:

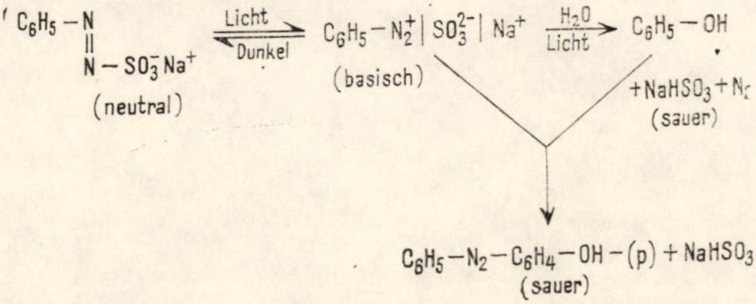
$C_6H_5-N=N-SO_3^-Na^+$
(neutral)
Licht
Dunkel
$C_6H_5-N_2^+|SO_3^{2-}|Na^+$
(basisch)
H_2O
Licht
C_6H_5-OH
$+NaHSO_3+N_2$
(sauer)
$C_6H_5-N_2-C_6H_4-OH-(p)+NaHSO_3$
(sauer)

Revue Roumaine de Chimie, 15, 1107–1119 (1970)

Revue Roumaine de Chimie, **15**, 1121–1125 (1970)

6-AZAURACIL DERIVATIVES WITH POTENTIAL CYTOSTATIC ACTIVITY. IX *

6-AZAURACIL-5-SULFONAMIDES

C. CRISTESCU

Chemical Pharmaceutical Reserach Institute, Bucharest,
Şos. Vitan 112

Received June 21, 1969

5-Mercapto-6-azauracil sodium salt is converted with chlorine in water, to 6-azauracil-5-sulfonyl chloride. This reacts with amino-compounds to form 6-azauracil-5-sulfonamides.

Recent works [1,2] on the antitumor activity of 6-azauracil (as-triazine-3,5 (2H, 4H) dione) have suggested that its various derivatives substituted in position 5 might prove of biological interest.

The previous papers [3,4] described the preparation of 5-mercapto-6-azauracil and some 5-substituted thioethers. The present paper deals with the preparation of several new 5-substituted-6-azauracil (6-substituted-as-triazine-3,5 (2H, 4H) dione) compounds.

When 5-mercapto-6-azauracil (I) was treated with chlorine in water and the temperature of the reaction mixture maintained at 2–4°, a 80% yield of crude 6-azauracil-5-sulfonyl chloride (II) was obtained.

A number of 6-azauracil-5-sulfonamides (III–VII) have been prepared by reaction of 6-azauracil-5-sulfonyl chloride with different amines.

The infrared spectra of these as-triazines show peaks in the 3200 cm^{-1} region and very sharp doublets in the 1700–1750 cm^{-1} region, because of the $-CO-NH-$ groups. The SO_2 group which normally has a strong peak at 1160 – 1180 cm^{-1} and 1330 – 1360 cm^{-1} shifts in the 1140 – 1160 cm^{-1} region for νs (SO_2). The C = N bond, between position 5 and 6 of 6-azauracil which normally[5] has a peak in the 1600 cm^{-1} region shows a shift in the 1570 – 1630 cm^{-1} region depending on the substitution in the 5-position.

---

* Part VIII : C. Cristescu and Marcela Lăzărescu, *Rv. Roumaine Chim.* (in press).

[1] J. Skoda, *Progr. Nucleic Acid Res.*, **3**, 197 (1963).

[2] G. B. Elion and H. G. Hitching , *Advan. Chemotherapy*, **2**, 91 (1965).

[3] C. Cristescu and J. Marcus, *Pharmazie*, **16**, 135 (1961).

[4] C. Cristescu and T. Panaitescu, *Pharmazie*, **17**, 209 (1962).

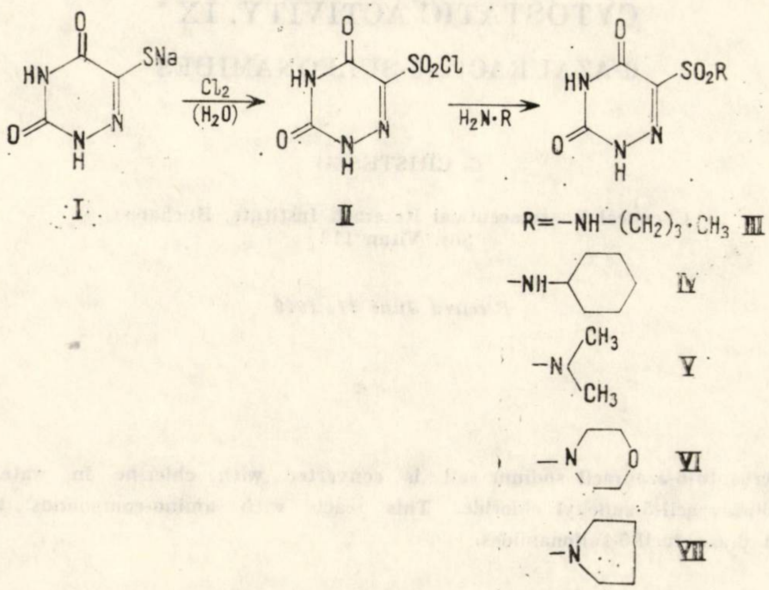

ANTITUMOR EVALUATION

The results obtained from the antitumor testing of compounds prepared in this investigation are shown in table 1. Testing was performed under the auspices of the Cancer Chemotherapy National Service Center C.C.N.S.C., Bethesda, Md. From the testing data so far available it is evident that this series possesses very little potential as inhibitory agents of L 1210 Lymphoid leukemia.

EXPERIMENTAL

Melting points were determined with a heating microscope stage. Analytical samples were dried at 20°/5 Torr 8 hours over P_2O_5. The infrared spectra were measured in pressed potassium bromide disks with a Zeiss Jena U.R. 10 spectrophotometer.

---

[5] M. Horák and J. Gut, *Coll. Czech. Chem. Comm.*, **28**, 3392 (1963).

Table 1

Screening data *a, b*

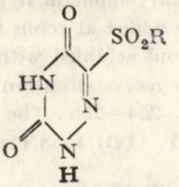

No	R	Test System [c]	Dose mg/kg	Survivors	Cures	Animal wt. dif. in g. (T−C)[d]	Tumor wt. g or Survival[e] days T/C	T/C[f] %
1	$-NH(CH_2)_3CH_3$	LE	400	3/4		0.0	8.3/8.9	93
			200	4/4		0.6	9.0/8.9	101
			100	4/4		0.3	9.3/8.9	104
			280	6/6	1	−1.1	11.5/8.7	132
2	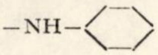	LE	400	4/4		0.9	9.8/8.9	110
			200	4/4		1.3	8.5/8.9	95
			100	4/4		0.8	9.0/8.9	101
3	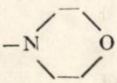	LE	400	4/4		0.4	8.3/8.6	96
			200	4/4		−0.8	8.3/8.6	96
			100	4/4		−0.3	8.3/8.6	96
4	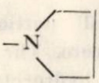	LE	400	3/4		1.1	8.3/8.9	93
			200	4/4		0.7	8.8/8.9	98
			100	4/4		0.8	8.8/8.9	98
			280	4/6		−2.2	8.8/8.7	91

a. Only part of the data are presented.

b. Assay performed according to specifications established by CCNSC as reported in *Cancer Chemotherapy Rept.*, **25**.1 (1962).

c. LE – L 1210 Lymphoid leukemia.

d. Average weight change of test group (T) minus average weight change of control (C) animals.

e. Survival days for LE test systems.

f. The requirements for passing different stages of the sequential screen given by the value of T/C in a single test at a nontoxic dose which should be: Stage 1 T/C ⩾ 125% and Stage 2 T/C ⩾ 156% (in L 1210 Lymphoid leukemia).

6-Azauracil-5-sulphonyl chloride (II)

A suspension of 5-mercapto-6-azauracil sodium salt (10.1 g; 0.05 M) in 35 ml water was treated with chlorine at 2–4⁰. Chlorine was bubbled through the mixture solution, until it became yellow-greenish (about 3 hours). The colourless crystalline product was filtered and dried over P_2O_5 on at diminished pressure at room temperature. Yield, 8.56 g (80%) crude 6-azauracil-5-sulphonyl chloride with m.p. 202–204⁰ (dec.). The product thus obtained was sufficiently pure for synthetic use. The analytical sample melted at 207–208⁰ (dec.) from glacial acetic acid.

$C_3H_2N_3O_4SCl$	*Calcd.*: N, 19.8: S, 15.1; Cl, 16.7%;
(211.5)	*Found*: N, 19.9: S, 15.2; Cl, 16.8%.

6-Azauracil-5(n-butyl) sulfonamide (III)

To a stirred solution of 2,2 g n-butylamine in 10 ml water in small portion, 2.1 g (0.01 M) 6-azauracil-5-sulphonyl chloride were added at room temperature. The reaction mixture was stirred 1 hour at 35°, cooled at 10° and acidified with 10% hydrochloric acid at pH 2. The solid precipitate was filtered off. After recrystallization from water, yield, 2 g (85%) 6-azauracil-5(n-butyl) sulfonamide with m.p. 254—255°. The analytical sample melted at 255—256° (from water) IR : 1695, 1745 (C = O); 1141, 1358 (SO_2); 1566 (C = N) cm^{-1}.

$C_7H_{12}N_4O_4S$	*Calcd.* : N, 22.5 S, 12.9%;
(248.2)	*Found.* : N, 22.6 S, 13.0%.

6-Azauracil-5-(N-cyclohexyl) sulfonamide (IV)

6-Azauracil-5-sulphonyl chloride (4.2 g; 0.02 M) was added to a solution of 10 g cyclohexylamine in 25 ml water, in small portions, at 40°. The reaction mixture was stirred 1 hour at 50°, diluted with 20 ml water, acidified with 10% hydrochloric acid at pH 2, then left standing overnight at 4°. The solid precipitate was filtered and recrystallized from water. Yield, 3 g (55%) 6-azauracil-5-(N-cyclohexyl) sulfonamide with m.p. 243—244°. A sample for analysis had m.p. 244—245° (from water). I.R : 1708, 1734 (C = O); 1158, 1350 (SO_2); 1130 (C = N) cm^{-1}.

$C_9H_{14}N_4O_1S$	*Calcd.* : N, 20.4 S, 11.7%;
(273.3)	*Found* : N, 20.6 S, 11.8%.

6-Azauracil-5 (N, N-dimethl) sulfonamide (V)

2.1 g (0.01 M) 6-azauracil-5-sulphonyl chloride was added, in small portions, to a stirred aqueous solution of 33% dimethylamine (10 ml) at 10° temperature. The reaction mixture was stirred 3 hours at room temperature, acidified with 10% hydrochloric acid at pH 2, then standing overnight at 4°. After recrystallization from water yield, 2 g (90%) 6-azauracil-5 (N, N-dimethyl) sulfonamide with m.p. 280—281° (dec.). IR : 1710, 1745 (C = O); 1145, 1346 (SO_2); 1583 (C = N) cm^{-1}.

$C_5H_8N_4O_4S$	*Calcd.* : N, 25.5 S, 14.5%;
(220.2)	*Found* : N, 25.7 S, 14.7%.

6-Azauracil-5 (N-morpholyl) sulfonamide (VI)

6-Azauracil-5-sulphonyl chloride (2.1 g; 0.01 M) was added, in small portions, to a solution of morpholine (7 g) in water (50 ml) at room temperature. The reaction mixture was stirred for 2 hours at 40°, and allowed to stand at room temperature for 3 hours. After acidifiation with 10% hydrochloric acid at pH 2, the white solid was collected and recrystallzed from water. Yield, 4.2 g (80.7%) 6-azauracil-5(N-morpholyl) sulfonamide with m.p. 289—290° (dec.). An analytical sample was melted at 292—293° (dec.) from water. IR : 1708, 1735 (C = O); 1158, 1350 (SO_2); 1574 (C = N) m^{-1}.

$C_7H_{10}N_4O_5S$	*Calcd.* : N, 21.3 S, 12.2%;
(262.2)	*Found* : N, 21.5 S, 12.4%.

6-Azauracil-5(N-pyrrolidyl) sulfonamide (VII)

6-Azauracil-5-sulphonyl chloride (2.1 g ; 0.01 M) was added, in small portions, to a solution of fresh distilled pyrrolidine (3 g) in water (25 ml) at a temperature below 35°. After the addition the reaction mixture was stirred 1 hour at 50°. Water (20 ml) was added and the solution was acidified at pH 2 with 10% hydrochloric acid. The solid precipitate was filtered and recrystallized from water. Yield, 2.3 g (95%) 6-azauracil-5(N-pyrrolidyl) sulfonamide with m.p. 272–273° (dec.). IR : 1704, 1741 (C = O) ; 1146, 1345 (SO_2) ; 1595 (C = N) cm^{-1}.

$C_7H_{10}N_4O_4S$	*Calcd.* : N, 22.7 S, 13.0% ;
(246.8)	*Found* : N, 22.9 S, 12.9%.

The author is grateful to Dr. Harry B. Wood Jr. of the Cancer Chemotherapy National Service Center, National Institutes of Health, Bethesda, Md., for the screening data. The analyses were made in the analytical department of this Institute by Mrs. Cornelia Ioan and Mrs. Sofia Arizan.

Revue Roumaine de Chimie, 15, 1127–1136 (1970)

QUARTÄRE AMMONIUMSALZE DES ACETAMIDO-BENZAL-FLUORENS

T. RĂDULESCU und H. D. SCHELL

aus dem Institut für Biochemie der Akademie
Bukarest, Str. Docenţilor 20

Eingegangen am 10. November 1969

Es wird die Darstellung einer Reihe von drei verschiedenen Typen quartärer Ammoniumsalze des Acetamido-benzal-fluorens beschrieben. Die Salze vom Typ I sind Abkömmlinge des 2-Acetamido-benzal-fluorens, dessen Benzolkern in *para*-Stellung entweder nicht oder mit einer Methoxy- oder Dimethylamino-Gruppe substituiert ist. Die Salze vom Typ II rühren vom 2,7-Bis-(chloracetamido)-benzal-fluoren her, dessen Benzolkern die *para*-Stellung ebenfalls substituiert oder nicht substituiert hat. Bei den Salzen vom Typ III schließlich, befindet sich die eine der quartären Ammoniumgruppen an den Fluorenkern und die andere an den Benzolkern in *ortho*-, *meta*- oder *para*-Stellung gebunden. Es werden auch 14 neue Nitro- und Aminoderivate des Benzalfluorens beschrieben, deren Darstellung für die Synthese der quartären Ammoniumsalze nötig war.

In Fortsetzung früherer Arbeiten über die Darstellung verschiedener quartärer Ammoniumsalze mit unterschiedlichem Lipophiliegrad,[1–4] beschreiben wir in der vorliegenden Arbeit eine neue Reihe, diesmal vom Acetamido-benzal-fluoren abstammende quartäre Ammoniumsalze. Die Verbindungen wurden im Hinblick auf die Erzielung neuer Daten über die zwischen chemischer Struktur und biologischer Wirkung bestehenden Beziehungen synthetisiert. Zur Zeit werden die quartären Ammoniumsalze mit Erfolg nicht nur in der Klinik als Muskelrelaxantien oder als Bakteriostatika oder sogar Bakterizide, sondern auch auf verschiedenen anderen Gebieten angewandt, wie z. B. in der chemischen und Textilindustrie als Detergenzien, in den Laboratorien für Genetik als Mutagene usw.

In der vorliegenden Arbeit werden folgende drei Typen von Verbindungen beschrieben :

---

[1] H. D. Schell, *Comunicările Acad. R.P.R.*, **5**, 1071 (1955).

[2] S. D. Gheorghe und H. D. Schell, *Studii Cercetări Biochim. Acad. R.P.R.*, **1**, 247 (1958).

[3] T. Rădulescu und S. Vasu, *Comunicările Acad. R.P.R.*, **8**, 793 (1958).

[4] H. D. Schell, *Studii şi Cercetări Chim,. Acad. R.P.R.*, **9**, 681 (1961).

— monoquartäre Ammoniumsalze des Acetamido-benzal-fluorens (Typ I), dessen Benzolkern in der *para*-Stellung entweder nicht oder mit einer Methoxy- oder Dimethylamino-Gruppe substituiert ist:

Verbindungen vom Typ I

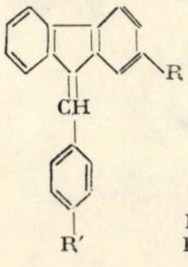

Verbindungen vom Typ II

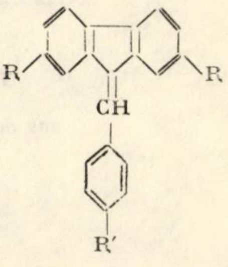

$R = -NH-CO-CH_2-N^+(CH_3)_3Cl^-$

$R' = H, OCH_3, N(CH_3)_2$

— diquartäre Ammoniumsalze des Acetamido-benzal-fluorens (Typ II), bei welchen die zwei quartären Ammoniumgruppen beide an den Fluorenkern gebunden sind und der Benzolkern ebenfalls — wie auch im Falle der Verbindungen vom Typ I — seine *para*-Stellung nicht oder mit einer Methoxy- oder Dimethylamino-Gruppe substituiert hat;

— diquartäre Ammoniumsalze des Acetamido-benzal-fluorens (Typ III), bei denen die eine der quartären Ammoniumgruppen an den Fluorenkern und die andere an den Benzolkern in *ortho*-, *meta*- oder *para*-Stellung gebunden ist.

Verbindungen vom Typ III

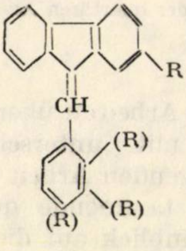

$R = -NH-CO-CH_2-N^+(CH_3)_3Cl^-$

Der bei der Synthese der obenerwähnten Ammoniumsalze eingeschlagene Weg bestand in der Kondensation des 2-Nitro- bzw. 2,7-Dinitro-fluorens mit substituiertem oder nicht substituiertem Benzaldehyd, gefolgt von der Reduktion der erhaltenen Nitroderivate zu den entsprechenden Aminen, die dann mit Hilfe des Säurechlorides der Monochloressigsäure chloracetyliert wurden. Durch Anlagerung von Trimethylamin an die erzielten Chloracetylderivate wurden dann schließlich die betreffenden mono- und diquartären Ammoniumsalze erhalten (siehe Reaktionsschema).

Die erhaltenen Ammoniumsalze bilden kristalline oder mikrokristalline wasserlösliche Stoffe, mit relativ hohen Schmelzpunkten, deren Farbe — je nach dem Substituenten aus der *para*-Stellung —

zwischen strohgelb und kaffeebraun liegt. Die wäßrigen Lösungen der Salze sind oberflächenaktiv und kurarewirksam.

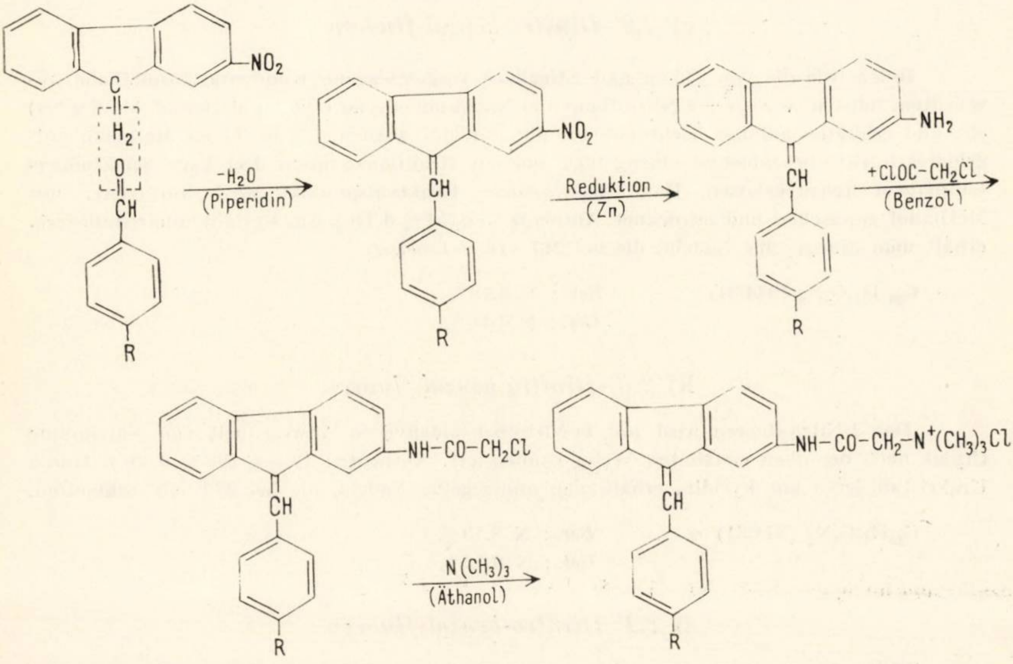
NO2
C
H2
O
CH
R
-H2O
(Piperidin)
NO2
CH
R
Reduktion
(Zn)
NH2
CH
R
+ClOC-CH2Cl
(Benzol)
NH-CO-CH2Cl
CH
R
N(CH3)3
(Äthanol)
NH-CO-CH2-N+(CH3)3Cl-
CH
R

In der vorliegenden Arbeit werden im Ganzen 23 neue Verbindungen beschrieben, davon 9 quartäre Ammoniumsalze sind ; es wurden außerdem auch 13 in der Fachliteratur schon bekannte Zwischenprodukte dargestellt.

EXPERIMENTELLES

1. – NITRODERIVATE

Die Mehrzahl der Nitroderivate, die zur Herstellung der in dieser Arbeit beschriebenen quartären Ammoniumsalze nötig waren, und zwar die des 2-Amino- und 2,7-Diamino-benzalfluorens, sind schon bekannt und wurden nach Angaben der erwähnten Fachliteratur dargestellt.

a) *2-Nitro-benzal-fluoren* [5,6]
b) *2-Nitro-4'-methoxy-benzal-fluoren* [7]

---

[5] C. CÂNDEA und E. MACOVSCHI, *Bull. Soc. chim. France*, **2**, 1703 (1935).
[6] L. GUGLIALMELI, J. COSOLOSA und Z. LUGONES, *Rev. Brasil. Chim.*, **4**, 192 (1937).
[7] F. DOBRESCU, *Studii și Cercetări Ști. Chim., Baza Cercetări Ști., Timișoara*, **3**, 45 (1956).

c) *2-Nitro-4'-dimethylamino-benzal-fluoren*[7]
d) *2,7-Dinitro-benzal-fluoren*[8]
e) *2,7-Dinitro-4'-methoxy-benzal-fluoren*[8]
f) *2,7-Dinitro-4'-dimethylamino-benzal-fluoren*[7]

g) *2,2'-Dinitro-benzal-fluoren*

Indem wir die von Thiele und Stieglitz[9] vorgeschlagene Kondensationsmethode anwandten, führten wir 8,4 g 2-Nitro-fluoren in Natriummethylat (100 ml Methanol + 1,6 g Na) ein und erhitzten anfangs leicht auf 40—50°. Sodann werden 6 g in 30 ml Methanol aufgelöstes *o*-Nitro-benzaldehyd hinzugefügt und das Reaktionsgemisch drei Tage bei Zimmertemperatur stehen gelassen. Das ausgeschiedene Reaktionsprodukt wird abfiltriert, mit Methanol gewaschen und getrocknet. Ausbeute : 7 g (51 % d.Th.). Aus Pyridin umkristallisiert, erhält man orangegelbe Nadeln, die bei 217—18° schmelzen.

$C_{20}H_{12}O_4N_2$ (344,31) *Ber.* : N 8,13 %
Gef. : N 8,18 %

h) *2,3'-Dinitro-benzal-fluoren*

Das 2-Nitro-fluoren wird mit *m*-Nitro-benzaldehyd in Anwesenheit von Natriummethylat nach der oben erwähnten Weise kondensiert. Ausbeute : 13,6 g (98 % d.Th.). Durch Umkristallisieren aus Pyridin, erhält man orangegelbe Nadeln, die bei 272—75° schmelzen.

$C_{20}H_{12}O_4N_2$ (344,31) *Ber.* : N 8,13 %
Gef. : N 8,19 %

i) *2,4'-Dinitro-benzal-fluoren*

2-Nitro-fluoren wird mit *p*-Nitro-benzaldehyd nach Vorschrift 1 g) kondensiert. Ausbeute : 12 g (87 % d.Th.). Aus Pyridin kristallisiert das Produkt in orangegelben Nadeln aus, die bei 274° schmelzen. Es ist zu erwähnen, daß Fischer und Bergmann,[10] indem sie diese Kondensation im Butylester der Essigsäure ausführten, den *cis*- (Schmp. 251—52°) und *trans*-Isomer (Schmp. 287—88°) isolieren konnten, da der erstere im verwendeten Kondensationsmilieu löslich und der letztere unlöslich ist.

$C_{20}H_{12}O_4N_2$ (344,31) *Ber.* : N 8,13 %
Gef. : N 8,20 %

2. — AMINODERIVATE

Durch Reduktion der obenerwähnten Nitroderivate wurden die entsprechenden Aminoderivate erhalten, von denen die ersten sechs ebenfalls in der Fachliteratur schon bekannt sind.

a) *2-Amino-benzal-fluoren*[11]
b) *2-Amino-4'-methoxy-benzal-fluoren*[7]
c) *2-Amino-4'-dimethylamino-benzal-fluoren*[7]

---

[8] F. Dobrescu, Teză, Iaşi (1964).

[9] J. Thiele und A. Stieglitz, *Ber. dtsch. chem. Ges.*, **52**, 1513 (1919).

[10] E. Fischer und E. D. Bergmann, *Bull. Research Council, Israel*, **1**, 136 (1951).

[11] B. A. Porai-Kositch und A. M. Efros, *Doklady Akad. Nauk S.S.S.R.*, **3**, 43 (1938).

d) *2,7-Diamino-benzal-fluoren*[8]

e) *2,7-Diamino-4'-methoxy-benzal-fluoren*[8]

f) *2,7-Diamino-4'-dimethylamino-benzal-fluoren*[7]

g) *2,2'-Diamino-benzal-fluoren*

Das 2,2'-Dinitro-benzal-fluoren wurde nach der von Diels[12] angegebenen Methode reduziert, indem 2 g des Dinitroderivates mit 22 g Zinkpulver gut vermengt und in 100 ml Äthanol zusammen mit 0,4 g in 1,5 ml Wasser aufgelöstem $CaCl_2$ vier Stunden auf dem Wasserbad in einem mit Rückflußkühler versehenen Kolben gekocht wurden. Es wird sodann heiß filtriert, das Zinkpulver einige Male mit heißem Äthanol gewaschen und das Amin durch Verdünnen des Alkoholfiltrates ausgefällt. Ausbeute : 1,4 g (85 % d.Th.). Das orangegelbe Amin schmilzt bei 175°.

$C_{20}H_{16}N_2$ (284,34)	*Ber.* : N 9,84 %
	Gef. : N 9,96 %

h) *2,3'-Diamino-benzal-fluoren*

Es wird wie in Vorschrift 2 *g)* verfahren, indem von 2 g 2,3'-Dinitro-benzal-fluoren ausgegangen wird. Durch Verdünnen des Alkoholfiltrates scheidet sich das Amin in orangegelben Flocken aus, die bei 115–117° schmelzen. Ausbeute : 1,5 g (90 % d.Th.).

$C_{20}H_{16}N_2$ (284,34)	*Ber.* : N 9,84 %
	Gef. : N 9,93 %

i) *2,4'-Diamino-benzal-fluoren*

Es wird nach Vorschrift 2 *g)* verfahren und von 2 g 2,4'-Dinitro-benzal-fluoren ausgegangen. Das aus dem eingeengten Alkoholfiltrat durch Verdünnen mit Wasser in gelben Flocken ausgeschiedene Amin schmilzt bei 115–120°. Ausbeute : 1,5 g (90 % d.Th.).

$C_{20}H_{16}N_2$ (284,34)	*Ber.* : N 9,84 %
	Gef. : N 9,91 %

3. — CHLORACETAMIDODERIVATE

a) *2-Chloracetamido-benzal-fluoren*

2 g 2-Amino-benzal-fluoren werden in 30 ml wasserfreiem Benzol gelöst und portionsweise mit 2,5 ml Säurechlorid der Monochloressigsäure versetzt, das mit 3 ml Benzol verdünnt worden war. Nach 4–6 stdg. Rückflußkochen wird das Reaktionsgemisch in einer Schale auf dem Wasserbad abgedampft, der harzige Rückstand mit heißem Wasser gewaschen, dann mit Äthanol versetzt und durch Reiben mit einem Glasstab in eine gelbe pulvrige Masse überführt. Ausbeute : 1,9 g (76 % d.Th.). Durch Umkristallisieren aus Eisessig, werden kurze, gelbe Nadeln erhalten, die oft rosettenförmig angeordnet sind und bei 146–147° unter Zersetzung schmelzen.

$C_{22}H_{16}ONCl$ (345,81)	*Ber.* : N 4,05 %
	Gef. : N 4,13 %

---

[12] O. Diels, *Ber. dtsch. chem. Ges.*, 34, 1759 (1907).

b) *2-Chloracetamido-4′-methoxy-benzal-fluoren*

Es wird von 2 g 2-Amino-4′-methoxy-benzal-fluoren ausgegangen und wie in Vorschrift 3 *a*) verfahren. Ausbeute: 1,9 g (76% d.Th.). Durch Umkristallisieren aus Eisessig werden gelbe, glänzende Nadeln erhalten, die bei 191–193° unter Zersetzung schmelzen.

$C_{23}H_{18}O_2NCl$ (375,83) *Ber.*: N 3,72%
Gef.: N 3,83%

c) *2-Chloracetamido-4′-dimethylamino-benzal-fluoren*

Es wird wie in Vorschrift 3 *a*) verfahren und von 2 g 2-Amino-4′-dimethylamino-benzal-fluoren ausgegangen. Nach Beendigung der Reaktion wird die Benzollösung abgegossen, der Niederschlag in Wasser suspendiert, filtriert, mit heißem Wasser und darauf mit etwas Äthanol gewaschen und im Trockenschrank getrocknet. Ausbeute: 1,3 g (54% d.Th.). Aus Eisessig oder Äthanol kristallisiert die Verbindung als orange mikrokristalline Substanz aus, und aus Aceton durch Verdünnen mit Wasser in orangegelben Nadeln. Schmp. 180–81° (Zers.).

$C_{24}H_{21}ON_2Cl$ (388,88) *Ber.*: N 7,20%
Gef.: N 7,29%

d) *2,7-Bis-(chloracetamido)-benzal-fluoren*

2 g 2,7-Diamino-benzal-fluoren werden in 75–100 ml wasserfreiem Benzol gelöst und mit einem Überschuß frisch zubereitetem Säurechlorid der Monochloressigsäure (4 ml Säurechlorid gelöst in 4 ml wasserfreiem Benzol) versetzt. Die Reaktion setzt sofort unter Ausscheidung des Chloracetamidoderivates ein und wird durch 1 stdg. Rückflußkochen auf dem Wasserbad beendet. Man filtriert an der Wasserstrahlpumpe, wäscht das braungelbe pulvrige Produkt mit viel heißem Wasser und trocknet im Trockenschrank. Ausbeute: 2 g (64% d.Th.). Aus Eisessig werden gelbe, glänzende Blättchen erhalten, die bei 244–45° unter Zersetzung schmelzen.

$C_{24}H_{18}O_2N_2Cl_2$ (437,31) *Ber.*: N 6,46%
Gef.: N 6,57%

e) *2,7-Bis-(chloracetamido)-4′-methoxy-benzal-fluoren*

Es wird von 2 g 2,7-Diamino-4′-methoxy-benzal-fluoren ausgegangen und nach Vorschrift 3 *d*) verfahren. Ausbeute: 2 g (64% d.Th.). Durch Umkristallisieren aus Eisessig, werden gelbe, glänzende Blättchen erhalten. Schmp. 241–42° (Zers.).

$C_{25}H_{20}O_3N_2Cl_2$ (467,34) *Ber.*: N 5,99%
Gef.: N 6,12%

f) *2,7-Bis-(chloracetamido)-4′-dimethylamino-benzal-fluoren*

Es wird von 2 g 2,7-Diamino-4′-dimethylamino-benzal-fluoren ausgegangen und wie in Vorschrift 3 *d*) verfahren. Das ziegelbraune Reaktionsprodukt ist in den gebräuchlichen organischen Lösungsmitteln praktisch unlöslich und schmilzt bis zu 340° nicht. Durch Kochen in Eisessig klebt es an den Boden des Gefäßes an, ohne in Lösung zu gehen. Ausbeute: 2g (64% d.Th.).

$C_{26}H_{23}O_2N_3Cl_2$ (480,36) *Ber.*: N 8,74%
Gef.: N 8,87%

g) *2,2′-Bis-(chloracetamido)-benzal-fluoren*

Es wird nach Vorschrift 3 *d*) verfahren und von 2 g 2,2′-Diamino-benzal-fluoren ausgegangen. Nach Beendigung der Reaktion wird das Reaktionsgemisch auf dem Wasserbad zur Trockene abgedampft und mit Äthanol versetzt. Durch Reiben des braunen, harzigen Rückstandes mit einem Glasstab, geht er in ein gelbes, pulvriges Produkt über. Ausbeute: 0,8 g (25% d.Th.). Schmp. 234° (Zers.).

$C_{24}H_{18}O_2N_2Cl_2$ (437,31) *Ber.*: N 6,46%
Gef.: N 6,55%

h) *2,3′-Bis-(chloracetamido)-benzal-fluoren*

Es wird von 2 g 2,3′-Diamino-benzal-fluoren ausgegangen und nach Vorschrift 3 *d*) verfahren. Ausbeute: 2,8 g (89% d.Th.). Durch Umkristallisieren aus Eisessig, erhält man ein gelbes, mikrokristallines Produkt, das bei 236–237° unter Zersetzung schmilzt.

$C_{24}H_{18}O_2N_2Cl_2$ (437,31) *Ber.*: N 6,46%
Gef.: N 6,59%

i) *2,4′-Bis-(chloracetamido)-benzal-fluoren*

2 g 2,4′-Diamino-benzal-fluoren werden nach Vorschrift 3 *d*) behandelt. Ausbeute: 2,3 g (73% d.Th.). Aus Eisessig umkristallisiert, erhält man ein grünlichgelbes, mikrokristallines Produkt, das bei 227–228° unter Zersetzung schmilzt.

$C_{24}H_{18}O_2N_2Cl_2$ (437,31) *Ber.*: N 6,46%
Gef.: N 6,54%

4. – QUARTÄRE AMMONIUMSALZE

a) *2-(Trimethylammonium-acetamido)-benzal-fluoren-chlorid*

0,5 g 2-Chloracetamido-benzal-fluoren werden zusammen mit einem Überschuß an Trimethylamin (2 ml alkoholische 21proz. Trimethylamin-Lösung) in geschlossenem Rohr im kochenden Wasserbad erhitzt. Nach 8–10 stdg. Erhitzen wird der Inhalt des Rohres auf dem Wasserbad zur Trockne eingedampft (0,7 g), in Äthanol gelöst, mit Kohle entfärbt und heiß filtriert. Beim Abkühlen scheidet sich das quartäre Salz in Form feiner zitronengelber Nadeln ab, die sich in heißem Wasser und verdünntem Äthanol äußerst gut, in kaltem Wasser und absolutem Äthanol aber schwerer lösen und bei 237–38° unter Zersetzung und vorangehendem Erweichen schmelzen.

$C_{25}H_{25}ON_2Cl$ (404,92) *Ber.*: N 6,91; Cl 8,76%
Gef.: N 6,99; Cl 8,75%

b) *2-(Trimethylammonium-acetamido)-4'-methoxy-benzal-fluoren-chlorid*

Das Trimethylamin wird unter den oben beschriebenen Bedingungen an 2-Chloracetamido-4'-methoxy-benzal-fluoren angelagert. Das aus 96proz. Äthanol umkristallisierte Produkt bildet gelblichrosa Nadeln, die gewöhnlich rosettenartig angeordnet sind, sich in Wasser und absolutem Äthanol schwer, in verdünntem Äthanol aber leicht lösen. Ausbeute : 0,6 g (86 % d.Th.). Schmp. 267—68° (Zers.).

$C_{26}H_{27}O_2N_2Cl$ (434,93) *Ber.* : N 6,44 ; Cl 8,16 %
Gef. : N 6,56 ; Cl 8,60 %

c) *2-(Trimethylammonium-acetamido)-4'-dimethylamino-benzal-fluoren-chlorid*

Das Trimethylamin wird in der in Vorschrift 4 *a*) angegebenen Weise an 2 Chlor acetamido-4'-dimethylamino-benzal-fluoren angelagert. Ausbeute : 0,5 g (87 % d.Th.). Aus Äthanol kristallisiert das quartäre Salz in orangefarbenen Blättchen aus, die in Wasser und absolutem Äthanol mäßig und in verdünntem Äthanol äußerst löslich sind. Schmp. 234—35° (Zers.). Interessant zu erwähnen ist, daß dieses Produkt lichtempfindlich ist : unter Lichteinfluß wechselt das Salz seine Farbe von orangegelb in kaffeebraun.

$C_{27}H_{30}ON_3Cl$ (447,94) *Ber.* : N 9,38 ; Cl 7,91 %
Gef. : N 9,50 ; Cl 8,06 %

d) *2,7-Bis-(trimethylammonium-acetamido)-benzal-fluoren-dichlorid*

Es wird von 0,5 g 2,7-Bis-(chloracetamido)-benzal-fluoren ausgegangen und nach Vorschrift 4 *a*) verfahren. Der nach Abdampfen des Reaktionsgemisches erhaltene Rückstand wird in heißem Äthanol aufgenommen, mit etwas Tierkohle gekocht und heiß filtriert. Durch Hinzufügen von Aceton zum Alkoholfiltrat, scheidet sich das Salz als klebrige Maße ab, die durch Reiben mittels Glasstab in Aceton in ein ziegelfarbenes Pulver übergeht. Ausbeute : 0,45 g (71 % d.Th.). Schmp. 112—15°. Das Produkt ist in Wasser und verdünntem Äthanol leicht löslich, schwer in absolutem Äthanol.

$C_{30}H_{36}O_2N_4Cl_2$ (555,53) *Ber.* : N 10,08 ; Cl 12,76 %
Gef. : N 10,19 ; Cl 12,89 %

e) *2,7-Bis-(trimethylammonium-acetamido)-4'-methoxy-benzal-fluoren-dichlorid*

Es wird von 0,5 g 2,7-Bis-(chloracetamido) -4'-methoxy-benzal-fluoren ausgegangen und wie in Vorschrift 4 *a*) verfahren. Ausbeute : 0,5 g (82 % d.Th.). Durch Umkristallisieren aus Äthanol mit Äther, scheidet sich das quartäre Salz als dunkelziegelroter, mikrokristalliner Stoff ab, der schwach hygroskopisch ist, sich in absolutem Äthanol schwer, in Wasser und verdünntem Äthanol sehr leicht löst. Schmp. 237—38° (Zers.).

$C_{31}H_{38}O_3N_4Cl_2$ (585,54) *Ber.* : N 9,56 ; Cl 12,11 %
Gef. : N 9,69 ; Cl 12,19 %

f) *2,7-Bis-(trimethylammonium-acetamido)-4'-dimethylamino-benzal-fluoren-dichlorid*

Man verfährt wie in Vorschrift 4 *a*) und erhitzt das 2,7-Bis-(chloracetamido)-4'-dimethylamino-benzal-fluoren mit einem Überschuß an Trimethylamin 20 Std. Durch Abdampfen des Reaktionsgemisches auf dem Wasserbad erhält man ein rotbraunes, dickflüssiges Produkt, das in einem Minimum von Äthanol aufgenommen und mit Aceton gefällt wird. Ausbeute : 0,5 g (80% d.Th.). Das rötlichbraune mikrokristalline, schwach hygroskopische Salz ist in Wasser und Äthanol löslich und schmilzt bis 325° nicht.

$C_{32}H_{41}O_2N_5Cl_2$ (598,59) *Ber.* : N 11,70 ; Cl 11,84 %
Gef. : N 11,79 ; Cl 11,98 %

g) *2,2'-Bis-(trimethylammonium-acetamido)-benzal-fluoren-dichlorid*

0,5 g 2,2'-Bis-(chloracetamido)-benzal-fluoren werden mit 2,5 ml alkoholischer 21proz. Trimethylamin-Lösung unter den in Vorschrift 4 *a*) gezeigten Bedingungen erhitzt. Ausbeute : 0,4 g (66% d.Th.). Aus Äthanol scheidet sich das Salz mit Äther in gelber mikrokristalliner Form ab. Schmp. über 300°.

$C_{30}H_{36}O_2N_4Cl_2$ (555,53) *Ber.* : N 10,08 ; Cl 12,76 %
Gef. : N 10,20 ; Cl 12,51 %

h) *2,3'-Bis-(trimethylammonium-acetamido)-benzal-fluoren-dichlorid*

Trimethylamin wird an 2,3'-Bis-(chloracetamido)-benzal-fluoren unter den weiter oben beschriebenen Bedingungen angelagert. Das entstandene Ammoniumsalz (0,3 g, 50% d.Th.) wird aus Äthanol mit Äther umkristallisiert. Das gelbe, mikrokristalline, schwach hygroskopische Produkt ist in Wasser und verdünntem Äthanol leicht löslich und schmilzt nicht unter 300°.

$C_{30}H_{36}O_2N_4Cl_2$ (555,53) *Ber.* : N 10,08 ; Cl 12,76 %
Gef. : N 10,18 ; Cl 12,44 %

i) *2,4'-Bis(trimethylammonium-acetamido)-benzal-fluoren-dichlorid*

Das Trimethylamin wird in der oben erwähnten Weise an das 2,4'-Bis-(chlor-acetamido) benzal-fluoren angelagert. Ausbeute : 0,3 g (50% d.Th.). Aus Äthanol mit Aceton erhält man gelbe Nadeln, die gewöhnlich rosettenförmig angeordnet sind, unter 300° nicht schmelzen, in absolutem Äthanol schwer, in verdünntem Ätahnol und Wasser aber leicht löslich sind.

$C_{30}H_{36}O_2N_4Cl_2$ (555,53) *Ber.* : N 10,08 ; Cl 12,76 %
Gef. : N 10,16 ; Cl 12,35 %

Die vorläufig an Fröschen ausgeführten pharmakodynamischen Teste haben gezeigt, daß alle dargestellten Ammoniumsalze kurarewirksam sind, doch verglichen mit D-Tubocurarin (D-Tc), eine schwache Aktivität aufweisen. Die schwächste Wirkung wurde – wie auch zu erwarten war – bei den monoquartären Salzen beobachtet. Es folgen dann die diquartären Salze vom Typ II, die ungefähr 30 mal schwächer und schließlich die Salze vom Typ III, die ungefähr 25 mal schwächer als D-Tc sind. Es konnte weiterhin auch festgestellt werden, daß, während bei den diquartären Ammoniumsalzen die Kurarewirkung kaum vom Substituenten der 4′-Stellung oder von der Stellung der quartären Ammoniumgruppe im Benzolkern beeinflußt wird, bei den monoquartären Ammoniumsalzen aber die höchste Aktivität bei der mit Dimethylamin substituierten und die schwächste bei der nicht substituierten Verbindung beobachtet wird.

Revue Roumaine de Chimie, **15**, 1137–1140 (1970)

LE MARQUAGE DU DIPHOLATAN AVEC ^{35}S PAR SYNTHÈSE

MARIA SZABO
Institut de Physique Atomique,
Boite postale 35, Bucarest

Reçu le 11 septembre 1969

On effectue le marquage du dipholatan avec ^{35}S par synthèse à partir du monochlorure de soufre marqué avec ^{35}S et du trichloréthylène. Les rendements chimiques et radiochimiques sont compris entre 51 et 82 %, en fonction de la difficulté de l'étape respective.

Le dipholatan est un fongicide de synthèse relativement récente (préparé en 1962) d'un potentiel fongique élevé.

Sa formule chimique

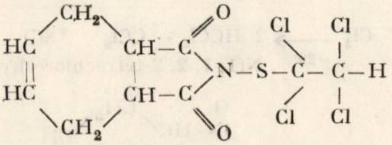

N(1, 1, 2, 2-tétrachloréthylthiotétrahydrophtalimide)

Il a un spectre large d'activité, actionnant sur 288 organismes phytopathogènes divisés en trois groupes selon le degré d'efficience du dipholatan.

Le dipholatan inhibe la germination des spores fongiques ayant une action plus persistante que les autres fongicides bien plus connus et utilisés couramment.

Les résidus sont assez réduits et il assure une protection efficace, de longue durée dans des conditions d'utilisation très sévères.

Son action persistante est expliquée, d'une part, par sa bonne efficacité intrinsèque et d'autre part par la ténacité du dépôt de pulvérisation.

Le dipholatan est une substance blanche, cristalline,[1] inodore, au point de fusion à 159–161°, insoluble dans l'eau, soluble dans des solvants organiques, stable à l'action de la lumière, en UV, à l'hydrolyse et à la chaleur.

Le dipholatan inhibe aussi bien les enzymes oxydatifs que les carboxylases des spores fongiques.

---

[1] G. E. ETTER, *Medeb. Werensch. Gent.*, **31**, 837 (1966).

Son métabolisme dans les organismes phyto-pathogènes, selon certains auteurs, serait le suivant : la dégradation du radical tétrachloréthylthioimidique dans des composés minéraux du soufre comme : sulfates, sulfites et thiosulfates.

Le cycle de l'imide donne un métabolisme inoffensif, mais il règle le mouvement du groupement toxophore dans la cellule fongique.

Dans le présent travail nous nous sommes proposé de marquer le dipholatan avec ^{35}S par synthèse.

Le produit marqué est utilisé pour établir le métabolisme d'action du toxique sur les spores fongiques.

La littérature ne mentionne pas l'obtention du dipholatan marqué. Il y a un patent sur la méthode d'obtention d'un fongicide mixte, dipholatan et captane non marqué[2].

Sur les étapes de synthèse du dipholatan, la littérature ne fait mention que de données insuffisantes.[3-5]

PARTIE EXPÉRIMENTALE

La synthèse du dipholatan marqué a été effectuée selon les étapes suivantes :

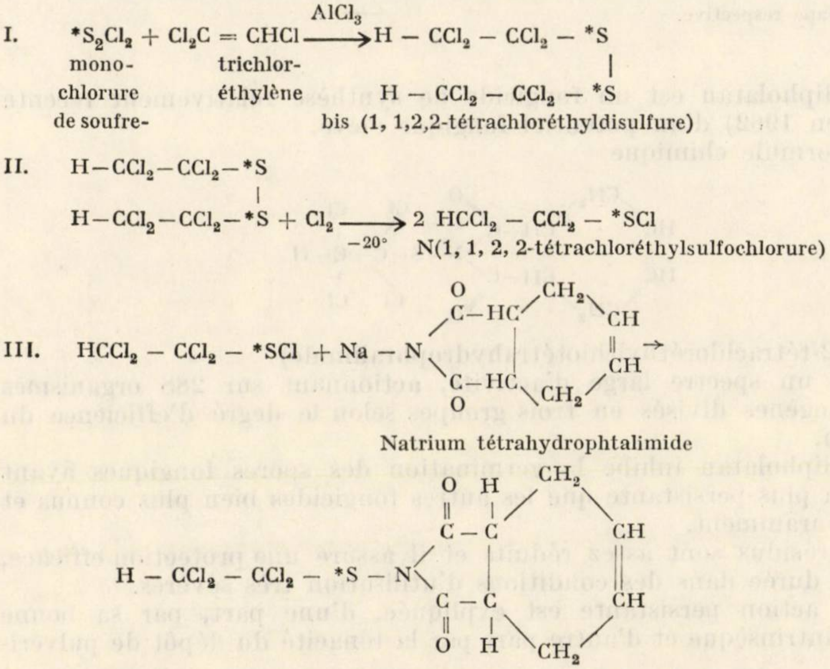
I.
*S₂Cl₂ + Cl₂C = CHCl
AlCl₃
H – CCl₂ – CCl₂ – *S
H – CCl₂ – CCl₂ – *S
mono-chlorure de soufre-
trichlor-éthylène
bis (1, 1,2,2-tétrachloréthyldisulfure)
II.
H–CCl₂–CCl₂–*S
H–CCl₂–CCl₂–*S + Cl₂
–20°
2 HCCl₂ – CCl₂ – *SCl
N(1, 1, 2, 2-tétrachloréthylsulfochlorure)
III.
HCCl₂ – CCl₂ – *SCl + Na – N
O
C–HC
CH₂
CH
CH
C–HC
O
CH₂
Natrium tétrahydrophtalimide
O H CH₂
C – C
CH
H – CCl₂ – CCl₂ – *S – N
C – C
CH
O H CH₂

Le dipholatan N (1, 1, 2, 2-tétrachloréthylthiotétrahydrophtalimide)

---

[2] G. K. Kohn (to Chenron Research Co), U.S. Patent 3 226 290, 28 sept. 1965, *Chem. Abstr.* **64**, , 8055 d (1966).

[3] J. Geering (to Hooker Chem. Corp.), U.S. Patent 3 088 818, 7 mai 1963; *Chem. Abstr.*, **59**, 11 258 a (1963).

[4] J. Geering (to Hooker Chem. Corp.), Ger. Patent 1 121 607, 21 mars 1960; *Chem. Abstr.*, **57**, 4548 e (1962).

[5] J. Geering (to Hooker Chem. Corp.), Fr. Addn. Patent 85 696, 27 sept. 1965; *Chem. Abstr.*, **64**, 3355 a (1966).

(Pour chaque expérience on a effectué deux épreuves).

Nous décrirons ci-après les étapes d'obtention du dipholatan marqué.

Première étape. Pour l'obtention du bis-tétrachloréthyldisulfure ont été pesés 58,8 g de trichloréthylène et 2,66 g de chlorure d'aluminium. Cette mixture a été homogénéisé par agitation et refroidie à 5° ; 3 heures après, on y a ajouté 27,02 g de $^{35}S_2Cl_2$ marqué avec ^{35}S par la méthode[6] d'activité totale 1,84 mCi et 7,64 mCi.

Après la réaction, la mixture a été filtrée et au filtrat on a ajouté de l'eau, une solution diluée de Na_2CO_3 et de nouveau de l'eau.

La mixture obtenue n'étant pas miscible, on a effectué facilement la séparation, dans un entonnoir de séparation. Finalement, au produit on a ajouté de l'alcool éthylique et de l'eau. Les couches ont été séparées et séchées sur du $CaSO_4$. Le produit a été distillé à 180–185° et à une pression de 3 mm.

La densité du produit à t = 23, 3° a été de d = 1,785.

On a déterminé aussi le rendement chimique et radiochimique. Les résultats sont présentés dans le tableau 1.

Tableau 1

Les rendements chimiques et radiochimiques obtenus par la synthèse du dipholatan

Etapes / Rendements %	I	II	III
Rendem. chimiques	72 76	81 72	55 54
Rendem. radiochimiques	75 79	82 71	51 53

Seconde étape. On a traité 39,8 parties de tétrachloréthyldisulfure marqué avec ^{35}S avec du chlore sous agitation et refroidissement à – 20°.

Au moment où le poids de la substance est le même que le poids du tétrachloréthylsulfochlorure (respectivement 46,9 g), la mixture que l'on a laissée réchauffer à la température de la chambre est distillée à la pression de 0,5 mm et à la température de 53–57°, par une colonne Vigreux. Le produit obtenu a une densité de 1,76, à 23°.

La synthèse de la Δ^4-tétrahydrophtalimide comporte deux phases[7] :

1. La synthèse de l'anhydride Δ^4-tétrahydrophtalique ;
2. La synthèse de la Δ^4-tétrahydrophtalimide.

La première phase est réalisée par une synthèse entre l'anhydride maléique et le butadiène.

Le processus est réalisé à 110° par barbotage du butadiène dans l'anhydride maléique. Sitôt que le point de fusion de la mixture atteint 97° (la température de fusion de l'anhydride tétrahydrophtalique) au ballon on a attaché un réfrigérant descendant et on a introduit du gaz ammoniac.

La température a été élevée jusqu'à 190–200°.

On a continué le barbotage de l'ammoniac jusqu'au moment où de la réaction se dégage la quantité d'eau théorique.

---

[6] V. N. Vasilieva et E. N. Gurianova, *Zhur. obschei Khim.*, **36**, 677 (1956).

[7] T. Ambruş, L. Tincu, A. Velniceru et L. Gavăt, *Rev. Chim.* (*Bucureşti*), **13**, 275 (1962).

Le produit obtenu est blanc, cristallin, au Pf à 125°. La recristallisation a été effectuée dans de l'alcool éthylique absolu.

Les rendements chimiques ont été de 70 à 80%.

Troisième étape. La littérature ne donne aucune indication sur le couplage de la tétrahydrophtalimide de sodium, avec le 1, 1, 2, 2-tétrachlor-éthylsulfochlorure, pour obtenir le dipholatan. C'est pourquoi cette étape a été effectuée par analogie avec la préparation d'un fongicide mixte.[2]

Ainsi, à une quantité déterminée de tétrahydrophtalimide, on a ajouté une solution de NaOH 50% en quantité stœchiométrique, en y ajoutant sous agitation continue, de l'eau et de la glace, jusqu'à la dissolution complète de la mixture.

Le tétrachloréthylsulfochlorure marqué a été aussi ajouté par agitation, la mixture étant maintenue pendant une heure à 2°.

Le précipité obtenu a été filtré, lavé avec de l'eau chaude, de l'alcool méthylique et de l'éther. Le produit obtenu étant séché, il en résulte une substance blanche, cristalline au P_f à 158° ayant les caractéristiques du dipholatan.

L'activité spécifique du dipholatan a été de 0,235 mCi/g.

L'analyse du produit final a été effectuée par la détermination du soufre, en oxydant le produit avec de l'acide azotique fumant.

Aux produits intermédiaires obtenus au cours du travail on a déterminé également la pureté radiochimique par chromatographie sur papier Schleicher — Schull 2040 A dans un bain d'acétone-toluène (2 : 3). Le spot a été développé avec de l'$AgNO_3$ et exposition en UV. On a obtenu, pour chaque produit, un seul spot radioactif coloré en gri sur fond noir.

Détermination de l'activité des produits

Tous les produits marqués avec ^{35}S, obtenus par la synthèse du dipholatan, ainsi que la substance initiale ont été oxydés avec de l'acide azotique fumant en présence du NaCl[8].

L'oxydation a été effectuée dans une fiole de verre fermée chauffée à 250—280°.

La quantité de substance prise pour l'oxydation, ainsi que la durée d'oxydation ont été établies pour chaque substance à part, par des essais préliminaires. Le dipholatan a été oxydé sans être dissous au préalable dans quelque solvant organique.

RÉSULTATS ET DISCUSSION

Du tableau 1 il résulte que les rendements chimique et radiochimique pour les deux premières étapes sont compris entre 72—81%.

Le rendement de 72%, respectivement de 71% de la deuxième étape est dû à la chloruration discontinue du tétrachloréthylsulfochlorure.

Les rendements de l'étape de couplage de la Δ^4-tétrahydrophtalimide de sodium au tétrachloréthylsulfochlorure sont de moins de 50%.

On doit relever le fait que les rendements chimiques et radiochimiques des deux premières étapes sont très bons, compte tenu que, en général, les rendements radiochimiques par synthèse sont petits. Le marquage du dipholatan avec ^{35}S par échange isotopique est difficile, du fait que le soufre se trouve dans le centre de la molécule et il n'est pas labile.

Le présent travail a aussi de très importantes et utiles contributions du point de vue de la détermination de l'activité du ^{35}S dans les molécules organiques insolubles dans l'eau.

---

[8] J. S. Fritz et G. S. Hammond « Quantitative Organic Analysis », Ed. John Wiley and Sons Inc., Londres, 1957, p. 137.

NOTE POUR LES AUTEURS

La *Revue Roumaine de Chimie* publie des articles en anglais, français, russe, allemand ou espagnol. Les auteurs sont priés d'envoyer des articles, notes, communications et comptes rendus inédits.

Les manuscrits seront dactylographiés à deux intervalles. Les tableaux seront dactylographiés sur feuilles séparées, de même que la légende des figures. Les diagrammes seront tracés à l'encre de Chine sur papier calque. Les tableaux et les figures seront numérotés par des chiffres arabes, en nombre strictement nécessaire. Prière de ne pas inscrire les mêmes données dans les tableaux et les figures. Les formules chimiques seront incluses dans le texte ; en outre, elles seront transcrites sur des feuilles séparées. Les auteurs sont priés d'indiquer les caractères italiques (en soulignant les lettres au crayon), ainsi que tout autre caractère spécial. L'ordre des références bibliographiques sera celui de leur mention dans le texte ; le nom de l'auteur sera précédé de l'initiale du prénom ; les publications périodiques seront présentées suivant les prescriptions internationales. Les références seront ajoutées à la fin de l'article ; elles paraîtront comme des notes, au bas de la page. Le texte sera précédé d'un résumé, comprenant 15 lignes au maximum.

L'entière responsabilité du contenu des articles appartient aux auteurs. On publie des articles dus aux collaborateurs roumains ou étrangers. Les auteurs recevront 50 tirés à part.

PRINTED IN ROMANIA

1970 OKT 14

TRAVAUX PARUS AUX ÉDITIONS DE L'ACADÉMIE DE LA RÉPUBLIQUE SOCIALISTE DE ROUMANIE

CORNEL BODEA et collab., **Tratat de biochimie vegetală**, partea I, **Fitochimie** (Traité de biochimie végétale, Ire partie, Phytochimie), Ier vol., 1964, 747 p. + 4 annexes + 2 pl., 41 lei ; IIe vol., 1265, 1962, p., 1 pl., 56 lei ; III vol., 1967, 773 p., 35 lei.

V. GHEȚIE et V. MICUȘAN, **Analiza imunochimică. Teorie și practică** (Analyse immunochimique. Théorie et pratique), 1966, 369 p., 28 lei.

R. PORTOCALĂ et L. POPA, **Acizii ribonucleici celulari și virali** (Les acides ribonucléiques cellulaires et viraux), 1966, 375 p., + 8 pl., 26 lei.

D. PURDELA et R. VÎLCEANU, **Chimia compușilor organici ai fosforului și ai acizilor lui** (La chimie des composés organiques du phosphore et de ses acides), 1965, 540 p., 37 lei.

CRISTOFOR SIMIONESCU, MARGARETA GRIGORAȘ et AGATA CERNĂTESCU-ASANDEI, **Chimia lemnului din R.P.R.** (La chimie du bois en Roumanie), 1964, 239 p. + 6 pl., 27 lei.

CRISTOFOR SIMIONESCU et CLEOPATRA VASILIU OPREA, **Mecanochimia compușilor macromoleculari** (La mécanochimie des composés macromoléculaires), 1967, 344 p., 23,50 lei.

CARMEN SABĂU, **Schimbul ionic, teoria și aplicațiile sale in chimia analitică** (L'échange ionique, Théorie et applications à la chimie analytique), 1967, 307 p., 12 lei.

I. V. MAXIM, **Materiale nucleare** (Matériaux nucléaires), 1969, 444 p., 30 lei.

CR. SIMIONESCU, C. UGLEA, **Fracționarea compușilor macromoleculari** (Le fractionnement des composés macromoléculaires), 1969, 292 p., 18,50 lei.

I.P.I. – c. 5396

43 426

Lei 25.—

F 1103

04

REVUE ROUMAINE DE CHIMIE

TOME 15

Nº 8

Août 1970

ÉDITIONS DE L'ACADÉMIE DE LA RÉPUBLIQUE SOCIALISTE DE ROUMANIE

Rev. Roumaine Chim.

15, 1141–1274 (1970), Bucarest

COMITÉ DE RÉDACTION

Rédacteur en chef:

C. D. NENIŢESCU, membre de l'Académie de la République Socialiste de Roumanie.

Rédacteurs en chef adjoints:

A. T. BALABAN et V. E. SAHINI, membres correspondants de l'Académie de la République Socialiste de Roumanie.

Collège de rédaction:

C. DRĂGULESCU, RALUCA RIPAN, CR. SIMIONESCU, membres de l'Académie de la République Socialiste de Roumanie; EM. BRATU, membre correspondant de l'Académie de la République Socialiste de Roumanie; Pr G. OSTROGOVICH, MARG. AVRAM, F. BADEA, I. D. MARCHIDAN, D. NEGOIU et D. SĂNDULESCU.

Les manuscrits, les livres et les revues proposés en échange, ainsi que toute correspondance seront envoyés à la rédaction :

REVUE ROUMAINE DE CHIMIE

23, str. Dumbrava Roşie, Bucarest, Roumanie.

REVUE ROUMAINE DE CHIMIE

ORSZÁGOS MŰSZAKI KÖNYVTÁR ÉS DOKUMENTÁCIÓS KÖZPONT 1883

Tome 15, N° 8 Août 1970

Page

COSTIN D. NENITZEZSCU I—III

I. G. MURGULESCU and M. I. VASS, Surface potential variation at successive carbon monoxide and oxygen adsorption on thin silver films . . . . . . 1143—1151

O. RADOVICI and VICTORIA SURDEANU, Passivity of steel in monoethanolamine solutions . . . . 1153—1161 R

D. CISMARU and STELA ZERVUDIS, Kinetics of the Al_2O_3+CoO reaction at high temperature accompanied by spinel formation in oxygen atmosphere 1163—1167

S. STERNBERG et I. GALASIU, L'électrode halogène — charbon dans les électrolytes fondus. VI. L'adsorption du chlore et de l'iode sur l'électrode de charbon activé . . . . 1169—1176

D. I. MARCHIDAN and M. CIOPEC, Thermal properties of potassium chloride High temperature heat content . . . . 1177—1180

D. COSTACHE, Kinetic measurement of cobalt traces. IV. With hematoxylin . 1181—1185 R

AL. ŞUTEU, I. AL. CRIŞAN und ELEONORA MÎNDRUŢIU, Die kinetische Bestimmung des Hydrazins mit Bromat und Amidol . . . . 1187—1190 R

CAMELIA BELDIE, Salting-in effects in organic solvent-water-organic electrolyte systems. Molecular weight of the organic electrolytes . . . . 1191—1196

A. POPESCU and A. SZABO, The activity of molybdenum oxide—bismuth oxide catalysts and the influence of metallic oxide mixtures . . . . 1197—1200 R

C. CHIRIAC et I. ZUGRĂVESCU, Pyrazoles. III. N-arylation des N-acylpyrazoles avec le chlorure de picryle . . . . 1201—1205

MARGARETA AVRAM, I. POGANY, I. G. DINULESCU, F. CHIRALEU and D. NENITZESCU, Investigations in the cyclobutane series. XXVIII. The reaction of *endo* and *exo*-3.4-benzotricyclo[4.2.1.$0^{2,5}$]nona-3.7-dienes with electrophylic reagents . . . . 1207—1218

MARGARETA AVRAM, F. CHIRALEU and I. POGANY, Investigations in the cyclobutane series. XXIX. NMR spectra studies of some 3.4-benzotricyclo [4.2.1.$0^{2,5}$]nona-3.7-diene derivatives . . . . 1219—1225

J. REICHEL und R. VIDAC, Untersuchungen über Aryldiazosulfonate und Aryldiazosulfonsäuren. II. Herstellung und photochemisches Verhalten der Benzoldiazosulfonsäure . . . . 1227—1232

ILEANA GOIA and MARIA IONESCU, Acridones. XXXV. The iodination of acridone . . . . 1233—1242

A. T. BALABAN, Chemical graphs. X. (Aromaticity. VIII) Resonance energies of *cata*-condensed benzenoid polycyclic hydrocarbons . . . . 1243—1250

Rev. Roumaine Chim. 15, 1141—1274 (1970), Bucarest

A. T. BALABAN, Chemical graphs. XI. (Aromaticity. IX) Isomerism and topology of non-branched *cata*-condensed polycyclic conjugated non-benzenoid hydrocarbons . . . . 1251—1262
IOANA ARSENIE et I. LEUCĂ, Contribution à la séparation du zirconium d'avec le hafnium par cristallisation fractionnée de l'hexafluozirconate de potassium . . . . 1263—1287

COSTIN D. NENITZESCU

MŰSZAKI KÖNYV
1983

COSTIN D. NENITZESCU

On the dawn of 28 July 1970, Professor Costin D. Nenitzescu, the outstanding figure of Romanian chemistry for many decades, died at Buşteni, in the midst of the mountains he loved so much.

Death took him from his friends and colleagues unexpectedly, bringing to a close a career of exceptional service and great distinction.

Costin D. Nenitzescu was born in Bucharest on 15 July 1902. He attended the university courses at the Polytechnics of Zurich and Munich, obtaining in 1925 his doctor's degree under the known scientist Hans Fischer. After his return to Romania, he gradually mounted all the steps of university teaching. In 1935 he was appointed Professor of Organic Chemistry at the Polytechnic Institute of Bucharest, a position which he held until his death.

In the course of 45 years of teaching, Costin D. Nenitzescu showed an untiring, passionate love of work, devoted to the education of future engineers, research workers or teachers. None of those who listened to his lectures will forget his lively spirit, proper to a man opening up new roads in science. He not only gave his students an outline of the great achievements in chemistry, but also showed them the subtle ways leading to them, raising in his listeners the wish to follow in the steps of their great forerunners in chemistry.

His treatise on organic chemistry, which was brought up to date in six successive editions and after which 42 generations of students have been learning, is considered one of the best works in this field. Highly appreciated abroad, it has been translated and published in several other languages.

A broad-minded scientist, with a wide scientific horizon, he viewed his tasks from angles that greatly exceeded the limits of organic chemistry. This may be seen from his treatise on general chemistry at which he worked, writing it again in a new form, up to the last day of his life. The high school chemistry teaching benefited from his rich scientific and didactic experience through the textbooks which he wrote, guiding beginners up the first steps of chemistry, contributing to the general education of the youth of our country.

Throughout his entire activity, Costin D. Nenitzescu was guided by the idea of combining the work of education with that of research. "You cannot teach others a science – he would say – if you are not yourself a creator of science". Moreover, he had a very clear conception of the relations between fundamental and applied research, considering that the progress of the former necessarily conditions the success of the latter. These principles were constantly confirmed by the results of his whole activity obtained in education, research and industry.

With a power of comprehension seldom encountered and an enthusiasm that he knew to impart to his collaborators, Costin D. Nenitzescu investigated successfully an unusually wide range of areas of organic chemistry : the Friedel-Crafts reaction of aliphatic and alicyclic compounds, isomerization of saturated aliphatic and alicyclic hydrocarbons, hydride ion transfer reactions, syntheses in the cyclobutane series, syntheses of pyrylium salts, reversible rearrangements through carbonium ions, oxidation of hydrocarbons, elimination and addition reactions to the olefinic double bond, syntheses in the indole and pyrrole series *). This brief list of the main fields in which Costin D. Nenitzescu brought fundamental contributions, hides behind it the enthusiastic, tremendous capacity for hard work and sustained effort he displayed at the head of the research group e created and whose very soul he was.

By the fundamental character of his work, by his original ideas — which many chemists from all over the world subsequently developed, Costin D. Nenitzescu opened up new roads and prospects in organic chemistry. "Nenitzescu reactions", "Nenitzescu compounds" are names currently used in chemical literature, indicating some of his original achievements. The interest his work awoke among the scientists of other countries is reflected in the numerous references encountered in the chemical literature, in his scientific correspondence with many great personalities of organic chemistry throughout the world, the countless invitations received to hold lectures, to participate in congresses or cooperate with laboratories of other countries.

Costin D. Nenitzescu founded the Romanian school of organic chemistry. His didactic and scientific work was always combined with the idea of creating new centers of research. Next to the Chair of Organic Chemistry of the Polytechnic Institute he formed several groups of chemical research, which later on developed independently. Thus, in 1948 the first center of research of the Ministry of Chemical Industry was founded; in 1949 he organized the first group of organic chemical research of the Academy, which later became the actual Center of Organic Chemistry whose director he was up to the day of his death.

A faithful son of his people, Costin D. Nenitzescu devoted his skill and knowledge, coupled with a rare abnegation, to the promotion of the chemical industry in Romania. Numerous original procedures used in the manufacture of drugs, dyes, plastics etc. have been developed under his direct supervision.

For his outstanding, many-sided activity, Costin D. Nenitzescu received awards, medals and orders of the Socialist Republic of Romania. In 1940 he was elected corresponding member of the Academy, then full member and president of the section of chemical sciences in 1955. He was also a member of several academies and honorary member of chemical societies abroad. As a recognition of his important contribution to the development of chemistry, he was awarded, in the last year of his life, one of the greatest scientific distinctions: the "A. W. von Hofmann" medal.

---

*) A more detailed account of the scientific activity and the list of publications of Costin D. Nenitzescu will appear in a forthcoming issue of this journal.

Endowed with unusual spiritual resources, receptive to all that was interesting and beautiful, Costin D. Nenitzescu would astound others, especially those who were acquainted with his wide range of professional concerns, by his humanistic and scientific erudition, by the diversity of his interests.

His prominent personality, his life of hard struggles, his outstanding achievements made those who knew him to love and admire him as he was ready to be near them, to understand them, with all his kindness and friendship.

The departure of Professor Costin D. Nenitzescu is for the science and especially for the Romanian science an enormous loss. Costin D. Nenitzescu continues to live on in his work, example and spiritual inheritance handed to his students.

one of the greatest scientific distinctions: the "A. W. von Hofmann" medal.

Endowed with unusual spiritual resources, receptive to all that was interesting and beautiful, Costin D. Nenitzescu would astound others, especially those who were acquainted with his wide range of professional concerns, by his humanistic and scientific erudition, by the diversity of his interests.

His profound personality, his life of hard struggles, his outstanding achievements made those who knew him to love and admire him, as he was ready to be near them, to understand them, with all his kindness and friendship.

The departure of Professor Costin D. Nenitzescu is for the science and especially for the Romanian science an enormous loss. Costin D. Nenitzescu continues to live on in his work, example and spiritual inheritance handed to his students.

Revue Roumaine de Chimie, **15**, 1143–1151 (1970)

SURFACE POTENTIAL VARIATION AT SUCCESSIVE CARBON MONOXIDE AND OXYGEN ADSORPTION ON THIN SILVER FILMS

I. G. MURGULESCU and M. I. VASS

Institute of Physical Chemistry, Bucharest, str. Dumbrava Roşie 23

Received December 29, 1969

The surface potential variations produced by successive adsorption of carbon monoxide and oxygen on thin silver films are reported. From the values obtained as well as from the behaviour of the systems at different operations, the structure of the surface complexes is inferred.

The reaction between two gases, catalysed by a solid surface, takes place by intermediate stages, the first being the adsorption of at least one of the reactants. There is only few information about the compound formed between the adsorbed gas and the other gas, which can be also adsorbed (on the metallic surface or over the first adsorbed layer) or free. Besides the methods which provide direct indication about intermediate compounds—infrared spectroscopy, mass-spectrometry—the method of surface potential determination gives complementary information on the complex charge, dipole moment value, the orientation of the molecular groups against the surface. Initially, the method was used by Tompkins and co-workers [1] to infer the structure of the complexes formed on the nickel and copper films at the successive adsorption of gases as CO, O_2, H_2 and later on [2] to the N_2 and H_2 adsorption on iron and nickel films, or O_2 and H_2 on nickel and molybden. [3] On porous silver catalyst, correlations between the rate of oxygen removing by CO or H_2 with the work function variations were established. [4]

The success of the method depends on the existence of a difference between the values of the surface potential of the two gases (if it is possible even with opposite signs) for the same metal. The forming of complexes on surface is revealed by the discrepancy between the observed value of the surface potential for the mixed layer and the value calculated with additivity rule from the dipole moment and the number of adsorbed molecules.

---

[1] M. M. Siddiqui and F. C. Tompkins, *Proc. Roy. Soc.*, **A. 268**, 412 (1962).

[2] P. M. Gundry, J. Haber and F. C. Tompkins, *J. Catalysis*, **1**, 363 (1962).

[3] Z. Knor and V. Ponec, *Coll. Czech. Chem. Comm.*, **31**, 1172 (1966).

[4] L. A. Rudnitskii, L. I. Shakovskaia, N. V. Kulkova and M. I. Tempkin, *Doklady Akad. Nauk S.S.S.R.*, **182**, 1358 (1968).

In a previous paper [5] we have studied the forming of the bonds in the oxygen adsorbed layer on silver films at 77°K. In the present one, being known [6,7] the silver activity in the carbon monoxide oxidation reaction, we have followed the ΔV modifications produced by previous or subsequent CO adsorption.

EXPERIMENTAL

Retarding field diode was used for the study of the surface potential variations in the mixed carbon monoxide-oxygen system. Complete experimental details on the vacuum installation, measuring circuits, oxygen preparation, working method were described elsewhere. [8,9] Silver films of about 600 Å thickness (deduced from the known Johnson & Matthey evaporated silver quantity and geometrical area) were deposited at 77°K and $2-5\times10^{-9}$ torr. After deposition the films were sinterized by heating at 353°K for 5—7 min to stabilize the crystalline lattice. The carbon monoxide used was prepared by thermal decomposition of calcium oxalate (reagent grade) purified by passing over a KOH column and a liquid nitrogen trap.

The experiments were carried out only at 77°K; after the saturation of the surface with one of the gases, the excess was pumped off and then doses from the second gas were introduced until the saturation is reached again. In the absence of a mass-spectrometer analyser for the study of desorption products the subsequent operations were intended to precise the interaction mechanism; heating at 298°K, pumping of the desorbed gases, readsorption of CO or O_2, returning at 77° K.

RESULTS AND DISCUSSION

Table 1 contains the values obtained for the surface potential (ΔV) in the studied systems.

Table 1

Values obtained for the surface potential variations in the systems: $Ag-O_2-CO$ and $Ag-CO-O_2$

System	ΔV (volts)		
		Adsorption of CO	Adsorption of O_2
O_2-Ag	-1.44	-0.60	—
$CO-Ag$	$+0.20$	—	$-1.2(-0.6)$

---

[5] I. G. Murgulescu and M. I. Vass, *Rev. Roumaine Chim.*, **13**, 1521 (1968).

[6] G. M. Schwab and K. Gosner, *Z. phys. Chem.* (*Frankfurt*), **16**, 39 (1958).

[7] A. F. Benton and T. R. Bell, *J. Amer. Chem. Soc.*, **56**, 501 (1934).

[8] I. G. Murgulescu and M. I. Vass, *Rev. Roumaine Chim.*, **11**, 266 (1966).

[9] I. G. Murgulescu and M. I. Vass, *Rev. Roumaine Chim.*, **13**, 373 (1968).

1. *System Ag—O$_2$—CO*

a) As we have found in the previous paper [5] the adsorbed oxygen on thin silver films produces a ΔV of $-$ 1.44 V for a maximum coverage og 8.1 $\times 10^{14}$ molec/cm^2. We supposed that for these values the adsorbed layer has a mixed composition : most of the adsorption sites are covered with oxygen molecules bound in the 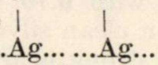 $\begin{array}{cc} O & \!\!\text{———}\!\! O \\ | & | \\ \text{...Ag...} & \text{...Ag...} \end{array}$ form, and only a small part as simple undissociated molecules 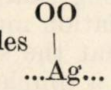 $\begin{array}{c} OO \\ | \\ \text{...Ag...} \end{array}$. The subsequent adsorption

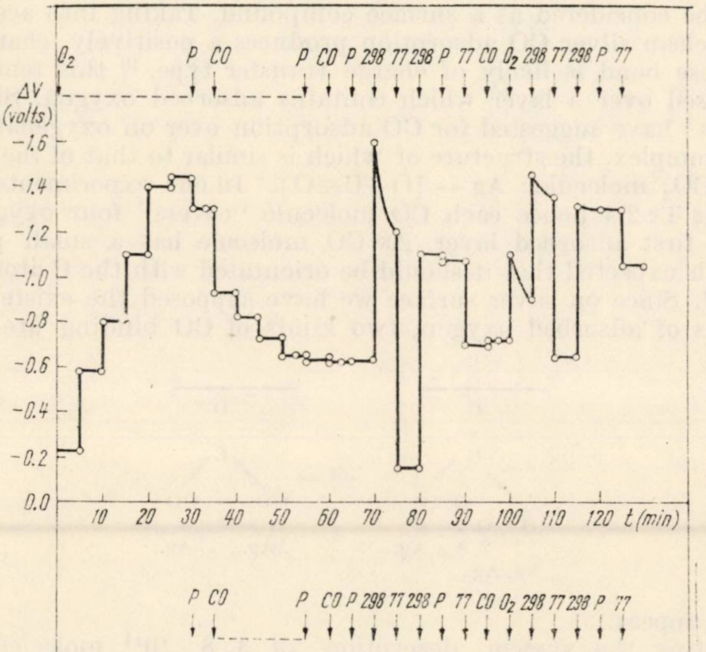

Fig. 1.— Surface potential variations in time, at 77°K for dose interaction in the system Ag$-$O$_2-$CO : in the low part simultaneous pressure variation is plotted.

of CO produces a 0.70 V positivation ot ΔV. The saturation values is obtained for the adsorption of 3.2×10^{14} molec/cm^2, namely a CO : O_2 rate of about 1 : 2.4. The introduction of a new CO quantity does not bring about any ΔV change, and the system may be considered CO-saturated. Because we consider also the oxygen monolayer complete it remains that the CO molecules must be adsorbed over the oxygen layer.

The ΔV increase with 0.70 V (given the + 0.20 V, ΔV increase for the CO adsorption on clean silver) points out the forming of the surface complex positively strong charged. Considering that additivity rule cab be applied, the ΔV variation must be 0.147 V, namely about 5 times smaller. We can suppose that the species appeared after CO adsorption is completely different from a simple superposition of the two components and can be considered as a surface compound. Taking into account that even for clean silver CO adsorption produces a positively charged complex, whose bond is likely of charge transfer type,[10] this tendency will be increased over a layer which contains adsorbed oxygen. Siddiqi and Tompkins[1] have suggested for CO adsorption over on oxygenated copper layer, a complex, the structure of which is similar to that of the resonance form of CO_2 molecule : $Ag \leftarrow [O-C\equiv O]^{+}$. In our experiments the rate CO : O_2 is 1 : 2.4 hence each CO molecule "covers" four oxygen atoms from the first adsorbed layer. As CO molecule has a small permanent dipole it is expected that it should be orientated with the C atom towards the metal. Since on silver surface we have supposed the existence of the two forms of adsorbed oxygen, two kinds of CO binding are also very

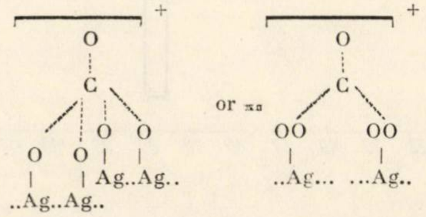

likely to appear.

Heating the system, desorption of 3.8×10^{14} molec/cm^2 is observed. It is known that CO is desorbed at room temperature, hence at least in the gaseous phase 3.2×10^{14} molec/cm^2 are CO molecules. There are two reasons for CO_2 forming as a result of this transformation : the great positive value of the charge of adsorbed complex formed by CO adsorption on oxygen layer, and the observation that the above mentioned heating, as well as the subsequent cooling at 77°K produce ΔV variations completely different from the observed value of the same modification with O_2—Ag system. The heating produces a decrease of 0.24 V and the cooling 1.2 V, as compared to 0.02 V and 0.6 V for the O_2—Ag system respectively.

The 0.24 V decrease of ΔV on heating, corresponds to the removing from the surface of about 7×10^{15} molecules (total quantity). Hence supposing that each removed molecule reacts with the CO, it follows that in the desorbed gas approximately 48 per cent are CO_2 molecules, the remaining being unreacted CO. The cooling of the system in the presence of desorbed gases, leads to only 15×10^{15} molecules readsorption, but ΔV decreases with 1. 2 V (twofold the value for the adsorption of CO on O_2—Ag layer). To explain this moditication we must take into account two elements : firstly, as a result of heating and the removing of some oxygen from the surface, the structure of oxygen-silver surface bonds might change and bonds of 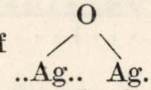 and 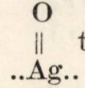 $\overset{O}{\underset{..Ag..}{\|}}$ type appear. Secondly, owing to the difference between the freezing points of the two gases it is expected that CO_2 must be adsorbed and CO remains free (which corresponds to the estimation from pressure value). The values for CO_2—Ag and CO_2—O—Ag systems are unknown but are probably great and positive like those found for the CO_2—Cu system.

The pumping of the gas phase and cooling, brings a decrease of 0.25 V. The new CO doses do not produce any change in ΔV but one oxygen dose gives a usual increase of 0.20 V.

b) If the silver film saturated with oxygen at 77°K is heated at 298°K and again cooled at 77°K a decrease of about 0.6 V takes place, as previously found. We suppose that this change is produced by the adsorption of molecular oxygen layer bond by charge transfer to the initial one. We have followed the effect of CO adsorption on this system. After the CO introduction, though the same CO quantity is adsorbed (as in a) 3.5×10^{14} molec/cm^2), the total ΔV decrease is 1.30 V, that means CO produces only a 0.50 V decrease compared to the 0.75 V decrease in a) — see fig. 2 —. It is interesting to notice that the effects are cumulative. It was expected that the bond between 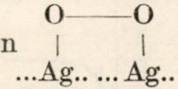 and CO be stronger than between the same layer and molecular oxygen. Consequently the latter must be destroyed and the ΔV total decrease be of 0.70 V. Unlike that observed in a), the ΔV evolution in time at CO introduction is different (fig. 2). In the first interval ΔV increases to negative values and the decreased value is reached after 5 min. It is clear that the initial ΔV increase may be produced by the destruction of the weak bond between molecular oxygen and the first adsorbed oxygen layer and the rebuilding of the common structure of the O_2— Ag system at 77°K. The CO molecules that start this change are readsorbed on the new layer, that means a ΔV decrease. However, to explain the great ΔV total decrease, two hypotheses may be advanced : *1.* the surface potential of CO_2 on an oxygen-covered silver film at 298°K (as a result of heating) is greater than the same magnitude for a film saturated with oxygen at 77°K; or *2.* during the above mentioned change, CO_2 forming is possible with a great and positive ΔV. A proof for the latter hypothesis is that the newly introduced oxygen doses produce a ΔV increase and are followed by a gas release. There are no reasons that an oxygen saturated layer should adsorb new oxygen quantities or that molecular oxygen should form a negatively charged layer on the initial one. We must conclude that CO_2 (and possibly CO) replacing by oxygen takes place. As a matter of fact the heating of the system restores the initial ΔV value and does not bring about a decrease of 0.24 V as in a).

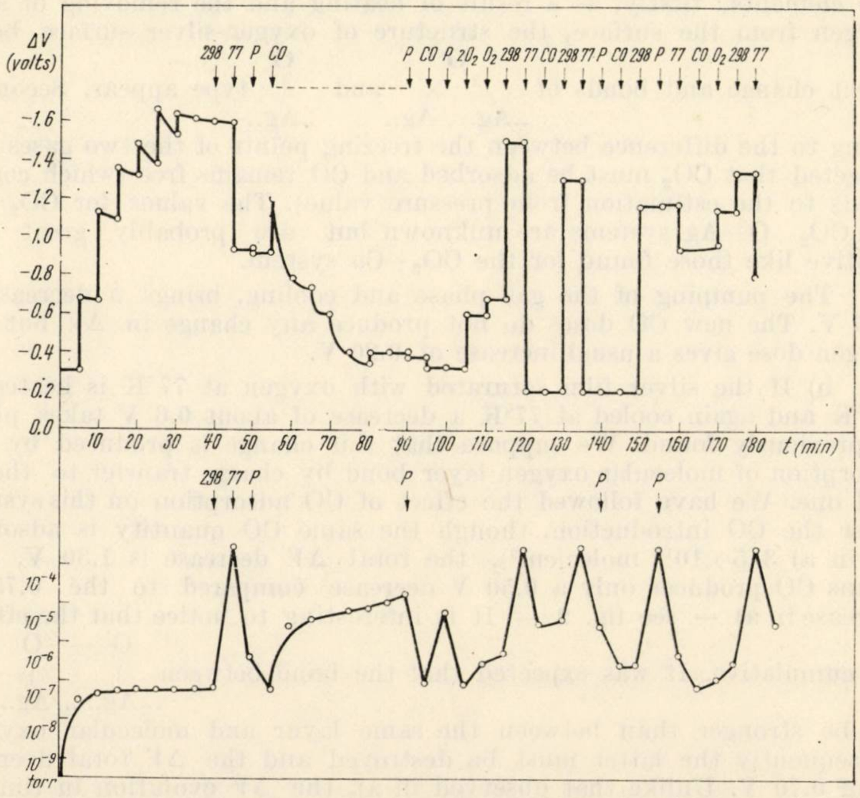

Fig. 2. — Surface potential variation in time, at 77°K for dose interaction in the system $Ag-O_2-CO$; CO introduction was effected after the O_2-Ag system was heated to 298°K and again cooled at 77°K ; in the low part simultaneous pressure variation is plotted.

Hence the silver surface remains covered with oxygen as a result of the desorption of the mixture $CO_2 + CO$. The returning to 77°K produces a $\Delta V = -0.20$ V as in a), namely a prevailing adsorption of CO_2.

2. *System* $Ag-CO-O_2$

CO adsorption on a clean silver surface produces ΔV variation of $+0.20$ V for a surface concentration of 4.5×10^{14} molec/cm². Our value is close to that found by other authors[10] (+ 0.30 V). In contrast with the value of n_{CO} for oxygen-covered silver surface, n_{CO} is greater in this case. From figure 3 one can see that n_{CO} reaches values of 6.4×10^{14} molec/cm², though ΔV does not increase. From physical adsorption experiments on the inert surfaces it is known[11] that CO molecule has an area of 16.8 Å^2, hence the maximum n_{CO} found by us corresponds to a monolayer (from n_{CO} an area of 84 cm^2 is found as compared to the 79 cm^2, the geometrical area). The difference between the maximum adsorbed quantity and that for which ΔV_{max} is reached, may be considered as reversibly adsorbed and at temperatures not too much above 77°K, is likely to be desorbed without any ΔV change. However, this quantity is not reversible on pumping.

---

[10] R. V. Culver, J. Pritchard and F. C. Tompkins, *Z. Elektrochem.*, **63**, 741 (1959).

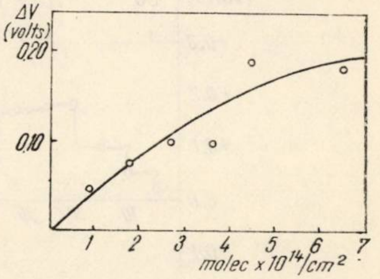

Fig. 3. — Surface potential variation with the number of CO adsorbed molecules on thin silver films at 77° K.

Introducing oxygen into the system, two groups of results were obtained. In one group ΔV increases to $-$ 0.6 V namely it reaches the same value as in a), which means total replacing of CO by oxygen and CO readsorption over this layer. In the other group described below, oxygen adsorption produces a ΔV of $-$ 1.2 V. Similar behaviours were found by the Hall effect and electrical resistance variations measurements on the same system[12]. We suggest that these two different groups of results should be related with different kinds of CO binding found for the adsorption of CO on polycrystalline surfaces.

As can be seen on figure 4 this change is unusual. For example, at the first dose of oxygen the ΔV variation is of 0.40 V and at the equilibrium it is by 0.25 V smaller. Towards completion of the saturation in oxygen , the returns are below 10%. The final value of ΔV is close to that found in the O_2-Ag system ($-$ 1.2 V against $-$ 1.44 V) and it is clear that the oxygen partially replaces the adsorbed CO. As in pressure evolution no increase is observed, namely no CO desorption, it follows that CO is readsorbed over the layer. The ΔV return for the first dose shows that CO readsorption takes place on the recently occupied side because the ΔV variation for a single dose ($+$ 0.25 V) is greater than ΔV_{max} for the CO$-$Ag system. It results that the CO readsorption on silver is not possible. It is difficult to explain the kinds of CO binding when oxygen saturation is reached. The final ΔV value does not correspond to that found for the $Ag-O_2-CO$ system as expected if the

---

[11] D. M. Young, and A. D. Crowell, "Physical Adsorption of Gases", Butterworth, London, 1962, p. 226.

[12] I. G. Murgulescu and G. Comşa, *Rev. Roumaine Chim.*, (in print).

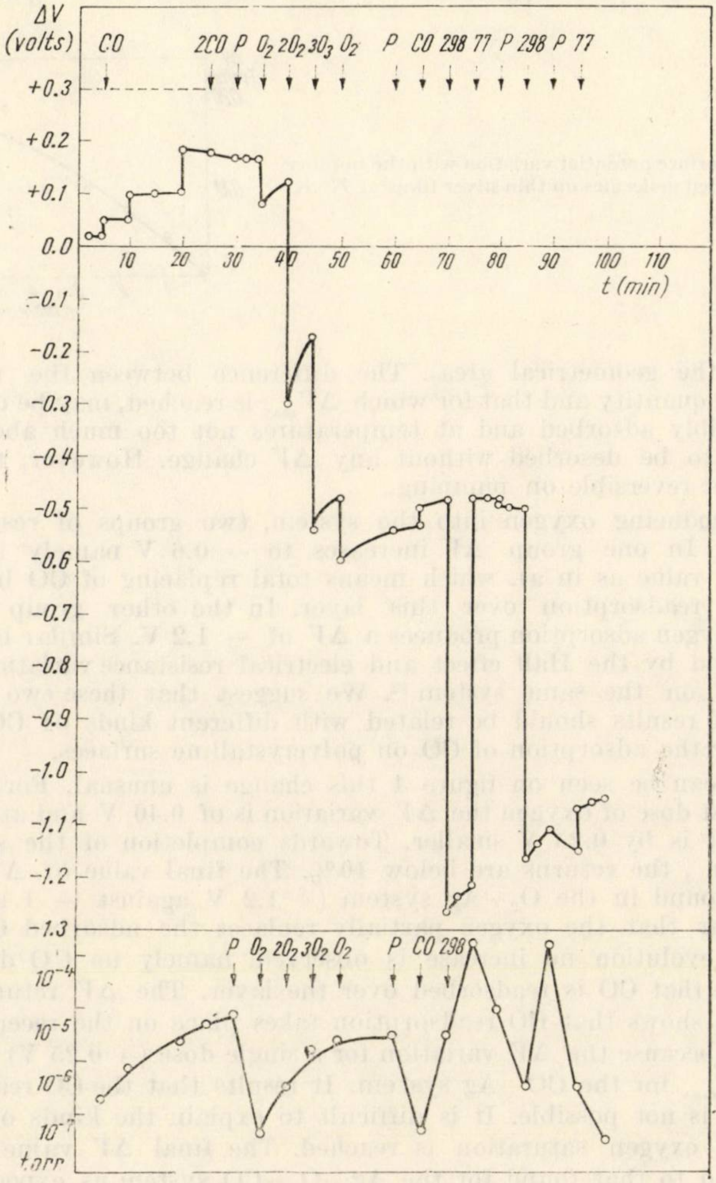

Fig. 4. — Surface potential variation in time, at 77°K for dose interaction, in the system $Ag-CO-O_2$; in the low part simultaneous pressure variation is plotted.

CO readsorption over the 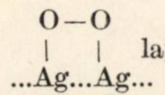 $\begin{array}{c}\mathrm{O-O}\\ |\quad\;|\\ \mathrm{...Ag...Ag...}\end{array}$ layer would take place. Moreover, the system so formed can adsorb new CO doses (producing increases of + 0.36 V for 1.8×10^{14} molec/cm^2). An oxygen adsorption over the CO molecules in the domains where the CO density is greater, is likely to take place at the same time with CO replacing. This would lead to the

complexes of 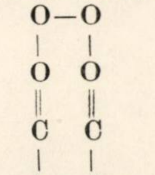 $\begin{array}{c}\mathrm{O-O}\\ |\quad\;|\\ \mathrm{O}\quad\mathrm{O}\\ \|\quad\;\|\\ \mathrm{C}\quad\mathrm{C}\\ |\quad\;|\\ \mathrm{...Ag...Ag...}\end{array}$ type, which would give ΔV negative too. The forming of such complexes clears up the possibility of subsequent adsorption of CO on the part covered only with the 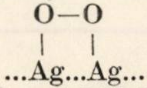 $\begin{array}{c}\mathrm{O-O}\\ |\quad\;|\\ \mathrm{...Ag...Ag...}\end{array}$ form.

The heating of the system produces a ΔV of -1.2 V, the maximum value for oxygen adsorption, but the pressure rise does not correspond to an additional oxygen desorption. In other words we cannot admit the CO_2 yield at the same rate as for the $Ag-O_2-CO$ system. The ulterior cooling brings a 1.0 V return; besides the + 0.6 V, due to CO adsorption over 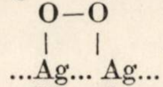 $\begin{array}{c}\mathrm{O-O}\\ |\quad\;|\\ \mathrm{...Ag...\,Ag...}\end{array}$, a difference of + 0.4 V appears; this could be ascribed to CO_2-adsorption on the same structure.

CO readsorption over the $\begin{array}{c}O-O\\ |\quad\ |\\ \ldots Ag\ldots Ag\ldots\end{array}$ layer would take place. Moreover, the system so formed can adsorb new CO doses (producing increases of + 0.36 V for 1.8×10^{14} molec/cm^2). An oxygen adsorption over the CO molecules in the domains where the CO density is greater, is likely to take place at the same time with CO replacing. This would lead to the complexes of $\begin{array}{c}O-O\\ |\quad\ |\\ O\quad O\\ |\quad\ |\\ C\quad C\\ |\quad\ |\\ \ldots Ag\ldots Ag\ldots\end{array}$ type, which would give ΔV negative too. The forming of such complexes clears up the possibility of subsequent adsorption of CO on the part covered only with the $\begin{array}{c}O-O\\ |\quad\ |\\ \ldots Ag\ldots Ag\ldots\end{array}$ form.

The heating of the system produces a ΔV of − 1.2 V, the maximum value for oxygen adsorption, but the pressure rise does not correspond to an additional oxygen desorption. In other words we cannot admit the CO_2 yield at the same rate as for the $Ag-O_2-CO$ system. The ulterior cooling brings a 1.0 V return; besides the + 0.6 V, due to CO adsorption over $\begin{array}{c}O-O\\ |\quad\ |\\ \ldots Ag\ldots Ag\ldots\end{array}$; a difference of + 0.4 V appears; this could be ascribed to CO_2 adsorption on the same structure.

Revue roumaine de Chimie, 15, 1173–1181 (1970).

Revue Roumaine de Chimie, 15, 1153–1161 (1970)

PASSIVITY OF STEEL IN MONOETHANOLAMINE SOLUTIONS

O. RADOVICI and VICTORIA SURDEANU

Institute of Physical Chemistry, str. Galaţi 31
Bucharest

Received June 17, 1969

The anodic behaviour of carbon steel has been studied in monoethanolamine (MEA) solution at 100 (as used in chemical industry). Potentiostatic measurements have shown that in deaerated solutions typical active-passive behaviour occurs. In aerated solution the shape of the anodic polarization curve shows a limiting value of the current density. The value of the limiting current density depends on the temperature, the presence of some adding agents : Fe^{++} ions, $NaVO_3$, CO_2, in MEA solutions. It was shown that $NaVO_3$ behaves as a corrosion inhibitor acting very slowly in time. The electrochemical data were compared with weight loss measurements, and Pourbaix diagrams. The dissolution of the passive film is accelerated by the presence of CO_2. The presence of Fe^{++} ions does not accelerate very much the dissolution of steel in MEA solutions. Based on the experimental results a mechanism of protective film formation is proposed.

INTRODUCTION

The monoethanolamine solutions are frequently used to purify many gases, which are necessary in numerous industrial processes, by the absorption of their CO_2 and H_2S content. At the same time in many plants of the chemical industry, the corrosion of the absorption towers, heat exchangers, etc. through which the MEA solution with absorbed CO_2 and H_2S flows, is observed.

In some papers several mechanisms for these corrosion processes have been proposed and different factors which influence the corrosion process, the inhibitors and degradation products are described.

Many authors have studied MEA corrosion by the weight loss measurements considering always systems containing both H_2S and CO_2 in different ratios.

Thus Froning and Jones [1] have observed the existence of pitting corrosion, while Suddbury, Riggs and Leterle [2] studying the corrosion of iron in some alcoholamine systems, one of them being the monoethanolamine, have proved the existence of a special type of filiform corrosion.

---

[1] H. R. Froning and J. H. Jones, *Ind. Eng. Chem.*, **50**, 1737 (1958).

[2] J. D. Suddbury, O.L. Riggs and J.F. Leterle, *Petroleum Refiner*, **37**, 183 (1958).

It has also been shown that the corrosion effect of aqueous MEA solutions is influenced by the presence in the solution of MEA oxidation or thermal degradation products, which gradually store in the system.

Polderman et al. [3] have observed the formation of hydroxyethyl-ethylene diamine by the thermal degradation of MEA. The growth of the corrosion rate while increasing the duration of action of the corrosion agent is accounted for by the presence within the system of the product of thermal degradation. The effect has been noticed in MEA solutions when CO_2 was present.

In this paper the steel corrosion determined by MEA aqueous solutions and by MEA with CO_2 but without H_2S systems is considered.

EXPERIMENTAL

In the experiments carbon steel and stainless Cr—Ni steel electrodes with an 1 cm^2 surface have been used.

The electrodes have been polished with metallographic paper, washed in distilled water, degreased with benzene and rinsed with acetone.

The following solutions have been considered: MEA 25%; MEA 25% with $NaVO_3$ admixtures in different concentrations; MEA 25% + CO_2 5%; MEA 25% + CO_2 5% with $NaVO_3$ admixtures in different concentrations; MEA 25% + CO_2 5% + $FeSO_4$ M/100. Undistilled and freshly distilled (in the laboratory MEA) solutions have been used parallelly. The measurements were carried out on a thermostat bath at 100 ± 0.5 using the glass cell shown in figure 1.

The potentials have been determined using a saturated calomel electrode as reference. The polarization curves have been obtained with a usual potentiostatic circuit (fig. 2). All the measurements were performed in aerated solutions.

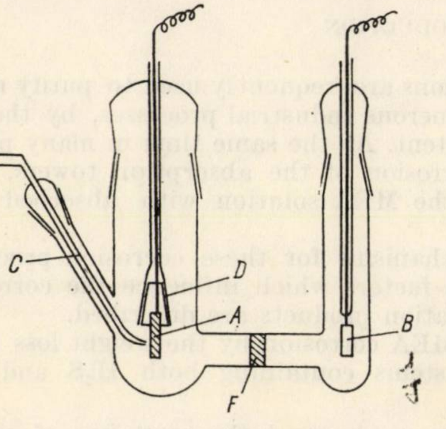

Fig. 1. — Working cell.
A – steel electrode; *B* – platinum electrode; *C* – Haber-Luggin capillary; *D* – teflon plug; *F* – gas frite.

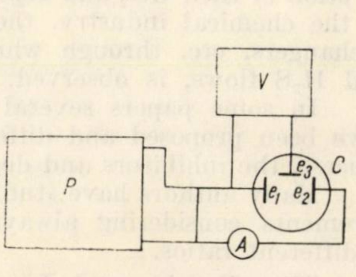

Fig. 2. — Potentiostatic circuit.
e_1 – steel electrode; e_2 – platinum electrode; e_3 – saturated calomel electrode; *A* – ampermeter; *C* – working cell; *P* – potentiostat; *V* – electronic voltmeter.

---

[3] L. D. Polderman, C. P. Dillon and A. B. Steele, *Oil Gas J.*, **54**, 180 (1955).

RESULTS AND DISCUSSION

1. *The anodic behaviour of steel in MEA solutions*

In figure 3 the anodic polarisation curve of carbon steel is shown. To reduce the oxide film produced in the air, a cathodic polarisation was applied. The Flade potential is −740 mV and the passivity current density i_p (corresponding to the dissolution of the passivisation film) is 20−24.7 μA/cm² in a large range of the potential. Comparing this curve with the corresponding one for iron in NaOH,[4] one observes a great similitude in the shape of the curve and quite the same values for the Flade potential and for the potential corresponding to the transpassivity state.

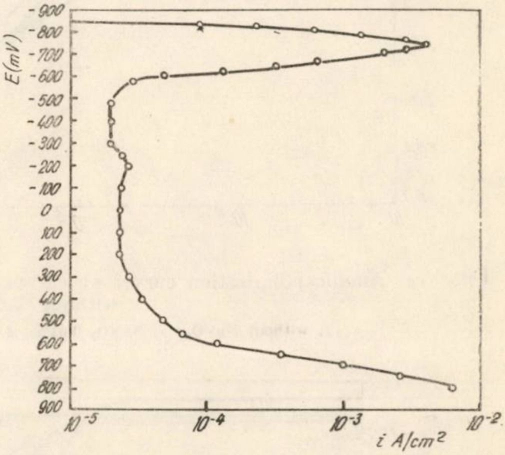

Fig. 3. — Anodic polarisation curve of carbon steel in MEA 25% + CO_2 5% solution.

One may conclude that the mechanism of the anodic process is identical with that in the above mentioned paper, being characterized by the formation of a passivisation film. A difference in the magnitude of the anodic current corresponding to the dissolution of the passivity film has however been observed. This current is greater for solutions containing CO_2 than that for alkaline or pure MEA solutions. This seems to prove that the main corrosive agent is CO_2 dissolved in the MEA solution.

In figure 4 (curve 1) and figure 5 (curve 1) are shown the anodic polarisation curves without the previous reduction in the oxide film present on the surface of the electrode.

One observes that only in the passive state these curves have the same shape as the preceding ones. This is due to the fact that in this case, the film formed in the alkaline solution prior to the anodic polarization, has not been dissolved. In fact, the whole curve starts from the passivisation domain. This is a limiting current density which shows the rate of

---

[4] I. G. Murgulescu, O. Radovici and S. Ciolac, *Studii și Cercetări Chim. Acad. București*, **13**, 839 (1965).

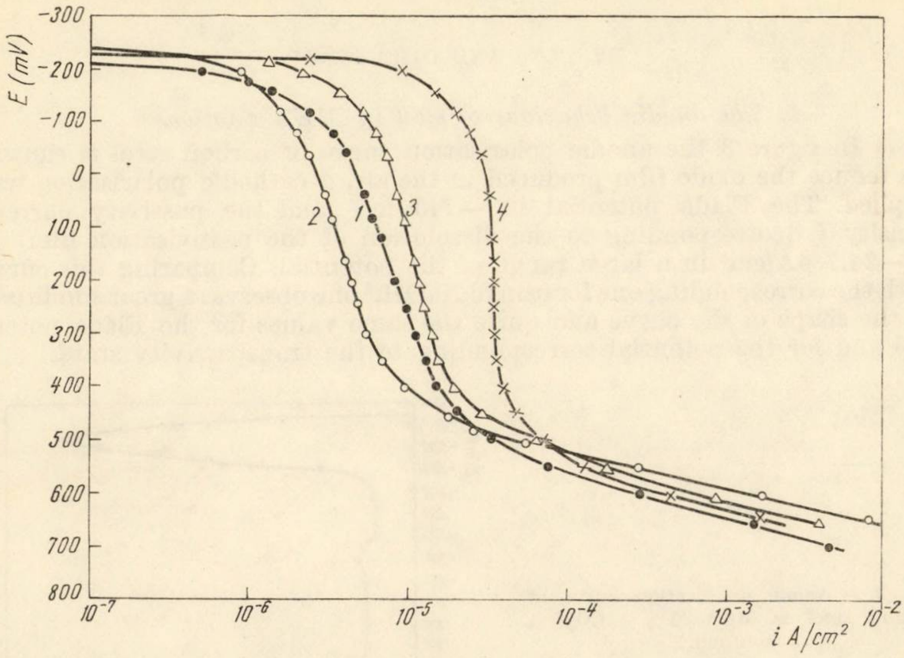

Fig. 4. — Anodic polarisation curves of carbon steel in MEA 25% solution with and without $NaVO_3$.

1, without $NaVO_3$; *2*, $NaVO_3$ 0.01%; *3*, $NaVO_3$ 0.1%; *4*, $NaVO_3$ 0.5%.

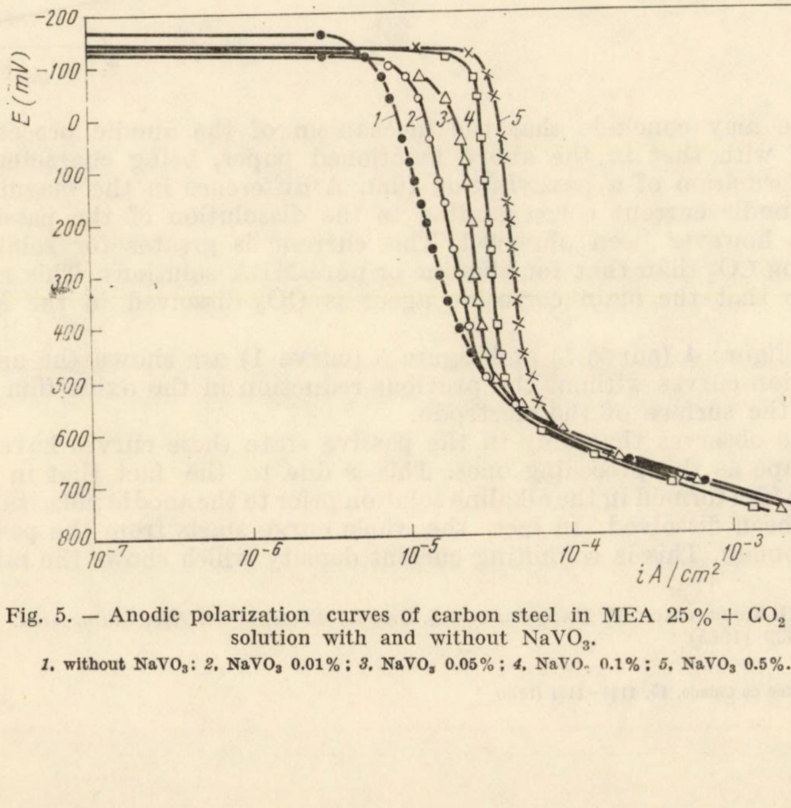

Fig. 5. — Anodic polarization curves of carbon steel in MEA 25% + CO_2 5% solution with and without $NaVO_3$.

1, without $NaVO_3$; *2*, $NaVO_3$ 0.01%; *3*, $NaVO_3$ 0.05%; *4*, $NaVO_3$ 0.1%; *5*, $NaVO_3$ 0.5%.

film repairing. As in the former case, one observes that the value of the passivisation current is greater for the solution containing CO_2 than for the solution without CO_2 (tables 1 and 2).

Table 1

Passivisation currents i_p of the carbon steel in MEA 25% solutions with and without $NaVO_3$

$NaVO_3$ %	0	0.01	0.1	0.5
i_p μA/cm²	2.6	1.6	5.3	32.3

Table 2

Passivisation currents i_p of carbon steel in MEA 25% + CO_2 5% solutions with and without $NaVO_3$

$NaVO_3$ %	0	0.01	0.05	0.1	0.5
i_p μA/cm²	6.14	11.3	23	28.1	34.6

2. *The impurities effects (Fe^{++} ions)*

Analysing the anodic polarization curves shown in figure 6 one may conclude that the presence of the Fe^{++} ions in the MEA solution containing CO_2 has no effects on the shape of the polarization curves and thus does not change the mechanism of the anodic process. The existence of the Fe^{++} ions has only a slight influence on the growth of the dissolution current of the passivisation film.

Many chemical reactions are involved in the process of CO_2 removal by aqueous solution of monoethanolamine. These reactions have been studied extensively by different authors.[5] The kinetics of these reactions is responsible for the corrosion of iron in the MEA + CO_2 system.

Monoethanolamine $H_2N-CH_2-CH_2-OH$ has two functional groups $-NH_2$ and $-OH$ which are likely to react with CO_2 according to the reactions :

$$-NH_2 + CO_2 \rightarrow -NHCOOH \text{ substituted carbamic acid,}$$

$$-OH + CO_2 \rightarrow -OCOOH \text{ substituted carbonic acid.}$$

Both products are acid, and can be neutralized by $-NH_2$ group when it hydrolizes to NH_3^+.

The reaction mechanism depends on the concentration of amine (a_0) and of CO_2 (θ). It was shown by Astarita and coworkers [5] that when $\theta < 0.5$ the favoured reaction is the carbamate.

$$CO_2 + 2\,RNH_2 \rightarrow RNHCOO.RNH_3 \quad (1)$$

---

[5] G. Astarita, "Mass Transfer with Chemical Reactions", Elsevier Amsterdam, 1967, p. 153.

and when $\theta > 0.5$ the overall reaction of CO_2 absorption is:

$$2\,H_2O + CO_2 + RNHCOO \cdot RNH_3 \rightarrow 2\,HCO_3 \cdot RNH_3 \qquad (2)$$

The reaction mechanism of (1) is expressed by the following steps

$$CO_2 + RNH_2 \rightarrow RNHCOO^- + H^+ \qquad \text{slow}$$
$$RNH_2 + H^+ \rightarrow RNH_3^+ \qquad \text{fast}$$

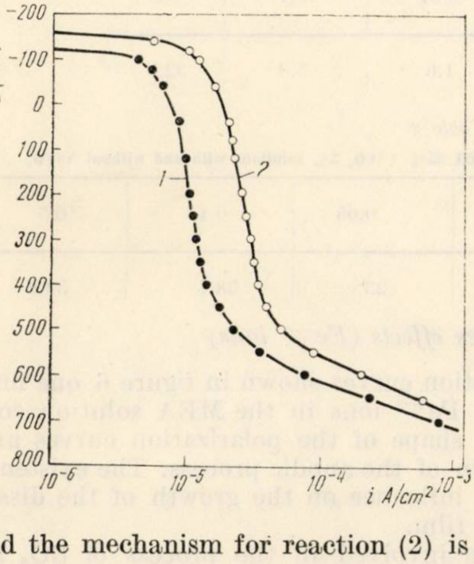

Fig. 6. — Anodic polarisation curves of carbon steel in MEA 25% + CO_2 5% solution with and without Fe^{++} ions. *1*, without Fe^{++} ions; *2*, with $FeSO_4$ M/100.

and the mechanism for reaction (2) is given by the following equations:

$$CO_2 + OH^- \rightarrow HCO_3^- \qquad \text{slow}$$
$$RNHCOO^- + H^+ \rightarrow RNH_2 + CO_2 \qquad \text{fast}$$
$$RNH_2 + H^+ \rightarrow RNH_3^+ \qquad \text{fast}$$
$$CO_2 + OH^- \rightarrow HCO_3^- \qquad \text{slow}$$
$$2\,H_2O \rightarrow 2H^+ + 2OH^- \qquad \text{fast}$$

When highly carbonated amine solutions are considered, the concentration of hydroxyl ions is so low that the direct reaction of CO_2 with water occurs:

$$CO_2 + H_2O = HCO_3^- + H^+ \qquad (3)$$

The analysis of possible regimes of the chemical absorption of CO_2 in the two cases $\theta < 0.5$ and $\theta > 0.5$ shows[5] that when $\theta < 0.5$ the reaction time is given by equation:

$$t_r = \frac{1}{K\,[RNH_2]} \qquad (4)$$

This equation shows that both last reaction and instantaneous reaction can be encountered when $\theta < 0.5$.

When $\theta > 0.5$ a completely different situation arises, and the reaction time is given by:

$$t_r = \frac{1}{K_c + K_a[OH^-]} \tag{5}$$

where K_c is of the order of 0.02 sec, while K_a is about 5,000 l/g mol. sec. Hence, the reaction time seems to be of the order of 40 sec which attests that slow reaction chemical absorption will be encountered in most practical cases. From the corrosion point of view, this means that during absorption of CO_2 in monoethanolamine solution, there is enough time for CO_2 to react, accordingly to equation (3) and consequently to produce locally the dissolution of the passive film on iron as observed in our experiments. This film on iron is observed in our experiments. This proves that neither the oxidation nor the thermal degradation products are responsible for the corrosion of iron in the MEA systems, but mainly the highly carbonated amine which gradually stores in the system and possibly gives reaction (3).

3. The anodic behaviour of stainless Cr–Ni steel

From the curves shown in figure 7 we may conclude that the stainless Cr–Ni steel has a different behaviour when compared with the carbon steel, the dissolution rate of the passivity film in the case of the Cr–Ni steel being much lower. This observation is consistent with the experimental data which show that the stainless steel is much more resistent to the action of CO_2 than the carbon steel.

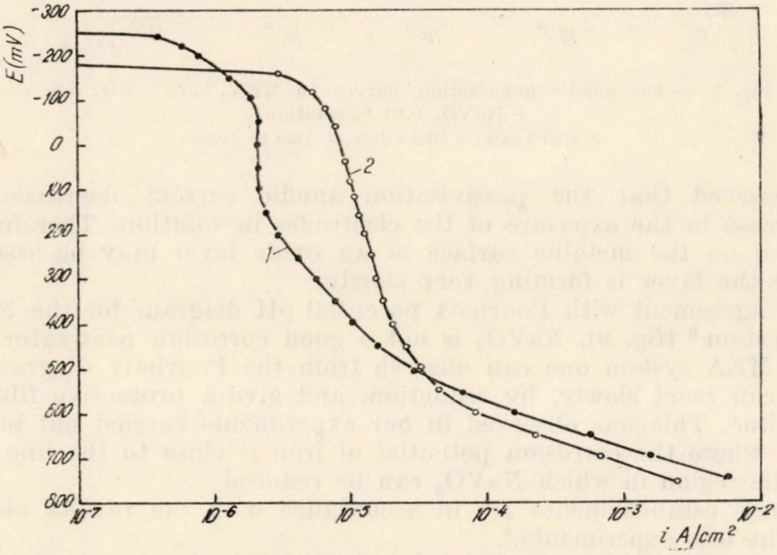

Fig. 7. — Anodic polarization curves in MEA 25% + CO_2 5% solution.
1, stainless steel Cr–Ni; *2*, carbon steel.

4. *The influence of $NaVO_3$*

The results obtained using electrodes freshly introduced into 25% MEA solutions in presence of CO_2 and of different concentrations of $NaVO_3$ are shown in figure 4 (curves 2, 3, 4) and figure 5 (curves 2, 3, 4, 5). From these figures as well as from tables 1 and 2, one observes that the dissolution anodic current is greater in presence of $NaVO_3$ than in its absence.

The polarization curves obtained for electrodes held in solution, under the respective conditions, for some days, are presented in figure 8.

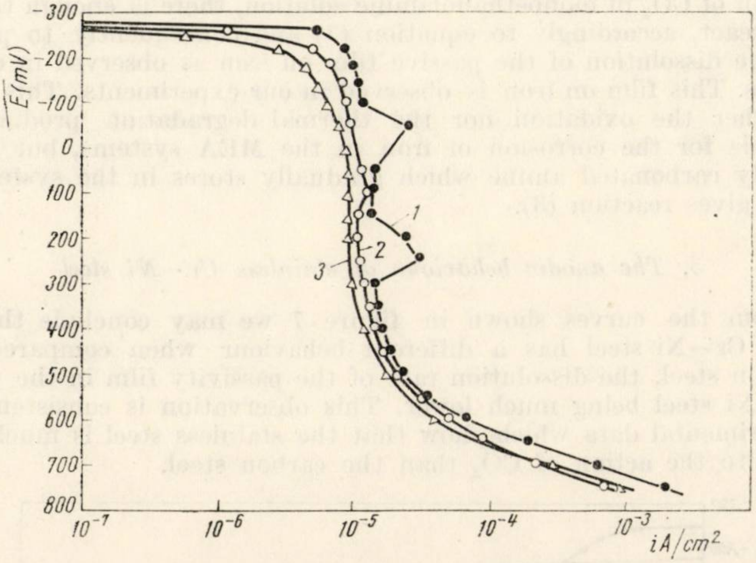

Fig. 8. — The anodic polarization curves in MEA 25% + CO_2 5% + + $NaVO_3$ 0.01 % solution.
1, after 3 days; *2*, after 6 days; *3*, after 12 days.

One observed that the passivisation anodic current decreases with the increase in the exposure of the electrodes in solution. Therefore the formation on the metallic surface of an oxide layer may be assumed; however the layer is forming very slowly.

In agreement with Pourbaix potential-pH diagram for the $NaVO_3$-water system[6] (fig. 9), $NaVO_3$ is not a good corrosion passivator. Still, for the MEA system one can observe from the Pourbaix diagram that $NaVO_3$ can react slowly, by reduction, and give a protective film in a longer time. This was observed in our experiments carried out in MEA solution where the corrosion potential of iron is close to the line which shows the region in which $NaVO_3$ can be reduced.

These establishments are in accordance with the results obtained by weight loss experiments.[7]

[6] M. Pourbaix, "Atlas d'équilibres électrochimiques", Gauthier-Villars & Cie, Paris, 1963, p. 75.

[7] I. I. Perin and A. R. Valieva, *Khim. Prom.*, **43**, 50 (1967).

In this way the $NaVO_3$ achieves the protection of steel against corrosion in a MEA + CO_2 mixture.

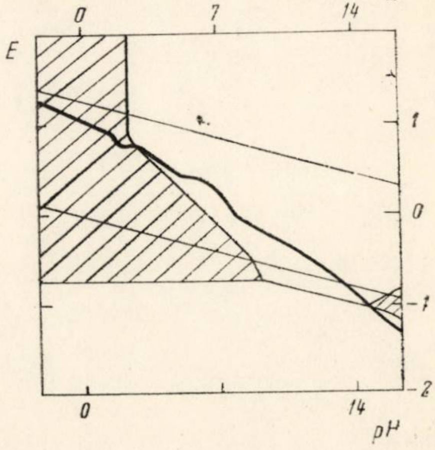

Fig. 9. — Potential-pH diagram for vanadates. The striped surfaces show the theoretical corrosion domains in presence of 0.01 M vanadate solution.

CONCLUSIONS

Our results seem to indicate that the mechanism of iron corrosion in MEA solutions is similar to the KOH, NaOH solutions. We noticed that the corrosion rates are higher in the presence of CO_2 and this component is the main agent in the corrosion of iron in the MEA system.

Revue Roumaine de Chimie, **15**, 1163–1167 (1970)

KINETICS OF THE Al_2O_3 + CoO REACTION AT HIGH TEMPERATURE ACCOMPANIED BY SPINEL FORMATION IN OXYGEN ATMOSPHERE

D. CISMARU and STELA ZERVUDIS

Centre of Physical Chemistry
Bucharest, str. Dumbrava Roşie 23

Received August 2, 1969

The kinetics of the Al_2O_3 + CoO reaction in a stoichiometric ratio of 1 : 1 mole between 900° and 1050° in oxygen atmosphere has been studied. The equation of the rate constant and activation energy has been established.

In a previous paper[1] we had tried to study the reaction of the Al_2O_3 + CoO mixture in a 1 : 1 mole ratio, as pelletted powder and in nitrogen atmosphere between 900° and 1050°.

The present contribution aims at studying the same reaction, in the same ratio and within the same temperature range but in powder form and in oxygen atmosphere.

Investigations of the formation reaction of the alumina double oxide with metallic oxides, with special emphasis on the qualities of the final product, have been carried out by some authors[2–14] too.

[1] D. Cismaru and S. Zervudis, *Rev. Roumaine Chim.*, **13**, 275 (1968).

[2] H. Werner-Tromnau, "Neues Jahrbuch für Mineralogie, Geologie und Paläontologie", Ab. A. B. Stuttgart, 1934, p. 349.

[3] G. Matto and L. Porserini, *Gazz. chim. Ital.*, **59**, 280 (1929).

[4] K. Linder, *Z. phys. Chem. (Frankfurt)*, **6**, 162 (1956).

[5] W. Jander, *Z. anorg. Chem.*, **163**, 1 (1927).

[6] K. Düweld and C. Wagner, *Z. phys. Chem.*, **24**, 53 (1934).

[7] K. L. Mampel, *Z. phys. Chem.*, **187**, A. 43, 235 (1940).

[8] G. Segawa, *J. Ceram. Assoc. Japan*, **56**, 59 (1948).

[9] S. Miyacl, *J. Ceram. Assoc. Japan*, **59**, 132 (1951).

[10] K. Shiuiki and T. Kuba, *J. Chem. Soc. Japan. Ind. Chem. Sect.*, **57**, 617 (1954).

[11] R. E. Carter, *J. Chem. Phys.*, **34**, 2010 (1961) ; **35**, 1137 (1961).

[12] R. I. Gallagher, "5-th Intern. Symposium on the Reactivity of Solids", Elsevier Public Comp. München, 1964, p. 192.

[13] W. Komatosu, "5-th Intern. Symposium on the Reactivity of Solids", Elsevier Public. Comp., München, 1965, p. 182.

[14] J. Hlavéc, "Proc. of 4-th Intern. Symposium on the Reactivity of Solids", Amsterdam, 1960.

Others [15–20] have dealt even with the $Al_2O_3 + CoO$ mixture also with a view to the final product, and Hedwall and Leffler [21] have studied the reaction in oxygen flow, too, dwelling especially upon the effect at the conversion temperature of Co_3O_4 in CoO.

In the present paper we attempted to start from Al_2O_3 and from CoO made by heating Co_3O_4 at 1000° in nitrogen atmosphere, therefore from well known structures. In the case when in the oxygen atmosphere CoO is converted, during the reaction, into Co_3O_4 according to reaction $3CoO + 1/2\ O_2 = Co_3O_4$ crystallographic conversion will also occur in the spinel lattice and therefore a different reactivity. If the conversion did not take place, reaction rates equal to those for the reaction in nitrogen atmosphere at the same temperature should be found.

For the $Al_2O_3 + CoO$ reaction in nitrogen atmosphere between 900° and 1050° the rate constant may be given by equation

$$Kt = 1 - (1 - z)^{2/3} - 2/3\ z \tag{1}$$

deduced by Ghinstling and Braunstein [22] and for other reactions in solid media by the equation found by Cismaru [23] for the first part of the $SiO_2 + CaSO_4$ as well as by equation

$$Z = 1 - \frac{6}{2} \sum_{n=1}^{n=\infty} \frac{1}{n} \exp(n^2 - Kt) \tag{2}$$

inferred by Serin-Ellickson. [24]

Here Z stands for that part of substance that had reacted (Al_2O_3 or CoO), K is the rate constant, t represents the time (expressed by us in minutes) and n in equation (2) appears as a whole number assuming values from 1 to ∞.

EXPERIMENTAL

The molar mixture of Al_2O_3 and CoO is that used in the previous paper[1] except that it has been kept in powder form.

The thermal treatment of the samples occurred in the same installation but operating in oxygen atmosphere.

The weighed samples have been thermally treated in platinum crucible, in an oven with quartz tube at the same temperatures i.e. 900°, 1000° and 1050° and within the same time intervals i.e. 1, 3, 5, 6, 7 and 9 h.

---

[15] H. Schmalzried, *Z. Phys. Chem.*, **25**, 170 (1960).
[16] H. Schmalzried, *Z. phys. Chem. (Frankfurt)*, **28**, 203 (1961).
[17] A. Markel, H. Schmalzried, *Z. phys. Chem. (Frankfurt)*, **32**, 76 (1962).
[18] H. Schmalzried, *Z. phys. Chem. (Frankfurt)*, **33**, 111 (1962).
[19] W. Rogola and H. Schmalzried, *Naturwiss.*, **50**, 593 (1967).
[20] H. Schmalzried, *Ber. dtsch. keram. Ges.*, **1**, 11 (1965).
[21] A. J. Hedwall and L. Leffler, *Z. anorg. Chem.*, **234**, 235 (1937).
[22] A.M. Ghinstling and E. I. Braunstein, *Zhur. priklad. Khim.*, **23**, 1249 (1950).
[23] D. Cismaru, *Studii și Cercetări Fiz. Acad. R. P.Română*, **3**, 435 (1955).
[24] B. Serin and R. T. Ellickson, *J. Chem. Phys.*, **9**, 742 (1941).

After weighing, the sample has been introduced into the oven with the prescribed temperature and with constant oxygen flow. Prior to the introduction into the oven, the oxygen passed a battery with vessels in order to be washed with conc. SO_4H_2, $CaCl_2$ and $Mg(ClO_4)_3$.

During the whole thermal treatment, temperature and oxygen pressure have been kept constant. After the programmed time had elapsed, the reaction tube has been removed without cutting the oxygen flow and left to cool on ceramic carriers. During the thermal treatment alumina and cobalt oxide reacted in accordance with the ratio characteristic of every temperature and heating time as shown by the tables. As compared to that obtained on thermal treatment in nitrogen it is somewhat smaller.

The CoO left free has been dosed in order to establish the reaction extent.

Dosage occurred after separation of the formed spinel and of the alumina unreacted by dissolution in 1 : 1 hydrochloric acid and filtration.

The filtrate had the Co^{2+} ion dosed with dipyridyl.[25] The CoO amount converted into spinel has been calculated.

RESULTS

The results which have been obtained were used for the calculation of the reaction rate K accordingto two equations : Ghinstling and Serin Ellickson K_G and K_{SE} as shown in table 1.

Table 1

Al_2O_3+CoO system in O_2 atmosphere k_G and k_{SE} values

Temperature °C	Time min.	z %	$k_G \cdot 10^6$	$k_{SE} \cdot 10^5$
900	60	0.45	0.25	0.17
	180	1.65	0.25	0.27
	300	2.53	0.26	0.28
	360	3.04	0.27	0.28
	420	3.40	0.27	0.28
	540	3.54	0.26	0.26
			$m = 0.25$	$m = 0.27$
1000	60	3.03	2.50	2.00
	180	5.70	2.20	2.00
	300	8.11	2.40	2.00
	360	9.38	2.40	2.20
	420	10.67	2.54	2.10
	540	12.03	2.40	2.40
			$m = 2.40$	$m = 2.13$
1050	60	5.60	6.00	4.50
	180	9.54	5.50	4.60
	300	12.54	6.02	5.00
	360	14.02	6.60	5.00
	420	14.99	6.00	5.00
	540	16.96	6.30	5.24
			$m = 6.02$	$m = 4.89$

---

[25] Th. PIRTEA, D. CRIVĂŢ and E. BLĂNARU, *Analele Univ. Buc. seria St. Nat.*, **XI**, 97 (1962).

By applying Arrhenius equation

$$K = A\,\mathrm{e}^{-E/RT}$$

he activation energy of the system may be determined. The value of K_G and K_{SE} has been made use of.

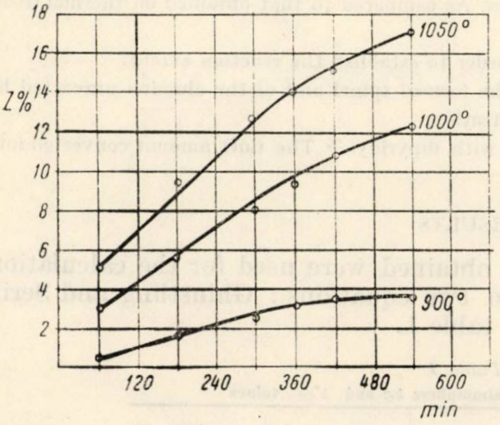

Fig. 1. — Diagram z % time in minutes for various temperatures.

Table 2

$Al_2O_3 + CoO$ system in O_2 atmosphere. $1/T$, log k_G and log k_{SE} values

Temperature °C	$10^4 . 1/T$	$k_G . 10^7$	$\log k_G + 7$	$k_{SE} . 10^6$	$\log k_{SE} + 6$
900	8.52	2.5	0.3979	2.70	0.4341
1000	7.85	24.0	1.3802	21.3	1.3284
1050	7.55	60.0	1.7782	48.9	1.6893

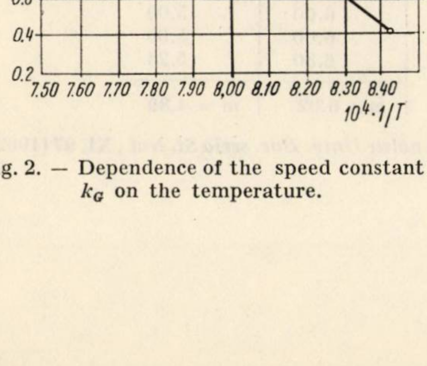

Fig. 2. — Dependence of the speed constant k_G on the temperature.

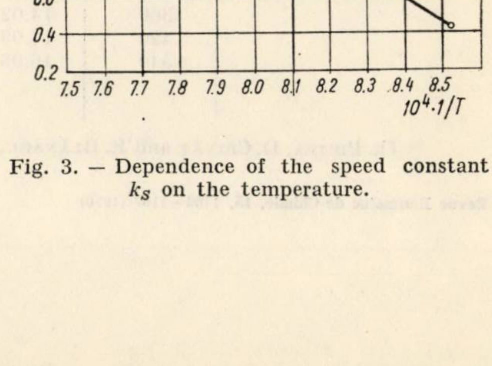

Fig. 3. — Dependence of the speed constant k_S on the temperature.

The activation energy resulting from the variation in the rate constant K_G and K_{SE} is 63.000 cal/mole.

Table 3 lists the comparative results of the rate constant of the Al_2O_3 + CoO reaction in nitrogen and oxygen.

Table 3

Al_2O_2+CoO system in N_2 and O_2 atmosphere

Temperature °C	N_2 atmosphere		O_2 atmosphere	
	$k_{G_{med}} \cdot 10^6$	$k_{SE_{med}} \cdot 10^5$	$k_{G_{med}} \cdot 10^6$	$k_{SE_{med}} \cdot 10^5$
900	0.30	0.28	0.25	0.27
1000	3.40	2.66	2.40	2.13
1050	7.90	6.20	6.02	4.89

The activation energy in nitrogen atmosphere was $E_G = 57.500$ cal/mole and $E_{SE} = 63.000$ cal/mole; in O_2 atmosphere: $E_G = 57.187$ cal/mole and $E_{SE} = 63.000$ cal/mole.

Similar values of the reaction rate while reacting in nitrogen or oxygen atmosphere, led us to the inference that at 900°, 1000° and 1050°, CoO is stable and consequently the oxygen atmosphere did not influence them.

The activation energy resulting from the variation in the rate constant K_1 and K_{II} is 63.000 cal/mole.

Table 3 lists the comparative results of the rate constant of the Al_2O_3 + CoO reaction in nitrogen and oxygen.

Table 3

[illegible] in N_2 and O_2 atmosphere

O_2 atmosphere		N_2 atmosphere		Temperature, °C
[illegible]	[illegible]	[illegible]	[illegible]	
0.27	0.25	0.29	[illegible]	950
3.13	2.40	2.80	[illegible]	1000
4.93	5.92	[illegible]	[illegible]	1050

The activation energy in nitrogen atmosphere was E_I = 57.500 cal/mole and E_{II} = 63.000 cal/mole, in O_2 atmosphere: E_I = 57.157 cal/mole and E_{II} = 64.000 cal/mole.

Similar values of the reaction rate while working in nitrogen or oxygen atmosphere led us to the inference that at 950°, 1000° and 1050°, CoO is stable and consequently the oxygen atmosphere did not influence them.

Revue Roumaine de Chimie, 15, 1169–1176 (1970)

L'ÉLECTRODE HALOGÈNE — CHARBON DANS LES ÉLECTROLYTES FONDUS. VI[1]

L'ADSORPTION DU CHLORE ET DE L'IODE SUR L'ÉLECTRODE DE CHARBON ACTIVÉ

S. STERNBERG et I. GALASIU
Centre de Chimie physique de l'Académie, Bucarest,
31, str. Galați

Reçu le 10 juin 1969

On étudie l'adsorption du chlore sur les électrodes de charbon actif dans les électrolytes fondus en fonction de la surface spécifique des charbons. On détermine aussi les isobares et les isothermes de l'adsorption de l'iode sur le même type d'électrodes.

Dans des travaux antérieurs [1, 2] nous avons présenté une méthode électrochimique pour l'étude de l'adsorption du chlore sur des électrodes de charbon actif dans des électrolytes fondus. Nous avons proposé, en outre, [1] un procédé pour la correction de l'autodésorption thermique du chlore sur l'électrode, étant donné que celle-ci se superpose à la désorption électrochimique et affecte ainsi l'exactitude des mesures.

Dans le présent travail nous continuons l'étude de l'adsorption du chlore sur le charbon actif en fonction de la surface spécifique des charbons et l'adsorption de l'iode sur le même type d'électrodes.

PARTIE EXPÉRIMENTALE

Le charbon actif a été préparé à partir d'un mélange homogène de poudre de charbon et de goudron de hêtre qu'on a ensuite pressé à environ 700 atmosphères dans une matrice de forme correspondante et puis calciné à environ 500° dans une atmosphère de gaz inerte pour éliminer les produits volatils.

Ces électrodes que nous considérons comme « semi-activées » ont une surface spécifique d'environ 10 – 15 m^2/g.

Pour obtenir une meilleure surface spécifique, on peut activer les charbons en les traitant à 800° avec des vapeurs d'eau mélangées avec du bioxyde de charbon. En fonction de la durée du traitement on peut obtenir des charbons actifs d'une surface spécifique de quelques centaines de mètres carrés par gramme.

---

[1] Ve Partie : S. STERNBERG et I. GALASIU, *Rev. Roumaine Chim.*, **13**, 991 (1968).

[2] I. G. MURGULESCU, S. STERNBERG et L. BEJAN, *Rev. Roumaine Chim.*, **11**, 447 (1966)

La surface spécifique des charbons a été déterminée en faisant passer des vapeurs de benzène sur une quantité déterminée de charbon actif à de diverses pressions relatives par rapport à un gaz porteur et en déterminant ainsi la quantité de benzène adsorbée à chaque pression relative. Dans la représentation graphique des deux variables on aperçoit que la courbe présente un palier qui indique la quantité de benzène nécessaire pour obtenir une couche adsorbée monomoléculaire. A partir de cette quantité et en connaissant aussi la surface couverte par une molécule de benzène, on calcule la surface spécifique du charbon actif.

La description détaillée de la méthode a été donnée par Rubinstein et Afanasyev [3].

La technique expérimentale est la suivante : la cathode est formée d'une barre en argent de 1mm de diamètre, l'anode d'une barre en charbon activé, l'électrolyte fondu étant un mélange de KCl ($x = 0{,}3$) + AgCl ($x = 0{,}7$) ou KI ($x = 0{,}3$) + AgI($x = 0{,}7$)

Pour saturer l'électrode de charbon avec l'halogène on a fait une électrolyse préliminaire durant 20 — 30 minutes à potentiel réversible. Pour éliminer de la cellule l'halogène produit pendant l'électrolyse préliminaire, on a mené les expériences dans un fort courant d'argon. Après avoir terminé la polarisation anodique, on a connecté la cellule à un schéma de polarisation cathodique galvanostatique à l'aide d'un commutateur double qui permet l'inversion de la polarité. On a ainsi déterminé les courbes : potentiel d'électrode (φ)-temps, à une intensité constante de courant, et la quantité d'halogène a été calculée des relations

$$Q = I \times t \quad \text{et} \quad a = \frac{Q}{F}$$

où

Q = quantité de courant exprimée en coulombs ;
F = constante de Faraday ;
I = intensité du courant de polarisation cathodique ;
t = temps de la polarisation cathodique ;
a = atome — grammes d'halogène.

Le potentiel φ a été mesuré à l'aide d'un oscillographe cathodique à trace rémanente.

Pour l'évaluation de l'autodécharge on a aussi enregistré des courbes potentiel — temps en circuit ouvert.

Le charbon activé a été immergé entièrement dans l'électrolyte à l'aide d'une barre de charbon spectral. On a constaté que la quantité de l'halogène adsorbée sur l'électrode spectrale est négligeable.

Une description plus détaillée de la technique expérimentale a été donnée dans nos travaux antérieurs. [1,2]

RÉSULTATS ET DISCUSSIONS

Dans le tableau 1 on compare les quantités de chlore adsorbées sur une électrode de charbon semi-activé et sur une électrode de charbon activé au potentiel réversible. Les déterminations ont été effectuées à la température à laquelle la quantité de chlore adsorbée présente une valeur maximum [1].

Bien que la surface spécifique du charbon activé soit environ 40 fois plus grande que celle du charbon semi-activé, on constate que la quantité de chlore adsorbée augmente seulement de 1,3 fois, ce qui pourrait être expliqué par le fait que l'adsorption du chlore a lieu, pour la plupart, à la surface de contact entre l'électrolyte et l'électrode et on peut supposer que cette surface ne diffère pas beaucoup pour les deux catégories d'électrodes. Par l'activation du charbon semi-activé on fait augmenter la longueur et le diamètre des pores à l'intérieur de l'électrode de charbon, etc., mais il paraît que la surface de contact entre l'électrolyte et l'électrode ne soit pas modifiée beaucoup.

---

[3] M. Rubinstein et I. Afanasyev, *Izvest. Akad. Nauk S.S.S.R., Otdel. khim. Nauk*, **11**, 1294 (1956).

Tableau 1

Degré de recouvrement des charbons activés et semi-activés en fonction de la surface spécifique

	Surface spécifique	Quantité de chlore adsorbée / charbon g	Surface occupée par le chlore	Degré apparent de recouvrement θ
charbon semicativé	14 m^2/g	$6{,}84.10^{-4}$ atome-grammes	12,7 m^2/g	0,907
charbon actif	550 m^2/g	$9{,}01{,}10^{-4}$ atome grammes	16,7 m^2/g	0,030

Cette hypothèse est schématiquement illustrée dans la figure 1 où l'on voit que tant au pore « long et ramifié », qu'au pore « court » les surfaces de contacts ne diffèrent pas beaucoup entre elles.

Dans nos expériences, la pression partielle du chlore dans la cellule d'électrolyse est maintenue quasi nulle grâce au barbotage d'argon. Dans ces conditions il est possible que la quantité de chlore qui pénètre à l'intérieur de l'électrode soit petite (mais non pas nulle comme on démontrera plus loin) et que la plus grande partie du chlore mesurée par nous provienne de l'adsorption électrochimique.

L'augmentation de 30% environ observée pour le chlore adsorbé sur charbon activé peut être expliquée par l'augmentation du nombre des pores et du diamètre de ceux-ci à l'activation.

Durant nos expériences on a remarqué qu'après la décharge cathodique, l'électrode se « repose », c'est-à-dire qu'après un certain laps de temps le potentiel de l'électrode augmente jusqu'à 0,4—0,5 V. Après quelques décharges cathodiques et « repos » successifs ce « potentiel rémanent » devient très petit ce qui démontre qu'une certaine quantité de chlore a pénétré aussi à l'intérieur de l'électrode. Après la polarisation cathodique, le chlore diffuse à l'interface de contact et confère à l'électrode « un potentiel rémanent »,

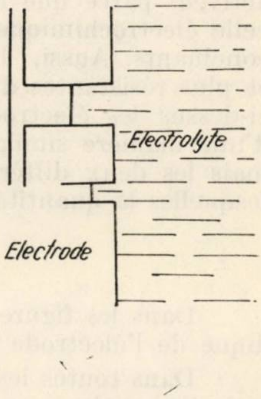

Fig. 1. — Schéma de la pénétration de l'électrolyte dans les pores du charbon actif.

ce qui est aussi confirmé par le fait que la quantité de chlore (a') correspondant au potentiel rémanent est plus grande aux électrodes activées qu'à celles non activées. Le chlore correspondant au « potentiel rémanent » (a') n'a pas été inclus dans le calcul de la quantité de chlore notée par a.

En considérant que le chlore adsorbé sur l'électrode se trouve à l'état atomique et en prenant 1Å comme rayon atomique du chlore on a calculé la surface couverte par le chlore et le « degré apparent de recouvrement (θ) ». A l'électrode activée, ce degré de recouvrement est très petit ce qui démontre dans ce cas que seulement une partie réduite de la surface spécifique est impliquée dans le processus d'adsorption électrochimique. De même, le degré de recouvrement du charbon semi-activé calculé par nous n'a qu'un caractère orientatif parce qu'on ne connaît pas exactement la surface de contact électrode-électrolyte. Il est possible que par l'électrolyse, la surface spécifique de l'électrode augmente [1, 2] et qu'en réalité le degré de recouvrement soit plus petit que celui calculé par nous. Tout de même, le fait que le degré de recouvrement soit voisin de l'unité révèle que chez le charbon semi-activé une grande partie de la surface spécifique prend part au processus de l'électrode.

Pendant ces expériences on a fait encore les observations suivantes : aux électrodes de charbon spectral il suffit une polarisation de 5 minutes environ pour que l'électrode arrive au potentiel réversible aux densités anodiques de courant entre 0,5 – 1 A/cm^2. Dans le cas des charbons semi-activés on a besoin d'un temps beaucoup plus long pour obtenir un potentiel réversible, environ 10 – 15 heures pour les premiers et 30 – 40 heures pour les derniers. Après que l'électrode soit ainsi « formée » il suffit de 20 – 30 minutes d'électrolyse pour arriver au potentiel réversible et à une quantité constante de chlore adsorbée.

Pour nos expériences on a choisi les électrodes de charbon semi-activées parce que leur surface spécifique est beaucoup plus proche de celle électrochimiquement active et les résultats ainsi obtenus sont plus concluants. Aussi, les électrodes semi-activées sont-elles plus stables et plus résistantes du point de vue mécanique. Ainsi que l'on a montré ci-dessus les électrodes semi-activées et celles activées se comportent d'une manière similaire en ce qui concerne l'adsorption électrochimique mais les deux diffèrent essentiellement des électrodes de graphite pour lesquelles la quantité de chlore adsorbée est 200 fois plus réduite. [2]

L'électrode d'iode

Dans les figures 2*a*–*f* on a donné les courbes de polarisation cathodique de l'électrode d'iode entre les températures de 300° et 800°.

Dans toutes les six figures, la courbe 1 représente la courbe de polarisation cathodique déterminée expérimentalement, tandis que la courbe 2 représente la courbe d'autodécharge. A cause des températures élevées, dans les sels fondus, à la différence des solutions aqueuses, a lieu une autodésorption thermique sur l'électrode, qui se superpose à la désorption électrochimique et affecte ainsi l'exactitude des mesures. Pour connaître le plus exactement possible la quantité d'iode adsorbée sur l'électrode, il faut faire une correction, en ajoutant à la quantité d'iode obtenue à l'aide de la polarisation cathodique galvanostatique, la quantité d'iode perdue entre-temps par l'autodésorption.

Cette correction a été faite de la manière suivante : Pour une certaine température, par exemple 600° (figure 2*d*), la polarisation cathodique

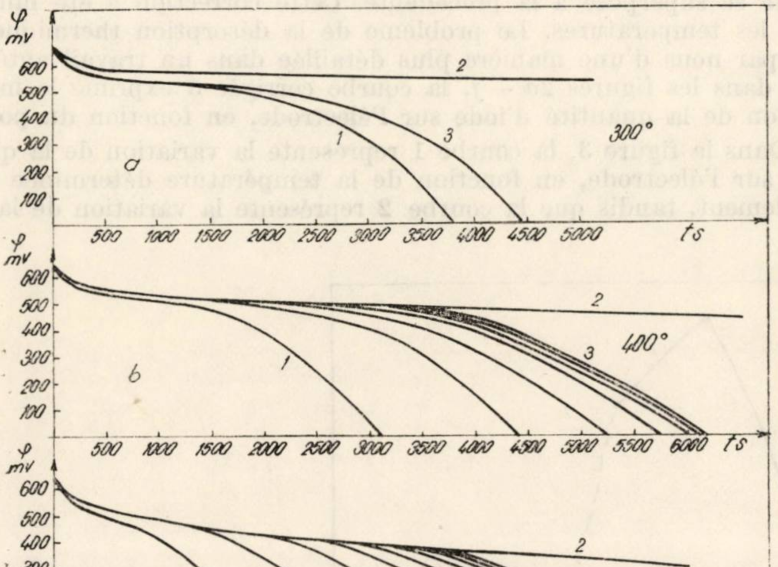

Fig. 2. — Courbes potentiel-temps à la décharge de l'électrode d'iode entre les températures de 300° et 800° avec la correction d'autodécharge.

1, Courbes de polarisation cathodique galvanostatique. Intensité du courant de polarisation = = 0,1A. *2*, Courbes d'autodécharge ; *3*, Courbes de polarisation cathodique corrigées.

dure τ secondes. A ce temps correspond le potentiel φ autodécharge sur la courbe d'autodécharge. Sur la courbe de polarisation cathodique, à ce potentiel correspond le temps τ' qui doit être ajouté au temps de polarisation cathodique. On procède de la même manière avec tous les points de la courbe 1, en obtenant ainsi une nouvelle courbe $\varphi - t$ corrigée, la courbe 1*a*. On répète les corrections jusqu'à ce que la dernière courbe obtenue se superpose à la précédente. Cette correction a été faite pour toutes les températures. Le problème de la désorption thermique a été traité par nous d'une manière plus détaillée dans un travail antérieur[1]. Donc, dans les figures 2*a* — *f*, la courbe corrigée 3 exprime le mieux la variation de la quantité d'iode sur l'électrode, en fonction du potentiel.

Dans la figure 3, la courbe 1 représente la variation de la quantité d'iode sur l'électrode, en fonction de la température déterminée expérimentalement, tandis que la courbe 2 représente la variation de la même quantité après avoir fait la correction d'autodécharge. On observe que l'allure des deux courbes est tout à fait différente, sur la courbe corrigée il y a un maximum qui n'existe pas sur celle non corrigée. On observe aussi, que, entre les températures de 500° et 600°, il y a une décroissance brusque, discontinuité qui peut être expliquée par le fait que la température critique de l'iode est de 511°. Il est possible qu'à une température

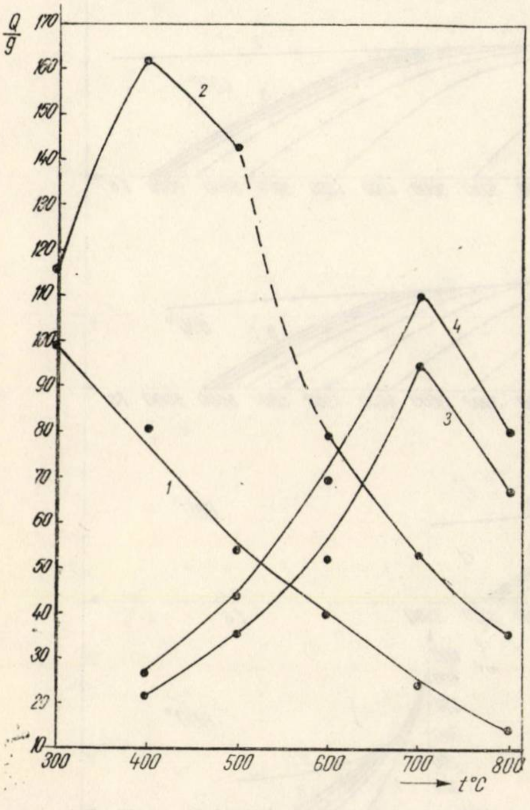

Fig. 3. — Variation de la quantité d'halogène adsorbée en fonction de la température.

1, Courbe expérimentale pour l'iode ; *2*, Courbe corrigée pour l'iode ; *3*, Courbe expérimentale pour le chlore ; *4*, Courbe corrigée pour le chlore.

inférieure à la température critique, l'iode se trouvant à l'état de vapeurs, l'adsorption ait lieu d'après un schéma polymoléculaire. Dans ce cas $\theta > 1$ comme on remarque aussi dans le tableau 2.

Dans la figure 3, on a représenté aussi l'isobare d'adsorption du chlore sur une électrode de charbon semi-activé identique à celui utilisé pour l'iode (la courbe 3 est déterminée expérimentalement, et la courbe 4 est la courbe corrigée). Comme on peut voir, à des températures plus réduites que la température critique de l'iode, $a_I > a_{Cl}$. Pour des températures supérieures à la température critique de l'iode, $a_I < a_{Cl}$. Il y a tout lieu de croire que dans ce cas pour les deux gaz il y a une adsorption monomoléculaire. Si l'on admet que le degré de recouvrement est approximativement égal pour les deux gaz, il résulte que

$$\frac{a_{Cl}}{a_I} \approx \frac{r_I^2}{r_{Cl}^2}$$

Tableau 2

Degré de recouvrement avec de l'iode de l'électrode de charbon semi-activé en fonction de la température

t°C	θ
300	2,9
400	3,3
500	2,8
600	1,3
700	0,9
800	0,6

A la température de 800° cette relation se vérifie approximativement c'est-à-dire

$$\frac{a_{Cl}}{a_I} = 2{,}2 \quad \text{et} \quad \frac{r_I^2}{r_{Cl}^2} = 1{,}8$$

Les courbes de la figure 3 représentent les valeurs moyennes pour quelques déterminations faites avec des électrodes préparées de la même manière.

Comme on le voit dans les figures 2*a*—*f* l'allure même des courbes de polarisation cathodique est différente pour les deux intervalles de température. On observe jusqu'à 500° un palier qui disparaît pour les températures plus élevées.

On ne peut pas encore donner une explication au maximum observé sur l'isobare d'adsorption de l'iode, ainsi que, d'ailleurs, du chlore.[1] Ce maximum pourrait être causé par un changement du caractère de l'interaction halogène adsorbé — charbon, mais aussi par une augmentation de l'interface de contact électrode — électrolyte en fonction de la température.[1]

Il faut mentionner que l'allure des isobares d'adsorption est la même pour toutes les sortes de charbons actifs que nous avons utilisés, les valeurs absolues variant en fonction de la surface des charbons et du mode de préparation de ceux-ci.

Enfin, dans la figure 4 la courbe 1 représente la valeur de la correction pour l'autodésorption de l'iode à toutes les températures. La valeur de cette correction est déterminée par deux facteurs. Le premier c'est le temps de polarisation cathodique. Celui-ci, d'après ce que l'on voit dans les figures 2*a* — *f* (courbes 1), diminue avec la température. Le second facteur, c'est la vitesse de l'autodécharge, qui augmente avec la température comme on le voit dans les figures $2a - f$ (courbes 2). Le résultat de la combinaison de ces deux facteurs est le maximum que l'on observe sur la courbe 1 de la figure 4. La courbe 2 de la figure 4 représente la valeur de la correction de l'autodésorption du chlore. Celle-ci est plus petite pour le chlore que pour l'iode, à cause du fait que le temps de polarisation cathodique du chlore est plus réduit.

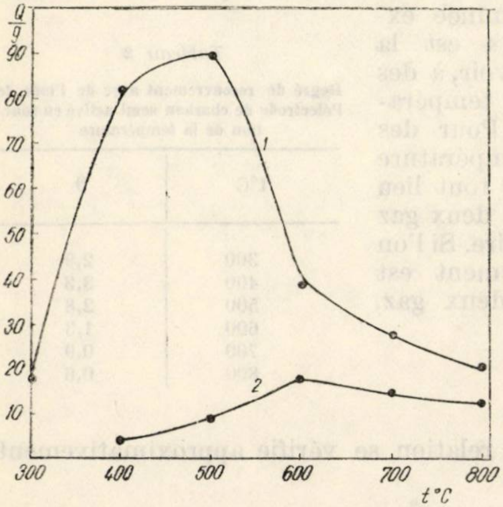

Fig. 4. — Variation de la correction pour l'autodécharge en fonction de la température.
1, pour l'iode; *2*, pour le chlore.

Revue Roumaine de Chimie, 15, 1177 – 1180 (1970)

THERMAL PROPERTIES OF POTASSIUM CHLORIDE
HIGH TEMPERATURE HEAT CONTENT

D. I. MARCHIDAN and M. CIOPEC

Institute of Physical Chemistry
Str. Galaţi 31, Bucharest 13

Received February 14, 1970

The heat content of KCl has been determined from 400° to 700° K using a copper-block drop calorimeter. The results of this investigation were correlated with comparable studies from the literature. A tabulation of thermodynamic values is presented.

Heat capacities, entropies and free energy functions at high temperature are usually derived from the experimentally determined enthalpy values. These data are required for the study of many problems in high-temperature chemistry and, in particular, constitute the basic data used by the powerful tool of equilibrium thermodynamics.

In this paper a description is given of the method and the experimental procedure used in enthalpy determinations.

The drop calorimeter technique continues to be the most reliable method for determining these heat contents. Such a calorimeter has been constructed using a rather simple bridge, having a thermistor as one arm, to measure temperature changes with high precision.

EXPERIMENTAL PROCEDURES

The experimental technique has been described in detail in a previous paper [1] and the accuracy of the measurements is considered to be within the reproducibility, which was ± 0.4 per cent. In brief, this method is as follows. The sample, sealed in this container, is suspended in a furnace until it comes to a constant known temperature. It is then dropped into a copper-block calorimeter, which measures the heat evolved by the sample plus container in cooling to 25°. In order to account for the heat capacity of the container and the heat lost during the drop, a similar experiment is made with the empty container at the same temperature. The difference between the two values of heat is a measure of the change in enthalpy of the sample between 25° and the temperature in the furnace. From enthalpy values of the sample so determined, for a series of temperatures, the heat capacity can be derived.

Many of the details of the copper-block calorimeter and furnace and their operation have been given in previous publications.[1,2]

---

[1] D. I. MARCHIDAN and M. CIOPEC, *Studii Cercetări Chim. Acad. Romania* **17**, 737 (1969).

[2] D. I. MARCHIDAN and M. CIOPEC, *Rev. Roumaine Chim.* (in print).

Electrical calibrations of the calorimeter gave an energy equivalent of 300 cal per °K with a standard deviation of ±0.62 cal per °K.

Containers were constructed of aluminum in an attempt to find a substitute for platinum. High purity aluminum with known heat capacity was machined into cylinders to fit the crucibles (containers).

The potassium chloride used, with a purity "specpure" (Johnson, Matthey & Co) were dried before being introduced into the container.

RESULTS AND DISCUSSIONS

The first determinations were carried out on the empty aluminum container by measuring the temperature change (ΔT_2) of the calorimetric block (table 1). Subsequently, the temperature change (ΔT_1) of the calorimetric block due to the container with potassium chloride was measured.

Table 1

Observed temperature of calorimeter for empty container

No.	Temperature °K	ΔT calorimeter-block °C
1	383.64	0.230
2	385.49	0.239
3	386.59	0.242
4	486.32	0.533
5	489.32	0.532
6	490.56	0.535
7	599.73	0.856
8	602.67	0.874
9	604.16	0.870
10	665.63	1.056
11	667.80	1.080
12	668.96	1.082
13	714.25	1.230
14	719.99	1.245
15	720.71	1.241

The difference ($\Delta T_1 - \Delta T_2$) for a given temperature represents the increase of calorimetric temperature due to the substance heated at the given temperature. The $(\Delta T_1 - \Delta T_2)/n$ value multiplied by the energy equivalent represents the value of the $H_T - H_{298.15}$ function.

Within the experimental temperature range, the following equation, obtained by the method of least squares, can be used to represent these data :

$$H_T - H_{298.15} = -3440.6 + 11.075 . T + 1.8868 \times 10^{-3} T^2 \qquad (1)$$

The deviations ot experimental data from the calculated curve are given in table 2. The comparison of the calculated data on the basis of equation (1) with data[3] in literature (JANAF tables) which follow an equation of the type:

$$H_T - H_{298.15} = -3518 + 11.235\, T + 1.85 \times 10^{-3}\, T^2 \qquad (2)$$

indicates a good agreement (table 3)

Table 2

Enthalpy of potassium chloride

Temperature °K	$H_T - H_{298.15}$ cal/mol		Deviation	
	Observed	Calculated eq(1)	cal/mol	%
387.16	1167.7	1130.0	+37.7	+3.3
491.80	2387.2	2462.2	−75.2	−3.1
601.98	3889.0	3910.0	−21.0	−0.5
603.12	3906.3	3925.2	−18.9	−0.5
662.09	4691.7	4719.1	−27.4	−0.6
713.66	5435.8	5424.1	+11.7	+0.2
714.16	5425.4	5431.0	−5.6	−0.1

Table 3

Departure from JANAF data

Temperature °K	$H_T - H_{298.15}$ cal/mol		Departure	
	Eq (1)	JANAF Eq(2)	cal/mol	%
400	1291.3	1272	+19.3	+1.5
500	2568.6	2562	+ 6.6	+0.24
600	3883.6	3889	− 5.4	−0.14
700	5236.4	5255	−18.6	−0.35

The results are better than those for aluminum and this is probably due to the fact that the errors mentioned in the case of aluminum have been eliminated by measuring the heat content of the container with and without substance, only the difference of these values being used in the calculations. That is why the deduced equation (1) is very close to that which fits JANAF data (2).

The temperature dependence of heat capacity for potassium chloride is obtained by differentiating equation (1), respectively:

$$C_p = 11.075 + 3.7736 \times 10^{-3}\, T \qquad (3)$$

Table 4 gives the computed values of heat capacity, enthalpy, entropy and the free energy function in the range 400° to 700° K at 50° intervals.

The $S_{298.15}$ value for potassium chloride is 19.773 e.u.

---

[3] "JANAF Thermochemical Tables" (ed. D. R. Stull).
Dow Chemical Company, Midland, Mich., Aug. 1965, Nr. PB 168−370.

Table 4

Thermodynamic functions for potassium chloride

Temperature °K	C_p cal/mol.deg.	$H_T - H_{298.15}$ cal/mol	S_T e. u. cal/mol. deg.	$-\frac{G_T - H_{298.15}}{T}$ e.u.
400	12.58	1291.3	23.38	20.15
450	12.77	1925.2	24.86	20.59
500	12.96	2568.6	26.22	21.08
550	13.15	3221.1	27.47	21.61
600	13.34	3883.6	28.62	22.14
650	13.53	4555.3	29.32	22.31
700	13.72	5236.4	30.70	23.22

Acknowledgements. We wish to express our deep gratitude to Professor I. G. Murgulescu for the help and the interest he has shown in our work. Our thanks are also due to the tehnician C. Volcovici.

Revue Roumaine de Chimie, **15**, 1181 – 1185 (1970)

KINETIC MEASUREMENT OF COBALT TRACES. IV*
WITH HEMATOXYLIN

D. COSTACHE

Department of Analytical Chemistry, University of Bucharest
Splaiul Independenţei 89

Received July 29, 1969

Cobalt is measured kinetically, by making use of its catalytic action on the oxidation reaction of hematoxylin with peroxide in an alkaline medium. One studies the influence of the pH, of the peroxide concentration, one gives the values of the rate constants, one draws up the calibration graphs, studies the influence of alien ions and the reproductivity of the method. The method may be applied in the concentration range of 1.55×10^{-11} to 7.75×10^{-11} g Co/cm^3.

The kinetic method, recently adopted for analytical measurements, is based on a proportionality between the reaction rate, and the concentration of a compound to be measured. The compounds which are measured are substances of a catalytic character.

In the case of cobalt, one could establish that the oxidizing rate with peroxide in alkaline medium of some organic compounds containing two hydroxyl groups in *ortho* position is influenced by the presence of cobalt traces. Such measurements are known in the speciality literature and may be found in the papers.[1–15]

---

* Part III: D. Costache, *Rev. Roumaine Chim.* **15**, 945 (1970).

[1] J. Bognar and O. Jellinek, *Acta Chim. Acad. Hung.*, **29**, 121 (1961).

[2] E. Schulek and J. Laslovski, *Mikrochim. Acta*, 1, 41 (1960).

[3] N. B. Parhomenko, G. A. Prik and K. B. Iatsimirski, *Zhur. analit. Khim.*, 16, 599 (1961).

[4] J. Bognar, *Magyar Kém. Folyóirat*, **59**, 24 (1953).

[5] J. Bognar and O. Jellinek, *Acta Chim. Acad. Hung.*, **29**, 319 (1961).

[6] J. Bognar, *Mikrochim. Acta*, **4**, 801 (1963).

[7] J. Bognar, *Mikrochim. Acta*, **5**, 901 (1961).

[8] J. Laszovski, *Mikrochim. Acta*, **2**, 289 (1961).

[9] A. K. Babko and J. Lukovskaia, *Ukrain. khim. Zhur.*, **28**, 968 (1962).

[10] V. M. Peskova, J. F. Dolmanova and N. M. Chemenova, *Zhur. analit. Khim.*, **18**, 1228 (1963).

[11] J. Bognar and L. Sipos, *Mikrochim. Acta*, **5**, 442 (1963).

[12] Gr. Popa and D. Costache, *Rev. Roumaine Chim.*, **8**, 963 (1967).

[13] Gr. Popa and D. Costache, *Analele Univ. Bucureşti*, **16**, 107 (1967).

[14] D. Costache and Gr. Popa, *Anal. Univ. Bucureşti*, **17**, 21 (1968).

[15] Gr. Popa and D. Costache, *Anal. Univ. Bucureşti*, **17**, 55 (1968).

In the present contribution the reactive used is hematoxylin, the structural formula of which is:

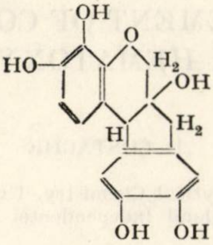

Its oxidation by peroxide in alkaline medium leads to colourless reaction products.

EXPERIMENTAL

Reactives: The reactive solution was obtained by solving hematoxylin in ethylic alcohol (0.024%).

The peroxide obtained from hydrogen peroxide had a 1.83% concentration, verified every hour by titration in acid medium with potassium permanganate.

The reaction medium used was a buffer solution, obtained by solving 5 gr of Sörensen boric acid in 1000 cm^3 of NaOH 0.24 N.

The cobalt solution was obtained by solving spectrally pure metallic cobalt in dilute sulphuric acid.

Tridistilled water was used for all solutions.

Apparatus: The reaction rate was measured spectrophotometrically, by watching the variation in time of the optical density of the reaction mixture at a horizontal Pulfrich Zeiss Jena spectrophotometer, and a wavelength of $\lambda = 533$ nm. The measurements were carried out at 25°, by adopting a thermostatic device to the spectrophotometer.

Working method: we have added in 25 cm^3 flasks the reactive, buffer, peroxide and cobalt solutions. After mixing and bringing to mark, one starts the chronometer, stirs well the content of the flask, which is then transferred into the spectrophotometer's cell, and the optical density is read every minute, with water as blank.

The concentration of the solutions in the cell is:

Hematoxylin	9.60×10^{-6} g/cm^3
Peroxide	4.32×10^{-4} g/cm^3
Cobalt	$1.55 \times 10^{-11} - 7.75 \times 10^{-11}$ g Co/cm^3

To find out the optimum reaction conditions, we have first carried out a preliminary kinetic study, consisting of: the study of the influence of the pH and of the influence of the peroxide's concentration, the finding out of the rate constants, the influence of temperature on those constants, the reaction order for a correct application of the corresponding kinetic relationships.

The influence of the pH can be seen in graph 1.

It results that the reaction rate is the highest in the alkaline range from 11.5 to 13.5 pH units.

The influence of peroxide is given in graph 2.

This shows that the reaction rate depends on the concentration of peroxide, having also a relatively stable interval between 2.80 and 5.10 g $H_2O_2/cm^3 . 10^{-4}$.

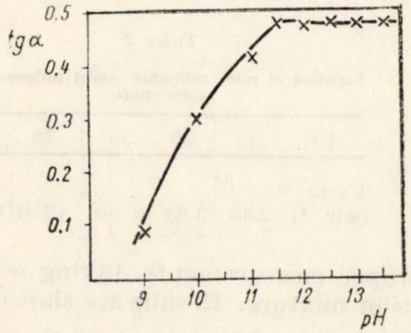

Fig. 1. — Influence of pH on the reaction rate.

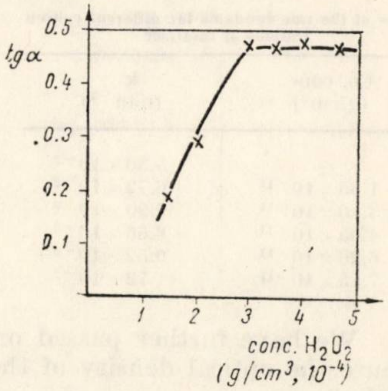

Fig. 2. — Influence of peroxide concentration on the reaction rate.

Based on the experimental data (graph 3), we have studied the reaction order, which was found to be of the first order and the corresponding kinetic relationship which is

$$\ln \frac{a}{a - x} = kt \tag{1}$$

We have thus a pseudomonomolecular reaction as against the concentration of the coloured organic reactive.

We relate the concentration of the organic reactive to the optical density by means of the Lambert-Beer relationship, obtaining

$$\ln \frac{D_0}{D} = kt \tag{2}$$

or

$$\ln D = \ln D_0 - kt \tag{3}$$

where D_0 and D represent the optical densities at the initial moment, and at a certain moment, t. We consider two successive readings, and eliminate the optical density at the initial moment, obtaining:

$$k = \frac{\lg D_1 - \lg D_2}{t_2 - t_1} \cdot 2.303 \tag{4}$$

which represents the relationship by means of which we shall calculate the rate constants of uncatalytic and catalytic reactions. Results can be seen on table 1.

The reaction rate is strongly influenced by temperature, thus affecting the value of the rate constants. Results are given on table 2

It henceforth results that the measurements must be carried out at a certain temperature.

Table 1

Values of the rate constants for different concentrations of catalyser

Co. conc. (g/cm^3)	k (min^{-1})
—	5.30×10^{-2}
1.55×10^{-11}	6.72×10^{-2}
3.10×10^{-11}	7.90×10^{-2}
4.65×10^{-11}	8.66×10^{-2}
6.20×10^{-11}	9.52×10^{-2}
7.75×10^{-11}	11.72×10^{-2}

Table 2

Variation of rate constants under influence of temperature

t°C	15	20	25	30	35
$k \times 10^{-2}$ (min^{-1})	2.35	3.98	5.30	12.41	19.47

We have further passed on to proper measurements, taking every minute the optical density of the reaction mixture. Results are shown on graph 3.

We have choosen the "tangent method" for the measurement of the cobalt, representing in semilogarithmic coordinates the optical density *versus* time, as in graph 3, after which, according to relation (3) one obtains straight lines.

Measuring the angles of these lines with the abscissa, finding out the value of their tangents and representing these as a function of the cobalt concentration, one obtains graph 4, which can be used as a working graph.

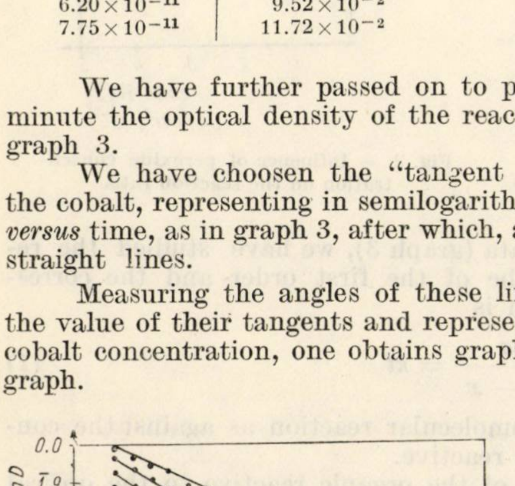

Fig. 3. — Variation of D in time.

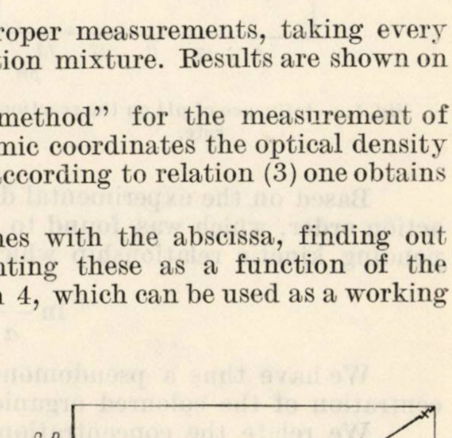

Fig. 4. — Dependency of tg α on cobalt concentration.

In the case of unknown sample, one adopts the same working technique and by means of graph 4 finds out the cobalt concentration. We have further studied the influence of alien ions, and found that following ions affect the reaction rate : Fe^{2+}, Fe^{3+}, V^{5+}, Pd^{2+}, if their ratio to cobalt exceeds the value of 1,000 to 1.

Some measurements regarding the reproducibility of the method are given further in table 3.

It results that the measurement of cobalt by this method has a good reproducibility.

Table 3

Reproducibility of the method

No. of measurements	Co analysed (g/cm^3)	$\sphericalangle \alpha^\circ$	tg α	Co found in analysis (g/cm$^3 \times 10^{-11}$)	Difference (g/cm$^3 \times 10^{-11}$)
	1.55×10^{-11}	30	0.577	—	—
1		30	0.577	1.70	0.15
2		31	0.600	2.01	0.46
3		29	0.554	1.40	0.15
4		30	0.577	1.70	0.15
5		30	0.577	1.70	0.15
	3.10×10^{-11}	34	0.674	—	—
1		33	0.649	2.87	0.23
2		34	0.674	3.33	0.23
3		35	0.700	3.72	0.62
4		34	0.674	3.33	0.23
5		34	0.674	3.33	0.23
	4.65×10^{-11}	37	0.753	—	—
1		37	0.753	4.65	—
2		38	0.781	4.96	0.31
3		37	0.753	4.65	—
4		36	0.726	4.19	0.46
5		37	0.753	4.65	—
	6.20×10^{-11}	40	0.839	—	—
1		41	0.869	6.35	0.15
2		39	0.809	5.58	0.62
3		40	0.839	5.97	0.23
4		40	0.839	5.97	0.23
5		39	0.809	5.58	0.62
	7.75×10^{-11}	44	0.965	—	—
1		45	1.000	8.37	0.62
2		43	0.932	7.44	0.31
3		44	0.965	7.90	0.15
4		44	0.965	7.90	0.15
5		43	0.932	7.44	0.31

The period for one determination is 20 min.

Concluding, we can state that by the kinetic method with hematoxylin one can measure cobalt in the concentration range 1.55×10^{-11} to $7.75 \times \times 10^{-11}$ g Co/cm^3 with a good reproducibility.

Revue Roumaine de Chimie, **15**, 1181–1185 (1970)

Revue Roumaine de Chimie, 15, 1187–1190 (1970)

DIE KINETISCHE BESTIMMUNG DES HYDRAZINS MIT BROMAT UND AMIDOL

AL. ŞUTEU, I. AL. CRIŞAN und ELEONORA MÎNDRUŢIU

vom Lehrstuhl für Analytische Chemie der ,,Babeş-Bolyai''-Universität Cluj,
str. Arany Janos, 11.

Eingegangen am 27. Februar 1969

In dieser Arbeit werden die theoretischen Grundlagen einer neuen Art von kinetischen Analysenmethoden vorgelegt, die bei der kinetischen Bestimmung des Hydrazins angewendet werden. Die Hydrazinbestimmung hat die auch experimetell beobachtete lineare Abhängigkeit zwischen dem Zeitpunkt des Beginns der Indikationsreaktion zwischen Bromat und Amidol und die Menge des zu bestimmenden Hydrazins, zur Grundlage. Das Bromat oxydiert Amidol (*p*-2,1-Diaminophenol) zu einer rot gefärbten Verbindung, die durch λ_{max} = 510 nm und den molaren Extinktionskoeffizienten 881,9 gekennzeichnet ist.

Bei der kolorimetrischen Bestimmung des Hydrazins wurden bis jetzt verschiedene organische Reagenzien verwendet. So bestimmten Watt und Chrisp [1] Hydrazin, indem sie als Reagens Dimethylazobenzaldehyd in alkoholischer Lösung verwenden. Dieses bildet mit Hydrazin *p*-Dimethylaminobenzaldehyd, das kräftig rot gefärbt ist und bei $\lambda =$ $= 458$ nm kolorimetriert wird. Dieselbe Reaktion wurde auch von Freier und Resch[2] für die Bestimmung von Hydrazinspuren in Wasser verwendet. Diese Reaktion wurde auch von Dombrauskos und Herbert [3] in einer abgeänderten Wattschen Methode zur Bestimmung von Hydrazin aus verschiedenen Materialien, angewendet. Riley [4] bestimmte Hydrazin mit Pikrylchlorid (2, 4, 8-Trinitrochlorbenzol), welches mit Hydrazin in Chloroformlösung Hexanitrohydrazobenzol von violetter Farbe bildet, das bei 494 nm kolorimetriert wird.

PRINZIP DER METHODE

Eine Analysenmethode mit großen Aussichten für die Bestimmung kleiner Mengen von Substanzen ist die katalytische Titration. In der katalytischen Titration wird eine gewisse Substanz in Gegenwart anderer

---

[1] C. W. Watt und D. Chrisp, *Analyt. Chem.*, **24**, 2006 (1952).
[2] R. Freier und G. Pesch, *Z. analyt. Chem.*, **149**, 177 (1956).
[3] T. Dombrauskos und H. Herbert, *Ann. Ind. Hyg. Assoc. J.*, **23**, 151 (1962).
[4] J. P. Riley, *Analyst*, **79**, 76 (1954).

Substanzen bestimmt, deren Reaktion durch eine Titrationsagens katalysiert werden kann. Auf dieser Grundlage wurden[5] kleine Mengen von J^- bestimmt, indem man mit Ag^+ in Gegenwart von AsO_3^{3-} und Ce^{4+} titrierte. Dieses Prinzip ist in folgendem verallgemeinert und bei der kinetischen Bestimmung des Hydrazins in Gegenwart von Amidol und Bromat angewendet. Betrachtet man zwei Redox-Reaktionen:

$$\text{red}_1 + \text{ox}_2 \rightleftharpoons \text{ox}_1 + \text{red}_2 \tag{1}$$

$$\text{red}_3 + \text{ox}_2 \rightleftharpoons \text{ox}_3 + \text{red}_2 \tag{2}$$

welche dank der Differenzen zwischen den normalen Redoxpotentialen der reagierenden Systeme nur aufeinanderfolgend stattfinden können, so sieht man, daß die zweite Redoxreaktion zeitlich um so später beginnen wird je größer die Konzentration von red_1 ist (wenn man einen konstanten Überschuß von red_3 und ox_2 in Betracht zieht). Man kann die Gleichung:

$$\Delta t = a' + b'.x \tag{3}$$

annehmen, wo Δt die Zeit ist, nach der die Reaktion (2) beginnt, die von dem Anfang der Reaktion (1) markiert wird, x ist die Konzentration von red_1 der zu bestimmenden Substanz und a und b sind konstant. Es ist ersichtlich, daß man diese Beziehung auch auf die Bestimmung der Oxydationsmittel anwenden kann, wie zum Beispiel:

$$\text{ox}_1 + \text{red}_2 \rightleftharpoons \text{red}_1 + \text{ox}_2 \tag{4}$$

$$\text{ox}_3 + \text{red}_2 \rightleftharpoons \text{red}_3 + \text{ox}_2 \tag{5}$$

wie auch in einigen folgenden Arbeiten gezeigt wird.

Falls eines der Reaktionsprodukte gefärbt ist, so kann, anstatt der Messung des Parameters Δt, die Zeit gemessen werden, in welcher eine gewisse willkürlich gewählte Absorbanz der Lösung (mit E bezeichnet) erreicht wird. In diesem Fall schreibt man die Beziehung (3):

$$E = a + b \cdot x \tag{6}$$

Auf dieser Grundlage wurde die Möglichkeit der kinetischen Bestimmung des Hydrazins untersucht, die Tatsache beachtend, daß Hydrazin von Bromat, entsprechend der Reaktion:

$$3\ N_2H_4 + 2\ KBrO_3 \rightleftharpoons 3N_2 + 2KBr + 6H_2O \tag{7}$$

oxydiert wird. In gewissen pH-und Konzentrationsverhältnissen verläuft obige Reaktion mit meßbarer Geschwindigkeit und ihre Dauer ist eine lineare Funktion der Hydrazinmenge.

Durch die Verwendung einer entsprechenden Indikatorreaktion, die es ermöglicht den Titrationsschluß der Reaktion zu bemerken, kann die Hydrazinmenge leicht mit Hilfe einer Titrationskurve ermittelt werden. Eine solche Indikatorreaktion dürfte nicht stattfinden, so lange noch

---

[5] K. B. Jatsimirskii und T.I. Fedorowa, *Doklady Akad. Nauk. S.S.S.R.*, **1962**, 143.

Hydrazin vorhanden ist und müßte schnell mit einer brüsken Eigenschaftsänderung (Farbe) verlaufen, sobald die ganze Hydrazinmenge oxydiert wurde. Als Indikatorreaktion wählten wir die Reaktion zwischen Bromat und Amidol (*p*-2,4-Diaminophenol), da die vorher ausgeführten Versuche zeigten, daß diese Reaktion sich sehr gut zu diesem Zweck eignet. Die oben genannten Bedingungen erfüllend, wird Amidol durch $KBrO_3$ zu einer rot-violetten Verbindung oxydiert, die ein Absorptionsmaximum bei 510 nm hat. Die Absorptionskurve des erhaltenen Färbmittels, das durch die Oxydation des Amidols erhalten wurde, wird in Abbildung 1 gezeigt.

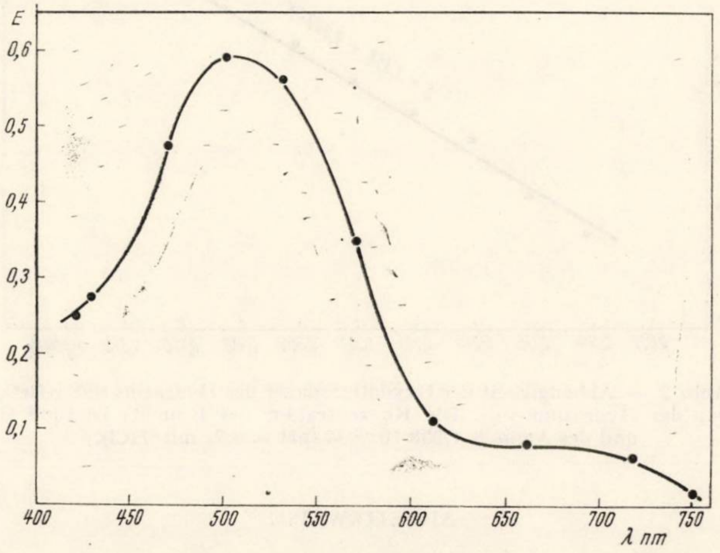

Abb. 1. — Absorbanz der Amidollösung (mit $KBrO_3$ oxydiert) in Funktion von λ(nm). Die Konzentration des Amidols ist $c = 1{,}338.10^{-3}$ Mol/1000 cm^3, die Küvette von 1 cm.

Der molare Extinktionskoeffizient, der bei $\lambda = 510$ nm bestimmt wurde ist : $\varepsilon_{\lambda_{\max}} = 881{,}\ 9$.

Die Oxydationsreaktion des Hydrazins hängt sehr stark von dem Säuregehalt der Lösung ab, ihre Geschwindigkeit ist bei pH= 1 beinahe null. Bei pH = 0,5 zeigten die Versuche, daß die Reaktionsgeschwindigkeit sehr steigt, so daß zwischen der Reaktionsdauer und den Hydrazinmengen keine lineare Beziehung gefunden wurde. Die vorteilhaftesten Bedingungen, bei denen eine solche Linearität zwischen der Hydrazinmenge und der Reaktionsdauer besteht, wurden bei pH = 0,7 gefunden. Als beste $KBrO_3$-Konzentration fanden wir 10^{-3} M. Die Abhängigkeit der Reaktionsdauer von der Hydrazinmenge wird in Abbildung 2 gezeigt. Aus der Abbildung sieht man, daß zwischen 0,05 — 0,5 mg Hydrazin/ /30 ml und der Reaktionsdauer eine lineare Abhängigkeit besteht.

Mit Hilfe der Statistik der geraden Linie wurde die Gleichung der wahrscheinlichsten Eichgeraden berechnet:

$$E = 1{,}558 \times 4{,}943 .\, x \qquad (8)$$

(wo E = Absorbanz und x = Hydrazinmenge ist), aus welcher, durch eine einfache Berechnung die Hydrazinmenge bestimmt werden kann.

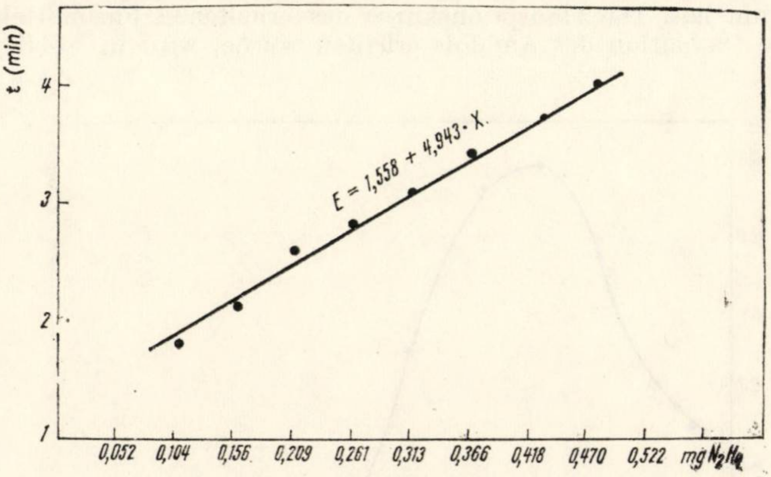

Abb. 2. — Abhängigkeit der Oxydationsdauer des Hydrazins mit $KBrO_3$ von der Hydrazinmenge. Die Konzentration des Bromats ist 10^{-3} M und des Amidols $1{,}338 . 10^{-3}$ M (pH = 0,7, mit HCl).

ARBEITSWEISE

Der 0,05—0,5 mg enthaltende Hydrazinlösung werden 5 ml 0,2 M HCl, 5 ml 0,1% Amidol, 10 ml 10^{-3} M $KBrO_3$ hinzugefügt und wird dann mit Wasser auf 30 ml Endvolumen aufgefüllt. Es wird dann gut vermengt und die Zeit bis zum Farbauftritt chronometriert. Auf Grund einer Eichkurve kann die Hydrazinmenge mit einem Fehler von — 1,2% bestimmt werden.

Andere Reduktionsmittel wie NH_2OH, Ascorbinsäure usw. interferieren und verändern die Ergebnisse.

Ein pH-Wechsel von 0,1 pH Einheiten. So wie ein Temperaturwechsel von ± 2° beeinflußt die Ergebnisse nicht. Die Bestimmungen wurden bei 22° durchgeführt.

Aus den Ausführungen folgt, daß Hydrazin in bestimmten kinetischen Bedingungen auf Grund einer linearen Abhängigkeit zwischen der Hydrazinmenge und dem Zeitpunkt des Beginns der Indikatorreaktion (Bromat + Amidol) bestimmt werden kann.

Revue Roumaine de Chimie, **15**, 1191–1196 (1970)

SALTING-IN EFFECTS IN ORGANIC SOLVENT-WATER-ORGANIC ELECTROLYTE SYSTEMS. MOLECULAR WEIGHT OF THE ORGANIC ELECTROLYTES

CAMELIA BELDIE

Department of Physical Chemistry
University of Jassy
Calea 23 August No. 11

Received July 30, 1969

Experimental data with respect to the salting-in effects produced by some organic electrolytes on the binary cyclohexanone-water system are presented. The data are compared with those obtained in phenol-water- and furfural-water-organic electrolyte mixtures, which also obey the expression $\Delta t = am$. This relation suitably expressed could lead to the determination of the molecular weight of the electrolytes with large ions, from salting-in data. The experimental data are discussed based on existing theories. Some considerations are advanced about the influence of the solvent on the interaction parameter k_s.

The problem of the relation of the solubility to the salt effect was the investigation object of several authors among whom two apparently different points of view [1-3] predominated.

Janaszewski [4] in a very interesting discussion concerning the relation between salting out effects and solubility accorded the two points of view which in fact do not exclude each other.

The conclusions are supported by purely thermodynamic arguments by means of which Janaszewski developed an equation that can be experimentally tested. [5]

The results of Janaszewski's thermodynamic discussion are similar with those of Kogan, [3] namely in a ternary system 1–2–3, a salting-out of the component 2 caused by addition of 3 to the binary mixture 1–2 is to be expected when the binary 2–3 is much more positive than 1–3 in the deviations from Raoult's law. At sufficiently high deviations this would correspond to a phase separation and thus it would be evident that a decreased solubility of 3 in 2 than of 3 in 1 is a necessary condition for a salting-out of 2 to occur according to the scheme given above.

---

[1] E. C. Novella and J. M. Tarroso, *Anales real. Soc. españ. Fis. Quim.*,

[2] A. Miro Rius, *Ibid.*, **53B**, 171 (1957); *Ibid.*, **56B**, 629 (1960); *Ibid.*, **57B**, 219 (1961).

[3] V. B. Kogan, S. F. Bulushev, V. T. Safranov and O. F. Moskovets, *Zhur. priklad. Khim.*, **32**, 2409 (1959); R. R. Tursi and A. R. Thomson, *Chem. Eng. Progr.*, **47**, 304 (1951)

[4] B. Janaszewski, *Roczniki Chem.*, **40**, 117 (1966).

[5] B. Janaszewski, *Ibid.*, **40**, 109 (1966).

This statement is true for a salting-out obtained by ordinary electrolytes whose ions are small and in which the solvent 1 is water.

In our case this is not true as we shall see further.

EXPERIMENTAL RESULTS AND DISCUSSION

In two previous papers we found that some organic electrolytes produce a salting-in on the binary phenol-water [6] and furfural-water [7] systems. These are : oxalic, malonic, succinic, adipic acid, pirocatechin, resorcine, hydroquinone, citric and benzilic acid.

These results, as we shall see, can have practical applications and for this reason we extended our study upon other solvent -solvent or solvent-nonelectrolyte couples.

In this paper we present the data obtained for the cyclohexanone-water mixture in which we added the above organic substances. We used a turbidimetric nonisothermal method, described previously, [6] using an ultrathermostater U_{10}.

The purity of the solvents used was verified by measuring the refractive index for cyclohexanone and the ionic conductivity for water.

In all investigations the cyclohexanone-water composition was. maintained constant (saturated solution at 25°) and we measured Δt—the displacement ot the equilibrium temperature, by adding various electrolyte concentrations.

In this case as in previous studies, [6,7], the salt effects obey the Hamilton-Hickson's [8] empirical equation

$$\Delta t = ac^b \tag{1}$$

We applied this expression as

$$\Delta t = am \tag{2}$$

Equation (2) applies to all electrolytes that give a salting-in. In this equation Δt has the significance shown above, c — the electrolyte concentration in moles/*l*, *m*-the same concentration expressed in molalities, *a* and *b* are two constants, *a*, *a* constant specific to an electrolyte and *b* another constant specific to the liquid mixture.

The values of *a* for the electrolytes used are listed in table 1.

In order to compare the solvent influence we also listed in the same table the data of phenol and furfural as solvents.

We found that the constant *b* is equal to 1 for all electrolytes producing a salting-in.

This fact can be seen by plotting log *m* versus log Δt. The plots are straight lines, the slopes of which are equal to the unity (Fig. 1—3).

---

[6] C. Beldie and E. Papafil, *Anal. Sti. Univ.* "Al. I. Cuza" *Iaşi Sect. 1.* **11**, 117 (1965)

[7] C. Beldie and Fl. Bărbulescu, *Rev. Roumaine Chim.*, (in print).

[8] H. J. Carrington, L. R. Hickson and W. Hamilton Patterson, *J. Chem. Soc.*, **1925**, 2544.

Table 1

Values of the constant *a*

Solvent mixture	Phenol-water 25°	Cyclohexanone-Water 25°	Furfural-water 25°
Electrolyte			
Oxalic acid	—	130.7	107.3
Malonic acid	91.2	—	93.3
Succinic acid	128.7	109.3	115.7
Adipic acid	—	123.6	126.5
Pirocatechin	—	81.8	48.8
Resorcine	93.0	101.8	74.9
Hydroquinone	57.1	34.37	66.0
Benzilic acid	17.4	—	78.5
Camphoric acid	28.3	132.4	—
Picric acid	21.5	—	—
Citric acid	67.0	391.0	158.0

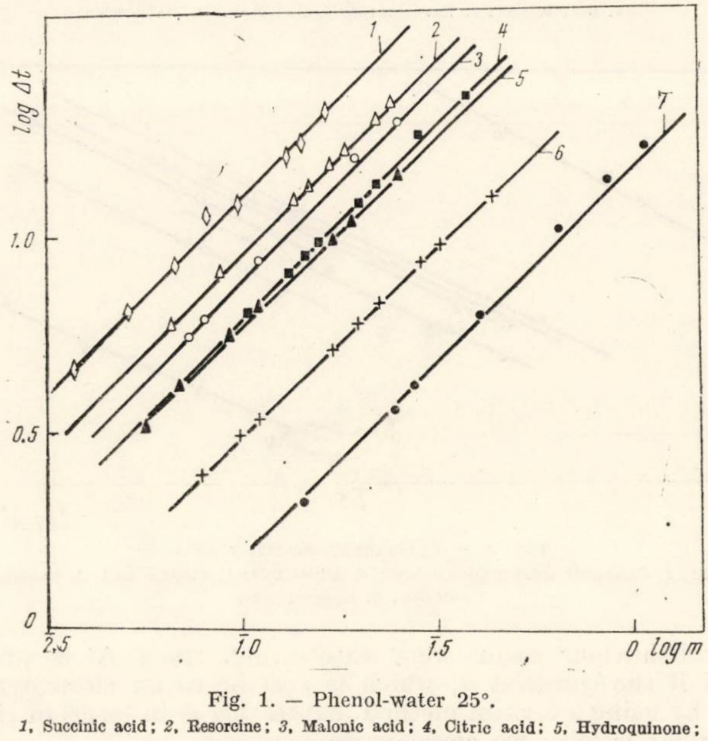

Fig. 1. — Phenol-water 25°.
1, Succinic acid; *2*, Resorcine; *3*, Malonic acid; *4*, Citric acid; *5*, Hydroquinone; *6*, Camphoric acid; *7*, Benzilic acid.

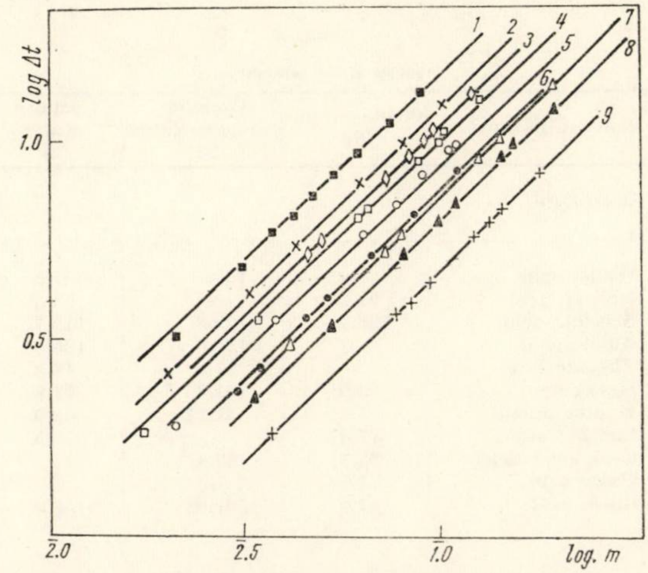

Fig. 2. — Furfural-water 25°.

1, Citric acid; *2*, Adipic acid; *3*, Succinic acid; *4*, Oxalic acid; *5*, Malonic acid; *6*, Benzilic acid; *7*, Resorcine; *8*, Hydroquinone; *9*, Pirocatechin.

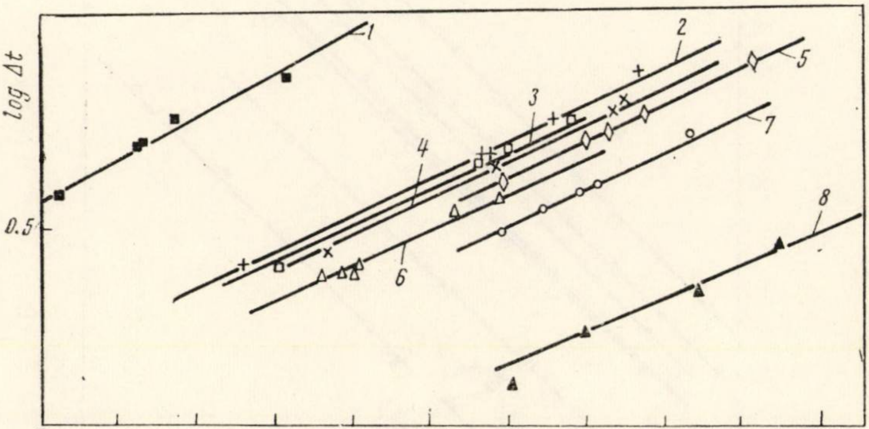

Fig. 3. — Cyclohexanone-water 25°.

1, Citric acid; *2*, Camphoric acid; *3*, Oxalic acid; *4*, Adipic acid; *5*, Succinic acid; *6*, Resorcine; *7*, Pirocatechin; *8*, Hydroquinone.

This behaviour seems very interesting, since Δt is proportional to m, and if the constant a, which is specific to an electrolyte, can be estimated by using a certain method, expressing m in terms of the electrolyte molecular weight, we could write

$$\Delta t = 1000\, a\, g/G_s M \tag{3}$$

where g is the amount of electrolyte in grammes, G_s — the solvent mixture in grammes and M—the electrolyte molecular weight.

In such a case the salting-in measurements could give directly the molecular weight of the electrolyte.

The constant a which represents in fact the molecular lowering of the equilibrium temperature, and is different for each electrolyte, is hard to be found.

In the first approximation it can be found by the trial and error method.

It must be also mentioned, that although so far one thought that b is a constant depending only on the liquid mixture, it is equal to the unity for all electrolytes producing a salting-in, irrespective of the solvent mixture.

This statement can be proved by using the experimental data obtained for organic substances in the binary systems discussed above (Fig. 1 — 3).

From the same data we came to the conclusion that Janaszewski's expression which was tested for water-alcohol-NaCl and -KCl mixtures, [5] is not valid for our data. When one uses as main solvent an organic one such as phenol, furfural, cyclohexanone which mixes with water in limited proportions, the theoretical thermodynamic conclusions developed by Janaszewsky have no validity.

Organic substances such as oxalic, malonic, succinic, adipic acids, pyrocatechin, resorcine, hydroquinone, citric and camphoric acid all are less soluble in water than in the organic solvents given above. Therefore, if we add one of the organic substances used to the organic solvent-water mixture, it produces a salting-in and not a salting-out as it would be expected if Janaszewski's relation, [4] were applied.

This equation in its final form, is :

$$(\partial m/\partial z_2)_{\mu_3, T, p} = m/M_{1,2}\,[\partial(M_1\,\mu_2 - M_2\,\mu_1)/\,\partial(z_1\,\mu_1 + z_2\mu_2)]_{z_2, T, p} \qquad (4)$$

where $M_{1,2} = z_1M_1 + z_2M_2$ is the "mean molecular weight" of the solvent having the composition z_2.

Therefore to compare the behaviour of the systems shown by us, we must also consider other properties of the saturate ternary solutions such as the difference $(V_s - \overline{V}_s^0)$ of Long and McDevit's expression [9]

$$k_s = \overline{V}_s^0\,(V_s - \overline{V}_s^0)/2.303RT\beta_0 \qquad (5)$$

The difference $(V_s - \overline{V}_s^0)$, in the case of the organic electrolytes recalled above, must have a negative value and the result will be a salting-in.

The values of the interaction parameter k_s calculated with the help of the expression,

$$\log S_0/S = k_s\,c_s \qquad (6)$$

where S_0 — the nonelectrolyte solubility in pure solvent

---

[9] F. A. Long and W. F. Mc Devit, *Chem. Rev.*, **51**, 119 (1952).

S — the nonelectrolyte solubility in salt solution

c_s — the electrolyte solubility in moles$^0/_{00}$ g solvent mixture, are negative and are also listed in table 2 together with the corresponding data of the other two systems, in order to be compared.

Table 2

k_s Values at 20°

Solvent mixture	Phenol-water	Cyclohexanone-water	Furfural-water
Electrolyte			
Citric acid	−0.208	−1.359	−1.120
Camphoric acid	−0.109	−0.484	—
Oxalic acid	—	−0.458	−0.757
Adipic acid	—	−0.431	−0.916
Succinic acid	−0.430	−0.392	−0.815
Resorcine	−0.311	−0.350	−0.534
Pirocatechin	—	−0.289	−0.347
Hydroquinone	−0.204	−0.118	−0.467
Benzilic acid	−0.054	—	−0.564
Malonic acid	−0.263	—	−0.660

As it can be seen relation (5) can explain the experimental data qualitatively only. We were not able to use expression (5) for computation, because V_s and $\overline{V}_s^0$ values are not known.

From the same table 2 it can be seen that an influence of the solvent on the interaction parameter k_s exists, since for the same electrolyte-nonelectrolyte couple in different solvents, the parameter k_s has different values.

If we consider the dipole moments and dielectric constants of the three solvents, which are :

phenol—1.56 D; 9.68
cyclohexanone—2.9 D; 18.2
furfura—3.57 Dl; 41.7

we do not find the same order for the k_s parameter. Therefore we came to the conclusion that, beside the physical properties such as dipole moments, dielectric constants and molecular volumes, the chemical properties must also be considered.

We must also consider the eventuality that the large ions can disturb the ordered structure of the solvent, fact which so far has been observed for water only,[10] but which is likely to exist for other solvents, too, having a structure similar to water.

In conclusion we think that this determination method of the molecular weight of the organic electrolytes with large ions, could be extended to polyelectrolytes, too, for which a salting-in must also be obtained.

This statement is supported by some preliminary data using polyacrylic acid. The results in this direction will be given in a next paper.

---

[10] R. M. DIAMOND, *J. Phys. Chem.*, **67**, 2513 (1963).

Revue Roumaine de Chimie, **15**, 1197–1200 (1970)

THE ACTIVITY OF MOLYBDENUM OXIDE–BISMUTH OXIDE CATALYSTS AND THE INFLUENCE OF METALLIC OXIDE MIXTURES

A. POPESCU and A. SZABO

University of Bucharest
Faculty of Chemistry, Laboratory of Catalysis, Splaiul Independenţei, 89

Received December 10, 1969

One has studied the influence of admixtures of vanadium, manganese, iron, cobalt, nickel, copper and zinc oxides on the activity of the $MoO_3-Bi_2O_3$ catalyst (55.30% MoO_3 and 44.70% Bi_2O_3) in the oxidation reaction of methylic alcohol *via* formaldehyde. Of all the catalysts only those containing iron oxide lead to a noticeable increase of the catalytic activity (25%). Cobalt and copper oxides do not practically influence this activity and vanadium, manganese, nickel and zinc oxides even decrease the yield. The positive influence of iron oxide on the $MoO_3-Bi_2O_3$ catalyst may be explained by the simultaneous presence of the following components in the catalyst: bismuth molybdate, iron molybdate and molybdenum oxide.

Oxide catalysts and mixed catalysts used in the catalytic oxidation of organic compounds have been the object of investigations in the last ten years.[1–10]

Studying the catalytic oxidation of methylic alcohol *via* formaldehyde[5,8,10–12] one has noticed the high activity of mixed catalysts: $MoO_3-Cr_2O_3$, $MoO_3-La_2O_3$, MoO_3-MnO_2, $MoO_3-Bi_2O_3$.

---

[1] P. Jiru, B. Wichterlowa and J. Tichy, *Proc. Intern. Congr. Catalysis*, Amsterdam. 1964, North-Holland Publ. Co. Amsterdam, **1**, 199 (1965).

[2] M. Dente, R. Pappi and I. Pasquon, *Chimica e Industria*, **46**, 1326 (1964).

[3] G. K. Boreskov, G. D. Kolovertnov, L. M. Kefeli, L. M. Pleasova, L. G. Karokciev, V. N. Mostihin, B. I. Popov, V. A. Dzisko and D. I. Tarasova, *Kinetica i Kataliz*, **7**, 144 (1966).

[4] D. G. Klisourski, *Compt. Rend. Acad. Bulg. Sci.*, **19**, 1159 (1966).

[5] G. Bliznakov, P. Jiru and D.G. Klisourski, *Coll. Czech. Chem. Comm.*, **31**, 2995 (1966)

[6] A. Popescu, A. Szabo and I. V. Nicolescu, *Rev. Chim.* (*Bucureşti*), **17**, 602 (1966).

[7] A. Popescu, A. Szabo, A. Ionescu and A. Stănculescu, *Analele Univ. Bucureşti, Seria St. Naturii-Chimie*, **16**, 9 (1967).

[8] N. Pipercone, G. Liberti, L. Ernisi and G. Donegani, "The 4th Intern. Congr. Catalysis", Moscow, 1968, Preprint of the paper 21.

[9] V. N. Bibin and B. I. Popov, *Kinetica i Kataliz*, **9**, 618 (1968).

[10] A. Popescu, E. Segal, A. Ionescu and A. Szabo, *Rev. Roumaine Chim.*, **14**, 79 (1969).

[11] A. Popescu, A. Szabo and A. Ionescu, *Analele Univ. Bucureşti, Seria St. Naturii-Chimie*, **16**, 33 (1967).

[12] P. Jiru, F. Trifiro, D. G. Klisourski and I. Pasquon, *Corsi e Seminari di Chimica*, **5**, 313 (1966).

In previous works concerning this reaction we have studied the activity of the catalytic systems $MoO_3-Fe_2O_3$ and Bi_2O_3 [6,10,11] as well as the influence of some metallic admixtures on the catalytic activity of the system $MoO_3-Fe_2O_3$. [7,13]

In order to obtain more data concerning the influence of some oxides, namely : vanadium, manganese, iron, cobalt, nickel, copper and zinc oxides, on the activity of the catalysts, of the $MoO_3-Bi_2O_3$ system, one has studied in the present work catalysts with the following composition : 55.30% MoO_3 and 44.70 % Bi_2O_3, with, or without admixtures of oxides.

The choice of a basic catalyst of this composition, leading to a 70% yield in formaldehyde, [11] was necessary for a better information on the increase or decrease of the catalytic activity under the influence of oxides admixtures. We mention the fact that in the speciality literature no data can be found on the behaviour of the ternary systems $MoO_3-Bi_2O_3$ with oxides admixtures, in the oxidation reaction of methylic alcohol *via* formaldehyde.

EXPERIMENTAL

The $MoO_3-Bi_2O_3$ catalyst was obtained by the coprecipitation of an ammonium molybdate and bismuth nitrate [11] solution. The different oxides admixtures were introduced by impregnating the catalyst samples with the solutions of vanadium, manganese, iron, cobalt, nickel, copper and zinc salts, which were thus calculated that after drying and calcinating at 420° during 5 h, the catalysts should contain 0.095 moles of added oxide per 1 mole of molybdenum oxide. Table 1 shows the chemical composition of the prepared catalysts.

The catalytic activity was estimated during the reaction of methylic alcohol oxidation *via* formaldehyde at the temperature of 220, 260 and 300° and with the space velocity ranging

Table 1

Chemical composition of catalysts

No Catalyst	% MoO_3	% Bi_2O_3	% oxide added
1	55.30	44.70	—
2	51.86	41.92	6.22 vanadium
3	53.90	43.57	2.53 manganese
4	52.25	42.23	5.52 iron
5	53.83	43.51	2.66 cobalt
6	53.83	43.51	2.66 nickel
7	53.74	43.44	2.82 copper
8	53.70	43.41	2.89 zinc

---

[13] A. Popescu, A. Szabo and I. V. Nicolescu, *Analele Univ. București, Seria St. Naturii-Chimie*, **15**, 93 (1966).

from 4 to 8 N 1 admixtures/g. cat. h. The composition of reactant mixture corresponds to the ratio g air/g methylic alcohol, 15/1. The experiments were carried out with the laboratory apparatus described previously[6] and the real activity of the catalysts was estimated with respect to the yield of formaldehyde.

$$\eta = \frac{\text{moles formaldehyde obtained}}{\text{moles methylic alcohol introduced}}$$

RESULTS AND DISCUSSION

The influence of metallic oxides admixtures on the $MoO_3 - Bi_2O_3$ catalyst is shown in figure 1.

One has found that for the optimal temperature condition (300°) only the iron oxide admixture bring about an important increase (about 25–27%) in the yield. In the same reaction conditions, cobalt and copper oxides lead to an increase of only 3–4%, while the vanadium, manganese, nickel and zinc oxides are unfavourable. The peculiar behaviour of a catalyst with iron oxide admixture is more evident in figure 2 where the activity was plotted *versus* the space velocity variation for all the three reaction temperatures.

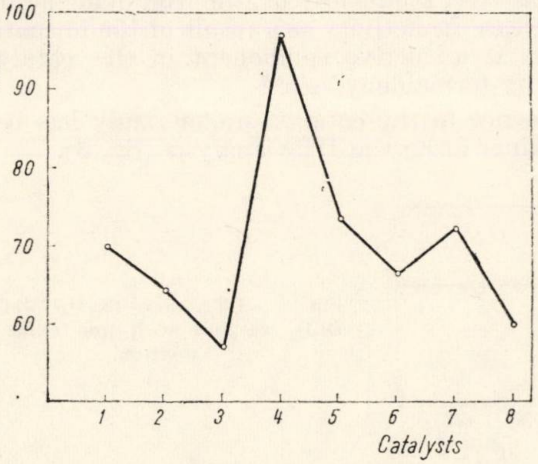

Fig. 1. – Activity variation of the $MoO_3 - Bi_2O_3$ catalyst *versus* the nature of the metallic oxides admixtures. Reaction temperature 300°.

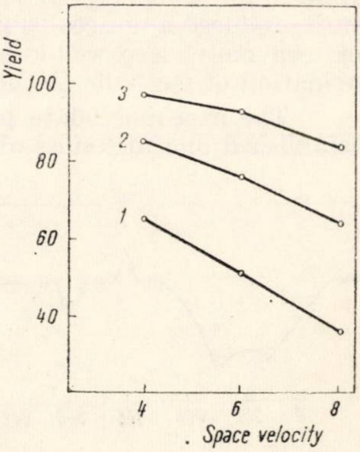

Fig. 2. – Activity of $MoO_3 - Bi_2O_3$ catalyst containing iron oxide admixture, *versus* the space velocity. The reaction temperature: 1–220°, 2–260° and 3–300°.

One notices, that irrespective of the space velocity magnitude, the catalysts activity increases with the increase in the reaction temperature. On the other hand, at all studied reaction temperatures, the activity of the catalyst decreases simultaneously to the space velocity increase. One may notice that the magnitude of this decrease diminishes parallelly to the increase in the reaction temperature, which can be noticed also from the slope of the three curves.

The influence of the space velocity on the activity of catalysts may be explained taking into account the intermediate stages which occur during the reaction. [1,2,6]

1. $CH_3OH_{(g)} + Cat_{ox} \longrightarrow CH_2O_{(g)} + H_2O_{(g)} + Cat_{red}$
2. $Cat_{red} + O_{2(g)} \longrightarrow Cat_{ox}$

When reaching an optimal air/methylic alcohol ratio and a relatively high contact time (space velocity = 4), the reoxidation of the catalysts is promoted and thus the formation of by-products is avoided.

The influence of a different metallic oxide admixture on the activity of $MoO_3 - Bi_2O_3$ catalyst may be assigned to the fact that in the composition of the latter, besides the main component — bismuth molybdate — a small excess of molybdenum oxide is present. When the metallic oxides admixtures are introduced, and as a consequence of thermal treatment, metallic molybdates which are formed due to molybdenum excess appear in the catalyst's composition. Among the molybdates thus formed, some may perform a proper catalytic activity, increasing the yield of formaldehyde, while others, being unselective for this reaction, will decrease it. Indeed, for the $MoO_3-Bi_2O_3$ catalyst studied by us, the iron oxide admixture produced a noticeable increase in activity as a result of the formation of iron molybdate well-known as an active component in the catalytic oxidation of methylic alcohol by formaldehyde. [3,6,7]

The iron molybdate presence in the catalyst under study has been established due to results obtained from the DTA analysis (fig. 3).

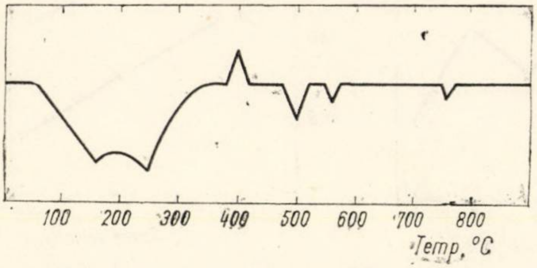

Fig. 3. — DTA curve for the $MoO_3-Bi_2O_3$ catalyst with iron oxide admixture.

One notices a strong endothermic effect in the 60 — 350° range, which corresponds to the processus of water removal. The other present endothermic effects, on the DTA curve, may be assigned to the polymorphous transformations of the iron molybdate (500°), the bismuth molybdate (560°) and the melting of molybdenum oxide (760°). [3,14] The exothermic effect at 400° corresponds to the iron molybdate crystallization. [3,14]

The above results show that in the $MoO_3-Bi_2O_3$ catalyst with iron oxide admixture, there exists simultaneously, as active components, iron and bismuth molybdates, as well as molybdenum oxide.

---

[14] A. Popescu, E. Segal, E. Bădărău and D. Fătu, *Rev. Roumaine Chim.*, **12**, 471 (1967).

Revue de Chimie, **15**, 1201–1205 (1970)

PYRAZOLES. III[1]

N-ARYLATION DES N-ACYLPYRAZOLES AVEC LE CHLORURE DE PICRYLE

C. CHIRIAC et I. ZUGRĂVESCU

Institut de Chimie macromoléculaire « P. Poni » de l'Académie, Filiale de Jassy,
41 A, Aleea Gr. Ghica-Vodă

Reçu le 17 octobre 1969

On étudie les réactions de N-arylation des N-acylpyrazoles avec le chlorure de picryle, qui ont lieu par le chauffage des produits fondus, avec élimination de chlorure d'acyle. Le 4-nitrochlorobenzène et le 2,4-dinitrochlorobenzène ne donnent pas cette réaction. On étudie le mécanisme de la réaction.

INTRODUCTION

Dans une note antérieure, [1] nous avons étudié les réactions de N-arylation des pyrazoles avec les dérivés chlorurés aromatiques suivants : 4-nitrochlorobenzène (NCB), 2,4-dinitrochlorobenzène (DNCB) et chlorure de picryle (TNCB).

La réactivité remarquable des N-acylpyrazoles (pyrazolide) [2] nous a déterminé d'essayer les réactions de N-arylation de ces composés. Nous avons constaté que par le chauffage des pyrazoles N-acylés avec le chlorure de picryle en quantités équimoléculaires à 160–170°, pendant 5–6 h, il résulte des N-arylpyrazoles. Nous avons effectué une étude détaillée de cette réaction et de son mécanisme.

RÉSULTATS ET DISCUSSIONS

Parmi les dérivés chlorurés aromatiques étudiés : NCB, DNCB et TNCB, seulement le TNCB réagit avec les pyrazoles N-acylés, celui-ci étant le plus réactif. La N-arylation des N-acylpyrazoles avec le TNCB a lieu avec élimination des chlorures acides. Ces chlorures ont été séparés et identifiés.

Par exemple, dans le cas de 1-acétyl-3,5-diméthylpyrazole, on a séparé le chlorure d'acétyle. La fin de la réaction a été mise en évidence par la formation du 1-picryl-3,5-diméthylpyrazole solide (avec un point de fusion plus haut que la température de réaction). Les réactions de N-arylation des N-acylpyrazoles avec TNCB ont lieu d'après le schéma 1.

---

[1] IIe Partie C. Chiriac et I. Zugrăvescu, *Rev. Roumaine Chim.*, **14**, 1263 (1969).
[2] H. A. Staab, *Angew. Chem.*, **74**, 418 (1962).

Schéma 1

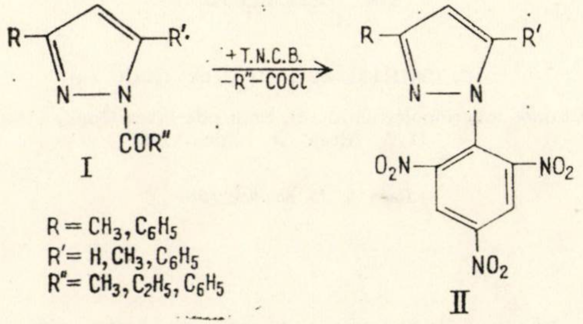

$R = CH_3, C_6H_5$
$R' = H, CH_3, C_6H_5$
$R'' = CH_3, C_2H_5, C_6H_5$

Les résultats de l'étude de ces réactions sont présentés dans le tableau 1.

Tableau 1

N-arylation des N-acylpyrazoles avec le chlorure de picryle

N°	pyrazole I R, R', R"	temps de réaction h	t°C	pyrazole II p.t.°C	rend. %
1	CH_3, CH_3, CH_3	5−6	160−170	220−222[3]	93
2	CH_3, H, CH_3	,,	,,	174−175[3]	87
3	CH_3, CH_3, C_2H_5	,,	,,	220−222[3]	91,5
4	CH_3, CH_3, C_6H_5	,,	,,	,, ,, [3]	85,7
5	CH_3, H, C_6H_5	,,	,,	174−175[3]	86

Les substitutions de ce genre avec le TNCB ne sont pas connues; nos investigations ont été dirigées sur les possibilités d'élucidation du mécanisme de cette réaction. Le TNCB peut réagir sur les acylpyrazoles, avec la substitution du radical picryle, à l'atome d'azote de la position 1 (réaction a) ou de la position 2 (réaction b).

Dans le cas particulier de 1-acétyl-3-méthylpyrazole, il peut résulter deux composés différents : 1-picryl-3-méthylpyrazole (IV) ou 1-picryl-5-méthylpyrazole (VI), conformément au schéma 2.

---

[3] J. Elguero et R. Jacquier, *Bull. Soc. chim. France*, **1966**, 2837.

Schéma 2

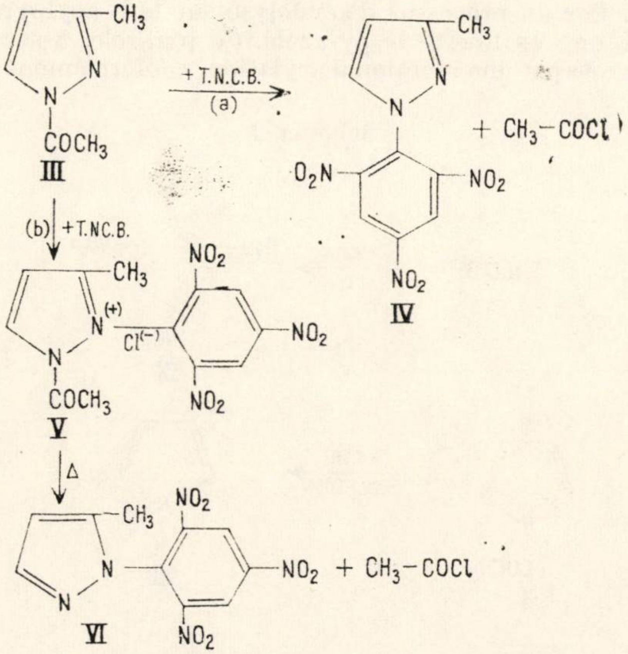
CH3
N
N
COCH3
III
+ T.N.C.B.
(a)
CH3
N
N
O2N
NO2
NO2
IV
+ CH3–COCl
(b) + T.N.C.B.
CH3
N(+)
N
Cl(–)
NO2
NO2
NO2
COCH3
V
Δ
CH3
N
N
NO2
NO2
NO2
VI
+ CH3–COCl

En réalité, on obtient une seule substance, 1-picryl-3-méthylpyrazole (IV). Donc la réaction est une substitution du groupement acétyle avec le groupement picryle à l'atome d'azote de la position 1.

La manière dont a lieu la substitution du groupement acétyle de la position 1 par le groupement picryle est un problème relativement compliqué.

Compte tenu du fait que les pyrazolides et les imidazolides peuvent réagir [4] avec l'acide chlorhydrique d'après le schéma 3, nous avons été tentés au commencement d'attribuer à notre réaction un mécanisme semblable.

Schéma 3

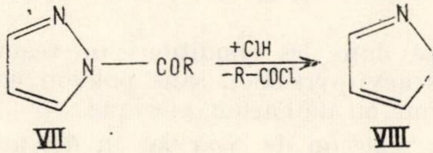
N
N
COR
+ ClH
–R–COCl
N
NH
VII
VIII

---

[4] H. A. Staab et A. P. Datta, *Angew. Chem.* (*Internat. Ed.*), **3**, 132 (1964).

Dans le cas de la réaction étudiée par nous, on peut envisager la possibilité de formation de l'acide chlorhydrique par l'action de l'eau sur le TNCB. Par un processus d'acydolyse sur le N-acylpyrazole, l'acide chlorhydrique met en liberté le pyrazole. Ce pyrazole, à son tour, forme le N-arylpyrazole par une réaction d'arylation, conformément au schéma 4.

Schéma 4

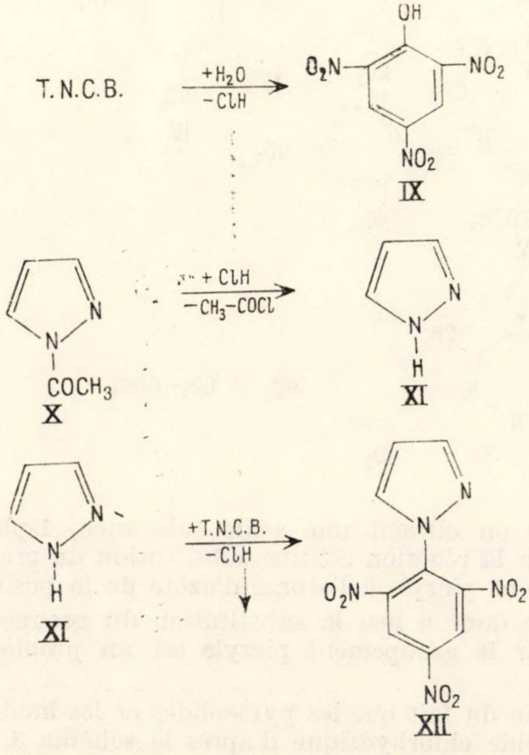

Dans le cas de ce mécanisme il est nécessaire d'une très petite quantité (catalytique) d'acide chlorhydrique, pour amorcer la réaction. Ce mécanisme, peu justifié d'ailleurs, ne pouvait être repoussé dès le début, vu que des traces d'humidité sont suffisantes pour cette réaction.

Pour élucider ce mécanisme nous avons procédé de la manière suivante :

— On a chauffé dans les conditions de réaction indiquées plus haut, le TNCB (sans acyl-pyrazole), sans pouvoir constater la présence de l'acide chlorhydrique ou de l'acide picrique.

— En outre, la réaction de N-arylation des acylpyrazoles avec le TNCB a été effectuée avec succès, dans une atmosphère d'azote spécialement anhydrisé, pour éviter les traces d'humidité qui pourraient générer l'acide chlorhydrique nécessaire à la réaction d'après le mécanisme présenté dans le schéma 4.

Ces faits, ainsi que l'analogie avec une réaction d'acylation de N-triméthylsilyl-pyrazole avec le chlorure d'acétyle,[5] plaident pour un mécanisme concerté, d'après le schéma 5.

Schéma 5

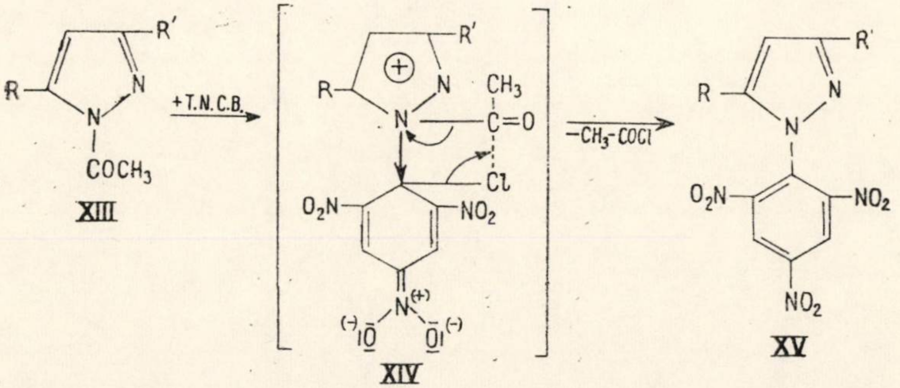

Le mécanisme conformément au schéma 4 pourrait être attribué aussi à la réaction de N-acylation de N-triméthylsilyl-pyrazole, pourtant Birkofer et Ritter,[5] les auteurs de cette réaction, ont proposé un mécanisme concerté, semblable à celui proposé par nous dans le cas de la N-arylation des N-acylpyrazoles avec le TNCB.

PARTIE EXPÉRIMENTALE

Produits intermédiaires

1-Acétyl-3,5-diméthylpyrazole (I_1). On le prépare à partir de 3,5-diméthylpyrazole et de chlorure d'acétyle.[6]

1-Acétyl-3-méthylpyrazole (I_2). On le prépare de 3(5)-méthylpyrazole et d'anhydride acétique.[7]

1-Propionyl-3,5-diméthylpyrazole (I_3). On le prépare comme le dérivé (I_1) en partant de 3,5-diméthylpyrazole et de chlorure de propionyle.[8]

Les dérivés pyrazoliques N-arylés, présentés dans le tableau 1, ont été préparés par le chauffage des N-acylpyrazoles avec le TNCB, en petit excès, dans les conditions indiquées dans ce tableau. Nous donnons à titre d'exemple, le cas suivant :

1-Picryl-3,5-diméthylpyrazole (II_1). 1-Acétyl-3,5-diméthylpyrazole, 1,38 g (0,01 mole) et le chlorure de picryle 2,5 g (0,011 mole) sont chauffés dans un ballon, muni d'un réfrigérateur et d'un tube de $CaCl_2$, à 150—160° , pendant 5—6 h. On laisse refroidir. On recristallise du benzène, P_f 220—222°, rendement 93 %.

---

[5] L. Birkofer et A. Ritter, *Chem. Ber.*, **93**, 2804 (1960).

[6] R. Hüttel, *Chem. Ber.*, **92**, 2019 (1959).

[7] K. von Auwers et W. Daniel, *J. prakt. Chem.*, **110**, 257 (1925).

[8] W. Ried et F. J. Konigstein, *Liebings Ann. Chem.*, **622**, 40 (1959).

Revue Roumaine de Chimie, 15, 1207–1218 (1970)

INVESTIGATIONS IN THE CYCLOBUTANE SERIES. XXVIII[1]

THE REACTION OF *endo* AND *exo*-3.4-BENZOTRICYCLO [4.2.1.$0^{2,5}$]NONA-3.7-DIENES WITH ELECTROPHYLIC REAGENTS

MARGARETA AVRAM, I. POGANY, I. G. DINULESCU, F. CHIRALEU and
C. D. NENITZESCU

Institute of Organic Chemistry, Bucharest, Splaiul Independenţei, 202 B

Received October 18, 1969

The reaction of *endo*-3.4-benzotricyclo[4.2.1.$0^{2,5}$]nona-3.7-diene (**1**) with electrophilic reactants takes place with rearrangement of the skeleton to *exo*-7.9-disubstituted compounds. The isomeric *exo*-hydrocarbon (**2**) reacts with electrophyls without rearrangement, leading to *trans*-7.8-disubstituted compounds. The configuration of the addition products was established by means of NMR spectroscopy. *)

The mechanism of the addition reaction to **1** and **2** is discussed.

As a continuation of former observations [2] on halogen and hydrogen halide elimination form, and addition to, strained ring systems we report now the behaviour of 3.4-benzotricyclo[4.2.1.$0^{2,5}$]nona-3.7-diene (benzocyclobutenonorbornene) system. We were especially interested to note the different behaviour of the *endo* and of the *exo*-benzocyclobuteno isomers.

The *endo*-isomer (**1**) was prepared by us [3] by treating benzocyclobutadiene with cyclopentadiene while the *exo*-isomer (**2**) was obtained according to Simmons,[4] by cycloaddition of benzyne to norbornadiene.

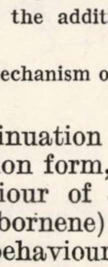

1

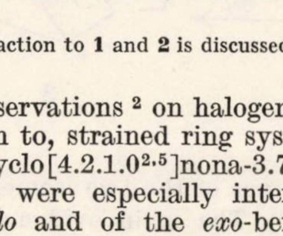

2

---

*) See the following paper in this issue.

[1] Part XXVII: M. Avram, D. Constantinescu, I. G. Dinulescu, O. Constantinescu-Simon, G. D. Mateescu and C. D. Nenitzescu, *Rev. Roumaine Chim.*, **15**, 1097 (1970).

[2] M. Avram, G. D. Mateescu, I. G. Dinulescu, A. Juvara and C. D. Nenitzescu, *Rev. Roumaine Chim.*, **13**, 1075 (1968); M. Avram, G. D. Mateescu, I. G. Dinulescu, I. Pogany and C. D. Nenitzescu, *ibidem*, **13**, 1085 (1968); M. Avram, G. D. Mateescu, M. Rentzea, I. G. Dinulescu and C. D. Nenitzescu, *ibidem*, **13**, 1097 (1968).

[3] C. D. Nenitzescu, M. Avram and D. Dinu, *Chem. Ber.*, **90**, 2541 (1957).

[4] H. Simmons, *J. Amer. Chem. Soc.*, **83**, 1657 (1961).

In the following we present the results of the addition of bromine and chlorine to the two isomers **1** and **2** as well as their reaction with performic acid.

Reactions of endo-3.4-benzotricyclo[$4.2.1.0^{2,5}$]nona-3.7-diene (**1**).

Bromine addition. When hydrocarbon **1** was treated with bromine in dichloromethane, a mixture of dibromo-derivatives was obtained in 91% yield. This mixture was found to contain 83.5% 7-*endo*-9-*syn*-dibromo-*exo*-3.4-benzotricyclo[$4.2.1.0^{2,5}$]non-3-ene (**3**), and 16.5% 7-*exo*-9-*syn*-dibromo-*exo*-3.4-benzotricyclo[$4.2.1.0^{2,5}$]non-3-ene (**4**).

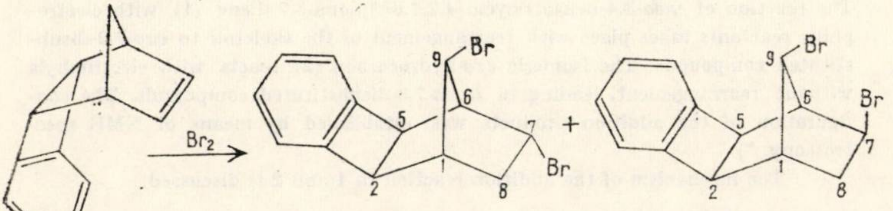

1 **3** **4**

The structure of the two isomers was ascribed on the basis of their NMR spectra *). The main evidence for the *exo* configuration of the benzocyclobutene ring comes from the absence of coupling between the protons H_1-H_2 and H_6-H_5 respectively. The 7-*endo*-9-*syn*-configuration of the two bromine atoms in **3** is evidenced by the lack of long-range coupling between the *anti*-H_9 and *exo*-H_7 protons. Such a coupling of 2 Hz is actually found between the *anti*-H_9 and *exo*-H_8 protons.

In the case of the dibromo-derivative **4** the *exo* configuration of the bromine atom of 7 position determines a long-range coupling between the *anti*-H_9 and the *endo*-H_7 ($J = 1.3$ Hz). The absence of coupling between the $H_1(H_6)$ and H_2 (H_5) protons indicates the *exo* orientation of the benzocyclobutene ring.

The formation of products **3** and **4** from **1** involves a rearrangement of the skeleton. In order to explain this result we admit the formation of a nonclassical ion **7**, possibly *via* the bromonium ion **5** or the open ion **6**. The ion **7** accounts for the 7-*exo*-9-*syn*-dibromoderivative **4**.

The absence of a *trans*-7.8-dibromo-product is probably due to the electronic shielding caused by the benzene ring which prevents an *endo* attack on the bromonium ion (**5**).

---

*) See also the following paper, in this issue

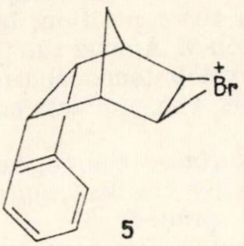

5

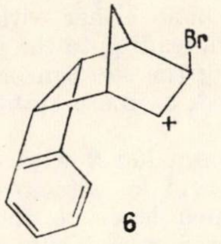

6

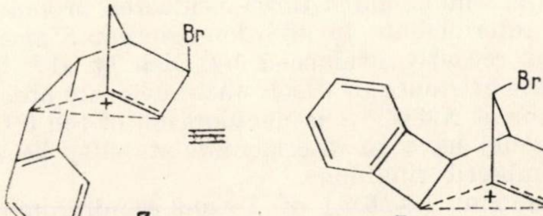

7 7

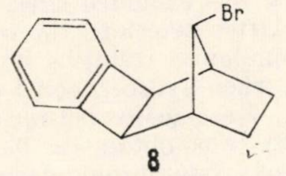

8

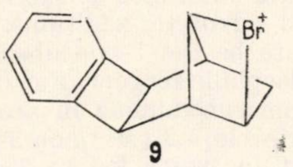

9

We may assume therefore the participation of the σ 1.2 bond leading to the non-classical ion **7**. The formation of the nonclassical ion **7** from the bromonium ion **5** is a normal reaction of the 2-norbornyl derivatives. An ion similar to **7** is also encountered during solvolyses. Such a transformation is admitted for the additions to norbornenes.[5] It seems therefore plausible that the ion **7** arises during the transformation **5** → **9**, the latter species being probably the more stable. The ion **7** can explain the formation of the dibromo-derivative **4** by a normal *exo* attack on the 1 position but cannot account for the dibromo-derivative **3**. The alternative rearranged (classical) ion **8** is unlikely because it should lead mainly to **4**, by preferential *exo* attack.

In order to account for product **3** we checked the possibility of the epimerisation **3** ⇄ **4**. However, we actually found that the dibromo-compounds **3** and **4** are not interconvertible under the reaction conditions.

We believe that formation of the dibromide **3** as the main reaction product is explained by the intermediate intervention of the bromonium ion **9**. The latter should arise by compensation of the electron-deficit of the 7 position of the nonclassical ion **7** by the unshielded electrons of the bromine atom. This is made possible by the proximity of the bromine atom and its great volume as well as by the rigidity of the system. An equilibrium **7** $\rightleftarrows$ **9** is very plausible. In the norbornyl ion **7** the bromine atom can form a bond either with the 1-position, leading back to **5**, or with the 7-position, leading to the ion **9**. Among the three possible species, the ions containing the *exo*-benzocyclobutenonorbornyl system (**7** and **9**) should be preferred, as more stable. The products actually isolated arise from these ions.

---

[5] T. G. Traylor, *Accounts Chem. Res.*, **2**, 152 (1969).

The bromonium ion **9** with diffused charge, favoured by the non-polar medium, should be attacked by the Br^- anion exclusively in the *endo* position, which leads to the product **3**.

Four-membered ring bromonium ions have not been reported so far in the literature. The common three-membered bromonium ion generally admited as intermediate in addition-reactions[6] or in nucleophilic substitutions,[7] was recently evidenced by Olah et al.[8] Five-membered bromonium ions, the existence of which was previously observed,[9] was also evidenced by means of NMR.[10] A bromonium ion of the **9** type with four-membered ring should have an intermediate stability between the three and the five membered ring ions.

The little amount (~16%) of 7-*exo*-9-*syn*-dibromo compound **4** results very likely from the reaction of the nonclassical ion **7**.

A steric hindrance of the *exo* attack was excluded since it was not observed in solvolytic additions. In the latter reactions the only product was found to be the 7-*exo*-substituted compound resulting by *exo* attack of the nucleophilic reagent. For instance, when hydrocarbon **1** was treated with N-bromosuccinimide in acetic acid, 7-*exo*-acetoxy-9-*syn*-bromo-*exo*-3.4-benzotricyclo[$4.2.1.0^{2.5}$]non-3-ene (**10**) was obtained. The reaction carried out in water led to 7-*exo*-hydroxy-7-*syn*-bromo-derivative (**11**). Acetylation of the alcohol **11** yielded the acetoxy-derivative **10**.

On oxidation with chromic anhydride-pyridine complex the alcohol **11** gave the bromo-ketone **12**.

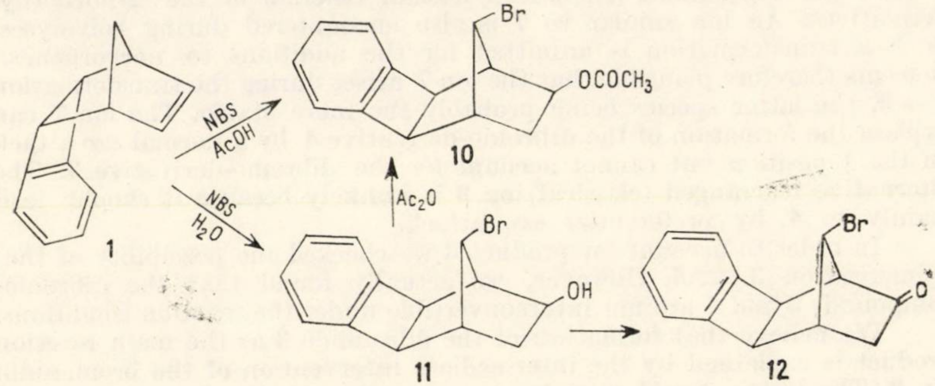

---

[6] J. Roberts and J. E. Kimball, *J. Amer. Chem. Soc.*, **59**, 947 (1937).

[7] S. Winstein and H. J. Lucas, *J. Amer. Chem. Soc.*, **61**, 1576, 2845 (1939).

[8] G. A. Olah and J. M. Bollinger, *J. Amer. Chem. Soc.*, **89**, 4744 (1967); *ibidem*, **90**, 2587 (1968).

[9] P. E. Peterson and F. J. Slama, *J. Amer. Chem. Soc.*, **90**, 6516 (1968) and the literature therein cited.

[10] G. A. Olah and P. E. Peterson, *J. Amer. Chem. Soc.*, **90**, 4675 (1968).

The NMR spectrum of the acetoxy-derivative **10** reveals the absence of the couplings H_1-H_2, respectively H_6-H_5, indicating *exo* configuration for the benzocyclobutene ring. The weak long-range coupling of 1.2 Hz between the *anti*-H_9 and *endo*-H_7 protons indicates *endo* configuration for the H_7 proton and implicitly *exo* configuration for the acetoxy group. In the IR spectrum of the ketone **12** the ν_{CO} frequency appears at 1765 cm^{-1}, indicating that the carbonyl group is located on the cyclopentane ring.[11]

Chlorine addition. Hydrocarbon **1** treated with a dichloromethane solution of chlorine yielded a mixture of 47% 7-*endo*-9-*syn*-dichloroderivative **13**, 36% 7-*exo*-9-*syn*-dichloro-derivative **14** and 17% unidentified compounds. The proportion of the two isomers formed by *endo* and by *exo* attack is respectively 56.5% **13** to 43.3% **14**.

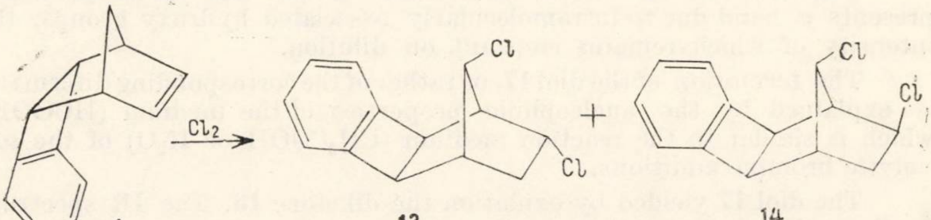

1 13 14

The almost equal amounts of the *exo* and *endo* products seem to indicate that the four-membered ring chloronium ion **16** is less stable that the analogous bromonium ion **9**, just as other chloronium ions are less stable as compared with bromonium ions with similar structures. We expect therefore a more pronounced contribution from the classical ion **15**.

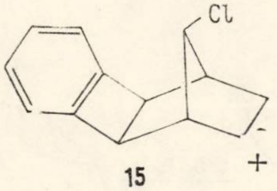

15

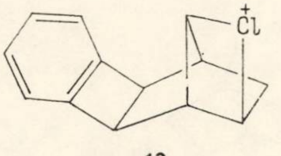

16

The reaction with performic acid. By treating hydrocarbon **1** with formic acid and hydrogen peroxide[12] (performic acid) followed by hydrolysis, a diol was obtained with molecular formula $C_{13}H_{14}O_2$. On the basis of the NMR spectra the product was ascribed the structure of 7-*exo*-9-*syn*-dihydroxy-*exo*-3.4-benzotricyclo$[4.2.1.0^{2,5}]$non-3-ene (**17**).

---

[11] M. Avram and G. D. Mateescu, "Spectroscopia în infraroşu. Aplicaţii în Chimia Organică", Ed. Tehnică, Bucharest, 1966.

[12] H. Kwart and W. C. Vosburgh, *J. Amer. Chem. Soc.*, **76**, 5400 (1954).

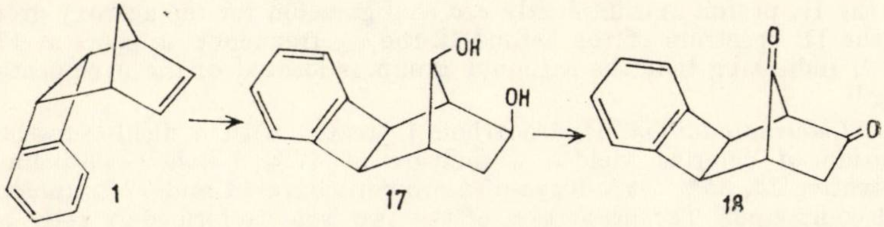

The structure **17** is also confirmed by the IR spectrum which presents a band due to intramolecularly associated hydroxy groups, the intensity of which remains constant on dilution.

The formation of the diol **17**, or rather of the corresponding diformate, is explained by the nucleophilic properties of the medium (HCOOH) which is similar to the reaction medium (CH_3COOH or H_2O) of the solvolytic bromine additions.

The diol **17** yielded by oxidation the diketone **18**. The IR spectrum confirms the ascribed structure : it contains two ν_{CO} bands at 1740 cm^{-1} and 1800 cm^{-1}. The former band corresponds to the carbonyl group of the 7 position while the latter, typical to bridgehead ketones, corresponds to the carbonyl group in the 9 position. The NMR spectrum is also in agreement with the formula **18**.

Hydroboration reaction. By treating hydrocarbon **1** with diborane and then with hydrogen peroxide, the hydroxy derivative **19** was obtained. The latter was converted into ketone **20** by oxidation with chromic acid-pyridine complex. Both **19** and **20** compounds preserved unrearranged *endo*-tricyclononene skeleton.

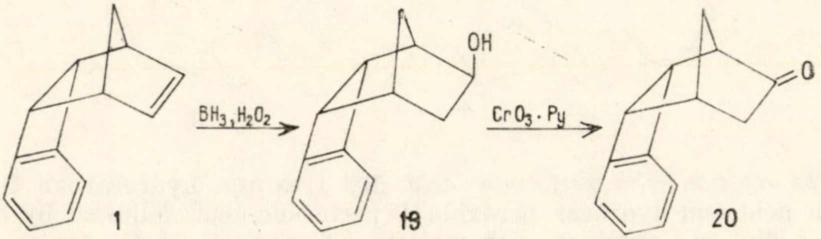

Reactions of exo-3.4-benzotricyclo$[4.2.1.0^{2,5}]$*nona-3.7-diene* (**2**).

When hydrocarbon **2** was treated with a dichloromethane solution of bromine, a dibromo-derivative $C_{13}H_{12}Br_2$ was obtained. The NMR spectrum of the compound corresponds to a normal *trans* addition product namely *trans*-7.8-dibromo-*exo*-3.4-benzotricyclo[4.2.1.0^{2,5}]non-3-ene (**21**).

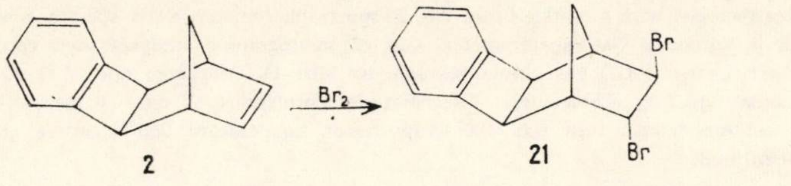

2 21

We assume that the bromonium ion **22** is the intermediate of the reaction.

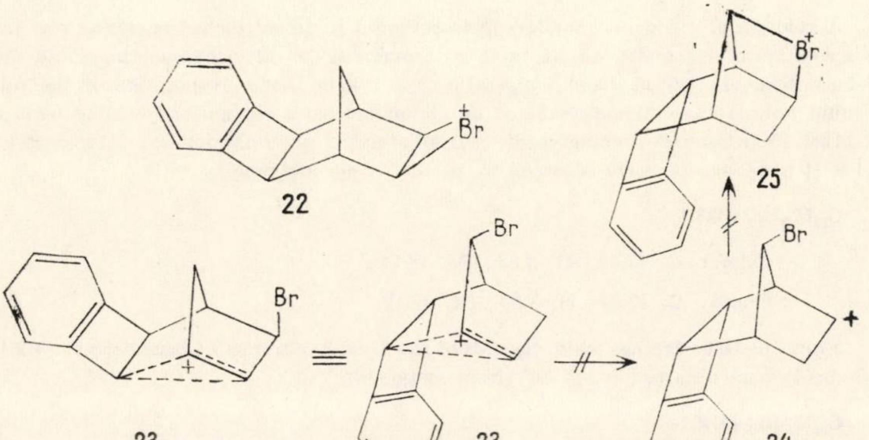

22 25 23 23 24

Unlike the case of the bromonium ion **5**, in the ion **22** there is no strain or electronic hindering to prevent a normal reaction with Br$^-$ ion. The formation of a bromonium ion **25** (*via* the nonclassical ion **23** or the ion **24**) cannot be excluded but, as we have shown before, in the case of such an ion there can be no *endo* attack of the Br$^-$ ion. Since only one product, namely **21**, was isolated, we are bound to assume that even if the ions **22**, **23**, **24** and **25** equilibrate only the ion **22** reacts.

The reaction of the hydrocarbon **2** with performic acid proceeds in a similar way. This reaction, in which the epoxide **26** appears as an intermediate, leads only to the *trans*-diol **27** which possesses unrearranged skeleton according to NMR data.

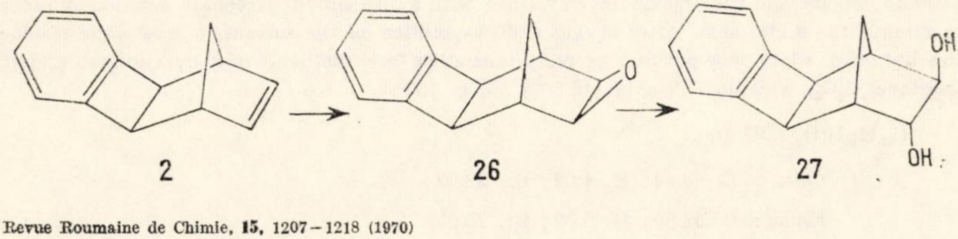

2 26 27.

EXPERIMENTAL

Microanalyses were performed by Miss E. Sliam and Mrs. V. Daniel. IR spectra were recorded with a double beam UR 20 spectrophotometer. NMR spectra were determined with a Varian A-60A spectrometer. Gas chromatographic analyses were carried out on a Carlo Erba model GD gas chromatograph, by Miss D. Georgescu and Miss J. Nicoară. The columns were 20% ethylene-glycol succinate on Chromosorb W (60–80 mesh), 1.5m × 2 mm; the column temperature was 190° (vaporizator temperature 250°); carrier gas: hydrogen, 63.9 ml/min.

Addition of bromine to endo-3.4-benzotricyclo[4.2.1.$0^{2,5}$]nona-3.7-diene (**1**)

A solution of 1.7 g (10 mmoles) hydrocarbon **1** in 10 ml dichloromethane was treated with a solution of 1.9 g (0.6 ml, 12 mmoles) bromine in 10 ml dichloromethane and the obtained solution was left at room temperature for 1 hour. After evaporation of the solvent, the liquid residue was chromatographied on aluminium oxide column and eluated with petroleum ether. From the first runnings white crystals of *endo*-7-*syn*-9-dibromo-*exo*-3.4-benzotricyclo-[4.2.1.$0^{2,5}$] non-3-ene (**3**) were isolated; m. p. 108° (from methanol).

$C_{13}H_{12}Br_2$ (328.1)

Calcd.: C, 47.59; H, 3.68; Br, 48.71;

Found: C, 47.64; H, 3.80; Br, 49.12.

From the last runnings white crystals of *exo*-7-*syn*-9-dibromo-3.4-benzotricyclo[4.2.1.$0^{2,5}$] non-3-ene(**4**) were isolated; m. p. 76° (from methanol).

$C_{13}H_{12}Br_2$ (328.1)

Calcd.: C, 47.59; H, 3.68; Br, 48.71;

Found; C, 47.76; H. 3.94; Br, 48.93.

In another experience the product obtained by addition of bromine to hydrocarbon **1** was analysed by means of gas chromatography. It was found that the reaction mixture contained 76% *endo*-7-*syn*-9-dibromo-isomer (**3**), 15% *exo*-7-*syn*-9-dibromo-isomer (**4**), together with 9% unidentified byproducts.

exo-7-Acetoxy-syn-9-bromo-exo-3.4-benzotricyclo[4.2.1.0 ^{2,5}]non-3-ene (**10**)

A solution of 0.8 g (5 mmoles) **1** in 20 ml acetic acid was treated with 0.9 g (5 mmoles) of N-bromosucinimide and the mixture was left at room temperature. Soon afterwards the solution became green. After one hour water was added, the product was extracted with dichloromethane and the organic layer washed with a 5% sodium carbonate solution in order to remove the acetic acid. After drying and evaporation of the solvent, a crystalline residue was obtained, which was purified by recrystallization from methanol and by chromatography (pentane/Al_2O_3), yielding 0.7 g **10** (46.5%), m. p. 122°.

$C_{15}H_{15}BrO_2$ (307.2)

Calcd.: C, 58.64; H, 4.92; Br, 26.02;

Found: C, 58.60; H, 5.07; Br, 26.39.

exo-7-Hydroxy-syn-9-bromo-exo-3.4-benzotricyclo[4.2.1.$0^{2,5}$]non-3-ene (11)

A solution of 1.68 g (10 mmoles) **1** in 40 ml tetrahydrofuran and 10 ml water was treated with 1.78 g (10 mmoles) N-bromosuccinimide and the mixture was left at room temperature. After 24 hours water was added and the product was extracted with ether. After evaporation of the ether a waxy crystalline residue with m. p. 118–120° was obtained. Purification by chromatography on aluminium oxide (cyclohexane) yielded 2.3 g (87%) **11**, m. p. 126°.

$C_{13}H_{13}BrO$ (265.1)

Calcd.; C, 58.89; H, 4.94; Br, 30.14;

Found; C, 58.24; H, 5.31; Br, 31.99.

By treating 0.1 g of the alcohol **11** with 5 ml acetic anhydride and a drop of pyridine the bromacetoxy-derivative **10** was obtained (identified by means of IR and NMR spectra).

syn-9-Bromo-exo-3.4-benzotricyclo[4.2.1.$0^{2,5}$]non-3-en-7-one (12)

A solution of 1.3 g (5 mmoles) **11** in 13 ml anhydrous pyridine was added to a suspension of chromic anhydride-pyridine complex obtained from 1.3 g chromic anhydride and 13 ml pyridine. The mixture was left at room temperature for 24 hours with occasional shaking. Water was added and the product was extracted with ether. In order to remove the pyridine the ethereal solution was washed several times with a 2% hydrochloric acid solution. After washing with water and drying, the ether was removed by distillation and the crude crystalline residue was purified by chromatography on aluminium oxide with cyclohexane, yielding 0.9 g (70%) **12**, m. p. 110°.

$C_{13}H_{14}BrO$ (263.1)

Calcd.: C, 59,34; H, 4.21; Br, 30.38;

Found: C, 58.39; H, 4.51; Br, 32.35.

Chlorine addition to endo-3.4-benzotricyclo[4.2.1.$0^{2,5}$]nona-3.7-diene (1)

A solution of 1.7 g (10 mmoles) **1** in 10 ml dichloromethane was treated with an excess of solution of chlorine in dichloromethane. After 2 hours the solvent was removed and a liquid residue remained, which did not crystallize and which could not be separated by column chromatography. Gas-chromatographic analysis indicated a content of 47% *endo-syn*-dichloro-derivative (**13**) and 36% *exo-syn*-derivative (14) together with 17% unidentified products.

The separation of the two dichloro-derivatives was carried out by preparative gas-chromatography on a Fractovap GV device (Carlo Erba) (2 m length, 5 mm diameter, column filled with 20% ethyleneglycol-adipate on Chromosorb P 60–80 mesh, at 210°, carrier gas 300 ml/min hydrogen).

endo-7-*syn*-9-Dichloro-*exo*-3.4-benzotricyclo[4.2.1.$0^{2,5}$]non-3-ene (**13**), m. p. 50°.

$C_{13}H_{12}Cl_2$ (239.2)

Calcd.: C, 65.29; H, 5.06; Cl, 29.65;

Found: C, 65.01; H, 5.25; Cl, 30.29.

exo-7-*syn*-9-Dichloro-*exo*-3.4-benzotricyclo[4.2.1.0 ^{2,5}]non-3-ene (**14**), m. p. 74°.

$C_{13}H_{12}Cl_2$ (239.2)

Calcd.: C, 65.29; H, 5.06; Cl, 29.65;

Found: C, 64.48; H, 5.25; Cl, 30.33.

exo-7-syn-9-Dihydroxy-exo-3.4-benzotricyclo[4.2.1.0^{2,5}]non-3-ene (17)

2. 1 g (12.3 mmoles) **1** were added dropwise to a vigorously stirred solution of 1.75 ml 30% hydrogen-peroxide in 7.5 ml 90% formic acid, the temperature being maintained at 40–45°. The reaction mixture was stirred for 2 hours at this temperature. The non-homogeneous reaction product was evaporated to dry in vacuum and the oily residue was treated slowly with a solution of 1.5 g sodium hydroxide in 3 ml water. The resulting solution was extracted with ether and the ethereal layer dried. After evaporation of the solvent the oily residue was purified by chromatography (ether/Al_2O_3). There remained 1.8 g (74%) **17**, m. p. 115°.

$C_{13}H_{14}O_2$ (202.2)

Calcd.: C, 77.20; H, 6.98;

Found: C, 76.98; H, 7.24.

exo-3.4-Benzotricyclo[4.2.1.0^{2,5}]non-3-en- 7.9-dione (18)

2.0 g (10 mmoles) **17** in 20 ml pyridine were added to a suspension of a complex prepared from 4 g chromic anhydride and 40 ml anhydrous pyridine, and the mixture was left for 24 hours at room temperature. Water was added and the mixture extracted with ether. The ethereal solution was washed with dilute hydrochloric acid solution. Evaporation of the ether and recrystallization of the residue from methanol yielded 0.8 g (40%) **18**, m. p. 134°.

$C_{13}H_{10}O_2$ (198.2)

Calcd.: C, 78.77; H, 5.10;

Found: C, 78.15; H, 5.49.

exo-7-Hydroxy-endo-3.4-benzotricyclo[4.2.1.0^{2,5}]non-3-ene (19)

The solution of 3.4 g boron trifluoride etherate in 3 ml diglyme was added dropwise to a solution of 0.5 g sodium borohydride in 12.5 ml diglyme. The evolving diborane was passed for 2 hours, at room temperature, through a solution of 2.2 g (13 mmoles) **1** in 10 ml tetrahydrofuran. Then 1 ml of water, 1.5 ml 12% sodium hydroxide solution and 1.5 ml hydrogen peroxide 30% were carefully added and the mixture extracted with ether. The evaporation of the ether yielded 2.2 g (91%) **19**, m. p. 85°.

$C_{13}H_{14}O$ (186.3)

Calcd.: C, 83.84: H, 7.57;

Found: C, 83.66; H, 7.67.

endo-3.4-Benzotricyclo[4.2.1.$0^{2,5}$]non-3-en-7-one (**20**)

Into a suspension of complex obtained from 1.0 g chromic anhydride and 10 ml pyridine, the solution of 1.0 g (5.4 mmoles) of alcohol **19** in 10 ml pyridine was introduced and the mixture was left for 24 hours at room temperature.

Water was added and the mixture extracted with ether. The ethereal layer was washed several times with 2% hydrochloric acid until all pyridine was removed. The colourless oil remaining after evaporation of the solvent was distilled in vacuum, yielding 0.7 g (70%) **20**, m. p. 84° (cyclohexane); b. p. 140°/5 mm.

$C_{13}H_{12}O$ (184.2)

Calcd.: C, 84.75; H, 6.56;

Found: C, 83.89; H, 6.92;

2.4-Dinitrophenylhydrazone, yellow crystals, m. p. 180°.

$C_{19}H_{16}N_4O_4$ (364.4)

Calcd.: C, 62.63; H, 4.42; N, 15.38;

Found: C, 62.81; H, 4.60; N, 15.31.

exo-3.4-Benzotricyclo[4.2.1.$0^{2,5}$]nona-3.7-diene (**2**)

The hydrocarbon **2** was prepared after Simmons [4] by reaction of benzyne with bicyclo [2.2.1] hepta-2.5-diene. Benzyne was generated from antranylic acid by treatment with amyl nitrite. [13] The product **2** resulted together with phenyl amyl ether which could not be separated by distillation. Isolation of the pure hydrocarbon **2** was carried out by means of preparative gas-chromatography on a Fractovap GV device from Carlo Erba, using a 2 m × 5 mm diameter column filled with 25% apiezon L on Chromosorb P 30—60 mesh at 170° and 300 ml/min hydrogen as carrier gas.

Addition of bromine to exo-3.4-benzotricyclo[4.2.1.$0^{2,5}$]nona-3.7-diene (**2**)

A solution of 0.8 g (5 mmoles) **2** in 10 ml dichloromethane was treated at low temperature with a solution of 0.9 g (0.3 ml, 6 mmoles) bromine in 10 ml dichloromethane. The mixture was left for 1 hour at room temperature. A residue of 1.1 g (67%) *trans*-7.8-dibromo-*exo*-3.4-benzotricyclo[4.2.1.$0^{2,5}$]non-3-ene (**21**) remained after evaporation of the solvent. Recrystallization from methanol and chromatography on aluminium oxide column, eluted with petroleum ether, yielded the pure product **21** with m. p. 84°.

$C_{13}H_{12}Br_2$ (328.1)

Calcd.: C, 47.59; H, 3.68; Br, 48.71;

Found: C, 47.87; H, 3.90; Br, 47.85.

---

[13] T. F. Mich, E. J. Nienhouse, T. E. Farina and J. Tufariello, *J. Chem. Educ.*, **45**, 272 (1968).

trans-7.8-Dihydroxy-exo-3.4-benzotricyclo[4.2.1.$0^{2,5}$*]non-3-ene* (27)

In a solution of 0.7 ml 30% hydrogen peroxide and 3 ml 90% formic acid, 0.8 g (5 mmoles) were added **2** dropwise in such a rate as to maintain the temperature at 40—45°. The homogeneous solution was left for 3 hours at 45° with occasional shaking and then concentrated in vacuum. The residue was treated with a solution of 0.6 g sodium hydroxide in 1.3 ml water, with vigorous stirring and the mixture extracted 4 times with 25 ml ether. The ethereal extract was chromatographied on aluminium oxide column. Evaporation of the solvent yielded 0.5 g (50%) **27**, m. p. 87° (cyclohexane).

$C_{13}H_{14}O_2$ (202.2)

Calcd.: C, 77.20; H, 6.98;
Found: C, 76.80; H, 7.04.

Revue Roumaine de Chimie, **15**, 1219–1225 (1970)

INVESTIGATIONS IN THE CYCLOBUTANE SERIES. XXIX[1]

NMR SPECTRA STUDIES OF SOME 3.4-BENZOTRICYCLO[4.2.1.$0^{2,5}$]NONA-3.7-DIENE DERIVATIVES

MARGARETA AVRAM, F. CHIRALEU and I. POGANY

Institute of Organic Chemistry, Bucharest
Splaiul Independenţei, 202 B

Received February 19, 1970

The structure and stereochemistry of some 3.4-benzotricyclo[4.2.1.0 ^{2,5}]nona-3.7-diene dibromides are established by means of NMR spectroscopy.

In the previous paper [1] it was shown that the addition of bromine to *endo*-3.4-benzotricyclo[4.2.1.$0^{2,5}$]nona-3.7-diene (**1**) *) was found to be accompanied by a rearrangement, while the reaction of the *exo* isomer **2** took place without rearrangement.

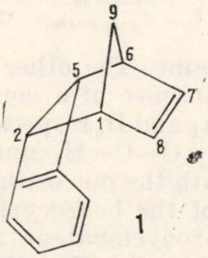

1

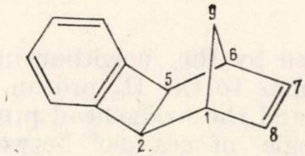

2

In this paper we present the NMR spectroscopy results on the basis of which we ascribed the structure and configuration of the dibromides **3**, **4** and **21** and of the bromoacetoxy-derivative **10**.

7-endo-9-syn-Dibromo-exo-3.4-benzotricyclo[4.2.1.$0^{2,5}$]non-3-ene (3)

The NMR spectrum of the dibromo-derivative **3**, recorded in deuterochloroform, is shown in Fig. 1; the interpretation of the signals is presented in Table 1.

---

*) In this paper the formulas are assigned the same numbers as in the previous paper.[1]

[1] Part XXVIII: M. Avram, I. Pogany, I. G. Dinulescu, F. Chiraleu and C. D. Nenitzescu, *Rev. Roumaine Chim.*, **15**, 1213 (1970).

The multiplet at δ 6.9 – 7.4 ppm corresponds to the four aromatic protons. The doublet at δ 4.14 ppm and the doublet at δ 3.44 ppm form an AB system with a coupling constant of 4 Hz as shown by double resonance. When a doublet is irradiated the other one becomes a singlet (Fig. 1b and 1c).

In dibromide **3** the only protons which can form an AB system without being coupled with the other protons of the molecule are H_2 and H_5. The signal at lower field (δ 4.14 ppm) belongs to the benzylic proton H_5 more deshielded by the neighbouring bromine. The other signal (δ 3.44 ppm) corresponds to the H_2 proton. The absence of a coupling between these protons and the bridgehead protons H_1 and H_6 respectively indicates a dihedral angle of cca. 90° between $H_5-C-C-H_6$ and respectively $H_1-C-C-H_2$. The value is in agreement with the one estimated from the Dreiding models for an *exo* configuration of the benzocyclobutene ring.l For the parent compound **2** with *exo* benzocyclobutene ring (dihedra angle ~90°) a coupling $J_{1.6}$ ($J_{2.5}$) = 0 was found.[2] For the *endo* isomer **(1)** (estimated dihedral angle ~35°) this coupling is 4.0 Hz. These values are in agreement with the Karplus relationship for the variation of the coupling constants *versus* the dihedral angle.[3,4]

Table 1

NMR spectral parameters of the dibromide 3

δ ppm	Pattern	Number of protons	Assignment	Coupling Hz
7,4 – 6,9	multiplet	4	aromatics	
4,82	two triplets	1	H_7	$J_{6.7} = 4$ $J_{7.8\text{-}endo} = 4$ $J_{7.8\text{-}exo} = 10$
4,14	doublet	1	H_5	$J_{2.5} = 4$
3,6	broadened singlet	1	$H_{9\text{-}anti}$	$J_{8\text{-}endo.9\text{-}anti} = 2$
3,44	doublet	1	H_2	$J_{2.5} = 4$
2,82	octet	1	$H_{8\text{-}exo}$	$J_{1.8\text{-}exo} = 4,8$ $J_{7.8\text{-}exo} = 10$ $J_{8\text{-}exo.8\text{-}endo} = 13,5$
2,66	doublet	1	H_6	$J_{6.7} = 4$
2,42	doublet	1	H_1	$J_{1.8\text{-}exo} = 4,8$
1,56	two quartets	1	$H_{8\text{-}endo}$	$J_{7.8\text{-}endo} = 4$ $J_{8\text{-}endo.9\text{-}anti} = 2$ $J_{8\text{-}exo.8\text{-}endo} = 13,5$

The double triplet at δ 4.82 ppm corresponds to the proton H_7 near the bromine atom. The analysis of the coupling of all the protons shows that the proton H_7 is coupled with H_6($J_{6.7}$=4.0 Hz), with H_{8-endo}($J_{7.8-endo}$ =4.0 Hz) and with H_{8-exo}($J_{7.8-exo}$ = 10 Hz).[5] The couplings were confirmed by double resonance. One of this experiments, namely the decoupling between H_7 and H_6, is shown in Fig. 1d.

---

[2] H. E. Simmons, *J. Amer. Chem. Soc.*, **84**, 1657 (1961).

[3] M. Karplus, *J. Chem. Phys.* **30**, 11 (1959).

[4] P. Laszlo and P. v. R. Schleyer, *J. Amer. Chem. Soc.*, **86**, 1171 (1964).

[5] F. A. Anet, *Canad. J. Chem.*, **39**, 789 (1961); M. M. Anderson and P. M. Henry, *Chem. and Ind.*, **1961**, 2053.

The signal at δ 3.6 ppm was atributed to the proton H_9 on the basis of chemical shift and the decoupling experiments. The protons H_9 and H_{8-endo} form a long range coupling of 2.0 Hz.[6] By irradiating the proton H_9 the multiplets of H_{8-endo} are modified without disturbing the signals of the other protons of the molecule. This confirms the *anti* configuration of the proton H_9 and consequently the *syn* configuration of the bromine atom of the 9 position. The absence of coupling between H_{9-anti} and H_7 indicates *exo* configuration for the proton H_7 and therefore *endo* configuration for the bromine atom of the 7 position.

The complex signal between δ 2.35 and 3.08 ppm is constituted by a group of 10 signals. Eight of these signals belong to the proton H_{8-exo} (centered at δ 2.82 ppm). The latter is coupled with H_1 ($J_{1.8-exo}$ = = 4.8 Hz), with H_7 ($J_{7.8-exo}$ = 10 Hz) and with H_{8-endo} ($J_{8-exo.8-endo}$ = = 13.5 Hz).[5,7]

Over this octet is superposed a doublet centered at δ 2.66 ppm belonging to the bridged proton H_6 which in turn is coupled with H_7 ($J_{6.7}$ = 4.0 Hz). The decoupling of the proton H_6 by irradiation of H_7 is shown in the double-resonance spectrum of the Fig. 1d.

The neighbouring doublet at higher field, δ 2.42, ppm, corresponds to the proton H_1 coupled with H_{8-exo} ($J_{1.8-exo}$ = 4.8 Hz).

The doubled quartet at δ 1.56 ppm corresponds to the proton H_{8-endo}. The 8 signals result from the coupling of this proton with H_{8-exo} ($J_{8-exo.8-endo}$ = 13.5 Hz), with H_7 ($J_{7.8-endo}$ = 4.0 Hz) and with H_9 ($J_{9.8-endo}$ = 2.0 Hz). By irradiating H_9 the signal H_{8-endo} becomes a double doublet in which the couplings $J_{8-exo.8-endo}$ of 13.5 Hz and $J_{7.8-endo}$ of 4.0 Hz are maintained; the long range coupling disappears (Fig. 1e).

On the basis of the above data the compound with m.p. 108° was ascribed the formula **3** of 7-*endo*-9-*syn*-dibromo-3.4-*exo*-benzotricyclo [4.2.1.$0^{2,5}$]non-3-ene.

7-exo-9-syn-Dibromo-exo-3,4-bezontricyclo[4.2.1.$0^{2,5}$]non-3-ene (**4**)

The NMR spectrum of the dibromo-derivative with m.p. 78°, recorded in deuterochloroform, is shown in Fig. 2. The signals and the couplings are presented in Table 2.

The singlet at δ 3.32 ppm corresponds to the protons H_2 and H_5 which are equivalent as far as chemical shift and structure are concerned.

The absence of a coupling with the neighbouring protons, H_1 and H_6 respectively, indicates a dihedral angle of $\sim$90° between the plans formed by the atoms $H_2-C-C-H_1$ and $H_5-C-C-H_6$, and therefore *exo* configuration for the benzocyclobutene ring.

In the complex signal between δ 3.60 and δ 4.00 ppm (2 H) a wide singlet can be distinguished at δ 3.67 ppm, corresponding to the proton H_9; over this singlet a splitted quartet (octet) id superposed, centered at

---

[6] J. I. Musher, *Mol. Phys.*, **6**, 93 (1963); J. Meinwald and J. C. Meinwald, *J. Amer. Chem. Soc.*, **85**, 2514 (1963).

[7] P. Laszlo and P. v. R. Schleyer, *J. Amer. Chem. Soc.*, **85**, 2709 (1963); K. L. Williamson, *ibidem* **85**, 516 (1963).

δ 3.88 ppm and corresponding to the proton H_7. As it can be seen from Table 2 and Fig. 2, in the octet due to the H_7 proton three couplings can be distinguished; the lower one, of 1.3 Hz, is possibly a long-range coupling between the protons H_{9-anti} and H_{7-endo}.

Table 2

meters of the dibromide 4

δ ppm	Pattern	Number of protons	Assignment	Coupling Hz
7,32−6,9	multiplet	4	aromatics	
3,88	octet	1	H_7	$J_{7.8\text{-}endo} = 8$ $J_{7.8\text{-}exo} = 4{,}5$ $J_{7.9\text{-}anti} = 1{,}3$
3,67	broadened singlet	1	H_9	
3,32	singlet	2	H_2, H_5	
2,87	singlet	1	H_6	
2,77	two triplets	1	$H_{8\text{-}exo}$	$J_{1.8\text{-}exo} = 4$ $J_{7.8\text{-}exo} = 4{,}5$ $J_{8\text{-}exo.8\text{-}endo} = 13{,}5$
2,52	doublet	1	H_1	$J_{1.8\text{-}exo} = 4$
2,20	dedoubled quartet	1	$H_{8\text{-}endo}$	$J_{8\text{-}endo.9\text{-}anti} = 1{,}5$ $J_{7.8\text{-}endo} = 8{,}0$ $J_{8\text{-}exo.8\text{-}endo} = 13{,}5$

The signal at δ 2.87 ppm was attributed to the proton H_6. It appears as a singlet because the *endo* configuration of the proton H_7 determines a dihedral angle of ~90° between $H_9-C-C-H_7$ and therefore no coupling is possible between these protons. [3]

In the previous case of the dibromo compound **3** with H_{7-exo} and therefore *endo* bromine, the estimated dihedral angle of 35° determines a coupling $J_{6,7}$ of 4.0 Hz. These two facts lead to the conclusion that in compound **4** the bromine atom of the 7 position has *exo* configuration.

The doublet from δ 2.52 ppm was attributed to the proton H_1 which can be coupled only with the proton H_{8-exo} as in the dibromide **3**.

Over these signals a complex signal is superposed constituted of a splitted quartet with a low coupling constant and centered at δ 2.20 ppm, which was attributed to the proton H_{8-endo}, and a double triplet centered at δ 2.77 ppm due to the proton H_{8-exo}.

The splitted quartet at δ 2.20, belonging to the proton H_{8-endo}, is coupled with H_{8-exo} ($J_{8-exo.8-endo} = 13.5$ Hz), with H_7 ($J_{7.8-endo} = 8.0$ Hz) and, by a long-range coupling of 1.5 Hz, with H_9.

The multiplet of the proton H_{8-exo} centered at δ 2.77 ppm presents couplings with H_{8-endo} ($J_{8-exo.8-endo} = 13.5$ Hz) and with H_{7-endo} ($J_{8-exo.7-endo} = 4.5$ Hz). It has also a coupling with H_1 ($J_{1.8-exo} = 4.0$ Hz).

As shown in the above analysis, the spectrum corresponds to the structure of 7-*syn*-9-*exo*-dibromo-3.4-*exo*-benzotricyclo[$4.2.1.0^{2,5}$]non-3-ene (**4**).

7.8-trans-Dibromo-exo-3.4-benzotricyclo[4.2.1.0$^{2.5}$]non-3-ene (**21**)

The NMR spectrum recorded in deuterochloroform is shown in Fig. 3a. The proton signals are presented in Table 3.

Table 3

NMR spectral parameters of the dibromide 21

δ ppm	Pattern	Number of protons	Assignment	Coupling Hz
6,92−7,36	multiplet	4	aromatics	
4,55	quartet	1	H_8	$J_{1.8} = 4,2$ $J_{7.8} = 3$
3,95	doublet	1	H_2	$J_{2.5} = 3,8$
3,88	triplet	1	H_7	$J_{7.8} = 3$ $J_{7.9\text{-}sin} = 3$
3,37	doublet	1	H_5	$J_{5.2} = 3,8$
2,60	broad	2	H_1, H_6	
1,78	doublet AB	1	$H_{9\text{-}anti}$	$J_{9\text{-}sin.9\text{-}anti} = 11,5$ $J_{7.9\text{-}anti} = 3$ $J_{1.9\text{-}anti} = 1,5$
1,10	doublet	1	$H_{9\text{-}sin}$	

The quartet at δ 4.55 ppm was attributed to the proton H_{8-exo} on the basis of chemical shift, at lower field as compared with the *endo* proton of 7 position; the latter forms a triplet at δ 3.88 ppm.

The quartet of the proton H_{8-exo} results from coupling with the bridgehead proton H_1 ($J_{1.8-exo} = 4.2$ Hz) and with the vicinal proton H_7 ($J_{7.8-exo}=3.0$ Hz). In order to ascribe these signals to the corresponding protons, double resonance measurements were used. The figures 3b and 3c present the transformations of the quartet of the proton H_{8-exo} into a doublet when the proton H_1 or the proton H_{7-endo} are irradiated. The couplings of 4.2 Hz and 3.0 Hz respectively disappear.

The signal due to the proton H_{7-endo} at δ 3.88 ppm appears as a triplet (at 60 MHz) as a result of equal couplings with H_{8-exo} ($J_{7.8-exo} = 3.0$ Hz) and H_{9-anti} ($J_{7.9-anti} = 3.0$ Hz). Over the triplet due to the proton H_7 are superposed the signals of the protons H_2 at δ 3.95 ppm which form an AB system with the proton H_5 at δ 3.37 ppm. The signal at δ 3.95 ppm was attributed to the proton H_2 deshielded by the neighbouring bromine atom.

The absence of couplings with the protons H_1 (H_6) support the ascribed configuration of the protons H_2 (H_5) and therefore the *exo* configuration of the benzocyclobutene ring.

The protons H_{9-anti} and H_{9-syn} of the methylene bridge form a complex AB system between δ 1.10 and δ 1.78 ppm. This system presents a coupling of 11.5 Hz corresponding rather to a geminal coupling of the methylene bridge group than to a CH_2 group of a six-membered ring.[8] Since the *exo* benzocyclobutene ring must have magnetical anisotropy, the doublet at δ 1.78 ppm was attributed to the proton H_{9-syn}, and the doublet at higher field, at δ 1.10 ppm, to the proton H_{9-anti}.

In addition to the geminal coupling of 11.5 Hz ($J_{9-syn.9-anti}$) the proton H_{9-anti} presents also a coupling $J_{7.9-anti}$ of 3.0 Hz as well as a coupling of 1.5 Hz with the proton H_1 and H_6. In the case of the other dibromo isomers previously studied, the coupling H_1-H_{9-anti}, of a lower value, could not be evidenced under the conditions used. The doublet at δ 1.78 ppm attributed to the proton H_{9-syn} presents a complex structure and with the resolution of our instruments it was not possible to evidence the low couplings between H_{9-syn} and the protons H_2, H_5 on the one hand, and H_1, H_6 on the other hand.

7-exo-Acetoxy-9-syn-bromo-exo-3.4-benzotricyclo[*4.2.1.*$0^{2,5}$]*non-3-ene* (10)

The NMR spectrum of the compound **10** recorded in $CDCl_3$ is shown in Fig. 4. The signals, the couplings and the attributions of the protons are shown in Table 4.

Table 4

NMR spectral parameters of the bromo-acetoxy-derivative 10

δ ppm	Pattern	Number of protons	Assignment	Coupling Hz
7,33–6,9	multiplet	4	aromatics	
4,63	octet	1	H_7	$J_{7.9-anti}$ = 1,2 $J_{7.8-exo}$ = 3,8 $J_{7.8-endo}$ = 7,5
3,54	singlet (triplet)	1	H_{9-anti}	$J_{7.9-anti}$ = 1,2 $J_{9.8-endo}$ = 1,2
3,29	singlet	2	H_2, H_5	—
2,74	singlet	1	H_6	—
2,55	doublet	1	H_1	$J_{1.8-exo}$ = 4
2,26	double triplet	1	H_{8-exo}	$J_{1.8-exo}$ = 4 $J_{7-endo.8-exo}$ = 3,8 $J_{8-exo.8-endo}$ = 14
2,05	singlet	3	acetoxy	
1,93	two dedoubled doublets	1	H_{8-endo}	$J_{8-endo.9-anti}$ = 1,2 $J_{7-endo.8-endo}$ = 7,5 $J_{8-exo.8-endo}$ = 14

The comparison of the spectrum of the acetoxy derivative **10** with that of the dibromide **4** clearly indicates a structural similarity. The singlet at δ 3.29 ppm was attributed to the benzylic protons H_2 and H_5; as it was shown for the other compounds, this confirms the *exo* configuration of the benzocyclobutene ring.

---

[8] R. C. COOKSON, T. A. CRABB, J. J. FRANKEL and J. HUDEC, *Tetrahedron suppl.*, no. 7, 355 (1966).

The octet at δ 4.63 ppm, which on the basis of chemical shift was attributed to the proton H_7 situated near the acetoxy group, presents three couplings among which one of low value, namely 1.2 Hz. This low coupling corresponding to a "long range" is found again in the case of the splitted quartet attributed to proton H_{8-endo} at δ 1.93 ppm which is partially covered by the singlet of the acetoxy group at δ 2.05 ppm. The bridgehead proton H_6, more deshielded than H_1, appears as a singlet. The above facts indicate *exo* configuration for the acetoxy group and therefore *endo* configuration for H_7.

The very narrow triplet at δ 3.54 ppm has a chemical shift very similar to the signals attributed to the protons H_{9-anti} of the bromo-compounds **3** and **4**.

Consequently this signal was attributed to the proton H_{9-anti}. It appears as a triplet as a result of equal low couplings of 1.2 Hz with H_{7-endo} and H_{8-endo}.

The protons H_1, H_{8-exo} and H_{8-endo} have signals similar to those of the corresponding protons of the dibromo compound **4**; however the triplet of H_{8-exo} appears much more clearly (see Fig. 4 and Table 4).

The spectrum corresponds to the proposed structure of 7-*exo*-acetoxy-9-*syn*-bromo-derivative (**10**).

EXPERIMENTAL

The NMR spectra were recorded with a Varian A–60A spectrometer. The decoupling experiments were performed with the same instrument using a spin-decoupler device.

The bromo-compounds were prepared according to the indications given in the previous paper [1] from *endo*- and from *exo*-3.4-benzotricyclo[4.2.1.0 ^{2,5}]nona-3.7-dienes.

7-*endo*-9-*syn*-Dibromo-*exo*-3.4-benzotricyclo[4.2.1.0 ^{2,5}]non-3-ene (**3**), m. p. 108° (methanol).

7-*exo*-9-*syn*-Dibromo-*exo*-3.4-benzotricyclo[4.2.1.0 ^{2,5}]non-3-ene (**4**), m. p. 76° (methanol).

7.8-*trans*-Dibromo-*exo*-3.4-benzotricyclo[4.2.1.0 ^{2,5}]non-3-ene (**21**), m. p. 84° (methanol).

7-*exo*-Acetoxy-9-*syn*-bromo-*exo*-3.4-benzotricyclo[4.2.1.0 ^{2,5}]non-3-ene (**10**), m. p. 122° (methanol).

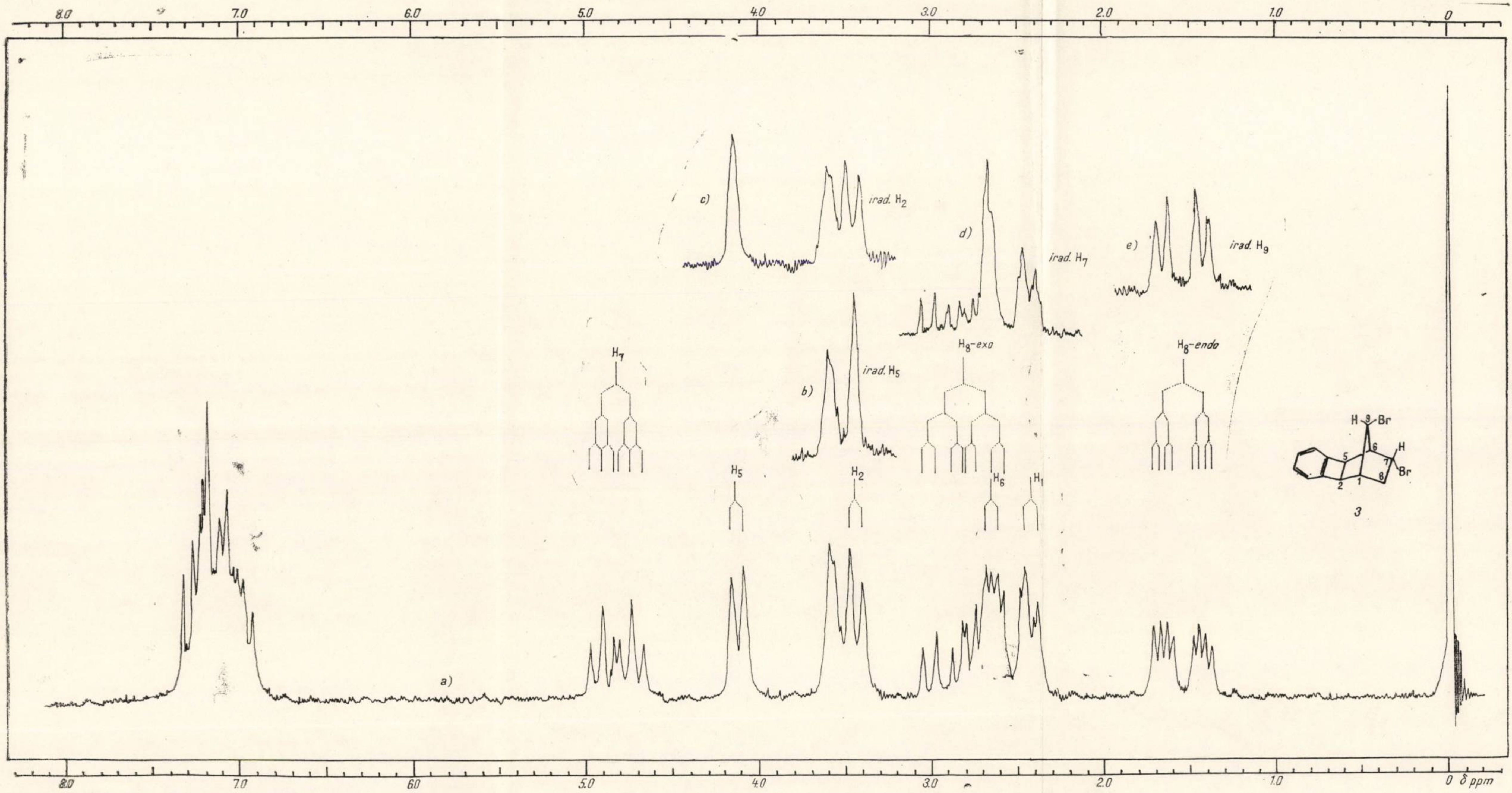

Fig. 1. — NMR spectrum of the dibromide 3.

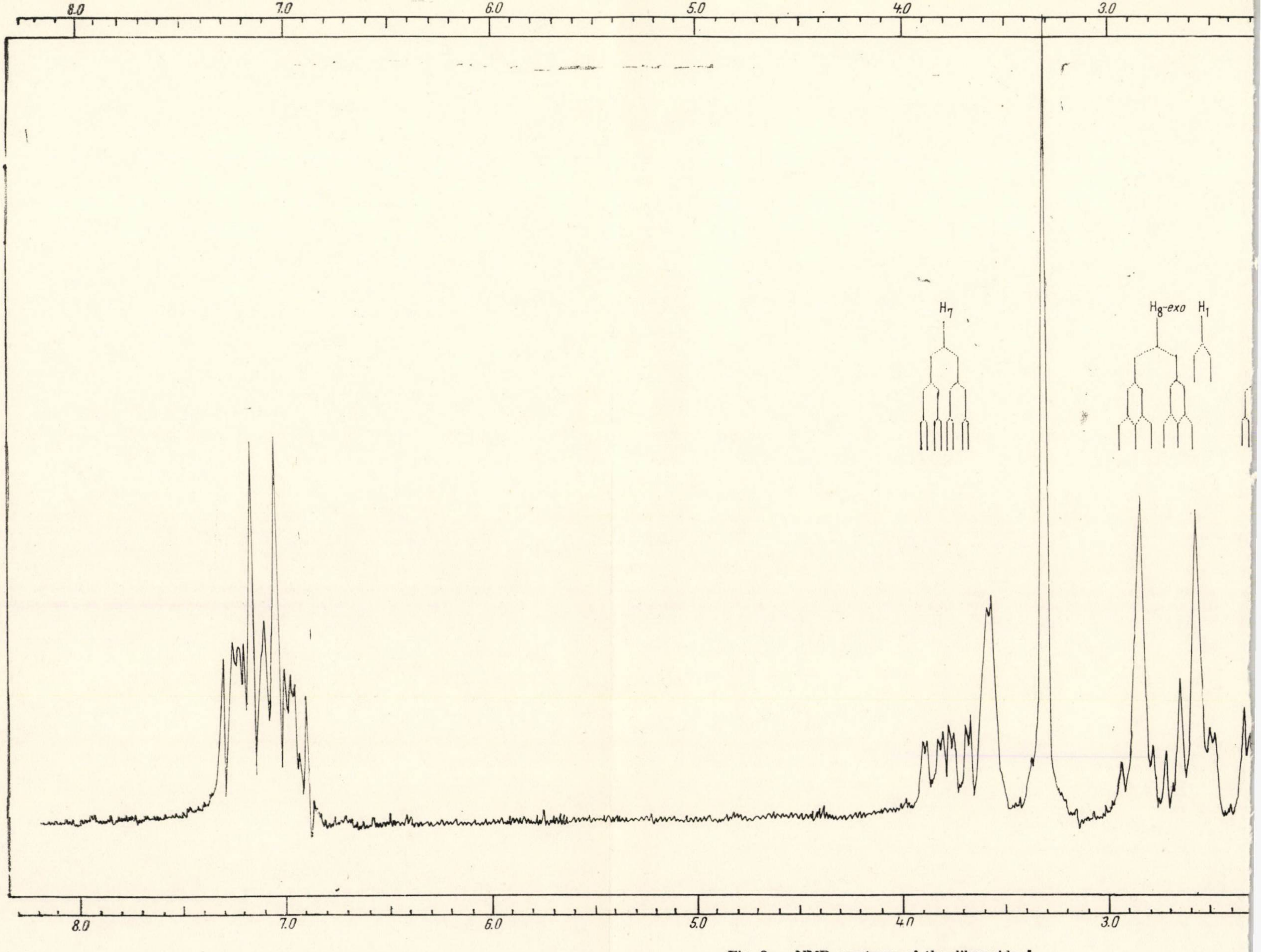

Fig. 2. — NMR spectrum of the dibromide **4**.

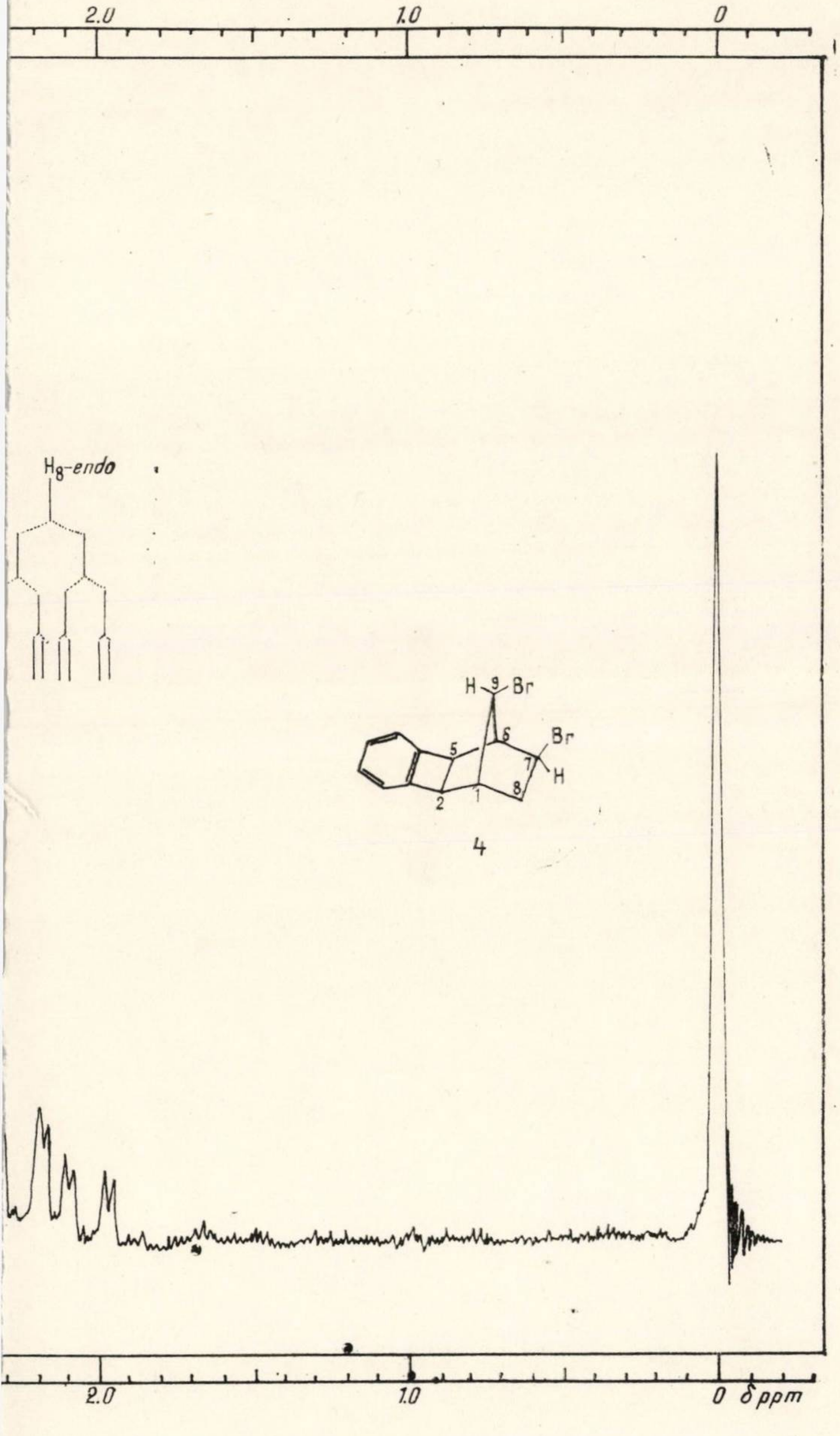
2.0
1.0
0
H_8-endo
H
9
Br
5
6
Br
7
H
8
2
1
4
2.0
1.0
0 δ ppm

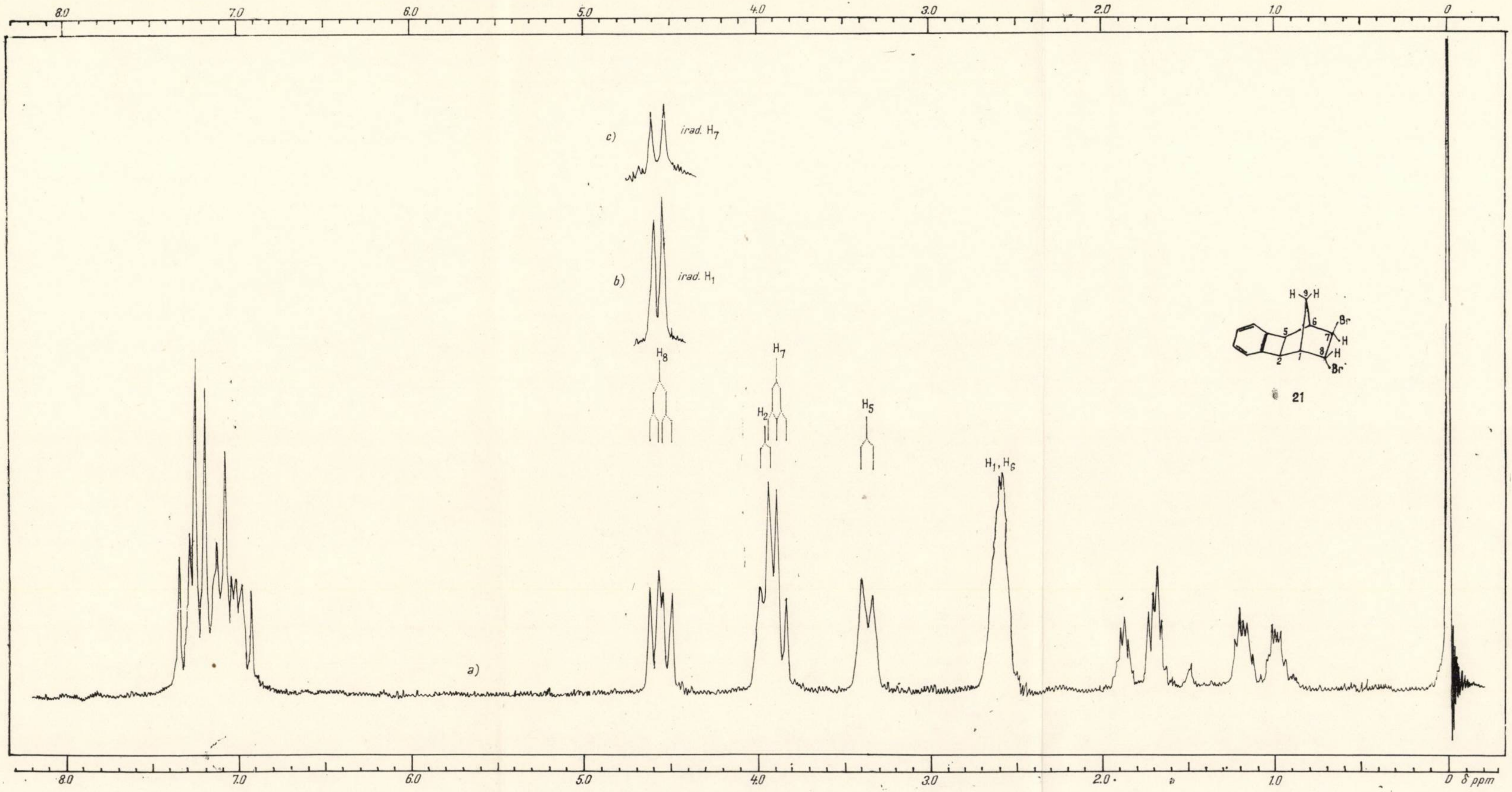

Fig. 3. — NMR spectrum of the dibromide **21**.

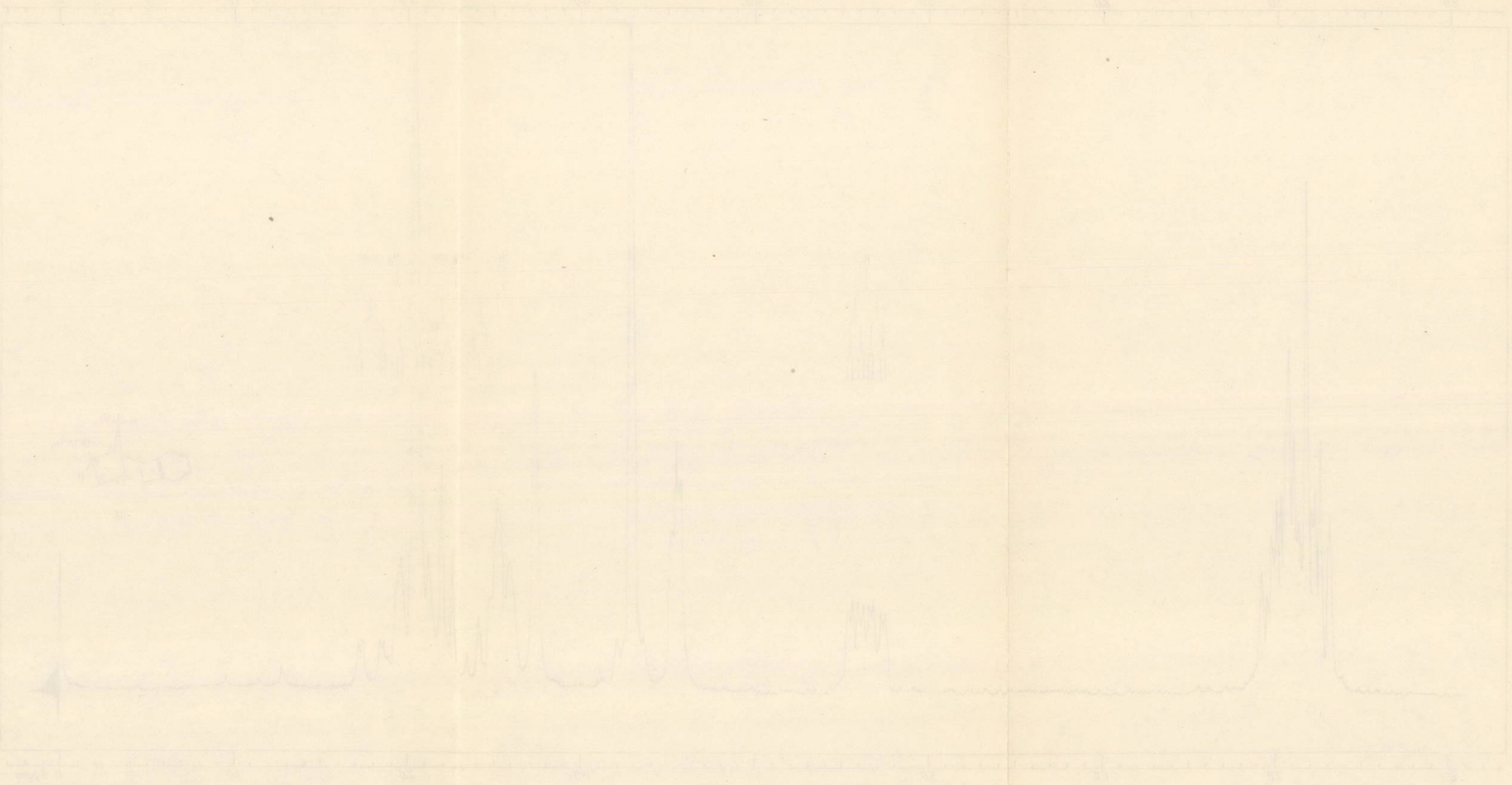

Fig. 4. — NMR spectrum of the bromo-acetoxy derivative 19.

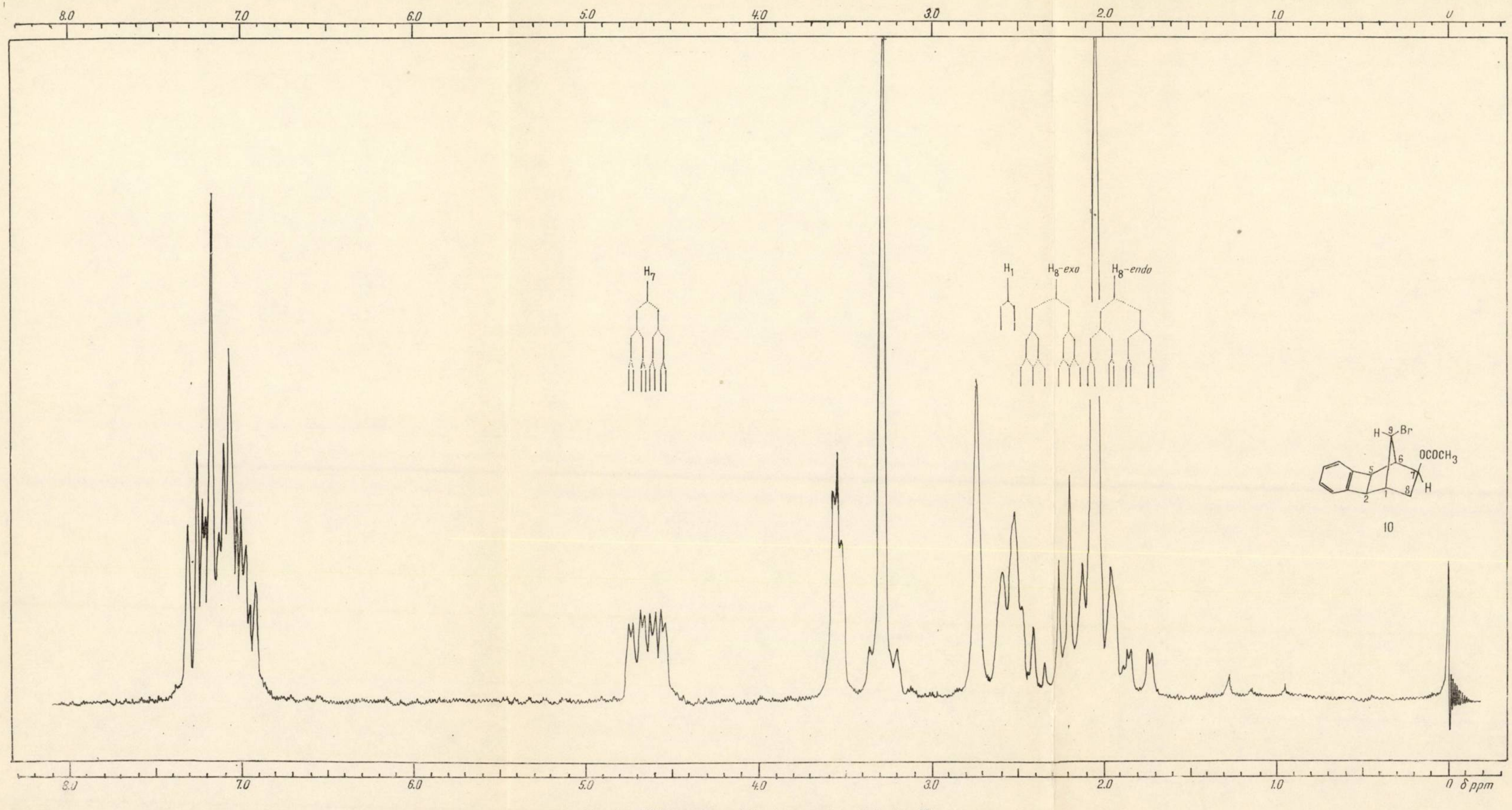

Fig. 4. — NMR spectrum of the bromo-acetoxy-derivative **10**.

Revue Roumaine de Chimie, **15**, 1227–1232 (1970)

UNTERSUCHUNGEN ÜBER ARYLDIAZOSULFONATE UND ARYLDIAZOSULFONSÄUREN. II[1]

HERSTELLUNG UND PHOTOCHEMISCHES VERHALTEN DER BENZOLDIAZOSULFONSÄURE

| J. REICHEL | und R. VIDAC

aus dem Laboratorium für Farbstoffe und Zwischenprodukte der Technischen Hochschule, Timişoara Bd. 30 Decembrie, 2 und aus dem Laboratorium für Angewandte Chemie der Universität Timişoara, str. Pestalozzi, 16

Eingegangen am 31. März 1969

Die in verdünnten wäßrigen Lösungen stabile Benzoldiazosulfonsäure wurde aus benzoldiazosulfonsaurem Natrium oder Kalium mit Hilfe stark saurer Ionenaustauscher erhalten. Die durch die ultraviolette Bestrahlung der wäßrigen Benzoldiazosulfonsäurelösungen hervorgerufenen spektralen Veränderungen *im ultravioletten Bereich,* die der Bildung von Diazoniumionen und Phenol zugeschrieben werden, unterscheiden sich nicht von jenen, die durch Bestrahlung der alkalischen Benzoldiazosulfonate hervorgerufen werden, ein Beweis dafür, daß auch die primäre photochemische Umwandlung der letzteren nicht in ihrer Isomerisierung zu syn-Diazosulfonaten besteht. Zum Unterschied von der Benzoldiazosulfonaten wird *im sichtbaren Bereich* keine Bildung des *p*-Hydroxyazobenzols festgestellt, sondern erst nachdem die ganze Diazosulfonsäure sich in das Benzoldiazoniumsalz der Benzoldiazosulfonsäure, in Diazoniumsulfit und Phenol umgesetzt hat, in welchem Falle die Wasserstoffionenkonzentration Werte annimmt, die eine Azokupplung erlauben.

★

Durch die Einwirkung von Mineralsäuren zersetzen sich die Aryl-syn-diazosulfonate sofort in ein Diazoniumsalz und Schwefeldioxid, weil die Aryl-syn-diazosulfonsäuren nicht frei existieren können.[2]

Bis jetzt wurden die Aryl-anti-diazosulfonsäuren nur mit Hilfe der Silbersalze erhalten. Diese Herstellungsvariante einiger Aryl-anti-diazosulfonsäuren wurde von Hantzsch und Schmiedel [3] beschrieben : die aus Diazoniumsalzen und Sulfit hergestellten Kalium-Diazosulfonate werden mit Silbernitrat in stabile Silber-Diazosulfonate umgesetzt und aus warmem Wasser umkristallisiert:

---

[1] I. Mitteil. : J. Reichel und R. Vidac, *Rev. Roumaine Chim.* (unter Druck) **15**, 000 (1970).

[2] R. Pütter, „Methoden der organischen Chemie", Band X/3, IV. Auflage, Georg Thieme Verlag, Stuttgart, 1965, S. 576.

[3] A. Hantzsch und M. Schmiedel, *Ber. dtsch. chem. Ges.*, **30**, 71 (1897).

$$Ar-N_2-SO_3K + AgNO_3 \longrightarrow Ar-N_2-SO_3Ag + KNO_3$$

Die Silber-diazosulfonate werden in Wasser suspendiert und mit berechneten Mengen von Salzsäure zersetzt:

$$Ar-N_2-SO_3Ag + HCl \longrightarrow Ar-N_2-SO_3H + AgCl$$

Nach dem Abfiltrieren des Silberchlorids wird die Lösung bei niedrigen Temperaturen über Schwefelsäure verdampft und man erhält auf diese Weise gelbe kristalline Prismen der Diazosulfonsäuren.

So wurde die 4-Brom-, 2,4-Dibrom-, 4-Methyl-benzoldiazosulfonsäure[3] und die 2-Chlor-benzoldiazosulfonsäure [4] hergestellt. Die beiden ersten und die letzte Säure können in reinem und wasserfreiem Zustand erhalten werden, während die dritte Säure sich teilweise zersetzt, wenn ihre Trocknung vollständig ausgeführt wird. Frisch hergestellt, kuppeln sie nicht mit β-Naphthol. Nach einigen Tagen aber bilden sich unlösliche Zersetzungsprodukte, welche mehr oder weniger mit β-Naphthol kuppeln, ein Beweis dafür, daß sich auch Diazoniumsalze gebildet hatten.

Die Benzoldiazosulfonsäure konnte nicht erhalten werden, weil sie sich schon während der Herstellung zersetzte.[2, 3, 5]

DIE HERSTELLUNG DER ARYLDIAZOSULFONSÄUREN MIT HILFE VON IONENAUSTAUSCHERN

Wir stellten fest, daß die Aryldiazosulfonsäuren direkt aus den Natrium- oder Kalium-Diazosulfonaten, mit Hilfe stark saurer Ionenaustauscher hergestellt werden können, und daß auf diese Weise der Umweg über die Silbersalze nach der klassischen Methode vermieden werden kann.

$$n Ar-N_2-SO_3Na + RH_n \longrightarrow n Ar-N_2-SO_3H + RNa_n$$

RH_n ist der Ionenaustauscher in der Form der freien Säure

Auf diese Weise können wir auch reine wäßrige Benzoldiazosulfonsäurelösungen, von bis 10%igen Konzentrationen und mit einer Ausbeute von 100% erhalten. Als stark sauren Ionenaustauscher benützten wir ein Merckprodukt — Ionenaustauscher I und ein Kationit rumänischer Fabrikation-Vionit CS-2.

Die so erhaltenen Benzoldiazosulfonsäurelösungen sind stark sauer, stabil in der Zeit und beim Erhitzen und kuppeln nicht mit Naphtholen. Eine leichte Zersetzung, bemerkbar durch eine geringe Kupplung mit β-Naphthol, wird bei Konzentrationen über 10% beobachtet. Mit wachsender Konzentration der Lösungen wird die Kupplung stärker, selbst im Exsikkator um 0°. Bei großen Konzentrationen wird aus der Lösung Schwefeldioxid freigesetzt. Durch Trocknen erhält man eine orange Masse welche prismatische hygroskopische Kristalle enthält, die sehr stark mit Naphtholen kuppeln. Wir schreiben dieses Verhalten der Bildung des Benzoldiazonium-Benzoldiazosulfonates, infolge der Instabilität der nichtdissozierten Benzoldiazosulfonsäure zu:

---

[4] H. C. Freeman und R. J. W. Le Fèvre, *J. Chem. Soc.*, **1951**, 415.

[5] C. Paal und F. Kretschmer, *Ber. dtsch. chem. Ges.*, **27**, 1241 (1894).

$$C_6H_5-N_2-SO_3H \rightarrow C_6H_5-N_2^+SO_3H^- \xrightarrow{+C_6H_5-N_2-SO_3^-H^+}$$

$$\rightarrow (C_6H_5-N_2-SO_3)^- (C_6H_5-N_2)^+ + SO_2 + H_2O$$

DIE PHOTOCHEMISCHE UMWANDLUNG DER BENZOLDIAZOSULFONSAURE

Freeman und Le Fèvre [4] untersuchten spektroskopisch das photochemische Verhalten der *o*-Chlorbenzoldiazosulfonsäure, publizierten aber nur die Feststellung, daß sie keine Beweise für die Bildung eines hypothetischen „syn"-Isomeren gefunden hätten.

In vorliegender Arbeit untersuchten wir spektroskopisch, im ultravioletten und sichtbaren Bereich, die photochemische Umwandlung der Benzoldiazosulfonsäure im ultravioletten Licht, in wäßriger Lösung.

Die Absorptionsspektren in Abbildung 1 wurden mit Hilfe eines Spektrophotometers Unicam SP. 800 erhalten. Die Extinktionskoeffizienten der dem Licht ausgesetzten Lösungen wurden auf Grund der Benzoldiazosulfonsäurekonzentration der ursprünglich nichtbestrahlten Lösung berechnet.

Die Kurve 1 stellt das Absorptionsspektrum im ultravioletten-sichtbaren Bereich für die Benzoldiazosulfonsäure dar. Infolge der Tatsache, daß die Benzoldiazosulfonsäure bei der verwendeten Verdünnung total ionisiert ist, erwies sich ihr Absorptionsspektrum identisch mit dem des benzoldiazosulfonsauren Natriums.[1]

Die Kurven 2–5 wurden durch das Studium einiger Benzoldiazosulfonsäurelösungen, nach der ultravioletten Bestrahlung erhalten, bei Konzentrationen von 5.10^{-3} mol/1, nach 2 (Kurve *2*), 5 (Kurve *3*), 9 (Kurve *4*) und 12 (Kurve *5*) Minuten, bei einer Schichtdicke von 1 mm, bei 20 cm Abstand von einer Quecksilberdampflampe VEB (K) Thelta Zella-Mehlis, Typ Q 99.

Aus den Kurven 2–5 folgt, daß die spektralen Veränderungen im *ultravioletten Bereich*, hervorgerufen durch die ultraviolette Bestrahlung, die gleichen sind, sowohl für die Benzoldiazosulfonsäure, als auch für das Natrium-Benzoldiazosulfonat [1]. Da es bekannt ist, daß die Diazosulfonsäuren nur in der „anti"-Form existieren können, sehen wir in dieser Tatsache eine Bestätigung unserer in einer früheren Arbeit aufgestellten [1] Behauptung, und zwar *daß auch die primäre photochemische Umsetzung des Benzol-*

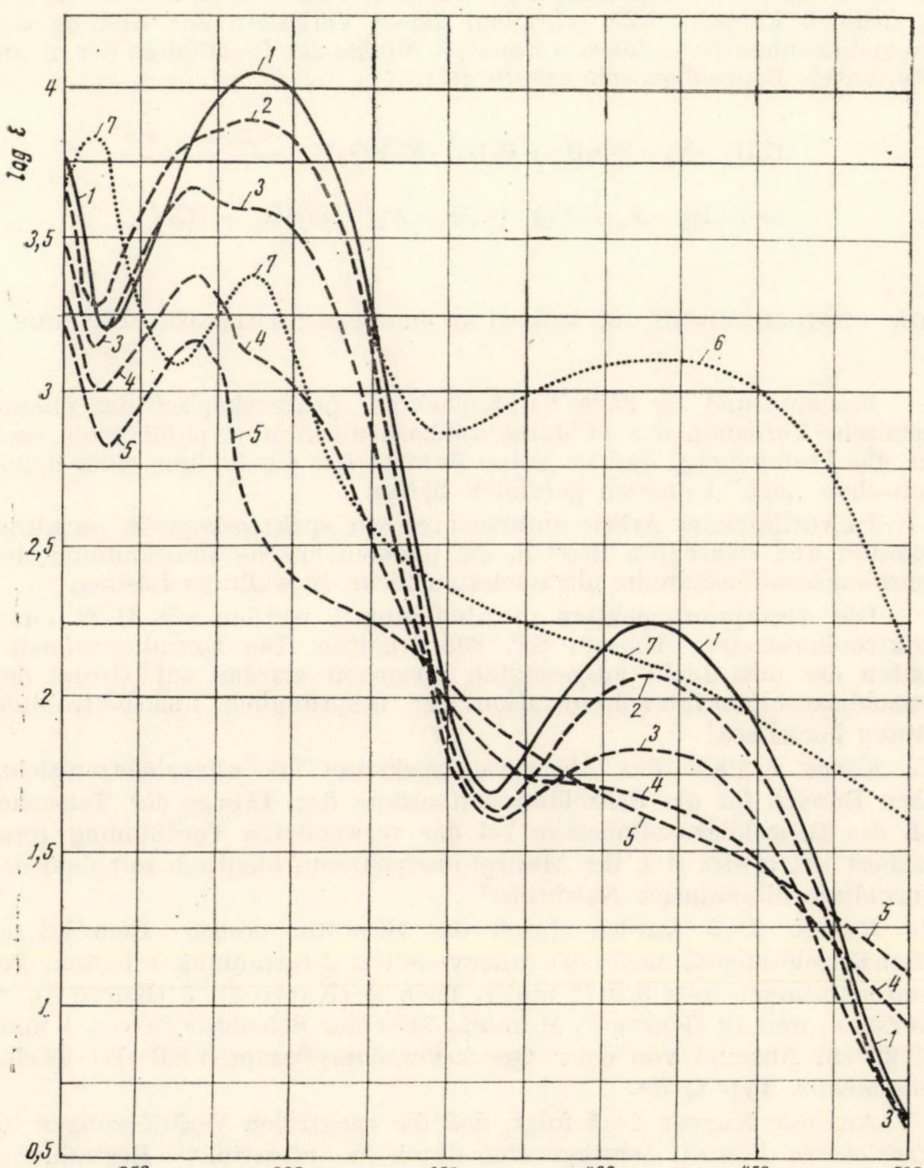

Abb. 1. — Die Absorptionsspektren im ultraviolett-sichtbaren Bereich.

1. Benzoldiazosulfonsäure im Wasser. *2–5.* Wäßrige Benzoldiazosulfonsäurelösungen bei einer Konzentration von 5.10^{-3} mol/1, Schichtdicke 1 mm, während 2 (2), 5 (*3*), 9 (*4*) und 12 (*5*) Min. dem ultravioletten Licht ausgesetzt. **6.** Eine 2 Minuten lang bestrahlte, dann auf pH–12 alkanisierte Probe. **7.** Eine 12 Minuten lang bestrahlte, dann auf pH–12 alkanisierte Probe.

anti-Diazosulfonates ebenfalls in einer Dissoziation in Diazoniumionen und nicht in einer Isomerisierung zu syn-Diazosulfonat, besteht.

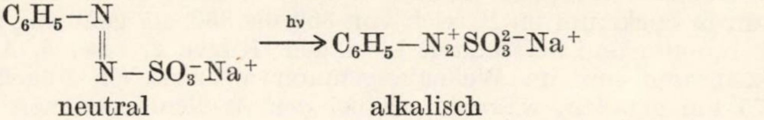

$$\begin{array}{l} C_6H_5-N \\ \quad\| \\ N-SO_3^-Na^+ \end{array} \xrightarrow{h\nu} C_6H_5-N_2^+SO_3^{2-}Na^+$$

neutral alkalisch

Die Dissoziation der freien Säure in Diazoniumione :

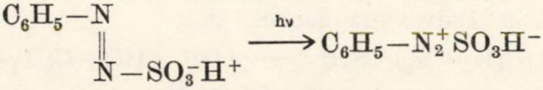

$$\begin{array}{l} C_6H_5-N \\ \quad\| \\ N-SO_3^-H^+ \end{array} \xrightarrow{h\nu} C_6H_5-N_2^+SO_3H^-$$

bewiesen durch eine Verstärkung der Absorption im Bereich von 235–266 mμ der 2 minutenlang bestrahlten Lösung (Kurve *2*, Abb. 1) wird von einer Ersetzung der schwefeligen Säure mit noch unzersetzter Diazosulfonsäure gefolgt.

$$C_6H_5-N_2-SO_3H + C_6H_5-N_2^+SO_3H^- \rightarrow$$
$$\rightarrow (C_6H_5-N_2-SO_3)^- \; (C_6H_5-N_2)^+ + SO_2 + H_2O$$

neutral

Nur die bestrahlte Diazosulfonatlösung wird basisch, schon von Anfang des photochemischen Vorganges an, nicht aber auch die Diazosulfonsäurelösung.

Die stufenweise photolytische Umwandlung in Phenol, welche in beiden Fällen stattfindet und welche aus dem Spektrum der länger bestrahlten Lösungen, durch das Maximum von 269 mμ, sichtbar wird, stellt den Benzoldiazoniumionen — die während der

$$C_6H_5-N_2^+(SO_3)^{2-}Na^+ + H_2O \xrightarrow{h\nu} C_6H_5OH + N_2 + NaHSO_3$$

$$(C_6H_5-N_2)^+(C_6H_5-N_2-SO_3)^- + H_2O \xrightarrow{h\nu} C_6H_5OH + N_2 +$$
$$+ C_6H_5-N_2-SO_3H$$

primären photochemischen Umwandlung gebildet werden — eine Azokupplungskomponente zur Verfügung, mit der sie *p*-Hydroxyazobenzol bilden können, wenn die Lösung schwach basisch ist. Die Azokupplung findet im Falle der Bestrahlung des Diazosulfonates schon zu Beginn des Vorganges statt, während im Falle der Diazosulfonsäure diese stattfinden kann nachdem die ganze Säure in Benzoldiazonium-benzoldiazosulfonat und Diazoniumsulfit übergegangen ist, wodurch die Lösung basisch wurde :

$$(C_6H_5-N_2-SO_3)^- (C_6H_5-N_2)^+ \xrightarrow{h\nu} 2\,(C_6H_5-N_2)^+ SO_3^{2-}$$

basisch

Die spektralen Modifikationen aus dem *sichtbaren Bereich* bestätigen die obenaufgestellte Annahme, und zwar: bei den 2 und 5 minutenlang bestrahlten Lösungen (Kurve *2*, bzw. *3*, Abb. 1) ist die Extinktion im ganzen Spektrum im Bereich von 500 bis 350 mμ gefallen; bei den 9 und 12 minutenlang bestrahlten Lösungen (Kurve *4*, bzw. *5*, Abb. 1) ist die Extinktion nur im Wellenlängenintervall zwischen ungefähr 375 und 475 mμ gefallen, während sie bei den Wellenlängen von 350—375 mμ und bei höheren als 475 mμ, stark angestiegen ist, analog mit dem infolge der Bestrahlung des Benzoldiazosulfonates gemessenen Anstieg.[1] Wie auch im Falle des Natrium-Benzoldiazosulfonates schreiben wir diesen Extinktionsanstieg dem *p*-Hydroxyazobenzol zu:

$$\mathrm{HO{-}C_6H_5} + 2\,(\mathrm{C_6H_5{-}N_2})^+\,\mathrm{SO_3^{2-}} \longrightarrow (p)\ \mathrm{{-}HO{-}C_6H_4{-}N_2{-}C_6H_5} + \\ + \mathrm{C_6H_5{-}N_2}^+\mathrm{HSO_3^-}$$

Die in *Kurven 6 und 7*, Abb. 1 wiedergegebenen Spektren bestätigen diese Tatsache:

Kurve 6, die durch spektroskopische Untersuchung im sichtbaren Bereich der 2 Minuten lang bestrahlten und dann auf pH-12 alkalinisierten Benzoldiazosulfonsäurelösung (Kurve *2*) aufgestellt wurde, zeigt einen sehr klaren Extinktionsaufstieg im Gebiete der intensiven Absorption des *p*-Hydroxyazobenzols, in basischer Lösung (siehe Abb. 3 aus Lit.[1]).

Kurve 7, die aufgestellt wurde für die 12 Minuten lang bestrahlte und dann auf pH = 12 alkalinisierte Benzoldiazosulfonsäurelösung, zeigt im sichtbaren Gebiet die zusätzliche Bildung eines Azofarbstoffes, dessen Konzentration aber doch kleiner als im vorherigen Fall bleibt (Kurve *6*), infolge der kleineren Verfügbarkeit der Benzoldiazoniumionen, die sich in einem größeren Ausmaß in Phenol umgewandelt haben. Letzteres ist als Hauptprodukt der vorgeschrittenen Bestrahlung durch die Maxima von 269 mμ (Kurve *5*-Phenol) und von 235 und 287 mμ (Kurve *7*-Phenoxid) hervorgehoben.

SCHLUSSFOLGERUNGEN

Die Modifikationen die sich im Absorptionsspektrum im ultravioletten Bereich durch eine ultraviolette Bestrahlung der Benzoldiazosulfonsäure ergeben, sind gleich mit denen die bei der Bestrahlung des benzoldiazosulfonsauren Natriums[1] festgestellt wurden und wir schreiben sie der direkten Dissoziation in Diazoniumsalze und deren Photolyse zu Phenol zu. Es wurde kein Beweis für eine vorherige Umwandlung in das „syn"-Isomer erhalten.

Die spektralen Veränderungen aus dem sichtbaren Bereich sind analog mit denen, die bei der Bestrahlung des Benzoldiazosulfonates nur nach längerer Lichtaussetzung festgestellt wurden, weil dann das Anwachsen des pH-Wertes eine teilweise Azokupplung der Diazoniumione mit Phenol ermöglicht, eine Kupplung die im Falle des Benzoldiazosulfonates[1] am Anfang des photochemischen Prozesses stattgefunden hatte.

Die für das photochemische Studium verwendete Benzoldiazosulfonsäure erhielten wir nach einer neuen, eingangs beschriebenen Methode und zwar direkt aus ihrem Natriumsalz, mit Hilfe stark saurer Ionenaustauscher.

Revue Roumaine de Chimie, 15, 1233–1242 (1970)

ACRIDONES. XXXV*
THE IODINATION OF ACRIDONE

ILEANA GOIA and MARIA IONESCU
Institute of Chemistry of the Academy, Cluj, str. Donath, 59–65

Received August 30, 1969

The action of iodine chloride on acridone in different conditions of reaction has been investigated and unitary iodo-, mixed iodo-chloro-acridone, and the corresponding 9-chloro-acridines and 9-thioacridones have been obtained.

Direct iodination of aromatic compounds reveals special problems.[1–13] Since molecular iodine is the least reactive as compared to bromine and chlorine, we used iodine chloride which is, however, an iodinating species. Dissociation of ICl molecule either heterolytically (causing iodination, eqn. 1) or homolytically (causing chlorination, eqn. 2) depends, among others, on the polarity of the reaction medium.[14]

$$ICl \rightleftharpoons I^+ + Cl^- \quad (1)$$

$$2ICl \rightleftharpoons I_2 + Cl_2 \quad (2)$$

In the media of higher polarity such as acetic acid, nitrobenzene, iodine chloride can act as an iodinating species, while in carbon tetrachloride, a medium of low polarity, it acts as a chlorinating agent.

---

[*] See XXXIV. M. Ionescu and I. Meşter, *Rev. Roumaine Chim.*, (in press).

[1] P.S. D. De La Mare and J. H. Ridd, "Aromatic Substitution", Buterworth, London, 1959, p. 110, 125.

[2] E. Grovenstein and N. S. Aprohamian, *J. Amer. Chem. Soc.*, **84**, 212 (1962).

[3] R.O.C. Norman and R. Taylor, "Electrophilic Substitution in Benzenoid Compounds", Amsterdam, Elsevier Publishing Company, 1965, Chap. 1, 2, 5.

[4] A. R. Katritzky, "Advances in Heterocyclic Chemistry", vol. 7, Academic Press; London, 1966, p. 1.

[5] R. M. Keefer and L. J. Andrews, *J. Amer. Chem. Soc.*, **78**, 5623 (1956).

[6] E. Berliner, *J. Amer. Chem. Soc.*, **78**, 3632 (1956).

[7] E. Grovenstein and D. C. Kilby, *J. Amer. Chem. Soc.*, **79**, 2972 (1957).

[8] A. Grimison and J. H. Ridd, *J. Chem. Soc.*, **1959**, 3019.

[9] H. P. Braendlin and E. T. Mc. Bee, "Friedel-Crafts and Related Reactions", vol. 3, Interscience Publishers New York, 1964, p. 1517, 1521.

[10] E. Schulek and K. Burger, *Acta Chim. Acad. Sci. Hung.*, **19**, 453 (1959).

[11] B. Jones and E. N. Richardson, *J. Chem. Soc.*, **1953**, 713.

[12] E. A. Shilov and F. W. Weinstein, *Nature*, **182**, 1300 (1958), *Doklady Akad. Nauk S.S.S.R.*, **123**, 93 (1958).

[13] L. J. Lambourne and P. W. Robertson, *J. Chem. Soc.*, **1947**, 1167.

[14] T. W. Bennett and A. G. Sharpe, *J. Chem. Soc.*, **1950**, 1383.

The action of iodine chloride on acridone in different media (acetic acid, nitrobenzene, dimethylsulfoxide, carbontetrachloride) led to multiple iodination and chlorination reactions having resulted in iodo- and iodo-chloro-acridone derivatives. See scheme 1 and tables 1, 2, 3.

SCHEME I

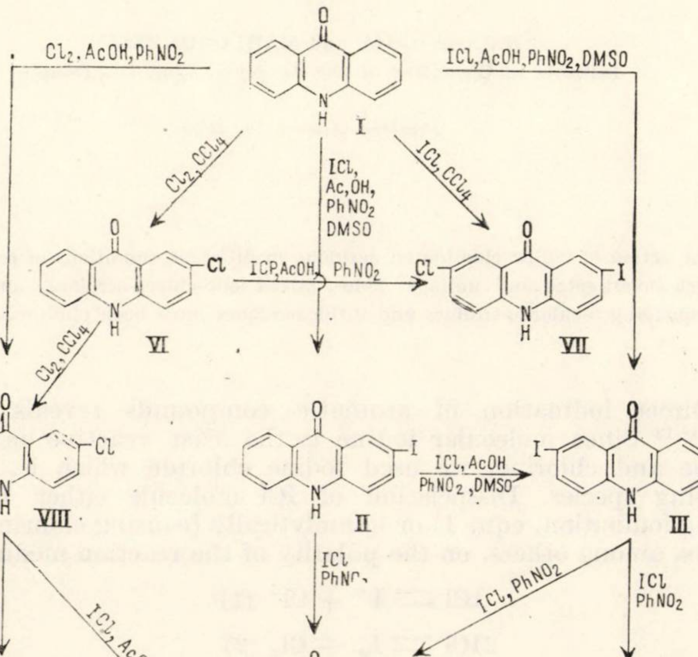
Cl₂, AcOH, PhNO₂
ICl, AcOH, PhNO₂, DMSO
I
Cl₂, CCl₄
ICl, Ac,OH, PhNO₂ DMSO
ICl, CCl₄
ICP, AcOH, PhNO₂
VI
VII
Cl₂, CCl₄
VIII
II
III
ICl, AcOH PhNO₂, DMSO
ICl AcOH PhNO₂
ICl₂, AcOH, PhNO₂
ICl PhNO₂
ICl, PhNO₂
ICl PhNO₂
IX
IV
V
X

Electrophilic substitution of acridone by ICl, takes place in the same positions of the molecule, as in the case of the direct bromination and chlorination.[15, 16] Thus, in polar solvents, iodination at C_2, $C_{2,7}$ takes place first forming mono-iodo-acridone (II) and diiodo-acridone (III), in different amounts depending on temperature, solvent, and reaction time. Iodinated derivatives, with more than two iodine atoms, even in prolonged reaction conditions and high temperature could not be isolated.

---

[15] M. Ionescu and I. Goia, *Rev. Chim. Acad. R.P.R.*, **5**, 85 (1960).

[16] R. M. Acheson and M. J. T. Robinson, *J. Chem. Soc.*, **1953**, 232.

Table 1

Iodination of acridone with ICl in glacial acetic acid

Compound	g	Solvent ml	Reagent ml	Temp.	Time h	Product	g
Acridone (I)	1.0	100	0.5	boiling	0.25	2-iodo-acridone (II) 2.7-diiodo-acridone (III)	0.47 0.35
Acridone (I)	1.0	100	0.5	boiling	1	2-iodo-acridone (II) 2.7-diiodo-acridone (III)	0.30 0.65
Acridone (I)	1.0	100	0.5	room temp.	1	2-iodo-acridone (II)	0.05
Acridone (I)	1.0	100	0.5	boiling	4	2-iodo-acridone (II) 2.7-diiodo-acridone (III)	0.30 1.00
Acridone (I)	1.0	100	0.25×2	boiling	4	2-iodo-acridone (II) 2.7-diiodo-acridone (III)	0.15 0.80
Acridone (I)	1.0	100	0.25×3	boiling	4	2-iodo-acridone (II) 2.7-diiodo-acridone (III)	0.05 1.50
Acridone (I)	1.0	100	1.0	boiling	2	2-iodo-acridone (II) 2.7-diiodo-acridone (III)	0.20 0.90
Acridone (I)	1.0	100	2.0	boiling	12	2.7-diiodo-acridone (III) 2.7-diiodo-4-chloro-acridone (IV) 2.7-diiodo-4.5-dichloro-acridone (V)	1.60 0.10 0.05
Acridone (I)	1.0	100	2.0	boiling	40	2.7-diiodo-acridone (III) 2.7-diiodo-4-chloro-acridone (IV) 2.7-diiodo-4.5-dichloro-acridone (V)	1.85 0.05 0.05
Acridone (I)	1.0	100	2.0	boiling	24	2.7-diiodo-acridone (III) 2.7-diiodo-4-chloro-acridone (IV)	1.70 trace
2-Iodo-acridone (II)	0.5	150	0.75	boiling	1	2.7-diiodo-acridone (III) 2.7-diiodo-4-chloro-acridone (IV)	0.35 0.05
2-Chloro-acridone (VI)	0.5	100	0.5	boiling	1.5	2-chloro-7-iodo-acridone (VII)	0.40
2.7-Dichloro-acridone (VIII)	0.5	150	0.5	boiling	1.5	2.4.7-trichloro-acridone (IX)	0.40
2.7-Diiodo-acridone (III)	0.5	60	0.5	boiling	5	2.7-diiodo-acridone (III) 2.7-diiodo-4-chloro-acridone (IV)	0.45 0.03
2.7-Diiodo-acridone (III)	0.5	150	0.5	boiling	2	2.7-diiodo-acridone (III) 2.7-diiodo-4-chloro-acridone (IV)	0.45 0.02
2.7-Diiodo-acridone (III)	0.5	100	0.5	boiling	6	2.7-diiodo-acridone (III) 2.7-diiodo-4-chloro-acridone (IV)	0.47 0.02
2,7-Diiodo-acridone (III)	0.5	150	1.0	boiling	40	2.7-diiodo-acridone (III) 2.7-diiodo-4-chloro-acridone (IV)	0.48 0.03

Table 2

Iodination of acridone with ICl in nitrobenzene

Compound	g	Solvent ml	Reagent ml	Temp.	Time h	Product	g
Acridone (I)	1.0	50	0.5	120	1	2-iodo-acridone (II) 2.7-diiodo-acridone (III)	0.50 0.55
Acridone (I)	1.0	50	0.5	120	4	2-iodo-acridone (II) 2.7-diiodo-acridone (III) 2.7-diiodo-4-chloro-acridone (IV)	0.60 0.70 0.07
Acridone (I)	1.0	50	2.5	75	12	2.7-diiodo-acridone (III) 2.7-diiodo-4-chloro-acridone (IV) 2.7-diiodo-4.5-dichloro-acridone (V)	0.90 0.20 0.20
2-Iodo-acridone (II)	0.5	50	0.5	120	1.5	2.7-diiodo-acridone (III) 2.7-diiodo-4-chloro-acridone (IV)	0.10 0.30
2.7-Diiodo-acridone (III)	0.5	50	0.5	120	1.5	2.7-diiodo-acridone (III) 2.7-diiodo-4-chloro-acridone (IV) 2.7-diiodo-4.5-dichloro-acridone (V)	0.10 0.25 trace
2.7-Diiodo-acridone (III)	0.5	50	0.5	120	2	2.7-diiodo-acridone (III) 2.7-diiodo-4-chloro-acridone (IV) 2.7-diiodo-4.5-dichloro-acridone (V)	0.10 0.40 0.05
2.7-Diiodo-acridone (III)	0.5	50	0.5	120	6	2.7-diiodo-4-chloro-acridone (IV) 2.7-diiodo-4.5-dichloro-acridone (V)	0.10 0.20
2.7-Diiodo-acridone (III)	0.3	30	0.35	75	5.5	2.7-diiodo-acridone (III) 2.7-diiodo-4-chloro-acridone (IV) 2.7-diiodo-4.5-dichloro-acridone (V)	0.06 0.10 0.10
2.7-Diiodo-acridone (III)	0.3	30	1.2	75	12	2.7-diiodo-4-chloro-acridone (IV) 2.7-diiodo-4.5-dichloro-acridone (V)	0.10 0.10
2.7-Diiodo-acridone (III)	0.5	50	2.0	75	12	2.7-diiodo-4-chloro-acridone (IV) 2.7-diiodo-4.5-dichloro-acridone (V)	0.10 0.15
2-Chloro-acridone (VI)	0.5	50	0.5	120	1.5	2-chloro-7-iodo-acridone (VII)	0.35
2.7-Dichloro-acridone (VIII)	0.5	50	0.5	120	1.5	2.4.7-trichloro-acridone (IX) 2.4.5.7-tetrachloro-acridone (X)	0.35 0.05

Table 3

Iodination of acridone with ICl in CCl_4 and DMSO

No	g	Solvent	ml	Re-agent ml	Temp.	Time h	Product	g
1	1	CCl_4	80	0.75	boiling	1.5	2-chloro-7-iodo-acridone (VII)	0.07
2	2	CCl_4	80	1.0	boiling	0.75	acridone (I)	1.90
							2-chloro-7-iodo-acridone (VII)	trace
3	1	DMSO	50	1.0	75	5	acridone (I)	0.95
4	1	DMSO	40	0.5	75	1	2-iodo-acridone (II)	0.35
					189	0.25	2.7-diiodo-acridone (III)	0.12

This led us to the presumption, without excluding other factors, that the difficulty of the introduction of large iodine atoms in positions 4 and 5 of the acridone molecule is the result of a steric hindrance. The data in table 4 show the difficulty to obtain, in this position, halogenated products with larger and larger halogen atoms.

Table 4

Halogenation in acetic acid

Compound	Re-agent	Time h	Product
2.7-dichloro-acridone	Cl_2	0.5	2.4.5.7-tetrachloroacridone
2.7-dibromo-acridone	Br_2	48	2.4.5.7-tetrabromoacridone
2.7-diiodo-acridone	ICl	64	2.7-diiodo-4-chloroacridone (trace)

Besides, when the reaction with ICl is performed on acridone whose positions 2 and 7 are occupied by iodine (experimental conditions similar to diiodo-derivative) the substitution in position 4 and 5 of the acridone molecule, is a chlorination and not an iodination and corresponding chlorinated derivatives are obtained — (IV), (V), and (X). If the substituent (chlorine or iodine) is to be found only in position 2 of the acridone molecule, then iodination occurs in position 7 with results of 2-chloro-7-iodo-acridone or 2,7-diiodo-acridone and afterwards in position 4 and 5 a chlorination process occurs.

In the reaction mixture, both chlorine as chlorinating agent and I^+ species as iodinating agent are perhaps present as a consequence of the two types of dissociation of iodine chloride (eqn. 1 and eqn. 2). This is why in the first stage of the reaction iodination of the acridone molecule occurs in positions 2 and 7 and when this is not possible any more because of the steric hindrance, iodination subsequently ceases and the chlorination takes place in position 4 and 5 and iodo-chloro-acridone derivatives are obtained.

The yields of iodo-acridone derivatives, in these reactions, depend on the solvent.

Protic or aprotic solvents can influence the iodination reaction through their dielectric constant and their capacity to solvate anions through hydrogen bonds.[17]

Though acetic acid has a small dielectric constant ($\varepsilon \sim 6$) it increases the iodination possibility of the ICl agent (eqn. 1) by its specific capacity to solvate anions through the hydrogen bonds, and in this way the yields of iodo-derivatives are similar to, or higher than, those in nitrobenzene.

In carbontetrachloride medium, we obtained only a small amount of monochloro-monoiodo-acridone, though in this medium the chlorination process is favoured.

In dimethylsulfoxide medium though with a high ε, the iodination of the acridone hardly takes place, and the yield in mono- and diiodo-acridone is very low. This is probably a consequence of the great capacity of the DMSO to solvate specifically the cations owing to its bipolar ion structure — in which the negative charge is concentrated on the oxygen atom (this being such an easy access to the cations) — while the positive charge being concentrated on the sulphur atom is sterically hindered by the methyl groups. The chlorination process, on the one hand, does not take place, probably because the homolytic dissociation through eqn. 2 is weak, and on the other hand, the chlorine resulted through oxidation by DMSO is present in an insufficient quantity to effect the chlorination of the acridone.

All these facts led to the conclusion that the action of ICl on the acridone molecule is a complex one; nevertheless we could establish the conditions (solvent, time, temperature) to obtain some halogenated-acridone derivatives.

We also mention that some iodo-acridone derivatives (2-iodo- (II), 2-iodo-7-chloro- (VII), and 2.7-diiodo-acridone (III)) were obtained by Singh[18] through ring closure of substituted diphenylamine carboxylic acids, but the melting points of compounds (III) and (VII) were given erroneously.

Iodo- and iodo-chloro-acridones like acridone itself are characterized by high melting points owing to the existence of the intermolecular associations. The only exceptions are the tetrahalogen-derivatives, with low melting points because they are not able to form the associations owing to the C_4, C_5 substituent steric effect over the hydrogen atom attached to nitrogen, which forms these molecular associations.

The solubility in organic solvents of the halogenated-acridone derivatives increases thus: di- < mono- < tri- < tetra-halogen derivatives and these compounds also have the fluorescence in the solution.

---

[17] B. Tchoubar, *Bull. Soc. chim. France*, **1964**, 2069; M. L. Schlafer and Schaffernicht, *Angew. Chem.*, **72**, 618 (1960); C. Agami, *Bull. Soc. chim. France*, **1965**, 1021; W. W. Epstein and F. W. Sweat, *Chem. Rev.*, **67**, 247 (1967).

[18] S. Singh and M. Singh, *J. Sci. Ind. Research*, **10B**, 298 (1951); **11B**, 102 (1952); *Chem. Abstr.*, **48**, 8786 (1954).

Halogen-substituted acridones (iodo-, iodo-chloro) being treated with $POCl_3$ give corresponding 9-chloro-acridine derivatives,which are useful for the characterization of acridones and in the synthesis of halogenated thioacridones. 9-Chloro-acridines are more soluble, have lower melting points and thus they can be used for molecular weight determinations. See table 5.

Table 5

9-Chloro-halogenated-acridines

Compound	Recrystallized from	Molecular weight		Analysis	
		Calcd.	Found	Calcd.	Found
2.9-Dichloro-acridine	aq. ethanol	$C_{13}H_7Cl_2N$ 248.10	—	C 62.92 H 2.84 Cl 28.58	C 63.09 H 2.86 Cl 28.20
2.7.9-Trichloro-acridine	benzene-ethanol	$C_{13}H_6Cl_3N$ 282.20	—	C 55.25 H 2.14 Cl 37.63	C 55.07 H 2.25 Cl 37.75
2.4.7.9.-Tetrachloro-acridine	aq. dioxane	$C_{13}H_5Cl_4N$ 316.97	321.6	C 49.26 H 1.59 Cl 44.74	C 49.21 H 1.87 Cl 45.00
2.4.5.7.9-Pentachloro-acridine	benzene-ethanol	$C_{13}H_4Cl_5N$ 366.45	370.5	C 44.42 H 1.15 Cl 50.49	C 44.80 H 1.50 Cl 50.41
2-Iodo-9-chloro-acridine	aq. dioxane	$C_{13}H_7ClIN$ 339.55	—	C 45.97 H 2.07	C 45.80 H 2.15
2.7-Diiodo-9-chloro-acridine	aq. dioxane	$C_{13}H_6ClI_2N$ 465.42	—	C 33.54 H 0.91	C 33.20 H 1.37
7-Iodo-2.9-dichloro-acridine	aq. dioxane	$C_{13}H_6Cl_2IN$ 373.97	—	C 41.75 H 1.61	C 41.50 H 2.17
2.7-Diiodo-4.9-dichloro-acridine	aq. dioxane	$C_{13}H_5Cl_2I_2N$ 499.87	495.5	C 31.23 H 1.00	C 31.09 H 1.04
2.7-Diiodo-4.5.9-trichloro-acridine	aq. dioxane	$C_{13}H_4Cl_3I_2N$ 534.31	528.0	C 29.22 H 0.75	C 29.54 H 0.90
2-Iodo-4.5.7.9-tetrachloro-acridine	aq. dioxane	$C_{13}H_4Cl_4IN$ 442.86	436.0	C 32.43 H 1.25	C 32.70 H 1.20

Halogenated-9-thioacridones cannot be obtained by direct halogenation of the thioacridone since the substitution of the sulphur by halogen occurs first.[19] Therefore they are prepared from the preceding 9-chloro-acridines by sodium sulphide treatment. Their physical and chemical behaviour differs from that of the corresponding acridones but the effect of halogen atoms on thioacridone molecule is the same. See table 6.

---

[19] M. Ionescu, H. Mantsch and I. Goia, *Studii și Cercetări Chim. Fil. Cluj*, **12**, 135 (1961).

Table 6

9-Thio-halogenated-acridones

Compound	M.p. C°	Colour	Molecular weight	Analysis	
				Calcd.	Found
2-Chloro-9-thio-acridone	273	red	$C_{13}H_8ClNS$ 245.60	C 63.57 H 3.28 N 5.70	C 63.32 H 3.46 N 5.86
2.7-Dichloro-9-thio-acridone	314	red	$C_{13}H_7Cl_2NS$ 280.00	C 55.59 H 2.51 N 4.99	C 55.75 H 2.60 N 5.05
2.4.7-Trichloro-9-thio-acridone	325	red	$C_{13}H_6Cl_3NS$ 314.52	C 49.64 H 1.92 N 4.45	C 49.35 H 1.87 N 4.30
2.4.5.7-Tetrachloro-9-thio-acridone	235	brown	$C_{13}H_5Cl_4NS$ 348.90	C 44.74 H 1.34 N 4.82	C 44.60 H 1.50 N 4.30
2-Iodo-9-thio-acridone	262	red	$C_{13}H_8INS$ 337.09	C 46.32 H 2.39 N 4.15	C 46.50 H 2.30 N 4.35
2.7-Diiodo-9-thio-acridone	291	red	$C_{13}H_7I_2NS$ 462.98	C 33.72 H 1.52 N 3.02	C 33.95 H 1.97 N 3.00
2-Chloro-7-iodo-9-thio-acridone	309	red	$C_{13}H_7ClINS$ 371.53	C 42.02 H 1.90 N 3.76	C 41.90 H 1.63 N 3.90
2.7-Diiodo-4-chloro-9-thio-acridone	264	red	$C_{13}H_6ClI_2NS$ 497.42	C 31.39 H 1.21	C 31.18 H 1.65
2.7-Diiodo-4.5-dichloro-9-thio-acridone	308	red	$C_{13}H_5Cl_2I_2NS$ 531.87	C 29.35 H 0.94	C 29.50 H 1.00
2-Iodo-4.5.7-trichloro-9-thio-acridone	271	red	$C_{13}H_5Cl_3INS$ 439.41	C 35.53 H 0.91	C 35.70 H 0.80

EXPERIMENTAL

The melting points are uncorrected. In all iodination reactions we used glacial acetic acid and fresh distilled iodine chloride.[20]

The microanalytical determinations were carried out in the microanalytical laboratory of the Institute.

2-Iodo-acridone (II)

1. Into a boiling solution of 1 g pure acridone and 100 ml acetic acid, fresh distilled 0.5 ml ICl is added and for 15 minutes boiling is continued. The hot solution is filtered.

a. The precipitate is washed with some acetic acid and then with dilute sodium thiosulphate, water, and dried. The soluble compounds are extracted with acetic acid and the insoluble 2,7-diiodo-acridone, m. p. 437°, (0.35 g), is obtained.

---

[20] A. I. VOGEL, "Practical Organic Chemistry", 3rd ed., Longmans, 1956, p. 974.

b. From the cold mother liquor 2-iodo-acridone is deposited. This is washed with some acetic acid, then with dilute sodium thiosulphate solution, water, and is recrystallized from acetic acid. Yellow needles, (0.47 g), m. p. 365°. *Found*: C, 48.48; H, 2.86; *Calcd.*: for $C_{13}H_8INO$ (321.09); C, 48.61; H, 2.51.

2. Into a solution of 1 g pure acridone in 50 ml nitrobenzene at 120° under mechanical stirring 0.5 ml ICl are added. The heating and stirring are maintained for 1 hour. After cooling the precipitate is filtered, washed with some alcohol, dilute sodium thiosulphate solution, water and after drying it is extracted with 2×100 ml hot acetic acid. The part of undissolved substance was 2,7-diiodo-acridone, m. p. 437°, (0.5 g). The cold extract (200 ml) deposited 2-iodo-acridone, recrystallized from acetic acid, m. p. 365°, (0.28 g). After steam-distillation of nitrobenzene still 0.25 g of 2-iodo-acridone is isolated.

2.7-Diiodo-acridone (*III*)

1. Into a boiling solution of 1 g pure acridone in 100 ml acetic acid 0.5 ml (2×0.25 ml) ICl is added and the mixture is refluxed for 4 hours. The reaction mixture, still hot, is filtered.

a. The undissolved substance is dried after washing with dilute sodium thiosulphate solution, water. This is extracted with 2×150 ml hot acetic acid. The part of undissolved substance is 2,7-diiodo-acridone, m. p. 438°, (1 g). *Found*: C, 35.33; H, 1.67; *Calcd.*: for $C_{13}H_7I_2NO$ (446.85); C, 34.94; H, 1.57.

b. From the mother liquor and extracts, after cooling, 2-iodo-acridone is deposited. This is washed with dilute thiosulphate solution, water, and is recrystallized from acetic acid, m. p. 365°, (0.3 g).

2. Into a solution of 1 g pure acridone in 50 ml nitrobenzene at 120° under mechanical stirring, 0.5 ml ICl is added. The heating and stirring are maintained for 1 hour. After cooling the deposited yellow substance is washed with some alcohol. Then, with 2×100 ml hot acetic acid, 2-iodo-acridone is extracted, and the part of undissolved substance is 2,7-diiodo-acridone, m. p. 437°, (0.5 g). 2,7-Diiodo-acridone is hardly soluble in organic solvent, but can be recrystallized from alkaline alcohol.

2-Chloro-7-iodo-acridone (*VII*)

Into a boiling solution of 0.5 g 2-chloro-acridone in 100 ml acetic acid, 0.5 ml ICl is added and the boiling is maintained for 1 : 30 h. After cooling, the precipitate is filtered, washed with acetic acid, dilute sodium thiosulphate and water. The part of substance more soluble is extracted with 75 ml acetic acid, and the part of substance left is 2-chloro-7-iodo-acridone which is twice recrystallized from acetic acid, m. p. 405°, (0.35 g). *Found*: C, 44.10; H, 1.84; *Calcd.*: for $C_{13}H_7ClINO$ (355.53), C, 43.80; H, 1.98.

2.7-Diiodo-4-chloro-acridone (*IV*)

Into a suspension of 0.5 g 2.7-diiodo-acridone in 50 ml nitrobenzene heated at 120° under mechanical stirring 0.5 ml ICl is added. The heating and stirring are maintained for 2 hours. After cooling 800 ml light petroleum (b. p. 70—90°) is added, and the yellow precipitate is filtered and washed with light petroleum. The dried precipitate is tritured with dilute sodium thiosulphate solution, filtered and washed with water, then solved in 250 ml hot acetic acid; 100 ml water are added, and after cooling 2,7-diiodo-4-chloro-acridone deposits, which is recrystallized from acetic acid. Yellow needles, m. p. 367°, (0.4 g). *Found*: C, 32.95; H, 1.55. *Calcd.*: for $C_{13}H_6ClI_2NO$ (481.42), C, 32.43; H, 1.25.

2.4.7-Trichloro-acridone (IX)

1. Into a boiling suspension of 0.5 g 2,7-dichloro-acridone in 150 ml acetic acid 0.5 ml ICl is added and the mixture is refluxed for 1 : 30 h. After cooling the precipitate is filtered, washed with dilute sodium thiosulphate solution and water. It is several times recrystallized from acetic acid. Yellow needles, m. p. 410°, (0.35 g). *Found*: C, 51.93; H, 2.37; *Calcd.* for $C_{13}H_6Cl_3NO$ (298.52); C, 52.29; H, 2.02.

2. Into a suspension of 0.5 g 2,7-dichloro-acridone in 50 ml nitrobenzene at 120° under mechanical stirring, 0.5 ml ICl is added and the heating and stirring are maintained for 1 : 30 h. After cooling the precipitate is filtered, washed with alcohol and several times recrystallized from acetic acid, m. p. 412°, (0.35 g).

2.7-Diiodo-4.5-dichloro-acridone (V)

0.5 ml ICl is added into a suspension of 0.5 g 2.7-diiodo-acridone in 50 ml nitrobenzene at 120° under mechanical stirring. The heating and stirring are maintained for 6 hours. After cooling 500 ml light petroleum (b. p. 70—90°) is added and the precipitate is filtered and washed with some alcohol. From yellow substance with m.p. 315—320° after several extractions with acetic acid, 0.10 g of 2.7-diiodo-4.5-dichloro-acridone m. p. 292° is isolated. *Found*: C, 30.80; H, 1.40; *Calcd.*: for $C_{13}H_5Cl_2I_2NO$ (515.87); C, 30.27; H, 0.97.

9-Chloro-halogenated-acridine

General method

0.1 g halogenated acridone with 6 ml fresh distilled $POCl_3$ is kept on boiling for 2 hours. The reaction mixture after cooling is poured into a mixture of ice and ammonia (75 g, 25 ml) under strong stirring. The yellow precipitate is filtered, washed with water and recrystallized.

9-Thio-halogenated-acridone

General method

0.1 g of 9-chloro-halogenated-acridine in 15 ml ethanol with an excess of sodium sulphide is kept on boiling for 1—2 hours. The hot solution is filtered, after cooling is acidulated with dilute HCl and the red precipitate is recrystallized from aqueous-pyridine.

Revue Roumaine de Chimie, **15**, 1243 – 1250 (1970)

CHEMICAL GRAPHS. X.[1] (AROMATICITY. VIII*) RESONANCE ENERGIES OF *CATA*-CONDENSED BENZENOID POLYCYCLIC HYDROCARBONS

A. T. BALABAN

Institute of Atomic Physics, P.O.B. 35, Bucharest

Received March 16, 1969

The resonance energies of *cata*-condensed benzenoid polycyclic hydrocarbons depend in the first approximation only on the topology of the molecule. Procedures are proposed for calculating resonance energies after Sahini (formula 1), or Dewar resonance energies after Baird (formula 3), without having recourse to limiting structures but making use instead of the (much simpler) associated characteristic graph of the molecule.

In earlier papers,[2,3] benzenoid polycyclic hydrocarbons (named polyhexes henceforth for abbreviation) were classified by means of the associated characteristic graph formed by joining the centers of adjacent condensed hexagons **: when this graph is a tree (for graph-theoretical definitions cf. ref. 4) the polyhex is *cata*-condensed and is termed catafusene; when this graph is not a tree (i.e. when it contains rings) the polyhex is *peri*-condensed and is named perifusene.

Non-branched [2] and branched [3,5] catafusenes were enumerated and a shorthand notation based on digits 0, 1, and 2 was proposed for discriminating among possible isomeric polyhexes. These earlier papers only considered the general topology of the molecule, disregarding the arrangement of double bonds and other electron-dependent features.

The present paper extends this graph-theoretical treatment to calculating properties of these molecules which depend on their molecular orbitals, such as resonance energy or polarographic half-wave reduction potential. Further properties of this type are the electron affinity, ionization potential, energies of electronic transitions[6]. In the class of catafusenes these properties can be satisfactorily correlated with the topology of the molecule.

---

* Preceding part in the Aromaticity series is the paper by A. T. Balaban *Rev. Roumaine Chim.*, **14**, 1201 (1969) which was mistakenly listed as part VI in this series, Part VI is the paper by A. T. Balaban and F. Harary, *ibid.*, **12**, 1511 (1967).

** This is the dual graph from which the point corresponding to the external region and all adges incident with it have been omitted. Unlike usual graphs or trees. in the associated characteristic graph, angles between lines (120° or 180°) are importat.

[1] Part IX, A. T. Balaban, D. Farcasiu and F. Harary, *J. Labelled Comp.*, (in press).

[2] A. T. Balaban and F. Harary, *Tetrahedron*, **24**, 2505 (1968).

[3] A. T. Balaban, *Tetrahedron*, **25**, 2949 (1969).

[4] F. Harary, "Graph Theory", Addison-Wesley Publ. Comp., Reading, Mass., 1969

[5] F. Harary and R. C. Read, *Commun. Assoc. Computing Machinery* (in press).

As shown by Sahini,[7-9] a good agreement with resonance energies calculated for catafusenes by the simple Hückel molecular orbital method,[10,11] by the valence bond method,[12] or by Daudel's method [13-15] can be achieved by means of a simple formula (1) giving the resonance energy R (in beta-units),[7] as a function of the number n of rings in the catafusene and the number a of "imperfectly aromatic rings", i.e. the number of hexagons which accomodate less than three double bonds in the limiting structure with the maximum number of "perfectly aromatic rings" (i.e. rings which accomodate three double bonds). As customary, double bonds common to two condensed rings are counted twice.

It is readily apparent that the number of "imperfectly aromatic rings", a, equals the number of zero digits in the proposed shorthand notation of the catafusene [2,3] (cf. tables 1 and 2). Hence the tedious procedure of writing limiting structures [16] (especially for higher numbers n of rings in the polyhex) can be dispensed with in calculating resonance energies R. An analogous formula (2) was proposed [9] for the polarographic half-wave reduction potential E (in volts versus the saturated calomel electrode) of catafusenes, the constant b depending on the mode of annelation, i.e. on the topology of the molecule.

$$R = 1.75\,n - 0.15\,a + 0.25 \tag{1}$$

$$E = -\,0.403\,n + 0.034\,a + b \tag{2}$$

$$R' = 21.0\,n_3 + 12.5\,n_2 + 8.0\,n_1\,(+\,0.0\,n_0) \tag{3}$$

Recently, Baird [17] showed that resonance energies R' of catafusenes * (in kcal/mole), agreeing well with resonance energies obtained by

---

[6] E. Clar, "Polycyclic Hydrocarbons". Academic Press – Springer Verlag, London, 1964.

[7] V. E. Sahini, *J. chim. phys.*, **59**, 177 (1962).

[8] V. E. Sahini, *Rev. Chim. Acad. R. P. Roumaine*, **7**, 1265 (1962).

[9] V. E. Sahini, *Rev. Chim. (Bucuresti)*, **15**, 551 (1964).

[10] E. Heilbronner and P. A. Straub, „Hückel Molecular Orbitals", Springer Verlag, Heidelberg, 1966 ; E. Heilbronner and H. Bock, "The HMO (Hückel Molecular Orbital) Model and Its Application . Vol. 1. Principles and Operation", Verlag Chemie, Weinheim, 1968.

[11] A. Streitwieser, "Molecular Orbital Theory for Organic Chemists", Wiley, New York, 1961.

[12] G. W. Wheland, "Resonance in Organic Chemistry", Wiley, New York, 1955.

[13] R. Daudel, "Structure électronique des molécules", Gauthier-Villars, Paris, 1962 ; *Adv. Quantum Chem.* **1**, 115 (1964).

[14] R. Daudel and A. Pullman, *J. Phys. radium*, **7**, 74 (1946) ; O. Chalvet, *Rec. trav. chim.* **75**, 385 (1956).

[15] R. Daudel, R. Lefèvre and C. Moser, "Quantum Chemistry", Interscience Publ., New York, 1959.

[16] M. Gordon and W. H. T. Davison, *J. Chem. Phys.*, **20**, 428 (1952) ; H. Sofer, G. Derflinger and O. E. Polansky, *Monatsh. Chem.* **99**, 1895 (1968), and previous papers in the series.

[17] N. C. Baird, *Canad. J. Chem.* **47**, 3535 (1969).

* Baird's procedure applies equally well to *peri*-condensed systems.

Table 1

Resonance energies of all possible catafusenes with n = 2,3,4, or 5 benzenoid rings

n	Graphs and indices [a]	Notation	$\underline{a}$	R (beta units)		R' (k cal/mole)	
				Formula (1)	Daudel	Formula (3)	Dewar-Baird
2	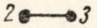	•	0	3.75	3.52	33.5	34.2
3	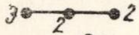	0	1	5.35	5.24	46.0	43.9
	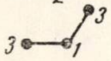	1	0	5.50	5.33	50.0	49.6
4	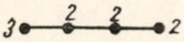	00	2	6.95	6.94	58.5	60.5
	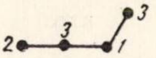	01	1	7.10	7.05	62.5	61.2
	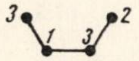	11	0	7.25	7.14	62.5	58.6
	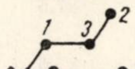	12	0	7.25	—	62.5	65.3
	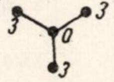	1(.)	0	7.25	7.21	63.0	66.7
5	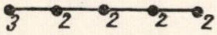	000	3	8.55	8.65	71.0	—
	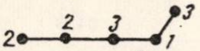	001	2	8.70[b]	8.78	75.0	—
	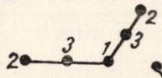	010	2	8.70	—	75.0	—
	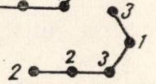	011	1	8.85	—	75.0	—
	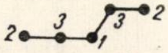	012	1	8.85	—	75.0	—
	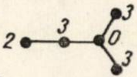	01(.)	1	8.85	—	75.5	—
	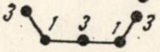	101	1	8.85	8.85	79.0	—
	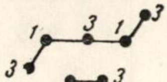	102	1	8.85	—	79.0	—
	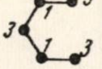	111	0	9.00	—	79.0	—
	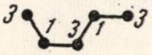	112	0	9.00	—	79.0	—
	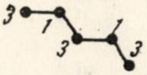	121	0	9.00	—	79.0	—
	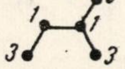	11(.)	0	9.00	—	79.0	—

---

[a] Only one assignment of indices to points is shown, from the several possible ones, all having the minimum allowed number of indices 2.

[b] Corrected value (of. ref. 7).

Table 2

Resonance energies of all possible hexacatafusenes ($n=6$)

Graphs and indices	Notation	a	R (formula 1) beta units	R' (formula 2) $\frac{\text{kcal}}{\text{mole}}$
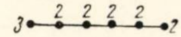	0000	4	10.15	83.5
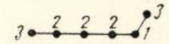	0001	3	10.30	87.5
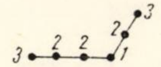	0010	3	10.30	87.5
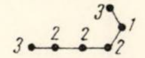	0011	2	10.45	87.5
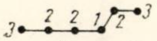	0012	2	10.45	87.5
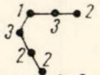	0110	2	10.45	87.5
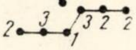	0120	2	10.45	87.5
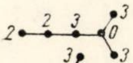	001(.)	2	10.45	88.0
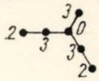	01(.)0	2	10.45	88.0
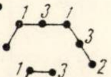	0101	2	10.45	91.5
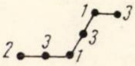	0102	2	10.45	91.5
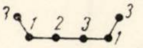	1001	2	10.45	91.5
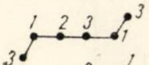	1002	2	10.45	91.5
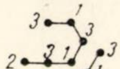	0111	1	10.60	91.5
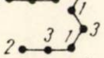	0112	1	10.60	91.5
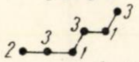	0121	1	10.60	91.5
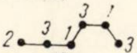	0122	1	10.60	91.5
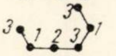	1011	1	10.60	91.5
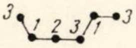	1012	1	10.60	91.5
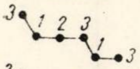	1021	1	10.60	91.5
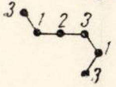	1022	1	10.60	91.5

Table 2 (continued)

Graphs and indices	Notation	a	R (formula 1) beta units	R' (formula 2) $\frac{\text{kcal}}{\text{mole}}$
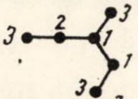	01(.)1	1	10.60	91.5
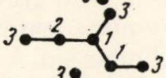	01(.)2	1	10.60	91.5
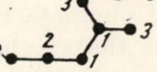	011(.)	1	10.60	91.5
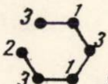	1111	0	10.75	91.5
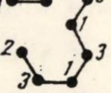	1112	0	10.75	91.5
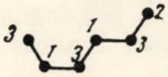	1121	0	10.75	91.5
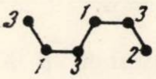	1122	0	10.75	91.5
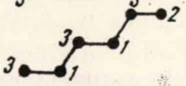	1212	0	10.75	91.5
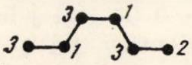	1221	0	10.75	91.5
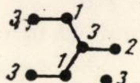	11(.)1	0	10.75	91.5
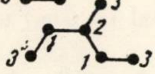	11(.)2	0	10.75	91.5
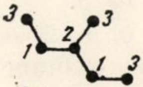	12(.)1	0	10.75	91.5
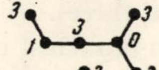	101(.)[a]	1	10.60	92.0
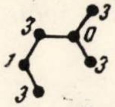	111(.)	0	10.75	92.0
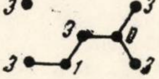	1(.)12	0	10.75	92.0
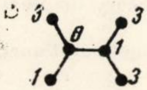	1(.)1(.)	0	10.75	92.0

---

[a] See discussion in text.

Dewar's procedure,[18-20] can be calculated additively. Baird's procedure can be represented by formula (3), where n_i (i = 0, 1, 2, or 3) is the number of condensed benzenoid rings accomodating *i* double bonds in the optimal limiting structure which gives the maximum value for R′. Of course, $\sum_{i=0}^{3} n_i = n$. The constants in formula (3) correspond to resonance energies of i double bonds in polyenes, therefore a comparison with Hückel resonance energies is not expected to be exact. A double bond is counted, however, only once even when it is common to two condensed rings. Translated into conditions imposed on the associated characteristic graph of the polyhex, this involves assigning each point of the graph an index from the set i = 0, 1, 2, or 3 (corresponding to the number of double bonds assigned to the respective hexagon in the optimal limiting structure) according to the following rules.

1. Given a catafusene with *n* hexagons, i.e. a tree with *n* points, the number of double bonds, i.e. the sum of all its indices, is $\sum_{i=0}^{3} i n_i = 2n+1$.

2. Each point of the associated characteristic graph is assigned an index from the set i = 0, 1, 2, or 3 according to items 1 above and 3–10 below. One obtains thus n_i points of index i, $\sum_{i=0}^{4} n_i = n$.

3. There exist several possible partitions [21,22] of the number 2n + 1 as a sum of *n* terms which may only have the values 0, 1, 2, or 3 (cf. table 1) to be used as indices. These partitions can all be deduced from the identity $2n + 1 \equiv 1 \cdot 3 + (n - 1) \cdot 2$: through k replacements of 2 + 2 by 3 + 1 and/or j replacements of 2 + 1 by 3 + 0 (k and j bein arbitrary non-negative integers) one obtains the identity $2n + 1 \equiv$ $\equiv (k + j + 1) \cdot 3 + (n - 2k - j - 1) \cdot 2 + (k - j) \cdot 1 + j . 0$ where all coefficients n_i of 3, 2, 1, and 0 must be non-negative integers. This identity satisfies the two sum rules 1 and 2 above.

4. An endpoint (with local degree, or valence, equal to one) of the graph has an index 2 or 3.

5. A point with local degree two has an index 1, 2, or 3.

6. A point with local degree three has an index 0, 1, 2, or 3, therefore partitions involving zero terms can only apply to branched catafusenes (branching points have local degrees equal to three).

7. The sum of two indices of adjacent points in non-branched catafusenes is 4 or 5, therefore no adjacent pair of points can have indices 3 for both points.

---

[18] M. J. S. Dewar and G. J. Gleicher, *J. Amer. Chem. Soc.* **87**, 692 (1965).

[19] M. J. S. Dewar and C. De Llano, *J. Amer. Chem. Soc.* **91**, 789 (1969).

[20] M.J.S.Dewar, "The Molecular Orbital Theory of Organic Chemistry", ch.5, McGraw-Hill Book Comp., New York, 1969.

[21] G. H. Hardy and E. M. Wright, "An Introduction to the Theory of Numbers", 3rd Ed., Oxford Univ. Press, chapter 19, 1954.

[22] M. A. Abramowitz and I. A. Stegun, "Handbook of Mathematical Functions", Natl. Bureau of Standards, Washington, D. C., 1964.

8. When there is a non-branched subgraph with three collinear points, the middle point cannot have index 1, but only 2 or 3.

9. The number of indices 2 must be minimized when the preceding rules allow alternative solutions.

10. As a thumb rule for assigning indices to points of associated characteristic graphs, for non-branched free-end subgraphs consisting of m collinear points one has to assign m − 2 indices 2. When such subgraphs continue at both ends, one has to assign m − 3 indices 2.

11. The resonance energy R′ is calculated after formula (3).

Examples for the application of all these rules can be found in tables 1 and 2.

From the parameters in Baird's procedure which amount to a resonance energy per double bond of 7, 6.25, and 8 kcal/mole for cycles with 3, 2, and 1 double bonds, respectively, and from the request that R′ be maximal, condition 9 is derived. Practically, replacement of an adjacent pair of indices $1+2$ by $0+3$, increasing the total resonance energy by 0.5 kcal/mole, is not significant; however, replacement of a pair of indices $2+2$ by $1+3$ does increase markedly the total resonance energy (by 4 kcal/mole).

Thus the calculation of resonance energies R′ too is simplified by the use of the associated characteristic graph, without having recourse to writing limiting structures.

As seen from table 1 in the case of catafusenes with $n = 2$ to 5, and from table 2 for $n = 6$ hexagons, though there is a good correlation between the results of the two procedures for calculating resonance energies R and R′, there exist some differences. Whereas the first approach simply relates the resonance energy to the number of linearly annelated subsystems (e.g. the number of distinct subgraphs with three collinear points), the second approach is more subtle: collinear subgraphs of 3 or more points decrease the resonance energy only if they occur at a free end of the graph. An illustration is provided by the compounds with note[a] in table 2, where the former, but not the latter, procedure assigns a lower resonance energy if a collinear subgraph of three points is present.

Assuming that two from the four coefficients n_3, n_2, n_1 and n_0 are zero, one obtains from rules 1—3 : $n_3 = (2n - in + 1)/(3 - i)$, $n_i = (n - 1)/(3 - i)$ which gives the following three particular cases when i equals 0, 1, and 2, respectively:

n-Acenes with notation $\{0\}_{n-1}$ have $a = n - 2$, $n_1 = n_0 = 0$, $n_3 = 1$, $n_2 = n - 1$;

$$R = 1.60\,n + 0.55 \text{ beta-units}$$

$$R' = 12.5\,n - 4.5 \text{ kcal/mole}$$

Highly branched n-catafusenes with notation $1(\cdot)\{12(\cdot)\}_{(n-7)/3}11(\cdot)$ (e.g. triphenylene)have $a = 0$, $n_2 = n_1 = 0$, $n_3 = (2n+1)/3$, $n_0 = (n - 1)/3$;

$$R = 1.75\,n + 0.25 \text{ beta-units}$$

$$R' = 14n + 7 \text{ kcal/mole}$$

Non-branched zigzag n-catafusenes with notation $1\,\{21\}_{(n-3)/2}$ (e.g. phenanthrene, picene) have $a = 0$, $n_2 = n_0 = 0$, $n_3 = (n + 1)/2$, $n_1 = (n - 1)/2$;

$$\mathrm{R} = 1.75\,\mathrm{n} + 0.25 \text{ beta-units}$$

$$\mathrm{R}' = 14.5\,\mathrm{n} + 6.5 \text{ kcal/mole}$$

In all these cases the correlation between R and R′ holds fairly well with $\beta = 8.2$ kcal/mole.

The above treatment of polyhexes is generalized in the following paper to *cata*-condensed systems with various ring sizes, including non-alternant compounds.

Revue Roumaine de Chimie, **15**, 1251–1262 (1970)

CHEMICAL GRAPHS. XI. (AROMATICITY. IX)[1] ISOMERISM AND TOPOLOGY OF NON-BRANCHED *CATA*-CONDENSED POLYCYCLIC CONJUGATED NON-BENZENOID HYDROCARBONS

A. T. BALABAN
Institute of Atomic Physics, P.O.B. 35, Bucharest, Romania

Received March 16, 1970

Formulas are devised for calculating the numbers of isomers for conjugated non-branched *cata*-condensed polycyclic hydrocarbons formed from rings of any size. The topology of the system introduces additional criteria for aromaticity, along with the Hückel rule.

INTRODUCTION

Previous papers in the series on chemical graphs enumerated all possible isomers of non-branched [2] or branched [3,4] *cata*-condensed * benzenoid polycyclic aromatic systems (for short, polyhexes, which consist of *cata*-condensed six-membered aromatic rings). It was shown [1] that resonance energies and other properties such as polarographic reduction potentials depend mainly on the topology of these systems, and that graph-theoretical algorithms can be devised for approximating these properties without having recourse to elaborate calculations.

The present paper generalizes this treatment to conjugated non-benzenoid *cata*-condensed systems consisting of any kind of condensed rings (alternant systems, possessing only even-membered rings, or non-alternant systems which include also odd-membered rings [5]).

We shall designate by "class" all polycyclic compounds which possess a given set of unordered ring sizes; a "subclass" contains polycyclic compounds possessing a given set of ring sizes in a specified order; every polycyclic system within a subclass is an individual compound distinguished by the mode of linking of the condensed rings. Both the arrangement of ring sizes, and the mode of linking, determine the symmetry of the system. The number of subclasses belonging to the same class of non-branched systems equals the number of distinct arrangements of ring sizes.

---

* Two condensed rings possess in common two adjacent atoms. Definitions of *cata*- and *peri*-condensation are given in reference 2.

[1] Previous parts in both series, A. T. Balaban, preceding paper.

[2] A. T. Balaban and F. Harary, *Tetrahedron*, **24**, 2505 (1968).

[3] A. T. Balaban, *Tetrahedron*, **25**, 2949 (1969).

[4] F. Harary and R. Read, *Commun. Assoc. Computing Machinery* (in press).

[5] C. A. Coulson and G. S. Rushbrooke, *Proc. Cambridge Phil. Soc.*, **36**, 193 (1940); H. C. Longuet-Higgins, *J. Chem. Phys.*, **18**, 275 (1950).

Only *cata*-condensed systems are considered since only in this case is it possible to extend the validity of the Hückel $4r + 2$ π-electron rule to polycyclics;* this rule is strictly valid only for monocyclic compounds, but *cata*-condensed systems are essentially * bridged annulenes, where the bridges have a pronounced single-bond character. Also, only for *cata*-condensed compounds belonging to a given class (i.e. consisting of a given set of n ring sizes z_i) are all possible systems formed from these rings isomeric, irrespective of the order of z_i values and irrespective whether the system is branched or non-branched. In the present paper we shall restrict the discussion to non-branched systems, which represent a string of condensed rings, and in which any given ring is condensed with at most two other rings.

NOTATIONS

Let n be the total number of condensed rings in the system. Ring sizes will be denoted by z (general notation, irrespective of the parity of z), x (for even-membered rings) or y (for odd-membered rings). A class of isomeric systems is thus defined by the unordered set $z_1, z_2, \ldots, z_n$. A subclass of unsymmetrical non-branched *cata*-condensed systems can therefore be noted by the ordered sequence $z_1z_2z_3 \ldots z_{n-1}z_n$ (I). The subclass of symmetrical systems (relatively to the arrangement of ring sizes) containing an even number ($n = 2\,m$) of rings will be denoted $z_1z_2 \ldots z_{m-1}z_mz_mz_{m-1} \ldots z_2z_1$ (II), whereas for odd n ($n = 2m + 1$) the notation will be $z_1z_2 \ldots z_{m-1}z_mz_0\,z_mz_{m-1} \ldots z_2z_1$ (III).

A subclass such as (I) with a given set and order of z_i values contains several isomeric systems. It is the purpose of this paper to calculate the number of these possible isomers, assuming that the molecules are planar (enantiomers of helicene-like structures are disregarded in this treatment).

It is assumed that n, m, r, x, y, and z are positive integers. Ring sizes z will be generally taken to be greater than 3 : little is known on the chemistry of compounds with condensed cyclopropene rings; they are possible only as uninteresting marginal rings on the non-branched string of condensed rings; the considerable steric strain and Bredt's rule tend to make such compounds rather unstable.

The following notations will be employed:

n = number of condensed rings (parity expressed by $2m$ or $2m + 1$)
z = ring size (parity expressed by x when z is even, or y when it is odd)

---

* Limitations of the Hückel rule "monocyclic aromatics have 2 (mod 4) π-electrons" are discussed in the last section of this paper.

p = number of ring (carbon) atoms (expressed as $4r + 2$ in systems obeying the Hückel rule)

u = number of asymmetric isomers of a given subclass (point group C_1), either with an asymmetrical arrangement of z values (e.g.I), or with a symmetrical arrangement (II or III) but with an asymmetrical mode of linking, e.g. IV.

c = number of centre-symmetric isomers (point group C_{2h}) with a symmetry axis C_2 perpendicular to the plane of the molecule, e.g.V.*

s = number of plane-symmetric isomers (point group C_{2v}) with a symmetry axis C_2 in the plane of the molecule, e.g.VI.*

a = number of linearly-condensed isomers (point group D_{2h}, combining the symmetry elements of the above two types), e.g. VII*.

K = total number of isomers of a subclass (consisting in a given set of n condensed rings ordered in a specified manner).

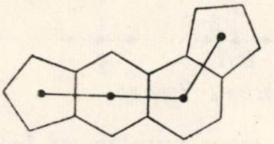

56^06^15
(56^06^25, 56^16^05, 56^26^05)
IV

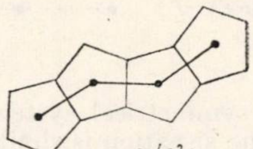

55^15^25
(55^25^15)
V

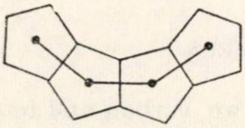

55^15^15
(55^25^25)
VI

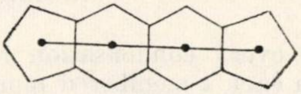

56^06^05
VII

The symmetry in the mode of linking of condensed rings in the system is expressed by conditions imposed to its adjacency matrix. If the central link in a symmetric system (II) with an odd number of bridging links obeying the Hückel rule, hence containing $p = 4r + 2$ atoms, is placed between atoms numbered 1 and $2r + 2$ (numbering in agreement with the IUPAC nomenclature rules), then any further link between two atoms numbered f and g leads, by the symmetry of the particular mode of linking, to another link between atoms f' and g' where the numbers f' and g' are given by the following relationships.

---

* A symmetrical arrangement of z values (II or III) is a prerequisite for types c, s, or a of isomers, which are distinguished by the symmetry of their mode of linking.

$$f' = 2r + f + 1$$

$$g' = 2r + g + 1$$

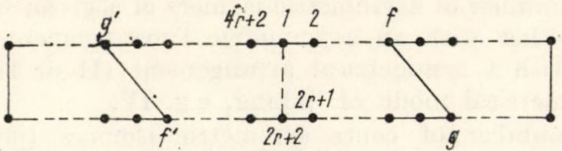

Centre-symmetry VIII (type c)

$$f' = 4r + 4 - f$$

$$g' = 4r + 4 - g$$

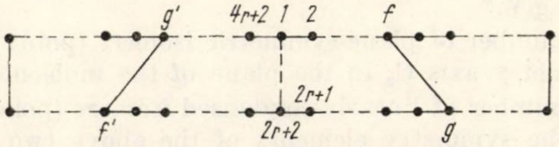

Plane-symmetry IX (type s)

$$g = 2r + 3 - f$$

$$f' = 2r + 1 + f$$

$$g' = 4r + 4 - f$$

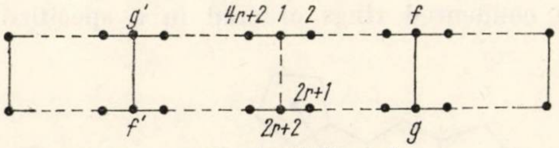

Linear condensation X (type a)

If the symmetrical system has an even number of bridging links (III), then the situation is similar to that depicted above, but the central link between atoms 1 and $2r + 2$ is missing (the above numering is now no longer in agreement with established rules).

NUMBER OF ISOMERS

Since every condensation removes two carbon and four hydrogen atoms from each z-membered monocyclic ring, the *cata*-condensed hydrocarbon formed from n condensed z_i-membered rings possesses $p = \sum_{i=1}^{n} z_i - 2\,(n - 1)$ ring (carbon) atoms, and $\sum_{i=1}^{n} z_i - 4\,(n - 1)$ hydrogen atoms.

To allow continuous conjugation in systems devoid of charge or with an even number of electrical charges, the number of ring atoms must be even, hence $\sum_{i=1}^{n} z_i$ must be even. Since, however, z can be either even (x) or odd (y), the above condition reduces to the necessity that the number of odd-membered rings should be even. For systems with an odd number of electrical charges, the number of odd-membered rings should be odd.

To every condensed system we associate a characteristic graph (the dual graph, in the accepted nomenclature,[6] without the vertex corresponding to the external region and all edges incident with this vertex), consisting of a vertex in the centre of each ring, and of edges connecting pairs of vertices if they occur in adjacent condensed rings. Unlike usual graphs where angles are unimportant, in characteristic graphs the angles discriminate among various isomers. For non-branched *cata*-condensed systems consisting of n rings, the characteristic graph is a path with n vertices and $n-1$ edges.

---

[6] F. Harary, "Graph Theory", Addison-Wesley Publ. Comp., Reading, Mass. 1969; O. Ore, "Theory of Graphs", Amer. Math. Soc. Coll. Publ. N° 38, Providence, Rhode Island, 1962; R. G. Busacker and T. L. Saaty, "Finite Graphs and Networks. An Introduction with Applications", McGraw-Hill, New York, 1965.

Since a marginal z-membered ring can be annelated in $z-3$ different ways to yield a *cata*-condensed system with one more ring, we associate to each vertex in the centre of a z-membered ring, $z-3$ possible powers of z for each possible angle of the characteristic graph at that vertex, as shown by XI and XII. For odd y-membered rings (XI) these powers range from 1 to $y-3$, while for even x-membered rings (XII) they range from 0 to $x-4$, where 0 stands for an angle of 180°. Even and odd powers are used for angles smaller and greater than 180°, respectively (alternatively, one could use positive and negative exponents for this purpose).

Thus every isomer from a subclass of *cata*-condensed non-branched systems (I) can be symbolized by a sequence of n figures z_i; all but the first and last figures have exponents indicating the angles at vertices $z_2 z_3 \ldots z_{n-1}$ of the characteristic associated graph. Since a linearly condensed system (e.g. VII) has one possible notation only, i.e. $z\,(x^0)_{n-2}z$, we obtain for such a system $a = 1$. Systems with a symmetry plane perpendicular to the molecular plane (e.g. VI) or a centre of symmetry (e.g. V) can each be symbolized by two different notations on interchanging the corresponding even and odd exponents (or, in the alternative notation, the signs of the exponents). Unsymmetrical systems belonging to subclass I, or to subclasses II or III but linked asymmetrically like IV, can be symbolized by four different notations (in addition to the above interchange, one can start the enumeration from the other end of the system). When more than one notation is possible, that sequence of exponents is selected which yields the lowest number, disregarding the z values. Examples IV—VII illustrate the selected symbol (the rejected notations are enclosed in brackets).

For an unsymmetrical system, $a = c = s = 0$, and the number of isomers is, when some non-marginal rings are odd-membered,

$$K = u = \frac{1}{2} \prod_{i=2}^{n-1} (z_i - 3) \tag{1}$$

or, when all non-marginal rings are even-membered,

$$K = u = \frac{1}{2}\left(\prod_{i=2}^{n-1} (x_i - 3) + 1 \right) \tag{1'}$$

Indeed, one can write $2\prod_{i=2}^{n-1}(z_i-3)$ different notations according to the above rules, by starting from each of the two ends of the path;

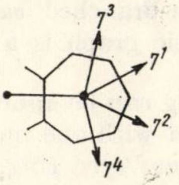

XI

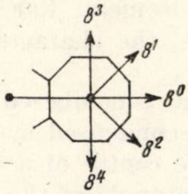

XII

every isomer can be symbolized by four of these notations, hence formula (1). When all non-marginal rings are even-membered, one linear isomer has to be added, hence formula (1′).

For symmetrical systems, it makes no difference from which end one starts. The following general relationships are valid:

$$K = a + s + c + u \tag{2}$$

$$\prod_{i=2}^{n-1}(z_i-3) = a + 2s + 2c + 4u \tag{3}$$

If a symmetrical system with $n-2$ condensed rings is annelated at both ends to afford a symmetrical system with n rings, one can demonstrate by induction the following recurrence relationships, where the number of rings is shown as an index in brackets:

$$c_{(n)} = (z_{n-1}-3)\,c_{(n-2)} + \frac{1}{2}(z_{n-1}-4)\,a_{(n-2)} \tag{4}$$

$$s_{(n)} = (z_{n-1}-3)\,s_{(n-2)} + \frac{1}{2}(z_{n-1}-4)\,a_{(n-2)} \tag{5}$$

Five different cases, *a*–*e*, of symmetrical systems have to be discussed.

I. Odd number of rings, $n = 2m+1$, system belonging to subclass (III).

Ia. Odd-membered central ring, y_0.

There can be no linear or center-symmetrical system, therefore

$$a = 0 \tag{6a}$$

$$c = 0 \tag{7a}$$

Relationship (3) is in this case

$$(y_0-3)\prod_{i=2}^{m}(z_i-3)^2 = 2s + 4u \tag{3a}$$

The recurrence (5) becomes

$$s_{(n)} = (z_{n-1} - 3)\, s_{(n-2)} \tag{5a}$$

which leads to

$$s_{(2m+1)} = \frac{1}{2}(y_0 - 3)\prod_{i=2}^{m}(z_i - 3) \tag{8a}$$

From the above relationships we obtain

$$u = \frac{1}{4}(y_0 - 3)\prod_{i=2}^{m}(z_i - 3)\left[\prod_{i=2}^{m}(z_i - 3) - 1\right] \tag{9a}$$

$$K = \frac{1}{4}(y_0 - 3)\prod_{i=2}^{m}(z_i - 3)\left[\prod_{i=2}^{m}(z_i - 3) + 1\right] \tag{10a}$$

Ib. Even-membered central ring, x_0; some non-marginal rings are odd-membered.

The above relationships become in this case :

$$(x_0 - 3)\prod_{i=2}^{m}(z_i - 3)^2 = a + 2s + 2c + 4u \tag{3b}$$

$$a = 0 \tag{6b}$$

$$c = \frac{1}{2}\prod_{i=2}^{m}(z_i - 3) \tag{7b}$$

$$s = \frac{1}{2}(x_0 - 3)\prod_{i=2}^{m}(z_i - 3) \tag{8b}$$

From these equations we obtain

$$u = \frac{1}{4}(x_0 - 3)\prod_{i=2}^{m}(z_i - 3)^2 - \frac{1}{4}(x_0 - 2)\prod_{i=2}^{m}(z_i - 3) \tag{9b}$$

$$K = \frac{1}{4}(x_0 - 3)\prod_{i=2}^{m}(z_i - 3)^2 + \frac{1}{4}(x_0 - 2)\prod_{i=2}^{m}(z_i - 3) \tag{10b}$$

Ic. In case when all non-marginal rings are even-membered, these formulas are replaced by : $a = 1$ (6c)

$$u = \frac{1}{4}(x_0 - 3)\prod_{i=2}^{m}(x_i - 3)^2 - \frac{1}{4}(x_0 - 2)\prod_{i=2}^{m}(x_i - 3) - \frac{1}{4} \tag{9c}$$

$$K = \frac{1}{4}\left[(x_0 - 3)\prod_{i=2}^{m}(x_i - 3)^2 + (x_0 - 2)\prod_{i=2}^{m}(x_i - 3) + 1\right] \tag{10c}$$

II. Even number of rings, $n = 2m$. No central ring exists in this subclass (II).

IId. If some of the non-marginal rings are odd-membered, then

$$a = 0 \tag{6d}$$

$$s = c = \frac{1}{2}\prod_{i=2}^{m}(z_i - 3) \tag{7d, 8d}$$

$$\text{hence } u = \frac{1}{4}\prod_{i=2}^{m}(z_i - 3)\left[\prod_{i=2}^{m}(z_i - 3) - 2\right] \tag{9d}$$

$$K = \frac{1}{4}\prod_{i=2}^{m}(z_i - 3)\left[\prod_{i=2}^{m}(z_i - 3) + 2\right] \tag{10d}$$

IIe. If all non-marginal rings are even-membered, then

$$a = 1 \tag{6e}$$

$$s = c = \frac{1}{2}\left[\prod_{i=2}^{m}(x_i - 3) - 1\right] \tag{7e, 8e}$$

$$u = \frac{1}{4}\left[\prod_{i=2}^{m}(x_i - 3) - 1\right]^2 \tag{9e}$$

$$K = \frac{1}{4}\left[\prod_{i=2}^{m}(x_i - 3) + 1\right]^2 \tag{10e}$$

Cases *c* and *e* above reduce to the polyhex problem if all $x_i = 6$, as it can be easily shown. The five formulas 10a—10e above exhaust all possible cases of symmetrical subclasses (II or III).

To summarize, the number K of isomers of any non-branched *cata*-condensed system formed from z_i-membered rings (where the z_i's are integers greater than 3, and $i = 1, 2, \ldots, n$) in a specified sequence, depends on several factors : (i) whether the sequence of z_i values gives rise to an unsymmetrical (I) or symmetrical arrangement (II or III) ; (ii) whether the total number n of rings is even or odd ; (iii) whether all non-marginal z_i values are, or are not, even ; (iv) whether the central ring z_0 in the symmetrical arrangement with odd n (III) is even- or odd-membered. The dichotomic derivation of the various formulas for K is presented in the following flowsheet.

Unsymmetrical arrangement (I)
    At least one non-marginal ring is odd-membered : formula (1)
    All non-marginal rings are even-membered : formula (1′)
Symmetrical arrangement
    Odd number of rings (III)
        Central ring is odd-membered : formula (10a)
        Central ring is even-membered

Some non-marginal rings are odd-membered : formula (10b)
All non-marginal rings are even-membered : formula (10c)
Even number of rings (II)
Some non-marginal rings are odd-membered : formula (10d)
All non-marginal rings are even-membered : formula (10e)

APPLICATIONS

Five illustrations for the application of these formulas are provided.

(i) Electrically neutral systems consisting only of five-membered rings. Since the number n of rings must be even, formulas d afford :

$$s = c = \frac{1}{2}(y-3)^{m-1} = 2^{m-2}$$

$$4u = (y-3)^{2m-2} - 2(y-3)^{m-1} = 2^{m}(2^{m-2}-1)$$

$$4K = (y-3)^{2m-2} + 2(y-3)^{m-1} = 2^{m}(2^{m-2}+1)$$

Results are presented in table 1.

Table 1

Number of isomers of systems formed from 5-membered rings

Subclass	$n = 2m$	c	s	u	K
5555	4	1	1	0	2
555555	6	2	2	2	6
55555555	8	4	4	12	20

(ii) Neutral systems containing only seven-membered rings. According to case d,

$$s = c = \frac{1}{2}.4^{m-1} = 2.4^{m-2}$$

$$u = 4^{m-2}(4^{m-1}-2)$$

$$K = 4^{m-2}(4^{m-1}+2)$$

Results are presented in table 2.

Table 2

Number of isomers of systems formed from 7-membered rings

Subclass	$n = 2m$	c	s	u	K
7777	4	2	2	2	6
777777	6	8	8	56	72
77777777	8	32	32	992	1056

(iii) Tetracyclic systems consisting of 5-, 6-, and 7-membered rings ($n = 4$). Results are given in table 3.

Table 3

Number of isomers of tetracyclic systems

Subclass	Formulas	a	c	s	u	K
5555, 6556, 7557	d	0	1	1	0	2
5557	1	0	0	0	2	2
5656, 6657, 6567	1	0	0	0	3	3
5665, 6666, 7667	e	1	1	1	1	4
5577, 7575, 5575, 6576, 7577	1	0	0	0	4	4
5667	1	0	0	0	5	5
5676, 5766, 7676	1	0	0	0	6	6
5775, 6776, 7777	d	0	2	2	2	6
5777	1	0	0	0	8	8

(iv) For symmetrical hexacyclic systems (II) obeying the Hückel rule and containing 5-, 6-, and 7-membered rings, the results are presented in table 4.

Table 4

Number of isomers of hexacyclic systems

Subclass	Formulas	a	c	s	u	K
655556	d	0	2	2	2	6
565565, 765567, 556655, 756657	d	0	3	3	6	12
675576, 657756	d	0	4	4	12	20
666666	e	1	4	4	16	25
576675, 776677, 567765, 767767	d	0	6	6	30	42
677776	d	0	8	8	56	72

(v) Hexacyclic systems formed from three 5-membered and three 7-membered rings. Formula (1) indicates that for such subclasses, which can only give rise to unsymmetrical arrangements, the numbers of isomers are: 16 (for subclasses 755577 or 755757), 32 (for 575577, 555777, 557577, 557757 or 575757), and 64 (for 557775 or 575775).

TOPOLOGY AND THE HÜCKEL AND CRAIG RULES

For *cata*-condensed systems, in the symmetrical cases when the Craig rule [7] can be applied, it gives equivalent results to the Hückel rule. Therefore, since the Hückel rule can also be applied to unsymmetrical systems, only this latter, more general, rule need be examined.

---

[7] D. P. Craig, in "Theoretical Organic Chemistry", Kekulé Symposium, Butterworths, London, 1959.

Apart from steric factors, there exist three limitations which make the Hückel rule a necessary but insufficient condition for aromaticity in electrically neutral *cata*-condensed hydrocarbons.

1. Presence of large rings. It is well known that for monocyclic rings obeying the Hückel rule and possessing more than ca. 14 atoms, bond alternation occurs.[8] Their resonance energy drops asymptotically, becoming negligible for rings with more than ca. 22 atoms.[9] For the known Hückel-type annulenes, the diamagnetic ring current persists, however, even in large rings.[10]

2. Presence of 3- and 4-membered rings. Theoretical calculations support what was said earlier on the effect of condensed 3-membered cyclopropene rings.[11] It was also argued on the basis of theoretical calculations that *cata*-condensed systems containing 4-membered rings do not possess aromatic character.[12,13] This theoretical result is borne out by the few experimental data available, for instance for bicyclo [6.2.0]-decapentaene,[14] which unlike the isomeric naphthalene or azulene, appears to be non-aromatic.

3. Centre-symmetrical structure C_{2h} in non-alternant systems possessing $2\ k$ pairs of 1(mod 4)-or 3(mod 4)-membered rings ($k = 1, 2$, etc.). As it was observed by Bochvar and coworkers for system V using the simple Hückel molecular orbital method, the energy levels are such that this molecule does not possess a closed electronic shell.[15] This is a general property of non-alternant systems VIII with a centre of symmetry, containing $4k$ odd-membered rings with the same z-value, for example the centre-symmetrical systems belonging to classes 5, 5, 5, 5, (V),[15] 7, 7, 7, 7, 5, 5, 5, 5, 6, 5, 5, 5, 5, 6, 6, 5, 5, 5, 5, 7, 7, 7, 7, 5, 5, 5, 5, 5, 5, 5, 5, etc. (but not 5, 5, 7, 7, 5, 5, 6, 7, 7, 5, 5, 6, 6, 7, 7, etc. which have closed electronic shells). With $p = 4r + 2$ ring atoms, and π-electrons, a closed electronic shell requires $2r + 1$ bonding molecular orbitals to be occupied and $2r + 1$ antibonding molecular orbitals to be vacant. In the above cases of systems containing $4k$ odd-membered rings with the same value arranged symmetrically and linked centre-symmetrically, two sets of eigenvalues of opposite signs are obtained : one set has $2r$ and the other $2r + 2$

---

[8] H. C. Longuet-Higgins and L. Salem, *Proc. Roy. Soc.*, **A 251**, 172 (1959); **A 257**, 445 (1960); G. BINSCH and I. TAMIR, *J. Amer. Chem. Soc.*, **91**, 2450 (1969).

[9] M. J. S. Dewar and G. J. Gleicher, *J. Amer. Chem. Soc.*, **87**, 685 (1965); cf. also R. Zahradník, *Angew. Chem., Internat. Ed.*, **4**, 1039 (1965); D. M. G. Lloyd, "Carbocyclic Non-Benzenoid Aromatic Compounds", Elsevier, Amsterdam, 1966; G. M. Badger, "Aromatic Character and Aromaticity", Cambridge Univ. Press, 1969.

[10] F. Sondheimer *et al.*, in "Aromaticity", Chem. Soc. Special Publ. No. 21, p. 75. London, 1967; cf. also J. A. Elix, *Austral. J. Chem.*, **22**, 1951 (1969).

[11] D. A. Bochvar and A. V. Tutkevich, *Izv. Akad. Nauk, Ser. Khim.*, **1966**, 756.

[12] C. F. Wilcox Jr., *Tetrahedron Letters*, **1968**, 795; *J. Amer. Chem. Soc.*, **91**, 2732 (1969).

[13] M. J. S. Dewar and N. Trinajstic, *Tetrahedron Letters*, **1969**, 2129.

[14] G. Schröder and H. Röttele, *Angew. Chem.*, **80**, 665 (1968).

[15] D.A. Bochvar, I. V. Stankevich and A. V. Tutkevich, *Izv. Akad. Nauk., Ser. Khim.*, **1969**, 1185.

eigenvalues, leading to an occupied antibonding orbital, or to an empty bonding orbital. In addition, system XIII (but not its three other centre-symmetrical isomers, cf. table 1) has a non-bonding orbital.

Simple Hückel molecular calculations for all systems quoted in the preceding paragraph were performed on an IBM 360—30 computer using the programme kindly made available by Miss K. Göttler.

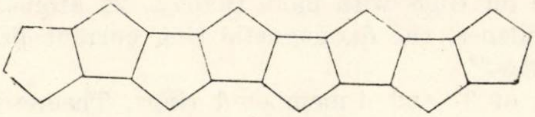

XIII ($55^1 5^2 5^1 5^2 5^1 5^2 5$)

Revue Roumaine de Chimie, 15, 1263–1273 (1970)

CONTRIBUTION À LA SÉPARATION DU ZIRCONIUM D'AVEC LE HAFNIUM PAR CRISTALLISATION FRACTIONNÉE DE L'HEXAFLUOZIRCONATE DE POTASSIUM

IOANA ARSENIE
Institut de Physique Atomique, Bucarest, B.P. 35

I. LEUCĂ
Faculté de Physique Nucléaire, Bucarest

Reçu le 16 septembre 1969

L'ouvrage présente certaines données obtenues par le développement du procédé de séparation du zirconium d'avec le hafnium par cristallisation fractionnée du $K_2Zr/Hf/F_6$. On développe un schéma technologique de cristallisation successive pour atteindre une pureté de 0,01% Hf/Zr (η = 80%) et on met en évidence l'influence des paramètres sur le processus de séparation, à savoir : pH, température, concentration et vitesse de cristallisation.

I. INTRODUCTION

Le zirconium (et ses alliages) peut être considéré actuellement comme matériel classique [1] pour les réacteurs nucléaires, étant donné ses propriétés, notamment excellente résistance à la corrosion, bonnes propriétés mécaniques et propriétés nucléaires favorables. La plus précieuse propriété nucléaire du zirconium est la section d'absorption des neutrons thermiques (σ = 0,18 barn) de beaucoup inférieure à celle de l'acier inoxydable (σ= 3 barn).

Toutefois, l'emploi du zirconium dans la technique nucléaire a nécessité l'élaboration de méthodes pour la séparation[2] des impuretés qui accroissent considérablement la section efficace, impuretés dont la plus nocive est le hafnium (σ = 115 barn). Etant donné que le hafnium est l'homologue supérieur du zirconium ayant des rayons ioniques de dimensions semblables et des propriétés chimiques semblables, leur séparation devient un problème principal (et difficile) pour l'obtention du zirconium de pureté nucléaire.[3]

---

[1] «Zirconium», Conference on the Use of Zirconium Alloys in Nuclear Reactors, octombre 21–26 1966, Marianské Lazné, Tchécoslovaquie.

[2] W. Schreiter, «Metale rare», Editura tehnică, Bucarest, 1966, p. 375.

[3] Edwin M. Larsen, *J. Chem. Educ.*, **28**, 529 (1951).

Pour la séparation de ces deux éléments on emploie les petites différences de certaines propriétés [4] comme la solubilité, l'absorption et la température d'ébullition des composés de zirconium et de hafnium, les principaux procédés de séparation étant : cristallisation fractionnée, extraction par solvants organiques et échange ionique.

La cristallisation fractionnée, comme procédé de séparation du zirconium d'avec le hafnium, est basée sur la solubilité différente de certains composés du zirconium et du hafnium, tels que [5] : oxychlorures, sulfates, phosphates, citrates et fluoro-composés.

La solubilité d'une substance dans un solvant est fortement influencée par la présence d'autres substances dissoutes. Par l'influence « mutuelle » de la solubilité des deux substances dissoutes, et par la variation de la température ou de la vitesse de cristallisation, l'une des substances peut cristalliser seule, les autres impuretés restant en solution, dont la concentration a été choisie telle qu'elle n'atteigne pas la concentration de saturation.[6,7]

Dans le présent ouvrage on a développé le procédé de séparation par cristallisation fractionnée du $K_2Zr/Hf/F_6$, d'après un schéma technologique de cristallisations multiples (en travaillant également sur les eaux mères) et on a étudié l'influence des principaux paramètres : pH, température, concentration, vitesse de cristallisation. On a ainsi obtenu un hexafluozirconate de potassium avec 0,0077% hafnium/zirconium, après quinze cristallisations, en partant d'un hexafluozirconate de potassium initial avec 2,5 Hf/Zr, à une température de 100—35° et un pH inférieur à 3.

Les données obtenues ont de l'importance pour le développement du procédé de séparation du zirconium d'avec le hafnium par cristallisation fractionnée à une échelle semi-industrielle.

II. STADE DU PROBLÈME

La séparation du zirconium d'avec le hafnium par le procédé de cristallisation fractionnée a été développée à une échelle semi-industrielle aux Etats-Unis,[8] en U.R.S.S.[9] et aux Indes.[10]

Dans l'ouvrage mentionné [8] on spécifie qu'on part de l'hexafluozirconate de potassium ayant 1,5% Hf/Zr et par 10 cristallisations on arrive à 0,01% Hf/Zr. La température de travail est de 100°—35° et le pH = 3.

Dans l'ouvrage [9] on emploie de l'hexafluozirconate de potassium avec 2,5% Hf/Zr et par 16—18 cristallisations on arrive à 0,01% Hf/Zr à une température de 80—90°—20° et un pH = 3.

---

[4] F. Hudowell et J. H. Hutcheon, Conf. Int. Appl. Pac. Energ. Atom., Genève, 8/409, 1955.

[5] G. Henesy, *Chem. Rev.*, **2**, 1 (1926).

[6] A. G. Kasatkin, «Procedee și aparate principale în tehnologia chimică», Ed. tehnică, Bucarest, 1963, p. 737.

[7] E. Bratu, « Aparate și procedee în industria chimică », Ed. tehnică, 1969.

[8] W. W. Beaver, BBC, 54, 28 août, 1950.

[9] N. P. Sajin et E. Pepelyaeva, Conf. Int. Appl. Pac. Energ. Atom., Genève, 8, P/34, 1955.

[10] *Trans. Indian Inst. Metalls*, **19**, 9 (1966).

Des données de la littérature,[11,12] il ressort que parmi les composés de Zr et Hf, les hexafluoro composés de potassium et d'ammonium présentent une stabilité dans le temps et aussi une différence de solubilité.

L'hexafluozirconate de potassium purifié (déhafnié), peut être utilisé comme tel dans le procédé de préparation du zirconium métallique par électrolyse [13], ou peut être passé sous forme d'oxyde de zirconium et après en zirconium métallique par le procédé classique Kroll.[14]

III. RÉSULTATS EXPÉRIMENTAUX

Les expériences ont porté sur de hexafluozirconate de potassium ayant la composition chimique en pour-cent suivante :

Zr —30—32%
Hf — 2,48
Cu — 10^{-3}
Pb — 10^{-3}
Fe — 10^{-2}
Al — 10^{-2}
Si — 10^{-1}
Mn — 10^{-3} — 10^{-4}
Mg — 10^{-2}

Pratiquement on a recherché :

1. Le développement d'un schéma technologique de cristallisation multiple pour obtenir une haute pureté (0,01% Hf/Zr) et un bon rendement (au-dessus de 80%).
2. L'influence des paramètres principaux : pH, concentration, température, vitesse de refroidissement ou cristallisation.

1. SCHÉMA TECHNOLOGIQUE

Le schéma technologique détaillé est présenté dans la figure 1, et comprend 15 degrés (cristallisation pour une charge S_1) et 15 cycles résultant du traitement des eaux mères.

La charge S_1—250 g $K_2Zr/Hf/F_6$ est dissoute dans un litre de solvant (de l'eau déionisée, acidulée avec du HF à un pH inférieur à 3 qui ne dépasse pas une concentration du HF de 1%), chaufée à 100° et après refroidie à une vitesse de 1°/mn jusqu'à 35°.

On obtient ainsi un degré de cristallisation. Les cristaux S_{1-1} sont séparés des eaux mères A_{1-1} et soumis à une nouvelle opération.

Les eaux mères A_{1-1} et A_{1-2} sont concentrées par évaporation et on obtient une nouvelle charge de cristallisation S_2 qui est traitée en passant les eaux mères A_{1-3}, A_{1-4} et ainsi de suite.

---

[11] N. V. Sidgwick, « The Chemical Elements and Their Compounds », Ier vol., Oxford University Press, Londres, 1962, p. 629.

[12] R. D. Peacock, « Some Florine Compounds of the Transition Metals in « Progress in Inorganic Chemistry », IIe vol., Ed. F. Albert Cotton, New York, 1960, p. 194.

[13] A. Călușaru, « Depunerea electrolitică a metalelor în formă dispersă », Ed. Acad., 1962, p. 205.

[14] G. L. Miller, « Zirconium », Butterworths, Scientifics Publications, Londres, 1954, p. 74.

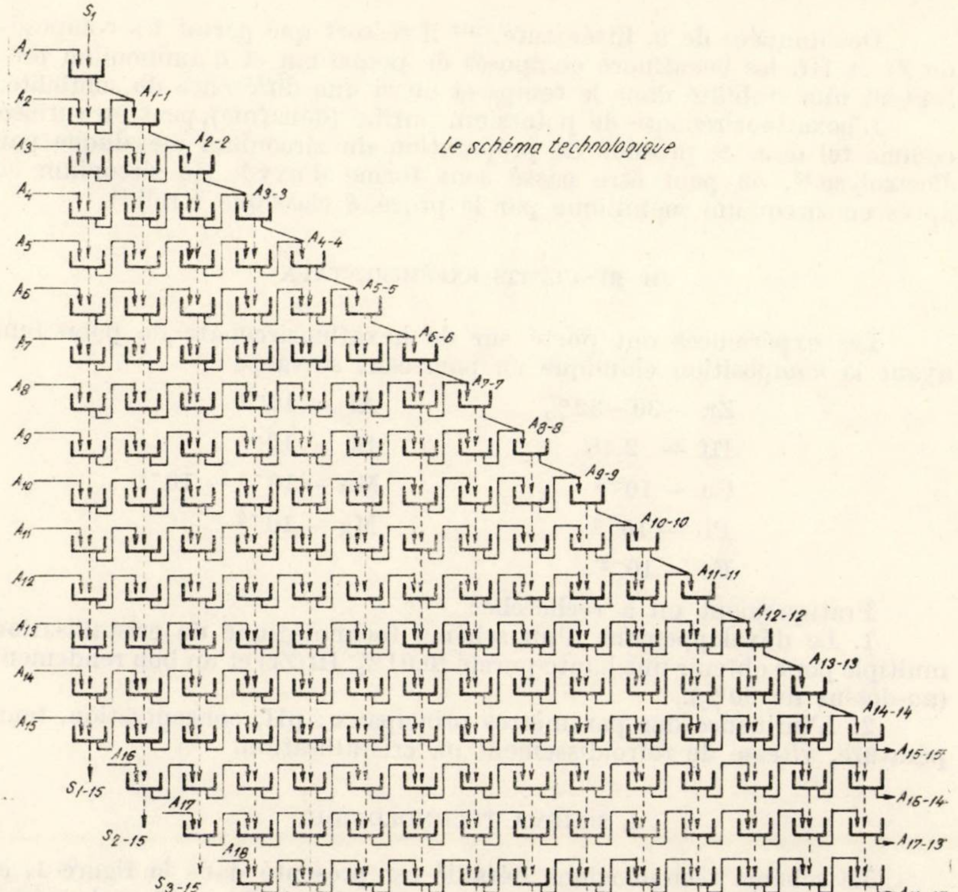
S1
A1
A1-1
A2
A2-2
Le schéma technologique
A3
A3-3
A4
A4-4
A5
A5-5
A6
A6-6
A7
A7-7
A8
A8-8
A9
A9-9
A10
A10-10
A11
A11-11
A12
A12-12
A13
A13-13
A14
A14-14
A15
A15-15
A16
S1-15
A16-14
A17
S2-15
A17-13
A18
S3-15
A18-12
A19
S4-15
A19-11
A20
S5-15
A20-10
A21
S6-15
A21-9
A22
S7-15
A22-8
A23
S8-15
A23-7
A24
S9-15
A24-6
A25
S10-15
A25-5
A26
S11-15
A26-4
A27
S12-15
A27-3
A28
S13-15
A28-2
A29
S14-15
A29-1
S15-15
1
2

Fig. 1. — Schéma technologique:
1, circulation des cristaux; *2*, circulation des eaux mères.

On continue selon le schéma proposé qui a les avantages suivants :

— par le traitement des eaux mères le rendement en K_2ZrF_6 purifié augmente ;

— on peut récupérer aussi le hafnium retenu dans les solutions finales, par échange ionique ou extraction par solvants organiques.

La figure 2 nous montre la variation de la teneur en hafnium avec le nombre de dégrés de la charge S_1, et le tableau 1 nous donne la teneur en hafnium des charges (S_{1-15}, S_{2-15}, S_{3-15} . . . S_{15-15}), d'où il ressort qu'on peut atteindre le même degré de pureté par cycles si on traite le même nombre de degrés.

Les eaux mères concentrées ont accumulé finalement 5% Hf/Zr.

Le tableau 2 nous donne l'analyse spectrographique de l'hexafluozirconate de potassium déhafnié et des eaux mères.

Dans l'ouvrage [15] on montre que dans le développement du processus de cristallisation il est important de connaître la solubilité de la substance soumise à l'opération de cristallisation.

En tenant compte de la solubilité pour la température de séparation des cristaux de solution mère (35°) par cycle on atteint un rendement de 10—12%. En obtenant la même pureté par cycles, le rendement global est de 75—80% en hexafluozirconate de potassium déhafnié.

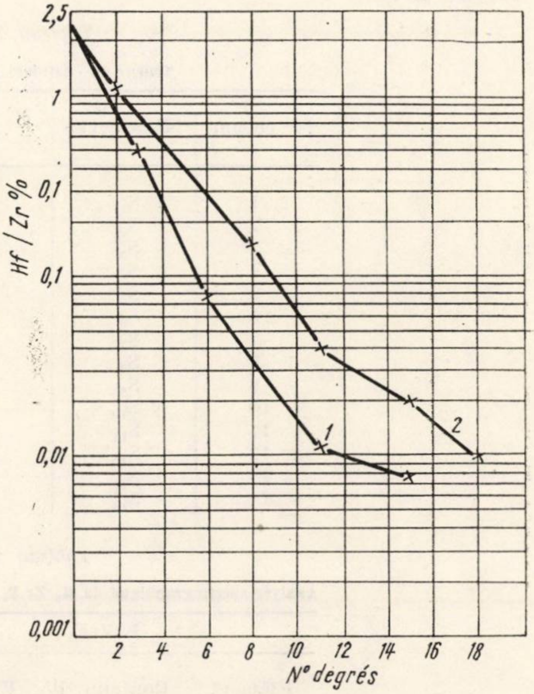

Fig. 2. — Variation de la teneur en hafnium avec le nombre de degrés.
1, pH = 3 ; 2, pH = 4,5.

2. INFLUENCE DES PARAMÈTRES PRINCIPAUX SUR LE PROCESSUS DE SÉPARATION DU ZIRCONIUM D'AVEC LE HAFNIUM PAR CRISTALLISATION FRACTIONNÉE

a) *Influence du PH*

Pour mettre en évidence l'influence du pH dans le processus de séparation du zirconium d'avec le hafnium par cristallisation fractionnée on a fait des expériences pour différentes valeurs de celui-ci et notamment : pH = 1,5 ; 3 ; 4,5 ; 7.

---

[15] J. W. Mullin, « Cristallization », Butterworths, Londres, 1961, p. 21—136.

La figure 3 montre l'influence du pH de la solution sur le processus de séparation du zirconium d'avec le hafnium et notamment : l'établissement du nombre de degrés pour atteindre la même teneur en hafnium.

Il ressort que le pH optimum va jusqu'à 3, un nombre inférieur de degrés étant nécessaire pour atteindre un contenu de moins de 0,01% Hf de Zr.

Tableau 1

Teneur en hafnium par cycles

N° échant.	N° de cycles	N° degrés final	Teneur en Hf en ppm
1	S_1	15	77
2	S_2	14	92
3	S_3	14	96
4	S_4	14	100
5	S_5	14	98
6	S_6	14	93
7	S_7	14	94
8	S_8	12	100
9	S_9	11	150
10	S_{10}	11	160
11	S_{11}	11	150
12	S_{12}	10	170
13	S_{13}	10	180
14	S_{14}	9	210

Tableau 2

Analyse spectrographique du K_2ZrF_6 déhafnié et des eaux mères

K_2ZrF_6		Les eaux mères	
Elément	Contenu %	Elément	Contenu %
Si	$10^{-1}-10^{-2}$	Si	10^{-2}
Fe	$10^{-3}-10^{-4}$	Fe	$10^{-1}-10^{-2}$
Al	$10^{-2}-10^{-3}$	Al	10^{-1}
Mg	$10^{-2}-10^{-3}$	Mg	10^{-1}
Cu	10^{-4}	Cu	—
Hf	$77\ 10^{-4}$	Hf	5
Na	—	Na	1
Ca	—	Ca	10^{-4}
B	—	B	10^{-2}
Mn	—	Mn	10^{-2}

En partant d'un pH = 3, on arrive à 92–96 ppm Hf/Zr en 14 degrés, pour un pH = 4,5 toujours en 14 degrés à un contenu de 170–180 ppm Hf/Zr, et pour un pH = 7, en 15 degrés, on arrive à 300 ppm Hf/Zr.

La valeur pH = 3 comme point optimum est indiquée dans l'ouvrage[16] et est en même temps justifiée par les faits suivants :

---

[16] P. PASCAL, « Nouveau Traité de Chimie Minérale », IXe vol., Masson Cie, Paris, 1963, p. 611.

— La différence de solubilité entre l'hexafluozirconate de potassium et l'hexafluohafniate de potassium croît avec l'acidité. L'ouvrage [17] et le tableau 3 montrent ces différences.

— Le zirconium et certaines impuretés hydrolysent [18,19] à un pH = = 3 encore plus grand. Le tableau 4 nous donne le domaine du pH dans lequel certains éléments sont hydrolysés.

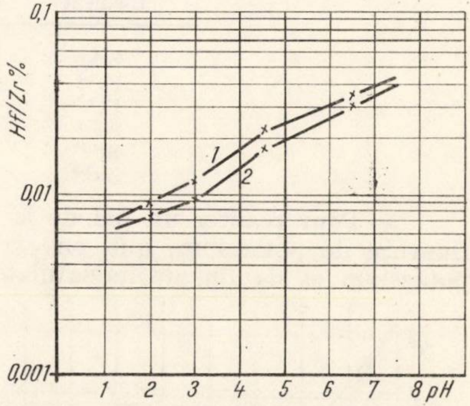

Fig. 3. — Influence du pH de la solution dans le processus de séparation du Zr d'avec le Hf.
1, température 80° – 20°; 2, température 100° – 35°.

L'hydrolyse n'est pas souhaitable étant donné que les impuretés restent dans le produit final, et le zirconium se transforme en oxyde de zirconium dans l'hexafluozirconate de potassium déhafnié et incommode le processus d'électrolyse de celui-ci pour l'obtention du zirconium métallique.

Tableau 3

Solubilité du K_2ZrF_6 en solution Hf à la température de 20°

Composé K_2MF_6	Solvant Hf	Solubilité de l'élément g/100 ml solution	
		Hf	Zr
,,	0,125 N	3,74	1,86
,,	5,89	7,2	3,68
,,	H_2O	—	1,55

Le tableau 5 nous donne l'analyse spectrographique de l'hexafluozirconate de potassium initial et de celui déhafnié à pH = 3, de la comparaison desquels il ressort que les impuretés sont restées dans l'hexafluozirconate déhafnié, en se concentrant même.

— On réalise le pH = 3 en ajoutant de l'acide fluorhydrique sans dépasser une concentration de 1%, étant donné qu'une concentration supérieure mène à la formation de l'acide hexafluozirconique.[20]

---

[17] G. Henesy, *Chem. News*, **127**, 33 (1923).

[18] B. A. Lister, A.E.R.E., C/R 801, 1951.

[19] Const. Gh. Macarovici, « Chimie analitică cantitativă », Ed. tehnică, Bucarest, 1959, p. 72–81.

[20] I. Tananaev, *Zuhr. neorg. Khim.*, **1**, 274 (1956).

— On doit encore ajouter que par la dissolution de l'hexafluozirconate dans l'eau pour la réalisation de la solution de séparation, celle-ci a un pH $\simeq$ 4,5.

Tableau 4

Le domaine du pH d'hydrolyse de certains éléments

Elément	Domaine du pH
Zr^{4+}	2,8–4,5
Fe^{2+}	5,5–8,5
Fe^{3+}	3 –7
Al^{2+}	4,1–6,5
Si^{4+}	4 –4,5
Zn^{2+}	6 –7

— Pour réaliser un pH de la solution supérieur on peut ajouter du fluorure de potassium, qui, en excès, donne de l'heptafluozirconate de potassium et de l'heptafluohafniate de potassium ayant des solubilités proches,[21] ce qui a été mis en évidence par les expériences au pH = 7 (cristallisant en cube).

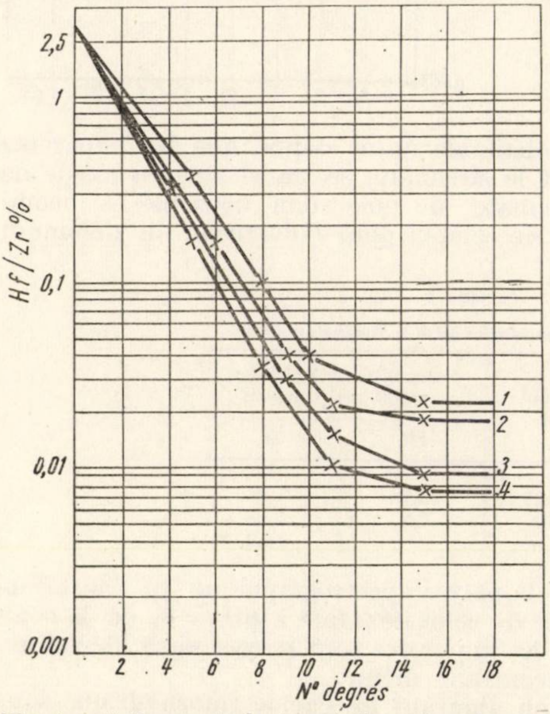

Fig. 4. — Influence de la température dans le processus de séparation du Zr d'avec le Hf.

1, température 80–20° – pH = 4,5 : *2*, température 80–20° – – pH = 3 ; *3*, température 100 – 35° – pH = 4,5 ; *4*, température 100 – 35° – pH = 3.

b) *L'influence de la température*

Par certaines expériences effectuées à différentes températures et par le maintien des autres paramètres constants, on a étudié l'influence de la température.

La figure 4 nous montre l'influence de la température dans le processus de séparation du zirconium du hafnium.

De l'analyse des données pratiques il ressort que la température optimum de travail peut être considérée 100° pour réaliser la solution sursaturée et jusqu'à 35° la température de refroidissement.

Dans les expériences à la température de travail de 100° (la réalisation de la solution sursaturée) et 35° (le refroidissement pour la cristallisation) au pH = 4,5 on est arrivé à une teneur de 170 — 180 ppm en Hf/Zr en 15 degrés, en comparaison des expériences où la température a été de 80°–20° et où l'on a obtenu

---

[21] R. N. Haszeldine et G. Sharpe, « Fluorine and its Compounds », Methuen Co LTD, Londres, 1951, p. 48.

Tableau 5

Analyse spectrographique du K_2ZrF_6

K_2ZrF_6 initial		K_2ZrF_6 déhafnié	
élément	contenu %	élément	contenu %
Hf	2,48	Hf	18.10^{-3}
Cu	10^{-3}	Cu	$10^{-3}-10^{-4}$
Mg	10^{-2}	Mg	10^{-2}
Mn	10^{-4}	Mn	10^{-4}
Al	10^{-2}	Al	10^{-1}
Fe	10^{-3}	Fe	10^{-3}
Si	10^{-1}	Si	10^{-1}
Pb	10^{-3}	Pb	10^{-3}

210—220 ppm Hf/Zr. Les expériences au pH = 3, ont donné de meilleurs résultats en ce qui concerne la teneur en hafnium, mais il existe des différences entre les épreuves obtenues à différentes températures, conformément aux courbes b et d de la figure 4.

La littérature [22] nous indique une température plus élevée (100° et 65°), étant donné que la solubilité augmente avec la température.

c) *Influence de la concentration de la solution*

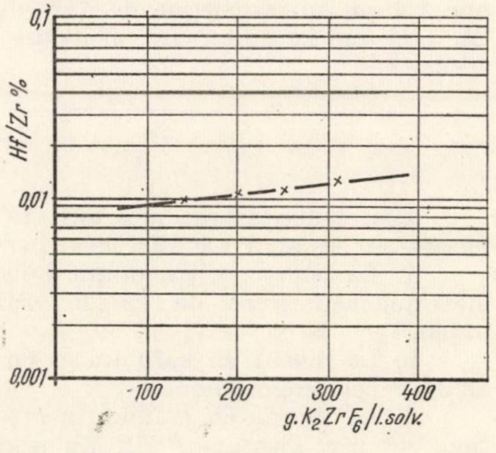

Fig. 5. — Influence de la concentration dans le processus de séparation du Zr d'avec le Hf.

La figure 5 nous donne l'influence de la concentration de la solution à séparer dans le processus de purification du zirconium et du hafnium, les autres paramètres étant maintenus constants.

Le tableau 6 indique la concentration et la teneur finale en hafnium.

Il ressort qu'on peut traiter des solutions ayant des concentrations supérieures à 250 g/l de solvant, et même 300 g/l de solvant, en arrivant par le même nombre de degrés à un contenu proche de hafnium.

---

[22] I. V. Maxim, « Materiale nucleare », Ed. Academiei, Bucarest, 1969, p. 117.

Tableau 6

Concentration des solutions à 100° et contenu final du Hf/Zr

Concentration en K_2ZrF_6 g/l solvant	Contenu % Hf/Zr
140	$96\ 10^{-4}$
250	$110\ 10^{-3}$
300	$120\ 10^{-3}$

Les ouvrages [7,23] spécifient que le degré de sursaturation est essentiel dans le processus de cristallisation, mais il doit être choisi de telle sorte que les impuretés finales n'atteignent pas la concentration de saturation (dans les eaux mères), ce qui d'ailleurs dans le cas de la séparation par cristallisation du zirconium et du hafnium n'a jamais lieu, l'hexafluozirconate de potassium initial ayant 2,5% Hf/Zr, et la solubilité de l'hexafluohafniate de potassium étant plusieurs fois supérieure à celle de l'hexafluozirconate de potassium.

d) *Influence de la vitesse de refroidissement des solutions*

La vitesse de refroidissement (cristallisation) a de l'influence en ce qui concerne la dimension des cristaux, notamment à des vitesses de refroidissement au-dessus de 3°/mn on obtient des cristaux plus grands que 1,4 cm en proportion de 60% du poids total des cristaux (K_2ZrF_6). On sait que la pureté est meilleure dans le cas de l'obtention de gros cristaux.

IV. ANALYSE

Les résultats pratiques ont été interprétés dans la partie III en se basant sur les analyses effectuées par trois méthodes :

1. La teneur en zirconium dans la solution a été déterminée gravimétriquement avec de l'acide mandélique [24,25] et de l'acide flavianique.[26]

2. La teneur en hafnium et en autres impuretés a été étudiée par analyse spectrographique.[27]

3. La teneur en hafnium a été étudiée aussi par analyse d'activation,[28,29] par l'isotope ^{181}Hf. En principe, pour l'analyse d'activation on a procédé comme suit :

---

[23] G. Henesy, *J. Chem. Soc.*, **1924**, 2372.

[24] N. Howell Furmann, « Standard Methods of Chemical Analysis », Ier vol., D. von Nostrand Company/N. C., New Jersey, New York, 1962, p. 1266.

[25] Cl. J. Rodden, « Analysis of Essential Nuclear Reactor Materials », U.S.A.E.C., Washington, 1964.

[26] T. Născuţiu et G. Baiulescu, *Studii şi Cercetări Chim., Acad.* (*Bucureşti*), **6**, 31 (1958).

[27] W. T. Elwell et D. V. Wood, «The Analysis of Titanium of Zirconium and their Alloys », John Willey et Sons Limited, Birmingham, 1961, p. 117.

[28] L. Fournet et Ph. Albert, *Compt. rend.*, **254**, 1076 (1962).

[29] W. D. Mackintosh et R. F. Jerners, *Analyt. Chem.*, **7**, 9 (1953).

Les échantillons sous forme d'oxyde avec les étalons de hafnium ont été irradiés (en fiole d'aluminium) pendant 2,30 heures dans un flux de 10^{13}n/cm^{2}s et ensuite mesurés à l'aide d'un compteur d'impulsions — scintillateur INa (Tl) et un analyseur à 400 canaux SA-40 type Intertechnique.

V. CONCLUSIONS

1. Le nombre de degrés nécessaires pour atteindre une pureté inférieure à 0,01% Hf/Zr varie en fonction de la teneur initiale en hafnium et de la variation des paramètres accompagnant le processus de séparation.

2. Les paramètres optima de développement du procédé de séparation par cristallisation fractionnée pour obtenir une pureté avancée ont été établis comme suit :

— pH = 3
— concentration 250—310 g/l du solvant,
— température ⟨ réalisation de la solution sursaturée 100°
réalisation de la cristallisation 35°
— vitesse de refroidissement inférieure à 1°/mn

3. Le produit final contient 0,0077 % hafnium/zirconium comparé au 2,5 %Hf/Zr initial atteignant ce contenu en 15 degrés, et peut être utilisé à l'obtention du zirconium métallique ; donc par le procédé de l'électrolyse, ou sous forme d'oxyde de Zr par le procédé Kroll.

4. Les eaux mères ont cumulé 5% Hf/Zr qui peut être traité par échange ionique pour l'obtention du hafnium.

CORRECTION

The title of the paper "Aromaticity. VI" by A.T. Balaban published in Revue Roumaine de Chimie, **14**, *10*, 1323 (1969) should correctly read AROMATICITY. VII.

Revue Roumaine de Chimie, 15, 1263—1273 (1970).

La *Revue Roumaine de Chimie* paraît 12 fois par an. Le prix d'un abonnement annuel est de £ 5.0.0 ; $ 12, — ; FF 60, — ; D.M. 48, — . Toute commande de l'étranger (fascicules ou abonnements) sera adressée à Intreprinderea de comerţ exterior — LIBRI, Boîte postale 134—135, Bucarest, Calea Victoriei 126, Roumanie, ou à ses représentants à l'étranger :

ALBANIA Ndermarja Shtetetrore E. Tregetimit Te Librit Tirana ; AUSTRIA Globus Buchvertrieb Salzgries 16 Wien I ; BELGIUM Du Monde Entier 5, Place St. Jean Bruxelles ; Librairie Claeys-Verheughe 8, Volderstraat Gand ; Maison des Langues Vivantes 65, Rue du Midi Bruxelles ; Office International de Librairie 30, Av. Marnix Bruxelles 5 ; Vander Editeur 10, Munstraat Louvain; BULGARIA Hemus Pl. Slaveikov 11-Sofia ; CANADA Canadian Slavic Studies Loyola Colege Montreal 262 ; Librairie Lidec Inc. 1083 Van Home Montreal ; Panonia Books 2, Spadina Road Toronto 4 Ontario ; CHINA Waiwen Shudian P.O. Box 88 Peking ; COLOMBIA Libreria Karl-Bucholz Av. Jimenzez 8—40 Bogota ; CUBA Cubartimpex P.O. Box 6540 La Habana ; CZECHOSLOVAKIA Artia Ve Smerckach 30 Praha I ; DENMARK Munksgaard 6 Norregade Copenhagen K ; N. J. Hasses-Bogimport 8, Loerstraede Copenhagen K. ; FINLAND Akateeminen Kirjakauppa Postfach 10128 Helsinki 10 ; FRANCE Agence Littéraire et Artistique Parisienne 7, Rue Debelleyme Paris 3-e ; Eyrolles Editeur 61, Boulevard Saint-Germain Paris 5-e ; Librairie de l'enseignement technique (Stand permanent des livres techniques et scientifiques roumains) 61, Boul. Saint-Germain, Paris 5-e ; Librairie Hachette 25, Rue des Cévennes Paris 5-e ; Librairie Joseph Gibert 26—30, Boul. Saint-Michel Paris 6-e ; Libella 12, Rue Saint-Louis-en-l'Ile Paris 4-e ; Maison du Livre Italien 46, Rue des Ecoles Paris 5-e ; Office International de Documentation et Librairie 48, Rue Gay Lussac Paris 5-e ; Presses Universitaires de France 17, Rue Soufflot Paris 5- ; THE GERMAN DEMOCRATIC REPUBLIC Deutscher Buch-Export-und-Import Leninstrasse 16 Leipzig C. 1 ; THE FEDERAL REPUBLIC OF GERMANY Kubon Sagner P.O. Box 68 München 34 ; Reise und Verkehrsverlag Hönigwiesenstrasse, 25 7 Stuttgart-Veihingen ; Zumsteins Landkartenhaus Liebherrstrasse, 5 8 München 22 ; GREAT BRITAIN Bailey Bros Swinfen Ltd. Warner House 48, Upper Thames Street London E.C. 4 City 6521 ; Blackwell's Foreign Department Broad Street Oxford ; Central Books Ltd. 37, Grays Inn Road London W.C. 1 ; Collet's Holdings Ltd. Denington Estate London Road Wellingborough Northans N G Goyle Ltd. 119—125 Charring Cross Road London W.C. 2 ; Parker Son 103, Walton Street Oxford ; HOLLAND Antiquariat Junk Walderstraat 10 Lochem ; Boekhandel Pegasus Leidsestraat 25 Amsterdam ; Intertaal Van Baerlesstraat 150 Amsterdam Zuit ; Meulenhoff Beulingstraat 2 Amsterdam C ; Swets Zeitlinger Keizersgracht 471—487 Amsterdam ; HUNGARY Kultura Fö utca 32 Budapest 1 ; ISRAEL Haiflepac Ltd. 11, Arlosorov St. Haifa ; Lepac Ltd, 15, Rambam St. Tel-Aviv ; Lotus Ltd. Achad Haam St. Tel-Aviv ; ITALY SO, CO, LIB, RI Export-Import Piazza Margana 33 Roma ; JAPAN Maruzen Ltd. 6 Tory Michome Nihombashi Tokyo ; Nauka Ltd. Imp. Departm. 30—19 Minami Ikebukuro 2, Chome, Toshima-Ku Tokyo ; DEMOCRATIC PEOPLE'S REPUBLIC OF KOREA Chulpanmul ; MEXICO Editorial Grijalbo S. A. Aparatado 28568 Mexico. 17.D.F. ; MONGOLIA Mongolgosknigotorg Ulan Bator ; NORWAY Norsk Bokimport Postboks 3267 Oslo ; POLAND Ars Polona Krakowskie Przedmiescie 7 Warszawa ; PORTUGAL Libreria Bucholz Avenida Libertade Lisboa ; SPAIN Libreria Bucholz Paseo de Recoletos Madrid ; Libreria Cientifics General Preciados no. 48 Madrid 13 ; SWEDEN Almqvist Wiksell 26, Gamla Brogatan Stockholm 8. ; C. E. Fritze Fredgatan 2 Stockholm 16 ; Gumperts AB P. O. Box 346 Göteborg I ; SWITZERLAND Fachbucherei Postfach 1420 3001-Berna ; Herbert-Lang Ecke Munzgraben 2 Berna ; Librairie Payot 1-Rue de Bourg Ch-1002 Lausanne ; Librairie Rousseau 36, Rue Jean-Jacques Rousseau Genève ; Pinkus Co. Froschaugasse 7 Zurich I ; THE UNITED ARAB REPUBLIC Dar ElTahrir et Publishing 21 Kasr el Nil St. (Dar el Shark Bookshop Cairo ; THE U.S.A. Angelescu Book Service 3645, Barham Street Detroit 24 Michigan ; American Chemical Society 1155, Sixteenth Street NWWashington DC 20036 ; Fam Book Service 69, Fifth Avenue Suite 8 F ; New York 10003, N.Y. Franklin Square-Subscription Agency Teaneck (New Jersey 07666) ; W. S. Heinman 400, East 72nd Street New York, 21, N. Y. ; McGraw-Hill Book Company 330, West 42nd Street New York, N.Y. 10036 ; Moore-Cottrell Subser. Agency Worth Cohocton, New York 14868 ; Nicoară Travel Service 17432, Woodward Ave. Detroit Michigan 48203 ; Shoenhof's Foreign Books, Inc. 1280, Massachusetts Avenue Cambridge, Massachusetts 02138 ; Henry M. Snyder Co. Inc. 440 Fourth Avenue New York, N.Y. 10016 ; Twayne Publishers, Inc. 31 Union Square West New York 3, N. Y. ; Zeitein Ver Brugge Booksellers 815 No. La Cienaga BLVD Los Angeles 69, California ; THE U.S.S.R. Mejdunarodnaia Kniga Moscow C. 200 ; THE DEMOCRATIC REPUBLIC OF VIET-NAM Xunhasaba 32, Hai Ba Trung Hanoi ; YUGOSLAVIA Forum V. Misica, 1 Novi Sad ; Jugoslovenska Knjiga Terazije, 27 Beograd ; Libertatea Z. Zrenjanina, 7 Pancevo ; Prosveta Terazije 16 I Beograd.

NOTE POUR LES AUTEURS

La *Revue Roumaine de Chimie* publie des articles en anglais, français, russe, allemand ou espagnol. Les auteurs sont priés d'envoyer des articles, notes, communications et comptes rendus inédits.

Les manuscrits seront dactylographiés à deux intervalles. Les tableaux seront dactylographiés sur feuilles séparées, de même que la légende des figures. Les diagrammes seront tracés à l'encre de Chine sur papier calque. Les tableaux et les figures seront numérotés par des chiffres arabes, en nombre strictement nécessaire. Prière de ne pas inscrire les mêmes données dans les tableaux et les figures. Les formules chimiques seront incluses dans le texte ; en outre, elles seront transcrites sur des feuilles séparées. Les auteurs sont priés d'indiquer les caractères italiques (en soulignant les lettres au crayon), ainsi que tout autre caractère spécial. L'ordre des références bibliographiques sera celui de leur mention dans le texte ; le nom de l'auteur sera précédé de l'initiale du prénom ; les publications périodiques seront présentées suivant les prescriptions internationales. Les références seront ajoutées à la fin de l'article ; elles paraîtront comme des notes, au bas de la page. Le texte sera précédé d'un résumé, comprenant 15 lignes au maximum.

L'entière responsabilité du contenu des articles appartient aux auteurs. On publie des articles dus aux collaborateurs roumains ou étrangers. Les auteurs recevront 50 tirés à part.

PRINTED IN ROMANIA

TRAVAUX PARUS AUX ÉDITIONS DE L'ACADÉMIE DE LA RÉPUBLIQUE SOCIALISTE DE ROUMANIE

CORNEL BODEA et collab., **Tratat de biochimie vegetală**, partea I, **Fitochimie** (Traité de biochimie végétale, Ire partie, Phytochimie), Ier vol., 1964, 747 p. + 4 annexes + 2 pl., 41 lei, IIe vol., 1965, 1962 p., 1 pl., 56 lei, IIIe vol., 1967, 773 p., 35 lei.

V. GHEŢIE et V. MICUŞAN, **Analiza imunochimică. Teorie şi practică** (Analyse immunochimique. Théorie et pratique), 1966, 369 p., 28 lei.

SILVIA IONESCU, **Reacţii chimice induse de radiaţiile ionizante** (Réactions chimiques produites par les radiations ionisantes), 1963, 271 p., 15 lei.

MARIETA NICOLAE, **Fizico-chimia proceselor fotografice** (Physico-chimie des processus photographiques), 1964, 426 p. + 4 pl., 35 lei.

R. PORTOCALĂ et L. POPA, **Acizii ribonucleici celulari şi virali** (Les acides ribonucléiques cellulaires et viraux), 1966, 375 p. + 8 pl., 26 lei.

D. PURDELA et R. VÎLCEANU, **Chimia compuşilor organici ai fosforului şi ai acizilor lui** (La chimie des composés organiques du phosphore et de ses acides), 1965, 540 p., 37 lei.

CRISTOFOR SIMIONESCU, MARGARETA GRIGORAŞ et AGATA CERNĂTESCU-ASANDEI, **Chimia lemnului din R.P.R.** (La chimie du bois en Roumanie), 1964, 239 p. + 6 pl., 27 lei.

CRISTOFOR SIMIONESCU et CLEOPATRA VASILIU-OPREA, **Mecanochimia compuşilor macromoleculari** (La mécanochimie des composés macromoléculaires), 1967, 344 p., 23,50 lei.

I. V. MAXIM, **Materiale nucleare** (Matériaux nucléaires), 1969, 444 p., 4 pl., 30 lei.

I. P. I. c. 5504 | 43 436 | Lei 25

F 1103

R

REVUE ROUMAINE DE CHIMIE

04

REZERVA

TOME 15
N° 9
Septembre 1970

ÉDITIONS DE L'ACADÉMIE DE LA RÉPUBLIQUE SOCIALISTE DE ROUMANIE

Rev. Roumaine Chim. 15, 1275–1460 (1970), Bucarest

COMITÉ DE RÉDACTION

Redacteur en chef :

C. D. NENIȚESCU, membre de l'Académie de la République Socialiste de Roumanie

Redacteurs en chef adjoints :

A. T. BALABAN et V. E. SAHINI, membres correspondants de l'Académie de la République Socialiste de Roumanie

Collège de rédaction :

C. DRĂGULESCU, RALUCA RIPAN, CR. SIMIONESCU, membres de l'Académie de la République Socialiste de Roumanie; EM. BRATU, membre correspondant de l'Académie de la République Socialiste de Roumanie, Pr G. OSTROGOVICH, MARGARETA AVRAM, F. BADEA, D. I. MARCHIDAN, D. NEGOIU et D. SĂNDULESCU.

Les manuscrits, les livres et les revues proposés en échange, ainsi que toute correspondance seront envoyés à la rédaction :

REVUE ROUMAINE DE CHIMIE

23, str. Dumbrava Roșie, Bucarest, 9, Roumanie.

REVUE ROUMAINE DE CHIMIE

ORSZÁGOS MŰSZAKI KÖNYVTÁR ÉS DOKUMENTÁCIÓS KÖZPONT 1883

Tome 15, N° 9 Septembre 1970

Page

STEFANIA ZUCA, Viscosity of some molten nitrates 1277–1286

D. I. MARCHIDAN and M. CIOPEC, High temperature enthalpy and related thermodynamic functions of some materials from the uranium-oxygen system 1287–1301

T. CHIRULESCU, Nickel ferrite-oxygen magnetization-volume adsorption isotherm 1303–1305

N. BONCIOCAT, L. CHIOSA, FLORICA MIHĂILESCU and M. OLTEANU, Chemical reactions in liquid junctions. I. The expression of the liquid-junction potential 1307–1317

FLORICA POPEA und A.-C. BANCIU, Spektrophotometrische Untersuchung im System $Th(NO_3)_4$–Violursäure 1319–1329

C. LITEANU et ELENA HOPÎRTEAN, Etude sur les électrodes-membranes polymère + plastifiant. III. L'utilisation de l'électrode-membrane en PCV et tricrésylphosphate dans le titrage potentiométrique des acides et bases forts 1331–1336

A. ŞUTEU, I. AL. CRIŞAN und ELISABETA POP, Die kinetische Bestimmung des Kupfers (II) mit Bromat und Amidol . . . . 1337–1341 R

I. GĂNESCU et Al. POPESCU, Complexes thiocyanato-chromiques dans l'analyse chimique. I 1343–1348

D. COSTACHE and GR. POPA, Kinetic determination of cobalt traces. V. With brompyrogallol red 1349–1353

FL. POPESCU, Polymères organiques phosphorylés. III. Phosphorylation du polystyrène dans des hydrocarbures aliphatiques (C_6–C_8) . . . . . . 1355–1364 R

M. MARCU and M. DIMA, Coordination polymers. IV. Polycoordination of 4,4'-[*p*-phenylene-bis(methyliden-nitrilo)]-di-methyl salicylate with cobalt, nickel and copper . . . . 1365–1373 R

A. BALOG, D. BREAZU, E. VARGHA, F. GÖNCZY and LUCIA BEU, Peptides. VIII. Some β-dicarbonyl N-protected aminoacids and model dipeptides 1375–1390

A. BALOG, E. VARGHA, D. BREAZU, LUCIA BEU and F. GÖNCZY, Peptides. IX. The activation and protection of the carboxyl group in the β-dicarbonyl N-protected aminoacid series 1391–1407

C. CRISTESCU, As-triazine derivatives with potential therapeutic action. X. 6-Carboxyhydrazide-as-triazines 1409–1414

Rev. Roumaine Chim. 15, 1275–1460 (1970), Bucarest

Page

FELICIA CORNEA, CORNELIA FULEA et S. MOLDOVEANU, Complexes moléculaires des thioamides. I. Complexes de transfert de charge entre le thiobenzamide, la thiobenzpipéridine et l'iode 1415–1426

T. RĂDULESCU und H. D. SCHELL, Mono- und diquartäre Ammoniumsalze des Benzal-Fluorens 1427–1431

V. FĂRCĂŞAN, I. OPREAN et C. BODEA, Sur la formylation des méthyl-10-phénothiazines 1433–1439

D. AUSLÄNDER, CORINA ŞERBAN et IOANA DĂBALĂ, Action des ultrasons sur un processus de carbonatation 1441–1446

E. POPPER, The microanalysis of cobalt by electrophoretic focussing with radioactive tracer 1447–1451

G. OSTROGOVICH, Z. SIMON and F. KEREK, Stereochemistry of imine systems. III. Mechanism of their uncatalysed *syn-anti* isomerization. The influence of the substituent on the activation energy 1453–1459

Revue Roumaine de Chimie, **15**, 1277 – 1286 (1970)

ORSZÁGOS MŰSZAKI KÖNYVTÁR ÉS DOKUMENTÁCIÓS KÖZPONT
1883

VISCOSITY OF SOME MOLTEN NITRATES

STEFANIA ZUCA
Institute of Physical Chemistry, str. Galaţi 31,
Bucharest

Received February 26, 1970

The density and viscosity of the following molten nitrates : $LiNO_3$, $NaNO_3$, KNO_3, $RbNO_3$, $CsNO_3$, $AgNO_3$ are reported for the temperature range of 150° above their melting point. The obtained results are discussed in the light of current views on viscous flow in ionic liquids.

Our recent papers [1,2] were concerned with the density and viscosity of binary alkali nitrate systems and of silver nitrate – alkali nitrate systems. On that occasion it was evident that a better knowledge of the magnitude of these properties of pure salts could provide interesting results on their structure.

Numerous authors [3–10] have previously reported on these properties but, in general, there has been considerable disagreement in the data of various investigators. Thus it has been proved expedient to measure the density and viscosity of all alkali nitrates and silver nitrates in order to obtain a self-consistent and perhaps a more accurate set of data.

EXPERIMENTAL RESULTS

The oscillating sphere method has been employed for viscosity measurements. The experimental set up was basically similar to that described elsewhere. [11] We note that the damping oscillations were this time automatically recorded by means of a PHD 8 Photodyne which has resulted in a higher precision in the determination of the logarithmic decreament and hence of the viscosity (error in viscosity is 2–3 %).

---

[1] I. G. Murgulescu and S. Zuca, *Electrochim. Acta*, **11**, 1483 (1966) ; **14**, 519 (1968)

[2] S. Zuca and R. Borcan, *ibid.*, in press.

[3] H. M. Goodwin and R. D. Mailey, *Phys. Rev.*, **23**, 22 (1906) ; **25**, 469 (1907) ; **26**, 28 (1908).

[4] R. S. Dantuma, *Z. anorg. Chem.* **175**, 1 (1928).

[5] F. A. Pugsley and F. E. W. Wetmore, *Canad. J. Chem.* **32**, 839 (1954).

[6] B. R. Sundheim and A. Berlin, *J. Phys. Chem.* **68**, 1266 (1964).

[7] G. J. Janz and R. D. Reeves, *Trans. Faraday Soc.* **61**, 2305 (1965).

[8] P. I. Protsenko and O. N. Razumovskaya, *Zhur. priklad. Khim.* **38**, 2355 (1965).

[9] R. E. Wellman, R. De Vitt and R. B. Ellis, *J. chem. Engng. Data*, **11**, 156 (1966).

[10] V. C. Reinsborough, *Austral. J. Chem.* **20**, 1037 (1967).

[11] I. G. Murgulescu and S. Zuca, *Z. phys. Chem.*, (Leipzig) **218**, 379 (1961).

The density has been determined by the hydrostatic method with a precision of 0.1–0.2%.

A constant temperature of the furnace to within ± 0.2°C was obtained, by use of a photothermoregulator. The temperature has been measured by means of a calibrated Pt/Pt–10% Rh thermocouple immersed directly into the studied molten nitrate.

An inert atmosphere of nitrogen gas was provided inside the furnace during the experiment.

The alkali nitrates were Merck or B.D.H. *p.a.* reagents. But samples of $RbNO_3$ and $CsNO_3$ were obtained also by direct synthesis from purified corresponding carbonate and nitric acid.

All salts were purified by recristallizing once from distilled water, dried for 24 h at 150° and melted under an inert atmosphere of thoroughly dried nitrogen gas. The melts were a clear colourless liquid.

Highly purified silver nitrate was prepared by adding to a saturated solution of *p.a.* reagent silver nitrate, an equal volume of concentrated nitric acid to effect crystallization of the salt. By drying and melting the crystals, the excess of nitric acid is completely eliminated, obtaining finally a clear slightly yellowish liquid.

As a further check of the purity of the salts used, the melting points were determined. The observed melting points are listed in table 1. They are not lower, within experimental error, than those generally accepted.

Table 1

Melting point (°C) of various molten nitrates

Salt	Our *) results	N.B.S.[12]	Other values
$LiNO_3$	254	254	253[13]
$NaNO_3$	307	310	306[13], 306.5[14]
KNO_3	334	337	333[13], 334[14]
$RbNO_3$	314	316	313[8]
$CsNO_3$	410	414	410[8]
$AgNO_3$	210	210	210.6[13]

*) Estimated accuracy ± 2°.

The salts were checked for alkalinity (loss of nitrate ion by hydrolysis) with phenolphthalein, both before and after experiment, but they were consistently neutral.

For each salt the density *d*, and the viscosity η, have been measured, in general, over a temperature range of about 150° above their melting point.

The results obtained for the density are summarized in the form of linear function of temperature in Table 2. These equations represent the observed points within experimental error, as indicated in the root mean square deviations column. The temperature ranges indicated are those within which the data were obtained. A comparison with the most recently reported data[12] shows that the agreement is very good and the differences do not exceed ± 0.2% except $RbNO_3$ where they are of +0.8%.

---

[12] G. J. Janz, F. W. Dampier, G. R. Lakshminarayanan, P. K. Lorenz and R.P.T. Tomkins, "Molten Salts", vol. 1, N.S.R.D.S., N.B.S., 15, 1968.

[13] P. Franzosini and C. Sinistry, *Ricerca Scient.* **Re** (**II**) **A3**, 411 (1963).

[14] V. A. Sokolov and N. E. Schmidt, *Izvest. Sekt. fiz. khim. Analiza Inst. Obshcheinorg. Khim.*, **26**, 123 (1953).

Table 2

Density equations of molten nitrates

Salts	Density *) eqs.	Standard deviations	Temperature range °C
$LiNO_3$	$d = 1.9238-0.5457\ t.10^{-3}$	0.0003	275 − 428
$NaNO_3$	$d = 2.1337-0.7319\ t.10^{-3}$	0.0008	326 − 469
KNO_3	$d = 2.1289-0.7592\ t.10^{-3}$	0.0001	353 − 483
$RbNO_3$	$d = 2.8141-1.0062\ t.10^{-3}$	0.0006	319 − 460
$CsNO_3$	$d = 3.2767-1.1269\ t.10^{-3}$	0.0007	419 − 524
$AgNO_3$	$d = 4.2016-1.0969\ t.10^{-3}$	0.0012	226 − 383

*) d is given in g/cm^3

Usually, the viscosity was measured in the same temperature range as the density. The results obtained are given in table 3.

The present data are compared to the values of viscosity obtained by other workers in figures 1 − 6. Generally three experimental methods were previously used, for measuring the viscosity of the presently studied molten nitrates :

— capillary method,[3, 5, 6, 8, 9, 10]
— oscillating sphere method, [4]
— oscillating hollow sphere. [7]

Table 3

Viscosity of molten nitrates

$LiNO_3$		$NaNO_3$		KNO_3		$RbNO_3$		$CsNO_3$		$AgNO_3$	
t°C	$\eta\cdot$cP	t°C	$\eta\cdot$cP	t°C	$\eta\cdot$cP	t°C	$\eta\cdot$cP	t°C	$\eta\cdot$cP	t°C	$\eta\cdot$cP
264.8	5.44	325	2.73	342	2.845	322	3.81	423.2	2.38	217.6	4.935
275	5.02	342	2.51	350	2.72	325.3	3.72	425	2.34	225.6	4.61
281.5	4.84	350	2.415	357.5	2.58	332.6	3.575	438.1	2.155	239	4.145
293	4.475	355.8	2.34	359	2.52	344	3.25	447	2.045	246	3.86
300.1	4.235	369.8	2.18	375	2.35	350.2	3.195	450	2.02	249.5	3.855
311.6	4.00	375	2.12	378.2	2.31	359	2.995	456.2	1.925	250	3.73
325.3	3.60	384.7	1.995	380.1	2.33	370.3	2.86	467.4	1.84	255.6	3.68
340.2	3.30	392.1	1.93	383.6	2.26	375	2.60	471.9	1.795	260.6	3.50
350	3.09	400	1.88	387	2.20	389.2	2.63	475	1.805	263	3.525
365	2.86	415.3	1.76	395	2.11	396	2.55	482	1.74	267.8	3.395
373.6	2.66	425	1.68	400	2.065	400.1	2.535	489.9	1.70	271.2	3.32
375	2.65	450	1.55	404.6	2.06	405.5	2.505	500	1.65	275	3.22
382	2.56	450.5	1.545	408.9	2.005	411.5	2.45			279.3	3.165
387.3	2.41	475	1.46	421	1.87	424.6	2.38			289.5	2.98
391	2.43			425	1.84	433	2.25			300	2.84
400.2	2.35			443.2	1.705	448.6	2.09			310	2.72
412.1	2.245			450.3	1.64	450	2.08			325	2.52
424.3	2.155			462	1.56	462.3	1.98			334	2.42
				472.6	1.50	469	1.91			350	2.24
				475	1.47	473	1.89			352.3	2.23
				484	1.43					363.1	2.09
				491.1	1.40					375	2.04
										376.2	2.04

From the data illustrated in figures 1—6, it is evident that there is a considerable disagreement among various laboratories especially concerning the viscosity of $LiNO_3$.

The dependence of viscosity on temperature for $LiNO_3$ (fig. 1) differs by as much as +8% from the values of Goodwin and Mailey[3] and those of Protsenko and Razumovskaia.[8] However except for Dantuma's[4] work the relative shape of the curves is approximately the same. Dantuma's data[4] indicate a stronger temperature dependence and with increasing temperature the percent difference diminishes from −14% to −3%.

We note here that the percent difference is calculated as :

$$\left[\frac{\text{Our Value} - \text{Literature Value}}{\text{Literature Value}}\right] 100.$$

The present results for $NaNO_3$ (fig. 2) agree within experimental error very closely with the values of viscosity obtained by the other workers.[3, 4, 8] The percent difference is of ±1% from the values reported by Dantuma[4] and by Protsenko and Razumovskaia[8] but reaches at a higher temperature, + 3% from the values of Goodwin and Mailey.[3]

KNO_3 is often used as a standard for the calibration of viscometers for use at high temperatures since it is stable material and its viscosity is generally accepted as being well established with Dantuma's values[4] which are the most reliable. Figure 3 shows clearly the close agreement between different laboratories[3, 4, 7, 8] and present data. The maximum percent difference is of +1.5%, −1.4%, −0.5%, −1.9% respectively. A slightly lower temperature dependence is indicated in a more recent work by Welleman, De Witt and Ellis.[9] Thus, at temperatures ranging from 460—490° the percent difference reaches −5.5% while from 340—450° it does not exceed ± 1%.

Only one investigation on the viscosity of $RbNO_3$ and $CsNO_3$ has been reported in literature.[8]

As it can be seen in figure 4, the agreement between the two sets of values for $RbNO_3$ is good +2.5% at lower temperature, but with increasing temperature the difference increases steadily to + 8%.

A contrary development is observed in figure 5 for $CsNO_3$. The present data indicate a stronger temperature dependence and while in the vicinity of 425° the percent difference is of +12.5% at a higher temperature there seems to be a very good agreement and the percent difference diminishes to 2%.

For $AgNO_3$ (fig. 6) the present results are in reasonable agreement ± 3% with the more recently measured values.[5, 8, 10] The percent difference is higher compared with the other data quoted in literature,[3, 6] namely of +6% and −6.3% respectively.

Surveying the different papers[3−10] in this field, we tried to examine the causes to which could be assigned the above observed discrepancies. An analysis of the techniques used by earlier investigators did not provide any explanation. It could be, either an error in method due to some unrecognized effects or to the purity of the reagent used. Nevertheless, we consider that with the oscillating sphere method which is an absolute method, any error of calibration met with capillary type instruments, be avoided.

DISCUSSIONS

A graphical analysis of log η against $1/T(°K)$ showed that all studied nitrates gave straight lines, i.e, the Arrhenius equation :

$$\eta = A \exp\ (E_\eta/RT) \tag{1}$$

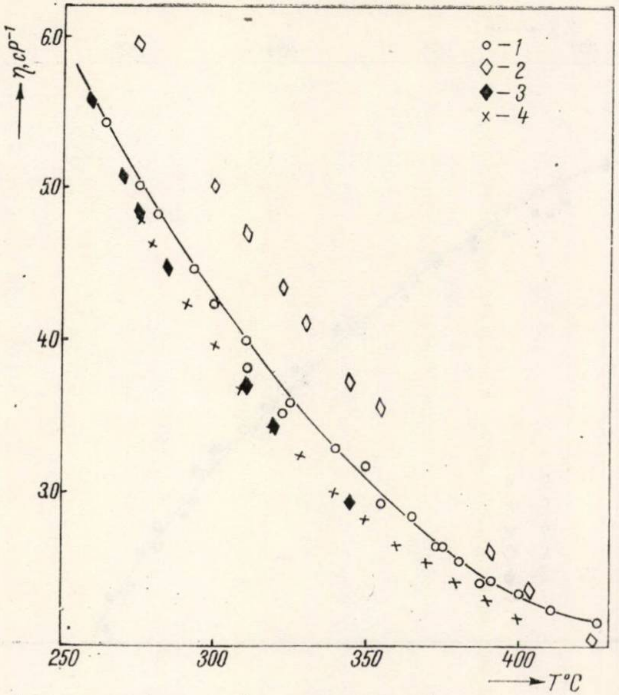

Fig. 1. — Viscosity of molten $LiNO_3$.

1, present data; *2*, Goodwin and Mailey [3]; *3*, Dantuma[4]; *4*, Protsenko and Razumovskaia.[8]

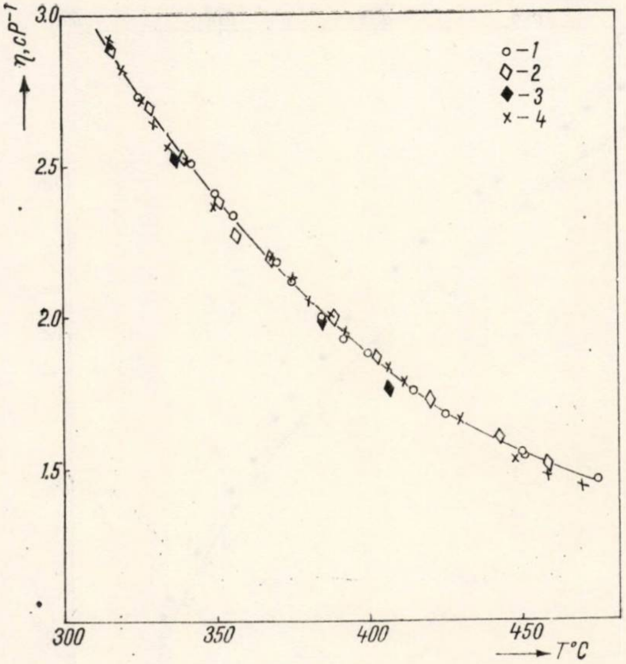

Fig. 2. — Viscosity of molten $NaNO_3$.

1, present data; *2*, Goodwin and Mailey [3]; *3*, Dantuma [4]; *4*, Protsenko and Razumovskaia[8].

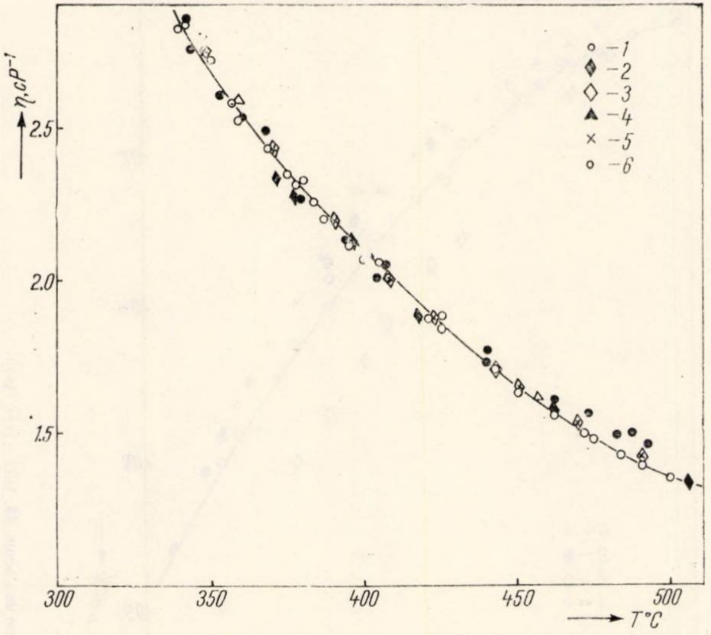

Fig. 3. — Viscosity of molten KNO_3.

1, present data; *2*, Goodwin and Mailey[3]; *3*, Dantuma[4]; *4*, Janz and Reeves[7]; *5*, Protsenko and Razumovskaia[8]; *6*, Wellman, De Witt and Ellis.[9]

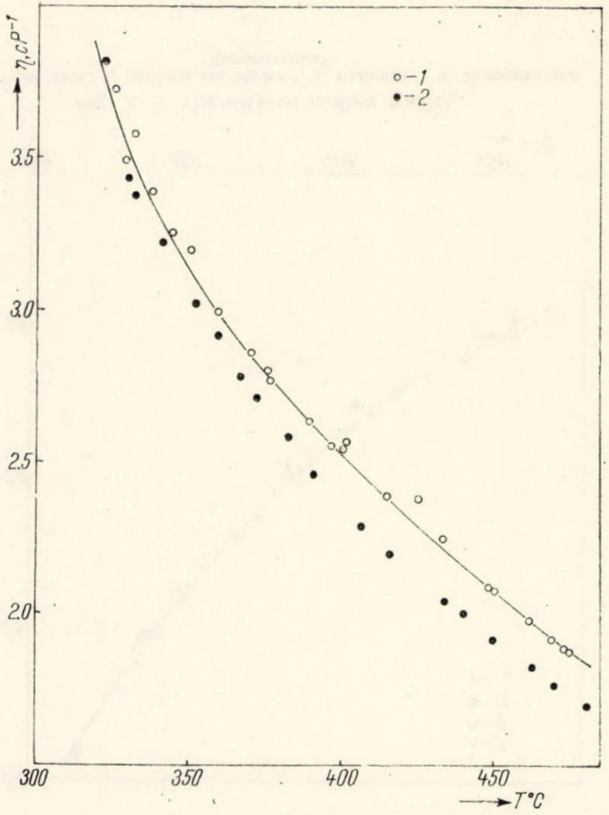

Fig. 4. — Viscosity of molten $RbNO_3$.

1, present data; *2*, Protsenko and Razumovskaia.[8]

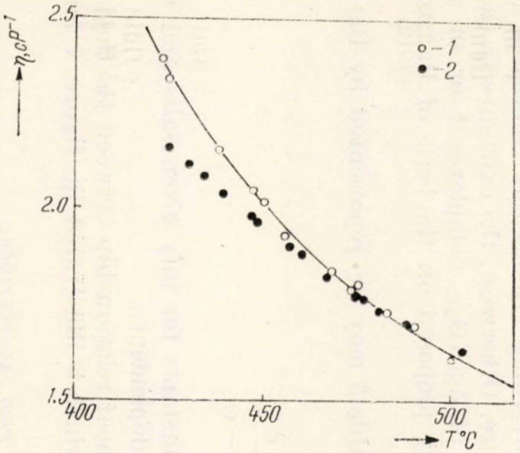

Fig. 5. — Viscosity of molten $CsNO_3$.
1, present data ; *2*, Protsenko and Razumovskaia. [8]

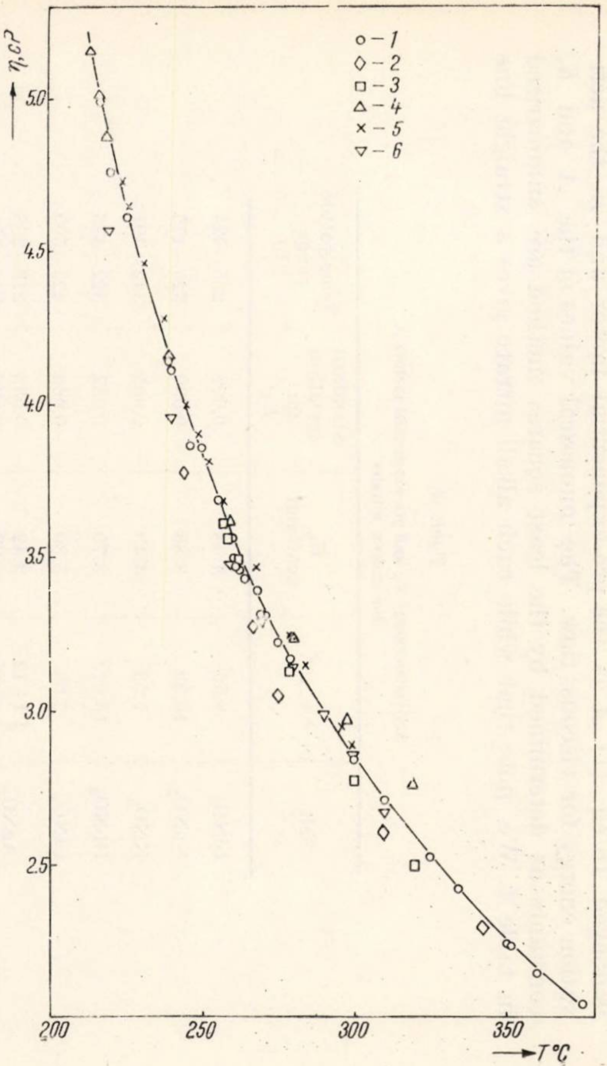

Fig. 6. — Viscosity of molten $AgNO_3$.
1, present data ; *2*, Goodwin and Mailey[3] ; *3*, Pugsley and Wetmore[5] ; *4*, Sundheim and Berlin[6] ; *5*, Protsenko and Razumovskaia[8] ; *6*, Reinsborough. [10]

is obeyed. In eq. (1) A is the pre-exponential factor and E_η the activation energy for viscous flow. The numerical values of the A and E_η constants as determined by the least squares method are summarized in table 4. We note that while each alkali nitrate gives a straight line

Table 4

Activation energy E_η and pre-exponential factors A for molten nitrates

Salt	*$A . 10^2$	E_η kcal/mol	Standard deviation for E_η	Temperature range (°C)
$LiNO_3$	8.56	4.44	0.009	265–424
$NaNO_3$	10.39	3.88	0.030	325–475
KNO_3	7.53	4.43	0.005	342–491
$RbNO_3$	13.67	3.79	0.032	322–473
$CsNO_3$	5.08	5.30	0.069	423–500
$AgNO_3$	{ 14.12 8.76	3.42 3.93	0.035 0.030	218–268 263–376

*) η is given in cP.

Arrhenius viscosity plot, for silver nitrate there is a noticeable change in slope and two straight lines which intersect at about 260° are obtained. A similar behaviour was previously noticed by Reinsborough.[10] It can be interpreted as indicating Arrhenius flow at all temperatures, but that at ~260° the structural unit governing viscous flow increases in size on cooling through this temperature. Otherwise, the existence in the melted silver nitrate of ion-pairing, [15] of $Ag(NO_3)_2^-$ complexes [16] or of a cubic close packing [17] has been already proposed on the basis of Raman and infrared spectra results.

Alternately, the data given in table 3 may be represented by Batchinskii equation :

$$\eta = \frac{c}{v - \omega}$$

where c and ω are characteristic constants for any given salts and v is the specific volume (temperature dependent).

According to eq. (2) there is a linear relationship between the fluidity $(1/\eta)$ and the specific volume v, which is illustrated in figure 7 for the six presently investigated nitrates. The slope and interception of each straight line in figure 7, give the c and ω values as shown in table 5.

---

[15] S. C. Wait and A. T. Ward, *J. Chem. Phys.*, **44**, 448 (1966).

[16] J. P. Delvin, K. Williamson and G. Austin, *ibid.*, **44**, 2203 (1966).

[17] G. J. Janz and D. W. James, *ibid.*, **35**, 739 (1961).

The constant ω in eq. (2) frequently is named the limit specific volume because it represents the specific volume at which the viscosity becomes infinite i.e. the liquid solidifies. Consequently the constant ω represents the specific volume of the solid at the freezing point and the difference $v-\omega$ may be regarded as the free volume available for viscous flow. The validity of Batchinskii equation proves that the free volume plays an important part in the viscous flow in the pure molten nitrates

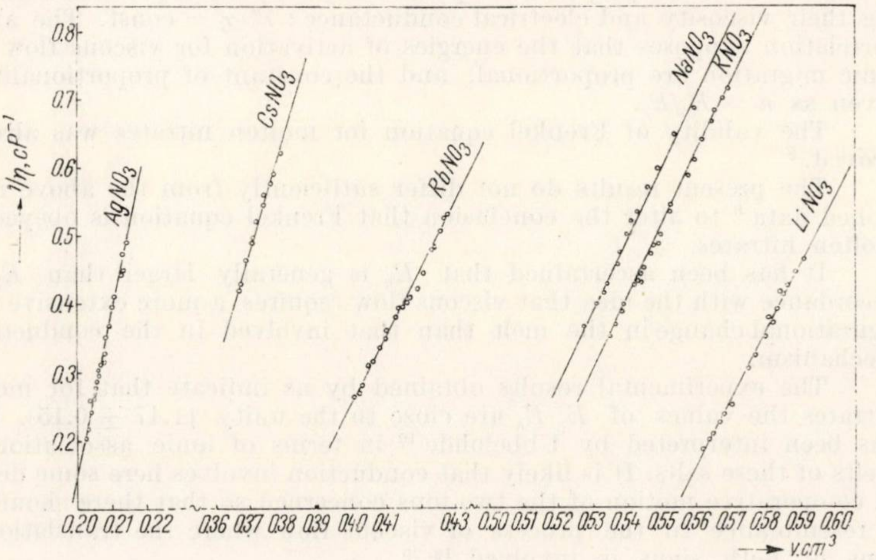

Fig. 7. — **Dependence of** fluidity ($1/\eta$) against specific volume v in molten alkali nitrates and silver nitrate.

Table 5

Batchinskii equation parameters for molten nitrates

Salt	*c.10^2	ω
$LiNO_3$	9.852	0.5448
$NaNO_3$	9.521	0.4938
KNO_3	9.229	0.5032
$RbNO_3$	10.320	0.3739
$CsNO_3$	6.003	0.3316
$AgNO_3$	2.560	0.2489

*) η is given in cP.

In addition to the dependence upon free volume, we may expect the viscosity to be some function of the size and mass of ions in the melt. However, the plot of η against r, $1/r$, $1/m$, $1/m^2$ gave no smooth curves, and no quantitative correlation could be established.

Frenkel[18] has proposed for pure molten salts an expression connecting their viscosity and electrical conductance : $\lambda^n \cdot \eta = \text{const}$. The above correlation supposes that the energies of activation for viscous flow and ionic migration are proportional, and the constant of proportionality is given as $n = E_\eta / E_\lambda$.

The validity of Frenkel equation for molten nitrates was already proved.[8]

The present results do not differ sufficiently from the above mentioned data[8] to alter the conclusion that Frenkel equation is obeyed by molten nitrates.

It has been ascertained that E_η is generally larger than E_λ in accordance with the idea that viscous flow requires a more extensive configurational change in the melt than that involved in the conductance mechanism.

The experimental results obtained by us indicate that for molten nitrates the values of E_η/E_λ are close to the unity (1.47 ± 0.15). This has been interpreted by Ubbelohde[19] in terms of ionic association in melts of these salts. It is likely that conduction involves here some degree of co-operative motion of the two ions concerned so that there should be a resemblance to the process of viscous flow where the translation of ions of both signs is involved.[12, 20]

[18] J. Frenkel, "Kinetic Theory of Liquids", Oxford University Press, London, 1946, p. 441.

[19] J. Davies, S. E. Rogers and A. R. Ubbelohde, *Proc. Roy Soc.*, **A 220**, 14 (1953).

[20] I. G. Murgulescu and S. Zuca, *Z. phys. Chem.* (Leipzig) **222**, 300 (1962) ; *Rev. Roumaine Chim.* **10**, 123 (1965).

Revue Roumaine de Chimie, **15**, 1287-1301 (1970)

HIGH TEMPERATURE ENTHALPY AND RELATED THERMODYNAMIC FUNCTIONS OF SOME MATERIALS FROM THE URANIUM-OXYGEN SYSTEM

D. I. MARCHIDAN and M. CIOPEC

Centre of Physical Chemistry, Str. Galaţi 31
Bucharest, Romania

Received February 25, 1970

Enthalpy data are reported for $UO_{2.125}$ and $UO_{2.63}$ over a temperature range from 300 to 1300°K. To this purpose $UO_{2.125}$ was sealed in a quartz capsule evacuated under argon subsequently introduced into a platinum container; $UO_{2.63}$ was inserted into a platinum capsule sealed in the air. A drop technique was employed in conjunction with an isothermal-jacket, block-type calorimeter in order to measure the heat release which was then converted into enthalpies. Prior to these tests similar measurements were carried out on the enthalpy of alpha-alumina (NBS standard substance) up to 1300°K. The results were found to be in good agreement with the existing high temperature data and hence the accuracy of the technique. The thermodynamic functions have been calculated from experimental results. A comparison is made between the observed data and the previous values.

Enthalpy measurements are customarily used to obtain thermodynamic functions for compounds above the ambient temperature. If these data could fit an analytical expression, C_p, $S_T - S_{298.15}$, and $(G_T - H_{298.15})/T$ (if $S_{298.15}$ is known) would be obtained quite easily at temperatures over the measurement range.

The derived functions are required for the treatment of other high temperature thermodynamic data.

Many of the thermodynamic data for uranium compounds are reliable and consistent, but a number of inconsistencies still remain such as those existing in the uranium-oxygen system.

The high temperature enthalpy of the compounds in the uranium-oxygen system is of interest both for theoretical and practical reasons.

For this reason our laboratories have initiated the investigation of the uranium-oxygen system with special emphasis on the thermodynamics of nonstoichiometric compounds between UO_2 and U_3O_8.

APPARATUS AND PROCEDURE

The enthalpy measurements in the high temperature range (25 to 1000°) were made by drop calorimetry. The experimental technique has been described in detail in a previous paper.[1]

The determination procedure is the following.

The capsule-sealed sample is suspended in a furnace until a known constant temperature.The sample is then droped into the block-type calorimeter with isothermal jacket which measures the heat evolved by the sample and the container, due to the cooling to 25°. In order to account for the heat content of the capsule and the heat lost while droping, a similar experiment is made with the empty capsule at the same temperature. The difference between the two heat values is a measure of the change in the heat content of the sample from the furnace temperature up to 25°. The values obtained for a series of temperatures, enable to calculate the enthalpy, whereby the heat capacity, increment in entropy, and free energy functions can be derived.

The block-type calorimeter with isothermal jacket consists of a copper block in a brass container. The calorimetric block is chromium coated, as is the inside of the container surrounding the block. A copper gate covers the central receiving "well", thereby preventing the energy loss by the sample radiation. The copper block rests on three Teflon supports and has no contact with any of the surrounding metal surface.

The calibration factor of the calorimeter was determined periodically by supplying with a known amount of electrical energy a Kanthal heater, wound on the alumina tube inserted into the copper block.

The change in the block temperature is determined with a thermistor immersed in a calorimeter's hole subsequently filled with Wood alloy.

The measurement of the temperature increase occurred by considering the resistance of a thermistor (CICE, type CS, made in France) introduced into a Wheatstone bridge. The resistance of the thermistor was followed manually with a VEB Mellenbach bridge. At 25⁰ the thermistor's resistance is 29 293 ohms. A 0.001° change brings about a 1.0 ohm change in the thermistor resistance. Usually some difficulties occur as regards the stability of thermistors which are solved by maintaining continuously constant day-and night, [1] the current supply within ± 0.05%. The bridge supply was held below 0.1 mA by placing a 2 kilohm series resistor, fed from a 2 V low discharge storage cell. The bridge unbalance was determined with a Multiflex galvanometer Lange, type MG-2. One unit of the galvanometer scale is equivalent to a change of approximately 1 ohm or 0.001°. The thermistor was calibrated against a calibrated Beckman thermometer. Although the thermistor resistance does drift after several months, the entire calibration curve is shifted almost parallelly so that no recalibrations become necessary. The uncertainty due to this drift, corresponding to a temperature change of 5°, does not go beyond some thousandths of degree and is proportionally smaller for small temperature changes.

The calorimeter set up was immersed into a well-stirred water bath the temperature of which was controlled up to ±0.005° by means of a mercury regulator (Höppler).

The furnace consists of an alumina tube with Kanthal electric resistance. The furnace core contains a metallic block, the temperature of which was maintained within ± 0.5° by a proportional controller, using a Pt–PtRh control thermocouple. The temperature of the sample was measured by another Pt–PtRh thermocouple. These thermocouples are close to the sample, which is suspended in the central well of the metallic block by a 0.1 mm diameter Cronix wire, clamped between two solid Kanthal electrodes. These electrodes are fixed in a motion-device shifting towards X – Y that allows adjustment of the positions of the heated sample from outside. The device is bound by flexible copper straps to an electrical source. In order to accurately release the sample the current is passed through the suspension wire causing it to vaporize rapidly. Experiments have shown that no heat correction is required for this discharge energy. The measuring thermocouple was checked against a Degussa (Germany) calibrated thermocouple.

---

[1] D. I. Marchidan and M. Ciopec, *Studii şi Cercetări Chim. Acad.*, **17**, 737 (1969).

EXPERIMENTAL RESULTS

The calibration factor of the calorimeter block was determined by supplying with a known amount of electrical energy from the calibration heater and observing the temperature change of the block which corrects for heat losses to the isothermal surrounding.

Prior to energy input the voltage from the storage batteries was stabilized by switching it into a circuit with a dummy resistance with the same value as the calibration heater. The total time t of the energy input was measured on a stop watch with a 0.05 sec accuracy. The stop watch was switched on and off exactly in time with the energy input by means of a mechanical device. The potential drops V and I across the heater were measured with high precision at 30-sec intervals. The heat developed in the leads is negligible[2] and the heat liberated in the calorimeter is then given by:

$$Q = 0.239 \quad V.I.t \text{ (calories)} \tag{1}$$

Calibration factor of the calorimeter is given by:

$$W = Q/\Delta\theta \tag{2}$$

where $\Delta\theta$ is observing the temperature change of the block.

Correction of the $\Delta\theta$ value for the heat exchange of the block with the isothermal surroundings was made with the equation[3]

$$\mathrm{d}\theta/\mathrm{d}t = K\,(\theta - 25) \tag{3}$$

Where $\mathrm{d}\theta/\mathrm{d}t$ is the measured cooling rate in degrees per minute, K is Newton's constant, θ is the calorimeter temperature in degrees Celsius, and 25 is the temperature, also in degrees Celsius, at which the heat exchange rate is zero. The magnitude of Newton's constant depends mainly upon the heat capacity of the block, the thermal conductivity of the gas and the metal leads between block and jacket, and the distance between them.

For each calibration (or drop) experiment a plot was made of the temperature increment of the block *versus* time and the K value was calculated from initial and final periods. In a second step, $\mathrm{d}\theta/\mathrm{d}t$ was calculated for each interval between two experimental points of the principal period (fig. 1). The total correction for the experimental $\Delta\theta$ value was obtained from the integration of these values.

---

[2] D. C. Ginnings and E. D. West, *Rev. Sci. Instr.*, **35**, 965 (1964).

[3] T. B. Douglas and E. G. King in J. P. Mc Cullough and D. W. Scott, "Experimental Thermodynamics", Butterworths, London, 1968, p. 293.

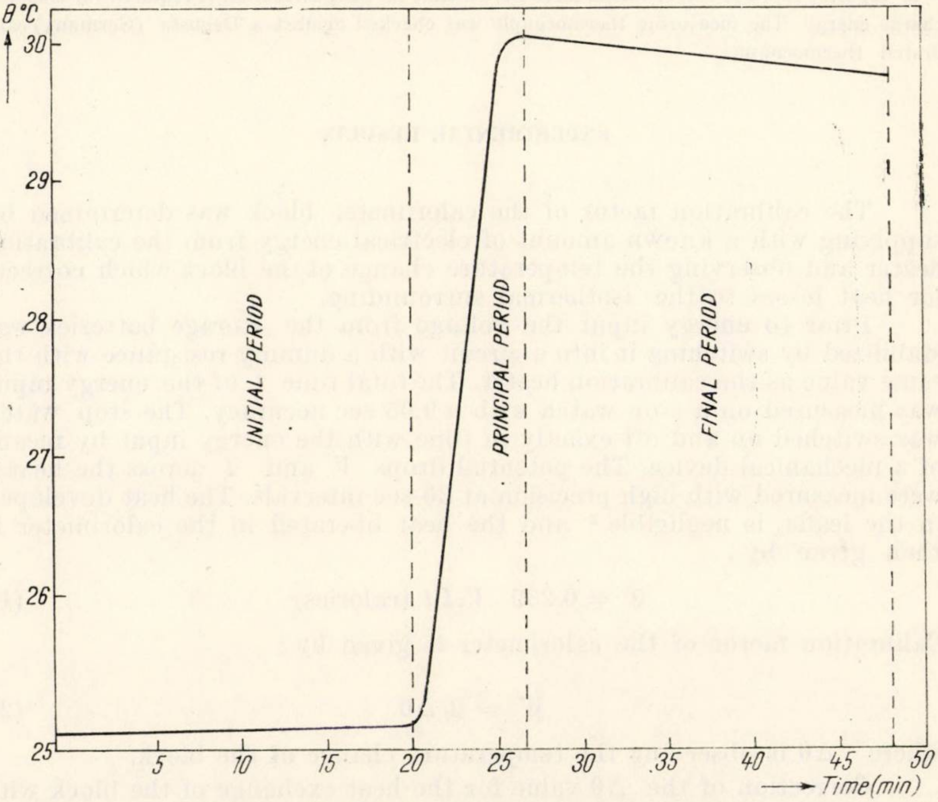

Fig. 1. — Typical diagram for a drop experiment.

A series of ten runs with temperature increase from 0.7 to 4.5° gave a calibration factor $W = 300$ calories/degree with an average deviation of $\pm 0.3\%$ (Table 1).

Table 1

Experimental values for calibration factor (W)

Run No	$\Delta\theta$ (degrees)	Q (calories)	W (calories)
1	0.778	233.90	300.65
2	0.945	284.14	300.68
3	1.557	468.62	300.98
4	1.823	545.86	299.43
5	2.261	677.42	299.61
6	2.447	733.29	299.67
7	2.600	778.23	299.32
8	3.023	907.90	300.33
9	3.756	1124.17	299.30
10	4.526	1357.26	299.88

ENTHALPY DATA FOR STANDARD SUBSTANCE

The reliability of the enthalpy data determined in the calorimeter was established by measuring the enthalpy of a standard substance for the experimental measurement of heat capacity in a high temperature range.

The synthetic sapphire (alpha-Al_2O_3) used as a standard substance was recommended by the Fourth Calorimetry Conference in 1949.[4] It was obtained from the U.S. Bureau of Standards, Washington. The material was used as received.

The enthalpy of alpha-alumina was determined with high accuracy by Furukawa ,[5] Macleod[6] and Chekhovskoi[7] using the drop method. A recent complete review of experimental data on the specific heat of aluminum oxide was made by Buyco.[8]

The equation for the enthalpy in calories/mole of aluminum oxide from 298.15°K was to T°K found to be

$$H_T - H_{298.15} = 35.5092\ T - 4.0884\ (10^{-4})\ T^2 - 11232.04 \log\ T + 17242.22 \qquad (4)$$

A sample of the synthetic sapphire, Calorimetry Conference, (7.1362 g) was enclosed in a platinum capsule and held in the furnace at constant temperature for at least thirty minutes and then droped into calorimeter.

The increase in temperature of the copper block due to the sample and the capsule was determined at 41 temperatures between 350 and 1250°K. Subsequently 41 determinations were carried out with the empty capsule at the same temperature, and each experimental $\Delta\theta$ value was corrected with equations (3). The increase in temperature due to the sample was obtained as the difference between the two sets of measurements.

From these data the heat content of the sample and the enthalpy of alpha-alumina are then obtained. Correction of the enthalpies occurred because the final calorimeter temperatures were above 25°; the data $(H_T - H_{298.15})$ are shown in Table 2 and compared with NBS data calculated by equation (4).

---

[4] * * * *Chem. Eng. News*, **27**, 2772 (1949).

[5] G. T. Furukawa, T. B. Douglas, R. E. Mc Coskey and D. C. Ginnings, *J. Res. Nat. Bur. Stand.*, **57**, 67 (1965).

[6] A. C. Macleod, *Trans. Faraday Soc.*, **63**, 300 (1967).

[7] V. Ya. Chekhovskoi, *Teplofiz. Vysokikh Temp.*, **2**, 296 (1964).

[8] E. H. Buyco in "Proc. Fourth Symp. on Thermophys. Properties", Univ. of Maryland, College Park, Maryland, 1968, p. 161.

Table 2

Enthalpy of synthetic sapphire Calorimetry Conference sample
(mol. wt. = 101.96)

T (°K)	$(H_T - H_{2915\cdot8})$ cal. mol^{-1}		Deviation cal. mol^{-1}	Deviation %
	obs.	calc. NBS eqn. (4)		
362.3	1304	1310	− 6	−0.46
364.4	1350	1356	− 6	−0.42
398.6	2123	2121	+ 2	+0.10
438.8	3047	3067	−20	−0.65
474.9	3963	3950	+15	+0.33
475.4	3967	3962	+ 5	+0.13
577.0	6614	6581	+33	+0.50
617.7	7705	7674	+31	+0.40
623.5	7851	7831	+20	+0.25
624.2	7863	7851	+12	+0.15
664.5	9031	9016	+15	+0.17
671.3	9155	9140	+15	+0.16
671.6	9163	9148	+15	+0.16
723.9	10561	10613	−52	−0.49
725.3	10634	10652	−18	−0.17
729.6	10822	10774	+48	+0.44
769.7	11908	11916	−10	−0.08
771.2	11963	11955	+ 8	+0.07
773.4	12019	12016	+ 1	+0.01
823.9	13460	13470	−10	−0.07
830.5	13675	13660	+15	+0.11
832.0	13748	13704	+44	+0.32
836.5	13860	13834	+26	+0.19
875.6	15031	14972	+59	+0.39
876.0	15031	14982	+49	+0.33
876.5	15066	14999	+67	+0.45
878.6	15135	15060	+75	+0.50
924.8	16431	16417	+14	+0.09
982.1	18091	18113	−22	−0.12
990.1	18316	18351	−35	−0.19
993.2	18476	18444	+32	+0.17
1048.5	20074	20097	−23	−0.11
1049.9	20100	20138	−38	−0.19
1056.5	20260	20337	−77	−0.38
1099.0	21608	21611	− 3	−0.01
1107.5	21795	21873	−78	−0.36
1108.2	21864	21894	−30	−0.14
1173.8	23947	23882	+65	+0.27
1174.9	24000	23915	+85	+0.35
1175.9	23982	23946	+41	+0.17
1234.1	25787	25719	+68	+0.26
				±0.25 %

In columns 4 and 5 the difference between present values and those calculated from the equation (4) representing the NBS-1956 smoothed data are listed. The mean deviation are less than ± 0.3% and show a slightly positive trend.

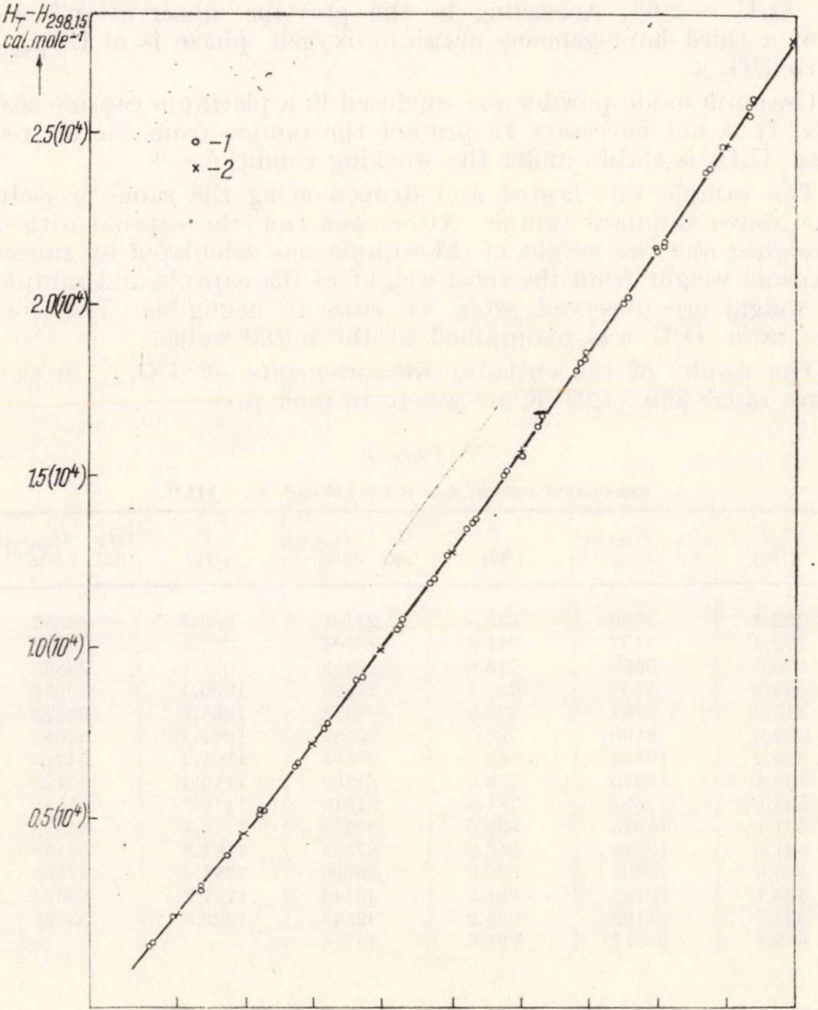

Fig. 2. — Enthalpy data for the sample at synthetic sapphire (Calorimetry Conference).

1, present work (experimental values);

2, NBS – 1956 data calc. by eq. (4).

The present results for the enthalpy of alpha Al_2O_3 are in good agreement with the NBS-1956 ones (Fig. 2), hence the accuracy of the technique seems to be of ± 0.3%.

ENTHALPY DATA FOR U_3O_8

Enthalpy was measured using 4.5 g U_3O_8 powder, 99% purity, with 83.89% uranium. The stoichiometry of this oxide was established to be $O/U = 2.63$. According to the previous observation[9] a lower limit of a third homogeneous uranium-oxygen phase is at $UO_{2.62}$ quite close to $UO_{2.67}$.

Uranium oxide powder was enclosed in a platinum capsule sealed in the air. It is not necessary to protect the sample from the air reaction because U_3O_8 is stable under the working conditions.[10]

The sample was heated and droped using the same procedure as for the above standard sample. After each run the capsule with sample was weighed and the weight of the sample was calculated by subtracting the capsule weight from the total weight of the capsule and sample. The total weight loss observed after 44 runs is negligible. Therefore the atomic ratio O/U was maintained at the initial value.

The results of the enthalpy measurements of $UO_{2.63}$ in the temperature range 350—1250°K are given in table 3.

Table 3

Experimental enthalpy data of UO 2.63 (mol. wt. = 842.1)

T (°K)	$(H_T - H_{298 \cdot 15})$ cal. mole^{-1}	T (°K)	$(H_T - H_{298.15})$ cal. mole^{-1}	T (°K)	$(H_T - H_{298 \cdot 15})$ cal. mole^{-1}
332.3	2720	673.3	24101	983.2	46382
352.2	4197	711.8	26784	999.5	47684
379.4	5509	716.8	27353	1021.1	48893
385.2	5734	721.5	27696	1030.4	49681
416.8	7791	725.8	28378	1088.2	53229
424.6	8190	760.5	30157	1095.5	53685
454.2	10134	763.6	30385	1101.2	54426
508.1	13270	773.5	31360	1113.4	55122
528.5	14851	781.8	31816	1116.7	55521
531.1	15078	838.9	36213	1174.7	59356
581.6	18229	854.2	37524	1181.4	59459
585.6	18404	872.5	38606	1211.6	61605
589.1	19143	921.2	42143	1217.3	62062
624.7	21195	925.2	42543	1226.8	63021
668.1	23817	928.6	42714		

ENTHALPY DATA FOR UO_{2+x} $(x = 0.125)$

A sample of 5 g UO_{2+x} powder, 98% purity, with 85.70% uranium was sealed in a quartz (vitreous glass) capsule under purified argon at 10^{-2}torr. The quartz capsule was enclosed in a platinum capsule for mechanical protection while droping.

[9] J. J. Katz and E. Rabinovitch, "The Chemistry of Uranium", Dover Publications, Inc., N. Y., 1951, p. 244.

[10] P. Pascal, "Nouveau Traité de Chimie Minérale", Tome XV, deuxième fascicule, Masson et Cie, 1961, p. 243.

The increase in temperature of the calorimeter block due to the empty quartz capsule enclosed in the platinum capsule, together with the small heat loss during the droping, have been determined by separate blank experiments. Another set of experiments was made with uranium oxide sealed in the platinum-enclosed quartz capsule. These experimental data have led to the calculation, as above, of enthalpy data for uranium oxide sample.

The stoichiometry of the sample was established to be O/U = 2.125. At this O/U ratio the system is homogeneously monophasic.[11]

After each run the capsule was weighed and the weight of the sample calculated as above. The total weight loss observed after 33 runs was negligible. Therefore the atomic ratio O/U was maintained at the initial value.

The results of the enthalpy measurements of $UO_{2.125}$ in the temperature range 350–1250°K are given in Table 4.

Table 4

Experimental enthalpy data of $UO_{2.125}$ (mol. wt. = 272.00)

T (°K)	$(H_T - H_{298.15})$ cal. mole^{-1}	T (°K)	$(H_T - H_{298.15})$ cal. mole^{-1}
354.9	934	750.4	8868
362.0	966	791.7	9660
379.6	1410	844.7	10959
396.0	1790	850.0	11054
397.7	1837	901.0	12194
451.1	2930	938.7	12700
452.4	3120	949.4	12859
493.3	3595	957.4	13001
499.3	3833	994.2	13761
550.4	4909	1047.6	14869
588.9	5765	1102.5	16245
590.4	5780	1137.9	16894
645.8	6825	1143.1	17197
647.0	6936	1152.3	17371
684.7	7696	1189.3	18248
743.6	8726	1190.8	18396
		1222.4	19084

---

[11] * * * "Thermodynamic and Transport Properties of Uranium Dioxide and Related Phases" Technical Reports Series No. 39, I AEA, Vienna, 1965, p. 7.

ANALYSIS AND TREATMENT OF THE DATA

The enthalpies of $UO_{2.63}$ and $UO_{2.125}$ were subjected to the least squares analysis in order to obtain a mathematical relationship between enthalpy and temperature.

A program was written for the least square analysis, which was performed on a CET 500 Romanian computer.

The best fit of several empirical equations for $H_T - H_{298.15}$ (cal.mole^{-1}) was obtained with an equation of the form :

for $UO_{2.63}$

$$H_T - H_{298.15} = -16173.786 + 56.174\ T + 7.294\ (10^{-3})\ T^2 - 0.865\ (10^{-6})\ T^3 \tag{5}$$

for $UO_{2.125}$

$$H_T - H_{298.15} = 3845.429 + 9.658\ T + 11.762\ (10^{-3})\ T^2 - 3.007\ (10^{-6})\ T^3 \tag{6}$$

Other equations of second and fourth degree polynomials in T, resulted in a poorer fit with the data.

The enthalpy equations and the observed data are plotted in figures 3 and 4 so that the reader might estimate their agreement.

The estimated deviation of experimental enthalpy values from the smoothed curve is 0.5%.

Differentiation of these enthalpy equations yielded the following heat capacity equations which are plotted in figure 5 :

for $UO_{2.63}$

$$C_p = 56.174 + 14.588\ (10^{-3})\ T - 2.595\ (10^{-6})\ T^2 \tag{7}$$

for $UO_{2.125}$

$$C_p = 9.658 + 23.524\ (10^{-3})\ T - 9.021\ (10^{-6})\ T^2 \tag{8}$$

From these equations the increment in entropy $S_T - S_{298.15}$ was calculated which is listed in tables 5 and 6 together with values calculated for the increment in enthalpy and heat capacity.

The equations were the following :

for $UO_{2.63}$

$$S_T - S_{298.15} = 56.174\ \ln\ (T/298.15) + 14.589\ (10^{-3})\ T - 1.297\ (10^{-6})\ T^2 - 4.234 \tag{9}$$

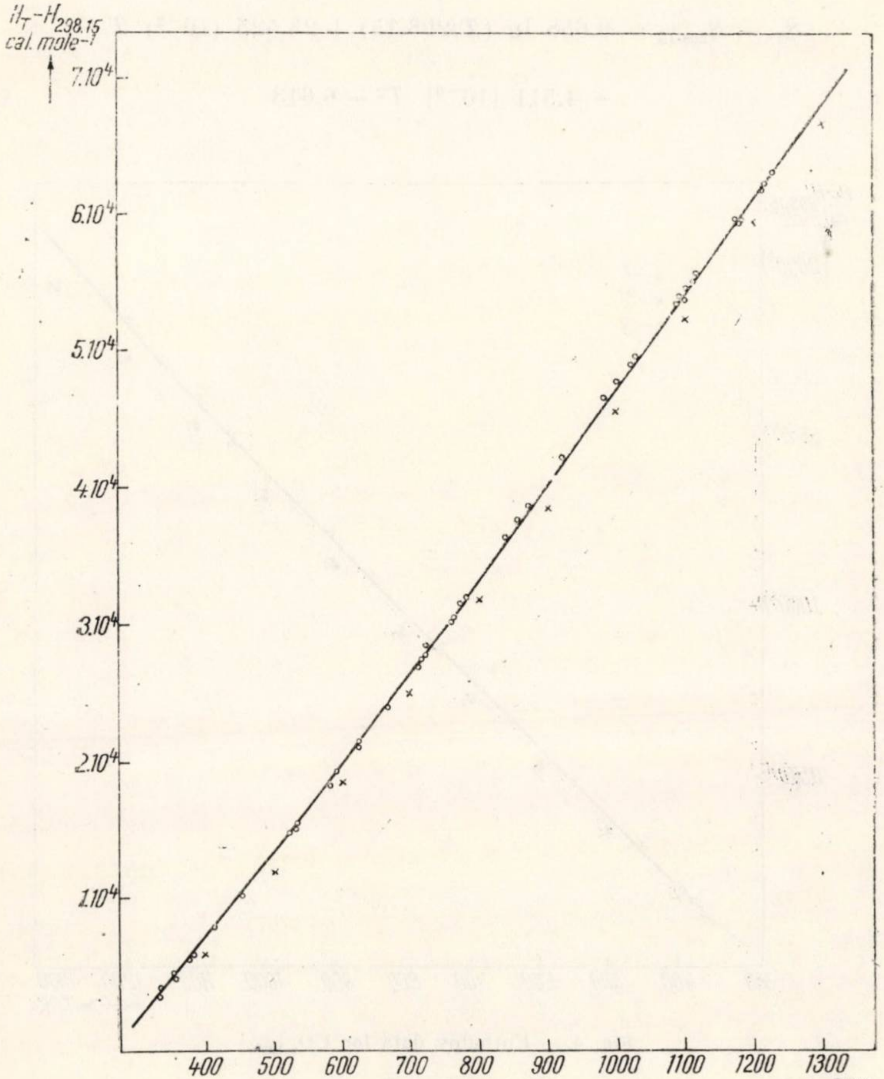

Fig. 3. – Enthalpy data for $UO_{2.63}$.

U_3O_8 { O/U = 2.66 → x from [12]
O/U = 2.63 → ○ experimental
– calculated (present paper)

---

[12] C. E. Wicks and F. E. Block, "Bulletin 605, Bureau of Mines", U. S. Gov't. Print. Off., Washington, 1963, p. 128.

for $UO_{2.125}$

$$S_T - S_{298.15} = 9.658 \ln (T/298.15) + 23.525\,(10^{-3})\,T - 4.511\,(10^{-6})\,T^2 - 6.613 \qquad (10)$$

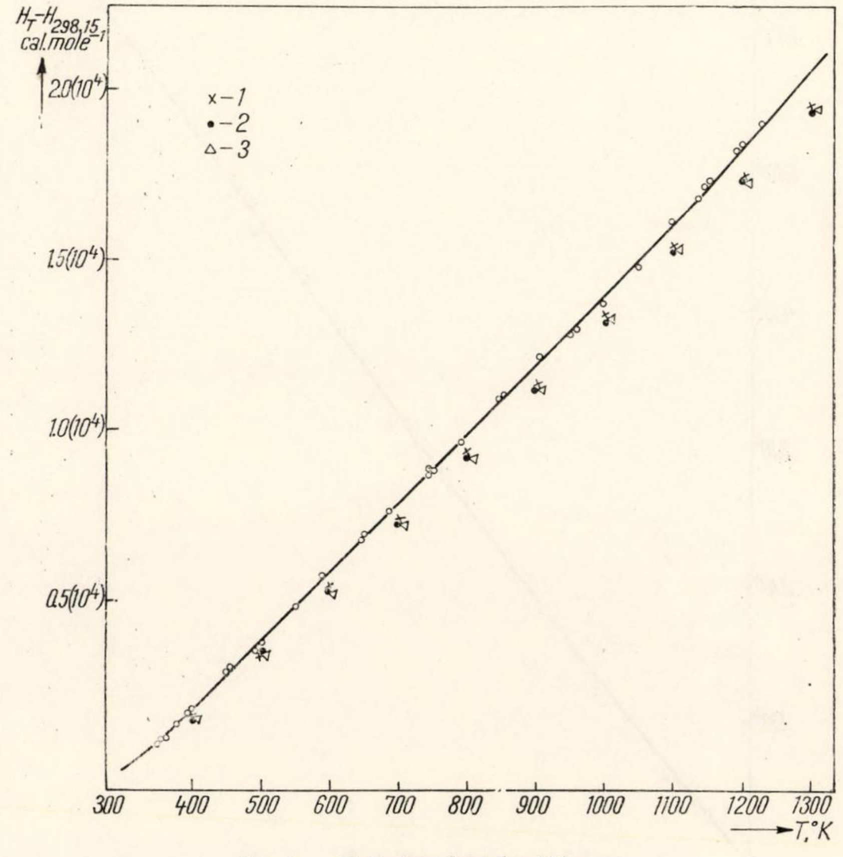

Fig. 4. — Enthalpy data for $UO_{2.125}$.

UO_2 { *1*, from [13]; *2*, from [14]; *3*, from [15].

$UO_{2.125}$ { O experimental (present paper) – calculated

---

[13] T. G. Godfrey, J. A. Woolley and J. M. Leitnaker, U. S. At. Energy Comm., 1966, ORNL–TM–1596.

[14] * * * "Thermodynamics of Nuclear Materials, 1967", IAEA, 1968, p. 651.

[15] G. E. Moore and K. K. Kelley, *J. Amer. Chem. Soc.*, **69**, 2105 (1947).

For U_3O_8 (O/U = 2.66) the value of $S_{298.15} = 67.5$ e.u.[18] has not been used in tabulating the free energy function $-(G_T - H_{298.15})/T$ because the stoichiometry of our oxide was O/U = 2.63. For this reason we tabulated the values of function

$$[(G_T - H_{298.15})/T] + S_T = (H_T - H_{298.15})/T.$$

For $UO_{2.125}$ the value of $S_{298.15}$ is not available and the tabulation of the data was made in the same manner as for $UO_{2.63}$.

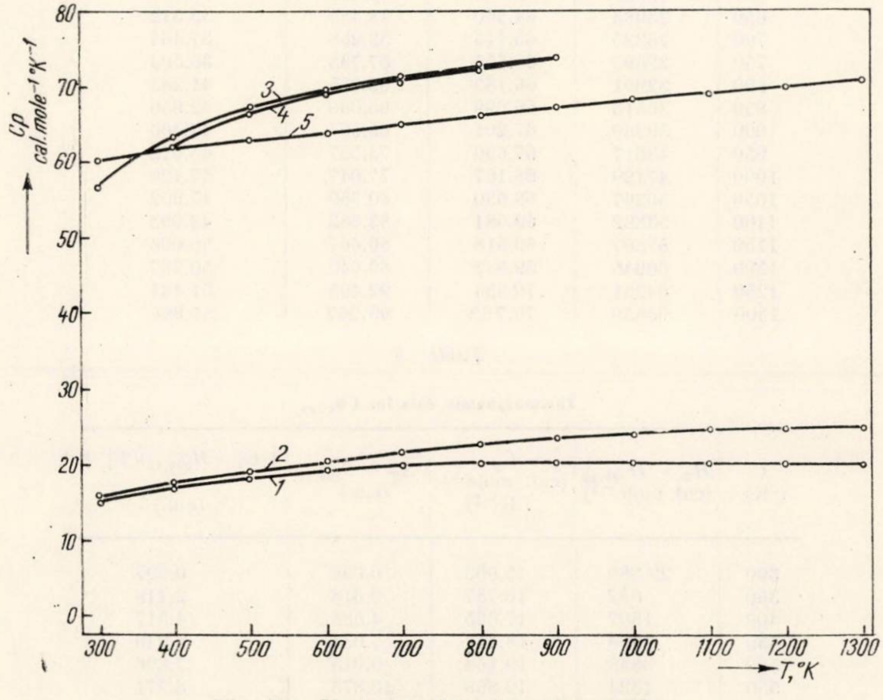

Fig. 5. — Heat capacity of uranium oxides.

1. C_p data for UO_2[13]; *2.* C_p data for $UO_{2.125}$ (present paper) ; *3.* C_p data for U_3O_8[16]; *4.* C_p data for U_3O_8[17]; *5.* C_p data for $UO_{2.63}$ (present paper).

---

[16] M. M. Popov, G. L. Gal'cenko and M. D. Senin, *Zhur. neorg. Khim.*, **3**, 1734 (1958)

[17] M. H. Rand and O. Kubaschewski, "The Thermal Properties of Uranium Compounds", Interscience Ltd., London, 1963, p. 70.

[18] E. F. Westrum Jr. and F. Gronvold, *J. Amer. Chem. Soc.*, **81**, 1777 (1959).

Table 5

Thermodynamic data for $UO_{2.63}$

T (°K)	$H_T - H_{298.15}$ (cal. mole^{-1})	C_p (cal. mole^{-1} °K^{-1})	$S_T - S_{298.15}$ (e.u.)	$[(G_T - H_{298.15})/T] + S_T$ (e.u.)
300	1011	60.317	0.361	3.370
350	4143	60.962	9.725	11.837
400	7127	61.594	16.585	17.817
450	10202	62.213	25.184	22.671
500	13328	62.819	31.782	26.656
550	16584	63.412	37.777	30.152
600	19869	63.993	43.331	33.115
650	23083	64.560	48.485	35.512
700	26225	65.115	53.298	37.464
750	29695	65.655	57.793	39.593
800	32991	66.183	62.055	41.283
850	36513	66.699	66.090	42.956
900	39960	67.201	69.904	44.400
950	43617	67.690	73.557	45.912
1000	47129	68.167	77.047	47.129
1050	50297	68.630	80.389	47.902
1100	53892	69.081	83.582	48.993
1150	57507	69.518	86.667	50.006
1200	60945	69.942	89.640	50.787
1250	64351	70.354	92.495	51.481
1300	68859	70.753	95.267	51.968

Table 6

Thermodynamic data for $UO_{2.125}$

T (°K)	$H_T - H_{298.15}$ (cal. mole^{-1})	C_p (cal. mole^{-1}. °K^{-1})	$S_T - S_{298.15}$ (e.u.)	$[(G_T - H_{298.15})/T] + S_T$ (e.u.)
300	29.389	15.903	0.096	0.097
350	847	16.787	2.618	2.419
400	1807	17.625	4.688	4.517
450	2808	18.417	7.034	6.240
500	3848	19.164	9.015	7.696
550	4824	19.868	10.873	8.771
600	5834	20.525	12.631	9.723
650	6825	21.137	14.300	10.500
700	7907	21.704	15.889	11.296
750	8905	22.227	17.403	11.873
800	9919	22.704	18.853	12.399
850	10955	23.135	20.244	12.888
900	11965	23.521	21.775	13.294
950	13006	23.864	22.858	13.690
1000	14067	24.160	24.058	14.067
1050	15081	24.411	25.276	14.363
1100	16157	24.617	26.414	14.688
1150	17200	24.778	27.513	14.956
1200	18484	24.895	28.572	15.403
1250	19731	24.966	29.588	15.784
1300	20680	24.991	30.568	15.907

CONCLUSIONS

Thermodynamic data obtained for non-stoichiometric oxides of uranium (enthalpy and heat capacity) are compared with available similar data for stoichiometric oxides in figures 3–5.

The figures seemingly show that the thermodynamic behaviour of non-stoichiometric oxides is similar to that of the corresponding stoichiometric oxides except for the heat capacity of $UO_{2.63}$ that increases more slowly with temperature.

A quantitative analysis of the departure in the behaviour of stoichiometric oxides is impossible for the time being, because the data available for non-stoichiometric oxides are insufficient and, moreover, our oxides were not very pure.

Present thermodynamic data for non-stoichiometric uranium oxides wholly confirm the fact that any alteration in the oxygen content as against the stoichiometric composition brings about the change in the heat content. This difference is significant as compared to the combined accuracy of the experiments and it is reproducible when different samples are used.

Acknowledgments. The work was performed under an I.A.E.A. contract 695/RB. The authors are grateful to the International Atomic Energy Agency for the permission to publish this paper. We wish to express our deep gratitude to Professor I. G. Murgulescu for his interest in our work and to C. Volcovici for his help in the equipment construction.

Revue Roumaine de Chimie, **15**, 1303–1305 (1970)

NICKEL FERRITE-OXYGEN MAGNETIZATION-VOLUME ADSORPTION ISOTHERM

T. CHIRULESCU
Institute of Physical Chemistry of the Academy, str. Dumbrava Roşie 23, Bucharest

Received January 12, 1970

The magnetization-volume isotherms derived in the case of oxygen adsorption are applied to oxygen adsorption on a nonstoichiometric nickel ferrite. The simplification of the problem is justified by a good agreement between theoretical and experimental data.

The effect of different adsorbed gases on the magnetization of finely divided nonstoichiometric nickel ferrite has been investigated in another paper.[1] In the present paper we present the application of the magnetization-volume isotherms[2] to the oxygen adsorption on the nonstoichiometric nickel ferrite. Three assumptions are made.

1. The adsorptive behaviour of nonstoichiometric nickel ferrite may be approximated by the behaviour of nickel ferrite with stoichiometric composition.
2. All the particles of the nickel ferrite have the same size.
3. The adsorbed molecules are uniformly distributed on the surface of all ferrite particles.
4. Approximately, the volume of introduced gas is equal to the adsorbed volume.

Let us consider the magnetization-volume isotherm corresponding to the cation vacancies distributed in the octahedral sites only. For this distribution the spinel structure remains unchanged after adsorption[3]; the experimental data support this distribution.[2,4,5] The equation of this isotherm is[2] :

$$\frac{\Delta M}{M} = \frac{1}{4}\,\frac{m}{n}\,\frac{1.5M^{3+} - 2M^{2+}}{M^{2+}} + \frac{1}{64}\,\frac{m^2}{n^2}\,\frac{(1.5M^{3+} - 2M^{2+})^2}{(M^{2+})^2} \qquad (1)$$

---

[1] T. Chirulescu and E. Segal, *Rev. Roumaine Chim.*, **15**, 000 (1970)

[2] T. Chirulescu, (under press).

[3] G. Parravano, "Fourth Intl. Congress on Catalysis", Moscow, 1968, paper no. 11.

[4] G. Ferguson and M. J. Hass, *Phys. Rev.*, **112**, 1130 (1958).

[5] W. E. Henry and M. J. Boehm, *Phys. Rev.*, **101**, 1253 (1957).

where M^{2+} and M^{3+} are the magnetic moments of a divalent cation, respectively trivalent one. Let us consider only the first term of eq. (1)

$$\frac{\Delta M}{M} = \frac{1}{4}\,\frac{m}{n}\,\frac{1.5M^{3+} - 2M^{2+}}{M^{2+}} \tag{2}$$

In the case of the nickel ferrite $M^{2+} = 2\ \beta$ (the magnetic moment of the nickel divalent ion) and $M^{3+} = 5\ \beta$ (the magnetic moment of the trivalent iron ion). Thus eq. (2) becomes :

$$\frac{\Delta M}{M} = 4.4 \times 10^{-1}\frac{m}{n} \tag{3}$$

where m represents the number of the oxygen atoms adsorbed on n surface molecules of the ferrite. Also we consider that m represents the number of oxygen atoms in the volume $v(cc)$ (STP) of gas. Then we can write :

$$m = 2 \times 6.023 \times 10^{23} \times v/22.4 \times 10^{3} = 5.40 \times 10^{19} v \tag{4}$$

Let N be the number of the molecules in one gram of nickel ferrite. One mole of this ferrite has a mass of 234 g, therefore,

$$N = 6.023 \times 10^{23}/234 = 2.57 \times 10^{21} \tag{5}$$

The number, N, of molecules in a sphere of radius r is found by dividing the volume of the sphere by the effective volume of one ferrite molecule, $5.66\ (a/2)^3$, for close packed structure, where a is the lattice parameter of the nickel ferrite (the cubic lattice of the nickel ferrite was approximated to a sphere of radius a/2); for the nickel ferrite is obtained[6] :

$$N = (4\pi/3)r^3/5.66(a/2)^3 = 5.90\ (r/a)^3 \tag{6}$$

The surface of a sphere of radius r may be written as :

$$A = 4\pi r^2 \tag{7}$$

Let $s(\mathrm{m}^2/\mathrm{g})$ be the value of the surface area of the sphere of radius r. Then,

$$s = 4\pi r^2 (10^{-10})^2 \times 6.023 \times 10^{23}/234N = 17a^3/r \tag{8}$$

where eq. (6) was used and the term $(10^{-10})^2$ comes from $r(\text{Å}) = 10^{-10} r(m)$.

For the number, n, of ferrite molecules on the surface of the sphere of radius r, one may obtain :

$$n = 4\pi r^2/2\pi(a/2)^2 = 8(r/a)^2 \tag{9}$$

---

[6] P. W. Selwood, S. Adler and T. R. Phillips, *J. Amer. Chem. Soc.*, **77**, 1462 (1955).

By dividing eq, (9) by eq. (6), one may obtain :

$$n/N = 8(r/a)^2 (5.90)^{-1} (a/r)^3 = 1.35a/r \qquad (10)$$

but taking into account the value of ratio a/r from eq. (8), eq. (10) becomes :

$$n/N = 1.35s/17\pi a^2 = 2.55 \times 10^{-2} s/a^2 \qquad (11)$$

The lattice parameter of nickel ferrite is $a = 8.33$ Å, therefore from eq. (11) it results :

$$n/N = 3.70 \times 10^{-4} s \qquad (12)$$

or,

$$n = 3.70 \times 10^{-4} sN \qquad (13)$$

Taking into account eq. (5), one obtains :

$$n = 9.50 \times 10^{17}\, s \qquad (14)$$

The ratio m/n may be obtained by dividing eq. (4) by q. 14 thus,

$$m/n = 5.40 \times 10^{19} v/9.50 \times 10^{17} s = 5.70 \times 10 v/s \qquad (15)$$

The equation of magnetization-volume isotherm results by introducing the m/n ratio into eq. (3) :

$$\frac{\Delta M}{M} = 4.40 \times 10^{-1} m/n = 4.40 \times 10^{-1} \times 5.70 \times 10 v/s \qquad (16)$$

or,

$$\frac{\Delta M}{M} = 2.50 \times 10 v/s \qquad (17)$$

where $v(cc, STP)$ is the volume of gas adsorbed by one gram of the nickel ferrite and s represents the surface area of sample, determined by the BET-standard method (low-temperature nitrogen adsorption). In the case of our sample of 0.9 m²/g, the initial slope of the magnetization-volume isotherm, derived from eq. (17), is :

$$\frac{\Delta M}{M} = 2.77 \times 10 v \qquad (18)$$

This value is in good agreement with the experimental value. [1]

Finally, it should be pointed out that the expression $(1.5M^{3+} - 2M^{2+})/M^{2+}$ in eqs. (1) and (2) is greater than zero. Therefore, the initial slope of the magnetization-volume isotherm is positive ; this means that oxygen adsorption on the nickel ferrite brings about an increase in the magnetization. This conclusion supports the mechanism proposed.

Revue Roumaine de Chimie, 15, 1303 – 1305 (1970)

Revue Roumaine de Chimie, **15**, 1307–1317 (1970)

CHEMICAL REACTIONS IN LIQUID JUNCTIONS. I

THE EXPRESSION OF THE LIQUID-JUNCTION POTENTIAL

N. BONCIOCAT, L. CHIOSA, FLORICA MIHĂILESCU and M. OLTEANU

Institute for State Control of Drugs and Pharmaceutical Researches,
str. Sfîntul Ion Nou, 14, Bucharest, Romania

Received January 20, 1970

A theoretical examination of the liquid junction HCl $(c_1)\parallel$ NaOH $((Vc_2-vc_1)/(V+v))+$ NaCl$(vc_1/(V+v))$; $vc_1<Vc_2$ has been carried out. The concentration profiles along the liquid junction double layer and the liquid-junction potential expression are deduced by taking into account the chemical reaction $H^+ + OH^- \rightarrow$ $\rightarrow H_2O$. This reaction is assumed to be very fast and quantitative. The liquid junction NaOH$(c_1)\parallel$ NaCl$(vc_1/(V+v))+$HCl$((Vc_2-vc_1)/(V+v))$; $vc_1<Vc_2$, which can be considered as the "dual" of the first junction, is also examined. The properties of these two "dual" liquid junctions are then generalized obtaining thus the general properties of two "dual" classes of liquid junctions. The experimental data obtained by the authors prove the validity of the theoretically deduced results.

1. INTRODUCTION

The liquid-junction potential is a hypothetical quantity, impossible to evaluate by any thermodynamic experimental method. Indeed, Guggenheim[1] has arrived at the negative conclusion that the electric potential difference between two points in different media has not yet been defined in terms of measurable quantities. This point of view was anticipated by Gibbs.[2] A similar negative result, namely that measurements of cells with or without liquid junctions can yield no information concerning ionic free energies, has been obtained by Taylor.[3]

---

[1] E. A. Guggenheim, *J. Phys. Chem.*, **33**, 842 (1929); **34**, 1540 (1930).

[2] "The Collected Works of J. Willard Gibbs" 1st vol., Longmans Green Co., New York, 1928, p. 429.

[3] P. B. Taylor, *J. Phys. Chem.*, **31**, 1478 (1927).

Equations for liquid-junction potentials, such as Planck's [4-7], and Henderson's, [8,9] do not solve the difficulties. In reality, these formulas were obtained by assuming the ionic activity coefficients to be equal with 1.

For this reason, the investigations concerning the liquid-junction potentials have been focussed especially on the major problem of reducing the uncertainty that liquid junctions produce in the thermodynamic experimental measurements. Three principal research trends can be distinguished :

— the use of special cells with liquid junctions in modern measurements of pH. Under special experimental conditions, the measurements of such cells can yield results of thermodynamic significance. These conditions are concerned with the elimination, by extrapolations based upon a series of measurements, of liquid-junction potentials and not with their evaluation. [10-16]

— the experimental estimation of liquid-junction potentials for different liquid junctions. [17-20]

— theoretical studies, in order to improve the Henderson's and Planck's formulas. [21-24]

The present paper is referring to another research trend, concerning the liquid-junction potentials, which has not yet been thoroughly studied, namely the influence of a chemical reaction, taking place within a liquid junction, on the concentration profiles along the liquid junction double layer and on the liquid-junction potential value.

In other research fields the influence of chemical equilibriums on the display of different processes was thoroughly investigated. For instance, Vetter [25-27] and Vetter and Manecke [28] have studied the influence

---

[4] M. Planck, *Ann. Physik*, **39**, 161 (1890); **40**, 561 (1890).

[5] H. A. Fales and W. C. Vosburg, *J. Amer. Soc.*, **40**, 1291 (1918).

[6] J. J. Hermans, *Rec. Trav. chim.*, **57**, 1373 (1938).

[7] D. A. MacInnes, "The Principles of Electrochemistry", Reinhold Publ. Corp., New York, 1939, p. 461.

[8] P. Henderson, *Z. phys. Chem.*, **59**, 118 (1907); **63**, 325 (1908).

[9] J. J. Hermans, *Rec. Trav. chim.*, **57**, 1373 (1938); **58**, 99 (1939).

[10] D. I. Hitchcock and A. C. Taylor, *J. Amer. Chem. Soc.*, **59**, 1812 (1937).

[11] H. S. Harned and R. A. Robinson, *J. Amer. Chem. Soc.*, **50**, 3157 (1928).

[12] E. Güntelberg and E. Schiodt, *Z. phys. Chem.*, **135**, 393 (1928).

[13] E. Larsson and B. Adell, *Z. phys. Chem.*, **A156**, 352 (1931).

[14] B. B. Owen, *J. Amer. Chem. Soc.*, **60**, 2229 (1938).

[15] B. B. Owen and E. J. King, *J. Amer. Chem. Soc.*, **63**, 1717 (1941).

[16] B. B. Owen and S. R. Brinkley, Jr., *J. Amer. Chem. Soc.*, **60**, 2233 (1938); **64**, 2171 (1942).

[17] Monique Dupeyrat, *Compt. rend.*, **252**, 269 (1961).

[18] I. V. Nelson and R. T. Iwamoto, *Analyt. Chem.*, **33**, 1795 (1961); **35**, 867 (1963).

[19] P. B. Mathur, *Indian J. Appl. Chem.*, **22**, 173 (1959).

[20] K. Schwabe and H. Geisler, *Electrochim. Acta*, **12**, 147 (1967).

[21] T. Foerland, *Acta Chem. Scand.*, **14**, 1381 (1960).

[22] J. P. Schwing, *J. Chim. phys.*, **61**, 491 (1964).

[23] G. Bianchi, G. Faita, R. Galli and T. Mussini, *Electrochim. Acta*, **12**, 439 (1967).

[24] P. A. Rock, *Electrochim. Acta*, **12**, 1531 (1967).

[25] K. J. Vetter, *Z. Elektrochem.*, **55**, 121 (1951).

[26] K. J. Vetter, *Z. phys. Chem. (Frankfurt)*, **199**, 22 (1952).

[27] K. J. Vetter, "Elektrochemische Kinetik", Springer, Berlin-Göttingen, 1961, chapter 2, paragraph 57 and 58.

[28] K. J. Vetter and G. Manecke, *Z. phys. Chem. (Frankfurt)*, **195**, 337 (1950).

of the equilibrium $Ag^+ + 2(CN^-) \rightleftharpoons Ag(CN)_2^-$ on the anodic dissolution of Ag in a cyanide solution, as well as the influence of the equilibrium $2Mn^{3+} \rightleftharpoons Mn^{2+} + Mn^{4+}$ on the diffusion processes at the Mn^{4+}/Mn^{3+} redox electrode. As for the electrical phenomena associated with the transport of ions and ion pairs in liquid ion-exchange membranes, a theoretical examination has been carried out by Sandblom, Eisenman and Walker,[29] of the steady-state properties of a homogeneous, ideally permselective, liquid ion-exchange membrane in which sites and counterions are incompletely dissociated. Dissociated species were assumed to be in chemical equilibrium with neutral ion pairs at every point in the membrane.

In this paper several systems of the aqueous solution 1 ‖ aqueous solution 2 type are analysed, having as principal feature the presence within the liquid junction of a chemical reaction. In this reaction, one component of the first and one component of the second solution take part as reactants.

For the theoretical treatment, the following system was chosen:

$$\mathrm{HCl}\,(c_1)\,\|\,\mathrm{Na\,OH}\left(\frac{Vc_2 - vc_1}{V+v}\right) + \mathrm{NaCl}\left(\frac{vc_1}{V+v}\right); \quad vc_1 < Vc_2 \qquad (1)$$

The chemical reaction taking place within the liquid junction is evidently $H^+ + OH^- \rightarrow (H_2O)_r$. We shall suppose that this reaction is a very fast and quantitative one; r is used to make a distinction between this water and the "solvent", though from the chemical point of view they are identical.

In the case of the system (1) the Henderson's or Planck's formulas for the liquid-junction potential cannot be used. Indeed, they suppose that chemical equilibriums do not occur within the liquid junction. A comparative analysis of the two formulas was made by Cumming and Gilcrist.[30]

For the system (1) the concentration profiles along the liquid-junction double layer are discussed and on their basis an expression of the liquid-junction potential is obtained. This formula leads to values in very good agreement with the experimental data obtained by the authors

The theoretical conclusions, concerning the system (1), are then generalized for a whole class of systems, analogous to the system (1).

The system

$$\mathrm{NaOH}\,(c_1)\,\|\,\mathrm{NaCl}\left(\frac{vc_1}{V+v}\right) + \mathrm{HCl}\left(\frac{Vc_2 - vc_1}{V+v}\right); \quad vc_1 < Vc_2 \qquad (2)$$

can be considered as the "dual" of the system (1). It belongs to another class, which is the "dual" of the first class. The concentration profiles.

---

[29] J. Sandblom, G. Eisenman and J. L. Walker, Jr., *J. Phys. Chem.*, **71**, 3862, 3871 (1967).

[30] A. C. Cumming and E. Gilcrist, *Trans. Faraday Soc.*, **9**, 174 (1913).

and the expression of the liquid-junction potential, which are representative for this second class, are also obtained.

2. THE CONCENTRATION PROFILES WITHIN THE JUNCTION

$$\mathrm{HCl}\,(c_1)\,\|\,\mathrm{NaOH}\left(\frac{Vc_2 - vc_1}{V + v}\right) + \mathrm{NaCl}\left(\frac{vc_1}{V + v}\right); \quad vc_1 < Vc_2$$

IN THE ASSUMPTION $K_{H_2O} = 0$

Let us suppose that the chemical reaction $H^+ + OH^- \rightarrow (H_2O)_r$ is not taken into account. Then, the concentration profiles can be obtained using the Henderson's or Planck's conception. For the sake of simplicity, the Henderson's conception was chosen and the concentration profiles are shown in fig. 1

They correspond to the linear relationship

$$c_k = c_{k.1} + (c_{k.2} - c_{k.1})\,x \tag{3}$$

where, $c_{k.1}$, $c_{k,2}$ are the concentration of k ion in the two solutions and x is the Henderson's mixture ratio (in 1 ml mixture, x ml are from the second solution).

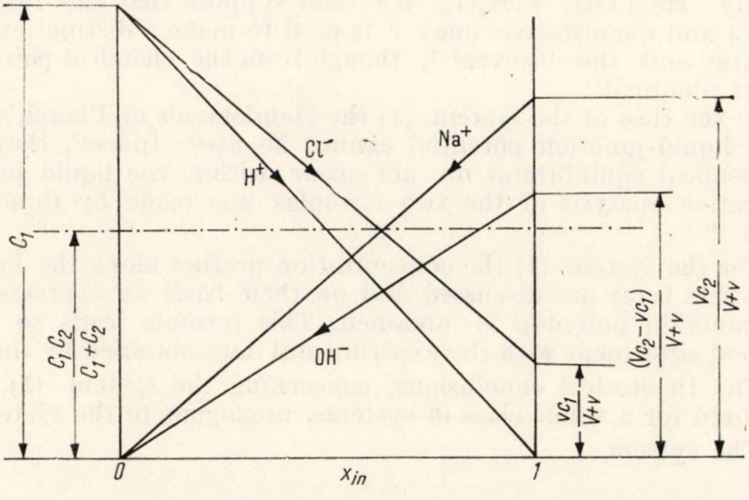

Fig. 1. — Concentration profiles along the liquid junction : $\mathrm{HCl}(c_1)\,\|$ $\|\,\mathrm{NaOH}\left(\frac{Vc_2 - vc_1}{V + v}\right) + \mathrm{NaCl}\left(\frac{vc_1}{V + v}\right)$; $vc_1 < Vc_2$, without considering the water formation within the junction.

It is easy to see that the value of x for which $c_{OH^-} = c_{H^+}$ is equal to :

$$x_{in} = (V + v)c_1/V\,(c_1 + c_2) \tag{4}$$

If we take now into account the chemical reaction $H^+ + OH^- \rightarrow$ $\rightarrow (H_2O)_r$ within the junction, it results that c_{OH^-} is zero for $x \leqslant x_{in}$, c_{H^+}

is zero for $x \geqslant x_{in}$ and, as a consequence, we have to modify the concentration profiles for H^+ and OH^- ions and to indicate a new concentration profile for $c_{(H_2O)_r}$.

The new concentration profiles thus obtained, are shown in figure 2.

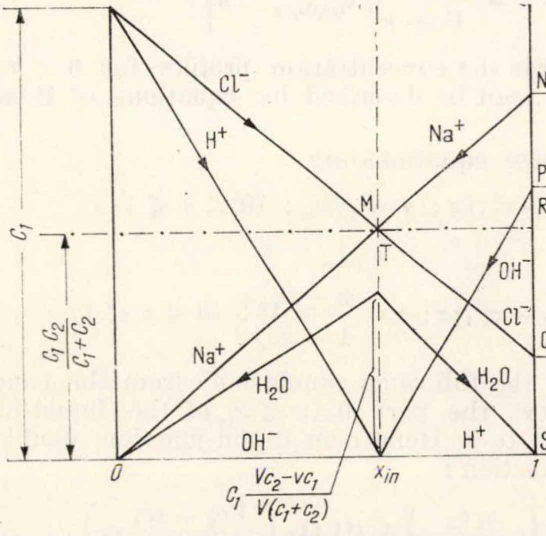
Cl^-
N
H^+
Na^+
P
M
R
C_1
T
OH^-
Cl^-
Q
$\frac{C_1C_2}{C_1+C_2}$
Na^+
H_2O
H_2O
OH^-
H^+
S
O
x_{in}
I
$C_1\frac{Vc_2-vc_1}{V(c_1+c_2)}$
$\frac{vc_1}{V+v}$
$\frac{Vc_2-vc_1}{V+v}$
$\frac{Vc_2}{V+v}$

Fig. 2. — Concentration profiles along the liquid junction: $HCl(c_1) \| NaOH \left(\frac{Vc_2 - vc_1}{V+v}\right) + NaCl \left(\frac{vc_1}{V+v}\right)$; $vc_1 < Vc_2$, when the water formation within the junction is taken into account.

The equations (3) can be used only for Cl^- and Na^+ ions. It results that the liquid-junction double layer is not of a Henderson type. Let $\{c^{I}_{k,1}\}$; $\{c^{I}_{k,2}\}$; $\{c^{II}_{k,1}\}$; $\{c^{II}_{k,2}\}$ be the following sets:

$$\{c^{I}_{k,1}\} = \{c^{I}_{H^+,1} = c_1,\ c^{I}_{Cl^-,1} = c_1,\ c^{I}_{Na^+,1} = 0,\ c^{I}_{(H_2O)_r,1} = 0\}$$

$$\{c^{I}_{k,2}\} = \left\{c^{I}_{H^+,2} = 0,\ c^{I}_{Cl^-,2} = \frac{c_1 c_2}{c_1 + c_2},\ c^{I}_{Na^+,2} = \frac{c_1 c_2}{c_1 + c_2},\ c^{I}_{(H_2O)_r,2} = \right.$$
$$\left. = \frac{Vc_2 - vc_1}{V(c_1 + c_2)}\, c_1 \right\} \tag{5}$$
$$\{c^{II}_{k,1}\} = \left\{c^{II}_{OH^-,1} = 0,\ c^{II}_{Cl^-,1} = \frac{c_1 c_2}{c_1 + c_2},\ c^{II}_{Na^+,1} = \frac{c_1 c_2}{c_1 + c_2},\ c^{II}_{(H_2O)_r,1} = \right.$$
$$\left. = \frac{Vc_2 - vc_1}{V\,(c_1 + c_2)}\, c_1 \right\}$$

$$\{c^{\mathrm{II}}_{k,2}\} = \left\{ c^{\mathrm{II}}_{\mathrm{OH^-},2} = \frac{Vc_2 - vc_1}{V + v},\ c^{\mathrm{II}}_{\mathrm{Cl^-},2} = \frac{vc_1}{V + v},\ c^{\mathrm{II}}_{\mathrm{Na^+},2} = \right. \tag{5}$$

$$\left. = \frac{Vc_2}{V + v},\ c^{\mathrm{II}}_{(\mathrm{H_2O})_r,2} = 0 \right\}$$

It is easy to prove that the concentration profiles for $0 \leqslant x \leqslant x_{in}$, as well as for $x_{in} \leqslant x \leqslant 1$, can be described by equations of Henderson type.

For $0 \leqslant x \leqslant x_{in}$ these equations are

$$c^{\mathrm{I}}_k = c^{\mathrm{I}}_{k,1} + (c^{\mathrm{I}}_{k,2} - c^{\mathrm{I}}_{k,1})\,y\,;\ y = x/x_{in}\,;\ (0 \leqslant y \leqslant 1) \tag{6}$$

and for $x_{in} \leqslant x \leqslant 1$

$$c^{\mathrm{II}}_k = c^{\mathrm{II}}_{k,1} + (c^{\mathrm{II}}_{k,2} - c^{\mathrm{II}}_{k,1})\,z\,;\ z = \frac{x - x_{in}}{1 - x_{in}}\,;\ (0 \leqslant z \leqslant 1) \tag{7}$$

Therefore, it results the following conclusion: from the concentration profiles point of view, the part $0 \leqslant x \leqslant x_{in}$ of the liquid-junction double layer is equivalent to a Henderson liquid-junction double layer corresponding to the junction:

$$\mathrm{HCl}\,(c_1)\,\|\,\mathrm{NaCl}\left(\frac{c_1\,c_2}{c_1 + c_2}\right) + (\mathrm{H_2O})_r\left(\frac{Vc_2 - vc_1}{V\,(c_1 + c_2)}\,c_1\right) \tag{8}$$

and the part $x_{in} \leqslant x \leqslant 1$, with one corresponding to the junction:

$$\mathrm{NaCl}\left(\frac{c_1c_2}{c_1 + c_2}\right) + (\mathrm{H_2O})_r\left(\frac{Vc_2 - vc_1}{V\,(c_1 + c_2)}\,c_1\right) \| \ \mathrm{NaCl}\left(\frac{vc_1}{V + v}\right) + \tag{9}$$

$$+ \ \mathrm{NaOH}\left(\frac{Vc_2 - vc_1}{V + v}\right)$$

This conclusion expresses the influence of the chemical reaction $\mathrm{H^+} + \mathrm{OH^-} \rightarrow (\mathrm{H_2O})_r$ on the liquid-junction double layer structure.

3. THE DEDUCTION OF THE LIQUID-JUNCTION POTENTIAL EXPRESSION

To obtain this expression, it is necessary to integrate, along the liquid-junction double layer (fig. 2), the differential equation:

$$F\mathrm{d}\,\Phi = -\,RT \sum_i \omega_i\,\mathrm{d}\ln a_i - RT \sum_k (t_k/z_k)\,\mathrm{d}\ln a_k \tag{10}$$

which gives the isotherm diffusion elementary potential. In this equation, the second term on the right-hand side is referring to the charged components and the first one, to the uncharged components; ω_i is the Washburn's number of the uncharged component i and is defined by means of the relation :

$$dJ_i = \omega_i \, (dI/F) \tag{11}$$

where J_i is the flux density of the i component and I the current density.[31-34]

From the relation (11), it results that the Washburn's number is zero, for an uncharged component i, if a variation of the current density in the system is not reflecting in a variation of the flux density of this component.

In our case, $(H_2O)_r$ is the uncharged component whose contribution to the value of the liquid-junction potential must be analysed. Consequently, it is necessary to obtain the value of $\omega_{(H_2O)_r}$. It is easy to show that in the assumption $K_{H_2O} = 0$, the Washburn's number $\omega_{(H_2O)_r}$ is zero.

Indeed, the application of an electrical field variation to the system will modify the ionic components fluxes such that $F \sum\limits_k z_k \, dJ_k = dI$, but it will not influence directly the $(H_2O)_r$ flux (uncharged component). The $(H_2O)_r$ flux is not modified nor indirectly, that is as a consequence of the variation of H^+ and OH^- fluxes, because there is no place within the liquid-junction double layer in which the two ions H^+, OH^- should be simultaneously present (fig. 2).

Consequently, to obtain the expression of the liquid-junction potential, only the charged components must be taken into account. Then, the part $0 \leqslant x \leqslant x_{in}$ of the liquid-junction double layer can be equated with a Henderson liquid-junction double layer corresponding to the junction $HCl\,(c_1)\,\|\,NaCl\left(\frac{c_1c_2}{c_1 + c_2}\right)$ and the part $x_{in} \leqslant x \leqslant 1$ with one corresponding to the junction $NaCl\left(\frac{c_1\,c_2}{c_1 + c_2}\right)\|\,NaCl\left(\frac{vc_1}{V + v}\right) + NaOH\left(\frac{Vc_2 - vc_1}{V + v}\right)$.

We shall apply the Henderson's formula to these two parts and then we shall add the expressions thus obtained. It results :

$$E_J = \frac{RT}{F}\,\frac{(c_1 + c_2)\,u_H - c_1u_{Cl} - c_2\,u_{Na}}{(c_1 + c_2)\,u_H + c_1u_{Cl} - c_2\,u_{Na}}\,\ln\frac{(c_1 + c_2)\,(u_H + u_{Cl})}{c_2\,(u_{Cl} + u_{Na})} + \tag{12}$$

$$+ \frac{RT}{F}\,\frac{(c_1 + c_2)\,u_{OH} - c_1\,u_{Cl} - c_2\,u_{Na}}{(c_1 + c_2)\,u_{OH} - c_1\,u_{Cl} + c_2\,u_{Na}}\,\ln\frac{(vc_1\,u_{Cl} + (Vc_2 - vc_1)\,u_{OH} + Vc_2\,u_{Na})}{(c_1\,c_2/(c_1 + c_2))\,(V + v)\,(u_{Cl} + u_{Na})}$$

$$(vc_1 \leqslant Vc_2)$$

---

[31] G. SCHATCHARD, *J. Amer. Chem. Soc.*, **75**, 2883 (1953).

[32] H. S. HARNED and B. B. OWEN, "The Physical Chemistry of Electrolytic Solutions", (3rd ed.), Reinhold Publ. Corp., New York, 1958, p. 38.

[33] S. R. DE GROOT and P. MAZUR, "Non-Equilibrium Thermodynamics", North-Holland Publ. Co., Amsterdam, 1963, p. 367.

[34] J. N. AGAR, "Thermogalvanic Cells" in "Advances in Electrochemistry and Electrochemical Engineering", 3rd vol., Interscience Publishers, New York, London, 1963.

In this expression, the first term is referring to the part $0 \leqslant x \leqslant x_{in}$ and as one can see is independent of v (the height of M point in figure 2 is independent of v). The second term expresses the potential jump along the part $x_{in} \leqslant x \leqslant 1$ and is dependent on v (the heights of N, P, Q points are dependent on v). For $Vc_2 = vc_1$ this second term is zero. In this situation, the part $x_{in} \leqslant x \leqslant 1$ disappears, the points M, N, Q reach R and the points P, T reach S.

The theoretical results obtained for the system (1), concerning the concentration profiles and the expression of the liquid-junction potential, can be generalized becoming thus representative for a whole class of systems analogous to the system (1).

Thus, the general expression for the liquid-junction potential is

$$E_J = \frac{RT}{F} \frac{(c_1 + c_2)\dfrac{u_C}{z_C} - c_1 \dfrac{u_A}{|z_A|} - c_2 \dfrac{u_{C^*}}{z_{C^*}}}{(c_1 + c_2)\, u_C + c_1 u_A - c_2 u_{C^*}} \ln \frac{(c_1 + c_2)(u_C + u_A)}{c_2 (u_A + u_{C^*})} + \tag{13}$$

$$+ \frac{RT}{F} \frac{(c_1 + c_2)\dfrac{u_{A^*}}{|z_{A^*}|} - c_1 \dfrac{u_A}{|z_A|} - c_2 \dfrac{u_{C^*}}{z_{C^*}}}{(c_1 + c_2)\, u_{A^*} - c_1 u_A + c_2 u_{C^*}} \ln \frac{(vc_1 u_A + (Vc_2 - vc_1) u_{A^*} + Vc_2 u_{C^*})}{(c_1 c_2/(c_1 + c_2))(V + v)(u_A + u_{C^*})}$$

$$(vc_1 \leqslant Vc_2)$$

In this relation, by C, C^* are indicated the quantities which correspond to the cation present in the first solution, respectively to the cation present in the second solution. Similarly, by A, A^* those which correspond to the anion present in both solutions, respectively to the anion present only in the second solution; $z_C, z_{C^*}, z_A, z_{A^*}$ are the corresponding valences and c_1, c_2 the concentrations (equiv./ml) of the two solutions, for $v = 0$. The chemical reaction, within the liquid junction, is now $\nu_1 C^{z_C+} + \nu_2 A^{*\,|z_{A^*}|-} \rightarrow C_{\nu_1} A^*_{\nu_2}$; $(\nu_1 z_C + \nu_2 z_{A^*} = 0)$. The $C_{\nu_1} A^*_{\nu_2}$ molecules either remain in the solution, or leave the solution by precipitation.

The concentration profiles within the liquid-junction double layer, remain described by the figure 2, but the straight line segments which correspond to H^+, Cl^-, Na^+, OH^- and $(H_2O)_r$, will correspond now to C^{z_C+}, $A^{|z_A|-}$, $C^{*\,z_{C^*}+}$, $A^{*\,|z_{A^*}|-}$ and $C_{\nu_1} A^*_{\nu_2}$. If $C_{\nu_1} A^*_{\nu_2}$ is practically insoluble, it will leave the solution by precipitation and, evidently, the problem of its concentration profile, is no more actual.

The general formula for E_J, corresponding to the "dual" class of the systems analogous to the system (2), can be obtained from the relation (13) by making the following changes:

$$u_C \rightarrow u_{A^*}\,;\; u_{A^*} \rightarrow u_C\,;\; u_A \rightarrow u_{C^*}\,;\; u_{C^*} \rightarrow u_A\,;\; z_C \rightarrow |z_{A^*}| \tag{14}$$

$$|z_{A^*}| \rightarrow z_C\,;\;\; |z_A| \rightarrow z_{C^*}\,;\; z_{C^*} \rightarrow |z_A|\,;\; E_J \rightarrow -E_J$$

This time, A^* is the anion present only in the first solution, C^* is the cation present in both solutions and C, A are the cation, respectively the anion, present only in the second solution.

The concentration profiles for this "dual" class, remain described in figure 2, but the straight line segments which correspond to H^+, Cl^-, Na^+, OH^- and $(H_2O)_,$, will correspond now to $A^{*^{|z_{A^*}|-}}$, $C^{*^{z_{C^*}+}}$, $A^{^{|z_A|-}}$, $C^{^{z_C+}}$ and $C_{\nu_1} A^*_{\nu_2}$.

4. EXPERIMENTAL

In table 1 are shown the experimental emf values, at 18°, for 20 concentration cells of the type :

$$Hg|Hg_2Cl_2|\,KCl\,(sat)\,||\,HCl\,(c_1)\,||\,10\text{ ml }NaOH\,(c_2) + v\text{ ml }HCl\,(c_1)\,||\,KCl\,(sat)\;|\,Hg_2Cl_2|Hg \qquad (15)$$

The following systems of values (c_1, c_2, v) were used :

a. $c_1 = c_2 = 0.1$ M ; $v = 0,1,\ldots,10$ ml ; b. $c_1 = 0.1$ M ; $c_2 = 0.05$ M ; $v = 0,1,\ldots,5$ ml ; c. $c_1 = 0.1$ M ; $c_2 = 0.02$ M ; $v = 0,1,2$ ml. Consequently, the condition $vc_1 \leqslant Vc_2$ is fulfilled.

A pH-meter "MV 11 S Clamann & Grahnert, Dresden G.D.R.", coupled through a sensitivity reducer (piece belonging to a polarograph HEYROVSKY V 301) to a recorder "GRAPHISPOT SEFRAM type GRVAJ, Paris" was used. The emf values were read on the linear scale of the recorder, previously calibrated in mV.

Table 1

Calculated $E_J(v)$ values, for the liquid junction HCl (c_1) || 10 ml NaOH (c_2) + v ml HCl (c_1), comparatively with the experimental emf values of the cells Hg|Hg_2Cl_2|KCl (sat)||HCl (c_1)||10 ml NaOH (c_2) + v ml HCl(c_1)|| KCl (sat) |Hg_2Cl_2|Hg

v	$c_1 = c_2 = 0.1$M			$c_1 = 0.1$M ; $c_2 = 0.05$M			c_1=0.1M ; c_2=0.02M		
	E_J (mV) (1)	E_J (mV) (2)	E (mV)	E_J (mV) (1)	E_J (mV) (2)	E (mV)	E_J (mV) (1)	E_J (mV) (2)	E (mV)
0	67.4	34.0	67.5	68.7	37.7	67.0	75.4	45.8	73.4
1	64.5	34.3	65.0	59.4	38.6	61.5	66.8	49.5	61.2
2	62.0	34.5	61.8	56.4	39.9	58.7	55.5	55.5	56.0
3	59.2	35.2	61.2	53.2	41.7	55.5			
4	56.6	35.5	58.5	50.6	43.4	51.3			
5	54.0	36.3	56.3	46.0	46.0	49.5			
6	51.5	36.8	53.6						
7	49.0	37.7	51.0						
8	46.3	38.7	48.5						
9	43.6	39.8	46.0						
10	40.7	40.8	46.0						

(1) Calculated on the basis of (12) ; (2) Calculated on the basis of (16).

In the same table are also given the values of E_J, calculated on the basis of formula (12), respectively on the basis of formula :

$$E_J = \frac{RT}{F} \frac{V\left(\frac{c_1}{c_2}(u_{\mathrm{H}} - u_{\mathrm{Cl}}) + u_{\mathrm{OH}} - u_{\mathrm{Na}}\right) + v\frac{c_1}{c_2}(u_{\mathrm{H}} - u_{\mathrm{OH}})}{V\left(\frac{c_1}{c_2}(u_{\mathrm{H}} + u_{\mathrm{Cl}}) - u_{\mathrm{OH}} - u_{\mathrm{Na}}\right) + v\frac{c_1}{c_2}(u_{\mathrm{H}} + u_{\mathrm{OH}})} \ln \frac{(V+v)\frac{c_1}{c_2}(u_{\mathrm{H}} + u_{\mathrm{Cl}})}{V(u_{\mathrm{Na}} + u_{\mathrm{OH}}) - v\frac{c_1}{c_2}(u_{\mathrm{OH}} - u_{\mathrm{Cl}})}$$

(16

$$(vc_1 \leqslant Vc_2)$$

The latter results from the application of Henderson's formula to the liquid junction $\mathrm{HCl}(c_1) \parallel 10$ ml $\mathrm{NaOH}(c_2) + v$ ml $\mathrm{HCl}\,(c_1)$, without taking into account the water formation within the liquid junction (fig. 1).

To calculate the E_J values on the basis of formulas (12) and (16), data concerning the ionic mobility values were necessary.

If the ionic strength $J = \frac{1}{2}\sum_i m_i z_i^2 \simeq \frac{1}{2}\sum_i c_i z_i^2$ is calculated for the two parts of the liquid-junction double layer, it results :

Part $(0, x_{in})$

$$J_{\mathrm{I}} = c_1 - (Vc_1/(V+v))\,x;\ 0 \leqslant x \leqslant x_{in} \tag{17}$$

Mean value $\overline{J}_{\mathrm{I}} = \frac{c_1}{2}(1 + c_2/(c_1 + c_2))$

Part $(x_{in}, 1)$

$$J_{\mathrm{II}} = (Vc_2/(V+v))\,x;\ x_{in} \leqslant x \leqslant 1 \tag{18}$$

Mean value $\overline{J}_{\mathrm{II}} = \frac{c_1}{2}(c_1 / (c_1 + c_2) + V/(V+v))$

Similarly, in the case of figure 1 :

$$J = c_1(1 - x) + (Vc_2/(V+v))x;\ 0 \leqslant x \leqslant 1 \tag{19}$$

Mean value $\overline{J} = \frac{1}{2}(c_1 + Vc_2/(V+v))$

Then, on the basis of the mobility values at 18° and 0.1 M, 0.01 M concentrations, taken from tables,[35] the values used in calculations were obtained by interpolation corresponding to the following concentrations : $c_{\mathrm{I}} = \overline{J}_{\mathrm{I}}$ and $c_{II}(v) = \overline{J}_{\mathrm{II}}(v)$ in the case of the first respectively the second term on the right-hand side of (12) and $c(v) = \overline{J}(v)$ in the case of (16).

[35] T. Erdey-Grúz and G. Schay, "Chimie Fizică Teoretică", (Romanian edition) 2nd vol., Ed. tehnică, Bucharest, 1958, p. 640.

From the table 1, it results that the values predicted by (12) are in very good agreement with the experimentally obtained values $E = E(v)$, but the agreement between the experimental values and those predicted by (16) is completely unsatisfactory.

In conclusion, the experimental data, confirm the validity of our conception with regard to the liquid-junction double layer structure and the fact that the formula (12) which is a consequence of this conception, expresses quite exactly the $E = E(v)$ values.

In the next paper, starting from the expressions (12) and (13), several other expressions are derived and on their basis a new potentiometric titration method is founded. This method is not affected by the uncertainty that an experimental evaluation of a liquid-junction potential implies.

Revue Roumaine de Chimie. **15**, 1319–1329 (1970)

SPEKTROPHOTOMETRISCHE UNTERSUCHUNG IM SYSTEM $Th(NO_3)_4$ – VIOLURSÄURE *

FLORICA POPEA und A.-C. BANCIU
Institut für Physikalische Chemie der Akademie,
Bucarest, Str. Dumbrava Roşie, 23

Eingegangen am 29. November 1969

Die Komplexbildung in wäßrigen Lösungen von $Th(NO_3)_4$ und Violursäure wird spektrophotometrisch untersucht. Die Anwendung mehrerer Methoden, die für die Untersuchung im Falle der Bildung eines einzigen Komplexes geeignet sind, führt zu keinen klaren Ergebnissen, sondern läßt die Bildung mehrerer gleichzeitig anwesender Komplexe vermuten. Mit Hilfe der Methode des „molaren Verhältnisses" können mehrere einkernige Komplexe, und zwar der Zusammensetzung Metall : Ligand = 1 : 1, 1 : 2, 1 : 3 und 1 : 4 nachgewiesen werden. Die Anwendung einer Variante der Jazimirskij-Methode zur Bestimmung der Bildungskonstanten mehrerer gleichzeitig anwesender einkerniger Komplexe führt zur Berechnung der Beständigkeitskonstanten aller dieser Komplexe, die von der Größenordnung 10^2, 10^5, 10^7 und 10^{10} sind.

EINLEITUNG

Von der Violursäure (5-Isonitrosobarbitursäure), die eine Keto-Enol-Tautomerie aufweist

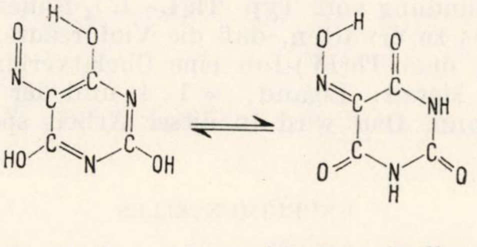

ist bekannt, daß sie dank der benachbarten Stellungen der Isonitrosogruppe mit einer Keto- bzw. Enolgruppe, mit Metallionen einen stabilen Chelatring von fünf oder sechs Atomen bilden kann. In der freien Säure kann das Proton als pendelnd zwischen den beiden Atomen mit Elektronendonoreigenschaften die an Chelatringbildung teilnehmen können, d.h. zwei O-Atome, oder ein N- und ein O-Atom, betrachtet werden.

---

* Diese Arbeit wurde auf dem internationalen Symposium „Koordinationschemie der Übergangselemente" in Jena (DDR) im September 1969 vorgetragen.

Wird dieses Proton durch ein Metallion ersetzt, so entsteht die Chelatverbindung. Die Fachliteratur erwähnt einige spektrophotometrische Untersuchungen über die Chelatverbindungen der Violursäure mit Übergangsmettallionen wie Kupfer [1], Palladium [2], Eisen und Kobalt[3] und mit einigen Ionen der seltenen Erden [4].

In allen diesen Untersuchungen ist aber nicht festgestellt worden, ob die Chelatverbindung Fünf- oder Sechsringe bildet, d.h. ob bei der Isonitrosogruppe das Sauerstoff- oder das Stickstoffatom als Bindungsatom zum Metallion fungiert und sich Komplexe der Formel (I) oder (II) bilden.

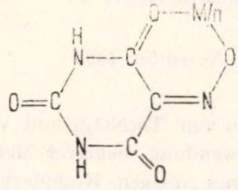

I

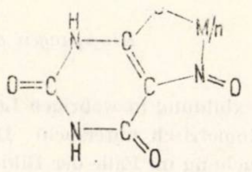

II

Dies hängt von mehreren Faktoren und nicht zuletzt von der Natur des entsprechenden Metallions ab.

Vom Thoriumion, welches eine hohe Wertigkeitsstufe (+4) hat, ist bekannt, daß es die Elektronenkonfiguration $6s^2$ $6p^6$ besitzt, in der die Orbitale 6d, 7s und 7p völlig unbesetzt sind, so daß es sogar 16 Elektronen aufnehmen kann und auf diese Weise auch Chelatverbindungen, welche die Koordinationszahl acht aufweisen, von Typ $Th(L-L')_4$ (wobei mit $L-L'$ ein bidentater Ligand, wie es z.B. die Violursäure ist, bezeichnet wurde) bilden kann. Am bekanntesten sind die Chelate des Thoriums von diesem Typ mit Acetylaceton (als Anion) und seinen Derivaten, sowie neuerlich mit dem Tropolonanion [5]. Es sei zu erwähnen daß von einigen Derivaten der Violursäure, wie die 1,3-Di-*p*-tolyl-violursäure [6], welche mit Metallionen schwerlösliche Chelatverbindungen bildet, auch die Verbindung vom Typ $Th(L-L')_4$ isoliert wurde. An Hand dieser Daten ist es zu erwarten, daß die Violursäure, besser gesagt das Anion dieser, mit dem Th(IV)-Ion eine Chelatverbindung der Bruttozusammensetzung Metall: Ligand = 1 : 4, und der Strukturformel (I) oder(II) bilden kann. Dies wird in dieser Arbeit spektrophotometrisch untersucht.

EXPERIMENTELLES

Reagenzien. $Th(NO_3)_4.5H_2O$ *p.a* (Merck-Reagens), Gehalt: 99,1 % und Violursäure *p.a.* (Austranal-Reagens). Der genaue Gehalt an Violursäure von 92,5 %, wurde nach dem experimentell ermittelten Gesamtkohlenstoffgehalt von 28,29 % berechnet.

---

[1] M. Ziegler, *Z. analyt. Chem*,. **164**, 387 (1958).

[2] M. Ziegler und O. Glemser, *Mikrochim. Acta*, **1956**, 1152.

[3] P. A. Leermakers und A. W. Hoffman, *J. Amer. Chem. Soc.*, **80**, 5663 (1958).

[4] E. Antonescu und S. Ploştinaru, *Rev. Roumaine Chim.*, **11**, 947 (1966).

[5] E. L. Muetterties und C. M. Wright, *J. Amer. Chem. Soc.*, **87**, 4706 (1965).

[6] R. P. Singh, *J. Indian Chem. Soc.*, **37**, 569 (1960).

Die Messungen wurden mit wäßrigen Lösungen dieser Reagenzien, im allgemeinen von der Konzentration $1,5.10^{-2}$ Mol/l, durchgeführt. Die Absorptionskurven wurden mit einem VSU-1-Carl Zeiss-Spektrophotometer aufgenommen.

Experimentelles. Die wäßrige Violursäure-Lösung ist schwach rosa gefärbt. Beim starken Ansäuern mit Mineralsäuren tritt allmählich Entfärbung ein, bis die Farbe völlig verschwindet. Das Absorptionsspektrum dieser bei Wellenlängen die größer sind als 360 nm wird in Abb. 1 gezeichnet. Beim Zusammenmischen einer Violursäure-Lösung mit der farbolsen Lösung des $Th(NO_3)_4$ tritt augenblicklich eine bleibende gelbe grünstichige Farbe auf, welche nicht von einer pH-Änderung verursacht werden kann und auf Komplexbildung hindeutet. Diese Farbe zeigt, daß die Absorption bei Wellenlängen von etwa 400 nm stattfinden muß. Außerdem ist zu erwähnen, daß das Zusammenmischen der Violursäure mit der $Th(NO_3)_4$-Lösung von einer kleinen Änderung des pH-Wertes begleitet wird. Die $1,5.10^{-2}$ Mol/l-Lösung von Violursäure hat den pH-Wert 2,6, die $Th(NO_3)_4$-Lösung gleicher Konzentration hat den pH-Wert 2,2 und der pH-Wert verschiedener gebrauchter Mischungen dieser Stammlösungen variiert zwischen 2,4 und 4,1.

Die kleine pH-Änderung hat keinen nennenswerten Einfluß auf die Farbintensität der eventuell im Überschuß anwesenden Violursäure.

ERGEBNISSE UND DISKUSSION

Um Hinweise über die Absorptionsverhältnisse zu gewinnen, wurden die Spektren verschiedener Mischungen von Lösungen gleicher Konzentration ($1,5.10^{-2}$Mol/l) an $Th(NO_3)_4$ und Violursäure, bei denen x Volumenteile $Th(NO_3)_4$-Lösung zu $(1-x)$ Volumenteilen Violursäure-Lösung hinzugefügt wurden, gemessen. Diese Spektren werden in der Abb. 1 gezeichnet.

Man merkt, daß bei Wellenlängen die größer sind als 390 nm die Eigenabsorption der Violursäure kleiner als die Absorption der Mischungen mit $Th(NO_3)_4$ ist, aber trotzdem in derselben Größenordnung wie diese liegt und nicht vernachläßigt werden kann. Man hat also mit dem Fall zu tun, indem neben der Komplexverbindung (oder neben den Komplexverbindungen) auch der Ligand absorbiert. Von Abb. 1 sieht man, daß sich die Absorptionskurven mehrerer Mischungen, die einem Molverhältnis $Th(NO_3)_4$: Violursäure $= 1:4$; $3:7$; $2:3$ und $1:1$ entsprechen, in einem größeren Wellenlängenbereich — von etwa 380 bis 460 nm — überlagern.

Dies wäre keinesfalls im Falle der Existenz einer beständigen Komplexverbindung möglich und zeigt, daß in diesem Bereich mehrere gleichzeitig anwesende Komplexverbindungen absorbieren.

Die Anwendung mehrerer Methoden, die zur Untersuchung der Komplexbildung im Falle der Existenz einer Komplexverbindung geeignet sind — der Methode der „kontinuierlichen Variationen"[7] der „logarithmischen" von Bent und French[8], der „des Neigungsverhältnisses" von Harvey und Manning[9], und der „Geraden" — Methode von

---

[7] P. Job, *Ann. Chim. Phys.*, *9*, 113 (1928).

[8] H. E. Bent und C. L. French, *J. Amer. Chem. Soc.*, **63**, 568 (1941).

[9] A. E. Harvey und D. L. Manning, *J. Amer. Chem. Soc.*, **72**, 4488 (1950).

Asmus[10] führt zu keinen eindeutigen Ergebnissen, was erneut auf die gleichzeitige Anwesenheit mehrerer Komplexspezien schließen läßt.

Im Falle der Existenz mehrerer Komplexverbindungen erscheint die Methode „des molaren Verhältnisses" von Meyer und Ayres[11] als besonders geeignet, wenn die entsprechenden Komplexverbindungen stabil sind. Von mehreren Messungen, die nach dieser Methode durchgeführt wurden, sind einige in den Abb. 2 bis 5 wiedergegeben. Alle diese Extinktionen wurden an Mischungen der Stammlösungen von der Konzentration $1{,}5.10^{-2}$ Mol/l gemessen. Man merkt, daß auf diese Weise die Chelatverbindungen der Bruttozusammensetzung Th^{4+} : Violursäure = 1 : 4 (Abb. 2 und 5), 1 : 3 (Abb. 3), und 1 : 2 (Abb. 2,4 und 5) identifiziert sind. Bei fast allen untersuchten Mischungen tritt beim Molverhältnis Th^{4+} : Violursäure = 1 : 1 keine sprunghafte Änderung der Steigung zweier Geraden auf, sondern eine kontinuierlich gekrümmte Kurve, was darauf schließen läßt, daß die Chelatverbindung der Zusammensetzung Th : Violursäure = 1 : 1 unbeständig ist. In keinem der Fälle aus Abb. 2—5, sowie in keiner der anderen nach dieser Methode untersuchten Mischungen konnten mehrkernige Komplexe identifiziert werden. Die Anwendung der Methode des molaren Verhältnisses hat also nicht nur die Existenz der Verbindung Th : Violursäure = 1 : 4 (siehe Abb. 2 und 5)

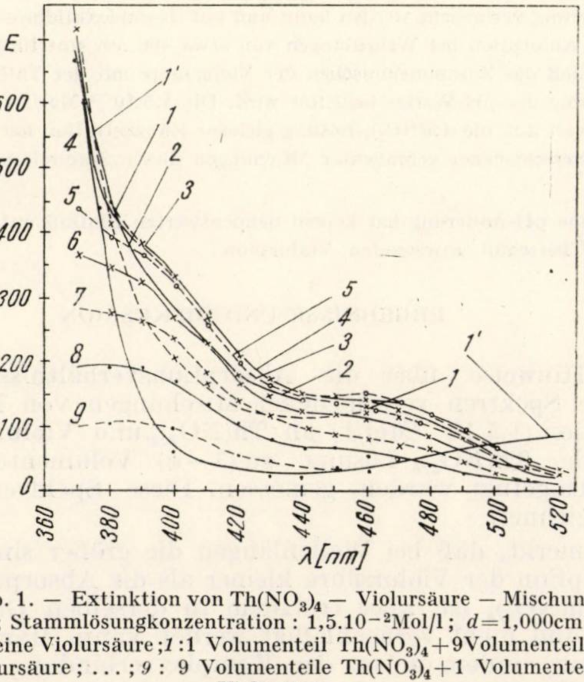

Abb. 1. — Extinktion von $Th(NO_3)_4$ — Violursäure — Mischungen; Stammlösungkonzentration: $1{,}5.10^{-2}$Mol/l; $d = 1{,}000$cm; *1'*: reine Violursäure; *1*: 1 Volumenteil $Th(NO_3)_4 + 9$ Volumenteile Violursäure; . . . ; *9*: 9 Volumenteile $Th(NO_3)_4 + 1$ Volumenteil Violursäure.

---

[10] E. Asmus, *Z. analyt. Chem*, **178**, 104 (1960).

[11] A. S. Meyer und G. H. Ayres, *J. Amer. Chem. Soc.* **79**,49 (1957).

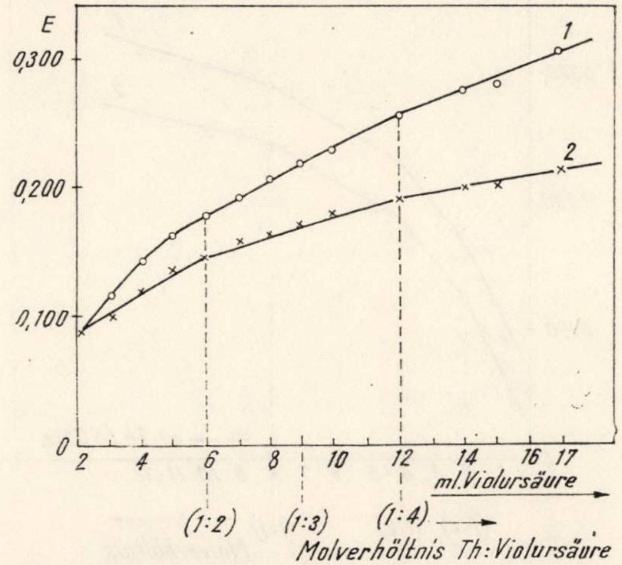

Abb. 2. – Extinktion von $Th(NO_3)_4$ – Violursäure – Mischungen; Stammlösungkonzentration: $1{,}5.10^{-2}$ Mol/l; $d = 1{,}000$ cm; 3 ml $Th(NO_3)_4$ – Lösung (konstant) + 0. . .17 ml Violursäurelösung; *1*, $\lambda = 387$ nm; *2*, $\lambda = 400$ nm.

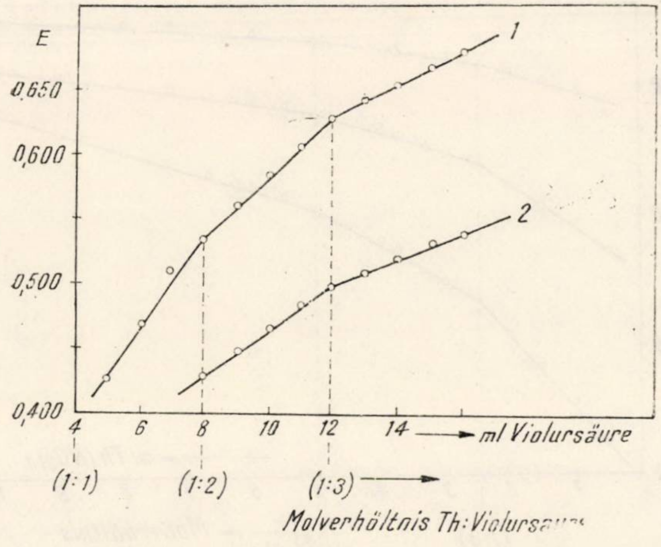

Abb. 3. – Extinktion von $Th(NO_3)_4$ – Violursäure – Mischungen; Stammlösungkonzentration: $1{,}5.10^{-2}$ Mol/l: $d = 2{,}997$ cm; 4 ml $Th(NO_3)_4$ – Lösung (konstant) + 0. . .16 ml Violursäurelösung; *1*, $\lambda = 400$ nm; *2*, $\lambda = 410$ nm.

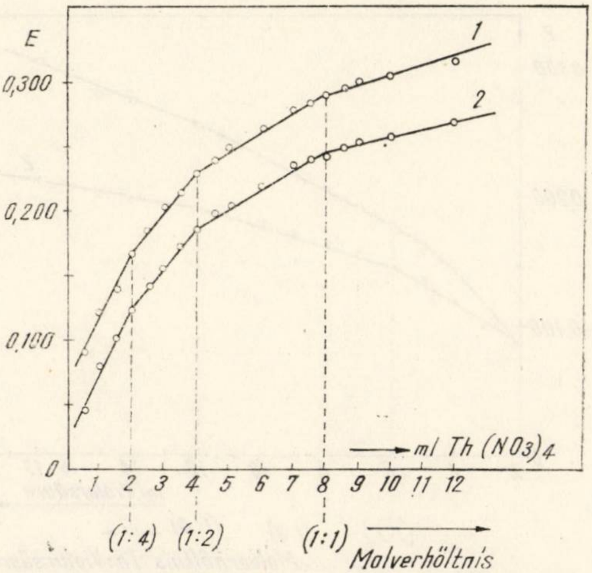

Abb. 4.— Extinktion von $Th(NO_3)_4$—Violursäure — Mischungen; Stammlösungkonzentration: $1{,}5.10^{-2}$ Mol/l; $d = 1{,}000$ cm; 8 ml Violursäure — Lösung (konstant) + 0...12 ml $Th(NO_3)_4$ — Lösung: *1*, $\lambda = 387$ nm; *2*, $\lambda = 400$ nm.

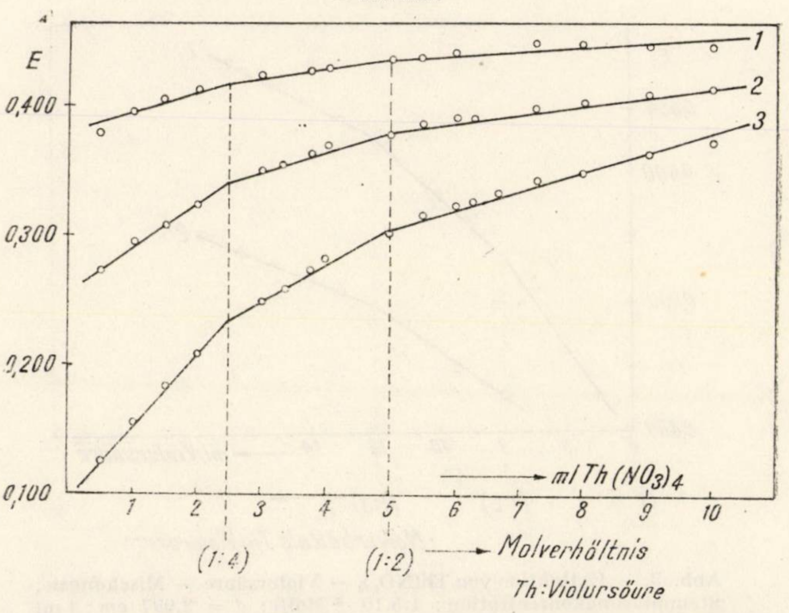

Abb. 5. — Extinktion von $Th(NO_3)_4$ — Violursäure — Mischungen; Stammlösungkonzentration: $1{,}5.10^{-2}$/Mol/l; $d = 1{,}000$ cm; 10 ml Violursäure — Lösung (konstant) + 0...10 ml $Th(NO_3)_4$ — Lösung; *1*, $\lambda = 370$ nm; *2*, $\lambda = 375$ nm; *3*, $\lambda = 387$ nm.

bewiesen, sondern hat auch gezeigt, daß neben dieser auch die Verbindungen von der Zusammensetzung Th^{4+} : Violursäure $= 1:3$ und $1:2$ existieren. Da die Bildung eines solchen Komplexes wie Th : Violursäure $= 1:4$ in Stufen verläuft, kann auch das erste Glied der Reihe, die Verbindung Th: Violursäure $= 1:1$, als existierend betrachtet werden, wenn schon die erzielten Ergebnisse zeigen, daß diese sehr dissoziiert sein soll. Es war interessant zu erfahren, wie sich die Stabilitätskonstanten der gleichzeitig anwesenden Chelattverbindungen verhalten: Wie schon erwähnt, absorbiert im untersuchten Fall neben den gebildeten Komplexen das Metallion nicht, aber der Ligand hat eine Absorption, die nicht vernachlässigt werden kann, da sie in derselben Größenordung wie die Absorption der Komplexe liegt.

Es wurde kürzlich gezeigt, [12] daß die Methode der Untersuchung stufenweiser Komplexbildung von Jazimirskij [13] auch in dem Falle anwendbar ist, in dem im untersuchten Spektralbereich neben den gebildeten Komplexen auch der Ligand absorbiert.

Durch Anwendung dieser Methode werden im Falle der Existenz von vier einkernigen Komplexen folgende Ausdrücke der Koeffizienten a_i :

$$\begin{aligned}
a_1 &= \frac{\varepsilon_A}{[M]} + \varepsilon_1 K_1 \\
a_2 &= \varepsilon_2 K_2 - \frac{\varepsilon_A}{[M]} K_1 - \varepsilon_1 K_1^2 \\
a_3 &= \varepsilon_3 K_3 - (\varepsilon_1 + \varepsilon_2) K_1 K_2 - \frac{\varepsilon_A}{[M]} (K_2 - K_1^2) + \varepsilon_1 K_1^3 \\
a_4 &= \varepsilon_4 K_4 + \frac{\varepsilon_A}{[M]} (2K_1 K_2 - K_1^3 - K_3) - (\varepsilon_1 + \varepsilon_3) K_1 K_3 + \\
&\quad + (2\varepsilon_1 + \varepsilon_2) K_1^2 K_2 - \varepsilon_2 K_2^2 - \varepsilon_1 K_1^4
\end{aligned} \tag{1}$$

und b_i

$$\begin{aligned}
b_1 &= \varepsilon_4 \\
b_2 &= (\varepsilon_3 - \varepsilon_4) \frac{K_3}{K_4} \\
b_3 &= (\varepsilon_2 - \varepsilon_4) \frac{K_2}{K_4} - (\varepsilon_3 - \varepsilon_4) \frac{K_3^2}{K_4^2} \\
b_4 &= (\varepsilon_1 - \varepsilon_4) \frac{K_1}{K_4} + \frac{\varepsilon_A}{[M]} \frac{1}{K_4} - (\varepsilon_2 + \varepsilon_3 - 2\varepsilon_4) \frac{K_2 K_3}{K_4^2} + (\varepsilon_3 - \varepsilon_4) \frac{K_3^3}{K_4^3}
\end{aligned} \tag{2}$$

---

[12] A-C. Banciu, *Rev. Roumaine Chim.*, **14**, 1019 (1969).

[13] K. B. Jazimirskij, *Zhur. Neorg. Khim.*, **1**, *10*, 2306 (1956).

erhalten, wobei $\varepsilon_1 \ldots \varepsilon_4$ die individuellen Extinktionskoeffizienten und $K_1 \ldots K_4$ die Bildungskonstanten der Komplexe der Zusammensetzung Metall : Ligand $= 1:1, \ldots 1:4$ sind, während ε_A der Extinktionskoeffizient des Liganden und $[M]$ die Gleichgewichtkonzentration des Metallions bedeuten.

Durch Umformen und Kombinieren der Gleichungen (1) und (2) erhält man zuletzt folgendes System von vier Lineargleichungen mit vier Unbekannten (die Bildungskonstanten $K_1 \ldots K_4$) welches praktisch immer lösbar ist, am besten auf Grund der Determinantentheorie

$$\begin{aligned}
\varepsilon_1 K_1 &= a_1 - \frac{\varepsilon_A}{[M]} = b_4 K_4 + b_3 K_3 + b_2 K_2 + b_1 K_1 - \frac{\varepsilon_A}{[M]} \\
\varepsilon_2 K_2 &= a_2 + a_1 K_1 = b_3 K_4 + b_2 K_3 + b_1 K_2 \\
\varepsilon_3 K_3 &= a_3 + a_2 K_1 + a_1 K_2 = b_2 K_4 + b_1 K_3 \\
\varepsilon_4 K_4 &= a_4 + a_3 K_1 + a_2 K_2 + a_1 K_3 = b_1 K_4
\end{aligned} \tag{3}$$

Unter der Annahme, daß man in den Rechnungen zur Ermittlung der Koeffizienten a_i und b_i die Gleichgewichtskonzentration des Liganden, $[A]$, durch dessen Gesamtkonzentration c_A ersetzen kann, wurden nach diesem Rechnungsverfahren durch Extinktionsmessungen bei $\lambda = 400$ nm die in den Tabellen 1 und 2 zusammengefaßten Werte der angewandten Hilfsfunktionen berechnet, und durch Extrapolation dieser auf den Wert Null der Variablen die in denselben Tabellen angegebenen Werte der Koeffizienten $a_1 \ldots a_4$ und $b_1 \ldots b_4$ bestimmt.

Durch Einführen dieser Werte in das Gleichungssystem (3) und durch Lösen dieses Systems wurden für die (Brutto) Bildungskonstanten $K_1 \ldots K_4$ der Chelatverbindungen der Zusammensetzung Th : Violursäure $= 1:1$, $1:2$, $1:3$ und $1:4$, folgende Werte ermittelt :

$$K_1 = 8.10^2$$

$$K_2 = 2.10^5$$

$$K_3 = 5.10^7$$

$$K_4 = 1.10^{10}$$

Der kleine Wert der Konstante K_1, von der Größenordnung 10^2, zeigt daß der Komplex Metall : Ligand $= 1:1$ recht unbeständig ist ; dies erklärt, warum diese Verbindung nicht durch die Anwendung der Methode des „molaren Verhältnisses" nachgewiesen werden konnte, denn diese Methode ist nur für beständige Komplexe anwendbar. Es sei zu erwähnen, daß mit Hilfe der „Geraden"-Methode von Asmus nur dieser Komplex nachgewiesen wurde, und es ließ sich für ihn nach Asmus eine Dissoziationskonstante in der Größenordnung von 10^{-2} berechnen, welche im Einklang mit diesem Ergebnis steht.

Der genaue Wert dieser Konstanten kann natürlich nicht genau ermittelt werden, denn auch die Extrapolationskoeffizienten $a_1 \ldots a_4$ und $b_1 \ldots b_4$ können nicht mit beliebiger Genauigkeit berechnet werden. Es ließ sich trotzdem überprüfen, daß die Größenordnung dieser Konstanten als korrekt ermittelt betrachtet werden kann. So konnten durch Einführen in das Gleichungssystem (3) von Koeffizienten $a_1 \ldots a_4$ und $b_1 \ldots b_4$ deren Wert sich von dem der oben angegebenen Koeffizienten etwas unterscheidet, d.h. von Koeffizienten die durch von diesen etwas unterschiedlichen Extrapolationsergebnisse ermittelt wurden, für die Bruttobildungskonstanten $K_1 \ldots K_4$ dieselben Größenordnungen von $10^2, 10^5$, 10^7 und 10^{10} berechnet werden.

Die obigen Berechnungen wurden auch unter der Annahme durchgeführt, daß man mit Konzentrationen statt Aktivitäten arbeiten kann, d.h. daß die Konzentration klein ist, oder, wenn das nicht der Fall ist, daß die Ionenstärke konstant ist. Dies ist auch der Fall gewesen, den man hat mit ziemlich verdünnten Lösungen gearbeitet. Außerdem, wenn man eine Berechnung der Ionenstärke durchführt, unter der Annahme, daß sich die Violursäure als ein ein-einwertiger Elektrolyt verhält, kommt man zum Ergebnis, daß im untersuchten Fall (Tabellen 1 und 2) die Ionenstärke höchstens zwischen 0,031 und 0,042 variiert hat.

Tabelle 1

Ermittlung der Koeffizienten $a_1 \ldots a_4$

$c_M = 3.10^{-3}$ Mol/1 ; $d = 2{,}997$ cm ; $[A] \approx C_A$, $\lambda = 400$ nm

$C_A \approx [A]$ Mol/l	E	$\bar{\varepsilon} = \frac{E}{c_M . \alpha}$	$f_1 = \frac{\bar{\varepsilon}}{[A]}$	$f_2 = \frac{f_1 - a_1}{[A]}$	$f_3 = \frac{f_2 - a_2}{[A]}$	$f_4 = \frac{f_3 - a_3}{[A]}$
$7{,}5.10^{-4}$	0,128	14,22	$1{,}89.10^4$	$-5{,}33.10^6$	$+2{,}21.10^9$	
$11{,}25.10^{-4}$	0,178	19,77	$1{,}76.10^4$	$-4{,}80.10^6$	$+1{,}88.10^9$	
$15{,}10^{-4}$	0,228	25,33	$1{,}69.10^4$	$-4{,}00.10^6$	$+2{,}00.10^9$	
$18{,}75.10^{-4}$	0,271	30,11	$1{,}60.10^4$	$-3{,}73.10^6$	$+1{,}74.10^9$	
$22{,}5.10^{-4}$	0,310	34,44	$1{,}53.10^4$	$-3{,}42.10^6$	$+1{,}60.10^9$	
$26{,}25.10^{-4}$	0,342	38,00	$1{,}45.10^4$	$-3{,}03.10^6$	$+1{,}33.10^9$	

Der Wert der Koeffizienten $a_i = \lim\limits_{[A] \to 0} f_i : a_1 = +2{,}3.10^4 ; \ a_2 = -7{,}0.10^6 ; \ a_3 = +2{,}5.10^9$

Der Wert des Koeffizienten $a_4 = \lim\limits_{[A] \to 0} \frac{\mathrm{d}f_3}{\mathrm{d}[A]} ; \quad a_4 = -4{,}1.10^{11}$

Die Jazimirskij-Methode empfiehlt die Überprüfung der gefundenen Koeffizienten, indem man in gesamten Konzentrationsbereich des Liganden die berechneten Werte mit den experimentellen vergleicht. Man führt dafür die ermittelten Koeffizienten und Bildungskonstanten in

Tabelle 2

Ermittlung der Koeffizienten $b_1 \ldots b_4$

$c_M = 3.10^{-3}$ Mol/1 ; d = 2,997 cm ; [A] $\approx C_A$; $\lambda = 400$ nm

$C_A \approx [A]$ Mol/l	$y = \frac{1}{[A]}$	E	$\bar{\varepsilon} = \frac{E}{d.C_M}$	$\varphi_1 = \frac{\bar{\varepsilon} - b_1}{y}$	$\varphi_2 = \frac{\varphi_1 - b_2}{y}$	$\varphi_3 = \frac{\varphi_2 - b_3}{y}$
90.10^{-4}	$1{,}111.10^2$	0,630	69,77	−0,209	$+0{,}9.10^5$	$+0{,}8.10^{-7}$
$93{,}75.10^{-4}$	$1{,}066.10^2$	0,635	70,55	−0,210		
$97.5.10^{-4}$	$1{,}026.10^2$	0,646	71,77	−0,207	$+2{,}8.10^{-5}$	$+2{,}7.10^{-7}$
105.10^{-4}	$0{,}952.10^2$	0,657	73,00	−0,210		
$112{,}5.10^{-4}$	$0{,}888.10^2$	0,670	74,44	−0,208	$+1{,}9.10^{-5}$	$+2{,}1.10^{-7}$
120.10^{-4}	$0{,}833.10^2$	0,680	75,55	−0,209	$+1{,}2.10^{-5}$	$+1{,}4.10^{-7}$
Der Wert der Koeffizienten b_i :			$b_1 = \lim\limits_{y \to 0} \bar{\varepsilon} = 9{,}3.10^1$	$b_2 = \lim\limits_{y \to 0} \varphi_1 = -2{,}1{,}10^{-1}$	$b_3 = \lim\limits_{y \to 0} \varphi_2 = \cong 0$	$b_4 = \lim\limits_{y \to 0} \varphi_3 = \cong 0$

den Ausdruck des mittleren molaren Extinktionskoeffizienten, $\bar{\varepsilon}$, und man vergleicht den so berechneten $\bar{\varepsilon}$-Wert mit den experimentell gemessenen $\bar{\varepsilon}$-Wert.

Eine Überprüfung dieser Art, für verschiedene Werte der Ligandenkonzentration wird in der Tabelle 3 wiedergegeben.

Tabelle 3

Vergleichen der Werte von $\bar{\varepsilon}_{exp}$ und $\bar{\varepsilon}_{ber}$

$[A] \approx C_A$	$\bar{\varepsilon}_{exp} = \frac{E}{d.\,C_M}$	$\bar{\varepsilon}_{ber}$	$\Delta\bar{\varepsilon} = = \bar{\varepsilon}_{ber} - \bar{\varepsilon}_{exp}$
$7{,}5.10^{-4}$	14,22	14,23	0
$3{,}10^{-3}$	41,77	40,90	−0,87
$6{,}10^{-3}$	59,44	60,97	+1,53
$9{,}10^{-3}$	69,77	64,62	−5,15
$1{,}2.10^{-2}$	75,55	80,50	+5,0

Man merkt, daß sich $\bar{\varepsilon}_{ber}$ von $\bar{\varepsilon}_{exp}$ nicht stark unterscheidet.

Um zu erfahren, wie sich die Stabilitätskonstanten der Komplexe in Gegenwart eines inerten Elektrolyten verhalten, wurde eine der in den Tabellen 1 und 2 zusammengefaßten Reihe hinsichtlich Konzentration der Reagenzien, Wellenlänge und Schichtdicke völlig entsprechende Reihe von Extinktionsmessungen in Anwesenheit von $NaClO_4$ durchgeführt. Man hat dafür die Violursäure als einen wohl definierten ein-einwertigen Elektolyt betrachtet und den Mischungen von Violursäure- und $Th(NO_3)_4$-Lösungen die Mengen von einer 0,3 Mol/1−$NaClO_4$ Lösung, die zu einer konstanten Ionenstärke von 0,192 führen würden, hinzugefügt. Die in der Anwesenheit solcher Mengen von $NaClO_4$ gemessenen Extinktionen unterscheiden sich nur wenig von denen die in Tabellen 1 und 2 angegeben sind, und dies galt auch für die in diesem Falle ermittelten Koeffizienten $a_1 \ldots a_4$ und $b_1 \ldots b_4$, die vomselben Vorzeichen und von der gleichen Größenordnung wie die aus den Tabellen 1 und 2 waren. Durch Einsetzen dieser in die Gleichungen (3) und lösen des Systems wurden für die Bildungskonstanten $K_1 \ldots K_4$ Werte in derselben Größenordnung wie die der oben angegebenen erhalten. In den angewandten Konzentrationen hat also der neutrale Elektrolyt keinen großen Einfluß auf die Stabilitätkonstanten.

Zusammenfassend wurden im wäßrigen System $Th(NO_3)_4$ — Violursäure vier einkernige Komplexe der Zusammensetzung Metall : Ligand = 1 : 1; 1 : 2; 1 : 3 und 1 : 4 ermittelt, und die Bildungskonstanten aller dieser, die von der Größenordnung 10^2, 10^5, 10^7 und 10^{10} sind, berechnet.

Revue Roumaine de Chimie, **15**, 1331 – 1336 (1970)

ÉTUDE SUR LES ÉLECTRODES-MEMBRANES POLYMÈRE + PLASTIFIANT. III[1]

L'UTILISATION DE L'ÉLECTRODE-MEMBRANE EN PCV ET TRICRÉSYLPHOSPHATE DANS LE TITRAGE POTENTIOMÉTRIQUE DES ACIDES ET BASES FORTS

C. LITEANU et ELENA HOPÎRTEAN

Chaire de Chimie analytique de l'Université « Babeş-Bolyai »,
Cluj, 11, str. Arany János

Reçu le 5 mars 1970

L'ouvrage présente les résultats obtenus par l'utilisation de l'électrode-membrane en PCV+ tricrésylphosphate dans le titrage potentiométrique de quelques acides et bases forts. L'asymétrie prononcée de quelques courbes de titrage ainsi que la variation relativement faible du potentiel autour du point d'équivalence dans le cas du titrage de l'acide fluorhydrique et de l'hydroxyde de tétraméthylammonium dénotent une appréciable interaction de la membrane et des ions F^-, respectivement $[N(CH_3)_4]^+$.

Les membranes ionitiques ont été utilisées par plusieurs auteurs[2-5] comme électrodes indicatrices dans le titrage potentiométrique acido-basique. La forme des courbes de titrage obtenues est généralement différente de celle des titrages potentiométriques classiques, dans quelques cas la détermination du point final du titrage étant assez difficile.

Dans un ouvrage antérieur[6] on a décrit un nouveau type d'électrode indicatrice utilisable dans des titrages potentiométriques acido-basiques, formée d'une membrane obtenue par la plastification du polychlorure de vinyle par le tricrésylphosphate.

Dans le présent ouvrage on expose les résultats de l'utilisation de l'électrode-membrane mentionnée dans le titrage potentiométrique de quelques acides et bases forts.

---

[1] C. Liteanu et E. Hopîrtean, *Talanta*, **17**, (1970).
[2] S. K. Sinha, *J. Indian Chem. Soc.*, **31**, 572 (1954) ; **32**, 75 (1955).
[3] R. Geyer et P. Nicklas, *Z. analyt. Chem.*, **177**, 166 (1960).
[4] E. A. Materova, J. Iurchenko, *Zhur. analit. Khim.*, **16**, 388 (1961).
[5] F. P. Ijsseling et E. van Dalen, *Analyt. Chim. Acta*, **42**, 77 (1968).
[6] C. Liteanu et E. Hopîrtean, *Rev. Roumaine Chim.*, **15**, 749 (1970).

PARTIE EXPÉRIMENTALE ET DISCUSSIONS

Les mesures du potentiel ont été effectuées avec un pH-mètre MV−11 en utilisant la chaîne électrolytique

$$(-)\ \text{ESC} \mid \text{solution interne HCl } 10^{-4}\text{N} \mid \text{membrane} \mid \text{solution externe (à titrer)} \mid \text{ESC}\ (+)$$

La membrane utilisée était en boule. Les titrages ont été conduits à la température ambiante et les valeurs du potentiel ont été lues en conditions d'agitation (magnétique). Pour les volumes d'équivalence on considère les volumes d'inflexion calculés d'après la méthode Hahn-Weiler. [7] Pour la caractérisation de la précision des titrages, on a déterminé graphiquement la variation du potentiel autour du point d'équivalence, pour la précision de ± 1 %, c'est-à-dire $(\Delta E)_{\pm 1\%} = |E_{99\%} - E_{101\%}|$.

1. LE TITRAGE DE QUELQUES ACIDES FORTS

Sur la figure 1 sont présentées les courbes de titrage des acides halogénés 10^{-2} N, par l'hydroxyde de sodium 2.10^{-1} N. Le titrage de l'acide fluorhydrique a été effectué dans un récipient en plastique. L'extrémité de l'électrode standard de calomel a été aussi recouverte par un tube en plastique. La localisation du volume d'équivalence sur la courbe 1 est facile, celle-ci présentant une variation assez grande du potentiel autour du point d'équivalence $(\Delta E)_{\pm 1\%} = 28$ mV.

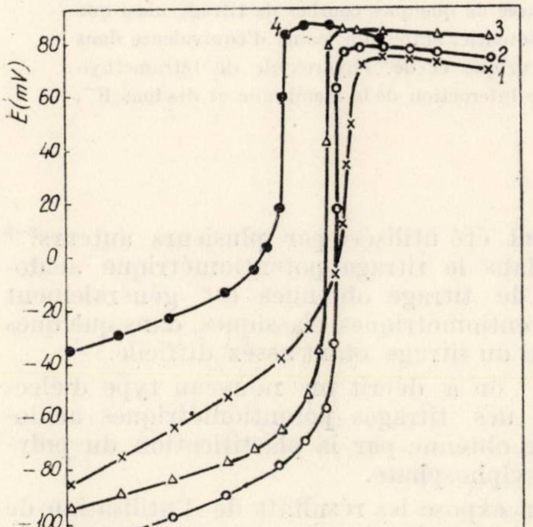

Fig. 1. — Titrage des acides halogénés en concentration 10^{-2} N par hydroxyde de sodium 2.10^{-1}N.

1, acide fluorhydrique ; $(\Delta E)_{\pm 1\%}$ = 28 mV ;
2 acide chlorhydrique ; $(\Delta E)_{\pm 1\%}$ = 72 mV ;
3, acide bromhydrique ; $(\Delta E)_{\pm 1\%}$ = 62 mV ;
4, acide iodhydrique ; $(\Delta E)_{\pm 1\%}$ = 42 mV ;

Le titrage de l'acide chlorhydrique et celui de l'acide bromhydrique (courbe *2*, respectivement *3*) découlent très bien, les courbes de titrage obtenues étant semblables. La variation du potentiel autour du point d'équivalence pour ces deux acides est beaucoup plus grande que dans le titrage de l'acide fluorhydrique, ce qui a pour effet une bonne précision. L'acide iodhydrique est titré avec une précision moindre, $(\Delta E)_{\pm 1\%} = 42$ mV, que les acides chlorhydrique et bromhydrique, mais plus grande que l'acide fluorhydrique, dû certainement à l'effet dépressif de potentiel de l'anion I^-, ainsi que l'on a montré dans un ouvrage antérieur ^{1}.

---

[7] F. L. Hahn et G. Weiler, *Z. analyt. Chem.*, **69**, 417 (1926).

Sur la figure 2 on présente les courbes de titrage des autres acides forts : sulfurique, azotique et perchlorique. Dans tous les cas, la variation du potentiel autour du point d'équivalence est assez grande, $(\Delta E)_{\pm 1\%} = 55-75$ m V, ce qui permet une localisation facile (par calcul ^{7}) du volume d'inflexion.

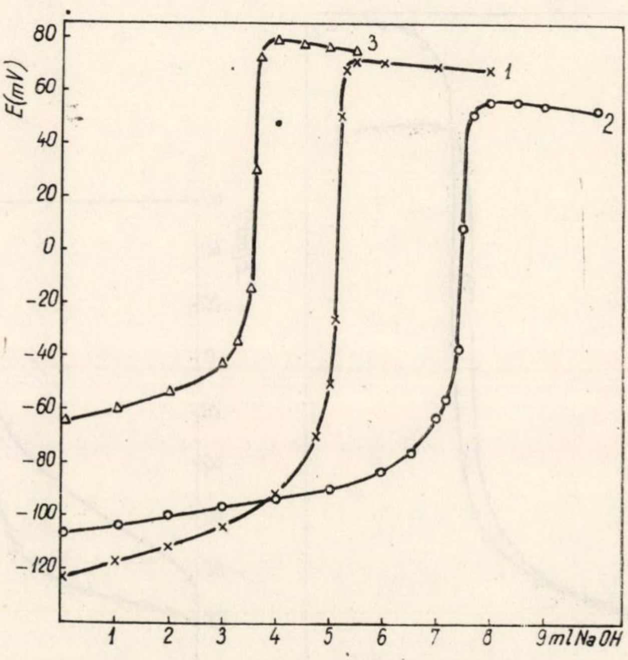

Fig. 2. — Titrage de quelques acides forts par hydroxyde de sodium 2.10^{-1}N.

1, acide sulfurique; $(\Delta E)_{\pm 1\%} = 76$ mV;

2, acide azotique; $(\Delta E)_{\pm 1\%} = 68$ mV;

3, acide perchlorique; $(\Delta E)_{\pm 1\%} = 52$ mV.

Sur la figure 3 sont présentées les courbes de titrage de l'acide sulfurique 5.10^{-3} N par l'hydroxyde de sodium 5.10^{-2} N (courbe *1*) et par l'hydroxyde de baryum 5.10^{-2} N (courbe *2*). On remarque que si on utilise l'hydroxyde de baryum comme titrant (le sulfate de baryum étant peu soluble), la variation du potentiel autour du point d'équivalence est plus grande que si la neutralisation a lieu par l'hydroxyde de sodium ; cela s'explique par l'effet dépressif de potentiel de l'électrolyte résulté (Na_2SO_4).

Les courbes de titrage des acides chlorhydrique et fluorhydrique par l'hydroxyde d'ammonium sont présentées sur la figure 4. Bien que le saut de potentiel autour du point d'équivalence soit plus petit (surtout pour le HCl) que si l'on utilise de l'hydroxyde de sodium comme titrant, il reste toutefois assez grand pour qu'on puisse facilement localiser le point final des titrages.

On remarque aussi dans le cas du titrage de l'acide fluorhydrique par l'hydroxyde de sodium (fig. 1, courbe *1*), une asymétrie accentuée de la courbe, ce qui indique une forte interaction en milieu acide de l'anion F^- avec la membrane.

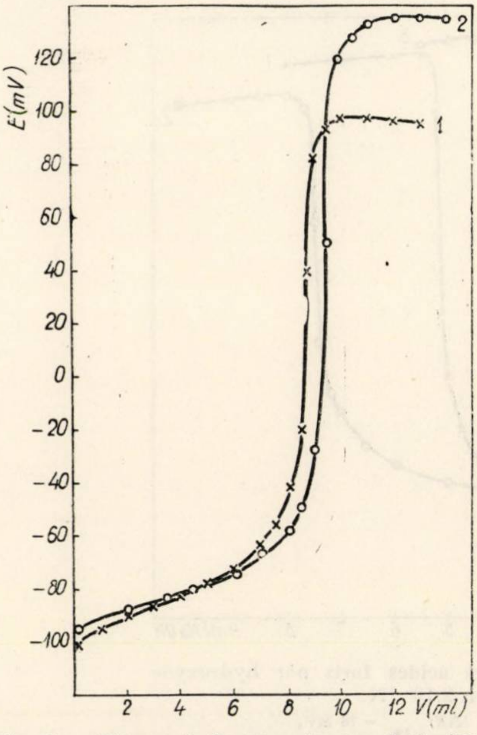

Fig. 3. — Titrage de l'acide sulfurique 5.10^{-3}N par différents titrants.

1. NaOH 5.10^{-2} N ; $(\Delta E)_{\pm 1\%} = 62$ mV

2. $Ba(OH)_2$ 5.10^{-2} N ; $(\Delta E)_{\pm 1\%} = 84$ mV.

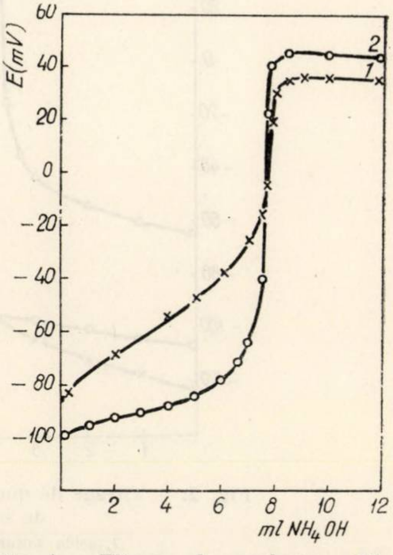

Fig. 4. — Titrage de quelques acides par hydroxyde d'ammonium 10^{-1}N.

1. acide fluorhydrique ; $(\Delta E)_{\pm 1\%} = 24$ mV ;

2. acide chlorhydrique ; $(\Delta E)_{\pm 1\%} = 55$ mV.

2. TITRAGE DE QUELQUES BASES FORTES

Sur la figure 5 sont présentées les courbes de titrage des hydroxydes de sodium, de baryum et de tétraméthylammonium, par l'acide chlorhydrique.

Pour éviter la carbonatation de la solution, le titrage de l'hydroxyde de baryum a été conduit sous de l'huile de paraffine. Le saut du potentiel autour du point d'équivalence, ($\Delta E_{\pm 1\%} = 90$ mV) est plus grand que pour le titrage de l'hydroxyde de sodium par le même acide ($\Delta E)_{\pm 1\%} = 60$ mV.

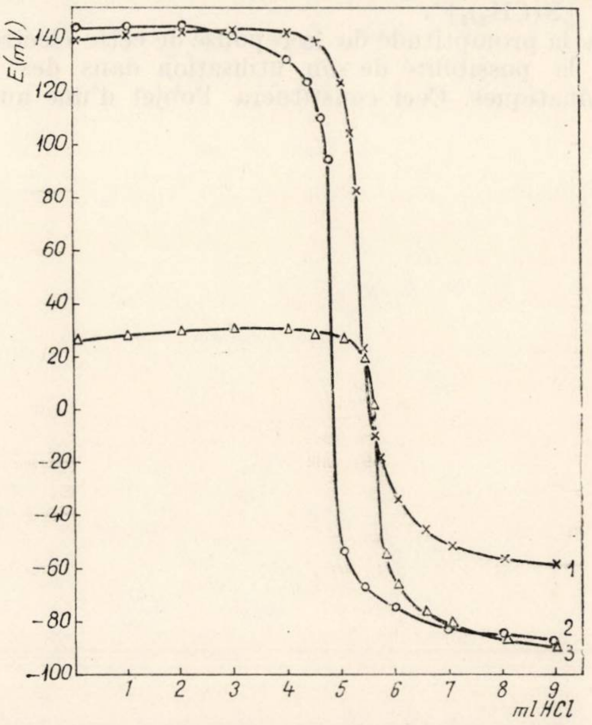

Fig. 5. — Titrage de quelques bases fortes 10^{-2}N par acide chlorhydrique 2.10^{-1} N

1. hydroxyde de sodium ; $(\Delta E)_{\pm 1\%} = 55$ mV ;
2. hydroxyde de baryum ; $(\Delta E)_{\pm 1\%} = 90$ mV ;
3. hydroxyde de tétraméthylammonium ; $(\Delta E)_{\pm 1\%} = 45$ mV.

Le titrage de l'hydroxyde de tétraméthylammonium (courbe *3*) découle bien, mais la variation du potentiel autour du point d'équivalence est plus petite que celle escomptée pour une base forte, ce qui indique aussi une interaction prononcée de la membrane et du cation organique.

En conclusion, on peut affirmer que l'électrode-membrane obtenue par plastification du polychlorure de vinyle par le tricrésylphosphate peut être utilisée avec succès au titrage potentiométrique des acides et bases forts. L'asymétrie prononcée de quelques courbes de titrage, ainsi que la petite variation du potentiel autour du point d'équivalence dans le titrage de l'acide fluorhydrique et de l'hydroxyde de tétraméthylammonium prouvent une appréciable interaction de la membrane avec les ions F^- et $[N(CH_3)_4]^+$.

Grâce à la promptitude de la réponse de cette électrode-membrane, on entrevoit la possibilité de son utilisation dans des titrages acido-basiques automatiques. Ceci constituera l'objet d'une autre étude.

Revue Roumaine de Chimie, 15, 1337–1341 (1970)

DIE KINETISCHE BESTIMMUNG DES KUPFERS (II) MIT BROMAT UND AMIDOL

A. ŞUTEU, I. AL. CRIŞAN und ELISABETA POP
vom Lehrstuhl für Analytische Chemie der „Babeş-Bolyai"-Universität Cluj,
str. Arany János, 11

Eingegangen am 31. März 1969

In der vorliegenden Arbeit wird eine neue kinetische Analysenmethode beschrieben, die sich auf die katalytische Wirkung der Cu^{2+}-Ionen in der Oxidationsreaktion des Amidols (*p*-2,1-Diaminophenol) stützt. Es können 0,5–5μg Cu^{2+}/30 ml bestimmt werden, wenn die Tangentenmethode verwendet wird.

In der Fachliteratur sind mehrere Bestimmungsmethoden des Cu^{2+} beschrieben, welche sich auf seine katalytische Wirkung in verschiedenen Reaktionen stützt. So bestimmen Kupinskaia und Schulow[1] Cu^{2+} auf Grund seiner katalytischen Wirkung in der Zersetzungsreaktion des Wasserstoffsuperoxids. Lambert [2] beschreibt mehrere Methoden auf Grund der katalytischen Wirkung des Cu^{2+} in verschiedenen Oxidationsreaktionen der organischen Substanzen mit dem Sauerstoff aus der Atmosphäre. Die organischen Substanzen, deren Oxidation von Lambert studiert wurde sind : α-Thiosäuren, Ascorbinsäure, das Na-Salz der Arsenilsäure, die Leukobase des Methylenblaus, 6,7-Dioxy-4-methylenmarin, 0-Aminophenol und Resorzin. Jatsimirskii und Drobischewa [3], stützen sich auf die katalytische Wirkung des Cu^{2+} in der Reaktion

$$2\,Fe^{3+} + 2\,S_2O_3^{2-} = 2\,Fe^{2+} + S_4O_6^{2-} \qquad (1)$$

und beschreiben eine andere Methode für die kinetische Bestimmung des Kupfers, indem sie die Geschwindigkeit dieser Reaktion auf kolorimetrischem Weg verfolgen. Hahn [4] gibt eine andere Methode, indem er die Reaktionsgeschwindigkeit auf potentiometrischem Weg verfolgt, während Czarmecki[5] die Geschwindigkeit derselben Reaktion polarographisch verfolgt.

---

[1] G. V. Kupinskaia und E. A. Schulow, *Referaty Trud. Ironovskogo Khimiko-technologitscheskogo Instituta*, **4**, 27 (1949).

[2] R. H. Lambert, *Analyt. Chem.*, **24**, 868 (1952).

[3] K. B. Jatsimirskii, O. M. Drobischewa und V. Rigin, *Zhur. neorg. Khim.*, **14**, 60 (1959).

[4] F. L. Hahn, *Analyt. Chim. Acta*, **11**, 482 (1954)

Von unserer Feststellung ausgehend, daß die Cu^{2+}-Ionen in der Oxidationsreaktion des Amidols mit Bromat katalytische Wirkung haben, wurden in vorliegender Arbeit die Bedingungen festgelegt, in welchen die Reaktion ausgeführt werden muß, um zur kinetischen Bestimmung des Cu^{2+} dienen zu können.

$KBrO_3$ oxidiert Amidol (2,4-Dioxyaminophenol) zu einer Verbindung von roter Farbe mit einem Absorptionsmaximum bei 510 nm. In Abbildung 1 wird die Absorptionskurve dieser Verbindung gegeben.

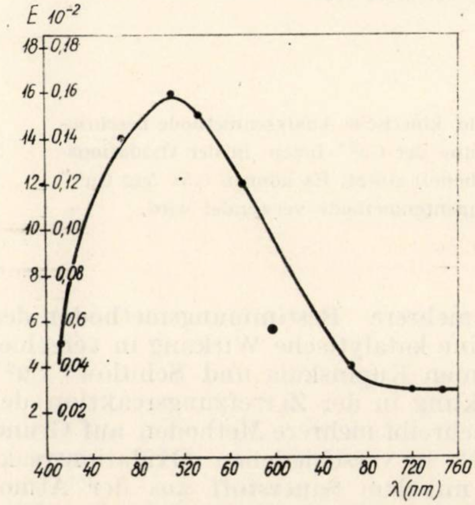

Abb. 1. — Die Absorbanz der (mit $KBrO_3$ oxidierten) Amidollösung in Funktion der Wellenlange (nm). Konzentration des Amidols : $1{,}614.10^{-3}$ M.

Der berechnete molare Extinktionskoeffizent ist $\varepsilon_{\lambda_{max}} = 881{,}9$ cm²/Mol. Weil die Geschwindigkeit der Oxidationsreaktion des Amidols mit Bromat jedoch von dem Säuregrad des Mittels sehr abhängig ist, so wurde in erster Reihe das pH untersucht, bei welchem die Geschwindigkeit dieser Reaktion in Abwesenheit des Cu^{2+} praktisch Null ist, aber genügend groß ist in seiner Anwesenheit. Die Versuche zeigten, daß bei pH $= 2$ das 0,05 M Bromat das Amidol auch in Abwesenheit des Cu^{2+} oxidiert, aber bei pH $= 7$ ist die katalytische Wirkung des Cu^{2+} vernachlässigbar. Die beste katalytische Wirkung des Cu^{2+} wurde bei pH $= 4{,}6$ beobachtet, daher wurde bei den Messungen eine Essigsäure-Ammoniumazetat-Pufferlösung vom pH $= 4{,}6$ (die Ammoniumazetat-Lösung wurde mit Essigsäure auf pH $= 4{,}6$ gebracht) verwendet.

Die Oxidationsgeschwindigkeit des Amidols mit Bromat hängt von der Konzentration des Bromats ab. Es wurde festgestellt, daß bei größeren Konzentrationen als 0,1 M oxidiert das Amidol gerade auch in Abwesenheit des Cu^{2+}. Es wurde festgestellt, daß die treffendste Bromatkonzentration 0,016 M ist, bei der die katalytische Wirkung des Cu^{2+} am besten ist, während die Reaktionsgeschwindigkeit zwischen Bromat und Amidol in Abwesenheit des Cu^{2+} am kleinsten ist.

---

[5] K. Czarmecki, *Chem. Analit.* **5**, 377 (1960).

Auf Grund des oben wiedergegebenen Vorstudiums, wurde festgestellt, daß die Möglichkeit besteht, Cu^{2+} durch eine kinetische Analysenmethode zu bestimmen. Die Tatsache ist bekannt, [6,7] daß den kinetischen Analysenmethoden die Verfolgung der Zeit und der Konzentration einer Substanz mit katalytischer Wirkung zu Grunde liegt. Alle praktischen Varianten der kinetischen Analysenmethoden haben eine allgemeine Gleichung der Art:

$$\frac{\mathrm{d}P}{\mathrm{d}t} = ax + b \tag{2}$$

zu Grunde, in der P der verfolgte Parameter ist, wie zum Beispiel die Absorbanz, t ist die Zeit, x die Konzentration des Katalysators, während a und b Konstanten sind, welche alle bekannten Parameter eines gegebenen konkreten Bereiches einschließt.

Durch die graphische Darstellung der Änderung der Absorbanzien E in Funktion von t für Proben mit veränderlichen Konzentrationen x von Cu^{2+}, wobei die Konzentration des Bromats und des Amidols bei demselben pH gehalten wurden, erhielt man die Geraden aus Abbildung 2.

Stellt man die Neigung der Kurven in Funktion von der Konzentration des Katalysators, entsprechend den allgemeinen Gleichungen:

$$\mathrm{tg}\alpha = a'x + b' \tag{3}$$

(falls ein von der Konzentration eines Reaktionsproduktes abhängiger Parameter verfolgt wird) oder entsprechend:

$$-\,\mathrm{tg}\alpha = a'x + b' \tag{4}$$

(falls ein von der Konzentration eines Reaktionspartners abhängiger Parameter verfolgt wird), dar, so erhält man eine typische Eichkurve. In unserem Fall hat die Gleichung (3) die konkrete Form aus Abbildung 3. Aus Abbildung 3 ist ersichtlich, daß eine lineare Abhängigkeit zwischen $\mathrm{tg}\alpha$ und der Konzentration Cu^{2+} in den Konzentrationsgrenzen von 0,5 — 5,0 μg Cu^{2+}/30 ml besteht.

---

[6] K. B. Jatsimirskii, „Kinetitcheskie metody analisa", Goskhimisdat, Moskau, 1963, S. 69.

[7] Gr. Popa und D. Costache, *Rev. Roumaine Chim.*, **12**, 964 (1967).

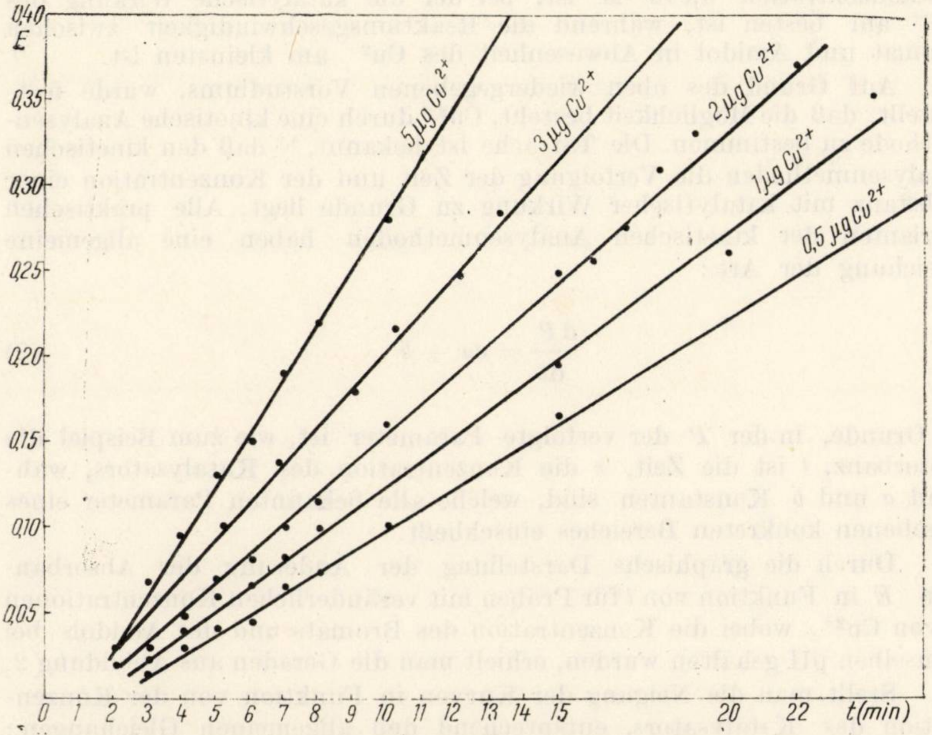

Abb. 2. — Abhängigkeit der Absorbanz in Funktion der Zeit für verschiedene Cu^{2+}-Mengen ($KBrO_3$ 0,016 M und Amidol $1{,}613.10^{-4}$ M).

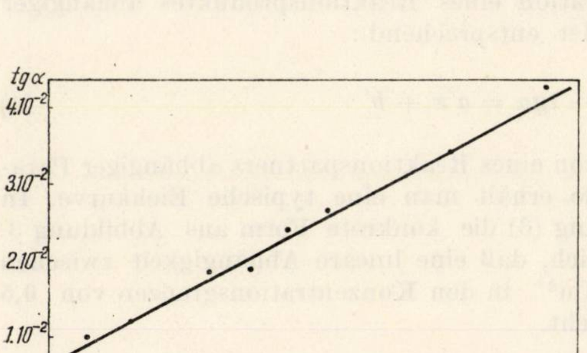

Abb. 3. — Abhängigkeit des tgα in Funktion der Cu^{2+}-Menge

Arbeitsweise. Eine Probe, welche 0,5—5,0 μg Cu^{2+} enthält, wird in die Küvette (30 ml) des Kolorimeters gebracht und, 10 ml $KBrO_3$ 0,05 M, 5 ml Azetatpuffer, 5 ml 0,1 % ige Amidollösung hinzugefügt und dann mit Wasser auf 30 ml aufgefüllt. Es wird die Absorption bei 510 nm in Funktion der Zeit gemessen.

Es wird $E = f(t)$ graphisch dargestellt, $tg\alpha$ bestimmt und auf Grund der Eichgeraden $tg\alpha = f([Cu^{2+}])$ wird die Cu^{2+} Menge aus der unbekannten Probe bestimmt.

Diese Methode kann in Anwesenheit anderer Ionen, welche auf die Reaktion zwischen Bromat und Amidol katalytische Wirkung haben, nicht verwendet werden. Beispiele sind: V^{5+}, Fe^{3+}, Mo^{6+}. $Cr_2O_7^{2-}$.

Ein pH-Wechsel von 0,1 pH Einheiten, sowie ein Temperaturwechsel von ± 2° beeinflußt die Ergebnisse nicht. Die Bestimmungen wurden bei 22° durchgeführt.

Man bemerkt also, bei Verwendung der katalytischen Wirkung des Cu^{2+} in der Oxidationsreaktion des Amidols mit Bromat, daß Cu^{2+} in den Konzentrationsgrenzen von 0,5—5,0 μg Cu^{2+}/30 ml bestimmt werden kann.

Revue Roumaine de Chimie, 15, 1343–1348 (1970)

COMPLEXES THIOCYANATO-CHROMIQUES DANS L'ANALYSE CHIMIQUE. I

DÉTERMINATION GRAVIMÉTRIQUE ET COLORIMÉTRIQUE DE LA PIPÉRAZINE AVEC LES ANALOGUES DU SEL DE REINECKE.

I. GĂNESCU et AL. POPESCU

Laboratoire de Chimie inorganique et analytique de
l'Université de Craiova, 165, str. Calea București

Reçu le 10 mars 1969

On a élaboré une méthode gravimétrique et une méthode colorimétrique de dosage de la pipérazine du produit chimique pur, ainsi que du produit CIF sous la forme

$$\text{Pip.H[Cr (NCS)}_4\text{ (aniline)}_2\text{] et}$$

$$\text{Pip.H[Cr (NCS)}_4\text{ (benzylamine)}_2\text{]}$$

Dans ces méthodes on utilise pour la première fois comme réactifs les analogues du sel de Reinecke.

La pipérazine ou l'hexahydropyrazine avec la formule brute $C_4H_{10}N_2$ est une substance cristalline, incolore, très soluble dans l'eau, particulièrement importante du point de vue pharmaceutique.

Pour sa détermination dans différents médicaments, dans les matériaux biologiques, on a élaboré plusieurs méthodes volumétriques et gravimétriques.

Parmi les méthodes volumétriques d'analyse, on connaît les méthodes acidimétriques dans les solutions d'eau ou dans les milieux non aqueux. Dans les solutions d'eau la pipérazine peut être dosée par titrage avec la solution de H_2SO_4 0,1N en présence du méthylorange comme indicateur.[1]

Dans un milieu de CH_3COOH glacial on a titré avec $HClO_4$[2]. Maybury et collaborateurs[3] utilisent $CHCl_3$ dans une solution aqueuse comme milieu pour le titrage avec du $HClO_4$.

---

[1] «Farmacopeea română», VIIIe éd., Ed. medicală, Bucarest, 1967, p. 541.

[2] ER. VASILIEV, J. FRUDITER et M. JECU, *Farmacia* (*București*), **13**, 203 (1965).

[3] B. MAYBURY, J. P. BARETTA et R. PYFER, *J. Assoc. Offic. Agr. Chemists*, **46**, 1060 (1963).

Les méthodes gravimétriques de détermination de la pipérazine sont basées sur la formation de certains sels peu solubles avec de différents acides, tels que l'acide picrique,[4] l'acide tétraphénylborique,[5] ou avec des hétéropolyacides, tel l'acide silicowolframique[6].

Bond[7] et Myrand[8] déterminent gravimétriquement la substance mentionnée sous forme d'un produit acétylé.

Grecu et ses collaborateurs ont remarqué que la pipérazine peut fonctionner comme un générateur de complexes, en présence de certains métaux de transition. Ils ont constaté que les substances [Cd(pipérazine)]I_2[9] et [Cd(pipérazine)] $(NCS)_2$[10,11] sont peu solubles dans les conditions bien choisies et en conséquence pour cette raison ils peuvent être utilisés au dosage gravimétrique de cette base.

Les complexes thiocyanato-chromiques comme $K_3[Cr(NCS)_6]$ et $NH_4[Cr(NCS)_4(NH_3)_2]H_2O$ sont ceux qui forment en général des sels peu solubles avec les amines hétérocycles et avec des alcaloïdes à formule générale : Amine $H[Cr(NCS)_4(NH_3)_2]$[12] respectivement $(Amine)_3H_3[Cr(NCS)_6]$.[13]

Bondel[14] a élaboré une méthode de détermination gravimétrique de la pipérazine sous forme de Reinecke-at.

Ripan et ses collaborateurs[15,16] ont réussi à obtenir une série de complexes thiocyanato-chromique par une réaction de substitution entre $K_3[Cr(NCS)_6]$ et les amines aromatiques et hétérocycliques conformément à l'équation

$$K_3[Cr(NCS)_6] + 2\,\text{amine} = K[Cr(NCS)_4(\text{amine})_2] + 2\,KCNS$$

Ces complexes analogues au sel Reinecke forment des combinaisons peu solubles avec les alcaloïdes et avec d'autres N-bases hétérocycliques.

Leurs sels avec la pipérazine ont la formule générale : $C_4H_{10}N_2H[Cr(NCS)_4(\text{amine})_2]$ où « amine » est aniline, *p*-toluidine, *p*-anisidine, benzylamine, etc.

Les combinaisons formées avec les dérivés de l'aniline et de la benzylamine sont des combinaisons microcristallines de couleur rose qui précipitent d'une solution de pipérazine acidulée d'acide chlorhydrique.

Les dérivés de la pipérazine ont des propriétés favorables du point de vue analytique. C'est pourquoi nous les avons utilisés pour le dosage gravimétrique et colorimétrique de la base citée.

[4] M. L. Leng, *J. Assoc. Offic. Agr. Chemists*, **40**, 1059 (1957).

[5] M. Hadicke, *Pharm. Zentralhalle*, **97**, 375 (1958).

[6] A. Gastiglioni, *Z. analit. Chem.*, **25**, 117 (1939).

[7] G. R. Boond, *Analyt. Chem.*, **32**, 1332 (1960).

[8] W. R. Mayrand, *J. Assoc. Offic. Agr. Chemists*, **42**, 610 (1959).

[9] I. Grecu, E. Curea et M. Pitiş, *Studii şi Cercetări Chim. Fil. Cluj*, **13**, 35 (1962).

[10] I. Grecu, E. Curea et M. Neamţu, *Farmacia (Bucureşti)*, **14**, 361 (1966).

[11] I. Grecu, *Farmacia (Bucureşti)*, **3**, 261 (1960).

[12] G. Boda, Cs. Várhelyi et A. Mostis, *Stud. Univ. Babeş-Bolyai, Chem.*, **10**, 63 (1965).

[13] R. Ripan, I. Gănescu et Cs. Várhelyi, *Rev. Roumaine Chim.*, **11**, 1051 (1966).

[14] H. Bandel, *Z. analyt. Chem.*, **163**, 235 (1958).

[15] R. Ripan, I. Gănescu et Cs. Várhelyi, *Z. anorg. Chem.*, **357**, 140 (1968).

[16] I. Gănescu et Cs. Várhelyi, *Rev. Roumaine Chim.*, **12**, 395 (1967).

PARTIE EXPÉRIMENTALE

Les réactifs : $NH_4[Cr(NCS)_4$ (aniline)$_2]H_2O$ et $NH_4[Cr(NCS)_4$ (benzylamine)$_2]H_2O$ ont été préparés selon la méthode de Gănescu.[17]

On mélange 0,1 mole $K_3[Cr(NCS)_6]$ finement trituré avec 0,6 mole d'aniline, respectivement 0,3 mole de benzylamine, et on les introduits dans un ballon muni d'un bouchon sur un bain d'eau bouillante pendant quatre heures.

Il se forme un produit visqueux de couleur rouge. On le traite avec de l'acide acétique 50%, puis on filtre la masse microcristalline formée, dissoute dans 250 ml de méthanol à froid et versée par petites portions dans une solution saturée de NH_4Cl. Dans un court intervalle précipitent les sels d'ammonium. On filtre, après on lave avec de l'eau.

$NH_4[Cr(NCS)_4$ (aniline)$_2]H_2O$ /M = 506,6/.

$NH_4[Cr(NCS)_4$ (benzylamine)$_2]H_2O$ /M = 534,5/.

Réactifs: Solutions de 3% dans l'éthanol de 50%.

Pip.H[Cr (NCS)$_4$ (aniline)$_2$]

Analyse :

trouvé Cr = 9,36%, S = 22,84%

calculé pour C_4H_{10} $N_2H[Cr(NCS)_4(C_6H_5-NH_2)_2]$.

(M = 557,7), Cr = 9,32% S = 22,96%

Pip.H [Cr(NCS)$_4$ (benzylamine)$_2$]

Analyse :

trouvé Cr = 8,82%, S = 21,86%

calculé pour : C_4H_{10} $N_2H[Cr(NCS)_4(C_6H_5-CH_2-NH_2)_2]$.

(M = 585,6), Cr = 8,88%, S = 21,91%.

Dosage gravimétrique de la pipérazine sous forme de Pip. H[Cr(NCS)$_4$(aniline)$_2$] respectivement de Pip. H[Cr(NCS)$_4$(benzylamine)$_2$]

On traite une solution qui contient 58–43,00 mg de pipérazine avec 5–10 ml de HCl conc. puis on y ajoute le réactif en excès. Après un repos de 15–20 mn, on filtre le précipité cristallin de couleur rouge violacée par le creuset G_4. On lave avec un mélange de méthanol-eau 20% pour le composé avec le rhodanylate d'ammonium et respectivement de 40% méthanol-eau pour le composé de benzylamine, jusqu'à ce que le filtré coule incolore. On le sèche en étuve pendant 30′ à 80′ et on le pèse.

Les facteurs gravimétriques

$$\frac{\text{Pip.6 } H_2O}{\text{Pip.}[HCr(NCS)_4(\text{aniline})_2]} = 0{,}3479$$

respectivement

$$\frac{\text{Pip.6 } H_2O}{\text{Pip.}H[Cr(NCS)_4(\text{benzylamine})_2]} = 0{,}3319$$

Les résultats des déterminations sont inscrits dans les tableaux 1 et 2.

---

[17] I. Gănescu, *Stud. Univ. Babeş-Bolyai, Chem.*, **12**, 103 (1967).

Tableau 1

Dosage gravimétrique de la pipérazine sous forme de $Pip.H[Cr(NCS)_4(aniline)_2]$

N^{o} crt.	mg Pip. pris	g^{r}Cx. trouvé	mg Pip. trouvé	ΔH(mg)	Err. %
1	2,58	0,0074	2,57	0,01	$-0{,}38$
2	4,30	0,0125	4,35	0,05	$+1{,}16$
3	6,02	0,0175	6,08	0,06	$+0{,}99$
4	8,60	0,0250	8,69	0,09	$+1{,}00$
5	11,18	0,0324	11,27	0,09	$-0{,}80$
6	13,76	0,0398	13,84	0,08	$+0{,}57$
7	17,20	0,0497	17,28	0,08	$+0{,}46$
8	20,64	0,0596	20,73	0,09	$+0{,}43$
9	24,94	0,0719	25,01	0,07	$+0{,}28$
10	29,25	0,0843	29,32	0,08	$+0{,}27$
11	34,40	0,0991	34,47	0,07	$+0{,}23$
12	43,00	1,2362	43,007	0,007	$+0{,}16$

La méthode gravimétrique appliquée par nous peut être utilisée seulement dans le cas des produits pharmaceutiques qui ne contiennent pas d'alcaloïde ou autres N-bases organiques avec un squelette hétérocyclique.

Tableau 2

Dosage gravimétrique de la pipérazine sous forme de $Pip.H[Cr(NCS)_4(benzylamine)_2]$

N^{o} crt.	mg Pip. pris	g^{r} Cx. trouvé	mg Pip. trouvé	ΔH (mg)	Err. %
1	2,58	0,0076	2,64	0,06	$+2.32$
2	4,30	0,0132	4,38	0,08	$+1{,}86$
3	6,02	0,0184	6,10	0,08	$+1{,}32$
4	8.60	0,0262	8,69	0,09	$+1{,}04$
5	11,18	0,0339	11,25	0,07	$+0{,}62$
6	13,76	0,0417	13,84	0,08	$+0{,}58$
7	17,20	0,0521	17,29	0,09	$+0{,}52$
8	20,64	0,0624	20,71	0,07	$+0{,}33$
9	24,94	0,0755	25,08	0,11	$+0{,}44$
10	29,24	0,0884	29,33	0,09	$+0{,}30$
11	34,40	0,1036	34,48	0,08	$+0{,}23$
12	43,00	0,1295	43,11	0,11	$+0{,}27$

Détermination colorimétrique

Les complexes thiocyanato-chromiques sont intensément colorés en rouge violacé avec un maximum d'absorption dans la partie visible du spectre à 535 nm. La solution des complexes avec pipérazine en acétone suit la loi Lambert — Beer dans l'intervalle des concentrations de $10^{-4} - 10^{-2}$ g/ml de pipérazine (intervalle imposé par la sensibilité de l'appareil).

La courbe d'étalonnage s'établit soit avec Pip.H $[Cr(NCS)_4(aniline)_2]$ soit avec Pip.H $[Cr(NCS)_4(benzylamine)_2]$, l'aniline ou la benzylamine des réactifs utilisés ne produisant pas le déplacement des bandes d'absorption.

Les résultats des déterminations sont inscrits dans les tableaux 3 et 4.

Tableau 3

Dosage colorimétrique de la pipérazine sous forme de Pip.H$[Cr(NCS)_4(aniline)_2]$

N° crt.	mg Pip. pris	mg Pip. trouvé	ΔH(mg)	Err. %
1	0,86	0,8668	0,0068	+0,78
2	1,72	1,7251	0,0051	+0,29
3	2,58	2,5954	0,0154	+0,59
4	4,30	4,3172	0,0172	+0,40
5	6,02	6,0212	0,0012	+0,019
6	8,60	8,6058	0,0058	+0,06
7	11,18	11,1911	0,0111	+0,09
8	13,76	13,7637	0,0037	+0,02
9	17,20	17,2050	0,0050	+0,02
10	20,64	20,6565	0,0165	−0,07
11	24,94	24,9549	0,0149	+0,05
12	29,24	29,2575	0,0175	+0,059

Nous avons préféré la méthode colorimétrique à la détermination de l'hydrate de pipérazine du produit CIF « Nematocton » qui se trouve dans le commerce en concentration de 10 % et de 25 %. Dans nos déterminations, nous avons utilisé « Nematocton » 10 %.

Tableau 4

Dosage colorimétrique de la pipérazine sous forme de Pip.H$[Cr(NCS)_4(benzylamine)_2]$

N° crt.	mg Pip. pris	mg Pip. trouvé	ΔH(mg)	Err. %
1	0,86	0,8668	0,0068	+0,78
2	1,72	1,7251	0,0051	+0,29
3	2,58	2,5800	—	—
4	4,30	4,3172	0,0172	+0,59
5	6.02	6,0212	0,0012	+0,019
6	8,60	8,6058	0,0058	+0,06
7	11,18	11,1911	0,0111	+0,09
8	13,76	13,7637	0,0037	+0,02
9	17,20	17,1832	0,0168	−0,009
10	20,64	20,6369	0,0031	−0,01
11	24,94	24,9549	0,0149	+0,05
12	29,24	29,2575	0,0175	+0,059

Les résultats des déterminations sont inscrits dans le tableau 5 et confirment que le produit correspond aux prévisions de « Farmacopeea română », VIIIe éd.

Tableau 5

Dosage colorimétrique de la pipérazine du produit CIF «Nematocton» 10% sous forme de Pip. H [Cr(NCS)$_4$ (aniline)$_2$]

N° crt.	mg Pip. pris	mg Pip. trouvé	ΔH(mg)	Err. %	Pip. % trouvé
1	5	4,9905	0,0095	−0,19	9,981
2	10	9,9960	0,0040	−0,04	9,996
3	20	19,9920	0,0080	−0,04	9,996
4	30	30,0880	0,0880	+0,29	10,029

Pour une meilleure interprétation des résultats obtenus par la méthode gravimétrique, nous avons effectué, un calcul statistique.[18] Finalement nous avons obtenu pour le tableau 1 :

$t_a = 0{,}35$ et pour le tableau 2 : $t_a = 0{,}04$

$t_b = 0{,}15$ $t_b = 0{,}01$

La valeur tabulée $t_{n-2,\,\alpha}$ dans laquelle $\alpha = 90\,\%$ est 1,81.

En conséquence dans chacun des deux cas t_a et t_b étant $< t_{n-2,\alpha}$, on conclut que la méthode utilisée n'est pas affectée d'erreurs systématiques.

Des conclusions similaires nous pouvons tirer également pour la méthode colorimétrique, aussi bien pour le tableau 3

$t_a = 2{,}57$ que pour le tableau 4 $t_a = 0{,}18$

$t_b = 1{,}00$ $t_b = 0{,}07$

La valeur tabulée $t_{n-2,\,\alpha}$ dans laquelle $\alpha = 98\,\%$ est 2,76.

---

[18] W. J. Jouden, «Statistical Methods for Chemist», John Wiley & Sons, Inc. New York, 2nd priting, 1955, p. 40−44.

Revue Roumaine de Chimie, **15**, 1349–1353 (1970)

KINETIC DETERMINATION OF COBALT TRACES. V.* WITH BROMPYROGALLOL RED

D. COSTACHE and GR. POPA

Department of Analytical Chemistry
University of Bucharest, Splaiul Independenţei 89

Received July 29, 1969

For the analytical determination of cobalt, one makes use of its catalytic effect on the oxidizing reaction of brompyrogallol red with peroxide in an alkaline medium. One gives the value of the rate constants and studies the influence of the concentration of reactives and temperature. The method may be applied in the range of 7.76×10^{-10} g Co/cm^3 to 38.80×10^{-10} g Co/cm^3.

It is well known in the speciality literature that organic substances having two hydroxyls in *ortho* position lead, in alkaline medium and under the influence of peroxide, to colourless products, and that the rate of these reactions is influenced by the presence of cobalt traces. Based on the catalytic effect of cobalt on the above mentioned oxidizing reactions one has established dosing methods of the cobalt. Some of them are mentioned in works. [1–15]

---

* Part IV: D. Costache, *Rev. Roumaine Chim.*, **15**, 1187 (1970).

[1] J. Bognar, *Mikrochim. Acta*, **5**, 901 (1961).

[2] J. Bognar and O. Jellinek, *Acta Chim. Acad. Sci. Hung.*, **29**, 2, 131, (1961); **29**, 2, 139, (1961); **29**, 4, 319, (1961).

[3] J. Bognar and O. Jellinek, *Acta Chim. Acad. Sci. Hung.*, **29**, 21 (1961).

[4] E. Schulek and J. Laszlovski; *Mikrochim. Acta*, **1**, 41 (1960).

[5] N. B. Parhomenko, G. A. Prik and K. B. Iaţimirski, *Zhur. analit. Khim.*, **16**, 599 (1961).

[6] V. M. Peşcova, J. F. Dolmanova and N. M. Cemenova, *Zhur. analit. Khim.*, **18**, *10*, 1228 (1963).

[7] A. K. Babko and N. M. Lukocskaia, *Ukrain. khim. Zhur.*, **28**, 968, (1962).

[8] S. G. Oradovski, *Khim. Protsesy Moyakh Okeankh Acad. Nauk.*, **1966**, 78.

[9] J. Laszlovski, *Magyar Kém, Folyóirat*, **71**, 260 (1965); **71**, 99 (1965).

[10] J. Bognar and L. Sipoş, *Mikrochim. Acta*, **5**, 442, (1963).

[11] J. Bognar, *Mikrochim. Acta*, **4**, 801 (1963).

[12] Gr. Popa and D. Costache, *Analele Universităţii Bucureşti*, **16**, 107, (1967).

[13] Gr. Popa and D. Costache, *Rev. Roumaine Chim.*, **12**, 963 (1967).

[14] Gr. Popa and D. Costache, *Analele Universităţii Bucureşti*, **17**, 21 (1968).

[15] D. Costache and Gr. Popa, *Analele Universităţii Bucureşti*, **17**, 55 (1968).

In the present paper one makes use of the reaction between brompyrogallol red and peroxide in alkaline medium, catalysed by the cobalt ions. The reactive has the following formula :

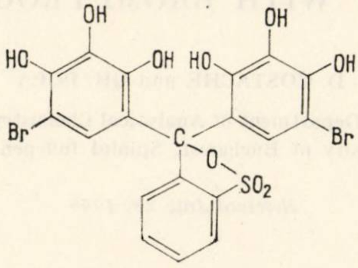

EXPERIMENTAL

Reactives : the reactive solution was obtained by solving brompyrogallol red in water (0.014 %).

The peroxide, obtained by diluting hydrogen peroxide, had a 5.04 % concentration. This was controlled by titration with potassium permanganate in acid medium.

To maintain the reaction medium, one has made use of a buffer solution obtained by solving 5 g Sörensen boric acid in 1000 cm^3 0.4 N.

The cobalt solution was obtained by solving the spectrally pure metallic cobalt in dilute sulphuric acid.

Tridistilled water was used for all solutions.

Working method : The reaction mixture was prepared in 25 cm^3 flasks, adding the constituent parts in the following order : buffer solution, brompirogallol red, peroxide, varied quantities of cobalt so that, after bringing to mark, we had the following concentrations in the reacting medium :

Brompyrogallol red	2.80×10^{-5} g/cm^3
Peroxide	4.00×10^{-3} g/cm^3
Cobalt	38.80×10^{-10} g/cm^3

After stirring, the mixture is transferred into the spectrophotometer cell, and the optical density is read every minute for twenty minutes, having water for control. Determinations were made at a $\lambda = 533$ nm wavelength with a horizontal Pulfrich Zeiss Jena spectrophotometer, provided with a thermostating device.

To find out the optimum reaction conditions we have first watched the influence of the pH on the reaction rate. Results are given in graph 1.

It henceforth results that the reaction rate is the highest in the pH range 11.5 to 13.4.

The influence of the peroxide's concentration on the reaction rate is shown on graph 2.

Graph 2 shows that the reaction rate increases with the concentration of the peroxide, and remains constant in the range $3.25 \times 10^{-3} - 4.80 \times 10^{-3}$ g H_2O_2/cm^3.

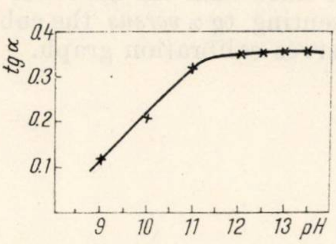

Fig. 1. — Influence of pH on reaction rate.

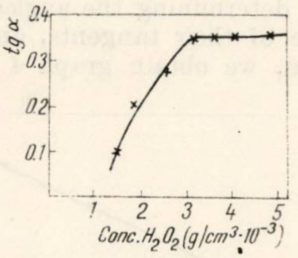

Fig. 2. — Influence of peroxide concentration on reaction rate.

RESULTS AND DISCUSSIONS

We had first to establish the reaction succession in order to apply correctly the kinetic relationships. This we made based on experimental data (table 1) by means of the fixed time method and the graphic method. Results led to the conclusion that we have a pseudomonomolecular reaction.

The reaction rate is expressed in this case by the relationship:

$$\ln \frac{a}{a - x} = kt \tag{1}$$

We express the concentration of the coloured organic reactive by the optical density according to Lambert-Beer's relationship, obtaining

$$\ln D = \ln D_0 - kt \tag{2}$$

For the proper determination, we have watched the variation of the optical density of the reaction mixture for 20 minutes. Experimental results are shown on graph 3.

The graph 3 shows according to relation (3) a beam of lines differing through their slope.

Fig. 3. — Variation in time of ln D value:
1, g Co $\times 10^{-10}$/cm^3; *2*, 7.76 $\times 10^{-10}$ g Co/cm^3; *3*, 15.52 $\times 10^{-10}$ g Co/cm^3; *4*, 23.28 $\times 10^{-10}$ g Co/cm^3; *5*, 31.04 $\times 10^{-10}$ g Co/cm^3; *6*, 38.80 $\times 10^{-10}$ g Co/cm^3.

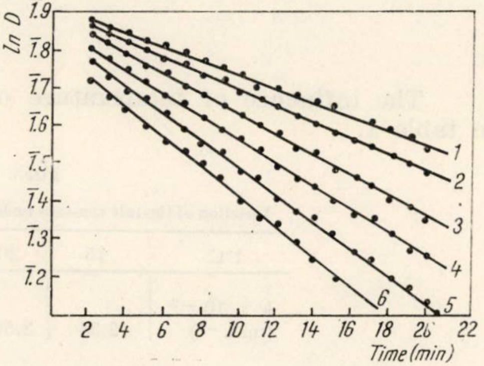

By determining the angles of these lines with the abscissa, we find the value of their tangents, and representing tg α *versus* the cobalt concentration, we obtain graph 4 which serves calibration graph.

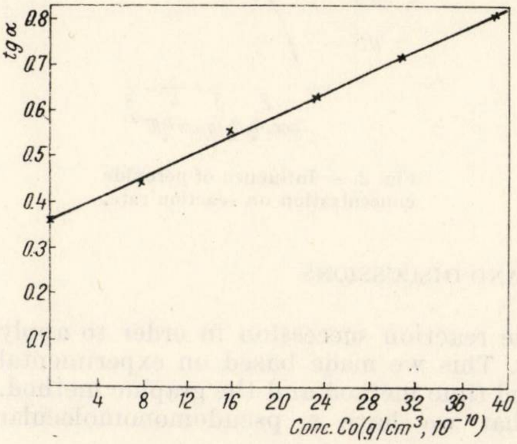

Fig. 4. — Dependency of tg α on cobalt concentration.

We have aimed at finding a proportionality relationship between the principal parameter of the reaction rate — the rate constant k — and the concentration of the cobalt, and therefore we have also drawn up a graph in these coordinates (graph 5). This can also serve as calibration graph.

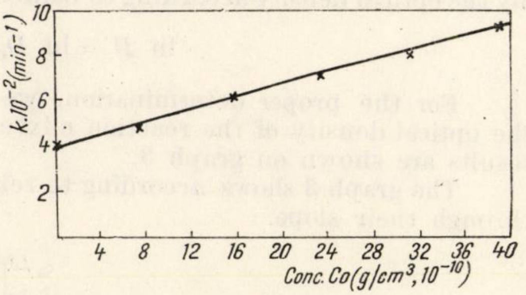

Fig. 5. — Dependency of rate constant on cobalt concentration.

The influence of temperature on the reaction rate may be seen in table 1.

Table 1

Variation of the rate constant under the influence of temperature

t°C	15	20	25	30	35
$k \times 10^{-2}$ (min.$^{-1}$)	2.04	3.56	4.19	6.93	8.57

Alien ions, influencing the determinations are: Ni^{2+}, Fe^{2+}, V^{5+} if their ratio as against cobalt is higher than 1.000 : 1.

A table with the reproducibility of the method is further given (table 2). The period for one determination is 20 minutes.

Table 2

Reproducibility of the method

No of determinations	Co analysed (g/cm^3)	α°	tg α	Co found in analysis (g/cm$^3 \times 10^{-10}$)	Difference (g/cm$^3 \times 10^{-10}$)
	7.76×10^{-10}	24	0.445	—	—
1		25	0.466	8.92	1.16
2		23	0.424	5.43	2.33
3		24	0.445	7.37	0.39
4		24	0.445	7.37	0.39
5		24	0.445	7.37	0.39
	15.52×10^{-10}	29	0.554	—	—
1		29	0.554	16.68	1.16
2		28	0.531	14.75	0.77
3		29	0.554	16.68	1.16
4		30	0.577	18.21	2.69
5		28	0.531	14.75	0.77
	23.28×10^{-10}	32	0.624	—	—
1		33	0.649	24.83	1.55
2		31	0.600	20.95	2.33
3		32	0.624	22.90	0.38
4		32	0.624	22.90	0.38
5		32	0.624	22.90	0.38
	31.04×10^{-10}	36	0.726	—	—
1		35	0.700	29.49	1.55
2		36	0.726	31.81	0.77
3		37	0.753	33.37	2.33
4		36	0.726	31.81	0.77
5		36	0.726	31.81	0.77
	38.80×10^{-10}	39	0.809	—	—
1		40	0.839	41.90	3.10
2		39	0.809	38.80	—
3		41	0.869	44.23	5.43
4		39	0.809	38.80	—
5		39	0.809	38.80	—

In conclusion, the method with brompyrogallol red is applicable in the concentration range $7.76 \times 10^{-10} - 38.80 \times 10^{-10}$ g Co/cm^3, with a good reproducibility.

Revue Roumaine de Chimie, **15**, 1355–1364 (1970)

POLYMÈRES ORGANIQUES PHOSPHORYLÉS. III *

PHOSPHORYLATION DU POLYSTYRÈNE DANS DES HYDROCARBURES ALIPHATIQUES ($C_6 - C_8$)

FL. POPESCU
Institut de Chimie macromoléculaire «P. Poni»
41 A, Aleea Gr. Ghica Vodă, Jassy

Reçu le 14 juin 1969

Par la phosphorylation dans le hexane, heptane ou octane du polystyrène imbibé avec du trichlorure de phosphore il résulte du polystyrène phosphorylé réticulé par le phosphore dans une proportion de 98 %. Les produits ainsi obtenus ont une capacité d'échange jusqu'à 4,5 meq/g résine sèche et une bonne résistance thermique.

L'introduction du phosphore dans les polymères par (co)polymérisation ou (co)polycondensation est difficile et, à l'exception de quelques rares cas, on obtient des produits ayant une petite teneur en phosphore, un petit poids moléculaire, de mauvaises propriétés mécaniques ainsi qu'une mauvaise stabilité hydrolytique [1].

La phosphorylation des polymères a donné de bons résultats et on obtient par des méthodes de synthèse relativement simples des produits à une teneur élevée en phosphore. On a obtenu ainsi des produits avec des propriétés intéressantes et des auteurs comme Gefter, [2] Marhol, [3] Steiniger et Sander [4] ont fait des exposés détaillés sur les synthèses et les propriétés des polymères phosphorylés.

La méthode la plus utilisée consiste dans la phosphorylation par le trichlorure de phosphore d'un copolymère de styrène-divinylbenzène en présence du trichlorure d'aluminium, suivie de l'hydrolyse et de l'oxydation du produit obtenu. [5,6] Le copolymère, réticulé par le divinylbenzène est aussi partiellement réticulé par le phosphore. [7]

---

* Notes I et II, Fl. Popescu (voir réf. 7 et 8).

[1] M. Sander et E. Steiniger, *J. Macromol. Sci.* (*rev*)., C_1, 7 (1967).

[2] E. I. Gefter, «Fosfororganicheskye monomery i polimery» Izdatelstvo Akademii Nauk S.S.S.R., Moscou, 1960, p. 144.

[3] M. Marhol, *Chem. listy*, **58**, 713 (1964).

[4] E. Steiniger et M. Sander, *J. Macromol. Sci.* (*Rev*), C_2, 57 (1968).

[5] E. V. Trostyanskaya, Lu-Sian Jao, A. S. Tevlina et I. P. Losev, *Vysokomol. Soedinenya*, **3**, 41 (1961).

[6] K. Lohz (VEB Fabriken Wolfen) Ger (Est) 11083, 22 déc. 1954.

[7] Fl. Popescu, *Rev. Roumaine Chim.*, **13**, 977 (1968).

La phosphorylation en présence de trichlorure d'aluminium du polystyrène dissous dans le trichlorure de phosphore mène à un mélange de produits qui diffèrent entre eux par la teneur en phosphore et aussi à une quantité de polystyrène insoluble réticulé par le phosphore.[8].

La phosphorylation du copolymère réticulé styrène-divinylbenzène, donne de meilleurs résultats que la phosphorylation du polystyrène dissous dans le trichlorure de phosphore, puisque ce dernier précipite partiellement pendant la synthèse et change ainsi les conditions de la réaction.

Dans le présent travail, afin d'obtenir des produits homogènes on a phosphorylé du polystyrène introduit dans un mélange de hexane, heptane ou octane avec une quantité limitée de trichlorure de phosphore. Le polystyrène ne se dissout pas dans le mélange et peut être phosphorylé tout aussi facilement que le copolymère insoluble styrène-divinylbenzène. On obtient comme principal produit, du polystyrène phosphorylé réticulé par le phosphore et en conséquence insoluble.

MODE DE TRAVAIL

Dans un ballon à trois tubulures, muni d'un agitateur, d'un réfrigérant ascendant avec tube à chlorure de calcium, et d'une ampoule à brome, on place successivement 6 gr de polystyrène en perles ($\theta < 1$ mm), 10 gr de trichlorure d'aluminium en poudre sublimé et 60 ml hexane, heptane ou octane. On ajoute lentement par l'empoule à brome 17 ml de trichlorure de phosphore, sous une forte agitation et à une température inférieure à 20°. On chauffe ensuite à 70° pendant 45 minutes.

Le rapport molaire entre les réactants $AlCl_3$: polystyrène (unité structurelle) : PCl_3 est de 1,3 : 1 : 3,43.

Le contenu du ballon refroidi est transvasé dans un Berzelius contenant 300 ml d'alcool méthylique ou d'alcool éthylique.

Après filtration, les produits de la réaction sont broyés, lavés avec de l'acide chlorhydrique 10 % et puis avec de l'eau jusqu'à la neutralité. Les produits sont séchés à 65° dans une étuve à circulation d'air. Les composants solubles sont éliminés par extractions successives avec du chloroforme et de la solution de soude 10 %.

Les produits phosphorylés séparés par filtration sont traités avec de l'acide chlorhydrique 10 % pour les transformer sous forme hydrogène, ensuite lavés avec de l'eau jusqu'à neutralité et séchés selon le mode indiqué.

La capacité d'échange a été déterminée statiquement avec de l'hydroxyde de sodium 0,1 n pour les produits insolubles broyés ($\theta \approx 0,05$ mm) et pour les mêmes produits oxydés par l'acide azotique 63 % pendant 6 h à 20°.

Le titrage potentiométrique a été réalisé dans des solutions de chlorure de sodium 0,5 n avec de l'hydroxyde de sodium 0,5 n.

On a utilisé la méthode de K. Ziegler et coll. [9] pour les analyses de phosphore.

Le polystyrène utilisé ($\overline{M}_v = 144.700$) a été obtenu par la polymérisation en suspension, sous forme de perles avec un diamètre compris entre 0,1 et 1,2 mm.

Les déterminations comparatives ont été faites avec un copolymère de styrène avec 8 % divinylbenzène. Pour la phosphorylation du copolymère on a utilisé un rapport molaire $AlCl_3$: unité structurelle de polystyrène : PCl_3 de 1,1 : 1 : 9.[7]

---

[8] Fl. Popescu, *Rev. Roumaine Chim.*, **14**, 1525 (1969).

[9] K. Ziegler, H. Till et H. Schindlbauer, *Microchim. Acta*, **1963**, 1144.

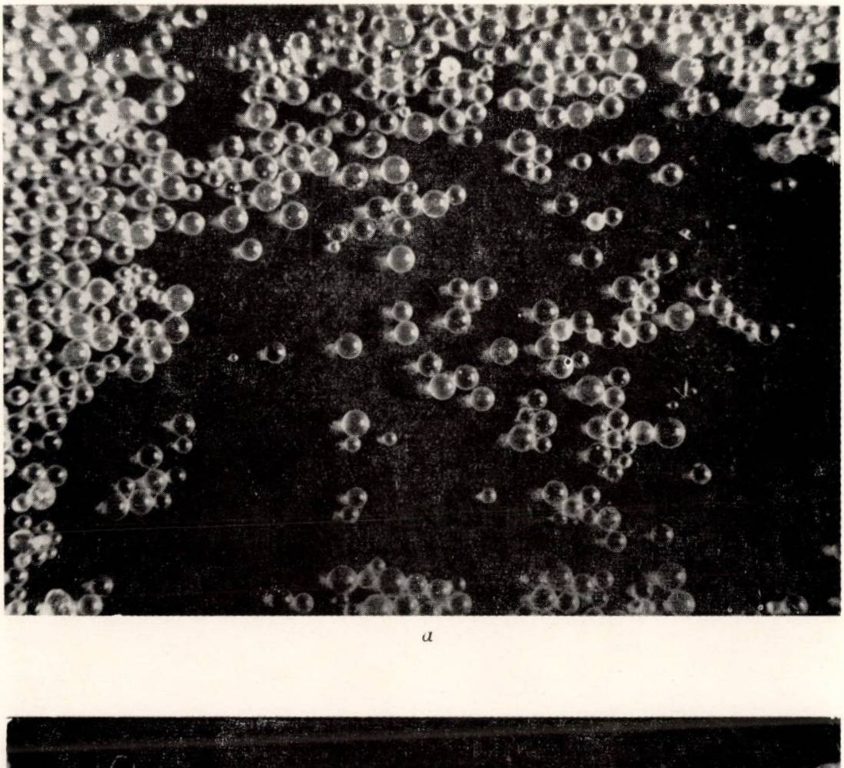

Fig. 1. — Produits de la phosphorylation.

a, perles de polystyrène ; *b*, produits obtenus après la phosphorylation des perles de polystyrène.

RÉSULTATS

Les perles de polystyrène introduites dans le mélange hydrocarbure-trichlorure de phosphore absorbent du trichlorure de phosphore, se gonflent et s'agglomèrent. L'agglomération est favorisée par l'élévation de la température et l'agitation.

Si l'on ajoute sous agitation du trichlorure de phosphore au mélange de polystyrène et du trichlorure d'aluminium en poudre dans l'hydrocarbure, les perles ne s'agglomèrent plus, puisque le trichlorure d'aluminium qui les couvre empêche le contact.

Le mode de synthèse décrit peut être employé pour la phosphorylation du polystyrène ayant un poids moléculaire ($\overline{M}_v$) supérieur à 100 000. Les perles de polystyrène de poids moléculaire inférieur ne restent pas distinctes dans le mélange indiqué même si l'on accroît la quantité d'hydrocarbure ou la quantité de trichlorure d'aluminium.

Les perles de polystyrène ($\overline{M}_v > 100\,000$) soumises à la phosphorylation modifient leur forme initiale. Pendant les 15 premières minutes de synthèse les perles se déforment et se transforment en pellicules de forme irrégulière ayant l'aspect de croûtes (fig.1).

La teneur en phosphore baisse avec la croissance du diamètre des perles (fig. 2 ; 1). Dans la figure 2 est donnée aussi comparativement la variation de la teneur en phosphore dans le cas du polystyrène réticulé avec 8% divinylbenzène, pour une durée de synthèse égale et pour une durée de synthèse 8 fois plus longue (fig.2, 2 et 3).

Dans les 45 premières minutes de la synthèse le contenu en phosphore augmente rapidement. Entre 45 minutes et 3 heures, l'augmentation de la teneur en phosphore est beaucoup plus petite (fig.3).

Si la synthèse dure plus de trois heures, on constate des dégradations dues à l'action du trichlorure d'aluminium qui couvre la surface du polystyrène.[10] Les produits se colorent en jaune et le spectre en IR présente les modifications suivantes : la bande d'absorption de la vibration C—H située à 700 cm^{-1} baisse en intensité, la vibration C—C (aromatique) située à 1493 cm^{-1} n'est plus visible et par contre l'absorption due au groupement CH_2 augmente en intensité à 2924 cm^{-1}. Les indications fournies par le spectre en IR nous mènent à la conclusion que les modifications ont lieu au noyau benzénique.

Dans la figure 5 est donnée la variation de la teneur en phosphore en fonction de la quantité de trichlorure d'aluminium utilisée. A un rapport molaire $AlCl_3$: unité structurelle de polystyrène supérieur à 2,6 : 1 la teneur en phosphore reste approximativement constante. La tendance d'agglomération des perles de polystyrène se manifeste à un rapport molaire plus petit que 1,2 : 1.

---

[10] H. .P. Frank, *Makromol. Chem.*, **64**, 213 (1963).

Les possibilités de variation de la quantité de trichlorure de phosphore sont limitées :

Si le rapport molaire $AlCl_3 : PCl_3$ est inférieur à 1 : 1 moles, le polystyrène se dégrade partiellement. Les produits se colorent en jaune-brun et le spectre en IR présente les modifications signalées dans le cas de la prolongation du temps de synthèse à plus de 3 heures.

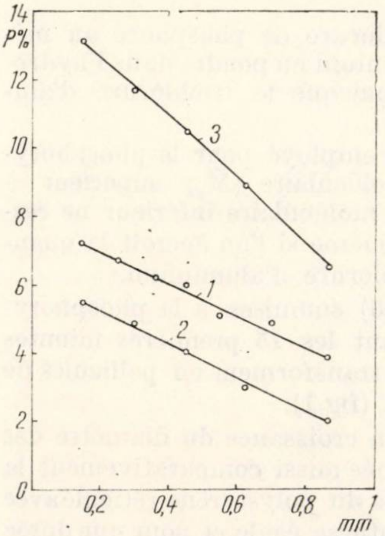

Fig. 2. — Variation de la teneur en phosphore en fonction du diamètre des perles.

1, polystyrène ($\overline{M}_v$ = 144.700) Durée de la synthèse : 45 mn ; *2*, copolymère styrène — 8 % divinylbenzène. Durée de la synthèse : 45 mn ; *3*, copolymère styrène — 8 % divinylbenzène. Durée de la synthèse : 6 h.

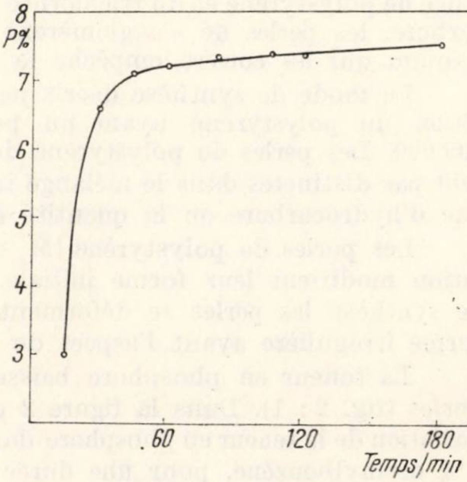

Fig. 3. — Variation de la teneur en phosphore en fonction de la durée de synthèse.

À un rapport molaire PCl_3 : unité structurelle de polystyrène supérieur à 5 : 1, les perles s'unissent et incorporent partiellement le trichlorure d'aluminium. Le contenu en phosphore augmente (fig. 6).

La quantité de produits phosphorylés solubles (non réticulés) qu'on obtient dans diverses conditions de synthèse est réduite.

Les produits solubles en chloroforme ne dépassent pas la valeur de 1,8 %, à l'exception des synthèses ayant une durée inférieure à 15 minutes. Les quantités des produits solubles dans la soude 10 % varient entre 0,2 et 0,3 % quand on soumet à la phosphorylation des perles ayant le diamètre plus petit que 0,3 mm et 7 % pour les perles d'un diamètre ≈ 1 mm.

En phosphorylant des perles ($\varnothing < 0,3$ mm) de polystyrène dans les conditions indiquées dans le mode de travail, on obtient du polystyrène phosphorylé insoluble (réticulé) dans une proportion de 98 %.

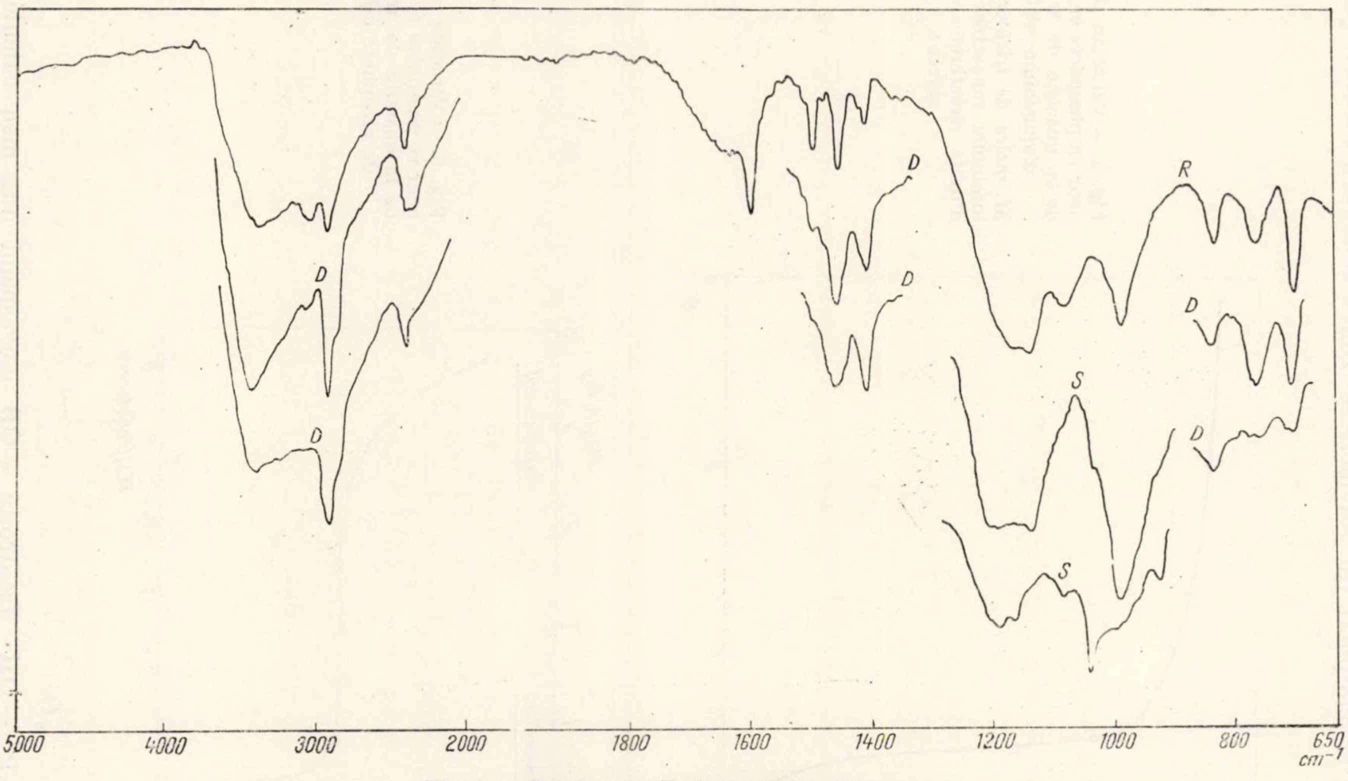

Fig. 4. — Spectres en IR des produits obtenus.

R, polymère phosphorylé insoluble (réticulé par le phosphore) ; S, polymère phosphorylé soluble ; D, modifications dues à la dégradation du produit phosphorylé.

La droite OA de la figure 7 correspond aux meq calculés au cas où tout le phosphore du polymère se trouve sous forme d'acide phospho-

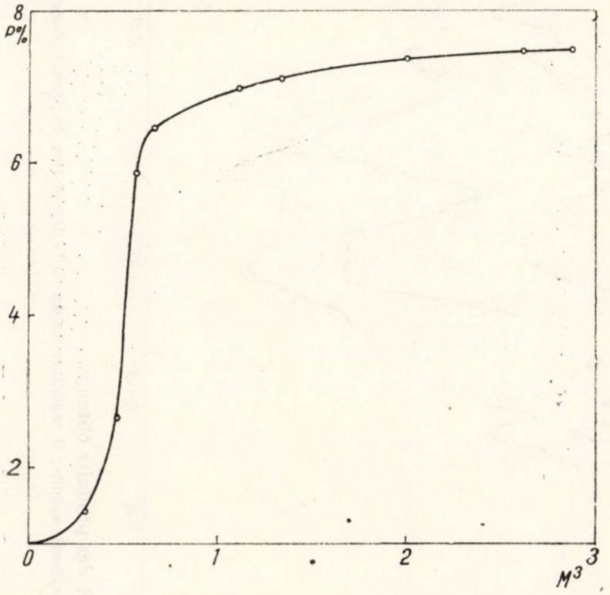

Fig. 5. — Variation de la teneur en phosphore en fonction de la quantité de trichlorure d'aluminium utilisée.

M, moles de trichlorure d'aluminium rapportées à 1 mole d'unité structurelle de polystyrène.

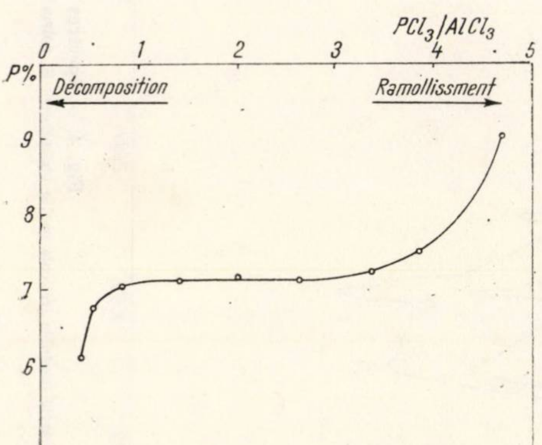

Fig. 6. — Variation de la teneur en phosphore en fonction de la quantité de trichlorure de phosphore utilisée.

nique
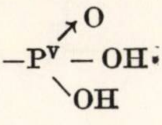
$-\overset{\nearrow O}{P^{V}}\underset{\searrow OH}{-OH}$. La droite —OB correspond aux meq calculés pour

l'acide phosphoneux 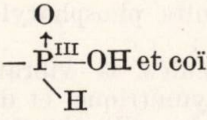 $-\underset{\diagdown H}{\overset{\overset{O}{\uparrow}}{P^{III}}}-OH$ et coïncide avec les valeurs calculées pour P^{V} dans le cas d'une totale réticulation (acide phosphinique 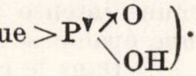 $>P^{V}\begin{smallmatrix}\nearrow O\\ \diagdown OH\end{smallmatrix}$).

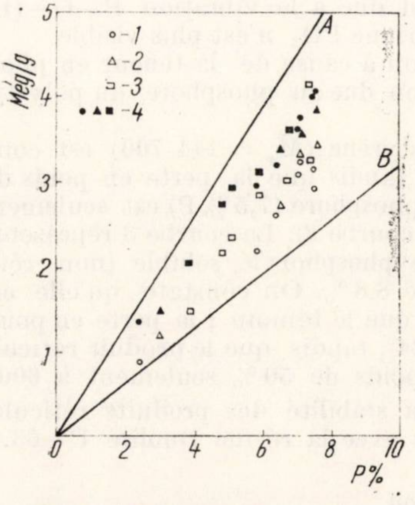

Fig. 7. — Valeurs de la capacité d'échange.

OA — meq calculés pour l'acide phosphonique. OB — meq calculés pour les acides phosphoneux et phosphiniques *1*, synthèses avec des quantités différentes de trichlorure d'aluminium ; *2*, synthèses de différentes durées ; *3*, synthèses avec des perles de différents diamètres ; *7*, les mêmes produits après l'oxydation par l'acide azotique.

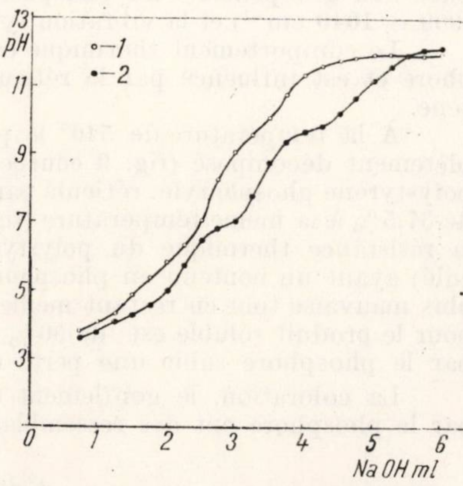

Fig. 8. — Courbes de titrage potentiométrique pour le polystyrène phosphorylé réticulé par le phosphore (8 % P).

***1*, produits oxydés par air chaud ; *2*, produits oxydés par acide azotique.**

La capacité d'échange pour les produits insolubles oxydés avec de l'acide azotique est plus grande, comparativement aux mêmes produits oxydés seulement avec de l'air chaud (fig. 7). La plus grande valeur est de 4,5 meq/g. Les résultats indiquent l'existence de la réticulation dans le premier cas, et une oxydation incomplète dans le second.

Le titrage potentiométrique a été réalisé comparativement pour le polystyrène phosphorylé insoluble, oxydé avec de l'air chaud et pour le même polystyrène oxydé avec de l'acide azotique. On peut constater que les inflexions de la courbe de titrage sont bien plus marquées dans le deuxième cas. Les courbes obtenues diffèrent de celles indiquées dans la littérature pour les copolymères de styrène-divinylbenzène à polarité phosphonique[2,5] (on constate l'existence de trois inflexions à cause de la présence de l'acide phosphinique). On a déjà comparé les courbes de titrage du polystyrène phosphorylé et d'une résine dans laquelle prédomine l'acide phosphinique.[7]

Les spectres en IR des produits phosphorylés insolubles (fig. 4) présentent les différences suivantes :

Dans le cas des produits réticulés, la vibration P → O (réticulé) est superposée à la vibration PO_2^- asymétrique et donne une bande commune intense à 1100 – 1230 cm^{-1}. La vibration symétrique PO_2^- forme une épaule à 1100 cm^{-1}.

Dans le cas des produits solubles, la bande la plus intense attribuée aux groupements du phosphore est due à la vibration P–O–(H) (909 – 1040 cm^{-1}) et la vibration symétrique PO_2^- n'est plus visible.

Le comportement thermique est bon à cause de la teneur en phosphore et est influencé par la réticulation due au phosphore du polystyrène.

À la température de 540° le polystyrène ($\overline{M}_v = 144\ 700$) est complètement décomposé (fig. 9 courbe *1*), tandis que la perte en poids du polystyrène phosphorylé, réticulé par le phosphore (7,5 % P) est seulement de 37,5 % à la même température (fig. 9 courbe *2*). La courbe 3 représente la résistance thermique du polystyrène phosphorylé soluble (non réticulé) ayant un contenu en phosphore de 8,8 %. On constate qu'elle est plus mauvaise tout en restant meilleure que le témoin ; la perte en poids pour le produit soluble est de 50 % à 524°, tandis que le produit réticulé par le phosphore subit une perte en poids de 50 % seulement à 600°.

La coloration, le gonflement et la stabilité des produits réticulés par le phosphore ont des ressemblances avec la résine Duolite C–63.[11]

Coloration

Les produits phosphorylés sont blancs. Après oxydation par l'acide azotique ils sont de couleur orange sous forme d'hydrogène, brune sous forme de sodium et verdâtre sous forme de cuivre

Stabilité

Les produits sous forme de sodium, tenus à 100° pendant 120 heures, ne modifient pas leur capacité d'échange. La résistance thermique ne change pas après l'oxydation par l'acide azotique (fig. 9).

Gonflement

Le gonflement est considérable sous forme de sodium. En notant avec 100 le volume sous forme d'hydrogène, le volume sous la forme de sodium est d'environ 220 et seulement ≈ 130 sous forme de cuivre, pour une granulation de 0,05 – 0,1 mm et une teneur en phosphore de 7 %.

Gonflés dans l'eau, les produits sont friables sous forme d'hydrogène et élastiques sous forme de sodium.

Les produits peuvent être pastillés à une pression de 12 atm. En acides, les pastilles obtenues ne changent pas de forme. En milieu alcalin les pastilles se gonflent initialement et puis se divisent graduellement en particules de petites dimensions ($\emptyset < 1$ mm).

---

[11] J. Persoz et R. Rosset, *Bull. Soc. Chim. France*, **1964**, 2197.

CONCLUSIONS

La phosphorylation du polystyrène dans un milieu où celui-ci ne se dissout pas permet le maintien des mêmes conditions de réaction pendant tout l'intervalle de la synthèse, à l'encontre de la phosphorylation du polystyrène dissout dans le trichlorure de phosphore. [8]

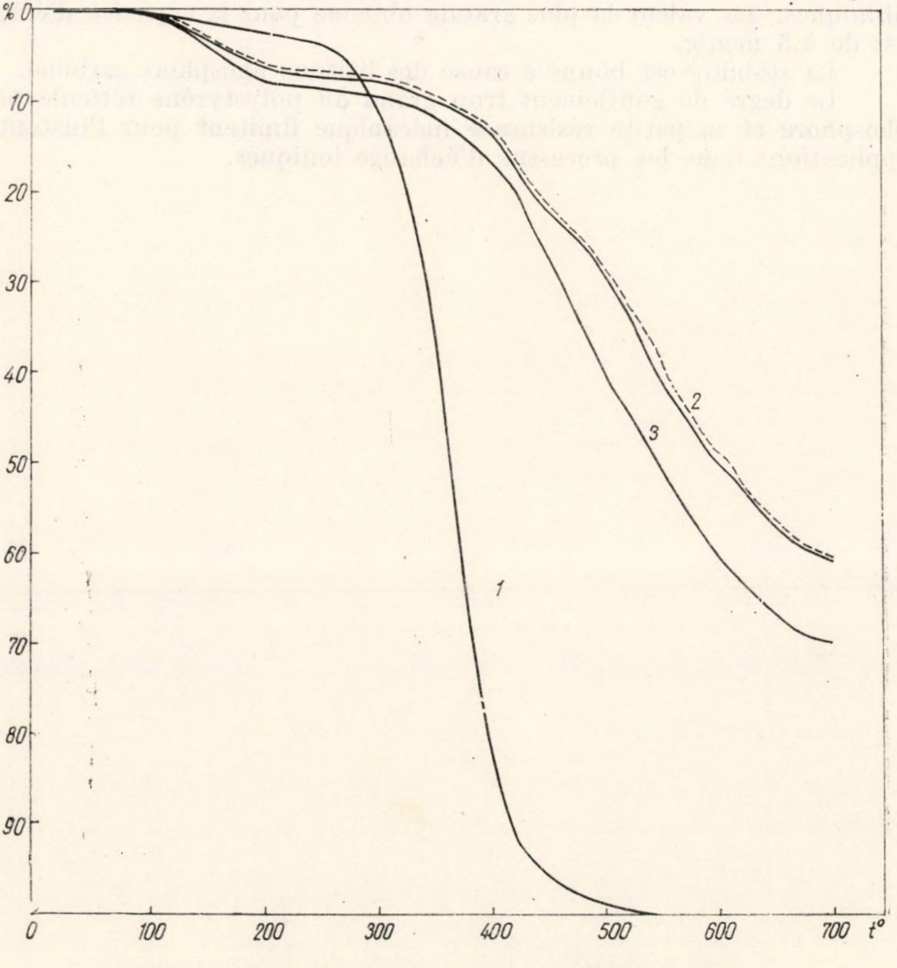

Fig. 9. — Résistance thermique des produits phosphorylés.

1, polystyrène de référence ($\overline{M}_y$ = 144.700) ; *2*, (ligne ininterrompue), produit phosphorylé réticulé par le phosphore (7,5% P) ; *2* (pointes), le même produit après oxydation par acide azotique 63% pendant 12 h, à 20° ; *3*, produit phosphorylé non réticulé (8,8 % P).

Comme produit principal, on obtient du polystyrène phosphorylé insoluble réticulé par le phosphore.

La quantité de trichlorure de phosphore ne peut être réduite à moins de 1 : 1 moles PCl_3 : $AlCl_3$ et le temps de réaction ne peut être prolongé à plus de 3 heures, du fait de la dégradation des produits phosphorylés.

Le polystyrène phosphorylé oxydé, réticulé par le phosphore est un polyélectrolyte qui possède des groupements phosphoniques et phosphiniques. La valeur la plus grande obtenue pour la capacité d'échange est de 4,5 meq/g.

La stabilité est bonne à cause des liaisons phosphore-carbone.

Le degré de gonflement trop grand du polystyrène réticulé par le phosphore et sa petite résistance mécanique limitent pour l'instant ses applications dans les processus d'échange ioniques.

Revue Roumaine de Chimie, **15**, 1365–1373 (1970)

COORDINATION POLYMERS. IV

POLYCOORDINATION OF 4,4'-[*p*-PHENYLENE-BIS(METHYLIDEN-NITRILO)]-DI-METHYL SALICYLATE WITH COBALT, NICKEL AND COPPER

M. MARCU and M. DIMA

Institute of Macromolecular Chemistry "P. Poni"
Jassy, aleea Grigore Ghica Vodă 41 A

Received January 16, 1970

By reacting stoichiometric quantities of 4,4'-[*p*-phenylene-bis(methyliden-nitrilo)]-di-methyl salicylate in DMF at 60 to 80° with cobalt, nickel and copper acetates in DMF, one obtains coordination polymers as coloured powders. Elementary analysis, IR and ESR spectra confirm the structure of the obtained polymers. One has studied the thermic stability in air, the X-ray spectra and the variation of the electric conductivity *versus* temperature, reaching the conclusion that polymers are semiconductors.

In 1960 Kubo and coworkers [1] have synthetized a series of coordination polymers of dicarboxylic acids with copper. Based on the IR spectra, the authors reach the conclusion that the polymers obtained from dicarboxylic acids, with pair number of carbon atoms, have a reticular structure.

Korsak and coworkers [2] investigated the coordination polymers obtained through the reaction of 2,5-dihydroxyterephthalic, 4,4'-dimetoxytriphenylmethane-3,3'-dicarboxylic acids, and its methylic ster, with transitional metals.

The same authors [3] studied the coordination polymers obtained from aliphatic dicarboxylic acids and transitional metals.

Subsequently, one studies the reaction between phenyltaliumdiisobutyrate and the adipic, azelaic, and sebacic acids, [4] as well as the reaction between the organostanic compounds and sebacic, α, α'-dioxysebacic and α,α'-dimetoxysebacic acid, [5] to obtain coordination polymers.

[1] M. Kubo, M. Kishita and M. Kuroda, "Mezhdunarodnîi simpozion po macromol. khimia," Moscow, 1960, p. 85; *Uspekhi Khim*, **12**, 1487 (1963).

[2] V. V. Korşak, S. V. Rogovin and V. I. Volkov, *Vysokomol. Soedineniya*, **3**, 1808 (1961).

[3] V. V. Korşak, S. V. Rogovin and V. I. Volkov, *Vysokomol. Soedineniya*, **4**, 20 (1962).

[4] V. V. Korşak, S. V. Rogovin and T. A. Markova, *Vysokomol. Soedinenya*, **4**, 1137 (1962).

[5] V. V. Korşak, S. V. Rogovin and T. A. Markova, *Vysokomol. Soedineniya*, **4**, 1297 (1962).

In the present paper one presents the reaction between stoichiometric quantities of 4,4'-[*p*-phenylen-bis (methyliden-nitrilo)]-di-methyl salicylate in DMF at 60—80° and cobalt, nickel and copper acetates in DMF, when coordination polymers according to the following reaction diagram are obtained, separating from the reaction medium as coloured powders.

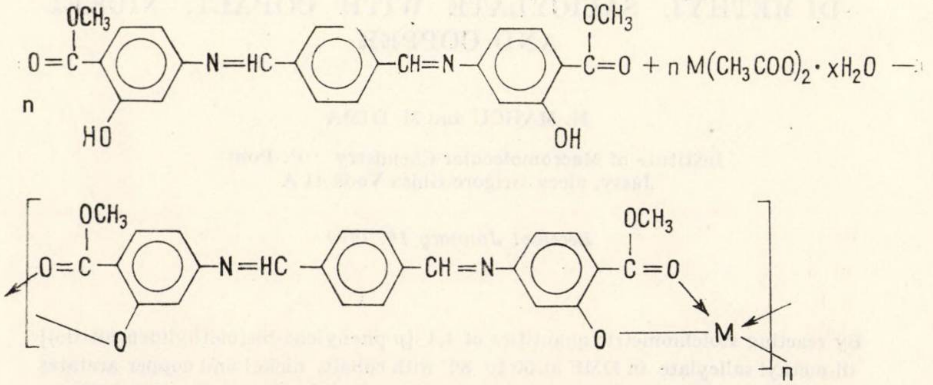

$+2n\ CH_3COOH + nxH_2O$
in which M is Co^{2+}, Ni^{2+}, Cu^{2+}.

The polymer with cobalt is mustard-yellow, that with nickel is green-yellow and the one with copper is dark green.

All polymers are not soluble in known organic solvents and water, which makes the determination of their molecular weight through known methods impossible. Estimates on their polymerization degree are made from the data of elementary analysis.

Taking into account the fact that synthetized coordination polymers have at their ends active ligand groups (a fact proved by IR spectra) schematically we may write the macromolecular chain as :

$$\ldots > L < M > L < M > L < M > L < M > L < M \ldots$$

in which one has denoted by $> L <$ the bifunctional ligand, and by M the tetracoordinated metal ion.

We may thus write the following relations, which modifiy the calculation formula of the polymerization degree given by Korşak[6] for this case :

$$nM + (n - 1)L - 2(n - 1) + 2L - 2 = M_n$$

where :

n — the polymerization degree
M — the metal ion
L — the ligand
M_n — molecular weight of the polymer

---

[6] V. V. Korşak, E. S. Krongauz, A. M. Sladkov, V. E. Seina and L. K. Luneva, *Vysokomol. Soedineniya*, **12**, 1764 (1959).

On the other hand, we may write the relation :

$$M_n = n \cdot 100 \ M/M \ \%$$

where $M\%$ is the metal percentage in the polymer.

One can then calculate the polymerization degree from the relation :

$$n(M + L - 2) = n \cdot 100 \ M/M \ \%$$

Thus, for the polymers synthetized by us one has obtained

$$(C_{24}H_{18}N_2O_6Co)_n \ \ldots \ n = 72$$

$$(C_{24}H_{18}N_2O_6Ni)_n \ \ldots \ n = 123$$

$$(C_{24}H_{18}N_2O_6Cu)_n \ \ldots \ n = 106$$

EXPERIMENTAL

One has synthetized the methylic ester of the *p*-aminosalicylic acid after Drain,[7] which reacted with terephthalic aldehyde to obtain the 4,4′-[*p*-phenylene-bis(methylidennitrylo)]-di-methyl salicylate ligand.[8]

1. *Synthesis of the polymer with cobalt*

One introduces 0.864 g (0.002 mol) of ligand, solved in 75 ml DMF at 80°, into a 250 ml flask, provided with reflux refrigerent, drop-funnel and stirrer. To this solution one adds, under stirring, drop by drop, a 0.4982 g (0.002 mol) solution in 50 ml DMF of tetrahydrated cobalt acetate. After the first drops of cobalt salt, a mustard-yellow suspension readily forms. This suspension is stirred for half an hour at 80°, cooled, washed with alcohol, dryed at 110° and in vacuum.

Analysis : $(C_{24}H_{18}N_2O_6Co)_n$	C%	H%	N%	Co%
Calcd. :	58.90 ;	3.68 ;	5.72 ;	12.05 ;
Found :	58.55 ;	3.85 ;	5.75 ;	11.92.

2. *Synthesis of the polymer with nickel*

One proceeds as for the polymer with cobalt with the difference that the ligand solution and the polymer suspension in solvent is heated to 60–65°. The polymer with nickel separates from the solution, towards completion of the nickel salt addition over the ligand solution in DMF. A green-yellowish product is obtained.

Analysis $(C_{24}H_{18}N_2O_6Ni)$	C%	H%	N%	Ni%
Calcd. :	58.07 ;	3.69 ;	5.72 ;	12.01 :
Found :	58.53 ;	3.88 ;	5.00 ;	11.90.

---

[7] D. J. Drain, D. D. Martin, B. W. Mitchell, D. E. Seymour and F. S. Spring, *J. Chem. Soc.*, **1949**, 1498.

[8] E. Massarani, D. Nardi and L. Mauri, *Boll. chim. farm.*, **104**, 155 (1965).

3. *Synthesis of the polymer with copper*

The same procedure as in the synthesis of the polymer with cobalt is used. A dark green product is obtained.

Analysis $(C_{24}H_{18}N_2O_6Cu)_n$	C%	H%	N%	Cu%
Calcd. :	58.35 ;	3.64 ;	5.67 ;	12.86 ;
Found :	58.10 ;	3.76 ;	5.41 ;	12.77.

RESULTS AND DISCUSSION

IR spectra

The IR spectra of the 4,4′- [*p*-phenylene- bis (methyliden-nitrilo)] — di-methyl salicylate ligand are significant in three regions, namely: 3000–3500 cm^{-1}, 1600–1700 cm^{-1} and 1000–1300 cm^{-1} which shall be discussed below.

Brooks and coworkers[9] show that in the methylsalicylate, the carbonyl group of the ester forms intramolecular hydrogen bonds (chelatic) with phenolic hydroxyl, and that the frequency $\nu_{(CO)}$ decreases to 1681 cm^{-1}, against $\nu_{(CO)}$ of the methyl benzoate at 1730 cm^{-1}. The same authors show that the chelatic $\nu_{(OH)}$ in the methyl salicylate moves towards higher wavelengths, namely to 3200 cm^{-1}.

In the case of our ligand, we find $\nu_{(CO)} = 1670$ cm^{-1}, therefore displace towards higher wavelengths owing to the intramolecular (chelatic) hydrogen bond with the phenylic hydroxyl, and the chelatic $\nu_{(OH)}$ at 3180 cm. The vibration band lowered from 1635 cm^{-1} corresponds to the $\nu_{(CN)}$ frequency, and is somehow associated to the vibration of the (C=C) bond from 1600 cm^{-1}. Between 1000 and 1300 cm^{-1} the spectra of the carboxylic acids esters present several more or less intensive bands. The bands were associated to the different coupled vibration ways of the C = O and O − R bonds of the COOR group. [10,11] Thus the bands at 1100, 1145, 1160, 1220 and 1260 cm^{-1} are responsible for the vibrations C = O and O − CH_3 of $COOCH_3$.

The IR spectra of the coordination polymers with cobalt, nickel and copper, will be discussed below, in the same regions as the ligand's spectrum.

The band due to the $\nu_{(OH)}$ vibration in the ligand is shifted towards smaller wavelengths and is far less intensive, a fact demonstrating that the chelation phenomenon observed for the ligand, between C = O and OH, does no longer exist in polymers, this time the free $\nu_{(OH)}$ band at the ends of the coordination polymers being at stake. We have thus: $\nu_{(OH)} = 3450$ cm^{-1} for the polymer with Co^{2+} and Ni^{2+} and $\nu_{(OH)} = 3500$ cm^{-1} for the polymer with Cu^{2+}.

The band due to the vibration of the carbonylic group in the polymers is each time associated to the band due to the vibration of the (C = N) bond, and is displaced towards higher wavelengths, a fact demonstrating the existence of the coordinative bond formed between the esteric carbonyl and the metal ion in the polymer. In the case of the polymer with

---

[9] C. J. W. Brooks, G. Eglinton and J. F. Mormann, *J. Chem. Soc.*, **1961**, 661.
[10] H. W. Thompson and D. Torkington, *J. Chem. Soc.*, **1945**, 640.
[11] R. N. Russel and H. W. Thompson, *J. Chem. Soc.*, **1955**, 479.

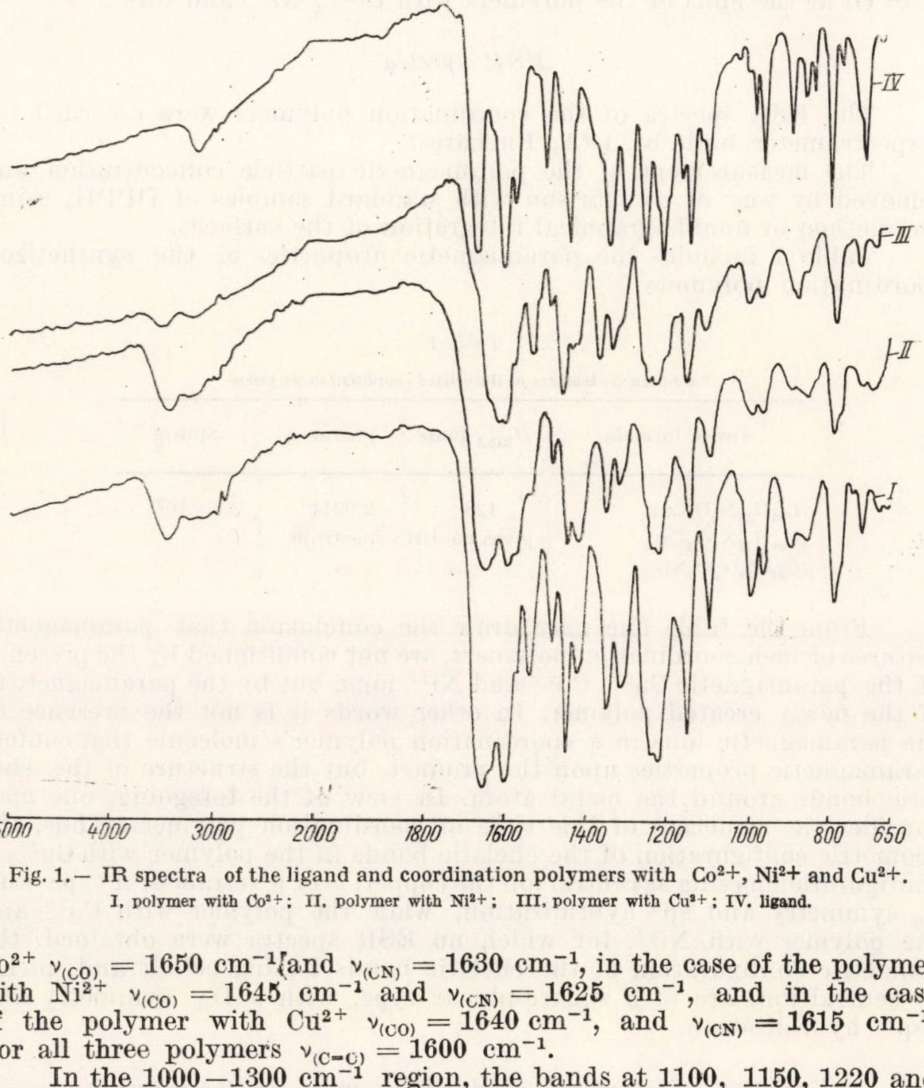

Fig. 1.— IR spectra of the ligand and coordination polymers with Co^{2+}, Ni^{2+} and Cu^{2+}.
I, polymer with Co^{2+}; II, polymer with Ni^{2+}; III, polymer with Cu^{2+}; IV, ligand.

Co^{2+} $\nu_{(CO)} = 1650$ cm^{-1} and $\nu_{(CN)} = 1630$ cm^{-1}, in the case of the polymer with Ni^{2+} $\nu_{(CO)} = 1645$ cm^{-1} and $\nu_{(CN)} = 1625$ cm^{-1}, and in the case of the polymer with Cu^{2+} $\nu_{(CO)} = 1640$ cm^{-1}, and $\nu_{(CN)} = 1615$ cm^{-1}. For all three polymers $\nu_{(C=C)} = 1600$ cm^{-1}.

In the 1000–1300 cm^{-1} region, the bands at 1100, 1150, 1220 and 1240 cm^{-1} for the polymer with Co^{2+}, the bands at 1000, 1150, 1220 and 1235 cm^{-1} for the polymer with Ni^{2+}, and the bands at 1100, 1150, 1230 and 1245 cm^{-1} for the polymer with Cu^{2+} are responsible for the coupled vibrations of the C = O and O – CH_3 bonds in $COOCH_3$.

The fact that in the IR spectra of the coordination polymers the $\nu_{(OH)}$ vibration is found at smaller wavelengths than in the ligand, and the band's intensity is lower, and the fact that the band due to the $\nu_{(C=O)}$ vibration in polymers is shifted towards higher wavelengths than in the ligand, confirms the suggested structure of the macromolecular chain unit; it also confirms the existence of the active groups in the ligand (OH) and (C = O) at the ends of the polymers with Co^{2+}, Ni^{2+} and Cu^{2+}.

ESR spectra

The ESR spectra of the coordination polymers were recorded by a spectrometer built by IFA, Bucharest.

The measurement of the paramagnetic particle concentration was achieved by way of comparison with standard samples of DPPH, using the method of double graphical integration of the surfaces.

Table 1 includes the paramagnetic properties of the synthetized coordination polymers

Table 1

Paramagnetic features of sinthetized coordination polymers

Gross formula	$H_{\mathbf{max}}$ gauss	Factor g	Spin/g
$(C_{24}H_{18}N_2O_6Cu)_2$	128	2.0211	3.4×10^{21}
$(C_{24}H_{18}N_2O_6Co)_n$	gives no ERS spectrum		
$(C_{24}H_{18}N_2O_6Ni)_n$	,, ,, ,, ,,		

From the table one may draw the conclusion that paramagnetic features of such coordination polymers, are not conditioned by the presence of the paramagnetic Cu^{2+}, Co^{2+} and Ni^{2+} ions, but by the paramagnetism of the newly created polymer. In other words it is not the presence of the paramagnetic ions in a coordination polymer's molecule that confers paramagnetic properties upon the product, but the structure of the chelatic bonds around the metal atom. In view of the foregoing, one may consider the structure of this type of coordination polymers. Thus, the geometric configuration of the chelatic bonds in the polymer with Cu^{2+}, a configuration having as central ion the copper, is of a tetrahedral type with T_d symmetry and sp^3 hybridization, while the polymer with Co^{2+} and the polymer with Ni^{2+}, for which no ESR spectra were obtained, the geometric configuration of the chelatic bonds having cobalt and nickel as central ion, are of a square-planar type, with a D_{4h} symmetry and dsp^2 hybridization.

Variation of electrical conductivity with the temperature

The measurements of the electrical conductivity were carried out in the temperature range 25—200° on polymer tablets obtained by pressing at 10 t/cm². The measurements were used to draw the curves $\ln\sigma = f(1/T)$, according to relation:

$$\sigma=\sigma_0\exp\left(-\Delta E/2kT\right)$$

whence the activation energy ΔE (eV) and σ_0 (ohm^{-1} cm^{-1}) was calculated by extrapolation for $1/T = 0$.

Table 2 gives the results of the electrical conductivity measurements for coordination polymers, as well as for ΔE(eV) and σ_0 (ohm^{-1} cm^{-1}).

Table 2

Electric conductivity and activation energy of coordination polymers

Gross formula	σ_T°K ohm^{-1} cm^{-1}	σ_0 ohm^{-1} cm^{-1}	ΔEeV
$(C_{24}H_{18}N_2O_6Co)\ Co)_n$	1.80×10^{-15}	4.18×10^{-9}	0.91
$(C_{24}H_{18}N_2O_6Ni)_n$	3.50×10^{-15}	4.21×10^{-10}	0.79
$(C_{24}H_{18}N_2O_6Cu)_n$	10.90×10^{-15}	8.69×10^{-10}	0.74

Figure 2 gives the variation of the electrical conductivity with the temperature for the coordination polymers with Co^{2+}, Ni^{2+} and Cu^{2+}.

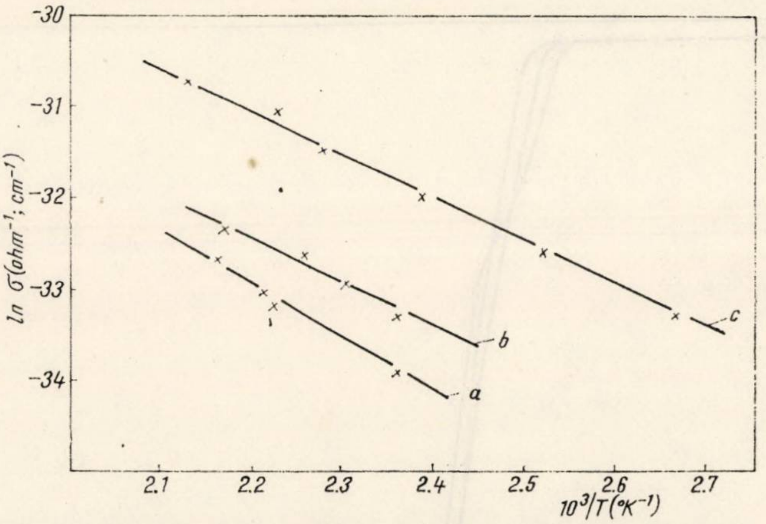

Fig. 2. — Variation of the electrical conductivity with the temperature for the coordination polymers with Co^{2+}, Ni^{2+} and Cu^{2+}.
a) polymer with Co^{2+}; b, polymer with Ni^{2+}; c, polymer with Cu^{2+}.

In the temperature range $10^3/T = 2.13 - 2.67$ °K^{-1}, the coordination polymer with copper behaves as semiconductor, since the variation of the electrical conductivity with the temperature is an exponential function. The polymers with cobalt and nickel behave like semiconductors in the temperature range $10^3/T = 2.17 - 2.36$°K^{-1}. The computed values of σ_0 and ΔE are given in table 2. By analysing table 2 and figure 2, one notices that for the same ligand, but according to the metal of the macromolecular chain, the electrical conductivity changes, meaning that the activation energy increases with the decrease in the electrical conductivity. This remark is still better confirmed by figure 3, which shows the dependency of the electrical conductivity on the activation energy.

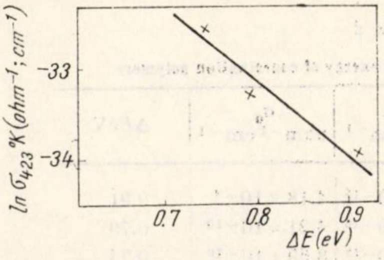

Fig. 3. — Variation of the electrical conductivity with the activation energy for the coordination polymers with Co^{2+}, Ni^{2+} and Cu^{2+}.

Moreover, the dependency $\ln \sigma = f(\Delta E)$ shows that the three points corresponding to the pairs of values for the three polymers, adopt, with sufficient approximation, a straight line.

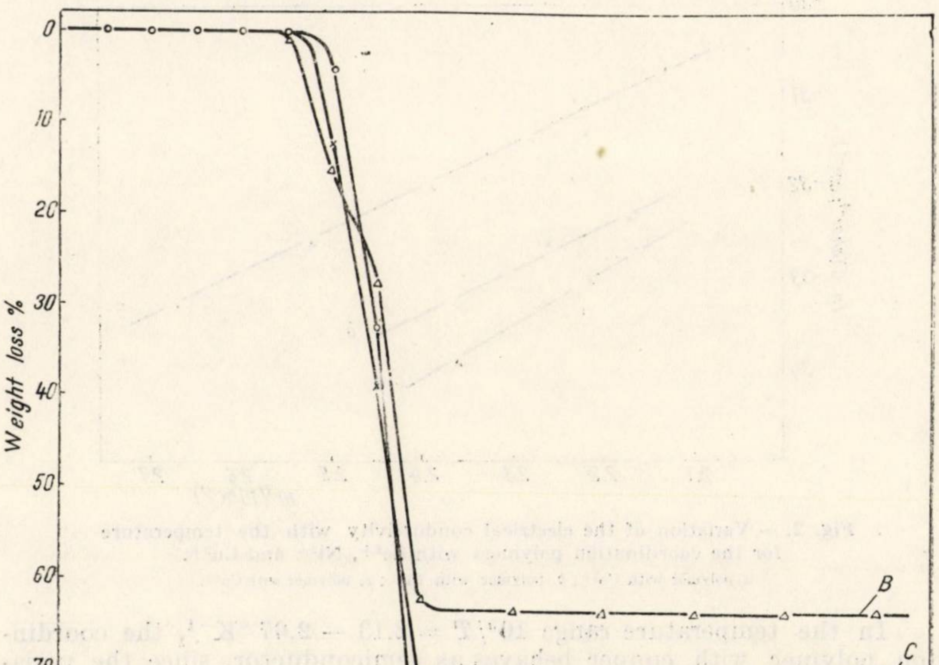

Fig. 4. — Thermogramms of the coordination polymers with Co^{2+}, N^{2+} and Cu^{2+}

A, polymer with Co^{2+}; *B*, polymer with Ni^{2+}; *C*, polymer with Cu^{2+}.

Thermogravimetric analysis

The polymers with Co^{2+}, Ni^{2+} and Cu^{2+} of this ligand, have a good thermal stability. Thus, the polymer with cobalt has a disintegration temperature of 295°, the polymer with nickel, 250° and the polymer with copper, 275°. For the same ligand the thermal stability of the polymers, according to the metal contained by the macromolecular chain, decreases in the following order $Co > Cu > Ni$.

The polymers do not loose weight till they reach the disingration temperature, but then the loss is sudden : in one stage for the polymers with cobalt and copper, and in two stages for the polymers with nickel. Then total loss in weight is of 71.8 % for the polymer with cobalt, 70.5 % for the polymer with copper and 63.0 % for the polymer with nickel, at 400°. Between 400 and 900°, owing to the metal oxides formed, the polymers do not loose weight anymore.

X-ray spectra

To appreciate the degree of order of the synthetized coordination polymers, one has recorded the diffraction spectra of polymers powders, making use of the Debye-Scherrer method. The diffraction images with X-rays were obtained by means of a $TURM_{60}$ type apparatus. To calculate the crystallinity of the polymers, the diffraction images by X-rays were photometrically determined by means of the Lirepho-2 microphotometer. The calculation of the crystallinity was carried out according to the Hermans [12] method.

The synthethized polymers can be classified as follows :

a) coordination polymers with Co and Ni in which only a local order (amorphous) exists,

b) the polymer with Cu, with a biphasic character, which besides the local order state, also presents diffraction lines characteristic of the crystalline state (cristallinity 89 %).

---

[12] P. H. Hermans and W. D. Weidinger, *J. Polymer Sci.*, **4**, 709 (1960).

Revue Roumaine de Chimie, 15, 1375–1390 (1970)

PEPTIDES. VIII*

SOME β-DICARBONYL N-PROTECTED AMINOACIDS AND MODEL DIPEPTIDES**

A. BALOG, D. BREAZU, E. VARGHA***, F. GÖNCZY and LUCIA BEU

Institute for Chemical and Pharmaceutical Research,
Str. Karl Marx 93, Cluj, Romania

Received July 24, 1969

The field of application of β-dicarbonyl compounds to the protection of α-aminoacids has been enlarged. The enaminic salts III have been obtained in relatively pure state from potassium or sodium derivatives of the β-dicarbonyls, isolated or formed *in situ* (methods B, C and D). In the given conditions the protection occurs without racemization. Suitable methods have been elaborated for the synthesis and purification of analogous salts of organic bases, especially of dicyclohexylamine. The salts III have been used in the synthesis of some model dipeptides, by applying the method of mixed anhydrides and by using ethyl glycinate as amine component.

The use of β-dicarbonyl compounds or of β-ketoesters in the protection of the amino group as a step in the peptide synthesis is a relatively recent development.[1-3] The method is based on the condensation of aminoacids II with β-dicarbonyl derivatives I in the presence of a stoichiometrical quantity of base. The Schiff base is present in the enamine form III, stabilised by a hydrogen bond:

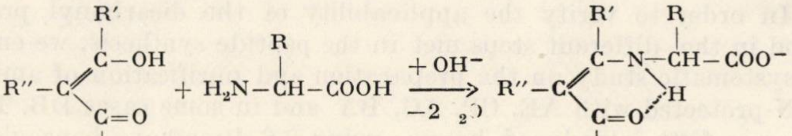

$$R''-C(=C(OH)R')-C(=O)R''' + H_2N-CH(R)-COOH \xrightarrow[-2H_2O]{+OH^-} R''-C(=C(R')-NH-CH(R)-COO^-)-C=O\cdots H\,R'''$$

I II III

---

[*] Part VII: A. Balog, E. Vargha, V. Voinescu, M. Herman, R. Ramonţian and L. Moraru, *Stud. Univ. Babeş-Bolyai, Chem.*, **14** (2), 137 (1969).

[**] The work described in this paper was ptesented in part at the 5th International Symposium on the Chemistry of Natural Products, IUPAC, London, July 1968.

[***] The Department of Organic Chemistry, Babeş-Bolyai University, Cluj, Str. Arany János, 11.

[1] E. Dane, F. Drees P. Konrad and T. Dockner, *Angew. Chem.*, **74**, 873 (1962).

[2] E. Dane and T. Dockner, *Chem. Ber.*, **98**, 789 (1965).

[3] R. G. Hiskey and G. I. Southard, *J. Org. Chem.*, **31**, 3582 (1966).

Because of the ease with which the above protective group is eliminated under the action of diluted acids, the salts of the type III have been used e.g. in the synthesis of semisynthetic penicillins.[2,4-7] In the use of salts III for the peptide bond formation[1-3] the protection of the aminoacids has been carried out with ethyl acetoacetate, ethyl cyclopentanone-2-carboxylate, acetylacetone and benzoylacetone. The protective group derived from β-dicarbonyl compounds, their names and the symbols used are presented in table 1.

Table 1

Protective groups derived from β-dicarbonyl compounds

No	R′	R″	R‴	Dicarbonyl protective group	Abbreviation of protective group
1	CH_3	H	OC_2H_5	1-Ethoxycarbonyl-propen-2-yl	AE*
2	$CH_2-CH_2-CH_2$		OC_2H_5	2-Ethoxycarbonyl-cyclopenten-1-yl	CP*
3	CH_3	H	CH_3	1-Acetylpropen-2-yl	AC*
4	CH_3	H	C_6H_5	1-Benzoylpropen-2-yl	BA*
5	CH_3	H	$C_6H_3(OCH_3)_2$	1-(2′,6′-Dimethoxy-benzoyl)-propen-2-yl	DB

* Symbols used by Dane.[1,5]

Hiskey and Southard[3] in their various attempts in peptide synthesis have used such derivatives as BA−Gly−OK, BA−L−Ala−OK and BA−Cys(Tr)−OK, but they emphasize that these salts are unstable and were therefore unable to isolate them in a suitable purity for elementary analysis. This fact is mentioned as the main inconveniency in the handling of dicarbonyl-N-protected aminoacids and even Dane and co-workers[1] did not succeed in the analytical and especially optical characterization of aminoacids salts protected with such groups as BA, AC and CP. These compounds were used without purification in the synthesis of dipeptide esters.

In order to verify the applicability of the dicarbonyl protection method in the different steps met in the peptide synthesis, we embarked on a systematic study on the preparation and purification of aminoacids salts N-protected with AE, CP, AC, BA and in some cases DB. This last group was first introduced by us, using 2,6-dimethoxy-benzoylacetone.

The method proposed by Dane,[2,5] for the preparation of potassium salts III mainly consists in the treatment of warm alcoholic solutions of aminoacid salt with the β-dicarbonyl compound (*method A*).

---

[4] V. Voinescu, E. Ramonţian, M. Herman and A. Balog, "The 4th Session of Scientific Communications I.C.C.F.", Bucharest, 1965.

[5] E. Dane and T. Dockner, *Angew. Chem.*, **76**, 342 (1964).

[6] G. R. Fosker, J. H. C. Nayler and J. A. Wilcox, Brit. Pat. 991,586, Beecham Research Laboratories Ltd., Brentford, 1962, *Chem. Zentr.*, **1967**, 33−1856.

[7] G. S. Postnikova, M. S. Rabinovich and P. S. Braginskaya, *Khim. Pharm. Zhur.*, **2** (1), 39 (1968).

We adopted a modified and general method which uses potassium or sodium derivatives of the dicarbonyl compounds, either *in situ* (method B and D) or in isolated form (method C). In *method B* the potassium salts III were obtained by adding a 10–15% excess of the aminoacid to the dicarbonyl compound dissolved in ethanolic or methanolic potassium hydroxide. The mixture is then refluxed until practically the whole aminoacid is dissolved.

Method C consists in the protection of the aminoacid with the previously isolated potassium derivative of dicarbonyl compounds. This method seems to be extremely convenient when acetylacetone, benzoylacetone or 2-ethoxycarbonyl-cyclopentanone are used, these compounds being easily separated as potassium derivatives from an ethanolic solution of potassium hydroxide.[8, 9]

Sodium salts[6] corresponding to formula III have been also prepared by the condensation of the aminoacid with the β-dicarbonyl agent in the presence of sodium methoxide or ethoxide in absolute alcohol (*method D*).

Despite the observations of Hiskey and Southard[3] that isolation in a pure form of these dicarbonyl N-protected aminoacids is very difficult, we succeeded in separating them in almost every case in a crystalline form. When benzoylacetone was used for protection, the protected aminoacid sodium salts were not purified by recrystallization but were isolated by concentration *in vacuo* of the reaction mixture and subsequent azeotropic elimination of water. Similar procedures were used in the case of dicarbonyl protected valine, leucine and isoleucine salts. All the protected derivatives were characterized by elementary analysis and optical rotation (table 2).

Some difficulties met in the purification of potassium and sodium salts prompted us to consider the use of several organic bases in the formation of enamino acid salts III. Based on the excellent results obtained by Klieger and Gibian,[10] who isolated the α-esters of N-acylmonoamino dicarboxylic acids in the form of dicyclohexylammonium salts, we performed the condensation of aminoacids with β-diketones or β-ketoesters in the presence of dicyclohexylamine, piperidine, N-methyl morpholine etc. The dicyclohexylammonium and related salts III were obtained in good yields and further purification was performed by recrystallization from ethyl acetate, ethyl acetate-petroleum ether or, in some instances, from ethyl ether (table 3). We mention that the isolation of N-protected γ-benzylglutamate was possible only as dicyclohexylammonium salts.

Dicyclohexylammonium salts were also prepared by the reaction of dicyclohexylamine hydrochloride with the corresponding alkaline salts III, suspended in ethyl acetate. In some cases the ammonium salts formation was performed also starting from the free acids IV.

---

[8] L. Beu, A. Balog and F. Gönczy, *Rev. Chim.* (*Bucureşti*), **20**, 28 (1969).

[9] R. Mayer, G. Wenschuch and W. Töpelman, *Chem. Ber.*, **91**, 1616 (1968).

[10] E. Klieger and H. Gibian, *Liebigs Ann. Chem.*, **673**, 196 (1964).

Table 2

Alkaline salts of some N-(oxopropenyl)-aminoacids

No	$\overset{\text{R}}{\overset{\vert}{\text{QNH}-\text{CH}-\text{COO}^-}}$	Method	Yield	M.p. °C	$[\alpha]_D^{20-22}$ (c = 1, methanol)	Formula (M. weight)	Analysis Metal % Calc.	Analysis Metal % Found.	Analysis N % Calc.	Analysis N % Found
1	AE–Gly–OK	B	80	172–174	–	$C_8H_{12}NO_4K$ (225.3)	17.35	17.20	6.22	5.91
2	CP–Gly–OK	B	85	196–200	–	$C_{10}H_{14}NO_4K$ (251.3)	15.53	15.20	5.57	5.26
3	AC–Gly–OK	B	85	233–235	–	$C_7H_{10}NO_3K$ (195.3)	–	–	7.16	7.20
4	BA–Gly–OK a)	B	75	253–256	–	$C_{12}H_{12}NO_3K$ (257.3)	15.20	14.80	5.44	5.32
5	AE–L–Ala–OK	B	95	205–208	+125.3	$C_9H_{14}NO_4K$ (239.3)	16.34	15.80	5.85	5.90
6	CP–L–Ala–OK a)	B, C	82	185–189	+105.1	$C_{11}H_{16}NO_4K$ (265.4)	14.73	15.00	5.28	5.00
7	AC–L–Ala–OK	B, C	88	214–216	+208.4	$C_8H_{12}NO_3K$ (209.3)	18.68	18.20	6.70	6.20
8	BA–L–Ala–OK a)	C	85	223–225	+189	$C_{13}H_{14}NO_3K$ (271.4)	14.41	13.83	5.16	4.90
9	BA–L–Ala–ONa	C, D	72	102–108	+143.5	$C_{13}H_{14}NO_3Na$ (255.2)	9.01	9.56	5.49	5.24
10	AE–L–Val–OK	B	67	126–130	+154.8	$C_{11}H_{18}NO_4K$ (267.4)	14.62	14.24	5.24	4.96
11	AE–D–Val–OK	B	70	125–130	–156.6	,,		14.40		5.02
12	AE–DL–Val–OK	B	80	175–180	–	,,		14.30		4.92
13	CP–L–Val–OK	B	85	191–195	+ 86	$C_{13}H_{20}NO_4K$ (293.4)	13.32	12.90	4.77	5.45
14	AC–L–Val–OK b)	B, C	83	165–167	+178.5	$C_{10}H_{16}NO_3K$ (237.3)	16.47	16.20	5.90	5.80
15	BA–L–Val–ONa	D	73	100–105	+137	$C_{15}H_{18}NO_3Na$ (283.3)	8.12	8.50	4.94	4.50
16	AE–L–Leu–ONa	A, D	72	155–158	+ 95.3	$C_{12}H_{20}NO_4Na$ (265.3)	8.67	8.90	5.28	5.21
17	CP–L–Leu–OK	B	82	175–180	+ 76.1	$C_{14}H_{22}NO_4K$ (307.4)	12.72	11.56	4.56	4.50
18	AC–L–Leu–OK	A, B	87	196–198	+141.4	$C_{11}H_{18}NO_3K$ (251.4)	15.55	14.90	5.57	5.21

19	BA–L–Leu–OK	B	50	243–245	+153.5	$C_{16}H_{20}NO_3K$ (313.4)	12.48	11.90	4.47	4.50
20	BA–L–Leu–ONa	D	52	220–228	+113	$C_{16}H_{20}NO_3Na$ (297.3)	7.73	8.70	4.71	4.40
21	AE–L–Phe–OK	B	85	149–150	−277	$C_{15}H_{18}NO_4K$ (315.4)	12.40	12.30	4.44	4.25
22	AE–D–Phe–OK	B	87	150–152	+265	,,		12.80		4.50
23	AE–DL–Phe–OK	B	85	182–183	—	,,		—	—	4.60
24	CP–L–Phe–OK	B, C	98	146–147	−228.8	$C_{17}H_{20}NO_4K$ (341.5)	11.45	11.35	4.10	3.70
25	AC–L–Phe–OK	B, C	70	214–216	−322.2	$C_{14}H_{16}NO_3K$ (285.4)	13.70	13.50	4.91	4.87
26	BA–L–Phe–OK	B	85.7	100 (dec)	−320	$C_{19}H_{18}NO_3K$ (347.5)	11.20	10.50	4.03	4.10
27	BA–L–Phe–ONa	D	90	115 (dec)	−273	$C_{19}H_{18}NO_3Na$ (331.3)	6.94	7.90	4.23	4.51
28	AE–L–Phg–OK	A	71	218–219	−285 c)	$C_{14}H_{16}NO_4K$ (301.4)	12.97	13.01		
29	AE–D–Phg–OK[2,5,6,7]	A, B	88	216–218	+273 d)	,,		12.80		
30	AE–DL–Phg–OK[7]	A	75	160–162 e)	—	,,		13.00		
31	AE–L–Phg–ONa	D	70	235–236	−303	$C_{14}H_{16}NO_4Na$ (285.3)	8.06	8.05		
32	AE–D–Phg–ONa[6]	D	72	232–233 f)	+301	,,		8.37		
33	AE–DL–Phg–ONa	D	75	192–195	—	,,		7.76		
34	CP–L–Phg–OK	B	76	240–241	−206	$C_{16}H_{18}NO_4K$ (327.4)	11.94	12.20		
35	CP–D–Phg–OK[6]	B, C	80	240–242 g)	+208	,,		12.10		
36	CP–DL–Phg–OK	B, C	82	245–246	—	,,		11.90		
37	AC–L–Phg–OK	A, C	92	222–223	−357	$C_{13}H_{14}NO_3K$ (271.4)	14.41	14.08		
38	AC–D–Phg–OK[2,5]	A, B, C	96	224–225 h)	+355	,,		14.90		
39	AC–DL–Phg–OK	B	85	222–224	—	,,		14.00		
40	BA–L–Phg–OK	A, B, C	70	224–225	−330.9	$C_{18}H_{16}NO_3K$ (333.4)	11.72	11.40	4.20	4.01
41	BA–D–Phg–OK[2,5,6]	A, B, C	72	224–225 i)	+317.8	$C_{18}H_{16}NO_3K$ (333.4)	11.72	11.70	4.20	3.98
42	BA–DL–Phg–OK	A, B, C	68	241–242	—	,,		11.80		4.09
43	DB–L–Phg–OK	A, B	80	116–119	+180.8	$C_{20}H_{20}NO_5K$ (393.5)	9.94	10.06	3.56	3.50
44	DB–D–Phg–OK	A, D	83	115–120	−195.5	,,		10.02		3.40

a) In the lit.[1,4] reported without physical and analytical data; b) In the lit.[1] reported only the D-isomer, without analytical data; c) In lit.[7] m.p. 224–5°, $[\alpha]_D^{20} = -280 \pm 5°$ (c = 0.5, EtOH); d) In lit. m.p. 229–233[2,3], 225–226[7], 234–236[6], $[\alpha]_D^{20} = +275° \pm 5°$ (c = 0,5, EtOH)[7]; e) Lit.[7] m.p. 163–6°; f) Lit.[6] 255–6°; g) Lit.[6] 243–5°; h) Lit.[2,5] m.p. 222–4 resp.[2] 232–233°; i) Lit.[2] m.p. 231–234° resp.[6] 190–192°.

Table 3

Alkylammonium salts of some N-(oxopropenyl)-aminoacids*

No	Salt	Yield %	M.p. °C	$[\alpha]_D^{20-24}$ (c = 1, MeOH)	Formula (M. Weight)	Analysis Calc. / Found		
						C	H	N
1	AE–Gly–OH. DCHA	80	166–168 (EtOH)	—	$C_{20}H_{36}N_2O_4$ (368.5)	65.19 65.48	9.85 10.20	7.60 7.50
2	BA–Gly–OH.DCHA	58	165–167 (AcOEt)	—	$C_{24}H_{36}N_2O_3$ (400.6)	71.96 71.84	9.06 9.14	6.99 6.75
3	AE–L–Ala–OH.DCHA	78	132–133 (Et_2O)	+ 69.1	$C_{21}H_{38}N_2O_4$ (382.6)	65.93 66.12	10.01 10.32	7.32 7.18
4	BA–L–Ala–OH.DCHA	65	163–165 (AcOEt)	+165.6	$C_{25}H_{38}N_2O_3$ (414.6)	72.43 72.70	9.24 9.78	6.76 7.03
5	AE–L–Val–OH. DCHA	78	123–124 (Et_2O)	+ 68.5	$C_{23}H_{42}N_2O_4$ (410.6)	67.28 67.70	10.30 10.56	6.82 6.99
6	BA–L–Val–OH.DCHA	73	160–161 (AcOEt)	+139.5	$C_{27}H_{42}N_2O_3$ (442.7)	73.26 73.80	9.56 10.00	6.33 6.20
7	AE–L–Leu–OH. DCHA	55	124–126 (Et_2O)	+ 47.2	$C_{24}H_{44}N_2O_4$ (424.6)	67.89 68.40	10.44 10.87	6.60 6.73
8	BA–L–Leu–OH. DCHA	80	158–160 (AcOEt)	+116.9	$C_{28}H_{44}N_2O_3$ (456.7)	73.64 73.42	9.71 10.16	6.13 6.02
9	AC–L–Leu–OH.DCHA	87	134–135 (LP)	+108.8	$C_{23}H_{42}N_2O_3$ (394.6)	70.01 70.21	10.73 11.20	7.09 7.30
10	AE–L–Ile–OH.DCHA	82	124–125 (Et_2O)	+ 55	$C_{24}H_{44}N_2O_4$ (424.6)	67.89 68.65	10.44 10.60	6.60 6.87
11	CP–L–Ile–OH.DCHA	—	119–121 (Et_2O)	+ 40.3	$C_{26}H_{46}N_2O_4$ (450.7)	69.28 69.19	10.29 10.53	6.22 6.34
12	AC–L–Ile–OH.DCHA	62	122–124 (Et_2O)	+117.8	$C_{23}H_{42}N_2O_3$ (394.6)	70.01 70.40	10.73 10.90	7.09 7.17
13	BA–L–Ile–OH.DCHA	68	151–152 (AcOEt)	+136.6	$C_{28}H_{44}N_2O_3$ (456.7)	73.64 73.53	9.71 9.90	6.13 5.78

14	AE–D–Phg–OH.DCHA	84	120–124[a] (AcOEt)	+157	$C_{26}H_{40}N_2O_4$ (444.6)	70.24 70.39	9.07 9.57	6.30 6.50
15	CP–D–Phg–OH.DCHA	80	153–154 (AcOEt)	+151.4	$C_{28}H_{42}N_2O_4$ (470.7)	71.45 71.78	9.00 10.10	5.95 5.52
16	AC–D–Phg–OH.DCHA	70	124–125 (n-hexan)	+224.5	$C_{25}H_{38}N_2O_3$ (414.6)	72.43 72.35	9.24 9.71	6.76 6.80
17	BA–D–Phg–OH.DCHA	98	140–141 (AcOEt)	+208.6	$C_{30}H_{40}N_2O_3$ (476.7)	75.59 74.97	8.46 8.52	5.87 5.30
18	BA–D–Phg–OH.MePp	95	153–155 (Et_2O)	+115.3	$C_{24}H_{30}N_2O_3$ (394.5)	73.07 73.16	7.66 8.14	7.10 7.05
19	BA–D–Phg–OH. MeMph	92	214–218 (MeOH–Et_2O)	+308.6	$C_{23}H_{28}N_2O_4$ (396.5)	69.67 69.94	7.12 7.36	7.07 7.13
20	AE–L–Phe–OH.DCHA	67	128–130 (Et_2O)	–134.8	$C_{27}H_{42}N_2O_4$ (458.7)	70.70 70.87	9.23 9.59	6.11 6.50
21	BA–L–Phe–OH.DCHA	80	158–160 (MeOH)	–249	$C_{31}H_{42}N_2O_3$ (490.7)	75.88 75.20	8.63 8.66	5.71 5.67
22	BA–L–Phe–OH.Pp	80	142–145 (Me_2CO)	–305.7	$C_{24}H_{30}N_2O_3$ (394.5)	73.07 73.35	7.66 8.10	7.10 6.80
23	AE–L–Glu(Bzl)–OH.DCHA	93.5	118–119 (Et_2O)	–7.7	$C_{30}H_{46}N_2O_6$ (530.7)	67.90 68.30	8.74 9.05	5.27 5.51
24	CP–L–Glu(Bzl)–OH.DCHA	75	118–120 (Et_2O)	–12.9	$C_{32}H_{48}N_2O_6$ (556.8)	69.04 69.00	8.69 8.95	5.03 5.04
25	AC–L–Glu(Bzl)–OH.DCHA	92	114–116 (Et_2O)	+ 9.3	$C_{29}H_{44}N_2O_5$ (500.7)	69.56 70.00	8.86 9.16	5.60 5.76
26	BA–L–Glu(Bzl)–OH.DCHA	87.5	139–140 (AcOEt–Et_2O)	+14.8	$C_{34}H_{46}N_2O_5$ (562.8)	72.56 72.80	8.24 8.80	4.98 5.33
27	AE–DL–Try–OH.DCHA	75.8	163–164 (AcOEt–PE)	—	$C_{29}H_{43}N_3O_4$ (497.7)	70.02 69.70	8.71 9.01	8.44 8.31

---

* *Abbreviations*: 1. DCHA = dicyclohexylamine; Pp = piperidine; MePp = N-methylpiperidine; MeMph = N-methylmorpholine; Bzl = benzyl.
2. Solvents: EtOH = ethanol; MeOH = methanol; PE = petroleum ether; AcOEt = ethyl acetate; LP = Light petroleum of b.p. 60–80°C; Et_2O = ethyl ether; Me_2CO = acetone; DIOX = dioxan.
a) Isolated sirup which on inoculating became crystalline.

In all instances the salts were characterized by melting points and specific rotations (table 2 and 3). While the potassium and sodium salts do not have sharp melting points the dicyclohexyl-ammonium salts melt in a narrow range.

By treating the aminoacid salts III protected with groups such as AE, CP or AC, with diluted acids (normal hydrogen chloride, at room temperature) deprotection takes place and the corresponding aminoacid hydrochloride is formed.[1-5] A certain stability can be remarked in the case of enamines formed by C-phenylglycine [2] and phenylalanine with benzoylacetone and 2,6-dimethoxybenzoylacetone respectively. These protected salts, when treated with diluted acids (pH = 4–5) form the corresponding N-protected free aminoacid IV; at a lower pH the protective group splits:

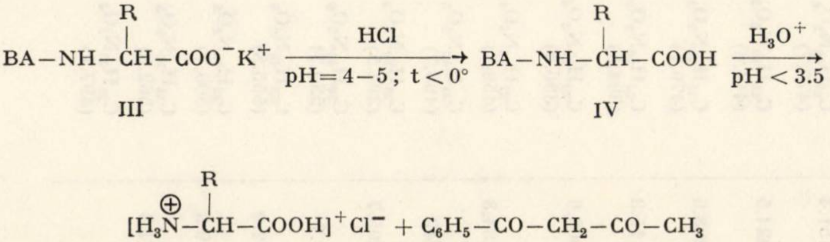

$$\underset{\text{III}}{BA-NH-\overset{R}{\overset{|}{C}}H-COO^-K^+} \xrightarrow[pH=4-5;\ t<0^\circ]{HCl} \underset{\text{IV}}{BA-NH-\overset{R}{\overset{|}{C}}H-COOH} \xrightarrow[pH<3.5]{H_3O^+}$$

$$[H_3\overset{\oplus}{N}-\overset{R}{\overset{|}{C}}H-COOH]^+Cl^- + C_6H_5-CO-CH_2-CO-CH_3$$

Owing to the mild conditions in which protection and deprotection take place, the dicarbonyl method has the advantage of avoiding racemization of the optically active aminoacids. This holds true even when dealing with C-phenylglycine, which has a special sensitivity towards racemization.[11] Thus, starting with the optical antipodes of C-phenylglycine with different optical purities (D(−) : 98%; L(+) : 89%) by their protection with acetylacetone we obtained the AC-Phg-OK antipodes with almost identical specific rotations: −355°, 6 for D(−) and +357° for L(+) (c = 1, in methanol). Not only the dicarbonyl method is free of racemization, but this method of protection, leads after deprotection to an aminoacid with a higher specific rotation than the initial value. Using, for instance, an initial L(+) phenylglycine with $[\alpha]_D: +145^\circ$, after protection with ethyl acetoacetate and subsequent deprotection, the aminoacid was obtained with $[\alpha]_D: +165^\circ$ (c = 2, in 10% hydrogen chloride).

The applicability of dicarbonyl N-protected aminoacid salts in the peptide bond formation through the mixed anhydride method, was demonstrated by the synthesis of a series of model dipeptides of type VII. Good yields were obtained when trimethylacetyl chloride (pivaloyl chloride (V))[12] was used for the preparation of the mixed anhydrides VI. The same advantage is presented by the benzoic [13] and the *p*-nitrobenzoic mixed anhydrides; as a coupling partner ethyl glycinate was used.

[11] D. G. Neilson and D. F. Ewing, *J. Chem. Soc.*, **1966**, 393.

[12] M. Zaoral, *Coll. Czeh. Chem. Comm.*, **27**, 1273 (1962); J. R. Vaughan Jr. and R. L. Osato, *J. Amer. Chem. Soc.*, **73**, 5553 (1951).

[13] Th. Wieland, W. Kern and R. Sehring, *Liebigs Ann. Chem.*, **569**, 117 (1950); Th. Wieland and R. Sehring, *ibid.*, **569**, 122 (1950).

The ethoxycarbonyl mixed anhydride method with the modification recommended by Fosker and coworkers[6] with catalytical amounts of N-methylmorpholine furnished very good yields and high purity of VII dipeptides.

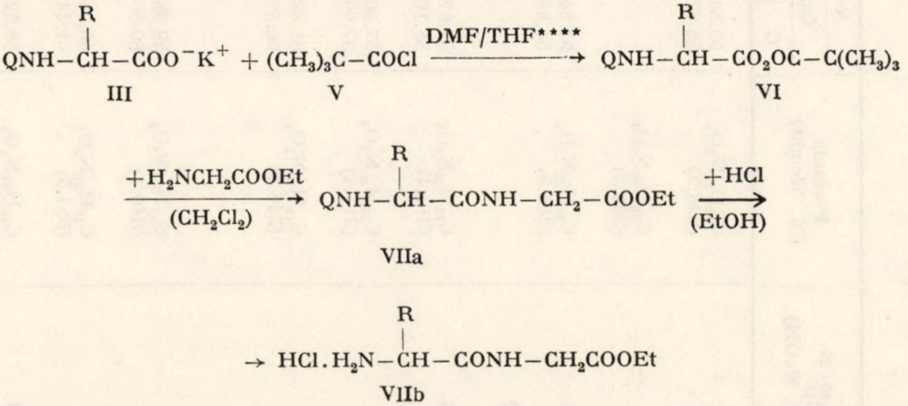

$$\underset{\text{III}}{\mathrm{QNH{-}\overset{R}{\overset{|}{C}}H{-}COO^-K^+}} + \underset{\text{V}}{\mathrm{(CH_3)_3C{-}COCl}} \xrightarrow{\text{DMF/THF}^{****}} \underset{\text{VI}}{\mathrm{QNH{-}\overset{R}{\overset{|}{C}}H{-}CO_2OC{-}C(CH_3)_3}}$$

$$\xrightarrow[\mathrm{(CH_2Cl_2)}]{\mathrm{+H_2NCH_2COOEt}} \underset{\text{VIIa}}{\mathrm{QNH{-}\overset{R}{\overset{|}{C}}H{-}CONH{-}CH_2{-}COOEt}} \xrightarrow[\mathrm{(EtOH)}]{\mathrm{+HCl}}$$

$$\rightarrow \underset{\text{VIIb}}{\mathrm{HCl.H_2N{-}\overset{R}{\overset{|}{C}}H{-}CONH{-}CH_2COOEt}}$$

Q = dicarbonyl protective rest.

In all instances the peptide bond formation took place without racemization. The results are listed in table 4.

The dicyclohexylcarbodiimide method[14] can also be used for the peptide synthesis in the case of dicarbonyl N-protected aminoacids. If BA—DL—Phg — OH was used as a starting material, by the DCC method the dipeptide ester BA—DL—Phg—Gly—OEt was obtained with an yield of 84%.

The cleavage of the protective dicarbonyl group in the dipeptide series was performed in ethanolic solution, at room temperature, by treatment with a 20% ethanolic hydrogen chloride. For identification purposes, the dipeptide esters hydrochlorides have been transformed in some cases in N-acetyl derivatives. Alkaline hydrolysis of the N-protected dipeptide esters leads to the formation of the corresponding dipeptides. Starting from the optically active dipeptide ester (i.e. AE—Phg—Gly—OEt) the hydrolysis is accompanied by total racemization.

EXPERIMENTAL

Melting points were taken in capillary tubes and are uncorrected. Specific rotations were measured in a Polarimeter type Metra 400/*a* Praha in a 2 dm tube at 20—24° in methanol, unless otherwise recorded.

**** For abbreviations see table 3 and 4.

[14] J. C. SHEEHAN and G. P. HESS, *J. Amer. Chem. Soc.*, **77**, 1067 (1955).

Table 4

Model dipeptides with ethyl glycinate*

No	Dipeptide derivatives	Method	Yield %	M.p. °C (Solvent)	$[\alpha]_D^{20-25}$ (c = 1, MeOH)	Formula (M. Weight)	Analysis Calc. / Found		
							C	H	N
1	CP–Gly–Gly–OEt	PIV	89	138–140 (EtOH–PE)	–	$C_{14}H_{22}N_2O_5$ (298.3)	56.34 56.82	7.43 7.89	9.39 9.25
2	BA–Gly–Gly–OEt	pNB	72	135–136 a) (EtOH)	–	$C_{16}H_{20}N_2O_4$ (304.3)			9.21 8.90
3	AE–L–Ala–Gly–OEt	PIV	78.5	142–145	+264.3	$C_{13}H_{22}N_2O_5$ (286.3,	54.54 54.88	7.75 8.11	9.78 9.76
		BZ	78	136–138 (MeOH)	+268.2				
4	CP–L–Ala–Gly–OEt	PIV	83	140–140.5b) (EtOH–H_2O)	+191.5	$C_{15}H_{24}N_2O_5$ (312.4)	57.67 58.10	7.74 8.26	8.97 8.78
5	AE–D–Val–Gly–OEt	BZ	89	111–111.5 (AcOEt–LP)	–162	$C_{15}H_{26}N_2O_5$ (314.4)	57.30 57.00	8.34 8.60	8.91 8.84
6	BA–L–Val–Gly–OEt c)	PIV	88	101–102d)	+300	$C_{19}H_{26}N_2O_4$ (346.4)	65.88 66.39	7.57 8.05	8.09 7.90
		BZ	56	98–99 (EtOH–H_2O)					
7	CP–L–Val–Gly–OEt	PIV	87.5	111–112 (EtOH–H_2O)	+115	$C_{17}H_{28}N_2O_5$ (340.4)	59.98 60.50	8.29 8.69	8.23 8.06
8	CP–L–Leu–Gly–OEt	PIV	73.5	71–71.5 (AcOEt–LP)	+111	$C_{18}H_{30}N_2O_5$ (354.5)	60.99 61.44	8.53 8.61	7.90 8.20
9	AE–L–Ile–Gly–OEte)	BZ	84	109–111 (AcOEt–PE)	+156.8	$C_{16}H_{28}N_2O_5$ (328.4)	58.52 59.22	8.60 9.07	8.53 8.50

10	AE–Phg–Gly–OEt[4]	(L)	PIV	32 (recr)	129–130 (EtOH)	−58.7	$C_{18}H_{24}N_2O_5$ (348.4)	62.06 61.72	6.94 7.15	8.04 8.23
		(D)		84	124–125f) (EtOH)	+57.2 (c = 1, EtOH)				7.84
		(DL)		83	103–105 (EtOH–H_2O)					8.13
11	CP–Phg–Gly–OEt[4]	(L)	PIV	32 (recr)	128–128.5 (EtOH–H_2O)	−35 (c = 1, EtOH)	$C_{20}H_{26}N_2O_5$ (374.4)	64.16	7.00	7.48 7.55
		(D)		50	130–131 (EtOH–H_2O)	+36.7 (c=1, EtOH)		64.50	7.16	7.87
		(DL)		92	129–130 (EtOH)	—				7.23
12	AC–D–Phg–Gly–OEt[4]		PIV	72	158–160g) (EtOH)	+85.3				
13	BA–Phg–Gly–OEt[4]	(L)	PIV	68	126–127 (EtOH–H_2O)	−110.4 (c = 1, EtOH)	$C_{22}H_{24}N_2O_4$ (380.4)	69.47	6.36	7.36 7.31
		(D)		89	127–130h) (EtOH–H_2O)	+107.8h) (c = 1, EtOH)				7.42
		(DL)	PIV DCC	67 84	170–173i) (EtOH)	—		69.64	6.72	7.26
14	DB–D–Phg–Gly–OEt[4]		PIV	61	185–186 (EtOH)	+12 (c = 0.5, EtOH)	$C_{24}H_{28}N_2O_6$ (440.5)	65.44 65.68	6.41 6.52	6.36 6.24
15	AE–L–Phe–Gly–OEt		BZ	91	109–110.5 (EtOH)	−64.6	$C_{19}H_{26}N_2O_5$ (362.4)	62.97 63.02	7.23 7.39	7.73 7.96
16	AE–DL–Try–Gly–OEt		BZ	73.5	136–137 (AcOEt–PE)	—	$C_{21}H_{27}N_3O_5$ (401.5)	62.82 63.13	6.78 7.29	10.46 10.00

* *Abbreviations*: 1. Mixed carboxylic anhydrides: PIV = pivaloyl; pNB = *p*-nitrobenzoyl; BZ = benzoyl; DCC = dicyclohexyl carbodiimide;
2. Solvents: See table 3. a) Lit.[1] M.p. 133–134°; b) Lit.[1] M.p. 138–140°; c) Prepared with freshly distilled ethyl glycinate; d) In lit.[1] the D-isomer is described, M.p. 97–98°; e) Prepared from the corresponding dicyclohexylammonium salt; f) Lit.[4] M.p. 125–127°; g) Lit.[2] M.p. 162–164°; h) Lit.[2] M.p. 126–128°, $[\alpha]_D^{20} = +108.9$ (c = 1, EtOH); i) Lit.[2] M.p. 174–175.

MATERIALS *DL-C-phenylglycine* was prepared after Klosa[15] and resolved in D and L isomers by the Ingersolls method,[16] having the following values of rotation:

D(−): $[\alpha]_D^{20} - 160°$ (c = 1, in HCl 10%).

L(+): $[\alpha]_D^{20} + 154°$ (c = 1, in HCl 10%).

2,6-Dimethoxy-benzoylacetone.[4] To a suspension of methanol-free sodium methoxyde (11.8 g, 220 mmoles) in ethyl acetate (40 ml), cooled below −5° a solution of dimethoxyacetophenone[17] (20 g, 110 mmoles) in ethyl acetate (40 ml) was added under vigorous stirring. Stirring was continued for 4−5 hours and the mixture was allowed to reach room temperature. The solution was hydrolysed with cold water (150 ml), and the separated organic (layer washed with water (100 ml). The aqueous portions were combined, washed with ether (150 ml) and acidified with ice and hydrochloric acid (pH = 1.5−2). An oil separated, which was extracted in ethyl acetate and dried over Na_2SO_4. The solvent was removed by distillation and the residue distilled under reduced pressure at 178−180° (5−6 Torr. Yield, 14.6 g (60%).

Anal: *Found*: C, 64.70; H, 5.50; *Calcd.* for $C_{12}H_{14}O_4$ (222.2):
C, 64.85; H, 6.35.

Benzoylacetone was obtained in a similar way in a 75−80% yield; m.p. 58—61° (ethanol). (Lit.[18] 54−60°).

I. Potassium, sodium and alkylammonium salts of N-(1-acylpropen-2-yl)-aminoacids (III)

Method A[1,2]

1. *Potassium N-(1-acetylpropen-2-yl)-L-leucinate* (**2.18**).[*****] Potassium L-leucinate was prepared from L-leucine (2.6 g, 20 mmoles) in ethanolic potassium hydroxide (18.5 ml, 6.2% 20 mmoles). To this solution acetylacetone (2.2 g, 22 mmoles) was added and refluxed for 50−60 minutes. By azeotrope distillation according to (5), a syrup was obtained. This was dissolved in dry ether, after 24 hours crystals separated. Yield, 2.3 g.

Method B

2. *Potassium N-(1-ethoxycarbonyl-propen-2-yl)-L-alaninate* (**2.5**). A solution of potassium ethyl acetoacetate prepared from ethyl acetoacetate (8 ml, 60 mmoles) in ethanolic potassium hydroxide (40 ml, 7.2%, 52 mmoles), was treated with L-alanine (5 g, 56 mmoles) and refluxed for 20−30 minutes. The almost clear solution was filtered and set aside. Aciform crystals were separated. Yield, 10.5 g (78%); $[\alpha]_D^{22}$: +125.3° (c = 1% in methanol), recrystallized from ethanol: $[\alpha]_D^{22}$: +123.9°.

---

[15] J. Klosa, *Arch. Pharmaz. Ber. dtsch. pharmaz. Ges.*, **285/57**, 278 (1952); *Chem. Zentr.*, **1952**, II, 551.

[16] A. W. Ingersoll, *J. Amer. Chem. Soc.*, **47**, 1168 (1925).

[17] N. J. Cartwright, J. J. Jones and D. Marmion, *J. Chem. Soc.*, **1952**, 3499.

[18] J. M. Sprague, L. J. Beckham and H. Adkins, *J. Amer. Chem. Soc.*, **56**, 2665 (1934).

[*****] First figure represents number of table, second one refers to the position of substance in the table.

3. *Potassium N-(2-ethoxycarbonyl-cyclopenten-1-yl)-L-phenylalaninate* (**2.24**). A suspension of potassium compound of 2-ethoxycarbonyl-cyclopentanone, prepared from 2-ethoxycarbonyl-cyclopentanone (5 ml) in ethanolic potassium hydroxide (24 ml, 7.2%, 30 mmoles), was treated with L-phenylalanine (5.2 g, 31.4 mmoles). After refluxing for 90 minutes the almost clear solution was filtered and evaporated to dryness under reduced pressure. Dry benzene was added to the residue and the distillation repeated twice. After recrystallization from ethanol, yield, 10 g; $[\alpha]_D^{22}$: $-228°$ ($c = 1\%$ in methanol).

4. *Potassium N-(1-acetylpropen-2-yl)-L-alaninate* (**2.7**). Acetylacetone (4.5 ml) and L-alanine (3.7 g, 31.6 mmoles) were added to a well cooled ethanolic potassium hydroxide (29 ml, 7.75%, 40 mmoles). After refluxing for 30 minutes the reaction mixture was filtered and evaporated to dryness under reduced pressure. The residue was triturated with hot ethyl acetate to yield 8.2 g, m.p. 214—218°; after recrystallization from ethanol, m.p. 214—216°.

5. *Potassium N-(1-ethoxycarbonyl-propen-2-yl)-D-valinate* (**2.11**). Ethyl acetoacetate (7.5 ml) and D-valine (6 g, 51.2 mmoles) in ethanolic potassium hydroxide (40 ml, 7%, 50 mmoles) were refluxed 30 minutes. The almost clear solution was filtered and evaporated to dryness under reduced pressure and the syrupy residue was refluxed for a few minutes with hexane or anhydrous acetone, when it became crystalline. Yield, 9.4 g.

Method C

6. *Potassium N-(2-ethoxycarbonyl-cyclopenten-1-yl)-D-C-phenylglycinate* (**2.35**). Potassium compound of 2-ethoxycarbonyl-cyclopentanone[9] (6 g) dissolved in hot ethanol (30 ml) was treated with D(—)-C-phenylglycine (4.7 g) and refluxed for one hour. After filtration, on cooling, crystals separated; yield: 5 g.

Method D

7. *Sodium N-(1-benzoylpropen-2-yl)-L-leucinate* (**2.20**). Sodium methoxide solution was prepared from sodium (0.46 g, 20 mmoles) in dry methanol (30 ml), and was treated with benzoylacetone (3.24 g, 20 mmoles) and L-leucine (2.8 g, 22 mmoles). The mixture was refluxed 30 minutes and then worked up as described at (5). The product remained as a glassy substance, but triturated with n-hexane, became crystalline. It was dried over paraffin and phosphorous pentoxide in vacuum desiccator. Yield, 3 g.

General method for preparing dicyclohexylammonium salts

8. *Dicyclohexylammonium salts of N-(1-acylpropen-2-yl)-aminoacids.* A suspension of the aminoacid (20 mmoles) in methanol (50 ml) is treated with the dicarbonyl compound (22—25 mmoles) and refluxed. Freshly distilled dicyclohexylamine (4 ml) is added from a dropping funnel in 10—15 minutes by maintaining the refluxation. If necessary refluxing is prolonged till an almost clear solution results. The solution is filtered and evaporated to dryness under reduced pressure by adding n-hexane, or dry benzene.

Dicyclohexylammonium salts of the N-(1-benzoylpropen-2-yl)-aminoacids were recrystallized from ethyl acetate-light petroleum solution; on the other hand the same N-(1-ethoxycarbonyl-propen-2-yl)-derivatives are purified by dissolving them in dry ether, filtering off and allowing the evaporation of the solution (table 3).

9. *N'-Methylmorpholinium N-(1-benzoylpropen-2-yl)-D(+)-C-phenylglycinate* (**3.18**). A suspension of N-(1-benzoylpropen-2-yl)-D(+)-C-phenylglycine (1.3 g, 4.3 mmoles) in ethyl

acetate (50 ml) was treated with N′-methylmorpholine (0.43 g, 4.25 mmoles). The next day the solvent was evaporated and the isolated crystalline substance recrystallized from ethyl acetate-light petroleum. Yield, 1.45 g (92 %); m.p., 214–218°; $[\alpha]_D^{22}$: +308° (c = 1, in methanol). A sample prepared by the general method was less pure, m.p., 150–154°, $[\alpha]_D^{25}$: +287° (c = 1, in methanol).

10. *Dicyclohexylammonium N-(1-benzoylpropen-2-yl)-D(+)-C-phenylglycinate* **(3.16)**. Potassium N-(1-benzoylpropen-2-yl)-D(+)-C-phenylglycinate **(2.41)** (3.4 g, 10 mmoles) was suspended in 50 ml ethyl acetate and treated with dicyclohexylamine hydrochloride (2.2 g, 10 mmoles). After stirring for 3 hours at room-temperature the reaction mixture was filtered and the filtrate was worked up as described in the general method. Yield, nearly quantitatively, m.p., 138–140° (after recrystallization 140–141°); $[\alpha]_D^{23}$: +208.6° (c = 1, in methanol).

After the general method: yield, 68 %; m.p., 138–140°; $[\alpha]_D^{18}$: + 189.2°.

II. *N-(1-Benzoylpropen-2-yl)-aminoacids (IV)*

11. *N-(1-Benzoylpropen-2-yl)-L(–)-phenylalanine.* Potassium N-(1-benzoylpropene-2-yl)-L-phenylalaninate **(2.26)** (3.5 g, 10 mmoles) was dissolved in water (100 ml), cooled to 0° and 0.1 normal aqueous HCl was added until the pH reached 4–4.5. The white precipitate was filtered and repeatedly washed with water and with ether. The dry substance was dissolved in ethyl acetate (30 ml) and dried over sodium sulfate. The solvent was evaporated in a vacuum desiccator. Yield, 2.2 g (70 %); m.p., 152–153°; $[\alpha]_D^{22}$: –393° (c = 1, in ethyl acetate).

Anal: *Found*: C, 73.43; H, 6.70; N, 4.20. *Calcd.*: for $C_{19}H_{26}NO_3$ (309.4): C, 73.74; H, 6.20; N, 4.53.

DL-isomer: yield, 60 %, m.p., 145–146°. *Found*, N, 4.38.

In a similar way was prepared:

12. *N-[1-(2′,6′-Dimethoxybenzoyl)-propen-2-yl]-D-C-phenylglycine*, yield, 86 %; m.p., 150–152°; $[\alpha]_D^{22}$: +155° (c = 0.5, in acetic acid).

Anal.: *Found*: C, 67.18; H, 6.22; N, 4.27. *Calcd.*: for $C_{20}H_{21}NO_5$ (355.4): C, 67.58; H, 5.96; N, 3.95.

13. *N-(1-Benzoylpropen-2-yl)-D-C-phenylglycine*, yield, 87 %, m.p., 141–142° (Lit.[2] 142–145°); $[\alpha]_D$: +429.8° (c = 1, in ethyl acetate); +379° (c = 0.5, in acetic acid).

Anal.: *Found*: N, 4.92. *Calcd.*: for $C_{18}H_{17}NO_3$ (295.3): N, 4.74.

DL-isomer: m.p., 152–154°. *Found*: N, 4.73.

III. *Dipeptides (VII)*

Pivaloyl chloride method

14. *N-(2-Ethoxycarbonyl-cyclopenten-1-yl)-glycyl-glycine ethyl ester* **(4.1)**. A suspension of potassium N-(2-ethoxycarbonyl-cyclopenten-1-yl)-glycinate **(2.2)** (2.6 g, 10.4 mmoles) in tetrahydrofurane (40 ml) was cooled to –8–10° and treated with N-methyl-morpholine (1–2 drops). The mixture was stirred and pivaloyl chloride (1.5 ml) was added durring 2–5

minutes, then stirred for other 15 minutes. The resulting mixture contained the reactive pivaloyl mixed anhydride in solution and potassium chloride in suspension. Meanwhile a solution of glycine ethyl ester was prepared from glycine ethyl ester hydrochloride (1.7 g, 12.2 mmoles) and triethylamine (1.7 ml, 12.2 mmoles) in dichlormethane (30 ml). The mixed anhydride solution was then added to this solution with vigorous stirring during 2–3 minutes and the mixture was stirred further in an ice-salt bath for 1 hour and 2 hours at room temperature. A solution of saturated sodium hydrogen carbonate (50 ml) was added and the organic layer removed by distillation under reduced pressure (20–50 Torr). The separated white crystals were isolated by filtration. Yield, 3.2 g.

15. *Glycylglycine ethyl ester hydrochloride.* A solution of N-(2-ethoxycarbonyl-cyclopenten-1-yl)-glycyl-glycine ethyl ester (**4.1**) (3.2 g) in ethyl acetate (70 ml) was treated with ethanolic hydrogen chloride (17.5 ml, 3 %). Solvents were removed by distillation under reduced pressure and the crystalline residue recrystallized from ethanol-ether. Yield, 1.7 g (72 %); m.p. 179–181°. (Lit.[19] 182°).

16. *D-C-Phenylglycyl-glycine ethyl ester hydrochloride.* [4] N-(1-Ethoxycarbonyl-propen-2-yl)-D-C-phenylglycyl-glycine ethyl ester (**4.10**) (0.6 g, 7.3 mmoles) suspended in ethanol (20 ml) was triturated with ethanolic hydrogen chloride (3 ml, 20 %). After 4 hours standing at room temperature the solvent was eliminated by distillation and the crystalline residue washed with dry ether on a Buchner-funnel. Yield, 0.26 g (100 %); m.p. 168–171°.

17. *N-Acetyl-D-C-phenylglycyl-glycine ethyl ester.* [4] *a.* A suspension of the above dipeptide ester hydrochloride [16] (0.2 g) in dry benzene (60 ml) was treated with acetic anhydride (0.5 ml) and triethylamine (0.6 ml). After 12 hours standing at room temperature crystals deposited in 98 % yield. M.p., 170–173° (water); $[\alpha]_D^{22}$: $-120°$ (c = 0.36, in water).

b. Pivaloyl mixed anhydride was prepared from N-acetyl-D-phenylglycine[20] (2 g, 10 mmoles) and pivaloyl chloride (1.2 ml) in tetrahydrofurane (30 ml). The reactive mixed anhydride was added to a solution of glycine ethyl ester prepared from glycine ethyl ester hydrochloride (1.4 g, 10 mmoles) and triethylamine (1.4 ml), in tetrahydrofurane (30 ml). Worked up as usually, yield, 1.2 g (43 %), after recrystallization from water, m.p., 173–174°, without depression with the above specimen $[\alpha]_D^{22}$: $-117°$ (c = 0.36, in water).

Anal. : *Found* : C, 60.45 ; H, 6.87 ; N, 9.96. *Calcd.* : for $C_{14}H_{18}N_2O_4$
(278.3) : C, 60.42 ; H, 6.52 ; N, 10.57.
L- and DL-isomers : N, 9.68 resp. 9.82.

Benzoyl chloride method [13]

18. *N-(1-Ethoxycarbonyl-propen-2-yl)-D-valyl-glycine ethylester* (**4.5**). Benzoyl mixed anhydride was prepared from potassium N-(1-ethoxycarbonyl-propen-2-yl)-D-valinate (8 g, 30 mmoles) and benzoyl chloride (3.6 ml, 30 mmoles) in tetrahydrofurane (50 ml) as described for the N-(2-ethoxycarbonyl-cyclopenten-1-yl)-derivative **4.1**, and the peptide bond was formed with freshly distilled glycine ethyl ester (3.1 g). The product was worked up as in the case of the quoted example. Yield, 8.4 g; m.p. 108–110°; recrystallized from ethyl acetate-light petroleum : 7.2 g; m.p. 111–111.5° (Anschütz).

---

[19] E. Fischer and E. Fourneau, *Ber. dtsch. chem. Ges.*, **34**, 2868 (1901).

[20] O. Neubauer and O. Warburg, *Z. physiol. Chem.*, **70**, 1 (1910).

19. *N-(1-Ethoxycarbonyl-propen-2-yl)-L-isoleucyl-glycine ethyl ester* (**4.9**). A solution of dicyclohexylammonium N-(1-ethoxycarbonyl-propen-2-yl)-L-isoleucinate (**3.9**) (4.3 g, 10 mmoles) in tetrahydrofurane (50 ml) was treated with N-methylmorpholine (1—2 drops) and under vigorous stirring at —8—12° benzoyl chloride (1.2 ml, 10 mmoles) was added. After 15 minutes stirring the separated dicyclohexylamine hydrochloride was eliminated by filtration and to the mixed anhydride solution freshly distilled glycine ethyl ester (1.1 g, 11 mmoles) was added at once. Stirring was continued in the ice-salt bath for 1 hour and at room temperature for 3 hours. Worked up as described for the synthesis of N-(2-ethoxycarbonyl-cyclopenten-1-yl)-glycyl-glycine ethyl ester (**4.1**), yield, 3 g (91%); m.p., 109—111°.

20. *N-(1-Benzoylpropen-2-yl)-DL-C-phenylglycyl-glycine ethyl ester* (**4.13**).[4] To a solution of N-(1-benzoylpropen-2-yl)-DL-C-phenylglycine (0.6 g, 2 mmoles) in tetrahydrofurane (6 ml) freshly distilled glycine ethyl ester (0.3 ml) was added and subsequently treated with N,N′-dicyclohexylcarbodiimide (0.4 g, 2 mmoles). The solution was allowed to stand at room temperature for 18 hours, treated with a small amount of acetic acid to decompose the excess reagent. The insoluble urea was removed by filtration and the solvent replaced by ethyl acetate. The ethyl acetate solution was washed with a dilute solution of sodium hydrogen carbonate and water and dried over Na_2SO_4. The solvent was eliminated by distillation under reduced pressure; yield 0.64 g; m.p. 170—173° (ethanol), without depression on mixing with an authentical sample.

Saponification

21. *DL-C-Phenylglycyl-glycine.*[4] A solution of N-(1-ethoxycarbonyl-propen-2-yl)-D-C-phenylglycyl-glycine ethyl ester (**4.10**) (1.3 g, 3.7 mmoles) in dioxane (12 ml) was treated with a N sodium hydroxide solution (4.6 ml) and was kept at room temperature for 6 hours. Upon acidification of the alkaline reaction mixture with hydrochloric acid the dipeptide separated (0.75 g, 100%). M.p., 243—243.5° (recrystallized twice from water). (Lit.[19] 248°).

Revue Roumaine de Chimie, 15, 1391–1407 (1970)

PEPTIDES. IX[1]

THE ACTIVATION AND PROTECTION OF THE CARBOXYL GROUP IN THE β-DICARBONYL N-PROTECTED AMINOACID SERIES *

A. BALOG, E. VARGHA**, D. BREAZU, LUCIA BEU and F. GÖNCZY

Institute for Chemical and Pharmaceutical Research,
Str. Karl Marx 93, Cluj, Romania

Received July 24, 1969

Cyanomethyl and phenacyl esters of N-(oxopropenyl)-aminoacids were prepared. The N-protecting group can be removed selectively by treating of these esters with dilute ethanolic hydrochloric acid. The isolated ester hydrochlorides were used for preparing peptides by Goodman's "backing off procedure". The optical behaviour of the prepared esters also was observed.

In a previous paper [1] conditions have been presented under which the protection of the amino group with β-dicarbonyl compounds in the monoamino monocarboxylic acids series (I) can be applied with advantages in peptide synthesis *via* the mixed anhydride method. As the cyanomethyl esters method [2] has an outstanding importance in the peptide bond formation for synthetic and optical reasons, a study of these activated esters (III) was undertaken with dicarbonyl N-protected aminoacids.

The most frequently used cyanomethylating agent is chloroacetonitrile [3] requiring drastic conditions — refluxing for 14 hours — under which some aminoacids suffer racemization. An attempt to prepare by this route from BA–D–phenylglycine *** the corresponding cyanomethyl ester was met with a total racemization. Quite recently Taschner [4] proposed the use of bromoacetonitrile to reduce the degree of racemization.

---

* The work described in this paper was presented in part at the 5th International Symposium on the Chemistry of Natural Products, IUPAC, London. July 1968.

** The Department of Organic Chemistry, Babeş-Bolyai University, Cluj, Str. Arany János, 11.

[1] Previous paper: A. Balog, D. Breazu, E. Vargha, F. Gönczy and L. Beu, *Rev. Roumaine Chim.*, **15**, 1389 (1970).

[2] M. Bodanszky and M. Ondetti, "Peptide Synthesis", Interscience Publishers, John Wiley and Sons, New York-London-Sydney, 1966, p. 98.

[3] R. Schwyzer, B. Iselin and M. Feurer, *Helv. Chim. Acta*, **38**, 69 (1955); *ibidem*, **38**, 80 and 83 (1955).

*** For abbreviations see tables 1 and 2.

[4] E. Taschner, M. Rzeszotarska and A. Kuziel, *Acta Chim. Acad. Sci. Hung.*, **44**, 67 (1965).

A new method is described here in which the above mentioned cyanomethylating agents are replaced by cyanomethyl tosylate (II) previously prepared by the authors.[5]

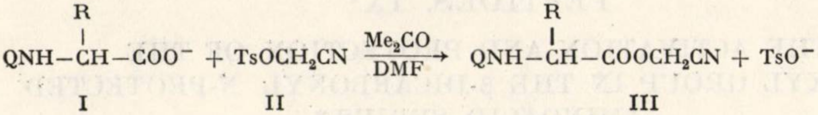

$$\underset{\text{I}}{\text{QNH}-\overset{\text{R}}{\overset{|}{\text{C}}}\text{H}-\text{COO}^-} + \underset{\text{II}}{\text{TsOCH}_2\text{CN}} \xrightarrow[\text{DMF}]{\text{Me}_2\text{CO}} \underset{\text{III}}{\text{QNH}-\overset{\text{R}}{\overset{|}{\text{C}}}\text{H}-\text{COOCH}_2\text{CN}} + \text{TsO}^- \qquad (1)$$

Q = Dicarbonyl protective group (See table 1).

The reaction takes place under very mild conditions. A mixture of acetone and dimethylformamide (2 : 1) is used at room temperature and for relatively short reaction time (3—4 hours). In these conditions a high optical purity and good yields are obtained (80—90 %). Usually at the end of the reaction on dilution with water the ester separates in a syrupy form, but crystallizes on standing overnight in a refrigerator. Recrystallization can be performed in an appropriate solvent usually with an increase of the optical purity (table 1).

Through this method even cyanomethyl esters of phenylglycine have been prepared without racemization. This was controlled by their transformation into derivatives with a known optical activity. Cyanomethylesters of valine and leucine could not be isolated in crystalline form but were found to be suitable as such for the preparation of the crystalline hydrochlorides.

This method can be extended for the synthesis of cyanomethyl esters of N-phthalyl or N-tosyl aminoacids but in this case from triethyl ammonium salts of N-protected aminoacids (table 1). In a similar way the methyl, ethyl and benzyl tosylates proved to be convenient reactants for the synthesis of the methyl (see table 5), ethyl and benzyl esters of the β-dicarbonyl N-protected C-phenylglycine. A similar method was used by Theodoropoulos and Tsangaris[6] for the esterification of N-protected aminoacids and dipeptides with the *p*-nitrobenzyl tosylate.

The removal of the β-dicarbonyl protective group takes place in very mild conditions, by treatment with one equivalent of 3 % ethanolic hydrogen chloride. The respective hydrochlorides V are readily obtained in crystalline form and in good yields (table 3). These types of hydrochlorides of cyanomethyl esters, which are so important in peptide synthesis, are rarely quoted and only in the case of some formyl-[7] and furfuryloxycarbonyl[8]-protected esters, where a permanent danger of hydrolysis of the nitrile group exists during removal of the protective group.

Special attention was given to the preparation and behaviour of esters in the N-protected C-phenylglycine because of the ease with which derivatives of this aminoacid are racemized.[9,10] Attempts to recrystallize N-protected C-phenylglycine esters from methanol or light petroleum were associated with a considerable lowering of optical activity. For example, in the case of AE—L—Phg—OCH_2CN first isolated with $[\alpha]_D^{22}$: —92°, by a recrystallization from methanol $[\alpha]_D$ lowers to —33°, and after a new recrystallization, this time from light petroleum, $[\alpha]_D$ reaches the value of —21° (c = 1, in methanol). We succeeded in improving the optical purity from a specific rotation of —92° to —139,2° (c = 1, in methanol) by dissolution of the crude ester in cold ethyl acetate and subsequent precipitation with petroleum ether. The hydrochlorides isolated by deprotection in the whole series of N-protected-D-phenylglycine cyanomethyl esters have a molecular rotation which ranges from —186° to —202° (c = 1, in water). The optical data for the methyl esters hydrochlorides, prepared in the above mentioned way correspond, in the limits of determination errors, to those given in literature.[11]

---

[5] Cl. Schönberger, V. Voinescu and A. Balog, *Rev. Chim.* (Bucharest), **14**, 688 (1963); A. Balog, Cl. Schönberger, L. Moraru and E. Vargha, "The 3rd Republican Conference for Chemistry", Timişoara, June, 1966.

[6] D. Theodoropoulos and J. Tsangaris, *J. Org. Chem.*, **29**, 2272 (1964).

[7] M. Goodman and K. C. Stueben, *J. Amer. Chem. Soc.*, **81**, 3980 (1959).

[8] H. Jeschkeit, G. Losse and K. Neubert, *Chem. Ber.*, **99**, 2083 (1966).

[9] D. G. Neilson and D. F. Ewing, *J. Chem. Soc.* (C), **1966**, 393.

[10] E. Dane and T. Dockner, *Chem. Ber.*, **98**, 789 (1965).

β-Dicarbonyl N-protected cyanomethyl esters (III) have been used as N-terminal aminoacids in peptide synthesis. As a model AE—L—Ala—Gly—OEt was synthesized through the cyanomethyl ester method (yield, 75%, $[\alpha]_D^{20}$: +267°) as well as through the mixed pivaloyl anhidride method[1] (yield, 85%, $[\alpha]_D^{20}$: + 264°, c = 1, in methanol). Furthermore CP—Gly—Gly—OEt[1] was also prepared, which after removal of the protective group led to the corresponding hydrochloride, with an yield of 85%, identical with that given in other references.[12]

For the study of racemization during peptide bond formation we performed the condensation of cyanomethyl esters of optically active C-phenylglycine, protected with the four β-dicarbonyl groups presented in table 1, with benzylamine and ethyl glycinate as amine components. Although the reactions were carried out at room temperature the benzylamides and dipeptide esters were completely racemized.

We believe that in these cases racemization is due on the one hand to a —I effect of α- phenyl group, on the other hand to the basicity of the amine partners which causes the direct proton abstraction from the asymmetric α-carbon atom.[13]

For this explanation pleads also the fact that the cyanomethyl esters of other aminoacids N-protected with dicarbonyl group form with freshly distilled ethyl glycinate (and in equimolecular quantities) optically active peptide esters. At the same time, on the basis of some observations from our laboratory[14], Z—D—Phg—OCH_2CN and H—Gly—OC_2H_5 in a molar ratio of 1 : 1.1 in ethyl acetate form the corresponding dipeptide ester with a total racemization. But if in this reaction the molar ratio is reversed (i.e. cyanomethylester in excess is used) the dipeptide ester is obtained only with a partial racemization: $[\alpha]_D^{20}$: $-63°$ while the same derivative prepared through the mixed pivaloyl anhydride method had $[\alpha]_D^{20}$: $-118°$ ($c = 1$, in methanol). Similar observations were made in the case of the synthesis of N–etoxicarbonyl–D–Phg–GlyOEt. Using the cyanomethyl ester in excess the dipeptide ester has $[\alpha]_D^{20}$: $-108°$ ($c = 0.8$, in methanol), while the mixed anhydride method leads to $[\alpha]_D^{20}$: $-93°$ ($c = 1$, in methanol).

---

[11] "Dictionary of Organic Compounds", vol. 1, ed. J. Heilbron and M. M. Bunbury, London, 1946, p. 112.

[12] E. Fischer and E. Fourneau, *Ber. dtsch. chem. Ges.*, **34**, 2868 (1901); A. H. Cook and A. L. Levy, *J. Chem. Soc.*, **1950**, 646.

[13] G. W. Anderson, J. E. Zimmerman and F. M. Callahan, *J. Amer. Chem. Soc.*, **89**, 5012 (1967).

[14] A. Balog, E. Vargha, V. Voinescu, M. Herman, E. Ramonţian and L. Moraru, *Stud. Univ. Babeş-Bolyai, Chem.*, **14** (2), 137 (1969).

On the other hand the cyanomethyl ester hydrochlorides (V) can be used for the formation of dipeptide esters VI having an activated carboxyl. The method used was first introduced by Balog and Vargha[15] and consists in the benzene (or dioxane) refluxing of the cyanomethyl ester hydrochloride with the N-protected (phthalyl or tosyl) aminoacid chloride IV.

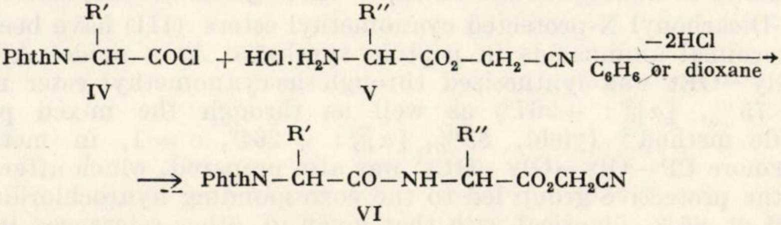

$$\underset{\text{IV}}{\text{PhthN}-\overset{\overset{\text{R}'}{|}}{\text{CH}}-\text{COCl}} + \underset{\text{V}}{\text{HCl.H}_2\text{N}-\overset{\overset{\text{R}''}{|}}{\text{CH}}-\text{CO}_2-\text{CH}_2-\text{CN}} \xrightarrow[\text{C}_6\text{H}_6 \text{ or dioxane}]{-2\text{HCl}}$$

$$\longrightarrow \underset{\text{VI}}{\text{PhthN}-\overset{\overset{\text{R}'}{|}}{\text{CH}}-\text{CO}-\text{NH}-\overset{\overset{\text{R}''}{|}}{\text{CH}}-\text{CO}_2\text{CH}_2\text{CN}} \qquad (2)$$

Table 4 lists some carboxyl activated dipeptides prepared as above.

These activated dipeptides (VI) are suitable for the elongation of the peptide chain through fragment condensation. The following simple tripeptide has been prepared: Phth–Gly–Gly–Gly–OEt.

In the elongation of the peptide chain, starting from C-terminal aminoacids, of special interest are the carboxyl protected aminoacids. One of the most recently introduced group for the protection of the carboxyl is the phenacyl group.[16] Again, the potassium or dicyclohexylammonium salts of dicarbonyl N-protected aminoacids proved to be extremely suitable for the synthesis of phenacyl esters VIII. These esters are easily obtained by treating the potassium salts I in acetone with phenacyl bromide (VIIIa) or *p*-nitro-phenacyl bromide (VIIIb) at room temperature:

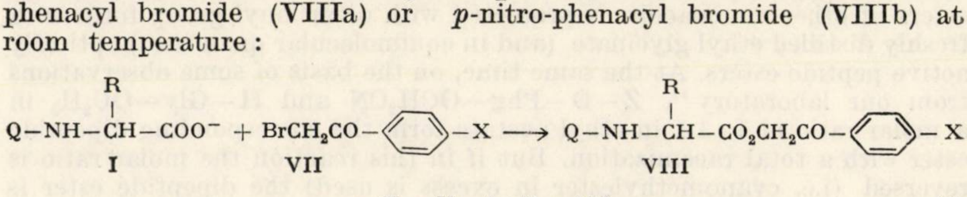

(3)

High optical purity and yields are obtained (table 2).

After selective removal of the N-protective group with diluted ethanolic hydrochloric acid, the corresponding hydrochlorides of phenacyl [illegible]

[15] A. Balog, E. Vargha and I. Balázs, *Stud. Univ. Babeş-Bolyai, Chem.*, **3** (2), 17 (1958).

[16] J. C. Sheehan and G. D. Daves Jr, *J. Org. Chem.*, **29**, 2006 (1964), G. C. Stelakatos, A. Paganou and L. Zervas, *J. Chem. Soc.* (C), **1966**, 1191; J. Taylor-Papadimitriou. C, Yovanidis, A. Paganou and L. Zervas, *J. Chem. Soc.* (C), **1967**, 1830.

esters are obtained (table 3) which can be used for the synthesis of carboxyl protected dipeptides, following the same condensation technique as in equation (2) (table 4).

The same method (equation 3) can be used for the preparation of *p*-nitrobenzyl esters employing the *p*-nitrobenzyl bromide. As a model we prepared $AE-L-Ala-OCH_2-C_6H_4-NO_2(p)$ and $BA-L-Ala-OCH_2-C_6H_4-NO_2(p)$, after deprotection with 3% ethanolic hydrogen chloride *p*-nitrobenzyl alaninate hydrochloride identical with the specimen described in literature[17] was obtained.

Among the already well known methods for the synthesis of *p*-nitrophenyl esters we used so far only the carbodiimide method given by Rothe-Kunitz and Elliot-Russel[18] in the case of BA–L–Phe–OH esterification. In this way the field of applicability of β-dicarbonyl compounds in the peptide synthesis enlarges very much. In this respect, results obtained with cyanomethyl esters prove that activated esters in the dicarbonyl N-protected series can be used in the stepwise peptide synthesis and especially with the "backing off procedure" of Goodmann,[7,19] having the advantage of an easy deprotection. Our method, in the case of hydrochlorides of activated or of carboxyl-protected esters seems to be more advantageous than those given in literature. At the same time the method is useful in the case of the tripeptide synthesis following Goodmann's procedure, that is in the first stage the acylation of the bifunctional aminoacid with chlorides of N-phthalyl or N-tosyl aminoacids in anhydrous media, method which has given good results in the case of cyanomethyl esters of protected dipeptides. In the second stage the use of phenacyl esters simplifies the operation for the preparation of tripeptides.

EXPERIMENTAL

Melting points were taken in capillary tubes and are uncorrected. Samples for analysis were dried for 2–4 hours at 64° and 16–30 Torr over P_2O_5. Specific rotations were measured in a polarimeter type Metra 400/a Praha in a 2 dm tube at 20–24° in methanol, except otherwise stated.

I. CYANOMETHYLATING REACTIONS THROUGH CYANOMETHYL *p*-TOLUENE SULFONATE (Table 1)

1. *Cyanomethyl p-toluenesulfonate.*[5] A solution of potassium cyanide (130 g, 2.0 moles) in water (250 ml) is cooled in a ice-salt bath. With stirring a solution of commercial 37% formaldehyde solution (170 ml, 2.0 moles) and water (130 ml) is admitted slowly from the dropping funnel at such a rate, that the temperature never rises above 10° (about 60 minutes are required). The mixture is cooled to –10° and a solution of tosylchloride (380 g, 2.0 moles) and acetone (320 ml) is added with vigorous stirring, maintaining the internal

---

[17] G. Losse and H. Vietmeyer, *J. prakt. Chem.*, **32** (3–4), 204 (1966).

[18] M. Rothe and F. Kunitz, *Liebigs Ann. Chem.*, **609**, 88 (1957); D.F. Elliot and D. W. Russel, *Biochem. J.*, **66**, 49P (1957).

[19] J. Kovács and R. L. Rodin, *J. Org. Chem.*, **33**, 2418 (1968).

Table 1

N – Protected cyanomethyl esters*

$R-COO^{-} + Ts-OCH_2CN \longrightarrow R-COOCH_2CN + Ts-O^{-}$

No	Cyanomethyl ester	Yield %	M.p. °C (solvent)	$[\alpha]_D^{20-25}$	Formula	Calcd./Found C	H	N
1.1	AE–Gly–OCM	55	73–74 (AcOEt–LP)	—	$C_{10}H_{14}N_2O_4$ (226,2)	53.09 53.38	6.24 6.51	12.38 12.21
1.2	CP–Gly–OCM	94	87–88 (AcOEt–LP)	—	$C_{12}H_{16}N_2O_4$ (252.3)	57.13 57.22	6.40 6.75	11.10 11.21
1.3	AE–L–Ala–OCM	71	61.5–62.5 (EtOH)	+194 (c=1,MeOH)	$C_{11}H_{16}N_2O_4$ (240.3)	54.98 54.40	6.70 7.12	11.65 11.49
1.4	CP–L–Ala–OCM	67	62–64 (AcOEt–LP)	+127 (c = 1, MeOH)	$C_{13}H_{18}N_2O_4$ (266.3)	58.64 58.25	6.81 7.02	10.52 10.15
1.5	CP–L–Phe–OCM	95	72–74 (EtOH)	–109 (c = 1, MeOH)	$C_{19}H_{22}N_2O_4$ (342.4)	66.65 66.05	6.48 6.66	8.18 8.10
1.6	AE–Phg–OCM[5]	(L) 90	83–84 (Et_2O)	–108 (c = 1,MeOH)	$C_{16}H_{18}N_2O_4$ (302.3)	63.56 63.39	6.00 6.64	9.26 9.37
		(D) 86	82–84 (Et_2O)	+139 (c = 1,MeOH)		—	—	9.06
		(DL) 85	86–88 (Et_2O)	—		—	—	9.08
1.7	CP–Phg–OCM[5]	(L) 90	76–78 (LP)	–90 (c = 1,MeOH)	$C_{18}H_{20}N_2O_4$ (328.4)	65.84	6.14	8.53 8.03
		(D) 83	75–76 (LP)	+90,5 (c = 1,MeOH)		65.73	6.40	8.24
		(DL) 90	78–79 (EtOH–H_2O)	—				8.24

1.8	AC–DL–Phg–OCM^5		82	98–99 (LP)	–	$C_{15}H_{16}N_2O_3$ (272.3)	66.16 66.48	5.93 6.21	10.29 10.41
1.9	BA–Phg–OCM^5	(L)	75	108–109 (LP)	–93.4 (c=1,MeOH)	$C_{20}H_{18}N_2O_3$ (334.4)	71.84 71.57	5.42 5.67	8.38 8.26
		(D)	72	106–107 (Et_2O–LP)	+123.6 (c = 1,MeOH)				8.72
		(DL)	80	104–105$^{a)}$ (EtOH)	–				8.18
1.10	DB–L–Phg–OCM^5		57	133–134 (Et_2O)	–15.6 (c = 1,MeOH)	$C_{22}H_{22}N_2O_5$ (394.4)	67.00 67.22	5.61 5.95	7.10 6.86
1.11	Z–Gly–OCM		64	74–80$^{b)}$ (Et_2O–PE)		$C_{12}H_{12}N_2O_4$ (248.2)			
1.12	Phth–Gly–OCM		77	132–134$^{c)}$ (Me_2CO)		$C_{12}H_8N_2O_4$ (244.2)			
1.13	Ts–Ala–OCM	(L)	87.5	82–84 (AcOEt–LP)	–31.3 (c= 1, Diox.)	$C_{12}H_{14}N_2O_4S$ (282.3)	51.06 51.12	4.99 5.30	9.92 9.72
		(DL)	88.6	100–101.5 (AcOEt–LP)			51.40	5.44	9.50
1.14	Phth–L–Phe–OCM		89	140–142 (EtOH)	–192 (c=1, Diox.)	$C_{19}H_{14}N_2O_4$ (334.3)	68.27 68.10	4.21 4.63	8.39 8.60

* *Abbreviations* : CM = cyanomethyl ; AE = 1-Ethoxycarbonyl-propen-2-yl ; CP = 2-Ethoxycarbonyl-cyclopenten-1-yl ; AC = 1-acetyl-propen-2-yl ; BA = 1-benzoyl-propen-2-yl ; DB = 1-(2,6-Dimethoxybenzoyl)-propen-2yl ; Z = benzyloxycarbonyl ; Phth = phthaloyl ; Ts = *p*-toluene sulfonyl.

Solvents : AcOEt = ethyl acetate ; LP = light petroleum, b.p. 60–80° ; PE = petroleum ether ; EtOH = ethanol ; MeOH = methanol ; Et_2O = ethyl-ether, Me_2 CO = acetone ; Diox. = dioxane. a) Lit. [10] 106–108°, b) Lit. [3] 69–70° ; c) Lit. [20] 132–133.5°.

---

[20] B. Helferich, P. Schellenberg and J. Ulbrich, *Chem. Ber.*, **90**, 700 (1957).

temperature between —5° and —10° (about 3 hours). Simultaneously the pH of the reaction mixture must be taken between 7 and 9 adding a N potassium hydroxide solution. The flask is then removed from the cooling bath, and after standing over night, 1200 ml of water are added with stirring. After 30 minutes the precipitate is filtered, washed thoroughly with cold water (5 × 50 ml) and dried at room temperature. The crude material melts at 44—47° and weighs 400 g. It is purified by recrystallization from ethanol (600 ml) using decolorizing charcoal (20 g), refluxing 1 hour, filtering and then cooling the solution in an ice-box. The product is filtered, washed with cold water and dried. The recrystallized *p*-toluenesulfonyl cyanomethyl ester melts at 47—48°. Yield : 272 g . A second crop of 30 g (total yield 71,5%) was secured by working up the mother liquor.

2. *N—(2-Ethoxycarbonyl-cyclopenten-1-yl)-glycine cyanomethyl ester* (**1.2**). A solution of potassium N—(2-ethoxycarbonyl cyclopenten-1-yl)-glycinate (10 g, 40 mmoles/ in N,N-dimethyl-formamide (25 ml) and acetone (50 ml) with cyanomethyl *p*-toluene-sulfonate (7 g, 33 mmoles) was refluxed for three hours. After dilution with water (1200 ml) the separated crystals were filtered (7.8 g, 94%).

3. *N—(1-Ethoxycarbonyl-propen-2-yl)-D—C—phenylglcine cyanomethyl ester* (**1.6**). To a solution of potassium N—(1-ethoxycarbonyl-propen-2-yl)-D—C-phenylgylcinate (9.05 g, 30 mmoles) in acetone (50 ml) and N,N-dimethylformamide (50 ml), cyanomethyl *p*-toluenesulfonate (6 g, 28 mmoles) was added. After 3 hours at room temperature the solution was diluted with water (1000 ml); yield, 7.7 g, (90%), m.p., 83—84°; $[\alpha]_D^{23}$: +92,6° (c = 1, in methanol), purified by reprecipitation with petroleum ether from a solution in ethylacetate, m.p., 86—88°; $[\alpha]_D^{22}$: +139,2°. Recrystallization from ethanol and then from benzine shows : $[\alpha]_D^{22}$: + 35°, respectively + 21°.

4. *D(—)-C-phenylglycine cyanomethyl ester hydrochloride* (**3.6**). The above ester (**1.6**) (3 g, 10 mmoles) was introduced in to ethanolic HCl 3% (15 ml). Crystals of the hydrochloride separated. Diluted with anhydrous ether there were isolated 1.9 g of the hydrochloride, m.p., 175—177° (Table 3).

5. *L-Valine cyanomethyl ester hydrochloride* (**3.3**). Potassium N-(2-ethoxycarbonyl-cyclopenten-1-yl)-L-valinate (8,8 g, 30 mmoles) and cyanomethyl *p*-toluenesulfonate (6.3 g, 30 mmoles) were dissolved in tetrahydrofurane (50 ml). After 12 hours at room temperature the solution was filtered and poured into water (100 ml), the organic solvent evaporated under reduced pressure and the remaining water layer extracted with ethyl acetate, dried over Na_2SO_4 and treated with ethanolic hydrogen chloride 18% (8 ml). The precipitate was filtered and washed with anhydrous ether. Yield, 3.2 g (55%) (Table 3).

6. *N-Benzyloxycarbonyl-glycine cyanomethyl ester* (**1.11**). N—Benzyolxycarbonyl-glycine (4.2 g, 20 mmoles) was dissolved in acetone (50 ml) containing triethylamine (2,4 ml) and this was followed by the addition of cyanomethyl *p*-toluenesulfonate (4 g, 19 mmoles). After being kept for 5 hours at room temperature ethyl acetate (100 ml) was added and the resulting solution washed with water, dried (Na_2SO_4) and the solvent evaporated to give a syrupy residue which in a few days crystallized. Yield, 3 g (64%); m.p. 74—80°. Recrystallized from ether-petroleum ether, 69—70° (Lit. [3]69—70°).

7. *N-Phthalyl-L-phenylalanine cyanomethyl ester* (**1.14**). N-Phthalyl-L-phenylalanine (4.4 g, 15 mmoles) was dissolved in acetone (50 ml), containing triethylamine (2,1 ml) and cyanomethyl *p*-toluenesulfonate (3 g, 14 mmoles) were added. After being kept for 4 hours at room temperature the solution was poured into water (500 ml). Yield, 3 g (87%); m.p. 122—124°. Recrystallized from ethanol m.p. 140—142°.

II. *p*-NITROPHENYL ESTER WITH DCC-METHOD.[18]

8. *N-(1-Benzoyl-propen-2-yl)-L-phylalanine p-nitrophenyl ester.* To a solution of N-(1-benzoyl-propen-2-yl)-L-phenylalanine[1] (4.5 g, 15 mmoles) and *p*-nitrophenol (2.3 g, 18 mmoles) in ethyl acetate (50 ml), N,N′-dicyclohexylcarbodiimide (4 g, 15 mmoles) was added at 0°. After 30 minutes the mixture was allowed to reach the room temperature and was kept for 1 hour. The N,N′-dicyclohexylurea was filtered off and washed with ethyl acetate. The combined filtrate and washings were evaporated to dryness and the crystalline residue recrystallized from hot ethanol. Yield, 3.6 g (55%); m.p., 115–116°; $[\alpha]_D^{22}$: —42,2° (c = 1, in methanol).

Anal. *Calcd.*: for $C_{21}H_{22}N_2O_5$(382.4) C, 69.73; H, 5.15; N, 6.51;

Found: C, 70.30; H, 5.56; N, 6.26.

III. PHENACYL AND ANALOGOUS ESTERS OF DICARBONYL N-PROTECTED AMINOACIDS (Table 2)

9. *N-(1-Ethoxycarbonyl-propen-2-yl)-L-alanine phenacyl ester* (**2.2**). A suspension of potassium N—(1-ethoxycarbonyl-propen-2-yl)-L-alaninate[1] (12 g, 50 mmoles) in acetone-dimethylformamide (30—30 ml) was treated with ω-bromoacetophenone (10 g, 50 mmoles) and stirred for 3 hours at room temperature. The reaction mixture was diluted with water (500 ml) and the initially oily substance became crystallin. Yield nearly quantitative. M.p., 94—96° (ethyl acetate-light petroleum).

10. *L-Alanine phenacil ester hydrochloride* (**3.2**). The above ester (**2.2**) (6.4 g, 20 mmoles) was dissolved in dry ethanol (50 ml) and treated with ethanolic hydrogen chloride (5 ml, 18%). The reaction mixture was allowed to stand at room temperature for 1.5 minutes, after which the solvent was evaporated to dryness under reduced pressure. The residue was crystallized from ethanol-ether. Yield, 2.2 g m.p. 158—159°, $[\alpha]_D^{24}$: +1.9 (c = 2, in methanol) (Table 3).

11. *N-(1-Benzoyl-propen-2-yl)-D-valine phenacyl ester* (**2.5**). Potassium N-(1-benzoyl-propen-2-yl)-D- valine (15 mmoles) was prepared according the method described before[1] without isolation and to the ethanolic solution ω-bromoacetophenone was added (3 g, 15 mmoles). Worked up as in 9, 4.5 g of the phenacyl ester were obtained. M.p., 96—97° (from ethanol).

12. *D-Valine phenacyl ester hydrochloride* (**3.9**). D-Valine (3.2 g, 25 mmoles) and potassium 2-ethoxycarbonyl-cyclopentanone (5.2 g, 25 mmoles) in methanol (50 ml) was refluxed until complete dissolution occurred. To the hot solution ω-bromoacetophenone (5 g, 25 mmoles) was added and then heated under reflux on a water bath for one hour. Upon addition of water (750 ml) a syrup separated which was extracted twice with ethyl acetate (50 ml). The organic layer was washed with water, dilute sodium hydrogen carbonate solution, water and then dried (Na_2SO_4) and a solution of dry hydrogen chloride in ethanol (18%, 5 ml) was added. The solvent was then removed under reduced pressure and the residue taken up in anhydrous ethanol (25 ml) and anhydrous ether (25 ml). Yield, 3.4 g (70%) (Table 3).

Table 2

With β-dicarbonil N-protected amino acid phenacyl esters and some analogous esters*

$R-COO^{-}K^{+} + Br-CH_2-R' \rightarrow R-COOCH_2R'$

1–10 : $R' = COC_6H_5$
11 : $R' = COC_6H_4NO_2(p)$
12–13 : $R' = C_6H_4NO_2(p)$

No	Aminoacid ester	Yield %	M.p.°C (solvent)	$[\alpha]_D^{20-25}$	Formula	Calcd./Found		
						C	H	N
2.1	AE–Gly–OPAc	86	101–102 (MeOH)	—	$C_{16}H_{19}NO_5$ (305,3)	62.94 62.74	6.27 6.90	4.58 4.40
2.2	AE–L–Ala–OPAc	98	94–96 (AcOEt–LP)	+225.5 (c = 1,AcOEt)	$C_{17}H_{21}NO_5$ (319.4)	63.94 64.07	6.63 6.79	4.38 4.45
2.3	CP–L–Ala–OPAc	77	89–92 (AcOEt–LP)	+97.3 (c = 1,AcOEt)	$C_{19}H_{23}NO_5$ (345.4)	66.07 65.50	6.70 6.94	4.06 4.10
2.4	CP–D–Val–OPAc	93.7	65–66 (AcOEt–LP)	+131.1 (c= 1,MeOH)	$C_{21}H_{27}NO_5$ (373.5)	67.53 67.68	7.28 7.68	3.75 3.62
2.5	BA–D–Val–OPAc	88	96–97 (EtOH)	+259 (c = 1,MeOH)	$C_{23}H_{25}NO_4$ (379.5)	72.80 72.67	6.64 7.20	3.69 3.67
2.6	AE–L–Leu–OPAc	88	62–64 (EtOH)	+132.6 (c = 1,MeOH)	$C_{20}H_{27}NO_5$ (361.4)	66.46 66.00	7.53 7.71	3.87 3.85
2.7	CP–L–Leu–OPAc	100	94–96 (EtOH)	+100.6 (c=1,MeOH)	$C_{22}H_{29}NO_5$ (387.5)	68.20 68.24	7.54 7.70	3.63 3.80
2.8	AE–L–Phe–OPAc	95.5	94–95 (AcOEt–LP)	–92.8 (c = 1,MeOH)	$C_{23}H_{25}NO_5$ (395.5)	69.85 70.44	6.37 6.70	3.54 3.36
2.9	CP–L–Phe–OPAc	100	94–96 (AcOEt–LP)	–86.9 (c = 1,MeOH)	$C_{25}H_{27}NO_5$ (421.5)	71.23 71.85	6.46 6.58	3.32 3.87
2.10	AE–D–Phg–OPAc	85	120–122 (AcOEt–LP)	–25.1 (c = 1,MeOH)	$C_{22}H_{23}NO_5$ (381.4)	69.28 68.72	6.09 6.23	3.67 3.55
2.11	AE–L–Ala–ONPA	87.5	92–93.5 (EtOH)	+196.6 (c = 1,Diox)	$C_{17}H_{20}N_2O_7$ (364.4)	56.03 56.63	5.53 5.88	7.70 7.43
2.12	AE–L–Ala–ONBzl	80	91–91.5 (EtOH)	+194 (c = 1,MeOH)	$C_{16}H_{20}N_2O_6$ (336.3)	57.14 57.62	6.00 6.38	8.33 8.57
2.13	BA–L–Ala–ONBzl	80	115–116 (EtOH)	+242 (c = 1, Diox)	$C_{20}H_{20}N_2O_5$ (368.4)	65.21 65.70	5.47 5.75	7.61 7.57

* *Abbreviations*: See table 1; PAc = $CH_2COC_6H_5$; NPA = $CH_2COC_6H_4-NO_2$ (p); NBzl = $CH_2C_6H_4-NO_2$ (p).

13. *N-(1-Ethoxycarbonyl-propen-2-yl)-L-alanine p-nitrochenacyl ester* (**2.11**). Potassium N-(1-ethoxycarbonyl-propen-2-yl)-L-alaninate[1] (1.2 g, 5 mmoles) and ω-bromo-*p*-niroacetophenone (1.2 g, 5 mmoles) was stirred in acetone (25 ml) for one hour. The reaction mixture was diluted with water (500 ml). A syrup separates which readily crystallizes. Yield, 1.6 g; m.p., 92–93,5°.

14. *L-Alanine p-nitrophenacyl ester hydrochloride* (**3.13**). To a solution of N–(1-ethoxycarbonyl-propen-2-yl)-L-alanine *p*-nitro-phenacyl ester (2.9 g, 10 mmoles) in ethyl acetate (50 ml), ethanolic hydrogen chloride (5 ml, 18 %) was added. After 45 minutes at room temperature the precipitate was filtered and washed twice with anhydrous ether. Yield, 2.2 g; m.p., 165.5–166°.

15. *N–(1-Ethoxycarbonyl-propen-2-yl)-L-alanine p-nitrobenzyl* ester (**2.12**). Potassium N–(1-ethoxycarbonyl-propen-2-yl)-L-alaninate[1] (2.4 g, 10 mmoles) and *p*-nitrobenzyl bromide (2.4 g, 10 mmoles) were suspended in dry acetone (60 ml) and stirred at room temperature for three hours. Poured into water (400 ml) a syrup separates which readily crystallizes. Working up in the usual manner 2.7 g (80 %); m.p. 87–89° are obtained. Recrystallized from ethanol m.p., 91–91.5°.

16. *L-Alamine p-nitrobenzyl ester hydrochloride* (**3.14**) was obtained by the removal of N-protecting group in ethanolic dry hydrogen chloride; yield 90 %; m.p. 202–204° (lit.[17] 198–200°).

IV. AMIDE FORMATION WITH BENZYLAMINE ON THE C-PHENYLGLYCINE SERIES

17. *N – (1-Ethoxycarbonyl-propen-2-yl)-DL – C-phenylglycine benzylamide.* N – (1-Ethoxycarbonyl-propen-2-yl)–D–C-phenylglycine cyanomethyl ester (3 g, $[\alpha]_D^{25}$: + 91.7°, c = 1 in methanol) was treated with freshly distilled benzylamine (1 ml) in anhydrous ethyl acetate (10 ml). After being kept over night at room temperature, the solution was washed with sodium hydrogen carbonate solution (5 %, 8–10 ml) and the solvent of the dried organic layer distilled under reduced pressure. Yield, 2.4 g (68.6 %); m.p. 149–150° (ethanol).

Anal.: *Calcd.* for $C_{21}H_{24}N_2O_3$ (352.4) C, 71.56; H, 6.86; N, 7.95;
Found: C, 71.80; H, 6.36; N, 8.04.

The same substance was obtained from racemic cyanomethyl ester. Yield, 71 %, m. p., 148–150°, without depression when mixed with the above substance.

18. *N-(-1-Ethoxycarbonyl-propen-2-yl)-D-C-phenylglycine benzylamide.* Pivaloyl-mixed anhydride was prepared starting from potassium N-(1-ethoxycarbonyl-propen-2-yl)-D-C-phenylglycinate (1.6 g) and pivaloyl chloride (0,7 ml) in dry acetone (30 ml) at –5°. It was treated with benzylamine (0.6 ml). The mixture was allowed to stand at room temperature for 3 hours. Poured into water an oil separated which ready crystallized. Yield, 1.5 g (80 %), m. p., 121–122° (ethanol); $[\alpha]_D^{22}$: + 123° (c = 1, in ethanol).

Anal. Calcd.: for $C_{21}H_{24}N_2O_3$ (352.4) N, 7.95. *Found*: N, 7.68.

19. *N-(2-Ethoxycarbonyl-cyclopenten-1-yl)-DL-C-phenylglycine benzylamide* was obtained from N-(2-ethoxycarbonyl-cyclopenten-1-yl)-D-C-phenylglycine cyanomethyl ester ($[\alpha]_D$: + 117°; c = 1, in ethanol) and benzylamine as described by.[17] Yield, 74 %; m.p. 156–160° (ethanol).

Anal. *Calcd.* for $C_{23}H_{26}N_2O_3$ (378,5) C, 72.99; H, 6.99; N, 7.40;
Found: C, 73.01; H, 7.36; N, 7.44.

Table 3

Aminoacid ester hydrochlorides*

$$Q - NHCH(R)COOR' \xrightarrow[(EtOH)]{HCl} HCl.H_2NCH(R)COOR' \quad Q = AE,\ CP,\ BA$$

No	Ester hydrochlorides	Yield %	M.p. °C (solvent)	$[\alpha]_D^{20-25}$	Formula	Calcd/Found			
						C	H	N	Cl
				a) *Cyanomethyl Esters*					
3.1	H−Gly−OCM.HCl	80	170−172 (EtOH)	−	$C_4H_7ClN_2O_2$ (150.6)	31.90 31.98	4.68 4.99	18.60 18.70	23.54 23.50
3.2	H−L−Ala−OCM.HCl	65	158−159 (EtOH−Et_2O)	+18 (c = 2,H_2O)	$C_5H_9ClN_2O_2$ (164.6)	36.50 37.00	5.50 6.30	17.02 16.80	21.52 21.80
3.3	H−Val−OCM.HCl	(L) 55	144−146 (EtOH−Et_2O)	+13,0 (c=2,H_2O)	$C_7H_{13}ClN_2O_2$ (192.6)	43.66 43.75	6.80 7.08	14.55 14.80	18.40 18.32
		(D) 43	144−146 (EtOH−Et_2O)	−9.5 (c=2,H_2O)					18.30
		(DL) 52	145−147 (EtOH−Et_2O)	−					17.84
3.4	H−L−Leu−OCM.HCl	68	163−165 (EtOH−Et_2O)	+8.75 (c = 1.6,H_2O)	$C_8H_{15}ClN_2O_2$ (206.7)	46.48 46.16	7.32 7.72	13.54 13.30	17.15 17.62
3.5	H−L−Phe−OCM.HCl	73	185−186[a] (EtOH)	−1,25 (c = 4,H_2O)	$C_{11}H_{13}ClN_2O_2$ (240.7)				14.73 14.93
3.6	H−D−Phg−OCM.HCl	83	175−177 (EtOH−Et_2O)	−89.4 (c = 1,H_2O)	$C_{10}H_{11}ClN_2O_2$ (226.7)	52.98 53.02	4.88 5.05	12.36 11.86	15.64 15.70

b) *Phenacyl and some p-Nitrophenacyl and p-Nitrobenzyl Esters*

3.7	H−Gly−OPAC.HCl	82	178−180 (i−PrOH)	−	$C_{10}H_{12}ClNO_3$ (229.7)	52.29 52.52	5.26 5.70	6.09 5.91	15.43 15.45
3.8	H−L−Ala−OPAC.HCl	85	184−185 (EtOH−Et_2O)	+4.8 (c = 2,H_2O)	$C_{11}H_{14}ClNO_3$ (243.7)	54.21 53.82	5.79 6.15	5.75 5.44	14.57 14.89
3.9	H−D−Val−OPAC.HCl	79	182−183 (EtOH−Et_2O)	−11.4 (c=0.7, H_2O)	$C_{13}H_{18}ClNO_3$ (271.7)	57.46 57.78	6.68 6.88	5.15 4.73	13.05 13.28
3.10	H−L−Leu−OPAC.HCl	69	151−153 (EtOH−Et_2O)	+17 (c=2,H_2O)	$C_{14}H_{20}ClNO_3$ (285.8)	58.83 58.32	7.05 6.92	4.90 5.32	12.41 12.92
3.11	H−L−Phe−OPAC.HCl	78	156−158 (EtOH−Et_2O)	+6.4 (c=2,H_2O)	$C_{17}H_{18}ClNO_3$ (319.8)	63.85 64.01	5.67 6.12	4.38 4.77	11.09 11.87
3.12	H−D−Phg−OPAC.HCl	83	182−185 (EtOH−Et_2O)	−112.5 (c = 2,H_2O)	$C_{16}H_{16}ClNO_3$ (305.8)	62.85	5.27	4.58 4.27	11.58 12.30
3.13	H−L−Ala−ONPA.HCl	75.3	165.5−166 (EtOH)	+10.5 (c = 2,H_2O)	$C_{11}H_{13}ClN_2O_5$ (288.7)	45.77 46.21	4.54 4.80	9.70 9.54	12.28 12.33
3.14	H−L−Ala−ONBzl.HCl	90	202−204[b]	−10 (c = 4,H_2O)					

* Abbreviations : See Table 1−2. i−PrOH = 2 − propanol

a) Reported[7] : 186.5−188.5°

b) Reported[17] : m.p. 198−200°; $[\alpha]_D^{20}$: −2.45° (in dimethyl-formamide).

The *D-isomer* was prepared by the pivaloyl mixed anhydride method as described by.[18] Yield, 81 %; m. p., 135.5—136°; $[\alpha]^{22}_{D}$: + 65° (c = 1 in ethanol). *Found* : N 7.19.

20. *N-(Benzoil-propen-2-yl)-DL-C-phenylgycine benzylamide* was obtained starting from the N-(1-benzoyl-propen-2-yl)-D-C-phenylglycine cyanomethyl ester and freshly distilled benzylamine as described by.[17] Yield, 61.5 %; m.p., 183—184° (ethanol).

Anal. *Calcd.* for $C_{25}H_{24}N_2O_2$ (384.4) C, 78.09; H, 6.20; N, 7.28;
Found : C, 78.41; H, 6.60; N, 7.47.

V. PEPTIDE FORMATION

A. Cyanomethyl ester method.[3]

21. *N-(1-Ethoxycarbonyl-propen-2-yl)-L-alanylglycine ethyl ester..* N-(1-Ethoxycarbonyl-propen-2-yl)-L-alanine cyanomethyl ester (6 g, 25 mmoles) was dissolved in ethyl acetate (25 ml) and glycine ethyl ester (2.5 ml) was added. Next day ethyl acetate (75 ml) was added to dissolve separated crystals and the product was then isolated in the usual manner. Yield, 4.2 g (58.3%); m. p., 145—146° (ethyl acetate); $[\alpha]^{23}_{D}$: + 254° (c = 1, in methanol), identical with a sample obtained through the mixed anhydride method.[1]

22. *N-Phthalyl-triglycyl ethyl ester* was prepared from N-phthalyl-glycyl-glycine cyanomethyl ester (0.6 g, 2 mmoles) and ethyl glycinate (0.2 ml, 2 mmoles) according to Schwyzers indications[3]; yield, 63 %; m.p., 219—221° (lit.[3] 232—233°).

B. Acid chloride method.[15]

23. *Phthalylglycyl-glycine cyanomethyl ester* (**4.1**). *a.* Glycine cyanomethyl ester hydrochloride (3.5 g, 20 mmoles) and phthaliminoacetyl chloride (4.5 g, 20 mmoles) was refluxed in benzene (150 ml) until hydrogen chloride evolution ceased (4 hours). After cooling to room temperature the crystalline material was filtered and recrystallized from ethyl acetate-ligroin. Yield, 5.25 g (87%), m. p., 203—204°.

b. Phthalylglycyl-glycine (0.8 g, 3 mmoles) was dissolved in dry acetone (10 ml) containing triethylamine (0,45 ml, 3 mmoles) and cyanomethyl *p*-toluenesulfonate (0.63 g, 3 mmoles) was added. Worked up in the usual manner 0.8 g (80 %) of dipeptide cyanomethyl ester was obtained, m.p. 203—204°; mixed m.p. with **4.1** *a* 203—204°.

24. *N-(p-Toluenesulfonyl)-L-anayl-D-C-phyenylglycine phenacyl ester* (**4.12**). Tosyl-L-alanyl chloride (2.6 g, 10 mmoles) and D-C-phenyl-glycine phenacyl ester hydrochloride (3 g, 10 mmoles) were refluxed in dioxan (50 ml) until HCl-evolution ceased. Poured into water (500 ml) crystals were separated. Yield, 3.9 g (78 %), m.p. 141—142°.

C. Mixed-anhydride method

25. *N-(1-Ethoxycarbonyl-propen-2-yl)-L-γ-benzylglutamyl-L-valine phenacyl ester.* Dicyclohexylammonium N-(1-ethoxycarbonyl-propen-2-yl)-L-γ-benzyl glutamate[1] (9.6 g, 18 mmoles) in dry tetrahydrofurane (50 ml) was cooled to —5° —8° and treated with benzoyl chloride (2.5 g, 18 mmoles) and 2—3 drops of N-methylmorpholine. After 15 minutes the separated dicyclohexylamine hydrochloride was removed by filtration and a solution of L-valine phenacyl ester, prepared from the hydrochloride (**3.3**) (4 g) on treating it with N-methylpiperidine (1.8 ml) in dichlormethan (10 ml), was added. The reaction mixture was

Table 4

Carboxyl activated or protected dipeptides *

$$\mathrm{R-COCl + HCl.H_2NCH(R')CO_2R'' \xrightarrow[(C_6H_6)]{-2HCl} R-CO-NHCH(R')CO_2R''}$$

No	N-Protected dipeptide ester	Yield %	M.p.°C (solvent)	$[\alpha]_D^{20}$	Formula	Calcd./Found		
						C	H	N
4.1	Phth−Gly−Gly−OCM	80	203−205 (EtOH ; EtOAc−LP)	—	$C_{14}H_{11}N_3O_5$ (301.3)	55.82 55.70	3.69 4.29	13.96 13.50
4.2	Phth−Gly−Gly−OPAc	95	235−242 (AcOEt−PE)	—	$C_{20}H_{16}N_2O_6$ (380.4)	63.15 63.20	4.24 4.78	7.36 7.40
4.3	Phth−Gly−L−Ala−OCM	82	182−184 (AcOEt−LP)	−67.6 (c = 1,MeOH)	$C_{15}H_{13}N_3O_5$ (315.5)	57.14 56.92	4.15 4.40	13.32 13.40
4.4	Phth−Gly−L−Val−OCM	55	168−170 (AcOEt−LP)	−49.7 (c=1,MeOH)	$C_{17}H_{17}N_3O_5$ (343.3)	59.46 60.00	5.00 5.35	12.24 11.84
4.5	Phth−Gly−DL−Val−OCM	50	162−164 (AcOEt−LP)	—		59.79	5.67	11.73
4.6	Phth−Gly−L−Leu−OCM	67	158−159 (AcOEt−LP)	−38.9 (c=1,MeOH)	$C_{18}H_{19}N_3O_5$ (357.4)	60.50 61.10	5.36 5.93	11.75 11.12
4.7	Phth−Gly−L−Phe−OCM	81	183−184 (AcOEt−LP)	+31.05 (c = 1,Diox)	$C_{21}H_{17}N_3O_5$ (391.4)	64.45 64.67	4.37 4.89	10.73 10.58
4.8	Phth−Gly−DL−Phe−OCM		180−182 (AcOEt−LP)	—		64.64	4.81	10.21
4.9	Ts−L−Ala−Gly−OCM	94	141−143 (AcOEt−PE)	−51.7 (c=1,MeOH) −42.5 (c = 1, Diox)	$C_{14}H_{17}N_3O_5S$ (339.4)	49.55 50.00	5.04 5.57	12.38 11.95
4.10	Ts−L−Ala−Gly−OEt	72	105−106 (AcOEt−PE)	−15.7 (c = 1,AcOEt)	$C_{14}H_{20}N_2O_5S$ (328.4)	51.21 51.13	6.14 6.22	8.53 8.05
4.11	Ts−L−Ala−D−Phg−OCM	92	138−140 (AcOEt−PE)	−94.8 (c = 1,Diox)	$C_{20}H_{21}N_3O_5S$ (415.5)	57.82 57.85	5.09 5.65	10.11 10.30
4.12	Ts−L−Ala−D−Phg−OPAc	78	141−142 (AcOEt−LP)	−119 (c=1, Diox)	$C_{26}H_{26}N_2O_6S$ (494.6)	63.14 63.54	5.30 5.57	5.66 5.40
4.13	Phth−L−Phe−L−Ala−OCM	50	163−164 (EtOH)	−157.7 (c = 1,MeOH)	$C_{22}H_{19}N_3O_5$ (405.4)	65.18 65.56	4.72 5.02	10.36 9.91

* Abbreviations : See tables 1−3.

Table 5

With β-dicarbonyl N-protected C-phenylglycine methyl esters*[5]

$Q - NHCH(C_6H_5)COO^-K^+ + Ts-OCH_3 \rightarrow Q - NHCH(C_6H_5)COOCH_3 + TsO^-K^+$

No	Q	Isomeric form	Yield %	M.p.°C	$[\alpha]_D^{20-22}$ (c = 1, MeOH)	Formula	Calcd/Found		
							C	H	N
5.1	AE	L	94	80−82 (LP)	−238	$C_{15}H_{19}NO_4$ (277.3)	64.96	6.90	5.05 5.02
5.2		D	80	80−81 (LP)	+259 a)		64.90	7.12	4.93
5.3		DL	85.7	104−105 (LP)			—	—	5.12
5.4	CP	L	87	82−83 (LP)	−188	$C_{17}H_{21}NO_4$ (303.4)	67.31 —	6.97 —	4.60 4.44
5.5		D	65	82−83 (EtOH+H_2O)	+176.7		67.49	7.24	4.40
5.6		DL	95	68−70 (EtOH+H_2O)	—		—	—	4.63
5.7	AC	L	85	103−107 (Bz)	−391.5	$C_{14}H_{17}NO_3$ (247.3)	67.99 67.92	6.93 7.43	5.66 5.62
5.8	BA	L	98	125−126 (LP)	−417	$C_{19}H_{19}NO_3$ (309.4)	73.76 —	6.20 —	4.52 4.65
5.9		D b)	98	124−125 (EtOH+H_2O)	+424		73.98	6.95	4.45
5.10		DL	60	126−127 (EtOH+H_2O)					4.72
5.11	DB	L		146−147 (EtOH−PE)	−261	$C_{21}H_{23}NO_5$ (369.4)	68.28	6.27	3.79 3.80
5.12		D b)		145−146 (Bz−PE)	+254		68.75	6.78	3.73

* Abbreviations : See tables 1−3 ; LP = light petroleum b.p. 80−100 ; Bz = benzene

a) After a second recryst from LP : M.p., 78° ; $[\alpha]_D^{20} = +222°$;

b) Prepared from the corresponding acid through esterification with ethereal diazomethane.

kept at room temperature overnight and worked up in the usual manner. Yield, 7.5 g (75 %), m. p., 79—81°. Recrystallized from methanol and once more from ethyl acetate-light petroleum, m.p., 92—94°; $[\alpha]_D^{23}$: + 10.2° (c = 1, in methanol).

Anal. *Calcd.* for $C_{31}H_{38}N_2O_8$(546.4) C, 65.70 ; H, 6.76 ; N, 4.95 ;
Found : C, 66.02 ; H, 7.24 ; N, 4.93.

VI. ESTERIFICATIONS WITH TOSYL ESTERS ON THE C-PHENYLGLYCINE SERIES[5]

26. *N-(1-Benzoyl-propen-2-yl)-L-Cp-henylglycine methil ester* (**5.8**). *a.* Potassium N-(1-benzoyl-propen-2-yl)-L-C-phenylglycinate[1] (6.7 g, 20 mmoles) was dissolved in dry acetone (50 ml) and N,N-dimethylformamide (25 ml) and followed immediately by the addition of methyl *p*-toluenesulfonate (4.2 g, 20 mmoles). After being kept for 5 hours at room temperature water (750 ml) was added. A syrup separates, which on standing crystallized. Yield, 5.5 g ; m.p., 126—127° (from aq. ethanol) ; $[\alpha]_D^{22}$: — 417° (c = 1, in methanol).

b. D-isomer (**5.9**). — N-(1-Benzoyl-propen-2-yl)-D-C-phenylglycine[1] (3 g, 10 mmoles) was suspended in ether (50 ml) and treated with an etheral diazomethane solution (100 ml, 0.8 %) until gas evolution ceased. After evaporation the solvent crystals remained. Yield, 2.6 g (84 %) ; m.p., 126—128° (from aq. ethanol) ; $[\alpha]_D^{23}$: +424° (c = 1, in methanol).

27. *D-C-Phenylglycine methyl ester hydrochloride. a.* The above methyl ester **5.9** (3 g, 10 mmoles) was suspended in ethanol (10 ml) and treated with dry hydrogen chloride in ethanol (2 ml, 10 %). A precipitate of the ester hydrochloride began to appear in a few minutes. Dry ether (50 ml) was added to complete the precipitation, which was collected, washed with dry ether. Yield : 76 % ; m.p., 196—202° (lit.[11] 202°). $[M]_D^{23}$: —238° (c = 2, in water) (lit.[11] — 247° in water).

b. This ester hydrochloride was also prepared in a similar way starting from N-(2-ethoxycarbonyl-cyclopenten-1-yl)-derivative **5.4** as described before. Yield, 0.5 g (76 %) ; m. p. 225—227° (lit.[11] 202°), unchanged on crystallization from ethanol ether ; $[M]_D^{23}$: — 243.5°.

28. *N-(1-Ethoxycarbonyl-propen-2-yl)-L-C-phenylglycine benzyl ester.* Potassium N-(1-ethoxycarbonyl-propen-2-yl)-L-C-phenylglycinate[1] (3 g, 10 mmoles) and benzyl *p*-toluenesulfonate[21](2.1 g, 10 mmoles) were dissolved in dry acetone and worked up as at 26. Yield, 2.7 g (77 %) ; m.p., 80—82° (ethyl acetate-light petroleum) $[\alpha]_D^{21}$: — 192.5° (c = 1, in methanol).

Anal. Calcd. for $C_{21}H_{23}NO_4$ (353.4), C, 71.33 ; N, 6.56 ; N, 3.96 ;
Found : C, 71.99 ; N, 7.06 ; N, 4.14.

---

[21] F. DRAHOWZAHL and D. KLAMANN, *Monatsh.*, **82**, 452 (1951) ; *Chem. Zentr.*, **1955**, 8132.

kept at room temperature overnight and worked up in the usual manner. Yield 7.5 g (73%), m. p. 78–81°. Recrystallized from methanol and once more from ethyl acetate-light petroleum, m. p. 82–84°; $[\alpha]_D^{20}$ = –30.7 (c = 1, in methanol).
Anal. — [illegible]: C, 66.70; H, 6.79; N, 4.30;
Found: C, 66.92; H, 7.14; N, 4.35.

◆

VI. PREPARATIONS WITH TOSYL ESTERS OF THE L-PHENYLGLYCINE SERIES*

24. [illegible] methyl ester ([illegible]). [illegible] was dissolved in dry acetone (50 ml), and N,N-dimethylformamide (25 ml) and followed successively by the addition of [illegible] p-toluenesulfonate (4.2 g, 20 mmoles). After being kept for 5 hours at room temperature water (250 ml) was added. A syrup separated which on standing crystallized. Yield 5.5 g; m. p. 120–122° (from aq. ethanol); $[\alpha]_D^{20}$ = –41° (c = 1, in methanol).

b. [illegible]-D-phenylglycine (8 g, 10 mmoles) was suspended in ether (50 ml) and treated with an ethereal diazomethane solution (100 ml, 0.8 N) until gas evolution ceased. After evaporation the solvent crystals remained. Yield 8.0 g (94%); m. p. 126–128° (from aq. ethanol); $[\alpha]_D^{20}$ = +41° (c = 1, in methanol).

25. D-(–)-Phenylglycine methyl ester hydrochloride. a. The above methyl ester 5.9 (2 g, 20 mmoles) was suspended in ethanol (10 ml) and treated with dry hydrogen chloride in ethanol (2 ml, 10 N). A precipitate of the ester hydrochloride began to appear in a few minutes. Dry ether (50 ml) was added to complete the precipitation, which was collected, washed with dry ether. Yield: 75 %; m. p. 198–202 (dec.) (lit. [illegible]); $[\alpha]_D^{20}$ = [illegible] (c = 2, in water) (lit. [illegible] –247° in water).

b. This ester hydrochloride was also prepared in a similar way starting from N-[illegible]-D-phenylglycine as described before. Yield 6.3 g (70%), m. p. 195–200° (lit. [illegible]), unchanged on recrystallization from ethanol-ether; $[\alpha]_D^{20}$ = [illegible] 118.5°.

26. [illegible] phenylglycine [illegible] ester [illegible] (2 g, 10 mmoles) and hexyl p-toluenesulfonate (2.1 g, 10 mmoles) were dissolved in dry acetone and worked up as usual. Yield 2.5 g (77%); m. p. 80–83° (from ethyl acetate-light petroleum); $[\alpha]_D^{20}$ = –102.7° (c = 1, in methanol).
Anal. Calcd. for [illegible]: C, 71.23; H, 6.95; N, 3.96;
Found: C, 71.17; H, 7.05; N, 4.13.

---

* [illegible] Angew. Chem. [illegible]; Chem. Zentr. 1966, [illegible].

[illegible] 15, [illegible]

Revue Roumaine de Chimie, **15**, 1409 – 1414 (1970)

AS-TRIAZINE DERIVATIVES WITH POTENTIAL THERAPEUTIC ACTION. X[1]

6-CARBOXYHYDRAZIDE-AS-TRIAZINES

C. CRISTESCU
Chemical Pharmaceutical Research Institute, Bucharest
Şos. Vitan 112

Received October 27, 1969

In view of obtaining compounds with potential cytostatic and antitubercular activity, a series of as-triazines possessing 6-carbethoxy, 6-carboxyhydrazide and 3 and/or 5 oxo, thioxo, methylthio, hydrazine groups, were synthetized.

As a result of the similarity of the as-triazine ring with that of pyrimidine, the research in the field of synthesis and pharmacology of as-triazine derivatives to obtain compounds with potential cytostatic and antibacterial activity, has developed more and more in the last years.[2–4].

In this work, the synthesis of one series of as-triazine derivatives, where C_6 of the ring is substituted by $-COOC_2H_5$ or $-CONHNH_2$ and C_3 and/or C_5 by oxo, thioxo, methylthio and hydrazine, are described. These derivatives were prepared in order to investigate the two therapeutical possibilities as A/. antimetabolite like as-triazine-3,5(2H,4H) dione (6-Azauracile) derivatives and as B/. inhibitors of the growth of the *Mycobacterium tuberculosis*, having hydrazidic structure.

Our starting materials, 3-thioxo-6-carbethoxy-as-triazine-3,5(2H,4H) dione (I) and as-triazine-3,5(2H,4H) dione-6-carboxylic acid (VII) were synthesized according to the sequence of reaction reported by Falco and coworkers[5] and improved in our laboratory.[6]

Thionation of I was effected in pyridine with a content of 0.2% water. It yielded 85% in 3,5-dithioxo-6-carbethoxy-as-triazine-3,5 (2H,4H) dithione (II) at a molar ratio of substance : P_2S_5 of 2 : 1; II with two equivalents of methyliodide in hydroalcoholic solution of sodium hydroxide yields 3,5-dimethylthio-6-carbethoxy-as-triazine (III). Compound III may be subjected to acid hydrolysis to give as-triazine-3,5(2H,4H)dione-6-carboxylic acid, identical in all respects with VII prepared through the above mentioned unequivocal sequence.[5,6]

---

[1] Part IX : *Rev. Roumaine Chim.*, (in press).

[2] G. B. Elion and H. G. Hitchings, *Adv. Chemotherapy*, **2**, 91 (1965).

[3] S. Bresnik, S. Singer and G. H. Hitchings, *Biochim. Biophys. Acta*, **37**, 251 (1960).

[4] A. Čihák, J. Veselý and F. Šorm, *Coll. Czech. Chem. Comm.*, **31**, 1124 (1966).

[5] E. A. Falco, E. Pappas and G. H. Hitchings, *J. Amer. Chem. Soc.*, **78**, 1938 (1956).

[6] C. Cristescu and T. Panaitescu, *Pharmazie*, **18**, 336 (1963).

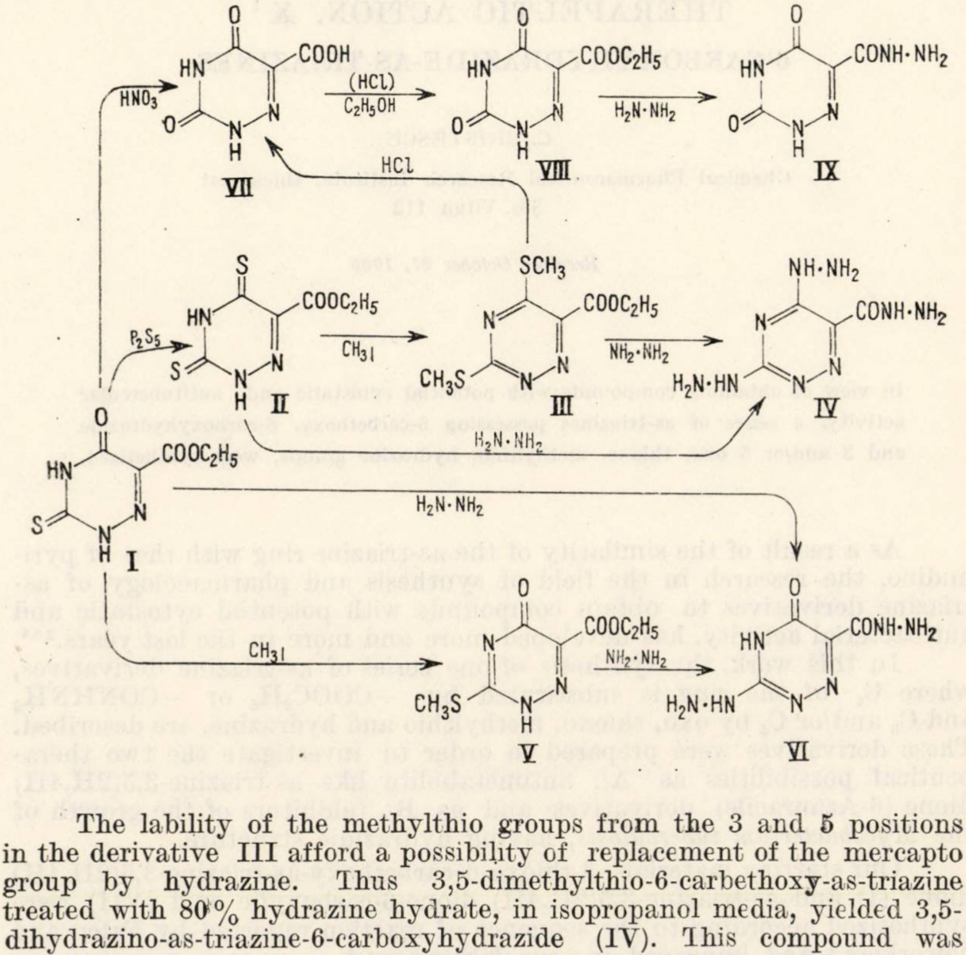

The lability of the methylthio groups from the 3 and 5 positions in the derivative III afford a possibility of replacement of the mercapto group by hydrazine. Thus 3,5-dimethylthio-6-carbethoxy-as-triazine treated with 80% hydrazine hydrate, in isopropanol media, yielded 3,5-dihydrazino-as-triazine-6-carboxyhydrazide (IV). This compound was also obtained, in a low yield, from II with 100% hydrazine hydrate in anhydrous medium.

Methylation of I with methyliodide in hydroalcoholic solution of sodium hydroxide gave 3-methylthio-6-carbethoxy-as-triazine-5(2H) one (V), which, upon treatment with hydrazine hydrate in refluxing isopropanol, underwent a rapid displacement of methylthio- and carbethoxy groups to yield 5-hydrazino-as-triazine-5(4H)one-6-carboxyhydrazide (VI). The latter was also prepared, in a low yield, by an alternative sequence. Thus starting material I and 100% hydrazine hydrate in refluxing isopropanol yields 5-hydrazino-as-triazine-5(4H)one-6-carboxyhydrazide identical in all respects with VI prepared through the methylthio derivative.

Esterification of carboxylic acid VII yielded 6-carbethoxy-as-triazine-3,5(2H,4H) dione (VIII), which, upon treatment with hydrazine hydrate in refluxing ethanol, gave as-triazine-3,5(2H,4H)dione-6-carboxyhydrazide (IX).

Antitumorous evaluation

The results obtained from the testing of compounds prepared in this investigation are shown in table 1. Testing was performed under the auspices of the Cancer Chemotherapy National Service Center (C.C.N.S.C.), Bethesda, Md. From the testing data available at the present time it is evident that the compounds II–V possess a very small potential as inhibitory agents of L 1210 Lymphoid leukemia.

Antitubercular activity

In vitro antitubercular activity was determined against *Micobacterium tuberculosis* var. *hominus* strain $H_{37}Rv$ by the serial dilution technique. The results are shown in table 2.

Table 1

Screening data[a,b]

Compound	Test system[c]	Dose mg/kg	Survivors	Animal wt. dif. in g $(T - C)^d$	Tumor wt. in g. or Survival[e] days T/C	T/C[f] %
II	LE	400	5/5	−0.7	9.8/9.1	107
		200	6/6	−1.7	9.2/9.1	101
		100	6/6	−1.3	9.3/9.1	102
III	LE	400	0/6	1.3	0.0/9.3	
		300	2/6	−2.5	11.0/9.7	
		150	6/6	0.6	10.5/9.7	108
		75	6/6	0.6	9.7/9.7	100
V	LE	400	6/6	−0.3	9.5/9.3	102
IV	LE	400	6/6	0.4	9.0/9.3	97

a. Only a part of the data are presented

b. Assay were performed according to specifications established by CCNSC as reported in *Cancer Chemotherapy Rept*,. **25**. 1 (1962).

c. LE – L 1210 Lymphoid leukemia.

d. Average weight change of test group (T) minus average weight change of control (C) animals.

e. Survival days for LE test systems.

f. The requirements for passing different stages of the sequential screen where the value of T/C in a single test at a nontoxic dose must be as follows : Stage 1 T/C ⩾ 125 % and Stage 2T/C ⩾ 156 % (in L 1210 Lymphoid leukemia).

Table 2

Antitubercular activity

Compound	Required for inhibition of growth γ/ml
H.I.N[a]	0.03
IX	> 10
VI	> 10
IV	2

a – Isonicotinic acid hydrazide

EXPERIMENTAL

Melting points were determined on heating stage microscope. Analytical samples were dried at 20°/5 Torr for 8 hours over P_2O_5.

3,5-Dithioxo-6-carbethoxy-as-triazine-3,5 (2H, 4H) dithione (II)

3-Thioxo-6-carbethoxy-as-triazine-3,5 (2H, 4H) dione (9,55 g; 0.05 M) and phosphorus pentasulphide (5.5 g; 0.025 M) were boiled in 150 ml pyridine, with a content of 0.2 % water for 3 hours. The clear brown-red solution was decanted after cooling at room temperature and concentrated at 50°, under reduced pressure. The dry residue was dissolved in boiling water (400 ml), filtered and adjusted to pH 4, with 10 % hydrochloric acid. After cooling at 4° over night, the product was recrystallized from ethanol-water (1 : 2) to yield 9.2 g (85 %) 3,5-dithioxo-6-carbethoxy-as-triazine-3,5 (2H,4H) dithione, brown-red needles, m. p: 172–174°. The analytical sample melted at 178–180° from ethanol water (1 : 2).

$C_6H_7N_3O_2S_2$ *Calcd.*: C, 33.16; H, 3.24; N, 19.34; S, 29.51 %;
(217.26) *Found*: C, 33.30; H, 3.20; N, 19.50; S, 29.70 %.

3,5-Dimethylthio-6-carbethoxy-as-triazine (III)

3,5-Dithioxo-6-carbethoxy-as-triazine-3,5 (2H, 4H) dithione (10.84 g; 0.05 M) was dissolved at 35° in 150 ml ethanol and 100 ml N/1 sodium hydroxide. A solution of methyliodide (14.3 g; 0.1 M) in 10 ml ethanol was added. The mixture was stirred at room temperature for 1 hour, cooled at 4° and filtered. The product was recrystallized from ethanol-water (1 :1) to yield 11.6 g (95 %) 3,5-dimethylthio-6-carbethoxy-as-triazine with m.p.: 75–77°. The analytical sample melted at 78–80° from isopropanol.

$C_8H_{11}N_3O_2S_2$ *Calcd.*: C, 39.16; H, 4.52; N, 17.13; S, 26.13 %;
(245.32) *Found*: C, 39.30; H, 4.60; N, 17.30; S, 26.30 %.

Hydrolysis: 0.5 g of III was boiled with 5 ml ethanol-water (1 : 2) and 0.5 ml of hydrochloric acid conc,. for 1 hour; as-triazine-3,5 (2H, 4H) dione-6 carboxylic acid precipitated after cooling. Yield, 0.25 g (80 %) with m.p : 238–239° (dec.) (from water), without depression when mixed with an authentic sample.

3,5-Dihydrazino-as-triazine-6-carboxyhydrazide (IV)

A. — 3,5-Dimethylthio-6-carbethoxy-as-triazine (7,35; 0.03 M) was dissolved in 150 ml isopropanol and 80 % hydrazine hydrate (8 g of 100 %; 0.16 M) was added at 50°. The mixture was heated under reflux for 6 hours with stirring. After cooling, the solid was filtered and recrystallized from water, yielding 4.8 g (80 %) 3,5-dihydrazino- as-triazine-6-carboxyhydrazide with m.p. > 300°. A sample for analysis was obtained by two recrystallizations from water.

$C_4H_9N_9O$ *Calcd.*: C, 24.11; H, 4.55; N. 63.29 %;
(199.18) *Found*: C, 14.30; H, 4.70; N, 63.40 %.

B. — 3.5-Dithioxo-6-carbethoxy-as-triazine-3,5 (2H, 4H) dithione (2.17 g; 0.01 M) was dissolved in 50 ml absolute ethanol and a total of 100 % hydrazine hydrate (25 g; 0,5 M) was added. The mixture was heated under reflux for 10 hours with stirring. The hydrazine hydrate was added portionwise in the following manner: 5 ml were added at the beginning and then other 2 ml at approximately every hour. After cooling, the precipitate is filtered off, washed twice with ethanol and recrystallized from water. Yield, 0.79 g (40 %) 3,5-dihydrazino-as-triazine-6-carboxyhydrazide with m. p > 300°. The infrared spectrum of this material was essentially identical with that of the product of method A and distinctly different from that of the starting material.

Found: C, 24.20; H, 4.60; B, 63.50%

3-Methylthio-6-carbethoxy-as-triazine-5 (2H) one (V)

Starting material I (10.5 g; 0.05 M) was dissolved in 100 ml of N/1 sodium hydroxide. The ice-cooled solution was treated by rapid addition of methyliodide (7.10 g; 0.055 M) with vigorous stirring. The mixture was stirred for 1 hour at 10° and 1 hour at room temperature, adjusted to pH 2 with 10% hydrochloric acid and maintained at 4° over night. After recrystallization from water yield 10 g (93%) 3-methylthio-6-carbethoxy-as-triazine-5 (2H) one with m. p: 136—138°. The analytical sample melted at 139—140° from water.

$C_7H_9N_3O_3S$ *Calcd.*: C, 39.07; H, 4.22; N, 19.52; S, 14.90 %;

(215.22) *Found*: C, 39.20; H, 4.10; N, 19.70; S, 14.60%.

3-Hydrazino-as-triazine-5 (4H) one-6-carboxyhydrazide (VI)

A. — 3-Methylthio-6-carbethoxy-as-triazine-5 (2H) one (4.2 g; 0.02 M) was dissolved in ethanol (200 ml) and 100% hydrazine hydrate (5g; 0.1 M) was added at 50°. The mixture was heated under reflux for 3 hours with stirring. After cooling, the precipitate was filtered and recrystallized from water. Yield, 3 g (80%) 3-hydrazino-as-triazine-5 (4H) one-6-carboxyhydrazide with m. p > 300°. A sample for analysis was obtained by two recrystallizations from water.

$C_4H_7N_7O_2$ *Calcd.*: C, 25.81; H, 3.79; N, 52.94%;

(185.14) *Found*: C, 25.90; H, 4.00; N, 53.00%.

B. — Starting material I (2.01 g; 0.01 M) was dissolved in 100 ml isopropanol and a total of 100% hydrazine hydrate (12.5g; 0.25 M) was added. The mixture was heated under reflux for 10 hours with stirring. The hydrazine hydrate was added portionwise in the followed manner: 2.5 ml were added at the beginning and afterwards 1 ml was added approximately every hour. After cooling, the product is filtered off, washed twice with isopropanol and recrystallized from water. Yield, 0.85 g (45%) 3-hydrazino-as-triazine-5 (4H) one-6-carboxyhydrazide with m.p. > > 300°. The infrared spectrum of this material was essentialy identical with that of the product from method A and distinctly different from that of the starting material.

Found: C, 25.80; H, 3.90; N, 52.80%

6-Carbethoxy-as-triazine-3,5 (2H, 4H) dione (VIII)

A suspension of as-triazine-3,5 (2H, 4H) dione- 6-carboxylic acid (15.7 g; 0.1 M) in absolute ethanol (225 ml) was treated with dry hydrochloric acid. The acid was bubbled about 75 minutes at 15° and the mixture was heated under reflux for 1 hour. Concentration to 30 ml and chilling at —5° gave a solid which was collected by filtration and recrystallized from water. Yield, 12 g (65%) 6-carbethoxy-as-triazine-3,5 (2H, 4H) dione with m.p: 180—181°. The analytical sample melted at 181—183° (from water):

$C_6H_7N_3O_4$ *Calcd.*: C, 38.92; H, 3.81; N, 22.69%;

(185.13) *Found*: C, 39.10; H, 3.80; N, 22.80%

As-triazine-3,5 (2H, 4H) dione-5-carboxyhydrazide (IX)

A mixture of 6-carbethoxy-as-triazine-3,5 (2H, 4H) dione (3.60 g 0.02 M) in ethanol. (100 ml) and 100% hydrazine hydrate (3 g; 0.06 M) was heated at reflux for 30 minutes. The solid, precipitating on cooling, was filtered off. The crude product was dissolved in boiling water (55 ml) and acidified with acetic acid to pH 4. After cooling, the precipitate was filtered and recrystallized from water. Yield, 3.1 g (90%) as-triazine-3,5 (2H, 4H) dione-6-carboxyhydrazide with m.p : 302—304° (dec.).

$C_4H_5N_5O_3$ *Calcd.* : C, 28.07 ; H, 2.94 ; N, 40.95 %;
(171.12) *Found* : C, 28.20 ; H. 3.00 ; N, 41.10 %.

The authors are indebdted to Dr. Harry B. Wood Jr. of the Cancer Chemotherapy National Service Center, National Institute of Health, Bethesda, Md., for the antitumor screening data. Analyses were performed in the Analytical Department of our Institute by Mrs. Cornelia Ioan.

Revue Roumaine de Chimie, **15**, 1415–1426 (1970)

COMPLEXES MOLÉCULAIRES DES THIOAMIDES. I

COMPLEXES DE TRANSFERT DE CHARGE ENTRE LE THIOBENZAMIDE, LA THIOBENZPIPÉRIDIDE ET L'IODE

FELICIA CORNEA, CORNELIA FULEA et S. MOLDOVEANU *

Laboratoire de Chimie organique, Faculté de Chimie,
Université de Bucarest, 89, Spl. Independenţei

Reçu le 22 novembre 1969

Cette étude met en évidence la capacité du thiobenzamide et de la thiobenzpipéridide de fonctionner comme donneurs d'électrons dans la formation des complexes moléculaires avec l'iode. Les complexes formés sont étudiés par spectroscopie en UV, en visible et en IR. On détermine les paramètres thermodynamiques caractéristiques des complexes obtenus. La chaleur de la formation du complexe du thiobenzamide avec l'iode a la plus grande valeur, en comparaison d'autres complexes connus de ce type. La distribution électronique qui existe dans la molécule du thiobenzamide et la structure spatiale de la molécule peuvent expliquer cette constatation.

La propriété de fonctionner comme donneurs d'électrons dans l'interaction avec l'iode, présentée par quelques substances organiques qui contiennent dans la molécule un atome de soufre, a été mise en évidence jusqu'à présent pour un nombre relativement réduit de composés.

Bien que les recherches effectuées dans ce domaine soient restreintes, cependant elles ont montré, en général, que les composés soufrés sont des donneurs beaucoup plus forts que leurs analogues avec oxygène.

Ce comportement s'explique par la valeur plus petite du potentiel d'ionisation du soufre comparativement au potentiel de l'oxygène.

On pourrait encore expliquer ce comportement par la polarisabilité plus grande des électrons qui se trouvent sur la dernière couche d'atome de soufre en comparaison des électrons d'oxygène.

On a étudié les complexes formés par l'interaction de l'iode et des différents composés organosulfurés [1-4] et en ce qui concerne les thioamides on a étudié les complexes des thioacétamide et thiourée,[5-8] N-méthylthioacétamide[1], NN-diméthylthioacétamide, N-tétraméthylthiourée[9] et thio-carbanilide.[8]

---

* Laboratoire de Chimie analytique, Faculté de Chimie, 89, Spl. Independenţei.

[1] K. R. Bhaskar, S. N. Bhat, A.S.N. Murthy et C.N.R., Rao, *Trans. Faraday Soc.*, **62**, 788 (1966).

[2] H. Tsubomura et R.P. Lang, *J. Amer Chem. Soc.*, **83**, 2085 (1961).

[3] R. L. Middaugh, R. S. Drago et R. J. Niedzielski, *J. Amer. Chem. Soc.*, **86**, 388 (1964).

[4] A. F. Grand, *Diss. Abstr.*., **29**, 961 (B 1968). In : *Chem. Abstr.*, **70**, 7054 z (1969).

L'existence dans le groupement fonctionnel thioamidique de deux atomes qui possèdent des électrons p (l'azote et le soufre) et qui peuvent fonctionner comme donneurs dans l'interaction avec les accepteurs conduit à la nécessité d'établir l'atome donneur.

Les études par spectroscopie en IR de quelques complexes moléculaires de ce type on montré que l'atome donneur c'est l'oxygène et respectivement le soufre et non l'atome d'azote.[10,11,1,5,8]

La conjugaison qui s'établit entre les électrons p de l'atome d'azote et les électrons π de la double liaison $> C = S$ a comme effet la diminution de la basicité de l'atome d'azote du groupement thioamidique et en même temps l'augmentation de la basicité de l'atome de soufre qui devient donneur.

Si à l'atome d'azote thioamidique sont liés des substituants qui exercent un effet + I, la conjugaison $p\pi$ est augmentée et la substance devient un donneur plus fort, fait confirmé expérimentalement.[8]

Les complexes moléculaires que nous avons obtenus par l'interaction du thiobenzamide (TB) et de la thiobenzpipéridide (TBP) avec l'iode ont été étudiés par des méthodes spectrales.

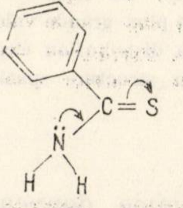

TB

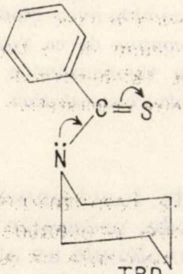

TBP

ÉTUDE SPECTROPHOTOMÉTRIQUE DES COMPLEXES $TB-I_2$ ET $TBP-I_2$ EN VISIBLE ET EN UV

Le complexe $TB-I_2$

La comparaison du spectre d'absorption en visible de quelques solutions de TB et de l'iode en tétrachlorure de carbone avec le spectre d'un mélange des deux solutions mentionnées a mis en évidence des différences dans l'allure des courbes.

[5] R. P. Lang, *J. Amer. Chem. Soc.*, **84**, 1185 (1962).

[6] M. M. Gerbier et J. Gerbier, *Compt. Rend.*, **263 A**, 1057 (1966).

[7] P. Klaboe, *J. Amer. Chem. Soc.*, **89**, 3667 (1967).

[8] K. R. Bhaskar, R. K. Gosavi et C. N.R. Rao, *Trans. Faraday Soc.*, **62**, 29 (1966)

[9] R. J. Niedzielski, R. S. Drago et R. L. Middaugh, *J. Amer. Chem. Soc.*, **86**, 1694 (1964).

[10] M. Zackrisson et J. J. Lindqvist, *J. Inorg. Nuclear Chem.*, **17**, 69 (1961).

[11] W. Gerrard, M. F. Lappert, H. Pyszora et J. W. Wallis, *J. Chem, Soc.*, **1963**, 2144.

Si l'on mélange une solution de TB et une solution d'iode en tétrachlorure de carbone, on observe l'apparition d'une autre coloration.

Dans la figure 1, on observe facilement que la courbe d'absorption de la solution de TB (courbe *2*) en tétrachlorure de carbone présente un maximum à 412 mμ et un minimum à 380 mμ. Dans le domaine du minimum, la solution d'iode (courbe *1*) n'absorbe pas, tandis que le mélange (courbe *3*) présente une plus forte absorption.

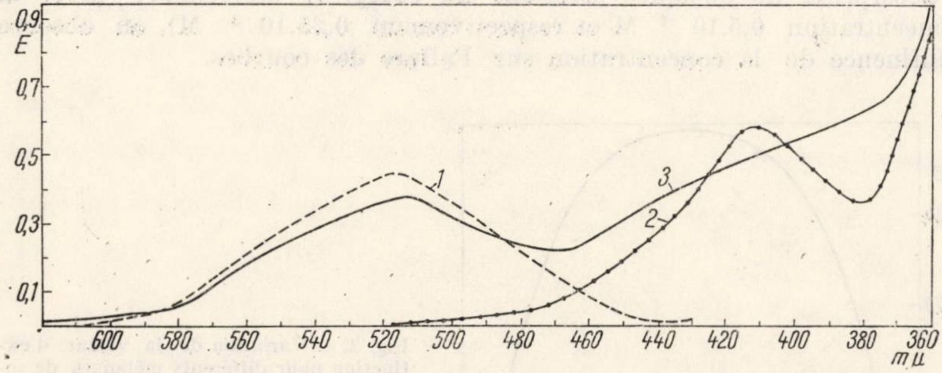

Fig. 1. — Absorption en visible et en UV de quelques solutions d'iode (1), TB (2) et TB — I_2 en CCl_4 (3).

L'allure des courbes *1*, *2* et *3* permet de conclure que, dans les conditions mentionnées, en solution se forme un complexe moléculaire. Nous avons obtenu ce complexe à l'état cristallin.

En déterminant d'une part le spectre en visible et en UV d'une solution du complexe moléculaire solide en CCl_4 (de conc. $0{,}5.10^{-4}$ M) et d'autre part le spectre d'une solution de complexe moléculaire (de conc. $0{,}5.10^{-4}$M), obtenue par le mélange des solutions de TB et d'iode dans le CCl_4, on a trouvé des spectres identiques.

Nous avons déterminé ensuite dans quel rapport le thiobenzamide se combine avec l'iode, en apppliquant la méthode des séries isomolaires de Job, par la détermination des extinctions des différentes solutions à $\lambda = 380$ mμ, longueur d'onde où la solution de thiobenzamide présente un minimum, la solution d'iode n'absorbe pas, tandis que la solution du complexe présente une absorption appréciable.

Dans la figure 2 on observe que le rapport donneur-accepteur est 1 : 1 (pour lequel l'extinction est maximum) étant donc le même que dans le cas d'autres complexes moléculaires des thioamides avec l'iode.

Dans la figure 3 on observe les maximums d'absorptions et les valeurs des extinctions en différents domaines soit pour les solutions de différentes concentrations des composés initiaux (donneurs) soit pour le complexe moléculaire.

Les courbes qui correspondent à des solutions de concentrations assez grandes (courbes *3* et *5*) ne sont pas représentées complètement, le maximum étant situé à l'extinction plus grande où l'erreur de détermination est appréciable.

Nous avons présenté ces courbes en vue de certaines comparaisons pour le domaine respectif.

Si l'on compare les courbes *2* et *3* (fig. 3) qui représentent le spectre d'une solution de TB en tétrachlorure de carbone de concentration $0{,}5.10^{-4}$ M et $0{,}25.10^{-3}$M et les courbes *4* et *5* qui représentent le spectre d'absorption de quelques solutions du complexe moléculaire (avec la concentration $0{,}5.10^{-4}$ M et respectivement $0{,}25.10^{-3}$ M), on observe l'influence de la concentration sur l'allure des courbes.

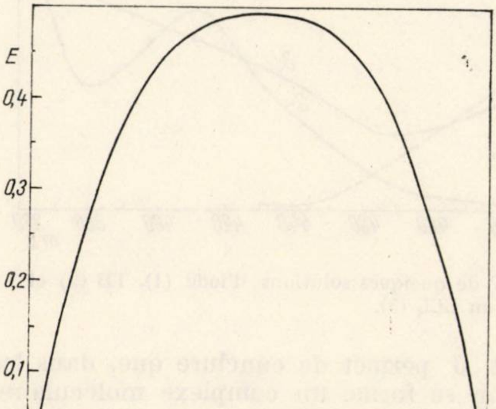

Fig. 2. — Variation de la valeur d'extinction pour différents mélanges de solutions isomolaires de TB et I_2 en CCl_4.

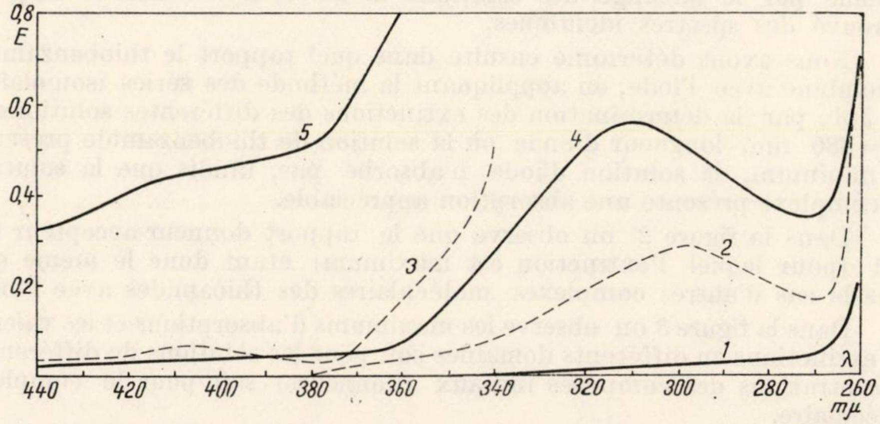

Fig. 3. — Absorption en visible et en UV de quelques solutions d'iode, TB et TB$-I_2$ en CCl_4, de différentes concentrations.

1, I_2 conc. $0{,}5.10^{-3}$ M ; *2*, TB conc. $0{,}5.10^{-1}$ M ; *3*, TB conc. $0{,}25.10^{-3}$M ; *4*, TB $-$ I_2 conc. $0{,}5\cdot10^{-4}$ M; *5*, TB $-$ I_2 conc. $0{,}25.10^{-3}$ M.

Les courbes *2* et *4* indiquent que le thiobenzamide présente dans le domaine ultraviolet un maximum à 298 mμ, tandis que le complexe présente un maximum à 312 mμ.

Les coefficients molaires d'extinction pour le TB et pour le complexe sont

$$\underset{\text{TB}}{\varepsilon_{\max} = 0{,}56.10^4} \qquad \underset{\text{TB}-\text{I}_2}{\varepsilon_{\max} = 1{,}01.10^4}$$

La bande située à 312 mμ peut être associée avec la bande de transfert de charge entre TB et I_2.

Les bandes d'absorption au-delà de 266 mμ sont dues à l'absorption du solvant et à la présence du noyau benzénique substitué.

Nous avons déterminé ensuite la constante de stabilité du complexe TB-I_2 par la méthode de Sakellaridis [12] qui utilise des solutions isomolaires et qui s'applique quand le rapport de combinaison, donneur-accepteur, est 1 : 1. Les déterminations ont été effectuées à 25,5°, 34,5° et 40,5°.

Dans le tableau 1 sont données les valeurs moyennes des extinctions, déterminées à la longueur d'onde de 380 mμ, pour des mélanges de solutions isomolaires de TB et d'iode en tétrachlorure de carbone, de concentration $0{,}5.10^{-3}$ M, prises en différentes proportions.

Dans le tableau 2 sont donnés les mêmes types de valeurs mais pour les solutions de concentrations $0{,}3.10^{-3}$ M.

Tableau 1

Valeurs des extinctions de quelques mélanges de solutions de TB et I_2 en CCl_4 de concentration $0{,}5.10^{-3}$ M

	Rapport TB : I_2	$E_{25.5}$°C	$E_{34.5}$°C	$E_{40.5}$°C
1	1 : 1	0,495	0.380	0.310
2	1 : 2	0,420	0,345	0,280
3	2 : 1	0,420	0,345	0,280
4	3 : 2	0,460	0,365	0,300
5	2 : 3	0,460	0,365	0,300
6	1 : 3	0,340	0,290	0,235
7	3 : 1	0,345	0,295	0,240
8	1 : 4	0,280	0,235	1,190
9	1 : 7	0,170	0,145	0,115

Les valeurs moyennes de la constante d'instabilité et de stabilité obtenues par la méthode graphique [12] sont indiquées dans le tableau 3.

On observe une décroissance de la stabilité du complexe par l'augmentation de la température.

---

[12] P. Sakellaridis, *Bull. Soc. chim. France*, **1958**, 282.

Tableau 2

Valeurs des extinctions de quelques mélanges de solutions de TB et I_2 en CCl_4 de concentration 0 3.10⁻³M

	Rapport TB : I_2	$E_{25,5}$ °C	$E_{34,5}$ °C	$E_{40,5}$ °C
1	1 : 1	0,225	0,170	0,130
2	1 : 2	0,200	0,145	0,110
3	2 : 1	0,200	0,145	0,110
4	3 : 2	0,215	0,160	0,120
5	2 : 3	0,215	0,160	0,120
6	1 : 3	0,165	0,110	0,090
7	3 : 1	0.170	0,115	0,090
8	1 : 4	0,135	0,086	0,070
9	1 : 7	0,082	0,055	0,042

Tableau 3

Valeurs moyennes des constantes d'instabilité et stabilité du complexe TB – I_2

t°C	25,5	34,5	40,5
$\overline{K}_{\text{instable}}$	$1.02.10^{-4}$	$4{,}47.10^{-4}$	$7{,}63.10^{-4}$
$\overline{K}_{\text{stable}}$	$0{,}98.10^{4}$	$0{,}22.10^{4}$	$0{,}13.10^{4}$

Le complexe TBP – I_2

L'étude du complexe TBP – I_2 a été faite de la même manière que l'étude du complexe TB – I_2.

La courbe *3* (fig. 4) qui correspond à la solution de TBP en tétrachlorure de carbone possède un minimum situé à 360 mμ, tandis que le complexe TBP-I_2 absorbe assez fort dans ce domaine (fig. 4, c. *5*).

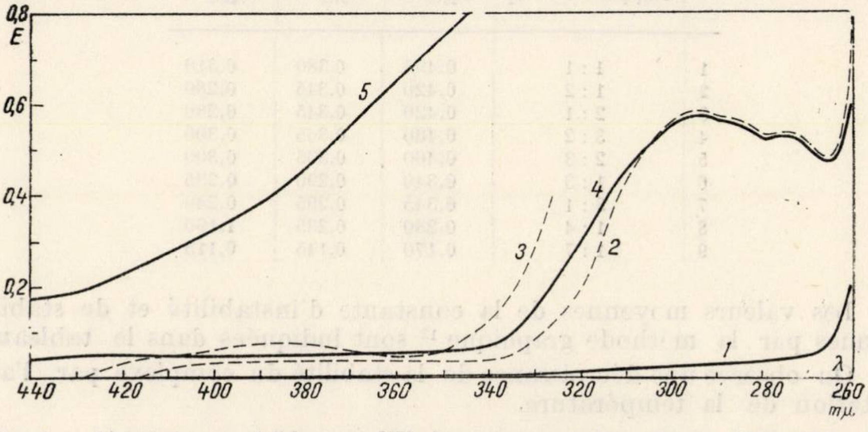

Fig. 4. — Absorption en visible et en UV de quelques solutions d'iode, TBP, TBP – I_2 en CCl_4, de différentes concentrations.

1, I_2 conc. $0{,}5.10^{-3}$ M; *2*, TBP conc. $0{,}5.10^{-4}$ M ; *3*, TBP conc. $0{,}25.10^{-3}$ M; *4*, TBP – I_2 conc. $0{,}5.10^{-4}$ M; *5*, TBP – I_2 conc. $0{,}25.10^{-3}$ M.

Les déterminations ultérieures ont été faites à $\lambda = 360$ mμ. Le rapport de combinaison du TBP avec l'iode est aussi 1 : 1.

Dans le domaine en UV les spectres de la solution de TBP en tétrachlorure de carbon et du complexe $TBP-I_2$ sont très semblables. La TBP présente un maximum d'absorption situé à 292 mμ, tandis que le complexe $TBP-I_2$ présente le maximum à 294 mμ.

Le déplacement de la bande n'est que de 2 mμ, tandis que dans le premier cas il était de 14 mμ.

Les coefficients molaires d'extinction pour TBP et $TBP-I_2$ sont approximativement les mêmes et ont la valeur de $1{,}20 \cdot 10^4$.

La constante de stabilité du complexe $TBP-I_2$ a été déterminée par la méthode mentionnée au cas du complexe $TB-I_2$, les résultats obtenus étant indiqués dans les tableaux 4–6.

Tableau 4

Valeurs des extinctions de quelques mélanges de solutions de TBP et I_2 en CCl_4 de concentration 0.5.10^{-3} M

	Rapport $TBP-I_2$	E_{26}°C	$E_{34,5}$°C	E_{40}°C
1	1 : 1	0,755	0,565	0,500
2	1 : 2	0,650	0,520	0,410
3	2 : 1	0,650	0,520	0,410
4	3 : 2	0,715	0,550	0,460
5	2 : 3	0,715	0,550	0,460
6	1 : 3	0,565	0,425	0,340
7	3 : 1	0,570	0,430	0,340
8	1 : 4	0,485	0.360	0,280
9	1 : 7	0,305	0,220	0,180

Tableau 5

Valeurs des extinctions de quelques mélanges de solutions de TBP et I_2 en CCl_4 de concentration 0,3.10^{-3} M

	Rapport $TBP-I_2$	E_{26}°C	$E_{34,5}$°C	E_{40}°C
1	1 : 1	0,335	0,245	0,190
2	1 : 2	0,290	0,210	0,170
3	2 : 1	0,290	0,210	0,170
4	3 : 2	0,320	0,235	0,185
5	2 : 3	0,320	0,235	0,185
6	1 : 3	0,240	0,170	0,130
7	3 : 1	0,245	0,175	0,135
8	1 : 4	0,200	0,135	0,100
9	1 : 7	0,120	0,080	0,060

Tableau 6

Valeurs moyennes des constantes d'instabilité et stabilité du complexe TBP $-I_2$

t°C	26	34,5	40
$\overline{K}_{\text{instable}}$	$4{,}11.10^{-4}$	$7{,}16.10^{-4}$	$10{,}60.10^{-4}$
$\overline{K}_{\text{stable}}$	$0{,}243{,}10^{4}$	$0{,}139.10^{4}$	$0{,}094.10^{4}$

Pour le complexe TBP$-I_2$, ainsi que pour le complexe TB$-I_2$ la valeur de la constante d'instabilité augmente avec la température. La comparaison des valeurs des constantes de stabilité et d'instabilité obtenues pour ces deux complexes met en évidence une différence marquante entre celles-ci, qui s'explique par la structure des thiobenzamide et thiobenzpipéridide, structure qui a une influence importante sur le pouvoir donneur du soufre.

Les paramètres thermodynamiques

Les valeurs des constantes de stabilité des complexes mentionnées étant déterminées, nous avons calculé l'énergie libre de formation des complexes, par la relation $\Delta F = - RT \ln \mathrm{K}$.

Les valeurs de ΔF obtenues pour trois températures différentes nous ont permis d'écrire l'équation de la droite $\Delta F = \Delta H - T\,\Delta S$, où ΔH représente l'ordonnée à l'origine et ΔS la pente de la droite.

La valeur du ΔH peut être encore obtenue en utilisant la relation

$$2{,}303 \log \frac{K_2}{K_1} = \frac{-\Delta H}{R} \left(\frac{1}{T_2} - \frac{1}{T_1} \right)$$

Nous avons ensuite calculé l'enthalpie et l'entropie des complexes TB$-I_2$ et TBP$-I_2$, les valeurs obtenues étant indiquées dans les tableaux 7 et 8.

Tableau 7

Paramètres thermodynamiques du complexe TB $-$ I_2

t°C	$-\Delta F$ cal/mole	$-\Delta H$ cal/mole	$-\Delta S$ cal/degré-mole
25,5	5440	25.738	68
34,5	4750		
40,5	4420		

Tableau 8

Paramètres thermodynamiques du complexe TBP $-I_2$

t°C	$-\Delta F$cal/mole	$-\Delta H$ cal/mole	$-\Delta S$ cal/degré-mole
26	4637	11 500	23,3
34,5	4419		
40	4255		

Les études effectuées par Mullinken et coll. [13,14] ont montré que la stabilité thermodynamique des complexes n donneur — σ accepteur est plus grande que la stabilité thermodynamique des complexes de types différents, dans lesquels existent d'autres interactions donneurs-accepteurs.

Les valeurs les plus grandes connues jusqu'à présent sont celles obtenues pour les complexes d'amines [13,14] et de thiocarbanilide [8] avec l'iode, pour ce dernier la valeur étant de — 18,6 kcal/mole.

Les valeurs des paramètres thermodynamiques obtenues pour le complexe $TB-I_2$ dépassent les valeurs les plus grandes connues, d'où on peut tirer la conclusion que le thiobenzamide est un donneur beaucoup plus fort que les donneurs étudiés jusqu'à présent.

En ce qui concerne la stabilité des complexes de thioamides avec l'iode les données obtenues indiquent l'ordre suivant :

$$TB - I_2 > \text{thiocarbanilide} - I_2 > TBP - I_2$$

En considérant les complexes $TB-I_2$ et $TBP-I_2$ du point de vue de leur stabilité thermodynamique, on peut conclure que l'atome de soufre est un donneur plus fort dans la molécule du thiobenzamide, que dans la molécule de la thiobenzpipéridide.

Cette différence est due à la distribution électronique existante dans les molécules de ces deux thioamides, comme une conséquence de l'influence du radical lié au groupement fonctionnel thioamidique ainsi que de l'influence de la nature des atomes ou des radicaux liés à l'atome d'azote.

Dans le cas du thiobenzamide, le radical phényl peut être orienté dans le même plan que le groupement thioamidique. Les électrons p de l'atome d'azote et les électrons π du radical phényl peuvent participer à la conjugaison avec les électrons π de la double liaison $C = S$, augmentant de cette façon le caractère basique de l'atome de soufre.

Dans la molécule de la TBP l'effet de la conjugaison est plus faible, comme une conséquence de l'influence stérique du cycle pipéridinique. Le déplacement du maximum d'absorption dans le cas de la TBP vers les longueurs d'onde plus petites, à 292 mμ, comparativement à celui de la TB situé à 298 mμ (fig. 4 et 3) met en évidence une diminution de la conjugaison dans la molécule de TBP, tel qu'il a été d'ailleurs constaté pour le N,N-diméthylthiobenzamide.[15]

Le cycle pipéridinique par sa structure spatiale et le mode d'orientation dans la molécule peut encore rendre difficile l'interaction de la molécule de la TBP et de l'iode, donc la formation du complexe $TBP-I_2$.

---

[13] R. S. Mulliken et W. B Person, *Ann. Rev. Phys. Chem.*, **13**, 107 (1962).

[14] R. S. Mulliken, *J. Chem. Phys.*, 1963, 20.

[15] J. Sandstrom, *Acta Chem. Scand.*, **16**, 1616 (1962).

Les spectres en IR

Les thioamides absorbent en IR et leurs spectres présentent des bandes complexes auxquelles contribuent les vibrations des atomes du groupement fonctionnel thioamidique.[16]

La formation des complexes détermine des changements dans les spectres en IR qui se traduisent par la modification de l'intensité et de la position des bandes caractéristiques.

Les spectres en IR des complexes avec transfert de charge étudiés par nous diffèrent des spectres des donneurs, surtout par la diminution de l'intensité des bandes.

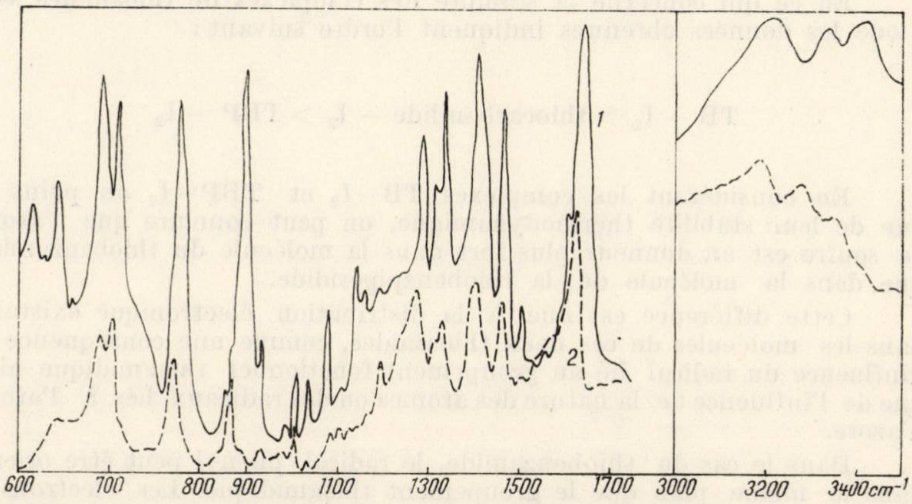

Fig. 5. — Spectres en IR du TB (1) et du complexe TB$-I_2$ (2) en pastilles de KBr.

Le spectre du complexe solide TB$-I_2$ (déterminé rapidement après la préparation) présente les trois bandes caractéristiques de vibration de valence du groupement $-NH_2$, déplacées vers les fréquences plus petites. Cela constitue une preuve que le donneur n'est pas l'atome d'azote et que le déplacement vers les fréquences plus petites est une conséquence du fait que la liaison N$-$H dans le complexe, est un peu plus longue que dans le thioamide à cause de la conjugaison $p-\pi$ qui existe dans la molécule. L'apparition d'une bande faible, située à 1565 cm^{-1} peut être attribuée à la vibration de la liaison C$-$N qui possède dans le complexe un caractère de double liaison beaucoup plus accentuée que dans la molécule du thioamide.

Les autres bandes caractéristiques sont aussi un peu déplacées vers les valeurs plus petites de la fréquence.

---

[16] K. A. Jensen et P. H. Nielsen, *Acta Chem. Scand.*, **20**, 597 (1966).

Le spectre en IR du complexe TBP$-I_2$ diffère de celui de la TBP par la diminution de l'intensité des bandes caractéristiques, la position étant, proprement dit, presque la même.

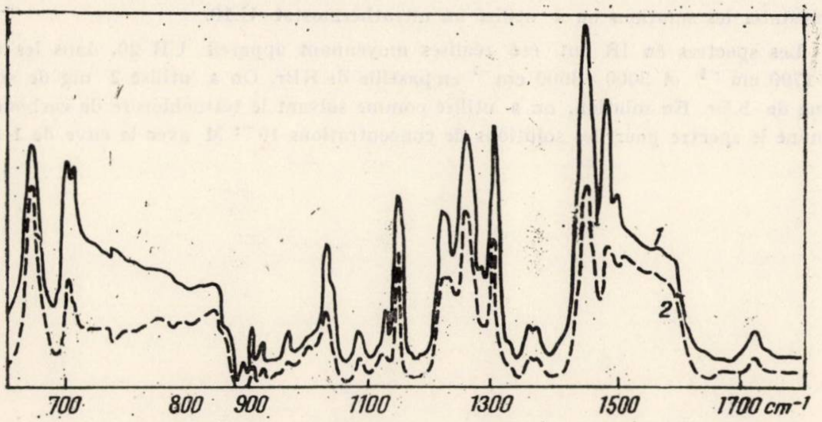

Fig. 6. — Spectres en IR du TBP (1) et du complexe TBP$-I_2$ (2) en CCl_4.

Pour le complexe TBP$-I_2$ le spectre en IR est moins concluant, mais pour le complexe TB$-I_2$ on peut conclure avec certitude que la coordination a lieu par l'intermédiaire de l'atome de soufre.

PARTIE EXPÉRIMENTALE

Le thiobenzamide a été préparé par la réaction du benzonitrile avec le thioacétamide en présence de chlorhydrate de diméthylformamide.[17]

La thiobenzpipéridide a été obtenue en appliquant la réaction Willgerodt-Kindler.[18] Ces deux thioamides ont été purifiés par recristallisations répétées jusqu'à un point de fusion constant.

$$\text{TB } P_f = 115 - 116°; \quad \text{TBP } P_f = 63 - 64°.$$

L'iode a été purifié par sublimation répétée.

Le tétrachlorure de carbonate utilisé comme solvant a été séché et distillé sur une colonne Vigreux de 60 cm.

Le complexe moléculaire TB$-I_2$ a été obtenu en mélangeant des solutions concentrées de TB en CCl_4 et l'iode en CCl_4, quand il se forme un précipité, microcristallin de couleur vert foncé, $P_f = 88-91°$ avec décomposition.

---

[17] E. Taylor et Z. Zolthewich, *J. Amer. Chem. Soc.*, **82**, 2656 (1960).

[18] A. Carayon-Gentil, M. Minot et P. Chabrier, *Bull. Soc. chim. France*, **1964**, 1420

Le complexe moléculaire TBP$-I_2$ a été obtenu seulement en solution, en mélangeant des volumes égaux de solutions isomolaires de TBP et I_2, en tétrachlorure de carbone.

Les spectres en visible et UV ont été effectués avec un spectrophotomètre Beckmann, type DB. Les extinctions ont été vérifiées sur un spectrophotomètre Karl-Zeiss VSU2. Pour thermostater les solutions on a utilisé un ultrathermostat U.10.

Les spectres en IR ont été réalisés moyennant appareil UR 20, dans les domaines 600$-$1700 cm^{-1} et 3000$-$3600 cm^{-1} en pastille de KBr. On a utilisé 2 mg de substance/ 800 mg de KBr. En solution, on a utilisé comme solvant le tétrachlorure de carbone et on a déterminé le spectre pour des solutions de concentrations 10^{-2} M avec la cuve de 1 mm.

Revue Roumaine de Chimie, **15**, 1427–1431 (1970)

MONO- UND DIQUARTÄRE AMMONIUMSALZE DES BENZAL-FLUORENS

T. RĂDULESCU und H. D. SCHELL

Aus dem Institut für Biochemie der Akademie Bukarest, Str. Docenţilor, 20

Eingegangen am 3. November 1969

Es wird die Herstellung einiger Ammoniumsalze des 2-Amino-benzal-fluorens und des 2,2′-, 2,3′- sowie des 2,4′-Diamino-benzal-fluorens beschrieben. Vorläufige pharmakodynamische Teste zeigten, daß die erhaltenen Stoffe Curarewirkung aufweisen.

Zur Untersuchung einiger Beziehungen, die zwischen chemischer Struktur und biologischer Wirkung bestehen, wurden in Fortsetzung früherer Arbeiten[1,2] neue quartäre Ammoniumsalze vom Benzal-fluoren dargestellt. Bekanntlich sind Verbindungen dieser Art sowohl für die Klinik, als auch für verschiedene Zweige der Industrie und für biologische, physiologische u.a. Forschungslaboratorien von Bedeutung.

In der vorliegenden Arbeit werden mono- (I) und diquartäre (II) Ammoniumsalze des Benzal-fluorens beschrieben, von denen die ersteren die 4′-Stellung entweder nicht oder mit einer Methoxy-Gruppe — welche, wie bekannt, die Curarewirkung in verstärkendem Sinne beeinflußt — substituiert haben und

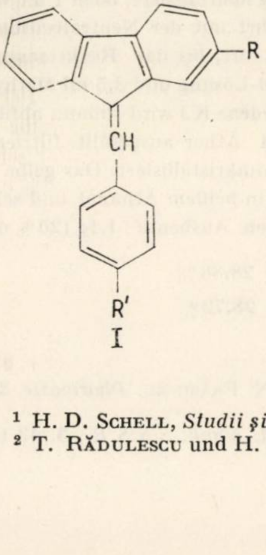

I

$$R = \overset{+}{N}(CH_3)_3\ X^-$$
$$X = I, Cl$$
$$R' = OCH_3, H$$

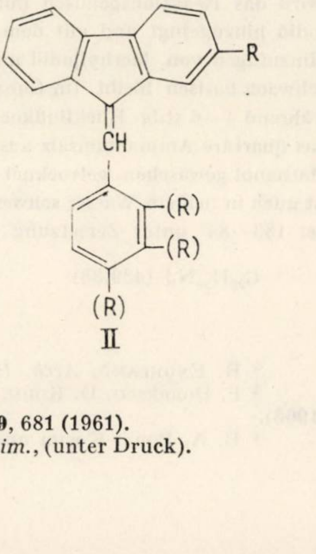

II

---

[1] H. D. Schell, *Studii şi Cerc. Chim., Acad. R.P.R.*, **9**, 681 (1961).

[2] T. Rădulescu und H. D. Schell, *Rev. Roumaine Chim.*, (unter Druck).

die letzteren ein zweites quartäres Stickstoffatom in verschiedengroßen Abständen vom ersteren entfernt enthalten.

Die quartären Ammoniumsalze wurden durch Methylierung der betreffenden Amine mittels Methyljodid nach Engeland[3] in Anwesenheit von Kaliumhydroxid hergestellt und die dazu nötigen Amine nach den in einer früheren Arbeit[2] erwähnten Angaben erhalten.

Da die Jodide in Wasser schwer löslich sind, wurden sie mittels frisch zubereitetem Silberchlorid in die in Wasser leicht löslichen Chloride überführt. Sowohl die Jodide, als auch die Chloride bilden gelbe kristalline Stoffe, deren wäßrige Lösungen oberflächenaktiv sind.

Die vorläufigen, an Fröschen ausgeführten pharmakodynamischen Teste ergaben, daß sämtliche Chloride curarewirksam sind, die monoquartären ungefähr 30 mal, die diquartären ungefähr 16—18 mal schwächer als d-Tubocurarin, also eine größere Aktivität als die entsprechenden, in einer früheren Arbeit[2] beschriebenen Ammoniumsalze aufweisen, deren quartäre Ammoniumgruppe nicht direkt, sondern durch eine Acetamid-Brücke an den Benzal-fluoren-Kern gebunden sind.

In der vorliegenden Arbeit werden 10 quartäre Ammoniumsalze beschrieben. Zwei von ihnen und zwar das 2,4′-Bis-(trimethylammonium) benzal-fluoren-dijodid und -dichlorid wurden auch von Dobrescu und Mitarb.[4], jedoch auf anderem Wege hergestellt.

EXPERIMENTELLES

1. JODIDE

a) *2-Trimethylammonium-benzal-fluoren-jodid*

1,2 g nach Porai und Efros[5] hergestelltes 2-Amino-benzal-fluoren werden zusammen mit 5 ml einer methanolischen 5proz. KOH-Lösung und 1,5 ml Methyljodid in einem mit Rückflußkühler versehenen Kolben auf dem Wasserbad erhitzt. Nach 30 minutenlangem Erhitzen wird das Reaktionsgemisch mit 5 ml der 5proz. KOH-Lösung neutralisiert, noch 1 ml Methyljodid hinzugefügt und mit dem Erhitzen fortgesetzt. Man fährt mit der Neutralisation, dem Hinzufügen von Methyljodid und dem Erhitzen nun so lange fort, bis das Reaktionsgemisch schwach basisch bleibt. Im Ganzen wurden 17 ml 5 proz. KOH-Lösung und 3,5 ml Methyljodid während 4—6 stdg. Rückflußkochen verwendet. Das ausgeschiedene KJ wird sodann abfiltriert, das quartäre Ammoniumsalz aus dem alkoholischen Filtrat mit Äther ausgefällt, filtriert, mit Mathanol gewaschen, getrocknet und aus Methanol mit Äther umkristallisiert. Das gelbe Jodid ist auch in heißem Wasser schwer löslich, etwas leichter löslich in heißem Äthanol und schmilzt bei 183—84° unter Zersetzung nach vorangehendem Erweichen. Ausbeute : 1,1g (20 % d.Th.) .

$C_{23}H_{22}NJ$ (439,33)	*Ber.* :	N 3,19	J 28,88 %
	Gef. :	N 3,30	J 28,72 %

---

[3] R. Engeland, *Arch. Pharm*,. **237**, 353 (1909).

[4] F. Dobrescu, D. Kohn, A. Martin, M. Zalman und N. Frăsinel, *Pharmazie*, **21**, 214 (1966).

[5] B. A. Porai-Kosici und A. M. Efros, *Doklady Akad. Nauk. S.S.S.R.*, **3**, 43 (1938).

b) *2-Trimethylammonium-4'-methoxy-benzal-fluoren-jodid*

Man verfährt wie oben, doch von 1,5 g nach Dobrescu [6] dargestelltem 2-Amino-4'-methoxy-benzal-fluoren ausgehend. Ausbeute : 1,4 g (23% d.Th.). Das aus Äthanol mit Äther in gelben Nadeln auskristallisierende Jodid ist in Wasser schwer löslich, leichter in heißem 96proz. Äthanol und schmiltz bei 155° unter Zersetzung nach vorangehendem Erweichen.

$C_{24}H_{24}ONJ$ (469,35) *Ber.* : N 2,98 J 27,04%
Gef. : N 3,07 J 27,12%

c) *2,2'-Bis-(trimethylammonium)-benzal-fluoren-dijodid*

In einem mit Rückflußkühler versehenen Kolben werden 1,5 g von Rădulescu und Schell[2] dargestelltes 2,2'-Diamino-benzal-fluoren zusammen mit 10 ml methanolischer 5proz. KOH-Lösung und 3 ml Methyljodid auf dem kochenden Wasserbad erhitzt und weiter, wie in Vorschrift 1 a verfahren, wobei im ganzen aber 34 ml KOH-Lösung und 6 ml Methyljodid verbraucht wurden. Der sich nach Beendigung der Reaktion bei Erkalten des Reaktionsgemisches ausscheidende Niederschlag wird zwecks Entfernung der nicht aufgebrauchten KOH-Reste auf einem Büchner-Filter mit Methanol gewaschen und dann getrocknet. Darauf wird das Ammoniumsalz mit heißem Methanol aufgenommen, das unlösliche KJ abfiltriert und durch Behandeln des alkoholischen Filtrates durch Äther das Dijodid ausgefällt. Ausbeute : 1,5 g (46% d.Th.). Das Ammoniumsalz ist in Äthanol und kaltem Wasser schwer löslich, löst sich aber leicht in heißem Wasser und verdünntem Äthanol. Durch Umkristallisieren aus Äthanol werden gelbe, glänzende Nadeln erhalten, die bei 182—183° mit Zersetzung nach vorangehendem Erweichen schmelzen.

$C_{26}H_{30}N_2J_2$ (624,35) *Ber.* : N 4,48 J 40,65%
Gef: N 4,56 J 40,50%

d) *2,3'-Bis-(trimethylammonium)-benzal-fluoren-dijodid*

Es wird wie in Vorschrift 1 c verfahren, indem aber von 1,5 g von Rădulescu und Schell[2] dargestelltem 2,3'-Diamino-benzal-fluoren ausgegangen wird. Ausbeute : 1,3 g (40% d.Th.). Das hellgelbe Dijodid ist in Wasser und absolutem Äthanol schwer löslich, leicht aber in verdünntem Äthanol. Aus Äthanol mit Äther umkristallisiert, werden hellgelbe Nadeln erhalten, die bei 187—88° unter Zersetzung und vorangehendem Erweichen schmelzen.

$C_{26}H_{30}N_2J_2$ (624,35) *Ber.* : N 4,48 J 40,65%
Gef: N 4,59 J 40,51%

e) *2,4'-Bis-(trimethylammonium)-benzal-fluoren-dijodid*

Die Quaternierung des von Rădulescu und Schell[2] dargestellten 2,4'-Diamino-benzalfluorens und die Isolierung des entstandenen Dijodides wird nach den in Vorschrift 1 c erwähnten Anweisungen ausgeführt. Von 1,5 g Diamin ausgehend, wurden 1,5 g (Ausbeute : 46%

---

[6] F. Dobrescu, *Studii şi Cercetări Şti. Chim., Baza Cercetări Şti., Timişoara,* **3**, 45, (1956).

d.Th.) Ammoniumsalz erhalten, das in Äthanol und kaltem Wasser schwer löslich ist, sich aber in heißem Wasser und verdünnten Äthanol leicht löst. Durch Umkristallisieren aus Äther erhält man gelbe Nadeln, die nach vorangehendem Erweichen bei 177° unter Zersetzung schmelzen.

$C_{26}H_{30}N_2J_2$ (624,35)	*Ber.* : N	4,48	J	40,65 %
	Gef. : N	4,55	J	40,55 %

2. CHLORIDE

a) *2-Trimethylammonium-benzal-fluoren-chlorid*

1 g 2-Trimethylammonium-benzal-fluoren-jodid werden in 50 ml 80 proz. Äthanol gelöst und zusammen mit 1,5 g frisch hergestelltem Silberchlorid 5 Std. auf dem kochenden Wasserbad in einem mit Rückflußkühler versehenen Kolben erhitzt. Es wird heiß filtriert, mit etwas heißem Äthanol nachgewaschen und das Filtrat auf dem Wasserbade zur Trockne eingedampft. Der dickflüssige Rückstand wird in Äthanol aufgenommen und mit Äther gefällt. Das Chlorid kristallisiert schwer in mikrokristallinen hygroskopischen Flocken aus, die bei 82° unter Zersetzung und vorangehendem Erweichen schmelzen. Ausbeute : 0,5 g (63 % d.Th.).

$C_{23}H_{22}NCl$ (347,87)	*Ber.* : N	4,02	Cl	10,19 %
	Gef. : N	4,09	Cl	10,08 %

b) *2-Trimethylammonium-4'-methoxy-benzal-fluoren-jodid*

Es wird von 1 g 2-Trimethylammonium-4′-methoxy-benzal-fluoren-jodid ausgegangen und nach der vorangehenden Vorschrift verfahren. Das entstandene Chlorid kristallisiert ebenfalls schwer aus, ist hygroskopisch und schmilzt bei 84—87° unter Zersetzung und vorangehendem Erweichen. Ausbeute : 0,55 g (70 % d.Th.).

$C_{24}H_{24}ONCl$ (377,89)	*Ber.* : N	3,70	Cl	9,38 %
	Gef. : N	3,79	Cl	9,21 %

c) *2,2'-Bis-(trimethylammonium)-benzal-fluoren-dichlorid*

Es wird von 1 g 2,2′-Bis-(trimethylammonium)-benzal-fluoren-dijodid ausgegangen und nach Vorschrift 2 a verfahren. Der nach Abdampfen des Filtrates erhaltene Rückstand wird in Äthanol gelöst und mit Äther ausgefällt. Die erhaltenen gelben, schwach hygroskopischen Nadeln schmelzen bei 175° unter Zusetzung und vorangehendem Erweichen. Ausbeute : 0,68 g (89 % d.Th.).

$C_{26}H_{30}N_2Cl_2$ (441,42)	*Ber.* : N	6,34	Cl	16,06 %
	Gef. : N	6,42	Cl	16,00 %

d) *2,3'-Bis-(trimethylammonium)-benzal-fluoren-dichlorid*

Die Umwandlung des 2,3′-Bis-(trimethylammonium)-benzal-fluoren-dijodids in das entsprechende Dichlorid findet unter den in Vorschrift 2 a gezeigten Bedingungen statt. Aus Äthanol mit Aceton umkristallisiert erhält man das Dichlorid als eine gelbliche, mikrokristalline, schwach hygroskopische Substanz, die bei 190—91° unter Zersetzung und vorangehendem Erweichen schmilzt. Ausbeute: 0,68 g (89 % d.Th.).

$C_{26}H_{30}N_2Cl_2$ (441,42)	*Ber.*:	N 6,34	Cl 16,06 %
	Gef.:	N 6,38	Cl 16,01 %

e) *2,4'-Bis-(trimethylammonium)-benzal-fluoren-dichlorid*

Es wird von 1 g 2,4'-Bis-(trimethylammonium)-benzal-fluoren-dijodid ausgegangen und nach Vorschrift 2 a verfahren. Durch Umkristallisieren aus Äthanol mit Aceton, scheidet das Dichlorid in gelben, mikrokristallinen, schwach hygroskopischen Flocken aus (Nadeln), die bei 163° unter Zersetzung und vorangehendem Erweichen schmelzen. Ausbeute: 0,55 g (72 % d.Th.).

$C_{26}H_{30}N_2Cl_2$ (441,42)	*Ber.*:	N 6,34	Cl 16,06 %
	Gef.:	N 6,40	Cl 16,03 %

Revue Roumaine de Chimie, **15**, 1433—1439 (1970)

SUR LA FORMYLATION DES MÉTHYL-10-PHÉNOTHIAZINES

V. FĂRCĂŞAN, I. OPREAN et C. BODEA

Institut de Chimie de l'Académie, Cluj, 59—65, str. Donath

Reçu le 7 mars 1970

La formylation par la méthode de Vilsmeier a été effectuée sur la méthyl-10-phénothiazine (I), la chloro-3-méthyl-10-phénothiazine (XII) et la nitro-3-méthyl-10-phénothiazine (XIV). Dans le premier cas on a isolé à côté d'un monoformyldérivé (II) la diformyl-3,7-méthyl-10-phénothiazine (III). On compare le comportement de la substance I au comportement de la méthyl-N-diphénylamine (VIII) et on cherche à expliquer les différences observées.

La réaction de formylation par la méthode de Vilsmeier[1] a été effectuée sur la méthyl-10-phénothiazine (I) et quelques-uns de ses dérivés,[2,3] et on a constaté que la substitution a toujours lieu sur le carbone en position *para* par rapport à l'atome d'azote de l'hétérocycle, les composés obtenus étant des monoformyl-dérivés.

Dans un travail antérieur,[4] en modifiant la méthode de Buu-Hoï et Hoan[5] pour la formylation de la méthyl-10-phénothiazine(I), nous avons obtenu la formyl-3-méthyl-10-phénothiazine(II) dans des conditions plus avantageuses. Dans la masse de réaction, par chromatographie en couche mince nous avons mis en évidence la présence de plusieurs composants, parmi lesquels I et II, et de petites quantités d'un produit de couleur jaune. La détermination de la structure de ce produit fait le premier objet de ce mémoire.

Le comportement chromatographique, la masse moléculaire, les données de l'analyse centésimale correspondent pour le diformyl-3,7-méthyl-10-phénothiazine (III).

La présence de la fonction aldéhyde a été prouvée par le spectre en IR et par les réactions avec l'hydroxylamine et la dinitro-2,4-phénylhydrazine. L'obtention d'une dioxime sous l'action de l'hydroxylamine et le redoublement du coefficient molaire d'extinction pour les bandes caractéristiques observé lorsqu'on compare les spectres électroniques des

---

[1] A. Vilsmeier et A. Haack, *Chem. Ber.*, **69**, 119 (1927),.

[2] G. Cauquil et A. Casadevall, *Compt. rend.*, **240**, 1784 (1953).

[3] G. Cauquil, E. Casadevall et R. Greze, *Bull. Soc. chim. France*, **1964**, 590.

[4] C. Bodea, V. Fărcăşan et I. Oprean, *Rev. Roumaine Chim*,. **10**, 1103 (1956).

[5] N. P. Buu-Hoï et N. Hoán, *J. Chem. Soc.*, **1951**, 1834.

SCHÉMA 1

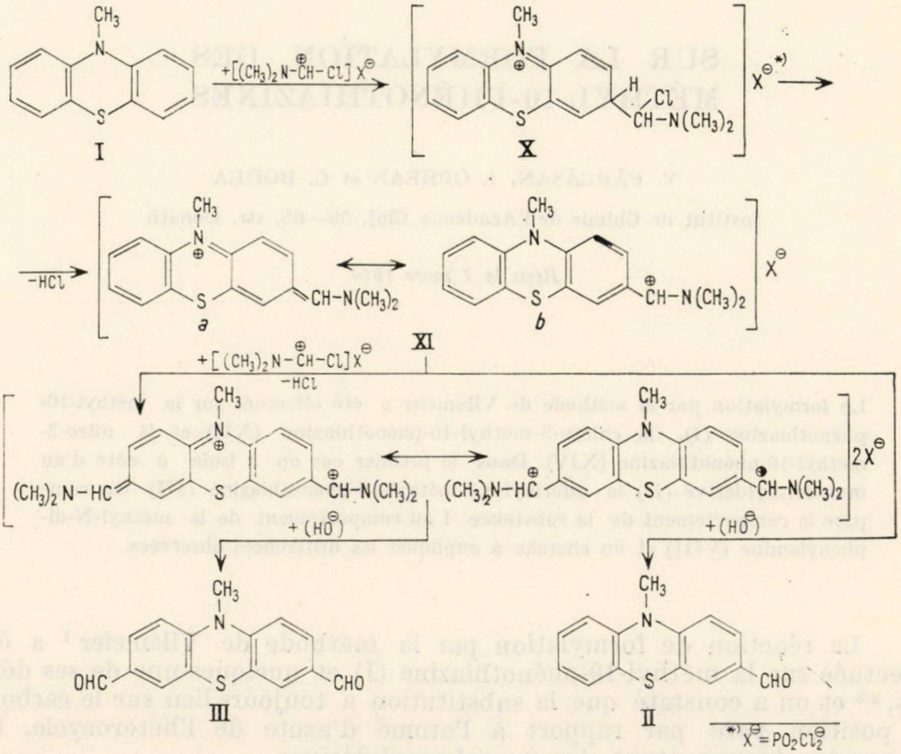

*) $X^{\ominus} = PO_2Cl_2^{\ominus}$

substances II et III attestent l'existence de deux fonctions aldéhydes. La preuve définitive de la structure est fournie par la réduction Huang-Minlon [6] qui a mené à la triméthyl-3,7,10-phénothiazine (IV) identique au produit obtenu par la même méthode, en partant de la diméthyl-3,10-formyl-7-phénothiazine(V), ou par la méthylation de la diméthyl-3,7-phénothiazine(VI). [7]

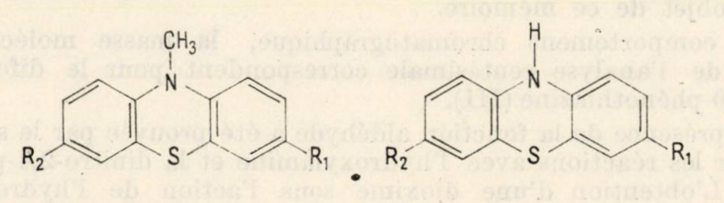

I : $R_1 = R_2 = H$

II : $R_1 = CHO$; $R_2 = H$

III : $R_1 = R_2 = CHO$

VI : $R_1 = R_2 = CH_3$

---

[6] Huang-Minlon, *J. Amer. Chem. Soc.*, **68**, 2487 (1946).

[7] G. Cauquil, A. Casadevall et E. Casadevall, *Compt. rend.*, **236**, 1363 (1953).

IV : $R_1 = R_2 = CH_3$

V : $R_1 = CH_3$; $R_2 = CHO$

VII : $R_1 = CHO$; $R_2 = CHN{-}NHC_6H_3(NO_2)_2$

XII : $R_1 = Cl$; $R_2 = H$

XIII : $R_1 = Cl$; $R_2 = CHO$

XIV : $R_1 = NO_2$; $R_2 = H$

XV : $R_1 = NO_2$; $R_2 = CHO$

XVII : $R_1 = R_2 = CNOH$

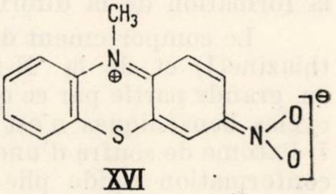
XVI

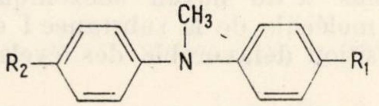

VIII : $R_1 = R_2 = H$

IX : $R_1 = R_2 = CHO$

On remarque que seulement l'un des deux groupements formyl réagit avec la dinitro-2,4-phénylhydrazine pour donner un monohydrazone (VII) dont le spectre en IR présente les fréquences $\nu_{C=O}$ à 1690 cm^{-1} et $\nu_{C=N}$ à 1620 cm^{-1}. Ce comportement doit être attribué à la solubilité très réduite du VII, qui précipite du milieu de réaction et échappe par suite à l'action du réactif.

Il s'ensuit que par la formylation de la méthyl-10-phénothiazine (I) dans les conditions décrites dans l'ouvrage antérieur, une quantité appréciable de substance initiale n'est pas transformée. Afin de trouver les conditions qui permettraient la transformation totale de la méthyl-10-phénothiazine (I) d'une part et l'amélioration du rendement en dialdéhyde d'autre part, nous avons modifié quelques paramètres de la réaction. Si sous l'action d'un excès de réactif, I est totalement consumé, nous n'avons pas pu observer une augmentation sensible de la quantité de diformyl-3,7-méthyl-10-phénothiazine(III), ce qui prouve que l'introduction d'un deuxième groupement formyl se heurte à des difficultés.

Par la formylation dans les mêmes conditions de la méthyl-N-diphénylamine(VIII), nous avons obtenu le diformyl dérivé IX comme il était à prévoir, compte tenu des ouvrages de Wilson.[8]

Le comportement différent des substances I et VIII soulève quelques problèmes que nous traiterons par la suite.

---

[8] C. D. Wilson, USA. Pat,. 2.558 285, 26 juin 1951 ; *Chem. Abstr.*, 46, 1041f (1952).

Faisant état du mécanisme de la réaction Vilsmeier [9] et en admettant pour l'agent de formylation la structure suggérée par Wizinger, [10] confirmée par les ouvrages de Arnold et Holy,[11] la formation de la diformyl-3,7-méthyl-10-phénothiazine (III) peut être exprimée par le schéma 1, qui — si l'on néglige l'atome de soufre — reste valable aussi pour la formation de la diformyl-4,4'-N-méthyl-diphénylamine (IX).

Le comportement différent à la formylation de la méthyl-10-phénothiazine(I) et de la N-méthyl-diphénylamine(VIII) peut être expliqué en grande partie par ce que dans la molécule du VIII la libre rotation des cycles benzéniques n'est pas entravée tandis que, dans la molécule du I, l'atome de soufre d'une part et le méthyl de l'autre part imposent une conformation rigide plié CH_3 extra.[12, 13] Dans ces conditions tandis que dans le cas de la substance VIII, l'interaction des électrons non appariés présents sur l'azote et les électrons π du noyau benzénique peut se manifester sans contrainte, dans la molécule de la substance I elle est en grande mesure entravée par la position défavorable des cycles (benzéniques).

C'est pourquoi la densité électronique en position *para* par rapport à l'atome d'azote est plus forte chez le dérivé diphénylaminique(VIII), que chez le dérivé phénothiazinique (I) et une attaque électrophile sur VIII est ainsi favorisée.

Ainsi qu'il résulte du schéma 1 par la perte d'acide chlorhydrique, X engendre l'intermédiaire XI. Le même empêchement de la libre rotation du cycle benzénique fait que la forme XIa soit favorisée du point de vue énergétique et qu'elle ait par conséquent une contribution plus importante à l'état réel de XI que la forme correspondante dans le cas du dérivé diphénylaminique. Une preuve dans ce sens est fournie par les spectres électroniques enregistrés pour les mélanges de réaction obtenus dans les mêmes conditions avant l'hydrolyse, en partant des substances I et VIII. Dans le premier cas la bande de la longueur d'onde la plus élevée est déplacée bathochrome (max. 456 resp. 390 mμ). Cela explique au moins en partie pourquoi la deuxième attaque électrophile peut s'effectuer plus facilement à la formylation du VIII.

En appliquant la réaction de Vilsmeier à d'autres dérivés de la méthyl-10-phénothiazine(I) substitués en position 3, nous avons constaté que tandis que la chloro-3-méthyl-10-phénothiazine(XII) peut être formylée dans les conditions habituelles pour engendrer la chloro-3-formyl-7-méthyl-10-phénothiazine (XIII), la nitro-3-méthyl-10-phénothiazine (XIV), même traitée avec un excès de réactif, est formylée avec de très faibles rendements, pour former très probablement la nitro-3-formyl-7-méthyl-10-phénothiazine (XV).XV a été identifiée par chromatographie et la réaction avec la dinitro-2,4-phénylhydrazine.

---

[9] G. A. Olah, « Friedel-Crafts and Related Reactions », IIIe vol., 2e part., Interscience publishers a division of John Wiley et Sons. Inc., New York — Londres — Sydney, 1964, p. 1211.

[10] R. Wizinger, *J. prakt. Chem.*, **154**, 25 (1939).

[11] Z. Arnold et A. Holy, *Coll. Czech. Chem. Comm.*, **27**, 2886 (1962).

[12] N. J. Leonard et L. E. Sutton, *J. Amer. Chem. Soc.*, **70**, 1564 (1948).

[13] J. P. Malrieu et B. Pullman, *Theoret. Chim. Acta*, **2**, 293 (1964).

Le comportement de XIV permet de supposer que de même que dans le cas bien connu de la nitro-4-diméthylaniline, la répartition des électrons est semblable à celle présentée par la formule XVI, structure qui ressemble beaucoup à l'intermédiaire XIa et pour les mêmes raisons que celles mentionnées c'est à prévoir que la formylation se heurte à des difficultés.

Les données obtenues dans le présent ouvrage, sur le comportement de quelques méthyl-10-phénothiazines à la formylation révèlent aussi la complexité du problème de la transmission des effets des substituants d'un noyau dans l'autre dans la classe des phénothiazines, relevée parmi d'autres par Azzaro et collab. [14]

PARTIE EXPÉRIMENTALE

Diformyl-3,7-méthyl-10-phénothiazine (*III*)

A 80 ml de diméthylformamide refroidis dans la glace, on ajoute, goutte à goutte, et sous agitation 40 ml d'oxychlorure de phosphore fraîchement distillé. On agite 1/2 h, puis on ajoute 18 g de méthyl-10-phénothiazine (I) et on chauffe 2 h au bain-marie bouillant. On verse sur 500 g de glace pilée et on ajoute une solution saturée d'acétate de sodium jusqu'au pH = 6. On sépare le résidu brun verdâtre visqueux par décantation et on le dissout dans 1000 ml de toluène. Après séchage sur sulfate de sodium sicc., la solution est concentrée sous vide à 100 ml, et on chromatographie sur 1250 g d'alumine (Brockmann III), sur colonne, l'éluant étant le toluène. On obtient 11 g de formyl-3-méthyl-10-phénothiazine (II) et 0,8 g de diformyl-3,7-méthyl-10-phénothiazine (III). III est recristallisée dans le benzène et on isole ainsi la substance pure : plaques jaunes, qui fondent à 202—3°. Elle est soluble dans du chloroforme, de la diméthyl-formamide et très peu dans de l'éthanol et dans de l'éther éthylique

$C_{15}H_{11}NO_2S$ (269,3)

calculé :	C 66,79 ;	H 4,12 ;	N 5,21
trouvé :	C 66,79 ;	H 4,62 ;	N 5,87

Masse moléculaire (Rast) : 270

IR ν_{CO} 1685 cm^{-1}

UV λ_{max} 289 mμ ε 51000

Pour II λ_{max} 287,7 mμ ε 23100

Dioxime (*XVII*)

On chauffe au bain-marie 0,1 g III, 0,4 d'hydroxylamine chlorhydratée et 2 ml de pyridine durant 45 mn. On verse dans de l'eau. On dissout le précipité dans 2 ml de diméthyl-formamide et on ajoute de l'eau jusqu'au dépôt de cristaux—aiguilles jaunes—qui fondent à 224—5°.XVII est peu soluble dans de l'éthanol mais elle se dissout dans de l'acétone.

---

[14] M. Azzaro, A. Cambon, F. Guezo et R. Guedj, *Bull. Soc. chim. France*, **1967**, 1977.

$C_{15}H_{13}N_3O_2S$ (299,4)

calculé : N 14,06

trouvé : N 14,04

Monohydrazone (*VII*)

On travaille dans les conditions habituelles, en partant de la diformyl-3,7-méthyl-10-phénothiazine (III). Après recristallisation dans la diméthylformamide, on obtient des cristaux bruns qui fondent à 272—3°. VII est peu soluble dans les dissolvants usuels.

$C_{21}H_{15}N_5O_5S$ (449,4)

calculé : N 15,6

trouvé : N 15,75

IR ν_{CO} 1690 cm^{-1} $\nu_{C=N}$ 1620 cm^{-1}

Triméthyl-3,7,10-phénothiazine (*IV*)

a) A une solution de 0,1 g de diformyl-3,7-méthyl-10-phénothiazine (III) dans 5 ml de diéthylène-glycol bouillant on ajoute 0,5 ml d'hydrazine hydratée à 98% et 0,2g de potasse dissous dans la quantité minime d'eau. On maintient à reflux pendant 4 h. Après cet intervalle on ajoute 0,5 ml d'hydrazine hydratée et 0,2 g de potasse et on continue à chauffer à reflux encore 4 h. On distille l'eau formée. Après refroidissement on précipite IV avec de l'eau sous forme de plaques incolores. $P_f = 79-80°$ (recristallisé dans de l'éthanol-eau). Pour le produit obtenu par méthylation de la diméthyl-3,7-phénothiazine (VI) $P_f = 81°$.[7]

b) Par la réduction de la diméthyl-3,10-formyl-7-phénothiazine (V)[2] dans des conditions similaires à celles pour la réduction de III on obtient la même substance.

$P_f = 80°$.

Epreuve du mélange $P_f = 80°$.

Diformyl-4,4'-méthyl-N-diphénylamine (*IX*)

On travaille dans les conditions décrites pour III en partant de VIII. On obtient IX avec les propriétés décrites par Wilson.[8]

Chloro-3-formyl-7-méthyl-10-phénothiazine (*XIII*)

En partant de 4,2 g de chloro-3-méthyl-10-phénothiazine (XII) dans les conditions décrites pour la préparation de III, on obtient 1,5 g de XIII. Après recristallisation dans de l'éthanol, la substance pure, sous forme d'aiguilles jaunes, fonde à 153—154°.

$C_{14}H_{10}ClNOS$ (275,7)

calculé : C 60,96 ; H 3,66 ; Cl 12,86

trouvé : C 61,12 ; H 3,76 ; Cl 13,47

Nitro-3-formyl-7-méthyl-10-phénothiazine (*XV*)

En partant de la nitro-3-méthyl-10-phénothiazine (XIV), dans les mêmes conditions que pour la formylation de I, on isole la substance initiale et par chromatographie en couche mince sur silicagel G (éluant = toluène-éthanol 2 : 1) une très petite quantité d'une substance jaune-brune, qui donne les réactions spécifiques des aldéhydes (hydrazone, etc.).

Les points de fusion ont été déterminés en tube capillaire et n'ont pas été corrigés.

Les spectres en IR ont été enregistrés à l'appareil Karl Zeiss Iéna UR-10. Les échantillons ont été préparés à partir de pastilles de bromure de potassium.

Les spectres électroniques ont été effectués dans du chloroforme comme solvant, à l'aide d'un appareil Beckmann DK-2A.

Nous remercions Mme F. Teodoru et M. V. Voivod qui ont enregistré les spectres électroniques et IR.

Revue Roumaine de Chimie, 15, 1441–1446 (1970)

ACTION DES ULTRASONS SUR UN PROCESSUS DE CARBONATATION

DESIDERIU AUSLÄNDER, CORINA ŞERBAN et IOANA DĂBALĂ

Laboratoire d'ultra-acoustique, Institut Pédagogique, Cluj, 4, Piaţa Ştefan cel Mare

Reçu le 12 décembre 1969

Les auteurs étudient l'effet des ultrasons sur la réaction de précipitation du bicarbonate de sodium par la carbonatation de la solution de carbonate de sodium, prenant en considération les possibilités de modification de la vitesse de réaction et des dimensions des cristaux obtenus. Les expériences, effectuées à l'aide d'un générateur hydrodynamique d'ultrasons, démontrent l'effet d'accélération considérable de la vitesse de réaction, ainsi que l'effet de déplacement de la distribution granulométrique vers des dimensions plus réduites.

Le processus de fabrication du bicarbonate de sodium dans les conditions technologiques de l'usine[1] mène à l'obtention d'un produit dont l'analyse granulométrique indique la prédominance des cristaux ayant des dimensions de plus de 100 μ.

Dans le dessein d'une amélioration qualitative par l'augmentation de la surface spécifique sous l'influence de l'action de l'énergie ultrasonique, nous avons entrepris des études sur le flux technologique de la production du bicarbonate de sodium. Il s'ensuit que l'étape optimale est la phase de carbonatation :

$$Na_2CO_3+H_2O+CO_2=2\ NaHCO_3$$

L'effet des ultrasons se manifestera ainsi sur toutes les étapes du processus : réaction chimique, augmentation de la concentration jusqu'à la sursaturation, formation des germes et croissance des cristaux.

Cette situation exige d'atteindre le but poursuivi, c'est-à-dire la diminution des cristaux, tout en évitant les préjudices qui pourraient résulter de l'action des ultrasons pour les autres étapes du processus, surtout en ce qui concerne le rendement. Compte tenu que dans les conditions expérimentales données, le paramètre le plus important qui pourrait en être affecté est la vitesse de réaction, les recherches ont porté sur le mécanisme de modification de ce paramètre par le champ ultrasonique.

---

[1] S. I. Volfkovici, A. P. Egorov, et D. A. Epstein, « Tehnologie chimică generală », 1er vol.. Ed. tehnică, Bucarest, 1955, p. 540.

A une température constante et une concentration donnée, on s'attendrait à ce que par la destruction de l'écoulement laminaire et l'apparition de l'écoulement turbulent les ultrasons agissent dans le sens d'agrandir la surface de contact des réactants et implicitement de la vitesse de réaction ; le développement dynamique de la surface des réactants par leur continuel renouvellement pendant l'ultrasonorisation mène également au même effet.

Les ultrasons, agissant par une plus grande probabilité des molécules et des réactants de s'entre-heurter, provoquent le même effet en ce qui concerne la vitesse de réaction dans un processus hétérogène de même que l'accroissement de la concentration dans un processus homogène.

Nous estimons également que le niveau énergétique des molécules s'élève par l'ultrasonorisation, qui facilite de surmonter les barrières de potentiel entre les différents états, ce qui se reflétera pendant la durée du processus par l'augmentation de la vitesse de réaction. [2,3]

Il est évident que l'évacuation continuelle du produit au cours du processus contribuera par le renouvellement des surfaces de contact à augmenter la vitesse de réaction, indifféremment de la présence ou l'absence du champ des ultrasons.

Quant à l'étape de la formation du précipité, il est bien connu que pour obtenir des cristaux de dimensions plus réduites il faut soit diminuer la concentration des réactants, soit abaisser la température. [4] Toutes les deux méthodes ont cependant des effets défavorables sur le rendement du processus.

L'action des ultrasons favorisant les étapes antérieures, conformément à ce qui vient d'être dit plus haut, exercera de l'influence autant sur le processus de formation des germes de cristallisation, que sur le processus de croissance des cristaux. C'est à cause des fluctuations de densité que se forment les germes de cristallisation dans la solution sursaturée instable du précipité. La propagation de l'onde ultrasonique étant caractérisée par des gradients de pression appréciable contribuera à l'accélération du processus, de même qu'à l'augmentation du nombre de germes dont la conséquence sera la diminution des dimensions des cristaux. [5]

Etant donné que les variations des dimensions sont inversement proportionnelles à la vitesse de formation du précipité, l'action positive des ultrasons sera déterminée par la modification de la vitesse de cette étape dans le sens de son accélération. Du fait que la vitesse d'un processus dans son ensemble est déterminée par la vitesse de l'étape la plus lente, ce qui décidera de la vitesse de croissance des cristaux ce sera la valeur de la vitesse de diffusion, dont l'expression selon la loi de Fick [4] est

$$\frac{\mathrm{d}n}{\mathrm{d}t} = \frac{D}{l} S\,(C_1 - C_2)$$

---

[2] J. Blitz, « Fundamentals of Ultrasonics », Butterworths, Londres, 1967, p. 132.

[3] Warren P. Mason, « Physical Acoustics », IIe vol., part. A, Academic Press, Londres, 1965, p. 298.

[4] Al. Codarcea, « Mineralogie », Ed. didactică și pedagogică, Bucarest, 1965, p. 172.

[5] V. Fridman, 5e Congrès International d'Acoustique, Liège, **1 A**, D 23, 1965.

où

D = coefficient de diffusion;
S = surface de contact des réactants;
l = grosseur de la couche de diffusion;
C_1 = concentration moyenne de la solution sursaturée dont elle précipite la phase solide;
C_2 = concentration de la solution saturée à la surface des particules solides.

Dans les conditions du maintien de la température à une valeur constante pour des concentrations données, l'action des ultrasons se manifestera sur les grandeurs : S, D et l.

L'influence sur la surface de contact S sera reflétée par l'augmentation de la vitesse, pour les motifs déjà mentionnés.

Le coefficient de diffusion D augmentera sous l'action des ultrasons, d à l'accélération des vitesses moléculaires, l'effet de l'agitation des ultrasons étant analogue à celui produit par l'élévation de la température.

La grosseur de la couche de diffusion l varie proportionnellement à la racine carrée de la vitesse de déplacement des réactants; sa valeur diminuera donc à la suite de l'ultrasonorisation.[6]

Par conséquent, par l'augmentation du nombre de germes et l'accélération de la vitesse du processus de formation des cristaux les ultrasons, en dehors de l'accélération du processus tout entier, mèneront à la formation d'un produit à petites dimensions.

PARTIE EXPÉRIMENTALE

En vue de réaliser des conditions de travail analogues au processus technologique de l'usine, on a effectué une colonne de carbonatation d'une hauteur de 1 m et du diamètre de 14,5 cm, munie de spirales de refroidissement, respectivement de chauffage, reliée à un réservoir, afin de permettre la recirculation de la solution.

La solution à la densité de 21° Bé provenue de l'usine a passé dans le circuit : réservoir→colonne→réservoir, par le générateur hydrodynamique d'ultrasons placé dans la partie supérieure de la colonne. Le faisceau d'ultrasons à la fréquence de 20—25 kHz a été orienté le long de la verticale sur le liquide de la colonne, tandis que dans sa partie inférieure on a introduit CO_2 à la pression de 1,5—2,5 atmosphères.

L'effet produit par les ultrasons a été poursuivi dans différentes conditions de travail, telles que : ultrasonorisation de la solution avant la carbonatation, ultrasonorisation de la solution de précipité après la fin de la réaction de carbonatation, ultrasonorisation intermittente alternant avec le passage du bioxyde de carbone et ultrasonorisation continuelle pendant toute la durée du processus. Ont été également observés les effets en fonction de la fréquence du vibrateur et en fonction de la température.

Dans les conditions mentionnées, on a effectué au cours du processus des mesurages concernant la densité, le coefficient de viscosité et la distribution granulométrique du produit par des méthodes de sédimentation, ainsi que des microphotographies dans le but illustratif.

Toute la gamme de déterminations a été évaluée comparativement à celles qui correspondent aux conditions identiques en l'absence de l'ultrasonorisation.

[6] N. P. CHUGUNOV, *Akust. Z.*, **2**, 10. (1964).

RÉSULTATS

La totalité des données expérimentales confirme l'hypothèse concernant les effets des ultrasons sur le processus recherché et l'analyse des différentes conditions de travail plaide pour la variante de l'ultrasonorisation pendant toute la durée du processus.

Dans ce qui suit seront présentés les résultats obtenus dans ces conditions expérimentales de travail, d'après le graphique de la figure 1. Les deux courbes représentent la solution à concentration diminuée, après la filtration du précipité, en fonction du temps, aux épreuves extraites sans ultrasonorisation (%) 1, respectivement avec ultrasonorisation; 2, à la même température de 42°. Le comportement de ces courbes met en évidence l'augmentation appréciable du rendement sous l'action des ultrasons.

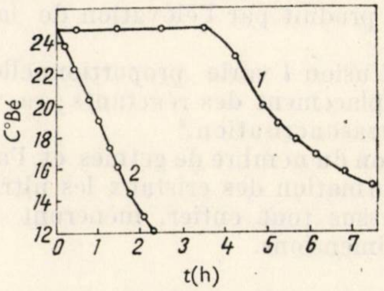

Fig. 1. — Variation de la concentration de la solution au cours de la précipitation en fonction du temps.
Courbe *1*, solution non ultrasonorisée ; Courbe *2*, solution ultrasonorisée :

Le moment initial ($t = 0$) correspond au commencement de l'administration du bioxyde de carbone et au couplage du générateur d'ultrasons dans le cas du processus décrit par la courbe *2*.

On peut constater qu'à la différence du témoin, où la formation du précipité apparaît après une longue période pendant laquelle se déroule la réaction, la saturation et la sursaturation de la solution correspondant à la portion horizontale de la courbe 1, dans le cas de l'ultrasonorisation le processus a lieu rapidement, le précipité étant mis en évidence déjà après les premières minutes.

Les tangentes à la courbe indiquent dans le cas 2 le maintien d'une vitesse supérieure et constante jusqu'à $1^1/_2$ h, tandis que, à défaut d'ultrasonorisation, le processus découle de plus en plus lentement et marque une diminution du rendement.

Mentionnons que dans nos expériences le précipité formé n'a pas été éliminé pendant le processus, n'étant extraites que les épreuves nécessaires aux mesurages. La filtration concomittante contribuera à l'augmentation du rendement en présence autant qu'en l'absence du champ ultrasonique.

La distribution des cristaux par dimensions est présentée dans le tableau 1 pour trois variantes : dans la première colonne sont inscrites les données correspondant au produit usinier, dans la colonne II celles du témoin obtenu à la température de 42° et dans la colonne III les données concernant les cristaux obtenus à 42° dans les conditions d'ultrasonorisation.

Tableau 1

Distribution des cristaux par dimensions

Diamètre μ	Produit		
	Usine	Témoin $t = 42°$	Ultrasonorisé $t = 42°$
>65	98 %	61 %	9 %
40–65	5 %	15 %	37 %
30–40	1 %	7 %	33 %
<30		17 %	21 %

Les différences de granulation entre le produit de l'usine et celui non ultrasonorisé du laboratoire proviennent probablement des différences de température, le processus de fabrication ayant lieu à des températures supérieures à 42°.

L'effet des ultrasons résulte de la comparaison des deux dernières colonnes, les procédés de préparation étant absolument identiques. On peut remarquer la formation, de préférence, des cristaux de dimensions réduites ; par exemple, la quantité des cristaux ayant un diamètre de 30 μ à 65 μ atteint par l'ultrasonorisation 70 % par rapport à 22 % au témoin.

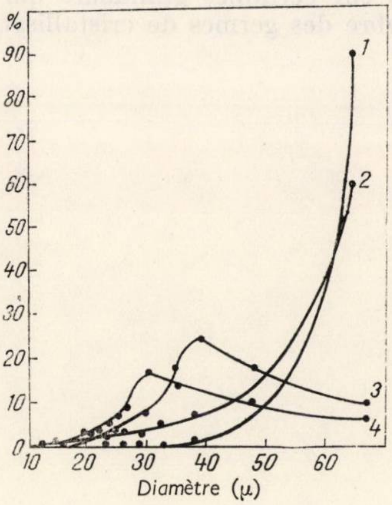

Fig. 2. — Distribution des cristaux par dimensions.

Courbe *1*, cristaux obtenus dans les conditions de l'usine ; Courbe *2*, cristaux témoins ; Courbe *3* ; cristaux obtenus dans le champ ultrasonorisé pour $t = 42°$; Courbe *4*, cristaux obtenus dans le champ ultrasonorisé pour $t = 32°$.

Les courbes granulométriques[7] représentées sur la figure 2 sont données pour des variantes différentes, en fonction des conditions de travail respectives, à savoir :
la courbe *1* est donnée pour la distribution des dimensions fournies par l'usine, la courbe *2* pour la température de 42° sans ultrasonorisation,

---

[7] A. F. Strickland, Constable « Kinetics and Mechanism of Crystallization », Londres, 1958, p. 98.

qui sert de témoin, la courbe *3* pour l'ultrasonorisation à 42° et la courbe *4* pour l'ultrasonorisation à 32°.

Les différences entre les distributions 1 et 4 ont été déjà mentionnées plus haut ; la courbe *3* démontre l'effet produit par les ultrasons, le maximum se situant à une valeur de 40 μ. Il est évident qu'à une température plus réduite, à 32° comme l'indique la courbe *4*, a lieu un déplacement dans le domaine des dimensions plus petites, le maximum se situant à environ 30 μ.

Les microphotographies des cristaux présentées sur les figures 3 et 4 ont été effectuées pour illustrer les différences de granulation entre le produit usinier (fig. 3) et le produit obtenu dans les conditions d'ultrasonorisation à 42°.

CONCLUSIONS

1. La carbonatation de la solution de soude calcinée sous l'action des ultrasons est caractérisée par l'augmentation appréciable du rendement.
2. L'effet des ultrasons se manifeste par la réduction des dimensions des cristaux, ce qui contribue à l'amélioration qualitative du produit.
3. Les effets obtenus sont expliqués par l'intervention des ultrasons sur certaines grandeurs qui déterminent la vitesse de réaction, le nombre des germes de cristallisation et la vitesse de diffusion.

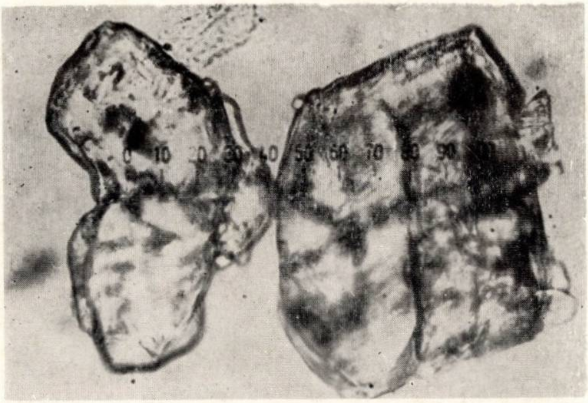
10
40
50
60
70
90

Fig. 3. — Microphotographie du bicarbonate de sodium produit par l'usine.

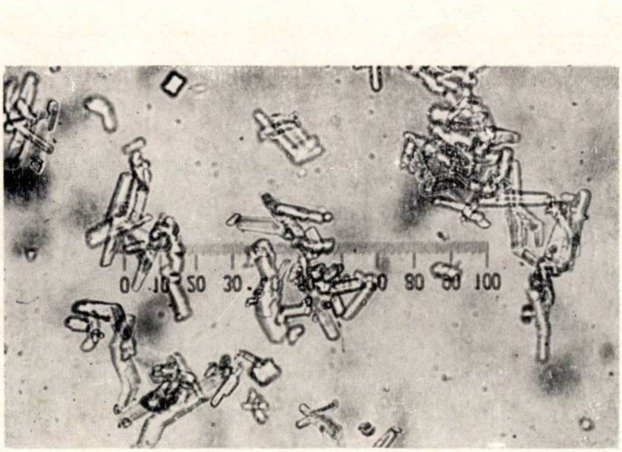
0
10
50
30
80
80
100

Fig. 4. — Microphotographie du bicarbonate de sodium obtenu dans des conditions d'ultrasonorisation.

Revue Roumaine de Chimie, 15, 1447 – 1451 (1970)

THE MICROANALYSIS OF COBALT BY ELECTROPHORETIC FOCUSSING WITH RADIOACTIVE TRACER

E. POPPER

Institute of Medicine and Pharmacy, str. Pasteur 4, Cluj, Romania

A. SZABO and P. SZENTGYÖRGYI

Institute for Atomic Physics, str. Donath 59, Cluj, Romania

Received September 11, 1969

The paper presents an isotopical dilution method combined with electrophoretic focussing on paper, for cobalt microanalyses. These analyses may be carried out with small volume of samples using Co^{60} as tracer. The solution to be analysed is labelled with radioactive cobalt, the cobalt is substoichiometrically complexed with EDTA solution and then the complexed anions and noncomplexed cations are separated by electrophoretic focussing. The concentration of cobalt is calculated knowing the radioactivities of both anions and cations and the concentration of the EDTA solution. The sensitivity of the method is 0.5×10^{-4} atom-grams Co per litre.

INTRODUCTION

Some toxicological, biochemical and chemical studies need analyses of small liquid samples containing trace amounts of heavy metals, either the untreated solution or the fractions obtained after their chromatographic processing being analysed. Usually liquid samples of 0.1 – 0.5 ml are analysed, containing heavy metals, especially cobalt in amounts of about 10 – 100 micrograms. Since these analyses take place in series, the methods involved must be simple, fast and accurate at the same time. For the determination of cobalt in aqueous solutions a method suggested by Fuchs[1] may be used. According to this author a substoichiometric amount of EDTA solution and a solution labelled with Co^{60} are added to the sample to be analysed for cobalt. The separation of the complexed and noncomplexed cobalt is made by electrophoretic focussing, method elaborated by Schumacher.[2] The percents of the radioactive cobalt in the complexed and noncomplexed fragments are the same because no isotope separation takes place. Therefore, measuring the ratio of the radioactivity of the two fragments, the complexed/noncomplexed metal ratio is determined and from this ratio the concentration of cobalt in the solution to be analysed may be calculated. [3]

---

[1] A. Fuchs, *Helv. Chim. Acta*, **49**, 1023 (1966).

[2] E. Schumacher and H. J. Streiff, *Helv. Chim. Acta*, **40**, 228 (1957).

In the present paper this method is adapted to the requirements of some microanalyses of liquid samples of biological origin or effluent drops from chromatographic columns. The method and its performance are described in the following.

EXPERIMENTAL

About 0.1 ml of EDTA solutions were added to the samples of 0.1 ml containing different amounts of cobalt. The concentration of the complexing solution was chosen so that substoichiometric complexing of the metal should take place. Other quantities of 0.1 ml buffer solution of pH = 5 and 0.5 ml of radioactive cobalt solution were added, too. A drop of about 0.5 ml of the solution prepared as above was put on a strip of chromatographic Whatman paper, 10 mm wide. This was fixed and introduced into the electrophoresis apparatus (Fig. 1). At the beginning the two ends of the paper were immersed into the electrolyte contained in the electrode holder without switching on the current. Thereby the paper was soaked with electrolyte (a 0.5 M sodium nitrate solution). Afterwards cyclohexane was poured over the paper and 150 V were applied between its ends, so that about 5–15 mA d.c. passed through the strip. Cyclohexane was needed for cooling the paper and prevent evaporation during the experiment. Due to the electric current and the migration of sodium and nitrate ions, the $[Co]^{2+}$ cation and $[CoY]^{2-}$ anion shifted to opposite directions. After 15 minutes the current was switched off and the paper strip was removed from the electrolysis apparatus. After fast drying by an infrared lamp, the strip was cut in pieces of 2.5 mm length, put on small aluminium planchets and measured with a window G.M. counter of VAZ-320 type coupled at a scaler of Cuanta type. Plotting the results, a radioelectrophoretic curve was received with two peaks corresponding respectively to the cations and anions. The ratio of the activity of these ions was determined estimating the areas under the corresponding peaks. The cobalt concentration in the sample was calculated with the aid of this ratio and of the concentration of EDTA solution, using the following equation:

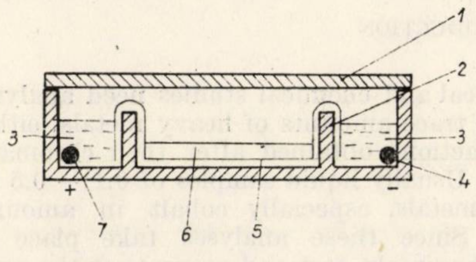

Fig. 1. — Electrophoresis apparatus. *1*, the cover of the apparatus; *2*, electrophoretic tank made of plastics; *3*, sodium nitrate solution; *4*, platinum cathode; *5*, electrophoretic paper fixed on plastic support; *6*, cyclohexane; *7*, platinum anode.

$$[Co]^{2+} = [EDTA]\,\frac{P_{anion} - P_{cation}}{P_{anion}}$$

---

[3] E. Schumacher and W. Friedli, *Helv. Chim. Acta*, **43**, 1013 (1960).

where :

$[Co]^{2+}$ = the concentration of cobalt in the solution to be analysed, mol/litre ;

[EDTA] = the concentration of the complexant solution added to the sample to be analysed, mol/litre ;

P_{anion} = the activity of the anion peak, counts per minute ;

P_{cation} = the activity of the cation peak, counts per minute.

RESULTS

Preliminary experiments have shown that the shift of the focussed zones is faster and more reproducible if cyclohexane were used as cooling liquid. With carbon tetrachloride the migration rate was slower and the border of the focussed zones was more confused, thereby cyclohexane appeared to be more suitable. It must be noticed that this liquid was not used till now as a cooling agent for paper electrophoresis. In the first set of experiments the influence of the electrophoresis time on the separation of the zones was studied. It was clear that separation took place after 10 minutes (Fig. 2). The extension of the electrophoresis time did not improve the separation. The diminution in the solution's concentration of about 100 times had no influence (Fig. 3). Another factor that was studied was the influence of the kind of anion accompanying the cation. It was established that in the case of both nitrate and chloride anions good separations were obtained after 15 minutes. These experiments concluded as to an optimum electrophoresis time of 15 minutes.

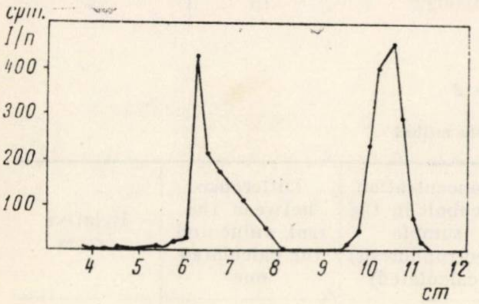

Fig. 2. — Repartition curve of the radioactivity.

Electrophoresis time : 10 minutes ; Concentration : 0.2 M/l ; Cation : nitrate.

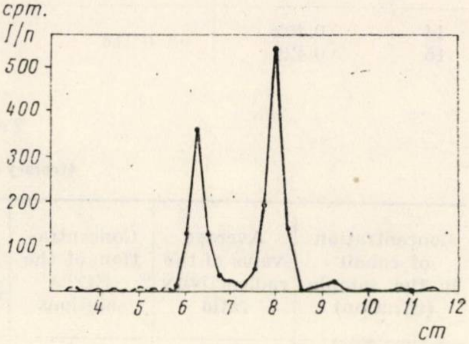

Fig. 3. — Repartition curve of the radioactivity.

Electrophoresis time : 15 minutes ; Concentration : 0.002 M/l ; Anion : chloride.

Another set of experiments has studied the reproducibility of the method, performing the electrophoresis with cyclohexane as cooling agent. The results obtained are shown in table 1. It has been found that, for

Table 1

Reproducibility of the electrophoretic separation

No	Ratio of the radioactivity	Average value of the radioactivity ratio	Concentration of cobalt in the sample	Amount of cobalt in the sample	Amount of cobalt taken for analysis
	R	$\bar{R}$	c		m
			mol/l	micrograms	micrograms
			Cobalt nitrate		
1	0.458	0.442	0.236	1390	205
2	0.415				
3	0.450				
4	0.443				
5	0.438	0.441	0.0236	139	21
6	0.443				
7	0.419	0.436	0.00437	26	4
8	0.453				
			Cobalt chloride		
9	0.45	0.443	0.220	1300	191
10	0.48				
11	0.40				
12	0.450	0.448	0.022	130	19
13	0.446				
14	0.402	0.416	0.0022	13	2
15	0.429				

Table 2

Accuracy of the method

Concentration of cobalt in the sample (titration)	Average value of the radioactivity ratio	Concentration of the EDTA solutions	Concentration of cobalt in the sample (electrophoresis) (calculated)	Difference between the real value and the calculated one	Relative errors
mol/l		mol/l			%
			Cobalt nitrate		
0.236	0.443	0.1	0.0225	0.011	4.7
0.236	0.441	0.01	0.0226	0.0010	4.2
0.00437	0.436	0.00185	0.00424	0.0013	3.5
			Cobalt chloride		
0.220	0.443	0.1	0.225	0.005	2.3
0.022	0.0448	0.01	0.0223	0.003	1.4
0.0022	0.416	0.001	0.0024	0.0002	9.1

the same sample and for the same run, the change of the radioactivity ratio agrees with the statistical fluctuations of the radioactive decay. That shows a good reproducibility of both the substoichiometric complexing of cobalt and its separation from the noncomplexed ions. It is clear from the table that the reproducibility is as well for cobalt nitrate as for cobalt chloride. The concentration diminution of the solution to be analysed did not influence the reproducibility of the complexing and separation.

In order to study the accuracy of the method the concentration of some cobalt nitrate and cobalt chloride solutions was determined using the electrophoretic focussing method described above, as well as titrating some samples of 5 – 10 ml with EDTA solution. The results obtained are given in table 2. It is obvious that the electrophoretic focussing method has given relative errors smaller than 5%, that may be considered satisfactory taking into account the small volume of the cobalt samples to be analysed. Under the described experimental conditions, the accuracy of the method has depended neither on concentration nor on anions accompanying the cobalt ions.

There are some indications in the literature that the electrophoretic focussing method may be applied to analyses of other heavy metal ions using cobalt as radioactive tracer. [3] In spite of this assertion our experiments have shown that neither the complexing reproducibility nor the accuracy were satisfactory when analysing by this method mercury, lead and other metal ions.

CONCLUSIONS

1. The electrophoretic separation of cobalt ions complexed with EDTA solution from noncomplexed ions takes place with higher rate if cyclohexane is used instead of carbon tetrachloride as cooling liquid.

2. Under the experimental conditions described in this paper, the voltage applied between the ends of the paper strip may be relatively small (150 volts) in comparison with that used by other investigators (1500 volts).

3. Due to the mentioned advantages, a very simple apparatus may be used to achieve electrophoretic focussing.

4. The optimum time for separating the focussed zones is 15 minutes. This time does not depend on the solution concentration or on the anions accompanying cobalt.

5. The reproducibility and the accuracy of the method are good, the relative errors being below 5%. One may use solutions more concentrated (2×10^{-1} M) as well as diluted ones (2×10^{-3} M), the minimum value of the required samples being of about 0,1 ml.

6. For the analysis of heavy metal ions by the isotopic dilution method and electrophoretic focussing, the radioactive tracer must belong to the metal to be analysed. It is not possible to use another tracer because the different complexing of the metals makes the method unreproducible.

---

[4] R. Pribil, "Complexonii în chimia analitică", Ed. tehnică, Bucharest, 1961, p. 283.

Revue Roumaine de Chimie, 15, 1447–1451 (1970)

Revue Roumaine de Chimie, 15, 1453–1459 (1970)

STEREOCHEMISTRY OF IMINE SYSTEMS. III[1]. MECHANISM OF THEIR UNCATALYSED *SYN-ANTI* ISOMERIZATION. THE INFLUENCE OF THE SUBSTITUENT ON THE ACTIVATION ENERGY

G. OSTROGOVICH *, Z. SIMON ** and F. KEREK *

* Laboratory for Organic Chemistry of the Polytechnic Institute, str. Bocşei 6 and
** Department for Organic Chemistry of the University, Bd. V. Pârvan 4
Timişoara, Romania

Received April 7, 1969

A simple HMO calculation, concerning the steric isomerization of benzalaniline (III) and its related compounds supported the isomerization mechanism by the "lateral shift" of the N-bonded substituent. A similar calculation applied for phenyliminodimethyl-carbonate (IV) suggests the possibility of an isomerization by means of a "torsional motion" allowed by the π (C=N) bond splitting in those cases when the intermediate complex is sufficiently stabilized by conjugative effects. For the "lateral shift" mechanism a quantitative correlation was obtained between the activation energy and the electronegativity of the N-bonded substituent which seems to be in agreement with experimental data.

1. — The specific configuration of the $>C=N\diagup$ bond confers to all imine compounds, $R_1R_2C=N-X$, the possibility to exist in two diastereoisomeric configurations, usually denoted by *syn* and *anti*. For the similar ethylene derivatives, due to their greater configurational stability, the isomers are generally separable (at common temperature and pressure). This kind of stability is usually not found for imines, where only the derivatives with an electronegative group (as $-OH$; $-OR$; $-Cl$; $-Br$; $-NH_2$; $-NHR$) bonded to the N atom, have stable isomers.[2a, 3-7]

---

[1] Previous papers of this series were headed "Stereochemistry of carbodiimides and ketenimines" I (ref. 2a); II (ref. 2b), but they referred also to the general problem of the imine systems configurational stability.

[2a] G. Ostrogovich and F. Kerek, *Studii şi Cercetări Chim. Acad. RSR*, **16**, 923, (1968).

[b] Z. Simon, F. Kerek and G. Ostrogovich, *Revue Roumaine Chim.*, **13**, 381 (1968).

[3] A. W. Stewart, "Stereochemie", Springer Verlag, Berlin, 1908, chap. III.

[4] J. Meisenheimer and W. Theilacker, "Stereochemie", edited by K. Freudenberg, F. Deuticke Verlag, Leipzig-Wien, 1933, 3. Buch, p. 974–81.

Most part of imines (especially the Schiff bases) possess a lower activation energy for the *syn-anti* isomerization ($\Delta E^{\ddagger} < 23$ kcal/mol). Thus they occur in liquid phase as equilibrium mixtures of the two isomers in ratios which vary from : 1/1 ($R_1 = R_2$) until below 1/100 when $\Delta F > 3$ kcal/mol and only the thermodynamical more stable isomer is isolable.[2a]

The uncatalytic (thermic) interconversion of the imine stereoisomers may take place in the following two ways (Fig. 1) :

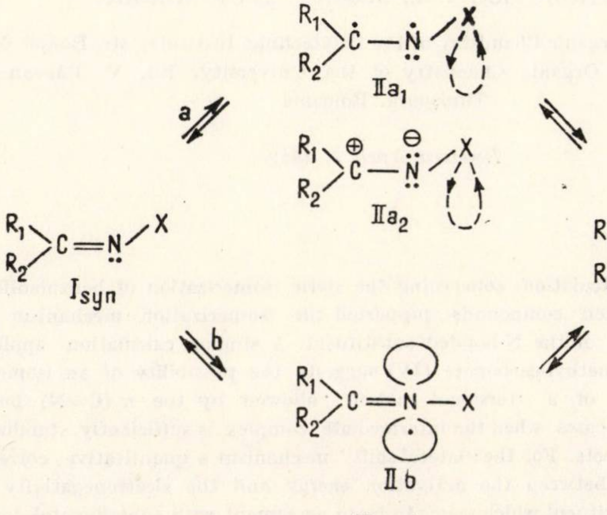

Fig. 1

a) *Torsional motion* around the C—N bond as axis allowed by splitting of the C=N π bond (by decoupling II_a or by strong polarization II_{a_2} of the π electrons).

b) *Lateral shift* of the X group (I) in the molecular plane (determined by R_1, R_2 and C—N) through the intermediate complex II_b in which the N atom has an sp hybridization (The initially sp^2 hybridized unshared electrons are promoted to a pure "p" orbital without any change in the C=N double bond).

The last of these ways was imagined as possible and even probable by E. Hückel in 1930.[8]

---

[5] C. S. Marvel, "*Cis-trans* Isomerism" in "Organic Chemistry", vol. 1, edited by H. Gilman, J. Wiley, 1953, p. 465.

[6] R. W. Layer, *Chem. Rev.*, **63**, 489 (1963).

[7a] D. Y. Curtin and J. W. Hauser, *J. Amer. Chem. Soc.*, **83**, 3474 (1961).

[b] D. Y. Curtin and C. G. Mc Carty, *Tetrahedron Letters*, **26**, 1269 (1962).

[c] D. Y. Curtin, E. J. Grubbs and C. G. Mc Carty, *J. Amer. Chem. Soc.*, **88**, 2775 (1966).

[8] E. Hückel, *Z. Physik*, **1930**, 423.

It is evident that the thermal isomerization of ethylene compounds may take place according only to the first route (a). Hückel calculations for substituted stilbene derivatives (i.e. subtracting the total π electron energy of the initial compound from that of the intermediate complex with interrupted conjugation) gave several activation energy values in good agreement with those experimentally determined.[9a]

When the same method was used for azobenzene there appeared a great difference between the calculated activation energy ($\Delta E^{\ddagger} = 47.3$ kcal/mol) and the experimental obtained value of 23 ± 2 kcal/mol for seven substituted azobenzenes.[9b] This disagreement supports undoubtedly the "lateral shift" isomerization route, as well as the relatively small substituent influence (the substituent influence is great for the torsional mechanism [2b]).

Based on these facts we performed a similar LCAO—MO calculation for imine systems. We tried also to obtain for the lateral shift mechanism a quantitative correlation between the X group electronegativity and the isomerization rate.

2. – RESULTS AND DISCUSSION

2.1. – *Hückel calculation*

By means of the Hückel method using the parameters given in table 1 we calculated the total π electron energy (E_π^{AB}) for benzalaniline (III AB) as well as for both molecular fragments A and B of its intermediate complex generated by the C=N π bond splitting. For the activation energy the value $\Delta E^{\ddagger} = (E_\pi^A + E_\pi^B) - E_\pi^{AB} = 34.6 \div 36.8$ kcal/mol results using the $\beta = -27.1$ kcal/mol from the *cis-trans* isomerization of stilbene derivatives.[9]

This value is much greater than the experimentally obtained activation energy for benzalaniline in cyclohexane solution (16—17 kcal/mol).[10] Thus, benzalaniline and its substituted derivatives are isomerized most probably through the lateral shift of the N-bonded substituent.

We may nevertheless not exclude for all cases the possibility of the "torsional" route which may become probable if the R_1, R_2 and X groups stabilize the decoupled or polarized intermediate by strong conjugative effect. Using the same calculation method for the phenyliminodimethylcarbonate IV there results an activation energy $\Delta E^{\ddagger} = -0.724\ \beta = 19.5$ kcal/mol comparable with that determined in $CHCl_3$ solution: 14.4 kcal/mol.[11]

[9a] I. G. Murgulescu and Z. Simon, *Z. phys. Chem.* (*Leipzig*), **221**, 29 (1962).

[b] I. G. Murgulescu and Z. Simon, *Rev. Roumaine Chim.*, **10**, 423 (1963).

[10] E. Fischer and Y. Frei, *J. Chem. Phys.*, **27**, 808 (1957).

[11] N. P. Marullo and E. H. Wagener, *J. Amer. Chem. Soc.*, **88**, 5034 (1966).

Table 1

Parameters for HMO-calculations* and π-electron-energy values obtained

Formula	Parameters	E_π^{AB}	E_π^{A}	E_π^{B}	$\Delta E^{\ddagger} = (E_\pi^{A} + E_\pi^{B}) - E_\pi^{AB}$
III		$C_6H_5-CH=N-C_6H_5$	$C_6H_5-\dot{C}H-\dot{N}-C_6H_5$		
III−1	$\alpha_N = \alpha + 0.5\,\beta$; $\beta_{C=N} = 1.2\,\beta$ $\beta_{ring-C} = 0.8\,\beta$; $\beta_{ring-N} = 0.8\,\beta$	$14\,\alpha + 19.31\,\beta$	$6\,\alpha + 8.60\,\beta$	$8\,\alpha + 9.35\,\beta$	$-1.36\,\beta = 36.8\,\frac{kcal}{mol}$
III−2	$\alpha_N = \alpha + 0.5\,\beta$; $\beta_{xy} = 1\,\beta$	$14\,\alpha + 19.53\,\beta$	$6\,\alpha + 8.72\,\beta$	$8\,\alpha + 9.53\,\beta$	$-1.28\,\beta = 34.6\,\frac{kcal}{mol}$
IV		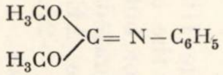 $(H_3CO)_2C=N-C_6H_5$	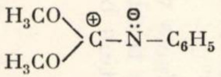 $(H_3CO)_2\overset{\oplus}{C}-\overset{\ominus}{\ddot{N}}-C_6H_5$		
IV−1	$\alpha_N = \alpha + 0.5\,\beta$; $\alpha_{O-CH_3} = \alpha + 2\,\beta$ $\beta_{O-C} = 0.8\,\beta$; $\beta_{N-ring} = 0.8\,\beta$ $\beta_{C=N} = 1.2\,\beta$	$12\,\alpha + 19.56\,\beta$	$4\,\alpha + 9.02\,\beta$	$8\,\alpha + 9.83\,\beta$	$-0.72\,\beta = 19.5\,\frac{kcal}{mol}$

* Calculations were performed on the MECIPT−1 computer of the Polytechnic Institute, Timişoara.

2.2. — *The influence of the substituent on the activation energy for the lateral shift mechanism*

As shown in our previous papers[2] the height of the energy barrier for the "lateral shift" route is determined mainly by the energy necessary for the $sp^2 \rightarrow sp$ hybridization change of the N atom.

In order to compute the difference between these two hybridization states we used the following notations for their electron-repartition:

$$(tr)^{n^{\sigma}_{(C)}}; \quad (tr)^{n^{\sigma}_{(X)}}; \quad (tr)^2; \quad (\pi)^{n^{\pi}_{(C)}} \text{ for } sp^2 \text{ state}$$

$$\text{and } (di)^{n^{\sigma}_{(C)}}; \quad (di)^{n^{\sigma}_{(X)}}; \quad (p_y)^2; \quad (\pi)^{n^{\pi}_{(C)}} \text{ for } sp \text{ state}$$

where: — (tr) are the sp^2 hybridized trigonal orbitals, (di) the sp hybridized digonal orbitals

— n the "occupation numbers" [12]; those with the σ superscript refer to the σ orbitals with the imino carbon and the X group, while those labelled with π to the π orbital with the imino carbon.

— the two unshared nitrogen electrons are promoted from a trigonal to a pure p orbital denoted by p_y.

According to the definition given by Hinze et al.[13] the orbital electronegativity is:

$$\chi_j = \frac{\partial E}{\partial n_j} \tag{1}$$

where — $\partial E/\partial n_j$ is the derivative of the given atom's total energy for the j-th orbital.

— n_j — the occupation number of the j-th orbital.

For small changes of the n value we may write:

$$\Delta E_j = \Delta n_j \chi_j \tag{2}$$

Using the χ values for the nitrogen atom's valence state orbitals, given by Hinze and Jaffe [14] (in eV)

$\chi_\sigma(tr) = -25.74$; $\chi_\pi = -15.90$ for the (tr^2, tr, tr, π) hybridization

$\chi_\sigma(di) = -28.94$; $\chi'_\pi = -16.25$ for the (di, di, p_y^2, π) hybridization

we obtained the total energy of the nitrogen electrons at the initial (3) and at the intermediate state (4)

$$-E_{sp^2} = (n^{\sigma}_{(X)} + n^{\sigma}_{(C)})\,25.74 + 2\,\chi_{tr^2} + n^{\pi}_{(C)}\,15.90 \tag{3}$$

$$-E_{sp} = (n^{\sigma}_{(X)} + n^{\sigma}_{(C)})\,28.94 + 2\,\chi_{p_y^2} + n^{\pi}_{(C)}\,16.25 \tag{4}$$

---

[12] J. Hinze, *Fortschr. der chem. Forschung*, **9** (3), 448 (1968).

[13] J. Hinze, M. A. Whitehead and H. H. Jaffe, *J. Amer. Chem. Soc.*, **85**, 148 (1963).

[14] J. Hinze and H. H. Jaffe, *J. Amer. Chem. Soc.*, **84**, 540 (1962).

The activation energy of *syn-anti* isomerization will be:

$$\Delta E^{\ddagger} = E_{sp} - E_{sp^2} = -2\,(\chi_{p_y^2} - \chi_{tr^2}) - 3.2\,(n^{\sigma}_{(X)} + n^{\sigma}_{(C)}) - 0.35\ n^{\pi}_{(C)} \qquad (5)$$

The $-2\,(\chi_{p_y^2} - \chi_{tr^2})$ term (eq. 5) represents the promotion energy of two unshared electrons from a trigonal to a pure p orbital, which certainly is an endothermal process. Since it is difficult to compute its exact value we denote this energy difference by $\delta\varepsilon$.

As the $n^{\sigma}_{(C)}$ from eq. (5) is practically constant we may include the $-3.2\ n^{\sigma}_{(C)}$ value in a constant C together with $2\,\delta\varepsilon$:

$$C = 2\,\delta\varepsilon - 3.2\,n^{\sigma}_{(C)} \qquad (6)$$

In order to study the influence of the X substituents we may use the relation (7) for the occupation number[12]

$$n^{\sigma}_{(X)} = \frac{2\chi_N}{\chi_N + \chi_X} \qquad (7)$$

With equations (6) and (7) equation (5) becomes:

$$\Delta E^{\ddagger} = C - 6.4\,\frac{\chi_N}{\chi_N + \chi_X} - 0.35\,n^{\pi}_{(C)} \qquad (8)$$

It results from equation (8) that the height of the energy barrier is determined by:

— the energy, necessary for promotion of the unshared electrons from a trigonal to a p orbital ($2\,\delta\varepsilon$),

— $[-3.2\ n^{\sigma}_{(C)}]$ which practically does not depend on the X substituent,

— $[-0.35\,n^{\pi}_{(C)}]$ whose variation with substituents due to the 0.35 factor's small value, may be neglected,

— $[6.4\ \chi_N/(\chi_N + \chi_X)]$ term whose value is inversely proportional to the electronegativity of the X substituent.

In figure 2 (kinetic results for isomerization of imine,[7,10,15] hydrazone and semicarbazone,[16] oxyme,[17] oxyme-ether,[7c] brom- and chlorimine[7c] compounds) the logarithms of rate constants $k(\mathrm{sec}^{-1})$ are plotted against the corresponding $\chi_N/(\chi_N + \chi_X)$ values.[12,18]

If we take into account that $\log k = \log A - \Delta E^{\ddagger}/4.575\ T$ and that the temperature was of the order of 300°K, a log k unit corresponds to 1.37 kcal/mol. The slope of diagram 2 (10 log k units for 0.09 $\chi_N/\chi_N + \chi_X$ units) corresponds to 150 kcal/mol (6.5 eV) in very good agreement with the 6.4 eV factor from the eq. (8).

One can remark that the same variation of the configurational stability was recently observed for several azyridine derivatives[19,20]

---

[15] H. A. Staab, F. Vögtle and A. Mannschrecke, *Tetrahedron Letters*, **12**, 697 (1965).

[16] G. J. Karabatsos, F. M. Vane, A. Taller and N. Hsi, *J. Amer. Chem. Soc.*, **86**, 3351 (1964).

[17] J. W. LeFevre and J. Northcott, *J. Chem. Soc.*, **1949**, 2235.

[18] For the χ_X values see also: A. Batzanov, "The Elements Electronegativity" (in Russian), Novosibirsk, 1962.

[19] J. M. Lehn and J. Wagner, *Chem. Communications*, **1968**, 148.

[20] S. J. Brois, *J. Amer. Chem. Soc.*, **90**, 506; 508 (1968); *Tetrahedron Letters*, **1968**, 5997.

where the isomerization mechanism is related to those discussed in the present paper.

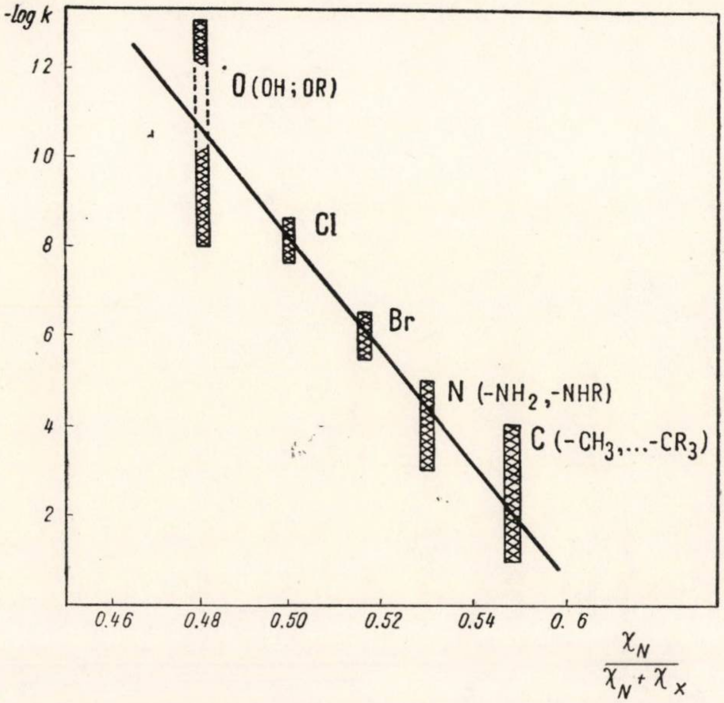

Fig. 2. — Logk *versus* ($\chi_N/\chi_N + \chi_X$) values plot for the *syn-anti* isomerization of some substituted imine derivatives ($R_1R_2C=N-X$).

3. — CONCLUSIONS

— The Hückel calculation supports the lateral shift isomerization mechanism for benzalaniline and its analogues.

— If the activated complex, formed through a splitting of the C=N π bond were sufficiently stabilized by conjugation (i.e. compound IV) there appears the possibility of a torsional isomerization mechanism.

— Relation (8) is in good agreement with the experimentally observed facts i.e. the increase of configurational stability of the imino compounds together with the increase of the electronegativity for the N-bonded substituents.

Revue Roumaine de Chimie, **15**, 1453–1459 (1970)

ORSZÁGOS MŰSZAKI KÖNYVTÁR
DOKUMENTÁCIÓS KÖZPONT

where the isomerization mechanism is related to those discussed in the present paper.

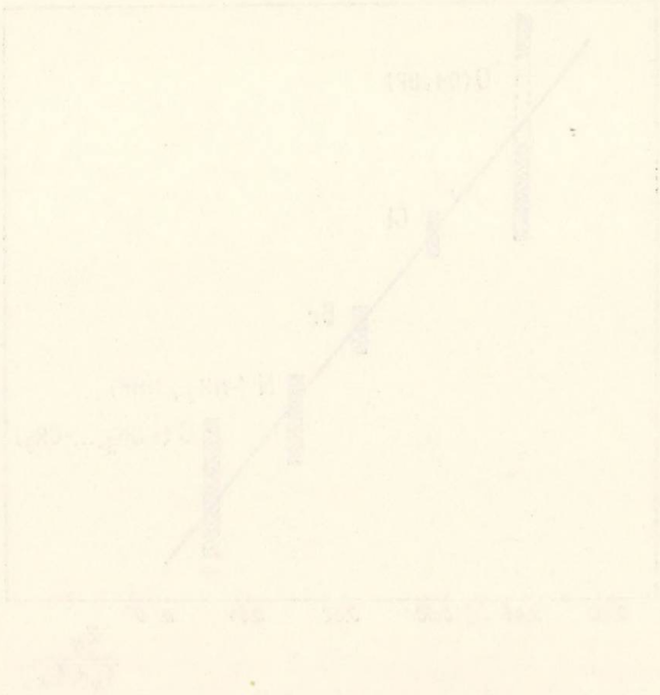

Fig. 3. — [illegible]

5. — CONCLUSIONS

The Hückel calculation supports the belief that isomerization mechanism for benzaldehyde and its analogues.

If the activated complex formed through a splitting of the C = N bond were sufficiently stabilized by conjugation (i.e. compound IV), then appears the possibility of a different isomerization mechanism.

— Relation (8) is in good agreement with the experimentally observed facts i.e. the increase of configurational stability of the [illegible] compounds together with the increase of the electronegativity for the Z-bonded substituents.

La *Revue Roumaine de Chimie* paraît 12 fois par an. Le prix d'un abonnement annuel est de £ 5.0.0 ; $ 12,— ; FF 60,— ; DM 48,—. Toute commande de l'étranger (fascicules ou abonnements) sera adressée à Centrala Cărţii, Oficiul de comerţ exterior, Boîte postale 134—135, Bucarest, Roumanie, ou à ses représentants à l'étranger :

ALBANIA Ndërmarja Shtetëtrore E. Tregëtimit Të Librit Tirana ; AUSTRIA Globus Buchvertrieb Salzgries 16 Wien I ; BELGIUM Du Monde Entier 5, Place St. Jean Bruxelles ; Librairie Claeys-Verheughe 8, Volderstraat Gand ; Maison des Langues Vivantes 65, Rue du Midi Bruxelles ; Office International de Librairie 30, Av. Marnix Bruxelles 5 ; Vander Editeur 10, Munstraat Louvain ; BULGARIA Hemus Pl. Slaveikov 11-Sofia ; CANADA Canadian Slavic Studies Loyola College Montreal 262 ; Librairie Lidec Inc. 1083 Van Home Montreal ; Pannonia Books 2, Spadina Road Toronto 4 Ontario ; CHINA Waiwen Shudian P.O. Box 88 Peking ; COLOMBIA Libreria Karl-Bucholz Av. Jimenez 8—40 Bgoota ; CUBA Cubartimpex P.O. Box 6540 La Habana ; CZECHOSLOVAKIA Artia Ve Smerckach 30 Praha I ; DENMARK Munksgaard 6 Norregade Copenhagen K ; N. J. Hasses-Bogimport 8, Loerstraede Copenhagen K. ; FINLAND Akateeminen Kirjakauppa Postfach 10128 Helsinki 10 ; FRANCE Agence Littéraire et Artistique Parisienne 7, Rue Debelleyme Paris 3-e ; Eyrolles Editeur 61, Boulevard Saint-Germain Paris 5-e ; Librairie de l'enseignement technique (Stand permanent des livres techniques et scientifiques roumains) 61, Boul. Saint-Germain, Paris 5-e ; Librairie Hachette 25, Rue des Cévennes Paris 5-e ; Librairie Joseph Gibert 26—30, Boul. Saint-Michel Paris 6-e ; Libella 12, Rue Saint-Louis-en-l'Ile Paris 4-e ; Maison du Livre Italien 46, Rue des Ecoles Paris 5-e ; Office International de Documentation et Librairie 48, Rue Gay-Lussac Paris 5-e ; Presses Universitaires de France 17, Rue Soufflot Paris 5-e; THE GERMAN DEMOCRATIC REPUBLIC Deutscher Buch-Export- und -Import Leninstrasse 16 Leipzig C. 1 ; THE FEDERAL REPUBLIC OF GERMANY Kubon & Sagner P.O. Box 68 München 34 ; Reise und Verkehrsverlag Hönigwiesenstrasse, 25 7 Stuttgart-Veihingen ; Zumsteins Landkartenhaus Liebherrstrasse, 5 8 München 22 ; GREAT BRITAIN Bailey Bros & Swinfen Ltd. Warner House 48, Upper Thames Street London E.C. 4 City 6521 ; Blackwell's Foreign Department Broad Street Oxford ; Central Books Ltd. 37, Grays Inn Road London W.C.1 ; Collet's Holdings Ltd. Denington Estate London Road Wellingborough Northans N & G Goyle Ltd. 119—125 Charring Cross Road London W.C. 2 ; Parker & Son 103, Walton Street Oxford ; HOLLAND Antiquariat Junk Walderstraat 10 Lochem ; Boekhandel Pegasus Leidsestraat 25 Amsterdam ; Intertaal Van Baerlesstraat 150 Amsterdam Zuit; Meulenhoff Beulingstraat 2 Amsterdam C ; Swets & Zeitlinger Keizersgracht 471—487 Amsterdam ; HUNGARY Kultura Fö utca 32 Budapest 1 ; ISRAEL Haiflepac Ltd. 11, Arlosorov St. Haifa ; Lepac Ltd, 15, Rambam St. Tel-Aviv ; Lotus Ltd. Achad Haam St. Tel-Aviv ; ITALY SO, CO, LIB, RI Export-Import Piazza Margana 33 Roma ; JAPAN Maruzen Ltd. 6 Tory Michome Nihombashi Tokyo ; Nauka Ltd. Imp. Departm. 30—19 Minami Ikebukuro 2, Chome, Toshima-Ku Tokyo ; DEMOCRATIC PEOPLE'S REPUBLIC OF KOREA Chulpanmul ; MEXICO Editorial Grijalbo S. A. Aparatado 28568 Mexico. 17.D.F. ; MONGOLIA Mongolgosknigotorg Ulan Bator ; NORWAY Norsk Bokimport Postboks 3267 Oslo ; POLAND Ars Polona Krakowskie Przedmiescie 7 Warszawa ; PORTUGAL Libreria Bucholz Avenida Libertade Lisboa ; SPAIN Libreria Bucholz Paseo de Recoletos Madrid ; Libreria Cientifica General Preciados no. 48 Madrid 13 ; SWEDEN Almqvist & Wiksell 26, Gamla Brogatan Stockholm k.; C. E. Fritze Fredgatan 2 Stockholm 16 ; Gumperts AB P. O. Box 346 Göteborg I ; SWITZERLAND Fachbücherei Postfach 1420 3001-Berna ; Herbert-Lang Ecke Munzgraben 2 Berna ; Librairie Payot 1-Rue de Bourg Ch-1002 Lausanne ; Librairie Rousseau 36, Rue Jean-Jacques Rousseau Genève ; Pinkus & Co. Froschaugasse 7 Zürich I ; THE UNITED ARAB REPUBLIC Dar El Tahrir et Publishing 21 Kasr el Nil St. (Dar el Shark Bookshop) Cairo ; THE U.S.A. Angelescu Book Service 3645, Barham Street Detroit 24 Michigan ; American Chemical Society 1155, Sixteenth Street NW Washington DC 20036 ; Fam Book Service 69, Fifth Avenue Suite 8 F ; New York 10003, N.Y. Franklin Square-Subscription Agency Teaneck (New Jersey 07666) ; W. S. Heinman 400, East 72nd Street New York, 21, N. Y. ; McGraw-Hill Book Company 330, West 42nd Street New York, N.Y. 10036 ; Moore-Cottrell Subscr. Agency Worth Cohocton, New York 14868 ; Nicoară Travel Service 17432, Woodward Ave. Detroit Michigan 48203 ; Shoenhof's Foreign Books, Inc. 1280, Massachusetts Avenue Cambridge, Massachusetts 02138 ; Henry M. Snyder & Co. Inc. 440 Fourth Avenue New York, N.Y. 10016 ; Twayne Publishers, Inc. 31 Union Square West New York 3, N. Y. ; Zeitein & Ver Brugge Booksellers 815 No. La Cienaga BLVD Los Angeles 69, California ; THE U.S.S.R. Mejdunarodnaia Kniga Moscow C. 200 ; THE DEMOCRATIC REPUBLIC OF VIET-NAM Xunhasaba 32, Hai Ba Trung Hanoi ; YUGOSLAVIA Forum V. Misica, 1 Novi Sad ; Jugoslovenska Knjiga Terazije, 27 Beograd ; Libertatea Z. Zrenjanina, 7 Pancevo ; Prosveta Terazije 16 I Beograd.

La Revue Roumaine de Chimie paraît 12 fois par an. Le prix d'un abonnement annuel est de £ 5.00 ; $ 12.— ; Ff 60.— ; DM 45.— Toute commande de l'étranger (fascicules ou abonnements) sera adressée à Centrala Cărţii, Oficiul de comerţ exterior, Boîte postale 134-135, Bucarest, Roumanie, ou à ses représentants à l'étranger :

ALBANIA Ndermarja Shtetërore E Tregtimit Te Librit Tirana ; AUSTRIA Globus Buchvertrieb Salzgries 16 Wien I ; BELGIUM Du Monde Entier 5, Place St. Jean Bruxelles ; Librairie Claeys-Verheughe 8, Koloniestraat Gand ; Maison des Langues Vivantes 65, Rue du Midi Bruxelles ; Office International de Librairie 30, Av. Marnix Bruxelles 5 ; Vander Editeur 10, Muntstraat Louvain ; BULGARIA Hemus 6, Ruskey Blvd. Sofia ; CANADA Canadian Slavic Studies Loyola College Montreal 262 ; Librairie Liddec Inc. 1083 Van Horne Montreal ; Pannonia Books 2, Spadina Road Toronto 4 Ontario ; CHINA Waiwen Shudian P.O. Box 88 Peking ; COLOMBIA Libreria Karl Buchholz Av. Jimenez 8—40 Bogota ; CUBA Cubartimpex P.O. Box 6540 La Habana ; CZECHOSLOVAKIA Artia Ve Smeckach 30 Praha 1 ; DENMARK Munksgaard 6 Nørregade Copenhagen K ; N. J. [illegible] 2, Løvstræde Copenhagen K ; FINLAND Akateeminen Kirjakauppa Postbox 10128 Helsinki 10 ; FRANCE Agence Littéraire et Artistique Parisienne 7, Rue Debelleyme Paris 3-e ; Eyrolles Editeur 61, Boulevard Saint-Germain Paris 5-e ; Librairie de l'enseignement technique (Stand permanent des livres techniques et scientifiques roumains) 61, Boul. Saint-Germain, Paris 5-e ; Librairie Mesnil 25, Rue des Cévennes Paris 5-e ; Librairie Joseph Gibert 26—30, Boul. Saint-Michel Paris 6-e ; Lipsia 12, Rue Saint-Louis-en-l'Île Paris 4-e ; Maison du Livre Italien 45, Rue des Écoles Paris 5-e ; Office International de Documentation et Librairie 48, Rue Gay-Lussac Paris 5-e ; Presses Universitaires de France 17, Rue Soufflot Paris 5-e ; THE GERMAN DEMOCRATIC REPUBLIC Deutscher Buch-Export und -Import Leninstrasse 16 Leipzig C 1 ; THE FEDERAL REPUBLIC OF GERMANY Kubon & Sagner P.O. Box 68 München 34 ; Reise und Verkehrsverlag Hönigvogelstrasse 15, 7 Stuttgart-Vaihingen ; Zumsteins Landkartenhaus Liebherrstrasse 5, 8 München 22 ; GREAT BRITAIN Bailey Bros. & Swinfen Ltd. Warner House 48, Upper Thames Street London E.C. 4 City 8822 ; Blackwell's Foreign Department Broad Street Oxford ; Central Books Ltd. 37, Grays Inn Road London W.C. 1 ; Collet's Holdings Ltd. Denington Estate London Road Wellingborough Northants ; W. & G. Foyle Ltd. 119—125 Charing Cross Road London W.C. 2 ; Parker & Son 103, Walton Street Oxford ; HOLLAND Antiquariaat Junk Waldestraat 10 Lochem ; Boekhandel Pegasus Leidsestraat 25 Amsterdam ; Intertaal Van Baerlestraat 150 Amsterdam Zuid ; Meulenhoff Bruna Beulingstraat 2 Amsterdam C ; Swets & Zeitlinger Keizersgracht 471—487 Amsterdam ; HUNGARY Kultura Fö utca 32 Budapest 1 ; ISRAEL [illegible] Ltd. 1 A, Arlosorov St. Haifa ; Lepac Ltd. 15, Rambam St. Tel-Aviv ; Lepac Ltd. Achad Haam St. Tel-Aviv ; ITALY SO.CO.LIB. RI Export-Import Piazza Margana 33 Roma ; JAPAN Maruzen Ltd. 6 Tori Nichome Nihonbashi Tokyo ; Nauka Ltd. Exp. Departm. 30—19, Minami Ikebukuro 2, Chome, Toshima-Ku Tokyo ; DEMOCRATIC PEOPLE'S REPUBLIC OF KOREA Chulpanmul ; MEXICO Editorial Cartago S. A. Apartado 28568 Mexico 17 D.F. ; MONGOLIA Mongolgosknigotorg Ulan Bator ; NORWAY Narvesens Kioskkompani Postboks 125 Oslo ; POLAND Ars Polona Krakowskie Przedmiescie 7 Warszawa ; PORTUGAL Livraria Buchholz Avenida Liberdade Lisboa ; SPAIN Libreria Buchholz Paseo de Recoletos Madrid ; Libreria Cientifica General Preciados no. 48 Madrid 12 ; SWEDEN Almqvist & Wiksell 26, Gamla Brogatan Stockholm 1 ; C. E. Fritze Fredsgatan 2 Stockholm 16 ; Gumperts AB. P. O. Box 346 Göteborg 1 ; SWITZERLAND Parlamentsbuchhandlung Postfach 1400 3001 Berna ; Herbert Lang & Cie Münzgraben 2 Berna ; Librairie Payot 1 Rue de Bourg CH-1002 Lausanne ; Librairie Rousseau 36, Rue Jean-Jacques Rousseau Genève ; Pinkus & Co. Froschaugasse 7 Zürich 1 ; THE UNITED ARAB REPUBLIC Dar El Tahrir el Hadietha 21 Kasr el Nil St. Cairo ; Shark Bookshop Cairo ; THE U.S.A. [illegible] Book Service 3005 Woodward Street Detroit 24 Michigan ; American Chemical Society 1155 Sixteenth Street N.W. Washington DC 20036 ; Fam Book Service 69, Fifth Avenue New York ; New York 10003 N.Y. ; Franklin Square-Subscription Agency [illegible] (New Jersey) [illegible] 400 East 72nd Street New York, 21 N.Y. ; McGraw-Hill Book Company 330 West 42nd Street New York, N.Y. 10036 ; Moore-Cottrell Subscr. Agency North Cohocton New York 14868 ; [illegible] Travel Service 17422 Woodward Ave. Detroit Michigan 48203 ; Schoenhof's Foreign Books, Inc. 1280 Massachusetts Avenue Cambridge Massachusetts 02138 ; Henry M. Snyder & Co. Inc. 440 South Avenue New York, N.Y. 10016 ; Twayne Publishers Inc. 31 Union Square West New York 3, N. Y. ; Zeitlin & Ver Brugge Booksellers 815 No. La Cienega Blvd. Los Angeles 69, California ; THE U.S.S.R. Mezhdunarodnaja Kniga Moscow G 200 ; THE DEMOCRATIC REPUBLIC OF VIETNAM Xunhasaba 32, Hai Ba Trung Hanoi ; YUGOSLAVIA Forum V. Mišića 1 Novi Sad ; Jugoslovenska Knjiga Terazije 27 Beograd ; Libertatea 2, Zrenjanin, 7 Pančevo ; Prosveta Terazije 16 Beograd

NOTE POUR LES AUTEURS

La *Revue Roumaine de Chimie* publie des articles en anglais, français, russe, allemand ou espagnol. Les auteurs sont priés d'envoyer des articles, notes, communications et comptes rendus inédits.

Les manuscrits seront dactylographiés à deux intervalles. Les tableaux seront dactylographiés sur feuilles séparées, de même que la légende des figures. Les diagrammes seront tracés à l'encre de Chine sur papier calque. Les tableaux et les figures seront numérotés par des chiffres arabes, en nombre strictement nécessaire. Prière de ne pas inscrire les mêmes données dans les tableaux et les figures. Les formules chimiques seront incluses dans le texte ; en outre, elles seront transcrites sur des feuilles séparées. Les auteurs sont priés d'indiquer les caractères italiques (en soulignant les lettres au crayon), ainsi que tout autre caractère spécial. L'ordre des références bibliographiques sera celui de leur mention dans le texte ; le nom de l'auteur sera précédé de l'initiale du prénom ; les publications périodiques seront présentées suivant les prescriptions internationales. Les références seront ajoutées à la fin de l'article ; elles paraîtront comme des notes, au bas de la page. Le texte sera précédé d'un résumé, comprenant 15 lignes au maximum.

L'entière responsabilité du contenu des articles appartient aux auteurs. On publie des articles dus aux collaborateurs roumains ou étrangers. Les auteurs recevront 50 tirés à part.

PRINTED IN ROMANIA

1970 NOV 13

TRAVAUX PARUS AUX ÉDITIONS DE L'ACADÉMIE DE LA RÉPUBLIQUE SOCIALISTE DE ROUMANIE

CORNEL BODEA et collab., **Tratat de biochimie vegetală**, partea I, **Fitochimie** (Traité de biochimie végétale, Ire partie, Phytochimie), Ier vol., 1964, 747 p. + 4 annexes + 2 pl., 41 lei, IIe vol., 1965, 1262 p., 1 pl., 56 lei, IIIe vol., 1967, 773 p., 35 lei.

V. GHEŢIE et V. MICUŞAN, **Analiza imunochimică. Teorie şi practică** (Analyse immunochimique. Théorie et pratique), 1966, 369 p., 28 lei.

R. PORTOCALĂ et L. POPA, **Acizii ribonucleici celulari şi virali** (Les acides ribonucléiques cellulaires et viraux), 1966, 375 p. + 8 pl., 26 lei.

D. PURDELA et R. VÎLCEANU, **Chimia compuşilor organici ai fosforului şi ai acizilor lui** (La chimie des composés organiques du phosphore et de ses acides), 1965, 540 p., 37 lei.

CRISTOFOR SIMIONESCU, MARGARETA GRIGORAŞ et AGATA CERNĂTESCU-ASANDEI, **Chimia lemnului din R.P.R.** (La chimie du bois en Roumanie), 1964, 239 p. + 6 pl., 27 lei.

CRISTOFOR SIMIONESCU et CLEOPATRA VASILIU-OPREA, **Mecanochimia compuşilor macromoleculari** (La mécanochimie des composés macromoléculaires), 1967, 344 p., 23,50 lei.

CARMEN SABĂU, **Schimbul ionic, teoria şi aplicaţiile sale în chimia analitică** (L'échange ionique, théorie et applications à la chimie analytique), 1967, 307 p., 12 lei.

I. MAXIM, **Materiale nucleare** (Matériaux nucléaires), 1969, 444 p., 30 lei.

CR. SIMIONESCU, C. UGLEA, **Fracţionarea compuşilor macromoleculari** (Le fractionnement des composés macromoléculaires), 1969, 292 p., 18,50 lei.

I.P. „Informaţia" c. 5626

43 426

Lei 25

F 1103

R

REVUE ROUMAINE DE CHIMIE

REFERÁLVA

TOME 15
N° 10
Octobre 1970

ÉDITIONS DE L'ACADÉMIE DE LA RÉPUBLIQUE SOCIALISTE DE ROUMANIE

Rev. Roumaine Chim. 15, 1461–1632 (1970), Bucarest

COMITÉ DE RÉDACTION

Rédacteur en chef :

C. D. NENIȚESCU, membre de l'Académie de la République Socialiste de Roumanie

Rédacteurs en chef adjoints :

A. T. BALABAN et V. E. SAHINI, membres correspondants de l'Académie de la République Socialiste de Roumanie

Collège de rédaction :

C. DRĂGULESCU, RALUCA RIPAN, CR. SIMIONESCU, membres de l'Académie de la République Socialiste de Roumanie ; EM. BRATU, membre correspondant de l'Académie de la République Socialiste de Roumanie ; Pr G. OSTROGOVICH, MARGARETA AVRAM, F. BADEA, I. D. MARCHIDAN, D. NEGOIU et D. SĂNDULESCU.

La REVUE ROUMAINE DE CHIMIE paraît 12 fois par an. Le prix d'un abonnement annuel est de : £ 5.0.0 ; $ 12,– ; FF 60,– ; DM 48,–. Toute commande de l'étranger (fascicules ou abonnements) sera adressée à Întreprinderea de Comerț exterior, «LIBRI», Boîte postale 134–135, Bucarest, Roumanie, ou à ses représentants à l'étranger.

Les manuscrits, les livres et les revues proposés en échange, ainsi que toute correspondance seront envoyés à la rédaction :

REVUE ROUMAINE DE CHIMIE

23, str. Dumbrava Roșie, Bucarest, 9, Roumanie.

REVUE ROUMAINE DE CHIMIE

ORSZÁGOS MŰSZAKI

Tome 15, No 10 Octobre 1970

Page

I. G. MURGULESCU, Some physico-chemical properties of simple molten salts. II 1463–1471

I. G. MURGULESCU and DOINA TODOR-BOGDAN, Kinetics of reaction between 1-phenyl-azo-2-naphthol and copper chloride 1473–1483

D. CISMARU, AL. FRUMA and D. CRĂCIUNESCU, Determining the size of metal particles in hydrogen chemisorption measurements 1485–1489

D. I. MARCHIDAN and SPERANȚA MATEI, High-temperature thermodynamic properties of some uranium oxides from EMF measurements on solid electrolyte galvanic cells 1491–1502

ȘTEFANIA ZUCA and M. OLTEANU, Electrical conductivity of binary molten alkali halide systems as a function of anion polarization . . . . 1503–1511 R

N. BONCIOCAT, L. CHIOSA, FLORICA MIHĂILESCU and M. OLTEANU, Chemical reactions in liquid junctions. II. A new potentiometric titration method 1513–1523

N. I. IONESCU, About the electrical resistance variations in thin iron films during water chemisorption and decomposition 1525–1528

RALUCA RIPAN und A. BOTAR, Eine neue Gruppe von Heteropolyverbindungen des U(IV). I. Uran(IV)-Oktowolframanion, Synthese der Alkalisalze und Bestimmung ihrer Basizität 1529–1535

RALUCA RIPAN und A. BOTAR, Eine neue Gruppe von Heteropolyverbindungen des U(IV). II. Photokolorimetrische Studien der Bildung des $[UW_8O_{28}]^{4-}$ in Abhängigkeit von pH, Temperatur und Zeit 1537–1541

C. DRĂGULESCU, R. POMOJE, I. MENESSY und MARIA PÎRLEA, Metallkomplexe der Anthranyldiessigsäure (ANDA). IX. Das System Al–ANDA 1543–1546

T. GOINA and MARIA OLARU, Formation of aluminium complexes with pyrogallol . . . . 1547–1554 R

CANDIN LITEANU and IOVANCA HAIDUC, Pretreated indicating electrodes in potentiometric titrations. II. Bright palladium-hydrogen electrode in acid-base titration . . . . 1555–1561 R

A. ȘUTEU et LUCREȚIA MÎRZA, L'étude röntgénostructurale des trihétéropolyacides 1563–1572

I. PETRARIU, CORNELIA LUCA and M. DIMA, Quaternary basic ammonium polyelectrolytes. II. Chlorination with thionyl chloride of some quaternary basic ammonium polyelectrolytes containing hydroxylic groupings 1573–1580

Rev. Roumaine Chim. **15,** 1461–1632 (1970), Bucarest

Page

DIANA GIURGIU, I. POPESCU, AGLAIA CIOBANU, M. BOSTAN, N. VOICULESCU und LUCIA ROMAN, Arylaluminium-Phosphin Verbindungen 1581–1589

GH. FURNICĂ, Recherches sur la dégradation des macromolécules polysulfoniques au moyen des isotopes radioactifs 1591–1599

N. BĂRBULESCU und F. POTMISCHIL, Darstellung und Untersuchung der Hydroacridine. VII. Ein direkt-Verfahren zur Darstellung von N-Alkyl- und N-Aryl-Perhydroacridinen 1601–1610

S. H. DOSS and M. S. AHMAD, New synthetic chemical compounds with expected schistosomicidal activity 1611–1614

L. SZOTYORI, L. FEY and AL. KÖVENDI, The reaction between sodium alcoxides and α-haloketones. VII. The action of sodium methoxide on *p*-chloro-ω-bromoacetophenone 1615–1622

CĂTĂLINA DEMETRESCO, VIORICA MANU et M. VANGHELOVICI, Contribution à la chimie des phényl-2-benzylidène-4-azlactones-5. Synthèses de nouvelles hydrazides substituées douées d'action psychoénergisante et parasympathicolytique 1623–1631

Revue Roumaine de Chimie, **15**, 1463–1471 (1970)

SOME PHYSICO-CHEMICAL PROPERTIES OF SIMPLE MOLTEN SALTS. II [1]

I. G. MURGULESCU

Center of Physical Chemistry
str. Galaţi 31, Bucharest, Romania

Received August 26, 1970

The substitution of internal pressure into Buehler, Hirschfelder and Curtis equation [2] leads to useful equations of state for molten salts. The relations obtained for the expansion and compressibility coefficients with these equations of state give values which at melting point are in good agreement with experimental data.

In a previous paper [1] the Buehler, Hirschfelder and Curtis [1] equation :

$$PV\left(1-\frac{\sigma}{a}\right)=RT$$

was shown to be applicable to molten salts. In this equation σ represents the molecular diameter while a, being the shortest distance between particles, is correlated with the volume occupied by a particle, v, by the equation :

$$a^3=\sqrt{2}\,v$$

For molten salts, the Buehler, Hirschfelder and Curtis [1] equation may be written as :

$$PV\left(1-\frac{2^{5/6}\,\nu^{1/3}\,N^{1/3}}{V^{1/3}}\,\bar{r}\right)=\nu RT \qquad (1)$$

when V is the molar volume, ν the number of ions resulting from the dissociation of a fused salt molecule and $\bar{r}$ the average radius of the constituent ions.

The validity of equation (1) for molten salts, assimilated to ionic liquids, results from the satisfactory agreement existing between the values of expansion coefficient α and compressibility coefficient β_T calculated with the equations :

---

[1] I. G. Murgulescu, *Rev. Roumaine Chim.*, **14**, 965 (1969).

[2] J. O. Hirschfelder, C. F. Curtis and R. Byron Bird, "Molecular Theory of Gases and Liquids", New York, London, 1954, p. 286.

$$\alpha = \frac{1}{V}\left(\frac{\partial V}{\partial T}\right)_P = \frac{1}{T}\,\frac{1 - \dfrac{2^{5/6}\,\nu^{1/3}\,N^{1/3}}{V^{1/3}}\,\bar{r}}{1 - \dfrac{2}{3}\,\dfrac{2^{5/6}\,\nu^{1/3}\,N^{1/3}}{V^{1/3}}\,\bar{r}} \tag{2}$$

$$\beta_T = -\frac{1}{V}\left(\frac{\partial V}{\partial P}\right)_T = \frac{V}{\nu R T}\,\frac{\left(1 - \dfrac{2^{5/6}\,\nu^{1/3}\,N^{1/3}}{V^{1/3}}\,\bar{r}\right)^2}{1 - \dfrac{2}{3}\,\dfrac{2^{5/6}\,\nu^{1/3}\,N^{1/3}}{V^{1/3}}\,\bar{r}} \tag{3}$$

which were deduced from equation (1) and the experimental values. In the following an attempt is made to change equations (1) – (3) into other useful equations by introducing the internal pressure and the heat of vaporization.

INTERNAL PRESSURES. HEATS OF VAPORIZATION

The thermal pressure in equation (1) is equal to the sum of two terms :

$$P = P_i + P_a$$

the internal pressure P_i and the applied pressure P_a. In normal working conditions with molten salts the applied pressure does not exceed one atmosphere and is negligible in comparison with P_i which passes beyond 10,000 atmospheres. This latter may be approximated by the well known equation

$$P_i = \left(\frac{\partial E}{\partial V}\right)_T \tag{4}$$

E being the internal energy of the system.

Let us consider a molten salt in equilibrium with its vapours at the melting temperature. At temperatures higher than the melting point the vapours consist both of monomers and polymers : dimers and trimers.[3] We assume that the condensation of vapours takes place only by the liquefactions of polymeric species according to the scheme :

$$M_n\,(g) \rightleftarrows n\,M\,(2)$$

Since only data on fused alkali halides are available, in the following only these systems are considered. The vapours of these systems are formed only of monomers and dimers so that the condensation process may be regarded as a transition of dimers from gaseous to liquid state.

---

[3] S. H. Bauer and R. F. Porter in "Molten Salt Chemistry", Edited by Milton Blander, New York, London, Sydney, 1964, p. 607.

In these circumstances the condensation of one mole of dimer of an alkali halide may be represented by the scheme :

$$M_2(g) \rightleftarrows 2\,M(l) \qquad \text{(I)}$$

M being the corresponding monomer. In this way the internal energy of fused halide increases with

$$2\,V\left(\frac{\partial E}{\partial V}\right)_T$$

where V is the mole volume of the liquid salt. As the considered energy is equal to the molar heat or molar enthalpy of vaporization λ of the dimer, the following equation is obtained if relation (4) is taken into account :

$$P_i = \frac{\lambda}{2V} \qquad (5)$$

Thus equation (1) for alkali halides and generally for molten binary salts ($\nu = 2$) takes the form :

$$\lambda\left(1 - \frac{2^{5/6}\,2^{1/3}\,N^{1/3}}{V^{1/3}}\,\bar{r}\right) = 4\,RT \qquad (6)$$

This equation is equivalent to the Buehler, Hirschfelder and Curtis equation.

The internal pressure for fused alkali halides may be evaluated either by means of equation (1) (with $\nu = 2$) or by making use of equation (5). In table 1 the values obtained from these equations at melting point are listed. The enthalpies of vaporization for dimers have been taken from Bauer and Porter's data. [3,4] The agreement between the two series of values calculated for the internal pressure is satisfactory if the simplifying assumptions involved in the deduction of equation (5) as well as the errors in vaporization enthalpies determinations are taken into account. For K, Rb and Cs halides, this agreement is even very good.

---

[4] G. J. Janz, "Molten Salts Handbook", Academic Press, New York, London, 1967, p. 205.

Table 1

Internal pressures in alkali halides at fusion temperatures

Salt	T_f °K	V cm³	$\bar{r}$ Å	λ cal. mol⁻¹	P_i atmosphere According to (1)	According to (5)
LiF	1121	14.2	0.98	48600	55630	63390
LiCl	883	28.2	1.21	36300	20850	26210
LiBr	823	34.3	1.28	37200	15550	22390
LiI	742	43.1	1.38	33900	11130	16240
NaF	1268	21.0	1.16	51900	48820	51020
NaCl	1073	37.6	1.38	42600	21360	23390
NaBr	1020	44.0	1.45	39600	17230	18580
NaI	933	54.7	1.56	36700	12670	13850
KF	1131	30.4	1.35	42700	33900	29000
KCl	1043	48.9	1.57	44500	18110	18790
KBr	1007	56.0	1.64	42400	15740	15630
KI	954	67.8	1.75	42200	12340	12850
RbCl	995	53.8	1.65	44700	17700	17150
RbBr	965	60.9	1.72	42700	15260	14480
RbI	920	73.4	1.82	43000	11690	12090
CsF	976	41.6	1.53	39700	23620	19700
CsCl	918	60.3	1.75	44300	15070	15170
CsBr	909	67.9	1.82	40500	14230	12320
CsI	899	81.8	1.93	43700	11470	11550

Equation (6) may be used in the evaluation of molar heat of vaporization of dimers. Solving in terms of λ one obtains:

$$\lambda = \frac{4\,RT}{1 - \dfrac{2^{5/6}\,2^{1/3}\,N^{1/3}}{V^{1/3}}\,\bar{r}} \tag{7}$$

In table 2 are given, besides the experimental data, the enthalpies of vaporization for dimers of alkali halides at melting temperature.

Important differences between experimental data and those calculated with equation (7) are found for lithium halides while for the other halides the difference between experimental and calculated enthalpies of vaporization is acceptable.

Table 2

Heats of vaporization for dimers at melting point

Salt	T_f °K	V cm^3	$\bar{r}$ Å	λ, cal. mol^{-1} Exp. *B.* and *P.*^{3}	Exp. *M.* and *T.*^{5}	According to (7)	According to (8)
LiF	1121	14.2	0.98	48600	—	32260	38240
LiCl	883	28.2	1.21	36300	—	28480	28450
LiBr	823	34.3	1.28	37200	—	25840	25820
LiI	742	43.1	1.38	33800	—	23230	23210
NaF	1268	21.0	1.16	51900	—	49650	49620
NaCl	1073	37.6	1.38	36300	48100	38910	38890
NaBr	1020	44.0	1.45	39600	44700	36720	36690
NaI	933	54.7	1.56	36700	41300	33560	33530
KF	1131	30.4	1.35	42700	—	49920	49890
KCl	1043	48.9	1.57	44500	40300	44550	44550
KBr	1007	56.0	1.64	42400	43350	42700	42720
KI	954	67.8	1.75	42200	39600	40510	40480
RbCl	995	53.8	1.65	44700	39200	46120	46090
RbBr	965	60.9	1.72	42700	44300	45020	44990
RbI	920	73.4	1.82	43000	43500	41550	41530
CsF	976	41.6	1.53	39700	—	47600	47570
CsCl	918	60.3	1.75	44300	45500	44020	43990
CsBr	909	67.9	1.82	40500	49700	46790	46770
CsI	899	81.8	1.93	43700	41500	45460	45440

The enthalpy of vaporization of all alkali halides, with dimer formation, may also be calculated having as basis the enthalpy corresponding to one of halides. Thus if λ_1 denotes this enthalpy, V_1 the molar volume of that halide at its melting point (T_1) the following equation is easily obtained :

$$\lambda = \lambda_1 \frac{T}{T_1} \frac{1 - \dfrac{2^{5/6}\,2^{1/3}\,N^{1/3}}{V_1^{1/3}}\bar{r}_1}{1 - \dfrac{2^{5/6}\,2^{1/3}\,N^{1/3}}{V^{1/3}}\bar{r}} \tag{8}$$

---

[5] I. G. Murgulescu and L. Topor, *Rev. Roumaine Chim.*, **13**, 1109 (1968).

which means that the heat of vaporization of a halide (λ) may be found out if its volume at melting point (V), and its average molecular radius $\bar{r}$ are known.

In the last column of table 2 the enthalpies of vaporization calculated according to equation (8) with data for potassium chloride as basis are given ; potassium chloride was chosen since for this salt better experimental data seem to have been obtained.

The results are very close to those obtained with equation (7). The two methods are equivalent.

THE EXPANSION COEFFICIENT

By differentiating relation (6) with respect to temperature the expansion coefficients are obtained. For alkali halides ($\nu = 2$) it results :

$$\alpha = \frac{4\,R - \left(1 - \dfrac{2^{5/6}\,2^{1/3}\,N^{1/3}}{V^{1/3}}\,\bar{r}\right)\dfrac{\partial \lambda}{\partial T}}{\dfrac{2^{5/6}\,2^{1/3}\,N^{1/3}}{3\,V^{1/3}}\,\bar{r}}$$

Since according to the vaporization process (I) :

$$\frac{\partial \lambda}{\partial T} = \Delta\, C_P = 2\, C_P(l) - C_P(g)$$

the expression of expansion coefficients becomes :

$$\alpha = \frac{4\,R - \left(1 - \dfrac{2^{5/6}\,2^{1/3}\,N^{1/3}}{V^{1/3}}\,\bar{r}\right)[2\,C_P(l) - C_P(g)]}{\dfrac{2^{5/6}\,2^{1/3}\,N^{1/3}}{3\,V^{1/3}}\,\bar{r}\,\lambda} \tag{9}$$

where $C_P(l)$ represents the heat capacity of molten salts and $C_P(g)$ the heat capacity of dimer vapours. Equation (9) is equivalent to equation (2) for $\nu = 2$; it presents no practical advantages over equation (2) since it needs additional physical constants — heat capacities, enthalpies of vaporization — which are very often subject to experimental errors. Therefore we compare the expansion coefficients calculated according to equation (9) with their experimental values in order to prove that the assumptions used in deducing equation (6) are founded.

The values of heat capacities $C_P(l)$ required by the application of equation (9) have been available in papers already mentioned.[3,4]

A 16.0 cal mol^{-1} value was considered as most probable for $C_p(l)$ in those alkali halides for which such data are missing.

It seems more difficult to choose the acceptable value for the $C_p(g)$ heat capacity of dimer vapours for which there are no data. The contribution of molecular translation and rotation to $C_p(g)$ is 8 $R/2$ that is 8 cal. mol^{-1}. The contribution of atomic vibrations remains uncertain. We can only approximate it noticing that only part of the 6 normal vibrations of the dimers are active at low fusion temperatures. In gases formed of tetra-atomic molecules (the case under study) as ammonia at temperature of about 1500°K, there are actually only 3 vibrations almost completely active. If this situation is accepted for vapours of alkali halides, too, the contribution of atomic vibrations at melting temperature could not go beyond 6 $R/2$ namely 6 cal. mol^{-1}.

According to these considerations a value of 14 cal. mol^{-1} may be accepted as plausible for the heat capacity of dimer vapours. It was of this value that we made use in calculating the expansion coefficients by equation (9). For the enthalpies of vaporization the experimental values given by Bauer and Porter and listed in table 2 have been used.

Table 3

Expansion coefficients of alkali halides at fusion temperature

Salt	T_f °K	V cm^3	$\bar{r}$ Å	$C_P(l)$ cal. mol^{-1}	ΔC_P cal. mol^{-1}	$\alpha \times 10^4$ grad^{-1}		
						Exp.	Eq(2)	Eq(4)
LiF	1121	14.2	0.98	15.5	17.0	2.71	4.25	3.21
LiCl	883	28.2	1.21	15.0	16.0	2.87	5.61	4.39
LiBr	823	34.3	1.28	16.0	18.0	2.59	6.13	3.19
LiI	742	43.1	1.38	16.0	18.0	2.96	7.09	4.00
NaF	1268	21.0	1.16	16.4	18.8	2.89	3.42	3.86
NaCl	1073	37.6	1.38	16.0	18.0	3.49	4.25	3.61
NaBr	1020	44.0	1.45	16.0	18.0	3.50	4.52	3.85
NaI	933	54.7	1.56	16.0	18.0	3.48	4.92	4.17
KF	1131	30.4	1.35	16.0	18.0	3.41	3.51	4.03
KCl	1043	48.9	1.57	16.0	18.0	3.84	3.90	3.81
KBr	1007	56.0	1.64	16.0	18.0	3.91	4.06	3.98
KI	954	67.8	1.75	16.0	18.0	3.89	4.27	4.01
RbCl	905	53.8	1.65	16.0	18.0	3.95	3.85	3.94
RbBr	965	60.9	1.72	16.0	18.0	3.95	3.96	4.13
RbI	920	73.4	1.82	16.0	18.0	3.96	4.27	4.05
CsF	976	41.6	1.53	16.0	18.0	3.52	3.78	4.53
CsCl	918	60.3	1.75	18.0	22.0	3.84	3.85	3.60
CsBr	909	67.9	1.82	16.0	18.0	3.89	3.85	4.54
CsI	899	81.8	1.93	17.2	20.4	3.74	3.99	3.87

Table 3 allows the comparison between the values calculated by equations (2) and (9) and the experimental ones. As may be easily seen equation (9) leads to results which are as exact as those obtained with equation (2) in spite of the uncertainties affecting the values of heat capacities and enthalpies of vaporization of dimers. The equations (2) and (9) are wholly equivalent from the point of view of their accuracy. It is worth noticing that in equation (9) the expansion coefficients depend on temperature only implicitly through the volume V, the heat of vaporization λ and the heat capacities $C_p(l)$ and $C_p(g)$.

THE COMPRESSIBILITY COEFFICIENTS

The differentiation of equation (6) with respect to P leads for binary salts ($\nu = 2$) to the equation:

$$\frac{\partial \lambda}{\partial P}\left(1 - \frac{2^{5/6}\,2^{1/3}\,N^{1/3}}{V^{1/3}}\,\bar{r}\right) + \frac{2^{5/6}\,2^{1/3}\,N^{1/3}}{3\,V^{4/3}}\,\bar{r}\,\lambda\,\frac{\partial V}{\partial P} = 0$$

On the other hand equation (5) gives:

$$\frac{\partial \lambda}{\partial P} = 2V$$

Taking into account this relation and writing the compressibility coefficient one obtains:

$$\beta_T = \frac{2V\left(1 - \dfrac{2^{5/6}\,2^{1/3}\,N^{1/3}}{V^{1/3}}\,\bar{r}\right)}{\dfrac{2^{5/6}\,2^{1/3}\,N^{1/3}}{3\,V^{1/3}}\,\bar{r}\,\lambda} \tag{10}$$

which is valid at fusion temperature, for alkali halides whose vapours are formed of dimers.

Table 4

Compressibilities of some alkali halides at melting point

Salt	T_f °K	V cm^3	$\bar{r}$ Å	$\beta_T \cdot 10^{11}$ cm^2 dyn^{-1}		
				Exp.	Eq(3)	Eq(10)
LiCl	883	28.2	1.21	2.14	2.40	3.65
LiBr	823	34.5	1.28	2.27	3.07	4.81
NaCl	1073	37.6	1.38	2.87	2.10	3.56
NaBr	1020	44.0	1.45	2.83	—	4.64
NaI	933	54.7	1.56	3.73	—	6.06
KCl	1043	48.9	1.57	3.95	2.13	3.61
KBr	1007	56.0	1.64	3.90	—	4.36
KI	954	67.8	1.75	4.87	3.27	5.29
CsCl	918	60.3	1.75	4.95	2.15	3.90

In table 4 the compressibility coefficients according to equation (10) together with those calculated with equation (3) and the experimental ones are given. As easily seen on the table the results obtained with equation (10) are not better than those to which equation (3) leads. The former are slightly higher than the latter.

Given the uncertainty attached to the values of enthalpies of vaporization the agreement between the experimental data and those predicted by calculations must be considered good.

ANOTHER FORMULATION OF EQUATION (1)

Equation (6) represents a simplified form of equation (1) which is valid for low applied pressures. When this latter, which we denote by p, takes important values the overall pressure becomes :

$$P = p + P_i = p + \frac{\lambda}{nV}$$

for molten salts the vapours of which are formed of n-mers. Equation (1) is then written as :

$$\left(p + \frac{\lambda}{nV}\right)(V - 2^{5/6}\,\nu^{1/3}\,N^{1/3}\,\bar{r}\,V^{2/3}) = \nu RT \qquad (11)$$

This is another expression of Buehler, Hirschfelder and Curtis equation applied to molten salts. For alkali halides ($\nu = 2$) $n = 2$ at melting point and equation (11) becomes :

$$\left(p + \frac{\lambda}{2V}\right)(V - 2^{5/6}\,2^{1/3}\,N^{1/3}\,\bar{r}\,V^{2/3}) = 2RT \qquad (12)$$

Equations (11) and (12) are quite similar to Eyring equation of state[6] for molecular liquids. The resemblance may be underlined by introducing the covolume, b :

$$b = 4\frac{4\pi}{3}N\bar{r}^3$$

In this case one obtains instead of (11) and (12) :

$$\left(p + \frac{\lambda}{nV}\right)(V - 0.6945\,\nu^{1/3}\,b^{1/3}\,V^{2/3}) = \nu RT \qquad (11')$$

$$\left(p + \frac{\lambda}{2V}\right)(V - 0.87746\,b^{1/3}\,V^{2/3}) = 2RT \qquad (12')$$

These equations are both equivalent with Buehler, Hirschfelder and Curtis equation.

---

[6] J. O. Hirschfelder, C. F. Curtis and R. Byron Bird, *op. cit.*, p. 281.

Revue Roumaine de Chimie, **15**, 1463–1471 (1970)

Revue Roumaine de Chimie, **15**, 1473 – 1483 (1970)

KINETICS OF REACTION BETWEEN 1-PHENYL-AZO-2-NAPHTHOL AND COPPER CHLORIDE

I. G. MURGULESCU and DOINA TODOR-BOGDAN

Faculty of Chemistry, Bucharest University, Physical Chemistry Department,
Bd. Republicii 13

Received April 17, 1970

The present paper presents the results obtained by studying the reaction between 1-phenyl-azo-2-naphthol and copper chloride in an alcoholic solution as well as the study of the same reaction in the presence of hydrochloric acid.

INTRODUCTION

Isolate trimolecular reactions are not very numerous even in solutions where conditions for their occurrence are more favourable. It is therefore particularly interesting to signal out and study their kinetics.

The reaction between 1-phenyl-azo-2-naphthol (Sudan I) and copper chloride in ethylic alcohol solution takes place according to a third order kinetics. In the absence of metallic salts, the alcoholic solutions of the dye are very stable thermally as well as photochemically. The dye, like other ortho-hydroxi-azo derivates, forms with metallic salts stable complexes called "coloured lacquer".[1] With copper chloride in alcoholic solution the reaction taking place may be represented by the equation

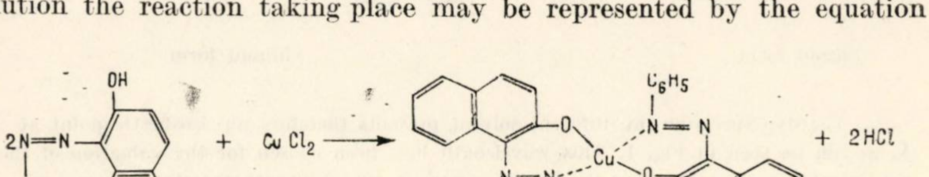

(I)

At room temperature the reaction product separates as a slightly soluble brown precipitate. Elementary analysis and determination through the cryoscopic method of the molecular weight confirm the formulation of equation (I). When carrying out the reaction at temperatures over

---

[1] A. Burawoy, A. G. Salem and A. R. Thompson, *J. Chem. Soc.*, **1952**, 4793.

50° one notices that the precipitate no longer separates because the copper complex decomposes

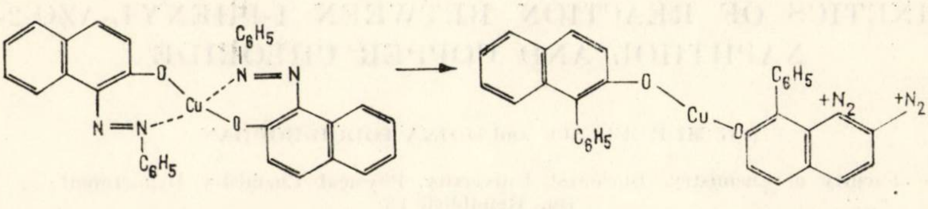

(II)

and the solution loses its colour. While reaction (I) is slow and may be followed by the conventional kynetic methods, reaction (II), in the above temperature conditions, is quick. The present paper gives the results obtained through the kinetic study of reaction (I), which proves to be a trimolecular reaction of the type 2A + B → Products.

EXPERIMENTAL

To study the kinetics of reaction (I) we have examined the decrease of the dye concentration through spectrophotometric measurements at a wavelength of 4700 Å, by means of a UNICAM Sp 800 photometer.

It is well known that 1-phenyl-azo-2-naphthol in solution, like other ortho-hydroxi derivatives, consists of two tautomer forms in equilibrium

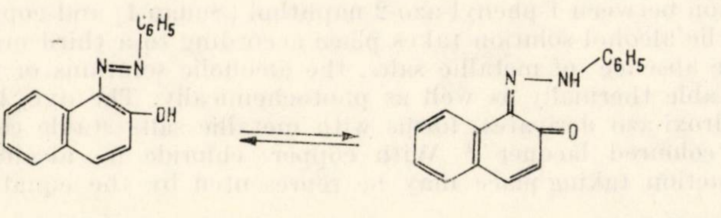

(III)

azoid form chinoid form

The dye spectrum in different solvent presents therefore an isosbestic point at 4500 Å, as can be seen in Fig. 1. This wavelength has been chosen for the valuation of the dye concentrations by measuring the transparence at the spectrophotometer.

To obtain a suitable reaction rate one has worked at temperatures between 70 and 100°. By means of a Höppler thermostat the experimental temperature could be maintained constant with a ±0.02° approximation.

The reaction was watched in sealed phials with a central tube in which the alcoholic solution with $CuCl_2$ is inserted, while the dye solution whose transparence is to be measured is poured into the surrounding space (Fig. 2).

After sealing the phial is left in the thermostat to reach its proper temperature, after which one shakes the solutions. After the known experimental time the phial is suddenly cooled, opened, and the transparence of the solution is measured with the spectrophotometer.

RESULTS

The studied reaction being of the 2 A + B → Products type, the rate constant is generally given by the equation

$$k_3 = \frac{2}{t(a-2b)^2}\left[\,2.303\,\log\frac{2b\,(a\text{-}x)}{a\,(2b\text{-}x)} + (2b-a)\left(\frac{1}{a-x}-\frac{1}{a}\right)\right] \qquad (1)$$

in which a and b represent the initial concentration of the dye and of the copper chloride and x the decrease in the dye concentration.

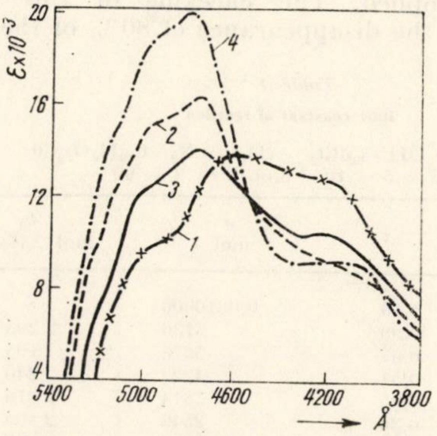

Fig. 1. — The absorption spectrum of 1-phenyl-azo-2-naphthol in different solvents.

1, hexan; *2*, chloroform; *3*, ethyl alcohol; *4*, 50% ethyl alcohol.

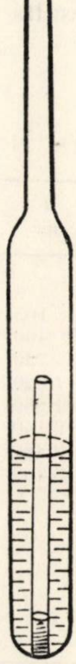

Fig. 2. — Sealed ampoule with two concentric compartments used as reaction vessel.

When $a = 2b$, meaning that the reactants are taken in stoichiometric proportions, the rate constant becomes

$$k_3 = \frac{1}{t}\left[\frac{1}{(a-x)^2} - \frac{1}{a^2}\right]. \qquad (2)$$

In the presence of a great copper chloride excess ($b \gg x$) the rate constant satisfies the equation

$$k_3 = \frac{1}{bt}\left[\frac{1}{(a-x)} - \frac{1}{a}\right]. \qquad (3)$$

In these conditions one works to establish the reaction order according to the dye.

When the dye is in excess ($a \gg x$) the following equation is valid

$$k_3 = \frac{2 \times 2.303}{a^2 t} \log \frac{2b}{2b - x} \tag{4}$$

which permits the checking of the reaction order according to the copper chloride.

All these equations have been used to draw the conclusion that reaction (I) is trimolecular.

Table 1 gives the progress of a determination for the ratio $a : b = 1$, when equation (1) is applied. The checking of this equation gives satisfactory results up to the disappearance of 80% of the dye.

Table 1

Rate constant of reaction

$2H_5C_6-N_2-C_{10}H_6-OH+CuCl_2 \rightarrow (H_5C_6-N_2-C_{10}H_6O)_2Cu + 2\ HCl$
$a = b = 10^{-3}$ mol. l^{-1} T = 90°

t sec	ε	$a - x$ mol. l^{-1}	k_3 $mol^{-2}\ l^2\ s^{-1}$
0	1.18	0.0010006	—
105	0.96	8136	2 295
400	0.67	5678	2 193
720	0.51	4322	2 246
1 020	0.45	3814	2 016
1 930	0.30	2542	2 105
2 160	0.28	2373	2 089
3 480	0.20	1695	2 104
5 100	0.15	1271	2 109

Media = 2 145

Table 2

Rate constant of reaction

$2H_5C_6-N_2-C_{10}H_6OH-CuCl_2 \rightarrow (H_5C_6-N_2-C_{10}H_6O)_2Cu + 2HCl$
$a = 10^{-3}$ mol l^{-1}; $b = 0{,}5 . 10^{-3}$ mol. l^{-1} T = 90°

t sec.	ε	$a - x$ mol. l^{-1}	k_3 $mol^{-2}\ l^2\ s^{-1}$
0	1.26	0.0010000	—
100	1.15	9127	2 004
900	0.76	6032	1 943
1 200	0.68	5397	2 028
1 800	0.56	4444	2 257
2 400	0.52	4127	2 030
4 200	0.41	3254	2 010
7 200	0.32	2540	2 013
14 400	0.23	1825	2 009

Media = 2037

Table 2 gives the progress of a measurement, at the same temperature, the reactant being in stoichiometric proportions ($a = 2b$) when equation (2) is now applied. Tables 3 and 4 refer to reactions carried out in the presence of an excess of one of the reactants, either $CuCl_2$ or dye. The kinetic constants were calculated in these cases by means of equations (3) and (4)

Table 3

Rate constant of reaction

$$2H_5C_6-N_2-C_{10}H_6-OH+CuCl_2 \rightarrow (H_5C_6-N_2-C_{10}H_6O)_2Cu+2HCl$$
$$a = 10^{-3}\ \mathrm{mol\ l^{-1}},\ b = 10^{-2}\ \mathrm{mol.\ l^{-1}}\quad T = 90°$$

t sec	ε	$a - x$ mol. l^{-1}	k_3 $\mathrm{mol^{-3}\ l^2\ s^{-1}}$
0	1.11	0.0010000	—
12	0.90	8108	1 940
32	0.77	6937	2 090
38	0.63	5676	2 050
60	0.50	4505	2 030
100	0.34	3063	2 265
270	0.17	1532	2 040
		Media	2 069

Table 4

Rate constant of reaction

$$2H_5C_6-N_2-C_{10}H_6-OH + CuCl_2 \rightarrow (H_5C_6-N_2-C_{10}H_6O)_2Cu+2HCl$$
$$a = 10^{-3}\ \mathrm{mol\ l^{-1}},\ b = 0{,}25\ 10^{-3}\ \mathrm{mol.\ l^{-1}}\quad T = 90°$$

t sec	ε	$a - x$ mol l^{-1}	k_3 mol. $l^2\ s^{-1}$
0	1.26	0.0010000	—
270	1.10	8730	2 170
600	0.96	7619	2 156
900	0.88	6984	2 054
1 200	0.80	6349	2 183
1 500	0.74	5873	2 327
		Media	2 198

The data given in these tables show that whatever be the ratio between the reactants, reaction (1) remains on the whole trimolecular : of order two regarding the dye and order one regarding the copper chloride.

Table 5 gives the value of the rate constants for experimental temperatures between 70 and 100°.

Table 5

Rate constants k_3 as function of T

Temp. °C	k_3 $\mathrm{mol^{-2}\ l^{-2}\ s^{-1}}$	log A
70	324	17.07
80	745	17.02
90	2 037	17.06
100	4 048	17.05

Figure 3 shows the logarithm of the kinetic constants as a function of the inverse value of absolute temperature. There results an activation energy of 22850 cal/mol.

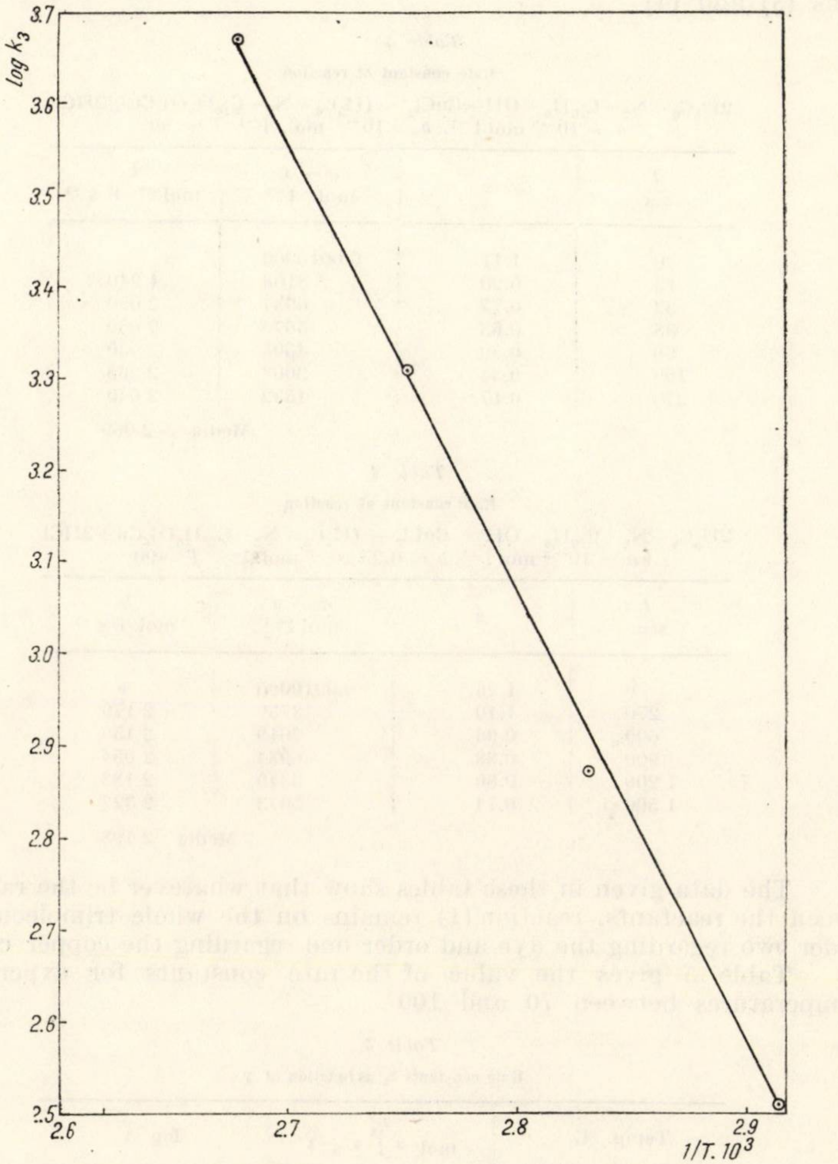

Fig. 3. — Influence of temperature on the rate of reaction.

The last column of Table 5 gives the value of the pre-exponential factors A of Arrhenius'equation : $k_3 = \text{aexp}(-E/RT)$.

Both the activation energy and the pre-exponential factor are higher than the expected values.

As it results from Tables 1,2 and 3, the kinetics of the reaction verifies order III up to the conversion of about 80–85% of the dye. From here on the rate constant increases rapidly, the absorption band shifts from 4700 Å towards 5300 Å and the solution becomes slightly red-violet. The same colouring is produced when the dye solution is treated with concentrated hydrochloric acid.

To elucidate this behaviour we have watched the kinetics of the decomposition reaction of the dye under the impact of hydrochloric acid. In the presence of copper chloride, the decomposition of the dye in alcoholic solution of hydrochloric acid verifies the reaction of order I. In Table 6 the progress of one of the determinations is given.

Table 6

Rate constant of reaction

$2H_5C_6-N_2-C_{10}H_6-OH + CuCl_2 \rightarrow (H_5C_6-N_2-C_{10}H_6O)_2\,Cu + 2HCl$

$a = 10^{-3}$ mol l^{-1}, $b = 0.5.10^{-3}$ mol. l^{-1} $c_{HCl} = 5.10^{-3}$ mol^{-1}

t sec	ε ($\lambda = 4700$Å)	$10.\,\frac{2,303}{t}\log\frac{a}{a-x}$
0	1.26	—
1 500	1.20	27.11
6 000	1.065	28.03
13 530	0.875	26.33
22 380	0.690	26.90
31440	0.545	26.65
36 780	0.46	27.38
43 500	0.385	27.24
73 740	0.17	27.76
		Media 27.18

In Table 7 we give the results obtained for hydrochloric acid concentrations between 2×10^{-3} and 2.4×10^{-1} mol/l. As the table shows, the rate constant calculated by means of the kinetic equation of order I (column 2) decreases rapidly when the concentration of the hydrochloric acid increases.

Table 7

Rate constant of reaction

$2H_5C_6-N_2-C_{10}H_6-OH + CuCl_2 \rightarrow (H_5C_6-N_2-C_{10}H_6O)_2Cu +$
$+ 2HCl$ for different HCl concentrations

$a = 10^{-3}$ mol l^{-1} $b = 0.5.10^{-3}$ mol. l^{-1}; $T = 90°$

Conc. HCl mol l^{-1}	$10^6\,\frac{2.303}{t}\log\frac{a}{a-x}$	$k_1 10^4$	$k_2.10^4$
2.10^{-3}	80.60	2.415	—
5.10^{-3}	27.18	2.446	—
7.10^{-3}	18.62	2.420	—
$1.6.10^{-2}$	16.30	—	—
$1.6.10^{-1}$	8.84	—	4.526
$2.4.10^{-1}$	4.03	—	4.640

DISCUSSION OF RESULTS

The values of the activation energy and of the Arrhenius factor characterizing the kinetics of reaction (I) exceed the probable values of trimolecular reactions. It is therefore possible that reaction (I) should actually consist of two consecutive bimolecular processes

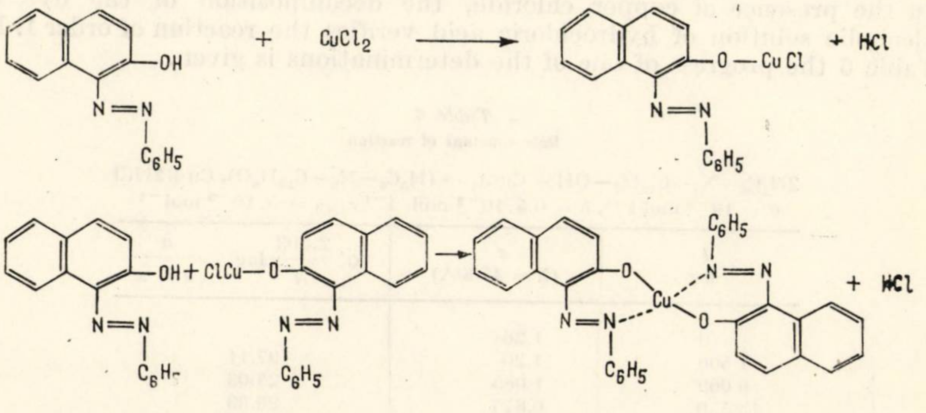

of which (for instance) the first is very rapid.

Towards the end of reaction (I), when the hydrochloric acid reaches a sufficiently high concentration, reaction (I) replaced by the reaction system

$$F + CuCl_2 \rightleftarrows [CuF]\ Cl_2 \qquad \text{(fast reactions)} \qquad \text{(IV)}$$

$$[CuF]Cl_2 \rightarrow CuCl_2 + \text{Prod.} \qquad \text{(slow reaction)} \qquad \text{(V)}$$

in which F represents a molecule of the dye. In these conditions the reaction (IV) determines the kinetics of the system

$$\frac{dx}{dt} = k.c_{(CuF)Cl_2}$$

x being as before the decrease in concentration of the dye. As $CuCl_2$ is divided between the two preceding reactions and the reactions

$$CuCl_2 + HCl \rightleftarrows [CuCl_3\ ]H \qquad \text{(fast reactions)} \qquad \text{(VI)}$$

$$CuCl_2 + 2\ HCl \rightleftarrows [CuCl_4]\ H_2 \qquad \text{(fast reactions)} \qquad \text{(VII)}$$

the concentration of the complex (CuF) Cl_2 remains all the time at low values, comparable to the equilibrium reactions (IV), (VI) and (VII), and we can write successively

$$\frac{c_{[CuF]Cl_2}}{c_F \cdot c_{CuCl_2}} = \frac{c_{[CuF]Cl_2}}{c_{CuCl_2} \cdot (a-x)} = K; \quad c_{[CuF]Cl_2} = K \cdot c_{CuCl_2} \cdot (a-x)$$

$$\frac{c_{[CuCl_3]H}}{c_{CuCl_2} \cdot c_{HCl}} = K_1 \quad ; \quad c_{CuCl_2} = \frac{c_{[CuCl_3]H}}{K_1 \cdot c_{HCl}}$$

$$\frac{c_{[CuCl_4]H_2}}{c_{CuCl_2} \cdot c^2_{HCl}} = K_2 \quad ; \quad c_{CuCl_2} = \frac{c_{[CuCl_4]H}}{K_2 \cdot c^2_{HC}}$$

Consequently

$$\frac{dx}{dt} = k.K.c_{CuCl_2} \cdot (a-x).$$

For low concentrations of hydrochloric acid, when reaction (VI) prevails, there results

$$\frac{dx}{dt} = \frac{kK}{K_1} \frac{c_{[CuCl_3]H}}{c_{HCl}} (a-x) = k_1 \frac{c_{[CuCl_3]H}}{c_{HCl}} (a\text{-}x),$$

the expression kK/K_1 being replaced by the constant k_1. In experimental conditions $c_{[CuCl_3]H}$ remains practically constant and equal to the concentration b of copper chloride. The concentration of the hydrochloric acid becomes equal to $c^0_{HCl} - b$ where c^0_{HCl} is the initial concentration of the acid. By integrating in these conditions the preceding equation, one obtains

$$k_1 = \frac{c^0_{HCl} - b}{b} \left(\frac{2.303}{t} \log \frac{a}{a-x} \right). \tag{5}$$

The third column of Table 7 gives the rate constants k_1 calculated by means of the equation for the first three concentrations of hydrochloric acid, when one can suppose that only reaction (VI) takes place simultaneously with the equilibrium reaction. The concordance of the three values of the constant k_1, confirms the adopted reaction device.

For high concentrations of hydrochloric acid, one can suppose that reaction (VII) prevails. In this case

$$\frac{dx}{dt} = \frac{k.K}{K_2} \cdot \frac{c_{[CuCl_4]H_2}}{c^2_{HCl}} (a-x) = k_2 \cdot \frac{c_{[CuCl_4]H_2}}{c^2_{HCl}} (a-x)$$

where $k_2 = kK/K_2$. By integrating these results

$$k_2 = \frac{c^{02}_{\mathrm{HCl}}}{b} \cdot \frac{2.303}{t} \log \frac{a}{a-x}, \tag{6}$$

In the last column of table 7 the value of the constant k_2 is given for the maximum concentration of hydrochloric acid 1.6×10^{-1} as well as for the value 2.4×10^{-1} mol/l, at which we may imagine that reaction (VII) takes place exclusively. The initial concentration of hydrochloric acid being high compared to b, one has neglected b in comparison to c^0_{HCl}

Taking into account the significance of constants k_1, k_2 and their value one obtains

$$\frac{k_2}{k_1} = \frac{K_1}{K_2} = \frac{4.583}{2.427} = 1.888.$$

As expected, the stability constant of reaction (VI) is higher than that of reaction (VII).

For intermediate concentrations of hydrochloric acid, as for instance 1.6×10^{-2}, reactions (VI) and (VII) take place at a comparable scale. In these conditions

$$\frac{\mathrm{d}x}{\mathrm{d}t} = \left[k_1 \frac{c_{[\mathrm{CuCl_3}]\mathrm{H}}}{c_{\mathrm{HCl}}} + k_2 \frac{c_{[\mathrm{CuCl_4}]\mathrm{H_2}}}{c^2_{\mathrm{HCl}}} \right] (a-x).$$

By integrating and retaining the validity of the above simplifying hypotheses, then results :

$$k_1 \frac{c_{[\mathrm{CuCl_3}]\mathrm{H}}}{c_{\mathrm{HCl}}} + k_2 \frac{c_{[\mathrm{CuCl_4}]\mathrm{H_2}}}{c^2_{\mathrm{HCl}}} = \frac{2.303}{t} \log \frac{a}{a-x}. \tag{7}$$

The right hand side of equation (7) obtained experimentally equals 16.30×10^{-6}. For the valuation of the left hand side, the equilibrium equations give successively

$$\frac{c_{[\mathrm{CuCl_3}]\mathrm{H}}}{K_1 \cdot c_{\mathrm{HCl}}} = \frac{c_{[\mathrm{CuCl_4}]\mathrm{H_2}}}{K_2 \cdot c^2_{\mathrm{HCl}}}\,; \quad \frac{c_{[\mathrm{CuCl_3}]\mathrm{H}}}{c_{[\mathrm{CuCl_4}]\mathrm{H_2}}} = \frac{K_1}{K_2 \cdot c_{\mathrm{HCl}}} = \frac{1.888}{c^0_{\mathrm{HCl}} - b} = \frac{1.888}{0.0155} = 121.8 \cdot$$

On the other hand, by neglecting the concentration of the complex $[\mathrm{CuF}]\mathrm{Cl_2}$ one can write

$$c_{[\mathrm{CuCl_3}]\mathrm{H}} + c_{[\mathrm{CuCl_4}]\mathrm{H_2}} = b = 0.0005.$$

Knowing the sum and the ratio of the two concentrations one obtains

$$c_{[\mathrm{CuCl_3}]\mathrm{H}} = 0.0004959 \qquad c_{[\mathrm{CuCl_4}]\mathrm{H_2}} = 0.0000041$$

The balance is much shifted towards $(\mathrm{CuCl_3})\mathrm{H}$.

Calculating, there results

$$k_1 \frac{c_{[CuCl_3]H}}{c_{HCl}} + k_2 \frac{c_{[CuCl_4]H_2}}{c^2_{HCl}} = 14.88.10^{-6} \qquad \text{(a)},$$

while

$$\frac{2.303}{t} \log \frac{a}{a - x} = 16.30.10^{-6} \qquad \text{(b)}.$$

Taking into account the approximations introduced in calculations, one may consider the agreement of the last two figures (a) and (b) as satisfactory. The kinetic device proposed cannot contribute to the establishment of the compound [CuF]Cl_2 structure. Only its separation at lower temperatures could offer the solution to this problem.

Revue Roumaine de Chimie, **15**, 1485–1489 (1970)

DETERMINING THE SIZE OF METAL PARTICLES IN HYDROGEN CHEMISORPTION MEASUREMENTS

D. CISMARU, AL. FRUMA and D. CRĂCIUNESCU

Institute of Physical Chemistry

Bucharest, str. Dumbrava Roşie 23

Received September 9, 1969

A formula has been deduced for computing the size of the metal powder particles in hydrogen chemisorption measurements. The formula deduced was applied to aluminium and molybdenum powders. The results obtained were comparable with microscope observations.

The microscope method,[1] and more recently the X-ray diffraction method[2–4] and the chemisorption method,[1,5] are currently used for determining the size of metal powder particles. The chemisorption method was used particularly in the study of catalysts, the dispersion of the supported metal particles being determined.[5–7] The preferential use of hydrogen as adsorbed gas can be explained owing to the fact that hydrogen is strongly adsorbed by most metals while its adsorption is very weak on the usual supports (alumina, silica).[5,6,8]

The authors suggest a method hereunder, for computing the size of unsupported, pure metal powder particles. This method, in comparison with the X-ray diffraction and the electronic microscope methods, has the advantage of requiring a relatively simple and inexpensive installation. Likewise, due to the fact that hydrogen is adsorbed on the surface of the particles no matter whether the latter are clustered or not, one of the main sources of errors of other methods is eliminated.

---

[1] R. G. Haldemann and M. C. Botty, *J. Phys. Chem.*, **63**, 489 (1959).

[2] C. R. Adams, R. Curtis, K. P. Benesi and R. Meisenheimer, *J. Catalysis*, **1**, 366 (1962).

[3] I. A. Dorling and R. L. Moss, *J. Catalysis*, **7**, 378 (1967).

[4] L. E. Alexander and E. C. Sommer, *J. Phys. Chem.*, **60**, 1640 (1956).

[5] H. J. Gruber, *J. Phys. Chem.*, **66**, 68 (1961).

[6] I. Spenadel and M. Boudart, *J. Phys. Chem.*, **64**, 204 (1960).

[7] D. Cismaru and Al. Fruma, *Rev. Roumaine Chim.*, **13**, 1277 (1968).

[8] D. Cismaru and Al. Fruma, *Rev. Roumaine Chim.*, **13**, 139 (1968).

EXPERIMENTAL

A volumetric vacuum installation was used for the static determination of hydrogen adsorption on powders. The installation, previously used in studying catalysts of the metal-on-support type, has been described in an earlier paper.[8]

The equilibrium pressure at which the quantity of chemisorbed hydrogen was measured, was 100 torr. At this pressure there is a certainty of having saturation adsorption. The working temperature was 25° since this temperature is very favourable for chemisorption measurements.[9] The aluminium and molybdenum metal powders were first sifted through a 330-mesh sieve. A 250 x "Polmi A" microscope was used for the microscope estimation of particle size.

RESULTS AND DISCUSSION

The following hypotheses were used as a starting point for computing particle diameter :

1. On reaching saturation the hydrogen is found adsorbed in the form of a single compact layer, each metal atom receiving one hydrogen atom.

2. Hydrogen distribution is uniform on the entire area of the particles.

3. The distance between any two hydrogen atoms is equal to the diameter of the adsorbant metal atom.

G grams of metal in powder form adsorb, at saturation, A hydrogen atoms. If d is the diameter (in Å) of the metal atom, then, keeping the hypothesis that one hydrogen atom is adsorbed on one metal atom, there results that along a distance of 1 cm there will be $\frac{10^8}{d}$ hydrogen atoms or $10^{16}\, d^{-2}$ hydrogen atoms per 1 cm^2.

The area of the hydrogen adsorbed by G grams of metal, i.e. the area occupied by A hydrogen atoms will be

$$S_1 = \frac{A}{10^{16}\, d^{-2}} = 10^{-16}\, d^2\, A \text{ cm}^2. \tag{1}$$

Should the G grams of metal be a single sphere, its surface would be

$$S_2 = 4\pi r^2 \text{ and the radius } r = (S_2/4\pi)^{1/2}.$$

The volume of this hypothetical sphere would be

$$V = \mathrm{G}/\rho = \frac{4\pi r^3}{3} \tag{2}$$

where ρ is the metal density.

---

[9] D. Cismaru and Fl. Fruma, *Rev. Roumaine Chim.*, **13**, 679 (1968).

From expression (2) we obtain the radius

$$r = (3\,G/4\,\pi\,\rho)^{1/3}$$

and hence the surface

$$S_2 = 4\,\pi\left(\frac{3G}{4\pi\rho}\right)^{2/3}. \tag{3}$$

Obviously S_2 differs from S_1 since the G grams of metal powder do not form a single sphere of surface S_2, but several, (n), spheres, each of which has the surface S_n. The sum of the surfaces of these small spheres must be equal to the surface on which hydrogen is adsorbed, i.e. S_1.

Hence

$$S_1 = n\,S_n. \tag{4}$$

On the other hand, the sum of the volumes of the small spheres must be equal to the volume of the hypothetical sphere, i.e. to V yielded by formula (2)

$$V = n\,V_n. \tag{5}$$

Since the radius of the hypothetical sphere and the radius of the particle are, respectively

$$r = \left(\frac{S_2}{4\pi}\right)^{1/2}; \quad r_n = \left(\frac{S_n}{4\pi}\right)^{1/2}$$

there results from (5)

$$\frac{4\pi}{3}\left(\frac{S_2}{4\pi}\right)^{3/2} = n\,\frac{4\pi}{3}\left(\frac{S_n}{4\pi}\right)^{3/2}$$

i.e.

$$n\,S_n^{3/2} = S_2^{3/2}. \tag{7}$$

Substituting $n = \frac{S_1}{S_n}$ for n in (4), there results from (7)

$$\frac{S_1 \cdot S_n^{3/2}}{S_n} = S_2 \qquad \text{i.e.} \quad S_n = \frac{S_2^3}{S_1^2}. \tag{8}$$

Consequently, the particle radius is

$$r_n = \left(\frac{S_n}{4\pi}\right)^{1/2} = \left(\frac{S_2^3}{4\pi S_1^2}\right)^{1/2} = \frac{S_2^{3/2}}{(4\pi)^{1/2} S_1}. \tag{9}$$

In this expression the respective equations (2) and (3) are substituted for the values S_1 and S_2. The particle diameter is thus obtained

$$\varnothing = 2\, r_n = \frac{2}{(4\pi)^{1/2}} \cdot \frac{(4\pi)^{3/2}\left(\frac{3G}{4\pi\rho}\right)}{10^{-16}\, d^2 A}.$$

By simplifying, one finally obtains

$$\varnothing = 6 \cdot 10^{16}\, \rho^{-1} A^{-1} d^{-2} G \text{ cm}.$$

We have thus obtained a formula allowing to compute the mean diameter of the metal powder particles — considered to be spheres — when we know the quantity of hydrogen chemisorbed at saturation, the density and the weight of the metal sample, as well as the diameter of the metal atom. The only size to be experimentally determined is therefore the quantity of hydrogen chemisorbed at saturation.

The fact that the particles are considered as being spheric in shape obviously introduces a factor of idealization. However, this conception already made its appearance in Turkevich's works[10] for supported metal particles, and it constitutes an acceptable approximation.

The formula was applied experimentally for two metals for which the certainty exists that they do not solve hydrogen : aluminium and molybdenum. The results obtained are listed in the table hereunder.

Table 1

Computation of aluminum and molybdenum powder particle size

Metal	G grams	Quant. of H_2 adsorbed μ mol/g	A H atoms adsorbed	ρ g/cm³	d Å	(Ø) μ
Al	1	16.2	9.757 10^{18}	2.7	1.43	11.163
Mo	1	13.3	8.01 10^{18}	10.2	1.40	3.75

So far, we have only been able to check the accuracy of the results by means of optical microscope observations. We thus noticed that although the particles differ very much from one another as regards the shape and size, most of them are of a size comparable to the computed size. An X-ray or electron microscope check might lead to an improvement of the formula by establishing eventual corrections, so that it should become a useful and practical instrument for determining particle size.

---

[10] J. Turkevich and P. C. Stenson and J. Hillier, *Discuss. Faraday Soc.*, **11**, 55 (1951).

CONCLUSIONS

A relation was found between the adsorption capacity of metal powders and particle diameter. The formula obtained was applied to some aluminium and molybdenum powders. Although the three stated hypotheses are used, the computation of particle size is based on a plausible physical model.

Revue Roumaine de Chimie, 15, 1491–1502 (1970)

HIGH-TEMPERATURE THERMODYNAMIC PROPERTIES OF SOME URANIUM OXIDES FROM EMF MEASUREMENTS ON SOLID ELECTROLYTE GALVANIC CELLS

D. I. MARCHIDAN and SPERANŢA MATEI

Centre of Physical Chemistry, str. Galaţi 31, Bucharest, Romania

Received March 13, 1970

Electromotive force measurements on high temperature galvanic cells containing solid electrolyte have been made in order to obtain the thermodynamic data for uranium oxides with O/U ratio 2.125 and 2.63 at temperatures between 1073 to 1373°K. Partial molar free energies, enthalpies and entropies of solution of oxygen in $UO_{2.125}$ and $UO_{2.63}$ and the corresponding relative integral quantities as a function of the temperature, as well as the equilibrium pressures of oxygen over the two oxides have been calculated.

The uranium-oxygen system is one of the most complex metal-oxygen systems ever known. It has been the object of investigations carried out by means of different experimental techniques and methods : high-temperature X-ray techniques, tensimetric, thermogravimetric and effusion methods, calorimetric techniques, EMF measurements, etc. Some of these investigations did not lead to concordant results, so that the available information is neither complete nor accurate enough to provide an exact and reliable set of the thermodynamic data of the system.

The potentialities of EMF measurements on galvanic cells involving solid electrolytes for the determination of the thermodynamic properties of uranium compounds at elevated temperatures were previously shown.[1-3]

In our laboratory an investigation of the uranium-oxygen system between UO_2 and U_3O_8 in the temperature range 1073 to 1373°K by EMF measurements was initiated. The purpose of the present paper is to report the results obtained in the study about the thermodynamic properties of two oxides having a non-stoichiometric composition : $UO_{2.125}$ and $UO_{2.63}$.

The used electrochemical cells with solid electrolyte were of the type :

$$\text{Fe, Wüstite} \mid (0.85\ ZrO_2 + 0.15\ CaO) \mid \text{Uranium oxide}$$

---

[1] S. Aronson and J. Belle, *J. Chem. Phys.*, **29**, 151 (1958).

[2] K. Kiukkola, *Acta Chem. Scand.*, **16**, 327 (1962).

[3] T. L. Markin, L. E. Roberts and A. Walter, "Thermodynamics of nuclear materials", Ed. I.A.E.A., Vienna, 1962, p. 693.

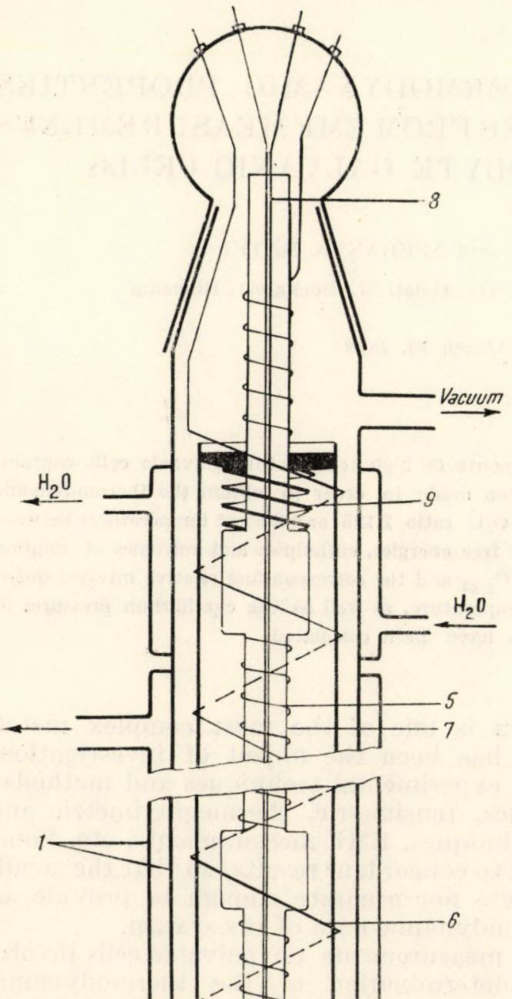

Fig. 1. — Work cell.

1, The walls of the quartz cell; *2*, electrode pellets; *3*, electrolyte pellet; *4*, platinum discs; *5*, *6*, platinum leads; *7*, quartz tube; *8*, thermocouple; *9*, spring.

The cells involve an iron-wüstite reference electrode with a known relative partial molar free energy of oxygen and a solid electrolyte which, as previously shown,[4] presents an anionic conductivity due to the presence of vacancies in the oxygen lattice. The right-hand electrode is made of uranium oxide with a predetermined O/U ratio.

In order to verify that our equipment and experimental procedure were adequate for the proposed research, and following previous suggestions, [1,2] we measured the standard molar free energy of the formation of NiO in cells of the type:

$$\text{Fe, Wüstite} \mid (0.85\ \text{ZrO}_2 + 0.15\ \text{CaO}) \mid \text{NiO, Ni}$$

in the temperature range of 1023 – 1323°K.

EXPERIMENTAL AND MATERIALS

The EMF measurements were effected in a vacuum installation at the residual gas pressure of about 10^{-6} torr. The apparatus and the experimental procedure are described in detail in a previous work.[5]

Arrangement of the cell

The arrangement of the cell is shown in figure 1.

The cell assembly consisting of the electrolyte tablet between the two electrode tablets was inserted into a quartz cell placed in a vertical electrically heated furnace. The structure of the quartz cell is partly similar to that of the cell used by Rezukhina in the study of

[4] F. Hund, *Z. phys. Chem.* (*Leipzig*), **199**, 142 (1952).

[5] D. I. Marchidan and S. Matei, *Studii și Cercetări de Chim. Acad.* R. S. Român ia (in press).

solid electrolytes cells.[6] The work cell is provided with two walls between which vacuum is produced, in order to avoid air penetration through quartz, into the installation, at high temperatures (1173–1373°K).

The tablets were clamped between two horizontal platinum discs which were provided with platinum connecting leads to the potentiometer. In order to maintain the best possible contact between the electrode tablets and the electrolyte, a quartz tube, propelled by a spring, presses the upper electrode. This tube also contains the Pt, Pt+10% Rh thermocouple which is used for measuring the temperature. The thermocouple length is calculated in such a way that, when the cell is assembled, it may find itself at 1–2 mm from the upper electrode surface. The small distance between the electrodes minimizes local temperature differences within the cell and therefrom eventually resulting thermoelectric forces.

The cell is welded within the vacuum instalation, the schedule and description of which are presented in the above mentioned paper.[5]

Preparation of the tablets

When preparing the electrodes and electrolyte tablets, the literature indications were taken into account.[1,6–8]

The reference electrode was prepared from electrolytic iron and Fe_2O_3 powders, pressed at 100–150 atm after mixing and sintered at 1000–1100° under vacuum for about three days.

To prepare the electrolyte we mixed and pressed ZrO_2 and CaO powders in amounts corresponding to the composition 0.85 ZrO_2 + 0.15 CaO. The tablets were then dried at about 150° for about three hours and finally sintered in air at 1200°.

The uranium oxide tablets were prepared by pressing the powder of the known composition into cylindrical tablets and by their sintering at 1250–1300°.

The Ni, NiO electrode used in the checking preliminary studies was prepared by pressing an equimolar mixture of Ni and NiO powders and by sintering tablets at 1100–1200°.

The electrolyte and electrode pellets had the same size (2 to 3 mm thickness and 8 mm diameter).

Measurements

The EMF measurements were taken with a Digital Voltmeter "Solartron" of a great inner resistance ($10^{10}\Omega$), type LM 1440.2.

Before starting the experiments, the installation is emptied for a long time, beginning from the room temperature, then by the slow heating of the cell. The heating was gradually effected at a constant increase, so that the rest of pressure in the apparatus would not pass over $2-3\times10^{-5}$ mm Hg.

The electromotive force was measured at approximately 50°, every time waiting sufficiently till the equilibrium values were recorded. Practically, it is considered that EMF attained the equilibrium value when three readings at 30 min intervals varied by less than 0.5 mV. In each run, the EMF of the cell was measured at rising and falling temperature, in the temperature range of 1073–1373°K. Generally, steady potentials were attained more rapidly at higher than at lower temperatures. A single run lasted one day or even longer. The determi-

---

[6] T. N. Rezukhina, Thesis, The University of Moscow, 1968.

[7] K. Kiukkola and C. Wagner, *J. Amer. Chem. Soc.*, **104**, 379 (1957).

[8] W. A. Yuill, Thesis, The University of Iowa, Ph. D., 1967.

nations were considered to be satisfactory when values for ascending and descending temperatures agreed within 1 or 2 mV.

In some runs, irreproducible and erratic potentials were attained. As Kiukkola and Wagner[7] supposed this could be explained by the penetration of the constituents of the electrodes into the electrolyte tablet in case the electrolyte was not sufficiently dense, or because of the contained impurities in the oxides used for preparing the electrolyte.

When iron-wüstite and ZrO_2—CaO pellets were used for some runs, after each run the surfaces were polished to remove surface contamination.

RESULTS AND DISCUSSION

The cell chosen to verify the equipment and the experimental procedure was:

$$\text{Fe, wüstite} \mid (0.85\ ZrO_2 + 0.15\ CaO) \mid \text{NiO, Ni} \qquad \text{(I)}$$

The EMF measurements were effected within the temperature range 1023 – 1323°K. The EMF values corresponding for each of the read temperatures are shown in the table 1. By the least squares analysis we obtained that the representation of the cell (I) be given by a straight line, the equation of which is:

Table 1

Electromotive force of the cell:
Fe, wüstite | (0.85 ZrO_2 + 0.15 CaO) | NiO, Ni

Temp. °K	E_{obs} (mV)	E_{calc} (mV)	Deviations	
			mV	%
1 023	250	254.53	−4.53	−0.99
1 073	267	261.78	+5.22	+1.9
1 123	269	269.03	−0.03	−0.1
1 173	276	276.28	−0.28	−0.2
1 223	287	283.53	+3.47	+1.2
1 273	286	290.78	−4.78	−0.7
1 323	299	298.03	+0.97	+1

$$E = 0.1062 + 0.145 \times 10^{-3} T \qquad (1)$$

The deviations in mV and percent of the observed electromotive force against the values which were calculated following equation (1) are listed in table 1. The electrolyte of the cell shows only predominant ionic conduction due to migration of oxygen ions from the electrode having a greater partial molar free energy to the electrode having a smaller partial molar free energy. The EMF can thus be noted[7]:

$$E = [(\overline{G}''_{O_2} - G^0_{O_2}) - (G'_{O_2} - G^0_{O_2})]/nF, \qquad (2)$$

where $\overline{G}'_{O_2}$ and $\overline{G}''_{O_2}$, respectively, are the partial molar free energies of oxygen on the left-hand and the right-hand side of the cell, $G^0_{O_2}$ is the standard molar free energy of oxygen, F is the Faraday constant and n is the number of equivalents of oxygen ion transferred.

Using the free energy values for the system iron + wüstite evaluated from gas equilibrium measurements[7] the standard molar free energy of formation of NiO in the temperature range 1023-1323° K could be computed (table 2). For a comparison, table 2 lists standard molar free energies of the formation of nickel oxide obtained by Kiukkola and Wagner[7] (who studied the same cell but by means of another type of installation), as well as the values of $\Delta G^0_{\mathrm{N_iO}}$ calculated by Coughlin[9] from gas equilibrium measurements. The accordance is satisfactory.

Table 2

Standard free energy change ΔG^0 of the reaction $Ni + 1/2O_2 = NiO$

Temp. °K	$-\Delta G^\circ$ (kcal/mol)			$-\log p_{O_2}$	
	This work	Kiukkola and Wagner[7]	Coughlin [9]	This work	Kiukkola and Wagner [7]
1 023	35.58	35.20	34.58	15.20	15.03
1 073	34.46	34.20	33.49	14.03	13.94
1 123	33.29	33.29	32.40	12.95	12.95
1 173	32.15	32.15	31.31	11.99	11.99
1 223	31.10	31.19	30.22	11.12	11.14
1 273	29.97	30.15	29.14	10.29	10.35
1 323	28.86	29.12	28.07	9.54	9.62

The temperature dependence is given by a straight line the equation of which, computed from the data obtained by us, is:

$$\Delta G^0_{\mathrm{NiO}}\,(\mathrm{kcal/mol}) = -\,58.343 + 0.0223\,T \tag{3}$$

Rizzo, Bidwell and Frank[10] suggest for the free energy of formation of NiO, the equation:

$$\Delta G^0_{\mathrm{NiO}} = -\,56.450 + 0.02075\,T \tag{4}$$

but do not specify in which range of temperatures their measurements were effected.

The expression indicated by Wicks and Block[11] for the free energy of formation of NiO in the temperature range 633 – 1725°K (taken account, for a first consideration, two terms only), is:

$$\Delta G^0_{\mathrm{NiO}} = -\,57.6 + 0.03282\,T \tag{5}$$

Considering that the temperature range in which our measurements were effected is not perfectly equivalent to the temperature range investigated in the above mentioned paper, we can come to the conclusion that the expression we obtained for ΔG^0_{NiO} is in good accordance with the expressions obtained by other authors.

---

[9] J. P. Coughlin, *U.S. Bur. Mines Bull.*, 542 (1954).

[10] F. E. Rizzo, L. R. Bidwell and D. F. Frank, *Trans. Met. Soc. A.I.M.E.*, **239**, 593 (1967).

[11] C. E. Wicks and F. E. Block, *U. S. Bur. Mines Bull.*, 605 (1963).

Also, the values for ΔH° and ΔS°, obtained from equation (3) (-58.343 kcal/mol, respectively -22.3 e.u.) are in good accordance to the values $-$ 56.45 kcal/mol, respectively $-$ 20.75 e.u., obtained from equation (4).

Table 2 also presents the values for the partial pressure of oxygen over the Ni, NiO electrode calculated from our data and, for a comparison, the values calculated from the data of Kiukkola and Wagner.[7] The accordance is good.

Since the results obtained in this paper are satisfactorily in accordance with the data existing in the literature, this allows to affirm that the experimental equipment and the working technique that were used are suitable for the following step in the research we enterprised — to determine the thermodynamic properties of uranium oxides, starting from measurements of EMF on galvanic cells with solid electrolyte.

Calculation of thermodynamic quantities for $UO_{2.125}$ and $UO_{2.63}$

The free energy change of a cell of the type :

$$\text{Fe, wüstite} \mid (0.85\ ZrO_2 + 0.15\ CaO) \mid UO_{2+x} \tag{II}$$

is given by the expression :

$$\Delta G_{cell} = -\ 4\ FE \tag{6}$$

where E is the cell EMF in volts and $F = 23.066$ Kcal/volt.equiv. As follows from equation (6), an uncertainty of 0.001 V in the EMF corresponds to an uncertainty of $4F = 92.264$ cal in ΔG_{cell}. The free energy change can also be written :

$$\Delta G_{cell} = 2\ \Delta G^0_{wüstite} - \Delta\overline{G}_{C_2} \tag{7}$$

where $\Delta G^0_{wüstite}$ is the standard free energy of formation of wüstite in equilibrium with iron and $\Delta\overline{G}_{O_2}$ is the partial molar free energy of the solution of oxygen in UO_{2+x}. By combining the standard free energy of formation of wüstite known from equilibrium measurements in gas,[7] with the measured free energy change of the cell, the partial molar free energy of oxygen in equilibrium with the uranium oxide may be obtained.

Partial molar free enthalpies and entropies and the values of the equilibrium oxygen partial pressure may also be calculated from the thermodynamic relations :

$$\frac{\partial\left(\frac{\Delta\overline{G}}{T}\right)}{\partial T} = -\frac{\Delta\overline{H}_{O_2}}{T^2} \tag{8}$$

$$\Delta\overline{G}_{O_2} = \Delta\overline{H}_{O_2} - T\Delta\overline{S}_{O_2} \tag{9}$$

$$\Delta\overline{G}_{O_2} = \overline{G}_{O_2} - G^0_{O_2} = RTlnp_{O_2} \tag{10}$$

The integral molar thermodynamic quantities may be computed from partial molar quantities. Thus, the relative integral molar free energy, ΔG, for the formation of uranium oxide of any composition from the UO_2 of ideal composition and oxygen gas may be calculated from the measured values of the relative partial molar free energy of oxygen, $\Delta \overline{G}_{O_2}$, by using the equation[2] :

$$\Delta G = (1 - n_{O_2}) \int_0^{n_{O_2}} \frac{\Delta \overline{G}_{O_2}}{(1 - n_{O_2})^2} \, \mathrm{d}nO_2 \qquad (11)$$

where n_{O_2} is the mole fraction of oxygen in UO_{2+x}. If the O/U atomic ratio in the oxide is $2 + x$, then $n_{UO_2} = 2\,(2 + x)$ and $n_{O_2} = x\,(2 + x)$.

Using a similar equation to (11), the relative integral molar heat ΔH is obtained.

The values of ΔG and ΔH being known, the relative integral molar entropy ΔS, may be computed using the known equation :

$$\Delta G = \Delta H - T\Delta S. \qquad (12)$$

From the values ΔG, ΔH and ΔS one can infer the relative integral molar quantities per gram atom of uranium : $\Delta G/n_{UO_2}$, $\Delta H/n_{UO_2}$ and $\Delta S/n_{UO_2}$.

Thermodynamic data for $UO_{2.125}$

The EMF measurements about the cell :

$$\text{Fe, wüstite} \mid (0.85\ ZrO_2 + 0.15\ CaO) \mid UO_{2.125} \qquad (III)$$

were effected within the temperature range of 1073—1373°K (table 3) and we found that in this range, EMF varied linearly with the temperature.

Table 3

Electromotive force of the cell: Fe, wüstite|(0.85 ZrO_2 + 0.15 CaO)| $UO_{2.125}$

Temp. °K	E_{obs} (mV)	E_{calc}(mV)	Deviations	
			mV	%
1 073	476	476.41	−0.41	−0.09
1 123	472	472.80	−0.80	−0.17
1 173	468	469.30	−1.30	−0.28
1 223	466	465.72	+0.28	+0.06
1 273	462	462.27	−0.27	−0.05
1 323	458	458.66	−0.66	−0.14
1 373	454	455.10	−1.10	−0.25

By the least squares analysis we obtained the equation which gives the dependence of EMF on temperature, from 1073 to 1373°K :

$$E = 0.552 - 0.071 \times 10^{-3}T \qquad (13)$$

In table 3 are shown the EMF values observed and computed following to equation (13), as well as the deviations in mV and percent of the observed electromotive force as against the values which were calculated following equation (13).

The partial molar free energy of oxygen in equilibrium with the uranium oxide was calculated from the equation (7). We found that the temperature dependence is given by a straight line, the equation of which is :

$$\Delta\overline{G}_{O_2}\ (\text{kcal/mol}) = -\ 75.85 + 0.025\,T \tag{14}$$

The fact $\Delta\overline{G}_{O_2}$ linearly varies with the temperature is in accordance with Aronson and Belle.[1] Studying the thermodynamic properties variation as against the atomic ratio O/U for a series of oxides having a non-stoichiometric composition comprised between 2.00 - 2.20 these authors also found a linear variation of the partial molar free energy as against the temperature.

Since the partial molar free energy is a linear function of the temperature at constant composition, this means that the partial molar entropy and enthalpy are independent against the temperature. Their values for the temperature range of 1073 — 1373°K, calculated from the equation (8) and (9), as well as the log p values computed from the equation (10) are shown in table 4.

Table 4

Thermodynamic data for $UO_{2.125}$

Temp. °K	$-\Delta\overline{G}_{O_2}$ (kcal/mol)	$-\Delta G$ (kcal/mol)	$-\Delta G\, n_{UO_2}$ (kcal/g.atom) uranium	$-\log p_{O_2}$ (atm)
1 073	49.03	2.882	3.063	9.98
1 123	47.78	2.809	2.985	9.29
1 173	46.53	2.735	2.906	8.66
1 223	45.28	2.662	2.828	8.09
1 273	44.03	2.588	2.750	7.55
1 323	42.78	2.515	2.672	7.06
1 373	41.53	2.441	2.594	6.61

$-\Delta\overline{H}_{O_2}$ (kcal/mol) = 75.85
$-\Delta H$ (kcal/mol) = 4.46
$-\Delta H/n_{UO_2}$(kcal/g. atom uranium) = 4.73

$-\Delta\overline{S}_{O_2}$ (e.u.) = 25
$-\Delta S$ (e.u.) = 1.47
$-\Delta S/n_{UO_2}$(e.u.) = 1.56

The integral molar thermodynamic quantities were calculated from partial molar quantities by using the equations above mentioned. Table 4 includes a complete list of all thermodynamic data.

The accuracy of the free energy values estimated by making use of the standard error of EMF and the deviation of the observed values from the calculated ones is about ± 2.5 kcal/mol. The limits of errors were estimated to be ± 4.5 kcal/mol for the enthalpies and ± 2.5 e.u. for the entropies.

The high-temperature phase diagram [12-14] shows that the non-stoichiometric oxide $UO_{2.125}$ is part of the series of non-stoichiometric

---

[12] L. E. J. Roberts and A. Walter, *J. Inorg. Nucl. Chem.*, **22**, 213 (1961).

[13] M. H. Rand and O. Kubaschewski, "The Thermochemical Properties of Uranium Compounds", Oliver and Boyd, Edinburgh, **1963**, p. 26.

[14] "Thermodynamic and transport properties of uranium dioxide and related phases" Technical Report Series Nr. 39, Ed. I.A.E.A., Vienna, **1965**, p. 3.

oxides UO_{2+x} comprised between UO_2 and U_4O_9 which make up a single phase at high temperatures, with the fluorite-type structure. Several authors investigated this domain having a single phase UO_{2+x} within certain ranges of temperature and composition.[1-3, 12, 15, 16]

As for the atomic ratio 2.125 we did not find in the literature complete and tabulated thermodynamic data. For comparison, we chose from the values reported by Aronson and Belle, the molar partial free energies values, corresponding to some non-stoichiometric oxides having an atomic ratio O/U near to 2.125 for three temperatures. On the same diagram (figure 2) we also inscribed the values obtained by us for 2.125 at the same temperatures. One can observe that the values of the partial molar free energies obtained by us inscribe themselves in the series of the molar partial free energies values of the oxides existing in this single phase region.

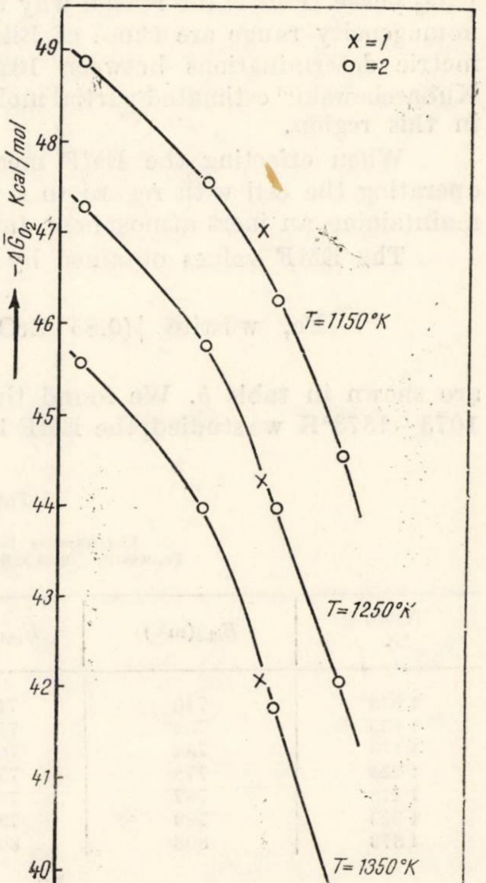

Fig. 2. — $\Delta\overline{G}_{O_2}$ *versus* O/U ratio at 1150°, 1250° and 1350°K.

1 obtained by authors for $UO_{2.125}$; *2*, obtained by Aronson and Belle[1] for some compositions near to $UO_{2.125}$.

Thermodynamic data for $UO_{2.63}$

The non-stoichiometric oxide $UO_{2.63}$ is part of the series of non-stoichiometric oxides U_3O_{8-y} comprised between U_4O_9 and U_3O_8 which form a single phase with orthorhombic structure at high temperatures. It is generally admitted that the single phase region stretches from $UO_{2.61}$ to $UO_{2.67}$, but the phase boundaries depend on the temperature.

In the U_3O_{8-y} region few data exist concerning the partial molar quantities at all temperatures. This is due to high oxygen partial pressure (especially from $UO_{2.65}$ to $UO_{2.67}$), which renders more difficult the obtaining of reproducible results. As long as the oxygen pressures are high, the tensimetric method is one of the best to study the sub-stoichiometric

---

[15] F. Grønvold, *J. Inorg. Nucl. Chem.*, **1**, 357 (1955).

[16] P. E. Blackburn, *J. Phys. Chem.*, **62**, 897 (1958).

U_3O_8 phase. This is the reason why the most complete data for the U_3O_{8-y} homogeneity range are those of Biltz and Müller[17] (who effected tensimetric determinations between 1023 — 1433°K), of which Rand and Kubaschewski[13] estimated partial molar free energy curves for compositions in this region.

When effecting the EMF measurements, cautions were taken on operating the cell with regard to a very slow temperature rising and to maintaining an inert atmosphere during the experiments.

The EMF values obtained by measurements about the cell:

$$\text{Fe, wüstite} \mid (0.85\ ZrO_2 + 0.15\ CaO) \mid UO_{2.63} \qquad \text{(IV)}$$

are shown in table 5. We found that within the temperature range of 1073—1373°K we studied, the EMF linearly varies with the temperature.

Table 5

Electromotive force of the cell:
Fe, wüstite |(0.85 ZrO_2 + 0.15 CaO) | $UO_{2.63}$

Temp. °K	E_{obs}(mV)	E_{calc} (mV)	Deviations	
			mV	%
1 073	740	740.71	−0.71	−0.10
1 123	752	752.16	−0.16	−0.30
1 173	764	763.61	+0.39	+0.05
1 223	778	775.06	+2.94	+0.3
1 273	787	786.51	+0.94	+0.06
1 323	799	797.96	+1.04	+0.13
1 373	808	809.41	−1.41	−0.18

The EMF dependence against the temperature from 1073 to 1373° K is given by the equation:

$$E = 0.495 + 0.229 \times 10^{-3} T \qquad (15)$$

obtained by applying the least squares analysis to our data. Table 5 also shows the deviations in mV and percent of the observed electromotive force against the values which were calculated following equation (15).

Following the same computing procedure as that which was previously indicated for $UO_{2.125}$, we could compute the thermodynamic properties of $UO_{2.63}$ within the temperature range of 1073—1373° K. These are shown in table 6.

Calculating the values of the thermodynamic properties from our EMF data we stated that for the temperatures comprised between 1073—

---

[17] W. Biltz and H. Müller, *Z. anorg. Chem.*, **163**, 257 (1927).

1373° K, the molar partial free energy presents a linear dependence against the temperature given by the equation :

$$\Delta\overline{G}_{O_2}\ (\text{kcal/mol}) = -81.109 + 0.0526\,T \tag{16}$$

Table 6

Thermodynamic data for $UO_{2.63}$

Temp. °K	$-\Delta\overline{G}_{O_2}$ (kcal/mol)		$-\Delta G$ (kcal/mol)	$-\Delta G/n_{UO_2}$ (kcal/g. atom uranium)	$-\log p_{O_2}$ (atm)
	This work	Rand and Kubaschewski[13]			
1 073	24.67	24.430	5.89	7.75	5.02
1 123	22.04	21.811	5.26	6.93	4.28
1 173	19.41	19.205	4.63	6.10	3.61
1 223	16.78	16.610	4.01	5.27	2.99
1 273	14.15	14.024	3.38	4.44	2.42
1 323	11.52	11.465	2.75	3.62	1.90
1 373	8.89	8.911	3.12	2.79	1.41

$-\Delta\overline{H}_{O_2}$ (kcal/mol) = 81.109
$-\Delta H$ (kcal/mol) = 19.38
$-\Delta H/n_{UO_2}$(kcal/g.atom uranium) = 25.5

$-\Delta\overline{S}_{O_2}$ (e.u.) = 52
$-\Delta S$ (e.u.) = 12.428
$-\Delta S/n_{UO_2}$(e.u.) = 16.3

Referring to a wider temperature range (525 – 1750°K), Rand and Kubaschewski[13] indicated that the dependence of the molar partial free energy, enthalpy and entropy on the temperature for the $UO_{2.63}$ composition in this temperature range is well rendered by the following equations :

$$\Delta\overline{G}_{O_2} = -88.400 + 0.1084\ T - 0.0161\ T \times \log T \tag{17}$$

$$\Delta\overline{H}_{O_2} = -88.400 + 0.007\ T \tag{18}$$

$$\Delta\overline{S}_{O_2} = 0.1014 + 0.0161 \log T \tag{19}$$

Calculating the values of $\Delta\overline{G}_{O_2}$ for a series of temperatures comprised between 1073 and 1373° K from the equation of Rand and Kubaschewski and representing them in the same way as the values obtained from the equation (16), we can observe an accordance of the data (figure 3), which verifies the availability of the equation obtained by us, showing at the same time that the deviation from linearity is due to lower or higher temperatures.

In the same way as that for $UO_{2.125}$, the accuracy of the free energy values in table 6 is estimated to be ± 1.5 kcal/mol. The limits of error for the enthalpy were estimated to be ± 3 kcal/mol and for the entropy ± 1.5 e.u.

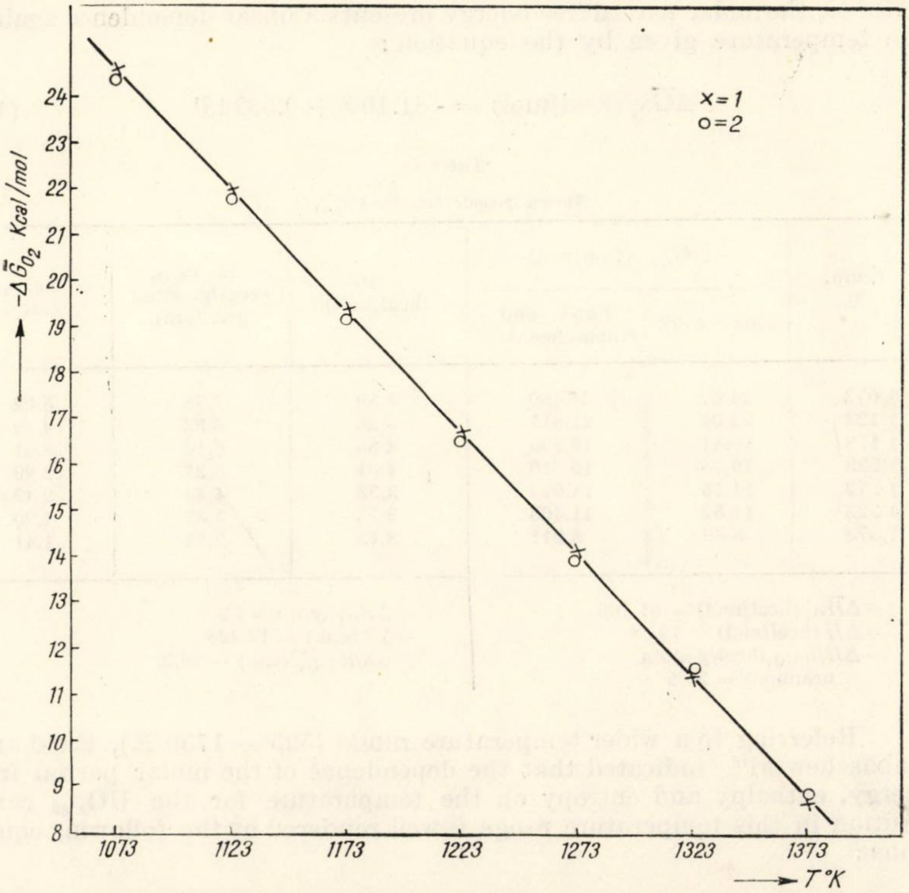

Fig. 3. — $\Delta\overline{G}_{O_2}$ *versus* temperature for $UO_{2.63}$ in the temperature range 1073 — 1373°K.
1, calculated from the equation (16) ; *2*, calculated from the equation (17).

Acknowledgements. This work was performed under contract I.A.E.A. 695/RB. The authors are grateful to the International Atomic Energy Agency for permission to publish this paper.

We wish to express our deep gratitude to Professor I.G. Murgulescu for his interest in our work and to C. Volcovici, for his help in the construction of equipment.

Revue Roumaine de Chimie, 15, 1503–1511 (1970)

ELECTRICAL CONDUCTIVITY OF BINARY MOLTEN ALKALI HALIDE SYSTEMS AS A FUNCTION OF ANION POLARIZATION

ŞTEFANIA ZUCA and M. OLTEANU

Institute of Physical Chemistry, Str. Galaţi, 31, Bucharest

Received April 16, 1970

The density and electrical conductivity of equimolecular mixtures of (Li–Na) Cl, (Li–Rb)Cl, (Li–Cs)Cl, (Li–Na)Br, (Li–K)Br, (Li–Rb)Br, (Na–K) Br, (Na–Rb)Br, (K–Rb)Br, (Na–Rb)I, (K–Rb)I systems are reported.

The electrical conductivity deviations from additivity are found to obey the equation :

$$\Delta\lambda = -a\alpha\left[\frac{1}{(r_{\mathrm{Me_I X}} - d)^2} - \frac{1}{(r_{\mathrm{Me_{II} X}} + d)^2}\right]^2$$

thus indicating that the polarization of common anion owing to the different cation sizes, is the main hindrance to electrical transport in mixture.

A previous paper by the authors[1] concerned the conductivity of some binary alkali chloride systems. From a study of the data presented in that paper it was evident that the features of the electrical conductivity isotherms of the investigated mixtures, were consistent with the anion polarization model of Lumsden.[2,3] The polarization effect occurs because the common anion, X^-, is subject to an unsymmetrical electric field due to the different sizes of the two cations in the melt, $\mathrm{Me_I^+}$ and $\mathrm{Me_{II}^+}$, the polarization energy being:

$$E_p = -\frac{\alpha e^2}{2}\left[\frac{1}{r^2_{\mathrm{Me_I X}}} - \frac{1}{r^2_{\mathrm{Me_{II} X}}}\right]^2 \qquad (1)$$

where α is the polarizability of the common anion and $r_{\mathrm{Me_I X}}$ and $r_{\mathrm{Me_{II} X}}$ refer to the interionic separation in single salts. According to this model, the main hindrance to electrical transport in mixture is the polarization of common anion and the mixtures where E_p is comparable are expected to exhibit a similar development of the isotherms of conductivity.

---

[1] Şt. Zuca and M. Olteanu, *Rev. Roumaine Chim.*, **15**, 357 (1970).

[2] J. Lumsden, *Discuss. Faraday Soc.*, **32**, 138 (1961).

[3] J. Lumsden, "Thermodynamics of Molten Salt Mixtures". Academic Press, London, 1966, p. 70.

To check up this supposition we have extended our former study [1] to other fused binary systems formed by the alkali halides.

Presently we report the density and conductivity data of the following eleven binary alkali halide systems : (Li - Na)Cl ; (Li - Rb)Cl ; (Li - Cs)Cl ; (Li - Na) Br ; (Li - K) Br ; (Li - Rb) Br ; (Na - K) Br ; (Na - Rb) Br ; (K - Rb)Br ; (Na - Rb)I ; (K - Rb)I.

RESULTS AND DISCUSSIONS

The experimental set up for the density and conductivity is simila to the one previously employed. [1]

The alkali halides were the same reagent grade quality as the salts used in our earlier works.[1,4] Regarding the lithium halides more detailed information is given elsewhere. [5]

For each investigated system the density and specific conductivity have been measured in equimolecular mixture over a temperature range of about 200° above their melting point.

All salts were tested for alkalinity with phenolphthalein both before and after the experiment and they were consistently neutral.

The results obtained for the density are summarized in the form of linear function of temperature in Table 1. These equations represent the points observed within experimental error as indicated in the root mean square deviations column. The temperature ranges indicated are those over which the data were obtained.

Table 2 gives the experimentally determined specific conductivity, $\varkappa$, at different temperatures for each investigated equimolecular mixture.

Table 1

Density equations of equimolecular alkali halide mixtures

System	Density eqs.	Standard deviations	Temperature range °C
(Li—Na) Cl	$d = 1.8794 - 0.4858\ t \times 10^{-3}$	0.0006	620—850
(Li—Rb) Cl	$d = 2.4816 - 0.7384 . t \times 10^{-3}$	0.0008	615—855
(Li—Cs) Cl	$d = 2.9260 - 0.8833\ t \times 10^{-3}$	0.0007	660—855
(Li—Na) Br	$d = 2.9460 - 0.7821\ t \times 10^{-3}$	0.0010	730—830
(Li—K) Br	$d = 2.7949 - 0.7688\ t \times 10^{-3}$	0.0016	600—765
(Li—Rb) Br	$d = 3.2468 - 0.9522\ t \times 10^{-3}$	0.0008	640—760
(Na—K) Br	$d = 2.8183 - 0.8356\ t \times 10^{-3}$	0.0006	710—860
(Na—Rb) Br	$d = 3.2561 - 0.9885\ t \times 10^{-3}$	0.0008	690—860
(K—Rb) Br	$d = 3.0998 - 0.9628\ t \times 10^{-3}$	0.0004	750—850
(Na—Rb) I	$d = 3.5062 - 1.0695\ t \times 10^{-3}$	0.0010	690—860
(K—Rb) I	$d = 3.3911 - 1.0801\ t \times 10^{-3}$	0.0009	685—865

---

[4] ŞT. ZUCA and M. OLTEANU, *Rev. Roumaine Chim.*, **12**, 1285 (1967) ; **13**, 1567 (1968).

[5] ŞT. ZUCA and M. OLTEANU, *Rev. Roumaine Chim.*, **15**, 357 (1970).

Table 2

Specific conductivity, $\varkappa$, of equimolecular alkali halide mixtures

0.5 (Li–Na) Cl		0.5 (Li – Rb) Cl		0.5 (Li – Cs) Cl		0.5 (Li – Na) Br		0.5 (Li – K) Br		0.5 (Li – Rb) Br	
$t°$	$\varkappa$, ohm.$^{-1}$cm^{-1}	$t°$	$\varkappa$, ohm^{-1}.cm^{-1}	$t°$	$\varkappa$, ohm^{-1}. cm^{-1}	$t°$	$\varkappa$, ohm^{-1}. cm^{-1}	$t°$	$\varkappa$, ohm^{-1}. cm^{-1}	$t°$	$\varkappa$, ohm^{-1}.cm^{-1}
638.5	3.979	630.7	1.738	644.6	1.378	649.5	3.382	603	1.903	564.6	1.322
646.3	4.000	664.5	1.762	659	1.431	655.8	3.408	615.2	1.949	582	1.375
650.8	4.029	466	1.859	665	1.438	665.2	3.437	627	1.987	596	1.423
660.2	4.064	669.8	1.867	673.2	1.474	670	3.448	640.5	2.034	601.2	1.436
678.2	4.148	675	1.899	694.7	1.523	683.3	3.490	652	2.074	607	1.454
686.7	4.164	682.8	1.906	702.4	1.560	688.3	3.502	664.2	2.111	617.5	1.482
694.2	4.212	702	1.970	711	1.567	697.6	3.530	675	2.141	627.6	1.512
705.7	4.242	714.3	2.008	718	1.594	707	3.567	691	2.187	634.6	1.530
710.2	4.275	729	2.065	725	1.607	713.3	3.589	705.7	2.228	642.2	1.548
725	4.325	742	2.105	732.5	1.618	721.8	3.608	719.5	2.264	648	1.563
734.8	4.343	748	2.111	747	1.641	730	3.628	732.6	2.298	657.3	1.589
746.3	4.394	754.8	2.140	751	1.673	745.5	3.667	748.6	2.341	665	1.609
750.7	4.398	761	2.147	759.8	1.697	752	3.687	760.7	2.387	675	1.636
763	4.455	768.5	2.178	767	1.713	762	3.708	764.7	2.390	682	1.652
778.8	4.502	775.5	2.188	773.7	1.731	771	3.735	773.5	2.345	694	1.682
785	4.521	785.3	2.223	783.2	1.752	776	3.741	780.6	2.347	704.3	1.704
798	4.562	790.8	2.227	791.5	1.773	785	3.763	788	2.349	713	1.728
803	4.573	803.6	2.273	807.7	1.812	796.8	3.794			721.8	1.747
817.8	4.614	807.5	2.286	818.7	1.838	801.8	3.809			732	1.774
829	4.647	840.3	2.395	837.3	1.877	817.8	3.849			742	1.790
838	4.682	862.2	2.447	847.5	1.902	820	3.856			756.3	1.829
856.8	4.700										

(continued Table 2)

0.5 (Na − K) Br		0.5 (Na − Rb) Br		0.5 (K − Rb) Br		0.5 (Na − Rb) I		0.5 (K − Rb) I	
$t°$	$\varkappa$, $ohm^{-1}.cm^{-1}$	$t°$	$\varkappa$, $ohm^{-1}.cm^{-1}$	$t°$	$\varkappa$, $ohm^{-1}.cm^{-1}$	$t°$	$\varkappa$. $ohm^{-1}.cm^{-1}$	$t°$	$\varkappa$· $ohm^{-1}.cm^{-1}$
720.4	1.955	685.7	1.551	700.7	1.326	655	1.312	674.4	1.068
726.2	1.968	697.0	1.576	707	1.346	669.5	1.338	681	1.081
734.5	1.987	707.6	1.601	710.2	1.351	671.6	1.341	692	1.099
741.6	2.002	718	1.621	719.5	1.370	681.4	1.357	699.5	1.113
749.3	2.016	727	1.642	724	1.383	689	1.370	705	1.123
755.6	2.032	739	1.665	728.6	1.389	699	1.388	714.5	1.140
767.7	2.057	749	1.687	735.8	1.404	708.5	1.403	717.8	1.144
778.6	2.083	759.6	1.706	742	1.416	714.3	1.414	730.8	1.164
783.5	2.089	765	1.713	750.7	1.434	728.2	1.435	735	1.171
788.2	2.101	776	1.736	756.5	1.445	733.6	1.444	744.6	1.187
791.7	2.108	789.2	1.762	766.4	1.464	742.3	1.455	751	1.197
804.3	2.133	795.4	1.777	775.5	1.480	753.3	1.467	759.6	1.211
813	2.149	801	1.783	791.0	1.508	761.4	1.482	763.2	1.216
820	2.163	805	1.793	802.5	1.529	770	1.498	773.7	1.233
827.8	2.175	811.2	1.801	807.5	1.537	775	1.506	783	1.247
832.8	2.185	819.6	1.817	814	1.549	782.4	1.515	791.5	1.258
837.6	2.193	831.5	1.835	820	1.558	788	1.524	795.6	1.264
842	2.203	838.8	1.847	831.5	1.578	799.3	1.539	802.8	1.276
848	2.213	848.2	1.863	842.6	1.596	807	1.550	817	1.297
858.3	2.230	865.3	1.888	853.8	1.616	813.7	1.557	828	1.315
864	2.243	876	1.902	860	1.626	821.5	1.570	832	1.320
871	2.261	881.4	1.909			830.8	1.582	839.5	1.331
						839.8	1.593	850.5	1.347
						852.0	1.604		

The data in tables 1 and 2 were used for the subsequent calculations of molar volume $V_m = M/d$ (M denoting the molecular weight of equimolecular mixture) and of the equivalent conductivity $\lambda = V_m \varkappa$.

A graphical analysis of log λ against $1/T$ (°K) plot indicated that all studied mixtures gave straight lines, i.e., the Arrhenius equation :

$$\lambda = A e^{-E_\lambda/RT} \qquad (2)$$

is obeyed. The numerical values of pre-exponential factor A, and of activation energy E_λ, as determined by the least squares method, are summarized in table 3 along with applicable temperature range. Simultaneously the corresponding standard deviations in E_λ are given.

Table 3

Activation energy E_λ and pre-exponential factor A for equimolecular alkali halide mixtures

System	$A.10^{-2}$	E_λ kcal/mol	Standard deviations for E_λ	Temperature range °C
(Li−Na) Cl	4.49	2.28	0.005	630−860
(Li−Rb) Cl	5.68	3.75	0.008	630−865
(Li−Cs) Cl	5.39	3.93	0.010	640−850
(Li−Na)Br	4.32	2.18	0.004	650−820
(Li−K) Br	5.09	3.13	0.009	600−790
(Li−Rb) Br	4.97	3.46	0.004	560−760
(Na−K) Br	4.50	3.02	0.003	720−870
(Na−Rb) Br	4.16	3.12	0.003	665−890
(K−Rb) Br	5.20	3.66	0.004	700−860
(Na−Rb) I	4.35	3.02	0.004	645−855
(K−Rb) I	5,31	3.66	0.003	670−850

For pure halides the conductivity has been in many cases measured by different investigators. This however does not always apply for the halide mixtures. According to the authors' present knowledge the conductivity of the systems in discussion has been very little investigated so far.

The only available data refer to the systems : (Li−Cs)Cl[6] and (Li - K) Br.[7]

The present results for equimolecular mixture of (Li−K)Br system differ from the values of Mehta, Lantelme and Chemla[7] by 1% while for (Li - Cs)Cl system the percent difference from the data of Smirnov and coworkers,[6] is of about 20%. In both situations these differences can be explained in terms of the data obtained for the conductivity of pure components which are discussed elsewhere.[5]

Table 4 gives the molar volume of the presently investigated mixtures, V_m, as well as the percent deviation from the additive values, V_{ad}.

---

[6] M. V. Smirnov, V. A. Khoklov and T. A. Puzanova, *Tr. Inst. Elektrochim. Akad. Nauk. S.S.S.R., Ural. Filial.*, **9**, 21 (1966).

[7] O. P. Mehta, F. Lantelme and M. Chemla, *Electrochim. Acta*, **14**, 505 (1969).

Table 4

Molar volume of equimolecular alkali halide mixtures

System	750°			800°			850°		
	V_{ad}	V_m	$100 \frac{\Delta V}{V_{ad}}$	V_{ad}	V_m	$100 \frac{\Delta V}{V_{ad}}$	V_{ad}	V_m	$100 \frac{\Delta V}{V_{ad}}$
(Li–Na) Cl	—	—	—	—	—	—	34.32	34.38	0.2
(Li–Rb) Cl	42.04	42.36	0.7	42.79	43.19	0.9	43.58	44.05	1.07
(Li–Cs) Cl	46.05	46.56	1.1	46.91	47.48	1.2	47.82	48.45	1.30
(Li–Na) Br	40.19	40.21	0.05	40.84	40.89	0.1	41.61	41.69	0.2
(Li–K) Br	46.33	46.35	0.06	47.20	47.24	0.1	48.09	48.15	0.1
(Li–Rb) Br	49.49	49.79	0.6	50.45	50.77	0.6	51.43	51.77	0.65
(Na–K) Br	50.15	50.17	0.04	51.09	51.13	0.08	52.08	52.14	0.1
(Na–Rb) Br	53.30	53.35	0.1	54.34	54.41	0.14	55.42	55.53	0.2
(K–Rb) Br	59.45	59.83	0.6	60.65	61.04	0.65	61.90	61.34	0.7
(Na–Rb) I	66.48	67.00	0.8	67.80	68.35	0.8	69.19	69.76	0.8
(K–Rb) I	73.04	73.30	0.3	74.56	74.87	0.4	76.14	76.51	0.5

We note here that for (Li—Na, K, Rb) Br mixtures, which possess very low melting temperatures, it was difficult to perform experimental measurements at higher temperatures. That is why for these mixtures we calculated the V_m as well as λ values for 800° and 850° by means of the equations reported in tables 1 and 3, extending their validity over the applicable temperature range. We consider that the obtained data could not be affected by significant errors, but their precision is to some extent connected to a certain approximation.

From the data in table 4 it is evident that the additivity of molar volume is verified for most cases of binary alkali halide systems, particularly for the mixtures formed by salts of adjacent elements. A similar behaviour is observed for the already studied alkali chloride systems.[1] As a rule in these cases, the values of excess volume ΔV are positive and do not exceed additivity by more than 0.5%. In the mixtures where the two uncommon cations differ considerably by their size, a more marked increase of volume occurs by mixing and the deviation of molar volume from additivity becomes appreciable. Thus in (Li - Cs)Cl, (Na - Cs)Cl and (Li - Rb)Cl systems the ΔV values go beyond 1% from the values of molar volume of the mixture. This behaviour can be assigned to the ionic interactions in the mixtures which are all the more marked as the difference between the two uncommon cations becomes greater.

According to the data reported in table 3, the equivalent conductivity shows the usual negative deviations from additivity. Table 5 gives the $\Delta\lambda$ values at the temperatures of 750°, 800° and 850° for the presently investigated systems as well as for the previously reported alkali chloride mixtures.[1] It was then established that, $\Delta\lambda$ may be expressed as :

$$\Delta\lambda = -\,a\alpha\left[\frac{1}{(r_{\mathrm{Me_I X}} - d)^2} - \frac{1}{(r_{\mathrm{Me_{II} X}} + d)^2}\right]^2 \tag{3}$$

where

$$d = 0.1274\,\frac{r_{\mathrm{Me_I X}} - r_{\mathrm{Me_{II} X}}}{r_{\mathrm{X^-}}} \tag{4}$$

is a packing parameter, introduced in the expression of the polarization energy by Sternberg and Herdlicka,[8]

"a" is a factor changing very little with temperature and the molar fraction of the mixture. The other terms in eq. (3) preserve their above mentioned significance.

The parameter $P = \alpha\left[\frac{1}{(r_{\mathrm{Me_I X}} - d)^2} - \frac{1}{(r_{\mathrm{Me_{II} X}} + d)^2}\right]^2$ is given in the last but one column of table 5 and has been calculated using the values of Kordes[9] for the anion polarizability and those of Wyckoff[10] for interionic separation.

---

[8] S. Sternberg and C. Herdlicka, *Rev. Roumaine Chim.*, **13**, 13 (1968).

[9] E. Kordes, *Z. Electrochem.*, **59**, 551 (1955).

[10] R. W. G. Wyckoff, "Crystal Structure", Interscience, New York, 1948.

According to (3), if $\Delta\lambda$ is plotted against the parameter P a straight line with a numerical value of the slope equal to "a", will be obtained. Figure 1 illustrates the results for equimolecular mixtures at 850°. From this figure it is evident that making allowance for the relative error in $\Delta\lambda_{0.5}$ a straight line can be drawn through the obtained points and the origin of the coordinate system. The values of "a" are of 0.7988 at 850°, 0.7780 at 800° and 0.7197 at 750°.

Table 5

$\Delta\lambda$ values for equimolecular alkali halide mixtures

System	$-\Delta\lambda$ ohm^{-1} cm^2			$P.10^4$	ΔE_λ kcal/mol
	750°	800°	850°		
(Li—Na) Cl	—	—	13.90	19.30	0.07
(Li—K) Cl	—	39.97	42.50	56.94	0.74
(Li—Rb) Cl	50.05	50.15	50.09	70.00	0.93
(Li—Cs) Cl	61.19	62.19	63.03	96.40	0.98
(Na—K) Cl	—	—	8.20	12.73	0.18
(Na—Rb) Cl	—	—	16.73	22.24	0.36
(Na—Cs) Cl	—	—	20.19	38.46	0.39
(K—Rb) Cl	—	1.57	1.33	1.33	0.09
(K—Cs) Cl	—	3.89	3.74	7.09	0.18
(Rb—Cs) Cl	1.30	1.47	2.03	2.28	0.01
(Li—Na) Br	15.67	15.83	15.96	11.75	0.04
(Li—K) Br	37.91	37.95	38.09	46.60	0.31
(Li—Rb) Br	47.50	47.63	48.63	64.01	0.65
(Na—K) Br	8.29	8.65	9.07	11.86	0.01
(Na—Rb) Br	11.52	11.76	12.00	21.60	0.10
(K—Rb) Br	1.21	1.21	1.19	1.42	0.00
(Na—Rb) I	12.73	13.15	13.55	20.65	0.09
(K—Rb) I	1.07	0.96	0.86	1.65	0.07

The data in figure 1 illustrate convincingly that the anion polarization effect plays an important part in the electrical transport of binary molten alkali halide mixtures.

As already stated[1] as a result of anion polarization, sort of associated cation-anion groups, e.g.. Me_I-X - Me_{II}, appear in the melt, the common anion being displaced towards the smaller cation. As a consequence its mobility relative to the anion is reduced compared with the pure salts, and implicitly the electrical conductivity of the mixture decreases. The effect being more marked as the difference between the two cations is greater, we expect $\Delta\lambda$ to increase in the same way, which is proved by the results in figure 1.

A special remark concerning (Li—Cs)Cl and (Li—Na)Cl systems is worth to be made here. These two systems can be looked upon as the most notable exception in figure 1.

A possible explanation for this behaviour may lie in the fact that the differences between the two uncommon cations in the mixture (Li^+ and Cs^+ or Na^+ and Cs^+) are now extremely large. Thus, it is possible that the ionic interactions intensify to such an extent that the complex ions arise in these melts instead of simple associated cation-anion groups. We recall here the molar volume behaviour which certifies also the peculiarity of these systems. Work is in progress on the corresponding bromide and iodide mixtures and similar results are awaited.

From figure 1 another characteristic fact may be brought into evidence, namely, according to our expectation, the systems having a similar energy of polarization exhibit Δλ values which are equal within experimental error.

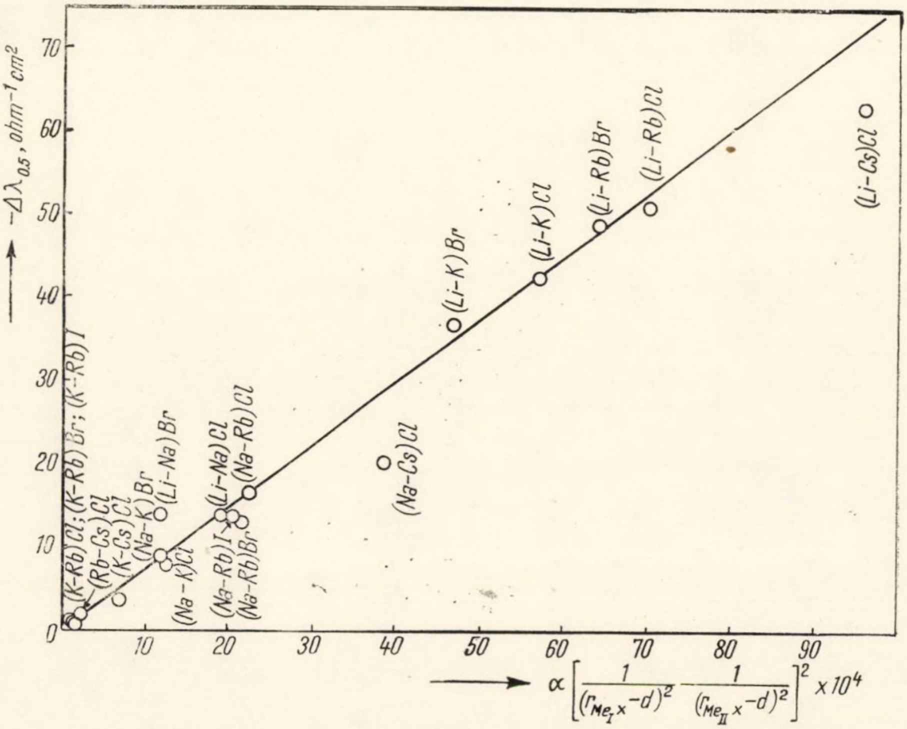

Fig. 1. — Δλ deviations for equimolecular mixtures at 850°.

In conclusion, it is worth noting that the excess activation energy for the electrical conductivity, ΔE_λ, exhibits, as can be seen in the last column of table 5, positive deviations from ideality. The ΔE_λ values are higher especially as the electrical conductivity deviates more from additivity. This can be looked upon as an argument speaking for the interpretation that the changes in relative mobility of the ions are to be attributed to the changes in the cation — anion bonding energy.

Revue Roumaine de Chimie, 15, 1513–1523 (1970)

CHEMICAL REACTIONS IN LIQUID JUNCTIONS. II[1]. A NEW POTENTIOMETRIC TITRATION METHOD

N. BONCIOCAT, L. CHIOSA, FLORICA MIHĂILESCU and M. OLTEANU

The Institute for State Control of Drugs and Pharmaceutical Researches
Str. Sfîntul Ion Nou, 14, Bucharest, Romania

Received February 3, 1970

This paper continues the examination of the chemical reactions in liquid junctions. Starting from the results obtained in the preceding paper, a new potentiometric titration method is theoretically and experimentally elaborated. The method is based on the continuous variation, during the titration, of the liquid-junction potential, as a consequence of the continuous variation of the liquid-junction double layer structure. Several experimental titration curves are given for neutralization and precipitation reactions. The accuracy and the reproducibility of the method are also discussed.

1. INTRODUCTION

In the preceding paper two "dual" classes of systems of the aqueous solution 1 || aqueous solution 2 type were analysed.[1] The first class is composed of the system :

$$\mathrm{HCl}(c_1) \,\|\, \mathrm{NaCl}\left(\frac{vc_1}{V+v}\right) + \mathrm{NaOH}\left(\frac{Vc_2 - vc_1}{V+v}\right);\ vc_1 < Vc_2 \qquad (1)$$

and all the systems analogous to the system (1). The second class is composed of the system :

$$\mathrm{NaOH}(c_1) \,\|\, \mathrm{NaCl}\left(\frac{vc_1}{V+v}\right) + \mathrm{HCl}\left(\frac{Vc_2 - vc_1}{V+v}\right);\ vc_1 < Vc_2 \qquad (2)$$

and all the systems analogous to the system (2).

The concentration profiles along the liquid-junction double layer, as well as the expression of the liquid-junction potential, representative for each of these two classes, were deduced.

---

[1] N. Bonciocat, L. Chiosa, F. Mihăilescu and M. Olteanu, *Rev. Roumaine Chim.*, (to appear).

In this paper, starting from the results obtained in the preceding paper, a new potentiometric titration method is theoretically and experimentally elaborated, for the class of chemical reactions, which fulfil the following conditions : in the reaction, the cation (anion) of the titrated solution and the anion (cation) of the solution to be analysed take part as reactants ; as a result of the chemical reaction an uncharged molecule is formed, which can pass into solution, or be precipitated ; the chemical reaction is a very fast and a quantitative one. The neutralization reactions and the reactions forming compounds with very small solubility products, or complex combinations with very great stability constants, are examples of chemical reactions belonging to this class.

The potentiometric titration methods with their different variants, described in the literature, are based on the chemical tension variation of a suitable indicating electrode introduced into the solution to be analysed, when to this solution the titrated solution is gradually added [2-12].

Unlike these, the proposed method is based on the continuous variation, during the titration, of the liquid-junction potential corresponding to the contact between two compartments, as a result of the continuous variations of the liquid-junction double layer structure and of the second compartment composition. The first compartment does not modify its composition during the titration.

The principle scheme of this method is shown in figure 1 (Experimental). At the initial moment in the first compartment are found V_1 ml of the titrated solution and in the second one V ml of the solution to be analysed. The titrated solution is penetrating, at a constant flow, into the solution to be analysed, just through the liquid junction establishing the contact between the two compartments. In each compartment a saturated calomel electrode is introduced, thus forming a concentration cell with transport. Evidently, during the titration, the second compartment is continually stirred. By means of a potentiometer with high input ohmical resistance, coupled to a suitable recorder, the EMF (E) of the cell is recorded as a function of the variable volume v.

If the flow the titrated solution is penetrating into the second compartment, is sufficiently slow and the stirring of the second compartment sufficiently intense to ensure a uniformity of the practically instantaneous composition, the experimental device will realize a continuous passage through an infinite range of instantaneous liquid junctions of a static type. By this it differs from the models described in literature i.e. static

---

[2] J. Cihalik, "Potenciometrie", Publ. House of the Czech. Acad. of Sci., Prague, 1961.

[3] R. W. Murray and C. N. Reilley, *Analyt. Chem.*, **34**, 313R (1962); **36**, 370R (1964).

[4] D. K. Roe, *Analyt. Chem.*, **38**, 461 R (1966).

[5] E. Clifford Toren, Jr., *Analyt. Chem.*, **40**, 402 R (1968).

[6] J. Coursier, *Analyt. Chim. Acta*, **7**, 77, 585 (1952); **10**, 182, 265 (1954).

[7] C. N. Reilley, R. W. Schmid and D. W. Lamson, *Analyt. Chem.*, **30**, 953 (1958).

[8] I. M. Kolthoff and E. R. Nightingale, Jr., *Analyt. Chim. Acta*, **19**, 593 (1958).

[9] E. Bishop, *Mikrochim. Acta*, **1960**, 803.

[10] G. D. Short and E. Bishop, *Analyt. Chem.*, **37**, 962 (1965).

[11] F. Conti and G. Eisenman, *Biophys. J.*, **5**, 247 (1965).

[12] E. Pungor, K. Toth and J. Havas, *Acta Chim. Acad. Sci. Hung.*, **48**, 17 (1966).

liquid junctions,[13] liquid junctions with continuous flow resulting from the meeting of two liquids[14-17] or semiflowing liquid junctions in which only one liquid is poured at a controlled rate.[18]

The injection flow value of the titrated solution is selected on the basis of previous experiments, with the purpose of establishing the conditions of the best reproducibility. Generally, for concentrations, lower than 0.1 M, the injection flow of 1 ml/minute ensures a good reproducibility of the curves. As a matter of fact, this is the magnitude order of the flows used in the case of the continually flowing junctions.[19]

2. THE THEORETICAL BASIS OF THE METHOD

Let us consider the titration of a $NaOH(c_2)$ solution with $HCl\ (c_1)$. Before the equivalence point ($vc_1 < Vc_2$) we have to consider the system (1) and after the equivalence point ($vc_1 > Vc_2$) the system

$$\mathrm{HCl}(c_1)\,\|\,\mathrm{NaCl}\left(\frac{Vc_2}{V+v}\right)+\mathrm{HCl}\left(\frac{vc_1-Vc_2}{V+v}\right);\ vc_1 > Vc_2 \tag{3}$$

The expression of the liquid-junction potential for the system (1) was obtained in the preceding paper:

$$\begin{aligned}E_J = {} & \frac{RT}{F}\,\frac{(c_1+c_2)\,u_{\mathrm{H}}-c_1\,u_{\mathrm{Cl}}-c_2\,u_{\mathrm{Na}}}{(c_1+c_2)\,u_{\mathrm{H}}+c_1\,u_{\mathrm{Cl}}-c_2\,u_{\mathrm{Na}}}\ln\frac{(c_1+c_2)\,(u_{\mathrm{H}}+u_{\mathrm{Cl}})}{c_2\,(u_{\mathrm{Cl}}+u_{\mathrm{Na}})}+\\ & +\frac{RT}{F}\,\frac{(c_1+c_2)\,u_{\mathrm{OH}}-c_1\,u_{\mathrm{Cl}}-c_2\,u_{\mathrm{Na}}}{(c_1+c_2)\,u_{\mathrm{OH}}-c_1\,u_{\mathrm{Cl}}+c_2\,u_{\mathrm{Na}}}\ln\frac{(vc_1\,u_{\mathrm{Cl}}+(Vc_2-vc_1)\,u_{\mathrm{OH}}+Vc_2\,u_{\mathrm{Na}})}{(c_1\,c_2/(c_1+c_2))\,(V+v)\,(u_{\mathrm{Cl}}+u_{\mathrm{Na}})}\end{aligned} \tag{4}$$

The liquid junction of the system (3) is a liquid junction without chemical reactions and consequently, to obtain the expression of the liquid-junction potential, we can apply the general formula of Henderson.[20, 21] It thus results:

$$E_J=\frac{RT}{F}\,\frac{(c_1+c_2)\,u_{\mathrm{H}}-c_2\,u_{\mathrm{Na}}-c_1\,u_{\mathrm{Cl}}}{(c_1+c_2)\,u_{\mathrm{H}}-c_2\,u_{\mathrm{Na}}+c_1\,u_{\mathrm{Cl}}}\ln\frac{(V+v)\,c_1\,(u_{\mathrm{H}}+u_{\mathrm{Cl}})}{(vc_1-Vc_2)\,u_{\mathrm{H}}+Vc_2\,u_{\mathrm{Na}}+vc_1\,u_{\mathrm{Cl}}} \tag{5}$$

---

[13] G. N. Lewis, T. B. Brighton and R. L. Sebastian, *J. Amer. Chem. Soc.*, **39**, 2245 (1917).

[14] A. B. Lamb and A. T. Larson, *J. Amer. Chem. Soc.*, **42**, 229 (1920).

[15] D. A. Mac Innes and Y. L. Yeh, *J. Amer. Chem. Soc.*, **43**, 2563 (1921).

[16] E. J. Roberts and F. Fenwick, *J. Amer. Chem. Soc.*, **49**, 2787 (1927).

[17] J. V. Lekhani, *J. Chem. Soc.*, **1932**, 179.

[18] P. B. Mathur, *Indian J. Appl. Chem.*, **22**, 173 (1959).

[19] D. A. Mac Innes, "The Principles of Electrochemistry", Reinhold Publ. Corp., New York, 1939, ch. 13, fig. 5.

[20] P. Henderson, *Z. phys. Chem.*, **59**, 118 (1907); **63**, 325 (1908).

[21] J. J. Hermans, *Rec. Trav. chim.*, **57**, 1373 (1938); **58**, 99 (1939).

It is easy to see that for $vc_1 = Vc_2$ the two formulas (4) and (5) lead to the same value for E_J. Therefore, the function $E_J = E_J(v)$ given by (4) and (5) is continuous in the equivalence point. But it is not differentiable in this point. Indeed one can easily obtain :

$$\frac{F}{RT}\frac{\partial E_J}{\partial v} = \begin{cases} \dfrac{V(c_1 u_{\mathrm{Cl}} + c_2 u_{\mathrm{Na}} - (c_1 + c_2) u_{\mathrm{OH}})}{(V+v)(vc_1 u_{\mathrm{Cl}} + (Vc_2 - vc_1) u_{\mathrm{OH}} + Vc_2 u_{\mathrm{Na}})}; & vc_1 < Vc_2 \\[2ex] \dfrac{V(c_1 u_{\mathrm{Cl}} + c_2 u_{\mathrm{Na}} - (c_1 + c_2) u_{\mathrm{H}})}{(V+v)(vc_1 u_{\mathrm{Cl}} + (vc_1 - Vc_2) u_{\mathrm{H}} + Vc_2 u_{\mathrm{Na}})}; & vc_1 > Vc_2 \end{cases} \tag{6}$$

It thus results :

$$\alpha = \frac{\left(\dfrac{\partial E_J}{\partial v}\right) v = (Vc_2/c_1) + 0}{\left(\dfrac{\partial E_J}{\partial v}\right) v = (Vc_2/c_1) - 0} = \frac{(c_1 + c_2) u_{\mathrm{H}} - c_1 u_{\mathrm{Cl}} - c_2 u_{\mathrm{Na}}}{(c_1 + c_2) u_{\mathrm{OH}} - c_1 u_{\mathrm{Cl}} - c_2 u_{\mathrm{Na}}} > 1 \tag{7}$$

The function $E_J = E_J(v)$ will have an angular point at the equivalence. The new potentiometric titration method is based just on this fact.

Because $u_{\mathrm{H}} > u_{\mathrm{OH}} > u_{\mathrm{Cl}} > u_{\mathrm{Na}}$, one can see from (6) that $E_J = E_J(v)$ is decreasing before as well as after the equivalence point. It means that the two potential jumps along the two parts $(0, x_{\mathrm{in}})$ and $(x_{\mathrm{in}}, 1)$ of the liquid-junction double layer (fig.2 in the preceding paper) have the same polarity.

On the basis of (6) it is possible to calculate $\partial^2 E_J / \partial v^2$ for the two periods. Studying the sign of the functions thus obtained, we arrive at the conclusions :

— $E_J = E_J(v)$ may have for $vc_1 < Vc_2$ an inflexion point, if the ratio c_1/c_2 satisfies the double inequality :

$$(u_{\mathrm{Na}} + 2u_{\mathrm{Cl}} - u_{\mathrm{OH}})/(u_{\mathrm{OH}} - u_{\mathrm{Cl}}) < c_1/c_2 < (u_{\mathrm{OH}} + u_{\mathrm{Na}})/(u_{\mathrm{OH}} - u_{\mathrm{Cl}}) \tag{8}$$

The value of v corresponding to this inflexions point is given by :

$$2v/V = (c_2 (u_{\mathrm{OH}} + u_{\mathrm{Na}})/c_1(u_{\mathrm{OH}} - u_{\mathrm{Cl}})) - 1 \tag{9}$$

Before this inflexion point the curve $E_J = E_J(v)$ is concave and after it, it is convex.

— After the equivalence point, irrespective of the values c_1 and c_2, the curve $E_J = E_J(v)$ cannot have an inflexion point, remaining all the time concave.

The relation (7) leads to :

$$\left(\frac{\partial \alpha}{\partial c_2}\right)_{c_1} = \frac{c_1 (u_{\mathrm{H}} - u_{\mathrm{OH}})(u_{\mathrm{Na}} - u_{\mathrm{Cl}})}{((c_1 + c_2) u_{\mathrm{OH}} - c_1 u_{\mathrm{Cl}} - c_2 u_{\mathrm{Na}})^2} < 0 \tag{10}$$

Therefore, the ratio of the two slopes, which can be considered as a measure of the accuracy of the method, grows when the ratio c_2/c_1 decreases (for a fixed c_1).

Let us observe that the function $E=E(v)$ and not $E_J=E_J(v)$ is graphically recorded. E differs from E_J by the potential jumps E_{J1}, E_{J2} along the liquid junctions : KCl (sat) $\|$ first compartment, respectively second compartment $\|$ KCl (sat). E_{J1} remains constant during the titration, because the first compartment does not modify its composition. Therefore, $dE_{J1}/dv = 0$. E_{J2} depends on v. For $vc_1 < Vc_2$ it represents the liquid-junction potential corresponding to the liquid junction : variable mixture NaOH + NaCl $\|$ KCl (sat) and for $vc_1 > Vc_2$ the liquid-junction potential corresponding to the liquid junction : variable mixture NaCl + HCl $\|$ KCl (sat). It is evident that dE_{J2}/dv is continuously varying before as well as after the equivalence point and consequently, the discontinuity point of dE_{J2}/dv is just the equivalence point. In conclusion, the functions dE_J/dv, dE_{J2}/dv and dE/dv have only one discontinuity point, which is just the equivalence point. In addition, E_{J1}, E_{J2} are very small and we can suppose that $E=E(v)$ estimates quite exactly the function $E_J = E_J(v)$.

The relation (7) is a particular case of the following general relation :

$$\alpha = \frac{(c_1+c_2)\,u_C/z_C - c_1\,u_A/|z_A| - c_2\,u_{C*}/z_{C*}}{(c_1+c_2)\,u_{A*}/|z_{A*}| - c_1\,u_A/|z_A| - c_2 u_{C*}/z_{C*}} \qquad (11)$$

Indeed, relation (11) can be applied to any system which is analogous, before the equivalence point to the system (1) and after the equivalence point to the system (3). C^{z_C+}, $A^{|z_A|-}$ are the ions of the titrated solution, $C^{*z_{C*}+}$, $A^{*|z_{A*}|-}$ of the solution to be analysed and the chemical reaction in the liquid junction is $\nu_1\,C^{z_C+} + \nu_2\,A^{*|z_{A*}|-} \rightarrow C_{\nu_1}A^*_{\nu_2}$.

If the potential jumps along the two parts $(0, x_{in})$, $(x_{in}, 1)$, of the liquid-junction double layer, have the same polarity, α is positive and if they have an opposite polarity, α is negative. The case $\alpha < 0$ leads to curves $E=E(v)$ which are increasing (decreasing) before the equivalence and decreasing (increasing) after the equivalence. In this case, the position of the equivalence point is very well marked.

Sometimes α remains positive (or negative) irrespective of the values c_1, c_2, at other times, the sign of α depends on the pair c_1, c_2 chosen to carry out the experiment. Evidently, in the latter case it is desirable to choose such values for c_1, c_2, so that they would lead to a negative values for α.

Similarly, the relation.

$$\tilde{\alpha} = \frac{(c_1+c_2)u_{A*}/|z_{A*}| - c_1\,u_{C*}/z_{C*} - c_2\,u_A/|z_A|}{(c_1+c_2)\,u_C/z_C - c_1\,u_{C*}/z_{C*} - c_2\,u_A/|z_A|} \qquad (12)$$

can be applied to any system which is analogous, before the equivalence point to the system (2) and after the equivalence point to the system :

$$\mathrm{NaOH}\,(c_1)\,\|\,\mathrm{NaOH}\left(\frac{vc_1 - Vc_2}{V+v}\right) + \mathrm{NaCl}\left(\frac{Vc_2}{V+v}\right);\quad vc_1 > Vc_2 \qquad (13)$$

This time, $A^{*|z_{A^*}|-}$, $C^{*z_{C^*}+}$ are the ions of the titrated solution, $A^{|z_A|-}$, C^{z_C+} of the solution to be analysed and the chemical reaction in the liquid junction is $\nu_2 A^{*|z_{A^*}|-} + \nu_1 C^{z_C+} \rightarrow C_{\nu_1} A^{*}_{\nu_2}$. In conclusion, relations (11) and (12) are referring to the situation in which the anion, respectively the cation of the solution to be analysed is the ion which is titrated.

3. EXPERIMENTAL

The experimental device which was used is shown in figure 1.

A perfusion pump "B. Braun Apparatebau, type, Unita I, Melsungen G.F.R" acts the plunger of a 10 ml glass syringe, injecting, through a small glass cylindrical vessel (height : 5 cm ; inner diameter : 8.5 mm ; wall thickness : 2 mm) and thereafter through a glass capillary (inner diameter : 1 mm ; wall thickness : 2 mm), the titrated solution into the solution to be analysed, contained in a 50 ml reaction cell. The set syringe, glass cylindrical vessel, glass capillary and the two connecting rubber tubes formed the first compartment and the

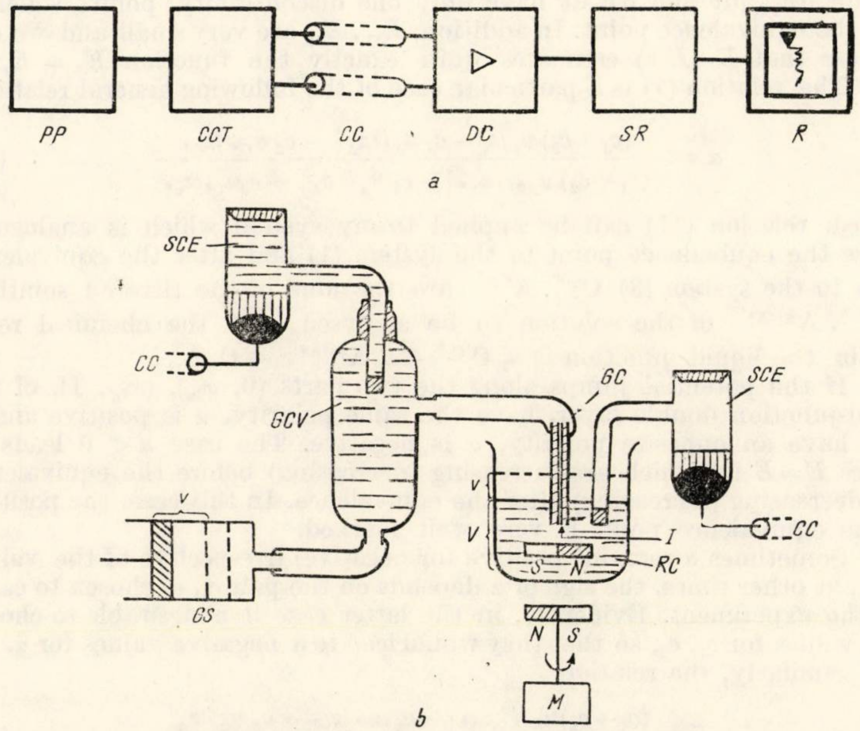

Fig. 1. — *a* : *PP*, perfusion pump ; *CCT*, concentration cell with transport ; *CC*, coaxial cables ; *DC*, amplifier ; *SR*, sensitivity reducing piece ; *R*, recorder *b* (the concentration cell with transport) ; *GS*, glass syringe ; *GCV*, glass cylindrical vessel ; *GC*, glass capillary ; *RC*, reaction cell ; *M*, magnetic stirrer ; *SCE* saturated calomel electrodes ; *J*, the liquid junction ; *V*, ml of the solution to be analysed, at the initial moment ; *v*, ml of the titrated solution injected into the second compartment.

reaction cell the second one. The liquid junction is formed at the lower extremity level of the glass capillary when this is introduced into the solution to be analysed. The latter solution was magnetically stirred. A saturated calomel electrode is introduced into the solution to be analysed and another one into the titrated solution, namely in the cylindrical vessel. The insertion of the second saturated calomel electrode is tightly closing the cylindrical vessel. The EMF of the cell was recorded by means of a pH-meter "MV 11 S Clamann & Grahnert, Dresden, G.D.R", coupled through a sensitivity reducing piece (belonging to a polarograph" Heyrovsky V 301") to a recorder "Graphispot Sefram, type Grvaj, Paris".

In figure 2 are reproduced 3 experimental curves $E=E(v)$, obtained at room temperature ($\simeq 20°$), corresponding to the titration of NaOH (c_2) with HCL (c_1).

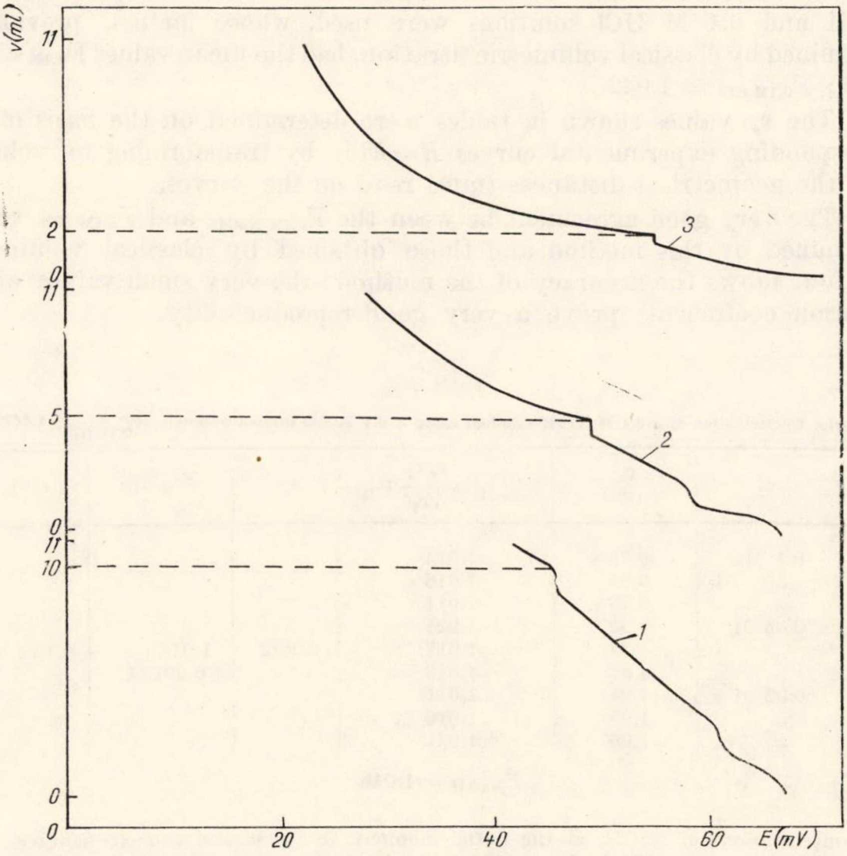

Fig. 2. — Titration curves of NaOH (c_2) with HCl (c_1), at room temperature ($\simeq$20°), corresponding to the pairs of values : *1*, $c_1=0.1$ M, $c_2=0.1$ M ; *2*, $c_1=0.1$ M ; $c_2=0.05$ M, *3*, $c_1=0.1$ M, $c_2=0.02$ M. The first compartment (HCl) is negative as compared to the second compartment.

The recorder rolling rate was 6 mm / minute and the injection flow of the titrated solution 1.19 ml/minute.

One can see that the equivalence point is marked on the $E=E(v)$ curves by angular points. The curves are decreasing before as well as after the equivalence point. All three curves are concave after the equivalence, but before the equivalence the first two have an inflexion point, by which they are passing, becoming from concave, convex ones, accordingly to the theoretical predictions. It is thus easy to see, using for the ionic mobilities, values taken from tables,[22] that for the first two curves the double inequality (8) is satisfied, but not for the third curve.

In tables 1 and 2 experimental data obtained by this method are given, regarding the determination of the factors and of their confidence intervals for 0.1 M NaOH and 0.1 MHCl solutions. For this purpose 0.1 M NaOH and 0.1 M HCl solutions were used, whose factors, previously determined by classical volumetric titration, had the mean values $\overline{F}_{0.1\text{M NaOH}} = 1.015$; $\overline{F}_{0.1\text{M HCl}} = 1.042$

The v_e values shown in tables were determined on the basis of the corresponding experimental curves $E=E(v)$, by transforming in volumes (ml), the geometrical distances (mm) read on the curves.

The very good agreement between the $\overline{F}_{0.1\text{M NaOH}}$ and $\overline{F}_{0.1\text{M HCl}}$ values determined by this method and those obtained by classical volumetric titration, shows the accuracy of the method; the very small values of the variation coefficients prove a very good reproducibility.

Table 1

Factor determination of a 0.1 M NaOH solution, using a 0.1 M HCl titrated solution ($\overline{F}_{0.1\text{MHCl}} = 1.042$)

No.	c_2	v_e (ml)	$F_{\text{NaOH}} = \frac{v_e c_1}{V c_2} F_{\text{HCl}}$	$s_{\overline{F}}$	$\overline{F} \pm ts_{\overline{F}}$	$C.V\%$
1	0.1 M	9.73	1.014	0.0013	1.016± ±0.0013 t	0.13
2	,,	9.75	1.016			
3	,,	9.70	1.011			
4	0.05 M	4.90	1.021			
5	,,	4.88	1.017			
6	,,	4.86	1.013			
7	0.02 M	1.94	1.011			
8	,,	1.95	1.016			
9	,,	1.96	1.021			

$\overline{F}_{\text{NaOH}} = 1.016$

c_2 = concentrations of NaOH, at the initial moment, in the second compartment; v_e = ml HCl 0.1 M ($\overline{F}_{\text{HCl}} = 1.042$) used up to the equivalence; $s_{\overline{F}}$=experimental standard error of the mean value; $\overline{F} \pm ts_{\overline{F}}$ = fiducial interval of the factor true value; $C.V\% = (s_{\overline{F}}/\overline{F})\,100 =$ =coefficient of variation; t = student t-deviate[23]; V = volume of NaOH introduced in the second compartment = 10 ml in all experiments.

---

[22] T. Erdey-Gruz and G. Schay, "Chimie Fizică Teoretică", vol. 2, (Romanian edition, after Hung. 2nd edn), Editura Tehnică, Bucharest, 1958, p. 640.

[23] D. J. Finney, "Statistical Method in Biological Assay", (2nd edn), Charles Griffin and Company Limited, London 1966, p. 625.

Table 2

Factor determination of a 0.1 M HCl solution, using a 0.1 M NaOH titrated solution ($\overline{F}_{0.1\text{MNaOH}} = 1.015$

No.	c_2	v_c (ml)	$F_{\text{HCl}} = \frac{v_e c_1}{V c_2} F_{\text{NaOH}}$	$s_{\overline{F}}$	$\overline{F} \pm ts_{\overline{F}}$	$C.V\%$
1	0.1 M	10.28	1.043	0.0022	$1.043 \pm$ ± 0.0022 t	0.21
2	,,	10.31	1.046			
3	,,	10.24	1.039			
4	0.05 M	5.16	1.047			
5	,,	5.11	1.037			
6	,,	5.17	1.050			
7	0.02 M	2.07	1.051			
8	,,	2.05	1.040			
9	,,	2.03	1.030			

$$\overline{F}_{\text{HCl}} = 1.043$$

c_2= concentrations of HCl, at the initial moment, in the second compartment ; v_e= ml NaOH 0.1M ($\overline{F}_{\text{NaOH}}=1.015$) used up to the equivalence ; $s_{\overline{F}}$= experimental standard error of the mean value ; $\overline{F} \pm ts_{\overline{F}}$ = fiducial interval of the factor true value ; C.V% = $(s_{\overline{F}}/\overline{F})\,100$ = coefficient of variation ; t = student t-deviate [23]; V = volume of HCl introduced in the second compartment = 10 ml in all experiments

In figures 3, 5, are shown other titration curves obtained by this method. As we can see, in the case of the reaction $Ba^{2+} + SO_4^{2-} \rightarrow BaSO_4 \downarrow$ the position of the equivalence point is very well marked when the concentration of $BaCl_2$ is lower than the concentration of Na_2SO_4 and in the case of the reaction $Ag^+ + Cl^- \rightarrow AgCl \downarrow$, when the concentration of $AgNO_3$ is lower than the concentration of KCl.

The example of THAM (tris(hydroxymethyl) aminomethane), shown in figure 5, belongs to another class of chemical reactions which will be examined in a further paper. Indeed, H^+ and THAM (uncharged molecule) are the reactants and as a result of the chemical reaction a supplementary ionic species (THAM-H^+) is formed.

In this paper we only mention that two parts $(0, x_{\text{in}})$ and $(x_{\text{in}}, 1)$ can also be distinguished in the liquid-junction double layer structure and the potential jumps along these two parts have an opposite polarity.

In figure 6 are shown three titration curves for different mixtures of NaOH and THAM.

In this case, three parts $(0, x'_{\text{in}})$, $(x'_{\text{n}}, x''_{\text{in}})$ and $(x''_{\text{in}}, 1)$ can be distinguished in the liquid-junction double layer structure, because two chemical reactions take place within the liquid junction. The potential jumps along the parts $(0, x'_{\text{in}})$ and $(x''_{\text{in}}, 1)$ have the same polarity, but the potential jump along the part $(x'_{\text{in}}, x''_{\text{in}})$ has an opposite polarity. Since the reaction $H^+ + OH^- \rightarrow H_2O$ is much more shifted to the right than the reaction $H^+ + \text{THAM} \rightleftharpoons \text{THAM-}H^+$, the transformation of THAM into THAM-HCL will begin practically only after the complete transformation of NaOH in NaCl. For this reason, the curve $E = E(v)$ has three parts : the first decreasing. the second increasing and the third one also decreasing. At the end of

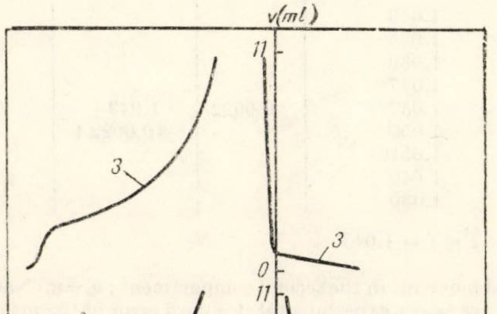

Fig. 3. — *a*: Titration curves of Na_2SO_4 (c_2) with $BaCl_2$ (c_1), at room temperature (≃20°), corresponding to the pairs of values :

1, $c_1 = 0.1$ N, $c_2 = 0.1$ N; *2*, $c_1 = 0.1$ N, $c_2 = 0.05$ N; *3*, $c_1 = 0.1$N, $c_2 = 0.02$ N. The first compartment ($BaCl_2$) is positive as compared to the second compartment *b* : Titration curves of $BaCl_2$ (c_2) with Na_2SO_4 (c_1), at room temperature (≃20°), corresponding to the pairs of values: *1*, $c_1 = 0.1$ N, $c_2 = 0.05$ N; *2*, $c_1 = 0.1$ N, $c_2 = 0.02$ N; *3*, $c_1 = 0.1$ N, $c_2 = 0.01$ N. The first compartment (Na_2SO_4) is negative as compared to the second compartment.

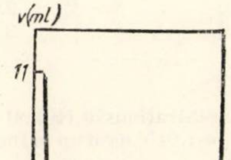

Fig.4. — Titration curves of $AgNO_3$ (c_2) with KCl (c_1), at room temperature (≃20°), corresponding to the pairs of values :

1, $c_1 = 0.1$M, $c_2 = 0.05$ M; *2*, $c_1 = 0.1$ M, $c_2 = 0.02$ M. The first compartment (KCl) is negative as compared to the second compartment.

the first part, when NaOH is transformed into NaCl, x''_{in} becomes equal to 1 and at the end of the second one, when THAM is transformed into THAM-HCl, x'_{in} becomes equal to 1. It thus results that a small amount of THAM increases the precision of the equivalence point determination, for the titration of a strong base with a strong acid.

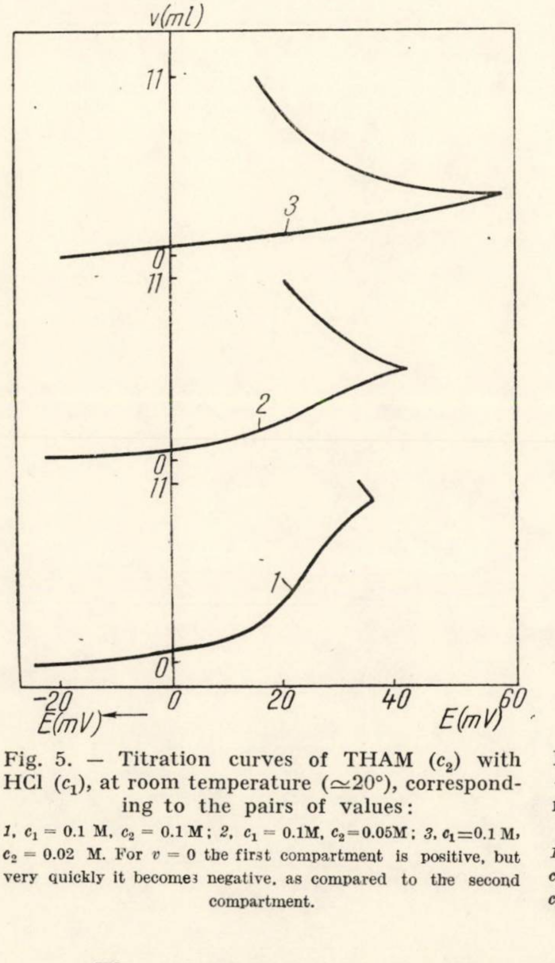

Fig. 5. — Titration curves of THAM (c_2) with HCl (c_1), at room temperature ($\simeq 20°$), corresponding to the pairs of values:

1, $c_1 = 0.1$ M, $c_2 = 0.1$ M; 2, $c_1 = 0.1$M, $c_2 = 0.05$M; 3, $c_1 = 0.1$ M, $c_2 = 0.02$ M. For $v = 0$ the first compartment is positive, but very quickly it becomes negative, as compared to the second compartment.

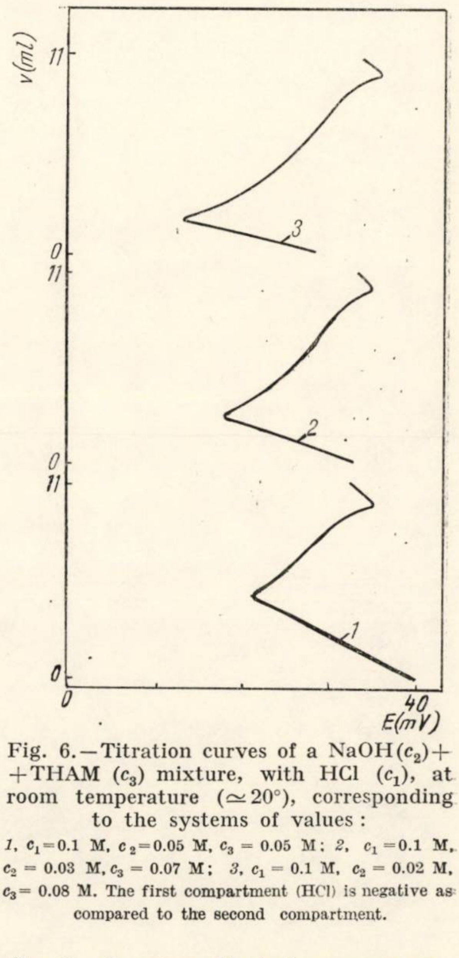

Fig. 6.—Titration curves of a NaOH(c_2)+ +THAM (c_3) mixture, with HCl (c_1), at room temperature ($\simeq 20°$), corresponding to the systems of values:

1, $c_1 = 0.1$ M, $c_2 = 0.05$ M, $c_3 = 0.05$ M; 2, $c_1 = 0.1$ M, $c_2 = 0.03$ M, $c_3 = 0.07$ M; 3, $c_1 = 0.1$ M, $c_2 = 0.02$ M, $c_3 = 0.08$ M. The first compartment (HCl) is negative as compared to the second compartment.

The experimental curves, shown in fig. 2—6, prove that the accuracy of the method depends on the value of the ratio c_1/c_2. For every particular chemical reaction, it is possible to choose such values for c_1/c_2, so that, on the $E=E(v)$ curve, the position of the equivalence point should be very well marked.

Revue Roumaine de Chimie, **15**, 1525–1528 (1970)

ABOUT THE ELECTRICAL RESISTANCE VARIATIONS IN THIN IRON FILMS DURING WATER CHEMISORPTION AND DECOMPOSITION

N. I. IONESCU

Institute of Physical Chemistry of the Academy
Bucharest, str. Dumbrava Roşie 23

Received March 27, 1970

The analysis of the results concerning the electrical resistance variations in thin iron films during water chemisorption and decomposition has shown that the observed effect can be explained, very probably, by the action of two simultaneous mechanisms : the decrease in the film thickness and the change in the electrons mobility of the metal.

The variation in the electrical resistance of thin metallic films in the gas chemisorption process can be explained by three main hypotheses.

I. The decrease in the number of conduction electrons in the metal,[1]

II. The decrease in the effective film thickness,[2]

III. The change in the electrons mobility of the metal. [3,4]

In a previous paper we have shown[5] that for the explanation of the recorded electrical resistance variation in thin copper and silver films during oxygen chemisorption it is necessary to consider the simultaneous existence of two mechanisms from the three above mentioned.

The present paper aims at investigating whether our conclusions can be extended to some recent results[6] concerning the water chemisorption and decomposition in thin iron films.

RESULTS AND DISCUSSION

The experiments performed by Suhrmann, Heras, de Heras and Wedler in order to determine the change in the temperature coefficient of the electrical resistance (T.C.R.) in thin iron films have shown[6] that, as a consequence of water chemisorption and decomposition, this becomes smaller than that corresponding to a clean film. The obtained results are listed in table 1, columns 1—7.

---

[1] R. Suhrmann and K. Schulz, *Z. phys. Chem. (Frankfurt)*, **1**, 69 (1954).

[2] W. M. H. Sachtler and G. J. H. Dorgelo, *Z. phys. Chem. (Frankfurt)*, **25**, 69 (1960).

[3] T. Toya, *J. Res. Inst. Cat.*, **10**, 236 (1962).

[4] O. A. Pancenko and Iu. G. Ptushinski, *Izvest. Akad. Nauk S.S.S.R., seria fiz.*, **28**, 1466 (1964).

[5] N. I. Ionescu, *Rev. Roumaine Chim.*, **15**, 273 (1970).

[6] R. Suhrmann, J. M. Heras, L. V. de Heras and J. Wedler, *Z. Elektrochem.*, **72**, 854 (1968).

Table 1

Resistance increases depending on temperature and temperature coefficient α in thin iron films after water chemisorption and decomposition

Experiment	T °K	R_0 Ω	ΔR Ω	R Ω	$\alpha_0 . 10^3$ degree $^{-1}$	$\alpha_1 . 10^3$ degree $^{-1}$	$\frac{\Delta R_{77}}{\Delta R_{273}}$	$\frac{(\Delta R/R)_{77}}{(\Delta R/R)_{273}}$
1	2	3	4	5	6	7	8	9
1	77	39.230	7.541	46.771	1.877	1.657	1.049	1.553
	273	62.045	7.185	69.230				
2	77	50.171	8.284	58.455	1.623	1.437	1.059	1.474
	273	73.519	7.824	81.343				
3	77	43.498	7.682	51.180	1.782	1.584	1.035	1.501
	273	66.810	7.420	74.230				

R_0 is the resistance of the clean film, R the resistance of the covered one, α_0 and α_1 the T.C.R. before and after water chemisorption and decomposition and $\Delta R = R - R_0$.

In the first two experiments the adsorption of water took place first at 77°K and the last one first at 273°K.

A similar behaviour has been observed for the nickel-oxygen,[7] silver-oxygen[8] and copper-oxygen[9] systems.

If we admit that the structure of the film, uninvolved in chemisorption does not change during the process, then on considering the relation :

$$\alpha = \frac{\alpha_\infty}{\ln \beta \dfrac{1}{d}} \tag{1}$$

where β is a constant, d the thickness of the film and α_∞ and 1 the T.C.R. respectively the mean free path of electrons in the bulk which has the same structure as the thin film, it results that a decrease in the coefficient α can be assigned only to a decrease in the thickness d.

It is worth mentioning, that relation (1) complies with the condition $d/1 \leqslant 0.2$.[10,11] At 273°K the mean free path of iron electrons is 440 Å[12] and the greatest film thickness 98.5 Å,[6] leading to a value of $d/1 = 0.223$, which can be considered to integrate within given limits.

---

[7] R. Suhrmann, J. M. Heras, L. V. de Heras and G. Wedler, *Z. Elektrochem.*, **68**, 990 (1964).

[8] I. G. Murgulescu and N. I. Ionescu, *Rev. Roumaine Chim.*, **11**, 1267 (1966).

[9] I. G. Murgulescu and N. I. Ionescu, *Rev. Roumaine Chim.*, **14**, 681 (1969).

[10] H. Mayer, "Physik dünner Schichten", vol. 2, Wissenschaftliche Verlagsgesellschaft m.b.H., Stuttgart, 1955, p. 216.

[11] D. S. Campbell, "The Use of Thin Films in Physical Investigations", Ed. J. C. Anderson, Academic Press, London and New York, 1966, p. 299.

[12] N. F. Mott and H. Jones, "The Theory of the Properties of Metals and Alloys", Dover Publications Inc., New York, 1958, p. 268.

Supplementary data concerning the mechanisms which bring about the conductivity variations in thin iron films during water chemisorption and decomposition can be obtained by considering the temperature dependences of the electrical resistance increases.

As we have previously shown[8,13] the mechanism I or I and II producing the resistance variations are expressed by the relation:

$$\frac{\left(\frac{\Delta R}{R}\right)_{273}}{\left(\frac{\Delta R}{R}\right)_{77}} = 1 \qquad (2)$$

whereas the mechanism III leads to the expression:

$$\frac{\Delta R_{273}}{\Delta R_{77}} = 1 \qquad (3)$$

As seen in table 1, columns 8 and 9, the obtained results advocate for the mechanism III producing the electrical resistance variations in the gas chemisorption process.

In order to explain the resistance variations, with the same results, it was obtained by one method, the mechanism II through a decrease in the thickness, and by another one, the mechanism III through a change in the electrons mobility of the metal. As both ways of obtaining the results are equally efficient, the most probable explanation implies the coexistence of two mechanisms.

The results obtained so far are synthesized in table 2.

Table 2

Mechanisms determining the variation in the electrical resistance in thin iron films during water chemisorption

Sense of the temperature variation	Variation in the temperature coefficient of the electrical resistance	$\frac{\Delta R_{273}}{\Delta R_{77}}$	$\frac{(\Delta R/R)_{273}}{(\Delta R/R)_{77}}$	Mechanisms explaining the observed variations in the electrical resistance
1	2	3	4	5
77 ↓ 273	diminishes	$=1$	$\neq 1$	II and III
273 ↓ 77	diminishes	$=1$	$\neq 1$	II and III

[13] I. G. Murgulescu and N. I. Ionescu, *Rev. Roumaine Chim.*, **14**, 1073 (1969).

The mechanisms determining the variations of the electrical resistance in thin iron films during water chemisorption and decomposition do not appear individually but grouped according to the data shown in table 2.

This conclusion could be also found in the systems copper-oxygen[5] and silver-oxygen.[5]

The picture of the interaction between iron and water in accordance with the above data might be the following : a superficial combination tends to form either with water or with its products of decomposition. This combination remains adsorbed on the surface and by introducing a number of supplementary defects into the lattice, increases concomitantly the residual resistance.

From the presented data we can conclude that the variations in the electrical resistance in thin iron films during water chemisorption and decomposition can be explained very probably, by the action of two simultaneous mechanisms : the decrease in the thickness of the thin film and the change in the electrons mobility of the metal.

Revue Roumaine de Chimie, **15**, 1529–1535(1970)

EINE NEUE GRUPPE VON HETEROPOLYVERBINDUNGEN DES U(IV). I

URAN(IV)-OKTOWOLFRAMANION, SYNTHESE DER ALKALISALZE UND BESTIMMUNG IHRER BASIZITÄT

RALUCA RIPAN und A. BOTAR

Aus dem Chemischen Institut der Akademie, Zweigstelle Cluj, str. Donath, 59–65

Eingegangen am 18. November 1969

Es wurde eine neue Gruppe von Heteropolywolframaten mit U(IV) als Zentralion synthetisiert, deren Generalformel Me^{I}_{4} $[UW_{8}O_{28}]\cdot XH_{2}O$ ($Me^{I} = Na^{+}$, K^{+}, Rb^{+}, Cs^{+}und NH_{4}^{+}) ist. Es wurden die chemische und thermogravimetrische Analyse dieser Salze, sowie die physikalischen und chemischen Eigenschaften untersucht. Die $H_{4}[UW_{8}O_{28}]$-Säure wurde in der wäßrigen Lösung mit Hilfe der Methode der Ionenaustausch-Chromatographie hergestellt und die Basizität durch die konduktometrischen Titrationen mit dem einwertigen Thalliumacetat bestimmt. Die erhaltene Basizität ist vier und sie ist gleich mit der Basizität der Alkalisalze.

Die praktische und theoretische Bedeutung der Heteropolyelektrolyte führte in der letzten Zeit zur Entwicklung der Chemie dieser Verbindungen. Zu diesem Zweck versuchten wir die Heteropolywolframate mit dem Zentralion U(IV) zu gewinnen, die bisher in der Fachliteratur unbekannt sind.

Im Polykondensationsverlauf der Wolframanionen, werden unter dem Einfluß der Wasserstoffionen, in Anwesenheit eines Metallionerzeugerkomplexes, in Abhängigkeit von der Koordinationsfähigkeit des Metallions, sowie von den Bedingungen in denen die Kondensationsreaktion verläuft, Heteropolywolframate erhalten, in denen das Verhältnis Me : W = 1 : 6, 1 : 9, 1 : 12 und 1 : 8 ist.[1–11]

---

[1] L. C. BAKER, G. A. GALLAGHER und T. P. MCCUTCHEON, *J. Amer. Chem. Soc.*, **75**, 2493 (1955).

[2] L. C. W. BAKER, G. FOSTER, W. TAN, F. SCHOLNIK und T. P. MCCUTCHEON, *J. Amer. Chem. Soc.*, **77**, 2136 (1955).

[3] L. C. W. BAKER und T. P. MCCUTCHEON, *J. Amer. Chem. Soc.*, **78**, 4503 (1966).

[4] J. A. MAIR, *J. Chem. Soc.*, **1950**, 2364.

[5] J. A. MAIR, und J. L. T. VAUGH, *J. Chem. Soc.*, **1950**, 2372.

[6] D. H. BROWN und J. A. MAIR, *J. Chem. Soc.*, **1958**, 2597.

[7] D. H. BROWN und J. A. MAIR, *J. Chem. Soc.*, **1962**, 3946.

[8] D. H. BROWN, *J. Chem. Soc.*, 1962, 3322.

[9] R. RIPAN und I. TODORUŢ, *Roczniki Chem.*, **38**, 1787 (1964).

[10] R. RIPAN und I. TODORUŢ, *Rev. Roumaine Chim.*, **11**, 691 (1966).

[11] R. RIPAN und I. TODORUŢ, Die dritte chemische Landeskonferenz, Zusammenfassungen, Timişoara, 39, 20 (1966).

Wenn im Polykondensationsverlauf gleichzeitig zwei Metallionen anwesend sind, dann erhält man Heteropolywolframate, die jeweils ein Metallion oder beide Metallionen im Komplexanion enthalten.[12-18]

Unsere Studien zeigten, daß die Heteropolywolframate vom Typ $Me^{I}_{4}[UW_8\,O_{28}].\,XH_2O$, wo $Me^{I} = Na^+, K^+, Rb^+, Cs^+, NH_4^+, Ag^+$, usw. vom selben Typ wie die Heteropolywolframate sind, in denen das zentrale Metallion Ce (IV), Ce (III) und Th (IV) ist.[9-11] Die IR-Spektren der erwähnten Heteropolywolframate weisen eigentlich auch eine große Ähnlichkeit untereinander auf.

In vorliegender Arbeit werden die Synthesebedingungen und einige physikalischen und chemischen Eigenschaften der Heteropolywolframate mit dem Zentralion U(IV) gebracht.

Die Darstellungsmethoden der Heteropolywolframate mit dem metallischen Zentralion U(IV) sind leicht auszuführen. Für die Bestimmung der bestmöglichen Synthesebedingungen haben wir das Studium durch Papierelektrophorese bei Hochspannung vorgenommen und photokolorimetrisch die Bildung des $[UW_8\,O_{28}]^{4-}$ in Abhängigkeit von pH, Konzentration, Rea- genzien, Temperatur und Zeit verfolgt.

Die charakteristischen physikalischen und chemischen Eigenschaften dieser Klasse sind einerseits von der kleinen Basizität und der großen Löslichkeitszunahme mit der Temperatur und andererseits vom Molekulargewicht bestimmt.

Die obenerwähnten Alkalisalze sind dunkelbraune, gut gebildete Makrokristalle, die mit einer großen Anzahl von Wassermolekülen (10-30 H_2O) kristallisieren und im Wasser leicht löslich sind.

Das $[UW_8\,O_{28}]^{4-}$-Heteropolyanion bildet mit den schweren Metallkationen oder anderen Komplexkationen amorphe Niederschläge, die im Wasser wenig löslich und analytisch interessant sind.

EXPERIMENTELLES

A. Darstellungen

1. *$Na_4[UW_8\,O_{28}].24\,H_2O$.* 50 g $Na_2WO_4.2H_2O$ löst man in 100 ml Wasser und stellt den pH-Wert der erhaltenen Lsg mit Eisessig auf 7,5—8,0 ein. Man stellt aus 8g $UO_2SO_4.3H_2O$ eine U(IV)-Lsg her, indem man an einer Säule mit Amalgamzink[19] U(VI) zu

[12] Z. F. S. Shakhova und S. A. Gavrilova, *Zhur. neorg. Khim.*, **3**, 1370 (1958).

[13] L. C. W. Baker, V. Simmon-Baker, K. Eriks, M. T. Pope, M. Shibata, O. W. Rollins, J. H. Fang und L. L. Koh, Proceedings 9th I.C.C.C., St. Moritz-Switzerland, Sept. 1966, 1 Fri 6 S. 421.

[14] L. C. W. Baker, V. Simmons-Baker, K. Eriks, M. T. Pope, M. Shibata, O. W. Rollins, J. H. Fang und L. L. Koh, *J. Amer. Chem. Soc.*, **88**, 2329 (1966).

[15] V. E. Simmons und L. C. W. Baker, Proceedings 7th I.C.C.C., Stokholm and Upsala-Sweden, 1966, 4D6, S. 195.

[16] T. J. R. Weakley und S. A. Malik, *J. Inorg. Nucl. Chem.*, **29**, 2935 (1967).

[17] R. Ripan und M. Puscaşiu, *Z. anorg. Chem.*, **358**, 82 (1968).

[18] M. Puşcaşiu, *Doklady Akad. Nauk S.S.S.R.*, **182**, 634 (1968).

[19] C. W. Sill und H. Peterson, *Anlayt. Chem.*, **24**, 1175 (1952).

U(IV) reduziert. Die auf diese Weise erhaltene Lsg fügt man tropfenweise und unter ständigem Umrühren zu einer heißen Natriumwolframatlösung hinzu.

Zuletzt wird die dunkelbraune Lösung, die den pH-Wert 5,0–5,5 haben muß, 1–2 Min. gekaht. Nach Abkühlung auf Zimmertemperatur filtriet man die Lsg vom unlöslichen Produkt ab. Nach 10–12 Std. scheiden die dunkelbraunen Kristalle $Na_4[UW_8O_{28}].24H_2O$, mit gut gebildeten Flächen und monoklinischem Aspekt aus. Ausb. 75–80 %d.Th.

Das Produkt wurde zweimal aus 75 ml heißem Wasser mit pH-Wert 5,5 umkristallisiert. Die Kristalle wurden 4 Std. an der Luft gelassen und dann chemisch analysiert. Die analytische Berechnung zeigt folgende Zusammensetzung:

$$Na_4[UW_8O_{28}].24H_2O$$

Gef.: Na 3,42; U 8,85; W 55,28; H_2O 16,14%

Ber.: Na 3,43; U 8,88; W 54,85; H_2O 16,12%

2. *$K_4[UW_8O_{28}].14H_2O$.* Man löst 10 g KCl in warmem Wasser und fügt die gesättigte Lsg zu einer heißen Lsg, die man aus 14 g $Na_4[UW_8O_{28}].24H_2O$ in 100 ml Wasser erhält. Nach Abkühlen und Filtrieren bei Zimmertemperatur scheiden dunkelbraune Kristalle mit gut gebildeten Flächen und mit triklinischem Aspekt aus. Ausb. 75% d.Th.

Die Kristalle wurden zweimal aus heißem Wasser umkristallisiert, 4 Std. an der Luft gelassen und chemisch analysiert. Die analytische Berechnung ergibt folgende Zusammensetzung:

$$K_4[UW_8O_{28}].14H_2O$$

Gef.: K 6,13; U 9,17; W 58,36; H_2O 10,20%

Ber.: K 6,09; U 9,28; W 57,34; H_2O 10,13%

3. *$Rb_4[UW_8O_{28}].15H_2O$.* Man löst 4,5 g RbCl in Wasser und fügt die gesättigte Lsg zu einer heißen Lsg, die man aus 15 g $Na_4[UW_8O_{28}].24H_8O$ in 100 ml Wasser erhält. Nach Abkühlen und Filtrieren bei Zimmertemperatur und nach Stehenlassen erscheinen dunkelbraune gut ausgebildete Kristalle mit triklinischem Aspekt. Ausb. 75% d.Th.

Nach Umkristallisieren aus Wasser läßt man die erhaltenen Makrokristalle 4 Std. an der Luft stehen und analysiert sie chemisch. Die analytische Berechnung zeigt folgende Zusammensetzung:

$$Rb_4[UW_8O_{28}].15H_2O$$

Gef.: Rb 11,97; U 8,80; W 54,71; H_2O 9,64%.

Ber.: Rb 12,34; U 8,51; W 53,12; H_2O 9,79%.

4. *$Cs_4[UW_8O_{28}].11H_2O$.* Man löst 7,5 g CsCl in warmem Wasser und fügt die gesättigte Lsg zu einer heißen Lösung, die man aus 15 g $Na_4[UW_8O_{28}].24H_2O$ in 100 ml Wasser erhält. Nach Abkühlen und Filtrieren bei Zimmertemperatur scheiden nach einiger Zeit dunkelbraune Kristalle, mit rhombischem Aspekt aus. Ausb. ungefähr 60–65 %d. Th. Nach Umkristallisieren aus Wasser wurden die Kristalle 4 Std. an der Luft gelassen und chemisch analysiert. Die analytische Berechnung zeigt folgende Zusammensetzung:

$$Cs_4[UW_8O_{28}].11H_2O$$

Gef.: Cs 19,52; U 8,36; W 53,73; H_2O 6,84%.

Ber.: Cs 18,42; U 8,24; W 50,97; H_2O 6,86%.

5. $(NH_4)_4\,[UW_8O_{28}].14H_2O$. Man löst 26 g Ammoniumazetat in warmem Wasser und fügt die gesättigte Lsg zu einer heißen Lsg, die man aus 20g $Na_4\,[UW_8O_{28}].24H_2O$ in 100 ml Wasser erhält. Nach Abkühlen und Filtrieren, bei Zimmertemperatur scheiden nach einiger Zeit dunkelbraune Kristalle mit triklinischem Aspekt aus Ausb. ungefähr 60—65% d.Th. Nach Umkristallisieren aus dest. Wasser läßt man die Kristalle 10 Std. an der Luft und analysiert sie chemisch. Die analytische Berechnung zeigt folgende Zusammensetzung:

$$(NH_4)_4[UW_8O_{28}].14H_2O$$

Gef.: N 2,13: U 9,12; W 58,81; H_2O 9,92%.
Ber.: N 2,25; U 9,58: W 59,28; H_2O 10,16%.

B. *Thermogravimetrische Analyse*

Die Thermogramme der $Me^{I}_{4}[UW_8O_{28}].XH_2O$-Salze, wo $Me^{I} = Na^+, K^+, Rb^+, Cs^+$ und NH_4^+, erlauben die direkte Bestimmung des in jedem Komplex, enthaltenen Wassers sowie die Art und Weise seiner Entfernung in Abhängigkeit von der Temperatur (Abb. 1—5). Aus dem Verlauf der Thermogramme entnimmt man, daß die Höchstgeschwindigkeit der Wasserausscheidung zwischen 80—100° und der Schluß der Wasserausscheidung zwischen 250—300° liegt.

Die Versuchsergebnisse sind weiter unten gezeigt:

C. *Chemische Grundanalyse*

Die synthetisierten Komplexverbindungen wurden in warmer konzentrierter Natronlauge zersetzt und jedes Element wurde folgenderweise bestimmt:

— Uran photokolorimetrisch mit Morin,[20] oder gravimetrisch.[21]

— Alkalimetalle flammphotometrisch (Na und K) und mit Tetraphenylborat-(Rb und Cs).

— Stickstoff nach Kjeldhal.

— Wolfram gravimetrisch durch Abwägen von WO_3, Fällung mit Cinconin und konzentrierter Salzsäure und Kalzinierung.

— Die Anzahl der Wassermoleküle thermogravimetrisch (s. Tabelle 1)

D. *Synthese der $H_4[UW_8O_{28}]$-Heteropolysäure und Bestimmung ihrer Basizität*

Die $H_4[UW_8O_{28}]$-Säure wurde aus der wäßr. Lsg von $Na_4\,[UW_8O_{28}].xH_2O$ hergestellt, dessen Synthese oben gezeigt worden ist, und zwar durch Ionenaustausch-chromatographische Methoden.[3,22,23] Bisher konnte die Heteropolysäure in festem Zustand nicht hergestellt werden, weil eben so wie im Falle der anderen bekannten Heteropolysäuren die wäßr. Lsgen sich mit der Zeit zersetzen.

[20] GY. ALMASSY, Z. NAGY und J. STRAUB, *Acta Chim. Hung.*, **7**, 317 (1955).
[21] R. RIPAN und V. SECELEANU, *Talanta*, **12**, 69 (1965).
[22] E. MATIYEVICI und M. KERKER, *J. Amer. Chem. Soc.*, **81**, 5560 (1959).
[23] R. RIPAN und I. TODORUŢ, *Rev. Roumaine Chim.*, **11**, 1279 (1960).

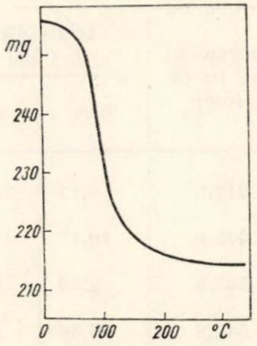

Abb. 1. — Thermogravimetrische Kurve von $Na_4[UW_8O_{28}] \cdot 24H_2O$.

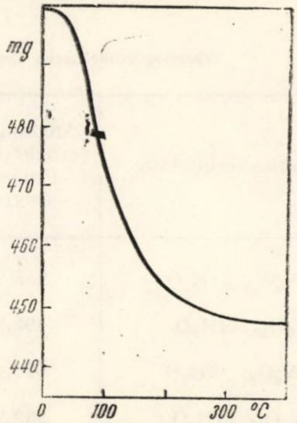

Abb. 2. — Thermogravimetrische Kurve von $K_4[UW_8O_{28}] \cdot 14H_2O$.

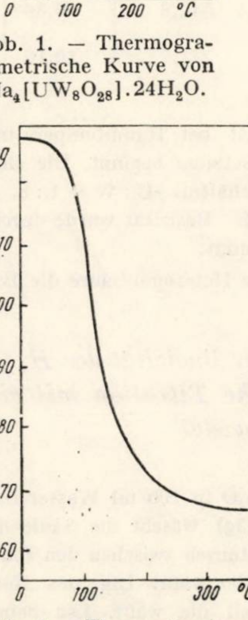

Abb. 3. — Thermogravimetrische Kurve von $Rb_4[UW_8O_{28}] \cdot 15H_2O$.

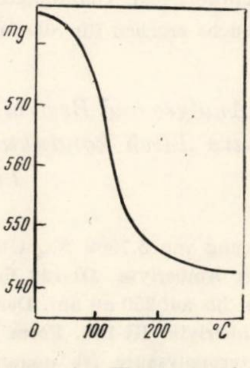

Abb. 4. — Thermogravimetrische Kurve von $Cs_4[UW_8O_{28}] \cdot 11H_2O$.

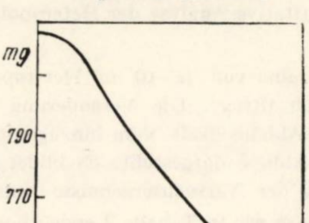

Abb. 5. — Thermogravimetrische Kurve von $(NH_4)_4[UW_8O_{28}] \cdot 14H_2O$.

Tabelle 1

Thermogravimetrische Bestimmung der Wassermolekülzahl

Lfd. Nr.	Komplexverbindung	Angfangsgewicht der Probe (mg)	Endgewicht der Probe (mg)	Verlustgewicht (%)		H_2O-Moleküle
				Ber.	*Gef.*	
1	$Na_4UW_8O_{28}.24H_2O$	255,2	214,0	16,12	16,14	24
2	$K_4UW_8O_{28}.14H_2O$	499,3	448,6	10,13	10,20	14
3	$Rb_4UW_8O_{28}.15H_2O$	627,0	567,5	9,79	9,64	15
4	$Cs_4UW_8O_{28}.11H_2O$	582,7	542,8	6,86	6,84	11
5	$(NH_4)_4UW_8O_{28}.14H_2O$	823,5	741,7	10,16	9,92	14

Die wäßr. Lsg der $H_4[UW_8O_{28}]$-Säure ist bei Raumtemperatur eine Woche lang beständig, nachher trübt sie sich, denn die Zersetzung beginnt. Die chemische Analyse der Lösung der Heteropolysäure zeigt, daß das Verhältnis U : W = 1 : 8, was auch bei der Analyse der alkalischen Salze gefunden wurde. Die Basizität wurde durch konduktometrische Titration mit einwertigem Thalliumacetat bestimmt.

Die Versuche ergeben für die untersuchte Heteropolysäure die Basizität vier.

E. *Synthese, Analyse und Bestimmung der Basizität der $H_4[UW_8O_{28}]$-Heteropolysäure durch konduktometrische Titration mit einwertigem Thalliumazetat*

Eine Lösung von 5,7909 Na_4 $UW_8O_{28}.23H_2O$ in 100 ml Wasser leitet man durch den Ionenaustauscher Amberlyte IR-120 Form H (5g) wäscht die Säule mit dest Wasser und füllt mit Wasser bis auf 250 ml auf. Der Ionenaustausch zwischen den Ionen H^+ des Kationenaustauschers Amberlyte IR-120, Form H^+ und der wäßr. Lsg des Natriumsalzes der entsprechenden Heteropolysäure ist quantitativ, weil die wäßr. Lsg beim Flammphotometer für Natrium eine negative Reaktion zeigt. Vor dem Ionenaustausch der wäßr. Lsg des Natriumsalzes war der pH-Wert ungefähr 6 und nach dem Ionenaustausch ungefähr 2.

Die quantitative Analyse der Heteropolysäure zeigt, daß das Verhältnis U : W = 1 : 8 beträgt.

Die Volumina von je 10 ml Heteropolysäure wurden mit einer Thalliumacetatlösung konduktometrisch titriert. Die Veränderung des elektrischen Widerstands der Heteropolysäurelösung in Abhängigkeit vom hinzugefügten Volumen (ml) der einwertigen Thalliumacetatlösung ist in Abb. 6 dargestellt. Es bildet sich ein voluminöser orangegelber Niederschlag.

Aufgrund der Versuchsergebnisse wurde die Basizität der $H_4[UW_8O_{28}]$-Heteropolysäure berechnet, so wie in Tabelle 2 ersichtlich.

Die Basizität der H_4 $[UW\ O_{28}]$-Säurelösung wurde nicht durch konduktometrische Titration mit Natriumhydroxidlösung bestimmt, weil sich die Heteropolysäure durch Hinzufügen von Natronlauge teilweise zersetzt. Durch Titrationen mit $AgNO_3$ wurde derselbe Wert der Basizität der Heteropolysäure erhalten.

Tabelle 2

Konduktometrische Bestimmung der Basizität der H_4 [UW_8O_{28}]-Säure mit $TlCH_3-COO$

Lfd. Nr.	$H_4[UW_8O_{28}]$-Lösung für die Titration	Titer der $H_4[UW_8O_{28}]$-Lösung	$TlCH_3COO$-Menge verbraucht von $H_4[UW_8O_{28}]$		Basizität
			Ber.	*Gef.*	
1	10				
2	10				
3	10	0,015302	0,07614	0,07665	4
4	10				
5	10				

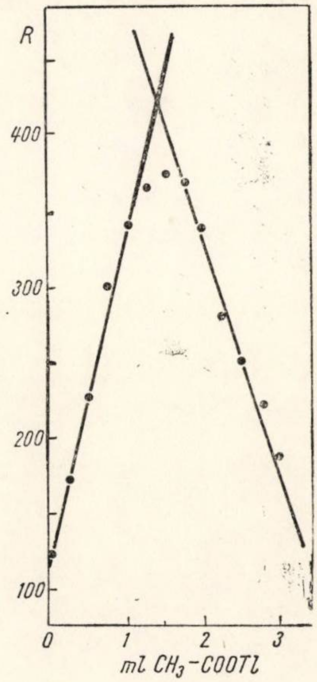

Abb. 6. — Konduktometrische Titration einer $H_4[UW_8O_{28}]$-Lösung mit einer $TlCH_3-COO$-Lösung.

SCHLUSSFOLGERUNGEN

— Es wurde zum ersten Mal eine neue Gruppe von Heteropolywolframaten mit U(IV) als Zentralion von der allgemeinen Formel Me^I_4 [UW_8O_{28}]. XH_2 O, wo $Me^I = Na^+$, K^+, Rb^+, Cs^+, NH^4_+, dargestellt.

Die entsprechende Heteropolysäure wurde in wäßriger Lösung hergestellt und ihre Basizität wurde durch konduktometrische Titrationen mit einwertigem Thalliumacetat bestimmt. Die Basizität ist 4.

Revue Roumaine de Chimie, **15**, 1537–1541, 1970

EINE NEUE GRUPPE VON HETEROPOLYVERBINDUNGEN DES U(IV). II

PHOTOKOLORIMETRISCHE STUDIEN DER BILDUNG DES $[UW_8O_{28}]^{4-}$ IN ABHÄNGIGKEIT VON pH, TEMPERATUR UND ZEIT

RALUCA RIPAN und A. BOTAR
Aus dem Chemischen Institut der Akademie, Zweigstelle Cluj, str. Donath, 59–65

Eingegangen am 24.Dezember 1969

Es wurde der pH-Bereich und die optimale Ausbeute des $[UW_8O_{28}]^{4-}$ in Abhängigkeit von pH, Temperatur und Zeit, der Reaktion zwischen WO_4^{2-} und U^{4+} bestimmt. Die Höchstausbeute (ungefähr 80% d.Th.) des Heteropolywolframates von U(IV) erhält man, wenn man mit den Natriumwolframatlösungen bei pH = 6–8 arbeitet. Die Ausbeute des $[UW_8\ O_{28}]^{4-}$ ändert sich sehr wenig in Abhängigkeit von Zeit und Temperatur (Tabelle 1).

In einer früheren Arbeit[1] wurden die Synthesemethoden und einige physikalische und chemische Eigenschaften der Heteropolywolframate von U(IV) mit der allgemeinen Formel $Me_4^I\ [UW_8O_{28}]\cdot XH_2O$ wobei $Me^I = Na^+$, K^+, Rb^+, Cs^+, und NH_4^+ dargestellt.

In der vorliegenden Arbeit wurde der pH-Bereich und die optimale Ausbeute des $[UW_2O_{28}]^{4-}$-Ions in Abhängigkeit von pH, Temperatur und Zeit, durch ein photokolorimetrisches Studium der Reaktion zwischen WO_4^{2-} und U^{4+} bestimmt.

Wenn man zu einer Natriumwolframatlösung (bei verschiedenen pH-Werten) steigende Mengen von U^{4+} hinzufügt, dann bildet sich das obenerwähnte dunkelbraune Heteropolywolframat und folglich steigt die Extinktion der Lösung. Wenn das ganze Natriumwolframat für die Bildung des $[UW_8O_{23}]^{4-}$-Ions verbraucht ist, reagiert das hinzugefügte U^{4+} mit diesem Heteropolyanion, es entsteht ein Niederschlag von $U[UW_8O_{28}]\cdot xH_2O$ und infolgedessen nimmt die Extinktion der Lösung ab.

Stellt man die Extinktionsveränderung der Lösung in Abhängigkeit von der hinzugefügten Menge von U^{4+} bei einer bekannten Menge von Natriumwolframat graphisch dar, so kann man die Menge des durch Natriumwolframat bei der Bildung des $[UW_8O_{28}]^{4-}$ gebundenen U^{4+} berechnen und folglich die Ausbeute dieses Heteropolyanions bestimmen.

---

[1] I. Mitt. R. Ripan und A. Botar, *Rev. Roumaine Chim.* **15**, 1529 (1970)

EXPERIMENTELLES

Durch Lösen von 20,5 g $Na_2WO_4.2H_2O$ in 400—450 ml Wasser wurde eine 0,05M Na_2WO_4-Lsg bereitet, deren pH-Wert mit $HClO_4$ (1 : 2) oder NaOH auf die Werte 2,3,4,... 9 eingestellt und die nachher in einem Kolben auf 500 ml verdünnt wurde. Auf diese Weise erhält man eine Natriumwolframatlösung mit $T_W = 0{,}0228$.

Für das Bereiten der U^{4+} -Lsg löst man 6g $UO_2SO_4.3H_2O$ in 45 ml Wasser, versetzt mit 1,5 ml konzentrierter Schwefelsäure und leitet die erhaltene Lsg durch eine mit Zinkamalgam gefüllte Säule.[2]

Schließlich bringt man die Lsg in einen Kolben und verdünnt mit Wasser auf 200ml. Die Lsg hat den Titer $T_U = 0{,}0168$.

Von der Natriumwolframatlösung mit dem pH-Wert 2,3,4, ... 9, wurden Proben von je 10 ml genommen, denen steigende Mengen von U^{4+} hinzugefügt wurden. Die Proben wurden sehr gut geschüttelt der pH-Wert der Lsg von neuem auf die Anfangswerte von 2,3,4, ... 9, eingestellt, und in Meßkolben bis auf 25 ml aufgefüllt. Man filtriert auf Papier und mißt die Extinktion.

Der pH-Wert wurde mit einem pH-Meter Typ L.P.Y. und die Extinktion mit einem Photokolorimeter FEK-M (Blaufilter und Kuvetten von 1 cm) gemessen.

DISKUSSION

In der Fortsetzung werden wir nur einige der bedeutendsten experimentellen Ergebnisse bekanntmachen.

1. Photokolorimetrische Untersuchung beim pH-Wert = 7,6

Sofort nach Ansäuerung der Natriumwolframatlösung. In Abb. 1. sind die erhaltenen Ergebnisse dargestellt.

2. Photokolorimetrische Untersuchung beim pH-Wert = 7,0

Sofort nach Ansäuerung der Natriumwolframatlösung. In Abb. 2. sind die erhaltenen Ergebnisse dargestellt.

3. Photokolorimetrische Untersuchung beim pH-Wert = 6,0

Sofort nach Ansäuerung der Natriumwolframatlösung. In Abb. 3 sind die experimentellen Ergebnisse dargestellt.

4. Photokolorimetrische Untersuchung beim pH-Wert = 5,0

Sofort nach Ansäuerung der Natriumwolframatlösung. In Abb. 4 sind die experimentellen Ergebnisse dargestellt.

Wir erwähnen, daß das photokolorimetrische Studium der Bildung von $[UW_8O_{28}]^{4-}$ auch in Abhängigkeit von der Temperatur und der Zeit verfolgt wurde : erstens sofort nach Ansäuerung der Natriumwolframatlösung und zweitens, sofort nach Ansäuerung und Kochen (fünf Minuten) der Lösung. Gleichzeitig wurde die Komplexbildung für jeden der pH-Werte 7, 24 und 48 Stunden nach Ansäuerung der Natriumwolframatlösung verfolgt.

---

[2] C. W. Sill und H. E. Petersen, Analyt. Chem., **24**, 1175 (1952).

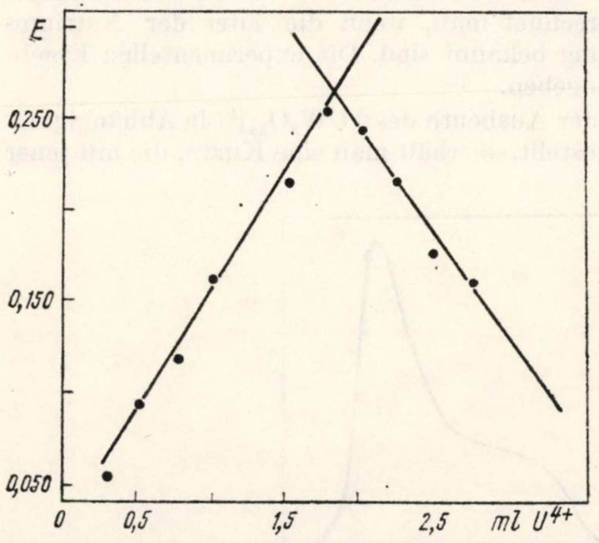

Abb. 1. — Die photokolorimetrische Titration der Natriumwolframatlösung (sofort nach Ansäuerung) mit einer U^{4+}-Lösung, beim pH-Wert = 7,6.

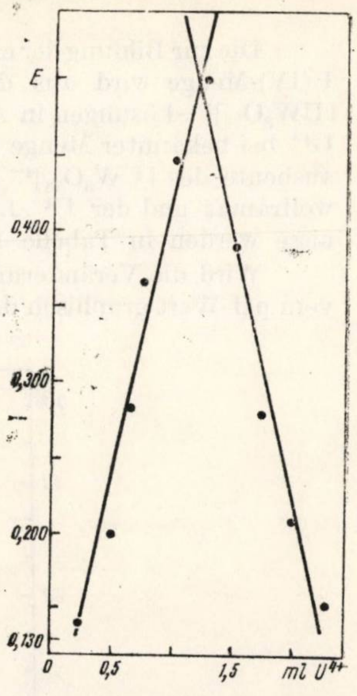

Abb. 2. — Die photokolorimetrische Titration der Natriumwolframatlösung (sofort nach Ansäuerung) mit einer U^{4+}-Lösung, beim pH-Wert = 7,0.

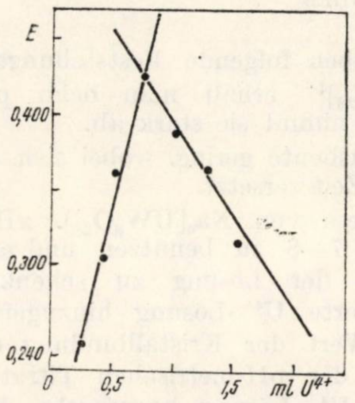

Abb. 3. — Die photokolorimetrische Titration der Natriumwolframatlösung (sofort nach Ansäuerung) mit einer U^{4+}-Lösung, beim pH-Wert = 6,0.

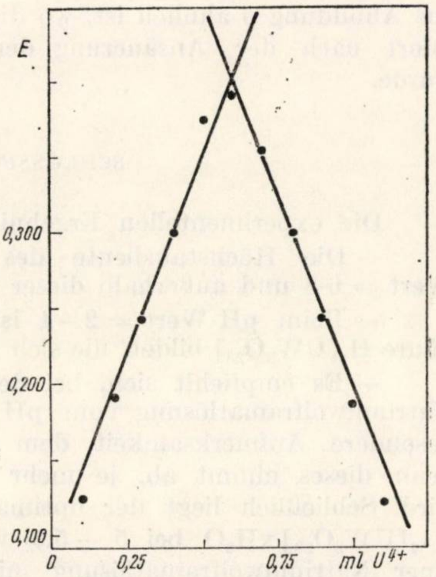

Abb. 4. — Die photokolorimetrische Titration der Natriumwolframatlösung (sofort nach Ansäuerung) mit einer U^{4+}-Lösung, beim pH-Wert = 5,0.

Die zur Bildung der entsprechenden Heteropolyverbindung notwendige U(IV)-Menge wird aus der graphischen Darstellung der Extinktion der $[UW_8O_{28}]^{4-}$-Lösungen in Abhängigkeit von der hinzugefügten Menge von U^{4+} bei bekannter Menge von Natriumwolframat bestimmt. Die Bildungsausbeute des $[UW_8O_{28}]^{4-}$ berechnet man, wenn die Titer der Natriumwolframat- und der U^{4+}-Lösung bekannt sind. Die experimentellen Ergebnisse werden in Tabelle 1 angeben.

Wird die Veränderung der Ausbeute des $[UW_8O_{28}]^{4-}$ in Abhängigkeit vom pH-Wert graphisch dargestellt, so erhält man eine Kurve, die mit jener aus Abbildung 5 ähnlich ist, wo diese Abhängigkeit beim pH-Wert = 7,6 sofort nach der Ansäuerung der Natriumwolframatlösung dargestellt wurde.

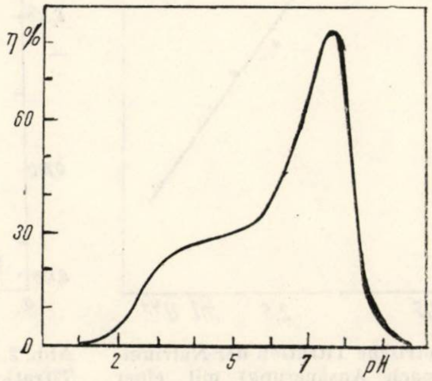

Abb. 5. — Die Veränderung der Bildungsausbeute des $[UW_8O_{28}]^{4-}$ in Abhängigkeit von der Zeit, beim pH-Wert = 7,6.

SCHLUSSFOLGERUNGEN

Die experimentellen Ergebnisse erlauben folgende Feststellungen:

— Die Höchstausbeute des $[UW_8O_{28}]^{4-}$ erhält man beim pH-Wert = 6-8 und außerhalb dieser Grenzen nimmt sie stark ab.

— Beim pH-Wert = 2—4 ist die Ausbeute gering, wobei sich die Säure $H_4[UW_8O_{28}]$ bildet, die sich mit der Zeit zersetzt.

— Es empfiehlt sich, bei der Synthese von $Na_4[UW_8O_{28}]. xH_2O$ Natriumwolframatlösung vom pH-Wert = 7—8 zu benützen und eine besondere Aufmerksamkeit dem End-pH der Lösung zu schenken, denn dieses nimmt ab, je mehr angesäuerte U^{4+}-Lösung hinzugefügt wird. Schließlich liegt der optimale pH-Wert der Kristallbindung des $Na_4[UW_8O_{28}].xH_2O$ bei 5 — 5,5 was aus der pH-metrischen Titration einer Natriumwolframatlösung mit einer U^{4+}-Lösung hervorgeht. Wir haben diese Tatsache experimentell kontrolliert.

— Beim entsprechenden pH-Wert befindet sich nicht das gesamte in Arbeit genommene Natriumwolframat in aktiver Form, das mit U^{4+} unter Bildung von $[UW_8O_{28}]^{4-}$ zu reagieren fähig ist (Tabelle 1.)

Tabelle 1

Die Ausbeute des $[UW_8O_{28}]^{4-}$ in Abhängigkeit von pH, Temperatur und Zeit

Lfd. Nr.	pH	Ausbeute %				
		Sofort nach der Ansäuerung des Wolframates	Sofort nach Ansäuerung und Kochen (5 Minuten) des Wolframates	7 Stunden nach Ansäuerung des Wolframates	24 Stunden nach Ansäuerung des Wolframates	48 Stunden nach Ansäuerung des Wolframates
1	2	0	0	0	0	0
2	3	20,53	22,81	20,53	20,53	20,56
3	4	26,01	20,95	24,18	21,44	20,53
4	5	27,37	22,81	26,46	26,46	26,01
5	6	34,22	27,37	34,22	34,22	32,85
6	7	54,73	57,93	52,45	50,61	50,17
7	7,6	83,01	82,09	82,09	74,07	72,79
8	9	0	0	0	0	0

— Die Ausbeute verändert sich sehr wenig in Abhängigkeit von Temperatur und Zeit.

— Aus den photokolorimetrischen Bestimmungen findet man das Verbindungsverhältnis U : W=1 : 8, was auch durch die chemische Grundanalyse der Alkalisalze dieser Klasse von Heteropolyverbindungen gefunden wurde.

Revue Roumaine de Chimie, **15**, 1537–1541, 1970

— c. 5716

Revue Roumaine de Chimie **15**, 1543–1546 (1970)

METALLKOMPLEXE DER ANTHRANYLDIESSIGSÄURE (ANDA). IX[*]

DAS SYSTEM AL – ANDA

C. DRĂGULESCU, R. POMOJE, I. MENESSY und MARIA PÎRLEA

von der Fakultät für Angewandte Chemie der Technischen Hochschule, Timişoara, str. Bocşei, 6

Eingegangen am 27. April 1970

Es werden die Komplexierungsgleichgewichte im System Al(III)–ANDA–H^+ untersucht. Aufgrund von spektralphotometrischen Bestimmungen wurde festgestellt, daß sich eine einzige Komplexverbindung im Verhältnis 1 : 1 bildet, deren Dissoziationskonstante bei pH = 3 den Wert $K = 2{,}5 \cdot 10^{-5}$ hat.

Anthranyldiessigsäure (ANDA) bildet mit Metallionen Komplexe im Verhältnis 1 : 1 und wirkt in den meisten Fällen als ein vierzähniger Ligand.[1] Die Vierzähnigkeit des Liganden kommt im UV-Spektrum durch das Auftreten einer Bande im Bereich 275-290 mμ zum Ausdruck[2]; diese Tatsache ermöglicht es die Komplexbildung mit farblosen Kationen zu erforschen. In Abhängigkeit vom Metall treten kleine Abweichungen in der Lage und Intensität dieser Bande auf.[3,4]

Um das Bestehen von Komplexen in dem untersuchten System zu bestätigen, wurden die Lichtabsorptionskurven von $Al_2(SO_4)_3$-Lösungen, von ANDA sowie von ihrem Gemisch im UV-Bereich (220–360 mμ) verfolgt. Die Messungen wurden mit einem Spektralphotometer UNICAM SP 800 durchgeführt, während zur Bestimmungen der pH-Werte der Proben ein pH-Meßgerät MV 11 mit Glas- und Kalomelelektrode verwendet wurde. Zur genauen Einstellung der pH-Werte wurde $HClO_4$ oder NaOH hinzugefügt.

Bei $Al_2(SO_4)_3$-Lösungen findet praktisch keine Lichtabsorption im Bereich 220-360 mμ statt.

Die Absorptionskurven einer ANDA-Lösung bei pH = 3 und die einer Al(III) + ANDA-Lösung bei demselben pH sind in Abbildung 1 dargestellt.

---

[*] VIII. C. Drăgulescu, R. Pomoje, I. Menessy und M. Pîrlea, *Rev. Roumaine Chim.*

[1] C. Drăgulescu, R. Pomoje und I. Menessy, Omagiu Acad. Prof. Raluca Ripan. Ed. Acad., Bukarest, 1966, S. 225.

[2] C. Drăgulescu, R. Pomoje, I. Menessy und C. Mihăescu, *Revue Roumaine Chim.*, **12**, 553 (1967).

[3] C. Drăgulescu, I. Menessy, M. Pîrlea und A. Ferencz. *Bull. Soc. chim. France*, **1967**, 4740.

[4] C. Drăgulescu, S. Policec und T. Simonescu, *Talanta*, **13**, 1451 (1966); **13**, 1543 (1966).

Wie aus Abb. 1 ersichtlich ist, besitzt die Absorptionskurve in Gegenwart von Al(III) ein charakteristisches Maximum bei 277 mμ, wodurch die Bildung einer Komplexverbindung bestätigt wird.

Die Wasserstoffionenkonzentration beeinflußt wesentlich die Lichtabsorption der Lösungen (Abb. 2).

Aus Abb. 2 ergibt sich, daß im pH-Bereich von 2 bis 7 (Kurven *2-7*) die Lichtabsoptionskurven einen für den Komplex charakteristischen Verlauf haben. Bei pH < 2 (Kurve *1*) weist die Lichtabsorptionskurve kleine Unterschiede gegenüber der Kurve auf, die für Lösungen des Liganden bei gleichem pH erhalten wurden.[5] In basischen Lösungen (pH > 8) haben die Absorptionskurven (Kurven *8-11*) das Bestreben sich dem Verlauf, der für den freien Liganden charakteristischen Kurven zu nähern, was durch das Auftreten der Maxima bei ~260 und ~310 mμ gekennzeichnet wird. Durch diesen Verlauf der Lichtabsorptionskurven wird die Bildung einer einzigen Komplexverbindung in dem untersuchten System angezeigt, deren Beständigkeit gleichzeitig mit steigenden pH-Werten der Lösung zwischen 2 und 7 zunimmt. Der identische Verlauf der Absorptionskurven in Gegenwart von Al(III) bei pH-Werten unter 2 und über 8, mit denen des Liganden wird durch die Zersetzung des Komplexes infolge Protonierung des Liganden in saurem Medium und durch Hydrolyse von Aluminium unter Bildung von $Al(OH)_3$, bzw. $Al(OH)_4^-$ in alkalischem Medium erklärt.

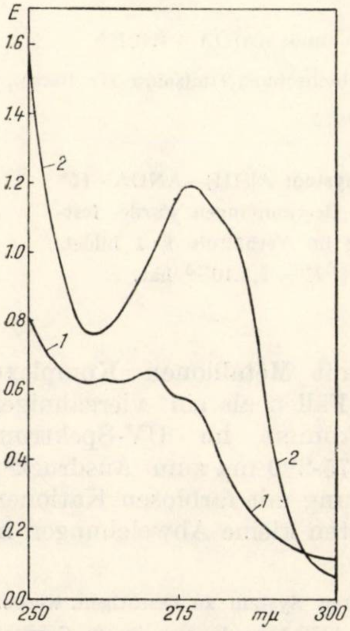

Abb. 1.—Lichtabsorption der Lösungen von:
1. [ANDA]$=2.10^{-4}$ M; l$=4{,}0$ cm; pH$=2{,}83$
2. [ANDA] $=$ [Al] $= 10^{-3}$ M; l $= 1{,}0$ cm; pH $= 2{,}85_5$

Zur Bestimmung der Verbindungsverhältinsse wurde die Methode der kontinuierlichen Veränderungen und des molaren Verhältnisses verwendet. In Abb. 3 sind die Lichtabsorptionskurven von Lösungen dargestellt worden, die den Liganden in einem konstanten, Al dagegen in veränderlichem Verhältnis bei pH $= 3$ enthalten. Es kann beobachtet werden, daß mit zunehmender Al-Konzentration, die Absoptionskurven allmählich ihren Verlauf ändern und von der für den Liganden charakteristischen Kurvenform zur Kurvenform des Komplexes übergehen.

Das Anwachsen der Extinktion im Bereiche des Maximums zeigt selbst bei großen Werten des Verhältnisses Al : ANDA eine geringe Beständigkeit des Komplexes bei diesem pH an. Aus diesen Versuchsergebnissen sowie aus den Daten, die mit der Methode der kontinuierlichen Veränderungen erhalten wurden, ist ersichtlich, daß sich in dem untersuchten

---

[5] C. Drăgulescu, R. Pomoje, I. Menessy, M. Pîrlea und C. Mihăescu, *Rev. Roumaine Chim.*, **14**, 1595 (1969).

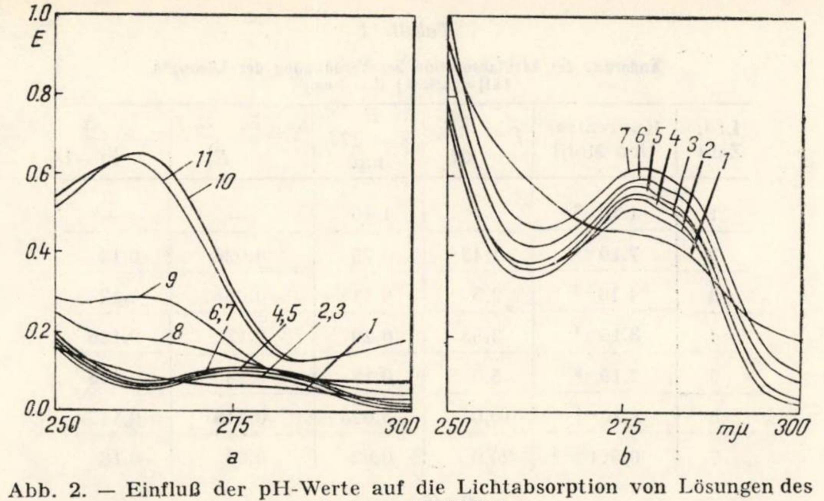

Abb. 2. – Einfluß der pH-Werte auf die Lichtabsorption von Lösungen des Systems Al-ANDA

[Al] = [ANDA] = 10^{-3} M
a, l = 0,1 cm; *b*, l = 0,5 cm.
1, pH = 0,9; *2*, pH = 2; *3*, pH = 2,9; *4*, pH = 4,4; *5*, pH = 5,1; *6*, pH = 6,07; *7*, pH = 7,05; *8*, pH = 8,15; 9, pH = 8,7; *10*, pH = 9,7; *11*, pH = 12.

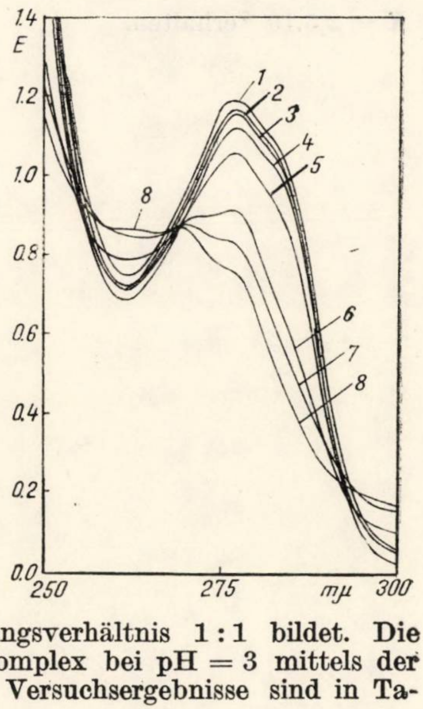

Abb. 3. — Lichtabsorptionskurven von Lösungen mit konstanter ANDA-Konzentration und veränderlicher Konzentration von Al

[ANDA] = 10^{-3} M; pH = 3; l = 1 cm
1, [Al] = 10^{-1} M; *2*, [Al] = 5.10^{-2} M; *3*, [Al] = 10^{-3} M; *4*, [Al] = 8.10^{-4} N; *5*, [Al] = 5.10^{-4} M; *6*, [Al] = 2,4.10^{-4} M; *7*, [Al] = 1.10^{-4} M; *8*, [Al] = 0

System ein Komplex mit dem Verbindungsverhältnis 1 : 1 bildet. Die Stabilitätskonstante wurde für diesen Komplex bei pH = 3 mittels der Verdünnungs methode bestimmt.[6] Die Versuchsergebnisse sind in Tabelle 1 angeführt.

---

[6] A. K. Babko, „Fisiko khimicheskii analiz komplexnykh soedinenii v rastvorakh", Isd. Akad. Nauk USSR, Kiev, 1955, S. 119.

Tabelle 1

Änderung der Lichtabsorption bei Verdünnung der Lösungen
[Al] = [ANDA] (l = 1 cm)

Lfd. Zahl	Konzentration Mol/l	$f = \frac{C_1}{Ci}$	E $\lambda = 277$ mμ	$\Delta = \frac{E_1 - E_i \cdot f}{E_1}$	$\alpha_1 = \frac{\Delta}{\sqrt{f} - 1}$
1	1.10^{-3}	—	1,10	—	—
2	7.10^{-4}	1,43	0,75	0,026	0,13
3	4.10^{-4}	2,5	0,41	0,068	0,12
4	3.10^{-4}	3,33	0,29	0,12	0,146
5	2.10^{-4}	5,0	0,18	0,18	0,145
6	1.10^{-4}	10,0	0,075	0,318	0,147
7	$0{,}5.10^{-4}$	20,0	0,02	0,63	0,18

$\alpha_m = 0{,}146$

Aus der Beziehung $K = \frac{\alpha^2 \cdot c}{1 - \alpha}$ wird bei pH = 3 der Wert $K = 2{,}5.10^{-5}$ erhalten.

Revue Roumaine de Chimie, **15**, 1547– 1554 (1970)

FORMATION OF ALUMINIUM COMPLEXES WITH PYROGALLOL

T. GOINA and MARIA OLARU

Laboratory of inorganic chemistry, Institute of Medicine and Pharmacy,
Tg. Mureş, Str. Gh. Marinescu 38

Received July 2, 1969

The authors study the formation of soluble chelatic compounds of the aluminium ion with pyrogallol in aqueous solution by means of potentiometric titration and thermic determinations. They conclude that stable compounds are formed in a pyrogallol : Al ratio of 1, 2, 3. By applying Bjerrum's computing method of formation constants, one obtains respectively the values $pK_1 = -24.5$, $pK_2 = -21.0$ and $pK_3 = -13.4$.

Pyrogallol forms complexions with a large number of ions of trivalent,[1] tetravalent [2] and even pentavalent[3] metals. The combining ratio depends on the nature of the metal. For pyrogallol, one indicates in all cases the same anion participation in the formation of the complex $[C_6H_3(OH)O_2]^{2-}$. According to the Czech authors Bartusec and Zelinka,[4] pyrogallol has $pK_1 = 9.05$, $pK_2 = 11.9$ and $pK_3 = 14$.

In our paper we have studied the formation of aluminium ion complexes with pyrogallol, by thermic and potentiometric measurements.

EXPERIMENTAL

Thermic measurements were carried out at a 25 ± 0.005° temperature, according to a technique described by us previously. [5, 6]

We have first determined the caloric effect obtained at continuous stirring of some aqueous solutions of 0.25 M pyrogallol and alkaline aluminate, a reaction that takes place with a considerable liberation of heat. The results are given in figure 1, (curve 1) which attests a maximum of thermic uneveness ($+\Delta T°$) for a molar ratio close to 2 pyrogallol : 1 Al.

---

[1] N. S. Poluectov and K. V. Cercasevici, *Zhur. neorg. Khim.*, **12** 1862 (1967).

[2] S. J. Snaiderman and I. V. Cernaia, *Zhur. neorg. Khim.* **10**, 224 (1965).

[3] A. I. Busev and Z. P. Kariakina, *Zhur. neorg. Khim.*, **12**, 1603 (1968).

[4] M. Bartušek and J. Zelinka, *Coll. Czech. Chem. Comm.*, **32**, 1022 (1967).

[5] I. Cădariu and T. Goina, *Stud. Univ. Babeş Bolyai Chem.* Ser. I, fasc. 2, 25, (1961).

[6] T. Goina, I. Ristea and M. Munteanu, *Studii şi Cercetări Chim. Acad. R.P.R.*, **13**, 1209, (1965).

The computed reaction heat amounts to a mean value of -27.7 Kcal/mol of aluminate.

By proceeding similarly with continuous pyrogallol-$AlCl_3$ 0.5 M mixtures, one obtains equally exothermic, but very small effects (Fig. 1, curve 2). The maximum thermic uneveness is to be found exactly for the ratio 2 pyrogallol : 1 Al.

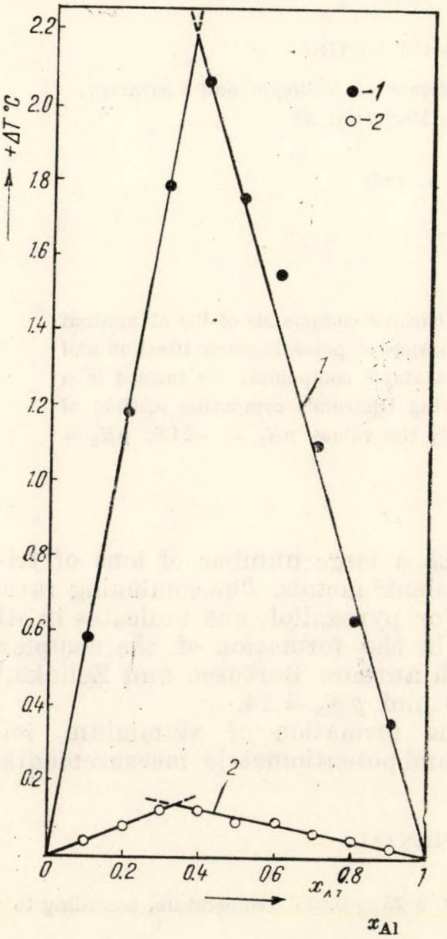

Fig. 1. — Isomolar series :

1, pyrogallol 0.25 M — sodium aluminate 0.25 M;
2, pyrogallol 0.50M — $AlCl_3$ 0.50 M.

Fig. 2. — Isomolar series :

1, ($AlCl_3$ 0.25 M + pyrogallol 0.25 M) — NaOH 0.25 M;
2, ($AlCl_3$ 0.25 M + pyrogallol 0.50 M) — NaOH 0.25 M;
3, ($AlCl_3$ 0.25 + pyrogallol 0.75 M) — NaOH 0.25 M.

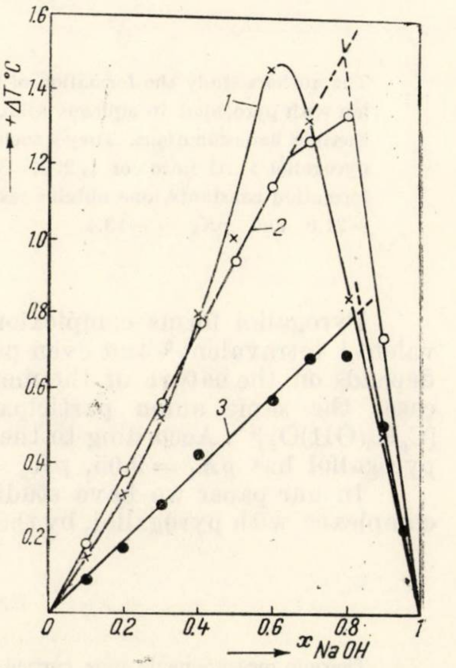

The neutralization heats with NaOH solutions of some mixtures of $AlCl_3$ with pyrogallol in various ratios of 1 : 1, 1 : 2 and 1 : 3 were determined in the same way. The results are given in Fig. 2; one notices that the maxima of the curves shift towards a greater basic consumption with the increase of the pyrogallol proportion. The shifting takes place from 2 towards 4, respectively 5 basic equivalents (extrapolated values).

The mean value of neutralization heats computed, on the left branches of the curves in figure 2, are equal to -8.8 Kcal/mol Al for the ratios $AlCl_3$ pyrogallol 1 : 1 and 1 : 2, and much smaller for the ratio 1 : 3 (respectively -4.3 Kcal/mol Al) but distinctly different to the neutralization-heat of pyrogallol, equal to -5.8 Kcal/equivalent.[7]

---

[7] T. Goina, I. Ristea and M. Munteanu, *Rev. Roum. Chim.*, **12**, 1095 (1967).

The results of the potentiometric measurements for the same solutions are given in figure 3, which shows that the mixture in the ratio pyrogallol : aluminium = 1 is distinctly titrated at $pH = 7$ with a consumption of 2 basic equivalents, and for the other two mixtures the consumption is slightly higher (∼ 2.2 basic equivalents).

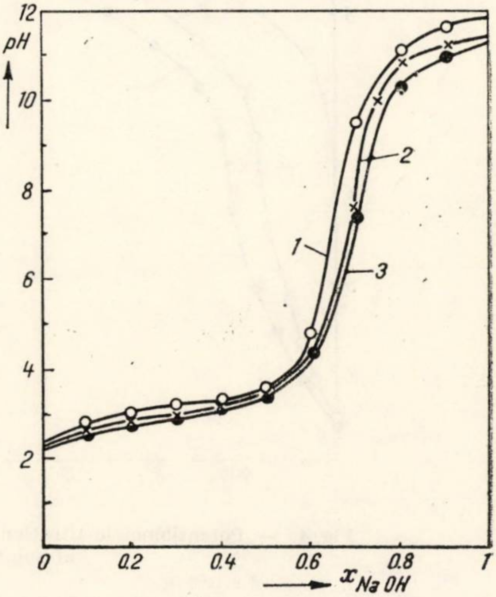

Fig. 3. — Isomolar series :
1. ($AlCl_3$ 0.25 M + Pyrogallol 0.25 M) – NaOH 0.25 M;
2. ($AlCl_3$ 0.25 M + Pyrogallol 0.50 M) – NaCH 0.25 M;
3. ($AlCl_3$ 0.25 M + Pyrogallol 0.75 M) – NaOH 0.25 M.

We have used a Clamann-Grahnert *pH*-meter MV-11, standardized on the scale *pH* : 0–14, at room temperature (∼ 22°).

The above experiments have suggested that we are dealing with equilibrium between several sorts of compounds, successive complexes, for the analysis of which a Bjerrum study would be suitable. We have thus proceeded to carry out certain potentiometric measurements needed for the calculation of the formation constants, according to Bjerrum's method .[8] The *pH* variation of a pyrogallol 2×10^{-2} M solution at the adding of NaOH (Fig. 4, curve 1) respectively after the adding of $AlCl_3$ so as to have an excess of 15 moles pyrogallol (Fig. 4, curve 2), respectively 10 moles pyrogallol (Fig. 4, curve 3) was watched in separate samples. In all samples a constant ion force was ensured by using KCl 2×10^{-1} M solutions. The titration was carried out with a NaOH solution devoid of carbonate.

The shape of the curves in Fig. 4, has induced us to work in the *pH* range between 3.75 and 8.

---

[8] J. Bjerrum "Metal Ammine Formation in Aqueous Solution", P. Haase and Son, Copenhagen, 1941.

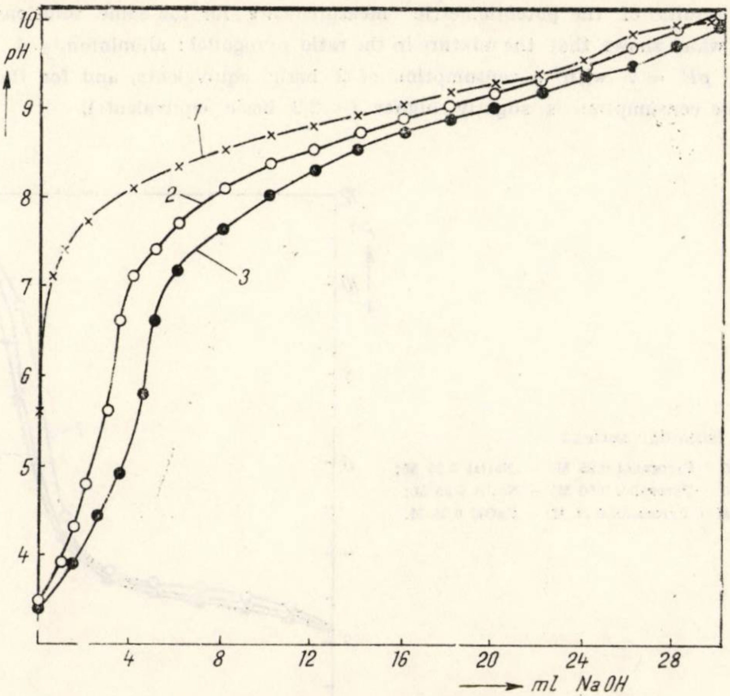

Fig. 4. — Potentiometric titration with NaOH 2.10^{-2} M a 25 ml of solutions.

1. Pyrogallol 2.10^{-2} M;
2. Pyrogallol 2.10^{-2} M + $AlCl_3$ $1.3.10^{-3}$ M (15 : 1);
3. Pyrogallol 2.10^{-2} M + $AlCl_3$ 2.10^{-3} M (10 : 1).

To calculate the necessary data for plotting the formation curve in accordance with Bjerrum's theory (the formation of successive complexes 1 : 1, 2 : 1, 3 : 1) we have supposed that the following reactions would take place in the system

$$H_3Pir + OH^- \rightleftarrows H_2Pir^- + H_2O$$

$$H_2Pir^- + Al^{3+} + OH^- \rightleftarrows H\ Pir\ Al^+ + H_2O$$

$$HPir\ Al^+ + H_2Pir^- + OH^- \rightleftarrows (H\ Pir)_2Al^- + H_2O$$

$$(H\ Pir)_2Al^- + H_2Pir^- + OH^- \rightleftarrows (H\ Pir)_3Al^{3\,-} + H_2O$$

We have then plotted the formation curve (Fig. 5) from which we have read the approximate values of the successive formation constants for $n = 0.5$, 1.5 and 2.5, which have afterwards been corrected by means of the convergence formulae given by Bjerrum.

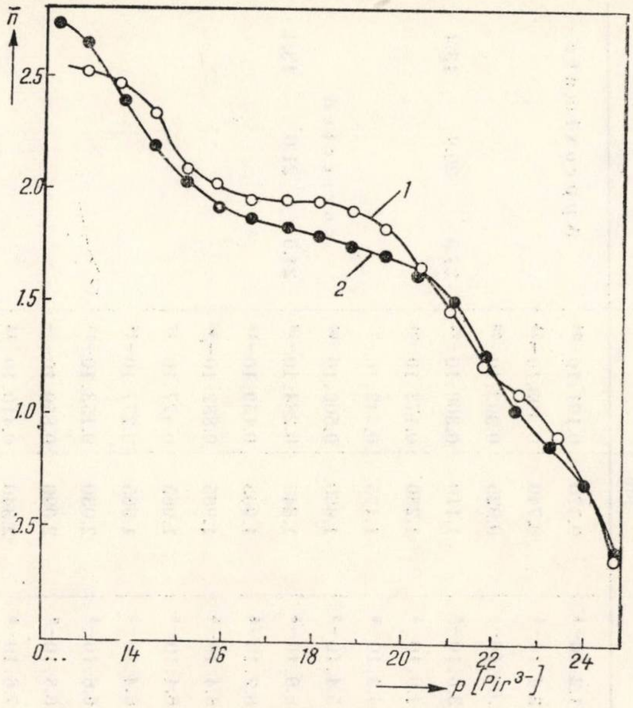

Fig. 5. — Formation curve:
1, Pyrogallol : Al^{3+} = 15;
2, Pyrogallol : Al^{3+} = 10.

In Tables 1 and 2 we have listed the experimental and computed data as well as the *pK* values of the approximate formation constants corrected for the two different concentrations in $AlCl_3$. For the complexes in the ratios 1 : 1 and 2 : 1 there result close values for the formation constants differing however sensibly from the value of the complex in the 3 : 1 ratio, which, however, is sufficiently high.

DISCUSSION

The use of Bjerrum's potentiometric method for the formation of the aluminium ion complexes with pyrogallol shows the formation of stable compounds in the ratio pyrogallol : Al = 1,2,3 characterized by the values $pK_1 = -24.50$, $pK_2 = -20.05$ and $pK_3 = -13.40$.

Qualitative indications at the same meaning are also given by the measurements of the reaction heat at the mixing of pyrogallol solutions with aluminium salts, in acid and alkaline medium. The maximum thermic unevenness found for the ratio 2 pyrogallol : 1 aluminium, draws our attention to the fact that aluminium can coordinate at least 2 molecules of pyrogallol. On the other hand, the almost identical values of the neutralizing heats ($\Delta H = -8.8$ Kcal/mol Al) of the pyrogallol—aluminium salt

Table 1

1 Al : 15 H_3 Pir. 25 ml; μ = 0.2; [H_3Pir] = 2.10^{-2} M; [Al^{3+}] = 1.3.10^{-3}M

pH	[H^+]	n_{Me}	n_A	ml_{NaOH}	n_{NaOH}	$\overline{n} = \frac{^nNaOH}{^nMe}$	[Pir^{3-}]	log K_1	log K_2	log K_3
3.75	1.78.10^{-4}	3.25.10^{-5}	5.10^{-4}	0.6	1.2.10^{-5}	0.370	0.191.10^{-24}	Approximate		
4.00	1.00.10^{-4}	,,	,,	1.2	2.4.10^{-5}	0.740	0.103.10^{-25}			
4.25	5.62.10^{-5}	,,	,,	1.5	3.00.10^{-5}	0.925	0.392.10^{-23}			
4.50	3.16.10^{-5}	,,	,,	1.8	3.6.10^{-5}	1.110	0.300.10^{-22}	24.5	20.9	13.4
4.75	1.78.10^{-5}	,,	,,	2.0	4.0.10^{-5}	1.230	0.173.10^{-21}			
5.00	1.00.10^{-5}	,,	,,	2.4	4.8.10^{-5}	1.475	0.943.10^{-21}			
5.25	5.62.10^{-6}	,,	,,	2.7	5.4.10^{-5}	1.660	0.509.10^{-20}	corrected		
5.50	3.16.10^{-6}	,,	,,	3.0	6.0.10^{-5}	1.845	0.284.10^{-19}	24.5	21.0	13.4
5.75	1.78.10^{-6}	,,	,,	3.1	6.2.10^{-5}	1.905	0.159.10^{-18}			
6.00	1.00.10^{-6}	,,	,,	3.2	6.4.10^{-5}	1.965	0.882.10^{-18}			
6.25	5.62.10^{-7}	,,	,,	3.2	6.4.10^{-5}	1.965	0.477.10^{-17}			
6.50	3.16.10^{-7}	,,	,,	3.2	6.4.10^{-5}	1.965	0.277.10^{-16}			
6.75	1.78.10^{-7}	,,	,,	3.5	6.6.10^{-5}	2.030	0.153.10^{-15}			
7.00	1.00.10^{-7}	,,	,,	3.4	6.8.10^{-6}	2.090	0.850.10^{-15}			
7.25	5.62.10^{-8}	,,	,,	3.8	7.6.10^{-5}	2.340	0.410.10^{-14}			
7.50	3.16.10^{-8}	,,	,,	4.0	8.1.10^{-5}	2.460	0.249.10^{-13}			
7.75	1.78.10^{-8}	,,	,,	4.1	8.2.10^{-5}	2.520	0.130.10^{-12}			
8.00	1.00.10^{-8}	,,	,,	4.1	8.2.10^{-5}	2.520	0.247.10^{-12}			

Table 2

1 Al : 10 H_3 Pir. 25 ml; μ = 0.2; [H_3 Pir] = 2.10^{-2}M; [Al^{3+}] = 2.10^{-3} M

pH	[H^+]	n_{Me}	n_A	ml_{NaOH}	n_{NaOH}	$\bar{n}=\frac{n_{NaOH}}{n_{Me}}$	[Pir^{3-}]	log K_1	log K_2	log K_3
3.75	$1.78.10^{-4}$	5.10^{-5}	5.10^{-4}	1.0	$2.0.10^{-5}$	0.40	$0.187.10^{-24}$			
4.00	$1.00.10^{-4}$	,,	,,	1.8	$3.6.10^{-5}$	0.72	$0.985.10^{-24}$			
4.25	$5.62.10^{-5}$	,,	,,	2.2	$4.4.10^{-5}$	0.88	$0.554.10^{-23}$			
4.50	$3.16.10^{-5}$	,,	,,	2.6	$5.2.10^{-5}$	1.04	$0.293.10^{-22}$		Approximate	
4.75	$1.78.10^{-5}$	,,	,,	3.2	$6.4.10^{-5}$	1.28	$0.156.10^{-21}$	24.5	21.1	13.4
5.00	$1.00.10^{-5}$	,,	,,	3.8	$7.6.10^{-5}$	1.52	$0.842.10^{-21}$			
5.25	$5.62.10^{-6}$	,,	,,	4.1	$8.2.10^{-5}$	1.64	$0.469.10^{-20}$			
5.50	$3.16.10^{-6}$	,,	,,	4.3	$8.6.10^{-5}$	1.72	$0.256.10^{-19}$			
5.75	$1.78.10^{-6}$	,,	,,	4.4	$8.8.10^{-5}$	1.76	$0.142.10^{-18}$		Corrected	
6.00	$1.00.11^{-6}$	,,	,,	4.5	$9.0.10^{-5}$	1.80	$0.795.10^{-18}$	24.5	21.0	13.4
6.25	$5.62.10^{-7}$	,,	,,	4.6	$9.2.10^{-5}$	1.84	$0.435.10^{-17}$			
6.50	$3.16.10^{-7}$	,,	,,	4.7	$9.4.10^{-5}$	1.88	$0.245.10^{-16}$			
6.75	$1.78.10^{-7}$	,,	,,	4.8	$9.6.10^{-5}$	1.92	$0.137.10^{-15}$			
7.00	$1.00.10^{-7}$	,,	,,	5.1	$10.2.10^{-5}$	2.04	$0.735.10^{-15}$			
7.25	$5.62.10^{-8}$	,,	,,	5.5	$11.0.10^{-5}$	2.20	$0.386.10^{-14}$			
7.50	$3.16.10^{-8}$	,,	,,	6.0	$12.0.10^{-5}$	2.40	$0.216.10^{-13}$			
7.75	$1.78.10^{-8}$	,,	,,	6.4	$12.8.10^{-5}$	2.56	$0.116.10^{-12}$			
8.00	$1.00.10^{-8}$	,,	,,	6.6	$13.2.10^{-5}$	2.64	$0.551.10^{-12}$			

mixtures in the ratio 1 :1 and 2 :1 are a clear indication that the two complexes formed have close stabilities. The fact that the mixture with pyrogallol in excess (3 :1) develops a lower neutralization heat (ΔH=−4.3 Kcal/equiv. Al) shows that the third complex formed is less stable. The last value of the neutralization heat being, in absolute value, smaller than the neutralization heat of the pyrogallol itself (ΔH =−5.8 Kcal/equiv.) shows that this complex is nevertheless formed.

Thermometric titration proves able to register with greater precision the phenomena taking place in these systems than potentiometric titration. It shows an increasing basic consumption with the increase of the proportion of ligand, corresponding to 2, 4, 5 equivalents of hydrogen ions, as the reactions supposed to take place in the systems point out.

Revue Roumaine de Chimie, **15**, 1555–1561 (1970)

PRETREATED INDICATING ELECTRODES IN POTENTIOMETRIC TITRATIONS. II*)

BRIGHT PALLADIUM-HYDROGEN ELECTRODE IN ACID-BASE TITRATION

CANDIN LITEANU and IOVANCA HAIDUC

Babeş-Bolyai University, Analytical Chemistry
Research Center, Cluj, str. Arany J. 11

Received March 30, 1970

Palladium-hydrogen electrodes were prepared by activating bright palladium metal by pre-anodization, followed by electrolytic saturation of the metal with hydrogen in a cathodization of the electrode. Electrodes prepeared in this way can be used as indicating electrodes in several successive acid-base titrations, within a few days, without bubbling gaseous hydrogen. The presence of oxidizing and reducing agents does not influence the acid-base titration with pre-cathodised palladium electrodes.

INTRODUCTION

The capacity of palladium metal to absorb large amounts of hydrogen has been observed for a long time[1] and the state of the hydrogen absorbed on the metal was subjected to extensive investigations.[2] Thus, different ways of introducing hydrogen into palladium, pressure-composition-temperature relationships and electrochemical properties of the palladium - hydrogen system were investigated in some detail.[2] It was found that the Pd-H_2 system consists of two phases : α—which is a homogeneous solution of hydrogen in palladium, and β—a homogeneous solution of palladium in non-stoichiometric palladium hydride.[3]

Several of the studies on the Pd-H_2 system have great electrochemical interest. Gaseous hydrogen can be readily absorbed from aqueous solution, thus affording preparation of "hydrogen electrodes on palladium", somewhat similar to the well known hydrogen electrode on platinum; subsequently, the potential of such palladium-hydrogen electrodes

---

*) Part I: C. Liteanu and Iov Haiduc, *Revue Roumaine Chim.*, **14**, 1039 (1969).

[1] T. Graham, *Phil. Trans. Roy. Soc.*, **156**, 415 (1866).

[2] F. A. Lewis, "The Palladium-Hydrogen System", Academic Press, London, New York, 1967, Chapter 2.

[3] R. V. Bucur, *Studii şi Cercetări Chim. Acad. RPR*, **12**, 171 (1964).

has been studied by several authors[4-7] and the use of palladium-hydrogen system as reference electrode [8-15] or as indicating electrode in acid-base titrations [16,17] has been reported.

For practical purposes palladium-hydrogen electrodes were prepared by using deposits of palladium black on platinum, [16,18,19] gold, [16,18] glass [20] or palladium metal. [16-18,21] The hydrogen can be introduced into palladium either by absorbtion of gaseous hydrogen from aqueous solution, or better electrolytically, using palladium black as cathode.[16,17,22-25]

Although the above quoted studies afforded important knowledge of the electrochemical behaviour of palladium-hydrogen system, the exploitation of this electrode for analytical purposes is rather limited. An idea was that the great absorbtive capacity of palladium for hydrogen might permit such electrodes to replace the standard platinum-hydrogen electrodes without bubbling hydrogen (gaseous or generated electrolytically) over the surface during the measurement.[16]

We attempted to use *bright* palladium, preliminary saturated electrolytically with hydrogen, as indicating electrode in acid-base titrations. This requires a preliminary anodic treatment of the electrode (pre-anodization) in order to activate the surface, followed by cathodic pre-polarization, which results in the saturation of the electrode with hydrogen. A bright palladium electrode thus prepared can be used in several successive acid-base titrations within 6 — 7 days, without bubbling hydrogen over its surface. We investigated the variation of the potential in time and the use as indicating electrode in acid-base titration in the presence of oxidizing and reducing reagents.

---

[4] S. Schuldiner, G. Castellan and J. P. Hoare, *J. Chem. Phys.*, **28**, 16 (1958).

[5] T. B. Flanagan and F. A. Lewis, *Trans. Faraday Soc.*, **55**, 1409 (1959).

[6] P. C. Aben and W. G. Burger, *Trans. Faraday Soc.*, **58**, 1989 (1962).

[7] J. P. Hoare and S. Schuldiner, *J. Phys. Chem.*, **61**, 399 (1957).

[8] M. Fleischmann and H. Thirsk, *Trans. Faraday Soc.*, **51**, 71 (1955).

[9] S. Schuldiner and J. P. Hoare, *Canad. J. Chem.*, **37**, 228 (1959).

[9a] H. Shiratori, *J. Electrochem. Soc. Japan*, **29**, E 161 (1961); *Chem. Abstr.*, **61**, 3918 (1964).

[10] J. P. Hoare, *Gen. Motors Eng. J.*, **9**, 14 (1962).

[11] J. P. Hoare, *J. Electrochem. Soc.*, **110**, 245 (1963).

[12] M. J. Vasile and C. G. Enke, *J. Electrochem. Soc.*, **112**, 865 (1965).

[13] R. V. Bucur and L. Stoicovici, *J. Electroanalyt. Chem.*, **11**, 152 (1966).

[14] C. Bifano and F. Brito, *Ann. Quim.*, **64**, 301 (1968); *Chem. Abstr.*, **68**, 11820 (1968).

[15] D. J. G. Ivers and G. J. Janz, ,,Reference Electrodes'', Academic Press, New York and London, 1961, p. 111.

[16] J. P. Schwing and L. B. Rogers, *Analyt. Chim. Acta*, **15**, 379 (1956).

[17] J. T. Stock, W. C. Purdy and T. R. Williams, *Analyt. Chim. Acta*, **20**, 73 (1959) and references cited therein.

[18] W. Bottger, *Z. Phys. Chem.*, **24**, 255, 260 (1897).

[19] P. Nylén, *Z. Elektrochem*,. **43**, 915 (1937).

[20] E. Newbery, *Trans. Electrochem. Soc.*, **64**, 209 (1933).

[21] B. Neumann, *Z. Phys. Chem.*, **14**, 201 (1894).

[22] T. Graham, *Proc. Roy. Soc.*, **16**, 422 (1968).

[23] A. Frumkin and N. A. Aladzhalova, *Acta Physico-Chim. USSR*, **19**, 1 (1944).

[24] P. Nylén, *Z. Electrochem.*, **43**, 915 (1937).

[25] G. W. Castellan, *J. Electrochem. Soc.*, **111**, 1273 (1964).

EXPERIMENTAL

In the experiments described here a bright palladium plate of 0.5 cm^2 was used as indicating electrode in acid-base titration; as reference a standard calomel electrode was used. The palladium-hydrogen electrode was prepared as follows: the palladium plate was introduced in 1N H_2SO_4 solution and subjected to an anodic current of 16 mA/cm^2 during 30 s to activate the metal surface. Then, the sense of the current was reversed and the palladium plate was subjected to a cathodic current of $16mA/cm^2$ during 5 min. During this process the superficial layer of oxide (formed during pre-anodization) was reduced, and hydrogen generated electrolytically saturated the metal. The electrode thus treated was kept in distilled water until use. Between two successive titrations the electrode was carefully washed and kept in distilled watter.

The solutions were prepared and standardized according to common procedures. The titration curves were determined with the aid of an MV–11S pH-meter, used for the measurement of the potential.

The titrations were caried out at 22±1°, without removal of the atmospheric oxygen. Literature data [16] and preliminary experiments showed that the air over unprotected and unstirred solutions does not affect the titration results.

RESULTS AND DISCUSSION

Electrode pretreatment. It was shown that the potential of a palladium-hydrogen electrode depends upon the concentration of absorbed hydrogen, and remains constant for some time, according to the surface-volume ratio of the electrode and the surface activity.[3,26] These properties are in turn influenced by the electrode pretreatment. On the other hand, for the indicating electrode in titrations, a stable constant electrode potential is required. Therefore, we followed the stability of electrode potential in time, after different pre-cathodizations at various current densities; these experiments showed that a current density of ca. 15 mA/cm^2 gives a stable potential, which changes little in time, as shown in figure 1. Stirring of the solution results in an increase of the potential, but after stopping the stirring the original value of the electrode potential is resumed. At low current densities used in pre-cathodization, e.g. of the order of 0.1 mA/cm^2 the electrode potential changes rapidly and is strongly influenced by stirring of the solution. Thus a palladium-hydrogen electrode treated in this way (0.1 mA/cm^2), dipped in a 0.1N H_2SO_4, solution, changes its potential from −200mV (*vs.* standard calomel electrode) to + 100mV in only 3 min, under stirring. This variation in fact depends upon the stirring rate and growths with the increase in the stirring rate. At larger current densities, e.g. of the order of 10^2 mA/cm^2, the electrode absorbs too large amounts of hydrogen and after dipping into solution, gas bubbles appear around it. The potential of such an electrode changes slightly when the solution is stirred, but the original value is not resumed after stopping

---

[26] J. P. Hoare, *J. Electrochem. Soc.*, **106**, 640 (1959).

the stirring. Therefore, in our experiments, a current density of 16 mA/cm² was used in the cathodic pretreatment of the palladium electrode, for electrolytical saturation with hydrogen.

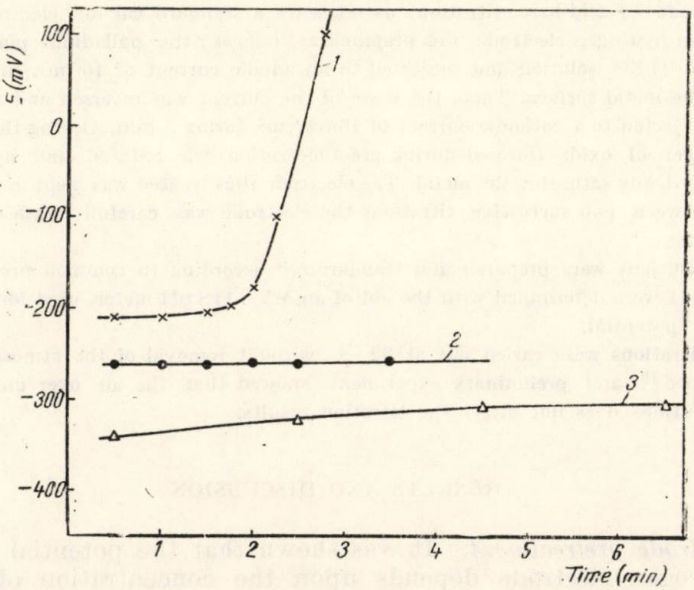

Fig. 1. — Variation of palladium-hydrogen electrode potential (*vs.* SCE) after various cathodic pretreatments.

1, electrode treated at 0.1 mA/cm²; *2*, electrode treated at 16 mA/cm²; *3*, electrode treated at 150 mA/cm².

In alkaline solution the electrode potential increases slowly in time during stirring. In titrations it was necessary to wait 30—40 seconds after each addition of the titrating reagent and to stop the stirring, in order to obtain a constant potential.

Titration of 0.1N H_2SO_4 with 0.1N NaOH. Successive titrations of sulphuric acid solution (0.1N) with 0.1N sodium hydroxide were made, using a palladium-hydrogen electrode treated as mentioned above. The titration curves are shown in figure 2. Between two successive titrations the electrode was kept in distilled water, without any other treatment. A number of 7-8 titrations were made within 6 days. The first 4-5 titration curves were practically superposable and in figure 2 they are shown by curve 1. For the characterization of the behaviour of the indicating electrode, the potential variation ΔE in the vicinity of the equivalence point (the sharpness index)[27], when passing from the stage of (100-*e*)% to the stage of (100+*e*)% (where *e* is the accepted error), has to be used. In our case we choosed $e = 1$, therefore $\Delta E_{\pm 1\%}$ was used. In the first titrations (curve 1 in fig. 2) $\Delta E_{\pm 1\%}$ was 350 mV, but ΔE decreased to about 100 mV after eigth successive titrations, made whithin six days, but remained still significant even on the 8th titration (see Fig. 3). In this case $\Delta E_{\pm 1\%}$ being relatively small, the equivalence point can be readily calculated by the method of Hahn and Weiler.[28] This shows that the deterioration of the palladium-hydrogen electrode occurs rather slowly. Therefore, a bright palladium-hydrogen electrode, in which the hydrogen absorbed in the metal was generated electrolytically during the cathodic pre-treatment can

---

[27] M. Tanaka and G. Nakagawa, *Analyt. Chim. Acta*, **32**, 123 (1965).

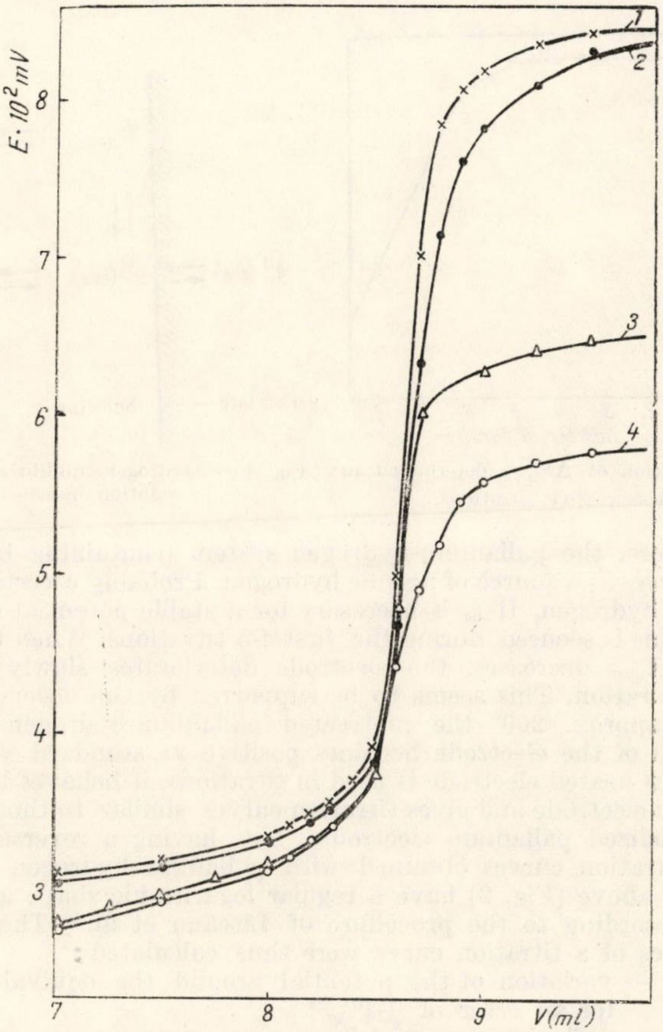

Fig. 2. — Successive titration curves obtained with an electrode pretreated at 16 mA/cm².

1, first 4–5 titrations in a series (superposed curves); *2–4*, individual titrations made successively at about 1 day interval.

---

[28] F. L. Hahn and G. Weiler, *Z. analyt. Chem.*, **69**, 417 (1926).

be successfully used as indicating electrode in acid-base titration without bubbling gaseous hydrogen during the measurements.

The behaviour of palladium-hydrogen electrode can be probably explained[3] by the equilibrium $H_{2(ads)} \rightleftarrows 2H^+_{(aq)} + 2e^-$, in which $H_{2(ads)}$ at the electrode surface is in equilibrium with the hydrogen absorbed at the palladium surface $H_{(ads)}$ and absorbed in the metal volume, $H_{(abs)}$ (partly as non-stoichiometric palladium hydride), as shown in figure 4.

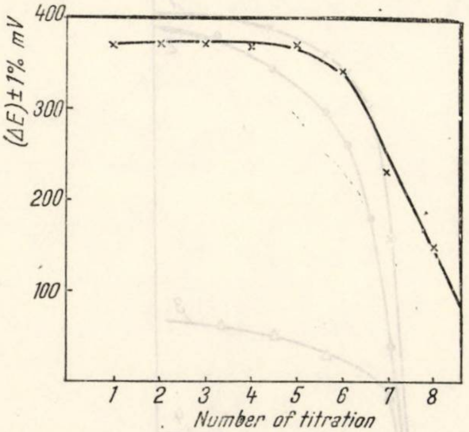

Fig. 3. — Variation of $\Delta E_{\pm 1\%}$ determined in several successive titrations.

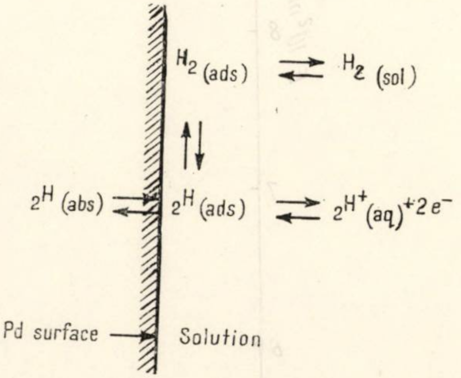

Fig. 4. — Hydrogen equilibria at electrode-solution interface.

Therefore, the palladium-hydrogen system (containing both α and β phases) serves as a source of atomic hydrogen. Probably a certain amount of absorbed hydrogen, $H_{(abs)}$ is necessary for a stable potential of the electrode, and this is secured during the first 4-5 titrations. When the concentration of $H_{(abs)}$ decreases, the electrode deteriorates slowly with each successive titration. This seems to be supported by the observation that heating at approx. 200° the pretreated palladium-hydrogen electrode, the potential of the electrode becomes positive *vs.* standard calomel electrode. If this heated electrode is used in titrations, it behaves like a palladium-oxygen electrode and gives titration curves similar to those obtained with pre-anodized palladium electrodes, but having a reversed shape.

The titration curves obtained with palladium-hydrogen electrodes, as described above (Fig. 2) have a regular logarithmic shape and can be linearized according to the procedure of Liteanu et al.[29] The following characteristics of a titration curve were thus calculated:

$\Delta E_{\pm 1\%}$ — variation of the potential around the equivalence point for an error of $\pm 1\%$,[29]
E_i — inflexion potential,[29]
u — real asymmetry coefficient,[30]
V_i — analytical inflexion volume,[31]
V_e — equivalence volume.[31]

---

[29] C. Liteanu and M. Mioscu, *Rev. Roumaine Chim.*, **13**, 899 (1968).

[30] C. Liteanu and D. Cörmös, *Talanta*, **7**, 25 (1960).

[31] C. Liteanu and D. Cörmös, *Talanta*, **7**, 32 (1960).

These are given in table 1 and allow to estimate the precision of the titration.

Table 1

Statistical treatment of titration curves shown in figure 3

Electrode used in titration	Titration curve (in Fig. 3)	V_i ml	u	$V_e - V_i$ ml	E_i mV	E_e mV	$\Delta E_{\pm 1\%}$ mV
Precathodised	curve 1	8.51	1.16	1.23×10^{-4}	593	593	361
$(Pd-H)/H_2$	curve 3	8.51	0.99	1.5×10^{-3}	500	499	215
electrode	curve 4	8.50	1.43	8.6×10^{-4}	430	439	130
Standard hydrogen electrode* Pt/Pt black/H_2	—	8.50	1.07	1.1×10^{-4}	631	632	381

* Some data obtained with a standard platinum-hydrogen electrode are given for comparison.

The electrode function in the titration of sulphuric acid with sodium hydroxyde for the palladium-hydrogen electrode, was found to be 60 mV/pH unit (in the pH range from 1 to 10), calculated from the data of curve 1 in figure 2.

Titration of sulphuric acid in the presence of oxidizing and reducing agents. Some titrations of sulphuric acid solutions (0.1 N) were made in the presence of oxidizing agents such as MnO_4^- (1.6×10^{-3}N), CrO_4^{2-} (4×10^{-3}N), and Ce^{4+} (4×10^{-3}N), by using pretreated palladium-hydrogen electrodes, prepared as described above. It was found that the behaviour of the electrode is not affected by the presence of the oxidizing agents in solution, at least at the concentrations shown. Titration curves almost superposable to those obtained in the absence of oxidizing agents were obtained. The data are given in table 2. It can be seen that the potential variation (ΔE) at the equivalence point (sharpness index) is practically the same in both cases.

Table 2

Titration data in the presence of oxidation reagents *

Electrode		V_i	E_i	$\Delta E_{\pm 1\%}$
$(Pd-H)/H_2$	in absence of oxidant	8.51	593	351
	in the presence of MnO_4^-	8.51	585	341
	in absence of oxidant	8.50	553	335
	in the presence of $CrO_4{}^{2-}$	8.50	560	337

*) Treatment of data according to Hahn and Weiler[27]

In the presence of scorbic acid the titration curve of sulphuric acid also remained unchanged (the value of ΔE was practically the same). However, in this particular case the values of the inflexion volume (V_i) and equivalence volume (V_e) were slightly larger, due to consumption of part of the titrating agent (sodium hydroxide) by the scorbic acid.

Revue Roumaine de Chimie, 15, 1563–1572 (1970)

L'ÉTUDE RÖNTGÉNOSTRUCTURALE DES TRIHÉTÉROPOLYACIDES

A. ŞUTEU et LUCREŢIA MÎRZA

Université «Babeş-Bolyai», Cluj, Faculté de Chimie,
Chaire de Chimie analytique et Chaire de minéralogie, 11, str. Arany János

Reçu le 31 mars 1969

On démontre que les acides $H_5[PMo_1OV_2O_{40}].30H_2O$ et $H_5[PW_{10}V_2O_{40}].30\ H_2O$ cristallisent dans le système cubique le groupe spécial $O_h^2 - Pn\ 3\ n$. La cellule élémentaire des deux hétéropolyacides est formée de 8 molécules. Le paramètre de l'acide $H_5[PMo_{10}V_2O_{40}].30\ H_2O$ est égal à 22,456±0,00435 Å et également pour l'acide $H_5[PW_{10}V_2O_{40}].30\ H_2O$ il est égal à 22,426±0,00125 Å. L'étude systématique d'extinction montre que la moitié du nombre total des molécules est orientée dans une certaine direction, tandis que l'orientation de la seconde moitié est diamétralement opposée.

Les acides phosphomolybdovanadique et phosphowolframovanadique ont été synthétisés pour la première fois par Kokorine et Polotebnova.[1, 2] Ces auteurs ont attribué à ces acides les formules suivantes : $H_7\ [P(Mo_2O_7)_5\ V_2O_6].x\,H_2O$ et $H_7\ [P(W_2O_7)_5\ V_2O_6].\ x\ H_2O$, en conformité avec l'hypothèse de Miolati-Rosenheim. Le titrage potentiométrique par KOH en solution aqueuse, effectué par Kokorine et Polotebnova[3] sur l'acide phosphomolybdovanadique, a mis en évidence une basicité de 5. Courtin et Chauveau,[4] par titrage cryoscopique en solution saline, ont retrouvé pour l'acide phosphomolybdovanadique la même basicité que Polotebnova et Meimark[5] au titrage potentiométrique par KOH de l'acide phosphowolframovanadique dissous en alcool amylique.

Cette basicité, déterminée par les auteurs cités pour les deux hétéropolyacides, ne correspond pas aux formules de type Miolati-Rosenheim, mais elle est en concordance avec une représentation de type Keggine.[6]

Conformément à celle-ci, les hétéropolyacides phosphomolybdovanadique et phosphowolframovanadique ont les formules suivantes :

$$H_5[PMo_{10}V_2O_{40}]\cdot x\ H_2O \text{ et } H_5[PW_{10}V_2O_{40}]\cdot xH_2O.$$

---

[1] A. I. KOKORIN et N. A. POLOTEBNOVA, *Zhur. obshchei Khim.*, **24**, 1818 (1954).

[2] A. I. KOKORIN et N. A. POLOTEBNOVA, *Uchenye Zapiski Kishinev. Univ.*, **6**, 63 (1953).

[3] A. I. KOKORIN et N. A. POLOTEBNOVA, *Zhur. obshchei Khim.*, **27**, 549 (1957).

[4] P. COURTIN et F. CHAUVEAU, *Bull. Soc. chim. France*, 1947, 2461.

[5] N. A. POLOTEBNOVA et W. A. NEIMARK, *Zhur. neorg. Khim.*, **11**, 1406 (1966).

[6] I. F. KEGGIN, *Proc. Roy. Soc.*, **144**, 75 (1934.)

Les études structurales effectuées par Keggine sur l'acide $H_3[PW_{12}O_{40}]$ ont démontré que, dans cet acide, l'atome de phosphore occupe le centre d'un tétraèdre régulier, dont les coins sont occupés par les atomes d'oxygène en formant ainsi le tétraèdre central PO_4, ce tétraèdre étant entouré de 22 octaèdres, déformés de WO_6, répartis autour du tétraèdre central selon quatre groupes, dont chacun comporte trois octaèdres de WO_6. Sur la base de ces données, Keggine a attribué à l'acide phospho-12-wolframique la formule suivante : $H_3[P(W_3O_{10})_4]\cdot xH_2O$. L'étude röntgénostructurale effectuée par Hoard[7] à l'aide de la méthode de Laue, sur l'acide phospho-12-molybdénique hydraté avec 30 molécules d'eau, a démontré que cet acide aussi a une structure du même type. Ablov, Alinovsky et Dediu[8], en effectuant une étude röntgénographique à l'aide de la méthode de Debye-Scherrer, sur le sel $Cs_3H_2[PMo_{10}V_2O_{40}]\cdot 2H_2O$, sont arrivés à la conclusion que l'anion de trihétéropolyacide de ce sel est construit pareillement à l'anion de l'acide phospho-12-molybdénique, donc d'après une structure de type Keggine.

Dans un travail précédent[9] on a étudié, par la méthode de la résonance électronique de spin, l'acide $H_5[PW_{10}V_2O_{40}]\cdot 26H_2O$, en obtenant de nouvelles données qui confirment que l'anion de ce hétéropolyacide aussi est construit d'après une structure de type Keggine. Conformément aux données du travail susmentionné, les deux atomes de vanadium sont répartis selon deux groupes dont chacun comporte trois octaèdres, coordinés tétraédriquement autour de l'atome central de P.

Etant donné que l'étude röntgénographique des trihétéropolyacides (hétéropolyacides mixtes) se limite seulement au sel $Cs_3H_2[PMo_{10}V_2O_{40}]\cdot 2H_2O$, dans le présent travail nous nous sommes proposé d'étudier les cristallohydrates riches en eau des hétéropolyacides phosphomolybdovanadique et phosphowolframovanadique des formules : $H_5[PMo_{10}V_2O_{40}]\cdot 30H_2O$ et $H_5[PW_{10}V_2O_{40}]\cdot 30H_2O$. Les études röntgénographiques de ces hétéropolyacides ont été précédées d'observations goniométriques qui nous ont fourni des données obtenues sont reproduites dans le tableau 1.

Tableau 1

Étude röntgénographique des acides

$H_5[PMo_{10}V_2O_{40}].30H_2O$ et $H_5[PW_{10}V_2O_{40}].30H_2O$	
Faces observées	Angle complémentaire
100–111	54°42′
100–010	90°
100–001	90°
111–111	70°30′

Les valeurs goniométriques obtenues inscrivent les cristaux du point de vue cristallographique dans le système cubique, la classe hexachisoctaédrique. Les cristaux des deux hétéropolyacides présentent les faces suivantes : (111) faces d'octaèdre bien développées et (100) faces de cube faiblement développées, spécialement dans le cas de l'acide $H_5[PMo_{10}V_2O_{40}]\cdot 30H_2O$.

---

[7] I. Hoard, *Z. Krist.*, **81**, 217 (1953).

[8] A. V. Ablov, T. V. Alinovsky et V. I. Dediu, *Zhur. neorg. Khim.*, **4**, 397 (1959).

[9] A. Şuteu et G. Cristea, *Rev. Roumaine Chim.*, **14**, 209 (1969).

ÉTUDES RÖNTGÉNOGRAPHIQUES

Toutes les déterminations röntgénostructurales ont été effectuées par la méthode Debye-Scherrer. Les röntgénogrammes ont été obtenus à un appareil röntgen TuR—M—60 à anticathode de Co et Cr. La tension et l'intensité utilisées pour les deux anticathodes sont de 50 Kw, respectivement de 7 mA. Pour la filtration des radiations on a employé, dans le cas de l'anticathode de Co, un filtre de Fe et pour celui de Cr un filtre de V. Le diamètre de la caméra Debye-Scherrer de l'appareil est de 57,5 mm, le temps d'exposition variant de 8 à 12 heures.

Les préparations de l'acide $H_5[PMo_{10}V_2O_{40}] \cdot 30H_2O$ et $H_5[PW_{10}V_2O_{40}] \cdot 30H_2O$ ont été couvertes d'une couche mince de polystyrène pour éviter pendant les déterminations des processus de déshydratation. Après avoir obtenu les röntgénogrammes, on n'a pas constaté de changements de couleur ou de transparence aux préparations exposées, ce qui prouve que pendant l'exposition, à l'intérieur des préparations, des phénomènes de réduction ou de déshydratation ne se produisent pas.

Les données röntgénostructurales obtenues sont reproduites dans le tableaux 3 et 5, où l'on trouve les valeurs θ, la constante Q, les indices des plans de réflexion, l'intensité et les valeurs $d\alpha/n$ et $d\beta/n$.

Pour déterminer les poids spécifiques, on s'est servi de la méthode picnométrique, en employant l'*o*-xylène, en raison d'une faible tension superficielle, d'une bonne humectation et d'une moindre volatilité par rapport à celle du benzène, qui est le plus souvent employé dans ce but.

A. *Étude röntgénostructurale de l'acide*

$H_5[PMo_{10}V_2O_{40}]\cdot 30H_2O$.

L'acide phosphomolybdovanadique a été synthétisé par nous à l'aide de la méthode décrite par Kokorin et Polotebnova.[10]

L'analyse de l'hétéropolyacide était conforme à la formule : $H_5[PMo_{10}V_2O_{40}]\cdot 30H_2O$, comme on peut voir des données du tableau 2.

Tableau 2

Analyse de l'acide $H_5\ [PMo_{10}\ V_2\ O_{40}]\ 30\ H_2O$

Pourcentage	P	M_0	V	H_2O	
Calculé	1,36	42,14	4,47	23,7	$G_m = 2\,277,40$
Déterminé	1,30	42,30	4,51	22,95	

Le dosage du molybdène a été exécuté gravimétriquement par précipitation avec de l'oxynate, après avoir, au préalable, réduit le vanadium au vanadium tétravalent et après que celui-ci s'est complexé avec l'EDTA pour ne pas précipiter lui aussi, comme oxynate[11]. Le vanadium a été déterminé par une autre épreuve, à savoir par la différence de la somme des oxynates de molybdène et de vanadium ou de la somme des oxydes après calcination des oxynates par oxydes. Le phosphore a été déterminé colorimétriquement, d'après la méthode colorimétrique décrite par B. Charretton et ses collaborateurs,[12] et l'eau par la méthode thermogravimétrique.

---

[10] L. Erdey, « A kémiai analizis súlyszerinti módszerei », vol. 2, Akad. Kiadó, Budapest, 1960, p. 527.

Au tableau 3 on trouve les données obtenues après l'étude des röntgénogrammes et le calcul des valeurs respectives.

Les röntgénogrammes de l'acides $H_5[PMo_{10}V_2O_{40}] \cdot 30H_2O$ mettent en évidence pour un angle 2 θ variant entre 0 - 80° 30 réflexes.

Des valeurs angulaires θ tirées des röntgénogrammes on a calculé le plus grand diviseur commun pour $\sin^2\theta$, Q_m, et la valeur de la constante réticulaire a. L'erreur a été calculée pour $K = n - 1$ degrés de liberté, la valeur correspondant à k de la variable t prise des tableaux,[12] l'erreur moyenne-carrée du moyen de sélection $S\bar{x}$ et la probabilité choisie $\alpha = 0{,}95$.

En vertu de ces données on obtient :

$$Q \text{ moyen} = 0{,}001580 \pm 7{,}33.10^{-6}\text{ ; } K = 29,\ t\alpha = 2{,}04,\ \alpha = 0{,}95$$

$$a = 22{,}456 \pm 0{,}0439 \text{ Ä ; } S\bar{x} = 3{,}56 \cdot 10^{-6}$$

le poids spécifique déterminé $= 2{,}681$, le nombre de molécules dans la cellule élémentaire $n = \dfrac{11390 \cdot 2{,}68}{2277{,}4 \cdot 1{,}662} = 8{,}35$, le poids spécifique calculé $\dfrac{8}{8{,}35} \cdot 2{,}68 = 2{,}57$.

Etant donné que dans la série des numéros qui représentent $\sum h_i^2$ apparaissent les valeurs 61 et 91, quoique représentant de faibles réflexes, il faut admettre qu'à la base de la structure se trouve un réseau cubique primitif. En tenant compte des autres extinctions qui indiquent des plans de translation diagonaux tant sur les faces 100 (quand on éteind les plans de type hkO qui ont la condition d'extinction comme $h + k$ = nombre impair), que sur les faces hlO (quand on éteind les plans hhO qui respectent la condition $h + 1$ = nombre impair), il faut admettre le groupe spatial O_h^2 ou Pn 3 n.

B. *Étude röntgénostructurale de l'acide*

L'acide phosphowolframovanadique de cette composition a été synthétisé par nous à l'aide de la méthode décrite par Kokorine et Polotebnova[13].

---

[11] B. Charretton, F. Chauveau, G. Bertho et P. Courtin, *Chem. analyt.*, **470**, 17 (1965).

[12] V. V. Nalimov, « Primenenye matematicheskoi statistiki pri analize veshestve », Gosudarstvenoe izdatelistvo fizicomatematicheskoi literatury, Moscou, 1960, p. 375.

[13] A. I. Bradley et I. W. Illingworth, *Proc. Roy. Soc.*, **157**, 113 (1936).

Tableau 3

Étude röntgénographique de l'acide $H_5[PMo_{10}V_2O_{40}]\cdot 30H_2O$ (Φ = 0,86; anticathode Co)

N	θ	Q	$\sum h_i^2$	I	h k l	$\frac{d\alpha}{n}$	$\frac{d\beta}{n}$
1	4°30′	0,001550	4	ffi	200	11,377	(10,307)
2	7°57′36″	0,00160	12	fs	222	6,4459	(5,8399)
3	9°03′36″	0,001550	16	fs	400	5,6687	(5,1357)
4	10°10′12″	0,001561	20	fs	420	5,0555	(4,5801)
5	11°49′12″	0,001613	26	m	510 431	4,3578	(3,9480)
6	12°52′48″	0,001552	32	fs	440	4,0045	(3,6279)
7	14°17′24″	0,001600	38	ffs	532	3,6164	(3,2764)
8	15°11′24″	0,001569	44	m	622	3,4068	(3,0864)
9	16°03′	0,001592	48	fi	444	3,2287	(2,9250)
10	16°45′	0,001597	52	i	640	3,0973	(2,8061)
11	18°03′36″	0,001575	61	fs	650;643	2,8794	(2,6086)
12	18°27′36″	0,001567	64	m	800	2,8191	(2,5540)
13	19°28′12″	0,001595	70	s	653	2,6781	(2,4263)
14	21°04′48″	0,001577	82	s	910	2,4818	(2,2485)
15	21°19′48″	0,001575	84	s	842	2,4541	(2,2233)
16	22°17′24″	0,001581	91	s	931	2,3534	(2,1321)
17	23°57′	0,001583	104	ffs	10.2.0	2,1989	(1,9922)
18	25°21′36″	0,001581	116	s	862 ; 10.4.0	2,0841	(1,8882)
19	26°40′12″	0,001574	128	fs	864	1,9887	(1,8017)
20	27°07′48″	0,001575	132	m	880	1,9575	(1,7735)
21	27°52′48″	0,001584	138	s	10.4.4 ; 882	1,9089	(1,7294)
22	28°20′24″	0,001587	142	fs	11.4.1 ; 875	1,8804	(1,7036)
23	30°51′36″	0,001584	166	s	965	1,7402	(1,5766)
24	31°43′12″	0,001582	174	i	11.6.3 ; 976 13.2.1 ; 11.7.2 ;	1,6978	(1,5381)
25	32°24′	0,001577	182	m	10.7.5 ; 13.3.2 ; 11.5.6 ;	1,6659	(1,5093)
26	33°06′	0,001570	190	s	10.9.1 ;	1,6346	(1,4809)
27	33°28′48″	0,001584	192	fs	10.9.3 ;	1,6182	(1,4660)
28	35°22′48″	0,001581	212	s	888	1,5417	(1,3967)
29	36°21′36″	0,001583	222	s	14.4.0 ; 12.8.2 ; 14.5.1 ; 13.7.2 ; 11.10.1	1,5057	(1,3641
30	37°52′48″	0,001583	238	s	15.3.2 ;	1,4538	(1,3171)

L'analyse de l'hétéropolyacide était conforme à la formule: $H_5[PW_{10}V_2O_{40}]\cdot 30H_2O$, comme on peut le constater des données réportées au tableau 4.

Tableau 4

Analyse de l'acide $H_5[PW_{10}V_2O_{40}]\cdot 30H_2O$

Pourcentage	P	W	V	H_2O	
Calculé	0,97	58,58	3,24	17,77	$G_M = 31, 38, 40$
Déterminé	0,95	39,02	3,18	57,34	

L'analyse de la substance a été effectuée par le même procédé que celui décrit dans le cas de l'acide phosphomolybdovanadique.

Le tableau 5 présente les données obtenues après l'examen des röntgénogrammes.

$$Q_{\text{moyen}} = 0{,}0015842 \pm 3{,}595.10^{-6},\ K = 41,\ t_\alpha = 2{,}02,$$

$$\alpha = 0{,}95,\ a = 22{,}426 \pm 0{,}00125\ \text{Ä},\ S_{\bar{x}} = 1{,}78.10^{-6}$$

Le poids spécifique déterminé = 3,82, nombre de molécules $n = \dfrac{11268.3{,}82}{3138{,}40.1{,}662} = 8{,}23$, qui donne $n = 8$, le poids spécifique calculé $\dfrac{8}{8{,}23}\cdot 3{,}98 = 3{,}71$.

Dans le cas de cette combinaison dans la série des numéros $\sum h_i^2$ apparaissent les valeurs 21 et 61, ce qui nous fait considérer, comme dans le cas précédent, qu'à la base de cette structure se trouve un réseau cubique primitif.

Sur la base des autres extinctions qui indiquent les mêmes plans de translation que dans le cas de l'acide phosphomolybdovanadique, nous considérons que cette combinaison cristallise dans le même groupe spatial $O_h^2 - Pn3n$.

Tableau 5

Étude röntgénographique de l'acide $H_5[PW_{10}V_2O_{40}]\cdot 30H_2O$ ($\Phi = 71$, anticathode Co)

Nº	θ	Q	Σh_i^2	I	$h\ k\ l$	$\frac{d\alpha}{n}$	$\frac{d\beta}{n}$
1	4°39′	0,001637	4	10	200	11,011	(9,9456)
2	9°12′38″	0,001603	16	5	400	5,5762	(5,0527)
3	9°45′36″	0,001598	18	1	330	5,2657	(4,7704)
4	10°30′36″	0,001584	21	3	421	4,8937	(4,4335)
5	11°16′12″	0,001591	24	3	422	4,5675	(4,1380)
6	12°32′24″	0,001571	30	5	521	4,1113	(3,7247)
7	13°47′24″	0,001578	36	1	442	3,7448	(3,3928)
8	14°31′12″	0,001572	40	2	620	3,5604	(3,2255)
9	15°18′	0,001583	44	8	622	3,3829	(3,0647)
10	16°02′24″	0,001591	48	7	444	3,2306	(2,9268)

Tableau 5 (suite)

N°	θ	Q	$\sum h_i^2$	I	$h\ k\ l$	$d\alpha/n$	$d\beta/n$
11	16°47′24″	0,001604	52	9	640	3,0902	(2,7936)
12	17°21′00″	0,001787	56	1	642	2,9933	(2,7119)
13	18°03′	0,001574	61	1	643	2,8809	(2,6100)
14	18°28′48″	0,001570	64	6	800	2,8161	(2,5514)
15	19°06′	0,001575	68	3	820 644	2,7280	(2,4714)
16	20°22′12″	0,001594	76	5	622	2,5645	(2,3233)
17	21°34′48″	0,001573	86	1	921 761	2,4270	(2,1987)
18	22°04′48″	0,001570	90	1	930 851 754	2,3747	(2,1513)
19	22°44′24″	0,001589	94	1	932 763	2,3093	(2,0921)
20	23°11′24″	0,001582	98	2	941 853 770	2,2669	(2,0537)
21	23°35′24″	0,001571	102	2	10.1.1 772	2,2306	(2,0208)
22	24°05′24″	0,001572	106	3	950 943	2,1869	(1,9813)
23	25°50′24″	0,001583	120	1	10.4.2 ;	2,0480	(1,8555)
26	29°13′48″	0,001589	150	2	11.5.2 ;	1,8280	(1,6561)
27	29°34′48″	0,001582	154	5	12.3.1 ; 583	1,8083	(1,6383)
28	30°23′24″	0,001580	162	4	11.5.4 ; 990	1,7645	(1,5986)
29	30°56′24″	0,01592	166	4	11.6.3 ; 976	1,7362	(1,5729)
30	31°51′	0,001582	176	3	12.4.4 ; 14.4.0 ; 12.8.3 ;	1,6916	(1,5325)
31	32°36′36″	0,001578	184	1	12.6.2 ; 14.5.5 ; 13.7.2 ; 11.10.5 888	1,6563	(1.5006)
					15.3.0 ; 13.8.1 ;	1,6190	(1,4668)
32	33°27′36″	0,001583	192	2	13.7.4 ; 12.9.3 ; 11.8.7 ;		
34	35°27′36″	0,001587	212	6	14.4.0 ; 12.8.2	1,5387	(1,3876)
35	36°24′36″	0,001586	222	8	14.5.1 ; 13.7.2 ; 11.10.1	1,4898	(1,3625)
36	37°26′24″	0,001579	234	5	15.3.0 ; 13.8.1 ; 13.7.4 ; 12.9.3 ; 11.8.7 ;	1,4683	(1,3303)
37	38°15′	0,001583	242	1	15.4.1 ; 13.8.3 ; 11.11.0 ;	1,4418	(1,3063)
38	39°24′36″	0,001586	254	3	15.5.2 ; 14.7.3 ; 13.9.9 ; 13.7.6 ;	1,4060	(1,2738)
39	40°09′36″	0,001587	262	4	15.6.1 ;	1,3841	(1,2539)
40	41°07′12″	0,01589	272	3	16.4.0 ; 12.8.8 ;	1,3573	(1,2297)
41	42°19′48″	0,001585	286	2	15.6.5 ; 14.9.3 ; 13.9.6 ;	1,3255	(1,2009)
42	43°11′24″	0,001582	296	1	16.6.2 ; 14.10.0 ; 14.8.6 ;	1,3042	(1,1816)

$Q_{\text{moyen}} = 0{,}0001584.$

Vu que les deux hétéropolyacides $H_5[PMo_{10}V_2O_{40}] \cdot 30H_2O$ et $H_5[PW_{10}V_2O_{40}] \cdot 30H_2O$ ont la composition semblable et appartiennent au groupe spatial O_h^2 – Pn 3*n*, nous supposons que l'arrangement spatial des molécules dans la cellule élémentaire est le même, et c'est pour cette raison que nous traitons aussi ce problème.

Conformément aux données obtenues, les cellules élémentaires comportent 8 molécules et ont à la base un réseau cubique primitif, l'arrangement des 8 molécules dans la cellule élémentaire étant le suivant : un réseau cubique primitif formé de 8 molécules à appartenance 1/8, placées aux coins, centré par interpénétration avec 1/2 , 1/2, 1/2 avec un autre réseau primitif, ayant les molécules placées en position inverse. Ce réseau, ainsi obtenu, par une translation de 1/2,0,0 suivant les trois directions nous donnera la structure de la substance. Il résulte donc que tant les faces h00, que celles hh0 sont des plans de translation, donnés par les molécules en position inverse du centre de la cellule élémentaire et des faces de celle-ci.

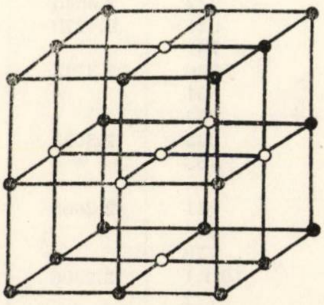

Fig. 1. — Le réseau des acides $H_5[PMo_{10}V_2O_{40}] \cdot 30H_2O$ et $H_5[PW_{10}V_2O_{40}] \cdot 30H_2O$.

Le réseau est représenté dans la figure 1.

De la cellule élémentaire il résulte que la moitié du nombre total de molécules est orientée dans une certaine direction (étant représentée dans la figure par des points noirs), l'autre moitié ayant une orientation opposée à la première (représentée par des billes blanches). A l'appui de cette affirmation nous fournisons aussi les données obtenues par la méthode RES d'où il ressort que pour n'importe quel des axes [111] on obtient le même spectre RES. Cela démontre que dans la cellule élémentaire, les molécules d'hétéropolyacide sont placées de façon que les atomes de vanadium soient également distribués le long de n'importe quel axe [111].

Compte tenu du fait démontré dans le même travail, que les deux atomes de vanadium font partie de deux groupes composés des 3 octaèdres coordinés tétraédriquement autour de l'atome central, si toutes les molécules avaient la même orientation on devrait avoir le même spectre pour deux des axes [111]. L'existance du même spectre RES pour tous les quatre axes [111] montre que la moitié du nombre total des molécules de l'hétéropolyacide sont arrangées de façon que les atomes de vanadium soient orientés vers une direction suivant deux des axes [111] de la cellule élémentaire, les atomes de vanadium de l'autre moitié des molécules étant orientés d'après les deux autres axes [111].

Dans le tableau 6 nous donnons les valeurs des paramétres *a* et *n* obtenus par nous en comparaison des valeurs obtenues dans la littérature pour les hétéropolyacides simples.

Tableau 6

Valeurs des paramètres *a* et *n* déterminées par nous dans le cas du trihétéropolyacide et les valeurs correspondantes prises de la littérature pour le hétéropolyacide simples

Formule	*a*	*n*	Bibliographie
$H_3[PMo_{12}O_{40}].30H_2O$	23,1 A	8	I. Hoard, [7]
$H_3[PW_{12}O_{40}].29\ H_2O$	23,28 A	8	A. I. Bradley, I. W. Illingweth [13]
$H_5[PMo_{10}V_2O_{40}].30\ H_2O$	22,45 A	8	
$H_5[PW_{10}V_2O_{40}].20\ H_2O$	22,42 A	8	

Ainsi qu'il résulte du tableau 6, nos données montrent que les hétéropolyacides mixtes aussi ont la dimension de la cellule élémentaire proche de celle obtenue par d'autres auteurs pour les hétéropolyacides simples, et que tant les hétéropolyacides mixtes que ceux simples cristallisent toujours dans le système cubique à une appartenance de 8 molécules sur la cellule élémentaire.

Par la suite on a construit la cellule élémentaire en entier qui est représentée dans les figures 2 et 3.

Les molécules d'hétéropolyacides sont liées entre elles à l'aide des molécules d'eau qui complètent le réseau de l'édifice cristallin. Pour y arriver, les molécules d'eau sont réparties sur la surface des molécules d'hétéropolyacide de façon qu'elles réalisent un cube. La répartition des molécules d'eau rapportée à une seule molécule d'hétéropolyacide est la suivante :

8 × 1 = 8 à appartenance 1/8 = 1 aux coins du cube
12 × 3 = 36 à appartenance 1/4 = 9 sur les arêtes du cube
6 × 5 = 30 à appartenance 1/2 = 15 sur les faces du cube
4 × 1 = 4 à appartenance 1 = 4 à l'intérieur du cube

Total 29 molécules d'eau

Les cubes ainsi complétés sont rangés dans la cellule élémentaire, les molécules d'hétéropolyacide présentant les deux orientations révélées par les figures 2 et 3.

Les molécules d'eau complètent le réseau dans les places occupées par Mo et V, en formant des cubes centrés sur les faces ; y font exception les quatre molécules d'eau trouvées à l'intérieur des cubes, occupant la place de l'oxygène, et six des 36 molécules placées sur les arêtes qui occupent les places vides également du plan V et Mo, mais qui centrent des cubes centrés sur les faces. Il est probable que ces six molécules d'eau soient plus faiblement reliées, ce qui explique la stabilité relative du cristallohydrate avec 23 molécules d'eau. Outre l'eau qui participe à la réalisation du réseau, il existe la possibilité de retenir une quantité variable d'eau de type zéolitique qui pénètre dans le réseau par les canaux hexagonaux que l'on peut remarquer dans la direction [110] (fig. 3).

CONCLUSIONS

Des données présentées dans ce travail il résulte :

1. Les acides $H_5[PMo_{10}V_2O_{40}]\cdot 30H_2O$ et $H_5[PW_{10}V_2O_{40}]\cdot 30H_2O$ cristallisent dans le système cubique le groupe spatial O_h^2 — Pn $3n$.

2. La dimension de la cellule élémentaire de l'acide $H_5[PMo_{10}V_2O_{40}]\cdot 30H_2O$ est de : a = 22,456 ± 0,00435 Å, et aussi pour l'acide : $H_5[PW_{10}V_2O_{40}]\cdot 30\ H_2O$ de : a = 22,426 ± 0,00125 Å.

3. La cellule élémentaire des deux hétéropolyacides est formée de 8 molécules.

4. Les cellules élémentaires ont à leur base un réseau cubique primitif formé de 8 molécules d'hétéropolyacide, placées aux coins, centré par interpénétration de 1/2, 1/2, 1/2, avec un autre réseau primitif aux molécules placées en position inverse.

Fig. 2. — La cellule élémentaire, en entier, des acides $H_5[PMo_{10}V_2O_{40}]\cdot 30H_2O$ et $H_5[PW_{10}V_2O_{40}]\cdot 30H_2O$, vue dans la direction (100).

1, molécules d'eau; *2*, atomes de vanadium; *3*, atomes de molybdène ou de tungstène; *4*, atomes d'oxygène: bille noire = atomes de phosphore.

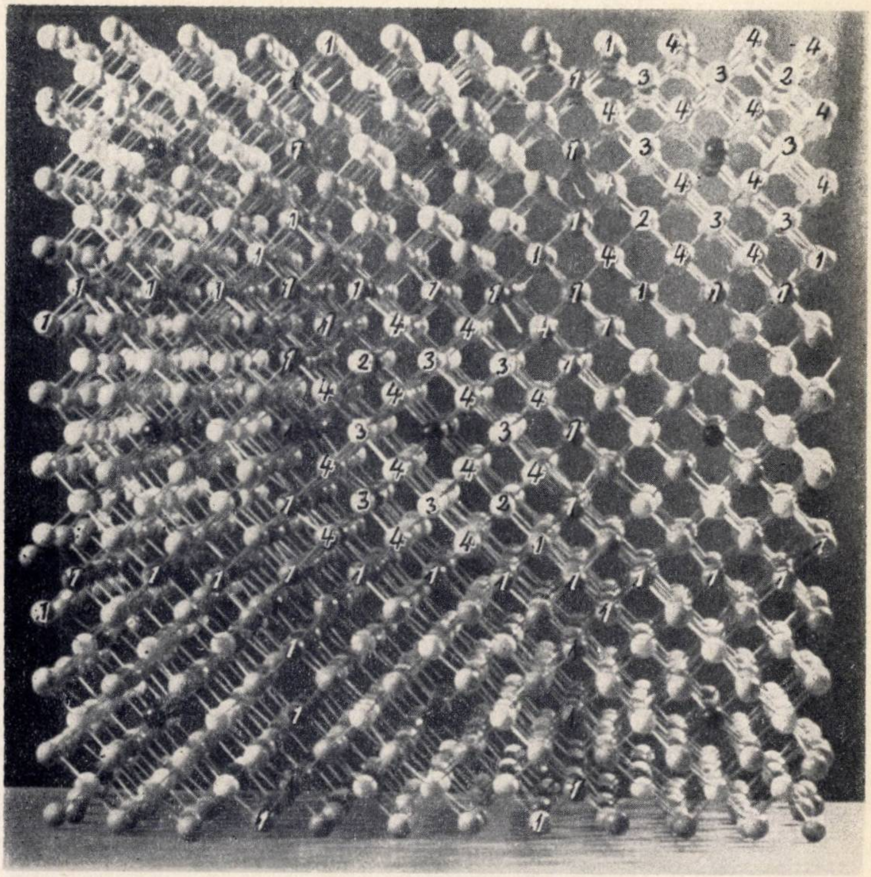

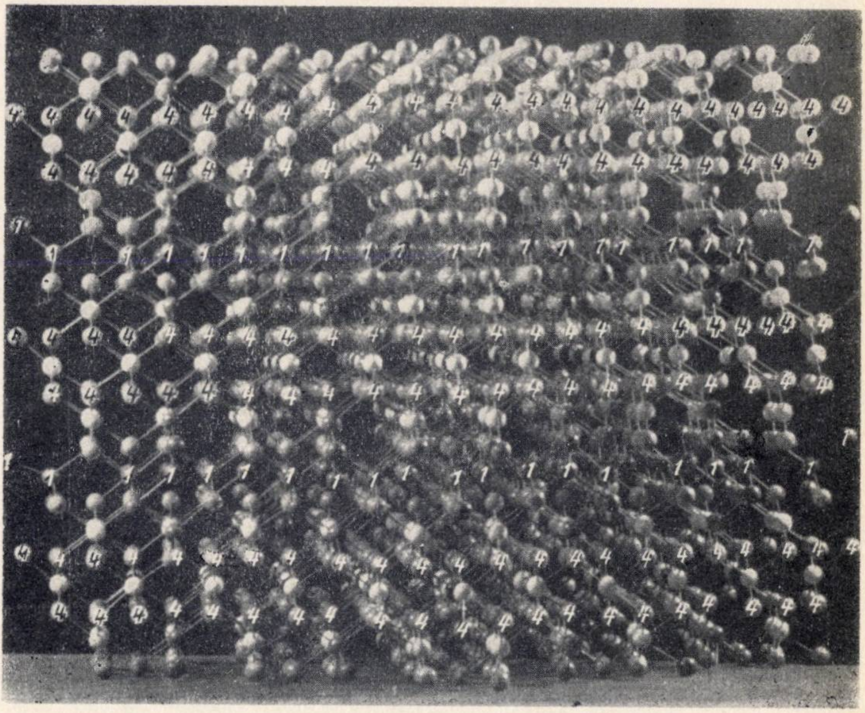

Fig. 3. — Cellule élémentaire, en entier, des acides $H_5[PMo_{10}V_2O_{40}]\cdot 30H_2O$ et $H_5[PW_{10}V_2O_{40}]\cdot 30H_2O$ vue dans la direction (110).

Revue Roumaine de Chimie, **15**, 1573 – 1580 (1970)

QUATERNARY BASIC AMMONIUM POLYELECTROLYTES. II

CHLORINATION WITH THIONYL CHLORIDE OF SOME QUATERNARY BASIC AMMONIUM POLYELECTROLYTES CONTAINING HYDROXYLIC GROUPINGS

I. PETRARIU, CORNELIA LUCA and M. DIMA

Institute of Macromolecular Chemistry "P. Poni",
Aleea Grigore Ghica Vodă 41 A, Jassy, Romania

Received July 23, 1969

The chlorination reactions of the poly[(*p*-vinylbenzyl)diethyl-β-hydroxyethylammonium chloride] and poly[(*p*-vinylbenzyl)dimethyl-2-hydroxypropylammonium chloride] with thionyl chloride have been studied and new polyelectrolytes of the type poly[(*p*-vinylbenzyl)diethyl-β-chlorethylammonium chloride] and poly[(*p*-vinylbenzyl)dimethyl-2-chlor-propylammonium chloride] have been obtained. The reactions took place in a heterogeneous medium and a 87% conversion degree of the OH groupings with Cl was attained for the first polyelectrolyte and 83% for the second polyelectrolyte.

A series of papers dealing with highly basic quaternary ammonium polyelectrolytes, soluble as well as insoluble, largely used in different domains, have appeared lately.

These polymers are used, for instance, as anion exchangers for the sorption of weak acids in dilute solutions, as catalysts in different chemical reactions, absorbents in chromatography[1] etc.

The polyelectrolytes of this type can also be used successfully as coagulation agents to remove acid substances of aqueous solutions, a feature used in the sugar industry to separate the acid coloured substances from the aqueous sugar or molasses syrups.

In a recent work, one has shown the optimum synthesis conditions of the type poly[(*p*-vinylbenzyl)dimethyl-β-hydroxyethylammonium chloride] of polyelectrolyte, as well as the factors determining approximately 99% replacement of the OH groups with Cl and obtaining a new type of polyelectrolyte, namely the poly[(*p*-vinylbenzyl)dimethyl-β-chlorethylammonium chloride][2].

---

[1] E. B. Trostianskaia, S. B. Makarova and A. S. Tevlina, *Vysokomol. Soedineniya*, **9**, 1358 (1961).

[2] M. Dima and I. Petrariu, *Rev. Roum. Chim.*, **13**, 611 (1968).

In the present paper this study was extended to two other polyelectrolytes of the type poly[(*p*-vinylbenzyl)dimethyl-β-hydroxyethylammonium chloride] and poly[(*p*-vinylbenzyl)dimethyl-2-hydroxypropylammonium chloride], by watching the substitution degree of the OH groups by Cl, using thionyl chloride as reactant to obtain chlorinated soluble polyelectrolytes.

One has studied in the meantime the thermal stability of these chlorinated and unchlorinated polyelectrolytes as well as their behaviour in solution.

General reactions would be the following

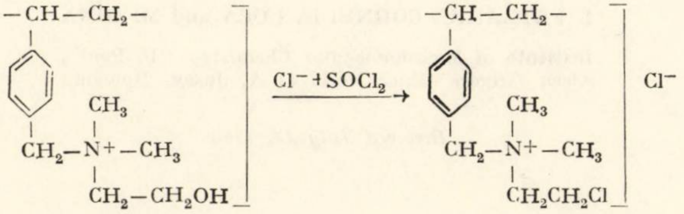
–CH–CH₂–
CH₃
CH₂–N⁺–CH₃
CH₂–CH₂OH
Cl⁻ + SOCl₂
–CH–CH₂–
CH₃
CH₂–N⁺–CH₃
CH₂CH₂Cl
Cl⁻

I

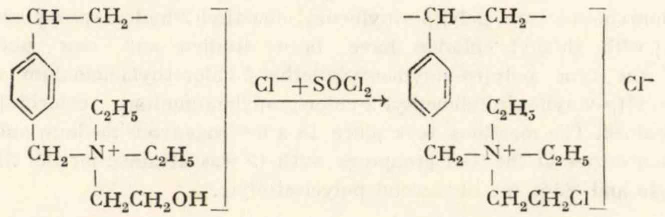
–CH–CH₂–
C₂H₅
CH₂–N⁺–C₂H₅
CH₂CH₂OH
Cl⁻ + SOCl₂
–CH–CH₂–
C₂H₅
CH₂–N⁺–C₂H₅
CH₂CH₂Cl
Cl⁻

II

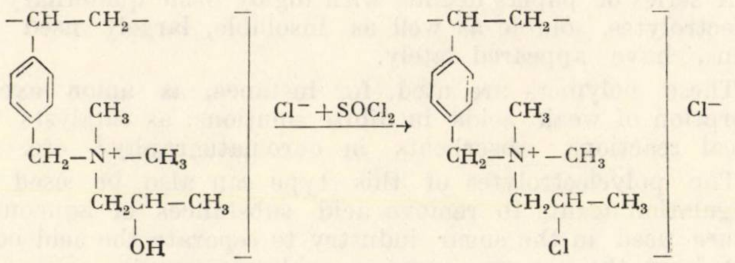
–CH–CH₂–
CH₃
CH₂–N⁺–CH₃
CH₂CH–CH₃
OH
Cl⁻ + SOCl₂
–CH–CH₂–
CH₃
CH₂–N⁺–CH₃
CH₂CH–CH₃
Cl
Cl⁻

III

MATERIALS AND METHODS

The poly[(*p*-vinylbenzyl)diethyl-β-hydroxyethylammonium chloride] II and the poly[(*p*-vinylbenzyl)dimethyl-2-hydroxypropylammonium chloride] III were obtained through amination of the chloromethylated polystyrene with diethylethanolamine and dimethyl-2-hydroxypropylamine.[3]

---

[3] I. Petrariu, Cornelia Luca and M. Dima, (in print).

The thionyl chloride (Loba-Chemie, Wien Fischamend), was redistilled before use, and the fraction with a melting point of 75.7° has been used.

The solvents were benzene made anhydrous on metallic sodium, and CCl_4 made anhydrous on $CaCl_2$.

The IR spectra were obtained with a UNICAM SP-200 spectrophotometer (pelleting with potassium bromide).

The derivatograms were obtained with the F. Paulik, J. Paulik and L. Erdey derivatograph, in air atmosphere, with a heating regime of 13.4°/min.

Viscosimetric measurements were carried out at 25° by means of an Ubbelohde viscosimeter with suspended level, on chlorinated polyelectrolytes at 40° and 70°, during 5 hours, with a 1 : 2 molar ratio of polymer type I, II, III : $SOCl_2$, as well as on unchlorinated electrolytes.

The substitution of Cl for the OH groups was also evidenced spectrally. The chlorination, as well as the calculation of the percentage of OH groups replaced by Cl was made according to a previously published method.

RESULTS AND DISCUSSIONS

To find the optimum conditions for the chlorination of the above mentioned polyelectrolytes, one has first watched the replacement degree of OH groupings by Cl versus temperature (Fig. 1).

As the reaction takes place in a heterogeneous medium, an efficient stirring of the reaction medium was necessary, as well as a very advanced degree of crushing of the polymer subject to chlorination. The data in Fig. 2 show that the optimum conversion temperature should be 70°, when the polymers are still stable (as proved by spectral analysis) and the conversion degree is at its maximum.

While the polymers of type I and II reach, at this temperature, conversion values between 62–68%, the polymer of type III suffers a transformation degree of only 32.5%.

The variation of the conversion degree versus reaction time has been concomitantly followed.

Figure 2 shows that for a 1 : 2 molar ratio, polymer I, II or III : $SOCl_2$, and a reaction temperature of 40°, the polymer with type I structure proves to be the most reactive, reaching in 8 hours a transformation degree of 70%, while the type II polymer attains 50% and the type III, 45%.

To increase the conversion degree, the chlorination reaction of the three polymers was carried out at a much higher molar ratio, namely polymer I, II, III : $SOCl_2 = 1 : 15$ (a necessary condition, considering that the reaction takes place in a heterogeneous medium), reaction time 5 hours and temperature 40°.

Reactions were carried out in a benzene and anhydrous carbontetrachloride medium.

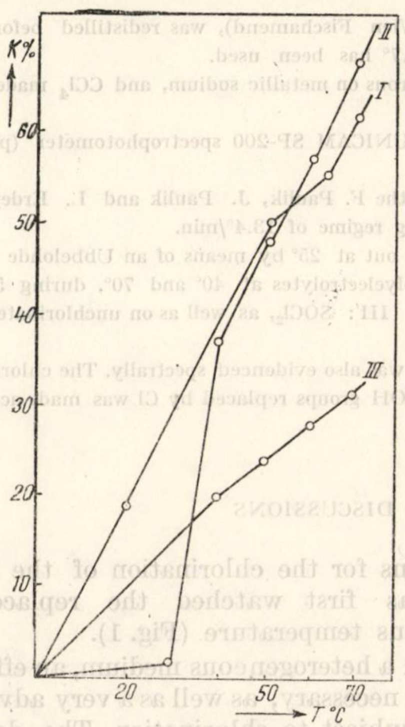

Fig. 1. — Variation of the conversion degree *versus* temperature.
K = conversion % of the theoretical value. Reaction conditions: 5 hours, molar ratio 1 : 2 polymer type I, II, III : $SOCl_2$. Reaction medium: anhydrous benzene.

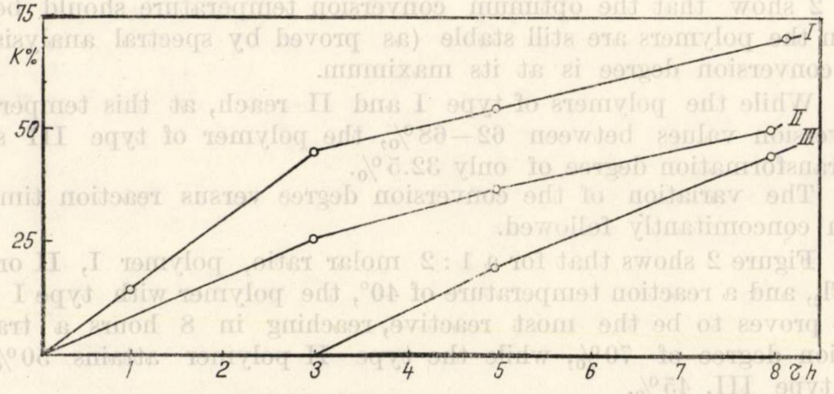

Fig. 2. — Influence of the chlorination time on the conversion degree.
K = conversion % of the theoretical value; τ = reaction time in hours. Reaction conditions: molar ratio 1 : 2 polymer type I, II, III : $SOCl_2$, 40%, reaction medium: anhydrous benzene.

When the reaction takes place in anhydrous benzene (Fig. 3) the substitution degree is 97% for polymer I, 87% for polymer II and 83% for polymer III.

If the reaction takes place in carbon tetrachloride medium (Fig. 4) the conversion degree for polymer I is of 99%, while for the other two (II and III) the conversion is of only 80% and 53%, values inferior to those obtained in benzene.

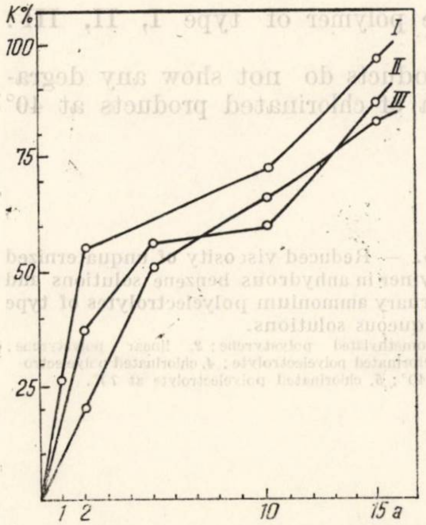

Fig. 3. — Variation of conversion degree *versus* molar ratio of type I, II, III : $SOCl_2$ in anhydrous benzene.

K = conversion % of the theoretical value; a = $SOCl_2$ moles for 1 mole of polymer I, II, III. Reaction conditions : 40°; 5 hours.

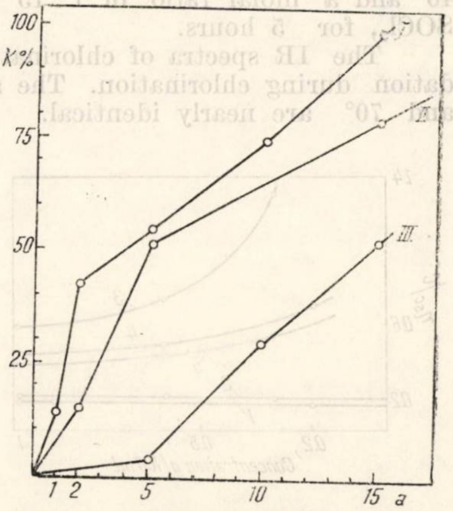

Fig. 4. — Variation of conversion degree *versus* molar ratio of polymer type I, II, III polymer : $SOCl_2$ in anhydrous carbon tetrachloride.

K = conversion % of theoretical value a = $SOCl_2$ moles for 1 mole of polymer I, II, III. Reaction conditions : 40°; 5 hours.

A clearer image of the maximum chlorination conditions of these three polyelectrolyte types results from the analysis of data shown in Table 1.

Table 1

Variation of the maximum substitution degree of Cl for the OH groups according to the kind of polyelectrolyt and solvent for a molar ratio 1 : 15 of : polymer I, II, III / $SOCl_2$ for 5 hours at 40°

Polyelectrolyte	Reaction Medium	% of Maximum Conversion
Poly[(*p*-vinylbenzyl)dimethyl-β-hydroxyethylammonium chloride] I	CCl_4	99
Poly[(*p*-vinylbenzyl)diethyl-β-hydroxyethylammonium chloride]II	benzene	87
Poly[(*p*-vinylbenzyl)dimethyl-2-hydroxypropylammonium chloride]III	benzene	83

One notices a decrease in the conversion degree parallel to the increase in the volume of radicals bound to the quaternary nitrogen. This goes from 99% for the type I polyelectrolyte, to 83% in the case of type III polyelectrolyte.

One can conclude that to attain high conversion values of OH groups to Cl, the reaction should be carried out in anhydrous benzene at

40° and a molar ratio of 1 : 15 of the polymer of type I, II, III : $SOCl_2$, for 5 hours.

The IR spectra of chlorinated products do not show any degradation during chlorination. The spectra of chlorinated products at 40° and 70° are nearly identical.

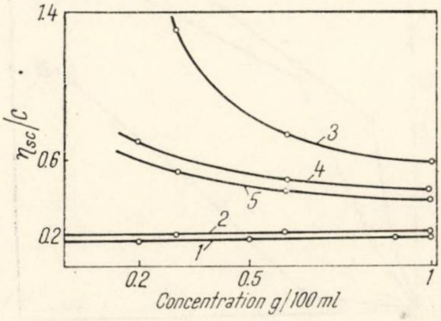

Fig. 5. — Reduced viscosity of unquaternized polymer in anhydrous benzene solutions and quaternary ammonium polyelectrolytes of type I in aqueous solutions.

1, chloromethylated polystyrene; *2*, linear polystyrene; *3*, unchlorinated polyelectrolyte; *4*, chlorinated polyelectrolyte at 40°; *5*, chlorinated polyelectrolyte at 70°.

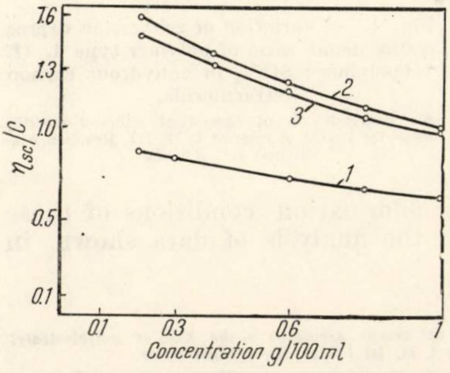

Fig. 6. — Reduced viscosity of type II ammonium quaternary polyelectrolytes in aqueous solutions.

1, unchlorinated polyelectrolyte; *2*, chlorinated polyelectrolyte at 40°; *3*, chlorinated polyelectrolyte at 70°.

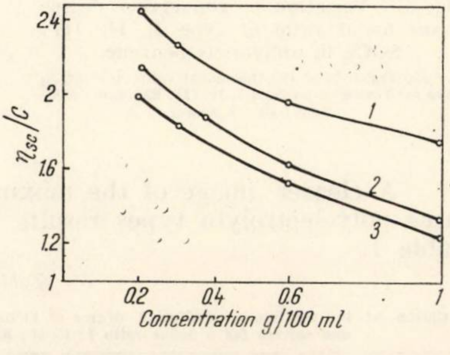

Fig. 7. — Reduced viscosity of aqueous solutions of type III ammonium quaternary polyelectrolytes.

1, unchlorinated polyelectrolyte; *2*, chlorinated polyelectrolyte at 40°; *3*, chlorinated polyelectrolyte at 70°.

A series of viscosimetric measurements of aqueous solutions of type I, II, III quaternized polymers were carried out in parallel. These have shown that the reduced viscosity η_{sc}/C increases with the decrease in the concentration (Figs. 5, 6, 7). For low concentrations, the reduced viscosity reaches considerably high values as compared to the unquaternized polymers (Fig. 5), a fact showing that polymers of type I, II and III are polyelectrolytes.

This is explained by the fact that for high concentrations, the molecules of the quaternized polymer are most compactly gathered, and the reduced viscosity η_{sc}/C represents normal values.

On increasing the dilution, the molecules of quaternized polymers begin to space out, and due to the positive charge of the nitrogen atom, they start stretching. For a still higher degree of dilution, electrostatic forces are great enough to produce a maximum stretching of the molecule.

This finding was also proved on other cationic polyelectrolytes of the type polyvinyl-chloracetate quaternary salts.[4]

Analysing the data presented in Figs. 5 and 7, one notices that the reduced viscosity of the aqueous solution of polymers of the type I and III, decreases with the increase in chlorine content in the polymer, respectively with the disappearance of the OH groupings. Thus, maximum values of reduced viscosity are obtained in the case of unchlorinated polyelectrolyte, followed in decreasing order by the product chlorinated at 40° and slightly lower values for the product chlorinated at 70°, where the chlorine content is the highest.

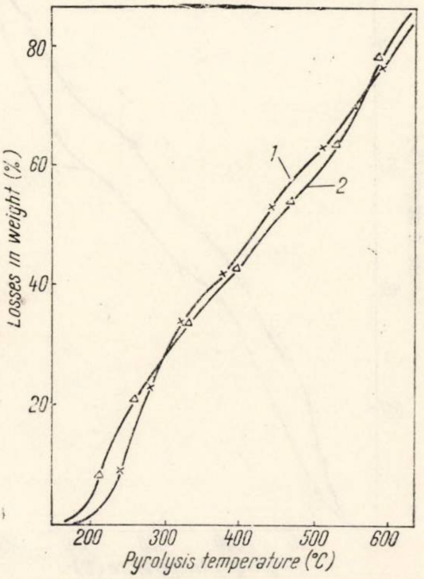

Fig. 8. — Thermogravimetric curves of polymer type I.
1, × = unchlorinated; 2, Δ = chlorinated at 70°.

A particular case is somehow presented by the reduced viscosity of polyelectrolyte II (Fig. 6) which increases with the increase of the dilution, to a greater extent for chlorinated products, than for the unchlorinated ones. This might be due to the nature of the radicals bound to the quaternary nitrogen which induce the appearance of electrostatic forces among the quaternary ammonium groupings, stretching more or less the molecule.

Synthetized polymers of type I, II and III, chlorinated as well as unchlorinated ones, were also studied from the point of view of the thermal decomposition, and the losses in weight according to the pyrolisis temperature have been determined.

Analysing the data shown in Figs. 8, 9 and 10, one may draw the following conclusions :

---

[4] J. P. Newport and R. J. Reynolds, *S.C.I. Monograph*, **26**, 131–142 (1967).

— The replacement of the OH groups by Cl does not produce essential changes as to the thermal stability of polymers I, II and III.

— The unchlorinated polymers present, with small exceptions, a higher thermal stability than the chlorinated ones.

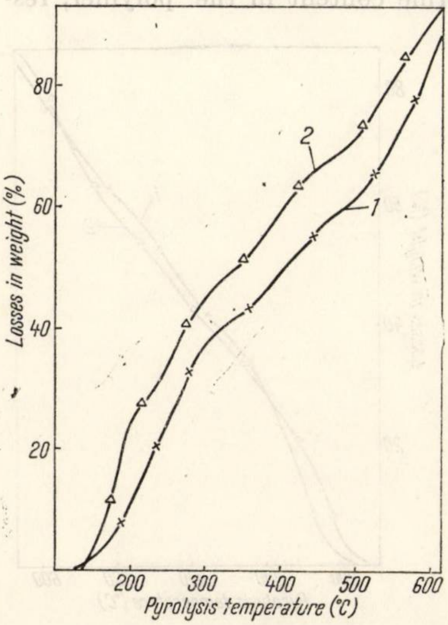

Fig. 9. — Thermogravimetric curves of polymer type II.
1, × = unchlorinated; 2, Δ = chlorinated at 70°.

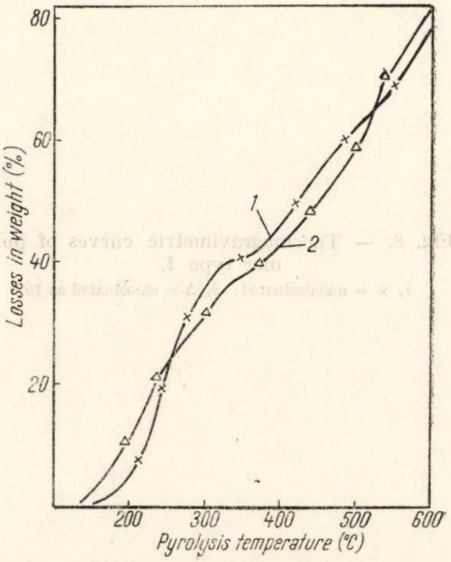

Fig. 10. — Thermogravimetric curves of polymer type III.
1, × = unchlorinated; 2, Δ = chlorinated at 70°.

— According to the kind of polymer subject to degradation, one can state that up to 300° the thermal stability increases in the following order: polymer I >III >II, from 300° to 550° the order is III >I >II.

All products obtained, the polymers of the type I, II and III as well as those chlorinated in different proportions are completely soluble in water, methanol and ethanol.

CONCLUSIONS

One has studied the chlorination reaction of the poly[(*p*-vinylbenzyl)diethyl-β-hydroxyethylammonium chloride] and poly[(*p*-vinylbenzyl)dimethyl-2-hydroxypropylammonium chloride] with thionyl chloride, obtaining new polyelectrolytes of the type poly[(*p*-vinylbenzyl) diethyl-β-chlorethylammonium chloride] and poly[(*p*-vinylbenzyl) dimethyl-2-chlorpropylammonium chloride].

The polyelectrolytes were characterised from the point of view of their thermal stability and their behaviour in aqueous solutions.

Revue Roumaine de Chimie, 15, 1581–1589 (1970)

ARYLALUMINIUM-PHOSPHIN VERBINDUNGEN

DIANA GIURGIU, I. POPESCU, AGLAIA CIOBANU, M. BOSTAN,
N. VOICULESCU und LUCIA ROMAN

vom Institut für Makromolekuläre Chemie „P. Poni", Abteilung für anorganische makromolekulare Verbindungen (Polymere), Aleea Gr. Ghica Vodă 41 A, Iassy

Eingegangen am 6. Oktober 1969

Durch die Reaktion von Triarylaluminium (Aryl = Phenyl, *o*-Tolyl, α-Naphthyl) mit Diphenylphosphin wurden die dimeren Substitutionsverbindungen $[(C_6H_5)_2Al-P(C_6H_5)_2]_2[(CH_3C_6H_4)_2Al-P(C_6H_5)_2]_2$ und das Addukt $(C_{10}H_7)_2Al-P(C_6H_5)_2.$ $.Al(C_{10}H_7H)_3$ erhalten. Die Reaktion von $[(C_6H_5)_2Al-P(C_6H_5)_2]_2$ mit *o*-Phenantrolin und Acridin ergab Additionsprodukte im Molverhältnis von 2 : 1, 1 : 1. Die Verbindungen wurden spektrophotometrisch untersucht und mit den Ausgangsprodukten verglichen. Röntgenaufnahmen zeigen amorphe Strukturen für die Substitutionsprodukte und eine kristalline Struktur für das Additionsprodukt.

Die Reaktionen des Alkyl- bzw. Arylaluminiums mit sekundären und tertiären Phosphinen wurden erst in letzter Zeit untersucht.

Die bekannten Versuche betreffen sowohl Additionsprodukte des Donor-Acceptor Typs wie z.B. das $Al(C_6H_5)_3.P(C_6H_5)_3$, welches von Neunhoeffer in Benzol bei 300° dargestellt wurde,[1] als auch Substitutionsverbindungen der Formel $(R_2Al-PR'_2)_n$ (R = Methyl, Äthyl, R′ = Äthyl, Phenyl). Fritz und Trenczek [2] stellten das $[Cl_2Al-P(C_6H_5)_2]_3$ aus $AlCl_3$ und $LiP(C_6H_5)_2$ in verschiedenen Al : P Molverhältnissen dar. Von den Verbindungen, die die Al—P Bindung enthalten,[3] ist das Trimere $(Me_2Al-PMe_2)_3$ bekannt, für welches eine cyclische Struktur angenommen wird.

Issleib und Mitarb.[4] erhielten das $Et_2Al-PEt_2$, welches sich in Benzol als Dimer befindet, oder in monomolekularer Form in Dioxan, oder als $Et_2Al-PEt_2.OEt_2$ in kristalliner Form dargestellt werden kann. Es kann noch das von Issleib[5] durch thermische Spaltung bei 180° erhaltene $Et_2Al-PEt_2.OEt_2$ erwähnt werden, für welches die Autoren keine Struktur angeben.

---

[1] O. Neunhoeffer und W. Wiegel, *J. prakt. Chem.*, **4**, 201 (1957).

[2] G. Fritz und G. Trenczek, *Z. anorg. Chem.*, **313**, 236 (1961).

[3] N. Davidson und H. C. Brown, *J. Amer. Chem. Soc.*, **64**, 316 (1942).

[4] K. Issleib und H. I. Deylig, *Z. Naturforsch.*, **17 b**, 198 (1962).

[5] K. Issleib und F. Krech, *Z. anorg. Chem.*, **328**, 21 (1964).

In einer Reihe von Arbeiten befaßten sich Coates und Mitarb.[6] mit amorphen oder glasartigen Dimeren und Trimeren des $(R_2M-DR'_2)_n$ Typs (M = Element der III-Gruppe und D = Donorelement der V-Gruppe).

Jonson und Mitarb.[7] erhielten das $[Et_2Al-PhP_2]_2$ und untersuchten dessen Eigenschaften.

In Folge des Lewis-Säure-Charakters des Al-Atoms,[8] trachtet dieses seine Oktettlücke mit dem einsamen Elektronenpaar des P-Atoms zu ergänzen, welches seinerseits unter diesem Einfluß eine tetraedrische Verwitterung eingeht und mit dem Al-Atom eines anderen Moleküls, welches als Lewis-Base wirkt, dimere oder trimere Verbindungen bildet. Für die freihe monomolekulare Form liegen keine Beweise vor. Es müßte eine Al—P Doppelbindung nach dem Jonson-Schema

$$R_2Al-\ddot{P}R_2 \rightleftarrows R_2\overset{(-)}{Al}=\overset{(+)}{P}R_2$$

vorhanden sein.

Im folgenden befaßten wir uns mit den Reaktionen der Triphenyl-Tri-*o*-tolyl- und Tri-α-naphthylaluminium mit Diphenylphosphin und, Substitutionsverbindungen des Ar_2Al-PR_2 Typs wobei Ar = Phenyl, *o*-Tolyl, α-Naphthyl erhalten wurden

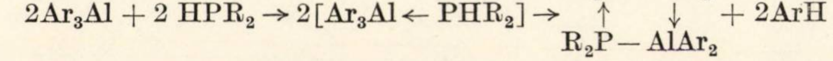

$$2Ar_3Al + 2\,HPR_2 \rightarrow 2[Ar_3Al \leftarrow PHR_2] \rightarrow \begin{array}{ccc} Ar_2Al & - & PR_2 \\ \uparrow & & \downarrow \\ R_2P & - & AlAr_2 \end{array} + 2ArH$$

Eine Ausnahme bildet das Tri-α-naphthylaluminium, welches mit Diphenylphosphin das Additionsprodukt $(C_{10}H_7)_2Al-P(C_6H_5)_2.Al(C_{10}H_7)_3$, mit einem Al/P Molverhältnis von 2 : 1, ergibt.

Die Umsetzungen erfolgten bei Zimmertemperatur und gegen Ende der Reaktion wurde auf 120° erwärmt.

Bei der Umsetzung von $[(C_6H_5)_2Al-P(C_6H_5)_2]_2$ mit *o*-Phenantrolin und Acridin, die stärkere Lewis-Basen sind, zersetzt sich das Dimere und es bilden sich $[(C_6H_5)_2Al-P(C_6H_5)_2]_2.N_2C_{12}H_8$ und $(C_6H_5)_2Al-P(C_6H_5)_2.NC_{13}H_9$ Addukte.

VERSUCHSTEIL

Die Arbeit mit Organoaluminium-Verbindungen und Phosphinen benötigt sorgfältigen Luft- und Feuchtigkeitsausschluß. Die Synthesen erfolgten in Schlenk-Glasgeräten in sauerstofffreiem trockenem Stickstoffstrom.

Die Ausgangsprodukte wurden in unserem Labor dargestellt und gereinigt.

Die Lösungsmittel wurden unter Zusatz von Benzophenon über Na destilliert.

---

[6] G. E. Coates und J. Graham, *J. Chem. Soc.*, **1963**, 233.

[7] A. W. Jonson, W. D. Larson und G. H. Dohl, *Canad. J. Chem.*, **43**, 1338 (1965).

[8] F. G. A. Stone, *Chem. Rev.*, **58**, 101 (1958).

Triphenyl-, Tri-*o*-tolyl- und Tri-α-naphthylaluminium werden nach Krause[9] durch Schmelzen von körnigem Aluminium[10] und der entsprechenden Arylquecksilber-Verbindungen erhalten. Die Masse wird in Benzol gelöst und mit n-Hexan versetzt. Das Triarylaluminium wird mit n-Hexan gewaschen und unter Vakuum getrocknet.

Diphenylphosphin wurde durch Hydrolyse aus $KP(C_6H_5)_2$.Diox dargestellt.[11]

Die Einwaagen für die Analysen wurden ebenfalls in N_2-Strom durchgeführt. Die IR-Spektren wurden unter Luft- und Feuchtigkeitsausschluß in Nujol (zwischen KBr-Platten) mit einem Unicam SP-200 Spektrophotometer aufgenommen. Röntgenaufnahmen wurden mit Cu-Kα-Strahlung (1,5418 A); 40 KV; 12 mA; und 4 Std. Bestrahlungsdauer, mit einem TUR M-60 Röntgenapparat, erhalten.

Die thermogravimetrischen Analysen wurden ebenfalls in N_2-Strom durchgeführt.

I. $[(C_6H_5)_2Al-P(C_6H_5)_2]_2$. Zu 2g (7,75 mMol) Triphenylaluminium werden 1,6 g (8,60 mMol) Diphenylphosphin (Überschuß) tropfenweise eingetragen. Es findet eine exotherme Reaktion unter Benzolabspaltung statt. Schließlich erwärmt man 30 Min. auf 120° zur Beendigung der Reaktion. Das Reaktionsgemisch wird mit 10 ml Benzol verdünnt und mit n-Hexan versetzt. Das ausgebildete Diphenylaluminium-diphenylphosphin wird viermal mit jeweils 25 ml n-Hexan gewaschen, um das überschüssige Diphenylphosphin zu entfernen, und unter Vakuum getrocknet. Das Podukt ist ein weißes Pulver, stark luft- und feuchtigkeitsempfindlich, in Benzol, Nitrobenzol und Toluol wenig löslich, in Äther, Hexan, Petroläther unlöslich. Es zersetzt sich mit Wasser und Alkohol unter Phosphin- und $Al(OH)_3$-Bildung. In oxidierender Salpetersäure-Perchlorsäure-Mischung entzündet es sich explosionsartig.

Analysen für $C_{24}H_{20}AlP$

gef.:	Al 7,41	P 8,25%
ber.:	Al 7,37	P 8,47%

Das Molekulargewicht wurde kryoskopisch in Benzol bestimmt und betrug 665 statt 366, wie für die Minimalzusammensetzung $C_{24}H_{20}AlP$ berechnet wurde. Dem entspricht ein Assoziationsgrad von 1,81, etwa 2.

II. $[(CH_3C_6H_4)_2Al-P(C_6H_5)_2]_2$ wird in der oben angeführten Vorschrift aus 2,5 g (8,21 mMol) Tri-*o*-tolylaluminium und 1,85 g (9,9 mMol) Diphenylphosphin dargestellt. Das Produkt ist weißgelblich, sehr unbeständig, luft- und lichtempfindlich. Löslichkeit in Benzol und Toluol gering, unlöslich in Äther, Petroläther und Hexan.

Analysen für $C_{26}H_{24}AlP$

gef.:	Al 7,06	P 7,90%
ber.:	Al 6,83	P 7,84%

III. $(C_{10}H_7)_2Al-P(C_6H_5)_2.Al(C_{10}H_7)_3$. Zu einer benzolischen Lsg von 2 g (4,9 mol) Tri-α-naphthylaluminium werden 1,5 g Diphenylphosphin eingetragen. Es wird 1 Std. unter Rückfluß erwärmt und mit n-Hexan versetzt. Der ausgebildete Niederschlag wird mit n-Hexan gewaschen und im Vakuum getrocknet. Das kristalline, sandartige Produkt ist in Benzol und Toluol löslich und in Äther und Hexan unlöslich.

Analysen für $C_{62}H_{45}Al_2P$

gef.	Al 6,08	P 3,49%
ber.	Al 6,17	P 3,54%

Das Molekulargewicht wurde kryoskopisch in Benzol bestimmt und betrug 562 (ber. 874) mit dem Dissoziationsgrad $\alpha = 0{,}555$.

---

[9] E. Krause und P. Dittmar, *Ber. dtsch. chem. Ges.*, **63**, 2401 (1930).

[10] T. Mole, *Austral. J. Chem.*, **16**, 798 (1963).

[11] K. Issleib und A. Tzschach, *Chem. Ber.*, **92**, 1118 (1959).

IV. $[(C_6H_5)_2Al-P(C_6H_5)_2]_2N_2C_{12}H_8$. Zu 1,5 g I in 10ml Benzol werden 0,37 g *o*-Phenantrolin in Ätherlsg eingetragen. Es bildet sich sofort ein roter Niederschlag, welcher mit kalter Äther-Benzol Mischung gewaschen und im Vakuum getrocknet wird.

Analysen für $C_{60}H_{11}Al_2P_2N_2$

gef. :	Al 6,34	P 7,10	N 2,72 %
ber. :	Al 5,90	P 6,78	N 3,06 %
gef. ; MG	852		
ber. :MG	912		

V. $(C_6H_5)_2Al-P(C_6H_5)_2.NC_{13}H_9$. Zu 1,5 g I in benzolischer Lsg werden 1 g festes Acridin eingetragen. Der ausgebildete gelbe Niederschlag wird in 25 ml Benzol gelöst und 1 Std. unter Rückfluß erwärmt. Es kristallisiert das gelbe Produkt, welches mit Petroläther und Benzol gewaschen und in Vakuum getrocknet wird.

Analysen für $C_{37}H_{29}AlPN$

gef. :	Al 4,51	P 6,07	N 2,70 %
ber. :	Al 4,95	P 5,68	N 2,56 %

DISKUSSION

Bekanntlich besitzt das Al-Atom in den dimeren Verbindungen $Al_2(CH_3)_6$, $Al_2(C_2H_5)_6$, $Al_2(C_3H_7)_6$, Al_2X_6 (X = Halogen) vier sp^3 Atomorbitale, die nach den Ecken eines Tetraeders gerichtet sind.

Die röntgenographische Analyse des kristallinen $Al_2(CH_3)_6$ weist auf eine dimere Struktur,[12] die durch die Bildung von „three-centred bond" erklärt wird.[13] Diese Tatsache entspricht einer Auffüllung der Elektronenlücke des Al-Atoms in den AlR_3 Verbindungen (R = Alkyl, Aryl, Halogen), welche durch die doppelte Funktion der Molekülorbitale erfolgt, und zu einer Brückenbindung führt.

Andererseits sind die aluminiumorganischen Verbindungen, die verzweigte Alkylreste enthalten, monomer, was durch die sterische Hinderung der organischen Liganden erklärt wird (z.B. $Al(i-C_4H_9)_3$).

Die bisherigen Röntgenuntersuchungen[14] beweisen, daß auch das Triphenylaluminium in dimerer Form vorliegt.

Die Phenylgruppen der Brücke sind stark deformiert und bilden mit dem Al_2C_2 Ring einen Winkel von 84,4°, so daß die π-Elektronen der Phenylreste teilweise an der Al—C Bindung lokalisiert wurden und die Unvollständigkeit der Elektronenkonfiguration verhindern.[15]

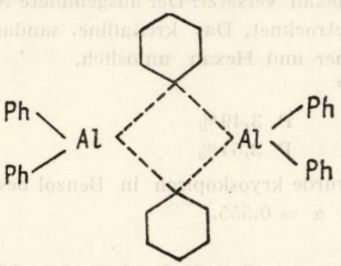

---

[12] P. H. Lewis und R. E. Rundle, *J. Chem. Phys.*, **21**, 986 (1953).

[13] E. A. Jeffery, T. Mole und J. K. Saunders, *Austral. J. Chem.*, **21**, 137.

[14] J. F. Malone und W. S. McDonald, *Chem. Commun.*, **1967**, 444.

[15] K. Wade, *Chemistry in Britain*, **4**, **11**, 503 (1968).

Die Elemente der V. Gruppe (außer Bi) sind in den $EH_{3-n}-R_n$ ($E = N$, P, As, Sb) Verbindungen tetraedrisch verzwittert und besitzen zwei ungepaarte Elektronen, die als Elektronendonor in der D—A -Bindung eintreten können.

In Folge der Anwesenheit des Elementes E in den Molekülen vom Typ $[R_{3-n}Al(EH_{3-p}R_p)_n]_2$ (p, $n = 1,2,3$) liegen diese in normalem Zustand als Dimere vor.[16]

Die sterische Hinderung kann[16] die Donor-Acceptor Komplexbildung abschirmen. Die Elektronenlücke der sp^3 Elektronenkonfiguration des Al-Atoms wurde mit dem einsamen Elektronenpaar des Elements E eines anderen Moleküls aufgefüllt, um dimere oder polymere Verbindungen zu bilden.

Die röntgenographische Untersuchung des $(RNAlPh)_4$ weist eine kubische Struktur auf.[17,18]

Die von uns synthetisierten aluminiumorganischen Verbindungen enthalten das P^{III} Atom (Phosphin), dessen einsames Elektronenpaar eine Donor-Acceptor-Bindung bildet. Die Synthese derartiger Verbindungen erfolgt über das $R_3Al \leftarrow PHR_2$ Addukt, welches unter RH Abspaltung in eine kovalente Verbindung übergeht.

In die Substitutionsreihe der Lewis-Basen, die von Davidson und Brown[3,19] aufgestellt wurde, befinden sich die PR_3 Basen zwischen Äther und Aminen $R_2O < R_3P < NR_3$ wonach die Reaktionsfähigkeit des P-Atoms kleiner als die des N-Atoms ist. So erklärt sich die Notwendigkeit der direkten Einwirkung des Phosphins auf das Triphenylaluminium in festem Zustand oder in benzolischer Lösung. Bei dem $AlPh_3.OEt_2$ ist der Äther fest gebunden und wird durch das Phosphin nicht ersetzt. Der schwache thermische Effekt der direkten Reaktion wurde durch die Bildung des $R_3Al \leftarrow PPh_2H$ Addukts erklärt, welches unter Kohlenwasserstoffabspaltung in die dimere Form übergeht, wobei sich die Koordinationsbindung in eine kovalente Bindung umwandelt.

Die vier verzwitterten Atomorbitale des Al-Atoms bzw. Molekülorbitale der Moleküle mit identischen Partnern sind gleichwertig. Im Falle der Umsetzungsreaktion mit Radikalen oder mit einem Element E ($E = P$) wächst die Bindungsenergie der Partner, und eine nachfolgende Umsetzung erfolgt viel schwerer oder wird ganz unmöglich. So erklärt sich die Tatsache, daß in der Literatur nur Substitutionsprodukte der Formel $(R_2Al-PR'_2)_n$ ($n = 2,3$)[2,6] beschrieben werden.

Ziegler und Gellert[20] haben festgestellt, daß auch im Fall $E = N$ bei der Titration des Dialkylaluminiums mit NH_3, mono- und dimere Substitutionsverbindungen entstehen. Dennoch kann der kleine Radius von 0,71 Å des Stickstoffatoms in der tetragonalen Konfiguration im

---

[16] I. Popescu, A. Ciobanu, D. Giurgiu und M. Bostan, *Rev. Roumaine Chim.*, **12**, 1251 (1967).

[17] T. R. McDonald und W. S. McDonald, *Proc. Chem. Soc.*, **1963**, 382.

[18] H. Schmidbaur und G. Jonas, *Angew. Chem.*, **79**, *9*, 413 (1964).

[19] H. Lehmkuhl, *Angew. Chem.*, **75**, 1090 (1963).

[20] K. Ziegler und H. G. Gellert, *Liebigs Ann. Chem.*, **629**, 20 (1960)

Verhältnis zu 1,10 Å des P-Atoms und seine große Elektronegativität 3,0 im Verhältnis zu 2,10 des P-Atoms in diesem Fall die vollständige Umsetzung erklären[16]:

$$2\,(R')_3Al + 6NH_2R \rightarrow [Al\,(NHR)_3]_2 + 6R'H$$

(R = Alkyl, Aryl)

Die kryoskopische Molekulargewichtsbestimmung des I in Benzol ergab 665 statt 366, wie für die monomere Form berechnet wurde; dieses zeigt einen Assoziationsgrad von $1{,}81 \sim 2$.

Das geringe Molekulargewicht von III wurde durch die große Löslichkeit des $Al(C_{10}H_7)_3$ in Benzol in Folge der Dissoziation dieser Verbindung erklärt. Der gefundene Wert 562 statt 874 liegt zwischen den Werten 408 für $Al(C_{10}H_7)_3$ bzw. 466 für $(C_{10}H_7)_2Al-P(C_6H_5)_2$ der beiden Partnern entspridt und 874 der für $(C_{10}H_7)_2Al-P(C_6H_5)_2.Al(C_{10}H_7)_3$ berechnet wurde.

Die Reaktion des *o*-Phenantrolins bzw. Acridins mit I in benzolischer Lösung ersetzt die $Al \leftarrow P$ koordinative Bindung der dimeren Form mit einer $Al \leftarrow N$ Bindung. Es bilden sich die Addukte IV und V.

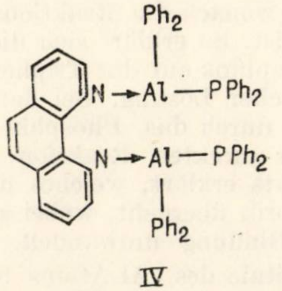

IV

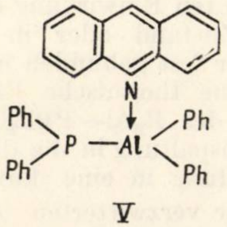

V

Die Verbindungen die durch Analysen und Molekulargewichtsbestimmungen festgelegt wurden, bestätigen die Substitutionsreihe der Lewis-Basen.[3,19]

Die thermische Zersetzungskurve von I (Abb.1) zeigte fünf Temperaturgebiete zwischen 100—216°, 216—330°, 330—426°, 426—500° und über 500°. Der erste Bereich zeigte einen mittleren Verlustgradienten von 0,092% g/Gr(d (Punktl), welcher einem Gesamtverlust von 10,70% entspricht. Die Neigung der Kurve zeigt das Ende eines thermolytischen Phänomens an, welches der Abspaltung einer Phenylgruppe entspricht.

Zwischen 216—330° zeigt die Neigung der Kurve einen kleineren Verlustgradienten von 0,0812% g/Grad. Bei 330° (Punkt 2) entspricht dem Gesamtverlust von 19,98% eine Abspaltung von 1,90—2 Phenylgruppen. Der geringe Gradient bzw. die geringe Neigung der Kurve benötigt eine kleine Geschwindigkeit der Thermolyse bzw. eine große Energie für die Spaltung der Bindungen und Neuordnung der Moleküle.

Das Gebiet 330–426° mit einem Verlustgradienten von 0,230% g/Grad und Gesamtverlust von 42,10% (Punkt 3) entspricht der Spaltung von vier Phenylgruppen. Die Kurve verläuft gerade und die Enthalpie bleibt konstant. Bei 426–500° beträgt der mittlere Gradient 0,122% g/Grad mit einer kleineren Verlustgeschwindigkeit. Einem Verlust von 51,12% bei 500° (Punkt 4) entspricht die Abspaltung von fünf Phenylgruppen. Über 500° verläuft die Kurve gerade und das thermische Geschehen findet ununterbrochen statt. Die Abspaltung einer Phenylgruppe vom Ausgangsmolekül, welche dann durch Kupplung Diphenyl bildet und durch Sublimation das System verläßt, führt zu einer Neuordnung des Moleküls und zur Bildung neuer Bindungen.

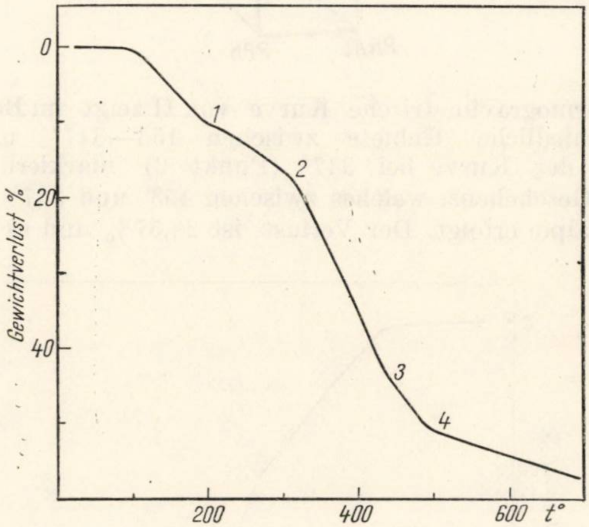

Abb. 1. – Die thermogravimetrische Kurve von $[(C_6H_5)_2Al-P(C_6H_5)_2]_2$.

Der Verlust zweier Phenylgruppen wird durch eine Umsetzung der Donor-Acceptor-Bindung in eine kovalente Bindung erklärt.

Gleichzeitig bilden sich zwei neue Donor-Acceptor-Bindungen, die die Elektronenlücke auffüllen, und es entsteht die Verbindung

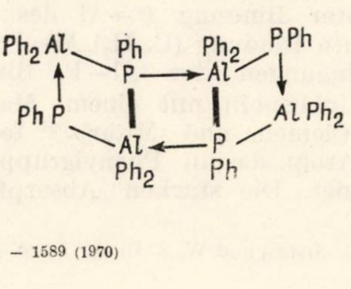

Der Aufbau der Verbindung nach der Abspaltung von vier Phenylgruppen könnte durch eine kubische Struktur erklärt werden:

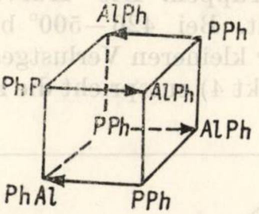

Die thermogravimetrische Kurve von II zeigt im Bereich 50—600° zwei unterschiedliche Gebiete zwischen 153—347° und 347—600°. Die Neigung der Kurve bei 347° (Punkt 2) markiert das Ende des thermischen Geschehens, welches zwischen 153° und 347° mit einer konstanten Enthalpie erfolgt. Der Verlust ist 23,57 % und es wird angenommen, daß eine simultane Abspaltung einer Phenyl- und einer Naphthylgruppe stattfindet. Der berechnete Verlust ist 23,34 %, In diesem Fall geht die Donor-Acceptor Bindung P→Al des $(C_{10}H_7)_2Al-P(C_6H_5)_2.Al(C_{10}H_7)_3$ in die kovalente Bindung $(C_{10}H_7)_2Al-P(C_6H_5)-Al(C_{10}H_7)_2$ über.

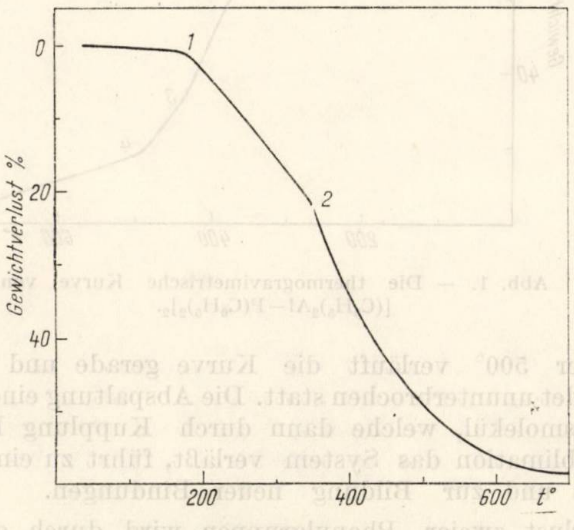

Abb. 2. — Die thermogravimetrische Kurve von $(C_{10}H_7)_2Al-P(C_6H_5)_2.Al(C_{10}H_7)_3$.

Die Valenzschwingungen der Al—P Bindung des Triphenylaluminiumtetraphenyldiphosphins mit einem Maximum im Bereich von 1120 cm^{-1} wird, wie Clemens und Mitarb. [21] feststellten, dem koordinativ-vierwertigem P-Atom, das an Phenylgruppen und an ein Al-Atom gebunden ist, zugeordnet. Die starken Absorptionsbanden bei 1450—

---

[21] D. F. Clemens, H. H. Sisler und W. S. Brey, *Inorg. Chem.*, **5**, 527 (1966).

Tabelle 1

Die IR Spektren der untersuchten Verbindungen

Verbindung	IR-Spektren, cm^{-1}
1. $[(C_6H_5)_2Al-P(C_6H_5)_2]_2$	2850 (i), 1470 (i), (1400 (i) 1160 (s), 1140 (s), 1100 (m)
2. $[(CH_3C_6H_4)_2Al-P(C_6H_5)_2]_2$	2850 (i), 1480 (i) , 1395 (i) 1180 (s), 1160 (s)
3. $(C_{10}H_7)_2Al-P(C_6H_5)_2 . Al(C_{10}H_7)_2$	2920 (i), 1460(i), 1380 (i) 1135 (s), 1125 (s)
,, 4. in benzolischer Lösung	2940 (i), 1480 (i), 1400 (m) 1160 (m)
5. $HP(C_6H_5)_2$	1430 (i), 1200 (i), 1120 (i)

1430 cm^{-1} der P-Phenyl-Bindung werden auch dem koordinativ-vierwertigen P-Atom[22] zugeschrieben.

Für die Verbindungen des Typs $(R_2M-PR'_2)_n$ wo M = Al, Ga, In, fanden Beachley und Coates [23] die Valenzschwingungen der $P^{III}-CH_3$ Bindungen im Bereich 1299—1278 cm^{-1}.

In Übereinstimmung mit diesen Ergebnissen zeigen die IR-Spektren der Dimeren I und II starke Absorptionsbanden bei 3000—2850 cm^{-1} und 1480—1460 cm^{-1} und ein schwächeres Maximum im Gebiet 1160—1140 cm^{-1}. Die zwei starken Maxima des koordinativ-vierwertigen P-Atoms decken sich mit den Absorptionsbanden des Nujols, welche unvollständig kompensiert wurden. Im Falle von III, wurde gleichzeitig mit dem IR-Spektrum in Nujol auch eines in benzolischer Lösung aufgenommen. (Die Verbindung III ist in Benzol ohne Zersetzung leicht löslich.) Die oben angeführten Absorptionsbanden wurden der Anwesenheit des koordinativ-vierwertigen P-Atoms im Molekül zugeordnet. Die dimeren Substitutionsprodukte I und II zeigen im Gebiet 1160—1140 cm^{-1} schwache Maxima, welche den Valenzschwingungen des koordinativ-vierwertigen P-Atoms zugeordnet wurden. Diese Voraussetzung wird dadurch unterstützt, daß das IR-Spektrum des Diphenylphosphins zwei starke Absorptionsbanden im Gebiet 1200—1120 cm^{-1} aufweist. Die Bildung einer Al$\leftarrow$P Bindung vermindert die Elektronendichte des P-Atoms und in Folge der Anwesenheit eines Al-Atoms werden die Absorptionsbanden verringert.

Im Falle der Verbindung III, wo das P-Atom auch koordinativ-vierwertig gebunden ist, zeigen die IR-Spektren Schwingungen im Bereich 1135—1125 cm^{-1}.

Die Röntgenaufnahmen sprechen im Falle der Verbindungen I und II für eine amorphe und bei dem Addukt III für eine kristalline Struktur.

---

[22] W. A. Hart und H. H. Sisler, *Inorg. Chem.*, **3**, 617 (1964).

[23] B. O. Beachley und G. E. Coates, *J. Chem. Soc.*, **1965**, 3241.

Revue Roumaine de Chimie, **15**, 1581 – 1589 (1970)

Revue Roumaine de Chimie **15**, 1591–1599 (1970)

RECHERCHES SUR LA DÉGRADATION DES MACROMOLÉCULES POLYSULFONIQUES AU MOYEN DES ISOTOPES RADIOACTIFS

GH. FURNICĂ
Laboratoire des rayonnements ionisants, Institut d'Hygiène, Bucarest 15, 1, str. Leonte

Reçu le 5 août 1969

Des macromolécules polyphénol-sulfoniques marquées au S–35 à la fonction $-SO_3H$ et aux isotopes Na–22 ou bien Cs–137 au « contre-ion » mobile du même polymère ont été conservées à sec ou bien exposées aux rayons ionisants émis par Co–60. On a continué l'étude de l'élimination des isotopes radioactifs contenus dans la structure macromoléculaire en mesurant dans ce but la radioactivité de la solution externe. Les résultats obtenus confirment le processus de désulfonation des polymères étudiés à la suite de l'action des radiations ionisantes.

La conservation prolongée et surtout l'irradiation par de fortes doses de rayonnement ionisant [1–16] modifient les principales propriétés des macromolécules polyphénol-sulfoniques, ou polystyrène-sulfoniques. Les travaux publiés qui donnent les résultats des recherches effectuées sur le mécanisme de ces transformations portent soit sur la dégradation des échangeurs d'ions[1–5] soit sur leur dégradation par irradiation.[4–16]

---

[1] J. G. Morralli, *J. Rech. Centre nat. Rech. Sci.*, **26**, 277, 289 (1954).

[2] G. M. Kline, « Analytical Chemistry of Polymers », vol. 1, 2 and 3 Interscience Publish., New York, 1959–1963.

[3] W. Foerst, « Ulmans Encyklopädie der technischen Chemie », VIIIe vol., 1917, p. 787.

[4] F. A. Bovey, « The Effects of Ionizing Radiation on Natural Synthetic high Polymers », Interscience Publish, New York, 1958, p. 182.

[5] T. D. Ionescu, « Schimbători de ioni », Ed. tehnică, Bucarest, 1961, p. 143.

[6] R. O. Bolt et J. G. Carrol, « Radiation Effects on Organic Materials », Acad. Press., New York, 1963, p. 127.

[7] A. Chapiro, « Radiation Chemistry of Polymeric Systems », Interscience Publish. New York, 1962, p. 488.

[8] J. Higgins, « U.S.A.E.C. », ORNL, **1352** (1962).

[9] C. Cathers, « Actes de la Conf. Internat. Nat. Unies », IIIe vol., Genève, 1954, p. 569.

[10] O. Costachel et Gh. Furnică, « Deux Conf. Internat. Nat. Unies », Genève, 1958. **29**, p. 246 (1958).

[11] Gh. Furnica et A. Drăguț, *Studii și Cercetări chim.*, Acad. R.P.R., **7**, 399 (1959),

[12] P. H. Kasai, *J. Chem. Phys.*, **43**, 3322 (1965).

[13] E. D. Kiseleva et K. V. Ciumutov, *Zhur. fiz. Khim.*, **37**, 1926 (1963).

[14] A. El. Guebeily et N. Sauka, *J. Chem. U.A.R.*, **8**, 269 (1965).

[15] H. Julien, *Comp. rend.* (*C*), **263**, 1514 (1966) ; **264**, 1039 (1967).

[16] J. P. Menin et T. Kiridai, *Comp. rend.* (*C*). **264**, 1963 ; **265**, 129 (1967).

Le mécanisme établi démontre des processus de fragmentation de la macromolécule, ou de réticulation de la structure macromoléculaire, ainsi que des transformations de la structure chimique au niveau des fonctions organiques ionogènes.[11-16]

Compte tenu du fait que l'une des principales caractéristiques des polyélectrolytes macromoléculaires synthétiques dépend de la présence des fonctions ionogènes, nous avons entrepris des recherches sur les transformations éventuelles induites au niveau de ces fonctions dans la structure des macromolécules sulfoniques par les rayonnements ionisants.

Les transformations chimiques de la structure des fonctions dissociables de la macromolécule peuvent être étudiées, à part d'autres méthodes, aussi au moyen des atomes radioactifs. Le marquage radioactif au S—35 de la fonction $-SO_3H$ a permis l'étude des transformations structurelles subies par l'ion solide (le macro-anion). Le marquage de l'ion métallique qui fait partie du contre-ion, au Na—22 ou au Cs—137 permet l'étude du processus d'échange ionique dépendant des transformations qui se passent dans la fonction ionogène.

MÉTHODE DE TRAVAIL

La vitesse à laquelle s'établit l'équilibre d'échange ionique entre la solution et la résine a été déterminée au moyen des radionucléides Na — 22 et Cs — 137 qui se trouvaient dans la solution externe sous forme d'ions Na^+ et Cs^+ (NaCl et CsCl). On a mesuré l'évolution de la radioactivité *gamma* à des intervalles de 22 minutes, séparément pour la résine humide, isolée de la solution externe, et pour la solution externe, à l'aide d'un compteur à scintillations, muni d'un cristal de NaI (Tl) en forme de puits. L'efficience du compteur a été de 27% pour le Cs—137 et de 32% pour le Na—22, étant déterminée avec des sources étalon AIEA.

Le polymère a été isolé, après avoir retenu au moment de l'équilibre chimique une certaine quantité de Na—22 ou de Cs—137 ; ensuite il a été lavé à l'eau bidistillée, jusqu'à ce que la solution ne contenait pas plus de radioactivité que le fonds radioactif naturel du compteur. La résine obtenue ainsi a été soumise à l'action du rayonnement *gamma* émis par une source de Co—60, à l'activité de 400 Ci, avec une dose de $2,5.10^6$ R ($2,84.10^{20}$eV/g résine). La dose d'irradiation a été mesurée au moyen d'une solution de $[Fe(NH_4)_2]\ (SO_4)_2$.[17]

Le comportement de l'ion «fixe» $R-SO_3^-$ a été étudié après le marquage par échange isotopique de la fonction ionogène avec du S—35.[18] La résine marquée de cette manière a été soumise à l'action des rayons d'une source de Co—60 avec une dose de $2,5.10^6$ R ($2.84.10^{20}$ e V/g). On a mesuré la radioactivité du résidu de l'eau de lavage, avant et après l'irradiation de la résine. Les observations ont été effectuées avec un compteur à circulation de CH_4, géométrie 50% et une efficience de 11% en rapport avec une source étalon à S—35 AIEA.

---

[17] E. M. Fettes, "Chemical Reactions of Polymers" Interscience Publish. New York 1964, p. 648.

[18] Gh. Furnică et V. Voicu, *Radiochimica Acta*, **7**, 164 (1967).

RÉSULTATS EXPÉRIMENTAUX

L'équilibre d'échange ionique entre la résine Ph_2S formaldéhyde-ortho-phénol-sulfonique ($R_{34}H$) synthétisée conformément à un procédé publié précédemment[19] est présenté dans la figure 1. On observe que cet équilibre est atteint dans un intervalle de 8 à 12 minutes pour le Cs^+ et de 14 à 18 minutes pour le Na^+. En tenant compte de la dilution isotopique utilisée

$0{,}855$ pCi $^{137}Cs/1$ ng ^{132}Cs

$12{,}5$ pCi $^{22}Na/1$ ng ^{23}Na

on peut calculer au moyen des données de la figure 1 et du tableau 1 les valeurs des rendements radiochimiques des processus induits par le rayonnement.

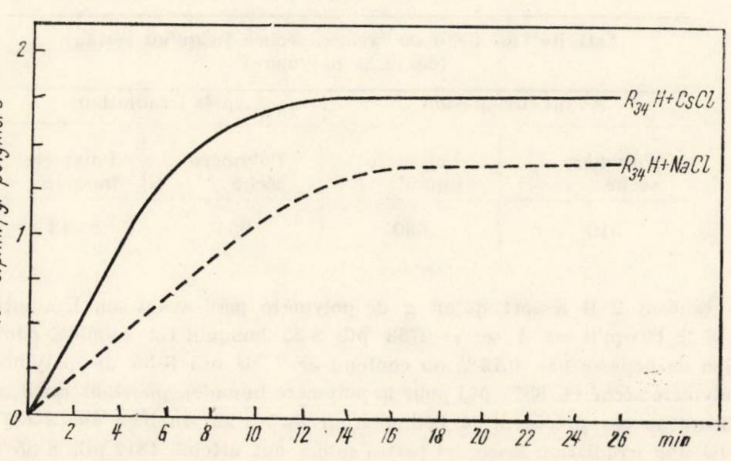

Fig. 1. — Variation de l'activité de la macromolécule Ph_2S lors du processus d'échange ionique entre RH + CsCl au RH + NaCl (la dilution isotopique : 6,8 pCi Cs-137/1ng CsCl et 12,5 pCiNa-22/1ng NaCl).

Tableau 1

Contenu radioactif de Na-22 et Cs-137 déterminé dans la solution extérieure du polymère Ph_2S irradiée avec la dose de $2{,}84.10^{20}$ eV/g. lavée avec 5×2 ml eau

	Activité de la résine c.p.m./g. résine	Activité de l'eau de lavage de la résine (c.p.m. /10 ml)			
		Avant irradiation		Après irradiation	
		Résine séchée	Résine humide	Résine séchée	Résine humide
$R-Na^{22}$	50.751	19.3	9,4	76.8	51,3
$R-Cs^{137}$	6 308	0,7	0,9	5,8	7,3

---

[19] D. A. Isăcescu, S. Păucescu et Gh. Furnică, *Studii și cercet. chimie*, 5, 355, 655 (1957).

A sec, le polymère perd après son irradiation 80,6 pCi Na-22 et 8,5 pCi Cs-137 ; imbibé d'eau, le polymère perd après son irradiation 58,66 pCi Na-22 et 10,6 pCi Cs-137. L'activité retenue par 1 g de résine est de 71 440 pCi pour le Na-22 et de 10 524 pour le Cs-137 ; cette activité correspond, pour les dilutions mentionnées, aux poids suivants : 5715,2 ng Na-23 et 1535,2 ng Cs-132. L'élimination, après irradiation, du Na-22 ou bien du Cs-137 ne dépasse pas 0,12 % du total de la quantité retenue. On constate que la résine non irradiée élimine aussi une petite part d'isotope radioactif dans la solution externe (27 pCi Na-22 et 1,1 pCi Cs-137 pour la résine séchée et 13 pCi Na-22 et 1,2 pCi Cs-137 pour la résine humide).

Tableau 2

Contenu en S-35 déterminé dans l'eau de lavage (25 ml) du polymère Ph_2S (marqué au S-35 en proportion de $1.9.10^6$ c.p.m./g) irradié avec la dose de $2,84.10^{20}$eV/g polymère

Activité de l'eau de lavage, séchée jusqu'au résidu (c.p.m./g polymère)			
Avant irradiation		Après irradiation	
Polymère séché	Polymère humide	Polymère séché	Polymère humide
510	680	954	2 043

Du tableau 2 il ressort qu'un g de polymère perd avant son irradiation seulement 2088 pCi S-35 lorsqu'il est à sec et 2783 pCi S-35 lorsqu'il est humide. Après irradiation l'élimination ne dépasse pas 0,15 % du contenu de 7 764 nCi S-35 du polymère (3905 pCi pour le polymère séché et 8378 pCi pour le polymère humide), pourtant cette quantité n'est pas supérieure au cas précédent de l'élimination du Na-22 ou bien du Cs-137 par le polymère irradié. Par irradiation à sec les pertes subies ont atteint 1817 pCi S-35 ($4,25.10^{-14}$g), tandis qu'à l'état humide 5595 pCi S-35 ($13,09.10^{-14}$g). La valeur du rendement G est donnée par la formule :

$$G = \frac{g.S-35/g \text{ polymère}}{100 \text{ eV}} =$$

ce qui représente : $G_{sec} = 1,49.10^{-32}$ et $G_{humide} = 4,60.10^{-32}$.

Le polymère utilisé (Ph_2S) avant l'irradiation contient 5,1 % S, et après l'irradiation il contient 4,9 % S (à sec) et 4,5 % S (humide). Le polymère a un pouvoir d'échange de 1,96 méquival/g pour un pH = 7 et 2,90 méquival/g pour un pH = 10, sa capacité d'imbibition hydrique étant de 140 %. Nous mentionnons que le calcul donne pour 5,1 % S un pouvoir d'échange théorique de 1,62 méquival/g résine.[19] Par dessiccation sous vide de 2 mm Hg en présence de P_2O_5 le polymère ne retient plus d'eau, tandis que le séchage à l'air détermine une rémanence dans le polymère de 8,7—9,8 % H_2O[20]. La valeur du rendement *G* calculée par la variation du pouvoir d'échange ionique est donnée par la formule

$$G = \frac{\text{méquival/g}}{100 \text{ eV}}$$

En mesurant le pouvoir d'échange ionique avant et après l'irradiation de la résine, par rapport au NaCl ou au NaOH, on a obtenu les résultats suivants :

$K_{NaCl} = 1{,}96$ (non irradié) ; $K_{NaCl} = 1{,}36$ (irradié à sec)
$K_{NaCl} = 1{,}90$ (irradié humide)
$K_{NaOH} = 2{,}90$ (non irradié) ; $K_{NaOH} = 5{,}40$ (irradié humide)
$K_{NaOH} = 2{,}10$ (irradié à sec)

En calculant les valeurs G dans ces conditions, pour les rendements radiochimiques après l'irradiation du polymère, on obtient les résultats suivants :

$G_{NaCl} = 2{,}11.10^{-19}$ (à sec) ; $G_{NaCl} = 2{,}11.10^{-20}$ (humide)
$G_{NaOH} = 8{,}8.10^{-19}$ (à sec) ; $G_{NaOH} = 2{,}8.10^{-19}$ (humide)

Les valeurs G par rapport au contenu de S-32 ou S-35 sont données par la formule :

$$G = \frac{\text{Nombre d'atomes S/g de polymère}}{100 \text{ eV}}$$

On a obtenu les résultats suivants :

$G_{S-32} = 13{,}2$ (à sec) ; $G_{S-32} = 43{,}2$ (humide)
$G_{S-35} = 2{,}5.10^{-10}$ (à sec) ; $G_{S-35} = 7{,}9.10^{-10}$ (humide)

En calculant la dilution isotopique de la résine, on a obtenu les résultats suivants :

avant irradiation : $1{,}785.10^{-10}$g S−35/5,1.10^{-2}g S−32
après irradiation : $1{,}784.10^{-10}$g S−35/4,9.10^{-2}g S−32 (à sec)
$1{,}7837.10^{-10}$g S−35/4,5.10^{-2}g S−32 (humide)

DISCUSSION DES RÉSULTATS EXPÉRIMENTAUX

La recherche sur l'échange ionique au moyen des isotopes radioactifs est apparue dans la littérature dès 1954, lorsqu'on utilisa en guise d'ions mobiles les radionucléides Na−22 et Sr−90.[2]

Les résultats mentionnés dans la présente recherche démontrent le pouvoir d'échange ionique du polymère Ph_2S qui, par ses ions mobiles H^+ se comporte comme un macro-acide (fig. 2).

En conditions statiques d'échange ionique entre le polymère et les ions de la solution externe, l'équilibre est atteint après 10−20 mn de contact, au cours duquel le processus se déroule de la manière suivante

$$[R - SO_3^- + H^+] + [Na^+ + Cl^-] \rightleftharpoons [R - SO_3^- + Na^+] + [H^+ + Cl^-]$$

La réaction a lieu dans un milieu hétérogène, à l'interface solide-liquide, qui est très étendue grâce à la structure poreuse du polymère. La présence des fonctions polaires $-SO_3H$ dans la macromolécule, et, dans une certaine mesure, celle des fonctions phénoliques −OH, détermine un comportement de la résine[15] analogue à celui d'un polyélectrolyte.

Le domaine dans lequel se passe la réaction d'échange ionique est situé entre les limites du pH = 1,5 et pH = 14 pour les fonctions $-SO_3H$, tandis que pour les fonctions phénoliques −OH isolées, ces limites du pH sont de 8,5 à 14. L'influence réciproque entre $-SO_3H$ et $-OH$ augmente l'acidité des fonctions $-OH$, ce qui diminue la valeur du pH pour laquelle la fonction $-OH$ participe au processus d'échange ionique avec le NaCl (fig. 3).

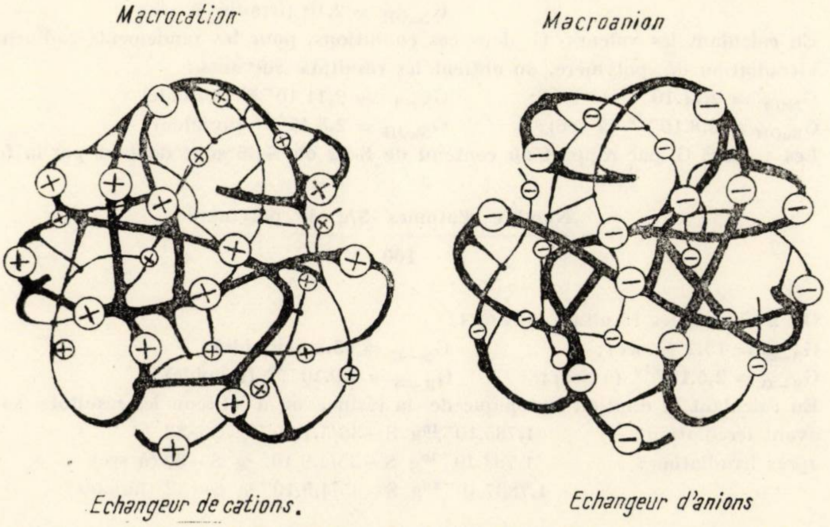
Macrocation
Macroanion
Echangeur de cations.
Echangeur d'anions

Fig. 2. — Schéma de la distribution des ions mobiles (H^+) dans une particule de résine échangeuse d'ions.

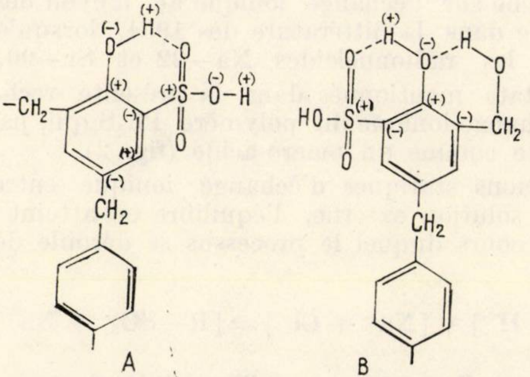
(–)
O
(+)
H
O
(+)
S
(–)
O
(+)
H
O
–CH₂
(+)
(–)
(+)
(–)
CH₂
A
(+)
H
(–)
O
H
O
HO
S
(+)
O
O
(+)
(–)
(–)
CH₂
CH₂
B

Fig. 3. — Schéma de l'influence réciproque entre les groupements $-OH$ et $-SO_3H$ dans la position *ortho* (A) ou aux extrémités de la chaîne macromoléculaire (B).

Le comportement différent par rapport aux ions Na^+ et Cs^+ signalé dans la figure 1 s'explique par la diffusion des « contre-ions » (les ions mobiles) dans la solution interne de la résine. Le volume de la solution interne varie avec le degré d'imbibition du polymère ; ce degré est modifié, à son tour, sous l'influence de la concentration de la solution extérieure et de la nature de l'ion mobile.[20] La forme R-Na retient 6,6% d'eau, tandis que la forme R-Cs retient seulement 4,5%, après avoir été séchée à l'air. Ainsi, les ions différents agiront sur le processus d'échange ionique par leurs dimensions différentes ; ceux à grand volume diffuseront plus difficilement à travers la solution interne et seront retenus en moindre quantité. Il est bien connu que l'ion Na^+ hydraté a les dimensions plus grandes que l'ion Cs^+ hydraté.[3]

Le fait que le polymère au « contre - ion » marqué par du Na-22 ou du Cs—137 libère une petite quantité d'isotope dans la solution externe démontre le processus de dissociation, ou, plus correctement, la migration des contre-ions de la solution interne dans la solution externe, c'est-à-dire 0,018% Na-22 et 0,014% Cs—137 dans le cas de la résine maintenue humide. Après avoir été séchée à l'air, la résine cède à la solution externe 0,038% Na-22 et 0,011% Cs—137. Par rapport aux quantités totales d'ions Na^+ et Cs^+, les valeurs respectives du poids sont petites (conformément à la dilution isotopique mentionnée), mais elles restent sous la limite de sensibilité des méthodes analytiques usuelles. Ces résultats soulignent la rétention plus marquée des ions Cs^+ dont le caractère électropositif est plus accentué que celui des ions Na^+. De même, la conservation de la résine à sec détermine une dégradation de la macromolécule, par la perte de ses fonctions dissociables, le polymère étant d'autant plus stable que les contre-ions sont plus électropositifs. Il paraît que le processus est dû au détachement des fonctions $-SO_3H$ de la macromolécule, par la formation de radicaux libres, sous la forme suivante[20]

$$R - SO_3H \rightleftharpoons R\cdot + \cdot SO_3H$$

Ce phénomène a été démontré à l'aide des spectres RES dans une publication précédente[20] et dans la recherche qui fait l'objet de cette publication, ce même phénomène a été démontré par le marquage de l'« ion solide » (l'ion fixe) à l'isotope S—35. De cette manière on a constaté que le polymère Ph_2S marqué à la fonction dissociable perd 0,026% S—35 dans la solution externe après sa conservation à sec, tandis qu'il perd 0,035% S—35 après la conservation à l'état humide de la résine. Ainsi se trouve confirmé une fois de plus le fait que la stabilité de la liaison $C-SO_3H$ diminue avec l'affaiblissement du caractère électropositif du contre-ion (fig. 3).

Les équilibres chimiques qui décrivent le détachement de la fonction $-SO_3H$ de la molécule du dérivé sulfonique ont été mentionnés depuis longtemps dans la littérature. On a formulé les réactions suivantes[21-23]

$$R - SO_3H + H_2SO_4 \rightleftharpoons RH + H_2S_2O_7 \ \text{(sulfolyse)}$$
$$R - SO_3H + H_2O \rightleftharpoons RH + H_2SO_4 \ (R - SO_3H \rightleftharpoons R^- + SO_3H^+)$$

---

[20] GH. FURNICĂ et C. CONSTANTINESCU, *Radiochimica Acta*, **12**, 669 (1969).

[21] C. D. NENIŢESCU, « Tratat elementar de chimie organică », Ed. tehnică, Bucarest, Ier vol., p. 424 (1956) ; IIe vol., 1958, p. 13.

[22] E. A. SHILOV et F. M. VAINSTEIN, *Ukrain. Khim. Zhur.*, **21**, 58 (1955).

[23] A. E. BRODSKY, « Isotopenchemie », Akad. Verlag, Berlin, 1961, p. 371.

En analysant l'action du rayonnement ionisant du Co—60 sur le polymère Ph_2S, on peut affirmer que les pertes plus élevées de Na—22 et Cs—137 dans la solution externe, après l'irradiation, pourraient être dues au détachement de l'ion mobile avec toute la fonction dissociable; ce phénomène est décrit par les équilibres suivants :

$$R - SO_3Me \rightleftharpoons R\cdot + \cdot SO_3Me$$

$$[R\cdot + \cdot SO_3Me] + H_2O \rightarrow R\,H + Me\,H\,SO_4$$

Certains auteurs admettent même deux possibilités de réaction avec l'eau du radical sulfonique [24,25]; celui-ci, en se transformant du point de vue chimque, ne peut plus se recombiner avec la macromolécule :

$$\begin{array}{ll} & \nearrow SO_3 + Me\,(.SO_3Me + H_2O = MeHSO_4) \\ .SO_3Me & \\ & \searrow SO_2 + MeO\left(\begin{array}{l} SO_2 + H_2O = H_2SO_3 \searrow \\ MeO + H_2O = MeOH \nearrow \end{array} MeHSO_3 + H_2O\right) \end{array}$$

Le rayonnement ionisant peut agir sur le polymère en attaquant simultanément plusieurs points de la macromolécule, de la manière démontrée dans le schéma de la figure 4.

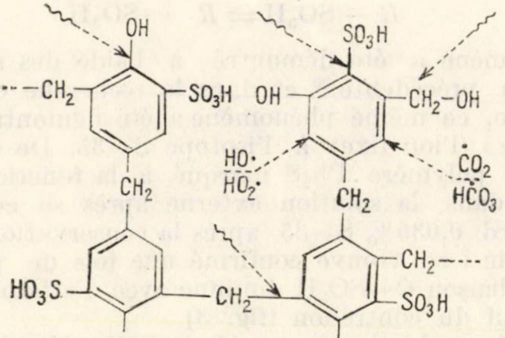

Fig. 4. — Schéma des positions de la macromolécule polyphénol-sulfonique attaquées probablement par les rayonnements ionisants.

La réaction de désulfonation constitue un des principaux processus qui se passent sous l'action du rayonnement; elle a été démontrée aussi dans des publications précédentes [10-12] et vient d'être confirmée de nouveau maintenant à l'aide du radionucléide S—35, isotope qui

[24] E. D. Kiseleva, K. V. Ciumutov et V. N. Krupnova, *Zhur. fiz. Khim.*, **35**, 1816, 1822 (1961).

[25] A. M. Shemushin, I. A. Kuzin et V. E. Edokimov, *Zhur. fiz. Khim.*, **36**, 1959 (1962).

marque l'ion solide $R-SO_3^-$. L'irradiation du polymère Ph_2S, marqué au S—35, est la cause de la présence en plus grande quantité de l'isotope radioactif dans la solution externe, que dans le cas du polymère non irradié (tabl. 2). Pendant la simple conservation à l'air, la macromolécule perd 0,026% de S—35, et pendant la conservation humide, 0,035% de S—35. En irradiant le polymère on constate que cette perte augmente. Le polymère séché et irradié élimine, au total, 0,036% de S—35 (c'est-à-dire encore 0,010% en surcroît), et le polymère irradié humide élimine après irradiation 0,107% de S—35 (c'est-à-dire 0,072% en surcroît). On constate donc que l'irradiation en état d'imbibition hydrique est suivie de la perte d'un nombre considérable de fonctions $-SO_3H$, qui, en se détachant de la macromolécule sous forme de radicaux, réagissent avec l'eau et se transforment du point de vue chimique.

Par conséquent, la réaction de désulfonation constitue un important processus chimique de dégradation des macromolécules polysulfoniques, qui est provoqué par la dissociation même de la fonction $-SO_3H$ comprise dans la structure du polymère. Ce processus est amplifié par le rayonnement ionisant, qui favorise la rupture d'un nombre accru de liaisons $C-SO_3H$.

Revue Roumaine de Chimie, **15**, 1591–1599 (1970)

Revue Roumaine de Chimie, 15, 1601–1610 (1970)

DARSTELLUNG UND UNTERSUCHUNG DER HYDROACRIDINE. VII[1]

EIN DIREKT-VERFAHREN ZUR DARSTELLUNG VON N-ALKYL- UND N-ARYL-PERHYDROACRIDINEN

N. BĂRBULESCU und F. POTMISCHIL

aus dem Organisch-Chemischen Laboratorium der Universität Bukarest,
Spl. Independenţei, 89

Eingegangen am 7. April 1970

Von 2,2'-Methylen-bis-cyclohexanon (**I**) und primären Alkyl- oder Arylaminen ausgehend werden entsprechend N-substituierte Perhydroacridine (**II**) und *symm*-Oktahydroacridiniumperchlorate (**III**) erhalten; die Konfiguration und Ausbeute der entstandenen Perhydroacridine ist von der Art des eingesetzten Amins abhängig. Es werden die NMR-Spektren der dargestellten Verbindungen besprochen.

2,2'-Methylen-bis-cyclohexanon (**I**) ist bereits als vorteilhaftes Ausgangsmaterial zur Darstellung unsubstituierter Perhydroacridine gut bekannt.[2–5] Die Fähigkeit der Ameisensäure enaminische C—C-Doppelbindungen zu reduzieren[6] veranlaßte uns zu Versuchen aus (**I**) und primären Aminen, in Ameisensäure als Reaktionsmedium, geradewegs entsprechend N-substituierte Perhydroacridine (**II**) zu gewinnen.

Die erwarteten Perhydroacridine bilden sich tatsächlich, doch (trotz der Anwendung eines ausreichenden Überschusses an Ameisensäure) immer nur in Begleitung eines mittels Überchlorsäure als entsprechend N-substituiertes *symm*-Oktahydroacridiniumperchlorat (**III**) trennbaren Nebenproduktes:

---

[1] VI. Mitteilung: N. Bărbulescu und F. Potmischil, *Tetrahedron Letters*, **1969**, 5275.

[2] J. Colonge, J. Dreux und H. Delplace, *Bull. Soc. chim. France*, **1957**, 447.

[3] M. N. Tilitschenko und V. I. Vyssotzkiy, *Doklady Akad. Nauk. S.S.S.R.*, **119**, 1162 (1958).

[4] V. I. Vyssotzkiy, *Zhur. org. Khim.*, **4**, 1494 (1968).

[5] N. Bărbulescu und F. Potmischil, *Rev. Roumaine Chim.*, **14**, 1427 (1969).

[6] P. L. De Benneville und J. H. Macartney, *J. Amer. Chem. Soc.*, **72**, 3073 (1950).

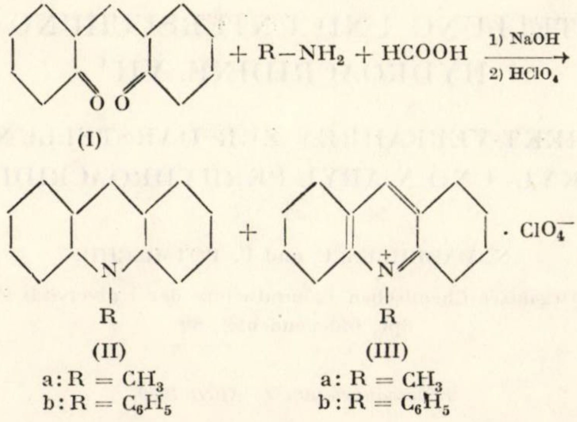

Indem die Reaktion sowohl mit Methylamin wie mit Anilin ausgeführt wurde, konnte ein bedeutender Einfluß der Art des Amins auf Konfiguration und Ausbeute der entstandenen Perhydroacridine festgestellt werden.

Unter Anwendung des Methylamins wurde ein Gemisch vier stereoisomerer N-Methyl-perhydroacridine (**II a**) in 46%iger Gesamtausbeute und N-Methyl-*symm*-oktahydroacridiniumperchlorat (**III a**) in 40%iger Ausbeute erhalten. Die Zahl der Stereoisomere (**II a**) wurde nach den vier verschiedenen N-Methyl-Signalen im NMR-Spektrum ihres Gemisches festgestellt: 2,07—2,11—2,20 und bzw. 2,23 δ (in CCl_4 mit TMS als innerem Standard).

Zur Identifizierung der vier Isomere wurde das Gemisch über die Nitrosamine (**IV**) entalkyliert *):

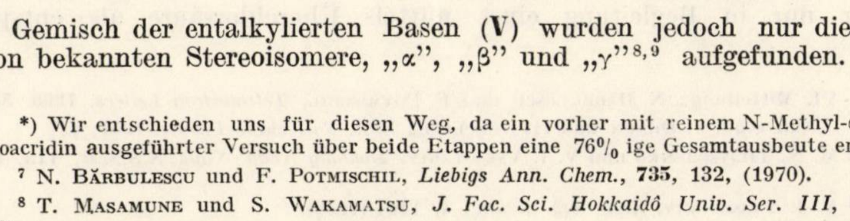

Im Gemisch der entalkylierten Basen (**V**) wurden jedoch nur die drei schon bekannten Stereoisomere, „α“, „β“ und „γ“[8,9] aufgefunden. Das vierte N-Methylderivat ist höchstwahrscheinlich identisch mit dem N-Methyl-δ-perhydrocridin, das von Masamune und Mitarb. dargestellt, aber nicht charakterisiert wurde.[9] Der Verlust des vierten Isomers könnte einer besonders niedrigen Reaktionsfähigkeit des N-Methylderivats in der Etappe (**IIa** → **IV**) zugeschrieben werden; dadurch wäre auch die geringe Gesamtausbeute dieser Etappe zu erklären.

---

*) Wir entschieden uns für diesen Weg, da ein vorher mit reinem N-Methyl-α-perhydroacridin ausgeführter Versuch über beide Etappen eine 76%ige Gesamtausbeute ergab.[7]

[7] N. BĂRBULESCU und F. POTMISCHIL, *Liebigs Ann. Chem.*, **735**, 132, (1970).

[8] T. MASAMUNE und S. WAKAMATSU, *J. Fac. Sci. Hokkaidô Univ. Ser. III*, **5**, 47 (1957).

[9] T. MASAMUNE, M. OHNO, K. TAKEMURA und S. OHUCHI, *Bull. Chem. Soc. Japan*, **41**, 2458 (1968).

Unter Anwendung des Anilins wurde ein einziges Isomer des N-Phenyl-perhydroacridins (**IIb**, Schmp. 132,5–133°)*) in 9%iger Ausbeute und N-Phenyl-*symm*-oktahydroacridiniumperchlorat (**IIIb**) in 52%iger Ausbeute erhalten.

Da das NMR-Spektrum des N-Phenyl-perhydroacridins keine eindeutige Aussage über dessen Konformation und Konfiguration erlaubt, und da wir hinsichtlich der NMR-Spektren unsubstituierter Perhydroacridine schon einige Erfahrung haben,[1,11] beabsichtigten wir die N-Phenylgruppe abzuspalten, was über das *p*-Nitrosoderivat sehr einfach auszuführen schien. Das N-(*p*-Nitrosophenyl)-perhydroacridin wurde auch recht glatt erhalten, doch erwies sich dieses gegen Natriumhydroxid vollkommen unempfindlich und die Bisulfit-Methode[12] war ebenso erfolglos. Die außergewöhnliche Beständigkeit dieses *p*-Nitroso-N,N-dialkylanilins wäre dadurch zu erklären, daß der Angriff am aminischen Stickstoffatom sterisch stark verhindert ist; diese Hinderung wird auch durch die große Schwierigkeit mit welcher sich das Jodmethylat des N-Phenyl-perhydroacridins (**IIb**, Schmp. 132,5 – 133°) bildet erkenntlich (ca. 6%ige Ausb. nach über 600 Reaktionsstunden bei 90°).

Die Zn/HCl-Reduktion des Perchlorats (**IIIb**) führte zu einem Gemisch aus dem ein anderes N-Phenyl-perhydroacridin (**IIb**, Schmp. 105–106°) in reinem Zustand getrennt werden konnte. Diesem kann anhand seines NMR- und IR-Spektrums die Konfiguration „*trans-syn-trans*" zugeordnet, und somit die Benennung N-Phenyl-α-perhydroacridin gegeben werden.

DISKUSSION DER SPEKTREN

Die Konformation und Konfiguration der drei unsubstituierten Perhydroacridine, „α", „β" und „γ", konnte NMR-spektroskopisch, aufgrund der Multiplizität und chemischen Verschiebung der Signale der beiden mit dem Stickstoffatom benachbarten Protone, H_{4a} und H_{10a} bestimmt werden.[1,11]

---

*) Dieses wurde schon von Kaminskiy und Tilitschenko beschrieben (Schmp. 129–130°)[10].

[10] V. A. KAMINSKIY und M. N. TILITSCHENKO, *Zhur. org. Khim.*, **5**, 186 (1969).

[11] N. BĂRBULESCU und F. POTMISCHIL, *Tetrahedron Letters*, **1969**, 2309.

[12] J. v. BRAUN, K. HEIDER und E. MÜLLER, *Ber. dtsch. chem. Ges.*, **51**, 737 (1918).

N-Phenyl-perhydroacridin (**IIb**, *Schmp. 132,5–133°*)

Das NMR-Spektrum dieser Verbindung (Abb. 1) ermöglicht es nicht festzustellen von welchem der Stereoisomere des Perhydroacridins dieses N-Phenylderivat abstammt. Die Signale der mit dem Stickstoffatom benachbarten Protone, H_{4a} und H_{10a}, bilden ein gemeinsames, bei 3,42 δ zentriertes Multiplett (anscheinend Quintett). Da seine fünf Spitzen als das Ergebnis entweder der Überdeckung eines Tripletts ($J \cong 8$ Hz, Intensitätsverhältnis 1 : 2 : 1) mit einem Dublett ($J \cong 8$ Hz, Intensitätsverhältnis 1 : 1) oder der Überdeckung zweier Tripletts ($J \cong 4$Hz, Intensitätsverhältnis 1 : 2 : 1) betrachtet werden können, ist es nicht möglich die Multiplizität der einzelnen Komponenten eindeutig zu bestimmen. Außerdem, kann der hohe Raumanspruch der Phenylgruppe bei manchen Stereoisomeren Konformationveränderungen verursachen*) und dadurch zu falschen Folgerungen führen.

Ein zweites, bei 2,29 δ zentriertes Multiplett (2H) stammt wahrscheinlich von den Protonen einer der Methylengruppen C-4 oder C-5. Die aromatischen Protone sind in zwei spitzige, bei 7,18 δ (2H) und bzw. 6,83 δ (3H) zentrierte Multipletts aufgespalten.

Im IR-Spektrum dieses N-Phenyl-perhydroacridins ist kein „Bohlmann"-Band vorhanden. **)

*N-(*p*-Nitrosophenyl)-perhydroacridin* (*Schmp. 188°*)

Von den chemischen Verschiebungen abgesehen, unterscheidet sich das NMR-Spektrum (in $CDCl_3$) des N-(*p*-Nitrosophenyl)-perhydroacridins nicht von dem des ursprünglichen N-Phenyl-perhydroacridins: die Protone H_{4a} und H_{10a} erscheinen ebenfalls als gemeinsames Multiplett, bei 3,70 δ zentriert.

N-Phenyl-N-methyl-perhydroacridiniumjodid (*Schmp. 105–108°*)

Die Signale der Protone H_{4a} und H_{10a} sind im NMR-Spektrum (in $CDCl_3$) des Jodmethylats getrennt. Erkennbar ist aber nur ein Dublett (1H, $J \cong 11$ Hz), bei 4,53 δ zentriert, dessen Zweige zusätzlich zu je einem Multiplett aufgespalten sind; das andere Signal ist in einer ununterbrochenen, zwischen 4,20 — 0,80 δ ausgedehnten Kette von Signalen enthalten. Die aromatischen Protone bilden ein schmales, bei 7,53 δ zentriertes Multiplett. Die Abwesenheit eines scharfen Singuletts weist auf eine starke sterische Hinderung der N^+-Methylgruppe hin.

---

*) Im N-Nitroso-β-perhydroacridin und einigen N-Acylderivate des β-Perhydroacridins, z. B., hat der Piperidinring wegen sterischer Hinderung eine verzerrte Wannenkonformation.[13]

**) Die „Bohlmann"-Banden treten in Piperidinderivaten nur dann auf wenn mindestens zwei mit dem Stickstoffatom benachbarte axiale C—H-Bindungen zum einsamen Elektronenpaar am Stickstoff in *trans*-Stellung stehen.[14]

[13] N. Bărbulescu und F. Potmischil, *Rev. Chim.* (*București*), **21**, 451 (1970).

[14] F. Bohlmann, *Chem. Ber.*, **91**, 2157 (1958).

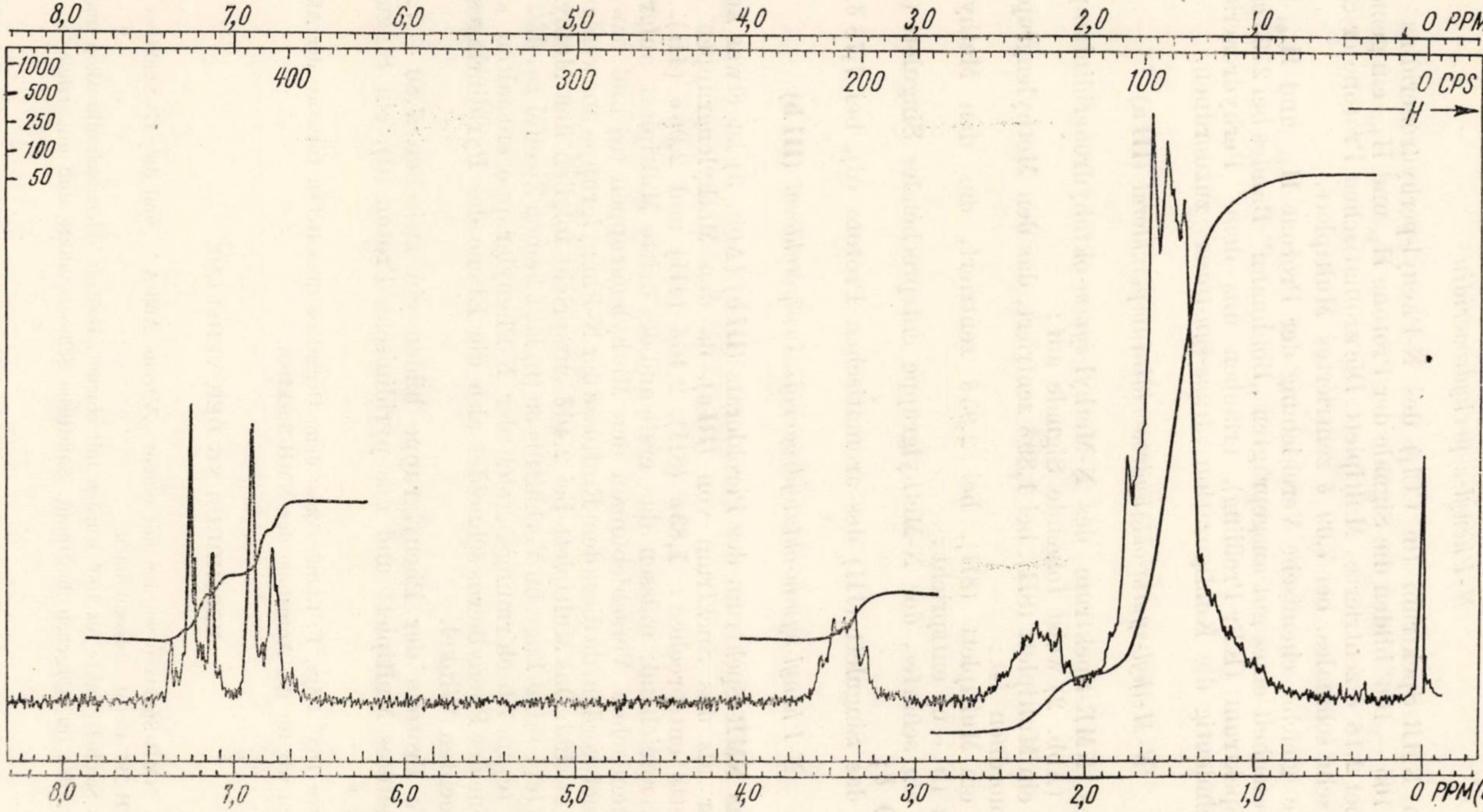

Abb. 1. — 60 MHz-NMR-Spektrum des N-Phenyl-perhydroacridins (**IIb**, Schmp. 132,5–133°), in $CDCl_3$ mit TMS als innerem Standard.

N-Phenyl-α-perhydroacridin

Im NMR-Spektrum (in CCl_4) des N-Phenyl-perhydroacridins mit Schmp. 105 — 106° bilden die Signale der Protone H_{4a} und H_{10a} ein gemeinsames, bei 2,18 δ zentriertes Multiplett. Die aromatischen Protone erscheinen als sehr schmales, bei 7,09 δ zentriertes Multiplett.

Die gleiche chemische Verchiebung der Protone H_{4a} und H_{10a} und die Anwesenheit eines gut ausgeprägten „Bohlmann"-Bandes bei 2793 cm^{-1} im IR-Spektrum (KBr-Preßling), erlauben uns dem Perhydroacridingerüst eindeutig die Konfiguration „*trans-syn-trans*" zuzuordnen.

N-Methyl-symm-oktahydroacridiniumperchlorat (**III a**)

Das NMR-Spektrum des N-Methyl-*symm*-oktahydroacridiniumperchlorats (Abb. 2) weist folgende Signale auf:

— ein Multiplett (8H), bei 1,89 δ zentriert, das den Methylengruppen (a) zuzuordnen ist;

— ein Multiplett (8H), bei 2,95 δ zentriert, das den Methylengruppen (b + c) entspricht;

- ein scharfes, der N-Methylgruppe entsprechendes Singulett (3H) bei 4,00 δ;

— das Singulett (1H) des aromatischen Protons (d), bei 7,78 δ.

N-Phenyl-symm-oktahydroacridiniumperchlorat (**III b**)

Das NMR-Spektrum des Perchlorats (**III b**) (Abb. 3) ist etwas komplizierter als das Spektrum von (**III a**), da den Methylengruppen drei Multipletts entsprechen: 1,83 δ (8H), 2,46 δ (4H) und 2,96 δ (4H). Mit (**III a**) vergleichend, müssen das erste und das dritte Multiplett aufgrund ihrer chemischen Verschiebungen den Methylengruppen (a) und bzw. (b) zugeordnet werden, da diese dem Einflusse der N-Phenylgruppe am wenigsten ausgesetzt sind. Das Multiplett bei 2,46 δ entspricht folglich den Methylengruppen (c); seine Lage im Verhältnis zu (b) läßt keinen Zweifel zu, daß die Protone (c) im Abschirmungsbereich der N-Phenylgruppe enthalten sind. Die Ebene des Phenylkerns schneidet also die Ebene des Pyridinringes in einem rechten Winkel.

Die Protone der Phenylgruppe bilden ein zwischen 7,80 — 7,33 δ ausgebreitetes Multiplett und das pyridinische Proton (d), ein Singulett bei 7,94 δ.

Herrn Dipl.-Phys. F. Chiraleu aus dem Organisch-Chemischen Institut der Akademie danken wir für die Aufnahme der NMR-Spektren.

BESCHREIBUNG DER VERSUCHE

Die NMR-Spektren wurden mit einem „Varian A60-A"- und die IR-Spektren mit einem „UR-20"-Gerät aufgenommen.

Die Schmelzpunkte bis 100° wurden mit einem „Boëtius"-Heiztischmikroskop und die ab 100° wurden im Röhrchen bestimmt. Sämtliche Schmelzpunkte sind unkorrigiert.

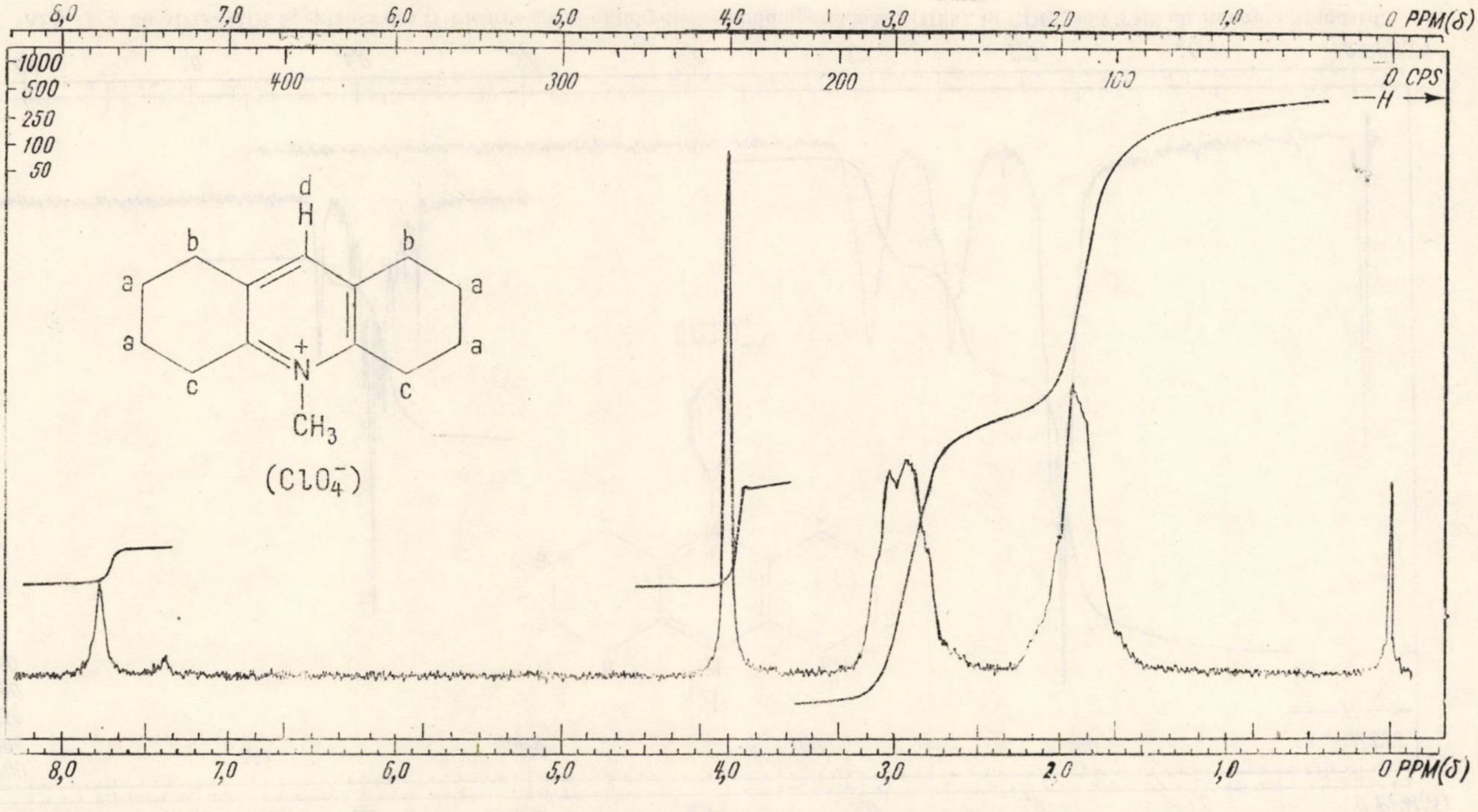

Abb. 2. — 60 MHz-NMR-Spektrum des N-Methyl-*symm*-oktahydroacridiniumperchlorats (**III a**), in $CDCl_3$ mit TMS als innerem Standard.

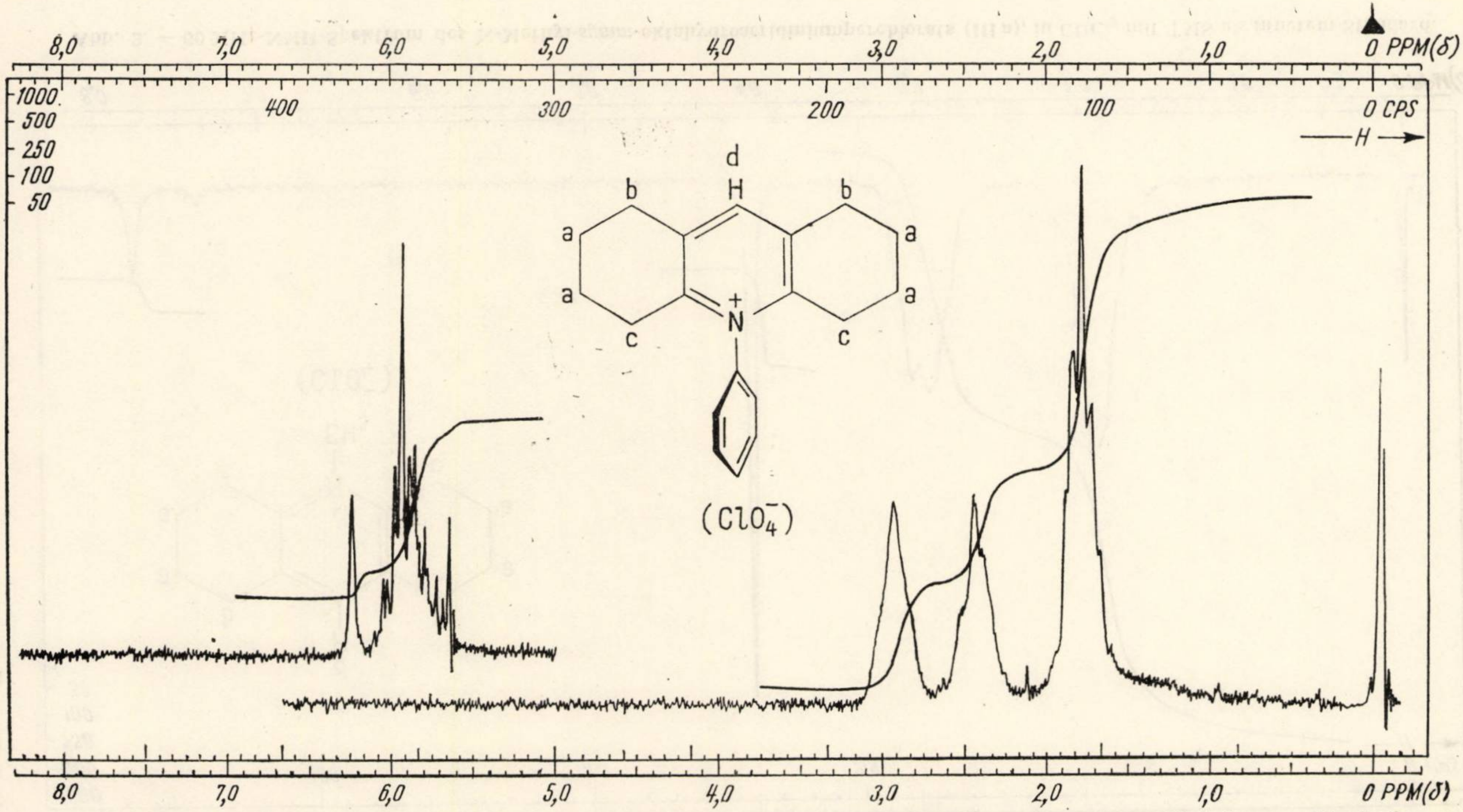

Abb. 3. — 60 MHz-NMR-Spektrum des N-Phenyl-*symm*-oktahydroacridiniumperchlorats (**III b**), in $CDCl_3$ mit TMS als innerem Standard.

Das Gemisch der vier N-Methyl-perhydroacridine (**II a**) *und N-Methyl*-symm-*oktahydroacridiniumperchlorat* (**III a**) : Aus 34 g (0,5 Mol) Methylaminhydrochlorid wurde das Amin befreit und in 300 ml 80 proz. Ameisensäure absorbiert. Zur erhaltenen Lsg. wurden 104 g (0,5 Mol) (I) gegeben, und das Gemisch 8 Std. unter Rückfluß erwärmt. Nach Erkalten wurde mit 40 proz. wäßr. Natriumhydroxidlsg. stark alkalisiert, abermals gekühlt und ausgeäthert. Die blutrote äther. Lsg. wurde kurz über Kaliumcarbonat getrocknet und, unter Rühren, tropfenweise mit einem Gemisch von 70 proz. Überchlorsäure — Äthanol (1 : 1) bis zum Verschwinden der roten Farbe versetzt. Dabei schlug das rohe Perchlorat (**III a**) als grauer Kristallbrei nieder. Nach Filtrieren wurde die äther. Lsg. auf ca. 350 ml eingeengt und mit trockener Salzsäure gesättigt. Die als schweres Öl abgeschiedenen Hydrochloride wurden mit Wasser ausgezogen. Nach Alkalisieren des wäßr. Auszuges wurden 48 g (46 % d.Th.) an rohem N-Methyl-perhydroacridinen-Gemisch erhalten. Das Gemisch ging unter Vakuum einheitlich bei 116—117°/0,3 Torr (im Ölbad 150°) über: $n_D^{25} = 1{,}5069$, $d_4^{25} = 0.9678$; $MR_{ber.}$ 64,2, $MR_{gef.}$ 63,7.

$C_{14}H_{25}N$ (207,36) *Ber.* : N 6,75 *Gef.* : N 7,08

Nach Absaugen des Perchloratbreis wurden 60 g (40 % d.Th.) an rohen Kristallen erhalten. Diese wurden wiederhohlt aus Aceton umkristallisiert (das erste Mal durch Tiefkühlen, nachher durch Äther-Zugabe gefällt): Schmp. 122—124°.

$C_{14}H_{20}ClNO_4$ (301,77) *Ber.* : N 4,64 *Gef.* : N 4,89

α-, β- *und* γ-*Perhydroacridin* (**α-, β- *und* γ-V**) : 35 g (0,17 Mol) des Gemisches (**II a**) wurden in 435 ml Eisessig und 750 ml Wasser gelöst. Die Lsg. wurde am siedenden Wasserbad erwärmt, während 2,5 Std. mit einer Lsg. von 245 g (3,2 Mol) Natriumnitrit in 330 ml Wasser versetzt, und noch 1 Std. am Wasserbad gehalten. Anschließend wurden noch 435 ml Eisessig und 750 ml Wasser dazugegeben, und mit anderen 490 g (6,4 Mol) Natriumnitrit in 670 ml Wasser unter den obigen Bedingungen versetzt. Nach Erkalten wurden die Nitrosamine mit Äther ausgezogen und der Auszug mit 15 proz. wäßr. Natriumhydroxidlösung so oft gewaschen bis die Lauge farblos blieb. Nach Trocknen über Magnesiumsulfat und Entfernung des Äthers wurden 21 g (56 % d.Th.) an Nitrosaminen erhalten (bei einer Wiederhohlung des Versuches unter gleichen Bedingungen betrug die Ausb. 22,5 g : 60 % d.Th.).

Von dem Nitrosaminen-Gemisch wurden 43 g in 50 ml warmem Äthanol gelöst, mit 400 ml 36 proz. Salzsäure versetzt und 30 Min. unter Rückfluß erwärmt. Nach Entfernung des Alkohols wurde alkalisiert, wodurch sich eine bedeutende Menge dunkler Harze bildete. Das Perhydroacridinen-Gemisch wurde zur Reinigung mit Wasserdampf destilliert: 26,8 g (71 % d.Th., auf die Nitrosamine bezogen).

Die Perhydroacridine wurden in Methanol gelöst und bis zu schwach saurer Reaktion mit 36 proz. Salzsäure versetzt. Das uns gut bekannte, schwer lösliche α-Perhydroacridinhydrochlorid [5] (13 g) wurde von den übrigen durch stufenweises Einengen getrennt. Aus den übrigen Hydrochloriden wurden die Amine wieder freigesetzt, in Methanol gelöst und mit Pikrinsäure versetzt. Es entstanden 10,9 g eines kristallisierten Pikrats (Rohschmp. 198—199°); dieses ergab nach Umkristallisieren aus Methanol 8,4 g γ-Perhydroacridinpikrat mit Schmp. 208—209° (Lit.[8] : 211—213°). Dieses wurde mit Natriumhydroxidlsg. in Überschuß versetzt, und das freiwerdende Amin mit Wasserdampf destilliert. Es wurden 3,4 g γ-Perhydroacridin mit Schmp. 72—73° (Lit. [7] : 72,5—74°) erhalten. Nach völligem Eintrocknen der Mutterlauge vom rohen γ-Perhydroacridinpikrat hinterblieb ein harziges Pikrat, aus welchem 0,3 g an (mit γ-Isomer schwach verunreinigtem) β-Perhydroacridin gewonnen wurden: Schmp. 43–46° (Lit.[5,9]: 49,5–50° und bzw. 51–53°). Die Identität des Isomers wurde durch das NMR-Spektrum bestätigt.

N-Phenyl-perhydroacridin (**II b**, *Schmp. 132,5–133°*) *und N-Phenyl-*symm*-oktahydroacridiniumperchlorat* (**III b**): Mit 104 g (0,5 Mol) (**I**) und 46,5 g (0,5 Mol) Anilin, in 300 ml 80 proz. Ameisensäure, wurde bis einschließlich zur Fällung des Perchlorats (**III b**) wie für (**II a** und **III a**) beschrieben verfahren; nach Trennung des Perchlorats wurde die äther. Lsg. vollständig eingeengt. Der Rückstand ergab 12,5 g (9% d.Th.) (**II b**), Rohschmp. 125°. Nach Umkristallisieren aus Äther-Methanol Schmp. 132,5–133°. Pikrat-Schmp. 198–200° (Zers.) aus Methanol.

$C_{19}H_{27}N$ (269,4) *Ber.*: N 5,19 *Gef.*: N 5,41

Das Perchlorat (**IIIb**) entstand schon in rohem Zustand gut kristallisiert: 97 g (52% d.Th.), Rohschmp. 184–185°; nach Umkristallisieren aus Methanol Schmp. 194–195° (Lit.[10]: 199–200°).

N–(p-Nitrosophenyl)-perhydroacridin (*Schmp. 188°*): 1 g (3,7 mMol) (**II b**, Schmp. 132,5–133°) wurde unter wärmen in 10 ml konz. Salzsäure und 240 ml Wasser gelöst. Die Lsg. wurde auf unter 5° gekühlt, 10 g Eis dazugegeben und unter Rühren, tropfenweise, mit einer Lsg. von 3 g Natriumnitrit in 10 ml Wasser versetzt und eine Std. stehen gelassen. Nach Alkalisieren mit Natriumcarbonat (bis pH = 10) wurde ausgeäthert. Nach vollständigem Einengen der olivbraunen äther. Lsg. hinterblieben 0,8 g (72% d.Th.) an feinen olivgrünen Kristallen. Schmp. 188° (Äthanol).

$C_{19}H_{26}N_2O$ (298,4) *Ber.*: N 9,38 *Gef.*: N 9,38

N-Phenyl-N-methyl-perhydroacridiniumjodid (*Schmp. 205–208°*): 0,93 g (3,4 mMol) (**II b**, Schmp. 132,5–133°) und 5 ml Methyljodid, in 30 ml Aceton, wurden 314 Std. bei Raumtemperatur und 653 Std. im Wärmeschrank bei 90° im geschlossenen Rohr aufbewahrt. Das Salz wurde, zusammen mit einer ansehnlichen Menge harzigem Produkt, durch Ätherzugabe gefällt. Die Kristalle behielten selbst nach einer Rekristallisation aus Methanol (+Äther) eine rötlich-gelbe Farbe: 0,082 g (6% d.Th.) Schmp. 205–208°. Die ganze Menge wurde zur Aufnahme des NMR-Spektrums verbraucht.

N-Phenyl-α-perhydroacridin (**α-II b**): 10 g (27,4 mMol) (**III b**) wurden in 550 ml konz. Salzsäure gelöst und bei Raumtemperatur portionenweise, unter Rühren, mit 107 g (1,63 g-Atom) Zinkstaub versetzt und das Rühren noch 2 Std. bei Raumtemperatur und 4 Std. am Wasserbad fortgesetzt. Es wurde heiß filtriert und auf Raumtemperatur gekühlt, wodurch sich farblose Kristalle bildeten. Es wurde abermals filtriert und die Kristalle wurden in Wasser (ca. 2 l) gelöst, die Lsg. alkalisiert und das gebildete Öl mit Äther ausgezogen. Nach Entfernung des Äthers hinterblieben 3 g (dicker öliger) Rückstand. Aus diesem bildete sich während ca. 2 Wochen eine kleine Menge farbloser Nadeln. Diese wurden abgesaugt und mit Aceton gewaschen: 0,22 g (3% d.Th.), Rohschmp. 94–101°; nach einmaligem Umkristallisieren aus Aceton Schmp. 105–106°.

$C_{19}H_{27}N$ (269,4) *Ber.*: N 5,19 *Gef.*: N 5,66

Revue Roumaine de Chimie, **15**, 1611–1614 (1970)

NEW SYNTHETIC CHEMICAL COMPOUNDS WITH EXPECTED SCHISTOSOMICIDAL ACTIVITY

S. H. DOSS* and M. S. AHMAD

Bilharz Institute National Research Centre, Cairo, U.A.R.

Received March 28, 1970

On pharmacological basis of activity the following new amino naphthalene derivatives which may possess schistosomicidal activity were prepared :

6-Dimethylamino-4-acetoxy-2-methylnaphthoate IV,

6-Dimethylamino-4-hydroxy-2-naphthoic acid V,

Methyl-6-dimethylamino-4-methoxy-2-naphthoate VI,

6-Dimethylamino-4-methoxy-2-naphthoic acid VII,

4-Acetoxy-6-dimethylamino-naphthalene-2-carboxylic acid hydrazide VIII.

It was postulated[1] that an association of ring moities with a cationic center at physiological pH values might confer anthelmentic properties on molecules.

A variety of naphthalene compounds possessing an amino group[2] were synthesized, some of them possessed schistosomicidal effect especially against schistosoma mansoni infected mice, hamsters and monkeys.

Different hydroxy naphthoic acid derivatives were patented[3] as intermediates in the preparation of compounds possessing antiparasitic and chemotherapeutic properties in forming salts with amines as thickening agents.

On these bases the synthesis of some amino naphthalene derivatives has been carried out *via* the Stobbe Condensation[4, 5] of *p*-dimethylamino-benzaldehyde and dimethyl succinate giving rise to the halfester, 4-*p*-N-dimethylanilo-3-methoxycarbonyl-buten-3-oic acid (I). Cyclization of the crude halfester using fused sodium acetate in acetic anhydride gave a mixture of acid and neutral fractions, the acid fraction, probably unreacted half ester, was a viscous red brownish oil, which on hydrolysis with baryta solution gave the dibasic acid (II). The neutral fraction was found to be 6-dimethylamino-4-acetoxy-2-methyl-naphthoate (IV) which on alkaline hydrolysis afforded 6-dimethylamino-4-hydroxy-2-naphthoic acid (V), this was treated with dimethylsulphate and potassium carbonate in acetone to give methyl-6-dimethylamine-4-methoxy-2-naphthoate (VI). Alkaline hydrolysis of (VI) yielded 6-dimethylamino-4-methoxy-2-naphthoic acid (VII). Treatment of the acetoxy-ester (IV) with hydrazine hydrate gave 4-acetoxy-6-dimethylamino-naphthalene-2-carboxylic acid hydrazide (VIII) as golden yellow needles.

---

* Present adress: Organisch-Chemisches Institut der Universität Bonn, W/Germany.

[1] M. Harfenist, *J. Amer. Chem. Soc.*, **79**, 2211 (1957); *J. Med. Chem.*, **6**, 361 (1963).

[2] E. F. Elslager et al., *J. Med. Chem.*, **6**, 217, 444 (1963), **7**, 487, 658, 663 (1964).

[3] E. F. Elslager, U. S. Pat. 3, 248, 422; 3, 161, 641; 3, 264, 296.

[4] H. Stobbe and K. Niedenzu, *Liebigs Ann. Chem.*, **321**, 94 (1902).

[5] A. M. Elabbady and S. H. Doss, *Canad. J. Chem.*, **43**, 2408 (1965); *J. chem. U.A.R.*, **11**, No. 1, 35 (1968).

These new synthetic compounds especially compound (VIII) fulfill the requirements of a cationic center, which may have activity at the neuro-muscular junction in nematodes, and the ring structure, which is necessary to prevent destruction of the compound or to cover a large fixed area on some enzyme onto which the compounds are held by their positive charge.[1]

The pharmacological effects of these compounds are still under investigation. Finally the diacid (II) and its anhydride (III) were prepared.

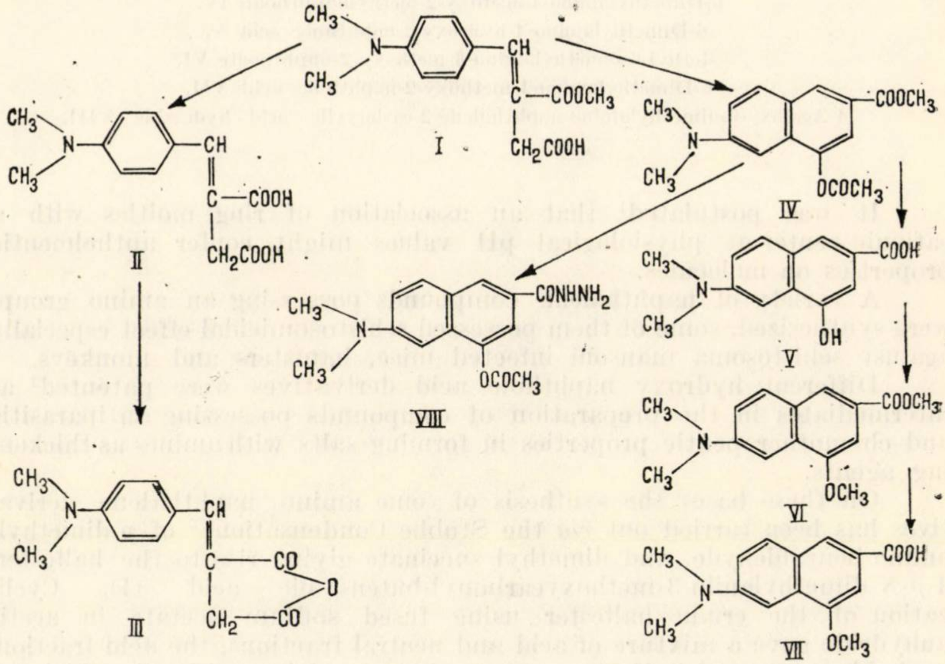

EXPERIMENTAL *)

α-p-N-Dimethylanilo-3-methoxycarbonyl-butin-3-oic-acid (I)

A mixture of *p*-dimethylaminobenzaldehyde (50 g 0.33 Mol), dimethylsuccinate (50 g 0.34 Mol) and tert. butanol (20 ml) was added under nitrogen to a boiling solution of

---

*) all melting points are uncorrected.

potassium tert. butoxide (from potassium 6.2 g 0.15 Mol, in dry *tert.* butanol 150 ml) during 50 min. The whole mixture was then refluxed under nitrogen for 60 min the cold brownish red mixture was acidified with ice cold dilute acetic acid. Removal of *tert.* butanol *in vacuo* left the brownish oil which was extracted with ether. The ethereal solution was extracted with cold saturated sodium hydrogen carbonate solution, the alkaline extract was acidified with acetic acid, the resulting oil was extracted with ether, dried over anhydrous sodium sulphate, after evaporation of ether a reddish brown oil was formed, which solidified into reddish brown crystals from pet. ether 60–80, m.p. 62°, yield (82 g, nearly 92%).
Anal. calcd. for. $C_{14}H_{17}NO_4$ (263.28) : C, 63.86 ; H, 6.51 ; N, 5.32% ;
Found : C, 63.72 ; H, 6.40 ; N, 5.50%.

Hydrolysis of the halfester I (3 g 0.013 Mol) with sodium hydroxide solution 10% (40 ml) for 4 hrs gave after extraction with ether and acidification with acetic acid the diacid (II, 2.7 g, nearly 90%) which was crystallized from methanol into yellow brown crystals, m.p. 216°.
Anal. calcd. for $C_{13}H_{15}NO_4$ (249.26) . C, 62.64 ; H, 6.07 ; N, 5.62% ;
Found : C, 62.70 ; H, 6.30 ; N, 5.80%.

On refluxing the diacid (II, 2 g, 0.008 Mol) with acetic anhydride (15 ml) and acetyl chloride (10 ml) for 3 hrs, evaporation of the mixture under reduced pressure gave rise to the anhydride (III, 1.7 g, nearly 88%) which was crystallized from xylene into yellow crystals of m.p. 240°.
Anal. calcd. for. $C_{13}H_{13}NO_3$ (231.24) : C, 67.52 ; H, 5.67 ; N, 6.06 ;
Found : C, 67.34 ; H, 5.90 ; N, 6.52.

6-Dimethylamino-4-acetoxy-2-methylnaphthoate (IV)

Crude halfester (I, 5.3 g, 0.02 Mol) and anhydrous sodium acetate (2 g, 0.02 Mol) in acetic anhydride (25 ml) were refluxed or 6 hrs. The acetic anhydride was then removed under reduced pressure and the residue extracted with ether. The ethereal extract was washed with sodium carbonate solution, then water and dried (Na_2SO_4). Evaporation of the solvent left the acetoxy ester (3.7 g, nearly 68%) which was crystallized from pet. ether 60–80 into yellow red crystals of m.p. 140°.
Anal. calcd. for. $C_{16}H_{17}NO_4$ (287.30) : C, 66.88 ; H, 5.96 ; N, 4.88 ;
Found : C, 66.89 ; H, 5.92 ; N, 4.87.

The carbonate solution was washed with ether acidified with acetic acid and then reextracted with ether. Evaporation of the organic solvent left an oily residue which was hydrolysed with 10% sodium hydroxide solution (10 ml), 3 hrs refluxing. A solid acid was formed (0.9 g) crystallized from methyl alcohol, m.p. 215° this was undepressed on admixture with a specimen of the dibasic acid (II), m.p. 216°.

6-Dimethyl-4-hydroxy-2-naphthoic acid (V)

The acetoxy naphthoate (3 g, 0.012 Mol) was refluxed with 10% sodium hydroxide solution (40 ml) for 6 hrs ; then the alkaline solution was extracted with ether and acidified with cold dilute acetic acid to yield V ; this was crystallized from ether as pale brown crystals (2.6 g, 89%) m.p. 250°.
Anal. calcd. for $C_{13}H_{13}NO_3$ (231.24) : C, 67.52 ; H, 5.67 ; N, 6.06 ;
Found : C, 67.52 ; H, 5.62 ; N, 6.34.

Methyl-6-dimethylamino-4-methoxy-2-naphthoate (VI)

The phenolic acid (6 g, 0.023 Mol), dimethylsulphate (18 g, 0.14 Mol) and anhydrous potassium carbonate (24 g) in acetone (150 ml) were refluxed for 18 hrs on water bath, after the evaporation of acetone, the resulting solid was dissolved in water, then extracted with ether, the ethereal layer was dried, after evaporation of ether, brownish oil (5 g, 90 %) was crystallized from pet. ether 60–80 into yellow crystals m.p. 74°

Anal. calcd. for $C_{15}H_{17}NO_3$ (259.29) : C, 69.48 ; H, 6.61 ; N, 5.40 ;

Found : C, 69.22 ; H, 6.44 ; N, 5.80.

6-Dimethylamino-4-methoxy-2-naphthoic acid (VII)

The methoxy ester (VI, 1 g, 0.006 Mol) was refluxed with sodium hydroxide solution 10 % for 6 hrs after cooling extraction with ether then acidification with acetic acid, then crystallization of the resulting solid from pet. ether 60–80, a yellowish brown crystals (0.8 g, nearly 76 %) m.p. 147° was formed.

Anal. calcd. for $C_{14}H_{15}NO_3$ (245.27) : C, 68.55 ; H, 6.16 ; N, 5.71 ;

Found : C, 68.52 ; H, 6.15 ; N, 5.20.

4-Acetoxy-6-dimethylamino-naphthalene-2-carboxylic acid hydrazide (VIII)

Acetoxy ester (IV, 2 g, 0.018 Mol) was refluxed with hydrazine hydrate (10 ml, 0.2 80 %) for 2 1/2 hrs, evaporation of hydrazine hydrate gave the solid hydrazide (1.7 g, 82%), which was crystallized from methyl alcohol as yellowish green crystals, m.p. 264°.

Anal. calcd. for. $C_{15}H_{17}N_3O_3$ (287.31) : C, 62.70 ; H, 5.96 ; N, 14.63 ;

Found : C, 63.00 ; H, 6.10 ; N, 14.89.

Acknowledgment: The authors thank Prof. Dr. B. Helferich for revising the manuscript and Prof. Dr. El Abbady for his interest in this work.

Revue Roumaine de Chimie, **15**, 1615 – 1622 (1970)

THE REACTION BETWEEN SODIUM ALCOXIDES AND α-HALOKETONES. VII*.

THE ACTION OF SODIUM METHOXIDE ON *p*-CHLORO-ω-BROMOACETOPHENONE

L. SZOTYORI, L. FEY and AL. KÖVENDI

Laboratory of Organic Chemistry of the "Babeş-Bolyai" University, Str. Arany János 11
and Chemical-Pharmaceutical Research Institute, Str. Fabricii 126, Cluj, Romania

Received September 29, 1969

The reaction between sodium methoxide and *p*-chloro-ω-bromoacetophenone dependent on the experimental conditions produces either isomers *cis* and *trans* of the 1-*p*-chlorobenzoyl-2-*p*-chlorophenyl-1,2-epoxy-3-bromopropane — (*p*-chloro-bromodiphenacyl)-(II and III), or a mixture of dimethylketal of *p*-chloro-benzoylcarbinol (VII) and *p*-chloro-ω-methoxy-acetophenone (VIII); the latter ones were separated chromatographically. The epoxy compound is transformed by the sodium methoxide into 2-methoxy-2,4-di-(*p*-chlorophenyl)-3,4-epoxy-tetrahydrofuran (VI).

It is known[1] that ω-bromoacetophenone under the action, of sodium alkoxide is transformed into *cis* and *trans* (or α and β, respectively) isomers of bromodiphenacyl, with m.p. 128–130° and 163–164° respectively.

A.

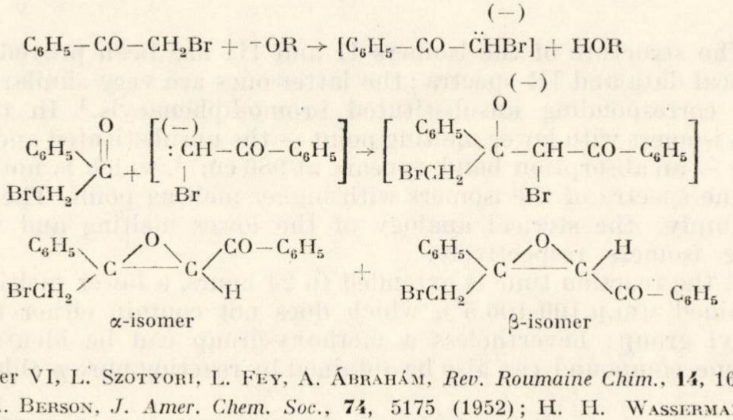

---

* Paper VI, L. Szotyori, L. Fey, A. Ábrahám, *Rev. Roumaine Chim.*, **14**, 1621 (1969).

[1] J. A. Berson, *J. Amer. Chem. Soc.*, **74**, 5175 (1952); H. H. Wasserman, N. E. Aubrey and H. E. Zimmerman, *J. Amer. Chem. Soc.*, **75**, 96 (1953).

In a previous paper[2] we have shown that by changing the experimental conditions from ω - bromoacetophenone and sodium methoxide we can obtain dimethylketal of benzoylcarbinol and in addition ω - methoxy-acetophenone, according to a completely different mechanism :

B.

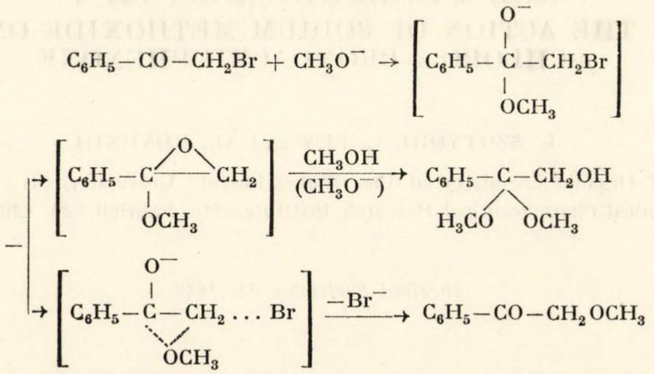
$C_6H_5-CO-CH_2Br + CH_3O^- \rightarrow$
O^-
$C_6H_5-C-CH_2Br$
OCH_3
O
C_6H_5-C
CH_2
OCH_3
CH_3OH
(CH_3O^-)
$C_6H_5-C-CH_2OH$
H_3CO
OCH_3
O^-
$C_6H_5-C-CH_2 \ldots Br$
OCH_3
$-Br^-$
$C_6H_5-CO-CH_2OCH_3$

In the present paper we report the results obtained in the case of *p*-chloro-ω-bromoacetophenone. The reaction was carried out at low temperature, using equimolecular reactant quantities. After a short while the reaction was interrupted and the two isomers of *p*-chloro-bromodiphenacyl — (II and III) — could be isolated (m.p.106.5.-107° and 130.5-131° respectively).

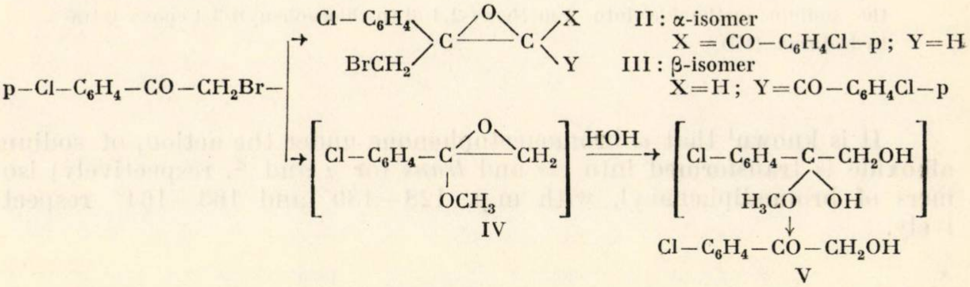
$p-Cl-C_6H_4-CO-CH_2Br-$
$Cl-C_6H_4$
O
C
C
X
$BrCH_2$
Y
II : α-isomer
$X = CO-C_6H_4Cl-p$; $Y=H$
III : β-isomer
$X=H$; $Y=CO-C_6H_4Cl-p$
$Cl-C_6H_4-C$
O
CH_2
OCH_3
IV
HOH
$Cl-C_6H_4-C-CH_2OH$
H_3CO
OH
$Cl-C_6H_4-CO-CH_2OH$
V

The structure of the isomers II and III has been proved by microanalytical data and IR spectra ; the latter ones are very similar to spectra of the corresponding unsubstituted bromodiphenacyls.[1] In the spectra of both isomers with lower melting point — the unsubstituted and substituted ones — an absorption band appears at 980 cm^{-1}, which is not present at all in the spectra of the isomers with higher melting point. These observations imply the sterical analogy of the lower melting and the higher melting isomers respectively.

If the reaction time is extended to 24 hours, a lower melting product is obtained -(m.p.100-100.5°), which does not contain either bromine or carbonyl group ; nevertheless a methoxy-group can be identified in it. The same compound can also be obtained by reacting pure *p*-chloro-bromo-

[2] L. Szotyori, L. Fey and A. Ábrahám, *Rev. Roumaine Chim.*, **14**, 1621 (1969).

diphenacyl with sodium methoxide. On the basis of these observations, as well as of the microanalytical data, we concluded that this compound is 2-methoxy-2,4-di-(*p*-chlorophenyl)-3, 4-epoxy-tetrahydrofuran (VI). On the ground of the preceeding arguments and by establishing the structure of the product VI, as well as by taking into consideration the formal analogy with the formation of the epoxyether I,[3] we assumed that the formation of VI from bromodiphenacyl takes place according to the following mechanism :

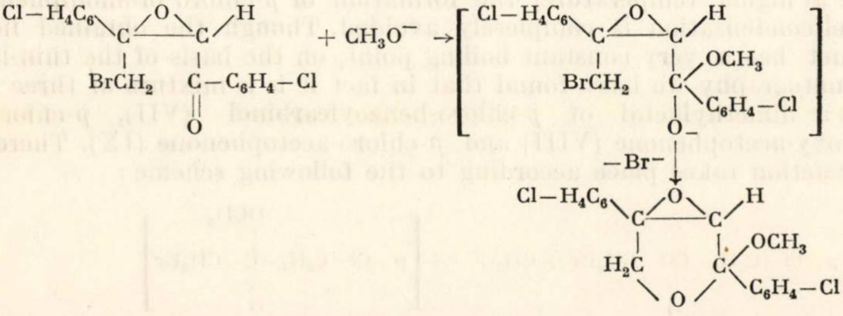

VI

As the tetrahydrofuran ring is practically tensionless, its formation might take easily place. The IR spectrum of the compound VI is in a perfect agreement with the proposed structure. From its spectrum the absorption band typical of carbonyl group and present in the spectrum of *p*-chloro-bromodiphenacyl at 1710 cm^{-1}, is wanting. On the other hand the maxima, characteristic of the epoxyde ring are maintained, and in addition an absorption band appears at 1139 cm^{-1}, which indicates the presence of a methoxy group. The new, very intense band at 1058 cm^{-1} is characteristic of the tetrahydrofuran ring.[4] The form and the position of this latter band correspond exactly to that of tetrahydrofuran, registered by us in similar conditions, namely in chloroform.

According to the above mechanism the intermediate *p*-chloro-bromodiphenacyl is transformed into VI by the excess methoxide. If this is true, then it would be recommendable to use 1/2 mole of sodium methoxide for 1 mole of bromoacetophenone in order to isolate the intermediate. Indeed, in these conditions, the compounds, II, III were obtained with higher yield. On the other hand in order to isolate VI without difficulty, it is even better to carry out the reaction in two steps, isolating the intermediates II, III, which afterwards are transformed quantitatively into the final product VI, using an excess of sodium methoxide.

By reacting at low temperature *p*-chloro-ω-bromoacetophenone either with 1 or with 1/2 mole of sodium methoxide, *p*-chloro-benzoylcarbinol (V) can also be isolated. The formation of this by-product can only be explained by the appearance of the intermediate epoxyether IV, a compound structurally analogous with I. Owing to the high reactivity of the intermediate IV, this is hydrolized during the isolating process. Consequently the reaction always takes place in part according to the mechanism B. Moreover, the reaction can be completely pushed in this direction by changing the reaction conditions. Thus, dropping slowly the highly diluted bromoketone solution in a solution of sodium methoxide at higher temperature, the formation of *p*-chloro-bromodiphenacyl by selfcondensation is completely avoided. Though the obtained liquid product has a very constant boiling point, on the basis of the thin-layer chromatography we have found that in fact it is a mixture of three products: dimethylketal of *p*-chloro-benzoylcarbinol (VII), *p*-chloro-ω-methoxy-acetophenone (VIII) and *p*-chloro-acetophenone (IX). Therefore the reaction takes place according to the following scheme:

---

[3] A. M. Ward, *J. Chem. Soc.*, **136**, 1541 (1929) ; T. I. Temnikowa and E. N. Kropachewa, *Journ. obshchei Khim.*, **19**, 1917 (1949) ; C. L. Stevens, W. Malik and R. Pratt, *J. Amer. Chem. Soc.*, **72**, 4758 (1950) ; M. Almási, L. Szotyori and M. Domokos, *Journ. prakt. Chem.*, **23**, 1 (1964).

[4] G. M. Barrow and S. Searles, *J. Amer. Chem. Soc.*, **75**, 1175 (1953).

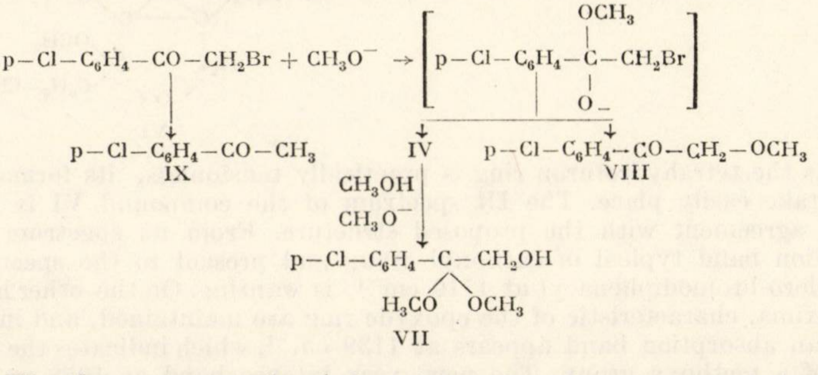

The three compounds of the mixture have been separated chromatographically on aluminium oxide.

The structure of the main product VII was proved microanalytically by the determination of chlorine, of methoxy group and of hydrogen mobile, and then spectroscopically in IR by comparing its spectrum with that of the unsubstituted compound[2] as well as by some reactions. Thus, with acid hydrosysis the compound VII is transformed into *p*-chloro-benzoylcarbinol (V), on the other hand by the action of hydrochloric acid in methanol 2,5-di-(*p*-chlorophenyl)-2,5-dimethoxy-dioxane (X) is formed, which can also be obtained from *p*-chloro-benzoylcarbinol in similar conditions:

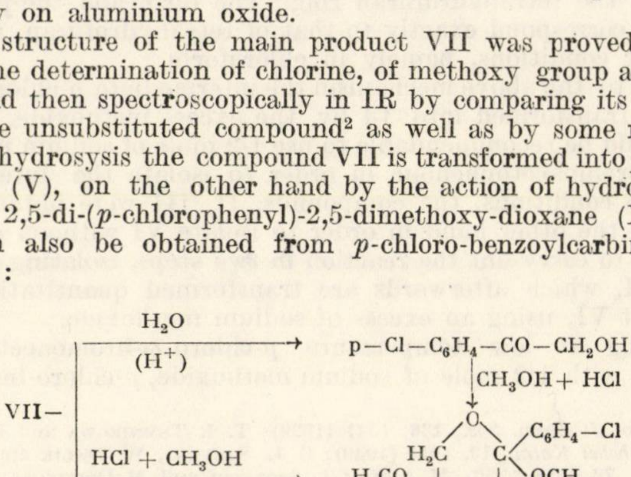

The compound VIII has been identified spectroscopically, by thin-layer chromatography and polarographically by comparison to the reference substance (VIII a) prepared separately according to the following scheme :

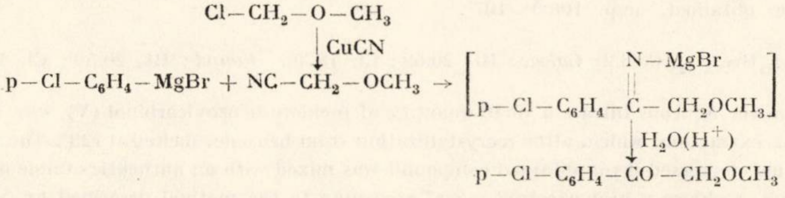

$$Cl-CH_2-O-CH_3$$

$$\downarrow \text{CuCN}$$

$$p-Cl-C_6H_4-MgBr + NC-CH_2-OCH_3 \rightarrow \left[p-Cl-C_6H_4-\overset{\overset{N-MgBr}{\|}}{C}-CH_2OCH_3 \right]$$

$$\downarrow H_2O(H^+)$$

$$p-Cl-C_6H_4-CO-CH_2OCH_3$$

VIIIa

The third product is *p*-chloro-acetophenone (IX), which is identified chromatographically, spectroscopically as well as polarographically by comparing it with a pure chloroketone. The partial reduction of *p*-chloro-ω-bromoacetophenone is explained by the well known[5] reducing action of the methoxide-methanol system ; we observed this reducing action also in the case of the reaction between α-bromopropiophenone and sodium methoxide.[6]

In order to determine the relative ratio of the three compounds in the mixture, this was subjected to spectral analyses in UV and to a polarographic analyses. Thus, comparing the intensities of the absorption bands at 251 nm in the spectrum of the mixture and the reference *p*-chloro-ω-methoxyacetophenone (VIIIa), respectively, it was found, that the mixture contains 14 per cent of aromatic ketones. The polarogram of the mixture shows two waves, the first, a well formed one, was identified as being the reduction of carbonyl group of the *p*-chloro-ω-methoxy-acetophenone, which corresponds to a 10 per cent ratio of this product in the mixture. Therefore the ratio of *p*-chloro-acetophenone is about 4 per cent.

On the other hand the compounds VIII and IX could be identified polarographically directly from the mixture by the method of feeding, because the waves, corresponding to the reduction of the oxo-groups from them are well separated. Adding to the test pure *p*-chloro-ω-methoxy -acetophenone only the height of the first wave increases, while introducing p-chloro-acetophenone only the second wave increases.

EXPERIMENTAL

*1-*p*-chlorobenzoyl-2-*p*-chlorophenyl-1,2-epoxy-3-bromopropane (α-and β-*p*-chloro-bromodiphenacyl) (II and III)*

a., 5.8 g (0.025 mole) of *p*-chloro-ω-bromoacetophenone were dissolved in 400 ml methanol, the solution was cooled to 0°, and then 0.025 mole of sodium methoxide in 25 ml methanol was introduced during 5 minutes under vigorous stirring. After 10 more minutes the reaction mixture was poured into water, the separated solid was filtered and recrystallized from methanol. The yield of the β-isomer was 1 g (21 %), m.p. 130.5–131°.

---

[5] Houben-Weyl, "Methoden der Organischen Chemie", Ed. 4, Vol. 6/2, Georg Thieme, Stuttgart, 1963, p. 68.

[6] L. Szotyori and L. Fey, *Rev. Roumaine Chim.*, **9**, 843 (1964) ; L. Szotyori, L. Fey, N. Almási and E. Hamburg, *Rev. Roumaine Chim.*, **12**, 1155 (1967).

The filtrate from the recrystallization was concentrated, the crystalline solid was collected and then twice recrystallized from methanol. Thus, 0.4 g (8.4 %) of α-*p*-chloro-bromodiphenacyl were obtained, m.p. 106.5–107°.

$C_{16}H_{11}BrCl_2O_2$ (386.2) *Calcd.* : Br, 20.69 ; Cl, 18.36. *Found* : Br, 20.50 ; Cl, 18.40 %.

From the aqueous filtrate a small quantity of *p*-chloro-benzoylcarbinol (V) was isolated by ethereal extraction, which, after recrystallization from benzene, melted at 123°. The melting point was not depressed if the obtained compound was mixed with an authentic sample of V, obtained from *p*-chloro-ω-bromoacetophenone according to the method described by Straus.[7]

b., The β-*p*-chloro-bromodiphenacyl was prepared with a yield of 44 per cent by introducing during 40 minutes, 0.0128 mole of sodium methoxide in 50 ml methanol into a solution of 0.025 mole of *p*-chloro-ω-bromoacetophenone in 250 ml of methanol. The mixture was then stirred at 0° for further 80 minutes, and the β-isomer was isolated according to the method *a.* The formation of the *p*-chloro-bromodiphenacyl was followed polarographically in the following conditions : Electrolyte : methanol 90 %, KBr 0.5 % ; depolarizing substance $1-3.10^{-3}$ mole/l ; $E_{1/2}$ (p-chloro-bromodiphenacyl) -0.98 ; -1.34 ; -1.46V ; $E_{1/2}$ (*p*-chloro-ω-bromoacetophenone) -0.15 ; -1.46 V, compared to the immobile mercury anode. The oxygen was removed by passing through the solution a current of inert gas. From the polarographical determinations resulted that under the above conditions, the compound III was formed with a yield of 48 per cent. The measurements were effected directly on the reaction mixture. After the concentration of the reaction mixture and the separation of the *p*-chloro-bromodiphenacyl, the filtrate was treated with gaseous hydrochloric acid dissolved in methanol, and we obtained in this way the same compound X, which was prepared from VII.

*2-methoxy-2,4-di-(*p*-chlorophenyl)-3,4-epoxy-tetrahydrofuran (VI)*

To 5.8 g (0.025 mole) of *p*-chloro-ω-bromoacetophenone dissolved in 250 ml methanol, a solution of 0.025 mole of sodium methoxide in 50 ml methanol was added at 0° under stirring, dropwise, during 30 minutes. After 24 hours the mixture was concentrated under reduced pressure, the residue was poured into water and the oily product extracted with ether. The ethereal solution was dried over sodium sulphate, then after the removing of ether, an oily product was obtained which did not crystallize, even if kept at low temperature (below 0°) for a long time. By addition a small quantity of methanol the compound VI however separated within one hour as a crystalline solid, which, after recrystallization from methanol, melted at 100–100.5°. The yield : 0.8 g (19.1 %).

$C_{17}H_{14}Cl_2O_3$ (337.2) *Calcd.* : Cl, 21.03 ; OCH_3, 9.20. *Found* : Cl, 21.48 ; OCH_3, 9.47 %.

On the other hand, compound VI was obtained almost quantitatively by treating the methanolic solution of β-*p*-chloro-bromodiphenacyl with three moles of sodium methoxide. Next day the solvent was removed under reduced pressure and the residue was recrystallized from methanol. In this manner the yield calculated for the *p*-chloro-ω-bromoacetophenone rose to 44 per cent.

---

[7] F. Straus, *Liebigs Ann. Chem.*, **393**, 330 (1912).

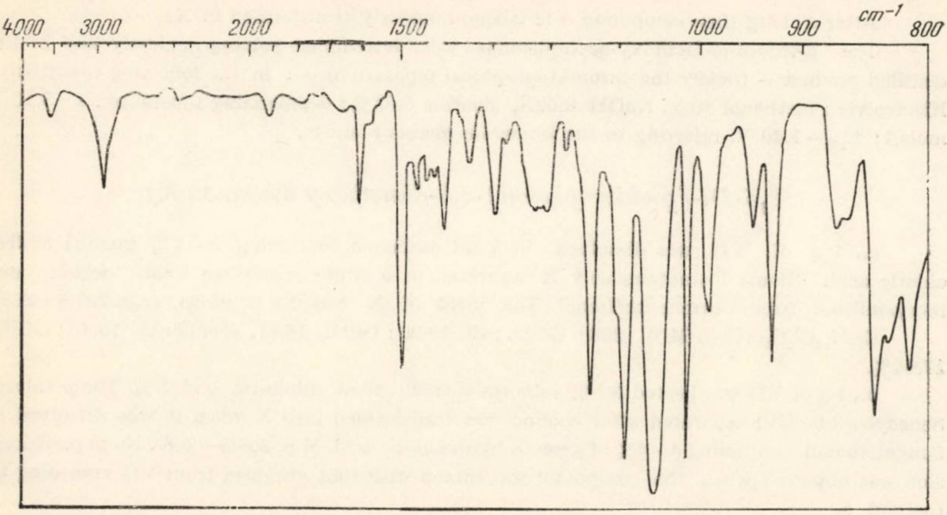

Fig. 1. — IR spectrum of the compound VI.

Dimethylketal of p-*chloro-benzoylcarbinol (VII)*

To a solution of 11.6 g (0.05 mole) of *p*-chloro-ω-bromoacetophenone in 500 ml methanol there were added dropwise 0.05 moles of sodium methoxide dissolved in 70 ml methanol during 90 minutes, at 30–35°. During addition the mixture was vigorously stirred. The solution was then concentrated under reduced pressure, keeping the temperature of the water-bath below 30°. The oily residue was poured into water, extracted with ether and then the ethereal solution was diluted with benzene, and dried over sodium sulphate. The solvents were removed in vacuum at room temperature and the residue was distilled under reduced pressure. The obtained 6.5 g of colourless, pleasantly odorous oil distilled very uniformly, b.p.$_2$ 114.5°, (n_D^{20} 1.5334), nevertheless, it could be separated chromatographically, — (on aluminium oxide Brockman II/III grade, with chloroform, using a 60×4 cm column)- obtaining three pure compounds, 0.2 g of *p*-chloroacetophenone, 0.6 g of *p*-chloro-ω-methoxy-acetophenone and 5 g (46.3%) of compound VII.n_D^{20} 1.5060*).

$C_{10}H_{13}ClO_3$(216.7) *Calcd.* : Cl, 16.36 ; OCH_3, 28.64. *Found* : Cl, 16.00 ; OCH_3, 28.40% ; Hydrogen mobile, 1.02.

*) In the same way the product obtained from ω-bromoacetophenone and sodium methoxide, described in a previous paper, [2] was also separated. Two pure compounds could be identified from the mixture :

1., The dimethylketal of benzoylcarbinol, n_D^{20} 1.5125

$C_{10}H_{14}O_3$ (182.2) *Calcd.* : OCH_3, 34.06. *Found* : OCH_3, 34.36% ; Hydrogen mobile 1.04 ; IR spectrum : maxima at 1036, 1080, 1140 and 1176 cm^{-1} (characteristic of the acetal group), 3425 cm^{-1} (characteristic of the hydroxy group), but no maximum was found at 1695 cm^{-1} -(characteristic of the carbonyl group)-which is present in the spectrum of the mixture ;

2., The ω-methoxy-acetophenone, n_D^{20} 1.5350 ; Lit. [8] n_D^{20} 1.5338. Its IR spectrum is identical with that of the pure methoxyketone prepared according to the method described by Pratt and Robinson. [9]

[8] C. Dufraisse and R. Chaux, *Bull. Soc. chim. France*, **39**, 443 (1926) ; *Chem. Zentr.*, **1926**, I 3222.

[9] D. D. Pratt and R. Robinson, *J. Chem. Soc.*, **123**, 745 (1923).

Revue Roumaine de Chimie, **15**, 1615–1622(1970)

After a long time compound VII is spontaneously transformed in X.

The *p*-chloro-ω-methoxy-acetophenone was determined polarographically also in the distilled product — (before the chromatographical separation) —, in the following conditions: Electrolyte : methanol 80 %, NaOH 0.02N, gelatine 0.02 %; depolarizing substance : $1-3.10^{-4}$ mole/l; $E_{1/2}$ -1.40 V, referring to the immobile mercury anode.

*2,5-Di-(*p*-chlorophenyl)-2,5-dimethoxy-dioxane (X)*

a., 1 g of VII was dissolved in 5 ml methanol containing 3–4 % gaseous hydrochloric acid. Almost instantaneously X separated as a white crystalline solid, which was recrystallized from benzene-methanol. The yield of X was 0.8 g (95 %), m.p. 207.5–208°.

$C_{18}H_{18}Cl_2O_4$(369.3) M.W. 358; *Calcd.* : Cl, 19.20; OCH_3, 16.81. *Found* : Cl, 19.45; OCH_3, 17.04 %.

b., 1 g of VII was heated for 30 minutes with 20 ml of sulphuric acid 5 %. The *p*-chlorobenzoylcarbinol(V) separated after cooling was transformed into X when it was dissolved in 5 ml methanol containing 3–4 % of gaseous hydrochloric acid. M.p. 207.5–208°. No m.p. depression was observed when this compound was mixed with that obtained from VII according to method *a.*

p-*Chloro-ω-methoxy-acetophenone (VIII)*

This ketone was obtained by using the procedure given for the preparation of the p-chloro-α-methoxy-propiophenone.[10] Thus, from 3.9 g (0.055 mole) of methoxyacetonytrile[11] and *p*-chloro-phenyl-magnesiumbromide corresponding to 9.5 g (0.05 mole) of *p*-chloro-bromobenzene,[12] was obtained 4.6 g (50 %) of methoxyketone VIII, b.p.$_3$ 106°. The distilled oily product was solidifying almost instantaneously. M.p., 67.5–68°, after recrystallization from n-heptane.

$C_9H_9ClO_2$ (184.6) *Calcd.* : Cl, 19.20; OCH_3, 16.81. *Found* : Cl, 19.71; OCH_3, 17.07 %.

[10] L. Szotyori and E. Hamburg, *J. prakt. Chem.*, **22**, 202 (1963).

[11] D. Gauthier, *Compt. rend.*, **143**, 831 (1906); *Chem. Zentr.*, **1907**, I 400.

[12] A. Mouneyrat and Ch. Pouret, *Compt. rend.*, **129**, 605 (1899).

Revue Roumaine de Chimie, **15**, 1623–1631 (1970)

CONTRIBUTION À LA CHIMIE DES PHÉNYL-2-BENZYLIDÈNE-4-AZLACTONES-5

SYNTHÈSES DE NOUVELLES HYDRAZIDES SUBSTITUÉES DOUÉES D'ACTION PSYCHOÉNERGISANTE ET PARASYMPATHICOLYTIQUE

CĂTĂLINA DEMETRESCO*, VIORICA MANU** et M. VANGHELOVICI***

Reçu le 15 août 1969

Par la décyclisation de l'anneau azlactonique sous l'action de l'hydrazine (hydrazinolyse), les auteurs ont synthétisé 10 nouveaux composés — hydrazides de l'acide α-benzoylamino-cinnamique — doués d'effet spasmolytique *in vitro* et d'une intense action antidépressive, probablement par inhibition de la monoaminoxidase (MAO) *in vivo*. La constitution chimique de ces hydrazides a été établie par analyse élémentaire (N et S) et par étude spectroscopique en IR.

Ces derniers temps, la chimie des benzylidène-azlactones a pris un grand développement, surtout grâce à l'importance pratique de différents types de composés, qu'on obtient convenablement. Nous pouvons indiquer, par exemple, la synthèse des aminoacides aryliques ou hétérocycliques — constituants des protéines cellulaires et la synthèse des polypeptides ou bien de certains dérivés de l'acide cinnamique, qui possèdent la capacité de régler la fonction cellulaire hépatique, ainsi que des différentes hormones thyroïdiennes.[1,2]

Toutes ces multiples possibilités de synthèse sont dues à la réactivité chimique tout à fait particulière des benzylidène-azlactones, composés ayant une structure lactonique, qui peuvent subir très facilement une réaction de cyclolyse commode, dans différentes conditions expérimentales.

Les données de la littérature[3-5] mettent en évidence l'importance thérapeutique remarquable de la fonction hydrazine ($-NH-NH_2$) capable d'entraîner une action antidépressive, tranquillisante-sédative, antibactérienne ou spasmolytique. Dans des recherches antérieures[6,7] nous avons

---

* Laboratoire de Chimie Organique de la Faculté de Pharmacie de l'Institut Médico-Pharmaceutique de Bucarest, 19–20, Str. Alex. Sahia.

** Laboratoire de Chimie Générale de la Faculté de Chimie Industrielle de l'Institut Polytechnique de Bucarest, 1, str. Polizu.

*** Laboratoire de Chimie Biologique de la Faculté de Médecine de Timişoara, 2, Piaţa 23 August.

[1] E. L. Benett et C. Niemann, *J. Amer. Chem. Soc.*, **72**, 1806 (1950).

[2] W. F. Dunn, *J. Biol. Chem.*, **234**, 802 (1959).

[3] R. Granger, J. Giroux, J. Lanet et M. Corbier, *Bull. Soc. Chim. France*, **1160**, 1958.

[4] A. E. Drukker, P. A. Shore, S. Spector et B. B. Brodie, *J. Amer. Chem. Soc.*, **15**, 19 (1958).

[5] E. Grünberg et R. Schintzer, *Quart. Bull. of Sea vicio Hosp.*, **13**, 3 (1952).

[6] M. Vanghelovici et C. Demetresco, *Studii şi Cercetări Chim. Acad. Bucureşti*, **8**, 157 (1960).

[7] C. Demetresco, A. Popa et M. Vanghelovici, *Studii şi Cercetări Chim. Acad. Bucureşti*, **10**, 189 (1963).

montré que la présence du groupe hydrazine dans les molécules ayant une structure vinylogue (riche en électrons π polyconjugués) a pour effet une réduction prononcée de la toxicité de ce groupe.

En partant de ces idées, nous nous sommes proposé dans le présent travail d'effectuer la synthèse de nouvelles classes d'hydrazides de l'acide cinnamique α-benzoylaminé, par décyclisation de l'anneau azlactonique.

Dans leurs recherches sur les benzylidène-azlactones, Blaise[8] et Schröter[9] ont montré que sous l'action de l'hydrate d'hydrazine, l'anneau azlactonique reste toujours intact et qu'il se produit tout au plus une simple addition de l'hydrazine au groupe carbonyle de l'oxazolone.

En 1941, Vanghelovici et A. Ştefănesco[10] en reprenant ces recherches aboutissent à la conclusion que l'hydrate d'hydrazine agit différemment sur l'anneau azlactonique, en fonction des conditions expérimentales de réaction, plus ou moins énergiques. Vanghelovici et Moise[11] obtiennent par une simple agitation des benzylidène-oxazolones, à froid, avec de l'hydrate d'hydrazine à 100% ou 50%, en milieu d'éthanol absolu, des composés d'addition au groupe carbonyle de l'oxazolone, dénommés isomères B

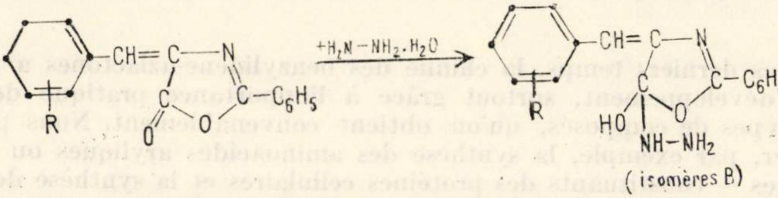

C'est une réaction analogue à celle indiquée par Blaise pour les azlactones aliphatiques.

En conditions de réaction énergiques toutefois, c'est-à-dire par ébullition pendant 30 minutes, dans un milieu d'éthanol absolu, on obtient des isomères acycliques, dénommés isomères A. Ces composés avec des points de fusion beaucoup plus élevés correspondent à la même formule structurelle, à laquelle on peut aboutir à partir des isomères B, par une transposition intramoléculaire, réalisée par la migration d'un proton, accompagnée par l'ouverture du cycle azlactonique :

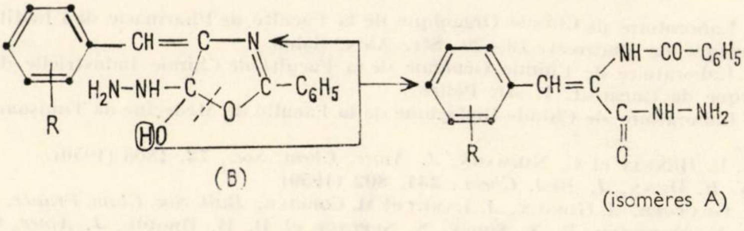

---

[8] R. Blaise, *Bull. Soc. Chim. France*, **33**, 1093 (1905) ; **4**, 7 (1910).

[9] E. Schröter, *Chem. Ber.*, **53**, 230 (1920).

[10] M. Vanghelovici et A. Ştefănesco, *Bul. Soc. Chim. Rom.*, **3**, 159 (1941–1942) ; *Chem. Abstr.*, **38**, 550 (1944).

[11] M. Vanghelovici et I. Moise, *Bul. Soc. Chim. Rom.*, **3**, 85 (1941–42) ; *Chem. Zentr.*, **II**, 1275 (1943).

Pour établir une corrélation entre l'influence des substituants R, doués d'intenses effets électromères ou inductifs, qui peuvent être greffés facilement sur le noyau benzénique des benzylidène-oxazolones et la capacité de décyclisation de l'anneau azlactonique, nous avons étendu dans ce travail l'étude de l'action de l'hydrazine sur l'anneau des phényl-2-benzylidène-4-oxazolones-5, convenablement substitués par des groupes polaires dans les positions-clef de leur noyau benzénique.

De cette manière, les substituants que nous avons choisis peuvent influencer considérablement, par leur nature, la distribution des densités électroniques dans la molécule des hydrazides, résultées par décyclisation. Par l'intermédiaire du système vinylogue de la molécule, l'influence électrique des substituants peut se transmettre jusqu'au niveau de la fonction hydrazide, modifiant la nucléophicité de l'atome d'azote terminal de la fonction hydrazide ($-CO-NH-NH_2$).

Nous avons démontré ce fait par des études récentes, effectuées sur la capacité complexante de telles hydrazides, qui peuvent fonctionner comme des ligands organiques bidentés. [12]

Au cours des recherches systématiques antérieures [13,14] nous avons réussi à mettre en évidence certains effets pharmacodynamiques importants, à savoir une action antibacillaire, antihelmintique, antidépressive, etc., effets qui apparaissent dans le cas de quelques nouvelles hydrazides substituées de l'acide α-benzoylamino-cinnamique, dans lesquelles nous avons introduit, par l'intermédiaire de la décyclisation de l'anneau azlactonique, la fonction déterminante

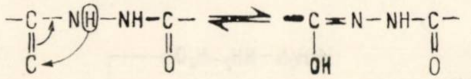

Cette fonction peut subir tant *in vitro*, que *in vivo*, une tautomérie céto-énolique, tautomérie qui, évidemment, peut apparaître aussi dans le cas des hydrazides libres, mentionnées ci-dessous

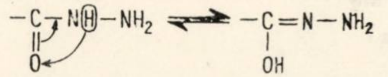

Ceci rend possible la formation de combinaisons complexes avec certains ions métalliques d'importance biologique. La chélation a lieu par cyclisation, avec l'apparition des cycles penta-atomiques stables.

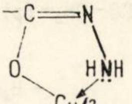

---

[12] N. Teodoresco, C. Demetresco et M. Vanghelovici, *Rev. Roumaine Chim.*, **8**, 1049 (1967).

[13] C. Marcu, M. Manuchian, C. Demetresco et D. Dobresco, *Thérapie*, **21**, 1483 (1966).

[14] C. Demetresco, « Thèse », Bucarest, mai 1962, Université de Bucarest.

Or, la capacité donatrice d'électrons non participants (*p*) du groupe $-NH_2$ terminal de la fonction hydrazide est évidemment en étroite relation avec la nucléophicité de l'atome d'azote, exprimée par la force avec laquelle ce dernier attire son doublet électronique, non participant, qui intervient dans la liaison coordinative avec les cations métalliques. La nucléophicité du groupe $-NH_2$ peut être évidemment sensiblement et systématiquement influencée, par l'intermédiaire des substituants polaires, introduits sur le noyau benzénique de l'acide α-benzoyl-amino-cinnamique, par la substitution convenable des benzylidène-oxazolones, à partir desquels on exécute la synthèse par décyclisation.

Vu que les bioéléments (Cu^{2+}, Co^{2+}, Cr^{3+}, Fe^{3+}, Zn^{2+}, etc.) jouent souvent un rôle extrêmement important, dans la vie d'un grand nombre de bactéries, leurs systèmes enzymatiques étant inactifs en leur absence, nous avons abouti à la conclusion que la possibilité de complexer spécifiquement confère aux substances à structure hydrazidique un rôle thérapeutique essentiel. Le groupement hydrazide accomplit ainsi le rôle de centre biologique actif des molécules organiques à structure vinylogue, permettant des interrelations sélectives au niveau des pharmorécepteurs biologiques cellulaires, en fonction de la nature des substituants greffés à ce groupement.

Conformément aux schémas de réaction, indiqués ci-dessous, nous avons obtenu par synthèse 10 nouvelles hydrazides substituées de l'acide α-benzoylamino-cinnamique, qui correspondent aux formules I_A et I_B.

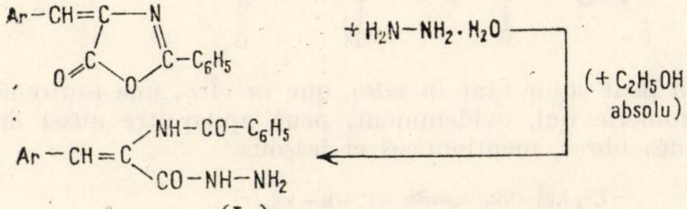

(I_A)

où

$Ar = C_6H_4-Cl\ (o);\ -C_6H_4-O-CO-CH_3-(o);\ -C_6H_4-O-CO-CH_3-(m)$;

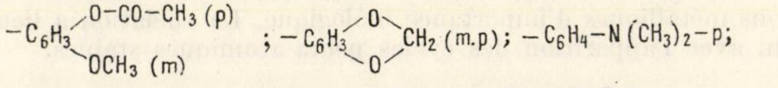

$-C_6H_3\begin{matrix}O-CO-CH_3\ (p)\\ OCH_3\ (m)\end{matrix}$; $-C_6H_3\begin{matrix}O\\ O\end{matrix}CH_2\ (m.p)$; $-C_6H_4-N(CH_3)_2-p$;

$-C_6H_4-N(C_2H_5)_2-p$; $C_6H_4-NH-CO-CH_3-(p)$;$-CH=CH-C_6H_5$

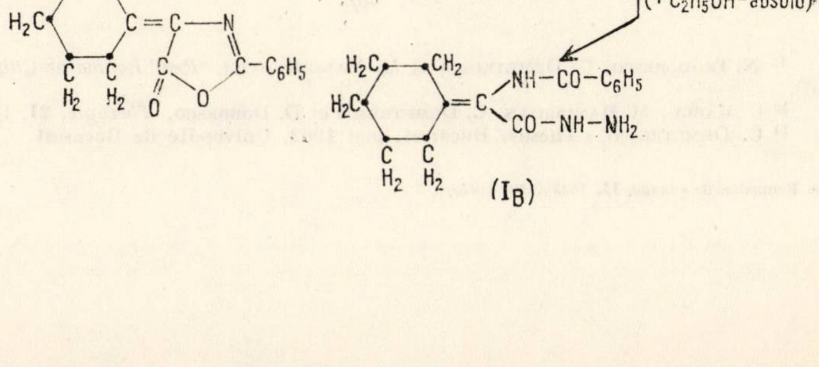

(I_B)

Les nouveaux composés synthétisés se présentent sous forme de microcristaux aciculaires, incolores ou colorés, aux points de fusion bien précisés, très stables à la longue.

Pour la réaction de décyclisation des benzylidène-hydrazides, sous l'action de l'hydrazine, nous suggérons un mécanisme nucléophyle, par l'attaque nucléophyle de l'hydrazine à l'atome de carbone carbonylique de l'azlactone, suivie d'une transposition intramoléculaire du proton, selon le schéma

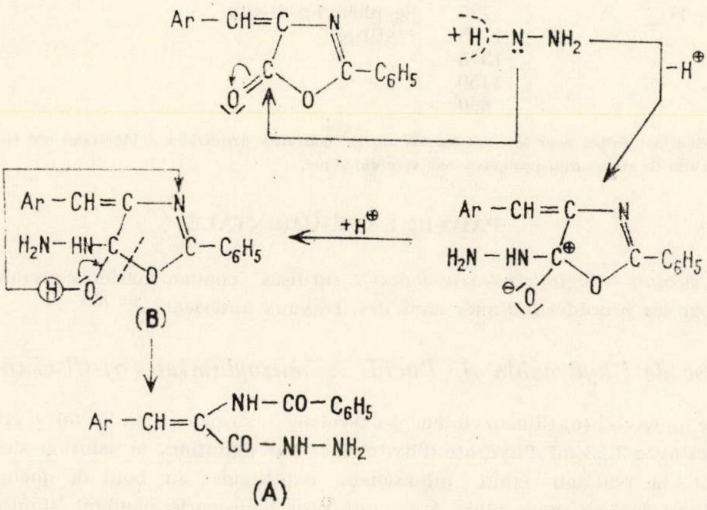

La structure chimique des nouveaux composés synthétisés a été déterminée par analyse élémentaire et par des études spectroscopiques en IR.

ANALYSE SPECTRALE EN IR DE LA STRUCTURE MOLÉCULAIRE *

On a effectué l'étude spectroscopique des nouveaux composés synthétisés, dans le domaine spectral compris entre 400 et 4000 cm^{-1}, par la technique du pastillage en KBr, en utilisant pour les déterminations un spectrophotomètre automatique du type UR_{10}, à double faisceau.

Nous présentons en guise d'exemple, dans la figure 1 et le tableau 1, les attributions que nous avons pu faire pour les bandes correspondant aux principaux groupements actifs en IR, dans le cas de l'hydrazide au n° 8.

---

* Les spectres d'absorption en IR ont été effectués en collaboration avec le physicien Florin Coman que nous remercions vivement.

Tableau 1

Les bandes correspondant aux groupements actifs en IR

($\tilde{\nu}$ cm^{-1})

Attributions	Composé au n° 8	Attributions	Composé au n° 8
C=O Am. I	1660	l'anneau benzénique ν_4 : /C−H/$\perp$ pl.	695
δ/O=C−N/ Am. IV	757	ν_{14} : /C−H/$\parallel$ pl.	1030
	835	ν_{12} : /C−H/ def.	3090
δ/N−H/ def.	3340		
	3210		
amide Vδ/N−H/$\perp$	725	le phényl *p*-di-substitué	820
/N−N/ v.	1105		
δ/CH_3/ sym.	1375		
δ/CH_3/ asym.	1450		
δ/=CH/	860		

Les attributions faites pour les bandes des autres nouvelles hydrazides synthétisées ont tout à fait correspondu aux formules de structures, proposées par voie chimique.

PARTIE EXPÉRIMENTALE

Les phényl-2-benzylidène-4-oxazolones-5, utilisés comme matières premières, ont été synthétisés par les procédés indiqués dans des travaux antérieurs. [12, 15]

Synthèse de l'hydrazide de l'acide α-benzoylamino-(o)-Cl-cinnamique

5 g de phényl-2-(o)-Cl-benzylidène-4-oxazolone-5, suspendus en 50 ml d'éthanol absolu, ont été traités avec 3,53 ml d'hydrate d'hydrazine. Par agitation, la solution s'est réchauffée spontanément, la réaction étant intensément exotherme ; au bout de quelques minutes, le mélange s'est coloré en rouge-rubis. Après reflux au bain-marie, pendant 50 minutes et après la concentration de la solution, des cristaux incolores se sont déposés, par refroidissement, au P_f = 150° (éthanol). Rend. = 61 %

$C_{16}H_{14}O_2N_3Cl$	*Calculé* : N 13,30 %
(M = 315,74)	*Trouvé* : N 13,35 %

Synthèse de l'hydrazide de l'acide α-benzoylamino-p-diméthylamino-cinnamique

2,92 g de phényl-2-*p*-diméthylamino-benzylidène-4-oxazolone-5, suspendus en 24 ml d'éthanol absolu, ont été traités avec 1,60 ml d'hydrate d'hydrazine à 100 %. La solution s'est colorée en rouge violacé et s'est réchauffée spontanément. On l'a refluxée au bain-marie, pendant 20 minutes. Le précipité gélatineux obtenu et maintenu pendant deux jours sur glace, a déposé des cristaux, sous forme de feuillets jaune canari, à reflets soyeux ; P_f = 136° (éthanol). Rend. = 79 %

$C_{18}H_{20}O_2N_4$	*Calculé* : N 17,27 %
(M = 324,37)	*Trouvé* : N 17,35 %

Les autres composés, synthétisés par des procédés similaires sont indiqués dans le tableau synoptique 2, ci-joint.

---

[15] C. Demetrescu, C. Chiriţă et V. Ion, *Rev. Roumaine Chim.*, **12**, 1039 (1967).

Tableau Synoptique 2

des nouveaux composés synthétisés

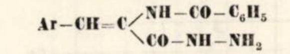

$$Ar-CH=C\begin{cases}NH-CO-C_6H_5\\CO-NH-NH_2\end{cases}$$

N°	Ar	Formule et poids moléculaire	Point de fusion et solvant de cristallisation	Rend. %	N %	
					Calculé	Trouvé
1	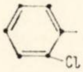	$C_{16}H_{14}O_2N_3Cl$ (315,74)	150° (éthanol)	61	13,30	13,35
2	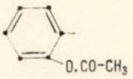	$C_{18}H_{17}O_4N_3$ (339,34)	197° (éthanol)	68	12,38	12,53
3	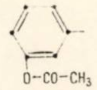	$C_{18}H_{17}O_4N_3$ (339,34)	217° (éthanol)	60	12,38	12,44
4	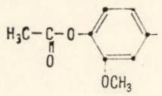	$C_{19}H_{19}O_5N_5$ (369,36)	206° (éthanol)	78	11,37	11,45
5	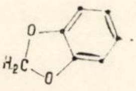	$C_{17}H_{15}O_4N_3$ (325,31)	198° (éthanol)	82	12,91	13,06
6	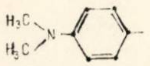	$C_{18}H_{20}O_2N_4$ (324,37)	156° (éthanol)	79	17,27	17,35
7	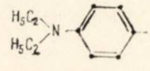	$C_{20}H_{24}O_2N_4$ (352,42)	184° (éthanol)	88	15,90	15,91
8	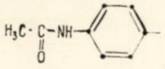	$C_{18}H_{18}O_3N_4$ (338,35)	212° (éthanol)	49	16,56	16,68
9	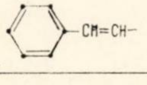	$C_{18}H_{17}O_2N_3$ (307,34)	203° (éthanol)	69	13,67	13,71
10	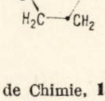	$C_{15}H_{19}O_2N_3$ (273,32)	224° (éthanol)	42	15,37	15,38

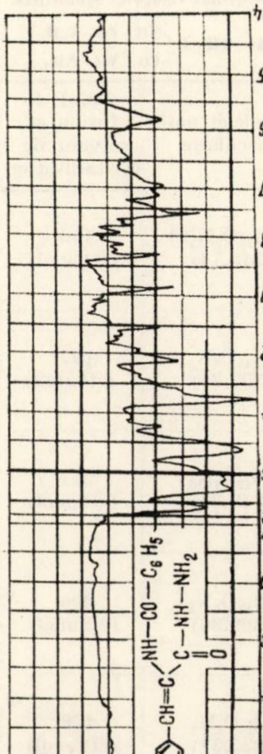
N4
N5
N6
N7
N8
N10
N12
N14
N16
N18
L10
L20
L22
L24
L26
L28
L30
L32
L34
L36
L38
L40
K4
L30 K5
L32 K5
N34
$H_3C-C(=O)-HN-C_6H_4-CH=C(NH-CO-C_6H_5)-C(=O)-NH-NH_2$

Fig. 1

DONNÉES PRÉLIMINAIRES SUR LA TOXICITÉ DES COMPOSÉS ET SUR LEUR ACTIVITÉ PHARMACODYNAMIQUE *

On a étudié l'action spasmolytique *in vitro* des nouvelles hydrazides sur le duodénum de chien *in situ* et on a constaté un effet relaxant, à des doses de 10—15 mg/kilocorps. Ainsi, par exemple, le composé au n° 8 (l'hydrazide de l'acide α-benzoylamino-*p*-nitro-cinnamique) exerce un intense effet relaxant, sans influencer la tension artérielle.

Administrées i.v. sous forme de feuilles en propylenglycol, ces hydrazides exercent aussi une action stimulatrice sur le système nerveux central, probablement par un mécanisme d'inhibition de la monoaminoxidase (MAO).

Nous nous attendions à cet effet car les nouvelles hydrazides synthétisées correspondent du point de vue structurel à la classe des hydrazines alcoylées, intéressant la thérapie des médicaments psychoénergisants, qui sont utilisés à présent sur une grande échelle dans le traitement des psychoses dépressives.

On a également étudié la toxicité des nouveaux composés sur des lots de souriceaux blancs. Des doses jusqu'à 500 mg/kgc n'ont pas provoqué d'effets toxiques, au bout de 48 heures aucun cas léthal n'étant enregistré.

Des recherches pharmacodynamiques approfondies sont en cours.

CONCLUSION

On a synthétisé dans ce travail 10 nouvelles hydrazides de l'acide α-benzoylamino-cinnamique, par décyclisation de l'anneau azlactonique sous l'action de l'hydrazine (hydrazinolyse).

La structure de ces nouveaux composés a été confirmée par analyse chimique élémentaire (N et S) et par une étude spectroscopique en IR.

Pour la décyclisation des azlactones sous l'action de l'hydrazine, nous avons suggéré un mécanisme nucléophile d'addition au groupe carbonyle, suivie de la migration intramoléculaire d'un proton. Confirmé expérimentalement, ce mécanisme peut expliquer l'obtention des isomères acycliques de type A, mis en évidence aussi dans d'autres recherches, effectuées par nous antérieurement.

La toxicité pratiquement négligeable des nouvelles hydrazides et les données pharmacologiques, obtenues jusqu'à présent, laissent entrevoir l'intérêt qu'elles présentent pour la chimiothérapie des psychoses dépressives.

---

* L'action spasmolytique et antidépressive a été expérimentée par le Dr Valentin Stroescu et A. Granici (Chaire de Pharmacologie de la Faculté de Médecine de Bucarest), que nous remercions vivement.

Revue Roumaine de Chimie, **15**, 1623—1631 (1970)

ORSZ. MŰSZAKI KÖNYVTÁR ÉS DOKUMENTÁCIÓS KÖZPONT 1883

1963

NOTE POUR LES AUTEURS

La *Revue Roumaine de Chimie* publie des articles en anglais, français, russe, allemand ou espagnol. Les auteurs sont priés d'envoyer des articles, notes, communications et comptes rendus inédits.

Les manuscrits seront dactylographiés à deux intervalles. Les tableaux seront dactylographiés sur feuilles séparées, de même que la légende des figures. Les diagrammes seront tracés à l'encre de Chine sur papier calque. Les tableaux et les figures seront numérotés par des chiffres arabes, en nombre strictement nécessaire. Prière de ne pas inscrire les mêmes données dans les tableaux et les figures. Les formules chimiques seront incluses dans le texte ; en outre, elles seront transcrites sur des feuilles séparées. Les auteurs sont priés d'indiquer les caractères italiques (en soulignant les lettres au crayon), ainsi que tout autre caractère spécial. L'ordre des références bibliographiques sera celui de leur mention dans le texte ; le nom de l'auteur sera précédé de l'initiale du prénom ; les publications périodiques seront présentées suivant les prescriptions internationales. Les références seront ajoutées à la fin de l'article ; elles paraîtront comme des notes, au bas de la page. Le texte sera précédé d'un résumé, comprenant 15 lignes au maximum.

L'entière responsabilité du contenu des articles appartient aux auteurs. On publie des articles dus aux collaborateurs roumains ou étrangers. Les auteurs recevront 50 tirés à part.

PRINTED IN ROMANIA

TRAVAUX PARUS AUX ÉDITIONS DE L'ACADÉMIE DE LA RÉPUBLIQUE SOCIALISTE DE ROUMANIE

CORNEL BODEA et collab., **Tratat de biochimie vegetală**, partea I, **Fitochimie** (Traité de biochimie végétale, Ire partie, Phytochimie), Ier vol., 1964, 747 p. + 4 annexes + 2 pl., 41 lei; IIe vol., ,1962 1265 p., 1 pl., 56 lei, IIIe vol., 1967, 773 p., 35 lei.

V. GHEŢIE et V. MICUŞAN, **Analiza imunochimică. Teorie şi practică** (Analyse immunochimique. Théorie et pratique), 1966, 369 p., 28 lei.

SILVIA IONESCU, **Reacţii chimice induse de radiaţiile ionizante** (Réactions chimiques produites par les radiations ionisantes), 1963, 271 p., 15 lei.

MARIETA NICOLAE, **Fizico-chimia proceselor fotografice** (Physico-chimie des processus photographiques), 1964, 426 p. + 4 pl., 35 lei.

R. PORTOCALĂ et L. POPA, **Acizii ribonucleici celulari şi virali** (Les acides ribonucléiques cellulaires et viraux), 1966, 375 p. + 8 pl., 26 lei.

D. PURDELA et R. VÎLCEANU, **Chimia compuşilor organici ai fosforului şi ai acizilor lui** (La chimie des composés organiques du phosphore et de ses acides), 1965, 540 p., 37 lei.

CRISTOFOR SIMIONESCU, MARGARETA GRIGORAŞ et AGATA CERNĂTESCU-ASANDEI, **Chimia lemnului din R.P.R.** (La chimie du bois en Roumanie), 1964, 239 p. + 6 pl., 27 lei.

CRISTOFOR SIMIONESCU et CLEOPATRA VASILIU-OPREA, **Mecanochimia compuşilor macromoleculari** (La mécanochimie des composés macromoléculaires), 1967, 344 p., 23,50 lei.

I. V. MAXIM, **Materiale nucleare** (Matériaux nucléaires), 1969, 444 p., 4 pl., 30 lei.

CRISTOFOR SIMIONESCU et CONST. UGLEA, **Fracţionarea compuşilor macromoleculari** (Fractionnement des composés macromoléculaires), 1969, 292 p., 18,50 lei.

1971 JAN 29

I. P. I. c. 5716 | 43 436 | Lei 25

F 1103

0 R

REVUE ROUMAINE DE CHIMIE

REFERÁLVA

TOME 15
N° 11
Novembre 1970

ÉDITIONS DE L'ACADÉMIE DE LA RÉPUBLIQUE SOCIALISTE DE ROUMANIE

Rev. Roumaine Chim. **15, 1633–1792 (1970), Bucarest**

COMITÉ DE RÉDACTION

Rédacteur en chef :

C. D. NENIȚESCU, membre de l'Académie de la République Socialiste de Roumanie

Rédacteurs en chef adjoints :

A. T. BALABAN et V. E. SAHINI, membres correspondants de l'Académie de la République Socialiste de Roumanie

Collège de rédaction :

C. DRĂGULESCU, RALUCA RIPAN, CR. SIMIONESCU, membres de l'Académie de la République Socialiste de Roumanie ; EM. BRATU, membre correspondant de l'Académie de la République Socialiste de Roumanie, Pr G. OSTROGOVICH, MARGARETA AVRAM, F. BADEA, D. I. MARCHIDAN, D. NEGOIU et D. SĂNDULESCU.

Les manuscrits, les livres et les revues proposés en échange, ainsi que toute correspondance seront envoyés à la rédaction :

REVUE ROUMAINE DE CHIMIE

23, str. Dumbrava Roşie, Bucarest, 9, Roumanie.

REVUE ROUMAINE DE CHIMIE

Tome 15, N° 11 Novembre 1970

Page

I. G. MURGULESCU and D. OANCEA, Nucleophilic substitutions. III. The kinetics of the reactions between benzyl iodide and sodium alcoxides . . 1635–1646

LUCIA ODOCHIAN and I. A. SCHNEIDER, Some aspects of methane cracking kinetics in static conditions. I. The influence of the initial pressure of methane . . . . 1647–1651 R

M. ARSHAD A. BEG and M. S. SIDDIQUI, Spectroscopic studies of organophosphorus compounds. Ultraviolet spectra of phosphine-quinone adducts 1653–1663

S. STERNBERG and V. VASILESCU, Ultrasonic velocity, compressibility and excess volume of molten salts : $NaCl + (Li, K, Rb, Cs) Cl$ 1665–1673

D. I. MARCHIDAN and CR. TELEA, The heat of mixing in binary systems of molten salts : $KCl + RbBr$ and $KBr + RbCl$ 1675–1680

ŞTEFANIA ZUCA and RODICA BORCAN, Viscosity of molten $(Li-K)Cl$ mixtures 1681–1687

M. I. VASS, The influence of rapid temperature changes on the surface potential variation in the system oxygen-thin copper films 1689–1698

IULIANA VARTIRES, On the standard potential of thin lead films 1699–1706

E. POPA, EUGENIA IVANA and S. V. VOLKOV, Electronic absorption spectra of $ZnCl_2$, $CdCl_2$ and $AgCl$ in passing from solid to molten state 1707–1711

ELISABETA NICOLOIU, LUCIA GANOVICI und I. GANOVICI, Die Selbstdiffusion des flüssigen Tellurs im Temperaturbereich von 460–600° . . 1713–1720

IOANA DEMETRESCU, The effect of electrostatic energy in reactions between benzhydryl chloride and normal alcohols 1721–1725

T. CHIRULESCU and E. SEGAL, Adsorptive properties of a nickel ferrite . . . 1727–1733

V. M. BHATNAGAR, The cell parameters of synthetic calcium apatites . . . 1735–1739

L. CZEGLÉDI et CONST. GH. MACAROVICI, Combinaisons complexes avec des hydroxyacides. XIV. L'étude spectrophotométrique du système $ZrOCl_2$ – acide D-gluconique 1741–1750

C. LITEANU, S. GOCAN et T. HODIŞAN, La thermochromatographie sur papier. XIV. La possibilité de séparer certains ions ayant les valeurs R_f pratiquement égales en chromatographie isotherme 1751–1758

AL. ŞUTEU and H. NAŞCU, Catalytic determination of vanadium V(V) with amidol . . . . 1759–1765 R

Rev. Roumaine Chim.

15, p. 1633–1792 (1970) Bucarest

Page

MARGARETA AVRAM, F. CHIRALEU, I. POGANY, I. G. DINULESCU, Investigations in the cyclobutane series. XXX. NMR spectral parameters of some compounds with benzocyclobuteno-norbornene and -norbornane skeleton 1767–1776

D. CHRISTOV und N. NENOV, Über die Darstellung des 3,7-Dichlorphenothiazins durch die Reduktion seines Oxides mit Stannochlorid 1777–1783

MARIA IONESCU, ILEANA GOIA and M. VLASSA, Acridone. XXXVI. The chlorination of iodo-acridones. 1785–1791

Revue Roumaine de Chimie, **15**, 1635–1646 (1970)

NUCLEOPHILIC SUBSTITUTIONS.
III[1] THE KINETICS OF THE REACTIONS BETWEEN BENZYL IODIDE AND SODIUM ALCOXIDES

I. G. MURGULESCU and D. OANCEA

Faculty of Chemistry of the Bucharest University, Physical Chemistry Department,
Bucharest, Bd. Republicii 13

Received June 22, 1970

The kinetics of the reactions between benzyl iodide and sodium alcoxides in alcoholic solutions, using normal saturated alcohols from methyl to n-hexyl alcohol, was studied. The rate constants in the temperature range 30°–80° verify both the simple electrostatic and the Benson equations which account for the solvent effect on the reaction rate. In the series of benzyl halides, the activation energy does not reflect the stability of carbon-halogen bond energy.

In two previous works [1,2] the kinetics of the reactions between benzyl chloride or bromide with sodium alcoxides was studied. It was found that the logarithms of the rate constants show a linear dependence upon the reciprocal of dielectric constant and the activation energy referring to benzyl bromide reactions is smaller than the corresponding value for benzyl chloride, according to carbon-halogen bond energy change. In order to find and explain benzyl halides reactivity order towards alcoxide ions in alcoholic solutions, the present paper deals with the kinetics of the reactions between benzyl iodide and sodium alcoxides. The first paper dealing with the reaction between benzyl iodide and sodium ethoxide has been reported by Conrad and Brückner,[3] which found a rate constant at 0°, $k^{\circ} = 0.148\ \mathrm{cm^3\,mol^{-1}\,sec^{-1}}$ (for 0.5 M concentrations of both reactants), a figure which is in good agreement with that found by us, namely $k^{\circ} = 0.126\ \mathrm{cm^3\,mol^{-1}\,sec^{-1}}$ (extrapolated value). Although the kinetic parameters of the reaction between benzyl iodide and sodium ethoxide are specified in two books devoted to chemical kinetics, [4,5] the literature cited (W. Hecht, M. Conrad and C. Brückner, *Z. Phys. Chem.*, **4**, 273 (1889)) contains no data regarding this reaction.

[1] III part: I. G. Murgulescu and D. Oancea, *Rev. Roumaine Chim.*, **15**, 299 (1970).

[2] I. G. Murgulescu, D. Oancea and G. Mincu, *ibid.*, **14**, 3 (1969).

[3] M. Conrad and C. Brückner, *Z. phys. Chem.*, **4**, 631 (1889).

[4] E. A. Moelwyn-Hughes, "The Kinetics of Reaction in Solution", 2nd ed., Oxford University Press, Oxford 1947, p. 71.

[5] A. A. Frost and R. G. Pearson, "Kinetics and Mechanism", Wiley and Sons, New York, 1961, p. 148.

The result found in the present paper confirms the order of benzyl-halides reactivities reported by Conrad and Brückner,[3] namely $PhCH_2I > PhCH_2Br > PhCH_2Cl$, but shows that there is no direct correlation between activation energy and halogen-carbon bond energy.

A linear dependence of log k_2 *versus* $1/D$ has been found as well as for the other benzyl halides.[1,2]

EXPERIMENTAL

Benzyl iodide was prepared by the reaction of benzyl chloride with sodium iodide in acetone solution.[6] The raw product was recrystallized three times from absolute ethanol, obtaining a crystalline and colourless product (m.p. 27°). Sodium alcoxides were obtained as previously reported.[2] All the kinetic runs were performed by titrating unreactioned alcoxide.[1,2] Since the reactions were fast enough, for all working temperatures, a special reaction vessel [1] was used (which permits a quick mixing of reactants and a short time for the aliquots taking). All reagents used in the present investigation were of analytical reagent grade.

RESULTS

The rate constants of the reactions between benzyl iodide and sodium alcoxides in methyl, ethyl, n-propyl, n-butyl, n-amyl and n-hexyl alcohols have been determined within the temperature range 30°—80°. As previously pointed out,[1,2] the following simultaneous reactions occur under these circumstances:

$$PhCH_2I + RONa \xrightarrow{k_2} PhCH_2OR + NaI \tag{a}$$

$$PhCH_2I + ROH \xrightarrow{k_1} PhCH_2OR + HI \tag{b}$$

$$RONa + HI \xrightarrow{fast} ROH + NaI \tag{c}$$

A 0.1 M solution of $PhCH_2I$ in ethyl alcohol at 50°, does not show any acidity increasing an hour after mixing. Under the same conditions, the reaction (a) shows a 50% conversion 1/2 hour after mixing. This behaviour proves that the reaction (b), and consequently the reaction (c) has a much smaller contribution as compared to the reaction (a) and can be neglected. Hence, the chemical process can be rightly described only by equation (a). The kinetic measurements showed that the process is bimolecular and verifies the equation:

$$k_2 = \frac{2.303}{t(a-b)} \cdot \log \frac{(a-x)b}{(b-x)a} \tag{1}$$

---

[6] G. H. Coleman and C. R. Hauser, *J. Amer. Chem. Soc.*, **50**, 1196 (1928).

or equation :

$$k_2 = \frac{1}{t}\left(\frac{1}{a-x} - \frac{1}{a}\right) \tag{2}$$

when the reactants are in equimolar concentrations. Here, the time was expressed in seconds and the concentrations in mol/cm³. In tables 1 and 2 are given two kinetic runs referring to the reaction between benzyl iodide and sodium methoxide or hexoxide, respectively. The relative deviations ($C = S \,.\, 100/X$) for these kinetic runs are 3.14% and 4.66%, respectively. S stands for standard deviation $S = [\Sigma(X - X_i)^2/(n-1)]^{1/2}$, assuming validity of normal distribution law.

Table 3 gives the rate constants for the reaction under investigation. Each of these values is an average value of three kinetic runs. The relative deviation for the average value is maximum 2%.

Table 1

Kinetic run for the reaction between benzyl iodide ($b = 0.0601 \times 10^{-3}$ mol/cm³) and sodium methoxide ($a = 0.1005 \times 10^{-3}$ mol/cm³). $T = 50°$

t(sec)	$(a-x)$ (mol.cm^{-3}) × 10³	k_2 (cm³ mol^{-1} sec^{-1})
300	0.0749	21.53
900	0.0563	20.63
1200	0.0507	22.27
1500	0.0487	20.72
1800	0.0462	21.47
		$(k_2)_m = 21.32 \pm 0.67$

Table 2

Kinetic run for the reaction between benzyl iodide ($b = 0.0669 \times 10^{-3}$ mol/cm³) and sodium n-hexoxide ($a = 0.1035 \times 10^{-3}$ mol/cm³) $T = 50°$

t(sec)	$(a-x)$ (mol . cm^{-3}) × 10³	k_2 (cm³ mol^{-1} sec^{-1})
600	0.0761	9.98
1320	0.0610	9.93
2400	0.0497	10.22
3000	0.0461	10.40
3600	0.0429	11.19
4200	0.0419	10.58
4800	0.0404	10.98
		$(k_2)_m = 10.47 \pm 0.48$

Table 3

Rate constants of the reactions between benzyl iodide and sodium alcoxides at different temperatures (cm³ mol^{-1}-sec^{-1})

Temperature / Alcoxide	30°	40°	50°	60°	70°	80°
CH_3ONa	3.312	8.512	21.38	50.12	136.4	—
C_2H_5ONa	4.416	12.16	32.36	81.30	—	—
$n-C_3H_7ONa$	3.820	10.00	25.12	60.94	142.8	—
$n-C_4H_9ONa$	2.820	7.674	18.71	45.18	83.18	—
$n-C_5H_{11}ONa$	1.950	4.842	12.60	29.17	67.71	136.5
$n-C_6H_{13}ONa$	1.699	4.467	10.48	24.00	55.57	109.7

Because the similar reactions of benzyl chloride and benzyl bromide[1,2] did not show any variation of the rate constant on the initial concentration of alcoxide (for initial concentrations 0.05 ; 0.1 ; 0.2 ; 0.3 M), in the present work the alcoxide concentration was kept constant, namely around 0.1 M, while the benzyl iodide concentration was taken between 0.05 and 0.1 M. The dependence of the rate constant on the temperature was investigated by using Arrhenius equation. For all systems a linear dependence of log k_2 *versus* $1/T$ was found (Fig. 1). Within the temperature range 30°—80° the activation energy did not show any variation. The experimental values of the activation energies and of the pre-exponential factors, calculated by the least squares method, are given in table 4.

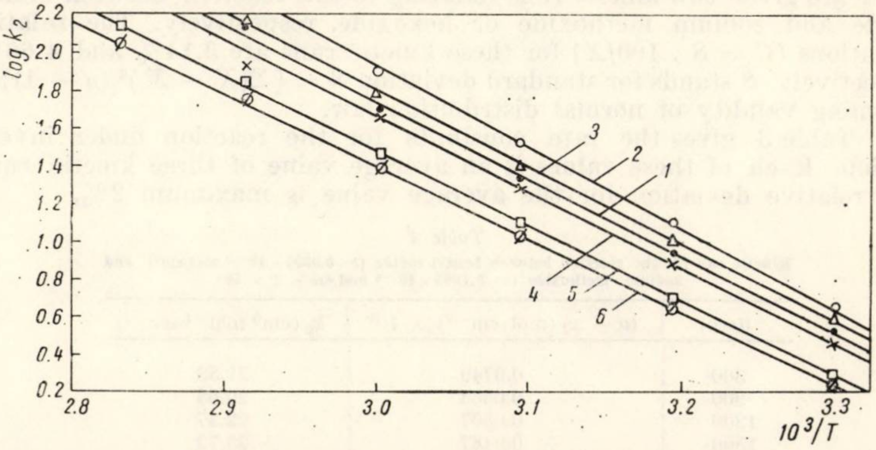

Fig. 1. — Influence of the temperature on the rate of the reactions between benzyl iodide and sodium alcoxides $(RO^-) \cdot R =$

1, CH_3 ; *2*, C_2H_5 ; *3*, nC_3H_7 ; *4*, nC_4H_9 ; *5*, nC_5H_{11} ; *6*, nC_6H_{13}.

Table 4

Kinetic parameters of the reactions between benzyl iodide and sodium alcoxides

	CH_3O^-	$C_2H_5O^-$	$nC_3H_7O^-$	$nC_4H_9O^-$	$nC_5H_{11}O^-$	$nC_6H_{13}O^-$
E_A (kcal . mol^{-1})	18.650	19.310	18.350	17.460	18.120	17.660
log A^*	13.988	14.613	13.846	13.106	13.422	13.018

$^*A$ is given in $cm^3 \cdot mol^{-1} \cdot sec^{-1}$

Except for the reaction occurring in methyl alcohol the reaction rate decreases when the hydrocarbonate chain of alcohol increases. Although in the same series the activation energy decreases slowly, at the same time, the pre-exponential factor decreases, leading to an overall decrease in the reaction rate.

DISCUSSIONS

Numerous experimental observations, based on the conductivity measurements, [7,8] showed that the dilute solutions of sodium alcoxides were entirely ionized in respective parent alcohols. This behaviour results, to a great extent, from the great solvation ability of these hydroxilic solvents which form hydrogen bridges with alcoxide ions. At the same time, sodium ion is well solvated because it interacts stronger with alcohols than with water [9].

The significant increase (with approximately four orders of magnitude) of the rate constant for the reaction between sodium alcoxides and benzyl halides, as compared to the corresponding alcoholysis reactions [1,2] suggests that the rate determining step in these reactions is nucleophilic attack of the alcoxide ion on the saturated carbon atom, as shows the following mechanism :

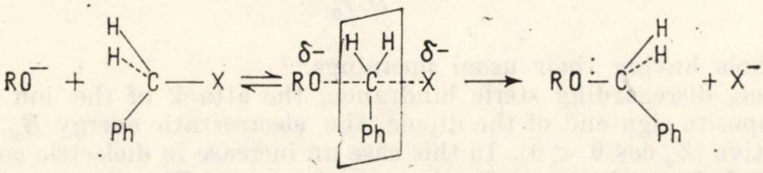

The reaction rate is strongly influenced by the solvent because of the solvation of both reactants and transition state and, on the other hand, because of modified electrostatic interactions. The study of the solvent effects on the reactions between ions and dipolar molecules has shown that the solvent produces a retardation of the chemical process because of the solvation of the reacting species.[10] This point of view is supported by the fact that numerous reactions between ions and molecules in the gas phase have a nearly null activation energy.[11] Also, the null activation energy of the reaction between hydroxide ion and alkyl halides in the gas phase, calculated on the basis of the complete potential energy surfaces,[12] justifies the hypothesis that the rate determining step at which the activation energy of the reactions between ions and dipolar molecules refers is the escape of the ion from its solvation sheath.[10] By transferring a reaction between an anion and a dipolar molecule from a protic to a dipolar aprotic solvent, the reaction rate increases usually with some orders of magnitude. This behaviour was explained [13,14] in view of the fact that

---

[7] G. E. M. Jones and O. L. Hughes, *J. Chem. Soc.*, **1934**, 1197.

[8] D. C. Bradley, "Metal Alcoxides" in "Progress in Inorganic Chemistry", Vol. 2, Ed. by A. Cotton, 1960.

[9] O. Jardetzky and J. W. Wertz, *J. Amer. Chem. Soc.*, **82**, 318 (1960).

[10] E. A. Moelwyn-Hughes, "Physical Chemistry", 2nd ed., Pergamon Press, 1961, Chap. 24.

[11] F. W. Lampe, J. L. Franklin and F. H. Field, *Progr. React. Kinetics*, **1**, 67 (1961).

[12] R. Hurst, "Thesis", Cambridge, 1948; "Corso Estivo di Chimica", Varenna, 1957, Cf. 10.

[13] A. J. Parker, *Quart. Revs.*, **16**, 163 (1962).

[14] A. J. Parker, *Chem. Revs.*, **69**, 1 (1969).

in dipolar aprotic solvents the anions are much less solvated than in protic solvents.

The variation of the rate constant for a reaction between ions and dipolar molecules when the solvent changes is usually correlated with the modification of the dielectric constant of the medium, taking into account that electrostatic interactions between ions and dipoles are altered by the solvent, looked as a continuous dielectric.[15] For a reaction between an ion $A^{Z\varepsilon}$ and a dipole μ_B immersed in a continuous dielectric, the rate constant is given by the equation :

$$\ln\left(\frac{k}{k_0}\right) = -\frac{E_{el}}{RT} \tag{3}$$

where

$$E_{el} = \frac{NZ_A \varepsilon \mu_B \cos\theta}{D \cdot r_0^2} \tag{4}$$

the symbols having their usual meanings.[1,2]

Since, disregarding steric hindrance, the attack of the ion occurs at the opposite sign end of the dipole, the electrostatic energy E_{el} should be attractive ($Z_A \cos\theta < 0$). In this case an increase in dielectric constant should lead to a decrease in the reaction rate. The same conclusion arises from the fact that in transition state the charge is more dispersed than in initial state. Such a correlation is not always found,[14] and there are cases when the behaviour is in opposite direction than that predicted.[15,16] Amis [15] showed that for positive and negative ions the dependence of log k_2 against $1/D$ sould have the slopes of opposite signs (positive and negative, respectively). The reactions between alcoxide ions and benzyl halides [1,2] showed indeed such a behaviour. For the reactions between benzyl iodide and sodium alcoxides in alcoholic solutions a linear dependence of log k_2 *versus* $1/D$ was found, as the eq. (5) shows

$$\log k_2 = \log k_0 - \frac{NZ_A \varepsilon \mu_B \cos\theta}{2.303 \cdot D r_0^2 \cdot RT} \tag{5}$$

By plotting log k_2 against $1/D$, straight lines result, given by the equation (6) :

$$\log k_2 = \log k_0 - \frac{B}{D} \tag{6}$$

The plots described by equation (6) are given in fig. (2), at all working temperatures.

The dielectric constants were taken from a previous work.[2] Except for the reaction between sodium methoxide and benzyl iodide in methyl alcohol, a good linear dependence was found. Disregarding the values for this system, the slopes B and the intercepts $\log k_0$ of these lines were calculated by the least squares method. The results are given in table 5.

---

[15] E. S. Amis, "Solvent Effects on Reaction Rates and Mechanisms", Academic Press, New York, 1966, p. 42.

[16] R. Fuchs and A. Nisbet, *J. Amer. Chem. Soc.*, **81**, 2371 (1959).

From the equation (5) it follows that k_0 stands for extrapolated value of the experimental rate constant k_2 when $D \to \infty$, as it were in the absence of the electrostatic interactions. Since the rate constant does not depend on the initial concentration of alcoxide, the influence of the ionic strength on these reactions was ignored, considering that the experimental values of k_2 are identical with the corresponding values at infinite dilution.

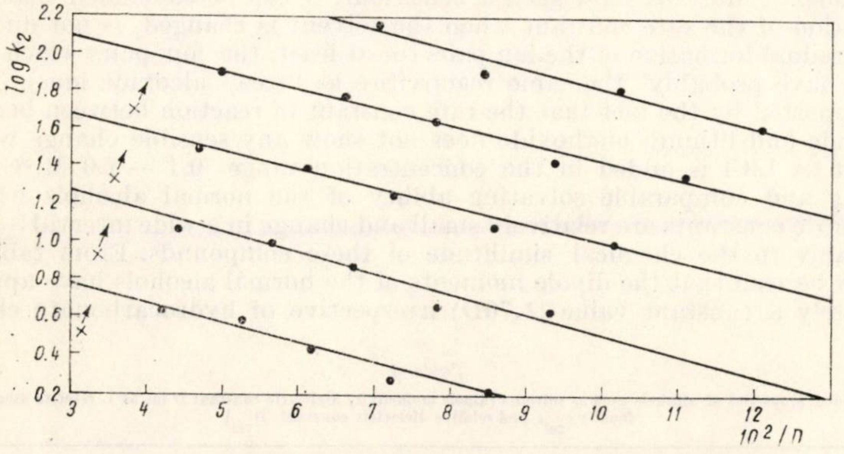

Fig. 2. — Influence of the dielectric constant on the rate of the reaction between benzyl iodide and sodium alcoxides (simple electrostatic equation)
× $CH_3O^- + PhCH_2I$

Table 5

Values of B, $\log k_0$ and r_0 for the reaction between benzyl iodide and sodium alcoxides at different temperatures

$T°$	B	$\log k_0$	r_0(Å)
30	10.484	1.0988	2.19
40	9.848	1.5305	2.23
50	9.485	1.9571	2.23
60	9.126	2.3630	2.24
70	7.610	2.6290	2.42

The change of the dielectric constant from 23.75 for ethyl alcohol at 30°, to 7.65 for n-hexyl alcohol at 80°, raises another problem connected with the possibility that ionic pairing occurs in these solvents. Ionic pairing effect on the reaction between ions and dipolar molecules in solvents of low polarity is not yet entirely elucidated. [17] Many workers in the field consider that the ion pair is less reactive than the "free" ion (in solution the ion is actually in solvated form), ionic pairing leading to a decrease of the rate constant. Although this opinion is not unanimously admitted and was even criticized occasionally,[18] a series of experimental studies showed that the rate constant for some reactions between ions and dipolar molecules decreases when ionofor concentration increases.[4, 17, 19] Since the reactions between benzyl chloride or benzyl bromide with sodium alcoxides [1, 2] did not show such a behaviour, it can be concluded that the variation of the rate constant when the solvent is changed, is not due to the gradual formation of the ion pairs (or at least, the ion pairs which can form have probably the same reactivities as "free" alcoxide ions). This is supported by the fact that the rate constant of reaction between benzyl chloride and lithium methoxide does not show any sensible change when a salt as LiCl is added in the concentration range 0.1 – 1.0 M.[20] The strong and comparable solvating ability of the normal alcohols whose dielectric constants are relatively small and change in a wide interval is due probably to the chemical similitude of these compounds. From table 6 it can be seen that the dipole moments of the normal alcohols have approximately a constant value (1.70D) irrespective of hydrocarbonate chain length. The change of the dielectric constant in this series arises probably from a decrease in the number of dipoles per unit volume (ρ) when the chain of the alcohol increases. Comparing $\rho_{relative} = \rho / \rho$ ethyl alcohol with the relative dielectric constant D relative $= D/D$ ethyl alcohol, a good agreement results (table 6). These results confirm the view that the solvent "polarity" can be poorly described only by the dielectric constant, but properly by the magnitude of the dipole moment of the solvent molecule and the screening of the dipole charges [22] which do not changes appreciably for normal alcohols.

---

[17] N. N. Lichtin and K. N. Rao, *J. Amer. Chem. Soc.*, **83**, 2417 (1961).

Table 6

Physical properties of alcohols used as solvents [dipole moment μ, dielectric constant D (at 50°), relative dipole density ρ_{rel}, and relative dielectric constant D_{rel}]

	CH_3OH	C_2H_5OH	nC_3H_7OH	nC_4H_9OH	$nC_5H_{11}OH$	$nC_6H_{13}OH$
$\mu^*(D)$	1.70±0.01	1.70±0.01	1.69±0.03	1.67±0.02	—	—
$D^{**}_{50°}$	28.00	21.25	16.40	13.85	11.75	9.88
ρ_{rel}	1.44	1.00	0.78	0.64	0.54	0.47
D_{rel}	1.31	1.00	0.77	0.65	0.55	0.46

* Cf. 21
** Cf. 1

From experimental slopes, B, given in table 5, and their theoretical expressions given by equation 5, it is possible to calculate the reaction parameter r_0. The values thus obtained are recorded in the last column of table 5. In the theoretical expression of B (eq. 5), cos θ was taken as its mean value,[2] namely $\cos\theta = 2/\pi$, and the dipole moment of benzyl iodide as $\mu_B = 1.59$ D.[23]

---

[18] J. N. Brönsted and E. A. Guggenheim, *J. Amer. Chem. Soc.*, **49**, 2557 (1927), cf. 17.

[19] K. B. Wiberg, "Physical Organic Chemistry", Wiley and Sons, New York, 1964, Part 3.

[20] I. G. Murgulescu and D. Oancea, unpublished results, communicated at the 1st General and Applied Republican Conference of Physical Chemistry, Bucharest, 2–5 September, 1968.

[21] Handbook of Chemistry and Physics, 41st ed., Chemical Rubber Publishing, 1959–1960, Cleveland, Ohio.

[22] Y. Pocker, *Progr. React. Kinetics*, **1**, 215 (1961).

The intercepts log k_0 (table 5) at different working temperatures were plotted against $1/T$ in figure 3.

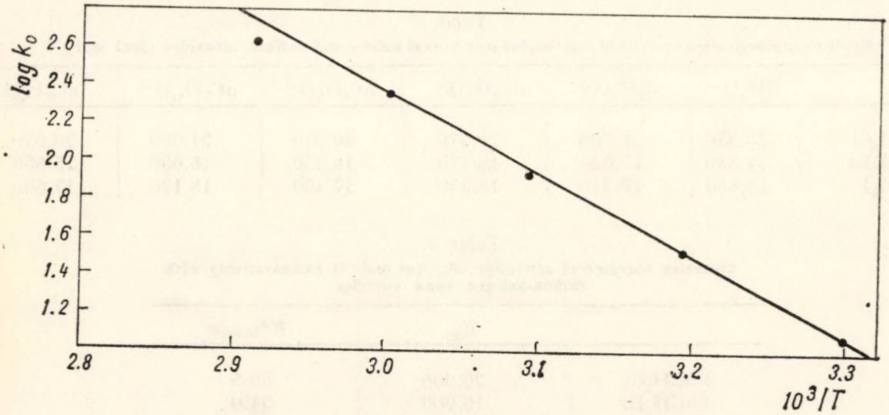

Fig. 3. — Influence of the temperature on the rate constants corrected for electrostatic interactions (simple electrostatic equation).

A good linear dependence results. The activation energy E_0 and the pre-exponential factor log A_0 can be calculated from this plot, by using the least squares method. The results are 19.420 cal. mol^{-1} and 15.15, respectively. According to the above, E_0 and A_0 stand for Arrhenius parameters when $D \to \infty$, i.e. in the absence of electrostatic interactions.

Using these results and those previously reported[1, 2] a survey on benzyl halides reactivities towards sodium alcoxides in alcoholic solution can be made. In table 7 are recorded the relative rate constants at 50° (the relative rate constant for benzyl iodide was taken as 1,000). For the sodium ethoxide system a comparison can be made with the corresponding values found by Conrad and Brückner at 0° : $k(PhCH_2I) : k(PhCH_2Br) : k(PhCH_2Cl) = 1{,}000 : 604 : 10.28$. The agreement with our results is satisfactory. An examination of experimental activation energies (table 8)

Table 7

Relative rate constants of benzyl halides at 50°

	CH_3O-	C_2H_5O-	nC_3H_7O-	nC_4H_9O-	$nC_5H_{11}O-$	$nC_6H_{13}O$
$PhCH_2Cl$	26	18	21	24	27	25
$PhCH_2Br$	770	651	740	747	710	743
$PhCH_2I$	1,000	1,000	1,000	1,000	1,000	1,000

---

[23] I. G. Murgulescu and D. Oancea, to be published.

or of E_0 energies (table 9) shows that the reactivity order $PhCH_2I >$ $> PhCH_2Br >$ $PhCH_2Cl$ is not the same as the activation energy decreasing order E $(PhCH_2Br) < E(PhCH_2I) < E(PhCH_2Cl)$. Although it is to be expected that the energies corresponding to bond breaking and forming, constitute a part of the activation energy, [25] for many chemical reactions in solution, there is no correlation between these quantities. [10]

Table 8

Experimental activation energies of reaction between benzyl halides and sodium alcoxides ($kcal\ mol^{-1}$)

	CH_3O-	C_2H_5O-	nC_3H_7O-	nC_4H_9O-	$nC_5H_{11}O-$	$nC_6H_{13}O-$
$PhCH_2Cl$	20.370	21.760	20.570	20.780	21.000	20.970
$PhCH_2Br$	17.380	17.020	16.470	16.250	16.090	15.850
$PhCH_2I$	18.650	19.310	18.350	17.460	18.120	17.660

Table 9

Corrected energies of activation, E_0($kcal\ mol^{-1}$) comparatively with carbon-halogen bond energies

	E_0	$E^{*}_{\mathrm{bond}^{24}}$
$PhCH_2Cl$	20.900	66.5
$PhCH_2Br$	16.000	54.0
$PhCH_2I$	19.420	45.5

* Cf.[24]

Comparing the activation energies with halogene-carbon bond energies (table 9) it can be seen that the activation energy does not reflect the stability of covalent bond which is broken during the course of the reaction. This behaviour proves that for a better understanding of the complex nature of the activation energies referring to these reactions, it must be taken into account the solvation and desolvation process of both reactants and transition state. The solvation of reagents can easily be made evident, at least qualitatively. Thus, alcoxide ions are strongly solvated in alcoholic since, in addition to purely electrostatic contribution, hydrogen bonding arises, too. At the same time, the organic halides give hydrogen bonds with the alcohols, whose strength depends on the kind of halogene and his chemical neighbourhood. [26] Transition state solvation remains, however, a supposition field. The relative contribution of the solvation energies for reactants and activated complex should probably be able to explain the behaviour of the activation energies obtained from this study. The influence of halogen nature on the benzyl halides reactivities towards sodium alcoxides shows that, in the rate determining step, in addition to the desolvation energy of ion, it must make allowance for the chemical nature of the desolvating molecule. Benson [27] suggests that a fairer model for the formation of the transition complex for anion-dipolar molecule reaction might result from considering it as resulting from the displacement in the solvent sheath of the ion of a solvent molecule of dipole moment μ_s by a reactant molecule of dipole moment μ_B. The free energy of formation of the transition state, neglecting dipole-dipole interaction is :

---

[24] O. A. Reutov "Probleme teoretice ale chimiei organice", Ed. Acad. Bucharest, 1964, Translation from Russian, Anexe, Table 4.

[25] E. F. Caldin, *J. Chem. Soc.*, **1959,** 3345.

[26] P. J. Krueger and H. D. Metee, *Canad. J. Chem.*, **42,** 288 (1964).

[27] S. W. Benson, "The Foundations of Chemical Kinetics", McGraw-Hill Book Company, New York, 1960, chap. 15.

$$\Delta F = \frac{Z_A \varepsilon \mu_B \cos\theta}{D r_B^2}\left(1 - \frac{\mu_s \cdot r_B^2}{\mu_B \cdot r_S^2}\right) \tag{7}$$

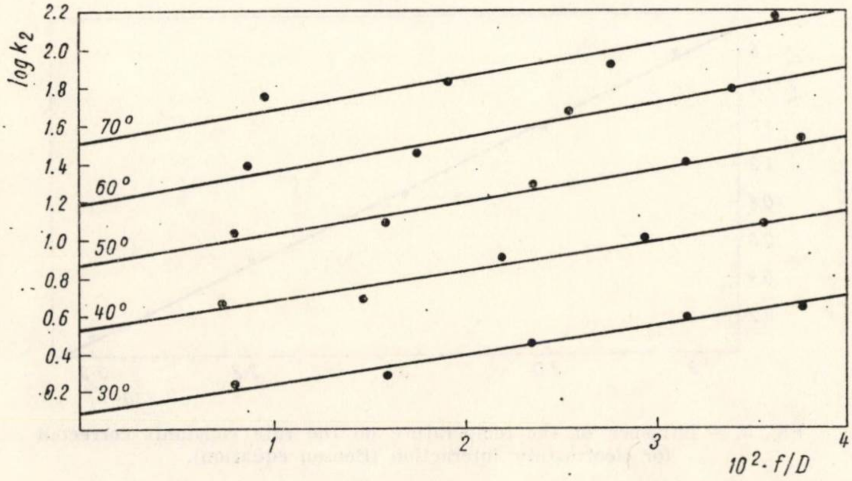

Fig. 4. — Influence of the dielectric constant on the reaction rate (Benson equation).

In this case the rate constant is given by :

$$\log k_2 = \log k'_0 - \frac{N Z_A \mu_B \varepsilon \cos\theta}{2.303\, D r_B^2 R T}\left(1 - \frac{\mu_s}{\mu_B} \cdot \frac{r_B^2}{r_S^2}\right) \tag{8}$$

By plotting log k_2 against f/D, where $f = \left(1 - \frac{\mu_S}{\mu_B} \cdot \frac{r_B^2}{r_S^2}\right)$, straight lines result, at all working temperatures (fig. 4). In calculating the expression given in brackets (denoted by f), μ_s value was taken as the same for all alcohols, namely 1.70 D. (table 6). The radius, r_s, of the alcohol molecules was taken from a previous work. [2] The benzyl iodide radius was calculated by using the equation $2r = \sigma = 1.184 \times 10^{-8}\ (M/d)$, and taking benzyl iodide density at 40°, namely 1.7146^{23} ($r_{\mathrm{PhCH_2I}} = 2.98$ Å).

The slopes and intercepts of the lines given in figure 4, calculated by the least squares method, are recorded in table 10, at different working temperatures.

The plot of log k'_0 against $1/T$ (figure 5) gives a straight line from which activation energy $E_0 = 17{,}100$ cal. mol^{-1} and pre-exponential factor log $A_0 = 12.483$ were calculates by using the least squares method. The slopes of the lines plotted in figure 4 are about 16.3, a figure which is about

Table 10

Slopes and intercepts of lines given in figure 4 at different temperatures

	30°	40°	50°	60°	70°
B'	15.11	16.71	17.18	17.66	14.87
$\log k'_0$	0.086	0.496	0.858	1.196	1.567

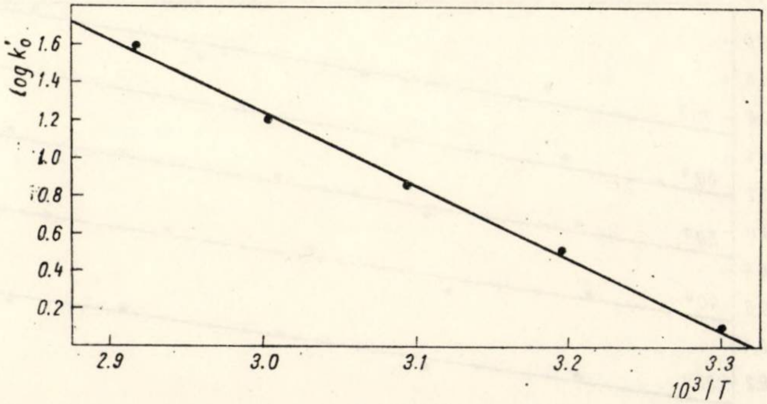

Fig. 5. — Influence of the temperature on the rate constants corrected for electrostatic interaction (Benson equation).

twice greater than the theoretical value resulted from eq. 8($B_{\text{theor}} = 8.37$ when $\cos \theta = 1$). This discrepancy arises probably from the utilization of the macroscopic dielectric constant D which is too great comparatively with the "effective" dielectric constants applicable to ion-dipole interaction at short distances. The slopes of the lines plotted in figure 2 and 4 have opposite signs because of the negative sign of f quantity.

CONCLUSIONS

The reactions between sodium alcoxides, resulted from normal aliphatic alcohols and benzyl iodide proceed through the SN_2 mechanism.

The effect of the solvent on these reactions is satisfactorily described by both simple electrostatic equation, which correlates ion-dipolar molecule reaction rate with dielectric constant of the medium, and the Benson equation which accounts for the desolvation of the ion by the reactant molecule.

Comparing the activation energies of different benzyl halides it can be seen that they do not reflect the stability of the carbon-halogen bond which breaks in the course of the reaction.

Revue Roumaine de Chimie, **15**, 1647 – 1651 (1970)

SOME ASPECTS OF METHANE CRACKING KINETICS IN STATIC CONDITIONS. I

LUCIA ODOCHIAN and I. A. SCHNEIDER

Department of Physical Chemistry, "Al. I. Cuza" University, Jassy, Romania,
Calea 23 August 11

Received March 17, 1970

The study of the methane cracking in static conditions at temperatures between 913°–973°K and at pressures from 10 to 760 mm Hg., shows a serious influence of the wall which increases with the decrease in the initial pressure of methane, determining a diminution of the overall reaction order.

Many works have already dealt with the kinetics of the methane cracking. However, because of the complexity of the reaction there are still enough contradictions concerning the interpretation of the experimental data.

Some of these works accept that the methane cracking takes place by a branching [1] chain reaction, the ethane having an important role as branching agent. [2,3] However there are works which do not make any difference between the action of ethane and that of other C_2 hydrocarbons [4,5] and there are also indications that ethane is not the primary intermediate product in any conditions of reaction and that C_2 hydrocarbons may be formed in parallel reactions, mainly at higher temperatures.

The aim of the present paper is to bring additional data regarding mainly the initial period of methane cracking at low temperatures.

EXPERIMENTAL

As it has been shown in another paper,[6] if we consider the mechanism of C_2 hydroarbon formation :

$$2\,CH_4 \rightarrow C_2H_6 + H_2$$

$$2\,CH_4 \rightarrow C_2H_4 + 2H_2$$

$$2\,CH_4 \rightarrow C_2H_2 + 3H_2$$

---

[1] I. A. SCHNEIDER, *Z. phys. Chem.* (*Leipzig*), **223**, 234 (1963).

[2] I. A. SCHNEIDER, Dissertation, Polytechnic Institute of Timişoara, Romania, 1962.

[3] J. E. GERMAIN and C. VANISCOTTE, *Bull. Soc. chim. France*, **1968**, 964.

[4] A. S. GORDON, *J. Amer. Chem. Soc.*, **70**, 395 (1948).

[5] P. S. SANTAROVICI and B. V. PAVLOV, *Zhur, fiz. Khim.*, **30**, 811 (1956).

[6] I. A. SCHNEIDER, *Rev. Roumaine Chim.*, **5**, 227 (1960).

we may notice that ethane formation occurs without change of the moles number, so that a common manometric static equipment used by earlier workers [7,8] really does not permit to observe the methane cracking in the initial period.

For a kinetical interpretation of the process, only the use of another physical characteristic of the reaction mixture will lead to satisfactory results.

Taking into account that the hydrogen is the main product of the methane cracking and that it has a much higher thermal conductivity than the other participants in the reaction, we have thought to use its characteristic to study the methane cracking in static conditions.

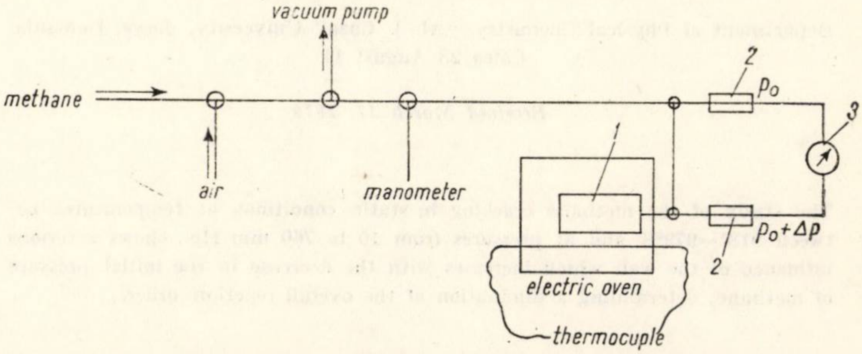

Fig. 1.—Equipement used for the thermal decomposition of methane in static conditions.
1, reactor ; *2*, thermal conductivity cells ; *3*, zero manometer.

Combining the thermal conductivity measurements with the usual manometric method for the study of the methane cracking, differences will appear if the ethane is the primary product of methane decomposition in our conditions of reaction.

Schematically the equipment is presented in figure 1.

The main parts of the above installation are : *1*, a quartz 225 cm^3 reactor ; *2*, two cells for measuring the thermal conductivity of the mixture comparative to that of methane ; *3*, a U tube manometer for measuring the pressure variation ΔP.

The two thermal conductivity cells had both a platinum wire of $\Phi = 0.05$ mm with a resistance of 1.60 Ω and 1.80 Ω respectively, which put into a Weston bridge supplied by a 4V battery. The variation of the thermal conductivity of the reaction mixture compared to that of the pure methane in initial conditions was recorded by a 10 mV Leads-Northrup recorder. A 0.1 mm platinum wire was placed in the branch of the manometer and connected to the part of the apparatus under initial pressure P_0. The platinum wire resistance of 3Ω was connected to a second Wheatstone bridge supplied by a rectifier of the Glow-Mac-Instrument Model 9999 type. The resistance variation of the platinum wire due to the shift of the mercury level in the U tube manometer under the influence of the increasing pressure of the reaction mixture was recorded by a 1 mV EKB/T recorder. The sensitivity of this manometer was of 10^{-4} mmHg.

The purity of the methane was higher than 99.3 %, the impurities being nitrogen as found by G. C. analysis.

---

[7] L. S. Kassel, *J. Amer. Chem. Soc.*, **54**, 3149 (1932).

[8] S. Kodama, K. Tarama, S. Katoa and S. Hayokawa, *J. Chem. Soc. Japan pure Chem. Sect.*, **70**, 421 (1949) ; **71**, 389 (1950).

RESULTS AND DISCUSSIONS

The records showed that there was a clear difference between the thermal conductivity variation of the reaction mixture and the increase in its pressure.

This fact is emphasized by the great differences concerning the induction period of the cracking process as it results from figures 2 and 3.

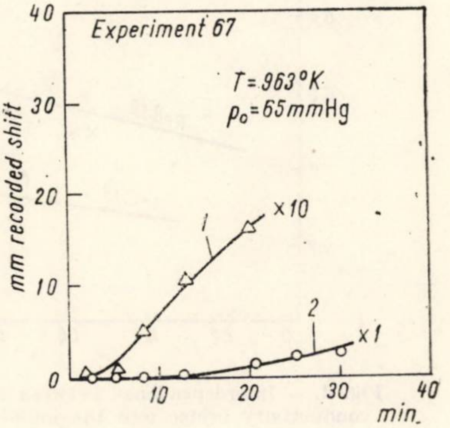

Fig. 2. — Typical recording of the kinetical curves obtained by the two methods at an initial pressure of $P = 65$ mmHg and at 943°K.
1, thermal conductivity; *2*, pressure.

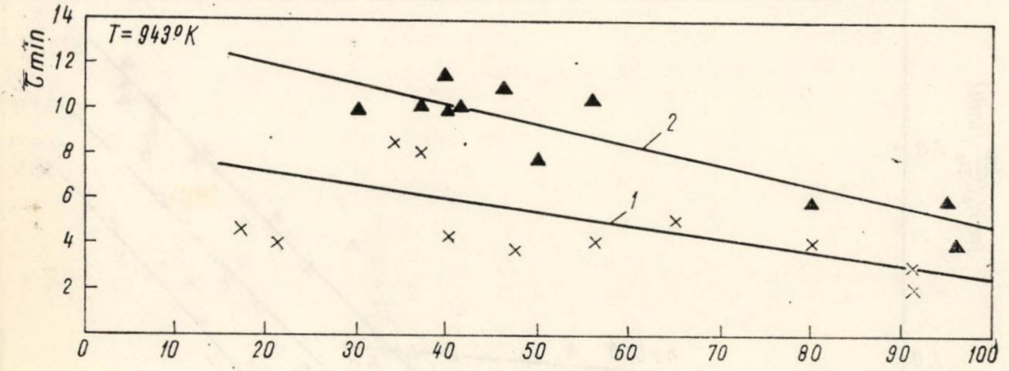

Fig. 3. — Variation of the induction period function of the initial pressure of methane at 943°K.
1, thermal conductivity; *2*, pressure.

It has been noticed that the induction period measured with the pressure bridge is much greater than that measured with the thermal conductivity bridge, a fact which may be considered as an evidence that ethane is the primary intermediate product under the reaction conditions.

The dependence on the pressure of the initial rate evaluated according to the two series of results at different temperatures, shows different straight lines indicating different reaction orders for the methane decompo-

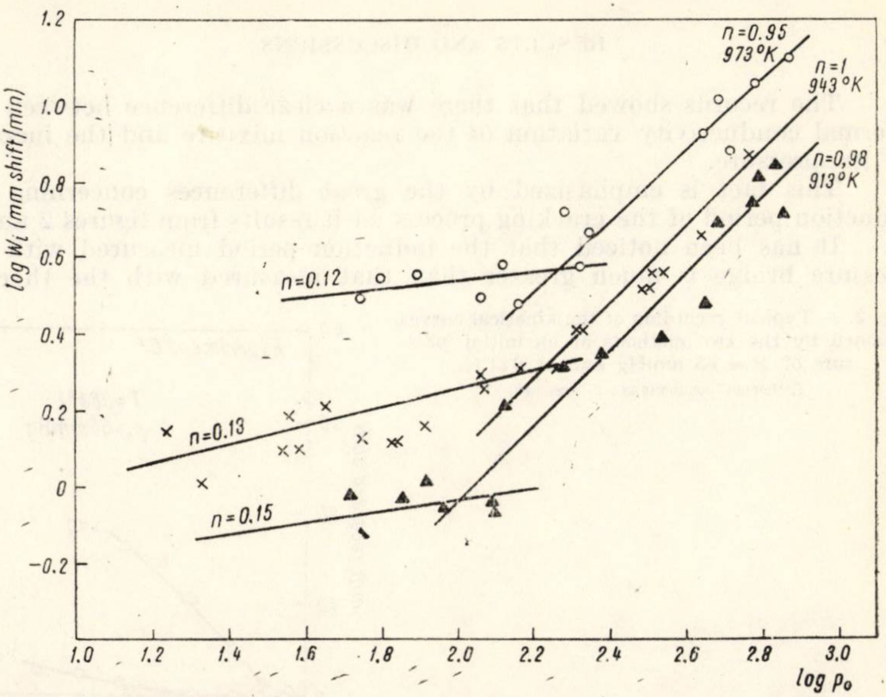

Fig. 4. — Interdependence between the initial rate expressed in mm/min shift of the conductivity bridge and the initial pressure of methane at different temperatures.

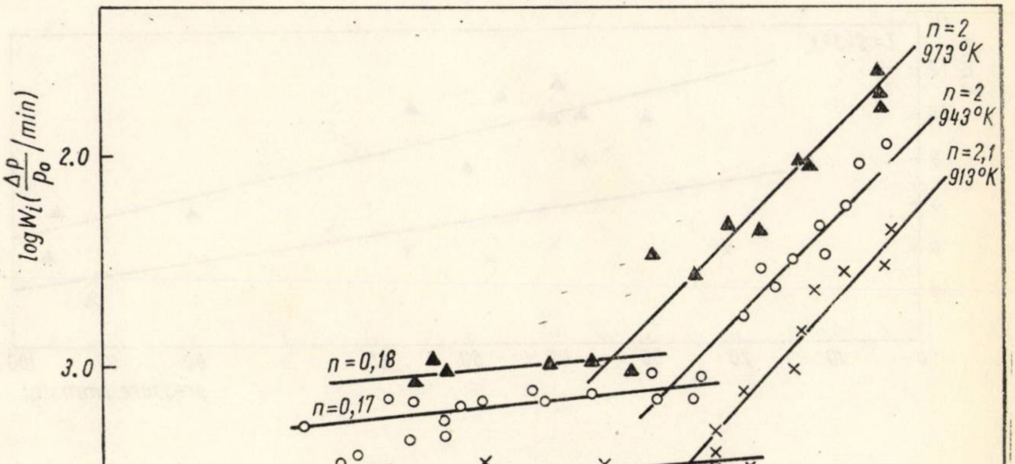

Fig. 5. — Interdependence between the initial rate expressed in $\Delta P/P_0$/min and the initial pressure of methane at different temperatures.

sition (figure 4 and figure 5). At the same time the plots show a significant dependence of the overall reaction order on the initial pressure.

We remark that reproductible results could be obtained only by heating in air of the reactor after each experiment.

Regarding the wall influence, also suggested by other workers [9, 10] the effect of the initiation reaction on the wall increases at low pressures, the reaction order being modified as one can see in the figures below.

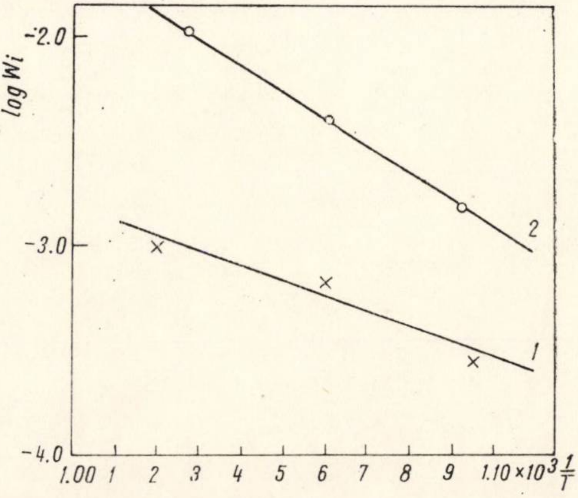

Fig. 6. — Arrhenius diagram for high (*1*) and low (*2*) initial pressures.

These results as well as the small activation energy found for the low pressure reaction ($E_a = 36.8$ kcal/mol) may be considered as an argument for a homogeneous-heterogeneous mechanism of the methane cracking reaction.

Using the values of the initial rate W_i calculated for the pressure variation at high initial pressures, the Arrhenius plot (figure 6), leads to an overall activation energy of 59.3 kcal/mol. This value corresponds satisfactorily to that indicated by Germain and Sueur [11] for the branching process ($E_a = 60$ kcal/mol). Nonetheless this confirms the branching effect of the ethane because the pressure variation of the reaction mixture will be observed only after ethane formation as stated before.

In conclusion we wish to remark that the results obtained using the thermal conductivity method could not be used for quantitative calculations because the calibration of the thermal conductivity bridge could not be made.

---

[9] J. E. Germain and C. Vaniscotte, *Bull. Soc. chim. France*, **1957**, 692.
[10] I. Iosif and I. A. Schneider, *Z. phys. Chem.* (*Leipzig*), **237**, 81 (1968).
[11] J. E. Germain and R. Sueur, *Compt., rend.*, **257**, 3881 (1963).

Revue Roumaine de Chimie, **15**, 1653–1663 (1970)

SPECTROSCOPIC STUDIES OF ORGANOPHOSPHORUS COMPOUNDS. VI
ULTRAVIOLET SPECTRA OF PHOSPHINE-QUINONE ADDUCTS

M. ARSHAD A. BEG and M. S. SIDDIQUI

Pakistan Council of Scientific and Industrial Research Laboratories, Karachi-39, Pakistan

Received January 12, 1970

The UV spectra of the adducts of trimethyl, phenyldimethyl, triphenyl and tri-*p*-tolyl phosphines with toluquinone and naphthoquinone have been recorded at pH 2, 6 and 8. A systematic shift is noted in each case at pH 8 while at pH 2 there is only a reduction in intensity. It is possible to explain these variations in terms of a zwitterionic structure so that in the acid medium the carbonyl group is ionized thus reducing the transition dipole moment and hence the lower intensity. The high intensity in the basic medium however, suggests a more phenolic character and the shifts pertain to a quinonoid effect, indicating a phosphinemethylene structure at higher pH.

In our previous publication [1] the UV spectra of the adducts of phosphines and *p*-benzoquinone were discussed. Typical shifts in the frequency were noted with a variation in the pH of the solution. The spectra were interpreted in terms of a dipolar structure for the adducts. Here we describe the spectra of the phosphine adducts with mono-and di-substituted quinones viz. toluquinone and naphthoquinone.

For a mono-substituted quinone we had described three main maxima, I at 240 mμ, II at 280–320 mμ, and III at 420–500 mμ. In the present series of compounds, we would expect features similar to a di-substituted quinone in the case of toluquinone adducts where a further shift in the band position is anticipated [2] and band I may be found at 260–270 mμ, band II at 310–320 mμ and band III between 430 – 480mμ. For naphthoquinone adducts the situation would be similar to trisubstituted quinones where the position of band I would be further shifted to 280 mμ and band II and III to 330 and 420 mμ respectively. For a comparison of the effect of substitution and to determine the nature of the compound that is whether zwitterionic or otherwise we have also recorded the spectra of the quinones and the corresponding hydroquinones.

---

[1] M. A. A. Beg and M. S. Siddiqui, *P. J. Sci. Ind. Res.*, **12**, 334, 1970.

[2] R. A. Morton, "Biochemistry of Quinones", Academic Press, London, 1965, p. 23–65.

Toluquinone: In the spectra of the toluquinone and *p*-dihydroxytoluene it is observed that with a decrease in the pH of the solution there is a decrease in the intensity, but the feature remains nearly the same as in the original solution with pH 6. Upon a increase in the pH of the solution, however it is found that the spectrum is very much altered as would be evident from the spectra recorded in figures 1—8. This feature is quite similar to that found in the case of hydroquinones, particularly so in the basic medium. It is known that phenols are ionized in the basic medium, and their ionization leads to an increase in the intensity accompanied with a red shift.[3] Consequently the observation of the bands at 385 and 480 mμ in the basic medium (these bands are absent at pH 2 and pH 6 for the dihydroxytoluene) should be attributed to this ionization.

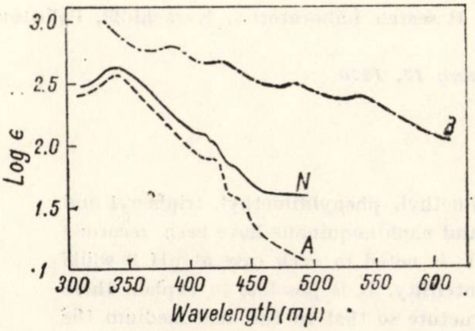

Fig. 1. — Spectrum of toluquinone in the 300—650 mμ region.

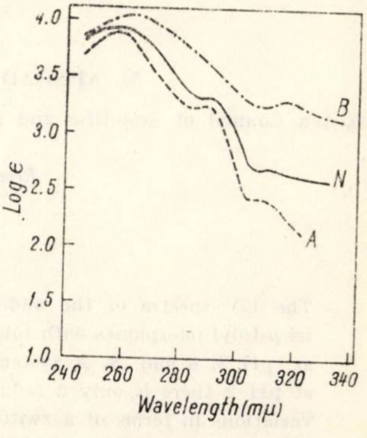

Fig. 2. — Spectrum of toluquinone in the 240—340 mμ region.

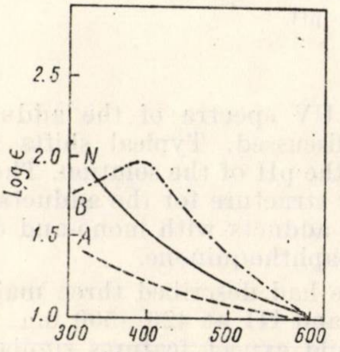

Fig. 3. — Spectrum of dihydroxytoluquinone in the 300—600 mμ region.

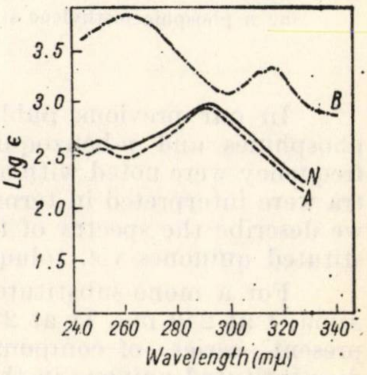

Fig. 4. — Spectrum of dihydroxytoluquinone in the 240—340 mμ region.

---

[3] G. Schwarzenbach and H. Suter, *Helv. Chim. Acta*, **24**, 617 (1941).

Toluquinone Adducts: In all the spectra of the adducts we note the 260 mμ band. This absorption is also found in the Me_3P adducts and a set of 2 to 3 bands is a common feature between 230—265 mμ region. The pattern is similar to the π→π* transition of the benzenoid. The spectra of the phosphine-toluquinone adducts recorded in figures 9—16 show three bands at 320 ± 10, 450 ± 20, and 650 ± 20 mμ, particularly at pH 2 and pH 6. The band positions are in accord with those noted above for a di-substituted quinone. At pH 8 the 320 mμ band disappears but those at 450 ± 20 and 650 ± 20 mμ have an enhanced intensity. Similar enhancement in intensity of these two bands was noted above for dihydroxytoluene. In the adducts therefore, these bands should be due to

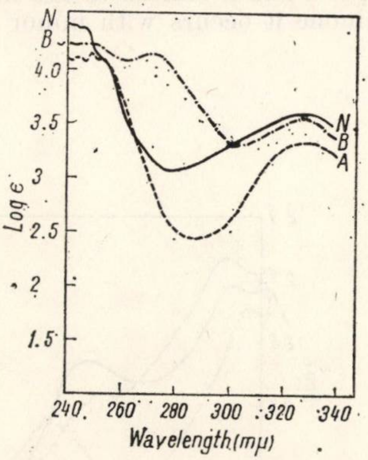

Fig. 5. — Spectrum of *p*-naphthoquinone in the 240—340 mμ region.

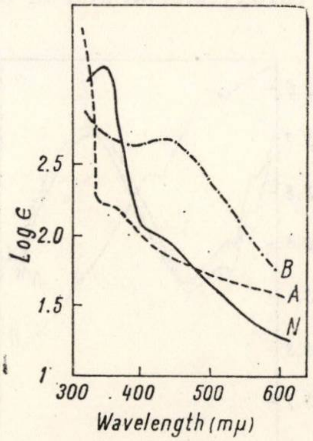

Fig. 6. — Spectrum of *p*-naphthoquinone in the 340—700 mμ region.

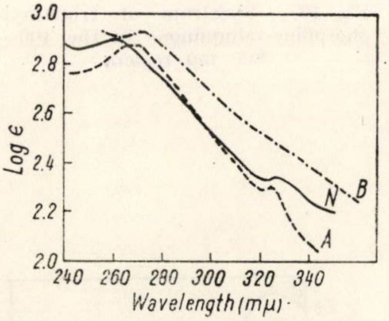

Fig. 7. — Spectrum of hydronaphthoquinone in the 240—340 mμ region.

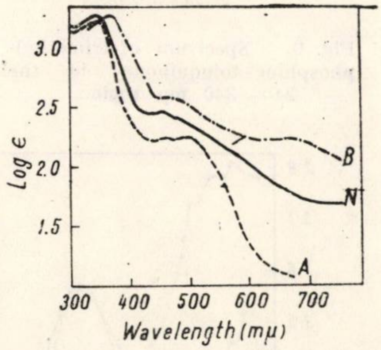

Fig. 8. — Spectrum of hydronaphthoquinone in the 300—700 mμ region.

the ionization of the phenolic group. Although the 320 mμ band is absent at pH 8 for all the adducts it is recorded in the spectra of dihydroxytoluene and toluquinone. If this band is due to the ionization of the phenolic group, it should appear at pH 8 in the phenol as well as in the quinone. The band occurs at 290 mμ at pH 2 and is shifted to 310 mμ at pH 8 in dihydroxytoluene and in toluquinone it occurs with minor shifts in

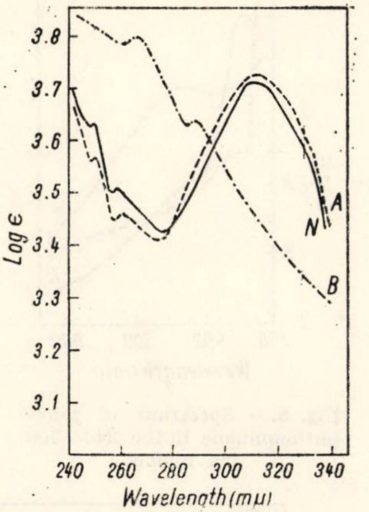

Fig. 9. — Spectrum of trimethylphosphine-toluquinone in the 240—340 mμ region.

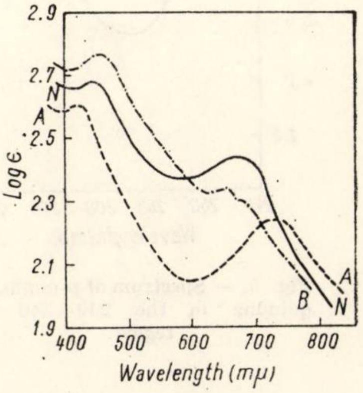

Fig. 10. — Spectrum of trimethylphosphine-toluquinone in the 400—800 mμ region.

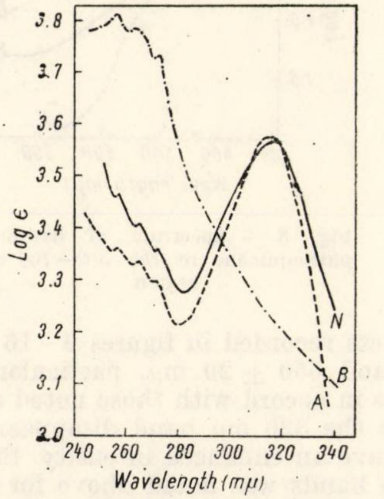

Fig. 11. — Spectrum of phenyldimethylphosphine-toluquinone in the 240—340 mμ region.

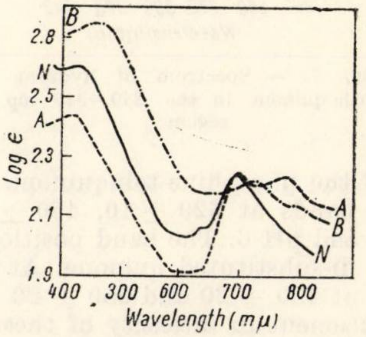

Fig. 12. — Spectrum of phenyldimethylphosphine-toluquinone in the 400—800 mμ region.

the acid as well as basic medium along with the band at 290 mμ observed only at pH 2 and pH 6. This is opposite to the spectra of the adducts where the 320 mμ band appears at pH 2 and pH 6 and the 290 mμ band appears at pH 8. It appears that at pH 2 and pH 6, the carbonyl group is ionized while at pH 8, a phenolic group is ionized. The occurrence of the 290 mμ in the basic medium is similar to that for the toluquinone at pH 2 and pH 6.

Naphthoquinone: The quinone itself has three main maxima at (I) 250, consisting of three peaks at 244, 249 and 254 mμ (II) at 330 and

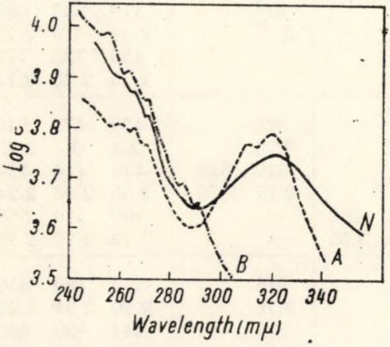

Fig. 13. — Spectrum of triphenylphosphine-toluquinone in the 240—340 mμ region.

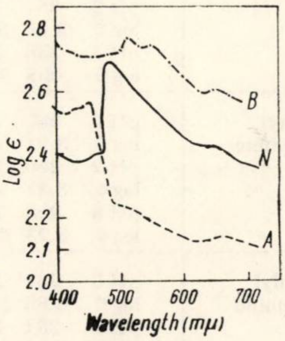

Fig. 14. — Spectrum of triphenylphosphine-toluquinone in the 400—800 mμ region.

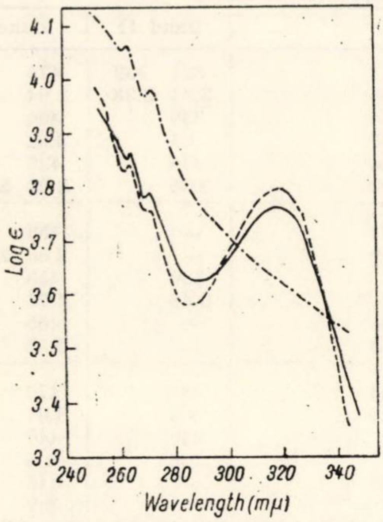

Fig. 15. — Spectrum of tri-p-tolylphosphine-toluquinone in the 240—340 mμ region.

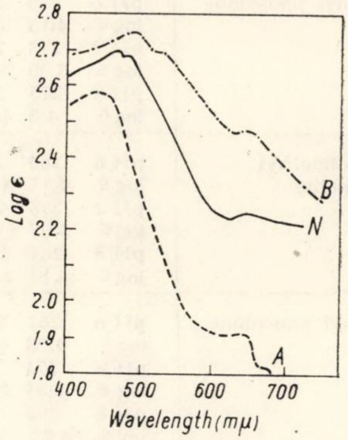

Fig. 16. — Spectrum of tri-p-tolylphosphine-toluquinone in the 400—700 mμ region.

Table 1

UV spectra of phosphine – toluquinone adducts

		Band I					Band II		Band III			
Trimethyl phosphine	pH 6	249	258				310		452	675		
	log ∈	3.63	3.51				3.7		2.69	2.44		
	pH 2	250	260				310		424	730		
	log ∈	3.57	3.46				3.73		2.61	2.24		
	pH 8	266	289				—		458	655	675	
	log ∈	3.8	3.64				—		2.77	2.34	2.3	
Phenyldimethyl phosphine	pH 6	257	265	272			315		428	635	690	
	log ∈	3.46	3.41	3.36			3.57		2.6	2.06	2.25	
	pH 2	257	265	272			314		416	635	695	775
	log ∈	3.36	3.34	3.3			3.57		2.44	1.9	2.25	2.2
	pH 8	256	264	272			—		458	725	777	
	log ∈	3.8	3.79	3.73		—			2.75	2.23	2.14	
Triphenyl phosphine	pH 6	260	266	271			320		470	478	645	
	log ∈	3.91	3.87	3.8			3.75		2.4	2.7	2.43	
	pH 2	260	266	270			310	320	440	446	494	660
	log ∈	3.81	3.80	3.77			3.77	3.79	2.55	2.56	2.24	2.14
	pH 8	256	264	271	285	290	—		490	510	550	648
	log ∈	3.93	3.91	3.86	3.69	3.65	—		2.72	2.77	2.75	2.6
Tri-*p*-tolyl phosphine	pH 6	264	271				318		470	480	650	
	log ∈	3.86	3.79				3.76		2.70	2.69	2.25	
	pH 2	264	271				319		444	450	650	675
	log ∈	3.84	3.76				3.79		2.58	2.5	1.9	1.81
	pH 8	263	272				—		490	518	650	
	log ∈	4.04	3.98				—		2.75	2.73	2.48	

Table 2

UT spectra of phosphine-naphthoquinone adducts

		Band I					Band II		Band III		
Trimethyl phosphine	pH 6	273	283	284			322	332	475		
	log ∈	4.15	3.94	3.96			3.44	3.38	2.94		
	pH 2	273	283	284			330		400		
	log ∈	3.99	3.86	3.87			3.4		3.98		
	pH 8	273	283	284			330		425	480	
	log ∈	4.2	4.02	4.02			3.38		3.08	2.98	
Phenyldimethyl phosphine	pH 6	266	271	284			—		450	465	
	log ∈	4.11	4.12	3.9			—		2.60	2.57	
	pH 2	273	284				330		450		
	log ∈	3.97	3.9				3.46		1.77		
	pH 8	264	271	284			—		465		
	log ∈	4.14	1.15	3.98			—		2.57		
Triphenyl phosphine	pH 6	264	266	284			330		470		
	log ∈	4.23	4.22	3.9			3.5		3.07		
	pH 2	274	287				330		440		
	log ∈	3.88	3.88				3.6		2.6		
	pH 8	262	269	286			—		445		
	log ∈	4.22	4.2	4.01			—		3.2		
Tri-*p*-tolyl phosphine	pH 6	267	271	283	284	287	330		490	520	640
	log ∈	4.24	4.2	4.08	4.07	4.06	3.7		2.7	2.76	2.6
	pH 2	271	283	284	287		310	330	460	625	
	log ∈	4.13	4.04	4.04	4.03		3.7	3.7	2.68	2.46	
	pH 8	260	273	285			310	330	555	635	
	log ∈	4.29	4.27	4.18			3.85	3.55	2.78	2.61	

Table 3

UV spectra of quinone and hydroquinone naphtoquinone

	Band I			Band II		Band III		
pH 6	244	249	254	330	350	420		
log ∈	4.16	4.27	4.17	3.57	3.23	2.00		
pH 2	244	249	254	330	350	—		
log ∈	4.35	4.23	4.11	3.34	3.2	—		
pH 8	241	246	268	325		440		
log ∈	4.25	4.25	4.16	3.53		2.68		
Naphtho Hydro Quinone								
pH 6	260			326	346	455	485	
log ∈	2.9			2.35	3.26	3.11	2.44	
pH 2	267			324	346	455	485	
log ∈	2.88			2.25	2.26	2.25	2.25	
pH 8	270			370		460	660	
log ∈	2.92			3.29		2.60	2.27	
Toluquinone								
pH 6	256	290		309	343	415	422	435
log ∈	3.95	3.33		2.69	2.64	2.11	2.00	1.84
pH 2	256	290		309	343	415	422	435
log ∈	3.93	3.25		2.47	2.60	1.95	1.84	1.60
pH 8	262			314	385	428	480	540
log ∈	3.79			3.32	2.84	2.70	2.51	2.43
p-Dihydroxy Toluene								
pH 6	250	292		—		—		
log ∈	2.63	2.99		—		—		
pH 2	250	292		—		—		
log ∈	2.59	2.96		—		—		
pH 8	262			310	317	400		
log ∈	3.84			3.30	3.35	1.99		

350 and (III) at 420 mμ. In the acid medium band III disappears. At pH 8 a new band appears at 269 mμ while the III band is shifted to 440 mμ. It is of interest to see that naphthohydroquinone also has a set of three bands (1) at 260 mμ (2) at 326 and 346 mμ and (3) at 455 and 485 mμ. The band at 246 mμ is shifted at pH 8 to 370 mμ, and a new band appears in this medium at 660 mμ.

Naphthoquinone Adducts: The spectra are recorded in figure 17 — 24. In the aryl phosphine adducts a band is recorded at 265 ± 2 mμ, which is absent in the trimethylphosphine showing that this band is due to the $\pi \rightarrow \pi^*$ transition of the aryl group on phosphorus. The other bands occur at 270 ± 2 mμ. The intensity in each case is highest for the basic medium, followed by those at pH 6 and pH 2. Since the bands in this region are due to the benzenoid absorption, not much variation is anticipated any way.

The pattern regarding the pH sensitive 320 mμ band in toluquinone is followed in the naphthoquinone adducts also except those of trimethyl

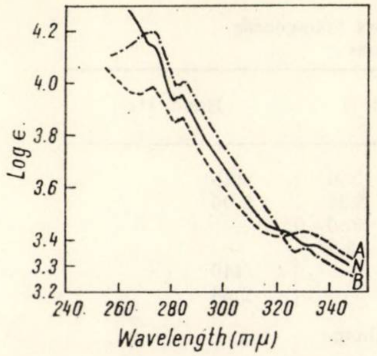

Fig. 17. — Spectrum of trimethylphosphine-naphthoquinone in the 240—340 mμ region.

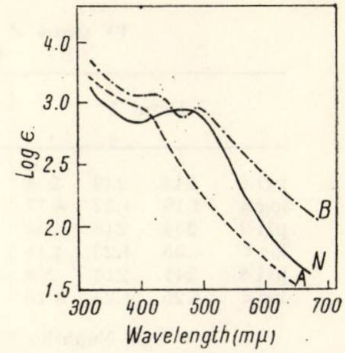

Fig. 18. — Spectrum of trimethylphosphine-naphthoquinone in the 300—700 mμ region.

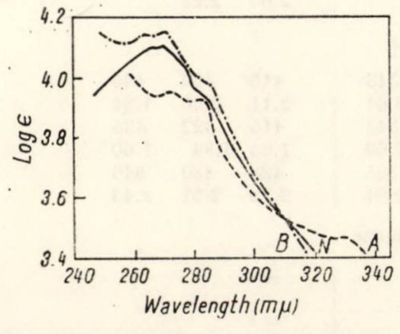

Fig. 19. — Spectrum of phenyldimethylphosphine-naphthoquinone in the 240—340 mμ region.

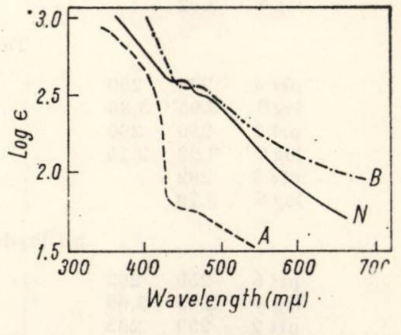

Fig. 20. — Spectrum of phenyldimethyl phosphine - naphthoquinone in the 300—700 mμ region.

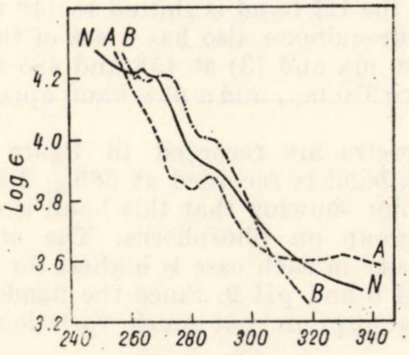

Fig. 21. — Spectrum of triphenylphosphine-naphthoquinone in the 240—340 mμ region.

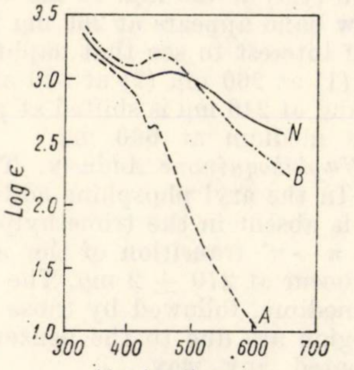

Fig. 22. — Spectrum of triphenylphosphine-naphthoquinone in the 300—700 mμ region.

and tritolylphosphines, where we note a considerable decrease in intensity. This possibly indicates only partial ionization of the phenolic hydroxyl in these two compounds at pH 8. In these adducts the third set of bands occurring at 480 mμ is susceptible of pH variation as noted for toluquinone. In the trimethyl phosphine adducts a single band at 480 mμ is shifted to lower wavelengths and occurs at 400 mμ at pH 2, while at pH 8 it is split into two which occur at 425 and 480 mμ. In the phenyldimethylphosphine adduct, pH 6 records two maxima at 450 and 465 mμ. At pH 2 the intensity of the former is very much lower while at pH 8 there is only one band at 465 mμ with approximately the same intensity. In the triphenyl phosphine adducts the band is observed at 470 mμ, which is shifted to 440 mμ at pH 8 and in the acid medium only the 440 mμ band is observed. Similarly the tritolylphosphine adduct has a band at 510 mμ with a shoulder at 490 mμ at pH 6, and another one at 640 mμ. At pH 2 these bands are shifted to 460 and 625 mμ respectively, while at pH 8, the bands occur at 555 and 635 mμ.

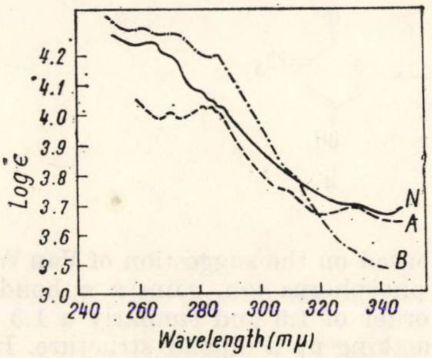

Fig. 23. — Spectrum of tri-*p*-tolylphosphine-naphthoquinone in the 240—340 mμ region.

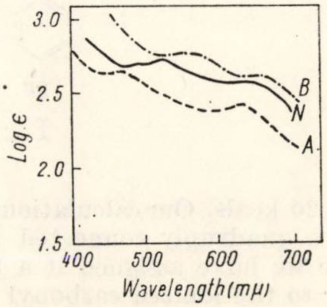

Fig. 24. — Spectrum of tri-*p*-tolylphosphine-naphthoquinone in the 400—700 mμ region.

The naphthoquinone adducts with trimethyl and tritolyl phosphines seem to be more stable since they are rather insensitive to pH variation particularly in the 320 mμ region. It must be realized that the oxidation potential of this quinone is much lower than that of benzoquinone and toluquinone. It is therefore quite likely that a phosphinemethylene structure is more favorable in these cases.

It is tempting to make a comparison of these spectra with those of tautomeric systems like pyridine carboxylic acids where also the position and intensity of the bands are pH dependent. [4] The phenolic hydroxyl group is ionized at higher pH and since a red shift with enhanced intensity is characteristic of phenols it is suggested that at lower hydrogen ion concentrations we should expect a phenolic character as obtained in phosphinemethylenes. Band III here is due to n→π transition [5] and a decrease in intensity only implies that the carbonyl group is being ionized in the acid medium.

---

[4] H. P. Stephenson and H. Sponer, *J. Amer. Chem. Soc.*, **79**, 2050 (1957).

[5] J. W. Sidman, *J. Amer. Chem. Soc.*, **78**, 2363 (1956).

On the basis of energetics structure II should be more stable by at least 20 kcals. Our calculations are based on the suggestion of Van Wazer[6] that a quadruply connected ionic phosphorus ion, gains a π bond and hence we have assigned it a bond order of 1.5 and similarly a 1.5 bond order to the ionized carbonyl thus making up a dipolar structure. In our earlier paper [7] also we had seen that there are evidences for an ylid structure, II. We may therefore, explain the present results by keeping in view three sets of chromophores, 1) the benzenoid, 2) the quinonoids and 3) the phenolics. The benzenoids absorb at 250–270mμ. The quinonoids absorb at 260–290 and 400–450 mμ and the phenolic hydroxyl at 270 and 320 mμ with the latter shifting to 400 mμ with enhanced intensity [8]. These assignments are borne out from the spectra of the quinones and hydroquinones. The quinones absorb at the same position, in the acid medium. There is however, a decrease in intensity suggesting partial ionization. The phenols are ionised in the basic medium and the pattern of absorption is completely changed. The spectra of the adducts also indicate similar changes. It may be seen that both structures I and II have an O–H group. Therefore in the acid medium both should have similar patterns since phenols are not ionized in this medium. The reduction in intensity is due to protonation which blocks the lone pair interaction with the π electrons.

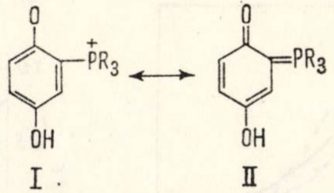

I. II

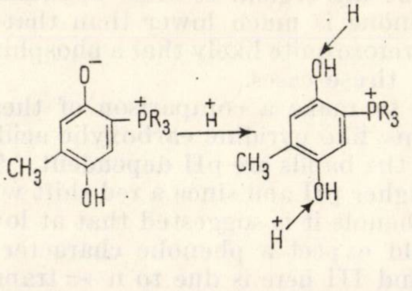

---

[6] J. Van Wazer, "Phosphorus and its Compounds" vol. 1, Interscience Publishers Inc., New York, 1958, p. 42–43.

[7] M. A. A. Beg and M. S. Siddiqui, *Tetrahedron*, **22**, 2203 (1966).

[8] W. Baker and W. D. Ollis, "Recent Developments in the Chemistry of Natural Phenolic Compounds", Edited by W. D. Ollis, Pergamon Press, Oxford, 1961.

The ionization of phenols in the basic medium changes the spectrum.

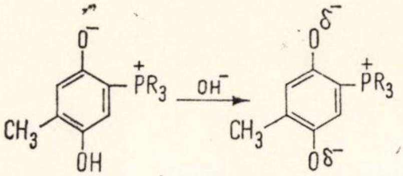

This ionization leads to the stabilization of the ylid structure since energetically this is more stable.

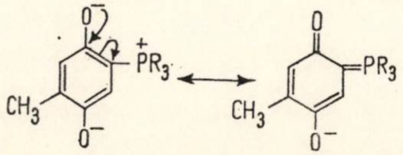

From a comparison with the data from α haloketones also we find that there would be an intensification accompanied by a red shift if there is an orbital situated so as to overlap with the π orbital[9]. This supports an *o*-quinonoid structure for the compound in the basic medium.

Conclusion : The UV study of the phosphine adducts with the *p*-quinones in general suggests that the equilibrium between the phosphobetaine and the phosphinemethylene is pH dependent.

EXPERIMENTAL

The phosphines and the adducts were prepared as described earlier.[7] Toluquinone was prepared by the oxidation of *m*-toluidine and the hydroquinones by the reduction of quinones.

The spectra were recorded on a Beckman DK-2 spectrophotometer in methanol solutions. The pH of the solutions was altered by adding a drop of HCl or NaOH to the original solution and the pH was measured by a pH-meter.

[9] N. L. Allinger, J. C. Tal and M. A. Miller, *J. Amer. Chem. Soc.*, **88**, 4495 (1966).

Revue Roumaine de Chimie, **15**, 1665 – 1673 (1970)

ULTRASONIC VELOCITY, COMPRESSIBILITY AND EXCESS VOLUME OF MOLTEN SALTS : NaCl + (Li, K, Rb, Cs) Cl

S. STERNBERG and V. VASILESCU

Institute of Physical Chemistry, Bucharest Str. Galaţi 31

Received March 10, 1970

The velocities of ultrasonic waves in NaCl + XCl (X = Li, K, Rb, Cs) mixtures have been measured and adiabatic and isothermal, compressibilities have been calculated. Some considerations on the correlation between the excess compressibility and excess volume in molten salts mixtures are presented; use has been made of Hildebrand-Scatchard theory as well as of the hole theory.

In previously published papers,[1-3] the ultrasonic velocity and the compressibility of binary mixtures KCl + KBr, $PbCl_2$ + (Li, Na, K, Rb, Cs) Cl, $MgCl_2 + BaCl_2$, $MgCl_2$ + KCl have been studied.[1-3]

In the present paper similar results are given for the systems NaCl + XCl (X = Li, K, Rb, Cs). These systems present positive excess volumes increasing in Li to Cs order. Some considerations on excess isothermal compressibility β^E, excess volume V^E, excess expansion coefficient α^E, as well as the molar sound velocity R and its excess value R^E, are also given.

EXPERIMENTAL

Ultrasonic waves of 1 M Hz were passed into the melt and picked up by silica rods.[1-7] Measurements were carried out in a silica crucible soldered at the lower silica rod.[1-3] A pulse, phase interference method (20 μ s pulses with 200 Hz repetition frequency) was used.

---

[1] S. Sternberg and V. Vasilescu, *Rev. Roumaine Chim.*, **12**, 1187 (1967).

[2] S. Sternberg and V. Vasilescu, *Rev. Roumaine Chim.*, **13**, 266 (1968).

[3] S. Sternberg and V. Vasilescu, *J. Chem.-Thermodynamics*, **1**, 595 (1969).

[4] N. E. Richard, E. J. Brauner and J. O'M. Bockris, *Brit. J. Appl. Phys.*, **6**, 387 (1956).

[5] J.O'M Bockris and N. E. Richards, *Proc. Roy Soc.*, A, **241**, 44 (1957).

[6] J. O'M Bockris, A. Pilla, J. L. Barton, *Rev. Chim. Acad. R.P.R.*, **2**, 69 (1962).

[7] J.O'M Bockris, T. L. White and T. O. Mackenzie, "Physico-Chemical Measurements at High Temperatures", Butterworths, London, 1959, p. 284.

The maximum error in individual velocity determinations was ±5 ms^{-1} (approximately 0.3 %) while the temperature gradient through the sample was of up to 0.5° K cm^{-1}. A more detailed description of the device used and of the method, was given elsewhere.[1] The salts used in measurements were prepared from Merck reagents by recrystallization, gradual heating in vacuum, melting and bubbling with CCl_4 and argon. LiCl was prepared by the same method, and the solid salt was kept over P_2O_5 in a vacuum desiccator.

RESULTS

A linear dependence of velocity on temperature[1-3] holds for the systems studied in the present paper:

$$u = u_0 - at \tag{1}$$

where u and u_0 are the ultrasonic velocities at t and $t = 0°C$ respectively while a, is the temperature coefficient of the velocity. The u_0 and a values are given in table 1.

Table 1

Temperature variation of ultrasonic velocity in simple salts and mixtures

NaCl+LiCl			NaCl+KCl		
X_{NaCl}	u_0/m.s^{-1}	a/m.s^{-1}.K^{-1}	X_{NaCl}	u_0	a
0	2572	0.846	0	2273	0.865
0.5	2449	0.818	0.207	2272	0.872
1	2405	0.811	0.512	2316	0.875
			0.729	2322	0.818
			1.0	2405	0.811
NaCl+RbCl			NaCl+CsCl		
X_{NaCl}	u_0	a	X_{NaCl}	u_0	a
0	1804	0.714	0	1558	0.636
0.25	1878	0.743	0.25	1671	0.715
0.50	1957	0.733	0.50	1758	0.667
0.57	2149	0.792	0.75	1967	0.724
1.0	2405	0.811	1	2405	0.811

The adiabatic compressibility was calculated according to the well known relation $\beta_s = 1/u^2\rho$ where ρ is the density; use was made of Zuca's[8] density data for NaCl + (Li,Rb, Cs) Cl systems and of Van Artsdalen's[9] for NaCl + KCl. The adiabatic compressibilities for the 4 systems at 1073°K are represented on figure 1. The isothermal compressibility was calculated from the equation

$$\beta = \gamma\,\beta_s \text{ where } \gamma \text{ is the } C_p/C_v \text{ ratio.}$$

---

[8] S. Zuca and M. Olteanu, *Rev. Roumaine Chim.* (in press).

[9] E. R. Van Artsdalen and I. S. Yaffe, *J. Phys. Chem.*, **59**, 118 (1955).

For the calculation of γ in simple melts the following equation was used :

$$\gamma - 1 = \frac{u^2\,\alpha^2\,T\,M}{C_p} \tag{2}$$

where α is the thermal expansion coefficient, and M is the molecular mass.

Equation (2) is no longer valuable for γ calculations in molten salts mixtures as their heat capacities have not been determined so far.

In our previous papers the γ values for the mixtures have been calculated from those for simple melts by an additivity rule.

An approximate evaluation of γ is possible with C_V considered additive : $C_V = X_1C_{V1} + X_2C_{V2}$ where X_1 and X_2 are the molar fractions and C_{V1} and C_{V2} are the heat capacity at constant volume for the pure molten salts. This approximation is plausible for those mixtures in which no new molecular species occur. With this assumption, equation (2) gives :

$$C_p = \frac{C_V \pm C_V^2 + \dfrac{4\alpha^2\,TV}{\beta_s}\,C_V}{2} \tag{3}$$

where V is the molar volume and the sign which makes physical sense is plus. The γ values calculated by help of equation (3) are very sensitive to the variation of thermal expansion coefficient α, magnitude which is subject to errors as it is calculated from density change *versus* temperature. That is why, we preferred to calculate γ according to the additivity relation we have been using so far ($\gamma = X_1\gamma_1 + X_2\gamma_2$). In table 2 the values of γ additively calculated and those calculated by making use of equation (3), are compared. One can see the good agreement between the two sets of values, but those for 0.75 NaCl + RbCl and 0.50 NaCl—CsCl. It is evident that the discrepancy could be ascribed to errors in α determinations. C_p values given in references [10] and [5] have been used in calculations.

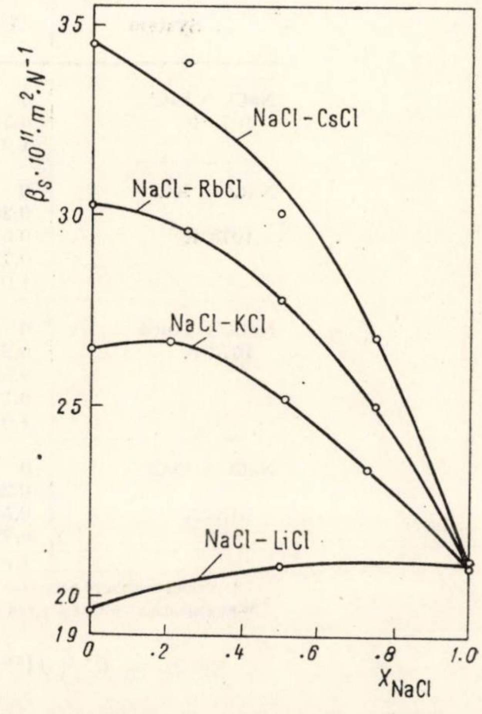

Fig. 1. — Adiabatic compressibility of NaCl + + XCl (X = Li, K, Rb, Cs) at 1073°K.

---

[10] O. Kubaschewski, E. L. Evans and C. B. Alcock, "Metallurgical Thermochemistry", Pergamon Press, New York, 1967, pp. 396, 401, 404.

To make a more complete characterization of these systems, the pressure and temperature coefficients of the excess volume $(\partial V^E/\partial p)_T$ and $(\partial V^E/\partial T)_p$ respectively, have been calculated too. For the pressure coefficients the following equation was used.[3,11]

Table 2

Values of γ for the systems under study

System	X_{NaCl}	$\gamma^{*)}$	$\gamma^{**)}$
NaCl + LiCl	0	1.23	1.23
1073°K	0.50	1.29	1.28
	1.0	1.35	1.35
NaCl + KCl	0	1.45	1.45
	0.207	1.43	1.43
1073°K	0.512	1.40	1.39
	0.729	1.38	1.37
	1.0	1.35	1.35
NaCl + RbCl	0	1.47	1.47
1073°K	0.25	1.44	1.44
	0.50	1.41	1.40
	0.75	1.38	1.52
	1.0	1.35	1.35
NaCl + CsCl	0	1.44	1.44
	0.25	1.42	1.41
1073°K	0.50	1.40	1.45
	0.75	1.37	1.41
	1.0	1.35	1.35

*) Values calculated according to the additivity rule.

**) Calculated with C_p given by equation (3).

$$\beta^E = -V^{-1}(\partial V^E/\partial p)_T - \beta_0 V^E/V_0 \tag{4}$$

The excess volume was calculated according to an equation previously deduced by us[3] on the basis of Hildebrand's theory:

$$V^E = -V\left[\frac{(\partial V^E/\partial p)_T}{\beta V} + 1\right] + V\left[\left\{\frac{(\partial V^E/\partial p)_T}{\beta V} + 1\right\}^2 + \right.$$
$$\left. + \frac{2}{V}\{V_I^E + TV_0\alpha^E\}\right]^{1/2} \tag{5}$$

the term V_I^v being given by the equation:

$$V_I^E = -V_0\beta_0 T\left(\frac{\alpha}{\beta} - \frac{\alpha_0}{\beta_0}\right) \tag{6}$$

---

[11] I. Prigogine, "The Molecular Theory of Solutions", North Holland Publishing Company, Amsterdam 1957, p. 16

and V_0, α_0 and β_0 representing the ideal values of molar volume, expansion coefficient and compressibility respectively. Equation (6) was found out [3] by starting from Hildebrand's formula and making the substitution :

$$(\partial E/\partial V)_T = T\frac{\alpha}{\beta} \tag{7}$$

where E is the internal energy.

The hole theory in the form given by Bockris [5] was used and we obtained for the $\frac{\beta}{\beta_0}$ ratio the relation :

$$\frac{\beta}{\beta_0} = \frac{\frac{\beta'}{\beta_0'} + \theta\frac{\beta_{(s)}}{\beta_0'}}{1 + \theta\frac{\beta_{(s)}}{\beta_0'}} \tag{8}$$

where β' and β_0' are the real and ideal contributions of holes to the compressibility, $\beta_{(s)}$ and $\beta_{(s)0}$ the similar values due to the liquid lattice, while θ is a coefficient whose value lies between 0 and 1. Finally, use was made of Rao's equation [12] in the form which fits molten salts [13-15, 1,2] and the molar ultrasonic velocity (R) was calculated :

$$R = Vu^{2/3} \tag{9}$$

In table 3 the R values for the four systems at 3 temperatures are given ; as expected R does not depend on temperature.

The excess ultrasonic molar velocity $R^E = R - R_0$ was also calculated ; R_0 the ideal value of R was given by :

$$R_0 = V_0 u_0^{2/3} \tag{10}$$

where $V_0 = X_1V_1 + X_2V_2$ and u_0 (the ideal value of ultrasonic velocity) was calculated according to the equation :

$$u_0^2 = \frac{1}{\beta_{s0}\,\rho_0} \tag{11}$$

β_{s0} and ρ_0 are the ideal adiabatic compressibility and density respectively ;

$$\beta_{(s)0} = \varphi_1\beta_{s1} + \varphi_2\beta_{s2}\,, \quad \rho_0 = \varphi_1\rho_1 + \varphi_2\rho_2$$

---

[12] R. Rao, *Indian J. Phys.*, **14**, 109 (1940).

[13] S. V. Subrahnanyam and T. Bhimasenachor, *J. Phys. Soc. Japan*, **17**, 1447 (1961).

[14] R. W. Higgs and T. A. Litovitz, *J. Acoust. Soc. America*, **32**, 1108 (1960).

[15] A. V. Satyavati, *Acustica*, **21**, 51, (1969).

φ_1 and φ_2 are the volume fractions, β_{s1}, β_{s2} the compressibilities of simple melts, ρ_1, ρ_2 the densities of simple melts.

Table 3

Values of molar ultrasonic velocity at 1073, 1173, 1273° K for the four systems under study

System	X_{NaCl}	$10^3 R$ MKS units		
		1073°K	1173°K	1273°K
NaCl + LiCl	0	4.58	4.58	4.58
	0.50	5.00	5.01	5.01
	1.0	5.47	5.49	5.52
NaCl + KCl	0	6.70	6.71	6.72
	0.207	6.38	6.39	6.40
	0.512	6.00	6.01	6.01
	0.729	5.75	5.77	5.78
	1.0	5.46	5.49	5.51
NaCl + RbCl	0	6.40	6.40	6.40
	0.25	6.07	6.07	6.07
	0.50	5.79	5.80	5.81
	0.75	5.59	5.66	5.72
	1	5.47	5.49	5.52
NaCl + CsCl	0	6.60	6.60	6.60
	0.25	6.15	6.13	6.10
	0.50	5.87	5.91	5.94
	0.75	5.53	5.55	5.57
	1.0	5.47	5.49	5.52

Subrahmanyam [13] and Satyavati [15] introduced R^+ and R^- values for the ions of simple molten salt and considered $R = R^+ + R^-$. This assumption suggests a very simple additivity rule for mixtures:

$$R_{\text{add}} = X_1 R_1 + X_2 R_2 \tag{12}$$

R_1 and R_2 representing the molar velocities of simple salts. We attempted to check this rule by calculating

$$\Delta R = R - R_{\text{add}} \tag{13}$$

It is worth to be mentioned that R_{add} is different from R_0. In tables 4—7 the following data for the studied systems are given: γ, β, β^E, α, α^E, β^E/β_0, $(\beta^E/\beta_0)_{\text{calc}}$ (according to (8)), $(\partial V^E/\partial p)_T$, $(\partial V^E/\partial T)_p$, V^E, V^E_I, V^E_{calc} (according to (5)), R, R_{add}, ΔR, R_0 and R^E. The compressibilities of solid salts used in calculations were taken from reference [16] and θ in equation (8) was considered 0.5.

---

[16] International Critical Tables of Numerical Data, Physics, Chemistry and Technology, Vol. 3, McGraw-Hill, New York — London, 1928, p. 49.

DISCUSSION

The systems under consideration do not form complex combinations in molten state, their phase diagrams indicating the formation of solid solutions for systems NaCl + LiCl (I), NaCl + KCl (II) and eutectics for systems NaCl + RbCl (III) and NaCl + CsCl (IV).

Table 4

Excess quantities for NaCl + LiCl at 1073° K

X_{NaCl}	0.0	0.50	1.0
γ	1.23	1.29	1.35
$10^{11} . \beta m^2 N^{-1}$	24.2	26.8	28.2
$10^{11} . \beta^E \ m^2 N^{-1}$	0	0.4	0
$10^4 . \alpha K^{-1}$	2.99	3.26	3.50
$10^4 . (\alpha^E K^{-1}$	0	0.01	0
$100 \, \beta^E / \beta_0)$	0	1	0
$100 \, (\beta^E / \beta_0)$*)	0	1	0
$10^{15} (\partial V^E / \partial p)_T m^5 N^{-1} \mathrm{mol}^{-1}$	0	−0.16	0
$10^{10} (\partial V^E / \partial T)_p m^3 K^{-1} \mathrm{mol}^{-1}$	0	0	0
$10^6 V^E m^3 \ \mathrm{mol}^{-1}$	0	0.06	0
$10^6 V_I^E m^3 \mathrm{mol}^{=1}$**)	0	0.14	0
$10^6 V^E m^3 \mathrm{mol}^{-1}$***)	0	0.09	0
$10^3 R$ MKS units	4.58	5.00	5.47
$10^3 R_{\mathrm{add}}$ MKS units	4.58	5.03	5.47
$10^3 \Delta R$ MKS units	0	−0.03	0
$10^3 \ R_0$ MKS units	4.58	5.02	5.47
$10^3 \ R^E$ MKS units	0	−0.02	0

*) according to equation (8)

**) according to equation (6)

***) according to equation (5)

Table 5

Excess quantities for NaCl + KCl at 1073° K

X_{NaCl}	0	0.207	0.512	0.729	1.0
γ	1.45	1.43	1.40	1.38	1.35
$10^{11} \cdot \beta m^2 N^{-1}$	38.4	38.2	35.3	32.3	28.1
$10^{11} \cdot \beta^E m^2 N^{-1}$	0	1.5	1.5	0.8	0
$10^4 \cdot \alpha K^{-1}$	3.86	3.88	3.73	3.64	3.49
$10^4 \cdot \alpha^E K^{-1}$	0	0.08	0.03	0.03	0
$100 (\beta^E / \beta_0)$	0	4	4	3	0
$100 (\beta^E / \beta_0)$*)	0	3	3	1	0
$10^{15} (\partial V^E / \partial p)_T m^5 N^{-1} \mathrm{mol}^{-1}$	0	−0.79	−0.74	−0.36	0
$10^{10} (\partial V^E / \partial T)_p m^3 K^{-1} \mathrm{mol}^{-1}$	0	6	3	3	0
$10^6 V^E m^3 \mathrm{mol}^{-1}$	0	0.22	0.25	0.10	0
$10^6 V_I^E m^3 \mathrm{mol}^{-1}$ **)	0	0.35	0.60	0.26	0
$10^6 V^E m^3 \mathrm{mol}^{-1}$ ***)	0	0.78	0.77	0.40	0
$10^3 \ R$ MKS units	6.70	6.38	6.00	5.75	5.46
$10^3 \ R_{\mathrm{add}}$ MKS units	6.70	6.44	6.07	5.80	5.46
$10^3 \ \Delta R$ MKS units	0	−0.06	−0.07	−0.05	0
$10^3 \ R_0$ MKS units	6.70	6.44	6.04	5.78	5.46
$10^3 \ R^E$ MKS units	0	−0.05	−0.04	−0.03	0

*) according to equation (8)

**) according to equation (6)

***) according to equation (5)

Table 6

Excess quantities for NaCl + RbCl at 1073° K

X_{NaCl}	0	0.25	0.50	0.75	1.0
γ	1.47	1.44	1.41	1.38	1.35
$10^{11} \cdot \beta m^2 N^{-1}$	44.5	42.6	39.2	34.5	28.2
$10^{11} \beta^E m^2 N^{-1}$	0	1.1	1.3	0.9	0
$10^4 \cdot \alpha K^{-1}$	3.92	3.89	3.82	4.58	3.52
$10^4 \alpha^E K^{-1}$	0	0.04	0.06	0.93	0
$100\ (\beta^E/\beta_0)$	0	3	3	3	0
$100\ (\beta^E/\beta_0)$*)	0	3	3	3	0
$10^{15}\,(\partial V^E/\partial p)_T m^5 N^{-1} \mathrm{mol}^{-1}$	0	−0.66	−0.72	−0.48	0
$10^{10} (\partial V^E/\partial T)_p m^3 K^{-1} \mathrm{mol}^{-1}$	0	8	4	42	0
$10^6 V^E m^3\ \mathrm{mol}^{-1}$	0	0.23	0.29	0.30	0
$10^6 V_I^E m^3\ \mathrm{mol}^{-1}$**)	0	0.34	0.34	−3.67	0
$10^6 V^E m^3\ \mathrm{mol}^{-1}$***)	0	0.58	0.66	0.54	0
$10^3\ R$ MKS units	6.40	6.07	5.79	5.59	5.47
$10^3\ R_{\mathrm{add}}$MKS units	6.40	6.17	5.94	5.70	5.47
$10^3\ \Delta R$ MKS units	0	−0.10	−0.15	−0.11	0
$10^3\ R_0$ MKS units	6.40	6.10	5.84	5.61	5.47
$10^3\ R^E$ MKS units	0	−0.03	−0.05	−0.02	0

*) according to equation (8)
**) according to equation (6)
***) according to equation (5)

Table 7

Excess quantities for NaCl + CsCl at 1073°K

X_{NaCl}	0	0.25	0.50	0.75	1.0
γ	1.44	1.42	1.40	1.37	1.35
$10^{11} . \beta\, m^2\, N^{-1}$	49.7	48.3	42.1	36.7	28.2
$10^{11} . \beta^E\ m^2\, N^{-1}$	0	2.1	3.1	0.7	0
$10^4 . \alpha\ K^{-1}$	4.12	4.06	4.26	4.06	3.52
$10^4\ \alpha^E\ K^{-1}$	0	0.04	0.36	0.32	0
$100\ (\beta^E/\beta_0)$	0	5	8	2	0
$100\ (\beta^E/\beta_0)$*)	0	6	6	2	0
$10^{15} . (\partial V^E/\partial p)_T\ \mathrm{m}^5\ N^{-1}$ mol^{-1}	0	−1.43	−1.80	−0.38	0
$10^{10}\ (\partial V^E/\partial T)_p\ m^3\ K^{-1}$ mol^{-1}	0	4	34	16	0
$10^6\ .\ V^E\ m^3\ \mathrm{mol}^{-1}$	0	0.46	0.52	0.21	0
$10^6\ .\ V_I^E\ m^3\ \mathrm{mol}^{-1}$**)	0	0.82	−0.26	−1.14	0
$10^6\ .\ V^E\ m^3\ \mathrm{mol}^{-1}$***)	0	1.11	1.82	0.39	0
$10^3\ R$ MKS units	6.60	6.15	5.87	5.53	5.47
$10^3\ R_{\mathrm{add}}$ MKS units	6.60	6.32	6.04	5.75	5.47
$10^3 \Delta R$ MKS units	0	−0.17	−0.17	−0.22	0
$10^3\ R_0$ MKS units	6.60	6.19	5.83	5.56	5.47
$10^3\ R^E$ MKS units	0	−0.04	0.04	−0.03	0

*) according to equation (8)
**) according to equation (6)
***) according to equation (5)

In this series the excess volumes increase in the sequence (I)—(IV) while the excess compressibilities increase in the same order, confirming a parallelism previously established.[1–3] It is also visible that the excess volumetric properties, V^E, β^E, α^E increase as the interionic separations increase. As the radius of changeable cation increases in the series (from

Li to Cs) the packing at mixing is more imperfect, the excess volume greater and as a consequence the excess compressibility increases. The values of $(\partial V^E/\partial p)_T$ are negative in all the studied systems and the absolute values increase in the same order. On the other hand $(\partial V^E/\partial T)_p$ is positive in all systems, its sign being the same with that of α^E.

The $\frac{\beta^E}{\beta_0}$ values calculated from the hole theory by equation (8) agree with the experimental data and this confirm the hypothesis we made about the origin of excess volume and excess compressibility in molten salts. In these mixtures, too, it is very likely that the greatest part of the positive excess volume comes from the increased overall hole volume. This brings in the rapid increase of compressibility and this explains the fact that β^E/β_0 is 4–6 times higher than V^E/V_0.

For "normal" mixtures of molecular liquids, Hildebrand assumed the relation $V = \beta_0 H^E$, which correlates the excess volume and heat of mixing. This equation does not hold for the systems under consideration: they all have positive V^E values, while H^E is negative in all of them: H^E_{05} is -280 cal for (I),[17] -130.5 cal for (II),[17] -238 cal for (III)[18] and -245 cal for (IV).[17]

The excess volumes calculated by equation (5) give a good sign agreement with experimental data; the equation (6) gives in many cases a better numeric agreement than (5), but the sign agreement is poorer.

As one can see in tables 4–7 the additivity of molar velocities which was stated for simple melts, does not hold for binary mixtures of molten salts, even if these are very simple ones; ΔR takes always considerable values.

As already underlined above, the molar velocity, R is constant on a wide range of temperatures both in simple salts and mixtures; this was to be expected since equation (9) is based upon temperature dependence of density and ultrasonic velocity. On the other hand, the low values of R are remarkable; this behaviour could be better understood by means of the relation:

$$(V/_{V_0})^4 = \beta/_{\beta_0}\,(R/_{R_0})^3 \tag{14}$$

which is easily obtained from equation (9). From the results we present in this paper, as well as from previous ones,[2,2] it results that in many molten salts mixtures the β/β_0 ratio, is only a little larger than $(V/V_0)^4$ while $(R/R_0)^3$ is a correction term only slightly smaller than unit.

---

[17] O. J. Kleppa, L. S. Hersh and J. M. Toguri, *Acta Chem. Scand.*, **17**, 2681 (1963).

[18] J. G. Murgulescu, D. I. Marchidan and C. Telea, *Rev. Roumaine Chim.*, **11**, 1031 (1966).

Revue Roumaine de Chimie, **15**, 1675–1680 (1970)

THE HEAT OF MIXING IN BINARY SYSTEMS OF MOLTEN SALTS : KCl + RbBr AND KBr + RbCl

D. I. MARCHIDAN and CR. TELEA

Institute of Physical Chemistry, Bucharest, Str. Galaţi 31

Received April 3, 1970

The dependence of heat of mixing on concentration was determined in the systems KCl + RbBr and KBr + RbCl with a platinum isoperibol calorimeter for high temperatures. The values obtained for 860° are relatively small and of opposite sign. The sign of the heat of mixing is given by the reciprocal Coulombian effect. The processing of data evidenced an unlike coordination of the ions in mixture.

For a ternary system containing the A^+, B^+, C^- and D^- ions, the heat of mixing could be expressed by the sum of the heat of mixing of the respective binary systems and an additional term which is called excess ternary enthalpy. On the other hand the values of excess ternary enthalpy may be obtained from the theory of conformal solutions [1] and the quasichemical approximation.[2,3]

The study of the system with about equally sized ions showed that this approximation accounts well enough for the experimental values obtained.[4,5]

Whenever the ions have significantly different sizes, the deviations from the random mixing are proportional with the difference between the ionic size and ionic asymmetry.[6]

Taking into account Blander's [2] asymmetric approximation in the form given by Førland,[3] the thernary excess enthalpy for K—Rb—Br—Cl system was calculated. The comparison with experimental data and with the values obtained from the symmetric approximation put into evidence an additional factor that is the unlike coordination capacity of ions in the mixture.

---

[1] M. Blander, "Advances in Chemical Physics", vol. 2, Ed. by I. Prigogine, Interscience, London, 1967, p. 112.

[2] M. Blander and L. E. Topol, *Electrochim. Acta*, **10**, 1161 (1960).
M. Blander and J. Braunstein, *Ann. New York Acad. Sci.*, **79**, 838 (1960).
M. Blander, *J. Chem. Phys.*, **34**, 432 (1961).

[3] H. Flood, T. Førland and K. Grjotheim, *Z. anorg. Chem*, **276**, 289 (1954).
T. Førland," Fused Salts" McGraw-Hill, New York, 1964, p. 63—64.

[4] O. J. Kleppa and J. M. Toguri, "Selected Topics in High Temperature Chemistry", Ed. by T. Førland, Universitetsforlaget, Oslo, 1966, p. 15—26.

[5] D. I. Marchidan and Cr. Telea, *Rev. Roumaine Chimie*, **14**, 1495 (1969).

[6] S. V. Meschel, J. M. Toguri, O. J. Kleppa, *J. Chem. Phys.*, **45**, 3075 (1966).

EXPERIMENTAL

The heat of mixing of the reciprocal K-Rb-Cl-Br system was directly determined with an isoperibol calorimeter described elsewhere .[7] The salts were dried at 125°, then melted in purified nitrogen atmosphere.

The provenance and purity of the salts were the following ;

- Potassium chloride — p.a. Austranal.
- Potassium bromide — p.a. E. Merck.
- Rubidium chloride — c.p. Chemapol.
- Rubidium bromide — p.a. Schuchard, Munich.

The dried salts were stored in vacuum over P_2O_5.

The thermal effects have been recorded on X — Y Luxytrace (SEFRAM-France) recorder (fig. 1). An increasing voltage produced by a circular-linear potentiometer actuated by a clockwork mechanism was fed into the X input. The sensitivity of the recorder was 10^{-6}V/mm ; the recording speed was conveniently chosen by changing the voltage applied to the potentiometer and the speed of the clockwork mechanism.

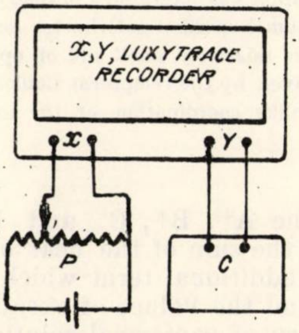

Fig. 1. — P — potentiometric scheme with rising voltage ; C — calorimeter.

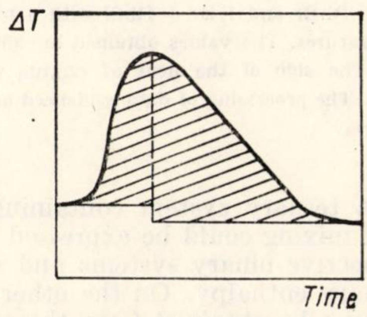

Fig. 2. — The shape of the surface obtained when determining the heat of mixing.

The caloric equivalent of the surface area obtained (figure 2) was determined by electric calibration after each mixing. In the meantime calibration experiments have been carried out by using systems the heat of mixing of which was known.

RESULTS AND DISCUSSION

For a quasi-binary mixture of $A^+ - B^+ - C^- - D^-$ type one can choose as independent variables any 3 of the 4 components of the system AC, AD, BC, BD. In this case the heat of mixing of the ternary system can be written as a sum of six terms [4] :

$$\Delta H^M_{\text{tern}} = x_B x_C \, \Delta H^0 + x_A \, \Delta H^M_{A(C+D)} + x_B \, \Delta H^M_{B(C+D)} + \\ + x_C \, \Delta H^M_{C(A+B)} + x_D \, \Delta H^M_{D(A+B)} + \Delta H^E_{\text{tern}} \qquad (1)$$

---

[7] I. G. Murgulescu and D. I. Marchidan, *Rev. Roumaine Chimie*, **9**, 793 (1964).

if the molar fraction of AC, AD and BD are considered as independent variables. In equation (1), ΔH° is the enthalpy change of the reaction:

$$AC + BD = AD + BC \tag{2}$$

The obtained values for the heat of mixing in the systems KCl + + RbBr and KBr + RbCl are given in table 1. On figure 3 the dependence of the heat of mixing on concentration is drawn.

Table 1

Heat of mixing of binary mixtures KCl + RbBr and KBr + RbCl, at 860°

System	KCl + RbBr				
x_{KCl}	0.2	0.4	0.5	0.6	0.8
ΔH^M (cal/mol)	+132	+152	+158	+124	+71
System	KBr + RbCl				
x_{KBr}	0.2	0.4	0.5	0.6	0.8
ΔH^M (cal/mol)	−65	−101	−115	−99	−54

Making use of the data in table 2 for $x = 0.5$ we can get the change of standard enthalpy of the reaction:

Table 2

Heat of mixing of equimolecular systems K (Cl + Br) Rb (Cl + Br), Cl (K + Rb) and Br (K + Rb) at 860°

System		K (Cl + Br)	Rb (Cl + Br)	Cl(K + Rb)	Br (K + Rb)
ΔH^M $x = 0.5$ (cal/mol)	Kleppa	+15	+12	+ 5	0
	Our results	+59	+63	+21	—

$$\begin{gathered} KCl + RbBr = KBr + RbCl + \Delta H^0 \\ \Delta H^0 = 2\,(115 + 158) = 546 \text{ cal/mol} \end{gathered} \tag{3}$$

On the other hand, Kleppa [6] carried out measurements of heats of mixing in the reciprocal systems: Na^+, Rb^+, Cl^-, Br^- and Na^+, K^+, Cl^-, Br^- and from these should be obtained the ΔH^0 for the respective reactions:

$$NaCl + KBr = NaBr + KCl + 1503 \text{ cal} \tag{4}$$

$$NaBr + RbCl = NaCl + RbBr - 2134 \text{ cal} \tag{5}$$

If for equation (4) use is made of the standard enthalpy which we previously measured,[5] we get:

$$\mathrm{NaCl} + \mathrm{KBr} = \mathrm{NaBr} + \mathrm{KCl} + 1678 \text{ cal} \qquad (4')$$

$$\mathrm{NaBr} + \mathrm{RbCl} = \mathrm{NaCl} + \mathrm{RbBr} - 2134 \text{ cal} \qquad (5')$$

Adding (4) and (5) and separately (4′) and (5′) the reaction (3) is obtained.

The three values obtained for ΔH^0 (table 3) are very close to each other, taking into account that there is only one obtained by direct measurements (+546) while the others are obtained on the basis of a thermochemical cycle.

The excess ternary enthalpy may be calculated from the relation (1) which for our system becomes:

$$\Delta H^M_{\mathrm{KCl+RbBr}} = x_{\mathrm{RbBr}} x_{\mathrm{KCl}} \Delta H^0 + x_{\mathrm{K^+}} \Delta H^M_{\mathrm{K(Cl+Br)}} + x_{\mathrm{Rb^+}} \Delta H^M_{\mathrm{Rb(Cl+Br)}} + x_{\mathrm{Cl^-}} \Delta H^M_{\mathrm{(K+Rb)Cl}} + x_{\mathrm{Br^-}} \Delta H^M_{\mathrm{(K+Rb)Br}} + \Delta H^E_{\mathrm{tern}}. \qquad (1')$$

Introducing in equation (1′), ΔH^0 from table 3 and the heats of mixing for the respective bynary systems at equimolecular concentrations, (table 2), the excess ternary enthalpy at molar fraction 0.5 is obtained.

From the theory of conformal solutions for reciprocal mixtures[1] one obtains:

$$\Delta H^E_{\mathrm{ternar}} = x_{\mathrm{K^+}} x_{\mathrm{Rb^+}} x_{\mathrm{Cl^-}} x_{\mathrm{Br^-}} P[(g_1 + g_4 - g_2 - g_3)^2] \qquad (6)$$

where P is a constant which depends only on the properties of "comparison salt". A useful approximation for P is obtained only by comparison with the similar term in the quasi-lattice theory[2]:

$$P[(g_1 + g_4 - g_3 - g_2)^2] = -\frac{(\Delta H^0)^2}{ZRT} \qquad (7)$$

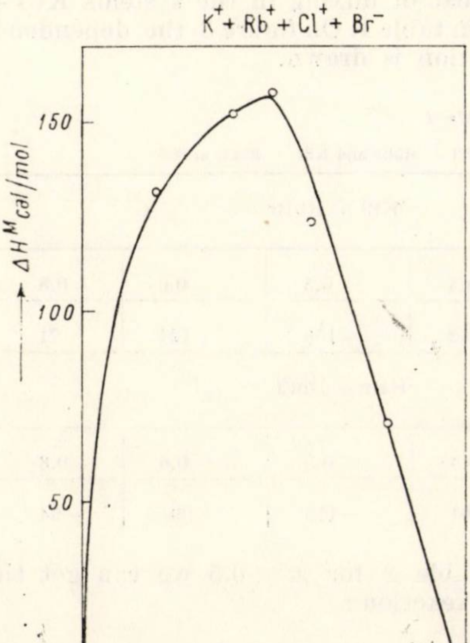

Fig. 3. — Molar enthalpies of mixing at 860° in fused salt systems: KCl + RbBr and KBr + RbCl.

Table 3

Values of ΔH^0 and $\Delta H^E_{\text{tern.}}$ for $x = 0.5$

	From $\Delta H^M_{\text{tern.}}$ (table 1)	From eq. (4) and (5)	From eq. (4′) and (5′)
ΔH^0	+546	+630	+456
$\Delta H^E_{\text{tern.}}$ calc. from eq. (8)	≈−2	≈2.5	—
$\Delta H^E_{\text{tern.}}$ calc. from eq. (11)	−20	−23	—
$\Delta H^E_{\text{tern.}}$ alc. from eq. (1′)	−50	−16	—

Accordingly :

$$\Delta H^E_{1234} = - x_{\text{K}^+} x_{\text{Rb}^+} x_{\text{Cl}^-} x_{\text{Br}^-} \frac{(\Delta H^0)^2}{ZRT} \tag{8}$$

If use is made now of the quasi-chemical approximation in the form given by Førland, [3] we get :

$$\frac{(x_A x_D + y)(x_B x_C + y)}{(x_A x_C - y)(x_B x_D - y)} = \exp\left[-\frac{(\Delta H^0)^2}{ZRT}\right] \tag{9}$$

and so

$$\Delta H^E_{\text{tern}} = y \cdot \Delta H^0 \tag{10}$$

Here y indicates the deviation from the chaotic mixing of ions in the mixture and directly determines the value of excess ternary enthalpy. If only the first terms of the expansion in power series of equation (9) are considered, one obtains :

$$y = - x_A x_B x_C x_D \frac{\Delta H^0}{ZRT}$$

so that the two equations (8)and (9) are identical in a first approximation. The values of excess ternary enthalpy obtained from this equations for equimolecular concentrations are also given in table 3.

The values corresponding to y are very small ($3-4 \times 10^{-3}$) indicating, according to the quasi-chemical theory, small deviations from the chaotic behaviour that is excess ternary enthalpies much smaller than those experimentally obtained. This means that to the excess ternary enthalpy besides the deviations from chaotic behaviour there are some other contributions.

A first correction will be the considering of collective interactions. As is known, the formation of a new bond, between the ions in mixture requires the same energy, according to the quasi-chemical theory, irrespective of the number of existing links. The consideration of the possibilities of interference of the new formed bonds in the mixture was achieved by Blander [2] within the frame of asymmetric approximation by calculating the number of ways the ions could be distributed in the mixture for a given value of y and so the entropy of mixing.

A somewhat similar statistic treatment is used by Førland who obtained the following equation for the law of mass action, taking into consideration the unlike coordination capacity of ions in the mixture:

$$\frac{(Zx_A x_C + Z_y)[(1 - Zx_A)x_D + Z_y]}{[(1 - Zx_A)x_C - Z_y](Zx_A x_D - Z_y)} = \exp\left[-\frac{\Delta H^0}{ZRT}\right] \tag{11}$$

and

$$\Delta H^E_{\text{tern}} = y \, . \, \Delta H^0 \tag{12}$$

For $x_A = x_B = x_C = x_D = 0.5$ the values given in table 3 were obtained. If $Zx_A = x_A^*$, $1 - Zx_A = x_B^*$ and $Zy = y^*$, the same form of equation (9) is obtained.

This could be interpreted as formally indicating a deviation from chaotic distribution of $y^* = Zy = 4.5 \times 0.036$. In fact this value of y^* takes into account according to the initial assumptions a coordination capacity which is different for the ions in the mixture.

It is worth to be mentioned that the use of upper terms of the expansion in power series of equation (9) or (11) alter but very slightly the results of the first order approximation.

We can state in conclusion that the deviations from the quasi-chemical theory or in other words the contributions to the excess ternary enthalpy result from the non-chaotic mixing of ions in the mixture as well as from the interference of new formed bonds between ions in the mixture (collective interactions).

Acknowledgements. We wish to express our deep gratitude to Professor I.G. Murgulescu Head of the Institute of Physical Chemistry, for his great interest in our work.

Revue Roumaine de Chimie, **15**, 1681–1688 (1970)

VISCOSITY OF MOLTEN (Li–K)Cl MIXTURES

ŞTEFANIA ZUCA and RODICA BORCAN

Institute of Physical-Chemistry, Bucharest, str. Galaţi 31

Received April 16, 1970

The density and viscosity of the molten (Li–K)Cl system have been investigated as a function of both temperature and molar fraction and the activation energy for viscous flow was calculated. While the molar volume varies nearly linearly with composition the viscosity and the activation energy show negative deviations from additivity. These deviations are caused by the ionic interaction occurring by mixing and are found to obey the formula $\Delta\eta = ax_1x_2$.

It is known that both viscosity and conductivity isotherms in binary fused salts mixtures usually exhibit negative deviations from the additivity. This is the opposite of what would be predicted by Walden's rule, $\lambda \cdot \eta = \text{const.}$, which has been verified in pure molten salts by the modified relation $\lambda^n \cdot \eta = \text{const.}$ proposed by Frenkel.[1]

Many authors[2-4] showed that in (Li–K)Cl system which should be a typical ionic melt the deviations of electrical conductivity from additivity are so large that the istoherm actually passes through a minimum at about 80% mole KCl.

The results on the viscosity of this system obtained by Karpachev and co-workers [5] and by Matsumura and co-workers [6] exhibit generally negative deviations from additivity, but no concludent results can be drawn from the shape of their isotherms of viscosity. The obtained curves present some peculiar breaks. At the same time the two sets of data differ very much from each other. Therefore it was thought worthy of reinvestigation.

---

[1] J. Frenkel, "Kinetic Theory of Liquids", Oxford University Press, London, 1946, p. 441.

[2] E. R. Van Artsdalen and L. S. Yaffe, *J. Phys. Chem.*, **59**, 119 (1955).

[3] F. R. Duke and L. Bissell, *J. Electrochem. Soc.*, **111**, 717 (1964).

[4] J. Matsumura, M. Mizuno and K. Nishihara, *Memoirs of the Faculty of Engineering, Kyoto University*, **vol. 29**, Part 4, 462, (1967).

[5] I. V. Karpachev, A. Stromberg and V. N. Podchainova, *Zhur. Obshchei. Khim.*, **5**, 1517 (1935).

[6] J. Matsumura, M. Mizuno and K. Nishihara, *Memoirs of the Faculty of Engineering, Kyoto University*, **vol. 28**, Part 4, 404 (1966).

The purpose of this work was to determine whether more reliable values of viscosity could be obtained for (Li—K)Cl mixtures.

RESULTS AND DISCUSSIONS

Both density and viscosity of the pure salts and six of their mixtures (mole fraction $x_{\mathrm{LiCl}} = 0.2 ; 0.3 ; 0.4 ; 0.5 ; 0.6 ; 0.8 ;$) were determined at several temperatures.

The experimental set up and method of operation used in this work are described in a previous paper.[7]

The lithium and potassium chlorides were the same reagent grade quality as the salts used in our earlier work.[7] The LiCl was prepared by a special technique described elsewhere.[8]

The results obtained for the density, *d*, are summarized in the form of linear function of temperature, *t*°C, in table 1. These equations represent the observed points within experimental error, as indicated in the root mean square deviations column. The temperature ranges are those within which the data were obtained.

The variation of viscosity, η, with both temperature and molar composition of (Li—K)Cl system are shown in table 2.

Table 1

Density of the (Li – K)Cl system

Composition X_{LiCl}	Density eqs.	Standard deviation	Temperature range, °C
0	$d = 1.9564 - 0.5583 \times 10^{-3}t$	0.0002	780—900
0.2	$d = 1.9465 - 0.5649 \times 10^{-3}t$	0.0003	685—806
0.3	$d = 1.9372 - 0.5668 \times 10^{-3}t$	0.0004	645—798
0.4	$d = 1.9113 - 0.5429 \times 10^{-3}t$	0.0005	605—800
0.5	$d = 1.8824 - 0.5217 \times 10^{-3}t$	0.0004	610—796
0.6	$d = 1.8840 - 0.5354 \times 10^{-3}t$	0.0005	616—800
0.8	$d = 1.8213 - 0.4814 \times 10^{-3}t$	0.0003	600—797
0	$d = 1.7562 - 0.4243 \times 10^{-3}t$	0.0003	605—800

The activation energy for viscous flow, E_η, was calculated by the least squares method, for each investigated mixture over the temperature range covered in this work.

The Arrhenius equation:

$$\eta = Ae^{E\eta/RT} \tag{1}$$

---

[7] I. G. Murgulescu and Ş. Zuca, *Z. Phys. Chem. (Leipzig)*, **218**, 397 (1961); **222**, 300 (1962).

[8] Ş. Zuca and M. Olteanu, *Rev. Roumaine Chim.*, in press.

Table 2

Viscosity of the (Li – K)Cl system

X_{LiCl}	$t°$	η, cP	X_{LiCl}	$t°$	η, cP
0	812	1.06	0.5	760	1.03
	823.7	1.02		773.3	0.99
	852.7	0.94		775	0.97
	857.2	0.93		785.3	0.94
	883	0.89		800	0.92
0.2	695.7	1.37		805.5	0.91
	701	1.35	0.6	616.3	1.47
	708.5	1.31		639.4	1.37
	735	1.20		664.5	1.25
	764.8	1.12		696	1.15
	778.8	1.08		721.8	1.07
	788.5	1.05		724.7	1.07
	815.5	0.99		761	0.98
0.3	642.2	1.51		784	0.94
	661.5	1.40		801.8	0.91
	680	1.32	0.8	629.5	1.43
	691	1.26		666.5	1.29
	724.6	1.19		678	1.23
	757.4	1.11		704.7	1.17
	783	1.01		718	1.11
	807.4	0.97		727.5	1.07
0.4	638.4	1.50		763	1.00
	650	1.44		787	0.95
	665.5	1.35		805.5	0.91
	695.3	1.23	1	619	1.66
	724	1.15		627.5	1.60
	759	1.06		6.54	1.44
	765.8	1.03		678	1.31
	792	0.97		685	1.30
	803.5	0.95		699	1.25
0.5	653.4	1.35		705	1.18
	670	1.31		716	1.17
	694.7	1.20		734.6	1.13
	703.8	1.17		748	1.08
	717	1.14		770	1.02
	721.8	1.10		783.5	1.00
	747.5	1.06		797	0.96

was used, where A is the pre-exponential factor. Table 3 gives the obtained values as well as the standard deviation in E_η.

The agreement between this work and the previously mentioned publications, [5,6] on pure components is illustrated in figures 1 and 2.

From figure 1 it is evident that for KCl there is a close agreement with Karpachev and co-workers' data [5] while considerable higher values (+20%) are given by Matsumura, Mizuno and Nishihara.[6]

However for LiCl (fig. 2) the agreement with both above mentioned works [5, 6] is poor. A stronger temperature dependence is indicated

Table 3

Activation energy E_η and pre- exponential factor A

X_{LiCl}	$^*A.10^2$	E_η kcal/mol	Standard deviation in E_η kcal/mol	Temperature range, °C
0	5.38	6.42	0.030	780–928
0.2	7.31	5.62	0.032	695–815
0.3	7.77	5.07	0.042	642–807
0.4	7.82	4.97	0.053	613–803
0.5	7.79	4.91	0.034	653–800
0.6	7.71	4.94	0.012	616–805
0.8	7.56	5.14	0.030	600–805
1	5.01	6.20	0.064	618–809

* η is given in cP.

by [5] so that at temperatures ranging from 750°–800° the differences reach 10%. The values of Matsumura and co-workers [6] are very much higher (+25%) in the whole temperature range covered by them.

We notice here that in figures 1 and 2 are given the present results as well as our earlier data, [7]and the figures in table 3 were obtained taking into account both sets of data.

Figure 3 shows the isotherm of viscosity and of molar volume of (Li–K) Cl system plotted against molar fraction of LiCl in the mixture, x_{LiCl}, at 800° together with activation energy for viscous flow. As

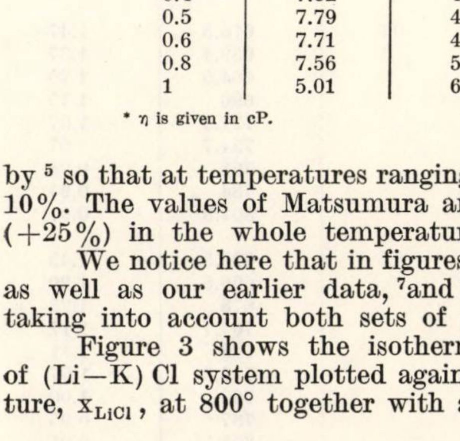

Fig. 1. — Viscosity *vs.* temperature for pure KCl

1, our data; *2*, data from Karpachev, Stromberg and Podchainova [5]; *3*, data from Matsumura, Mizuno and Nishihara [6]

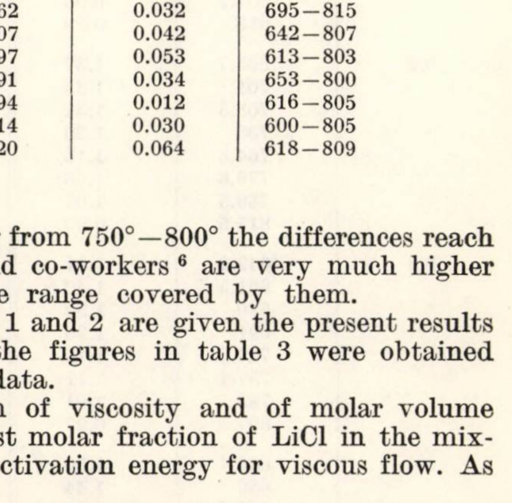

Fig. 2. — Viscosity *vs.* temperature for pure LiCl

1, our data; *2*, data from Karpachev, Stromberg and Podchainova[5]; *3* data from Matsumura, Mizuno and Nishihara[6] it can be seen in figure, the additivity is accomplished by the molar volume (differences do not exceed 0.20%), but the isotherm of viscosity shows systematic negative deviations from linearity and the activation energy is always smaller than that calculated additively.

The viscosity *vs.* composition at 800° is compared with those values reported in the above mentioned papers [5,6] in figure 4. The difference in the three curves is astonishing. A smooth curve can be drawn through the values determined by us, while there appears to be some discontinuities in the other two curves. In our opinion no realistic explanation can be found for the features of the isotherm obtained by Karpachev and co-workers.[5] It is also difficult to explain the inflection points on the curve of Matsumura, Mizuno and Nishihara.[6]

We recall here that a characteristic development was observed on the equivalent conductivity isotherm [2–4] namely a marked minimum point at 80% mole KCl. Such behaviour has been frequently ascribed to the complex ion presence in the melts. However, according to the available phase diagram information [9] there is no evidence for the formation of complex ions in (Li—K)Cl system and a simple eutectic point is formed. At the same time, figure 3 illustrates in a convincing way that this system is ideal in its molar volume relationship. From this point of view (Li—K)Cl mixtures behave like simple ionic melts. The observed development of the electrical conductivity isotherms could satisfactorily be explained [10] in terms of a relatively simple model involving a kind of cation-anion associated groups due to the common anion polarization effect.

As a result of ionic interactions, we expect the isotherm of viscosity not to reach additivity. However, ionic associations will not inhibit viscous flow as they inhibit electrical conduction, since viscous flow in molten salts involves the translation of ions of both signs.[7] Therefore no marked maximum points are expected to be formed on the isotherm of viscosity of the simple ionic melts. The monotonic isotherms of viscosity obtained by us (fig. 3) support this point of view.

If the deviation of viscosity from additivity $\Delta\eta = \eta_{ad} - \eta_{exp}$ ($\eta_{ad} = x_1\eta_1 + x_2\eta_2$, denotes the additive value and η_{exp} the observed one), is plotted against mole fraction, as shown in figure 5, it is possible to draw for each temperature a symmetrical curve with a maximum at $x_{LiCl} = x_{KCl} = 0.5$. There is a marked resemblance with the behaviour observed for binary alkali nitrate systems.[11]

The curves in figure 5 can be expressed by the following equation:

$$\Delta\eta = ax_1x_2 \tag{2}$$

where "*a*" is a constant determined by temperature. The numerical values of "*a*" are equal to 0.391 and 0.302 at 775° and 800°, respectively. Eq. (2) allows us to calculate easily the viscosity of the mixture from the

---

[9] E. Elchardus and P. Laffitte, *Bull. Soc. chim. France*, **51**, 1572 (1932).

[10] Ş. Zuca and M. Olteanu, *Rev. Roumaine Chim.*, **15**, 357 (1970).

[11] I. G. Murgulescu and Ş. Zuca, *Electrochim. Acta* **11**, 1383 (1966); **14**, 519 (1969

Fig. 3. — Molar volume, viscosity and activation energy for viscous flow for (Li—K)Cl system.

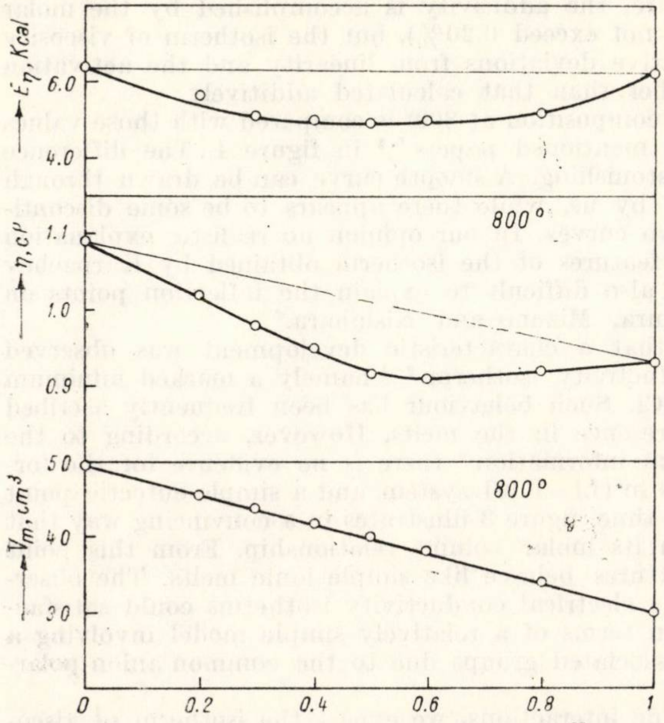

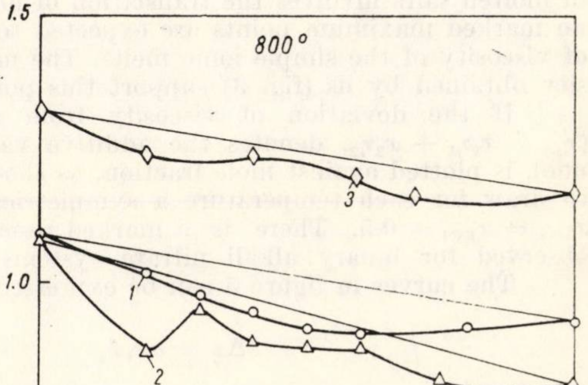

Fig. 4. — Isotherm of viscosity of (Li—K)Cl system at 800°.
1, our data; *2*, data from Karpachev Stromberg and Podchainova[5]; *3*, data from Matsumura, Mizuno, Nishihara[6]

viscosity of the pure component by subtracting $\Delta\eta$ value calculated with (2) from the additive value.

From the data registered in Table 4 it is clear that the observed values of viscosity are thus rendered within experimental error (precision of $\mp 1\%$).

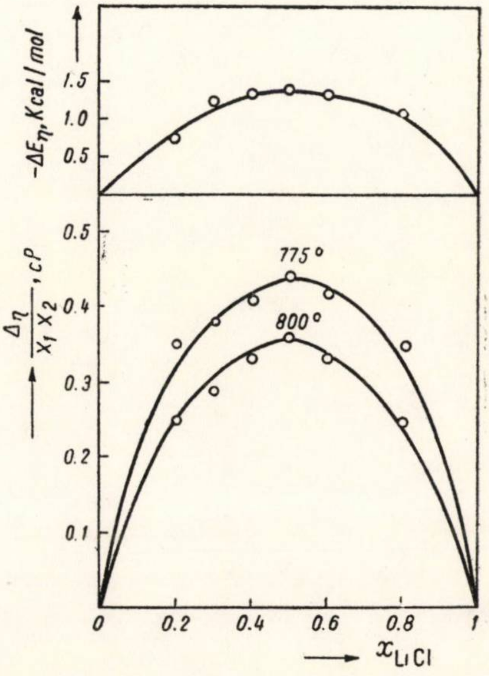

Fig. 5. $\frac{\Delta\eta}{x_1x_2}$ and $-\Delta E_\eta$ *vs* molar fraction for (Li−K)Cl system.

Table 4

Validity of eq (2) for the (Li−K)Cl system

X_{LiCl}	775°, a = 0.391			800°, a = 0.302		
	η exp, cP	η calc cP	Dif. %	η exp, cP	η calc cP	Dif. %
0	1.17	1.17	0	1.09	1.09	0
0.2	1.08	1.075	−0.4	1.02	1.012	−0.7
0.3	1.04	1.038	−0.2	0.98	0.977	−0.3
0.4	1.00	1.006	+0.6	0.95	0.958	+0.8
0.5	0.97	0.982	+1.2	0.92	0.931	+1.1
0.6	0.96	0.966	+0.6	0.91	0.918	+0.8
0.8	0.97	0.965	−0.5	0.92	0.912	−0.8
1	0.99	0.99	0	0.93	0.93	0

Finally, a special remark concerning the activation energy for viscous flow must be made. If the changes in the viscosity are caused by the interaction between the different types of ions in the melts we also expect the activation energy of the mixture to be influenced. The development observed in figure 3 proves that there is an important negative deviation of the activation energy from additivty.

The decrease of excess energy, $\Delta E\eta$ follows generally the development observed for $\Delta\eta$ reaching a minimum value in equimolecular mixtures (fig. 4).

Revue Roumaine de Chimie, **15**, 1689 —1698 (1970)

THE INFLUENCE OF RAPID TEMPERATURE CHANGES ON THE SURFACE POTENTIAL VARIATION IN THE SYSTEM OXYGEN-THIN COPPER FILMS

M. I. VASS

Institute of Physical Chemistry, Bucharest, str. Dumbrava Roşie 23

Received November 22, 1969

Surface potential variations produced by oxygen adsorption on copper films at 77°K and 298°K as well as by the rapid temperature changes, using the retarding field diode method are reported. The "surface reference change" hypothesis is assumed to explain the special behaviour of the oxygen-covered copper films on temperature changes.

In previous papers [1,2] we have studied the surface potential variation at sudden temperature changes in oxygen adsorbed on thin gold and silver films systems. To explain the observed variations we suggested a model supposing weak bonds of the charge transfer type between the first and the subsequent adsorbed layer.

The study of the same modification in the oxygen adsorbed on copper films system, is the purpose of the present paper, the reactivity of this metal towards the oxygen as compared with the two previously studied metals being well known. It is also a continuation of a previous paper [3] on the same system.

EXPERIMENTAL

The retarding field diode in the initial current domain has been used for measurements of the surface potential variations. The cell, the measuring circuits, the vacuum installation, the gas handling and the working method were previously described. [2,3] The copper was Johnson & Matthey spectroscopically pure. The film deposition (of approx. 600 Å thickness) was effected at a pressure of $2-5 \times 10^{-9}$ torr and 77°K, and was followed by a sinterization at 353°K for the lattice structure stabilization. The precision of the measurements deduced from the parallelism of family curves representing the retarding potential *versus* the anodic current, was $\pm$ 0.01 V.

---

[1] I. G. Murgulescu and M. I. Vass, *Rev. Roumaine Chim.*, **13**, 373, (1968).

[2] I. G. Murgulescu and M. I. Vass, *Rev. Roumaine Chim.*, **13**, 1521 (1968).

[3] I. G. Murgulescu and M. I. Vass, *Rev. Roumaine Chim.*, **11**, 299 (1966).

RESULTS AND DISCUSSION

Two groups of measurements have been performed : starting from an oxygen covered at 77°K copper film (ΔV constant) or from a copper film saturated with oxygen at 298°K. To define more accurately the modifications of the system, a set of different operations as : gas excess pumping, new oxygen doses introduction (at 298°K or 77°K) repeating of heating or cooling, were carried out after the temperature change 77°K → 298°K or 298°K → 77°K.

Since in the present paper we used the retarding field diode method whereas in the previous one[3] the space charge limited diode method, to emphasize some differences, we shall firstly relate the results concerning ΔV variations with the number of adsorbed molecules (n_a). The following table gives the results obtained. The previous obtained values were -0.32 V at 77°K and -0.56 V at 298°K. There are small differrences between the two methods ; the values obtained with space charge diode are to a certain extent greater a fact which agrees with the results of other authors.[4] On figure 1, ΔV *versus* n_a curves for both temperatures are given. The following observations can be made : *1*, the maximum number of adsorbed molecules (ΔV saturation) at 77°K is

Table 1

Values obtained for the surface potential and number of adsorbed molecules at 77° K and 298° K and the equilibrium pressure

	77°K	298°K
$\Delta V_{\max}$ (average, in volts)	-0.30	-0.50
$n_{a\,\max}$ (average, in molecules/cm^{2}x 10^{14})	7.8	4.35
$p_{\text{eq.}}$ torr	1×10^{-6}	1×10^{-4}

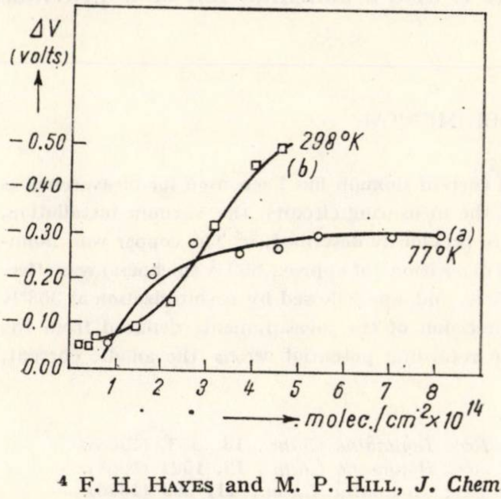

Fig. 1. — Surface potential variation with the number of adsorbed oxygen molecules at 77°K (a) and 298°K (b).

---

[4] F. H. Hayes and M. P. Hill, *J. Chem. Phys.*, **42**, 2919 (1965).

greater than that obtained at 298°K ; *2*, the value of the ΔV obtained at 77°K is lower than the same value for 298°K and *3*, the ΔV value for one oxygen dose is not always constant in time.

Adsorption at 77°K

To explain the saturation with oxygen of the copper film surface for the values given in table 1, we must assume, taking into account that there are approximately 1.5×10^{15} atoms per cm^2 of metallic copper surface, that oxygen molecule at 77°K forms bonds with two copper atoms. The area occupied by one adsorbed molecule of oxygen at 77°K is[5] 14.1 Å^2, that gives an 86 cm^2 area — deduced from the total number of adsorbed molecules 61 x lo^{15} — against the 80 cm^2 of geometrical area. From this agreement we can conclude that the oxygen layer is the molecular one and the bonds could be of the 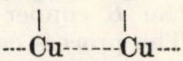 $\begin{array}{ccc} \mathrm{O} & — & \mathrm{O} \\ | & & | \\ \cdots\mathrm{Cu} & \cdots & \mathrm{Cu}\cdots \end{array}$ type, the molecule being only partially dissociated. The dipole moment variation of the bond (μ)-deduced assuming the covalent character of the bond and the applicability of Helmholtz equation at low coverage — shows that unimportant modifications take place. The μ value oscillates around 0.35 D (fig. 2, curve a) and this observation supports the previous assumption, since low μ value are specific of the weak molecular bonds.

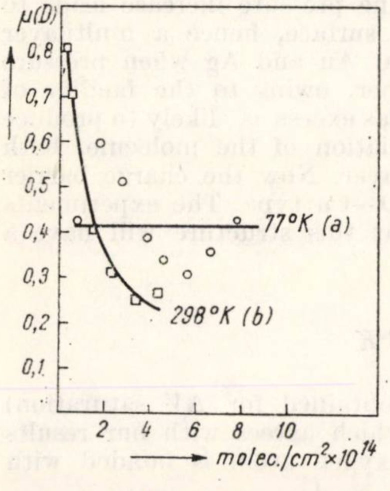

Fig. 2. — Variation of the dipole moment of the bond with the number of adsorbed oxygen molecules at 77°K (a) and 298° K(b).

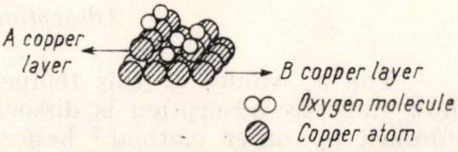

Fig. 3. — Model for the copper surface coverage with oxygen at 77°K.

Taking into account the distribution of the copper atoms on a surface which should expose[6] the 110 plane, we can suppose that the coverage takes place as in figure 3, namely part of molecules are adsorbed on the first layer of the copper atoms — layer *A* — and the other part on the next nearest layer, *B*. This distribution of the adsorbed molecules could explain also the ΔV decrease in time. This decrease points out a rearrangement in the adsorbed layer. Since the μ value is not increasing concomitantly, we can assign the ΔV decrease to the oxygen molecules migration towards the *B* layer, without penetration into the metallic lattice. This produces vacancies in the charge barrier structure, that means evidently lower ΔV. The same mobility of the molecules can explain ΔV increases above the average value, found in some experiments by excess gas dosing. The pressure increase leads to the oxygen concentration increase on the surface, hence a multilayer adsorption. We have found this situation at Au and Ag when pressure increase leaves ΔV unchanged. With copper, owing to the facility of oxygen molecule to pass to the *B* layer, the gas excess is likely to produce finally a lattice spacing, possibly a dissociation of the molecule, both leading to the penetration under the *A* layer. Now the charge barrier will include mixed layers of the $O_2-Cu-O-Cu$ type. The experiments described below enable us to conclude that this structure will have a greater ΔV.

---

[5] D. M. Young and A. D. Crowell, "Physical Adsorption of Gases", Butterworth, London, 1962, p. 226.

[6] D. Brennan and M. J. Graham, *Discuss. Faradays Soc.* **1966**, 95.

Adsorption at 298°K

The n_a values at this temperature (obtained for ΔV saturation) show that the adsorption is dissociative, which agrees with our results obtained by other method [7] hence each oxygen atom is bonded with two copper atoms, supposedly in the 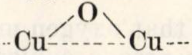 $\cdots Cu\overset{O}{\cdots\cdots}Cu\cdots$ form. If we follow the ΔV variation with n_a (fig. 1 b) we can see that unlike what is observed at 77°K for small oxygen doses (approx. 0.2×10^{14} molec/cm^2) ΔV oscillates around a constant value. Only after greater doses ΔV rises and reaches the saturation. Keeping in view the previous conclusion we assume that the atomic oxygen can easier penetrate towards the *B* copper atoms, thus even if n_a increases, ΔV remains constant. The process can be promoted by the structure inhomogenities of the film surface or by cracks. The appearance of mixed structures previously mentioned supports the same hypothesis; ΔV increases in time at subsequent gas introduction.

On figure 2 (curve b) the μ variation with n_a is plotted (the applicability of Helmholtz equation being admitted for low coverages). For the first doses its value is 0.7 D and then decreases to 0.23 D. Undoubtedly the great value is assigned to the bond of adsorbed oxygen atoms on a copper layer, and it might be really greater because atomic oxygen partially migrated towards the *B* layer.

Drawing a parallel between the ΔV variations at the initial stages for the two temperatures, one can see that, though the doses are 0.9×10^{14} molec/cm^2 and 0.2×10^{14} molec/cm^2 for 77°K and 298°K respectively, the ΔV value is approximately the same 0.05 V. Let us assume that the formed layer contains the same species; for the calculation of ΔV_{298} the μ value deduced from ΔV_{77} (in covalent adsorption) was used and a value of 0.013 V was found. Admitting the dissociative adsorption the number of dipoles will be $2 \times n_a$ and $\Delta V \rightarrow 0.026$ V. To obtain the experimental value it is necessary to assume that the adsorbed species at 298°K has $\mu = 0.7$ D, namely twice that obtained at 77°K. This means that the μ value for the 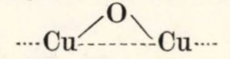 $\cdots\mathrm{Cu}\overset{\mathrm{O}}{\diagup\cdots\cdots\diagdown}\mathrm{Cu}\cdots$ form is twice that for the 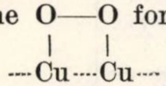 $\begin{array}{c}\mathrm{O}-\mathrm{O}\\ |\quad\;|\\ \cdots\mathrm{Cu}\cdots\mathrm{Cu}\cdots\end{array}$ form.

---

[7] I. G. Murgulescu and M. I. Vass, *Rev. Roumaine Chim.*, **14**, 1201 (1969).

The dipole moment can be written, for a partial ionic bond as: $\mu = ze \times d$, where z is the fractional charge on the oxygen atom, e — electronic charge and d, the distance between atom and surface. Taking for d, the covalent radius of the oxygen, as 0.66 Å and assuming that electrical conduction continues to take place at the metallic surface, from the experimentally determined μ at low coverages, one can easily obtain the fractional charge on the oxygen atom. This is 0.22 e ($\theta \rightarrow 0$) and 0.17 e ($\theta \rightarrow 1$). This value is close to that given by Delchar and Tompkins,[8] 0.3 e for the oxygen adsorption on nickel films.

The change 77°K → 298°K (fig. 4)

The sudden heating of an oxygen-saturated copper film at 77°K leads invariably to the ΔV increase to a value of about -0.80 V and is accompanied by the desorption of 0.8×10^{14} molec/cm^2. These values are not characteristic of the 298°K adsorption, contrary to the expectation. The ΔV increase is also different from that observed for O_2—Au and O_2—Ag systems when on rising the temperature, ΔV remains constant. The number of the molecules remaining on the surface is by $2.5 \times \times 10^{14}$ molec/cm^2 larger than that observed for the 298°K adsorption. First we must agree that at the end of this operation the oxygen is atomically adsorbed. There are two possibilities to explain this change: the excess observed can form an atomic oxygen-adsorbed layer with bonds of the 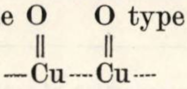 $\begin{array}{c}\mathrm{O}\quad\;\mathrm{O}\\ \|\quad\;\|\\ -\mathrm{Cu}\cdots\mathrm{Cu}\cdots\end{array}$ type (I) or the excess can penetrate under the *A* layer (II).

The remaining 7×10^{14} molec/cm^2 dissociated molecules will cover 1.4×10^{15} copper atoms/cm^2 from the geometrical area of the film namely an oxygen atoms/copper atoms ratio of approx. one. In the dipole moment calculation, care must be taken that the density be double and though ΔV increases by 0.4 V, μ remains constant at about 0.3 D.

---

[8] T. A. Delchar and F. C. Tompkins, *Proc. Roy. Soc.*, **A 300**, 141, (1967).

This means that μ for the $\overset{\mathrm{O}}{\underset{\cdots\mathrm{Cu}}{\|}}\overset{\mathrm{O}}{\underset{\cdots\mathrm{Cu}\cdots}{\|}}$ form is equal to that of the $\underset{\cdots\mathrm{Cu}\cdots\mathrm{Cu}\cdots}{\mathrm{O}-\mathrm{O}-}$ and half of the value for the $\cdots\mathrm{Cu}\overset{\mathrm{O}}{\diagup\;\diagdown}\mathrm{Cu}\cdots$ form, which is a hardly

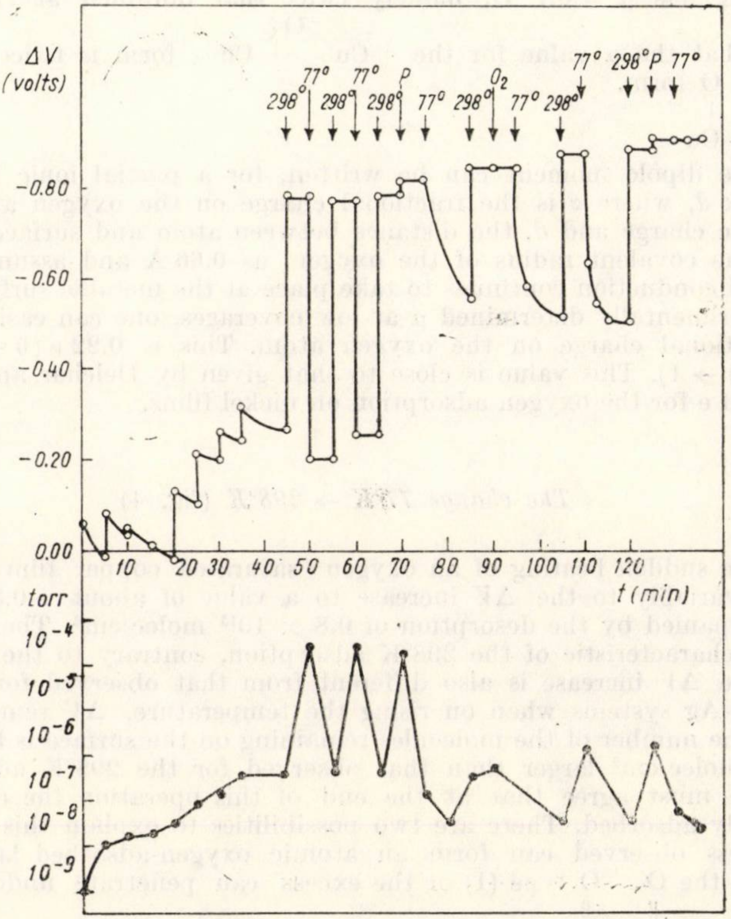

Fig. 4. — Surface potential variation in time on introduction of oxygen doses at 77° K for sudden temperature change (298°K) and gas excess pumping (P) for a typical experiment ; in the lower part the simultaneous pressure variation in the system is plotted.

conceivable conclusion. Moreover, we must assume that at 298°K two different structures for the adsorbed layer with different oxygen concentrations are formed on the surface, according to the way the adsorption is achieved.

The second hypothesis is the penetration of the 2.5×10^{14} molec/cm^2 into the film, the so-called oxygen incorporation.[7-10] According to other authors'[7-10] observations, the oxygen incorporation is accompanied by a positive change in ΔV, which is not observed with copper. But in the quoted papers, the incorporation is considered as an oxygen vanishing into the metallic bulk and thus the surface is regenerated. If we consider

Fig. 5. — Model for oxygen atoms migration and for "surface reference" modification.

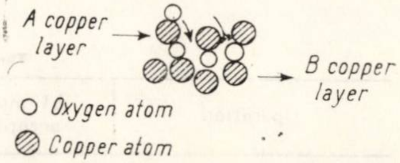

that oxygen migrates under the first metallic layer — as figure 5 shows — then the reference surface, whose work function is changing after adsorption, has no homogeneous composition, containing oxygen atoms. It is clear that a surface without a definite work function, will produce surface potential variations depending on the incorporated oxygen concentration. The first consequence is that ΔV will be influenced by the pumping of gas excess. Another consequence would be the possibility of obtaining continuous ΔV variations, due to the subsequent oxygen adsorption, a process facilitated by the repeated heating-cooling cycles.

If such a system is set back to the initial temperature (77°K) the readsorption of 0.8×10^{14} molec/cm^2 takes place and ΔV decreases to -0.20 V. Both hypotheses can be used to explain this modification: assuming that the excess is adsorbed as oxygen molecules on the layer of the 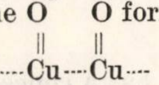 $\overset{\overset{\displaystyle O}{\|}}{\cdots Cu}\cdots\overset{\overset{\displaystyle O}{\|}}{Cu}\cdots$ form or on the copper atoms which become free as a result of a migration to the B layer. However the observed gas quantity is too small to explain the ΔV decrease (approx. 40% from the initial value). Very likely the temperature change is accompanied by lattice modifications which result in the oxygen molecules returning on the surface.

The returning to 77°K in the absence of the gas excess produces a ΔV decrease of only 0.25 V. This might be attributed to the temperature influence upon the crystalline lattice structure or to the oxygen rearrangement in the adsorbed layer. The heating leads to the ΔV increase ($\Delta V \rightarrow -0.84$ V) a proof that new oxygen atoms penetrate towards the *B* layer, process which is strenghtened by the addition of new oxygen doses ($\Delta V \rightarrow 0.90$ V), a new cooling leads to $\Delta V \rightarrow 0.51$ V. By this method one can cause the ΔV to increase up to -1.10 V a value evidently different from those for copper clean surface saturation at 77°K or 298°K. The final value is close to those reported by Roberts

---

[9] J. S. Anderson and D. F. Klemperer, *Proc. Roy. Soc.*, **A 258**, 350 (1960).

[10] L. A. Rudnitzki and N. V. Kulkova, *Doklady Akad. Nauk S.S.S.R.*, **162**, 617 (1965).

and Quinn,[11] −0.8 V, for a copper surface exposed at 40 torr oxygen pressure, value assigned by the authors to the Cu_2O forming.

From the above we conclude that the hypothesis of surface reference changing can explain the observed ΔV modifications and for clarity scheme 1 gives the ΔV variations according to the two hypotheses as well as the experimental values.

Scheme 1

The change 77° K → 298° K

Operation	ΔV modification according to I	ΔV modification according to II	ΔV exp. (in volts)
1. Film saturated at 77°K	constant	decreases tendency	−0.40→0.35
2. Heating to 298°K	increases	increases	−0.80
3. Cooling to 77°K	decreases	decreases	−0.20
3′ Pumping at 298°K	constant	increases	−0.82
3″ Cooling to 77°K	decreases	decreases	−0.57
4 Heating to 298°K	constant	increases	−0.84
5 New oxygen doses	constant	increases	−0.90
6 Cooling to 77°K	decreases	decreases	−0.51

The change 298°K → 77°K (fig. 6)

The oxygen adsorbed on the copper films at 298°K has a concentration of 4.35×10^{14} molec/cm^2 and produces a ΔV change of −0.50 V. The equilibrium pressure is 1×10^{-4} torr. Cooling the system this excess is adsorbed, and n_a becomes 5.05×10^{14} molec/cm^2 and $\Delta V \rightarrow 0.33$ V. The obtained ΔV value is close to that obtained for saturation at 77°K, but the concentration is considerably different. If the gas excess is evacuated, the cooling produces a ΔV change to 0.40 V. Hence, only 0.07 V must be assigned to readsorption. the difference remains to be attributed to the layers rearrangements.

Additional doses (on the cooled system) produce transient increases of ΔV (0.50 → 0.38 V) and $n_a \rightarrow 7.1 \times 10^{14}$ molec/cm^2. Both values are specific of the 77°K adsorption. Only now the return to 298°K is accompanied by 0.8×10^{14} molec/cm^2 desorption, and ΔV increases to −0.70 V a state similar to that found for the 77°K → 298°K change. Consequently we consider that subsequent ΔV changes due to other operations with the system, support the previous explanations too. See scheme 2.

The previous finding shows that there is a critical concentration of oxygen on the surface or a certain configuration of the bonds which leads to the reference surface transformation. It seems that oxygen migration towards the second metallic layer is possible only after the

---

[11] M. W. Roberts and C. M. Quinn, *Trans. Faraday Soc.*, **60**, 899 (1964).

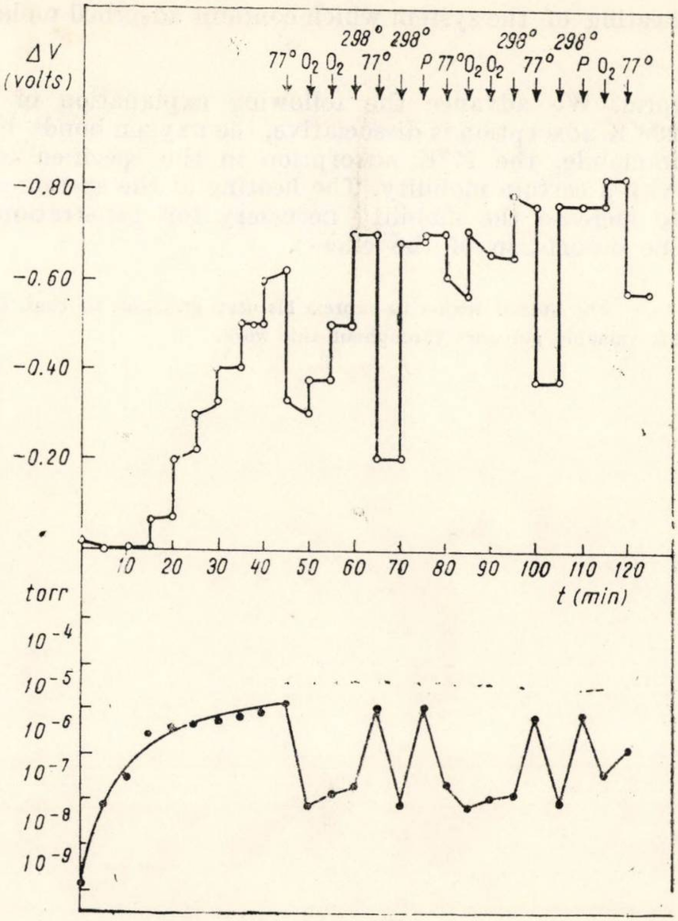

Fig. 6. — Surface potential variation in time for on introduction of oxygen doses at 298°K and at steep temperature change to 77°K and at gas excess pumping (P) for a typical experiment; in the lower part the simultaneous pressure variation in the system is plotted.

Scheme 2

The change 298°K→77°K

Operation	ΔV modification according to I	ΔV modification according to II	ΔV exp. (in volts)
1. Film saturated at 298°K	constant	increases tendency	−0.43→−0.50
2. Cooling to 77°K	decreases	decreases	−0.33
2′. Pumping at 298°	constant	increases	−0.37
3′. Cooling to 77°K	decreases	decreases	−0.40
3. New oxygen doses	constant	transient increases	−0.50→−0.38
4. Heating to 298°K	constant	increases	−0.70
5. Cooling to 77°K	decreases	decreases	−0.20

heating of the system which contains adsorbed molecules in the 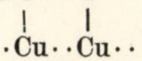 $\begin{array}{cc} \mathrm{O}- & \mathrm{O} \\ | & | \\ \cdot\cdot\mathrm{Cu}\cdot\cdot & \mathrm{Cu}\cdot\cdot \end{array}$ form. We advance the following explanation of this fact: while the 298°K adsorption is dissociative, the oxygen bonds being strong and hence immobile, the 77°K adsorption in the specified form leads to a layer with a certain mobility. The heating of the system gives sufficient energy to increase the mobility necessary for penetration but insufficient for the desorption of the excess.

The author wishes to express his deep gratitude to Prof. Dr. Doc. I.G.Murgulescu for his valuable guidance throughout this work.

Revue Roumaine de Chimie, **15**, 1699–1706 (1970)

ON THE STANDARD POTENTIAL OF THIN LEAD FILMS

IULIANA VARTIRES

Institute of Physical Chemistry, Bucharest, Str. Galaţi 31

Received May 15, 1970

The standard potential of the system Pb/Pb^{++} has been determined by e.m.f. measurements for the following electrochemical cells :

$$Pb \mid PbCl_{2(sat)} HCl_{(m)} Hg_2Cl_{2(sat)} \mid Hg^+$$

$$Pb \mid PbCl_{2(sat)}\ HCl_{(m)} \mid Pt_{(H_2\ 1\ atm)}$$

The lead electrode was made of thin metallic films of various thickness, obtained by vacuum evaporation on a glass support. The resulting value differs from that obtained by using bulk lead electrodes. The differences are growing when the films get thinner. The explanation of the phenomenon is given and the correlation between the decrease in the standard potential and the lowering of the heat of sublimation of the metal in thin films is shown.

INTRODUCTION

The study of the standard potential of thin lead films adds to our previous papers, with respect to the electrochemical behaviour of very thin films formed by vacuum evaporation.[1-4]

The early papers show that both the films of group 1 B monovalent metals and those of cadmium divalent metal, from the electrochemical point of view, have a deviation of the electrode equilibrium towards the formation of metallic ions. The deviation depends on the chemical nature of the metal and especially on the obtaining conditions of the films.

In choosing lead among the other tetravalent metals its wide utilization in the chemical current sources has been considered.

On the thin lead films both the studies on the structure [5-6] and those relating to the other kind of determination, like the measurements on

---

[1] I. G. Murgulescu, I. Vartires and O. Radovici, *Rev. Roumaine Chim.*, **12**, 215 (1967).

[2] I. G. Murgulescu and I. Vartires, *Rev. Roumaine Chim.*, **12**, 1069 (1967).

[3] I. G. Murgulescu and I. Vartires, *Rev. Roumaine Chim.*, **13**, 1397 (1968).

[4] I. G. Murgulescu and I. Vartires, *Rev Roumaine Chim.*, **14**, 1479 (1969).

[5] R. Grigorovici, N. Croitoru and A. Dévényi, *Z. Physik.*, **154**, 160 (1959).

[6] R. Grigorovici, N. Croitoru and A. Dévényi, *Studii şi Cercetări de Fiz. Acad. R.P.R.*, 4, 897 (1960).

the work functions by Gorodatskii,[7] proved the existence of a disorganization of the metal's crystalline lattice.

In the present paper we intend to study the electrochemical behaviour of lead films obtained by vacuum evaporation on a glass support by measuring their standard potential. Films with thickness from 150—1450 Å have been used.

The standard potential of the bulk metal of which the thin films were made, has also been determined. In this respect we used exactly the same couple $Pb/PbCl_2$ substances and device to avoid errors when comparing the values of the standard potential of thin films and of bulk metal. The differences pointed out in this case are only due to the partial disorganization of the crystalline lattice forming the films.

EXPERIMENTAL

The lead electrode is made of lead films obtained by vacuum evaporation by means of a device manufactured according to the general constructive principles of such devices.

At the vacuum installation is connected the cell in which the thin metallic films and the electrochemical measurements are made. In this way the lead film has been obtained avoiding the influence at atmospheric oxygen. The cell was represented in a previous paper.[4]

To obtain an inert atmosphere in the evaporation cell of the device, one introduces previously for half an hour purified argon. The output of the argon is arranged in such a way as to maintain a constant pressure of approximately 10^{-1} torr in the installation. The degassing of the supports occurs at 350° during 4 hours at 10^{-5} torr. The deposition rate is around 70 — 100Å/minute. The support's temperature during deposition is of about 140Å K.

The main parameters influencing the film's structure are kept constant, changing only the depositing duration from one measurement to another, in view of obtaining different thicknesses of the films. The bulk thickness of the films was determined by a spectrophotometrical method.

MATERIALS

Bulk lead metal is spectral pure (Johnson Matthey). The measurement medium, was a solution of very pure HCl in tridistilled water. The $PbCl_2$ *p.a.* has been purified from triply distilled water and three times recrystallized substances.

All determinations of standard potentials of the cell were achieved in deaerated solutions with purified argon.

THE ELECTROCHEMICAL MEASUREMENTS

In the cell where the thin metal films with a certain thickness were prepared (after a previous standardization bulk thickness-electric resistence), one proceeds to the electrochemical measurements that were carried out in the same conditions as those described in our early paper.[4]

---

[7] D. A. Gorodatskii, *Fiz. Tverd. Tela*, **11**, 790 (1969).

We pointed out that both the compensation of the vacuum and introduction of the solutions into the measuring cell, were made under a stream of purified argon.

The reference electrode was both the hydrogen electrode (to avoid the diffusion potentials) and the calomel electrode. The measurements were almost the same against both electrodes. The same observation was pointed out by Belew.[8]

In this way galvanic piles are made of :

$$Pb\,|PbCl_{2(sat)}HCl_{(m)}\,|\,Pt_{(H_2 1.\ atm)} \tag{1}$$

$$Pb\,|PbCl_{2(sat)}HCl_{(m)}\,Hg_2Cl_{2(sat)}\,|Hg \tag{2}$$

where m = 0.1 N. This HCl concentration was selected so as to avoid the formation of the complex ions of $PbCl_3^-$, $PbCl_4^{--}$ etc.

The e.m.f. was measured with a Feussener potentiometer to a precision of 0.01 mV. The determinations were made at 25° ± 0.02 by means of a U_{10} thermostat.

The experiments of the standard potential for bulk lead were performed in an electrochemical cell described in [4] under the same conditions as those described for films.

Galvanic piles :

$$Pb_xHg\,|PbCl_{2(sat)}HCl_{(m)}\,|\,Pt_{(H_2 1.\ atm)} \tag{3}$$

$$Pb_xHg\,|PbCl_{2(sat)}\,HCl_{(m)}\,Hg_2Cl_{2(sat)}\,|Hg \tag{4}$$

are also built.

The lead amalgam has been obtained according to the method described by Treadwell[9] where x = 1.8 – 2%.

RESULTS AND DISCUSSION

The basic reaction, for the galvanic cell (1) is :

$$Pb^0 + 2H^+ \rightleftharpoons Pb^{++} + H_{2(g)} \tag{5}$$

the e.m.f. of which is given by equation :

$$E = -E^0_{Pb,Pb^{++}} + \frac{2RT}{F}\ln f(m) - \frac{RT}{2F}\ln K_{PbCl_2} \tag{6}$$

at 25° the standard potential's expression becomes :

$$E^0_{Pb,Pb^{++}} = -E + 0.1183 \log f(m) - 0.02957 \log K_{PbCl_2} \tag{7}$$

---

[8] W. L. Belew and H. P. Raaen, *J. Electroanalyt. Chem.*, 8, 475 (1964).

[9] W. D. Treadwell, "Electroanalytische Methoden" Verlag von Gebrüder Borntraeger, Berlin 1915, p. 147.

where "*m*" is the molar concentration and "*f*" the activity coefficient of HCl . K_{PbCl_2} the equilibrium constant of $PbCl_2$ has been calculated from the solubility data of $PbCl_2$ in different concentrations of HCl by Ende [10] and it was found equal to 2.126×10^{-5}.

For the galvanic cell (2) the equation is:

$$Pb^0 + Hg_2^{++} \rightleftharpoons Pb^{++} + 2\,Hg^0 \qquad (8)$$

but the e.m.f. is given by the expression:

$$E = E^0_{Hg,Hg_2^{++}} - E^0_{Pb,Pb^{++}} - \frac{RT}{2F} \ln \left(\frac{K_{PbCl_2}}{K_{Hg_2Cl_2}} \right) \qquad (9)$$

at 25° the standard potential's expression becomes:

$$E^0_{Pb,Pb^{++}} = E^0_{Hg,Hg^{++}} - E - 0.02957 \log \left(\frac{K_{PbCl_2}}{K_{Hg_2Cl_2}} \right) \qquad (10)$$

From tables we found: $E^0_{Hg,Hg^{++}} = 0.7986$ V and $K_{Hg_2Cl_2} = 1.15 \times 10^{-18}$. One may readily estimate the value of standard potential $E^0_{Pb,Pb^{++}}$ from equations (7) and (10).

In table 1 are given the values of standard potentials of bulk lead for one concentration of HCl for both galvanic cells (1) and (2).

Table 1

Standard potential of bulk lead T = 25°

No	Reference electrode	HCl concentration	e.m.f. in V	E° Pb,Pb++ in V	Standard deviation in V
1	S.H.E.	0.1 N	0.1340	0.1258	±0.0004
2	S.C.E	0.1N	0.5323	0.1260	±0.0002

$E^0_{Pb,Pb^{++}} = 0.1259$ V

In the estimation of the standard potential for the electrode amalgam the amalgamated metals were considered with a behaviour similar to that of as the single crystals.

The values found by us were in good agreement with those mentioned in literature.[11-13]

The results of the measurements on the lead thin films are given in table 2. Here the values of the standard potentials depending on the film thickness in Å are given, computed from experimental (limit) value of e.m.f. (E) by means of equation (10).

---

[10] C. L. Ende, *Z. anorg. Chem.*, **26**, 148 (1901).

[11] K. Faragó, *Acta lit. Sci. regiae. Univ. Francesco-Josephinae Sect. Chem. Mineral Phys.*, 5, 193 (1937).

[12] H. Fromherz, *Z. physik. Chem.*, 153, 383 (1931).

[13] I. G. Murgulescu and E. Constantinescu, *Rev. Chim.* Acad. R.P.R., **8**, 5 (1963).

Figure 1 illustrates the plots of the experimental results. The mean reproducibility of the potentials for thinner films is up to ± 0.002 V, for thicker films (over 1000 Å) it reaches ± 0.001 V.

Table 2

$E^0_{Pb,Pb^{++}}$ in HCl 0.1 N for unstabilized and stabilized films

No	Thickness in Å	e.m.f. in V	$E^0_{Pb,Pb^{++}}$ in V	Standard deviation in V	Molal heat of sublimation λ° in kcal/mol
1	150	0.4452	0.0389	±0.0025	42.980
2	160	0.4466	0.0403	±0.0025	42.940
3	165	0.4492	0.0429	±0.0020	43.160
4	185	0.4589	0.0526	±0.0018	43.610
5	200	0.4600	0.0537	±0.0025	43.660
6	220	0.4643	0.0580	±0.0020	43.890
7	230	0.4667	0.0610	±0.0029	44.090
8	240	0.4699	0.0636	±0.0019	44.120
9	250	0.4740	0.0677	±0.0015	44.310
10	335	0.4825	0.0762	±0.0023	44.700
11	450	0.5004	0.0941	±0.0015	45.520
12	625	0.5141	0.1070	±0.0014	46.190
13	1 400	0.5323	0.1260	±0.0010	46.990
			for stabilized films		
14	1200	0.5360	0.1297	±0.0010	

As it results from the data provided by table 2 as well as from figure 1, normal potentials decrease with the increasing thickness of the films, becoming more negative. The phenomenon can be more easily seen for very thin films. For thicker films, the standard potential approaches the normal values of the amalgamated lead electrodes.

Table 2 also presents the standard potential obtained on a stabilized film. The stabilization was obtained thermally by heating previously the film at 350° for 15 min. The value of its standard potential is practically identical to that of the standard potential of a bulk electrode.

Figure 2 represents the standard potentials depending on the reciprocal of the thickness of the film, for thicker than 150 Å. Hence a dependence with the form :

$$E^0 = 0.1220 - \frac{A}{x} \qquad (11)$$

where x is the thickness of the film. When this is expressed in Å the constant A takes the value 13.17. The value 0.1220 represents the standard potential of a bulk electrode ($x \to \infty$) obtained by extrapolation as one sees in figure 2.

The result agrees with the value of the normal potential of a bulk electrode (0.1259 V) as well as with that of the standard potential of a stabilized film (0.1297 V).

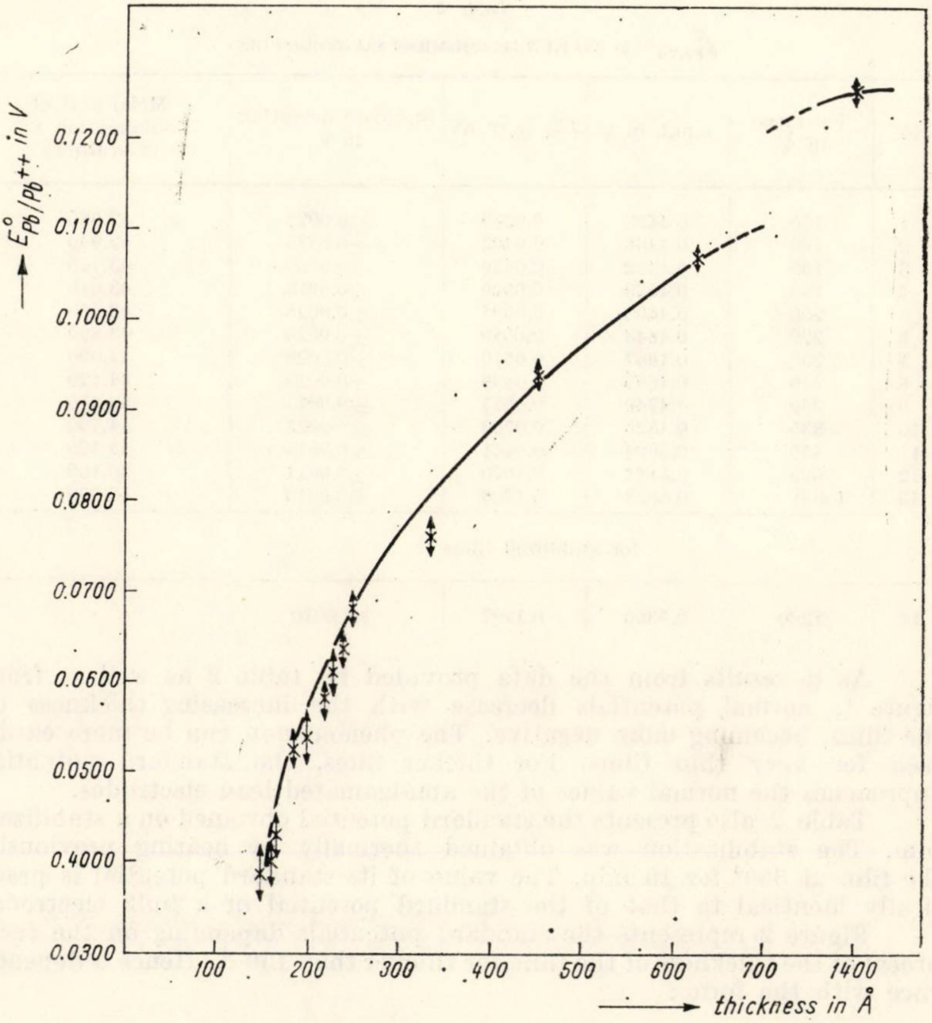

Fig. 1. – Dependency of the $E^0_{\mathrm{Pb,Pb}}{}^{++}$ on the film thickness in Å in HCl 0.1 N.

The deviation of the standard potential of the lead thin films electrode towards more negative values is due to the partial disorganization of the crystal lattice which forms the film. In such conditions the energy of the ions of the lattice increases, resulting in an increase in the "electrolytical dissolution tension" of the metal rendered by a negativation of the electrode potential.

The disorganization of the crystal lattice and the volatility of the metal increase and its sublimation heat decreases. For the calculation of the sublimation heat, in the case of thin films, one resorts to equation (12) deduced from a previous paper[14] which relates the electrode

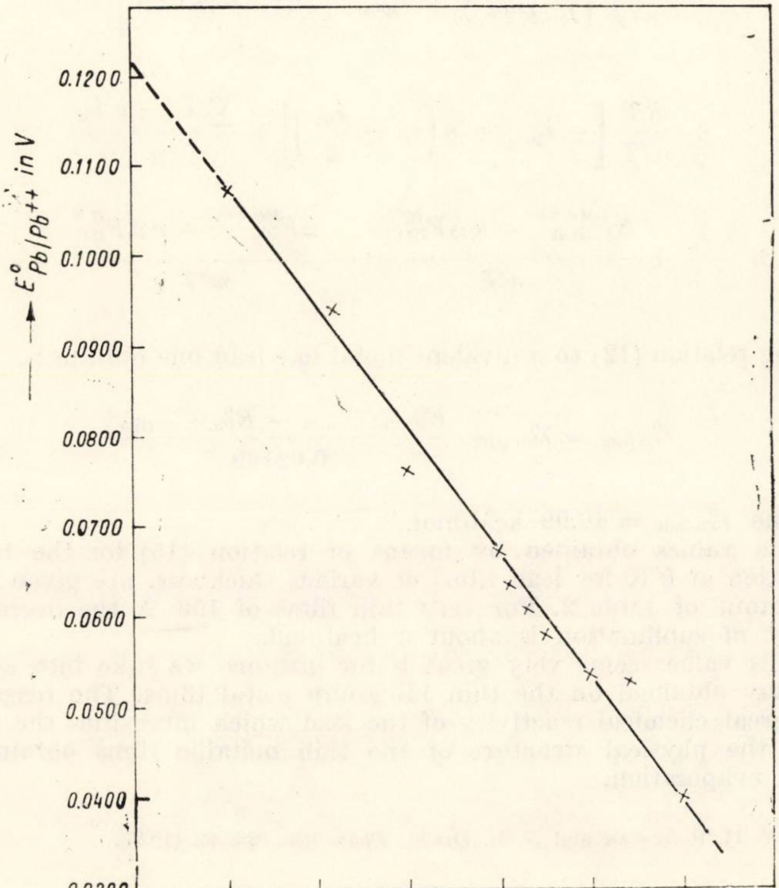

Fig. 2. — Variation of the $E_{Pb,Pb}^{++}$ potential function of the reverse film thickness in Å^{-1}.

---

[14] I. G. Murgulescu and E. Constantinescu, *Rev. Chim. Acad. R.P.R.* **12**, 339 (1967).

potential to the sublimation heat. The symbols appearing in (12) have their significance shown in the respective paper.

$$E^0_{\mathrm{Me,\,Me}^{(+)n}} = \frac{\lambda^0_{\mathrm{Me}} + n/2\,D^0_{\mathrm{H}_2}}{n\mathcal{F}} + \frac{5/2\,(n-1)\,RT\ln T}{n\mathcal{F}} + \frac{RT}{n\mathcal{F}}\left[\int_0^T \frac{\mathrm{d}T}{RT^2}\int_0^T (C_{p_{\mathrm{Me(s)}}} - n/2\; C_{p_{\mathrm{H}_2(\mathrm{g})}})\,dT\right] + \frac{RT}{n\mathcal{F}}\left[-\,i_{\mathrm{Me(g)}} + n\left(i_H - \frac{i_{\mathrm{H}_2}}{2}\right)\right] + \frac{\sum^n I_i - n\,I_H}{n} + \frac{\Delta F^{\mathrm{Me}(+)n}_{\mathrm{Hydr.}} - n\,\Delta F^{\mathrm{H}^+}_{\mathrm{Hydr.}}}{n\mathcal{F}} + \frac{\Delta F^{\mathrm{Me}(+)n}_{\mathrm{Dil.}} - n\,\Delta F^{H^+}_{\mathrm{Dil}}}{n\mathcal{F}} \tag{12}$$

Applying relation (12) to a divalent metal like lead one obtains :

$$\lambda^0_{\mathrm{Pb\,film}} = \lambda^0_{\mathrm{Pb\,bulk}} - \frac{E^0_{\mathrm{Pb,Pb}^{++}\,\mathrm{bulk}} - E^0_{\mathrm{Pb,Pb}^{++}\,\mathrm{film}}}{0.02169} \tag{13}$$

the value $\lambda^0_{\mathrm{Pb\,bulk}} = 46.99$ kcal/mol.[15]

The values obtained by means of relation (15) for the heat of sublimation at 0°K for lead films of various thickness, are given in the last column of table 2. For very thin films of 150 Å the decrease in the heat of sublimation is about 4 kcal/mol.

This value seems very great if for instance we take into account the values obtained on the thin 1B group metal films. The reason lies in the great chemical reactivity of the lead which intensifies the alteration in the physical structure of the thin metallic films obtained by vacuum evaporation.

---

[15] W. H. Rodebush and A. L. Dixon, *Phys. Rev.*, **26**, 85 (1925).

Revue Roumaine de Chimie, 15, 1707–1711 (1970)

ELECTRONIC ABSORPTION SPECTRA OF $ZnCl_2$, $CdCl_2$ AND AgCl IN PASSING FROM SOLID TO MOLTEN STATE

E. POPA, EUGENIA IVANA and S. V. VOLKOV*
Institute of Physical Chemistry, Bucharest, Dumbrava Roşie, 23

Received February 16, 1970

UV and visible absorption spectra of $ZnCl_2$, $CdCl_2$ and AgCl un passing from solid to molten state were obtained. The modifications of the absorption spectrum of $ZnCl_2$ in passing from solid to molten state are attributed to the gradual destruction of the crystalline structure and to the presence of $(ZnCl_2)n$ clusters. The important bathochromic shifts observed when fusion of $CdCl_2$ and AgCl takes place are being explained as a result of the disorder and of the increasing dissociation, in spite of the fact that for these salts the presence of clusters is characteristic, either.

INTRODUCTION

The modifications of the absorption spectra of the salts in passing from solid to melt have been noticed for the first time in Retschinsky' s[1] work that broke new ground. This work shows that a 5000–8000 cm^{-1} shift of the absorption edge towards lower energies appears for molten NaCl, NaBr, KCl, KBr.

Later on, a similar shift of about 5600 cm^{-1} has been found by Mollwo [2] for KI. In 1959, precise measurements made by Ubbelohde and Rhodes [3] with thin layers of LiI have shown the same shift towards red, the order of magnitude being 1400 cm^{-1}. These facts allow to conclude that the fusion of alkali-halides is generally accompanied by an important shift of the ultraviolet absorption bands towards longer wavelengths. This has been correlated mainly with the considerable positional disorders during fusion.

At the same time, Ubbelohde and Rhodes have established that salts like KNO_3, $NaNO_3$, $LiNO_3$, $AgNO_3$, KCNS show at fusion an important hypsochromic shift, though at a lesser extent as compared with the bathochromic shift of alkali halides. This shift, as well as the mechanism of fusion itself, has been interpreted on the basis of intensive ion pair and association formation in the melt. For analogue salts, e.g. $RbNO_3$, $CsNO_3$, NH_4NO_3, no blue shift has been observed, [4] as expected.

---

[1] T. Retschinsky, *Ann. Phys.*, **27**, 100 (1908).
[2] E. Mollwo, *Z. Physik*, **124** 118 (1947).
[3] E. Rhodes and A. R. Ubbelohde, *Proc. Roy. Soc.*, **A251**, 156 (1959).

* Institute of General and Inorganic Chemistry, Kiev.

Doucet and al.[5] have repeated some of the measurements and confirmed the two mentioned types of shifts :

— a hypsochromic shift for $LiNO_3$, $NaNO_3$, KNO_3 and $TlNO_3$

— a bathochromic shift for LiI and, surprisingly, for $ZnCl_2$.

This is essentially all the available information in the field of absorption spectra in passing from crystals to molten salts.

The purpose of the present work is to investigate the absorption spectra of molten $ZnCl_2$, $CdCl_2$ and AgCl, salts known for their strong trend for association in molten state.[6–8]

EXPERIMENTAL

The electronic absorption spectra were measured on a DK-2 Beckmann spectrophotometer, the cell being placed in a thermostated furnace. The temperature was measured by means of a Pt-Pt(Rn) thermocouple and was kept steady within ± 2°.

Due to the strong absorption of molten salts, silica cells with very thin layers of about 12 to 200μ were used. The cells were filled and sealed under vacuum, to avoid contact with moisture ($ZnCl_2$ being very hygroscopic).

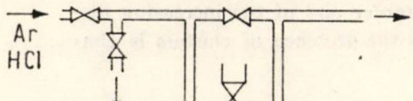

Fig. 1. — Apparatus for drying and purifying salts.

A particular attention was paid to salt preparations. $ZnCl_2$ and $CdCl_2$ were recrystallized, then dried and melted by bubbling dry Ar. $ZnCl_2$ was dried once more using the apparatus shown in figure 1 and then filtered directly into the cell. AgCl was obtained from recrystallized $AgNO_3$ and KCl, then dried and purified by bubbling gaseous HCl in the melt.

RESULTS AND DISCUSSIONS

The absorption spectra of $ZnCl_2$, $CdCl_2$ and AgCl show two sharply different and characteristic absorptions : one of total transmittance, and the other, of total absorbance.

The figures 2 to 4 show the dependence of the wavelength of the absorption band's edge on the temperature.

Consideration of this dependence in the $ZnCl_2$ case leads to the following conclusions :

---

[4] K. Sakai, *J. Phys. Chem.*, **61**, 1131 (1957).

[5] Y. Doucet, R. Bailleux and A. Lacroix, *Compt. rend.*, **259**, 1403 (1964).

[6] B. F. Markov and S. V. Volkov "Fizicheskaya khimia rasplavlenih solei", Metalurgizdat, Moscow, 1965, p. 211.

[7] E. R. van Artsdalen, *J. Phys. Chem.*, **60**, 172 (1965).

[8] *** "Stroenie rasplavlenih solei", Izd. Mir., Moscow, 1966.

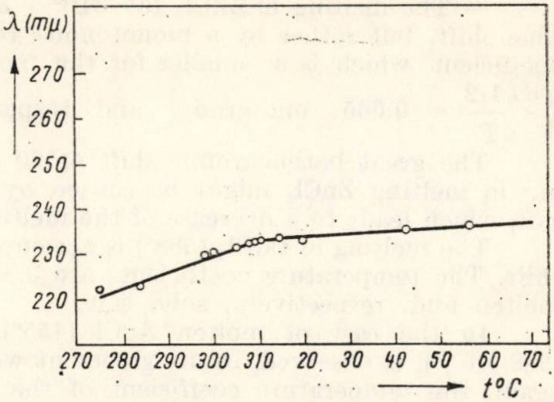

Fig. 2. — Temperature dependence of $\lambda\ 1/2$ for $ZnCl_2$.

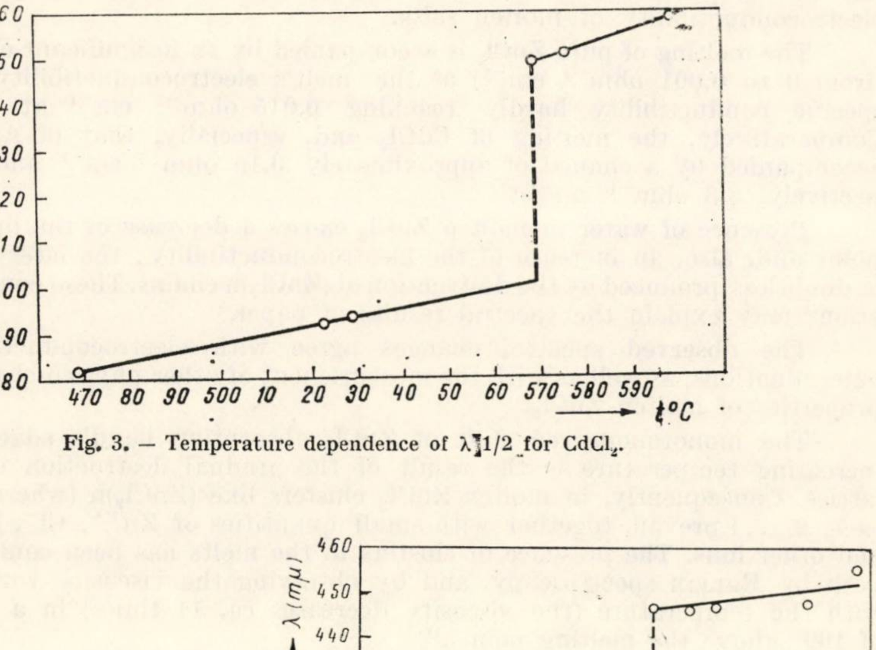

Fig. 3. — Temperature dependence of $\lambda 1/2$ for $CdCl_2$.

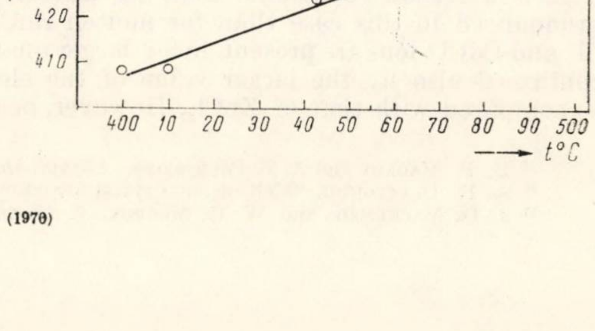

Fig. 4. — Temperature dependence of $\lambda 1/2$ for AgCl.

— The melting of $ZnCl_2$ (at $310^0 \pm 5^0$) is not accompanied by a blue shift, but rather by a monotonous red shift, with a temperature coefficient which is a smaller for the molten than for the solid $ZnCl_2$ $\left(\frac{d\lambda 1/2}{dT} = 0.065 \text{ m}\mu \text{ grad}^{-1} \text{ and respectively } 0.313\text{m}\mu \text{ grad}^{-1}\right)$.

The great bathochromic shift (4500 cm^{-1}) observed by Doucet et al.[5] in melting $ZnCl_2$ might be caused by the presence of water in the salt, which leads to a decrease of the melting point down to 262°.

The melting of $CdCl_2$ (568°) is accompanied by a great bathochromic shift. The temperature coefficients are 0.316 and 0.19 m $grad^{-1}$ for the molten and, respectively, solid salt.

In the case of molten AgCl (455°), a small bathochromic shift (982 cm^{-1}), is observed, in disagreement with results of the paper.[1] Here again, the temperature coefficient of the shift of band's edge for melt (0.2 mμ $grad^{-1}$) is lower than for the solid AgCl (0.363 mμ $grad^{-1}$).

From the viewpoint of association-dissociation processes, it is interesting to compare our results with the data obtained by studying of electroconductibility of molten salts.

The melting of pure $ZnCl_2$ is accompanied by an insignificant change (from 0 to 0.001 ohm^{-1} cm^{-1}) of the melt's electroconductibility, the specific conductibility hardly reaching 0.015 ohm^{-1} cm^{-1} at 400°.[9] Comparatively, the melting of $CdCl_2$ and, especially, that of AgCl is accompanied by a change of approximately 0.15 ohm^{-1} cm^{-1} and, respectively, 3.8 ohm^{-1} cm^{-1}.[10]

Presence of water in molten $ZnCl_2$ causes a decrease of the melting point and, also, an increase of the electroconductibility; the later effect is doubtless produced by the destruction of $(ZnCl_2)n$ chains. These considerations may explain the spectral results of paper.[5]

The observed spectral changes agree with electroconductibility determinations, as well as with the measurement of other physico-chemical properties of molten $ZnCl_2$.

The monotonous red shift of $ZnCl_2$ absorption band's edge with increasing temperature is the result of the gradual destruction of the lattice. Consequently, in molten $ZnCl_2$ clusters like $(ZnCl_2)n$ (where $n = 1, 2, \ldots$) prevail, together with small quantities of Zn^{++}, Cl^-, $ZnCl^+$ and other ions. The presence of clusters in the melts has been confirmed both by Raman spectroscopy, and by observing the viscosity variation with the temperature (the viscosity decreases ca. 11 times) in a range of 100° above the melting point).[11]

The 4570 cm^{-1} bathochromic shift of the $CdCl_2$ absorption band's edge is a reason to assume that the dissociation process is much more pronounced in this case than for molten $ZnCl_2$. This means that Cd^{++}, Cl^- and $CdCl^+$ ions are present in far larger quantities, fact which is being confirmed also by the larger value of the electroconductibility of $CdCl_2$ as compared with that of $ZnCl_2$. However, because $CdCl_2$ has got a significant tendency to form covalent bands and molecular associations, one should not exclude the cluster's presence. Theire xistence has been confirmed in fact, in the Raman spectra, even at temperatures far above the melting point.[8]

---

[9] B. F. Markov and A. T. Polishchyk, *Ukrain. khim. Zhur.*, **31**, 1133 (1965).

[10] A. R. Ubbelohde, "Melting and Crystal Structure", Oxford Univ. Press, 1965, p. 50.

[11] J. D. Mackenzie and W. K. Murphy, *J. Chem. Phys.*, **33**, 366 (1960).

The bathochromic effect of 982 cm^{-1} of the absorption band's edge of AgCl, correlated with the large value of electroconductibility, leads to the conclusion that in the melt, together with Ag^+ and Cl^- ions, autocomplexes of the form $(Ag_nCl_{n+1})^-$ and $(Ag_nCl_{n-1})^+$ are being present too.

Revue Roumaine de Chimie, **15**, 1713–1720 (1970)

DIE SELBSTDIFFUSION DES FLÜSSIGEN TELLURS IM TEMPERATURBEREICH VON 460–600°

ELISABETA NICOLOIU, LUCIA GANOVICI und I. GANOVICI

aus dem Forschungszentrum für Physikalische Chemie der Akademie Bukarest,
str. Galaţi, 31

Eingegangen am 31. Januar 1970

Es wurden die Selbstdiffusionskoeffizienten des flüssigen Tellurs im Temperaturbereich von 470–600° mit Hilfe der Kapillar-Reservoirmethode und der Tracer-Methode bestimmt. Die Temperaturabhängigkeit ergibt sich aus der Gleichung $D = 12,\ 9.10^{-2}$ exp. $(-5550/RT)$, Es wurde der Radius der diffundierenden Teilchen bestimmt.

EINLEITUNG

Die vorliegende Arbeit hat den Zweck die experimentellen Kenntnisse hinsichtlich der Selbstdiffusion in flüssigen reinen Metallen zu bereichern. Die Fachliteratur bringt wenig Daten über das flüssige Tellur, von welchen die meisten Fragen der Densität und der Viskosität behandeln. Über die Diffusion des Tellurs in flüssigem Kupfer und Silber hat Inagaki u. Mitarb.[1,2] berichtet.

Zieht man die wichtige Rolle in Betracht, die das Tellur in der Herstellung der flüssigen Halbleiter spielt, so wird der praktische Wert der Diffusionsbestimmungen ersichtlich. Desgleichen trägt die genaue Bestimmung der Diffusionskoeffizienten in flüssigen Metallen zur Erläuterung des flüssigen Zustandes bei.

ARBEITSMETHODE

Die Diffusionsmessungen des flüssigen Tellurs wurden nach der allgemein gebräuchlichen Kapillar-Reservoirmethode in Kombination mit der Tracer-Methode durchgeführt. Die dazu verwendete Apparatur wurde in einer vorhergehenden Arbeit genau beschrieben.[3]

Die Reservoirschmelze bestand aus ungefähr 50g Tellur mit einem Reinheitsgrad von 99,999 %, der 5g radioaktives Te von derselben Reinheit zugesetzt wurde. Die Radioaktivität

---

[1] Noboru Inagaki, Tatsuhiko Ejima und Mitsu Kameda, *Nippon Kogyo Kaishi*, **81**, (12), 29 (1965).

[2] Noboru Inagaki, Tatsuhiko Ejima und Mitsu Kameda, *Nippon Kogyo Kaishi*, **82**, (4), 17 (1966).

[3] N. Petrescu, St. Zămarcă, Lucia Ganovici und I. Ganovici, *Rev. Roumaine Chim.*, **13**, 865 (1968).

der Schmelze war ca. 2mCi. Die zur Diffusion verwendeten Kapillaren bestanden aus spektralreinem Graphit und hatten eine Länge von 20 mm und einen Durchmesser von 1mm.

Die Kapillaren wurden mit in Vakuum geschmolzenem Tellur unter Argondruck gefüllt. [3] Die gefüllten Kapillaren wurden röntgenologisch geprüft, nachdem Proben, die Hohlräume aufwiesen, ausgeschlossen wurden. Die Kapillaren wurden am freien Ende zugespitzt, um zu verhindern, daß Teilchen der radioaktiven Schmelze mitgerissen werden .

Die Diffusionen wurden in einem Temperaturbereich von 470—600° durchgeführt. Die Temperatur wurde mit einem Pt-PtRh Thermoelement, mit einer Genauigkeit von ±1 gemessen. Der große Dampfdruck des Te bei Temperaturen von über 600° (bei 604° — 5,98mm, bei 700° schon 28,97mm[4]) verursacht große Schwierigkeiten bei den Messungen des Selbstdiffusionskoeffizienten bei höheren Temperaturen.

Die Diffusionen wurden in reinem Argon durchgeführt um das Oxidieren der Metalloberfläche zu verhindern. Die Diffusionszeit war 1 Std.

Nach der Diffusion wurden die Metallstäbchen aus den Graphitkapillaren entfernt und gewogen. Die Radioaktivität wurde mit einem Geiger-Müllerkontor bei gleichen geometrischen Bedingungen gemessen. Die Aktivität der Tellurproben wurde auf die aus der Reservoir-Schmelze erhaltenen Proben von derselben Größe und geometrischen Form bezogen. Die Bezugsproben wurden nach jeder Diffusion aus der Schmelze entnommen, indem man die ganze Installation auf einen Unterdruck von 0,2 atm brachte ; mit Hilfe eines Argonüberdruckes wurden dann die Graphitkapillaren mit geschmolzenem Tellur gefüllt.

Die Selbstdiffusionskoeffizienten wurden so berechnet indem man die integrale Radioaktivität der Proben nach der Diffusion ($\overline{C}$) auf die Radioaktivität der Tellurschmelze im Reservoir (C_0) nach folgender Gleichung bezog

$$\frac{\overline{C}}{C_0} = 1 - \frac{8}{\pi^2}\sum_{n=0}^{\infty}\frac{1}{(2n+1)^2}\cdot\exp\left[-\frac{(2n+1)^2\pi^2}{4}\cdot\frac{Dt}{l^2}\right] \qquad (1)$$

wo t — Diffusionszeit in Sek, l — Länge der Kapillaren in cm und D Selbstdiffusionskoeffizient in cm/s.

Die Gleichung wurde durch die Integration des zweiten Fickschen Gesetzes in bezug auf Anfangs- und Endbedingungen unserer Experimente erhalten :

$$\begin{array}{llll} \text{Wenn} & t = 0 & C = 0 & \text{für} \quad 0 < x < 1 \\ & t > 0 & C = C_0 & \text{für} \quad x = 0 \\ & \dfrac{\partial C}{\partial x} = 0 & & \text{für} \quad x = 1 \end{array} \qquad (2)$$

Die Gleichung wurde mit Hilfe eines Elektronenrechners C.E.T. —500 in bezug auf den Parameter $\theta = Dt/l^2$ tabelliert.

RESULTATE, DISKUSSIONEN

Wir haben die Selbstdiffusionskoeffizienten des flüssigen Tellurs für sieben Temperaturpunkte im Bereiche von 470—600° bestimmt. Die in Tabelle 1 angeführten Daten stellen ein Mittel von mindestens 4 Messungen dar. Ungefähr 40 % der Proben wurden wegen zu kleiner Radioaktivität nicht in Betracht gezogen. (Zu kleine Radioaktivität zeigt, daß die Diffusion nicht stattgefunden hat.)

---

[4] A. N. Nesmeianov, „Davlenie para khimicheskikh elementov", Izd. AN SSSR Moskau, 1961, S. 286.

Um die Genauigkeit der Meßergebnisse zu bestimmen wurde der Wert des relativen Gesamtfehlers 20 %, wie auch der des mittleren quadratischen Fehlers für jeden Temperaturpunkt berechnet.

Tabelle 1

Selbstdiffusionskoeffizienten des flüssigen Tellur :
Experimentelle und berechnete Daten

Diffusions-temperatur, °C	$D_{\text{exp}} \pm \Delta D$ $10^5 \text{cm}^2/\text{s}$	D_{ber} $10^5 \text{cm}^2/\text{s}$
470	3,03 ± 0,28	3,32
480	3,20 ± 0,32	3,44
500	3,44 ± 0338	3,68
530	4,06 ± 0,50	4,05
560	4,30 ± 1,1	4.43
580	5,00 ± 2,1	4,68
600	5,35 ± 2,9	4,94

• $D = 3{,}38.10^{-4}.1{,}43.\ \exp(-3950\ RT)$

In Tabelle 1 sind neben den von uns gemessenen Werten auch die nach der Frenkelschen Gleichung[5] berechneten Daten angegeben.

$$D = D_0^{theor} e^{-\gamma} e^{-E_{vD}/RT} \tag{3}$$

D_0, $e^{-\gamma}$ und E_{vD} wurden auf folgende Art bestimmt

$$D_0^{theor} = \frac{K\theta}{6h}\left(\frac{V_{at}}{N_A}\right)^{2/3} = 3{,}38 \cdot 10^{-4}\ \text{cm}^2/\text{s} \tag{4}$$

K = Boltzmann-Konstante, h = Plank-Konstante, $V_{at} = 22{,}01$ cm (Atomvolumen des flüssigen Te bei seinem Schmelzpunkt[6])

N = Avogadro-Zahl, θ = Debye-Temperatur wurde nach Lindemann berechnet

$$\theta = 0{,}866 \sqrt{T_m / A V_{at}^{2/3}} \tag{5}$$

A = Atomgewicht des Te, $e^{\gamma} = 1{,}43$ ein Entropie-Faktor berechnet aus Viskositätsdaten des flüssigen Tellurs.[5, 6]

---

[5] A. V. Grosse, *Rev. Inst. Haute Temper. Refract.*, **4**, 171 (1967).

[6] V. M. Glasov, S. A. Chzhevskaia und H. N. Glagoleva, „Zhidkie poluprovodniki", Izd. Nauka, Moskau 1967, S. 222, 228.

Der Wert der Aktivierungsenergie E_{vs} wurde desgleichen aus Viskositätsdaten des flüssigen Te bestimmt.[6] Sie stellt die Neigung der Geraden $\log \theta = f(1/T)$ dar; und wurde aus experimentellen Ergebnissen nach der Methode der kleinsten Quadrate errechnet. Der gefundene Wert 3950 cal/Mol diente zur Berechnung der Diffusionskoeffizienten von Tabelle 1. Wie aus dem Vergleich ersichtlich, sind die berechneten Daten den experimentellen annähernd gleich. Die Differenzen reichen bis zu maximum $\pm 10\%$, was sich im Rahmen des experimentellen Fehlerbereiches der Methode befindet.

Den Radius des diffundierenden Teilchens haben wir an Hand der Gleichung von Sutherland berechnet

$$D = \frac{kT}{4\pi\eta r} \tag{6}$$

welche den Diffusionskoeffizienten im Verhältnis zur dynamischen Viskosität ausdrückt. Wir erhielten für r einen Wert von 1,31 Å. Der Radius wurde für $T = 773°\text{K}$ berechnet. Zu seiner Bestimmung haben wir den experimentell gefundenen Wert des Diffusionskoeffizienten und die dynamische Viskosität des flüssigen Te aus [6] gebraucht. Der gefundene Radius des diffundierenden Teilchens hat einen annähernden Wert zu dem des metallischen Radius [7] ($r = 1{,}37$ Å).

Im allgemeinen wird der Diffusionsprozeß in Flüssigkeiten in Analogie zum festen Zustande als ein „aktivierter" Prozeß betrachtet. Dem zu Folge sind die meisten experimentellen Daten in Abhängigkeit von den Parametern D_0 und E_v dargestellt. Eventuelle Abweichungen von dem Gesetze

$$D = D_0 \exp\,(-E \exp\,(-E_{vD}/RT) \tag{7}$$

werden so sehr leicht übersehen.

Auch werden auf diese Weise andere Prozesse, die desgleichen einen Aufschluß über die Struktur der flüssigen Metalle, wie auch die Art der Atombewegungen geben könnten, in den Schatten gestellt.

In der vorliegenden Arbeit wurden die experimentellen Daten als erstes von dem Standpunkte des aktivierten Prozesses aus bearbeitet. Mit Hilfe der Methode der kleinsten Quadrate haben wir an Hand unserer Daten folgende Gleichung zur Bestimmung der Diffusionskoeffizienten in Abhängigkeit von der Temperatur erhalten.

$$D = 12{,}9 \cdot 10^{-4}\ \exp.\ (-5550/RT) \tag{8}$$

Ein graphischer Vergleich mit anderen Metallen [8] auf Grund ihrer Schmelzpunkte (Abb. 1) zeigt, daß der von uns gefundene Wert der Aktivierungsenergie für flüssiges Te (5553 kal/Mol) als gut bewertet werden kann.

---

[7] L. PAULING, „The Nature of the Chemical Bond", Ausg. III, CORNELL, Univ. Press, New York, 1962, S. 410.

In Tabelle 2 sind unsere Werte für D_0 und E_v mit denen in der Literatur für die Diffusion des Te in flüssigem Kupfer und Silber verglichen.[1, 2]

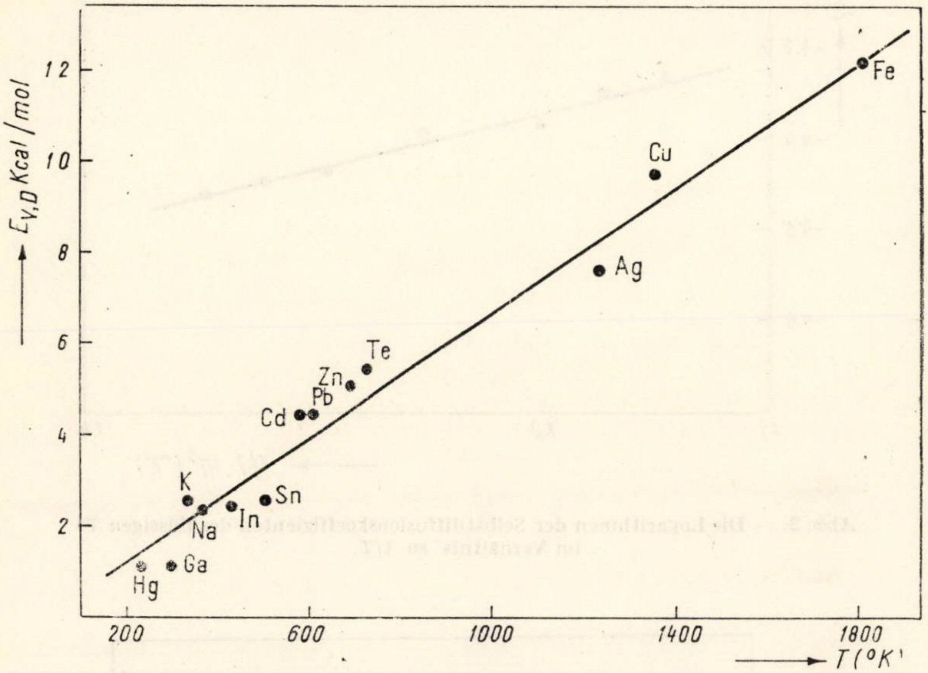

Abb. 1. — Die Aktivierungsenergie verschiedener Metalle im Verhältnis zu ihrem Schmelzpunkt.

Tabelle 2

Die Werte von $_{VD}$ D_0 für die Diffus[illegible]
Te, Cu und Ag

Das Element in welchem Te diffundiert	Schmelztemp. °K	E_{vD} Kal/Mol	$D_o 10^{-4}$ m^2/s
Tellur	725	5 550	12,9
Silber	1 234	9 200	9,9
Kupfer	1 356	12 800	3,4

Man kann aus Tabelle 2 feststellen, daß die Aktivierungsenergie der Diffussion mit dem ansteigenden Schmelzpunkt der Metalle, in welchen das Tellur diffundiert, zunimmt, während der D_0-Wert abnimmt. Die Fehler in der Bestimmung des D_0 sind im allgemeinen größer, da dieser Wert durch Extrapolation auf den Nullwert der Geraden $\log D = f\left(\frac{1}{T}\right)$ berechnet wird. Die Gerade ist ihrerseits nur für begrenzte Temperaturintervalle bestimmt. Die Darstellung der Logarithmen der

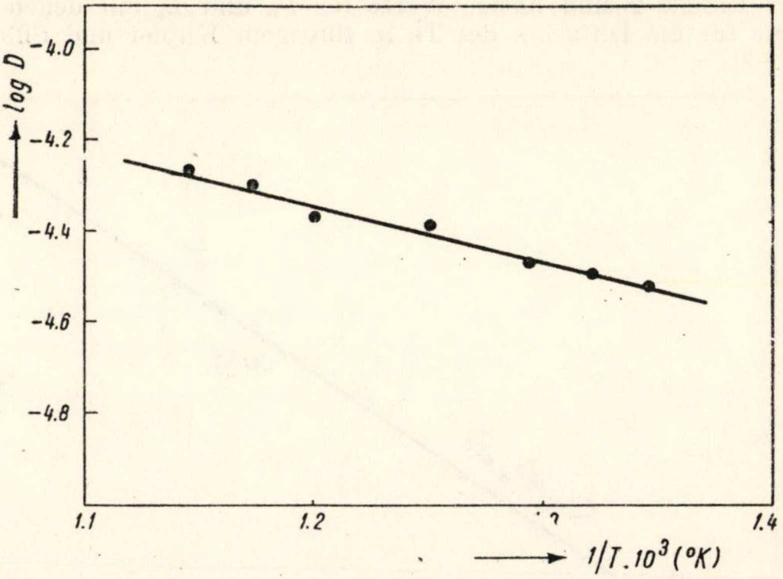

Abb. 2. — Die Logarithmen der Selbstdiffusionskoeffizienten des flüssigen Te im Verhältnis zu $1/T$.

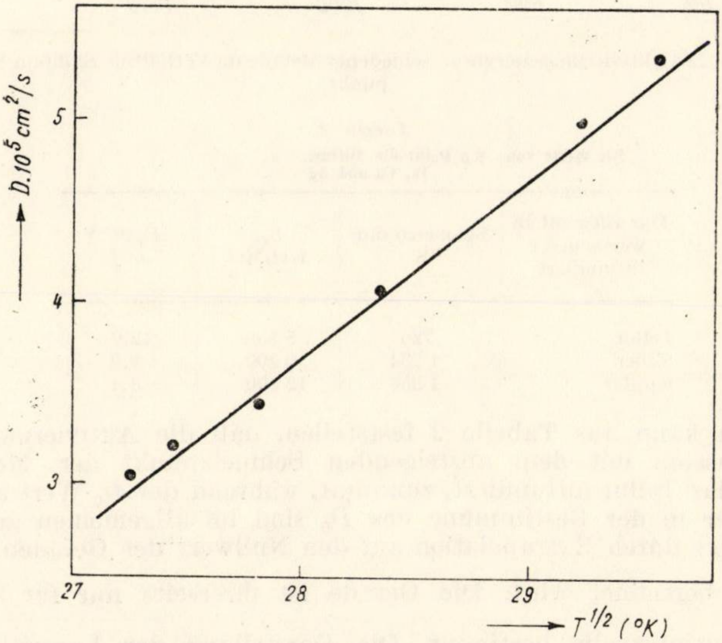

Abb. 3. — Die Selbstdiffusionskoeffizienten des flüssigen Te im Verhältnis zu $T^{1/2}$.

Selbstdiffusionskoeffizienten des flüssigen Tellurs im Verhältnis zu $1/T°$ K ist in Abb. 2 abgebildet.

In Abb. 3, 4 und 5 haben wir das graphische Verhalten der Diffusionskoeffizienten im Verhältnis zu T, $T^{1/2}$ und T^2 dargestellt. Im

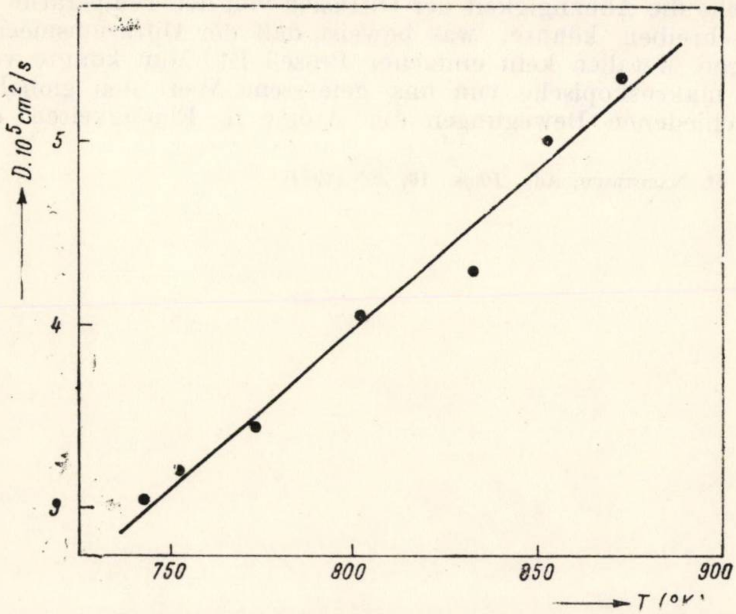

Abb. 4. — Die Selbstdiffusionskoeffizienten des flüssigen Te im Verhältniss zu T.

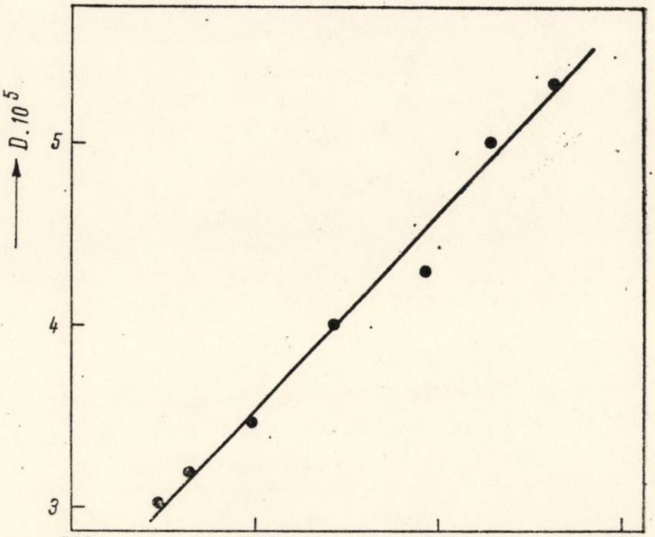

Abb. 5. — Die Selbstdiffusion skoeffizienten des flüssigen Te im Verhältnis zu T^2.

Rahmen des experimentellen Fehlerbereiches stellen die Punkte in allen Fällen eine Gerade dar, was die Tatsache zum Ausdruck bringt, daß jede der Darstellungen die Abhängigkeit der Diffusion von der Temperatur bezeichnen könnte. Es ist schwer eine einfache Funktion zu finden, welche die Abhängigkeit der Diffusion von der Temperatur vollkommen beschreiben könnte, was beweist daß der Diffusionsmechanismus in flüssigen Metallen kein einfacher Prozeß ist. Man könnte vermuten, daß der makroskopische von uns gemessene Wert den globalen Wert der verschiedenen Bewegungen der Atome in Flüssigkeiten darstellt.

---

[8] N. H. Nachtrieb, *Adv. Phys.*, **16**, 309 (1967).

Revue Roumaine de Chimie, 15, 1721–1725 (1970)

THE EFFECT OF ELECTROSTATIC ENERGY IN REACTIONS BETWEEN BENZHYDRYL CHLORIDE AND NORMAL ALCOHOLS

IOANA DEMETRESCU

Physical Chemistry II Department, Bucharest University,
Bd. Republicii 13

Received January 30, 1970

The effect of electrostatic interactions in reactions between benzhydryl chloride and normal alcohols is made evident. For the reactions with the first six normal alcohols the corrected activation energies are calculated by taking into account this effect.

The reactions between benzhydryl chloride and alcohols were studied by many research workers. Most of them [1,2] turned their attention to alcohol-water mixtures, dealing to a smaller extent with systems containing pure alcohols.

In the following, starting from a previous work, [3] we tried to make evident the effect of electrostatic interactions in reactions between benzhydryl chloride and normal alcohols :

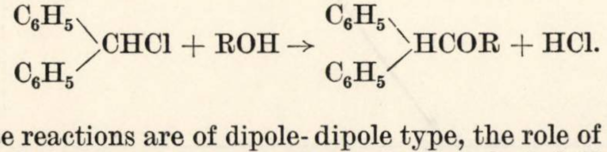

$$\begin{matrix}C_6H_5\\ C_6H_5\end{matrix}\!>\!CHCl + ROH \rightarrow \begin{matrix}C_6H_5\\ C_6H_5\end{matrix}\!>\!HCOR + HCl. \qquad (1)$$

These reactions are of dipole-dipole type, the role of the solvent being played by the partner in excess, that is by the alcohol. For these reactions Eyring and Polany have established the well known equation (2), [4] on the basis of a result obtained from Kirkwood's equation giving the free energy of transferring a dipole from vacuum into a medium with a dielectric constant as great as D :

$$\log k = \log k_0 + C\,\frac{D-1}{2D+1}\cdot \qquad (2)$$

---

[1] J. Norris and A. Morton, *J. Amer. Chem. Soc.*, **50**, 1795 (1928).

[2] F. King Jons and A. Ward, *J. Amer. Chem. Soc.*, **58**, 2394 (1935).

[3] I. G. Murgulescu and Fl. Bărbulescu, *Rev. Roumaine Chim.*, **8**, 153 (1963).

[4] S. Glasstone, K. J. Laidler, and H. Eyring, "The Theory of Rate Processes", New York – London, 1941, p. 419.

The constant C is given by :

$$C = -\frac{N}{2.303\,RT}\left(\frac{\mu_1^2}{r_1^3} + \frac{\mu_2^2}{r_2^3} - \frac{\mu^{*2}}{r^{*3}}\right), \tag{3}$$

in which μ_1 and μ_2 are the moments of the two dipoles, r_1 and r_2 the molecular distances containing them, and μ^* and r^* the moment and the radius of the activated complex.

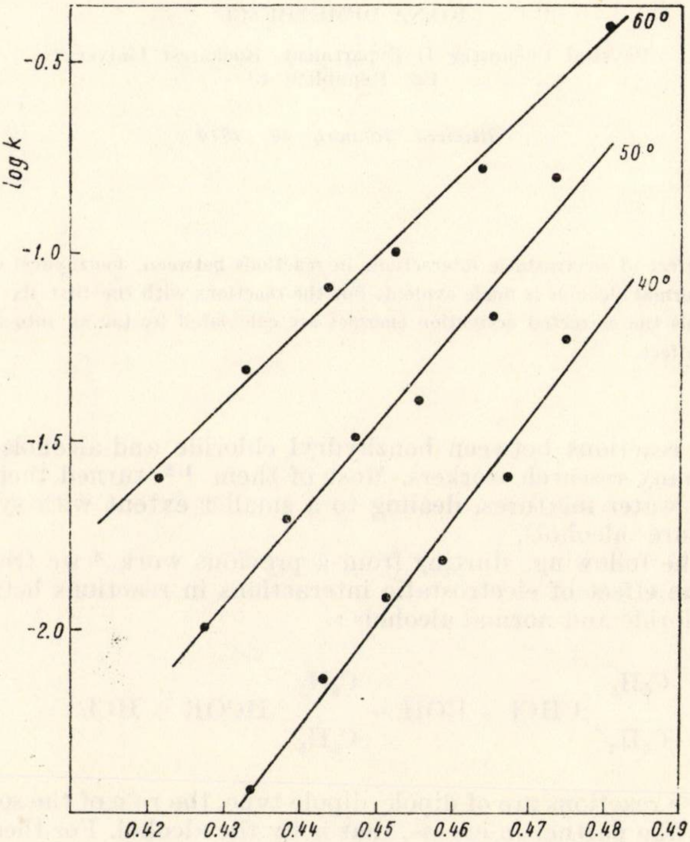

Fig. 1. — Log k as a function of $(D-1)/(2D+1)$ for reactions between benzhydryl chloride and normal alcohols at various temperatures.

The replacement of an alcohol by another being accompanied by the change of the dielectric constant, we tried to plot log k as a function of $(D-1)/(2D+1)$. The values of the dielectric constant D were taken from a previous work.[5]

---

[5] I. G. Murgulescu, D. Oancea, and G. Mincu, *Rev. Roumaine Chim.*, **14**, 3 (1969).

As it can be seen in figure 1, at each temperature taken into account (40°. 50°. 60°) this plot is a straight line, that is the studied system fits in the equation (2).

The slopes of these straight lines, determined through the least squares method, were found to be as great as 26.0 (at 40°), 23.8 (at 50°) and 19.3 (at 60°). For a mean value of 23.0, (3) becomes :

$$-\frac{N}{2.303\ RT}\left(\frac{\mu_1^2}{r_1^3}+\frac{\mu_2^2}{r_2^3}-\frac{\mu^{*2}}{r^{*3}}\right)=23.0 \tag{4}$$

Assuming that the distances r_1, r_2, and r^* are roughly of the same size r, and μ^* can be replaced by the sum $(\mu_1+\mu_2)$ of the two dipoles, (4) becomes :

$$\frac{2N\,\mu_1\,\mu_2}{2.303\,RTr^3}=23.0 \tag{5}$$

By taking μ_1, the dipole moment of benzhydryl chloride, being as great as $1.89D$ and μ_2, the dipole moment of alcohols, as great as $1.88D$, we have found $r = 1.45$ Å. Having in view the simplifying assumptions we have made, this plausible result proves the usefulness of equation (2).

In table 1 we give a comparison between the experimentally found rate constants [3] and those calculated by means of (2). Though the agreement is rather good, the differences existing between the values of k allow us to correct the activation energy.

To evaluate the real activation energy, E, we have to add to the apparent activation energy, E_{exp} the energy which appears as a result of the interaction between dipoles.

The potential of the interaction between two dipoles being given by :

$$\Phi = -\frac{\mu_1\mu_2}{DR^3}(2\cos\theta_1,\cos\theta_2-\sin\theta_1\sin\theta_2\cos\varphi), \tag{6}$$

where θ_1 and θ_2 are the angles between the two dipoles and the axis joining them, φ is the angle between the planes containing the dipoles, and R is the distance between the dipoles, we find :

$$E = E_{\text{exp}}+\frac{N\,\mu_1\,\mu_2}{4.18\times10^7\,DR^3}(2\cos\theta_1\cos\theta_2-\sin\theta_1\sin\theta_2\cos\varphi). \tag{7}$$

Adopting the maximum correction, which occurs if $\theta_1=\theta_2=0$, and taking R as great as the minimum distance $2r$ between the dipoles, we get :

$$E = E_{\text{exp}}+\frac{4\,236}{D} \tag{8}$$

Table

Comparison between the experimental kinetic

Alcohol	40°C				50°C	
	log k_0	D	log k		log k_0	D
			exp.	calc.		
CH_3OH	−13.9213	29.58	−1.2528	−1.3322	−12.850	27.95
C_2H_5OH		22.50	−1.6173	−1.5355		21.34
C_3H_7OH		17.65	−1.8317	−1.7665		16.44
C_4H_9OH		14.91	−1.9329	−1.9611		13.85
$C_5H_{11}OH$		12.70	−2.1482	−2.1770		11.65
$C_6H_{13}OH$		10.75	−2.4373	−2.4381		9.86

Table 2

Comparison between the experimental activation energies and the corrected ones, for the first six normal alcohols

Alcohol	$E_{exp.}$	Correction	$E_{corr.}$
CH_3OH	19560	152	19712
C_2H_5OH	19500	198	19698
C_3H_7OH	19400	258	19658
C_4H_9OH	19370	306	19676
$C_5H_{11}OH$	19530	364	19894
$C_6H_{13}OH$	19040	430	19470

In table 2 we give the activation energies experimentally found in the previous work we mentioned above, together with the corrections and the corrected activation energies. As we can see, the correction made for the effect of electrostatic interactions diminishes the differences between the activation energies. We specify that these corrections are however small, and in case of systems formed with the first alcohols of the series, they fall within the range of the errors affecting the activation energy.

In the last time it was tried to correlate the solvolysis rate with other quantities without a certain physical meaning but which have the advantage of being intuitive. Several works [6-9] have tried to apply this idea to systems formed by benzhydryl chloride and bromide and normal alcohols. Thus, by using Swain's equation, the parameter Y, indicating the ionizing power, was calculated. Because of the fact that the plot of Y as a function of $(D-1)/(2D+1)$ is approximately linear for many systems, it follows that these attempts to correlate the solvolysis rate with

---

[6] E. Grunwald and S. Winstein, *J. Amer. Chem. Soc.*, **70**, 846 (1948).

[7] S. Winstein, A. Fainberg, and E. Grunwald, *J. Amer. Chem. Soc.*, **79**, 4146 (1957)

[8] A. Fainberg and S. Winstein, *J. Amer. Chem. Soc.*, **79**, 1602, 1608 (1957).

[9] A. Streitwieser, *Chem. Revs.*, **56**, 620 (1956).

1

constants and those computed according to (2)

50C°		60°C			
log k		log k_0	D	log k	
exp.	calc.			exp.	calc.
−0.8298	−0.9210	−9.7209	26.31	−0.4323	−0.4423
−1.1956	−1.1110		20.24	−0.7993	−0.7733
−1.4122	−1.3470		15.31	−1.0179	−0.9907
−1.5141	−1.5370		12.84	−1.1204	−1.1603
−1.7297	−1.7620		10.70	−1.3364	−1.3536
−2.0150	−2.0160		9.04	−1.6181	−1.5922

other parameters do not refute but they also strengthen the image adopted by us, concerning the influence of the dielectric constant in systems consisting of benzhydryl chloride and normal alcohols.

Revue Roumaine de Chimie, 15, 1727–1733 (1970)

ADSORPTIVE PROPERTIES OF A NICKEL FERRITE

T. CHIRULESCU and E. SEGAL

Institute of Physical Chemistry of the Academy, Bucharest, str. Dumbrava Roşie 23

Received January 19, 1970

The gas adsorption on a nonstoichiometric nickel ferrite is investigated by following the variations in the magnetization of the sample at 296°K. The influence of the thermal treatment and slight sintering on the initial slope of the magnetization-volume isotherms is also studied. The adsorption of any (donor or acceptor) gas on the surface of the nickel ferrite brings about an increase in the magnetization. The interpretations of variations in magnetization is made on the basis of two different standpoints.

In the previous papers, the gas adsorption on the perminvar ferrites has been investigated.[1–3] In order to obtain more accurate information about the mechanism of the gas adsorption on ferrites, the adsorptive properties of a ferrite with a more simple chemical structure have been studied. To this purpose, a nonstoichiometric nickel ferrite, $Ni_{0.98}Fe_{2.02}O_4$, was used. The modifications in the magnetization of the nickel ferrite induced by gas adsorption was followed by means of a d. c. permeameter.[4,5]

EXPERIMENTAL

The experimental device and preparation of gases were described elsewhere.[1,2,6,7]

The nickel ferrite used has been prepared and analysed in the chemical laboratory of IFB.[8] It has been obtained by thermal decomposition of nickel-iron double oxalate[9] according to the reaction:

$$NiFe_2(C_2O_4)_3 + 1/2\ O_2 = NiOFe_2O_3 + 3CO + 3CO_2$$

[1] T. Chirulescu and E. Segal, *Rev. Roumaine Chim.*, **12**, 1295 (1967).

[2] T. Chirulescu and E. Segal, *ibid.*, **13**, 1577 (1968).

[3] T. Chirulescu and E. Segal, *ibid.*, **15**, 67 (1970).

[4] P. W. Selwood, "Adsorption and Collective Paramagnetism", Academic Press, New York and London, 1962, p. 89.

[5] T. Chirulescu, *Studii Cercetări Chim.* Acad. RSR, **17**, 43 (1969).

[6] T. Chirulescu and E. Segal., *Rev. Roumaine Chim.*, **11**, 1367 (1966).

[7] Al. I. Fruma, (private communication).

[8] A. Cormoş and E. Vărzaru, *Rev. Chim.* (*Bucureşti*), 1970 (under press).

[9] W. J. Schuele, *J. Phys. Chem.*, **63**, 83(1959).

This reaction took place at 500°, in air, the liberation of the gases assuring a permanent breaking up of the sample. This was calcinated at 1100°, for 1 h and at 1200°, for 10 h, for obtaining the complete spinel structure. The BET surface area of the sample, determined by low-temperature nitrogen adsorption, [10] has been found to be 0.9 m^2/g.

RESULTS AND DISCUSSION

The magnetization curve of the sample at 296° K is plotted in figure 1. This curve was obtained in the range of 50 — 500 oe and was extrapolated to H = 0.

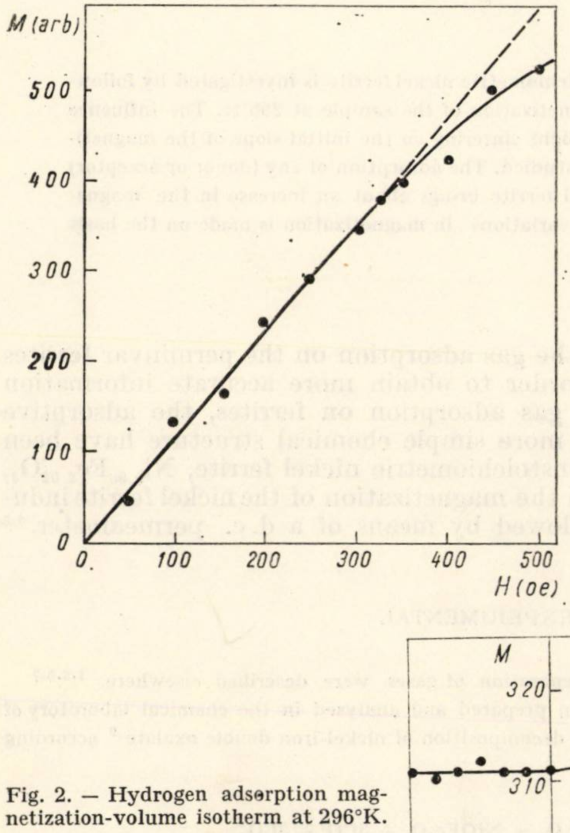

Fig. 1. — Magnetization curve of the sample at 296°K.

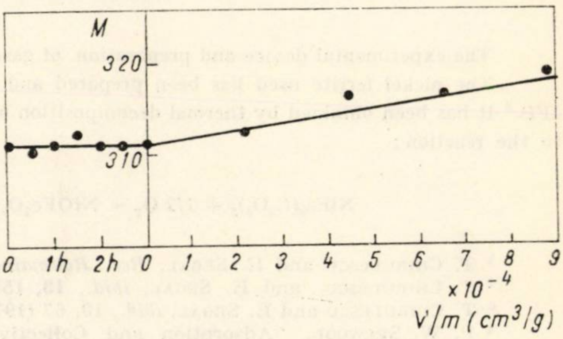

Fig. 2. — Hydrogen adsorption magnetization-volume isotherm at 296°K.

The magnetization curve shows no remanent behaviour; this curve is, approximately, a straight line.

---

[10] S. Brunauer, P. H. Emmett and E. Teller, *J. Amer. Chem. Soc.*, **60**, 309 (1938).

Figure 2 presents the magnetization-volume isotherm for hydrogen adsorption on the sample at room temperature. The sample was outgassed at 400°, for 4 h. From the examination of this isotherm it may be concluded that the hydrogen adsorption leads to an increase in the magnetization of the sample.

Besides the mechanism of oxygen adsorption on nickel ferrite, the effect of thermal treatment and slight sintering on the initial slope of the magnetization-volume isotherm was followed. For this purpose, six experiments on the same sample were performed. The influence of the temperature of the thermal treatment on the initial slope is pointed out by the first three runs performed at three different temperatures (Fig.3).

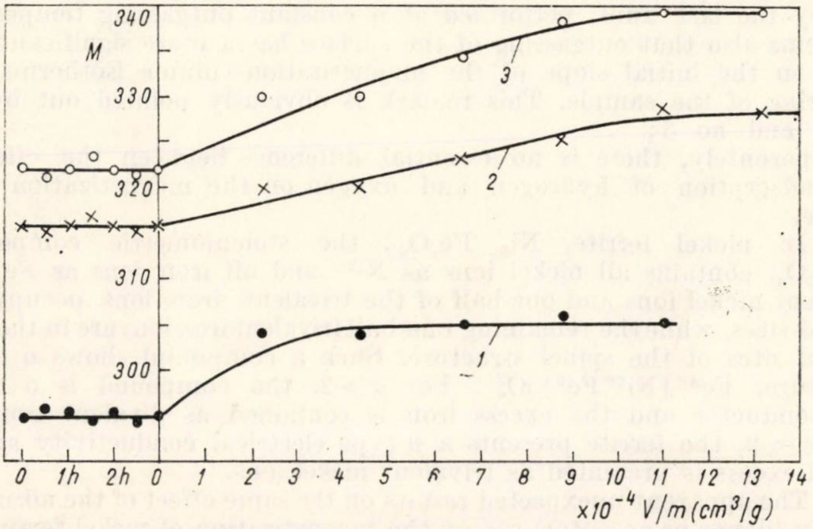

Fig. 3. — Oxygen adsorption magnetization-volume isotherms at 296°K. Sample outgassed at : *1*, 600° ; *2*, 300° ; *3*, 200°.

The effect of a slight sintering on the initial value of the magnetization and initial slope of the magnetization-volume isotherm has resulted rom the following runs. The results are presented in table 1.

Table 1

Effect of a slight sintering on the initial value of the magnetization and initial slope of the magnetization-volume isotherm.

Run no	Outgassing temperature (°C)	M_0(mm)	Initial slope of magnetization-volume isotherms
1	600	310	$+1.11\times10^{-2}$
2	200	315	$+0.75\times10^{-2}$
3	300	322	$+0.88\times10^{-2}$
4	300	324	$+0.62\times10^{-2}$
5	300	327	$+0.50\times10^{-2}$
6	300	325	$+0.40\times10^{-2}$

The results and conclusions on the effect of the gas adsorption on the magnetization of the sample may be summarized as follows:
1. the oxygen adsorption on the nickel ferrite leads, at room temperature, to an increase in the magnetization of the sample;
2. in the course of the six runs, it has been found that initial magnetization, M_0, presents a slight increase. This increase may be interpreted as a slight successive sintering of the sample;
3. generally, the initial slope of the magnetization-volume isotherms is dependent upon the sintering of the sample. This conclusion is supported by the last runs, performed at a constant outgassing temperature. It seems also that outgassing of the surface has a more significant influence on the initial slope of the magnetization-volume isotherms, than sintering of the sample. This remark is obviously pointed out by runs no 2 and no 3;
4. apparentely, there is no essential difference between the effects of the adsorption of hydrogen and oxygen on the magnetization of the ferrite.

In nickel ferrite, $Ni_{3-x}Fe_xO_4$, the stoichiometric composition, $NiFe_2O_4$, contains all nickel ions as Ni^{2+} and all iron ions as Fe^{+3}. All divalent nickel ions and one-half of the trivalent iron ions occupy octahedral sites, while the remaining one-half trivalent iron ions are in the tetrahedral sites of the spinel structure. Such a compound shows a inverse structure, $Fe^{3+}[Ni^{2+}Fe^{3+}]O_4^{2-}$. For $x > 2$, the compound is a n-type semiconductor and the excess iron is contained as divalent iron ions. For $x < 2$, the ferrite presents a *p*-type electrical conductivity and the nickel excess is presented as trivalent nickel ions.

The apparent unexpected results on the same effect of the adsorption of any (donor or acceptor) gas on the magnetization of nickel ferrite may be interpreted from two different standpoints.

1. According to Squires and Parravano the gas interaction with a ferrite takes place substantially in the octahedral sites (sublattice B), because the cations of different electrical charges may be easily accomodated in these sites. [11]

On the original surface of the ferrite, covered with oxygen, each surface cation is likely to be fully coordinated. The thermal treatment of the surface with hydrogen leads to a surface reduction by loss of water. This conclusion has been established for several transition metal oxides. In the case of our ferrite, $x > 2$, the surface activation takes place according to the reaction [11]:

$$Fe^{3+}(O^{2-})_6 + H_2 \begin{array}{l} \rightarrow Fe^{3+}(O^{2-})_4(OH^-)_2 + 2e \\ \searrow Fe^{3+}(O^{2-})_5 + H_2O + 2e \end{array} \qquad (1)$$

Thus, the surface octahedral complex, $Fe^{3+}(O^{2-})_6$, is reduced to a lower coordination (square pyramid, tetrahedral). One can see that reaction (1) involves electron transfer to the substrate, in accordance with the experimental results. [11] This surface activation can also be obtained even without hydrogen, by vacuum treatment only. [12] But a lower coordination of the surface octahedral complexes means a reduction in the number of trivalent iron ions in octahedral sites. Therefore, a decrease in the magnetization will be expected after surface activation. This way, it is likely that gas adsorption consists in a restoration of the original octahedral coordination of surface cations. Thus, the hydrogen adsorption on a active surface of the nickel ferrite should take place according to one of the following reactions [11]:

---

[11] R. G. Squires and G. Parravano, *J. Catalysis*, **2**, 324 (1963).

[12] E. Molinari and G. Parravano, *J. Amer. Chem. Soc.*, **75**, 5233 (1953).

$$Fe^{3+}(O^{2-})_5 + H_2 \rightarrow Fe^{2+}(H)(OH^-)(O^{2-})_4 \qquad (2)$$

or,

$$Fe^{3+}(O^{2-})_5 + H_2 \rightarrow Fe^{3+}(O^{2-})_4(H^-)(OH^-) \qquad (3)$$

Thus, hydrogen adsorption leads to a restoration of the octahedral coordination of the trivalent iron ions on the surface. An enhancement of the number of trivalent iron ions in octahedral sites will be expected, followed by an increase of magnetization, after adsorption on ferrite.

However the two mechanisms of the hydrogen adsorption bring about an increase in the magnetization of nickel ferrite, the first mechanism being possibly to be less probable than the second one. The first reaction leads to an uncharged adsorbed species (H) on surface, while the second reaction brings about some charged adsorbed species on the surface of the sample. This interpretation is supported by the work on the transition metal hydrido-complexes. [13]

Also, the oxygen adsorption on the surface of the nickel ferrite is possibly determined by the tendency to restore at surface the sixfold coordination of the surface cations:

$$Fe^{3+}(O^{2-})_5 + 1/2\ O_2 + 2e \rightarrow Fe^{3+}(O^{2-})_4(O^{2-})_2 \qquad (4)$$

Similarly to the hydrogen adsorption, the oxygen adsorption brings about an enhancement in the number of the trivalent iron ions in the octahedral sites. Therefore, an increase in the magnetization will be obtained. Reaction (4) leads to some charged adsorbed species on the surface of the sample.

The model mentioned above is based on the assumption of Dowden and Wells. [14] According to this assumption the adsorption on the transition metal cations means an enhancement in the number of bonds in a complex and, consequently, an increase in coordination state. Commonly, this is an exothermal effect and called crystal field stabilization. A critical examination of the model mentioned above shows that:

---

[13] J. Chatt, *Proc. Chem. Soc.*, **1962**, 318; *J. Chem. Soc.*, **1962**, 5075.

[14] D. D. Dowden and D. Wells, in "Actes du Deuxième Congrès Intern. Catalyse", Editions Tchnip Paris, 1961, p. 1499.

a) the assumption of the ferrite-gas interactions in the octahedral sites only, is disputable;
b) it is impossible to discuss the gas adsorption without taking in account the electron interactions between gas and ferrite. In other words, it is impossible to reduce the chemisorption to a coordination question only;
c) from our model it results that the electron involved in the thermal treatment and adsorption (see reactions (1) and (4)) have no effect on the magnetic properties of the ferrite. This conclusion is scarcely acceptable.

2. From the above mentioned facts, we consider that our experimental data are also consistent with another interpretation, based on the electron interactions between adsorbent and adsorbat.[1-3] We shall assume that, as a rule, both sublattices may interact with the gas, and the geometric considerations may be invoked as a restriction only. In this case, the interaction of oxygen with the octahedral sublattice and hydrogen with the tetrahedral sublattice is a plausible assumption.

The size of the octahedral site is given by [15]

$$r_{\text{oct}} = 0.418\, r_{O^{2-}} \tag{5}$$

where $r_{O^{2-}}$ is the radius of O^{2-} ion. Similarly, the size of the tetrahedral site is

$$r_{\text{tetra}} = 0.227\, r_{O^{2-}} \tag{6}$$

It is possible that the passing of the divalent iron ions into the trivalent state brings about the appearence of O^{2-}, O_2^- or O^- ions on the surface of ferrite after chemisorption. Since the magnetic moments of the divalent and trivalent iron ions are 4.4 β, respectively, 5 β,[16] it results that the magnetic moment of the octahedral sublattice increases, and thus the magnetization of the ferrite also increases. This result is being in agreement with experimental data.

Since radius of the hydrogen ion is smaller than the radius of the oxygen ion, hydrogen may interact, as a donor, with the tetrahedral sublattice. Therefore, one part of the trivalent iron ions will be reduced by hydrogen. This reduction leads to a decrease in the magnetic moment of the tetrahedral sublattice and to an enhancement in the magnetization of the ferrite. This result is also in agreement with experimental data.

This model may be criticized too, because it tacitly assumes that the structure of the ferrite remained unchanged after vacuum treatment, even in a surface layer.

Our opinion is that both vacuum thermal treatment and gas adsorption are complex phenomena, in which the two mentioned effects have a certain importance. A quantitative estimation of coordination and electron effects will be possible by an important increase of the new experimental data. The significant theoretical results on the gas adsorption on the nickel ferrite may be summed up as follows :

---

[15] L. I. Rabkin, S. A. Soskin and B. S. Epstein, "Ferrity", Energia, Leningradskoie otdelenie, 1968, p. 34.

[16] J. P. Suchet, "Chemie physique des semiconducteurs", Monographies Dunod, Paris, 1962, p. 133.

1. The adsorption of any (donor or acceptor) gas on the surface of a nickel ferrite leads to an increase in magnetization of the sample.

2. The results may be interpreted on the basis of two different standpoints.

The authors are grateful to Miss E. Vărzaru for preparation and analysis of the nickel ferrite, and to Mr. G. Galaţki for BET measurement.

Revue Roumaine de Chimie, **15**, 1727–1733 (1970)

Revue Roumaine de Chimie, 15. 1735–1739 (1970)

THE CELL PARAMETERS OF SYNTHETIC CALCIUM APATITES

V. M. BHATNAGAR*)
Fisk University, Nashville, Tennessee 37203, USA

Received April 25, 1970

High-precision, computer-refined values of the cell parameters of three compounds with an apatite-type structure have been determined with an X-ray diffractometer, internally standardized by means of sodium chloride. The results obtained are as follows:

$Ca_{10}(PO_4)_6Cl_2$	a = 9.6420Å	c = 6.7756Å	c/a = 0.702
$Ca_{10}(PO_4)_6F_{0.554}Cl_{1.446}$	a = 9.5827Å	c = 6.8324Å	c/a = 0.712
$Ca_{10}(PO_4)_6F_{1.449}Cl_{0.579}$	a = 9.4512Å	c = 6.8639Å	c/a = 0.726

INTRODUCTION

This paper contains the results of a high-precision determination of the lattice parameters of three synthetic compounds with apatitic structures. The small amount of material available (generally less than 0.25 gram) suggested the use of either an 11 cm Debye-Scherrer powder camera or a diffractometer with a special sample preparation and loading technique. In the interests of high precision and resolution, the diffractometer was finally chosen in preference to the powder camera.

The use of a computer was considered mandatory, and a least-square refinement technique [1] was considered to be the best approach for the calculation and refinement of the cell parameters. Whenever possible, least-squares refinement was used on reflections that could be indexed unambiguously. There were never less than 36, and sometimes more than 40 reflections were used for the calculations.

The computer programmes, Celfit [2] and Genrat [3] were used for calculating the cell parameters of the compounds and for indexing the diffraction lines. The programmes had to be re-written into FORTRAN IV in order to be compatible with the IBM digital computer model 360/40.

---

* Present address: IROQUOIS CHEMICALS Ltd., Cornwall, Ontario Canada.

[1] L. I. Mirkin, "Handbook of X-ray Analysis of Polycrystalline Materials", Consultants Bureau, New York, 1964, pp. 523, 550.

[2] B. H. Bracher, U.K. Rept. AERE-R 5412 (1967).

[3] C.W.F.T. Pistorius, C.S.I.R. Pretoria (1968).

The CELFIT programme, when supplied with sets of Miller indices (h k l), corresponding values of the Bragg angle (θ) and a set of approximate unit cell dimensions (a, b, c, α, β, γ), refines any or all of the latter by the method of least-squares until the shifts in these parameters fall below specified limits.

The GENRAT programme, when supplied with sets of unit cell dimensions, generates all possible h k l reflections between two specified values of the Bragg angle. Reflections forbidden by space-group restrictions have then to be eliminated from the list by inspection.

EXPERIMENTAL

Sample Preparation

It was decided to use A.R. grade sodium chloride as an internal standard with each of the apatites being investigated in order to ensure the angular accuracy of all the measured peaks [1]. Preliminary investigations, in which sodium chloride with an initial grain size of less than 30 microns and finely powdered fluorapatite were used [4], indicated that a 1 :1 mixture by weight of sodium chloride and fluorapatite would yield peaks that could be measured accurately. The apatite to be investigated and sodium chloride were carefully mixed, in their correct proportions by weight, in an agate mortar to ensure an even distribution of sodium chloride before it was loaded onto the sample holders. The apatites of this investigation have been described earlier. [5]

Sample Loading

Since a maximum weight of only 0.3 gram of sample was available for analysis, a special sample-loading technique had to be devised for the X-ray diffraction analysis [6]. Sheets of brass were machined flat to a thickness of 1.5 mm, a length of 53.5 mm, and a width of 35 mm. Pressure-sensitive, self-adhesive paper labels were then attached with their adhesive surface downwards onto the brass plate. The mixture, consisting of apatite being investigated and sodium chloride, was then evenly sprinkled onto the gummed label to occupy an area of approximately 12.5 mm by 52 mm. The mixture was then smoothed with a clean, glass microscope-slide and firmly pressed by hand onto the paper to yield a smooth surface suitable for X-ray analysis.

Apparatus and Instrumental Settings

A Philips wide-range goniometer model PW-1050 was used for all the determinations.

X-ray generator =40 kV, 20 mA

Radiation =Copper with nickel filter

Goniometer scanning speed =1 degree 2θ per minute

Slits =1 degree divergence, 0.1 degree receiving, 1 degree scatter

Ratemeter settings =400 counts per second, time constant 2 seconds

Chart-recorder paper speed =26.5 mm per minute

Measurement of Angular Position of Peaks

The angular positions of all peaks were taken at points in the centre of the peaks, one-third of the distance between the actual top of the peaks and their base lines.

---

[4] V. M. Bhatnagar, *Rev. Roumaine Chim.*, **15**, 87 (1970).

[5] V. M. Bhatnagar, *Experientia*, **24**, 765 (1968).

[6] H.V.R. von Rahden, South Afr. Natl. Inst. Metal, Project. C. 66/67.

Intensity Measurements

Because of the variable degree of preferred orientation likely to be introduced as a result of the sample-loading technique used, the intensities listed for the various h k l reflections have not been given in terms of integrated intensities but rather in terms of their heights above background, taken relative to the strongest peak as intensity 1 0 0. These values could, however, be recalculated in terms of integrated intensities from the graph given by Swanson et al.[7]

RESULTS AND DISCUSSION

The results obtained during the present investigation are shown in Tables 1—3. The cell parameters quoted are based on the best fit obtained

Table 1

Cell parameters of $Ca_{10}(PO_4)_6Cl_2$ Radiation = Cuλ 1.54178Å ; I/I_1 = Diffractometer; System = Hexagonal; a = 9.6420 Å, c=6.7756 Å, c/a= 0.702; volume=545.5$Å^3$.

h k l	I/I_1	*d*Å (observed)	*d*Å (calculated)
010	5	8.33	8.35
011	5	5.25	5.26
111	2	3.921	3.928
021	2	3.551	3.554
002	19	3.381	3.388
120	6	3.156	3.156
121	54	2.860	2.861
030	100	2.779	2.783
022	6	2.627	2.631
031	3	2.572	2.575
130	19	2.316	2.316
131	4	2.191	2.191
032	5	2.148	2.151
113	2	2.045	2.045
222	16	1.964	1.964
230	9	1.917	1.916
132	8	1.912	1.912
231	16	1.843	1.843
123	14	1.835	1.837
140	15	1.824	1.822
042	3	1.779	1.777
033	2	1.754	1.754
014	1	1.664	1.660
133	3	1.618	1.617
142	3	1.605	1.605
052	5	1.499	1.498
124	3	1.492	1.493
332	3	1.453	1.452
034	3	1.447	1.447
015	6	1.339	1.338
243	2	1.294	1.294
125	10	1.245	1.245
144	8	1.242	1.241
244	3	1.155	1.155
154	2	1.123	1.123
235	2	1.106	1.106
046	3	0.993	0.993
117	2	0.949	0.949

[7] H. E. Swanson, M. C. Morris, R. P. Stinchfield and E. H. Evans, "Standard X-ray Diffraction Powder Patterns", Natl. Bur. Stand. Monograph 25, Sect. 1, 2—3 (1962).

by the least-squares programme. Both calculated and observed interplanar spacings have been reported for the sake of completeness.

Table 2

Cell parameters of $Ca_{10}(PO_4)_6F_{0\cdot554}$ $Cl_{1\cdot446}$ Radiation = Cuλ 1.54178Å ; I/I_1 = Diffractometer : System = Hexagonal ; a = 9.5827Å, c = 6.8324Å, c/a = 0.712 ; volume = 543.3Å³.

h k l	I/I_1	*d*Å (observed)	*d*Å (calculated)
010	5	8.28	8.30
111	4	3.914	3.923
021	3	3.534	3.547
002	15	3.406	3.416
120	19	3.125	3.137
121	67	2.844	2.851
112	41	2.787	2.782
030	100	2.761	2.766
022	8	2.631	2.637
031	7	2.559	2.564
030	47	2.297	2.302
132	10	1.906	1.909
230	12	1.901	1.904
123	21	1.840	1.843
231	17	1.835	1.834
050	3	1.660	1.660
051	3	1.612	1.613
240	4	1.567	1.568
150	9	1.491	1.491
151	4	1.458	1.456
034	9	1.455	1.453
332	4	1.448	1.447
242	4	1.424	1.425
341	4	1.336	1.338
250	3	1.329	1.329
251	3	1.304	1.304
243	3	1.290	1.292
153	4	1.247	1.247
440	3	1.197	1.198
135	3	1.177	1.175
351	1	1.169	1.168
071	1	1.169	1.168
334	3	1.167	1.167
261	1	1.134	1.135
154	3	1.122	1.123
064	1	1.075	1.075

Table 3

The cell parameters of $Ca_{10\cdot4}(PO_4)_6F_{1\cdot449}Cl_{0\cdot579}$. Radiation = Cuλ 1.54178Å ; I/I_1 = Diffractometer ; System = Hexagonal ; a = 9.4512Å, c = 6.8639Å, c/a = 0.726 ; volume = 531.0Å³.

h k l	I/I_1	*d*Å (observed)	*d*Å (calculated)
010	26	8.16	8.18
011	2	5.24	5.26
020	16	4.086	4.092
111	3	3.892	3.893
021	2	3.513	3.515
002	11	3.427	3.433
012	6	3.163	3.166

Table 3 *(continued)*

h k l	I/I_1	*d*Å (observed)	*d*Å (calculated)
120	20	3.089	3.094
112	25	2.774	2.777
030	100	2.723	2.728
022	9	2.628	2.630
122	2	2.296	2.298
130	26	2.268	2.270
131	7	2.155	2.155
113	2	2.064	2.060
040	6	2.046	2.046
222	12	1.945	1.946
132	4	1.892	1.893
230	3	1.877	1.877
123	9	1.839	1.840
231	12	1.810	1.811
140	18	1.785	1.786
042	5	1.757	1.758
004	6	1.717	1.716
232	4	1.649	1.647
223	3	1.645	1.644
330	3	1.576	1.575
240	4	1.548	1.547
331	2	1.534	1.535
241	2	1.509	1.509
052	2	1.477	1.478
150	2	1.470	1.470
034	5	1.453	1.453
233	4	1.450	1.452
151	6	1.439	1.437
341	3	1.322	1.320
115	2	1.319	1.320
243	2	1.282	1.282
342	2	1.253	1.253
160	2	1.249	1.248
144	5	1.238	1.237
334	2	1.161	1.161
235	4	1.108	1.108

Acknowledgements. The information contained in this article was obtained by Dr. S. A. Hiemstra and H. V. R. von Rahden of National Institute for Metallurgy, Johannesburg, South Africa; the text and data quoted in the article have been taken from Report no 375 of that Institute. The author thanks Dr. W. R. Liebenberg and Dr. R. E. Robinson for their interest and help and Prof. J. R. Lawson and Prof. N. Fuson of Fisk University for valuable discussions on apatites.

Revue Roumaine de Chimie, 15, 1735–1739 (1970)

Revue Roumaine de Chimie, **15**, 1741–1750 (1970)

COMBINAISONS COMPLEXES AVEC DES HYDROXYACIDES. XIV*

L'ÉTUDE SPECTROPHOTOMÉTRIQUE DU SYSTÈME $ZrOCl_2$ – ACIDE D-GLUCONIQUE

L. CZEGLÉDI et CONST. GH. MACAROVICI

Institut de Chimie de l'Académie, Filiale de Cluj, 59–65, str. Donath

Reçu le 29 janvier 1970

L'interaction de l'ion zirconyle et de l'acide D-gluconique est caractérisée par l'existence dans la solution d'un complexe du type $2ZrO^{2+} : 1HGH_4$**, complexe de stabilité moyenne dans le domaine du pH = 4 – 9. La constante de dissociation apparente calculée au pH = 3 ($\lambda = 220$ nm) a une valeur de $5{,}65.10^{-3}$ moles $0{,}5/l^{0,5}$. Le complexe est moins stable que le complexe formé par le titane et l'acide D-gluconique.

L'interaction du Zr(IV) et de l'acide D-gluconique a été étudiée par voie potentiométrique [1], échange ionique [2, 3] et par extraction[4].

Dans ce travail on étudie le système $ZrOCl_2$ – acide D-gluconique par voie spectrophotométrique. On se propose notamment d'obtenir une orientation générale sur le système en fonction de la variation du pH et de déceler (par différentes méthodes) le rapport de combinaison entre l'ion central et l'acide D-gluconique.

PARTIE EXPÉRIMENTALE

Appareillage. Les mesures d'absorption ont été faites au spectrophotomètre Beckman DK-2A, utilisant de cuvettes de quartz.

Le pH des solutions a été contrôlé à un potentiomètre LP–5, en utilisant des électrodes de verre et de calomel saturé.

---

* Const. Gh. Macarovici et E. Perţe, *Bul. Inst. Politeh. Iaşi* (sous presse).

** KGH_4 = gluconate de potassium; HGH_4 = acide D- gluconique.

[1] Const. Gh. Macarovici, H. Roth et L. Czeglédi, *Studii şi Cercetări Chim., Acad. R.P.R. Fil. Cluj*, **12**, 229 (1961).

[2] Const. Gh. Macarovici, H. Roth et L. Czeglédi, *Studii şi Cercetări Chim., Acad. R.P.R. Fil. Cluj*, **12**, 245 (1961).

[3] H. Roth, L. Czeglédi et Const. Gh. Macarovici, *Studii şi Cercetări Chim., Acad. R.P.R. Fil. Cluj*, **14**, 69 (1963).

[4] Const. Gh. Macarovici, E. Moţiu et E. Perţe, *Rev. Roumaine Chim.* (sous presse).

Solutions. a) On a préparé différentes solutions à diverses concentrations d'oxychlorure de zirconium à partir de $ZrOCl_2 . 8H_2O$ *p.a.*, par dissolution dans de l'eau bidistillée. La concentration du zirconium a été déterminée par la méthode de la précipitation par l'acide mandélique.

b) Les solutions d'acide D-gluconique, de différentes concentrations, ont été préparées par échange ionique à partir de gluconate de calcium sur le cationite Amberlite IR 120 forme hydrogène.

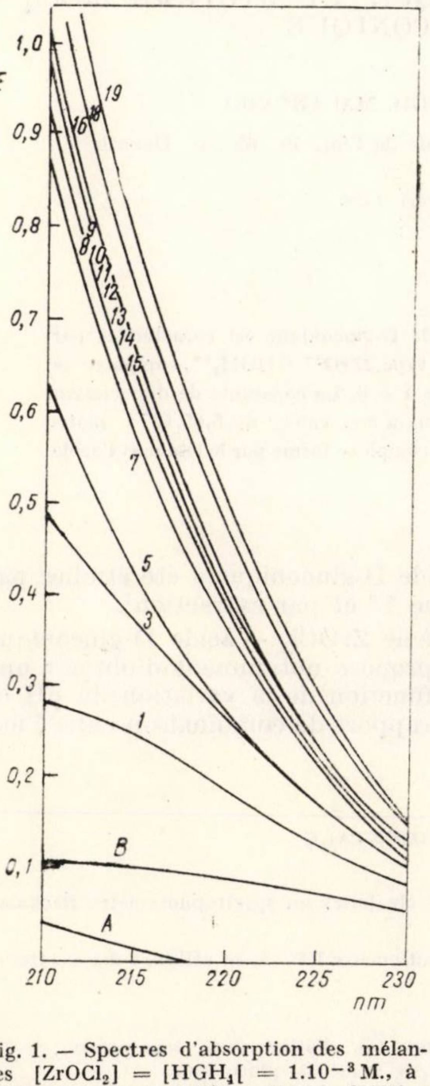

Fig. 1. — Spectres d'absorption des mélanges $[ZrOCl_2] = [HGH_4[= 1.10^{-3}$ M., à différents pH ; 1 : [HCl] = 2N ; 3 : [HCl] = = 1N ;

5 : pH = 1,20 ; 7 : pH = 3,07 ; 8 : pH = 3,63 ; 9 – 15 : pH = 4,32 – 8,20 ; 16 : pH = 8,40 ; 18 : [NaOH] = $= 10^{-2}$ M ; 19 : [NaOH] = 10^{-1} M. (A) = $[ZrOCl_2] = 1.10^{-3}$ M ; pH = 1,50. (B) = $[HGH_4] = 1.10^{-3}$ M ; pH = 0. – 9,5. Cuve = 1 cm ; μ = 2 – 0,05.

c) Le pH désiré a été réalisé au moyen de solutions d'hydroxyde de sodium.

d) La force ionique a été fixée par de l'acide chlorhydrique, du chlorure de sodium ou du perchlorate de sodium.

Les spectres d'absorption en fonction du pH

On a préparé trois séries de solutions en fonction du pH. La concentration de l'oxychlorure de zirconium était de 1.10^{-3} M dans chaque série. Dans la première série on n'a pas ajouté d'acide D-gluconique (1 : 0) ; dans la deuxième, la concentration de l'acide D-gluconique était de 1.10^{-3}M(1 :1) et dans la troisième elle était de 3.10^{-3} M(1 : 3). Les solutions ont été maintenues à la température ambiante, et les spectres d'absorption ont été répétés à des intervalles d'un jour.

Les solutions au pH > 3, qui ne contenaient que de l'oxychlorure de zirconium étaient instables ; l'hydroxyde de zirconium précipitait soit immédiatement, soit au bout de quelques heures.

L'oxychlorure de zirconium jusqu'au pH = 2, aux concentrations utilisées, absorbe moins de $E = 0,05$; aussi cette extinction n'a-t-elle pas été prise en considération. L'absorption de l'acide chlorhydrique (étant incomparablement plus grande) a été déduite des valeurs d'absorptions obtenues.

Sur la figure 1 sont représentés les spectres d'absorption des mélanges de 1 : 1 — $ZrOCl_2$ — acide D-gluconique (20 échantillons au pH variant de 2N HCl à pH ≅ 13), après une équilibration de 2 jours, en fonction de la longueur d'onde.

Les spectres des échantillons obtenus à différentes valeurs de concentration des ions d'hydrogène ne signalent pas un maximum d'absorption dans le domaine ultraviolet. L'augmentation de l'absorption des échantillons 1 — 9, à une longueur d'onde donnée, représente le domaine de formation d'un complexe. En l'absence de tout point isosbestique, on en déduit que dans la solution il y a un seul complexe dans le domaine de $[HCl] = 2N$ jusqu'au $pH \cong 9$. Il faut remarquer que les échantillons jusqu'au $pH = 4$ manifestent une tendance d'augmentation dans le temps des extinctions ; cependant, à mesure que le domaine de pH est atteint ($pH = 4 - 8$) où existe le complexe, E reste pour ainsi dire stable, à part quelques petites variations d'un jour à l'autre. On remarque aussi que jusqu'au point de neutralisation, le pH des solutions demeure constant dans le temps. Au $pH > 8$, les valeurs de pH diminuent dans le temps, ce qui s'explique par l'hydrolyse du complexe ou bien par son passage à un autre type de complexe.

La série des mélanges au rapport de 1 : 3 $ZrOCl_2$ — acide D-gluconique a un comportement similaire.

En représentant les absorptions en fonction du pH, à une longueur d'onde constante, on peut se rendre compte plus nettement du domaine d'existence du complexe formé.

Etant donné que l'acide D-gluconique présente une absorption quelconque, on a corrigé les extinctions pour les mélanges, en déduisant les valeurs d'extinction de l'acide D-gluconique des valeurs enregistrées pour le complexe ($E = E_{\text{compl.}} - E_{HGH_4}$).

Le domaine jusqu'au $pH \cong 4$ représente la formation d'un complexe. Dans la région entre $pH = 4 - 9$, les courbes d'absorption s'inscrivent presque parallèlement à l'axe du pH, ce qui révèle que le complexe est stable dans ce domaine de pH. Au $pH > 9$ il se forme un autre complexe ou bien il se produit un autre phénomène, tel que la condensation. On remarque aussi que la série des mélanges 1 Zr : 3 HGH_4 présente, en général, des extinctions plus grandes qu'au rapport de 1 :1 à la même longueur d'onde constante.

Sur la figure 3 sont représentés les spectres d'absorption de l'acide D-gluconique seul ($[HGH_4] = 3.10^{-3}$ M, $\mu = 0{,}05-0{,}5$) à différents pH en fonction de la longueur d'onde. On observe l'existence d'un groupe de courbes dans le domaine $pH < 3$, pour que, ensuite, au $pH = 3 - 4$, les absorptions des échantillons soient plus basses ; au $pH > 4$ il y a un autre groupe de courbes aux absorptions encore plus basses. Ce comportement de l'acide D-gluconique pourrait s'expliquer par l'existence de la lactone dans les solutions de l'acide, qui, avec l'augmentation du pH, se défait successivement pour passer à l'acide libre, puis à son sel de sodium. Au rapport de 1: 3 (fig. 2), les absorptions plus grandes dans le domaine de $pH = 1-3$ sont également dues à l'existence de la lactone non transformée en acide D-gluconique. Cette influence n'est pas manifestée dans le cas des courbes correspondant au rapport 1 : 1, à cause de l'absence d'un excès d'acide gluconique. Le complexe formé présente des extinctions constantes au pH $= 4 - 7$. Dans cet intervalle de pH, les solutions étant maintenues pendant 3 jours, il ne s'est produit aucun changement de pH ni d'extinction.

Dans le cas des solutions au $pH > 7$ on enregistre dans le temps aussi bien des baisses de pH que des modifications de l'extinction.

Ces constatations nous ont amenés à étudier le complexe qui existe dans la solution au $pH < 7$.

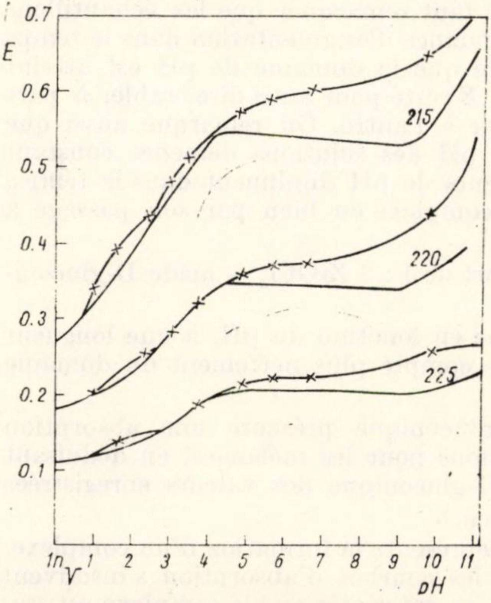

Fig. 2. — Courbes d'absorption à une longueur d'onde constante (représentées dans la partie droite de la figure), en fonction du pH.
($E = E_{\text{compl.}} - E_{HGH_4}$); —— $Zr : HGH_4 = 1 : 1$. × × × × $Zr : HGH_4 = 1 : 3$. Cuve = 1 cm.

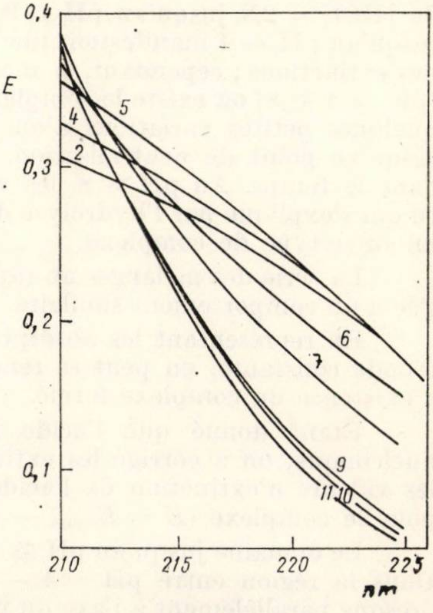

Fig. 3. — Les spectres d'absorption de l'acide D-gluconique.
($[HGH_4] = 3.10^{-3}$ M); $E = E_{HGH_4} - E_{HCl}$; 2 : pH = 1 ; 4 : pH = 2,53 ; 5 : pH = 2,97 ; 6 : pH = 3,37 ; 7 : pH = 3,88 9 : pH = 4,67 ; 10 : pH = 5,61 ; 11 : pH = 6,06 ; $\mu = 0{,}5 - 0{,}05$; Cuve = 1 cm.

Établissement de la composition du complexe et détermination de la constante de dissociation

En vue de déterminer le rapport de combinaison du complexe formé dans la solution, nous avons appliqué deux méthodes spectrophotométriques, à savoir : la « méthode du principe des variations continues » et la « méthode des droites ».

La méthode du principe des variations continues [5-7] s'applique dans le cas des composés stables. La composition du complexe s'établit difficilement si le rapport de combinaison est différent de 1 : 1.

Dans notre cas, à un petit excès d'ion central, il se produit une hydrolyse suivie de précipitation, ce qui empêche l'évaluation du rapport de combinaison dans le domaine de pH = 4 — 9.

---

[5] I. Ostromyslenski, *J. Russ. Phys. Chem. Soc.*, **42**, 1332, 1500 (1910).

[6] P. Job, *Compt. rend.*, **180**, 928 (1925).

[7] W. C. Vosburgh et C. R. Cooper, *J. Amer. Chem. Soc.*, **63**, 437 (1941).

Néanmoins, en vue de nous orienter en ce qui concerne le rapport de combinaison, nous avons effectué 3 séries isomolaires aux valeurs de $pH < 4$.

Sur la figure 4 sont représentées les séries isomolaires à $\lambda = 215$ nm. La concentration totale des composants dans chaque série était de 1.10^{-3} M. Dans les séries 1 et 3 le ligand était l'acide D-gluconique, et dans la 2ᵉ série le sel de potassium de l'acide ($[KGH_4] = 1.10^{-2}$ M; $pH = 6{,}40$)*. La force ionique ($\mu = 0{,}2$) a été fixée par du $NaClO_4$ dans le cas des séries 1 et 3. Dans la 2ᵉ série on n'a pas appliqué de force ionique constante. Le pH des séries 1 et 2 a

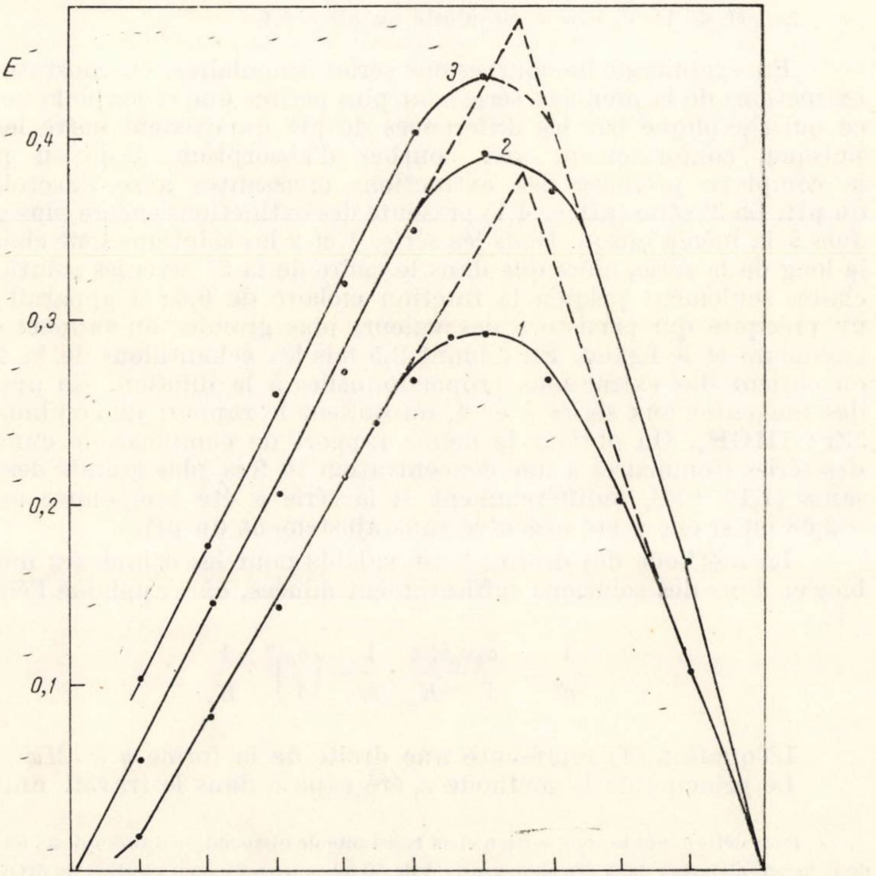

Fig. 4. — Séries isomolaires.

1 : $[Zr] + [HGH_4] = 1.10^{-3}$ M; $E = E_{compl.} - (E_{Zr} + E_{HGH_4} - NaClO_4)$

2 : $[Zr] + [KGH_4] = 1.10^{-3}$ M; $E = E_{compl.} - (E_{Zr} + E_{KGH_4})$;

3 : $[Zr] + [HGH_4] = 1.10^{-3}$ M; $E = E_{compl.} - E_{HGH_4}$;

Cuve = 2 cm; $\lambda = 215$ nm.

---

* KGH_4 = gluconate de potassium; HGH_4 = acide D-gluconique.

varié comme suit :

1. pH = 3,50 – 2,91 ; entre la fraction molaire 0,4 – 0,7 ; pH = 3,10 – 2,97 ;

2. pH = 5,09 – 2,92 ; entre la fraction molaire 0,4 – 0,7 ; pH = 3,40 – 3,03.

Le pH de la 3e série a été ajusté au pH = 4,1.

En examinant les courbes des séries isomolaires, on constate que les extinctions de la première série sont plus petites que celles de la deuxième, ce qui s'explique par les différences de pH qui existent entre les séries, puisque, conformément aux courbes d'absorption, jusqu'au pH = 4, le complexe présente des extinctions croissantes avec l'accroissement du pH. La 3e série (pH = 4,1) présente des extinctions encore plus grandes, dues à la même raison. Dans les séries 1 et 2 les solutions sont claires tout le long de la série, alors que dans le cadre de la 3e série les solutions sont claires seulement jusqu'à la fraction molaire de 0,6 ; il apparaît ensuite un précipité qui persiste à des valeurs plus grandes du rapport entre le zirconium et le ligand. En diluant 2,5 fois les échantillons de la 2e série, on obtient des extinctions proportionnelles à la dilution. En appliquant des tangentes aux séries 1 et 2, on obtient le rapport de combinaison de 2Zr : 1HGH_4. On obtient le même rapport de combinaison dans le cas des séries isomolaires à une concentration 10 fois plus grande des composants (1.10^{-2} M), indifféremment si la série a été tamponnée au pH = =2,08 ou si elle a été exécutée sans ajustement du pH.

La méthode des droites [8] est valable pour les complexes moins stables et dans des solutions suffisamment diluées, où s'applique l'équation :

$$\frac{1}{v^n} = \frac{a_0 v_0 b_0^n \varepsilon}{V^{n+1} K_c} \cdot \frac{1}{m} - \left(\frac{b_0}{V}\right)^n \cdot \frac{1}{K_c} \qquad (1)$$

L'équation (1) représente une droite de la forme $y = Mx - N$.

Le principe de la méthode a été exposé dans le travail antérieur. [9]

Pour déterminer la composition et la constante de dissociation du complexe, on a procédé de la façon suivante : dans des balons jaugés de 50 ml on prend 2,5 ml solution de $ZrOCl_2$ 1.10^{-2} M et 0,2 M en $NaClO_4$ et des volumes croissants d'une solution d'acide D-gluconique 2.10^{-2} M ; après une dilution proche du volume final on ajuste le pH avec NaOH 0,5 M et l'on complète le volume à 50 ml avec de l'eau distillée. Après une équilibration de deux jours, on lit l'extinction des échantillons.

Les essais d'effectuer une série au pH = 5 n'ont pas donné de résultats satisfaisants parce que, dans le domaine de pH = 4 – 8, à des rapports plus grands que 1 Me : 0,5 HGH_4, apparaissent des précipités qui empêchent l'évaluation des extinctions réelles, fait que l'on a constaté aussi aux titrages potentiométriques. C'est pourquoi, à l'évaluation du rapport de combinaison et de la constante de dissociation, on a utilisé la série au pH = 3, où les précipités n'apparaissent pas. Les résultats sont reportés dans le tableau 1.

---

[8] E. Asmus, U. Hinz, K. Ohls et W. Richley, *Z. analyt. Chem.*, **178**, 104 (1960).

[9] Const. Gh. Macarovici et L. Czeglédi, *Rev. Roumaine Chim.*, **14**, 57 (1969).

Tableau 1

1.10^{-2} M $ZrOCl_2$ et 0,2 M en $NaClO_4$ (v_0 = 2,5 ml) + 2.10^{-2} M acide D-gluconique (v ml) ; volume total V = 50 ml ; pH = 3 ; cuve 2 cm ; référence eau ; μ = 0,2 ; λ = 220 nm. $\overline{E} = E_{compl} - (E_{HGH_4} + E_{Zr} - E_{NaClO_4})$

v ml	$[HGH_4]$ 10^4	$\overline{E}$	$m = \frac{\overline{E}}{d}$ cm^{-1}	$\frac{1}{m} = \frac{d}{\overline{E}}$ cm	$\frac{1}{v^{0,5}} \cdot 10^{-1,5}$ $l^{-0,5}$	$\frac{1}{v} \cdot 10^{-3}$ l^{-1}	$\frac{1}{v^2} \cdot 10^{-6}$ l^{-2}	$\frac{1}{v^3} \cdot 10^{-9}$ l^{-3}
0,25	1	0,088	0,044	22,728	—	—	—	—
0,5	2	0,161	0,0805	12,423	1,414	2	4	8
0,75	3	0,170	0,085	11,765	1,155	1,333	1,778	2,370
1	4	0,176	0,088	11,364	1.—	1.—	1.—	1.—
1,25	5	0,180	0,090	11,112	0,894	0,800	0,640	0,512
1,875	7,5	0,188	0,094	10,639	0,730	0,533	0,284	0,152
2,5	10	0,191	0,095	10,472	0,632	0,400	0,160	0,064
3,75	15	0,193	0,096	10,363	0,516	0,267	0,071	0,019
5	20	0,198	0,099	10,101	0,447	0,200	0,040	0,008
7,5	30	0,192	0,096	10,417	—	—	—	—
12,5	50	0,250	0,125	8,000	—	—	—	—

En représentant graphiquement et en notant 1/m en abscisse et $1/v^n \cdot 10^{-3n}$ en ordonnée et en donnant à „n" des valeurs successives, on obtient une droite à la valeur de $n = 0,5$, représentant le nombre des ligands de la combinaison complexe. Cela signifie que dans la solution il existe le complexe au rapport de combinaison de 2 Zr : 1 HGH_4.

La valeur de la constante de dissociation apparente (K_c) peut être calculée à partir de la valeur de l'intersection de la droite avec l'axe de l'ordonnée (respectivement de la valeur négative de l'ordonnée), où

$$-\frac{1}{v^n} = -\left(\frac{b_0}{V}\right)^n \cdot \frac{1}{K_c} \qquad (2)$$

d'où

$$K_c = \left(\frac{b_0}{V}\right)^n \cdot v^n \qquad (3)$$

On obtient la valeur $-1/v^n$, qui entre dans les calculs de K_c en multipliant la valeur de la pente M par la valeur $1/m$ pour $-1/v^n = 0$, du graphique. De la première partie de l'équation (1) on a calculé la valeur du coefficient d'extinction molaire (ε apparent) et la valeur du module d'extinction („m") correspondant à la complexation totale des ions métalliques. C'est au tableau 2 que sont reportées ces données.

Tableau 2

Termes qui interviennent lors du calcul de la constante de dissociation

pH	λ nm	M $l^{-0,5}$ cm^{-1}	$-\frac{1}{v^n}$ $l^{-0,5}$	"m" cm^{-1}	ε 1/moles cm	K_c $moles^{0,5}/l^{0,5}$
3,0	220	$3,99 \cdot 10^{0,5}$	$3,54 \cdot 10^{1,5}$	0,1129	225,8	$5,65 \cdot 10^{-3}$

De la valeur de „m" on a calculé l'extinction correspondant aux conditions de la liaison totale du zirconium dans le complexe ($\overline{E}_n$ = m.d. = 0,2258).

La constante de dissociation apparente a été calculée aussi par la méthode du déplacement des équilibres [10]

$$K_c = \frac{[ZrO]^2 \cdot [GH_4^-]}{[(2ZrO).GH_4]}$$

On a calculé la concentration du complexe

$$[(2\,ZrO)\cdot GH_4] = \frac{1}{2}\,\frac{\overline{E}_1}{\overline{E}_n}\,[ZrO_{total}] \tag{4}$$

où $\overline{E}_1$ représente l'extinction d'un certain échantillon et $\overline{E}_n$ l'extinction dans les conditions de la complexation totale de l'ion métallique.

On a calculé la concentration de l'ion métallique qui ne réagit pas

$$[ZrO^{2+}] = [ZrO_{total}] - 2[(2ZrO)GH_4] \tag{5}$$

La concentration de l'ion gluconique se calcule par

$$[GH_4^-] = ([HGH_{4\,total}] - [(2ZrO)\cdot GH_4])\cdot\frac{K_1}{K_1 + [H^+]} \tag{6}$$

Les résultats obtenus sont consignés au tableau 3.

Tableau 3

$[ZrOCl_2] = 5\cdot10^{-4}$; pH = 3 ; λ = 220 nm ; cuve = 2 cm, $\mu = 0{,}2(NaClO_4)$; $\overline{E} = E_{compl.} - (E_{HGH_4} + E_{Zr} - E_{NaClO_4})$

$[HGH_4]$ 10^4	$\overline{E}_1$	$[(2ZrO)GH_4]$ 10^4	$[ZrO^{2+}]$ 10^4	$[GH_4^-]$ 10^5	$K_c = \frac{[ZrO^{2+}]^2[GH_4^-]}{[(2ZrO)GH_4]}$ moles^{0,5}/l^{0,5}
2	0,161	1,78	1,44	0,482	$4{,}86.10^{-3}$
3	0,170	1,88	1,24	2,461	$6{,}69.10^{-3}$
4	0,176	1,95	1,11	4,516	$7{,}30.10^{-3}$
5	0,180	1,99	1,02	6,619	$7{,}66.10^{-3}$
7,5	0,188	2,08	0,84	11,920	$7{,}98.10^{-3}$
					$K_c = 6{,}90.10^{-3}$

A partir de la série isomolaire (fig. 4, 2) où $[Zr] + [KGH_4] = 1.10^{-3}$M on a également calculé la constante d'instabilité du complexe à l'aide des valeurs obtenues à λ = 220 nm.

---

[10] A. K. Babko, «Physiko-himitcheskii analiz komplexnih soedinenii v rastvorah», Ed. Acad. Nauk Ukrain, S.S.S.R., Kiev, 1955, p. 130–138.

Le rapport de l'extinction maximum observée expérimentalement, E_1, à l'extinction du maximum interpolé, E_0 jusqu'au point d'intersection des premières parties de la courbe exprime la valeur du déplacement de l'équilibre du complexe formé.

En utilisant la relation [11] du degré de dissociation α

$$\alpha = \frac{E_0 - E_1}{E_0}. \tag{7}$$

et, pour le calcul de la constante de dissociation K_c la relation

$$K_c = \frac{\alpha^2 c}{(1 - \alpha)} \tag{8}$$

on obtient $K_c = 5{,}64.10^{-3}$ $\text{moles}^{0,5}/\text{l}^{0,5}$

En comparant les constantes de dissociation apparentes pour la même série par deux méthodes de calcul et par la méthode des séries isomolaires, on observe une concordance assez bonne :

$5{,}65.10^{-3}$ $\text{moles}^{0,5}/\text{l}^{0,5}$ par la méthode des droites
$6{,}90.10^{-3}$ ” ” ” du déplacement des équilibres
$5{,}64.10^{-3}$ ” ” ” des séries isomolaires

Plus la constante de dissociation d'un complexe est plus grande, plus le complexe est moins stable et plus dissocié.

Etant donné qu'à $\lambda = 220$, et le pH$= 3$ pour le système oxychlorure de zirconium — acide gluconique, la constante de dissociation apparente ($K_c = 5{,}65.10^{-3}$ $\text{moles}^{0,5}/\text{l}^{0,5}$) est comparativement plus grande que celle du système TiO — acide gluconique ($K_c = 2{,}20.10^{-5}$ moles/l)[9], on pourrait en déduire que le premier a une stabilité plus petite que le second.

Une telle comparaison ne serait juste que si les complexes étaient de la même composition et structure.

Afin de procéder correctement on peut prendre comme critère de comparaison des stabilités le logarithme de la valeur du degré de complexation du cation dans le complexe étudié, c'est-à-dire le logarithme du rapport de la concentration des ions métalliques dans le complexe et celle des ions libres, dans les mêmes conditions d'acidité [12]

$$\alpha = \frac{[\mathrm{Me\,L}]}{[\mathrm{Me}]} \tag{9}$$

où α est le degré de complexation.

Le rapport entre le logarithme de degré de complexation d'un complexe et d'un autre nous offre des indications quant à la stabilité relative des complexes.

---

[11] A. K. Babko, « Physiko-himitcheskii analiz komplexnih soedinenii v rastvorah », Ed. Acad. Nauk Ukrain, S.S.S.R., Kiev, 1955, p. 118.

[12] I. V. Piatnitski, *Zhur. neorg. Khim.*, **1**, 2368 (1956).

On calcule la concentration des ions métalliques de complexe à partir de l'équation

$$[\mathrm{MeL}] = \frac{\overline{E}_1}{\overline{E}_n} [\mathrm{Me_{total}}] \tag{10}$$

et la concentration de l'ion métallique non lié résulte de la relation

$$[\mathrm{Me}] = [\mathrm{Me_{total}}] - [\mathrm{MeL}] \tag{11}$$

Vu que dans le cas du titane et du zirconium pour obtenir la constante de dissociation on a opéré par séries au pH = 3, la comparaison dont il a été fait état est valable. Les résultats sont donnés dans le tableau 4.

Tableau 4

Comparaison du degré de complexation au pH = 3

$[\mathrm{HGH_4}]$ 10^4	$[\mathrm{TiO_{compl.}}]$ 10^4	$[\mathrm{TiO_{libre}}]$ 10^4	$[\mathrm{ZrO_{compl.}}]$ 10^4	$[\mathrm{ZrO_{libre}}]$ 10^4	$\log\alpha_{\mathrm{TiO}}$	$\log\alpha_{\mathrm{ZrO}}$	$\log\left(\frac{\alpha\mathrm{TiO}}{\alpha\mathrm{ZrO}}\right)$
2	1,80	0,20	3,56	1,44	0,954	0,394	0,560
3	1,86	0,14	3,76	1,24	1,123	0,482	0,641
4	1,90	0,10	3,89	1,11	1,278	0,547	0,731
				Moyenne	1,118	0,479	0,644

Il résulte des données de ce tableau qu'au pH = 3 et λ_{220}, le logarithme du degré de complexation du système titane — acide gluconique est plus grand ($\simeq$ 4,40 fois), ce qui nous permet de conclure que ce complexe est plus stable que celui avec le zirconium.

Cette constatation concorde avec celle de Rjabtchikow[13] et collaborateurs pour le cas des systèmes Ti(IV), Zr (IV), Hf(IV) avec de l'acide tartrique. La stabilité des complexes avec de l'acide tartrique est d'autant plus grande que l'ion métallique est plus hydrolysable ; l'ordre de la stabilité est Ti > Zr > Hf. Dans le 4ᵉ sous-groupe, la stabilité des complexes tartriques baisse donc du titane au zirconium et à l'hafnium.[13, 14]

Dans le cas des complexes du titane et du zirconium avec l'acide gluconique le comportement est similaire.

---

[13] D. I. Riabtchikov, A. N. Ermakov, V. K. Beliaeva et N. N. Marov, *Zhur. neorg. Khim.*, 4, 1814 (1959).

[14] J. V. Piatnitski, *Uspekhi Khim.*, 32, 93 (1963).

Revue Roumaine de Chimie, 15, 1751–1758 (1970)

LA THERMOCHROMATOGRAPHIE SUR PAPIER. XIV[1]

LA POSSIBILITÉ DE SÉPARER CERTAINS IONS AYANT LES VALEURS R_f PRATIQUEMENT ÉGALES EN CHROMATOGRAPHIE ISOTHERME

C. LITEANU, S. GOCAN et T. HODIŞAN

Chaire de Chimie Analytique de l'Université « Babeş-Bolyai », Cluj, 11, str. Arany János

Reçu le 4 mai 1970

On indique la possibilité de séparer les ions Ni^{2+} et Co^{2+}, à un certain gradient de température, dont la séparation en chromatographie isotherme n'a pu être obtenue même à 70°. Les expériences ont été faites sur papier Whatman n° 3, et comme éluant on a employé du *n*-butanol saturé de HCl 4N. En ce qui concerne le mécanisme d'action du gradient de température, on montre qu'on peut réaliser des colonnes de n'importe quelle « longueur », quoique la longueur géométrique de la colonne *l* soit limitée. Ce fait donne la possibilité de séparer certaines substances ayant des coefficients de répartition très proches.

Dans un ouvrage antérieur [1] on a étudié certains problèmes théoriques sur l'efficience de la séparation en chromatographie à gradient de température comparé à la chromatographie isotherme, et on a établi une série de relations. Ainsi le coefficient de séparation pour deux substances en fonction des valeurs R_f est

$$\beta = \frac{\alpha_1}{\alpha_2} = \frac{R_{f_2} - R_{f_1} R_{f_2}}{R_{f_1} - R_{f_1} R_{f_2}} \tag{1}$$

ou

$$\beta = 1 + \frac{d}{(R_{f_1} - R_{f_2}^2)\, l - R_{f_1} d} \tag{2}$$

d'où

$$l = \left(\frac{1}{\beta - 1} + R_{f_1}\right) \cdot \frac{d}{R_{f_1} - R_{f_1}^2} \tag{3}$$

---

[1] C. Liteanu et S. Gocan (sous presse)

où $l = v/A_M$ représente la longueur de la colonne de papier chromatographique entre le start et le front de l'éluant, v le volume de l'éluant de cette colonne, A_M la section de la phase mobile et d la distance entre les centres des spots quant ils sont tangents.

PARTIE EXPÉRIMENTALE

Pour démontrer la justesse de ces affirmations, on a choisi la séparation des ions Ni^{2+} et Co^{2+} qui, sur papier Whatman n° 3 et ayant comme éluant du *n*-butanol saturé de HCl 4 N, ont les valeurs R_f à 20° pratiquement égales.

Les développements isothermiques ont été effectués à l'aide d'éprouvettes spéciales décrites dans un ouvrage antérieur [2]. Les résultats sont donnés dans le tableau 1 et les figures 1 et 2.

Tableau 1

Valeurs R_f en fonction de la température pour les ions Ni^{2+} et Co^{2+}. Développement ascendant, éluant *n*-butanol saturé de HCl 4N, sur papier Whatman n° 3.

n° crt.	Temp. (°C)	R_f		
		Ni^{2+}	Co^{2+}	$Ni^{2+} + Co^{2+}$
1	20	0,03	0,03	0,03
2	30	0,03	0,03	0,03
3	40	0,03	0,04	0,03
4	50	0,04	0,05	0,05
5	60	0,06	0,07	0,06
6	70	0,09	0,11	0,08

Les développements en gradient de température ont été réalisés à l'aide d'une chambre chromatographique décrite dans un ouvrage antérieur. [3] Les résultats sont donnés dans les tableaux 2 et les figures 3 et 4.

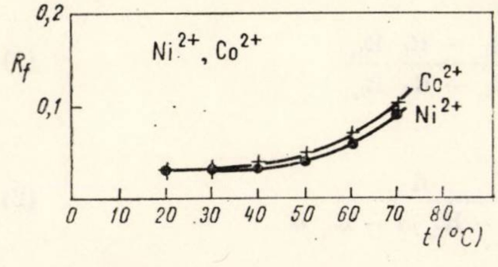

Fig. 1. — Variation des valeurs R_f, en fonction de la température des composants libres.

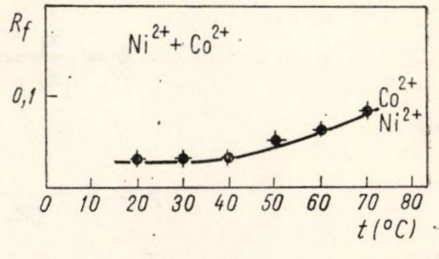

Fig. 2. — Variation des valeurs R_f, en fonction de la température des composants en mélange.

---

[2] C. Liteanu et S. Gocan, *Bull. Soc. chim. France*, **1967**, 3836.
[3] C. Liteanu et S. Gocan, *Bull. Soc. chim. France*, **1969**, 1416.

DISCUSSIONS DES RÉSULTATS ET CONCLUSIONS

L'examen du tableau 1 et des figures 1 et 2 ne révèle pas la séparation des deux ions. Les différences des valeurs R_f dues à la croissance de la température sont trop faibles pour permettre leur séparation.

Ainsi qu'on a démontré [1] théoriquement il ne peut pas exister deux ions ayant des valeurs R_f égales dans le même système phase mobile — — phase stationnaire, admettant une différence entre les valeurs R_f des deux ions à 20° pour $0{,}005 = (\Delta R_f)_{\text{isoth}}$. Cette différence évidemment est très petite et est comprise dans les valeurs des erreurs expérimentales. On a ainsi admis qu'à 20° le Ni^{2+} a la valeur $R_{f_1} = 0{,}030$ et le Co^{2+} la valeur $R_{f_2} = 0{,}035$. A l'aide de la relation (1) on a calculé le coefficient de séparation $\beta = 1{,}17$.

Tableau 2

Valeurs R_f en fonction du gradient de température pour les ions Ni^{2+} et Co^{2+}. Développement ascendant, éluant *n*-butanol saturé de HCl 4N, sur papier Whatman n° 3

n° crt.	temp. (°C)		grad. temp. (°C/cm)	R_f			Distance start-front cm
	t_s	t_i		Ni^{2+}	Co^{2+}	$Ni^{2+} + Co^{2+}$	
1	20	20	—	0,03	0,03	0,03	12
2	30	20	0,59	0,04	0,04	0,04	12
3	40	20	1,18	0,05	0,05	0,05	12
4	50	20	1,80	0,11	0,12	0,11	12
5				0,16	0,20	0,17 ; 0,20	11*
	55	20	2,06				
6				0,28	0,33	0,27 ; 0,33	11**

*) Durée de développement 14 heures ;
**) Durée de développement 36 heures.

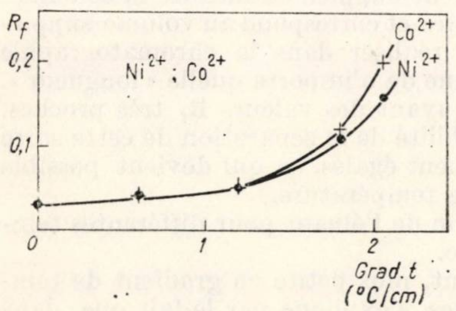

Fig. 3. — Variation des valeurs R_f, en fonction du gradient de température des composants libres.

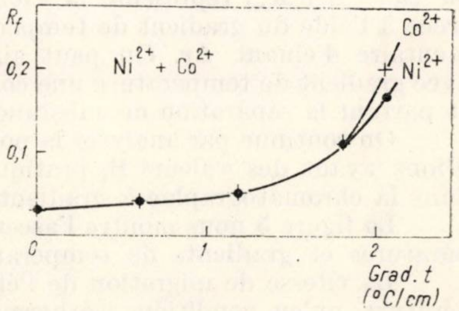

Fig. 4. — Variation des valeurs R_f, en fonction du gradient de température des composants en mélange.

La séparation des deux ions a été complète lorsque la distance entre leurs centres d = 0,7cm, valeur que l'on a obtenue par mesurages directs sur chromatogramme.

En remplaçant les données ci-dessus dans la relation (3), on obtient la valeur de la longueur de la colonne chromatographique, $l = 142$ cm, nécessaire à la séparation en conditions isothermiques à 20°. Cette longueur ne peut être pratiquement obtenue en chromatographie isothermique, étant donné que le papier chromatographique a une longueur maximum de 60 cm. D'autre part, généralement, on travaille en chromatographie isothermique sur des bandes de papier chromatographique ayant une longueur de tout au plus 35 cm. Il est évident que dans ces conditions leur séparation n'est pas possible.

Néanmoins, pour vérifier expérimentalement ce fait on a construit une éprouvette spéciale d'une longueur de 80 cm et aux parois doubles pour pouvoir être thermostatée, en y procédant à un développement avec le même éluant et le même papier que dans les expériences précédentes. La longueur du papier chromatographique a été d'approximativement 60 cm (longueur de la feuille) et la durée de développement de 240 heures, à 20°. Même dans ces conditions on n'a pu obtenir la séparation des deux ions (Ni^{2+} et Co^{2+}). En revanche on a constaté une diffusion latérale très prononcée des deux spots, ce qui s'explique par la longue durée d'immersion du papier chromatographique.

On a de même établi que pour une chromatographie avec gradient de température, on peut écrire la relation (2) comme suit

$$\beta = 1 + \frac{\mathrm{d}}{(\mathrm{R}_{\mathrm{f}_1} - \mathrm{R}_{\mathrm{f}_1}^2)(l + \Delta l) - \mathrm{R}_{\mathrm{f}_1}\mathrm{d}} \tag{4}$$

où $\Delta l = \Delta v / A_M$, représente la « longueur supplémentaire de la colonne » créée à l'aide du gradient de température et correspond au volume supplémentaire d'éluant Δv. On peut ainsi réaliser dans la chromatographie avec gradient de température une colonne de n'importe quelle « longueur », et partant la séparation de substances ayant des valeurs R_f très proches.

On continue par analyser la possibilité de la séparation de cette sorte d'ions ayant des valeurs R_f pratiquement égales, ce qui devient possible dans la chromatographie à gradient de température.

La figure 5 nous montre l'ascension de l'éluant pour différentes températures et gradients de température.

La vitesse de migration de l'éluant, plus petite en gradient de température qu'en conditions isothermiques, s'explique par le fait que, dans ces conditions, une partie de l'éluant qui émigre s'évapore de la colonne et est condensée dans la partie inférieure de la chambre chromatographique. [2] A l'intérieur de la chambre il existe de même un gradient de tension de vapeurs créant une diffusion de haut en bas, en même temps que la condensation de la phase de vapeur à la surface de l'éluant où la température est la plus basse.

Ainsi qu'il est connu, la vitesse d'évaporation est donnée par la relation

$$E_v = k \frac{F - f}{H} \tag{5}$$

où k est le coefficient de proportionnalité, S — la surface d'évaporation, F — la tension des vapeurs saturées à la température du liquide qui s'évapore, f — la tension des vapeurs se trouvant au-dessus du liquide et H — la pression atmosphérique.

En même temps que l'accroissement de la température dans la partie supérieure de la chambre chromatographique, le gradient de température croît évidemment aussi, ainsi que la tension des vapeurs saturées F, ce qui entraîne l'accroissement de la différence $F - f$, c'est-à-dire du gradient de la tension de vapeurs. Mais, ainsi qu'il résulte de la relation (5), la vitesse d'évaporation croît en même temps que la différence $F - f$, autrement dit le volume Δv de liquide quittant la colonne par unité de temps croît.

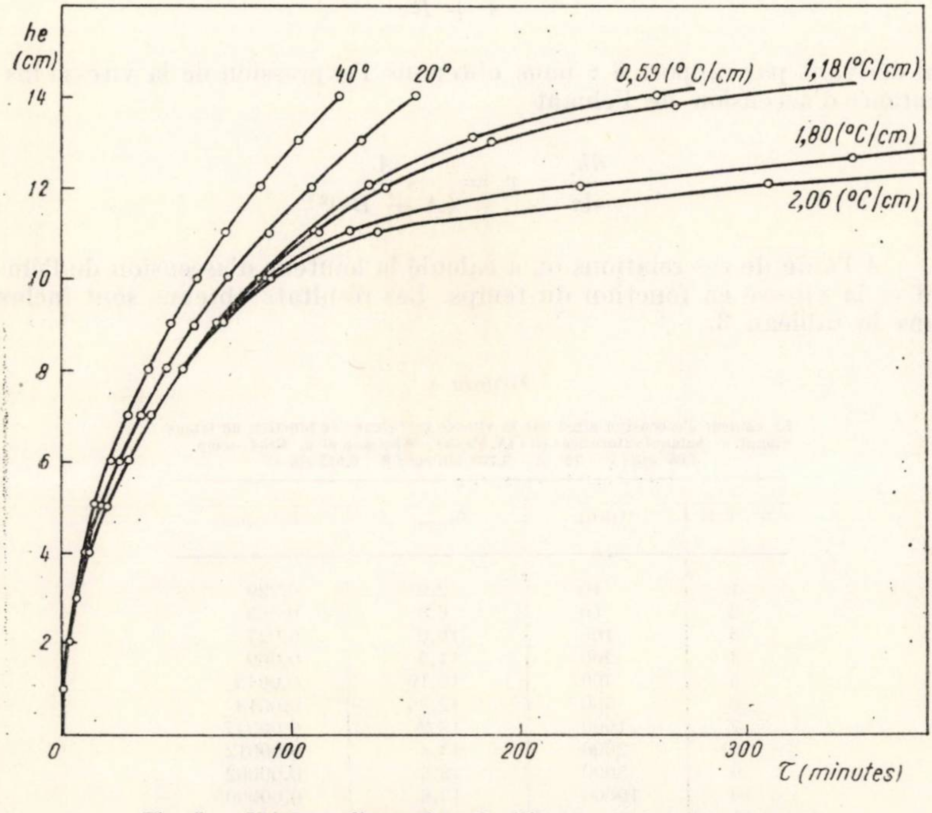

Fig. 5. — Hauteur d'ascension de l'éluant en fonction du temps. Eluant : n-buthanol saturé de HCl 4N ; Papier : Whatman n° 3 ; $t_i = 20°$.

Cette perte de l'éluant de la colonne est compensée par la pénétration d'une nouvelle quantité d'éluant dans la colonne. De cette manière, pour que l'éluant parcoure la même distance que dans le cas isotherme, il faut un volume plus grand d'éluant qui passe par la colonne, c'est-à-dire $v' = v + \Delta v$.

De la figure 5 il résulte que la vitesse d'ascension de l'éluant en gradient de température diminue avec le temps, étant d'autant plus petite à un moment donné que celui-ci a de plus petites valeurs.

Ainsi qu'il a été montré [4] l'ascension de l'éluant en fonction du temps a lieu selon une équation ayant la forme

$$h_e = \frac{\tau}{A + B\tau}$$

En dérivant par rapport à τ nous obtenons l'expression de la vitesse instantanée d'ascension de l'éluant

$$\frac{dh_e}{d\tau} = v_e = \frac{A}{(A + B\tau)^2}$$

A l'aide de ces relations on a calculé la hauteur d'ascension de l'éluant et la vitesse en fonction du temps. Les résultats obtenus sont inclus dans le tableau 3.

Tableau 3

La hauteur d'ascension ainsi que la vitesse de l'éluant en fonction du temps
Eluant: n – butanol saturé avec HCl 4N. Papier : Whatman n° 3. Grad. temp. = 2,06°/cm ; t_j = 20°. A = 2,702 mn/cm ; B = 0,073 cm^{-1}

n° crt.	(mn)	$h_{e(\text{cm})}$	v_{e}(cm/mn)
1	10	2,9	0,229
2	50	6,8	0,065
3	100	10,0	0,027
4	200	11,5	0,009
5	300	12,19	0,0045
6	500	12,75	0,0018
7	1000	13,2	0,00047
8	2000	13,4	0,00012
9	5000	13,5	0,00002
10	10000	13,6	0,000005
11	∞	13,7	0

Du tableau 3 on constate que la vitesse d'ascension de l'éluant diminue beaucoup avec le temps de développement. Théoriquement elle devient égale à zéro pour $\tau = \infty$, mais pratiquement on peut la considérer égale à zéro pour le présent exemple après approximativement 1000 minutes (16 heures et 40 minutes).

Cela ne signifie pas que le processus d'évaporation de l'éluant et de sa condensation, ainsi que la migration d'une nouvelle quantité cessent, mais constitue un processus qui continue même à $v_e = 0$. La quantité d'éluant, quittant la colonne, Δv est déterminée par la vitesse d'évaporation E_v, qui à son tour est fonction de la grandeur du gradient de température, ainsi que de la durée du processus chromatographique. Comme la durée du processus chromatographique peut avoir n'importe quelle longueur ($\tau = \infty$), nous obtenons pour $\Delta v = \tau E_e = \infty$, respectivement $\Delta l = \frac{\Delta v}{A_M} = \infty$.

---

[4] S. Gocan et C. Liteanu, *Bull. Soc. chim. France*, **1969**, 1409.

En conclusion, en chromatographie à gradient de température, on peut réaliser des colonnes de n'importe quelle « longueur », ce qui permet ainsi la séparation des substances ayant des valeurs de coefficients de partage aussi proches que possible, respectivement très près de l'unité, car, ainsi qu'il résulte de la relation (4), si $\Delta l \rightarrow \infty$, $\beta \rightarrow 1$.

Dans ces conditions limite, donc $\tau \rightarrow \infty$, il est évident que h_s spot tend vers h_e éluant, et par suite les spots se trouveront sur le front de l'éluant. Il en résulte que le processus chromatographique doit être arrêté à $\tau < \tau_\infty$ quand les conditions de séparation seront réalisées, à savoir lorsque $h_{s_2} - h_{s_1} = d$, où ainsi qu'il a été montré, d est la distance entre les centres des spots, lorsque ceux-ci sont au moins tangents.

Vu que tel qu'il a déjà été établi dans [2]

$$\mathrm{R}_{\mathrm{f}_{\mathrm{grad}}} = \mathrm{R}_{\mathrm{f}_{\mathrm{iso}}} \cdot \frac{v + v}{v} \tag{6}$$

$\mathrm{R}_{\mathrm{f}_{\mathrm{grad}}}$ croît avec l'augmentation de Δv, respectivement avec la durée de développement ainsi que le montre le tableau 2.

Les résultats du tableau 2 révèlent une séparation totale, à un gradient de température de 2,06°/cm, la distance start-front, $l = 11$ cm, et la distance entre les centres des spots des deux ions lorsqu'ils sont tangents, d $= 0{,}7$ cm, pour un temps de développement de 36 heures.

Après remplacement dans la relation (6) on obtient

$$0{,}06 = 0{,}005\left(1 + \frac{\Delta v}{v}\right)$$

ou

$$11v = \Delta\, v$$

où

$$v = l \cdot A_M,\ \Delta v = \Delta l \cdot A_M \text{ et donc}$$

$$11\, l = \Delta\, l$$

et étant donné que $l = 11$ cm, on obtient $\Delta l = 121$ cm.

Il s'ensuit qu'en chromatographie à gradient de température on a réalisé une « colonne supplémentaire » égale à 121 cm, à savoir onze fois plus grande que la colonne réelle. Ainsi, dans ce cas les choses se sont passées comme si on avait travaillé en réalité avec une colonne ayant la longueur de $l + \Delta l = 132$ cm, valeur en bonne concordance avec la valeur trouvée par chromatographie isothermique de 142 cm. Evidemment dans cette longueur est également incluse la croissance de la longueur supplémentaire due à l'éventuelle modification des coefficients de partage en gradient de température, un problème déjà [2] abordé et qui sera repris dans un ouvrage prochain.

Il résulte donc clairement que la chromatographie à gradient de température, sans faire appel à des gradients spéciaux, offre la possibilité de séparer des substances qui ne peuvent être séparées en chromatographie isotherme.

Revue Roumaine de Chimie, **15**, 1759–1765 (1970)

CATALYTIC DETERMINATION OF VANADIUM V(V) WITH AMIDOL

AL. ŞUTEU and H. NAŞCU

Chair of Analytical Chemistry, Cluj, str. Arany Ianos 11

Received March 21, 1970

The paper describes a kinetic colorimetric method, based on the catalytic action of V(V) ions on the oxidation reaction of amidol (*p*-diamino-phenol) with bromate in the presence of phenol. The reaction develops a violet-reddish compound ($\lambda = 510$ nm). The reaction is followed photocolorimetrically, using the tangent method, when a straight line tg $\alpha = f(c)$ is obtained. The quantities of the V(V) which can be determined are found within the range 0.05–0.5 μg V(V) (0.001 –0.01 μg/ml). In the absence of phenol tg $\alpha = f(c)$ is represented by a parabolic curve, which can be a straight line, by a logarithmic plot log tg $\alpha = f(\log c)$. In this case the determination range of V(V) are 0.5–8 μg V(V) (0.01–0.3 μg/ml).

The literature describes a number of catalytic determination methods of V(V), based mainly on its catalytic action in the oxidative reaction with different oxidants of certain colourless or coloured organic compounds. Thus Szebelledy and Ajtai [1,2] have used the oxidative reaction of chlorate with *p*-phenetidine, aniline, *p*-phenylene-diamine in the presence of naphthol or oxine as "activators". Nazarenko et al. have used the catalytic oxidation of aniline with chlorate, [3,4] for the determination of V(V) in semiconductors and titanium. Hiroshi Nishida describes a method based on the oxidation of aniline with H_2O_2,[5] and two others based on the oxidative action of hydrogen peroxide on diphenylamine[6] and diphenyl-carbazide.[7] Bontschev[8] recommended a method based on the oxidative effect of potassium chlorate on *p*-phenetidine in the presence of phenol as activator, studying at the same time the mechanism[9] and the kinetics of the reaction.[10]

---

[1] L. Szebelledy and M. Ajtai, *Mikrochemie ver Mikrochim. Acta*, **25**, 258 (1938).

[2] L. Szebelledy and M. Ajtai, *Mikrochemie ver Mikrochim. Acta*, **26**, 72 (1939); **26**, 87 (1939).

[3] V. A. Nazarenko and E. A. Birjuk, *Zhur. analit. Khim.*, **10**, 28 (1955).

[4] M. B. Schustova and V. A. Nazarenko, *Zavodskaya Lab.*, **26**, 1339 (1960).

[5] Hiroshi Nishida, *Bunseki Kagaku*, **14**, 1009 (1965); *Chem. Abstr.*, **64**, 5752a (1966).

[6] Hiroshi Nishida, *Bunseki Kagaku*, **13**, 1259 (1964); *Chem. Abstr.*, **62**, 8386c (1965).

[7] Hiroshi Nishida, *Bunseki Kagaku*, **14**, 301 (1965); *Chem. Abstr.*, **63**, 2383g (1965).

[8] P. R. Bontschev, *Mikrochim. Acta*, **1962**, 577.

[9] P. R. Bontschev, *Mikrochim. Acta*, **1962**, 584.

[10] P. R. Bontschev, *Mikrochim. Acta*, **1962**, 592.

Bognar and Jellinek have studied the catalytic activity of *V*(*V*) on the oxidation of ascorbic acid with the following oxidants: chlorate, [11,12] bromate [13,14] using the *p*-toluidine, azocarmine GX or a substance of the *p*-$R_2NC_6H_4NR'_2$ type [15] (where $R = H$, $R' =$ Me or Et or $R = R' =$ Me) as indicators. Based on the same catalytic action of V(V), on the oxidation of benzidine with potassium chlorate, in the presence of hydrochloric acid, Li-Ching-Tien and Wen-Ping-Chang describe a very sensitive determination method of V(V) 0.0001–10 μg/ml.[16] Another method based on the catalytic action of V(V) in oxidation with periodate [17] has also been reported. In all the above mentioned papers organic substances, which after oxidation develop coloured compounds, have been used as reductors. Methods using inorganic reductors as: thiosulphate [18] and stanium (II) ion [19] and as oxidants: hydrogen peroxide and potassium chlorate respectively, have also been reported. Budanov and Panfilova [20] have studied the kinetics of oxidation of indigocarmine with bromate in the presence of V(V) and recommended a sensitive method plotting the absorbance decrease as function of time.

Having in view the fact that the V(V) ions have a catalytic action in the oxidation of amidol (*p*-diamino-phenol) with potassium bromate the aim of the present work is to determine the special conditions under which the reaction must be performed for accurate V(V) determination. The amidol at optimum concentration 0.1% was prepared by solving pure amidol in 2n hydrochloric acid of high purity. It is necessary that the solution should be freshly prepared as its stability lasts but 3–4 days. The absorption curve of the compound resulting from the amidol oxidation with bromate was determined (fig. 1) at first.

Since the rate of the oxidative reaction between bromate and amidol is dependent to a great extent upon the pH, our investigations aimed at establishing the pH at which the rate of the reaction between bromate and amidol is negligible in the absence of the catalyst V(V) but sufficiently high in its presence.

Our experiments have shown that at pH lower than 1 the potassium bromate (at a concentration of 0.016 M) oxidized the amidol even in the absence of V(V), whereas at pH = 5 the catalytic activity of V(V) was negligible. In order to determine the most suitable pH conditions under which the V(V) promotes the highest catalytic activity we have plotted the absorbance as function of time (for potassium bromate and amidol

[11] J. Bognar and O. Jellinek, *Mikrochim. Acta*, **1964**, 317.

[12] J. Bognar, O. Jellinek and S. Sarosi, *Mikrochim. Acta*, **1965**, 708.

[13] J. Bognar and O. Jellinek, *Mikrochim. Acta*, **1964**, 1129.

[14] J. Bognar and O. Jellinek, *Mikrochim. Acta*, **1969**, 318.

[15] J. Bognar and O. Jellinek, *Mikrochim. Acta*, **1969**, 366.

[16] Li-Ching Tien and Wen-Ping Chang, *Hua Hsueh Hsueh Pao*, **30**, 101 (1964); *Chem. Abstr.* **61**, 6392g (1964).

[17] L. Markus, *Dissertation*, Budapest, 1943.

[18] K. B. Iatimirski and E. F. Narischina, *Zhur. neorg. Khim.*, **4**, 1548 (1959).

[19] J. Bognar and O. Jellinek, *Mikrochim. Acta*, **1967**, 193.

[20] V. V. Budanov and E. Panfilova, *Izvest. V.U.Z.M.V.O. S.S.S.R. Khim. i Khim. Tekhnol.*, **8**, 208 (1965).

solutions at concentrations of 0.016 M and 0.1 % respectively) at different pH values: the tg α for each pH level was separately calculated and we have plotted the dependence of the tg α on the pH (fig. 2).

As it may be seen in figure 2 the highest slope of the curve was obtained at pH = 2.2 (buffer 91.1 ml citric acid 0.1 M and 9.9 ml monopotassic citrate 0.1 M, after Kolthoff and Vleeschhouwer). At this pH the catalytic action of V(V) is high and the oxidative reaction of potassium bromate with amidol is negligible in the absence of the catalyst. A variation of ± 0.1 units of pH does not change the results.

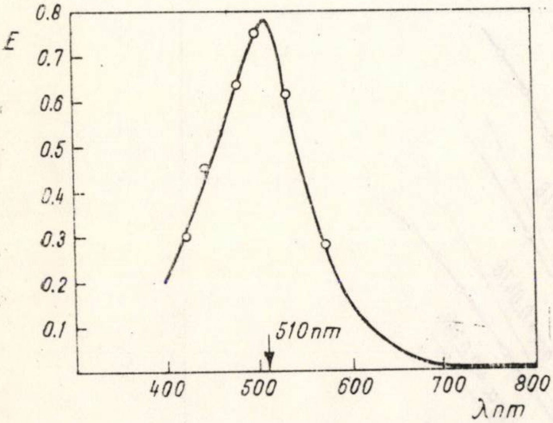

Fig. 1. — Absorbance of amidol solution (oxidized with $KBrO_3$) as function of λ (nm) for 0.1 μg V(V) in 30 ml after 30 minutes.
$KBrO_3$: 0.016 M at pH = 2.2 (buffer monopotassic citrate-citric acid)
Amidol : 0.1 %.

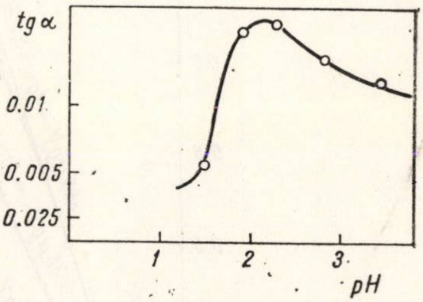

Fig. 2. — Plot of tg α as function of pH (buffer monopotassic citrate-citric acid)
$KBrO_3$: 0.016 M
Amidol : 0.1 %
V (V) : 1.0 μg.

Since the rate of the oxidative reaction between potassium bromate with amidol is also dependent upon the bromate concentration, we have investigated the optimal bromate concentration at which the reaction does not take place in the absence of V(V), but it is progressing at an adequate rate in its presence. Our experiments have shown that a 0.016 M concentration of potassium bromate is the most suitable. The determinations were carried out at 20° a variation of ± 0.1° being insignificant.

For V(V) determinations based on this reaction we have used the tangent method. Thus we have determined the dependence of absorbance on time, for solutions of various concentrations in V(V), but of the same concentration in potassium bromate (0.016 M), amidol (0.1 %) and with the same pH (2.2). Accordingly for each V(V) concentration a curve was obtained (see fig. 3).

The tangents of these curves, plotted just at 5 minutes after the beginning of the reaction were calculated and plotted as function of concentration tg α = f(conc V(V)) in fig. 4. These tangents build a parabolic curve. In order to obtain a straight line the tangents were represented logarithmically in coordinates log tg α = f (log conc V(V) in fig. 5 for V(V) concentrations within 0.6 – 8 μg V(V) in 30 ml.

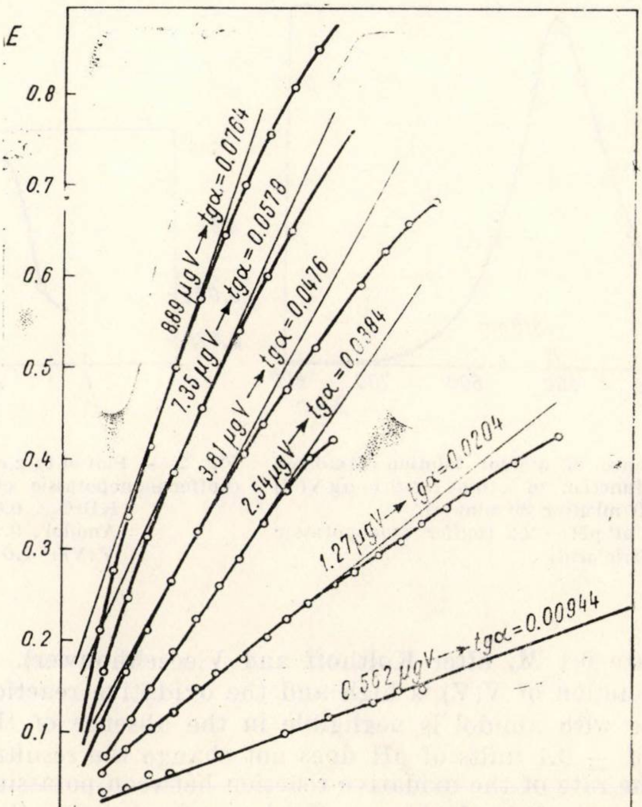

Fig. 3.– Absorbance variation as function of time for various amounts of V (V).
$KBrO_3$: 0.016 M at pH = 2.2 (buffer monopotassic citrate-citric acid)
Amidol : 0.1 %.

The parabolic curve may be explained through the interference during the reaction between bromate and amidol, of bromine which decolorize the product of oxidation. In order to avoid this reaction, we have tried, by adding a certain amount of phenol, to block up the bromine in the form of tribrom-phenol. Accordingly, we have studied the effect of different amounts of phenol on the catalytic reaction of amidol with bromate. Our experiments have shown that by increasing the amounts of phenol, an increased absorbance takes place, a fact which proves that

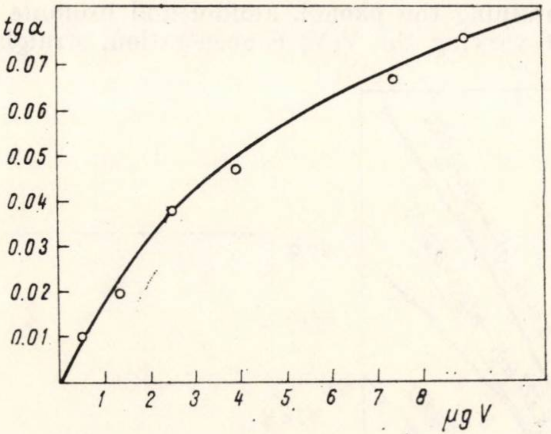

Fig. 4. – Plot of tg α as function of V(V) concentrations.

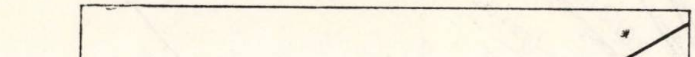

Fig. 5. – Plot of log tg α as function of log conc. V (V).

the phenol increases the catalytic action of V(V) in the oxidative reaction of bromate with amidol. At the same time, the linear portion of the curves is lengthening due to the bromine blockage. In order to determine the optimal amount of phenol, we have used the same quantity of V(V) but different phenol concentrations. Our experiments have shown that starting with concentrations higher than 0.003 %, the slopes of the curves remain actually constant, proving that beyond this level phenol becomes inactive. Further on, maintaining the phenol, amidol and bromate at a constant concentration but varying the V(V) concentration, straight lines (represented in fig. 6) have been obtained. By representing this time tg α as function of the V(V) concentration, a straight line was obtained (fig. 7) within the range 0.05—0.5 μg V(V) in 30 ml solution.

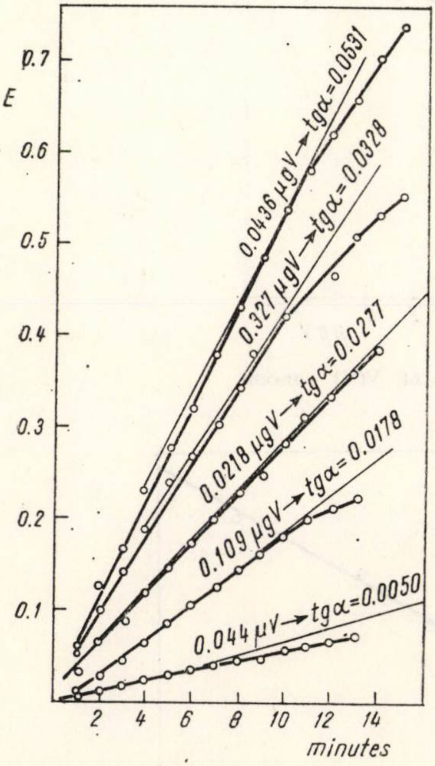

Fig. 6. — Absorbance variation as function of time for various amounts of V(V) in the presence of phenol (1 ml 0.003 %).

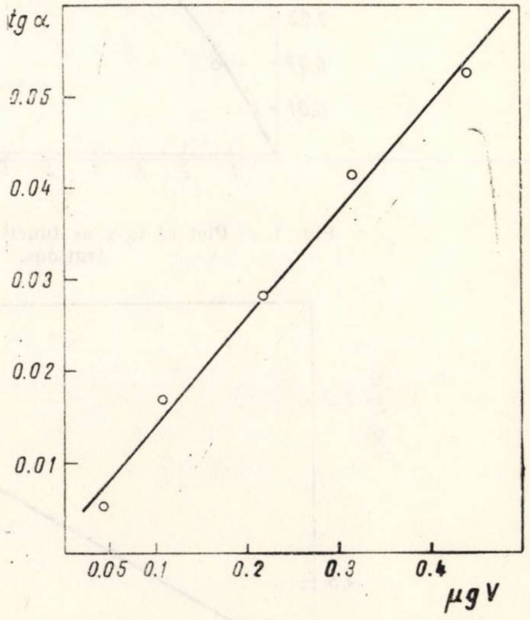

Fig. 7. — Plot of tg α as function of V (V) concentration in the presence of phenol (1 ml 0.003 %)

PROCEDURE

A sample of 0.05—0.5 μg V was placed in the colorimeter cell with 5 ml potassium bromate 0.1 M, 5 ml buffer solution of monopotassic citrate-citric acid (pH = 2.2), 1 ml phenol 0.003 % completed with 3 times distilled water to 29 ml and 1 ml fresh amidol solution (0.1 %). A photocolorimeter with blue philter (λ = 500 nm) was used for the interpretation of the absorbance as function of time *versus* a blank without V(V), the absorbance being plotted against time passing from the starting point of reaction.

A straight line was obtained the slope of which is proportional to the V(V) concentration.

The V(V) content of the unknown sample is found by interpolation from a standard curve obtained for various V(V) amounts under the experimental conditions.

In the method in which phenol was not used as activator the procedure was similar with the only difference that the phenol is replaced by the same amount of water and thus the amount of V(V) may be determined within the range of 0.5–8.0 μg V(V) in 30 ml.

These determinations cannot be obtained either in the presence of Fe^{3+}, Cu^{2+}, Ce^{4+} ions, which interfere with V(V) in the bromate-amidol reaction, or in the presence of oxidants such as H_2O_2, Cr^{6+}, Cl_2, Br_2, IO_3^- etc. which oxidize amidol interfering with the action of the bromate. Moreover, in the presence of complexants such as Kelaton-3, hexametaphosphate, F^-, the determination of V(V) is not possible, because of the V(V) blockage.

Revue Roumaine de Chimie, **15**, 1767–1776 (1970)

INVESTIGATIONS IN THE CYCLOBUTANE SERIES. XXX[1]

NMR SPECTRAL PARAMETERS OF SOME COMPOUNDS WITH BENZOCYCLOBUTENO-NORBORNENE AND -NORBORNANE SKELETON

MARGARETA AVRAM, F. CHIRALEU, I. POGANY, I. G. DINULESCU

Institute of Organic Chemistry, Bucharest, Splaiul Independenţei 202 B

Received June 16, 1970

NMR spectral parameters of *endo*- and *exo*-benzocyclobuteno-norbornene and of several substituted benzocyclobuteno-norbornanes are discussed. Chemical shifts and coupling constants are compared and correlated with sterical configurations of the respective compounds.

The bicyclo [2.2.1] heptane systems of norbornane, norbornene and norbornadiene,[2–4] along with the related benzobicyclo [2.2.1] heptane systems of benzonorbornene and benzonorbornadiene[5,6] have been thoroughly investigated by means of NMR spectroscopy. However, there are scarce spectroscopy data about norbornane systems condensed with a benzocyclobutene ring, namely 3.4-benzotricyclo $[4.2.1.0^{2,5}]$ non-7-ene (benzocyclobutenonorbornane) and 3.4-benzotricyclo $[4.2.1.0^{2,5}]$ nona-3,7-diene (benzocyclobutenonorbornene).[7]

In the course of our investigations on the reactions of *endo*- and *exo*-benzotricyclo $[4.2.1.0^{2,5}]$ nona-3,7-diene[8] we noted some typical aspects of the spectral parameters (chemical shift and coupling constant) of a number of derivatives of the benzocyclobuteno-norbornanes **1** and

---

[1] Part XXIX: M. Avram, F. Chiraleu and I. Pogany, *Rev. Roumaine Chim.*, **15** 1219 (1970).

[2] P. Laszlo and P. von R. Schleyer, *J. Amer. Chem. Soc.*, **86**, 1171 (1964) and the literature cited therein.

[3] E. I. Snyder and B. Franzus, *J. Amer. Chem. Soc.*, **86**, 1166 (1964) and the literature cited therein.

[4] K. L. Williamson, *J. Amer. Chem. Soc.*, **85**, 516 (1963).

[5] K. Tori, Y. Hata, R. Munekuki, I. Takamo, T. Tsuji and H. Tanida, *Canad. J. Chem.*, **42**, 928 (1964).

[6] K. Tori, K. Aono, Y. Hata, R. Munekuki, T. Tsuji and H. Tanida, *Tetrahedron Letters*, **1966**, 9.

[7] H. Simmons, *J. Amer. Chem. Soc.*, **83**, 1657 (1961).

[8] M. Avram, I. Pogany, F. Badea, I. G. Dinulescu and C. D. Nenitzescu, *Tetrahedron Leters*, **1969**, 3851.

2,[1,8,-10] depending on the molecule geometry and the nature of substituents. Some data on chloro-derivatives were recently reported.[11]

DISCUSSION OF SPECTRAL PARAMETERS

Chemical shift. In table 1 are presented the signals of the parent compounds *endo*- and *exo*-benzocyclobuteno-norbornanes **1** and **2**,[7] benzocyclobuteno-norbornenes **3** and **4**,[7] as well as of a series of benzocyclobuteno-norbornane derivatives with electron-withdrawing substituents (Cl, Br, OH, $OCOCH_3$, C = O) in 7, 8 and 9 positions.[1,8,-10] The spectral analysis of hydrocarbons **1** and **2** and of some bromo-derivatives was carried out previously.[1,9]

The H_1H_6 protons give generally rather wide signals due to small coupling constants with neighbouring protons. The position of these signals is influenced by the nature of the groups attached to the neighbouring 7, 8 and 9 carbon, and varies with the *endo* or *exo* configuration of the adjacent benzocyclobutene ring.

In the parent saturated hydrocarbons *endo*-**1** and *exo*-**2** the chemical shifts of the two equivalent bridgehead protons have practically the same value (δ 2.28 and 2.30 ppm).[7] In the case of the alkenes **3** and **4** the signal is shifted towards lower field, namely with 0.64 ppm for the *endo*-**3** and with 0.41 ppm for the *exo*-**4** isomer. The chemical shift values (δ 2.92 for **3** and 2.71 for **4**) are close to that previously found [7] for norbornene (δ 2.78 ppm). In the bromo-olefin **5**, the 9-*syn* bromine atom causes a shift of the signal towards lower field, at δ 3.03 ppm, providing an additional deshielding of 0.73 ppm with respect to the saturated compound **2** and of 0.32 ppm with respect to the alkene **4**.

When a substituent is introduced in the 7-position, the H_1H_6 protons become unequivalent. The H_6 proton is more influenced by the substituent than the more distant H_1 proton; the effect is similar to that observed with norbornenes.[2] Table 2 presents the chemical shifts of the H_1H_6 protons in some compounds 7-*endo*- or *exo*- substituted with bromine and chlorine, relative to the parent hydrocarbon **2**.

It was found that the deshielding caused by a 7-*endo*-halogen is three times stronger for the H_6 proton than for H_1 (compounds **6**, **8**). A more pronounced deshielding of both bridgehead protons is observed in 7-*exo*-substituted compounds (**7**, **10**); however, the difference between H_1 and H_6 is smaller. In the carbonyl compounds **12** and **14** the still more pronounced and nearly equal deshielding of the H_1 and H_6 protons is due to more profound structural changes, especially in hybridization of the bridgehead C—H bond in these strained systems. The effect of hybridization change on CH stretching frequencies has been discussed previously.[12]

---

[9] M. AVRAM, I. POGANY, I. G. DINULESCU, F. CHIRALEU and C. D. NENITZESCU, *Rev. Roumaine Chim.*, **15**, 1207 (1970).

[10] M. AVRAM, L. ENESCU and C. D. NENITZESCU, in press.

[11] R. BAKER, D. E. HALLIDAY and T. J. MASON, *Tetrahedron Letters*, **1970**, 591.

[12] M. AVRAM, GH. D. MATEESCU and I. POGANY, *Rev. Chim.*, **8**, 665 (1962).

Table 1

Chemical shift (δ)

		H_2	H_5	H_1	H_6	H_7	H_9-*anti*	H_9-*syn*	H_8-*exo*	H_8-*endo*	H_7, H_8 olefinic
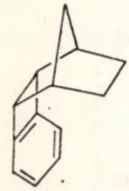	**1**	3.51	3.51	2.28	2.28	1.12	1.63	1.63			
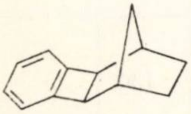	**2**	3.14	3.14	2.30	2.30	1.44	0.97	0.97			
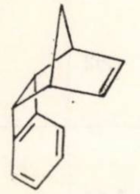	**3**	3.63	3.63	2.92	2.92		1.94	1.94			5.55
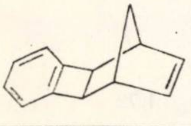	**4**	3.07	3.07	2.71	2.71		0.86	1.28			6.12
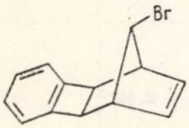	**5**	3.26	3.26	3.03	3.03		3.56				6.20
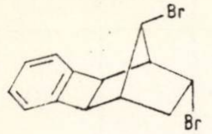	**6**	3.44	4.14	2.42	2.66	4.82	3.6		2.82	1.56	
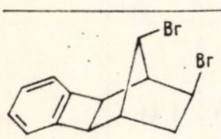	**7**	3.32	3.32	2.52	2.87	3.88	3.67		2.77	2.15	

Table 1 (*continued*)

		H_2	H_5	H_1	H_6	H_7	H_9-*anti*	H_9-*syn*	H_8-*exo*	H_8-*endo*	H_7, H_8 olefinic
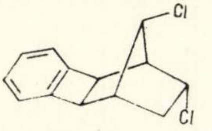	**8**	3.49	4.2	2.42	2.62	4.78	3.6		2.75	1.38	
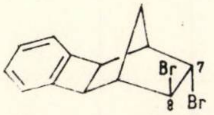	**9**	3.37	3.95	2.6		4.55	1.10	1.78		3.88	
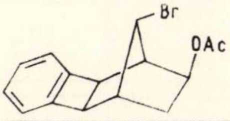	**10**	3.29	3.29	2.55	2.74	4.63	3.54		2.26	1.93	
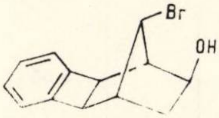	**11**	3.15	3.30	2.65		3.85	3.6		2.20	1.92	
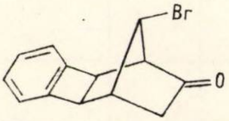	**12**	3.54	3.72	2.95	2.98		3.77		2.78	1.84	
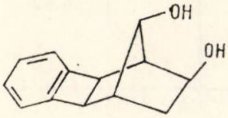	**13**	3.12	3.12	2.30–2.40		3.85	3.6		1.98	1.72	
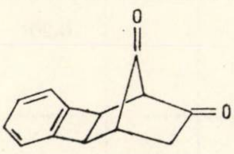	**14**	3.69	3.85	2.93	3.02				2.68	2.49	
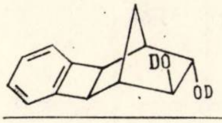	**15**	3.72–3.42		2.47	2.58	3.60	1.4	1.7	4.20		
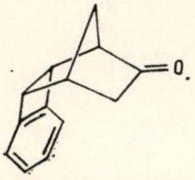	**16**	4.02	4.02	2.82			2.10		1.90	1.44	

Table 2

Deshielding of the protons H_1H_6 with respect to the parent compound 2

Compound No	Substituent		δH_1 ppm	ΔH_1 ppm	δH_6 ppm	ΔH_6 ppm
	7	9_{syn}				
2	—	—	2.30	0	2.30	0
6	Br_{endo}	Br	2.42	+0.12	2.66	+0.36
8	Cl_{endo}	Cl	2.42	+0.12	2.62	+0.32
7	Br_{exo}	Br	2.52	+0.22	2.87	+0.57
10	AcO_{exo}	Br	2.55	+0.25	2.74	+0.44
12	= o	Br	2.95	+0.65	2.98	+0.68
14	= o	= o	2.93	+0.63	3.02	+0.72

The H_2H_5 protons belong at the same time to a norbornane and to a benzocyclobutene system, possessing a benzyl-like character. The position of their signals corresponds to that found in the spectra of 1,2-dialkylbenzocyclobutenes (δ 3.00−3.30 ppm).[13]

A characteristic difference in chemical shift was noted between the *endo* H_2H_5 protons in *exo*-benzocyclobutenes (hydrocarbons **2**, **4** and halo-derivatives **5**—**9**) and the *exo* H_2H_5 protons in *endo*-benzocyclobutenes (**1**, **3**, **16**). Such a difference appeared very clearly when the spectra of **1** and **2** were compared with those of **3** and **4**. As in the case of other norbornane derivatives, the *endo* protons give signals at higher field (δ 3.07−3.26 ppm) than the *exo* protons (δ 3.5−3.6 ppm). The H_{exo}-H_{endo} difference in chemical shift is 0.37 ppm for the isomers **1** and **2**, and 0.56 ppm for the olefins **3** and **4**. The similar difference for the norbornane and norbornene systems is in the range 0.35−0.53 ppm.[2,3]

The shielding of the *endo*H_2H_5 protons in the alkenes **4** and **5** could have been attributed to an anisotropy effect of the neighbouring double-bond. The fact that the saturated hydrocarbons **1** and **2** display differences of the same order of magnitude is better explained by an anisotropy effect of the σ C—C bonds of the norbornane system, similarly to the differenciation of equatorial and axial protons in flexible cyclohexane systems.[2,14]

In the halo-compounds **6** and **8** the presence of a 7-*endo*-bromine brings about a deshielding of the opposite H_5 proton. No such effect is observed with a 7-*exo*-substituent (compound **7**). The H_2 proton is also not affected by these substituents. In the *trans*-7,8-dibromoderivative **9**, the 7-*endo*-bromine causes deshielding of the H_5 proton by a proximity effect, but does not modify the chemical shift of H_2. Here neither the 8-*exo*-bromine appears to have any influence on H_2 (table 3).

---

[13] M. Avram, D. Constantinescu, I. G. Dinulescu and C. D. Nenitzescu, *Tetrahedron Letters*, **1969**, 5215.

[14] N. S. Bacha and D. H. Williams, "Application of NMR Spectroscopy in Organic Chemistry", Holden-Day Inc., 1964, p. 49.

Table 3

Shielding differences between H_2 and H_5

Compound No	δ H_2 ppm	δ H_5 ppm	$\Delta H_5 - H_2$ ppm	$\Delta H_5 - H_2$ Hz
6	3.44	4.14	0.70	42.0
7	3.32	3.32	—	—
8	3.49	4.2	0.71	42.6
9	3.37	3.95	0.58	34.8

The shielding difference between H_2 and H_5 appears also in the ketones **12** and **14**, the neighbouring effects being due here to the orbitals of the 7-carbonyl group.

The olefinic H_7H_8 protons. The signal of the olefinic protons of the *exo*-benzocyclobuteno-norbornenes **2** and **5** appear at δ 6.11 ppm and δ 6.20 respectively. The chemical shift is close to that of norbornene (δ 5.98 ppm). In the case of the *endo*-benzocyclobutene **3** the olefinic signal is shifted to higher field, at δ 5.57 ppm. The different shielding of these protons is due to the vicinity of the benzene ring which includes differently the H_7H_8 protons in its shielding cone.

We calculated, according to Johnson and Bovey's method,[15] the deshielding produced by the benzene ring of the *endo* and the *exo* olefinic protons of benzocyclobutene. The benzene ring contribution to deshielding and to shielding was found to be 0.11 ppm for the *exo* isomer and -0.57 ppm for the *endo* isomer. The values experimentally found for compounds **4** and **3**, as compared to norbornene, are 0.13 ppm and -0.43 ppm respectively, which is in satisfactory agreement with the calculations.

The H_7 protons. In the 7-substituted benzocyclobutenonorbornanes the $H_{7\text{-}endo}$ gives a signal at higher field than $H_{7\text{-}exo}$. The shielding difference *exo-endo* is in the range 0.67–0.94 ppm. In the halides **6** and **8** one may note the influence of the *syn*-9-halogen on the $H_{7\text{-}exo}$ proton. However, the *syn*-9-bromine has no effect on the $H_{7\text{-}endo}$ proton. The electronegativity of the substituent on C_7 has only a minor influence on the chemical shift of H_7. The chemical shift difference of $H_{7\text{-}endo}$ in the dibromide **6** and the dichloride **8** is 0.03–0.04 ppm (1.8–2.4 Hz), although the difference in electronegativity between bromine (E = 2.96) and chlorine (E = 3.25) is 0.29.[16,17] The strong deshielding in the bromo-acetoxy derivative **10**, as compared to the bromo-hydroxy derivative **11** or the dibromide **6**, is mostly due to the change in electronic distribution at H_7 as a result of the acetoxy group resonance, and not to a difference in electronegativity.

---

[15] T. W. Emsley, J. Feeney and L. H. Sutcliffe, "High Resolution Nuclear Magnetic Resonance Spectroscopy", Pergamon Press, 1967, p. 595.

[16] P. Laszlo and P. von R. Schleyer, *J. Amer. Chem. Soc.*, **85**, 2709 (1963).

[17] R. C. Cookson, T. A. Crabb, J. J. Frankel and J. Hudec, *Tetrahedron Suppl*, **7**, 355 (1966).

The geminal $H_{8\text{-}endo}$ *and* $H_{8\text{-}exo}$ *protons* have different chemical shifts. In all compounds, the more shielded $H_{8\text{-}endo}$ proton gives signals at higher field. The chemical shift difference $H_{8\text{-}exo}-H_{8\text{-}endo}$ is in the range 1.37 – 0.19 ppm, depending on the nature and configuration of adjacent 7-substituents. If one takes into account the unsubstituted norbornane systems where the difference $H_{exo}-H_{endo}$ is 0.35 – 0.53 ppm,[2,3] it appears clearly that the 7-substituent has an effect on the chemical shift difference between $H_{8\text{-}exo}$ and $H_{8\text{-}endo}$. In the 7-*endo*-bromo-derivative **6** the $H_{8\text{-}endo}$ signal is shifted with 0.59 ppm towards higher field, with respect to the $H_{8\text{-}endo}$ signal of 7-*exo*-bromo-compound **7**.

The $H_{9\text{-}anti}$ *and* $H_{9\text{-}syn}$ *protons*. The geminal protons of the 9-position form an AB system. In the olefin **3**, the signal of $H_{9\text{-}syn}$, close to the double bond, appears at higher field than that of $H_{9\text{-}anti}$. In the isomeric *exo*-olefin **4** one may note a general shifting of the $H_{9\text{-}anti}-H_{9\text{-}syn}$ signals towards higher field. Both protons undergo shielding, by the double bond and by the benzene ring respectively. An examination of Dreiding models shows that in the *exo*-olefin **4** the $H_{9\text{-}anti}$ proton enters into the shielding cone of the benzene ring, appearing at a higher field than the $H_{9\text{-}syn}$ proton. The difference $H_{9\text{-}anti}-H_{9\text{-}syn}$ is 0.33 ppm for the *endo*-isomer **3** and 0.42 ppm for the *exo*-isomer **4**.

Coupling constants. In table 4 are given coupling constants of protons from the discussed compounds with benzocyclobuteno-norbornane skeleton.

The vicinal couplings $J_{1.2}$ *and* $J_{5.6}$. The vicinal coupling between the bridgehead protons $H_1(H_6)$ and the benzo-cyclobutene protons $H_2(H_5)$ depends on the dihedral angles $H_1-C-C-H_2$ and $H_5-C-C-H_6$ res-respectively. In the case of the *exo* benzocyclobuteno-norbornane isomers which possess *endo* H_2 and H_5 a value of nearly 90° for the dihedral angle can be estimated from the models. In accordance with the classical rules of the coupling constant dependence on the dihedral angle one should expect $J_{1.2} = J_{5.6} = 0$. For the compounds with *exo*-benzocyclobutene skeleton it was actually found that the couplings $J_{1.2}$ and $J_{5.6}$ are zero. However, it should be pointed out that in the diketone **14** the presence of the two carbonyl groups modifies angles and hybridization leading to a small coupling $J_{1.2} = J_{5.6} = 1$ Hz.

By using Dreiding models for the *endo*-benzocyclobuteno-norbornane systems, possessing *exo* oriented $H_2(H_5)$, the angle $H_1-C-C-H_2$ ($H_5-C-C-H_6$) was estimated to be about 35°, which corresponded to a coupling of 5 Hz. The value found experimentally for $J_{1.2} = J_{5.6}$, in the compounds **3** and **16**, was 4 Hz. The existence or the absence of this vicinal coupling is a sure means of extablishing the *endo* or the *exo* configuration of the benzocyclobutene ring with respect to the norbornane moiety, as previously pointed out by Simons.[7]

The vicinal coupling $J_{2.5}$. In the hydrocarbons **1**–**4** and the bromoalkene **5** the magnetic equivalence of the two protons H_2 and H_5 leads to $J_{2.5} = 0$.

A substituent in 7 makes the molecule unsymmetrical and the two protons H_2 and H_5 unequivalent. As it was shown above, only a 7-*endo*-

Table 4

Coupling constants (Hz)

	Comp. No	$J_{1.2}$ $J_{6.5}$	$J_{2.5}$	$J_{1.8}$ $J_{6.7}$	$J_{9\ syn\ 9\text{-}anti}$	$J_{7.9\text{-}anti}$ $J_{8\ 9\text{-}anti}$
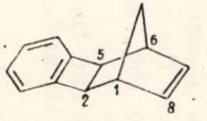	**4**			1.7	9.0	1.7
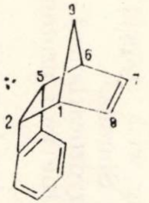	**3**	4.0		1.8	8.4	1.8

Table 4 (*continued*)

Comp. No.	$J_{1.2}$ $J_{6.5}$	$J_{2.5}$	$J_{1.8\text{-}exo}$	$J_{6.7\text{-}exo}$	$J_{8\text{-}exo.8\text{-}endo}$	$J_{9\text{-}syn.\ 9\text{-}anti}$	$J_{8\text{-}endo.9\text{-}anti}$	$J_{7endo.\ 9\text{-}anti}$	$J_{7.8}(exo\text{-}endo)$	
6		4.0	4.0	4.8	13.5		~2.0		4.0	$J_{7\text{-}exo.8\text{-}exo} = 10.0$
7			4.0		13.5		1.3	1.3	4.5	$J_{7\text{-}endo.8\text{-}endo} = 8.0$
8		4.5	4.0	4.2	13.5		2.0		4.0	$J_{7\text{-}exo.8\text{-}exo} = 10.0$
9		3.8		4.2		11.5	3.0		3.0	
10			4.0		14.0		1.2	1.2	3.8	$J_{7\text{-}endo\ 8\text{-}endo} = 7.5$
11		4.0			14.0			1.3		
12		4.2	4.2		18.5					
13					18.0					
14	1.0	4.5	4.0		18.5					$J_{1.8\text{-}endo} = 2.5$
15						12.0				
16	4,2		5,2		18.0					$J_{1.5} = J_{2.6} = 1,8$

halogen is capable of influencing sensibly the chemical shift of the neighbouring H_5 proton; a 7-*exo*-substituent is without effect on this proton. The 7-*endo*-substituted compounds (**6**, **8**, **9**) possess a $J_{2\cdot 5}$ coupling of 3.8–4.5 Hz. This coupling appears also in the carbonyl compounds **12** and **14** (4.2 Hz and 4.5 Hz respectively), but is absent in the 7-*exo*-substituted derivatives.

The protons H_2 and H_5 are members of both the benzocyclobutene and the norbornane moieties. The coupling $J_{2.5}$, although an *endo-endo* coupling, is actually smaller than the *endo-endo* coupling of the true norbornane systems.[2]

The vicinal couplings $J_{1.8}$ *and* $J_{6.7}$. In the alkenes **3** and **4** the olefinic protons H_7, H_8 are coupled with the neighbouring bridgehead protons: $J_{1.8} = J_{6.7} = 1.7$ Hz.

In the 7-*endo* substituted compounds with *exo*-benzocyclobuteno-norbornane skeleton (**6**, **8**, **9**) the coupling between H_6 and $H_{7\text{-}exo}$ is in the range 4.2–4.8 Hz. This coupling does not appear in the 7-*exo* substituted derivatives. The coupling $J_{1.8\text{-}exo}$ is 4.0 Hz for almost all compounds. A higher value, of 5.2 Hz, is encountered in the case of the ketone **16** with *endo*-benzocyclobuteno-norbornane skeleton.

The vicinal couplings $J_{1.8\text{-}endo}$ *and* $J_{6.7\text{-}endo}$. Since the dihedral angles $H_1-C-C-H_{8\text{-}endo}$ and $H_6-C-C-H_{7\text{-}endo}$ are about 90°, the respective couplings between these protons decrease to zero. In the diketon **14** the two carbonyl groups modify the angle $H_1-C-C-H_{8\text{-}endo}$ so that there is a coupling $J_{1.8\text{-}endo}$ of 2.5 Hz.

The vicinal coupling $J_{7\text{-}exo\cdot\ 8\text{-}exo}$. In the 7-*endo* substituted compounds there is a vicinal *exo-exo* $J_{7.8}$ coupling of 10 Hz. In norbornane systems with electron-attracting groups[3,14,16] $J_{exo\text{-}exo}$ is in the range 7.5–9.5 Hz, depending on the substituent electronegativity; for norbornenes the value increases to 9–11 Hz.

The vicinal coupling $J_{7\text{-}endo.8\text{-}endo}$. The *endo-endo* $J_{7.8}$ coupling has, like for norbornanes,[2-4] a lower value (5.6–7.7 Hz). For the dibromo-derivative **7** this coupling reaches 8.0 Hz, while for the bromo-acetoxy compound **10** it is 7.5 Hz, slightly increased as compared to unsubstituted systems.

The vicinal couplings $J_{7\text{-}exo.8\text{-}endo}$ *and* $J_{7\text{-}endo.8\text{-}exo}$. The *trans* coupling *exo-endo* $J_{7.8}$ would be expected to have lower values (for norbornanes it is in the range 2.1–5.8 Hz, depending on the substituents). For the *trans*-7.8-dibromide **9** this is 3.0 Hz. For the 7-*endo*-halides $J_{7\text{-}exo.8\text{-}endo}$ is 4.0 Hz. In the case of the 7-*exo*-substituted derivatives the coupling $J_{7\text{-}endo.8\text{-}exo}$ is 4.5 Hz (compound **7**) and 3.8 Hz (compound **10**).

The geminal couplings. In the molecules studied there are geminal couplings between the H_9 protons of the bridge as well as between H_8 protons of the norbornane ring. These two couplings differ in their values.[17]

$J_{9\text{-}syn.9\text{-}anti}$. The geminal protons of the 9-position in the *endo* olefin **3** form an AB system with J = 8.4 Hz. In the *exo*-isomer **4** $J_{9\text{-}syn.9\text{-}anti}$ is 9.0 Hz. For the *trans*-7,8-disubstituted compounds **9** and **15**, with *exo*-benzocyclobuteno-norbornane skeleton, the coupling constant reaches 11.5 Hz and 12.0 Hz respectively.

$J_{8\text{-}endo.8\text{-}exo}$. The geminal coupling of the protons of the 8-position is only slightly influenced by the nature of the adjacent 7-substituents. For all 7-chloro, -bromo or -acetoxy compounds, irrespective of the configuration of the substituent, the coupling $J_{8\text{-}endo.8\text{-}exo}$ is 13.5–14.0 Hz. In the carbonyl compounds **12, 14, 16** this coupling is 18.5 Hz. The J^{π} contribution of the carbonyl group in the rigid system leads to a higher value of J.[14] This J^{π} contribution of about 4.5 Hz indicates the symmetrical position of the methylene group of C_8 with respect to the carbonyl double bond.

Long range coupling. In the benzocyclobuteno-norbornenes **3** and **4** the long range coupling between the olefinic H_7H_8 protons and the $H_{9\text{-}anti}$ proton is 1.7 Hz. Since $J_{1.8} = J_{6.7}$ the signal of the H_7H_8 protons appears, at 60 MHz, as a triplet.

In the 9-*syn*-7-*endo*-disubstituted benzocyclobuteno-norbornanes **6** and **8** there is a long range coupling of 1.2–2 Hz between the $H_{9\text{-}anti}$ and the $H_{8\text{-}endo}$ protons. In the 9-*syn*-7-*exo*-disubstituted compounds **7, 10, 11** and **13**, in addition to the $J_{9\text{-}anti.8\text{-}endo}$ coupling of 1.2 Hz the $H_{9\text{-}anti}$ proton presents a long range coupling of 1.2–1.3 Hz with the $H_{7\text{-}endo}$ proton. This coupling is very useful for establishing the configuration of 7- and 9-substituents. In the *trans*-7, 8-dibromide **9** the $H_{8\text{-}endo}$ proton has a higher coupling, namely 3.0 Hz. This coupling is absent in the 9-*syn*-7-*endo*-disubstituted compounds (**6** and **8**).

EXPERIMENTAL

The NMR spectra of all the compounds (3–16) were recorded on a Varian A-60A spectrometer of 60 MHz in $CDCl_3$ solution. Some of the couplings were identified by means of the double resonance method.[1,9,10]

CONCLUSIONS

The spectral comparison of the compounds studied (substituted benzocyclobuteno-norbornanes) with norbornanes, norbornenes and similar compounds from the literature, revealed that the benzocyclobutene ring and the 7- and 9-substituents do not distort appreciably the norbornane skeleton. However, significant changes were found for the carbonyl derivatives.

The presence of electron-withdrawing substituents in the 9-*syn*- and the 7-*exo*- or 7-*endo*-positions leads to characteristic changes in the NMR spectra as compared to the spectra of the parent hydrocarbons.

The substituents in the 7-position reduce the symmetry of the molecule so that the H_1H_6 protons and the H_2H_5 protons become unequivalent, presenting different chemical shifts. At the same time, this leads to an additional vicinal coupling between the H_2 and H_5 protons.

Revue Roumaine de Chimie, 15, 1777–1783 (1970)

ÜBER DIE DARSTELLUNG DES 3,7-DICHLORPHENOTHIAZINS DURCH DIE REDUKTION SEINES OXIDES MIT STANNOCHLORID

D. CHRISTOV und N. NENOV

von der Physikalischen Fakultät der Universität „Kliment Ochridski" Lehrstuhl für Atomphysik, Sofia 26, Boul. Ivanov, 1, Bulgarien

Eingegangen am 11. Februar 1970

Es wird vorgeschlagen, die Reduktion des 3,7-Dichlorphenthiazin-5-Oxides mit Stannochlorid in homogenem Medium zu führen. Das erhaltene 3,7-Dichlorphenothiazin wird bequem durch eine einmalige Entfärbung seiner Benzollösung mittels aktivem Aluminiumoxid gereinigt. Die Ursachen der in der Literatur existierenden Gegensätze bezüglich der tatsächlichen Schmelzpunkte des Dichlorphenothiazins und seines Oxides sind festgelegt.

Die Darstellung eines Dichlorderivates des Phenothiazins wurde zum erstenmal von Unger und Hofmann[1] gemeldet. Dabei zeigt das Dichlorphenothiazin, in Abhängigkeit seiner Darstellung zwei Schmelzpunkte: 225–227° (unter Zersetzung) und 222°, was von den Autoren mit der Bildung von zwei Isomeren erklärt wurde.

Die späteren Untersuchungen anderer Autoren bestätigen nicht die Existenz von Dichlorphenothiazin-Isomeren. Ausgehend von der Methode von Page und Smiles[2] zur Darstellung des Tetrachlorphenothiazins durch die Oxidation von Phenothiazin mit Wasserstoffsuperoxid in einem mit Chlorwasserstoff gesättigten Alkohol-Medium, wählt Antonov[3] versuchsmäßig solche Reaktionsbedingungen, bei welchen der Prozeß der Bildung von Dichlorphenothiazinoxid mit Schmelzpunkt 232–233° aufhört. Bei der Reduktion einer Suspension des letzteren mit Stannochlorid wurde Dichlorphenothiazin mit einem Schmelzpunkt von 222° (unter Zersetzung) erhalten, das man später als 2,7-Dichlorphenothiazin identifizierte.[4] Derselbe Autor hält die Existenz von Dichlorphenothiazin mit einem Schmelzpunkt von 225–227° für fragwürdig und schließt die Möglichkeit nicht aus, daß das von Unger und Hofmann mit diesem Schmelzpunkt beschriebene Produkt mit Oxiden des Mono- und Dichlorphenothiazins verunreinigt ist. Beim Zugeben von Dichlorphenothiazinoxid zum Dichlorphenothiazin sollten Gemische erhalten werden, die bei 225—227° schmelzen.

---

[1] O. Unger u. K. A. Hofmann, *Ber. dtsch., chem. Ges.*, **29**, 1365 (1896).

[2] H. J. Page u. S. Smiles, *J. Chem. Soc.*, **97**, 1118 (1910).

[3] D. S. Antonov, Dissertat, Chemisch Technologisches Institut, Moskau 1950; *Bull. Institut chim. Acad. bulg. Sci.*, **2**, 75 (1953).

[4] D. S. Antonov, *C.R. Acad. bulg. Sci.*, **9**, 57 (1956).

Nach Antonov [3] ist die Darstellung des Dichlorphenothiazins durch eine direkte Chlorierung von in Chloroform aufgelöstem Phenothiazin [1] kein zuverlässiges Verfahren. Im Gegensatz zu dieser Behauptung haben aber Bodea und Răileanu [5] durch die Chlorierung von Phenothiazin mit Chlor in Essigsäure 3,7-Dichlorphenothiazin mit guter Ausbeute und mit einem Schmelzpunkt von 226—227° erhalten. Bei der Oxidation des Dichlorphenothiazins mit Kalium-Bichromat in Wasser-Azetonmedium, haben dieselben Autoren [6] 3,7-Dichlorphenothiazin-5-Oxid mit einem Schmelzpunkt von 242—243° erhalten. Hier ist zu bemerken, daß die von Antonov [3,4] erhaltenen 2,7-Dichlorphenothiazin (I) und sein Oxid (II), bei welchen, für das Schwefelatom die Stelle 9 angezeigt ist, identisch mit den von Bodea und Răileanu [5,6] erhaltenen 3.7-Dichlorphenothiazin (III) und sein Oxid (IV) sind, wobei bei den letzteren für das Schwefelatom die Stelle 5 angezeigt ist.

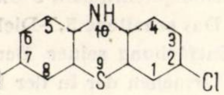

Smp 222°

I

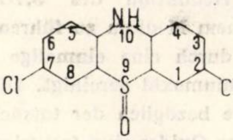

Smp 232-233°

II

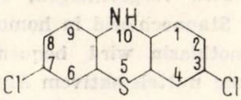

Smp 226-227°

III

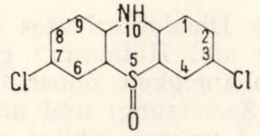

Smp 242-243°

IV

In beiden Fällen ist für das Stickstoffatom die Stelle 10 angewiesen.

Von allem bisher dargelegten ist ersichtlich, daß sich die Literaturangaben für die Schmelzpunkte des Dichlorphenothiazins und seines Oxides widersprechen. Die angegebenen Schmelzpunkte sind unkorrigiert, was die Möglichkeit für einen Vergleich noch mehr beschränkt. Bei der Darstellung des Dichlorphenothiazins und seines Oxides nach dem Verfahren von Antonov haben wir festgestellt, daß die Reaktionsprodukte bei ihrer sorgfältigen Reinigung höher liegende Schmelzpunkte aufweisen, welche mit diesen von Bodea und Răileanu angegebenen, in guter Vereinbarung stehen. Wenn jedoch berücksichtigt wird, daß Antonov in seiner Dissertation[3] der Frage des Schmelzpunktes des Dichlorphenothiazins besondere Aufmerksamkeit schenkt und die Möglichkeit, daß er höher als 222° liegt, ausschließt, ist die Notwendigkeit, die Ursachen dieser Gegensätze zu klären, leicht verständlich. Im Verlauf der Untersuchungen, Gegenstand dieser Mitteilung, wurden am Verfahren von Antonov [3] eine ganze Reihe von Unzulänglichkeiten bezüglich der Reduktion des Dichlorphenothiazinoxides in heterogenem Medium bei willkürlich gewählter Temperatur und bei längerer Dauer des Prozesses (5 bis 6 Stunden), sowie bezüglich der Reinigungsart und des Reinigungsgrades des rohen Dichlorphenothiazins festgestellt. Nach einer systematischen Untersuchung wurde festgestellt, daß die Reduktion des Dichlorphenothiazinoxides mit Stannochlorid in viel kürzerer Zeit (30 Minuten) vor sich geht, wenn die Reaktion beim Erhitzen in homogenem Medium verläuft. Die Reinigung des rohen Dichlorphenothiazins geschieht leicht durch eine einmalige Entfärbung seiner Benzollösung mit aktivem Aluminiumoxid.

---

[5] C. Bodea u. M. Răileanu, *Studii şi Cercetări Chim.* (*Fil. Cluj*), **9**, 162 (1958).

[6] C. Bodea u. M. Răileanu, *Liebigs Ann. Chem.*, **614**, 175 (1968).

ERGEBNISSE UND DISKUSSION

Zuerst sollte die Frage über die tatsächlichen Schmelzpunkte des 3,7-Dichlorphenothiazins und seines Oxides gelöst werden. Aus Tabelle 1 ist ersichtlich, daß das 3,7-Dichlorphenothiazin-5-Oxid einen Schmelzpunkt hat, der um 10° höher als der von Antonov angegebene liegt und der praktisch mit dem von Bodea und Răileanu bestimmten, zusammenfällt. Das Ergebnis von Antonov ist entweder auf eine unzulängliche Reinigung des Präparats, oder auf einen groben Fehler bei der Bestimmung des Schmelzpunktes zurückzuführen. Das Produkt der dritten und vierten Umkristallisation (Tabelle 1) schmilzt bei der von Antonov angegebenen Temperatur von 232–233°, erst wenn es bei dieser Temperatur im Verlauf von 4 bis 5 Minuten erhitzt wird. Das ist leicht erklärlich, wenn man berücksichtigt, daß eine teilweise thermische Zersetzung des Oxides noch lange vor seiner Schmelzung beginnt.

Tabelle 1

Reinigung des 3,7-Dichlorphenotiazin-5-Oxides

Nr. der Umkristallisierung	Umkristallisierungsweise	Schmelzpunkt in °C des Produktes der betreffenden Umkristallisierung	
		unkorrigiert	korrigiert
1	Aus Äthanol bei zweimaligem Auskochen der Lösung mit aktiver Kohle im Verlauf von je 30 Minuten	236–238	241–243
2	Aus Äthanol bei einmaligem Auskochen der Lösung mit aktiver Kohle im Verlauf von 30 Minuten	240–241	245–246
3	Aus Äthanol	241–242	246–247
4	Aus Äthanol	241–242	246–247

Tabelle 2 zeigt, daß der Schmelzpunkt des 3,7-Dichlorphenothiazins in Abhängigkeit von den verschiedenen Reinigungsverfahren bis zu 225–227° steigt (unkorrigiert). Bei Entfärbung der Benzollösung mit aktivem Aluminiumoxid (Probe 3) weist das Produkt schon nach seiner ersten Umkristallisierung den Schmelzpunkt der reinen Substanz auf. Diese Reinigungsart ist besonders geeignet für präparative Zwecke, da sie Zeit und Lösungsmittel erspart. Für die Erschmelzung des reinen Dichlorphenothiazins bei 221–222° ist es notwendig dasselbe bei dieser Temperatur 2 Minuten lang zu halten. Bei etwa 215° wird die Verbindung trübe. Es ist zu bemerken, daß Antonov keinen Schmelzpunkt des Dichlorphenothiazins im Intervall angibt, obwohl die Verbindung unter Zersetzung schmilzt. Die von ihm vorgeschlagene Abdestillierung des Lösungsmittels bis zum trockenen Zustand noch bei der ersten Umkristallisierung des rohen Dichlorphenothiazins aus Benzol ist unzweckmäßig, da dabei eigentlich keine Reinigung zustande kommt. Andere von uns durchgeführte Experimente zeigten, daß nach der ersten Umkristallisierung aus Benzol,

Tabelle 2

Reinigung des 3,7-Dichlorphenothiazins, erhalten durch Reduktion des Oxides in heterogenem Medium[3]

Proben-Nummer	Umkristallisierungsnummer	Umkristallisierungsart	Schmelzpunkte in °C des Produktes der Umkristallisierung	
			unkorrigiert	korrigiert
1	1.1	Aus Benzol	220–222	224–226
	1.2	Aus Äthanol mit Zugabe von 2–3 Tropfen Lösung aus 25%iger Stannochloridlösung in 25%iger alkoholischer Salzsäure	220–222	224–226
	1.3	Wie bei der Umkristallisierung 1.2	223–224	227–228
	1.4	Aus Äthanol	225–227	229–231
	1.5	Aus Äthanol	225–227	229–231
2	2.1	Aus Benzol	210–214	213–217,5
	2.2	Aus Benzol	215–217	218,5–221
	2.3	Aus Benzol	222–224	226–228
	2.4	Aus Benzol	225–227	229–231
	2.5	Aus Benzol	225–227	229–231
3	3.1	Aus Benzol bei Reinigung der Lösung mit aktivem Aluminiumoxid	225–227	229–231
	3.2	Aus Benzol	225–227	229–231

der Schmelzpunkt des auskristallisierten Dichlorphenothiazins sich in Abhängigkeit von dem Abdestillierungsgrad des Lösungsmittels von 210° bis 222° (unkorrigiert) ändert. Die Zugabe einiger Tropfen Stannochloridlösung zu der alkoholischen Dichlorphenothiazinlösung (Umkristallisierung 1.2 und 1.3) bildet noch einen Grund für das Erhalten eines niedrigeren Schmelzpunktes für das Dichlorphenothiazin von Antonov. Wenn das Produkt aus der Umkristallisation 1,5 noch einmal aus Äthanol unter Zugabe von einigen Tropfen Stannochloridlösung umkristallisiert wird, so erhält man wieder Dichlorphenothiazin mit einem niedrigeren Schmelzpunkt- nämlich 222° bis 224° (unkorrigiert).

Die Elementaranalyse der Präparate von Dichlorphenothiazin und Dichlorphenothiazinoxid, die die von uns bestimmten konstanten Schmelzpunkte aufweisen, bestätigt auch die Reinheit derselben. Die Vergleichsuntersuchungen der Infrarotspektren der Produkte aus den verschiedenen Umkristallisierungen der Probe 2 (Tabelle 2) zeigen, daß mit der Erhöhung des Schmelzpunktes, die Beimengung von Dichlorphenothiazinoxid bis Spuren herabfällt (Umkristallisierungen 2.4 und 2.5), die keine Wirkung mehr darauf haben. Trotzdem wurden auch Mischproben des Dichlorphenothiazins mit wachsenden Mengen von Dichlorphenothiazinoxid vorbereitet. Es wurde festgestellt – im Gegensatz zu der Behauptung von Antonov (Tabelle 3), daß die Beimengungen von Dichlorphenothiazinoxid den Schmelzpunkt des Dichlorphenothiazins nicht erhöhen, sondern herabsetzen. Die Beimengung von Dichlorphenothiazinoxid in Mengen von 0,01% haben keine Wirkung auf die Höhe des Schmelzpunktes des Dichlorphenothiazins, bestimmt nach dem konventionellen Verfahren in Schmelzröhrchen mit dem Thiele-Apparat.

Tabelle 3

Schmelzpunkte der Gemische aus 3,7-Dichlorphenothiazin (Schmelzpunkt 225–227° unkorrigiert) und dessen Oxid (Schmelzpunkt 241–242° unkorrigiert)

Nr. des Gemisches	Zusammensetzung des Gemisches in mg		Gehalt der Oxide im Gemisch in %	Schmelzpunkt des Gemisches in °C	
	3,7-Dichlorphenothiazin	3,7-Dichlorphenothiazin 5-Oxid		unkorrigiert	korrigiert
1	9999	1	0,01	225–227	229–231
2	999	1	0,1	223–225	227–229
3	990	10	1	221–223	225–227
4	900	100	10	214–216	217,5–219,5

Antonov [3] reduziert das Dichlorphenothiazinoxid mit in alkoholischer Salzsäure gelöstem Stannochlorid bei einer Temperatur von 50–60° im Verlauf von 5 bis 6 Stunden. Die lange Dauer des Prozesses erklärt er damit, daß das Oxid in Form von Niederschlag ist, d.h. daß die Reduktion in einem heterogenen Medium vor sich geht. In Wirklichkeit ist aber diese Zeit von 5–6 Stunden willkürlich gewählt. Beim Übergießen des Dichlorphenothiazinoxides mit einer Stannochloridlösung setzt eine exothermische Reaktion an, die Temperatur steigt bis auf 66–68° an und weiter finden keine äußeren Änderungen statt. Bei der Umkristallisierung des rohen Dichlorphenothiazins aus der Probe 1 (Tabelle 4), auf dem Filter bleibt eine kleine Menge unreagiertes Dichlorphenothiazinoxid. Wenn das Reaktionsgemisch im Laufe von 30 Minuten erhitzt wird (Proben 2 und 3), so löst sich der Niederschlag fast vollständig auf und die Reduktion findet im homogenen Medium statt. Von der abgekühlten Lösung kristallisiert nach einigen Stunden ein voluminöser Niederschlag von Dichlorphenothiazin aus, der sich in Benzol vollständig lösen läßt. Probe 3 zeigt, daß die Reduktion des Oxides auch ohne seine Isolierung aus dem Reaktionsgemisch und ohne Reinigung vor sich gehen kann. Das ist besonders vorteilhaft von präparativem Standpunkt aus.

Tabelle 4

Vergleich von verschiedenen Reduktionsbedingungen des 3,7-Dichlorphenothiazin-5-Oxids mit Stannochlorid

Nr. der Probe	Reduktionsbedingungen	Ukristallisierungsart	Unkorrig. Schmelzpunkt des Produktes der betreffenden Umkristallisierung in °C					Korrigierter Schmelzpunkt d. Produktes der letzten Umkristallisierung in °C
			I	II	III	IV	V	
1	Das Oxid wird übergossen mit einer Lösung von Stannochlorid in alkoholischer Salzsäure laut [3] und wird nach 10 Min. (ohne Erhitzen) filtriert	Wie Probe 3 aus Tabelle 2	225–227	225–227	–	–	–	229–231
2	Das Oxid wird übergossen mit Stannochloridlösung laut [3] und wird erhitzt beim Rückkühler 30 Min. über siedendem Wasserbad	Wie Probe 3 aus Tabelle 2	225–227	225–227	–	–	–	229–231
3	Zum Dichlorphenothiazinoxid, erhalten aus 20 g Phenothiazin laut [3] ohne Filtrierung wird 45 g $SnCl_2 \cdot 2H_2O$ zugeben und das Ganze wird bei Rückkühler 30 Min. über siedendem Wasserbad erhitzt	Wie Probe 3 aus Tabelle2	225–227	225–227	–	–	–	229–231
4	Wie bei Probe 3	aus Benzol	210–215	217–220	222–224	225–227	225–227	229–231

Antonov [3] nimmt an, ohne darüber irgendwelche Beweise anzuführen, daß die Reduktion des Dichlorphenothiazinoxides mit Stannochlorid beim Erhitzen zum Abspalten von Chlor-Atomen führen kann. Die Schmelzpunkte der Produkte der verschiedenen Umkristallisierungen der Probe 4 (Tabelle 4), reduziert beim Erhitzen, fallen aber mit diesen der Produkte der betreffenden Umkristallisierungen der Probe 2 (Tabelle 2), reduziert nach den Hinweisen von Antonov, zusammen. Daraus folgt, daß im rohen Dichlorphenothiazin, erhalten durch Reduktion in homogenem Medium (beim Erhitzen), keine anderen Beimengungen enthalten sind (in Mengen, die den Schmelzpunkt beeinflussen können), die im Produkt, erhalten bei der Reduktion in heterogenem Medium, fehlen. Die Infrarotspektren der Präparate in Tabelle 4 deuten ebenfalls nicht auf das Vorhandensein solcher Beimengungen.

BESCHREIBUNG DER VERSUCHE

Das 3,7-Dichlorphenothiazin-5-Oxid wurde nach der Anweisung in [3] dargestellt. Die Umkristallisierung des Dichlorphenothiazins und des Dichlorphenothiazinoxides (Tabelle 1 und 2) erfolgte beim Erhitzen. Für jede nachfolgende Umkristallisierung wurde nur das Produkt benutzt das beim Abkühlen der Lösung kristallisierte, und zwar, ohne Abdestillierung des Lösungsmittels. Die Reinigung der Benzollösung des rohen Dichlorphenothiazins erfolgte durch chromatographisches mit Salzsäure aktiviertes Aluminiumoxid. Für diesen Zweck wird zu der heißen Benzollösung unter Rühren portionenweise aktives Aluminiumoxid solange zugegeben, bis sich das letzte nicht mehr färbt und die Lösung eine dunkle, orange-rötliche Farbe annimmt. Das gefärbte Aluminiumoxid wird filtriert und bei der Abkühlung kristallisiert reines Dichlorphenothiazin aus. Für präparative Zwecke können selbstverständlich aus dem Filtrat noch zusätzliche Mengen der Substanz isoliert werden.

Die Gemische aus Dichlorphenothiazin und seinem Oxid wurden vorbereitet, indem man die in Tabelle 3 angezeigten Mengen in Äthanol auflöste und das Lösungsmittel in Wasserbad bis zur Trockene abdestillierte.

Die Bestimmung des Schmelzpunktes erfolgte im Kapillarröhrchen mit dem Thiele-Apparat, bei Einhaltung der betreffenden Anforderungen, die das Erhalten von richtigen und reproduzierbaren Ergebnissen sichern. Die Flüssigkeit im Apparat — flüssiges Paraffin — wurde nach einer Anweisung von Fischer [7] derweise erhitzt, daß die Temperatur um 1° in etwa 2 bis 3 Sekunden stieg. Ungefähr 5 bis 10° vor dem Schmelzen verzögert man die Erhitzung etwas ohne daß aber ein Stillstand oder eine Herabsetzung der Temperatur erfolgte. Als Schmelzpunkt unter Zersetzung wird der Temperaturbereich zwischen der Benetzung der Substanz (das erste Auftauchen von Flüssigkeit im Kapillarrohr) und der vollständigen Schmelzung mit der die Zersetzung beginnt, bezeichnet. Beim Beginn der Zersetzung darf das Quecksilber im Thermometer nicht steigen. Dieselben Ergebnisse werden erhalten, auch wenn das Thermometer, zusammen mit dem Schmelzröhrchen mit der Substanz, in das bis auf 200—210° erhitzte Paraffin getaucht wird und wie oben angegeben, erhitzt wird, nachdem das Quecksilber zu steigen aufhört.

Die Schmelzpunkte sind mit Hilfe der Eichkurve des Thermometers korrigiert.

Die Infrarotspektren wurden aufgenommen unter Anwendung der Preßtechnik zur Vorbereitung der Prüfmuster. Als Trägerstoff wurde Kaliumbromid benutzt, da sich das Oxid in Tetrachlormethan und in den anderen geeigneten Lösungsmitteln nicht lösen läßt.

---

[7] E. Fischer, *Ber. dtsch. chem. Ges.*, **41**, 76 (1908).

Revue Roumaine de Chimie, 15, 1785–1791 (1970)

ACRIDONE. XXXVI*
THE CHLORINATION OF IODO-ACRIDONES

MARIA IONESCU, ILEANA GOIA and M. VLASSA

Institute of Chemistry of the Academy, Cluj, Str. Donath 59–65

Received August 30, 1970

The action of chlorine on iodo-acridones was investigated. The vibrational spectra of halogenated acridones (chloro, bromo, iodo) was performed and different characteristic absorptions (νC=0, ν C=S, νNH, γCH) were identified.

In previous reports [1,2] of this series which dealt with the chlorination reactions of acridone, with good results mono- di- and tetra chloro-acridones were obtained the latter being the highest chlorinated derivative.

The chlorination process with gaseous chlorine of iodo-acridone derivatives, namely 2-iodo-(II), and 2,7-diiodo-acridone (III) (in different conditions of time, temperature, solvent, and concentration) leads to a wide variety of mixed halogenated acridone derivatives (iodo-chloro) and unitary halogenated acridone derivatives (only chloro) according to scheme 1 and tables 1, 2.

At the beginning the chlorine acts on the unoccupied positions of molecule, favourable to the chlorination, C_7, C_4, C_5. In the case of mono-iodo-derivative – depending on the reaction conditions – it acts first on C_7 forming 2-iodo-7-chloro-acridone (VII) and afterwards on C_4 and C_5 forming 2-iodo-7, 4, 5-trichloro-acridone (VI). In the case of diiodo-acridone, chlorine acts on C_4 and C_5, and 2,7-diiodo-4,5-dichloro-acridone (V) is obtained. A further action of the chlorine on these derivatives leads to a substitution process of the iodine from the molecule by the chlorine resulting thus first 2-iodo-4, 5, 7-trichloro-acridone (VI) and then 2, 4, 5, 7-tetrachloro-acridone (IV). Thus we could obtain the same mixed halogen-substituted acridones (iodo-chloro) as in the iodination reactions involving ICl reagent and so we could notice that these reactions developed in the same manner.* As in case of acridone chlorination no other more chlorinated derivative than tetra was isolated.

A detailed IR spectroscopic study of these series of unitary and mixed halogen substituted acridones (chloro, bromo, iodo) was carried out. The characteristic vibrations $\nu C = 0$, $\nu C = S$, νNH, γCH as well as the influence of the nature, position and number of halogen atoms in acridone molecule over these vibrations were identified.

---

* See XXXV. I. Goia and M. Ionescu, *Rev. Roumaine Chim.*, **8**, 1233 (1970).

[1] M. Ionescu and I. Goia, *Studii şi Cercetări Chim. Fil. Cluj*, **10**, 335 (1959).

[2] M. Ionescu and I. Goia, *Rev. Chim. Acad. R.P.R.*, **5**, 85 (1960).

Schema I

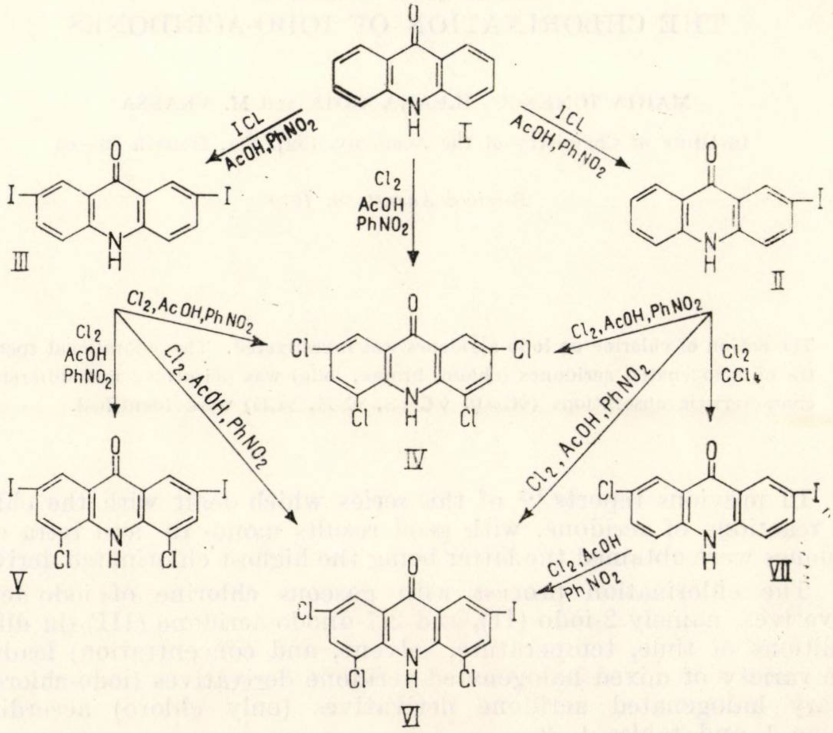

By introducing halogens (chloro, bromo, iodo), substituents having lone-pair electrons into acridone (thioacridone) nucleus as a result of their interaction with nucleus, the polarity of the carbonyl (thiocarbonyl) bond increases. Consequently a lower frequency shift of carbonyl (thiocarbonyl) vibration takes place in the case of mono-, di-, and tri-halogen-acridones (thioacridones), the lowest being with the iodo-acridone derivatives. (See tables 3,4).

In the IR absorption spectra of the unitary and mixed mono-, di-, and tri-halogen-acridone (thioacridone) there appears a relative large number of intensive and distinguished νNH vibrations (9–12) between 2600–3300 cm^{-1}, which indicate the presence of strong molecular associations as in the case of acridone (thioacridone) [3] also confirmed by a different behaviours (m.p. and solubility); the unitary and mixed tetra-halogenated acridones show only one band νNH at $\sim$3340 cm^{-1}, indicating the lack of such molecular associations (other behaviours : lower m.p. and higher solubility than the former).

---

[3] H. Mantsch, I. Goia and M. Ionescu, *Omagiu Raluca Ripan*, ed. Academiei, România, **1966**, 353; *Chem. Abstr.*, **67**, 73010 (1967).

Table 1

Chlorination of iodo-acridones with Cl_2 in acetic acid

Compound	g	Solvent ml	Temp. °C	Time m	Reaction product	Yield g
2-Iodo-acridone (II)	0.5	100	75	10	2-iodo-7-chloro-acridone (VII)	0.05
					2-iodo-4, 5, 7-trichloro-acridone (VI)	0.05
					2, 4, 5, 7-tetrachloro-acridone (IV)	traces
2-Iodo-acridone (II)	0.5	100	75	20	2-iodo-7-chloro-acridone (VII)	0.05
					2-iodo-4,5 7,-trichloro-acridone (VI)	0.10
					2, 4, 5, 7-tetrachloro-acridone (IV)	0.10
2-Iodo-acridone (II)	0.5	150	75	30	2-iodo-4, 5, 7-trichloro-acridone (VI)	0.20
					2, 4, 5, 7-tetrachloro-acridone (IV)	0.20
2,7-Diiodo-acridone (III)	0.5	100	75	20	2,7-diiodo-4,5-dichloro-acridone (V) .	0.10
					2-iodo-4, 5, 7-trichloro-acridone (VI)	0.10
					2, 4, 5, 7-tetrachloro-acridone (IV)	0.05
2,7-Diiodo-acridone (III)	0.5	150	75	30	2,7-diiodo-4-chloro-acridone	0.05
					2,7-diiodo-4,5-dichloro-acridone (V)	0.20
					2-iodo-4, 5, 7-trichloro-acridone (VI)	0.07
					2, 4, 5, 7-tetrachloro-acridone (IV)	0.05
2,7-Diiodo-acridone (III)	0.5	150	75	45	2,7-diiodo-4,5-dichloro-acridone (V)	0.20
					2-iodo-4, 5, 7-trichloro-acridone (VI)	0.20
					2, 4, 5, 7-tetrachloro-acridone (IV) .	0.05
2,7-Diiodo-acridone (III)	0.5	150	boiling	90	2,7-diiodo-4,5-dichloro-acridone (V)	0.10
					2-iodo-,4 ,5, 7-trichloro-acridone (VI)	0.20
					2, 4, 5, 7-tetrachloro-acridone (IV)	0.10

Table 2

Chlorination of iodo-acridones with Cl_2 in $PhNO_2$ and CCl_4

Compound	g	Solvent ml.	Temp. °C	Time m	Reaction product	Yield g
2-Iodo-acridone (II)	0.5	$PhNO_2$50	75	45	2-iodo-4, 5, 7-trichloro-acridone (VI)	0.10
					2,4,5, 7-tetrachloro-acridone (IV)	0.20
2,7-Diiodo-acridone (III)	0.5	$PhNO_2$50	75	45	2,7-diiodo-4, 5-dichloro-acridone (V)	0.05
					2-iodo-4, 5, 7-trichloro-acridone (VI)	0.05
					2, 4, 5, 7-tetrachloro-acridone (IV)	0.10
2-Iodo-acridone (II)	0.5	$CCl_4$80	boiling	40	2-iodo-acridone (II)	0.35
					2-iodo-7-chloro-acridone (VII)	0.10

Table 3

νNH and νCO vibrations of the halogenated acridones

No	-acridone	νNH cm^{-1}			νC = 0	Δν C = 0
		no. of bands 2800 – 3400	the most intensive	the highest		
1	unsubstituted	12	2940	3270	1638	0
2	2-chloro-	12	3120	3265	1641 1623	+ 3
3	2-bromo-	11	3130	3272	1641 1628	+ 3
4	2-iodo-	9	3160	3265	1629 1615	– 9
5	2,7-dichloro-	9	3160	3260	1634	– 4
6	2,7-dibromo-	9	3160	3255	1629	– 9
7	2,7-diiodo-	8	3160	3250	1625 1607	–13
8	2-chloro-7-iodo-	9	3180	3260	1628 1620	–10
9	2, 7, 4-trichloro-	9	3185	3270	1625	–13
10	2,7-diiodo-4-chloro-	9	3267	3267	1619 1616	–19
11	2, 4, 5, 7-tetrachloro-	1	3342	—	1664	+26
12	2, 4, 5, 7-tetrabromo-	1	3347	—	1647	+ 9
13	2, 7-dichloro-4,5-dibromo-	1	3352	—	1646	+ 8
14	2,7-dibromo-4,5-dichloro-	1	3346	—	1655	+17
15	2,7-diiodo-4,5-dichloro-	1	3356	—	1642 1635	+ 4
16	2-iodo-4, 5, 7-trichloro-	1	3355	—	1649 1640	+11
17	N-methyl-	—	—	—	1632	– 6

Table 4

νNH and νCS vibrations of the halogenated thioacridones

No	-thioacridone	νNH			νC = S	ΔνC = S
		no of bands 2800 – 3400	the most intensive	the highest		
1	unsubstituted	14	2960	3255	1215	0
2	2-chloro-	12	3265	3265	1209 1192	– 6
3	2-bromo-	11	3255	3255	1209 1191	– 6
4	2-iodo-	11	3265	3265	1209 1193	– 6
5	2,7-dichloro-	9	3275	3275	1203	–12
6	2,7-dibromo-	9	3265	3265	1201	–14
7	2,7-diiodo-	8	3275	3275	1203	–12
8	2-chloro-7-iodo-	9	3275	3275	1201	–14
9	2, 4, 7-trichloro-	9	3270	3270	1205	–10
10	2,7-diiodo-4-chloro-	8	3360	3360	1202	–13
11	2, 4, 5, 7-tetrachloro-	1	—	3368	1226 1204	+11
12	2, 4, 5, 7-tetrabromo-	1	—	3324	1219 1199	+ 4
13	2,7-dichloro-4,5-dibromo-	1	—	3327	1218 1200	+ 3
14	2,7-dibromo-4,5-dichloro-	1	—	3368	1226 1204	+11
15	2,7-diiodo-4,5-dichloro-	1	—	3372	1226 1207	+11
16	2-iodo-4, 5, 7-trichloro-	1	—	3362	1226 1204	+11

The halogen-substituted acridones, thioacridones and 9-chloro-acridines show in 700—900 cm^{-1} frequencies region a number of absorption bands with high intensities, the γCH bands being very characteristic of the substitution type in acridinic nucleus.[4] (See Tables 5, 6, 7).

Only one very intensive band appears in the IR spectra at about 750 cm^{-1}, in the case of C_9 substitution (O, S, Cl) of the acridinic nucleus, corresponding to the absorption *ortho*-disubstituted benzene ring.

The presence of one substituent in a carbocyclic ring in position 2 (2-chloro, -bromo, -iodo-acridone) gives rise to the appearance (besides the band from 750 cm^{-1}) to other sufficient intensive bands — at 812—825 cm^{-1} and 870—880 cm^{-1}— characteristic of the asymmetric trisubstituted benzene.

In the case of the spectra of symmetrical carbocyclic substituted ring, namely C_2, C_7 (2,7-dichloro, -dibromo, -diiodo-acridone) the intensive band from 750 cm^{-1} disappears, but the other two bands at about 808—829 cm^{-1}, and 870—886 cm^{-1} (characteristic of the asymmetric trisubstituted benzene) are kept.

The acridine derivatives with more halogens, in which each carbocyclic ring is asymmetrically tetrasubstituted ($C_{2,4,5,7}$ -tetrahalogen-acridines, -acridones, -thioacridones) have in the spectra only one band characteristic of this substitution at 860—880 cm^{-1}. At the same time with these halogenated derivatives an intensive band appears at about 790 cm^{-1} which is probably due to the C-halogen stretching vibration.

A comparison of these series of halogen substituted acridones, thioacridones, and 9-chloro-acridines shows that the γCH vibrations of the acridone and thioacridone derivatives are at higher frequencies. Besides

Table 5

γCH vibrations of the halogenated acridines

No	-9-chloroacridine	1,2 disubst.	1, 2, 4 (1, 2, 5) trisubstituted		1, 2, 4, 6 (1, 2, 3, 5) tetrasubstituted	
1	2-chloro-	757	825	870	—	—
2	2-bromo-	755	822	870	—	—
3	2-iodo-	742	822	872	—	—
4	2,7-dichloro-	—	829	872	—	—
5	2,7-dibromo-	—	827	872	—	—
6	2,7-diiodo-	—	820	872	—	—
7	2-chloro-7-iodo-	—	821	872	—	—
8	2, 7, 4-trichloro-	—	821	872	860	792
9	2,7-diiodo-4-chloro-	—	821	870	860	790
10	2, 4, 5, 7-tetrachloro-	—	—	—	862	790
11	2, 4, 5, 7-tetrabromo-	—	—	—	862	790
12	2,7-dichloro-4,5-dibromo-	—	—	—	860	788
13	2,7-dibromo-4,5-dichloro-	—	—	—	860	788
14	2,7-diiodo-4,5-dichloro-	—	—	—	862	790
15	2-iodo-4, 5, 7-trichloro-	—	—	—	857	793
16	9-chloroacridine	757	—	—	—	—

---

[4] H. MANTSCH, I. GOIA and M. IONESCU, *Studii și Cercetări Chim. Fil. Cluj*, **2**, 293 (1963).

Table 6

γ CH vibrations of the halogenated acridones

No	-acridone	1,2 disubstituted	1, 2, 4 (1, 2, 5) trisubstituted		1, 2, 4, 6, (1, 2, 3, 5) tetrasubstituted	
1	2-chloro-	758	818	876	—	—
2	2-bromo-	757	815	872	—	—
3	2-iodo-	758	812	868	—	—
4	2,7-dichloro-	—	818	886	—	—
5	2,7-dibromo-	—	815	877	—	—
6	2,7-diiodo-	—	810	864	—	—
7	2-chloro-7-iodo-	—	817	880	—	—
8	2, 4, 7-trichloro-	—	818	878	—	793
9	2,7-diiodo-4-chloro-	—	817	880	—	795 824
10	2, 4, 5, 7-tetrachloro-	—	—	—	878	790 825
11	2, 4, 5, 7-tetrabromo-.	—	—	—	880	793 858
12	2,7-diiodo-4,5-dichloro-	—	—	—	880	793 825
13	2,7-dibromo-4,5-dichloro-	—	—	—	881	792 827
14	2,7-dichloro-4,5-dibromo-	—	—	—	880	793
15	2-iodo-4, 5, 7-trichloro-	—	—	—	881	793 826
16	N-methyl-	758	—	—	—	—
17	unsubstituted	751	—	—	—	—

Table 7

γCH vibrations of the halogenated thioacridones

No	-thioacridone	1,2 disubstituted	1, 2, 4 (1, 2, 5) trisubstituted		1, 2, 4, 6 (1, 2, 3, 5) tetrasubstituted	
1	unsubstituted	750	—	—	—	—
2	2-chloro-	752	818	876	—	—
3	2-bromo-	755	815	875	—	—
4	2-iodo-	753	809	875	—	—
5	2,7-dichloro-	—	815	875	—	—
6	2,7-dibromo-	—	812	881	—	—
7	2,7-diiodo-	—	808	883	—	—
8	2-chloro-7-iodo-	—	813	883	—	—
9	2, 4, 7-trichloro-	—	813	883	—	792
10	2,7-diiodo-4-chloro-	—	812	877	—	795
11	2, 4, 5, 7-tetrachloro-	—	—	—	877	790
12	2, 4, 5, 7-tetrabromo-	—	—	—	878	790 858
13	2,7-dichloro-4,5-dibromo-	—	—	—	878	790 800
14	2,7-dibromo-4,5-dichloro-	—	—	—	878	790 822
15	2,7-diiodo-4,5-dichloro-	—	—	—	875	792 852
16	2-iodo-4, 5, 7-trichloro-	—	—	—	876	790 850

the $\sim$790 cm^{-1} absorption, presumably due to the C-halogen bonds a second band appears at $\sim$825 cm^{-1} for tetra-halogenated derivatives.

These γCH bands being sufficiently intensive, can serve as analytical bands in the determination of the substitution type in acridine series.

EXPERIMENTAL

A. Synthetical

The melting points are uncorrected. In all chlorination reactions we used glacial acetic acid. The microanalytical determinations were carried out in the microanalytical laboratory of the Institute.

2-Iodo-7-chloro-acridone.(*VII*). Into a suspension of 0.5g 2-iodo-acridone in 80 ml CCl_4 on a boiling water bath, a moderate gaseous chlorine current passed for 40 minutes. After cooling, filtration, washing with CCl_4 and drying, the precipitate was extracted with 40 ml acetic acid and the insoluble part was twice recrystallized from acetic acid. Yellow needles, m.p. 404°(0.10g). *Found* : C, 44.10 ; H, 1.84.*Calcd.* : for $C_{13}H_7ClINO$(355. 53) : C,43.80 ; H, 1.98.

2-Iodo-4,5,7-trichloro-acridone. (*VI*). Into a suspension of 0.5 g 2,7-diio do-acridone, finely powdered in 100 ml acetic acid on boiling, a moderate gaseous chlorine current passed for 1.30 h. After cooling, filtration, the precipitate was extracted with 50 ml acetic acid. This solution, after cooling, deposited 2-iodo-4,5,7-tricholoro-acridone (0.2 g) which is again recrystallized from 30 ml acetic acid. Yellow needles, m.p. 261—262°. *Found* : C, 36.20 ; H,1.69 ; *Calcd.* : for C_{13} H_5Cl_3INO (424.42) C,36.81 ; H, 1.18.

The insoluble substance from the first extraction was 2,7-diiodo-4,5-dichloroacridone with m.p.290° (0.1 g).

2,7-Diiodo-4,5-dichloro-acridone (*V*). Into a suspension of 0.5 g 2,7-diiodo-acridone, finely powdered in 150 ml acetic acid on boiling water bath, a moderate gaseous chlorine current passed for 30 minutes. The hot solution is filtered.

a) From the precipitate, with 50 ml acetic acid 2,7—diiodo—4,5—dichloro—acridone with m.p. 291° (0.04 g) was extracted and the insoluble substance was 2,7-diiodo-acridone unreacted.

b) From the mother liquor, after cooling, a mixture of 2-iodo-4,5,7-trichloro-and 2,7 -diiodo-4,5-dichloro-acridone separated. By boiling extraction with 30 ml acetic acid 2-iodo-4,5,7-tri-chloro-acridone with m.p. 262°(0.07 g) separated and the undissolved substance was 2,7-diiodo-4,5-dichloro-acridone with m.p. 293° (0.16 g). Yellow needles from acetic acid.*Found* : C, 30.75 ; H, 1.50 *Calcd.* : for $C_{13}H_5Cl_2I_2NO$ (515.87) C, 30.27 ; H, 0.97.

B. Infrared absorption spectra

The spectra were measured on a double beam Zeiss U.R.10 spectrophotometer on potassium bromide pellets, and the frequency was calibrated with a polystyrene film. (With technical assistance of Mrs. E. Hamburg and Mr.V.Voivod).

NOTE POUR LES AUTEURS

La *Revue Roumaine de Chimie* publie des articles en anglais, français, russe, allemand ou espagnol. Les auteurs sont priés d'envoyer des articles, notes, communications et comptes rendus inédits.

Les manuscrits seront dactylographiés à deux intervalles. Les tableaux seront dactylographiés sur feuilles séparées, de même que la légende des figures. Les diagrammes seront tracés à l'encre de Chine sur papier calque. Les tableaux et les figures seront numérotés par des chiffres arabes, en nombre strictement nécessaire. Prière de ne pas inscrire les mêmes données dans les tableaux et les figures. Les formules chimiques seront incluses dans le texte ; en outre, elles seront transcrites sur des feuilles séparées. Les auteurs sont priés d'indiquer les caractères italiques (en soulignant les lettres au crayon), ainsi que tout autre caractère spécial. L'ordre des références bibliographiques sera celui de leur mention dans le texte ; le nom de l'auteur sera précédé de l'initiale du prénom ; les publications périodiques seront présentées suivant les prescriptions internationales. Les références seront ajoutées à la fin de l'article ; elles paraîtront comme des notes, au bas de la page. Le texte sera précédé d'un résumé, comprenant 15 lignes au maximum.

L'entière responsabilité du contenu des articles appartient aux auteurs. On publie des articles dus aux collaborateurs roumains ou étrangers. Les auteurs recevront 50 tirés à part.

PRINTED IN ROMANIA

1971 JAN 20

TRAVAUX PARUS AUX ÉDITIONS DE L'ACADÉMIE DE LA RÉPUBLIQUE SOCIALISTE DE ROUMANIE

CORNEL BODEA et collab., **Tratat de biochimie vegetală**, partea I, **Fitochimie** (Traité de biochimie végétale, Ire partie, Phytochimie), Ier vol., 1964, 747 p. + 4 annexes +2 pl., 41 lei, IIe vol., 1965, 1962 p., 1 pl., 56 lei, IIIe vol., 1967, 773 p. 35 lei.

V. GHEŢIE et V. MICUŞAN, **Analiza imunochimică. Teorie şi practică** (Analyse immunochimique. Théorie et pratique), 1966, 369 p., 28 lei.

SILVIA IONESCU, **Reacţii chimice induse de radiaţiile ionizante** (Réactions chimiques produites par les radiations ionisantes), 1963, 271 p., 15 lei.

MARIETA NICOLAE, **Fizico-chimia proceselor fotografice** (Physico-chimie des processus photographiques), 1964, 426 p. + 4 pl., 35 lei.

R. PORTOCALĂ et L. POPA, **Acizii ribonucleici celulari şi virali** (Les acides ribonucléiques cellulaires et viraux), 1966, 375 p. + 8 pl., 26 lei.

D. PURDELA et R VÎLCEANU, **Chimia compuşilor organici ai fosforului şi ai acizilor lui** (La chimie des composés organiques du phosphore et de ses acides), 1965, 540 p., 37 lei.

CRISTOFOR SIMIONESCU, MARGARETA GRIGORAŞ et AGATA CERNĂTESCU-ASANDEI, **Chimia lemnului din R.P.R.** (La chimie du bois en Roumanie), 1964, 239 p. + 6 pl., 27 lei.

CRISTOFOR SIMIONESCU et CLEOPATRA VASILIU-OPREA, **Mecanochimia compuşilor macromoleculari** (La mécanochimie des composés macromoléculaires), 1967, 344 p., 23,50 lei.

I. V. MAXIM, **Materiale nucleare** (Matériaux nucléaires), 1969, 444 p., 4 pl. 30 lei.

I.P.I. – c. 5815

43 436

Lei 25.–

F 1103

04 R

REVUE ROUMAINE DE CHIMIE

TOME 15
N° 12
Décembre 1970

ÉDITIONS DE L'ACADÉMIE DE LA RÉPUBLIQUE SOCIALISTE DE ROUMANIE

Rev. Roumaine Chim.

15, 1793—2016 (1970), Bucarest

COMITÉ DE RÉDACTION

Rédacteur en chef :

C. D. NENIȚESCU, membre de l'Académie de la République Socialiste de Roumanie.

Rédacteurs en chef adjoints :

A. T. BALABAN et V. EM. SAHINI, membres correspondants de l'Académie de la République Socialiste de Roumanie.

Collège de rédaction :

C. DRĂGULESCU, RALUCA RIPAN, CR. SIMIONESCU, membres de l'Académie de la République Socialiste de Roumanie ; EM. BRATU, membre correspondant de l'Académie de la République Socialiste de Roumanie ; Pr G. OSTROGOVICH, MARG. AVRAM, F. BADEA, I. D. MARCHIDAN, D. NEGOIU et D. SĂNDULESCU.

Les manuscrits, les livres et les revues proposés en échange, ainsi que toute correspondance seront envoyés à la rédaction :

REVUE ROUMAINE DE CHIMIE

23, str. Dumbrava Roșie, Bucarest, Roumanie.

REVUE ROUMAINE
DE
CHIMIE

Tome 15, N° 12 Décembre 1970

Page

V. EM. SAHINI, C. BENDIC and MARIANA DOBRESCU, Electronic structure and vapour spectrum of carbazole 1795–1797

O. RADOVICI and BELARISA POPESCU, Corrosion and passivity of some Pb-Sn alloys in media of different pH 1799–1806

N. BODOR and N. TRINAJSTIĆ, Valence-shell MO calculations for formamide and related compounds 1807–1811

RODICA VÎLCU and AL. BÎRHALĂ, Vapour pressure osmometry. Thermodynamic properties of naphthalene and anthracene in $CHCl_3$ and naphthalene in CCl_4 solutions 1813–1818

V. VASILESCU, S. VOLKOV and S. STERNBERG, Ultrasonic velocity, compressibility and excess volume for binary mixtures of molten salts: $NaCl + ZnCl_2$, $KCl + ZnCl_2$ . . . . 1819–1825 R

ILEANA IOSIF and I. A. SCHNEIDER, On the cool flame in the reaction of methane oxidation . . . . 1827–1829 R

ŞTEFANIA ZUCA and RODICA COSTIN, Viscosity of some molten alkaline earth chlorides 1831–1837

RODICA VÎLCU and C. MISDOLEA, Excess thermodynamic functions for liquid binary mixtures of some alkali metals 1839–1845

N. I. IONESCU, On the Elovich equation 1847–1849

S. SOLACOLU et A. BĂRBULESCU, La détection des réactions ayant lieu dans les mélanges oxydiques pulvérulents du système $La_2O_3-TiO_2-ZrO_2$ par la mesure de la résistance électrique 1851–1855

M. ARSHAD, A. BEG and B. BILQUIS, Studies on coordination compounds. Cobalt (II) complexes of adipyl dihydrazide . . . . 1857–1862 R

CONST. GH. MACAROVICI et L. CZEGLÉDI, Combinaisons complexes avec des hydroxyacides. XV. L'étude potentiométrique du système $ZrOCl_2$-acide D-gluconique 1863–1869

C. LITEANU et LUCREŢIA GHERGARIU-MÎRZA, Titrage conductométrique à résistance indicatrice. II. Titrage de l'acide chlorhydrique en solutions concentrées de chlorure de sodium à résistance membrane PCV + plastifiant + montmorillonite — natrium 1871–1882

I. NANU and C. ANDREI, Copolymers of conjugated dienes with maleic acid monoesters. I. Isoprene copolymerization with the methylic monoester of the maleic acid 1883–1892

Rev. Roumaine Chim. **15**, 1793–000 (1970) Bucarest

Page

D. FELDMAN, NATALIA SIMIONESCU, C. CIUBOTARIU, MARTHA CIUBOTARIU, T. CRIŞAN and G. DRESSNANDT, Butadiene-styrene carboxylated copolymers 1893–1900

ANTOANETA SPINZI et I. V. NICOLESCU, Propriétés physico-structurales des catalyseurs utilisés pour l'oxydation des hydrocarbures. IV. Propriétés électriques des systèmes oxydiques à base de $V_2O_5 - Ga_2O_3$ 1901–1906

J. REICHEL und C. TĂRĂBĂŞANU, Forschungen in der indigoiden Serie. II. Neue gemischte kondensierte azo-indigoide Systeme 1907–1912

ELENA SOFRONIE, ECATERINA-TĂRĂBĂŞANU-MIHĂILĂ and C. TĂRĂBĂŞANU, Radiolytic oxidation of acenaphthene to naphthalic acid on the acenaphthene-potassium permanganate-pyridine system 1913–1922

C. BODEA, TEODORA PANEA and V. FĂRCĂŞAN, Synthetical phenothiazine glycosides. III. Oxidation reaction 1923–1929

SIMONA BĂDILESCU, Simultaneous vibrational transitions. II. Induced simultaneous vibrational transitions in some haloform — carbon disulfide mixtures 1931–1934

CORNELIA VASILE, ANA ONU et I. A. SCHNEIDER, L'étude thermodynamique des solutions de PVC 1935–1946

I. VODNÁR, Decomposition of hydroperoxides on activated kaolins. II. Decomposition of cumene hydroperoxide on activated Chinese kaolin, in static conditions 1947–1951

AL. MAVRODIN, CĂTĂLINA DEMETRESCU, C. CHIRIŢĂ et OLGUŢA MACOVSCHI, Recherches dans la classe des *p*-fluor-diphénylsulfones. I. Synthèses de nouveaux composés à efficience antibactérienne . . . 1953–1965

A. GIOABĂ and O. MAIOR, Condensed heteroaromatic systems. Halogenation and dehalogenation with phenoxathiine, phenoxaselenine, phenoxatellurine and phenothiatellurine 1967–1974

GH. CIURDARU, MARCELA FĂRCĂŞAN and VIORICA I. DÉNES, Methylene bases of heterocycles. IX. Spectral study of 2-acylmethyleneazolines and their protonated forms. 1975–1985

IOANA ARSENIE et I. LEUCA, Variation de certaines propriétés du $K_2Zr/Hf/$ $/F_6$ par déhafnisation 1987–1992

N.S. BIRADAR and V.H. KULKARNI, Schiff base complexes of Ti (IV) . . 1993–1998

INDEX DU TOME 15 (1970) 1999–2016

Revue Roumaine de Chimie, **15**, 1795–1797 (1970)

ELECTRONIC STRUCTURE AND VAPOUR SPECTRUM OF CARBAZOLE

V. EM. SAHINI, C. BENDIC and MARIANA DOBRESCU
Physical Chemistry Department
University of Bucharest, Bd Republicii 13

Received the July 3, 1970

The semiempirical Pariser-Parr method has been used to study the electronic structure of carbazole. The calculated frecvencies have been compared with the vapour spectrum of carbazole.

INTRODUCTION

The carbazole molecule has already been subject of some theoretical studies which made use either of the Hückel [1a, b] or of more elaborated methods [2a, b, 3]. Among these, the contributions aiming at the reproduction of spectral data led to an unsatisfactory consistency, calling for additional studies in order to assigne the carbazole spectrum.

The present paper is concerned with the study of the electronic structure of carbazole by the semiempirical Pariser-Parr method with configurational interaction. Since there are some differences among the results of the various authors who dealt with the ultraviolet spectrum of carbazole in solution [4a, b, c, 5] we have also carried out its vapour spectrum in order to avoid the influence of the solvent.

I. EXPERIMENTAL

The vapour spectrum of carbazole has been obtained at 80° using a PGS 2 m spectrograph and a deuterium DVS 25 lamp as a source. The samples have been purified by repeated recrystallization and sublimation.

---

[1] a) R. D. Brown and M. L. Hefferman, *Australian J. Chem.*, **12**, 152 (1959); b) C. A. Coulson and C. Longuet Higgins, *Trans. Faraday Soc.*, **43**, 87 (1947).

[2] a) N. Mataga, Y. Torihashi and K. Ezumi, *Theor. Chim. Acta.*, **2**, 158 (1964); b) Noboru Mataga and Y. Torihashi, *Bull. Chem. Soc. Japan*, **36**, 356 (1963).

[3] C. A. Pinkham and S. C. Wait, *J. Mol. Spectroscopy*, **27**, 326 (1968).

[4] a) A. V. Chernobai, A. E. Shepeleva and V. S. Zubkova, *Vysokomol. Soedineniya*, **7**, 1080 (1965); b) B. L. van Dunren, *J. Org. Chem.*, **1961**, 2955; c) E. Merkel, *Ber. Bunsensges. Physik. Chem.*, **69**, 716 (1965).

[5] W. A. Schroeder, P. E. Wilcox, K. N. Trueblood and A. O. Dekker, *Analyt. Chem.*, **23**, 1740 (1951).

The general shape of the vapour spectrum is close to that of the solution spectrum with some shifts of the absorption maxima (table 1). The main maxima occur at 325.1 ; 312.5 ; 285.5 and 231.5 nm (fig. 1). The band at 325.1 nm, assigned to the first electronic transition ($\Psi'_0 \to \Psi'_{68}$ is broad and of a relatively low intensity, without any noticeable vibrational structure. The band at 285.5 nm, assigned to the second electronic transition ($\Psi' \to \Psi'_{78}$) has a much greater intensity with maxima of vibrational bands at 285.5 ; 280.0 ; 276.7 and 272.6 nm.

We assume the maximum of 312.4 nm to be due to a sequence band of the same electronic transition, which is supported also by the fact that it has not been found theoretically. The broad intense band at 231.5 nm is assigned to a ($\Psi'_0 \to \Psi'_{58}$) transition, in accordance with our theoretical results.

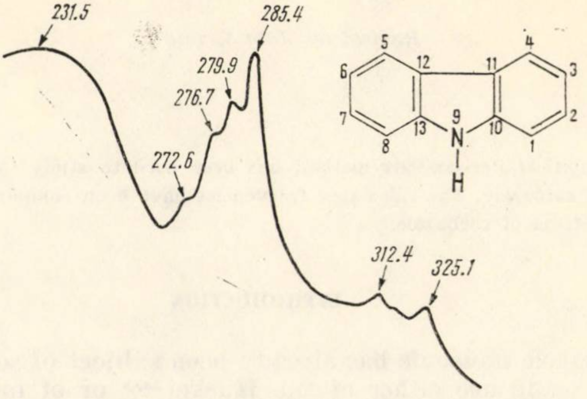

Fig. 1. — Vapour spectrum of carbazole.

II. THEORETICAL

We used as a starting point in our calculations the HMO obtained with the set of parameters that led to the best agreement with the experimental data ($h_{\ddot{N}} = 1.6$ and $k_{C\ddot{N}} = 1$).[6] The calculation was carried out by the Pariser-Parr method with the assumption of zero differential overlap.[7] The transition energies to the first three unfilled orbitals have been calculated including configuration interaction.

Since literature is but scarcely provided with X-ray data on carbazole geometry, we have used the bond lengths theoretically calculated by Dewar and Gleicher.[8]

In order to calculate the bicentric repulsion integrals we have employed the uniformly charged sphere approximation, the effective charge of the carbon and nitrogen being respectively $Z_{c^+} = 3.18$ and $Z_N^{++} =$ $= 4.80$.[6] The monocentric integrals have been calculated using the ionisation potentials recommended by Dewar and Gleicher.[8] In the calculation of resonance integrals β_{pq}, the approximation

$$\beta_{pq} = 1/2\ (W_p + W_q)\, S_{pq}$$

---

[6] W. P. Purcell and J. A. Singer, *J. Chem. Eng.*, **12**, 235 (1967).

[7] R. G. Parr and R. Pariser, *J. Chem. Phys.*, **21**, 466 (1953).

[8] M. J. S. Dewar and G. J. Gleicher, *J. Chem. Phys.*, **44**, 759 (1966).

has been used,[9] where the overlap integrals have been estimated using Preuss tables.[10] We have thus obtained $\beta_{c_1c_2} = -2.79$ eV; $\beta_{c_{10}N} = -2.997$ eV and $\beta_{c_{11}c_{12}} = -2.344$ eV (the numbering is that given in figure 1). The calculation has also considered the penetration integrals estimated according to.[11,12]

Table 1 lists the results obtained for the first electronic transitions, calculated under consideration of configurational interaction. There is a satisfactory general agreement between the calculated and observed wavelengths listed in the table. The calculated value for the first transition is rather large, but its relative arrangement tallies very well with the experimental assignments.

Table 1

Theoretical and experimental transitions of carbazole

λ (nm) Transition	$\lambda_{calc.}$	$\lambda_{exp.}$* (vapour)	$\lambda_{exp.}^{4b}$ (cyclohexane)	$\lambda_{exp.}^{5}$ (dioxane)	$\lambda_{exp.}^{3}$
$\Psi_0 \rightarrow \Psi_{68}$	345.6	325.1	330	336	326
$\Psi_0 \rightarrow \Psi_{78}$	277.7	285.5	289	292	275
$\Psi_0 \rightarrow \Psi_{58}$	233.5	231.5	231	235	—

* Present paper.

The good agreement between the calculated and experimental value for the third band supports its assignement to an electronic $\Psi_0 \rightarrow \Psi_{58}$ transition.

---

[9] Per Olöv Löwdin, "Advances in Quantum Chemistry", vol. 1, Acad. Press, New York, London 1964, p. 203.

[10] H. Preuss, "Integraltafeln zur Quantenchemie", vol. 2, Springer Verlag, Berlin-Göttingen-Heidelberg, 1957.

[11] R. Pariser and R. G. Parr, *J. Chem. Phys.*, **21**, 767 (1953); *J. Chem. Phys.*, **21**, 568 (1953).

[12] R. Parr, D. P. Craig and J. G. Ross, *J. Chem. Phys.*, **18**, 1561 (1950).

[illegible] while the overlap integrals have been estimated using [illegible] tables. We have then calculated [illegible] [illegible] eV [illegible] −2.5 eV (the numbering is that given in figure 1). The calculation has also considered the perturbation integrals evaluated according to [illegible]

[illegible] the values obtained for the first electronic transition [illegible] consideration of configuration interaction [illegible]. There is [illegible] good agreement between [illegible] and observed [illegible] in the table. The calculated value for the first transition [illegible] relative [illegible] very well with the experimental measurements.

Table 1

[illegible]

The good agreement between the calculated and experimental [illegible] to an [illegible].

[illegible] Chemistry [illegible]

[illegible]

[illegible]

[illegible]

Revue Roumaine de Chimie, 15, 1799–1806 (1970)

CORROSION AND PASSIVITY OF SOME Pb-Sn ALLOYS IN MEDIA OF DIFFERENT pH

O. RADOVICI and BELARISA POPESCU

Chair of the Chemical Thermodynamics and Electrochemistry,
University of Bucharest, Bd. Republicii 13

Received March 17, 1970

The electrochemical behaviour of five characteristic Pb-Sn alloys has been investigated in media of different pH. Potentiostatic method shows that the highest corrosion resistance is provided by the alloy possessing the eutectic composition.

INTRODUCTION

In spite of the wide application of the lead-tin alloys, there are few investigations as to their electrochemical behaviour.

This paper is an account of the results obtained from a study of anodic and cathodic behaviour under potentiostatic conditions of four Pb—Sn alloys representing under eutectic, approximately eutectic and above eutectic states, and of the pure metals.

EXPERIMENTS

The electrodes used were alloys of the following composition Sn 20 % – Pb 80 %, Sn 40 % – Pb 60 %; Sn 60 % – Pb 40 %, Sn 80 % – Pb 20 %, and pure Sn and Pb. The electrodes were in the form of rods, with the exposed area of 1 cm^2.

The buffer solutions were : citric acid and NaOH of pH 2,12 ; 3.15 ; 4.27 ; 6.15. The electrolytic cell was H shaped, to separate the anodic space from the cathodic one.

As auxiliary electrode Pt was used, and as reference electrode the saturated calomel electrode. The connections between the working electrode and the reference electrode were made with a Haber-Luggin capillary.

The solutions were deaerated by passing pure nitrogen.

All measurements were conducted at 25° ± 0.1°. Quasistationary polarization curves were obtained with an electronic potentiostat (Tacussel). The potentials applied to the working electrode were varied by steps of 0.1 V. For every potential step, the current value was read on a milliampermeter with a class sensitivity of 0.2. The imposed potential was verified by electronic millivoltmeter (fig. 1).

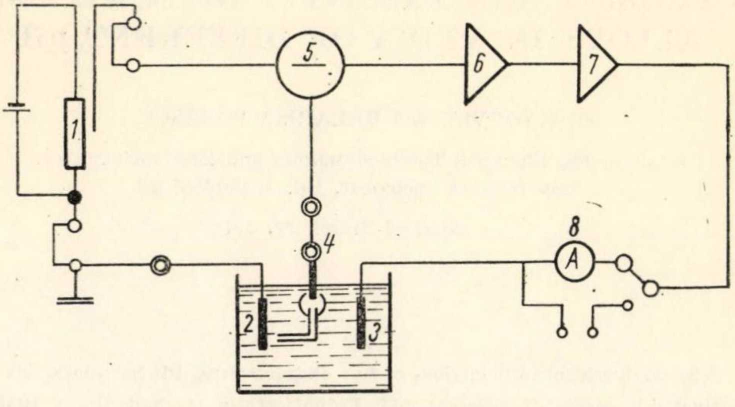

Fig. 1. — Experimental potentiostatic equipment.
1, Potentiometer; *2*, working electrode;
3, counter electrode; *4*, reference electrode;
5, comparator; *6*, voltage amplifier;
7, power amplifier; *8*, milliampermeter.

RESULTS AND DISCUSSION

Figures 2, 3, 4, 5 show the curves of anodic and cathodic polarization obtained for alloys and pure metals in all buffer solutions.

The cathodic curves have a slops of 0.1 V for all alloys in all solutions.

The values of the corrosion current were obtained by extrapolation of the cathodic curves at the corrosion potential.

The anodic polarization curves have the classical shape of passivation curve characterized by active, active-passive transition and passive region.

CORROSION POTENTIAL

The corrosion potentials — that is potentials for $i = 0$, have a linear dependence of pH for Sn and all alloys (fig. 6).
For lead, they have constant values, independent of the pH of the solution.

The potential of reaction

$$\mathrm{Sn} + \mathrm{H_2O} \rightarrow \mathrm{SnO} + 2\mathrm{H} + 2\mathrm{e}^- \qquad E_0 = -0.104 - 0.059\,\mathrm{pH}$$

was calculated from the Pourbaix [1] diagrams of Sn. The values obtained (table 1) are very close to the values of Sn corrosion potential for every buffer solution.

---

[1] M. Pourbaix, Atlas d'équilibres électrochimiques. Gauthier-Villars & Cie. 1963, Paris.

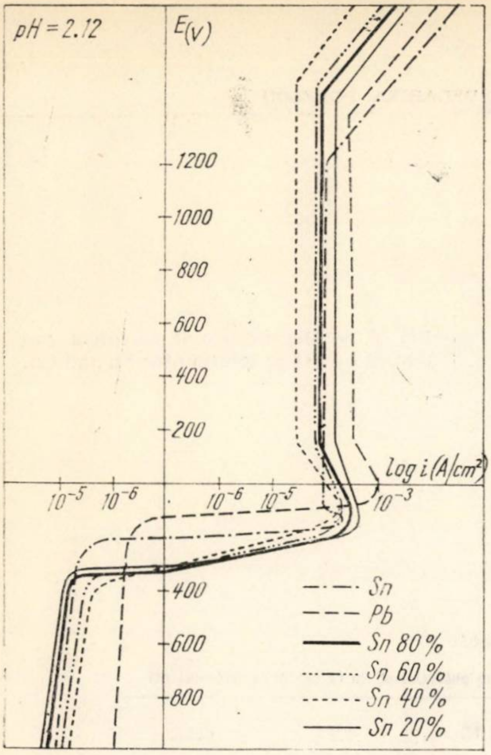

Fig. 2. — Anodic polarization curves for Sn, Pb and their alloys in solution of different pH.

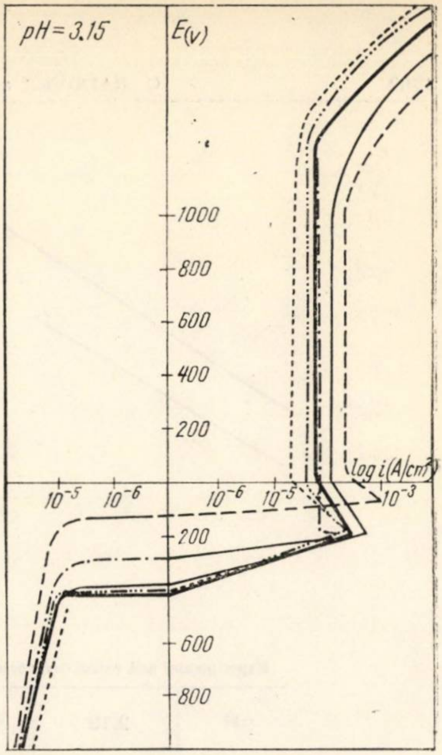

Fig. 3. — Anodic polarization curves for Sn, Pb and their alloys in solution of different pH.

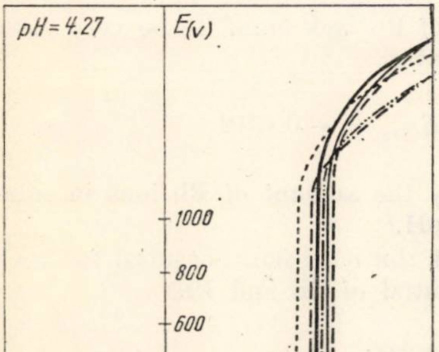

Fig. 4. — Anodic polarization curves for Sn, Pb and their alloys in solution of different pH.

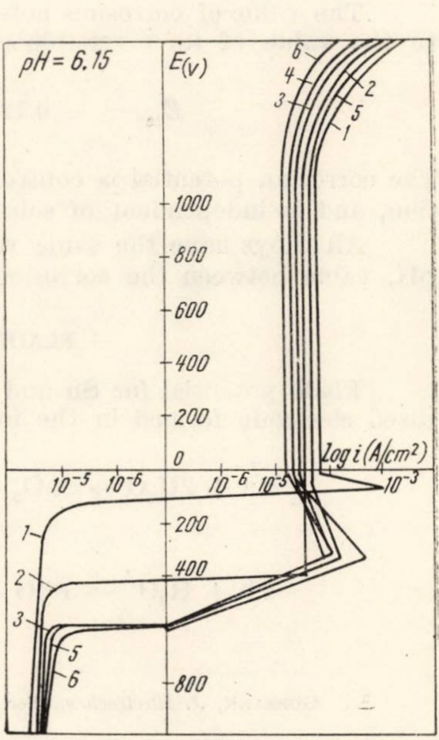

Fig. 5. — Anodic polarization curves for Sn, Pb and their alloys in solution of different pH.

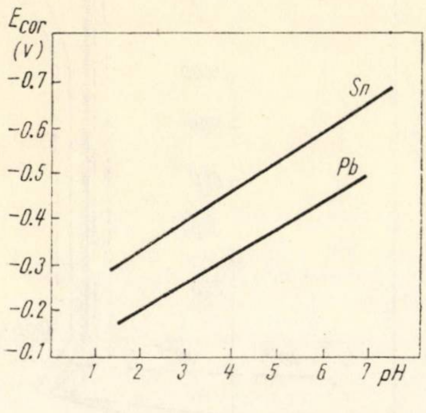

Fig. 6. — Dependence of corrosion potential by pH of solution for Sn and Pb.

Table 1

Experimental and calculated corrosion potential of Sn in media of different pH

pH	2.12	3.15	4.27	6.15
E_{corr}	−0.2112	−0.2712	−0.3512	−0.4312
$E_{Pourbaix}$	−0.21908	−0.2898	−0.35393	−0.46685

The value of corrosion potential of Pb was found to be very close to the value of its reversible potential.

$$E_{rev} = -0.126 \qquad E_{corr} = -0.1312$$

The corrosion potential is controlled by the amount of Pb ions in solution, and is independent of solutions pH.[2]

All alloys have the same value of the corrosion potential for each pH, value between the corrosion potential of Sn and Pb.

FLADE POTENTIAL

Flade potential for Sn and Pb is close to the potential of the oxidized electrode formed in the following reactions

$$Sn + 2H_2O \rightarrow SnO_2 + 4H^+ + 4e^-$$

$$E_0 = 0.008 - 0.059 \text{ pH}$$

$$Pb + H_2O \rightarrow PbO + 2H^+ + 2e^-$$

$$E_0 = 0.277 - 0.059 \text{ pH}$$

---

[2] J. Burbank, *J. Electrochem. Soc.*, **106**, 369 (1959).

—0.08 and 0.277 represent the potential of oxide electrodes. The experimental and calculated values of the Flade potentials for pure metals are given in table 2.

Table 2

Experimental and calculated Flade potential of Sn and Pb in media of different pH

pH	2.12		3.15		4.27		6.15	
	Sn	Pb	Sn	Pb	Sn	Pb	Sn	Pb
E_{Fl}	−0.121	+0.1588	−0.1812	0.0997	−0.2412	0.0406	−0.362	−0.062
E_{calc}	−0.1338	+0.15192	−0.19385	0.09115	−0.25793	0.0270	−0.37085	−0.08581

These values are in agreement with Vetter [3] relation

$$E = E_0 - 0.059 \text{ pH}$$

where E_0 represents the reversible potential of oxide electrodes.

The dependence of the Flade potential on the pH solution is linear (fig. 7).

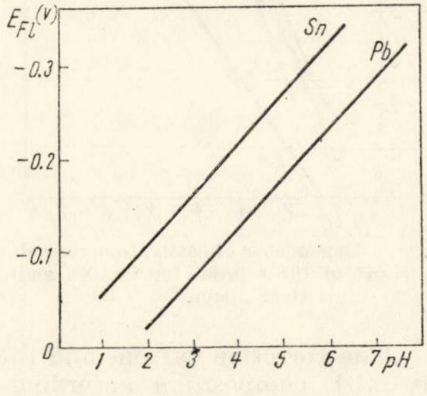

Fig. 7. — Dependence of Flade potential on the pH of the solution for Sn and Pb.

From the anodic polarization curves of the alloys it is obvious that the value of the potential at which the current starts to decrease corresponds to the Flade potential of Sn and the value of the potential at which the current attains a minimum and constant value corresponds to the Flade potential of Pb.

CORROSION CURRENT

The corrosion currents were obtained by extrapolation of the cathodic curves to the value of the corrosion potential.

---

[3] K. Arnold and K. J. Vetter, *Z. Electrochem.*, **64**, 407 (1960).

For all alloys and for the pure metals the dependence of the corrosion current on the pH is linear (fig. 8).

The maximum current of dissolution was estimated from the anodic polarization curves. The dependence of the maximum current of dissolution on the pH is also linear (fig. 9).

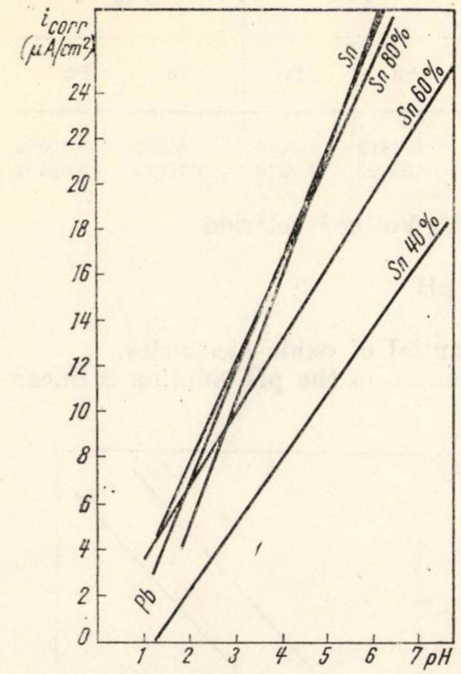

Fig. 8. — Dependence of passivation current on the pH of the solution for Pb, Sn and their alloys.

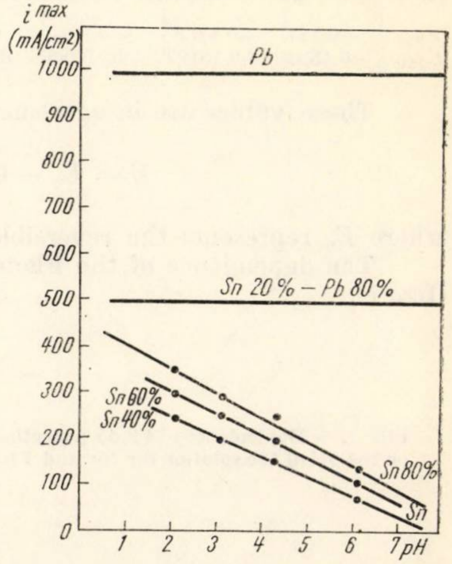

Fig. 9. — Dependence of corrosion current on the pH of the solution for Sn, Pb and their alloys.

The corrosion current and the maximum current of dissolution may vary with composition according to figures 10 and 11.

The results imply that the alloys with the composition near to eutectic composition have the lowest dissolution rate.

This may be ascribed to the circumstance that the eutectic alloys have the most homogeneous structure as compared to the other alloys in which pure metals will form as separate phases. The same observation was made by Abdul Azim and M. M. Anwar,[4] for Sn—Pb alloys in H_2SO_4.

THE PASSIVATION CURRENT

Figure 12 shows the linear dependence of the passivation current on the pH for pure metals and for all alloys.

---

[4] A. A. Abdul Azim and M. M. Anwar, *Corrosion Science*, **9**, 193 (1969).

An increase of the passivation current with acidity was observed.

The dependence of the passivation current on composition (figure 13) is the name as for the corrosion current. Eutectic alloys with homogeneous structures have the smallest value for the passivation current.

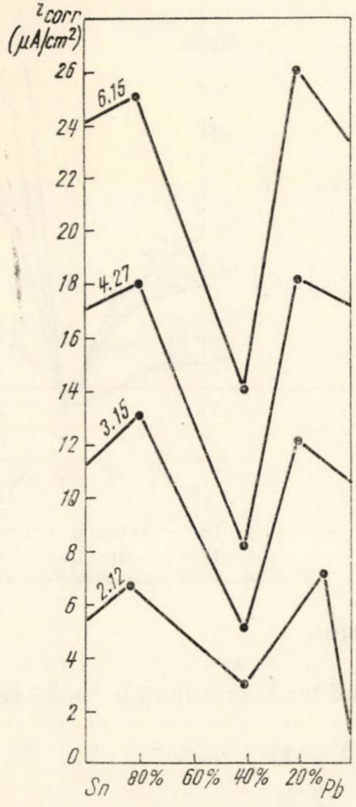

Fig. 10. — Relation between percentage composition of the alloys and corrosion current.

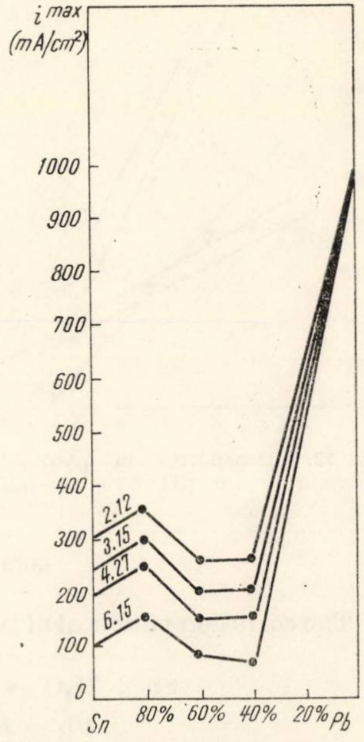

Fig. 11. — Relation between percentage composition of the alloys and maximum dissolution current.

It was noted, from the Flade potential, that Sn forms a superior hydrated oxide SnO_2, and Pb, the monoxide PbO.

These oxides have a high tendency to dissolve in acid media. The values of the maximum dissolution current are near to the values of the passivation current, that means that instead of metal dissolution there occurs a dissolution of the oxide. At the end of the anodic polarization, it was observed that the bright white electrode of tin and lead, became white opaque for tin, and gray for lead.

After anodic polarization the alloys present a surface with white and gray spots.

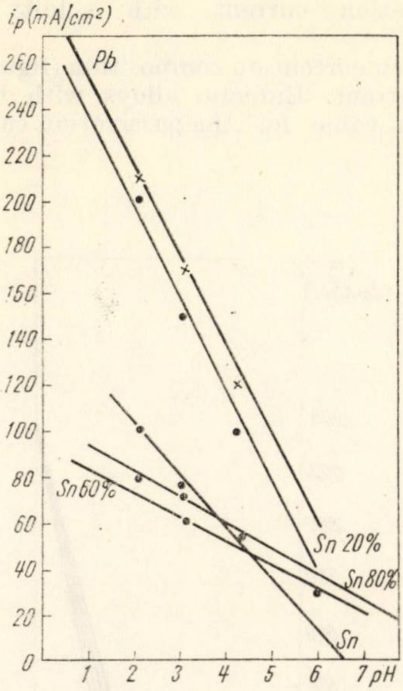

Fig. 12. — Dependence of passivation current on the pH of the solution

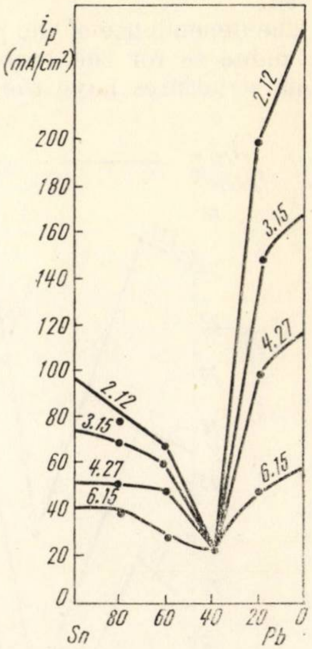

Fig. 13. — Relation between percentage composition of the alloys and passivation current.

CONCLUSION

1. The corrosion potential of tin and lead corresponds to the reaction :

$$Sn + H_2O \rightarrow SnO + 2H^+ + 2e^-$$
$$Pb \rightarrow Pb^{++} + 2e^-$$

The alloys have the same value of corrosion potential in every buffer solution value located between the corrosion potential of tin and lead.

2. The Flade potential of Sn and Pb has the values in agreement with Vetters relation.

$$E_{Fl} = E_0 = 0.059 \text{ pH}$$

E_0 — the potential of oxide electrode.

3. The corrosion current, the passivation current, and the maximum dissolution current show a linear dependence on the pH of the solution.

The dependence of this current on composition implies that the minimum velocity of corrosion is obtained by the eutectic composition.

4. The small difference between the passivation current and the maximum dissolution current, leads to the conclusion that at the Flade potential a steady state is established, in which the dissolution and the formation of films develop with the same velocity.

Revue Roumaine de Chimie, **15**, 1807–1811 (1970)

VALENCE-SHELL MO CALCULATIONS FOR FORMAMIDE AND RELATED COMPOUNDS

N. BODOR

Chemical—Pharmaceutical Research Institute, Cluj, Romania

and

N. TRINAJSTIĆ*

Department of Chemistry, The University of Texas at Austin,
Austin, Texas 78712

Received April 28, 1970

The principal ground state properties for formamide and related compounds were calculated using the MINDO/2 semiempirical all-valence-electrons SCF MO method. The calculated values are in good agreement with the corresponding experimental ones. The orbital ordering of the two highest occupied orbitals n_0 and π_2 are discussed.

Recent interest concerning the orbital ordering of the two highest occupied orbitals n_0 (the non-bonding orbital on oxygen) and π_2 (the antisymmetric pi MO) in formamide and N-methyl substituted formamides, both experimental [1] and theoretical [1], prompt us to report our semiempirical all-valence-electrons molecular orbital calculations in the framework of the MINDO (modified intermediate neglect of differential overlap) for these molecules.

The MINDO method is a semiempirical SCF MO procedure in which all-valence-electrons, both σ and π are included. In MINDO/1[2] the core-core repulsions are set equal to the electron-electron repulsions, and the energy minimum at the calculated equilibrium geometry does not correspond to the experimental molecular geometry. MINDO/1 is parametrized to give accurate heats of formation for a large variety of molecules, the molecular geometries used being the standard ones of Baird and Dewar.[2] In MINDO/2 the more realistic core-core repulsion term introduced by Dewar and Klopman [3] in their PNDO treatment is used, and the predicted geometries are consequently close to the experimental ones. The MINDO/2 method was recently parametrized for hydrocarbons [4] and then extended to compounds containing nitrogen and/or oxygen.[5] In this latter work [5] by including a set of 40 compounds containing carbon, hydrogen, oxygen, and nitrogen and various types of bonds, the degeneracy [4] of solutions for the parameters for carbon and hydrogen has been reduced, obtaining better results for hydrocarbons, than the earlier [4] treatment and it also gives generally good results for compounds containing nitrogen and/or oxygen. The MINDO/2 method gives very good estimates of the heats of formation, molecular geometries, and ionization potentials for various compounds containing carbon, hydrogen, nitrogen, and/or oxygen. We have used in the present work the latest version [5] of the MINDO method, whose detailed description was given elsewhere [4,5] and there is no need to be repeated here.

---

*) On leave of absence from The Rudjer Bosković Institute, Zagreb, Croatia, Yugoslavia.

[1] C. R. Brundle, D. W. Turner, M. B. Rubin, and H. Basch, *Chem. Phys. Letters*, **3**, 292 (1969).

[2] a) N. C. Baird, and M. J. S. Dewar, *J. Chem. Phys.*, **50**, 1262 (1969); b) N. C. Baird, M. J. S. Dewar, and R. Sustman, *ibid.*, **50**, 1275 (1969); c) M. J. S. Dewar, M. Shanshal, and S. D. Worley, *J. Amer. Chem. Soc.*, **91**, 3590 (1969).

The MINDO/2 method [5] has been successfully employed in predicting ionization potentials and heats of formation for a set of cyclic hydrocarbons, including adamantane and its derivatives.[6] Here we report calculations for the following molecules : formic acid, formamide, N-methyl-formamide, N,N-dimethyl-formamide, and methylformate. The calculated heats of formation, bond lengths, and first ionization potentials together with experimental data, where available, are shown in table 1.

The first ionization potentials were estimated in two ways :

(a) from Koopmans' theorem (the ionization potentials are equated to minus the corresponding calculated orbital energies), and

(b) from the relationship : $(IP)_1 = \Delta H_f\ (A^+) - \Delta H_f\ (A)$, where $\Delta H_f\,(A)$ and $\Delta H_f\,(A^+)$ are the calculated heats of formation of the neutral molecules and of the corresponding positive ions, respectively.

Ionization potentials predicted by any of the above methods should really be compared with vertical ionization potentials, since none of them does allow for changes in geometry or wave function upon ionization. (An adiabatic ionization potential is the difference in energy between the ground vibrational levels of the molecule and the ion, while a vertical ionization potential is the difference in energy between the ground vibrational level of the molecule and some vibrational level of the ion, the nature of which is dictated by the Franck-Condon Principle. The vertical ionization potentials are commonly only 0.1—0.3 eV higher than the corresponding adiabatic ones, which is, however, within the limits of error of all current theoretical procedures).

The two experimentally observed heats of formation (for formic acid and methyl formate) are in good agreement with the calculated values, the difference being less than 4 kcal/mole. The calculated bond lengths (for formic acid, formamide, and methyl formate) are in fair agreement with the experimental values. Similarly, the first ionization potentials are also reproduced fairly well, the difference being less than 0.5 eV.

---

[3] M. J. S. Dewar, and G. Klopman, *J. Amer. Chem. Soc.*, **89**, 3089 (1967).

[4] M. J. S. Dewar, and E. Haselbach, *ibid.*, **92**, 590 (1970).

[5] N. Bodor, M. J. S. Dewar, A. J. Harget, and E. Haselbach, *J. Amer. Chem. Soc.*, **92**, 3854 (1970).

[6] N. Bodor, M. J. S. Dewar, and S. D. Worley, *J. Amer. Chem. Soc.*, **92**, 19 (1970)

Detailed study of the photoelectron spectra of formic acid and its derivatives shows that in formic acid and formamide, ionization from n_0 preceds that from π_2, but in the case of formamide these two orbitals are nearly degenerate, while in formic acid the difference is considerable (of the order of 1 eV). The reverse order was obtained in N-methyl formamide and in N,N-dimethyl formamide (see table 2.)

Table 1

Calculated and observed heats of formation at 25° C (ΔH_f), bond lengths (l_{ij}), and first vertical ionization potentials ($(IP_1)_v$).

	ΔH_f (kcal/mole)			l_{ij} (Å)	$(IP_1)_v$ (eV)			
Molecule (A)	A		A^+	calc. (obs.)	obs. [(a)]	calculated		
	obs.	calc.	calc.			(b)	(c)	(d)
HCOOH	−90.5[(e)]	−90.67	156.89	C = O : 1.230 (1.245)[(f)] C − O : 1.338 (1.312)[(f)] C − H : 0.979 (0.950)[(f)]	11.51	10.74	11.24	12.05
$HCONH_2$		−50.68	189.16	N − H : 1.020 (0.995)[(g)] (1.014)[(h)] C − N : 1.380 (1.343)[(g)] (1.376)[(h)] C = O : 1.220 (1.243)[(g)] (1.193)[(h)]	10.32	10.40	10.83	10.90
$HCONHCH_3$		−44.02	182.21	(i)	9.87	9.81	10.37	
$HCON(CH_3)_2$		−31.35	179.71	(j)	9.25	9.15	9.93	
$HCOOCH_3$	−81.0[(e)]	−84.45	156.83	C =O: 1.224 (1.200)[(f)] C − O : 1.334 (1.334)[(f)] O − C; (methyl) : 1.392 (1.437)[(f)]		10.46	10.96	

(a) C. R. Brundle, D. W. Turner, M. B. Robin, and H. Basch, *Chem. Phys. Letters*, **3**, 292 (1969).
(b) Calculated from the relationship : $(IP)_1 = \Delta H_f(A+) - \Delta H_f(A)$
(c) Calculated from Koopmans' theorem.
(d) Calculated by using the double zeta GTO basis set in ref. (a) from Koopmans' theorem and reduced by 8%.
(e) L. H. S. Green, *Quart. Rev.*, **15**, 125 (1961).
(f) L. E. Sutton, Ed. *Tables of Interatomic Distances*, The Chemical Society, London (1958 and 1965).
(g) R. J. Kurland, and E. B. Wilson, *J. Chem. Phys.*, **27**, 585 (1957).
(h) C. C. Costain, and J. M. Dowling, *J. Chem. Phys.*, **32**, 158 (1960).
(i) Here the bond lengths used were those calculated for formamide, snd N−C (methyl) bond length (1.474 Å) from ref. (f).
(j) L. V. Vilkov, P. A. Akishin, and V. M. Presnyakova, *J. Struct. Chem.*, **3**, *3*, (1962). The measured values are close to those calculated for formamide. Thus we used latter values for all bonds and for the N−C (methyl) bond length the experimental value (1.45 Å).

Revue Roumaine de Chimie, **15**, 1807−1811 (1970)

Earlier calculations[1] were not complete because the method used there (SCF MO) using double zeta Gaussian-Type Orbitals basis set [7]) could handle only formic acid and formamide (these results are also given in table 2). Our values obtained from MINDO/2 calculations using Koopmans' theorem follow closely experimental results, i.e. we predicted that the ionization from the π_2 orbital should preced that from from the n_0 orbital in N-methyl formamide and in N,N-dimethyl formamide, while the reverse order is obtained in formic acid and formamide.

Table 2

Calculated and observed ionization potentials (eV).

Molecule	Orbital type	Observed		MINDO/2 results (Koop-mans'theorem)	SCF MO with GTO corrected for 8 % (ref. 1)
		vertical	adiabatic		
		(ref. 1)			
HCOOH	n_0	11.51	11.33	11.24	12.05
				12.22(σ?)	
	π_2	12.51	12.37	12.41	12.51
		14.74	≈14.2	14.61	15.07
		15.72	≈15.4	15.34	16.32
		17.13	16.97	16.17	17.87
		≈17.7 (?)		21.12	18.55
$HCONH_2$	n_0	10.32	10.13	10.83	10.90
	π_2	10.52	⩽10.52	11.01	10.41 (?)
				12.48(σ?)	
		14.18	13.76	13.96	15.02 (?)
		14.75	14.62	14.11	14.42
		16.30	16.16	16.23	16.80
		≈19		20.27	19.18
$HCONHCH_3$	π_2	9.87	9.79	10.37	
	n_0	10.05	10.05	10.60	
				11.95 (σ?)	
		13.20	≈12.6	13.24	
		14.3		14.64	
				14.84	
		15.7		15.10	
		18.3			
		≈20 (?)		20.97	
$HCONH(CH_3)_2$	π_2	9.25	9.14	9.93	
	n_0	9.77	⩾ 9.40	10.34	
				11.74 (σ?)	
				12.22	
				12.83	
		≈13.4	≈12.3	13.39	
		14.2		14.25	
		15.9		15.52	
		17.4		17.73	
		18.9		19.31	
		≈20.4			

---

[7] H. Basch, M. B. Robin, and N. A. Kuebler, *J. Chem. Phys.*, **47**, 1201 (1967); *ibid.*, **49**, 5007 (1968).

It can be seen in table 2., that there are few calculated energy levels (by MINDO/2), which do not have any corresponding ones in the photoelectron spectra of the molecules. In view of probable misunderstandings, it seems necessary to mention that because there are many closely spaced energy levels in a large organic molecule, particularly one with low symmetry, resolution in the photoelectron spectra can be poor, i.e. two of the closely spaced (but not degenerate) energy levels appear as a single peak in the photoelectron spectrum.

Revue Roumaine de Chimie, 15, 1813–1818 (1970)

VAPOUR PRESSURE OSMOMETRY. THERMODYNAMIC PROPERTIES OF NAPHTHALENE AND ANTHRACENE IN $CHCl_3$ AND NAPHTHALENE IN CCl_4 SOLUTIONS

RODICA VÎLCU and AL. BÎRHALĂ
Institute of Physical Chemistry, Bucharest, str. Galaţi 31

Received March 31, 1970

Making use of a vapourometer (own manufacture) the vapour pressures of naphthalene and anthracene in $CHCl_3$ and naphthalene in CCl_4 solutions, were measured, within the 0.01–0.1 mole/l concentration range at 298.59, 303.66 and 308.83°K. Gibbs free enthalpies of dilution and molal osmotic coefficients were calculated.

The vapourometric micromethod which was applied during the last years to the molecular weight determinations in polymers, has got important applications in the thermodynamic characterization of solutions, too. The number of works devoted to this aim has been limited to a few papers.[1-4] The present work deals with the estimation of some representative thermodynamic magnitudes in solutions formed by organic components.

The differential vapourometric method used, belongs to the static methods class, of determining vapour pressures and is based on the estimation of the differences between the vapour pressure of the solution and that of pure solvent, for both measurements only very small quantities of substances being needed (a droplet of each).

The fundamentals of the method, as well as a detailed description of the apparatus were given in a previous paper.[5]

The estimation of thermodynamic magnitudes from vapourometric data is based upon the proportionality between the solvent-solution temperature difference, caused by the different thermal effect of vapours condensation on the solvent and solution drops, respectively ΔT, and the pure solvent-solvent in solution, chemical potential difference $\Delta\mu_1$[3-4]:

$$\Delta T = K_2 \Delta \mu_1 \tag{1}$$

---

[1] C. G. Mc Gee and B. R. Y. Iyengar, *Indian J. Phys.*, **26**, 61 (1952).
[2] D. F. Burge, *J. Phys. Chem.*, **67**, 2590 (1963).
[3] R. D. Johnson and F. M. Goyan, *J. Pharm. Sci.*, **56**, 757 (1967).
[4] W. Brown, *J. Appl. Polymer Sci.* **11**, 2381 (1967).
[5] R. Vîlcu and Al. Bîrhală, *Rev. Roumaine Chim.*, **15**, 175 (1970).

To the ΔT difference corresponds a resistance difference ΔR, between the two thermistors on which the solvent and solution drops are placed, so that the following proportionality equation exists :

$$\Delta R = K_1 \Delta T \tag{2}$$

or equivalently :

$$\Delta R = K_1 K_2 \Delta\mu_1 = K_3 \Delta\mu_1 \tag{3}$$

The thermodynamic activity of the solvent, a_1, directly related to the chemical potential, is related to the $\Delta\mu_1$ change by :

$$\Delta\mu_1 = -RT \ln a_1 \tag{4}$$

Equations (3) and (4) give :

$$\Delta R = -K_4 \ln a_1 \tag{5}$$

where $K_4 = K_3 RT$, K_4 being a calibration constant characteristic of the solvent in solution at a certain temperature. In calculations of molecular weights from vapourometric data, one uses the molal constant k, which is related to the activity of the solvent by the relation :

$$-\ln a_1 = \frac{\Delta R M_1}{1000\, k} \tag{6}$$

The calibration constant is estimated from the graph. The molecular weight of the solute (M_2) is given by the relation :

$$M_2 = \frac{(K_4 - \Delta R)\, g_2 M_1}{\Delta R g_1} \tag{7}$$

where subscript 1 is for the solvent, while subscript 2 indicates the solute (g = weight in grams, M = molecular weight). As soon as the thermodynamic activity is known the molal variation of dilution free enthalpy, ΔG_1, is established :

$$\Delta G_1 = -RT \ln a_1 \tag{8}$$

From this equation the correspondence between different thermodynamic magnitudes could be deduced, aiming at the estimation of dilution magnitudes.

The ideality of the system in the range of low concentrations, approached in the present paper, could be confirmed by the values of molal osmotic coefficient, Φ, given by the equation:

$$\Phi = \frac{\Delta R}{km_2} \tag{9}$$

where m_2 is the molality of the solution, k the molal calibration constant and ΔR resistance difference.

APPARATUS

The vapourometer we worked with (own manufacture) has as temperature detectors high resistance thermistors (100,000 Ω at 25°) with thermal coefficient of the resistance of $-4.6\ \%/^\circ$; the working method and its characteristics are given elsewhere.[5] The calibration for different temperatures and for each solvent used was carried out with benzil within the concentration range of 0.01 – 0.12 mole/l. The benzil forms. with many organic solvents, perfect solutions within the quoted concentration range, so that the relation $\Delta R = KC$ (K is the apparatus constant and C the concentration) is valid.

The calibration constant K_4 and k (table 1), were determined as ordinates at origin in $\Delta R/x_2$ *versus* x_2 and $\Delta R/m_2$ *versus* m_2 diagrams, respectively; x_2 is the molar fraction while m_2 is the molality of the solution.

The values of calibration constants are given in table 1.

Table 1

Calibration constants

Solvent	298.59°K		303.66°K		308.83°K	
	K_4	k	K_4	k	K_4	k
$CHCl_3$	86,200	10,280	70,700	8,345	57,600	6,875
CCl_4	60,450	9,305	51,600	7,940	43,300	6,658

The measuring cell was thermoset within ±0.005° and ΔT was measured with a precision of $\pm 10^{-4}$°.

The ΔR differences corresponding to ΔT, were measured with a Wheatstone bridge.[5] The thermal equilibrium within the vapourometric cell was reached in 5 minutes for chloroform solutions and 7 minutes for carbon tetrachloride.

REAGENTS

Spectroscopically pure chloroform and carbon tetrachloride were used. The benzil used in calibrations was purified by reiterated recrystallizations from absolute ethanol. Naphthalene and anthracene were p.a. reagents.

RESULTS AND DISCUSSION

Vapour pressure measurements were carried out on solutions of naphthalene and anthracene in chloroform and carbon tetrachloride at 298.59, 303.66 and 308.83°K, at concentrations between 0.01 and 0.1 mole/l that is 0.0063—0.63 molal for chloroform solutions and 0.0068—0.068 molal for carbon tetrachloride solutions.

The validity of the experimental data was confirmed by the values obtained for molecular weights of solutes in the two solvents used. For calculations the equation (7) was used and the results are presented in tables 2 and 3.

Table 2

Determination of molecular weights in $CHCl_3$ at 303.66°K

Substance	g_2 (g)	ΔR (Ω)	M_2		Error (%)
			Theoretic	Experimental	
Naphthalene	0.0128	58	128.16	126.6	−1.2
	0.0320	143		128.2	+0.03
	0.0641	276		132.8	+3.5
	0.0961	415		132.2	+3.0
	0.1282	546		133.7	+4.1
Anthracene	0.0178	59	178.24	173.1	−2.9
	0.0446	145		176.2	−1.1
	0.0891	292		174.5	−2.1
	0.1337	436		175.0	−1.8
	0.1782	565		179.6	+0.7

Table 3

Determination of molecular weights in CCl_4 303.66 °K

Substance	g_2 (g)	ΔR (Ω)	M_2		Error (%)
			Theoretic	Experimental	
Naphthalene	0.0128	49	128.16	130.3	+1.6
	0.0320	124		128.5	+0.2
	0.0641	246		129.4	+0.9
	0.0961	362		131.6	+2.6
	0.1282	485		130.7	+1.9

The agreement of theoretic and experimental molecular weights lies within the limits of a percentage error of − 3 — +4 for chloroform and smaller ones for carbon tetrachloride. Tables 4 and 5 present the results of vapour pressure osmometry measurements.

These tables, identically formed contain in the first two columns, the experimental data and in the other columns the results of data processing as basic thermodynamic magnitudes : thermodynamic activities of the solvent, dilution free enthalpies and molal osmotic coefficients.

For the systems under study there are no available thermodynamic data which could be used to be compared to our data ; the confirmation

Table 4

Thermodynamic magnitudes of naphthalene and anthracene in $CHCl_3$ at different temperatures and concentrations

Substance	m_2	ΔR (Ω)			$-\ln a_1 \times 10^3$			$-\Delta G_1$ (cal/mol) $\times 10^3$			$\varnothing$		
		298.59°K	303.66	308.83	298.59	303.66	308.83	298.59	303.66	308.83	298.59	303.66	308.83
Naphthalene	0.0068	68	58	46	0.79	0.82	0.80	469	495	483	0.973	1.011	0.984
	0.0170	169	143	116	1.96	2.02	2.01	1,163	1,219	1,213	0.967	0.997	0.992
	0.0340	332	276	223	3.85	3.90	3.87	2,284	2,353	2,335	0.950	0.962	0.954
	0.0510	495	415	327	5.74	5.87	5.68	3,408	3,542	3,427	0.944	0.965	0.932
	0.0680	650	546	436	7.54	7.73	7.57	4,476	4,661	4,567	0.930	0.952	0.932
Anthracene	0.0068	66	59	46	0.76	0.83	0.80	451	501	483	0.944	1.028	0.984
	0.0170	170	145	120	1.97	2.05	2.08	1,169	1,237	1,255	0.973	1.011	1.027
	0.0340	347	292	237	4.03	4.13	4.11	2,388	2,492	2,480	0.993	1.018	1.014
	0.0510	520	436	357	6.04	6.17	6.20	3,580	3,720	3,741	0.992	1.013	1.018
	0.0680	681	565	458	7.91	7.99	7.95	4,690	4,821	4,797	0.974	0.985	0.980

Table 5

Thermodynamic magnitudes of naphthalene in CCl_4 at different temperatures and concentrations

Substance	m_2	Δ R (Ω)			$-\ln a_1 \times 10^3$			$-\Delta G_1$ (cal/mol) $\times 10^3$			$\varnothing$		
		298.59 °K	303.66 °K	308.83 °K	298.59 °K	303.66 °K	308.83 °K	298.59 °K	303.66 °K	308.83 °K	298.59 °K	303.66 °K	308.83 °K
Naphthalene	0.0062_9	58	49	41	0.96	0.95	0.95	569	573	583	0.989	0.979	0.977
	0.0157	140	124	103	2.31	2.40	2.38	1,370	1,448	1,460	0.958	0.995	0.985
	0.0314	282	246	204	4.66	4.77	4.71	2,765	2,878	2,890	0.965	0.987	0.976
	0.0471	407	362	305	6.73	7.01	7.04	3,993	4,229	4,320	0.928	0.968	0.972
	0.0629	540	485	402	8.93	9.40	9.29	5,298	5,672	5,698	0.923	0.971	0.960

of their validity is given by the molecular weights of naphthalene and anthracene which fit well those found by Müller and Stolten,[6] Neumayer,[7] and Kulkarin.[8] The existing differences can be considered very small if one takes into account the fact that the quantity of substance for one trial, is of about one hundredth of a milligram for the most diluted solution under study.

The values of molal osmotic coefficients listed in the last two columns of tables 4 and 5 are slightly different from the unit, thus confirming the character of diluted solutions of the systems in study, at concentrations between 0.0063—0.063 molal and 0.0068—0.068 molal. In this narrow concentration range no regularity concerning the dependence of osmotic coefficient on concentration or temperature, could be established. As easily seen the values of molal osmotic coefficients are very close to each other. In the case of naphthalene-chloroform solutions a slight decrease in the osmotic coefficient with the increase of concentration occurs; this renders evident a slight deviation from ideality which accompanies the dilution decrease.

The values of dilution free enthalpies are low and decrease with the increase in concentration in all cases under study.

The values obtained for molal osmotic coefficients in a concentration range, where no other experiments have been carried out so far, evince the performances of the vapourometric micro-method.

This method allows the thermodynamic characterization of solutions of certain substances which are hardly available or slightly soluble. To the rapidity of the method and to its wide field of application in a large variety of systems the advantage of working on a wide temperature range should be added.

---

[6] R. H. Müller and H. J. Stolten, *Analyt. Chem.*, **25**, 1103 (1953).

[7] J. J. Neumayer, *Analyt. Chim. Acta.*, **20**, 519 (1959).

[8] S. B. Kulkarni, *Nature*, **171**, 219 (1953).

Revue Roumaine de Chimie, **15**, 1819–1825 (1970)

ULTRASONIC VELOCITY, COMPRESSIBILITY AND EXCESS VOLUME FOR BINARY MIXTURES OF MOLTEN SALTS : $NaCl + ZnCl_2$, $KCl + ZnCl_2$

V. VASILESCU, S. VOLKOV*) and S. STERNBERG

Institute of Physical Chemistry, Bucharest
str. Galaţi 31

Received April 15, 1970

The velocities of ultrasonic waves in $NaCl + ZnCl_2$ and $KCl + ZnCl_2$ mixtures have been measured and adiabatic and isothermal compressibilities calculated. In the first system the excess compressibility as well as excess volume are negative. This behaviour is explained by the destruction of associated structure of $ZnCl_2$ on alkali chloride addition. In the second system the excess compressibility is negative while the excess volume is positive ; this was explained by the action of two opposite factors : the destruction of $ZnCl_2$ associated structure which leads to a compression of the solution and the complex ion formation whose effect is an expansion of the solution.

1. INTRODUCTION

In previously published papers[1–4] the ultrasonic velocity and compressibility of binary mixtures $KCl + KBr$, $PbCl_2 + XCl$ ($X = Li$, Na, K, Rb, Cs), $MgCl_2 + BaCl_2$, $MgCl_2 + KCl$, $NaCl + XCl$ ($X = Li$, K, Rb, Cs) have been studied.

In the present paper similar results for $NaCl + ZnCl_2$ and $KCl + ZnCl_2$ are given. The study of these mixtures is interesting because fused $ZnCl_2$ is an associated liquid and its interaction with alkali chlorides has a specific influence upon physico-chemical properties of these melts and their structure, which depends both on associated structure destruction and complex formation.

The first mixture has negative excess volume while the second one has, according to the density data we used, positive excess volume. The general considerations on excess compressibility, β^E and excess volume V^E are similar to those given in paper.[3]

---

*) Permanent address : Institute of General and Inorganic Chemistry, Academy of Science, Kiev, USSR.

[1] S. Sternberg and V. Vasilescu, *Rev. Roumaine Chim.*, **12**, 1187 (1967).

[2] S. Sternberg and V. Vasilescu, *Rev. Roumaine Chim.*, **13**, 265 (1968).

[3] S. Sternberg and V. Vasilescu, *J. Chem. Thermodynamics*, **1**, 595 (1969).

[4] S. Sternberg and V. Vasilescu, *Rev. Roumaine Chim.*, (in press).

2. EXPERIMENTAL

Ultrasonic waves of 1 MHz were passed into the melt and picked up by silica rods. Measurements were carried out under dry argon in a silica crucible soldered at the lower silica rod.[1−4]

Dried $ZnCl_2$ was prepared from Merck *p.a.* reagent : the salt was slowly heated in dry gaseous HCl stream up to the melting point and after melting bubbled with HCl and dry Ar for several hours. The solid salt was kept over P_2O_5 in a vacuum desicator. All solid mixtures for measurements were melted in HCl stream and, after melting, bubbled with HCl and Ar.

3. RESULTS

The ultrasonic velocity for molten $ZnCl_2$ as well as all studied mixtures has a linear dependence on temperature ; the values of the velocity for $T = 273°K$ (u_0) and the temperature coefficients of velocity (a) are listed in table 1. Similar values for pure $ZnCl_2$ found by Bockris[5] are given for comparison.

The adiabatic compressibilities together with the molar excess volume are represented on figure 1 for $NaCl + ZnCl_2$ and on figure 2

Table 1

Temperature variation of ultrasonic velocities in simple melts and mixtures

$NaCl + ZnCl_2$			$KCl + ZnCl_2$		
$XZnCl_2$	$u_0(m.s^{-1})$	$a(m.s^{-1}.K^{-1})$	$XZnCl_2$	$u_0\ (m.s^{-1})$	$a(m.s^{-1}.K^{-1})$
1	1123	−0.420	1	1123	−0.420
1*)	1108	−0.375	0.842	1286	−0.546
0.8	1275	−0.477	0.687	1500	−0.704
0.7	1399	−0.535	0.548	1691	−0.823
0.5	1716	−0.730	0.361	1857	−0.798
0.3	1951	−0.768	0.302	1896	−0.788
0	2405	−0.811	0.189	2026	−0.830
			0	2273	−0.865

*) According to reference.[5]

---

[5] J.O'M. Bockris, A. Pilla and J. L. Barton, *Rev. Chim. Acad. R.P.R.*, **7**, 59 (1962).

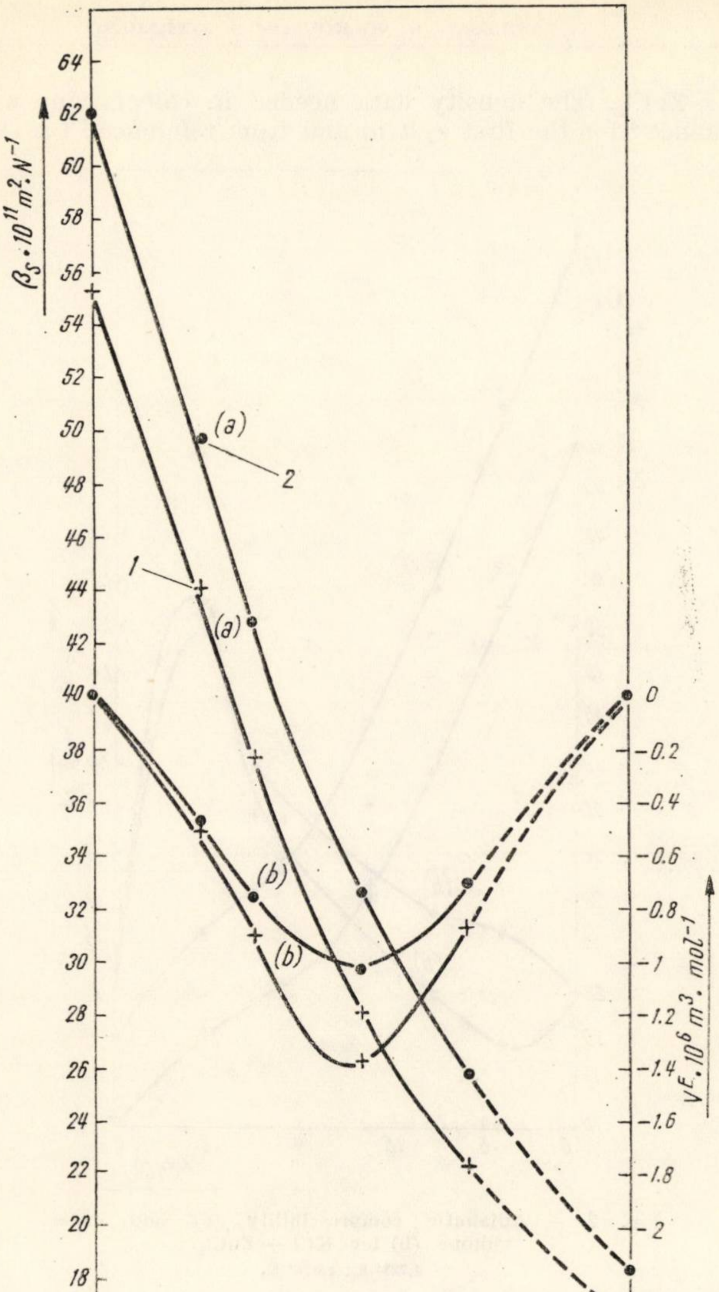

Fig. 1. — Adiabatic compressibility (a) and excess volume (b) for $NaCl + ZnCl_2$.
1, 873° K; *2*, 973° K.

for KCl + $ZnCl_2$. The density data needed in calculations were taken from reference[6] for the first system and from reference[7] for the second.

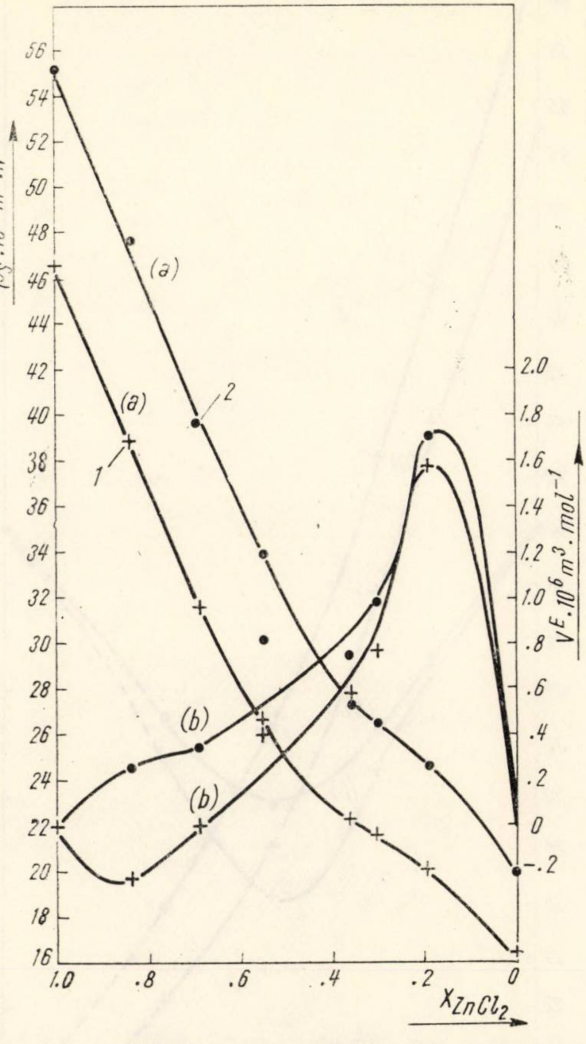

Fig. 2. — Adiabatic compressibility (a) and excess volume (b) for KCl + $ZnCl_2$.
1,723° K; *2*,873° K.

The values of the expansion coefficient (α), excess expansion coefficient (α^E), heat capacities ratio (γ), excess volume (V^E), isothermal and excess isothermal compressibilities (β and β^E respectively), the excess isothermal compressibility over ideal isothermal compressibility ratio

---

[6] M. F. Lantratov and T. N. Sevliakova, "Phys. Khim., Rasplavenikh Solei", Akad. Nauk Ukr. S.S.R., Metalurg Izdat., Moscow, 1965, p. 13.

[7] F. R. Duke and R. A. Fleming, *J. Electrochem. Soc.*, **104**, 251 (1957).

(β^E/β_0), the (β^E/β_0) value calculated according to the hole theory [3,8], the pressure and temperature coefficients of the excess volume ($(\partial V^E/\partial p)_T$ and $(\partial V^E/\partial T)_p$ respectively), the excess volume calculated according to the modified Hildebrand's theory [3,9] (V_I^E) and the excess volume calculated according to Sternberg's method [3] (V_{II}^E) for the two studied systems are given in tables 2 and 3. The following equations have been used for (β^E/β_0), V_I^E and V_{II}^E:

$$\beta^E/\beta_0 = \frac{\beta'/\beta'_0 + \theta\beta(s)/\beta'_0}{1 + \theta\beta(s)_0/\beta'_0} - 1 \tag{1}$$

$$V_I^E = -V_0\,\beta_0\,T\left[\frac{\alpha}{\beta} - \frac{\alpha_0}{\beta_0}\right] \tag{2}$$

$$V_{II}^E = -V\left[\frac{(\partial V^E/\partial p)_T}{\beta V} + 1\right] + V\left[\left\{\frac{(\partial V^E/\partial p)_T}{\beta V} + 1\right\}^2 + \frac{2}{V}\{V_I^E + T V_0\,\alpha^E\}\right]^{1/2} \tag{3}$$

Table 2

Excess quantities for NaCl + ZnCl$_2$ at 873° K.

$X\mathrm{ZnCl_2}$	1	0.8	0.7	0.5	0.3	0
$\alpha.10^4\mathrm{K}^{-1}$	1.96	2.36	2.73	3.52	3.55	3.38
$\alpha^E.10^4\ \mathrm{K}^{-1}$	0	0.21	0.47	1.02	0.75	0
γ	1.03	1.09	1.12	1.17	1.23	1.32
$V^E.10^6\mathrm{m^3mol^{-1}}$	0	−0.50	−0.90	−1.38	−0.87	0
$\beta.10^{11}\ \mathrm{m^2\ N^{-1}}$	56.9	48.1	42.2	32.8	27.4	21.5
$\beta^E.10^{11}\ \mathrm{m^2\ N^{-1}}$	0	−4.1	−7.3	−10.6	−8.6	0
$100\,(\beta^E/\beta_0)$	0	−0.08	−0.15	−0.24	−0.24	0
$100\,(\beta^E/\beta_0)^*)$	0	−0.07	−0.12	−0.18	−0.10	0
$(\partial V^E/\partial p)_T.10^{15}\mathrm{m^5\ N^{-1}\ mol^{-1}}$	0	2.39	4.05	5.31	3.80	0
$(\partial V^E/\partial T)_p.10^{10}\ \mathrm{m^3\ K^{-1}\ mol^{-1}}$	0	3	15	36	17	0
V_I^E **)	0	−1.88	−4.14	−8.66	−6.75	0
V_{II}^E ***)	0	−0.88	−1.77	−3.41	−3.10	0

*) according to equation (1);
**) according to equation (2);
***) according to equation (3).

---

[8] J. O'M. Bockris and N. E. Richards, *Proc. Roy. Soc.*, A, **241**, 44 (1957).

[9] J. H. Hildebrand and R. L. Scott, "The Solubility of Nonelectrolytes", Reinhold, New York, 1950, p. 136.

where : β', β'_0, $\beta_{(S)}$ and $\beta_{(S)_0}$ are the contributions of holes to the compressibility, its ideal value, the compressibility of the liquid lattice and its ideal value respectively, $0 < \theta < 1$ is a parameter which was approximated by 0.5, V_0 and α_0 the ideal values of V and α respectively.

For reasons widely exposed in a previous paper[4] the γ value was calculated according to an additivity rule. The C_p values for simple, molten salts were taken from reference [10] and the compressibilities of solid salts at working temperature from references.[5,11]

Table 3

Excess quantities for $KCl + ZnCl_2$ at 873°K.

$X\ ZnCl_2$	1.0	0.842	0.687	0.548	0.361	0.302	0.189	0.0
$\alpha . 10^4\ K^{-1}$	1.96	2.77	2.81	3.20	3.14	3.27	3.24	3.49
$\alpha^E . 10^4\ K^{-1}$	0	0.61	0.44	0.61	0.28	0.32	0.09	0
γ	1.03	1.08	1.14	1.17	1.24	1.26	1.29	1.36
$V^E . 10^6 m^3 . mol^{-1}$	0	0.26	0.35	0.82	0.75	0.99	1.71	0
$\beta . 10^{11} . m^2 N^{-1}$	56.9	51.7	45.3	39.8	34.1	33.5	31.9	27.2
$\beta^E . 10^{11}\ m^2 N^{-1}$	0	−1.3	−3.6	−5.3	−5.4	−4.0	−2.0	0
$100 \cdot (\beta^E/\beta_0)$	0	−0.03	−0.07	−0.12	−0.14	−0.11	−0.06	0
$100\ (\beta^E/\beta_0)$ *)	0	0.03	0.05	0.09	0.08	0.11	0.17	0
$(\partial V^E/\partial p)_T . 10^{15}\ m^5\ N^{-1}\ mol^{-1}$	0	0.58	1.78	2.43	2.43	1.63	0.39	0
$(\partial V^E/\partial T)_p . 10^{10} . m^3 K^{-1} mol^{-1}$	0	32	22	27	12	15	9.3	0
V^E_{I} **)	0	−3.28	−3.09	−4.71	−3.39	−3.05	−1.23	0
V^E_{II} ***)	0	−0.33	−0.81	−1.97	−1.92	−1.54	−0.82	0

*) according to equation (1);
**) according to equation (2);
***) according to equation (3).

4. DISCUSSION

As can be noticed on figure 1 the excess volume, as well as excess adiabatic compressibility for $NaCl + ZnCl_2$ have negative deviations from additivity in all concentration ranges. The negative excess volume could be explained by the destruction of the associated structure of $ZnCl_2$[12,13]

---

[10] O. Kubashewski, E. L. Evans and C. B. Alcock, "Metallurgical Thermochemistry", Pergamon Press, New York, 1967, p. 399, 401, 420.

[11] International Critical Tables of Numerical Data. Physics, Chemistry and Technology, Vol. 3, McGraw-Hill Book Comp., New York and London, 1928, p. 50.

[12] B. F. Markov and S. V. Volkov, "Phys. Khim. Rasplavenikh Solei", Akad. Nauk Ukr. S.S.R., Metallurg. Izdat. Moscow, 1965, p. 210.

[13] B. F. Markov and S. V. Volkov, Ukrain. Khim. Zhur., **34**, 1115 (1968).

which takes place on mixing. On the other hand the small radius of Na ion (the high ionic potential) prevents the system from complex ion formation. At the same time β also gives negative deviations from the additivity rule, a behaviour previously established for the system MgCl + + $BaCl_2$. The calculated V^E values which are given in table 2 are in a poor agreement with experimental data as long as V^E_{I} is concerned and in a better one when V^E_{II} is considered.

The experimental and calculated β^E/β_0 values are in good agreement. In this system (as well as in the other one) there is a good sign agreement between α^E and $(\partial V^E/\partial T)_p$.

The other system which is part of this study, broke the regularities established in all the series of mixtures studied so far : though the excess volume is positive, negative values are obtained for β^E. It seems that at lower temperatures (450° for instance), negative V^E values are found in mixtures richer in $ZnCl_2$[7,13]. V^E_{I}, V^E_{II} and β^E/β_0 give a very poor agreement with experimental data so much the more as even the sign agreement is no longer present.

In this system besides the associated structure destruction (which is accompanied by an increase in electro-valence), a complex ion formation phenomenon takes place, too (as it results from the phase diagram). The formation of complex ions is associated with positive excess compressibility and excess volume.[1-4] In case of KCl + $ZnCl_2$ the two above mentioned phenomena act against each other and the excess magnitudes can be written as :

$$\beta^E = \beta^E_{\text{ionic}} + \beta^E_{\text{complex}} \tag{4}$$

$$V^E = V^E_{\text{ionic}} + V^E_{\text{complex}} \tag{5}$$

where the values with "ionic" subscript are due to the increase in the ionic character of the melt on mixing while the "complex" subscript denotes the effect of complex ions formation. In equations (4) and (5) β^E_{ionic} and V^E_{ionic} are negative and β^E_{complex} and V^E_{complex} are positive.

It seems very likely that the ionizing effect has a stronger influence upon compressibility than upon the volume so that $|\beta^E_{\text{ionic}}| > |\beta^E_{\text{complex}}|$ and $|V^E_{\text{ionic}}| < |V^E_{\text{complex}}|$; it is in this way that the sign disagreement of β^E and V^E could be explained.

From the data presented above it results that the behaviour of NaCl + $ZnCl_2$ and KCl + $ZnCl_2$ systems differs from that of all the systems studied so far ; this seems to be due to a "compression" effect caused by the destruction of the stratified structure of zinc chloride occurring when alkali chloride is added. An increase in the ionic character of binding energies in zinc chloride — alkali chloride mixtures was evinced by other physico-chemical properties, too.

Revue Roumaine de Chimie, **15**, 1827–1829 (1970)

ON THE COOL FLAME IN THE REACTION OF METHANE OXIDATION

ILEANA IOSIF

Centre of Physical Chemistry, Bucharest, str. Galaţi 31

I. A. SCHNEIDER

"Al. I. Cuza" University, Chair of Physical Chemistry, Jassy,
str. 23 August 11

Received June 23, 1970

The nitric acid-initiated oxidation of methane has been studied in a flow system at 557°. The "cool flame" region was investigated and various parameters influencing it evinced.

In a series of previous papers it was shown that in case of low temperature — slow oxidation of methane, initiated by nitric acid or nitrogen oxides, a temperature maximum occurs in the dynamic conditions of reactants admission [1]; its position and shape depend on the initiator concentration and the flow rate of the reacting mixture.[2]

The formation of formaldehyde and hydrogen was proved to be directly dependent on this maximum [3] while the existing luminosity indicated the presence of a flame.[4]

The adiabatic character of this flame as well as the fact that at initial reactor temperature of 500° its top region did not go beyond 720—730° indicated the existence of a cool flame of methane. A kinetic interpretation was attempted on the basis of temperature increase curves [5]; it showed that the kinetic parameters lay within the limits indicated in literature.

To visualize the influence of different parameters upon the flame shape and position use has been made of an unfilled and uncoated (with potassium tetraborate) — silica reactor.

The reactor was shaped as a refrigerator, consisting of two silica coaxial tubes; the inner one was used for measuring and recording the temperature within the reactor with a chromel-alumel thermocouple.

---

[1] I. A. Schneider, O. S. Ivanov and A. B. Nalbadian, *Doklady Akad. Nauk S.S.S.R.* **180**. 626 (1968).

[2] A. B. Nalbadian, I. Iosif and I. A. Schneider. *Rev. Roumaine Chim.*, **13**, 671 (1968),

[3] I. Iosif, I. A. Schneider and A. B. Nalbadian, *Rev. Roumaine Chim.*, **13**, 867 (1968).

[4] D. P. Lazăr and I. A. Schneider, *Rev. Roumaine Chim.*, **13**, 1285 (1968)

[5] I. Iosif, D. P. Lazăr and I. A. Schneider, "Symposium on Gas Kinetics", Szeged, 1969.

The design and dimensions of the reactor are shown in figure 1.

The reactor was introduced into a horizontal furnace equipped with a silica window through which the light emission occurring on temperature maximum was studied.

RESULTS AND DISCUSSION

The influence of the flow rate of a CH_4/air $= 1/2$ mixture with 5% initiator (HNO_3) upon the position and shape of the resulting steady flame following a certain induction period is given in figure 2.

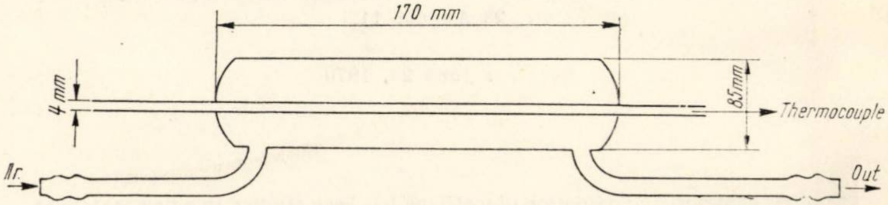

Fig. 1. — Silica reactor used in the reaction of methane oxidation.

It must be remarked that the so-called flame (encircled on the upper image of figure 2) is blue and appears instantaneously after the admission of the reaction mixture into the silica reactor.

The released heat produces a temperature increase and as the inner tube becomes incandescent the actual colour of the flame is partially hidden. It is in this way that the erroneous observation concerning the colour of the flame, which was given in reference,[4] could be explained. In that paper the flame formation was studied in a ground silica-filled tube. Since the external tube of the reactor remains cool all throughout the experiment, the flame has an adiabatic character.

The temperature distribution in steady flames is represented on figure 3 for three different flow rates.

The figure shows that the flame length is between 1 and 1.5 cm while the temperature difference between the top and the base of the flame is of about 200–225°.

It is worth mentioning that in all cases a reactor temperature of 557° was used.

The influence of CH_4/air ratio on the position and shape of the flame is represented in figure 4; a strengthening of the flame accompanied by a decrease in the CH_4 content in the reaction mixtures is generally observed.

These findings are much more evident on figure 5 which represents the flame obtained when cold air is blown into the inner tube to remove the heat produced by the flame; it is in this way that the silica tube is prevented from becoming incandescent and thus an undisturbed image of the blue flame is obtained.

Fig. 2. — Flow rate influence on the position and shape of the cool flame.

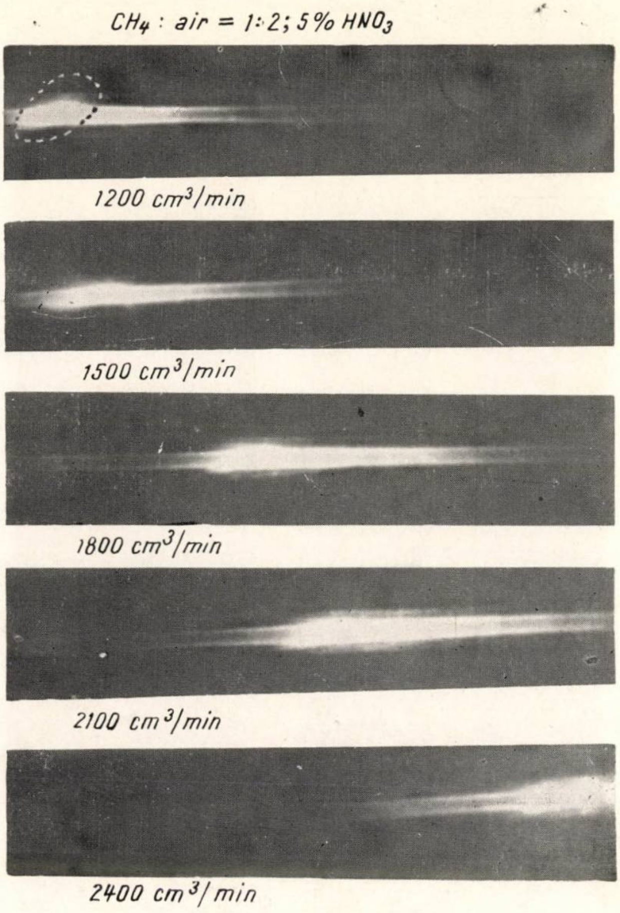
CH_4 : air = 1:2; 5% HNO_3
1200 cm³/min
1500 cm³/min
1800 cm³/min
2100 cm³/min
2400 cm³/min

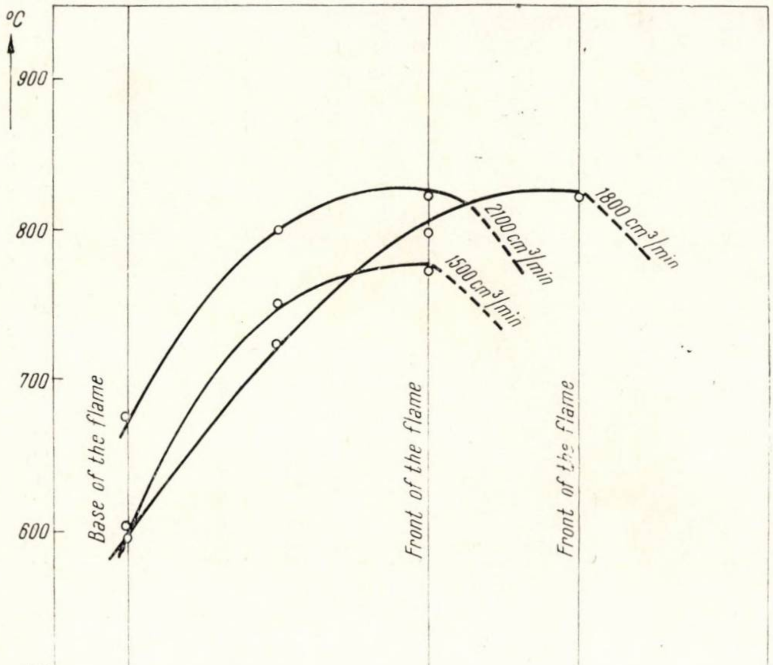

Fig. 3. — Temperature distribution along the flame.

1400 cm^3/min air, 5% HNO_3

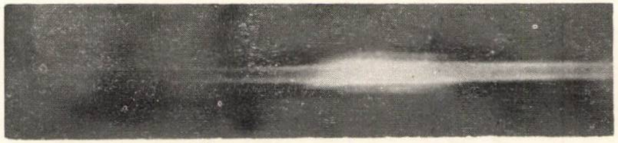

+ 700 cm^3/min CH_4

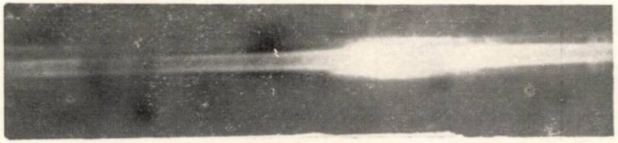

+ 500 cm^3/min CH_4

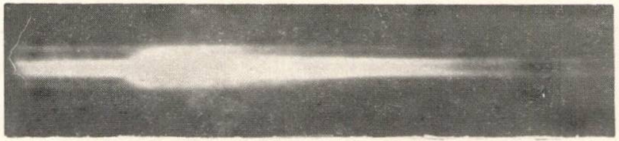

+ 350 cm^3/min CH_4

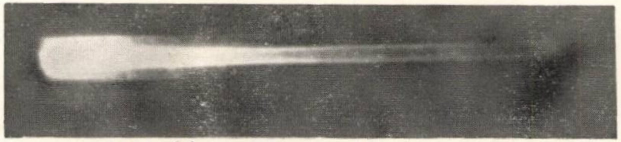

+ 225 cm^3/min CH_4

Fig. 4. — Influence of the ratio CH_4/air on the position and shape of the cool flame.

1000 cm^3/min air ; 5% HNO_3

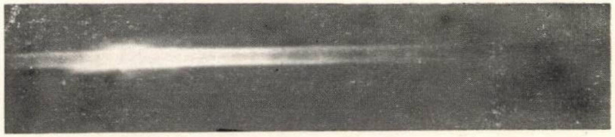

+ 500 cm^3/min CH_4

The same , cooled inner tube

+ 225 cm^3/min CH_4 , cooled inner tube

+ 70 cm^3/min CH_4 cooled inner tube

550 cm^3/min air + 70 cm^3/min CH_4 ; cooled inner tube

Fig. 5. — Cool flame image after the cooling of the inner tube.

This effect is evinced by a comparison of figures 1 and 2 with 5; this also indicates a displacement of the flame toward the reactor exit so that the displacement of the flame along the reactor caused by the flow rate increase, should be similarly explained by the increasing cooling effect of reacting gases introduced into the reactor.

The reduction of methane content (pictures 2—4) clearly causes the above mentioned strengthening; the clearest image of the flame was obtained for low flow rates and low CH_4 content (image 5—figure 5).

We finally mention that the attempt to further reduce the methane content in case of the last mixture (550 cm^3/min air + 70 cm^3/min CH_4; 5% HNO_3) leads to a two-stage ignition phenomenon; a flickering pale blue flame accompanied at random time intervals by bright ligthening which instantaneously crossed the whole reactor, was observed.

As the film available was not sensitive enough the phenomenon could not be recorded on a picture.

The [illegible] by a [illegible] of [illegible] and [illegible] a displacement of the flame toward the reactor [illegible] of the flame along the reactor [illegible] by the [illegible] caused by the [illegible] to the reactor.

[illegible] of [illegible] control [illegible] the [illegible] contact [illegible] of the flame [illegible] and [illegible]

We [illegible] that the [illegible] and [illegible] the [illegible] was observed.

[illegible] the phenomenon [illegible] not [illegible]

Revue Roumaine de Chimie, **15**, 1831–1837, (1970)

VISCOSITY OF SOME MOLTEN ALKALINE EARTH CHLORIDES

ŞTEFANIA ZUCA and RODICA COSTIN

Institute of Physical Chemistry, Bucharest, str. Galaţi 31

Received May 13, 1970

The viscosity of molten $CaCl_2$, $SrCl_2$ and $BaCl_2$ are reported for the temperature range of 100° above their melting point. The obtained results are discussed in the light of current views on viscous flow in ionic liquids.

The viscosity of molten alkaline earth halides has been very little investigated so far. This lack of data is due to the great experimental difficulties met with these melts, namely they have relatively high melting points and can with great difficulty be obtained free from compounds produced by hydrolisis within the salt upon melting. By the present time, the viscosity of molten $CaCl_2$, $SrCl_2$ and $BaCl_2$ has been investigated by some few groups,[1–5] but none of the earlier sets of data agree with each other. Therefore it was thought worthy of reinvestigation.

The experimental investigation reported in this paper concerns the viscosity of $CaCl_2$, $SrCl_2$ and $BaCl_2$.

RESULTS AND DISCUSSIONS

The oscillating sphere method has been employed for viscosity measurement. The experimental set up was basically similar to that described elsewhere [6]. Some refinements and modifications were effected. The damping oscillations were this time automatically recorded by means of a PHD 8 Photodyne, which enables a more accurate measurement of the amplitudes of oscillation to be made.

A vertical furnace provided for working in a controled atmosphere was used. Any contact with atmospheric oxygen and humidity was avoided and a permanent flow of throughly dried nitrogen gas free of oxygen was passed inside the furnace during the experiment.

A constant temperature of the furnace to within ±0.2°C was obtained by means of a photothermoregulator. The temperature uniformity was ±0.5°C over a 6 cm length. The

---

[1] S. Karpachev and A. Stromberg, *Zhur. fiz. Khim.*, **11**, 852 (1938).

[2] R. D. Reeves and G. J. Janz, *Trans. Faraday Soc.*, **61**, 2305 (1965).

[3] N. V. Bondareko and H. L. Streletz, "Fizicheskaia khimia i elektrokhimia rasplavenikh solei i schlakov", Izd. Khimia, Leningrad, 1968, p. 95.

[4] V. L. Barzakovsky, *Dissertation Akad. Nauk S.S.S.R.*, 1939

[5] V. T. Slavianski, *Doklady Akad. Nauk. S.S.S.R.*, **58**, 1077 (1948).

[6] I. G. Murgulescu and S. Zuca, *Z. phys. Chem. (Leipzig)*, **218**, 379 (1961).

temperature has been measured by means of a calibrated Pt/Pt–10 % Rh thermocouple immersed directly into the studied molten salts. The alkaline earth chlorides were p.a.reagent. Products of different sources have been used. All salts were purified by recristallizing twice from distilled water, dried for 24 h at 150° and melted to remove any compounds produced by hydrolysis within the slat upon heating.

The silica cell shown in fig. 1 was used with that end in view. The alkaline earth chloride contained in the silica tube A was slowly heated to the melting point alternatively under vacuum or in an inert atmosphere of dry argon gas saturated with CCl_4 vapours. The gas was bubbled through the molten salt for a further 1/4 h. The chlor obtained by decomposition of CCl_4 vapours, proved to be a very active purifying agent. By a change of gas pression into the cell the molten salt was evacuated by the capillary B into C where it was gathered and kept in liquid CCl_4 under the form of solid pellets. The obtained salts were checked for alkalinity with phenolphthalein and they were consistently neutral. Any subsequent handling of these salts was performed in a dry box.

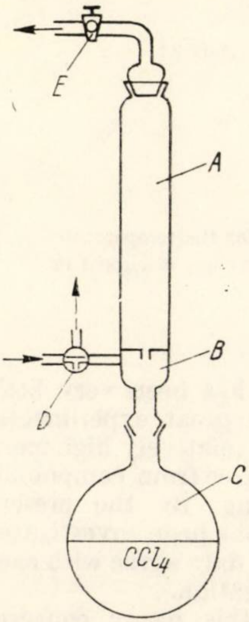

Fig. 1. – Scheme of melting cell.

A, silica melt container; *B*, evacuating capillary; *C*, receiving flask; *D*, stropcock for outlet to vacuum pump and inlet of argon + CCl_4; *E*, outlet of the gas.

The results obtained for the viscosity of investigated salts are given in Table 1. In all cases the density data quoted in literature [7] have been used in calculating the viscosity. The present data are compared to the values of viscosity obtained by other workers[1–5] in figs 2–4.

From the data illustrated on figs. 2–4 it is evident that there is a considerable desagreement among various laboratories.

The present data for $CaCl_2$ (fig. 2) indicate a lower temperature dependence than the other literature data [1,2]. The percent difference calculated as $100 \frac{\eta_{exp.} - \eta_{lit.}}{\eta_{lit.}}$, from the data of Karpachev and Stromberg (oscillating disc technique) [1] goes increasingly from +3% at 800° to +11% at 900°. Reeves and Janz[2] employed the oscillating hollow sphere technique and indicated values which agree very well at 790° (0%) but the percent difference rises with increasing temperature and reaches –43% at 980°.

For $SrCl_2$ the only data quoted in literature are those by Reeves and Janz [2]. As it can be seen in fig. 3 the agreement between the two sets of values is very poor. The present data indicate a lower temperature dependence and the percent difference increases steadly from +14% in vecinity of 880° to +55% at 950°.

The present results for $BaCl_2$ (fig. 4) agree within experimental error very closely with the values of viscosity obtained by Bondarenko and Streletz [3]. From fig. 3 it is obvious that a stronger temperature dependence and higher values of viscosity are indicated by Reeves and Janz [2]. The maximum percent difference is of – 20% at about 1000°

---

[7] G. J. Janz, F. W. Dampier, G. R. Lakshminaryanan, P. K. Lorenz and R. P. T. Tomkins, "Molten Salts", vol. 1, N.S.R.D.S.-N.B.S., 15, 1968.

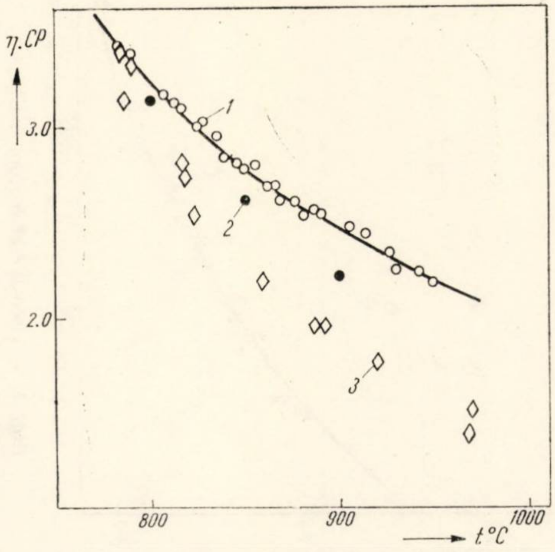

Fig. 2. — Viscosity of molten $CaCl_2$.

1, our data; , *2* Karpachev and Stromberg data [1]; *3*, Reeves and Janz data.[2]

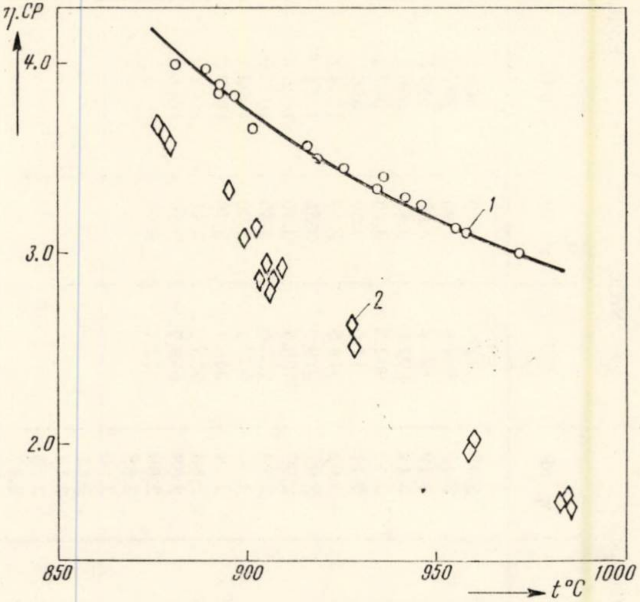

Fig. 3. — Viscosity of molten $SrCl_2$.

1, our data; *2*, Reeves and Janz data.[2]

Table 1

Viscosity of molten alkaline earth chlorides

$CaCl_2$		$SrCl_2$		$BaCl_2$	
t°C	η, cP	t°C	η, cP	t°C	η, cP
784.6	3.42	881.0	4.00	969.2	4.25
789.0	3.40	889.0	3.96	977.0	3.96
808.2	3.19	893.4	3.87	980.3	3.87
813.9	3.14	897.2	3.83	990.0	3.81
813.2	3.12	902.3	3.66	997.2	3.76
816.0	3.11	911.0	3.59	996.9	3.70
825.0	3.02	916.5	3.57	1008.1	3.63
826.2	3.03	919.0	3.51	1014.0	3.51
835.3	2.96	926.4	3.45	1023.6	3.44
839.0	2.83	935.0	3.35	1029.9	3.33
846.1	2.80	942.2	3.30	1032.1	3.28
851.7	2.78	946.1	3.26	1037.3	3.27
855.0	2.80	955.0	3.14	1052.0	3.10
861.3	2.68	958.7	3.10	1066.4	3.00
865.0	2.69	972.7	3.05		
870.2	2.63				
876.0	2.60				
879.3	2.61				
886.0	2.56				
891.4	2.53				
904.0	2.47				
914.7	2.43				
926.0	2.35				
929.0	2.27				
942.2	2.24				
948.0	2.19				

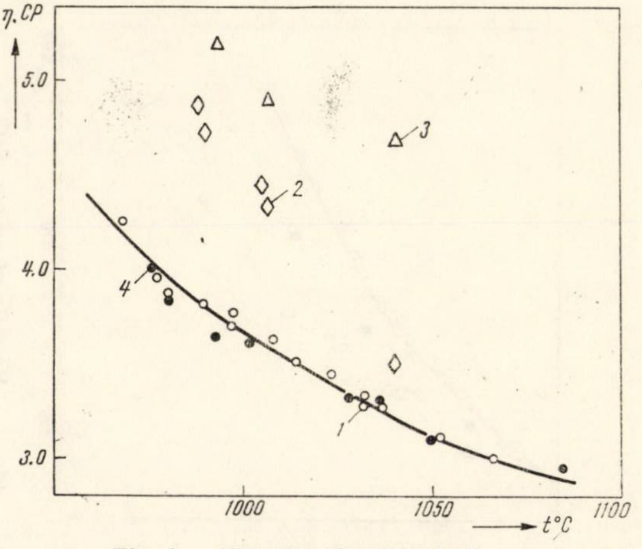

Fig. 4. — Viscosity of molten $BaCl_2$.
1, our data; *2*, Reeves and Janz data [2]; *3*, Slavianski data[3]; *4*, Bondarenko and Streletz data.[5]

and diminishes at -8% at a higher temperature. Barzakovsky [4] data can be very little relied on. They are quoted by Slavianski [5] in the form of a small graphic without any additional information. A difference of about -30% there seems to exist between the two sets of data.

We have made many attempts to measure the viscosity of molten $MgCl_2$, but no reproducible data could be obtained. It is most likely that the oxidation of molten $MgCl_2$ is not completely avoided and the very thin layer of MgO on the surface of the melts hinders the free damping of the sphere oscillations.

Fig. 5 illustrates that for all studied alkaline earth chlorides there is no important deviation from linearity of $\log\eta$ vs. $1/T$ plot, which proves that Arrhenius equation: $\eta = A \exp (E_\eta/RT)$ is obeyed. The slope of $\log\eta$ vs. $1/T$ lines gives the activation energy of viscous flow E_η: it is clear that it goes increasingly from $CaCl_2$ to $BaCl_2$.

The numerical values of A and E_η constants as determined by the east squares method are summarized in table 2.

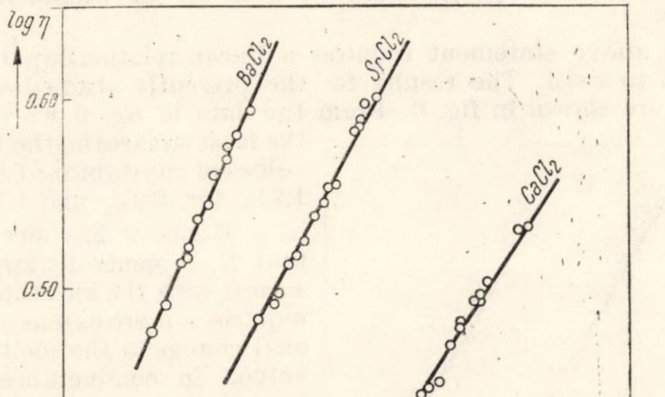

Fig. 5. — Graph of $\log \eta$ against reciprocal of the absolute temperature for molten $CaCl_2$, $SrCl_2$, $BaCl_2$.

The dependence of electrical conductivity of alkaline earth chlorides upon temperature can be expressed by a similar equation [8,9]. Fren-

---

[8] E. R. Van Artsdalen and I. S. Yaffe, "Chemistry Division, Semi-annual Progress Report", Oak Ridge National Laboratory, ORNL-2159, 80, 1956.

[9] J.O'M. Bockris, E. H. Crook, H. Bloom and N. E. Richards, *Proc. Roy, Soc.*, **A. 255**, 558 (1960).

Table 2

Pre-exponential factor A and the activation energy $E\eta$.

Salt	$^*A.10^2$	$E\eta$ kcal/mol	Standard deviation for $E\eta$ kcal/mol	Temperature range °C
$CaCl_2$	12.46	6.96	0.035	788–948
$SrCl_2$	6.07	9.63	0.076	893–972
$BaCl_2$	5.62	10.57	0.126	969–1066

* η is given in cP.

kel[10] has proved that the electrical conductivity and the viscosity of molten salts can be correlated by the following equation $\lambda^n . \eta = \text{const.}$ if the activation energy of viscous flow and of electrical conductivity are supposed to be proportional; the factor of proportionality being $n = E_\eta / E_\lambda$.

The above statement requires a linear relationship between log η and log λ to exist. The results for the presently studied alkaline earth chlorides are shown in fig. 6. From the data in fig. 6 we calculated, by the least squares method the following values of constant n : 1.333 for $CaCl_2$; 1.711 for $SrCl_2$ and 1.720 for $BaCl_2$.

Hence it has been ascertained that E_η is generally larger than E_λ in accord with the idea that viscous flow requires a more extensive configurational change in the melt than that involved in conductance mechanism. Nowadays it is accepted that the dominant entity in the transport of electrical charge is the more mobile ion — the cation — while the viscous flow involves the translation of ions of both signs[6]. However the value of factor n in $CaCl_2$, $SrCl_2$ and $BaCl_2$ melts is relatively close to the unity. It is likely that the rate determining entity in the conductive and viscous flow is somewhat similar and the conductance mechanism involves the motion of anion too.

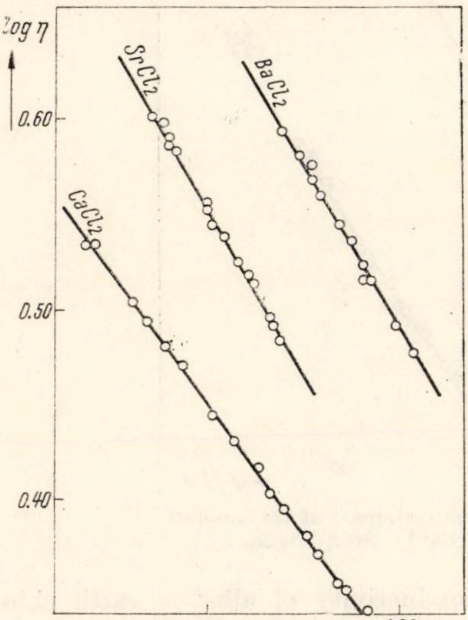

Fig. 6. — Log η plotted against log λ for molten $CaCl_2$, $SrCl_2$, $BaCl_2$.

Markov and Delimarski[11] proposed that in 2 : 1 salts two equilibria are present :

---

[10] J. FRENKEL, "Kinetic Theory of Liquids", Oxford University Press, London, 1946, p. 441.

[11] B. F. MARKOV and IU. K. DELIMARSKI, *Ukrain. Khim. Zhur.* **19**, 255 (1953).

$$MeX_2 \leftrightharpoons MeX^+ + X^- \tag{1}$$

$$MeX^+ \leftrightharpoons Me^{2+} + X^- \tag{2}$$

They calculated the degree of dissociation for molten $CaCl_2$, $SrCl_2$ and $BaCl_2$ and found that while the first dissociation scheme is total in all cases the second dissociation scheme takes place in proportion of 25, 43 and 70% respectively. Therefore the electrical conductivity increases from $CaCl_2$ to $BaCl_2$.

Batchinskii[12] has proposed for pure molten salts an expression connecting their viscosity with the free volume available for viscous flow :

$$\eta = \frac{c}{v - \omega} \tag{3}$$

where c and ω are characteristic constants for any given salts and v is the specific volume (temperature dependent).

The constant ω in eq. (3) frequently is named the limit specific volume because it represents the specific volume at which the viscosity becomes infinite i.e. the liquid solidifies. Consequently the constant ω represents the specific volume of the solid at the freezing point and the difference $v - \omega$ may be regarded as the free volume available for viscous flow.

According to (3) the plot of the fluidity $1/\eta$ vs. the specific volume v should yield for each salt a straight line with a numerical value of the slope and interception equal to c and ω respectively. When the experimental results for the studied liquids were leastsquared to (3) it was found to be obeyed to within an error of $\pm 2\%$. The obtained numerical values of constant c and ω are given in Table 3.

Table 3

Batchinskii equation parameters

Salt	*$c.10^2$	ω
$CaCl_2$	10.18	0.4513
$SrCl_2$	8.07	0.3475
$BaCl_2$	6.80	0.2993

* η is given in cP.

The validity of Batchinskii equation proves that the free volume plays an important part in the viscous flow in the pure molten alkaline earth chlorides.

---

[12] A. I. BATCHINSKII, *Z. phys. Chem.*, **34**, 634 (1913).

Revue Roumaine de Chimie, **15**, 1839–1845 (1970)

EXCESS THERMODYNAMIC FUNCTIONS FOR LIQUID BINARY MIXTURES OF SOME ALKALI METALS

RODICA VÎLCU and C. MISDOLEA

Institute of Physical Chemistry, Bucharest, str. Galaţi 31

Received may 13, 1970

The enthalpy of mixing and the excess free enthalpy, accompanying the formation of binaries Na–K, Na–Cs and K–Cs in the liquid phase, were statistically computed by applying an adaptation of the significant structure theory of liquids to the partition function formulation of molten metals, both isolated and mixed. The values of the thermodynamic quantities, computed for various temperatures, agree with the actual experimental data.

INTRODUCTION

Besides the scarce existing calorimetric information about the thermal effects accompanying the molten metals mixing,[1-4] we tried to compute the enthalpy of mixing by estimating, for a few bynary systems of alkali metals in the liquid phase, the components of interaction energy intervening at the mixing time.[5] Owing to this simple electronic structure, the alkali metals lend themselves quite well to theoretical studies while, by their physico-chemical behaviour, they offer a practical interest as well. Nevertheless, besides the numerical computations, given by Christmann [6] concerning the properties of some binary mixtures of molten alkali metals, we cannot mention but a few theoretical accounts in this domain. For instance, Cohen's paper [7] is devoted to some new theoretical methods of treating the non-transition metals, and Bellemans and De Leener [8] deal also with the theoretical aspect of the metallic solutions treatment. Cohen's theory is based upon a new dielectric formulation of the many-body problem, as well as upon the

---

[1] M. Kawakami, *Sci. Rept, Tohoku Univ., First Ser.*, **16**, 915 (1927).

[2] R. L. McKisson and L. A. Bromley, *J. Amer. Chem. Soc.*, **73**, 314 (1951).

[3] O. J. Kleppa, *J. Phys. Chem.*, **59**, 175 (1955).

[4] R. A. Oriani, *Acta Met.*, **7**, 808 (1959).

[5] T. Yokokawa and O. J. Kleppa, *J. Chem. Phys.*, **40**, 46 (1964).

[6] J. R. Christman, *Phys. Review.*, **153**, 225 (1967); **153**, 217 (1967).

[7] M. H. Cohen, *J. Phys. Radium*, **23**, 643 (1962).

[8] A. Bellemans and M. De Leener, *Phys. Rev. Letters*, **6**, 603 (1961). *Phys. Letters*, **4**, 157 (1963).

pseudopotential method with ion cores. Bellemans and De Leener deduced a formula for the fundamental state energy of metallic solutions as a function of composition.

In the present paper, we apply, to the binary solutions of molten alkali metals, the significant structure theory that, owing to its intuitive character, contributed to theoretical characterization of various category systems such as: moleculra liquids,[9] ionic liquids both isolated and mixed,[10,11] molten metals[12,13] and metal-metal salt systems.[14]

With a view to the thermodynamical treatment of binary mixtures of molten metals, the following expression was established for the partition function of metal in the liquid phase[12]:

$$Z = \left[\frac{e^{E_s/RT}}{(1-e^{-\theta/T})^3} \cdot \left(1 + n_h\, e^{-\frac{aE_s}{n_h RT}}\right)\right]^{N\frac{V_s}{V}} \left[\frac{(2\pi mkT)^{3/2}}{h^3}\frac{eV}{N}\right]^{2N\frac{V-V_s}{V}} \tag{1}$$

with the following symbols:

E_s denotes the sublimation energy at the melting point;

θ denotes the Einstein characteristic temperature of the solid at the melting point;

$n_h = \dfrac{n(V - V_s)}{V_s}$ denotes the accessible position number of a molecule outside the equilibrium position;

V, denotes the molar volume of the liquid;

a, denotes the molar volume of the solid at the melting point;

m, denotes the energy bound paramater, thanks to which a molecule can pass from a position to another one;

R, N, h, k denote the known universal constants.

The partition function given by equation (1), can be reduced to the form

$$Z = Z_s^{N\frac{V_s}{V}} \cdot Z_g^{N\frac{V-V_s}{V}} \tag{2}$$

Z_s denotes the partition function of the solid-like molecules, while Z_g denotes the partition function of gas-like molecules, as there results from formula (1).

In order to restrict the formality imposed by the statistic computation of thermodynamical computations, the partition function logarithm is expressed as follows:

$$\ln z = \frac{1}{x}(\sigma_1 + \sigma_2) + \left(1 - \frac{1}{x}\right)(\gamma + \ln x) \tag{3}$$

---

[9] Kay Liang, H. Eyring and Ray P. March, *Proc. Natl. Acad. Sci. U.S.A.*, **52**, 1107 (1964).

[10] C. M. Carlson, H. Eyring and T. Ree, *Proc. Natl. Acad. Sci. U.S.A.*, **46**, 333 (1960).

[11] R. Vîlcu and C. Misdolea, *J. Chem. Phys.*, **45**, 3414 (1916).

[12] C. M. Carlson, H. Eyring and T. Ree, *Proc. Natl. Acad. Sci. U.S.A.*, **46**, 649 (1960).

[13] R. Vîlcu and C. Misdolea, *J. Chem. Phys.*, **49**, 3179 (1968).

[14] R. Vîlcu and C. Misdolea, *Rev. Roumaine Chim.*, **13**, 281 (1968).

where

$$\sigma_1 = \frac{E_s}{RT} - 3\ln\,(1 - \mathrm{e}^{-\theta/T}) \tag{4}$$

$$\sigma_2 = \ln\,[1 + n\,(x - 1)\,\mathrm{e}^{-\frac{aE_s}{n(x-1)\,RT}}] \tag{5}$$

$$\gamma = \ln\left[\frac{(2\pi mkT)^{3/2}}{h^3}\frac{eV_s}{N}\right]^2 x\,; \qquad x = \frac{V}{V_s} \tag{6}$$

with $x = V/V_s$.

The partition function of the binary system of molten metals takes the form

$$Z_{12} = \left[\frac{(X_1+X_2)\,!}{X_1!\ X_2!}\overset{*}{Z}_{g_1}^{\,X_1\frac{V-V_s}{V}}\overset{*}{Z}_{s_1}^{\,X_1\frac{V_s}{V}}\overset{*}{Z}_{g_2}^{\,X_2\frac{V-V_s}{V}}\overset{*}{Z}_{s_2}^{\,X_2\frac{V_s}{V}}\right]^N \tag{7}$$

The quantities marked by an asterisk represent “solid-like” and “gas-like” partition functions of the pure liquids where the characteristic quantities of the mixture appear.

The statistic calculation of the excess thermodynamic functions is based upon the well-known thermodynamic relations :

$$G^E = RT\,[X_1 \ln Z_1 + X_2 \ln Z_2 - \ln Z_{12}] \tag{8}$$

where X_1 and X_2 are the molar fractions of the two components, while Z_1 and Z_2 are their partition functions :

$$H^M = RT^2\left[\frac{\partial \ln Z_{12}}{\partial T} - \left(X_1\frac{\partial \ln Z_1}{\partial T} + X_2\frac{\partial \ln Z_2}{\partial T}\right)\right] \tag{9}$$

CALCULATIONS AND RESULTS

The excess thermodynamic functions were computed for systems Na$-$K, Na$-$Cs and K$-$Cs at temperatures where the miscibility of the components is complete.[15-17] The values necessary to turn the partition functions into good account are taken from the available bibliographical sources.[12,13]

The Na$-$K system

The miscibility of this system is total at the 373°K; nevertheles the computations were made but for two molar fractions, for which we

---

[15] R. Hultgren and R. Orr “Selected Values of Thermodynamic Properties of Metals and Alloys”, John Wiley and Sons. Inc., New York, 1963, p. 828.

[16] C. Smithells “Metals Reference Book”, vol. 1, Buterworth Scientific Publications, London, 1955, p. 376.

[17] M. Hansen and K. Anderko, “Constitution of Binary Alloys”, McGraw-Hill Book Company, Inc., New York, 1958, p. 577.

disposed of data about the mixture[18] densities. In order to study the variation of the excess functions with temperature, we computed also their values at 523°K and 673°K.

The results are to be found in tables 1, 2 and 3.

Table 1

Excess thermodynamic functions for the Na – K system at 373°K

X_1 (Na)	H^M			G^E calc.	TS^E calc.
	calc.	calc.[7]	exptl.*[6]		
0.22	178	212	111**	43	135
0.56	318	192	182	72	246

* Values at 384°K
** Value for $X_{Na} = 0.238$.

Table 2

Excess thermodynamic functions for the Na – K system at 523°K

X_1 (Na)	H^M calc.	G^E calc.	TS^E calc.
	(cal/g.at)		
0.22	160	35	125
0.56	294	56	238

Table 3

Excess thermodynamic functions for the Na – K system at 673°K

X_1 (Na)	H^M calc.	G^E calc.	TS^E calc.
	(cal/g.at)		
0.22	150	26	124
0.56	274	36	238

The Na—Cs system

The computations were made at 384°K, 523°K, and 673°K. For this system, no data are available as to the densities of the mixture. The volume of the binary system was computed from density data of the pure components.[19] The sublimation energy was obtained from the following relation [9]:

---

[18] ⁂ "Liquid Metals Handbook," U.S. Government Printing Office, Washington, 1952.

$$E_s = X_1^2 E_{S_1} + X_2^2 E_{S_2} + 2X_1 X_2 \sqrt{E_{S_1} E_{S_2}} + \delta E_s \qquad (10)$$

where δE_s denotes a correction of the mixture sublimation energy. The results of these computations are given in tables 4, 5 and 6.

Table 4

Excess thermodynamic functions for the Na–Cs system at 384°K

X_1 (Na)	H^M calc.	H^M calc.[7]	H^M exptl.[6]	G^E calc.	TS^E calc.
	(cal/g.at)				
0.211	144	600	106	−203	347
0.346	217	724	167	−282	499
0.537	247	583	221	−361	608
0.669	234	380	243	−353	587
0.892	151	50	151	−200	351

Table 5

Excess thermodynamic functions for the Na–Cs system at 523°K

X_1 (Na)	H^M calc.	G^E calc.	TS^E calc.
	(cal/g.at)		
0.211	122	−271	393
0.346	189	−361	550
0.537	236	−437	673
0.669	217	−438	655
0.892	123	−235	358

Table 6

Excess thermodynamic functions for the Na–Cs system at 673°K

X_1 (Na)	H^M calc.	G^E calc.	TS^E calc.
	(cal/g.at)		
0.211	104	−297	401
0.346	148	−426	574
0.537	222	−464	686
0.669	181	−477	658
0.892	106	−231	337

---

[19] J. P. Stone, C. T. Ewing, J. R. Spann, E. W. Stenkuller, D. Williams and R. Miller, *J. Chem Eng. Data*, **11**, 320 (1966).

The K — Cs system

The calculating temperatures are the same as for the Na—Cs system. The calculating procedure of the volume and sublimation energy is also the same.

The liquid caesium density is available in reference 19. The results of these calculations are given in tables 7—9.

Table 7

Excess thermodynamic functions for the K – Cs system, at 384°K

X_1 (K)	H^M			G^E calc.	TS^E calc.
	calc.	calc.[7]	exp.[6]		
	(cal/g.at)				
0.186	12	47	14	−125	137
0.397	27	62	22	−193	220
0.485	30	70	25	−208	238
0.594	28	82	29	−218	246
0.778	13	83	25	−196	209

Table 8

Excess thermodynamic functions for the K – Cs system, at 523°K

X_1	H^M calc.	G^E calc.	TS^E calc.
	cal(g.at)		
0.186	6	−64	70
0.397	19	−83	102
0.485	25	−81	106
0.594	22	−82	104
0.778	8	−73	81

Table 9

Excess thermodynamic functions for the K – CS system, at 673°K

X_1 (K)	H^M calc.	G^E calc.	TS^E calc.
	cal/g.at		
0.186	4	− 70	74
0.397	15	−104	119
0.485	21	−106	127
0.594	16	−109	125
0.778	3	− 92	95

DISCUSSIONS AND CONCLUSIONS

The only recent data on the excess thermodynamic functions of the systems under study are the determinations of T. Yokohawa and O. J. Kleppa.[5] These data only refer to the 384°K temperature.

A theory on the mixing properties of the molten alkali metals was elaborated by J. R. Christman.[6]

This theory is based upon the augmented-plane-wave and quantum defect methods. Radial distribution functions are used and the heat of mixing results as a sum of contributions of coulombian, exchange-correlation and cell-cell interaction energies.

The valuation of these terms was made by taking into account the internal electronic structure of the molten metals : Na, K and Cs. To allow comparison, we gave also in the above tables the computed values on the basis of this theory.

The results of our computations of the mixture enthalpy agree satisfactorily with the experiments concerning systems Na—Cs and K—Cs, while the deviations are larger for system Na—K. With growing temperature, the systems come nearer to an excess function. In comparison with the other systems under study the K—Cs binary system is the nearest to an ideal behaviour.

The theoretical curves giving H^M as a function of composition are asymmetrical in the same way as the experimental ones : the heats of mixture are smaller for lower Na concentrations in the Na—Cs system and for lower K concentrations in the K—Cs system.

All the systems have their mixture enthalpies positive in concordance with the experimental data. Their values grow gradually as the metals composing the systems are further apart from one another in the periodic system of elements.

Revue Roumaine de Chimie, 15, 1847–1849 (1970)

ON THE ELOVICH EQUATION

N. I. IONESCU

Institute of Physical Chemistry, Bucharest
Str. Galaţi 31

Received May 23, 1970

The Elovich equation may be obtained, under certain circumstances, from the net rate of adsorption.

The kinetics of adsorption phenomena of gases onto solid surfaces is dominated by the equation first proposed by Roginsky and Zeldovich but now generally known as the Elovich equation:

$$\frac{d\theta}{dt} = \alpha \exp(-\beta\theta) \qquad (1)$$

where θ is the coverage degree of the surface and α and β are constants. In order to justify this equation many models were proposed,[1–7] which neglect the desorption.[8]

That is why, we proposed to show, in the present paper, that equation (1) may be obtained, under certain circumstances, in case desorption is considered, too.

RESULTS AND DISCUSSION

Let, at first, be the case with no dissociation of the absorbed molecules on the homogeneous surface. Each molecule is adsorbed on a surface site and the adsorbed layer is immobile. The net rate for the adsorption process is:

$$\frac{d\theta}{dt} = R_1(1-\theta) - k_1'\theta \qquad (2)$$

---

[1] H. A. Taylor and N. J. Thon, *J. Amer. Chem. Soc.*, **74**, 4169 (1952).

[2] P. T. Landsberg, *J. Chem. Phys.*, **23**, 1079 (1955).

[3] A. Cimino, E. Molinari and E. Cipollini, Actes Intern. Congr. Catalyse, 2-e, Paris 1960, Ed. Technip. Paris, 1961, vol. 1, p. 263.

[4] K. Hauffe, *Adv. Catalysis*, **7**, 213 (1955).

[5] A. S. Porter and F. C. Tompkins, *Proc. Roy. Soc.*, **A 217**, 529 (1953).

[6] F. S. Stone, in "Chemistry of the Solid State" (W. E. Garer Ed.) Butterworths, London, 1955, p. 384.

[7] A. M. Peers, *J. Catalysis*, **4**, 499 (1965).

[8] A. M. Peers, *J. Catalysis*, **4**, 672 (1965).

where k_1 is the overall constant of the adsorption and k_1' the same magnitude for the desorption. The k_1 and k_1' coefficients include the term $\exp\left(\frac{-E}{RT}\right)$ to allow for the possibility of activation energies of adsorption and desorption.

The relation (2) may be written under the form:

$$\frac{\mathrm{d}\theta}{\mathrm{d}t} = k_1\left(1 - \frac{k_1 + k_1'}{k_1}\,\theta\right) \tag{3}$$

If γ denotes the $\frac{k_1 + k_1'}{k_1}$ magnitude and the case $\gamma\theta \ll 1$ is considered, then $(1 - \gamma\theta)$ may be considered as equaling the first two terms of the expansion in series of the function $\exp(-\gamma\theta)$. Making this replacement in equation (3) one gets:

$$\frac{\mathrm{d}\theta}{\mathrm{d}t} = k_1 \exp(-\gamma\theta) \tag{4}$$

which is nothing else but the Elovich equation.

In this case, for the γ coefficient one obtains:

$$\gamma = 1 + \frac{K\,(2\,\pi\,m\,kT)^{1/2}}{\sigma p} \exp\left(\frac{-\Delta E}{RT}\right) \tag{5}$$

if for k_1 and k_1' the following expressions are used [9]:

$$k_1 = \frac{\sigma p}{(2\pi mkT)^{1/2}} \exp\left(\frac{-E_1}{RT}\right)$$

and

$$k_2 = K \exp\left(\frac{-E_1'}{RT}\right) \tag{6}$$

where K is the rate of desorption, σ, the condensation coefficient and $\Delta E = E_1' - E_1$, the other magnitudes having the known significance. For the σ and K magnitudes, the expression deduced by means of the absolute rates of surface reactions [9] can be used.

Let be now the case of a heterogeneous surface, formed, at first, of two sets of active sites. In these conditions:

$$\theta_1 + \theta_2 = \theta \tag{7}$$

and, as a consequence

$$\frac{\mathrm{d}\theta}{\mathrm{d}t} = \frac{\mathrm{d}\theta_1}{\mathrm{d}t} + \frac{\mathrm{d}\theta_2}{\mathrm{d}t} \tag{8}$$

---

[9] D. O. Hayward and B. M. W. Trapnell, "Chemisorption", Butterworths, London, 1964, p. 91.

From the expansion in series of the function

$$\frac{\mathrm{d}\theta}{\mathrm{d}t} = \varphi(t) \tag{9}$$

written for each coverage degree, only the first two terms are considered, in which case, taking into account expression (8) one gets :

$$\frac{\mathrm{d}\theta}{\mathrm{d}t} = k_1 + k_2 - (k_1^2\gamma_1 + k_2^2\gamma_2)\,t \tag{10}$$

For each coverage degree a relationship similar to (3) has been considered.

Relation (1) expressed also by means of the expansion in series according to eq. (9) leads to :

$$\frac{\mathrm{d}\theta}{\mathrm{d}t} = \alpha - \alpha^2\beta t \tag{11}$$

Equation (10) and (11) can be identified if

$$\alpha = k_1 + k_2 \quad \text{and} \quad \beta = \frac{k_1^2\gamma_1 + k_2^2\gamma_2}{(k_1 + k_2)^2} \tag{12}$$

An analogous treatment may be performed for a heterogeneous surface composed of n sets.

Thus, under certain circumstances, the Elovich equation may be obtained from the net rate of adsorption without any reference to a certain model (the variation of the activation energy with the coverage degree,[4-7,10,11] some dependences between the number of surfaces sites and the number of adsorbed molecules, [1-3] interaction between the molecules in the adsorption layer,[12] the creation of energetic chains on the solid surface [13]) or neglecting the desorption.[14]

---

[10] J. D. Halsey, *J. Phys. Chem.*, **55**, 21 (1951).
[11] Y. Kubokawa, *Bull. Chem. Soc. Japan*, **33**, 734 (1960).
[12] M. Boudart, *J. Amer. Chem. Soc.*, **74**, 3556 (1952).
[13] G. D. Sakharov, *Doklady Akad. Nauk S.S.S.R.*, **180**, 154 (1968).
[14] M. Bonnemay, G. Bronoel and D. Doniat, *Compt. rend.*, **268C**, 2262 (1969).

Revue Roumaine de Chimie, **15**, 1851–1855 (1970)

LA DÉTECTION DES RÉACTIONS AYANT LIEU DANS LES MÉLANGES OXYDIQUES PULVÉRULENTS DU SYSTÈME $La_2O_3-TiO_2-ZrO_2$ PAR LA MESURE DE LA RÉSISTANCE ÉLECTRIQUE

S. SOLACOLU et A. BĂRBULESCU

Institut Polytechnique de Bucarest,
Laboratoire de Chimie Physique des Silicates, 1,
str. Polizu, Bucarest, Roumanie

Reçu le 2 juillet 1970

En étudiant la variation de la résistance électrique quand on élève progressivement la température d'un mélange intime d'oxydes on a la possibilité de détecter les réactions en phase solide qui y ont lieu. C'est de cette manière qu'ont été mis en évidence les phénomènes apparaissant pendant le chauffage des mélanges oxydiques ayant une forte réactivité chimique qui font partie du système $La_2O_3 - TiO_2 - ZrO_2$. Dans le présent ouvrage une technique particulière de préparation des échantillons ainsi que les avantages qui en découlent sont décrits. Les résultats obtenus confirment les possibilités potentielles d'appliquer cette méthode à l'étude des réactions en phase solide.

1. INTRODUCTION

Les réactions qui ont lieu pendant le chauffage d'un système oxydique sont examinées le plus souvent par des méthodes ordinaires, comme, par exemple, l'analyse aux rayons X ou l'analyse thermique différentielle (ATD).

Mais il y a des cas où la possibilité d'appliquer ces méthodes est limitée par l'état de la structure cristalline ou par le caractère des effets thermiques. Un exemple est constitué par les matériels oxydiques amorphes obtenus par co-précipitation ; leur structure est pratiquement amorphe à travers des rayons X jusqu'à plusieurs centaines de degrés Celsius et la superposition ou la valeur des effets thermiques fournissent quelquefois des informations peu concluantes. Afin d'éviter les difficultés apparaissant dans ces situations, les auteurs de cet ouvrage se sont proposé d'examiner les réactions pendant le chauffage par la mesure de la résistance électrique, en fonction de la température. Cette méthode est basée sur la correspondance entre l'apparition d'un changement dans le mélange oxydique et la modification de pente de la courbe du logarithme de la résistivité en fonction de la température.[1] La formation d'un composant ou une transformation polymorphique peuvent modifier de façon appréciable le nombre n ou la mobilité μ des porteurs de charge, de manière que la modification de la valeur de la conductivité σ, exprimée par la relation

---

[1] A. N. Copp, M. Nakahira et G. W. Brindley, *J. Electrochem. Soc.*, **113**, 237 (1966).

$$\sigma = n\mu e$$

puisse être aperçue expérimentalement.

Jusqu'à présent, les auteurs qui ont entrepris des études de ce genre se sont limités seulement aux mélanges d'oxydes cristallins, pour détecter la réaction de formation en phase solide d'un composant chimique [2] ou, pour les masses céramiques ferroélectriques, afin de préciser le point de transformation polymorphique.[3]

Les mesures de la résistance électrique pour détecter une réaction ont été effectuées [1-5] sur des éprouvettes en forme de cylindre ou de disque ayant le diamètre de 10 à 20 mm et l'épaisseur de 3 à 15 mm; les échantillons ont été façonnés sans addition de liant, dans des moules métalliques, ensuite ils ont été montés sur des supports céramiques réfractaires (qui limitent la température maximale de travail à approximativement 1000°) et munis d'électrodes et d'armatures fixées mécaniquement sur les surfaces de contact. On a calculé la valeur de la résistivité électrique en utilisant les dimensions géométriques des éprouvettes avant le chauffage, ayant établi, au préalable, que l'effet de la modification des dimensions (due à la contraction pendant le frittage) sur les valeurs de la résistivité est négligeable. On a utilisé des fours électriques ayant une zone de température uniforme, où la vitesse d'augmentation de la température de 0,5° par minute représentait un compromis entre la mesure électrique dans des conditions de température assez bien définies et une température uniforme dans l'éprouvette.

2. TRAVAUX EXPÉRIMENTAUX

2.1. TECHNIQUE EXPÉRIMENTALE

Concernant la technique adoptée dans notre ouvrage, nous sommes partis des prémisses suivantes :

— La réduction de la masse et la simplification du système des contacts pourraient réduire l'inertie thermique et permettraient un rythme plus avantageux d'augmentation de la température.

— La détection d'un phénomène étant basée sur la détermination des discontinuités ou des changements de pente sur la courbe qui représente le logarithme de la résistivité en fonction de la température, il résulte que la variation de la résistance électrique R est également significative, compte tenu que dans la relation

$$\rho = \frac{l}{s} \cdot R, \qquad \frac{l}{s} \cong \text{constant}$$

---

[2] A. Bielanski, J. Deren, J. Haber et E. Polaczkawa, *Z. anorg. Chem.*, **294**, 269 (1958).

[3] P. D. Garn et S. S. Flaschen, *Analyt. Chem.*, **29**, 268 (1957).

[4] Z. G. Szabo et F. Solymosi, *Z. anorg. Chem.*, **301**, 225 (1959).

[5] R. Cypres et B. von Ommeslage, *Bull. Soc. Franç. Ceram.*, **54**, 65 (1962).

Par conséquent, les dimensions de l'éprouvette sont indifférentes.

Les deux observations exposées plus haut créent les prémisses d'une amélioration substantielle de la technique utilisée et c'est la formation d'une « perle » du matériel soumis aux essais, directement sur deux fils métalliques, qui remplaceront l'éprouvette à grandes dimensions et le système de fixer les contacts et de soutenir les éprouvettes.

La solution est extrêmement avantageuse parce que :

— on peut former des échantillons ayant seulement une masse de quelque dizaines de mg, donc des échantillons ayant une inertie thermique minime, négligeable ;

— on peut effectuer des déterminations jusqu'à 1500° ou même plus, en utilisant des fils en platine ou en platine allié avec du rhodium ;

— on réduit le temps nécessaire pour la détermination, attendu qu'il devient possible d'appliquer une vitesse d'augmentation de la température de 10° par minute ou même plus à la suite de la réduction considérable de l'inertie thermique de l'ensemble ;

— le chauffage de l'ensemble « perle-thermocouple » nécessite une température homogène dans un espace restreint, inférieur à un centimètre cube et par conséquent on peut utiliser des fours ordinaires à dimensions réduites.

Dans nos travaux, la perle de matériel a été formée par la compression isostatique, à 1000 atm, des matériels pulvérulents, directement sur deux fils en platine ayant le diamètre de 0,07 mm. L'ensemble perle-fils a une résistance mécanique suffisante pour les manipulations. Les deux fils en platine ayant le diamètre de 0,07 mm ont été connectés à deux fils en platine au diamètre de 0,8 mm. Une tige en céramique pour les thermocouples, ayant quatre canaux, a servi comme support pour les fils de platine et pour un thermocouple : Pt — PtRh10, dont le bulbe a été toujours placé dans le voisinage immédiat de la perle du matériel.

On a utilisé un four électrique horizontal à tube de quartz, muni d'un enroulement anti-inductif dont on a assuré une augmentation continuelle de la température de 10°/mn.

La résistance électrique des échantillons a été mesurée point par point en courant continu, à l'aide d'un pont permettant de mesurer la résistance jusqu'à 10^{10} ohm. Les phénomènes de polarisation enregistrés pendant les mesures sont négligeables, par rapport aux variations de résistance enregistrées en général.

Les déterminations ont été effectuées sur des masses oxydiques à activité élevée, préparées par co-précipitation.

Les poudres amorphes qui ont servi comme point de départ, constituées par des particules d'un ordre de grandeur de 100 Å et présentant des pertes à la calcination variant entre 25 et 30 %, ont été caractérisées préalablement par analyse thermique différentielle et analyse aux rayons X.

2.2. RÉSULTATS ET DISCUSSIONS

Les diagrammes indiqués dans la figure 1 montrent les résultats de l'analyse thermique différentielle comparés aux résultats des mesures de la résistance électrique en fonction de la température.

On constate que les effets thermiques enregistrés par l'ATD sont reflétés par les courbes $R = f(T)$ et que, de plus, l'évolution de la résistance électrique pendant l'augmentation de la température indique des phénomènes dont l'effet thermique n'a pas été aperçu à l'analyse thermique différentielle. Ainsi, dans le cas de TiO_2 jusqu'à approximativement 300°, sur la courbe ATD un large effet endothermique apparaît correspondant à la déshydratation des échantillons. Pour le même intervalle de tem-

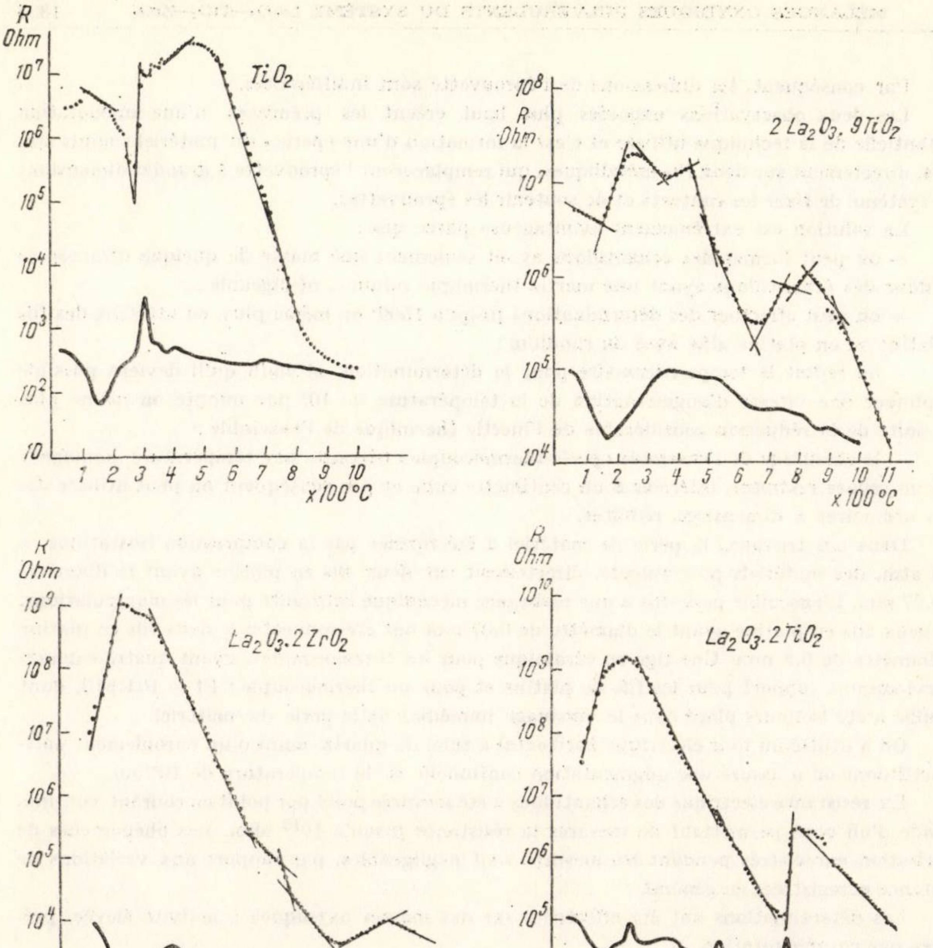

Fig. 1. — Les résistances électriques en fonction de la température (courbe pointillée) et les résultats l'ATD (courbe en trait plein) pour : TiO_2, $2\,La_2O_3 . 9\,TiO_2$, $La_2O_3 . 2\,ZrO_2$, $La_2O_3 . 2TiO_2$, $ZrO_2 . TiO_2$ et $La_2O_3 . TiO_2$.

pérature, la courbe $R = f(T)$ met en évidence des domaines de comportement différents. Le fait est intéressant, d'autant plus que, dans l'intervalle de température indiqué, la structure de l'échantillon ne peut être détectée par analyse aux rayons X. On observe un comportement semblable dans le cas de ZrO_2 . TiO_2 où la structure du matériel peut être analysée aux rayons X seulement après la cristallisation, qui a lieu à approximativement 600°.

Dans les deux cas, le moment de la structuration, signalé par un puissant effet exothermique dans l'ATD, est reflété sur la courbe $R = f(T)$ par une variation considérable de la concentration et de la mobilité des porteurs de charge.

On a obtenu aussi des résultats intéressants dans le cas des titanates de lanthane où la variation de la résistance en fonction de la température met en évidence de façon significative l'évolution thermique de ces matériels.

En observant comparativement l'évolution de TiO_2 et des composants à ZrO_2 ou La_2O_3 on peut apprécier que, du point de vue chimique, la formation des composants a lieu dès la période du processus de co-précipitation, donc avant l'application du traitement thermique. Un argument en ce sens peut être constitué par la variation de $R = f(T)$, qui indique le comportement particulier de chaque échantillon pris séparément.

CONCLUSIONS

Dans le présent ouvrage on a montré qu'il est possible de détecter les réactions dans les mélanges oxydiques, quel que soit le degré d'ordre cristallin, par la mesure de la résistance électrique en fonction de la température. Dans les conditions de la technique établie par les auteurs, la méthode est simple, rapide et sensible, sans nécessiter des appareillages prétentieux.

La caractérisation des échantillons par la détermination de la résistivité en fonction de la température peut être utilisée pour supplémenter les données obtenues par l'ATD et surtout pour obtenir des informations dans les domaines pour lesquels l'analyse aux rayons X ne donne pas de résultats. La méthode est particulièrement intéressante pour la caractérisation des matériaux oxydiques préparés par co-précipitation.

Revue Roumaine de Chimie, 15, 1857–1862 (1970)

STUDIES ON COORDINATION COMPOUNDS
COBALT (II) COMPLEXES OF ADIPYL DIHYDRAZIDE

M. ARSHAD, A. BEG * and B. BILQUIS **

Pakistan Council of Scientific and Industrial Research Laboratories,
Karachi–32, Pakistan

Received March 16, 1970

Adipyl dihydrazide (ADH) complexes of the type $[Co(ADH)_2.2H_2O]^+X_2$ where X is Cl^-, Br^-, NO_3^- or $^1/_2SO_4^-$ are reported. They are almost insoluble in all organic solvents. They have a magnetic moment of 4.4 to 5.5 BM and a molar conductivity corresponding to three ions. The infrared spectra suggest coordination through nitrogen. Their visible spectra have one strong band at 20000 cm^{-1}, a shoulder at 19000 cm^{-1} and a band of low intensity at 8600 cm^{-1}. These bands and the magnetic data fit in with a pseudo-octahedral structure. The ligand field parameter is 1030 cm^{-1} which is comparable with other ammines having the same structure type. The possibility of a coordination polymer formation is discussed.

INTRODUCTION

In the earlier paper [1] we have discussed the coordination compounds of adipyl dihydrazide (ADH) with nickel salts, which were shown to have an octahedral structure with tetragonal distortions. This paper reports the preparation of the cobalt (II) complexes. Adipyl dihydrazide has the hydrazide groups at the two ends. Such a structure is capable of forming a chelate as also a polymeric chain. Chelation demands planarity of the ring and this may not be possible with a ten-membered adipyl dihydrazide chain. However, if coordination could take place through the carbonyl group as in the case of the amides then a stable structure could have been obtained. But then the hydrazide group would be free and would be ready for coordination, thus giving rise to a cross-linked structure. Such a cross-linked structure would result in a completely insoluble compound and the spectra will also not be as simple as we have obtained. The evidence being discussed below all support the formation of a coordination polymer with a cross-linked chain for the complexes.

RESULTS

The compounds have a stoichiometry corresponding to $[Co(Adipyl\ dihydrazide)_2.2H_2O]^+X_2$ where X^- is Cl^-, Br^-, NO_3^- or $^1/_2SO_4^-$. The water molecules are not expelled easily and hence must be in the coordination sphere. Being insoluble in all organic solvents and to a certain extent in water also, they should be regarded polymeric in nature. As in nickel complexes the IR spectra of these compounds have the C—N frequency occurring at lower wavelengths indicating the participation of the amino groups in compound formation. The visible region spectra recorded in table 2 have three prominent bands at 490, 1100 and 1500 mμ or 2000, 8700 and 6700 cm^{-1} which is characteristic of an octahedral structure. There is also an inflexion on the 490 mμ band occurring on the higher wavelength side at 522 mμ or 19000 cm^{-1}. The intensities of these bands are quite low and these are listed in table 2. The magnetic susceptibility

---

* At present at the Dept. of Chemistry, University of Western Ontario, London, Ontario, Canada.

** Department of Chemistry, University of East Anglia, Norwich, U. K.

[1] M. A. A. Beg and B. Bilquis, *P.J. Sci. Ind. Res.*, (in press).

Table 1

Analysis, melting point and colour of the complexes

Compound	Co		Anion		Melting Point	Colour
	Calculated	Found	Calculated	Found		
$[Co(Adipyl\ Dihydrazide)_2.2H_2O]Cl_2$	11.46	11.25	13.8	13.33	270—75	Light Purple
$[Co(Adipyl\ Dihydrazide)_2.2H_2O]Br_2$	10.0	9.6	27.3	27.6	260—65	Bright Pink
$[Co(Adipyl\ Dihydrazide)_2.2H_2O](NO_3)_2$	10.39	10.21	—	—	165—70	Light Pink
$[Co(Adipyl\ Dihydrazide)_2.2H_2O]SO_4$	10.93	11.0	—	—	270—75	Pink

Table 2

Bands in the visible region and their assignments

Compound	Concentration (gms/litre)	Band		E	Assignment
		mμ	cm^{-1}		
$[Co(Adipyl\ Dihydrazide)_2.2H_2O]Cl_2$	22	495	20160	16	ν_3 or $4T_{1g} \rightarrow 4T_{1g}$ (P)
		522	19160	14	ν_2 or $4T_{1g} \rightarrow 4A_{2g}$ (F)
		1100	9090	4	
		1160	8620	4	ν_1 or $4T_{1g} \rightarrow 4T_{2g}$ (F)
		1490	6711	0.7	
$[Co(Adipyl\ Dihydrazide)_2.2H_2O]Br_2$	22	492	20330	19	ν_3 or $4T_{1g} \rightarrow 4T_{1g}$ (P)
		520	19230	10	ν_2 or $4T_{1g} \rightarrow 4A_{2g}$ (F)
		1100	9090	4	
		1150	8695	4	ν_1 or $4T_{1g} \rightarrow 4T_{2g}$ (F)
		1470	6803	1	
$[Co(Adipyl\ Dihydrazide)_2.2H_2O](NO_3)_2$	22	496	20160	16	ν_3 or $4T_{1g} \rightarrow 4T_{1g}$ (P)
		520	19230	8	ν_2 or $4T_{1g} \rightarrow 4A_{2g}$ (F)
		1110	9010	4	
		1160	8620	3	ν_1 or $4T_{1g} \rightarrow 4T_{2g}$ (F)
		1510	6621	0.5	
$[Co(Adipyl\ Dihydrazide)_2.2H_2O]SO_4$	22	494	20240	20	ν_3 or $4T_{1g} \rightarrow 4T_{1g}$ (P)
		530	18870	20	ν_2 or $4T_{1g} \rightarrow 4A_{2g}$ (F)
		1100	9090	5	
		1150	8695	5	ν_1 or $4T_{1g} \rightarrow 4T_{2g}$ (F)
		1520	6580	3	

of these compounds shows paramagnetism corresponding to three unpaired electrons and is listed in table 4. The electrical conductivity indicates the presence of three ions and is also listed in table 4.

Table 3

Calculated ligand field parameters

Compound	B'	β%	Dq	Dq/B	ν_2	
					Calculated	Observed
[Co(Adipyl Dihydrazide)$_2$.2H$_2$O]Cl$_2$	821.5	15.4	1019	1.24	19350	19160
[Co(Adipyl Dihydrazide)$_2$.2H$_2$O]Br$_2$	822.3	15.3	1036.5	1.26	19320	19230
[Co(Adipyl Dihydrazide)$_2$.2H$_2$O](NO$_3$)$_2$	815.1	16.1	1028	1.26	19170	19230
[Co(Adipyl Dihydrazide)$_2$.2H$_2$O]SO$_4$	822.0	15.4	1028	1.25	19330	18870

Table 4

Magnetic susceptibility and conductivity Λ 1000 of the compounds

Compound	Gram Suscepti-bility X_g $\times 10^{-6}$	Molar Suscepti-bility X_M $\times 10^{-6}$	X_M Corrected	μ_{eff} Bohr magneton	Λ 1000
[Co(Adipyl Dihydrazide)$_2$.2H$_2$O]Cl$_2$	15.5	7966.07	8111.97	4.43	323.7
[Co(Adipyl Dihydrazide)$_2$.2H$_2$O]Br$_2$	21.0	12657.54	12824.44	5.569	339.0
[Co(Adipyl Dihydrazide)$_2$.2H$_2$O](NO$_3$)$_2$	17.0	9637.98	9781.48	4.829	440.2
[Co(Adipyl Dihydrazide)$_2$.2H$_2$O]SO$_4$	16.0	8624.04	8769.84	4.606	267.9

DISCUSSION

The Fischer-Taylor-Hirschfelder model for these compounds suggests the participation of the amino groups as donors and a cross-linked structure if two ADH molecules are taking part in coordination. Such a structure will result in decreased solubility and it is found that the present series is less soluble than the nickel compounds. The IR spectra are almost the same as for the nickel compounds which support the earlier views regarding the participation of the amino groups and the polymeric structure. Figure 1 shows that the central atom is octahedrally surrounded by four amino and two water ligands and fits in with the observed stoichiometry. Polymeric structures have also been noted for aliphatic diamine complexes of chromium.[2] The ADH molecule also has two flanking amino groups and it would not be surprising if the structure of the present series of complexes is similar to those of the diamines giving a coordination polymer.

Visible spectra: The spectroscopy in this region records three main bands and a fourth of very low intensity. These bands occur at $20240 \pm \pm 80\ \mathrm{cm}^{-1}$, $19000 \pm 230\ \mathrm{cm}^{-1}$, $8600 \pm 33\ \mathrm{cm}^{-1}$ and 6500 to 6800 cm^{-1}. The second band is an inflexion on the low frequency side. The position of the bands suggests an octahedral structure but because of the unsym-

---

[2] H. L. Schlafer and O. Kling, *Z. anorg. Chem.*, **309**, 245 (1961).

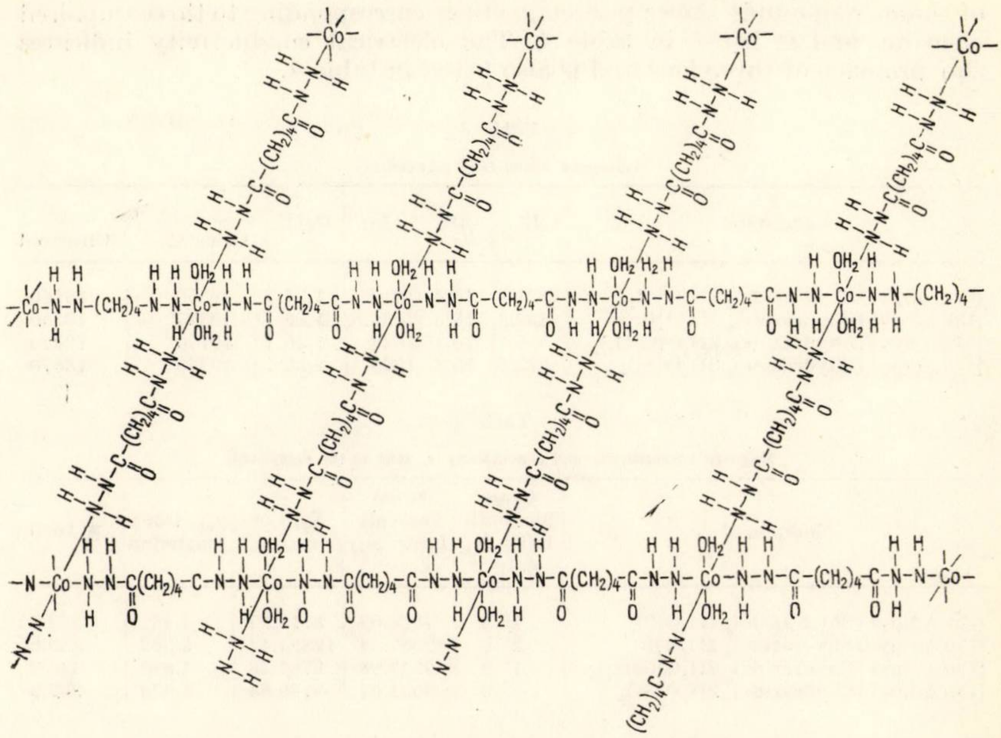

Fig. 1. — Possible polymeric structure of ADH complexes.

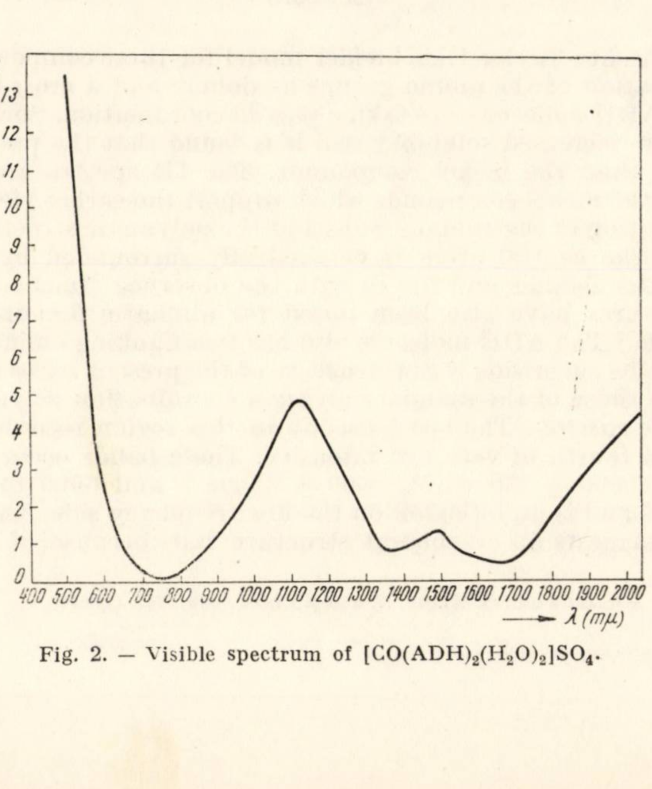

Fig. 2. — Visible spectrum of $[CO(ADH)_2(H_2O)_2]SO_4$.

metrical ligands the framework is suggested to suffer tetragonal distortions. The cross-linked structure noted above indicates that the water molecules in the coordination sphere might be symmetrically placed at the apical position.

From the position of the bands it is possible to assign the 20000 cm^{-1} band to ν_3 or $4T_{1g} \rightarrow 4T_{1g}(P)$, the 8600 cm^{-1} band to ν_1 or $4T_{1g} \rightarrow 4T_{2g}(F)$, and the 19000 cm^{-1} band to ν_2 or $4T_{1g} \rightarrow 4T_{2g}(F)$. The calculation of the parameters is usually difficult in the case of octahedral cobalt (II) complexes, hence the empirical approach adopted by Lever[3] has been used here in their calculation and we find that the predicted position of the ν_2 band is in close agreement with that observed. The method suggested by Reedijk, Driessen and Groeneveld[4] was also tried but it gave lower values for ν_2. The calculated value of Dq by the former method is 1028 cm^{-1} for the sulfate and nitrate and 1036 and 1042 cm^{-1} for bromide and chloride respectively. The Dq is quite high and is comparable but slightly lower than that for nickel. This lower value might be a result of the more symmetrical structure for the cobalt complexes. The high value, however, does suggest the participation of the terminal amino groups in coordination since these are of the same order as in other compounds where nitrogen is the donor.[5]

From the empirical method noted above B' is found to be $\sim$820. The calculation of $\beta = B'/B$ from this value compared with that of the free ion[6] is 15–16%. In the case of nickel the value was noted to be 17–19%. Here also we find larger values indicating larger interelectronic repulsions. This high value could be a result of Jahn-Teller distortions since the over-all spectrum is a picture of an octahedral structure with a superimposed tetragonal field.

The B value is high for the nitrate of both cobalt and nickel (19.94%). Also, since the Dq as well as the B' value change with the anion it is possible to suggest that the electrostatic perturbations of the anions too make significant contributions. For B' the sequence is $\mathrm{Br} > \mathrm{SO_4} > \mathrm{Cl} > \mathrm{NO_3}$ and for Dq it is $\mathrm{Cl} < \mathrm{SO_4} \approx \mathrm{NO_3} < \mathrm{Br}$. For nickel the sequence for B' was $\mathrm{Cl} > \mathrm{Br} > \mathrm{NO_3}$ and for Dq it was $\mathrm{Br} > \mathrm{Cl} > \mathrm{NO_3}$. Dq is dependent on the contributions from electrostatic perturbations as also interactions from σ and π bonding. The IR spectra do suggest the participation of the σ bonds and hence what is being observed from the spectra is due to a combination of the interelectronic forces including electrostatic perturbations from the anions.

If we consider the Dq/B values it would be clear that ADH is a strong field ligand and falls in the following sequence :

Dimethylcyanamide < Adipyl dihydrazide < Ethylenimine <
$\mathrm{CH_3CN}$ < Pyrazole < Hydrazine

Complexes of cobalt (II) have been studied extensively and it is agreed that cobalt assumes tetrahedral or octahedral symmetry. The magnetic moment data are within the range 4.3 – 5.2 BM observed for octahedral configurations. These values indicate that they are for spin free cobalt with a significant orbital contribution. This in turn suggests that the cobalt is in an octahedral framework with tetragonal distortions and that these distortions are not too large.

---

[3] A. B. P. Lever, *J. Chem. Educ.*, **45**, 711 (1968).

[4] J. Reedijk, W. L. Driessen and W. L. Groeneveld, *Rev. Trav. chim.*, **88**, 1095 (1969).

[5] R. W. Kiser and T. W. Lapp, *Inorg. Chem.*, **1**, 401 (1962).

[6] T. M. Dunn, *J. Chem. Soc.*, **1959**, 624.

EXPERIMENTAL

Adipyl dihydrazide was prepared by the method of Smith.[7] The complexes with the cobalt salts, cobalt chloride, bromide, nitrate and sulphate were prepared by mixing the saturated solution of cobalt salt with a saturated solution of ADH in 50% aqueous ethanol and refluxing the mixture for about three hours on a water bath. The solution so obtained was concentrated by distilling off some of the ethanol. On adding ether to the resulting solution a gel was obtained which when refluxed again with alcohol, deposited the complexes as amorphous solids. These were washed thoroughly with alcohol and ether and were desiccated over sulphuric acid. No loss in weight was observed even when stored for several days.

The analytical data, colour and melting points are reported in table 1. The IR spectra were run on a Beckman IR–4 spectrophotometer using aqueous solution. Magnetic susceptibility measurements were made on powdered samples, using a Newport Gouy balance system type C which was kindly made available to us through the CENTO Aid. The conductivity was measured on a WTW conductivity meter using conductivity water as solvent.

---

[7] A. S. Smith, *Org. Synthesis*, **36**, 69.

Revue Roumaine de Chimie, **15**, 1863–1869 (1970)

COMBINAISONS COMPLEXES AVEC DES HYDROXYACIDES. XV*

L'ÉTUDE POTENTIOMÉTRIQUE DU SYSTÈME $ZrOCl_2$-ACIDE D-GLUCONIQUE

CONST. GH. MACAROVICI et L. CZEGLÉDI
Institut de Chimie de l'Académie, Filiale de Cluj, 59–65, str. Donath

Reçu le 2 juin 1970

On étudie l'interaction de l'ion de zirconyle et de l'acide D-gluconique par voie potentiométrique. Dans la solution le rapport de combinaison des réactants est 2Zr : 1 HGH_4. On formule des considérations sur le mécanisme de réaction qui se produit dans la solution.

Dans les travaux antérieurs[1–5] on a étudié la formation des complexes des éléments tétravalents (Ti, Zr, Hf, Th) avec les acides gluconique et saccharique.

Dans ce travail on étudie l'interaction de l'oxychlorure de zirconium et de l'acide D-gluconique ou son sel de potassium, au moyen de la méthode potentiométrique.

PARTIE EXPÉRIMENTALE

Réactifs. La solution aqueuse de $ZrOCl_2$ 0,1 M a été préparée à partir de $ZrOCl_2 \cdot 8H_2O$ *p.a.* Le titre de la solution a été établi par la méthode de la précipitation par acide mandélique.

Les solutions d'acide D-gluconique de différentes concentrations ont été préparées par échange ionique à partir de gluconate de calcium sur Amberlite IR 120, forme hydrogène. On a contrôlé par voie potentiométrique le titre de la solution d'acide D-gluconique par addition de KOH 0,1 M en excès et retitrage par HCl 0,1 M.

---

[*] XIVe partie. L. Czeglédi et Const. Gh. Macarovici, *Rev. Roumaine Chim.* **15**, 1741 (1970).

[1] Const. Gh. Macarovici, H. Roth et L. Czeglédi, *Studii și Cercetări Chim. Acad. R.P.R. Fil. Cluj*, **12**, 229 (1961).

[2] Const. Gh. Macarovici, H. Roth et L. Czeglédi, *Studii și Cercetări Chim. Acad. R.P.R. Fil. Cluj*, **12**, 245 (1961).

[3] H. Roth, L. Czeglédi et Const. Gh. Macarovici, *Studii și Cercetări Chim. Acad. R.P.R. Fil. Cluj*, **14**, 69 (1963).

[4] Const. Gh. Macarovici et L. Czeglédi, *Rev. Roumaine Chim.*, **9**, 411 (1964).

[5] Const. Gh. Macarovici et L. Czeglédi, *Rev. Roumaine Chim.*, **14**, 57 (1969).

La solution de gluconate de potassium a été obtenue de la solution d'acide gluconique par neutralisation avec la quantité nécessaire de KOH. Pour le titrage des mélanges on a utilisé du KOH 0,1 M.

Appareillage. Le pH a été mesuré à un potentiomètre électronique LP-5 à électrode de verre et de calomel saturé. Au titrage on a employé un vase de 100 ml recouvert d'un disque en plexiglas, muni d'orifices pour les électrodes et la microburette. Pour agiter on a utilisé un agitateur magnétique et l'on a travaillé dans une chambre thermostatée à 20 ± 0,1°C.

On a procédé à trois types de titrages:

1. Les solutions aqueuses de $ZrOCl_2$, de l'acide gluconique et de leus mélanges en différentes proportions ont été titrées par du KOH 0,1 M de la façon suivante:

a) 40 ml de solution aqueuse de $ZrOCl_2$ à une concentration de $2{,}5 . 10^{-3}$ M;

b) 40 ml de solution, contenant de l'acide gluconique à une concentration de $2{,}5 . 10^{-3}$M;

c) 40 ml de solution contenant de l'ion métallique et de l'acide gluconique à différents rapports molaires (la concentration du métal étant de $2{,}5 . 10^{-3}$ M).

2. 40 ml de solution, contenant de l'ion métallique et du gluconate de potassium à différents rapports molaires (1 : 0,5; 1 : 1; 1 : 2; 1 : 3; Me = $2{,}5 . 10^{-3}$ M).

3. On a suivi la variation dans le temps du pH initialement fixé avec du KOH 0,1 M dans quatre séries dont chacune est formée de 15 échantillons contenant 40 ml de solution d'ion métallique et d'acide gluconique aux mêmes rapports molaires que sous le point 2. A chacun des échantillons des quatre séries on a ajouté des quantités variables de KOH nécessaires au tracement des courbes potentiométriques, mais la mesure du pH a été faite au bout de 20 et 48 heures.

A la représentation graphique on a inscrit en ordonnée le pH en fonction des moles de KOH additionnées pour 1 mole de métal, en notant ce rapport par „a" inscrit en abscisse.

RÉSULTATS ET DISCUSSIONS

Il est connu que la formation des combinaisons chélatiques des hydroxyacides avec les ions métalliques s'accompagne du déplacement des ions d'hydrogène de la molécule du ligand, et comme suite de ce fait le pH des solutions baisse et que même dans des solutions fortement acides de zirconium des processus d'hydrolyse, d'olation et d'oxolation se produisent avec formation de produits polymères. La mesure dans laquelle les processus mentionnés peuvent être entravés par la formation de complexes avec des ligands anioniques dépend de leur tendance à occuper des positions coordinatives autour des atomes centraux. Les anions peuvent pénétrer dans la sphère de coordination de l'ion métallique et déplacer des ponts oliques des composés polymères formés de l'ion métallique. Comme suite de cette pénétration des anions, il se produit d'abord une diminution des charges positives des ions complexes formés, puis la précipitation des agrégats de charge zéro. Si assez d'anions pénètrent, le processus conduit à la peptisation ou à la dissolution des précipités avec la formation de micelles, respectivement de complexes anioniques.[6]

Le système Zr(IV) — acide gluconique manifeste une tendance analogue, étant caractérisé par l'apparition de précipités blancs, abondants.[1]

Sur la figure 1 sont représentées les courbes de titrage de l'oxychlorure de zirconium (courbe *1*), de l'acide gluconique (courbe *2*) et de leurs mélanges aux rapports Zr : $HGH_4 = 1 : 0{,}5$; 1 : 1 ; 1 : 2 ; 1 : 3 (courbes 3—6) et les séries correspondantes où l'on a suivi la variation du pH avec le temps (courbes 3′—6′).

---

[6] J. C. Bailar Jr. «The Chemistry of the Coordination Compounds», Reinhold Publ. Corp., New York, 1956, p. 448–71.

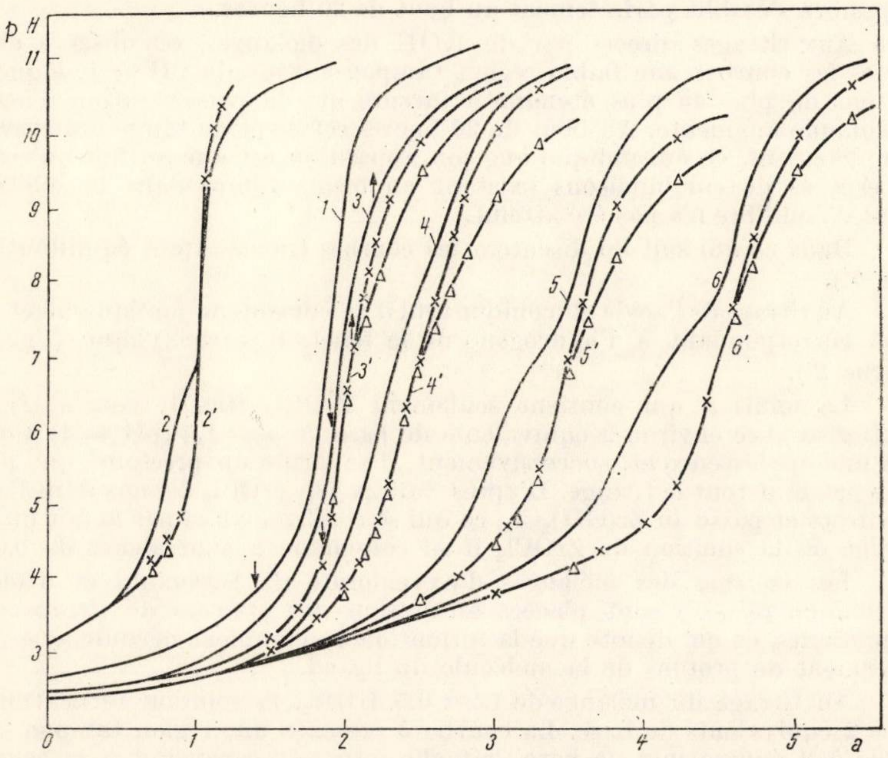

Fig. 1. — Titrage potentiométrique du système $ZrOCl_2$ — acide D-gluconique.
1, $ZrOCl_2$, 2.10^{-3} M ; *2*, acide gluconique ; *3—6*, $ZrOCl_2$ — acide D-gluconique aux rapports 1 : 0,5 ; 1 : 1 ; 1 : 2 ; 1 : 3.

——— titrage direct par KOH ;

2′—6′ = { xxx pH des mélanges au bout de 20 heures ;
Δ Δ Δ pH des mélanges au bout de 48 heures ;

↓ début de la précipitation ;

↑ dissolution du précipité.

Au titrage direct par du KOH du liant et des mélanges après chaque addition de KOH, le pH s'établit très lentement en raison de la difficulté qu'il y a d'établir avec le temps de l'équilibre entre l'hydroxyacide libre et la lactone de l'acide, respectivement avec les combinaisons complexes qui se forment en présence des métaux.[7] Dans le cas des courbes *1—6*, les déterminations du pH ont été faites 15 minutes après chaque addition de KOH, et dans le cas des courbes *2′—6′*, après 20 et 48 heures. Comme suite de l'hydrolyse des combinaisons en milieu alcalin, dans le cas des courbes tracées au bout de 48 heures, on observe une baisse du pH dans le domaine de $\text{pH} > 7$ par rapport à celles observées au bout de 20 heures. Jusqu'au $\text{pH} = 7$ les courbes des séries enregistrées après 20 heures se superposent à celles tracées après 48 heures, ce qui dénote qu'à un $\text{pH} < 7$ l'équilibre s'établit parfaitement au bout de 20 heures.

---

[7] R. L. Pecsok et J. Sandera, *J. Amer. Chem. Soc.*, **77**, 1489 (1955).

Aux titrages directs par du KOH des mélanges, on observe chez toutes les courbes une faible région tampon autour du $\text{pH} = 7$, laquelle devient de plus en plus étendue à mesure que la concentration d'acide gluconique augmente. Au bout de 20 heures cette région tampon disparaît complètement, ce qui indique que son apparition est due au fait qu'entre les espèces de combinaisons existant en même temps dans la solution l'état d'équilibre n'a pas été atteint.

Dans ce qui suit on discutera les courbes tracées après équilibration (*3'—6'*).

Au titrage de l'acide gluconique seul il se consomme un équivalent de base correspondant à l'hydrogène de la fonction carboxylique (fig. 1, courbe *2'*).

La solution qui contient seulement $ZrOCl_2$ (fig. 1, courbe *1*) se neutralise avec environ 2 équivalents de base. A $a = 1,5$ ($\text{pH} = 4$) apparaît une opalescence et, successivement, il se forme un précipité qui persiste pendant tout le titrage. D'après Zaïtsev [8] le $ZrOCl_2$ dissous dans l'eau s'hydrate et passe au $Zr(OH)_2Cl_2$, ce qui se confirme aussi par le fait qu'au titrage de la solution de $ZrOCl_2$ il se consomme 2 équivalents de base.

Les courbes des mélanges d'oxychlorure de zirconium et d'acide gluconique (3'—6') sont placées au-dessous des courbes de titrage des composants, ce qui dénote que la formation du complexe découle avec déplacement de protons de la molécule du ligand.

Au titrage du mélange de $1Zr : 0,5\ HGH_4$, la solution se neutralise avec 2 équivalents de base. La courbe *3* présente une région tampon très faible à 2 équivalents de base, laquelle disparaît cependant à la courbe (3'). Au $\text{pH} = 4,2$ commence la formation d'un précipité, suivie de sa dissolution au $\text{pH} > 7$. Aux mélanges de 1 : 1; 1 : 2 et 1 : 3 le précipité n'apparaît pas au cours du titrage.

L'allure des courbes nous permet de déduire qu'il se forme la combinaison au rapport de combinaison de $2Zr : 1HGH_4$. Le fait que le ligand en excès empêche la précipitation est en concordance avec la capacité connue des α-hydroxyacides d'inverser la charge des micelles d'oxydehydrate de zirconium,[6] avec formation d'anions complexes.

Au titrage des mélanges d'oxychlorure de zirconium et d'acide gluconique au rapport 1 : 1; 1 : 2 et 1 : 3, la consommation de base est égale à celle du rapport 1 : 0,5, plus un nombre d'équivalents de base correspondant à l'acide gluconique en excès.

En utilisant aux mélanges le sel de potassium de l'acide gluconique, il se consomme au titrage 1,5 équivalents de base pour tous les rapports de mélange entre les composants (fig. 2, courbes 1—4) et 3 équivalents de base pour le mélange de $2Zr : 1KGH_4$ (fig. 2, courbe *5*). Ce comportement confirme le fait qu'il se forme un seul complexe au rapport de combinaison 2Zr : 1HGH$_4$, conformément à la réaction globale

---

[8] L. M. ZAITSEV et G. S. BOTCHKAREV, *Zhur. neorg. Khim.*, **7**, 795 (1962).

$$C_6H_{12}O_7 + 2ZrOCl_2 + 2H_2O \rightleftharpoons 2Zr(OH)_2 . (C_6H_8O_7) + 4HCl \qquad (1)$$

L'acide gluconique entier est engagé dans le complexe, ce qui fait qu'il se consomme 2 équivalents de base pour un zirconium, comme dans le cas du titrage de la solution de $ZrOCl_2$ seule. Nous estimons que le précipité qui commence à apparaître au cours du titrage à pH $\cong$ 4,20 est le complexe électroneutral. Au pH $>$ 7 le précipité se dissout et il se forme le complexe anionique, consommant encore un équivalent de base

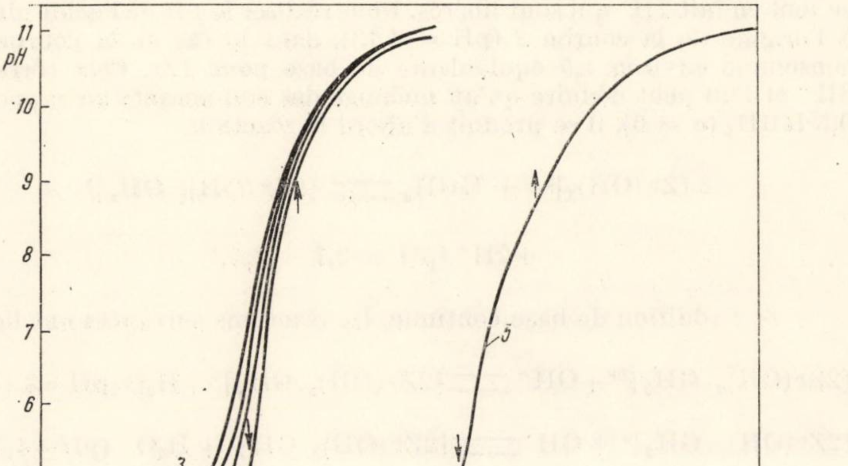

Fig. 2. — Titrage potentiométrique du système $ZrOCl_2$ — gluconate de potassium.

1–5 = $ZrOCl_2$ — gluconate de potassium aux rapports 1 : 0,5 ; 1 : 1 ; 1 : 2 ; 1 : 3 ; 2 : 1.
↓ début de la précipitation ;
↑ dissolution du précipité.

$$2Zr(OH)_2 . (C_6H_8O_7) + KOH \rightleftharpoons [2Zr(OH)_2 . (C_6H_7O_7)]\,K + H_2O \qquad (2)$$

Au rapport des réactants 1 : 1,1 : 2 et 1 : 3, les points d'équivalence se trouvent à 2,5, respectivement à 3,5 et 4,5 équivalents de base. Il se forme donc le même complexe, mais on titre en plus l'acide gluconique non engagé dans la formation du complexe.

En vertu de ce qui vient d'être exposé on peut faire quelques considérations sur le mécanisme des réactions qui ont lieu dans la solution à la formation de la combinaison complexe.

Pour réaliser le pH correspondant au point à l'origine ($a = 0$) de la figure 1, courbe *1* (pH = 2,70), dans le cas de la courbe *3'* (1Zr : 0,5HGH_4), il se consomme environ 1 équivalent de base, ce qui revient à dire qu'au mélange des réactants, quand se forme la combinaison de 2Zr : 1HGH_4, ce sont en fait $2H^+$ qui sont libérés. Pour réaliser le pH de l'acide gluconique à l'origine de la courbe *2* (pH = 3,13), dans le cas de la courbe *3'* il se consomme environ 1,5 équivalents de base pour 1Zr. Cela correspond à $3H^+$ et l'on peut déduire qu'au mélange des composants au rapport 1Zr : 0,5 HGH_4 ($a = 0$), il se produit d'abord la réaction.

$$2\,[Zr(OH)_2]^{2+} + HGH_4 \rightleftharpoons [2Zr(OH)_2.GH_3]^{2+} + +2H^+ \; (pH = 2,7 - 2,8)^* \qquad (3)$$

Si l'addition de base continue, les réactions suivantes ont lieu

$$[2Zr(OH)_2.GH_3]^{2+} + OH^- \rightleftharpoons [2Zr(OH)_2.GH_2]^+ + H_2O \; (pH = 3,13) \qquad (4)$$

$$[2Zr(OH)_2.GH_2]^+ + OH^- \rightleftharpoons [2Zr(OH)_2.GH]^0 + H_2O \quad (pH = 4,5-7) \quad (5)$$

$$[2Zr(OH)_2.GH]^0 + OH^- \rightleftharpoons [2Zr(OH)_2.G]^- + H_2O \quad (pH > 7) \qquad (6)$$

Dans le cas des mélanges avec le sel de potassium de l'acide gluconique et de l'oxychlorure de zirconium, le point d'équivalence se trouve toujours, quel que soit le rapport de mélange, à 1,5 équivalents de base, conformément à la réaction globale

$$KC_6H_{11}O_7 + 2ZrOCl_2 + 2H_2O \rightleftharpoons [2Zr(OH)_2.C_6H_8O_7] + 3HCl + KCl \quad (7)$$

A un équivalent de base en plus il se forme le complexe anionique (voir la réaction 2). Il se consomme donc 1,5 équivalents de base pour un zirconium (fig. 2, courbes *1—4*) ou 3 équivalents pour le mélange de 2Zr : 1HGH_4 (fig. 2, courbe *5*).

Le mécanisme donné par les réactions (3—6) est également valable si l'on prend en considération la formulation donnée par Ermakov en ce qui concerne la structure et l'état de l'oxychlorure de zirconium à l'état solide dissous dans l'eau.

S'appuyant sur les données Röntgen et de diffusion, Ermakov [9] montre qu'à l'état solide le $ZrOCl_2.8H_2O$ a la composition A et que, dissous dans l'eau par hydrolyse, il passe à B

---

* $HGH_4 = C_6H_{12}O_7$; $GH_4 = C_6H_{11}O_7$; $GH_3 = C_6H_{10}O_7$; $GH_2 = C_6H_9O_7$; $GH = C_6H_8O_7$; $G = C_6H_7O_7$.

[9] A. N. ERMAKOV, I. N. MAROV et V. K. BELIAEVA, *Zhur. neorg. Khim.*, **8**, 1623 (1963).

$$\underset{A}{[Zr_4(OH)_8 . 16H_2O]\,Cl_8 . 12H_2O} + aq \rightarrow \underset{B}{[Zr_4(OH)_8(OH)_4 . 12H_2O]\,Cl_4} . 12\,H_2Oaq + 4H^+\,aq + 4Cl^-\,aq \tag{8}$$

Dans le domaine des petites concentrations, cet agrégat se défait, formant des combinaisons polynucléaires à poids moléculaire plus petit, tandis que dans le domaine des concentrations plus grandes, deux ou plusieurs agrégats se lient par les OH non coordonnés.

Dans notre cas, les concentrations étant de l'ordre 10^{-3} M, on peut considérer que dans la solution est présent un agrégat binucléaire, donc

$$[Zr_2(OH)_4 . 8H_2O]\,Cl_4 . 6H_2O + aq \rightarrow \tag{9}$$

$$\rightarrow [Zr_2(OH)_4(OH)_2 . 6H_2O]\,Cl_2 . 6H_2O + 2H^+aq + 2Cl^-aq$$

C'est pourquoi au titrage du $ZrOCl_2$ par une base il se consomme deux équivalents de KOH.

Si l'on tient compte du fait que les anions pénètrent dans la sphère de coordination de l'ion métallique en déplaçant des ponts oliques des composés polymères formés, alors, par condensation s'éliminent $2H_2O$ et l'ion restera de charge +2 (voir la réaction 3)

$$[Zr_2\,(OH)_4\,(OH)_2]\,Cl_2 + HGH_4 \rightarrow [2Zr\,(OH)_2 . GH_3]\,Cl_2 + 2H_2O \tag{10}$$

Au titrage, il se consommera donc, au total, 2 équivalents de base pour le titrage de 2HCl mis en liberté à l'hydrolyse de l'agrégat binucléaire (voir la réaction 9) ; on passe ensuite à la condensation (10) et, par titrage par 2 équivalents de base, le complexe passe à la charge zéro, ce qui est en parfaite concordance avec les faits exposés ci-dessus.

On déduit des titrages potentiométriques que dans l'interaction du $ZrOCl_2$ et de l'acide gluconique il se forme dans la solution un seul type de complexe, dans lequel la complexation a lieu à la fois par le groupe carboxylique et par les groupes oliques du ligand.

En ce qui concerne l'origine des ions d'hydrogène, nous précisons que les $4H^+$ ($3H^+$ respectivement) proviennent du groupe carboxylique et des groupes oliques du ligand, parce que l'oxychlorure de zirconium ($ZrOCl_2$) ou l'oxychlorure hydraté ($Zr(OH)_2Cl_2$) se combinant à l'acide gluconique ne peut libérer $4H^+$ que par le scindement de $4H^+$ provenant des groupes carboxyliques et oliques. Si le complexe se formait seulement par les groupes hydroxyliques du ligand, aux titrages par la base des mélanges de $ZrOCl_2$ et d'acide gluconique, ou de gluconate de potassium, il devrait se consommer jusqu'au point d'équivalence 0,5 équivalents de base en plus pour 1 Zr.

Revue Roumaine de Chimie, 15, 1871–1882 (1970)

TITRAGE CONDUCTOMÉTRIQUE À RÉSISTANCE INDICATRICE. II[1]

TITRAGE DE L'ACIDE CHLORHYDRIQUE EN SOLUTIONS CONCENTRÉES DE CHLORURE DE SODIUM À RÉSISTANCE MEMBRANE PCV + PLASTIFIANT + MONTMORILLONITE – NATRIUM

C. LITEANU et LUCREȚIA GHERGARIU-MÎRZA

Chaire de Chimie Analytique de l'Université « Babeş-Bolyai », Cluj, 11, str. Arány Janos

Reçu le 6 juin 1970

L'ouvrage présente les résultats conductométriques du titrage de l'HCl, 0,04 n sur un fond de NaCl 3 n et 5 n, ainsi que de l'HCl 0,001 n + NaCl 5 n avec du NaOH 0,1 n, respectivement 0,01 n, en présence de la membrane indicatrice obtenue du PCV, de la montmorillonite–Na comme minéral échangeur d'ions et du dioctylphtalate comme plastifiant. La présence dans la solution à titrer de la membrane résoud la détermination du point d'équivalence avec précision et assez de sensibilité pour le titrage de l'HCl en présence d'un fond très conductible. Conformément aux données présentées, les titrages s'appliquent avec succès également pour les concentrations plus basses d'HCl (0,001 n) en solutions presque saturées de NaCl (5 n). Le titrage conductométrique réalisé en présence de la membrane chargée de montmorillonite–Na représente la variation de la conductibilité déterminée par les processus de réaction et d'échange ionique de celle-ci avec la solution, au cours du titrage.

L'application de la méthode de titrage conductométrique est limitée par le degré de mobilité des ions entrés et sortis de la réaction, et d'autre part par la concentration du fond de la solution. La présence dans la solution à titrer des ions ne participant pas à la réaction, en forte concentration, formant un fond très conductible, annihile partiellement ou totalement le changement de la conductibilité de la solution, comme conséquence de la différence entre la mobilité des ions entrés et sortis de la réaction. La courbe de titrage présente dans ce cas des droites délimitant un angle de forte aperture, ce qui rend impossible la détermination exacte du point d'équivalence.

Liteanu et Hopîrteanu [1] proposent, pour l'amélioration des courbes de titrage, l'introduction entre les deux électrodes d'une membrane indicatrice de polychlorure de vinyle imprégnée de cationite (Allassion CS sous forme R–H).

---

[1] C. Liteanu et El. Hopârtean, Ire Note, *Rev. Roumaine Chim.*, **12**, 517 (1967).

Dans le présent ouvrage on étudie le comportement de la membrane indicatrice de polychlorure de vinyle et imprégnée de montmorillonite—Na dans le titrage conductométrique de l'HCl par du NaOH en présence d'un fond de NaCl 3 n et 5 n.

On a choisi, pour imprégner la membrane, le minéral ayant la plus grande capacité d'échange, c'est-à-dire la montmorillonite, employée par nous comme échangeur d'ions, qui a été obtenue en extrayant la fraction $< 5.10^{-4}$ mm de la suspension dans de l'eau distillée de la bentonite de Valea Chioarului.

Le produit contient de la montmorillonite—Na en mélange avec 10—12% d'acide silicique libre (opale), ayant la composition suivante, établie par analyse chimique

$$Na_{0,13}\, K_{0,02}\, Ca_{0,08}\, (Mg_{0,48}\, Fe^{II}_{0.04}\, Fe^{III}_{0.07}\, Al_{1,37})[Si_{4,07}\, O_{10}]\, (OH)_2 \cdot$$

$$\cdot 2,38\, H_2O + 0,95\, SiO_2 \cdot 0,32\, H_2O$$

Du point de vue structural la montmorillonite employée est un minéral tristratifié, dioctaédrique, la distance entre les paquets étant de 15,55 Å (déterminée par nous). La forte capacité d'échange s'explique par un surplus de charge négative engendré par la caractéristique du réseau. Les ions d'échange pénètrent entre les couches, grâce à leur grande capacité de distancer.

La membrane indicatrice a été obtenue du polychlorure de vinyle (PCV) émulsion (Turda), de la montmorillonite — Na et du dioctylphtalate comme plastifiant.

On prépare une pâte homogène de 3 *p* PCV, 1 *p* montmorillonite—Na et 6 *p* dioctylphtalate. La pâte est travaillée en couche uniforme (épaisseur 0,1 — 0,2 mm), sur une plaque de verre et on chauffe graduellement (10°C/mn) dans une étuve, jusqu'à 175°, maintenue pendant 5 mn. Après refroidissement, on détache la membrane.

La cellule de conductibilité (fig. 1) à double paroi (thermostation) comprend deux pièces en verre jointes par un système (i) permettant la fixation de la membrane (m). L'étanchéité est réalisée au moyen d'une garniture en caoutchouc (d). Des deux côtés de la membrane, à distance égale sont fixées les deux électrodes (e) de platine platiné. La capacité de résistance de la cellule employée par nous est de $C = 1,9\ cm^{-1}$.

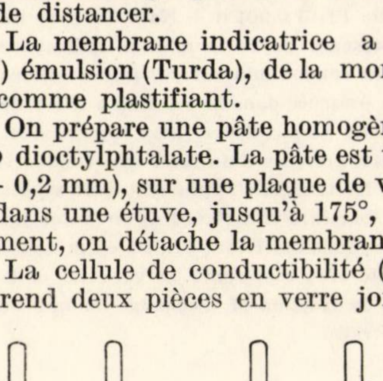

Fig. 1. — Cellule de conductibilité : *e*, électrodes de platine platiné. *m*, membrane, *i*, anneaux de fixation pour la membrane, *d*, garniture en caoutchouc.

L'enregistrement de la résistance de l'électrolyte de la cellule de conductibilité a été effectué à l'aide d'un pont RLC de type Tesla, fonctionnant en courant alternatif de 400 Hz.

DONNÉES EXPÉRIMENTALES

Les titrages conductométriques présentés par la suite ont été effectués par neutralisation par NaOH 0,1 n, respectivement 0,01 n des solutions d'HCl ayant les concentrations suivantes : 0,04 n et 0,001 n, sur un fond très conductible réalisé avec du NaCl 3 n et 5 n. Outre la concentration de 5 n NaCl, on a fait appel également à la concentration de 3 n étant donné d'une part qu'elle est suffisante pour changer la différence de pente de façon que l'application de la méthode classique de titrage conductométrique soit impossible, et d'autre part que le rapport des concentrations des ions H^+ et Na^+ de la solution est seulement légèrement supérieur au rapport de ces concentrations dans la solution de : HCl 0,1 n + NaCl 5 n (1 : 50) à laquelle on a travaillé dans le cas de la membrane imprégnée de cationite Allassion CS [1]. Les rapports des concentrations des ions H^+ et Na^+ dans les solutions de travail sont 1 : 75 (pour l'HCl 0,04 n avec du NaCl 3 n), 1 : 125 (pour l'HCl 0,04 n avec de l'HCl 5 n) et 1 : 5000 (pour l'HCl 0,001 n avec du NaCl 5 n).

Pour saisir les changements intervenus dans l'allure des courbes de titrage par l'introduction en plus de la solution acide d'un milieu très conductible (NaCl 3 n et 5 n), et par l'introduction entre les électrodes de la membrane indicatrice, on a effectué les titrages suivants :

a) le titrage d'HCl 0,04 n avec du NaOH, 1 n à 20°, 40° et 60°, en l'absence de la membrane ;

b) le titrage d'HCl 0,04 n sur un fond de NaCl 3 n avec du NaOH 0,1 n à 20°, 40° et 60° en présence et en l'absence de la membrane ;

c) le titrage d'HCl 0,04 n et d'HCl 0,001 n sur un fond de NaCl 5 n avec du NaOH 0,1 n respectivement 0,01 n à 20° en présence et en l'absence de la membrane.

Les courbes de titrage conductométriques ont été obtenues en figurant sur l'ordonnée la conductibilité λ ou $\lambda_c = \lambda \cdot \frac{v + V}{v}$ où v est le volume initial de la solution et V le volume total de la solution ajoutée.

Les solutions avec lesquelles on a travaillé ont présenté initialement, en l'absence de la membrane pour les trois températures données, les résistances suivantes : HCl 0,04 n à 20° 127,5 Ω ; à 40°, 105,5 Ω et à 60°, 80,8 Ω ; la solution résultant de l'HCl 0,04 n dans un milieu de NaCl 3 n à 20°, 10,5 Ω ; à 40°, 7,96 Ω et à 60°, 6,12 Ω ; la solution obtenue de l'HCl 0,04 n dans un milieu de NaCl 5 n à 20° manifeste une résistance de 8,95 Ω.

L'influence du milieu conductible sur l'allure des courbes de titrage conductométrique sont mises en évidence sur la figure 2, où les courbes de titrage sont représentées en l'absence de la membrane, avec et sans fond conductible. En l'absence du NaCl les courbes mettent clairement en évidence le point d'équivalence ; par contre, pour celles exécutées en présence d'un fond conductible (NaCl 3 n et 5 n) ce point ne peut être localisé.

Par l'introduction de la membrane entre les deux électrodes, apparaissent deux phénomènes, l'un consiste dans l'augmentation de la résistance enregistrée entre les deux électrodes (due évidemment à la membrane), et l'autre dans la variation de la résistance avec le temps.

Pour vérifier la reproductibilité du comportement de la membrane, on a exécuté des titrages répétés dans les mêmes conditions. On a remarqué qu'au cours du premier titrage (fig. 3, courbe *d*), la variation de la conductibilité de la membrane est légèrement plus importante que pour les titrages suivants. Après le premier titrage, le comportement de la membrane se maintient à peu près constant, mais sa résistance croît graduellement d'un titrage à l'autre. Ainsi, la résistance d'une membrane de la forme R-Na dans des conditions d'équilibre — c'est-à-dire en enregistrant la résistance de la membrane en contact avec une solution d'HCl 0,04 n + + NaCl 3 n après l'obtention d'une valeur pratiquement constante — est de 347 Ω au commencement du premier titrage, 681 Ω au commencement du second titrage et de 2375 Ω au 22e titrage. Cette augmentation de la résistance, due à la dégradation continuelle du minéral

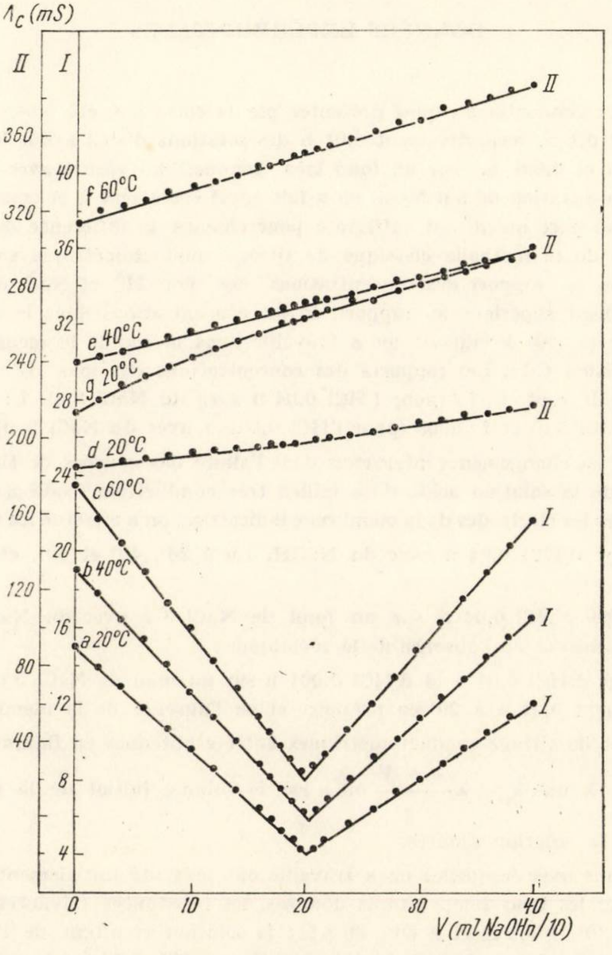

Fig. 2. — Courbes de titrage conductométrique obtenues en l'absence de la membrane :

I. courbes obtenues pour le titrage de l'HCl 0,04 n avec du NaOH 0,1 n, à 20°(a), 40° (b), 60° (c); II. courbes obtenues pour le titrage de l'HCl 0,04 n, sur un fond de NaCl 3 n avec du NaOH 0,1 n, à 20° (d), 40° (e), 60° (f) et de l'HCl 0,04 n+NaCl 5 n, à 20° (g).

argileux sous l'action des solutions acides et basiques du système, ne modifie pas essentiellement la variation de la conductibilité au cours d'un titrage. On peut considérer qu'exceptant le premier titrage, le comportement de la membrane est pratiquement le même dans les titrages suivants. Habituellement une membrane peut être utilisée pour environ 20 titrages. La membrane peut être utilisée pour plusieurs titrages à condition d'être préalablement maintenue, chaque fois, dans la solution à titrer jusqu'à conductibilité constante (équilibre), ce qui est réalisé en 1—2 heures. Après, on peut travailler dans les conditions suivantes :

1. On attend l'obtention d'une valeur de la conductibilité, pratiquement constante après chaque addition de réactif ; équilibre — équilibre (é—é).
2. On n'attend pas l'obtention d'une valeur constante de la conductibilité après chaque addition du réactif ; équilibre—non-équilibre (é—n).

On a également exécuté des titrages d'une troisième manière, c'est-à-dire :

3. La valeur de la résistance a été enregistrée dans des conditions de non-stabilisation de la conductibilité tant au commencement du titrage qu'après chaque addition de réactif ; ce genre de titrage est marqué : non-équilibre — non-équilibre (n—n). Mais dans ce cas, avant de commencer le titrage, la membrane fixée dans la cellule de conductibilité est amenée à la forme R-Na de la manière suivante : on la traite d'abord avec de l'HCl 0,01 n pour éliminer les ions OH^- restants du titrage antérieur, puis on la laisse pendant 8—10 heures avec les deux faces en contact avec une solution de NaCl 3 n.

1. *Titrage dans les conditions d'équilibre — équilibre* (*é—é*)

Les courbes de titrage conductométrique de l'HCl 0,04 n sur fond de NaCl 3 n à 20°, 40° et 60°, obtenues dans ces conditions, ainsi que de l'HCl 0,001 n + NaCl 5 n à 20° sont indiquées sur la figure 3. Le titrage a été effectué dans les deux compartiments de la cellule, et les valeurs de la résistance ont été enregistrées dans des conditions d'équilibre, c'est-à dire après l'obtention des valeurs pratiquement constantes.

Le temps nécessaire pour obtenir la constance de la conductibilité après l'addition de NaOH, varie de 2 à 15 mn, à l'exception des premières additions après le point d'équivalence, (30—60 mn).

Le temps nécessaire à l'équilibre diminue avec l'augmentation de la température. Ainsi, la durée totale d'un titrage é—é, exécuté à 20°, est d'environ 6 heures (fig. 3, courbe *b*) comparé à 5 heures pour le titrage exécuté à 60° (fig. 3, courbe *d*). On remarque que l'intervalle de temps nécessaire pour l'obtention de l'équilibre diminue et se maintient approximativement le même pour les additions au voisinage du point d'équivalence, dans le cas de la diminution de la concentration d'acide chlorhydrique dans la solution à titrer.

L'augmentation de la température, outre la diminution de la durée d'un titrage, a également un effet négatif de diminution du saut de la résistance au point d'équivalence. Ainsi, la courbe obtenue à 60° (*d*) ne peut être valorisée.

La comparaison des courbes de titrages obtenues dans des conditions d'équilibre-équilibre (fig. 3) révèle un changement net de leur allure dans le cas d'un changement du rapport des concentrations d'ions H^+ et Na^+. Pour le rapport 1 : 75 de ces concentrations, les courbes ont l'aspect des titrages potentiométriques (fig. 3, courbes *b*, *c*). Dans ce cas, la résistance de la solution varie légèrement tant avant qu'après la neutralisation. Le point d'équivalence peut être mis en évidence par une brusque diminution de la conductibilité. Pour un rapport 1 : 5000, le point d'équivalence est mis en évidence par l'intersection de deux droites comme pour les titrages classiques. La différence consiste dans le sens de variation de la résistance.

En effet, la courbe obtenue (fig. 3, courbe *a*) a une position inverse par rapport à celle exécutée en l'absence de la membrane et du fond conductible (fig. 2, courbes I). La croissance de la résistance après le point d'équivalence a lieu linéairement et représente dans le cas du titrage de l'HCl 0,001 n + NaCl 5 n avec du NaOH 0,01 n, le détaillage du brusque saut de résistance dans le titrage d'un acide plus concentré (HCl 0,04 n + NaCl 3 n) avec du NaOH 0,1 n.

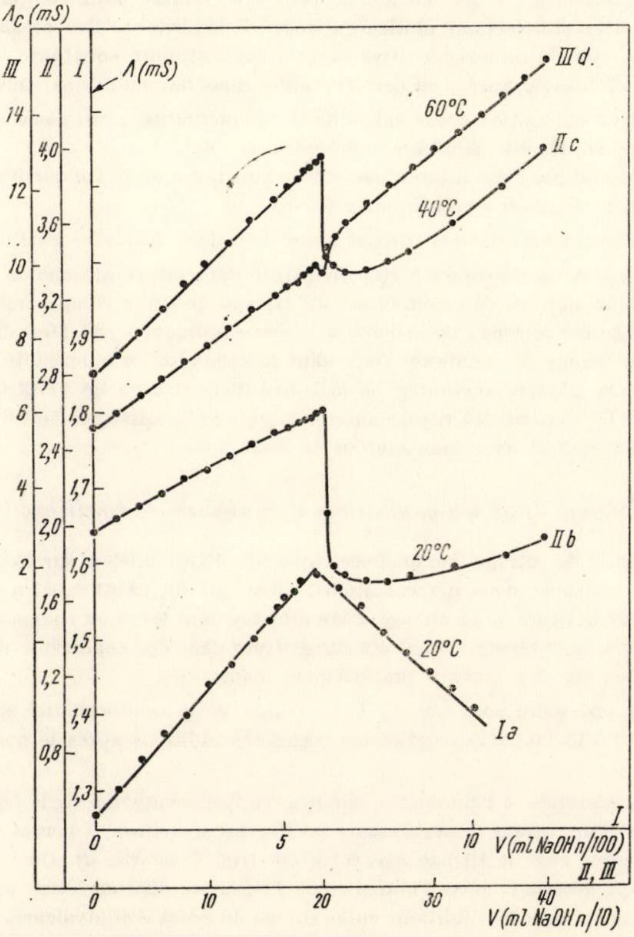

Fig. 3. — Courbes de titrage conductométrique obtenues en présence de la membrane imprégnée de montmorillonite — Na dans les conditions d'équilibre—équilibre.

a, courbe obtenue pour le titrage de l'HCl 0,001 n + NaCl 5 n avec du NaOH 0,01 n, à 20° ; *b,c,d*, courbes obtenues pour le titrage de l'HCl 0,04 n + NaCl 3 n avec du NaOH 0,1 n, à 20°, 40° et 60°.

2. *Titrage dans les conditions équilibre—non-équilibre (é—n)*

Les courbes de titrage conductométrique du type (é—n) (fig. 4) sont les suivantes :

a) Le titrage de la solution d'HCl 0,04 n sur fond de NaCl 3 n à 20°, 40° et 60°, avec du NaOH 0,1 n (fig 4, courbes *c*, *d*, *e*).

b) Le titrage de la solution d'HCl 0,04 n sur fond de NaCl 5 n à 20° avec du NaOH 0,1 n (fig. 4, courbe *b*).

c) Le titrage de la solution d'HCl 0,01 n sur fond de NaCl 5 n à 20° avec du NaOH 0,01 n (fig. 4, courbe *a*).

Les courbes de titrage é–n ont été effectuées afin de réduire le temps d'exécution. Pour ce type de courbes, ainsi qu'il a été montré (fig. 4), le titrage commence seulement après l'obtention d'une résistance constante au contact de la solution à titrer avec la membrane (équilibre).

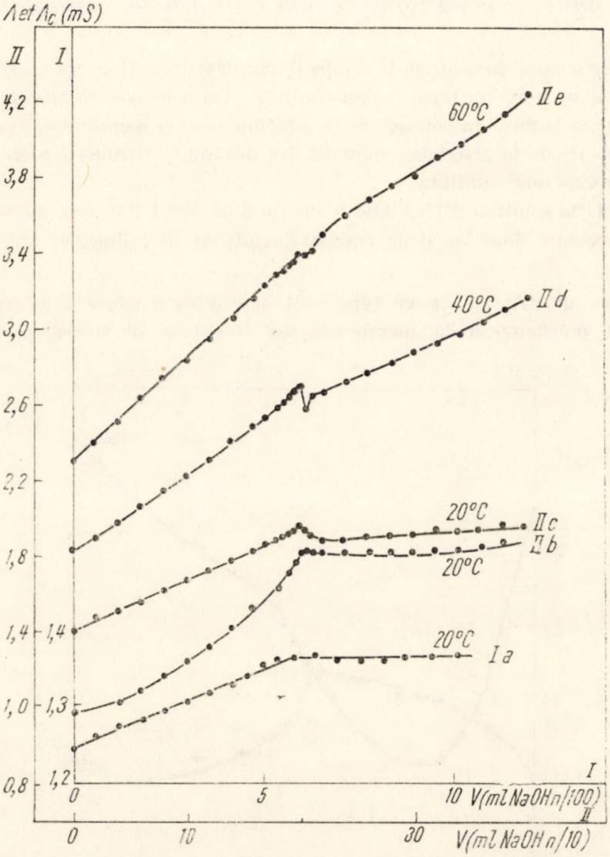

Fig. 4. — Courbes de titrage conductométrique obtenues en présence de la membrane imprégnée de montmorillonite–Na dans les conditions d'équilibre — non-équilibre.

a, courbe obtenue pour le titrage de l'HCl 0,001 n + NaCl 5 n avec du NaOH 0,01 n, à 20°. *b*, courbe obtenue pour le titrage de l'HCl 0,04 n + NaCl 5 n avec du NaOH 0,1 n, à 20°. *c*, *d*, *e*, courbes obtenues pour le titrage de l'HCl 0,04 n + NaCl 3 n, avec du NaOH 0,1 n, à 20°, 40° et 60°.

En analysant les courbes de titrage de type é–n de la figure 4, on remarque au point d'équivalence une brisure de la ligne donnée par la diminution de la conductibilité de la solution à la suite de l'apparition de l'ion OH^- dans le système. Le titrage étant exécuté dans des conditions de non-équilibre, la variation de la conductibilité au point d'équivalence est sensiblement diminuée.

Des courbes obtenues pour les trois températures on peut utiliser pour les déterminations seulement celles réalisées à 20°, avec le rapport H : Na variant de 1 : 75 à 1 : 5000. Dans le cas des courbes obtenues à 40°, respectivement à 60°, le point d'équivalence ne peut être déterminé avec une précision suffisante.

3. *Titrage dans les conditions de non-équilibre — non-équilibre (n—n)*

Pour réduire encore davantage le temps d'une détermination, on a exécuté des titrages dans des conditions de non-équilibre — non-équilibre. Dans ce cas, le titrage a été commencé immédiatement après la mise en contact de la solution avec la membrane, ayant lieu à vitesse constante. Les valeurs de la résistance enregistrées durant le titrage ont été prises également dans des conditions de non-équilibre.

Le titrage de la solution d'HCl 0,04 n sur fond de NaCl 3 n avec du NaOH 0,1 n à 20°, 40° et 60° a été exécuté dans les deux compartiments de la cellule, et est représenté sur la figure 5.

Les courbes de titrage de ce type sont déformées à cause à la superposition de la courbe de l'effet d'échange à la membrane, sur la courbe de titrage proprement dite. Le

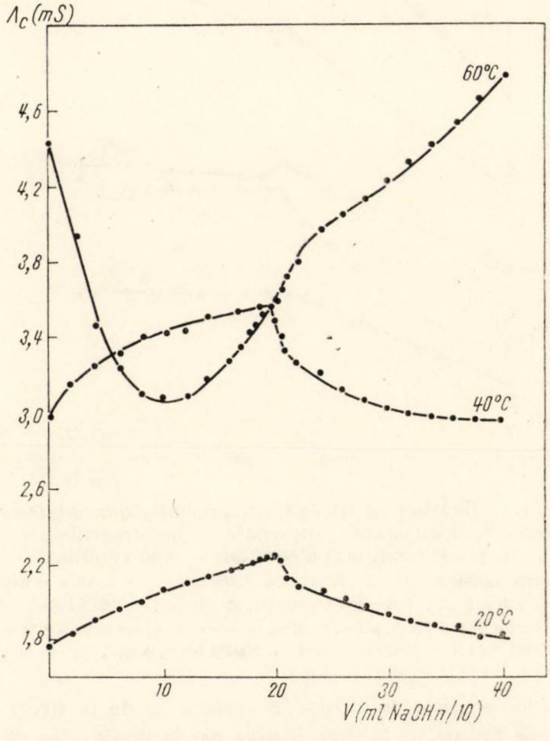

Fig. 5. — Courbes de titrage du type n—n obtenues en présence de la membrane chargée de montmorillonite—Na. On a titré par HCl 0,04 n + NaCl 3 n avec du NaOH 0,1 n à 20°, 40°, 60°.

point d'équivalence peut être localisé avec une exactitude et une précision satisfaisantes seulement pour les titrages exécutés à 20°. La durée d'une détermination est d'environ 30 mn.

Titrage dans un seul compartiment

Afin de simplifier les titrages conductométriques avec résistance indicatrice, pour son application dans des analyses courantes nous proposons les titrages d'un seul côté de la membrane, dans des conditions d'équilibre — non-équilibre et non-équilibre — non-équilibre. Les courbes obtenues de cette manière pour le titrage de l'HCl 0,04 n + NaCl 3 n avec du NaOH 0,1 n — dans l'autre compartiment se trouvant la solution à titrer (figures 6—8 ; courbes *c* et *d*) ou du NaCl 3 n (fig. 6—8 ; courbes *a* et *b*), sont représentées sur les figures 6 (20°), 7 (40°) et 8 (60°).

Le titrage d'un seul côté de la membrane améliore sensiblement l'allure des courbes. pe point d'équivalence peut être localisé avec précision pour toutes les trois températures Lans les titrages de type é—n et seulement pour 20° et 40° dans les titrages n—n. La durée du titrage proprement dit est d'environ 30 mn. Les courbes n—n exécutées à 60° présentent des inflexions non concluantes. En comparant les courbes *a*, *b* aux courbes *c*, *d*, on remarque une diminution de l'effet à l'équivalence dans le cas de la présence du NaCl 3 n dans le compartiment non titré.

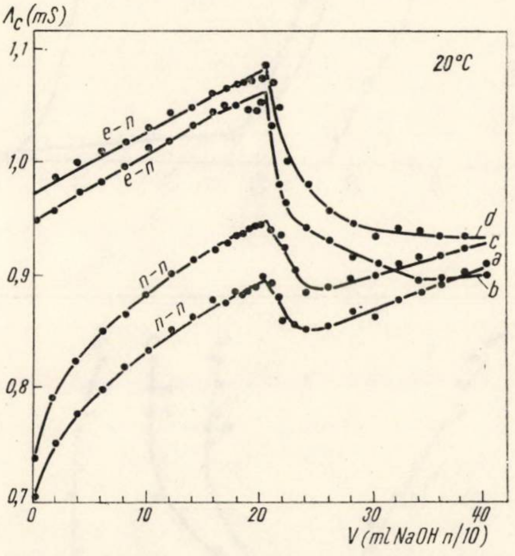

Fig. 6. — Courbes de titrage conductométrique obtenues à 20°, en présence de la membrane imprégnée de montmorillonite—Na de la solution d'HCl 0,04 n sur fond de NaCl 3 n (titrage d'un seul côté). Les courbes *a* (n—n) et *b* (é—n) ont, dans la partie non titrée, du NaCl 3 n. Les courbes *c* (n—n) et *d* (é—n) ont, dans la partie non titrée, de la solution à titrer.

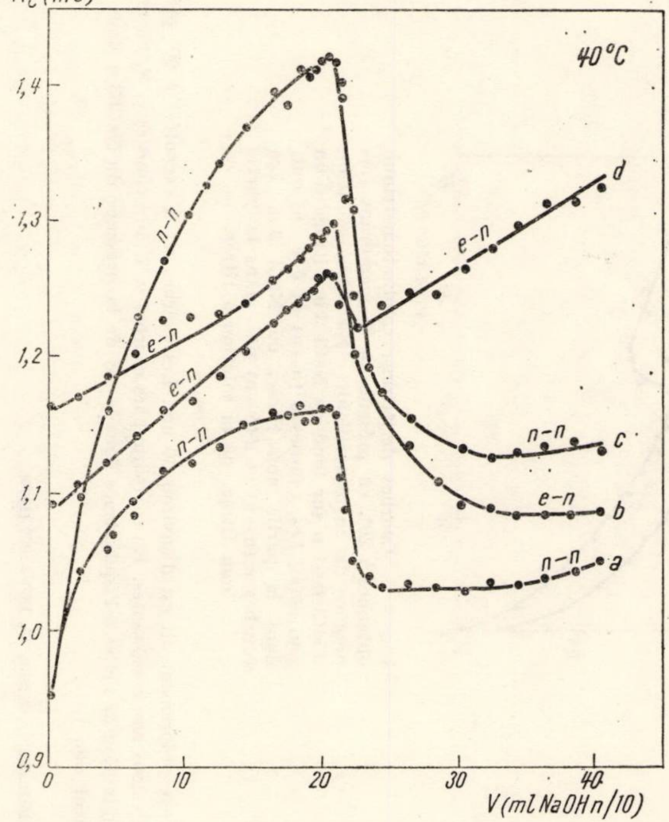

Fig. 7. — Les titrages donnés dans la figure 6, exécutés 40°.

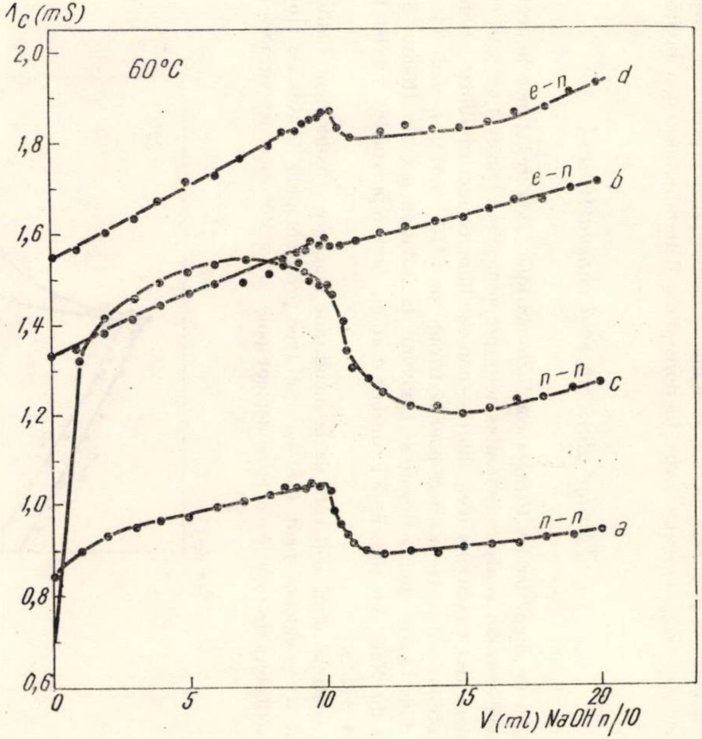

Fig. 8. — Les titrages donnés dans la figure 6, exécutés à 60°.

CONCLUSIONS

Des données expérimentales présentées il résulte que l'introduction d'une membrane imprégnée de montmorillonite—Na rend possible la détermination exacte du point d'équivalence dans le cas du titrage de l'acide chlorhydrique présent dans des solutions à haute conductibilité.

La membrane introduite entre les deux électrodes une résistance dont les variations pendant le titrage dépendent du type et de la concentration des ions présents, de la température et du temps, ainsi que de l'épaisseur de la membrane, respectivement de la quantité et de la qualité de la distribution de la montmorillonite. La résistance de la membrane pendant un titrage varie sensiblement, par exemple dans le titrage de l'HCl 0,04 n + + NaCl 3 n avec du NaOH 0,1 n (fig. 3, courbe *b*), elle atteint des valeurs minimales et maximales de 940 Ω et 1775 Ω (les valeurs sont prises au moment de l'équilibre dans la solution de titrage). Au cours d'un titrage, la variation de la résistance de la solution est négligeable (5 Ω ; fig. 2, courbe II, 20°) par rapport à la variation de la résistance de la membrane (environ 600 Ω). Les valeurs enregistrées pour les courbes de titrage peuvent être considérées donc comme représentant pratiquement la résistance seule de la membrane proprement dite, ce qui justifie leur nom de *resistances indicatrices*.

Outre les processus d'échange auxquels la membrane indicatrice participe, nous devons signaler le phénomène de dégradation de la montmorillonite par la réaction des ions OH^- avec les ions Al^{3+} des couches intérieures des paquets tristratifiés, produisant une diminution de la capacité d'échange du minéral. Le bloquage du minéral d'échange sous l'action des ions OH^- explique la diminution de la conductibilité à l'apparition de ces ions dans le système. Cette réaction est seulement partiellement réversible, car le contact ultérieur de la membrane avec le HCl ne régénère pas entièrement le minéral attaqué. La déterioration du minéral a lieu lentement puisqu'il est protégé par le PCV et est exprimée par la croissance graduelle de la résistance de la membrane après usages répétés. Une membrane imprégnée de montmorillonite peut être employée à environ 20 titrages.

Le titrage conductométrique réalisé en présence de la membrane indicatrice chargée de montomorillonite—Na résoud la détermination du point d'équivalence dans le cas des solutions d'HCl sur fond très conductible de NaCl. Cette méthode peut être appliquée pour des concentrations différentes d'HCl, notamment de 0,04 n à 0,001 n. Dans tous les cas, λ_c croît lors de l'addition du réactif avant la neutralisation de la solution acide et puis diminue. La diminution de la conductibilité après le point d'équivalence est plus importante ou plus faible, plus brusque ou plus lente, en fonction de la température, du temps d'exécution des déterminations, ainsi que des quantités de réactif ajouté.

Par la suite, le point d'équivalence peut être déterminé avec précision et suffisante sensibilité dans le cas des titrages exécutés à 20° et 40° dans les conditions é—é et é—n dans les deux compartiments de la cellule de conductibilité.

On obtient de bons résultats aussi pour le titrage du type é—n exécuté à 20° et 40° dans un seul compartiment. Le temps d'exécution diminue dans ce cas, et le point d'équivalence est mis clairement en évidence. La sensibilité du titrage croît si dans le compartiment non titré il y a également de la solution à analyser.

Revue Roumaine de Chimie, **15**, 1883–1892 (1970)

COPOLYMERS OF CONJUGATED DIENES WITH MALEIC ACID MONOESTERS I.

ISOPRENE COPOLYMERIZATION WITH THE METHYLIC MONOESTER OF THE MALEIC ACID

I. NANU * and C. ANDREI **

* Chair of Macromolecular Chemistry, Polytechnic Institute, Timişoara,
K. Marx Street, 3
and
** Research Laboratory, Combinatul Petrochimic Ploieşti, Brazi, Jud. Prahova

Received June 19, 1970

Isoprene copolymerization with monomethylmaleat in solution of cyclohexanone and in the presence of free radicals (A.I.B.N.) was studied. The copolymerization constants, determined by the Mayo-Lewis method $r_1 = 0.10 \pm 0.06$ and $r_2 = 0$ and by the Fineman-Ross method $r_1 = 0.151$ and $r_2 = 0$. show a marked trend towards alternating copolymerization. The copolymerization rate variation as a function of the isoprene-monomethylmaleate ($M_1 : M_2$) ratio also shows a trend towards alternating copolymerization. The determined apparent activation energy amounts to a value of $E_a = 22.4$ kcal/mole.

INTRODUCTION

The first information concerning the yield of copolymers of the conjugated dienes with dicarboxylic acids was found in the patent literature [1,2] and it points to the possibility of cpolymerizing isoprene, dimethylbutadiene and chloroprene with maleic, fumaric, chloromaleic and chlorofumaric acid, in order to obtain "carboxylic elastomers".

In 1939, Bacon and Farmer [3] presented a new possibility to introduce carboxylic functional groups into elastomers, by the interaction of maleic anhydride with rubbers in solvent medium and in the presence of benzoyl peroxide, with building up of a large series of products, such as carboxylic elastomers, and solid, fibrous and resinous products.

Along this line, research was continued by Compagnon and Bras [4,5] and published in an important amount of works, beginning with 1941.

[1] I. G. Farbenindustrie Aktiengesellschaft, Germ. Pat. 667.163, 1938.

[2] I. G. Farbenindustrie Aktiengesellschaft, Fr. Pat. 842.186, 1939.

[3] R. G. Bacon and E. H. Farmer, *Rubber Chem. Technol.*, **12**, 200 (1939).

[4] P. Compagnon and J. Bras, *Rev. Gen. Caoutchouc*, **18**, 89 (1941).

[5] P. Compagnon and O. Bonnet, *Rev. Gen. Caoutchouc*, **19**, 79 (1942).

The products obtained by alteration of rubbers with maleic anhydride (the term "alteration"[6] was accepted in order to differentiate the altered polymers from the block copolymers and graft copolymers, due to fact that the altered ones do not possess graft chain, branches, but only individual molecules) were called anhydride rubbers [4,7-10] which have the capacity of hydrolysing easily to carboxylic rubbers.

Though the patent literature shows that the carboxylic elastomers were obtained by copolymerizing conjugated dienes with unsaturated carboxylic acids, much before those obtained by altering rubbers with maleic anhydride or other unsaturated carboxylic acids, scientific work concerning the first process was published much later, after the industrialization of the carboxylic latexes.

The yield of carboxylic latexes on an industrial scale was carried out in 1949 by synthetizing a copolymer under the commercial denomination of "Hycar 1571" (latex based on acrylonitrile/butadiene copolymer, containing an acrylic-type comonomer: acrylic or metacrylic acid [10,11]).

The first scientific indications concerning the yield of copolymers from conjugated dienes and unsaturated carboxylic acids are found in the work of Frank, Kraus and Haefner [12] who studied the synthesis of the butadiene-metacrylic acid copolymers and their adhesive properties to steel, and in the work of Marvel and coworkers [13] which shows the possibility of copolymerizing butadiene and isoprene with cynamic acid and its derivatives, under different polymerization conditions.

These two works represent the beginning of a systematic study of the carboxylic elastomers, obtained by copolymerizing conjugated dienes with unsaturated monocarboxylic acids; this study was continued in a series of important works of Brown,[8,9,14] Marvel and coworkers,[15,16] Green and coworkers,[17] Dolgoplosk and coworkers [18,19] and Cooper.[20,21]

It is necessary to point out that in the field of copolymerization of conjugated dienes with unsaturated dicarboxylic acids and their derivatives, emphasized by the cited patents [1,2] and by a number of more recent

[6] A. Romanov, *Plaste und Kautschuk*, **12**, 521 (1965).

[7] P. Compagnon and O. Bonnet, *Rubber Chem. Technol.*, **19**, 319 (1946).

[8] H. P. Brown, *Rubber Chem. Technol.*, **28**, 937 (1955).

[9] H. P. Brown, *Rubber Chem. Technol.*, **30**, 1347 (1957).

[10] C. Andrei, "Study of Carboxylic Elastomers" unpublished synthesis work, Combinatul Petrochimic, Ploiești, 1969.

[11] G. E. Eilbeck and E. R. Urig, *Rubber World*, **148**, 38 (1963).

[12] C. F. Frank, A. J. Haefner and G. Kraus, *Ind. Eng. Chem.*, **44**, 1600 (1952).

[13] C. S. Marvel, G. H. McCain, M. Passer, W. K. Taft and B. G. Labbe, *Ind. Eng. Chem.*, **45**, 2311 (1953).

[14] H. P. Brown and M. G. Duke, *Rubber World*, **130**, 784 (1954).

[15] C. S. Marvel, W. S. Anderson, Barbara H. Weil, E. E. Ryder, H. K. Inskip and M. Passer, *Ind. Eng. Chem.*, **47**, 344 (1955).

[16] C. S. Marvel, R. Potts, J. Economy and G. P. Scott, *Ind. Eng. Chem.*, **47**, 2221 (1955).

[17] J. Green and F. E. Sverdrup, *Ind. Eng. Chem.*, **48**, 2139 (1956).

[18] B. A. Dolgoplosk, E. J. Tinyakova, V. N. Reikh, T. G. Juravleva and G. P. Belonovskaya, *Kautchuk i Rezina*, **16**, 11 (1957).

[19] B. A. Dolgoplosk, V. N. Reikh, E. J. Tinyakova, A. E. Kalays, Z. A. Korysenko and E. G. Sladkevici, *Rubber Chem. Technol.*, **32**, 328 (1959).

[20] W. Cooper, *Chem. and Ind.*, **74**, 1741 (1955).

[21] W. Cooper, *J. Polymer Sci.*, **28**, 195 (1958).

patents,[22-25] both in the field of obtaining carboxylic elastomers and in the field of obtaining some resines with high adhesive properties, there is lack of systematic scientific research.

The study of alternating copolymerization of 2,4-hexadiene with maleic anhydride[26] may be mentioned, but the huge number of works concerning the reaction of conjugated dienes with maleic anhydride and its derivatives deals with the yielding of Diels-Alder adducts and not with their copolymerization reaction.

The purpose of the present work was to study copolymerization of isoprene with monomethylmaleate, in the presence of radicalic initiators.

EXPERIMENTAL

Materials

The isoprene used (Fluka A. G. Buchs S. G.) was chemically pure with a concentration of 99% mol., Kp = 34–35°, $d_4^{20} = 0.681$ and $n_D^{20} = 1.422$.

Monomethylmaleate was prepared by us in the laboratory, from maleic anhydride *p.a.* (Union Chimique Belge) and absolute methyl alcohol („Reactivul", Bucharest) in a molar proportion of 1 : 1 and at 80° (we worked only with freshly prepared monoester, in order to exclude the possibility of its regrouping in time).[27] The characteristics of the obtained monoester had the following values :

– monoester concentration $> 99.5\%$

– $n_D^{20} = 1.4640$ and

– acidity index (A.I.) = 432–436.

As copolymerization medium, cyclohexanone *p.a.* („Reactivul", Bucharest) with a distillation interval of 154–156° and $n_D^{20} = 1.450-1.451$ was used, which is a good solvent, both for monomers and for the obtained copolymers.

As polymerization initiator, α, α'-azobisisobutyronitrile (A.I.B.N.) double-recrystallized in acetone or ethyl ether was used.

Procedure

The copolymerization process of isoprene with monomethylmaleate was carried out in Pyrex-phials.

After having been previously blown with nitrogen, the phials were filled with the components of the reaction mixture (cyclohexanone, A.I.B.N., monomethylmaleate and isoprene) at a filling rate of 0.5–0.6 and were sealed by welding.

---

[22] Y. Shinohara, Y. Tsuda and T. Sakai, Jap. Pat. 26.704, 1964; *Chem. Abstr.*, **68**, 87861 (1968).

[23] R. L. Zimmerman, M. Mich and G. B. Steling, Fr. Pat. 1.511.355, 1967; USA Pat. 3.311.584, 1967.

[24] H. Naarmann and E. Günther, West-German Pat. 1.227.243, 1966.

[25] W. T. Brady, SUA Pat., 3.250.751, 1966.

[26] M. Jwamoto and G. Yuguchi, *Bull. Chem. Soc. Japan*, **40**, 1272 (1967).

[27] S. N. Uşhakov, A. F. Nicolaev, A. M. Toroptseva and M. S. Trizno, *Zhur priklad. Khim.*, **32**, 667 (1959).

Copolymerization took place at well established temperatures, with a variation of ± 1°, in an oil bath; the stirring of the reaction mixture was carried out by rotating the phials.

After carrying out the reaction, the phials were suddenly cooled under the temperature of 0°, in order to break off copolymerization.

In order to separate the copolymer from the reaction mixture, the latter was introduced into a methanol-water mixture, reaching a reaction mixture : methanol-water rate of 1 : 8–15.

It must also be pointed out that the methanol-water ratio was varied as a function of the copolymer composition, between 85 : 15 and 25 : 75 vol. parts and this variation was established empirically.

The precipitated copolymer was separated by filtration in a filter crucible (G_4, G_5). Quantitative purification was carried out by solving the copolymer and precipitating it repeatedly with a methanol-water mixture; the control was carried out by comparing the results of the elementary analysis of the product after the first purification, with those obtained after a repeated purification.

Drying of the copolymer to constant weight was carried out at a temperature of 40–50°, under continuous air current or under vacuum and the conversion in the copolymerization process was calculated according to the obtained quantity.

RESULTS AND DISCUSSIONS

REACTIVITY RATIOS

Being a double bond conjugated system, isoprene is considered as a resonance hybrid of the structures (1), (2) and (3).

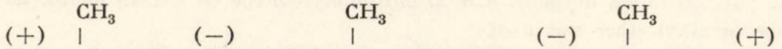

$$\overset{(+)}{H_2C} - \overset{CH_3}{C} = CH - \overset{(-)}{CH_2} \leftrightarrow H_2C = \overset{CH_3}{C} - CH = CH_2 \leftrightarrow \overset{(-)}{CH_2} - \overset{CH_3}{C} = CH - \overset{(+)}{CH_2}$$

(2) (1) (3)

Due to conjugation, the central bond shows a partially double bond characteristic, which forces the molecule to adopt two conformations : s-*trans* (transoidic) and s-*cis* (cisoidic).[28]

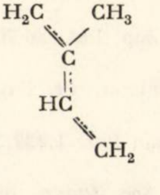

transoid

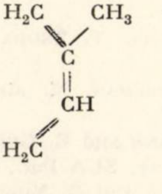

cisoid

---

[28] "Encyclopedia of Polymer Science and Technology", vol. 7, Interscience Publishers John Wiley, New York, 1967, p. 784.

More recent works,[29-31] contrary to older ones,[32] show clearly that the conformational shape of liquid isoprene (under normal conditions) is the transoidic one, as is the case of butadiene. The transoidic conformation is more stable than the cisoidic one, but with increasing temperature, transoidic form passes into cisoidic one.

The conclusions of the experimental research carried out on the stereochemistry of the Diels-Alder reaction, summarized the fact that the reaction may take place only when the diene has a s-*cis* (cisoidic) conformation.[33,34]

If the diene in the cisoidic conformation is substituted, and the substituents interfere, the diene synthesis is made difficult or may not take place at all.

Under these circumstances, the diene polymerization in the presence of the dienophile, accompanies sometimes the Diels-Alder reaction, or in other cases, it takes place even by excluding the latter.

The dienes with double substituted carbon atoms at the terminal positions of the conjugated system tend rather to yield polymers, than normal adducts.

Thus, 4-methyl-1,3-pentadiene, 2-methyl-2,4-hexadiene, 4-methyl-1,3-hexadiene, 2,5-dimethyl-2,4-hexadiene, 4-methyl-6-phenyl-1,3-hexadiene, 4-n-propyl-1,3-heptadiene yield with maleic anhydride, exclusively polymer products.[33]

Our experiments carried out in cyclohexanone medium and in the presence of a polymerization inhibitor, at a temperature up to 80° and a reaction time of 1—5 hours, in order to obtain Diels-Alder adducts of the isoprene with the monomethylmaleate, gave negative results.

Also, the quantitative determination of the monomethylmaleate, after its copolymerization reaction with isoprene, showed that this reaction was not accompanied by a Diels-Alder reaction, as there is a good agreement between the consumed quantity of monoester and the quantity refound in the copolymer.

Under these circumstances, we undertook the study of the copolymerization reaction.

In order to determine the reactivity ratios, the copolymerizations were stopped at conversions of less than 5%. The experimental results are presented in table 1.

---

[29] G. Szasz and N. Sheppard, *Trans. Faraday Soc.*, **49**, 358 (1953).

[30] M. I. Batuev, A. S. Onishchenko, A. D. Matreeva and N. I. Aronova, *Doklady Akad. Nauk. S.S.S.R.*, **132**, 581 (1960).

[31] D. Craig, J. J. Shipman and R. B. Fowler, *J. Amer. Chem. Soc.*, **83**, 2885 (1961).

[32] V. N. Nikitin and T. V. Yakovleva, *Zhur. fiz. Khim.*, **28**, 692 (1954); **28**, 697 (1954).

[33] R. Adams, W. E. Bachmann, A. H. Blatt, L. F. Fieser, J. R. Johnson and H. R. Snyder, "Organic Reactions", vol. 4, John Wiley, New York, 1948, p. 1—59.

[34] E. Angelescu and F. Cornea, "Probleme Teoretice de chimie organică", Ed. didactică şi pedagogică, Bucharest, 1969, p. 276—293.

Table 1

Radicalic Copolymerization of Isoprene (M_1) with Monomethylmaleate (M_2)

Test No	Feed composition		Copolymer composition		Reaction time min.	Conversion %	Copolymer analysis		F. $[M_1]_0 : [M_2]_0$	f. m_1/m_2
	$[M_1]_0$ Moles	$[M_2]_0$ Moles	m_1 Moles	m_2 Moles			C, %	H, %		
C_{38}	0.2470	0.0229	0.00688	0.00261	50	4.04	70.50	8.82	10.78	2.63
C_{40}	0.1452	0.0750	0.00322	0.00344	10	3.34	60.00	7.02	1.93	0.96
C_{41}	0.2178	0.0375	0.00496	0.00275	35	3.48	66.73	8.13	5.80	1.80
C_{42}	0.0703	0.1126	0.00480	0.00482	7	4.77	60.56	7.21	0.62	0.99
C_{43}	0.2760	0.0074	0.00490	0.00171	60	2.78	71.37	8.96	37.29	2.86
C_{44}	0.2833	0.0036	0.00136	0.00039	80	0.72	73.22	9.28	78.69	3.48
C_{50}	0.0365	0.1304	0.000838	0.000817	5	0.83	60.88	7.46	0.27	1.02
C_{51}	0.0137	0.1449	0.00485	0.000498	3.5	0.49	60.39	7.07	0.09	0.97

– Reaction temperature: 70°; Initiator $[AIBN] \times 10^3 = 0.91$ moles;
– Theoretical value of the C and H of an alternant copolymer: %C, 60.59; %H, 7.11.

Plotting the concentration value of the methylic monoester of the maleic acid in the copolymer, against its value in the feed composition, the copolymer composition diagram was obtained (fig. 1).

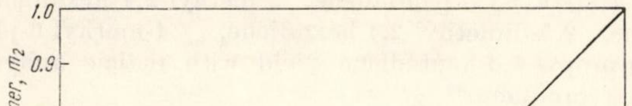

Fig. 1. — Composition diagram of the isoprene-monomethylmaleate copolymer.

From the diagram, an appreciable trend to build up some alternating copolymers is observed. When one works with very high ratios (isoprene-monomethylmaleate) in the feed composition, isoprene enriched copolymers may still be obtained, with properties tending towards those of the elastomers, but with a small molecular mass.

In order to determine the reactivity ratios, the results of table 1 were used applying both the intersection method of Mayo and Lewis [35] and the method of the linearized composition equation of Fineman and Ross.[36] This representation may be seen in figures 2 and 3.

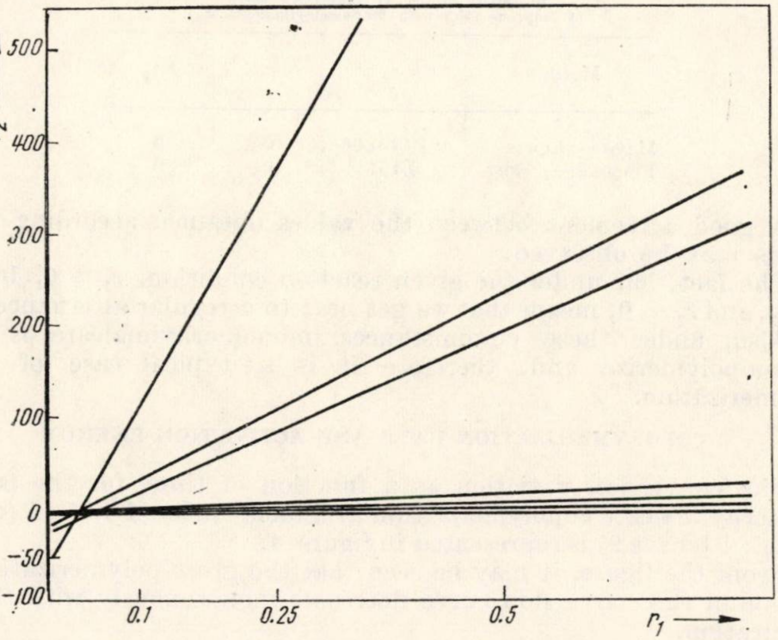

Fig. 2. — Determination of copolymerization constants by the Mayo-Lewis method for isoprene-monomethylmaleate.

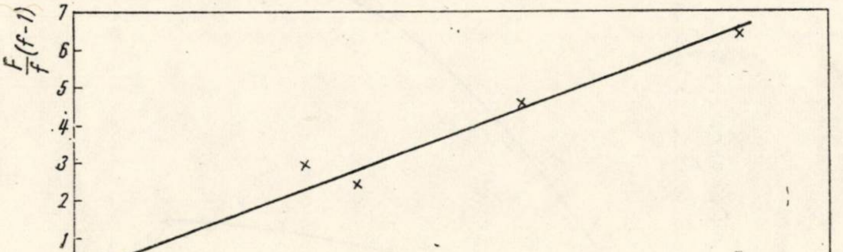

Fig. 3. — Fineman-Ross representation for determining the copolymerization constants of the isoprene-monomethylmaleate system.

---

[35] F. R. Mayo and F. M. Lewis, *J. Amer. Chem. Soc.*, **66**, 1594 (1944).

[36] M. Fineman and S. D. Ross, *J. Polymer Sci.*, **5**, 259 (1950).

The reactivity values obtained from these graphs, are presented in table 2.

Table 2

Reactivity Ratios in Copolymerization of Isoprene (M_1) with Monomethylmaleate (M_2).

Method	r_1	r_2	$r_1 r_2$
Mayo — Lewis	0.10 ± 0.06	0	0
Fineman — Ross	0.151	0	0

A good agreement between the values obtained according to both methods may be observed.

The fact that under the given reaction condition, $r_1 > 0$, but subunitary, and $r_2 = 0$, means that we get near to a regular alternance.

Also, under these circumstances, monomethylmaleate is unable to homopolymerize and therefore it is a typical case of heterocopolymerization.

COPOLYMERIZATION RATE AND ACTIVATION ENERGY

The conversion variation as a function of time, for the isoprene-monomethylmaleate copolymerization at a molar ratio of 4.95 : 1 (curve 1) and of 1 : 1 (curve 2) is represented in figure 4.

From the figure, it may be seen that the gross polymerization rate, the slope of the conversion curve decreases monotonously with the reaction duration.

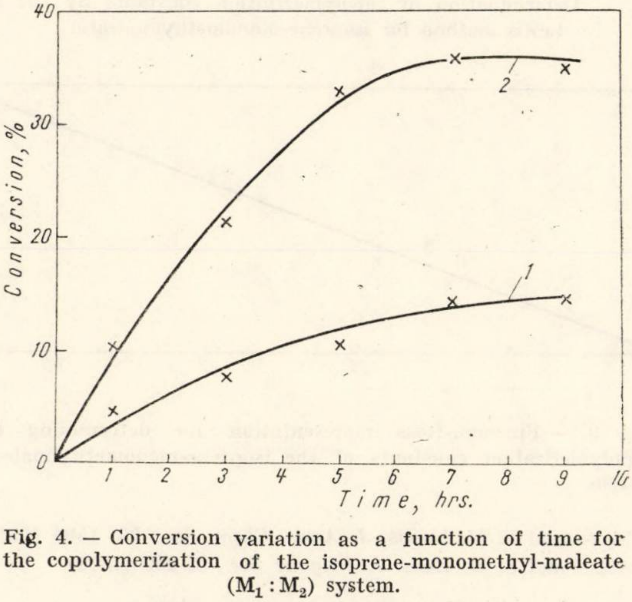

Fig. 4. — Conversion variation as a function of time for the copolymerization of the isoprene-monomethyl-maleate ($M_1 : M_2$) system.

1, Initial molar ratio, $[M_{10}] : [M_2]_0 : = 4.5 : 1$;

2, Initial molar ratio, $[M_{10} :] [M_2]_0 : = 1 : 1$.

Also, the lack of a marked conversion autoacceleration, during the studied period, known also under the term of "gel effect" can be observed.

In figure 5, the variation of the copolymerization speed (% hr^{-1}) as a function of the molar ratio isoprene-monomethylmaleate in the feed composition is represented.

The aspect of the curve also shows a marked trend towards alternating copolymerization.

The influence of temperature on copolymerization of isoprene with monomethylmaleate is given by the Arrhenius representation in figure 6.

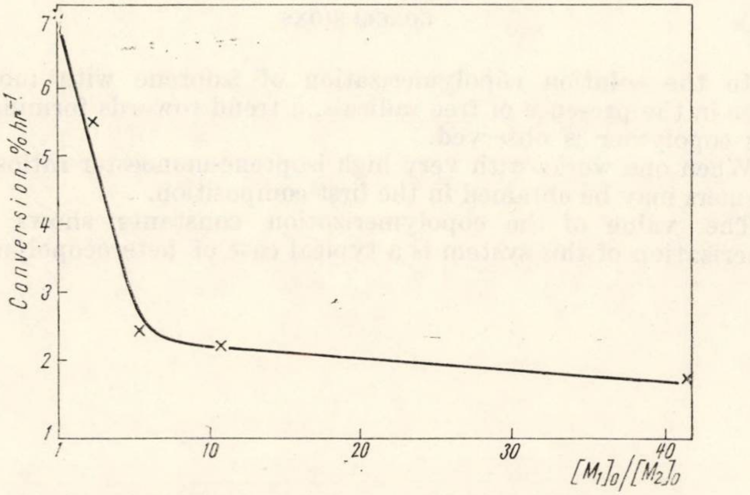

Fig. 5. – Conversion variation (% hr^{-1}) as a function of the isoprene-monomethylmaleate ratio ($M_1 : M_2$) in the initial polymerization composition.

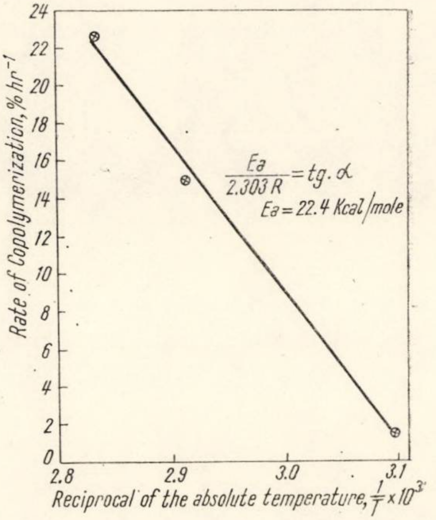

Fig. 6. – Effect of temperature on the reaction rate.

The calculated apparent activation energy is 22.4 kcal/mole, being much smaller than in the alternating copolymerization of ethylene with maleic anhydride.[37]

Taking into account that for the polymerization initiated with azocombinations for the majority of monomers $Ei = 30$ kcal/mole and $Ep - \alpha Er = 4 - 7$ kcal/mole, it can be observed that also the apparent activation energy, calculated for the copolymerization of the isoprene-monomethylmaleate system, is comprised between these limits.

CONCLUSIONS

In the solution copolymerization of isoprene with monomethylmaleate in the presence of free radicals, a trend towards forming an alternating copolymer is observed.

When one works with very high isoprene-monoester ratios, enriched copolymers may be obtained in the first composition.

The value of the copolymerization constants shows that the polymerization of this system is a typical case of heterocopolymerization.

---

[37] S. Machi, T. Sakai, M. Gotoda and T. Kagiya, *J. Polymer Sci. Part. A—1,* **4,** 821 (1966).

Revue Roumaine de Chimie, 15, 1893–1900 (1970)

BUTADIENE-STYRENE CARBOXYLATED COPOLYMERS

D. FELDMAN, NATALIA SIMIONESCU, C. CIUBOTARIU, MARTHA CIUBOTARIU,
T. CRIŞAN and G. DRESSNANDT

Institute of Macromolecular Chemistry "P. Poni",
Jassy, Aleea Grigore Ghica Vodă 41 A

Received March 23, 1970

The production by emulsion copolymerization of some terpolymers on the basis of butadiene, α-methyl styrene and unsaturated carboxylic acids (acrylic or methacrylic acid) was studied. Kinetics data permit the evaluation of the influence of some important factors as : nature and concentration of emulsifier, pH of reaction medium, nature and concentration of carboxylated monomers. Methacrylic acid shows a higher reactivity in comparison with acrylic acid ; some indications are given about the addition of acidic component when a terpolymer with a high content of carboxylic groups is to be otained.

I. INTRODUCTION

Nowadays the copolymerization is a usual way of great efficiency in order to obtain a large series of polymers with various physical and chemical properties. It permits the modification of the regularity of polymer microstructures and of their symmetry, thus favouring the decrease of polymer-polymer type interactions and respectively, the increase of elastic properties. On the other hand, the copolymerization can be used to introduce certain polar groups in the polymers with hydrocarbon character, this determining an increase of intermolecular forces. The presence of such groups is reflected in a series of main properties as : hardness of the product, its behaviour towards solvents, chemical agents and so on.

In recent years the copolymerization has been much applied to obtain carboxylated elastomers with good adhesive properties.

The presence of carboxylic monomers, modifies the regularity in the symmetry of the chains, by favouring, to the detriment of crystallinity, the elastic properties ; in addition, the introduced functional groups offer large possibilities for crosslinking.

The first carboxylic elastomer was obtained about thirty years ago.[1]

Copolymerization of the butadiene and of its homologous such as : isoprene, dimethyl-butadiene and chloroprene with dicarboxylic acids as: maleic, fumaric, chlormaleic, chlorfumaric acids was pointed out in a French patent which was published in 1939.[1]

---

[1] H. P. Brown, *Rubber Chem. Technol.*, **30**, 1347 (1957).

Later on,[2–15] a great number of copolymers were obtained from dienes, monocarboxylated vinylic monomers (acrylic, methacrylic, ethacrylic, α-chloracrylic acids) and a comonomer of ester, nytryl, amide etc. type.

Usually the obtaining of binary carboxylated copolymers, or of carboxylated terpolymers, is based on processes which occur in aqueous emulsions; less used is the method of grafting the monomers with carboxylic groups on elastomers in an organic solvents medium.

The increase in the content of carboxylated monomer of copolymers improves the resistance to abrasion, the adhesive properties, the sensitivity to alkalies and oxidants.

II. EXPERIMENTAL

In order to obtain the carboxylated butadiene-α-methyl-styrene terpolymers we have resorted to the usual method for the synthesis of binary butadiene-styrene copolymers which was adapted to the conditions of the present work.

The main components were used as follows:

Monomers	100	parts by weight
Emulsifiers	5–10	,, ,, ,,
Initiators	0.4–0.5	,, ,, ,,
Distilled water	200	,, ,, ,,

Copolymerization was effected at +5°, in bottles of soda water, in a rotative stirrer (60 rpm).

1. *Materials*

Monomers: Butadiene (B) (Borzeşti-Romania), technical purity; α-methyl-styrene (AMS) (Borzeşti-Romania) was used after the purification by distillation; anhydrous acrylic acid (AA) (Ugilor-Italy), anhydrous methacrylic acid (MAA) (Ugilor-Italy) was purified by vacuum distillation.

---

[2] D. B. Boguslavskii, B. Kutsenok, R. B. Uzina and M. D. Dostian, *Kautchiuk i Rezina*, **1959**, 6.

[3] D. B. Boguslavskii, M. S. Dostina and R. B. Uzina, *Kauciuk i Rezina*, **1959**, 27.

[4] Neth. Patent, 6, 506, 285, Nov. 21, 1966; *Chem. Abstr.*, **66**, 66475, (1967).

[5] L. F. Guziali and W. N. Maclay., U.S. Patent., 3, 301, 806., 31 Jan. 1967; *Chem. Abstr.*, **66**, (1967).

[6] Brit. Patent, 1, 063, 466. March, 30, 1967; *Chem. Abstr.*, **66**, 105747 (1967).

[7] D. A. Kardatov., "Sinteticheskie Klei", Izd. Khimia, 1964, p. 225.

[8] T. Kanzowa and Y. Sato., *Japan Chem. Quart.*, **2**, 41 (1966). In: *Chem. Abstr.*, **66**, 11647, (1967).

[9] E. Tsuchida, Y. Ohtoni, H. Nakadae and I. Shinohara, *Kogyo Kagaku Zasshy*, **70**, 573 (1967); *Chem. Abstr.* **68**, 40134 (1968).

[10] A. V. Riabov, Iu. D. Semchikov and N. N. Slovnitskaia, *Doklady Akad. Nauk, S.S.S.R.*, **145**, 822 (1962).

[11] G. J. Anderson and C. R. Williams, U.S. Patent. 3, 297,620., Jan. 10, 1967; *Chem. Abstr.*, **66**, 56176 (1967).

[12] D. D. Taft, U.S. Patent, 3, 297, 621., Jan. 10, 1967; *Chem. Abstr.*, **66**, 38509, (1967).

[13] J. C. Hwa and L. Miller, *J. Polymer Sci.*, **55**, 197 (1961).

[14] S. Eiichiro, and H. Shigaki, Japan Patent, 6, 950, 860; *Chem. Abstr.*, **70**, 106998 (1969).

[15] H. P. Brown, C. F. Gibbs, *Ind. Eng. Chem.*, **47**, 1006 (1955).

Emulsifiers : Natrium dresinate and Leucanol-technical product were used as aqueous solutions of 20% and 5% concentration respectively. Romopal LN (Azur-Romania) is a fatty alcohol ($C_{12}-C_{14}$) ethoxylated with 9 mols of ethylene oxide; it was used as aqueous solution of 30% concentration. Romopal O (Azur-Romania) is a fatty alcohol ($C_{12}-C_{18}$) ethoxylated with 22 mols of ethylene oxide and was used in the same concentration.

Initiators : Cumene hydroperoxide (CHP) (Borzeşti-Romania) was used as a solution of 5% in AMS; ferrous sulfate heptahydrate; Rrilon B and Rongalite-technical products were also used in aqueous solutions.

2. *Analysis*

a. Determination of total solids amount was carried out by evaporation and drying under vacuum of a determined quantity of latices.[16]

b. Content of acid monomer was determined by direct titration of carboxylic groups in diluted latices with solution of potassium hydroxide in ethanol.[17] To determine the content of $-COOH$ groups from unreacted acid, the measurement was effected at $pH = 6.85$, and for the determination of the total amount of carboxylic groups, the latice was titrated up to $pH = 9.85$. The calculation of the content of AA or MAA from the copolymer was realized by taking account of nonpolymer substances which enter the composition of initial mixture (respectively of lattice) and subsequently in the total solids.

3. *Copolymerization*

a. In alkaline medium. The attempt to use the common method of emulsion copolymerization in alkaline medium did not succeed due to the precipitation of dresinate after the addition of the acid ($pH = 9$). This fact determined the change of dresinate with nonionic emulsifier as Romopal LN and the using of the following method :

Monomers	100	parts by weight
Romopal LN	10	,, ,, ,,
Trilon B	0.066	,, ,, ,,
Ferrous sulfate. $7H_2O$	0.033	,, ,, ,,
Rongalite	0.1	,, ,, ,,
CHP	0.3	,, ,, ,,
Distilled water	200	,, ,, ,,

After copolymerization, dimethyldithiocarbamate and hydroquinone as inhibitors and Neozon D as stabilyzer were used.

b. In acid medium. In order to synthesize some terpolymers with a high content of bound acid, the copolymerization in acidic medium was experimented ($pH = 3-4$). The above method, with Romopal LN as emulsifier was used.

In all cases, unreacted monomers were removed from the latices by stripping.

---

[16] ⁂ "Standard Methods of Testing Synthetic Rubber Latices" ASTM, Designation D, 1417–61.

[17] A. I. Ezrielev, A. B. Peizner, and L. V. Utkina, *Izbret. Prom. Obraztsy Towarnye Znaki*, **45**, 94 (1968).

III. RESULTS AND DISCUSSIONS

At alkaline pH both binary and ternary copolymerization take place in satisfactory conditions; after a reaction time of 6 hours, a conversion of 65% and 75% respectively was achieved.

The curves in figure 1 represent the variation of conversion, function of emulsifier concentration and time.

Analysis of the plots shows that both in binary and ternary systems, the reaction rate increases with the emulsifier concentration.

Study of terpolymers, which are obtained in alkaline medium has proved that these are characterized by a low content of acidic comonomers. This fact confirms the data from the literature which recommend the copolymerization in acid medium [15] in order to obtain a high content of carboxylic groups in the copolymers.

Carrying out the copolymerization (in acid medium) at a ratio of comonomers of 50 : 40 : 10 (B : AMS : AA), and a copolymerization time of 8 hours, a diagram as in figure 2 was obtained.

These data show that the increase of emulsifier concentration determines the increase of the conversion, but at the same time the amount of precipitated terpolymer grows higher.

Maintaining unmodified both the emulsifier concentration and the temperature, the influence of the amount of acid component on the copolymerization rate was studied. The diagrams from figures 3 and 4 prove that the reaction rate decreases when greater amount of acid is used in the system (AA or MAA).

It was also interesting to study the participation of carboxylic monomers in the copolymerization as a function of the initial ratio of monomers and time, respectively.

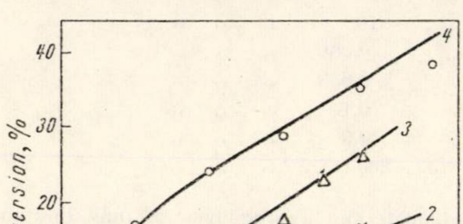

Fig. 1 — Variation of the conversion with copolymerization time at different concentrations of the emulsifier (Romopal LN).

1, 60 : 40 (B : AMS); 2.4% emulsifier; 2, 60 : 40 (B : AMS); 6.0% emulsifier; 3, 50 : 40 : 10 (B : AMS : AA); 2.5% emulsifier; 4, 50 : 40 : 10 (B : AMS : AA); 5.0% emulsifier.

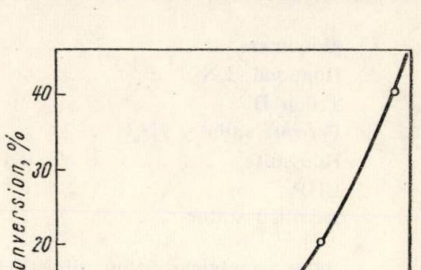

Fig. 2 — Variation of the conversion as a function of emulsifier concentration (Romopal LN) for the system 50 : 40 : 10 (B : AMS : AA), the copolymerization time 8 hours, temperature : +5°.

By using the above method with Romopal LN (10% as against monomers) for the B : AMS : MAA system, the results presented in figures 5, 6 and 7 were obtained. In these attempts the B : AMS ratio was maintained constant (50 : 40) but the amount of acid comonomers changed from 5 to 15 pc. All components were introduced in the reaction medium from the very beginning.

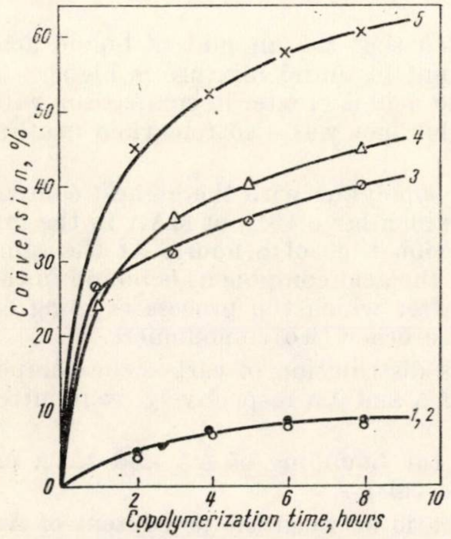

Fig. 3 — Variation in the time of the conversion as against the acid concentration from initial mixture. Temperature: +5°; emulsifier concentration: 9%.

1, MAA 15%; 2, AA 15%; 3, MAA 10%; 4, AA 7.5%; 5, MAA 7.5%.

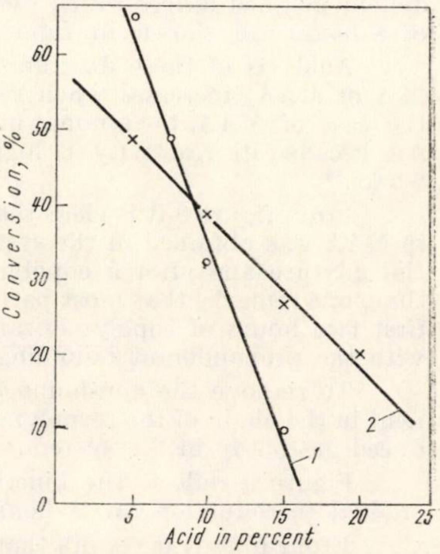

Fig. 4 — Variation of the conversion in the function of acid content initially introduced in the system. Time of copolymerization 8 hours; emulsifier concentration: 9%.

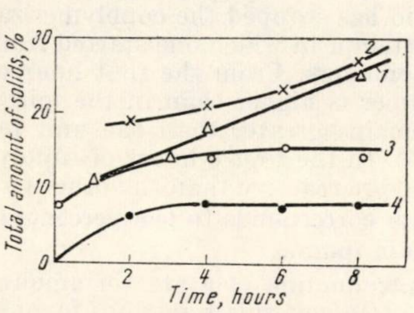

Fig. 5 — Variation of total solids content with copolymerization time.

1, MAA 5%; 2, MAA 7.5%; 3, MAA 10%; 4, MAA 15%.

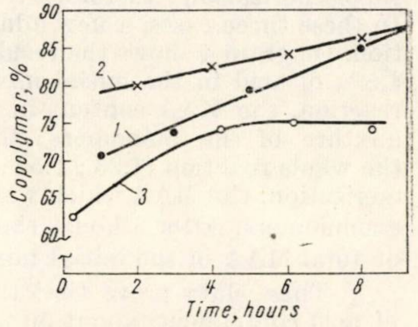

Fig. 6 — Variation of copolymer content from the total solids with copolymerization time.

1, MAA 5%; 2, MAA 7.5%; 3, MAA 10%.

From the diagrams in figures 5 and 6 one can see that both the content of total solids of latices and the content of the copolymer in total solids increase continuously with the copolymerization time for the experiments with 5% and 7.5% MAA. In the other cases (10% and 15% MAA) the highest conversion was attained after 6 and 2 hours, respectively.

Determinations of the content in acid comonomer in the case of some demonomerized latices which were obtained after a copolymerization time of 8 hours are shown in figure 7.

Analysis of these diagrams proved that the amount of bound acid (AA or MAA) increases when its content in initial mixture is higher; in the case of MAA, the amount of bound acid is greater in comparison with AA because its reactivity is higher. This fact was also remarked in other works.[18]

From figure 8 it is clear that the copolymer with the highest content in MAA was obtained in the systems which have 10% of MAA in the initial mixture and after a copolymerization time of 8 hours. At the same time, one remarks that most part from the acid component is bound in the first two hours of copolymerization, after which the process is going on with the preponderant bounding of the other two comonomers.

To remove the non-homogeneous distribution of carboxylic component in the chain of the terpolymer, MAA and AA respectively, were introduced gradually in the system.

Figure 9 reflects the kinetics of the bounding of AA and MAA on gradual introduction (at 2 hours intervals).

From plot 1, it results that the ratio between the pc content of AA in copolymer and that from initial mixture of monomers decreases from 0.33 for 1 hour of copolymerization, up to 0.162 for 5 hours, when small amounts of AA were gradually introduced. By adding MAA in the same amounts (diagram 2) this ratio stretches from 0.98 to 0.83 during the 6 hours of copolymerization. Starting from a MAA content in the mixture (diagram 3) the ratio varies from 0.6 for 1 hour to 0.88 for 5 hours of copolymerization; therefore it increases with the copolymerization time. In these three cases, a new addition of acid has stopped the copolymerization. Diagram 4 shows the results of the attempt in which one started from 4.5% of acid in the initial mixture of monomers. From the first hour of reaction, the MAA content in the copolymer is higher than in the initial mixture of the monomers; the ratio remains greater than the unit for the whole reaction (1.23 ; 1.52 ; 1.55 ; 1.05). In the first 6 hours of copolymerization, the MAA which was added is more reactive than the other two comonomers. After 8 hours the ratio which corresponds to the percentage of total MAA of the initial mixture is again found.

These data prove that the initial introduction of a greater amount of acid component (about 50%) and of subsequent small portions favours the binding of MAA in terpolymer, by obtaining at the same time a stable latice during the demonomerization. Experiments in which small amounts of acid were initially introduced and after 5 – 6 hours greater proportions were added, have given unstable latices. Although, by comparison of the diagrams 1 and 2 one can see that AA introduced in similar conditions, participates in the reaction to a smaller extent than MAA.

---

[18] A. Ia. Drinberg, B. M. Fundăler and E. A. Bolynscaia, *Zhur. priklad. khim.*, **32**, 2075 (1959).

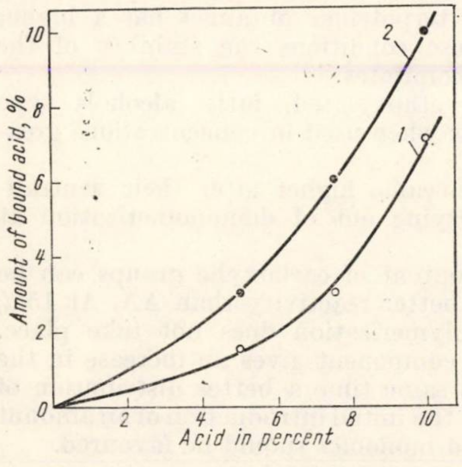

Fig. 7 – Variation of the content of bound acid, related to the total solids depending on the initial amount of acid.
1, AA; *2*, MAA.

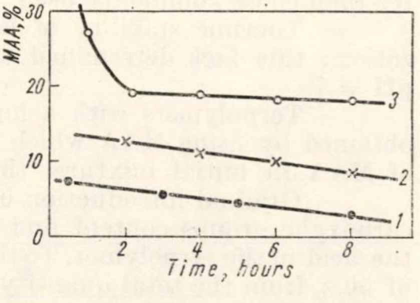

Fig. 8 – Variation of MAA content with copolymerization time.
1, MAA 5%; *2*, MAA 7.5%; *3*, MAA 10%.

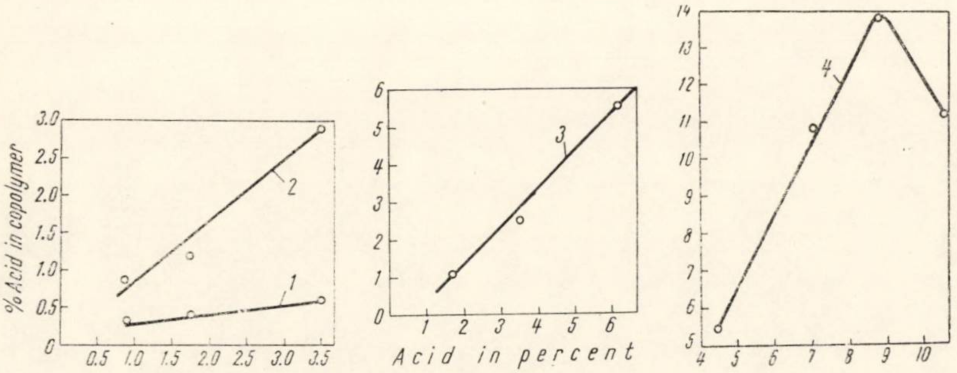

Fig. 9 – Variation of AA and MAA content in the copolymer, as against the acid percentage from monomers mixture and the introduction way.
1, AA after 1; 3 and 5 hours of copolymerization; *2*, MAA after 2;4 and 6 hours of copolymerization; *3*, MAA after 1;3 and 5 hours of copolymerization; *4*, MAA after 1; 3; 5 and 8 hours of copolymerization.

IV. CONCLUSIONS

The study carried out in the above-mentioned conditions, allows the following conclusions:

– Redox-initiating system – HPC – $SO_4Fe . 7H_2O$ – can be used to obtain the terpolymers of carboxylated butadiene-α-methyl-styrene type. Using this system, at +5° one can obtain the latices with conversions between 70% and 80%, after a copolymerization time of 8 and 10 hours respectively.

— For high pH values a great rate of the reaction can be reached, but the acid component is bound in small amounts. At low pH values, the reaction rate is smaller and the terpolymer obtained has a higher content of carboxylic groups. In these conditions the stability of the system is lower and the copolymer precipitates.

— Nonionic emulsifiers of the ethoxylated, fatty alcohols type (Romopal LN) give satisfactory results when used in concentrations greater than those commonly used.

— Thermic stability of latices became higher after their neutralization; this fact determined the carrying out of demonomerization at pH = 7.

— Terpolymers with a higher content of carboxylic groups can be obtained by using MAA which has a better reactivity than AA. At 15% of MAA in initial mixture, the copolymerization does not take place.

— Gradual introduction of acid component gives an increase in the carboxylic groups content and at the same time a better distribution of the acid in the terpolymer. To this end the initial introduction of an amount of 50% from the total quantity of acid monomer should be favoured.

Revue Roumaine de Chimie, **15**, 1901–1906 (1970)

PROPRIÉTÉS PHYSICO-STRUCTURALES DES CATALYSEURS UTILISÉS POUR L'OXYDATION DES HYDROCARBURES. IV.[1]

PROPRIÉTÉS ÉLECTRIQUES DES SYSTÈMES OXYDIQUES À BASE DE $V_2O_5 - Ga_2O_3$

ANTOANETA SPINZI et I. V. NICOLESCU

Centre de Recherches de Chimie Physique de l'Académie, Bucarest

Reçu le 21 mai 1970

On étudie la conductibilité électrique du système oxydique binaire $V_2O_5-Ga_2O_3$ de concentration 1 : 0,1 mole et 1 : 0,3 mole, en la rapportant au système de référence le V_2O_5. Les déterminations effectuées en air, jusqu'à 500°, ainsi que les isothermes en hydrogène de 360°, 380° et 400° indiquent une diminution de la conductivité électrique et une augmentation de la température de transition. L'interprétation des résultats comme variation relative de la résistance électrique ou bien comme vitesse relative de variation de la résistance électrique confirment le caractère accepteur du Ga_2O_3 par rapport au V_2O_5 ; l'effet est proportionnel à la concentration.

A la suite des travaux antérieurs [1-3] concernant le comportement électrique des catalyseurs oxydiques mixtes à base de V_2O_5, utilisés à l'oxydation des hydrocarbures, on a examiné ci-dessous le système binaire $V_2O_5-Ga_2O_3$. Le choix de ce système a été fait compte tenu de : a) la baisse de la concentration des électrons quasi libres du réseau de V_2O_5, par inclusion de certains ions à valence inférieure à celle de l'ion originaire ; b) la compatibilité des rayons ioniques de V^{5+} et Ga^{3+} ; c) la possibilité de formation des solutions solides de substitution, sans altération du réseau primaire de V_2O_5.

Conformément à la théorie zonaire, l'introduction des défauts d'impureté de ce type conduit à la diminution de la conductivité de type-n du V_2O_5, comme suite de la baisse de concentration des défauts de réseau. L'extension de la méthode de valence contrôlée au système $V_2O_5-Ga_2O_3$ pour lequel la littérature ne fournit pas encore de renseignements suffisants, confère la possibilité de présenter un tableau plus général des propriétés électriques des systèmes oxydiques mixtes à base de V_2O_5, éventuellement de les corréler avec l'activité catalytique présentée par les systèmes mentionnés, dans la réaction d'oxydation des hydrocarbures.

---

[1] A. Spinzi et I. V. Nicolescu, *Rev. Roumaine Chim.*, **15**, 451 (1970).

[2] A. Spinzi et I. V. Nicolescu, *Rev. Roumaine Chim.*, **14**, 903 (1969).

[3] I. V. Nicolescu et A. Suceveanu, *Rev. Roumaine Chim.*, **11**, 123 (1966).

Dans ce but, on a étudié la variation de la conductibilité électrique par rapport à la température et au milieu de réaction, pour le système binaire $V_2O_5 - Ga_2O_3$ de concentration 1 : 0,1 mole (9,4% mole) et 1 : 0,3 mole ($\sim$ 24% mole), par comparaison avec le système de référence, le V_2O_5 pur.

PARTIE EXPÉRIMENTALE

Les oxydes mixtes binaires $V_2O_5 - Ga_2O_3$ ont été préparés par imprégnation du V_2O_5 d'une solution de $Ga(NO_3)_3$, suivie de séchage à 110°, décomposition à 350°—2h et calcination à 500°—6h. Les poudres obtenues après broyage ont été pastillées à pression constante.

La préparation de V_2O_5 a été antérieurement décrite,[2] de même que l'appareil et la méthode utilisées à l'étude de la conductibilité électrique.[3]

Les déterminations de conductibilité électrique ont été effectuées en air, en fonction de la température, dans l'intervalle de 200 à 500°, et en hydrogène → azote → air, en fonction du temps à 360°, 380° et 400°.

RÉSULTATS ET DISCUSSIONS

Dans la figure 1 on représente la variation $\log \sigma = f(1/T)$ en air, pour le système $V_2O_5 - Ga_2O_3$ de concentration 1 : 0,1 mole (9,4% mole) et 1 : 0,3 mole ($\sim$24% mole) par comparaison à la variation $\log \sigma$ pour le V_2O_5 pur. On y remarque :

— la baisse de la conductivité électrique du V_2O_5 par dopage avec Ga_2O_3 ;

— la modification signalée est proportionnelle à la concentration de l'oxyde ajouté ;

— le déplacement de la température de transition suit l'ordre : $V_2O_5 < V_2O_5 - Ga_2O_3$ (1 : 0,1 mole) $< V_2O_5 - Ga_2O_3$ (1 : 0,3 mole).

Les résultats ci-dessus, mettent en évidence le rôle accepteur d'électrons du Ga_2O_3. On suppose[4] que le réseau du V_2O_5 pur présente un certain déficit stœchiométrique (vacances d'oxygène), engendrant initialement une concentration d'ions V^{4+}. L'inclusion de Ga_2O_3 dans le réseau du V_2O_5 tend à promouvoir la transition $V^{4+} \rightarrow V^{5+}$ en diminuant de la sorte la conductivité électrique. Le déplacement relatif des températures de transition (signalées sur le diagramme), reflète le même effet. L'additif accepteur, le Ga_2O_3, induit l'augmentation de la température de transformation de la conductivité d'impureté en conductivité propre ; l'effet est d'autant plus intense que la concentration de Ga_2O_3 s'accroît.

Le comportement du système $V_2O_5 - Ga_2O_3$ au traitement successif, hydrogène → azote → air, en temps, est présenté dans les figures 2a et 2b.

Les isothermes de 360°, 380° et 400° indiquent pour les deux concentrations une augmentation appréciable de la conductivité électrique en hydrogène. On considère que ce comportement ne peut être exclusive-

---

[4] J. D. Butter et B. G. Weston, *J. Catalysis*, **2**, 8 (1963).

Fig. 1. — Variation de la conductivité électrique en fonction de la température. *1*, V_2O_5 ; *2*, $V_2O_5 - Ga_2O_3$ (1 : 0,1 mole) ; *3*, — $V_2O_5 - Ga_2O_3$ (1 : 0,3 mole).

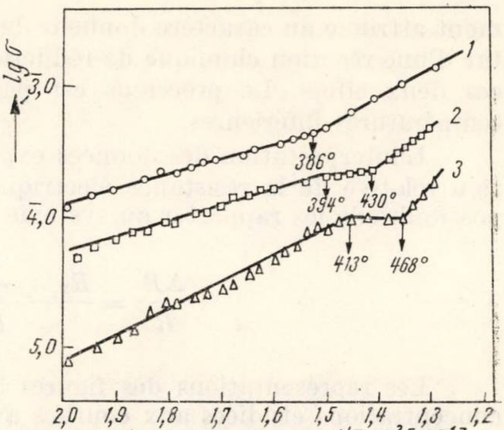

Fig. 2. — Isothermes de la conductivité électrique en fonction du temps, en courant d'hydrogène et en courant d'air *a*, $V_2O_5 - Ga_2O_3$ (1 : 0,1 mole) ; *b*. $V_2O_5 - Ga_2O_3$ (1 : 0,3 mole).

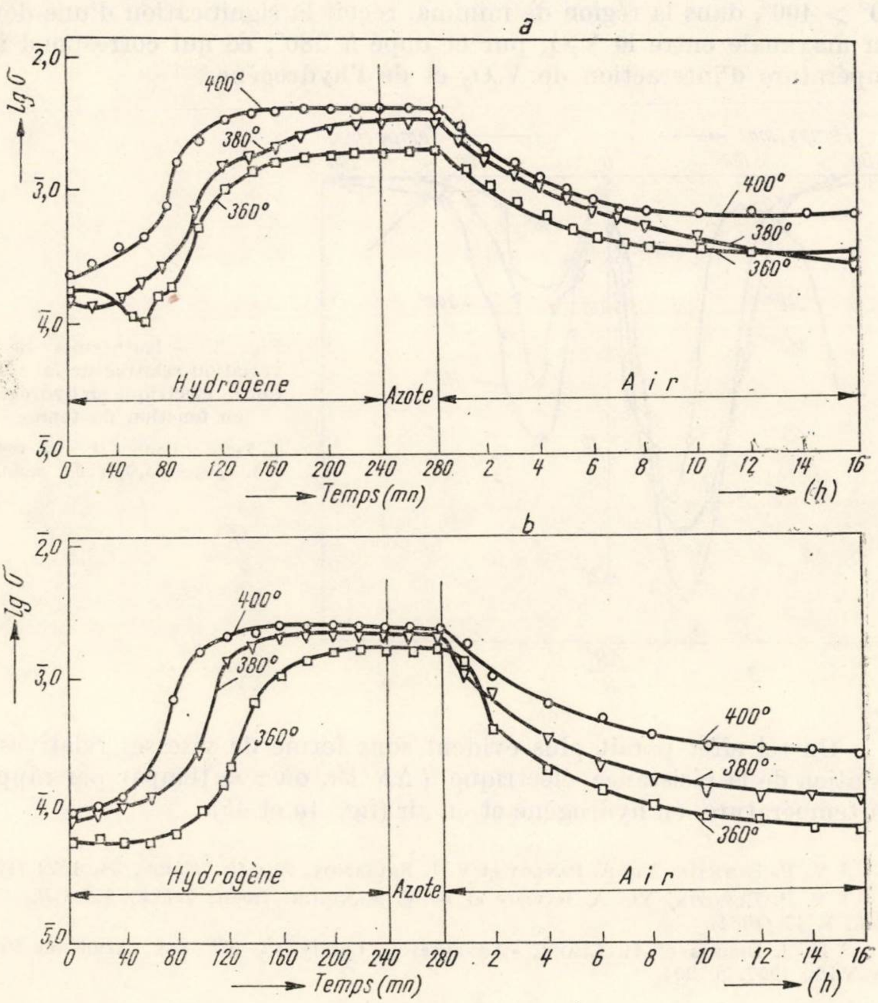

ment attribué au caractère donneur de l'hydrogène, étant surtout le résultat d'une réaction chimique de réduction. Il est difficile à distinguer entre ces deux effets. Le processus est partialement réversible, surtout aux températures inférieures.

L'interprétation des données expérimentales sous forme de la variation relative de la résistance électrique ($\Delta R/R$) en hydrogène donne la possibilité de les rapporter au système de référence, vu que

$$\frac{\Delta R}{R} = \frac{R_{V_2O_5} - R_{V_2O_5 \cdot Ga_2O_3}}{R_{V_2O_5}}$$

Les représentations des figures 3*a* et 3*b* conduisent pour les deux concentrations étudiées aux courbes avec maxima prononcée, située dans un intervalle de 40—60 mn. La variation $|\Delta R/R|$ selon l'ordre 380° $>$ 360° $>$ 400°, dans la région de minima, reçoit la signification d'une déviation maximale entre le V_2O_5 pur et dopé à 380°, ce qui correspond à la température d'interaction de V_2O_5 et de l'hydrogène.[5-7]

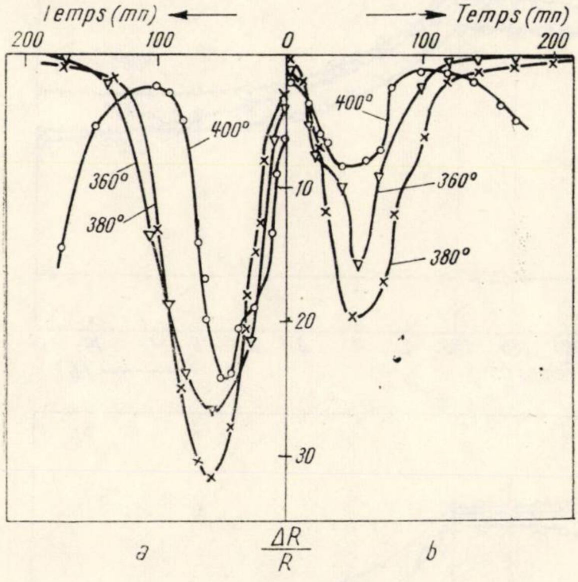

Fig. 3. — Isothermes de la variation relative de la résistance électrique en hydrogène en fonction du temps.

a, $V_2O_5 - Ga_2O_3$ (1 : 0,3 mole) ; *b*, $V_2O_5 - Ga_2O_3$ (1 : 0,1 mole).

Un tel effet paraît plus évident sous forme de vitesses relatives de variation de la résistance électrique ($\Delta R/R\tau$, où τ = temps) par rapport à la température, en hydrogène et en air (fig. 4*a* et 4*b*).

---

[5] V. P. Elyutin, Yu. A. Pavlov et V. I. Shulenov, *Zur fiz. Khim.*, **36**, 1524 (1962).

[6] V. P. Elyutin, Yu. A. Pavlov et A. V. Manuhin, *Izvest. V.U.Z. S.S.S.R., Cern. Metal.*, **5**, 17 (1964).

[7] D. J. Berets et H. Clark, «Advances in Catalysis», XIe vol., Academic Press, New York, 1957, p. 204.

Le processus en hydrogène est caractérisé par variations inverses par rapport au processus en air. La température de 380° souligne les déviations extrêmes ($<$ en H_2, $>$ en air). L'abaissement de la vitesse relative de variation de la résistance électrique est proportionnel à la concentration de Ga_2O_3 et inversement proportionnel au temps.

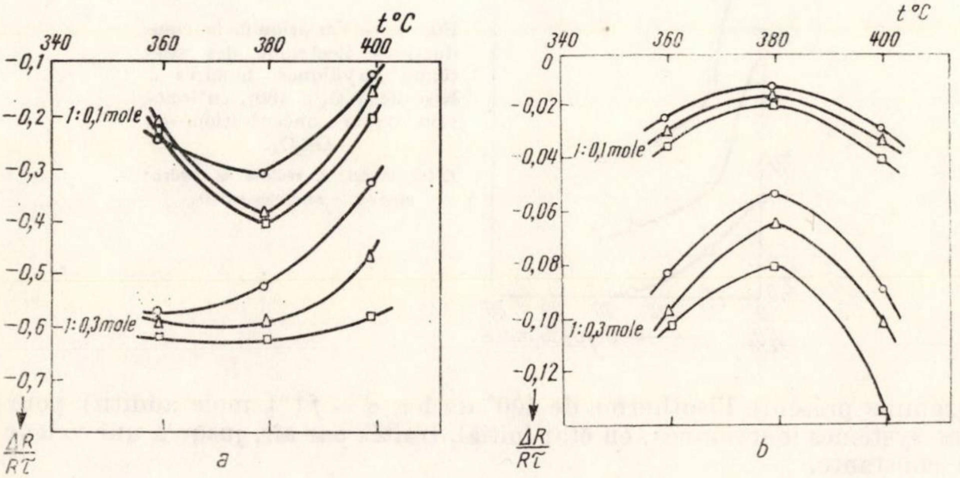

Fig. 4. — Vitesse relative de variation de la résistance électrique du système $V_2O_5-Ga_2O_3$ en fonction de la température.

a, hydrogène ; *b*, air.

Les vitesses négatives de variation de la résistance électrique ont la signification des valeurs supérieures des résistances pour le système $V_2O_5-Ga_2O_3$, comparativement au V_2O_5 pur.

Compte tenu du fait que la résistance électrique du semi-conducteur décroît avec la température, la déviation maximale négative qui a lieu à 380° en hydrogène, à 40,50 et 60 mn (échantillon L : 0,1 mole), doit être interprété comme un abaissement prononcé de la résistance électrique du V_2O_5. Ceci, reflète une interaction plus intense, $V_2O_5-H_2$. En air, les vitesses de variation de la résistance relative, beaucoup inférieures en valeurs absolues, montrent que le processus découle d'une façon contraire à celui en hydrogène. La température de 380° souligne une déviation négative minimale. Ceci, reflète en dernière instance, un abaissement de la résistance du système binaire.

Les effets mentionnés ci-dessus apparaissent plus évidents pour le système $V_2O_5-Ga_2O_3$ de concentration 1 : 0,3 mole, comme suite des valeurs inférieures de sa résistance électrique envers le même système de concentration 1 : 0,1 mole, dans tout l'intervalle de température étudié.

La généralisation des résultats obtenus par dopage du V_2O_5 à l'additif accepteur d'électrons (Ga_2O_3) est représentée dans la figure 5. Le diagramme présente l'isotherme de 400° de log $\sigma = f$ (% mole additif) pour les systèmes mentionnés, en état initial, traités par air, jusqu'à une valeur σ constante.

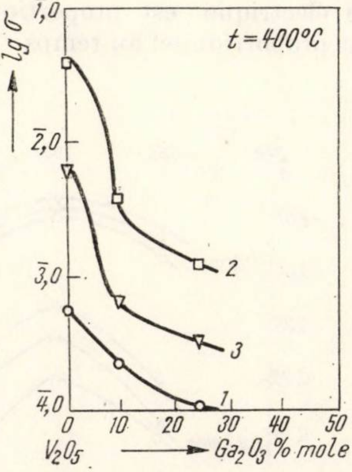

Fig. 5. — Variation de la conductivité électrique des systèmes oxydiques binaires à base de V_2O_5 à 400°, en fonction de la concentration en Ga_2O_3.

1, état initial; *2*, réduits en hydrogène; *3*, — réoxydés en air.

On confirme le caractère accepteur du Ga_2O_3 par rapport au V_2O_5, dans tout l'intervalle de concentration étudié.

Revue Roumaine de Chimie, **15**, 1907–1912 (1970)

FORSCHUNGEN IN DER INDIGOIDEN SERIE. II[1]

NEUE GEMISCHTE KONDENSIERTE AZO-INDIGOIDE SYSTEME

J. REICHEL und C. TĂRĂBĂŞANU

aus dem Laboratorium für Farbstoffe und Zwischenprodukte der Technischen Hochschule,
Bukarest, Calea Victoriei, 149

Eingegangen am 16. Februar 1970

Es wurden die Erhaltungsmöglichkeiten einiger Kupplungskomponenten mit indigoidem Rest durch die Kondensierung einiger Säurechloride, Sulfochloride oder chlormethylierten Derivaten des Indigos und Thioindigos mit verschiedenen Aminen untersucht. Durch Behandlung dieser Kupplungskomponenten mit diazotierten aromatischen Aminen auf Fasern als auch in Substanz ergeben sich echte Färbungen mit bemerkenswertem Widerstand.

In unserer ersten Mitteilung [1] wurde die Sulfonamidierungsreaktion des 5,5'-dichlorsulfonierten Indigos mit 2-Amino-5-naphthol-7-sulfonsäure geprüft. Die ausgezeichneten Färbeeigenschaften der erhaltenen sulfonamidischen Verbindung (Grünsäure) berechtigen unsere weiteren Nachforschungen auf diesem Gebiet.

In der vorliegenden Arbeit geben wir die Ergebnisse der experimentellen Untersuchungen bezüglich der Synthese und Anwendung anderer Verbindungen von allgemeiner Struktur (1) in ihrer Eigenschaft als Farbstoffe an:

$$Ar - NHY - Z - YNH - Ar \qquad (1)$$

wo:

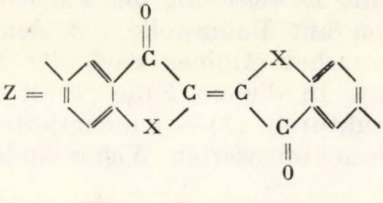

X = –NH–, –S–;

Y = $-SO_2-$, –CO–, CH_2-;

---

[1] J. Reichel und C. Tărăbăşanu, *Rev. Roumaine Chim.*, **11**, 1327, (1966).
J. Reichel und C. Tărăbăşanu, Brev. R.S.R. 500083, 12.12.1967.

Ar = aromatischer oder heterocyklischer Rest, fähig zu weiterer Kupplung.

VERSUCHE UND ERGEBNISSE

Der gewählte Weg der Synthese besteht in der Kondensierung einiger Komponenten mit der Struktur $Z(YCl)_2$ mit verschiedenen aromatischen oder heterocyklischen Aminen in einem Lösungsmittel (Aceton, Methyläthylketon, Dimethylformamid) oder in Wasser, in Gegenwart einiger salzsäureaufnahmefähigen Substanzen wie Pyridin, Pikolin, Chinolin, Triäthanolamin, Calciumkarbonat oder Mischungen von ihnen, bei Temperaturen zwischen 50 und 150°, in 5—36 Stunden:

$$2\,Ar - NH_2 + Z(YCl)_2 \xrightarrow{-2HCL} Ar - NHY - Z - YNH - Ar$$

In der ersten Tabelle sind unsere aus den Versuchen erhaltenen Ergebnisse in bezug auf die Synthese dargestellt, während Tabelle 2 die Ergebnisse der elementaren, chromatographischen und spektroskopischen Analyse für synthetisierte Verbindungen wiedergibt. Die Reinigung der Verbindungen so wie auch die Färbungen auf verschiedenen textilen Unterlagen mit oder ohne Entwicklung wurden in der in unserer ersten Mitteilung gezeigten Art ausgeführt.

Die ausgeführten Proben mit den neuen Verbindungen 1—15 bezüglich ihrer Anwendbarkeit als Farbstoffe für Wolle und synthetische Polyamidfasern sind in Tabelle 3 gezeigt. Man stellt eine völlige Übereinstimmung der Farben auf diesen textilen Unterlagen fest. Die Färbungen sind zwischen blau und grün für die indigoiden Derivate und zwischen rot und bordeau-violett für die thioindigoiden Derivate, in allen Fällen aber von einer beachtenswerten Reinheit. Diese Tatsache macht das Färben der Mischungen mit den Farbstoffen 1—15 möglich. Die Widerstände bei Naßbehandlung sind größer bei Wolle und synthetischen Polyamidfasern als bei Celluloseunterlagen.

Zur Vergrößerung des Widerstandes bei Naßbehandlung der Baumwolle so wie auch für die Erweiterung der Farbentöne, wurde die Entwicklung der Färbungen auf Baumwolle mit den Verbindungen 1—9, mit diazotierten aromatischen Aminen nach der Färbungsmethode mit Naphtholen verwirklicht. In diesem Falle erhält man auf den Fasern, Verbindungen mit Strukturen (2) — kondensierte gemischte azo-indigoide Systeme — mit beachtenswerten Widerständen.

$$Ar' - N = N - Ar - NHY - Z - YNH - Ar - N = N - Ar' \qquad (2)$$

Die erhaltenen Ergebnisse sind in Tabelle 4 angeführt.

Zu bemerken sind die großen Widerstände der Färbungen so wie auch die Klarheit der grünen Nuancen als Eigenschaften der Strukturen

Tabelle 1

Ergebnisse der Synthese einiger Verbindungen der Struktur (1)

Farbstoff Nr.	X	Y	Ar–NH–Rest von:	Grammol $Z(YCl)_2$: Grammol $Ar-NH_2$ in 100 ml Lösungsmittel	Lösungsmittel	Temperatur °C	Zeit h	Ausbeute %
1	–NH–	$-SO_2-$	2-Amino-8-naphthol-6-sulfonsäure	0,01 : 0,05	Dimethylformamid : Pyridin : Triäthanolamin = 1 : 1 : 1.	55	12	6
2	–NH–	$-SO_2-$	1-Amino-8-naphthol-3,6-disulfonsäure	0,01 : 0,025	Methyläthylketon Methylisobutylketon	60 60	14 6	11 78
3	–NH–	$-SO_2-$	*p*-Aminoazetoazetanilid	0,01 : 0,026				
4	–NH–	$-SO_2-$	1-(4′-Aminophenyl)-3-methyl-5-pyrasolon	0,01 : 0,026	Methylisobutylketon	60	6	81
5	–S–	$-SO_2-$	3-Amino-5-naphthol-7-sulfonsäure	0,01 : 0,030	Dimethylformamid	80	5	70
6	–S–	$-SO_2-$	2-Amino-8-naphthol-6-sulfonsäure	0,01 : 0,04	Dimethylformamid : Pyridin : Triäthanolamin = = 1 : 1 : 1.	Rückfluß	12	7,5
7	–S–	$-SO_2-$	1-Amino-8-naphthol-3,6-disulfonsäure	0,01 : 0,03	Pyridin : Dimethylformamid = 3 : 1. Methyläthylketon	Rückfluß 50 150	14 6 8	12,5 77 80
8	–S–	$-SO_2-$	*p*-Aminoazetoazetanilid	0,01 : 0,03	Dimethylformamid : Triäthanolamin = 10 : 1			
9	–S–	$-SO_2-$	1-(4′-Aminophenyl)-3-methyl-5-pyrasolon	0,01 : 0,045				
10	–NH-	–CO–	3-Amino-5-naphthol-7-sulfonsäure	0,01 : 0,03	Pyridin	Rückfluß	6	53
11	–NH–	–CO–	1-(4′-Aminophenyl)-3-methyl-5-pyrasolon	0,01 : 0,025	Pyridin	Rückfluß	6	73
12	–NH–	$-CH_2-$	3-Amino-5-naphthol-7-sulfonsäure	0,01 : 0,035	Wasser	95	36	65
13	–NH–	$-CH_2-$	1-(4′-Aminophenyl)-3-methyl-5-pyrasolon	0,01 : 0,04	Wasser	95	36	70
14	–S–	$-CH_2-$	3-Amino-5-naphthol-7-sulfonsäure	0,01 : 0,035	Wasser	95	36	57
15	–S–	$-CH_2-$	1-(4′-Aminophenyl)-3-methyl-5-pyrasolon	0,01 : 0,04	Wasser	95	36	81

Tabelle 2

Ergebnisse der elementaren, chromatographischen, spektroskopischen Analyse für die Farbstoffe 1–15

Farbstoff Nr.	Bruttoformel	N %		S %		Absteigende Papier Chromatographie Papier W2		Lichtabsorption in wässriger 5 % NaOH-Lösung	
		ber.	*gef.*	*ber.*	*gef.*	Eluent	Rf.	λ max.	log ε
1	$C_{36}N_4S_4O_{14}H_{24}$	6,48	6,35	14,48	14,61	F8*	0,61	610	3,52
2	$C_{36}N_4S_6O_{20}H_{24}$	5,46	5,32	18,75	18,62	F8	0,84	615	3,48
3	$C_{36}N_6S_2O_{10}H_{30}$	10,90	10,75	8,31	8,42	A**	0,42	605	3,32
4	$C_{34}N_8S_2O_8H_{24}$	15,21	15,36	8,69	8,52	B***	0,39	614	3,50
5	$C_{36}N_2S_6O_{14}H_{22}$	3,11	2,91	21,37	21,48	F8	0,65	541	3,51
6	$C_{36}N_2S_6O_{10}H_{22}$	3,11	2,95	21,37	21,50	F8	0,59	549	3,45
7	$C_{36}N_2S_8O_{20}H_{22}$	2,64	2,51	24,19	24,31	F8	0,77	555	3,47
8	$C_{36}N_4S_4O_{10}H_{28}$	6,96	7,20	15,91	15,71	A	0,22	544	3,39
9	$C_{34}N_6S_4O_8H_{22}$	10,90	11,10	16,62	16,73	B	0,43	554	3,52
10	$C_{38}N_4S_2O_{12}H_{24}$	7,07	6,91	—	—	C****	0,57	600	3,50
11	$C_{36}N_8O_6H_{24}$	16,86	16,69	—	—	C	0,61	603	3,47
12	$C_{38}N_4S_2O_{10}H_{28}$	7,32	7,19	8,37	8,50	F8	0,72	615	3,40
13	$C_{26}N_8O_4H_{24}$	21,70	21,59	—	—	F8	0,52	612	3,46
14	$C_{38}N_2S_4O_{10}H_{26}$	3,50	3,39	16,04	16,20	F8	0,81	568	3,50
15	$C_{26}N_6S_2O_4H_{26}$	15,27	15,13	11,63	11,84	F8	0,91	556	3,48

Eluent: F8*=25ml. Pyridin:70ml. Acetessigsäureäthylester:20ml. H_2O. in Volumen;
A**=BuOH:EtOH:H_2O=2:1:1 in Volumen; B***=BuOH:EtOH:H_2O=1:1:1, in Volumen;
C****=HCl 35% :BuOH=1:9

Tabelle 3

Die Eigenschaften der Färbungen mit den Farbstoffen 1–15 auf Wolle und synthetischen Polyamidfasern

Färbemittel Nr.	Farbe auf Wolle und Polyamidfasern	CI[2]	Lichtbeständigkeit	Beständigkeit für feuchte Behandlungen
1	grün-blau	42	4	4
2	grün-blau	16	4	3
3	blau-grün	16	7	5
4	blau-grün	16	7	5
5	dunkelrot	47	5	5
6	rot-dunkelrot	9	5	4
7	rot-dunkelrot	26	5	3
8	dunkelrot-violett	26	5	3
9	dunkelrot-violett	26	7	5
10	grün-blau	42	6	2
11	grün-blau	16	6	3
12	blau-grün	17	5	2
13	blau-grün	17	5	4
14	weichselrot	—	4	4
15	weichselrot	—	6	4

mit indigoidem Rest. Die Synthese der azo-indigoiden Produkte führt zu gleichartigen Farben wie jene auf den Fasern erhaltenen Farben, aber die Widerstände der auf Baumwolle erhaltenen Färbungen sind viel geringer als jene von Tabelle 3.

SCHLUSSFOLGERUNGEN

Die kondensierten gemischten azo-indigoiden Systeme bewiesen sich als eine neue Farbklasse mit beachtenswerten Färbeeigenschaften als solche (für Wolle und synthetische Polyamidfasern), als auch durch die Anwendung auf Fasern durch das Färbeverfahren mit Naphtholen und Entwicklung mit diazotierten aromatischen Aminen (für Baumwolle).

Die Widerstände sind gut und die Farbenskala ist sehr umfassend.

Dank der identischen Nuancen der Färbungen auf verschiedenen textilen Unterlagen, läßt sich diese Farbklasse für Färbung von natürlichen und synthetischen Polyamidmischungen verwenden.

---

[2] Colour Index, Ed. II., Bradford, 1958, Hue Indication Chart.

Tabelle 4

Die Ergebnisse der Färbeproben auf Baumwolle mit und ohne Entwicklung für die Farbstoffe 1–9

Farbstoff Nr.	Färbung auf Baumwolle mit schwach alkalischer Küpe		Entwicklung mit : 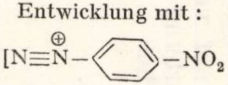				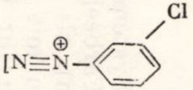				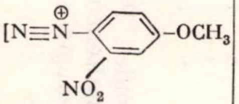				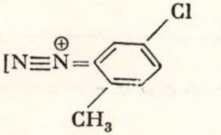				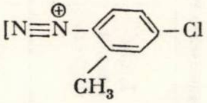			
	Farbe	CI[2]	Farbe	CI[2]	L*	S**	Farbe	CI[2]	L	S	Farbe	CI[2]	L	S	Farbe	CI[2]	L	S	Farbe	CI[2]	L	S
1	grün	17	braun	26	6	5	dunkel rot	9	4	4	dunkel rot	47	5	4	violett	10	5	2	braun	26	6	5
2	grün	16	violett	9	6	4	violett	35	5	4	dunkel rot	37	5	3	violett	35	6	5	violett	9	6	5
3	blau	16	grün	17	6	4	grün	17	7	5	grün	42	4	2	grün	17	7	5	blau	42	7	5
4	blau	16	grüu	17	6	5	grün	17	6	5	grün	42	3	2	grün	17	6	4	blau	42	7	5
5	rot	9	braun	26	3	2	braun	31	4	3	braun	26	4	5	braun	26	5	3	olive	29	4	3
6	dunkel rot	47	braun	29	4	3	braun	31	3	4	olive	30	5	5	dunkel rot	34	6	5	olive	29	6	5
7	rot	26	braun	26	2	2	braun	31	3	2	braun	26	3	4	braun	26	4	2	schwarz	—	4	1
8	violett	—	rot	***	5	4	rot	***	7	5	rot	***	5	4	rot	***	5	3	rot	***	5	4
9	violett	26	rot	***	6	5	rot	***	7	5	rot	***	6	4	rot	***	5	2	rot	***	5	5

L* Lichtbeständigkeit

S** Beständigkeit für feuchte Behandlungen

*** mit blauen Reflexen

Revue Roumaine de Chimie, 15, 1913–1922 (1970)

RADIOLYTIC OXIDATION OF ACENAPHTHENE TO NAPHTHALIC ACID ON THE ACENAPHTHENE-POTASSIUM PERMANGANATE-PYRIDINE SYSTEM

ELENA SOFRONIE, ECATERINA TĂRĂBĂŞANU-MIHĂILĂ and C. TĂRĂBĂŞANU

Institute of Atomic Physics, Bucharest, P. O. Box 35

Received February 5, 1970

The radiolytic oxidation of acenaphthene to naphthalic acid with ^{60}Co γ ray was studied. The dependence of the radiolytic yield of naphthalic acid formation on : dose rate, integral dose and reagent concentrations was investigated. The optimum conditions for the naphthalic acid formation were found. The oxidation reaction occurs by a chain free radical mechanism. The reaction kinetics is characteristic for consecutive reactions. The development of the oxidation reaction after the interruption of the irradiation was followed. It was established that the reaction chain proceeds after irradiation, too.

1. INTRODUCTION

An ever growing interest in the radiation synthesis of chemicals has been developing in recent years. There are many fields in which research has been carried out with some success. These are : the production of chemicals by halogenation, oxidation, sulfoxidation and many effects in catalytic reactions. The ability to bring about oxidation was early recognized as one of the characteristic features of high energy radiation. One of the first investigations aimed at studying the reaction of hydrocarbons with molecular oxygen, in the presence of ionizing radiation, was carried out by Bach and co-workers.[1]

The purpose of our work was to obtain naphthalic acid by the acenaphthene oxidation, in the presence of ^{60}Co γ ray.

Acenaphthene, $C_{12}H_{10}$, is a homologous of naphthalene and represents the residual product in the fractional distillation of coal tars, in the thermic and catalytic cracking of a few petroleum fractions and in the methane chemification process, in order to obtain acetylene. Naphthalic acid is an important acenaphthene oxidation product, constituting a precious intermediate in the vat dye synthesis.

---

[1] N. A. Bach, "Sbornik po radiatsionnoi khimii", Moscow, Izdat. Akad. Nauk S.S.S.R., 1955, p. 145.

The chemical oxidation of acenaphthene was investigated by many workers,[2-9] under different conditions but so far, the radiation induced oxidation has not been studied. We tried to obtain naphthalic acid by radiolytic oxidation hoping that the radiation energy should avoid the necessity of high temperatures and pressures as well as the presence of the catalysts.

2. EXPERIMENTAL

2.1. *Preparation of the samples*

The system we worked with was a solution of acenaphthene and potassium permanganate in pyridine. As it is known, pyridine is stable to the radiation,[10] so that we chose it as a solvent. On the other hand, we desired to have a homogeneous system. In this case, also, pyridine was the most adequate since both acenaphthene and potassium permanganate,[11] readily dissolve in it.

The permanganate part was to provide the oxygen quantity, necessary to the system. The potassium permanganate amount in comparison with that of acenaphthene was selected so that oxygen could be available all the time. On the other hand, this amount was limited by the maximum solubility of potassium permanganate in pyridine, at room temperature.

The experiments were carried out in glass bulbs of about 70 cc. capacity. In all attempts we used the same volume of solution, namely 40 cc.

2.2. *Irradiation technique*

The irradiations were accomplished by means of a 10,000 Ci ^{60}Co γ ray source. The dose rates were in the range: $2.6 \times 10^{17} - 1.09 \times 10^{18}$ eV/ml, min.

2.3. *Reagents. Analytical methods*

The reagents employed were: acenaphthene *p.a.* (VEB Laborchemie Apolda), potassium permanganate *p.a* .(E. Merck-Darmstadt) and anhydrous pyridine *p.a.* (U.C.B.).

Naphthalic acid was the only product of great interest to us and that we studied. The quantitative determination of naphthalic acid was effected gravimetrically, according to the method used by Wolff.[7] Its purity was verified by the determination of melting point which was found to be at 267°—269°, very close to the theoretical one (271°).

---

[2] Toshio Maki and Shunkichi Hashimoto, *J. Chem. Japan, Ind. Chem. Sect.*, **54**, 479 (1951).

[3] A. P. Karishin and T. P. Fedorenko, *Zhur. prikl. Khim.*, **29**, 955 (1956).

[4] Shimpachiro Kato, Hiroshi Yoshida and Mitsuharu Katagiri, *Yuky Gosei Kagaku Kiokai Shi*, **14**, 725—6 (1956); *Chem. Abstr.*, **51**, 8050 (1957).

[5] G. P. Petrenko and M. M. Dashevskhii, *Nauch. Zapiski, Odessk. Politech. Inst.*, **16**, 73—84 (1959).

[6] Yosuke Ishikawa, Yoshitaka Ito, Kenji Negoro and Hachiro Hiyama, *Kagaku to Kogyo* (*Osaka*), **34**, 20—5 (1960); *Chem. Abstr.*, **55**, 9357 (1961).

[7] M. Wolff, *Przemysl. Chem.*, **41**, 389—90 (1962).

[8] T. Urbanski and M. Wolff, *Roczniki Chem.*, **39**, 1447—53 (1965).

[9] J. Arient and J. Marhan, Czech. 114, 790 (cl. CO 7c), May 15 (1965).

[10] C. Pearce, U.S. Dept. Com. Office Tech. Serv., A.D., 286058, 1962, 13 pp.

[11] P. Pascal, "Nouveau Traité de Chimie Minérale", Tome XVI, Masson et Cie, Libraires de l'Académie de Médecine, 1960, p. 1046.

All irradiations were made at 22°. Blank experiments effected at this temperature gave no evidence for the oxidation process because in these conditions the system had no available oxygen.

3. RESULTS AND DISCUSSIONS

3.1. *Dose rate effect*

In order to perform the experiment, the dose rate varied between 2.6×10^{17} and 1.09×10^{18} eV/ml., min. The acenaphthene concentration was of 2.5×10^{-2} moles/liter and that of potassium permanganate, 1×10^{-1} moles/liter; the irradiation time, 5 minutes.

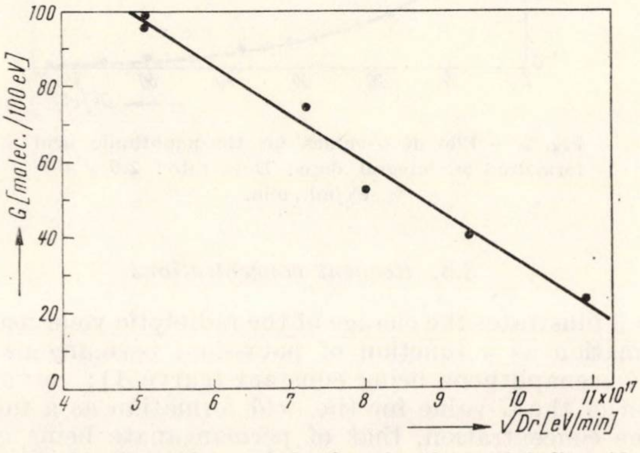

Fig. 1. — Dependence of *G*-values for the naphthalic acid formation on square root of the dose rate.

As one can see in figure 1, the radiolytic yield of the naphthalic acid formation shows a linear dependence on the square root of the dose rate. The fact that such a dependence represents a feature of the radiation induced chain reactions is well known. The variation with the dose rate as well as the high *G* values (> 100 molecules/100 eV), led us to the conclusion that the reaction of the acenaphthene oxidation takes place by a free radical chain process.

3.2. *Integral dose effect*

In figure 2 is represented the change of the radiolytic yield for the formation of naphthalic acid as a function of integral dose. The dose rate was of 2.6×10^{17} eV/ml., min., the other experimental conditions remaining unchanged. The radiolytic yield diminishes with integral dose,

this decrease being very stressed during the first five minutes of irradiation. Thus, it follows that the reaction is favoured by small irradiation doses for which high *G*-values ($>$ 400 molecules/100 eV), are obtained.

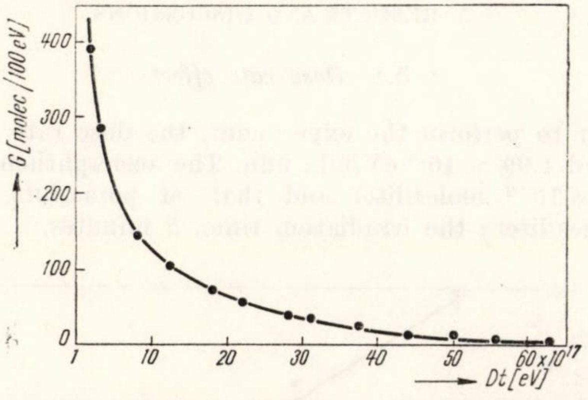

Fig. 2. — Plot of *G*-values for the naphthalic acid formation *vs.* integral dose; Dose rate: 2.6 × 10^{17} eV/ml., min.

3.3. *Reagent concentrations*

Figure 3 illustrates the change of the radiolytic yield for the naphthalic acid formation as a function of potassium permanganate concentration, that of acenaphthene being constant (curve 1); curve 2 represents the variation of the *G*-value for the acid formation as a function of the acenaphthene concentration, that of permanganate being constant. The selected concentration range was limited by the reasons exposed in Section 2.1. The *G*-values are increasing as the potassium permanganate amount increases, according to a curve which asymptotically tends to a constant value. For an acenaphthene constant concentration, an optimum ratio potassium permanganate — acenaphthene of 3 : 1 exists. Then, the increase of the potassium permanganate concentration does not lead to a further significant rise of the *G*-value for the naphthalic acid formation.

Regarding curve 2, the radiolytic yield of the acid formation shows a linear dependence on the acenaphthene concentration. This means that the greater the acenaphthene quantity in the system is, the greater the number of scavengeable free radicals, formed under irradiation. Nevertheless, it is not advisable to work with too large an acenaphthene amount because a great deal of it does not get into reaction. This happens since a constant quantity of oxygen exists in the system, for greater and greater acenaphthene quantities. Thus, the conversion into naphthalic acid for an acenaphthene concentration of 5 × 10^{-4} moles/liter is about 60 percent, while the corresponding conversion for the greatest acenaphthene concentration (2.5 × 10^{-2} moles/liter) employed by us, only represents 20 percent.

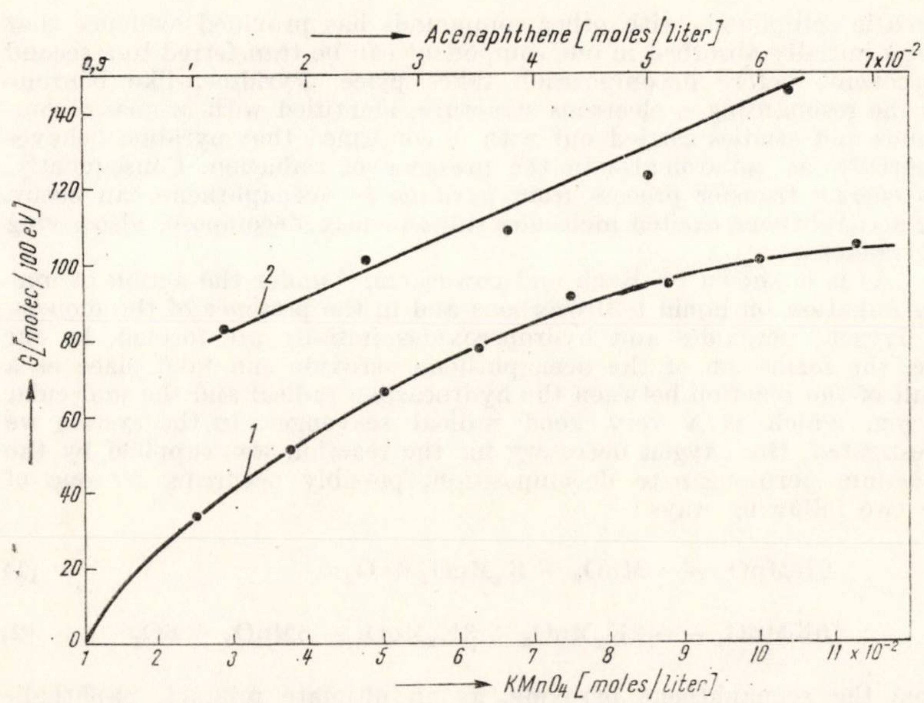

Fig. 3. — Dependence of G-values for the naphthalic acid formation on the reagent concentrations; curve 1, the potassium permanganate concentration; the acenaphthene concentration $= 2.5 \times 10^{-2}$ moles/liter; curve 2, the acenaphthene concentration; the potassium permanganate concentration $= 1 \times 10^{-1}$ moles/liter.

3.4. *Mechanism and kinetics of the reaction*

Generally, radiation may be used to accelerate normal thermal oxidations, although it is difficult in such systems to gain any understanding of the fundamental radiolytic processes. The oxidation reaction of hydrocarbons with molecular oxygen represents a chain radical process.[12] The experimental data exposed in Section 3.1. prove that the radiolytic oxidation of acenaphthene to naphthalic acid takes place by a chain reaction mechanism, but these data did not allow us to make it clear.

The radiation action on acenaphthene has as primary effect either the formation of free radicals, or the formation of excited molecules. The excited molecules are formed by the direct action of radiation which manifests either by the agency of slow secondary electrons or by the energy transfer process from the solvent molecules to those of the solute. Radiation could have a direct action on the acenaphthene molecules because its concentration always was great enough so that such an action could be possible. On the other hand, work on the irradiations of mixtures of aromatic compounds with other compounds has provided evidence that energy initially absorbed in one component can be transferred to a second component, before decomposition takes place. Pyridine, like benzene has the resonanting π electrons structure, identified with aromatic compounds and studies carried out with it confirmed that pyridine behaves essentially as an aromatic in the presence of radiation. Consequently, this energy transfer process from pyridine to acenaphthene can occur. The acenaphthene excited molecules subsequently decompose, also giving free radicals.

---

[12] N. N. Semenov, "Tsepnye reaktsii", Moscow, Goskhimtechizdat, 1934, p. 53.

As it is shown by Bach and coworkers, [13] under the action of ionizing radiation on liquid hydrocarbons and in the presence of the molecular oxygen, peroxides and hydroperoxides initially are formed. In our case, the formation of the acenaphthene peroxide can take place as a result of the reaction between the hydrocarbon radical and the molecular oxygen, which is a very good radical scavenger. In the system we investigated, the oxygen necessary for the reaction was supplied by the potassium permanganate decomposition, possibly occurring by one of the two following ways :

$$2KMnO_4 \rightsquigarrow MnO_2 + K_2MnO_4 + O_2 \qquad (1)$$

$$10KMnO_4 \rightsquigarrow 2K_2MnO_3 + 3K_2MnO_4 + 5MnO_2 + 6O_2 \qquad (2)$$

From the acenaphthene peroxide, as an ultimate product, naphthalic acid can be obtained.

The reaction of the acenaphthene radiolytic oxidation was investigated in the course of time. Figure 4 represents the variation of the

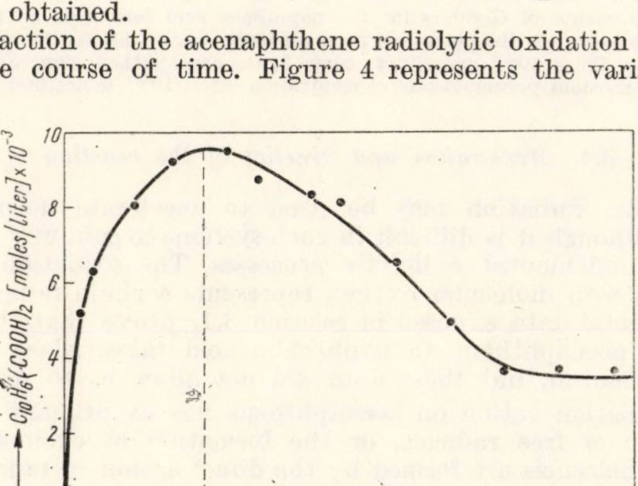

Fig. 4. — Variation of the naphthalic acid concentration as a function of the exposition time to radiation ; dose rate : 2.6×10^{17} eV/ml., min.

---

[13] N. A. Bach, "Sbornik po deistvie ioņiziruyushshikh izlucheņii na ņeorgaņicheskie i organicheskie sistemy", Moskva, Izdat. Akad. Nauk S.S.S.R., 1958, p. 117.

amount of naphthalic acid, formed as a function of the exposure time under the radiation. This quantity shows a marked increase during the first minute of reaction. In a second stage, the growth of the acid quantity is occurring with a smaller rate and at about six minutes of exposure, the maximum acid quantity is obtained. After this interval, the amount of the acid begins to diminish and after about twenty minutes it does not change any more, becoming constant.

The developing of the acenaphthene radiolytic oxidation in the course of time, takes place according to a kinetics which is characteristic of consecutive reactions. The process may be schematically represented as follows :

$$A \xrightarrow{k_1} B \xrightarrow{k_2} C$$

In our case A is acenaphthene, passing into B with a total rate constant, k_1. B is the intermediate product, that is the peroxide. As we have shown, it passes into acid or undergoes other reactions with a total rate constant, k_2, leading to the formation of secondary products (C). We denote by :

a : the acenaphthene initial concentration [moles/liter] ;

x : the amount of acenaphthene, transformed at the time t and equal to that of the peroxide quantity, formed at the time t ;

y : the peroxide amount changed into secondary products, at the time t ;

$x - y$: the peroxide quantity present at the time t and equal to that of the naphthalic acid, determined by us, [moles/liter].

The reaction rate of acenaphthene, A, is given by an equation under the form of :

$$\frac{\mathrm{d}x}{\mathrm{d}t} = k_1(a - x) \tag{3}$$

Integrating :

$$(a - x) = a \cdot \mathrm{e}^{-k_1 t} \tag{4}$$

The transformation rate of the intermediate product, B, is :

$$\frac{\mathrm{d}\,(x - y)}{\mathrm{d}t} = k_1(a - x) - k_2\,(x - y) \tag{5}$$

Effecting a series of intermediate operations and integrating, one obtains :

$$(x - y) = a\frac{k_2}{k_2 - k_1}\,(\mathrm{e}^{-k_1 t} - \mathrm{e}^{-k_2 t}) \tag{6}$$

The formation and decomposition rates of the intermediate product are identical when its maximum concentration is attained. Then, the decomposition rate becomes greater than the formation one and the concentration of the intermediate product begins to diminish. If $k_1 < k_2$, after a long enough time, $e^{-k_2 t} \ll e^{-k_1 t}$. Equation (6) changes in the following way:

$$(x - y) = a\,\frac{k_1}{k_2 - k_1}\,e^{-k_1 t} \text{ and} \tag{7}$$

$$\ln (x - y) = \ln \frac{ak_1}{k_2 - k_1} - k_1 t \tag{8}$$

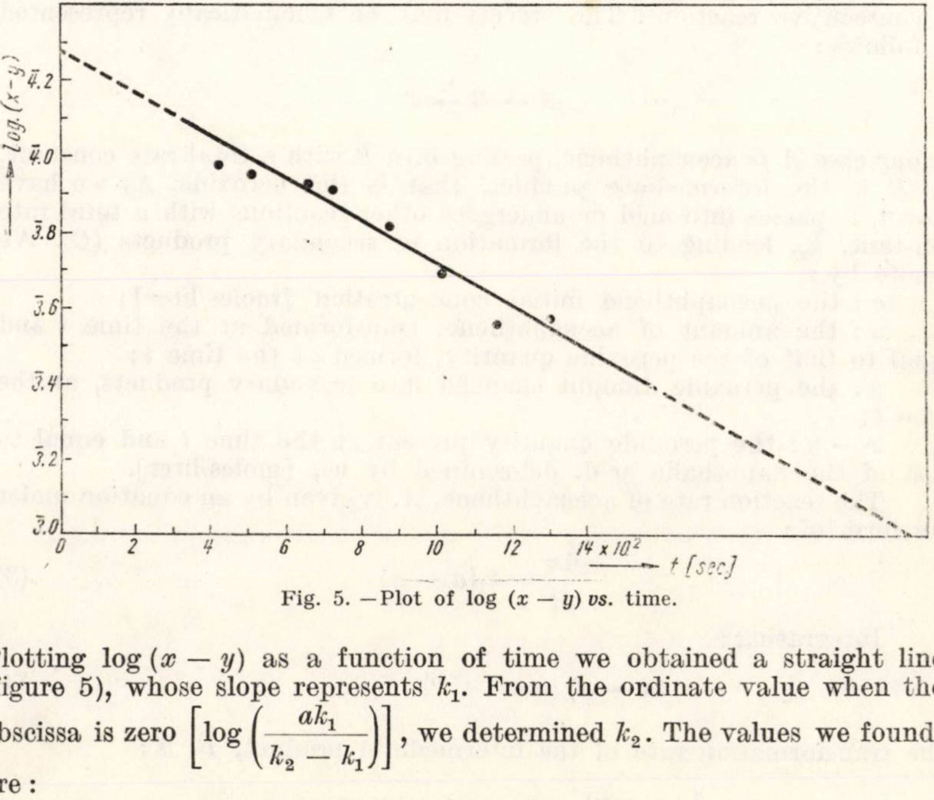

Fig. 5. —Plot of log $(x - y)$ *vs.* time.

Plotting log $(x - y)$ as a function of time we obtained a straight line (figure 5), whose slope represents k_1. From the ordinate value when the abscissa is zero $\left[\log\left(\frac{ak_1}{k_2 - k_1}\right)\right]$, we determined k_2. The values we found, are:

$$k_1 = 3.25 \times 10^{-4}\ [\text{sec}^{-1}]$$

$$k_2 = 1.033 \times 10^{-2}\ [\text{moles. sec}^{-1}\,.\,\text{l}^{-1}].$$

The time, $t_{\max}$, necessary for the intermediate product to reach maximum concentration, only depends on its formation and decomposition rate constants. Differentiating equation (6) and making equal to zero the obtained expression, we have for $t_{\max}$ the following relationship:

$$t_{\max} = \frac{\ln (k_2/k_1)}{\ln\,[(k_2/k_1) - 1]\,k_1} \tag{9}$$

Replacing k_1 and k_2 by the respective values found by us, we obtained $t_{\max} = 348$ sec; this value is very close to that indicated on the experimental curve in figure 4, namely 360 sec.

The development of the reaction of hydrocarbon chain oxidation involved serious problems and constituted the object of many studies.[14–18] As a conclusion, one can say that the radiation effect on the kinetics of the chain oxidation reaction is different from one system to another. But in all cases, the fact is obvious that at a certain dose, secondary reactions are occurring. These reactions are connected, especially, with the radiation action on the intermediate oxidation products. The fact that the concentration of the formed naphthalic acid begins to decrease after about 350 sec, can be explained by the existence of secondary reactions, whose extent increases as the absorbed dose increases. With regard to the kind of these reactions, we can say nothing since we have not determined other products which could be formed, except naphthalic acid.

3.5. *Investigation of the reaction after the interruption of irradiation*

As the reaction of the acenaphthene radiolytic oxidation occurs by a mechanism of chain radical reaction, we supposed that oxidation will proceed after the interruption of irradiation, too. In order to verify this supposition we followed the reaction in the course of time beginning with 30 minutes till 36 hours after interruption. Working with a potassium permanganate-acenaphthene ratio of 3 : 1, the acid amount obtained after 24 hours from interruption was about twice greater than that corresponding to the time of 30 minutes. Between 24 and 36 hours from the interruption of irradiation, the naphthalic acid concentration remained constant. This was the reason for which all samples were analysed after 24 hours from the interruption of irradiation. The oxidation rate in the absence of radiation is much smaller than during irradiation. The fact that the reaction of the acenaphthene oxidation proceeds after the irradiation interruption can be explained by carrying on the reaction chain, initiated by ionizing radiation. The necessary oxygen is available because potassium permangante continually decomposes. This decomposition is catalysed by the very manganese dioxide, formed under radiation.

Considering the results with respect to the radiolytic oxidation of acenaphthene to naphthalic acid, some conclusions can be drawn :

1. The oxidation reaction occurs according to a chain radical mechanism.

---

[14] M. Durup, J. Durup and M. Magat, "Conf. Application of Large Rad. Sources in Industry", Warsaw, 1959, p. 135.

[15] M. A. Proskurnin, Yu. L. Khmel'nitskii and E. B. Barelyu, *Doklady Akad. Nauk, S.S.S.R.*, **112**, 886 (1957).

[16] N. A. Emanuel, *Doklady Akad. Nauk, S.S.S.R.*, **111**, 1286 (1956).

[17] N. A. Slavinskaya, G. A. Kamenetskaya and S. Ya. Pshezhetskii, *Zhur. fiz. Khim.*, **34**, 1169 (1960).

[18] N. A. Slavinskaya, G. A. Jitneva, S. A. Kamenetskaya and S. Ya. Pshezhetskii, *Zhur. fiz. Khim.*, **36**, 1293 (1962).

2. The kinetics of the overall reaction is typical to consecutive reactions.

3. In our conditions, the optimum conversion of acenaphthene to naphthalic acid (about 55%) was obtained for short times of exposure to radiation (5 minutes), a dose rate of 2.6×10^{17} eV/min., ml and a potassium permanganate – acenaphthene ratio of 4.5 : 1.

Revue Roumaine de Chimie, **15**, 1923–1929 (1970)

SYNTHETICAL PHENOTHIAZINE GLYCOSIDES. III*
OXIDATION REACTION

C. BODEA, TEODORA PANEA and V. FĂRCĂŞAN

Institute of Chemistry, Cluj
Str. Donath 59–65

Received May 30, 1970

Oxidation of 3-(1,7,9-trichloro-phenothiazinyl)-β-D-2,3,4,6-tetra-O-acetyl-glucopyranoside (I) with potassium dichromate and with hydrogen peroxide yields 1,7,9-trichloro-phenothiazine-3 one (V), and 3-(1,7,9-trichloro-5,5-dioxi-phenothyazinyl)-β-D-2,3,4,6-tetra-O-acetyl-glucopyranoside (VII) respectively; VII obtained also on treating 1,7,9-trichloro-3-hydroxy-5,5-dioxi-phenothiazine (VIII) with α-glucoso-pentaacetate, was hydrolysed. The electronic spectra between 250 and 700 nm of the obtained compound and of some related compounds were recorded.

Previous investigations[1-3] have shown that the nature and number of substituents play an important role in the pathway the oxidation reaction of phenothiazine will follow, leading either to phenothiazone, or to phenothiazine-5-oxide or 5-dioxide. We have now investigated the action of oxidants on a phenothiazinyl-glycoside, namely 3-(1,7,9-trichloro-phenothiazinyl)-β-D-2,3,4,6-tetra-O - acetyl-glucopyranoside (I)[4] in which the sugar residue is not affected by oxidation. Glycosides of oxidated phenothiazines may show biological activities.

We first examined the action of $K_2Cr_2O_7$ on I. As it has been reported earlier[2] 3-methoxy- and 3-acetoxy-1,7,9-trichloro-phenothiazine II and III display a different behaviour with the brief action of $K_2Cr_2O_7$ in glacial acetic acid. Whilst the methoxy group is not affected, the acetoxy group is eliminated, the oxidation resulting in the formation of two different phenothiazones: 1,9-dichloro-3-methoxy-phenothiazine-7-one (IV) and 1,7,9-trichloro-phenothiazine-3-one (V). Considering, on the one hand, that the glycosides show from many points of view properties situated between those of ethers and esters and that, on the other hand, the big size of the acetylated sugar residue can involve sterical effects, it seems not possible to predict the way in which $K_2Cr_2O_7$ will act upon I.

---

* Part II: C. Bodea, V. Fărcăşan and T. Panea, *Rev. Roumaine Chim.*, **14**, 523 (1969).

[1] C. Bodea and. M. Răileanu, *Liebigs Ann. Chem.*, **614**, 171 (1958).

[2] C. Bodea and V. Fărcăşan, *Studii şi Cercetări Chim. Acad. Fil. Cluj*, **11**, 121 (1960).

[3] C. Bodea, V. Fărcăşan and T. Panea, *Rev. Roumaine Chim.*, **11**, 239 (1966).

[4] C. Bodea, V. Fărcăşan and T. Panea, *Rev. Roumaine Chim.*, **12**, 697 (1967).

Following by thin layer chromatography the oxidation of I by $K_2Cr_2O_7$ in glacial acetic acid we have found that the sugar residue is eliminated, I being almost quantitatively converted into 1,7,9-trichlorophenothiazine-3-one (V). That means that the O-glycoside I shows in this reaction the same behaviour as the ester III.

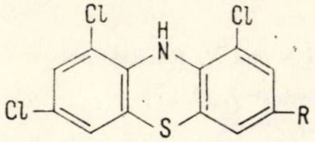

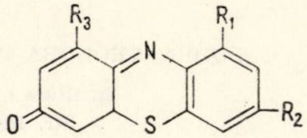

I : R = A X : R = OH IV : $R_1 = R_3 = Cl$; $R_2 = OCH_3$

II : R = OCH_3 XIII : R = Cl V : $R_1 = R_2 = R_3 = Cl$

III : R = $OCOCH_3$ VI : $R_1 = R_3 = Cl$; R_2 = A

A =

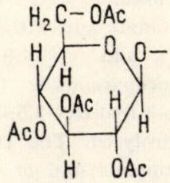

(Ac = $COCH_3$)

When I is treated with H_2O_2 in acetic acid, oxidation occurs at the sulfur atom. The oxidation product could not be reduced by Zn in acetic acid indicating that the substance is not a sulfoxide. From the elementary analysis and the IR spectrum showing bands at 1160 and 1310 cm^{-1} assigned to the symmetrical and asymmetrical ν_{SO_2} vibrations [5] it was deduced that the oxidation product is 3-(1,7,9-tricloro-5,5-dioxy-phenothiazinyl)-β-D-2,3,4,6-tetra-O-acetyl-glucopyranoside (VII). To confirm the

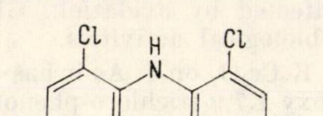

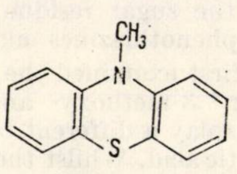

XIV

VII : R = A XII : R = Cl

VIII : R = OH XV : R = $OCOCH_3$

IX : R = B

B=

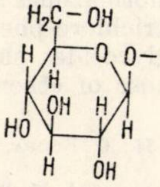

---

[5] C. N. R. Rao, "Chemical Application of Infrared Spectroscopy", Academic Press, New York and London, 1963, p. 304, 306.

structure we submitted VII to the acid catalysed hydrolysis. The eliberated aglycon proved to be identic with 1,7,9-trichloro-3-hydroxy-5,5-dioxy-phenothiazine VIII obtained by us in another way.[6]

On condensing VIII with α-aceto-bromo-glucose (IX) we isolated from the reaction products a substance showing the same properties as VII (m.p., IR spectrum). This demonstrates that during the oxidation of I with H_2O_2 the sugar residue remained unchanged.

Comparing the yields with which the glycosides of 1,7,9-trichloro-3-hydroxy-5,5-dioxy-phenothiazine (VIII) and of 1,7,9-trichloro-3-hydroxy-phenothiazine (X)[4] are obtained we see that they are much better in the case of VIII. This may be explained by the acid-stronging action of the SO_2 group on the $-OH$ group. Moreover the SO_2 group determines a marked increase of the redox potential of VIII, which prevents the oxidation of the $-OH$ group during the glycosidation reaction of VIII but observed in the case of X.

By basic hydrolysis VII was deacetylated yielding 3-(1,7,9-trichloro-5,5-dioxy-phenothiazinyl)-β-D-glucopyranoside (XI).

The good yields obtained in the condensation of VIII with IX permit to conclude that generally glycoside of hydroxy-phenothiazine-5,5- dioxides can much easier be prepared than glycosides of hydroxy-phenothiazines.

This opens the possibility to sinthesize by this way 5,5-dioxy-phenothiazinyl-glycosides and to investigate the influence of various substituents on the hydrolysis of the glycosidic linkage. To achieve the latter purpose it is important to find out whether the hydrolysis can be followed spectrophotometrically presuming the knowledge of the spectroscopic properties of the compounds.

The electronic spectrum of the glycoside XI shows four bands in the 220–400 nm region, similarly to other phenothiazine-5,5-dioxides[7] (table 1). The acetylation of the sugar residue (substance VII) does not affect the spectrum. In the spectra of the aglycon VIII, in comparison with XI, and of X compared with III a bathocromic shift, particularly for the first two maxima, can be observed. Comparison of the spectra of XI and VIII (fig. 1) shows that it is not possible to estimate quantitatively the two compounds in a mixture.

The addition of KOH to the methanolic solution of the aglycon VIII, causes a batochromic shift of all the four bands. This can be assigned to the halochromy due to the presence of the phenolic hydroxyl (table 1). In the same conditions the spectrum of the glycoside XI is also altered, but in this case only the first two maxima undergo a bathochromic shift, the third one is hypsochromically shifted. 1,3,7,9-Tetrachloro-phenothiazine-5,5-dioxide (XII) exhibits a similar behaviour as XI. In contrast to XII, the spectra of 1,3,7,9-tetrachloro-phenothiazine (XIII) and of 10-methyl-phenothiazine-5,5-dioxide (XIV) are not affected by the addition of KOH.

---

[6] T. PANEA and C. BODEA, Rom. pat. 60 238, 14 June, 1969.

[7] R. J. WARREN, I. B. EISDORFER, W. E. THOMPSON and J. E. ZAREMBO, *J. Pharm. Sci.*, **55**, 144 (1966).

Table 1

Electronic spectra. Absorption maxima and molar extinctions

Compound	$\lambda_{nm}(\varepsilon_{max} \times 10^{-3})$	
	In methanol	In methanol+KOH*
1,7,9-Trichloro-3-hydroxy-phenothiazine (X)	325 (5.84) 264.5 (40.00) 227^{S}	
1,7,9-Trichloro-3-acetoxy-phenothiazine (III)	323.8 (5,92) 262.8 (51.70)	
1,3,7,9-Tetrachloro-phenothiazine (XIII)**	326 264,5	326 264.5
1,3,7,9-Tetrachloro-phenothiazine-5,5-dioxide (XII)	344 (6.64) 312 (10.20) 279 (26.17) 227 (32.01)	364 (17.81) 320 (14.74) 267 (27.00) 230^{S}
10-Methyl-phenothiazine-5,5-dioxide (XIV)	333 (6.34) 295.5 (8.50) 269 (18.06) 238.5^{S}	333 (6.34) 295.5 (8.50) 268.8 (18.06) 238.5^{S}
1,7,9-Trichloro-3-hydroxy-phenothiazine-5,5-dioxide (VIII)	352 (6.63) 320 (6.70) 281 (22.65) 227 (30.72)	372 (5.01) 337 (7.36) 298 (15.27) 229.5 (25.05)
3-(1,7,9-Trichloro-5,5-dioxi-phenothiazinyl)-β-D-glucopyranoside (XI)	344 (6.74) 314 (8.14) 279 (25.10) 228 (32.54)	363 (17.16) 318 (18.48) 268.5 (15.84)
3-(1,7,9-Trichloro-5,5-dioxi-phenothiazinyl)-β-D-2,3,4,6-tetra-O-acetyl-glucopyranoside (VII)	345 (8.72) 314 (11.02) 278.5 (33.38) 227 (42.40)	360 (11.09) 317 (13.99) 278.5^{S} 271.5 (16.72) 227 (28.66)

S = shoulder

*) To 50 ml methanolic solution, 0.2 ml 10% KOH were added.

**) Molar extinctions were not registered.

From the data presented above, concerning the substances XII, XIII and XIV, it may be assumed that the changes in the spectrum of the glycoside XI occurring by addition of alkali to the methanolic solution, are due to the character of a vinylog sulfonamide of the phenothiazine-5,5-dioxides. This allows, if position 10 is free, the interaction with alkalis, characteristic of the primary and secondary sulfonamides. This point of view is supported by the spectral data obtained in the sulfonamide series. Thus for example Vignoli and coworkers[8] have registered for a series of seven sulfonamides the hypsochromic shift of the 270 nm band, on passing from neutral to alkaline medium.

---

[8] L. Vignoli, B. Cristan and J. P. Defretin, *Ann. pharm. franç.*, **21**, 477 (1963).

The different behaviour of XI and VIII, especially with regard to the shift of the third band in the presence of KOH, may be assigned to the appearance, by VIII in these conditions, of the phenoxidic ion, which disturbs deeply the vinylog-sulfonamide system.

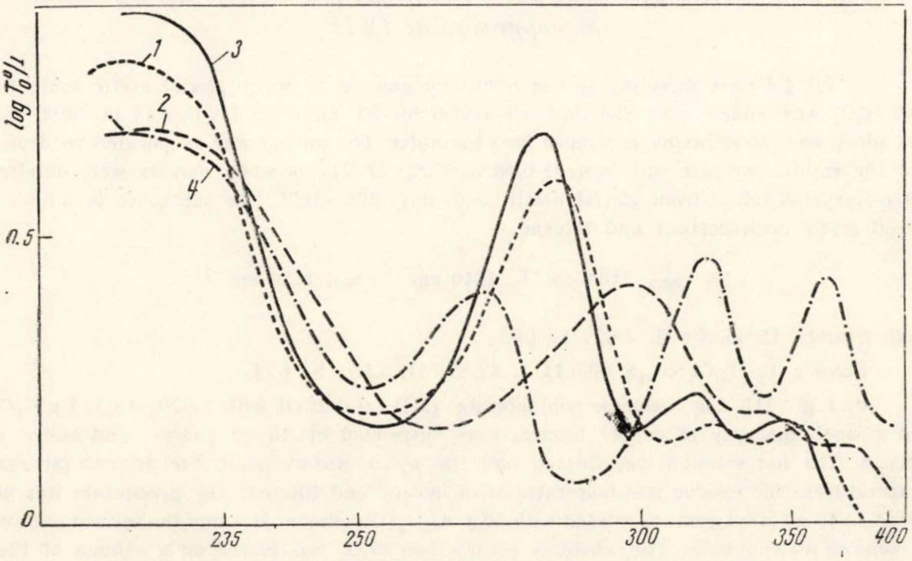

Fig. 1. — The electronic spectra of substances VIII and XI.

1, substance VIII in methanol; *2*, substance VIII in methanol + KOH; *3*, substance XI in methanol; *4*, substance XI in methanol + KOH.

Comparison of the spectra of the glucoside XI and of the aglycon VIII (fig. 1) recordered in methanolic alkaline solution, indicates that the 270 nm region, can serve to estimate quantitatively the two compounds present in a mixture.

It is to be noted that the addition of concentrated HCl to the methanolic solutions of the substances mentioned in table 1 (until the ~2% concentration is reached) does not affect the spectra.

The electronic spectra of phenothiazine-5,5-dioxides shall be considered extensively in another paper.

EXPERIMENTAL *

The action of $K_2Cr_2O_7$ on I

To a boiling solution I in glacial acetic acid, $K_2Cr_2O_7$ were added, and after one minute (boiling) poured into water. The precipitate was extracted with ethyl acetate. In this solution the 1,7,9-trichloro-phenothiazone (V) was indentified by thin layer chromatography, on silicagel G; developer toluene-ethyl-acetate 1 : 1. For comparison an authentic sample [1] was used. (*Obs.* On the plate another three very small spots were observed). Aspersing the plate with a saturated solution of ceric sulfate in concentrated sulfuric acid, no additional spots became visible.

---

* The melting points were determined in capillaries and are uncorrected.

3-(1,7,9-Trichloro-5,5-dioxi-phenothiazinyl)-β-D-2,3,4,6-tetra-O-acetyl-glucopyranoside (VII)

a) 0.1 g I were dissolved in the minimum amount of warm glacial acetic acid; 1 ml 30% H_2O_2 was added and the mixture boiled for 30 minutes. Another 1 ml 30% H_2O_2 was added and the refluxing continued for 15 minutes. The solvent was evaporated to dryness and the residue washed with water; 0.08 g (77%) of VII as white needles were obtained. After recrystallization from glacial acetic acid, m.p. 166—167°. The substance is soluble in glacial acetic acid, acetone and toluene.

IR ν_{SO_2} 1160 cm^{-1} 1310 cm^{-1} ν_{CO} 1750 cm^{-1}

Anal: *Found*: C, 45.60; H, 3.67; S, 4.62;

Calcd.: $C_{26}H_{24}Cl_3NO_{12}S$ (680.1) C, 45.85; H, 3.55; S, 4.72.

b) 1 g VIII, 2 g α-glucose pentaacetate (IX) (stabilized with $CaCO_3$ 1%), 1 g K_2CO_3 and a small quantity of copper bronze, were suspended in 10 ml xylene and boiled for 4 hours. The hot solution was filtered and the xylene was evaporated to dryness (at room temperature). The residue was macerated with hexane and filtered. The precipitate was dissolved in 10 ml ethyl acetate, mixted with 50 g Al_2O_3 (Brockman III) and the solvent removed *in vacuo* on a steam bath. The substance adsorbed on Al_2O_3 was placed on a column of 125 g Al_2O_3 (Brockman II/III) and eluated with toluene. After the removal of the toluene, 0.95 g (49%) pure substance, m.p. 166—167° were obtained. The mixed melting point with the substance prepared as described above shows no depression; the IR spectra of the two products are identical.

Anal.: *Found*: C, 45.62; H, 3.52; S, 4.34;

Calcd.: $C_{26}H_{24}Cl_3NO_{12}S$ (680.1); C, 45.85; H, 3.55; S, 4.72.

Action of zinc in acetic acid on VII

To a boiling solution of 0.05 g VII in 5 ml glacial acetic acid, 0.2 g zinc powder were added. After 15 minutes boiling, the hot mixture was filtered and the acetic acid evaporated. By thin layer chromatography exclusively VII was identified.

1,7,9-Trichloro-3-hydroxy-phenothiazine-5,5-dioxide (VIII)

A boiling solution of 0.05 g VII in 4 ml glacial acetic acid was treated successively during 5 minutes with three drops concentrated HCl and refluxed for 15 minutes. The acetic acid was evaporated and in the residue, VIII was identified by thin layer chromatography. For comparison an authentic sample of VIII [6] was used.

3-(1,7,9-Trichloro-5,5-dioxi-phenothiazinyl)-β-D-glucopyranoside (XI)

A mixture of 0.2 g VII, 3.5 ml N/10 solution of sodium methoxide (in methanol) and 8 ml dried methanol was refluxed for 30 minutes. The methanol was evaporated and the residue washed with water; 0.16 g XI were obtained. After recrystallization from ethanol m.p. 210–211°.

IR ν_{SO_2} 1162 cm^{-1} 1309 cm^{-1} ν_{OH} 3380 cm^{-1}

Anal. *Found*: C, 42.01; H, 3.21; S, 5.93;
Calcd.: $C_{18}H_{16}Cl_3NO_8S$ (512.7) C, 42.20; H, 3.15; S, 6.26.

Apparatus

For the recording of IR spectra, a double beam spectrophotometer Carl Zeiss Jena type UR-10 was used; the substances were prepared as KBr pellets.

The electronic spectra were recorded in a methanol solution on a DK-2A Beckmann spectrophotometer.

Revue Roumaine de Chimie, **15**, 1931–1934 (1970)

SIMULTANEOUS VIBRATIONAL TRANSITIONS. II.[1]
INDUCED SIMULTANEOUS VIBRATIONAL TRANSITIONS IN SOME HALOFORM – CARBON DISULFIDE MIXTURES

SIMONA BĂDILESCU

Research Department, Petrochemical Works, Piteşti Romania

Received June 23, 1970

The ST-bands arising from $\nu_{C-H(D)} + \nu_3\ (CS_2)$ combinations in chloroform, chloroform-*d*- and bromoform-carbon disulfide mixtures were studied. The asymmetrical ST-band in the $CHCl_3 - CS_2$ mixture was found to be a double unresolved ST-band. The induced nature of the supplementary band, fused to the main ST-band, was proved, and a mechanism of its engendering was outlined. Spectral measurements data concerning the ST-band in deuteriochloroform-carbon disulfide mixture that has not been previously reported are given.

INTRODUCTION

The simultaneous vibrational transitions (ST) in liquid mixtures of $CHHal_3 - CS_2$ type (Hal = Cl, Br) were studied by Hooge [2] only as regards the frequencies of the ST-bands appearance, but no peculiarity concerning the shape of bands was noted.

In connection with our studies on simultaneous vibrational transitions in liquid mixtures, [1] we investigated the ST-bands in chloroform –, and bromoform – carbon disulfide mixtures; a pronounced difference in the shape of the $ST_{CHCl_3-CS_2}$ and $ST_{CHBr_3-CS_2}$ bands (located at 4528 cm^{-1} and 4533 cm^{-1}, respectively) was noticed. This fact prompted us to study attentively these bands, in order to elucidate the origin of such a difference in the shape of the bands observed.

RESULTS AND DISCUSSIONS

Figure 1 shows the ST-bands of the $CHBr_3 - CS_2$ and $CHCl_3 - CS_2$ mixtures, one observes that while the $ST_{CHBr_3-CS_2}$ band appears as a whole symmetrical curve, the $ST_{CHCl_3-CS_2}$ band is asymmetrical. The asymmetry of the band was found to be dependent on the mixing ratio (m.r.) of the chloroform and carbon disulfide, and the maximum of the asymmetry coincides with the optimal m.r. for the most intense ST-band, i.e., mixing ratio equal to 0.5. These facts indicate that the asymmetry of the $ST_{CHCl_3-CS_2}$ band ought to be explained only within the framework of the ST-events.

---

[1] Part I., S. Bădilescu, *Rev. Roumaine Chim.*, **13**, 1297 (1968).

[2] F. N. Hooge, Thesis, Amsterdam, 1956.

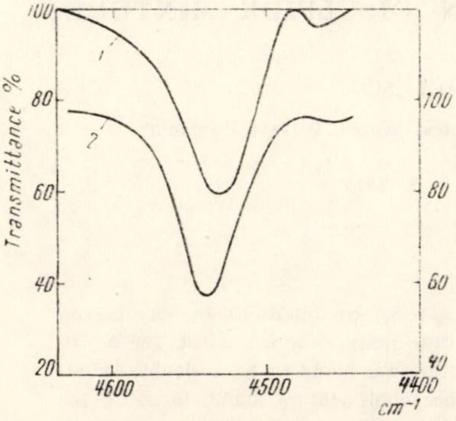

Fig. 1. — ST-bands of *1*) — $CHCl_3-CS_2$ and *2*) — $CHBr_3-CS_2$ mixtures.

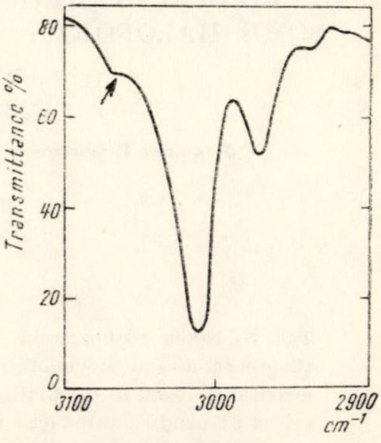

Fig. 2. — IR spectrum of chloroform in the 3000 cm^{-1} region. (Arrow shows the satellite band).

A first attempt to explain the observed asymmetry of $ST_{CHCl_3-CS_2}$ band arises from the examination of the absorption spectrum of chloroform in the 3000 cm^{-1} region (Figure 2). Indeed, a weak absorption band at 3060 cm^{-1} (which was assigned[3] to a combination of the $\nu_{C-Cl} + 2\ \delta_{CH}$ frequencies) may be suspected to be involved in a simultaneous vibration with the ν_3 frequency of carbon disulfide and, thus, the observed asymmetrical band at 4528 cm^{-1} would be an unresolved double ST-band. This assumption was proved by the following spectral evidences.

The related ST-band of the deuteriochloroform - carbon disulfide mixture (not previously reported) was also studied. This ST-band appears at 3760 cm^{-1} and, for comparison, figure 3 shows both $ST_{CHCl_3-CS_2}$ and

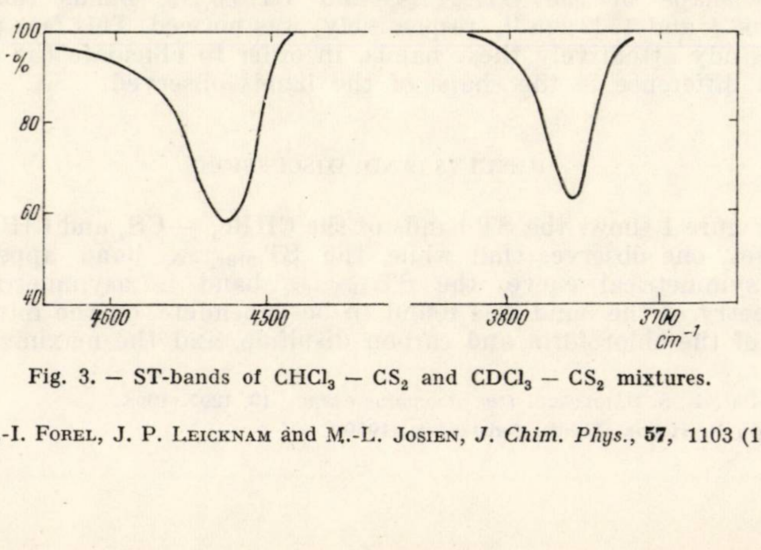

Fig. 3. — ST-bands of $CHCl_3 - CS_2$ and $CDCl_3 - CS_2$ mixtures.

---

[3] M.-I. Forel, J. P. Leicknam and M.-L. Josien, *J. Chim. Phys.*, **57**, 1103 (1960).

$ST_{CDCl_3-CS_2}$ bands, which were recorded in similar experimental conditions. Table 1 records the results of the spectral measurements obtained in this work and the available literature data concerning the ν_{C-D} frequency in liquid chloroform-*d* and its solutions, in nonpolar solvents. The value of the ST-band frequency in the $CDCl_3 - CS_2$ mixture, is quite equal to the sum of the ν_{C-D} and ν_3 (CS_2) frequencies which are combined.

Table 1

ν_{C-D} ($CDCl_3$)-and ν_{ST} ($CDCl_3 - CS_2$)-band frequency values

ν_{C-D} Stretching frequency value* (cm^{-1})		ν_{ST} Frequency value** (cm^{-1})	
neat liquid	soln. in CS_2	Found	Calculated***
2260	2254	3760	3769
2258[4]	*2260*[4]****	—	3775
2252[5]	*2244*[5]	—	3759
	2246[6]	—	3761
	2254[7]	—	3769

* Literature data in italics;
** $\nu_{ST} = \nu_{C-D} + \nu_3(CS_2)$;
*** From ν_{C-D} frequency values in solutions and the ν_3 (CS_2) frequency (taken[2] equal to 1515 cm^{-1});
**** Solution in carbon tetrachloride.

As it might be seen from figure 3, the $ST_{CDCl_3-CS_2}$ band is wholly symmetrical and, in addition, the half band width ($\Delta\nu_{1/2}$) value of this ST-band (of cca. 33 cm^{-1}) is slightly lower than that of the related $ST_{CHCl_3-CS_2}$ band ($\Delta\nu_{1/2}\sim 51$ cm^{-1}). The different spectral pattern of the $CDCl_3 - CS_2$ and $CHCl_3 - CS_2$ mixtures may be easily explained as follows. While the difference of the ν_{CH} frequency and its satellite band ($\nu_{C-Cl} + 2\delta_{CH}$) in chloroform is only of about 40 cm^{-1}, in deuteriochloroform the corresponding ν_{C-D} and $\nu_{C-Cl} + 2\delta_{CD}$ bands are remoted so much, that only the former mode of vibration leads to a ST-band with ν_3 (CS_2) mode; the later band, at about 2500 cm^{-1}, is too distant to be involved in such a type of ST with ν_3. Thus it can be readily seen that the symmetrical $ST_{CDCl_3-CS_2}$ band at 3760 cm^{-1} is due to the $\nu_{C-D} + \nu_3$ (CS_2) frequencies, while the $ST_{CHCl_3-CS_2}$ band at 4528 cm^{-1} arises from two fused ST-bands corresponding to $\nu_{C-H} + \nu_3$ (CS_2) and ($\nu_{C-Cl} + 2\delta_{CH}$) + ν_3 (CS_2) combinations.

---

[4] C. M. Huggins and G. C. Pimentel, *J. Chem. Phys.*, **23**, 896 (1955).
[5] M.-L. Josien, J. P. Leicknam and N. Fuson, *Bull. Soc. chim. France*, **1958**, 188.
[6] J. Lascombe, J. Devaure and M.-L. Josien, *J. Chim. phys.*, **61**, 1271 (1964).
[7] R. B. Bernstein and M. Tamres, *J. Chem. Phys.*, **23**, 2201 (1955).

As regards the mechanism of this unexpected doubly induced simultaneous vibrational transition, the following considerations are appropriate.

In the $CHCl_3 - CS_2$ system, the ν_{C-H} stretching frequency and its satellite band describe two oscillators of very close energies which can interact simultaneously with the oscillator corresponding to the ν_3 vibration of the CS_2 molecule. As a result, the $CHCl_3 - CS_2$ collision complex absorbs at the frequencies corresponding to the sums of $\nu_{1(CH)} + \nu_3(CS_2)$ and ($\nu_{C-Cl} + 2\delta_{CH}$) + ν_3 (CS_2), and the spectrum shows an asymmetrical (and little broadened) ST-band. Thus, the induced ST-band arises from the combination of two bands with the main vibration of the same symmetry (A_1).

Finally, it is of interest to show some observations concerning the intensity and frequency of the $ST_{CDCl_3-CS_2}$ band studied.

The ST-band in the $CDCl_3 - CS_2$ mixture is less intense than that observed for the $ST_{CHCl_3-CS_2}$ band and this fact agrees with literature data concerning the integrated intensities of the ν_{C-H} and ν_{C-D} bands. Indeed, Forel *et al.* [3] reported for those bands A = 230 and 650 ($1 \cdot mole^{-1} \cdot cm^{-2}$) for neat liquid $CDCl_3$ and $CHCl_3$, respectively, and A = 200 and 460 ($1 \cdot mol^{-1} \cdot cm^{-2}$) values for $CDCl_3$ and $CHCl_3$, respectively, in carbon disulfide solutions.

As concerns the frequency value of $ST_{CDCl_3-CS_2}$ band, it was found to change along with the mixing ratio, and this fact is in accordance with the general concept of the "collision complexes" in ST-events. [2] In the process of collision, the ondulatory functions of the molecules are strongly perturbed and consequently, frequency shift occurs. Bernstein and Tamres [7] reported that by progressive dilution of deuteriochloroform with carbon disulfide, the ν_{C-D} frequency value is linearly lowered, with respect to the ν_{C-D} value in neat $CDCl_3$ ($\nu_0 = 2260$ cm^{-1}).

EXPERIMENTAL

Materials used were of proper purities. Chloroform was freshly purified prior to use by the procedure described [1] which affords a very pure material (99.9 + % by v.p.c.). Carbon disulfide (Union Chimique Belge, spectroscopically grade), bromoform (Carlo Erba – Milano) and a 99.8 per cent chloroform-*d* (Serva) were used without supplementary purifications.

Spectral measurements. The spectra were recorded with a Carl Zeiss – Jena, Model UR-10, double beam spectrophotometer. Special cells [1] with a pathlength of 10.8 mm were used, and the measurements were carried out as reported in the previous paper. [1]

Acknowledgements. The author thanks Prof. V. Em. Sahini, Ph. D. (Centre of Physical Chemistry) for advice and helpful discussions.

Revue Roumaine de Chimie, **15**, 1935–1946 (1970)

L'ÉTUDE THERMODYNAMIQUE DES SOLUTIONS DE PVC

CORNELIA VASILE, ANA ONU et I. A. SCHNEIDER

Laboratoire de Chimie Physique, Université «Al. I. Cuza», Jassy, 11, 23 August

Reçu le 14 juillet 1970

Utilisant les méthodes viscosimétrique et la diffusion de la lumière on poursuit le comportement de la PVC-suspension et de la PVC-émulsion en différents solvants. On établit les fonctions thermodynamiques, les coefficients d'interaction, les paramètres dimensionnels dans les solvants respectifs. Les résultats obtenus par les deux méthodes concordent et s'encadrent entre les limites des valeurs données par la littérature de spécialité.

Les mesures viscosimétriques et de la diffusion de la lumière en solutions diluées permettent d'évaluer des dimensions non perturbées des chaînes polymères, des grandeurs thermodynamiques du processus de dissolution, etc., non seulement dans des conditions idéales — thêta [1] — mais aussi dans des conditions habituelles de température et de solvant, en utilisant les méthodes d'évaluation adaptées d'une manière correspondante. [2-4] Ces relations ont trouvé une large applicabilité dans la caractérisation des solutions diluées de polymères. [5-8]

Compte tenu qu'il y a un nombre relativement réduit de travaux concernant les propriétés thermodynamiques du polychlorure de vinyle (PVC), ce qui s'explique en partie par la grande tendance d'association des molécules de PVC, [9-12] qui rend difficiles les mesures de la diffusion de la lumière [13-15] et la corrélation des résultats obtenus par différentes méthodes, on essaie dans le présent travail une caractérisation des solutions de PVC en cyclohexanone par la technique viscosimétrique et celle de la diffusion de la lumière.

---

[1] P. J. Flory et T. G. Fox jr., *J. Amer. Chem. Soc.*, **73**, 1904 (1951).

[2] M. Kurata et W. H. Stockmayer, *Fortschr. Hochpolym.-Forsch.*, **3**, 196 (1963).

[2a] W. H. Stockmayer et M. Fixman, *J. Polymer Sci. C*, **1**, 137 (1963).

[3] M. Bohdanecky, *Coll. Czech. Chem. Comm.*, **30**, 1576 (1965).

[4] J. M. G. Cowie, *Polymer*, **7**, 487 (1966).

[5] T. G. Fox jr et P. J. Flory, *J. Amer. Chem. Soc.*, **73**, 1909 et 1915 (1951).

[6] H. A. Dieu, *J. Polymer Sci.*, **12**, 417 (1954).

[7] N. Kuvahara, K. Ogino, A. Kasai, S. Ueno et M. Kaneko, *J. Polymer Sci.* A, **3**, 985 (1965).

[8] W. Banks et C. T. Grenwood, *Makromol. Chem.*, **114**, 245 (1968).

[9] P. Doty et E. Mishuk, *J. Amer. Chem. Soc.*, **69**, 1631 (1947).

[10] D. J. Mead et R. M. Fuoss, *J. Amer. Chem. Soc.*, **64**, 277 (1942).

[11] R. Gaustron et G. Wippler, *J. Chim. phys.*, **58**, 754 (1961).

[12] A. Oth, 27 Congr. Inter. Chim. Industrielle, Bruxelles, 1954.

[13] D. Kratochvil, *Coll. Czech. Chem. Comm.*, **29**, 2767 (1964).

[14] J. Vavra, J. Lapcik et J. Sabados, *J. Polymer Sci. A*, **2**, 1305 (1967).

[15] G. Pezzin, G. Talamini et N. Gligo, *Chem. Ind.*, **46**, 648 (1964).

PARTIE EXPÉRIMENTALE

On a utilisé des échantillons de PVC polymérisé en suspension (PVC-suspensions) et PVC polymérisé en émulsion (PVC-émulsion) de différentes provenances, qui ont été purifiés par extraction avec un non-solvant. (Les échantillons de PVC-suspension ont été extraits pendant huit heures avec de l'éther de pétrole et de l'alcool méthylique ; celles de PVC-émulsion pendant huit heures avec de l'alcool méthylique.) Après dessèchement sous vide, les échantillons ont été fractionnés par la méthode d'extraction [16] ou par la méthode de précipitation fractionnée [17]. Après avoir été lavées avec de l'alcool méthylique, les fractions obtenues ont été séchées sous vide jusqu'à un poids constant. Les solvants utilisés à la préparation des solutions (cyclohexanone (CH), diméthylformamide (DMF) et orthodichlorobenzène (ODB)) ont été fraîchement distillés, la dissolution complète du polymère étant réalisée par le chauffage des solutions à 80° pendant 30 minutes. La purification optique des solutions et des solvants a été réalisée en les filtrant par filtres Iéna G5.

Les solutions utilisées aux mesures de la diffusion de la lumière avaient les concentrations entre $1 - 6 \cdot 10^{-3}$ g/ml, et celles pour les mesures viscosimétriques de $7{,}5 \cdot 10^{-4} - 1 \cdot 10^{-2}$ g/ml en polymère.

Les mesures viscosimétriques ont été effectuées à l'aide d'un viscosimètre à dilution et niveau suspendu PCL, adapté d'après le viscosimètre Ubbelhode. Le temps d'écoulement du solvant à 25° a été de 415,6 secondes, la thermostatation étant contrôlée avec une précision de ± 0,1°. Les corrections pour l'énergie cinétique et pour la densité ont été évaluées à l'aide des relations données dans la littérature, [18] pendant que les variations de la concentration avec la température ont été déduites à l'aide du coefficient de dilatation du solvant. La viscosité intrinsèque a été évaluée par extrapolation graphique des relations Huggins et respectivement Fuoss-Mead [17],

$$\text{a) } \eta\ \text{sp}/c = [\eta] + k'[\eta]^2 c \qquad (1)$$

$$\text{b) } \ln \eta\ \text{rel}/c = [\eta] + k''\ [\eta]^2 c$$

la concentration c étant exprimée en g/100 cm^3.

Les mesures de la diffusion de la lumière ont été réalisées à l'aide d'un photogoniodiffusiomètre de type Sofica, à 25 ± 0,05° et les angles de diffusion compris entre 30° et 150°. On a utilisé la lumière non polarisée, avec $\lambda = 5461$Å et le benzène comme liquide standard (distillé sur colonne après dessèchement sur $CaCl_2$, rapport Rayleigh $16{,}3 \cdot 10^{-6}$). Dans l'équation pour la diffusion de la lumière, on a utilisé pour la constante optique K la valeur de $4{,}28 \cdot 10^8$ pour CH et $5{,}42 \cdot 10^8$ pour DMF. La masse moléculaire moyenne gravimétrique a été obtenue par extrapolation des données représentées dans un diagramme Zimm, le rayon de giration du polymère dissous a été calculé à l'aide de la pente de la droite $c = 0$, et le deuxième coefficient du viriel à l'aide de la pente de la droite $\theta = 0°$.

---

[16] J. P. Benevisse, Thèse, Université de Lyon, 1960.

[17] G. Pezzin., G. Talamini et G. Vidotto, *Makromol. Chem.*, **43**, 12 (1961).

[18] L. Utracki, *J. Polymer Sci.*, *A*, **1**, 717 (1966).

RÉSULTATS ET DISCUSSIONS

Les mesures de l'intensité de la diffusion à différents intervalles de temps depuis la préparation de la solution de PVC ont montré que la solubilité complète, caractérisée par une constance de la valeur $\overline{M}_w$, se réalise seulement après quatre jours si la solution n'est pas chauffée. Cette solubilisation peut être assurée aussi par le chauffage de la solution à 80° pendant 30 minutes lorsqu'on obtient des résultats reproductibles (on a utilisé ce chauffage aussi, avant d'effectuer les mesures viscosimétriques).

On a également constaté que la filtration de la solution de départ par un filtre G5 et la dilution ultérieure avec du solvant filtré conduit à des graphiques Zimm distorsionnés qui rendent difficile l'extrapolation (fig. 1) et seulement la filtration de chaque solution à part directement dans la cuve conduit à des résultats satisfaisants (fig. 2).

Les solutions de PVC en cyclohexanone sont très stables présentant la même diffusion 30 jours après la filtration. Au contraire, les solutions de PVC en DMF sont instables, présentent une tendance à la séparation des phases, et la valeur plus grande de $\overline{M}_w$ indique une association des particules de polymère (tableau 1).

Tableau 1

Influence du solvant sur la valeur de la masse moléculaire, sur le second coefficient du viriel et sur le rayon de giration pour le PVC (Geon)

Solvant	$\overline{M}_w$	A_2	R_G(Å)
CH	150 000	$1{,}44 \cdot 10^{-3}$	210
DMF	890 000	$2{,}19 \cdot 10^{-4}$	350

Dans le tableau 2 on présente les résultats obtenus par les mesures de la viscosité et de la diffusion de la lumière pour les fractions d'une PVC-suspension (Geon), d'où on observe une inversion entre les fractions 2 et 3. Ce phénomène d'inversion a pu être observé pour la majorité des polymères de PVC fractionnés, indiféremment de la méthode de fractionnement utilisée.

Tableau 2

Viscosité intrinsèque et masse moléculaire moyenne gravimétrique pour les fractions obtenues dans le PVC (Geon)

Echantillon Grandeur	Fr.1	Fr.2	Fr.3	Fr. 4	Fr. 5	Fr. 6	Fr. 7	Fr.8 (reste)
$[\eta]$, (ml/g)	49,5	63,0	55,0	93,0	108,0	119,0	138,5	119,0
$M_w \cdot 10^{-3}$	49	67	63	108	117	152	173	143

Les valeurs différentes du deuxième coefficient viriel ($A_2 = 1.91\ 10^{-3}$ pour la deuxième fraction et $0{,}75\ 10^{-3}$ pour la troisième) suggèrent une différence en cristallinité ; pourtant les mesures en infrarouge, effectuées à un spectrophotomètre Perkin-Elmer 337, en comparaison de l'intensité d'absorption[19] à 690 cm^{-1} et 635 cm^{-1} ne sont pas suffisamment concluantes en ce sens.

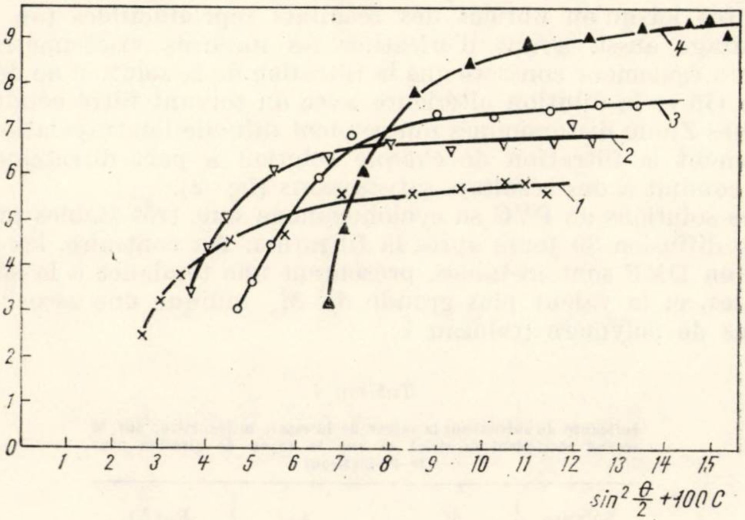

Fig. 1. — Graphique Zimm pour la PVC-suspension, obtenu après la filtration de la solution initiale, seulement.
1, $c = 2\ 10^{-3}$ g/ml ; 2, $c = 3\ 10^{-3}$ g/ml ; *3*, $c = 4\ 10^{-3}$ g/ml et *4*, $c = 6\ 10^{-3}$ g/ml

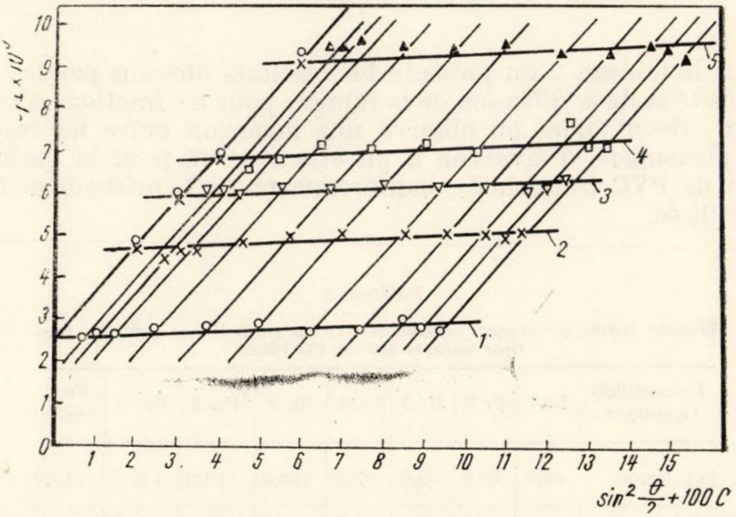

Fig. 2. — Graphique Zimm pour la PVC-suspension Geon obtenu après la filtration de chaque solution.
1, $c = 0$ g/ml ; *2*, $c = 2\ 10^{-3}$ g/ml ; *3*, $c = 3\ 10^{-3}$ g/ml ; *4*, $c = 4\ 10^{-3}$ g/ml ; *5*, $c = 6\ 10^{-3}$ g/ml.

---

[19] P. H. Burleigh, *J. Amer. Chem. Soc.*, **82**, 749 (1960).

Sur la base des données du tableau 2, on a pu déduire l'équation Mark-Houwing-Sakurada (M — H — S) suivante pour le polymère PVC-Geon étudié:

$$[\eta]^{25°\mathrm{C}}_{\mathrm{CH}} = 6{,}92\cdot 10^{-3}\,\overline{M}_w^{0{,}82}\ (\mathrm{ml/g}) \qquad (2)$$

qui est comparable aux équations données dans la littérature.[14, 15, 20, 21]

Compte tenu du grand nombre d'équations existant dans la littérature [22−29] il est assez difficile le choix d'une relation M—H—S ($[\eta]=kM^{\nu}$) pour l'évaluation de la masse moléculaire, au cas du PVC en CH à 25° ainsi qu'à d'autres températures. Vue que les relations de la littérature sont discutables, [25] on a choisi pour les calculs des relations par lesquelles on puisse faire la différence entre la PVC-suspension et la PVC-émulsion, de manière que l'exposant (ν) ait une valeur aussi proche que possible de la valeur théorique. [33] Compte tenu de ces considérations on a choisi les relations : — pour la PVC-suspension une équation [2] proche de l'équation obtenue par nous :

$$[\eta] = 12{,}3\cdot 10^{-5}\,\overline{M}_n\,0{,}82\ (100\ \mathrm{ml/g})$$

et pour la PVC-émulsion [25]

$$= 20{,}4\cdot 10^{-4}\,\overline{M}_n^{0{,}56}\,(100\mathrm{ml/g}) \qquad (3)$$

La concordance des valeurs K_θ obtenues par des mesures viscosimétriques et de diffusion de la lumière et le comportement évidemment différent des échantillons de PVC-suspension et de PVC-émulsion confirment le choix judicieux des relations.

Une première information sur le comportement thermodynamique des solutions de polymères s'obtient par l'évaluation de l'énergie d'activation de l'écoulement visqueux qui doit être indépendante de la masse moléculaire. Dans la figure 3 on a représenté graphiquement le log ($[\eta] \times \times 10$) en fonction de $1/T$ pour différentes fractions de PVC. Les pentes des droites sont approximativement constantes, la valeur moyenne de l'énergie d'activation étant de 1,035 kcal/mole.

---

[20] G. Pezzin, *J. Appl. Polymer Sci.*, **11**, 1539 (1967).

[21] M. Freeman et P. P. Manning, *J. Polymer Sci. A*, **2**, 2087 (1964).

[22] G. Pezzin, G. Sanmortin et F. Zilio Grandi, *J. Appl. Polymer Sci.*, **11**, 1539 (1967).

[23] G. Ciampa et H. Schwindt, *Makromol. Chem.*, **21**, 213 (1956).

[24] Z. Maneik, *Chem. listy*, **49**, 1598 (1955).

[25] G. Bier et H. Kramer, *Makromol. Chem.*, **18/19**, 154 (1956).

[26] H. Batzer et A. Nisch., *Makromol. Chem.*, **22**, 131 (1957).

[27] H. Staudinger et M. Hoberbe, *Makromol. Chem.*, **9**, 35 (1952).

[28] D. J. Mead et R. M. Fuoss, *J. Phys. Chem.*, **47**, 59 (1943).

[29] W. R. Moore et R. J. Hutchinson, *Nature*, **200**, 1095 (1963).

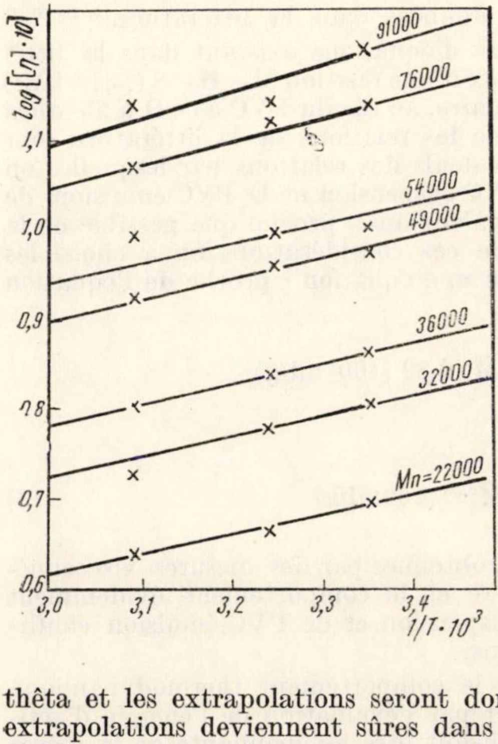

Fig. 3. – Variation de log $([\eta] \times 10)$ en fonction de la température pour les différentes fractions de PVC-suspension Shell.

Vu que la cyclohexanone est un bon solvant pour le PVC, on a utilisé pour l'évaluation des dimensions non perturbées les procédés d'extrapolation graphique de Bohdanecky-Cowie [4] et Stockmayer-Fixman [2] et pour comparaison on a effectué les représentations aussi d'après la méthode Flory-Fox-Schaefgen [1] qui est applicable seulement dans des conditions thêta et les extrapolations seront donc difficiles. Par cette méthode les extrapolations deviennent sûres dans les mauvais solvants comme l'orthodichlorobenzène. Les relations utilisées dans les représentations graphiques sont

Bohdanecky-Cowie [4]:

$$[\eta]/M^{1/2} = \Phi(\varepsilon)/\Phi(0) \times K_\theta + 0{,}9166\, \Phi(\varepsilon)/\Phi(0)\, K_\theta \times k^{7/20} M^{7/20} \quad (4)$$

Stockmayer-Fixman

$$[\eta]/M^{1/2} = K_\theta + 0{,}51\, \Phi_0\, B M^{1/2} \quad (5)$$

Flory-Fox-Schlaefgen [1]

$$[\eta]^{2/3}/M^{1/3} = K_\theta^{2/3} + 2C_M\,(1/2 - \chi_1)\, K_\theta^{5/3}\, M/[\eta] \quad (6)$$

où

$$K_\theta = \Phi_0\, [(\overline{R_0^2})/M]^{3/2} \quad (7)$$

Φ_0 étant la constante viscosimétrique universelle identique pour tous les polymères égale à 2,89. 10^{21}, et $[\overline{R}_0^2]$, la distance moyenne quadratique entre les bouts de chaîne en l'absence d'interaction (chaîne non perturbée)

$$\Phi(\varepsilon) = \Phi_0 (1 - 2{,}63\varepsilon + 2{,}86\varepsilon^2) \tag{8}$$

$$\varepsilon = (2\nu - 1)/3 \tag{9}$$

$$k = 0{,}33B(M/[\overline{R}_0^2])^{3/2} \tag{10}$$

$$B = v_2^2 (1 - 2\chi_1)/v_1 N_A \tag{11}$$

$$C_M = 3{,}3086 \cdot 10^{-3} v_2^2/v_1 \tag{12}$$

et

$$2C_M (1/2 - \chi_1) = C_T \tag{13}$$

v_2 le volume spécifique partiel du soluté, v_1 le volume molaire du solvant ; N_A, le nombre d'Avogadro ; χ_1 le paramètre d'interaction Flory. En portant sur un graphique $[\eta]/M^{1/2}$ (les relations 4 et 5) ou $[\eta]^{2/3}/M^{1/3}$ (la relation 6) en fonction de $M^{7/20}$; $M^{1/2}$ et respectivement $M/[\eta]$ nous avons obtenu dans les figures 4 *a*, *b*, et *c* des droites dont on peut obtenir simultanément les dimensions non perturbées de la chaîne, $[R^2{}_0]$, ainsi que le paramètre d'interaction Flory χ_1 qui nous ont permis d'estimer les fonctions thermodynamiques de la dilution.

Pour les représentations graphiques dans les figures 4 *a* et *b* on a utilisé aussi bien les masses moléculaires $\overline{M}_n$ évaluées à l'aide des relations (3) que les masses moléculaires $\overline{M}_w$ obtenues par la diffusion de la lumière, pour les échantillons de PVC-suspension et respectivement pour les PVC-émulsions. La différence entre les échantillons polymérisés en émulsions et ceux polymérisés en suspension est clairement représentée par le changement des pentes des droites, ce qui nous a permis de conclure que la solubilité, respectivement leur comportement thermodynamique est différent comme on pourra voir par la suite.

Les résultats obtenus par ces représentations graphiques comme le facteur de symétrie sont rassemblés dans le tableau 3. La figure 5 repré-

Tableau 3

Dimensions non perturbées des molécules de PVC obtenues par les données viscométriques à l'aide de différents procédés graphiques, à différentes températures.

Procédé Graphique	T (°C)	$K_\theta \cdot 10^3$	$([\overline{R}^2]_0/\overline{M})^{1/2} \cdot 10^{11}$ (cm)	σ
Flory	25	1,091	724,3	1,816
	35	0,9259	685,4	1,761
	50	0,7753	646,3	1,660
Bohdanecky-Cowie	25	1,2144	750,7	1,928
	35	1,0897	721,7	1,854
	50	0,9306	686,8	1,764
Stockmayer-Fixman	25	1,362	779,7	2,003
	35	1,243	756,54	1,943
	50	1,042	713,35	1,832

sente la variation de la constante K_θ en fonction de la température. Cette variation est la même indépendamment du procédé graphique utilisé pour l'obtention du K_θ.

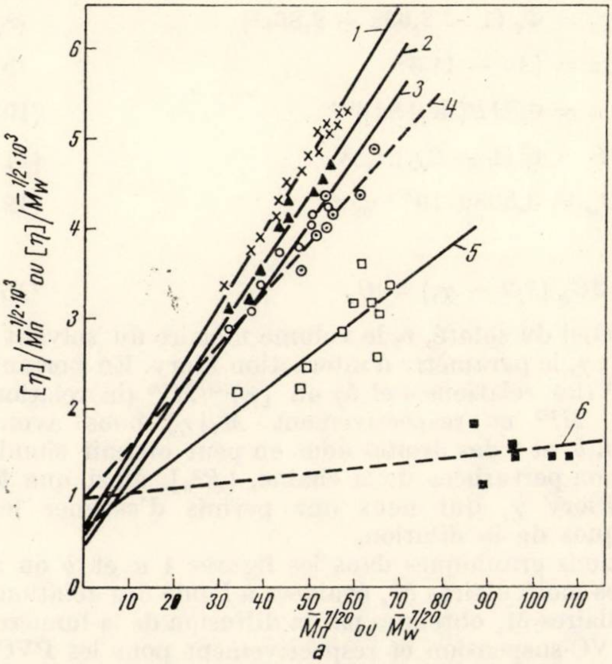

Fig. 4. — Représentations graphiques après :

a. Bohdanecky-Cowie. *1*, 2, et *3*, PVC-suspension à 25°, 35° et 50° respectivement ; *4*, PVC-émulsion à 25° ; *5*, et *6* dans les représentations on a utilisé la valeur M_w obtenue par la diffusion de la lumière. *b*. Stockmayer-Fixman : 1, *2*, et *3*, PVC-suspension à 25°, 35° et 50° respectivement ; *4*, PVC-émulsion à 25° ; *5*, et *6*, dans les représentations on a utilisé la valeur $\overline{M}_w$ obtenu par la diffusion de la lumière. c Fox-Flory-Schlaefgen, *1*, *2*, et *3* PVC-suspension en CH à 25°, 35° et 50° et *4*, *5*, et *6*, PVC-suspension en ODB à 50° 35° et 25° respectivement.

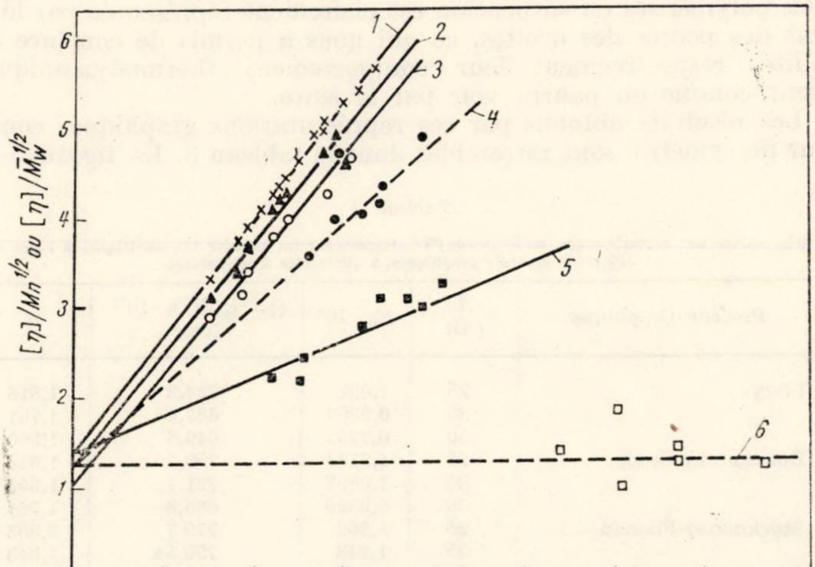

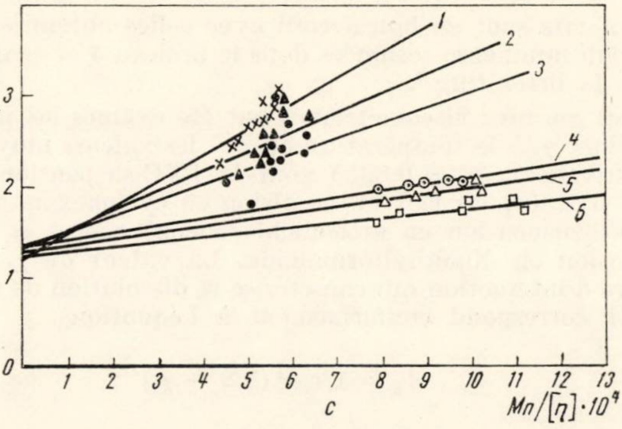

Tableau 4

Dépendance du rayon de giration de la masse moléculaire pour le PVC- Geon

Echantillon	$R_G/M_w^{0,5}$	$R_G/M_w^{0,6}$	$R_G/M_w\cdot 10^3$
Fract. 1	058	0,20	2,67
Fract. 2	1,03	0,34	4,01
Fract. 3	0,89	0,34	3,55
Fract. 4	0,65	0,20	2,00
Fract. 5	0,70	0,21	2,42
Fract. 6	0,54	0,17	1,40
Fract. 7	0,53	0,16	1,27
Fract. 8 (reste)	0,72	0,22	1,91

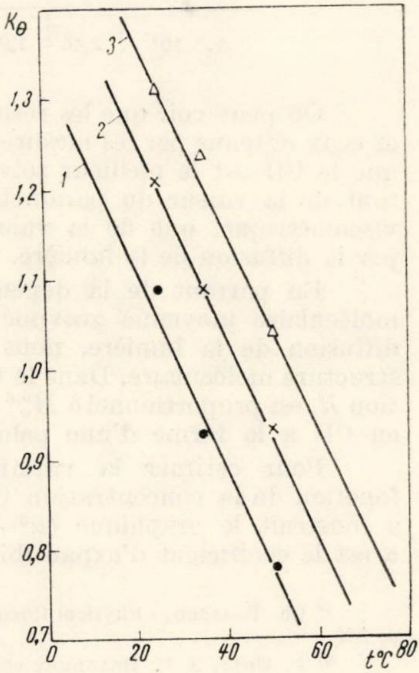

Fig. 5. — Variation de K_θ en fonction de la température

1. Flory-Fox ; 2. Bohdanecky-Cowie ; 3. Stockmayer-Fixman

Les valeurs sont en bon accord avec celles obtenues par la mesure de la diffusion lumineuse résumées dans le tableau 4 et également avec les données de la littérature[7].

Par les mesures viscométriques ont été évalués les paramètres d'interaction Flory χ_1 à la température de 25°, les valeurs moyennes obtenues étant les suivantes : $\chi_1 = 0,3255$ pour la PVC-suspension en cyclohexanone ; $\chi_1 = 0,3750$ pour la PVC-émulsion en cyclohexanone ; $\chi_1 = 0,4449$ pour la PVC-suspension en orthodichlorobenzène et $\chi_1 = 0,4662$ pour la PVC-suspension en diméthylformamide. La valeur de $\chi_1 = 0,3255$ pour le paramètre d'interaction qui caractérise la dissolution de la PVC-suspension en CH correspond conformément à l'équation

$$A_2 = 1/v_1 d^2 \, (1/2 - \chi_1) \tag{14}$$

(où v_1 est le volume molaire du solvant et d, la densité du polymère) à une valeur moyenne de $0,83 \cdot 10^{-3}$ pour le deuxième coefficient du viriel (A_2). La même valeur pour A_2 (second coefficient du viriel) on a obtenu par les mesures de la diffusion de la lumière. Ces valeurs sont présentées sur le tableau 5.

Tableau 5

Valeurs des seconds coefficients du viriel pour les fractions de PVC(Geon) en CH

Echantillon	Fr. 1	Fr. 2	Fr. 3	Fr.4	Fr .5	Fr. 6	Fr. 7	Fr. 8 (reste)
$A_2 \times 10^3$	2,46	1,91	0,75	1,36	0,956	0,734	1,244	1,14

On peut voir que les résultats obtenus par la diffusion de la lumière et ceux obtenus par les mesures viscométriques concordent, ce qui indique que le CH est le meilleur solvant pour le PVC. Cette conclusion résulte tant de la valeur du paramètre d'interaction Flory χ_1 obtenu par voie viscométrique, que de la valeur du second coefficient du viriel obtenu par la diffusion de la lumière.

En partant de la dépendance du rayon de giration de la masse moléculaire moyenne gravimétrique $\overline{M}_w$ obtenue par la mesure de la diffusion de la lumière, nous avons obtenu des renseignements sur la structure moléculaire. Dans le tableau 4 on remarque que le rayon de giration R_G est proportionnel à $M_w^{0,6}$; ce résultat indique que la molécule de PVC en CH a la forme d'une pelote désordonnée.[30-32]

Pour estimer la variation des fonctions thermodynamiques en fonction de la concentration pour les différents échantillons de PVC on a construit le graphique $(\alpha^3-\alpha^5)/M^{1/2} \cdot K_{\theta T}/K_{\theta T_0}$, en fonction de $1/T$ où α est le coefficient d'expansibilité du volume hydrodynamique et $K_{\theta T}$ et

---

[30] Ch. Tanford, « Physical Chemistry of Macromolecules », J. Wiley, New York, 1961, p. 309.

[31] P. Doty, J. H. Bradbury et A. M. Holtzer, *J. Amer. Chem. Soc.*, **78**, 947 (1956).

[32] P. Outer, C. I. Carr et B. H. Zimm, *J. Chem. Phys.*, **18**, 830 (1950).

$K_{\theta T_0}$ les constantes K_θ à une certaine température T et à une température de référence T_0 (298°K par exemple). A l'aide des données de la figure 6 qui représente un tel graphique on peut calculer la température thêta et le paramètre entropique ψ_1 respectivement par l'interception de l'abscisse à l'origine, la grandeur de $1/\theta$ et par la pente de la droite égale à $2\psi_1 C_M \theta$. Les droites 7 et 8 ont été obtenues en utilisant la pente du graphique Flory (la relation 13) ; sur l'ordonnée on représente $C_T K_{\theta T}/K_{\theta T_0}$ et l'abscisse reste la même ($1/T$). La température θ est de 153°K pour les échantillons de la PVC-suspension et de 174°K pour la PVC-émulsion. Il faut remarquer qu'il n'est pas possible d'obtenir un accord entre ces valeurs et celles qui sont évaluées dans les relations Krevelen-Hoftyzer [33] qui relient la température θ avec les paramètres de solubilité des composants du système. Ce désaccord se trouve aussi entre les valeurs calculées à l'aide des relations mentionnées et les valeurs obtenues par les mesures viscométriques ou par les mesures turbidimétriques pour le polystyrène, [5] la différence étant plus grande lorsque le rapport $(\delta_s - \delta_{\min})/(\delta_{\max} - \delta_{\min})$ s'approche de la valeur 0,33 qui résulte dans la condition $\delta_s = \delta_p$ où δ sont les paramètres de la solubilité pour le solvant et respectivement pour le polymère. Avec ces valeurs (θ et ψ_1) on peut ensuite calculer l'entropie, l'enthalpie et l'énergie Gibbs de dilution utilisant les relations bien connues. [4-6]

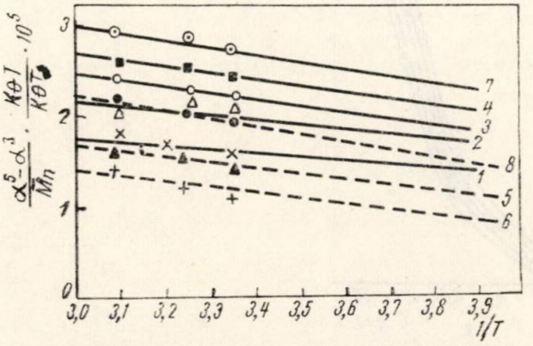

Fig. 6. — Représentation graphique pour l'évaluation de la température θ et du paramètre entropique ψ_1 pour la PVC-suspension avec $\overline{M}_n =$: *1*,22000 ; *2*, 32000 et 36000 ; *3*, 51000 et 54000 ; *4*. 72000 et pour la PVC-émulsion avec $\overline{M}n =$: *5*, 76000 et *6*, 64000 ; *7*, et *8*, graphique général pour la PVC-suspension et la PVC-émulsion respectivement.

La modification de ces grandeurs avec la concentration est représentée dans les figures 7*a*, *b* et *c* d'où on peut tirer des conclusions concernant la variation du comportement à la dissolution des échantillons de PVC en fonction des masses moléculaires et des provenances. On peut constater que si la masse moléculaire s'élève l'enthalpie s'accroît, l'entropie diminue et l'énergie Gibbs s'élève aussi vers des valeurs positives. Le comporte-

---

[33] D. W. van Krevelen et P. J. Hoftyzer, *J. Appl. Polymer. Sci.*, **11**, 1409,2189 (1967).

Fig. 7. — Variation des fonctions thermodynamiques avec la concentration : a) ΔH_1-enthalpie ; b) ΔS_1-entropie et c) ΔF_1-énergie Gibbs pour les échantillons de PVC-suspension avec $\overline{M}n$ = : *1*, 22000 ; *2*) 36000 ; *3*, 54000 ; *4*, 72000 et pour PVC-émulsion ; *5*, $\overline{M}n$ = 76000 ; *6*, 64000.

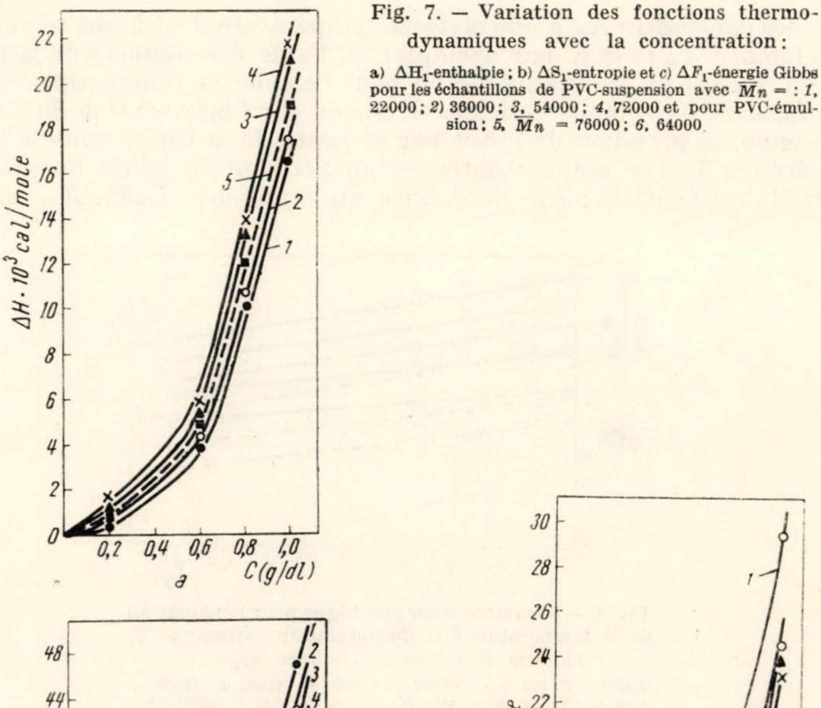

ment différent est le mieux exprimé par la variation de l'énergie Gibbs de dilution où la distinction entre les courbes caractéristiques pour chaque fraction est nette aussi bien en ce qui concerne la variation de celles-ci avec la masse moléculaire que la provenance de l'échantillon ; les échantillons de PVC-émulsion ayant les valeurs négatives plus petites de l'énergie Gibbs seront les moins solubles.

Revue Roumaine de Chimie, **15**, 1947–1951 (1970)

DECOMPOSITION OF HYDROPEROXIDES ON ACTIVATED KAOLINS. II[1]

DECOMPOSITION OF CUMENE HYDROPEROXIDE ON ACTIVATED CHINESE KAOLIN, IN STATIC CONDITIONS

I. VODNÁR
Babeş-Bolyai University, Department of Chemical Technology,
str. Arany János, 11, Cluj, Romania

Received March 7, 1970

The paper presents experimental results, obtained by the decomposition of cumene hydroperoxide into phenol and acetone by acidic catalysis, in static conditions. Activated Chinese kaolin has been used as catalyst ; its chemical and mineralogical composition was described in the first paper of this series. [1] The kaolin was activated with hydrochloric acid, [2] dried and treated with sulphuric acid. The catalyst prepared as above proved to be very efficient. Maximum conversions (97–99%) of cumene hydroperoxide into phenol can obtained when proceeding at low temperatures with dilute solutions of hydroperoxide. [3, 4]

The present paper is concerned with the catalytic decomposition of cumene hydroperoxide in cumene, by using activated Chinese kaolin as a catalyst. The reaction products are phenol and acetone. This is one of the most promising methods for producing these substances, but it also has some shortcomings which are described in the first paper of this series [1].

That is why the author tried to work out more economic methods for obtaining phenol and acetone.

Experimental

In this work there are presented the results obtained in the decomposition of cumene hydroperoxide on activated [2] Chinese kaolin, dried and treated with sulphuric acid. Kaolinite content of kaolin was approximately 97%. The granulation and chemical characteristics of the kaolin were described in the first paper of this series. [1]

---

[1] I. Vodnár, *Rev. Roumaine Chim.*, **14**, 803 (1969).

[2] B.A. Kopylev, D. G. Traber, M. M. Sychev and V. A. Grigor, "Rukovodstvo k prakticheskim zaniatiam po obshchei khimicheskoi technologhii", Goskimizdat, Moscow, 1953, p. 44.

[3] I. Vodnár, *Romanian Patent*, 49 843, 1967.

[4] I. Vodnár, *Romanian Patent*, 56 309, 1968.

Experiments have been carried out in static conditions, using 1 g of catalyst and 20 ml cumene solution of cumene hydroperoxide, concentration : 2,05 moles/l. The reaction mixture was stirred vigorously. The temperature was maintained constant by means of a Wobser U_8 ultrathermostat. Tests for dosing hydroperoxide[5] and phenol[6] are taken from the reaction mixture, periodically.

RESULTS AND DISCUSSION

Decomposition of cumene hydroperoxide has been studied in static conditions, in accordance with different parameters (temperature, concentration of hydroperoxide, quantity of catalyst, acid content of catalyst and activity of catalyst depending on the number of decomposition). Kinetic curves are designed on 7 values of temperature, between 30 and 90°.

Experimental results are illustrated in figures 1, 2, 3, 4, 5, 6 and 7.

Figure 1 shows the decomposition curves of cumene hydroperoxide in accordance with reaction time at different temperatures.

The curves show that cumene hydroperoxide decomposes with a great reaction rate ; at 90° cumene hydroperoxide is totally decomposed even during a reaction time of only 8 minutes (initial decomposition rate : 2.92 moles. l^{-1}. min^{-1}). It should be mentioned that the decomposition rate is great enough even at 30° (0.146 moles . l^{-1} . min^{-1}). Consequently, the catalyst used ensures opportune conditions in obtaining phenol and acetone.

In the following series of experiments the temperature was 50°, working with different quantities of catalyst (0.5 ; 1 and 2 g). Results are illustrated in figure 2.

We can state that initial rate of the reaction, increases from 0.227 moles/l . min to 1.36 moles/l . min if we use 0.5 g and respectively 2 g of catalyst.

The dependence between decomposition rate of cumene hydroperoxide and initial concentration of sample, is illustrated by the curves of figure 3. Samples of cumene hydroperoxide were used with the following initial concentrations : 1.4 ; 2.05 and 2.68 moles/1. The temperature was maintained constant at 50°.

The curves in figure 3 show that the decomposition rate of hydroperoxide depends on the initial concentration of samples which is characteristic of the first-order reactions.

In the following series of experiments, we studied the influence of sulphuric acid content of the catalyst, an important parameter of the decomposition process of hydroperoxide. The results obtained at 45° are illustrated in figure 4.

---

[5] H. Raley, F. Rust and W. Vaughan, *J. Amer. Chem. Soc.*, **70**, 1336 (1948).

[6] V. Ozhiganova and A. Martinenko, *Koks i Khimia*, **2**, 41 (1962).

Figure 4 shows that the stronger is the acidity of the catalyst, the greater is the rate of decomposition. Namely, if the sulphuric acid content of the catalyst is 0.63 %, the initial decomposition rate becomes 0.09 moles /l . min, and by a content of 2.89 % sulphuric acid, it raises to 0.854 moles /l . min.

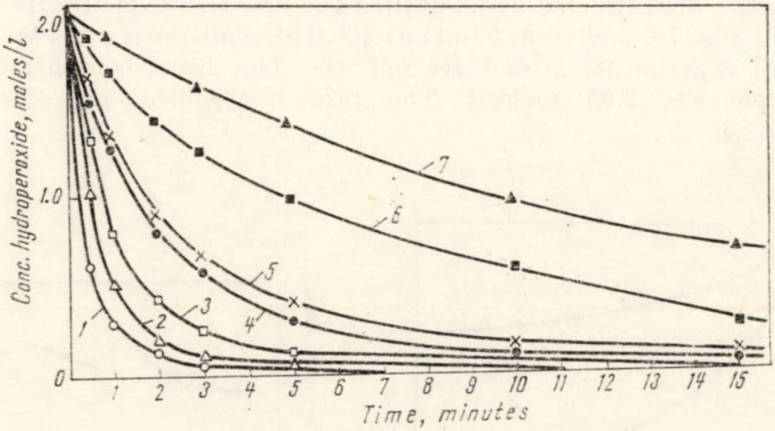

Fig. 1. — Relation between the content of the sample in cumene hydroperoxide and the decomposition time, at different temperatures :

1, 90° ; *2*, 80° ; *3*, 70° ; *4*, 60° ; *5*, 50° ; *6*, 40° ; *7*, 30°.

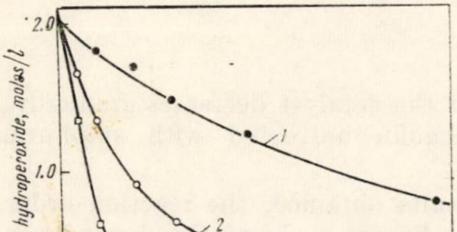

Fig. 2. — Relation between cumene hydroperoxide content of the sample and the decomposition time, using variable quantities of catalyst :

1, 0,5 g cat. ; *2*, 1 g cat. ; *3*, 2 g cat.

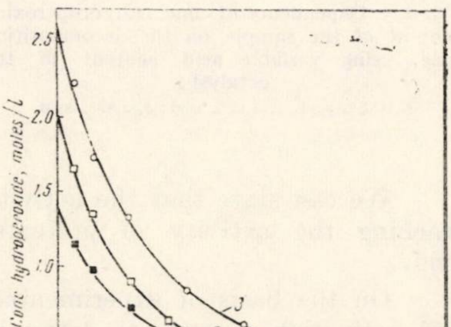

Fig. 3. — Dependence of cumene hydroperoxide content of the sample on the decomposition time, working at different initial concentration of cumene hydroperoxide :

1, 1,4 moles/l ; *2*, 2,05 moles/l ; *3*, 2,68 moles/l.

As a result of experiments we can state that when the sulphuric acid content of the catalyst exceeds 5%, the condensation of phenol with acetone occurs, yielding resinous substances.

The last parameter studied was the activity of the catalyst related to the number of the decomposition, using the same sample of catalyst. Experiments were effected as following : the first five experiments at 50°, from 6 to 8 at 70° and from 9 to 11 at 80°. The comparative test was taken out in all experiments after three minutes. The initial concentration of the sample was 2.05 moles/l. The results obtained are illustrated in figure 5.

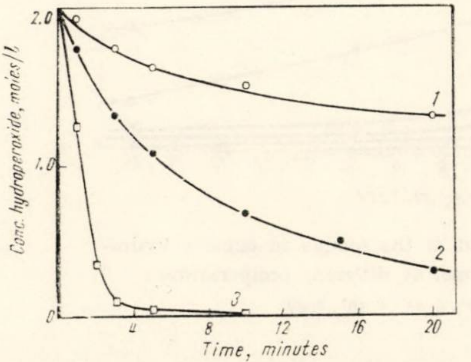

Fig. 4. — Dependence of cumene hydroperoxide content of the sample on the decomposition time, using variable acid content of the catalyst :

1, 0,63% acid ; *2*, 1,32% acid ; *3*, 2,89% acid.

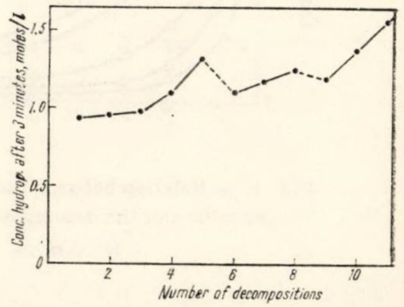

Fig. 5. — Dependence of the activity of catalyst on the number of decomposition.

We can state that the activity of the catalyst decreases gradually, reaching the activity of activated kaolin untreated with sulphuric acid.

On the basis of experimental results obtained, the reaction order and activation energy are determined. Figure 6 shows the dependence of lg $a/a\text{-}x$ on the reaction time.

Owing to their position, the points from figure 6 are sufficient to characterize the representative straight lines. This shows that the decomposition of cumene hydroperoxide on activated kaolins, acidulated with sulphuric acid is a first-order reaction. The same results should be obtained by using the half-life method (presenting the logarithm of half-life values function of initial concentration of the different samples).

The apparent activation energy of the decomposition process, as deduced from pairs of lg k and $1/T$ values, corresponding to the three chosen temperatures (see figure 7) becomes 14.5 kcal/mol.

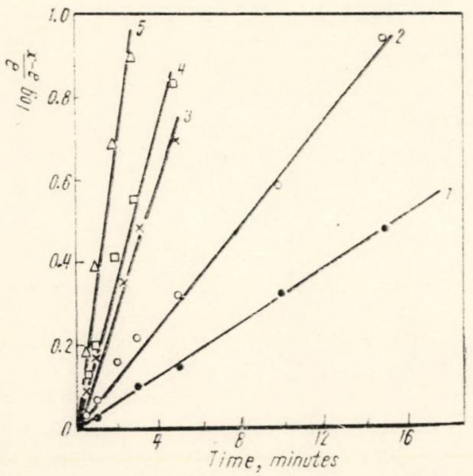

Fig. 6. — Dependence of lg a/a-x on decomposition time, at different temperatures : 1, 30°; 2, 40°; 3, 50°; 4, 60°; 5, 70°

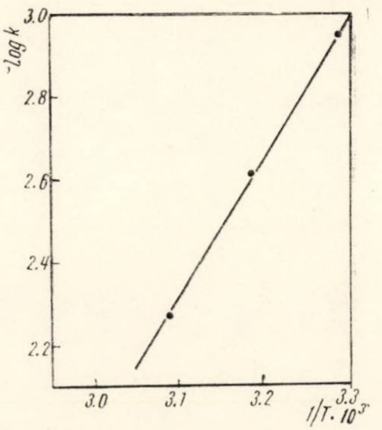

Fig. 7. — Dependence of lg k on $1/T$.

CONCLUSIONS

Acidic decomposition of cumene hydroperoxide in static conditions has been studied in order to obtain phenol that has an ever increasing industrial importance. At the same time, the kinetics of the reaction was cleared. We can draw the following conclusions :

— activated Chinese kaolin treated with sulphuric acid used as a catalyst, has proved to be perfectly fit to decomposition of cumene hydroperoxide ;

— maximum conversion of cumene hydroperoxide into phenol can be obtained if we work at low temperatures (30—60°) and the concentration of hydroperoxide does not exceed 20% ;

— decomposition of cumene hydroperoxide on used catalyst is a reaction of first-order and has an activation energy of 14.5 kcal/mol.

Revue Roumaine de Chimie, **15**, 1953–1965 (1970)

RECHERCHES DANS LA CLASSE DES *p*-FLUOR-DIPHÉNYLSULFONES. I

SYNTHÈSES DE NOUVEAUX COMPOSÉS À EFFICIENCE ANTIBACTÉRIENNE *

AL. MAVRODIN, CĂTĂLINA DEMETRESCU, C. CHIRIȚĂ
et OLGUȚA MACOVSCHI
Laboratoire de Chimie organique, Faculté de Pharmacie
de Bucarest, 19 – 21, str. Alex. Sahia

Reçu le 22 mai 1970

S'appuyant sur les considérations relatives à la structure électronique interne de l'atome de fluor, les auteurs synthétisent 12 nouveaux composés de la classe des *p*-fluor-diphénylsulfones, qui pourraient jouer le rôle d'antimétabolites à efficience thérapeutique. La formule de structure, proposée pour ces composés a été confirmée par dégradation, ainsi que par analyse chimique (N et S) et par études spectrales en IR. Les données pharmacodynamiques laissent envisager la possibilité d'utiliser certains composés en tant que substances antibactériennes, sélectives et efficientes.

Dans des recherches récentes, [1-3] nous avons essayé à établir une corrélation entre la structure électronique et l'effet mitodépressif, chez les composés dérivés de la diphénylsulfone, qui interviennent au niveau des systèmes enzymatiques, intéressés dans la division cellulaire. Les données concernant l'action antimitotique sur la cellule végétale en division, [4] ainsi que les résultats obtenus dans le traitement du cancer expérimental, [5-7] nous ont permis d'aboutir à la conclusion que les molécules vinylogues avec deux ou trois centres d'activité biologique — dont au moins un est représenté par le groupe diphénylsulfone : $-C_6H_4-SO_2-C_6H_4$ — possèdent une action antitumorale *in vitro* et *in vivo*. L'intensité de l'effet dépend en grande mesure de la densité électronique au niveau de ces centres. [1,2]

---

* Travail communiqué à la Session Scientifique Jubilaire de l'Institut de Médecine et de Pharmacie de Bucarest, 2–3 juillet 1969, à l'occasion du 25e anniversaire de la libération de la Roumanie.

[1] AL. MAVRODIN, C. DEMETRESCU, C. CHIRIȚĂ et V. ION, *Chim. Thérap.*, **2**, 125 (1968).

[2] C. DEMETRESCU, C. CHIRIȚĂ et R. DASCĂLU, *Chim. Thérap.*, **5**, 343 (1968).

[3] C. CHIRIȚĂ, C. DEMETRESCU, I. NICOARĂ, AL. MAVRODIN, *Pharmazie*, **23**, 360 (1968).

[4] AL. MAVRODIN, V. ZOTTA, C. DEMETRESCU, D. OȚELEANU, C. CHIRIȚĂ, A. MORAIT et E. LEHENE, *Pharmazie*, **19**, 448 (1964).

[5] A. TEITEL, C. DEMETRESCU, E. GÖRK, C. CHIRIȚĂ, P. GHEORGHIU et AL. MAVRODIN, *Acta biol. et med. germ.*, **15**, 329 (1965).

[6] C. DEMETRESCU, P. GHEORGHIU, E. GÖRK, C. CHIRIȚĂ, Al. MAVRODIN et A. TEITEL, *Pharmazie*, **10**, 634 (1965).

[7] A. TEITEL, C. CHIRIȚĂ, C. DEMETRESCU, E. GÖRK et AL. MAVRODIN, *Thérapie* (*Paris*), **20**, 1431 (1965).

En modifiant avec une certaine régularité la distribution de la densité électronique dans les zones actives de la molécule, par lesquelles celle-ci se rattache aux biorécepteurs enzymatiques cellulaires, nous pourrions influencer la corrélation entre la structure électronique et l'effet thérapeutique. Par conséquent, nous pourrions prévoir en lignes générales la structure des nouvelles molécules, à même d'intervenir par différents mécanismes compétitifs dans le métabolisme altéré de la cellule néoplasique.

Nos recherches antérieures sur la classe des diphénylsulfonyluréthannes *p*-X-substitués (où $X = -Cl$, $-Br$, $-OCH_3$, etc.) ont montré que l'effet antimitotique est en premier lieu influencé par la nature du substituant X, introduit en position *para* sur le noyau de la diphénylsulfone [1,3,8] et qu'il a une valeur optimum pour $X = -Cl$. Nous avons expliqué ce fait par l'effet de conjugaison électromère positif ($+E_s$), qui est plus fort pour l'halogène chlore que pour les autres substituants, introduits par nous sur la molécule.

Afin de vérifier exactement ces idées, nous avons élargi dans le présent travail notre domaine d'investigation, en utilisant comme substituant l'halogène fluor. Ce halogène, exerçant un effet électromère maximum, possède un volume atomique tellement petit, qu'il peut aisément substituer un atome d'hydrogène, sans que la structure de la molécule, sur laquelle il est attaché, soit perturbée.

De multiples recherches récentes, effectuées par Buu-Hoï et son école,[9] ainsi que par d'autres chimistes contemporains, [10-18] ont fait de la chimie des composés organofluorurés un point d'attraction particulièrement prometteur pour la chimiothérapie. Toutes les études dans ce domaine montrent que la présence de l'atome de fluor dans la molécule organique entraîne, presque sans exception, des effets thérapeutiques intenses et spécifiques, sans doute grâce à la configuration électronique de cet atome, c'est-à-dire à sa structure interne. Ainsi, parmi tous les halogènes, le fluor est le plus électronégatif, en vertu de son volume atomique minime, rapproché de celui de l'hydrogène et déterminé à l'aide de son rayon atomique, qui a été mesuré par des recherches cristallographiques. [19] Ceci explique pour-

---

[8] AL. MAVRODIN, C. DEMETRESCU, C. CHIRIŢĂ et O. MACOVSCHI, « Travaux du IIIe Congrès National des Pharmaciens », Bucarest, nov. 1968, p. 19.

[9] N. P. BUU-HOI, « Progress in Drug Research », tome 3, Ed. Birkhäuser, Basel — Stuttgart, 1961.

[10] V. P. MAMAEV, *Zhur. obschei Khim.*, **27**, 1290 (1951).

[11] R. DUSCHINSKY, E. PLEVEN et C. HEIDELBERGER, *J. Amer. Chem. Soc.*, **79**, 4559 (1957).

[12] A. GINER — SORELLA et A. BENDICH, *J. Amer. Chem. Soc.*, **80**, 5744 (1958).

[13] P. C. NOVELLO et J. M. SPRAGUE, *J. Amer. Chem. Soc.*, **79**, 2087 (1957).

[14] C. PELAYO, J. IRIARTE et H. RINGOLD, *J. Org. Chem.*, **25**, 1067 (1960).

[15] H. REIMANN, F. P. OLIVETO, R. NEVI, M. EISLER et P. PERLMAN, *J. Amer. Chem. Soc.*, **82**, 2308 (1960).

[16] J. A. EDWARDS, H. J. RINGOLD et C. DJERESSI, *J. Amer. Chem. Soc.*, **82**, 2318 (1960).

[17] S. BERNSTEIN et R. H. LENDARD, *J. Amer. Chem. Soc.*, **82**, 3680 (1960).

[18] A. L. YALE et F. SOWINSKY, *J. Amer. Chem. Soc.*, **82**, 2039 (1960).

[19] L. PAULING et M. L. HIGGINS, *Zeitschr. Kristalogr.*, **87**, 205 (1938).

quoi les composés organofluorurés accomplissent si facilement le rôle d'antimétabolites. Grâce à l'analogie de structure chimique entre l'hydrogène et le fluor, il existe une profonde similitude entre les composés organiques fluorurés et les métabolites de l'organisme, ces composés pouvant les substituer aisément, se fixant à leur place sur les biorécepteurs enzymatiques cellulaires, mais sans pouvoir exercer les fonctions spécifiques de ces métabolites. Les composés organiques qui contiennent d'autres halogènes comme substituants, à la place du fluor, interfèrent beaucoup plus difficilement dans cette compétition essentielle, à cause de leur grand volume atomique, qui rend la substitution difficile. D'autre part, n'ayant pas d'orbitales *d* disponibles, l'atome de fluor, contrairement aux atomes de chlore, brome ou d'iode,[20] ne peut étendre sa périphérie électronique de valence. Ces différences de structure électronique interne se traduisent sans doute aussi dans la spécificité des effets thérapeutiques des molécules fluorurées. En appliquant les données de la mécanique quantique à l'étude de la liaison C—F, on en a déduit la stabilité particulière de cette dernière, l'énergie nécessaire pour la rupture de cette liaison étant maximale dans la série des liaisons C—X et supérieure même à la liaison C—H. Toutes ces données, dues au volume atomique très petit du fluor, à son caractère intensément électronégatif et donc à la grande stabilité de la liaison C—F, expliquent pourquoi les composés fluorurés peuvent se fixer, par mécanisme compétitif, sur les enzymes et sur d'autres récepteurs biologiques cellulaires essentiels, actionnés par les métabolites de l'organisme.

En effet, par des recherches modernes, on a obtenu par synthèse de nombreux composés aromatiques fluorurés comme des amino-acides, les purines, des bases pyrimidiniques, des glucides ou des stéroïdes. On a synthétisé jusqu'à présent des classes entières de nouvelles substances à action antirhumatismale, antitumorale, antiinflammatoire, progestagène, anticonvulsivante, dépressive-centrale, relaxante musculaire, neuroleptique, analgétique, antihistaminique, antibactérienne, antivirale et hypoglycémiante. Tout ceci vient prouver qu'on a réussi à modifier favorablement, à l'aide du fluor, les propriétés de certains composés, qui ont acquis par fluoruration une action médicamenteuse.

Dans les recherches qui font l'objet de ce travail, nous avons tenu aussi compte de la constatation que l'halogénation peut influencer en général les propriétés physico-chimiques des composés organiques, avec augmentation de leur poids moléculaire, de leur point de fusion et de leur pouvoir narcotique. Mais en même temps, suite à l'halogénation, la stabilité des composés organiques diminue, fait qui entraîne certains effets toxiques, constatés surtout dans le cas des composés chlorurés ou bromurés. Or, cet inconvénient est éliminé par substitution du chlore et du brome, sans que les propriétés anesthésiques de la molécule soient conjointement supprimées.

Tout ce que nous venons d'exposer met en évidence l'intérêt thérapeutique tout particulier pour la synthèse de nouveaux composés (hydrazides, azides, amines, amides, esters carbamiques, etc.) dérivés de la diphénylsulfone, suivant le schéma général de réaction, indiqué ci-dessous :

---

[20] V. Baliah et M. Una, *Naturwiss.*, **45**, 512 (1958).

SCHÉMA 1

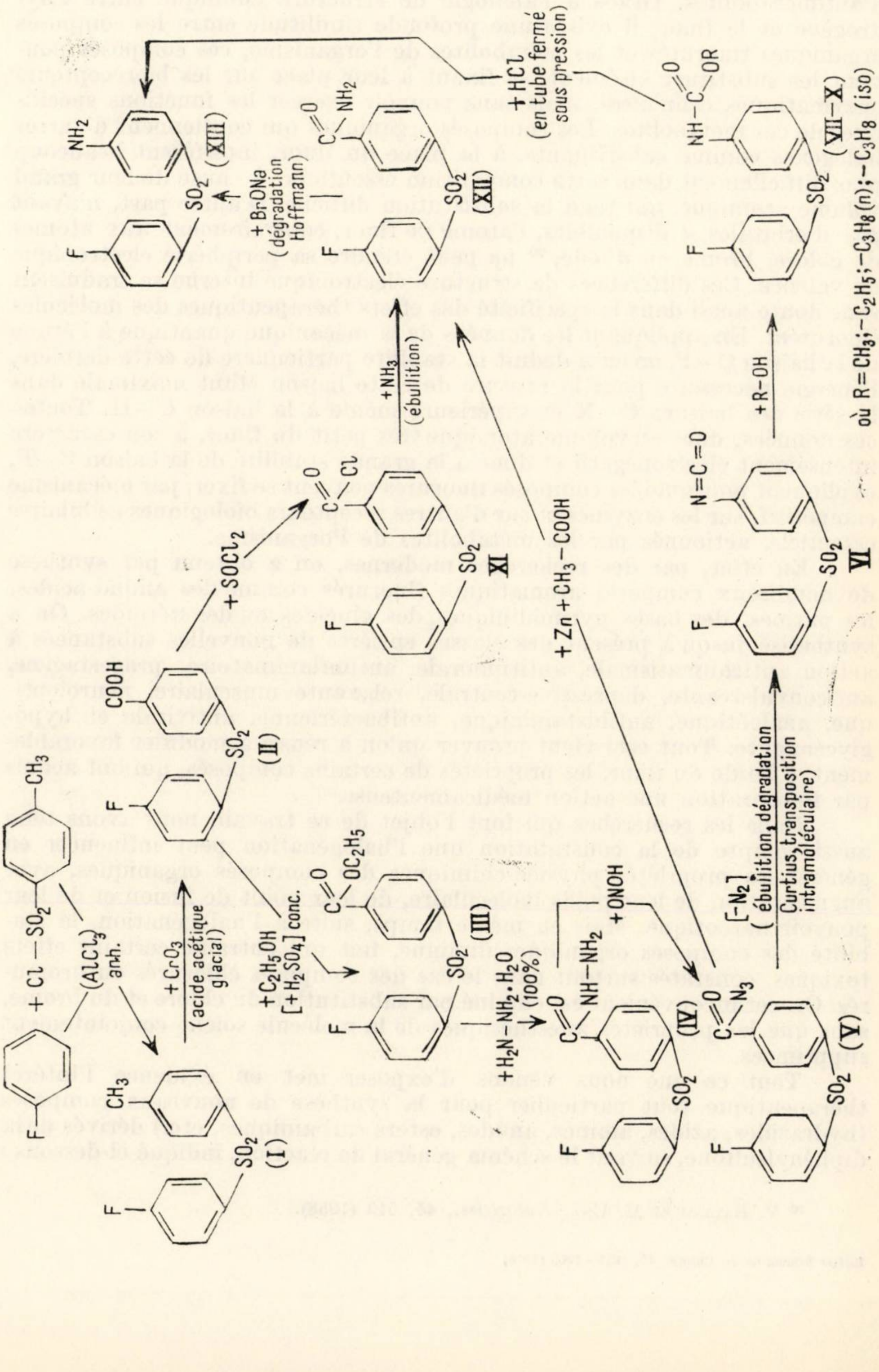
F
+ Cl SO2 — CH3
(AlCl3 anh.)
CH3
SO2
(I)
+ CrO3
acide acetique glacial)
COOH
SO2
(II)
+ C2H5OH
[+ H2SO4] conc.
C=O OC2H5
SO2 (III)
+ H2N·NH2·H2O
(100%)
C=O NH—NH2
SO2 (IV)
+ ONOH
C=O N3
SO2 (V)
(–N2↑)
(ébuition, dégradation
Curtius, transposition
intramoléculaire)
N=C=O
SO2
VI
+ R–OH
NH–C=O OR
SO2 (VII–X)
ou R = CH3; –C2H5; –C3H8 (n); –C3H8 (iso)
+ SOCl2
C=O Cl
SO2
XI
+ Zn + CH3 – COOH
+ NH3
(ébulition)
C=O NH2
SO2
(XII)
+ BrONa
dégradation
Hoffmann
NH2
SO2
(XIII)
+ HCl
(en tube fermé
sous pression)

Pour la synthèse, on part de la *p*-fluor-diphénylsulfone (I), qui a été soumise à la réaction d'oxydation avec du CrO_3 en milieu d'acide acétique glacial, aboutissant à l'acide *p*-F-diphénylsulfonyl-*p*'-carboxylique (II). Ce dernier a été estérifié avec de l'éthanol absolu, en milieu d'acide sulfurique concentré, conduisant à l'ester éthylique de l'acide *p*-F-diphénylsulfonyl-*p*'-carboxylique (III), qui a été transformé dans l'hydrazide correspondante (IV), par l'action de l'hydrate d'hydrazine à 100%, en milieu d'éthanol absolu. En présence de l'acide nitreux, l'hydrazide (IV) a conduit à l'azide (V), qui a été dégradée suivant Curtius, en milieu d'alcools aliphatiques inférieurs, avec la chaîne normale ou ramifiée. On a ainsi obtenu les esters carbamiques (VII—X), en passant par l'ester *p*-fluor-diphénylsulfonyl-*p*'-isocyanique (VI), obtenu par transposition intramoléculaire, au cours de la réaction de dégradation de Curtius de l'azide (V).

L'acide *p*-F-diphénylsulfonyl-*p*'-carboxylique a été ensuite refluxé avec un excès de chlorure de thionyle, jusqu'à dissolution complète, et transformé ainsi dans le chlorure de l'acide correspondant (XI). Celui-ci a été transformé dans l'amide correspondante (XII), par réchauffement à reflux, pendant 3 heures, avec de l'ammoniaque en excès.

C'est à la même amide (XII) que nous avons abouti aussi, par suite de la réduction de l'amide (V), par ébullition à reflux, avec du zinc poudre en acide acétique, pendant 14 heures.

L'amide (XII) a été dégradée par la méthode de Hoffmann avec de l'hypochlorite de sodium, conduisant à l'amine (XIII), qui a été synthétisée aussi par dégradation hydrolytique des uréthannes (VII—X), en présence de HCl concentré, par ébullition pendant 8 heures, dans un tube fermé, sous pression.

Nous avons synthétisé ainsi 12 nouveaux composés, dont la structure exacte a été établie par analyses élémentaires (microdosage de l'azote et semi-microdosage du soufre), ainsi que par des études spectrales en infrarouge.

ÉTUDE DE LA CONSTITUTION CHIMIQUE DES COMPOSÉS PAR ANALYSE SPECTRALE EN IR *

Pour la confirmation de la structure exacte, nous avons effectué les spectres d'absorption en IR, dans le domaine spectral compris entre 400 et 4000 cm^{-1}. Nous avons utilisé un spectromètre automatique à double faisceau, type UR_{10} et la technique du pastillage en bromure de potassium.

Dans le tableau 1, nous avons indiqué les attributions pour les bandes, correspondant aux principaux groupements caractéristiques, actifs en IR. De cette manière, l'étude spectrale a confirmé la formule structurelle, proposée par nous par voie chimique.

---

* Les spectres d'absorption en IR ont été exécutés en collaboration avec le Prof. Dr D. Bîrcă-Gălăţeanu et Dan Iordache, chef de travaux (Chaire de Physique de l'Institut Polytechnique de Bucarest), auxquels nous exprimons nos vifs remerciements.

Tableau

contenant les attributions pour les bandes

Nº crt.	Composé	C–F (1000–1400)	C_6H_5 –	
1	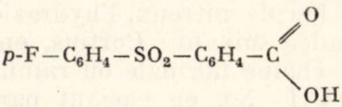 $p\text{-}F-C_6H_4-SO_2-C_6H_4-C(=O)OH$	1075 1095 1018 1405	ν_4 : (C–H)δ⊥pl. ν_{14} : (C–H)δ‖ pl. ν_{12} : (C–H) v. ν_{13} : (C–C) v.	690 1019 3095 1480
2	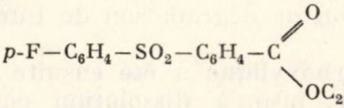 $p\text{-}F-C_6H_4-SO_2-C_6H_4-C(=O)OC_2H_5$	1075 1130 1240 1045	ν_4 : (C–H)δ⊥pl. ν_{14} : (C–H)δ‖ pl. ν_{12} : (C–H) v. ν_{13} : (C–C) v.	687 1020 3090 1480
3	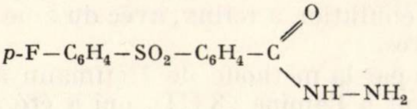 $p\text{-}F-C_6H_4-SO_2-C_6H_4-C(=O)NH-NH_2$	1090 1400	ν_4 : (C–H)δ⊥pl. ν_{14} : (C–H)δ‖ pl. ν_{12} : (C–H) v. ν_{13} : (C–C) v.	695 1020 3090 1485
4	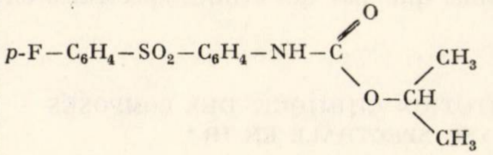 $p\text{-}F-C_6H_4-SO_2-C_6H_4-NH-C(=O)-O-CH(CH_3)_2$	1050 1095 1410	ν_4 : (C–H)δ⊥pl. ν_{14} : (C–H)δ‖ pl. ν_{12} : (C–H) v. ν_{13} : (C–C) v.	685 1018 3090 1480

ÉTUDE DE L'EFFET ANTIBACTÉRIEN DE CERTAINS COMPOSÉS

En collaboration avec le Dr Maria Mateescu, chercheur scientifique à la Chaire de Bactériologie (Directeur, le Prof. I. Mesrobeanu) de l'Institut « Dr I. Cantacuzino » de Bucarest, nous avons effectué le test de l'action antibactérienne sur quelques composés fluorurés, nouvellement synthétisés, en déterminant sur 12 souches bactériennes pathogènes, isolées des cas cliniques, l'effet inhibiteur de la croissance bactérienne.

On a utilisé la méthode diffusimétrique en agar, à l'aide de disques stériles sur du papier filtre, imprégnés extemporanément, à l'égard d'une

1

d'absorption des groupements actifs en IR (cm⁻¹)

SO_2	$-\mathrm{C}\genfrac{}{}{0pt}{}{/\!\!/\mathrm{O}}{\backslash\mathrm{OH}}$	$-\mathrm{C}\genfrac{}{}{0pt}{}{/\!\!/\mathrm{O}}{\backslash\mathrm{OC_2H_5}}$	$-\mathrm{C}\genfrac{}{}{0pt}{}{/\!\!/\mathrm{O}}{\backslash\mathrm{NH-NH_2}}$	$O=C-NH-$	$-CH_3$
déf. {500 {545 V_1 sym. 1168 V_2 asym. 1335	(C=O) : 1695 (C–O) : 1168	—	—		
déf. {520 {555 V_1 sym. 1160 V_2 asym. 1330	—	(–C=O) : 1740 $(-C_2H_5)$: {2805 {3105	—		
déf. {555 {580 V_1 sym. 1165 V_2 asym. 1325	—	—	(C=O) Am. I : {1670 {1640 (NH δ pl.) Am. II : 1535 δ(C–N) Am. III : 1295 δ(O=C–N) Am. IV 750 Am.V.. 705 NH v. 3320 (N–N) v. 1110		
déf. {545 {550 V_1 sym. 1165 V_2 asym. 1325	—			(C=O) Am. I {1775 {1770 (NH δ pl.) Am. III 1540 δ(C–N) Am. III {1270 {1280 δ(O=C–N) Am. IV 745 Am. V 710 NH v. 3360 (C–O) v. 1185	sym. : 1380 asym. : 1470 v : 2925

quantité de substance de 50 mg par disque (au niveau de la source de diffusion). Le diamètre des disques a été de 5 mm. On a utilisé des milieux nutritifs usuels, préparés suivant la formule de l'Institut « Dr. I. Cantacuzino », gelosés à 2 % et peptonnés à 1 %, à un pH = 7,2 — 7,4 (l'épaisseur de la couche du milieu, sur la plaque de Pétri, étant de 4 mm). On a utilisé comme inoculum des cultures en bouillon de 24 heures du germe isolé, dilué convenablement, afin d'obtenir sur la plaque-test la densité optimum de croissance.

Les plaques ont été inoculées par inondation.

Après l'application des disques, les plaques ont été incubées pendant 20 heures à 37°, la lecture des résultats étant indiquée par le diamètre des zones d'inhibition.

Les résultats obtenus, présentés dans le tableau 2, ci-dessous, ont mis en évidence une activité remarquable pour l'hydrazide de l'acide *p*-F-diphénylsulfonyl-*p'*-carboxylique, qui a manifesté un intense effet inhibiteur sur deux des trois souches de staphylocoque (doré et hémolytique) testées. Cette hydrazide a produit une zone d'inhibition appréciable, aussi bien sur la souche *Salmonella typhi murium*, agent des toxi-infections alimentaires, que sur le germe *Escherichia coli*, type sérologique O_{111} B_4 (souche pathogène, isolée d'un cas de syndrome toxicoseptique épidémique du nouveau-né) et sur la souche *Salmonella enteritidis* Gärtner, également isolée d'un cas de toxiinfection alimentaire. Enfin, l'action de ce nouveau composé s'est manifestée aussi sur la souche *Shigella Flexneri*, isolée d'une listériose humaine.

Tableau 2

Données sur l'effet inhibiteur de la croissance bactérienne, déterminé par la méthode diffusimétrique, à l'égard d'une dose-test de 50 mcg (diamètre du disque : ∅ = 5 mm), pour le composé (IV)

N° crt.	Espèce bactérienne	Souche	Diamètre de la surface d'inhibition ∅ (mm)
1	Staphylocoque (doré, hémolytique)	15 940	19
2	Staphylocoque (doré, hémolytique)	16 213	15
3	Staphylocoque (doré, hémolytique)	16 285	0
4	*Lysteria*	20 398	8
5	*Escherichia coli* (le type sérologique O_{111} B_4)	14 721	9
6	*Klebsiella*	7 356	0
7	Entérocoque	10 588	0
8	*Pseudomonas aeruginosa*	19 012	0
9	*Salmonella enteritidis* Gärtner	14 918	9
10	*Shigella Flexneri*	17 728	9
11	*Salmonella-typhi murium*	17 752	13
12	*Shigella Sonne*	14 993	0

Etant donné l'absence pratique de la toxicité des dérivés de la classe des diphénylsulfones, nous nous rendons compte de l'intérêt que présentent les nouveaux composés fluorurés synthétisés. Des investigations plus amples sont nécessaires à l'avenir, utilisant des doses-test encore plus élevées, ainsi que des quantités variables d'agent actif, au niveau de la source de diffusion.

En outre, d'amples recherches systématiques seront effectuées sur d'autres types d'effets pharmacodynamiques, l'activité cytostatique *in vivo* faisant l'objet d'études spéciales.

PARTIE EXPÉRIMENTALE

La *p*-fluor-*p*'-méthyl-diphénylsulfone (I) a été synthétisée par la réaction de Friedel-Crafts, en partant du *p*-toluènesulfochlorure et du fluor-benzène ; on a obtenu une substance, avec les mêmes constantes physiques que celles indiquées dans la littérature.[21]

L'acide p-*F-diphénylsulfonyl*-p'-*carboxylique* (*II*), Pf = 271°—2° (de l'acide acétique-glacial), a été obtenu avec un rendement de 69,2 %, par oxydation de la *p*-fluor-*p*'-méthyl-diphénylsulfone (I) avec CrO_3, en milieu d'acide acétique

$C_{13}H_9O_4FS$ *Calculé* : S 11,44 %

(M = 280,26) *Trouvé* : S 11,36 %

L'ester éthylique de l'acide p-*F-diphénylsulfonyl*-p'-*carboxylique* (*III*), Pf = 115° (de l'éthanol absolu), a été obtenu avec un rendement de 81,3 %, par ébullition, pendant 40 heures, de l'acide (III) avec de l'éthanol absolu et de l'acide sulfurique concentré

$C_{15}H_{13}O_4FS$ *Calculé* : S 10,40 %

(M = 308,32) *Trouvé* : S 10,36 %

L'hydrazide de l'acide p-*F-diphénylsulfonyl*-p'-*carboxylique* (*IV*), Pf = 223° (de l'éthanol), a été synthétisée par nous de l'ester (III), par traitement avec l'hydrate d'hydrazine à 100 %, en milieu d'éthanol absolu et ébullition à reflux, pendant 12 heures. Rend. = 89,1 %.

$C_{13}H_{11}O_3N_2FS$ *Calculé* : S 10,89 ; N 9,51 %

(M=294,30) *Trouvé* : S 10,77 ; N 9,64 %

L'azide de l'acide p-*F-diphénylsulfonyl*-p'-*carboxylique* (*V*), Pf = 116° a été synthétisée avec un rendement de 77 % en partant de l'hydrazide (IV), par traitement avec de l'acide nitreux, en milieu d'acide acétique glacial, à —4°

$C_{13}H_8O_3N_3FS$ *Calculé* : S 10,50 ; N 17,04 %

(M = 305,28) *Trouvé* : S 10,41 ; N 17,23 %

Le p-*F-diphénylsulfonyl*-p'-*isocyanate* (*VI*) a été synthétisé par ébullition à reflux de 2 g d'azide (V), en benzène anhydre, pendant 3 heures et refroidissement brusque de la solution filtrée. Pf = 165° (benzène anhydre). Rend. = 74,8 %

$C_{13}H_8O_3NFS$ *Calculé* : S 11,56 ; N 5,05 %

(M = 277,27) *Trouvé* : S 11,62 ; N 5,14 %

---

[21] K. WILGERODT et B. PLOCKSTIES, *J. prak. Chem.*, [21], **85**, 199 ; Blst., IV 208.

Le chlorure de l'acide p-*fluor-diphénylsulfonyl*-p'-*carboxylique* (XI) a été synthétisé par réchauffement à reflux de 3 g d'acide *p*-F-diphénylsulfonyl-*p'*-carboxylique (II) avec du $SOCl_2$ en excès, jusqu'à dissolution complète (environ 3 heures). On a refroidi la solution, on a distillé l'excès de chlorure de thionyle et on a essoré les cristaux de chlorure de l'acide, qui ont été bien séchés et ensuite recristallisés du chloroforme anhydre. On a obtenu des cristaux purs, blancs jaunâtres. Pf = 115°, Rend. = 73,6 %

$C_{13}H_8O_3SF\ Cl$	*Calculé* : S 10,74 %
(M = 298,72)	*Trouvé* : S 10,68 %

L'amide de l'acide p-*fluor-diphénylsulfonyl*-p'-*carboxylique* (*XII*) a été obtenue par deux méthodes, à savoir :

1. Par réchauffement, pendant 40 heures, de 3,05 g (0,05 moles) d'azide de l'acide *p*-fluor-diphénylsulfonyl-*p'*-carboxylique (V), avec 10 g de poudre de zinc, en 200 ml d'acide acétique. On a obtenu l'amide (XII), au Pf = 204° (de l'éthanol dilué). Rend. = 80,2 %.

2. Par ébullition à reflux de 3,05 g (0,01 moles) de chlorure de l'acide (XI) avec de l'ammoniaque concentré, en excès, pendant 12 heures. On a isolé des cristaux aciculaires, incolores, avec le même Pf = 204° (de l'éthanol dilué). Rend. = 85,1 %

$C_{13}H_{10}O_3N\ SF$	*Calculé* : S 11,48 ; N 5,01 %
(M = 279,28)	*Trouvé* : S 11,39 ; N 5,12 %

La p-*fluor-diphénylsulfonyl*-p'-*amine* (*XIII*) a été également synthétisée par deux voies, à savoir :

1. 5 g de N-[*p'*-(*p*-fluor-phénylsulfonyl)-phényle]-O-éthyl-uréthanne (VIII) ont été réchauffés avec 70 ml d'HCl conc., sur un bain d'huile, à 170°, sous pression, en bouteille fermée, pendant 8 heures. On a refroidi le mélange, on l'a dilué avec 250 ml d'eau, on l'a filtré et ensuite on l'a alcalisé avec une solution de NaOH 10 %. On a obtenu des cristaux aciculaires, incolores, au Pf = 174° (de l'éthanol). C'est en même temps une méthode de dégradation pour la confirmation de la structure des nouveaux uréthannes.

2. On a traité 7,8 g d'amide (XII) avec 4 g (0,65 ml) de brome et on a laissé dégoutter pendant 10 minutes, une solution refroidie, préparée par dissolution de 2,5 g NaOH dans 17,5 ml d'eau, jusqu'à ce que la couleur initiale rouge-brune, ait viré en jaune clair. Nous avons neutralisé alors avec une solution de 2,5 ml HCl conc. dans 2,5 ml d'eau. Ensuite nous avons évaporé la solution à sec sur un bain d'eau, en maintenant le résidu pendant quelques heures, dans un exsiccateur à vide, pour éloigner les traces d'eau. Après avoir adjoint 15 ml d'éthanol absolu, nous avons fait bouillir le mélange à reflux, pendant 10 minutes. Après filtration, nous avons concentré la solution à volume réduit et nous l'avons laissée au repos, à froid, pour que le chlorhydrate de l'amine puisse cristalliser.

Nous avons essoré et lavé les cristaux avec un peu d'éthanol. Rend. = 60,3 %

$C_{12}H_{10}O_2NFS$	*Calculé* : S 12,76 ; N 5,57 %
(M = 251,27)	*Trouvé* : S 12,71 ; N 5,62 %

Le N-[p'*-F-(phénylsulfonyl)-phényl*]*-O-iso propyl-uréthanne* (*X*) a été synthétisé de 2,5 g d'azide (V), dissoute en 50 ml d'alcool isopropylique anhydre, par ébullition à reflux, pendant 50 minutes. La solution a été filtrée chaude et ensuite refroidie brusquement. On l'a précipitée avec de l'éther en obtenant une poudre blanche jaunâtre, qui, recristallisée de l'éthanol, a déposé des cristaux aciculaires, incolores, Pf = 175° (de l'éthanol absolu)

$C_{16}H_{16}O_4NFS$	*Calculé* : S 9,50 ; N 4,15 %
(M = 337,36)	*Trouvé* : S 9,52 ; N 4,26 %

Les données analytiques et les constantes physiques pour les autres uréthannes, synthétisés par des méthodes similaires (VII, VIII et IX) sont indiquées dans le tableau 3.

La synthèse des uréthannes dans cette classe se heurte à certaines difficultés d'ordre expérimental, car on les obtient fréquemment impurifiés par des résines, ou ils se séparent sous forme huileuse, fait qui rend leur purification particulièrement difficile.

C'est pour cette raison que des recherches laborieuses ont été nécessaires pour séparer les composés, par des précipitations sélectives répétées, utilisant différents solvants, ou par des recristallisations répétées, en présence du charbon absorbant ou de certaines résines échangeurs d'ions.

CONCLUSIONS

Ce travail élargit le domaine d'investigation sur la classe des diphénylsulfones, par la synthèse de 12 nouveaux *p*-fluor-diphénylsulfonyl-dérivés, qui présentent de l'intérêt en tant qu'antimétabolites, en raison de l'atome de fluor, introduit comme substituant en position *para*. Celui-ci offre la possibilité de maintenir une formule structurelle, profondément similaire à celles des métabolites de l'organisme, mais n'étant plus capables d'exercer leur action biologique normale, spécifique.

La structure des nouveaux composés a été confirmée avec exactitude par méthodes de dégradation hydrolytique en catalyse acide, ainsi que par analyse chimique élémentaire du soufre et de l'azote, complétées par des études spectrales en infrarouge.

Les données pharmacologiques, obtenues jusqu'à présent, nous font supposer que les composés organofluorurés de cette classe pourraient présenter de l'intérêt pour la chimiothérapie antibactérienne. Des recherches détaillées restent à être effectuées aussi sur d'autres types d'effets biologiques.

Tableau

avec les données analytiques et les constantes

N°	COMPOSÉ	Formule et poids moléculaire
II	$p\text{-F}-C_6H_4-SO_2-C_6H_4-COOH$	$C_{31}H_9O_4FS$ (280,27)
III	$p\text{-F}-C_6H_4-SO_2-C_6H_4-COO-C_2H_5$	$C_{15}H_{13}O_4FS$ (308,32)
IV	$p\text{-F}-C_6H_4-SO_2-C_6H_4-CO-NH-NH_2$	$C_{13}H_{11}O_3N_2FS$ (294,30)
V	$p\text{-F}-C_6H_4-SO_2-C_6H_4-CO\cdot N_3$	$C_{13}H_8O_3N_3FS$ (305,28)
VI	$p\text{-F}-C_6H_4-SO_2-C_6H_4-N=C=O$	$C_{13}H_8O_3NFS$ (277,27)
VII	$p\text{-F}-C_6H_4-SO_2-C_6H_4-NH-COO-CH_3$	$C_{14}H_{12}O_4NFS$ (309,31)
VIII	$p\text{-F}-C_6H_4-SO_2-C_6H_4-NH-COO-C_2H_5$	$C_{15}H_{14}O_4\cdot NFS$ (337,36)
IX	$p\text{-F}-C_6H_4-SO_2-C_6H_4-NH-COO-(CH_2)_2-CH_3$	$C_{16}H_{16}O_4NFS$ (337,36)
X	$p\text{-F}-C_6H_4-SO_2-C_6H_4-NH-COO-CH(CH_3)_2$	$C_{16}H_{16}O_4NFS$ (337,36)
XI	$p\text{-F}-C_6H_4-SO_2-C_6H_4-CO-Cl$	$C_{13}H_8O_3FClS$ (298,72)
XII	$p\text{-F}-C_6H_4-SO_2-C_6H_4-CO-NH_2$	$C_{13}H_{10}O_3NFS$ (279,28)
XIII	$p\text{-F}-C_6H_4-SO_2-C_6H_4-NH_2\text{-}p'$	$C_{13}H_{10}O_2NFS$ (251,27)

Synoptique 3

physiques des nouveaux composés synthétisés

Rend. %	Point de fusion et solvant de cristallisation	N%		S%	
		Calculé	Trouvé	Calculé	Trouvé
69,2	271°–2° (acide acétique glac.)	—	—	11,44	11,36
81,1	115° (éthanol abs.)	—	—	10,40	10,36
89,1	223° (éthanol)	9,51	9,64	10,89	10,77
77	116°	17,04	17,23	10,50	10,41
74,8	165° (benzène anh.)	5,05	5,14	11,56	11,62
68,8	141° (éthanol abs.)	4,52	4,64	10,36	10,37
73,4	191° (éthanol abs.)	4,33	4,34	9,91	9,94
92,4	175° (éthanol abs.)	4,15	4,26	9,50	9,52
70,3	126° (éthanol abs.)	3,98	4,08	9,09	9,02
73,6	115°–6° (chloroforme anh.)	—	—	10,74	10,68
85,1	204° (éthanol dil.)	5,37	5,40	11,48	11,39
60,3	174° (éthanol)	5,57	5,62	12,76	12,71

Revue Roumaine de Chimie, **15**, 1967–1974 (1970)

CONDENSED HETEROAROMATIC SYSTEMS. HALOGENATION AND DEHALOGENATION WITH PHENOXATHIINE, PHENOXASELENINE, PHENOXATELLURINE AND PHENOTHIATELLURINE

A. GIOABĂ and O. MAIOR

Chair of Organic Chemistry
Bucharest University
Spl. Independenţei 89
Bucharest, Romania

Received June 15, 1970

The dehalogenating action of phenoxatellurine, as compared to phenoxaselenine and phenothiatellurine, on some dichlorinated and dibrominated derivatives has been shown. These reactions show that phenothiatellurine is a better dehalogenating agent than phenoxaselenine but weaker than phenoxatellurine. The action of phenoxatellurine and phenothiatellurine on some geminal dihalogenated derivatives has allowed to obtain a good yield of the corresponding alkenes. One has worked out a convenient method for separating phenoxaselenine-10.10-dibromide from phenoxatellurine-10.10-dibromide. A new method for the synthesis of phenothiatellurine-5,5-dichloride and thianthrene was described.

A previous paper has shown the dehalogenating action of phenoxatellurine on some vicinal dihalogenated derivatives, as well as the reaction of this substance with phenoxathiine-10.10-dichloride and phenoxathiine-10.10-dibromide.[1]

In the present paper we have extended this research to other isosteric heteroaromatic systems such as phenoxaselenine and phenothiatellurine. By treating phenoxathiine-10.10-dibromide (I) with phenoxaselenine (II) one obtains a good yield of phenoxaselenine-10.10-dibromide (III), and phenoxathiine (IV). By treating phenoxaselenine-10.10-dibromide in the same conditions with phenoxatellurine (V), one obtains phenoxatellurine-10.10-dibromide (VI) besides phenoxaselenine.

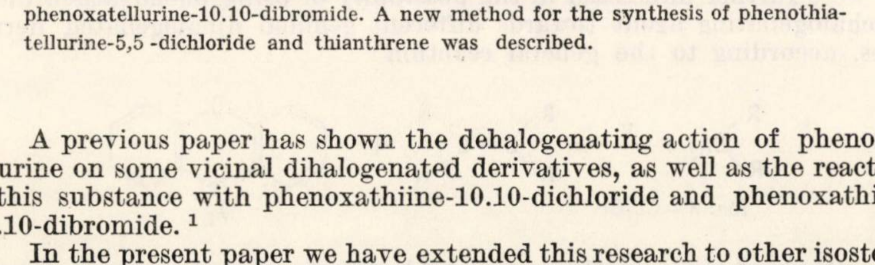

---

[1] A. Gioabă and O. Maior, *Rev. Chim.* (*Bucarest*), **21**, 131 (1970).

One notices that the transbromination reaction between the above mentioned heterocycles is favoured by the increase in the electropositivity of the heteroatoms (S $<$ Se $<$ Te). The dehalogenating capacity of these heterocycles also results from the thermic stability of the -10.10-dibromides (the strength of the ZBr_2bond) as the melting points (with decomposition) show : I (67°) $<$ III (172°) $<$ VI (295°).

From the above reactions one notices that phenoxaselenine acts as a dehalogenating agent towards (I). We have tested the behaviour of phenoxaselenine in reaction with 1,2-diiodophenylethene and 1,2-dibrommethane, finding that with these substances it has no dihalogenating effect. We nevertheless mention the fact that the above substances are dehalogenated by phenoxatellurine. [1]

On the other hand phenoxaselenine-10.10-dibromide brominates styrene and cyclopentene to the corresponding vicinaldibrom derivatives having a resemblance from this point of view with phenoxathiin -10.10-dibromide. [2]

On the basis of this feature we have worked out a new method of separating phenoxaselenine-10.10-dibromide (III) from phenoxatellurine-10.10-dibromide (VI), which can be applied to the synthesis of phenoxaselenine from phenoxatellurine according to the Drew method [3]

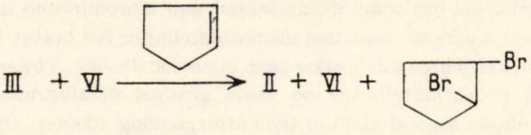

We were further interested in the possibility of using phenoxatellurine as a dehalogenating agent towards different geminal dihalogenated derivatives, according to the general reaction :

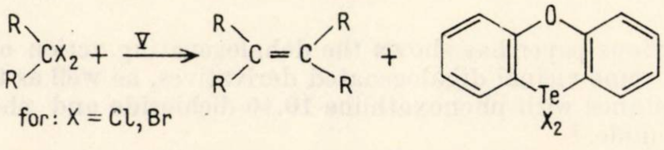

Some of these syntheses (see table 1) take place at a short interval and with a better yield than that known in literature. [4,5] Taking also into account the fact that the phenoxatellurine 10,10.dihalogenides resulting from the reaction can easily be quantitatively transformed into the initial phenoxatellurine (by reduction with potassium bisulphite) this method can be of some interest for the synthesis of some other substituted alkenes. We, nevertheless, mention the fact that the reaction of phenoxatellurine with benzylidenechloride and benzylidene bromide, has only led to stilbene traces.

[2] O. MAIOR, *Rev. Chim.* (*Bucarest*), **20**, 733 (1969).

[3] H. D. K. DREW, *J. Chem. Soc.*, **1928**, 511.

[4] M. HUDLICKY, "Preparativní reakce v organické chemii, II-Halogenace a dehalogenace", Ceskoslov. Akad. Ved., Prague, 1955.

[5] G. GRAEBE and B. MAN TZ, *Liebigs. Ann. Chem.*, **290**, 238 (1896).

Table 1

Dehalogenation reaction with phenoxatellurine

No	Geminal dihalogenated derivatives		Resulting unsaturated derivatives			Reaction time in min.	Reaction temp. in °C	Phenoxatellurine-10.10-dihalogenide resulting	
	Formula	Ref	Formula	Ref.	yield %			X	yield %
1	$(C_6H_5)_2CCl_2$	6	$(C_6H_5)_2C=C(C_6H_5)_2$	10,11	73	5–10	100–130	Cl	95
2	$(C_2H_5OOC)_2CBr_2$	7	$(C_2H_5OOC)_2C=C(COOC_2H_5)_2$	10	52	5–10	80–120	Br	91
3	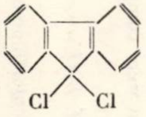	8	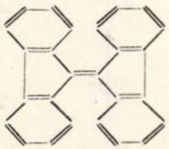	12	97	2–3	105–110	Cl	91
4	$C_6H_5-CHCl_2$		$C_6H_5-CH=CH-C_6H_5$ trans	13	traces	15–20	100–110	Cl	64
5	$C_6H_5-CHBr_2$	9	$C_6H_5-CH=CH-C_6H_5$ trans	13	id	45	120–140	Br	61

[6] * * * Org. Syntheses, Coll. II. John Wiley & Sons, p. 573.

[7] * * * Org. Syntheses Coll. I. John Wiley & Sons, p. 245.

[8] J. F. Norris, R. Thomas and M. Brown, *Ber. dtsch. chem. Ges.*, **43**, 2940 (1910).

[9] A. N. Costa, "Obschii praktikum po organicheskoikhimii", Izd. Mir., Moscow, 1965, p. 149.

[10] F. Weygand and H. G. Peine, *Rev. Chim. Acad. R.P.R.*, **7**, 1379 (1962).

[11] H. Low, *Ind. Eng. Chem. Product. Res. and Development*, **5**, 81 (1966).

[12] E. Campaigne and W. B. Reid, *J. Amer. Chem. Soc.*, **68**, 769 (1946).

[13] D. A. Ballard and W. M. Dehn, *J. Amer. Chem. Soc.*, **54**, 3969 (1932).

As could be expected, the iodobenzene dichloride is dehalogenated practically quantitatively in the presence of phenoxatellurine and the 1,2-diiodobenzene remains unaltered (it is therefore not possible to obtain benzyne in this way). In the same reaction conditions phenoxaselenine cannot dehalogenate-9.9-dichlorfluorene, thus showing a marked difference by comparison with phenoxatellurine.

We were also interested in the behaviour of phenothiatellurine as a dehalogenating agent, in other words the effect, on the reactivity, of the replacemnnt of the oxygen heteroatom by the sulphur heteroatom in a phenoxatellurine molecule.

Trying to synthetize phenothiatellurine-5.5-dichloride from diphenylthioether and tellurium tetrachloride in chloroform, we obtained negative results, in agreement with the literature.[14,15] Nevertheless, working without any solvent and with an excess of diphenylthioether, one obtains, with a low yield, phenothiatellurine-5.5-dichloride (VII), which, with potassium bisulphite, leads to phenothiatellurine (VIII). The structure of the compound (VIII) has been proved by transforming it into thianthrene (IX) by means of sulphur, this reaction being at the same time a new synthesis of the substance (IX). Table 2 shows the results of phenothiatellurine reactions with a series of dihalogenated compounds. By examining the data of table 2 one finds that phenothiatellurine is a better dihalogenating agent than phenoxaselenine, but weaker than phenoxatellurine.

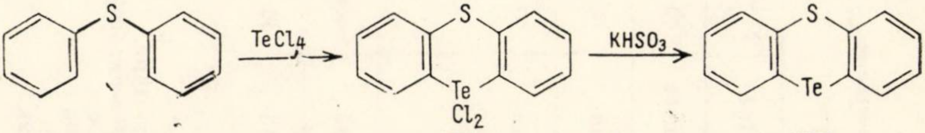

VII VIII

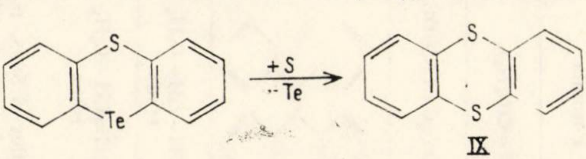

IX

EXPERIMENTAL

The raw materials have been synthetized according to literature data (tables 1 and 2) and the resulting compounds of the reaction were compared to authentic samples.

Synthesis of bifluorenilidene

A mixture of 3.96 g (0.016 mol) 9.9-dichlorfluorene with 5 g (0.016 mol) phenoxatellurine is gradually heated on a sieve in anhydrous conditions. At about 105° an exothermic

---

[14] N. Patragnani, *Tetrahedron*, **11**, 15 (1960).

[15] N. Petragnani and M. M. Campos, *Organometal. Chem. Rev.*, **2**, 61 (1967).

Table 2

Dehalogenation reaction with phenothiatellurine

No.	Initial halogenated product		Substances resulting from the reaction			Reaction time in min.	Reaction temp. in °C	Phenothiatellurine-5 ·5-dihalogenide resulting from the reaction	
	Formula	Ref.	Formula	Ref.	Yield. %			X	yield %
1	$(C_6H_5)_2CCCl_2$	6	$(C_6H_5)_2C=C(C_6H_5)_2$	10,11	71	5	100–120	Cl	93
2	$(C_2H_5OOC)_2CBr_2$	7	$(C_2H_5OOC)_2C=C(COOC_2H_5)_2$	10	52	5	105–110	Br	83
3	$C_6H_5-ICl_2$	16	C_6H_5-I	16		5–10	20	Cl	81
4	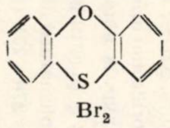	2	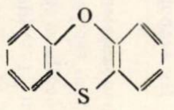	18		5–10	20	Br	80
5	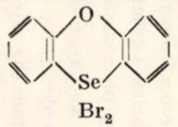	3	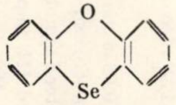	3		120	20	Br	66
6	$BrCH_2-CH_2Br$	17	—	—	—	60	131	—	—

[16] A. Vogel, "Practical Organic Chemistry", Longsman, London-New-York, 1967, p. 541.
[17] I. Tănăsescu and M. Ionescu, "Lucrări practice de chimie organică", Ed. Tehnică, Bucharest, 1957, p. 66.
[18] * * * Org. Syntheses, **18**, 64 (1938).

reaction starts (and the flame is removed). The reaction lasts 2—3 minutes, and the content of the flask forms a red crystalline mass. The bifluorenilidene is extracted by heating with 40 ml carbon tetrachloride. By filtering one separates 5,65 g phenoxatellurine-10.10-dichloride. The extract is concentrated nearly dry, obtaining 2.7 g of crude product with a 160—170° melting point. After recrystallizing from gasoline one obtains red bifluorenilidene needles with m.p. 189—190° in agreement with the literature [12] data for this substance obtained in another way.

Using phenoxaselenine instead of phenoxatellurine one has not obtained bifluorenilidene, the reaction mixture being decomposed. One obtains in the same way tetraphenylethene, m.p. 220—221°, from, diphenyldichloromethane and phenoxatellurine or phenothiatellurine.

The ethyl dibrommalonate treated with phenoxatellurine and respectively with phenothiatellurine in the same conditions as in the above syntheses, changes into tetracarbetoxiethene, m.p. 57—58°.

Benzylidene chloride or bromide reacts with phenoxatellurine leading to phenoxatellurine-10.10-corresponding dihalogenide, besides a resinous product from which only traces of stilbene were obtained by steam distillation.

In the above conditions by treating 1,2-dibromethane with phenoxaselenine or phenoxatellurine, the reaction does not take place, and the initial products are recovered. *Ortho*-diiodobenzene also does not react with phenoxatellurine.

Synthesis of phenoxaselenine-10.10-dibromide (III).

a) To 1 g (0.004 mol) phenoxaselenine dissolved in 12 ml of carbon tetrachloride one adds, at room temperature, 1.46 g (0.004 mol) phenoxathiine-10.10-dibromide. An orange precipitate of III settles immediateley. After 5 minutes one filters on Büchner, washes with 2 ml anhydrous carbontetrachloride and dries. The result is 1.5 g (yield 91.46%) of a red-orange product, m.p. 171—172° (decomp). By evaporating the filtrate one obtains 0.8 g (yield 98.76%) phenoxathiine.

b) to. 1.4 g (0.0056 mol) phenoxaselenine dissolved in 6 ml anhydrous carbontetrachloride one adds, under stirring, at room temperature, 0.3 ml (0.0058 mol) bromine in 2 ml carbontetrachloride. After 5 minutes one filters and dries the deposited precipitate. One has obtained 2 g (yield 86.95%) of III, m.p. 170—171° (decomp.); literature; 147—148° (decomp.) [3].

By repeating the synthesis of III in anhydrous chloroform (in literature conditions) one obtains a product with m.p. 170—171°. Consequently the melting point given by Drew is erroneous.

Halogenations with phenoxaselenine — 10.10-dibromide. Obtention of phenoxatellurine — 10.10. — dibromide (VI).

One treats 0.36 g (0.0012 mol) phenoxatellurine in 4 ml anhydrous benzene with 0.5 g (0.0012 mol) III at room temperature. After 7 hours one filters the deposited precipitate, washes it with anhydrous carbon tetrachloride and dries it. (Yield, 0.5 g (90.90%) VI). After evaporating the solvent, 0.24 g phenoxaselenine is obtained.

In the same way, from 0.8 g (0.0019 mol) III and 0.6 g (0.0019 mol) phenothiatellurine in 2 ml benzene one obtains 0.6 g phenothiatellurine-5.5-dibromide m.p. 268—270°. After recrystallization from acetone the m.p. is 270—271° (decomp.). From styrene and III, by using benzene as a solvent, one obtains 1.2-dibromo-1-phenylethane. Cyclopentene in excess and III lead, after fractionation in vacuum, to dibromocyclopentane; $n_{D^{25}} = 1.5450$ in agreement with literature. [19] The residue of the distillation contains phenoxaselenine.

---

[19] S. Winstein and R. M. Roberts, *J. Amer. Chem. Soc.*, **75**, 2299 (1953).

Separation of phenoxatellurine-10.10-dibromide of phenoxaselenine-10.10-dibromide.

A mixture of 1.6 g III and 1 g VI was refluxed for 20—30 minutes with 10 ml cyclopentene. After cooling it is filtered on a Büchner, obtaining VI with a practically quantitative yield. The filtrate is concentrated in vacuum, and the residue, after recrystallization from gasoline, leads to 0.8 g (yield 82.47 %) phenoxaselenine m.p. 88—89°.

Synthesis of phenothiatellurine-5.5-dichloride.

One introduces 40 g (0.1 mol) of tellurium tetrachloride and 27.5 g (0.14 mol) of diphenylthioether, in a round-bottomed flask provided with a reflux condenser equipped with a calcium chloride tube. The reaction mixture is gradually heated on an oil bath, under occasional stirring up to 190—200°,where it is maintained until the release of hydrochloric acid decreases markedly (10—12 hours) and a brown solid deposits on the flask's sides. After cooling, the reaction mixture is washed with 30—40 ml of ether, and then filtered with suction on a funnel with filtering mass. The solid product is washed with ether, dried, and then extracted with about 200 ml hot acetone. Thus phenothiatellurine-5.5-dichloride passes into the solution, being separated of the elementary tellurium (9.25 g) that results from the reaction. The nearly dry concentrated acetonic extract leads to 3.6 g (yield 6.33 %) of light yellow phenothiatellurine-5.5-dichloride with m.p. 205—215°. The crude product after recrystallization from acetone has a melting point at 264—266° (decomp.), in agreement with the same product obtained by an other method.

Synthesis of phenothiatellurine.

1.4 g phenothiatellurine-5.5-dichloride in suspension in 30 ml water is treated under ice-cooling, stirring in portions and for 25 minutes with 3 g of potassium metabisulphite. The reaction mixture is left at room temperature for 12 hours, filtered, washed with water and dried, giving 1.05 g (yield 92.1 %). Recrystallized from alcohol, one obtains light yellow needles with m. p. 123—124° in agreement with the same product obtained by Petragnani by reducing phenothiatellurine-5.5-dichloride with sodium sulphide. [14]

Synthesis of thiantrene (IX).

A mixture of 0.4 g phenothiatellurine and 0.1 g sulphur is gradually heated on a sieve, under hand-stirring until the reaction starts, noticeable by the darkening of the mixture's colour to brown, the increase of viscosity and the appearance of the elementary tellurium. The reaction lasts about 5 min. The reaction mixture is extracted after cooling with 30 ml benzene. The benzenic solution is treated with 0.5 ml thionyl chloride and after 30 minutes one filters the phenothiatellurine-5,5-dichloride. The filtrate is concentrated till it is almost dry, obtaining 0.15 g (yield 55.55 %) crude thianthrene. After two recrystallizations from glacial acetic acid the melting point is 156—157°. The mixed melting point with an authentic sample shows no drop and the IR spectrum is superposable.

Synthesis of phenothiatellurine-5.5-dibromide (X).

To 0.5 g (0.0016 mol) phenothiatellurine disolved in 9 ml, anhydrous carbon tetrachloride one adds in proportions and under stirring 0.6 g (0.0016 mol) I. The reaction takes place immediately; after 20 to 30 minutes the precipitate is filtered on a Büchner, washed with carbon tetrachloride and dried. The yield is 0.6 g (80 %) of a yellow product with m.p. 268–270°. Recrystallized in acetone, the m.p. becomes 270–271°.

Calc : for $C_{12}H_8STeBr_2$ ... Te % 27.05;
Found : for $C_{12}H_8S$ $TeBr_2$ ... Te % 26.74.

Reaction of iodobenzene dichloride with phenoxaselenine, phenoxatellurine and phenothiatellurine.

To 0.1 g of heterocyclic compound solved in 2–3 ml of anhydrous carbon tetrachloride one adds an equivalent quantity of iodobenzene dichloride under stirring. The reaction lasts for 5–10 minutes when the corresponding Te-dichlorides are precipitated. The reaction product is filtered under reduced pressure, washed with a small quantity of carbon tetrachloride and dried. Yields, 80–96 %.

Revue Roumaine de Chimie, 15, 1975–1985 (1970)

METHYLENE BASES OF HETEROCYCLES. IX[1]
SPECTRAL STUDY OF 2-ACYLMETHYLENEAZOLINES AND THEIR PROTONATED FORMS

GH. CIURDARU, MARCELA FĂRCĂŞAN and VIORICA I. DÉNES
Institute of Chemistry, Cluj, Str. Donath 65

Received August 18, 1970

In agreement with the chemical behaviour, spectral data support the zwitterionic structure of the acylmethyleneazolines. The protonated forms of these compounds in acid solution exist in a keto $\rightleftharpoons$ enol equilibrium mixture.

In a series of previously published papers [1–5] we have reported original routes leading to 3-alkyl-2-acylmethyleneazolines (A). From the structural point of view these compounds may be regarded as being cyclic keto-enamines. Coenen [6] and Katritzky [7] during their investigations about the ω-acylderivatives of cyclic enamines belonging to the series of 1,3,3-trimethylindole and pyridine, respectively, have pointed out that the dipolar resonance structure type B has an important contribution to the hybrid forms. An increase in the dipolar character is brought about by the insertion of a second heteroatom (X=O, S, Se, N) enabling an additional polarization pictured by the resonance structure C, as in the case of our 2-acylmethyleneazolines. The preferential attack of certain electrophiles such as alkyl [8] and acyl halides [9] to the carbonyl oxygen atom is a chemical evidence of the highly polarized character of these compounds.

The same conclusion arose from the IR spectrophotometric measurements. Thus in the spectra of 3-alkyl-2-acylmethyleneazolines (A) we found no absorption bands in the region 1800–1640 cm^{-1} in which the C=O stretching vibration usually appears. On the other hand we observed in a somewhat lower frequency range (1640–1540 cm^{-1}) two prominent bands, one of which must be produced by the carbonyl group and the other by the ethylene linkage. This remarkable downward shift agrees with the above stated dipolar character of these substances.

---

[1] Part VIII : Gh. Ciurdaru and V. I. Dénes, *Rev. Roumaine Chim.*, **14**, 1063 (1969).

[2] V. I. Dénes, Gh. Ciurdaru and M. Fărcăşan, *Chem. Ber.*, **96**, 2691 (1963).

[3] V. I. Dénes, Gh. Ciurdaru and M. Fărcăşan, *Rev. Roumaine Chim.*, **9**, 375 (1964).

[4] V. I. Dénes, Gh. Ciurdaru and M. Fărcăşan, *Rev. Roumaine Chim.*, **9**, 867 (1964).

[5] V. I. Dénes, Gh. Ciurdaru and M. Fărcăşan, *Rev. Roumaine Chim.*, **10**, 1045 (1965).

[6] M. Coenen, *Liebigs Ann. Chem.*, **633**, 92 (1960).

[7] A. R. Katritzky and J. D. Rowe, *Spectrochim. Acta*, **22**, 381 (1966).

[8] N. N. Sveshnikov, I. I. Levkoev, A. F. Vompe and B. S. Postnaia, *Doklady Akad. Nauk S.S.S.R.*, **88**, 281 (1953).

[9] V. I. Dénes and Gh. Ciurdaru, *Chem. Comm.*, **1970**, 510.

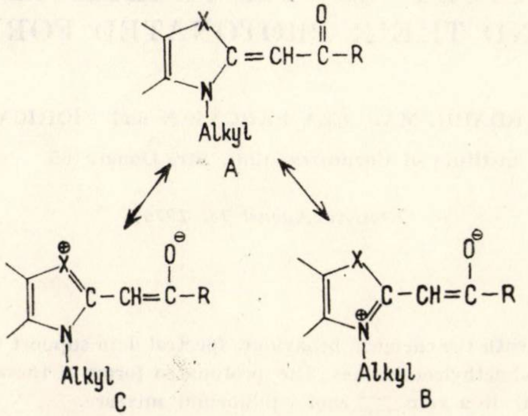

In order to obtain correct assignments of the bands mentioned, we investigated the spectral changes due to solvents. Since the 3-alkyl-2-acylmethyleneazolines (A) are in general sparingly soluble, a few compounds only could be examined. The solvent-induced frequency shifts exhibited by the bands appearing in the 1640–1540 cm^{-1} range are listed in table 1. It results from these data that in all but two cases the higher frequency band is more affected by the solvent change. Although the carbonyl group is usually regarded to be more solvent-sensitive than the C=C band, [10,11] in strongly conjugated systems the reverse seems to be true. [12–14] Since our substances possess strongly delocalized double bonds, we are entitled to assign the band exhibiting the larger solvent-shift to the ethylene absorption while the band less solvent-sensitive remains to be attributed to the carbonyl group.

The highly dipolar character of the 3-alkyl-2-acylmethyleneazolines (A) becomes apparent also in the electronic spectra. Thus we found that their absorption maximum is shifted toward shorter wavelengths with increasing polarity of the solvent (table 2), as do the merocyanine dyes. [15,16]

Similar to the common enamines, [12,17] the 3-alkyl-2-acylmethyleneazolines (A) react with strong electrophiles such as the diazonium salts

---

[10] L. J. Bellamy, *Spectrochim. Acta*, **13**, 60 (1958).

[11] L. J. Bellamy and P. E. Rogasch, *Spectrochim. Acta*, **16**, 30 (1960).

[12] P. J. Taylor, *Spectrochim. Acta*, **26A**, 153 (1970).

[13] J. Dabrowski and K. Kamienska-Trela, *Spectrochim. Acta*, **19**, 475 (1963).

[14] J. Dabrowski and K. Kamienska-Trela, *Spectrochim. Acta*, **22**, 211 (1966).

[15] L. G. S. Brooker, G. H. Heyes and D. W. Heseltine, *J. Amer. Chem. Soc.*, **73**, 535 (1951).

[16] E. G. McRae, *Spectrochim. Acta*, **12**, 192 (1958).

[17] G. Opitz and A. Griesinger, *Liebigs Ann. Chem.*, **665**, 101 (1963).

Table 1

Solvent effects on the 1540–1649 cm⁻¹ range bands

Compound	CCl_4	CH_2Cl_2	$CHCl_3$	(CCl_4-CHCl_3)
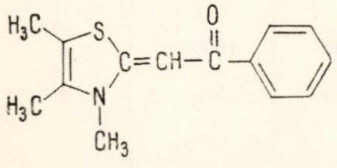	1640	—	1640	0
	—	1608	1606	2
	1599	1597	1595	4
	1568	1560	1558	10
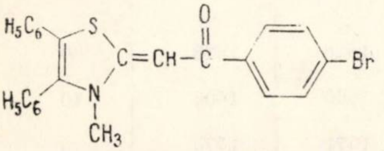	1605	1605	1605	0
	1590	1590	1588	2
	1560	1556	1553	7
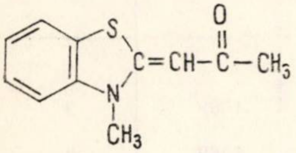	1627	1618	1610	17
	1590 sh	1590 sh	1590 sh	0
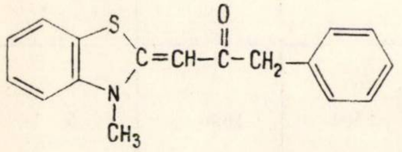	1622	1616	1610 sh	12
	1603	1603	1600	3
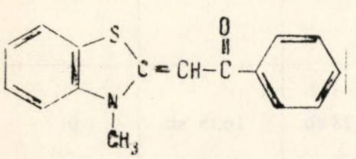	1614	1604	1603	11
	1578	1576	1575	3
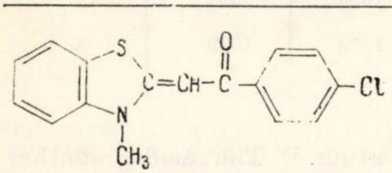	1615	1600	1598	17
	1600 sh	—	—	
	1570	1570	1568	2
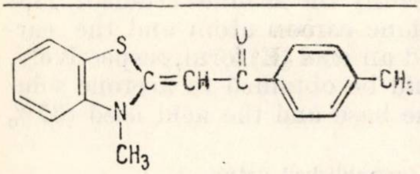	1610	1604	1603	7
	1571	1569	1569	2

Table 1 — continued

Compound	CCl_4	CH_2Cl_2	$CHCl_3$	(CCl_4-CHCl_3)
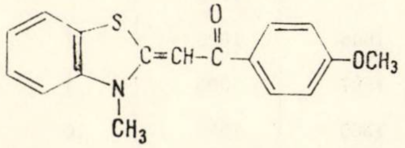	1604 1576	1602 1574	1600 1573	4 3
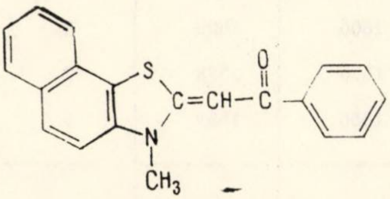	— 1610 1573	1628 1600 1571	1628 1600 1570	0 10 3
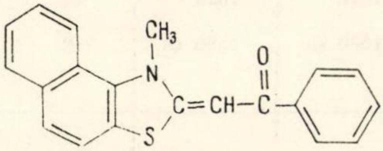	1609 1578	1603 1570	1600 1569	9 9
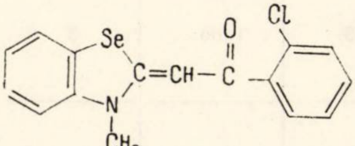	1595 1569	1594 1568	1590 1567	5 2
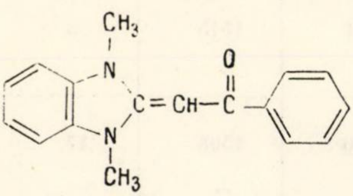	1628 sh 1606 1577	1628 sh 1600 1573	1628 sh 1595 1569	0 11 8

giving derivatives at the methine carbon atom.[18] The acids, another group of strong electrophiles, attack also readily the azolines studied. This protonation reaction affects both the methine carbon atom and the carbonyl oxygen atom affording a keto (D) and an enol (E) form, respectively. The crystalline protonated derivatives could be obtained in acetone solution. Depending on the starting methylene base and the acid used (37%

---

[18] M. FĂRCĂŞAN, R. CHIRA and V. I. DÉNES, (unpublished data).

Table 2

Solvent effects on the absorption maxima

Compound	DMF max. nm (∈)	DMF-water (16−84) max. nm (∈)	Δλ nm
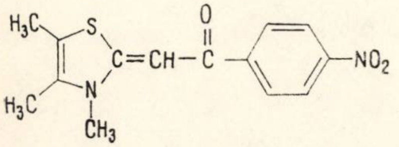	449.1 (14,000)	432.5 (20,000)	−16.6
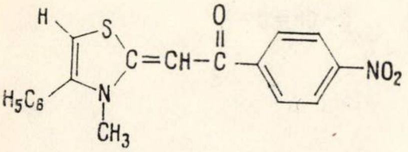	437 (14,700)	428 (14,800)	− 9
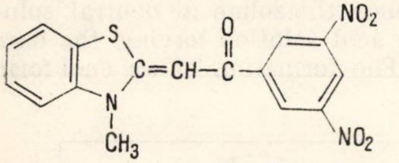	411.2 (21,800)	394.3 (24,500)	−16.9 —
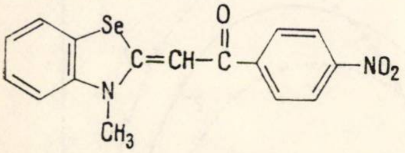	428 (20,200)	412 (12,400)	−16
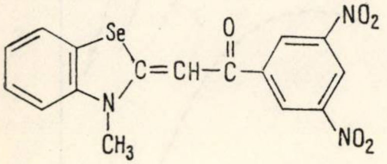	413.9 (21,000)	398 (26,300)	−15.9

hydrochloric acid or 70% perchloric acid) one could obtain one of the protonated forms (D) or (E), or a mixture of both (table 3).

The differentiation between the forms (D) and (E) was easily performed by IR spectrometry. In the enol form the C=C stretching vibration was found to appear as a strong band around 1620 cm^{-1}, while in keto form a strong C=O stretching band was observed around 1700 cm^{-1}.

Investigations with UV spectrometry in methanol solutions in the presence of increasing amounts of perchloric acid provided conclusive data about the protonation reaction. Figure 1 shows that the 384 nm band exhibited by 3-methyl-2-benzoylmethylenebenzthiazoline in neutral solution is shifted to 374 nm on passing to an acid solution having the base to acid molar ratio $1:3\times10^3$ (Table 4). The formation of an enol form

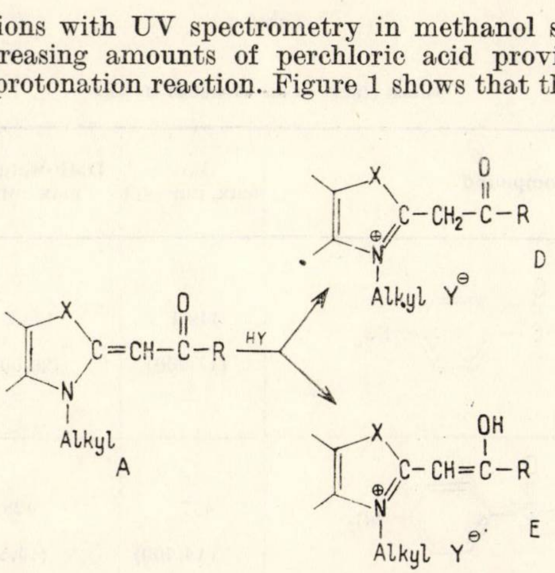

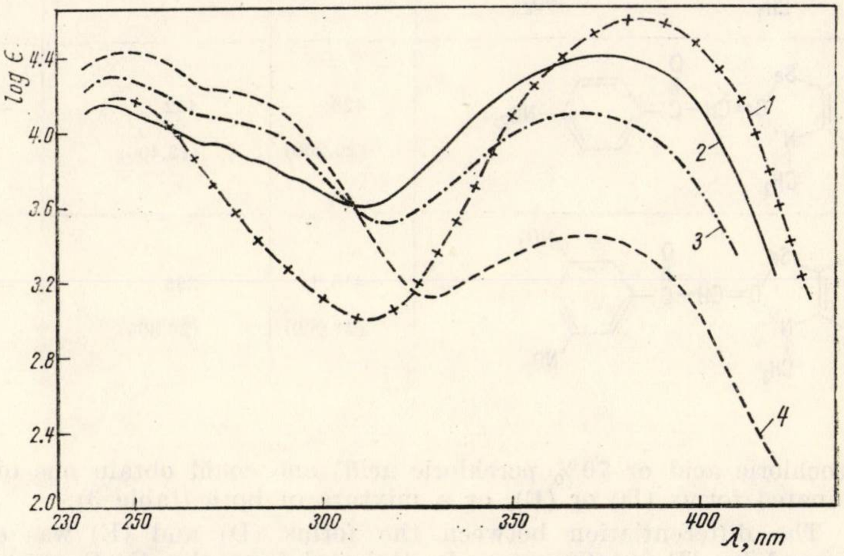

Fig. 1. — Electronic spectrum of the 3-methyl-2-benzoylmethylenebenzthiazoline in :

1, methanol-water (8 : 92) ; *2*, methanol-perchloric acid 1.5% (8 : 92) ; base-acid molar ratio $1:3,10^3$; *3*, methanol-perchloric acid 18% (8 : 92) ; base-acid molar ratio $1:3,10^4$; *4*, methanol-perchloric acid 46% (8 : 92) ; base-acid molar ratio $1:8,10^4$.

(E) accounts for this blue shift. On the analogy of the literature data, [19-21] the two inflexions at 274 and 285 nm may be regarded as being produced by the thiazolium ring included in a keto (D) and in an enol (E) form, respectively.

The curves obtained by increasing the acid concentration show an isobestic point (Fig. 1). At the same time a diminution in absorption at 374 nm and an accentuation of the absorption at 274 nm are to be seen.

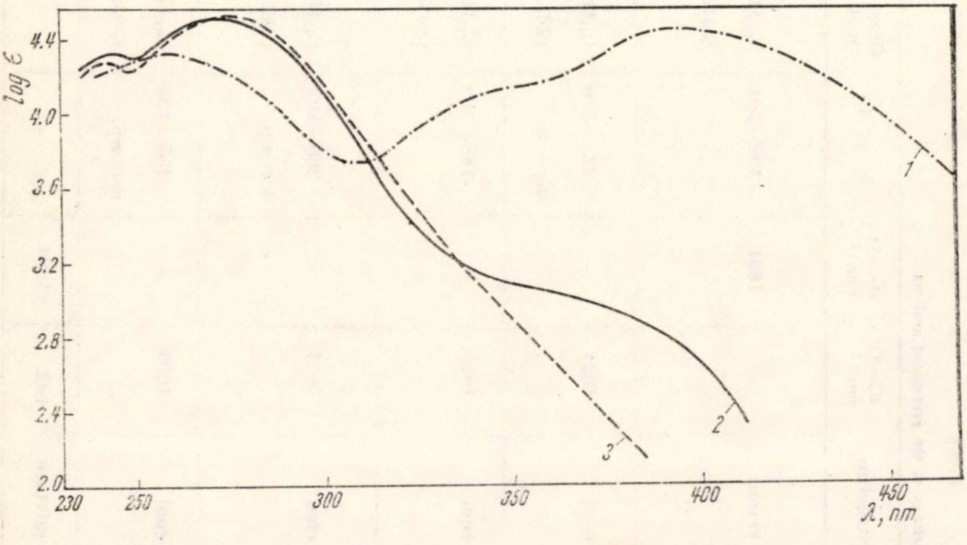

Fig. 2. — Electronic spectrum of the 3-methyl-2[methyl-(*p*-nitrobenzoyl)] methylenebenzthiazoline in:

1, methanol; *2*, methanol-perchloric acid 70% (84 : 16); base-acid molar ratio 1: 3,10^3; *3*, methanol-perchloric acid 70% (40 : 60); base-acid molar ratio : 1 :3,10^4.

These observations may be rationalised in terms of a pH-dependent equilibrium mixture of the keto (D) and enol (E) form. The increase in the hydrogen ions concentration displaces the equilibrium toward the keto form. In certain cases a sufficiently high pH value makes possible the complete conversion into the keto form as it was proved with 3-methyl-2[methyl-(*p*-nitrobenzoyl)]methylenebenzthiazoline (Fig. 2).

The fact that from acidified acetone solution either the one or the other protonated forms precipitate may be explained by the relative stability of the two isomers.

---

[19] J. L. Johnson, M. E. Herr, J. C. Babcock, A. E. Tonken, J. E. Stafford and F. W. Heyl, *J. Amer. Chem. Soc.*, **78**, 430 (1956).

[20] N. J. Leonard and J. A. Adamcik, *J. Amer. Chem. Soc.*, **81**, 595 (1959).

[21] R. Guglielmetti, E. Pretelli and J. Metzger, *Bull. Soc. chim. France*, **1967**, 2812.

Table 3

Characteristics of the protonated azolines

Compound	Acid used	Structure	νC=C cm^{-1}	νC=O cm^{-1}	M. p. °C	Gross formula (mol. weight)	Analysis N
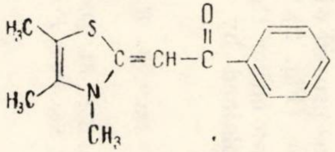	$HClO_4$	ketone	—	1691	199–201	$C_{14}H_{16}ClNO_5S$ (345.8)	calc. 4.05 found 4.39
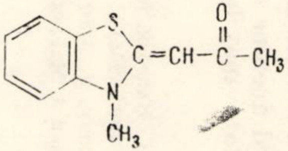	HCl	enol	1624	—	225–226 decomp.	$C_{11}H_{12}ClNOS$ (231.7)	calc. 6.04 found 5.87
	$HClO_4$	enol	1626	—	188–190	$C_{11}H_{12}ClNO_5S$ (305.7)	calc. 4.58 found 4.92
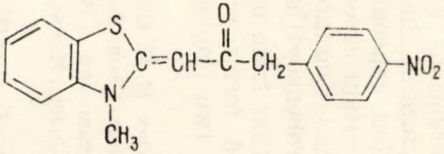	HCl	enol	1623	—	200–202 decomp.	$C_{17}H_{15}ClN_2O_3S$ (362.8)	calc. 7.72 found 7.50
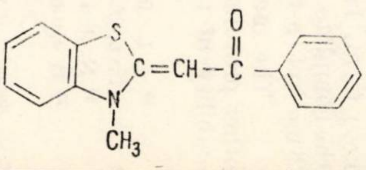	HCl	enol	1605	—	155–157 decomp.	$C_{16}H_{14}ClNOS$ (303.8)	calc. 4.76 found 4.75
	$HClO_4$	mixture	1623	1694	—	—	—

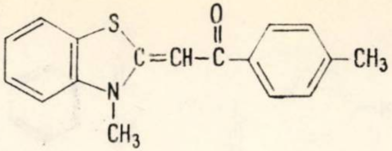	$HClO_4$	mixture	1609	1688	—	—	—
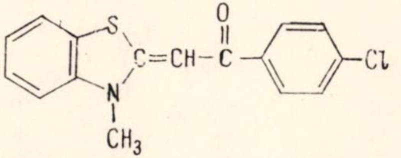	$HClO_4$	ketone	—	1693	234–237 decomp.	$C_{16}H_{13}Cl_2NO_5S$ (402.2)	calc. 3.49 found 3.47
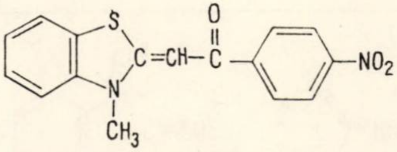	$HClO_4$	enol	1620	—	217–219	$C_{16}H_{13}ClN_2O_7S$ (412.8)	calc. 6.78 found 6.63
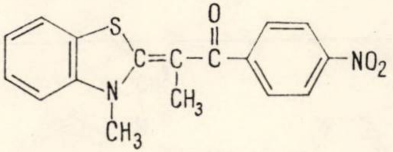	HCl	ketone	—	1695	190–192 decomp.	$C_{17}H_{15}ClN_2O_3S$ (362.8)	calc. 7.72 found 7.81
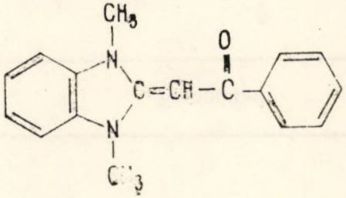	HJ[1]	ketone	—	1700			

Table 4

UV-absorption maxima of some azolines and of their protonated forms

Compound	Absorption maxima, nm (∈)	Solvent
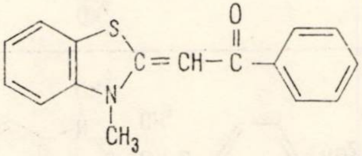	a) 384 (39,000) ; 248 (15,600).	CH_3OH-H_2O (8 : 92)
	b) 374 (25,200) ; 285i (6,600) ; 274i (8,300) ; 246 (14,100)	$CH_3OH-HClO_4$ 1.5 % (8 : 92)
	c) 370 (12,500) ; 274sh (11,400) ; 256–246 (20,000)	$CH_3OH-HClO_4$ 18 % (8 : 92)
	d) 370 (2,700) ; 274sh (16,600) ; 256–246 (27,000)	$CH_3OH-HClO_4$ 46 % (8 : 92)
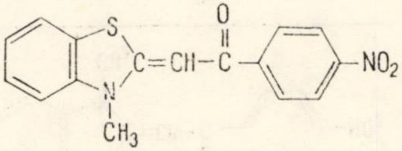	a) 411 (28,300) ; 317 (10,100) ; 264 (18,000)	CH_3OH
	b) 379 (38,100) ; 274 (12,500)	$CH_3OH-HClO_4$ 70 % (84 : 16)
	c) 379 (8,700) ; 276 (25,000) ; 243.5 (14,200)	$CH_3OH-HClO_4$ 70 % (40 : 60)
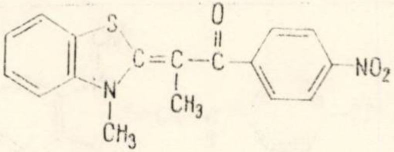	a) 392 (26,400) ; 354sh (13,700) ; 259 (20,100)	CH_3OH
	b) 355 (1,100) ; 271.5 (32,300) ; 243.8 (20,900)	$CH_3OH-HClO_4$ 70 % (84 : 16)
	c) 330–320i (2,100) ; 275 (32,800) ; 243 (19,100)	$CH_3OH-HClO_4$ 70 % (40 : 60)
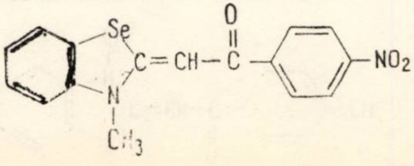	a) 414 (31,300) ; 316 (10,800) ; 262 (22,600)	CH_3OH
	b) 389 (40,300) ; 276 (13,000)	$CH_3OH-HClO_4$ 70 % (84 : 16)
	c) 389 (15,100) ; 278 (25,800) ; 248 (18,000)	$CH_3OH-HClO_4$ 70 % (40 : 60)

EXPERIMENTAL

3-Methyl-2-acylmethyleneazolines were prepared as described previously.[1–5]

Hydrochlorides. On treating with 37% HCl the acetone solution or suspension of the azolines or by bubbling gaseous hydrochloric acid through the acetone solution and adding ether the crystalline products precipitate. The characteristics of the compounds obtained are listed in table 3.

Perchlorates. On treating the acetone solution or suspension with some drops of 70% perchloric acid the addition products precipitate in crystalline form (Table 3).

The IR spectra of the hydrochlorides and perchlorates were performed in KBr pellets using a UR 10 Zeiss spectrophotometer. The bases were recorded in solution at a concentration of about 10^{-3} M except for the CCl_4 solutions where the concentrations were determined by the solubility of the substances studied; the path length: 0.4 mm.

The UV spectra were taken in methanol, in methanol with perchloric acid (Table 4) and in dry or aqueous dimethylformamide (Table 2). A Beckman DK-2A spectrophotometer was used.

Revue Roumaine de Chimie, 15. 1975–1985 (1970)

Revue Roumaine de Chimie, **15**, 1987 – 1992 (1970)

VARIATION DE CERTAINES PROPRIÉTÉS DU $K_2Zr/Hf/F_6$ PAR DÉHAFNISATION

IOANA ARSENIE * et I. LEUCA **

* Institut de Physique Atomique,
Bucarest, Măgurele, Boîte postale 135
** Faculté de Physique Nucléaire, 14, str. Academiei

Reçu le 19 août 1970

On présente la variation de certaines propriétés telles que : densité, solubilité en fonction « notamment » de la teneur en hafnium. Ceci a été réalisé au cours d'une étude de déhafnisation du zirconium par le procédé de cristallisation fractionnée du $K_2Zr/Hf/F_6$. (Objet d'un ouvrage sous presse.) On obtient une variation linéaire pour la densité en fonction de la teneur en hafnium et une différence de solubilité entre l'hexafluozirconate de potassium impur et celui déhafnié.

INTRODUCTION

L'hexafluozirconate de potassium est l'un des composés du zirconium qui présente une stabilité dans le temps.[1] L'hexafluozirconate de potassium déhafnié[2,3] peut être utilisé à l'obtention du zirconium métallique d'une pureté nucléaire tel quel, par le procédé de l'électrolyse,[4,5] ou peut être passé sous forme d'oxyde de zirconium qui sera traité par le procédé classique Kroll.[6]

Le zirconium de pureté nucléaire (un contenu de 0,01% de Hf/Zr) est considéré « matériel classique » pour les réacteurs nucléaires,[7] étant utilisé à la confection des gaines pour combustible nucléaire ou de différents détails et constructions des réacteurs nucléaires.[8]

---

[1] N. V. Sidgwick, « The Chemical Elements and Their Compounds ».I, Oxford University Press, Londres, 1962, p. 630.

[2] N. P. Sajin et A. Pepelyaeva, Conf. Int. Appl. Pac. En. Atom., Genève, **8**, 34 (1955).

[3] I. Arsenie et I. Leucă, *Rev. Roumaine Chim.*, **15**, 1277 (1970).

[4] A. Călușaru, « Depunerea electrolitică a metalelor sub formă dispersă », Ed. Academiei, Bucarest, 1962, p. 205.

[5] G. Mîndru, *Studii și Cercetări—Metalurgie*, **14**, 27 (1969).

[6] G. L. Miller, « Mettalurgy of the Rare Metals », 2 , Zirconium, Butterworths Scientific Publications, Londres, 1954, p. 74.

[7] W. Schreiter, « Metale rare », Ed. Tehnică, Bucarest, 1966, p. 370.

[8] * * * « Zirconium », Conference on the Use of Zirconium Alloys in Nuclear Reactors, octombre 21—26, 1966, Marianské Lazne, Czechoslovakia.

En connaissant la variation de la densité du K_2ZrF_6 en fonction de la teneur en hafnium on peut établir le degré de déhafnisation du zirconium par simple mesure de la densité.[9]

De même, l'établissement de l'isotherme du système K_2ZrF_6/H_2O est important pour le développement du procédé de séparation du zirconium d'avec le hafnium par cristallisation fractionnée du $K_2Zr/Hf/F_6$ pour réaliser des solutions sur-saturées, ceci étant l'essentiel du procédé de cristallisation.[2,10,9,3]

Les déterminations pratiques de densité et de solubilité ont été faites sur de l'hexafluozirconate de potassium ayant une composition connue d'avance.

Les analyses ont été effectuées spectrographiquement,[11] gravimétriquement[12] et par activation.[13] Pour l'analyse par activation les échantillons ont été irradiés pendant 2,30 h dans un canal dont le flux était de 10^{13} n/cm^2 s et mesurés à l'aide d'un compteur scintillateur NaI(Tl) et d'un analyseur à 400 canaux S.A. — 40 type Intertechnique.

PARTIE EXPÉRIMENTALE

Dans le cadre des recherches effectuées pour établir les conditions de séparation du zirconium d'avec le hafnium par le procédé de la cristallisation fractionnée du K_2ZrF_6, on a déterminé les propriétés suivantes :

1. la variation de la densité du K_2ZrF_6 avec la déhafnisation,
2. L'isotherme du système $K_2ZrF_6 - H_2O$.

1. *Variation de la densité du K_2ZrF_6 en fonction de la déhafnisation*

La figure 1 donne la courbe de déhafnisation du $K_2Zr/Hf/F_6$ obtenue par le procédé de séparation du zirconium d'avec le hafnium par cristallisation fractionnée.

Par l'étude de la variation de la densité du K_2ZrF_6 à travers les degrés de cristallisation, on a obtenu une variation linéaire de la densité de celui-ci conformément à la courbe présentée dans la figure 2, donc la décroissance de la teneur en hafnium entraîne également une diminution de la densité de l'hexafluozirconate.

Le tableau 1 présente quelques valeurs de la densité du K_2ZrF_6 à teneur en hafnium (connue).

Le tableau 2 donne de même l'analyse spectrographique du K_2ZrF_6 initial (2,48 % Hf/Zr) et déhafnié (0,0077 % Hf/Zr.

---

[9] J. W. Mullin, « Cristallization », Butterworths, Londres, 1961, p. 21.

[10] A. G. Kasatkin, « Procese și aparate în industria chimică », Ed. tehnică, Bucarest, 1963, p. 737.

[11] W. T. Elwell, « The Analysis of Titanium, Zirconium and Their Alloys », John Wiley & Sons LTD Publishers, Londres, 1961, p. 117.

[12] T. Născuțiu et G. Baiulescu, *Studii și Cercetări Chim. Ed. Acad. București*, **16**, 31 (1958).

[13] L. Fournet et Ph. Albert, *Compt. rend.*, **254**, 45 (1962).

Fig. 1. — Variation de la teneur en hafnium avec le nombre de cristallisations.

1. pH = 3 ; *2*. pH = 4,5.

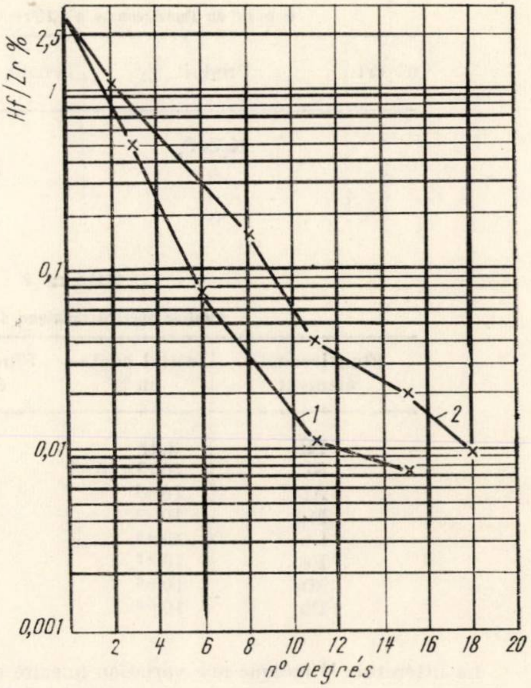

Fig. 2. — Variation de la solubilité de hexafluozirconate avec la température.

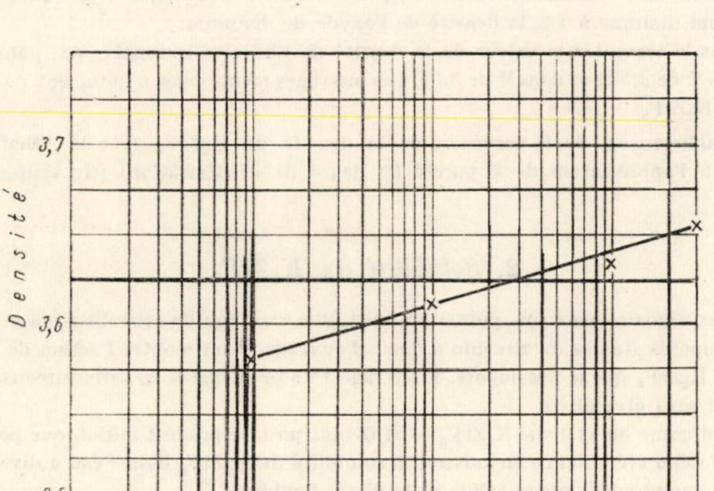

Tableau 1

Densité du fluozirconate à différentes teneurs en Hf

n° crt.	Produit	Teneur en Hf %	Valeur de la densité
1	K_2ZrF_6	2,5	3,657
2	,,	1	3,633
3	,,	0,1	3,611
4	,,	$77{,}10^{-4}$	3,578

Tableau 2

Analyse spectrographique du K_2ZrF_6

Fluozirconate élément	Initial contenu %	Fluozirconate élément	Déhafnié contenu %
Hf	2,48	Hf	0,0077
Si	10^{-1}-10^{-2}	Si	10^{-2}
Al	10^{-2}	Al	10^{-3}
Mg	10^{-2}	Mg	20^{-3}
Cu	10^{-3}	Cu	10_{-}^{4}
Fe	10^{-2}	Fe	10^{-3}
Mn	10^{-3}	Mn	10^{-4}
Pb	10^{-3}	Pb	10^{-4}

La littérature [14] indique une variation linéaire de la densité de l'oxyde de zirconium en fonction de la teneur en hafnium, tout en spécifiant qu'une addition de 1 % comme poids d'oxyde de zirconium diminue à 1 % la densité de l'oxyde de hafnium.

Dans le travail [14] la valeur de la densité de l'hexafluozirconate de potassium est de 3,656, dans [15] de 3,582 et dans [16] de 3,55. Les ouvrages mentionnés n'indiquent pas le degré de pureté du K_2ZrF_6.

L'établissement de la variation de la densité du K_2ZrF_6 avec la déhafnisation peut contribuer à l'appréciation de la pureté (le degré de déhafnisation) par simple mesure de la densité.

2. *Solubilité du K_2ZrF_6*

L'hexafluozirconate de potassium cristallise sans eau de cristallisation et est considéré l'un de composés stables du zirconium. Dans l'ouvrage, [17] on montre l'action de l'humidité de l'air sur le K_2ZrF_6 qui le décompose. L'ouvrage [18] admet que le hexafluozirconate peut être recristallisé sans être altéré.

L'isotherme du système K_2ZrF_6 — H_2O tant pour le produit initial, que pour le produit final (déhafnié) a été obtenue en suivant la solubilité du K_2ZrF_6 dans l'eau à diverses températures et en analysant la phase solide et la phase liquide.

---

[14] P. Pascal, « Nouveau Traité de Chimie Minérale », IXe vol. Masson et Cie, Paris, 1963, p. 490—524.

[15] W. W. Beaver, Brush Beryllium Co., Cleveland, Ohio BBC n° 54 août 1950.

[16] G. Hevesy, *J. Chem. Soc.*, 125, 2372 (1924).

[12] M. Jeanot et M. Chaigneau, *Compt. rend.*, **227**, 1402 (1948).

[18] R. H. Haszeldine et A. G. Sharpe, « Florine and its Compounds », Methuen co. LTD, Londres, 1951, p. 15—55.

Les résultats pratiques sont donnés par la figure 3 en comparaison des données de la littérature.

En comparant la solubilité de l'hexafluozirconate initial 2,48 % Hf/Zr et de celui déhafnié 0,0077 % Hf/Zr, il ressort que la solubilité diminue en même temps que la pureté, ce qui s'explique par l'influence réciproque des impuretés.

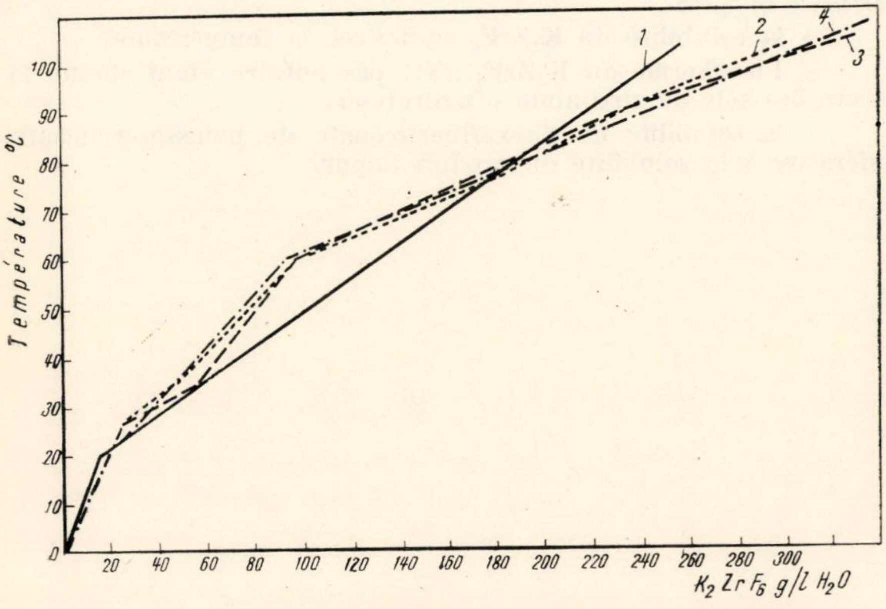

Fig. 3. — Variation de la densité du K_2ZrF_6 avec la teneur en hafnium.

1, isotherme prise de la littérature 2,6 ; *2*, isotherme prise de la littérature 5 ; *3*, isotherme obtenue pratiquement pour le K_2ZrF_6 impur ; *4*, isotherme obtenue pratiquement pour le K_2ZrF_6 purifié.

La solubilité dans l'eau du K_2ZrF_6 à différentes températures conformément aux données de la littérature[19] est indiquée dans le tableau 3. La pureté du K_2ZrF_6 n'est pas indiquée

Tableau 3

Solubilité du K_2ZrF_6 dans l'eau

Température	Solubilité g//l H_2O
20°	19,8
60	96
100	305

Les données sur la solubilité du K_2ZrF_6 mentionnées dans les ouvrages[16,14,2] diffèrent des données du tableau 3. Ces ouvrages ne nous indiquent pas la pureté du K_2ZrF_6.

---

[19] G. Hevesy, *Chem. Reviews*, **2**, 1 (1926).

CONCLUSIONS

On a mis en évidence une variation linéaire de la dénsite du K_2ZrF_6 à teneur en hafnium. On a ainsi obtenu pour le K_2ZrF_6 à 2,48% Hf/Zr une densité de 3,657 et pour le K_2ZrF_6 à 0,0077% Hf/Zr, $d = 3{,}578$.

— la solubilité du K_2ZrF_6 croît avec la température,

— l'isotherme du K_2ZrF_6 n'est pas linéaire étant donné la propriété des sels de zirconium d'hydrolyser,

— la solubilité de l'hexafluozirconate de potassium déhafnié est inférieure à la solubilité du produit impur.

Revue Roumaine de Chimie **15**, 1993–1997 (1970)

SCHIFF BASE COMPLEXES OF Ti (IV)

N. S. BIRADAR* and V. H. KULKARNI

Department of Chemistry, Karnatak University,
Dharwar-3, India

Received October 31, 1969

Four complexes of titanium (IV) with Schiff bases have been prepared in the pure form. The analytical data show 1 : 1 stoichiometry. These are dark coloured hygroscopic substances, in-soluble in almost all organic solvents. The infrared spectra of the complexes show the pattern for the hydrogen bonded OH. The phenolic C–O stretching frequency has not been much affected whereas the C=N stretching vibration shows considerable shift suggesting the possible co-ordination through the nitrogen of the azomethine group.

Recently the Schiff bases containing nitrogen and oxygen donor atoms have received considerable attention as the most promising reagents for the IV group metal ions. [1–13] The majority of the publications deal with bidentate Schiff bases and have shown that these ligands form 1 : 2 complexes with titanium (IV) chloride. Lapitskii et al.,[5] have shown that titanium (IV) forms 1 : 1 chelate with the tetradentate Schiff base i.e. bis (salicylidene) ethylenediamine. Garnovskii and coworkers[10] have prepared titanium (IV) complexes with heterocyclic azomethines and studied the possible co-ordination sites.

---

* To whom all the correspondence should be addressed.

[1] Ya Yü Chang, A. V. Lapitskii and I. A. Savich, *Vestnik Moskov. Univ., Ser. II*, **15**, 43 (1963), in *Chem. Abstr.*, **55**, 7968b(1961).

[2] Ya Yü Chang, I. A. Savich, A. V. Lapitskii, V. R. Samorukov and L. G. Titov, *Vestnik Moskov. Univ., Ser. II*, **15**, 40 (1960) in *Chem. Abstr.*, **55**, 9141d (1961).

[3] A. S. Kudryavtsev and I. A. Savich, *Zhur. Vseses. Khim. Obshchestva im. D. I. Mendeleeva*, **7**, 591 (1962), in *Chem. Abstr.*, **58**, 2121 b (1963).

[4] A. S. Kudryavtsev and I. A. Savich, *Vestnik Moskov. Univ. Ser. II. Khim.*, **18**, 32 (1963), in *Chem. Abstr.*, **58**, 8616d(1963).

[5] A. V. Lapitskii, Ya Yü Chang and I. A. Savich, *Zhur. neorg. Khim.*, **6**, 653 (1961), in *Chem. Abstr.*, **56**, 9706f(1962).

[6] A. S. Kudryavtsev and I. A. Savich, *Zhur. obshchei Khim.*, **33**, 3763 (1963), in *Chem. Abstr.*, **60**, 8873a(1964).

[7] V. A. Kogan, O. A. Osipov, V. I. Minkin and V. P. Sokolov, *Zhur. neorg. Khim.*, **10**, 83 (1965), in *Chem. Abstr.*, **62**, 7362a (1965).

[8] A. S. Kudryavtsev and I. A. Savich, *Zhur. Vseses. Khim. Obshchestva im. D. I. Mendeleeva*, **7**, 591 (1962), in *Chem. Abstr.*, **63**, 17461f(1965).

[9] P. Prashar and J. P. Tondon, *J. Less Common Metals*, **13**, 541 (1967), in *Chem. Abstr.*, **68**, 8893t(1968).

[10] L. V. Orlova, A. D. Garnovskii, O. A. Osipov and O. A. Raevskii, *Zhur. obshchei Khim.*, **37**, 1787 (1967), in *Chem. Abstr.*, **68**, 8897 (1968).

[11] A. D. Garnovskii, V. I. Minkin, O. A. Osipov, V. T. Panyushkin, L. K. Isaeva and M. I. Knyazhanskii, *Zhur. neorg. Khim.*, **12**, 2443(1967), in *Chem. Abstr.*, **68**, 8894u (1968).

[12] T. N. Malskevich, E. P. Trailina and I. A. Savich, *Vestn. Moskov. Univ. Khim.*, **23**, 31 (1968), in *Chem. Abstr.*, **69**, 113017d(1968).

[13] L. V. Orlova, A. D. Garnovskii, O. A. Osipov and I.I. Kukushkina, *Zhur. obshchei Khim.*, **38**, 1850 (1968), in *Chem. Abstr.*, **69**, 113055q (1968).

In the present paper we intend to report the preparation and properties of four titanium (IV) complexes.

The following ligands have been prepared for the preparation of complexes :

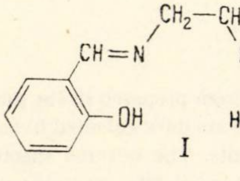

I

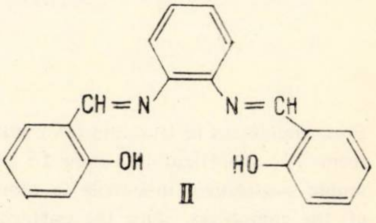

II

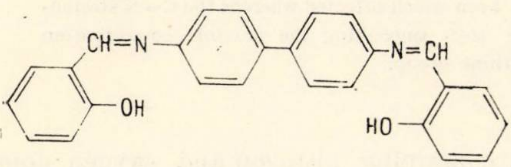

III

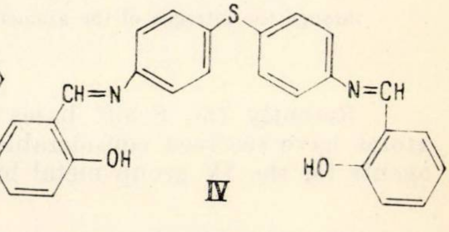

IV

EXPERIMENTAL

The chemicals used were of reagent grade.

p,p′-Dinitrodiphenyl sulphide[14] was prepared by the known method and reduced to its amine with stannous chloride.[15] Salicylaldehyde was distilled before use and anhydrous titanium (IV) chloride of Reidel grade was used as such. Benzene was distilled repeatedly and stored over sodium metal and the same was used as a solvent for the reactions.

All the Schiff bases were prepared by refluxing the diamines with salicylaldehyde in 1 : 2 molar ratio in an alcohol medium. The Schiff bases thus separated were filtered and recrystallized from alcohol.

General preparation and properties

All the complexes were prepared by treating a benzene solution of titanium (IV) chloride with a slight excess of Schiff base in the same solvent. The resulted precipitate was kept under stirring for about 3 hours at room temperature. The precipitate was filtered, washed free from reagent with benzene, and then with ether, and dried in vacuum over anhydrous calcium chloride.

---

[14] C. C. Price and G. W. Stacy, *Org. Synthesis*, **28**, 8233 (1948).

[15] S. R. Safir, S. Kuschner, L. M. Braucone and Y. Subbarao, *J. Org. Chem.*, 924 (1948).

All the complexes are dark coloured, highly hygroscopic and insoluble in almost all organic solvents. Water immediately hydrolyses them and precipitates titanium hydroxide.

Analysis

In the complexes titanium was estimated gravimetrically as TiO_2 and chloride gravimetrically as AgCl. Nitrogen was estimated by the Kjeldahl method. The results of the elemental analyses are given in table 1.

Physical measurements

The infrared spectra of the ligands and the complexes in nujol mull were taken with a Perkin Elmer infracord in the range of $4000-700\ cm^{-1}$.

Table 1

Elemental analysis

Ligand No.	Complex No.	% Titanium		% Nitrogen		% Chloride	
		Found	Calc.	Found	Calc.	Found	Calc.
I	V	10.66	10.45	5.99	6.11	38.50	39.04
II	VI	9.90	9.46	5.60	5.53	27.82	28.06
III	VII	7.98	8.23	4.88	4.81	24.05	24.40
IV	VIII	7.58	7.80	4.34	4.56	22.90	23.13

Table 2

The infrared frequencies (in cm^{-1}) and their assignments

I	V	II	VI	III	VII	IV	VIII	
2632	2597	2778	2667	2646	2646	2703	2632	Inframolecular H-bonded OH
1274	1280	1274	1269	1280	1280	1282	1282	C–O stretching vibration
1618	1626	1616	1600	1618	1642	1616	1639	C=N stretching vibration

RESULTS AND DISCUSSION

The Schiff bases under investigation can take the following course of reaction with titanium (IV) chloride.

a) An addition reaction may occur where the ligand molecule could co-ordinate to the metal ion through the azomethine group.

b) A substitution reaction through the *ortho* hydroxy group and co-ordination through the azomethine group may take place at the same time.

The probability (b) can be ruled out on the strength of the following observations :

1. No HCl gas was evolved during the preparation of the complexes.

2. The analytical data in Table 1 supports the formation of 1 : 1 adducts. A further support for the probability (a) is sought in the comparative study or the infrared spectra of the ligands and the complexes.

The pertinent IR data obtained in the course of this study are summarised in table 2. Tentative band assignments have been made and the following comments have been advanced in support of the assignments.

The ligands are capable of forming intramolecular hydrogen bonds with the azomethine group. This being the case of no absorption, one cannot observe the band due to the free OH stretching vibration in the spectra of the ligands. Instead, the spectra of the ligands show a broad weak band having fine structure in the region of 2800–2600 cm^{-1} and this is attributed to the intramolecular hydrogen bonded OH stretching vibration. This assignment agrees well with that given by Baker and Shulgin,[16] Freedman,[17] Ueno and Martell[18] in the case of salicylideneanilines. A comparison of the spectra of the ligands with the spectra of the complexes indicates that in all the complexes the pattern for the intramolecular hydrogen bonded OH is retained.

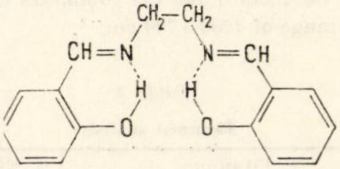

Marvel et al.,[19] have assigned the phenolic C—O vibration in the complexes to the region between 1310 and 1390 cm^{-1}. The phenolic C—O in the free Schiffr bases is usually found near 1280 cm^{-1}. Kovacic[20] finds a strong band for the salicylideneanilines in the same region, and furthermore, he observes shift of this band towards higher frequency in the complexes. In the present work a strong band found around 1280 cm^{-1} in the ligands is ascribed to the phenolic C—O and the absence of this band in the benzylideneaniline confirms the assignment. In the titanium (IV) complexes of these ligands the absorption band due to the C—O stretching vibration is found between 1282 to 1269 cm^{-1}.

A strong band in the region 1618–1613 cm^{-1} in the spectra of the ligands is assigned to the C=N stretching vibration in view of the assignment made by the other workers.[19,20] In the complexes V, VII and VIII, it is found in the region 1642–1626 cm^{-1} and in the complex VI, it is observed at 1600 cm^{-1}.

The above observations help us to come to the following conclusions. The retainment of the pattern in the region 2800–2600 cm^{-1}, and the observed non-shift of the C$-$O stretching vibration induce us to believe that the $-$OH's of the ligands have not taken part in the complex formation and the hydrogen bond existing in the ligands is also maintained in the complexes.

---

[16] A. W. Baker and A. T. Shulgin, *J. Amer. Chem. Soc.*, **81**, 1523 (1959).

[17] H. H. Freedman, *J. Amer. Chem. Soc.*, **83**, 2900 (1961).

[18] K. Ueno and A. E. Martell, *J. Phys. Chem.*, **60**, 1270 (1956).

[19] C. S. Marvel, S. A. Aspey and E. A. Dudley, *J. Amer. Chem. Soc.*, **78**, 4909 (1956).

[20] J. E. Kovacic, *Spectrochim. Acta*, **23A**, 183 (1967).

The shift observed in the C$=$N stretching vibration suggests the possible co-ordination through the nitrogen of the azomethine group.

The insolubility of the complexes in the organic solvents and their hygroscopic nature have made the further studies difficult. However, in view of the hexacovalency of titanium (IV) these may be regarded as the complexes of co-ordination number six.

Acknowledgement. The authors wish to thank Professor D. K. Banerjee I. I. Sc., Bangalore, for the infrared spectra. One of the authors (V.H.K.) is grateful to the authorities of the Karnatak University for the financial support.

F 1103

Revue Roumaine de Chimie, 15, 1999–2016 (1970)

INDEX DES AUTEURS

A.

page

ACHOUR M., voir BENALI BAITICH O. . . . 15
AHMAD M. S., voir DOSS S. H. 1611
ALBERT F. M. and A. MEGHEA, Electron spin resonance (ESR) study of the oxidation of some aromatic amines with sodium chlorite. 395
ANDREI C. and D. MIHĂIȚĂ, I. HOGEA, D. MUNTEANU, Grafting of maleic anhydride on ethylene vinyl acetate copolymer in homogeneous medium in presence of peroxide initiators 239
— voir NANU I. 1883
ANTONESCU E., voir SPACU P. 731
ARMEANU V. and L. M. BĂLOIU, Contributions to the study of the system dicyanoaurous acid-isoamyl alcohol-water 1057
ARSENE A., voir BALABAN A. T. . . . 635
— and M. PARASCHIV, A. T. BALABAN, Reaction of ethyl *o*-phenylene arsenite with tropolone 247
ARSENIE I. et I. LEUCĂ, Contribution à la séparation du zirconium d'avec le hafnium par cristallisation fractionnée de l'hexafluozirconate de potassium 1263
— et I. LEUCĂ, Variation de certaines propriétés du $K_2Zr(Hf)F_6$ par déhafnisation 1987
ARSHAD M. and A. BEG, B. BILQUIS, Studies on coordination compounds. Cobalt (II) complexes of adipyl dihydrazides 1857
and A. BEG, M. S. SIDDIQUI, Spectroscopic studies of organophosphorus compounds. Ultraviolet spectra of phosphine-quinone adducts . 1653
AUSLÄNDER D. et C. ȘERBAN, I. DĂBALĂ, Action des ultrasons sur un processus de carbonatation. 1441
AVRAM M. and F. CHIRALEU, I. POGANY, Investigations in the cyclobutane series. XXIX. NMR spectra studies of some 3.4-benzo-tricyclo [4.2.1.0^{2,5}] nona-3.7-diene derivatives 1219
— and F. CHIRALEU, I. POGANY, I. G. DINULESCU, Investigations in the cyclobutane series. XXX. NMR spectral parameters of some compounds with benzocyclobuteno-norbornene and -norbornane skeleton 1767
— and D. CONSTANTINESCU, I. G. DINULESCU, OANA CONSTANTINESCU-SIMON, GH. D. MATEESCU, C. D. NENITZESCU, Investigations in the cyclobutane series. XXVII. Attempted synthesis of 4.6-dimethyl-1-tert-butyl-benzo-cyclobutadiene and 4.6-dimethyl-1-chloro-benzo-cyclobutadiene 1097
— and I. POGANY, I. G. DINULESCU, F. CHIRALEU, C. D. NENITZESCU, Investigations in the cyclobutane series. XXVIII. The reaction of *endo* and *exo*-3.4-benzotricyclo [4.2.1.0^{2,5}] nona-3.7-dienes with electrophylic reagents 1207

B.

BADEA M., voir HÖRER O. L. 829
BĂDILESCU I. I., Hydrogen bonds. III. HMO treatment of some chelated compounds related to 2-hydroxyacetophenone 873
BĂDILESCU S., Simultaneous vibrational transitions. II. Induced simultaneous vibrational transitions in some haloform — carbon disulfide mixtures 1931
BALABAN A. T., Chemical graphs. VIII. Valence isomerism and general cubic graphs 463
— Chemical graphs. X. (Aromaticity. VIII) Resonance energies of *cata*-condensed benzenoid polycyclic hydrocarbons 1243
— Chemical graphs. XI. (Aromaticity. IX.) Isomerism and topology of non-branched *cata*-condensed polycyclic conjugated non-benzenoid hydrocarbons 1251
— voir ARSENE A. 247
— and A. ARSENE, I. BALLY, A. BARABÁS, M. PARASCHIV, M. ROMAN, E. ROMAȘ, Heterocyclic organoboron compounds. XII. 2,4,6-Trisubstituted -1,3,2-dioxaborinium salts . 635
BALABÁN L. and L. PREISLER, The evolution of gaseous products during

page

the photo-oxidative degradation of polypropylene 123

Balint A., The synthesis of some new 3,6-dichloro-2,5-bisphenylamino-1,4-benzoquinone derivatives with electron-donor and electron-acceptor groups 627

— and Z. Simon, M. Mracec, Molecular orbital calculations in the 2,5-diamino-1,4-benzoquinone series. III. Pariser-Parr-Pople calculations for 2,5-bisphenylamino-1,4-benzoquinone 511

Bally I., voir Balaban A. T. 635

Balog A. and D. Breazu, E. Vargha, F. Gönczy, L. Beu, Peptides. VIII. Some β-dicarbonyl N-protected aminoacids and model dipeptides 1375

— and E. Vargha, D. Breazu, L. Beu, F. Gönczy, Peptides. IX. The activation and protection of the carboxyl group in the β-dicarbonyl N-protected aminoacid series . . . 1391

Băloiu L. M., voir Armeanu V. . . . 1057

Baltă P., voir Solacolu S. 91, 741, 957

Banciu A.-C., voir Popea F. 1319

Barabás A., voir Balaban A. T. . . . 635

Bărbulescu A., voir Solacolu S. 1851

Bărbulescu F., voir Beldie C. . . . 385, 847

Bărbulescu N. und F. Potmischil, Darstellung und Untersuchung der Hydroacridine. VII. Ein Direkt-Verfahren zur Darstellung von N-Alkyl-und N-Aryl-Perhydroacridine 1601

Beg A., voir Arshad M. 1653, 1857

Beldie C., Activity coefficients in ternary systems phenol-water-electrolyte 221

— Salting-in effects in organic solvent-water-organic electrolyte systems. Molecular weight of the organic electrolytes 1191

— and F. Bărbulescu, Salt effects in ternary systems furfural-water-electrolyte. I. Ternary systems furfural-water-uni-univalent electrolyte 385

— and F. Bărbulescu, Salt effects in ternary systems furfural-water-electrolyte. II. Ternary systems furfural-water-organic electrolyte . . 847

Benali Baitich O. et M. Meklati, M. Achour, Interprétation des spectres électroniques d'ions complexes cyanes de fer (II) et de fer (III) dans l'approximation de la théorie du champ cristallin 15

page

Bendic C., voir Sahini V. E. 1795

Beu L., voir Balog A. 1375, 1391

Bhatnagar V. M., The cell parameters of synthetic fluorapatite, $Ca_{10}(PO_4)_6F_2$ 87

— The cell parameters of strontium hydroxy-apatite, $Sr_{10}(PO_4)_6(OH)_2$. 951

— The cell parameters of synthetic calcium apatites 1735

— New observations on lead apatites 955

Bilquis B., voir Arshad M. 1857

Biradar N. S. and V. H. Kulkarni, Schiff base complexes of Ti (IV) 1993

Bîrhală Al., voir Vîlcu R. 175, 1813

Bocaniciu L., voir Goina T. 1049

Bodea C., voir Fărcăşan V. 1433

— voir Nicoară E. 965

— voir Oprean I. 135

— and T. Panea, V. Fărcăşan, Synthetical phenothiazine glycosides. III. Oxidation reaction . . . 1923,

— voir Tămaş V. 655, 819

Bodor N. and N. Trinajstić, Valence-shell MO calculations for formamide and related compounds 1807

Bonciocat N. and L. Chiosa, F. Mihăilescu, M. Olteanu, Chemical reactions in liquid junctions. I. The expression of the liquid-junction potential 1307

— and L. Chiosa, F. Mihăilescu, M. Olteanu, Chemical reactions in liquid junctions. II. A new potentiometric titration method . . . 1513

Borcan R., voir Zuca Şt. 1681

Bostan M., voir Giurgiu D. 1581

Bostan M., voir Ciobanu A. 783

Botar A., voir Ripan R. 1529, 1537

Breazu D., voir Balog A. 1375, 1391

C.

Caproşu M. et M. Petrovanu, I. Zugrăvescu, L'addition des philodiènes sur la 1-méthyl-phtalazine et sur la β-phényl-vinyl-phtalazine . 619

Carpov A., voir Poinescu Ig. . . . 441

Chiorean L., voir Popper E. 115

Chiosa L., voir Bonciocat N. 1307, 1513

Chiraleu F., voir Avram M. 1207, 1219, 1767

Chiriac C. et I. Zugrăvescu, Pyrazoles. I. N-arylation des pyrazoles avec

page
des dérivés chlorurés aromatiques activés par les groupements nitro 789
— et I. Zugrăvescu, Pyrazoles. II. Aminolyse des 1-(2,4-dinitrophényl)-pyrazoles 1065
— et I. Zugrăvescu, Pyrazoles. III. N-arylation de N-acylpyrazoles avec le chlorure de picryle 1201
Chiriţă C., voir Mavrodin Al. 1953
Chirulescu T., Nickel ferrite-oxygen magnetization-volume adsorption isotherm 1303
— and E. Segal, Adsorptive properties of a nickel ferrite 1727
— and E. Segal, Gas chemisorption on ferromagnetic powder. IV. Hydrogen, oxygen ferrites system at liquid nitrogen temperature 67
Christov D. und N. Nenov, Über die Darstellung des 3,7-dichlorphenthiazins durch die Reduktion seines Oxides mit Stannochlorid 1777
Ciobanu A., voir Giurgiu D. 1581
— et L. Roman, M. Bostan, N. Voiculescu, D. Giurgiu, Combinaisons zinc-diarylamides. II. L'échange entre le diphénylzinc et les amines aromatiques primaires 783
Ciopec M., voir Marchidan D. I. 1005, 1177, 1287
Cismaru D. and Al. Fruma, D. Crăciunescu, Determining the size of metal particles in hydrogen chemisorption measurements 1485
— and D. Manolescu, Crystal structure studies of solid solutions in the system Al_2O_3-Cr_2O_3-Li_2O 291
— et E. Segal, S. Fătu, Étude de la chimisorption de l'oxygène sur des couches minces d'argent par des mesures de force thermoélectromotrice 161
— and S. Zervudis, Kinetics of the Al_2O_3+CoO reaction at high temperature accompanied by spinel formation in oxygen atmosphere 1163
Ciubotariu C., voir Feldman D. 1893
Ciubotariu M., voir Feldman D. 1893
Ciuhandu G. et M. Mracec, Dosage photométrique du benzène et de la *m*-phénylènediamine 757
Ciurdaru Gh. and M. Fărcăşan, V. I. Dénes, Methylene bases of heterocycles. IX. Spectral study of 2-acylmethyleneazolines and their protonated forms 1975
Comşa G., voir Murgulescu I. G. 987
Constantin V., voir Sahini V. E. 495

page
Constantinescu D., voir Avram M. 1097
Constantinescu E. and T. Marian, The anodic behaviour of pure aluminium in acidic solutions of potassium halides 333
Constantinescu-Simon O., voir Avram M. 1097
Cordiş V., voir Ripan R. 559, 719
Cordoş E., An automatic ratemeter for consecutive slope measurements 661
— voir Liteanu C. 583
Cornea F. et C. Fulea, S. Moldoveanu, Complexes moléculaires des thioamides. I. Complexes de transfert de charge entre le thiobenzamide, la thiobenzpipéridine et l'iode 1415
Costache D., Kinetic measurement of cobalt traces. III. With ponceau red 945
— Kinetic measurement of cobalt traces. IV. With hematoxylin 1181
— and Gr. Popa,Kinetic determination of cobalt traces. V. With brompyrogallol red 1349
— and P. Junie, Kinetic measurement of cobalt traces. I. With magnezon 1 597
— and Gr. Popa, Kinetic determination of cobalt traces. II. With tropeoline 0 761
— and Gr. Popa, Kinetic dosing of the cobalt in vitamine B_{12} 1061
Costeanu G. et O. Landauer, C. Mateescu, L'influence du solvant sur la vitesse de réaction. L'hydrolyse alcaline de l'acétate de *n*-butyle dans le solvant mixte eau-dioxane 27
Costin R., voir Zuca Şt. 1831
Crăciunescu D., voir Cismaru D. 1485
— voir Fruma Al. 71
Craiu M., voir Sahini V. E. 675
Crişan I. Al., voir Şuteu A. 1187, 1337
Crişan T., voir Feldman D. 1893
Cristescu C., As-triazine derivatives with potential therapeutic action.X. 6-Carboxyhydrazide-as-triazines 1409
— 6-azauracil derivatives with potential cytostatic activity. IX. 6-azauracil-5-sulfonamides 1121
Curea E., voir Grecu I. 409
Czeglédi L. et Const. Gh. Macarovici, Combinaisons complexes avec des hydroxyacides. XIV. L'étude spectrophotométrique du système $ZrOCl_2$- acide D-gluconique 1741
— voir Macarovici Const. Gh. 1863

Revue Roumaine de Chimie, 15, 1999–2016 (1970)

page

D.

Dăbală I., voir Ausländer D. 1441
Demetresco C. et V. Manu, M. Vanghelovici, Contribution à la chimie des phényl-2-benzylidène-4-azlactones-5. Synthèses de nouvelles hydrazydes substituées douées d'action psychoénergisante et parasympathicolytique 1623
— voir Mavrodin Al. 1953
Demetrescu I., The effect of electrostatic energy in reactions between benzhydril chloride and normal alcohols 1721
— voir Murgulescu I. G. 141
Dénes V. I., voir Ciurdaru Gh. 1975
Dick J. and A. Maurer, Neue Komplexverbindungen der Pyrazolonreihe. VI. 103
— und A. Maurer, Z. Szabadai, Neue Komplexverbindungen der Pyrazolonreihe. VII. Sichtbare-und UV-Spektren 917
Dima M., voir Marcu M. 423, 1365
— Petrariu I. 1573
Dinescu R., voir Solacolu S. . . . 401
Dinulescu I. G., voir Avram M. . . . 1097, 1207, 1767
Dobre E., voir Răileanu M. 823
Dobrescu M., voir Sahini V. E. . . . 679, 1795
Doss S. H. and M. S. Ahmad, New synthetic chemical compounds with expected schistosomicidal activity . 1611
Drăgulescu C. und R. Pomoje, I. Menessy, M. Pîrlea, Metallkomplexe der Anthranylessigsäure (ANDA). IX. Das System Al-ANDA . . . 1543
— und R. Pomoje, I. Menessy, M. Pîrlea, C. Mihăescu, Metallkomplexe der Anthranyldiessigsäure (ANDA). VIII. Über Cr(III)-ANDA-Komplexe 1029
— und T. Simonescu, G. Nemes, M. Totan, Untersuchungen der Komplexe Th-Alizarin und Th-Chinalizarin durch Extraktion mit Butanol-1 563
Dressnandt G., voir Feldman D. . . 1893

F.

Fărcăşan M., voir Ciurdaru Gh. . . 1975
Fărcăşan V., voir Bodea C. 1923
— voir Oprean I. 135
— et I. Oprean, C. Bodea, Sur la formylation des méthyl-10-phénothiazines 1433

page

Fărcaşiu M. and R. Istrăţoiu, The donor-acceptor complexes of N-substituted maleimides with amines, and their role in nucleophilic addition reaction 253
Fătu D. et S. Fătu, A. Teodorescu, E. Segal, Cinétique de la décomposition thermique de quelques combinaisons complexes des halogénures de cadmium avec des picolines . . . 855
Fătu S., voir Cismaru D. 161
— voir Fătu D. 855
Feldman D. and N. Simionescu, C. Ciubotariu, M. Ciubotariu, T. Crişan, G. Dressnandt, Butadiene-styrene carboxylated copolymers 1893
Fey L., voir Szotyori L. 1615
Fişel S. und G. Nemes, M. Totan, T. Simonescu, Der Einfluß der Trichloressigsäure (TCE) auf die Thorium-extraktion aus wäßrigen Lösungen mit Butanol-1 1043
Fiti M., La cinétique de compétition dans l'étude des intermédiaires instables. I. Les ions Co^{+}, Mn^{+}, Zn^{+}, Cd^{+} et Ni^{+}. 77
Fruma Al., voir Cismaru D. 1485
— et D. L. Crăciunescu, C. I. Ghirvu, L'influence de la structure électronique sur l'effet catalytique des complexes cuivre-aniline substituée 71
Fulea C., voir Cornea F. 1415
Furnică Gh., Recherches sur la dégradation des macromolécules polysulfoniques au moyen des isotopes radioactifs 1591
— et V. Voicu, Rétention de certains ions radioactifs par les macromolécules inorganiques naturelles des suspensions des bassins de surface et de certaines terres actives . . . 1087

G.

Galasiu I., voir Sternberg S. 1169
Gănescu I. et Al. Popescu, Complexes thiocyanato-chromiques dans l'analyse chimique. I. Détermination gravimétrique et colorimétrique de la pypérazine avec les analogues du sel de Reinecke 1343
Ganovici I. and L. Ganovici, Self-diffusion of liquid cadmium from its melting point to 500°. 213
— voir Nicoloiu E. 1713
Ganovici L., voir Ganovici I. . . . 213
— voir Nicoloiu E. 1713
Ghergariu-Mîrza L., voir Liteanu C. 1871
Ghirvu C. I., voir Fruma Al. . . . 71
— voir Sahini V. E. 11

page

Gioabă A. and O. Maior, Condensed heteroaromatic systems. Halogenation and dehalogenation with phenoxathiine, phenoxaselenine, phenoxatellurine and phenothiatellurine 1967
— and V. Em. Sahini, E. Volanschi, Charge transfer complexes of the aromatic heterocycles. II. CT-complexes of phenoxatellurine and some of its derivatives with TCNE . . 309
— and V. E. Sahini, E. Volanschi, Spectral study of phenoxatellurine and some of its derivatives . . . 501
Giurgiu D., voir Ciobanu A. 783
— und I. Popescu, A. Ciobanu, M. Bostan, N. Voiculescu, L. Roman, Arylaluminium-Phosphin Verbindungen 1581
Gocan S., voir Liteanu C. 1751
Goia I. and M. Ionescu, Acridones. XXXV. The iodination of acridone 1233
— voir Ionescu M. 1785
Goina T. and M. Olaru, Formation of aluminium complexes with pyrogallol 1547
— and M. Olaru, L. Bocaniciu, Formation constants of the aluminium ion chelates with pyrocatechol and pyrocatechol violet 1049
Gönczy F., voir Balog A. 1375, 1391
Görbe I., voir Nagy P. 881
— voir Nemes V. 711
Gorea V., voir Hodişan T. 615
Grecu I. et E. Curea, Combinaisons complexes de la dihydrazinophtalazine (DHF). Les sélénocyanates dihydrazinophtalazino-métalliques . 409
Gropşianu Z. und D. Kohn, A. Iovi, Wärmeübergangszahlen beim Verdampfen von Kaliumnitratlösungen 887
Gruia M. and O. Körner, A. Nicolescu, The variation of physico-structural properties of some aluminium hydroxides as against their formation conditions 457

H.

Haiduc I., voir Liteanu C. 1555
Herdlicka C., voir Sternberg S. . . 343
Hillebrand M. and O. Maior, V. Em. Sahini, Charge transfer complexes of the aromatic heterocycles. I. CT-complexes of some phenoxathiin derivatives 149
Hodişan T., voir Liteanu C. 1751
— und A. Şuteu, V. Gorea, Eine neue kolorimetrische Bestimmungsmethode des Urans (VI) 615
Hogea I., voir Andrei C. 239
Hopîrtean E., voir Liteanu C. . . . 749, 1331
Hörer O. L. and M. Badea, UV irradiation of UMP on paper 829

I.

Ionescu M., voir Goia I. 1233
— and I. Goia, M. Vlassa, Acridone. XXXVI. The chlorination of iodo-acridones 1785
— und K. Makkay, Das Verhalten einiger Oxazolidone-(4). VIII. Über den Reaktionsmechanismus bei der Bildung der 2,5-disubstituierten Oxazolidone-(4) 265
Ionescu N. I., About the mechanism of electrical resistance variations in thin copper and silver films during oxygen chemisorption 273
— About the electrical resistance variations in thin iron films during water chemisorption and decomposition 1525
— On the Ellovich equation . . . 1847
Iosif I. and I. A. Schneider, On the cool flame in the reaction of methane oxidation 1827
Iovi A., voir Gropşianu Z. 887
Irinei F., voir Vîlcu R. 43
Istrăţoiu R., voir Fărcaşiu M. . . . 253
Ivana E., voir Murgulescu I. G. 669
— voir Popa E. 1707

J.

Jitianu G., voir Solacolu S. . . . 91, 741, 957
Junie P., voir Costache D. 597

K.

Kékedy E., voir Zsakó J. 865
Kerek F., voir Ostrogovich G. . . . 1453
Kohn D., voir Gropşianu Z. 887
Körner O., voir Gruia M. 457
Kövendi Al., voir Szotyori L. . . . 1615
Kulkarni V. H., voir Biradar N. S. 1993

L.

Landauer O., voir Costeanu G. . . . 27
Leucă I., voir Arsenie I. 1263, 1987

page

Levison K. A. and P. G. Perkins, The electronic structure and geometry of aluminium borohydride 153

Lică S., L'électrolyte pâteux utilisable dans les accumulateurs électriques 543

Liteanu C. and E. Cordoş, L. Mărgineanu, Automatic potentiometric titration in molten media. I. A. new automatic continuous procedure for potentiometric titration in molten media with solid standard . . . 583

— et L. Ghergariu-Mîrza, Titrage conductométrique à résistance indicatrice. II. Titrage de l'acide chlorhydrique en solutions concentrées de chlorures de sodium à résistance membrane PCV + plastifiant + montmorillonite-natrium 1871

— et S. Gocan, T. Hodişan, La thermochromatographie sur papier. XIV. La possibilité de séparer certains ions ayant les valeurs R$_f$ pratiquement égales en chromatographie isotherme 1751

— and I. Haiduc, Pretreated indicating electrodes in potentiometric titrations. II. Bright palladium-hydrogen electrode in acid-base titration 1555

— et E. Hopîrtean, Étude sur les électrodes-membranes polymère + plastifiant. I. L'obtention et le comportement électrodique de la membrane de PCV et tricrésyl-phosphate sensible aux ions d'hydrogène . . 749

— et E. Hopîrtean, Étude sur les électrodes-membranes polymère + plastifiant. III. L'utilisation de l'électrode-membrane en PCV et tricrésylphosphate dans le titrage potentiométrique des acides et bases forts 1331

— voir Lukács I. 935

— and I. C. Popescu, The use of membranes to indicate the equivalence point. V. The parchment-paper membrane impregnated with BaSO$_4$, indicating electrode in Cl$^-$, Br$^-$, I$^-$ titration 973

Luca C., voir Petrariu I. 1573

Lukács I. et C. Strusievici, C. Liteanu, Sur les vanadates. XVIII. Composés mixtes V^{5+} — V^{4+} obtenus en solutions aqueuses 935

Lupu D., Magnetic exchange in a heterogeneous trinuclear system . . 417

M.

Macarovici Const. Gh., voir Czeglédi L. 1741

page

— et L. Czeglédi, Combinaisons complexes avec des hydroxyacides. XV. L'étude potentiométrique du système ZrOCl$_2$-acide D-gluconique 1863

— und F. Mánok, Cs. Várhelyi, Polarographische Untersuchung der Reaktion zwischen Pentachloro-aquo-platin(IV)-Säure und 1,2-Cyclohexandiondioxim 895

Macovschi M. E, and V. Niţu, Photometric determination of copper traces without extraction 605

— voir Radovici O. 167

Macovschi O., voir Mavrodin Al. . . 1953

Maior O., voir Gioabă A. 1967

— voir Hillebrand M. 149

Makkay K., voir Ionescu M. 265

Malinovský M., voir Paučirová M. 33, 201

Maniu C., voir A. Şuteu 119

Mánok F., voir Macarovici Const. Gh. 895

Manolescu D., voir Cismaru D. . . 291

Mântăluţă E., voir Stoicescu-Crivetz L. 129

Manu V., voir Demetrescu C. 1623

Marchidan D. I. and M. Ciopec, High temperature enthalpy and related thermodynamic functions of some materials from the uranium-oxygen system 1287

— and M. Ciopec, Thermal properties of aluminium. High-temperature heat content 1005

— and M. Ciopec, Thermal properties of potassium chloride. High temperature heat content 1177

— and S. Matei, High temperature thermodynamic properties of some uranium oxides from EMF measurements on solid electrolyte galvanic cells 1491

— and Cr. Telea, The heat of mixing in binary systems of molten salts : KCl + RbBr and KBr + RbCl 1675

Marcu M. and M. Dima, Coordination polymers. III. Polycoordination of 4,4'-diphenylsulphonedicarboxyldehyde bis (thiosemicarbazone) with cadmium and mercury 423

— and M. Dima, Coordination polymers. IV. Polycoordination of 4,4'-[p-phenylene-bis(methyliden-nitrilo)]-dimethyl salicylate with cobalt, nickel and copper 1365

Mărgineanu L., voir Liteanu C. . . 583

Marian T., voir Constantinescu E. 333

Mateescu C., voir Costeanu G. . . . 27

Mateescu Gh. D., voir Avram M. . . 1097

Matei S., voir Marchidan D. I.. . . 1491

page

MÁTHÉ J., Evidence of neighbour cation influence and correlation effect from ligand field calculations 283
MATIAŠOVSKÝ K., voir PAUČIROVÁ M. 33, 201
MAURER A., voir DICK J. 103, 917
MAVRODIN AL. et C. DEMETRESCU, C. CHIRIȚĂ, O. MACOVSCHI, Recherches dans la classe des *p*-fluor-diphényl-sulfones. I. Synthèses de nouveaux composés à l'efficience antibactérienne 1953
MAXIM S., voir POINESCU IG. 441
MEGHEA A., voir ALBERT F. M. . . . 395
MEKLATI M., voir BENALI BAITICI O. 15
MENESSY I., voir DRĂGULESCU C. . . . 1029, 1543
MIHĂESCU C., voir DRĂGULESCU C. . 1029
MIHAI FR. und R. NUȚIU, Verbindungen der Dilitursäure mit Anilin und Phenylendiaminen 573
MIHĂILESCU F., voir BONCIOCAT N. . . 1307, 1513
MIHĂIȚĂ D., voir ANDREI C. 239
MIHALCEA I., voir MURGULESCU I. G. 3
MINCU M. et E. SEGAL, Propriétés magnétiques des combinaisons complexes des halogénures des métaux bivalents avec des composés pyridiniques 539,
MÎNDRU I., Surface-active cationic substances of the type alkyl-ether-trimethylammonium and alkyl-ether-pyridinium halides. II. Study on the micelle formation of the dodecylpolyoxiethylene-trimethyl-ammonium and dodecylpolyoxiethylene-pyridinium chlorides 775
MÎNDRUȚIU E., voir ȘUTEU A. 1187
MÎRZA L., voir ȘUTEU A. 1563
MISDOLEA C., voir VÎLCU R. 1839
MOLDOVEANU S., voir CORNEA F. . . . 1415
MRACEC M., voir BALINT A. 511
— voir CIUHANDU G. 757
MUNTEANU D., voir ANDREI C. . . . 239
MURGULESCU I. G., Some physico-chemical properties of simple molten salts. II. 1463
— und G. COMȘA, Adsorption von Kohlenmonoxid an dünnen Silberschichten 987
— and I. DEMETRESCU, Kinetics of the reactions between benzyl bromide and normal alcohols 141
— and I. MIHALCEA, Radiolysis of the hexamminocobaltic nitrate in aqueous solutions 3
— and D. OANCEA, Nucleophilic substitutions. II. Reactions between benzyl bromide and alkali alcoxides 299
— and D. OANCEA, Nucleophilic substitutions. III. The kinetics of the reactions between benzyliodide and sodium alcoxides 1635
— et E. POPA, E. IVANA, Le spectre d'absorption des halogénures de plomb fondus 669
— and D. TODOR-BOGDAN, Kinetics of reaction between 1-phenyl-azo-2-naphthol and copper chloride . . 1473
— et D. TOPOR, Electromigration dans les nitrates monovalents fondus. Les ions de strontium et de baryum 843
— et L. TOPOR, L'association moléculaire des iodures alcalins en phase gazeuse 997
— and M. I. VASS, Surface potential variations during nitrogen adsorption on thin copper films 489
— and M. I. VASS, Surface potential variation at successive carbon monoxide and oxygen adsorption on thin silver films 1143
— and L. VASU, Correlations between electrical conductivity and diffusion in molten salts 837
MUSA M., Absorption spectra of $CoCl_2$ and $CoBr_2$ isolated in benzene matrix 705

N.

NAGY P. and I. GÖRBE, A. SZURKOS, The substituent effects on the halfwave potentials of the *p*-dimethyl-amino-*o′*, -*m′*, -*p′*-substituted azobenzenes 881
— voir NEMES V. 711
— voir SZURKOS A. 607
NANU I. and C. ANDREI, Copolymers of conjugated dienes with maleic acid monoesters. I. Isoprene copolymerization with the methylic monoester of the maleic acid 1883
NAȘCU H, voir ȘUTEU AL. 1759
NEBELL H., Thermodynamic properties of liquid magnesium-lead, magnesium-indium and magnesium-gallium alloys 59
NEMES G., voir DRĂGULESCU C. . . . 563
— voir FIȘEL S. 1043
NEMES V. and I. GÖRBE, P. NAGY, Correlation between the structure and basicity constants of the *p*-dimethylamino-*p′*-*m′*-X-azobenzenes based

page

on Hammett and Ismailow equations 711
Nenitzescu C. D., voir Avram M. . . 1097, 1207
— voir Roşca S. 259
Nenov N., voir Christov D. 1777
Nicoară E. and D. Oşianu, C. Bodea, Inchain epoxides on carotenoids. I. 9,10-and13,14-epoxy-canthaxanthin 965
Nicolescu A., voir Gruia M. 457
Nicolescu I. V., voir Spinzi A.. . . 451, 1901
Nicoloiu E. und L. Ganovici, I. Ganovici, Die Selbstdiffusion des flüssigen Tellurs im Temperaturbereich von 460—600° C 1713
Niculescu E., voir Stanciu-Stoian E. 1077
Niţu V., voir Macovschi M. 605
Nuţiu R., voir Mihai Fr. 573

O.

Oancea D., voir Murgulescu I. G. 299, 1635
Odochian L. and I. A. Schneider, Some aspects of methane cracking kinetics in static conditions, I. The influence of the initial pressure of methane 1647
Olaru M., voir Goina T. 1049, 1547
Olteanu M., voir Bonciocat N. . . . 1307, 1513
Olteanu M., voir Zuca Şt. 357, 1503
Oncescu T., On the intermediate in the reaction mechanism of Me(III) oxalato complexes decomposition. . . 209
Onu A., voir Vasile C. 1935
Oprean I. and C. Bodea, V. Fărcăşan, On the synthesis of 3-nitro-10-methyl-phenothiazine 135
— voir Fărcăşan V. 1433
Oşianu D., voir Nicoară E. 965
Ostrogovich G. und M. Safta, Studien auf dem Gebiet der symmetrischen Triazine (Neue Serie). IV. 2,4-Dioxo-6-(*p*-X-β-styryl)-tetrahydro-s-triazine; Elektronenspektroskopie der Basen und ihrer Protonierung 799
— and Z. Simon, F. Kerek, Stereochemistry of imine systems. III. Mechanism of their uncatalysed *syn-anti*-isomerization. The influence of the substituent on the activation energy 1453

P.

Panea T., voir Bodea C. 1923
Paralescu I., The molar absorptivity and stability of some complex compounds of the BA_n form 901
Paraschiv M., voir Arsene A. 247
— voir Balaban A. T. 635
Pascu N., voir R. Ripan 719
Paučirová M. and K. Matiašovský, M. Malinovský, Contribution to the study of the structure of molten $LiF—AlF_3$ and $NaF-AlF_3$ mixtures 201
— and K. Matiašovský, M. Malinovský, Volume properties of the melts of the systems $LiF—AlF_3$ and $NaF-AlF_3$ 33
Pavlovič and R. Popovič, Thermodynamics of the behaviour of Pb(II)-ions in acid and alkaline solution 313
Perkins P. G., voir Levison K. A. . . 153
Petrariu I. and C. Luca, M. Dima, Quaternary basic ammonium polyelectrolytes. II. Chlorination with thionyl chloride of some quaternary basic ammonium polyelectrolytes containing hydroxylic groupings 1573
Petrescu M., voir Petrescu N. 189
Petrescu N. and M. Petrescu, Self-diffusion of liquid bismuth from its melting point to 700° 189
Petrovanu M., voir Caproşu M. . . 619
Petruş I., Reactions in solid media. II. Kinetics of the formation of the double oxide of powder mixtures in nitrogen atmosphere 53
— voir Stanciu-Stoian E. . . . 1077
Pîrlea M., voir Drăgulescu C. . . 1029, 1543
Pitea I., voir Popper E. 115
Podină C., voir Sahini V. E. 495
Pogany I., voir Avram M. 1207, 1219, 1767
Poinescu Ig. and S. Maxim, A. Carpov, Synthesis of the sulphuric ester of poly(vinyl alcohol) 441
Pomoje R., voir Drăgulescu C. . . . 1029, 1543
Pop E., voir Şuteu A. 1337
Popa E. and E. Ivana, S. V. Volkov, Electronic absorption spectra of $ZnCl_2$, $CdCl_2$ and AgCl in passing from solid to molten state 1707
— voir Murgulescu I. G. 669
Popa Gr., voir Costache D. 761, 1061, 1349
— and D. M. Todor, Determination of the siderite and ankerite content by thermal analysis methods 589
Popa M. V., voir Radovici O. . . . 515
Popea F. und A.-C. Banciu, Spektrophotometrische Untersuchung im System $Th(NO_3)_4$-Violursäure 1319

page

Popescu A. and A. Szabo, The activity of molybdenun oxide-bismuth oxide catalysts and the influence of metallic oxide mixtures 1197

Popescu Al., voir Gănescu I. 1343

Popescu B., voir Radovici O. 1799

Popescu Fl., Polymères organiques phosphorylés. III. Phosphorylation du polystyrène dans les hydrocarbures aliphatiques (C_6-C_8). 1355

Popescu G., L'étude de la viscosité de structure des solutions de stéarate d'aluminium dans les hydrocarbures. L'Influence de quelques composés polaires 431

Popescu I., voir Giurgiu D. 1581

Popescu I. C., voir Liteanu C. 973

Popović R., voir Pavlović Z. 313

Popper E. and L. Chiorean, I. Pitea, Photocolorimetric study of Pd(II) and the α-ethyl-isonicotinic acid thioamide 115

— and A. Szabo, P. Szentgyörgyi, The microanalysis of cobalt by electrophoretic focussing with radioactive tracer 1447

Potmischil F., voir Bărbulescu N. 1601

Preisler L., voir Balaban L. 123

R.

Radovici O. and M. Macovschi, Hydrogen overvoltage on thin evaporated metal films. II. Application of Tafel equation to thin metal films . 167

— and M. V. Popa, The kinetics of cobalt corrosion process 515

— and B. Popescu, Corrosion and passivity of some Pb-Sn alloys in media of different pH 1799

— and V. Surdeanu, Passivity of steel in monoethanolamine solutions 1153

— and N. Totir, The anodic oxidation of acetylene and methane on porous platinum and palladium electrodes 683

— and V. Tucsek, The potential distribution and the surface charge at the silicon-hydrofluoric acid interface 325

Răileanu M. and E. Dobre, Volumetric dosage with phenothiazone-(3). III. The dosage of the thiolic compounds with phenothiazone-(3) 823

Radu M., Electrical conductivity in relation with dispersion degree of lyophilic colloids. XI. 0.2 Sodium stearate aqueous solutions with additions of *o*-cresol and various hydrocarbons 767

Rădulescu T. und H. D. Schell, Quartäre Ammoniumsalze des Acetamido-benzal-fluorens 1127

— und H. D. Schell, Mono- und diquartäre Ammoniumsalze des Benzal-Fluorens. 1427

Reichel J. und C. Tărăbăşanu Forschungen in der indigoiden Serie. II. Neue gemischte kondensierte azo-indigoide Systeme 1907

— und R. Vidac, Untersuchungen über Aryldiazosulfonate und Aryldiazosulfonsäuren. I. Über das photochemische Verhalten des benzoldiazosulfonsauren Natriums. . . . 1107

— und R. Vidac, Untersuchungen über Aryldiazosulfonate und Aryldiazosulfonsäuren. II. Herstellung und photochemisches Verhalten der Benzoldiazosulfonsäure 1227

Ripan R. und A. Botar, Eine neue Gruppe von Heteropolyverbindungen des U(IV). I. Uran(IV)-Oktowolframanion, Synthese der Alkalisalze und die Bestimmung ihrer Basizität 1529

— und A. Botar, Eine neue Gruppe von Heteropolyverbindungen des U(IV). II. Photokolorimetrische Studien der Bildung des $[UW_8O_{28}]^{4-}$in Abhängikeit von pH, Temperatur und Zeit 1537

— et V. Cordiş, Une nouvelle synthèse de l'acide phospho-12-vanadique au moyen des échangeurs d'ions 559

— et N. Pascu, A. Ungureanu, V. Cordiş, Contribution à l'étude de la cyanuration et du conditionnement des minerais aurifères de type Baia de Arieş 719

— et A. Şuteu, Utilisation des hétéropolycombinaisons comme échangeurs d'électrons. IV. L'utilisation du phospho-8-molybdo-2-tungsto-2-vanadate de nitron comme échangeurs d'électrons 1039

Roman L., voir Ciobanu A.. 783

— voir Giurgiu D. 1581

Roman M., voir Balaban A.T. 635

Romaş E., voir Balaban A. T. . . . 635

Roşca S. and C. D. Nenitzescu, The resolution of enantiomeric aminoderivatives of arene-tricarbonylchromium (O) 259

page

S.

SAFTA M., voir OSTROGOVICH C. . . 799

SAHINI V. E. and C. BENDIC, M. DOBRESCU, Electronic structure and vapour spectrum of carbazole . . . 1795

— and M. CRAIU, Depolarization ratio of the Raman lines of molecules containing carbonyl group 675

— and M. DOBRESCU, On the carbonyl stretching frequency of halogen-substituted benzophenones 679

— and C. I. GHIRVU, Pariser-Par-treatment of substituted benzenes. II. Charge transfer configurations of the benzenesulphonic acid . . . 11

— voir GIOABĂ A. 309,501

— voir HILLEBRAND M. 149

— et C. PODINĂ, V. CONSTANTIN, L'étude des picolines par spectrométrie de masse 495

SCHELL H. D., voir RĂDULESCU T. . . . 1127, 1427

SCHNEIDER I. A., voir IOSIF I. 1827

— voir ODOCHIAN L. 1647

— voir VASILE C. 1935

SEGAL E., voir CHIRULESCU T. . . 67,1727

— voir CISMARU D. 161

— voir FĂTU D. 855

— voir MINCU V. 539

— voir TEODORESCU M.. 371

ŞERBAN C., voir AUSLÄNDER D. . . . 1441

SIDDIQUI M. S., voir ARSHAD M. . . . 1653

SIMIONESCU N., voir FELDMAN D. . . 1893

SIMON Z., voir BALINT A. 511

— voir OSTROGOVICH G. 1453

SIMONESCU T., voir DRĂGULESCU C.. . 563

— voir FIŞEL S.. 1043

SOFRONIE E. and E. TĂRĂBĂŞANU—MIHĂILĂ, C. TĂRĂBĂŞANU, Radiolytic oxidation of acenaphthene to naphthalic acid on the acenaphthene-potassium permanganate-pyridine system 1913

SOLACOLU Ş. et P. BALTĂ, G. JITIANU, L'analyse elcothermique — méthode d'étude des transformations structurales dans les verres 741

— and P. BALTĂ, G. JITIANU, The influence of phosphorous pentoxide on the crystallization process of some lithium silicate glasses . . . 957

— and P. BALTĂ, G. JITIANU, The kinetics of changes of the vitreous structures in some lithium-silicate glasses 91

pag

— et A. BĂRBULESCU, La détection des réactions ayant lieu dans les mélanges oxydiques pulvérulents du système $La_2O_3-TiO_2-ZrO_2$ par la mesure de la résistance électrique 1851

— und R. DINESCU, M. ZAHARESCU, Die thermischen Phasengleichgewichte des Systems $BaO-TiO_2-V_2O_5$ 401

SPACU P. and E. ANTONESCU, Complexes of lanthanide halogenoacetates with 1,10-phenanthroline and 2,2'-dipyridyl 731

SPINZI A. et NICOLESCU I. V., Propriétés physico-structurales des catalyseurs utilisés à l'oxydation des hydrocarbures. III. Propriétés électriques des systèmes oxydiques à base de $V_2O_5-MoO_3-P_2O_5$ par rapport au milieu de réaction 451

— et I. V. NICOLESCU, Propriétés physico-structurales des catalyseurs utilisés pour l'oxydation des hydrocarbures. IV. Propriétés électriques des systèmes oxydiques à base de $V_2O_5-Ga_2O_3$ 1901

STANCIU-STOIAN E. and I. VLAGIU, I. PETRUŞ, E. NICULESCU, Radiochemical grafting of acrylonitrile on textile material in heterogeneous system 1077

STERNBERG S. et I. GALAŞIU, L'électrode halogène — charbon dans les électrolytes fondus. VI. L'adsorption du chlore et de l'iode sur l'électrode de charbon activé 1169

— and C. HERDLICKA, Interdiffusion coefficient of silver ion in molten alkali nitrates by the chronopotentiometric method. 343

— and M. TERZI, The surface tension of binary molten mixtures of silver chloride with sodium and potassium chloride 527

— voir VASILESCU V. 1819

— and V. VASILESCU, Ultrasonic velocity, compressibility and excess volume of molten salts: NaCl+(Li, K, Rb, Cs)Cl 1665

STOICESCU-CRIVETZ L. et E. MĂNTĂLUŢĂ, I. ZUGRĂVESCU, Polyhydantoïnes-Triazines 129

STRUSIEVICI C., voir LUKÁCS I. . . . 935

SURDEANU V., voir RADOVICI O. . . 1153

ŞUTEU A. und I. AL. CRIŞAN, E. MÎNDRUŢIU, Die kinetische Bestimmung des Hydrazins mit Bromat und Amidol 1187

— und I. AL. CRIŞAN, E. POP, Die

page

kinetische Bestimmung des Kupfers(II) mit Bromat und Amidol . . 1337
— voir Hodişan T. 615
— und C. Maniu, Kolorimetrische Bestimmung des Hydrazins mit Phosphomolybdowolframsäure. . . 119
— et L. Mîrza, L'étude röntgenostructurale des trihétéropolyacides . 1563
— and H. Naşcu, Catalytic determination of vanadium V(V) with amidol 1759
— voir Ripan R. 1039
Szabadai Z., voir Dick J. 917
Szabo A., voir Popescu A. 1197
— voir Popper E. 1447
Szabo M., Le marquage du dipholatan avec ^{35}S par synthèse 1137
— Szentgyörgyi P., voir Popper E. 1447
Szotyori L. and L. Fey, Al. Kövendi, The reaction between sodium alcoxides and α-haloketones. VII. The action of sodium methoxide on p-chloro-ω-bromoacetophenone . . . 1615
Szurkos A., voir Nagy P. 881
— and P. Nagy, A polarographic study on styrilcyanines. I. Substituent effects in the polarographic reduction of the styrilcyanines according to Brown-Okamoto equation 607

T.

Tămaş V. and C. Bodea, $TiCl_4$-carotenoid complexes. VII. Action of $TiCl_4$ on 5,8-epoxy-carotenoids (5,8-epoxy-β-carotene, 5,8-epoxy-cryptoxanthin and 5,8-epoxy-zeaxanthin) . 655
— and C. Bodea, $TiCl_4$-Carotenoid complexes. VIII. Cyclization of lycopene and δ-carotene 819
Tărăbăşanu C., voir Reichel J. . . . 1907
— voir Sofronie E. 1913
Tărăbăşanu-Mihăilă E., voir Sofronie E. 1913
Telea Cr., voir Marchidan D. I. . . 1675
Teodorescu A., voir Fătu D. . . . 855
Teodorescu M. and E. Segal, The effect of pretreatment on the electrical resistance variation of zinc oxide thin films, under irradiation and carbon monoxide chemisorption . 371
Teoreanu I. and Tran van Huinh, The mineralizing influence of apatite on the formation of portland cement clinker 229
Terzi M., voir Sternberg S. 527
Ţilenschi S. und A. Wohl, Prinzipielles über die Wirksamkeit einiger Reinigungsmethoden durch Adsorption 1017
Todor D. M., voir Popa Gr. 589
Todor-Bogdan D., voir Murgulescu I. G. 1473
Tomuş E. J., Heat of dilution of aqueous solutions of potassium, silver and lead nitrates. 377
Topor D., voir Murgulescu I. G. . . 843
Topor L., voir Murgulescu I. G. . 997
Totan M., voir Drăgulescu C. . . . 563
— voir Fişel S.. 1043
Totir N., voir Radovici O. 683
Tran van Huinh, voir Teoreanu I. 229
Trinajstić N., voir Bodor N. . . . 1807
Tucsek V., voir Radovici O. 325
Tudor L., Radiolysis processes in aqueous solution of KI in the presence of KH_2PO_4 and $NaNO_3$ . . 553

U.

Ungureanu A., voir Ripan R. . . . 719

V.

Vanghelovici M., voir Demetresco C. 1623
Vargha E., voir Balog A. . . . 1375, 1391
Várhelyi Cs., voir Macarovici Const. Gh. 895
— voir Zsakó J. 865
Vartires I., On the standard potential of thin lead films 1699
Vasile C. et A. Onu, I. A. Schneider, L'étude thermodynamique des solutions de PVC 1935
Vasilescu V. voir Sternberg S. . . 1665
— and S. Volkov, S. Sternberg, Ultrasonic velocity, compressibility and excess volume for binary mixtures of molten salts : $NaCl+ZnCl_2$, $KCl+ZnCl_2$ 1819
Vass M. I., The influence of rapid temperature changes on the surface potential variation in the system oxygen-thin copper films 1689
— voir Murgulescu I. G. . . . 489, 1143
Vasu G., Thermal conductivity of real dense fluids : hard sphere approximation. 1011

page

Vasu L., voir Murgulescu I. G. . . 837

Vidac R., voir Reichel J. 1107, 1227

Vîlcu R. and Al. Bîrhală, Differential vapour-pressure measurements and the thermodynamic properties of benzil-CCl_4, benzil-$CHCl_3$, biphenyl-CCl_4 and biphenyl-$CHCl_3$ solutions 175

— and Al. Bîrhală, Vapour pressure osmometry. Thermodynamic properties of naphthalene and anthracene in $CHCl_3$ and naphthalene in CCl_4 solutions 1813

— and F. Irinei, Excess functions for mixed electrolyte solutions . . 43

— and C. Misdolea, Excess thermodynamic functions for liquid binary mixtures of some alkali metals . . 1839

Vlagiu I., voir Stanciu-Stoian E. . 1077

Vlassa M., voir Ionescu M. 1785

Vodnar I., Decomposition of hydroperoxides on activated kaolins. II. Decomposition of cumene hydroperoxide on activated Chinese kaolin, in static conditions 1947

Voicu V., voir Furnică Gh. 1087

Voiculescu N., voir Ciobanu A. . . 783

— voir Giurgiu D. 1581

Volkov S. V., voir Popa E. 1707

— voir Vasilescu V. 1819

Volanschi E., voir Gioabă A. . . . 309, 501

W.

Wohl A., voir Ţilenschi S. 1017

page

Z.

Zaharescu M., voir Solacolu S. . . 401

Zervudis S., voir Cismaru D. . . . 1163

Zsakó J., Kinetic analysis of thermogravimetric data. II. Improvement of T. Ozawa's integral method . . 693

— and E. Kékedy, Cs. Várhelyi, Kinetics and mechanism of substitution reactions of complexes. XIX. Influence of heating rate on the thermal decomposition of $[Co(DH)_2(amine)_2]$ I type complexes in the conditions of thermogravimetric analysis 865

Zuca Şt., Viscosity of some molten nitrates. 1277

— and R. Borcan, Viscosity of molten (Li−K)Cl mixtures 1681

— and R. Costin, Viscosity of some molten alkaline earth chlorides . . 1831

— and M. Olteanu, The electrical conductivity of binary molten alkali chloride systems as a function of anion polarization 357

— and M. Olteanu, Electrical conductivity of binary molten alkali halide systems as a function of anion polarization 1503

Zugrăvescu I., voir Caproşu M. . . . 619

— voir Chiriac C. 789, 1065, 1201

— voir Stoicescu-Crivetz L. . . 129

INDEX DES SUJETS

A.

— Absorption spectra of $CoCl_2$ and $CoBr_2$ isolated in benzene matrix, M. Musa 705

— Acetamido-benzal-fluoren, Quartäre Ammoniumsalze des —, T. Rădulescu und H. D. Schell . 1127

— Acide phospho-12 vanadique, l'—, R. Ripan et V. Cordiş 559

— Acridone. XXXV., M. Ionescu, I. Goia 1233

— Acridone. XXXVI., M. Ionescu, I. Goia and M. Vlassa 1785

— Activity coefficients in ternary systems, C. Beldie 221

— Adsorption von Kohlenmonoxid an dünnen Silberschichten, I. G. Murgulescu und G. Comşa 987

— Adsorptive properties of a nickel ferrite, T. Chirulescu and E. Segal 1727

— Aluminium complexes with pyrogallol, Formation of—, T. Goina and M. Olaru 1547

— Aluminium hydroxides, Physico-structural properties of—, M. Gruia, O. Körner and A. Nicolescu . . 457

— Amino-derivatives of arene-tricar-

page

bonyl-chromium (O), S. Roşca and C. D. Nenitzescu 259
— Analyse elcothermique dans les verres, L'—, Ş. Solacolu, P. Baltă et G. Jitianu 741
— Anodic behaviour of pure aluminium, The—, E. Constantinescu and T. Marian 333
— Anodic oxydation of acetylene and methane, The—, O. Radovici and N. Totir 683
— Apatite, The mineralizing influence of—, I. Teodoreanu and Tran van Huinh 229
— Arylaluminium-Phosphin Verbindungen, D. Giurgiu, I. Popescu, A. Ciobanu, M. Bostan, N. Voiculescu und L. Roman 1581
— Aryldiazosulfonate und Aryldiazosulfonsäuren. I., II., J. Reichel und R. Vidac 1107, 1227
— Association moléculaire des iodures alcalins, L'—, I. G. Murgulescu et L. Topor 997
— Automatic ratemeter, E. Cordoş . 661
— Automatic titration in molten media. I., C. Liteanu, E. Cordoş und L. Mărgineanu 583
— Azauracil derivatives. IX., C. Cristescu 1121

B.

— Benzal-fluoren, Mono- und diquartäre Ammoniumsalze des— T. Rădulescu und H. D. Schell . . . 1427
— Benzenes. II., Priser-Parr treatment of substituted—, V. E. Sahini and C. I. Ghirvu 11
— Benzyl bromide and alkali alcoxides, Reactions between—, I. G. Murgulescu and D. Oancea . . . 299
— Benzyl bromide and normal alcohols, The kinetics of the reactions between—, I. G. Murgulescu and I. Demetrescu 141
— Butadiene-styrene carboxylated copolymers, D. Feldman, N. Simionescu, C. Ciubotariu, M. Ciubotariu, T. Crişan and G. Dressnandt 1893

C.

— Calcium apatites, The cell parameters of synthetic —, V. M. Bhatnagar 1735

page

— Carbonyl stretching frequency, On the—, V. E. Sahini and M. Dobrescu 679
— Carotenoids. I., Inchain epoxides on—, E. Nicoară, D. Oşianu and C. Bodea 965
— Catalyseurs pour l'oxydation des hydrocarbures. III., A. Spinzi et I. V. Nicolescu 451
— Catalyseurs pour l'oxydation des hydrocarbures. IV., A. Spinzi et I. V. Nicolescu 1901
— Catalytic determination of vanadium V(V) with amidol, A. Şuteu and H. Naşcu 1759
— Charge transfer complexes of the aromatic heterocycles. I., M. Hillebrand, O. Maior and V. E. Sahini 149
— Charge transfer complexes of the aromatic heterocycles. II., A. Gioabă, V. E. Sahini and E. Volanschi . . 309
— Chelates with pyrocatechol and pyrocatechol violet, T. Goina, M. Olariu and L. Bocaniciu 1049
— Chemical graphs. VIII., A. T. Balaban 463
— Chemical graphs. X., A. T. Balaban 1243
— Chemical graphs. XI., A. T. Balaban 1251
— Chemical reactions in liquid junctions. I. N. Bonciocat, L. Chiosa, F. Mihăilescu and M. Olteanu . . 1307
— Chemical reaction in liquid junctions. II., N. Bonciocat, L. Chiosa, F. Mihăilescu and M. Olteanu . . 1513
— Chimisorption par des mesures de force thermoélectromotrices, D. Cismaru, E. Segal et S. Fătu . . 161
— Cobalt, Microanalysis of—, E. Popper, A. Szabó and P. Szentgyörgyi . . 1447
— Cobalt (II) complexes of adipyl dihydrazide, M. Arshad, A. Beg and B. Bilquis 1857
— Cobalt corrosion process, The kinetics of—, O. Radovici and M. V. Popa 515
— Cobalt traces. I., Kinetic measurement of—, D. Costache and P. Junie 597
— Cobalt traces. II., Kinetic determination of—, D. Costache and Gr. Popa 761
— Cobalt traces. III., Kinetic measurement of—, D. Costache . . . 945
— Cobalt traces. IV., Kinetic measurement of—, D. Costache . . . 1181
— Cobalt traces. V., Kinetic determination of—, D. Costache and Gr. Popa 1349

page

— Cobalt in vitamine B_{12}, Kinetic dosing of the —, D. Costache and Gr. Popa 1061
— Combinaisons complexes avec des hydroxyacides. XIV., L. Czeglédi et Const. Gh. Macarovici 1741
— Combinaisons zinc-diaryl-amides. II., A. Ciobanu, L. Roman, N. Bostan, N. Voiculescu et D. Giurgiu . . . 783
— Complexes cuivre-aniline substituée, L'effet catalytique des —, Al. Fruma, D. L. Crăciunescu et C. I. Ghirvu 71
— Complexes of lanthanide halogenoacetates, P. Spacu and E. Antonescu 731
— Complexes moléculaires des thioamides. I., F. Cornea, C. Fulea et S. Moldoveanu 1415
— Complexes thiocyanato-chromiques dans l'analyse chimique. I., I. Gănescu et Al. Popescu 1343
— Coordination polymers. III., M. Marcu and M. Dima 423
— Coordination polymers. IV., M. Marcu and M. Dima 1365
— Copolymers of conjugated dienes with maleic acid monoesters. I., I. Nanu and C. Andrei 1883
— Copper traces, Photometric determination of —, M. Macovschi and V. Niţu 605
— Corrosion and passivity of some Pb—Sn alloys, O. Radovici and B. Popescu 1799
— Crystal structure of solid solutions, D. Cismaru and D. Manolescu . . 291
— Cyanuration des minérais aurifères, La —, R. Ripan, N. Pascu, A. Ungureanu et V. Cordiş . . . 719
— Cyclobutane series. XXVII., Investigations in the —, M. Avram, D. Constantinescu, I. G. Dinulescu, O. Constantinescu-Simon, Gh, D. Mateescu and C. D. Nenitzescu . 1097
— Cyclobutane series. XXVIII, Investigations in the —, M. Avram, I. Pogany. I. G. Dinulescu, F. Chiraleu and C. D. Nenitzescu . . 1207
— Cyclobutane series. XXIX, Investigations in the —, M. Avram, F. Chiraleu and I. Pogany. 1219
— Cyclobutane series. XXX. Investigations in the —, M. Avram, F. Chiraleu, I. Pogany and I. G. Dinulescu 1767

D.

— Décomposition thermique des halogénures complexes, D. Fătu, S. Fătu, A. Teodorescu et E. Segal 855

page

— Déhafnisation, Variations de certaines propriétés du $K_2Zr(Hf)F_6$ par —, I. Arsenie et I. Leucă 1987
— Depolarization ratio of the Raman lines. V. E. Sahini and M. Craiu . 675
— 3,6-Dichloro-2,5-bisphenyl-amino-1,4-benzoquinone derivatives, A. Balint 627
— 3,7-Dichlorphenthiazins, Über die Darstellung des —, D. Christov und N. Nenov 1777
— Dicyanoaurous acid-isoamyl alcohol — water, The study of the system —, V. Armeanu and L. M. Băloiu 1057
— Differential vapour — pressure measurements, R. Vîlcu and Al. Bîrhală 175
— Dilitursäure mit Anilin, Verbindungen der —, Fr. Mihai und R. Nuţiu 573
— 2,4-Dioxo-6-(*p*-X-β-styryl-tetrahydro-s-triazine, G. Ostrogovich und M. Safta. 799
— Dipholatan à ^{35}S par synthèse, Le marquage du —, M. Szabo . . . 1137
— Donnor-acceptor complexes of N-substituted maleimides, The —, M. Fărcaşu and R. Istrăţoiu 253
— Dosage photométrique du benzène et de la *m*-phenylènediamine, G. Ciuhandu et M. Mracec 757

E.

— Electrical conductivity of binary molten alkali chlorides, Şt. Zuca and M. Olteanu 357
— Electrical conductivity of binary molten alkali halide systems, Şt. Zuca and M. Olteanu 1503
— Electrical conductivity and diffusion in molten salts, I. G. Murgulescu and L. Vasu 837
— Electrical conductivity of lyophilic colloids. XI., M. Radu 767
— Electrode halogène-charbon dans les électrolytes fondus. VI., L'—, S. Sternberg et I. Galasiu 1169
— Electrodes membranes polymère + plastifiant. I., C. Liteanu et E. Hopîrtean 749
— Electrodes-membranes polymères + plastifiant. III., C. Liteanu et E. Hopîrtean 1331
— Electrolyte pâteux dans les accumulateurs électriques, L' —, S. Lică 543
— Electrolyte solutions, Excess functions for mixed —, R. Vîlcu and F. Irinei 43
— Electromigration dans les nitrates monovalents fondus, I. G. Murgulescu et D. Topor 843

page

— Electron spin resonance study of the oxidation of some aromatic amines, F. M. Albert and A. Meghea 395
— Electronic absorption spectra of $ZnCl_2$, $CdCl_2$ and AgCl, E. Popa, E. Ivana, and S. V. Volkov 1707
— Electronic structure of aluminium borohydride, The —, K. A. Levison and P. G. Perkins 153
— Electronic structure and vapour spectrum of carbazole, V. E. Sahini, C. Bendic and M. Dobrescu 1795
— Electrostatic energy in reactions between benzhydril chloride and normal alcohols, The effect of —, I. Demetrescu 1721
— Elovich equation, On the —, N. I. Ionescu 1847
— Equivalence point. V., The use of membranes to indicate the —, C. Liteanu and C. I. Popescu 973
— Evidence of neighbour cation influence, J. Máthé 283
— Excess thermodynamic functions for liquid binary mixtures of some alkali metals, R. Vîlcu and C. Misdolea 1839
— Extraktion von Th(IV), C. Drăgulescu, T. Simionescu, G. Nemes und M. Totan 563

F.

— Fluoropotite, The cell parameters of synthetic —, V. M. Bhatnagar 87
— *p*-Fluordiphenylsulfones. I., Al. Mavrodin, C. Demetrescu, C. Chiriță et O. Macovschi 1953
— Furan(VI), Eine neue kalorimetrische Bestimmungsmethode des —, T. Hodișan, A. Șuteu und V. Gorea 615

G.

— Gas chemisorption on ferromagnetic powder. IV., T. Chirulescu and E. Segal 67
— Graphting of maleic anhydride on ethylene vinyl acetate, C. Andrei, M. Mihăiță, I. Hogea and D. Munteanu 239

H.

— Heat of dilution of aqueous solutions of nitrates, E. J. Tomuș 377
— Heteroaromatic system, Condensed, A. Gioabă and O. Maior 1967
— Heterocycles, IX., Methylene bases of —, Gh. Ciurdaru, M. Fărcășan and V. I. Dénes 1975
— Heterocyclic organoboron compounds, XXII., A. T. Balaban, A. Arsene, I. Bally, A. Barabas, M. Paraschiv, M. Roman and E. Romaș 635
— Hétéropolycombinaisons comme échangeurs d'électrons. IV, R. Ripan et A. Șuteu 1039
— Heteropolyverbindungen des U(IV). I., II Eine neue Gruppe von —, R. Ripan und A. Botar 1529, 1537
— High temperature thermodynamic properties of some uranium oxides, D. I. Marchidan and S. Matei 1491
— Hydrazin, Die kinetische Bestimmung des, A. Șuteu, I. Al. Crișan und E. Mîndruțiu 1187
— Hydrazydes à action pharmacodynamique, Nouvelles —, C. Demetrescu, V. Manu et M. Vanghelovici 1623
— Hydroacridine. VII., Darstellung und Untersuchung der —, N. Bărbulescu und F. Potmischil 1601
— Hydrogen bonds. III., I. I. Bădilescu 873
— Hydrogen obervoltage on thin evaporated metal films. II., O. Radovici and M. Macovschi 167
— Hydrolyse alcaline de l'acétate de *n*-butyle, L'—, G. Costeanu, O. Landauer et C. Mateescu 27
— Hydroperoxides on activated kaolins. II., Decomposition of —, I. Vodnar 1947
— Hydroxyacides. XV., Combinaisons complexes avec des —, Const. Gh. Macarovici et L. Czeglédi 1863

I.

— Imine systems. III., Stereochemistry of —, G. Ostrogovich, Z. Simon and F. Kerek 1453
— Indigoiden Serie II., Forschungen in der —, J. Reichel und C. Tărăbășanu 1907
— Interdiffusion coefficient of silver ion in molten salts, S. Sternberg and C. Herdlicka 343

page

— Intermédiaires instables. I., L'étude des —, M. Fiti 77
— Ions radioactifs par les macromolécules inorganiques, Rétention de certains —, Gh. Furnică et V. Voicu 1087

K.

— Kinetic analysis of thermogravimetric data. II., J. Zsakó 693
— Kinetics of the Al_2O_3+CoO reaction in oxygen atmosphere, D. Cismaru and S. Zervudis 1163
— Kinetics and mechanism of substitution reactions of complexes. XIX., J. Zsakó, E. Kékedy and Cs. Várhelyi 865
— Kolorimetrische Bestimmung des Hydrazins, A. Şuteu und C. Maniu 119
— Komplexverbindungen der Pyrazolonreihe. VI., Neue —, J. Dick und A. Maurer 103
— Kupfer(II) mit Bromat und Amidol, Die kinetische Bestimmung des -s, A. Şuteu, I. Al. Crişan und E. Pop 1337

L.

— Lead apatites, New observations on —, V. M. Bhatnagar 955
— Lithium silicate glasses, Crystallization of —, S. Solacolu, P. Baltă and G. Jitianu 957
— Lithium-silicate glasses, Vitreous structures in some —, S. Solacolu, P. Baltă and G. Jitianu 91

M.

— Macromolécules polysulfoniques, La dégradation des —, Gh. Furnică . . 1591
— Magnetic exchange in a heterogeneous trinuclear system, D. Lupu . . 417
— Mélanges oxydiques pulvérulents du système $La_2O_3-TiO_2-ZrO_2$, S. Solacolu et A. Bărbulescu . . 1851
— Metal particles size determination in hydrogen chemisorption measurements, D. Cismaru, Al. Fruma and D. Crăciunescu 1485
— Metallic oxides mixtures influence, A. Popescu and A. Szabo . . . 1197
— Metallkomplexe der Anthranyldiessigsäure (ANDA). VIII., C. Drăgulescu, R. Pomoje, I. Menessy, M. Pîrlea und C. Mihăescu . . . 1029
— Metallkomplexe der Anthranylessigsäure (ANDA). IX., C. Drăgulescu, R. Pomoje, I. Menessy und M. Pîrlea 1543

page

— Methane cracking kinetics in static conditions. I., L. Odochian and I. A. Schneider. 1647
— Methane oxidation, On the cool flame in the reaction of —, I. Iosif and I. A. Schneider 1827
— Méthyl-10-phénothiazines, Sur la formylation de —, V. Fărcăşan, I. Oprean et C. Bodea 1433
— 1-Méthyl-phtalazine, L'addition des philodiènes sur la —, M. Caproşu, M. Petrovanu et I. Zugrăvescu . . 619
— Molar absorptivity and stability of some complex compounds, I. Paralescu 901
— Molecular orbital calculations in the 2,5-diamino-1,4-benzoquinone series. III., A. Balint, Z. Simon and M. Mracec 511
— Molecular weight from salting-in data, C. Beldie 1191
— Molten (Li—K) Cl mixtures, Viscosity of —, Şt. Zuca and R. Borcan 1681
— Molten salts, Heat of mixing in binary systems of —, D. I. Marchidan and Cr. Telea 1675
— Molten salts. II., Physico-chemical properties of simple —, I. G. Murgulescu 1463
— Molten salts, Ultrasonic velocity and compressibility for binary mixtures of —, V. Vasilescu, S. Volkov and S. Sternberg 1819
— Molten salts, Ultrasonic velocity, compressibility and excess volume of —, S. Sternberg and V. Vasilescu 1665

N.

— New synthetic chemical compounds with schistosomicidal activity, S. H. Doss and M. S. Ahmad 1611
— Nickel ferrite-oxygen magnetization — volume adsorption isotherm, T. Chirulescu 1303
— 3-Nitro-10-methyl-phenothiazine, I. Oprean, C. Bodea and V. Fărcăşan 135
— Nucleophilic substitutions. III., I. G. Murgulescu and D. Oancea . . 1635

O.

— Organophosphorus compounds, Spectroscopic studies of —, M. Arshad, A. Beg and M. S. Siddiqui . . . 1653
— Oxalato-complexes decomposition, Intermediate in the —, T. Oncescu 209
— Oxazolidone — (4). VIII., M. Ionescu und K. Makkay 265
— Oxygen chemisorption on copper and silver films, N. I. Ionescu 273

page

P.

— Passivity of steel in monoethanoamine solutions, O. Radovici and V. Surdeanu 1153
— Peptides. VIII., A. Balog, D. Breazu, E. Vargha, F. Gönczy and L. Beu 1375
— Peptides. IX. A. Balog, E. Vargha, D. Breazu, L. Beu and F. Gönczy 1391
— Phasengleichgewichte des Systems BaO$-$TiO$_2$$-V_2O_5$, Die —, S. Solacolu, R. Dinescu und M. Zaharescu 401
— Phenothiazine glycosides. III., Synthetical —, C. Bodea, T. Panea and V. Fărcăşan 1923
— Phenothiazone—(3). III., Volumetric dosage with —, M. Răileanu and E. Dobre 823
— Phenoxatellurine, Spectral study of —, A. Gioabă, V. E. Sahini and E. Volanschi 501
— 1-Phenyl-azo-2-naphthol and copper chloride, Reaction between —, I. G. Murgulescu and D. Todor-Bogdan 1473
— Photocolorimetric study of Pd(II) and the α-ethyl-isonicotinic acid thioamide, E. Popper, L. Chiorean and I. Pitea 115
— Picolines par spectrométrie de masse, L'étude des —, V. E. Sahini, C. Podină et V. Constantin . . . 495
— Polarographische Untersuchung der Reaktion zwischen der Pentachloro-aquo-platin (IV)-Säure und 1,2-Cyclohexandiondioxim, Const. Gh. Macarovici, F. Mánok und Cs. Várhelyi 895
— Polarography of substituted azobenzenes, P. Nagy, I. Görbe and A. Szurkos 881
— Polyelectrolytes. II., Quaternary basic ammonium —, I. Petrariu, C. Luca and M. Dima 1573
— Polyhydantoïnes-Triazines, L. Stoicescu-Crivetz, E. Măntăluţă et I. Zugrăvescu 129
— Polymères organiques phosphorylés. III., Fl. Popescu 1355
— Polypropylene, Photo-oxydative degradation of —, L. Balabán and L. Preisler 123
— Potential distribution at the silicon-hydrofluoric acid interface, O. Radovici and V. Tucsek 325
— Potentiometric titrations. II., Pretreated indicating electrodes in —, C. Liteanu and I. Haiduc. . . . 1555
— Propriétés magnétiques des combinaisons complexes, V. Mincu et E. Segal 539
— Pyrazoles. I., II., III., C. Chiriac et I. Zugrăvescu 789, 1065, 1201
— Pyrazolonreihe. VII. Neue Komplexverbindungen der —, J. Dick, A. Maurer und Z. Szabadai . . . 917

R.

— Radiochemical grafting of acrylonitrile, E. Stanciu-Stoian. I. Vlagiu, I. Petruş and E. Niculescu . . 1077
— Radiolysis of the hexamminocobaltic nitrate, I. G. Murgulescu and I. Mihalcea 3
— Radiolysis processes in aqueous solution of KI, L. Tudor 553
— Radiolytic oxidation of acenaphthene to naphthalic acid, E. Sofronie, E. Tărăbăşanu-Mihăilă and C. Tărăbăşanu 1913
— Reinigungsmethoden durch Adsorption. Die Wirksamkeit einiger —, S. Ţilenschi und A. Wohl . . . 1017

S.

— Salt effects in furfural-water-electrolyte systems. I., C. Beldie and F. Bărbulescu. 385
— Salt effects in furfural-water-electrolyte systems. II., C. Beldie and F. Bărbulescu 847
— Schiff base complexes of Ti(IV), N. S. Biradar and V. H. Kulkarni 1993
— Selbstdiffusion des flüssigen Tellurs, E. Nicoloiu, L. Ganovici und I. Ganovici 1713
— Sélénocyanates dihydrazino-phtalazino-métalliques, Les —, I. Grecu et E. Curea 409
— Self-diffusion of liquid bismuth, N. Petrescu and M. Petrescu . . 189
— Self-diffusion of liquid cadmium, I. Ganovici and L. Ganovici. . . 213
— Séparation du zirconium d'avec le hafnium, I. Arsenie et I. Leucă . 1263
— Siderite and ankerite content, Determination of the —, Gr. Popa and D. M. Todor 589
— Simultaneous vibrational transitions. II., S. Bădilescu 1931
— Sodium alcoxides and α-haloketones. VII., The reaction between —, L. Szotyori, L. Fey and Al. Kövendi 1615
— Solid media. II. Reactions in —, I. Petruş 53

page

— Spectre d'absorption des halogénures de plomb fondus, Le —, I. G. MURGULESCU, E. POPA et E. IVANA 669
— Spectres électroniques d'ions complexes cyanes de fer, O. BENALI BAITICH, M. MEKLATI et M. ACHOUR . 15
— Spectrophotometrische Untersuchung im System $Th(NO_3)_4$ - Violursäure, F. POPEA und A.-C. BANCIU 1319
— Standard potential of thin lead films, On the, — I. VARTIRES 1699
— Strontium hydroxyapatite, The cell parameters of —, V. M. BHATNAGAR 951
— Structure of molten $LiF-AlF_3$ and $NaF-AlF_3$ mixtures, M. PAUČIROVÁ, K. MATIAŠOVSKÝ and M. MALINOVSKÝ 201
— Styrilcyanines. I., A polarographic study on —, A. SZURKOS and P. NAGY 607
— Substituent effects on the protonization of azoderivatives, V. NEMES, I. GÖRBE and P. NAGY 711
— Sulphuric ester of poly(vinyl alcohol), IG. POINESCU, S. MAXIM and A. CARPOV 441
— Surface-active cationic substances. II., I. MÎNDRU 775
— Surface potential variation at CO and O_2 adsorption on silver films, I. G MURGULESCU and M. I. VASS . . . 1143
— Surface potential variation during nitrogen adsorption, I. G. MURGULESCU and M. I. VASS 489
— Surface tension of binary molten mixtures, The —, S. STERNBERG and M. TERZI 527

T.

— Temperature changes on the surface potential variation, M. I. VASS . . 1689
— Thermal conductivity of real dense fluids, G. VASU 1011
— Thermal properties of aluminium, D. I. MARCHIDAN and M. CIOPEC . . 1005
— Thermal properties of potassium chloride, D. MARCHIDAN and M. CIOPEC 1177
— Thermochromatographie sur papier. XIV., La —, C. LITEANU, S. GOCAN et T. HODIŞAN 1751
— Thermodynamic functions of some materials from the uranium-oxygen system, D. I. MARCHIDAN and M. CIOPEC 1287
— Thermodynamic properties of li- [illegible] magnesium-lead alloys, H. NEBELL 59
— Thermodynamics of the behaviour of the Pb(II)-ions, Z. PAVLOVIĆ and R. POPOVIĆ 313
— Thermodynamique des solutions de PVC, L'étude —, C. VASILE, A. ONU et I. A. SCHNEIDER . . . 1935
— Thoriumextraktion aus wäßrigen Lösungen mit Butanol-1, Der Einflu der Trichloressigsäure auf die —, S. FIŞEL, G. NEMEŞ, M. TOTAN und T. SIMONESCU 1043
— $TiCl_4$-Carotenoid complexes. VII., VIII., V. TĂMAŞ and C. BODEA . . . 655, 819
— Titrage conductométrique à résistance indicatrice. II., C. LITEANU et L. GHERGARIU-MÎRZA 1871
— Triazine derivatives. X., C. CRISTESCU 1409
— Trihétéropolyacides, L'étude röntgéno-structurale des —, A. ŞUTEU et L. MÎRZA 1563
— Tropolone, Reaction of ethyl *o*-phenylene arsenite with —, A. ARSENE, M. PARASCHIV and A. T. BALABAN . . 247
— Ultrasons sur un processus de carbonatation, Action des —, D. AUSLÄNDER, C. ŞEREAN et I. DĂBALĂ . 1441
— UV irradiation of UMP on paper, O. L. HÖRER and M. BADEA . . . 829

V.

— Valence-shell MO calculations for formamide and related compounds, N. BODOR and N. TRINAJSTIĆ . . 1807
— Vanadates. XVIII., I. LUKÁCS, C. STRUSIEVICI et C. LITEANU 935
— Vapour pressure osmometry, R. VÎLCU and AL. BÎRHALĂ 1813
— Viscosité de structure du stéarate d'aluminium, G. POPESCU 431
— Viscosity of some molten alkaline earth chlorides, ŞT. ZUCA and R. COSTIN 1831
— Viscosity of some molten nitrates, ŞT. ZUCA 1277
— Volume properties of the $LiF-AlF_3$ and $NaF-AlF_3$ mixtures, M. PAUČIROVA, K. MATIAŠOVKÝ and M. MALINOVSKÝ 33

W.

— Wärmeübergangszahlen von Kaliumnitratlösungen, Z. CROPŞIANU, D. KOHN und A. IOVI 887
— Water chemisorption in iron films, N. I. IONESCU 1525

Z.

— Zinc oxide thin films, The effect of pretreatment of —, M. TEODORESCU and E. SEGAL 371

NOTE POUR LES AUTEURS

La *Revue Roumaine de Chimie* publie des articles en anglais, français, russe, allemand ou espagnol. Les auteurs sont priés d'envoyer des articles, notes, communications et comptes rendus inédits.

Les manuscrits seront dactylographiés à deux intervalles. Les tableaux seront dactylographiés sur feuilles séparées, de même que la légende des figures. Les diagrammes seront tracés à l'encre de Chine sur papier calque. Les tableaux et les figures seront numérotés par des chiffres arabes, en nombre strictement nécessaire. Prière de ne pas inscrire les mêmes données dans les tableaux et les figures. Les formules chimiques seront incluses dans le texte ; en outre, elles seront transcrites sur des feuilles séparées. Les auteurs sont priés d'indiquer les caractères italiques (en soulignant les lettres au crayon), ainsi que tout autre caractère spécial. L'ordre des références bibliographiques sera celui de leur mention dans le texte ; le nom de l'auteur sera précédé de l'initiale du prénom ; les publications périodiques seront présentées suivant les prescriptions internationales. Les références seront ajoutées à la fin de l'article ; elles paraîtront comme des notes, au bas de la page. Le texte sera précédé d'un résumé, comprenant 15 lignes au maximum.

L'entière responsabilité du contenu des articles appartient aux auteurs. On publie des articles dus aux collaborateurs roumains ou étrangers. Les auteurs recevront 50 tirés à part.

PRINTED IN ROMANIA

1971 FEB 24

TRAVAUX PARUS AUX ÉDITIONS DE L'ACADÉMIE DE LA RÉPUBLIQUE SOCIALISTE DE ROUMANIE

CORNEL BODEA et collab., **Tratat de biochimie vegetală**, partea I, **Fitochimie** (Traité de biochimie végétale, Ire partie, Phytochimie), Ier vol., 1964, 747 p. + 4 annexes + 2 pl., 41 lei ; IIe vol., 1965, 1962 p., 1 pl., 56 lei ; IIIe vol., 1967, 773 p., 35 lei.

V. GHEŢIE et V. MICUŞAN, **Analiza imunochimică. Teorie şi practică** (Analyse immunochimique. Théorie et pratique), 1966, 369 p., 28 lei.

R. PORTOCALĂ et L. POPA, **Acizii ribonucleici celulari şi virali** (Les acides ribonucléiques cellulaires et viraux), 1966, 375 p. + 8 pl., 26 lei.

D. PURDELA et R. VÎLCEANU, **Chimia compuşilor organici ai fosforului şi ai acizilor lui** (La chimie des composés organiques du phosphore et de ses acides), 1965, 540 p., 37 lei.

CRISTOFOR SIMIONESCU, MARGARETA GRIGORAŞ et AGATA CERNĂTESCU-ASANDEI, **Chimia lemnului din R.P.R.** (La chimie du bois en Roumanie), 1964, 239 p. + 6 pl., 27 lei.

CRISTOFOR SIMIONESCU et CLEOPATRA VASILIU OPREA, **Mecanochimia compuşilor macromoleculari** (La mécanochimie des composés macromoléculaires), 1967, 344 p., 23,50 lei.

CARMEN SABĂU, **Schimbul ionic, teoria şi aplicaţiile sale în chimia analitică** (L'échange ionique, Théorie et applications à la chimie analytique), 1967, 307 p., 12 lei.

I. V. MAXIM, **Materiale nucleare** (Matériaux nucléaires), 1969, 444 p., 30 lei.

CR. SIMIONESCU, C. UGLEA, **Fracţionarea compuşilor macromoleculari** (Le fractionnement des composés macromoléculaires), 1969, 292 p., 18,50 lei.

I.P.I. — c. 5913

43 426

Lei 25.—